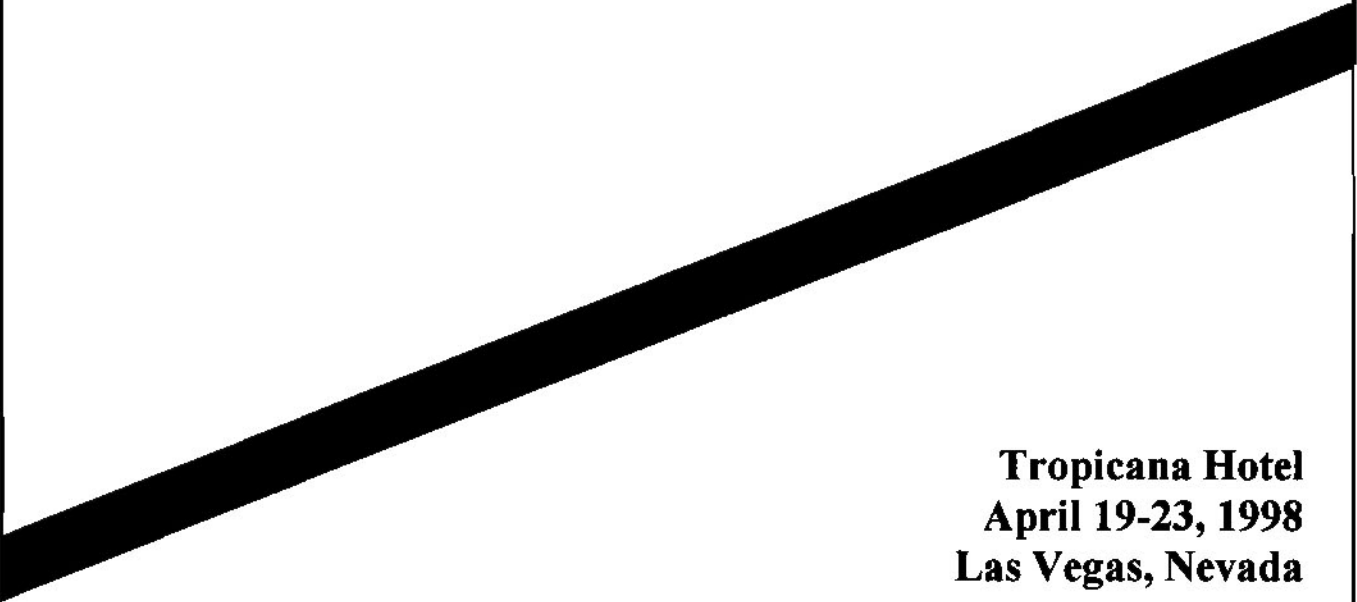


Proceedings of the First Federal Interagency Hydrologic Modeling Conference

*Theme: Bridging the Gap Between Technology and
Implementation of Surface Water Quantity and Quality Models
in the Next Century*



**Tropicana Hotel
April 19-23, 1998
Las Vegas, Nevada**

Prepared by the Subcommittee on Hydrology of the
Interagency Advisory Committee on Water Data

Proceedings of the First Federal Interagency Hydrologic Modeling Conference

*Theme: Bridging the Gap Between Technology and
Implementation of Surface Water Quantity and Quality
Models in the Next Century*

**Tropicana Hotel
April 19-23, 1998
Las Vegas, Nevada**

**Prepared by the Subcommittee on Hydrology of the
Interagency Advisory Committee on Water Data**

FOREWORD

The Federal Subcommittee on Hydrology published these proceedings and sponsored the associated First Federal Interagency Hydrologic Modeling Conference. The general purpose of the Subcommittee is to foster effective communication and collaboration for technical surface-water quantity activities. Representatives of more than a dozen Federal agencies participate on the Subcommittee. The Subcommittee currently sponsors or co-sponsors four subordinate groups: (1) the Flood Flow Frequency Analysis Work Group, (2) the Satellite Telemetry Interagency Work Group (STWIG) that is co-sponsored by the Interagency Coordination Committee on Meteorology and Supporting Research, (3) the Federal Hydrologic Radio Frequency Coordination Work Group, and (4) the Modeling Conference Work Group that planned this conference.

The Subcommittee is an interagency group that has operated within the Federal Government under a variety of authorities for about 50 years. In the early 1980's when the Reagan Administration disbanded the Water Resources Council, the Water Information Coordination Program (WICP) became the sponsor of the Subcommittee. Office of Management and Budget Memorandum No. 92-01 requires all Federal agencies to coordinate their water-information activities through the WICP and designates the U.S. Geological Survey to be the lead agency. The general purposes of the WICP are to ensure effective decision making for natural-resources management and environmental protection at all levels of government and in the private sector. Federal and non-Federal organizations that fund, collect, or use water-resources information work together to carry out the objectives of the WICP.

For additional information about the WICP and its committees and products, please write or telephone the Water Information Coordination Program, U. S. Geological Survey, 417 National Center, Reston, VA 20192. Telephone: (703)648-6832. Fax: (703) 648-5644. Information on the WICP is available on the World Wide Web at <<http://water.usgs.gov/public/wicp>>.

PREFACE

The Subcommittee on Hydrology, Interagency Advisory Committee on Water Data, held the Federal Interagency Workshop on Hydrologic Modeling Demands for the 90's in Fort Collins, Colorado, in June 1993. This highly successful workshop was limited to participants from various Federal agencies. One of the most significant products of the Workshop was a list of recommendations for Federal agencies to consider in implementing their hydrologic modeling research programs. Through the efforts of the Office of Water Data Coordination, some of these recommendations were adopted to guide interagency modeling activities since then. As we approach the 21st Century, we need new focus on hydrologic modeling techniques. The rapid advancement in computer and information technologies has profound effects on time and space scales of modeling. Not only is real-time modeling now a reality, modeling of large spatial scale watersheds with complex physical characteristics has also become practical. Federal agencies that are members of the Interagency Subcommittee on Hydrology expressed a strong desire to reconvene a modeling conference. The Subcommittee on Hydrology decided that this conference should be open to all interested parties and that the program should include models addressing surface water quality as well as quantity issues.

The primary purpose of the 1998 conference was to promote technology exchange among governmental agencies, academic institutions and private sectors in hydrologic modeling. The conference also provided opportunities for hydrologic modelers to share their existing models and exchange ideas of model development into the 21st Century. Major topics for the conference included new modeling systems from Federal agencies, hydrology, extreme events, river hydraulic and flow/stage forecasting, river and reservoir systems, erosion and sedimentation, and environmental/watershed. A model demonstration session was also incorporated in the program.

ACKNOWLEDGMENTS

Many people contributed to the success of the workshop. The following persons were responsible for the planning and organization of the workshop:

Ming T. Tseng, Conference Chair, U.S. Army Corps of Engineers, Washington, DC
Don Frevert, Technical Program Co-Chair, Bureau of Reclamation, Denver, CO
Don Woodward, Technical Program Co-Chair, Natural Resources Conservation Service,
Washington, DC

Doug Glysson, Operation Chair, U.S. Geological Survey, Reston, VA
Jim Thomas, Registration Chair, Bureau of Reclamation, Denver, CO

Robert Brose, Treasurer, Bureau of Reclamation, Boulder City, NV
Arlen Feldman, Technical Program, U.S. Army Corps of Engineers, Davis, CA
Marshall Flug, Technical Program, U.S. Geological Survey, Fort Collins, CO
Abbi Ginsberg, Demonstrations Chair, Federal Highway Administration, Washington, DC
Harvey Jobson, Technical Program, U.S. Geological Survey, Reston, VA
Marlene Johnson, Technical Program, Bureau of Reclamation, Denver, CO
Paula Makar, Registration, Bureau of Reclamation, Denver, CO
Mark Treviño, Audio-Video Chair, Bureau of Reclamation, Denver, CO

Foreword	ii
Preface	iii
Acknowledgments	iv

VOLUME 1

SECTION 1 – ENVIRONMENTAL WATERSHED
QUALITY AND QUANTITY

AgNPS
(Agricultural Non-Point Source)

Alonso, Carlos V.; Theurer, Fred D.; Havis, Robert N. – <i>Simulating Sedimentation in Salmonid Redds (see Section 8 - Demonstrations)</i>	
Chen, C. C.; Lee, C.Y. – <i>Using GIS and AgNPS Model to Study the Water Resources Conservation of Nan-Haw Reservoir Watershed in Taiwan</i>	1-1
Cronshey, Roger G.; Theurer, Fred D. – <i>AnnAGNPS -Non-Point Pollutant Loading Model</i>	1-9
Geter, W. Frank; Theurer, Fred D. – <i>AnnAGNPS - RUSLE Sheet & Rill Erosion</i>	1-17
Theurer, Fred D.; Cronshey, Roger G. – <i>AnnAGNPS - Reach Routing Processes</i>	1-25

Environmental Watershed Quality and Quantity

Altier, L.S.; Williams, R.G.; Lowrance, R.R.; Inamdar, S.P. – <i>The Riparian Ecosystem Management Model (REMM): Plant Growth Component</i>	1-33
Feaster, Toby D. – <i>Utilizing a Lagrangian-Eulerian Approach to Water-Quality Assessment of the Wateree River, South Carolina</i>	1-41
Garbrecht, Jürgen; Starks, Patrick J.; Williams, Robert – <i>A GIS-Numerical Modeling Approach to Identify Regions with Suitable Water Resources for a Dual Crop Rotation</i>	1-49
Hsu, Shiang-Kueen; Horng, Ming-Jame; Lee, Yau-Hui – <i>An Integrated Modeling for Water Resources Management Study in Taiwan</i>	1-57
Hung, C. Y. – <i>A Dynamic Model for Simulating the Long-Term Transport of Radionuclides from a Contaminated Land Surface to a Nearby Stream</i>	1-65
Inamdar, Shreeram; Altier, Lee; Lowrance, Richard; Williams, Randy; Hubbard, Robert – <i>The Riparian Ecosystem Management Model (REMM): Nutrient Dynamics</i>	1-73
Lowrance, R.; Altier, L.S.; Williams, R.G.; Inamdar, S.P.; Bosch, D.D.; Sheridan, J. M.; Thomas, D.L.; Hubbard, R.K. – <i>The Riparian Ecosystem Management Model: Simulator for Ecological Processes in Riparian Zones</i>	1-81
Mach, Rodney; Thibodeaux, Burnell – <i>An Innovative Approach to Improving Water Quality Through Stormwater Management</i>	1-89
Nicholson, J. Patrick – <i>Sustainable Soil, Water and Air Quality Mankind's Ultimate Challenge and Opportunity in the 21st Century</i>	1-95

CONTENTS - VOLUME 1

Schaffranek, Raymond W. – *Simulation Model for Open-Channel Flow and Transport* . . . 1-103
Shenk, G. W.; Linker, L.C.; Donigian, A.S. – *The Chesapeake Bay Program Models* 1-111
Slaughter, Charles W.; Goodwin, Peter – *Hydrologic Modeling Approaches for Integrated Management of Stream Systems* 1-119

General NPS

Ascough, James C. II; McMaster, Gregory S.; Shaffer, Marvin J.; Hanson, Jon D.; Ahuja, Lajpat R. – *Economic and Environmental Strategic Planning for the Whole Farm and Ranch: The GPFARM Decision Support System* 1-127
DiLuzio, M.; Arnold J. G.; Srinivasan, R.; Bingner, R.L. – *The Combination of a Rainfall Event Model and a Continuous Simulation Model for a Better Assessment of Nonpoint Source Pollution* 1-135
Preston, Stephen D.; Smith, Richard A.; Schwarz, Gregory E.; Alexander, Richard B.; Brakebill, John W. – *Spatially Referenced Regression Modeling of Nutrient Loading in the Chesapeake Bay Watershed* 1-143
Truman, Clint; Davis, Frank; Leonard, Ralph – *Influence of Rainfall Timing and Amount on Phosphorus Losses Associated with Runoff and Sediment - a GLEAMS Simulation* . . . 1-151

SECTION 2 – RIVER AND RESERVOIR SYSTEMS

Major River Systems

Chen, Songsheng; Zhang, Xuecheng – *Modeling on Closure Discharge of the Main Stream of TGP* 2-1
Feng, Xiangming – *Effects of Hydraulic Projects in San-Hua Reach of the Yellow River to Floods and Runoff* 2-7
Wang, Ling; Lin, Yingping; Chu, Yongwei; Cui, Qing – *Research on Flow Cut-outs in the Lower Yellow River* 2-13
Xiong, Ming; Ji, Xuewu – *A Comprehensive Summary on the Study of Flood Stochastic Simulation for Three Gorges Project* 2-21

Major River Systems/Reservoir System Operation

Hess, Glen W.; Berris, Steven N. – *Simulation of Selected Reservoir and River-Diversion Operations in the Truckee River and Carson River Basins, California and Nevada* 2-29
Huang, Wen-Cheng; Yang, Fu-Ti – *Applicability of Decision Support System for Reservoir Operation in Taiwan* 2-37
Ji, Xuewu – *Flood Disasters and the Three Gorges Projects on the Yangtze* 2-45
Malers, Steven; Bennett, Ray; Brazil, Larry – *Implementing a Water Resource Planning Model Within The Colorado River Decision Support System* 2-53

Reservoir System Operation

Bales, Jerad D.; Giorgino, Mary J. – *Dynamic Modeling of Water-Supply Reservoir Physical and Chemical Processes* 2-61
 Hayes, Richard J.; Bonner, Vernon R. – *Large-Scale Reservoir System Modeling* 2-69
 Jangaard, Loren – *Additional Storage Study of Hanson Reservoir, Green River, WA* 2-77
 Markstrom, Eric J.; Schwartz, Stuart, S.; Steger, Robert G.; Brazil, Larry E.; Day, Gerald N. – *Probabilistic Forecasts in Multiobjective Analysis for Reservoir Operations* 2-85

River/Estuary Water Quality

Conrads, Paul A. – *Effects of Model Output Time-Averaging on the Determination of the Assimilative Capacity of the Waccamaw River and Atlantic Intracoastal Waterway near Myrtle Beach, South Carolina* 2-93
 Dzedzic, M.; Fernandes, C.; Fill, H.; Tozzi, M. – *Environmental Assessment of the Barigui River Watershed* 2-101
 J. Izurieta D.; A. Ruiz L.; Ma. A. Gomez B.; P. Saldana F.; L. Marquez B.A. Lerdo de T.; R. Lopez – *Water Quality Simulation in the Cazonas River, Mexico* 2-109
 Mao, Hongmei; Ye, Shouze; Ji, Xuewu – *Water Quality Modeling of Maopingxi Pollution Zone in Three Gorges Project Construction Zone* 2-117
 Miller, William J.; Theurer, Fred D.; Alonso, Carlos V. – *A Computer Model to Predict Salmonid Fry Emergence* 2-125
 Rounds, Stewart; Wood, Tamara – *Using CE-QUAL-W2 to Assess the Ammonia Assimilative Capacity of the Tualatin River, Oregon* 2-133
 Thuc, Tran – *Development and Application of a Mud Transport and Bed Evolution Model for Estuary* 2-141
 Wood, Tamara; Rounds, Stewart – *Using CE-QUAL-W2 to Assess the Effect of Reduced Phosphorus Loads on Chlorophyll-a and Dissolved Oxygen in the Tualatin River, Oregon* 2-149

SECTION 3 – EROSION AND SEDIMENTATION

Bridge Scour and Channel Design

Dou, Xibing; Jia, Yafei; Wang, Sam S.Y.; Jones, J. Sterling – *An Alternative Methodology to Study Local Scour at Bridge Piers* 3-1
 Fripp, Jon B.; Halstead, Kenneth C.; Bhamidipaty, Surya; Webb, Jerry W. – *Sediment Transport Analysis of the Athens, Ohio, LPP and a Comparison of Two Corps Sediment Transport Computer Models* 3-9
 Johnson, Terry L.; Abt, Steven R. – *Design of Channel Riprap Using Overtopping Flow Methods* 3-17
 Richardson, J. R.; Roberts, David M. – *Reducing Local Pier Scour by Flow Redirection* . . . 3-23

Land Surface Erosion

Bosch, D. D.; Williams, R.G.; Inamdar, S.; Sheridan, J.M.; Lowrance, R.R. – *Erosion and Sediment Transport Through Riparian Forest Buffers* 3-31

Johnson, Billy E.; Julien, Pierre Y.; Watson, Chester C. – *Development of a Storm-Event Based Two-Dimensional Upland Erosion Model (CASC2D-SED)* 3-39

Oliveira, Maria da Gloria Braz de – *Analysis of the Temporal Evolution of the Sediment Production of the Pampulha Watershed and Evaluation of the Reservoir Silting* 3-47

Randle, Timothy J.; Yang, Chih Ted – *Predicting Sediment Yield From Arid Drainage Areas* 3-55

Sedimentation

Duizendstra, Don; Flokstra, Cor – *The Necessity of Modeling Non-Uniform Sediment in an 1-D Morphological Model for a Gravel Bed and a Sand Bed River in the Netherlands* 3-63

Klumpp, Cassie C.; Samad, Mohammed A. – *Stable Channel Analysis of the Rio Grande in the Upper Reaches of Elephant Butte Reservoir* 3-71

Langendoen, Eddy J.; Bingner, Ronald L.; Kuhnle, Roger A. – *Modeling of Long Term Changes of Unstable Streams* 3-79

Lee, Hong-Yuan; Hsieh, Hui-Ming; Lee, Sen-Yuan; Yang, Jinn-Chuang; Yang, Chih Ted – *Numerical Simulations of Scour and Deposition in a Channel Network* 3-87

Leput, Walter; Park, Howard – *Hildebrand Lock & Dam Sedimentation Problem and Solution* 3-95

Makar, Paula W.; Strand, Robert I.; Baird, Drew C. – *Geomorphic Analysis of the Rio Grande San Acacia to the Narrows of Elephant Butte Reservoir* 3-103

Sanchez, Viola – *River Channel Changes Downstream of Cochiti Dam, Middle Rio Grande, New Mexico* 3-111

Shea, Conor; Ports, Michael; Froehlich, David – *Alternatives Analysis for Reduction of Maintenance Dredging of a Tidal Inlet* 3-119

Sedimentation in Yellow River

Ke, Sujuan; Zhang, Xuecheng; Lu, Guangqi – *Research on Ice Regime in Yellow River* ... 3-127

Peng, Meixiang; Qiu, Shuhui; Zhao, Yingli – *Preliminary Analysis of the Influence of Climate Changes in Current Decade on Water and Sediment in the Upper and Middle Yellow River* 3-135

Qian, Yunping; Dong, Xuena; Lin, Jinping – *Analysis of Characteristics of Flow and Sediment in the Yellow River* 3-143

Xu, Jianhua; Li, Xuemei; Cui, Qing; Zhangzheng; Liu, Zhihong – *Inflow and Sediment Yield of the Yellow River Basin and Sediment Reduction Through Water Conservation* 3-151

SECTION 4 – EXTREME EVENTS

Drought Analysis

Burke, T.T., Jr.; Rao, A. Ramachandra; Hamed, Khaled – *Investigation of Physical Mechanisms Underlying the Predictability of Droughts* 4-1

Chang, Tiao J.; Germain, Richard; Bartrand, Timothy A. – *Applications of GIS for a Drought Study* 4-9

Gu, Ying – *Application of Simulating Method on the Regional Drought Analysis* 4-17

Zhang, Xuecheng; Zhu, Xiaoyuan – *The Application of Mean Value Generation Function Model in Regional Drought Research* 4-25

Flood Frequency

Dieckmann, Ronald J.; Dyhouse, Gary R. – *Changing History at St. Louis – Adjusting Historic Flows for Frequency Analysis* 4-31

England, John F. Jr.; Salas, Jose D.; Jarrett, Robert D. – *A Comparison of Moments-Based Estimators for Flood Frequency Analysis That Incorporate Historical Information* 4-37

Fan, Shou-shan – *Risk in Mitigating Hydrological Disasters* 4-45

Kosky, James A. – *Hydrologic Modeling of Tygart Lake for Dam Safety Assurance Evaluation Report* 4-53

Naghettini, Mauro – *The Relationship Between Extreme Rainfall Depths and Flood Volumes Under the Assumption of Exponentially-Tailed Probability Distributions* 4-61

Peck, Hilaire W.; Duffe, Bruce J. – *Cowlitz River Flood Hazard Study* 4-69

Webb, Jerry W. – *Regional Frequency & Extreme Event Analysis, Muskingum River Basin, Ohio* 4-77

Paleo Floods

Jarrett, Robert D. – *Paleoflood Investigations for Assessing Extreme Flooding for Elkhead Reservoir, Northwestern Colorado* 4-85

Levish, Daniel R.; Ostenaar, Dean A.; O'Connell, Daniel R.H. – *Paleohydrologic Bounds and Low Probability Floods* 4-93

O'Connell, D.R.H.; Levish, D. R.; Ostenaar, D. A. – *Risk-Based Hydrology: Bayesian Flood-Frequency Analyses Using Paleoflood Information and Data Uncertainties* . . . 4-101

Ostenaar, Dean A.; Levish, Daniel R. – *Paleohydrology: Long-Term Bounds on Unwarranted Extrapolation in Modeling* 4-109

VOLUME II
SECTION 5 – NEW MODELING SYSTEMS FROM THE AGENCIES

Corps HEC

(US Army Corps of Engineers Hydrologic Engineering Center)

Bonner, Vernon; Brunner, Gary – <i>HEC-RAS (River Analysis System)</i>	5-1
Carl, Robert; Burnham, Michael – <i>Next Generation Flood Damage Analysis Program</i>	5-9
Davis, Darryl W. – <i>The HEC Nexgen Software Development Project</i>	5-17
Peters, John C.; Feldman, Arlen D. – <i>Hydrologic Modeling System (HEC-HMS)</i>	5-25

Corps WES

(US Army Corps of Engineers Waterways Experiment Station)

Charley, William J.; Pabst, Arthur F. – <i>Hydrologic Engineering Center NEXGEN Data Storage System (HEC-DSS)</i>	5-33
Holland, J. P. – <i>Overview of Hydro-environmental Modeling and Simulation Systems for the U.S. Department of Defense</i>	5-41
Lin, H.C. Jerry; Richards, D. R.; Choate, M. – <i>Surface Water and Groundwater Interaction Modeling of South Florida</i>	5-49
Richards, D.R. – <i>Integration of Riverine, Estuarine, and Coastal Models into the Surface Water Modeling System</i>	5-57

USBR and USGS WARSMMP

(US Bureau of Reclamation and US Geological Survey
 Watershed and River Systems Management Program)

Davidson, P.; King, D. L.; Ozga, J.; Simons, J. – <i>Watershed and River Systems Planning Model in the San Juan River Basin, Colorado</i>	5-65
Fulp, Terrance J.; Frevert, Don K. – <i>Watershed and River Systems Management Program: Current and Future Applications in the Bureau of Reclamation</i>	5-71
King, D. L.; Parker, R. S.; Kuhn, Gerhard – <i>River Operations Modeling in the San Juan River Basin</i>	5-79
Kuhn, Gerhard; Parker, R. S.; Hay, L. E.; Leavesley, G. H. – <i>Precipitation Distribution Alternatives in Applying the Modular Modeling System in the San Juan River Basin, Colorado and New Mexico</i>	5-85
Leavesley, G. H.; Markstrom, S. L.; Brewer, M.S.; Viger, R. J. – <i>The Modular Modeling System (MMS) - The Physical Process Modeling Component of the Watershed and River System Management Program</i>	5-93
Lins, Harry; Frevert, Donald – <i>The Watershed and River Systems Management Program - An Overview</i>	5-101
Vaccaro, J. J.; Lynch, C. J.; Schurr, K. M.; Sharp, W.; Mastin, M.C.; Schramm, D. – <i>The Yakima River Basin Watershed and River System Management Program</i>	5-105
Zagona, Edith A.; Fulp, Terrance J.; Goranflo, H. Morgan; Shane, Richard M. – <i>RiverWare: A General River and Reservoir Modeling Environment</i>	5-113

**SECTION 6 – RIVER HYDRAULICS AND
FLOW/STAGE FORECASTING**

Flood Forecasting

Croley, Thomas E., II – <i>Great Lakes Advanced Hydrologic Prediction System</i>	6-1
Davis, Darryl W.; Pabst, Arthur F. – <i>Modernizing the US Army Corps of Engineers Water Control Data System</i>	6-9
Epstein, D. J.; Welles, E.; Day, G. N. – <i>Probabilistic Hydrologic Forecasting Methods and Tools</i>	6-17
Knapp, H. Vernon; Rice, William W. – <i>Application of a Continuous Simulation Watershed Model for Near Real-Time Flow Forecasting and Dam Operations</i>	6-25
Lai, Chintu; Wang, Tsan-Wen; Hsu, Nien-Sheng; Hsu, Shiang-Kueen – <i>A Comprehensive Flow Model for Flood Forecast/Hindcast for Tidal Reaches</i>	6-33
Larson, Lee; Welles, Edwin – <i>A Summary of the National Weather Service Advanced Hydrologic Prediction System Demonstration in Des Moines, Iowa</i>	6-41
Markus, M.; Salas, J. D. – <i>Comparing Methods for Forecasting Total Summer Flows on Tributaries of the Colorado-Big Thompson System</i>	6-49
Matthews, David; Hartzell, Curtis; Super, Arlin; Carroll, Tom; Schaake, John – <i>Integration of Quantitative Precipitation Forecasts with Hydrologic Models and River Basin Decision Support Systems</i>	6-57

River Hydraulics

Allison, Rebecca R. – <i>Development of an Unsteady Flow Hydraulic Model of the Lower Missouri River</i>	6-65
Babayan, A. V.; Nadolin, K.A. – <i>Modeling Substance Spreading in 2-D (in plane) Steady Stream</i>	6-73
Cheng, Haiyun; Rui, Xiaofang – <i>An Analytical Diffusion Model and Its Application to Water Level Forecast</i>	6-81
Denlinger, Roger P.; Walters, Roy A.; Levish, Dan; Ostenaar, Dean – <i>Robust Methods for Flood Routing Over Highly Irregular Terrain</i>	6-89
Gee, D. Michael; Tseng, Ming T. – <i>Unsteady Flow Model for Forecasting Missouri and Mississippi Rivers</i>	6-97
Holtschlag, D. J.; Grewal, M.S. – <i>Estimating Ice-Affected Streamflow by Extended Kalman Filtering</i>	6-105
Pridal, Daniel; Knofczynski, Joel – <i>Missouri River Forecast Model From Gavins Point Dam to Rulo, Nebraska</i>	6-113
Walters, Roy A. – <i>A Finite Element Model with Moving Boundaries: Application to Floods and Rumup</i>	6-121
Winer, Harley – <i>UNET Model of Connected Estuaries in Coastal Louisiana</i>	6-129
Wu, Reuy-Bean; Chang, Yao-Tser; Cheng, Yih-Pin – <i>Two-Dimensional Floodplain Modeling of Rivers in Taiwan</i>	6-137

SECTION 7 – HYDROLOGY

Data Input for Models

Davinroy, Robert D.; Gordon, David C.; Kreighbaum, David W. – *Remote Sensing of Detrimental Flow Conditions at Lock and Dam 24, Upper Mississippi River* 7-1

Flug, Marshall; Seitz, Heather L.H.; Scott, John – *A Data Gathering Technique for River Resource Identification* 7-9

Inamdar, Shreeram; Sheridan, Joseph; Williams, Randy; Bosch, David; Lowrance, Richard; Altier, L.S.; Thomas, Dan – *The Riparian Ecosystem Management Model (REMM): Evaluation of the Hydrology Component* 7-17

Straub, Timothy D.; Parmar, Paminder S. – *Comparison of Rainfall Records Collected by Different Rain-Gage Networks* 7-25

GIS Hydrology

Bullard, Kenneth L. – *Boise Five Mile Drain - Future Flooding and Old Canal Crossings* . 7-33

Chen, Wilson Huaisheng; Beschta, Robert L. – *Equivalent Rectangle Simplification (ERS) Method and Its Application in a Distributed Hydrologic Model* 7-41

Evans, Tom; Pabst, Art – *Standard Hydrologic Grid in Spatial Hydrologic Modeling* 7-49

Evans, Tom; Peters, John; Brunner, Gary – *GIS Data Exchange for Hydraulic and Hydrologic Modeling* 7-53

Kelly, Glenn G. – *Estimating Water Storage Potential in the Devils Lake Watershed Using High-Resolution, 7.5-minute U.S. Geological Survey Digital Elevation Models* 7-57

Quimpo, Rafael G.; Al-Medeij, Jaber – *Automatic Watershed Model Calibration with Geographic Information Systems* 7-65

Viger, R. J. Markstrom, S. L.; Leavesley, G. H. – *The GIS Weasel - An Interface for the Treatment of Spatial Information in Watershed Modeling and Water Resource Management* 7-73

Webb, Jerry W. – *ModClark Model Development, Muskingum River Basin, Ohio* 7-81

Hydrologic Modeling

Chen, Zhiming – *A Conceptual Monthly Rainfall Runoff Model* 7-89

Cheng, M.S.; Weinstein, N.; Victoria, C. – *Landscape Assessment of Wetland Functions (LAWF): A Geographic Information System (GIS) Model for the Evaluation of Wetland Functions* 7-97

Garen, David C.; Marks, Danny – *Spatially Distributed Energy Budget Snowmelt Modeling in Mountainous Regions of the Western United States* 7-101

Jackson, Thomas J. – *Satellite Based Soil Moisture Measurement for Hydrologic Modeling* 7-107

Kittle, John L.; Hummell, Paul R.; Duda, Paul; Lumb, Alan M. – *A Modular Approach to Interactive Watershed Modeling* 7-115

Prasad, S. N.; Romkens, M.J.M.; Helming, K. – *Rain Infiltration into Cracking Soils* 7-123

Savabi, M. R.; Richardson, C.W. – <i>Modeling Infiltration and Storm Runoff from Soils With Shrinkage Cracks</i>	7-131
Schumann, Andreas H.; Garen, David C. – <i>Spatially Distributed Hydrologic Modeling for Streamflow Simulation and Forecasting</i>	7-139
Sun, G.; Riekerk, H.; Comerford, N.B. – <i>Modeling the Hydrology of Wetland-Upland Systems on a Flat Terrain in Florida</i>	7-147
Van Mullem, Joseph A. – <i>Modeling Prairie Snowmelt Runoff</i>	7-155
Zarriello, Phillip J. – <i>Comparison of Nine Uncalibrated Runoff Models to Observed Flows in Two Small Urban Watersheds</i>	7-163

DEMONSTRATIONS

*(Those identified with an * are also oral presentations and are located in the previous sections of the proceedings.)*

Alonso, Carlos V.; Theurer, Fred D.; Havis, Robert N. <i>Simulating Sedimentation in Salmonid Redds</i>	8-1
Bingner, R. L.; Butoi-Stanescu, O.; Rodrique, P.B. <i>Internet-Based Decision Support Systems of Hydrology Tools for Wetland Determination</i>	8-9
Binger, R. L.; Darden, R.W.; Theurer, F.D.; Alonso, C.V.; Smith, P. <i>AnnAGNPS Input Parameter Editor Interface</i>	8-15
*Bonner, Vernon R.; Brunner, Gary <i>HEC-RAS (River Analysis System)</i>	5-1
Bowie, Randy; Khan, Abdul; Jia, Yafei; Wang, Sam <i>CCHE2D: A Two-dimensional Free Surface Flow and Sediment Transport Model for Natural Rivers</i>	8-19
*Carl, Robert; Burnham, Michael <i>Next Generation Flood Damage Analysis Program</i>	5-25
*Chen, Wilson Huaisheng; Beschta, Robert L. <i>Equivalent Rectangle Simplification (ERS) Method and Its Application in a Distributed Hydrologic Model</i>	7-41
Doe, William W. III; Julien, Pierre Y.; Ogden, Fred L.; Johnson, Billy E. <i>Spatially Distributed Modeling of the Hydrologic Effects of Mechanized Maneuvers on Military Training Lands</i>	8-27
Flerchinger, G. N.; Hardegree, S.P.; Johnson, G.L. <i>The Simultaneous Heat and Water (SHAW) Model: A Research Tool for Management Decisions</i>	8-35
Garcia, Luis; Patterson, David; Bender, Merlynn; Kinerson, Russell <i>Development of Water Quality Modeling Framework</i>	8-43
Ishii, A. L.; Charlton, T.J.; Ortel, T.W.; Vonnahme, C.C. <i>Modeling System for Near Real-Time Flood Simulation for Salt Creek in Du Page County, Illinois</i>	8-51
*Kittle, John L.; Hummell, Paul R.; Duda, Paul; Lumb, Alan M. <i>A Modular Approach to Interactive Watershed Modeling</i>	7-115

Kjelds, Jesper T. <i>Flood Plain Management, Integrating Numerical Models and GIS</i>	8-59
Lane, W. L.; Frevert, D. K.; Salas, J. D.; Chung, C. H. <i>Modeling of River Systems Using the SAMS Package</i>	8-65
Larson, Roger; Labadie, John; Baldo, Marc <i>MODSIM Decision Support System for River Basin Water Rights Administration</i>	8-73
*Leavesley, G. H.; Markstrom, S. L.; Brewer, M.S.; Viger, R. J. <i>The Modular Modeling System (MMS) - The Physical Process Modeling Component of the Watershed and River System Management Program</i>	5-93
*Lowrance, R.; Altier, L.S.; Williams, R.G.; Inamdar, S.P.; Bosch, D.D.; Sheridan, J. M.; Thomas, D.L.; Hubbard, R.K. <i>The Riparian Ecosystem Management Model: Simulator for Ecological Processes in Riparian Zones</i>	1-81
*Malers, Steven; Bennett, Ray; Brazil, Larry <i>Implementing a Water Resource Planning Model Within The Colorado River Decision Support System</i>	2-53
Marino, Laura; Crawford, Norman <i>Hydrologic Forecast and Analysis Modeling (HFAM)</i>	8-81
Parker, Nancy L., Patterson, David A. <i>PC HYDROSS Simulation System (PCHSS) A Graphical User Interface for the HYDROSS Model</i>	8-89
*Peters, John C.; Feldman, Arlen <i>Hydrologic Modeling System (HEC-HMS)</i>	5-17
Schornick, James <i>The U.S. Geological Survey Hydrologic Analysis Support Section Software Support Services for Hydrologic Modeling and Data Analysis</i>	8-95
Scott, John; Flug, Marshall <i>Modeling with MODSIM: Klamath River Water Quantity for Protecting Fish and Other Resource Values</i>	8-103
Thurman, Jane L.; Roberts, Ralph T. <i>Preparing the ARS Water Database for the Twenty-First Century</i>	8-111
Vieira, Dalmo A.; Langendoen, Eddy J.; Bingner, Ronald L. <i>FRAME - An Integrated Modeling System of Channel and Landscape Processes</i>	8-117
*Walters, Roy A. <i>A Finite Element Model with Moving Boundaries: Application to Floods and Runup</i> .	6-121
Weghorst, Paul; Ferrari, Ron; Nuanes, Sharon <i>Using ARC/INFO to Process and Analyze Reservoir Hydrographic Survey Information</i>	8-125
Williams, R. G.; Lowrance, R.R.; Altier, L. S.; Inamdar, S. P. <i>Riparian Ecosystem Management Model (REMM): A Demonstration</i>	8-133
Wisbith, Stanley M.; Buelow, David P. <i>Ohio River Division Real-Time Modeling/Forecasting System</i>	8-139
Yang, Chih Ted; Trevino, Mark A.; Simoes, Francisco J.M. <i>An Enhanced Generalized Stream Tube Model for Alluvial River Simulation</i>	8-143
*Zagona, Edith A.; Fulp, Terrance; Goranflo, H. Morgan; Shane, Richard M. <i>RiverWare: A General River and Reservoir Modeling Environment</i>	5-113

AnnAGNPS-REACH ROUTING PROCESSES

By Fred D. Theurer, Agricultural Engineer, Natural Resources Conservation Service, Beltsville, MD;
Roger G. Cronshey, Hydraulic Engineer, Natural Resources Conservation Service, Beltsville, MD

Abstract: The single-event Agricultural Non-Point Source Pollution (AGNPS) computer model has been replaced with a continuous simulation version called AnnAGNPS (Annualized AGNPS). AnnAGNPS will predict pollutant loadings (PL) anywhere within the watershed and identify their proportional contributions from selected points of origin. The reach routing processes are the set of technical procedures used to determine the fate & transport of the PL's once they are in the stream system.

The reach routing processes in AnnAGNPS track the fate & transport for the: (a) five sediment particle-size classes (clay, silt, sand, small aggregate, & large aggregate); and (b) absorbed and dissolved forms of the major chemical pollutants (nutrients, pesticides, & organic carbon). An accounting procedure is included that keeps track of the amount originating from within a field or stream reach of any given PL by erosion type or chemical form that arrives at any downstream point in the watershed.

The graphical peak discharge method in the Soil Conservation Service's TR-55 is limited to watershed drainage areas whose time of concentrations (T_c) do not exceed 10 hours (approximately 200 sq. mi.) and rainfall (P) to runoff relationships whose initial abstraction (I_a) is less than 50 percent of the rainfall ($0.1 \leq I_a/P \leq 0.5$). AnnAGNPS needs to operate satisfactorily for drainage areas up to 1000 sq. mi. (T_c 's up to 48 hr) and rainfall-runoff relationships that range between no runoff to total runoff ($0 \leq I_a/P \leq 1$). An extension of TR-55 is used to meet these requirements.

The sediment reach routing process accounts for deposition when there is an oversupply of a particular sediment class, and degradation when the particular sediment particle-size class transport is supply-limited and is available in the bed & bank. Amounts of erosion by type (sheet & rill, bed & bank, and gully) are tracked throughout the reach routing process. This allows the user to determine from where any particular sediment particle-size class originated by erosion type, and how much.

The major chemical reach routing processes have been updated to include partitioning between absorbed and dissolved states. The reach routing processes include: (a) the fate & transport of nitrogen & phosphorus; (b) a separate reach routing routine for organic carbon; and (c) the fate and transport for an unlimited number of individual pesticides.

INTRODUCTION

The reach routing processes are used in AnnAGNPS (Cronshey & Theurer 1998). Sediment from sheet & rill erosion is determined according to RUSLE (Geter & Theurer 1998). The results from AnnAGNPS are designed to be used by the other computer models such as the sediment intrusion into salmonid redds model (Alonso et al 1998) and the fry emergence model (Miller et al 1998).

The reach routing processes are assumed to be in an enclosed control volume. All inputs are total amounts (water, sediment, & chemicals) entering at the upstream end only. Chemicals are equilibrated—equilibrium balance between dissolved & adsorbed chemicals—immediately before routing begins. Sediments are routed by particle-size class where each particular size-class is deposited, more entrained, or simply transported unchanged depending upon the amount entering the reach, availability of that size class in the bed & banks, and the transport capacity of each size class. The chemicals are re-equilibrated at the downstream end to reflect possible changes in either the amount of water or fine sediment.

PL computer models require a water model component. The water model components needed by watershed-scale PL models must include a simple peak discharge procedure. A very simple and precise procedure with accepted credibility is the unit peak discharge (UPD) procedure included in Chapter 4, TR-55 (SCS 1986). However, TR-55 was developed primarily for use as an engineering field-level design tool rather than for inclusion in PL continuous-simulation, field- & watershed-level computer models. While applicable for the range of conditions for which it was developed, TR-55 does not cover the total range needed for such PL models.

HYDRAULICS

Rectangular shape channels offer computational efficiencies, especially when coupled with unit-width assumptions. Unit-width means dividing the respective parameter by the top width at the surface of the flow area.

For the hydraulic radius, use the hydraulic depth; i.e., let:

$$d_w = R = A/W \quad \text{Equation 1}$$

where: d_w = hydraulic depth, m;
 R = hydraulic radius, m;
 A = flow area, m^2 ; and
 W = flow width, m.

To solve for the velocity of flow when given the hydraulic depth of flow, use:

$$v_w = (1/n) \cdot d_w^{2/3} \cdot S_o^{1/2} \quad \text{Equation 2}$$

where: v_w = flow velocity of water, m/s;
 n = Manning's retardance;
 d_w = hydraulic depth, m; and
 S_o = channel slope, m/m.

To solve for the hydraulic depth and velocity when given the discharge, use:

$$d_w = [(n \cdot q_w) / (S_o^{1/2})]^{0.6} = n^{0.6} \cdot S_o^{-0.3} \cdot q_w^{0.6}$$

$$v_w = Q_w / (W \cdot d_w) = q_w / d_w \quad \text{Equation 3}$$

where: d_w = hydraulic depth, m;
 v_w = flow velocity of water, m/s;
 W = flow width of flow area, m;
 n = Manning's retardance;
 Q_w = water discharge, m^3/s ;
 $q_w = Q_w/W$, unit-width water discharge, $m^3/s/m$; and
 S_o = channel slope, m/m.

And the term $d_w \cdot S_o$, derived from Equation 4, will be used in subsequent formulas:

$$d_w \cdot S_o = n^{0.6} \cdot S_o^{0.7} \cdot q_w^{0.6} \quad \text{Equation 4}$$

where: d_w = hydraulic depth, m;
 v_w = flow velocity of water, m/s;
 W = flow width of flow area, m;
 n = Manning's retardance;
 $q_w = Q_w/W$, unit-width water discharge, $m^3/s/m$; and
 S_o = channel slope, m/m.

HYDROLOGY

Peak Discharge: The following set of regression coefficients were generated using the Extended TR55 (Theurer & Comer 1992) procedures and curve-fitted using TableCurve 2D version 4 by Jandel. UPD's were calculated for ninety-six I_d/P_{24} 's at 0.01 increments of I_d/P_{24} from 0 to 0.95 ($0 <= I_d/P_{24} <= 0.95$) and forty-one T_c 's from 0 to 48 hours using NEH-4 procedures (SCS 1972). The UPD at I_d/P_{24} equal one is zero because there is no surface runoff. The resulting data sets [(96+1)*41=3977 element values for each of the rainfall distribution types] became the basis for the extended TR-55 regression equations, error analyses, and subsequent findings. The mean error of the regression equations with respect to the NEH-4 (SCS 1972) values over the entire range of I_d/P_{24} & T_c conditions is approximately 0.5% and the standard deviation is less than approximately 2%. Table 1 show regression coefficients for each rainfall distribution. While AnnAGNPS uses I_d/P_{24} increments of 0.05, only increments of 0.20 are shown in Table 1.

Table 1: Unit Peak Discharge Regression Coefficients

Type	I/P_{24}	a	b	c	d	e	f
1 (I)	0.00	8.191203E-01	2.098577E+00	1.420600E-01	6.403418E-02	-1.798058E-03	-9.691654E-04
	0.20	2.881040E-01	2.269473E+00	3.648846E-02	3.394364E-02	1.194882E-03	3.185709E-03
	0.40	4.209120E-02	2.107367E+00	1.253109E-02	2.416459E-02	1.257576E-03	7.818349E-03
	0.60	4.166588E-03	2.719060E-02	1.090675E-04	3.126468E-03	7.904181E-06	1.235070E-04
	0.80	1.358244E-03	4.526567E-02	9.085505E-05	9.939561E-03	2.978380E-07	0.000000E+00
2 (Ia)	0.00	2.593320E-01	6.463246E-01	2.573810E-02	7.243833E-03	2.161611E-05	1.398574E-04
	0.20	7.630642E-02	6.560184E-01	2.566400E-03	-6.452636E-03	6.961028E-04	1.709310E-03
	0.40	9.523307E-03	3.028293E-02	2.788554E-04	2.240374E-03	1.933978E-05	1.080512E-04
	0.60	4.480394E-03	7.302563E-02	3.394787E-04	6.287665E-03	2.609098E-05	4.407477E-04
	0.80	1.741268E-03	8.602862E-02	1.642964E-04	1.576832E-02	2.481447E-07	0.000000E+00
3 (II)	0.00	1.519530E+00	2.112862E+00	7.955306E-02	6.263867E-02	8.513482E-03	6.758214E-03
	0.20	6.687890E-01	2.523586E+00	1.716150E-02	1.954410E-02	2.908914E-03	6.678482E-03
	0.40	2.272377E-01	3.907665E+00	3.469720E-02	1.245753E-01	9.446148E-04	6.197919E-03
	0.60	1.690395E-02	2.321569E+00	8.300435E-03	7.991502E-02	4.118532E-04	7.692973E-03
	0.80	1.042173E-03	-1.020764E-04	-3.811053E-06	2.567960E-03	9.359939E-09	-3.038358E-05
4 (III)	0.00	9.357636E-01	1.368530E+00	7.585186E-02	5.733524E-02	5.252073E-03	4.195782E-03
	0.20	4.129800E-01	1.675525E+00	3.451340E-02	5.585967E-02	8.903714E-04	2.210996E-03
	0.40	1.218296E-01	2.203114E+00	2.877259E-02	1.196262E-01	3.657518E-04	2.572314E-03
	0.60	1.103889E-02	7.637374E-01	2.652503E-03	3.138008E-02	2.008206E-04	3.555352E-03
	0.80	1.130600E-03	1.856640E-02	-1.739106E-05	1.191404E-03	2.667614E-06	1.966816E-04
5 (Uniform)	0.00	4.161024E-02	-2.291070E-02	-8.630791E-04	6.634947E-04	1.701998E-05	2.227598E-06
	0.20	2.878569E-02	8.682334E-02	2.068912E-03	4.156828E-03	7.760004E-05	1.814001E-04
	0.40	1.699438E-02	8.378853E-02	8.549266E-04	5.391781E-03	4.058543E-05	2.325788E-04
	0.60	9.214130E-03	1.278936E-01	6.050135E-04	1.159786E-02	4.280640E-05	7.157927E-04
	0.80	3.838705E-03	2.412793E-01	4.980051E-04	4.502355E-02	4.258091E-07	0.000000E+00
6 (II-a60)	0.00	2.889749E+00	3.273784E+00	1.446065E-01	1.008957E-01	0.000000E+00	0.000000E+00
	0.20	1.369500E+00	5.064453E+00	4.248368E-02	6.499361E-02	1.513193E-03	3.541284E-03
	0.40	6.334482E-01	1.025432E+01	8.351263E-02	3.603484E-01	-7.260700E-05	0.000000E+00
	0.60	6.916727E-02	9.339188E+00	2.710800E-02	2.062759E-01	-1.364500E-04	0.000000E+00
	0.80	6.231650E-04	-3.411600E-05	1.982740E-06	1.572730E-03	5.316790E-07	3.229390E-05
7 (II-a65)	0.00	3.105260E+00	3.109283E+00	1.921849E-02	2.558174E-03	0.000000E+00	0.000000E+00
	0.20	1.545424E+00	5.073367E+00	4.194001E-02	1.385273E-01	6.308154E-03	1.344247E-02
	0.40	-3.89279E-01	2.625254E+00	-8.147355E+00	3.551340E-01	-1.974840E+00	-6.946600E-04
	0.60	1.437442E-01	1.328429E+01	3.844520E-02	3.615960E-01	-1.330700E-04	0.000000E+00
	0.80	6.041370E-04	-1.627500E-05	-3.202300E-06	9.379760E-04	4.116320E-07	2.514860E-05
8 (II-a70)	0.00	3.431447E+00	3.225395E+00	1.107677E-02	0.000000E+00	0.000000E+00	0.000000E+00
	0.20	1.839241E+00	5.556090E+00	5.400739E-02	2.103572E-01	1.038225E-02	2.210380E-02
	0.40	7.815830E-01	8.413013E+00	3.026382E-02	4.524973E-02	-4.612800E-04	-1.478290E-03
	0.60	2.420561E-01	1.570367E+01	4.432599E-02	4.906144E-01	-9.166000E-05	0.000000E+00
	0.80	6.652130E-04	7.173470E-06	-2.262900E-05	-4.840900E-04	8.703930E-07	6.233150E-05
9 (II-a75)	0.00	3.774411E+00	3.340085E+00	5.425804E-03	0.000000E+00	0.000000E+00	0.000000E+00
	0.20	1.997334E+00	5.379884E+00	1.185453E-01	4.992425E-01	2.332722E-02	4.956452E-02
	0.40	8.924026E-01	8.062642E+00	1.867840E-02	9.565487E-02	2.095755E-03	1.197524E-02
	0.60	3.367238E-01	1.578486E+01	4.151122E-02	5.092234E-01	-4.802100E-05	0.000000E+00
	0.80	1.123760E-03	9.764010E-05	-1.679900E-04	-6.339630E-03	1.133440E-05	8.685300E-04

The general form for the regression equation to calculate the peak discharge is:

$$Q_p = 2.777777778 \cdot 10^{-3} \cdot P_{24} \cdot D_a \cdot \left[\frac{a + (c \cdot T_c) + (e \cdot T_c^2)}{1 + (b \cdot T_c) + (d \cdot T_c^2) + (f \cdot T_c^3)} \right] \quad \text{Equation 5}$$

where: Q_p = peak discharge, m^3/s ;
 D_a = total drainage area, hectares;
 P_{24} = 24-hour effective rainfall over the total drainage area mm;
 T_c = time of concentration hr; and
a, b, c, d, e, & f are the regression coefficients for a given I_p/P_{24} and rainfall distribution type.

Time of Concentration: Time of concentration is calculated according to the procedures described in TR-55 (SCS 1986).

Hydrograph Shape: A triangular shape is assumed. Since the sediment transport is only concerned with the duration for an average discharge, the time to peak is not important and a right triangle was used to calculate the sediment transport.

The time to base of the hydrograph (duration of surface runoff event) is:

$$t_b = 20 \cdot (R \cdot D_a / Q_p) \quad \text{Equation 6}$$

where: Q_p = peak discharge, m^3/s ;
 D_a = total drainage area, hectares;
R = surface runoff volume from upstream drainage area, mm; and
 t_b = time to base, s.

The hydrograph as a function of time is:

$$Q_w = (Q_p / t_b) \cdot t, \quad \text{for } 0 \leq t \leq t_b \quad \text{Equation 7}$$

where: Q_w = discharge as a function of time, m^3/s ;
 Q_p = peak discharge, m^3/s ;
 t_b = time to base, s; and
t = time from beginning of runoff, s.

And the unit-width peak discharge is:

$$q_p = Q_p / W \quad \text{Equation 8}$$

where: q_p = unit-width peak discharge, $m^3/s/m$;
 Q_p = peak discharge, m^3/s ; and
W = flow width, m.

SEDIMENT YIELD

All sediment routing in the concentrated flow channels is performed by the five particle-size classes (sand, large & small aggregates, silt, and clay) and for each increment of the hydrograph.

If the sum of all incoming sediment (q_{s1}) is greater than the sediment transport capacity (q_{sc}), then the sediment deposition algorithm is used. If that sum is less than or equal to the sediment transport capacity, the sediment discharge at the outlet of the reach (q_{s2}) will be equal to the sediment transport capacity for an erodible channel (by particle-size). Otherwise, if the upstream sediment discharge (q_{s1}) is less than or equal to the sediment transport capacity (q_{sc}) and the channel is non-erodible for that particular particle-size, the downstream sediment discharge (q_{s2}) is assumed equal to the upstream sediment discharge (q_{s1}).

- If $(q_{s1} - q_{sc}) \leq 0$ & the bed is erodible for the particular particle-size class, then $q_{s2} = q_{sc}$; or
- if $(q_{s1} - q_{sc}) \leq 0$ & the bed is non-erodible for the particular particle-size class, then $q_{s2} = q_{s1}$; or
- if $(q_{s1} - q_{sc}) > 0$, then the sediment deposition algorithm is used.

Sediment Concentration: The definition for sediment concentration is:

$$C_s = S/W \quad \text{Equation 9}$$

where: C_s = sediment concentration, Mg-sediment/Mg-water;
 S = sediment mass, Mg; and
 W = water mass from upstream drainage area, Mg.

Sediment concentration is assumed to be constant throughout the hydrograph; therefore, the sediment load for a given discharge at any time during the runoff hydrograph is:

$$q_s = C_s \cdot q_w \quad \text{Equation 10}$$

where: C_s = sediment concentration, Mg-sediment/Mg-water;
 q_s = unit-width sediment load, Mg/s/m; and
 q_w = unit-width water discharge at any time, Mg/s/m;

Sediment Transport Capacity Algorithm: The sediment transport capacity (q_{sc}) and the unit-width water discharge (q_w) are based upon the parameters at the upstream end of the reach (x_1).

The shear velocity, assuming unit-width, is based upon the parameters at the upstream end of the reach (x_1) and is defined to be:

$$U_* = [g \cdot d_w \cdot S_o]^{1/2} = g^{0.5} \cdot n^{0.3} \cdot S_o^{0.35} \cdot q_w^{0.3} \quad \text{Equation 11}$$

where: d_w = hydraulic depth at x_1 , m;
 g = gravitational constant, 9.81 m/sec²;
 n = Manning's retardance;
 q_w = unit-width water discharge at any time, Mg/s/m;
 S_o = channel slope, m/m; and
 U_* = shear velocity at x_1 , m/s.

For clay, silt, and small aggregates, use $A = 1$; for sand and large aggregates, use:

$$A = [(6 \cdot v_f) / (\kappa \cdot U_*)] / \{1 - \exp[-(6 \cdot v_f) / (\kappa \cdot U_*)]\} \quad \text{Equation 12}$$

where: A = constant of proportionality, for any flow and particle-size, between the depth-average suspended sediment concentration and the concentration at the laminar sub-layer plane, non-dimensional;
 κ = von Karman's turbulent-flow mixing-length constant (assume 0.4), non-dimensional;
 U_* = shear velocity at x_1 , m/s; and
 v_f = particle fall velocity (see Table 2), m/s.

For each particle-size, the sediment transport capacity is:

$$q_{sc} = k \cdot \tau \cdot v_w^2 / v_f \quad \text{Equation 13}$$

where: q_{sc} = unit-width sediment transport capacity, Mg/s/m;
 k = transport capacity factor (see Table 2), non-dimensional;
 τ = bed shear stress; Mg/m²
 v_w = flow velocity of water, m/s; and
 v_f = particle fall velocity (see Table 2), m/s.

The bed shear stress can be computed as follows:

$$\tau = \gamma_w \cdot d_w \cdot S_o \quad \text{Equation 14}$$

where: τ = bed shear stress; Mg/m²
 γ_w = 1.00, water density, Mg/m³;
 d_w = hydraulic depth at x_1 , m; and
 S_o = channel slope, m/m.

Table 2 contains the physical properties for each particle-size class (note D_p is in millimeters and v_f is in millimeters per second).

Table 2: Particle-size Class Physical Properties (after Young et al 1987)

Particle-size Class	Particle Size Range (mm)	Particle Density (γ_p) (Mg/m ³)	Fall Velocity (v_f) (mm/s)	Transport Capacity Factor (v_f)	Equivalent Sand Size (D_p) (mm)
clay	<0.002	2.60	$3.11 \cdot 10^{-3}$	$6.242 \cdot 10^{-3}$	$2.00 \cdot 10^{-3}$
silt	0.002-0.050	2.65	$8.02 \cdot 10^{-2}$	$6.053 \cdot 10^{-3}$	$1.00 \cdot 10^{-2}$
sand	0.050-2.000	2.65	$2.31 \cdot 10^{+1}$	$6.053 \cdot 10^{-3}$	$2.00 \cdot 10^{-1}$
small aggregates (SAGG)	0.020-0.075	1.80	$3.81 \cdot 10^{-1}$	$12.478 \cdot 10^{-3}$	$3.51 \cdot 10^{-2}$
large aggregates (LAGG)	0.200-1.000	1.60	$1.65 \cdot 10^{+1}$	$16.631 \cdot 10^{-3}$	$5.00 \cdot 10^{-1}$

Converting v_f in millimeters per second to meters per second, and using Equation 13 results in:

$$C = 322 \cdot k \cdot \gamma_w / v_f, \text{ and} \\ q_{sc} = C \cdot n^{-0.6} \cdot S_0^{1.3} \cdot q_w^{1.4} \quad \text{Equation 15}$$

where: q_{sc} = unit-width sediment transport capacity, Mg/s/m;
 C = particle-size class constant for the sediment transport capacity (see Table 3), Mg-s/m⁴;
 k = transport capacity factor (see Table 2), non-dimensional;
 n = Manning's retardance;
 q_w = unit-width water discharge, m³/s/m;
 S_0 = channel slope, m/m.
 v_f = particle fall velocity (see Table 2), mm/s; and
 $\gamma_w = 1.00$, water density, Mg/m³.

Using Equations 7, 8, & 15, the total sediment transport capacity for the hydrograph is:

$$S_{sc} = \int_0^{t_b} (W \cdot q_{sc}) dt = W \cdot C \cdot n^{-0.6} \cdot S_0^{1.3} \cdot q_p^{1.4} \cdot t_b / 2.4 \quad \text{Equation 16}$$

where: C = particle-size class constant for the sediment transport capacity (see Table 3), Mg-s/m⁴;
 n = Manning's retardance;
 q_p = unit-width peak discharge, m³/s/m;
 q_{sc} = unit-width sediment transport capacity, Mg/s/m;
 S_{sc} = total sediment transport capacity mass, Mg.
 S_0 = channel slope, m/m.
 t = time from beginning of runoff, s;
 t_b = time to base, s; and
 W = flow width, m.

Table 3 contains the sediment transport capacity constants for each particle-size class (note D_p is in millimeters and v_f is in millimeters per second).

Table 3: Particle-Size Class Sediment Transport Capacity

Sediment Class	D_p (mm)	γ_p (Mg/m ³)	v_f (mm/s)	k	C (Mg-s/m ⁴)
clay	$2.00 \cdot 10^{-3}$	2.60	$3.11 \cdot 10^{-3}$	$6.242 \cdot 10^{-3}$	$2.0071 \cdot 10^{+03}$
silt	$1.00 \cdot 10^{-2}$	2.65	$8.02 \cdot 10^{-2}$	$6.053 \cdot 10^{-3}$	$7.5474 \cdot 10^{+01}$
sand	$2.00 \cdot 10^{-1}$	2.65	$2.31 \cdot 10^{+1}$	$6.053 \cdot 10^{-3}$	$2.6203 \cdot 10^{+01}$
SAGG	$3.51 \cdot 10^{-2}$	1.80	$3.81 \cdot 10^{-1}$	$1.248 \cdot 10^{-2}$	$3.2756 \cdot 10^{+01}$
LAGG	$5.00 \cdot 10^{-1}$	1.60	$1.65 \cdot 10^{+1}$	$1.663 \cdot 10^{-2}$	$1.0079 \cdot 10^{+00}$

Sediment Deposition Algorithm: The sediment routing for each reach is done using the unit-width, steady-state, uniform, spatially-varied sediment discharge model.

The sediment routing for all reaches will be the same. All upstream sediment discharges ($q_{s,i}$) will be the sum of all incoming sediment from upstream reaches plus the local sediment associated with the upstream end of the current

reach. Primary cell upstream sediment discharges (q_{s1}) will consist only of local loadings since there is no incoming sediment from upstream reaches to a primary cell.

$$q_{s2} = q_{sc} + [(q_{s1} - q_{sc}) \cdot \exp(-N_d)] \quad \text{Equation 17}$$

where: A = Einstein's constant of proportionality, non-dimensional;
 L_2 = distance from x_1 to x_2 , m;
 $N_d = (A \cdot v_f \cdot L_2) / q_w$, deposition number, non-dimensional;
 q_{sc} = unit-width sediment transport capacity, Mg/s/m;
 q_{s1} = upstream unit-width sediment discharge at x_1 , Mg/s/m;
 q_{s2} = downstream unit-width sediment discharge at x_2 , Mg/s/m;
 q_w = unit-width water discharge, $m^3/s/m$; and
 v_f = particle fall velocity, m/s.

Table 4: 15-Point Gaussian-Legendra Quadrature for Numerical Integration

Point No.	t_i/t_0	ω_i
1	.006003741	.015376621
2	.031363304	.035183024
3	.075896109	.053579610
4	.137791135	.069785339
5	.214513914	.083134603
6	.302924330	.093080500
7	.399402954	.099215743
8	.500000000	.101289120
9	.600597047	.099215743
10	.697075674	.093080500
11	.785486087	.083134603
12	.862208866	.069785339
13	.924103292	.053579610
14	.968636696	.035183024
15	.993996259	.015376621

Einstein's constant of proportionality (A) is actually the ratio of the suspended sediment concentration at the bottom of the water column (near the bed surface) to the average concentration of suspended sediment throughout the water column.

For primary cells, the distance from x_1 to x_2 is the distance from the hydraulically most distant point (x_1) to the cell outlet (x_2).

For secondary cells, the distance from x_1 to x_2 is the length of the concentrated flow channel segment for the reach. The outlet for each reach is always x_2 in the above equations. All incoming sediment from upstream reaches is assumed to enter at the upstream end of the reach (x_1). Local loadings (originating within the associated cells) are assumed to be delivered to the downstream end of the cell's associated reach (x_2).

The channel dimensions for each reach are based upon the flow characteristics for the respective reach; and for the geomorphic option, the top width and depth are based upon the drainage area at the upstream end of each respective reach.

Gaussian-quadrature is used for numerical integration when closed form analytic solutions are not known. The subprogram GAULEG (Press et al 1987) generates the abscissas (t_i) & weights (ω_i) for a given N-point Gauss-Legendre quadrature. Points for the 15-point Gaussian-Legendra quadrature (Carnahan et al 1969) are shown in Table 4.

The N-point Gaussian-quadrature numerical integration of Q_s as a function of t is:

$$\int_{t_1}^{t_2} Q_s dt \cong (t_2 - t_1) \cdot \left[\sum_{i=1}^{i=N} (\omega_i \cdot Q_{s,i}) \right] \quad \text{Equation 18}$$

where: Q_s = sediment load as a function of time; Mg/sec;
 $Q_{s,i}$ = sediment load at Gauss-Legendre time point t_i ; Mg/sec;
 t_1 = time at beginning of time period, sec;
 t_2 = time at end of time period, sec;
 i = Gauss-Legendre point number;
 N = last Gauss-Legendre time point; and
 ω_i = Gauss-Legendre weight, non-dimensional.

CHEMICAL ROUTING

In general, chemicals exist in two phases: (1) dissolved (solution); and (2) attached (adsorbed) to clay-size particles.

Three nutrients are recognized by AnnAGNPS: (1) nitrogen; (2) phosphorous; & (3) organic carbon. Nitrogen & phosphorous are recognized as to be able to exist in both the soluble and adsorbed state. Organic phosphorous is assumed to be insoluble; therefore, only inorganic phosphorous is subject to equilibration. Organic carbon is assumed to be part of the clay-size particles with a known organic carbon to clay ratio.

AnnAGNPS allows any number of pesticides, each with their own independent chemical properties, but they are treated separately; i.e., there is no interaction assumed. Independent equilibration is assumed for each pesticide.

Adsorbed Chemicals: Conservation of mass calculations are made for any adsorbed chemicals if the clay-size particles are deposited within the stream reach. Re-equilibration, for the necessary chemicals, are repeated at the downstream end if clay-size particles are deposited or entrained from the bed & banks, or if there is any loss of water.

Solution Chemicals: Conservation of mass calculations are made for any chemicals in solution if there is any loss of water within the stream reach. Re-equilibration, for the necessary chemicals, are repeated at the downstream end if there is any change in the amount or source of clay-size, or if there is any loss of water.

Equilibration: A simple first order equilibration model for equilibration is used:

$$M_s = M_c / (1 + K_d) \quad \text{Equation 19}$$

where: K_d = partition coefficient of chemical, non-dimensional;
 M_c = total mass of chemical both adsorbed & in solution, Mg; and
 M_s = total mass of chemical in solution, Mg.

REFERENCES

- Alonso, C.V., Theurer, F.D., & Havis, R.N., 1998. Simulating sedimentation in salmonid redds. *In Proceedings First Federal Interagency Hydrologic Modeling Conference*, 19-23 April 1998, Las Vegas, NV.
- Carnahan, B., Luther, H.A., Wilkes, J. O., 1969, *Applied Numerical Methods*. John Wiley & Sons, Inc pg 100-116
- Cronshey, R.G. & Theurer, F.D., 1998. AnnAGNPS-non-point pollutant loading model. *In Proceedings First Federal Interagency Hydrologic Modeling Conference*, 19-23 April 1998, Las Vegas, NV.
- Geter, F. & Theurer, F.D., 1998. AnnAGNPS-RUSLE sheet & rill erosion. *In Proceedings First Federal Interagency Hydrologic Modeling Conference*, 19-23 April 1998, Las Vegas, NV.
- Miller, W.J., Theurer, F.D., & Alonso, C.V., 1998, A computer model to predict salmonid fry emergence, *In Proceedings First Federal Interagency Hydrologic Modeling Conference*, 19-23 April 1998, Las Vegas, NV.
- Press, W. H., Flannery, B. P., Teukolsky, S. A., Vetterling, W. T., 1987. *Numerical Recipes: The Art of Scientific Computing*. Cambridge University Press, pg 125-126
- SCS, 1972. *SCS National Engineering Handbook: Section 4, Hydrology*. Soil Conservation Service, USDA.
- SCS, 1986. *Technical Release 55: Urban hydrology for small watersheds*. Soil Conservation Service, USDA.
- Theurer, F.D., Comer, G.P., 1993. *Extended TR55*. 5 April 1992, USDA-SCS-ENG, Washington, DC. 308 pp.

Using GIS and AgNPS Model to Study the Water Resources Conservation of Nan-Haw Reservoir Watershed in Taiwan

By C.C. Chen, Associate Professor, Department of Forest Management, National Pingtung University of Science and Technology, Pingtung, Taiwan, R.O.C.; C.Y. Lee, Associate Professor, Department of Soil and water Conservation, National Pingtung University of Science and Technology, Pingtung, Taiwan, R.O.C.

Abstract

In this study, by using GIS and AgNPS as a tool and focusing our attention on the range of Nan-Haw reservoir watershed, the special distribution data of geology, soil, slope, aspect, land-use, and stream-order systems were built by ARC/INFO GIS. All of these data have something to do with that water resource conservation. With the established GIS database to match with AgNPS, we can figure out runoff volume and the transportation and product of pollutant at different grids, and we can also fully have the use condition of nutrient, mud, and sand of the whole area under control. In order to investigate how to make use of GIS database to monitor water resource conservation, this study, dividing the whole watershed into 18 sub-watersheds, according geographical traits, can figure out the characteristic parameters of each sub-watershed. Using the model output and geographical parameters of each sub-watershed, we can carry out, by means of correlation and regression analysis, a research into the problems of water resource conservation and monitor of Nan-Haw reservoir watershed.

Introduction

Water is increasing in great demand as the result of economical development in Taiwan, and this relatively makes water guilty in the reservoir go from bad to worse day after day. Watershed is the topographic unit of the rain's influx and output. To process a suitable management of land and resources in the watershed can provide not only good water quality and quantity distributed by timely but also continuous and desirable water quality at downstream area. Such factors inside the watershed as biological, physical, social, and economic one are the major items having influence on water resources in the watershed. Therefore, to figure out one desirable water resource management in the watershed, and to have basic data of environmental ecology under control is absolutely necessary for the process how to map out, supervise, and trace one watershed. Geographic information system is one effective tool of assistance to manipulate, store, and analyze spatial distribution data. This study, using GIS as a tool, with Nan-Haw Reservoir Watershed as its study area, has already set up spatially distribution data concerning that watershed and water resource conservation such as precipitation, discharge, soil, digital terrain, land use, and water system. With the already established GIS database matching AgNPS, it is possible to figure out different situations at various places for runoff, and transportation of sedimentation, chemical, and nutrient in the watershed. By doing so, the transportation trails of erosion and nutrient can be fully got under control. In addition, it is needed, with flood trace method and water

sampling, to collect factual materials of erosion and nutrient so as to verify the inferential result of water quality and quantity made by AgNPS in the reservoir watershed. The data concerning spatial runoff quantity and sedimentation distribution inferred by using GIS and AgNPS can provide this study as major data resource to quantify the water resource conservation practical effectiveness, and to investigate the hydrologic budget, and to evaluate the impact of water resource conservation before and after building a reservoir. This result can be taken as a reference when mapping out any water resource conservation in the reservoir watershed.

Study area description

The study area of this investigation, includes about 10,830 hectares in Nan-Haw county, southern Taiwan. Elevations ranged from 800 to 1000 m and mean annual precipitation is 2900mm, 90 percent of which comes between May and September, primarily resulting from typhoon and southwest monsoon. Average annual temperature is 25.6 °C and annual relative humidity is 84.5%. Soils within the study site are derived from sandy loam, loam and gravel. Geological distribution consists of argillite, slate complex and Phyllis, belonging to Nan-Zhuang formation.

Methods

AgNPS model

Watershed land-use management is one of the key issues in reservoir water quality control. Pollutants that affect reservoir water quality include sources and non-point sources. The Agricultural Non-point source Pollution Model, AgNPS, was developed by the Agricultural Research Service, Morris, Minnesota and the University of Minnesota for the Minnesota Pollution Control Agency (Young *et al.*, 1987). This model was designed to analyze the water quality impacts of non-point source pollution. It predicts runoff volume, peak rates, erosion, sediment, nitrogen, phosphorus, and chemical oxygen demand concentrations in the runoff (Vieux, 1994). The AgNPS model have adequate results in several watersheds in north of Taiwan (Sun *et al.*, 1992).

GIS implementation

Hydrologic processes are affected by the spatial variability of soils, topography, land use and cover, climate, and human-induced changes and management. The integration of distributed process models and Geographic Information Systems provide a powerful tool for decision making in the management, understanding, and control of non-point source water quality impacts (Vieux, 1994). For these reasons, a geographical information system (GIS) was implemented in this study. Arc/Info(ESRI, Redlands, California) software was used for the GIS. Several digital layers were generated to provide input for AgNPS model. These were (1) boundaries of watershed polygons; (2) boundaries of land-use polygons; (3) boundaries of soil type polygons; (4) digital elevation model (DEM); (5) stream. In Table 1, it shows the relationship between the parameters of AgNPS and geographic database.

Table 1. The relationship between the parameters of AgNPS and geographic database.

Number	Code	Cell Parameters	Geographic Database
1	CE	Cell number	watershed boundary
2	RC	Receiving cell number	digital elevation model
3	CN	SCS curve number	digital elevation model
4	LS	Land slope(percent)	digital elevation model
5	SF	Slope shape factor	digital elevation model
6	SL	Field slope length(feet)	digital elevation model
7	CS	Channel slope (percent)	river channel
8	CSS	Channel side-slope (percent)	river channel
9	N	Manning's roughness coefficient	land-use type
10	K	Soil erodibility factor	Soil type
11	C	Cover and management factor	land-use type
12	P	Support practice factor	land-use type
13	SCC	Surface condition constant	land-use type
14	A	Surface condition constant	land-use type
15	T	Soil texture	Soil type
16	F	Fertilization level	Land-use type
17	AF	Fertilizer availability factor	land-use type
18	PS	Point source indicator	other
19	GS	Gully source level(tons)	other
20	COD	Chemical oxygen demand factor	land-use type
21	IF	Impoundment factor	other
22	CI	Channel indicator	river channel

Integrate the geographic database to estimate the parameters of AgNPS

We use the PC ARC/INFO geographic information system's SML macro language to generate twenty-two parameters for AgNPS model from geographic database. The process of estimating the parameters of AgNPS are shown as Fig. 1.

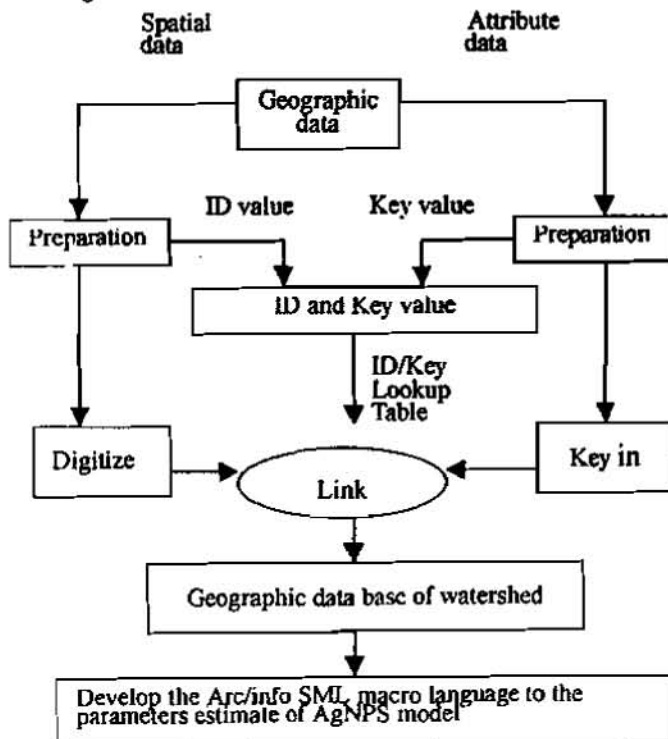


Figure 1. Process of estimating the parameters of AgNPS model.

Table 2. The output data of Sediment Analysis (R= 153 ; P = 1000mm)

(No)	Area Weighted Erosion Upland (T/ha)	Area Weighted Erosion Channel (T/ha)	Delivery Ratio (%)	Enrichment Ratio	Mean Concentration (PPM)	Area Weighted Yield (T/ha)	Yield (T/ha)
1	184.72	0.00	31	1	6934.26	56.58	81822.19
2	1369.12	0.00	15	1	24408.25	199.11	67006.41
3	163.29	0.00	26	1	5234.27	42.73	76348.84
4	2638.83	0.00	13	1	42466.93	347.81	124011.69
5	831.62	0.00	18	1	18110.07	150.56	18698.82
6	951.53	0.00	13	1	15001.54	122.85	51189.28
7	2244.37	0.00	52	1	135492.30	1165.62	303541.06
8	256.52	0.00	28	1	8784.95	72.32	34189.45
9	587.20	0.00	54	1	37978.95	316.44	65926.31
10	243.59	0.00	17	1	5187.60	42.35	9162.44
11	723.41	0.00	41	1	35611.64	299.65	164466.47
12	309.50	0.00	25	1	9518.21	78.01	46882.04
13	1160.51	0.00	20	1	27079.62	229.87	145503.12
14	858.19	0.00	18	1	18732.92	155.49	64785.61
15	750.33	0.02	16	1	14494.57	121.46	51579.56
16	1305.75	0.00	14	1	21470.69	183.80	194407.01
17	1140.62	0.02	32	1	41919.70	368.01	315505.17
18	1717.49	0.02	15	1	29617.80	256.70	174837.56

Table 3. The output data of nutrient analysis (R = 153 ; P = 1000.mm)

No	N-s	N-r	N-c	P-s	P-r	P-c	C-r	C-c
1	0.05	0.01	0.82	0.02	0.00	0.05	0.56	69
2	0.11	0.01	0.81	0.05	0.00	0.05	0.54	66
3	0.03	0.01	0.82	0.02	0.00	0.05	0.57	70
4	0.17	0.01	0.81	0.08	0.00	0.05	0.54	67
5	0.09	0.01	0.82	0.04	0.00	0.05	0.58	71
6	0.07	0.01	0.81	0.04	0.00	0.05	0.55	68
7	0.45	0.01	0.92	0.22	0.00	0.09	0.81	95
8	0.06	0.01	0.82	0.03	0.00	0.05	0.57	70
9	0.18	0.01	0.84	0.09	0.00	0.06	0.60	72
10	0.03	0.01	0.81	0.02	0.00	0.05	0.57	70
11	0.18	0.01	0.85	0.09	0.00	0.07	0.66	80
12	0.05	0.01	0.82	0.03	0.00	0.05	0.59	73
13	0.12	0.01	0.84	0.06	0.00	0.06	0.71	84
14	0.09	0.01	0.82	0.04	0.00	0.05	0.62	75
15	0.07	0.01	0.82	0.04	0.00	0.05	0.53	64
16	0.10	0.01	0.82	0.05	0.00	0.05	0.60	71
17	0.21	0.01	0.82	0.10	0.00	0.05	0.42	48
18	0.13	0.01	0.83	0.07	0.00	0.05	0.68	79

N-s: Total Nitrogen in Sediment(ton/ha)

N-r: Total soluble Nitrogen in Runoff(ton/ha)

N-c: Soluble nitrogen in Runoff(PPM)

P-s: Total Phosphorus in Sediment(ton/ha)

P-r: Total soluble Phosphorus in Runoff(ton/ha)

P-c: Soluble Phosphorus in Runoff(PPM)

COD-r: Total soluble Chemical oxygen demand in Runoff (Ton/ha)

COD-c: Soluble Chemical oxygen demand in Runoff(PPM)

Results and discussions

Geographic database and water quality modeling system

Traditionally, the use of GIS technology has been limited to manipulation geographic databases and producing maps. Recently, however, this rapidly emerging technology has been used extensively for planning water quality protection programs and in studying environmental processes (Goodchild, Parks, & Steyaert, 1993). In these applications, the GIS provides the tool to encode, spatially organize, manipulate, analyze, and present model input and output data. A number of papers have been developed to combine soil erosion and pollutant export models with ARC/INFO GIS software and graphic user interface (GUI) (Sun *et al.*, 1992; Tim & Liao, 1994).

To delineate the non-point source pollution of this study area, six basic maps, namely vegetation cover, slope, aspect, soil type (from Council of Agriculture), geological type (from Council of Agriculture), stream, boundary of watershed, have been prepared by integrating the data input from topographic map (1:250000). On the other hand, GRASS GIS use the digital elevation data of this area to divide watershed into 18 sub-watershed. For AgNPS modeling, the basic polygon coverage was converted to raster coverage by the POLYGRID command of ARC/INFO. The lookup table of AgNPS modeling parameters was built by referring to previously papers. By using raster coverage, lookup table as basic data and using ARC/INFO SML language as tool, the special parameters of AgNPS modeling has been produced.

Results of AgNPS modeling

This study collected the climatological data of Nan-Haw from 1984 to 1995, using Log-Pearson type III method to estimate the maximum precipitation in one day. The probability distribution of hydrologic frequency is shown as follows:

$$Y = 395.02 + 148.43 \ln(T) \quad r=0.99$$

$$T=14.79^{**} \quad T=11.41^{**}$$

Y : maximum probable rainfall in one day (mm)

T : return period (yr)

The rainfall-erosion factor R was obtained from the iso-erodent map of the Nan-Haw County. and a single-unit value of 153 was used for the watershed. If we set 25 years as return period, the maximum probable rainfall in one day can be estimated as 1000mm by the equation of hydrologic frequency. The entire database was manipulated and spatially organized in ARC/INFO as watershed modeling coverage. The simulation results for the Nan-Haw reservoir watershed are summarized in Table 2 and 3.

The Agricultural Research Service of United States of America developed AgNPS. In Taiwan, because of the different environment, so how to modify the output data of AgNPS is very important. Comparing the observed values with the predicted values (Line, *et al.*1991), had developed the modifying factor(0.15). Though some papers had proved that the predicted value of AgNPS was different from the observed value in Taiwan, we can use the predicted value as a relative value to compare the situation of water resources conservation in each sub-watershed.

Conclusions

High population density, and rapid economic development in Taiwan have resulted in changes so acute in land management, so that the land of reservoir watershed had been over-used. The objective of this study is to integrate the effective and powerful tools of Geographic Information System (GIS) and the Agricultural Non-point Source Pollution Model (AgNPS) to quantify erosion problems in the Nan-Haw reservoir watershed in Taiwan. The AgNPS model input data were obtained by GIS techniques. If we use 25-year frequency storm, 1000 mm/day to simulate one event storm, the results show that the soil erosion is 145.2 t/ha and the sedimentation is 35 t/ha. To prescribe appropriate soil and water conservation practices and controls the volume of soil loss within acceptable (or tolerable) limits. The model also has the capabilities of identifying areas within the watershed with high erosion and sediment yield. This provides a guide for government officials and decision-makers in formulating national policies and development plans to counteract erosion effects, to optimize farm output, and to stabilize economic development.

References

- Huggins, L.F. and Burney J.R. 1982. Surface runoff, storage and routing, Chapter 5, In Haan C.T. (Ed.) Hydrologic Modeling of Small Watershed, ASAE Monograph No.5 Agricultural Non-point Source Pollution Model. American Society of Agricultural Engineering, St.Joseph.Michigan. PP.160-170
- Knisel W.G.(Ed.) 1982. CREAMS:A Field-Scale Model for chemicals Runoff, and Erosion from Agricultural Management Systems. ASAE paper No.86 -2511. Winter Meeting,Chicago Illinois.
- Leonard, R.A.,Knisel W.G.,and still D.A. 1986. GLEAMS: Groundwater Loading Effects of Agricultural Management Systems. ASAE Paper No.86-2511. Winter Meeting,Chicago Illinois.
- Liao H.H., Tim U.S. 1994. Interactive Water Quality Modeling Within A GIS Environment. Comput. Environ. and Urban Systems Vol.18. No.5:343-363.
- Moore I.D.,Grayson R.B.,and Ladson A.R. 1991. Digital Terrain modeling Review of Hydrological, Geomorphologic, and Biological Applications. Hydrological Processes. Vol.5. 3-30.
- Needham S. and Vieux B.E. 1989 A GIS for the AgNPS parameter Input and Mapping Output. ASAE Paper No. 89-2673, Winter Meeting, Dec. 1989, Chicago,Illinois
- Ross B.B.,Contractor D.N. and Shanholtz V.O. 1979. A finite-element Model of Overland and Flow for Assessing the Hydrologic Impact of Land-use Change. Journal of Hydrology 41. 11-30.
- Speight J.G. 1974 A Parametric Approach to Landform Regions. Spewal Publication Institute of British Geographers. 7. 213-230.
- Sun C.H., Chan S.C., Yang M.C. 1992. Spatial Decision Support Systems for Reservoir Water Quality Management -A Prototype Study. Resource Technology 92 Taipei. November 16-18,1992, Taipei, Taiwan, R.O.C.

- Vieux B.E. 1988 Finite Element Analysis of Hydrological Response Areas Using Geographic Information Systems. An Unpublished ph.D. dissertation Department of Agricultural Engineering, Michigan state University East Lansing.
- Vieux B.E. 1991 Geographic Information Systems and Non-point Source Water Quality and Quantity Modelling. Hydrological Processes. Vol.5. 101-113.
- Young, R.A., Onstad C.A., Bosch D.D., and Anderson W.P. 1987. AgNPS Agricultural Non-Point-Source Pollution Model: A Watershed Analysis Tool, USDA-ARS. Conservation Research Report 35.

AnnAGNPS — NON-POINT POLLUTANT LOADING MODEL

By Roger G. Cronshey, Hydraulic Engineer, USDA Natural Resources Conservation Service, Beltsville, MD;
Fred D. Theurer, Agricultural Engineer, USDA Natural Resources Conservation Service, Beltsville, MD

INTRODUCTION

The continuous simulation Annualized Agricultural Non-Point Source pollution computer model (AnnAGNPS) is a replacement for the existing Agricultural Research Service (ARS) single-event AGNPS model (Young et al 1987). The development of AnnAGNPS was a partnering effort between the US Department of Agriculture's ARS and Natural Resources Conservation Service (NRCS). ARS provided the management support, funds for travel and some technical support personnel, and most of the research science that was used for the technology included in the model. NRCS provided most of the personnel to manage, plan, design, and develop the computer program, as well as refine the technology implemented.

AnnAGNPS simulates the movement of sediment and chemicals (nutrients and pesticides) in the surface water for a watershed over a user selected period of time using a daily time step. The pollutant loading can be expressed as quantities for a runoff producing event in selected stream reaches and as source contributions from a watershed component (specific land area, stream reach, feedlot, gully or point source) to the watershed outlet over the simulation period.

The computer model is written in ANSI standard Fortran 90, taking advantage of the latest Fortran features including runtime array allocation that utilizes only the computer memory required for the specific watershed being analyzed and is executed as a batch process. The use of standard Fortran makes the code extremely portable and it can be run on any computer platform that has a Fortran 90 compiler. Software to preprocess (prepare input data) and post-process AnnAGNPS data (sort, subdivide, and/or display output) are under separate development.

WATERSHED COMPONENTS

AnnAGNPS generates quantities of water, sediment and chemicals (nutrients and pesticides) leaving land areas (cells) and flowing into the watershed stream network at specific locations (reaches) on a daily basis. The cells can be of various sizes either square shaped (as was the case in AGNPS) or amorphous shaped (hydrologically based), provided each cell can be represented by a single land use, land management, and soil type. The water, sediment, and chemicals from the cells are then routed through the watershed reaches to the watershed outlet. The following specialized components are available to supplement the cells and reaches: **feedlots** (add nutrients from animal operations to the reaches); **gullies** (add sediment and attached chemicals to the reaches); **point sources** (add water and chemicals to the reaches); and **impoundments** (reduce sediment loads leaving storage reaches).

To simulate watershed variation during the simulation period, the following types of time variant data are entered: **daily climate** (precipitation, maximum and minimum air temperature, dew point temperature, sky cover, and wind speed and direction); **field operations** (schedules by land area detailing planting, harvesting, tillage, chemical applications (fertilizers and pesticides) and irrigation applications); and **feedlot operations** (schedules for each feedlot detailing changes in daily manure production rates and times of manure removal).

Each day the applied water and resulting runoff (if any) is routed through the watershed system before the next day is considered. Thus, no water except for that contained within the soil column is carried over from one day to the next. Chemicals in the cells and feedlots are also carried over from day to day after adjusting by appropriate daily decay rates.

MODEL INPUT

Input to the model is contained in three files. The files are: **AnnAGNPS input** which contains all watershed and time variant data except the climate data; **Climate input** which contains information on the climate station location and daily climate parameters for the simulation period; and **AnnAGNPS input filename** (optional) which contains the name of the AnnAGNPS input file. Each input file is either all English unit data or all SI (metric) unit data.

AnnAGNPS input file contains 34 different categories (Data Sections) of data used to describe the watershed and the time variant parameters. Not all 34 are needed for each job. For example, the optional program features: Feedlots; Fertilizers; and Pesticides each have two dedicated data sections, while the remaining optional features use only one. Most of the data sections are related (directly or indirectly) to the cells. Figure 1 shows the relationship between cell data and the other data sections, including the name of the data variable that makes the connection.

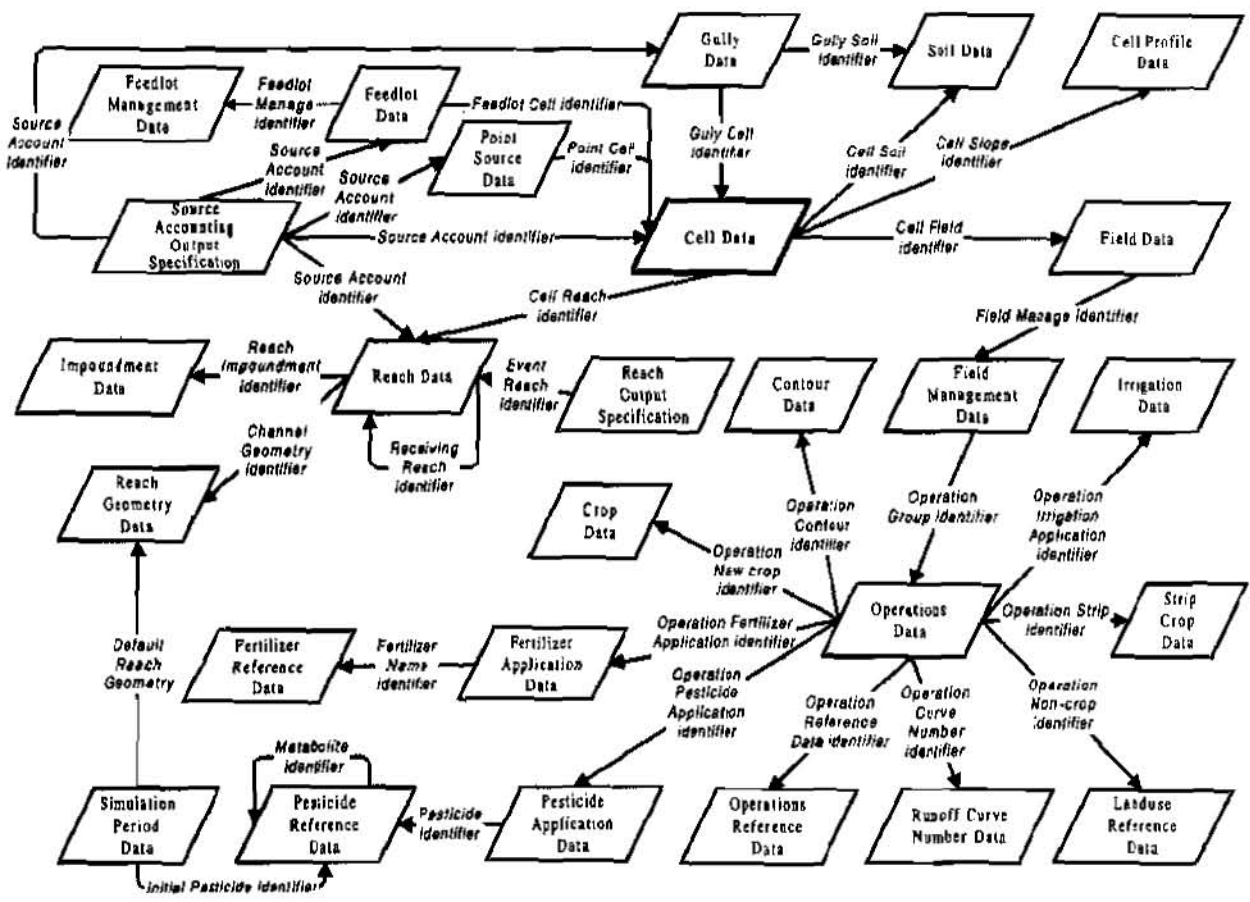


Figure 1 - AnnAGNPS input data sections as related to cell data

A special subset of the input file used to run a single event based on input data converted from the AGNPS program uses only a maximum of 20 of the input data sections. This special case does not use the climate input file and employs Universal Soil Loss Equation (USLE) based erosion and sediment as was done in AGNPS.

Climate input file is contained in one data section header. Climate station static parameters are on the first four records followed by one record of daily parameters for each day in the climate record. The climate record required may need to be longer than the simulation period. If the optional one-year parameter initialization simulation is to be used than daily climate data for that period must also be included. For short simulation period runs, climate data should be entered in complete months as average monthly values for several climate parameters are generated from the daily climate data provided. Climate data can be either from historically recorded data or from data generated with a climate generator.

AnnAGNPS input filename file is optional and contains the name of the AnnAGNPS input file. It is a one line file. If this file is not present the default AnnAGNPS file name (AnnAGNPS.inp) is used.

MODEL OUTPUT

There are four standard output files for the model. They are: **Error file**; **Debug file**; **Event file**; and **Source Accounting file**. The first three files are always present while the last is only created if source accounting information is specified. Output files are either all English unit data or all SI (metric) unit data.

Error file contains messages that define any errors encountered during: data preparation (reading and setting up the data for the simulation); simulation processing; or finishing source accounting data. Data preparation proceeds with as much error checking as possible. If any errors are found during data preparation, the run will terminate before any simulation processing. Most errors will occur during data preparation, and the error message text should lead directly to the offending (or missing) input. If an error is encountered during the simulation period, data up to the time of the error will have been written to the Event file but no data will be contained in the Source Accounting file. The Error file will have a file length of zero for a clean run using the model.

AnnAGNPS provides precise information on the error detected and, if appropriate, where the offending input is located. There are about 300 different error messages in AnnAGNPS and a sample message follows:

Value (90.) outside acceptable range (0.0 - 1.0) for 'Irrigated Area Fraction'
on record 3 of IRRIGATION APPLICATION DATA:

Debug file contains warning messages and most intermediate output requested by the user via the Verification Data section in the AnnAGNPS input file. There are almost 100 different flags that can be set with Verification Data allowing the control of warning message generation, subroutine traces, intermediate calculation output, and verification of input. If no Verification Data is requested, this file should have a zero length.

Event file contains information on user selected reaches for each runoff event during the simulation period. Data for the watershed outlet is automatically included. Specific information output can vary for each selected reach based on the following categories: water; sediment class and source; sediment class; sediment source; Nitrogen; Phosphorus; organic Carbon; and pesticides. Any of the codes for the categories that are blank in the Reach Output Specification (AnnAGNPS input file) for a given selected component will use the appropriate code from the Global Output Specification section data.

Source Accounting file contains information on the contribution for the selected component (specific cell, reach, feedlot, gully, or point source) to the watershed outlet over the simulation period. Values are expressed as a fraction of the outlet accumulation for a given parameter. (The outlet accumulations are also part of the file). Different information can be specified for each component selected based on the following categories: water; sediment class and source; sediment class; sediment source; nutrients; and pesticides. Any codes for the categories that are blank in the Source Accounting Output Specification (AnnAGNPS input file) for a given selected component will use the appropriate code from the Global Output Specification section data.

MODEL PROCESSING

Conceptually the computer model can be viewed as consisting of three parts: Data Preparation; Simulation Processing; and Source Accounting Output. **Data Preparation** encompasses: reading in data; error checking; setting internal pointers; establishing internal array sizes based on data read; initializing data required for the simulation (developing climate normals; soil compositing; determining cell and reach time of concentrations; establishing reach routing order and reach drainage areas, Revised Universal Soil Loss Equation (RUSLE) (Renard et al 1997) preprocessing, and optional one-year initialization). **Simulation Processing** includes processing climate information for each day of the simulation period and its impact on cells, feedlots, gullies point sources and reaches. Information concerning soil moisture, snow pack, crop growth, residue and chemicals are carried from one day to the next for each cell as are manure pack and nutrients for each feedlot. Reach and selected source accounting component data are accumulated from the events during the simulation processing. **Source Accounting Output** analyzes variable accumulations over the simulation period at upstream and downstream reach locations to determine outlet contribution from specific user selected components (cell, feedlot, gully, point source, or reach). Variables analyzed are user selected from input source accounting codes or global source accounting codes.

When the AGNPS to AnnAGNPS Converter is completed, the model will be capable of running in two modes. The RUSLE based continuous simulation mode which is the basis for AnnAGNPS and a USLE based AGNPS mode which will run the converted AGNPS input data without any additional data required. The AGNPS mode does NOT perform the same processing as was done in the older AGNPS program but adapts the AnnAGNPS technology to converted AGNPS input data. Many assumptions, which users should be aware of, will be made by the AGNPS Converter. In the following summary of major computational steps, some will be indicated as either AnnAGNPS or AGNPS which means the step only applies to that particular mode.

DATA PREPERATION

Read Input File Name - Name of the AnnAGNPS input file is read from the 'AnnAGNPS.fil' file if such file is available. If the file is not available, then the default AnnAGNPS input file name (AnnAGNPS.inp) is used.

Read AnnAGNPS Input File: AnnAGNPS input file is read a record at a time. The first record indicates the mode that will be used for the simulation run (AnnAGNPS or AGNPS). Remaining data is then read in the formats of the various data sections as described in the AnnAGNPS model documentation. The data sections can be read in any order the user chooses. Numeric data is checked for valid data type (integer or floating point). Numeric and some alphabetic data are checked for acceptable ranges. All required fields are checked for completeness.

Soil Composite Create: Entered soil layer data is reduced to a two layer soil profile for the use in the model. The top 200 mm are used as the top layer and the remaining soil profile comprises the second layer. Generally the values from the entered soil layer data are weighted by their relative thickness in either of the two composite layers.

Route Order: Receiving reach identifiers are used to construct the watershed flow network. From the network an order is determined that will be used for reach processing. The reach processing order ensures that all upstream reaches are processed prior to the current reach.

Reach Area: Cell areas are added to the reaches at the proper location (upstream or downstream) where they enter the watershed stream system. Using the routing order, the individual reach areas are accumulated in a downstream direction to define the entire upstream areas draining to each reach.

Read Climate Data (AnnAGNPS): Climate input file is read including climate station information and the daily climate parameters. The daily climate data time period must span the simulation period. Also for short simulation runs, data is best entered in complete months as monthly normal data is computed and used in the simulation processing.

Time Period Check (AnnAGNPS): The period of daily climate data entered is compared with that for the requested simulation run. Climate records which do not encompass the entire simulation period result in an error.

Create Normals: Daily climate data is used to produce average monthly values for most of the climate parameters. Annual average values are computed for precipitation and minimum and maximum temperature. Also using the individual monthly precipitation computed, a representative month of climate data (for each calendar month of the year) is selected. The daily values in the representative months will be used as the climate for the initialization year (if parameter initialization year is requested). Solar radiation (generated from daily sky cover) is reduced to an average value for each calendar day of the year and not monthly averages.

Cell T_c : If the cell time of concentration (T_c) was not entered with input, then it is calculated from the cell profile data. Cell time of concentration is the sum of the travel times for: overland flow; shallow concentrated flow; and concentrated flow within the cell. The first 50 m of flow length are treated as overland flow. The next 50 m are treated as shallow concentrated flow (with a maximum of .61 m/sec velocity). Cell flow length beyond 100 m is treated as concentrated flow. Calculations for the three flow types are based on procedures in Soil Conservation Service (SCS) TR-55 (SCS 1986). All three types may not be present in each cell.

Reach Geometry: If any or all the reach cross section parameters are missing from the input data, they are computed using the reach drainage area and power equations. The four reach geometry relationships included are: Reach Length; Reach Top Width; Reach Flow Depth; and Valley Width. The equation coefficient and exponent used for

each are based on the those associated with the Reach Channel Geometry Identifier for the reach or a default set if no identifier was provided.

Reach T_c : Each reach is processed in the reach routing order previously determined. The maximum single cell T_c directly contributing to the upstream end of the reach is determined. From each reach that flows into the current reach, two values are considered: the maximum single cell T_c that joins this reach at its downstream end; and the T_c at upstream end of the reach plus the travel time through the reach. Not all reaches have both a cell contributing at its upstream end or an upstream reach, but each reach must have at least one or the other.

Initialize Parameters: Starting conditions are established for most dynamic cell variables prior to the start of simulation period or one-year initialization. Information for initializing the variables comes from the initial Cropland and Non-crop information optionally entered as part of Simulation Period Data (AnnAGNPS input file) or from Operations Data which contains no operation date.

RUSLE Preprocess (AnnAGNPS): The required RUSLE parameters (K, LS, C, EI, and P) are established over the operation management cycle for each non-water cell. The K-factor is computed for each soil either as an annual value or a series of 24 15⁺ day values for a year depending on the specified Variable K-factor code and whether the EI Number supports variable K-factors. The C-factor is computed as an annual value for non-cropland and as a series of 24 15⁺ day values for each year in the operation management schedule for cropland. The LS-factor is computed for each cell. The P-factor is computed as an annual value for non-cropland and as a series of annual values (one for each year in the operation management schedule) for Cropland. The P-factor includes adjustments for contours, strip crops, and terraces contained in the cell, as well as sub-surface drainage. The EI-values used for the entire watershed are expressed as a series of 24 15⁺ day values in the calendar year.

Run Initialization Year (AnnAGNPS): If the initialization year is requested, the cell process portion of the simulation processing is run for a one year period ending at the start of the simulation period. The climate data used is for the days in the representative months selected from the climate data entered. The purpose of the initialization year is to stabilize the initial cell parameters before starting the actual simulation.

SIMULATION PROCESSING

Cell Processes: Each cell is processed on a daily basis. The following steps are used in the processing:

Adjust Weather: The daily climate station precipitation and temperatures are adjusted for the elevation difference between the climate station and the cell. All other climate data are taken directly from the climate station.

Potential Evapotranspiration (AnnAGNPS): Potential evapotranspiration is calculated with the Penman equation.

Select Operations (AnnAGNPS): The operation schedule is checked for any operations that occur for the cell on the current day. Any identified operations are set aside for incorporation into the remaining cell steps for the day.

Irrigation Applied (AnnAGNPS): Irrigation water is applied as identified in current day's operations or from previous operations if part of an irrigation interval. The applied irrigation can be either manual (fixed amount) or automatic (raise soil moisture to user supplied Irrigation Trigger). Only the applied water is determined, the amount that runs off is dependent on other daily factors. The irrigation runoff will be determined as part of the soil moisture balance.

Winter Routines (AnnAGNPS): Precipitation that occurs when average air temperature is below freezing (0° C) is treated as snow which accumulates on the cell. Existing snow packs are aged for the day (possibly producing snow melt) based on the climatic data and the soil temperature. Soil depth to frozen layers (up to 2) is also determined or adjusted. On any day that the winter routines are applied, irrigation amounts previously determined are ignored.

Soil Moisture (AnnAGNPS): Daily soil moisture accounting considers applied water (rainfall and irrigation or snow melt), runoff, evapotranspiration, and percolation in maintaining a water budget for the two-layer composite soil profile. Runoff is calculated using the SCS Runoff Curve Number equation, but may be modified if a shallow frozen soil layer exists. Curve numbers vary between the Antecedent Moisture Condition (AMC) I (dry) value and the

AMC III (wet) value using the procedure in the SWRRB (Arnold et al 1990) and EPIC (Williams et al 1989) models. Actual evapotranspiration is a function of potential evapotranspiration and soil moisture content. Percolation occurs at the rate of the hydraulic conductivity corresponding to the soil moisture content, calculated according to the Brooks-Corey equation. Runoff volume is stored separately for rainfall and snow melt or irrigation.

Revise Curve Number (AnnAGNPS): Revise the cell runoff curve number based on new curve number supplied with the day's operations (i.e. tillage, harvest etc.). If no new curve number is applied, adjust curve number if in a curve number transition period for crop "development" growth time.

RUSLE Sediment (AnnAGNPS): Sediment produced by the rainfall is generated from the user supplied rainfall distribution (code) and the current cell characteristics using RUSLE. Sediment from snow melt is also produced from RUSLE based on a uniform distribution. Sediment amount is divided into five particle size classes (clay, sand, silt, small aggregate, and large aggregate).

USLE Runoff and Sediment (AGNPS): The cell runoff is computed from the cell Runoff Curve Number and precipitation using the SCS rainfall-runoff equation. Sediment is calculated from the K (soil associated with cell), LS, P (field associated with cell), and C (landuse associated with cell) using the USLE equation. The computed sediment is distributed among the five particle size classes (silt, clay, sand, small aggregate, and large aggregate) for the cell soil.

Irrigation Runoff and Sediment: The portion of applied irrigation that runs off is determined. The sediment due to irrigation is computed using the irrigation runoff amount and the sediment concentration rate entered as input. Sediment amount is divided into five particle size classes (clay, sand, silt, small aggregate, and large aggregate).

Adjust Nutrients: The operation schedule is checked for addition of nutrients on the cell for the day. A daily mass balance for nitrogen (N), phosphorus (P), and organic carbon (OC) is computed for each. Major components considered are uptake of N and P by plants, application of fertilizers, residue decomposition, and downward movement of nitrogen and phosphorus. The day's sediment bound N, soluble N in runoff, sediment bound P, soluble P in runoff, and sediment bound OC are determined for the cell. Nitrogen and phosphorus are partitioned into organic and mineral parts and a separate mass balance computed for each. N and OC cycles are simplifications that track only major N transformations of mineralization from humified soil organic matter and plant residues, crop residue decay, and fertilizer and plant uptake. Plant uptake of N and P are modeled through a simple crop growth stage index.

Adjust Pesticides: The operation schedule is checked for addition of pesticides on the cell for the day. A daily mass balance adapted from the GLEAMS (Knisel 1993) model is computed for each pesticide. Major components considered are washoff from foliage, downward and upward pesticide movement in the soil profile, and degradation based on the pesticide half-life. The day's amounts of sediment bound and runoff soluble pesticide are computed.

Add Cell Data to Reach: Water, sediment by class, nutrients, and pesticide quantities leaving the cell are added to the appropriate stream reach at the proper location (upstream or downstream). Cell sediment is identified as "sheet and rill".

Feedlot Processes: Each feedlot is processed on a daily basis using the following steps.

Feedlot Event Calculations: If runoff occurs on the cell associated with the feedlot, then the portion of runoff that enters the feedlot area is routed. The amount of soluble nutrients (N, P, and OC) that are contained in the runoff are determined. The runoff and nutrients are then routed through any buffer area down slope of the feedlot which can reduce the nutrient quantities in the runoff. The resultant nutrient amounts are added to the appropriate stream reach for the cell containing the feedlot at the proper location (upstream or downstream). No water is added to the reach for the feedlot as it has already been accounted for with the cell runoff. Any nutrients that are picked up by runoff and leave the feedlot are subtracted from existing manure pack.

Feedlot Daily Calculations: The nutrients produced by the animals on the feedlot are added to the manure pack. The manure pack is decayed for the day using default decay rates for the different nutrients. The current daily change in nutrient production is added to the current days rate to define the new rate to apply to the feedlot the next

day. Check the feedlot operations for any operations today. If any operations are found, the daily rate and daily rate change for each of the nutrients is updated. These changes will take effect on the next day. If a scraping operation is indicated in a current day's operation (Pack Remove Ratio), the manure pack nutrients are adjusted.

Gully Processes: Each gully is processed on a daily basis. The runoff from the cell that drains through the gully is based on the ratio of the gully drainage area to the cell drainage area. The sediment total is determined from the gully runoff and a power equation using the user supplied coefficient and exponent. The sediment amount is divided into five particle size classes (clay, sand, silt, small aggregate, and large aggregate) using either the gully identified soil or the cell soil (if no gully soil was identified). Gully sediment is then added to the appropriate stream reach for the associated cell at the proper location (upstream or downstream). Gully sediment is identified as "gully". No water is added to the reach for the gully as it has already been accounted for with the cell runoff.

Point Source Processes: Each point source is processed on a daily basis. The user entered constant flow rate and nutrients are used to determine runoff volume and nutrient masses to be added to the reach associated with the cell containing the point source at the proper location (upstream or downstream).

Reach Processes: If runoff occurs from any cell (excluding point sources), then reach routing is performed. The routing is done in a reach routing sequence order that ensures all reaches upstream of a given reach are routed prior to it's routing. (Reaches with no water at the upstream end are not routed as there is nothing to route.) The following steps are used in the routing of a reach.

Water Routing: An equivalent Runoff Curve Number and associated Ia/P ratio are computed from the upstream runoff volume and the weighted rainfall (including rainfall and snow melt or irrigation). The Ia/P ratio along with the user defined rainfall type (Rainfall Distribution code) are used to determine a peak flow for the reach using an extension of the TR-55 Graphical Peak Discharge method (Theurer & Cronshey 1998). All water variables are then translated from the upstream end of the reach to the downstream end of the reach.

Sediment Routing: Sediment routing is done using the Bagnold equation. The water flow, if appropriate, is divided into within-bank-flow and out-of-bank flow for separate sediment load calculations. Sediment is routed by the five particle size class (clay, silt, sand, small aggregate, and large aggregate) with the three sediment sources (sheet and rill, gully, and bed and bank) combined together. After routing, the sediment sources are re-subdivided for each particle class as follows: decrease in reach (distribute decrease proportionally among the three sources); or increase in reach (all of the increase is bed and bank).

Nutrient Routing: Each nutrient (N, P, and OC) is subdivided into water borne (soluble) and sediment borne (attached). Attached P is further subdivided into organic and inorganic. Each nutrient subdivision is decayed based on the reach travel time, water temperature, and an appropriate decay constant. The soluble nutrients can be further reduced by the fraction of water that infiltrates through the bottom of the reach. The attached nutrients are adjusted by any change in clay sediment from the upstream to downstream end of the reach. Additionally an equilibration is done for the soluble and attached inorganic P at the beginning of the routing (upstream) and after the nutrients are routed (downstream). The upstream equilibration is required as water from several sources may converge at the upstream end of the reach, and while each may be in equilibrium, the aggregate may not.

Pesticide Routing: Each pesticide is subdivided into water borne (soluble) and sediment borne (attached). Each pesticide subdivision is decayed based on the reach travel time, water temperature, and the appropriate pesticide half-life. The soluble portion of each pesticide can be further reduced by the fraction of water that infiltrates through the bottom of the reach. The attached pesticides are adjusted by any change in clay sediment from the upstream to downstream end of the reach. Additionally an equilibration is done for each pesticide at the beginning of the routing (upstream) and after the pesticide is routed (downstream). The upstream equilibration is required as water from several sources may converge at the upstream end of the reach, and while each may be in equilibrium, the aggregate may not.

Update Receiving Reach: The routed water, sediment and chemical quantities are added to the upstream values for the next downstream reach (or to the outlet if at downstream end of watershed). Also added are any cell, feedlot, gully, and/or point source values that join the current reach at the downstream end. These added values were not included in the current reach routing but will contribute to any reaches downstream.

Output Event: At user selected reaches, if there is any water at the downstream end (routed or added from cells or point sources), then event information is written to the event file. Information on water, sediment, nutrients and pesticides can be included depending on the selections made by the user on either the Reach Output Specification or the Global Output Specification.

Simulation Accumulation: All information for the day's reach event is added to the simulation period accumulation for the reach. The data include the reach routed items (upstream and downstream) as well as the added items from cells, feedlots, gullies, and point sources that may join the reach at the downstream end but are not routed in the reach. This information will be used later for generating the source accounting information.

SOURCE ACCOUNTING OUTPUT

Reach Ratios: Ratios are computed from the simulation period accumulated data at each end of each reach. Which parameters (water, sediment, nutrients, and pesticides) have ratios computed depends on the composite selected output for the source accounting components. Upstream ratios are computed as the upstream parameter value / downstream parameter value. In situations where the upstream value is greater than the downstream value (loss due to infiltration or deposition), the upstream ratio is 1 (all downstream contribution to the outlet came from upstream). The downstream ratios are computed as the downstream value of the current reach / upstream value of the receiving reach. The watershed outlet is treated as the upstream end of a reach just downstream from the last reach and may include cell and other component contributions that are added after the last reach was routed.

Write Outlet Accumulation: The outlet accumulation information is written to the source accounting file. This will be used as the basis for applying the contributing ratios for the selected source accounting components that will be written to this file next.

Compute Source Accounting Ratios: Ratios are computed from the simulation period data for the source accounting component (other than a reach) and the previously computed reach ratios. The source accounting component ratio is computed as accumulated component value / upstream value (for components added at the upper end of a reach) and as accumulated component value / upstream value of receiving reach (for components added at the downstream end of a reach). The ratios are then multiplied by the upstream and downstream ratios for all reaches downstream of where the component enters the stream system. (Additions made at the upstream end of reach must also be multiplied by the current reach ratios, downstream additions do not.) For source accounting components added at the watershed outlet, the computation is simply the ratio of the accumulated value / outlet value.

Write Source Accounting Ratios: The computed source accounting ratios are written to the source accounting file based on the selected output for each component.

REFERENCES

- Arnold, J. G., Williams, J. R., Nicks, A. D., and Sammons, N. B., 1990, SWRRB A Basin Scale Simulation Model for Soil and Water Resources Management. Texas A&M University Press. ____ p
- Knisel, W. G., editor, 1993, GLEAMS: Groundwater Loading Effects of Agricultural Management Systems. University of Georgia, Coastal Plain Experiment Station, Biological and Agricultural Engineering Department, Publication No. 5, 260p
- Renard, K. G., Foster, G. R., Weesies, G. A., McCool, D. K., and Yoder, D. C., coordinators. 1997 Predicting Soil Erosion by Water: A Guide to Conservation Planning With the Revised Universal Loss Equation (RUSLE). USDA Agriculture Handbook No. 703, 404 p
- Soil Conservation Service, 1986 Urban Hydrology for Small Watersheds. USDA Soil Conservation Service Technical Release 55,
- Theurer, F.D., & Cronshey, R.G., 1998. AnnAGNPS-Reach Routing Processes. In *Proceedings First Federal Interagency Hydrologic Modeling Conference*, 19-23 April 1998, Las Vegas, NV.
- Williams, J.R., Dyke, P. T., Fuchs, W. W., Benson, V. W., Rice, O. W., and Taylor, F. D., 1989, EPIC — Erosion/Productivity Impact Calculator: 2, User Manual. Sharpley, A.N. and Williams, J. R., editors. USDA Technical Bulletin No. 1768. ____ p
- Young, R. A., Onstead, C. A., Bosch, D. D., Anderson, W. P., 1987, AGNPS, Agricultural Non-Point-Source Pollution Model. A Watershed Analysis Tool. USDA Conservation Research Report 35, 80p

AnnAGNPS—RUSLE SHEET & RILL EROSION

By W. Frank Geter, Environmental Modeling Specialist, USDA - NRCS, Fort Collins, CO;
Fred D. Theurer, Agricultural Engineer, USDA - NRCS, Beltsville, MD

Abstract This paper describes the design modifications to the Revised Universal Soil Loss Equation (RUSLE) to simplify and enhance its inclusion in the multi-cell continuous simulation model AnnAGNPS. These modifications include the: (a) ability to process multiple cells; (b) elimination of redundant calculations for cells with identical field management and soil conditions; (c) ability for contours and mechanical disturbances to rotate on non-cropland landuses; (d) calculation of sediment delivery ratio to the edge of the field for every cell; and (e) erosion modifications for frozen soil conditions.

INTRODUCTION

The Annualized Agricultural Non-Point Source Pollution Model (AnnAGNPS) (Cronshey & Theurer 1998) is a continuous simulation, daily time step, watershed scale, pollutant loading model. AnnAGNPS analyzes a watershed subdivided into suitably small cells of homogeneous landuse management, climate and soils which can adequately approximate site conditions. Runoff, sediment and other contaminants are routed from each cell through a channel network, including surface water impoundments, to the outlet of the watershed. A unique and powerful feature of AnnAGNPS is the ability to track the source and relative contribution of contaminants down through the channel network to the outlet of the watershed. This feature gives the user the ability to determine the source, and the relative contribution of that source, at any point in the watershed.

Soil detachment, deposition and transport are important considerations when modeling pollutant loads from agricultural watersheds. Detached soil particles are deleterious contaminants in downstream water courses causing a degradation in stream and lake habitat and can result in premature filling of lakes and reservoirs. In addition, detached soil particles are carriers of many other contaminants such as phosphorus and pesticides. Given the importance of soil erosion, deposition, and transport, it is critical that an appropriate level of technology be chosen to simulate these processes.

The Agricultural Non-Point Source Pollution Model (AGNPS) (Young et al 1987), the predecessor to AnnAGNPS, used the Universal Soils Loss Equation (USLE) (Wischmeier et al 1978) to predict soil erosion for a single storm event. Since AGNPS is a single storm event model, the fact that the soil erodibility factor (K factor), cover and management factor (C factor) and the practice factor (P factor) are fixed values, input by the user, is not a significant limitation. However, since AnnAGNPS is a continuous simulation model, temporal changes in cover, soil erodibility and conservation practices can have a significant impact on simulated pollutant loads. In addition, AnnAGNPS has virtually no limitation on the number of cells that can be defined by the user to make up a watershed, therefore manually estimating fixed USLE K, C, and P factors for each cell prior to simulation would impose a significant usability limitation. Several erosion prediction models and subroutines were considered in deciding which erosion technology should be incorporated into AnnAGNPS. Factors that were considered were; the number of inputs, time step, process detail, data availability, degree of model acceptance, and runtime.

The Revised Universal Soils Loss Equation (RUSLE) (Renard et al 1997) technology was selected as the most appropriate level of technology for the following reasons:

1. The number of inputs required did not significantly add to what was already required.
2. The minimum time step was 15 days. Although this is larger than the single day time step in AnnAGNPS it was not considered a significant limitation because RUSLE K and C factors do not vary significantly on a day to day basis and adjustments to K factor would be made on daily time step during the actual simulation.
3. The process detail was considerable but appropriate. The level of detail in calculating a time variant C factor in RUSLE is considerable because of the many processes involved such as; tillage effects, soil consolidation, and residue decomposition. This detail however was considered necessary and appropriate since cover conditions change frequently and tillage effects, soil consolidation and residue decomposition are critical factors.

4. Availability of data and broad model acceptance by an action agency were primary factors in the selection of RUSLE technology. At the time of consideration, Natural Resource Conservation Service (NRCS) agronomists were involved in an organized effort to collect tillage and crop management data across the country to enable RUSLE technology to be implemented in NRCS field offices. This indicated to the AnnAGNPS model developers a high degree of future data availability and a broad acceptance of RUSLE technology.
5. Model runtime was fairly low due to the fact that LS, K, C, and P factors are calculated at no less than a 15 day time step for only the length of the specified rotation. The calculation of the LS, K, C, and P factors is performed in a data preparation step in AnnAGNPS and not during the day to day simulation. However, during the AnnAGNPS simulation, the Erosion Index (EI) and K factor may be adjusted on a daily basis based on storm precipitation and frozen soil conditions respectively. This will be discussed in more detail later.

At the time of this writing, AnnAGNPS is currently a BETA release. RUSLE technology documented in this paper describes the current state of RUSLE technology in the BETA release of AnnAGNPS. However, upon review by the Agricultural Research Service Scientists and others, significant modifications to the code could be made before the first official release.

The remainder of this paper will primarily focus on how the technology from the RUSLE model was incorporated into the AnnAGNPS model and not discuss or debate the use or validity of RUSLE technology itself.

AnnAGNPS MODEL STRUCTURE

In order to understand how RUSLE technology is incorporated into AnnAGNPS it is important to have fundamental grasp of the basic structure of the AnnAGNPS model. From a high level, the AnnAGNPS model can be viewed as having three main parts that are processed in sequence: Data Preparation, Simulation Processing, and Source Accounting Output.

Data Preparation In the AnnAGNPS data preparation phase model input is read and verified, variables and arrays are initialized, input data rearranged into efficient data structures, various pointers are set and, germane to this discussion, RUSLE LS, K, C, P factors and a sediment delivery ratio to the edge of the field, are calculated. By far, the majority of the RUSLE technology has been incorporated in this step.

Simulation Processing During the simulation processing stage, the daily effects of climate on runoff, snow pack, crop growth, soil moisture, soil erosion, chemical transport, feedlots, impoundments and reach routing are determined. All AnnAGNPS cells are processed then reach routing performed. During the processing of individual cells, on days when a storm event and/or snow melt produces runoff, RUSLE factors that were calculated during the data preparation phase are used along with an estimate of the storm event EI to calculate the sediment delivery at the edge of the cell. No modification to RUSLE parameters occur with the exception of K factor which may be modified in some cases if frozen soil conditions exist.

Source Accounting Output The source accounting output phase is where accumulations of runoff and contaminants are analyzed over the entire simulation period to determine the contribution of a user identified cell(s) to a user identified location in the watershed.

RUSLE CODE IN AnnAGNPS

RUSLE code in AnnAGNPS was converted from the RUSLE Model, Version 1.5 pre.h, written in the 'C' programming language. The RUSLE Model, Version 1.5 pre.h will be referred to as the original RUSLE model for the remainder of the document. AnnAGNPS is written in Fortran90 therefore the original 'C' code had to be converted to Fortran90. In the process of converting the original RUSLE model code, significant organizational revisions were made to; separate the technology engine from the original RUSLE model user interface, simplify code maintenance, produce debug reports, and increase code readability. In essence, RUSLE code was basically re-written from scratch with a few exceptions. Every attempt was made to maintain the original technology contained in the code and where technical changes were made they are noted in this paper. Fortunately, few technology related changes were necessary.

ESTIMATION OF RUSLE FACTORS

During the data preparation step described above, RUSLE technology within AnnAGNPS calculates the LS, C, and P factors for each cell in the watershed and a K factor for each soil in the watershed. The highest level subroutine that controls the calculations of these parameters has the following flow control.

The remainder of the discussion describing the estimation of RUSLE parameters will follow the high level process control flow depicted in Figure 1.

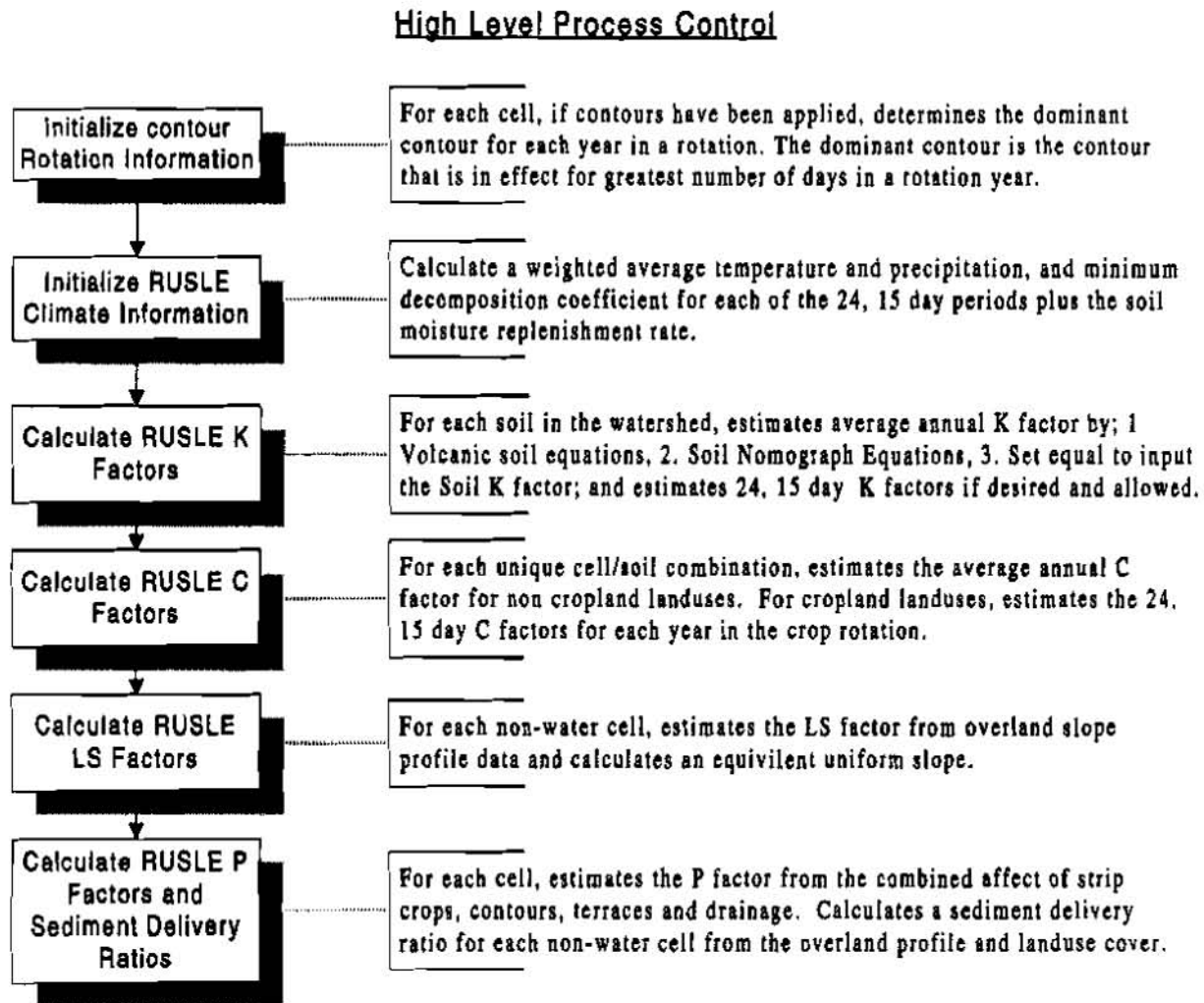


Figure 1

Initialize Contour Rotation Information: AnnAGNPS allows the user to specify the application of a contour or mechanical disturbance by month, day, and relative year in a rotation for every landuse. This capability is an enhancement to existing RUSLE technology. In the original RUSLE technology, only a single contour or mechanical application is allowed on a non-cropland landuse.

A contour and mechanical disturbance are both described in the AnnAGNPS input data under the contour data section. The only difference between the two is that mechanical disturbance has a ridge height of zero. For the remainder of this document, when a contour application or contour practice is mentioned, it applies to both a contour and a mechanical disturbance.

The routine to initialize contour rotation information results in information that will be used in later calculations to determine average annual C and P factors. For each non-water cell that has a rotation of operations with contours

specified, the contour rotation initialization routine sets a pointer to the dominant contour information for each year in the rotation and calculates the number of years since the dominant contour was first applied. The dominant contour is the contour that is on the ground for the greatest number of days in a rotation year. A contour applied in a previous rotation year will carry over into the current year and its days for the current year considered until a new contour is applied.

An example will help to explain. If there are two contour applications in four year rotation and the first contour was applied on day 100 in rotation year one and the second contour is applied on day 200 in rotation year 3, the resulting contour rotation information is in Table 1.

Table 1 Contour Rotation Example

Rotation Year	Pointer to Dominant Contour	Years Since Applied
1	contour 1	0
2	contour 1	1
3	contour 1	2
4	contour 2	1

Note that in rotation year three, when the second contour was actually applied, it is not the dominant contour for that year because it was on the ground for only 165 days where as the first contour was on the ground for 199 days.

Initialize RUSLE Climate Information: RUSLE requires certain climate related data that is common to most of the RUSLE routines. The logic and method used in each of these calculations is identical to that in the original RUSLE. These calculations are: 1) Calculating a weighted average temperature and precipitation for each of the 24, 15 day periods, 2) Derive a monthly non-cumulative EI distribution from the input monthly cumulative EI data, 3) Calculate the soil moisture replenishment rate based on average annual rainfall. (This is used in the computation of the soil moisture C sub-factor for the Pacific Northwest.)

RUSLE K Factors: For each unique soil in the watershed, K factor information is calculated. The only change from the original RUSLE model is the ability to cycle through all the soils in the watershed. The structure of the K factor computations in AnnAGNPS was changed significantly from the original model. Figure 2 illustrates the high level structure of the K factor routines used in AnnAGNPS.

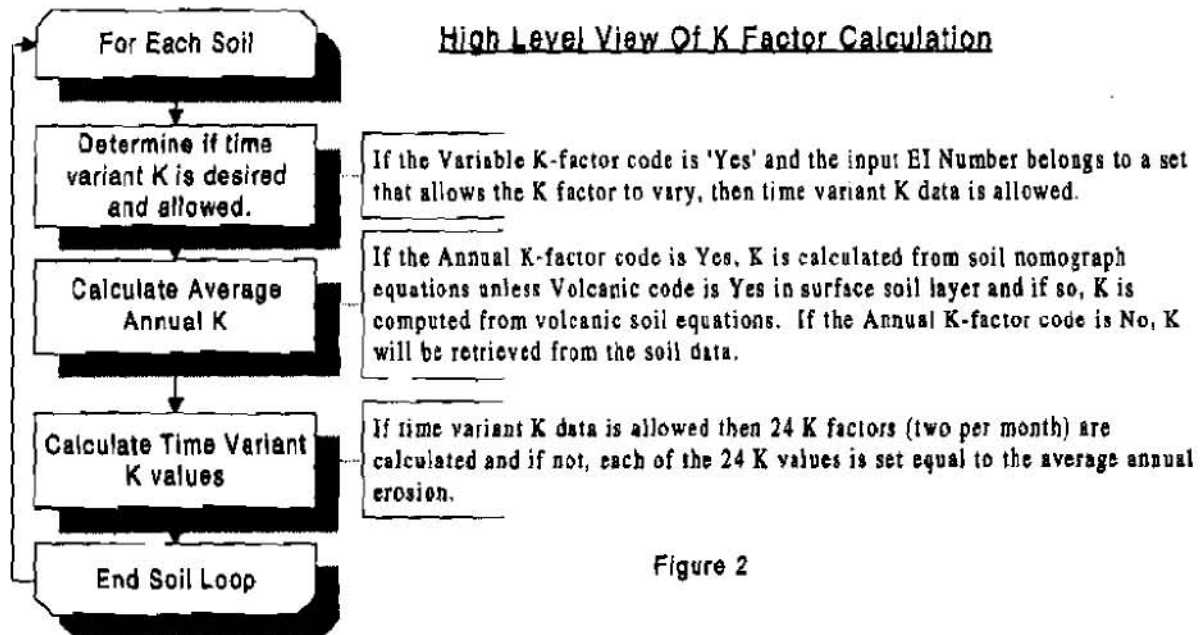


Figure 2

RUSLE C Factors: The computation of C factors in AnnAGNPS for a single cell is identical to that of the original model with one exception. The original RUSLE model only allowed one contour practice to be applied to a non-cropland cell. AnnAGNPS allows multiple contour practices to be applied in rotation on a non-cropland landuse.

In the original RUSLE model, when a contour is specified on a non-cropland landuse, the average annual C factors degrade over a period of time. The length of time is equal to the number of years it takes the soil to consolidate as specified in the soils data. For example, if it takes seven years for the soil to consolidate, the original RUSLE model will calculate seven average annual C factors with the C factor decreasing each successive year until it reaches its minimum value the seventh year.

The same algorithm is used in AnnAGNPS to degrade average annual C factors but since contours can be in a rotation on a non-cropland landuse, the C factor may not reach its fully degraded value before another contour is applied. The contour rotation information discussed under Initialize Contour Rotation Information is used to calculate the average annual C factors if contours have been applied. For each year in the rotation, the average annual C factor is calculated for the dominant contour. The number of years since the contour was first applied is used to determine the number of years the contour has degraded.

In implementing the C factor computations into AnnAGNPS it became obvious that computation time and memory requirements to store C factors for later use could be greatly reduced if redundant calculations and storage could be eliminated. An AnnAGNPS watershed can be subdivided into many cells that can either be square or amorphous in shape and each cell is assumed to have homogenous management and soil. Often the cell size will be substantially smaller than a field size resulting in many cells having identical management. If two or more fields have the same management, even more cells will have the same management. In addition, the smaller the cell size, the more likely the chance that two or more cells will have the same soil type. Therefore, in theory, as AnnAGNPS individual cell size decreases, the number of cells with the same management/soil combination increases.

To reduce the number of C factor computations and storage requirements, calculations are made only on cells where the management/soil combination has not been encountered previously. When a cell is encountered that has an identical management/soil combination that has already been computed, the calculations are skipped and that cell's pointer to its C factor data is set to point to the previous cell's C factor data that had the same management/soil combination. This dramatically reduces computation time since thousands of lines of code are skipped and reduces the internal storage requirements for C factor data as well.

In implementing C factor computations, major structural changes were made. The major difference between the original RUSLE model and AnnAGNPS is that, in AnnAGNPS, each C sub-factor is calculated individually for the entire rotation period. In the original RUSLE model, one large loop sequences through the rotation on 15 day increments and all the C sub-factors are calculated in succession. AnnAGNPS, however, has many small subroutines with each subroutine sequencing through the rotation. The advantage is that smaller subroutines are easier to code, verify, understand, and maintain. The disadvantage is that temporary storage requirements are higher since individual C sub-factors for the entire rotation period must be stored until all the other C sub-factors are computed and those results combined to compute the final C factor. Figure 3 depicts a high level view of the calculation of C factors in AnnAGNPS.

RUSLE LS Factor: Only a few minor structural changes were made to the LS factor code from the original model. The calculation of the LS factor in AnnAGNPS is the same as in the original model with the exception that the RUSLE 'Beta' code values that describe the rill to inter-rill ratio are mapped to the table codes required by the LS factor and shown in Table 2. The LS factor table code identifies which equation will be used to calculate the LS factor in RUSLE.

Table 2: Relationship Between Beta Codes and LS Factor Table Values

RUSLE Beta Code	LS Table Code
1 = rill/inter-rill erosion equal for bare soil (ratio = 0.035)	2 - moderate rill to inter-rill erosion
2 = inter-rill erosion dominant for bare soil (ratio = 0.025)	1 - low rill to inter-rill erosion
3 = rill erosion dominant for bare soil (ratio = 0.050)	3 - high rill to inter-rill erosion
4 = coarse soil, low ppt., cover strongly affects runoff (ratio = 0.045)	3 - high rill to inter-rill erosion

High Level View of C Factor Calculation

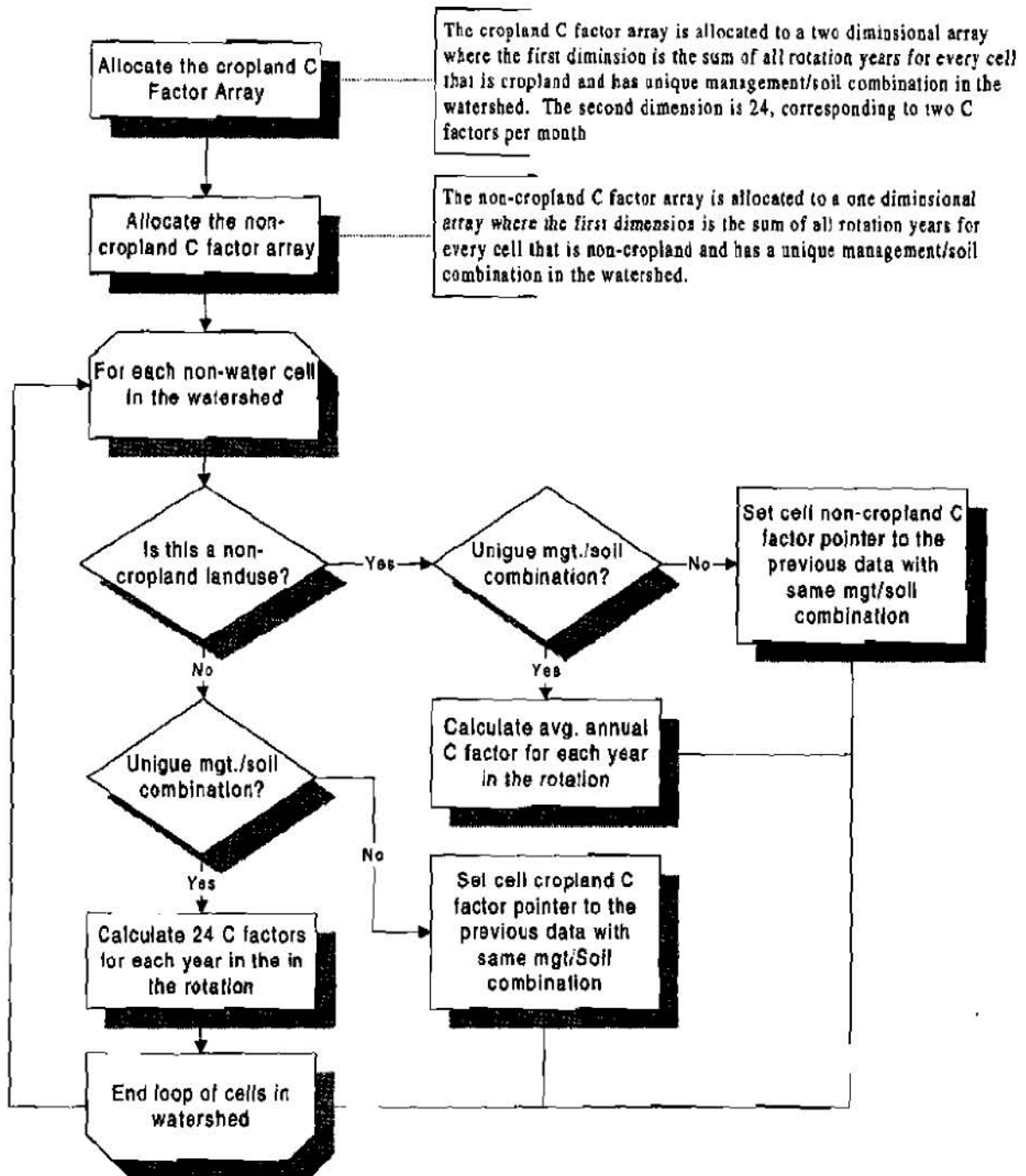


Figure 3

RUSLE P Factors and Sediment Delivery Ratio's: The calculation of RUSLE P factors and sediment delivery ratio's in AnnAGNPS are the same as in the original model with two exceptions. The original RUSLE model allowed only one contour practice to be applied on a non-cropland landuse and a sediment delivery ratio was calculated only when a strip crop conservation practice was applied. AnnAGNPS allows for the application of more than one contour practice to be applied in a rotation on a non-cropland landuse and a sediment delivery ratio is calculated for each non-water cell regardless of whether a strip crop has been applied or not.

In the original RUSLE model, when a contour is specified on a non-cropland landuse, the average annual contour P sub-factors degrade over a period of time. The length of time is equal to the number of years it takes the soil to consolidate as specified in the soils data. For example, if it takes seven years for the soil to consolidate, then the original RUSLE model will calculate seven average annual contour P sub-factors with the sub-factor decreasing each successive year until it reaches its minimum value the seventh year.

The same algorithm to degrade average annual contour P sub-factors is used in AnnAGNPS but since contours can be in a rotation, they may not reach their fully degraded value before another contour is applied. The contour rotation information discussed under Initialize Contour Rotation Information is used to calculate the average annual contour P sub-factors. For each year in the rotation, the average annual contour P sub-factor is calculated for the dominant contour. The number of years since the contour was first applied is used to determine the number of years the contour has degraded.

The same algorithm that was used in the original RUSLE model to calculate a sediment delivery ratio when a strip crop was applied is used in AnnAGNPS to calculate a sediment delivery ratio to the edge of the field for every non-water cell. If there is not a strip crop specified for a cell, AnnAGNPS assigns a RUSLE predefined cover code to each overland profile slope segment based on the type of landuse specified in the field data as shown in Table 3.

Table 3: Assigned Cover Code for Various Landuses

Landuse Specified in Field Data	RUSLE Predefined Cover Code
Cropland	5 - light cover and/or moderately rough
Pasture	1 - established sod-forming grass
Rangeland	4 - moderate cover and/or rough
Forest	3 - heavy cover and/or very rough
Urban	2 - 1st year grass or cut for hay

Figure 4 is a high level view of the process used in AnnAGNPS to calculate P factors.

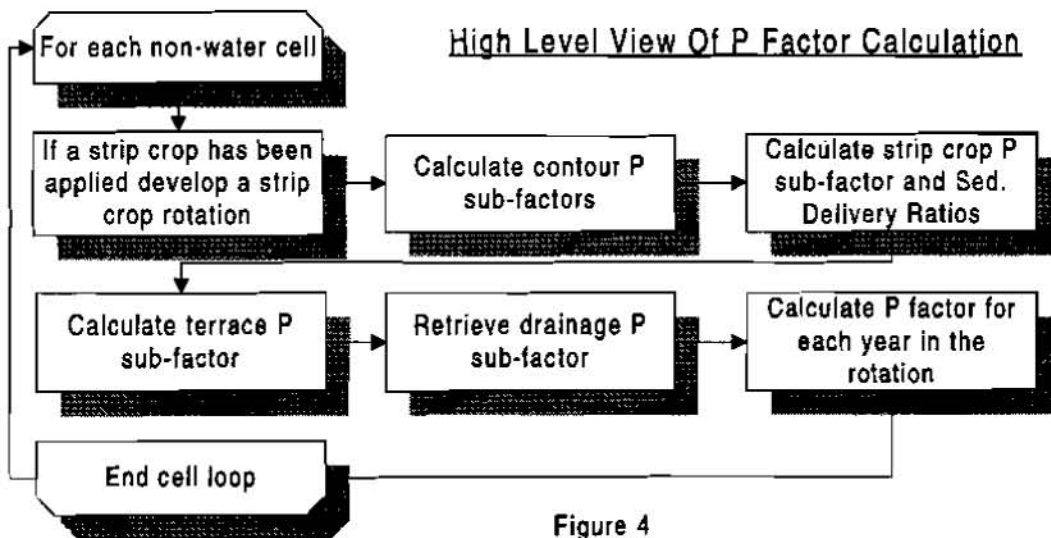


Figure 4

DAILY TIME STEP SEDIMENT DELIVERY CALCULATION

Sediment delivery to the edge of the field is calculated whenever a runoff event occurs from rainfall, irrigation, or snowmelt in the Simulation Processing phase of the AnnAGNPS model run. Each of the RUSLE parameters is either calculated or retrieved from previously calculated data.

The EI value is calculated given the rainfall distribution type and the rainfall amount using Equation 1 which is taken from AGNPS.

$$EI = \frac{A * \exp(2.119 * \log(R)) * \exp(0.0086 * \log(24))}{\exp(B * \log(24))} \quad \text{Equation 1}$$

Table 4: EI Coefficient and Exponent by Storm Type

where: R = Precipitation or Snowmelt in inches
 A = EI coefficient from Table 4
 B = EI exponent from Table 4

Storm Distribution Type	A	B
I	15.03	0.5780
IA	12.98	0.7488
II	17.90	0.4134
III	21.51	0.2811
Uniform	9.41	1.1401
IIA-60	20.99	0.2904
IIA-65	21.84	0.2631
IIA-70	22.87	0.2365
IIA-75	23.96	0.2118

Given each of the cumulative rainfall distributions, Keith Cooley, ARS Scientist, Boise ID, calculated the A and B coefficients to derive the storm EI value. For snowmelt, the Uniform distribution is used. If precipitation and snowmelt occur on the same day, their respective EI values summed together.

The K value is retrieved and modified for frozen soil conditions if the watershed is in the Palouse region using Equation 2 supplied by Don McCool, ARS Scientist, Pullman WA,:

$$K = K * (1 + 14 * (1 - \exp(-4 * (M - 0.5)))) \quad \text{Equation 2}$$

where: K = RUSLE K factor and,
 M = Moisture fraction in surface soil layer

The remaining RUSLE factors, LS, C, P, and sediment delivery ratio are retrieved from previously calculated data then the product of EI, LS, K, C and P is computed to determine the total potential erosion. This product is then compared to the amount of thawed soil available for erosion and the lesser of the two quantities is then multiplied by the sediment delivery ratio to determine the amount of sediment delivered to the edge of the field.

REFERENCES

- Wischmeier, W. H., Smith, D. D., 1978. Predicting Rainfall Erosion Losses-A Guide to Conservation Planning. U.S. Department of Agriculture, Agricultural Handbook No. 537
- Renard, K. G., Foster, G. R., Weesies, G. A., McCool, D. K., and Yoder, D. C., coordinators. 1997 Predicting Soil Erosion by Water: A Guide to Conservation Planning With the Revised Universal Loss Equation (RUSLE). USDA Agriculture Handbook No. 703, 404 p
- Cronshey, R.G., & Theurer, F.D., 1998. AnnAGNPS — NON-POINT POLLUTANT LOADING MODEL. *In Proceedings First Federal Interagency Hydrologic Modeling Conference, 19-23 April 1998, Las Vegas, NV.*
- Young, R. A., Onstead, C. A., Bosch, D. D., Anderson, W. P., 1987, *AGNPS, Agricultural Non-Point-Source Pollution Model. A Watershed Analysis Tool.* USDA Conservation Research Report 35, 80p

AnnAGNPS-REACH ROUTING PROCESSES

By Fred D. Theurer, Agricultural Engineer, Natural Resources Conservation Service, Beltsville, MD;
Roger G. Cronshey, Hydraulic Engineer, Natural Resources Conservation Service, Beltsville, MD

Abstract: The single-event Agricultural Non-Point Source Pollution (AGNPS) computer model has been replaced with a continuous simulation version called AnnAGNPS (Annualized AGNPS). AnnAGNPS will predict pollutant loadings (PL) anywhere within the watershed and identify their proportional contributions from selected points of origin. The reach routing processes are the set of technical procedures used to determine the fate & transport of the PL's once they are in the stream system.

The reach routing processes in AnnAGNPS track the fate & transport for the: (a) five sediment particle-size classes (clay, silt, sand, small aggregate, & large aggregate); and (b) absorbed and dissolved forms of the major chemical pollutants (nutrients, pesticides, & organic carbon). An accounting procedure is included that keeps track of the amount originating from within a field or stream reach of any given PL by erosion type or chemical form that arrives at any downstream point in the watershed.

The graphical peak discharge method in the Soil Conservation Service's TR-55 is limited to watershed drainage areas whose time of concentrations (T_c) do not exceed 10 hours (approximately 200 sq. mi.) and rainfall (P) to runoff relationships whose initial abstraction (I_a) is less than 50 percent of the rainfall ($0.1 \leq I_a/P \leq 0.5$). AnnAGNPS needs to operate satisfactorily for drainage areas up to 1000 sq. mi. (T_c 's up to 48 hr) and rainfall-runoff relationships that range between no runoff to total runoff ($0 \leq I_a/P \leq 1$). An extension of TR-55 is used to meet these requirements.

The sediment reach routing process accounts for deposition when there is an oversupply of a particular sediment class, and degradation when the particular sediment particle-size class transport is supply-limited and is available in the bed & bank. Amounts of erosion by type (sheet & rill, bed & bank, and gully) are tracked throughout the reach routing process. This allows the user to determine from where any particular sediment particle-size class originated by erosion type, and how much.

The major chemical reach routing processes have been updated to include partitioning between absorbed and dissolved states. The reach routing processes include: (a) the fate & transport of nitrogen & phosphorus; (b) a separate reach routing routine for organic carbon; and (c) the fate and transport for an unlimited number of individual pesticides.

INTRODUCTION

The reach routing processes are used in AnnAGNPS (Cronshey & Theurer 1998). Sediment from sheet & rill erosion is determined according to RUSLE (Geter & Theurer 1998). The results from AnnAGNPS are designed to be used by the other computer models such as the sediment intrusion into salmonid redds model (Alonso et al 1998) and the fry emergence model (Miller et al 1998).

The reach routing processes are assumed to be in an enclosed control volume. All inputs are total amounts (water, sediment, & chemicals) entering at the upstream end only. Chemicals are equilibrated—equilibrium balance between dissolved & adsorbed chemicals—immediately before routing begins. Sediments are routed by particle-size class where each particular size-class is deposited, more entrained, or simply transported unchanged depending upon the amount entering the reach, availability of that size class in the bed & banks, and the transport capacity of each size class. The chemicals are re-equilibrated at the downstream end to reflect possible changes in either the amount of water or fine sediment.

PL computer models require a water model component. The water model components needed by watershed-scale PL models must include a simple peak discharge procedure. A very simple and precise procedure with accepted credibility is the unit peak discharge (UPD) procedure included in Chapter 4, TR-55 (SCS 1986). However, TR-55 was developed primarily for use as an engineering field-level design tool rather than for inclusion in PL continuous-simulation, field- & watershed-level computer models. While applicable for the range of conditions for which it was developed, TR-55 does not cover the total range needed for such PL models.

HYDRAULICS

Rectangular shape channels offer computational efficiencies, especially when coupled with unit-width assumptions. Unit-width means dividing the respective parameter by the top width at the surface of the flow area.

For the hydraulic radius, use the hydraulic depth; i.e., let:

$$d_w = R = A/W \quad \text{Equation 1}$$

where: d_w = hydraulic depth, m;
 R = hydraulic radius, m;
 A = flow area, m^2 ; and
 W = flow width, m.

To solve for the velocity of flow when given the hydraulic depth of flow, use:

$$v_w = (1/n) \cdot d_w^{2/3} \cdot S_o^{1/2} \quad \text{Equation 2}$$

where: v_w = flow velocity of water, m/s;
 n = Manning's retardance;
 d_w = hydraulic depth, m; and
 S_o = channel slope, m/m.

To solve for the hydraulic depth and velocity when given the discharge, use:

$$d_w = [(n \cdot q_w) / (S_o^{1/2})]^{0.6} = n^{0.6} \cdot S_o^{-0.3} \cdot q_w^{0.6}$$

$$v_w = Q_w / (W \cdot d_w) = q_w / d_w \quad \text{Equation 3}$$

where: d_w = hydraulic depth, m;
 v_w = flow velocity of water, m/s;
 W = flow width of flow area, m;
 n = Manning's retardance;
 Q_w = water discharge, m^3/s ;
 $q_w = Q_w/W$, unit-width water discharge, $m^3/s/m$; and
 S_o = channel slope, m/m.

And the term $d_w \cdot S_o$, derived from Equation 4, will be used in subsequent formulas:

$$d_w \cdot S_o = n^{0.6} \cdot S_o^{0.7} \cdot q_w^{0.6} \quad \text{Equation 4}$$

where: d_w = hydraulic depth, m;
 v_w = flow velocity of water, m/s;
 W = flow width of flow area, m;
 n = Manning's retardance;
 $q_w = Q_w/W$, unit-width water discharge, $m^3/s/m$; and
 S_o = channel slope, m/m.

HYDROLOGY

Peak Discharge: The following set of regression coefficients were generated using the Extended TR55 (Theurer & Comer 1992) procedures and curve-fitted using TableCurve 2D version 4 by Jandel. UPD's were calculated for ninety-six I_d/P_{24} 's at 0.01 increments of I_d/P_{24} from 0 to 0.95 ($0 <= I_d/P_{24} <= 0.95$) and forty-one T_c 's from 0 to 48 hours using NEH-4 procedures (SCS 1972). The UPD at I_d/P_{24} equal one is zero because there is no surface runoff. The resulting data sets [(96+1)*41=3977 element values for each of the rainfall distribution types] became the basis for the extended TR-55 regression equations, error analyses, and subsequent findings. The mean error of the regression equations with respect to the NEH-4 (SCS 1972) values over the entire range of I_d/P_{24} & T_c conditions is approximately 0.5% and the standard deviation is less than approximately 2%. Table 1 show regression coefficients for each rainfall distribution. While AnnAGNPS uses I_d/P_{24} increments of 0.05, only increments of 0.20 are shown in Table 1.

Table 1: Unit Peak Discharge Regression Coefficients

Type	I/P_{24}	a	b	c	d	e	f
1 (I)	0.00	8.191203E-01	2.098577E+00	1.420600E-01	6.403418E-02	-1.798058E-03	-9.691654E-04
	0.20	2.881040E-01	2.269473E+00	3.648846E-02	3.394364E-02	1.194882E-03	3.185709E-03
	0.40	4.209120E-02	2.107367E+00	1.253109E-02	2.416459E-02	1.257576E-03	7.818349E-03
	0.60	4.166588E-03	2.719060E-02	1.090675E-04	3.126468E-03	7.904181E-06	1.235070E-04
	0.80	1.358244E-03	4.526567E-02	9.085505E-05	9.939561E-03	2.978380E-07	0.000000E+00
2 (Ia)	0.00	2.593320E-01	6.463246E-01	2.573810E-02	7.243833E-03	2.161611E-05	1.398574E-04
	0.20	7.630642E-02	6.560184E-01	2.566400E-03	-6.452636E-03	6.961028E-04	1.709310E-03
	0.40	9.523307E-03	3.028293E-02	2.788554E-04	2.240374E-03	1.933978E-05	1.080512E-04
	0.60	4.480394E-03	7.302563E-02	3.394787E-04	6.287665E-03	2.609098E-05	4.407477E-04
	0.80	1.741268E-03	8.602862E-02	1.642964E-04	1.576832E-02	2.481447E-07	0.000000E+00
3 (II)	0.00	1.519530E+00	2.112862E+00	7.955306E-02	6.263867E-02	8.513482E-03	6.758214E-03
	0.20	6.687890E-01	2.523586E+00	1.716150E-02	1.954410E-02	2.908914E-03	6.678482E-03
	0.40	2.272377E-01	3.907665E+00	3.469720E-02	1.245753E-01	9.446148E-04	6.197919E-03
	0.60	1.690395E-02	2.321569E+00	8.300435E-03	7.991502E-02	4.118532E-04	7.692973E-03
	0.80	1.042173E-03	-1.020764E-04	-3.811053E-06	2.567960E-03	9.359939E-09	-3.038358E-05
4 (III)	0.00	9.357636E-01	1.368530E+00	7.585186E-02	5.733524E-02	5.252073E-03	4.195782E-03
	0.20	4.129800E-01	1.675525E+00	3.451340E-02	5.585967E-02	8.903714E-04	2.210996E-03
	0.40	1.218296E-01	2.203114E+00	2.877259E-02	1.196262E-01	3.657518E-04	2.572314E-03
	0.60	1.103889E-02	7.637374E-01	2.652503E-03	3.138008E-02	2.008206E-04	3.555352E-03
	0.80	1.130600E-03	1.856640E-02	-1.739106E-05	1.191404E-03	2.667614E-06	1.966816E-04
5 (Uniform)	0.00	4.161024E-02	-2.291070E-02	-8.630791E-04	6.634947E-04	1.701998E-05	2.227598E-06
	0.20	2.878569E-02	8.682334E-02	2.068912E-03	4.156828E-03	7.760004E-05	1.814001E-04
	0.40	1.699438E-02	8.378853E-02	8.549266E-04	5.391781E-03	4.058543E-05	2.325788E-04
	0.60	9.214130E-03	1.278936E-01	6.050135E-04	1.159786E-02	4.280640E-05	7.157927E-04
	0.80	3.838705E-03	2.412793E-01	4.980051E-04	4.502355E-02	4.258091E-07	0.000000E+00
6 (II-a60)	0.00	2.889749E+00	3.273784E+00	1.446065E-01	1.008957E-01	0.000000E+00	0.000000E+00
	0.20	1.369500E+00	5.064453E+00	4.248368E-02	6.499361E-02	1.513193E-03	3.541284E-03
	0.40	6.334482E-01	1.025432E+01	8.351263E-02	3.603484E-01	-7.260700E-05	0.000000E+00
	0.60	6.916727E-02	9.339188E+00	2.710800E-02	2.062759E-01	-1.364500E-04	0.000000E+00
	0.80	6.231650E-04	-3.411600E-05	1.982740E-06	1.572730E-03	5.316790E-07	3.229390E-05
7 (II-a65)	0.00	3.105260E+00	3.109283E+00	1.921849E-02	2.558174E-03	0.000000E+00	0.000000E+00
	0.20	1.545424E+00	5.073367E+00	4.194001E-02	1.385273E-01	6.308154E-03	1.344247E-02
	0.40	-3.89279E-01	2.625254E+00	-8.147355E+00	3.551340E-01	-1.974840E+00	-6.946600E-04
	0.60	1.437442E-01	1.328429E+01	3.844520E-02	3.615960E-01	-1.330700E-04	0.000000E+00
	0.80	6.041370E-04	-1.627500E-05	-3.202300E-06	9.379760E-04	4.116320E-07	2.514860E-05
8 (II-a70)	0.00	3.431447E+00	3.225395E+00	1.107677E-02	0.000000E+00	0.000000E+00	0.000000E+00
	0.20	1.839241E+00	5.556090E+00	5.400739E-02	2.103572E-01	1.038225E-02	2.210380E-02
	0.40	7.815830E-01	8.413013E+00	3.026382E-02	4.524973E-02	-4.612800E-04	-1.478290E-03
	0.60	2.420561E-01	1.570367E+01	4.432599E-02	4.906144E-01	-9.166000E-05	0.000000E+00
	0.80	6.652130E-04	7.173470E-06	-2.262900E-05	-4.840900E-04	8.703930E-07	6.233150E-05
9 (II-a75)	0.00	3.774411E+00	3.340085E+00	5.425804E-03	0.000000E+00	0.000000E+00	0.000000E+00
	0.20	1.997334E+00	5.379884E+00	1.185453E-01	4.992425E-01	2.332722E-02	4.956452E-02
	0.40	8.924026E-01	8.062642E+00	1.867840E-02	9.565487E-02	2.095755E-03	1.197524E-02
	0.60	3.367238E-01	1.578486E+01	4.151122E-02	5.092234E-01	-4.802100E-05	0.000000E+00
	0.80	1.123760E-03	9.764010E-05	-1.679900E-04	-6.339630E-03	1.133440E-05	8.685300E-04

The general form for the regression equation to calculate the peak discharge is:

$$Q_p = 2.777777778 \cdot 10^{-3} \cdot P_{24} \cdot D_a \cdot \left[\frac{a + (c \cdot T_c) + (e \cdot T_c^2)}{1 + (b \cdot T_c) + (d \cdot T_c^2) + (f \cdot T_c^3)} \right] \quad \text{Equation 5}$$

where: Q_p = peak discharge, m^3/s ;
 D_a = total drainage area, hectares;
 P_{24} = 24-hour effective rainfall over the total drainage area mm;
 T_c = time of concentration hr; and
a, b, c, d, e, & f are the regression coefficients for a given I_p/P_{24} and rainfall distribution type.

Time of Concentration: Time of concentration is calculated according to the procedures described in TR-55 (SCS 1986).

Hydrograph Shape: A triangular shape is assumed. Since the sediment transport is only concerned with the duration for an average discharge, the time to peak is not important and a right triangle was used to calculate the sediment transport.

The time to base of the hydrograph (duration of surface runoff event) is:

$$t_b = 20 \cdot (R \cdot D_a / Q_p) \quad \text{Equation 6}$$

where: Q_p = peak discharge, m^3/s ;
 D_a = total drainage area, hectares;
R = surface runoff volume from upstream drainage area, mm; and
 t_b = time to base, s.

The hydrograph as a function of time is:

$$Q_w = (Q_p / t_b) \cdot t, \quad \text{for } 0 \leq t \leq t_b \quad \text{Equation 7}$$

where: Q_w = discharge as a function of time, m^3/s ;
 Q_p = peak discharge, m^3/s ;
 t_b = time to base, s; and
t = time from beginning of runoff, s.

And the unit-width peak discharge is:

$$q_p = Q_p / W \quad \text{Equation 8}$$

where: q_p = unit-width peak discharge, $m^3/s/m$;
 Q_p = peak discharge, m^3/s ; and
W = flow width, m.

SEDIMENT YIELD

All sediment routing in the concentrated flow channels is performed by the five particle-size classes (sand, large & small aggregates, silt, and clay) and for each increment of the hydrograph.

If the sum of all incoming sediment (q_{s1}) is greater than the sediment transport capacity (q_{sc}), then the sediment deposition algorithm is used. If that sum is less than or equal to the sediment transport capacity, the sediment discharge at the outlet of the reach (q_{s2}) will be equal to the sediment transport capacity for an erodible channel (by particle-size). Otherwise, if the upstream sediment discharge (q_{s1}) is less than or equal to the sediment transport capacity (q_{sc}) and the channel is non-erodible for that particular particle-size, the downstream sediment discharge (q_{s2}) is assumed equal to the upstream sediment discharge (q_{s1}).

- If $(q_{s1} - q_{sc}) \leq 0$ & the bed is erodible for the particular particle-size class, then $q_{s2} = q_{sc}$; or
- if $(q_{s1} - q_{sc}) \leq 0$ & the bed is non-erodible for the particular particle-size class, then $q_{s2} = q_{s1}$; or
- if $(q_{s1} - q_{sc}) > 0$, then the sediment deposition algorithm is used.

Sediment Concentration: The definition for sediment concentration is:

$$C_s = S/W \quad \text{Equation 9}$$

where: C_s = sediment concentration, Mg-sediment/Mg-water;
 S = sediment mass, Mg; and
 W = water mass from upstream drainage area, Mg.

Sediment concentration is assumed to be constant throughout the hydrograph; therefore, the sediment load for a given discharge at any time during the runoff hydrograph is:

$$q_s = C_s q_w \quad \text{Equation 10}$$

where: C_s = sediment concentration, Mg-sediment/Mg-water;
 q_s = unit-width sediment load, Mg/s/m; and
 q_w = unit-width water discharge at any time, Mg/s/m;

Sediment Transport Capacity Algorithm: The sediment transport capacity (q_{sc}) and the unit-width water discharge (q_w) are based upon the parameters at the upstream end of the reach (x_1).

The shear velocity, assuming unit-width, is based upon the parameters at the upstream end of the reach (x_1) and is defined to be:

$$U_* = [g \cdot d_w \cdot S_o]^{1/2} = g^{0.5} \cdot n^{0.3} \cdot S_o^{0.35} \cdot q_w^{0.3} \quad \text{Equation 11}$$

where: d_w = hydraulic depth at x_1 , m;
 g = gravitational constant, 9.81 m/sec²;
 n = Manning's retardance;
 q_w = unit-width water discharge at any time, Mg/s/m;
 S_o = channel slope, m/m; and
 U_* = shear velocity at x_1 , m/s.

For clay, silt, and small aggregates, use $A = 1$; for sand and large aggregates, use:

$$A = [(6 \cdot v_f) / (\kappa \cdot U_*)] / \{1 - \exp[-(6 \cdot v_f) / (\kappa \cdot U_*)]\} \quad \text{Equation 12}$$

where: A = constant of proportionality, for any flow and particle-size, between the depth-average suspended sediment concentration and the concentration at the laminar sub-layer plane, non-dimensional;
 κ = von Karman's turbulent-flow mixing-length constant (assume 0.4), non-dimensional;
 U_* = shear velocity at x_1 , m/s; and
 v_f = particle fall velocity (see Table 2), m/s.

For each particle-size, the sediment transport capacity is:

$$q_{sc} = k \cdot \tau \cdot v_w^2 / v_f \quad \text{Equation 13}$$

where: q_{sc} = unit-width sediment transport capacity, Mg/s/m;
 k = transport capacity factor (see Table 2), non-dimensional;
 τ = bed shear stress; Mg/m²
 v_w = flow velocity of water, m/s; and
 v_f = particle fall velocity (see Table 2), m/s.

The bed shear stress can be computed as follows:

$$\tau = \gamma_w \cdot d_w \cdot S_o \quad \text{Equation 14}$$

where: τ = bed shear stress; Mg/m²
 γ_w = 1.00, water density, Mg/m³;
 d_w = hydraulic depth at x_1 , m; and
 S_o = channel slope, m/m.

Table 2 contains the physical properties for each particle-size class (note D_p is in millimeters and v_f is in millimeters per second).

Table 2: Particle-size Class Physical Properties (after Young et al 1987)

Particle-size Class	Particle Size Range (mm)	Particle Density (γ_p) (Mg/m ³)	Fall Velocity (v_f) (mm/s)	Transport Capacity Factor (v_f)	Equivalent Sand Size (D_p) (mm)
clay	<0.002	2.60	$3.11 \cdot 10^{-3}$	$6.242 \cdot 10^{-3}$	$2.00 \cdot 10^{-3}$
silt	0.002-0.050	2.65	$8.02 \cdot 10^{-2}$	$6.053 \cdot 10^{-3}$	$1.00 \cdot 10^{-2}$
sand	0.050-2.000	2.65	$2.31 \cdot 10^{+1}$	$6.053 \cdot 10^{-3}$	$2.00 \cdot 10^{-1}$
small aggregates (SAGG)	0.020-0.075	1.80	$3.81 \cdot 10^{-1}$	$12.478 \cdot 10^{-3}$	$3.51 \cdot 10^{-2}$
large aggregates (LAGG)	0.200-1.000	1.60	$1.65 \cdot 10^{+1}$	$16.631 \cdot 10^{-3}$	$5.00 \cdot 10^{-1}$

Converting v_f in millimeters per second to meters per second, and using Equation 13 results in:

$$C = 322 \cdot k \cdot \gamma_w / v_f, \text{ and} \\ q_{sc} = C \cdot n^{-0.6} \cdot S_0^{1.3} \cdot q_w^{1.4} \quad \text{Equation 15}$$

where: q_{sc} = unit-width sediment transport capacity, Mg/s/m;
 C = particle-size class constant for the sediment transport capacity (see Table 3), Mg-s/m⁴;
 k = transport capacity factor (see Table 2), non-dimensional;
 n = Manning's retardance;
 q_w = unit-width water discharge, m³/s/m;
 S_0 = channel slope, m/m.
 v_f = particle fall velocity (see Table 2), mm/s; and
 $\gamma_w = 1.00$, water density, Mg/m³.

Using Equations 7, 8, & 15, the total sediment transport capacity for the hydrograph is:

$$S_{sc} = \int_0^{t_b} (W \cdot q_{sc}) dt = W \cdot C \cdot n^{-0.6} \cdot S_0^{1.3} \cdot q_p^{1.4} \cdot t_b / 2.4 \quad \text{Equation 16}$$

where: C = particle-size class constant for the sediment transport capacity (see Table 3), Mg-s/m⁴;
 n = Manning's retardance;
 q_p = unit-width peak discharge, m³/s/m;
 q_{sc} = unit-width sediment transport capacity, Mg/s/m;
 S_{sc} = total sediment transport capacity mass, Mg.
 S_0 = channel slope, m/m.
 t = time from beginning of runoff, s;
 t_b = time to base, s; and
 W = flow width, m.

Table 3 contains the sediment transport capacity constants for each particle-size class (note D_p is in millimeters and v_f is in millimeters per second).

Table 3: Particle-Size Class Sediment Transport Capacity

Sediment Class	D_p (mm)	γ_p (Mg/m ³)	v_f (mm/s)	k	C (Mg-s/m ⁴)
clay	$2.00 \cdot 10^{-3}$	2.60	$3.11 \cdot 10^{-3}$	$6.242 \cdot 10^{-3}$	$2.0071 \cdot 10^{+03}$
silt	$1.00 \cdot 10^{-2}$	2.65	$8.02 \cdot 10^{-2}$	$6.053 \cdot 10^{-3}$	$7.5474 \cdot 10^{+01}$
sand	$2.00 \cdot 10^{-1}$	2.65	$2.31 \cdot 10^{+1}$	$6.053 \cdot 10^{-3}$	$2.6203 \cdot 10^{+01}$
SAGG	$3.51 \cdot 10^{-2}$	1.80	$3.81 \cdot 10^{-1}$	$1.248 \cdot 10^{-2}$	$3.2756 \cdot 10^{+01}$
LAGG	$5.00 \cdot 10^{-1}$	1.60	$1.65 \cdot 10^{+1}$	$1.663 \cdot 10^{-2}$	$1.0079 \cdot 10^{+00}$

Sediment Deposition Algorithm: The sediment routing for each reach is done using the unit-width, steady-state, uniform, spatially-varied sediment discharge model.

The sediment routing for all reaches will be the same. All upstream sediment discharges ($q_{s,i}$) will be the sum of all incoming sediment from upstream reaches plus the local sediment associated with the upstream end of the current

reach. Primary cell upstream sediment discharges (q_{s1}) will consist only of local loadings since there is no incoming sediment from upstream reaches to a primary cell.

$$q_{s2} = q_{sc} + [(q_{s1} - q_{sc}) \cdot \exp(-N_d)] \quad \text{Equation 17}$$

where: A = Einstein's constant of proportionality, non-dimensional;
 L_2 = distance from x_1 to x_2 , m;
 $N_d = (A \cdot v_f \cdot L_2) / q_w$, deposition number, non-dimensional;
 q_{sc} = unit-width sediment transport capacity, Mg/s/m;
 q_{s1} = upstream unit-width sediment discharge at x_1 , Mg/s/m;
 q_{s2} = downstream unit-width sediment discharge at x_2 , Mg/s/m;
 q_w = unit-width water discharge, $m^3/s/m$; and
 v_f = particle fall velocity, m/s.

Table 4: 15-Point Gaussian-Legendra Quadrature for Numerical Integration

Point No.	t_i/t_0	ω_i
1	.006003741	.015376621
2	.031363304	.035183024
3	.075896109	.053579610
4	.137791135	.069785339
5	.214513914	.083134603
6	.302924330	.093080500
7	.399402954	.099215743
8	.500000000	.101289120
9	.600597047	.099215743
10	.697075674	.093080500
11	.785486087	.083134603
12	.862208866	.069785339
13	.924103292	.053579610
14	.968636696	.035183024
15	.993996259	.015376621

Einstein's constant of proportionality (A) is actually the ratio of the suspended sediment concentration at the bottom of the water column (near the bed surface) to the average concentration of suspended sediment throughout the water column.

For primary cells, the distance from x_1 to x_2 is the distance from the hydraulically most distant point (x_1) to the cell outlet (x_2).

For secondary cells, the distance from x_1 to x_2 is the length of the concentrated flow channel segment for the reach. The outlet for each reach is always x_2 in the above equations. All incoming sediment from upstream reaches is assumed to enter at the upstream end of the reach (x_1). Local loadings (originating within the associated cells) are assumed to be delivered to the downstream end of the cell's associated reach (x_2).

The channel dimensions for each reach are based upon the flow characteristics for the respective reach; and for the geomorphic option, the top width and depth are based upon the drainage area at the upstream end of each respective reach.

Gaussian-quadrature is used for numerical integration when closed form analytic solutions are not known. The subprogram GAULEG (Press et al 1987) generates the abscissas (t_i) & weights (ω_i) for a given N-point Gauss-Legendre quadrature. Points for the 15-point Gaussian-Legendra quadrature (Carnahan et al 1969) are shown in Table 4.

The N-point Gaussian-quadrature numerical integration of Q_s as a function of t is:

$$\int_{t_1}^{t_2} Q_s dt \cong (t_2 - t_1) \cdot \left[\sum_{i=1}^{i=N} (\omega_i \cdot Q_{s,i}) \right] \quad \text{Equation 18}$$

where: Q_s = sediment load as a function of time; Mg/sec;
 $Q_{s,i}$ = sediment load at Gauss-Legendre time point t_i ; Mg/sec;
 t_1 = time at beginning of time period, sec;
 t_2 = time at end of time period, sec;
 i = Gauss-Legendre point number;
 N = last Gauss-Legendre time point; and
 ω_i = Gauss-Legendre weight, non-dimensional.

CHEMICAL ROUTING

In general, chemicals exist in two phases: (1) dissolved (solution); and (2) attached (adsorbed) to clay-size particles.

Three nutrients are recognized by AnnAGNPS: (1) nitrogen; (2) phosphorous; & (3) organic carbon. Nitrogen & phosphorous are recognized as to be able to exist in both the soluble and adsorbed state. Organic phosphorous is assumed to be insoluble; therefore, only inorganic phosphorous is subject to equilibration. Organic carbon is assumed to be part of the clay-size particles with a known organic carbon to clay ratio.

AnnAGNPS allows any number of pesticides, each with their own independent chemical properties, but they are treated separately; i.e., there is no interaction assumed. Independent equilibration is assumed for each pesticide.

Adsorbed Chemicals: Conservation of mass calculations are made for any adsorbed chemicals if the clay-size particles are deposited within the stream reach. Re-equilibration, for the necessary chemicals, are repeated at the downstream end if clay-size particles are deposited or entrained from the bed & banks, or if there is any loss of water.

Solution Chemicals: Conservation of mass calculations are made for any chemicals in solution if there is any loss of water within the stream reach. Re-equilibration, for the necessary chemicals, are repeated at the downstream end if there is any change in the amount or source of clay-size, or if there is any loss of water.

Equilibration: A simple first order equilibration model for equilibration is used:

$$M_s = M_c / (1 + K_d) \quad \text{Equation 19}$$

where: K_d = partition coefficient of chemical, non-dimensional;
 M_c = total mass of chemical both adsorbed & in solution, Mg; and
 M_s = total mass of chemical in solution, Mg.

REFERENCES

- Alonso, C.V., Theurer, F.D., & Havis, R.N., 1998. Simulating sedimentation in salmonid redds. *In Proceedings First Federal Interagency Hydrologic Modeling Conference*, 19-23 April 1998, Las Vegas, NV.
- Carnahan, B., Luther, H.A., Wilkes, J. O., 1969, *Applied Numerical Methods*. John Wiley & Sons, Inc pg 100-116
- Cronshey, R.G. & Theurer, F.D., 1998. AnnAGNPS-non-point pollutant loading model. *In Proceedings First Federal Interagency Hydrologic Modeling Conference*, 19-23 April 1998, Las Vegas, NV.
- Geter, F. & Theurer, F.D., 1998. AnnAGNPS-RUSLE sheet & rill erosion. *In Proceedings First Federal Interagency Hydrologic Modeling Conference*, 19-23 April 1998, Las Vegas, NV.
- Miller, W.J., Theurer, F.D., & Alonso, C.V., 1998, A computer model to predict salmonid fry emergence, *In Proceedings First Federal Interagency Hydrologic Modeling Conference*, 19-23 April 1998, Las Vegas, NV.
- Press, W. H., Flannery, B. P., Teukolsky, S. A., Vetterling, W. T., 1987. *Numerical Recipes: The Art of Scientific Computing*. Cambridge University Press, pg 125-126
- SCS, 1972. *SCS National Engineering Handbook: Section 4, Hydrology*. Soil Conservation Service, USDA.
- SCS, 1986. *Technical Release 55: Urban hydrology for small watersheds*. Soil Conservation Service, USDA.
- Theurer, F.D., Comer, G.P., 1993. *Extended TR55*. 5 April 1992, USDA-SCS-ENG, Washington, DC. 308 pp.

THE RIPARIAN ECOSYSTEM MANAGEMENT MODEL (REMM): PLANT GROWTH COMPONENT

**L.S. Altier, Assistant Professor, California State Univ., Chico, CA;
R.G. Williams, Civil Engineer, USDA-ARS, Tifton, GA; R.R. Lowrance, Ecologist, USDA-ARS, Tifton, GA;
S.P. Inamdar, Post-Doctoral Associate, Univ. of Georgia, Tifton, GA**

INTRODUCTION

The Riparian Ecosystem Management Model (REMM) has been developed as a tool to aid natural resource agencies and others in making decisions regarding water quality management. It is also intended as a tool for researchers to aid in the study of the complex dynamics related to the water quality functions of riparian ecosystems. REMM is specifically designed to simulate processes in riparian buffer systems corresponding with specifications recommended by the U.S. Forest Service and the USDA-Natural Resource Conservation Service as a national standard (NRCS, 1995; Welsch, 1991).

Vegetation serves a critical role in riparian buffer systems for the control of water quality. Besides acting as a physical barrier to surface movement of water and associated pollutants, plants sequester potential pollutants such as N and P in standing biomass. The organic matter deposited in the soil by plants serves as a substrate for microbial transformations. Along the stream bank, large woody biomass is important for protecting aquatic habitat.

For these reasons, several aspects of plant growth are particularly important for simulating their water quality functions in a riparian ecosystem: the hydrology of the system is sensitive to water extraction from the soil by plant transpiration; soil nutrient dynamics are sensitive to rates of litter deposition above and below the ground surface; and nutrient uptake and sequestering by plants corresponds to plant growth rates. Another requirement of the model is the ability to simulate the management of riparian buffer systems involving one to many plant species growing in one or more canopies.

Numerous plant simulation models have been developed. Each has strengths in simulating aspects of plant growth. REMM relies on several of these for components of the plant module. The FOREST-BGC is growth model that simulates an even-aged forest stand (Running and Coughlan, 1988; Running and Gower, 1991). TREGRO is a single tree growth model that is very detailed in simulating phenological patterns (Weinstein and Beloin, 1990). It also employs a sink-based approach to growth and carbon partitioning, which makes it sensitive to environmental influences. SUCROS (Van Keulen et al., 1982) and SUCROS87 (Spitters et al., 1989) are models for herbaceous growth that employ a source-based approach to growth. A model by Jones et al. (1991) has provided an approach to simulating the response of root growth to environmental stresses. PAPRAN is a model simulating plant nutrient uptake (Seligman and van Keulen, 1981). Work by Mohren (1986) focused on the effects of nutrients on growth.

DESCRIPTION OF MODEL

The Riparian Ecosystem Management Model (REMM) simulates the growth of several types of herbaceous and woody vegetation in two canopy layers for even-aged forest stands. Feedback between vegetation and the environment allows sensitivity to changing resource levels. Carbohydrates are allocated dynamically to the plant organs or held in reserve according to the phenological and nutritional status of the plants. Generalizable for a wide variety of conditions and plant characteristics, the model enables evaluation of the effects of riparian management such as nutrient loads, choice of vegetation, and harvesting regimes on pollutant output into the stream.

There are several distinct submodules in REMM that simulate the growth of different types of plants. These plant types are identified in Table 1. In parameterizing the model for different plants, the most specificity is available in regards to the woody species. Because of the sensitivity of nutrient cycling to leaf longevity (Running and Gower, 1991), coniferous species are distinguished in the REMM user interface with respect to this factor. Several different deciduous plant types are distinguished with respect to their leaf drop pattern. However, individual species present in a particular buffer system may be characterized through the parameterization of many variables.

These variables represent values for the initial sizes of the plants, rates of photosynthesis, respiration requirements, rates of growth and mortality, sensitivity to light and temperature, response to nutrients, and timing of phenostages. The values of these variables for major riparian species are gradually being compiled into library files accessible in the REMM user interface.

Table 1. Vegetation types simulated in REMM.

Vegetation Type	Lower Canopy	Upper Canopy
Herbaceous Species		
1. annuals	X	
2. perennials	X	
Woody Deciduous Species		
3. autumn leaf drop	X	X
4. marscescent leaf drop		X
5. vernal leaf drop	X	X
Coniferous Species ¹		
6. short needle longevity	X	X
7. medium needle longevity	X	X
8. long needle longevity		X

¹Longevity of needles may vary from 2 to 20 years.

Photosynthesis

The calculations for photosynthesis follow the procedures described by Running and Coughlan (1988) in the FOREST-BGC model. For the purposes of determining photosynthesis and germination, solar radiation is sequentially intercepted through upper and lower plant canopies. Beer's law is used to calculate the extinction of light.

Photosynthesis is calculated as a function of leaf area index, daylength, mesophyll conductance of CO₂, and stomatal conductance of H₂O. Mesophyll and stomatal conductance are determined by adjusting a maximum rate by effects of nutrients, light, temperature, humidity, and leaf water potential.

Nutrient Uptake

The simulation of nutrient uptake and partitioning to plant parts follows the approach of the PAPRAN model (Seligman and van Keulen, 1981). It is based upon demands created by growth. The SPUR model for rangeland production (Hanson *et al.*, 1983), and models by Mohren (1986) and Chen *et al.* (1988) for tree growth also utilized this concept. The approach allows simulation of changing allocations of nitrogen and phosphorus to different plant organs, based upon availability and demand.

Although N affects both photosynthesis and growth, it has a relatively greater affect on growth. Low levels of nutrients in the plant will allow some photosynthesis to continue, but there may not be sufficient quantities to meet the growth demands by all the plant organs. Under these conditions, growth is favored in the lower parts of the plant that have priority access to nutrients.

Carbon Partitioning and Growth

The partitioning of nutrients and photosynthates for woody species in REMM corresponds with the concept of a functional equilibrium between roots and shoots described by Brouwer and De Wit (1968). According to this concept, plant organs are in competition for nutrients and photosynthates. A plant organ supplying a resource will have the first opportunity to fulfill its demand. If the supply organ is reduced in size, resulting in a reduced supply of a resource, growth of other dependent organs will slow down until the supply organ has recovered.

For woody species, C is dynamically allocated to maintenance respiration, shoot growth, root growth, and storage, in that order of priority, based upon sink strength. Demand by the plant organs for photosynthates is determined by relative growth rates modified by temperature, moisture, nutrient, and phenological effects. Stored C is used when the respiration and growth demands for photosynthates exceed daily rates of photosynthesis.

Woody plant growth follows an annual pattern of phenological stages described in the TREGRO model by Weinstein *et al.* (1992). The onset of cool, autumn weather or short daylengths can induce a dormancy condition in the aboveground parts of temperate plants. Only fine roots can remain active, and if temperatures are sufficiently high, their growth can occur throughout the year. Dormancy of upper plant parts continues until a chilling requirement has been satisfied. With increasing spring temperatures, buds swell and eventually open to begin leaf expansion. During the growing season, periods of branch and stem growth are signaled by accumulation of thermal units.

A simpler source-based approach is used for determining the growth of herbaceous annual and perennial plants. After maintenance respiration requirements are met, the amount of growth is dictated by the amount of photosynthates available, allocated to each plant organ according to fixed ratios.

Reproduction and Germination

Reproductive organs are not modeled explicitly. For most plant types, they are disregarded. For herbaceous annuals, after the plants reach reproductive stage, a relatively larger proportion of photosynthates are allocated to stem growth to represent the expenditure of carbohydrates on non-photosynthesizing tissue.

Germination is simulated for only the lower canopy vegetation. It is modeled as a function of moisture, light, and temperature effects as well as proportions of seed species in the soil. Shading by existing vegetation will tend to inhibit germination. However, once plants germinate, they become an indistinguishable part of the biomass of their respective plant type in the lower canopy.

Mortality

Plant parts die in different ways. Plant parts senesce as a result of annual cycles, such as with leaf drop of deciduous trees or the death of herbaceous plants. They may also die as a result of an inability to satisfy their maintenance respiration requirement due to lack of photosynthates. A shortage of photosynthates may result either directly from lack of light or indirectly from lack of water or nitrogen. During the winter, a shortage of stored carbohydrates may also reduce the ability of herbaceous perennials to emerge in the spring.

Another kind of mortality occurs on a regular basis as the sapwood of trees is converted into heartwood. REMM keeps track of annual cohorts of sapwood growth. When a cohort reaches a critical age, it becomes heartwood.

SIMULATION OF RIPARIAN BUFFER SYSTEM

Site Description

Initial testing of the model has been conducted using parameter values based upon the Gibbs Farm Experimental Riparian Site at the University of Georgia Coastal Plain Experiment Station near Tifton, GA. Extensive monitoring of this site has been conducted since 1992. The study area is located in the Tifton Upland in the drainage area of the Little River. The site has been managed as a three-zone buffer system. Zone 1 is a 10 m-wide strip of hardwoods, mostly yellow poplar (*Liriodendron tulipifera* L.) and black gum (*Nyssa sylvatica* Marsh.). Zone 2 is 40 to 55 m wide, consisting of conifers, primarily longleaf pine (*Pinus palustris* Mill.) and slash pine (*Pinus elliotti* Engelm.). Zone 3, the area of the buffer furthest away from the stream, is an 8 m strip of perennial grasses, mostly common Bermudagrass (*Cynodon dactylon* L. Pers.) and Bahia grass (*Paspalum notatum* Flugge.). Most of the riparian area is on Alapaha loamy sand (loamy, siliceous, thermic Arenic Plinthic Paleaquults). The upland fields are on Tifton loamy sand (fine-loamy, siliceous, thermic, Plinthic Kandudult) (Calhoun, 1983).

Lowrance *et al.* (1998), Sheridan *et al.* (1996, 1998) and Bosch *et al.* (1996) have provided detailed descriptions of this site and information regarding data collection. Evaluation of the hydrology, erosion, and nutrient components of the model have been described in companion papers to this one (Bosch *et al.* 1988; Inamdar *et al.*, 1998a,b). While there are several management treatments at the site, only data from the buffer system comprising the mature forest area have been used for initial evaluation of the model.

Parameterization

Input data requirements for REMM include: daily historical weather data for the site; daily surface and subsurface runoff loading from the contributing upland field; and topographic, soil, and vegetation information. Each zone was modeled with only one vegetation type. Initial estimates of vegetation biomass are associated nutrient contents are

necessary to get the model running. Parameter values were based upon data collected from the site or best estimates from literature values.

Table 2. Initial values of a few parameters concerning vegetation growth.

Parameter	Units	Zone 1		Zone 2		Zone 3	
		Hardwood Forest Upper Canopy	Lower Canopy	Pine Forest Upper Canopy	Lower Canopy	Perennial Grass Upper Canopy	Lower Canopy
Area Covered	%	100	0	100	0	0	100
LAI ¹		0	--	8.75	--	--	0
SLA ²	ha kg ⁻¹	0.0025	--	0.0025	--	--	0.0022
MaxRtDpth ³	cm	100	--	200	--	--	200
Leaves	kg ha ⁻¹	0	--	3,500	--	--	0
Branches	kg ha ⁻¹	20,000	--	20,000	--	--	--
Stem ⁴	kg ha ⁻¹	20,000	--	20,000	--	--	0
Stem Heartwood	kg ha ⁻¹	120,000	--	120,000	--	--	--
Coarse Roots	kg ha ⁻¹	80,000	--	8,000	--	--	--
Fine Roots	kg ha ⁻¹	3,000	--	3,000	--	--	1,000

¹Leaf area index

²Specific leaf area

³Maximum possible rooting depth

⁴Sapwood (woody species) or herbaceous stems

Since the trees were about 50 years old, it was assumed that net annual growth was close to zero. That is, annual respiration requirements plus tissue mortality was expected to nearly balance photosynthetic capacity. Some calibration of growth rates in the model was done to reflect this. Table 2 indicates some values used to parameterize the model for the Gibbs Farm Site. Because of the difficulty of accurately estimating existing plant biomass out in the field, especially of roots, simulated plant growth was seen to behave rather erratically for a few years until the masses of the plant parts reached an equilibrium. For that reason, the model was run for one hundred years with the same five-year data set before extracting the data shown in the results.

Results and Discussion

The figures below show the simulated patterns of leaf growth and corresponding uptake patterns of N and P for the three predominate vegetation types in the buffer system. They provide an indication of annual periods when different kinds of vegetation may be effective in reducing available nutrient loads in the soil. The grasses have very high rates of nutrient uptake, especially N for a relatively short period of time (Fig. 1). Increasing amounts of carbohydrate storage in the grasses correspond with a declining growth rate late in the season. Translocation of nutrients occurs from senescing plant parts at that time and uptake from the soil ceases.

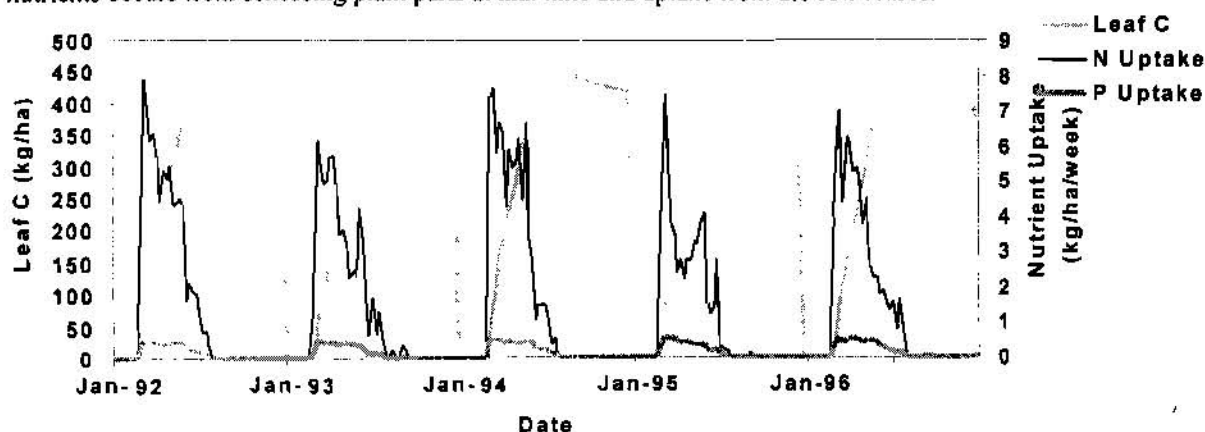


Figure 1. Simulated leaf C and nutrient uptake in the Zone 3 grass strip.

Figures 2 and 3 illustrate more even uptake patterns of nutrients throughout the year by the trees, albeit at much slower rates. Average annual uptakes of nutrients are shown in Table 3. It is apparent that grass has the capacity to extract relatively high total amounts of nutrients from the soil. However, unlike the trees, grass is of little benefit during the winter. Further, unless the grass were to be harvested from the site, with a short life span and a rapid decomposition rate in the soil, grasses would provide little long-term water quality benefits.

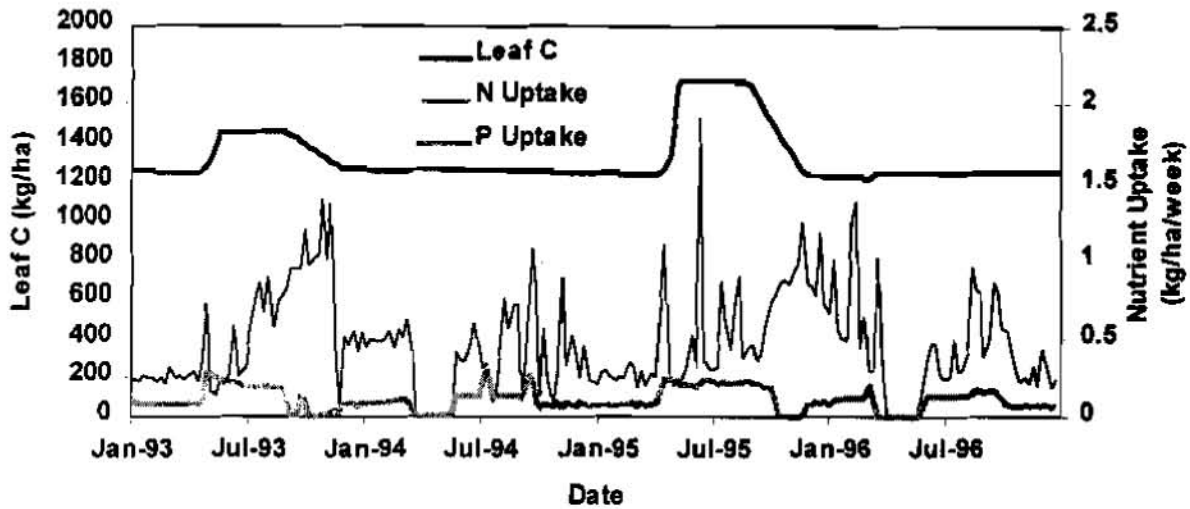


Figure 2. Simulated leaf C and nutrient uptake in the Zone 2 pine forest.

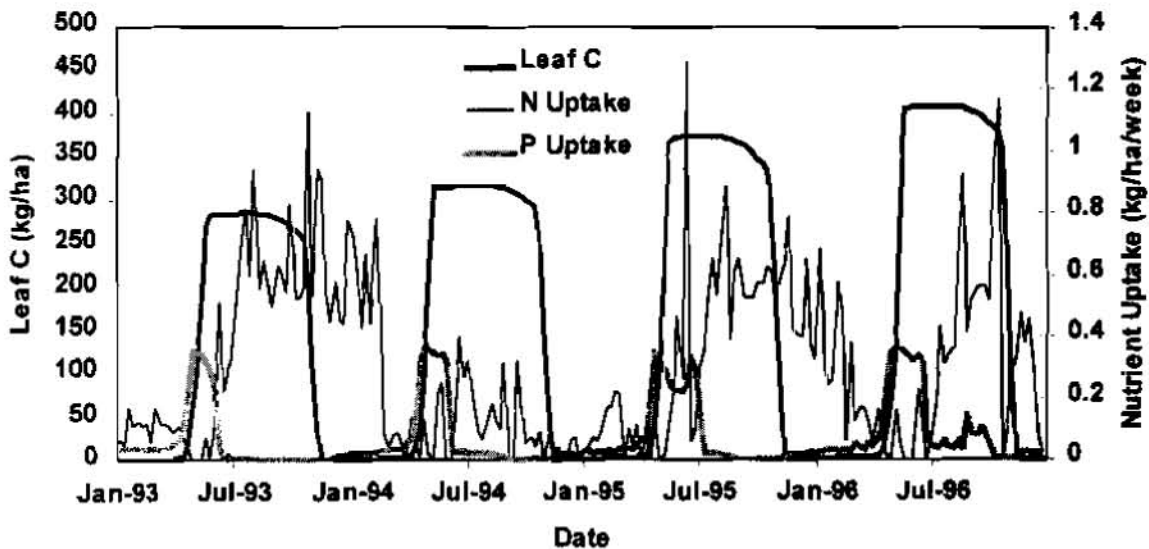


Figure 3. Simulated leaf biomass and nutrient uptake in the Zone 1

Table 3. Annual simulated uptake of N and P by the vegetation types in the buffer system (average over five years).

	Grass	Conifer	Deciduous
	----- kg ha ⁻¹ -----		
N	75	23	14
P	8	6	4

SUMMARY

The vegetation module simulates growth of annual and perennial herbaceous and woody plants in two canopies. Several different types of woody perennial plants are characterized in the model, corresponding to leaf fall patterns and leaf longevity of deciduous and evergreen species. There is no allowance in the current version of the model for succession of plants from the lower canopy into the upper canopy. It is also assumed that the upper canopy is entirely above the lower canopy. Incoming short-wave radiation is divided among vegetation types in the upper canopy according to the relative proportion of land covered by each stand. Radiation is divided among vegetation types in the lower canopy according to the relative sizes of their leaf area indices. Available moisture and nutrients in the soil are allocated to vegetation types according to relative demands and masses of roots in each soil layer. The resulting simulation model is very sensitive to changing environmental conditions. Comparisons in different locations with different plant species are ongoing to test the accuracy of the simulations.

REFERENCES

- Altier, L.S., R.R. Lowrance, R.G. Williams, J.M. Sheridan, D.D. Bosch, R.K. Hubbard, W.C. Mills, and D.L. Thomas. 1994. An ecosystem model for the management of riparian areas. p. 373-387. *In: Riparian ecosystems in the humid U.S.: functions values and management.* Nat. Assoc. Conserv. Districts, Washington, D.C.
- Bosch, D.D., Williams, R.G., Inamdar, S.P., Sheridan, J.M., and Lowrance, R.R. 1998. Erosion and sediment transport through riparian buffers. *In Proceedings of the First Federal Interagency Hydrologic Modeling Conference, Las Vegas, Nevada, (this volume).*
- Brouwer, R. and de Wit, C.T., 1968, A Simulation Model Of Plant Growth With Special Attention To Root Growth And Its Consequences. p. 224-242. *In: Proc. 15th Easter School Agric. Sci. Univ. of Nottingham.*
- Chen, C.W., Gomez, L.E., Fox, C.A., Goldstein, R.A., and Lucier, A.A., 1988, A Tree Growth Model With Multiple Stresses. USDA For. Serv. Gen. Tech. Report, No. Cent. For. Exp. Stn., St. Paul, MN.
- Dillaha, T.A., Reneau, R.B., Mostaghimi, S., and Lee, D., 1989, Vegetative Filter Strips for Agricultural Nonpoint Source Pollution Control. *Trans. ASAE* 32, 513-519.
- Hanson, J.D., Parton, W.J., and Skiles, J.W., 1983, SPUR Plant Growth Component, p. 68-73, *In: J.R. Wight (ed.) SPUR—Simulation of Production and Utilization of Rangelands: A Rangeland Model for Management and Research.* USDA, Misc. Pub. No. 1431.
- Inamdar, S.P., Altier, L.S., Lowrance, R.R., Williams, R.G., and Hubbard, R.K., 1998a. The Riparian Ecosystem Management Model (REMM): Nutrient Dynamics. *In Proceedings of the First Federal Interagency Hydrologic Modeling Conference, Las Vegas, NV (this volume).*
- Inamdar, S.P., Sheridan, J.M., Williams, R.G., Bosch, D.D., Lowrance, R.R., Altier, L.S., Thomas, D.L. 1998b. The Riparian Ecosystem Management Model (REMM): Evaluation of the hydrology component. *In Proceedings of the First Federal Interagency Hydrologic Modeling Conference, Las Vegas, NV (this volume).*
- Jones, C.A., Bland, W.L. and Ritchie, J.T., and Williams, J.R., 1991, Simulation of root growth. *In: J. Hanks and J.T. Ritchie (ed.) Modeling plant and soil systems.* Agronomy Monograph no. 31. ASA-CSSA-SSSA, Madison, WI.
- Lowrance, R.R., Altier, L.S., Williams, R.G., Inamdar, S.P., D.D. Bosch, Sheridan, J.M., Thomas, D.L., and Hubbard, R.K., 1998, The Riparian Ecosystem Management Model: Simulator for Ecological Process in Riparian Zones. *First Federal Interagency Hydrologic Modeling Conference, April 19-23, Las Vegas, NV (this volume).*
- Mohren, G.M.J. 1986. Modelling nutrient dynamics in forests, and the influence of nitrogen and phosphorus on growth. p. 105- 116. *In: G.I. Agren (ed.) Predicting consequences of intensive forest harvesting on long-term productivity.* Report no. 26. Dept. Ecology and Environmental Research, Swed. Univ. Agric. Sci.
- NRCS, 1995, Riparian Forest Buffer, 392. NRCS Watershed Science Institute, Seattle, WA.

- Running, S.W. and Coughlan, J.C., 1988, A general model of forest ecosystem processes for regional applications, I. Hydrologic balance, canopy gas exchange and primary production processes. *Ecol. Modelling* 42:125-154.
- Running, S.W. and Gower S.T., 1991, FOREST-BGC, A general model of forest ecosystem processes for regional applications. II. Dynamic carbon allocation and nitrogen budgets. *Tree Physiology* 9:147-160.
- Seligman, N.G. and Keulen, H. van, 1981. PAPRAN: A simulation model of annual pasture production limited by rainfall and nitrogen. p. 192-221. *In*: M.J. Frissel and J.A. van Veen (ed.) Simulation of nitrogen behavior in soil-plant systems. PUDOC, Wageningen, Netherlands.
- Spitters, C.J.T., Keulen, H. van, and Kraalingen, D.W.G. van, 1989, A simple and universal crop growth simulator: SUCRO87. p. 146-181. *In*: R. Rabbinge, S. R. Ward, and H.H. van Laar (ed.) Simulation Monographs. PUDOC, Wageningen, Netherlands.
- Van Keulen, H., Penning de Vries, F.W.T., and Drees, E.M., 1982, A summary model for crop growth. p. 87-97. *In*: F.W.T. Penning de Vries and H.H. van Laar (ed.) Simulation of plant growth and crop production. Centre for Agricultural Publishing and Documentation (Pudoc), Wageningen, Netherlands.
- Weinstein, D.A. and Beloin, R., 1990. Evaluating effects of pollutants on integrated tree processes: a model of carbon, water, and nutrient balances. P. 313-323. *In*: R.K. Dixon, R.S. Meidahl, G.A. Ruark, and W.G. Warren (ed.) Process modeling of forest growth responses to environmental stress. Timber Press, Portland, OR.
- Weinstein, D.A., Yanai, R.D., Beloin, R.M. and Zollweg, C.G., 1992, The Response of Plants to Interacting Stresses: TREGRO version 1.74 Description and Parameter Requirements. Res. Proj. 2799-01. Electric Power Res. Inst., Palo Alto, CA.

UTILIZING A LAGRANGIAN-EULERIAN APPROACH TO WATER-QUALITY ASSESSMENT OF THE WATeree RIVER, SOUTH CAROLINA

By Toby D. Feaster, P.E., Hydrologist, U.S. Geological Survey, Water Resources Division, Columbia, South Carolina

Abstract: In preparation for developing a dynamic streamflow and water-quality model to simulate flows and dissolved-oxygen concentrations in the Wateree River, South Carolina, a water-quality sampling scheme was designed based on Lagrangian and Eulerian reference frames. Designing a Lagrangian sampling scheme for the Wateree River was possible because data from a previous study were available, and the flows were known prior to the beginning of the study. By utilizing the previous data and models, the analytical laboratory cost for the sampling could be reduced by as much as 65 percent relative to an Eulerian sampling scheme. In addition, the water-quality data and field parameters for the Lagrangian water parcels could be used as a tool for assessing the major influences on the dissolved-oxygen concentrations before calibration of the model.

INTRODUCTION

In May 1996, the U.S. Geological Survey (USGS) entered into a cooperative agreement with the Kershaw County Water and Sewer Authority, South Carolina, to develop a streamflow and water-quality model to simulate dynamic flows and dissolved-oxygen (DO) concentrations in the Wateree River, South Carolina.

During a previous study of the Congaree, Wateree, and Santee Rivers, South Carolina (Hurley, 1991), the USGS used a one-dimensional numerical flow model for singular and interconnected channels (BRANCH) to simulate flow in the Wateree River (fig. 1) (Schaffranek and others, 1981). Hydraulic data computed by the BRANCH model were used as input for a one-dimensional transport model, the Branched Lagrangian Transport Model or BLTM (Jobson and Schoellhamer, 1987). The BLTM was used to simulate transport and dispersion of striped bass eggs in the Wateree, Congaree, and Santee Rivers.

Environmental monitoring and water-quality modeling can become an iterative process as a system is studied and better understood. In preparation for the intensive water-quality sampling necessary to properly model the DO concentrations, data from the Wateree River subreach of the previous models were used to develop a sampling schedule that combines the Lagrangian and Eulerian reference frames. In a Lagrangian reference frame, a parcel of water is followed through the system and sampled at predetermined locations to track the changes in that parcel. In an Eulerian reference frame, samples are collected at predetermined locations with time to document the changes at those locations.

The idea of using a Lagrangian sampling scheme on the Wateree River was conceived in an effort to reduce the sampling cost. According to USGS streamflow data, the travel

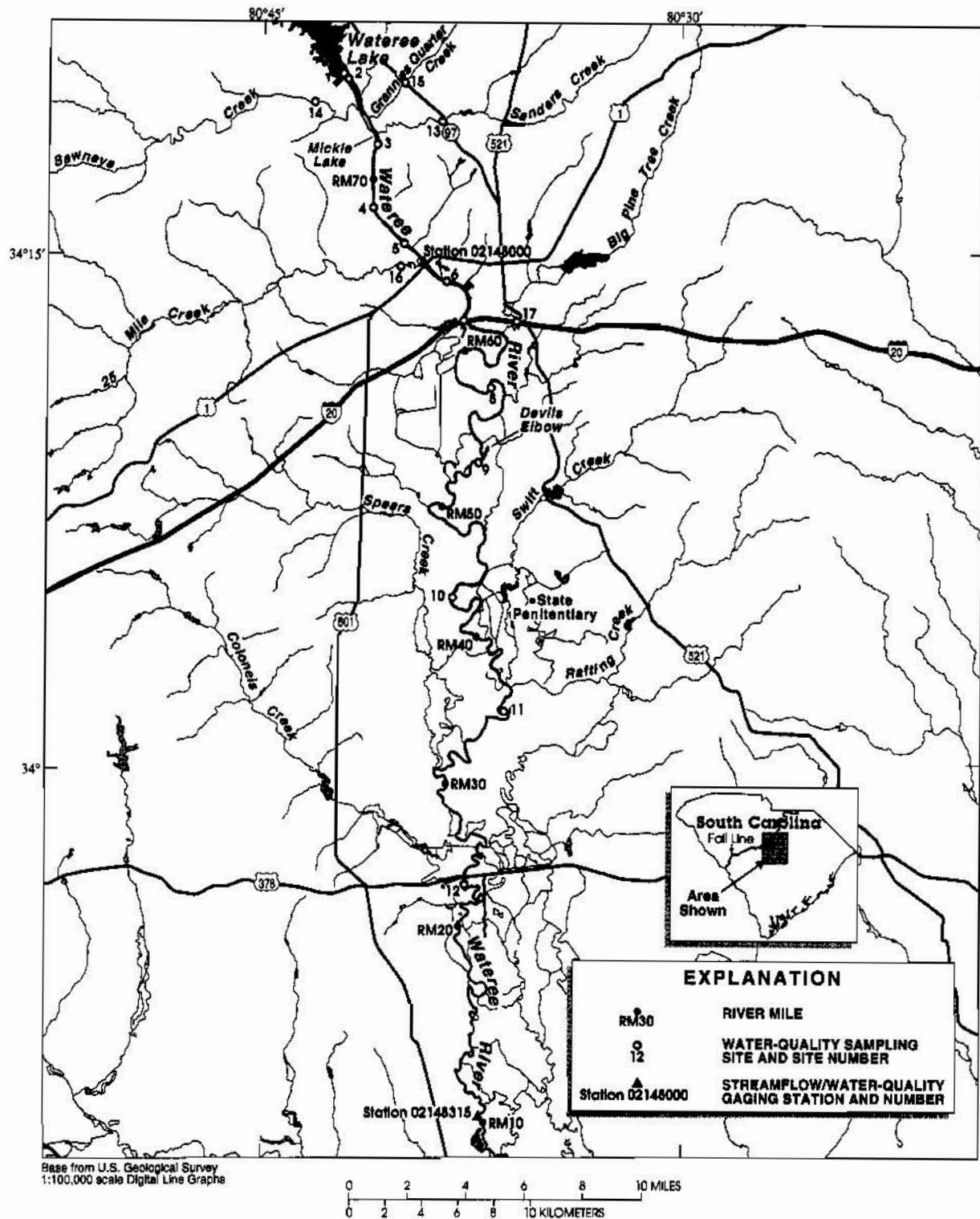


Figure 1. River miles, in-river and tributary water-quality sampling sites, and U.S. Geological Survey streamflow/water-quality gaging stations on the Wateree River, South Carolina.

time for the 50-mile reach from the Wateree Lake Dam to Site 12 for the flows of interest is approximately 2 days. Based on preliminary assessments of the system, 1 lake site, 11 in-river sites, and 5 major tributaries were selected to define the water quality in the Wateree River (fig. 1). If an Eulerian sampling scheme was applied with the goal of sampling 2 complete flushings of the system, this could be accomplished by collecting samples at each station at 6-hour intervals during a 4-day period for a total of 272 samples.

Utilizing data from the previous models on the Wateree River, a preliminary streamflow model and Lagrangian transport model were calibrated within acceptable limits for their intended use. Model simulations indicated that 3 complete flushings through the 50-mile study reach could be sampled over a 3-day period. If the lake and in-river sites were sampled so as to track 3 water parcels through the system and the tributaries were sampled 4 times per day, the total number of samples collected would be 96. Consequently, the Lagrangian sampling scheme could reduce the analytical laboratory cost by 65 percent relative to the Eulerian sampling scheme.

Intensive water-quality sampling requires much effort and resources. Although the Lagrangian sampling scheme would have reduced the analytical laboratory cost significantly, the other cost such as personnel and lodging would have been approximately the same. Therefore, it was concluded that in the larger objective of the project, a better sampling approach would be to utilize a combined Lagrangian-Eulerian sampling scheme. This approach would allow for some cost reduction and provide a larger set of data from which to calibrate and verify the water-quality model.

The Lagrangian-Eulerian sampling scheme would help optimize the limited sampling dollars. This sampling scheme would track 3 water parcels completely through the river system, track 6 water parcels partially through the river system, and then allow selected collection of additional samples to document changing conditions at the sampling sites. Once the data were collected, a well defined time-series data set would be available for model calibration. In addition, the water-quality constituents for each parcel could be plotted along with the DO concentrations soon after the data were received from the analytical laboratory. These plots could then be used as a tool for quickly assessing the major influences on the DO before beginning the modeling process.

DEVELOPING THE SAMPLING PLAN

In the previous study, Hurley (1991) had applied the BRANCH model to accommodate the backwater conditions at the downstream boundary on the Santee River. The Wateree reach of the system does not experience backwater, therefore the DAFLOW model (Jobson, 1989) was selected as the dynamic streamflow model for this study.

The Flow Model: The DAFLOW model was set up with 2 branches. Branch 1 has 21 segments and extends 50 miles from site 2 in the Wateree Lake Dam tailrace to site 12, just downstream from the U.S. 378 bridges. Branch 2 has 7 segments and extends 14

miles from site 12 to Station 02148315. During the previous study on the Wateree River, a time-of-travel study was made from Station 02148000 to the U.S. 378 bridges on August 19-21, 1987. Consequently, the period August 8-23, 1987, was selected to calibrate the DAFLOW model. Simulated and measured flows were compared at Stations 02148000 and 02148315. An optimization program provided with DAFLOW was used to improve the phase difference and the minimum and maximum computed flows until a reasonable calibration was obtained.

The Transport Model: Output from DAFLOW provided the hydraulic properties necessary for the BLTM. The BLTM was setup with the same grids and time steps as DAFLOW. Dye-concentration data were available near site 6. Because concentration data can not be input at internal grids except through tributary inflow, synthetic concentration data and tributary inflow were input at the appropriate time step at a grid near site 6. Therefore, calibration of the peak concentration and (or) dispersion of the dye was not possible. However, the measured and simulated peak travel times agreed within approximately 1 hour at sites 9 and 12. It was determined that the transport model calibration was adequate for its intended use: to develop a Lagrangian-Eulerian sampling scheme.

Streamflow versus Peak Travel Time: The BLTM was used to simulate the time of travel for the peak concentration of a conservative constituent injected in the tailrace of the Wateree Lake Dam. These travel times were obtained at 7 locations that corresponded with or were close to desired water-quality sampling locations. The travel times were simulated for 5 steady flows: 1,000; 2,000; 4,000; 6,000; and 10,000 cubic feet per second (ft^3/s). For each station, a streamflow versus travel time curve was developed using the 5 steady flows (fig. 2). These data were entered into a spreadsheet and regressed using a power-curve function. From these analyses, an equation was obtained for each of the 7 locations that would allow the peak travel time to be estimated for steady flows in the range of 1,000 to 10,000 ft^3/s .

Because a reaeration study, which required steady-flow conditions, was to be made during the same time period as the water-quality sampling, steady-flow releases were requested from the operator of the Wateree Lake Dam. Two flow rates were negotiated: approximately 2,000 and 3,000 ft^3/s . Tributary inflows were not included in the preliminary flow and transport models. Therefore, to account for slightly increasing flows in the downstream reaches, the flows used to calculate the peak travel times were increased by 10 percent (2,200 and 3,300 ft^3/s , respectively). Peak travel times were calculated at the 7 locations. The travel times for the other water-quality sampling locations were obtained by interpolation.

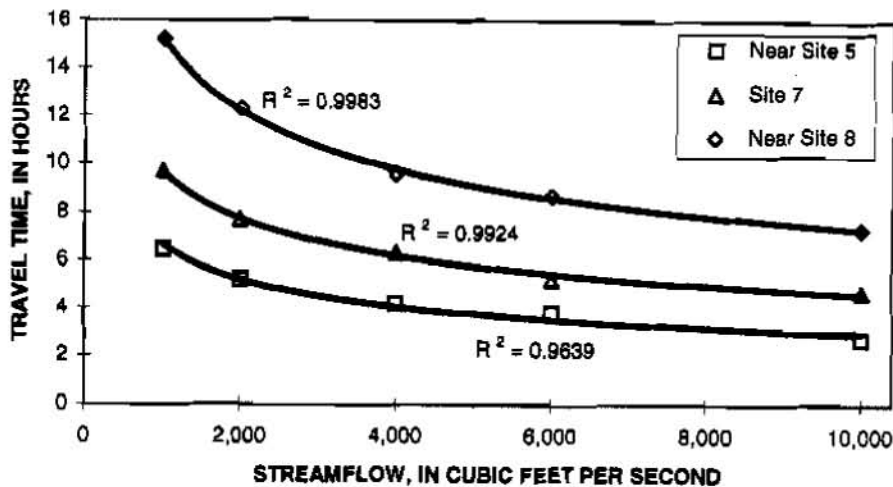


FIGURE 2. Regression of streamflow and travel time for selected sites on the Wateree River, South Carolina.

The Lagrangian-Eulerian Sampling Matrix: A sampling matrix was developed to aid in planning the logistics of sampling at 11 in-river and 5 tributary sites, and 1 lake site. The beginning times for the water parcels that were tracked through the system were 0600, 1200, and 1800 hours for the 3,300 ft³/s flow and 0600, 1100, and 1700 hours for the 2,200 ft³/s flow. These times were chosen for three reasons: (1) to allow enough time for the sampling teams to sample each station and be ready to sample the next parcel, (2) to record the influence of diurnal fluctuations, and (3) to minimize late-night sampling for safety concerns.

An initial sample at each site was collected to record background conditions. The collection times for the background samples were chosen so that all sites would have their first sample collected by 0600 hours, which was the beginning time for parcel 1. The tributary sample times were chosen to obtain a time series of data throughout the day without conflicting with in-river sample times. Because the peak travel times were based on some simplifying assumptions and to aid in logistics, all sample collection times were rounded to the nearest half hour.

RESULTS AND CONCLUSIONS

Time-of-travel studies were made during the water-quality samplings on June 23-25 and August 11-13, 1997, on the Wateree River. The results were used to assess the accuracy of the simulated water-parcel sample times. As previously discussed, the sample times were based on the time at which a parcel of water would reach a predetermined sample location. Plots of the DO concentrations measured at the in-river sampling stations for a simulated parcel of water departing from site 2 at 1500 hours on June 23, 1997, and at 1100 hours on August 11, 1997, are shown in figure 3. Also included in figure 3 is the actual location of the water parcels based on the time-of-travel studies from June and August 1997. The simulated sample times for the August study were improved based on

differences of the simulated and actual time of travel of peak-dye concentrations from the June study. Based on the data shown in figure 3, the simulated and actual parcel locations appeared to be reasonably close. Therefore, the data suggest that the Lagrangian-Eulerian sampling scheme was a success.

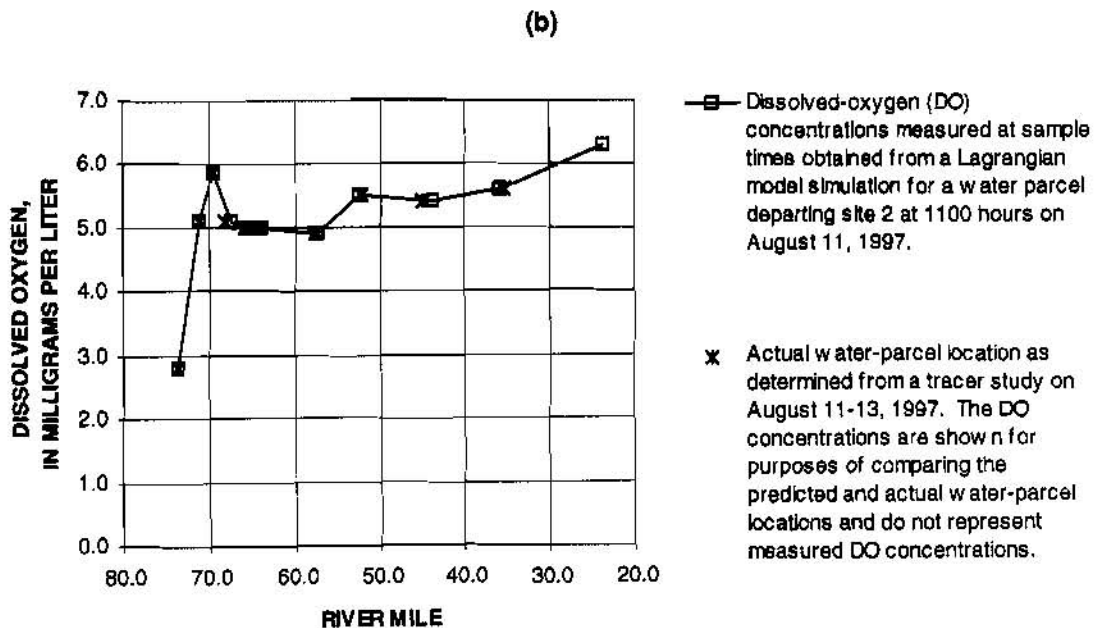
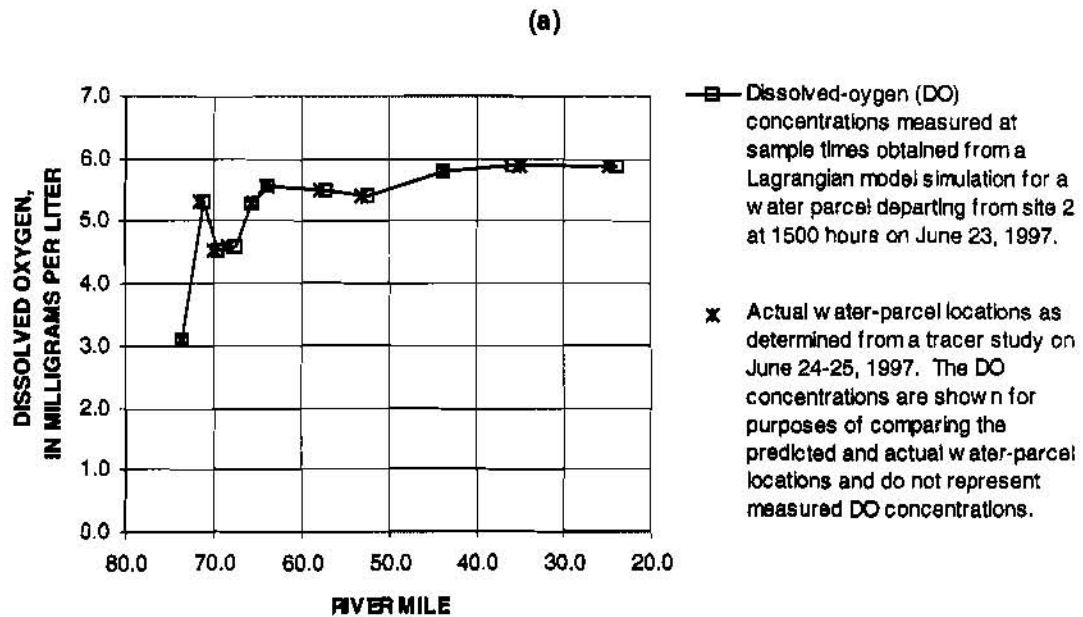


FIGURE 3. Dissolved-oxygen concentrations measured at simulated water-parcel locations versus actual water-parcel locations obtained from tracer studies on the Wateree River, South Carolina for (a) June 23-25, 1997 and (b) August 11-13, 1997.

Designing a Lagrangian-Eulerian sampling scheme for the Wateree River was possible because data from a previous study were available, and because the flows were known prior to the beginning of this study. By utilizing the previous data and models, the cost of the sampling was reduced. It is concluded that the water-quality data and field parameters for the Lagrangian water parcels can be used with confidence as a tool for assessing the major influences on the dissolved-oxygen concentrations before the actual modeling begins.

REFERENCES

- Hurley, N.M., Jr., 1991, Transport simulation of Striped Bass eggs in the Congaree, Wateree, and Santee Rivers, South Carolina: U.S. Geological Survey Water-Resources Investigations Report 91-4088, 57 p.
- Jobson, H.E., 1989, Users manual for an open-channel streamflow model based on the diffusion analogy: U.S. Geological Survey Water-Resources Investigations Report 89-4133, 73 p.
- Jobson, H.E., and Schoellhamer, D.H., 1987, User manual for a Branched Lagrangian Transport Model: U.S. Geological Survey Water-Resources Investigations Report 87-4163, 73 p.
- Schaffranek, R.W., Baltzer, R.A., and Goldberg, D.C., 1981, A model for simulation of flow in singular and interconnected channels: U.S. Geological Survey Techniques of Water-Resources Investigations book 7, chap. C3, 110 p.

A GIS - NUMERICAL MODELING APPROACH TO IDENTIFY REGIONS WITH SUITABLE WATER RESOURCES FOR A DUAL CROP ROTATION

**By Jurgen Garbrecht, Hydraulic Engineer, USDA-ARS, El Reno, Oklahoma;
Patrick J. Starks, Soil Scientists, USDA-ARS, El Reno, Oklahoma;
Robert Williams, Plant Physiologist, USDA-ARS, El Reno, Oklahoma**

Abstract: A GIS and numerical modeling approach to evaluate the water resources availability for a year-around forage production system is proposed for the Southern Great Plains (SGP). The GIS part of the approach identifies potentially suitable areas within the SGP based on climatic, physiographic and agricultural characteristics. Each of the GIS coverages is evaluated individually for suitability, and a final overlay analysis identifies those regions that are compatible for all GIS coverages. The subsequent numerical modeling part of the approach establishes the annual and seasonal soil water budget constraints for the forage production system in the regions identified by the GIS analysis. The soil water recharge, storage and losses are evaluated to establish the limits of water availability for the crop rotation. The study identifies a method to provide regional soil water estimates and is not intended for site specific estimation of crop productivity.

INTRODUCTION

The livestock industry in the Southern Great Plains (SGP) is concentrated around a few large feedlot operations. A decentralized cattle finishing system has been proposed in which cattle remains on the farm for forage-based on-farm-finishing (Phillips, 1997). Such a system has the potential to decrease the animal processing time at the feedlot, recycle a greater portion of animal waste onto farm pastures, and provide economic opportunities for livestock enterprises in rural communities.

This paper identifies soil water supply and availability issues for a year-round forage production system in the SGP and describes a practical approach to address these issues based on climate conditions in the SGP. The challenge of the approach is the diversity of the geographic area, the variability of the climate, and the necessity of a detailed soil water analysis to access the sustainability of the year-round forage production system. Soil water supply and availability, as opposed to crop water requirements and utilization, are emphasized in this study. This emphasis provides a broad framework to quantify the envelop of existing environmental constraints and evaluate alternative crop rotations with different water requirements. This paper presents the concepts and approach developed in the planning phase of the water resources evaluation project.

In the first section of this paper, the year-round, on-farm forage production system is described and the critical, water-limited component of this system is identified. In the second section the soil water issues, the framework and the objectives of the investigation are defined. Finally, the approach to address the soil water issues is described in the remainder of the paper. Findings and implications of the study will be presented at completion of the project.

PROPOSED DUAL CROP ROTATION

The traditional grazing system in the SGP relies on winter wheat and perennial summer grasses (Winter, 1994; Voigt and Sharp, 1995). This two component system results in forage production gaps in spring and fall that limit the potential for an on-farm cattle finishing system. A three component forage system that provides forage during the spring and fall forage gaps has been proposed by Rao, McKown and Williams (Phillips, 1997). It consists of (1) a winter wheat-pigeonpea (WW-PP) rotation, (2) warm-season grasses, and (3) a cool-season perennial chicory-pubescent wheat grass mixed pasture. This system provides year-round continuous supply of forage, and also allows livestock producers to switch from wheat graze-out to a graze-grain option under favorable grain market conditions.

Winter wheat and warm-season grasses have been grown for many years in the SGP under dry-land farming conditions. They represent a proven and sustainable forage source, exceptions being occasional severe droughts. As such, a soil water investigation is not warranted for these crops. The critical component of the forage production system is the added pigeonpea crop in the WW-PP rotation. This second crop is grown within the same year on the same acreage as the winter wheat. Winter wheat is grown from about mid-September through about mid-May, and pigeonpeas are grown after the winter wheat harvest through mid-September. Even though pigeonpeas have been proposed as the summer crop for the rotation, the approach described herein is applicable for other alternative summer crops. Thus, the fundamental question of this investigation is the soil water availability for a second crop during the summer fallow period of the winter wheat. In the following, the dual crop rotation is simply referred to as rotation, and summer crop refers to any alternative crop in rotation with the winter wheat.

STUDY OBJECTIVES AND SOIL WATER SUPPLY ISSUES

The main objective of the soil water supply investigation is the identification of regions in the SGP that have climate and soil water conditions that can sustain a rotation under dry-land farming conditions. This region identification is necessary to establish the geographic area that is suitable for the proposed on-farm cattle finishing system. The framework, boundary conditions and requirements for the investigation include: (1) consideration of a geographically diverse five state area that supports winter wheat and stocker cattle operations, (2) incorporation of a spatially and temporally variable climate, and, (3) need for a long term, annual and seasonal soil water supply analysis to insure sustainability of the rotation.

The soil water supply issues affecting the feasibility and sustainability of the rotation in the SGP are listed below in order of increasing restrictivity. The order is relevant, because the issues can be used as criteria to stepwise exclude unsuitable regions from the initial the five state area.

- 1) Mean annual precipitation must sustain the annual water requirements of the rotation: the mean annual precipitation is used as a gross estimation of potential annual soil water for crop consumption, independent of seasonal distribution. Seasonal distribution is disregarded here, because an inadequate total water supply remains inadequate no matter how it is distributed.

- 2) Mean seasonal precipitation regime must be compatible with plant water requirements of the rotation components: the mean seasonal pattern of precipitation is used as a gross estimation of seasonal distribution of potential soil water availability. The coincidence of seasonal soil water distribution with rotation water requirements is particularly relevant for regions with pronounced seasonal fluctuations of precipitation and soil water, as well as pronounced seasonal rotation water requirements.
- 3) Soil water storage capabilities must accommodate dry-season rotation water requirements: the precipitation pattern must allow for adequate soil water recharge and storage (with consideration for losses to surface runoff, deep percolation and evapotranspiration) to meet rotation water requirements through seasonal periods of reduced or no precipitation. The soil water dynamics (recharge, storage, losses and consumption) must be such that rotation water requirements can be sustained for consecutive average years.
- 4) Variability of annual and seasonal precipitation must permit a sustainable rotation: precipitation amount and distribution can vary considerably from one year to the next, and the probabilities of adequate soil water to sustain the rotation must be determined to establish the success/failure rates and the practicality of the rotation.

GENERAL APPROACH

Suitable regions for the summer crop are identified in two consecutive steps: first, a Geographic Information System (GIS) analysis, and, second, a numerical soil water analysis. In the GIS analysis, data coverages that represent suitable/unsuitable climate, agricultural and crop conditions are developed and used in an overlay analysis to identify those regions which are classified as suitable for all considered coverages. The careful selection of relevant GIS coverages and the overlay analysis are expected to significantly reduce the number of regions requiring a detailed soil water analysis.

In the second step, a numerical soil water analysis is conducted for those regions delineated as suitable by GIS analysis. A soil water flux model is used to simulate the soil water dynamics throughout the soil profile, and a winter wheat model is used to simulate the winter wheat plant parameters and soil water consumption. With these two models the soil water recharge, storage, consumption and losses are modeled for the entire winter wheat season and for average climate conditions. A detailed soil water budget for the summer crop season is developed to establish soil water availability. The soil water budget values include recharge, storage and losses, and lead to regional estimates for the range of soil water availability to meet the water requirements of the summer crop.

Finally, as part of the second step, those regions that are suitable under representative climate conditions are re-evaluated with recorded annual and seasonal climatic variations to establish the long term sustainability of the rotation. The probabilities of failure/success of the rotation on an

annual basis are derived from simulated winter wheat crop yields and soil water deficit values for the summer crop. This approach is believed to be adequate for the stated objective to identify regions that have suitable water resources for the rotation. Though modeling site-specific and local conditions would introduce additional accuracy, it would only be of local relevance and defeat the sought after objectives a regional analysis.

GIS ANALYSIS

The effectiveness of the GIS analysis depends on the choice of the GIS data coverages. A map of existing, non-irrigated winter wheat production areas is the first GIS coverage. The identified areas are assumed to represent regions with climatic, ecologic and economic conditions that are favorable for winter wheat production and potentially for the proposed rotation. Regions outside these areas are assumed to be un-favorable, and, therefore, highly unlikely to be able to support the more demanding needs of the rotation. For example, areas in south and south-west Texas will be excluded because winter wheat is poorly adapted to warm and moist climates without a cool dry season (Martin, Leonard and Stamp, 1976). Also, regions of New Mexico will likely be excluded because annual precipitation for many areas are at or below the lower limit of 380 mm needed for wheat production (Martin, Leonard and Stamp, 1976).

Spatial distribution of annual precipitation is the second GIS coverage. In the SGP the spatial variability of annual precipitation is very high. For example, annual precipitation in Oklahoma ranges from 380 mm in the west to 1400 mm in the east (Pettyjohn, White and Dunn, 1983). The high spatial gradient of the annual precipitation lends itself well to identify regions that can provide enough water to meet the annual water requirements of the rotation (first soil water issue).

The duration of the traditional summer fallow period of winter wheat is the third GIS coverage. The duration changes from north to south. It can be as short as two month in the north and as long as four months in the south (Martin, Leonard and Stamp, 1976). The spatial variation of the duration is used to identify regions with a summer fallow period long enough to accommodate the needs of the summer crop.

A GIS coverage is developed for the mean precipitation during the winter wheat growing season, and a second coverage for the mean precipitation for the summer fallow season. As noted above, the duration of the fallow period changes with geographic location. The two GIS coverages provide a gross estimation of precipitation and soil water availability during the growing season of each of the two crops (second soil water issue).

Additional climatic data coverages such as growing-degree days and photo-period, as well as coverages relating to topography or demographics of stocker cattle operations, are considered in the GIS analysis. These coverages, in conjunction with specific crop and on-farm finishing requirements, provide additional criteria for identifying regions that are suitable for the rotation. However, these coverages are not discussed in depth in this paper because they are of limited relevance to the soil water issues.

The last GIS coverage is the map of ecoregions and subregions of the United States (Bailey et al., 1994). This layer is used to define areas of similar climate, vegetation and soil characteristics (Bailey, 1983). This coverage is not used to define suitable/unsuitable regions, but to help subdivide large regions into subregions with similar eco-conditions. These subregions define uniform response areas for the subsequent detailed hydrologic modeling of soil water availability.

The above GIS coverages are largely independent of the summer crop selection and represent the environmental constraints for the summer crop. Thus, the GIS coverages remain constant and can be used repeatedly for different summer crops. Once a summer crop is selected, each of the coverages is processed to define regions that are either suitable or unsuitable for the corresponding crop requirements. Finally, all coverages are superposed to identify those regions that meet the crop and on-farm finishing requirements. These regions are retained for the subsequent numerical soil water analysis.

SOIL WATER ANALYSIS

The numerical soil water analysis accounts for seasonal distribution of precipitation, soil water storage effects and temporal soil water availability/consumption. The temporal scale of the numerical simulation is one day, and the result interpretation is performed on a weekly and monthly scale. This scale is consistent with the crop simulation objectives to establish soil water recharge, availability and consumption on a seasonal and annual basis.

A soil water flux model and a winter wheat model are used in the soil water analysis. The soil water flux model is the Simultaneous Heat and Water Model (SHAW) by Flerchinger and Saxton (1989). The model consists of a vertical, one-dimensional profile that includes canopy, snow, residue and soil layers. The strength of the model resides in the detailed and integrated physical representation of the energy and water fluxes through the soil-plant-atmosphere continuum. Even though the model has provisions to simulate water evapotranspiration by rangeland plant species, it does not have crop simulation capabilities. Winter wheat development and water consumption is simulated by a second model, the CERES-Wheat model (Ritchie, 1991). Winter wheat development is based on climate drivers, as well as water and temperature stress constraints. The weakness of the CERES-Wheat model, from a soil water perspective, is the empirical/conceptual representation of the soil water fluxes. The SHAW and CERES-Wheat models are used in a complementary fashion to quantify soil water availability and consumption.

The soil water analysis is conducted in two steps. In the first step, soil water values are quantified under consideration of the seasonal patterns of the climatic drivers. The climatic drivers are measured daily values corresponding to a year that has monthly mean precipitation values close to normal values for all or most months, and annual precipitation close to the long term annual mean. Soil characteristics are selected to reflect typical conditions for existing winter wheat production areas in the region under consideration.

With these boundary conditions, the components of the soil water budget are simulated for the winter wheat and the summer crop growing season. The water budget components include recharge, re-distribution in the profile, storage, losses at the bottom of the soil profile, surface runoff

and evapotranspiration. For the summer crop season, the soil water consumption by the crop is not simulated. Instead the potential soil water for consumption is inferred from recharge, losses and storage changes during the summer season. Of particular relevance to the objectives of this investigation are the following soil water values: (1) the amount of soil water at the time of winter wheat harvest and summer crop planting, (2) the soil water recharge, storage and losses during the summer crop growing season, and (3) the remaining soil water at the time of summer crop harvest and at the beginning of the next winter wheat crop. To estimate the last item, the soil water consumption by the summer crop is estimated using published values for the selected crop or for a closely related crop.

The suitability of a region for a summer crop is established by contrasting soil water recharge and storage with the water requirements for the selected summer crop (third soil water issue). The sustainability is achieved when the annual and seasonal soil water budget is balanced or positive (excess water). In addition to a balanced seasonal soil water budget, adequate soil water storage at crop transition times must also be insured. Of particular interest is the soil water storage at the end of the summer crop. In the presence of late or scarce fall precipitation, adequate soil water storage is required for establishment of winter wheat for grazing.

A negative soil water budget is likely for some regions. A soil water deficit does not necessarily imply that the summer crop or the rotation is unsustainable. It may simply result in a reduced crop production. Thus, the soil water budget values can also be used to estimate the reduction in crop production under limited soil water availability. The viability of a reduced crop production is not a water supply, but an economic issue, and is not further elaborated here. As a final note, the simulated soil water budget components for the summer season do not change with the selected summer crop. It is the crop water consumption/needs that change as a function of crop selection and desired productivity. Thus, the results of the numerical soil water simulation are not limited to establish the sustainability of a selected summer crop, but can also be used as a crop selection criterion.

The second step in this numerical analysis consists of establishing the sustainability of the rotation under annual climate variation. The same regions as in the first step are considered, unless soil water considerations have excluded some of these regions. The climatic drivers consist of historical climate data in excess of 30 to 50 years duration. The climate data are assumed to be representative of the frequency, severity, duration and timing of floods and droughts. The components of the annual and seasonal soil water budget are simulated and the annual variability of each component is established. Using cut-off values for soil water availability for adequate crop productivity, the success and failure rates can be computed. Regions that have excessive failure rates are considered as unsuitable. Even though the climate record is relatively short and confidence limits are expected to be large, the results will provide an indication of the vulnerability of the rotation to seasonal and annual climate variations.

The results of the numerical soil water analysis establishes regions that are suitable for the winter wheat-summer crop rotation. However, the decision of suitability and sustainability is not a yes or no issue as in the initial GIS analysis. Suitability and sustainability must be formulated in terms of productivity of the rotation which is a function of soil water availability.

FIELD EXPERIMENTS

The soil water flux simulation by the SHAW model is verified for known environmental and crop conditions at the USDA-ARS-Grazinglands Research Laboratory. Data are collected at Soil Heat and Water Measurement stations (SHAWMS) in native grassland, bare soil, winter wheat and pigeonpea field plots. The SHAWMS provides profile measurements of soil heat flux, soil temperature and soil water content at various depths in the root zone. Soil characteristics are also measured at these sites. Plant parameters (e.g., canopy traits, leaf litter, etc.) that are required by the models are measured or estimated as appropriate. With these data the soil water simulation is verified for local conditions. The SHAW model has also been successfully verified in semi-arid western and northwestern parts of the United States (Flerchinger, Hanson and Wight, 1996; Hayoe, 1994). The CERES-Wheat model has been applied to various wheat growing regions and shown to adequately approximate field conditions (French and Hodges, 1985). These verifications to a range of boundary conditions confirm the applicability of the models for this regional soil water investigation.

DISCUSSION AND SUMMARY

A GIS and numerical modeling approach to identify regions in a five state area that are suitable for an annual summer crop in rotation with winter wheat has been presented. Soil water availability was the central focus of the analysis. The approach consists of a GIS analysis of regional climatic, physiographic and agricultural characteristics, and of a numerical soil water analysis. The GIS analysis, based on a process of elimination, provides an initial, coarse screening that identifies regions in the five state geographic area of the SGP that are potentially suitable for a summer crop rotation. For these regions, a subsequent soil water budget analysis is conducted to establish the annual and seasonal soil water availability, as well as the long term sustainability of a summer crop. The soil water budget analysis includes water consumption by the winter wheat component of the rotation, and considers soil water recharge, storage and losses during the summer crop season. This approach provides a broad framework to define regional soil water constraints and evaluate alternative summer crops.

The soil water budget analysis for the summer crop season is based on precipitation input, soil water redistribution, storage, and losses (deep percolation, evaporation and surface runoff). Summation of initial soil water storage, precipitation input and losses provides the upper limit of available soil water for the summer crop. A more likely estimate of available soil water is based on the assumption that all deep percolation losses can be captured by the summer crop, but that surface runoff and evaporation losses are not recovered. Summer convective storms in the SGP are generally of high intensity and short duration and are likely to produce runoff with or without summer crop being present. Also, high summer temperatures and persistent winds in the SGP are expected to produce soil evaporation with and without a summer crop being present. Interpretations of individual water budget components are expected to lead to a relatively narrow window for regional soil water availability for a rotation. Such findings are believed to be adequate for a regional soil water analysis and are not intended for site-specific estimation of crop productivity.

The regional analysis should be followed by a site-specific investigation that accounts for local soil characteristics, topography and specific summer crop water requirements. In such a follow-up investigation the soil water consumption of the summer crop would be modeled explicitly and the sustainability of the rotation would be established for specific field sites.

REFERENCES

- Bailey, R. G. 1983. Delineation of Ecosystem Regions. *Environ. Management*, 7(4):365-373.
- Bailey, R. G., P. E. Avers, T. King, and W. H. McNab. 1994. Ecoregions and Subregions of the United States. U. S. Department of Agriculture, Forest Service.
- Flerchinger, G. N., and K. E. Saxton. 1989. Simultaneous Heat and Water Model of a Freezing Snow-Residue-Soil System I. Theory and Development. *Transactions of the ASAE*, 32(2):565-571.
- Flerchinger, G. N., C. L. Hanson, and J. R. Wight. 1996. Modeling Evapotranspiration and Surface Energy Budgets Across a Watershed. *Water Resources Research*, Vol. 32, No. 8, pp. 2539-2548.
- French, V., and T. Hogdes. 1985. Comparison of Crop Phenology Models. *Journal of Agronomy*, Vol. 77, pp 170-171.
- Hayhoe, H. N. 1994. Field Testing of Simulated Soil Freezing and Thawing by the SHAW Model. *Canadian Agricultural Engineering*, Vol. 36, No. 4, pp.279-285.
- Martin, J. H., W. H. Leonard and D. L. Stamp. 1976. Principles of Field Crop Production. Macmillan Publishing CO., Inc., New York and Collier Macmillan Publishers, London.
- Pettyjohn, W. A., H. White and S. Dunn. 1983. Water Atlas of Oklahoma. Published by the University Center for Water research, Oklahoma State University, Stillwater, Oklahoma.
- Phillips, W. A. 1997. Development of a Sustainable Decentralized Livestock Finishing System. Proposal for USDA Fund for Rural America.
- Ritchie, J. T. 1991. Wheat Phasic Development. In: *Modeling Plant and Soil Systems*, J. Hank and J. T. Ritchie (eds), Number 31 in the Series AGRONOMY; ASA, CSSA and SSSA, Madison, Wisconsin.
- Winter, S. R. 1994. Managing Wheat for Grazing and Grain. TX Agric. Exp. Stn. Bull. MP-1754.
- Voigt, P. W., and W. C. Sharp. 1995. Grasses of the Plains and Southwest. In R. F. Barnes, D. A. Miller, and C. J. Nelson (eds). *Forages: an Introduction to Grassland Agriculture*. Vol. I, p.395-408, Iowa State University Press, Ames, Ia.

AN INTEGRATED MODELING FOR WATER RESOURCES MANAGEMENT STUDY IN TAIWAN

**Shiang-Kueen Hsu, Director General; Ming-Jame Horng, Senior Engineer and Yau-Hui Lee, Research Engineer, Water Resources Bureau, MOEA
Taipei, Taiwan, ROC**

Abstract: In many places of Taiwan, an island country, the current supply of water is inadequate in satisfying the ever increasing quantity and quality demands for domestic and industrial water consumption. To cope this important issue, the former Water Resources Planning Commission (WRPC), now the Water Resources Bureau (WRB) in Taiwan has devoted much manpower and funding to cooperate with Delft Hydraulic to prepare management study for water resources .

The nature and extent of the problems in most of river basins in Taiwan, led to the conclusion that the management study of these problems should focus on the main questions: How can the future water supply be ensured and how can acceptable water quality be achieved and maintained? An integrated model for river-basin management is employed in this study for solving the complex situations, where conflicting interests demanding limited natural and economic resources. This paper describes the approach of the water resources management in Taiwan, and shows the results of integrated analysis for water quantity and quality of a study basin.

INTRODUCTION

Water resources management is the interaction of technology, economics, and institutions to balance water supply with demand. In many places of Taiwan, have completed the major developments of their water resources infrastructures. Water managers in Taiwan are faced with an increased population and pressure for the incorporation of environmental protection objectives into the operation of existing water resources system.

In many places of Taiwan, an island country, the current supply of water is inadequate in satisfying the ever increasing quantity and quality demands for domestic and industrial water consumption. To cope this important issue, the former WRPC, now the WRB in Taiwan has devoted much manpower and funding to cooperate with Delft Hydraulic to prepare management study for water resources .

The nature and extent of the problems in most of river basins in Taiwan, led to the conclusion that the management study of these problems should focus on the main questions: How can the future water supply be ensured and how can acceptable water quality be achieved and maintained? An integrated model for river-basin management is employed in this study for solving the complex situations, where conflicting interests demanding limited natural and economic resources. The following paper describes the approach of the water resources management in Taiwan, and shows the results of integrated analysis for water quantity and quality of a study basin.

WATER RESOURCES OVERVIEW

Water Supply: Taiwan's total area of roughly 36,000 km^2 is approximately 1/3 mountainous area above sea level (1,000m) contour; 1/3 hills and terraces, between 100 and 1,000m contours and 1/3 is a coastal plain. Most of population lives in the plain, which run predominantly along the western side of the island. On the northern plains, the climate is subtropical and its tropical in the south. The annual mean temperature ranges from 21^o to 24^o centigrade.

Average annual rainfall amounts to 2,500 mm over the entire island, and is between 1,000 and 2,000 mm over most of the coastal plains. The island is frequently subjected to typhoon, usually two to three each year. Typhoons are frequent in the north, where the annual average rainfall can be as high as 6,500mm. Reservoirs have been built for multipurpose, such as to meet the growing demands for water supply, flood control, and hydropower.

Water use: The current supply of water is inadequate in satisfying the ever increasing quantity and quality demands for domestic and industrial water consumption. The table summarizes the total volume of water used by the main categories of water consumers in Taiwan, for instance agriculture, public water supply (PWS), industrial plants, and so on. However, hydropower has not been included.

	1961	1981	1994	2001
Water use, billion cu. m.				
Total	10.4	16.6	17.6	20.7
Irrigation	9.8	13.7	13.2	15.0
Industry	0.2	1.8	1.6	2.2
Domestic & Community	0.4	1.1	2.8	3.5
Sources (%)				
Surface water	93	77	64	78
Groundwater	7	23	36	22

Water quality: Pollution of rivers and coastal waters increased rapidly over the past two decades. Taiwan has 21 major rivers, 29 minor rivers, and 79 common rivers. A 1994 survey used four water quality parameters to indicate the condition of the river water; dissolved oxygen, biochemical oxygen demand, suspended solids, and ammonia nitrogen. The survey results on the downstream reaches of the 50 major and minor rivers indicated that 22(44%) are unpolluted, and 4(8%) are slightly polluted, 12(24%) are moderately polluted, and 12(24%) are severely polluted. Main pollutant sources are: industrial waste water, in terms of BOD loading 54%, urban sewage 23%, and livestock wastes 23%.

All these have been the result of population growth and industrial development, leading to an increase in water use and the worsening of water quality. The more the economic development progresses, the severer the water pollution becomes. Consequently a proper approach must be found to manage the problem created by population growth and industrial waste, so as to minimize pollution problems.

ANALYSIS FRAMEWORK

The planning difficulties and related issues on river-basin level are usually clear-cut; but the approach required to deal with such issues can be fairly complicated. This is inherent to the complex nature of water resources management, which may be more serious further by socio-economic developments leading to increase in water demands and production of materials, and also institutional and administrative changes, leading to stricter rules and regulations. As such, the scope of water resources planning has changed from local to regional, from single to multiple criteria, and from supply-oriented to both supply- and demand-oriented.

In Taiwan two major types of problems exist in the performance of a river basin. First, the situation when either quantitatively or qualitatively there is not enough water supply to satisfy human demands, either in a sense. Second, the situation when the condition of the river basin adversely affects the natural environment and human activities.

When problems are expected, measures and strategies to improve on the situation have to consider. River-basin planning deals with the identification, analysis and evaluation of such measures and strategies. The cooperation with Delft Hydraulic resulted in an integrated model facilitating the various analysis steps and the ensuring study of measures and strategies for water resources management.

River-basin-oriented modeling framework: The river-basin-oriented modeling framework includes the following inter-related main modules, as presented in the figure 1 :

- PROgram for the Domestic and Industrial Sector (PRODIS) : computation of present and future water demand for households and industry, both from PWS and self-supply, and computation for water shortages and cost of water supply.
- Agricultural District Model (ADIMO) : ADIMO computes agricultural water demand from surface water and groundwater (request mode). In the allocation mode, the model computes water shortages in fields and indicates the damages that result from these shortages.
- River basin Distribution Model (RIBASIM) : RIBASIM determines the overall surface water balance in the river basin, including the operation of the reservoirs and the distribution of water in the river network. The model tries to match supply and demand in the system.
- DISCHRG, RIBOUT and POSTOUT : the processing program for the output of RIBASIM model.
- TAIwan Water Quality model (TAIWAQ) : for water quality calculations in estuary, river and reservoir system under both steady and unsteady conditions. It is a modified version of DELWAQ program from Delft Hydraulics supplemented with the waste production model WASPRO, and the flow distribution model, RJBASIM.

- WASTE PRODUCTION model (WASPRO) : a model to calculate waste loads from domestic, industrial, non-point (agriculture) and livestock sources, where possible associated with water flows in the RIBASIM network schematization.
- Regional Model for Impact Assessment (REMIA) : REMIA processes selective outputs from PRODIS, ADIMO and RIBASIM in order to provide a comprehensive report of physical quantities and socioeconomic consequences for different cases. Such cases consist of a combination of a water resources management strategy and so-called scenario specification, reflecting a set of assumptions about economic developments or conditions that affect water demands or supply. These cases are always compared with a base case, in order to determine the specific effects of the strategy under investigation.

The integrated model was used to analyze the present and future water resources management in terms of water quantity and quality, such as the management of existing or additional reservoir, or scenarios for future water demands by industry and municipal.

WATER RESOURCES MANAGEMENT APPROACH

The nature and extent of the problems in most of river basins in Taiwan, led to the conclusion that the management study of these problems should focus on the main questions: How can the future water supply be ensured and how can acceptable water quality be achieved and maintained? The integrated analysis focuses on the future water supply and water quality situation. The basic steps in the execution of the integrated analysis are: analysis of effects of demand increase and identification of quantity problems; identification and screening of water quantity measures; analysis of effects of waste load increase, identification of quality problems; identification and screening of water quality control measures; and analysis and evaluation of integrated measures and strategies.

The preparation of an integrated analysis involves the specification of analysis conditions, water demand scenarios, hydrological scenarios and the definition of cases. A case is defined as a combination of projection year, a demand scenario, a hydrological scenario and a measure or strategy.

The specification of analysis conditions includes problems statement, possible measures, objectives and criteria, scenarios, time and cost aspects, assumptions and boundary conditions, and a well-defined analytical approach. It should be emphasized that the efforts involved in preparing the computational framework for use in the analysis have been very substantial. The major activities in this aspect shown as following include schematization of the study area, data collection, processing and screening and execution of analysis.

Schematization of the study area: For the purpose of the different models to be used, the study area has been schematized in various ways.

- **RIBASIM:** network structure of branches and nodes:
 - branches reflecting the river stretches and other waterways that are parts of the major surface water infrastructure in the study area;

- nodes representing the points of inflows, storage or demand.
- **ADIMO:** schematization of area into:
 - district;
 - subdistrict;
 - fields.
- **PRODIS:** schematization of the area into:
 - groundwater supply areas;
 - PWS supply system.
- **TAIWAQ:** schematization of the river into:
 - estuary;
 - river;
 - reservoir system.

Data collection, processing and screening: The data processing included the following activities:

- adjustment of "raw" data to input data file formats and proper aggregation levels according to schematizations used;
- adjustment to consistent units;
- simplification of input data based on computed results.

Data screening, in general, involves the following activities:

- checking of internal consistency of the data files;
- checking of consistency with other data sources;
- checking of input data based on computed results.

Execution of the analysis: The analysis of the water resources management strategies for a basin is to be considered as a first round integrated analysis and has the characteristics of a pilot analysis. The pilot analysis is based on realistic data and assumptions. As such it provided a number of findings and results, that may lead to some preliminary conclusions. Yet, it certainly does not cover the full scope of possible and realistic options to be considered in an overall integrated analysis. Before the results can be used for actual planning and decision making, the analysis has to be considerably extended. In order to structure the analysis, the following case groups have been distinguished.

- A: effects of demand increase;
- B: supply oriented measures;
- C: demand oriented measures;
- D: administrative measures.

Cases that emerge from group A can be considered as base cases. The formulation of cases in group B and C requires the specification of infrastructural measures (reservoirs and diversions, and combinations to be considered simultaneously), and the specification of demand oriented measures (in terms of demand reduction by user in time and space). The cases in group D need a specification of concrete actions to regulate and control the water users and water resources system.

The integrated analysis for several river basins in Taiwan has demonstrated suitability of the approach and the models for application on river basin level in a pre-feasibility planning stage. The whole model will be employed in the other areas and integrate the results to consider water resources management in Taiwan.

CONCLUSION

The resulting general integrated model for river basin analysis in terms of water demand, water supply, water quality, and economics is available for application with several river basins in Taiwan. To deal with an integrated analysis, Taiwan has been quite successful in hydrological data collection and analysis and water resources information compilation. However, practical analysis remains to be emphasized by means of establishment of hydroinformation center, computer simulation and data analysis for flood forecasting and water resources availability prediction for drought to ensure the water utilization safely in this island country.

REFERENCES

- Delft Hydraulics, the Netherlands, national master plan for water resources management, Taiwan, ROC; *Final Report I-V: Master Plan Study*; (1985-1987).
- W.R.P.C., MOEA, National Master Plan for water resources management - Chianan area (Chinese edition), Research Report, (1992).
- W.R.P.C., MOEA, National Master Plan for water resources management - Kaoping area (Chinese edition), Research Report, (1992).
- Wu, Chian Min, Regional Water Resources Development and Planning in Taiwan, Republic of China, Report of Water Resour. Plng. Commission, MOEA, (1994).
- W.R.P.C., MOEA, National Master Plan for water resources management - Choshui area (Chinese edition), Research Report, (1995).
- W.R.P.C., MOEA, National Master Plan for water resources management - Taichung area (Chinese edition), Research Report, (1996).

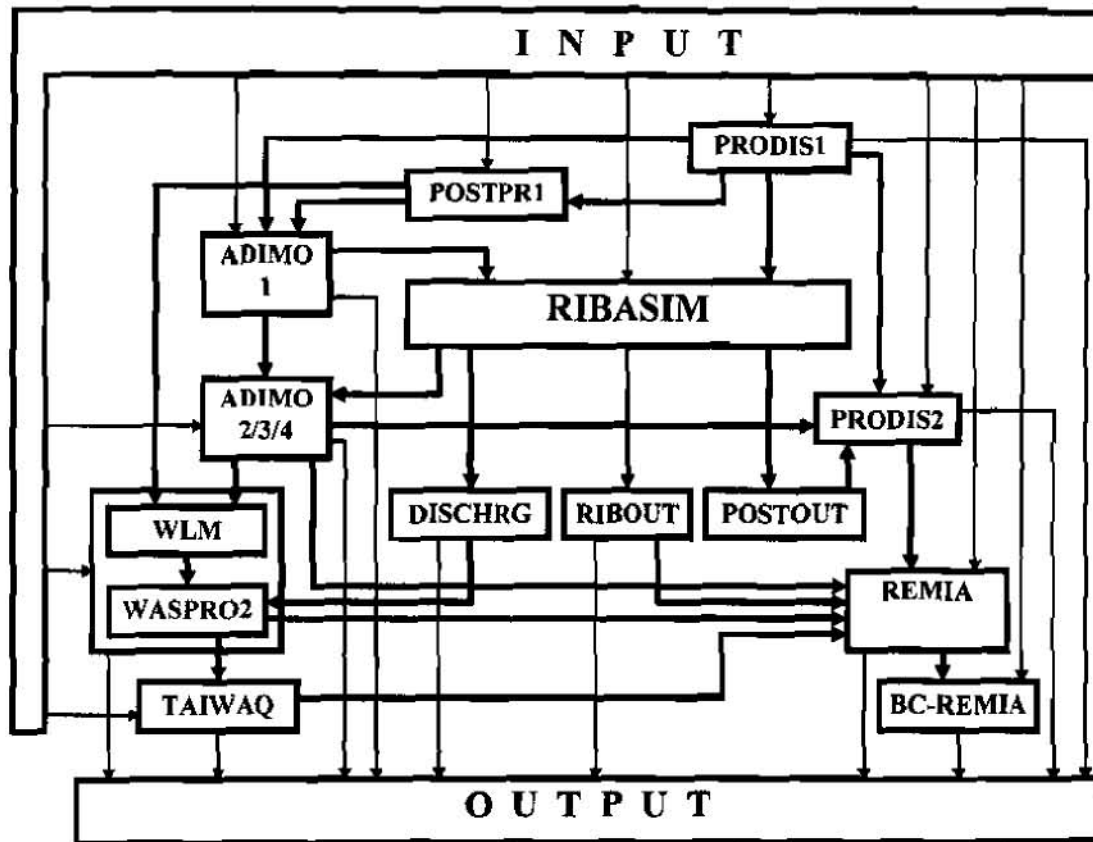


Figure 1. Computational framework of integrated model

A DYNAMIC MODEL FOR SIMULATING THE LONG-TERM TRANSPORT OF RADIONUCLIDES FROM A CONTAMINATED LAND SURFACE TO A NEARBY STREAM

**By C. Y. Hung, Hydrologist, Office of Radiation and Indoor Air,
Environmental Protection Agency, Washington, D.C.**

Abstract: This paper presents the theoretical background of the ORTER model used to simulate radionuclide transport via surface water. The theoretical background of this model is adopted from the existing PRESTO-EPA model. To demonstrate the model's applicability to an emergency spillage, a series of case studies are analyzed and results presented. The PRESTO-EPA model, published in 1987, was designed as a tool to assess the dose and risk to an individual due to the disposal of radioactive wastes in near surface trenches. The INFIL submodel was used to calculate the annual rate of infiltration to the waste matrix and the surface run-off to a nearby stream. The analysis involves complex mathematical processes for solving the partial differential equations representing the overland flow, subsurface flow and atmospheric diffusion systems. In developing the PRESTO-EPA model, the partial differential equations were transformed into ordinary differential equations, which improved the stability of the numerical calculation and reduced calculation time considerably. The ORTER model adopts the same methodology used in the PRESTO-EPA model to calculate the rate of radionuclide transport for deep infiltration to the aquifer and for surface runoff to a nearby stream. By ignoring the retardation effects in the distributing ditches, one can use this model to assess the impacts resulting from an emergency spillage of radioactivity onto the ground, or the effectiveness of a remediation measure, such as fixation of radionuclides, etc.

INTRODUCTION

A model to simulate the radionuclide transport from a contaminated land surface to a nearby stream is urgently needed today for protecting surface water. Unfortunately, there is no reliable model available. The purpose of this paper is to report on the US Environmental Protection Agency's effort in developing the ORTER model for use in an emergency response to protect the environment. The basic theoretical background is adopted from the existing PRESTO-EPA model.

The PRESTO-EPA model was designed as a tool to assess the dose and risk to an individual due to the disposal of radioactive waste in near surface trenches [EPA 1987a, 1987b, Hung 1989, 1992, 1996]. The INFIL submodel was used to calculate the annual rate of infiltration to the waste matrix and the surface run-off to a nearby stream. Since the infiltration flow and surface runoff are the driving forces for leaching radionuclides out of the waste matrix and the covering soil, the accuracy of the submodel is one of the important factors in determining the reliability of the entire transport model.

The analysis of the infiltration and surface runoff involves complex mathematical processes for solving the partial differential equations representing the overland flow, subsurface flow and atmospheric diffusion systems. During the process of developing the PRESTO-EPA model, the partial differential equations were transformed into ordinary differential equations, which

improved the stability of the numerical calculation and reduced the calculation time considerably [Hung 1983].

The ORTER model adopts the same methodology used in the PRESTO-EPA model to calculate the rates of radionuclide transport for deep infiltration to the aquifer and for surface runoff to a nearby stream. By ignoring the retardation effects in the distributing ditches, one can also use this model to assess the impacts resulting from an emergency spillage of radioactivity onto the ground, or the effectiveness of a remediation measure, such as fixation of radionuclides.

To demonstrate the application of the model to an emergency spillage, four cases studies (a basic case and three variations) normally considered in a response to a radioactivity spillage accident, are analyzed. The primary output of the analyses consists of the cumulative transport of radionuclides to the stream for the purpose of protecting a water supply intake.

MATHEMATICAL FORMULATION

Two submodels, INFIL and SURSOIL, are involved in the analysis of radionuclide transport via deep infiltration and surface runoff pathways. The INFIL submodel calculates fluid transport and the SURSOIL submodel calculates solute transport. The theoretical background of these two submodels are adopted from the PRESTO-EPA model with minor improvements.

INFIL Model: The INFIL submodel analyzes the fluid/moisture transport through overland flow, subsurface flow, and atmospheric diffusion systems. The basic equations for each system are described as follows:

Overland Flow System: The one-dimensional momentum and continuity equations governing an overland flow system are expressed by Iwasa [1964]:

$$\frac{1}{g} \frac{\partial u}{\partial t} + \frac{u}{g} \frac{\partial u}{\partial x} + \frac{\partial h}{\partial x} - \sin \alpha + \frac{n^2 u^2}{h^{4/3}} = 0 \quad (1)$$

$$\frac{\partial h}{\partial t} + h \frac{\partial u}{\partial x} + u \frac{\partial h}{\partial x} = P - E_0 - q_0 \quad (2)$$

where u = velocity of overland flow; h = depth of flow; α = average inclination of the slope; n = Manning's coefficient of roughness; P = rate of precipitation; E_0 = rate of evaporation; q_0 = rate of percolation; g = acceleration potential due to gravitational force; x = space coordinate along the slope of the trench cover; and t = time.

Subsurface Flow System: In general, the moisture in the soil is simultaneously transported in both liquid and vapor phases. The basic equations governing this system were derived by Currie [1961] and Hillel [1980] as:

$$q = -D_L(\theta) \frac{\partial \theta}{\partial z} + K(\theta) - \gamma D_v \frac{\partial p_v}{\partial z} \quad (3)$$

$$\frac{\partial \theta}{\partial t} = -\frac{\partial q}{\partial z} \quad (4)$$

where q = flux of moisture; θ = volumetric wetness of soil; K = hydraulic conductivity; D_L = hydraulic diffusivity; γ = conversion factor for transforming the vapor flux into liquid water flux; D_v = diffusivity for water vapor; and ρ_v = concentration of water vapor in the air-filled void.

Atmospheric Diffusion System: The atmospheric diffusion system transports water vapor through the turbulent boundary layer into the atmosphere. The analysis is extremely complicated. However, by assuming the system is quasi-steady, the solution of the system equation for the mass flux at the surface becomes obtainable. The "quasi-steady" technique assumes that within a small time increment the flow of the carrying fluid is steady and that the effect of the change from one flow state to the other due to the change in time step is negligible. By imposing the above assumption, the water vapor flux within the fully developed boundary layer was expressed by Bird [1966] based on Fick's law as:

$$J = -k^2 v^2 \left[\frac{dv}{dy} \right] \frac{d\rho}{dy} \quad (5)$$

where J = water vapor flux; k = Prandtl's mixing length coefficient; v = time averaged wind speed; ρ = concentration of water vapor in the boundary layer; y = distance from ground surface.

Theoretically, the above system equations can be solved numerically. However, the process requires extremely long calculation times and is vulnerable to the numerical calculation instability. To overcome these difficulties, the system equations can be simplified by transforming the space-dependent variables into space-independent variables. One attempt was made by Hung [1983] and was successfully used in the PRESTO-EPA model [EPA 1987a, 1987b, Hung 1989, 1992, 1996]. The results of the transformation are:

$$Q_0 = \{(\sin \alpha)^{1/3} H^{5/3}\} / n \quad (6)$$

$$dH/dt = P - E_o - q_o - Q_0/L \quad (7)$$

$$E_o = \begin{cases} E_p & \text{when } P + H/\Delta t > E_p \\ P + H/\Delta t & \text{when } E_p > P + H/\Delta t > 0 \\ 0 & \text{when } P + H/\Delta t = 0 \end{cases} \quad (8)$$

$$q_o = \begin{cases} K_s & \text{when } P - E_o + H/\Delta t > K_s \\ P - E_o + H/\Delta t & \text{when } K_s > P - E_o + H/\Delta t > 0 \\ 0 & \text{when } P - E_o + H/\Delta t = 0 \end{cases} \quad (9)$$

$$q_i = \begin{cases} K_s & \text{when } Z_g < Z_{\max} \\ 0 & \text{when } Z_g = Z_{\max} \end{cases} \quad (10)$$

$$dZ_g/dt = (q_i - q_o + q_0)/W_g \quad (11)$$

$$q_i = -D_e W_p / Z_p + K_e \quad (12)$$

$$q_i < E_p - E_o$$

$$q_v = -(E_p - E_o) \left[1 + \frac{0.5Z_p}{0.66(W_p + W_E)} \right]^{-1} \quad (13)$$

$$dZ_p/dt = -(q_p + q_i)/W_p \quad (14)$$

$$q_i = \begin{cases} q_o & \text{when } Z_p > 0 \\ 0 & \text{when } Z_p = 0 \end{cases} \quad (15)$$

$$q_p = -\text{Max}(|q_i|, |q_v|) \quad (16)$$

where Q_o = rate of overland flow per unit width, (m³/m-hr); H = average depth of overland flow over the slope (m); L = length of slope (m); n = Manning's coefficient of roughness; α = average inclination of the slope (m/m); P = rate of precipitation (m/hr); E_o = rate of evaporation from the overland flow (m/hr); q_o = rate of percolation from the overland flow system (m/hr); E_p = evaporation potential (m/hr); q_i = flux of moisture infiltrating into the trench (m/hr); q_l = flux of pellicular water transported in the liquid phase (m/hr); K_s = saturated hydraulic conductivity of the soil (m/hr); Z_g = deficit of gravity water (m); Z_{max} = maximum deficit of gravity water (m); W_g = component of wetness for the gravity water (unitless); W_p = component of wetness for the pellicular water (unitless); Z_p = deficit of the pellicular water (m); D_e = hydraulic diffusivity at equivalent wetness (m²/hr); K_e = hydraulic conductivity at equivalent wetness (m/hr); q_v = flux of moisture being transported in the vapor phase (m/hr); q_t = flux of moisture being transformed from gravity to pellicular water (m/hr); q_p = flux of pellicular water (m/hr); and Δt = time increment.

SURSOIL Model: The SURSOIL model considers the entire contaminated area with a presumed active depth as the control volume and employs a compartment type of model. The basic mass balance equation for the model is expressed as:

$$dI/dt = -A(Q_s + Q_d) C_w - \lambda_d I \quad (17)$$

where I = total inventory of activity in the control volume (Ci); A = the contaminated area (m²); Q_s = the rate of overland flow (m/hr); Q_d = the rate of deep infiltration (m/hr); C_w = the concentration of radionuclide dissolved in the water (Ci/m³); and λ_d = the decay constant (hr⁻¹).

By introducing the conventional definition of the distribution coefficient, K_d (cm³/g), one may obtain the retardation factor as:

$$R = 1 + (\rho_B K_d) / \phi \quad (18)$$

where R = the radionuclide retardation factor (unitless); ρ_B = the bulk density of the soil (g/cm^3); and ϕ = the porosity of the soil (unitless).

Substituting Equation 18 into Equation 17 and distributing the total inventory into the adsorbed and desorbed phase, One obtains

$$dC_w/dt = -\{(Q_s + Q_d)/(DR\phi)\} C_w - \lambda_d C_w \quad (19)$$

where D = depth of the active layer of mixing (m). Equation 19 can now be solved with known initial conditions.

DESCRIPTION AND DEVELOPMENT OF THE MODEL

The model is designed to calculate the radionuclide transport from a contaminated area to a nearby stream. It calculates the surface runoff and deep infiltration using the dynamic equations representing the overland flow, subsurface flow, and atmospheric diffusion systems. A compartment type of model is used to calculate the rates of radionuclide transport through overland flow and subsurface flow pathways.

The rates of radionuclide transport for overland and subsurface flow pathways are calculated at the boundary of the contaminated area. The rate of transport calculated for the surface runoff is assumed to be equal to the rate of transport at the confluence with the main stream. This assumption is acceptable because of the screening nature of the model. The same model can be applied for the forecast of the radionuclide transport to a stream as well as for the evaluation of a remedial action.

The model is coded in FORTRAN, and designed to be executed on a personal computer. For modeling convenience, three subroutines are used for the routing of the fluid flow. The time increment of the numerical calculation is fixed to one hour. Instability in numerical calculations may occasionally be seen at the transition from very small overland flow to no overland flow. However, the error in the mass balance is negligibly small in all cases studied. Therefore, from a practical viewpoint, the calculation is considered to be stable for all cases.

CASE STUDIES

In order to demonstrate the model functions, four cases are studied. For each case, 100 curies of Cs-137 is spilled on a 100 meter square slope. For the basic case (Case 1), it is assumed a 100-year 24 hour storm (total rainfall = 0.2 meter or approximately 8 inches) occurs approximately one month after the spillage. Case 2 assumes that the 100-year storm occurs right after the spillage; Case 3 assumes that the land is treated with chemical fixation (increase the distribution coefficient from $5 \text{ cm}^3/\text{g}$ to $10 \text{ cm}^3/\text{g}$); and Case 4 assumes that the area is plowed to 30 cm depth with mechanical fixation (increase the mixing depth from 10 cm to 30 cm).

The results of the analyses are shown in Figures 1, 2, 3, and 4 for Cases 1, 2, 3, and 4

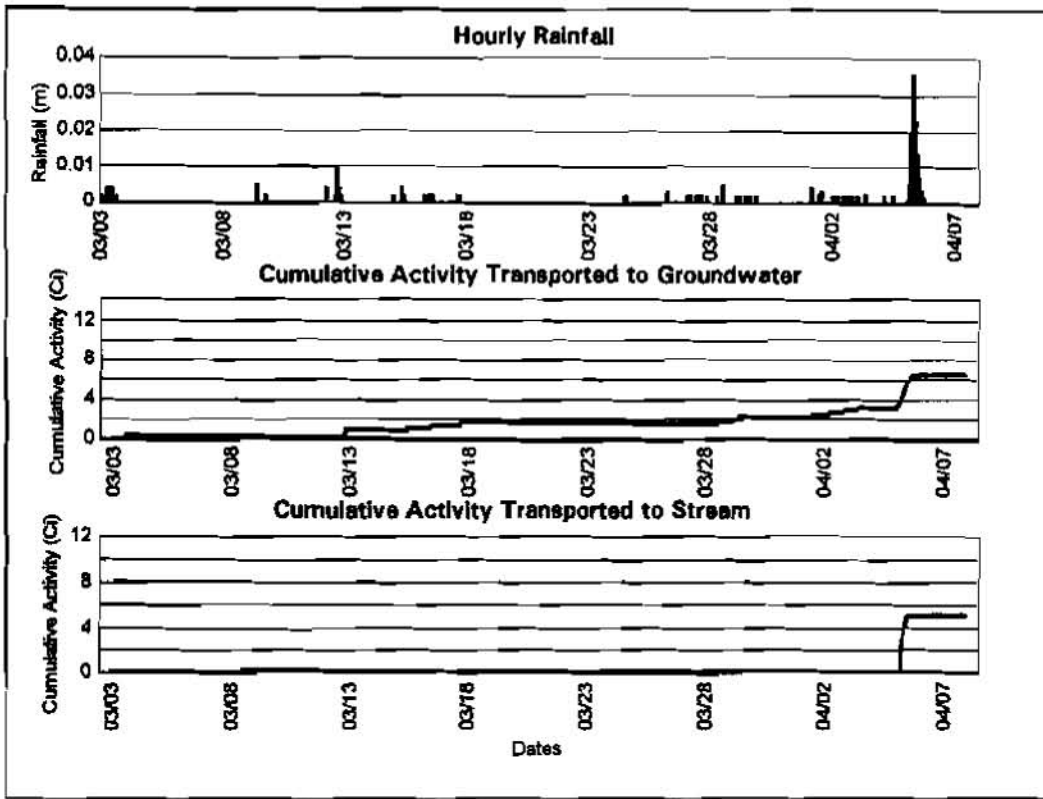


Figure 3. Results of Case 3 Analysis, With Chemical Fixation.

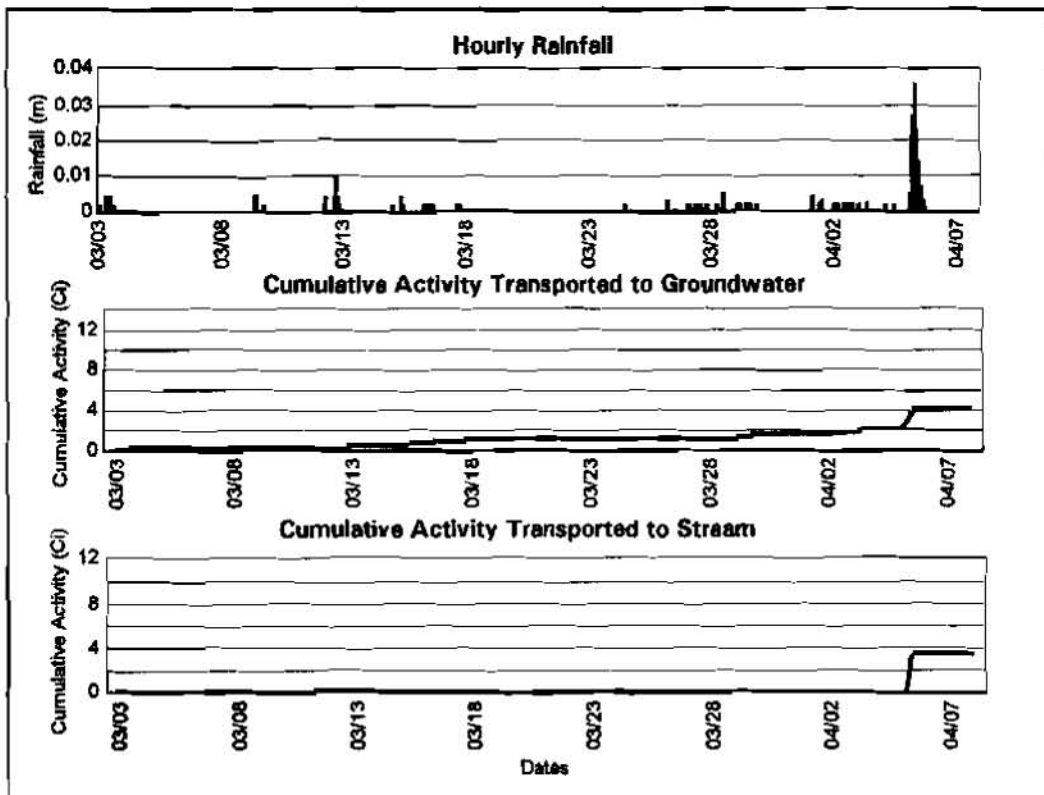


Figure 4. Results of Case 4 Analysis, With Mechanical Fixation.

respectively. The results indicate that the cumulative activity being transported into the stream for Case 2 increases from 9.20 Ci (basic case) to 10.7 Ci. By treating the area through chemical fixation, Case 3, could reduce the transported cumulative activity from 9.2 Ci to 5.05 Ci, and by plowing the area, Case 4, could reduce the transported cumulative activity from 9.20 Ci to 3.41 Ci.

CONCLUSIONS

A computational model designed to calculate the transport of radionuclides from a spillage area to a nearby stream is developed. The model can be used as a radionuclide transport forecasting model or a remediation measure evaluation model. The numerical calculation using a fixed one hour increment is judged to be stable and the mass balance is, in general, conserved. Sample case studies are also conducted for those potential application scenarios. The results indicated that the model responded to the test cases reasonably well.

REFERENCES

- Bird, R. B., Stewart, W. E., and Lightfoot, E. N., Transport Phenomena, John Wiley and Sons, Inc., New York, Seventh Edition, 1966.
- Currie, J.A., Gaseous Diffusion in Porous Media, Part 3 - Wet Granular Material, Brit. J. Appl. Phys. 12, 275-281, 1961.
- Hillel, D., Fundamentals of Soil Physics, Academic Press, New York 1980, pp. 221-223.
- Hung, C. Y., A Model to Simulate Infiltration of Rainwater Through the Cover of a Radioactive Trench Under Saturated and Unsaturated Conditions, in: Role of the Unsaturated Zone in Radioactive and Hazardous Waste Disposal, edited by James W. Mercer, et al., Ann Arbor Science, 1983.
- Hung, C.Y., User's Guide for the SYSCPG Program --- A PC Version of the PRESTO-EPA-CPG Operation System, EPA report, EPA 520/1-89-017, April 1989.
- Hung, C.Y., User's Guide for the SYSPOP Program --- A PC Version of the PRESTO-EPA-POP Operation System, EPA report, EPA 400-R-92-003, May 1992.
- Hung, C.Y., User's Guide for PRESTO-EPA-CPG Operation System, Version 2.1, EPA report, EPA 402-R-96-013, June 1996.
- Iwasa, Y., Fundamental Principles of Open-Channel Flow, published by Hydraulic Committee, Japan Society of Civil Engineers, 1964.
- U.S. Environmental Protection Agency, PRESTO-EPA-POP: A Low-Level Radioactive Waste Environmental Transport and Risk Assessment Code - Vol. 1, Methodology Manual, EPA 520/1-87-024-1, Washington, D.C., 1987.
- U.S. Environmental Protection Agency, PRESTO-EPA-CPG: A Low-Level Radioactive Waste Environmental Transport and Risk Assessment Code - Documentation and User's Manual, EPA 520/1-87-026, Washington, D.C., 1987.

THE RIPARIAN ECOSYSTEM MANAGEMENT MODEL (REMM): NUTRIENT DYNAMICS^{1,2}

Shreeram Inamdar, Postdoctoral Associate³; Lee Altier, Assistant Prof.⁴;
Richard Lowrance, Ecologist³; Randy Williams, Agricultural Engineer⁵;
and Robert Hubbard, Soil Scientist⁵.

³ University of Georgia, Tifton, GA; ⁴ College of Agriculture, California State University, Chico, CA;

⁵ Southeast Watershed Research Laboratory, USDA-ARS, Tifton, GA.

INTRODUCTION

The Riparian Ecosystem Management Model (REMM) has been developed as a tool to aid natural resource agencies and others in making decisions regarding water quality management. It is also intended as a tool for researchers to aid in the study of the complex dynamics related to the water quality functions of riparian ecosystems. REMM is specifically designed to simulate processes in riparian buffer systems corresponding with specifications recommended by the U.S. Forest Service and the USDA-Natural Resource Conservation Service as a national standard (USDA-NRCS, 1995).

The riparian system is characterized in the model as three zones parallel to the stream, representing increasing levels of management in the direction of the uplands (see Fig. 1 in Lowrance et al., 1998). The model provides the opportunity to analyze the effect of a variety of environmental and management scenarios. In general, however, buffer systems promote some common water quality functions. Vegetation and associated litter material provide physical barriers to water and sediment transport over the ground surface. Deposition of organic matter by plants provides a substrate supporting important biological transformations of chemicals in the soil. Plants also sequester nutrients such as nitrogen and phosphorus that contribute to water pollution. The zone immediately adjacent to the stream helps to protect the stream bank and aquatic habitat. The water quality functions of the three zones have been discussed in detail by Lowrance et al. (1995).

The model is also characterized by a litter layer and three soil layers through which vertical and lateral movement of water and associated dissolved nutrients are simulated. The litter layer is important as the locus for the mixing of surface water with the soil surface. This mixing process results in an equilibrium of dissolved and adsorbed chemical concentrations which determines amounts of chemicals that are subsequently leached, deposited on the ground surface, or carried along in surface runoff. Concentrations of dissolved and adsorbed chemicals are recalculated as water moves through each of the other soil layers.

As important contributors to water quality degradation, nitrogen, phosphorus, and sediment are the main foci of the REMM model. This paper describes soil nutrient processes simulated in REMM and describes an initial application of the model at a site in the Atlantic Coastal Plain Region of the United States in south Georgia. A more detailed description of the algorithms and equations is provided in the model documentation (Altier et al., in press).

DESCRIPTION OF MODEL

Nitrogen and phosphorus can enter into the buffer system in precipitation, dissolved in surface and subsurface water flow, and adsorbed to incoming sediment carried by surface flow. Their presence in different forms and the associated degree of physical and chemical stabilization influences their availability for microbial transformations and plant uptake.

¹ Contribution from the USDA-ARS, Southeast Watershed Research Laboratory, P.O. Box 946, Tifton, GA 31793, in cooperation with University of Georgia Coastal Plain Experiment Station and California State University.

² All programs and services of the USDA are offered on a nondiscriminatory basis without regard to race, color, national origin, religion, sex, age, marital status, or handicap.

³ Biological and Agricultural Engineering, University of Georgia, P.O. Box 745, Tifton, GA 31793; phone: (912) 386 7210; fax: (912) 386 7294; Email: rivers@tifton.cpes.peachnet.edu.

Organic Matter

The C cycle is fundamental for simulation of all organic matter dynamics and nutrient cycling processes in REMM. Stoichiometric relationships are assumed among C, N, and P in the organic matter. N and P are released and immobilized in proportion to transformations of C (Thompson et al., 1954; Sharpley et al., 1984). Simulation of C dynamics is largely based upon the Century Model (Parton et al., 1987, Parton et al., 1988). Five C pools comprising litter and soil organic matter are simulated, each characterized by a different rate of turnover and C:N and C:P ratios. The C:N ratios for these pools are a constant; the C:P ratios vary according to labile P level at the time of immobilization. Although the C pools would be difficult to distinguish and measure in the field, they represent portions of the total mass of soil carbonaceous material that must be accounted for in order to estimate mineralization and immobilization of nutrients (Jenkinson et al., 1987). The decomposition rates of the organic matter pools are calculated according to first-order rate equations modified by temperature, moisture, and in the case of litter residues, C:N and C:P ratios.

Although organic matter is largely insoluble, dissolution from the more labile pools into surface and subsurface water is simulated according to a relationship by McGill et al. (1981). Only small amounts of organic matter can enter solution. However, at depth in the soil where denitrification may be C limited, the presence of even small amounts of C could allow denitrification to occur.

Litter

As a simplification, instead of keeping track of many individual inputs of organic residues separately over time, daily inputs of fresh residue are mixed with existing pools of residue material. Depending on the source of vegetation (species and plant part), incoming litter is characterized by its C:N, C:P, and lignin:N ratios. The lignin:N ratio of fresh litter determines proportions that are allocated to a pool of quickly decomposed metabolic material or a more recalcitrant pool of structural material.

Exogenous sources of nutrients can facilitate the decomposition of litter (Alexander, 1977; Hart et al., 1993). Effective C:N and C:P ratios influencing residue decomposition are calculated as a function of the content of N and P in the litter as well as the content of available inorganic N and P in the soil. As decomposition of the litter takes place, C, N, and P are released. In satisfying the respiration requirements of the soil microbes, a portion of the C is lost in CO₂ to the atmosphere, and the remaining C is reimmobilized into humus. According to the requisite C:N and C:P ratios of the humus, corresponding amounts of N and P are immobilized with the C. The C:N and C:P ratios in plant residue are generally much higher than in the soil humus pools. As carbon is transformed from litter into humus, immobilization of exogenous inorganic N and P usually occurs from the soil. If amounts of available N and P are inadequate for synthesis with C into the humus, decomposition of the residue slows down, and immobilization of C, N, and P into humus stops.

Humus

Soil organic matter has been characterized as having active and stable components. The older fractions may be over 3000 years old (Jenkinson and Rayner, 1977). In REMM, based upon the Century model (Parton et al., 1987), plant residues are decomposed into three soil organic matter pools: 1) an active pool consisting of biomass and metabolites of biomass with a rapid decay rate; 2) a slow pool consisting of organic matter that has been partially stabilized either chemically or else physically by adsorption or entrapment within soil aggregates (Paul and van Veen, 1978); and 3) a passive pool of chemically stabilized organic matter having a very slow decay rate. Carbon is continually mineralized and reimmobilized among the soil organic matter pools.

In contrast to a fixed C:N ratio in the humus pools, the C:P ratio of newly formed soil organic material is allowed to vary, simulating a positive correlation between microbial P content and the content of labile inorganic P in the soil. This approach follows the Century model (Parton et al., 1988) and is based upon concepts of McGill and Cole (1981).

Inorganic Nutrients

Nitrogen

Ammonium and nitrate forms are both available for immobilization into soil organic matter. Immobilization of nitrate occurs only after all available ammonium has been used. Ammonium may be in solution or adsorbed to the soil matrix, according to an equilibrium equation.

Nitrification is calculated with a first-order rate equation influenced by temperature, moisture, and pH. The determination of the rate coefficient follows the approach of Reuss and Innis (1977) and Godwin and Jones (1991), based upon a Michaelis-Menten function described by McLaren (1970). With increasing amounts of substrate, the rate of nitrification is lagged to represent a delayed microbial response.

The calculation of denitrification is a function of the interaction of factors representing the degree of anaerobiosis, temperature, $\text{NO}_3\text{-N}$, and mineralizable C. At levels of nitrate concentration below 3 mg kg^{-1} , the denitrification rate is simulated as being limited by nitrate. At higher levels, the carbon concentration is limiting (Webster and Goulding, 1989; Yoshinari et al., 1977). Denitrification mostly occurs as water-filled pore space gets above 60%. However, the response to a sudden increase in anaerobiosis is lagged in order to account for the time required for bacterial enzyme production.

Phosphorus

Simulation of inorganic P follows the approach used in the EPIC model (Jones et al., 1984). Three pools of inorganic P are simulated in REMM. Besides a labile form, there are two pools representing increasing levels of chemical stabilization that are unavailable to plant uptake or microbial transformation. The labile form may be dissolved or adsorbed, according to a partitioning coefficient (Williams et al., 1984).

MODEL EVALUATION

Parameterization

REMM nutrient component was evaluated using data collected from experimental riparian buffer sites located at the University of Georgia Gibbs Farm near Tifton, Georgia. A detailed description of this site along with the type of data being collected and instrumentation is provided in Lowrance et al. (1998); Sheridan et al. (1996, 1998); and Bosch et al. (1996). The study area is located in the Tifton Upland in the drainage area of the Little River. The site has been managed as a three-zone buffer system. Zone 1 consists of hardwoods, mostly yellow poplar (*Liriodendron tulipifera* L.) and swamp black gum (*Nyssa sylvatica* var. *biflora* Marsh.). Zone 2 consists of conifers, primarily longleaf pine (*Pinus palustris* Mill.) and slash pine (*Pinus elliotti* Engelm.). Zone 3, the area of the buffer furthest away from the stream, consists of perennial grasses. Most of the riparian area is on Alapaha loamy sand (loamy, siliceous, thermic Arenic Plinthic Paleaquults). The upland fields are on Tifton loamy sand (Calhoun, 1983).

The most definite and explicit observation that was available to test the nutrient component was nitrate concentrations measured at recording wells located at different positions along the riparian transect (Hubbard and Lowrance, 1997). These wells were located at downslope edge of each zone and were assumed to monitor the nitrate concentration exiting each zone. Groundwater nitrate concentrations were collected biweekly from 92 through 96. The wells were screened at a depth of 2 m, so the measured nitrate concentrations represented the concentrations in the water table within the top 2 m of the soil profile. Other observations which were not as specific, that were available to compare against model predictions included: annual denitrification and plant uptake rates on a kg per hectare. In addition, an annual nitrogen budget of model predicted values was also prepared to compare against literature estimates from riparian areas and forests.

Prior to evaluation of the nutrient component, the hydrology and sediment components of the model were verified since the fate of nutrients is decided to a large extent by the spatial distribution and movement of water and sediment. Hydrology and sediment component evaluations were performed for a 5 year simulation period from 92 through 96 and have been presented in Inamdar et al. (1998) and Bosch et al. (1998) respectively. A description of the rainfall and runoff rates and hydrologic parameters required to initialize the model has also been presented in the above mentioned papers and hence is not repeated here. With respect to nutrient evaluation the model had to be initialized for: [a] daily nitrogen and phosphorus loadings from precipitation, and surface and subsurface runoff from contributing fields; and [b] values describing the carbon, nitrogen, and phosphorus pools in the riparian soil and vegetation.

Concentrations for organic nitrogen and phosphorus, ortho-P, nitrate, and ammonium entering in surface and subsurface runoff were available from the data collected at the site from 1992 through 1996 (Lowrance, Unpublished data). Atmospheric loadings of these parameters were estimated from values published by the National Atmospheric Deposition Program (NADP, 1997). Table 1 lists the estimated annual average concentrations of the nutrients entering in water and sediment. Carbon, nitrogen, and phosphorus pools were initialized based on measured data at Gibbs farm (Lowrance,

Unpublished data) and from previously published data from other riparian sites in the Little River Watershed (Fail et al., 1986; Fail, 1983).

Table 1: Annual average nutrient concentrations applied to the riparian buffer over the simulation period 92-96.

Nutrient forms	Precipitation (mg/L)	Surface runoff (mg/L)	Sediment (%) ¹	Subsurface flow (mg/L)
Nitrate-N	0.70	2.42	0.00	11.18
Ammonium-N	0.12	3.11	0.113	1.00
Ortho-P	0.0026	1.10	0.022	0.00
Carbon	1.00	11.00	2.31	20.00

¹ percent of sediment mass

Results and Discussion

Model predicted and observed monthly nitrate concentrations in subsurface flow exiting each zone are presented in Figure 1. Though simulations were performed for years 92 through 96, comparisons presented in Figure 1 start from year 93 since year 92 was assumed as a buffer year to allow the model to reach a pseudo-steady state condition. It is apparent from Figure 1 that predictions for zone 3 are excellent. For zone 2 the predictions were good, but for zone 1 model predicted values were significantly less than those observed. This indicates that processes and mechanisms that dictate nitrate concentrations in soil water are best simulated for zone 3, followed by zone 2 and 1.

Comparison of observed nitrate concentrations from the field and those exiting each of the zones (see Figure 1) reveals that zone 3 does not significantly influence the nitrate concentration in subsurface water. In contrast zone 2 which has the pine forest was responsible for the greatest drop in nitrate concentrations. This trend is also supported by model predictions. Although the grass buffer zone may be effective in reducing nutrients transported via surface runoff and sediment it may not be equally effective in sequestering nutrients such as nitrate-N traveling in subsurface flow. It is also possible that nitrate concentrations in subsurface water within zone 3 are augmented by nitrate additions from surface water since both field observations and model simulations indicate that most of the surface runoff that enters zone 3 from upland fields infiltrates in zone 3 (for hydrology results see Inamdar et al., [1998]).

Observed nitrate concentrations for zone 2 and 1 are very close and there seems to be no significant drop in nitrate concentration when subsurface flow moves through zone 1. Model results do not support this trend. Nitrate concentrations in the soil water within each zone as simulated in the model are influenced by external loadings, nitrification, denitrification, plant uptake, immobilization by microbes, and movement with water. External loadings and nitrification increase the nitrate levels whereas denitrification, plant uptake, immobilization by microbes, and movement with exiting water represents pathways through which soil water nitrate is lost or reduced. Considering the low levels of nitrate predicted for zone 1 compared to those observed, it is possible that the model is not adequately simulating additions of nitrate to the soil via processes such as mineralization and subsequent nitrification. Alternatively, the other possible reason for low simulated nitrate concentrations could be that simulated values of plant uptake and denitrification are higher than those occurring at the site. Though, this does not seem probable since simulated values for plant uptake and denitrification are close to those reported for this site (discussed below).

Model simulated annual nitrogen fluxes averaged over years 93-96 for each zone are presented in Figure 2. This allows comparison of annual estimates of processes such as denitrification and plant uptake with literature values. For the Gibbs farm riparian site Lowrance (Unpublished data) have found annual denitrification rates of 37, 19, and 17 kg N/ha/yr for zones 3, 2, and 1 respectively (rates for years 92 & 93 only). Observed rates were computed considering the top 1 m of the soil profile. Simulated denitrification rates of 23, 23, and 14 kg N/ha/yr for zones 3, 2, and 1 are close to the observed values (annual values averaged over 93-96). In model simulations, most of the denitrification occurred within the top two layers (1-1.5 m from the surface).

Estimates of other nitrogen cycling processes such as plant uptake, litterfall, mineralization, nitrification, etc., for the Gibbs

exiting zone 3

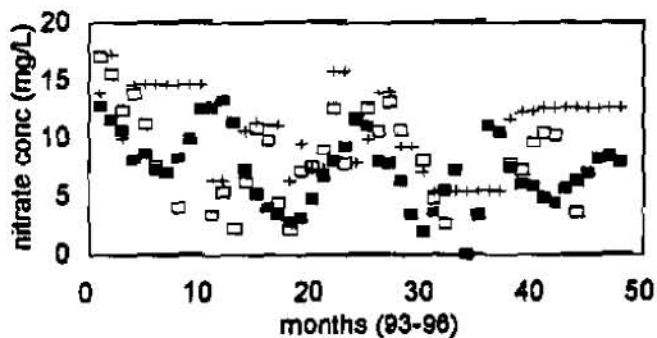
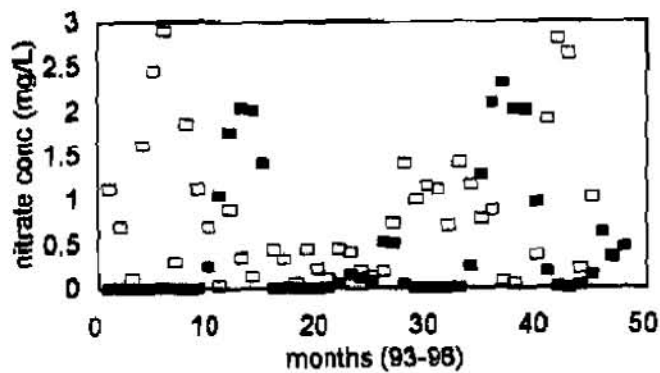


Figure 1: Nitrate concentrations in subsurface flow exiting zones 3, 2, and 1 respectively.

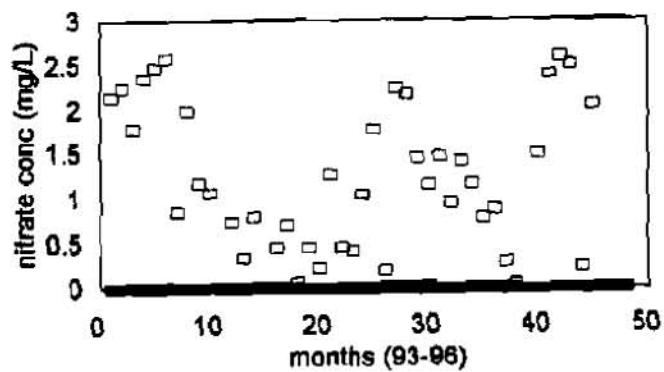
■ pred □ obs + field in

exiting zone 2

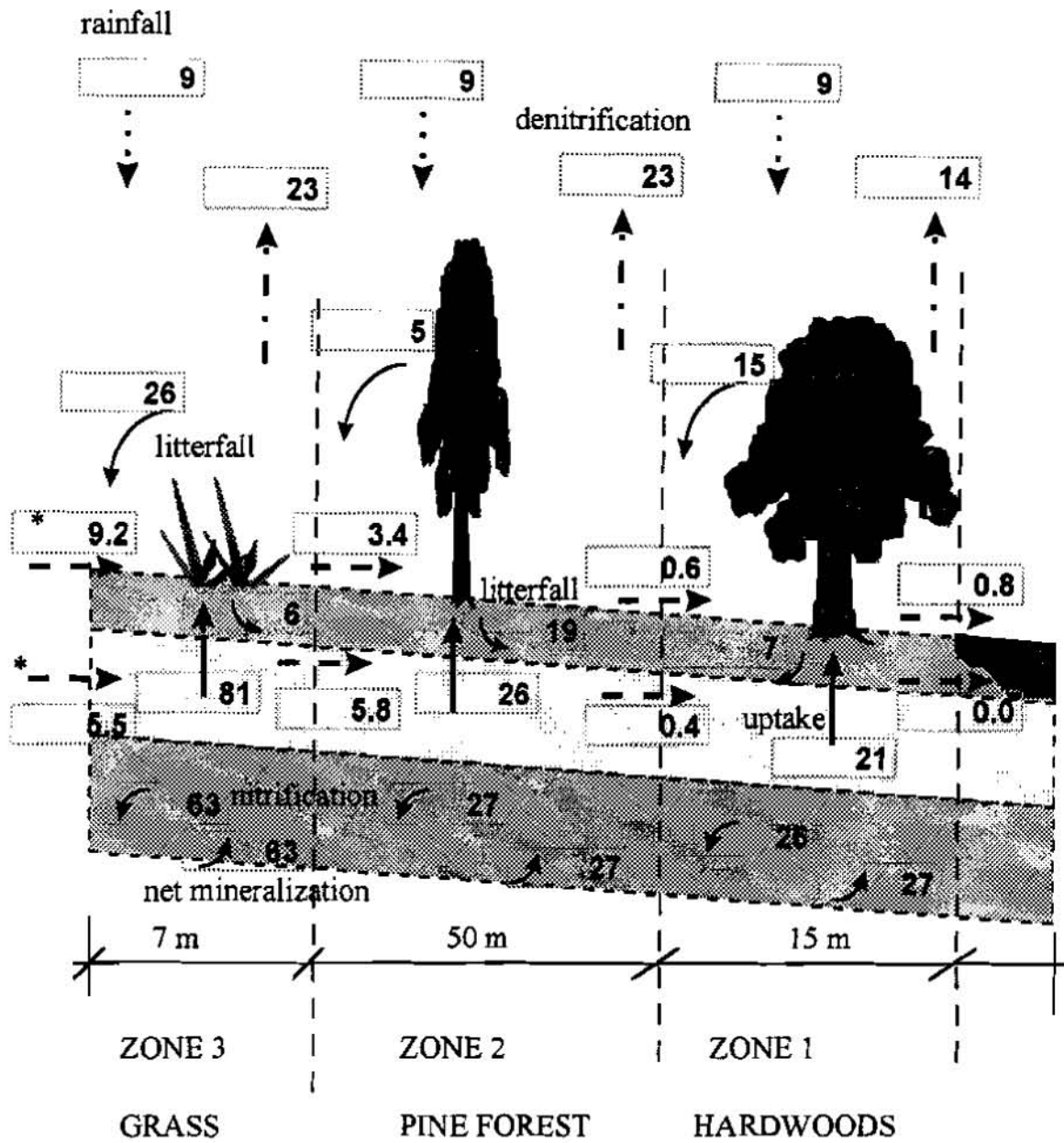


■ pred □ obs

exiting zone 1



■ pred □ obs



* - N in surface and subsurface flow is nitrate + ammonium only
 Values for each zone are summed across litter & all three soil layers
 Figure not to scale

Figure 2: Annual nitrogen fluxes averaged over the simulation period 93-96 (all values in kg/ha/yr).

farm were not available. To allow for some measure of verification of model simulations, predicted values for these processes were compared to literature estimates presented in Table 2. As is obvious from Table 2 there is a wide range for estimates on processes such as plant uptake, litterfall, and N-mineralization. Simulated plant uptake values seem to be within the bounds reported in literature. Conifer and deciduous vegetation simulated in the model was maintained at pseudo-steady state growth condition hence plant uptake values are expected to be smaller than those that would typically be observed for a growing forest. Litterfall and mineralization rates are similar to literature values.

Table 2: Literature estimates on nitrogen fluxes observed in riparian and upland forests.

Process	Units	Investigators	Location	Description	Estimates
Specific values:					
Denitrification	kgN/ha/yr	Lowrance, Unpublished data	Little River, GA	Riparian forest	37, 19, 17 ¹
Plant Uptake	kgN/ha/yr	Fail et al., 1986	Little River, GA.	Riparian forest	50
Plant Uptake	kgN/ha/yr	Peterjohn and Correll, 1984	Rhode River, MD	Riparian forest	77
Ranges: (mostly from upland forest studies) modified from Gosz, 1981.					
Litterfall N	kgN/ha/yr	--	--	Conifer forest	10 - 90
Litterfall N	kgN/ha/yr	--	--	Deciduous forest	45 - 90
Plant Uptake	kgN/ha/yr	--	--	Conifer forest	30 - 75
Plant Uptake	kgN/ha/yr	--	--	Deciduous forest	50 - 100
Mineralization	kgN/ha/yr	--	--	Conifer forest	50 - 100
Mineralization	kgN/ha/yr	--	--	Deciduous forest	100 - 300

¹ for zone 3, 2, and 1 respectively.

REFERENCES

- Alexander, M. 1977. Introduction to soil microbiology. John Wiley & Sons, New York, NY.
- Altier, L.S., Lowrance, R.R., Williams, R.G., Inamdar, S.P., Bosch, D.D., Sheridan, J.M., Hubbard, R.K., and Thomas, D.L. Riparian Ecosystem Management Model (REMM): Documentation. USDA Conservation Research Report, In Press.
- Bosch, D.D., Williams, R.G., Inamdar, S.P., Sheridan, J.M., and Lowrance, R.R. 1998. Erosion and sediment transport through riparian buffers. In Proceedings of the First Federal Interagency Hydrologic Modeling Conference, Las Vegas, Nevada, (this volume).
- Bosch, D.D., Sheridan, J.M., and Lowrance, R.R. 1996. Hydraulic gradients and flow rates of a shallow coastal plain aquifer in a forested riparian buffer. *Trans. of the ASAE*, Vol. 39(3):865-871.
- Calhoun, J.W., 1983, Soil Survey of Tift Co., GA. USDA-SCS, Washington, D.C.
- Fail, J.L., Haines, B.L., and Todd, R.L. 1986. Riparian forest communities and their role in nutrient conservation in an agricultural watershed. *American Journal of Alternative Agriculture*. Vol 2:114-121.
- Fail, J.L. 1983. Structure, biomass, production, and element accumulation in riparian forests of an agricultural watershed. Unpublished Ph.D. Dissertation. University of Georgia, Athens, GA.
- Godwin, D.C. and Jones, C.A. 1991. Nitrogen dynamics in soil-plant systems. In: J. Hanks and J.T. Ritchie (ed.) Modeling plant and soil systems. Agronomy Monograph no. 31. ASA-CSSA-SSSA, Madison, WI.
- Gosz, J.R., 1981. Nitrogen cycling in coniferous ecosystems. In *Terrestrial Nitrogen Cycles*, F.E. Clark, and T. Rosswall (eds.). *Ecol. Bull.* Vol. 33:405-426.
- Hart, S.C., Firestone, M.K., Eldor, P.A., and Smith, J.L. 1993. Flow and fate of soil nitrogen in an annual grassland and a young mixed-conifer forest. *Soil. Biol. Biochem.* 25:431-442.

- Hubbard, R.K., and Lowrance, R.R. 1997. Assessment of forest management effects on nitrate removal by riparian buffer systems. *Trans. ASAE*, Vol. 40:383-391.
- Inamdar, S.P., Sheridan, J.M., Williams, R.G., Bosch, D.D., Lowrance, R.R., Altier, L.S., Thomas, D.L. 1998. The Riparian Ecosystem Management Model (REMM): Evaluation of the hydrology component. In *Proceedings of the First Federal Interagency Hydrologic Modeling Conference, Las Vegas, NV (this volume)*.
- Jenkinson, D.S., Hart, P.B.S., Rayner, J.H., and Parry, L.C. 1987. Modelling the turnover of organic matter in long-term experiments at Rothamsted. *Intecol. Bull.* 15:1-8.
- Jenkinson, D.S., and Rayner, J.H. 1977. The turnover of soil organic matter in some of the Rothamsted classical experiments. *Soil Science* 123:298-305.
- Jones, C.A., Cole, C.B., Sharpley, A.N., and Williams, J.R., 1984, A Simplified Soil and Plant Phosphorus Model: I. Documentation. *Soil Sci. Soc. Am. J.* 48, 800-805.
- Lowrance, R.R., Altier, L.S., Williams, R.G., Inamdar, S.P., Bosch, D.D., Sheridan, J.M., and Thomas, D.L. 1998. The Riparian Ecosystem Management Model (REMM): Simulator for ecological processes in buffer systems. In *Proceedings of the First Federal Interagency Hydrologic Modeling Conference, Las Vegas, NV (this volume)*.
- Lowrance, R.R., Altier, L.S., Newbold, J.D., Schnabel, R.R., Groffman, P.M., Denver, J.M., Correll, D.L., Gilliam, J.W., Robinson, J.L., Brinsfield, R.B., Staver, K.W., Lucas, W.C., and Todd, A.H. 1995. *Water Quality Functions of Riparian Forest Buffer Systems in the Chesapeake Bay Watershed*. U.S. EPA Chesapeake Bay Program, Annapolis, MD.
- McGill, W.B., and Cole, C.V. 1981. Comparative aspects of cycling of organic C, N, S and P through soil organic matter. *Geoderma* 26:267-286.
- McGill, W.B., Hunt, H.W., Woodmansee, R.G., and Reuss, J.O. 1981. Phoenix, a model of the dynamics of carbon and nitrogen in grassland soils. p. 49-115. In: F.E. Clark and T. Rosswall (ed.) *Terrestrial nitrogen cycles*. *Ecol. Bull.*, Stockholm.
- McLaren, A.D. 1970. Temporal and vectorial reactions of nitrogen in soil: A review. *Can. J. Soil Sci.* 50:97-109.
- NADP. 1997. National Atmospheric Deposition Program. <http://nadp.nrel.colostate.edu/NADP/isopleth.maps>.
- Parton, W.J., Schimel, D.S., Cole, C.V., and Ojima, D.S. 1987. Analysis of factors controlling soil organic matter levels in Great Plains Grasslands. *SSAJ*. 51:1173-1179.
- Parton, W.J., Stewart, J.W.B., and Cole, C.V. 1988. Dynamics of C, N, P and S in grassland soils: a model. *Biogeochemistry* 5:109-131.
- Paul, E.A. and van Veen, J.A., 1978, The Use of Tracers to Determine the Dynamic Nature of Organic Matter. 11th International Congress of Soil Science, Transactions, 3, 61-102.
- Peterjohn, W.T., and Correll, D.L. 1984. Nutrient dynamics in an agricultural watershed: Observation on the role of a riparian forest. *Ecology*, Vol 65:1466-1475.
- Reuss, J.O. and Innis, G.S. 1977. A grassland nitrogen flow simulation model. *Ecology*. 58:379-388.
- Sharpley, A.N., Smith, S.J., Stewart, B.A., and Mathers, A.C. 1984. Forms of phosphorus in soil receiving cattle feedlot waste. *J. Environ. Qual.* 13:211-215.
- Sheridan, J.M., Lowrance, R.R., and Bosch, D.D. 1998. Management effects on runoff and sediment transport in riparian forest buffers. *Trans. Of the ASAE*. In review.
- Sheridan, J.M., Lowrance, R.R., and Henry, H.H. 1996. Surface flow sampler for riparian studies. *Applied Engineering in Agriculture*, Vol. 12(2):183-188.
- Thompson, L.M., Black, C.A., and Zoellner, J.A. 1954. Occurrence and mineralization of organic phosphorus in soils, with particular reference to associations with nitrogen, carbon, and pH. *Soil Sci.* 77:185-196.
- USDA-NRCS. 1995. *Riparian Forest Buffer, 391. Model State Standard and General Specifications*. NRCS Watershed Science Institute. Seattle, WA.
- Webster, C.P. and Goulding, K.W.T. 1989. Influence of soil carbon on denitrification from fallow land during autumn. *J. Sci. Food Agric.* 49:131-142.
- Williams, J.R., Jones, C.A., and Dyke, P.T., 1984, A Modeling Approach to Determining the Relationship Between Erosion and Soil Productivity. *Trans. ASAE* 27, 129-144.
- Yoshinari, T., Hynes, R., and Knowles, R. 1977. Acetylene inhibition of nitrous oxide reduction and measurement of denitrification and nitrogen fixation in soil. *Soil Biol. Biochem.* 9:177-183.

THE RIPARIAN ECOSYSTEM MANAGEMENT MODEL: SIMULATOR FOR ECOLOGICAL PROCESSES IN RIPARIAN ZONES¹²

R. Lowrance, Ecologist, USDA-ARS, Tifton, GA³; L. S. Altier, Assistant Professor, California State Univ., Chico, CA; R. G. Williams, Agricultural Engineer, USDA-ARS, Tifton, GA; S. P. Inamdar, Post-Doctoral Associate, Univ. of Georgia, Tifton, GA; D. D. Bosch, Hydrologist, USDA-ARS, Tifton, GA; J. M. Sheridan, Hydraulic Engineer, USDA-ARS, Tifton, GA; D. L. Thomas, Associate Professor, Univ. of Georgia, Tifton, GA; R. K. Hubbard, Soil Scientist, USDA-ARS, Tifton, GA

Abstract: The Riparian Ecosystem Management Model (REMM) is a simulation model developed by USDA and university cooperators to provide comparisons among different field-scale buffer systems. The primary uses of REMM will be to simulate the water quality impacts of riparian and other edge of field buffer systems of different lengths, slopes, soils, and vegetation. Agencies such as USDA-NRCS and USDA-FS need this type model in order to provide specific guidance to landowners needing edge of field buffer systems. Although designed to simulate the specific type of multiple-zone buffer system recommended by USDA agencies, REMM is flexible enough to accommodate a wide range of buffer systems in a variety of land use settings. If hydrologic and pollutant loadings to the buffer system are available or can be estimated or modeled, REMM can be used to represent most edge of field buffers receiving diffuse inputs of water. This paper presents the general structure of REMM and information on the initial field testing site for the model. Operational aspects and details of model components and test simulations for REMM using field data from a riparian buffer system in the southeastern coastal plain are presented in five other papers in these proceedings,

INTRODUCTION

Agriculture continues to be a major contributor of nonpoint source pollution to the nation's waters and continues to limit the attainment of designated uses in many rural watersheds (USEPA, 1997). There is a growing realization that for agricultural watersheds to meet designated uses as defined under the Clean Water Act (CWA), there must be a combination of efforts to both control nonpoint source pollution and to restore aquatic ecosystems. Restoration and management of riparian ecosystems are essential to restoration of aquatic ecosystems and to attainment of water quality goals because of the multiple water quality functions performed by riparian ecosystems. Riparian forests are known to reduce delivery of nonpoint source pollutants to streams and lakes in many types of watersheds (Lowrance et al., 1997). In addition, riparian forests are known to be important in controlling the physical and chemical environment of streams and in providing detritus and woody debris for streams and near-shore areas of large water bodies.

The major United States Department of Agriculture efforts to restore riparian ecosystems are funded through the continuous sign-up of the Conservation Reserve Program (CRP) and the Conservation Reserve Enhancement Program/State Enhancement Program (CREP/SEP) authorized in the 1996

¹ Contribution from the USDA-ARS, Southeast Watershed Research Laboratory, P.O. Box 946, Tifton, GA, 31793, in cooperation with the University of Georgia and California State University.

² All programs and services of the USDA are offered on a nondiscriminatory basis without regard to race, color, national origin, religion, sex, age, marital status, or handicap.

³ USDA-ARS-SEWRL, P.O. Box 946, Tifton, GA 31793. Phone: 912-386-3894; fax: 912-386-7294; e-mail: lorenz@tifton.cpes.peachnet.edu.

Farm Bill. The continuous sign-up allows landowners to offer lands with high Environmental Benefits for the CRP at any time. Efforts spearheaded by Vice-President Gore to address the nation's lack of progress toward CWA goals have focussed on use of the CREP/SEP mechanism to address critical agricultural water quality problems (White House Memorandum, 10/18/97). The first project funded for CREP/SEP is an effort to have up to 100,000 acres of riparian land along Maryland's streams and rivers set aside and maintained to protect water quality (White House Press Release, 10/20/97). The Maryland CREP/SEP will spend about \$200 million over 15 years to restore riparian ecosystems. Clearly, USDA is planning to make large investments of funds in restoring streamside (riparian) ecosystems to control nonpoint source pollution, increase attainment of designated uses of streams, to provide wildlife habitat, and to restore aquatic ecosystems. An evaluation of whether goals are being met and an evaluation of alternative scenarios for achieving the environmental goals should accompany expenditure of public money to achieve environmental goals. Restoration and management of riparian ecosystems, while generally good for water quality, should be evaluated for their efficacy in controlling specific nonpoint source pollution problems. Although general guidelines are available from USDA action agencies on the management of riparian buffers (Welsch, 1991; NRCS, 1995), information is lacking on how buffer zones should be designed and managed to meet site-specific needs.

The Riparian Ecosystem Management Model (REMM) has been developed by USDA and university cooperators in order to provide a tool to assess the nonpoint source pollution control functions of riparian buffer systems. Unlike pollution control practices, which depend on engineering structures to control water or water-borne pollutants, riparian buffer systems are complex ecosystems. The control of nonpoint source pollution in riparian ecosystems depends on interactions among the hydrology, soils, vegetation, management, and climate of a specific riparian buffer system. Models which cannot account for effects of these factors on water and chemical transport in riparian systems will not be useful for comparisons of different scenarios of riparian buffer use to control nonpoint pollution. The series of papers presented at this symposium describe the functional elements of REMM and present validation results for the model. A demonstration will provide details on initializing and running the model. In this paper we provide an overview of the conceptual basis for REMM. In addition, we describe the general characteristics of an experimental riparian buffer system used for validation studies presented in the other papers.

GENERAL FUNCTIONS OF RIPARIAN BUFFER SYSTEMS

Riparian forests were the original streamside vegetation in most humid and sub-humid regions of the world, including the Eastern and Midwestern United States. Riparian forest is generally distinct from the surrounding landscape, even when the adjacent areas are in forest. In more arid areas, the riparian forest may be the only forest in a landscape, for example the gallery forests of the tall-grass prairie. In most cases, regardless of original or native vegetation, riparian ecosystems form an ecotone or edge between upland vegetation and land uses and aquatic ecosystems.

The general functions of riparian forest ecosystems have been reviewed and ranked for the Chesapeake Bay Watershed from most to least general based on the available scientific literature (Lowrance et al., 1997). These buffer system concepts are based on field observations, process studies, and experimental manipulations in a number of different riparian ecosystem studies. Because of the diverse nature of the Chesapeake Bay Watershed, the rankings probably apply to many humid regions in the U.S. The most general water quality function of riparian forests is to provide control of the stream environment. These functions include modifying stream temperature; controlling light quantity and quality; enhancing habitat diversity; modifying channel morphology; and enhancing food webs and species richness. All of these factors are important to the ecological health of a stream and are best provided by a riparian forest that approximates the original native

vegetation (Sweeney, 1992). These functions occur along smaller streams regardless of physiographic region. These functions are most important on smaller streams, although they are important for bank and near-shore habitat on larger streams and the shoreline of lakes and bays. Riparian forests contribute to bank stability and thus minimize sediment loading due to instream bank erosion. Depending on bank stability and soil conditions in the area immediately adjacent to the stream, management of adjacent areas for long-term rotations may be necessary for sustainability of stream environment functions. The next most general water quality function of riparian forests is control of sediment and sediment-borne pollutants carried in surface runoff. Properly managed riparian forests should provide a high level of control of sediment and sediment borne chemicals regardless of physiographic region. Natural riparian forest studies indicate that forests are particularly effective in filtering fine sediments and promoting co-deposition of sediment as water infiltrates. The slope of the riparian forest, the available water storage capacity, and the soil cover by litter are the main factors determining the effectiveness of sediment removal in mature riparian forests. In restored riparian forests, the degree to which enhanced infiltration typical of forest soils has been established might also determine effectiveness in controlling surface runoff pollutants. In all physiographic settings it is important to convert concentrated flow to sheet flow in order to optimize riparian forest function. Conversion to sheet flow and deposition of coarse sediment that could damage young vegetation can be enhanced by a vegetated filter strip upslope from the riparian forest.

The next most general water quality function of riparian forests is to control nitrate in shallow groundwater moving toward streams. When groundwater moves in short, shallow flow paths, such as in many Coastal Plain watersheds, 90% of the nitrate input may be removed. In contrast, nitrate removal may be minimal in areas where water moves to regional groundwater such as in Piedmont and Valley and Ridge areas. The degree to which nitrate (or other groundwater pollutants) will be removed in the riparian forest depends on the proportion of groundwater moving in or near the biologically active root zone and on the residence time of the groundwater in these biologically active areas. The presence of wetlands and the hydrologic connection between source areas and wetlands enhances the removal of nitrate via denitrification.

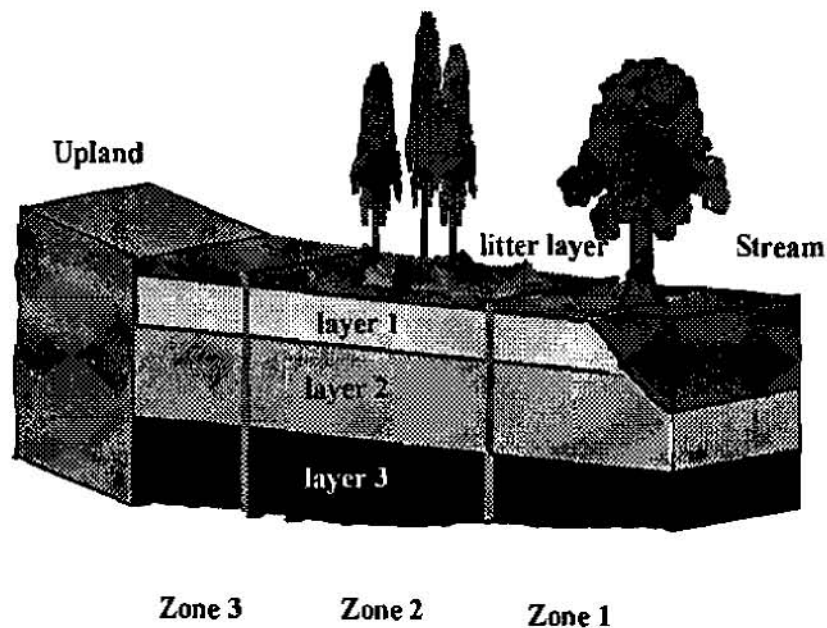
The least general function of riparian forests appears to be control of dissolved phosphorus in surface runoff or shallow groundwater. Control of sediment-borne P is generally effective. In certain situations, dissolved P can contribute a substantial amount of total P load. Most of the soluble P is bioavailable, so the potential impact of a unit of dissolved P on aquatic ecosystems is greater. It appears that natural riparian forests have very low net dissolved P retention. In managing for increased P retention, effective fine sediment control should be coupled with use of vegetation that can increase P uptake into plant tissue.

USDA's RIPARIAN FOREST BUFFER SPECIFICATION

Based on the general concepts described above, a riparian forest buffer system specification has been developed by USDA. (Welsch, 1991; Lowrance, 1992; NRCS, 1995) The riparian forest buffer specification is for a three zone riparian buffer system with each zone serving a particular major purpose and a number of secondary purposes (Figure 1). The buffer system consists of trees, shrubs, and herbaceous vegetation. The riparian forest buffer specification calls for a Zone 1 immediately adjacent to the stream which consists of permanent woody vegetation. In many cases, Zone 1 vegetation will be native hardwood species that occur on or near streambanks. The major purpose of Zone 1 is to provide shade and litter inputs for the aquatic ecosystem. The secondary function of Zone 2 is to retain nutrients. Zone 2 is on the upslope side of Zone 1. Zone 2 is an area of managed forest, which can be used for timber or biomass production by the landowner. The major function of Zone 2 is nutrient retention and infiltration of surface runoff. Secondary functions of

Zone 2 are to provide a buffer for Zone 1 vegetation and to retain sediment in surface runoff. Zone 3 is an herbaceous filter strip upslope from Zone 2. Zone 3 is similar to contour filter strips used as a field management practice. Management practices such as stiff grass buffers can also be incorporated in this zone. Zone 3 is generally immediately adjacent to the field or other pollutant source. The major functions of Zone 3 are sediment retention and conversion of channelized flow to sheet flow. Secondary functions of Zone 3 are infiltration of surface runoff and nutrient retention.

Figure 1: Cross section of riparian buffer system as simulated in REMM.



REMM was developed specifically to simulate hydrologic, chemical, physical, and biological processes in the type of riparian buffer system described above which has been adopted as a practice by USDA

agencies. REMM also provides flexibility to simulate functions of a wide variety of other field-edge and in-field buffer systems. Although the riparian forest buffer specification requires trees or shrubs in Zones 1 and 2, REMM can simulate up to twelve different vegetation types, and multiple vegetation types per zone. REMM can be used to simulate non-forest buffers and buffers in non-riparian positions, as long as the water, nutrient, and sediment inputs from the contributing area can be modeled or empirically determined.

GENERAL STRUCTURE AND FUNCTION OF REMM

REMM is designed to simulate daily processing of water, sediment, carbon, and nutrient inputs to a buffer system (Altier et al., In press). In general, inputs will be from agricultural lands, although inputs of water, sediment, and nutrients from other land uses could also be simulated. Water inputs are rainfall (or snowfall), surface runoff, subsurface flow (shallow groundwater), and seepage. Water outputs for each zone are calculated as subsurface flow, surface runoff, seepage, and evapotranspiration (ET). Nitrogen phosphorus, and carbon are input and output with each type of water input or output (except ET). Surface runoff carries sediment into and out of the zones. The output from Zone 1 is an estimate of the streamflow contribution of the entire contributing area, including the riparian buffer. In this sense, REMM is a watershed model when combined with modeled input from the upslope contributing area. REMM does not simulate the effects of channel expansion and overbank flooding during storm events. REMM assumes a lower confining layer for subsurface flow, although water can be allowed to move through the lower confining layer at a

constant rate. REMM does not allow simulation of groundwater flow paths that may make their way to stream discharge below the lower confining layer.

Much of the sediment transport module of REMM is based on AGNPS (Young et al, 1989). Sediment movement is simulated in rill and interrill erosion. Sediment is assumed to be composed of sand, large aggregate, small aggregate, silt, and clay. Sediment erosion, transport, deposition, and routing are done for each particle size class. Sediment deposition or transport is determined based on the transport capacity of the zone. Deposition or transport takes place through interaction with a litter layer, which is assumed to mix completely with surface runoff.

The dynamics of inorganic N and P in REMM are tied to estimates of either transformation rates or equilibrium concentrations for adsorbed ions. Nitrogen and phosphorus in initial soil organic matter (SOM) pools or N and P incorporated into plant biomass are cycled through SOM pools with different decomposition rates as done in the CENTURY model (Parton et al., 1987). N and P are mineralized as plant litter or SOM is re-synthesized into pools with a higher C/N or C/P ratio. N and P are immobilized from inorganic pools into either living plant biomass or SOM pools. As plant litter or soil organic matter are resynthesized into pools with higher C/N or C/P ratios, N and P are mineralized. Inorganic nutrients, whether from input sources or from mineralization of SOM, are available for plant uptake, microbial immobilization, water borne movement, or denitrification (N only). REMM does not simulate movement of pesticides, although it does simulate movement of dissolved and adsorbed carbon compounds that could be used as analogs of pesticides.

Vegetation growth is simulated on a stand basis. Vegetation in both an upper and lower canopy can be simulated for each zone and up to 12 different general vegetation types can be simulated. Plant growth is modeled based on estimates of the amount of gross photosynthesis and allocation of the photosynthate to growing plant parts and respiration depending on demand. If photosynthates are available, plant growth is limited by the availability of water and nutrients. Simulation of photosynthesis is based on the Forest-BGC model (Running and Coughlan, 1988).

TESTING AND VALIDATION OF REMM

Numerous research groups around the country where studies of riparian buffers in various settings have been conducted are currently testing REMM. Initial testing of REMM has been done by comparing simulated riparian buffers to data from actual riparian buffers studied by the Southeast Watershed Research Laboratory near Tifton, GA. This section of the paper describes the general characteristics of the field site used for validation of REMM. Subsequent papers in these proceedings will describe the specific results from the validation studies for hydrology, sediment transport, nutrient cycling, and plant growth.

Gibbs Farm Study Site: The study was done at a research farm (Gibbs Farm Site - GFS) which is part of the University of Georgia Coastal Plain Experiment Station near Tifton, GA. The site, referred to hereafter as the Gibbs Farm Site (GFS) is located in the Tifton-Vidalia Upland (TVU) portion of the Gulf-Atlantic Coastal Plain. The climate of the TVU is humid subtropical providing abundant rainfall and a long growing season. Because of both less permeable soil material at depth and the presence of a geologic formation (Hawthorn Formation) which limits deep recharge to the regional aquifer system, most of the excess precipitation in the TVU moves either laterally in shallow saturated flow or moves in surface runoff during storm events. The general hydrology of the region is reflected at the GFS and makes this region and the particular site ideal for the development of model testing data in a relatively simple hydrologic system.

The soil at the GFS riparian forest is an Alapaha loamy sand (fine-loamy, siliceous, acid, thermic Typic Fluvaquents). The soil of the adjacent upland area is a Tifton loamy sand (fine-loamy, siliceous, thermic, Plinthic Kandiudult). A three zone riparian buffer system as prescribed by the USDA-Forest Service specifications (Welsch, 1991) was established for this research project in 1992. Zone 3 is a herbaceous filter strip, Zone 2 is an area of managed forest where trees can be harvested, and Zone 1 is an area of permanent woody vegetation immediately adjacent to the stream channel. At the GFS (Figure 1), Zone 3 is an 8 m wide strip of common Bermudagrass (*Cynodon dactylon* L. Pers.) and Bahia grass (*Paspalum notatum* Flugge.). The grass strip was interplanted with perennial ryegrass (*Lolium perrene* L.) during its establishment. Zone 2 (before timber harvest) was a 40 to 55 m wide band of slash pine (*Pinus elliottii* Engelm.) and long leaf pine (*Pinus palustris* Mill.). Zone 1 is a 10-m wide band of trees with mostly hardwoods including yellow poplar (*Liriodendron tulipifera* L.) and swamp black gum (*Nyssa sylvatica* var *biflora* Marsh.). The entire buffer averages 55 m in width along an intermittent second-order stream channel. In early November 1992, one block of Zone 2 forest was clear-cut and one block was selectively cut. A third Zone 2 forest block was left as a reference area (Figure 2). The clear-cut Zone 2 blocks were replanted with improved slash pine in winter, 1993. No timber was harvested from Zone 1. The papers presented in this symposium will discuss model simulations and observations from the mature forest area only. The forest, with an average tree age of about 50 years, was considered to be in a steady state condition with very little net increase in biomass.

The field above the buffer system on the west side of the stream was in continuous corn (*Zea mays* L.) for the first three years of this study (1992-1994). In 1995, the field was planted in peanuts (*Arachis hypogea* L.). In 1996, the field was planted in millet (*Pennisetum glaucum* L.). All crops were grown using conventional tillage and conventional fertilizer and pesticide treatments. The exception is that the peanuts were grown in small test plots (4mx4m) which lead to high loadings of sediment in surface runoff.

Instrumentation and sample collection: Instrumentation at the experimental site was installed in late Fall, 1991 and Winter, 1992. Well sampling and surface runoff sampling began in January, 1992 and February, 1992, respectively. Recording well installations were completed in April, 1992. Samples were analyzed for sediment and N and P species using standard analytical techniques.

Surface runoff was collected using the dustpan shaped "Low-Impact Flow Event sampler (LIFE sampler, Sheridan et al, 1996). Two types of LIFE samplers are used to collect either 10% or 1% of the flow through a 30.48-cm wide dustpan. The 10% collection is made by splitting the flow into 10 pathways at the back of the collector and collecting flow from one pathway. The 1% sample is collected by connecting two 10% samples in series. The sample receptacle is large enough to contain runoff from approximately a 10-year return interval event in the 1% samplers. The receptacle is made from a 1m long piece of 10cm dia PVC pipe with capped openings at each end. PVC joints were welded using heated PVC to avoid possible interferences of solvents in PVC cement with the herbicide analysis. One of each type sampler is located at each zonal interface (six samplers per zonal interface). The samplers were positioned so as not to interfere with surface runoff collection at the next zonal interface (Figure 2). Six samplers are also in the middle of Zone 2. Having two types of samplers (10% and 1%) allows both large and small runoff events to be sampled and runoff volumes obtained. Surface runoff sample volumes were measured and subsamples collected for nutrient and sediment analysis on the work-day following each runoff event. Multiple events in a day were not collected separately. Samples were collected by pumping the receptacles with a peristaltic pump while agitating the sample by mixing with the inlet line of the pump.

Shallow groundwater movement of nutrients was determined using slotted monitor wells and a series of recording wells. A total of 115 slotted monitor wells were installed in the entire area (Figure 2) using Tri-loc slotted monitor pipe (Brainard-Kilman, Stone Mtn., GA). All PVC joints on monitor wells were welded using heated PVC. Paired wells were screened from 0-50 cm and 50-200 cm at

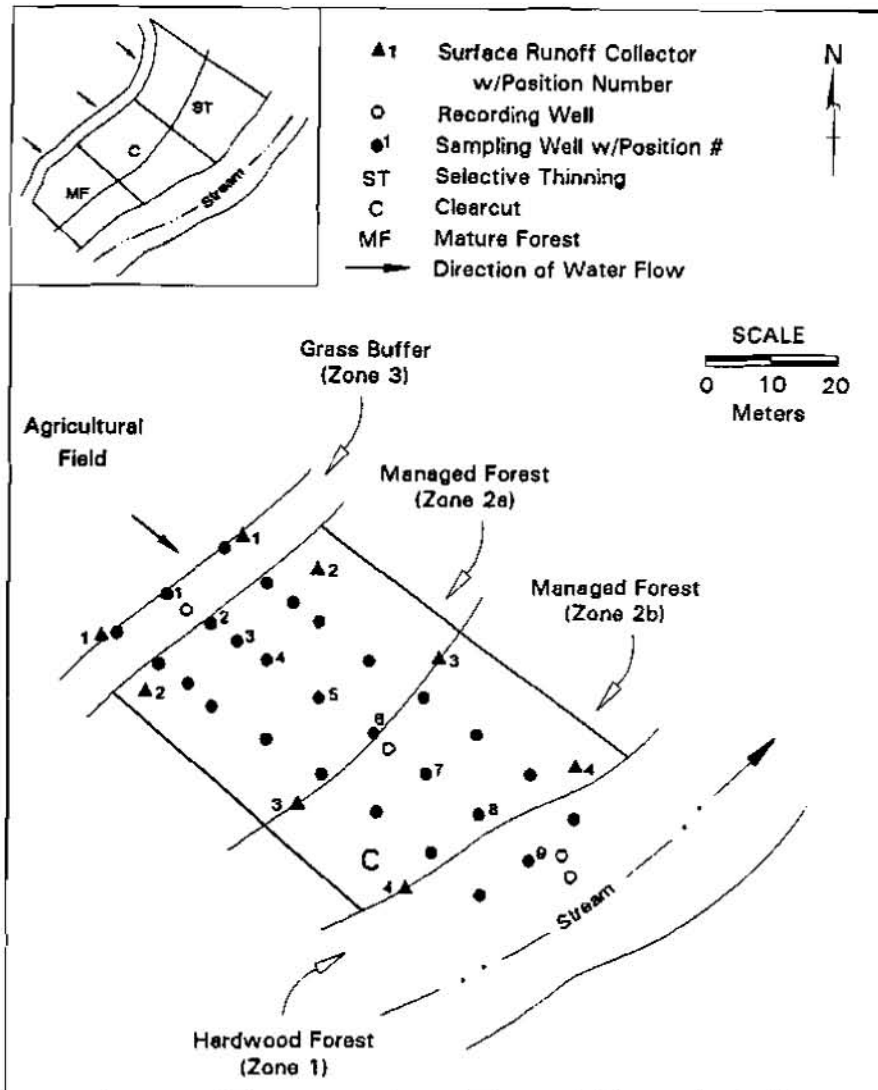


Figure 2. Layout of riparian forest plots in relation to upland field at the Gibbs Farm site.

the first four positions of each transect. The rest of the wells in each transect were screened from 0-200 cm depth. The first four positions are 5m apart and the rest of the well positions are 10m apart. Fully penetrating wells in the middle of each zone and the stream channel are instrumented with pressure transducers (Druck, Inc., New Fairfield, CT) connected to data loggers (Campbell Scientific, Logan, UT) so that water table levels can be monitored continuously. The soil water content and recording well data were used to calculate saturated thicknesses and ground water flux through the buffer system (Bosch et al., 1996). Wells were sampled bi-weekly. Before each well sampling, the depth of water below the ground surface was measured manually, and at least one well volume was removed and discarded.

Test Conditions and Reporting of Results: Four other papers presented as part of this symposium present simulation results for REMM with the model parameterized for the GFS. A final paper

discusses operational aspects of REMM. The test papers present results for hydrology, sediment transport, nutrient cycling, and plant growth for the mature riparian forest studied at the GFS. Where possible, key parameters from the GFS are compared to model simulation. For these tests of REMM, the GFS has been simulated as having a single vegetation type in each zone. Where possible, soil and water pools in REMM have been initialized with data from the GFS. When not possible, the pools were initialized from data collected at similar sites near the GFS or from literature values. Model simulations were done using weather data collected at the GFS and using estimates of upland inputs of water, sediment, and nutrients measured at the GFS. Very little calibration of REMM was necessary. Calibration of gross photosynthesis and soil organic matter turnover rates were done in order to stabilize the steady state or mature forest case. Other than that, the simulations presented in the companion papers are based on either field estimates of pools or rates or from literature values.

REFERENCES

- Altier, L.S., R. Lowrance, R.G. Williams, S. P. Inamdar, D.D. Bosch, J.M. Sheridan, R.K. Hubbard, and D.L. Thomas. Riparian Ecosystem Management Model (REMM): Documentation. USDA Conservation Research Report, In Press.
- Batten, H.L. 1980. Little River Research Watersheds. USDA Miscellaneous Publication, Southeast Watershed Research Lab, Tifton, GA. 17p.
- Bosch, D.D., J.M. Sheridan, and R. R. Lowrance. 1996. Hydraulic gradients and flow rates of a shallow coastal plain aquifer in a forested riparian buffer. Transactions of ASAE, 39, 865-871.
- Jacobs, T.C. and J.W. Gilliam. 1985. Riparian losses of nitrate from agricultural drainage waters. Journal of Environmental Quality 14, 472-478.
- Lowrance, R.R., R.L. Todd, J. Fail, Jr., O. Hendrickson, Jr., R. Leonard and L. Asmussen. 1984. Riparian forests as nutrient filters in agricultural watersheds. BioScience 34, 374-377.
- Lowrance, R., L.S. Altier, J.D. Newbold, R.R. Schnabel, P.M. Groffman, J.M. Denver, D.L. Correll, J.W. Gilliam, J. Robinson, R. Brinsfield, K. Staver, W. Lucas, and A. Todd. 1997. Water quality functions of riparian forest buffers in Chesapeake Bay watersheds Environmental Management 21, 687-712.
- NRCS. 1995. Riparian Forest Buffer, 392. United States Department of Agriculture/Natural Resources Conservation Service, Watershed Science Institute. Seattle, Washington.
- Parton, W.J., D.S. Schimel, C.V. Cole, and D.S. Ojima. 1987. Analysis of factors controlling soil organic matter levels in Great Plains grasslands. Soil Science Society of America Journal 51, 1173-1179.
- Peterjohn, W.T. and D.L. Correll. 1984. Nutrient dynamics in an agricultural watershed: Observation on the role of a riparian forest. Ecology 65, 1466-1475.
- Running, S.W. and J.C. Coughlan. 1988. A general model of forest ecosystem processes for regional applications I. Hydrologic balance, canopy gas exchange, and primary production processes. Ecological Modelling 42, 125-154.
- Sheridan, J.M., R.R. Lowrance, and H.H. Henry. Surface flow sampler for riparian studies. Applied Engineering in Agriculture 12, 183-188.
- Sweeney, B.W. 1992. Streamside forests and the physical, chemical, and trophic characteristics of Piedmont streams in eastern North America. Water Science & Technology 26, 2653-2673.
- USEPA. 1997. Clean Water Act Progress Report. United States Environmental Protection Agency, Office of Water. Washington, D.C.
- Welsch, D.W. 1991. Riparian Forest Buffers. USDA-Forest Service Publ. No. NA-PR-07-91.
- Young, R.A., C.A. Onstad, D.D. Bosch, and W.P. Anderson. 1989. AGNPS: A nonpoint-source model for evaluating agricultural watersheds. Journal of Soil and Water Conservation 44, 168-173.

AN INNOVATIVE APPROACH TO IMPROVING WATER QUALITY THROUGH STORMWATER MANAGEMENT

**By Rodney Mach, Environmental Engineer, US Army Engineer District, New Orleans,
Louisiana; Burnell Thibodeaux, Hydraulic Engineer, US Army Engineer District,
New Orleans, Louisiana**

Abstract: The Water Resources Development Act of 1992, Public Law 102-580, Section 307, authorized the Secretary of the Army to design and construct projects that address water quality problems associated with storm water discharges into Lake Pontchartrain and the Mississippi River. The purpose of this project is to demonstrate the capability of mitigating storm water impacts on Lake Pontchartrain water quality by collecting, storing, and removing runoff from the drainage system prior to its discharge to the Lake and to determine if this runoff can be effectively treated by existing treatment facilities that currently experience high infiltration inflows. New facilities to transport storm water can also be used to augment the capacity of existing sewage lift stations during wet weather to reduce the potential for sewage overflows from an overtaxed system. A monitoring and modeling program will be used to determine existing conditions and to validate the extent of anticipated improvements.

The Jefferson Parish Demonstration Project water quality monitoring/modeling program consists of two major components: the monitoring program and the modeling program. The monitoring program consists of collecting and compiling water quality, meteorologic, hydrologic, and hydraulic data which will be used in evaluating the demonstration project and for input to a receiving water quality simulation model. The modeling program will consist of a receiving water quality simulation model which will aid in evaluating the Project's impacts on Lake Pontchartrain for a wide range of conditions and in assessing potential alternatives and applications throughout Jefferson Parish.

This paper will explore the Corps' role in this cost shared project and describe in detail the monitoring and modeling programs which are planned to be implemented before and after construction. The paper will also describe the anticipated impacts to the lake, the challenges encountered in the water management process, and the conflicts that have been identified in the implementation of the operational management plan especially those related to flood control versus water quality. In addition the paper will address the development of the operational model for this unique and timely environmental and water control project.

INTRODUCTION

Background: The water surrounding any community is a natural treasure and the useability of that resource is always of great public concern. Concerns with urban runoff have primarily dealt with the prevention of localized flooding. Only recently has urban runoff been considered as a significant contributor to the degradation of the quality of receiving waters. Water quality problems are not always perceivable and are less dramatic than flood events. In some cases, the pollutant load applied to neighboring water bodies by runoff can be greater than point source loads.

Pollutants that are present between rainfall events prior to a storm accumulate on impervious surfaces

and are generally carried away in the first 1 inch of rainfall in moderate to heavy storms. Urban nonpoint source pollution is the result of rain washing the surfaces of urbanized areas. As this occurs, contaminants are picked up from the air; streets; sidewalks; petroleum residues from gas powered vehicles; exhaust products; heavy metals and tar residuals from the roads; chemicals applied for fertilization weed and insect control; and sediments from construction sites. The dumping of chemicals such as motor oil and antifreeze into storm drains is also a source of nonpoint pollution. Illicit hookups of storm drains to sanitary sewers result in increased volumes of flow to wastewater treatment plants causing more frequent overflows or bypasses of sewage flows into receiving waters.

A reconnaissance study of urban flood and water quality management for Jefferson and Orleans Parishes was completed and approved in December 1993. One purpose of the study was to improve the water quality of storm water runoff into Lake Pontchartrain. The study concluded that more data were needed and recommended the use of demonstration projects. In a "consensus agreement" between the New Orleans District and Jefferson Parish in July 1995, a plan developed by the parish to capture and treat storm runoff using excess capacity of the Parish's East Bank sewage treatment plant was adopted for a demonstration project.

Authority: The Water Resource Development Act of 1992, Public Law 102-580, Section 307, authorized the Secretary of the Army to design and construct projects that address water quality problems associated with storm water discharges into Lake Pontchartrain and the Mississippi River. The fiscal year 1994 Energy and Water Appropriations Bill provided \$2 million to prepare a Project Cooperation Agreement and technical documentation for a storm water management demonstration project proposed by Jefferson Parish officials. Senate Report 103-291, dated September 1994, allows cost reimbursement to the Parish for their design and construction of the facility, relegating the Corps to a technical management oversight role.

The recommended plan approved for implementation is to modify the existing storm water runoff collection system and pump, via a lift station, storm water from the drainage canals to the treatment plant for subsequent discharge to the Mississippi River.

PROJECT AREA

Description of Project Area: The project area is located in southeastern Louisiana in the vicinity of the city of New Orleans and includes the highly urbanized portion of Jefferson Parish on the east bank of the Mississippi River. The area is within the Pontchartrain Basin, situated near the center of the Gulf Coastal Plain in the lower reaches of the Mississippi embayment. The basin is a shallow depression lying between the alluvial ridge of the Mississippi River to the south, and sloping up on the north and west. The basin consists of lakes Maurepas, Pontchartrain, and Borgne. This system ultimately drains into the Gulf of Mexico via the Mississippi and Chandeleur Sounds.

In the project area the ground near the Mississippi River is above sea level and elevations decrease with distance from the river. The developed areas are protected from river and hurricane flooding by levee systems.

Description of Drainage System: The leveed areas are divided into many subbasins by natural and

man-made barriers and are webbed with drainage canals that terminate at pumping stations. The drainage system is an intertwined network of subsurface culverts, ditches, canals and pumping stations. In contrast to conventional systems which generally rely on gravity flow and free fall discharge, the Jefferson Parish drainage system depends on the collection and pumping of all storm water falling on the area to be drained by pumps which discharge into Lake Pontchartrain. The treated effluent from the sewage treatment plant is discharged into the Mississippi River.

Jefferson Parish operates their drainage pumping stations to maintain a specific water level in the major outfall canals. Once those elevations are exceeded the pumps are engaged to discharge the excess. Problems with subsidence have dictated this operation to ensure that ground water is not drawn out of areas adjacent to the canals.

The storage areas are laterally connected by a grid of canals. The lateral canals equalize flow between the major outfall canals. This allows rain water to flow in different directions depending on available capacities at the pumping stations and the location and areal extent of rainfall events over the parish.

PROJECT DESCRIPTION

The Jefferson Parish Waste Water Treatment Plant has a demonstrated wet weather capacity in excess of the required dry weather capacity. For the demonstration project this excess capacity will be used to treat the first runoff mixed with the contents of the drainage canals and, in dry weather a mixture of flow from the sewage system and drainage canal contents. A 20,000 gpm lift station and 54 in. diameter force main will be used to transport some of the storm water from the drainage system to the treatment facility as capacities allow and whenever water levels in the canal exceed a given criterion. The treatment plant is an activated sludge facility with an average capacity of 70 MGD.

Generally during wet weather peak flows, when infiltration and inflow cause an increase in treatment plant inflow, stormwater pumping to the treatment plant will be discontinued until dry weather conditions resume. Operation of the stormwater pumps will be closely interfaced with the existing Jefferson Parish control and monitoring systems of the drainage and sewerage departments.

MONITORING PROGRAM

A monitoring program will be conducted to evaluate the project and to provide data for input to a receiving water quality simulation model. The program involves collecting, compiling, and analyzing water quality, meteorologic, hydrologic, and hydraulic data. Monitoring will be conducted in two phases; pre and post-construction. The pre-construction phase will take place prior to completion of the project. The post-construction phase will begin after construction is complete.

Monitoring data will be used to determine existing and post construction storm water runoff quality in the Jefferson Parish drainage canal system. Existing and post construction Lake Pontchartrain water quality and the impact of storm water runoff on the Lake will also be evaluated. The program will define the characteristics (i.e. volume, duration, and pollutant concentrations) of stormwater runoff from a major portion of the urban area on the south shore of Lake Pontchartrain for both pre and post-construction conditions. It will also quantify the stormwater pollutant loading in this area

that is discharged to the Lake for pre and post-construction conditions.

Post-construction monitoring data will be compared to pre-construction monitoring data to evaluate the effectiveness of the demonstration project in improving stormwater quality and, especially, water quality in the Lake Pontchartrain receiving area.

It is anticipated that each of the phases of the monitoring program will be active for approximately a twelve month period. Within this time frame, data from ten to twelve rainfall events of varied intensity and duration will be collected and analyzed. The characteristics of runoff pollutant concentrations and loadings from these different events will be analyzed to determine if a first flush phenomenon occurs in this drainage system. These data will also be useful in optimizing operation of the project for maximum effectiveness.

Sampling: Water samples will be collected from interior drainage system canals and from the Lake Pontchartrain receiving area. Automatic water samplers will be utilized to collect water samples during rainfall events. Auto samplers will be positioned to obtain samples in the drainage canals on the intake side of three drainage pump stations. The samplers will be connected to rain gauges and area-velocity flow meters. This will facilitate the collection of samples based on drainage canal flow and rainfall. These sampling sites will provide information to characterize the composition and pollutant loading of storm water discharged to Lake Pontchartrain for pre and post-construction conditions. An auto sampler located at the intake of the proposed lift station will provide data about the composition and pollutant loading of storm water that will be pumped to the wastewater treatment plant via the proposed force main.

Water quality grab samples from the Lake Pontchartrain receiving area will be collected by watercraft. Samples will be collected from near and far shore sites located offshore of the three pump stations. Collection will take place prior, during, and after rainfall events. Data from these samples will establish baseline water quality conditions in the Lake. These data will also be used to assess the impacts of stormwater discharge from rainfall events on the receiving waters of Lake Pontchartrain.

Drainage canal grab samples will also be collected during dry periods. These samples will establish baseline ambient dry weather canal water quality.

Because of the great number of samples associated with this program a selective number of water quality parameters will be analyzed. Emphasis will be placed on pollutants that are common in storm water and on pollutants that affect the designated uses of Lake Pontchartrain.

The following parameters will be analyzed for all samples:

- Total Suspended Solids (TSS)
- Total Dissolved Solids (TDS)
- Total Volatile Solids (TVS)
- Chemical Oxygen Demand (COD)
- Total Phosphorus
- Dissolved Phosphorus

Total Ammonia
Nitrate + Nitrite
Total Kjeldahl Nitrogen (TKN)
Total Organic Carbon (TOC)
Dissolved Copper
Dissolved Lead
Dissolved Zinc
Hardness
Diazinon
Malathion
pH
Oil & Grease

Because of analyses holding times, only selected samples, including all grab samples, will be analyzed for Fecal Coliform, E. Coli, and BOD.

MODELING PROGRAM

A receiving area water quality model will be developed using WASP-5 to evaluate the impacts of the project on the Lake's water quality. The model has the capability of simulating the transport and transformation of conventional pollutants such as dissolved oxygen, biochemical oxygen demand, and bacteria in the water column. Data collected in the Lake during the monitoring program will be used to verify the model. The modeling will also provide information on the effectiveness of the demonstration project in improving the Lakes water quality. In addition, the model will be used to evaluate the project for a wide range of conditions and potential alternatives.

SUMMARY

The compelling issue which drove this project into being, improvement of the water quality of Lake Pontchartrain to support and sustain a resource available for use by the public at large with minimal risk to health, will soon have a satisfactory remedy in place. Cooperation between the Corps and Jefferson Parish has enabled this innovative landmark project to emerge. Continued cooperation during the various phases will ensure a successful, functioning project which will meet the expectations of all citizens.

REFERENCES

Lake Pontchartrain Storm Water Discharge, Louisiana, Technical Report, Jefferson Parish Demonstration Project, October 1996, US Army Engineer District, New Orleans, Louisiana

Louisiana Department of Environmental Quality, Office of Water Resources, Urban Nonpoint Source Pollution Program Information Pamphlet

SUSTAINABLE SOIL, WATER AND AIR QUALITY MANKIND'S ULTIMATE CHALLENGE AND OPPORTUNITY IN THE 21ST CENTURY

J. Patrick Nicholson, Chief Executive, N-Viro International Corporation, Toledo, Ohio

Abstract: The author, developer of the only water or wastewater technology to win the coveted President's Citation of Excellence in Environmental and Conservation Technology, identifies the major national and international problems associated with the management of over 10,000,000,000 (ten billion) wet tons of organic wastes annually generated in the USA alone. Pulp and paper, food process, and animal manures are the primary sources of these huge organic waste streams. The problems discussed in detail include significant, if not critical, public concern over pathogens in animal manures (over 2,000,000,000 wet tons), non-point source water pollution, and **unregulated** methane, CO₂, nitrous oxides, and hydrocarbon emissions exceeding 20 trillion cubic feet per year from organic landfills, lagoons, and surface impoundments. These gases exceed the emissions from the entire transportation industry of the United States.

The organic and mineral wastes now creating such immense public health, air, and water problems could be the cornerstone of a worldwide effort to provide sustainable soil fertility for mankind and the impending worldwide population explosion to 10 billion people by the middle of the 21st Century. Society has the science and technology to do the job and to do it right. All that is needed is political leadership and direction.

Compost and bio-mineral processes have already demonstrated the technology to pasteurize organic wastes to prevent manure pathogens from infecting our food supply and water quality. Such pathogens of critical concern include cryptosporidium parvum, E-Coli, salmonella and pfiesteria piscida.

Technologies, such as composting and bio-mineral processes that pasteurize, immobilize and stabilize organics and nutrients and provide "slow release" soil fertility through controlled mineralization, are discussed. The author feels technology transfer must be the essential component of the visionary bridge into the 21st Century. The bridge must be wide enough to allow environmental, agricultural and public communities to work together to do what is right. Political courage and leadership together with scientific truth are absolute vital components of that bridge structure. A sustainable national program of technology transfer is vital if such technologies are going to be understood, accepted and utilized.

This paper is a review of existing USA policies and practices with regard to the Earth's vital land, air and water resources and a recommendation of changes needed to ensure safe and sustainable soil fertility through responsible organic and mineral by-product management and technology.

INTRODUCTION

In the historic novel "A Tale of Two Cities", the author Charles Dickens, tells us "It was the best of times and it was the worst of times." As time runs out on the 20th Century, no words better describe the 20th Century's historic impact on civilization.

In the 20th Century, we witnessed unparalleled advances in science and technology, in the quality of life, in education, in communications, in medicine, and indeed in the very seeds of democracy.

Yet, in the 20th Century we also witnessed more bloodshed of man by man, more terror and the development of the tools of terror, more destruction of family life and human discipline, more crime, more drugs of all kinds, and finally, in the end, more greed and avarice than ever before witnessed in this country, if not in the world. Most importantly, we witnessed the unparalleled destruction by man of man's very home and environment. **We witnessed man's greed and power allowing man to pollute and harm the air we breathe and the soil and water so essential to our survival.** We began in this century to recognize the insanity of our actions, but these calls to action have been blunted and delayed and deliberately confused by the power of special interests to maintain the status quo **which is so profitable to so few and so destructive to so many.**

In the 1996 Presidential campaign, after all of the evidence of the past twenty-five years of abuse of the political process, we have witnessed an increase in political contributions of 2-3 times over any previous Presidential campaign. Where does the money come from? What do the contributors expect for their money? Are they

spending such money just because they love the candidates? Are they looking for invitations to parties at the White House? You and I both know what many of the contributors want. **They want the ability to control public decisions.** They want to maintain the status quo. They want the ability to pollute, to control prices, to sell drugs, to monopolize, to destroy values, and to ensure that the rights of special interests are preserved above all else. Can democracy survive in such an atmosphere of power and abuse? **Most importantly, can our planet earth survive the power and greed of these special interests?**

In the 20th Century thankfully, we have had Presidents in the United States who have had the vision and the courage to provide essential leadership to meet the critical challenges of their time. Theodore Roosevelt introduced conservation to protect our natural resources and fought the greed and power of monopolies. Woodrow Wilson gave us the vision of America's role in international leadership. Franklin Roosevelt, "all we have to fear is fear itself", uplifted our dreams, promoted the dignity and rights of the working man, and led America against the greatest evil of this century, Nazi Germany. Harry Truman gave us the courage and the leadership to fight Communism while he was condemned by right-wingers as a friend of Communism. Dwight Eisenhower recognized the essential dangers of fighting a land war in Asia, and the high risks of allowing the military-industrial complex to control America's foreign policy. John Kennedy lifted our vision of what America can and should be: "And so, my fellow Americans, ask not what your country can do for you, but what you can do for your country." Jimmy Carter made us all realize that human rights are important. Ronald Reagan, together with Pope John Paul II and Mikhail Gorbachev provided critical leadership at a point in time when the world could easily have experienced nuclear disaster. As a result of their efforts, the Cold War is over and I think we won. And George Bush united the free world against the greed and cruelty of a Mid-East maniac and restored American pride in our armed forces.

In today's society can any world leader build that bridge to the 21st Century? Can this President or any Chief of State provide the independent political leadership and courage to do what is critically necessary to sustain this planet earth for our children, our children's children and their children? This indeed is the ultimate challenge and opportunity in the 21st Century.

POPULATION GROWTH - FOOD REQUIREMENTS

It is now projected that by the middle of the 21st Century the world's population will nearly double to almost 10 billion people.

Today, we are not providing sufficient food for the world's population and today, in providing what we do provide, civilization is destroying the quality of earth's soils, earth's waters, and earth's air.

Let's spend a few minutes to seek the truth. First of all, let's look at the problem!

Mankind does not need to look to the future to see the folly of its actions, or more precisely, its inaction. The World Health Organization, and other respected public health institutions, are dedicated to forcing so-called intelligent industrial nations to recognize the terrible Third World devastation caused primarily by food shortages. Is society responding to this terrible human tragedy? **Malnutrition is the major contributing cause in the deaths of over 14,000 children per day.**

The Worldwatch Institute, in their 1994 *State of the World* report, said:

" ... Much of the land we continue to farm is losing its inherent productivity because of unsound agricultural practices and overuse. ... More than 550 million hectares (one third of all farmland) are losing topsoil or undergoing other forms of degradation as a direct result of poor agricultural methods."

" ... the huge amounts of fertilizers and pesticides now routinely used in agriculture frequently drain off into the groundwater beneath the fields, contaminating them for many centuries to come." Earth in the Balance: Ecology and the Human Spirit, Vice President Al Gore, 1992.

MANURES AND OTHER ORGANIC WASTE UTILIZATION

In 1993, the U.S. Department of Agriculture developed an excellent report titled "Agricultural Utilization of Municipal, Industrial and Animal Waste". In that report, USDA stated that "annual animal manure production exceeds 2.2 billion tons." This is 40-50 times more manure than human sludge or bio-solids waste. Moreover, the report showed that BOD levels from such wastes were 10-100 times higher than from treated bio-solids. In other words, manures are 500-5,000 times a bigger problem or opportunity than bio-solids. However, in all reality, manure management is non-existent because non-point source water pollution regulation is non-existent. We have spent billions on point source pollution prevention. And yet we have done practically nothing on non-point source water pollution. Why not? What special interests are preventing sound and scientific environmental and agricultural policies and practices? Why are these issues being ignored? All we seek is the truth!

The unpublished U.S. Department of Agriculture report states:

"Waste utilization problems present a challenge and an opportunity for U.S. agriculture. We are currently confronted with the long-term goal of developing crop production practices that promote sustainability. Animal wastes and many municipal and industrial wastes have substantial potential value for agricultural utilization. The development of methods to optimally integrate waste utilization into sustainable agricultural practices could provide a major part of the solution to urban and industrial waste disposal problems."

This excellent 1993 USDA report which so clearly identifies both the soil and water quality challenge and the opportunity, is now being published - finally! Hats off to Bob Wright and all others involved in an excellent report.

PUBLIC HEALTH CONCERNS

Two billion tons of manure are being generated annually. Three major concerns are obvious. They are public health, air emissions and water pollution. How can USDA, USEPA, U.S. Dept. of Health and the White House ignore these concerns?

1. How dangerous are farm-generated pathogens? The March 21, 1997 issue of *Science* tells us that indeed, as long suspected, the 1918 killer virus, that resulted in 675,000 deaths in the USA alone, "was a classical swine flu." Robert Webster, virologist at St. Jude Children's Research Hospital in Memphis, Tennessee states: "What this says is we had better watch what is happening in the pig population of the world."

On Sunday, March 23, 1997, Dateline and in Tuesday, March 25, 1997's Science Section of the *New York Times* we read and saw the wonderful work of Dr. JoAnn M. Burkholder of North Carolina State University. Dr. Burkholder has long been fighting a lonely battle against the "microscope killer", *Pfiesteria piscida*, and against a North Carolina power structure that has fought her heroic efforts in every possible way including threats to her life. The *Time's* story states "Pfiesteria is nourished by runoff from urban development and industries like hog farming." A CBS 60 Minutes December story was equally critical of pork power practices in North Carolina.

The excellent discussion draft for the president's conference on food safety discussed the well known problems of Salmonella and E-Coli. Last year in Florida, the orange juice industry was severely impacted by these pathogens. Many of those orange groves were fertilized by untreated chicken manure. A significant percentage of oranges are harvested from the ground.

Perhaps the greatest immediate fear is the parasite protozoan, *Cryptosporidium parvum*. A recent USDA survey showed that 100% of all states surveyed have a problem, 59% of all farms have a problem, and 22% of all calves have a problem. In 1993, *Cryptosporidium* infection impacted over 50% of the human population of Milwaukee.

How can animal manure disposal or utilization be ignored? Is the next case of "mad cow disease" about to take place in our USA? The Wall Street Journal recently reported a possible case in Indiana. With 2 billion tons of

untreated manure disposed annually near our water supplies, how are we, our children and our children's children protected without national reliance on demonstrated science and technology?

2. Manure disposal sites are a huge source of unrestricted emissions of hydrocarbons, methane, nitrous oxides and CO₂. Why are these point source emissions ignored?
3. **Unenforced** CAFO regulations only provide standards for NPDES water discharge permits. No federal laws or regulations now exist to provide manure management standards. Two billion tons of manure (50 times the volume of municipal sludge) containing organic and nutrient levels 10-100 times **per ton** greater than municipal sludge, are generated annually. Today there are no federal laws, no regulations, no standards, and precious little guidance or technology transfer relative to two billion tons of manure! Why?

Who made the decision that these waste manures were not covered by the Resource Conservation and Recovery Act? What was their authority?

IS CHANGE NECESSARY

The challenge and the opportunity have been well defined by other international authorities besides the U.S. Department of Agriculture.

"Manure supplies nitrogen, phosphorus, and other nutrients for crop growth; adds organic matter and improves soil structure and tilth; and increases the soil's ability to hold water and nutrients and to resist compaction and crusting. Disposal of manure as a waste often leads to both surface water and groundwater degradation. **Improved manure management can effectively capture the benefits of manure as an input to crop production and can reduce the environmental problems associated with manure disposal.**" *Soil and Water Quality: An Agenda for Agriculture*, National Research Council, 1993.

Let's summarize:

1. Our soils worldwide are losing their sustainability due to many factors, including an over-dependence on chemical fertilizers and pesticides, soil erosion, mismanagement, and diminishing organic and mineral content.
2. A great opportunity exists through proven established technology to utilize the huge quantities of organic and mineral wastes generated annually to compliment, not supplement, chemical fertilizers and pesticides, and to ensure worldwide sustainable soil fertility. However, the current uncontrolled use of such waste materials, creates immense water quality, sociological, and public health concerns and problems. Land application regulations of bio-solids and manures must require safe and inaccessible storage, pathogen reduction until time of use, responsible odor controls, and **management practices and technologies that control leaching to ground water and runoff to surface waters. Without enforcement there is no compliance. Without compliance, public health, social responsibility, and environmental protection are all seriously endangered with current land application practices.**

GLOBAL WARMING - GREENHOUSE CONCERNS

In 1988 USEPA published a report titled "Solid Waste Disposal in the USA." This report identified over 3 **billion dry tons** of organic wastes generated annually in the USA. Pulp and paper products, food and kindred products and animal manures constituted over 90% of this total. A vast majority of these organic wastes are disposed in landfills, lagoons, and surface impoundments. Regulations are either minimal or non-existent! Tragically, these organic wastes, as currently disposed, create immense quantities of CO₂, methane, and nitrous oxide emissions, which are the primary causes of global warming and ozone depletion, as well as other social problems as so well documented recently by CBS (60 Minutes - "Pork Power"). Moreover, these disposal facilities generate large amounts of soluble solutions with high BOD levels that overflow and leach into America's groundwater, waterways and wetlands, greatly increasing non-point source water pollution.

We estimate that the total gases generated from **the largest organic disposal facilities annually exceed fifteen trillion cubic feet**, which is equivalent to the gases generated by **two hundred million cars**.

MINERAL BY-PRODUCTS

Today, over 200,000,000 tons of boiler ash, fluidized bed ash, resource to energy ash, scrubber ash, lime kiln dust, cement kiln dust, and wood ash are **generated and wasted annually**. **This is tragic!** These materials have tremendous soil fertility value. They offer the **very best way to pasteurize, stabilize, and immobilize organics** so that organics can be effectively utilized to **reduce chemical dependency, increase soil fertility and greatly improve soil and water quality**. The importance of minerals in soils is well understood. The N-Viro process utilizes these by-products for pH elevation, exothermic heat, and drying. The N-Viro process is patented and N-Viro will defend its intellectual property.

UNLIMITED WORLD-WIDE OPPORTUNITY

The challenge is clear. Now let's emphasize the opportunities.

1. A classic example of what can be accomplished involves the sugar industry in the Pacific and Taiwan Sugar company. Last year while visiting Hawaii, I learned that Taiwan Sugar was dominating sugar sales in the Pacific to such extent that most sugar plantations in Hawaii were shutting down. While some blamed low labor rates in Taiwan, I questioned this position as Taiwan has a reasonably good standard of living. I visited Taiwan to seek the truth. Taiwan Sugar maintains a herd of over 500,000 hogs. **They compost the hog manure and use the compost almost exclusively as their source of both fertilizer and pesticide, thus greatly reducing their chemical input costs.** Moreover, the stabilization of composting allowed Taiwan Sugar to use the manure **without damaging either their precious surface or ground water resources**. This company is on the ball. Believe me, our challenge for economic leadership in the 21st Century is coming from the Pacific. Science and technology are our best ways of staying competitive, but we too had better be on the ball. **Science and technology, not political clout, must determine America's future agricultural, environmental, and economic policies and programs, or we can simply hand over world leadership to the Pacific Rim.**
2. In order for organic and mineral wastes to be utilized so as to not pollute either the water, the land, or the air, two requirements are absolutely necessary.
 - a. **Sound soil nutrient management practices**, including seasonal application, no till, zoning, crop rotation, etc., must be developed and implemented.
 - b. Technologies, such as compost and N-Viro Soil™, **that immobilize and stabilize organics and nutrients so that they provide "slow release" soil fertility through controlled mineralization, must be recognized and implemented.** In seeking solutions it is important to remember the words of Pope John Paul II: **"We are involved in a quest along with our fellow men ... let us avoid moralizing or suggesting that we have a monopoly on the truth."** Indeed, we welcome and encourage the development of alternative concepts or technologies that ensure results comparable to compost or N-Viro Soil™ and their ability to increase soil fertility while concurrently improving soil and water quality.
3. Technology transfer must be an essential component of that magnificent visionary bridge into the 21st Century. That bridge must be wide enough to allow the environmental, agricultural and public communities to work together to do what is right. **Political courage and leadership, together with scientific truth, are the absolutely vital components of that bridge structure.**

N-VIRO SOIL™

The House Agricultural Appropriations Sub-Committee, under the leadership of Chairman Joe Skeen and Minority Leader Marcy Kaptur, has appropriated \$900,000.00 to the U.S. Department of Agriculture to provide demonstration funds to the Rodale Institute, the Compost Council, and N-Viro International Corporation. The demonstration project is showing the ability of compost and N-Viro Soil™ technologies to utilize manure and bio-solids in such a manner as to provide **both sustainable soil fertility and reduced non-point source water pollution**. The two processes, i.e. compost and N-Viro Soil™, stabilize and immobilize nutrients and organics so that they are only available through the "slow release" mechanism of mineralization. **Moreover, they help reduce the leaching of chemical fertilizers, thus increasing their efficiency and they reduce the need for chemical pesticides.**

Compost is an established biological technology. N-Viro Soil™ is a new process with an established reference base and significant public recognition, that combines biological, chemical, and physical processes to pasteurize organic wastes, and convert to a stable, storable product that is capable of providing "slow release" soil fertility through immobilization and mineralization.

N-Viro International Corporation's patented N-Viro Soil™ and L-B Soil processes combine organic by-products with mineral by-products. The resultant products, which result from chemical, physical, and biological processes, are disinfected (N-Viro Soil achieves true pasteurization including total destruction of *Cryptosporidium* parasites), stabilized (immediate and long term odor suppression), and immobilized (nutrients, organics and metals remain insoluble and air emissions are greatly reduced).

Both N-Viro Soil and L-B Soil provide significant mineral benefits to the soil. Calcium and other critically need soil minerals such as salt, copper, selenium, magnesium and boron are readily available in N-Viro products. It is well recognized that agricultural soil mineral deficiencies are a major factor in human dietary problems and sustainable soil fertility concerns. N-Viro provides an aggressive answer to these concerns.

TIME FOR NATIONAL LEADERSHIP

A sustainable national program of technology transfer is absolutely vital if such technologies are going to be understood, accepted, and utilized.

The issue of air pollution caused by animal manures is clearly an EPA responsibility. However, beyond air pollution, we urge the Administration to encourage USDA to accept responsibility and authority for improved manure management and safety. Incentives, guidelines and standards, **not regulations**, are needed. **No one is more concerned about farm-generated diseases and water pollution than the American farmer.** Moreover, we have been most impressed by the concern and leadership at the American Farm Bureau and the Pork Producer's Council on this issue. USDA has the people, the technology, the credibility, and the trust of the American farmer to solve this problem and to convert these organic resources into safe sustainable soil fertility products. **All they need now is direction.**

The problems raised in this talk of public health, huge unregulated air emissions and non-point source water pollution are no more critical than the need for long-term sustainable soil fertility. The use of compost and bio-mineral technologies can create an unlimited worldwide opportunity to safely use animal and other organic by-products to provide fertility. The technology now exists to do the job and do it right. What is desperately needed is technology transfer and leadership from Washington. I urge the Administration to:

1. Give USDA full authority to manage animal manure with assistance from USEPA on risk analysis.
2. Either eliminate the placement of unstabilized organics in landfills, lagoons, surface impoundments or require gas collection systems.
3. Create an environmental technology transfer vehicle similar to the Transportation Research Board to ensure Federal - State, public - private, environmental - agricultural educational transfer. Set up Steering Committee: White House, USDA, USEPA, Water Environment Federation, American Farm Bureau.

As stated so well in "Earth in the Balance", leadership is the key. If leadership does not come from the United States, where will it come from?

Finally, I use the words of Senator Robert Kennedy, taken from George Bernard Shaw: **"Some people see things as they are and ask why. I dream of things that have never been and ask why not?"**

REFERENCES

Agenda 21: The Earth Summit Strategy to Save Our Planet, 1993, Introduction by U.S. Senator Paul Simon, Edited by Daniel Sitarz.

Agricultural and Food Processing Wastes, Proceedings of the Sixth International Symposium on Agricultural and Food Processing Wastes, December 17-18, 1990.

- Agricultural Utilization of Municipal, Animal and Industrial Wastes, United States Department of Agriculture, 1993, Draft Report, Edited by Robert J. Wright.
- Ausubel, K., 1994, *Seeds of Change: The Living Treasure: The Passionate Story of the Growing Movement to Restore Biodiversity and Revolutionize the Way We Think About Food.*
- Brown, L. R., 1994. *State of the World 1994: A Worldwatch Institute Report on Progress Toward a Sustainable Society.*
- Garst, R., Barry, T., 1992, *Feeding the Crisis: U.S. Food Aid and Farm Policy in Central America.*
- Gore, A., 1992, *Earth in the Balance: Ecology and the Human Spirit.*
- Hawken, P., 1993, *The Ecology of Commerce: A Declaration of Sustainability.*
- Jackson, W., 1980, *New Roots for Agriculture.*
- Magdoff, F., 1992, *Building Soils for Better Crops: Organic Matter Management.*
- Our Common Future*, World Commission on Environment and Development, 1987.
- Page, A. L., Logan, T. J., Ryan, J. A., 1987, *Land Application of Sludge: Food Chain Implications.*
- Polmet '91: *Pollution in the Metropolitan and Urban Environment, 1991*, Edited by John Boxall, Conference Proceedings of Polmet '91, held December 9-13, 1991.
- Schmidheiny, S., *Business Council for Sustainable Development, 1992, Changing Course: A Global Business Perspective on Development and the Environment.*
- Soil and Water Quality: An Agenda for Agriculture, 1993*, Committee on Long-Range Soil and Water Conservation, Board on Agriculture, National Research Council.
- U.S. Environmental Protection Agency, 1994, *Side-by-Side Analysis of S. 1114, the "Water Pollution Prevention and Control Act of 1994" Compared to President Clinton's Clean Water Initiative Compared to H.R. 3948, the "Water Quality Act of 1994".*
- Vlavianos-Arvanitis, A., Oleskin, A. V., 1992, *Biopolitics; The Bio-Environment; Bio-Syllabus: A Model Global Bio-Education Promoted by the International University for the Bio-Environment.*

SIMULATION MODEL FOR OPEN-CHANNEL FLOW AND TRANSPORT

by

Raymond W. Schaffranek, Hydrologist, U.S. Geological Survey, Reston, VA

Abstract: A flow-simulation model, formulated using an extended form of the one-dimensional de Saint Venant equations of unsteady open-channel flow, has been augmented to include solution of the advection-dispersion transport equation. The weighted, four-point implicit, finite-difference approximation of the unsteady-flow equations permits solutions at large time steps. The model is fully capable of simulating unsteady flow throughout a network of open channels connected in a dendritic or looped pattern. The flow model accommodates dynamic tributary flows and controlled diversions as well as lateral inflows and overbank storage. A mixed Eulerian/Lagrangian approach is used to solve the one-dimensional advection-dispersion equation for coupled simulation of solute transport. The transport solution technique avoids numerical dispersion associated with conventional finite-difference methods for advection-dominated problems. The technique is free of Courant number restrictions and can be applied using large time steps consistent with the flow-model discretization. Coupled solution of the unsteady flow and transport equations circumvents interpolation errors inherent in de-coupled simulation approaches and enables concurrent treatment of longitudinal pressure differentials due to variable density gradients.

INTRODUCTION

A Lagrangian particle-tracking scheme, previously developed and incorporated in the branch-network dynamic flow model, BRANCH, (Schaffranek et al. 1981, Schaffranek 1987a) permits examination of the retention times of parcels of water in open-channel networks. This particle-tracking scheme was first demonstrated in application to the tidal Potomac River (Schaffranek 1987b). The model was used to investigate the flushing capacity and retention properties of the tidal-river system for purposes of analyzing factors contributing to the development of algal blooms and the fate of phytoplankton. Retention times were found to vary considerably in response to changes in freshwater inflows, tidal dynamics, and meteorological conditions. Use of the model made it possible to identify local flow patterns under various combinations of boundary conditions and to investigate the role of tidal trapping in the fate of phytoplankton. Retention times in the main Potomac River channel were found to vary from weeks to months for moderate to low inflows, but to be of only several days duration for high inflows produced by upstream storm events.

In the effort described herein, the Lagrangian particle-tracking scheme of the dynamic flow model has been extended to include full solution of the transport equation by incorporating treatment of the physical process of dispersion. This direct coupling of the unsteady-flow and transport solutions eliminates the errors of numerical dispersion inherently introduced in de-coupled approaches wherein flow velocities must be interpolated to comply with the grid-point requirements of the transport scheme. Moreover, a coupled flow/transport simulation approach is required in situations where the fluid density varies longitudinally—as typically encountered in tidal-influenced, sediment-laden, or thermally-varying riverine flows—necessitating treatment of pressure differentials in the unsteady-flow equations.

In this paper, the BRANCH model of the tidal Potomac River network (Schaffranek 1987b) is used to demonstrate the coupled flow/transport simulation capability of the generic model. A previous numerical simulation, based on tracking parcels of water representing a conservative, non-dispersive constituent (Schaffranek 1987b), is repeated and revised to illustrate the capabilities of the model in simulating the combined effects of advection and dispersion on solute transport. Numerical simulations, conducted at varied Peclet numbers, illustrate the stability of the method when advection is the dominant process and the controlled response of the method for representation of physical dispersion without the introduction of numerical artifacts.

UNSTEADY FLOW EQUATIONS

Unsteady flow in open channels is governed principally by dynamic equilibrium of momentum changes due to inertial and convective accelerations, differential pressure forces, and gravitational and shear-stress effects of the bed and friction slopes. A variety of differential-equation sets can be derived for depicting unsteady open-channel flow (Lai 1986). The equation set employed in this model uses flow discharge, Q , and water-surface elevation above a horizontal datum (stage), Z , as the pair of dependent variables and longitudinal distance along the channel, x , and time, t , as the two independent variables:

$$B \frac{\partial Z}{\partial t} + \frac{\partial Q}{\partial x} - q = 0, \quad (1)$$

$$\frac{\partial Q}{\partial t} + \frac{\partial}{\partial x} \left(\beta \frac{Q^2}{A} \right) + gA \frac{\partial Z}{\partial x} + gAS_f - qu' - \xi BV_w^2 \cos \alpha = 0. \quad (2)$$

In derivation of these equations, a local Cartesian coordinate system was used in which x , y , and z are the streamwise, transverse, and vertical axes, respectively, and the flow discharge is normal to the y - z plane in the positive x direction. Assumptions used in their formulation are that the water is of homogeneous density, the vertical pressure gradient is hydrostatic, and the channel bottom is rigid—or relatively stable and fixed with respect to time—with a mild uniform slope. (The longitudinal pressure gradient term is not included in the equation set for this analysis.) Other symbols in the above equations, B , q , β , A , g , S_f , u' , ξ , and V_w , represent the channel top width, lateral inflow per unit length of channel, the Boussinesq momentum-correction coefficient, the cross-sectional area, gravitational acceleration, the friction slope, the x -component of lateral-inflow velocity, the wind-stress coefficient, and the wind velocity (occurring at an angle α to the longitudinal axis of the channel), respectively. The momentum coefficient, β , defined as $\int u^2 dA / U^2 A$, in which u is the velocity of water flowing through some finite elemental area dA and U is the mean flow velocity in the cross-sectional area A , is used to adjust for any nonuniform velocity distribution in the channel cross section. A Manning formulation of the friction-slope term is used in which S_f takes the form $(\eta/\lambda)^2 Q |Q| / A^2 R^{4/3}$, wherein $\lambda = 1.0$ for metric or 1.486 for foot-pound units, R is hydraulic radius, and the symbol η is used in place of the Manning n to indicate that the coefficient is being used to represent frictional resistance under unsteady-flow conditions. The dimensionless wind-stress coefficient, ξ , is a function of the water-surface drag coefficient, C_d , the water density, ρ , and atmospheric density, ρ_a , expressed as $C_d(\rho_a/\rho)$.

Four-Point Implicit Solution: The BRANCH model (Schaffranek et al. 1981, Schaffranek 1987a) uses a four-point, implicit, finite-difference approximation of the unsteady-flow equations (1) and (2). In the four-point, Preissmann (1961) or box scheme, spatial derivatives are centered in space and weighted in time according to a weighting factor θ . The finite-difference approximation of the spatial derivatives can vary from box-centered ($\theta = 0.5$) to fully forward ($\theta = 1$), which is the range for which its stability has been proven. See, for example, Fread (1974) for stability analysis using a linear wave approximation with a linearized form of the friction-slope term, and Samuels and Skeels (1990) for Fourier stability analysis of the linearized numerical equations including the general form of the friction term. To avoid computational-mode oscillations, a practical lower limit for θ appears to be 0.6 (Schaffranek et al. 1981). Time derivatives are centered in space; geometric properties and functional quantities are centered in space and time weighted according to θ . After the flow equations are coupled recursively to eliminate internal nodes, the matrix of flow and boundary-condition equations is solved in iterative fashion by Gaussian elimination using maximum pivot strategy.

TRANSPORT SIMULATION COMPONENT

The model solves the one-dimensional, advection-dispersion, transport equation describing the concentration of a solute as a function of time and distance, i.e.,

$$\frac{\partial C}{\partial t} + U \frac{\partial C}{\partial x} - D_x \frac{\partial^2 C}{\partial x^2} = 0 \quad (3)$$

in which $C(x, t)$ is the cross-sectional average concentration of a solute at location x along the longitudinal axis of channel at time t , U is the mean cross-sectional flow velocity (Q/A), and D_x is the longitudinal dispersion coefficient. Solution of the transport equation is directly coupled to the unsteady-flow model.

Transport Solution: The unknown flow conditions $Q(x, t)$ and $A(x, t)$ are provided directly by solution of the unsteady-flow equations (1) and (2); however, the transport equation (3) is not solved entirely by a Eulerian finite-difference technique. Instead, a mixed Eulerian/Lagrangian approach is used in which the advection and dispersion processes are treated separately and distinctly. The more difficult advection process ($U \frac{\partial C}{\partial x}$) is resolved by tracking particles representing parcels of water in a Lagrangian reference frame, whereas the dispersion process ($D_x \frac{\partial^2 C}{\partial x^2}$) is solved in a Eulerian framework by a finite-difference technique. A cubic spline is employed to interpolate the concentration profile of advected particles. An explicit, space-centered finite-difference scheme is used to represent the dispersion process. This solution approach avoids the well-known difficulties associated with numerical dispersion in advection-dominated systems introduced by pure Eulerian finite-difference solution methods. (See, for example, Gray and Pinder (1976).)

The cubic spline interpolant for the concentration profile is based on the method developed by Akima (1978). This spline interpolation technique has the desirable feature of minimizing the development of oscillations manifested as over- and under-shoot in the interpolated function. The Akima spline attempts to preserve the shape of the concentration profile as reflected by the data. The behavior of the Akima spline method is compared with a natural cubic spline

(de Boor 1978) interpolation of the same function, potentially representative of a temporal or spatial constituent concentration profile, in Fig. 1. Endpoint conditions are automatically determined by the Akima method, whereas values of zero are specified for second derivatives at the endpoints for the natural spline. The extraneous inflection points of the natural cubic spline (Fig. 1a), yielding over- and under-shoot in the interpolated function, are clearly illustrated in contrast to the smoother interpolant produced by the Akima spline method (Fig. 1b). Moreover, the Akima spline reduces the potential for the generation of negative concentrations as is evidenced in the interpolation produced by the natural spline (Fig. 1a). These attributes of the Akima spline interpolation method contribute to improved conservation properties for the transport-solution technique.

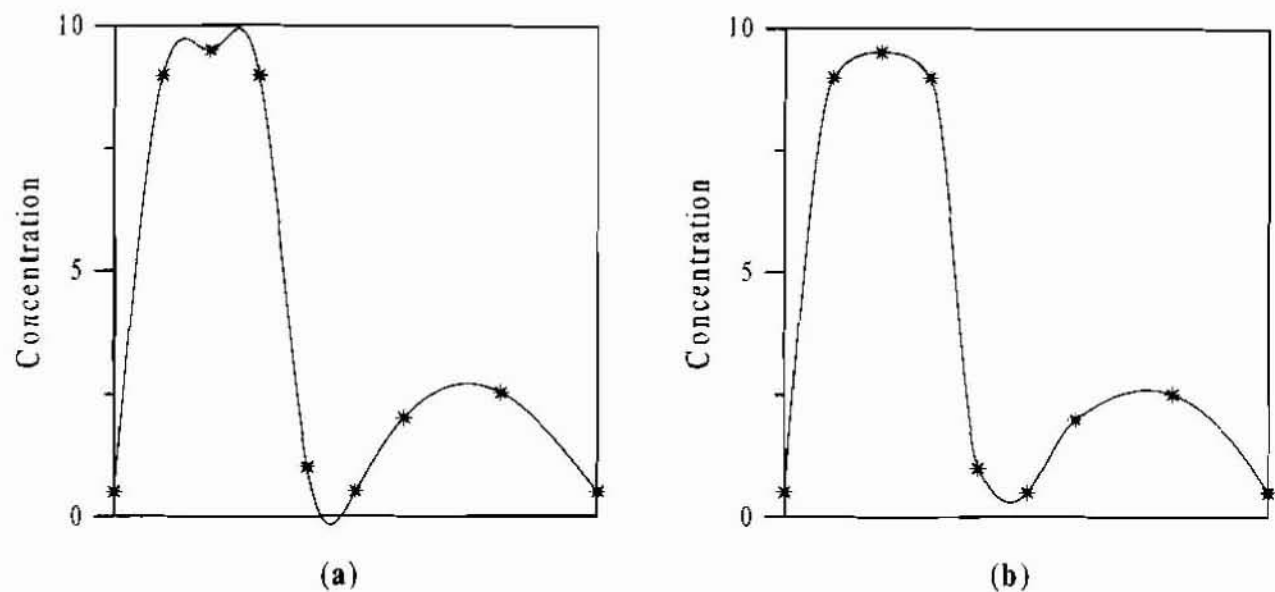


FIG. 1. Natural (a) and Akima (b) spline interpolants of hypothetical concentration profile.

THE TIDAL POTOMAC RIVER

The tidal-river segment of the Potomac River extends downstream from the head-of-tide, near Chain Bridge in the northwest quadrant of the District of Columbia, to Indian Head, Maryland, a distance of nearly 50 km. The cross-sectional area of the tidal river expands more than fortyfold between Chain Bridge and Indian Head, increasing from 232 to 9,960 m². The corresponding width increases from 44 to 1,950 m. Although the channel bottom is somewhat irregular depths, in general, range from about 9 m at Chain Bridge to 12 m at Indian Head. Several tributaries and tidal inlets, in which depths are typically 3 m or less, adjoin the main channel to form the tidal-river network.

Model Implementation: The model of the tidal Potomac River system was originally developed (Schaffranek 1987b) in order to study the flow dynamics of the network of channels. The model implementation consists of 25 branches joining or terminating at 25 nodes. A total of 66 cross sections, at intervals ranging from 0.7 to 4.8 km, are used to depict the irregular geometry of the tidal river and its tributaries and tidal inlets.

Boundary conditions used to conduct numerical simulations include zero discharges at the ends of tributaries and inlets, tide elevations recorded at Indian Head, and freshwater inflows derived from a rated gaging station near the head-of-tide. Freshwater inflows at the head-of-tide average $323 \text{ m}^3/\text{s}$, but have ranged from 3 to $13,700 \text{ m}^3/\text{s}$. Tidal amplitude at Indian Head is about 55 cm, but wind effects can significantly dampen tidal propagation. Wind speed and direction data collected at Indian Head are used to evaluate wind-forcing effects. Flow simulations are conducted using a 15-minute time step, which yields a Courant number $C_r \approx 6$. The model was calibrated and verified using five sets of tidal-cycle flow discharges measured at three different locations within the tidal-river system. Measured and model-computed flood and ebb flow volumes agree within 10 percent (Schaffranek 1987b).

Numerical Simulation Results: Flow data from the Potomac River, for the 30-day period beginning August 15 and ending September 13, 1981, are used to demonstrate the coupled flow and transport simulation capabilities of the model. These data are of particular interest due to the extremely low freshwater inflows that prevailed during the period. Inflows were less than the 5-year (1979-1983) average and less than $100 \text{ m}^3/\text{s}$, except for the last six days of the period. Ebb and flood tidal cycle discharges at Indian Head, as computed by the flow model, ranged from approximately $4,400$ to $4,700 \text{ m}^3/\text{s}$.

Particle Tracking: The transport of a conservative-type substance by advective processes alone is illustrated by the simulation results presented in Fig. 2. These results were obtained by tracking index particles representing parcels of water. In the simulation, nine index particles—potentially representing the location of a conservative, neutrally buoyant, passive solute or suspended particulate matter—were tracked through the main channel of the tidal river. The paths of travel of these particles are shown in the central graph of the figure. The vertical axis of the time-of-travel graph represents the main tidal Potomac River channel between Chain Bridge and Indian Head. The upper hydrograph in the figure shows the freshwater inflow recorded near Chain Bridge and lower hydrograph presents the tidal water-surface elevations simultaneously recorded at Indian Head. Together these hydrographs constitute the instantaneous boundary conditions used to solve the unsteady-flow equations.

The simulation results plotted in Fig. 2 demonstrate the combined effects of freshwater inflows and tidal forcing on the displacement of index particles and give indications of the retention properties and flushing characteristics of the tidal-river system. Throughout the period, the movement of index particles is variously influenced by the predominately semi-diurnal tides at Indian Head as they cycle through spring-neap variations and changing freshwater inflows at the head-of-tide. Near the end of the period, increased freshwater inflows, declining tidal elevations, and a significant wind event act to produce a pronounced downstream particle displacement. As is evident from the particle tracks, there is a tendency throughout the period for all particles to move closer to one another as they are advected along the channel. This variability in particle displacement can be attributed to the dynamic flow conditions and, in particular, to the magnitude and resultant dominance of the net tidal influx into the system as compared with the magnitude of freshwater inflows. This tidal dominance yields extended periods of little or no net downstream, and occasionally upstream, displacement of particles, which contributes to a diminished flushing capacity.

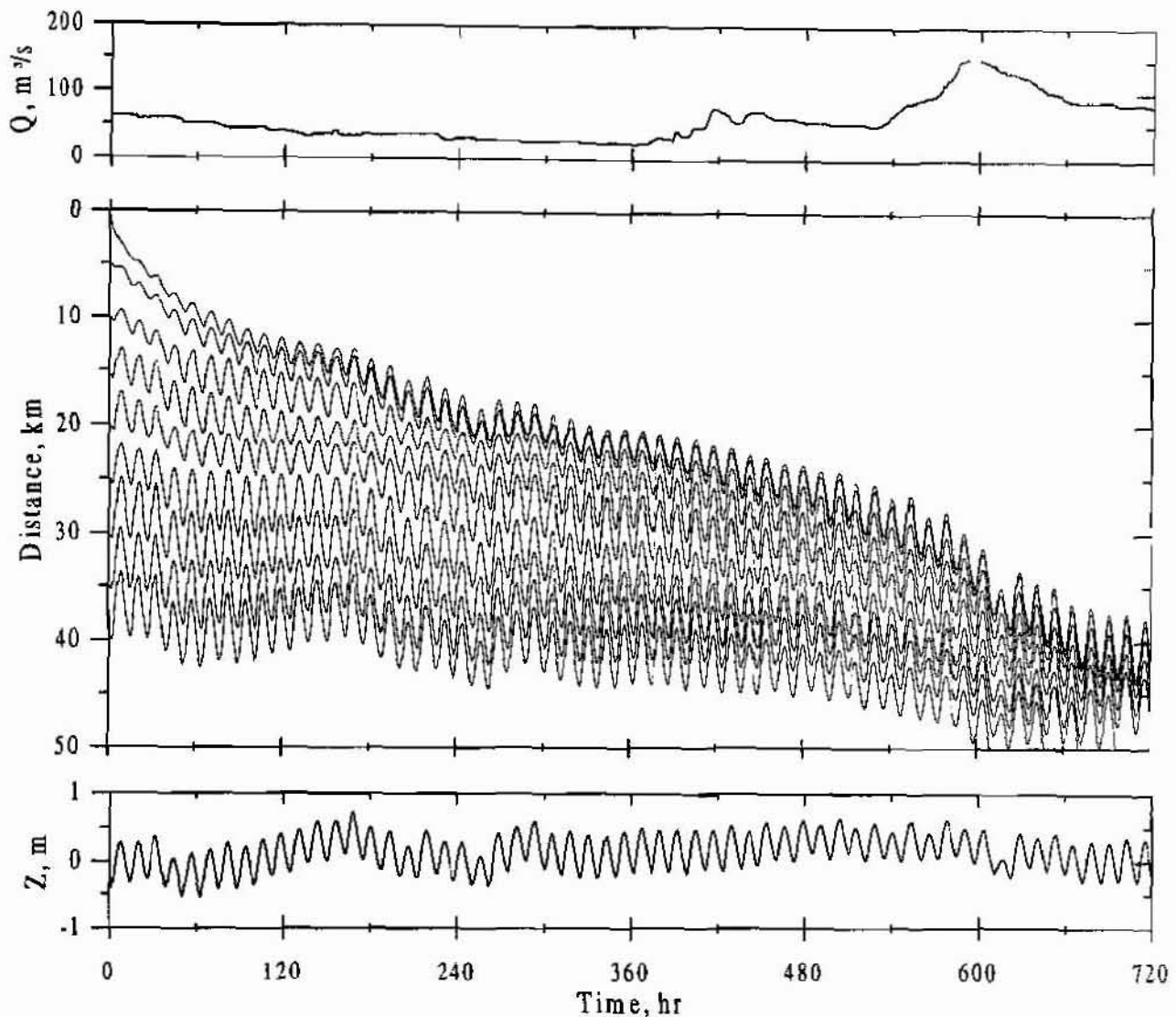


FIG. 2. Track of injected particles due to pure advection in the Potomac River for August 15 through September 13, 1981.

Constituent Transport: The transport of a conservative, non-reactive constituent along the tidal Potomac River, under the influences of both advection and longitudinal dispersion, is illustrated in Fig. 3. The results of four transport simulations are presented in Fig. 3b for the initial, hypothetical, constituent concentration profile presented in Fig. 3a. The transport simulation is for the same conditions as used to generate the particle-tracking results presented in Fig. 2. Distances on the horizontal axis of the figure are referenced to Chain Bridge. The four concentration profiles of a transported constituent, illustrated in Fig. 3b, present simulation results midway through the 30-day period at midnight on August 29. Values of 0, 1, 5, and 10 m^2/s were assigned to the dispersion coefficient, D_x . These coefficient values represent pure advection, $D_x = 0$, and mixed advection-dispersion conditions, $D_x = 1, 5, 10$, identified by Peclet numbers, $P_e = \frac{U\Delta x}{D_x}$, of 20, 4, and 2, respectively, for the mean flow velocity and 800 m grid-point spacing, Δx , of particles.

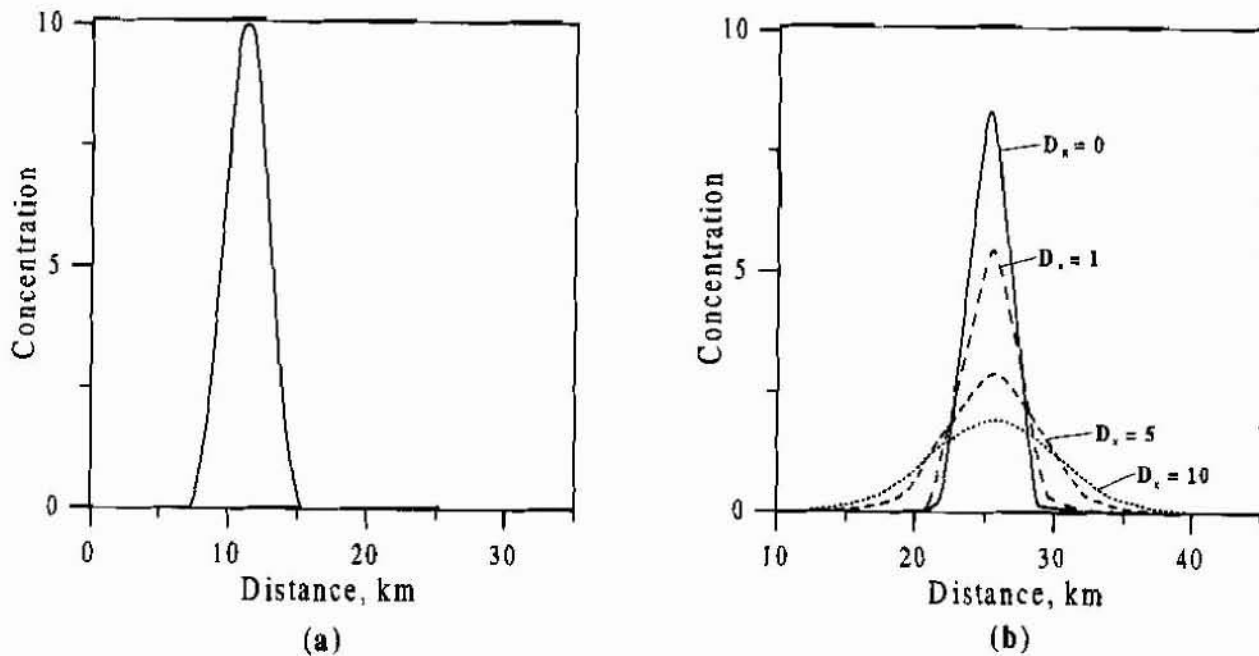


FIG. 3. Initial constituent concentration (a) and transported concentrations after 15 days (b) for varied longitudinal dispersion coefficients, $D_x = 0, 1, 5, 10$.

As Fig. 3 illustrates, the transport solution of the model yields stability in all four numerical simulations. In particular, no instabilities are visible and no numerical dispersion is evident in the simulation results in which pure advection is considered. The simulations, in which dispersive transport is also evaluated, i.e., $D_x = 1, 5, 10$ m²/s, illustrate that the attendant spreading of the concentration profiles can contribute to a lengthening of the retention time for a constituent within the system. Thus, the compression of the concentration profile as demonstrated in the pure advection results of the particle-tracking simulation will be diminished, and potentially overwhelmed, by the process of physical dispersion with resultant consequences on the evaluation of transport of a constituent through the system. By full consideration of advection and dispersion transport processes such as this, a more comprehensive analysis of the flushing capacity and retention properties of the tidal-river network can be conducted. This will lead to more definitive evaluations of the fate and resultant effects of constituents, potentially introduced or naturally occurring, within the system.

SUMMARY AND CONCLUSIONS

The branch-network dynamic flow model, BRANCH, has been extended to include coupled solution of the advection-dispersion equation for simulating solute transport within an open-channel system. The mixed Eulerian/Lagrangian, transport simulation approach yields stable solutions that are free of numerical dispersion introduced in pure Eulerian methods. Simulations, using the previously calibrated model as implemented for the tidal Potomac River, demonstrate the capabilities of the flow/transport model in evaluating constituent transport in a network of open channels. This transport simulation capability can be used to investigate the fate of constituents, such as pollutants or contaminants, potentially

introduced into an open-channel network. Coupled solution of the unsteady-flow and solute-transport equations permits evaluation and consideration of density effects on the flow and eliminates interpolation errors inherent in de-coupled flow/transport simulation approaches. The simulation model also can be used to investigate the retention time and flushing properties of coastal network systems composed of interconnected channels that are variously influenced by freshwater inflows, tidal forces, and the stochastic effects of weather fronts.

REFERENCES

- Akima, H. (1978). "A method of bivariate interpolation and smooth surface fitting for irregularly distributed data points." *ACM Transactions on Mathematical Software*, 4, 148-159.
- de Boor, C. (1978) *A practical Guide to Splines*, Springer-Verlag, New York, N.Y., 392 p.
- Fread, D.L. (1974). "Numerical properties of implicit four-point finite difference equations of unsteady flow." *Technical Memorandum NWS HYDRO-18*, U. S. National Oceanic and Atmospheric Admin., Silver Spring, Md., 38 p.
- Gray, W.G., and Pinder, G.F. (1976). "An analysis of the numerical solution of the transport equation." *Water Resources Research*, 12(3), 547-555.
- Lai, C. (1986). "Numerical modeling of unsteady open-channel flow." *Advances in Hydroscience*, V.T. Chow and B.C. Yen, eds., Vol. 14, Academic Press, Orlando, Fla., 163-333.
- Preissmann, A. (1961). "Propagation of translatory waves in channels and rivers." (in French), *Proc., First Congress of French Association for Computation (AFCAL)*, Grenoble, France, 433-442.
- Samuels, P.G., and Skeels, C.P. (1990). "Stability limits for Preissmann's scheme." *ASCE Journal of Hydraulic Engineering*, 116(8), 997-1012.
- Schaffranek, R.W. (1987a). "Flow model for open-channel reach or network." *Professional Paper 1384*, U.S. Geological Survey, Denver, Colo., 11 p.
- Schaffranek, R.W. (1987b). "A flow-simulation model of the tidal Potomac River." *Water-Supply Paper 2234-D*, U.S. Geological Survey, Denver, Colo., 41 p.
- Schaffranek, R.W., Baltzer, R.A., and Goldberg, D.E. (1981). "A model for simulation of flow in singular and interconnected channels." *Book 7, Chap. C3, Techniques of Water Resources Investigations*, U.S. Geological Survey, Denver, Colo., 110 p.

THE CHESAPEAKE BAY PROGRAM MODELS

G.W. Shenk*, L.C. Linker*, and A.S. Donigian**

*U.S. Environmental Protection Agency, Chesapeake Bay Program

410 Severn Ave., Annapolis, MD 21403

**Aqua Terra Consultants

2672 Bayshore Pkwy., Mountain View, CA 94043

ABSTRACT

The Chesapeake Bay Program (CBP) is a cooperative effort between state and local agencies to improve water quality in the Bay. One of the early findings is the expansion of anoxia in the Bay due to increasing eutrophication. In 1987 the goal of reducing by 40% nutrient loads to the Bay by the year 2000 was established. To track the achievement of this goal, and to examine ways to maintain a cap on nutrient loads beyond the year 2000, the Bay Program has developed linked models of the airshed, watershed, and estuary. The airshed model determines the percentage change in atmospheric loads to the watershed and estuary under different management strategies. The Chesapeake Bay Watershed Model is designed to simulate nutrient loads delivered to the estuary under different land- and air-based management scenarios. The Estuarine Model receives input from both models to determine the effects on water quality of varying nutrient inputs. Using the findings of earlier versions of these models, the Chesapeake Bay Program determined a nutrient cap that was feasible and would result in improved water quality in the Bay. The current airshed and watershed models are used to evaluate the effectiveness of various management practices in reaching the nutrient cap.

INTRODUCTION

The Chesapeake Bay is the largest estuary in the United States and one of the most productive in the world. The Bay has the highest watershed area per volume of water of any estuary in the United States. Shortly after the turn of the century, the Bay began a gradual decline in productivity. In the 1970s, the United States Congress directed the EPA to study the problem and develop solutions. The research phase completed in 1983 found that the decline in water quality was due to eutrophication brought on by excess nutrients entering the estuary from the watershed. In 1984 the Chesapeake Bay Program Office was established to coordinate the efforts of the individual states and federal agencies. In 1987, an agreement was signed with the intent of reducing "controllable" nutrients entering the Bay by 40% by the year 2000. In 1992 the Chesapeake Bay Program models were used to defined the controllable portion and established specific reduction goals.

The Chesapeake Bay watershed drains the waters (and nutrient loads) of six mid-Atlantic States from New York to Virginia plus the District of Columbia. The states of Pennsylvania, Maryland, and Virginia, the District of Columbia, and the Federal Government are partners in the Chesapeake Bay Agreement. The Agreement calls for a nutrient cap of 104.4 million kilograms of nitrogen (as N) and 7.00 million kilograms of phosphorus (as P) delivered to tidal waters during an average hydrology year. Average hydrology has been defined as the average of 1984 through 1987.

THE AIRSHED MODEL

The airshed model, known as the Regional Acid Deposition Model or RADM, is developed and applied by the National Exposure Research Laboratory in Research Triangle Park, NC. RADM is a three dimensional model which tracks nutrient emissions across the eastern United States. There are two RADM grids meeting various resolution needs. The large grid, covering the entire RADM domain contains 20,000 square cells of 6400 square kilometers each. Nested in the large grid, a fine grid of 60,000 cells, each covering 400 square kilometers, covers the mid-Atlantic region and Chesapeake Bay watershed. Vertically, the model domain is 15 cells high, reaching from ground level to the top of the free troposphere. The depth of the cells increases with altitude. A finding of the RADM model is that the Chesapeake Bay airshed, defined as the area accounting for 75% of the deposition in the watershed, is approximately 5.5 times the size of the watershed.

Airshed Model Scenarios: RADM is used for input data in scenarios associated with reductions in atmospheric deposition. The Reference Scenario (1985) deposition uses National Atmospheric Deposition Program observed data. All other scenarios of atmospheric deposition management use RADM derived reductions of the base load applied to each Watershed Model segment. RADM has supplied the Chesapeake Bay Program with reductions in wet and dry deposition for the Limit of Technology and Clean Air Act scenarios (see Table 1).

Table 1: Nitrogen Deposition under Varying Management Schemes

Scenario	Millions of Kg per Year
1985 Reference	204
Clean Air Act	178
Limit of Technology	128

Sources: Chesapeake Bay Program Phase IV watershed model and Regional Acid Deposition Model

THE WATERSHED MODEL

Code: The watershed model is an application of Hydrological Simulation Program - FORTRAN (HSPF). HSPF is a modular set of computer codes that simulates hydrology, nutrient, and sediment export from pervious and impervious land uses, and the transport of these loads in rivers and reservoirs. Versions of HSPF have been publicly available since 1980, and it is supported by the Environmental Protection Agency (ORD in Athens, Georgia). Applications of HSPF have included flood assessment, drainage design, nonpoint source nutrient evaluation, pesticide risk assessment, water resource planning, and water quality management. HSPF Release 11.1 was used for this application.

Model Segmentation: The Chesapeake watershed was divided into 86 model segments, each with an average area of 190,000 hectares. Segmentation, based on three tiers of criteria, partitioned the basin into regions of similar characteristics. The first criterion was segmentation of similar geographic and topographic areas. These were further delineated in terms of soil type, soil moisture holding capacity, infiltration rates, and uniformity of slope. The second criterion involved finer segmentation based on spatial patterns of rainfall. These criteria ensured that bankful channel travel time of each segment was about 24-72 hours (Hartigan, 1983). The third criteria was used to further delineate segments based on ease of simulation or calibration. Model segments that contained a reservoir were

separated into portions draining directly to the reservoir and portions draining into an upstream or downstream free-flowing river. This allowed more accurate reservoir simulation. Model segments were also created to take advantage of observed data locations, such that a model segment outlet was as close as possible to a particular station.

Hydrology Simulation: Data from a total of 178 precipitation stations were obtained from NOAA for the states of New York, Pennsylvania, West Virginia, Maryland, Delaware, and Virginia. Of the 178 stations, 105 recorded data hourly and 73 recorded data daily. Eight calendar years, 1984 through 1991, were simulated. Daily station data were converted to hourly data based on the time series data collected from the nearby hourly station which had a daily total closest to the daily data. The average precipitation for each model segment was based on the spatial distribution of the precipitation by the Thiessen polygon method. At least six precipitation stations were used for each model segment. Meteorologic data were obtained from the records of seven primary NOAA stations: Binghamton, NY (300687), Williamsport, PA (369728), Harrisburg, PA (363699), Elkins, WV (462718), Dulles Airport, VA (448903), Roanoke, VA (447285), and Richmond, VA (447201).

Nonpoint Source Load Simulation: Nutrient loads from the following sources were simulated: Forest, pasture, conventional-tilled cropland (conventionally tilled, fall plowed, and/or spring plowed cropland), conservation-tilled cropland (tillage practices that result in a residue cover of at least 30% at the time of planting), cropland in hay, animal waste areas (an average representation of manure piles, feed lots, and loafing areas), atmospheric deposition to water surfaces, pervious urban land, and impervious urban land.

Nutrient export loads from pervious land uses were simulated taking full advantage of the latest capabilities of HSPF. Nutrient cycling was simulated in forest using recent research of forest dynamics (Hunsaker, 1994). Cropland was simulated using a yield-based nutrient uptake algorithm to facilitate the simulation of nutrient management applications.

Land Use Data: A consistent land use data base was compiled for the entire basin. The methodology used provided particularly detailed information on agricultural lands. Principal sources were the U.S. Census Bureau series, Census of Agriculture for 1982, 1987, and 1992 (Volume 1, Geographic Area Series) published for each state. Tillage information on a county level was obtained for the conventional and conservation cropland distribution (CTIC). State agricultural engineers provided fertilizer and manure application rates and timing, crop rotations, and the timing of field operations. Soil characteristics for nutrient interaction were obtained from the Soils-5 data base (USDA, 1984). The USGS Land Use and Land Cover System (USGS LU/LC, Level II) was used to differentiate the urban land into five urban subcategories based on density. Other sources used to generate the 1990 land use data base were Soil Interpretations Records (SCS-SOI-5 data file)(1984), *National Resources Inventory (NRI)*(1984), *Forest Statistics for New York*, (1980), *Forest Statistics for Pennsylvania*, (1980), *Forest Resources of West Virginia*, (1978), and *Virginia's Timber*, (1978).

The 1990 land use data base was forecasted to 2020 and hindcasted to 1985 using the data sources indicated above and a statistical procedure based on population change and county-wide agricultural information.

Information on land slope and soil fines was provided by the National Resources Inventory (NRI) data base. Information on hydrologic characteristics of soils, such as percolation and reserve capacity, was obtained primarily from the SCS Soil Interpretation Records. Delivery of sediment from each land use was calibrated to that of the data base. The model was adjusted so that the average of the annual sediment loads from 1984-91 approached that of the NRI edge of field data, with a sediment delivery factor of 0.15.

Atmospheric Deposition: Watershed model inputs of nutrient atmospheric deposition were developed from the National Atmospheric Deposition Program (NADP) data base (NADP, 1982-1987). Annual atmospheric loads of wet fall ammonia and nitrate were obtained directly from NADP. Atmospheric loads of dry fall inorganic nitrogen were found using a segment-specific percentage of wet fall inorganic nitrogen determined by an application of RADM. Atmospheric loads of inorganic phosphate, organic phosphate and organic nitrogen were obtained from two state-operated atmospheric stations in Maryland. Phosphorus and organic nitrogen atmospheric loads were simulated as a load to the areas of water only in the model.

Point Source Inputs: Data for the eight-year record were obtained preferentially from the National Pollution Discharge Elimination System (NPDES). If no state NPDES data were available, state and year-specific default data were calculated for each missing parameter based on wastewater treatment plant flow. Septic systems were also included as a type of point source input. Septic system data were compiled using census figures and methodology suggested in Maizel and Muehlbach (1995).

Surface Water Diversions: The U.S. Geological Survey provided water diversion information. Only consumptive water use was counted as a diversion.

Calibration and Verification: The period of 1984 through 1991 was used as the calibration time period. This calibration was continually reviewed by a sub-committee of the Chesapeake Bay Program that was organized to oversee the modeling work. This group consists of representatives from the Chesapeake Bay Program signatory states and other interested parties as well as a specially-designated Model Evaluation Group (MEG). The MEG contains recognized academic experts in the environmental modeling field. Verification was performed on the period 1992 through 1995, without adjustment of the earlier calibration. The agreement with the observed data 1992-1995 was compared with the agreement with the 1984-1991 data, with no significant decrease in accuracy.

Management Scenarios: All scenarios are run on the same hydrology so that only the effects of management actions are recorded. The hydrology chosen was 1984 through 1987 to allow comparison with earlier Chesapeake Bay Program modeling efforts. Several key scenarios were completed in order to develop the basic inventory of loads under specific management conditions. The following scenarios are completed and scenario operations are ongoing at the time of this writing.

Base Case Scenario: This scenario is the base case year 1985 loads to the Chesapeake Bay. It differs from the calibration in that land use is set to 1985 values and point source loads are repeated at the 1985 level for each year of hydrology.

1996 Progress Scenario: This scenario describes the reductions made in nitrogen and phosphorus by

the year 1996 due to management actions taken by the states. The sources of input are state and federal Best Management Practice (BMP) implementation data.

Tributary Strategy / Year 2000 Progress Scenario: This scenario tests the plans that the states have submitted toward making their nutrient reduction goals. This is the expected year 2000 load to the Bay assuming representative hydrology and implementation of the state plans.

Limit of Technology Scenarios: Defined as the absolute limits of technology (LOT). These scenarios set a minimum on the amount of nutrients entering the Chesapeake Bay given reasonable limits on possible implementation. These scenarios include LOT air deposition and LOT point source scenarios.

BMP Methodology: Best Management Practices (BMPs) were implemented differentially in the watershed model depending on their type. Some nutrient reduction strategies were simply a land use change, others involved reducing the nutrients applied to the land or water surface, while still others depended on physical structures that reduced the eventual soil and/or nutrient loss.

Reductions in nutrient applications can be simulated directly within HSPF. Nutrient Management is the practice of applying only the fertilizer necessary such that the total available nutrients, including those from manure, mineralization, and atmospheric deposition meet the agronomic rate of the crops grown in that segment. Reductions averaged 33% for nitrogen and 10% for phosphorus, with variation depending on the type of crop grown, and amount of manure generated within the segment. Atmospheric deposition is also simulated as an hourly addition of dry NO_3 and a concentration in rainwater of NO_3 and NH_4 . These can be reduced by an arbitrary amount or by a segment specific percentage as determined by the Airshed Model.

A second type of BMP is a percentage reduction based on the BMP and land use. These percentage reductions were applied in the simulation between the land use and their connection to the river simulation or Bay Water Quality Model. The percentage reductions for each type of BMP and land use are determined by a committee of Chesapeake Bay Program experts through literature values and best professional judgement. A procedure was developed for land uses that had more than one type of BMP applied that assumed that certain types of BMPs could not be applied to the same acre of land. For example, a wet detention pond and a dry detention pond cannot be applied to the same acre of urban land. A second procedure was developed for types of BMPs that can overlap. For example a wet detention pond can service the same acre that is also receiving an urban nutrient management BMP.

A BMP can also take the form of a change from one land use to another. These are simulated simply by moving acres from one land use to another. For example, the addition of forest buffers includes a land use change from cropland to forest.

NUTRIENT LOADS

Nitrogen: Sources of delivered watershed nitrogen loads can be divided into those derived from forested, agricultural, and urban areas, with a small loading coming from atmospheric deposition directly to water surfaces. Agriculture accounts for largest amount of loads with 48.1% of the total in the 1985 reference case (see Table 2). Urban loads accounted for 36.4% and forest contributed 14.3% with the rest (1.2%) coming from atmospheric deposition to water. Forest contribution was relatively low even though it makes up 58% of the Chesapeake Bay watershed. Included in agricultural figures are loads arising from manure, fertilizer, and atmospheric deposition to land. The urban category includes all industrial and municipal point sources and septic loads.

In scenarios describing the state of the watershed in 1996 and the projected state in the year 2000, urban and forest play more significant roles while the influence of agriculture decreases somewhat. Urban rises to 37.5% of the delivered nitrogen in 1996, projected to 39.8% in 2000. Forest increased to 16.1% and 16.7% in 1996 and 2000 respectively. Actual forest acreage, and therefore loads, were reduced in the latter scenarios, but the BMP implementation in the other land uses caused the increase in forest percentage.

In terms of nitrogen kilograms per hectare at the edge-of-stream, urban is the highest loader with an average of 52.6 kilograms per hectare in the 1985 reference scenario. This figure drops to 44.3 kilograms per hectare in 1996 and is projected to 38.2 in the year 2000 scenario.

This decline is due almost exclusively to improvements in point source loads, with septic loads remaining approximately unchanged and nonpoint source loading rate declining slightly. Improvements in agricultural practices have a similar effect on agricultural loads. In 1985 the average acre of agriculture exported 18.3 kilograms of nitrogen which is projected to decline to 13.4 by the year 2000. Forest loads are constant at 3.4 kilograms per hectare.

Table 2: Nitrogen Loadings

Source	Percent of loading to bay	Edge-of-stream kg/ha
1985 Reference		
Agriculture	48.1	18.3
Urban	36.4	52.6
Forest	14.3	3.4
Atmos Dep to Water	1.2	11.8
1996 Progress		
Agriculture	45.2	15.6
Urban	37.5	44.3
Forest	16.1	3.4
Atmos Dep to Water	1.3	11.8
2000 Projection		
Agriculture	42.2	13.4
Urban	39.8	38.2
Forest	16.7	3.4
Atmos Dep to Water	1.4	11.8

Source: Chesapeake Bay Program Watershed Model Phase IV

Table 3: Phosphorus Loadings

Source	Percent of loading to bay	Edge-of-stream kg/ha
1985 Reference		
Agriculture	50.0	1.45
Urban	45.4	5.08
Forest	3.9	0.06
Atmos Dep to Water	0.8	0.63
1996 Progress		
Agriculture	58.1	1.24
Urban	35.5	2.62
Forest	5.2	0.06
Atmos Dep to Water	1.1	0.63
2000 Projection		
Agriculture	55.8	1.09
Urban	38.0	2.48
Forest	5.0	0.06
Atmos Dep to Water	1.2	0.63

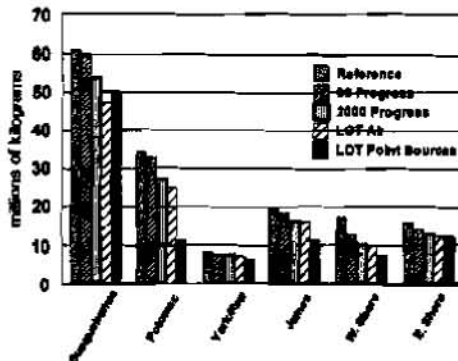
Source: Chesapeake Bay Program Watershed Model Phase IV

Phosphorus: Phosphorus loadings mirrored those of nitrogen (see Table 3) with agricultural loads being the largest source. With large reductions in point source phosphorus loadings, mostly due to a phosphate detergent ban, the contribution of urban to total loads decreased dramatically between 1985 and 1996. The increased controls on agricultural phosphorus in recent years combined with growth in urban areas has begun to reverse this trend, however. The phosphorus loading rates at the edge-of-stream show the large early gains in phosphorus, with a slowing in latter years. Reductions in agricultural phosphorus at the edge-of-stream are still continuing, with forests phosphorus remaining the same.

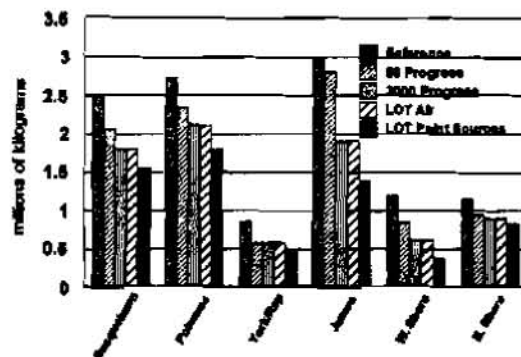
Comparison of Scenarios: Graphs below show the delivered loads of five scenarios for six major basins of the watershed. Large reductions have been made in phosphorus through 1996, but progress in nitrogen has been more modest. Nitrogen reductions are expected to increase through the year 2000 as the state agencies implement their plans. Further reductions in nitrogen are shown to be possible through limiting point sources or atmospheric deposition. Point source dominated basins such as the Potomac show the greatest potential for further reduction under the LOT point source run, while nonpoint source dominated systems, such as the Susquehanna, can achieve larger reductions through reductions in atmospheric deposition.

Nitrogen loads are correlated with flow. The Susquehanna, which supplies 50% of the fresh water

Total Nitrogen Loads Delivered to the Bay By Basin Under the 1985 Reference, 1996 Progress, 2000 Progress, LOT Air and LOT Point Source Scenarios



Total Phosphorus Loads Delivered to the Bay By Basin Under the 1985 Reference, 1996 Progress, 2000 Progress, LOT Air and LOT Point Source Scenarios



to the Bay, makes up the largest portion of the nitrogen loading. The Potomac and James rivers, respectively, make up the second and third largest flow and nitrogen inputs. Phosphorus is more likely to be bound on sediment and transported only during large flows, the loadings to the bay are driven more by the hydrology during the period studied. The Conowingo dam, near the mouth of the Susquehanna River, traps a large portion of the phosphorus which enters its reservoir.

Phosphorus reductions to point sources have been made to a large extent throughout the watershed but further gains will come with more difficulty.

More information can be found on the Chesapeake Bay Program modeling homepage at <http://www.chesapeakebay.net/bayprogram/committ/mdsc/model.htm>

CONCLUSION

The Chesapeake Bay Program Phase IV Watershed Model is a successful water quality simulation which quantifies the nonpoint source and point source nutrient loads from all basin sources. The model was essential in establishing a consistent method of accounting for the nutrient loads, among all sources, and among the basin jurisdictions of the Bay Program. The Chesapeake Bay Program has used the watershed model to examine the level of controls achievable from different management practices. The combination of the watershed model with the airshed and estuarine model provides a powerful tool to aid the Chesapeake Bay Program in meeting water quality objectives and do so in a cost-effective and equitable manner.

REFERENCES

- Donigian, Jr., A.S., and H.H. Davis (1978). *Users Manual for Agricultural Runoff Management (ARM) Model*. U.S. EPA Environmental Research Laboratory, Athens, GA.
- Donigian, Jr., A.S., B.R. Bicknell, L.C. Linker, J. Hannawald, C.H. Chang, and R. Reynolds (1990). *Watershed Model Application to Calculate Bay Nutrient Loads: Phase I Findings and Recommendations*. U.S. EPA Chesapeake Bay Program, Annapolis, MD.
- Donigian, Jr., A.S., B.R. Bicknell, L.C. Linker, C.H. Chang, and R. Reynolds (1991). *Watershed Model Application to Calculate Bay Nutrient Loads: Phase II Findings and Recommendations*, U.S. EPA Chesapeake Bay Program, Annapolis, MD. Conservation Technology Information Center (1985) 1985 Crop Tillage Data Base, West Lafayette, IN.
- Hartigan, J.P. (1983). *Chesapeake Bay Basin Model*. Final Report prepared by the Northern Virginia Planning District Commission for the U.S. EPA Chesapeake Bay Program, Annapolis, MD.
- Hunsaker, C.T., C.T. Garten, and Patrick J. Mulholland, (1994) Nitrogen Outputs from Forested Watersheds in the Chesapeake Bay Drainage Basin, EPA Oak Ridge National Laboratory, Oak Ridge, TN. Draft
- Johnson, R.C., J.C. Imhoff, J.L. Kittle, Jr. and A.S. Donigian, Jr. (1993). *Hydrologic Simulation Program - Fortran (HSPF): User's Manual for Release 11.0*. U.S. EPA Environmental Research Laboratory, Athens, GA.
- Maizel, M.S., A.G. Muehlbach, et al. (1995). "The Potential for Nutrient Loadings from Septic Systems to Ground and Surface Water Resources and the Chesapeake Bay." Report to Chesapeake Bay Program Office, Annapolis, MD.
- National Atmospheric Deposition Program (1982); (1983); (1984); (1985); (1986); 1997). (IR7)/National Trends Network. NADP/NTN Coordination Office, Natural Resource Ecology Laboratory, Colorado State University, Fort Collins, CO.
- U.S. Bureau of Census (1984). 1982 Census of Agriculture, Volume 1, Geographic Area Series, U.S. Department of Commerce, Washington, DC.
- U.S. Department of Agriculture (1984). Soil Interpretations Records (SCS-SOI-5 data file) and the National Resources Inventory (NRI), Soil Conservation Service, Washington, DC.
- U.S. Geological Service (1974) Geographic Information Retrieval and Analysis System (GIRAS) 1:125,000 land use/land cover (Anderson Level II classification). Washington, DC.

HYDROLOGIC MODELING APPROACHES FOR INTEGRATED MANAGEMENT OF STREAM SYSTEMS

Charles W. Slaughter
Northwest Watershed Research Center
USDA Agricultural Research Service
Boise, Idaho 83712
cslaugh@nwrc.ars.pn.usbr.gov

Peter Goodwin
Department of Civil Engineering
University of Idaho
Boise, Idaho 83712
pgoodwin@uidaho.edu

ABSTRACT

Serious recent flooding in the United States and Europe suggests a need for the re-evaluation of river management practices and in particular, attention has focussed on the interaction between rivers and their floodplains. These flood events have occurred during a period of increasing pressures on managers of river systems to meet new water quality standards (for example, TMDLs), fisheries enhancement, aesthetic and recreational needs as well as the more traditional objectives of flood 'control', power generation, navigation and water supply. In order to balance these diverse needs and uses, a comprehensive analysis approach is required which establishes the linkages between management actions and the watershed – or integrated watershed management. Implementation of integrated watershed management requires an understanding of the complex interactions between land use, water quality, flooding, sediment transport, geomorphology, ecology, economics and social issues. Application of an integrated hydrologic modeling approach to settings as diverse as second-order semi-arid rangeland watersheds and sixth order coastal river reaches is demonstrated. The connectivity of different river systems between different reaches, and the role of floodplains even in lower-order systems, are critical components of watershed processes influencing flood propagation, ecological characteristics and water quality buffering.

INTRODUCTION

Public awareness of the role of rivers in regional ecological systems, and concern for preserving, enhancing and restoring riparian corridors, is increasing. This concern is felt in both major river systems like the Columbia River and its tributaries, and in small headwater streams of western forests and rangelands. At the same time there are increasing pressures on all sectors of river systems, from headwater snowfields to tidal estuaries, to satisfy multiple objectives, e.g. flood control, power generation, recreation, navigation, fisheries, domestic and industrial water supplies, wildlife habitat and irrigation. One consequence of these coinciding pressures and needs has been a re-examination of traditional hydrologic and hydraulic approaches in river management (e.g., Hynes, 1975; Dunn: and Leopold, 1978; Havno and Goodwin; 1995).

Major floods in the US and Europe during the past five years have allowed an assessment of river management strategies and prior river restoration projects. Particular attention has focused on the interaction between the river and its floodplain for flood hazard reduction, water quality, sediment distribution, and the overall functioning of the riparian ecosystem. Examples include the restoration of floodplains along the River Rhine (Dister et al., 1990), consideration of floodplain restoration along the Mississippi River (Interagency Floodplain Management Review Committee, 1994), the 'Living River Strategy' (Napa River Community Coalition, 1996) and the Willamette River floodplain restoration strategy (Philip Williams and Associates, Ltd., 1996). These projects are attempting to provide a reduction in flood hazards through ecological restoration. There is extensive recent literature describing these new management strategies (for example, Friends of the River, 1997) and a range of new analysis techniques are emerging.

Management actions in flood control and structural flow regulation have more commonly focused on larger, downstream river reaches. Natural resource managers are increasingly concerned with relatively small, low-order stream systems and riparian environments located in the headwaters of river basins (e.g., Myers and Swanson, 1997). This paper describes initial efforts to apply a hydrologic modeling approach which was initially developed for large rivers to a low-order rangeland stream, and contrasts some of the physical processes in the two different types of systems.

REYNOLDS CREEK EXPERIMENTAL WATERSHED, IDAHO

Reynolds Creek Experimental Watershed (RCEW) was established in 1960 as a field laboratory to address issues of water supply, water quality, and rangeland hydrology in the semiarid rangelands of the interior Pacific Northwest (Robins et al. 1965). The 234 km² watershed (Figure 1) is located in the Owyhee Mountains of southwestern Idaho. Reynolds Creek is a third-order perennial stream that drains north to the Snake River. The basin ranges in elevation from 1100 m (at the lowest gauged point) to 2250 m. Precipitation varies from about 23 cm at the northern lower elevations, to over 100 cm in the higher regions at the southern and southwestern watershed boundaries. At these upper elevations about 75 percent of annual precipitation occurs as snowfall. About 77% of the watershed is federal or state lands, with the remainder under private ownership. The primary land use is livestock grazing, with some irrigated fields along the creek at the lower elevations and limited timber harvest in high-elevation forests. The Reynolds Creek basin and surrounding public lands are increasingly utilized for summer and winter outdoor recreation by the growing population of the nearby Boise metropolitan area.

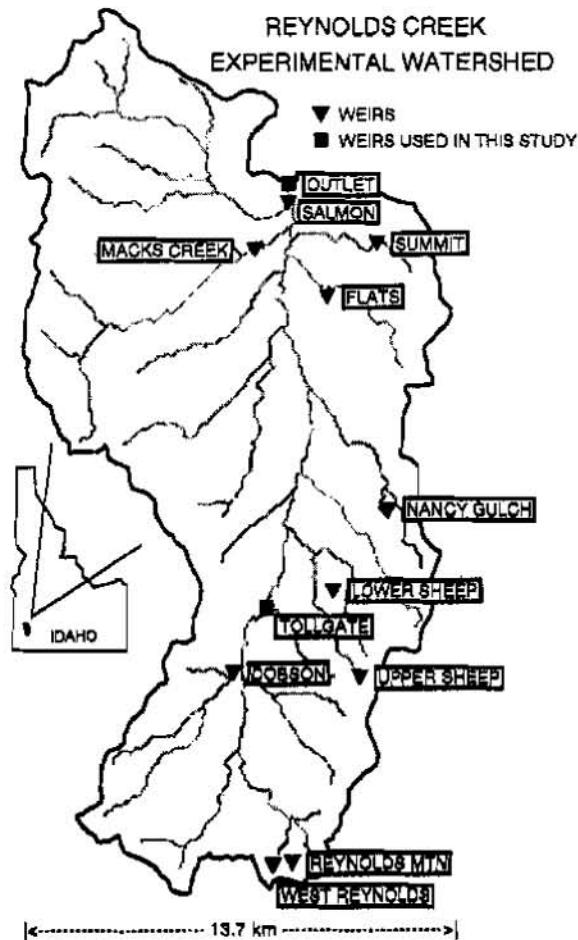


Figure 1: Location Map of Reynolds Creek

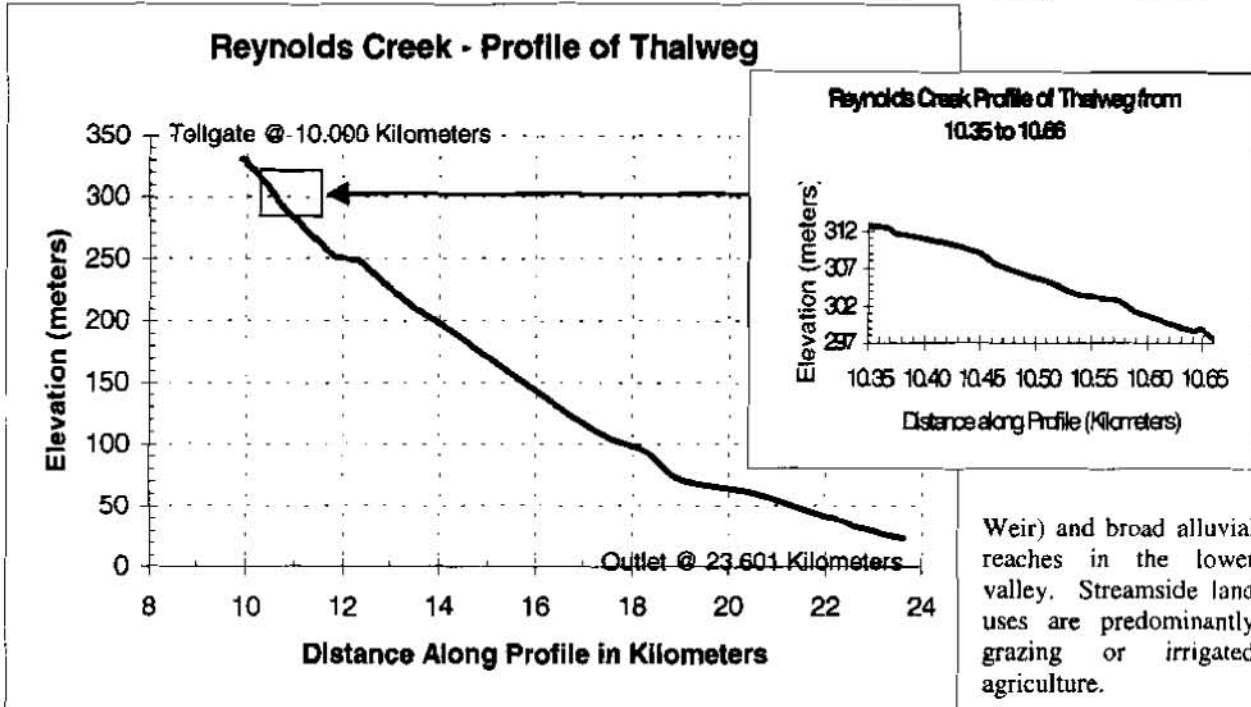
RCEW lies in an eroded structural basin, with late Tertiary volcanic and sedimentary rocks overlying Cretaceous granitic basement rocks. Soils range from shallow desertic soils at lower elevations to relatively deep organic soils in higher regions, the latter typically occupied by forest species. The primary vegetation cover types in RCEW are Wyoming big sagebrush (*Artemisia tridentata* subsp. *wyomingensis*); mountain big sagebrush (*Artemisia tridentata* subsp. *vesyana*); low sagebrush (*Artemisia arbuscula*); curleaf mountain mahogany (*Cercocarpus ledifolius*); bitterbrush (*Purshia tridentata*); quaking aspen (*Populus tremuloides*) woodland; bluebunch wheatgrass (*Pseudoroegneria spicata*)/Sandberg bluegrass (*Poa sandbergii*); Idaho fescue (*Festuca idahoensis*); bluebunch wheatgrass; salt desert shrub; alpine rangeland; subalpine fir (*Abies lasiocarpa*); Douglas fir (*Pseudotsuga menziesii*); and riparian communities (Stephenson 1977).

Extensive hydrologic data have been collected at RCEW since the early 1960's. There has been strong research emphasis on climate (Hanson 1989), seasonal snowpack accumulation and hydrologic regime (Wilcox et al., 1989), seasonally

frozen soils (Hanson and Flerchinger 1990; Seyfried et al. 1990), and on rangeland hydrology, soil erosion, and stream sediment processes (Blackburn et al. 1990; Pierson et al. 1994; Slaughter et al. 1996). Detailed meteorological measurements are collected at three sites on the watershed, representing low, middle, and high elevation areas. Continuous precipitation data are collected at 16 sites in the basin; streamflow is presently monitored at seven locations. Continuous records of historical streamflow and suspended sediment data are available from 1963 (Outlet Weir) and 1966 (Tollgate Weir) to present.

Physical Characteristics of the Site

The main channel of Reynolds Creek was chosen to test rangeland application of selected hydraulic and hydrologic models. The chosen sector is between Tollgate Weir (elevation 1412 m), above which the contributing drainage area is 5444 ha, and Outlet Weir (elevation 1108 m) which monitors streamflow from the entire RCEW (Figure 2). This stream sector includes both confined reaches with bedrock control (e.g. immediately downstream from Tollgate



A topographic survey control network was established for the study sector, providing a precise basis for linking subsequent channel geometry measurements. All control points were permanently monumented with concrete posts to facilitate a long-term monitoring program. Channel cross-sectional profiles were surveyed in selected reaches of this study sector. Each cross-section was tied directly to the control network, and left bank and right bank end points were marked on the ground with steel stakes for future re-location. Each measured channel cross-section extended across the immediate channel and sufficiently up-slope on either side define the flood channel and immediate floodplain geometry. Left edge of water and right edge of water at time of survey, and points of marked slope change, were specifically identified at each cross-section. Concurrent with cross-section surveying, the stream thalweg was surveyed. Digital photography was utilized to document current conditions at all 64 cross-sections surveyed in this phase.

INSTREAM HYDRAULIC CHARACTERISTICS

The model used to assess flood risk and mass transport may have a significant influence on the comparison of different management approaches. Some of the physical processes simulated by the models are well understood such as the attenuation of a floodwave in a one-dimensional system (e.g., Cunge et al., 1980) and the variation of roughness coefficients with stage (van Rijn, 1993). However, most of the research and model development has focussed on one-dimensional models and floodplains are treated as offstream storages or are incorporated into the conveyance of the main channel. The conveyance of the entire channel can be estimated as a single section with weighted hydraulic characteristics or by the 'method of slices'. In the method of offstream storage, there is no dynamic connection between the floodplain and river, and only the conservation of mass component of the St. Venant equations is considered (Cunge et al., 1980). In the method of slices, the channel cross-section is divided into regions of similar roughness, velocity and depth. The total channel flow is estimated by summing the regions or slices (Ackers, 1993). Recent findings from the Science and Engineering Research Council Flood Control Facility (FCF) at HR Wallingford, U.K. (Ackers, 1993; Greenhill and Sellin, 1993; Willetts and Hardwick, 1993) have

shown that errors using these methods can be significant. For example, predictions of discharge can be in error by as much as the bankfull discharge in the main channel (or up to 35% of the total discharge) under extreme circumstances.

Most research on the importance of floodplain function has concentrated on the lower reaches of large river systems. For example, the importance of the floodplain to travel time of floodwaves is shown in Figure 3a for the mainstem of the Willamette River, northwestern Oregon. The variation of the travel time is caused primarily by the flow going overbank and inundating the floodplain, and by variation of roughness with river stage. Questions being addressed in the present study include the role of floodplains in low-order tributaries and the influence of floodplain interaction on sediment transport. The bed slope of Reynolds Creek (in RCEW) is relatively steep and the ratio of the width of the floodplain to the bankfull channel width is much smaller than in higher-order reaches further downstream. The variation of travel time with peak flow rate for selected flood events in RCEW in which tributary inflows did not exhibit a major influence on the measured travel time is shown in Figure 3b. This preliminary analysis indicates that the variation in travel time could be significant in large as well as small scale river systems.

Typical spatial resolution of a one-dimensional model (i.e. spacing between cross-sections) might be 100m-1000m. At this resolution the modeled flow in the channel is supercritical, unless a very large lumped roughness coefficient is used. The travel time of floodwaves and channel depths can be adjusted through this lumped roughness coefficients which account for bedform roughness, particle size roughness, channel form roughness and vegetation roughness. The interactions between flow characteristics, channel morphology and sediment transport characteristics are less well understood in steeper channels in headwaters of watersheds than in sand bed low slope rivers.

Many researchers (e.g., Grant, 1997) have shown from observations of conditions in natural rivers that supercritical flows rarely exist except in local regions. Preliminary analysis of Reynolds Creek data confirms these observations, since the roughness coefficient (in this analysis, the Mannings n) to simulate subcritical flow conditions ranges from 0.05 to 0.1.

The problem of using a single lumped roughness coefficient to simulate the lumped effects of all roughness components is that it is difficult to replicate a wide range of hydrologic conditions. This gives a manager little confidence of the predictive capability of the model at any flow condition other than that used to estimate the global coefficient. A more detailed survey (Figure 2) shows that the actual bed slope is about 50% less than implied by the coarse survey; low-gradient reaches are punctuated by abrupt drops with local regions of supercritical flows. This more detailed representation shows that the roughness coefficient varies between 0.034 and 0.06 to create subcritical flows.

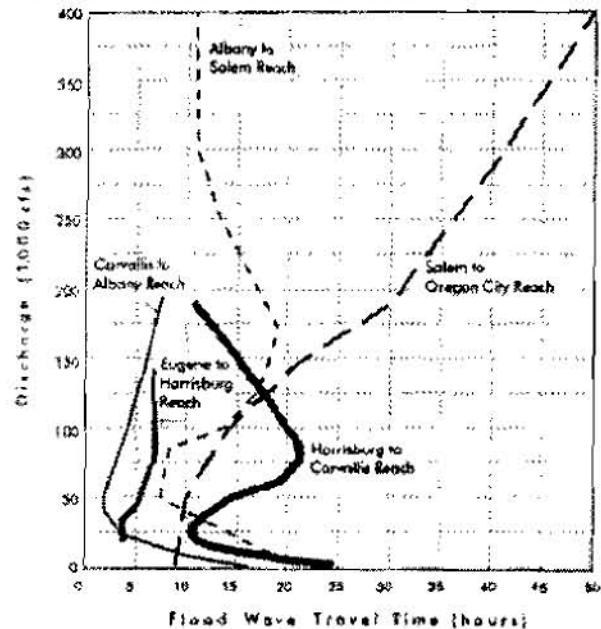


Figure 3a: Willamette River
Source: Philip Willaims & Associates

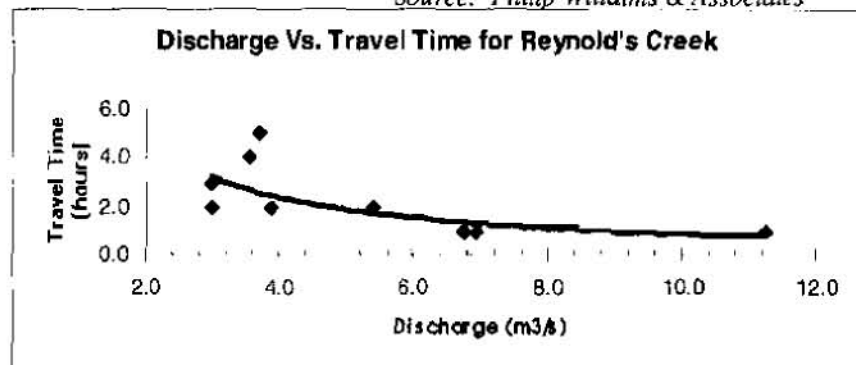


Figure 3b: Reynolds Creek

A third problem associated with the direct application of a conventional model is related to sediment transport. Using the lumped roughness coefficient to match hydrologic characteristics of the floodwave propagation and conventional sediment transport closure relations, such as a simple regression equation of sediment transport observations or other formulations (van Rijn, 1993) results in over-estimation of sediment transport at low flows. As an illustration, an estimate of the dominant discharge (or channel forming flow) for Reynolds Creek using the methodology of Wolman and Miller (1964), or Leopold et al. (1964) is shown in Figure 4. This shows that the estimate of the dominant discharge (or channel forming flow) derived using a sediment transport function using the lumped approximation of roughness is approximately $1.8 \text{ m}^3/\text{s}$. This calculation also assumes that sediment transport is not supply-limited. Preliminary results of a more detailed hydraulic simulation which considers sediment transport in each local reach and accounts for channel micro-topography alters the estimate of the dominant discharge significantly (Figure 4). In this latter case the total sediment transported during the period of record is an order of magnitude less than the lumped estimate, and the channel-forming flow in the alluvial reaches of the channel is estimated at approximately $2.8 \text{ m}^3/\text{s}$.

Continuing Research

Subsequent phases of this study will extend the model to the upper headwaters reaches of RCEW, and will include sediment transport and water quality in the model simulations. The purpose will be to understand how sediment and pollutant constituents are transported through these low-order streams and to develop a better understanding of the variability in boundary conditions used in models of the higher-order streams further downstream. The results will also help quantify the benefits and role of small tributary watersheds in downstream receiving waters.

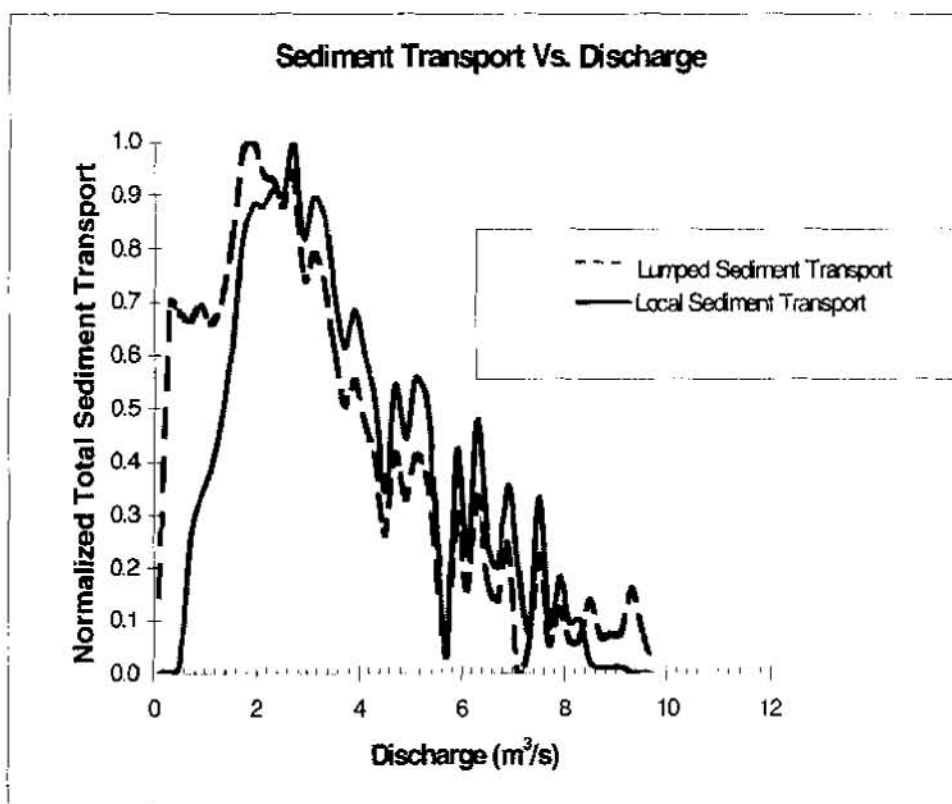


Figure 4: Dominant Discharge for Reynolds Creek Study Run

CONCLUSIONS

With an increasing emphasis on watershed analysis, it is often necessary to extend conventional unsteady mass transport and hydraulic computer models further into the upper reaches of watersheds either to understand local conditions or to understand the consequences of management strategies to downstream reaches. These more holistic approaches incorporate ecology, geomorphology, water quality, and land-use issues. The purpose of this study has been to illustrate that a coarse representation of the physical processes may lead to highly inaccurate predictions of the timing of tributary hydrographs and sediment transport delivery to downstream reaches. This may be important when assessing the impacts of different landuse practices in headwater regions of watersheds.

ACKNOWLEDGEMENTS

The authors wish to acknowledge the assistance of Dr. Leon Huber and Ron Hartzmann (ARS-NWRC), Rick Marbury (University of Idaho), and NWRC student interns Patty Rodriguez (Boise State University) and Jason Buttles (Northwest Nazarene College) in field survey, data processing and analysis.

REFERENCES

- Ackers, P., 1993, Stage-discharge functions for two stage channels: the impact of new research. *Journal IWEM* 7: 52-61.
- Blackburn, W.H., Pierson, F.B., and Seyfried, M.S., 1990, Spatial and temporal influence of soil frost on infiltration and erosion of sagebrush rangelands. *Water Resources Bulletin* 26:991-997.
- Cunge, J.A., Holly, F.M., and Verwey, A., 1980, *Practical Aspects of Computational River Hydraulics*. Monographs and Surveys in Water Resources Engineering, Vol. 3, Pitman. 240 p.
- Dister, E., Gomer, D., Obdrlik, P., Petermann, P., and Schneider, E., 1990, Water management and ecological perspectives of the Upper Rhine's floodplains. *Regulated Rivers: Research and Management* 5:1-15.
- Dunne, T., and Leopold, L.B., 1978, *Water in Environmental Planning*. W.H. Freeman, San Francisco. 818 p.
- Friends of the River, 1997. *Beyond flood control: flood management and river restoration*. Sacramento, Ca. 12p.
- Grant, G.E., 1997, Critical flow constraints flow hydraulics in mobile-bed streams: a new hypothesis. *Water Resources Research* 33(2):349-358.
- Greenhill, R.K., and Sellin, R.H.J., 1993, Development of a simple method to predict discharges in compound meandering channels. *Proc. Instn. Civ. Engrs. Wat. Marit, & Energy* 101:37-44.
- Hanson, C.L., 1989, Prediction of class A pan evaporation in southwest Idaho. *J. Irrigation and Drainage ASAE* 115:166-171.
- Hanson, C.L., and Flerchinger, G.N., 1990, Comparison of three methods for measuring depth of soil freezing. pp 257-262 *in* Frozen soil impacts on Agricultural, Range, and Forest Lands, Proc. of the International Symposium. CRREL Special Report 90-1. U.S. Army Cold Regions Research and Engineering Laboratory, Hanover, New Hampshire.
- Hynes, H.B.N., 1975, The stream and its valley. *Verh. Int. Verein. Limnol.* 19:1-15.
- Havno, K., and Goodwin, P., 1995, Towards an integrated approach for hydrologic, geomorphic and ecologic understanding of river corridors. Discussion Paper in Seminar 2: Hydraulic Modeling of Ecological Criteria. XXVI IAHR Congress, London. pp 1-6.
- Interagency Floodplain Management Review Committee, 1994, *Sharing the Challenge: floodplain management into the 21st century - a blueprint for change*. Report prepared for the Administration Floodplain Management Task Force. US Government Printing Office.
- Leopold, L.B., Wolman, M., and Miller, J.P., 1964, *Fluvial Processes in Geomorphology*. W.H. Freeman and Co., San Francisco, Ca. 522 pp.
- Myers, T. J., and Swanson, S., 1997, Stochastic modeling of transect-to-transect properties of Great Basin rangeland streams. *Water Resources Research* 33(4):853-864.
- Napa River Community Coalition, 1996, *Flood Management Plan for the Napa River*, Napa. Napa Valley Economic Development Corporation and Napa County Department of Public Works, California. 8 pp + appendices.

Philip Williams and Associates, Ltd., 1996, An evaluation of flood management benefits through floodplain restoration on the Willamette River, Oregon. Report #1082, San Francisco. Report prepared for River Network. 60 pp.

Pierson, F.B., Blackburn, W.H., Van Vactor, S.S., and Wood, J.C., 1994, Partitioning small scale spatial variability of runoff and erosion on sagebrush rangeland. *Water Resources Bulletin* 30:1081-1089.

Robins, J.S., Kelly, L.L., and Hamon, W.R., 1965, Reynolds Creek in Southwest Idaho: An outdoor hydrologic laboratory. *Water Resources Research* 1:407-413.

Seyfried, M.S., Wilcox, B.P., and Cooley, K.R., 1990, Environmental conditions and processes associated with runoff from frozen soil at Reynolds Creek Watershed. pp 125-134 in *Frozen soil impacts on Agricultural, Range, and Forest Lands*. K.R. Cooley (ed.). CRREL Spec. Rep. 90-1. U.S. Army Cold Regions Research and Engineering Laboratory, Hanover, New Hampshire

Slaughter, C.W., Cooley, K.R., Hanson, C.L., Pierson, F.B., Hartzmann, R.L., Huber, A.L., and Awang, J.B., 1996, Baseline sediment yield from dissimilar headwaters research watersheds. pp X30-X37 in *Proceedings of the Sixth Federal Interagency Sedimentation Conference, Sedimentation Technologies for Management of Natural Resources in the 21st Century*. Las Vegas, Nevada.

Stephenson, G.R., 1977, Soil-geology-vegetation inventories for Reynolds Creek Watershed. Miscellaneous series No. 42. Agric Exp. Sta., University of Idaho, Moscow, Idaho. 73 pp + appendices.

U.S. Army Corp of Engineers, 1996, Risk-based analysis for flood damage reduction studies. Engineer Manual, EM 1110-2-1619.

van Rijn, L.C., 1993, Principles of sediment transport in rivers, estuaries and coastal seas. Aqua Publications, Amsterdam. PAGES?

Willets, B.B., and Hardwick, R.I., 1993, Stage dependency for overbank flow in meandering channels. *Proc. Instn. Civ. Engrs. Wat., Marit. & Energy*, 101: 45-54.

Wilcox, B.P., Cooley, K.R., and Hanson, C.L., 1989, Predicting snowmelt runoff on sagebrush rangeland using a calibrated SPUR hydrology model. *Trans. ASAE* 32:1351-1357.

Wolman M.G. and Miller, J.P., 1960, Magnitude and frequency of forces of geomorphic processes. *Journal of Geology* 68:54-74.

ECONOMIC AND ENVIRONMENTAL STRATEGIC PLANNING FOR THE WHOLE FARM AND RANCH: THE GPFARM DECISION SUPPORT SYSTEM

By James C. Ascough II, Hydraulic Engineer; Gregory S. McMaster, Agronomist; Marvin J. Shaffer, Soil Scientist; Jon D. Hanson, Rangeland Ecologist; and Lajpat R. Ahuja, Soil Scientist

USDA-ARS Great Plains Systems Research Unit, Fort Collins, Colorado, U.S.A.

Abstract: The increasingly recognized need for an integrated systems approach towards agricultural research and management in the Great Plains dates back at least a decade or more. Sustainable agriculture has become a complex problem that demands consideration of many interrelated factors, processes, and institutions. Across the Great Plains, agriculture is challenged primarily by the availability of water and nitrogen. Central to meeting this challenge, the Microsoft Windows™ 95-based Great Plains Framework for Agricultural Resource Management (GPFARM) decision support system (DSS) was developed. GPFARM provides crop and livestock management support at the whole farm and ranch level with emphasis on water, nutrient, and pesticide management. In addition, GPFARM has strong links to economic and environmental analysis, site database generation, and site-specific management from which alternative farm and ranch agricultural management strategies can be developed and tested.

INTRODUCTION

The USDA-ARS Great Plains Systems Research Unit, in a collaborative effort with Colorado State University and other ARS units, has developed the Great Plains Framework for Agricultural Resource Management (GPFARM) decision support system (DSS). GPFARM is capable of analyzing both medium- and long-term whole farm and ranch management plans, based on the predicted productivity of selected management options and associated environmental and economic risks. GPFARM provides an operational framework for a whole farm and ranch DSS, and implements an integrated systems approach concept to address the problems of agriculture in the Great Plains. Specific features of the GPFARM DSS include:

- 1) The overall goal of GPFARM is to determine long-term effects of Great Plains current farming and ranching practices on environmental and economic sustainability in terms that targeted users understand and are familiar with. GPFARM combines site-specific databases and environmental modeling with economic analysis to provide whole farm and ranch strategic planning. Specifically, management changes and impacts of fertilizer and pesticide applications (including amendments such as manure and sewage sludge); soil productivity; wind and water erosion; and cropping, tillage, and livestock systems are simulated.
- 2) GPFARM is targeted for use at the individual whole farm and ranch level by agricultural consultants, computer-oriented producers, Extension personnel, and the NRCS. It has been designed for hardware platforms that are available to the majority of potential users, i.e., IBM compatible personal computers (PCs). GPFARM runs in the Microsoft Windows 95™ operating environment and is being developed with Microsoft Visual C++ 5.0™.
- 3) GPFARM consists of a graphical user interface (GUI), site-specific Microsoft Access™ databases (currently populated for Eastern Colorado climatic conditions and cropping systems), and an object-oriented (OO) framework encapsulating science (simulation) modules. Other stand-alone modules in GPFARM include economic analysis, information system, and record-keeping modules. Much of the scientific technology used in GPFARM was derived from existing decision support systems or ARS water quality computer models, and has required modification or enhancement before inclusion in GPFARM. To develop suitable management plans, GPFARM allows analysis and comparison of multiple management scenarios to determine which one is the "best." These analyses may be performed on individual management units (e.g., areas of similar soils or crop management) or combinations of management units up through the whole farm and ranch hierarchy. The target run-time goal for any given whole farm and ranch analysis is 30 minutes or less on a Pentium 90 PC. Initial setup of GPFARM is more time consuming, possibly on the order of many hours depending on the complexity of the farm/ranch, number of cropping systems, number of management operations for each cropping system, etc.

- 4) On-line documentation and help systems enable users unfamiliar with GPFARM to initialize and run GPFARM and interpret the results. The level of detail is sufficient to identify initial conditions for critical model parameters and to assign them reasonable preliminary values.
- 5) GPFARM is currently being tested on ARS farm cooperator sites in Eastern Colorado. Both irrigated and non-irrigated conditions are being tested. General experimental cropping systems include rotations containing dryland corn, wheat, and millet crops (e.g., wheat-fallow and wheat-corn-fallow rotations), and irrigated corn. In addition, GPFARM is being tested on an integrated dryland cropping (wheat, millet, and corn crops) and livestock production operation. General delivery of GPFARM will not occur until the initial farm cooperator sites have been thoroughly tested and analyzed.

BACKGROUND

GPFARM is applicable to Great Plains areas east of the Rockies to the eastern borders of North Dakota, South Dakota, Nebraska, Kansas, and Oklahoma, and from the southern portion of Manitoba and Saskatchewan, Canada to Northern Texas. Sustainable agriculture in the Great Plains is a complex problem that demands consideration of many interrelated factors, processes, and institutions. Across the Plains, agriculture is limited by the availability of water and nitrogen. Using and supplementing these resources to enhance production without damaging the environment is a major challenge. Past management practices and Federal programs have created special environmental, managerial, economic, and political considerations that must be addressed. Producers must be able to adapt to fluctuations in weather and commodity prices, react to trends in Federal and State legislation, and respond to perceptions by the urban public. The ability to wisely modify farm and ranch management practices to take advantage of:

- the global economy;
- new cropping, pest management, and tillage systems; and
- new legislation

while protecting soil, air, and water resources will determine whether an agricultural enterprise system survives or perishes.

The need for a systems approach and networking of scientists for agricultural research and management in the Great Plains dates back at least 10-15 years. The need was emphasized at a regional symposium "Sustainable Agriculture for the Great Plains" (Hanson et al. 1991) held in 1989 in Fort Collins, Colorado. Prior to the conference, a report titled "Great Plains Agroecosystems Project" outlined the basic components and key institutions needed in a regional project that would tie together research and development efforts across the Plains. Central to these efforts, a need was identified to develop a computer-based DSS for Great Plains agriculture. The system was to provide management support at the whole farm and ranch level with emphasis on cropping systems, crop and livestock integration, water and nutrient management, pest management, economics, environmental impacts, and risk analysis. It was hypothesized that the computer program would be most useful to agricultural consultants, computer-oriented producers, and action agencies.

Furthermore, potential users wanted to make better use of research results in applying new technology to their areas of interest. The reasons land managers could not use research data to solve current problems included:

- they could not locate the data or interpret the technical literature;
- they could not easily and reliably extrapolate data to specific sites or conditions;
- they found that key production components were not adequately researched; and
- they could not understand, synthesize, and implement solutions from the data.

Discussions with a number of producers in Eastern Colorado indicated that the inaccessibility of research data and the difficulties in synthesizing the various recommendations were the primary obstacles to using research results. Our observations supported the premise that many farmers and ranchers could improve the management of their production systems if these obstacles could be removed through an integrated approach, such as the GPFARM DSS.

GPFARM DEVELOPMENT

System Overview: GPFARM includes a soil-crop-animal simulation model, an environmental risk assessment module for evaluating pre-selected management options, various databases, an economic budgeting and analysis program, a record-keeping module, and an information delivery system for Great Plains agriculture. Figure 1 shows the user input data and information flow between the soil-crop-animal, economic, and environmental modules. GPFARM has been developed using object-oriented design, layout, and programming techniques (Booch, 1994) wherever feasible.

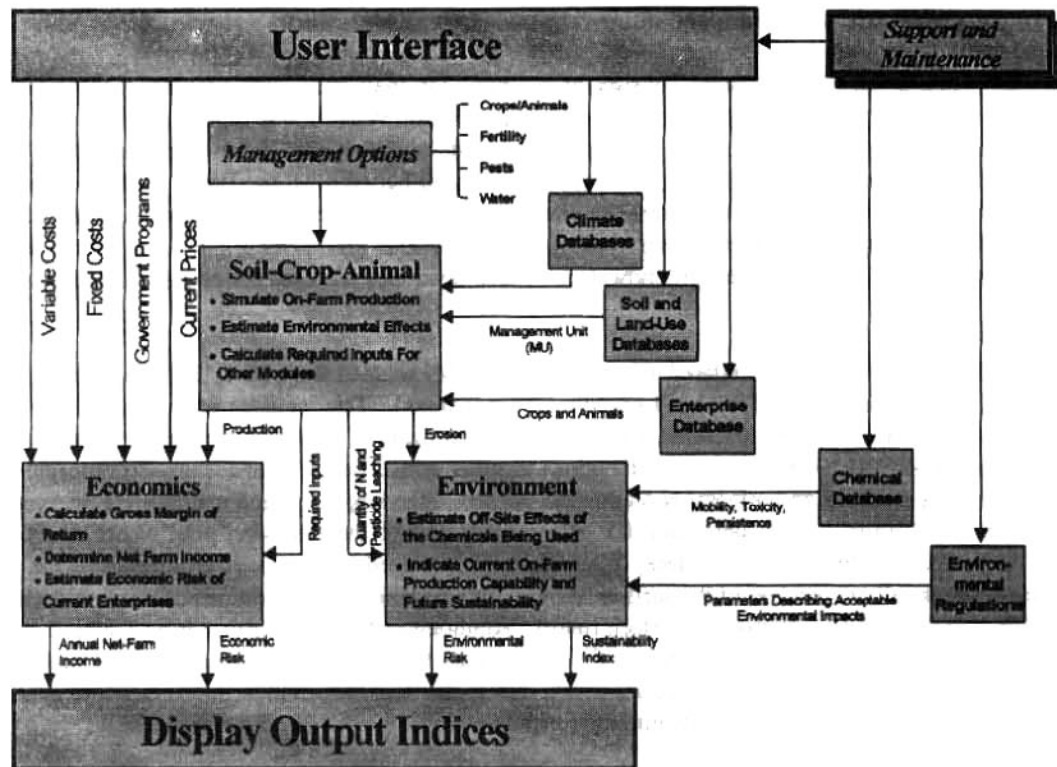


Figure 1. Modules within GPFARM.

Management options considered include integrated crop-livestock production, crop rotations, grazing, N fertilizer and pesticide applications, irrigation, yield reduction due to weeds, animal pests, residue cover, tillage practices, and snow-water conservation. Within the GUI, the user can select the climate, soils, crops, animal, equipment, prices (e.g., investments, equipment, and crops), and management parameters for the desired scenario. GPFARM databases include soils, land use, equipment, crop varieties, chemicals, climate, and various pre-set management options. Climatic data can either be obtained from the GPFARM climate database, entered by the user, or estimated using a weather generator for typical wet, average, and dry years, or any desired combination thereof.

Model parameters (e.g., coefficients describing various processes, acceptable chemical levels in the environment, etc.) are contained in a separate database that can be accessed by users through the GUI. Refinement and calibration of these parameters will be the responsibility of area or local managers that have the required technical expertise. Every effort will be made by the developers to supply customized sets of parameters that have application across sub-regions or areas of the Great Plains. Currently this has been accomplished for Eastern Colorado conditions only.

System Components

Simulation Model: The GPFARM science module framework uses the Booch (1994) OO design approach for identifying key places, players, and events in the whole farm system. The place (spatial hierarchy) where data information is stored includes the following levels or spatial units: whole farm, sub-farm, field, and management unit (MU). The MU, defined by a unique soil, management, or land use, is the basic spatial unit used for daily and event-based model simulation. Transient players on the MU's (e.g., animal herds), are simulated through the use of management events. The management event controller inherits information from the highest level in the framework. This control hierarchy allows events to be implemented by a calendar date, the firing of a system rule, or through interaction with another MU. In essence, the science module framework is responsible for controlling the simulation model and connecting it to the whole farm and ranch spatial system.

The soil-crop-animal simulation model consists of modules for mathematically simulating the various biological, physical, and chemical processes involved in crop-animal production systems; e.g. runoff, erosion, infiltration, ET, crop growth, nutrient cycling and uptake, deep percolation, pesticide transport, etc. Intra-farm transfers of resources (e.g., manure application, harvesting and feeding of forage) are allowed between MU's. Based on the selected management options and data from the various databases, the simulation model predicts crop and animal production, water use, nutrient cycling and uptake, nutrient losses (runoff, sediment, and groundwater), erosion (water and wind), and pesticide losses (runoff, sediment, and groundwater). These quantities are used for economic and environmental risk analysis.

Nutrient cycling in GPFARM is simulated using science modules adapted from NLEAP (Shaffer et al., 1991) for soil-incorporated residues, inorganic N, and soil organic matter (humus). This includes processes such as mineralization-immobilization, nitrification, denitrification, and ammonia volatilization. A surface residue decomposition model was developed that utilizes NLEAP base nutrient functions together with separate pool accounting procedures for standing dead and flat lying residues, and mineral N on the soil surface. Standing dead crop residues are decayed as a function of temperature and water content until they fall and become part of the flat lying pool where decay continues. A separate decay function based on stem decay rates and tillage is used to estimate the fall rate of the standing dead. Tillage incorporates all or a portion of the surface residues into the soil, and applications of water move surface NH₄-N and NO₃-N into the soil, and/or produce surface runoff. Ammonium-N on the surface is also subject to volatilization, nitrification, and immobilization; and surface NO₃-N also may be denitrified or immobilized. Each introduction of fresh dead residues on the surface is tracked separately during the decay process on the surface and after incorporation into the soil. Dead roots are added directly into the soil-incorporated residue pools for decay.

The rangeland (animal) component of the GPFARM science model consists of modules for simulating forage and beef cattle dynamics. The forage model simulates biomass production of five functional plant groups. These include warm-season grasses, cool-season grasses, legumes, shrubs (browse), and forbs (weeds). Each forage group is responsive to changes in soil moisture, plant-available nitrogen, and temperature. Live biomass accumulates at rates specific to the forage group. After senescence, the biomass falls as litter to the soil surface. Roots are produced in proportion to the amount of above-ground biomass and are exponentially distributed through the soil profile. Herd dynamics and animal growth are simulated by the livestock module. The herd consists of mature cows, pregnant cows, heifers, female calves, and male calves. Bulls are used to impregnate the cows, but their growth and dynamics are not simulated. Carrying capacity for the site is determined and the herd is culled so that overgrazing does not occur. The model does allow the user to preset a stocking rate, thereby overriding the safeguards of GPFARM, for testing the effect of overstocking. Replacement heifers are added to the herd each year at a rate set by the user. The remaining female calves are culled. All male calves are culled as steers. Any empty cows are culled and pregnant cows are culled to meet the site carrying capacity.

Cattle growth is determined by calculating the daily requirement for each class of animal. Demand for total digestible nutrient (TDN) is determined for each livestock class. This need can be met by either supplemental feed or forage. When grazing is allowed on a site (after forage production begins), both can be used to meet the animals demand. The maintenance energy requirement (as TDN) is also calculated based on the animal weight. Calves are given milk as the bulk of their diet. After weaning, the calves diet is determined the same as for the older classes of cattle.

Graphical User Interface (GUI): The GPFARM GUI runs in the Microsoft Windows 95™ operating environment and is being developed with Microsoft Visual C++ 5.0™. The GUI is the focal point of the system as it controls user interaction with the underlying databases and simulation model. The main screen of GPFARM is shown in Figure 2. It controls the input of information relating to the whole farm and ranch. This includes equipment, investments, climate, animal herds, and sub-farms (shown as a child window in Figure 2). New equipment can be defined, and parameters for default equipment (as taken from the equipment database) can be modified. Other GPFARM components can also be accessed in the main window, including a record-keeping module, and the GPFARM information system. The information system is a collection of over 2,500 pieces of information related to Great Plains agriculture, including research publications, Extension Fact sheets, Extension bulletins, NRCS data sheets, etc.



Figure 2. GPFARM whole farm/ranch level input screen.

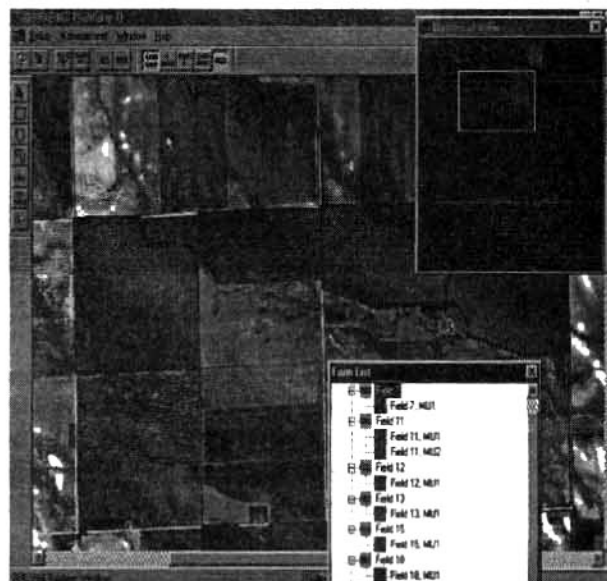


Figure 3. GPFARM sub-farm level input screen.

Fields and MU's are created in the sub-farm window and may overlay bitmap images such as aerial photographs (Figure 3). A shape palette allows the user to define a variety of field and MU shapes, including circles, squares, rectangles, and irregular polygons. The user can go to any location on the sub-farm by double-clicking on the appropriate field or MU listed in the Farm List window (Figure 3). The input of resources and management operations are also controlled in the sub-farm window. Figure 4 shows typical resource information required by GPFARM. Resources are considered to be time-invariant initial conditions, e.g., conservation structures, irrigation systems, residue cover, soil types, landscape topography, weed populations, etc. The primary management input screen is shown in Figure 5. The following information can be used to define a management operation: name, type, mode, equipment, date, properties, and materials. The management operation input mode may be either fixed-date or rule-based. If a rule-based operation is selected, a screen appears which allows the user to select from a pre-set rule base, or create their own custom rule base. The operation types available in GPFARM include planting; fertilizing; tillage; planting; weed, insect, and plant disease control; irrigation; and harvesting. Multiple operation types may be selected and they can be performed on the same day. The available equipment list is taken from the previously selected whole farm and ranch list. Similar to operation types, multiple pieces of equipment may be selected. The program calculates the operation time (acres/hour) based on the (limiting) speed of the slowest piece of equipment selected for that operation. Default machinery labor values can also be overwritten for individual management operations. Specific operation types (e.g., fertilizing and planting) also may have additional properties attached to them. For example, planting properties include seed variety information, row spacing, in-row plant spacing, seeding rates, and target yield goals.

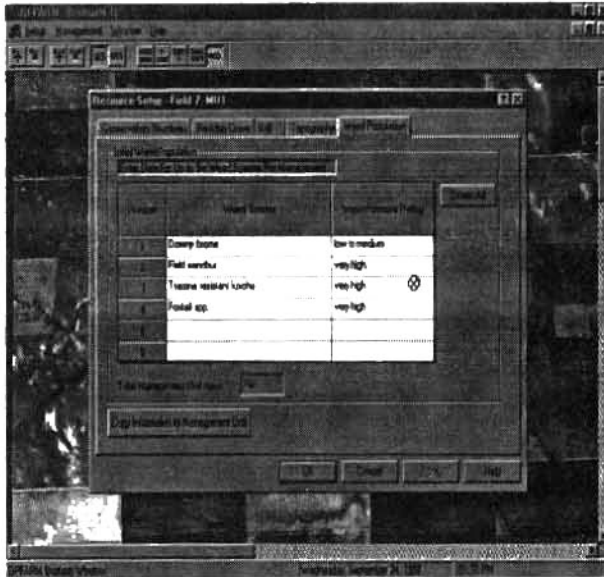


Figure 4. GPFARM resource setup screen.

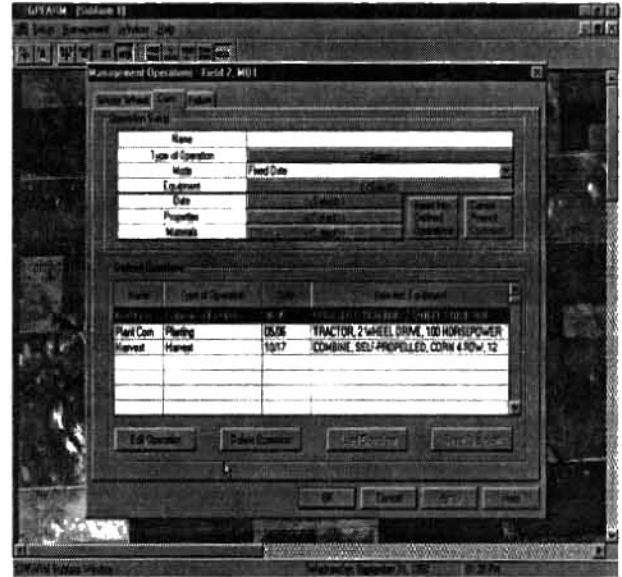


Figure 5. GPFARM management input screen.

Any additional materials needed for the management operations can also be entered. This information is then factored into the economic analysis. GPFARM output can be viewed in one of two ways: within a scenario or across scenarios. The output is presented spatially (across whole farm and ranch land units) if viewing within a scenario. If the user selects the view across scenarios option, the output is presented for a fixed land unit (e.g., an MU or a field) and shown for each scenario of interest. Figure 6 shows the main GPFARM output results screen.

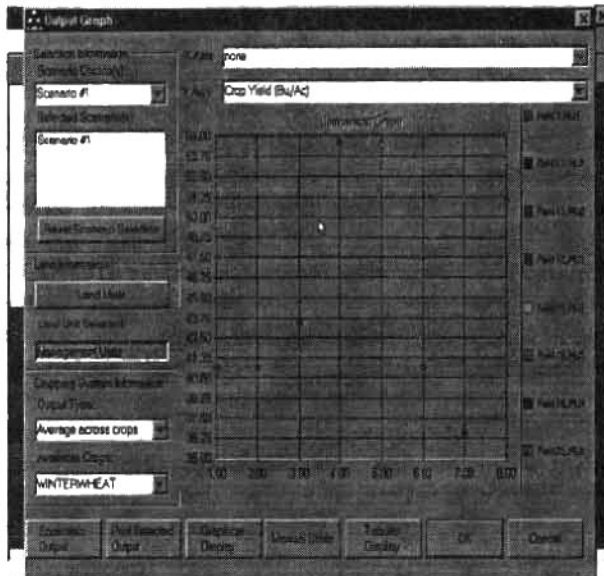


Figure 6. GPFARM main output display screen.

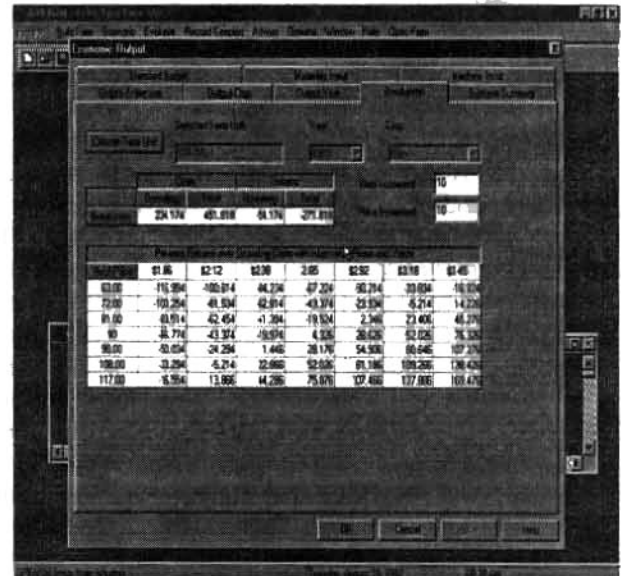


Figure 7. GPFARM break-even analysis economic output screen.

Economic Budgeting and Analysis: Farm enterprise budgeting procedures are used to determine farm profitability in terms of net farm costs and returns. The economic analysis module uses crop and animal production for each MU (from the simulation module or user-supplied) and user-supplied or on-line commodity prices to determine the gross income of each enterprise. Variable costs for each enterprise are calculated from the required production inputs. Detailed economic output is available for machine input, materials input, and a standard budget that shows

returns vs. costs. In addition, the user can also perform a breakeven analysis (Figure 7), and view costs vs. returns on an enterprise (crop rotation system), crop (individual crop) or temporal (year-by-year) basis.

Development Phases: GPFARM is being developed in three distinct phases because of the size and complexity of the problem, the need to deliver a quality product in a reasonable time frame, and the need to continuously interact with potential users. The goal of Phase 1 is to:

Build an initial version of GPFARM for strategic planning and analyzing medium- and long-term whole farm and ranch level management plans based on the predicted productivity of selected management options and associated environmental and economic risks. The initial version will consist of components from existing, familiar decision support systems and simulation models to demonstrate feasibility and usefulness of a Great Plains integrated DSS concept.

The GPFARM development effort is currently reaching the end of Phase 1. The objective of Phase 1 is to provide users an opportunity to develop an understanding of GPFARM, and to provide an opportunity for the beta-test cooperators have their production operations analyzed by GPFARM. An additional expected product from this phase is a final definition of the user requirements regarding the GUI, data inputs, and simulation model output of GPFARM. The final Phase 1 development release will be called Version 1.0 of GPFARM.

Phase 1 has been limited to dryland and irrigated cropping systems incorporating wheat, fallow, corn, proso millet and foxtail millet, and a livestock component of rangeland cattle. The region of emphasis includes only selected operations of Eastern Colorado. The time frame for completing Phase 1 Beta version is December, 1997. Users have interacted with the development team and supplied input requests including: farm layouts (aerial photos); historical precipitation data; historic county yield data; recommended application rates for manures, pesticides, and commercial fertilizers; information regarding experimental crop rotations and tillage practices; cattle herd information; production cost information; and government program information. The time frame for completing Phase 1 Version 1.0 is September, 1998. A workshop is planned at the end of Phase 1 to evaluate different components and linkages of Version 1.0, and the system as a whole. Experts in the various disciplines, prominent users, and database specialists will be invited to the workshop to critique different components and suggest improvements or better components.

Phase 2 will extend the GPFARM geographic area of consideration to the entire Great Plains, and will incorporate more crops (e.g., sorghum, soybeans, alfalfa, etc.) and range options. Integration of GPFARM into a geographic information system (GIS) framework is also being considered for Phase 2. The time frame for completing Phase 2 will be one to two years. The product at the end of Phase 2 will be Version 2.0 of GPFARM. This version will then be re-tested on ARS farm cooperator sites.

The objective of Phase 3 is to develop a DSS useful for real-time and short-term management of crop and animal production systems. The GUI for input and output of information will likely be derived and enhanced from Version 2.0 developed in Phase 2. Also, the underlying technology will be consistent with that used previously in Phase 2. The product produced in Phase 3 will be referred to as Version 3.0. Efficient collection and input of data will be crucial because these management decisions will be based in part on current conditions of the crop and animal production systems. A GIS will be used to manage the detailed information for describing field-level variability within an individual farm. Attribute maps of farm cooperators field boundaries, cropping system histories, land use, topography, soil and aquifer properties, conservation structures, etc. will be developed. The time frame for Phase 3 will be about two years. GPFARM could subsequently be modified as a template for agricultural systems beyond the Great Plains. Any work leading to this application would follow Phase 3.

SUMMARY

GPFARM integrates the most appropriate research findings and associated economic and environmental risks into a *whole farm and ranch system package*. Results from the DSS are providing agricultural consultants, producers, and action agencies with information for making management decisions that promote sustainable agriculture. In addition, GPFARM provides feedback concerning the most effective management technologies and assists in determining areas requiring further research and development. This is an evolutionary process that has tied research and technology transfer closely together. GPFARM will be developed over several years with a strong potential for extension to agricultural management support on a national basis. Scheduled dates for release of these components will be announced about three months in advance. Based on the current rates of advancement of computer technology (both hardware and software), the life expectancy of GPFARM is approximately ten years.

REFERENCES

- Booch, G. 1994. *Object-Oriented Analysis and Design*. Benjamin/Cummings Publishing Company, Redwood City, CA. 589pp.
- Hanson, J.D., Shaffer, M.J., Ball, D.A., Cole, C.V. 1991. *Sustainable Agriculture for the Great Plains*. Symposium Proceedings. USDA-ARS, ARS-89. 263 pp.
- Shaffer, M.J., Halvorson, A.D., Pierce, F.J. 1991. *Nitrate Leaching and Economic Analysis Package (NLEAP): Model description and application*. Chapter 13, pp. 285-322 In Follett et al. (Eds.) *Managing Nitrogen for Groundwater Quality and Farm Profitability*. Soil Science Society of America, Madison, WI.

For more information about GPFARM, please contact: James C. Ascough II, USDA-ARS-NPA, Great Plains Systems Research Unit, 301 S. Howes St., P.O. Box E, Fort Collins, Colorado 80522. Phone: (970) 490-8371; Fax: (970) 490-8310; E-mail: ascough@gpsr.colostate.edu

THE COMBINATION OF A RAINFALL EVENT MODEL AND A CONTINUOUS SIMULATION MODEL FOR A BETTER ASSESSMENT OF NONPOINT SOURCE POLLUTION

By M. Di Luzio, Post Doc. Res. Assoc., TA&M Blackland Research Center, Temple, Texas;
J.G. Arnold, Hydraulic Engineer, USDA-ARS, Grassland Research Lab., Temple, Texas;
R. Srinivasan, Prof. Assoc., TA&M Blackland Research Center, Temple, Texas;
R.L. Bingner, Agricultural Engineer, National Sedimentation Lab., Oxford, Mississippi.

Abstract: One method for the assessment of the release and movement of nutrients and pollutants within a watershed can be performed using hydrologically based simulation models. The main goal of modeling watershed hydrologic systems is the development of a mathematical structure that can be performed using the complexity of hydrological processes and their interrelations. To achieve this goal, state-of-the-art modeling techniques take advantage of GIS technology to provide a useful manner to collect, store and retrieve huge quantities of data for watershed scale assessments. GIS tools satisfy the assessment of distributed characteristics of the landscape and of the associated hydrological variables. This is particularly important using nonpoint pollution models for the assessment of the effects of agricultural activities that overlay intrinsic hydrological attributes. Temporal patterns of release of nutrient and chemicals is directly connected with rainfall events. Particularly, most chemicals are delivered to waterbodies during only a few large runoff events. Two USDA-ARS models have been developed for the assessment of nonpoint pollution loading from ungauged watersheds: SWAT (Soil and Water Assessment Tool) and AGNPS (Agricultural Nonpoint Pollution Source model). Each model performs distributed assessments on a watershed scale: with SWAT devoted to continuous long time simulations and AGNPS devoted to the analysis of the effect of single representative rainfall events. In this study the two models (SWAT and AGNPS) are considered complimentary and integrated in a single tool: SWAT provides the between-storm simulations of amount of seepage below the root zone and gives the initial condition for storm runoff simulation, AGNPS provides the short time storm simulation. The integration of the two models and the overlaying of simulations results show good prediction capabilities of runoff and sediment yield in the highly instrumented Goodwin Creek Watershed in northern Mississippi.

INTRODUCTION

Agriculture nonpoint pollution sources are spread over the land surface and the source flows originate from rainfall events following the spatial and temporal characteristics of rainfall. These aspects have been determining the high difficulty to assess the sediment and agro-chemical loads delivered by rainfall runoff water and the generated streamflow. Recent advances in hydrology, soil science, erosion mechanics, and computer technology have provided the basis for the development of distributed mathematical hydrological based models capable of a sophisticated and affordable method to assess the release and movement of nutrients and pollutants within a watershed. These simulation models have been developed as tools in developing management practices that can be used over various time periods. The uncertainty connected to the spatial variability of the territory attributes has been dealing with the use of the geographic information system (GIS) technology to easy handle mapped data and derive model input parameters. The erratic characteristic of the temporal pattern of precipitation has been dealing with designed raingage networks and remote sensing devices using short time sample patterns.

Watershed oriented erosion and nonpoint pollution models were developed with two different approaches:

- a) continuous long-term simulation models, such as model SWAT (Soil and Water Assessment Tool) (Arnold *et al.*, 1993), combine simplified assumptions to interpret many continuous and short time processes by using a daily simulation time step;
- b) event simulation models, such as AGNPS (Agricultural NonPoint Source) (Young *et al.*, 1989), have been developed for short term runoff simulations following single events of precipitation and do not include continuous processes that occur between them.

Both the model typologies are the result of focused targets, determining factors and practical compromises:

- a1) the necessity of tools to evaluate developing alternative management practices by hydrological models which could be used for long-term simulations on large ungauged watersheds with a minimal amount of user input data requirements;
- a2) the description of the involved processes, particularly in continuous, requires a complex set of input parameters;
- a3) long series of rainfall data are traditionally available with a fixed time step of 24 hours;

- b1) since the storm events are the phenomena driving most of the eroded sediment and agro-chemicals to the receiving waterbodies (Knisel, 1980), the simulation of the storm with as much detail as possible is of priority importance;
 - b2) In this case a reduced set of parameters is required supposing stationary the involved processes;
 - b3) representative events are selected with a design criteria (cumulates rainfall values with a design return period).
- Both the approaches show respective drawbacks:
- ai) the daily time step does not have a conceptual hydrologic content;
 - aii) the dynamic hydrologic processes during and following the storm event could be not sufficiently focused;
 - aiii) complex, detailed and long series of data are needed;
 - aiv) adequate statistical assessment of the watershed sediment yield and chemical loads responses are obtained with long term simulation of meteorological input data;
 - bi) temporal detailed rainfall data set need for an adequate description of the storm;
 - bii) difficulties arise setting the initial conditions of the watershed model system specially when the model is distributed;
 - biii) the prediction capabilities change for different storm sizes (Bingner *et al.*, 1992): large events generally produce large amounts of erosion, but smaller rainfalls control many of the antecedent parameters that effect erosion from large events;
 - biv) conservation cropping systems protect in different measure during different times of the year;
 - bv) there is not recognized standard in the choice of a representative design storm for watershed erosion and nonpoint pollution loading assessments.

Moreover inadequate experimental data of instream sediment loads and water quality variables to match models simulation results make their calibration and validation very doubtful. The uncertainty connected with erosion and water quality hydrologic processes and the points listed above can explain why these models have often shown their role as tools in the assessment of comparative trends obtainable with theoretical application of alternative agriculture management practices. The recent availability not only of data handling support tools (GIS technology), but the increasing of the number and quality of hydrologic data promises to improve the models performances.

The objectives of this study were to take advantage of the availability of rainfall data sets measured at short time intervals (break-point rainfall data) and check an effective method to safe the respective advantages of the approaches pointed above. The continuous model SWAT was applied with daily and break-point daily storm sets of rainfall data and an integrated continuous-event model system (SWAT-AGNPS) was developed and applied.

Goodwin Creek Watershed (GCW) experimental data sets were used to compare the simulation results for measured runoff and fine sediment yield at the watershed outlet.

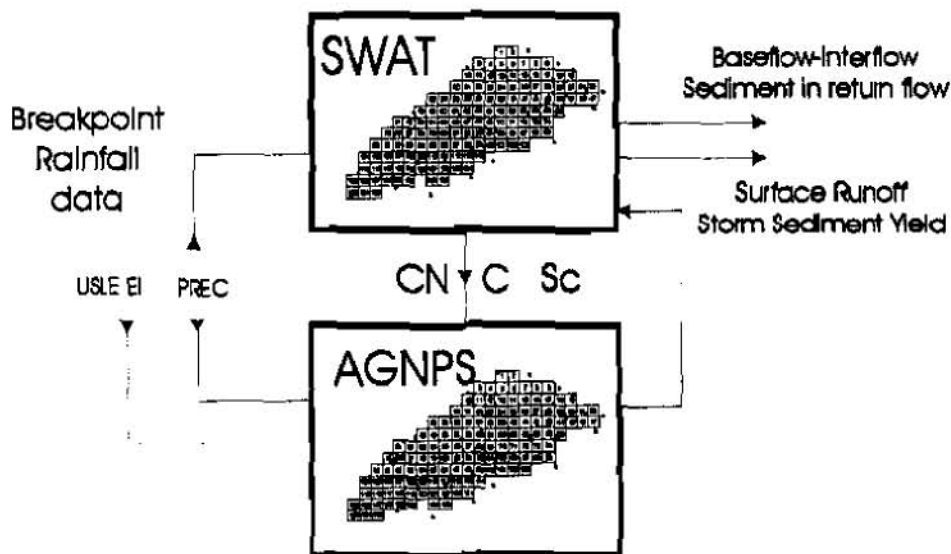


Figure 1 – Working scheme of the SWAT-AGNPS model system

MODEL SYSTEM DESCRIPTION

The system model developed in this study is a combination of the continuous model SWAT and event model AGNPS (fig 1).

Applying SWAT model (Arnold *et al.*, 1993) and the developed GRASS interface (Srinivasan and Arnold, 1994) the study watershed can be subdivided into many subbasins with any shape and size to simulate the spatial variability of a watershed. The model performs a characterization of lateral flow, groundwater flow, channel transmission losses, and routing of sediment and chemicals through the watershed. SWAT uses the SCS curve number (USDA-SCS, 1972) equation to estimate daily runoff. The curve number is adjusted according to the moisture conditions in the watershed. SWAT determines moisture conditions by simulating water infiltration into the soil, percolation losses, and evapotranspiration. AGNPS (Young *et al.*, 1989) can not simulate the continuous nature of plant growth so user inputs are required to inform the model of the crop's condition on the watershed at the time of the event. AGNPS requires that the Curve Number (CN), USLE crop factor (C) and a Surface Condition constant (SC) be updated for each event to describe the soil moisture content and the crop's condition (see Bingner, 1990 for details). Conceptually the developed model system is shown in figure 2: SWAT provides the between-storm simulations of amount of seepage below the root zone and gives the initial condition (CN, C and Sc) to AGNPS for the short time storm simulations.

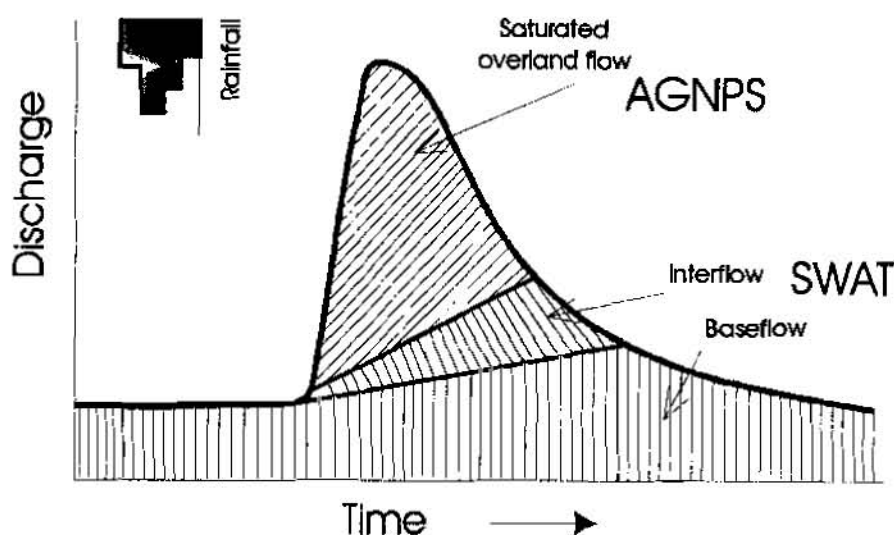


Figure 2 - Separation of sources of streamflow and sediment-chemicals on an idealized hydrograph

WATERSHED DESCRIPTION

Goodwin Creek Watershed (GCW) covers an area of 21.3 km² in the bluff hills region of the north central part of the state of Mississippi just east of the flood-plain of the Mississippi River (fig. 3). Many experimental and simulations studies have been applied to GCW (Alonso *et al.*, 1995; Kuhnle *et al.*, 1996; Bingner, 1996; Bingner *et al.*, 1997a; Bingner *et al.*, 1997b). Soils within GCW can generally be described as silt loams, with topography ranging from small alluvial valleys along the major channels to moderately hilly uplands. The land surface ranges in elevation from 71 to 128 m above the mean sea level, with a mean channel slope of 4 m/km. Simplified categories of land uses in GCW for 1987 included 48% Pasture/Idle, 26% forest and 15% cultivated. The normal annual rainfall is 1399 mm (Bingner, 1996).

DATA COLLECTION

GCW was instrumented in 1981 with fourteen streamflow measuring and sampling stations located through the watershed on the outlet of one or more nested subbasins (Alonso *et al.*, 1995), with 30 raingages located in or adjacent to the watershed (McGregor *et al.*, 1995). In this study values were used from the measured stream water flow and suspended sediment load (finer than 0.062mm) sampled at the outlet flume (the streamflow station located at 89°54'50" and long. 34°13'55") (Measuring Station #1) and the rainfall records of the 30 raingage stations

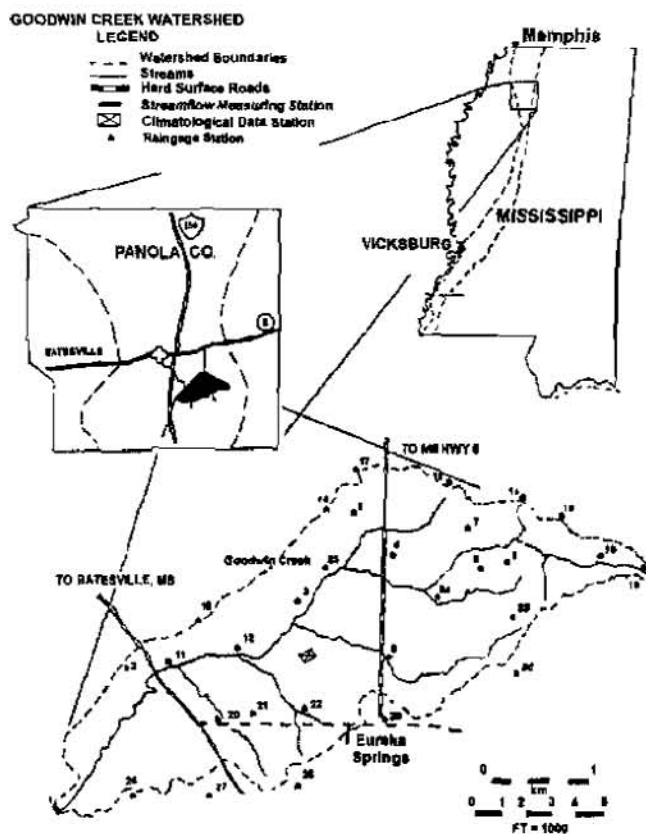


Figure 3 - Location of Goodwin Creek watershed with raingages and the streamflow measuring stations

located as shown in figure 3. GRASS-GIS (Shapiro *et al.*, 1992) data layers including elevations, landuse, and soil series types at a 30x30 m cell size were available from previously prepared U.S. Geological Survey (USGS) quad sheets, 1987 Landstat-5 thematic mapper image and NRCS soil surveys maps, respectively.

INPUT PARAMETERS

The simulation were performed using 135 square cells (subbasins) with 400 x 400 m size (fig.4). Parameters for each cell were estimated using SWAT/GRASS interface (Srinivasan and Arnold, 1994) based on the dominant land use or soil type described by GIS map layers within a cell. Bingner (1996) described a similar simulation process using SWAT to evaluate the runoff predicted at each of the GCW's fourteen instream measuring stations using the same number of correspondent subbasins to define the watershed. Kuhnle *et al.* (1996) and Bingner *et al.* (1997a) applied SWAT to evaluate fine sediment yield at the same locations using 138 subbasins. Bingner *et al.* (1997b) compared SWAT simulation with multiple numbers of subbasin subdivision. Since GCW was previously object of similar simulation process, the calibration was avoided; some model sensitive parameters were chosen following the observations reported in one of the previous applications of SWAT on the same watershed (Bingner *et al.*, 1997b):

- a) cotton was used to identify the crop land and ever green forest to identify forest;
 - b) the Universal Soil Loss Equation (USLE) (Wischmeier and Smith, 1978) support practice factors (P-factors) were chosen based on no support practices contained on pasture or forest land, resulting in a P-factor value of 1.0. Cropland areas were assigned a value of 0.5 for all fields, although the level of contour farming on GCW is not available;
 - c) the NRCS curve numbers (CN) values were chosen 89, 79 and 70, for cropland, pasture and forest respectively (these are medium values between the interface product values and values used in Bingner *et al.* (1997b));
 - d) the overland Manning's n values were chosen 0.07, 0.24 and 0.40, for cropland, pasture and forest respectively.
- A software program was developed to transfer the same set of parameters into AGNPS (version 5.0) input format. Slight modifications of the SWAT code (version 97.2) were performed to update the AGNPS input values of CN. C

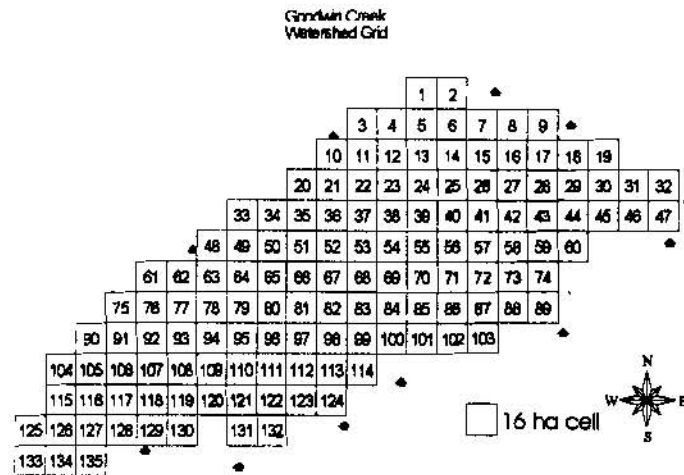


Figure 4 – Grid subdivision of Goodwin Creek Watershed (GCW)

and Surface Constant in occasion of each storm event, run AGNPS model with the storm data set (precipitation and Energy Intensity index of USLE) and feedback SWAT with AGNPS's cell based output data simulation (fig. 1).

Table 1 – Goodwin Creek Watershed: yearly average rainfall, average EI and observed total Runoff and fine Sediment yield at the outlet

Year	Average Rainfall [mm]	Average EI [MJ mm (ha h) ⁻¹]	Total Runoff [mm]	Fine Sediment Yield [t ha ⁻¹]
1982	1690.0	10726.97	735.0	17.6
1983	1658.7	10345.54	866.2	19.6
1984	1448.1	9489.774	551.3	16.5
1985	1201.9	7298.84	308.7	7.5
1986	1232.8	8064.042	319.7	5.2
1987	1160.3	5326.091	317.0	4.2
1988	1050.0	4941.068	282.5	3.0
1989	1785.1	10624.99	844.8	11.8
1990	1028.5	4648.024	669.2	9.3
1991	1990.4	14213.15	1155.9	20.0
1992	1120.4	6081.288	369.0	3.7
1993*	1065.6	4292.363	250.7	1.1

*Until september 1993

The precipitation data set were obtained elaborating short time rainfall data of 30 raingage stations located as shown in figure 3. Different set of precipitation data were prepared: daily time step (24 hours) and daily-storm (storms were defined as precipitation without a continuous break of 6 h with less than 0.25 mm and summarized on the day the storm started), average weighted watershed daily-storm precipitation and EI based on the single station data and on the station proximity areal coverage of the watershed area. The EI, for all storms with no limitations on storm size or intensity parameters, were computed using Agriculture Handbook 537 (Wischmeier and Smith, 1978) procedure in the SI metric units version of Foster *et al.* (1981). Measured total runoff and fine sediment watershed load were computed using the short time records registered at the outlet streamflow station (fig. 3). Table 1 reports a summary of the computed yearly average precipitation, average EI data and observed total runoff and fine sediment yield. The following section compares measured and simulated runoff and fine sediment yield data for the almost 12-year period January 1982 through September 1993.

RESULTS AND DISCUSSION

SWAT model was applied using traditional daily (SWAT) and daily-storm precipitations (SWAT-BRK) with the full available distributed data set (30 sets of rainfall data correspondent to the 30 stations of fig. 3). The results reported in Figures 5 show that total runoff simulated using SWAT are improved using daily-storm precipitation data instead of traditional daily data: for the whole period of analyses simulated total runoff was within 92% and 89% of the observed values respectively. Even the monthly based statistical comparison reported in table 2 show the improvement of the coefficient of determination (r^2), for the linear regression between the observed and simulated streamflow, and the simulation efficiency index of Nash-Sutcliffe (Nash and Sutcliffe, 1970).

An improvement of the statistical results was obtained for the simulation of sediment yield and the simulation of the accumulated fine sediment load passed to 69% from 62% of the observed value. However this last comparison is not completely meaningful because earlier studies in GCW watershed attribute a significant but not accurate portion of the fine sediment from channel and concentrated flows areas (Alonso *et al.*, 1995; Bingner *et al.*, 1997a; Kuhnle *et al.*, 1996).

When the SWAT-AGNPS model system was applied the results of the simulation were collected in two different manner, in fact while AGNPS computed the cell by cell runoff and sediment yield values, SWAT outlet output data (SWAT-AGNPS I) and AGNPS outlet output data (SWAT-AGNPS II) were collected. For an effective comparison, since AGNPS computes only the surface component of runoff and sediment yield, a portion loads were added computing the experimental subsurface and base flow runoff by an automatic digital filtering technique (Arnold *et al.*, 1995) and considering 100 mg/l the medium concentration of fine sediments in this components of runoff. The statistical results for the total runoff simulation showed further improvement (E and r^2 increase) while were simulated 90% and 92% of the observed accumulated value. Slight decreased of this last value could be due to the use of watershed average values of rainfall and EI data. The statistical results for the sediment yield were improved, while 67% and 29% of the observed accumulated value were simulated; a decreasing of the Nash-Sutcliffe coefficient of simulation efficiency for SWAT-AGNPS II was due to the remarkable lower values of the simulated sediment yields (see fig. 6 and table 2). In fact SWAT-AGNPS II model system simulated 29% of the observed accumulated fine sediment yield (AGNPS contains no channel bank erosion components) even if this value is supported by the data reported by Grissinger *et al.* (1991) who estimated that 75% of the fine material produced at the outlet of GCW from 1982 to 1987 originated from channel or gully sources. It needs to notice that the used landuse data are a picture of the 1987 survey and therefore the simulations did not take in account that the decrement of cultivated land in the GCW during the considered period reduced the sources and supply of fine sediment (Kuhnle *et al.*, 1996).

Table 2 – Nash-Sutcliffe index of efficiency (E) and r^2 for linear regression between monthly observed total runoff and fine sediment yield and simulated with SWAT, SWAT-BRK and daily-storm data, SWAT-AGNPS I and SWAT-AGNPS II

	SWAT		SWAT BRK		SWAT-AGNPS I		SWAT-AGNPS II	
	E	r^2	E	r^2	E	r^2	E	r^2
Monthly base								
Total Runoff	0.739	0.748	0.884	0.888	0.866	0.873	0.892	0.898
Fine Sediment Yield	0.365	0.452	0.573	0.687	0.623	0.774	0.167	0.717

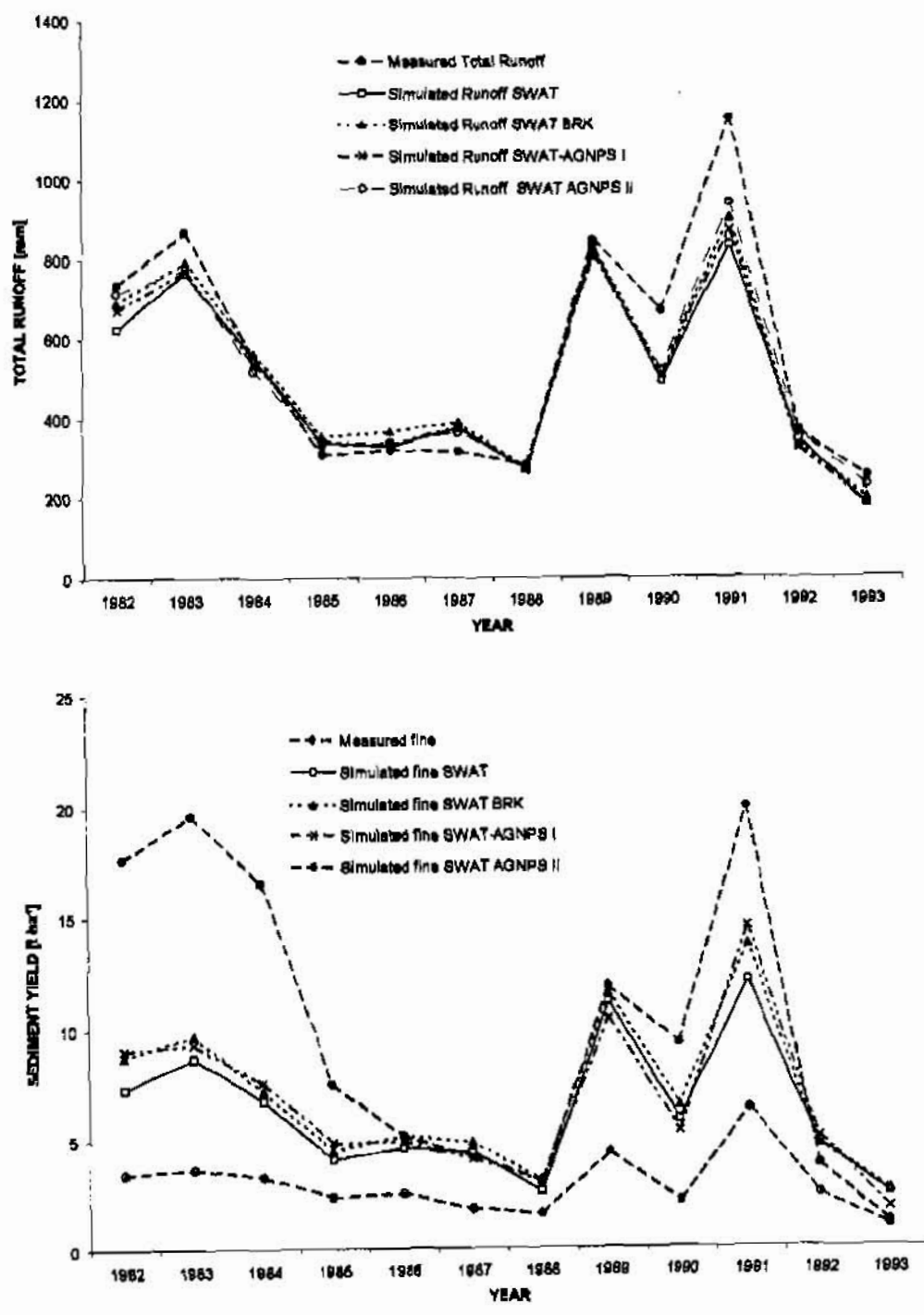
CONCLUSIONS

In this paper were described the steps followed to perform long-term sediment yield and water runoff simulations by the implementation of a SWAT-AGNPS system. The simulation results illustrated for the Goodwin Creek Watershed, even in the absence of the model system calibration, agree well with the measured values and previous experimental observations. For the almost twelve years period, the simulation of water runoff increased in efficiency and correlation with the observed data using SWAT with daily-storm data and linked with AGNPS model. In the same manner the simulated fine sediment yield showed statistical improvements. The SWAT-AGNPS II model system showed absolute remarkable lower values because AGNPS do not simulate channel erosion, but a real

comparison with observed results is actually difficult since in Goodwin Creek Watershed a dominant portion of fine material is originated from channel or gully sources that the two models did not simulate.

Daily-storm break-point cumulated rainfall data and the tested SWAT-AGNPS system revealed to be efficient for long term simulations encouraging furthermore comparison in different watersheds, considering simulated and measured chemical loads and storm by storm results. The study suggests that erosion and sediment yields (and nonpoint pollution) models should take advantage of the recent availability of enriched rainfall data (the forcing variable of the system) in temporal a spatial details, to improve the assessment of the process variables either between and during the rainfall events, for a global improvement of simulation results.

Figure 5 – Yearly measured total runoff, fine sediment yield and results of simulation with SWAT, SWAT-BRK daily-storm data, SWAT-AGNPS I and SWAT-AGNPS II



REFERENCES

- Alonso, C.V., Bingner R.L., Kuhnle R.A., 1995, Sediment yield from watersheds with eroding channels, In *Water Resources Engineering*, W.H. Espey, Jr., and P.G. Combs, Ed., ASCE, 2, 1183-1187.
- Arnold, J.G., Allen, P.M., Mutiah R., Bernhardt, G., 1995, Automated baseflow separation and Recession analysis techniques, *Ground Water*, 33(6), 1010-1018.
- Arnold, J. G., Engel, B. A., Srinivasan, R., 1993, Continuous time, grid cell watershed model. In *Application of Advanced Information Technologies for Management of Natural Resources*, Spokane, WA, 17-19 June 1993, 267-278.
- Bingner, R.L., 1990, Comparison of the components used in several sediment yield models. *Transactions of the ASAE* 33(4), 1229-1238.
- Bingner, R. L., 1996, Runoff simulated from Goodwin Creek Watershed using SWAT. *Transactions of the ASAE*, 39(1), 85-90.
- Bingner, R.L., Alonso, C.V., Arnold, J.G., Garbrecht, J., 1997a, Simulation of Fine Sediment Yield Within a DEC Watershed. In Wang, S.Y., Langendoen, E. and Shields, F. D. Jr., (eds.) *Management of Landscapes Disturbed by Channel Incision, Stabilization, Rehabilitation, and Restoration*, University of Mississippi, University, Mississippi. p. 1106-1110.
- Bingner, R.L., Garbrecht, J., Arnold J.G., Srinivasan R., 1997b, Effect of watershed subdivision on simulation runoff and fine sediment yield. *Trans. of the ASAE*, 40(5), 1329-1335.
- Bingner, R.L., Mutchler C.K., Murphee C.E., 1992, Predictive capabilities for erosion models for different storm sizes, *Transactions of the ASAE*, 35(2), 505-513.
- Knisel, W.G. CREAMS, 1980, A field scale model for chemicals, runoff, and erosion from agricultural management systems. U.S. Dept. Agric. Conserv. Res. Rept. No.26.
- Foster, G.R., McCool D.K., Renard K.G., Moldenhauer, W.C., 1981, Conversion of the universal soil loss equation to SI metric units, *Journal of Soil and Water Conservation*, 36(6), 355-359.
- Grissinger, E. H., Bowie, A. J., Murphey, J. B., 1991, Goodwin Creek bank instability and sediment yield. *Proceedings, Fifth Federal Interagency Sedimentation Conference*, PS32-PS39.
- Kuhnle, R.A., Bingner, R.L., Foster, G.R., Grissinger, E. H., 1996, Effect of land use changes on sediment transport in Goodwin Creek, *Water Resources Research*, 32(10), 3189-3196.
- McGregor, K.C., Bingner, R.L., Bowie, A.J., Foster., G.R., 1995, Annual and monthly variation of erosivity index in Northern Mississippi. *Transaction of the ASAE*, 38(4), 1039-1047.
- Nash, J.E., Sutcliffe, J.E., 1970, River flow forecasting through conceptual models, Part I – A discussion of principles, *Journal of Hydrology*, 10(3), 282-290.
- Shapiro, M. J., Westervelt, J., Gerdes, D., Larson, M., Brownfield, K. R., 1992, GRASS 4.0 Reference Manual. U. S. Army Corps of Engineers - CERL, Champaign, IL.
- Srinivasan, R., Arnold, J. G., 1994, Integration of a basin-scale water quality model with GIS. *Water Resources Bulletin*, 30(3), 453-462.
- USDA-Soil Conservation Service, 1972, *National Engineering Handbook. Hydrology Section 4, Chapter 4-10*, 19. USDA-SCS: Washington D.C.
- Wischmeier, W. H., and Smith, D.D., 1978, Predicting rainfall erosion losses. U.S. Dept. of Agriculture, *Agriculture Handbook No. 537*.
- Young, R.A., Onstad, C.A., Bosch, D.D., Anderson, W.P., 1989, AGNPS: A nonpoint-source pollution model for evaluating agricultural watersheds. *Journal of Soil and Water Conservation*, 44(2), 168-173.

SPATIALLY REFERENCED REGRESSION MODELING OF NUTRIENT LOADING IN THE CHESAPEAKE BAY WATERSHED

**Stephen D. Preston, Hydrologist, U.S. Geological Survey, Baltimore, Maryland;
Richard A. Smith, Hydrologist, U.S. Geological Survey, Reston, Virginia;
Gregory E. Schwarz, Economist, U.S. Geological Survey, Reston, Virginia;
Richard B. Alexander, Hydrologist, U.S. Geological Survey, Reston, Virginia;
John W. Brakebill, Geographer, U.S. Geological Survey, Baltimore, Maryland**

Abstract

A set of spatially referenced regression models is currently being developed to relate water quality in the Chesapeake Bay to sources of nutrients in the watershed and to factors that affect the transport of nutrients to the bay. Spatially referenced regression modeling is a statistical technique that uses spatial information to provide nutrient-load predictions that are more spatially detailed than those provided by other large-scale watershed models. Two applications of the technique for the determination of total nitrogen in the Chesapeake Bay watershed are described, including the estimation of incremental (local) yields and the estimation of yields delivered to the bay. The model shows that areas that are most important to the delivery of nutrients to the bay are those that drain directly to large streams or those that are near the bay. Instream loss of nutrients is minimal in both cases, thus enhancing nutrient delivery to the bay.

INTRODUCTION

Watershed modeling is commonly considered an essential tool for evaluating the sources and controls of nutrient loading to receiving waters. Watershed models provide a framework for integrating the data that describe the processes and land-surface characteristics that determine the amount of nutrients transported by streams. Development of watershed models is a difficult task, however, because of the broad spatial and temporal scales that must be considered and the large amount of information that must be integrated. Funding, time constraints and available information commonly limit the amount of spatial or temporal detail that can be considered by watershed models.

The Chesapeake Bay watershed is one area of the Nation where watershed modeling is being applied to evaluate nutrient loading (figure 1). Water quality and ecosystem integrity in the Chesapeake Bay have been affected by excessive nutrient loading, which has resulted in the depression of dissolved oxygen levels and the loss of submerged aquatic vegetation. These effects have impacted economically important aquatic species and have diminished the value of the bay as a recreational resource.

Watershed modeling has been an important component of the effort to understand nutrient loading to the Chesapeake Bay and to develop management strategies for controlling it. The Chesapeake Bay Program (CBP) is a multiagency taskforce that has been charged with coordinating and managing efforts to restore water quality in the bay. The CBP has developed a hydrologic and water-quality model for the Chesapeake Bay watershed using the Hydrologic Simulation Program - Fortran (HSPF) modeling framework (Donigian and others, 1994). Applications of the HSPF model

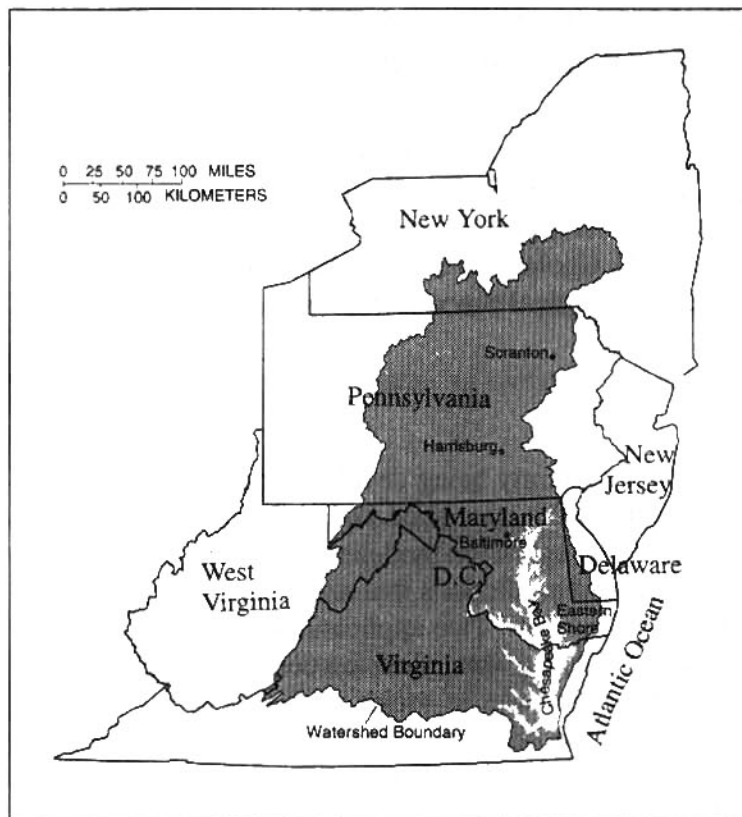


Figure 1. Chesapeake Bay watershed and surrounding area.

include (1) estimating nutrient loads from all areas of the watershed, (2) evaluating the impacts of land-use-change scenarios, and (3) evaluating the potential benefits of the implementation of Best Management Practices (BMP's). The Chesapeake Bay HSPF model is temporally detailed in that it is based on hourly time increments of streamflow and other environmental processes, but is limited in spatial detail and is based on 86 segments that average more than 700 square miles in area.

The HSPF modeling framework is deterministic in nature and includes a substantial amount of detail in the number of processes that are considered in simulating watershed hydrology and nutrient fate and trans-

port. The process detail included in HSPF is important for designing and evaluating nutrient management programs. The number of parameters in the model increases with the number of processes simulated, however, and determining appropriate values for those parameters can be difficult. The current Chesapeake Bay watershed model is manually calibrated at 14 sites. Parameter values are quantified by adjusting them to fit predicted values to measured data or by adopting published values for some parameters.

To support the CBP's modeling effort, the U.S. Geological Survey (USGS) has initiated the development of a set of spatially referenced regression models. These models can be used to provide a statistical basis to watershed modeling and additional spatial detail on nutrient sources and transport processes. The method used for developing the regression models is referred to as "SPARROW" (SPAtially-Referenced Regressions On Watershed attributes) (Smith and others, 1996). The SPARROW methodology is designed to provide statistically based relations between stream-water quality and environmental factors such as contaminant sources in the watershed, land-surface characteristics that affect contaminant delivery to streams, and instream contaminant losses. Because the regression models are linked to spatial information, predictions and subsequent analytical results can be illustrated through detailed maps that provide information about nutrient loading at multiple scales. The SPARROW methodology has been successfully applied at the national scale for estimating total nitrogen and total phosphorus loads for streams in the continental United States (Smith and others, 1996).

As an initial step in the development of SPARROW models for the Chesapeake Bay watershed, this paper describes an evaluation of the national scale model within the bay watershed. SPARROW regressions are currently being developed using data that are specific to the watershed, but the national model provides a useful preliminary view of nutrient loading to the bay. Specifically, this paper describes the results of two applications of the national SPARROW model for evaluating the important sources and controls of total nitrogen loads to the Chesapeake Bay.

METHODS

The SPARROW methodology consists of a nonlinear regression in which nutrient-load data are related to upstream sources and land-surface characteristics. Spatial referencing is accomplished by linking nutrient source, land-surface characteristic, and loading information to a geographically defined river-reach data set that serves as a network for relating upstream and downstream loads. Nutrient inputs to each river reach include loading from individual sources within the watershed that drains to the reach and loading from upstream. Land-surface characteristics that affect delivery of nutrients to the reach are included by linking the relative amount of the specific characteristic in the direct drainage area to the reach. All of the dependent and independent variables are spatially defined by point or polygon coverages that are related to the stream network, which defines the connectivity and allows predictions to be presented in a spatial context. Further details of the methodology are presented below; however, the reader is referred to Smith and others (1996) and Smith and others (1993) for a complete description.

The SPARROW statistical model includes three types of parameters: source, land-to-water delivery, and instream loss parameters. The basic form of the statistical model is:

$$L_i = \sum_{n=1}^N \sum_{j \in J(i)} \beta_n s_{n,j} e^{(-\alpha' Z_j)} e^{(-\delta' T_{i,j})} ,$$

where

L_i = load in reach i ;

n, N = source index where N is the total number of considered sources;

$J(i)$ = the set of all reaches upstream and including reach i , except those containing or upstream of monitoring stations upstream of reach i ;

β_n = estimated source parameter;

$s_{n,j}$ = contaminant mass from source n in drainage to reach j ;

α = estimated vector of land-to-water delivery parameters;

Z_j = land-surface characteristics associated with drainage to reach j ;

δ = estimated vector of instream loss parameters; and

$T_{i,j}$ = channel transport characteristics.

The source parameters (β_n) are included to determine the significance of individual sources in explaining the variation of loads among reaches. Sources considered in the national SPARROW model include point sources, fertilizer application rates, livestock production, atmospheric deposition and nonagricultural land. Additionally, in basins where load is monitored at some upstream location, the monitored load is considered an additional source with source parameter (β_n) set equal to one.

The land-to-water delivery parameters (α) determine the significance of different types of land-surface characteristics for increasing or decreasing the delivery of nutrients from the land surface to the stream reach. For example, relatively large percentages of impermeable surface area might be expected to increase delivery from the land surface to stream reaches. Land-surface characteristics (Z_j) that were considered in the national SPARROW model include temperature, slope, stream density, wetland, irrigated land, precipitation, and irrigated water use. Delivery of point-source loads to stream reaches was assumed to be unaffected by land-surface characteristics, and the value of the delivery term ($e^{(-\alpha Z_j)}$) for point sources is set equal to one.

Estimation of instream loss parameters (δ) is important for relating upstream sources to downstream loads. For the national SPARROW model, instream-loss parameters were estimated for three reach classes that were defined by discharge level. The classes were defined by the discharge intervals of less than 28 m³/s, between 28 and 283 m³/s, and greater than 283 m³/s.

All dependent and independent variable data sets were compiled from published data bases. Nutrient-loading data were derived from water-quality data collected as part of the USGS National Stream Quality Accounting Network (NASQAN). Load estimates were generated on the basis of total nitrogen measurements from 414 sites, including 13 sites from within the Chesapeake Bay drainage. Total nitrogen-source data were compiled primarily from published county-based data sets. Atmospheric deposition data, however, were generated through linear spatial interpolation of National Atmospheric Deposition Program (NADP) point measurements. Land surface-characteristics data were compiled from a variety of spatial data sets. Some variables were generated from county-based information (for example, wetlands, fraction of irrigated cropland). Others (soil permeability and slope), however, were compiled from the state-based soils data sets (STATSGO) (U.S. Soil Conservation Service, 1994) and published USGS data sets (temperature and precipitation). All dependent and independent variable data were compiled for calendar year 1987 or were generated to reflect conditions during that year.

The network for developing the national SPARROW model is based on River Reach File 1 (RF1) (DeWald and others, 1985) for model development and USGS hydrologic units for displaying model predictions. RF1 is a 1:500,000-scale, digital stream coverage that is attributed with reach length and average stream discharge and velocity. This information is used to classify reaches into size categories and to calculate traveltime (reach length/velocity) for estimating in-stream loss rates. Nationally, RF1 consists of approximately 60,000 stream reaches, which includes 1,366 stream reaches in the Chesapeake Bay watershed. Predicted total nitrogen loads and basin yields

for the continental United States were illustrated on the basis of 2,057 USGS hydrologic "cataloging" units. For the Chesapeake Bay watershed, the scale of the basin units was refined by delineating basin boundaries for each river reach based on a 1-km² digital elevation model (DEM). Basin delineation produced one basin unit for each reach, or 1,366 basins in all.

Model parameters in the national model were estimated by applying a nonlinear least-squares algorithm to the equation above. The error term in the model is assumed to be multiplicative and the estimation algorithm was applied after both sides of the equation were converted to logarithmic form. The robustness of the parameter estimates was evaluated by applying a bootstrap algorithm in which the model was repeatedly estimated based on subsamples of the load and predictor data. This procedure provided distributions of model parameters that could be used to evaluate the potential range of parameter estimates. Further details and results of the bootstrap analysis are described by Smith and others (1996).

RESULTS

Regression Results and Parameter Estimates

Results of model estimation for the total nitrogen national SPARROW model are summarized in table 1. Fit of the model is good with an R-squared value of 0.87 and a mean square error of 0.4544. Most of the independent variables considered were found to be significant; variables that were clearly not significant in exploratory regressions were left out of the final model. All parametric estimates of total nitrogen source parameters were found to be significant, although livestock waste production was only moderately significant (0.0632). All bootstrap estimates of total nitrogen source parameters were found to be highly significant. Three of the eight land-to-water delivery parameters were found to be significant by the parametric or bootstrap estimations. Temperature and soil permeability were inversely related to nitrogen loading possibly because higher temperature increases rates of denitrification and because higher soil permeability tends to shift nitrate transport to ground-water reservoirs. Stream density was implemented in the model in reciprocal form and is positively related to stream nitrogen loading because basins with higher stream density are expected, on average, to have shorter overland travel times than basins with lower stream density. Parametric estimates of instream loss parameters were highly significant for the two smaller stream-size classes. Instream loss rates are lower for larger stream sizes because larger (deeper) streams have less contact with sediment where denitrification is expected to occur.

Application of SPARROW for Spatial Nutrient Loading Analysis

To illustrate the benefit of spatial referencing, two applications of SPARROW in the Chesapeake Bay watershed are presented (figures 2 and 3). In both cases, total nitrogen yields are calculated by dividing the predicted load by the contributing area to calculate a per unit area load. Incremental yield (figure 2) is the load generated by the area that drains directly to the reach without loads from upstream. Input to the reach is assumed to occur at the middle of the reach and instream loss is calculated over half of the length to estimate loads at the end of the reach. Incremental loads provide an indication of the relative importance of local drainage areas to nitrogen loading and provide a common basis for evaluating source areas across the entire watershed. Incremental yields provide an indication of local influences on loading, but do not account for instream losses

Table 1. Parameter estimates, probability levels and regression results for national SPARROW model (modified from Smith and others, 1996).

Model parameters	Bootstrap Coefficient	Bootstrap p
Nitrogen Sources (β)		
Point sources	0.4331	<0.005
Fertilizer application	1.439	<0.005
Livestock waste production	1.060	0.005
Atmospheric deposition	6.538	<0.005
Nonagricultural land	16.71	<0.005
Land to water delivery (α)		
Temperature	0.0198	<0.005
Slope		
Soil permeability	0.0450	<0.005
Stream density	0.0244	0.025
Wetland		
Irrigated land		
Precipitation		
Irrigated water use		
Instream loss (δ)		
δ_1 ($Q < 28.3 \text{ m}^3/\text{s}$)	0.3843	<0.005
δ_2 ($28.3 \text{ m}^3/\text{s} < Q < 283 \text{ m}^3/\text{s}$)	0.1225	<0.005
δ_3 ($Q > 283 \text{ m}^3/\text{s}$)	0.0407	0.015
R-squared	0.8742	
Mean square error	0.4544	
Number of observations	414	

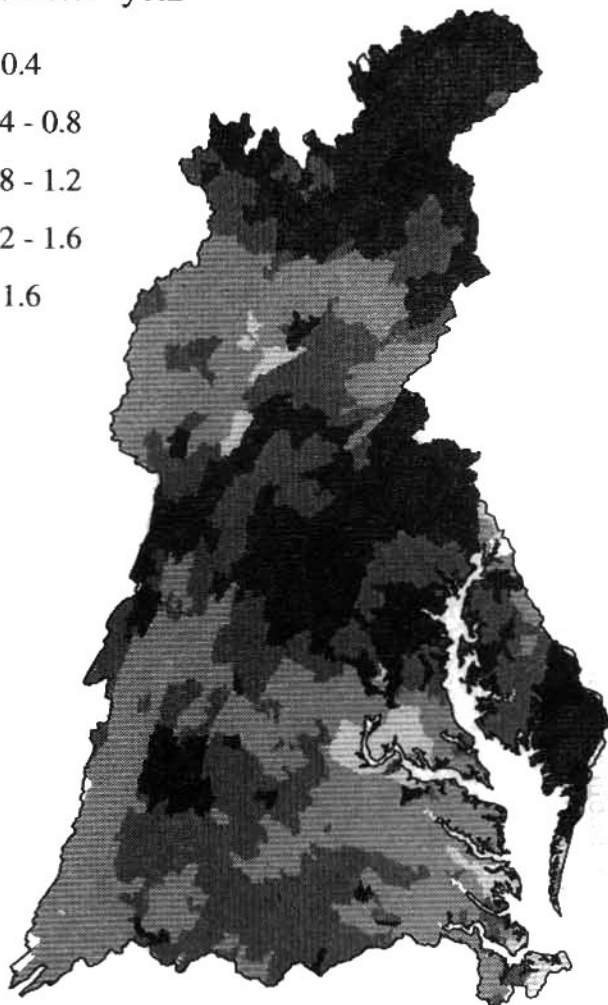
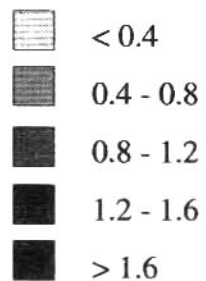
that occur as nitrogen is transported to the Chesapeake Bay. The effects of nutrient enrichment in the bay are a major concern and land-management agencies are seeking tools for prioritizing areas for the implementation of nutrient-reduction measures. If the bay is the primary area of concern, instream loss of nutrients is important because high local loading may become insignificant over distance and with long travel times. To account for instream losses, “delivered yields” (figure 3) were estimated by weighting the incremental loads by the instream loss that would occur over the distance from the end of each reach to the bay. Delivered yields provide a common basis for determining those areas in the entire watershed that are most important to the delivery of nitrogen to the bay.

Figures 2 and 3 illustrate incremental and delivered yields by shading basin areas by yield class. Areas with high incremental yields include the New York part of the watershed, southern Pennsylvania, central Maryland, western Virginia and the lower part

of the eastern shore of the bay. Causes of the high local loading in these areas vary by region. Agricultural sources (fertilizer application and livestock waste production) were important to the incremental yield in most of the areas mentioned, but especially in southern Pennsylvania, central Maryland, and the Eastern Shore. In New York, agricultural sources were important, but atmospheric deposition was the primary source of nitrogen. Point sources are important in many areas of the watershed where there are large population densities, but of the areas in figure 2 with high incremental yield, point-source loading is relatively high in the Scranton, and Harrisburg, Pa., and Baltimore, Md., areas.

Comparison of figures 2 and 3 illustrates the importance of the instream loss that occurs as nitrogen is transported to the bay. Most of the areas that had relatively high incremental (local) loading were much less important with respect to loading to the bay itself. Areas with the highest delivered nitrogen loading to the bay include northeastern and southern Pennsylvania, parts of central Maryland and parts of the lower Eastern Shore. Areas with high incremental yield and relatively low delivered yield include the New York part of the watershed and parts of central Maryland and western Virginia. The highest delivered yields are areas that drain directly to large streams or are

TOTAL NITROGEN
INCREMENTAL YIELD
gram/meter²-year



TOTAL NITROGEN
DELIVERED YIELD
gram/meter²-year

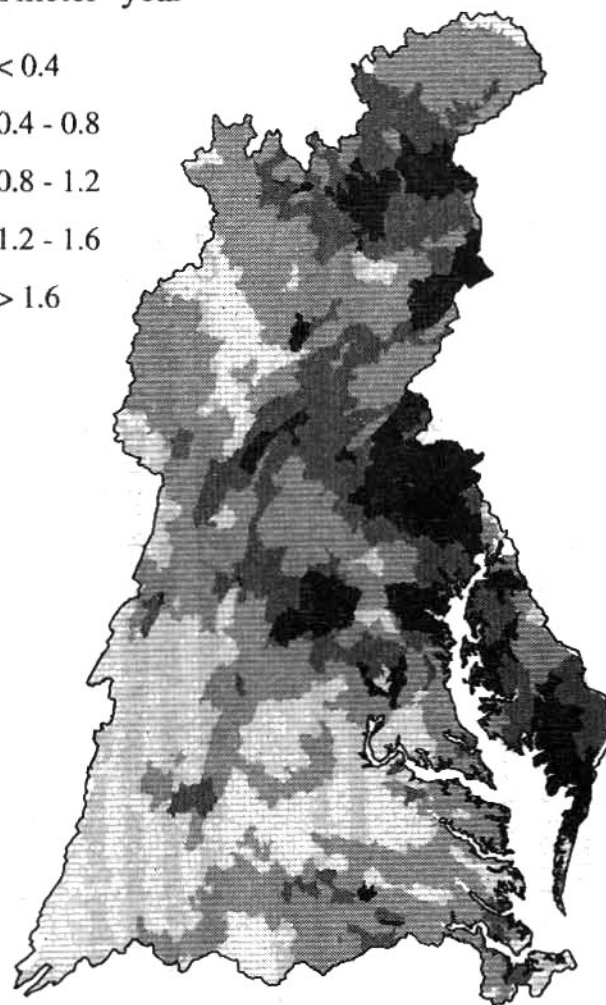
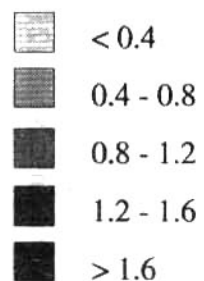


Figure 2. Incremental (local) total nitrogen yields to stream reaches in the Chesapeake Bay watershed.

Figure 3. Total nitrogen yields delivered from stream reach drainages to the Chesapeake Bay.

areas of high incremental loading that are close to the bay. Areas that drain directly to large streams have less instream loss due to lower loss rates (table 1), and for that reason those areas may be more important for delivery of nitrogen to the bay. Areas near the bay may be more important for nitrogen delivery because travel distances are short and the time for instream loss is short compared to other parts of the watershed.

REFERENCES

- Dewald, T., Horn, R., Greenspun, R., Taylor, P., Manning, L., and Montalbano, A., 1985, STORET Reach Retrieval Documentation, U.S. Environmental Protection Agency, Washington, D.C.
- Donigian, A.S., Bicknell, B.R., Patwardhan, A.S., Linker, L.C., and Chang, C., 1994, Chesapeake Bay Program Watershed Model Application to Calculate Bay Nutrient Loadings -- Final Facts and Recommendations. Report # EPA 903-R-94-042, U.S. Environmental Protection Agency Chesapeake Bay Program Office, Annapolis, Maryland, 283 p.
- Smith, R.A., Alexander, R.B., Tasker, G.D., Price, C.V., Robinson, K.W., and White, D.A., 1993, Statistical Modeling of Water Quality in Regional Watersheds. Proceedings of Watershed '93, A National Conference on Watershed Management. Alexandria, Virginia, March 21-24, 1993, 4 p.
- Smith, R.A., Schwarz, G.E., and Alexander, R.B., 1996, Regional Interpretation of Water-quality Monitoring Data. Water Resources Research, 33 (12).
- U.S. Soil Conservation Service, 1994, State Soil Geographic (STATSGO) Data Base. National Soil Survey Center. Publication number 1492, 88 p.

INFLUENCE OF RAINFALL TIMING AND AMOUNT ON PHOSPHORUS LOSSES ASSOCIATED WITH RUNOFF AND SEDIMENT - A GLEAMS SIMULATION

Dr. Clint Truman, Soil Scientist, USDA-ARS, Tifton, Georgia
Mr. Frank Davis, Computer Scientist, USDA-ARS, Tifton, Georgia
Dr. Ralph Leonard, Soil Scientist, USDA-ARS, Tifton, Georgia (Retired)

**Corresponding Author: Dr. Clinton C. Truman, USDA-ARS, Southeast Watershed
Research Lab., P. O. Box 946, Tifton, GA 31793; (912) 386-7174 or (912) 386-3515; FAX:
(912) 386-7294; Email: ctswrl@tifton.cpes.peachnet.edu.**

INTRODUCTION

Runoff leaving agricultural fields carries sediment and phosphorus (P) as nonpoint source pollutants. Millions of tons of sediment and nutrients (N and P) enter and degrade U.S. surface waters each year. Loss of P in runoff influences nutrient management strategies and has been associated with accelerated eutrophication in surface waters. Research and nutrient management guidelines presently focus on maximizing nutrient availability to meet crop nutrient requirements, while minimizing nutrient transport to reduce environmental contamination.

Losses of P in runoff (water and sediment) are influenced by rainfall and soil characteristics and fertilizer application timing relative to rainfall occurrence (Edwards and Owens, 1991; Smith et al., 1991; Edwards and Daniel, 1993; Truman et al., 1993; Pionke et al., 1996; Sharpley, 1997). For regulatory decisions, estimates of "worst-case" runoff are often sought. Majority of annual P losses associated with runoff generally occur during one or two "extreme" rainfall events immediately after fertilizer application. As a result, an increase in time between fertilizer application and a rainfall/runoff event reduces P losses in runoff.

Models can be used to help select management alternatives for reducing contaminant transport from agricultural production systems (Edwards et al., 1992; Leonard et al., 1992). For management questions, models are best used by comparing different alternatives in a relative manner rather than making interpretations based on absolute values or standards. Model output (annual totals, simulation period means, and single event amounts) due to precipitation patterns can be evaluated, especially P transport by surface runoff in relation to probability of or risks associated with off-site contamination and overall degradation of surface water quality.

Improved understanding and estimation of amounts, rates, and forms of P associated with solution and particulate phases leaving agricultural fields under different management and rainfall scenarios is needed. This study utilizes a modeling approach to evaluate the effect of rainfall timing/amount and fertilizer source on P losses in runoff and associated with sediment and soil P build up with continuous land application of commercial fertilizer or poultry litter.

PROCEDURES

When applying models to evaluate P and sediment delivery by runoff, a representative record of rainfall must be chosen. However, no generally accepted guidelines exist to describe what length of record is required to accurately represent expected future patterns and extremes in rainfall. Obviously, the "worst-case" for P associated with runoff will occur when the extreme event occurs on the day of fertilization. Representative periods of record should include these extreme events.

From expected recurrence intervals for rainfall of various amounts in 1-d periods in south Georgia (Sheridan et al., 1979), a worst-case was defined in terms of 2, 10, 25, 50, or 100-yr recurrence intervals assuming fertilization occurred immediately before these events.

The GLEAMS Model The GLEAMS (Groundwater Loading Effects of Agricultural Management Systems) model was developed by modifying the CREAMS model (Knisel, 1980) to evaluate agrichemical (nutrients and pesticides) losses in surface runoff and sediment from field-sized areas. GLEAMS was designed to provide relative comparisons among different management-climate-soil-chemical conditions.

GLEAMS consists of four major components: hydrology, erosion, pesticides, and nutrients. We will not discuss details of the pesticide component since we are interested in runoff, sediment, and associated phosphorus losses. The hydrology component uses daily precipitation inputs along with soil and crop characteristics to compute soil-water-balance in the root zone. Precipitation is partitioned between runoff and infiltration using a modification of the USDA-SCS curve number method (USDA, SCS, 1972; Williams and Nicks, 1982). Water in excess of storage is routed through the root zone, and total amount of percolation leaving the root zone is calculated.

The erosion component uses a modified Universal Soil Loss Equation (Wischmeier and Smith, 1978) for storm-by-storm simulation of rill and interrill erosion in overland flow areas (Foster et al., 1980). Sediment is routed with runoff by particle size (Foster et al., 1985) which allows for calculation of sediment enrichment ratios and simulation of adsorbed agrichemical transport.

The nutrient component (Knisel, 1993) monitors nitrogen and phosphorus cycles and describes how management practices affect daily nutrient status in the soil root zone and that associated with runoff, sediment, and leachate. The phosphorus model developed by Jones et al. (1984) and Sharpley et al. (1984) was incorporated into GLEAMS, with one notable modification in the mineralization of organic P in animal waste. The P section of the nutrient component has algorithms describing mineralization, uptake, leaching, P in runoff and attached to sediment. Management alternatives include fertigation, application of animal waste as solid, slurry, or liquid, and tillage.

Input requirements for GLEAMS include daily rainfall volumes, crop and management parameters, intrinsic soil physical and chemical properties with depth, soil detachment and transport parameters, and agrichemical properties. Output data include runoff, sediment, and percolation amounts, and agrichemical masses in runoff, sediment, and percolation.

In the simulations, fertilizer applications of a commercial fertilizer and poultry litter were applied to corn. Commercial fertilizer was applied in split applications: 1) at planting (56 kg/ha P), and 2) 45 days after planting (only N applied). Poultry litter (3% P and 2.5% organic P) was applied at planting at rates of 2 and 4 tons/A (4.5 and 9 t/ha). All fertilizer applications were incorporated by disking to a depth of 10 cm. A rectangular field of 4 ha consisting of a Cowarts loamy sand (Typic Kanhapludult) with uniform 4% slope with a single overland flow profile was assumed. Simulations were performed for a 50-yr period (1939-1988) using daily rainfall records from Tifton, GA. A 20-d planting window (March 20 - April 8) was assumed, and to ensure equal chance of fertilizer applications on days preceding extreme rainfall events during the 50-yr period, 20 repetitive simulations were performed moving ahead the application 1 d. Output files were created for annual totals and daily mass and concentrations in runoff for the entire year after application.

RESULTS AND DISCUSSION

In this study, we used a modeling approach to address the following questions: 1) How does rainfall timing/amount and fertilizer source influence P losses in runoff (water and sediment)?; 2) What is the probability of having a certain size storm capable of producing runoff and sediment that transports a specified amount of P?; and 3) How fast does soil P build up with continuous land application of commercial fertilizer or poultry litter?

Simulated P losses (kg/ha) associated with runoff (soluble P, SP) and that associated with sediment (SedP) during a 50-yr period for 20 consecutive application dates are given in Table 1. SP losses for the 4.5 and 9 tons/ha poultry litter applications were 1.4 and 2.5 times greater than SP losses for the commercial fertilizer application, whereas SedP losses for the same poultry litter applications were 2.7 and 5.3 times greater than that for the commercial fertilizer. Majority of P lost was in the SedP form. Annual P application rates for the commercial fertilizer and the 4.5 and 9 tons/ha poultry litter applications were 56, 135, and 270 kg/ha, respectively. In terms of percentage of application over the 50-yr simulation, SP losses were 0.2 to 0.4%, while SedP losses were 25 to 29%. Range of SP and SedP losses were relatively small, however, maximum and minimum losses did not necessarily occur for the same planting dates. Therefore, comparing only the twenty 50-yr annual means, application date was not important within the 20-d planting window. However, within each 50-yr simulation, year-to-year variation was relatively large as indicated by coefficient of variations (CV) about annual means. CV values for commercial fertilizer and the 4.5 and 9 tons/ha poultry litter applications ranged from 54-64, 57-100, and 60-89, respectively. Year-to-year variation was caused by different rainfall amounts and timing relative to fertilization.

The Gumbel extreme-value distribution was used to analyze annual P losses for planting (Julian) date 80. Probability plots (Figs. 1 and 2) in terms of "recurrence intervals" were produced which represent the average interval of time within which a value of specified magnitude will be equaled or exceeded, allowing point selection based on probability.

Much of the variation in annual means of P losses can be explained by the occurrence of major storm events near the day of fertilization. P losses for selected individual storm events are presented in Table 2. These 1-d storms were selected from a combination of 50 year rainfall records and different planting dates such that the event corresponded to the planting and fertilizer application

date. Storm event selection was also based on recurrence intervals expected for 1-d maximum rainfall based on the analysis by Sheridan et al. (1979) (Table 3). Rainfall events selected spanned the range from 2- to 100-yr recurrences. Results in Table 2 show that event SP and SedP losses generally increased as individual storm size increased. Exceptions were caused by different antecedent soil water conditions which affect runoff volumes (data not shown). Also, percent of total annual SP and SedP losses made up of the corresponding event losses increased with storm size. This was especially evident with SP losses.

Agricultural producers constantly seek answers to questions such as how much and for how long can they apply fertilizer and/or poultry litter to row-crop land without causing excess nutrient build up in the soil and/or off-site contamination, especially with continuous land application of the fertilizer sources. Simulated data representing P (PO_4 -P) build up in the 0-1 cm and 0-15 cm soil depths over a 10-yr period are shown in Figs. 3 and 4. As expected, P build up in the 0-1 cm soil layer shows much variations with no apparent trend (Fig. 3). The 0-1 cm soil depth is used by the GLEAMS model as an agrichemical source layer for agrichemicals transported in runoff (water and sediment). One would not expect P levels to reach elevated levels in this layer since many pathways exist for P to be removed from this layer (crop uptake, runoff, leaching). P accumulations for the 0-15 cm soil depth increased significantly over the 10-yr period (Fig. 4). For comparisons, soil test P (Mehlich I) levels (0-15 cm soil depth) for the state of Georgia are defined as low (0-34 kg/ha), medium (34-67 kg/ha), high (67-112 kg/ha), and very high (>112 kg/ha). Within the 10-yr period, all fertilizer sources approached or exceeded the high category for soil P build up. The 4.5 tons/ha poultry litter treatment extends well into the high range (max=90 kg/ha), while the 9 tons/ha poultry litter treatment (max=170 kg/ha) exceeds the very high category. Continuous application of fertilizers, especially poultry litter, can cause excess build up of P in a relatively short period of time. The 4.5 tons/ha poultry litter treatment reached/exceeded the high soil P category within 4 to 5 yrs, while the 9 tons/ha reached/exceeded the same level within 2 yrs.

Table 1. Runoff, sediment, soluble phosphorus (SP) and sediment-transported phosphorus (SedP) losses from 50-yr simulations covering the 20 planting dates.

Fertilizer Source	Runoff cm	Sedi-ment t/ha	SP		SP		SedP		SedP	
			Tot.	Range	Mean	Range	Tot.	Range	Mean	Range
			----- kg/ha-----							
Commercial	452	538	9.4	8.6-10.0	0.19	0.17-0.20	727	721-740	14.5	14.4-14.8
Poultry Litter (2 tons/A)	452	538	13.3	11.6-16.4	0.27	0.23-0.33	1978	1962-1991	39.6	57.3-60.8
(4 tons/A)	452	538	23.7	20.9-27.2	0.47	0.42-0.55	3841	3817-3876	76.8	76.4-77.5

Table 2. Phosphorus losses from selected rainfall events (rainfall events were selected so that the day of the rainfall event was the same as the planting date).

Planting Year	Planting Day	Rainfall mm	Event SP kg/ha	Event SP ppm	Event SedP kg/ha	Event SedP ppm	Annual SP kg/ha	Annual SedP kg/ha	% of Total SP	% of Total SedP
Commercial Fertilizer										
1941	80	41	0.02	0.35	0.02	41.5	0.66	4.4	2.5	0.4
1961	91	58	0.04	0.30	0.05	36.0	0.22	23.5	16.7	0.2
1964	98	67	0.06	0.39	0.09	46.7	0.39	27.2	15.8	0.3
1970	81	82	0.12	0.43	0.18	51.0	0.36	26.6	33.7	0.7
1960	93	89	0.12	0.37	0.18	44.2	0.19	8.6	62.7	2.1
1948	92	131	0.21	0.32	0.37	38.7	0.33	6.1	65.3	6.1
Poultry Litter (2t/A)										
1941	80	41	0.02	0.50	0.03	60.6	0.13	11.8	18.1	0.2
1961	91	58	0.08	0.65	0.12	78.1	0.50	69.3	16.3	0.2
1964	98	67	0.11	0.67	0.16	80.3	0.20	74.2	54.5	0.2
1970	81	82	0.20	0.70	0.30	83.4	0.45	75.9	43.5	0.4
1960	93	89	0.20	0.65	0.32	77.6	0.25	24.0	83.3	1.3
1948	92	131	0.37	0.56	0.64	66.9	0.46	19.7	79.5	3.3
Poultry Litter (4 t/A)										
1941	80	41	0.05	0.99	0.06	118.7	0.22	19.5	21.3	0.3
1961	91	58	0.16	1.30	0.23	155.7	0.86	136.2	18.9	0.2
1964	98	67	0.21	1.33	0.31	159.3	0.44	141.1	48.0	0.2
1970	81	82	0.39	1.39	0.59	167.2	0.94	146.5	42.0	0.4
1960	93	89	0.40	1.27	0.62	152.7	0.49	49.1	82.9	1.3
1948	92	131	0.73	1.10	1.28	132.5	0.96	39.1	76.0	3.3

Table 3. Maximum 1-d rainfall amounts for selected recurrence intervals at Tifton, Georgia (Sheridan, et al., 1979).

Recurrence Interval	Maximum 1-d Rainfall	
	March	April
Year	mm	mm
2	41	39
10	81	84
25	91	110
50	117	135
100	132	152

REFERENCES

- Edwards, W.M., and L.B. Owens. 1991. Large storm effects on total soil erosion. *J. Soil Water Conserv.* 46:75-77.
- Edwards, D.R., T.C. Daniels, and O. Marbun. 1992. Determination of best timing for poultry waste disposal: A modeling approach. *Water Res. Bull.* 28:487-494.
- Edwards, D.R., and T.C. Daniel. 1993. Drying interval effects on runoff from fescue plots receiving swine manure. *Trans. Am. Soc. Agric. Eng.* 36:1673-1678.
- Foster, G.R., L.J. Lane, J.D. Nowlin, J.M. Laflen, and R.A. Young. 1980. A model to estimate sediment yield from field-size areas: Development of model. *In* Knisel, W.G. (ed.) CREAMS: A field-scale model for chemicals, runoff, and erosion from agricultural management systems. USDA Sci. Educ. Admin., Conserv. Res. Rep. No. 26, p. 36-64.
- Foster, G.R., R.A. Young, and W.H. Neibling. 1985. Sediment composition for nonpoint source pollution analysis. *Trans. Am. Soc. Agric. Eng.* 28:133-139, 146.
- Jones, C.A., C.V. Cole, A.N. Sharpley, and J.R. Williams. 1984. A simplified soil and plant phosphorus model: I. Documentation. *Soil Sci. Soc. Am. J.*: 48:800-805.
- Knisel, W.G. 1980. CREAMS: A field-scale model for chemicals, runoff, and erosion from agricultural management systems. USDA Sci. Educ. Admin., Conserv. Res. Rep. No. 26.
- Knisel, W.G., 1993. GLEAMS (The GLEAMS model plant nutrient component). Univ. Of Georgia, Coastal Plain Experiment Station, Biological and Agricultural Engineering, Tifton, Ga. Pub. No. 5, 259 pp.
- Leonard, R.A., C.C. Truman, W.G. Knisel, and F.M. Davis. 1992. Pesticide runoff simulations: Long-term annual means vs. event extremes? *Weed Tech.* 6:725-730.
- Pionke, H.B., W.J. Gburek, A.N. Sharpley, and R.R. Schnabel. 1996. Flow and nutrient export patterns for an agricultural hill-land watershed. *Water Resour. Res.* 32:1795-1804.
- Sharpley, A.N., C.A. Jones, G. Gray, and C.V. Cole. 1984. A simplified soil and plant phosphorus model: II. Prediction of labile, organic, and sorbed phosphorus. *Soil Sci. Soc. Am. J.* 48:805-809.
- Sharpley, A.N., 1997. Rainfall frequency and nitrogen and phosphorus runoff from soil amended with poultry litter. *J. Environ. Qual.* 26:1127-1132.
- Sheridan, J.M., W.G. Knisel, T.K. Woody, and L.E. Asmussen. 1979. Seasonal variation in rainfall and rainfall-deficient periods in the Southern Coastal Plain and Flatwoods regions of Georgia. *Res. Bull.* 243, Univ. of Georgia, Coll. Agric. Exp. Stn., Athens, GA 73 p.
- Smith, S.J., A.N. Sharpley, J.R. Williams, W.A. Berg, and G.A. Coleman. 1991. Sediment-nutrient transport during severe storms. p. 48-55. *In* S.S. Fan and Y.H. Kuo (ed.) Fifth Interagency Sedimentation Conf., Las Vegas, NV. March 1991. Federal Energy Regulatory Commission, Washington, DC.
- Truman, C.C., G.J. Gascho, J.G. Davis, and R.D. Wauchope. 1993. Seasonal phosphorus losses in runoff from a Coastal Plain soil. *J. Prod. Agric.* 6:507-513.
- USDA, SCS. 1972. National Engineering Handbook: Sect. 4, Hydrology. Washington, DC. 548 p.
- Williams, J.R., and A.D. Nicks. 1982. CREAMS Hydrology Model - Option 1. *In* Proc. Int. Symp. on Rainfall-Runoff Modeling, p. 69-86. Littleton, CO: Water Res. Pub.
- Wischmeier, W.H., and D.D. Smith. 1978. Predicting rainfall erosion losses - A guide to conservation planning. *Agric. Handb. No. 537*, USDA, Sci. Educ. Admin. 58 p.

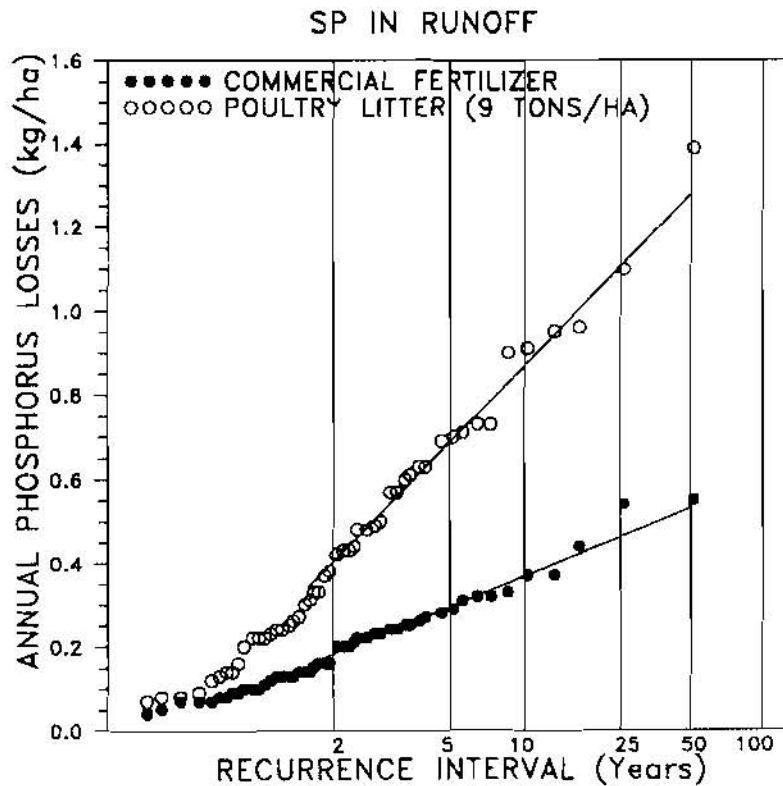


Figure 1. Gumbel extreme-value distributions of annual phosphorus losses (SP in runoff) for the inorganic fertilizer and poultry litter (9 tons/ha).

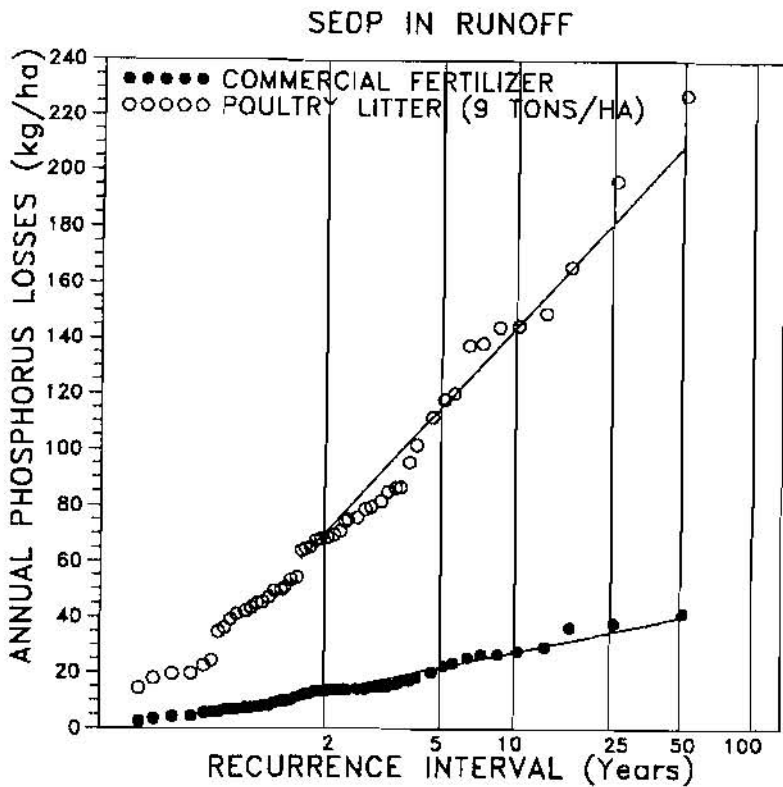


Figure 2. Gumbel extreme-value distributions of annual phosphorus losses (SedP in runoff) for the inorganic fertilizer and poultry litter (9 tons/ha).

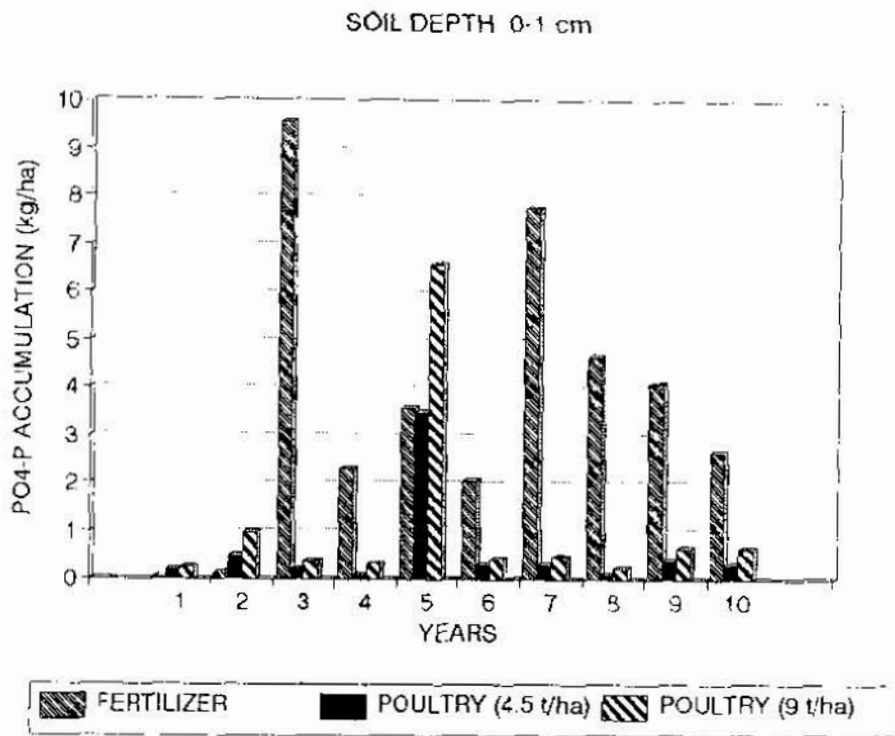


Figure 3. Soil P ($\text{PO}_4\text{-P}$) build-up in the 0-1 cm soil depth for the three fertilizer sources studied.

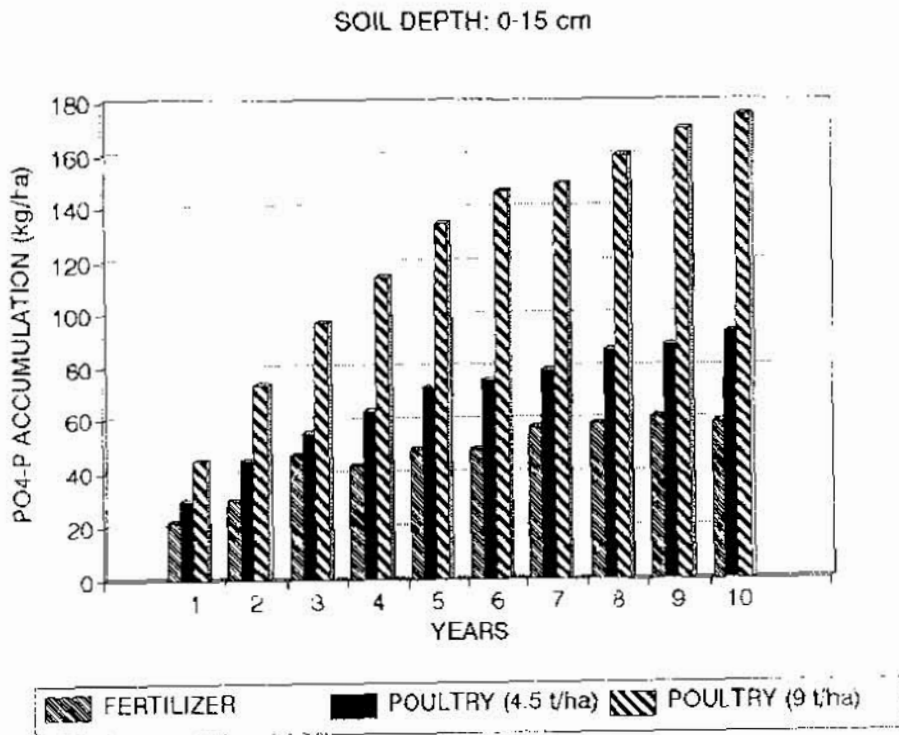


Figure 4. Soil P ($\text{PO}_4\text{-P}$) build-up in the 0-15 cm soil depth for the three fertilizer sources studied.

MODELING ON CLOSURE DISCHARGE OF THE MAIN STREAM OF TGP

By **Chen Songsheng**, Senior Engineer, Bureau of Hydrology, CWRC, Wuhan, China;
Zhang Xuecheng, Engineer, Bureau of Hydrology, YRCC, Zhengzhou, China

Abstract: In this paper, the change tendency of flow discharge at the closure mouth section during river closure of the Main Stream of TGP is studied with applying conventional hydrological measurement method. It is dangerous and difficult to measure discharge at narrower closure mouth cross section along with the progress of closure of the main stream. However, as the process of river closure is continuously developed, the evaluation of the closure mouth cross section can be considered from trapezoidal weir or broad crest weir to V shaped broad-crest weir, V shaped weir. Based on submerged discharge weir formulation, the model reflecting the dynamic variation of the closure mouth cross section and its relation to calculating discharge is established in this paper.

Key Words: TGP, closure discharge, calculation, closure mouth

RAISING PROBLEMS

Research on cross flow motion factors variation is the fundamental target of closure hydraulics in the cofferdam construction progress of hydraulic project. Many valuable hydrological data have been obtained in the past cofferdam construction progress of hydraulic project. But some information could not be observed, so it is quite dangerous to measure discharge with applying conventional hydrological measurement method at narrower closure mouth cross section along with the progress of closure of the main stream. In this paper, for providing hydrological data used in the decision process of river closure of the main stream of TGP, the closure discharge is simulated and calculated after analyzing the possibility of obtaining analysis information under the difficult condition by applying the weir formula.

GENERAL SITUATION OF TGP

TGP sites in Sannianping of Yichang city of Hubei Province. The watershed area is 10 million km² above the TGP dam site, and there is a middle-scale barrier island dividing Changjiang river into two forks at TGP dam site. The left fork is the main stream channel of Changjiang river and the right fork is called back river. At present, the vertical concrete cofferdam has been built at the middle-scale barrier, the back river has become as the pilot open-channel and water has passed.

In the main stream channel, the width of upstream cofferdam closure mouth gets 460m and the width of downstream cofferdam closure mouth gets 540m.

About the pilot open channel: The pilot open channel being the unique construction for flow diversion in the process of closure of the main stream is used as the flood passage and for navigation in the second stage progress of TGP. Design flow section is considered as lateral compound section (figure 1).

(4) Neglecting levee seepage discharge by caving while calculating water discharge at closure mouth.

The hydraulic characteristics of closure mouth reach: In closure process, flow diversion has been started at right pilot open channel. Inflow from Changjiang river flow toward downstream from the pilot open channel and closure mouth. When closure mouth begins to close, flow passing its section becomes neck current. Along with the closing progress, vertical and lateral contraction are taken place on closure mouth section and creating local energy loss. At the same time, parts of potential energy becomes as kinetic energy and flow state becomes as broad-crest weir flow state along with higher flow velocity and smaller section.

And flow on closure section becomes as three-dimensional flow along with the closing progress. Further, water body at closure mouth is divided into backflow area, turbulent current area and main current area by the action of the forward position of levee. Backflow is also formed at the middle site and downstream of the forward position of levee.

After analyzing the hydraulic characteristics of whole reach in different closing periods, we determine to apply water balance and energy balance principles to solve flow discharges passing open channel and main canal and relevant other hydraulic factors such as water stage, velocity etc. The basic equations are written as follows:

For water balance: $Q_o + Q_m = Q_d$

For energy balance: $\Delta Z_o = \Delta Z_m$

Where Q_o , Q_m and Q_d indicate discharges of open channel, main canal and dam site respectively. ΔZ_o and ΔZ_m indicate water heads between upstream and downstream of open channel and main canal reach respectively.

The calculation on closure mouth reach: As showed in above paragraph, flow passing closure mouth has become as free flow, i.e., weir flow. The hydraulic calculation of weir flow is mainly about the magnitude of flow capacity. The condition forming broad-crest weir flow is:

$2.5 < \sigma/H < 10$, where σ indicates weir top width, H indicates weir top water head. In this case, the jacking action of weir top thickness on flow has been become obvious. Because flow passing weir top is controlled by weir top vertical component, section passing flow becomes narrower and velocity becomes higher, so potential energy becomes lower with higher kinetic energy, thus water surface falling on closure mouth reach is formed with local energy loss creating as flow arrives at weir top in addition. If the downstream water stage is lower, flow over weir can take place falling in second time. But if the downstream water stage becomes higher, submerged discharge can be formed with wider section.

Here, water head loss is mainly considered as local water head loss and linear water head loss can be neglected with analyzing many experiential data.

The basic equation of weir flow: The equation can be written as:

$$Q = \epsilon \delta_i m b_r \sqrt{2g} H_o^{3/2}$$

Where Q indicates discharge; δ_i indicates submergence ratio decided by submergence area and section shape factors etc.; m indicates discharge coefficient being 0.30~0.33 if considering lateral contraction effect; ϵ indicates contraction ratio; b_r indicates the average water surface width of closure mouth (As showed in fig.2 and 3, for submerged flow, considering weir top water depth as downstream water depth, i.e., $b_r = Mh_n + b_o$; for non-submerged flow, considering

weir top water depth as critical water depth, i.e., $b_r = Mh_k + b_o$, if $h_k < h_n$, choosing h_n); h_n indicates downstream water depth from horizontal dumping bead top site; M indicates the side slope of closure mouth being 1.5; b_o indicates the height of closure mouth bottom; H_o indicates weir top water head.

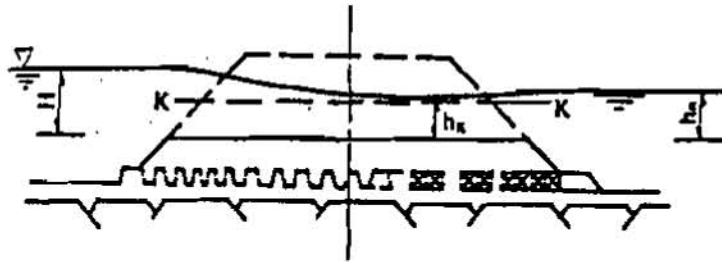


Figure 2. The schematic drawing of broad-crest weir submerged flow

When closure mouth section is considered as trapezoidal section, h_k is calculated by $Q_p^2/g = W_k^3/B_k$. Where B_k indicates closure mouth water surface height corresponding to critical water depth h_k , W_k indicates closure mouth section area corresponding to critical water depth h_k , Q_p and h_k are both determined by trial method.

When closure mouth section is considered as triangular section, h_k is calculated by $h_k = (2Q_p^2/gm^2)^{1/5}$.

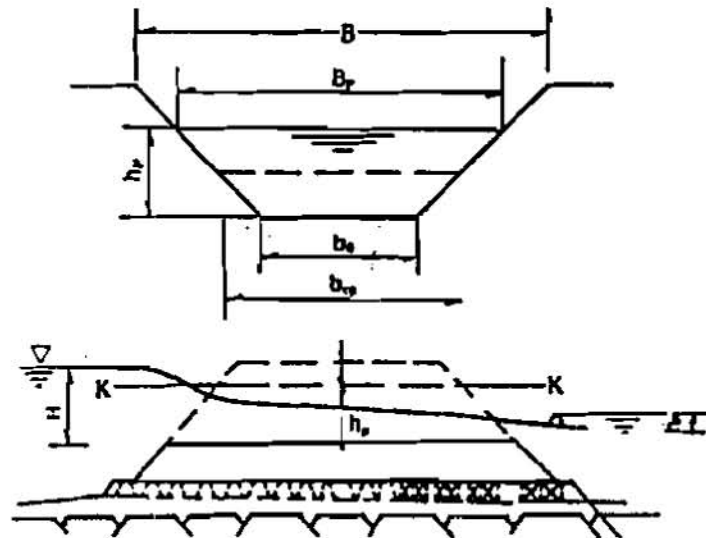


Figure 3. The schematic drawing of broad-crest weir section and non-submerged flow

CALCULATION RESULTS

According to above calculation method and conditions, calculation results of water stages, average velocities, the maximum point velocities, the maximum point discharges on various sections corresponding to upstream cofferdam mouth widths being 130m, 100m, 80m and 50m for open channel and main canal are showed in Table 1. (Notes: Suffixes a and m indicate average and maximum.)

Table 2 shows calculation results of hydrological factors for open channel when main canal is being closed completely in the closure progress of TGP.

Table 1. Calculation results of hydrological factors fro open channel and main canal corresponding various widths in the progress of closure of TGP

(1)B=130m

Discharge at dam site Q (m^3/s)	open channel Q (m^3/s)	main canal Q (m^3/s)	open channel flow diversion ratio (%)	open channel dam axis		open channel inlet		main canal		
				H (m)	V_a (m/s)	V_m (m/s)	V_a (m/s)	V_m (m/s)	V_a (m/s)	V_m (m/s)
10400	6800	3600	65.00	66.50	1.10	1.32	1.57	1.88	1.64	2.79
12400	8160	4210	66.00	66.62	1.31	1.57	1.86	2.23	1.92	3.26
14600	9650	4910	66.00	66.85	1.53	1.84	1.70	2.56	2.22	3.77
16300	10900	5410	67.00	67.07	1.71	2.05	2.35	2.82	2.42	4.11
19700	13300	6390	68.00	67.54	2.03	2.44	2.73	3.28	2.79	4.74

(2)B=100m

Discharge at dam site Q (m^3/s)	open channel Q (m^3/s)	main canal Q (m^3/s)	open channel flow diversion ratio (%)	open channel dam axis		open channel inlet		main canal		
				H (m)	V_a (m/s)	V_m (m/s)	V_a (m/s)	V_m (m/s)	V_a (m/s)	V_m (m/s)
10200	7600	2600	75.00	66.52	1.32	1.48	1.75	2.10	1.80	3.06
11900	9000	2900	75.00	66.64	1.46	1.75	2.07	2.48	2.12	3.60
14000	10600	3390	76.00	66.87	1.69	2.03	2.35	2.82	2.40	4.08
19200	14700	4450	77.00	67.59	2.24	2.69	3.01	3.61	3.02	5.13
21600	16700	4910	77.00	67.93	2.50	3.00	3.29	3.95	3.28	5.58

(3)B=80m

Discharge at dam site Q (m^3/s)	open channel Q (m^3/s)	main canal Q (m^3/s)	open channel flow diversion ratio (%)	open channel dam axis		open channel inlet		main canal		
				H (m)	V_a (m/s)	V_m (m/s)	V_a (m/s)	V_m (m/s)	V_a (m/s)	V_m (m/s)
10300	8300	2000	81.00	66.54	1.34	1.61	1.91	2.29	3.47	3.59
12360	9960	2400	81.00	66.57	1.60	1.92	2.25	2.70	3.11	4.25
14368	11620	2748	81.00	66.91	1.84	2.21	2.56	3.06	2.82	4.79
16359	13280	3079	81.00	67.16	2.07	2.48	2.83	3.40	3.11	5.29
19311	15770	3541	82.00	67.64	2.39	2.87	3.19	3.83	3.47	5.90

(4)B=50m

Discharge at dam site Q (m^3/s)	open channel Q (m^3/s)	main canal Q (m^3/s)	open channel flow diversion ratio (%)	open channel dam axis		open channel inlet		main canal		
				H (m)	V_a (m/s)	V_m (m/s)	V_a (m/s)	V_m (m/s)	V_a (m/s)	V_m (m/s)
10003	9250	753	92.00	66.57	1.49	1.79	2.11	2.53	1.35	2.30
12047	11160	887	93.00	66.71	1.78	2.14	2.50	3.00	1.57	2.67
13957	12950	1007	93.00	66.96	2.04	2.45	2.82	3.38	1.75	3.00
15927	14800	1127	93.00	67.23	2.30	2.76	3.12	3.74	1.92	3.26
19075	17760	1315	93.00	67.74	2.68	3.22	3.55	4.26	2.15	3.66

Table 2. Calculation results of hydrological factors for open channel

B=0.0m

Discharge at dam site Q (m^3/s)	open channel Q (m^3/s)	main canal Q (m^3/s)	open channel flow diversion ratio H (%)	H (m)	open channel			
					dam axis V_a (m/s)	V_m (m/s)	inlet V_a (m/s)	V_m (m/s)
8000	8000	0.00	100.00	66.42	1.30	1.56	1.86	2.23
10000	10000	0.00	100.00	66.59	1.61	1.93	2.28	2.74
12000	12000	0.00	100.00	66.75	1.92	2.30	2.67	3.20
14000	14000	0.00	100.00	67.01	2.20	2.64	3.02	3.62
16000	16000	0.00	100.00	67.29	2.48	2.98	3.35	4.02
19400	19400	0.00	100.00	67.83	2.91	3.49	3.82	4.58
22000	22000	0.00	100.00	68.22	3.24	3.89	4.16	4.99
25000	25000	0.00	100.00	68.79	3.57	4.28	4.48	5.38
30000	30000	0.00	100.00	69.77	4.08	4.90	4.89	5.87
35000	35000	0.00	100.00	80.84	4.52	5.42	5.22	6.26
40000	40000	0.00	100.00	71.85	4.93	5.92	5.53	6.64
45000	45000	0.00	100.00	72.89	5.30	6.36	5.80	6.96
50000	50000	0.00	100.00	73.99	5.62	6.74	6.01	7.21
55000	55000	0.00	100.00	74.96	5.94	7.15	6.24	7.49

CONCLUSION AND DISCUSSION

With analyzing above calculation results, we can conclude:

- (1)The hydraulic characteristics calculated for open channel, main canal and closure mouth reach in this paper are similar to results obtained by hydraulic test and simulation.
- (2)Calculated results of flow velocities for open channel and main canal are similar to observed values in 1997.
- (3)After main canal is closed completely, in contrast natural condition, water stage-discharge relation opposite curve for open channel moves up and approaches to natural condition.

Authors:

Chen Songsheng, Bureau of Hydrology, CWRC

Address:

No.1155, Jiangfang Street, Wuhan 430010, China

Zhang Xuecheng, Bureau of Hydrology, YRCC

Address: East No.12, Chengbei Road, Zhengzhou 450004, China

Tel: +86-10-63202623

Fax: +86-10-63202978

E-mail: Wangzhy@public3.bta.net.cn

EFFECTS OF HYDRAULIC PROJECTS IN SAN-HUA REACH OF THE YELLOW RIVER TO FLOODS AND RUNOFF

By Feng Xiangming, engineer, Hydrology Bureau, YRCC, Zhengzhou, China

Abstract: The two multi-purpose reservoirs of Luhun and Guxian can basically control the coming water from upper stream and can reduce flood peaks and flood volume of the San-Hua reach. The effects of medium and small-sized reservoirs in the San-Hua reach to floods are mainly function of retaining and storage and usually the function is small. Groups of medium small-sized reservoirs have greater influence to the peak discharge and runoff volume of an individual flood and smaller influence to an individual flood of continuous floods.

The reach between Sanmenxia and Huayuankou (San-Hua reach for short), with a area of 41,600 km², is one of main flood yielding areas of the lower Yellow River. Up to the end of 1991, there are 509 reservoirs set up in the area. The reservoirs have changed the phsiographic conditions of basin of the area, and then the hydrologic situation is influenced.

1 Basic condition of the reservoirs

All of the 509 reservoirs set up from 1953 to 1991 in the area, there are two multipurpose reservoirs of Luhun and Guxian, 19 medium reservoirs, 147 small-1 reservoirs and 341 small-2 reservoirs, reservoir volume is 3409 million m³. The reservoirs have been set up in which year and the reservoir volume is shown in statistical table 1.

Table 1 The Statistics Of Storage Of Reservoirs In The San-Hua Reach x10⁸m³

Years	Large sized		Medium sized		Small-1 sized		Total	
	number	storage	number	storage	number	storage	number	storage
1950-1959			2	0.3812	38	1.0378	40	1.4190
1960-1969	1	12.9	13	2.5944	58	1.7366	72	17.228
1970-1979			3	0.8755	46	1.4614	49	2.3329
1980-1989			1	1.0978	5	0.2190	6	0.3168
1990-1991	1	12.0					1	12.000
1950-1991	2	24.9	19	3.9498	147	4.4518	168	33.3007

The distribution of the reservoirs in the area is very non-uniform. The reservoirs of Guxian and Luhun lie in separately Luohe river and the middle of its channel segment - Yihe river, control drainage area are 5370km² and 3492km². Medium small-sized reservoirs situate mainly in the lower and middle of Luohe River and Qinhe river, i.e, the reach in Yihe river between Luhun and Longmenzhen(Lu-Long reach for short), and the reach in Luohe river between Changshui and Baimasi(Chang-Bai reach for short), and the reach in Qinhe river between Runcheng and Wulongkou(Run-Wu reach for short), as well as upper the Shanluping in the channel segment of Qinhe river. The four basins area is only 30% of San-Hua's, there are 13 medium reservoirs, 95 small-1 and 234 small-2 reservoirs, these

are 68.4% and 64.6 and 68.6% in all kinds of reservoirs; the 613 million m^3 for total reservoir volume is 66.7% in all of the reservoir volume.

2 Effects of reservoirs to floods

According to historical data statistics, the storm centre of San-Hua reach usually occur in the reach are four region as follows: Luanchuan、Luonan at the upper Yihe and Luohe River, Songxian, Yiyang and Xin'an at the lower and middle Yihe and Luohe river; Yuanqu, Balihutong in the reach between Sanmenxia and Xiaolangdi, Jiyuan, Wulongkou at the lower Qinhe river. Luhun and Guxian reservoirs can control the first storm center, the groups of medium and small-sized reservoirs can control the second, the forth storm center.

From the average annual flood peak discharge of the main control station in San-Hua reach(see table 2), we know that annual flood in 1950s are larger than other years in every station. Longmenzhen, Shanluping are 2.3 and 2.6 times of the average of years. Though this is related with precipitation, the effects of reservoirs are important. From table 2, we can see that the effects of the reservoirs to the controlled station of Longmenzhen and Shanluping are more obvious than others.

Table 2 The Average Of Annual Maximum Flood Of Main Control Station m^3/s

Years	Longmenzhen	Baimasi	Heishiguan	Wulongkou	Shanluping	Wuzhi
1950 ~ 1959	3000	3040	4290	1370	1030	1360
1960 ~ 1969	496	1530	1670	880	288	956
1970 ~ 1979	748	736	959	729	158	606
1980 ~ 1989	1030	1580	690	852	187	791
1950 ~ 1989	1320	1720	2150	958	416	928

2.1 Effects of large reservoirs to floods

Lunhun and Guxian reservoirs are large complex use ones with flood protection mainly as well as irrigation ,power generation, water provision, fish farming etc. Reservoir storage are 1,290 millions m^3 and 1,175 millions m^3 respectively.

Luhun reservoir was set up in August in 1965, there are two larger floods on 8,8,1975 and on 8,1,1982. Flood peak discharge for reservoir inter station Dongwan were 4200 and 3500 m^3/s , with subarea discharge formation reservoir inflow were 5640 and 5280 m^3/s , as well as design flood by the return period of in twenty years, after reservoir regulation, maximum discharge of outflow station were 1170 and 890 m^3/s , the reducing rate of peak is 79.2%, 83.1%. The reservoir inflow flood includes two peaks in 8,1982. The first peak discharge is 5280 m^3/s , by precipitation process for from Dongwan to Luhun formation; the last peak flow is 3500 m^3/s , by the peak discharge, there is a peak only in outflow, and maximum is only 890 m^3/s . During the flood, the storage of reservoirs reaches 2,120 millions and is 57.3% of the total of inflow—3,700 m^3

Obviously, Guxian reservoir, may also decrease the upstream peak and charge like Luhun reservoir. With operation of the Luhun and Sanmenxia reservoirs in union, it can improve the level of the downstream flood protection. So the two large reservoirs in the area are important parts in downstream flood protection project system.

2.2 Effects of medium and small reservoirs to floods

The water discharge equipment of reservoirs in the San-Hua reach only have spilldoor and no control. So the effects of medium and small reservoirs to flood are mainly retaining and storage. The use of reservoir is connected with its storage. As the statistical data of the 14 medium and small reservoirs and the operation case of the ones since 1982, the half of the total storage can be regarded as the storage of the flood protection.

$$R'_m = V_m/A \quad (1)$$

in which V_m ---storage of flood protection, A ---the control area of reservoir. The capacity of interception storage R_m is connected not with flood protection storage, but with initial storage of reservoir. If amount of antecedent influence rainfall I influences the initial storage of the reservoir,

$$R_m = R'_m(1 - P_a/I_m) \quad (2)$$

where I_m ---the maximum of P_a , normal $I_m=90\text{mm}$.

So, after long-time arid and non-rain and before the first flood during flood season, there is no water in the reservoir, $P_a \approx 0$, the capacity of interception is maximum; after one or two flood(s), the capacity of interception reduces smoothly; after serial floods or bigger floods, the reservoir is full basely, $P_a \approx I_m$, the capacity of interception nears zero.

In order to analysis and calculate, medium and small reservoirs in every regions may be regarded as a group of reservoirs. And use the proportion of flood protection storage of the reservoirs group and the area in the region to describe the maximum capacity of retaining and storage. As calculation, the capacity of interception of the reservoirs up the Yihe Lulong reach and Danhe Sanluping reach is bigger. They are 33.2 and 34.5mm separately. But, them of Luohe Changbai reach and Qinhe Runwu reach are smaller with 20.4 and 12.9mm separately. This is same as the result of table 3.

The influence of medium and small reservoirs to floods may also be analysed with rainfall-runoff relation. As the calculation of every rainfall's depth of runoff and the observation depth of runoff of the rainfall-runoff relation figure, before 1970, the deference of the two. The average is -0.4mm; after 1970, the calculated depth of runoff is bigger, the average is bigger 12mm, especially two floods "75.8", "82.8", bigger 25.6 and 40.5mm. This is also same as the result from the table 2 basely.

The table 3 is the calculated rainfall-runoff result of the three floods, R'_c is the volume of runoff not considered the influence of the reservoir by the forecasting figure. when the

rainfall is P , the reservoir's interception R_r can be calculated with the case

$$R_r = R_m(1 - e^{-P/R_m}) \quad (3)$$

Where R_m got with the case (2). The runoff R_c influenced by the reservoir is

$$R_c = R'c - R_r \quad (4)$$

Table 3 The Calculated Rainfall-runoff Result In Lulong reach mm

Time yr.mo	P	Pa	Rm	Ro	Unconsidered		Considered Reservoirs			Restored Value R'
					R'c	ΔR'	Rr	Rc	ΔR	
75.8	198.3	15.1	73.4	73.4	99.0	25.6	27.6	71.4	2.0	101.0
82.7	221.7	28.2	86.0	86.0	126.5	40.5	28.2	98.3	12.3	114.2
82.8	109.4	3.2	90.9	90.9	83.0	7.9	0	83.0	7.9	90.9

The table 3 shows that:

(1) Two floods "75.8" and "82.7", not considered the influence of reservoir, the calculated difference R' of runoff is bigger. The reason is mainly that the two floods are the first one in flood season. The antecedent influence rainfall amounts are 15.1 and 13.6 mm separately. It is very arid. So, the capacity of interception of reservoir is very big. As calculation, its depths of runoff of interception are 27.6 and 28.2mm separately, near its maximum of capacity of interception 33.2mm. Considered the effect of the capacity of the reservoir's interception, the calculated difference of depth of runoff reduces greatly.

Using the formula $R' = R_o + R_r$, the observed runoff depth (R_o) could be restored to natural one (R'), and be drawn on the relationship curve: $R = f(P, P_a)$, just as the dot A' and B' . The Figure shows that the simulation result A' and B' are better than A and B . It also shows that the influence of the reservoirs is the main reason which the observed runoff depth is less than that in the past.

(2) For the "82.8" flood, the runoff depth ($R'c$) which the influence of reservoirs are not considered corresponds to the observed value (R_o) well. That indicates the influence of reservoirs is small. This flood is the consistent one followed "82.7" flood, so the soil were very humid ($P_a = 81.4$ mm, is close to its maximum 90 mm), and all most reservoirs were full.

It is worth mentioning, moderate and small reservoirs can play great role in retaining flood for normal rainfall, but because of the flood protection standard of these reservoirs are not high, and the management is not better, so the probability which increase the flood peak

discharge if the large storm will be met and the reservoir will be dam-break. Is not to be ignored.

3 Effects of reservoirs to annual runoff

The influences of reservoirs to annual runoff are not obviously like those to flood mentioned above. But the law which the building of reservoirs decreased the annual runoff of the basin is right. It may be seen from table 4 that: under the condition of the annual precipitation were very close, but the annual runoff decreased progressively with years. That illustrates although the precipitation is the main factor of forming runoff, the reason which runoff decreased much more is chiefly due to the influence of reservoirs. Reservoirs have begun to affect annual runoff at 1970s, this is identical with the time of building reservoirs.

Table 4 The Statistics Of Precipitation And Runoff

Time	Heishiguan(Luohe River)		Wuzhi(Qinhe River)	
	P(mm)	R($\times 10^8$ mm)	P(mm)	R($\times 10^8$ mm)
1950 ~ 1959	680.1	41.73	646.5	16.16
1960 ~ 1969	653.5	35.48	650.3	14.03
1970 ~ 1979	624.8	20.46	594.9	6.15
1980 ~ 1989	678.8	29.9	590.6	5.41
1950 ~ 1989	659.3	31.89	620.6	10.44

4 Conclusion

(1) The two multi-purpose reservoirs of Luhun and Guxian can basically control the coming water from upper stream and can reduce flood peaks and flood volume of the San-Hua reach.

(2) The effects of medium and small-sized reservoirs in the San-Hua reach to floods are mainly function of retaining and storage and usually the function is small.

(3) Groups of medium small-sized reservoirs have greater influence to the peak discharge and runoff volume of an individual flood and smaller influence to an individual flood of continuous floods.

(4) The influence of reservoirs to annual runoff is very complicated , its influence obviously began at 1970s.

**Address: Hydrology Bureau, YRCC, No.12 Chengbei Road,
Zhengzhou,China**

Phone Number: 86-0371-6302051

Postcard: 450004

RESEARCH ON FLOW CUT-OUTS IN THE LOWER YELLOW RIVER

By Wang Ling, Engineer, Hydrology Bureau, YRCC, Zhengzhou, China; Lin
Yinping, Engineer, Hydrology Bureau, YRCC, Zhengzhou, China;
Chu Yongwei, Engineer, YRCC, Zhengzhou, China; Cui Qing,
Engineer, YRCC, Zhengzhou, China

Abstract: The flow cut-outs in the lower Yellow River are becoming more and more serious since the beginning of 1990s. This has drawn much attention and concern from all walks of life. Flow cut-outs have reflected the deteriorating situation caused by the contradiction between supply and demand of water resources. It is one of the latest and most notable problems we're meeting in development and regulation of the Yellow River. The Yellow River Conservation Commission has given top priority. Some measures have been taken in order to alleviate the bad effects that flow cut-outs have brought, meanwhile we are making a good study of this phenomenon, looking into the causes, analyzing the effects so that we may adopt effective measures to alleviate the situation and bring it under control.

1. Situations and characteristics of flow cut-outs

1.1 General Circumstances

In the past, the cut-outs of the lower Yellow River seldom taken place except damning the flow by SanMenXia Project at ice period in 1960. Frequent cut-outs began in seventies. From 1972 to 1996 flow cut-out had taken place in 19 years, by the average of four times in five years. Analyzing the observed data at Li Jin station, 57 times flow cut-outs had taken place in 19 years, the total days were 682, by an average of nearly 36days a year. Within them, the longest days was in 1996 which occupied the time 37% of the whole year. The longest reach was in 1996, i.e.,683 km from the mouth to Chenqiao which occupied 87% of the whole length of the low reaches.

1.2 Flow Cut-out Characteristics

From the statistic results, flow cut-outs characteristics include: In sixties and seventies, 13 years, totaling 191 days experienced cutouts at Lijin station site by an average of 15 days a year. In the 1990s, flow cut-outs has taken place six times in seven years at Linjin station site, totaling 491 days, by an average 82 days a year, nearly five times longer than that of 1960s, 1970s. In general, flow cut-outs in the lower Yellow River start from the mouth toward upper. The average length of cut-out is 242km in the 1970s, 256km in the 1980s, and has come to 392km in 1990s. The positions which cutouts frequent are located near LuoKou station site. The annual average length (about 295km) is also at LuoKou station site. So the river reach from Luokou down wards is quite vulnerable to cut-outs. Before nineties, cut-outs were liable to appear in mid-April. In the whole year, cut-out did not last more than 3 months, usually in May, June, and July, nearly occupying 86% of the total cut-out period. In the 1990s, cut-outs have been become earlier, about in mid-February. The cutouts in the whole year may last as long as six months, e.g., in 1996. Flow cut-out period is extended from March to July, holding up 92% of the whole period.

And flow cut-outs taken place is whole in June appeared in four years. In the 1970s, 1980s, only when monthly average discharge at HuaYuanKou station was less than $750\text{m}^3/\text{s}$, cut-outs would take place. But in the 1990s, even monthly average discharge increased to $1100\text{m}^3/\text{s}$ at HuaYuanKou station, cut-outs are still liable to appear.

2. Main reasons causing flow cut-outs

2.1 The poorer water resources in Yellow River are an important factor affecting fast growth of water demand.

The most areas in Yellow River basin belong to arid or semi-arid. The total area of the Yellow River basin is 795000km^2 , taking up 8% of China. The average natural annual inflow is 58 billion m^3 , only occupying 2% of the total in China. The average water consumption per person is 593m^3 , which is 25% of national average level. The average water use for one Mu cultivated land is 324m^3 , only 17% of the national average level. A lot of water conservancy projects have been implemented since the founding of the People's Republic of China. 3138 Reservoirs at different scales have been built on the branches and tributaries. The total reservoir capacity is 58.3 billion m^3 . We also have finished 9800 diversion projects, 23600 water-lifting works and 378000 motor-pumped wells. 122 stations for water-lifting, diversing, conveying have been built up in the lower Yellow River in order to diverse water to meet the demand of Hai River and Huai River areas. All these have provided the basic and fundamental facilities for development and utilization of water resources. They have played a very important part in pushing on social and economic development.

From statistic results, water consumption of the Yellow River for cultivating land, urban daily life, industries, and agriculture has been increased from 12.2 billion m^3 in the 1950s to 30 billion m^3 in 1990s, roughly 1.6 times. 33.4 billion m^3 in 1989 made the highest record. At present, the percentage of water resources utilization has exceeded 50%, which is higher, compared with many other large rivers at home and abroad as well. The regional distribution of water utilization is: In the upper reaches, the annual water consumption has increased from 7.3 billion m^3 in the 1950s to 13.2 billion m^3 in the 1990s, 0.8 times. In the middle reaches, it has reached 6 billion m^3 in the 1990s from 3 billion m^3 in the 1950s, it is doubled. In the lower Yellow River, in the nineties the annual water consumption has come to 10.8 billion m^3 from 1.9 billion m^3 of 1950s. The water supply of the Yellow River is mainly for agricultural irrigation, which holds up 90% of the total water consumption. The irrigation area depending mainly on the Yellow River's water has extended from 21.04 million Mu of 1950s to 73.06 million Mu in the 1990s. In the upper reaches, 12.2 million Mu in the 1950s has been increased to 19.73 million Mu in the 1990s; in the middle reaches, 6.34 million Mu to 20 million Mu; in the lower reaches, 4.50 million Mu to 33.34 million Mu.

The fast-growing water consumption and pressing water demand for irrigation by the regions and areas along the Yellow River had made the contradiction of supply and demand from bad to worse, and the Yellow River even poorer in water resources. This is the major reason accounting for the cut-outs. Especially, in the regions of the lower reaches, the total irrigated land relying on the Yellow River exceeds 35 million Mu.

There have 122 diversion works. The originally planned diversion capacity is $4000\text{m}^3/\text{s}$, excessively surpassing the water supply capacity of the Yellow River. In the 1990s, the water resources of the Yellow River terribly lack. The continuous dry climate often strikes the regions in the low reaches. So cut-outs are becoming more frequent, more serious day by day. In seventies and eighties, the scale of the cut-outs in terms of time, frequency and length were comparatively lower. However, in nineties, in order to alleviate the pressing situation caused by water deficiency, the regions and areas in the low reaches begin to store water in winter. They call the Project "Store in Winter, Use in Spring". This has inevitably aggravated the tense situation even in non-irrigating seasons. This also accounts for the deteriorating cut-out situation.

2.2 Decreasing natural runoff amount and decreasing rainfall

Statistics show that rainfall is decreasing along the Yellow River reaches from 1990 to 1995. The annual average rainfall from HuaYuanKou upwards is 388mm , taking up 89% of the previous years' average level. In the regions from HuaYuanKou downwards, the yearly average rainfall is 635.1mm , occupying 93.4% of the previous years' average level. In fifties, the rainfall and runoff quantity of the Yellow River almost reached the average level of recent years. Their changes had seldom affected by human activities. So the practical tests and statistics of 1950s and 1990s can act as a foundation for comparing and analyzing.

2.2.1. The runoff at LanZhou station

The annual runoff amount of 1990s has reduced by 3.86 billion m^3 compared with that of 1950s. 2.67 billion m^3 is lost, due to decreasing rainfall and vapouring. This does not include 1.19 billion m^3 of additional water consumption for industries and agriculture. As a result of the regulation of the LonYang Reservoir and the LiuJiaXia Reservoir, the runoff amount of 1990s in non-flood seasons is increased averagely 4.07 billion m^3 compared with that of 1950s.

2.2.2 The runoff at HeKouZhen station and water utilization at LanHeQiuJian

The runoff of 1990s at HeKouZhen is reduced by 6.94 billion m^3 , compared with that of 1950s. This is mainly due to the flow of 3.86 billion m^3 lost at LanZhou, and additional water use of 3.08 billion m^3 between LanZhou and HeKou reach. Thanks to additional 4.07 billion m^3 of water supply by the regulatin of the LongYan Reservoir and the LiuJiaXia reservoir, and also additional 2.7 billion m^3 of water consumption for industries and agriculture at LanHeQiuJian, so the wate discharge at HeKouZhen in non-flood seasons (mainly in April), has increased 1.37 billion m^3 in the 1990 s compared with that of 1950s. But the water discharge at HeKouZhen in flood seasons has decreased by an average of 8.31 billion m^3 in the 1990s, compared with that of 1950s. This also has affected the sediment transport in the lower Yellow River.

2.2.3 The runoff at HuaYuanKou station are decreased by an average of 19.45 billion m^3 per year, compared with that of 1950s.

The middle reaches regions from HeKouZhen to HuaYuanKou, the inflow is reduced by 12.51 billion m³. This does not include 6.94 billion m³ lost at HeKouZhen. All this are the results of runoff decrease in the regions of the middle reaches and fast-growing water consumption for industries and water preservation in the 1990s. on the base of statistics concerned, water consumption growth of 3.07 billion m³ in the middle reaches in nineties compared with that in fifties is due to fast-growing water demand of industries and urban daily life. The reduction of 9.44 billion m³ is mainly caused by little rainfall or some other reasons.

In contrast to the runoff in the 1950s, the annual runoff amount at HuaYuanKou station is reduced by 19.45 billion m³, among which 17 billion m³ is lost in flood seasons. The runoff reduction at HeKouZhen and HeHuaQuJian is 8.31 billion m³ and 8.69 billion m³ respectively. In non-flood seasons, the water flow decrease is 2.45 billion m³, among others, the runoff at HeKouZhen increased by 1.37 billion m³. There is 3.82 billion m³ water lost between Hekou and Hua yuankou reach.

2.2.4 in the areas along the lower Yellow River, from Huayuankou downwards, water consumption is growing very fast in the 1990s in contrast to that of 1950s.

The annual average increased water amount is 10.96 billion m³ among which, 8.15 billion m³ is in non-flood season, 2.81 billion m³ in flood seasons. The above analysis results show that the runoff at Huayuankou station in non-flood seasons is reduced by 2.45 billion m³ in the 1990s, compared with that of 1950s. the water consumption demand in the regions from Huayuankou downward is increased 81.50 billion m³. All this is the major reason accounting for the pressing situation of supply and demand of water resources and the frequent cut-outs in the lower Yellow River.

2.3 There was no a more unit integrated system for water resources regulation and management

The Yellow River is the most important water resource for North China and northwest China. The development of the Yellow River has played a major part in accelerating national economy and social progress of the provinces along the river. At the present, different departments, different regions and different provinces respectively administrate some backbone engineering and large irrigation projects. There has not an unit regulation and management system, which closely and uniformly integrats the central administration with the local one. So it is quite difficult to take the whole situation into consideration and plan accordingly. As there has no effective regulation and management for the backbone engineering and major diversion works, so long as dry climate comes water resources will be in short supply, sometimes may even result in water waste. All these account mainly for the recent cut-outs.

3. The effects of the cut-outs and the countermeasures to deal with the situation

Water resources development and utilization of the Yellow River have played an important role in boosting the economy of the provinces along the River. However, the limited water resources can not meet the fast-growing demand. Frequent cut-outs have

brought tremendous loss to the regions along the reaches, especially to industries and agriculture. The bad effects may be brought upon flood prevention and ecological balance of the delta at the river mouth.

3.1 The cut-out effects

To date, the cities, which depend on water supply of the Yellow River are Zhengzhou, Xinxiang, Kaifeng, Puyang in HeNan Province; Heze, LiaoCheng, Jinan, Dezhou, Zibo, BenzhouDongying in ShanDong Province, also the ZhongYuan Oil Field, and the ShengLi Oil Field. Some preliminary investigations show that industrial and agricultural loss (including the loss of the Oil fields) brought by the cut-outs and water deficiency in the lower Yellow River during the 1972-1996 period is 26.8 billion yuan, by an average of 1.4 billion yuan per year. In seventies and eighties, the annual average loss brought upon industry and agriculture in the lower reaches by the cut-outs is 400 million yuan. In nineties, the cut-outs have become more serious, the annual average loss has reached 3.6 billion yuan. Agriculture loss holds up 45.5% of the total loss. 70.42 million Mu of irrigated land is attacked by drought, reduction of output is 9.86 kg. Let's take 1995 for example. Linjin station experienced three times of cut-outs, totaling 122 days. Luokou, Aishan, Senkou, Gaocuen, Jiahetan tation also experienced cut-outs of respective 77 days , 62 days, 52 days, 8 days and 4 days. This year, 19 million Mu fields were stricken by drought in the lower Yellow River. The output was decreased by 2.7 billion kg. Investigation shows that 300000 Mu rice fields in Dongying, 100000 Mu in binzhou had failed to be transported rice seeding due to water deficiency. 850 million m³ of water failed to be diversified into Dezhou, so wheat output was cut down by 3400 million kgs. In Puyang, due to the cut-out, wheat output was reduced by 6.14 million kg. 200000 Mu of rice fields failed to be transported rice seeding on time, the farmers had to plant some other corns instead of rice. In Dezhou city, water supply for daily life was shrunk from 120000tons per day to 50000 tons per day. There had 139 factories that had to close down or reduce their production. The economic loss is 600 million yuan per year. Dongying city and the Shenli Oil Field had the Pingyuan reservoir to depend upon (storage capacity is 484 million m³), but due to the long time cut-out, water demand of 32 million m³ was still in short for industries. Most of the factories had to stop production. Economic loss had reached 960 million yuan. As the Shengli Oil Field lacked 2600000 m³ water, its crude oil production was cut down by 300000 tons. In Dongying city, Binzhou city and Dezhou city, on account of the pressing shortage of water, 100000 people had to be supplied with limited amount of water, at a fixed time every day. The residents had to queue up at a public tap, waiting for their shares of water. This had disturbed the residents' normal life and normal working and meanwhile brought unstability to society. Cut-outs make great impact environmental ecology in many ways. And the effects would be gradual, potential and irretrievable. So we should take it seriously and attach great importance to it. Runoff decrease and cut-outs of the Yellow River in non-flood seasons will make impact on environmental ecology in the following two aspects;

3.1.1 Water quality environment is deteriorating

Runoff amount of the Yellow River is decreasing, but the polluted and waste pouring in the Yellow River is increasing every year. And this has weakened the Yellow River's self-cleaning capacity. In 1993, waste discharge from cities and towns along the reaches was increased 60%, compared with that in early eighties. The pollutants from the branches of the Yellow River doubled or even more. Formerly, the water flow from Tongguan and Huayuankou was good and clear, now, is becoming worsen and difficult to meet water quality requirements. The most worrying thing is even when cutouts come, sewage discharge is still going on. For example, in June 1996, after 40 days' cutout near Jinan, the flow that people had long hoped for finally resumed. To their great disappointment, the water was not so clear and sweet as they had expected, the flow was blackened, on which were floating white foams and dead fish, smelling foul and terrible. Evidently this was the results of sewage and polluted water discharge from the upper reaches. In recent years, the kinds and types of fish in the lower Yellow River are shrinking rapidly, some even to extinction. And this has close connection with cut-outs and water quality.

3.1.2 Ecological environment of the river mouth delta is becoming worsen

Agricultural development zone at the Yellow River Delta is one of five newly built granaries in China. It is also an important protection zone confirmed by "China Protection Project for Biology Variety". It owns the international standard wet land, water ecological system and ocean-coast ecological system. Because of the frequent cutouts in the lower Yellow River and runoff decrease and sediment, agricultural development of this zone is badly affected, and vulnerable to sea tide attacks and salinization, grass strip at the delta would be degenerated into saline strip. This is quite disadvantageous to grassland ecology and presumably give rise to biological resources decline and species composition changes.

3.2. Counter-measures to alleviate cut-outs

3.2.1 To reinforce an unit regulation and management system for water resources of the yellow River

To date, diversion capacity of the Yellow River has far surpassed its water supply capacity in non-flood seasons. With the economic development in the upper and middle reaches, water demand will continue to rise. Water quantity to the lower reaches will continue to decline. In order to made the greatest advantage of the limited water resources, obtain overall benefits and alleviate cutouts in the lower of Yellow River, it is indispensable to implement an overall regulation system to control the total water amount and manage by different administrative levels.

3.2.2 To adopt effective measures and to economize on water

many irrigation zones along the Yellow River were built up in fifties and seventies. Due to a variety of reasons, the engineering standards were very low, conveyance systems were not very complete, and irrigation methods were out-of-date. At present, the conveyance area of the total irrigation zone in the upper and lower Yellow River has not

reached 20% of the planned goal. Some irrigation zones only have the main conveyance engineering without branches. Some even has not the key buildings on the main canals. Some irrigation projects were finished some 30 years ago, seriously deprecatory and out of repairs. Investigation shows depredeation percentage of the major irrigation zones has reached 28%-42%, depredeation percentage of the channels and canals is 38%-70%. Water resources have not been effectively utilized and waste of water is quite serious due to mismanagement. In some areas, irrigation water per Mu is high up to about 700 m³, but in some other economical area, only 200m³ per Mu. From this, we can see clearly the water resources potentiality.

In order to make good use of the limited water resources of the Yellow River, prevent unnecessary waste, first of all, we must attract more investment to improve save-on-water facilities of the irrigation zone. Water user, provinces and our government should make their own shares of investment contributions to accelerate the improvement of save-on-water technique and water conveyance facilities. Secondly, the non-gratuitous utilization system for water resources should be implemented as soon as possible. Law in order to develop and utilize the limited water resources reasonably and economically should impose reasonable fees. Thirdly, the confirmed prices should be reasonable, the diversion water should be well regulated.

3.2.3 To strengthen Scientific Research

The factors that make great impact on development of the Yellow River are multiplex and complicated. We should strengthen scientific researches, organize unified research centers. Some governmental departments concerned should organize scientific researches and made joint effects with local governments to push on the development and utilization of the Yellow River. At present,we have a lot to do in many scientific fields, for example, combination utilization of underground water and surface water, in some irrigation areas; implementation and population of save-on-water measures; reasonable regulation system for water inflow in the regions from Sanmenxia downwards in non-flood seasons; maintenance of the minimum inflow to the sea at river mouth areas.

There are vast lands and rich in mineral resources in Yellow River basin. The whole area is one of country's most potential development zones. On the long term vies point, in order to keep up with the social and economical development, to develop northwest China, to improve ecological environment, and to solve the problem of water shortage, we should build up gradually a big project to diverse the water of the upper ChangJiang river, to north China and meanwhile try our best to do a good job of save-on-water and reasonable regulatin of water.

Note: one hectare=15 Mu

Address: Hydrology Bureau, YRCC, No.12 Chengbei Road,

Zhengzhou, China

Phone Number: 86-0371- 6303419

Postcard: 450004

A COMPREHENSIVE SUMMARY ON THE STUDY OF FLOOD STOCHASTIC SIMULATION FOR THREE GORGES PROJECT

By Xiong Ming, Hydrology Bureau of Changjiang Water Resources Commission, Wuhan, China; Ji Xuewu, Hydrology Bureau of Changjiang Water Resources Commission, Wuhan, China

Abstract: In the planning and design of Three Gorges Project (TGP), to investigate the regional composition of design flood on TGP, the effect of proposed upstream (stem and tributaries) reservoirs on TGP, and the flood control benefit of Three Gorges reservoir (TGR) on midstream and downstream reaches, on the basis of existing short series observations and making use of the stochastic characteristics of flood variables, the flood stochastic models had been established separately for Yichang station or the representative station for Three Gorges damsite, the intervening area from Pingshan to Yichang or above the damsite, the intervening area from Yichang to Chenglingji or below the damsite, and the intervening area from Cuntan to Datong including the damsite. The models used were many and varied as many as possible, in which both the autoregression model and temporal disaggregation model for single site, and also the autoregression model and spatial disaggregation model for multi-site had been used. Only by the establishment of these models, can it be possible to work out the computation for the effect of cascade reservoirs on the design flood and the flood control benefits from flood control system formed by the reservoirs, dykes and flood diversion or storing works which were difficult to be performed by the representative year method of design flood. A pragmatically conclusion, such as the effect of upstream reservoirs (stem and tributaries) after construction of projects on the inflow flood of TGR, and the significance of TGR on the regulation of flood control at midstream and downstream reaches had been found, providing an important basis for the design of TGP.

INTRODUCTION

Long series of flood data will have a particular significance for the design flood analysis on TGP and the effect of TGR on midstream and downstream flood control system. However, due to the limited length of observed flood data series, the requirement of planning, design, operation and management of TGP can not be satisfied. the following methods are being used generally for the planning and design of the project nowadays: (1) Measured representative flood year method; (2) Frequency flood year method; (3) Measured flood data series method.

The above three methods used for determining the design flood will all have some definite deficiencies. In recent years, with the aid of statistic trial method, although the data series is short, as applying the stochastic characteristics of flood variables, the flood stochastic model can be established and the flood process of long series for single site or multi site can be simulated. By this method the deficiencies of short series and the complicated regional composition can be

avoided, so this method will have a great future.

In the design of TGP, the stochastic model method had been introduced earliest by Mr. Ding Jing, Ji Xuewu et, by whom the stochastic simulation of annual and monthly runoff for Yichang station on Changjiang river in 1984 had been performed. After that, the stochastic simulation had been gradually used for flood simulation. In the study on stochastic simulation for the flood on TGP, aiming at the different purposes and demands, the flood stochastic models had been made separately for the Three Gorges damsite or Yichang station, the intervening area from Pingshan to Yichang or above the damsite, the intervening area from Yichang to Chenglingji or below the damsite, and the intervening area from Cuntan to Datong including the damsite. The models used were many and varied, in which both the autoregression model and temporal disaggregation model for single site, and also the autoregression model and spatial disaggregation model for multi site were used. Only by the establishment of these models, can it be possible to work out the computation for the effect of cascade reservoirs on design flood, and for the flood control benefits from the flood control system formed by reservoirs, dykes, and flood diversion or storing works, which were difficult to be performed by the representative flood year method for design flood. The characteristics and applications of these models are described as follows.

STUDY ON FLOOD STOCHASTIC MODEL FOR YICHANG STATION

During the middle of eighties, in the demonstration and design of TGP, using the temporal disaggregation model, making the first trial on flood stochastic simulation. Its specific thinking was the dividing the simulation of flood process into two parts, i.e. at first to establish an absolute stochastic model for max. 60 days flood volume on Yichang station and then resolve the 60 days flood volume into daily discharge process by the disaggregation model.

In the absolute stochastic simulation for the max. 60 days flood volume on Yichang station, it was suggested that the model parameter was preliminary estimated by matrix, and to be modified, then a biased corrected formula for the parameter of P-III distribution had been proposed. In the correlative disaggregation model, to consider the bias characteristics of the data series, the equation set by Todini had been first used for the computation of stochastic figure on bias distribution.

On Yichang station there existed the continuous daily mean discharge hydrograph in flood period and also the rich historical flood investigation data, in which the max. 30 days discharge hydrograph for 1870 extraordinary historical flood had been estimated. Undoubtedly, these historical data was very important for the estimation of model parameter. Only by the continuous data series, can it be capable of establishing the model, so the following method of considering the historical flood had been proposed firstly in this study.

At first, the disaggregation model was established base on the 106 years of measured flood

process on Yichang station, with that model the data of flood process was extended for another 723 years, together with the above 106 years of measured data and that of 1870 historical flood, giving a total length of 830 years continuous flood data series (Long return period). Using this data series, the parameters for the model were estimated. Having the consideration of historical extraordinary flood information for the method of stochastic extrapolation, it will become more reliable on the estimation of model parameters.

In the study, altogether, 400 sets of flood process were simulated with a series length of 106 years. After determining the mean value and variance of the main statistic parameters by the computation for each set and compared with the main parameters in historical series, it was deemed that the flood process on Yichang station simulated by disaggregation model was adequate, of which the accuracy was relatively high, and the simulated flood process will provide a certain reference value to the hydrological design of TGP. It was also considered that the flood stochastic simulation for Yichang station was a successful trial, and the frequency calculation was only a simplest special case for the stochastic simulation.

STUDY ON FLOOD STOCHASTIC SIMULATION FOR THE INTERVENING AREA FROM CUNTAN TO DATONG

In order to study the flood control benefit of TGP on the midstream and downstream Changjiang, a study on flood stochastic simulation at multi site for the river reach from Cuntan to Datong including the damsite was arranged. According to the following principles, the above river reach for flood simulation was divided: (1) Considering the demand on flood control computation; (2) Distribution of hydrometric stations; (3) Demand on interpolation of discharge process on interval area; (4) The division of river reach being as simple as possible.

It was considered in the study that mostly the flood data series can not meet the need of normal distribution, but the statistic circle had provided a complete set of theory for the normal distribution, therefore the flood stochastic variables of abnormal distribution were transformed into that of normal distribution, and then according to the theory of normal distribution, the manipulation was performed. This, after all, was an effective way of manipulation. In this key project, through a large amount of analysis and investigation, a perfectly new conversion method was advanced, and the conversion equation was obtained as follows:

$$y = \text{Sign} [\ln(x-a)] \cdot |\ln(x-a)|^\lambda$$

in which, x is the original sequence; y is the sequence for normal distribution after conversion; λ is conversion exponent; a is the lower limit for the value x .

The significant advantage is that if the value of lower limit is ensured to be smaller than zero, the ratio of C_s/C_v will not be strictly limited and in general case the original sequence can be

converted into normal distribution sequence.

In this study, the simplification had been made on two ways for multi-dimension unsteady autoaggregation model, and the particle models applicable to Changjiang river (the large river) and reflecting the temporal and spatial characteristics of regional flood had been established, i.e. The multi-dimension unsteady autoregression model and the mixed regression model. The equation for estimating the least square parameter of multi-realities on steady autoregression model was derived, giving an equation for estimating the parameters of different lengths which will have the widely spreader value for application. Furthermore, the test on the steady field of parameter for the three order steady autoregression model selected was firstly performed, solving a difficult and unsettled problem on the steadiness of steady autoregression model that had been remained for more than one year. A universal form of considering the unsteady characteristics on autoregression coefficient for the mixed regression model was proposed, and also the equation for estimating the parameters of mixed regression model was derived.

In performing this key project, a concept that the model and simulation result should be widely and comprehensively examined was suggested and realized, including:(1)The characteristics of residual error for the model;(2)The hydrological characteristics of simulation result;(3)The principle of a least number of model parameters;(4)The effectiveness of model application.

The work amount of statistic for examination was seldom seen at home and abroad, especially, using the long series data of the control station on Changjiang stem creatively to make the comparison in the examination, the reasonableness and reliability of simulation result had been significantly tested and verified. It is shown by the examination that the simulated flood had reflected the main stochastic characteristics and the other characteristics of flood for this region; the adequate number of parameters; stable model; and the flood hydrograph comforting the inherent properties of natural flood. The verification by the experts firmly believed that this achievement had come up to advanced world standard, of which some parts were at the international leading position, which can be taken as the basis of computation on flood control benefit for Changjiang flood control system. There after, this achievement had been widely used in the computation on Changjiang flood control benefit, which gave a satisfactory result.

STUDY ON FLOOD STOCHASTIC SIMULATION FOR THE INTERVENING AREA FROM PINGSHAN TO YICHANG OR ABOVE THE TGR

A problem that whether or not the reservoirs on upstream Changjiang and its tributaries can replace the flood control function of TGP was proposed by some related experts, thus a research subject “ The effect of constructed TGR and the upstream reservoirs on the inflow flood of TGR ” was carried out by Hydrology Bureau of CWRC. To study this problem, three methods were used, such as regional computation method, frequency combination method, and stochastic

simulation method.

Some large size reservoirs which had played the flood control role, i.e. One reservoir on Yalongjiang river; two on Jinshajiang river, one on upstream Minjiang river; two on Daduhe river; three on Jialingjiang river; and five on Wujiang river had been planned to be constructed on the upstream river reaches of Three Gorges. Because the distribution of upstream reservoirs was scattered and each tributary had several reservoirs, of which the independent flood regulation was restricted by the limitation of data, as a result, a scheme of concentrated flood regulation for the reservoirs on each tributary was adopted: i.e. The cascade above Jinshajiang was concentrated at Xiangjiaba, controlled by Pingshan station; that on Daduhe and Minjiang were concentrated at Gongzui and Zipingpu, using the data at Tongjiezi and Zipingpu; that on Jialingjiang was concentrated at Tingzikou, of which the data was used; and that on Wujiang was concentrated at Pengshui, the data at Wulong was used. The selection of flood stochastic model, the preprocessing of basic data and the estimation of model parameter were the same as that for the method of multi-dimension steady autoregression model introduced on the above paragraph. The following indirect method was used for determining the inflow flood of TGR. At first, a sufficient length of flood data series for each site intervening area was simulated by the stochastic simulation method, and then the simulated flood data series of each reservoir control station was routed along the river course to the downstream inflow stations of TGR, Cuntan (stem) and Wulong (tributary) stations, superposing with the simulated flood data series on uncontrolled intervening area, a long data series of inflow flood hydrograph for TGR was determined. If the flood process of each reservoir station had not been regulated yet, the result obtained will be the material reservoir inflow flood hydrograph of TGR as after superposition, and if it had been regulated, that reservoir inflow flood hydrograph will be the one being affected by the upstream reservoirs.

The following principles should be considered for the flood control regulation of upstream reservoirs on stem and tributaries: (1) In accordance with its own flood control demands to make the downward releasing; (2) Guaranteed output of each power station itself can not be deteriorated; (3) Stepped regulation is adopted, and the flood control capacity reserved is divided into three steps for each reservoir (equivalent to 5%, 1%, and 0.1% respectively); (4) Assuming that each reservoir is at the limit water level for flood control, as the inflow is less than or equal to the probable max. releasing discharge, the discharge released will be made as the same value as the inflow, as the inflow is greater than probable max. releasing discharge of flood control limit, the operation is performed by a method so called "cutting and leveling the peak".

It was proved by this achievement that there will be the effect on inflow flood of TGR after the construction of upstream reservoirs. Because the flood occurred time of each tributary was not the same, the amount was also not the same, the flood was regulated individually for each tributary, and there was a function of inter-compensation between the reservoirs, resulting that for some reservoirs there was no flood to be regulated and for some there will be full filling

causing the disaster, it was shown that the regulation function of the entire controlled area was not significant. As a result, a conclusion was given that there will be the effect on inflow flood of TGR after the construction of upstream reservoirs, but it will not be significant.

In this study, the regional composition of flood upstream of Three Gorges and the effect of upstream reservoirs after construction on the inflow flood of TGR had been approached by the methods of flood regional composition method and frequency combination method. The results obtained from the above two methods were consistent to that from stochastic simulation method, while the later had overcome the deficiency on the restriction of representative process on the above two methods, giving a possibility of solving the problem on the encounter of complicated flood composition, and it will be the method existing a great future for determining the stepping inflow flood of reservoir. By this method the problem on inflow design flood of reservoir was being studied for the first time at home and abroad.

STUDY ON FLOOD STOCHASTIC SIMULATION FOR THE DAMSITE OF TGP AND THE INTERVENING AREA FROM YICHANG TO CHENGLINGJI

The major region for flood control on Changjiang is Jingjiang region on midstream Changjiang, as it relates to the inundation of 18 million mu of farmland on both banks of Jingjiang, the safety of more than 10 million people, and also the development of national economics. For this reason, in the flood control system on Changjiang, in order to investigate the flood control effect of TGP on the midstream and downstream Changjiang especially Jingjiang reach, a large amount and long series of flood data are required, including the flood hydrograph on TG damsite and the inflow hydrograph on the midstream control station and on the reach above the flood control sites. According to the basic condition, and the demands on flood control regulation of TGP, the study on flood stochastic simulation for the intervening area from Yichang to Chenglingji was performed including the following seven stations and intervening areas such as Yichang; Xiangtan; Taojiang; Taoyuan and Sanjiangkou stations; areas from Yichang to Shashi and of Dongtinghe.

Due to the complicated relation of water flow between Changjiang and Dongtinghe lake and the large amount of flood volume diverted and storage by the embankments on the intervening area from Yichang to Chenglingji, the flood routing will have been affected. According to these characteristics, the flood stochastic simulation for the intervening area from Yichang to Chenglingji was made by two steps. At first the total inflow at Luoshan was simulated by the steady autoregression model, and second, using the spatial disaggregation model, the total inflow at Luoshan simulated had been resolved into each station or area.

The model of total inflow at Luoshan was selected and determined as the four order steady autoregression model. The general form of disaggregation model had been expended by multi site model, both considering the characteristics of even distribution between the total amount and

the partial amount and also considering the correlation between each partial amount as the time delayed=1

$$Y_t = AX_t + B \varepsilon_t + CY_{t-1}$$

The expanding equation for estimating the parameter of disaggregation model had been derived. A great amount of examination had been made for model parameter and simulation result, by which the flood control effect of TGP on midstream and downstream Changjiang was determined. In the study two plans were adopted in flood control regulation for TPR: the first one was to use the compensated regulation for Chenglingji, and the second was to use compensated regulation for Jingjiang.

It was shown by the simulated 6000 years flood process and its flood regulation result that for the plan of compensated regulation at Chenglingji, TGR will have a definite reduction effect on the flood in different frequencies. It can be seen from the case of long-term annual average, that as for the max. one day flood, 1.212 billion m³ of water volume was reduced by TGR, conversion to water discharge being 14000m³/s. It can also be seen that the peak reducing ability was considerably great, and as the increase of time interval, the amount reduced by TGR was also increased, but the percentage was gradually decreased from 23.7% for max. 1 day to 8.3% for max. 60 days, conforming to the regularity of flood control regulation. As for the meeting a thousand years flood, the peak reduced was only 81 million m³ or 7880m³/s of discharge converted. The reducing amount was less than that for long-term annual average, while the reason investigated was that a great part of capacity was filled by the compensated regulation at Chenglingji in the antecedent period, giving a disadvantage to the protection against the extraordinary flood.

If the plan of compensated regulation at Jingjiang was adopted, as for max. daily value to meet a thousand years flood, the reduction range will be 3.089 billion m³, equivalent to the discharge 41500m³/s. As the increase of time interval, the reduction will be increased, but the percentage was decreased. It was shown by the result that this regulation plan will be adequate for protection against the extraordinary flood. Through the analysis on flood control regulation of TGR for simulated flood series, a conclusion that there will exist a significant effect of TGP on flood control of midstream and downstream Changjiang is given. Taking whatever scheme for flood control regulation you considered the flood regulating capability will be obviously existed in TGR for the floods of various frequencies. If the forecasting can be improved, the flood control effectiveness of TGP will be more outstanding.

CONCLUSION

The study on flood stochastic simulation for TGP plays an important role in the planning, design and scientific research of TGP. In the entire preparation, both the single site flood stochastic

model and multi-site flood stochastic model have been investigated. The models includes steady autoregression model, mixed regression model and also disaggregation model tried. In the study, a great deal of new thinking has been developed, proposing some new methods, successfully solving a series of difficult problems, and advancing the development of stochastic hydrology.

The utilization on the principle and method of historical extraordinary flood information in stochastic simulation for single site has been developed, while the historical extraordinary flood data will play a significant role in the estimation of parameters.

The result is satisfactory that in the stochastic simulation, successfully applying Bayesism statistic theory, the problem on uncertainty of stochastic figure has been considered.

A wholly new conversion method for logarithm and exponent has been proposed, solving the problem on deficiency in existing conversion method, capable of converting the bias distribution sequence into normal distribution sequence under the condition that no limitation is for the ratio of C_s and C_v .

The least square estimating formula, for steady multi-dimension autoregression model parameters under the condition of the multi-reality and the unequal length of the data at the site or the intervening area ,has been newly derived and proved to be effectiveness.

It is the first time to use the stability theory for multi-dimension ARMA(p,q) model parameter, that the parameters of steady multi-dimension autoregression model established are within the steady field has been demonstrated, and the mathematics strictness for flood simulation is ensured.

The method that the inflow flood of reservoir project is simulated by multi site flood stochastic model has been developed for the first time, to create a favorable condition for computing the effect of upstream reservoirs (stem and tributaries) on TGP.

An estimation formula of spatial disaggregation model expended by considering the characteristics of one order correlation has been derived, improving the accuracy of model computation.

Various examinations are performed widely and comprehensively on the simulated flood, of which the statistic work amount are so much and seldom presented in the documents at home and abroad. Especially, the check and examination are made intuitively by using the long series data on mainstream control station, effectively verifying the reasonableness and reliability of the simulated results.

SIMULATION OF SELECTED RESERVOIR AND RIVER-DIVERSION OPERATIONS IN THE TRUCKEE RIVER AND CARSON RIVER BASINS, CALIFORNIA AND NEVADA

by Glen W. Hess and Steven N. Berris, Hydrologists, U.S. Geological Survey, Carson City, Nev.

Abstract: The Truckee-Carson Program was established in 1992 to assist the U.S. Department of the Interior in implementing Public Law 101-618, the Truckee-Carson-Pyramid Lake Water Rights Settlement Act of 1990. An objective of the Truckee-Carson Program is to build, calibrate, test, and apply interbasin hydrologic computer models to support efficient water-resources planning, management, and allocation. Flow-routing computer models simulating storage and streamflow in the Truckee and Carson Rivers were modified to simulate reservoir and river-diversion operations for analysis of water-management scenarios. Examples of reservoir operations include reservoir releases based on flood-control criteria and water-storage priorities; reservoir releases to meet agricultural, municipal and industrial, and hydropower demands; exchanges of water categories between reservoirs; and reservoir releases to meet minimum flow requirements for fisheries. These models are coded with river-diversion operations for existing agricultural, municipal, and industrial demands and diversion operations used to fill reservoirs. The ability to simulate alternative management scenarios and compare simulation results will help users understand effects of changes in river/reservoir operations, land use, water-rights transfers, and irrigation practices on water quantity throughout the Truckee River and Carson River systems.

An interactive computer program is being developed to aid in the usage of these comprehensive and data-intensive river-basin models. The program will serve as a user interface enabling users to apply and analyze results from these complex models in an easy and efficient manner. Examples of the user/model interface are (1) to select, modify, and create a variety of model scenarios, (2) to run those various model scenarios, and (3) to analyze and compare the simulation results.

TRUCKEE-CARSON PROGRAM

The Truckee-Carson-Pyramid Lake Water Rights Settlement Act was passed in 1990, after decades of litigation and negotiation. The law provides a foundation for development of operating criteria for interstate allocation of water. These interstate allocations are to meet demands for municipal, irrigation, fisheries and wildlife, and recreational uses, as well as to meet water-quality standards in the approximately 7,000-square-mile Truckee River and Carson River Basins of eastern California and western Nevada (fig. 1). The Truckee-Carson Program of the U.S. Geological Survey (USGS) is assisting the U.S. Department of the Interior in implementing this act. The program has the following objectives: (1) Consolidate streamflow and water-quality data from several agencies into a single data base; (2) Establish new streamflow and water-quality gaging stations for more complete water-resources information and more-consistent support of river operations; and (3) Build, calibrate, test, and apply interbasin hydrologic computer models to support efficient water-resources planning, management, and allocation. Hess (1996, 1997), Berris (1996), and Berris and others (1996) describe the current progress of the Truckee-Carson Program objectives.

HYDROLOGICAL SIMULATION PROGRAM-FORTRAN

A computer model simulating storage, streamflow, and quality of the water in the Truckee River and Carson River Basins and in the Truckee Canal (fig. 1) is being developed to help meet an objective of the Truckee-Carson Program. The model, based on the Hydrological Simulation Program-FORTRAN (HSPF; see Bicknell and others, 1997), simulates reservoir and diversion operations to analyze alternative water-management scenarios.

This paper summarizes some of the capabilities that were added to HSPF to simulate complex reservoir and river-diversion operations in the Truckee River and upper Carson River Basins in eastern California and western Nevada. Reservoir operations include releases based on flood-control criteria and water-storage priorities; releases to meet instream flow requirements or agricultural, municipal and industrial (M&I), and hydropower demands; and exchanges of water categories¹ between reservoirs. River-diversion operations are the distribution of waters based on legal decrees that govern the right to beneficial use of water established in accordance with the system of appropriative water rights.² River-diversion operations include diversions to meet agricultural and M&I demands and operations used to fill reservoirs. In this summary, simplified or isolated examples are used to illustrate specific operations that can be

¹ A category of water is any block of water that is individually accounted for in an observed or simulated water budget. A single river, reservoir, lake, or diversion ditch may contain several categories. Water within a category may have specific ownership, such as "privately owned stored water," or have a designated use, such as "pooled water" (used to meet a minimum-flow requirement known as Floriston rates).

² Appropriative water rights such as those legally recognized in the Nevada part of the Carson River and Truckee River Basins, are based on the concept of "first in time, first in right." The first person to take a quantity of water and put it to beneficial use has a higher priority of right than a subsequent appropriative user. An appropriator usually is assigned a priority date (date of establishment of a water right) that is significant in relation to the dates assigned to other users from the same source of water. The priority date is important when the quantity of available water is insufficient to meet all the needs of legal users.

represented by HSPF. Actual day-to-day system management or simulation requires consideration of present and forecast flow conditions at various locations in the river basin as well as compliance with numerous legal agreements, legal decrees, and demands.

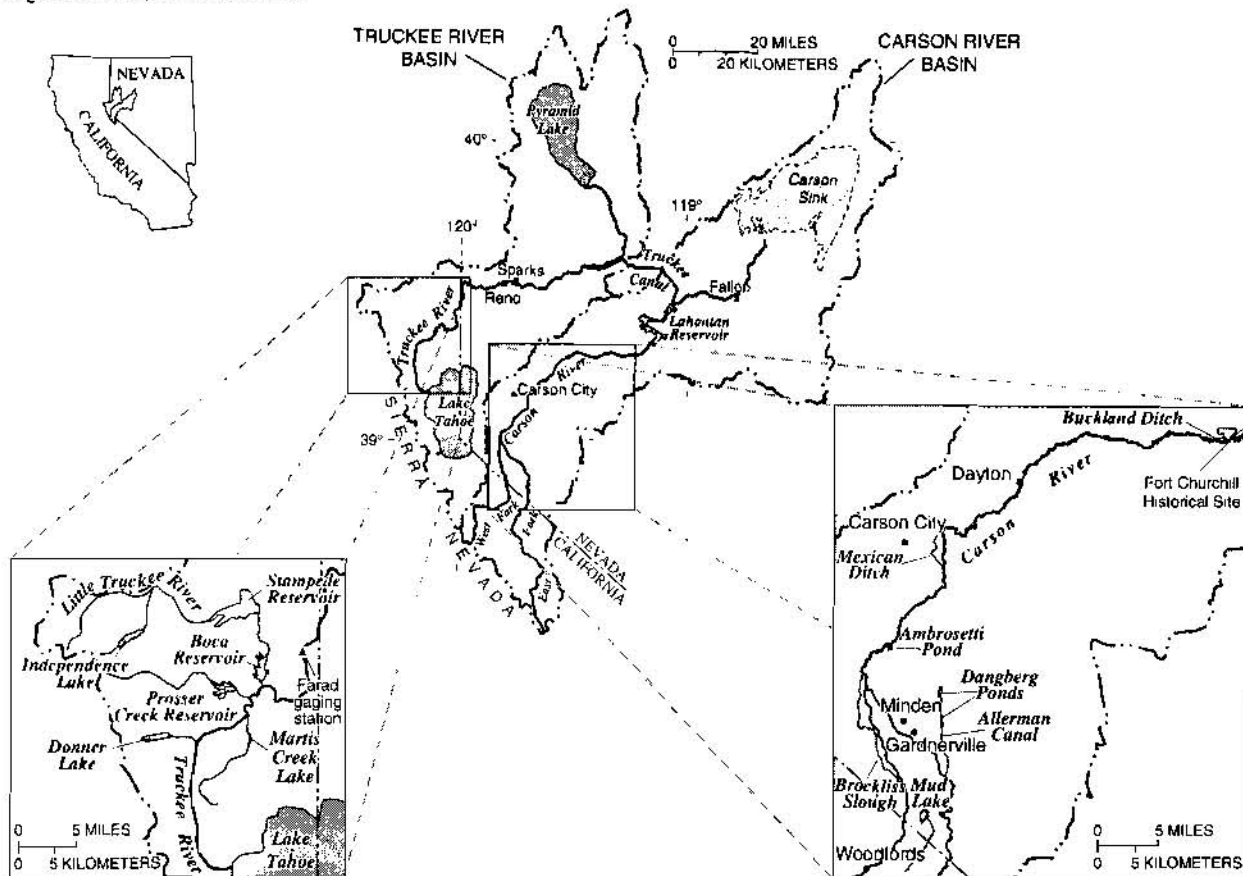


Figure 1. Geographic and hydrologic features of Truckee River and Carson River Basins.

HSPF was chosen to simulate Truckee River and Carson River reservoir and river-diversion operations primarily because it can (1) simulate streamflow continuously over time, including periods of storm runoff and low flows, (2) simulate streamflow at a variety of time steps, including daily and hourly, (3) simulate the hydraulics of complex natural and manmade drainage networks, (4) produce simulation results for many locations along a river and its tributaries, and (5) compute a detailed water budget that accounts for inflows and diversions as well as different categories of water in the river and associated reservoirs.

Use of such comprehensive river-basin models to assess hydrologic scenarios of reservoir and diversion operations requires advanced computer-processing capabilities. These advanced capabilities facilitate the summary and analysis of large volumes of input and output data.

The interactive computer program GENSCN (Generation and analysis of model simulation SCeNarios) was developed by J.L. Kittle, Jr., and others (U.S. Geological Survey, written commun., 1997). GENSCN aids the usage of the physically- and legally-based hydrologic models for the Truckee River and Carson River Basins. GENSCN allows the model user to (1) select, modify, and create a variety of model scenarios, (2) run the various models, and (3) analyze and compare simulation results from model scenarios in a variety of ways.

HSPF SIMULATIONS OF RESERVOIR AND RIVER-DIVERSION OPERATIONS

HSPF uses conditional logic³ to simulate operations. In the upper Truckee River Basin, seven dams are operated upstream from the Farad gaging station (fig.1), a USGS site on the Truckee River, to augment water supply and to minimize flood hazards. These dams control water releases from Lake Tahoe, Donner Lake, Martis Creek Lake, Prusser Creek Reservoir, Independence Lake, Stampede Reservoir, and Boca Reservoir. These lakes and reservoirs are

³ Conditional logic means that if certain conditions are met, then certain actions are taken. Conditions that are evaluated during simulations include the time of year; reservoir stage, reservoir storage, or volume of a given water category in a reservoir; streamflow magnitude at a given location; and fulfillment of water demands. HSPF models the operations by evaluating these conditions and simulating the designated action.

operated according to complex regulations and legal decrees that specify conditions for the storage and release of water. HSPF models the reservoir operations by evaluating the same conditions and simulating the designated action. In the upper Carson River Basin, ditch headgates along the East Fork Carson, West Fork Carson, and Carson Rivers also are operated according to complex regulations and legal decrees that specify conditions for the use of water.

The following examples show results from preliminary HSPF simulations of reservoir and river-diversion operations for the Truckee and Carson Rivers, based on selected existing regulations and legal decrees. These examples are intended only to illustrate how HSPF can simulate operations rather than to convey citable or quantitative model results.

Reservoir Operations Based on Flood-Control Criteria and Storage Priorities: Reservoir operations use flood-control criteria and storage priorities. Flood-control criteria are rules used to determine when and how much water must be released from reservoirs to maintain reservoir flood-control space. These rules of operation also minimize potential downstream flood damages. Once flood-control criteria have been met, a complex set of rules, derived from the Truckee River Agreement of 1935 and other legal decrees, governs the priority for storage of water of a particular water category within each reservoir. Storage priorities dictate when and how much water a reservoir may impound. Conditional-logic capabilities within HSPF allow the user to simulate reservoir operations based on the flood-control criteria and storage priorities.

Daily reservoir elevations simulated by HSPF on the basis of Prosser Creek Reservoir flood-control criteria are shown in figure 2. The span from August 7 to November 1 includes the space-drawdown period for flood control, during which the reservoir elevation is lowered to 5,703.7 feet to allow storage room for fall, winter, and spring inflows. This elevation is maintained from November 1 to April 10 by releasing all reservoir inflows. From April 10 through May 20, water storage is based on rules governing maximum daily storage. Finally, from May 21 through August 6, the reservoir typically is operated more to meet downstream water demands than to maintain flood-control space.

Daily water storage for Donner Lake and Prosser Creek Reservoir, simulated by HSPF on the basis of legally decreed storage priorities, is shown in figure 3. Donner Lake has an earlier storage priority than that for Prosser Creek Reservoir and, thus, can begin storing water sooner. During April 3-14, water volume remains constant at the winter-capacity storage of 2,500 acre-feet at Donner Lake and 9,800 acre-feet at Prosser Creek Reservoir. On April 15, Donner Lake storage begins to increase, while Prosser storage remains constant because of a later storage priority, which begins April 20.

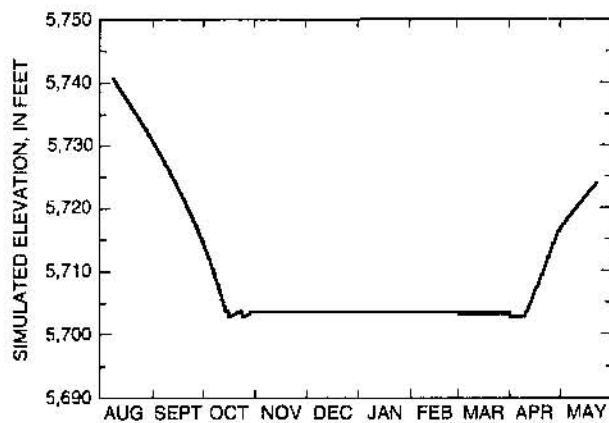


Figure 2. Prosser Creek Reservoir elevations simulated on basis of flood-control criteria.

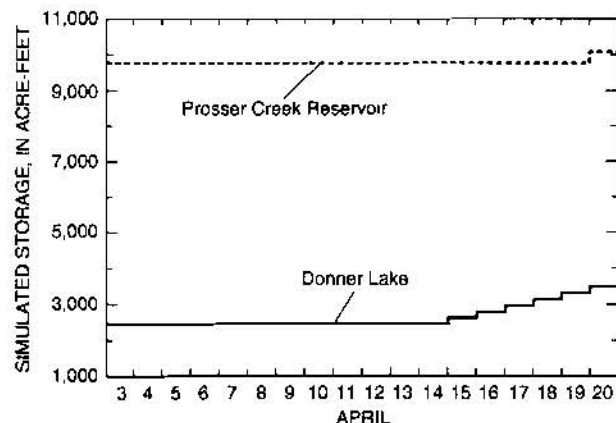


Figure 3. Donner Lake and Prosser Creek Reservoir water storage based on April storage criteria.

Reservoir Releases to Meet Demands: Using conditional logic, HSPF adjusts simulated releases from reservoirs to meet downstream demands, such as Floriston rates. Originally established by a Federal District Court decree in 1915 and revised in 1935, Floriston rates are minimum-flow criteria for the Truckee River at the California–Nevada State line and constitute the chief operational objective for the river. When flow rates (currently measured at the Farad gaging station, which is just upstream from the State line) meet Floriston rates, almost all downstream agricultural, municipal and industrial, and hydropower water rights are satisfied. According to the Truckee River Agreement of 1935, when these rates are not met by the natural flow of the river, categories of water designated for Floriston rates stored in Lake Tahoe and in Boca and Prosser Creek Reservoirs may be released to augment the natural flow in the river.

An HSPF simulation of how water stored in Lake Tahoe and in Boca and Prosser Creek Reservoirs can be released to attain Floriston rates for the period August through October is shown in figure 4. Simulated reservoir releases from pooled water compensate for and react to the variability of natural inflow to the Truckee River to approximate Floriston rates at the Farad gaging station. Simulated streamflow at the Farad gaging station consists of reservoir releases (fig. 4) and natural, unregulated inflow to the Truckee River which are routed downstream to the Farad gaging station.

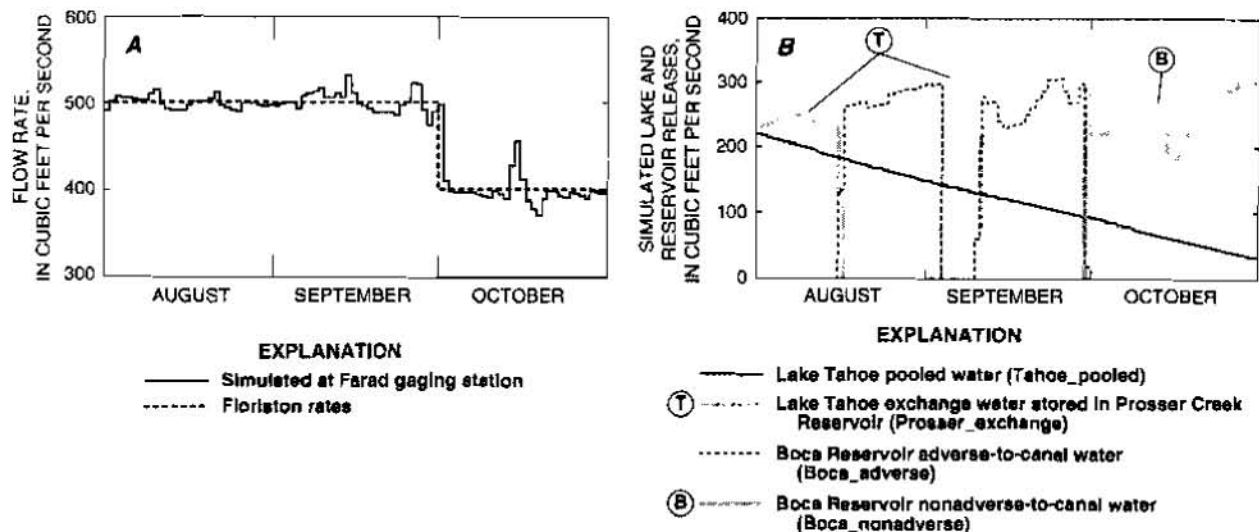


Figure 4. Lake and reservoir releases simulated to maintain Floriston rates at Farad gaging station. *A*, Simulated total flow at Farad gaging station compared to Floriston rates. *B*, Lake and reservoir releases necessary to augment natural Truckee River inflow.

Natural, unregulated inflow to the Truckee River can be augmented by four categories of pooled water stored within Boca and Prosser Creek Reservoirs and Lake Tahoe to maintain Floriston rates. These categories are Lake Tahoe pooled water (hereafter abbreviated Tahoe_pooled), Lake Tahoe exchange water stored in Prosser Creek Reservoir (Prosser_exchange), and two categories of Boca Reservoir water called adverse-to-canal (Boca_adverse) and nonadverse-to-canal (Boca_nonadverse). Under a complicated set of provisions within the Truckee River Agreement of 1935 and other legal decrees, orders of release to maintain Floriston rates are assigned to these water categories for different conditions and time periods of a given year (fig. 4).

If Floriston rates cannot be achieved by natural, unregulated inflow, Tahoe_pooled is the first choice for release only if the Lake Tahoe elevation is less than 6225.5 feet. However, hydraulic properties of the outlet, in terms of stage, may limit release rates from Lake Tahoe. Therefore, in this example, releases from Boca and Prosser Creek Reservoirs must augment Tahoe_pooled releases to maintain Floriston rates.

Water from the second category, Prosser_exchange, may be released to augment releases from Lake Tahoe. Although not formally addressed in legal decrees or regulations, the U.S. District Court Water Master currently attempts to maximize recreational use of Prosser Creek Reservoir from April 1 through Labor Day. Therefore, in this example, Prosser_exchange releases are made, if possible, only from nonrecreational storage in the reservoir to attain Floriston rates in the HSPF simulation. Nonrecreational storage in the reservoir is that volume of water in excess of 19,000 acre-feet, which is less important for recreational activities such as fishing, boating, and swimming. HSPF simulates this condition for the recreational season by the release of nonrecreational Prosser_exchange water, which has been assigned the second highest order of release to maintain Floriston rates.

The third water category for release to maintain Floriston rates is Boca_adverse water. Boca_adverse is the first 25,000 acre-feet of pooled water stored in Boca Reservoir. Therefore, as storage of nonrecreational Prosser_exchange water becomes depleted (mid-August in this example), Boca_adverse water is released.

In the model, Labor Day triggers a change in the choice for release from Boca_adverse water to recreational Prosser_exchange water (fig. 4). Boca_adverse water releases are reduced to zero while recreational Prosser_exchange water releases are increased to help achieve Floriston rates. As storage of recreational Prosser_exchange water becomes depleted, Boca_adverse water is released again. Finally, as Boca_adverse water becomes depleted, Boca_nonadverse water is released, which is pooled water in excess of the first 25,000 acre-feet.

Reservoir Operations Using Water Exchange: A commonly used operating method known as water exchange allows reservoir operators to meet multiple-use goals by transferring stored water from one reservoir to another. In this procedure, water is released from one reservoir in exchange for storage of an equal amount of water in another reservoir. In effect, the water is moved between the two reservoirs, even though the reservoirs may not be on the same tributary.

The Tahoe-Prosser Exchange Agreement of 1959 specifies the operation of Lake Tahoe and Prosser Creek Reservoir in order to meet multiple uses. This agreement requires releases of water from Lake Tahoe to maintain a minimum instream flow in the Truckee River below the lake during periods when water would otherwise be stored and accumulated for later release. In exchange, the agreement requires that an equivalent volume of water be stored in Prosser Creek Reservoir to compensate for the release from Lake Tahoe. Water stored in Prosser Creek Reservoir through this exchange is then used as though it were Lake Tahoe storage, and accounted for as a distinct water category called Prosser_exchange water.

HSPF simulates this linked operation of Lake Tahoe and Prosser Creek Reservoir, as shown in figure 5. The agreement requires a minimum instream flow below Lake Tahoe of 50 cubic feet per second between October 1 and March 31 and a flow of 70 cubic feet per second for the remainder of the year. In this simplified example, HSPF simulated the release of water from Lake Tahoe to maintain Floriston rates until May 25 and, thus, met the instream-flow requirement specified in the agreement. Therefore, storage of Prosser_exchange water remained constant through May 24. After May 24, most of the water released from Lake Tahoe was no longer required for Floriston rates, so Lake Tahoe outflows could have been reduced to zero on certain days. Instead, the release from Lake Tahoe was maintained at 70 cubic feet per second. Storage of Prosser_exchange water increased after May 24 at rates corresponding to that fraction of Lake Tahoe releases made solely to meet the instream-flow requirement.

To model this exchange of water, HSPF determines the minimum-flow requirement for a given date, the present rate of release from Lake Tahoe, and the availability of releasable storage in Lake Tahoe and of storable water in Prosser Creek Reservoir. If the conditional logic specified for the model determines that an exchange should and can be made, then Lake Tahoe releases for minimum instream flows are exchanged for Prosser Creek Reservoir water and designated as Prosser_exchange water. The model must track the accumulation and later release of this Lake Tahoe exchange water (stored in Prosser Creek Reservoir) through time.

Diversion Operations to Meet Agricultural or Municipal and Industrial Demands: The Alpine Decree separates the upper Carson River Basin into eight segments. Each segment is operated autonomously with respect to diversions. For lands within a segment, demand was tabulated according to (1) the consumptive-use duty⁴ specified as 4.5, 6.0, or 9.0 acre-feet per acre for agricultural demands and the net consumptive-use duty specified as 2.5 acre-feet per acre for M&I demands, and (2) the water-righted acreage (Garry Stone, U.S. District Court, written commun., 1995) using 1995 rights. In HSPF, each demand is separated according to priority date and the individual demands are grouped according to the ditch serving the lands. During the irrigation season, HSPF, using conditional logic, compares flow at the upstream boundary of the segment to the total amount of demands that could be satisfied based on priority dates. Those agricultural or M&I demands capable of being satisfied under current flow conditions are diverted from the mainstem Carson River to the appropriate ditch.

An HSPF simulation of how diversion operations of the Carson River are used to satisfy existing agricultural demands for the Buckland Ditch during April-October is shown in figure 6. For the period from April to mid-July, flow is available to satisfy all Buckland Ditch rights, which total about 23 cubic feet per second. Thereafter, flow in the river declines to a value of less than the amount required to satisfy all Buckland Ditch rights. Thus, the ditch diversion is reduced, satisfying increasingly fewer senior rights until late September, when no rights can be served by prevailing flow in the river.

Because of flexibility in programming operations in HSPF, alternative demand schedules can be simulated to analyze downstream effects on the Carson River. For example, a water right of 492.3 acres (only a part of the 838.3 acres of agricultural rights) served by the Mexican Ditch is hypothetically converted from agricultural to M&I use. Because of the difference between agricultural and M&I duties (in this case 6.0 and 2.5 acre-feet per acre, respectively), the agricultural diversion rate decreases from 26.0 to 18.8 cubic feet per second during the irrigation season from April through September. The downstream effect of the reduced diversion on Carson River flow near Fort Churchill for the period from July through October is shown in figure 7. The simulation indicates that only about half of the resulting 1,700 acre-feet per year of water savings is realized at Fort Churchill. The remainder is either consumed by the simulation of consumptive use by phreatophytes or used for irrigation by previously unsatisfied water-right holders between Mexican Ditch and Fort Churchill.

⁴ The consumptive-use duty for agriculture is the total volume of irrigation water required to mature a particular type of crop. The duty is the amount of water supplied to the land including transmission losses from the point of diversion at the river to the farm headgate, not the volume of water actually consumed by the plants. The consumptive-use duty for M&I has no transmission losses.

The Alpine Decree specifically defines operations of the East Fork Carson River when flow is less than 200 cubic feet per second during the irrigation season. One-third of the flow is directed to the Allerman Canal and two-thirds of the flow remains in the river. Conditional logic within the model separates flow according to these rules. Daily diversions to the Allerman Canal simulated by HSPF are shown in figure 8. For the period April 1 to late-July, Allerman Canal diversions are determined from operations based on agricultural demands. From late-July through September, when flow in the East Fork Carson River is less than 200 cubic feet per second, one-third of the flow is diverted into the Allerman Canal.

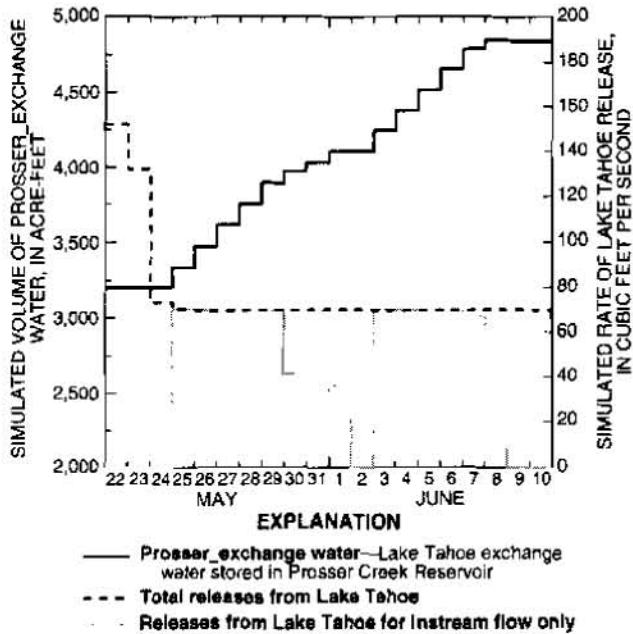


Figure 5. Prosser_exchange water category in Prosser Creek Reservoir and Lake Tahoe release simulated on basis of criteria in Tahoe_Prosser Exchange Agreement of 1959.

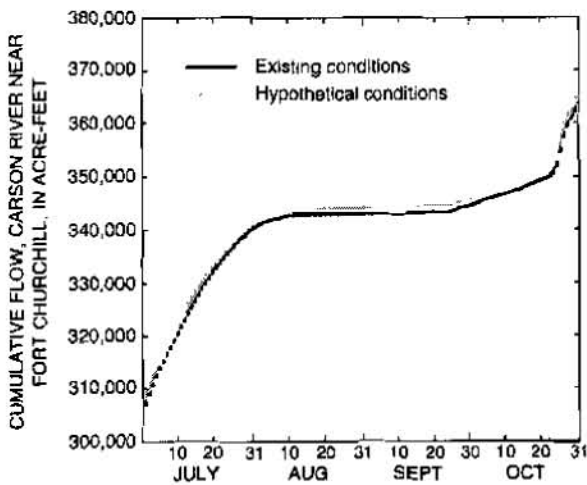


Figure 7. HSPF simulation of changes to Carson River flow near Fort Churchill that would occur if a portion of the water in Mexican Ditch were diverted for municipal and industrial water demands rather than for agricultural use.

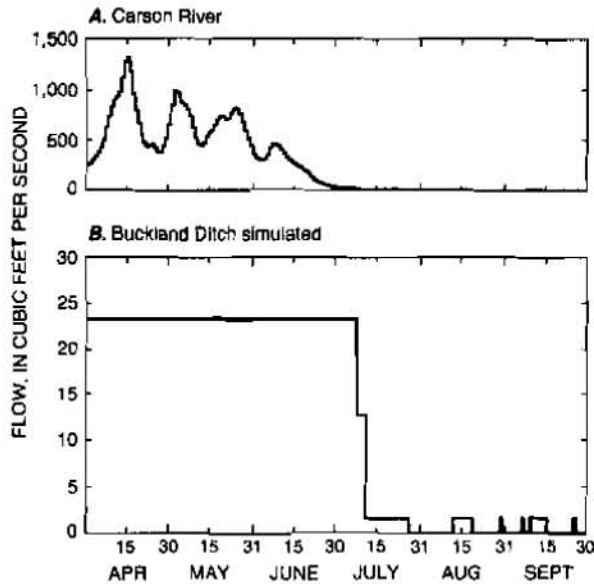


Figure 6. Carson River flow and diversion operations, Buckland Ditch. *A.* Carson River flow above ditch headgate. *B.* HSPF river diversions using existing agricultural water rights to simulate flow in Buckland Ditch.

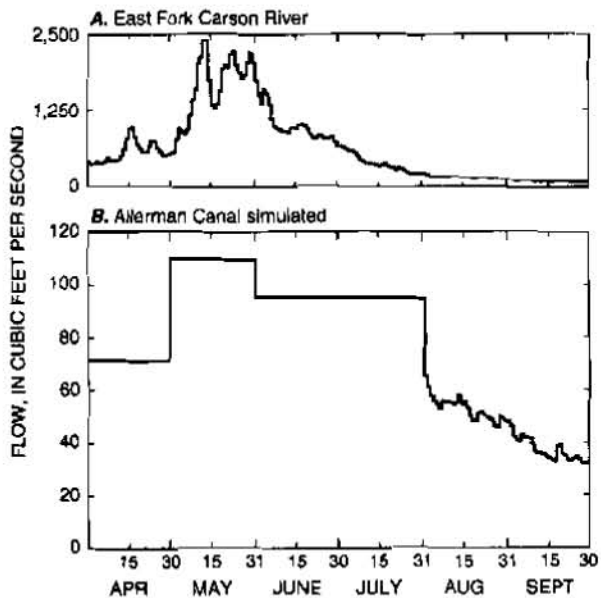


Figure 8. East Fork Carson River flow and diversion operations, Allerman Canal. *A.* East Fork Carson River flow. *B.* HSPF river diversions using Alpine Decree rules to simulate flow in Allerman Canal.

HSPF using conditional logic separates flow in the West Fork Carson River between segments in California and Nevada according to the Anderson-Bassman Decree rule of rotation. Weekly rotation takes place after June 1, if river flow is not sufficient to satisfy all rights (that is, if flow is less than about 180 cubic feet per second). Daily flows on the Brockliss Slough in Nevada simulated by HSPF are shown in figure 9. For the period June 1 to mid-June, flow is adequate to satisfy all rights, and no rotation occurs. From mid-June to late-September, when flows in the West Fork Carson River are less than about 180 cubic feet per second, weekly rotation between California and Nevada segments causes flows to fluctuate. Although not illustrated in figure 9, the rotation of the West Fork rights according to the Price Decree also is determined using conditional logic in the model.

Diversion Operations Used to Fill Reservoirs: Using conditional logic, HSPF can simulate river diversions to fill lateral reservoirs. The Alpine Decree allows the filling of Mud Lake during the nonirrigation season according to decreed storage rights. HSPF determines when and how much flow is needed to satisfy Mud Lake demands. Simulation of Mud Lake storage is shown in figure 10 for the period October 15 through December 31. On about December 20, Mud Lake has stored the legal limit of 3,172 acre-feet. For the period December 20-31, lake storage remains constant except for a slight increase in storage due to localized precipitation and runoff to Mud Lake. Similar logic, based on legal decrees, is used in filling Dangberg Ponds and Ambrosetti Pond in the Carson River Basin.

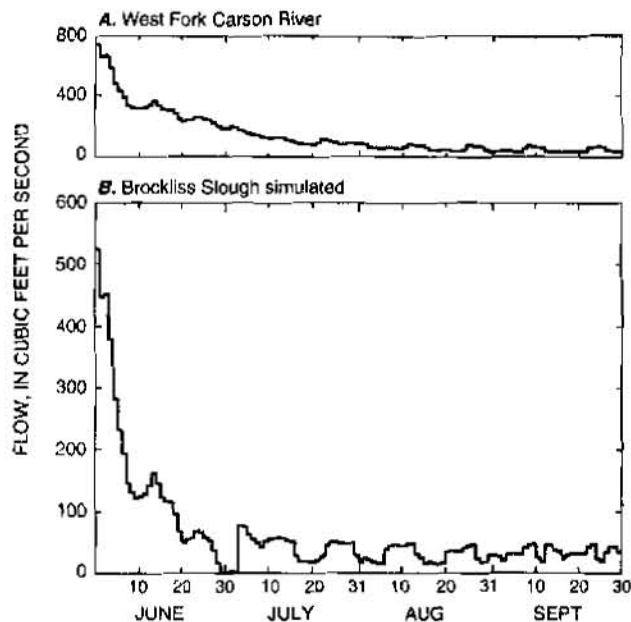


Figure 9. West Fork Carson River flow and diversion operations, Brockliss Slough. **A.** West Fork Carson River flow. **B.** HSPF river diversions using Anderson-Bassman Decree rule of rotation to simulate flow in Brockliss Slough.

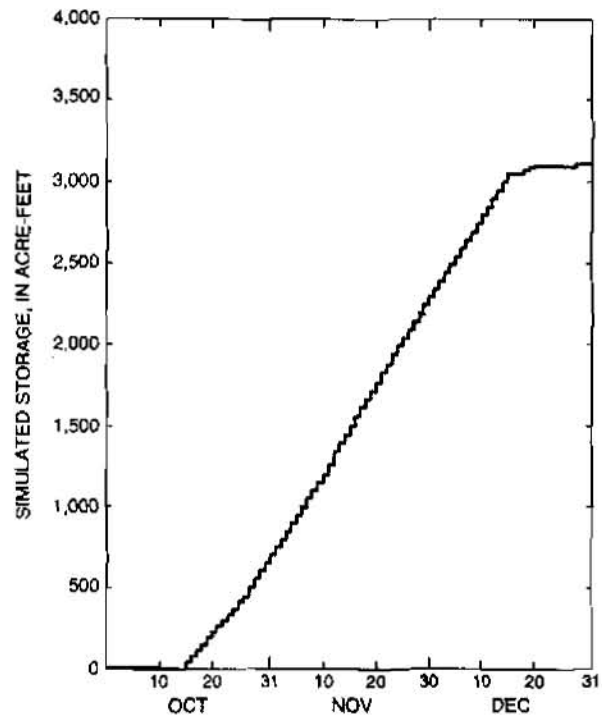


Figure 10. HSPF simulation of storage in Mud Lake based on Alpine Decree.

MODEL SCENARIOS

A scenario is a unique set of water-management operations, along with climate and physical characteristics, that simulate a proposed situation. A model scenario is defined by a coded input sequence (UCI file) containing user specifications, data regarding the river-system configuration, and input and output time series, applicable legal and operational constraints; and physically-based parameters that govern hydraulic or water-quality processes selected for simulation. After the model is run for a unique scenario, simulation results are stored as time-series data and are available for analysis using GENSCN.

An existing scenario may be activated by selecting it from a set of available scenarios. A "library" of commonly requested scenarios of Truckee River and Carson River models is beneficial to users who have little modeling expertise with HSPF and details of the UCI file.

Users with a moderate amount of modeling expertise can modify an existing scenario by varying the values of a variety of model specifications and parameters from an easy-to-use search and display feature. The user does not need to have specific knowledge of the format and structure of the UCI file. GENSCN displays a set of specifications and parameter values from a UCI file in an interactive setting for modification. This feature includes the specification or parameter name, definition, and maximum, minimum, and default (recommended) values.

Users having considerable experience with the HSPF program and a working knowledge of the structure and format of UCI files may edit the UCI file to create a new model scenario. Editing the UCI file provides the most flexibility for creating a custom scenario that may not be completely similar to previously developed scenarios.

Model Simulation: The activated scenario can be executed simply by selecting the simulate option within GENSCN. The progress status of a simulation is displayed on a window that indicates those operations and time periods that are completed, currently being simulated, and left to be simulated. Once the simulation is completed, users may analyze the results of a single run or compare the results of two or more scenarios.

Analysis of Simulation Results: GENSCN facilitates the selection and analysis of potentially large volumes of output data for the user after the simulation is complete. Three criteria (constituent, location, and scenario) are used in GENSCN to select the data to be analyzed. Data selected can range from all constituents at all locations for all scenarios to the smallest subset, such as observed stream temperature at a single gaging station. The user chooses the type of analysis to apply to the data selected. Tables, plots, and statistical analyses may be viewed on the display screen or printed as output files. In addition to these functions, the user interface can track water ownership in reservoirs and in river segments. Through animation, the user can view where, when, and how long critical thresholds are exceeded for any water ownership anywhere in the river systems.

OTHER MODELS UNDER DEVELOPMENT

The Truckee River and Carson River operations model is just one modular component in a comprehensive computer-modeling system being developed by the USGS Truckee-Carson Program. The modeling system integrates data management and analysis (Bohman and others, 1995) with the basin-operations model including reservoir operations and physically-based hydrologic models that simulate flow, stream temperature, precipitation-runoff relations, and selected water-quality characteristics. The modeling system, when calibrated and tested, will provide the tools necessary for modelers, as well as officials responsible for water-related policy, to examine many interrelated hydrologic and resources-management issues for the two river basins. The ability to simulate alternative management scenarios and compare the simulation results will help users understand the effects of changes in river/reservoir operations, land use, water-rights transfers, and irrigation practices on water quantity and quality throughout the system.

REFERENCES

- Berris, S.N., 1996, Daily flow-routing simulations for the Truckee River, California and Nevada. U.S. Geological Survey Water-Resources Investigations Report 96-4097, 83 p.
- Berris, S.N., Hess, G.W., and Cartier, K.D., 1996, Simulation of Selected Reservoir Operations in the Upper Truckee River Basin, California. U.S. Geological Survey Fact Sheet FS-082-96, 4 p.
- Bicknell, B.R., Imhoff, J.C., Kittle, J.L., Donigan, A.S., and Johanson, R.C., 1997, Hydrological Simulation Program—Fortran—User's manual for release 11. U.S. Environmental Protection Agency Report EPA/600/R-93/174, 755 p.
- Bohman, L.R., Berris, S.N., and Hess, G.W., 1995, Interactive computer program to simulate and analyze streamflow, Truckee and Carson River Basins, Nevada and California. U.S. Geological Survey Fact Sheet FS-165-95, 4 p.
- Hess, G.W., 1996, Progress report on daily flow-routing simulation for the Carson River, California and Nevada. U.S. Geological Survey Open-File Report 96-211, 41 p.
- Hess, G. W., 1997, Simulation of selected river diversion operations in the upper Carson River Basin, California and Nevada. U.S. Geological Survey Fact Sheet FS-240-96, 4 p.

Glen W. Hess, U.S. Geological Survey, 333 W. Nye Lane, Rm. 203, Carson City, NV 89706
Phone: (702) 887-7684, Fax: (702) 887-7629, email: gw Hess@usgs.gov

Steven N. Berris, U.S. Geological Survey, 333 W. Nye Lane, Rm. 203, Carson City, NV 89706
Phone: (702) 887-7693, Fax: (702) 887-7629, email: snberris@usgs.gov

APPLICABILITY OF DECISION SUPPORT SYSTEM FOR RESERVOIR OPERATION IN TAIWAN

By Wen-Cheng Huang, Associate Professor, National Taiwan Ocean University, Keelung, Taiwan; Fu-Ti Yang, Graduate Student, National Taiwan Ocean University, Keelung, Taiwan

Abstract: A user-friendly decision support system (DSS) for reservoir operation was introduced. The DSS model has been applied experimentally to the main reservoirs in Taiwan. In this study, the largest reservoir in southern Taiwan, the Tsengwen reservoir, was chosen to prove the applicability of the DSS model. The handy DSS was set on user-friendly computer interaction with Microsoft Excel in Windows system.

INTRODUCTION

In Taiwan, the total annual surface runoff is 67 km³/yr, of which 78% comes from the wet season (from May to October) and only 22% is available during the dry season (from November through April). Meanwhile, the total water demand is approximately 18 km³/yr. Taiwan uses almost 77% of its withdrawn water for irrigation, about 14% for domestic water supply, and about 9% for industry. If adequate water is not available, demand will be reduced by rationing among water users. Due to uneven distribution of water resources in Taiwan, droughts and floods frequently occur every year. A reservoir thus plays a very important part to retain excess surface water flows from wet season for use during the dry season. The Water Resources Bureau (WRB), the water authorities of the Republic of China, intends to develop a decision support system (DSS) used friendly and understood easily to assist the authorities for operational guidance of reservoirs, especially for use during periods of drought. The purpose of this paper is therefore to describe the framework of the DSS for application to reservoir operation.

STRUCTURE OF THE MODEL

Suppose that the average 10-day-long surface runoff in period t is of a continuous random variable, the exceedence probability of X exceeding or equaling a specific value $x_{(m)}$ in period t is

$$\Pr[X \geq x_{(m)}] = m/(n+1) \quad (1)$$

where

X = reservoir inflow, a random variable in period t

$x_{(m)}$ = a possible value of X , the m th largest observation

n = total number of observations

For a given inflow hydrograph with identical exceedence probability, a sequence of reservoir storage variation over a time space with ten-day time increment can be determined. The performance will show whether or not the water demand for each user is fulfilled. Reservoir operation obviously varies with different exceedence probability of inflow. The effects of this probable reservoir operation as time goes along may be examined according to the information provided by the DSS. If the operation indicates water shortage occurrences at any time of the year, then water demand for water users must be curtailed in advance to mitigate a probable drought loss. The amount to be reduced is up to the decision makers with specified values of rationing coefficient. Besides, the reservoir operation will be updated every time

increment. As a new observed inflow is obtained, the decision support system repeatedly activates its procedure to suggest suitable reservoir operating policy for the future.

Optimization models are studied mostly for planning purpose and often discarded because of a gap in existence between theory and practice on the real-time reservoir operation (Yeh 1985). In practical use, rule curves derived from simulation model are mostly used for reservoir operation in Taiwan. The reservoir operators prefer to use rule curves rather than optimization models due to its simplicity and reliability. The operation rules identify the storage zones associated with a certain operational behavior. In this research, a helpful decision support system for real-time long-term reservoir operation on the basis of exceedence probability of inflow is proposed here. The DSS providing more information would be a very useful booster to the authorities about how to adjust the operating policy.

It is anticipated that the developed DSS on real-time reservoir operation has the functions: (1) to provide available data such as the reservoir characteristics, inflow, water demand of each user in each period, (2) to examine the present status of reservoir storage and inflow, (3) to analyze the outlook of reservoir operation on the basis of varying exceedence probability of inflow, (4) to leave option to users for water rationing as drought happens, (5) to demonstrate results with useful tables and figures.

In accordance with the specified functions, The framework of the decision support system on real-time reservoir operation is shown in Figure 1. It shows an interaction between the user and the DSS while the reservoir operation is being executed. The worksheet of the DSS consists of three units: (1) database including the area and volume curves versus water level, rule curves, evaporation, exceedence probability of inflow, water rights and demands of each user over time, present inflow and reservoir storage, (2) data analysis including the reliability of specified water demand over a time space of a year with ten-day increment, current situations of inflow and reservoir storage, real-time reservoir operation, drought mitigation, (3) result output through a printer. The DSS was installed on user-friendly computer interaction based on Microsoft Excel for Windows system. As demonstrated in Figure 2, for example, the worksheet displays useful functions included in the DSS for the Tsengwen reservoir. Reservoir operators can easily key in the date where the operation starts and the actual reservoir storage and inflow at that time, then use the browser to pick any specific function encoded by Visual Basic.

Work on reservoir operation is usually repetitive and troublesome. For a handy decision support system installed in computer, a user-friendly interface is required to boost the system. Visual Basic is a programming language originally developed by Microsoft to assist programmers with a quick and easy way of developing Windows applications. It is an event-driven programming technique. Based on the integrated development environment provided by Visual Basic, a user interface can be created quickly and easily. Then a code to respond to specific events occurred as a result of user input can be written. Coupling with Microsoft Excel software using its powerful macro language for applications, a handy decision support system on reservoir operation can be definitely interesting and comfortable to reservoir operators in using the model. Detailed information on using Excel Visual Basic can be found from extensive books published by Microsoft Corporation (Microsoft 1994, 1995; Jacobson 1994; Wexler and Sharer 1992).

APPLICATION OF THE MODEL

Brief Introduction: To examine the applicability of the developed decision support system for long-term real-time reservoir operation, the experimental DSS model has been applied to several large reservoirs, e.g., Shihmen reservoir in northern Taiwan, Techii reservoir and Sun-Moon Lake in central Taiwan, and Tsengwen reservoir in southern Taiwan. In this study, the operation for the multipurpose Tsengwen reservoir (Figure 2) was introduced, the largest reservoir in Taiwan. Average annual rainfall of the area is 2612 mm corresponding to annual runoff 1.2 km^3 , of which 90% comes from the wet season and only 10% is available during the dry season. Severe droughts often occur provided that insufficient water is available in the preceding wet season. It is thus important to have a handy DSS for real-time reservoir operation about how to coordinate water, particularly during periods of drought. In addition to the rule curves presently used as operating policy for water allocation, the developed user-friendly DSS intends to provide more helpful information to reservoir operators. The reservoir with a catchment area of 481 km^2 is located at the upper reach of the Tsengwen river and about 60 km northeast of Tainan city. The reservoir capacity is 708 million cubic meters (MCM) with allowable maximum release of $9,470 \text{ m}^3/\text{s}$. Its primary purpose is to detain excess water from wet season for use during the dry season. It furnishes water to agriculture (irrigation area 67,000 ha), municipality ($400,000 \text{ m}^3/\text{day}$) and industry ($70,000 \text{ m}^3/\text{day}$). Of the water rights, agriculture holds 86%, domestic water supply has 11.5%, and industrial use only owns 2.5%. There is also a hydropower plant with 50,000 KW installed capacity. Aside from typhoon-borne floods, water through turbine is diverted to the Coral Lake, a small reservoir with storage capacity 84 MCM, and 6 km downstream from the Tsengwen reservoir. The active storage capacity of both reservoirs equals 693 MCM.

Cases of Real-Time Operation: Applicability of the real-time operation of the developed DSS model was tested with real-world cases. Prior to operation, the essential data installed at the database are required, such as the historical inflow ranging from 10% to 95% of the exceedence probability and water demand. The reliability of specified water demand over a year with ten-day increment clearly indicate that inadequate water is available during the dry season, particularly from January to April. This is due to the fact that irrigation for paddy fields requires more water throughout the growing season. So, the Tsengwen reservoir plays an important part on the regulation of water flows. The rule curves currently used at the Tsengwen reservoir have four storage zones in each of 36 periods within the year. Excluding zone A (the highest one for flood control), the reservoir storages within zone B, C, and D (the lowest one) correspond to the release policy ($k_a=k_m=k_i=1.0$), ($k_a=0.8$, $k_m=1.0$, $k_i=1.0$), and ($k_a=0.5$, $k_m=0.8$, $k_i=0.5$), respectively. And the parameters (k_a , k_m , k_i), express the ratio of water rationing separately for agriculture, municipality and industry.

Real-time operation on October 1995: At the end of the 28th ten-day period on October 1995 (initial winter season), the actual reservoir storage was 129.43 MCM within zone D, about 18.68% of the active storage. And the observed inflow equalled $11.06 \text{ m}^3/\text{s}$, approximately 89.24% of the exceedence probability at that time. The situation was crucial to the reservoir operation. The variation of reservoir storage over time shows that no matter what the future hydrologic status will be, severe drought with empty reservoir occurs at the end of January if demand was not curtailed (i.e., $k_a=k_m=k_i=1.0$). Obviously, water rationing among different water users is needed. In the case of drought condition, the releases based on the rule curves should be restricted with $k_a=0.5$, $k_m=0.8$ and $k_i=0.5$ for agriculture, municipality and industry separately. With the policy ($k_a=0.5$, $k_m=0.8$, $k_i=0.5$), however, serious water shortages may still exist after forthcoming February, as shown in Figure 3.

Obviously, the planting schedule of rice for the next growing season (from January through May) should be canceled to ease the drought situation. As a matter of fact, the drought forced the government to declare a regional emergency in water supply. WRB officials at that time decided to shorten demand with $k_a=0.5$, $k_m=0.8$ and $k_i=0.5$ till the end of the present growing season (end of November) and terminate the succeeding irrigation project for the paddy fields.

Real-time operation on January 1996: At the end of the first ten-day period on January 1996, the actual storage volume was 80.58 MCM, about 11.6% of the active storage. And the inflow approximates 1.96 m³/s, close to 85.67% of the exceedence probability at that time. The severity of water shortages still existed. Though the demand has been deducted by not irrigating as planned in the paddy fields, Figure 4 reveals that failures to meet targeted quantity of water ($k_a=0.5$, $k_m=0.8$ and $k_i=0.5$) occur in April as the exceedence probability exceeds 70%, where the targeted water with $k_a=0.5$ was delivered to irrigate any other crops than rice. It was found the risk of suffering reservoir emptiness may be reduced with $k_a=0.4$, $k_m=0.8$ and $k_i=0.5$. However, the delivered water to irrigate sugarcane and other crops as planned by the irrigation associations is insufficient. The effects of this disruption on water supply around the area can be devastating. Hence the decision makers, WRB officials, suspended the plan for the production of sugarcane and other crops. Meanwhile, the authorities coordinated the release policy with $k_a=0.0$, $k_m=1.0$ and $k_i=1.0$, as suggested by the DSS.

Real-time operation on June 1996: At the end of the 16th ten-day period on June 1996 (initial summer season), the current reservoir storage was 104.97 MCM, nearly 15.15% of the active storage. The storage volume is within zone B. According to the rule curves, the releases with $k_a=k_m=k_i=1.0$ would be allowable. It appears that the inflow approximates 25 m³/s, close to 85% of the exceedence probability at that time. The weather is dry. A prolonged dry condition in hydrology may persist, if typhoons with accompanying rainfall do not come within the wet season. With a lengthy dry weather, it was found in Figure 5 that the reservoir may become empty at the beginning of October and affect the crop harvest within the ongoing growing season (from June to November). The risk of suffering reservoir emptiness exists. Of course, WRB officials continuously keep an eye on the incoming hydrological sequences to adjust the operation.

Real-time operation on August 1996: A remarkable Typhoon Herb hit Taiwan and refilled the Tsengwen reservoir on August 1. At the end of the 22nd ten-day period, the remaining reservoir storage was 682.47 MCM. Most of the flood water was stored in the reservoir to be used for the following periods. Clearly, 100% of the targeted water within the summer's growing season can be fulfilled, as demonstrated in Figure 6.

CONCLUDING REMARKS

A user-friendly decision support system in determining appropriate reservoir releases for real-time long-term reservoir operation was developed. The DSS has been applied experimentally to the main reservoirs in Taiwan. During the experimental period, the DSS operated by the actual operators of the Tsengwen Reservoir Administration Bureau (TRAB) appears to have satisfactory performance on the reservoir operation. As the simulation results prove, the DSS is considerably suited to the reservoir operation. With the new storage volume and hydrological situation, the system operation can be renewed every time increment. It is thoroughly easy to run and understand the model. The handy DSS was installed on user-

friendly computer interaction with Microsoft Excel in Windows system. Furthermore, the users can survey on-line reservoir operation with browser on World Wide Web (WWW). The current uniform resource locator on WWW of the DSS is <http://wrm.hrc.ntou.edu.tw/>.

ACKNOWLEDGMENTS

The research was funded by the Water Resources Bureau, Ministry of Economic Affairs of the Republic of China.

REFERENCES

- Jacobson, R., 1994, *Microsoft Excel Visual Basic for applications step by step: version 5 for Windows*. Microsoft Press.
- Microsoft, 1994, *Microsoft Excel Visual Basic for applications reference*. Microsoft Press.
- Microsoft, 1995, *Microsoft Excel/Visual Basic programmer's guide*. Microsoft Press.
- Wexler, S. and Sharer, J., 1992, *Microsoft Excel macros version 4 step by step: for Windows and the Macintosh*. Microsoft Press.
- Yeh, W. W-G., 1985, Reservoir management and operations models: a state-of-the-art review. *Water Resources Research*, 21(12), 1797-1818.

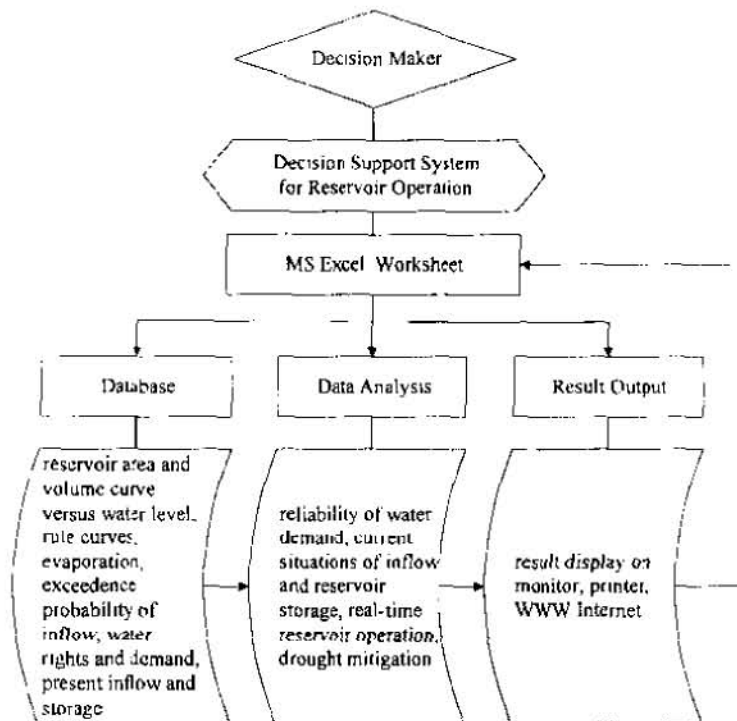


Figure 1. Framework of the decision support system for reservoir operation

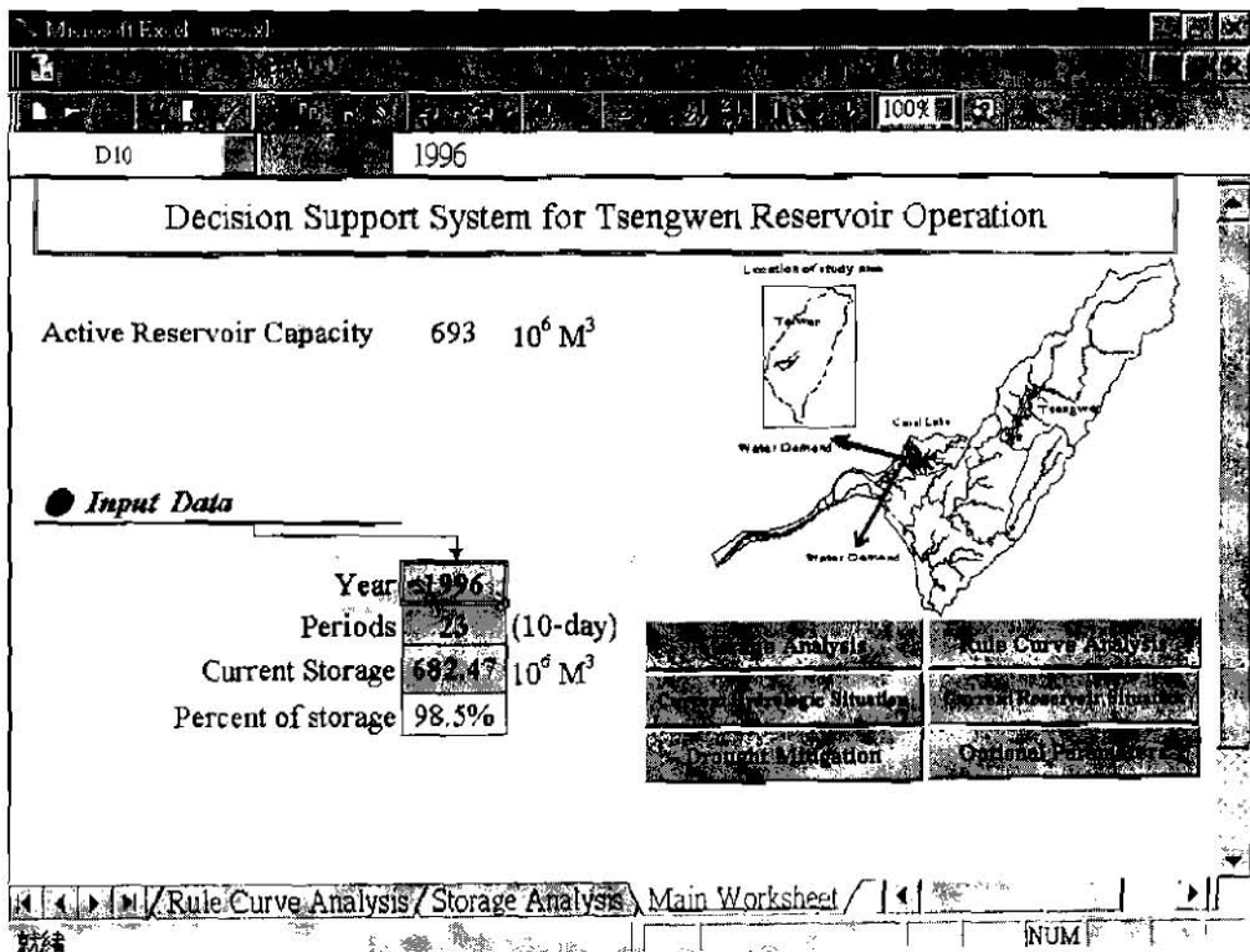


Figure 2. Worksheet in the decision support system

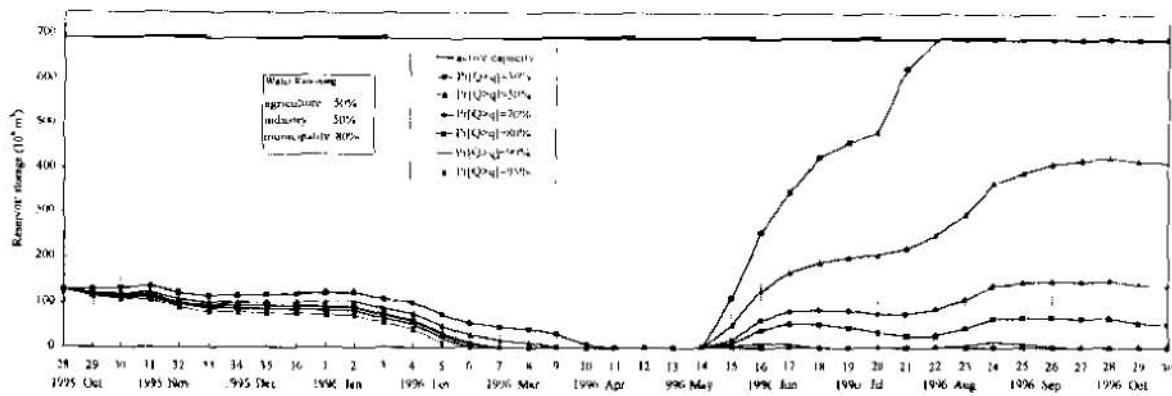


Figure 3 Probable storage variation over time at Tsengwen reservoir (Oct 1995 - Oct 1996)

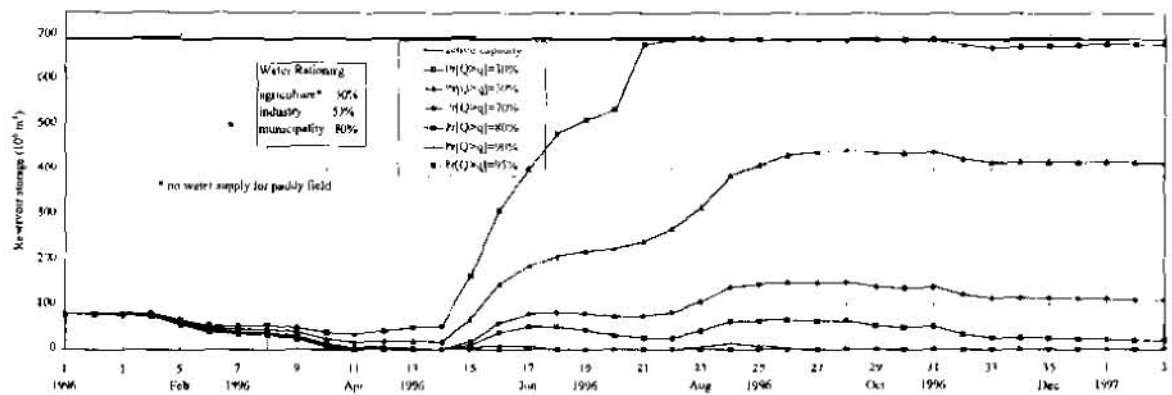


Figure 4 Probable storage variation over time at Tsengwen reservoir (Jan 1996 - Jan 1997)

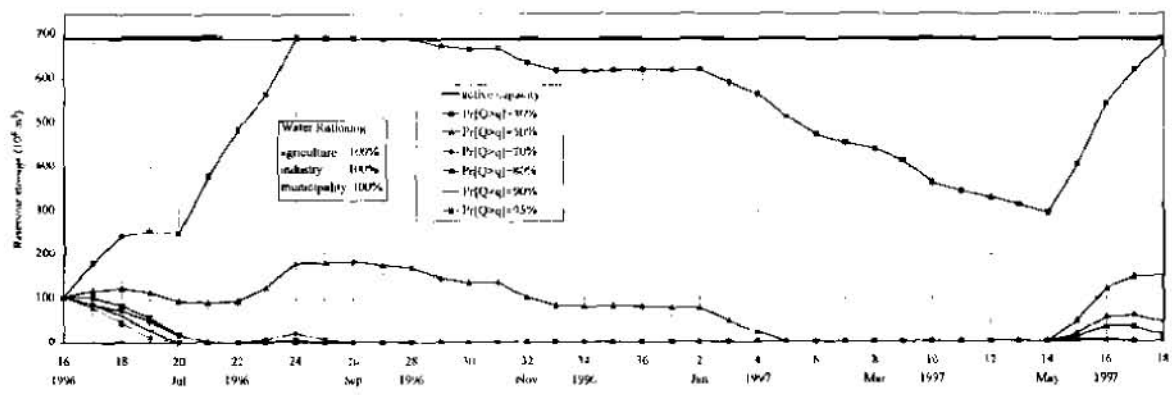


Figure 5 Probable storage variation over time at Tsengwen reservoir (Jun 1996 - Jun 1997)

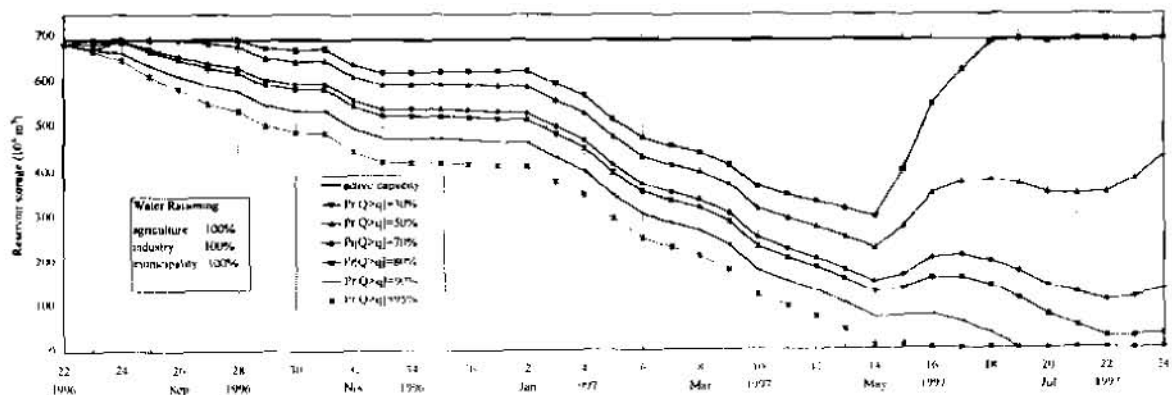


Figure 6 Probable storage variation over time at Tsengwen reservoir (Aug 1996 - Aug 1997)

FLOOD DISASTERS AND THE THREE GORGES PROJECT ON THE YANGTZE

JI Xuewu, Senior Engineer of Professorial Rank, Director-General Bureau of Hydrology, Changjiang Water Resources Commission, Ministry of Water Resources, P. R. China

Abstract: The Yangtze River is the largest river and one of the most flourishing area in the economics in China. However the plains in its middle and lower reaches are frequently threatened by stormflood hazards due to the ground surface being lower than the flood stages and depending mainly on 30,000 km long levees for their safeties. According to the historical records during the recent 2,000 years there occurred once of heavy flood disasters about every ten years in the area. In the 19th century there were two extraordinary floods, 1860 and 1870, producing peak discharges at Yichang of up to 92,500 m³/s and 105,000m³/s, respectively, which far exceeded the safety capacity 56,700-60,000m³/s at Zhicheng and caused extremely heavy damages. Untill recently, there existed flooding losses such as 1995 and 1996. Therefore, it is very important to establish the comprehensive flood control system which consists of engineering and non-engineering treatments including the key project, the Three Gorges Project(TGP) under construction, and flood monitor-forecasting warning system.

Based on the storm-flood properties and historical-palehydrological data in the Yangtze this paper deals with the TGP design floods comprised by frequency analysis, stochastic modeling and PMP/PMF estimation models, and with tremendous comprehensive benefits of TGP. In the paper the description will be made in some detail for the river monitor-forecasting warning procedure involving data collection transportation-processing and forecast model. Also the paper will introduce the progress of TGP after the start from 1993.

INTRODUCTION

Three Gorges Project(TGP) possesses enormous, comprehensive utilization benefits for flood control, power generation, navigation, irrigation, water supply and promoting economic development in the reservoir region. It is the key project to harness and develop the Yangtze (Changjiang) River, and the strategic measure to comprehensively use the rivers water resources.

NATURAL AND TOPOGRAPHIC CONDITIONS

The Yangtze River is the largest in china. The valley is located from 24 ° 27 ' to 35 ° 54 ' N latitude, and from 90 ° 33 ' to 122 ° 19 ' E longitude. It is long from west to east, and narrow from north to south, in the shape of a rectangular. The terrain of the valley slopes from northwest to southeast to the Pacific Ocean, which is favorable for the southeast and Southwest monsoons to bring great amount of warm moisture air into the valley. In the valley, the mountain area occupies 65 percent, which is mainly located in the west region and the boundary areas of

the valley, the hilly land 22 percent, mainly in Sichuan, Hunan and Jiangxi Provinces, and the plain 13 percent, mainly on the middle and lower reaches of the river.

The Yangtze River originates from the Qinghai-Xizhang(Tibet) Plateau. From the origin to Yichang, Hubei Province, is called the upper reach, with a length of 4,500km, and a catchment area of about 1 million km². The Three Gorges are located on the upper reach, starting from Fongjie, Sichuan Province to Yichang. The middle reach is from Yichang to Hukou, Jiangxi Province, with a length of 935 km and a catchment area of 680,000 km². From Hukou down to the river mouth is the lower reach. The Yangtze River has many tributaries. There are 8 of them with a basin area of over 80,000 km², 49 over 10,000 km² and 437 of 1,000 km².

The Yangtze valley is located in the subtropics region, with a climate of hot in summer and cold in winter. The mean annual temperature is between 15 to 19 °C, and the mean annual precipitation is 1,067 mm. Due to topographic impact, the regional distribution of precipitation is uneven. The precipitation decreases progressively from southeast to northwest. It precipitates more in the mountainous area than the plain area, more at the slope facing the wind than the leeslope. The distribution of precipitation is not even within a year. The precipitation in the dominant rain season (generally lasting four months) occupies 60 percent of that of the whole year. There are many rainstorm (the daily precipitation is ≥ 50 mm) areas in the valley, in which, the west Sichuan, Three Gorges area on the upper reach, the west parts of Hunan and Hubei, and parts of Jiangxi and Anhui are the major storm areas. In Lushan area of Jiangxi Province, the 24-h precipitation once reached 900 mm, and in Anxian, Sichuan Province, it was 577 mm.

FLOODS AND FLOOD DISASTERS ON THE YANGTZE RIVER

The floods on the Yangtze River are produced by rainstorms. The floods on the mainstream of the River and its tributaries on the upper reach always concentrate in the dominant flood season (three months), and the flood volume occupies more than 50 percent of that of the whole year. At Yichang, where the TGP locates and with a catchment area of 1 million km², the flood volume in the dominant flood season from July to September occupies 50.2 percent of that of the whole year, of which 32.4 percent is from Jinsha River, and 13.5 and 15.5 percent are from Minjiang R. and Jialin R. respectively. During the flood season from May to October, the flood volume at Yichang is 348.7 billion m³, which occupies 66.1 percent of that at Hankou (with a catchment area of 1,488,000 km²) and 59.0 percent of that at Datong (with a catchment area of 1.70 million km²). It is seen from the above mentioned data that the water from the upper reach is the major composition of floods on the middle and lower reaches. Where anomalous weather occurs, the floods from the middle and lower reaches of the River will meet that from the upper reach. Consequently, a disastrous flood appears on the middle and lower reaches. The 1931 and 1954 floods were typical examples of this kind of floods.

There are a wealth of reliable hydrological data in the valley. At Hankou, Yichang and Chongqing, there started water level observation in 1865, 1877 and 1892 respectively, and then have been continuous water level records since then. The Yangtze Valley has a long history. Flooding description appeared in the year of 966 B.C. (West Zhou Dynasty). A great number of tablets, stone inscription about floods have been found, along the mainstream and its tributaries the peak stage and discharge of any of floods can be reasonably worked out. In the Three Gorges areas, the earliest stone scripted flood stage was about a flood in 1153 (Song Dynasty). In recent year, paleoflood investigation has been carried out, the results of which have provided reference in estimating the flood frequency of the Yangtze River.

Comprehensive investigation and analysis have showed that there occurred over 214 big floods in the upper and middle reaches from the year of 185 B.C. (Han Dynasty to 1911 the end of Qing Dynasty), averagely once in about every ten years. There have occurred five extraordinary floods (1870, 1860, 1954, 1931 and 1935) since 1860, in which, the 1931 and 1935 floods each deprived about 140,000 people of the lives and 30,000 people was drowned by the 1954 flood. During the period from 1788 to 1870, there were four years in which discharge larger than 80,000 m³/s occurred (1788, 1796, 1860 and 1870) (See Table 1) at Yichang. From 1877 till now, however, the largest observed discharge is only 71,100 m³/s, which appeared in 1896. In the summers of 1995 and 1996, large floods occurred successively on the middle reach of the River, caused serious damages.

Table 1 Extraordinary historic floods at Yichang

order	year	discharge(m ³ /s)
1	1870	105,000
2	1227	96,000
3	1560	93,600
4	1153	92,800
5	1860	92,500
6	1788	86,000
7	1796	82,200
8	1613	81,000

The middle and lower reaches of the River is always threatened by flood disasters, and the losses are especially serious there due to fact that it is densely populated and with a developed economy. The Jingjiang reach of the River, from near Shashi, Hubei Province, to Chenglingji, Hunan Province, is frequently threatened by flood disasters in particular. The River near Shashi runs in a zigzag path and the capacity of the River there can only safely release a discharge of 50,000 m³/s. When the dyke there is heightened and reinforced, the safety capacity of this river reach is only 60,000 m³/s. If the flood diversion and storage measures are implemented, a maximum discharge

of 80,000 m³/s can pass through this river reach. At present, the dyke at Jingjiang River reach is generally 12m high and the crest is 15m high, while the flood water level in the flood season is over 10m higher than the ground elevation behind dyke. If the dyke were to be further heightened and reinforced, it is very difficult as well as risky. If floods to the scale of those in 1870 occurred, extraordinary disasters would be bound to hit both banks of the Jingjiang River reach. Wuhan City, the capital of Hubei Province, and the vital transportation center in central China, is seriously threatened. The national economic development of China will even be severely affected.

FLOOD CONTROL MEASURES ON THE MIDDLE AND LOWER REACHES AND THE THREE GORGES PROJECT

Flood control facilities on the middle and lower reaches have been greatly improved after some 50 years of efforts. The total length of dykes on the mainstream and the tributaries amounts to 30,000km, and many flood diversion works such as Jingjiang Diversion work on the Yangtze and Dujiatai Diversion work on the Hangjiang River and many other tempering flood diversion and storage areas have been constructed. And the flood forecasting and warning system have also been established. If a flood to the scale of that in 1954 (with a return period of 100 years near Wuhan) occurred, with all these measures implemented, devastating losses would not occur. But the Jingjiang River reach can only stand floods with a return period of 20 years. In the light of the flooding characteristics, that is, the storm comes mainly from the upper reach, the TGP is taken as the key structural measures for flood control on the River.

The TGP is sited at Sandouping, about 40 km above Yichang, and the catchment area is 1 million km². The designed elevation of the dam crest is 185 m above sea level, and the normal pool level is 175 m. This project is to bring enormous benefits for flood control, power generation, navigation, water supply and promoting economic development in the reservoir region. The total capacity of TGP reservoir is 39.3 billion m³ in which flood control storage capacity is 22.15 billion m³. The installed capacity is 17,680 mw, and the annual power generation is 84 billion kWh. 10,000-ton towboats will be able to sail right up to Chongqing, which is about 600 km above the damsite. Main features of the TGP is shown in Table 2. When completed, the TGP will bring enormous social, economic and environmental benefits. If a flood of the type of 1870 (about 1,000 years in return period) occurred, the TGP can be used together with the existing flood control facilities, and the discharge on the Jingjiang River reach can be kept below the safety capacity of the channel. If floods of the types of those in 1954, 1996 occurred, the TGP will also play a significant role in flood control.

TGP DESIGN FLOOD:

The main basis for design flood study is the observed data at Yichang Hydrometric Station and that at Cuntan Station (near Chongqing) with a catchment area of 867,000 km². A great amount of hydrological and meteorological data at the major hydrology stations and the important rain

gaging stations is also used for the sake of analyzing the storm flood characteristics, estimating the probable maximum flood (PMF) and for flood routing. Meanwhile, the investigated historical floods have also been fully considered.

Table 2 Main features of TGP

Name	Figure/Feature	Unit
Basin area	100	10 ⁴ km ²
Annual runoff	451.0	billion m ³
Suspend load of sediment	530	million t
Normal pool level	175	m
Total capacity of reservoir	39.3	billion m ³
Capacity for flood control	22.15	billion m ³
Area of reservoir	1,084	Km ²
Installed Power Capacity	17,680	mw
Annual Energy	84	billion kWh
Crest of Dam	185	m
Max height	175	m
Type of dam	concrete gravity	
Total axial length	2,335	m
Ship lock	double lines 5 steps	

Flood Frequency Analysis: By making use of 8 historical floods including the 1879 flood, the discharge of which is 105,000 m³/s, and the empirical return period is 840 years, and of the observed floods since 1877, an uncontinuous flood series is composed.

Plotting position formula: plotting position formula for historical floods

$$P_M = \frac{M}{N + 1}, \quad M=1,2 \dots a \quad (1)$$

plotting position formula for observed floods

$$P_m = \frac{1}{N + 1} \left[a + \frac{m(N - a + 1)}{n + 1} \right] \quad (2)$$

There, N=840; n=114(1877~1990); a=8, which is the number of historical floods; M, m are the ordinal numbers of historical and observed floods respectively.

Probability distribution model: The Pearson Type III distribution is adopted after a comparison of several distributions. And the Chi-square (X²) test is used to assess the goodness-

of-fit.

Flood statistical characteristics: The curve fitting methods are applied, and results are listed in Table 3.

Table 3 Flood statistical characteristics at Yichang

item	statistical characteristic			design value(%)		
	\bar{X}	C_v	C_s/C_v	0.01	0.1	1.0
Daily discharge	52,000	0.21	4.0	113,000	98,800	83,700
Flood volume in 7 days	27.50	0.19	3.5	54.72	48.68	42.08
Flood volume in 30 days	93.50	0.18	3.0	176.7	159.0	139.3

Note: daily discharge: m^3/s ; flood volume: billion m^3 ; \bar{X} : mean value; C_v : variation coefficient; C_s : skewness coefficient.

Design flood hydrograph: Based on an analysis of the flood characteristics, the flood hydrographs of 1981, 1982 and 1954 floods are chosen as three typical hydrographs. Then the discharges and flood volumes of the typical hydrographs are enlarged to the frequency of the design discharge and flood volumes. By this way, the design flood hydrograph at damsite is obtained.

Design hydrograph for reservoir inflow: The design hydrograph for reservoir inflow is derived by considering the changes in rainfall-runoff formation and flow concentration when the TGP is completed.

Flood Stochastic Modeling: The following stable multidimensional autoregressive model is applied.

$$Z_t = A_1 Z_{t-1} + A_2 Z_{t-2} + \dots + A_p Z_{t-p} + B \varepsilon_t \quad (3)$$

where Z_t is the multidimensional dynamic variable, ε_t is the white noise; A_p is the autoregressive coefficient with order P ; B is the residual error. Using the above mentioned model, the floods series in the flood season (180 days) at 8 stations (areas), that is, at both ends of the reservoir, on the reservoir surface, at the damsite and on the middle reaches, are modeled and obtained. This flood series can be used for reservoir operation and for calculating and assessing the flood control benefits.

Probable Maximum Precipitation (PMP) and Probable Maximum Flood (PMF): Due to the

fact that the catchment area above the damsite is large, the reservoir storage capacity is big, and the design duration is long, the method of precipitation process replacement in the typical flood years and the method of combination of the long term weather process's precipitation are used to derive the PMP series. Then through rainfall-runoff models and flow-concentration or routing computation, the PMFs at the TGP damsite are obtained. The estimated daily discharge is between 120,000 and 127,000 m³/s, and the flood volume in seven days is between 60.7 and 65.2 billion m³.

FLOOD FORECASTING AND WARNING (FF/W) SYSTEM FOR THE TGP

There are hydrological stations and rainfall gaging stations above the damsite. According to the temporal and spatial distribution of precipitation, and for the sake of reservoir operation, the inflows below Chongqing, which will have a direct impact on the reservoir, shall be monitored. Meanwhile, to meet the flood control needs on the middle and lower reaches, the inflows from the Dongting Lake, Hunan Province, shall also be forecasted. Accordingly, the FF/W System for the TGP shall be composed of four subsystems as follows.

Information collection subsystem: Around the damsite, 40 hydrological stations, 12 water level stations and 49 rainfall gaging stations are to be established within the FF/w system.

Data transmission subsystem: The water stage, discharge and rainfall data will be transmitted to 9 subcentres located in the reservoir region and on the river's middle reach via telemetry systems or the National Public Data Exchange Network (also known as cable communication), then further transmitted from the subcentres to the centers at the damsite and in Wuhan, which are connected with the National Flood Control Headquarters in Beijing. Communications between the major stations on the mainstream of the River and the subcenters are realized through INMARSAT-C, while that between subcentres and the System (or Beijing) via VSAT.

Hydrological Forecasting Subsystem: Precipitation forecasting is close linked with flood forecasting, and the medium-range forecasting with short-term one. Precipitation is forecasted quantitatively, focusing on the temporal and spatial distribution of rainfall. For rainfall-runoff models, the API, Xinanjiang model are used, and for flow-concentration routing the Sherman, Nash and flow-concentration coefficient are used. Stage-discharge relationship curves, Muskingum routing model have been used. In recent years, the real-time on line forecasting method based on the filter theory and the interactive forecasting programs have also been made use of.

Water information and flood warning service subsystem: Real-time hydrological data and the forecast on warning with specified duration, accuracy and criteria are disseminated to all the users and decision making units. Information monitoring and feed-back system is established.

THE TGP CONSTRUCTION PROGRESS AND SCHEDULE

The TGP started officially construction in December 1994. Up to now, on the right bank, the diversion channel has been excavated and lined. The longitudinal cofferdam has finished the concrete placement. On the left bank, the permanent navigation lock, double-line and five steps is being excavated, and the temporary navigation lock has been finished the concrete works and equipment being installed. The upper and lower cofferdams have been constructed, and the river was closed on November 8, 1997. The closure indicates the end of the first stage of the Project construction and the start of the second stage. In the years that follow, the powerhouse for the 14 generating units on the left bank will be constructed and equipment be installed. The permanent shiplock will be finished. the spillway and silt scouring sluice in the dam on the main channel will be constructed. By the year of 2003, the reservoir will store water to the water level of 135m above sea level, and start power generation of the first unit. The diversion channel will be closed. This closure will mark the beginning of the third stage of construction. During this stage, the powerhouse for the other 12 generating units on the right bank will be constructed and equipment installed. The placement of concrete in the dam will be finished. Up to now, all the works have been carried out smoothly as planned.

CONCLUSIONS

The middle and lower reaches of the Yangtze River is vulnerable to flood disasters. This storm flood comes mainly from the upper reaches of the River.

The TGP, when completed, will increase the flood control capacity on the Jingjiang River section to stand flood with a return period of 100 years. If the TGP is coordinately used with other flood diversion and storage facilities, this river section will be able to protect flood of 1,000 years in return period. Therefore, flood control and damage mitigation are the major tasks of the TGP.

The hydrological data series used for the TGP design flood studies is long, and with relatively high accuracy. The calculation methods are new and diverse. The results are fairly reliable and available.

The FF/W system for the TGP is an important nonstructural measure to enhance the benefits of the TGP and to mitigate flood damage on the middle and lower reaches of the Yangtze River.

IMPLEMENTING A WATER RESOURCE PLANNING MODEL WITHIN THE COLORADO RIVER DECISION SUPPORT SYSTEM

Steven Malers, Software Engineer, Riverside Technology, inc., Fort Collins, Colorado; Ray Bennett, CRDSS Project Manager, State of Colorado, Denver Colorado; Larry Brazil, President, Riverside Technology, inc., Fort Collins, Colorado

Abstract: The Colorado River Decision Support System (CRDSS) is a database and modeling system used by the State of Colorado to help water managers make informed decisions about Colorado water resources. Implementing the system has improved both the State's understanding of the data and its ability to analyze "what if" questions that are critical to water resources management in Colorado. The data-centered system allows different modeling and analysis tools to share the same data. This paper focuses on the implementation of the water resources planning component of the CRDSS.

INTRODUCTION

The CRDSS consists of databases and models that provide improved data and decision-making capability for the Colorado River and its tributaries within Colorado. It is being developed by the Colorado Water Conservation Board (CWCB) and the Division of Water Resources (DWR), under the overall guidance of the Department of Natural Resources. Initiated in 1993, the project is in the fifth and final year of development. The CRDSS Project Management Team consists of a contract project manager and senior staff of the CWCB and DWR. A Technical Advisory Committee of major Colorado River water users is helping guide the project. A consulting team headed by Riverside Technology, inc. (RTi) of Fort Collins was selected in January, 1994 to design and develop the CRDSS.

CRDSS was developed to allow Colorado to enter a new era of water management that emphasizes cooperation among state agencies, water providers, and water users. The CRDSS is a data-centered system that contains historic tabular data such as streamflow, climate and diversions; spatial data such as topography, hydrography, and irrigated acreage; and administrative data such as water rights and water management policies. Data are keyed to locations in the river basin using a geographic information system (GIS). This computer-based system allows decision makers to access water resource data, simulate potential decision and policies, and examine the consequences with regard to interstate compact policy, water resource planning, and water right administration.

This paper discusses one element of CRDSS: implementing a water resource planning (WRP) model using a data-centered approach. An extremely large scale application, CRDSS required the consistent development of five separate WRP model applications (White, Yampa, Colorado, Gunnison, and San Juan river basins) that, if desired, can be combined into one application that encompasses the entire western slope of the State of Colorado.

A DATA-CENTERED APPROACH

The CRDSS is a multi-year project requiring that various database and modeling components be developed and implemented over time. This required that the database design be scaleable and flexible enough to allow growth and enhancement. A model-generic approach was chosen, in which a core set of data are stored in a central database and are used by one or more applications. In this data-centered approach, the database becomes the repository for key data and consequently helps to maintain quality and consistency. **Figure 1** illustrates the CRDSS data-centered approach where various tools share common data.

In order to implement a data-centered system, there must be enough infrastructure in place to support and allow effective use of the system. The CRDSS database contains all of the key water resources data needed for planning and administrative purposes for the State of Colorado and allows for "one stop shopping" for Colorado water data users. Utilities have been written to format data files for models and provide effective data displays to users. Much of the data is available to Internet users via the CRDSS home page (see references). Utilities are available that allow users to quickly access and format data for use in other applications.

It is important to note that the implementation of a data-centered approach in the CRDSS has not precluded the use of modular tools. The WRP model and other tools can run stand-alone and are not tied directly to the database. This

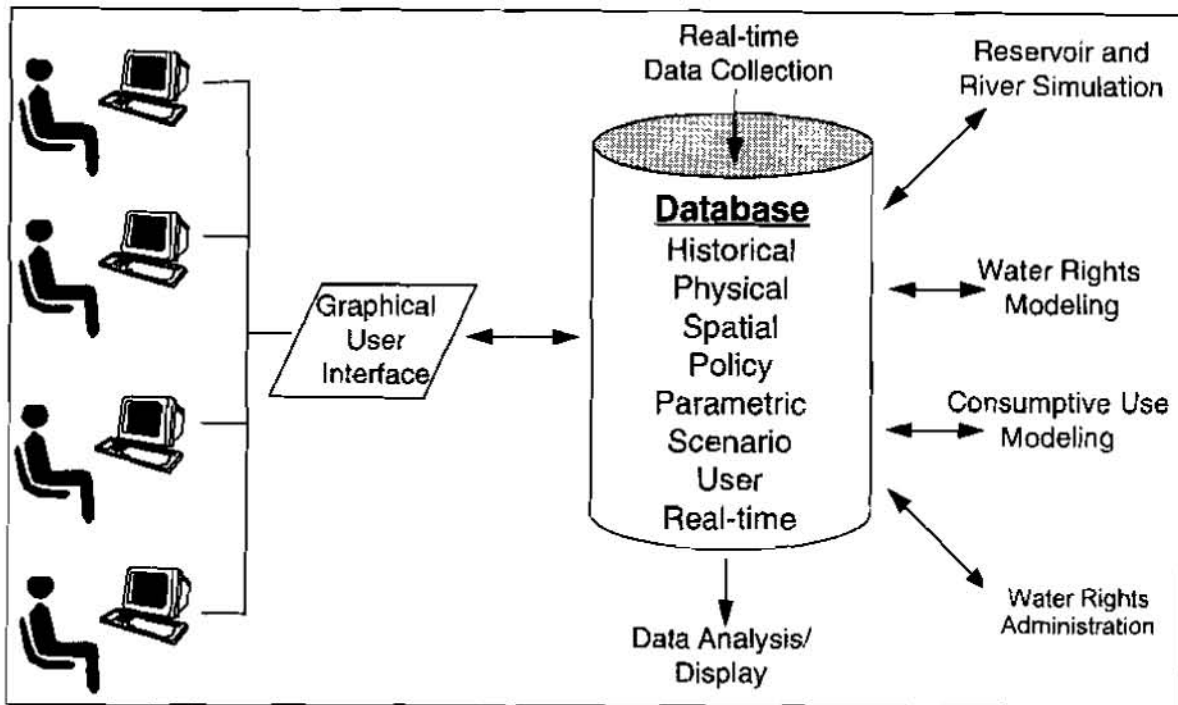


Figure 1. CRDSS Data-centered Approach

allows for distributed modeling efforts within the user community. In order to promote data sharing, standard data formats for time series and other data have been adopted. The data-centered approach, as adopted for the CRDSS, allows users to access data from a central location but perform analyses using accepted tools in a desktop environment. As a policy, model output is not currently stored in the database but is kept in the standard model output formats. This simplifies model use and database design and decreases the overall size of the database. Exchange of data between models occurs using standard data formats and file translation utilities, where necessary.

The main CRDSS database uses INFORMIX® on a server machine. Microsoft Access® versions of the database are being developed to further allow distribution and use of CRDSS data and tools for the PC environment. In this configuration, it is understood that the central database is the official repository of data for CRDSS that may only be changed by a database administrator.

Data Quality Issues: Despite the fact that State of Colorado staff had been maintaining a database of water rights and diversion data for many years, the CRDSS team quickly identified quality issues when data were loaded into the database and used for modeling. The new CRDSS database uses INFORMIX (which implements constraints and range checks), whereas the old database used a series of discrete files that often contained redundant data. The CRDSS team identified data coding problems such as miscoded structure types (a reservoir being called a diversion), use of the letter "O" instead of the number "0", and reservoir levels recorded as "full" or "half-full" instead of as a numeric value. Using a non-relational database resulted in a wide variety of data coding problems such as assigning the same structure different names ("XYZ DITCH" and "DITCH XYZ") and using different water coloring schemes (water coloring refers to the practice of identifying the different sources [river, storage, etc.] and uses [irrigation, power] of water). The CRDSS team detected some errors while populating the database, but often problems were detected only when the data was used for modeling. For example, if structure types were miscoded, then a request for all diversions might actually return a reservoir or instream flow. Some important (if simple) lessons were learned:

1. Ensure data quality, to the extent possible. For the State of Colorado, this meant using modern database tools to increase the scrutiny of data, as well as improving procedures to allow timely data corrections.

2. Enforce consistency and simplicity in data recording, to the extent possible. In a data-centered system, all data users and recorders should use standard practices so common tools can be used to share and use data, thus increasing efficiency.
3. Allow modeling tools to override official data, as needed. Because the modeling tools were meant to be generic, they could not effectively trap all data problems and implement fixes without becoming complicated and difficult to maintain. Therefore, utilities were implemented to allow the users to reset database values to correct problems. This overriding feature allows the State of Colorado to correct data problems in due time and lets modelers selectively edit data so that modeling can continue.
4. Understand the limitations of third-party data. The CRDSS database stores streamflow records from the U.S. Geological Survey (USGS), climate data from the National Oceanic and Atmospheric Administration (NOAA), and snow data from the Soil Conservation Service (SCS). In some cases, the CRDSS team found blatant errors in this data (for example, negative solar radiation, presumably from a badly calibrated gage). Rather than try to correct the data and compromise the tractability of the data, users of the system need to use good engineering judgment, as with any other engineering project.
5. Make the data available to as many people as possible. A common practice among the consulting community is to use USGS or other data and, if a problem is found (e.g., a water balance does not compute), make reasonable assumptions and continue with an analysis. There is seldom either time or budget to notify the data suppliers. However, for data that is controlled within the realm of the CRDSS (State of Colorado data), users (especially State of Colorado staff) who do find problems have a more direct channel of communication to allow data corrections. Additionally, CRDSS tools make it easier to detect data inconsistencies so that they can be corrected.

In summary, data quality problems were identified during both the database population and modeling activities. The quality problems have been prioritized, and the State of Colorado has invested resources to correct them. Techniques were developed to allow the modeling to proceed while data problems were corrected in a prioritized manner.

WATER RESOURCE PLANNING MODEL

The WRP model selected for use in CRDSS is called StateMod. This tool is a monthly water allocation and accounting model that had been developed for a series of projects by the State beginning in 1986. It is capable of making comparative analyses for the assessment of various historic and future water management policies in a river basin using the Prior Appropriation Doctrine (first in time, first in right). StateMod's operation is governed by hydrology, water rights, and operating rules. It recognizes four types of water rights: direct flow, instream flow, reservoir storage and operational. The direct flow, instream flow, and reservoir storage rights are self-explanatory. The operational rights are used to control complex, multi-structure activities associated with reservoir releases, exchanges, and carrier ditch systems. Key features of the model required to simulate the diverse operating conditions encountered on the western slope of Colorado include the following:

- Simulates tributaries and main stem river systems through the use of a tree-structured network
- Simulates direct flow, instream flow, storage and operation rights under the Prior Appropriation Doctrine as a function of water availability, priority, decreed amount, demand, structure capacity, and location
- Allows reservoirs to be operated with multiple accounts serving multiple users
- Allows instream flows to be operated as a point or river reach
- Simulates a wide variety of operating agreements and exchanges between several users or structures

- For a given structure, simulates one or more water rights, with one or more return flow patterns returning to one or more stream nodes
- Uses an efficient direct solution algorithm that recognizes the impact of a diversion's return flows during the current time step without having to iterate
- Estimates base or natural streamflows from gaged or estimated streamflow, diversion, and reservoir data

Baseflow Data: The generation of base or natural stream flows for a WRP application is necessary in order to analyze a "what if" scenario which includes a water right, structure, or operating strategy that might change in the future. Baseflow is a generic term defined herein to describe gaged stream flows that have been adjusted to remove a portion (0 to 100 percent) of human impact. If a user decides to remove all human activities (100 percent), then the baseflows generated are commonly called natural streamflow. If a user decides to remove only a portion of human impact, then the remaining impacts are "left in the gage."

Baseflows were created efficiently and consistently within CRDSS using the Baseflow module of StateMod. This module uses historic streamflow, diversion, and reservoir storage data to remove human impact for any number of structures that might be important for future development. Along with this historic data, the baseflow module uses the same water use parameters (efficiency, return flow timing, and return flow locations) that are used in the historic simulation. The key benefits resulting from the standard approach used to estimate baseflows within CRDSS include:

1. Parameter consistency: The same parameters used to estimate baseflows are used during the calibration to historic data.
2. Efficient baseflow generation: Baseflows can be quickly revised in response to calibration results or model refinements (e.g. include more historic structures).
3. Efficient calibration: Knowledge of historic data stored within the memory of the program provides an efficient mechanism to compare simulated to gaged stream flows, diversions and reservoir levels.

The Model Network: The model network describes the physical connectivity of the structures and gages being modeled. StateMod uses a network file that describes model nodes in an upstream to downstream fashion. **Figure 2** illustrates part of the network for the White River basin. This schematic representation of the network is useful for modeling and can be aligned to closely match the true orientation of the basin. Nodes are labeled with structure identifiers (State of Colorado identifiers or USGS stream gages). The figure illustrates the use of stream flow gages (e.g., 0903000), minimum streamflow reaches (e.g., upper terminus 432339 and lower terminus 432339_Dwn at top of figure), aggregate demands (e.g., node ADW_001 above the 09303000 gage), and the use of baseflow nodes, as discussed in the previous section.

The data used to plot the model network diagram shown in **Figure 2** is also used by utility programs to build most of the data files required by StateMod by querying the CRDSS database. The process begins with a single network file that describes the reaches and nodes in the model network. This file is processed to produce the network diagram, the StateMod-format network file, and several other files that contain structure and station information. These files are then processed by utility programs to create StateMod files containing data such as streamflow, diversion, demand, and water rights. During processing, command files can be used to override the database values, allowing the modeler to make adjustments for inaccurate or inappropriate data. The data flow sequence used to develop a StateMod network and supporting files has been fine-tuned to allow efficient modification and generation of data sets. Key benefits of this approach are the following:

1. Reproducibility: Model data sets can be reproduced quickly and accurately to react to new data, etc.
2. Documentation: Modeling assumptions are documented within the command files used to access the database.
3. Extensibility: Structures can be deleted or added and new data files build quickly and accurately.

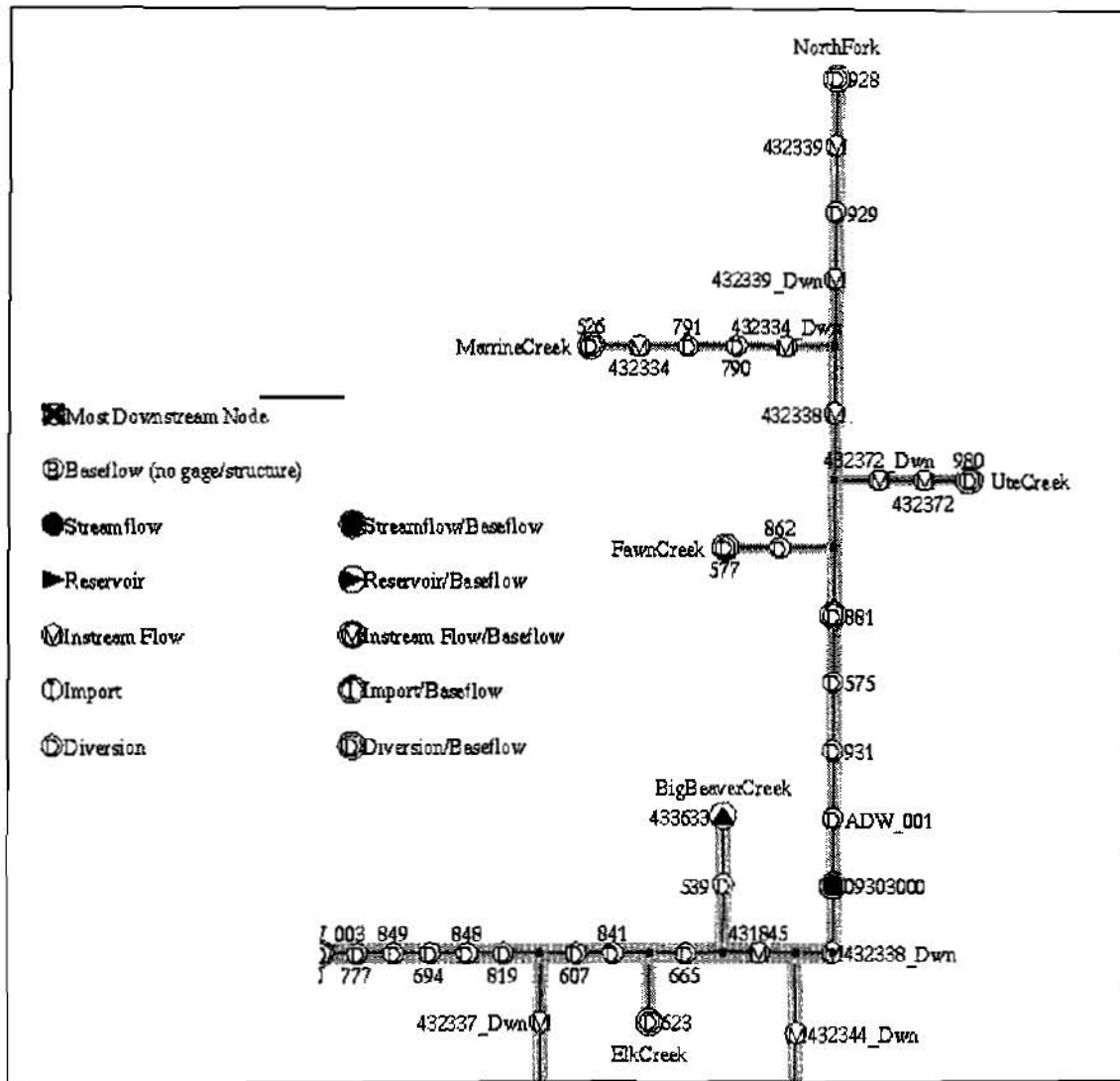


Figure 2. Example of Part of a StateMod Network Diagram - the North Fork of the White River

Model Size: To be cost-effective, meet deadlines, prove functionality, and meet the immediate needs of the State, the first phase of WRP development included only key structures. Key irrigation and municipal and industrial structures were selected for each river basin as follows:

1. A list of absolute decreed water rights for each structure was compiled and ranked.
2. The cumulative absolute decreed amount and percent of the basin total were determined.
3. Preliminary key structures were selected to represent 75 percent of the basin's cumulative absolute decreed amount.
4. Final key structures were determined after meeting with each basin's division and district engineers. These meetings resulted in the addition of new structures that were below the cut off but were considered important for administration. These meetings also resulted in the deletion of some structures that met the cutoff but which historically diverted significantly less than their decreed amount or they had been abandoned.

A similar approach was applied to reservoirs, instream flows, and stock ponds. The decision to explicitly model only key structures reduced the number of nodes included in each model from 80 to 90 percent, while simulating over 75

percent of each basin's water use. This version of modeling data used base flows that had been naturalized to 75 percent.

A second phase of WRP development, which is currently under development, is modeling the remaining water use in each basin by defining a number of spatially-located aggregated irrigation structures, reservoirs, stock ponds and municipal and industrial nodes. This version includes all instream flows that exist on the rivers and streams modeled. It includes aggregated irrigation structures, reservoirs, and stock ponds that were determined using GIS, based on their location relative to key streamflow gaging stations. It also includes aggregated municipal and industrial use that was determined to equal the difference between per capita water use estimates and explicitly modeled municipal and industrial structures. The enhancement from approximately 75 percent water use to 100 percent water use increased the number of modeled nodes by approximately 10 percent, still significantly less than explicitly modeling every structure. It was relatively easy to implement because of the data-centered approach discussed previously. Because this version of modeling data includes 100 percent of the basin water use, the base flows developed were natural flows.

Streamflow Data: Streamflow data is a key component to any WRP application. Unfortunately, it is typically available at a limited number of locations with a limited period of record. Therefore a mechanism is required to fill data gaps at gaged locations and distribute gaged data to ungaged portions of a watershed. To provide consistency and flexibility the following approach was used to develop streamflow data for the WRP within CRDSS:

1. Data filling parameters were developed. A control file containing data filling parameters was developed that allowed missing data at gaged locations to be filled on the fly when retrieving streamflow data from the centralized database. Key data filling parameters included the independent and dependent variables, regression type (linear or non-linear), and number of equations (annual - 1 equation versus monthly - 12 equations).
2. Proration factors were developed. For each gaged and ungaged location requiring streamflow data, the drainage area and average annual precipitation were developed using GIS. These proration factors thus provided a consistent, map-based approach to distribute gaged streamflow data to ungaged locations.

Diversion Data: Historic diversion data are used within the WRP model to estimate baseflows and to calibrate the model to historic observations. As discussed previously, one challenge was to develop a number of basin models in a cost-effective manner using data of varying quality. The diversion records available to CRDSS are of relatively high quality for large, key structures; small, less important structures typically have less frequent recordings. Similar to streamflow record filling, diversion records queried from the CRDSS database were filled on the fly using a control file provided by the user. Typical data filling approaches included the following:

1. If diversion records for a structure are not available at the beginning or end of the simulation period, fill with zeros.
2. If diversion records are unavailable during the study period, fill using the long-term historic average.
3. If neither of the simple data filling approaches just described are adequate, allow the user to provide a time series that overrides the information available in the database.

The last approach was used when the simpler data filling techniques were inadequate and when official database records were determined to be non-representative of current conditions. For example, the database records may indicate that a diversion was in place for 20 years with 3 years of missing record. Under the simple data filling approach, the missing years would be filled with the long-term average. However, if it is known that the diversion headgate was washed out during that period, a replacement time series having zeros during the 3 years could be specified.

Demand Data: Agricultural, municipal, and industrial demands are input to the StateMod model in order to divert and use water according to Prior Appropriation Doctrine. Demands are associated with diversions that are included in the network and may consist of explicitly modeled or aggregated structures. Municipal and industrial demands were estimated based on historic use. Irrigation demands were estimated from acreage, crop, and climate data.

Acreage data was developed in cooperation with the U.S. Bureau of Reclamation (USBR) by using aerial photography to construct GIS coverages of acreage for the entire western slope of Colorado for 1993. The State of Colorado then performed field surveys to verify the irrigated parcels, identify the crop grown, and tie each parcel of land to one or more headgates serving the land. The CRDSS team then assigned climate stations and weights to allow farm crop requirements to be estimated using the Blaney-Criddle approach. When combined with irrigation system efficiency estimates, river headgate demands were generated for each irrigation structure modeled.

System Efficiencies: One of the key pieces of data required by a WRP that is not generally gaged is the irrigation system efficiency (the ratio of water used to water diverted). For most WRP applications, irrigation system efficiencies are estimated based on agricultural practices, canal length, soil type, etc., but this approach requires significant knowledge of every diversion and can become highly subjective during the calibration process. As an alternative, the CRDSS team used consumptive use estimates in conjunction with historic diversion records to develop an average monthly efficiency for every irrigation structure modeled. For example, if a structure diverted 100 acre-feet of water in May, 1980, while the estimated demand is 30 acre-feet, then the system efficiency for that month is 30 percent (30/100). During a year, the annual efficiency might average 20 percent while monthly efficiencies might range from 10 to 40 percent. A similar range can be observed for one month from one year to the next. Therefore, these estimates could not be used without review because of data issues, irrigation practice variations, etc. However, once the data problems were resolved, the computed efficiencies seldom required adjustment during calibration.

One limitation of StateMod is that monthly efficiencies cannot currently be varied from one year to the next. Consequently, changing irrigation practices to reflect structural improvements or water management practices during water-short conditions cannot be fully reflected. A potential enhancement to StateMod might be to read in irrigation crop requirements and dynamically calculate monthly irrigation efficiencies.

SUMMARY

Previous sections illustrated some of the technical challenges that were addressed in implementing a WRP model into the CRDSS. Development efforts spent on constructing the centralized database and developing utility tools to access that data were only fully realized after applications to scenarios were implemented. For example, scenario data sets needed to be constructed to study different issues such as making a conditional water right absolute or inserting a new instream flow, diversion, or reservoir.

Figure 3 illustrates the Big Picture Plot feature of the StateMod graphical user interface (GUI). This graphic shows the difference in diversions between two scenarios, with upward bars indicating that the diversion received more water under the second scenario, and downward bars indicating a decrease. The size of the bar indicates the magnitude of the change. Consequently, WRP model users are able to see a basin's response to an input change. This type of display illustrates the power of the CRDSS and its potential for helping make decisions at different levels. The Big Picture Plot can be used by managers studying long-term average impacts, whereas hydrograph plots at a gage might be more useful to someone studying the time varying impact at a location on the river (such as an instream flow study). CRDSS offers display tools for various output levels to satisfy the needs of water managers.

REFERENCES

The CRDSS home page, <http://crdss.state.co.us>

Blaney(1952), Blaney, H.F., Rich, L. R., Criddle, W.D., et. al. (1952), "Consumptive use of water", Trans. ASCE, 117:948-967,

StateMod Users' Manual, on-line at <http://crdss.state.co.us/manuals/statemod/statemod.html>

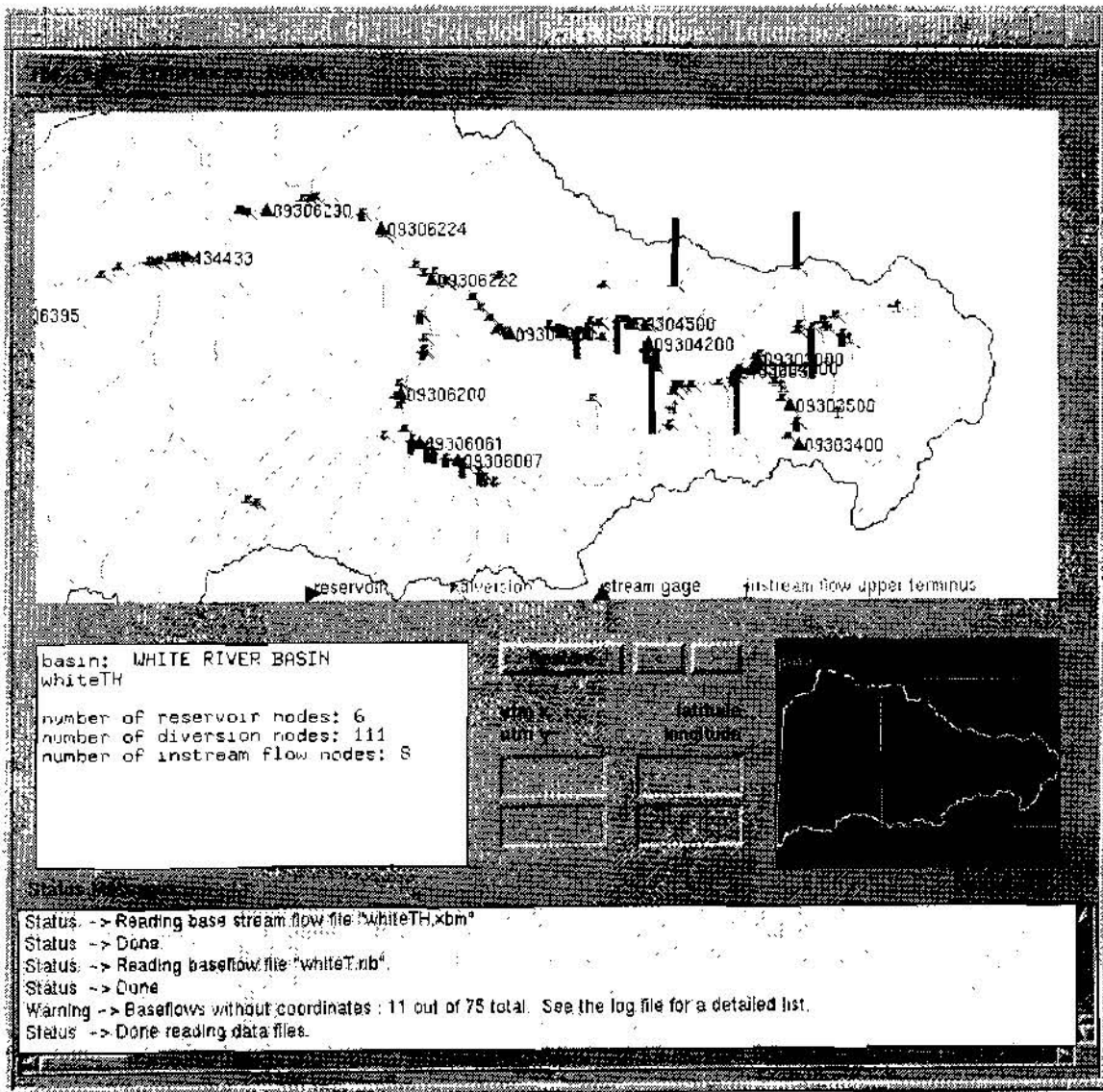


Figure 3. StateMod GUI Big Picture Plot

DYNAMIC MODELING OF WATER-SUPPLY RESERVOIR PHYSICAL AND CHEMICAL PROCESSES

Jerad D. Bales and Mary J. Giorgino, Hydrologists, U.S. Geological Survey,
Raleigh, North Carolina

Abstract: A spatially detailed hydrodynamic and chemical transport model was applied to Rhodhiss Lake, North Carolina. Rhodhiss Lake is about 22 kilometers long, has a maximum depth of 16 meters, is generally less than 700 meters wide, and has a theoretical mean retention time of 21 days. Monitoring data indicate that the reservoir is eutrophic. Data collected during a 15-month period in 1993-94 were used to calibrate and apply the model. The root mean square difference between measured and simulated water levels was 0.085 meter, and the mean difference between measured and simulated water temperatures was -0.24 degree Celsius. There was essentially no difference between the frequency of occurrence of measured and simulated dissolved-oxygen concentrations less than 5 milligrams per liter. The model was applied to demonstrate the transport of a neutrally buoyant, conservative tracer released into the headwaters of the reservoir during both stratified and unstratified conditions. During stratified conditions, about 40 days were required for the maximum concentration of the tracer at the dam to become less than one percent of the initial maximum concentration, whereas only 17 days were needed to reach the same condition during unstratified conditions.

INTRODUCTION

Rhodhiss Lake is an impoundment of the Catawba River in North Carolina (fig. 1) constructed in 1925. Information on hydraulic circulation and constituent transport in the reservoir is needed to more effectively manage the reservoir and its watershed, and to predict water-quality responses to changes in constituent loadings or hydrologic regime. Such changes could result from recently adopted State water-supply watershed regulations, proposed wastewater-treatment plant expansions in the watershed, and a new basinwide approach used by State regulators to permit point-source discharges.

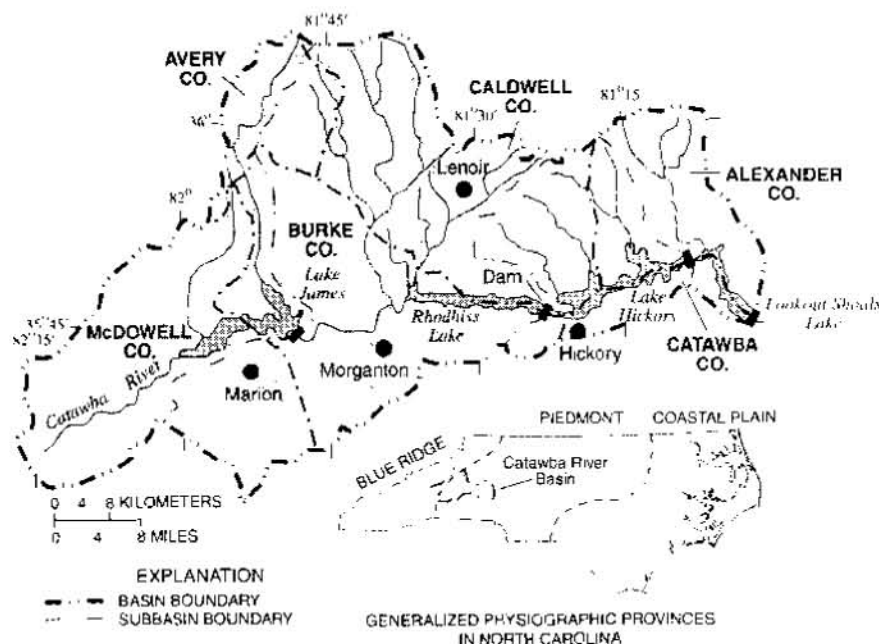


Figure 1. Location of Rhodhiss lake in the upper Catawba River Basin of North Carolina.

The U.S. Geological Survey (USGS), in cooperation with the Western Piedmont Council of Governments, conducted a 2-year investigation of water-quality conditions in Rhodhiss Lake. The investigation included intensive data collection during 15 months in 1993-94 to (1) quantify existing water-quality conditions and (2) provide data required for calibration and application of a dynamic water-quality model of the reservoir. The purpose of this paper is to describe the development and application of the dynamic water-quality model used to simulate physical and chemical processes in Rhodhiss Lake.

Physical and Chemical Characteristics: Rhodhiss Lake is about 22 km (kilometers) long and is less than about 700 m (meters) wide throughout the length of the reservoir. The surface area of the reservoir is 10.4 km² (square kilometers); the mean depth is 8.0 m; and the maximum depth is 16 m. The major inflow to the reservoir is the Catawba River, which has a drainage area of 2,650 km² at the reservoir headwaters. The drainage area of the reservoir increases only slightly to 2,830 km² at Rhodhiss Dam. Lake James, a mainstem reservoir on the Catawba River having a drainage area of 984 km², is located about 20 km upstream from Rhodhiss Lake. Streamflow into Rhodhiss Lake is somewhat regulated by releases from Lake James and typically varies between about 10 and 1,000 m³/s (cubic meters per second). The theoretical mean retention time of the reservoir is 21 days.

Three water-supply withdrawals are located in the reservoir. The total average withdrawal rate for 1993 was 0.67 m³/s. One permitted wastewater-treatment facility discharged an average of 0.21 m³/s directly to the reservoir in 1993.

During the data-collection period, median total phosphorus concentrations in the reservoir decreased from 0.053 mg/L (milligrams per liter) in the headwaters, to 0.044 mg/L at mid-reservoir and 0.034 mg/L in the forebay. Inorganic nutrients—nitrate, ammonia, and orthophosphate—were generally depleted from the epilimnion during the summer, probably by algal uptake. Concentrations of ammonia, and to a lesser extent total phosphorus, increased in the hypolimnion during summer anoxic conditions. However, nuisance levels of phytoplankton were rarely observed in the reservoir during the data-collection period, possibly because short residence time and mixing patterns suppressed algal growth. Mean chlorophyll a concentration at the mid-reservoir site during May-September 1993 was 10 µg/L (micrograms per liter), and the maximum concentration of 52 µg/L occurred during a late fall bloom.

RHODHISS LAKE MODEL DESCRIPTION

Study Objectives: Objectives of the reservoir modeling were to develop the capability to simulate (1) movement and mixing of spills or releases in the reservoir and (2) reservoir nutrient, algal, and DO (dissolved-oxygen) concentrations in response to possible changes in external loadings and flows. Because reservoir water-quality degradation often is first evident in coves, the capability for simulation of hydrodynamics and water-quality processes in coves and embayments, including exchange with the mainstem was needed. Rhodhiss Lake is relatively narrow, and temperature and DO data indicated that a laterally averaged formulation is appropriate for the reservoir. These functional requirements were considered when selecting the model CE-QUAL-W2 for application to Rhodhiss Lake.

Model Description: The model CE-QUAL-W2 has been under continuous development since at least 1975 (Edinger and Buchak, 1975). Complete details on model theory and structure, and an extensive bibliography for theoretical development and application are given in Cole and Buchak (1995).

Finite-difference forms of the complete laterally averaged equations of conservation of mass, conservation of momentum, and transport (one equation for each constituent) are solved using an efficient and accurate numerical scheme. The computational time step is variable throughout the simulation to ensure numerical stability, but typically is about 5 minutes for the Rhodhiss application. The modeled system is divided into a series of longitudinal segments, each of which may have a unique

length. Each segment is further subdivided into layers. All layers within a segment must have the same length, but each layer can have a unique width and thickness.

The Rhodhiss Lake model extends along the mainstem of the reservoir for a distance of 18.5 km. There are 37 computational segments along the mainstem. The model domain encompasses five embayments, and each embayment is represented by three segments. All segments are 500 m long. Each layer is 1 m thick. Distances from the spillway crest to the bottom of the channel ranged from 3 to 16 m.

Boundary Conditions: Upstream boundary conditions included estimated hourly streamflow, measured hourly water temperature, and estimated daily nutrient concentrations. Streamflow was measured from 70 percent of the basin upstream from Rhodhiss Lake, and inflows to the reservoir were estimated from these data. Monthly to semi-monthly measurements of nutrient concentrations were used with streamflow data to determine a relation between streamflow and nutrient levels. Daily streamflow was then used to estimate daily nutrient concentrations at the headwaters of the reservoir.

Local inflows from the 180 km² draining directly to the reservoir were estimated using measured streamflow data from a nearby gage. Recorded hourly releases from Rhodhiss Dam were used as the downstream boundary condition. No downstream thermal or chemical boundary conditions were required. Other boundary data included measured hourly meteorological conditions (wind speed and direction, air temperature, dewpoint temperature, and cloud cover), discharge to the reservoir (including temperature and nutrient concentrations), and withdrawals from the reservoir.

Model Parameters: Parameters are used to describe physical and chemical processes that are not explicitly modeled and to provide chemical kinetic rate information. Many parameters cannot be measured directly and are often adjusted during the model calibration process until simulated results agree with observations.

Most of the key hydrodynamic and thermal processes are modeled in CE-QUAL-W2, so there are relatively few adjustable hydraulic and thermal model parameters. Simulation results were generally insensitive to changes in the hydraulic and thermal model parameters, with the exception of the wind-sheltering coefficient, primarily because the detailed computational grid resolves small-scale physical processes. The dimensionless wind-sheltering coefficient, which is temporally variable, reduces the effects of wind on the reservoir because of topographic or vegetation sheltering of the water surface.

There are 57 chemical kinetic rate coefficients required for the Rhodhiss Lake application of CE-QUAL-W2 (Giorgino and Bales, 1997). Selection of most of the parameters was based on published information. All of the kinetic coefficients are temporally and spatially invariant.

DYNAMIC MODELING OF PHYSICAL AND CHEMICAL PROCESSES

Model calibration was achieved through adjustment of model parameters and estimated input data for the period April 1, 1993, through March 30, 1994. The model also was applied using boundary data from this period.

Hydrodynamics and Heat Transport: Simulated water levels were quite sensitive to inflow rates, so only relatively small adjustments were required in the original estimates of streamflow to achieve a good calibration. The root mean square difference between measured and simulated water levels for the 12-month calibration period was 0.085 m. Eighty percent of the differences between measured and simulated water levels were between 0.02 and 0.12 m. The total range in measured water level during the period was 1.32 m.

Simulated near-surface water-temperatures were generally within 1 °C (degrees Celsius) of measured values (fig. 2). Near-bottom water temperatures were underpredicted from mid-May through August, and larger differences between measured and simulated values occurred in the deeper waters. All of the water temperature data (177 observations) from the mid-reservoir site during the calibration period were compared with corresponding simulated values. The mean difference between the simulated and measured values was -0.24 °C, and 80 percent of the differences were between 1.26 and -1.80 °C. Simulated water temperatures were generally high relative to measured values when measured water temperature exceeded 20 °C. Most of the simulated temperatures underpredicted measured values when the measured water temperatures were less than 8 °C. Simulated water temperatures were equally overpredicted as underpredicted at a particular measurement depth, although simulation errors were smallest near the water surface, and greatest at about 3 m above the reservoir bottom.

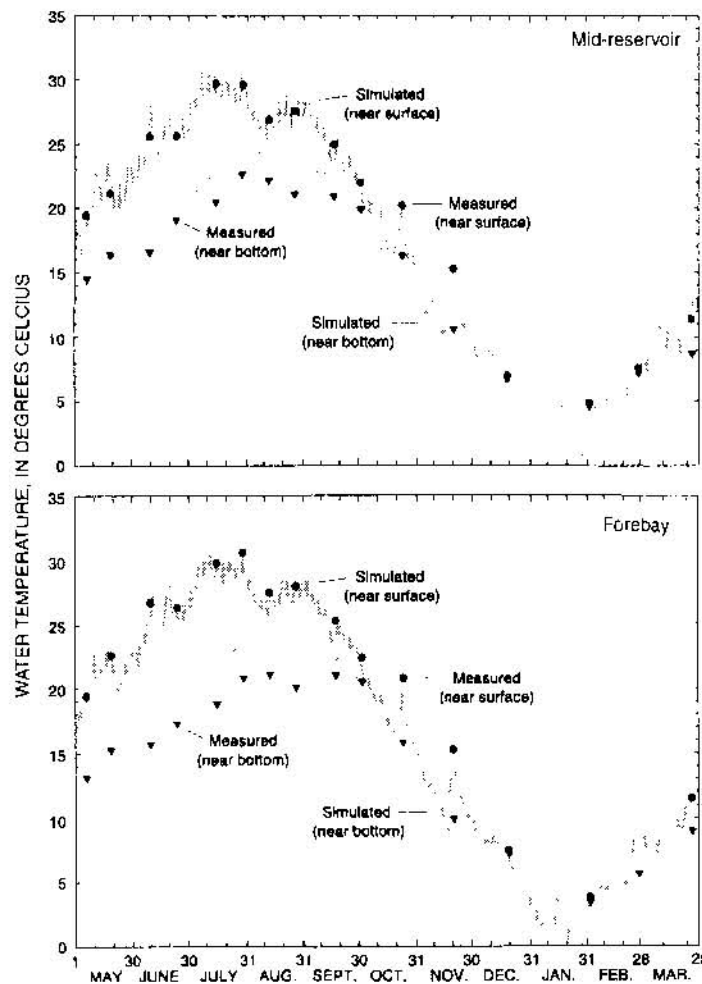


Figure 2. Measured and simulated water temperatures, May 1, 1993, through March 25, 1994, at mid-reservoir and forebay locations.

Results from the water temperature simulations provide information on physical characteristics and processes in the reservoir information that might not be obtained from periodic measurements. For example, water temperature data from September to November suggest that the reservoir was thermally stratified during the period (fig. 2). The simulations, however, indicate that the reservoir was continually mixing and stratifying during the period, probably as a result of changes in inflow conditions. Simulation results suggest that near-bottom water temperatures in the deeper part of the reservoir vary more

gradually than those in the shallower regions. Finally, the reservoir appears to thermally stratify and destratify rather quickly and often in the upstream reaches of the reservoir. Likewise, stratification and destratification appear to occur fairly often in the downstream reaches of the reservoir, in the fall and late winter.

Conservative Material Transport: The calibrated Rhodhiss Lake model was used to simulate the movement of a neutrally buoyant nonreactive material (or tracer) through the reservoir. Transport of material released from the upstream end of the reservoir at two different times (summer and winter) was simulated. The temporal distribution of the release was triangular in shape, with a time base of 2 days, and a maximum concentration of 1,000 ppt (parts per thousand). The inflow rate of the tracer was equal to the inflow rate of the water, which was between 16 and 27 m³/s during the winter period and between 12 and 40 m³/s during the summer period, resulting in a slightly greater mass of tracer released in the summer.

During the summer release, the influent Catawba River water temperature was colder than the near-surface water in the reservoir. Consequently, the tracer sank fairly rapidly as the material moved into the reservoir. The concentration of the tracer near the water surface 5 km downstream from the release was less than 5 percent of the initial peak concentration. Most of the sinking occurred between 2 and 5 km downstream from the release (fig. 3). The highest concentration at the dam was about 14 percent of the initial maximum concentration, occurred near mid-depth, and arrived at the dam 13 days after the release. The mid-depth peak likely reflects both an interflow phenomenon and, to a lesser degree, the effects of the mid-depth reservoir withdrawal on flow patterns. The effects of the interflow phenomenon are evident in the distribution of measured temperature and, to a lesser extent, DO data during selected periods in the summer of 1993 (Giorgino and Bales, 1997). The mid-depth tracer concentration at the dam remained greater than 1 percent of the initial concentration for about 40 days.

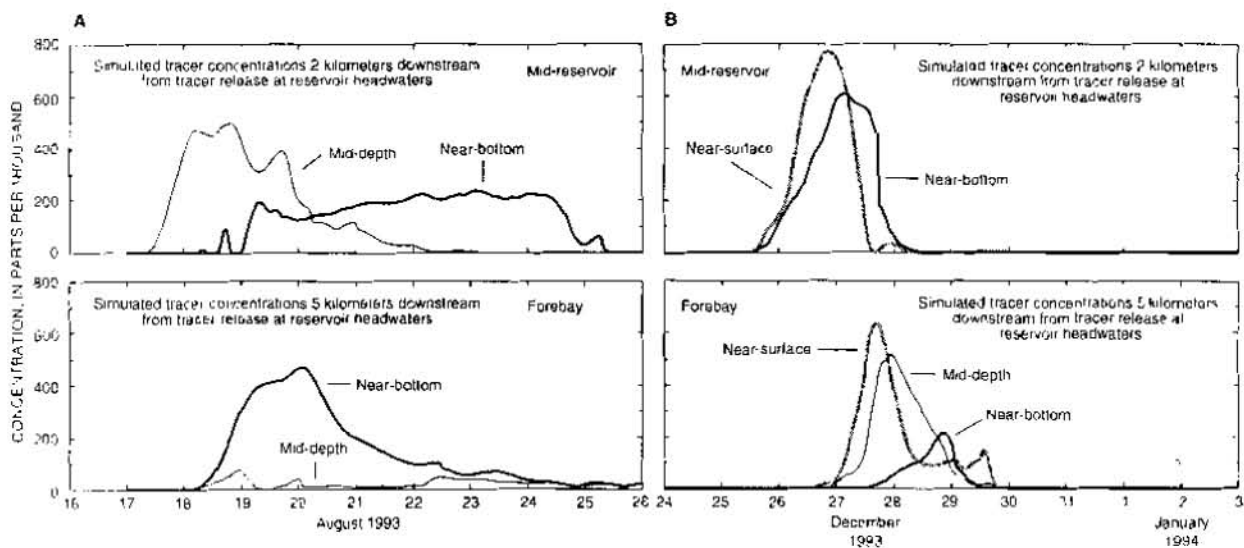


Figure 3. Simulated tracer concentrations at Rhodhiss Lake mid-reservoir and forebay locations for summer and winter.

Between 0 and 5 km downstream from the release, there was less attenuation of the peak concentration following the winter release than following the summer release (fig. 3). However, at Rhodhiss Dam, the peak concentration following the winter release was about half of the highest concentration after the summer release. The difference is the result of greater vertical mixing during the winter and, hence, greater dilution in the winter when the reservoir was less thermally stratified. Only about 17 days were required in the winter for the concentration at the dam to fall below 1 percent of the initial concentration.

These examples of simulation of the transport of a conservative material demonstrate (1) the use of the Rhodhiss Lake model in evaluating the movement of a brief or extended release of material into the reservoir; (2) the manner in which nonconservative materials move through the reservoir, without the confounding effects of chemical transformations, regeneration, and settling; (3) the difficulty in identifying a single residence time for the reservoir—residence times vary seasonally, as well as with depth; and (4) the effects of density stratification and vertical mixing on transport processes.

Chemical Transport: Eleven water-chemistry constituents were simulated in the Rhodhiss Lake model. These constituents included labile and refractory dissolved organic matter, volatile solids, organic bottom sediments, carbonaceous biological oxygen demand, DO, PO₄ (orthophosphate), ammonium, nitrate, iron, and algae.

The calibrated model provided a reasonable simulation of DO concentrations in Rhodhiss Lake. Near-surface and near-bottom DO appears to be predicted better than DO concentrations at mid-depth, where DO was typically overpredicted. The frequency of occurrence of DO concentrations less than 5 mg/L, the concentrations of most interest to regulators, was almost the same for measured and simulated DO. Simulation of the exact timing of low DO events was within about 5 days of the actual occurrence. Simulation results indicated that near-bottom DO concentrations were less than 4 mg/L only 2 percent of the time during April 1993 through March 1994 at the headwaters of the reservoir, compared to about 40 percent of the time at the forebay. Simulated near-bottom DO was less than 1 mg/L about 6 percent of the time at mid-reservoir, but near-bottom DO concentrations of 1 mg/L or less occurred about 30 percent of the time at the forebay.

Simulated algal concentrations generally agreed with measured values at the mid-reservoir site, with a few exceptions (fig. 4). Algal concentrations were overpredicted on July 14 and September 15, when PO₄ concentrations also were over-predicted. On November 17, 1993, when USGS data indicated a mid-reservoir algal concentration of 3.48 mg/L, data collected by the North Carolina Division of Environmental Management at the same location showed an algal concentration of 0.87 mg/L, which closely agrees with the simulated value. Accurate simulation of algal concentrations is very difficult for several reasons. First, algae are not uniformly distributed in the reservoir but often occur in patches. Consequently, obtaining a representative sample can be difficult, as suggested by the November 17 data. Second, phytoplankton is simulated by the Rhodhiss model as a single assemblage, so distinctions among algal types which bloom under different ambient conditions are not possible. Third, simulated algal concentrations represent the accumulated results of simulated solids concentrations, light penetration, water temperature, nutrient concentrations, and transport. Errors in simulations of each of these parameters are reflected in simulated algal concentrations. Finally, algal concentrations (biomass) are simulated, but chlorophyll *a* is measured as an indicator of biomass. For this application, biomass in milligrams per liter was obtained by multiplying chlorophyll *a* in micrograms per liter by 0.067 (American Public Health Association and others, 1992). This factor may not be appropriate for Rhodhiss Lake under all conditions.

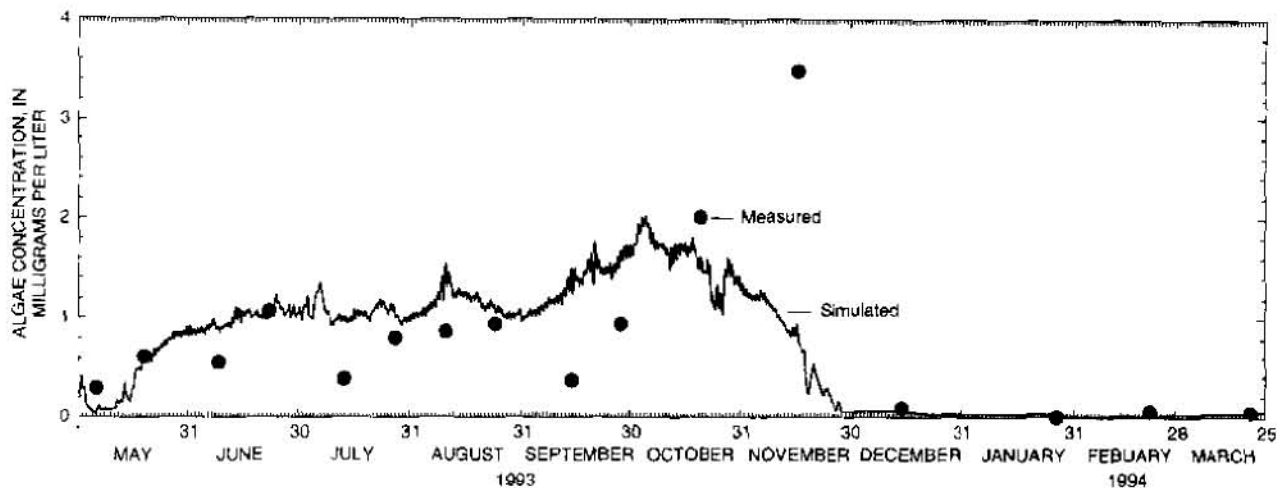


Figure 4. Measured and simulated algal concentrations at mid-reservoir location. May 1, 1993 through March 25, 1994.

SUMMARY

A spatially detailed hydrodynamic and chemical transport model was developed for Rhodhiss Lake, North Carolina. A laterally averaged formulation was used for the model, which consisted of 16 1-meter layers and 37 500-meter segments along the mainstem of the reservoir. The availability of comprehensive data for model calibration and testing was instrumental in obtaining good agreement between measured and simulated physical and chemical conditions. Predictions of physical conditions (water level and temperature) were better than predictions of chemical processes in the reservoir. The root mean square difference between measured and simulated water levels was 0.085 meter, and the mean difference between measured and simulated water temperatures was -0.24 degree Celsius. There was essentially no difference between the frequency of occurrence of measured and simulated DO concentrations less than 5 milligrams per liter. However, simulation of the exact timing of low DO events was only within about 5 days of the actual occurrence of such events. Reasonable simulations of algal concentrations were obtained. However, in general, highly accurate simulations of algae are difficult because of problems associated with obtaining representative samples, the accumulation of errors in the simulation of contributing physical and chemical processes, and simplifications made in the formulation of the algal simulation algorithms.

REFERENCES

- American Public Health Association, American Water Works Association, and Water Environment Federation. 1992. Standard methods for the examination of water and wastewater, 18th ed.: American Public Health Association, 981 p.
- Cole, T.M., and Buchak, E.M., 1995. CE-QUAL-W2: A two-dimensional, laterally averaged, hydrodynamic and water-quality model, version 2.0, user's manual: Vicksburg, Mississippi, Instruction Report EL-95-1, U.S. Army Engineer Waterways Experiment Station, 57 p. + app.
- Edinger, J.E., and Buchak, E.M., 1975. A hydrodynamic, two-dimensional reservoir model—The computational basis: Cincinnati, Ohio, U.S. Army Corps of Engineers, Ohio River Division.
- Giorgino, M.J., and Bales, J.D., 1997. Rhodhiss Lake, North Carolina: Analysis of ambient conditions and simulation of hydrodynamics, constituent transport, and water-quality characteristics: U.S. Geological Survey Water-Resources Investigations Report 97-4131, 62 p.

LARGE-SCALE RESERVOIR SYSTEM MODELING

Richard J. Hayes, P.E., Senior Hydraulic Engineer, and
Vernon R. Bonner, P.E., Chief, Training Division
Hydrologic Engineering Center, US Army Corps of Engineers
609 Second Street, Davis, CA, 95616

INTRODUCTION

In 1990, the US Congress authorized the Corps of Engineers to conduct a comprehensive study to evaluate the reservoir systems within two major river basins in Alabama, Georgia and Florida. The basins are: the Appalachicola-Chattahoochee-Flint (ACF) and the Alabama-Coosa-Tallapoosa (ACT). A schematic of the study region is shown in Figure 1. The development of comprehensive reservoir system models requires the development of two types of model data: the reservoir system model and the flow data to be applied to the system. The ACF/ACT basins are "blessed" with many stream gages, with long records of flow data. For this study, flow-data at more than 50 locations were developed for the period 1939 to 1993. Missing records were "filled in" based on flow correlation with observed data, or by transposing gaged data with drainage area adjustments and routing. Reservoir releases were computed based on ratings for the outlet works and reservoir inflows were computed based on pool levels and reservoir releases. Flow adjustments were made for data errors, initial reservoir filling, net diversions, reservoir evaporation losses and precipitation gains to estimate average daily, unimpaired flow. The flow data was processed using the Hydrologic Engineering Center's Data Storage System package of programs, HEC-DSS (HEC, 1995). The application of HEC-DSS to manage and process the flow data made processing almost 20,000 data values at each location manageable and provided a step-by-step record of the process, using macros with the DSSMATH program. Graphical presentations using HEC-DSPLAY facilitated review of the computed results and resolution of model problems. The flow data processing was a major study effort, which was documented in a separate study report, "Unimpaired Flow," (USACE, 1997).

The second study component is the data model representing the physical system and the operation policy. HEC-5, Simulation of Flood Control and Conservation Systems, (HEC, 1997) was selected at the simulation program for use in this study. The (ACF) and the (ACT) Rivers systems were developed as separate models. Several versions of these systems were developed to model aspects of the existing system with current and future demand scenarios. The two models simulate a total of 25 reservoirs operating primarily for hydropower, water supply, low-flow augmentation and navigation. Model data development was performed by Mobile District staff, in consultation with HEC. HEC staff also made several program modifications to better simulate operations of these complex systems. The general capability of the HEC-5 computer program and its application to the ACF/ACT River systems are described.

HEC-5 COMPUTER PROGRAM

The HEC-5 program is designed to simulate sequential reservoir operation based on specified project demands and constraints. Demands can be minimum channel flows, diversion requirements, and energy requirements. Operational constraints consist primarily of limiting channel capacities for flood control operation. Physical reservoir constraints define the available storage for flood control and conservation purposes, maximum outlet capability and rate-of-change limits to reservoir releases. Demands can be specified at the reservoir and at downstream locations (called Control Points). The simulation is performed with specified flow data in the time interval for simulation. The simulation process determines the reservoir release at each time step and the resulting downstream flows. Detailed output is available to evaluate the reservoir performance and resulting regulated flow.

Any dendritic reservoir system configuration may be used as long as dimension limits are not exceeded for number of reservoirs, control points, diversions, etc. Dimension limits for the PC-DOS version of HEC-5 are shown in Table 1.

Model data are defined starting at the upstream boundaries of the system, and data for each location are entered sequentially downstream. Each branch starts with a reservoir. For a reservoir, the primary physical data are the cumulative storage for each operational zone and the maximum outflow capability, given as a function of storage. Additional reservoir data includes: reservoir areas, elevations, and diversions as a function of reservoir storage. Area data are required to compute reservoir evaporation and elevation data are required for hydropower computations, otherwise, they are

40	Reservoirs
80	Control Points
40	Reservoir levels
60	Reservoir Storage - Outflow values
40	Diversions
35	Power Plants
18	Channel Storage - Outflow values

Table 1. HEC-5 Dimension Limits

informational only.

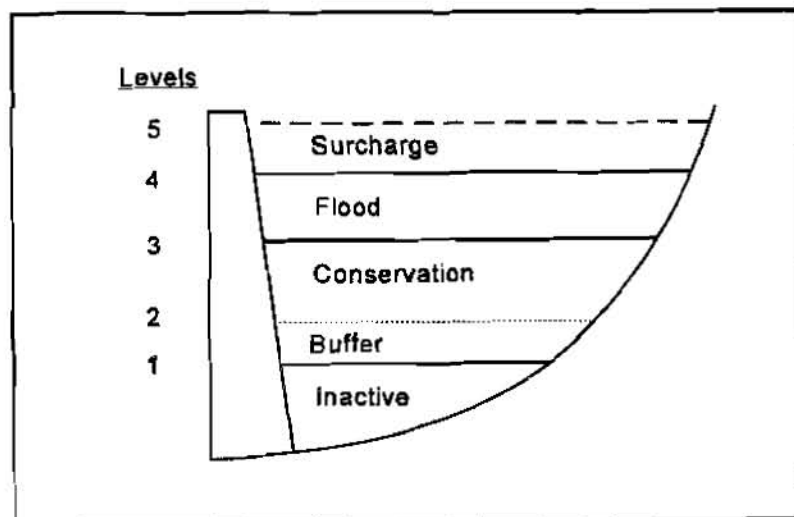


Figure 2. Reservoir Levels

An index level is associated with the primary reservoir storage zones: Inactive, Conservation, and Flood Control, see Figure 1. Up to 40 levels can be used.

The Inactive Pool is Level 1. No reservoir releases are made below this level. The storage at this level may be zero, or some minimum pool.

The Conservation Pool is next above Level 1. Level 2 could be the top of the pool, or the pool can be subdivided into multiple levels. A special subdivision of the Conservation Pool is the Buffer Pool, which could be Level 2. When the pool level drops into a Buffer Zone, a drought condition is indicated and only essential demands will be met (Required Flow). Above the Buffer Level, all conservation demands are met (Desired Flow). Additional levels can be used in the conservation pool to establish priorities among reservoirs in the system.

The Top of Flood Pool is the third operation zone; however it could be any Index Level. Typically, the zone between top of conservation and flood control is the active flood storage zone. Water is stored in this zone when it cannot be safely passed through the downstream channel system. If a reservoir in the system does not have flood control storage, the cumulative storage at the top of flood control would equal the storage at the top of conservation.

Typically, a reservoir has Surcharge Storage to accommodate water above the emergency spillway. In the surcharge zone, the outflow is determined by the spillway capacity; the reservoir no longer makes release decisions. The program can also perform gate regulation simulation to model induced surcharge routing with gated spillways, in accordance with Corps criteria. (USACE, 1987)

Every location in the reservoir system model has control point data. Minimum data requirements include an identifier number, channel capacity, a location name, and the connection to the next downstream location (routing information). Minimum flow requirements and diversion schedules are also defined at control points. The system configuration is defined by the routing reaches connecting a current location to a downstream control point. Hydrologic routing options provided are: Straddle-Stagger, Tatum, Muskingum, Modified Puls, Modified Puls as a function of inflow, Working R&D, SSARR Time-of-storage, and direct input of routing coefficients. The entire reservoir system model (reservoir and control point data) is defined in an ASCII (text) data file. Then, following the model data, the flow data for simulation are provided.

The program uses incremental local flows (flows between adjacent control points) in the system routings. The flow data set must be in the same regular time interval used in the simulation. The time interval can be in minutes, or hours up to one month. Incremental local flows can be computed from observed discharges and reservoir releases, or from natural flows. Flow data can be input as part of the model data, or read from an HEC-DSS file. Using DSS requires identification of the file and the data records to be associated with location flow. The HEC-5 program extracts the flow information from the DSS file and processes it at the start of model execution.

Reservoir routing is performed sequentially, in the order the reservoir data are given. The primary decision variable is the reservoir release for each time interval. The program considers 17 operational goals, demands and constraints in its release decision logic. Once the release is determined, the reservoir end-of-period storage is computed using storage accounting. However, when the proposed release exceeds the outlet capability of the reservoir, surcharge routing is used. When the flood control storage is going to fill to capacity, Emergency Release determination can be invoked.

Reservoir operation simulation primarily depends on the state of the reservoir at each time interval. The general goal is to keep the reservoir at the top of the conservation pool. As the pool level moves into flood control, conservation, and inactive storage zones, the operation goals change. If there is flood control storage and the pool level is in that zone, the reservoir will operate for flood control goals, maintaining the downstream flow within channel capacity to the extent possible. Once water is stored in the flood zone, the program will try to evacuate the excess water as quickly as possible. If the pool level is in the conservation storage zone, the program will only release water when it is necessary to meet specified conservation demands (e.g., minimum flow, diversions, or energy requirements) at the dam and designated downstream locations. If the reservoir is drawn down to the top of the inactive storage, no reservoir releases will be made. Only evaporation draws a reservoir below Level 1.

In addition to making the reservoir release decision for each time interval, the program provides output for a CASE variable to indicate the basis for the reservoir release. In some instances, there may be more than one reason; however, only one value can be shown. The basis for the release determination can be as important information as the actual release and resulting downstream flows.

Program output includes selectable standard tables and user-designed tables. Most of the output is time-series data which can also be written to an HEC-DSS file. The HEC-DSPLAY graphics program can be used to develop graphical and tabular displays of model output written to a DSS file.

ACF BASIN MODEL

The ACF basin model starts with Buford Dam on the Chattahoochee and the gage at Griffin on the Flint, and proceeds down both rivers to the junction near Jim Woodruff Dam, then down the Apalachicola to the gage at Sumatra, Florida. The Federal projects are: Buford, West Point, Walter F. George, and Jim Woodruff. Project operations are primarily for hydropower demands during the summer months and navigation during the fall. A unique operations feature is the simulation of navigation windows, which are two-week periods of guaranteed navigation depths on the lower Apalachicola River. Flood operations override all project purposes during high flows, and water supply and water quality are major concerns during drought.

Hydropower. There are three styles of at-site hydropower simulation in HEC-5: specified energy requirements, power guide curve, and run-of-river operation. *Specified energy* is an input requirement for energy in kWh or Plant Factor. Monthly energy requirements are distributed over a weekly schedule. The release for hydropower demand is met as long as there is sufficient water in storage. If downstream minimum flow and diversion requirements exceed the power release, additional flow will be released to meet those demands and to generate energy up to the plant capacity. *Power guide curve* defines the energy requirement dependent on the pool level. When the pool is high, a higher demand is applied; and, when it is low, the demand is reduced. Seasonal factors and daily distributions can be applied to the requirements to reflect the seasonal and weekly cycle of energy requirements. *Run-of-river* has no power demand. Energy is generated with the flows that pass through the reservoir, up to the maximum power capacity.

There are four Federal and five Georgia Power hydropower reservoirs in the basin model. Three of the Federal reservoirs operate with a power guide curve, and the fourth operates as run-of-river except that a small energy demand was defined to ensure energy generation during low flow periods. The Georgia Power projects have small storage pools and were modeled as run-of-river facilities.

Water Supply. Minimum flow targets and diversions are defined at control points. If releases for other purposes or locations are not sufficient to meet the target at a specified control point, additional water will be released from conservation storage. Low-flow demands were defined at Atlanta and Columbus, GA. Buford and Morgan Falls, a small Georgia Power impoundment, operate in tandem to meet Atlanta's minimum flow requirements. Index levels are used in the two reservoirs to define storage zones and to facilitate balancing. That is, both are considered balanced when at the same index level. Morgan Falls makes the releases to meet Atlanta requirement, and Buford makes hydropower releases and additional releases, if required to balance with Morgan Falls. Buford operates as a peaking hydropower facility Monday through Friday and during the weekend it makes a fixed release to provide project energy with the dam's small service unit. Buford's service unit discharge is modeled as leakage, which implies that the flow bypasses the main generation facility. This is appropriate in this instance since the energy generated is not furnished to the regional power grid. During the weekend, Morgan Falls releases from its limited storage to meet Atlanta demands. On Monday the two projects are out of balance, which means Buford needs to make added flow releases to refill Morgan Falls. Rather than balancing in one day, the program looks to the weekly energy schedule and distributes the balancing flow requirement over the power demand days. The goal is to refill the lower reservoir by Friday.

Navigation. The Apalachicola River requires flow to maintain navigation depth. Navigation can be treated as a minimum flow requirement. This works well when there is sufficient water. However, for low-flow periods, the concept of "navigation windows" has been adopted to maintain navigation depths for ten-day periods. Windows are scheduled every 30 days; however, they are also scheduled to avoid holidays when lake recreation would be hurt by falling lake levels.

Navigation windows are not a standard option in HEC-5. They are simulated by setting a seasonal minimum flow target that is dependent on the lake level. The seasons are defined to provide a navigation window the first 15 days of the summer and fall months, and to recover water in storage the second half of the month. West Point, Walter F. George and Jim Woodruff all support navigation windows until they reach a specified minimum elevation.

Flood Control. While flood reduction is an operation goal, the study focus and the 24 hour simulation interval do not support detailed flood operation simulation. The primary considerations are downstream channel capacity and reservoir outlet capability. When average daily flow approaches channel capacity, the program will limit releases to avoid contributing flow in excess of channel capacity. The outlet capability at Buford Dam was set to a lower value consistent with the average-daily flow during flood operation. The limited outflow capability replicated historic pool levels during high-flow periods.

ACT BASIN MODEL

The Alabama-Coosa-Tallapoosa (ACT) Basin contains challenging operation goals for the system analysis. There are five Corps multiple purpose projects and eleven Alabama Power Company (APC) projects. The projects operate for hydropower, flood control, low-flow augmentation, navigation, and recreation. The system can be subdivided into three logical subsystems; however, the HEC-5 model includes the entire basin.

Upper-Basin Projects. The upper basin cuts diagonally through north-western Georgia, with the Corps' Allatoona and Carters projects providing peaking hydropower generation and flood control. The Allatoona project on the Etowah River operates in a peaking mode Monday through Friday under a seasonal power guide curve that provides increased energy under full-pool conditions. Carters on the Coosawattee River operates as a peaking project, with a pump-back from a re-regulation reservoir that helps maintain Carters power pool, and operates to meet a downstream minimum flow goal. The Carters Re-reg. reservoir maintains sufficient storage in the buffer pool to meet the minimum flow target during the weekend. The two storage reservoirs also operate to reduce flood damage at Rome, GA.

Mid-Basin Projects. For the eleven APC peaking hydropower projects of the mid-basin, three subsystems of minimum-flow operation are modeled: the Coosa, Tallapoosa, and the combined system. The seven tandem APC projects on the Coosa River between Rome, GA and Montgomery, AL are required to meet a seasonally variable flow goal of 2,000 - 5,000 cfs at Jordan Dam, the lowest project on the Coosa. The upper two reservoirs operate with seasonal rule curves and a balancing strategy that moves water to Logan Martin, the primary storage facility in the system. The operation of the Coosa River projects for the Jordan Dam flow goal is complicated by Jordans interconnection with the Bouldin project, an off-stream impoundment. Coosa River flows greater than the Jordan flow target are released through the more modern generation facilities at Bouldin; however, flood flows in excess of Bouldins penstock capacity are released at Jordan. There are four APC projects on the Tallapoosa River. Harris Dam, the upper project, operates for a minimum flow target at the Wadley gage, and operates in tandem to balance with the largest APC project, Martin Dam. Martin operates to provide a minimum flow of 1,200 cfs at Thurlow Dam. The Coosa and Tallapoosa combine to form the Alabama River near Montgomery, AL. The combined system of Jordan, Bouldin and Thurlow Dams operate to provide a total minimum release of 4,640 cfs into the Alabama River. The simulation of the combined system was complicated by the fact that primary storage reservoirs, Logan Martin on the Coosa and Martin on the Tallapoosa, are situated in the middle of their respective stream reaches and must make release decisions with consideration for diversions and evaporative losses at downstream reservoirs while maintaining a balance with one another. Several new program features were developed to simulate the operation of these APC projects.

Lower-Basin Projects. The Corp's R. F. Henry and Millers Ferry Dams on the Alabama River are modeled as tandem reservoirs. Their operation re-regulates the releases from the APC projects to provide a minimum discharge from Millers Ferry of 6,600 cfs. The model represents the basic agreement between the Federal agencies and the Alabama Power Company to maintain a 7-day total release into the Alabama River of at least 32,480 dsf for navigation.

STUDY STATUS

The ACF/ACT reservoir system models, flow data and projected demand data have been completed and provided to the states. The Hydrologic Engineering Center has provided HEC-5 software and training to facilitate the development of water allocation formulas, by the states, which are to become the basis for an interstate compact. The Mobile District has begun an environmental assessment of anticipated operational changes at the Corps reservoirs using both HEC-5 and HEC-5Q, the water quality version of HEC-5. Computer program HEC-5, associated utility programs and documentation will be available at HEC's web site (www.wrc-hec.usace.army.mil).

ACKNOWLEDGMENT

The summary of basin model data and options is abstracted from the draft model report developed by the staff of Mobile District, USACE.

REFERENCES

Hydrologic Engineering Center (HEC), 1995, HEC-DSS User's Guide And Utility Manuals, User's Manual, Hydrologic Engineering Center, March, 1995.

HEC, 1997, HEC-5, Simulation of Flood Control and Conservation Systems, User's Manual, November 1997.

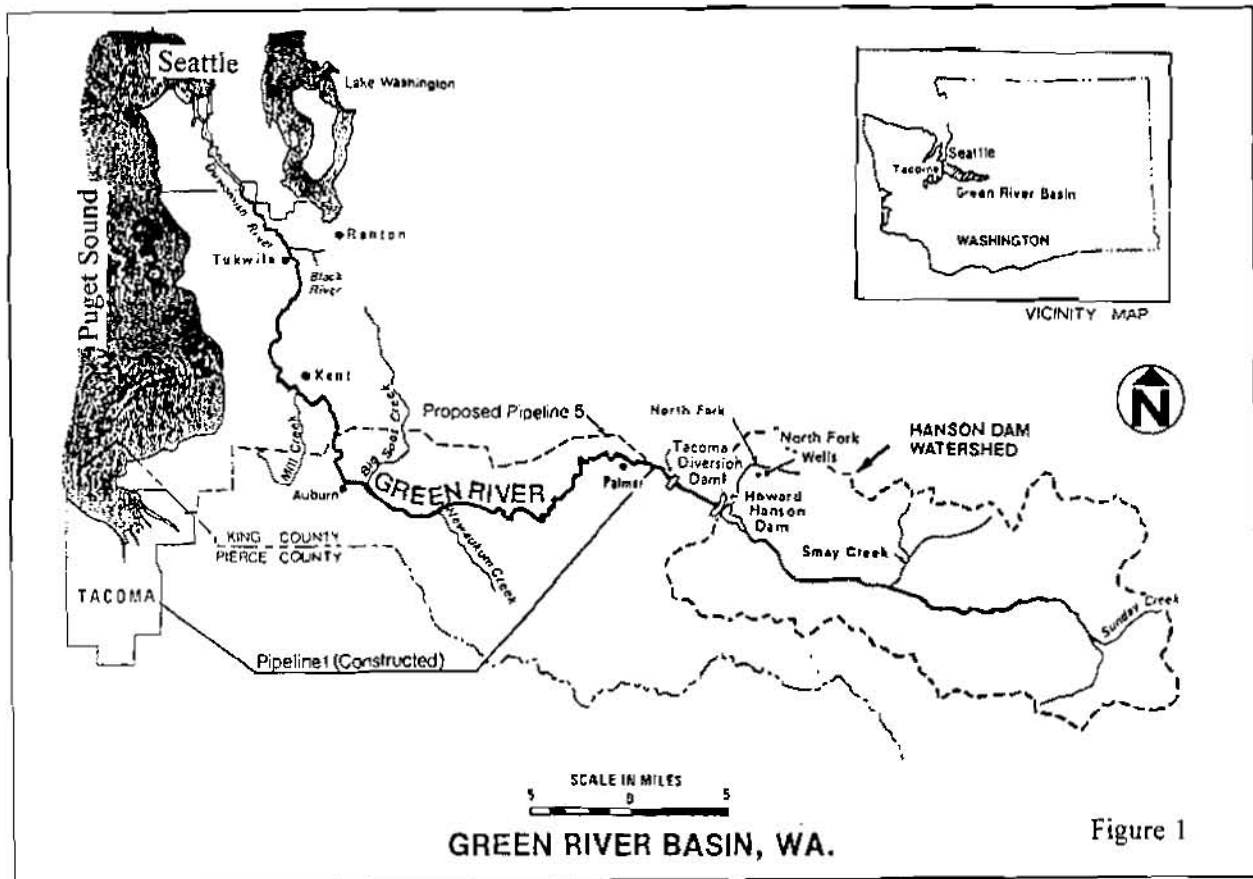
US Army Corps of Engineers (USACE), 1987, Management of Water Control Systems, EM 1110-2-3600, US Army Corps of Engineers, 30 November 1987.

USACE, 1997, Unimpaired Flow, ACT/ACF Comprehensive Water Resources Study, Surface Water Availability, Volume I, Mobile District and Hydrologic Engineering Center, July 8, 1997.

ADDITIONAL STORAGE STUDY OF HANSON RESERVOIR, GREEN RIVER, WA

Loren Jangaard, Hydraulic Engineer, U.S. Army Corps of Engineers,
Seattle District, Washington

Abstract: This paper describes how agencies with different responsibilities and priorities worked together with the hydrologic specialist and models to reach a consensus on the best operation plan for expanded utilization of the Corps reservoir storage space at Howard A. Hanson Dam near Seattle, Washington. The expanded utilization was formulated to include municipal and industrial water supply as a new project purpose. The existing reservoir project has been in place for 35 years and was designed as a flood control reservoir with about a quarter of the reservoir space used for summer fishery flow enhancement. Increased environmental awareness related to fishery needs opened up a relatively simple water management analysis to significant operational complications and constraints. Water supply utilization decisions were necessary among interests that competed for the natural resource limited by a finite reservoir storage. The willingness of the Corps and participants including the City of Tacoma, Muckleshoot Tribe, and Washington State Department of Fisheries to engage in adaptive and creative management techniques helped to make this project possible. The resolution strategy involved workshops to understand and respect the importance of each participant's needs and objectives; and an education process on hydrology, institutional priorities, and fishery life cycles. A key activity was the definition of optimum river flow for the fishery resource objective that was directly linked to the performance of an agreeable hydrologic flow scenario. Resolution of water releases became a negotiated



trade-off between performance levels of the various plans and operational constraints as demonstrated by the hydrologic model.

INTRODUCTION

Purpose: This was a study conducted by Hydrology and Hydraulics Branch for Planning Branch of Engineering Division, Seattle District Corps of Engineers. The local sponsor was the City of Tacoma Public Utilities (Tacoma). Hydrologists were interested in developing the capability to quantify storage amounts at the existing damsite required to meet a variety of downstream demands defined by fish biologists. Planners needed to investigate the environmental and economic impact of the formulated water supply development. The purpose of hydrologic computations was to determine how much additional storage was required for each of a variety of off-stream and instream demands beyond that needed to meet the current obligation to provide 110 cubic-feet-per-second (cfs) with 98% reliability.

Basin Characteristics: The Green River originates on the west side of the Cascade Range in Washington state. The river flows westward to Auburn, then northerly through the lower valley to Tukwila and Seattle. The river is 65 miles long between its mouth and Hanson Dam near Palmer. The area drained by the basin is 483 square miles. Floods in the basin occur generally as a result of warm rainstorms during the period from November to March. Snowmelt occurs from April through June. Minimum streamflows occur between July and November due to dry weather conditions. Figure 2 shows runoff for an annual season and illustrates the unusually long low-flow period experienced in year 1987 due to a low snowpack. The average annual flow recorded at Auburn is 1,300 cfs.

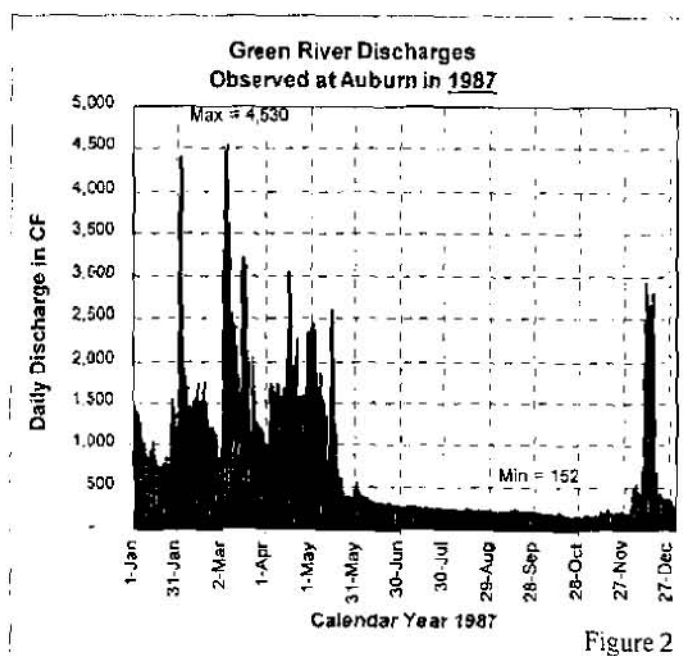


Figure 2

The average annual flow recorded at Auburn is 1,300 cfs.

RIVER FEATURES UNDER SYUDY

Existing Dam: Howard A. Hanson (Hanson) Dam was authorized in 1950 with project costs allocated to flood control and fisheries enhancement. Construction of the dam was completed to elevation 1228 feet in December 1961. The summer conservation pool was established at elevation 1141 feet (ft) with 25,400 acre-feet (ac.ft.) of storage. The flood control capacity was planned with 106,000 ac.ft. of storage at elevation 1206 feet. The purpose of the conservation pool is to provide for dam releases sufficient to assure with 98% reliability, the availability of at least 110 cfs in the river below Tacoma's diversion dam for fishery enhancement. Conservation storage is attained by June during the recession of the snowmelt runoff. Refill may begin as early

as March when low runoff is forecasted. The actual timing of storage accumulation depends on 98% assurance of refill, water quality, downstream fish passage, and fish residence below the dam. Reservoir drawdown is completed in the fall with the arrival of increased runoff from winter rains. Though the dam is a Federal project, and is exempt from State control, the storage of water is subject to the State's authority in issuing water rights.

Existing Water Supply Diversion: The City of Tacoma constructed a diversion dam and water delivery pipeline in 1913 to divert approximately 112 cfs for Municipal and Industrial (M&I) water supply. There is no active storage behind Tacoma's diversion dam due to its small size. The structure's main purpose is to provide a hydraulic head on the withdrawal pipeline. Tacoma is permitted to divert a maximum of 113 cfs or the sum of inflow to Hanson Dam and the local inflow between the two dams, whichever is least. The diversion site also receives water piped from a well field approximately 6½ miles away on the North Fork of the Green River. Six wells were placed into operation at the well field in late 1977 to use when the river flow is turbid.

Proposed Water Supply Diversion: Tacoma proposes to divert an additional 100 cfs from the Green River through a new gravity pipeline. The new pipeline would originate from the same location as the first pipeline and extend 33 miles along a northerly route that can provide water to new service areas. The new pipeline will be subject to flow restrictions in Washington State's instream resources protection program (1980). There is also an agreement between Tacoma and the Muckleshoot Indian Tribe that calls for diverted water to be returned to the river during certain periods of the year (1995). The additional storage project allows the use of water storage space in Hanson reservoir to store diverted water from the Green River for later withdrawal and diversion use by Tacoma later in summer.

Instream Flow: Instream flow is the discharge remaining in the river after off-stream water diversions. Instream flow criteria means that water right holders will not be allowed to continue diverting when streamflows fall below the dated flow quantities established by chapter 173-509 of the Washington Administrative Code. Previously stored water cannot be used to meet the instream flow quantity unless the water was previously stored for that purpose. Target instream

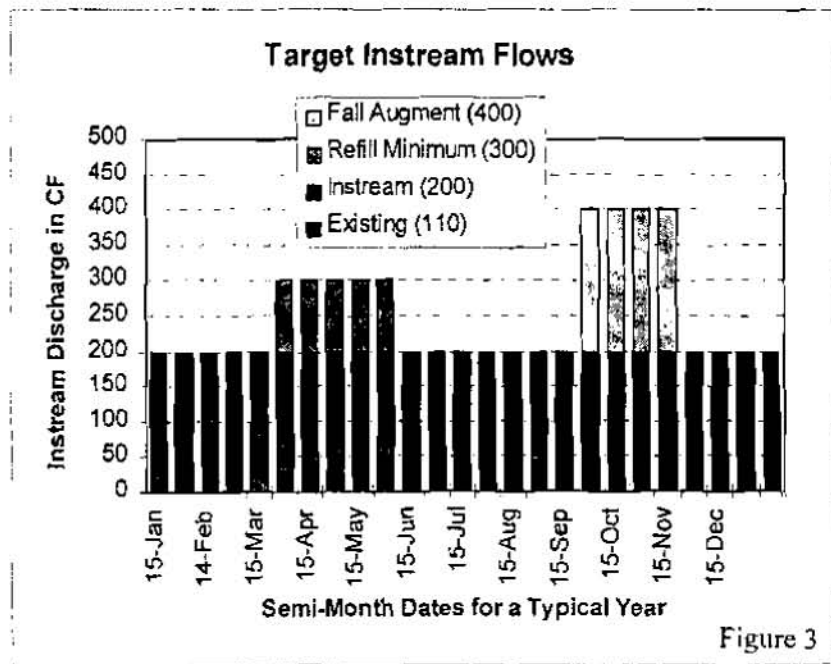


Figure 3

flows for this study are 200 cfs with an increase to 300 cfs during the snowmelt runoff and an increase to 400 cfs in fall just prior to the rainy season (Figure 3).

DATA AND MODELING

Database of Streamflows: Streamflow data for the additional storage study was determined in an earlier phase of the study in 1985. This work resulted in a 70-year time sequence of semi-monthly inflows to the reservoir, 1914-1985. During participation in a National Drought Study during 1990-1992, the data was updated through 1992 and converted to a weekly time step. The semi-month data was used during plan formulation of additional storage. The weekly data was used to illustrate the use of the storage and application of water deliveries downstream of the dam. During an environmental impact study, 32 years (1964-1995) of observed daily flows were used to better evaluate the change in outflows due to changing weather conditions from day-to-day.

River and Reservoir Modeling: The reservoir and river is a classical text book configuration with 3 control points. The reservoir is the primary control point with the source of data and water storage space. The other 2 control points are for the off-stream diversion flows and instream fishery flows. During the course of the study, Tacoma entered into an agreement with the Muckleshoot Indian Tribe to place further limitations on the operation of the 2nd diversion pipeline. An additional control point is added to bring in additional rules for controlling the river. A schematic view of the reservoir and control points is shown below. The groundwater and Tacoma well system did not need to be included in the modeling of Green River surface waters.

Schematic of River & Reservoir Model

<u>Schematic of Model</u>	<u>Purpose of Model Node</u>
Inflow Data	Observed & computed semi-month flows, also observed daily.
↓	
Flood Control Zone Additional Storage Existing Storage	106,000 acre-feet reserved for winter flood control at Hanson Dam. 25,400 acre-feet reserved for summer low-flow augmentation 37,000 acre-feet of expanded summer storage for water supply
↓	
Decision Model	HEC-5, then Spreadsheet.
↓	
Diversion Control Point	113 cfs or natural flow when less (existing) at Tacoma's structure. 100 cfs from additional storage (proposed).
↓	
Instream Control Point	110 cfs from existing storage (existing) at Palmer. State instream flows to control 2 nd diversion.
↓	
Additional Instream Control Point	More Instream rules for additional storage and diversions #1 & #2 from the Tacoma-Muckleshoot Agreement (at Auburn).

HEC-5 Computer Model: The generalized computer program HEC-5, "Simulation of Flood Control and Conservation Systems," was used to simulate the reservoir and river operations. The use of flood control space and reservoir refill was controlled by the application of rule curves that varied by calendar date. Early rules were applied with a priority over later rules. The Hydrologic Engineering Center (HEC) helped to alter the use of HEC-5 for the Green River.

Water Demands and Priorities: The priorities built-in to HEC-5 were difficult to modify for the simulation of the Green River. Instead of using a separate reservoir level to determine if the reservoir inflow was less than 113 cfs, the data base was examined with a separate data storage utility program to find the few occasions when streamflow was less than 113 cfs. A unique demand data set was then created as a time series of data to force the reservoir to release less than 113 cfs on appropriate dates. This meant that a reservoir curve did not need to be created for the 113 cfs decision. HEC-5's decision to release water for a diversion demand always had a higher priority over maintaining an instream flow amount. However for the Green River, instream flow has greater priority. A lower priority was applied in the model by using a lower diversion quantity than actually needed at a separate control point. Reservoir control by categorized weather seasons was not actually simulated within the model. The data set was preprocessed and segregated into low, average, and high runoff years. Appropriate demands could then be matched with the segregated years. Similar liberties were taken with other rules by processing data outside of the model and creating a separate time-series data set of demands to control the output of the reservoir. The hydrologist worked with minimal coordination with biologists. The hydrologist selected the 300 cfs spring target and the 200 cfs summer target. The biologist selected the fall augmentation of 400 cfs and it was up to the hydrologist to make it reliable. As additional time-series data-set demands were tabulated with modeled output, the results began to look more and more like spreadsheet output.

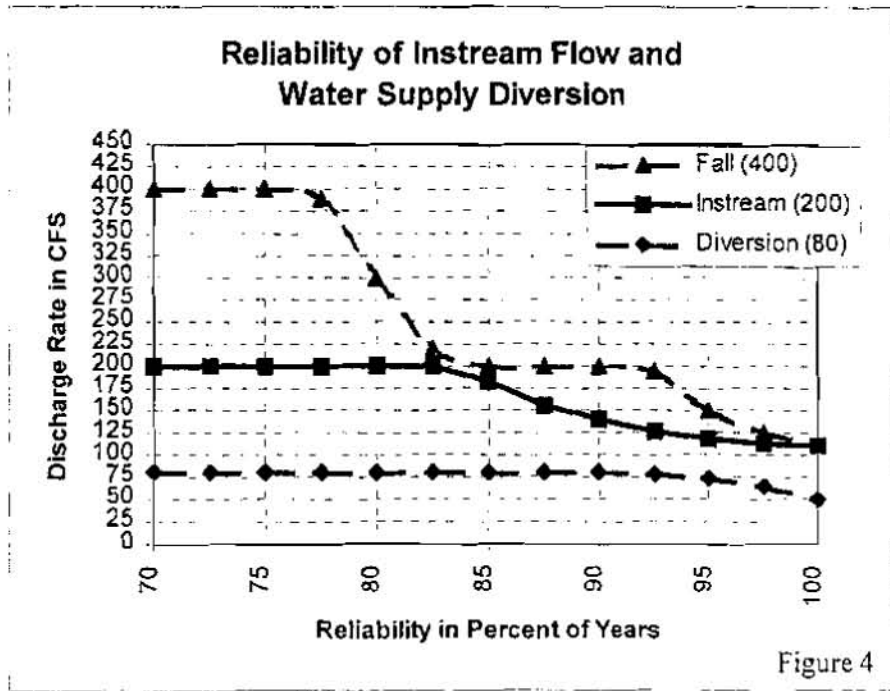


Figure 4

MODEL OUTPUT

Instream Flows: The final test of the appropriateness of reservoir decisions made by the model was to tabulate the resulting flows and determine how often the demands were met or failed. The reliability of maintaining a discharge was tabulated in terms of the percentage of years that all target flows were met or exceeded. Figure 4 shows the targeted discharge on the left scale and the modeled reliability on the bottom scale. The top curve is the reliability of providing 400 cfs for 6 weeks in the fall. There are a few years when the delivered flow is not quite 400 cfs, but is greater than 200 cfs. The second curve down shows the reliability of 200 cfs in the summer.

There are some failure periods of 200 cfs in the middle of the summer. The reliability of the 200 cfs flow comes back up in the fall as illustrated by the extension of the top curve at the discharge level of 200 cfs. Both instream flow curves converge at 110 cfs which is the base flow supplied by the existing storage. The bottom curve shows the reliability of the water supply diversion of 80 cfs. Fishery biologists accepted the modeled flows and returned to their own offices to do their own analysis of impacts.

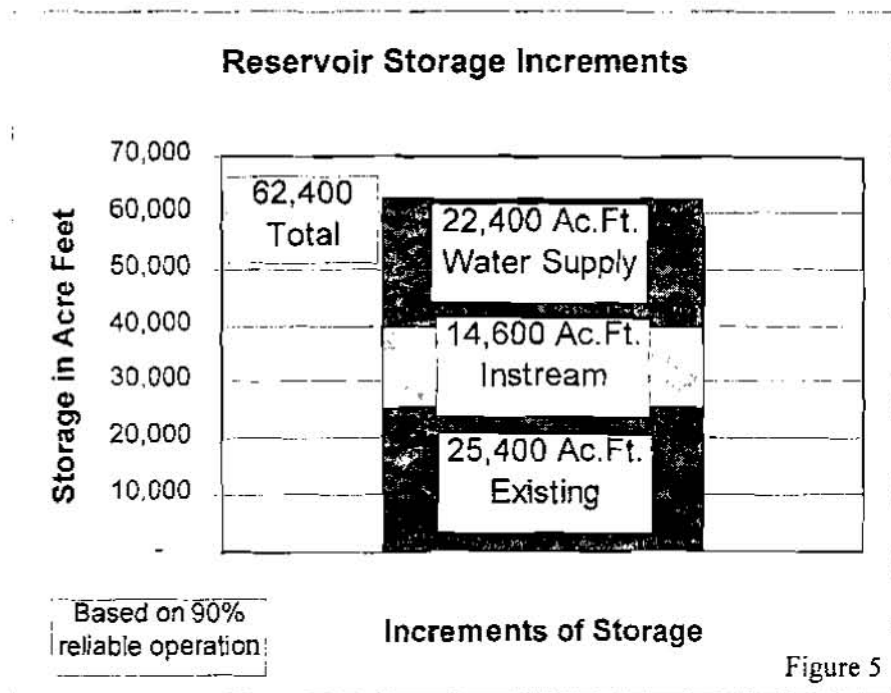
Water Supply Diversion Flows: The water supply diversion of 80 cfs was reliable for over 90% of the years as shown figure 4. This slightly exceeded the targeted reliability of 90%. Water supply shortages were modest as the pipeline was never less than at least half full. The water supply sponsor attended most of the coordination meetings to keep the priority of this purpose high.

Allocated Storage Amounts: The modeling summary output showed how the overall storage performed in terms of discharge with the given demands. The planners and economists needed to know precisely how much storage was used by each of the purposes. This question did not have an obvious answer because storage uses overlapped at some time periods and the variety of weather and snowmelt patterns caused different amounts of natural streamflows in the river for each of the years. The

diversion pipe was examined in detail to find out how much of the diverted water was from natural river flow, how much was from real-time "permitted" flow, and how much was from water stored in an earlier time period and released from the reservoir in the current time period. This type of computation was also done for the instream flow during years within the target range between 75% and 90% reliable operations.

The computation was done using a spreadsheet outside of the HEC-5 model. Figure 5 shows that 22,400 ac.ft. was allocated to the water supply purpose and 14,600 ac.ft. was allocated to the instream flow purpose. The existing storage allocation of 25,400 ac.ft. for 110 cfs did not change.

Other Effects on Storage: Small amounts of storage were used by operating conditions caused by other than the modeled purposes. A sedimentation survey had been performed during the study process during routine reservoir maintenance. This was compared with the initial survey



just after construction of the dam. The observed loss of storage caused by sedimentation was projected into the future 50-year economic life of the proposed project. The sedimentation projection was prorated among the 3 purposes so the existing storage would not suffer the entire loss of storage just because it was positioned in the lower zone where the actual sedimentation would likely reside. The error in accurately knowing the downstream gage discharges in real-time was indirectly included in modeling. During nearly all of the years, there was stored water remaining after all of the demands were met. During the more critical years when demands could not be met in all of the time periods, the outflows were carefully reduced along with the reservoir drawdown so the reservoir never completely emptied. The few thousand acre-feet that remained was allocated to gage error. In other words, the surplus storage could be converted to a few cfs of discharge over the critical drawdown period to give the reservoir operator some flexibility in precisely meeting downstream flows. This exercise usually needs to be done by the modeler to overcome the preciseness that is maintained by the math in the model which would bring critical year storage down to exactly zero.

MODEL REFINEMENTS

Adaptive Water Management: Once it was demonstrated that the proposal for the use of additional storage at Hanson Dam had some feasible merit, the examination of modeled output became much more intense. Modeling was done initially with a semi-month time step and later with a weekly time step. Technical reviewers wanted to see the fluctuations within the week such as between the weekend and mid-week periods. Daily flows were needed for detailed studies of fish habitat and populations. Reservoir operations during multiple critical years had been studied in detail. However, operations during average and high runoff years were provided only in the form of a single sample year. Biologists who wanted to know how the project was going to operate in the future were not satisfied to hear that a detailed reservoir regulation manual would be prepared later during design studies. They also did not like the presumption that the proposed operation would become scheduled and fixed for all years. Environmental planners were willing to do more detailed studies earlier in the planning phase. If the modeled outcome looked slightly undesirable, simulation rules could be changed, and a new outcome could be examined. A desired outcome was therefore adaptively managed with a succession of rules that would be flexible with the conditions of runoff and fish habitat that was present in the river. Hydrologists and reservoir regulators worked on the development of flow augmentation rules side-by-side with fish biologists in a series of weekly meetings over a 2-month period.

Remodeling by Spreadsheet: The formulation process was nearly completely redone with a large spreadsheet computation. Tacoma's Engineering consultant, CH2M Hill (1997), had previously modeled the Green River storage and river system with a spreadsheet model. This model was used again for the adaptive water management study. Water delivery instructions were derived in terms of specific flow amounts for specific times periods when certain fishery activities were predominant. Detailed water instructions were derived to fill the storage accounts during the spring runoff and draw out the water in the summer. HEC-5 was not used because it was not understandable by non water-resource engineers and was not very flexible to change. The spreadsheet process allowed rules to be examined as they were formulated. The plotted output revealed temporary storage zones where rules could be augmented. The modeling criteria

became a surrogate for applying fish life cycle and *behavior* information into the simulation. For instance, artificial freshets were delivered at 2-week intervals to accelerate the movement of downstream migrating fish. Figure 6 shows water demands plotted for a typical year spring refill period. The most important finding was the impact that reservoir refill has on fish survival in the river. Reservoir operations were altered to mimic the natural runoff pattern of the river. The effect still had enough of an impact to interrupt the plan formulation and create a two-phased implementation process. Environmental impacts would be carefully monitored and examined after a partial implementation (phase 1) prior to the development of the 2nd and final phase. Phase 1 includes the development of 34% of the instream flow storage and 89% of the water supply diversion storage. Details of Phase 1 are still being decided among the planners, biologists and hydrologists during the preparation of this paper.

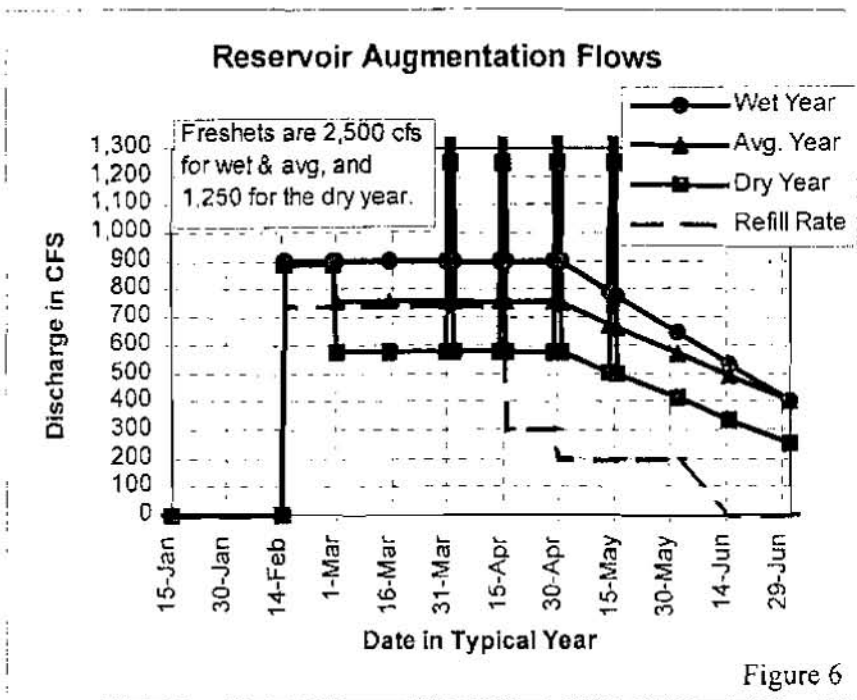


Figure 6

REFERENCES

CH2M Hill, 1997, Howard Hanson Dam Additional Water Storage Project: Modeling Results for Baseline, Phase 1, and Phase 2 Reservoir Operations, Bellevue Washington.

Tacoma Public Utilities, 1995, Agreement Between the Muckleshoot Indian Tribe and the City of Tacoma. Tacoma Washington.

U.S. Army Corps of Engineers, 1997, Howard Hanson Dam Additional Water Storage Project Draft Feasibility Report/EIS, Appendix D, Hydrology and Hydraulics, Seattle Washington.

Water Resources Policy Development Section, Washington State Department of Ecology, 1980, Green-Duwamish River Basin Instream Resources Protection Program. W.W.I.R.P. Series No.4, Chapter 173-509 WAC.

Loren Jangaard—Dept. of the Army, Seattle District, PO Box 3755 Seattle WA 98124-3755, phone 206-764-3591, fax 206-764-6678. www.nws.usace.army.mil

PROBABILISTIC FORECASTS IN MULTIOBJECTIVE ANALYSIS FOR RESERVOIR OPERATIONS

By Eric J. Markstrom, Systems Engineer, Riverside Technology, inc., Fort Collins, Colorado; Stuart S. Schwartz, Independent Consultant, Rockville, Maryland; Robert G. Steger, Water Resources Engineer, Denver Water Department, Denver, Colorado; Larry E. Brazil, President, Riverside Technology, inc., Fort Collins, Colorado; Gerald N. Day, Director, Riverside Technology, inc., Fort Collins, Colorado

INTRODUCTION

Because of increased, competing demands for reservoir benefits, decision makers are finding it increasingly more difficult to operate multipurpose reservoirs. Multipurpose reservoir operations call for strategic decisions that balance potentially competing goals and operational risks throughout the year. A risk-based, multiobjective decision framework that helps evaluate strategic tradeoffs for reservoir operations over both the long- and short-term operational horizon is the focus of this paper.

This paper highlights recent developments related to probabilistic forecasts in multiobjective reservoir analysis; a case study demonstrates the use of these forecasts at Dillon Reservoir. The paper first will present background information on Dillon Reservoir, including reservoir characteristics and operation objectives. Next, the paper will describe forecast information as related to reservoir operations and as model input for a stochastic linear reservoir optimization model. Finally, the paper will present a stochastic linear reservoir optimization model, along with the Stochastic Linear Binding Method (SLBM), as an effective reservoir management tool.

DILLON RESERVOIR BACKGROUND

The Denver Water Department is responsible for providing water for the City and County of Denver as well as 40 percent of the surrounding suburbs. To do this, Denver Water owns and manages 11 reservoirs on both the Eastern and Western slopes of the Continental Divide. Representing nearly half of Denver's raw water supply, Dillon Reservoir (*Figure 1*) is considered one of Denver Water's most important water supply facilities.

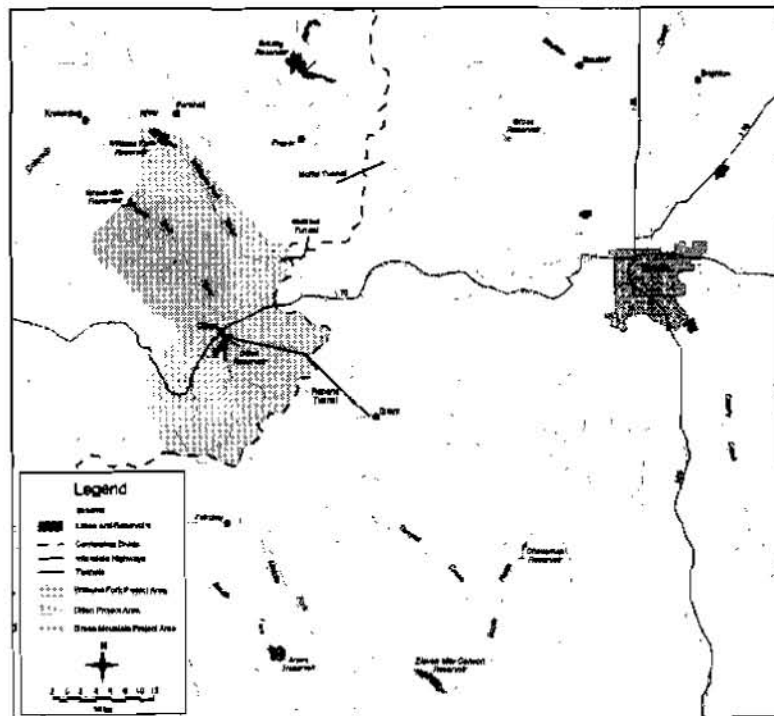


Figure 1. Dillon Reservoir

Located on the Western Slope's Blue River (Upper Colorado), with a live storage of 254,036 acre feet, Dillon reservoir is one of the largest lakes in Colorado. Water is diverted from Dillon Reservoir to Denver Water's treatment facilities via the 23.3 mile-long Roberts Tunnel under the Continental Divide. The water then flows into the North Fork of the South Platte River.

Although built and operated fundamentally for water supply, Dillon Reservoir offers many secondary benefits, including (1) downstream flood reduction for the town of Silverthorne, (2) in-lake recreation (boating, fishing, and camping), (3) downstream fisheries habitat augmentation, (4) downstream recreation (fly fishing and white water rafting), and (5) hydropower generation. A more detailed description of the downstream flood reduction and in-lake recreation benefits will appear later in this paper.

FORECAST INFORMATION FOR RESERVOIR OPERATIONS

Reservoir operators rely on a variety of forecast information as input into the decision-making process. Short-term forecasts (typically 3 to 5 days) give reservoir operators important information about reservoir inflows for real-time operations and short-term planning. Typically, short-term forecasts are deterministic in nature and represent the forecaster's best estimate of future reservoir inflow over several days. Extended probabilistic forecasts (1- to 3-month outlooks) give operators important information about the uncertainty and range of forecasts over an extended time horizon. The extended probabilistic forecasts give decision makers invaluable information about the distribution of possible reservoir inflows (i.e., timing and magnitude of peak inflow), as well as short-term and seasonal reservoir inflow volumes.

In the United States, the National Weather Service (NWS) issues short-term deterministic forecasts for over 3,000 forecast points daily. For many reservoir decision makers, these forecasts provide essential information used in immediate real-time operational decisions. In addition to short-term deterministic forecasts, the NWS also provides a number of longer-range forecast products for reservoir planning. Seasonal forecasts of water supply used in the western United States are prepared by the NWS and the Natural Resources Conservation Service (NRCS). These forecasts provide a most probable volumetric outlook along with reasonable minimum and maximum volumes. The reasonable minimum and maximum volumes represent inflow volumes that are expected to be exceeded 90 percent and 10 percent of the time, respectively.

An important forecast product used in reservoir operations and developed by the NWS is the Extended Streamflow Prediction (ESP) forecast. ESP forecasts are long-term stochastic forecasts, generated using conceptual hydrologic models and historical meteorological data. The ESP technique assumes that individual years of historical meteorological data define the potential distribution of possible future meteorology. The distribution of potential streamflow realizations is generated by inputting individual historical years of meteorological data to a conceptual hydrologic model. The model uses the current hydrologic states (i.e., soil moisture, snowpack, etc.) along with historical meteorological data (precipitation, temperature) and generates one potential streamflow realization for each year of historical meteorological data available. Each set of streamflow realizations provides information on the probabilities of future reservoir inflow volumes and peaks (*Figure 2*).

These probabilistic inflows are conditional and reflect the future variability of inflow based on current hydrological conditions. Once streamflow realizations have been generated, a forecaster can use the ESP Analysis and Display Program (ESPADP) to generate other helpful products. One such product is the Exceedance Probability Interval Plot displayed in *Figure 3*. This plot illustrates the weekly streamflow volumes that are expected to be exceeded, for several probability levels, for 8 weeks into the future.

Following is an example of a reservoir optimization model that uses ESP realizations of reservoir inflow to optimize operations at the multipurpose Dillon Reservoir.

RESERVOIR OPTIMIZATION MODEL

A wide variety of reservoir optimization models exists to help decision makers formulate reservoir release strategies. Each of these models provides different levels of information and utility, depending on reservoir system characteristics and operating goals. The SLBM and the associated stochastic linear reservoir optimization model discussed in this paper were developed to aid the operators of the multipurpose Dillon reservoir.

Currently, the NWS Colorado Basin River Forecast Center (CBRFC) provides Denver Water with ESP inflow forecasts for Dillon Reservoir during the spring and early summer runoff months. These forecasts include 40 daily streamflow realizations, and are typically downloaded two or three times per week by Dillon Reservoir operators as inputs into their models.

The stochastic linear reservoir optimization model was created to aid decision makers with both short-term (1 week) and long-term (seasonal) reservoir regulation decisions. The model helps reservoir decision makers explicitly quantify the benefits and risks associated with different operating policies by identifying tradeoffs of operating benefits. With 40 years of stochastic ESP inflows available for input, the reservoir optimization model was formulated as a multiobjective stochastic linear programming model, running on a daily time step. The following sections present an overview of the model through a discussion of model objectives and constraints.

Model Objectives: Although Dillon Reservoir is operated first and foremost for water supply, whenever early spring snowpack measurements indicate an above-average runoff year, reservoir operators make operational decisions to maximize secondary benefits. Flood reduction and in-lake recreation were chosen as principal objectives in this risk-based, multi-objective approach.

Because Dillon Reservoir is located immediately upstream of the city of Silverthorne, flooding and various property damage occur when releases from Dillon Reservoir exceed 1,800 cubic feet per second (cfs). Therefore, Denver Water attenuates the high inflows to Dillon Reservoir (whenever possible) to protect Silverthorne. In order to provide this benefit, a flood storage pool is maintained when inflow forecasts show a high probability of large runoff into Dillon Reservoir.

In-lake recreation is another important objective at Dillon Reservoir. Each summer, recreational pursuits (such as boating) generate hundreds of thousands of dollars in revenue for Summit County. A large part of this revenue can be attributed to Dillon Reservoir recreation. Decision makers seek to operate the reservoir so that the marinas in the cities of Dillon and Frisco can attain sufficiently deep water as early as possible during the summer recreation season.

Flood control and in-lake recreation are competing objectives. A flood pool must be reserved to store and attenuate high reservoir inflows to provide flood reduction for Silverthorne. During years of forecasted high runoff, however, maintaining a large flood pool delays filling the reservoir, which negatively impacts in-lake recreation in the early summer.

In the model's objective function, releases above a given flood threshold are subject to a release penalty that accounts for both magnitude and duration of releases over the specified threshold. Likewise, reservoir pool elevations below the minimum needed to float boats are subject to a recreation penalty.

Constraints: Several reservoir system constraints are included within the model and are described below. A continuity constraint ensures a mass balance for Dillon Reservoir. A flood penalty constraint assigns a release penalty decision variable when reservoir releases exceed the 1,800 cfs flood threshold. Maximum increase and decrease constraints limit the maximum daily change in release from the reservoir. A spillway constraint models Dillon's Morning Glory spillway by relating release to reservoir storage whenever Dillon's pool elevation exceeds the spillway elevation; it is represented by a piecewise linear approximation. The stochastic linear binding constraint allows the generation of one optimal release value for the first week of the run period. This particular constraint will be illustrated further in the Tradeoff Curves section below.

Tradeoff Curves: In the previous section, a multiobjective stochastic linear reservoir optimization model was introduced as an aid for reservoir decision makers. In this section, model results are presented through the tradeoff curve, a multiobjective and risk analysis tool.

The tradeoff curve helps decision makers make risk-based management decisions based on outputs generated by a multiobjective model. The tradeoff curve presented in Figure 4 illustrates a set of non-dominated (pareto) optimal solutions for Dillon Reservoir. Each point on the tradeoff curve defines an optimal alternative operating strategy, with each point representing a different preference between flood reduction and in-lake recreation benefits.

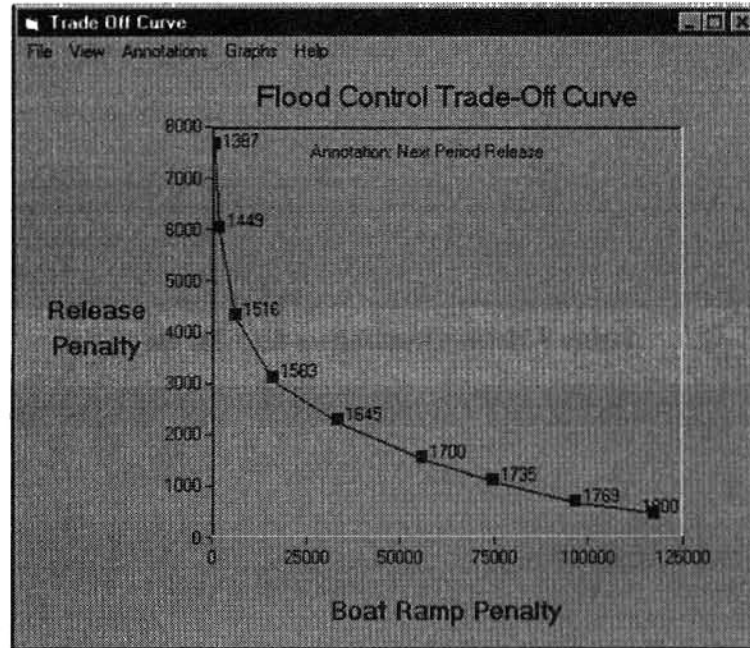


Figure 4. Tradeoff Curve

Because flood reduction and in-lake recreation are competing, noncommensurate benefits, a tradeoff curve is generated to compare alternative operations. In multiobjective analysis, a number of techniques are available to establish relative weights for objective terms. In this example, a hybrid of the a-posteriori weighting method was used. This technique assigns relative weights to each of the competing objectives (flood reduction and in-lake recreation) in order to formulate a single objective function. Once weights have been established, the model is run and the corresponding operating alternative is obtained. Model weights are varied until a representative non-dominated surface has been generated. Each point on the tradeoff curve is labeled with a model-generated, recommended reservoir release for the first week of the run period.

Figures 5 through 8 illustrate model results for two of the tradeoff curve points depicted in *Figure 4*.

Figures 5 and *6* represent model releases and storages for the tradeoff point corresponding to the release of 1,387 cfs during the first week of the run period. This point on the tradeoff curve represents the operational policy that minimizes the risk of not meeting in-lake recreation benefits, but has a corresponding large flood potential penalty. *Figure 5* illustrates the model behavior for the flood potential through depiction of the release realizations. First, the SLBM constant binds all of the release realizations to a release level of 1,387 cfs over the first week of the run period. By binding all of the future release realizations to this level, four of the realizations within the model are forced to eventually violate the 1,800 cfs threshold and increase the release penalty objective. On the other hand, *Figure 6* demonstrates that for the 1,387 cfs release schedule, none of the storage realizations are forced to fall below the minimum storage requirement (lower horizontal line). Therefore, a reservoir operator who chooses to make a release of 1,387 cfs over the first week of the run period is minimizing the risk of not meeting in-lake recreation demands at the expense of a large risk of potential future flooding.

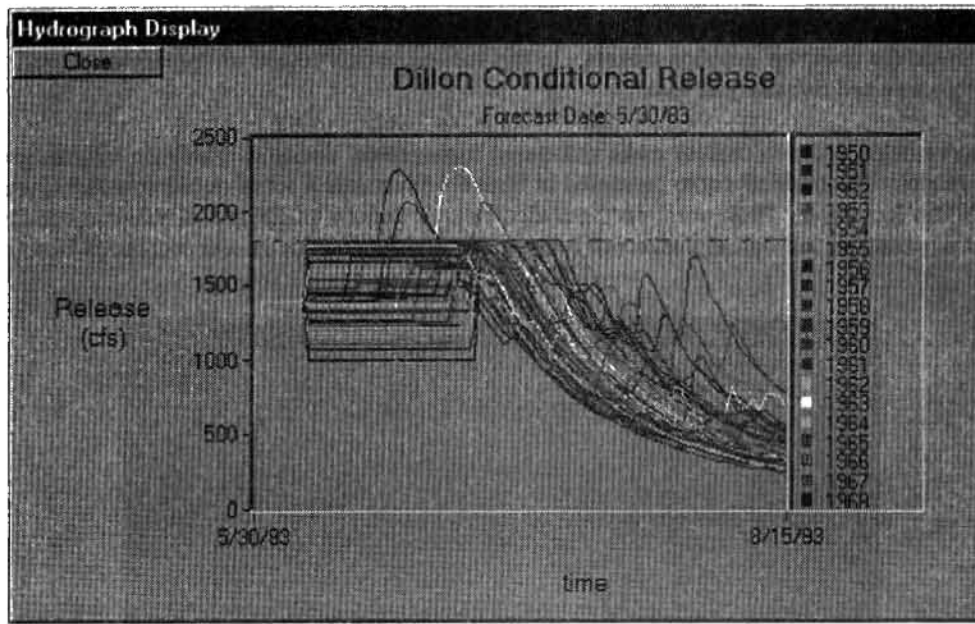


Figure 5. Release Realizations for 1,387 cfs

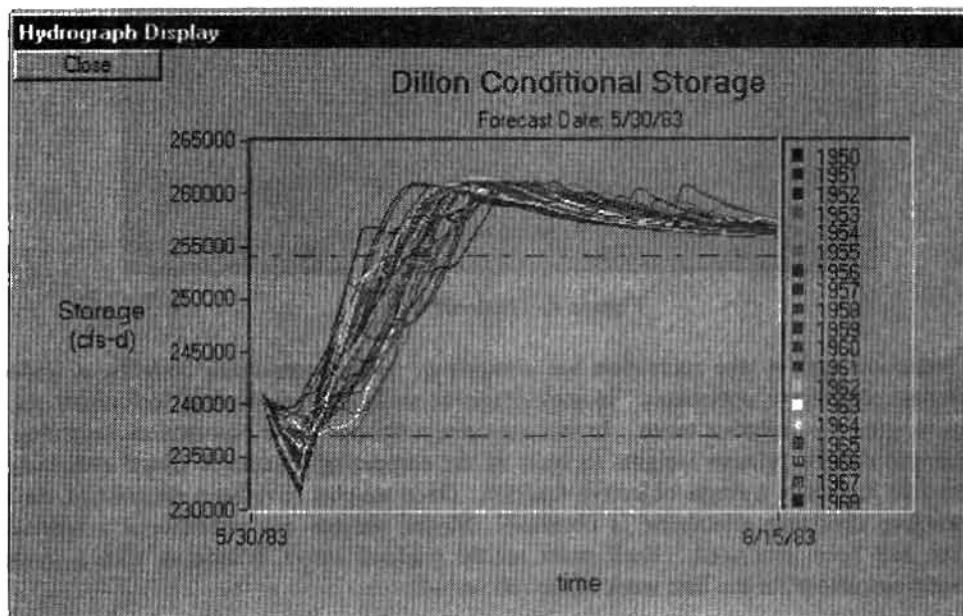


Figure 6. Storage Realizations for 1,387 cfs

Conversely, **Figures 7** and **8** represent the other extreme operating policy. By releasing 1,800 cfs, the reservoir operator is sacrificing in-lake recreation benefits to minimize the potential flood risk. **Figure 7** shows that by releasing 1,800 cfs over the first week of the run period, only one of future release realizations is forced to exceed the 1,800 cfs threshold. The potential flood risk has been reduced by increasing the risk of not meeting future in-lake recreation demands. **Figure 8** illustrates that in most of the storage realizations, a reservoir drawdown below the boat ramp elevation is required.

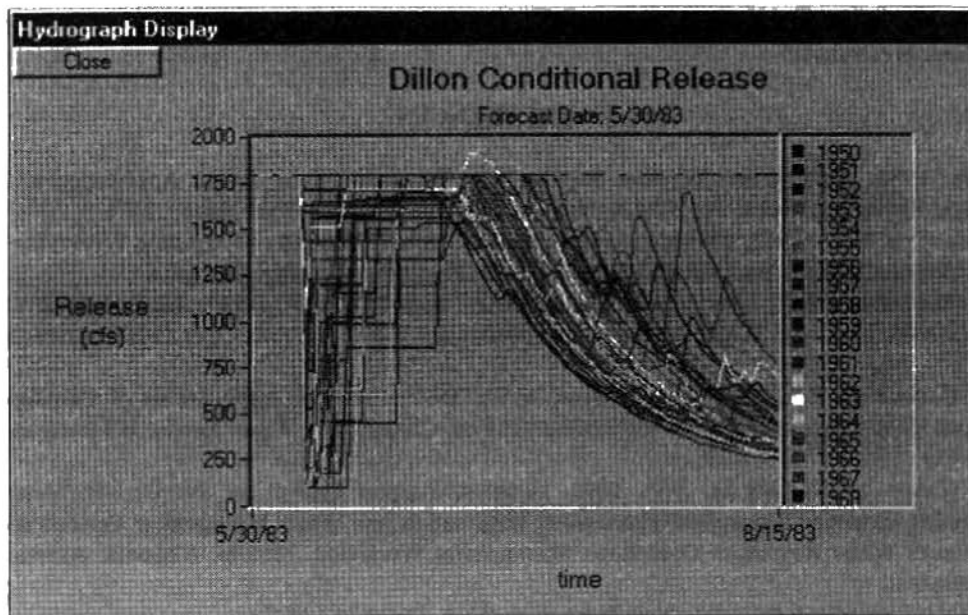


Figure 7. Release Realizations for 1,800 cfs

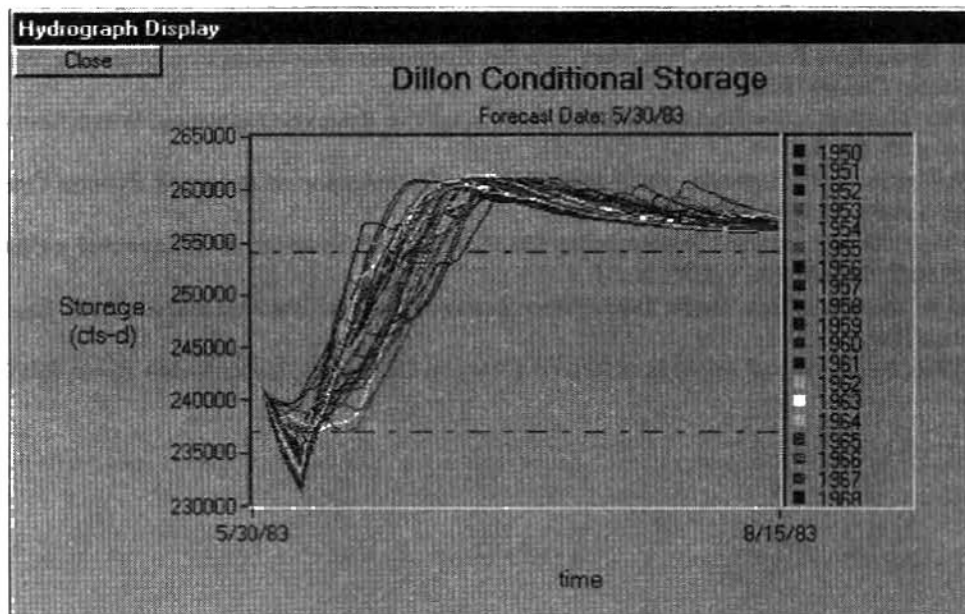


Figure 8. Storage Realizations for 1,800 cfs

CONCLUSION

This paper describes a risk-based approach to the operation of multipurpose reservoirs. A stochastic linear reservoir optimization model is presented as an effective means to balance operational tradeoffs for multipurpose reservoirs, using stochastic inflow forecasts as input.

Although the analysis presented in this paper focuses on tradeoffs between two benefits at Dillon Reservoir, there are also possible tradeoffs between other reservoir objectives, such as fish habitat augmentation, downstream recreation (fly fishing and white water rafting), and hydropower generation. Numerous tradeoffs exist for other reservoir

systems, each with varying importance according to the hydrological state, probabilistic inflow forecasts, and reservoir operator preference.

REFERENCES

- Anderson, E.A., 1986, The National Weather Service River Forecast System and its Application to Cold Regions. Hydrologic Research Laboratory, NOAA, National Weather Service, Silver Spring, MD.
- Brazil, L.E., Hudlow, M.D., 1982, Technological Developments in Hydrologic Forecasting Within the U.S. National Weather Service. AWRA International Symposium on Hydrometeorology, Denver, CO.
- Brazil, L.E., Markstrom, E.J., Day, G.N., Steger, R.G., Schwartz, S.S., 1997, Use of Hydrologic Forecast Information for Improved Water Management. Woodward Turbomachinery Controls Conference. Estes Park, CO.
- Brazil, L.E., Markstrom, E.J., Day, G.N., Waage, M.D., 1997, Practical Applications of Extended Streamflow Predictions. Symposium on Climate Variability, Climate Change, and Water Resource Management. Colorado Springs, CO.
- Brazil, L.E., Waage, M.D., Laurine, D.P., 1992, Decision Support System for the Denver Water Department: Incorporating Extended Streamflow Forecasting Information into Water Management Operations. Proceedings of the Fourth Water Resources Operations Management Workshop. Mobile, Alabama, American Society of Civil Engineers.
- Chvatal, V., 1983, Linear Programming. New York, NY: W.H. Freeman and Co.
- Dantzig, G.B., 1963, Linear Programming and Extensions. Princeton, NJ: Princeton University Press.
- Day, G.N., 1985, Extended Streamflow Forecasting Using NWSRFS. Journal of Water Resources Planning and Management. ASCE, Vol 111, No. 2.
- Day, G.N., Brazil, L.E., McCarthy, C.S., Laurine, D.P., 1992, Verification of the National Weather Service Extended Streamflow Prediction Procedure. AWRA Symposium Proceedings on Managing Water Resources During Global Change. Reno, NV.
- Harboe, R., 1992, Multiobjective Decision Making Techniques For Reservoir Operation. Water Resources Bulletin. AWRA, Vol 28, No. 1.
- Ko, S.K., D.G. Fontane, J.W. Labadie, 1992, Multiobjective Optimization of Reservoir Systems Operation. Water Resources Bulletin. AWRA, Vol 28, No. 1.
- Loucks, D.P., 1995, Developing and Implementing Decision Support Systems: A Critique and a Challenge. Water Resources Bulletin. AWRA, Vol 31, No. 4.
- Loucks, D.P., J.R. Stedinger, D.A. Haith, 1981, Water Resource Systems Planning and Analysis. Englewood Cliffs, NJ: Prentice Hall.
- Wurbs, R.A., 1996, Modeling and Analysis of Reservoir System Operations. Upper Saddle River, NJ: Prentice Hall.

EFFECTS OF MODEL OUTPUT TIME-AVERAGING ON THE DETERMINATION OF THE ASSIMILATIVE CAPACITY OF THE WACCAMAW RIVER AND ATLANTIC INTRACOASTAL WATERWAY NEAR MYRTLE BEACH, SOUTH CAROLINA

Paul A. Conrads, Hydrologist, U.S. Geological Survey-Water Resources Division,
Columbia, South Carolina

Abstract: A Branched Lagrangian Transport Model, was calibrated and validated for the tidally influenced portions of the Waccamaw and Pee Dee Rivers, Bull Creek, and the Atlantic Intracoastal Waterway near Myrtle Beach, South Carolina. In determining the assimilative capacity of the Atlantic Intracoastal Waterway, 1-hour, 24-hour, 14-day, and 30-day averaging intervals were used. For each averaging interval, point-source loadings in the model were increased until the State dissolved-oxygen standard was violated. Results of the averaging intervals and point-source loadings for two locations were evaluated by comparing time series of dissolved-oxygen concentration at critical locations and longitudinal profiles of average dissolved-oxygen concentration for particular reaches of the system. The concentrations of the oxygen-consuming constituents that can be assimilated vary by 180 percent, depending upon the averaging interval used for interpreting the simulation model output.

INTRODUCTION

The Grand Strand is a rapidly growing resort area on the northeastern coast of South Carolina (fig. 1). The municipalities of Myrtle Beach and North Myrtle Beach have experienced tremendous growth in the 1990's and have become one of the leading tourist destinations in the country. As the Grand Strand continues to grow, there are increasing demands on the water resources in the area. The Atlantic Intracoastal Waterway (AIW) and Bull Creek provide municipal source water and the AIW and Waccamaw River receive municipal wastewater-treatment effluent.

In order to protect the aquatic life in these receiving streams, the capacity to assimilate treated wastewater must be determined. For many reasons, the procedure for determining assimilative capacity for coastal waters is not well as established as compared to upland, riverine systems. The dynamic, oscillatory nature of flows in estuarine waterbodies makes statistically determined low-flow values very difficult to compute. Critical dissolved-oxygen concentrations may not occur during low-flow periods when estuarine waterbodies are influenced by ocean water which usually has dissolved-oxygen concentrations higher than those in the freshwater. Most water-quality standards in South Carolina were written for upland streams and not for coastal waters, where, in the case of South Carolina, the waters may not meet the dissolved-oxygen concentration standard due to natural conditions. For these waters in South Carolina, effluent releases are permitted only if the instream dissolved-oxygen concentration is minimally affected, which is quantified as less than a tenth of a milligram per liter decrease from the natural condition--also known as the point-one rule (South Carolina Department of Health and Environment Control, 1993).

For water-resource management, assimilative capacity is expressed as pounds per day (lbs/d) of ultimate oxygen demand (UOD) that can be assimilated without causing a violation of the State water-quality standard for dissolved oxygen. In municipal wastewater effluent, the principal oxygen-consuming constituents are ammonia and biodegradable organic substances. The UOD is the total, theoretical demand for oxygen from carbonaceous and nitrogenous sources. The South Carolina Department of Health and Environmental Control (SCDHEC) defines UOD by the equation (South Carolina Department of Health and Environment Control, 1991):

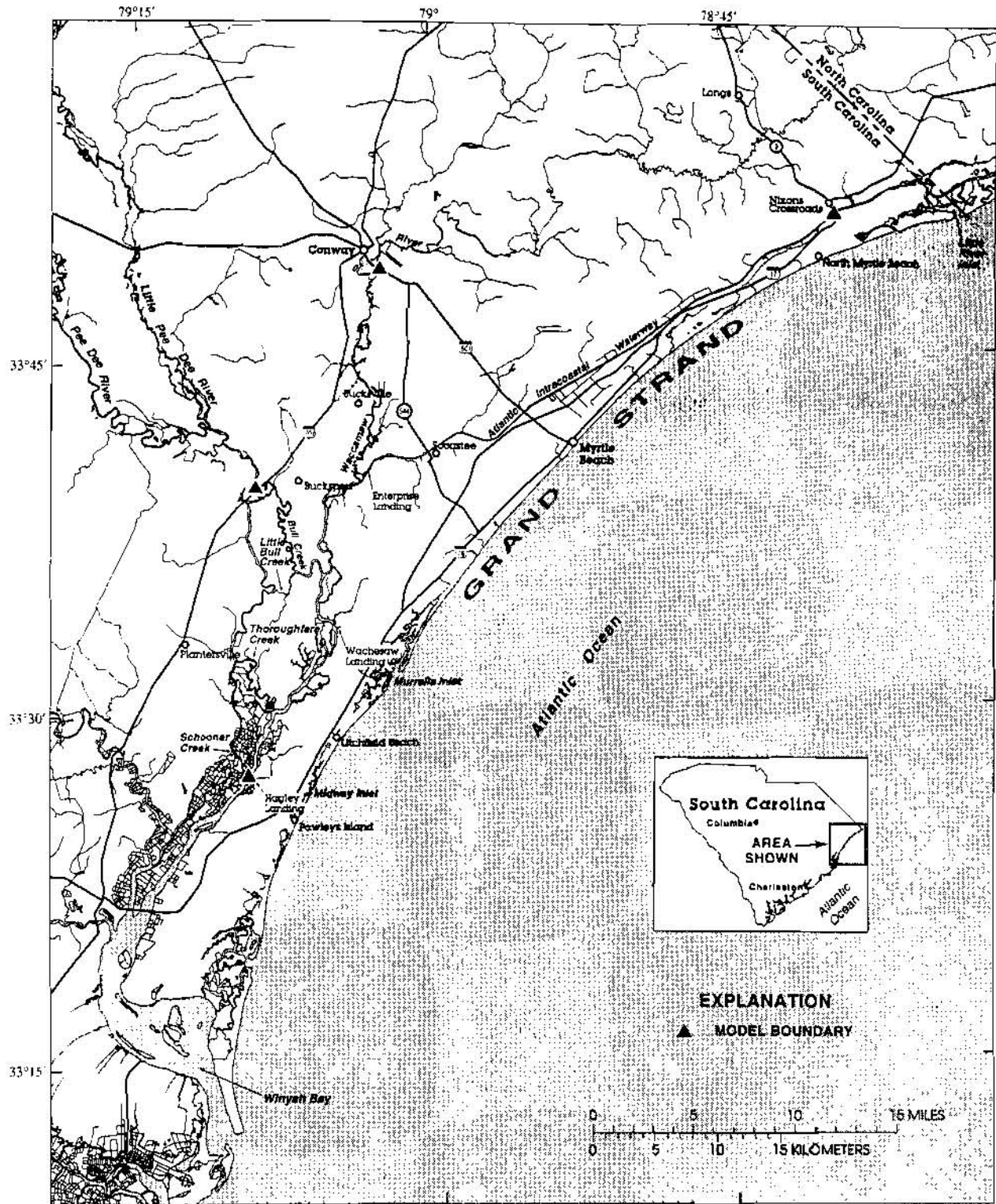


Figure 1. Location of study area and model boundaries.

$$\text{UOD} = (\text{BOD}_5 \times F_{\text{ratio}} + \text{NH}_3\text{-N} \times 4.57) \times \text{Flow} \times 8.34. \quad (1)$$

where

- UOD is the ultimate oxygen demand, in pounds per day;
- BOD₅ is the five-day carbonaceous biochemical oxygen demand, in milligram per liter;
- F_{ratio} is the conversion factor from BOD₅ to ultimate carbonaceous biochemical oxygen demand;
- NH₃-N is the ammonia concentration, in milligrams nitrogen per liter;
- 4.57 is the stoichiometric ratio of the milligrams of oxygen consumed per milligram of ammonia-nitrogen oxidized;
- Flow is wastewater flow, in million gallons per day; and
- 8.34 is the conversion factor to pounds per day.

The U.S. Geological Survey (USGS), in cooperation with the Waccamaw Regional Planning and Development Council, applied the one-dimensional dynamic flow model BRANCH (Schaffranek and others, 1981) and the dynamic mass transport and water-quality model Branched Lagrangian Transport Model (BLTM) (Jobson and Schoelhamer, 1987, Jobson 1997) to the Waccamaw River, Pee Dee River, Bull Creek, and Atlantic Intracoastal Waterway. Results from the model were used to determine the assimilative capacity for a range of streamflows of four reaches within the Grand Strand (Drewes and Conrads, 1995). Results from these models indicated that the assimilative capacity is dependent upon the flow conditions selected, the allowable dissolved-oxygen concentration decrease, and the averaging interval used in assessing the point-one rule.

The coastal waters of the Grand Strand experience forcing functions of various tidal frequencies: tidal days of 24.42 hours, spring/neap cycles of 14 days, and lunar cycles of 28 days. The state water-quality standard does not specify the appropriate averaging interval to use for interpretation of simulation model output. The U.S. Environmental Protection Agency has used 1-day, 7-day, and 30-day averaging intervals in developing national water-quality criteria (U.S. Environmental Protection Agency, 1986). There has been interest from various parties involved in the permitting process of these coastal waters that an averaging interval longer than 24-hours be used in determining the assimilative capacity for a tidal system due to the longer frequencies of the dominant driving forces of tidal waters. The purpose of this paper is to document the effects of averaging interval of modeling results on the determination of assimilative capacity in the AIW and Waccamaw River.

DESCRIPTION OF STUDY AREA

The Pee Dee River Basin, approximately 13,000 square miles (mi²), and the Waccamaw River Basin, approximately 1,300 mi², supply freshwater inflow to the Grand Strand. The Pee Dee River branches into three smaller creeks as it flows towards Winyah Bay. The first branch (south of the U.S. Highway 701 bridge) forms Bull Creek, the second branch forms Thoroughfare Creek, and the third branch forms Schooner Creek. The three creeks eventually flow into the Waccamaw River, and the net flow from these creeks is to the south through Winyah Bay. The Waccamaw River originates in North Carolina and enters the AIW about 10 miles north of the mouth of Bull Creek. Prior to the 1930's, the Waccamaw River flowed to the south towards Winyah Bay. In the 1930's the U.S. Army Corps of Engineers constructed a canal to form the AIW from Enterprise Landing to the Little River Inlet. After the construction of the canal, the flow of the Waccamaw River to the confluence with the AIW is north towards Little River Inlet.

The majority of the freshwater flow to the segment of Waccamaw River south of its junction with the AIW is from the Pee Dee River Basin and is carried by Bull Creek. The annual average streamflow from the Pee Dee Basin is about 14,100 ft³/s (cubic feet per second), which is the combined streamflow of the three major rivers (Pee Dee, Little Pee Dee, and Lynches Rivers) (Carswell and others, 1988). The Pee Dee River (below the confluence with the Little Pee Dee River), Bull Creek, and Thoroughfare Creek are tidally affected during low and medium streamflows. The annual average streamflow of the Waccamaw River at Longs, S.C., is 1,220 ft³/s, net flow of the AIW at the confluence with the Waccamaw River is north towards Little River Inlet from the Waccamaw River (Carswell and others, 1988).

Saltwater enters the system through Winyah Bay to the south and Little River Inlet to the north. The AIW is affected by semidiurnal tides throughout the entire reach with a mean tide-range of 4.0 ft (feet) at Nixons Crossroads and 3.5 ft at Hagley Landing (National Oceanic and Atmospheric Administration, 1995). The Pee Dee and Waccamaw Rivers are tidally affected during low and medium streamflows downstream of the U.S. Highway 701 bridge and U.S. Highway 501 bridge, respectively. The simulated streamflow for the Waccamaw River near Wachesaw Landing for July 1990 (fig. 2a) shows peak ebb flows are between 11,000 and 15,000 ft³/s, whereas peak flood flows are more variable and are between 5,000 and 15,000 ft³/s. The simulated streamflow for the AIW near S.C. Highway 544 for July 1990 (fig. 2b) shows peak ebb flows are between 1,800 and 2,800 ft³/s, whereas peak flood flows are more variable and are between 1,000 and 2,500 ft³/s.

METHODS

The BRANCH and BLTM models were used to simulate the streamflow and water-quality for the low-flow period of July 1990. For the purposes of this analysis, only two point-source discharges were included in the model; one on the Waccamaw River near Wachesaw Landing and the other on the Atlantic Intracoastal Waterway near S.C. Highway 544. The hydraulic data for the BLTM were simulated with the BRANCH model by using measured water-levels at the model boundaries. Steady-state water-quality boundary conditions for the BLTM were determined by SCDHEC as part of the wasteload allocation process. Boundary conditions for ammonia-nitrogen, nitrate-nitrogen, and ultimate carbonaceous biochemical oxygen demand represented the 95th percentile of the monthly monitoring data for SCDHEC stations near the model boundaries for the period 1980-1994. Boundary conditions for temperature and dissolved-

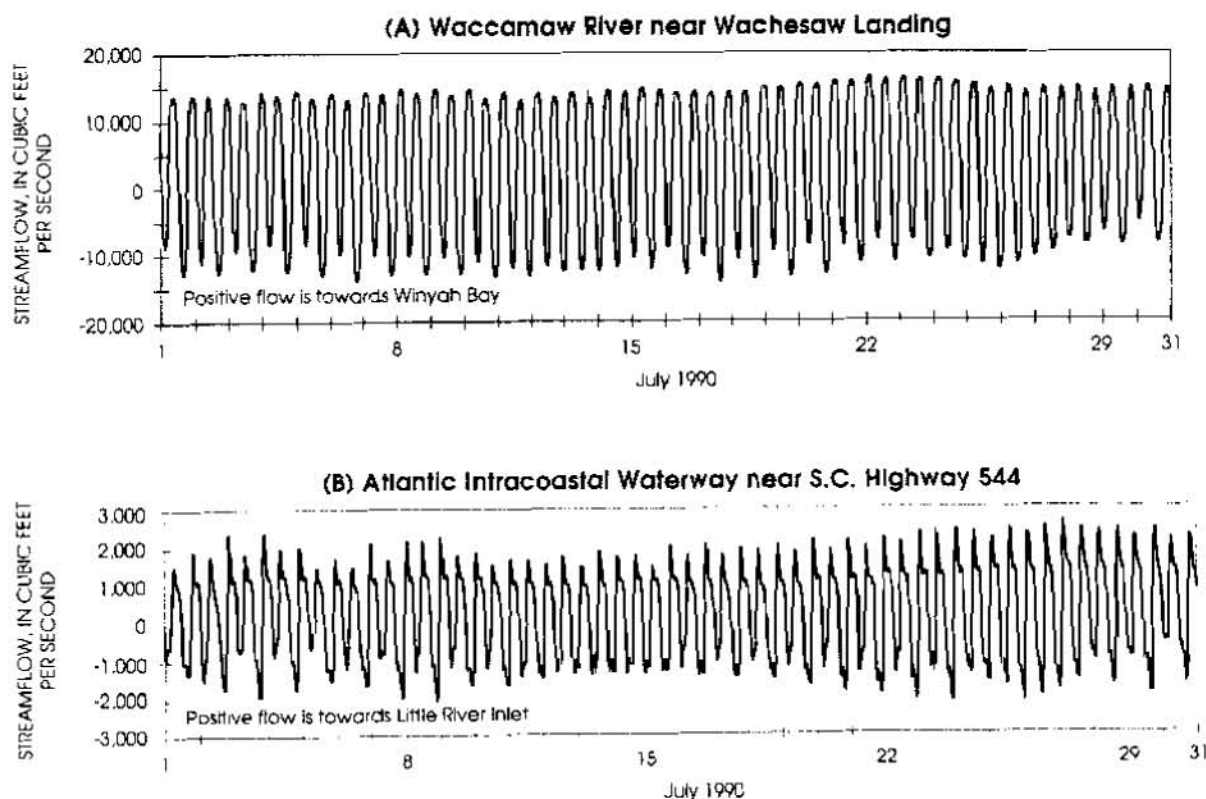


Figure 2. Simulated streamflow hydrographs for two locations on the Grand Strand, S.C., July 1990.

oxygen concentration represent the 95th and 5th percentiles, respectively, of the daily mean values from the USGS continuous monitors at the boundaries for the period 1990-1994.

Various point-source loading conditions are compared with a condition where there is no point-source discharge into the system, described to be a "no load" condition. The effects of the point-source loading conditions can be evaluated by comparing the differences in the dissolved-oxygen concentration for simulation. The model is used to compare relative differences between various point-source loading conditions rather than to predict the absolute dissolved-oxygen concentration of the system under a particular point-source loading condition. The modeled absolute value could be in error, but relative differences in the simulated results are more likely to be accurate.

A "no load" condition was simulated by omitting the point-source loadings. Simulations were made for the "load" condition. Point-source loadings (15 milligrams per liter [mg/L] ultimate carbonaceous oxygen demand, 1 mg/L ammonia-nitrogen, and 6 mg/L dissolved oxygen) were input to the system at the two discharge locations. The dissolved-oxygen concentration minimum (dissolved-oxygen sag) was located downstream of the discharge location. Model simulations were compared with the no-load simulation. For each averaging interval, point-source discharges were increased until the State dissolved-oxygen standard was violated. The UOD was determined for each averaging interval and loading condition (equation 1).

RESULTS

The simulated dissolved-oxygen concentrations for each averaging interval were evaluated to determine the extent of excursions from the no-load condition. For the Waccamaw River near Wachesaw Landing, the maximum hourly excursions from the no-load condition was 0.20 mg/L and the majority of the excursions were less than 0.1 mg/L for all the loading conditions. For the AIW at S.C. Highway 544, the maximum excursion from the no-load condition was 0.28 mg/L and majority of hourly excursions were less than 0.1 mg/L for all the loading conditions (table 1).

Table 1 Percent of hourly differences from no-load conditions for two locations on the Grand Strand.
[Mgal/d, million gallons per day; lbs/d, pounds per day; mg/L, milligrams per liter]

Averaging Interval	Effluent discharge ¹ (Mgal/d)	Ultimate Oxygen Demand (lbs/d)	Maximum difference from no-load condition (mg/L)	Percentage less than or equal 0.1 mg/L	Percentage between 0.1 and 0.2 mg/L	Percentage between 0.2 and 0.3 mg/L
<u>Waccamaw River near Wachesaw Landing</u>						
1-hr	20	4,030	0.10	100.0	0.0	0.0
24-hour	25	5,030	0.12	99.0	1.0	0.0
7-day	32.5	6,540	0.15	84.6	15.4	0.0
14-day	35	7,050	0.16	76.4	23.6	0.0
30-day	45	9,060	0.20	56.0	44.0	0.0
<u>Atlantic Intracoastal Waterway near S.C. Highway 544</u>						
1-hr	0.625	102	0.10	100	0	0
24-hour	0.75	122	0.13	97.4	2.6	0
7-day	1.25	204	0.20	79.0	21.0	0
14-day	1.5	245	0.24	73.9	23.8	2.3
30-day	1.75	286	0.28	59.5	37.6	2.9

¹ Effluent discharge at which the state dissolved-oxygen water quality standard was violated.

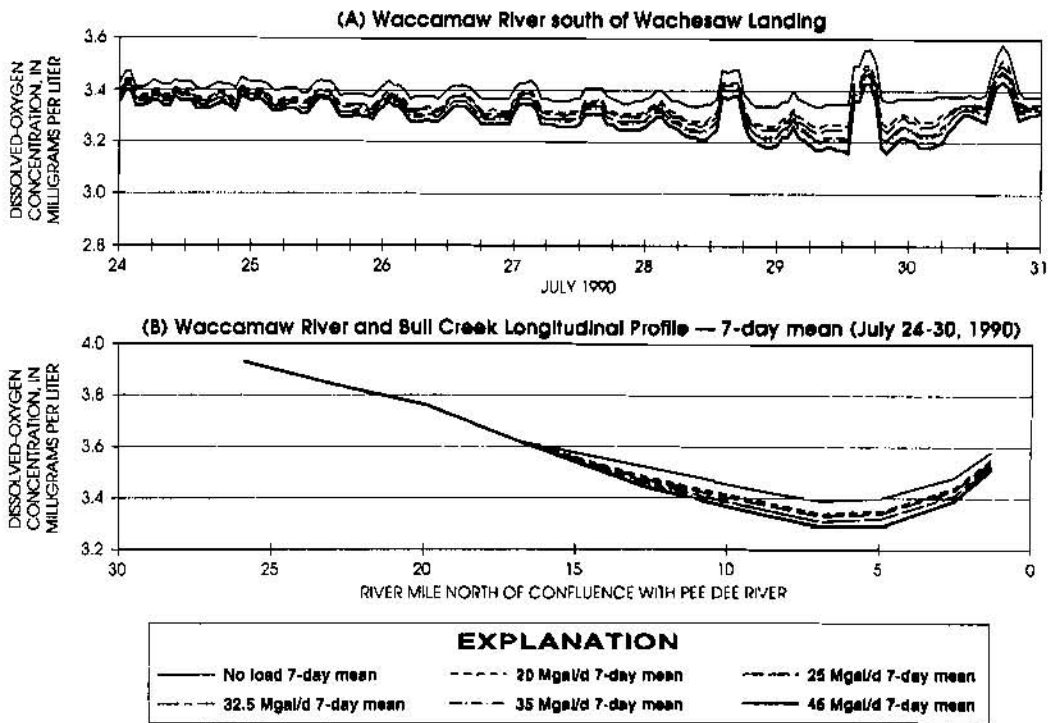


Figure 3. (A) Simulated dissolved-oxygen concentration for six loading conditions for the Waccamaw River south of Wachesaw Landing, July 24-30, 1990. (B) Longitudinal 7-day mean dissolved-oxygen concentration profile for the reach of the Waccamaw River and Bull Creek near Wachesaw Landing.

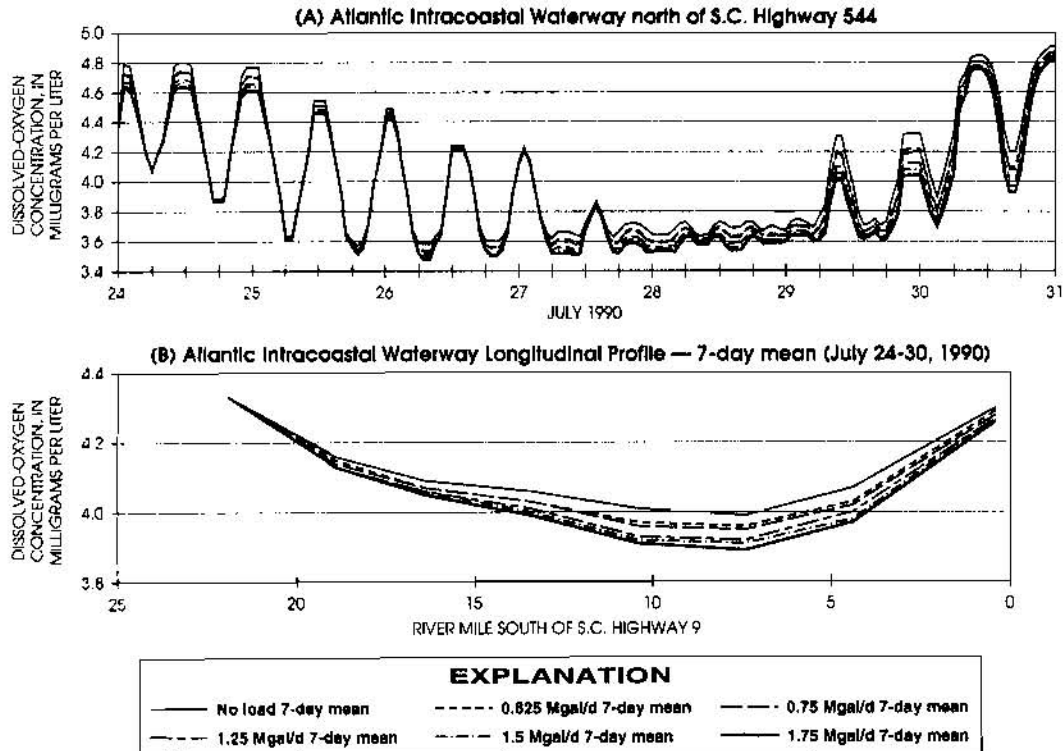


Figure 4. (A) Simulated dissolved-oxygen concentration for six loading conditions for the Atlantic Intracoastal Waterway north of S.C. Highway 544, July 24-30, 1990. (B) Longitudinal 7-day mean dissolved oxygen concentration profile for the reach of the Atlantic Intracoastal Waterway near S.C. Highway 544.

A time series of 7 days of the July 1990 simulation at the location of the sag downstream from Wachesaw Landing on the Waccamaw River (fig. 3a) shows that the loading to the system decreased the dissolved-oxygen concentration over the duration of the simulation, with the greatest excursion occurring on July 28 and 29. Loadings affect the dissolved-oxygen profile for approximately 18 miles for the Waccamaw River and Bull Creek reach (fig. 3b). A maximum 7-day mean difference of 0.11 mg/L from the no-load condition which occurred 4.9 miles upstream of the confluence of the Waccamaw River and the Pee Dee River.

The time series of dissolved-oxygen concentration for the AIW site north of S.C. Highway 544 (fig. 4a) show that the increased loading to the waterway had noticeably different effects there than at the site on the Waccamaw River. Rather than decreasing the dissolved-oxygen concentration for the entire simulation, significant differences occur at the peaks and troughs of the dissolved-oxygen concentration oscillations. Smaller differences occur on the rising and falling portions of the oscillation. The increased loading had an effect on the dissolved-oxygen profile for approximately 20 miles (fig 4b), with a maximum 7-day mean difference of 0.07 mg/L occurring 13.4 miles south of the S.C. Highway 544 bridge.

For the Waccamaw River near Wachesaw Landing, point-source loadings can increase by 125 percent with a maximum difference in dissolved-oxygen concentration from the no-load condition of 0.20 mg/L, or 5.9 percent of a 7-day mean dissolved-oxygen concentration of 3.4 mg/L (table 1, fig. 3b). For the AIW near S.C. Highway 544, point-source loadings can increase by 180 percent with a maximum difference in the dissolved-oxygen concentration of 0.28 mg/L, or 7.0 percent of a 7-day mean dissolved-oxygen concentration of 4.0 mg/L (table 1, fig. 3b).

DISCUSSION AND CONCLUSION

The ultimate goal of determining the assimilative capacity for wasteload allocations for a receiving stream is to protect the designated uses of the system. Water-resource managers must decide the allowable exposure from impacted waters that the aquatic community can accommodate and still be healthy. For two locations on the Grand Strand, the use of different averaging intervals resulted in increased loading by 125 percent for the Waccamaw River near Wachesaw Landing while having a maximum impact on the dissolved-oxygen concentration of 5.9 percent from the "natural" or no-load condition for the July 1990 simulation. For the AIW near S.C. Highway 544, the loading can increase by 180 percent, with a maximum impact of 7.0 percent on the no-load dissolved-oxygen concentrations by use of different averaging intervals. Water-resource managers must decide the excursion from a natural condition that is acceptable while balancing the environmental and economic consequences of the permitting point-source discharges. As the demographic and economic pressures on coastal areas continues to grow, there is a need to develop a more comprehensive procedure for determining wasteload allocations and total maximum daily loads for tidal waters to ensure integrity of the aquatic community.

REFERENCES

- Carswell, W.J., Sanders, C.L., and Johnson, D.M., 1988, Freshwater supply potential of the Atlantic Intracoastal Waterway near Myrtle Beach, South Carolina: U.S. Geological Survey Water-Resources Investigations Report 88-4066, 45 p.
- Drewes, P.A., and Conrads, P.A., 1995, Assimilative capacity of the Waccamaw River and the Atlantic Intracoastal Waterway near Myrtle Beach, South Carolina, 1989-92: U.S. Geological Survey Water-Resources Investigations Report 95-4111, 58 p.
- Jobson, H.E., 1997, Enhancements to the Branched Lagrangian Transport Modeling System: U.S. Geological Survey Water-Resources Investigation Report 97-4050, 56 p.
- Jobson, H.E., and Schoelhamer, D.H., 1987, Users manual for a Branched Lagrangian Transport Model: U.S. Geological Survey Water-Resources Investigation Report 87-4163, 73 p.

National Oceanic and Atmospheric Administration, 1995, Tide tables 1995, high and low predictions - East Coast of North and South America, Including Greenland: U.S. Department of Commerce, National Ocean Service, 301 p

Schaffranek, R.W., Baltzer, R.A. and Goldberg, D.E., 1981, A model for simulation of flow in singular and interconnected channels: U.S. Geological Survey Techniques of Water-Resource Investigation, book 7, chap. C3, 100 p.

South Carolina Department of Health and Environmental Control, 1991, Agreement on the development of wasteload allocations/total maximum daily loads and NPDES permit limitations, 43 p.

---- 1993, Water classifications and standards (Reg. 61-68) and classified waters (Reg. 61-69) for the State of South Carolina, 36 p.

U.S. Environmental Protection Agency, 1986, Ambient Water Quality Criteria for Dissolved Oxygen, pg. 33-36.

ENVIRONMENTAL ASSESSMENT OF THE BARIGÜI RIVER WATERSHED

By M. Dziejcz, Environmental Engineer; C. Fernandes, Professor; H. Fill, Director; M. Tozzi, Adjunct Director, CEHPAR (UFPR/COPEL), Curitiba, Paraná, Brazil

Abstract: The environmental assessment of the Barigüi river watershed, with preliminary results reported herein, represents a pioneering effort in Brazilian engineering teaching and research which aims to define tools for quantifying water pollution.

INTRODUCTION

Curitiba, capital of the Brazilian southern state of Paraná, has been touted worldwide as an "ecological" city, as well as one of the few large cities in Brazil in which it is relatively safe to live. All this publicity has caused the urban area to experience extraordinary growth in the past few years, a phenomenon which was clearly unplanned, and which has taken a noticeable toll on the quality of superficial waters.

The "Universidade Federal do Paraná", in the scope of a federal program for the improvement of engineering teaching, has undertaken the task of conducting the environmental assessment of the Barigüi river, one of the main rivers in the metropolitan region of Curitiba.

The initial stages of the work described herein involved the identification of the main sources of pollution, the selection of sites for the automated monitoring of hydrological and water quality data, viz. water level, air and water temperature, precipitation, concentration of dissolved oxygen, and conductivity. Periodical field activities were carried out for the measurement of flow rate and collection of water samples for *in situ* (DO, pH, and temperature) and laboratory analyses (BOD₅, total nitrogen, total phosphorus, suspended solids, coliforms). Field data were employed to calibrate EPA's QUAL2E computer model, which was used to help identify problems and simulate possible solutions.

In the beginning, when little field data were available, QUAL2E's simulation results were already important in the sense that they allowed the qualitative determination of the most important sources of pollution in the watershed, viz. raw domestic sewage, thereby pointing to the initial steps that have to be taken to improve the quality of water in the Barigüi river. The main outcome of the present study, regarding water quality in the river, shall be a recommendation of possible environmental recovery actions with their respective technical and financial feasibility analyses, and a definition of mechanisms for the management of the water resources.

A hydrological study of the watershed is also being carried out in order to determine the unit hydrograph, the precipitation-flow rate relationship, and to produce a flood prediction model which generates flood maps and can be used for planning flood prevention and site evacuation.

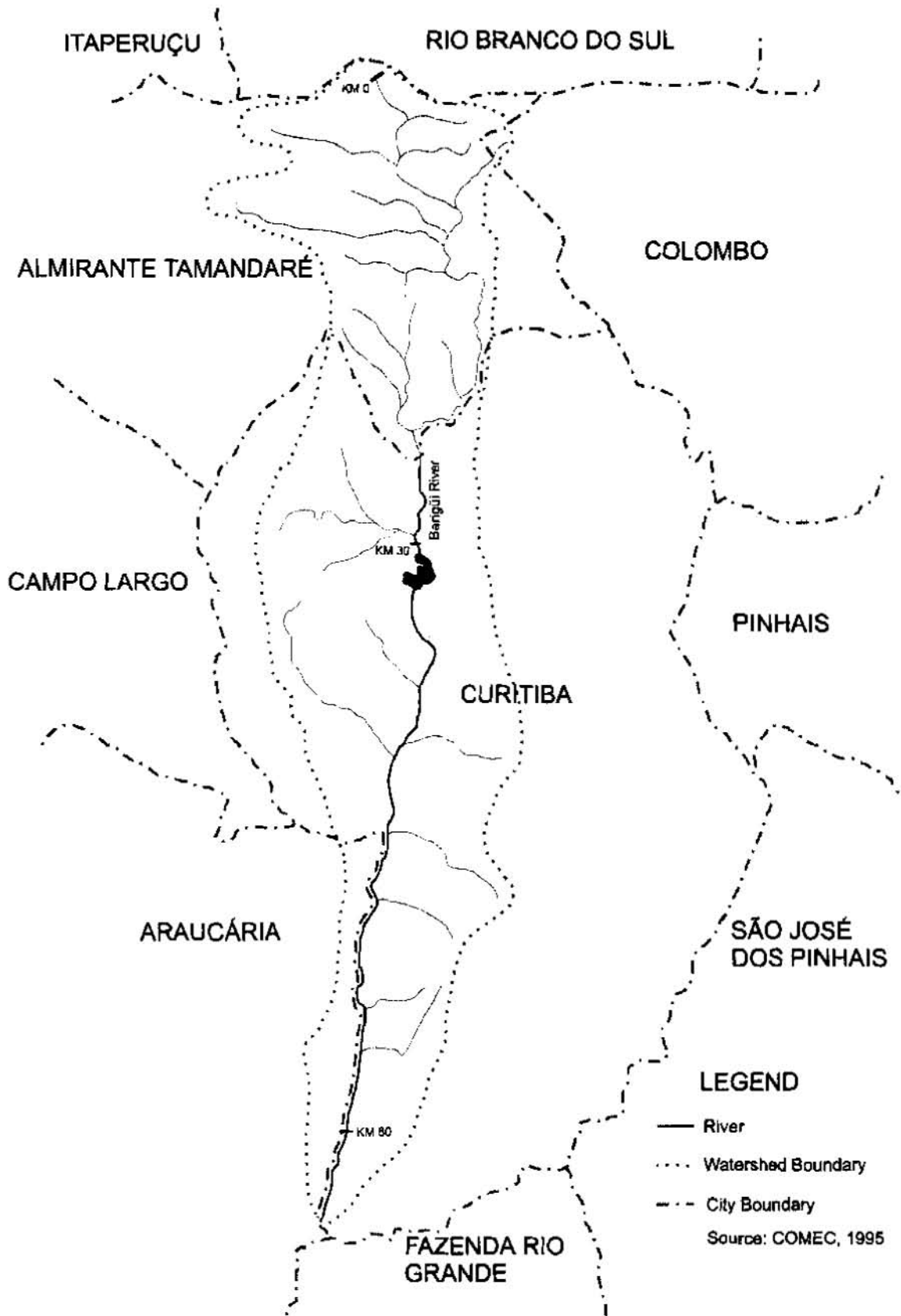


Figure 1 - The Barigüi river watershed.

RESIDENTIAL AND INDUSTRIAL ORGANIC SOURCES

The Barigüi river, as indicated in figure 1, flows south, discharging into the Iguaçú river (not shown). Its watershed encompasses 280 km², and is divided into three components, viz., rural, urban, and industrial, with the main canal being 66 km long. Data supplied by SANEPAR (Paraná's water utility company) show that, in 1991, 39% of the watershed population had its wastewater collected and partially treated by 35 FBAR (Fluidized Bed Anaerobic Reactor) units. Table 1 shows the predicted population growth, which underlines the need for planning in order to ensure the recovery and maintenance of water resources. Regarding land use, approximately 50% corresponds to urban areas, 16% to agricultural areas, there being about 193 industrial and commercial establishments in the watershed.

Year	Population	Collection (%)
1991	451,563	39
1995	576,845	65
2000	683,631	81
2005	769,667	84
2010	865,458	85
2015	963,710	85
2020	1,064,718	86
Saturation	2,894,207	89

Table 1 - Estimated population growth and wastewater collection/treatment in the watershed.

The first modelling task consisted of simulating dissolved oxygen (DO) and biochemical oxygen demand (BOD) concentrations along the Barigüi river with the aid of EPA's QUAL2E computer program. To that end, residential and industrial point sources were catalogued and the associated loads estimated. Lack of field data for the residential organic loads led to the adoption of average values *per capita*, viz., 54 g BOD/person/day, 9.8 g total nitrogen/person/day, 4×10^{11} coliforms/person/day, 2.7 g total phosphorus/person/day, and 54 g suspended solids/person/day. Thus, the population distribution in the watershed was determined and the associated loads estimated together with their discharge points in the riparian system.

Industrial activities in the Barigüi river watershed are fairly diversified, since it includes Curitiba's Industrial District, where a large number of galvanization and metal treatment industries are located. The main sources of pollution, however, are two paper mills, which account for almost 80 % of the total organic load in the watershed. Previous studies indicate that 23 industries in the watershed produce organic residues, with the associated load being in excess of 5300 kg BOD₅/day, while 22 industries dispose of heavy metals in the river (Fernandes et al., 1997).

Regarding agricultural-related pollution, a simplified analysis indicates that, while significant concentrations of pesticides are not suggested, it is certainly necessary to define eventually a monitoring policy.

RESULTS

The DO and BOD concentrations obtained are based on flow rates associated with a 30-day drought having a 5-year return period, $Q_{5,30}$ (Krüger, 1993), and the population of the year 1995. Since the industrial organic pollution data are far from complete, three types of simulation were carried out, considering, respectively, existing data, an increment of 50 % over the existing data, and an increment of 100 % over the existing data. During the initial stages of the project resources were very scarce, and field data difficult to obtain. Therefore, it is important to stress the qualitative nature of the results reported herein, which, nevertheless, are still important because they identify the main sources of pollution in the watershed.

Simulation results, considering only industrial sources, are presented in figures 2 and 3, for concentrations of DO and BOD, respectively, while figures 4 and 5 show a comparison of the effects of residential and industrial pollution. The horizontal lines depicted in these figures correspond to classes defined in Brazilian legislation (the lower the class number, the better the quality of the water). The classification is based upon the concentration of substances found in fresh waters and is used to indicate their possible use and necessary treatment.

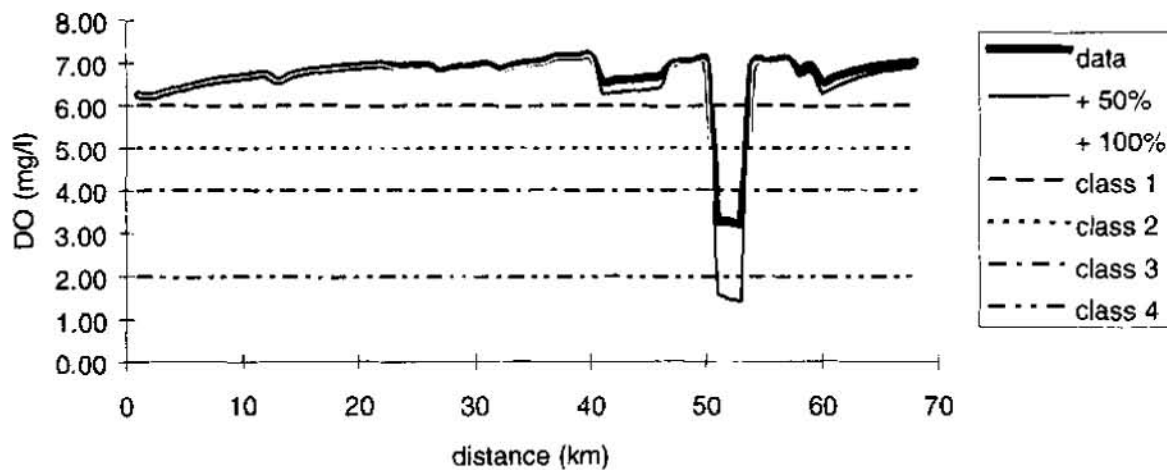


Figure 2 - DO concentration considering only industrial pollution.

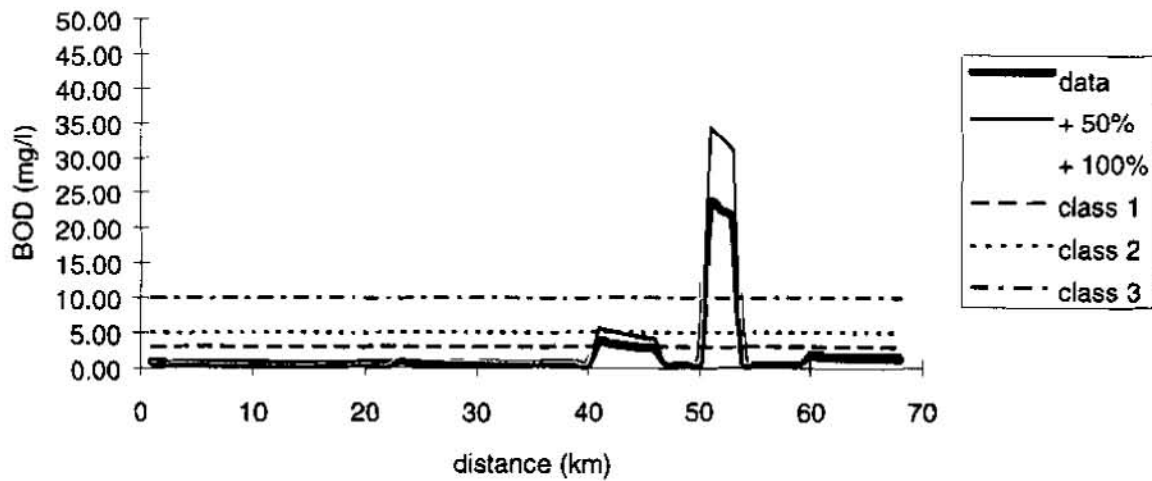


Figure 3 - BOD concentration considering only industrial pollution.

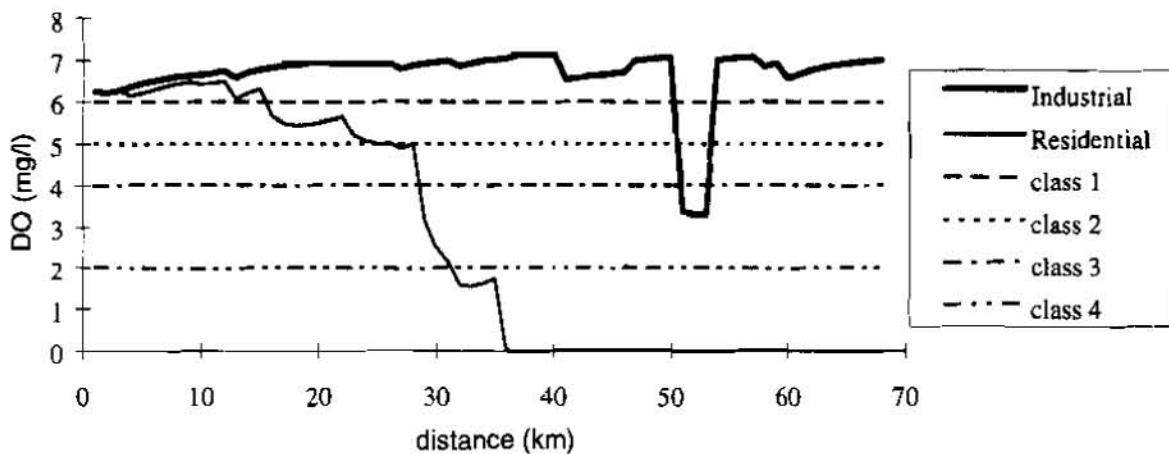


Figure 4 - Comparison of DO concentrations for industrial and residential pollution.

From figures 2 and 3, it is possible to conclude that the main impact of industrial pollution occurs between kilometers 40 and 60, being critical around kilometer 50. This corresponds to the location of Curitiba's industrial district and confirms the need for increased monitoring of effluents and improved treatment by the industries. On the other hand, figures 4 and 5 show that residential wastewater has a much bigger impact on water quality than the industries, and, therefore, increased wastewater collection and treatment should be a priority in the watershed.

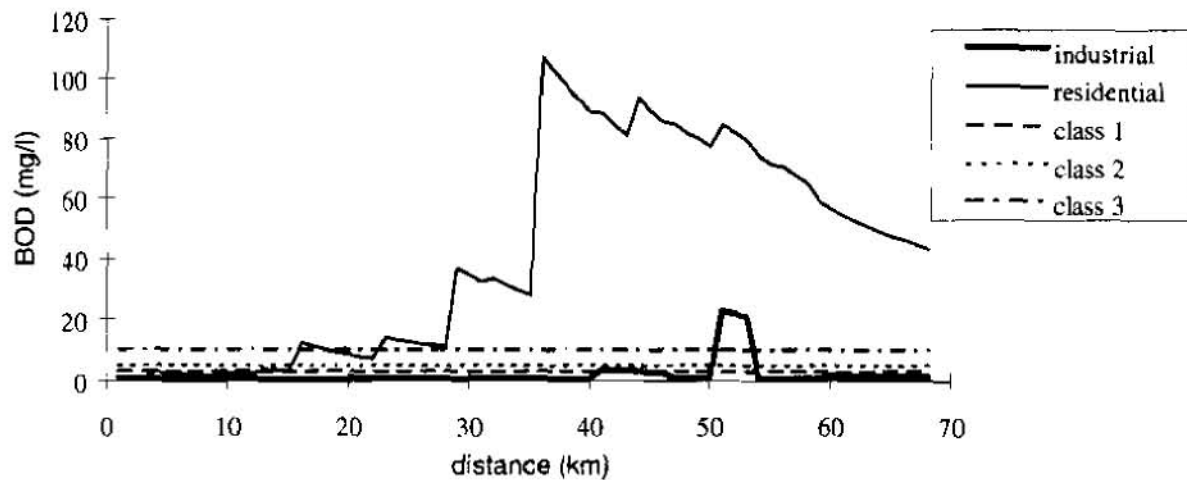


Figure 5 - Comparison of BOD concentrations for industrial and residential pollution.

FUTURE WORK

Despite lacking accuracy due to the scarcity of data, the results obtained are important to identify the main sources of pollution in the Barigüi watershed. Based on the information uncovered in the early stages of the project, an additional grant was approved which will warrant the continuity of the work, allowing to gain further much needed field data, and to purchase crucial equipment, such as automatic hydrologic and water quality monitoring stations.

REFERENCES

- FERNANDES, C.S., (Coord.), CARVALHO, M.C.F., RAMALHO, C, 1997. Diagnóstico ambiental da bacia do rio Barigüi. Curitiba; UFPR. 148p.
- KRÜGER, C. M., 1993. Projeto HG-77 - Regionalização de vazões em pequenas bacias hidrográficas do estado do Paraná, Relatório número 2 - Métodos de Regionalização, Centro de Hidráulica e Hidrologia Professor Parigot de Souza-CEHPAR.

Acknowledgements: The authors wish to thank the students involved in the work reported herein, Cristiane Ramalho and Maria C. F. Carvalho, and Professor Hans J. Leutheusser, of the University of Toronto, for proof-reading the original manuscript, and making valuable suggestions, during his stay at CEHPAR as a visiting professor.

The environmental assessment of the Barigüi river watershed is a joint effort of researchers and students of Universidade Federal do Paraná, municipal authorities of the Sanitation Secretariat,

and the state's electrical utility company COPEL, being supported by a grant from the Brazilian Federal Agency FINEP, in the context of a federal plan (REENGE) which aims to improve engineering teaching in Brazil.

Centro de Hidráulica e Hidrologia Prof. Parigot de Souza
Curitiba - Paraná - Brazil
C.P. 1309
80001-970
tel. +55 41 366-2020 x. 6313 fax +55 41 266-2935
dziedzic@cch.copel.br

WATER QUALITY SIMULATION IN THE CAZONES RIVER, MEXICO

By J. Izurieta D., A. Ruiz L., Ma. A. Gómez B., P. Saldaña F., L. Márquez B. A. Lerdo de T. and R. López.
Instituto Mexicano de Tecnología del Agua.- Jiutepec. Morelos, México.

Abstract : The Mexican Institute of Water Technology (IMTA) carried out an assessment of industrial and municipal discharges to the Cazonos River. in 1996. The main objective of this study was to quantify the reduction of pollutants in discharges to meet the new water standard, NOM-001-ECOL/96, and recommend treatments that could permit compliance with the standards foreseen for 2010.

The model, QUAL2E, of the Environmental Protection Agency (EPA), version 3.20 and 3.21 (for Windows™), was used to reproduce the physical and chemical processes in the river. Version 3.21 analyzes the alternatives more quickly. This model simulates stream water quality and the effect of one or several discharges on the river.

Simulated parameters included dissolved oxygen, biochemical oxygen demand, total nitrogen (nitrites, nitrates, N-organic and N-ammonia), fecal coliforms and total suspended solids. The model was calibrated with field and laboratory data determined from samples taken from April 27 to May 10, 1996.

Discharge concentrations, and dilution and assimilation capacities were simulated for all river segments. In general, the Cazonos River is capable of assimilating the discharges and maintaining a DO concentration higher than that set in the new regulation applicable to the year 2010.

A critical condition was projected for the area where the Salsipuedes Creek joins the Cazonos River. The Salsipuedes Creek carries high loads of municipal sewage and some industrial discharges from Poza Rica and the neighboring industrial complex.

INTRODUCTION

Many basins in Mexico receive wastewater from industries, agriculture and municipalities. Traditionally, receiving waters have been considered ecosystems with physical, chemical and biological mechanisms capable of diluting and assimilating wastes. High pollutant concentrations can surpass these mechanisms and provoke environmental degradation.

Current strategies for integrated river basin management involve the classification of the river according to its quality and uses, and then the specification of water quality standards for discharges.

Classification studies estimate the capacity of the receiving waters to dilute and assimilate wastes and predict critical organic loads. They also indicate point sources that should be controlled and levels of treatment. Within an integral planning strategy, these studies serve to establish quality goals that balance water uses and economic development without affecting environmental and social benefits.

The main objectives of this work were:

1. Determine assimilative capability of the Cazonos River in relation to its current uses and water quality.
2. Establish present and future admissible maximum organic loads in discharges to set water quality goals.
3. Provide data to monitor and establish discharge conditions for industries and municipal sewer systems in the basin.

STUDY AREA

The Cazonos River basin is located on the Gulf of Mexico coastal plain, on the border between states of Veracruz and Tamaulipas. Its total surface is 2,688 km², with an average annual volume of 1,354,000,000 m³. The average flow is 43 m³/s (17 year average). The river flows from an altitude of 350 masl to sea level. The average annual rainfall in Poza

Rica is 1,150 mm and the average annual temperature is 24.3 °C. The Cazones River has several tributaries near Poza Rica: the Cocinero, Salsipuedes, Totolapa and Acuatempa Creeks.

Water quality studies, carried out in 1973, identified suspended solids, grease and oils, and sulfates in high concentration as the main pollutants in water, and hydrocarbons and heavy metals in sediments. The extraction of petroleum and the production of polyethylene, sulfur and gasoline are the most important industrial activities in the area.

METHODOLOGY

For modeling purposes, the Cazones River was divided into ten reaches, based on the location of affluents and discharges (Table 1). Twenty-seven monitoring stations were placed in the area, from km 135 to km 32. From this point to the Gulf of Mexico, the river is considered an estuary. The main industrial and municipal discharges are between km 76 and km 56. Samples, taken during the critical flow period from April 29 to May 9, were analyzed for more than 30 parameters. Results were compared with the official discharge standard, NOM-001-ECOL/1996. The critical parameters included dissolved oxygen, chlorides, total nitrogen and fecal coliforms. The QUAL2E UNCAS (EPA, 1996) model was used to simulate the effects of the conventional critical parameters.

First, current river conditions were predicted from field and laboratory data to calibrate the model. The critical conditions were then defined for 7d10y minimum flow.

BOD decay coefficients were calculated using the Thomas and the Moments methods with 1, 3, 5 and 7 day incubation, BOD_0 and BOD_0/BOD_5 values. Reaeration coefficients were estimated from the O'Connor and Dobbins formula.

River reaches were represented as trapezoidal sections. Observed river flows were between 0.493 and 9.49 m³/s, with depths between 0.30 and 4.0 m., and an average velocity between 0.28 and 1.06 m/s.

Table 1. Cazones River data.

Reach	Stream station	Distance (Km)	Initial flow (m ³ /s)	Tributaries and discharges	Inflow (m ³ /s)
1	I - III	135.00 - 131.75	4.313	---	---
2	III - VII	131.75 - 110.00	5.175	Tlaxcalaltongo Creek El Metate Creek	0.674 0.302
3	VII - X	110.00 - 97.50	6.151	María Andrea Creek	0.011
4	X - Before XIII	97.50 - 77.00	9.949	Buenvista Creek	0.189
5	Before XIII - XIV	77.00 - 68.50	10.138	Poza Rica (withdrawal)	- 5.148
6	XIV - XVII	68.50 - 63.25	4.990	Cocinero Creek Petrochemical (withdrawal) Thermoelectric plant (withdrawal)	0.182 - 0.763 - 0.025
				Petrochemical Bottling industry Dehydrating plant Thermoelectric	0.048 0.006 0.001 0.011
7	XVII - XVIII	63.25 - 60.25	3.186	---	---
8	XVIII - XXI	60.25 - 56.50	0.493	Salsipuedes Creek	6.253
9	XXI - XXIV	56.50 - 45.50	4.163	Totolapa Creek	0.564
10	XXIV - XXVII	45.50 - 32.00	4.864	Acuatempa Creek	0.216

RESULTS AND DISCUSSION

River segmentation is indicated in Table 1. Table 2 shows monitoring data for the river stations used in the model; Table 3 monitoring data for the tributaries and Table 4, for industrial and municipal discharges.

Critical conditions

Historical data from the "Poza Rica" hydrometric station, located 4.5 km upstream of the affluence of the Cocinero Creek with the Cazonas River, was used to set the critical conditions (7d10y). A flow of 4.990 m³/s was observed during field studies. From historical data for the same point, the critical flow was calculated as 1.703 m³/s. To simulate critical conditions, the river flow was adjusted with a factor of 0.341 (1.703/4.990) and the discharges held at current values.

Table 2. Water quality parameters at monitoring stations.

Stream Station	Temperature (°C)	DO saturation (mg/L)	Dissolved oxygen (mg/L)			BOD ₅ (mg/L)		
			Aver	Min	Max	Aver	Min	Max
I	25.6	8.2	8.5	6.5	9.0	1.0	0.9	3.0
II	28.8	7.9	8.6	6.6	9.0	1.0	0.6	3.0
III	28.2	7.9	8.6	6.7	9.8	1.0	0.9	2.0
IV	28.6	7.9	8.6	8.0	8.8	2.0	1.0	4.0
VII	30.5	7.7	6.6	3.5	8.4	3.0	1.0	8.0
IX	30.3	7.8	6.4	6.0	9.2	4.0	2.0	4.0
X	29.8	7.8	6.8	5.1	11.5	5.0	2.0	9.0
XII	28.7	8.0	6.3	4.6	7.2	2.5	2.0	5.0
XIII	30.1	7.9	6.3	5.3	7.1	6.5	4.0	8.0
XIV	29.2	8.0	4.9	3.4	5.4	1.0	0.9	4.0
XVI	30.0	7.9	7.1	5.4	9.3	6.0	2.0	7.0
XVII	30.8	7.8	5.8	2.7	10.1	3.0	1.0	6.0
XVIII	30.6	7.8	10.1	8.8	15.3	3.5	2.0	4.0
XX	31.4	7.8	5.6	4.8	7.8	8.0	4.0	11.0
XXI	31.5	7.8	3.5	2.7	6.0	7.0	3.0	8.0
XXIII	32.0	7.7	5.8	3.7	6.3	6.5	5.0	8.0
XXIV	28.1	8.1	6.8	5.6	12.8	4.5	3.0	6.0
XXVI	29.6	8.0	7.3	4.6	8.7	5.5	4.0	7.0
XXVII	29.4	8.0	7.9	4.0	11.2	4.5	2.0	8.0
XXVIII	30.0	8.0	6.2	5.9	12.4	5.0	4.0	7.0

Table 3. Water quality parameters at tributaries.

Stream stations	Temperature (°C)	Dissolved oxygen (mg/L)			BOD ₅ (mg/L)			Flow (m ³ /s)
		Aver	Min	Max	Aver	Min	Max	
Tlaxcalaltongo	29.0	7.1	5.9	8.5	2.0	1.0	4.0	0.674
El Metate	31.9	6.6	6.0	10.8	1.0	0.9	2.0	0.302
María Andrea	30.0	1.4	1.2	3.9	8.0	6.0	10.0	0.011

Stream stations	Temperature (°C)	Dissolved oxygen (mg/L)			BOD ₅ (mg/L)			Flow (m ³ /s)
Buenavista	30.3	5.9	6.0	9.2	3.0	2.0	4.0	0.189
Cocinero	31.0	2.7	0.8	9.9	32.0	18.0	76.0	0.182
Salsipuedes	31.7	3.8	3.0	7.1	6.5	4.0	12.0	6.253
Totolapa	30.5	4.9	3.8	11.8	6.5	5.0	9.0	0.564
Acuatempa	29.0	9.1	5.5	14.2	4.5	4.0	6.0	0.216

Table 4. Water quality monitoring data for industrial discharges from Poza Rica complex.

Discharges	Temperature (°C)	Dissolved oxygen (mg/L)			BOD ₅ (mg/L)			Flow (L/s)
		Aver	Min	Max	Aver	Min	Max	
Thermoelectric plant	29.1	5.8	4.9	8.3	23.0	1.4	90.9	6.66
Bottling plant	31.7	2.2	0.9	4.2	618.0	406.8	1869.0	0.42
Petrochemical plant	26.1	3.4	2.9	5.6	8.0	4.2	12.3	1.00
Dehydrating plant	27.5	0.7	0.2	4.8	100.5	63.3	123.6	41.84

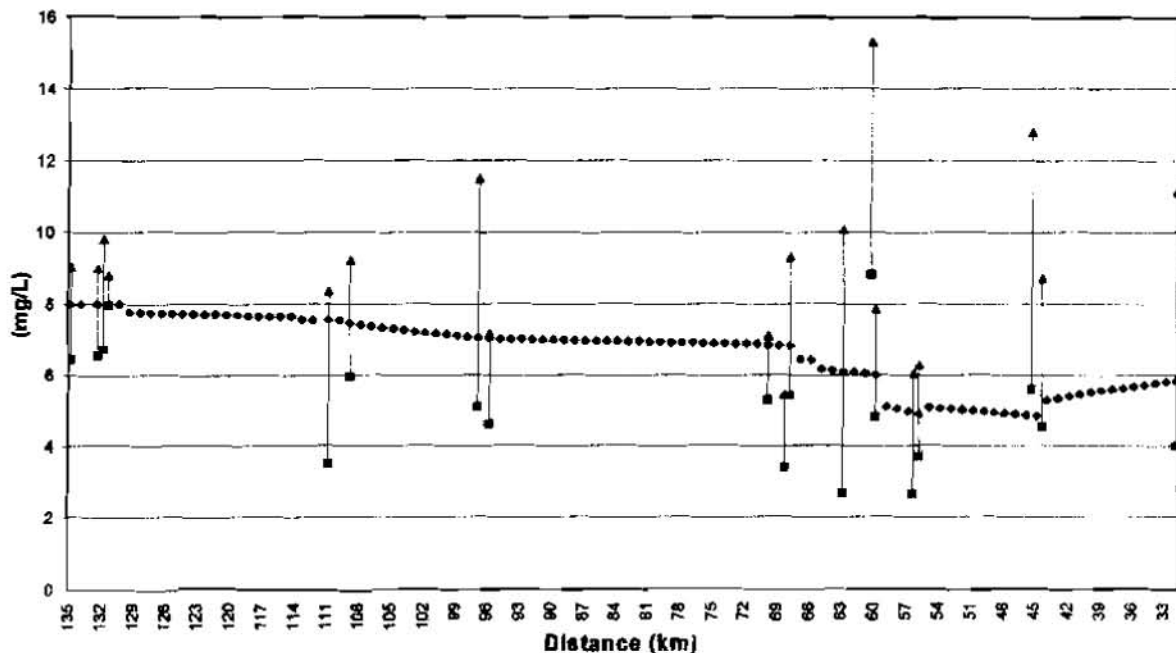


Figure 1. Critical conditions, plot for dissolved oxygen.

Under these conditions, the simulated river OD and BOD₅ behaved as shown in Figures 3 and 4. The minimum allowed OD for the Cazonos River is 5.0 mg/L upstream of km 68 and of 4 mg/L downstream of this point to km 55 where the greatest load of industrial wastes are discharged. Even under these critical conditions, the minimum OD limits can be satisfied (Figs. 1 and 2).

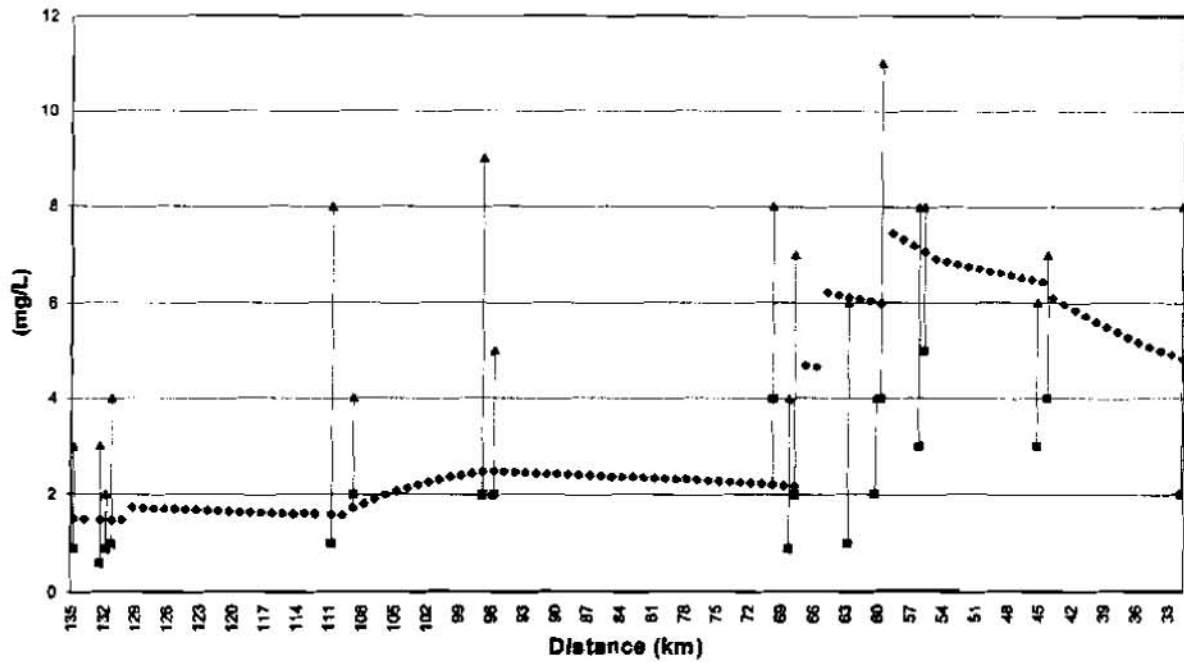


Figure 2. Critical conditions, plot for BOD₅

Assimilative capacity

The simulated assimilative capacity, when minimum acceptable OD values were 5.0 mg/L from stations I to XIV (above the affluence with the Cocinero Creek) and 4.0 mg/L from stations XIV to XXVII, is summarized in Figure 3.

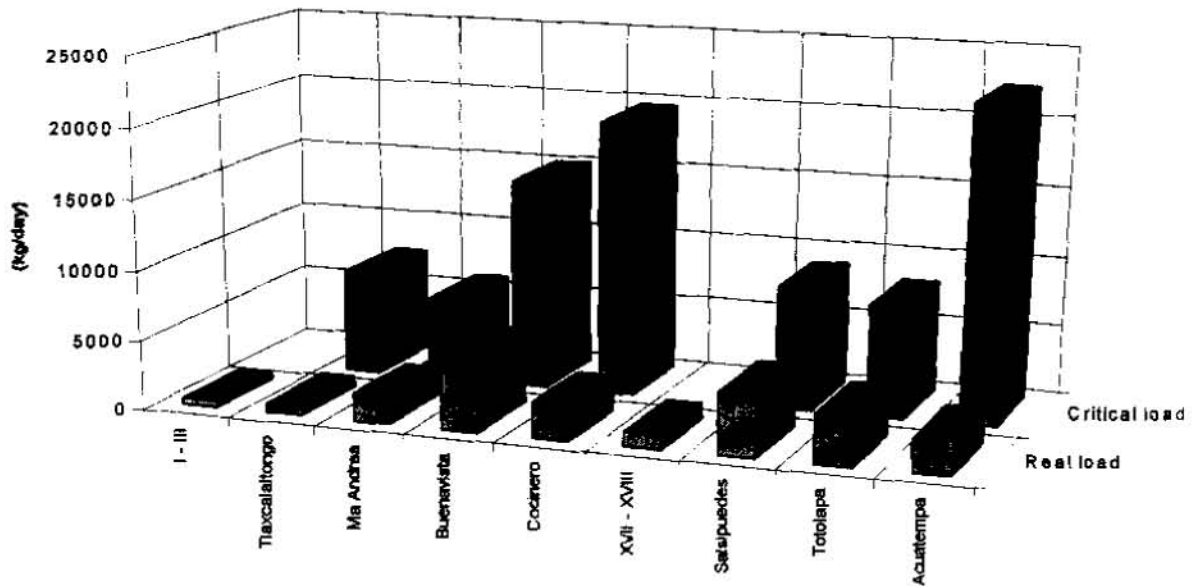


Figure 3. Real and critical transported loads.

Simulation of conventional parameters

The simulated values of key parameters were compared with the limits specified in the official standard, NOM-001-ECOL-1996. Total nitrogen, chlorides and fecal coliforms in tributaries and discharges exceeded the standards. (Tables 5 and 6).

Table 5. Average chloride and nitrogen concentrations in tributaries and discharges

Tributaries/Discharges	Chlorides (mg/L)	Ammonia (mg/L)	Total Nitrogen (mg/L)
Tlaxcalaltongo Creek	5.9	0.56	1.33
El Metate Creek	3.5	0.33	0.86
María Andrea Creek	40.1	2.99	4.82
Buenavista Creek	8.4	0.33	1.43
Cocinero Creek	69.8	2.90	6.81
Descargas (1)	13152.9	4.43	6.74
Salsipuedes Creek	208.0	2.16	3.82
Totolapa Creek	50.3	0.33	2.65
Acuatempa Creek	204.5	0.33	2.16

(1) Composite samples from petrochemical, dehydrating, thermoelectric and bottling plants.

Table 6. Fecal coliforms in tributaries and discharges

Tributaries/Discharges	Average	Minimum	Maximum
Tlaxcalaltongo	156000	6090	230000
El Metate	2900	434	18100
María Andrea	8360	1790	11000
Buenavista	320	18	41800
Cocinero	35400	5490	100000
Salsipuedes (1)	900000	730000	2500000
Totolapa	527	54	19900
Acuatempa	64	36	173
Thermoelectric plant	73800	(2)	(2)
Dehydrating plant	0	(2)	(2)
Petrochemical	0	(2)	(2)
Bottling plant	300000	(2)	(2)

(1) Poza Rica municipal discharge is included. (2) One sample was taken.

The river chloride concentration was clearly influenced by the discharges from the industrial complex in Poza Rica, the dehydrating plant and the Salsipuedes Creek. The main nitrogen sources are located on the María Andrea, Cocinero, Salsipuedes and Totolapa creeks, and within the Poza Rica industrial complex. The principal fecal coliform sources are on the Cocinero and Salsipuedes creeks, both of which receive municipal and industrial wastes. From this point downstream, high levels were observed. The limit for fecal coliforms is 2000 MPN/100 ml.

Comparative analyses of field results and model distribution curves for total nitrogen and fecal coliforms are shown in Figures 6 and 7.

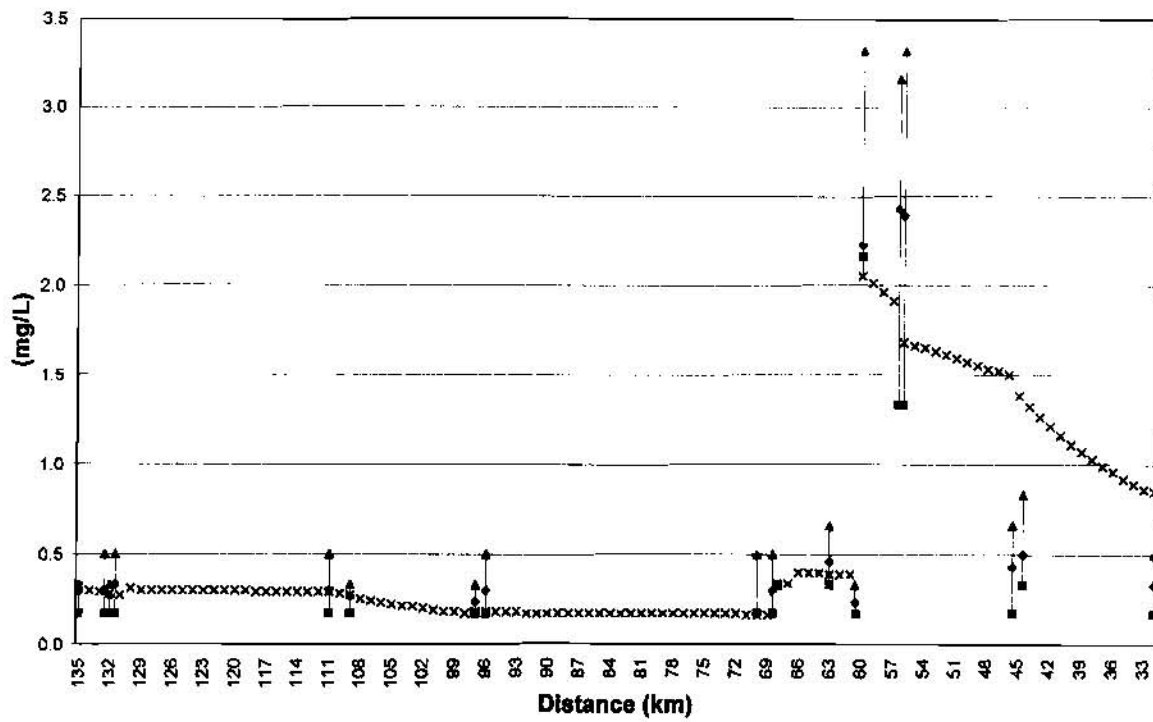


Figure 6. Calibration curve for ammonia.

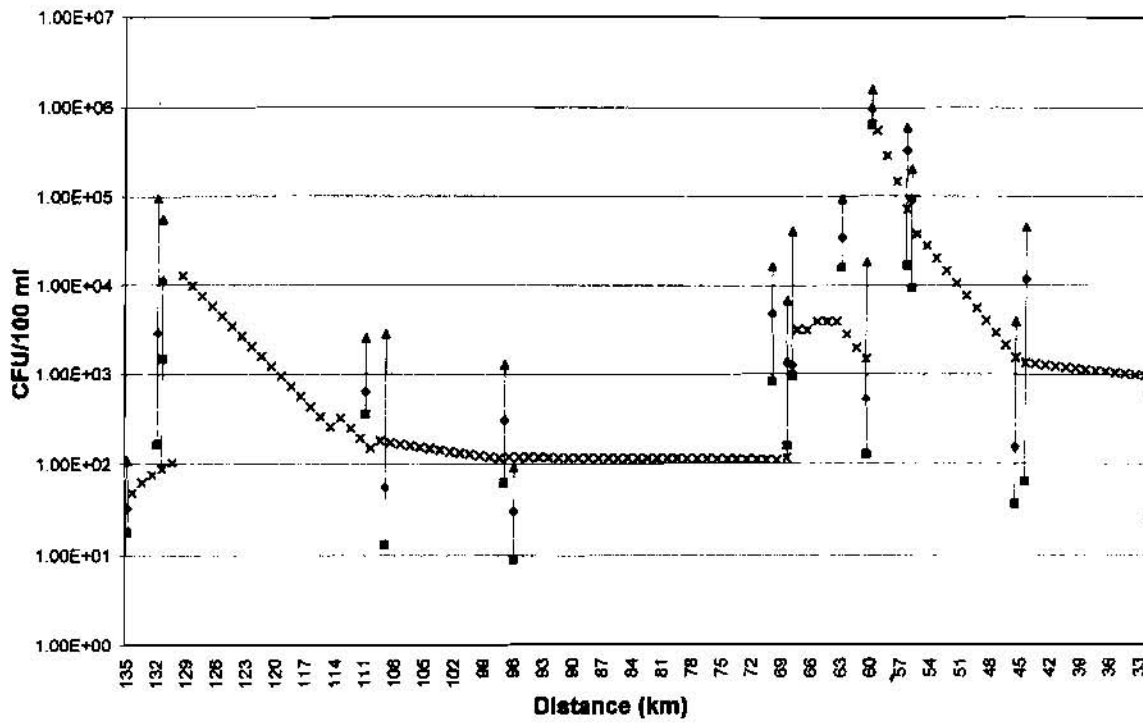


Figure 7. Calibration plot for fecal coliform.

Modeling results were used to suggest maximum levels for organic loads and other parameters for industrial and municipal discharges in the basin. In the classification statement for the Cazonos River, the proposed limits are as shown in Table 7.

Table 7 Maximum permitted limits in Cazonos River

	Limits
pH	6 to 9
Total suspended solids (mg/L)	15
BOD (mg/L)	15
Total nitrogen (mg/L)	40
Fecal coliforms MPN/100 mL	1000

The simulation of the conventional physical-chemical parameter simulations identified the Salsipuedes Creek as a major source of pollutants. From this point downstream water quality deteriorated. The Salsipuedes Creek, the largest single tributary to the Cazonos River, receives the municipal and industrial discharges from Poza Rica.

CONCLUSIONS

The water in the Cazonos River is acceptable for use as an aquatic habitat and a public water supply.

Analysis of alternatives indicates that 15 mg/L BOD₅, 40 mg/L total nitrogen and 1000 UFC/100 mL fecal coliforms are the maximum levels that may be accepted in discharges to the Cazonos River to meet the dissolved oxygen criterion of 5.0 and 4.0 mg/L in the long term (2010).

The QUAL2E system provided good simulated results for this tropical river with a moderate flow. During this study good agreement was observed between specific cases and model values.

Based on the results obtained in this study, QUAL2E was recommended for use by the National Water Commission for the classification of Mexico's rivers.

REFERENCES

EPA (Environmental Protection Agency), 1996. Exposure models library and integrated model evaluation system. Office of Research and Development. EPA7600/C-92/002. USA.

Nemerow N. L., 1991. Stream, lake, estuary and ocean pollution. Second edition. Environmental Engineering Series. Van Nostrand Reinhold. USA. 473 pp.

Comité Consultivo Nacional de Normalización para la Protección Ambiental. 1997, NOM-001-ECOL-1996.- (Lists the maximum. Diario Oficial de la Federación, January 6, 1997, 68-85 (Official Mexican standard: lists the maximum acceptable values for pollutants in waste waters discharged to water and public land)

Contact point: Instituto Mexicano de Tecnología del Agua. Subcoordinación de Impacto Ambiental. Paseo Cuauhnáhuac 8532. C.P. 62550. Col. Progreso, Jiutepec, Morelos. México. Tel. (+52)(73) 19 4000 ext 407 and 410. Fax (+52)(73) 19 4381. email : jizurieta@chac.imta.mx, email: ruizlo@letterbox.com, email: magomez@chac.imta.mx

WATER QUALITY MODELING OF MAOPINGXI POLLUTION ZONE IN THREE GORGES PROJECT CONSTRUCTION ZONE

By Mao Hongmei, Bureau of Hydrology, Changjiang Water Resources Commission, Wuhan, China; Ye Shouze, Wuhan University of Hydraulic and Electric Engineering, Wuhan, China; Ji Xuewu, Bureau of Hydrology, Changjiang Water Resources Commission, Wuhan, China.

Abstract: Simulation of the water quality of Maopingxi pollution zone, which is downstream the dam site and upstream a drinking water plant on the right bank in Three Gorges Project (TGP) construction zone, is presented in this paper. Being the biggest multipurpose water project in the world, the TGP will be constructed with a period of 17 years. According to the construction progress, water quality of Maopingxi pollution zone is modeled, so that the qualified water can be taken, and the construction can be carried out smoothly.

On the basis of flow characteristic and the polluted wastewater discharge conditions in the reach, the velocity distribution is derived through plotting flow plane chart by accumulated flow coordinate method, and the concentration distribution is obtained by a new method-Hybrid Finite Analytic Method coupled with Finite Difference Method. In accordance with river bed information and hydrological data of the reach, stream flow tubes in the reach are divided. The equation of water quality in the flow tubes is deduced, and the new method is applied to solve it. The numeric method is a combination of Hybrid Finite Analytic Method used in convection-dominated computer grid and Finite Difference Method used in diffusion-dominated computer grid. The model verification illustrated the new method can effectively simulate water quality of Maopingxi pollution zone. The modeled results show that Maopingxi pollution zone will not have great influence on water quality at the intake of the drinking water plant during the Yangtze River closure in a normal condition.

INTRODUCTION

Maopingxi is a small branch, Yangtze river at the confluence of which is located originally about 1 km upstream of Three Gorges Project dam site. After Three Gorges Project started construction, its course was diverted and the confluence is now located downstream the dam site, Sandouping, by outflow cavities. Maopingxi collect waste water from 22 paper-making factory in about 10 kilometer along the river at Chengjiaba, Wangjiaba, Jiuliping, Shixi. The sewage discharge is about 1600 thousand tons per year, where the mean annual discharge of COD is 130 ton, BOD₅, 870 ton, cyanide, 12 ton, and, alkali material, 1700 ton. A gold ore in Zigui county drains daily about 200 ton of hypertoxic sewage discharge of cyanide directly into Maopingxi. Some monitoring data have indicated that Maopingxi is a really sewage river.

With Three Gorges Project being constructed, more and more people and machine aggregated in the construction zone. According to the construction zone arrangement scheme, there will be a

drinking water plant at the right bank downstream the dam, which location is just downstream the pollution zone. This paper evaluated the influence of Maopingxi pollution zone on water quality at the intake of drinking water plant.

Maopingxi mean-annual discharge in flood period is about 3 to 4 cubic meter per second, yet the total amount of pollutant is very large, therefore in this paper the confluence of Maopingxi is simple regarded as a point pollution source. The flow field is completed through plotting flow plane chart by using accumulated flow coordinate method, the concentration distribution is obtained by a new method-Hybrid Finite analytic Method coupled with Finite difference Method. Finite difference method is a classic numerical method, which is often used in much literature and will be not introduced here.

Hybrid Finite Analytic Method can be introduced first by explaining the Finite Analytic Method. Finite Analytic Method was proposed by C. J. Chen (1979). Because of high degree of accuracy and keeping physical property of the problem in the construction of semi-analytical solution, automatic upwinding, the method has received considerable attention. Many related studies have been carried out. Also in china there were many developments about the method in the late 1980s. Hybrid Finite Analytic Method is one of those.

As an extension of Finite Analytic Method, Hybrid Finite Analytic Method is proposed in 1990. The principle of the method is: according to local linear operator superposition theorem, the solution of multidimensional problem is superposed on the analytic solution of linear ordinary differential equation in spatial one-dimensional partial cell. It can avoid of the series in the Finite Analytic Method, greatly simplified the mathematical formulation and at the same time keeping the property of automatic upwinding in Finite Analytic Method. Some related research indicated the method has special degree of accuracy in the modeling of larger Peclet number problem.

In the paper the new method, Hybrid Finite Analytic Method combined to Finite Difference Method, is proposed and applied to water quality modeling of Maopingxi pollution zone. According to hydraulic conditions in Yangtze river and diffusion conditions in near-bank pollution zone, the new method is proposed as a prelibation to simulation of near-bank pollution zone in Yangtze river.

MODEL

Model description: The waters of Maopingxi pollution zone is relatively shallow and board. Assuming vertical mixing, for a control volume of pollutant, the conservation equation of mass can be written as

$$\frac{\partial AC}{\partial t} + \frac{\partial}{\partial x}(QC) + \frac{\partial}{\partial y}(QC) = \frac{\partial}{\partial x}(AE_x \frac{\partial C}{\partial x}) + \frac{\partial}{\partial y}(AE_y \frac{\partial C}{\partial y}) + KCA \quad (1)$$

where

A is the cross-sectional area of the control element [L²],

Q is the flow rate of the control element [L³T⁻¹],

C is the concentration of the control element $[ML^{-3}]$,
 E_x is the longitudinal dispersion coefficient $[L^2T^{-1}]$,
 E_y is the lateral dispersion coefficient $[L^2T^{-1}]$,
 K is the decay coefficient of pollutant $[T^{-1}]$.

Due to the fact that the computing reach of Maopingxi pollution zone is very short and the advection item in cross direction is relatively small, the decay item and the cross-directional advection item are ignored.

Divide the reach along the cross direction into several flow tubes, the variable in the mass conservation equation is described by the mean value in the flow tube. In the same flow tube, the width, mean depth, velocity is different at the different cross section, but flow rate is kept constant. Assuming the width in the tube is B , and the left、right coordinate of the tube along the lateral direction is respectively a' 、 b' , the area A of the tube is multiplied by B and h . Integrating the equation in the flow tube can obtain the equation that describe pollutant transport in the nature river as follows

$$A \frac{\partial C}{\partial t} + \frac{\partial}{\partial x}(AuC) = \frac{\partial}{\partial x}(AE_x \frac{\partial C}{\partial x}) + hE_y \frac{\partial C}{\partial y} \Big|_{b'} - hE_y \frac{\partial C}{\partial y} \Big|_{a'} \quad (2)$$

where

A is the cross-sectional area of the tube $[L^2]$,
 u is the velocity of the tube $[LT^{-1}]$,
 h is the mean depth of the tube $[L]$.
 C is the concentration of the tube $[ML^{-3}]$.

Because the two-dimensional skew differential equation is difficult to solve directly, the equation is often disintegrated. In this paper according to split operator approach the equation is dissociated to direction x and direction y operator as follows

$$A \frac{\partial C}{\partial t} + \frac{\partial}{\partial x}(AuC) = \frac{\partial}{\partial x}(AE_x \frac{\partial C}{\partial x}) \quad (3)$$

$$A \frac{\partial C}{\partial t} = hE_y \frac{\partial C}{\partial y} \Big|_{b'} - hE_y \frac{\partial C}{\partial y} \Big|_{a'} \quad (4).$$

In a spatial step the concentration distribution caused by the advection and dispersion in direction x is first solved, and then in the same spatial step the distribution is regarded as a source to solve the concentration distribution caused by the advection and dispersion in direction y , so the concentration distribution caused by pollutant transport is obtained.

Numerical discretization: The flow rate of different cross section along the tube is kept constant. Equation (3) can be written as

$$A \frac{\partial C}{\partial t} + Q \frac{\partial C}{\partial x} = \frac{\partial}{\partial x}(AE_x \frac{\partial C}{\partial x}) \quad (5).$$

Neglecting longitudinal distribution of longitudinal mixing coefficient E_x , at the grid point X_i , (5) can be written as

$$\frac{\partial C}{\partial t} + u_i \frac{\partial C}{\partial x} = E_x \frac{\partial^2 C}{\partial x^2} \quad (6).$$

The formulation is a one-dimensional linear skew differential equation.

The value u_i in nature river is variable in different locations. Peclet (u_i / E_x) number is used to describe the intensity or weak of the advection. If Peclet number is larger, the advection is more intensive. In the modeling of this paper, the six points weighed half implicit formulation of HFA is used in the more intensive advection zone, the four points implicit formulation of FDA is used in the more intensive diffusion zone. The equation (6) is discretized as follows

$$VC_{i+1}^{n+1} + bC_i^{n+1} + aC_{i-1}^{n+1} = VVC_{i+1}^n + bbC_i^n + aaC_{i-1}^n \quad (7),$$

Where in the usage of the formulation of HFA

$$V = -qu_i e^{-P}, \quad a = -qu_i e^P, \quad b = 2qu_i ch(P) + \frac{2\Delta x}{\Delta t} sh(P),$$

$$VV' = (1-q)u_i e^{-P}, \quad aa' = (1-q)u_i e^P, \quad bb' = -2(1-q)u_i ch(P) + \frac{2\Delta x}{\Delta t} sh(P);$$

In the usage of the formulation of FDA

$$V = q\left(-\frac{E_x}{\Delta x^2}\right) + (1-q)\left(\frac{u_i}{\Delta x} - \frac{E_x}{\Delta x^2}\right), \quad a = -\frac{E_x}{\Delta x^2}, \quad VV' = 0,$$

$$b = \left(\frac{1}{\Delta t} + \frac{2E_x}{\Delta x^2}\right)q + \frac{1}{\Delta t}(1-q), \quad aa' = \frac{u_i}{\Delta x}, \quad bb' = (1-q)\left(q\frac{u_i}{\Delta x}\right) + \frac{1-q}{\Delta t}$$

where q is the weighed factor, defined by $P = \frac{u_i \Delta x}{2E_x}$.

Equation (4) is solved with an implicit finite difference scheme,

$$A_{ij} \frac{C_{ij}^{n+1} - C_{ij}^n}{\Delta t} = (hE_y)_{ij,j+1} \frac{C_{ij+1}^{n+1} - C_{ij}^{n+1}}{Y_{ij+1} - Y_{ij}} - (hE_y)_{ij,j-1} \frac{C_{ij}^{n+1} - C_{ij-1}^{n+1}}{Y_{ij} - Y_{ij-1}} \quad (8)$$

where

$(hE_y)_{ij,j+1}$ is the mean of which is multiplied by h and the lateral diffusion coefficient of tube j and tube $j+1$ in section i ,

$(hE_y)_{ij,j-1}$ is the mean of which is multiplied by h and the lateral diffusion coefficient of tube j and tube $j-1$ in section i ,

Y_{ij+1} , Y_{ij} , Y_{ij-1} is the center of tube $j+1$, j , $j-1$ in section i , respectively and

$$Y_{ij+1} - Y_{ij} = \frac{B_{j+1} + B_j}{2}, \quad Y_{ij} - Y_{ij-1} = \frac{B_j + B_{j-1}}{2}$$

Formulation constrains: The time interval is equivalent and constrained by the formulation convergent velocity and numerical dispersion. In this paper formulation of HFA used in direction x is stable under condition of

$$0 \leq q < \frac{1}{2}, \quad (1-2q) \frac{u\Delta t}{\Delta x} \operatorname{cth}\left(\frac{u\Delta x}{2E_x}\right) \leq 1 \quad (9);$$

$$\frac{1}{2} \leq q \leq 1.$$

If the weighed factor is the optimal factor q_0 , then

$$q_0 = \frac{1}{2} - \left(\frac{\Delta x}{2u\Delta t} \operatorname{cth}\left(\frac{u\Delta x}{2E_x}\right) - \frac{E_x}{u^2\Delta t} \right).$$

The formulation is four stepwise dissipation and three stepwise dispersion. The stable condition is

$$\left| \frac{\Delta x}{2u\Delta t} \operatorname{cth}\left(\frac{u\Delta x}{2E_x}\right) - \frac{E_x}{u^2\Delta t} \right| \leq \frac{1}{2} \quad (10).$$

The other two formulations are implicit format and are absolute stability. To avoid the numeral dispersion, it is required that

$$\frac{\Delta t}{\Delta x} \leq \frac{1}{u} \quad (11).$$

Model parameters: Flow tube is divided according to China Water Pollution Gross Capacity Control Technical Specification. The method of plotting flow plane chart is a simple and reliable method to obtain flow field in engineering design. Modifying Manning coefficient in consistent with different cross section style and calculating the accumulated value of flow rate, when the accumulated value is equal to the design value, the distribution curve of accumulated flow is obtained. Thereby according to the tube number to divide the curve of the accumulated flow rate, in different cross section chart and different flow velocity distribution, the width, depth and velocity of flow tube can be obtained. So the flow field of the reach is obtained. Flow tubes are divided as chart 1.

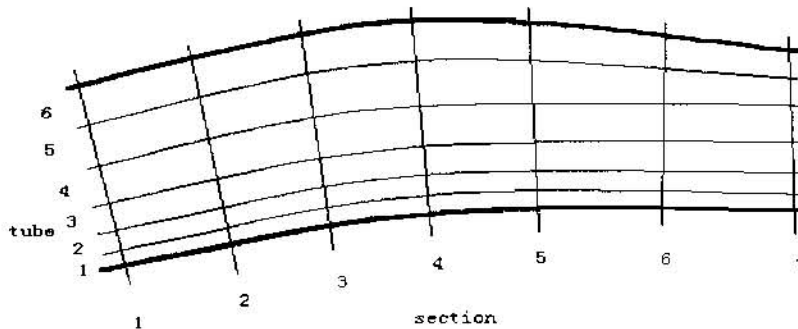


Chart 1 Diagrammatic representation of flow tubes.

In the model it is needed to solve the lateral diffusion coefficient E_y and the longitudinal

mixing coefficient E_x . Both of them, the parameter adjustment in the modeling is necessary.

The initial value of longitudinal dispersion coefficient is defined by the formulation in the shallow water near solid boradline proposed by Elder^[1]

$$E_x = 5.9hu, \quad (12)$$

and^{[2][3]}
$$E_x = 0.018u^{0.5}B^2u_*^{0.5}A^{-1} \quad (13)$$

$$E_x = 2.56nuh^{1.33} \quad (14)$$

where

u , is the bed shear velocity of the reach [LT⁻¹],

n is the Manning coefficient,

h is the mean depth of the reach,

B is the mean width of the reach,

A is the cross-sectional area.

On the basis of hydrometric records of Huanglingmiao hydrological station, 10 kilometers downstream the pollution zone, the reference value of E_x is obtained by calculating Fisher approximate difference formulation^[4],

$$E_x = -\frac{1}{A} \sum q'_k \Delta y_k \left[\sum_{j=2}^k \frac{\Delta y_j}{D_{y_j} h_j} \left(\sum_{i=1}^{j-1} q'_i \Delta y_i \right) \right] \quad (15),$$

where

A is the total cross-sectional area, defined by $A = \sum_{i=1}^n \bar{h}_i \Delta y_i$,

\bar{h}_i is the mean depth of unit i , defined by $\bar{h}_i = \frac{h_i + h_{i+1}}{2}$,

n is the number of unit which width is Δy in the cross section,

h_i 、 h_{i+1} is the depth of unit i 、 $i+1$, respectively,

u 、 \bar{u} is the mean velocity of unit i 、cross section,

q_i is the flow deviation per unit width in unit i , defined by $q' = \bar{h}_i (u_i - \bar{u})$,

d_{y_i} is the lateral diffusion.

Different from longitudinal and vertical diffusion coefficient, the lateral dispersion coefficient is variable and the error is up to 50%, and field observation is often needed. Lacking of the data, in the modeling of this paper the initial value of lateral dispersion coefficient is adapted according to the empirical formulation as follows^[4]

$$E_y = 0.67hu, \quad (16)$$

and empirical formulation used in Chongqin reach of Yangtze river^[5]

$$E_y = 0.228S^{1.67} \frac{u^{0.48}}{u_*^{0.24}} \left(\frac{B}{h} \right)^{0.089} hu, \quad (17)$$

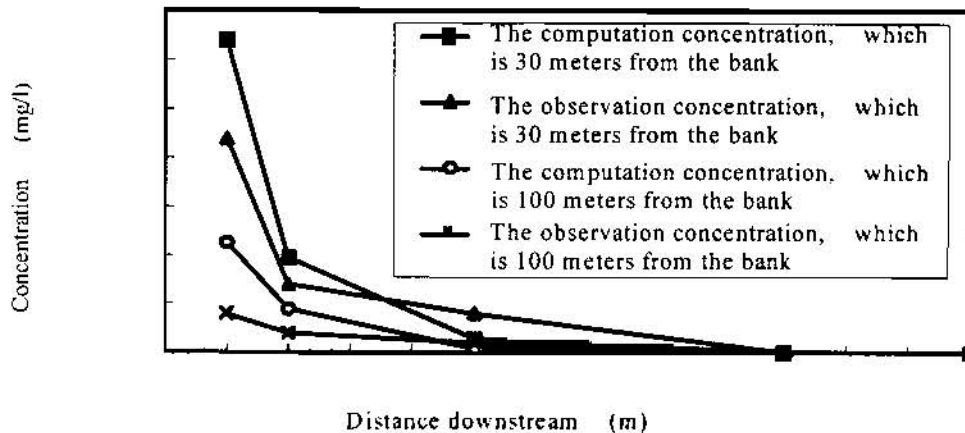
where h is the mean depth, B is the width, u , is the bed shear velocity, S is the flexibility of the

reach, u is the mean velocity.

RESULTS AND CONCLUSIONS

Modeling results: For model calibration, the measurements of cyanide in flood period of Maopingxi pollution zone are used. The time and longitudinal step are even intervals. The lateral step is obtained from the flow tube width, which in the paper there are 20 flow tubes divided by the hydraulic conditions and bed geography of the reach. The result is shown in chart 2

Chart 2 the result of cyanide in calibration of the quality model



The chart shows: near the sewage outlet the result is not satisfactory with the maximum error up to 36.4%, the further away from the outlet, the better the result is. The mean error is 10.8%. The phenomenon agrees closely with the general law of two-dimensional water quality model. The modeling result indicates the model is suitable and the numerical method is valid to modeling the pollution zone.

In the progress of the modeling two methods (HFA and FDM) are respectively used to solve the concentration distribution. The fact is founded that the method of HFA is used in intensive diffusion near-bank waters that will have unreasonable numerical reaction; the method of FDM is used in intensive advection waters that will not have good degree of accuracy. So the combination of HFA and FDM is proposed, and the result indicated the method is more suitable to model the Maopingxi pollution zone and have high degree of accuracy.

Predictions: The State Council requires that a paper factory with a capacity low then 5000 ton must be shut down by May,1996. Many of small paper factories along the bank of Maopingxi were closed, the quality of Maopingxi took a favorable turn. In this paper the quality of pollution zone caused by the sewage discharging from ore district is predicted. The parameter of pollutant is cyanide. The input of pollution source is the mean-annual discharge of pollutant. According to the construction progress, the right bank water plant is used only in the phases 1,2 of construction,

so the quality of pollution zone during the closure is received great attention. So the input of flow conditions is the combination of the mean-annual discharge of Maopingxi and the discharge with a frequency of 15% in November, which is just the closure period of Yangtze river. The prediction is as follows

Table 1 the prediction of cyanide in Maopingxi pollution zone unit meter

x \ y	100	200	300	400	500	1000
30	0.0612	0.0146	0.0046	0.0015	0.0005	0
100	0.0228	0.0085	0.0036	0.0015	0.0007	0

The location of Baimiaozi water plant is about 1300 meters downstream the confluence of Maopingxi and at least 30 meters away from the right bank of Yangtze river. Because of the significant self-purification of Yangtze river, according to the prediction in a general case Maopingxi pollution zone will not have great influence on the quality of Baimiaozi water plant.

Conclusion: According to flow characteristic and the polluted wastewater discharge conditions in the reach, the flow field is derived through plotting flow plane chart by accumulated flow coordinate method, and the concentration distribution is obtained by a new method-Hybrid Finite Analytic Method coupled with Finite Difference Method. The numerical method is a combination of Hybrid Finite Analytic Method used in convection-dominated computer grid and Finite Difference Method used in diffusion-dominated computer grid. The results indicated that the combination of HFA and FDM is more suitable to model the Maopingxi pollution zone and have high degree of accuracy. According to the prediction in a general case Maopingxi pollution zone will not have great influence on the quality of Baimiaozi water plant during Yangtze river closure. This is an explanation of the significant self-purification of Yangtze river.

REFERENCES

- Huang Pin, Water Environment Numerical Model and Applies, Guangzhou Press, 1996.
- Zhang Yongxing, Li Shushen, Wang Guangming, 1983. The Experiment Study on Dilution and Dispersion of Yangtze River in Yichang, Journal of Hydrology, 12.
- Guo Qingpin, Jiang Hao, Zhang Fang, 1994. The Discussion of Longitudinal Dispersion. Journal of Water Pollution and Protection.
- Fu Guowei, Stream Quality Model and Numerical Simulation. China Environment Science Press 1987.
- Xing zhiguo, Jiang Niangwei, 1994. Transverse Diffusion Coefficients of Yangtze River and Jialing River in Chongqin. Journal of Chongqin Environment Science 3.

A COMPUTER MODEL TO PREDICT SALMONID FRY EMERGENCE

By William J. Miller, Senior Aquatic Ecologist, Miller Ecological Consultants, Inc, Fort Collins, CO;
Fred D. Theurer, Agricultural Engineer, USDA Natural Resources Conservation Service, Beltsville,
MD; and Carlos V. Alonso, Research Hydraulic Engineer, USDA Agricultural Research Service,
Oxford, MS

Abstract: The salmonid fry emergence computer model was developed to determine fry survival and emergence as a function of physical parameters in the redd. The criteria in the percent fry emergence model were developed to reflect average habitat requirements that will provide realistic estimates of percent fry emergence. The model is applicable to rainbow trout (*Oncorhynchus mykiss*), steelhead trout (*O. mykiss*), and chinook salmon (*O. tshawytscha*). However, the concepts should be applicable to salmonid species, in general, after making the appropriate modifications for the species of interest. The model uses a binary criterion for survival due to temperature and dissolved oxygen with mortality calculated for the proportion of eggs exposed to lethal levels. The only physical parameter that fractional emergence values are derived from is substrate size and composition. This is a reflection of the amount of entrapment experienced by the emerging fry. Model predictive equations and survival criteria were incorporated into a Fortran 77 program.

INTRODUCTION

Natural resource managers responsible for maintaining or rehabilitating salmonid habitat frequently rely on models to assess changes in land use management practices. Models provide a method to assess several land use alternatives and then select the most appropriate alternative without collecting empirical data for each alternative. One example of this approach is the literature review of salmonid spawning habitat requirements (Chevalier *et al.*, 1984) and salmonid fry emergence model (Miller, 1985; Theurer and Miller, 1986) developed for the a pilot study in southeast Washington.

Recently, models that predict salmonid fry emergence as a function of percent fines in the redd have been developed to evaluate the effects watershed land use practices have on salmonid spawning habitat (Stowell *et al.*, 1983; Tappel and Bjornn, 1983; Raleigh *et al.*, 1986). The studies that were used as the basis for the models demonstrated that substrate size is important in determining salmonid emergence (Tappel and Bjornn, 1983; Irving and Bjornn, 1984). However, these models do not incorporate the effects of water temperature and dissolved oxygen (DO) on emergence. Previous studies have shown that both temperature and dissolved oxygen are important in determining salmonid embryo and larval survival (Silver *et al.*, 1963; Eddy, 1972; Miller, 1988). Colorado State University researchers developed an alternative model from existing research that incorporates water temperature, dissolved oxygen concentration and percent fines in a predictive fry emergence model (Miller, 1985; Theurer and Miller, 1986).

Salmonid Intragravel Habitat Requirements: Salmonids deposit their eggs in redds which they dig in the stream gravels. These eggs are then covered with up to several inches of gravel during the spawning process (Burner, 1951). The larvae remain in the gravel until the yolk is absorbed and then move up through the gravel at the onset of feeding. Incubation success depends on proper intragravel temperature, dissolved oxygen concentration, intragravel water velocity, and substrate particle size.

Intragravel temperatures influence developmental rates of incubating embryos and larvae. Temperature regimes and the accumulated temperature units are important for proper development. Water temperatures above normal in a particular stream can accelerate the developmental rate of embryos. The developmental rate is important for overall growth and formation of internal and external biological structures.

Dissolved oxygen levels have a direct effect on the quality of incubation habitat and salmonid survival. Silver *et al* (1963) and Shumway *et al* (1964) found a direct relationship between dissolved oxygen concentration and the size of salmonid fry at hatching. One researcher (Eddy 1972) studied the interactive effects of temperature and dissolved oxygen concentration on chinook salmon survival. Using the Eddy (1972) data and criteria from Miller (1985), survival ratios (percent) were computed for steelhead trout with the model of Theurer and Miller (1986). The ratios show the synergistic effects of temperature and dissolved oxygen.

Substrate size and composition, especially the amount of fine sediment, has a direct effect on the intragravel velocity and therefore the amount of dissolved oxygen carried to and metabolic wastes carried away from the embryos. Substrate size and composition, especially the degree of clogging of interstitial spaces, also is an important factor in determining fry emergence (Shirazi and Seim, 1981).

FRY EMERGENCE MODEL DESCRIPTION

Predictive Equation Development: The model development was an iterative process as follows. Data from Miller (1988) and from previous works were used to develop a model to predict emergence from a clean gravel substrate as a function of dissolved oxygen and temperature. First, a linear regression on the 15.2 C data and the 13.3 C values was used to predict values for 11.9 C. Second, a power curve was fit to the four DO levels at each temperature. Third, a linear equation was fit between temperatures at DO levels of 4.1 and 8.4 mg/l. Fourth, these regressions are used to solve for new coefficients at any intermediate temperature at 4.1 and 8.4 mg/l. Finally, the new coefficients are used to solve for emergence at any intermediate DO level.

The final predictive equation was a power curve fit based on DO level. The general equation used in the fit was:

$$\text{Percent Emergence} = a (\text{DO} - c)^b \quad (1)$$

where a, b, and c are coefficients specific for each temperature. This curve fitting resulted in three individual equations based on temperature. The 'c' coefficient is assumed constant at 2.4 based on the results of the emergence experiments. This was the oxygen concentration with no survival or emergence. The 'a' and 'b' coefficients varied for each temperature.

The power curve fit smoothed the adjusted and predicted data and, produced a better fit to the original data than the multiple linear regression. The equation used was forced to meet the zero survival conditions at 2.4mg/l DO. The power curve equation was a better predictor for the 15.2 C temperature at 8.4 mg/l than the linear equation, but did predict higher emergence than observed at both the 13.3 C and 15.2 C temperature for the 4.1 and 8.4 mg/l DO levels. The mean error for each equation ranged from 0.5 % at 15.2 C to 3.4 % at 11.9 C. The larger error at the 11.9 C temperature is probably due to the lack of accurate emergence data at that temperature. The overall mean error of estimate was 1.5 % with a standard error of the estimate of 7.7 %.

The power curve equations presented above predict percent emergence for rainbow incubated in a clean gravel substrate. The data analysis indicates that temperature and dissolved oxygen influence the percent emergence. Other researchers have shown that percent emergence at optimum dissolved oxygen and temperature conditions is strongly affected by substrate composition (Tappel and Bjornn, 1983; Witzel and MacCrimmon, 1981; Irving and Bjornn, 1984). There also may be other factors such as velocity that have a significant influence on emergence.

Model Components: This fry emergence model is similar to that used in the southeast Washington pilot study mentioned above. That study is an example of a watershed approach to assessing aquatic habitats. There are three variables included in the model determining fry emergence. These variables are water temperature, intragravel dissolved oxygen concentration, and substrate particle size and composition. The fry emergence

model has two main sections. The first section determines embryo mortality for rainbow trout based on water temperature and dissolved oxygen concentration. The second section determines larval mortality after the eggs hatch based on water temperature, dissolved oxygen concentration, and amount of fine sediment. This section also determines fry emergence based on sediment size and composition.

It is assumed that water temperature, dissolved oxygen concentration, and sediment composition in the physical environment of the spawning redd will be provided by sources external to this model. Intragravel velocity, substrate size, composition, and organic content are interrelated in that they determine the amount of dissolved oxygen carried to and waste products carried away from the embryos and fry. Embryo and pre-emergent fry survival is assumed primarily determined by dissolved oxygen concentration and temperature. Fry emergence is primarily dependent on dissolved oxygen concentration, water temperature and substrate particle size composition.

Embryo Mortality Component: The first input required is the daily water temperature. It is assumed that there is little or no influence from groundwater temperature in the redd, and that the instream water temperature and intragravel water temperature are the same. The criteria used for determining any mortality due to temperature were 15.5 C for eggs and 18.0 C for pre-emerged larvae. If the criterion is exceeded the eggs will die. The developmental stage of the embryos is computed from water temperature and days from fertilization using the formula obtained by Crisp (1981) to determine hatching dates for rainbow trout. This formula is a power-law model that accounts for over 97 % of the variance in the days from fertilization to hatching, and it has the form:

$$D_{\text{rainbow}} = a (T - R)^b \quad (2)$$

where

D_{rainbow} = days from fertilization to hatching

a = constant

b = constant

T = temperature (?C)

R = temperature correction factor

The equation from Crisp (1981) used to determine hatching date for steelhead embryos is:

$$D = 104.0313(T + 6.0)^{-2.0961} \quad (3)$$

To calculate the developmental phase, the daily developmental rate is calculated using the following equations:

$$R_d = 100/D \quad (4)$$

$$S_d = S_d + R_d \quad (5)$$

where

D = D_{rainbow}

R_d = daily development rate

S_d = sum of daily development rates

The hatch date is reached when the sum of the daily rates equals 100. The date is calculated by summing the days of development and adding the days to the fertilization date as follows.

$$J_d = J_d + 1 \quad (6)$$

$$J_h = J_f + J_d \quad (7)$$

where

Jd = days of development
Jf = fertilization date (Julian)
Jh = hatching date (Julian)

The degree-days (one degree-day is equivalent to one degree (C) above freezing for one day) are calculated and used to determine emergence dates. Degree-days are calculated by:

$$\text{Degree-day} = \text{degrec-day} + \text{daily degrees (C)} > 0 \text{ C} \quad (8)$$

Fry Emergence Dissolved Oxygen Model: The dissolved oxygen model determines the survival of the eggs based on the stage of development of the egg and the available oxygen concentration. The first check is made on the lower lethal limit of dissolved oxygen of 2.4 mg/l. If the average daily dissolved oxygen level is lower than 2.4 mg/l at any phase of development the eggs are considered dead. The criteria is based on the experimental study conducted by Miller (1988) and on research by Alderdice *et al* (1958), Silver *et al* (1963), and Shumway *et al* (1964) that report total mortality for steelhead and chinook at levels below 2.4 mg/l dissolved oxygen concentration.

Pre-emergent Fry Survival and Fry Emergence Component: After the eggs have hatched the fry remain in the gravel until the yolk is absorbed. Some previous research has reported that early emergence will occur if the dissolved oxygen level is less than the critical level (Tappel and Bjornn, 1983; Irving and Bjornn, 1984). To determine pre-emergent fry survival the variables of temperature, dissolved oxygen concentration, and the amount of fine sediment are used. Time of emergence is determined by degree-days. The average degrec day (C) value used in the model is 700 degree-days for rainbow emergence. This is based on results of Miller (1988) and Tappel and Bjornn (1983).

The first calculation made is a check on the average daily water temperature in reference to temperatures between 11.9 C and 15.2 C. Whence the reference temperature is determined, the power-law coefficients in Equation (1) are computed for the temperature based on the following algorithm: For 11.9 C < T < 13.3 C:

$$\text{PEMERG1} = 45.51 + (6.3429 * (T - 11.9)) \quad (9)$$

$$\text{PEMERG2} = 22.74 - (13.1643 * (T - 11.9)) \quad (10)$$

$$b(T) = \ln(\text{PEMERG1} / \text{PEMERG2}) / \ln(1.7 / 6)$$

$$a(T) = \text{PEMERG1}$$

$$c(T) = 2.4$$

and for 13.3 C < T < 15.2 C:

$$\text{PEMERG1} = 54.39 - (13.8211 * (T - 13.3)) \quad (11)$$

$$\text{PEMERG2} = 4.31 - (1.5158 * (T - 13.3)) \quad (12)$$

$$b(T) = \ln(\text{PEMERG1} / \text{PEMERG2}) / \ln(1.7 / 6)$$

$$a(T) = \text{PEMERG1}$$

$$c(T) = 2.4$$

where

PEMERG1 = emergence at DO = 4.1 mg/l;

PEMERG2 = emergence at DO = 8.4 mg/l;

a(T) = first coefficient in Equation (1);

b(T) = exponent in Equation (1);
c(T) = second coefficient in Equation (1);
T = water temperature, degrees (C).

The above equations can be used to predict emergence from a clean gravel within the range of dissolved oxygen and temperatures listed. The equations for percent emergence were developed in a laboratory apparatus where the substrate size composition was varied and dissolved oxygen and temperature held within the optimum range for development. The differences in percent emergence are assumed to be due to entrapment by fine sediment and not due to lack of dissolved oxygen or unsuitable temperatures. It is recognized that the intragravel hydraulic characteristics change as substrate size compositions change but process-based models such as SIDO (Alonso *et al.* 1996) should reflect the changes in its dissolved oxygen predictions and the predicted dissolved oxygen levels determine the survival of the fry.

FRY EMERGENCE COMPUTER PROGRAM

Program Sequence: The fry emergence model is dependent on other data sources such as the SIDO model for input parameters. The program is written in ANSI standard Fortran 77. The program consists of the mainline fry emergence program and subprograms for incubation temperature, dissolved oxygen concentration, substrate particle size composition, and total fry emergence. The percent survival and emergence are determined for a typical redd.

Mainline program. This portion of the program contains all of the variables and conditions that determine embryo and fry survival. There are also a set of Fortran logical flags that keep a record of total mortality for the redd caused by the physical factors of water temperature, dissolved oxygen concentration or total sediment blockage.

Dissolved oxygen and temperature subprogram. The dissolved oxygen and temperature subprogram is the first subprogram called by the main program. The temperature subroutine computes the degree-days for the incubation period and determine the hatching date for the eggs and emergence date for the fry (Equations 3-8). The temperature subprogram determines mortality caused by extreme temperatures. There is a logical flag that is specific to the temperature subprogram and indicates when total mortality occurs in the redd. The developmental stage is passed to the dissolved oxygen subprogram and substrate particle size distribution subprogram.

Substrate Particle size subprogram. The final subprogram called is the substrate particle size subprogram. The particle size distribution for each read is checked for the percent particle size less than 9.5 mm and the percent less than 0.85 mm. The percent emergence is calculated for the cell based on the criteria of Tappel and Bjornn (1983).

Total fry emergence subprogram. The total fry emergence for the read is calculated by multiplying the percent emergence due to temperature and dissolved oxygen by the sediment adjustment factor for particle size.

DISCUSSION

Model results versus observed results. An error analysis comparing model results with observed results showed that predicted values were generally within 10 percent of the observed emergence values. The assumptions made in the construction of the model probably contributed to the error. The fact that the model is within 10 percent of the actual values indicates that the estimated parameters are close to the actual values. The emergence data when plotted as a continuous surface has the highest emergence at the lowest temperature and highest DO level. The power curve model seems to accurately represent the shape of the actual data (Figure 1). The model developed in this study can be used to evaluate management alternatives. However, the potential user

is cautioned to evaluate the model results carefully. The model is a synthesis of available literature on emergence for several species. This synthesis required the aggregation of data for a variety of salmonid species. The basic data used in the experiment had a degree of variability due to experimental conditions as well as species variability. It has been assumed that the majority of the variability in the model can be explained by dissolved oxygen and temperature conditions.

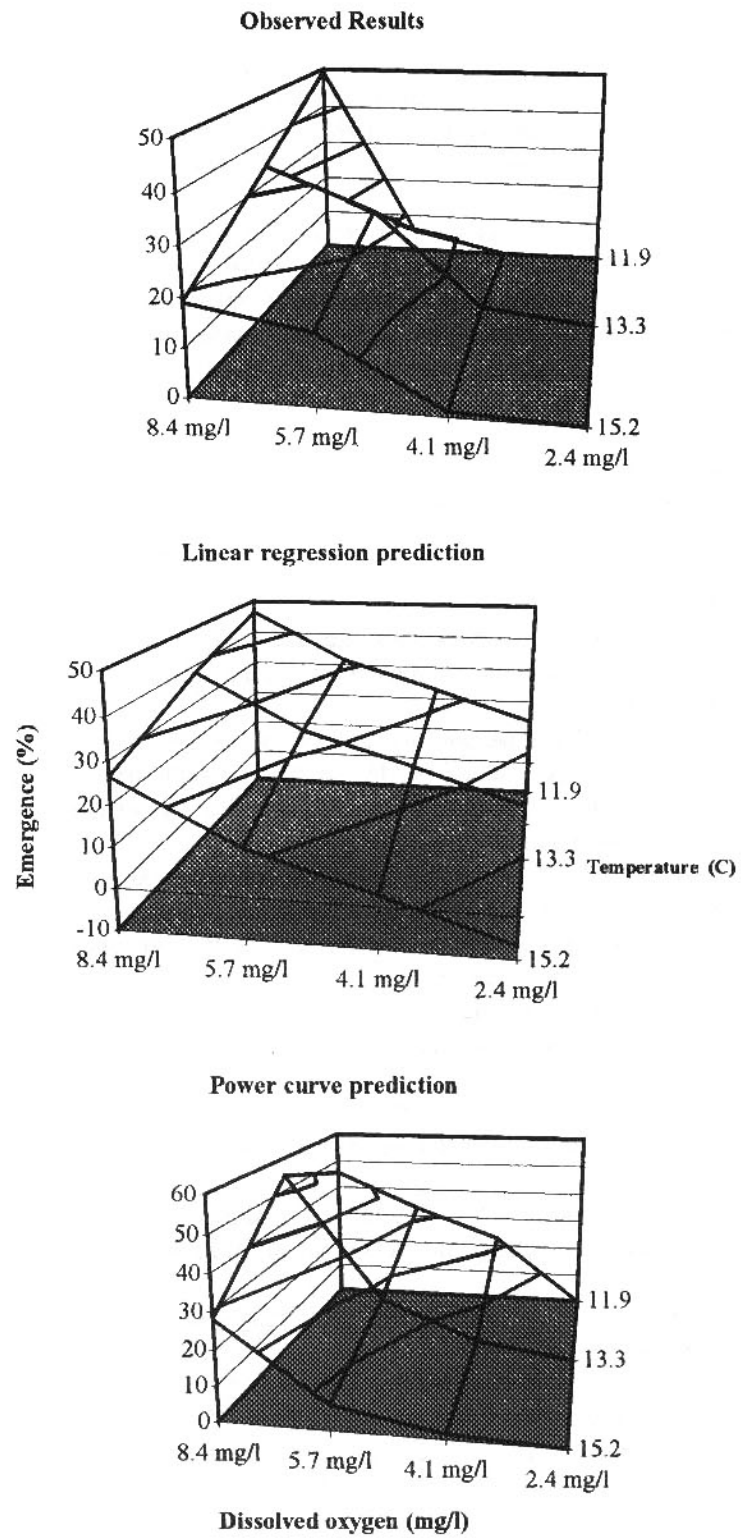
SUMMARY

The salmonid fry emergence computer model was developed to determine fry survival and emergence as a function of physical parameters in the redd. The criteria used in this model were developed after reviewing literature pertaining to salmonid embryo habitat requirements. Salmonid habitat requisites cover a wide range of conditions. The criteria in the percent fry emergence model were developed to reflect average habitat requirements that will provide realistic estimates of percent fry emergence. The concepts should be applicable to salmonid species, in general, after making the appropriate modifications for the species of interest.

The parameters used for the predictions of embryo survival and fry emergence are water temperature, intragravel dissolved oxygen concentration and substrate particle size composition. The fry emergence model uses the SIDO physical-process model to provide the required input values for intragravel water temperature sediment composition, and dissolved oxygen. The survival and emergence criteria for each parameter were developed from existing information in the literature and refined in laboratory studies using rainbow trout, *Oncorhynchus mykiss*. The model was developed to predict rainbow trout percent emergence for temperatures between 11.9 C and 15.2 C and dissolved oxygen concentrations between 2.4 mg/l and 8.4 mg/l. Model predictive equations and survival criteria were incorporated into a Fortran program. A previous version of the model was used to predict survival and emergence for steelhead trout, *O. mykiss* and chinook salmon, *O. tshawytscha*.

The model uses a binary criterion for survival due to temperature and dissolved oxygen with mortality calculated for the proportion of eggs exposed to lethal levels. The only physical parameter that fractional emergence values are derived from is substrate size and composition. This is a reflection of the amount of entrapment experienced by the emerging fry.

Figure 1. Comparison of observed emergence, linear regression and power curve predictive equations.



LITERATURE CITED

- Alderdice, D.F., W.P. Wickett, and J.R. Brett. 1958. Some effects of temporary exposure to low dissolved oxygen levels on Pacific salmon eggs. *Journal of the Fisheries Research Board of Canada*, 15(2):229-249.
- Alonso, C.V., Theurer, F.D., and Zachmann, D.W., 1996, Sediment Intrusion and Dissolved-Oxygen Transport Model — SIDO, *Technical Report No. 5*, USDA-ARS National Sedimentation Laboratory, Oxford, Mississippi, 269 pp.
- Burner, C.J. 1951. Characteristics of spawning nests of Columbia River salmon. *U.S. Fish and Wildlife Service Fishery Bulletin*, 52:97-110.
- Chapman, D.W. 1988. Critical review of variables used to define effects of fines in redds of large salmonids. *Transactions of the American Fisheries Society*, 117:1-21.
- Chevalier, B., C. Carson, and W.J. Miller. 1984. Report of engineering and biological literature pertaining to the aquatic environment: with special emphasis on dissolved oxygen and sediment effects on salmonid habitat. USDA-ARS project no. 5602-20813-008A. USDA Agricultural Research Service, Fort Collins, Colorado, 250pp.
- Crisp, D.T. 1981. A desk study of the relationship between temperature and hatching time for the eggs of five species of salmonid fishes. *Freshwater Biology*, 11:361-368.
- Eddy, R.M. 1972. The influence of dissolved oxygen concentration and temperature on the survival and growth of chinook salmon embryos and fry. Master's Thesis, Department of Fisheries and Wildlife, Oregon State University, Corvallis, Oregon.
- Irving, J.S. and T.C. Bjornn. 1984. Effects of substrate size composition on survival of kokanee salmon and cutthroat and rainbow trout embryos. University of Idaho, Idaho Cooperative Fishery Research Unit. Technical Report 84-6, 21pp.
- Miller, W.J., 1985. Tucannon River percent fry emergence model. Completion report submitted to the USDA-Soil Conservation Service. ARS CWU No. 5402-20810-004-01S. October, 1985. 83pp
- Miller, W.J., 1988. Rainbow trout survival to emergence as a function of temperature and dissolved oxygen. Doctoral Dissertation. Colorado State University.
- Raleigh, R.F., W.J. Miller, and P.C. Nelson. 1986. Habitat suitability index models and instream flow suitability curves: chinook salmon. *U.S. Fish and Wildlife Service Biological Report* 82(10.122).
- Shirazi, M.A. and W.K. Seim. 1981. Stream system evaluation with emphasis on spawning habitat for salmonids. *Water Res. Research*, 17(3):592-594.
- Shunway, D.L., C.E. Warren, and P. Dourdoroff. 1964. Influence of oxygen concentration and water movement on the growth of steelhead trout and coho salmon embryos. *Transactions of the American Fisheries Society*, 93:342-356.
- Silver, S.J., C.E. Warren, and P. Dourdoroff. 1963. Dissolved oxygen requirements of steelhead trout and chinook salmon embryos at different water velocities. *Transactions of the American Fisheries Society*, 92:327-343.
- Stowell, R., A. Espinosa, T.C. Bjornn, W.S. Platts, D.C. Burns, J.S. Irving. 1983. Guide for predicting salmonid response to sediment yields in Idaho batholith watersheds. U.S. Forest Service, Northern Region, Intermountain Region. 95pp.
- Tappel, P.D. and T.C. Bjornn. 1983. A new method of relating size of spawning gravel to salmonid embryo survival. *North American Journal of Fisheries Management*, 3:123-125.
- Theurer, F.D., and W.J. Miller. 1986. Tucannon River Offsite Study: Fry emergence model report. Submitted to USDA-ARS, Hydro-ecosystems Research Unit, Fort Collins, CO. August, 1986 54pp.
- Witzel, L.D., and H.R. MacCrimmon. 1981. Role of gravel substrate on ova survival and alevin emergence of rainbow trout, *Salmo gairdneri*. *Canadian Journal of Zoology* 59:629-636.

USING CE-QUAL-W2 TO ASSESS THE AMMONIA ASSIMILATIVE CAPACITY OF THE TUALATIN RIVER, OREGON

Stewart Rounds, Hydrologist, U.S. Geological Survey, Portland, Oregon;
Tamara Wood, Hydrologist, U.S. Geological Survey, Portland, Oregon

Abstract

A modified version of the U.S. Army Corps of Engineers model CE-QUAL-W2 was used to simulate flow, temperature, and water quality in the lower reaches of the Tualatin River, a low-gradient stream that meanders through a mixture of urban and rural landscapes on the western side of the Portland, Oregon metropolitan area. Simulated water-quality constituents included nutrients (nitrogen and phosphorus), phytoplankton, and dissolved oxygen. Once calibrated, the model was used to quantify the river's ability to assimilate ammonia wasteloads from the basin's two largest wastewater treatment plants without causing violations of the State of Oregon minimum dissolved oxygen standard. This assimilative capacity increases with increasing river discharge and solar insolation, and decreases with increasing water temperature. Model simulations were used to determine that the 30-day mean dissolved oxygen concentration would decrease by only about 0.2 milligrams per liter under the most sensitive observed conditions when each of the wastewater treatment plants releases a constant load of 100 pounds per day of ammonia nitrogen. This determination of the ammonia assimilative capacity will aid in the ongoing reassessment of a Total Maximum Daily Load for ammonia in the Tualatin River.

INTRODUCTION

During the warm, sunny, and dry conditions characteristic of summer in northwestern Oregon, discharge in the reservoir reach of the Tualatin River (fig. 1, river miles [RM] 3.0 to 3.4) typically decreases to less than 150 ft³/s (cubic feet per second), and concentrations of dissolved oxygen (DO) sometimes decrease to levels that violate the State of Oregon minimum DO standard (6.5 mg/L [milligrams per liter] as a 30-day mean). Oxygen demands that combine to cause these problems include sediment oxygen demand, carbonaceous biochemical oxygen demand, phytoplankton and zooplankton respiration, and instream nitrification of ammonia. The most significant point sources of ammonia to the river are the two large wastewater treatment plants (WWTPs) operated by the Unified Sewerage Agency (USA). Prior to upgrades at the WWTPs in the late 1980s and early 1990s, ammonia loads from these plants caused a very large instream oxygen demand when nitrifying bacteria converted the ammonia to nitrate; this demand was typically large enough to produce violations of the minimum DO standard. To prevent these violations and to protect the river's designated beneficial uses, the Oregon Department of Environmental Quality (ODEQ) in 1988 established a Total Maximum Daily Load (TMDL) for ammonia nitrogen in the Tualatin River, including ammonia wasteload allocations for the WWTPs. Since that time, ODEQ personnel have determined that the ammonia TMDL does not adequately protect the river against ammonia-related DO violations; the ammonia TMDL is currently being revised. This modeling work, performed in collaboration with both USA and ODEQ, was designed to aid in the revision of this TMDL.

MODEL CALIBRATION AND LOADING SCENARIOS

CE-QUAL-W2, a two-dimensional, laterally-averaged reservoir model (Cole and Buchak, 1995) was used to simulate flow, water temperature, and water quality in the lower Tualatin River from RM 38.4, a point just upstream of one of the WWTPs, to a low-head dam at RM 3.4, downstream of the second WWTP (fig. 1). Some modifications of the model code were required to simulate flow past the dam and to allow one-dimensional transport in several shallow reaches of the river (S.A. Rounds, U.S. Geological Survey, unpub. data). The model was calibrated to the summer low-flow conditions observed from May 1 through October 31 of 1991, 1992, and 1993, and then used to evaluate the effects of hypothetical WWTP ammonia loads on DO concentrations in the Tualatin River. These model simulations were run using the same hydrologic and meteorological conditions under which the model was calibrated, thus providing a wide range of imposed conditions, from the low-flow drought conditions of 1992 to the wet conditions of 1993. Ammonia loads from the two WWTPs were held constant in each simulation. Loads of 0, 50, 100, 250, 500, 750, 1000, 1250, and 1500 lb/d (pounds per day) of ammonia nitrogen from each plant were evaluated. (Typical WWTP ammonia loads are in this range, depending on the nitrification efficiency of the plant.) These simulations were designed to keep all other factors as constant as possible from simulation to simulation to minimize changes in other components of the oxygen budget. Therefore, to keep the availability of nutrient nitrogen identical to that of the calibration, the total inorganic nitrogen load (ammonia plus nitrate) from each plant was not changed. When the

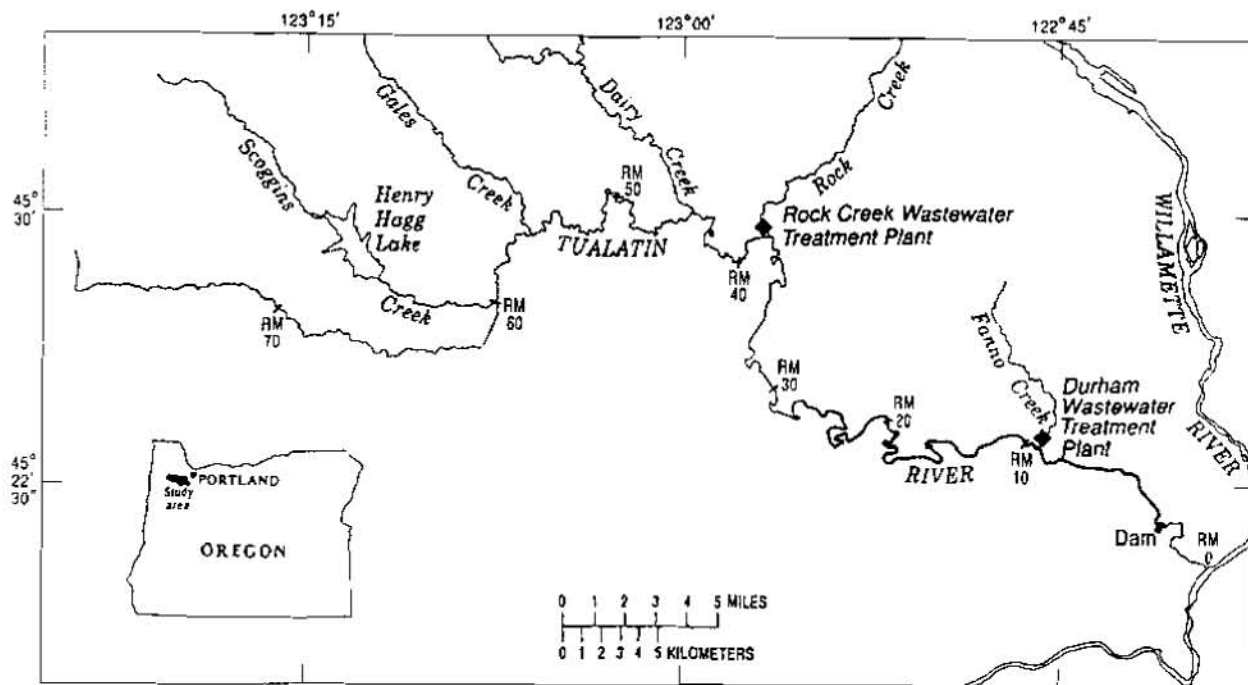


Figure 1. Map of the Tualatin River, Oregon, showing the location of the two largest wastewater treatment plants. The model extends from RM (river mile) 38.4 to the low-head dam at RM 3.4.

imposed ammonia load exceeded the observed load, the load of nitrate nitrogen was decreased to compensate; when the imposed ammonia load was less than the observed load, the nitrate load was increased accordingly. An instream nitrification rate of 0.11 day^{-1} was used for each simulation, based on instream ammonia data collected during a period of high ammonia concentrations in the summer of 1995.

FACTORS AFFECTING DISSOLVED OXYGEN

Several important factors control the effect of the imposed WWTP ammonia loads on the simulated DO concentrations, including the magnitude of the loads, river discharge, water temperature, and solar insolation. The effects of several of these factors are apparent when the simulated DO concentrations are analyzed for violations of the minimum DO standard. The DO standard for the Tualatin River has several parts, but the most frequently violated clause states that the 30-day mean DO concentration, with no credit for supersaturation, shall not be less than 6.5 mg/L (Oregon Department of Environmental Quality, 1997a). Violations of the DO standard usually occur within the reservoir reach of the river (RMs 30–3.4, fig. 1); representative monitoring sites within that reach are located at RMs 16.2 and 5.5. Table 1 shows the percentage of time that the simulated 30-day mean DO concentrations at RMs 16.2 and 5.5 violated the standard as a function of WWTP ammonia load and month during the low-flow summer period.

Ammonia Load

Increases in the simulated ammonia load from each of the WWTPs give rise to an increasing frequency of simulated DO violations (table 1). For example, the simulated frequency of violation at RM 5.5 in the months of September for 1991–1993 increases from 0 to 67 percent as the ammonia load from each WWTP increases from 0 to 1500 lb/d. As the imposed ammonia load is increased, the amount of DO consumed through instream ammonia nitrification increases, and the magnitude of the DO loss can be large. Even averaged over the entire May–October period, nitrification-caused decreases in the simulated DO concentration downstream of the WWTPs can be more than 1 mg/L for ammonia loads greater than 1000 lb/d (fig. 2). The slight increase in the mean DO concentration in figure 2 at RM 9 is due to the effect of dilution; both Fanno Creek and the Durham WWTP discharge into the Tualatin River at that point (fig. 1). Note that the incremental change in DO concentration for each additional 250 lb/d of ammonia load is similar, indicating that the relation between ammonia load and DO loss is approximately linear in this range of WWTP ammonia load. Although the reaeration rate must increase as the DO deficit increases, reaeration is slow enough in this reach that it does not offer much protection from DO violations under these ammonia loads.

Table 1. Percentage of time that the running 30-day mean of the simulated dissolved oxygen concentration was in violation of the State of Oregon standard, based on simulated hourly concentrations averaged vertically over the top 10 feet of the water column. (lb/d, pounds per day; WWTP, wastewater treatment plant)

WWTP Ammonia Load (lb/d)	Percentage of time in violation of the 30-day mean dissolved oxygen standard											
	River Mile 16.2						River Mile 5.5					
	May	Jun	Jul	Aug	Sep	Oct	May	Jun	Jul	Aug	Sep	Oct
0	0	0	0	0	0	18	0	0	0	0	0	21
50	0	0	0	0	0	20	0	0	0	0	0	22
100	0	0	0	0	0	22	0	0	0	0	0	24
250	0	0	0	0	0	30	0	0	0	0	0	34
500	0	0	0	0	7	33	0	0	0	1	7	44
750	0	0	0	0	14	33	0	0	0	22	32	63
1000	0	0	0	9	47	76	0	0	3	42	45	77
1250	0	0	0	36	59	100	0	0	17	53	57	89
1500	0	0	1	53	78	100	0	0	32	60	67	100

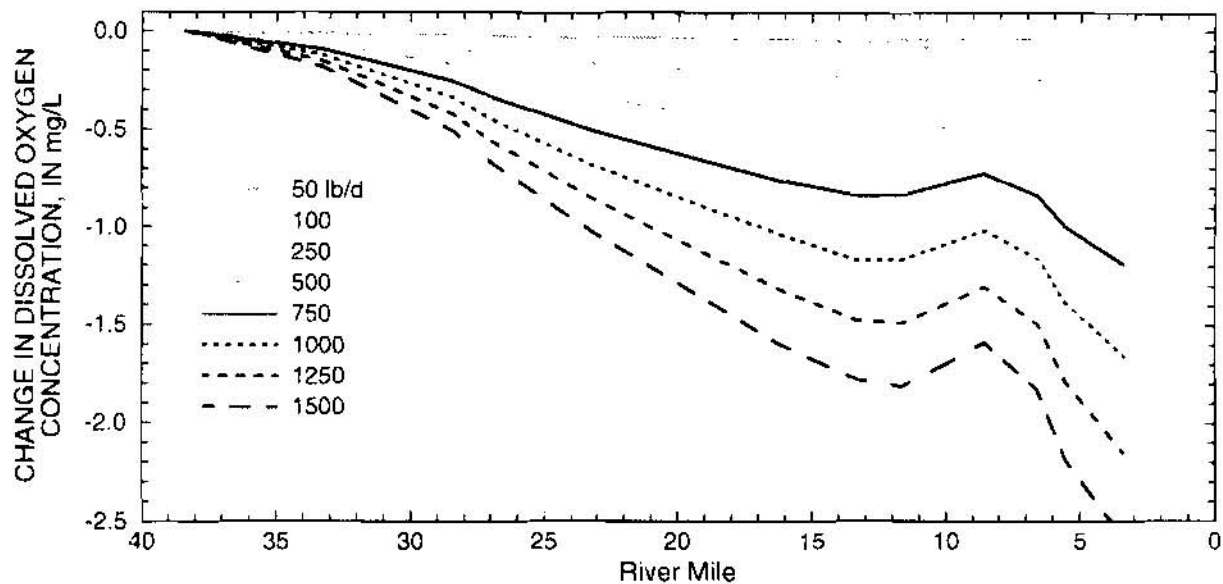


Figure 2. Simulated change in the mean dissolved oxygen concentration (May–October, 1991–1993) as a function of river mile for WWTP ammonia loads between 50 and 1500 pounds per day, relative to zero WWTP ammonia loads. (mg/L, milligrams per liter; lb/d, pounds per day; WWTP, wastewater treatment plant)

River Discharge and Water Temperature

River discharge and water temperature are important factors in determining the effect of WWTP ammonia loads on Tualatin River DO concentrations. Lower river flows result in longer travel times through the reservoir reach of the river, where slow moving water reduces the effectiveness of reaeration. As the travel time lengthens, more of the nitrogenous oxygen demand will be exerted in the reservoir reach, where most of the DO violations typically occur. Travel times through the reservoir reach can be as long as 14 days when river discharge decreases to 150 ft³/s. Under those conditions, about 80 percent of the nitrogenous oxygen demand from the Rock Creek WWTP will be realized within the reservoir reach. In contrast, when river discharge is high, the travel time is short and the amount of oxygen demand exerted by instream ammonia nitrification within the reservoir reach will be a small fraction of the possible

nitrogenous oxygen demand. Higher flows also carry larger loads of oxygen, resulting in smaller DO concentration decreases for the same mass of DO consumed. The effect of water temperature is important mainly because it influences the rate of ammonia nitrification; the reaction proceeds faster in warmer water.

Both river discharge and water temperature have predictable seasonal trends. Flow in the Tualatin River reflects the regional precipitation pattern; most of the rain falls between November and April, and the lowest flows are observed in July and August — the months that typically receive the least precipitation. Water temperature is normally greatest during midsummer as a result of long sunny days and low flow conditions. The effects of river discharge and water temperature are illustrated in figure 3 for a WWTP ammonia load of 1500 lb/d from each plant. The effect of this ammonia load is smallest during May because river discharge typically is highest in May. As the flow decreases from May through August, the amount of DO consumed in the reservoir reach through nitrification increases due to lengthening travel times and faster nitrification rates in the warmer water. During September and October, the flow typically remains low, but the water becomes slightly cooler, resulting in slightly less DO consumption in parts of the reservoir reach. The month of September and October are critical periods for DO due to typically low river flow.

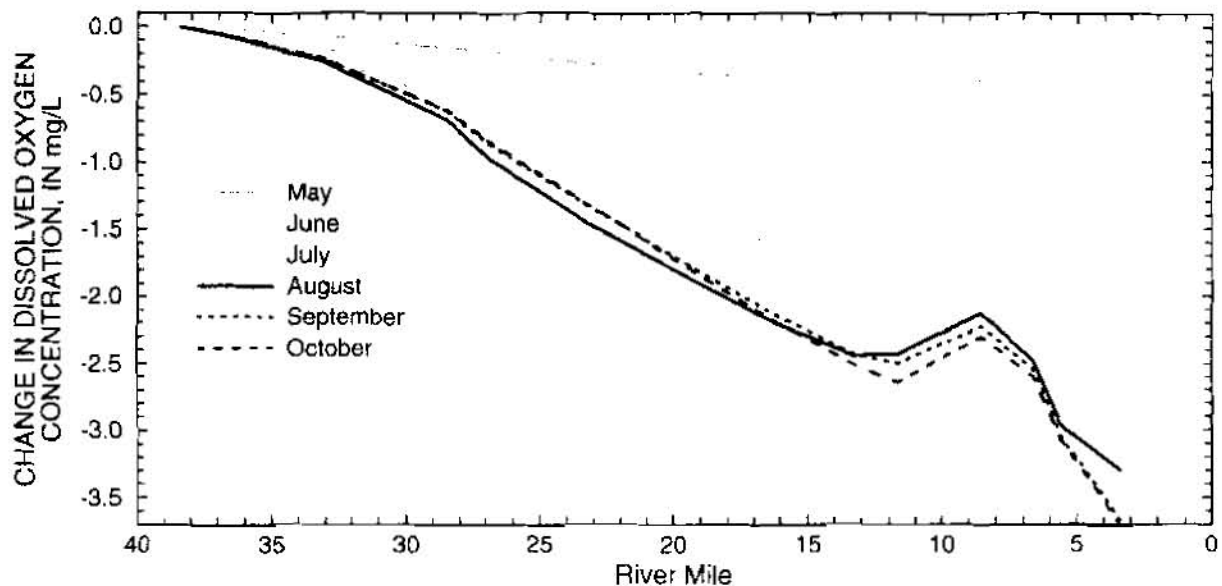


Figure 3. Simulated change in the monthly mean dissolved oxygen concentration (1991–1993) as a function of river mile using WWTP ammonia loads of 1500 pounds per day, relative to zero WWTP ammonia loads. (mg/L, milligrams per liter; WWTP, wastewater treatment plant)

Although more than 2.5 mg/L of DO can be consumed through the nitrification of a 1500 lb/d ammonia load during August, that consumption may or may not result in a DO violation. The results in table 1, for example, indicate that a 1500 lb/d ammonia load from both WWTPs produced August DO violations at RM 5.5 60 percent of the time, for the conditions observed in 1991–1993. Violations were not produced more frequently because the low flows of August also encourage the growth of large blooms of phytoplankton. The amount of DO produced through the photosynthetic activity of these algae often is large enough to offset a large nitrogenous oxygen demand and keep the DO concentration above the standard.

In an attempt to quantify how compliance with or violation of the 30-day mean DO standard varies with river discharge, the distribution of 30-day mean discharge was plotted against the imposed WWTP ammonia load for periods of both compliance and violation in the entire 18 month simulation period (fig. 4). Although river discharge and the ammonia load are not the only factors determining compliance or violation, figure 4 does suggest that violations are more likely to occur at the lowest flows and less likely to occur above certain levels of discharge for a given ammonia load. For example, most of the simulated violations for WWTP ammonia loads of 750 lb/d or less coincide with flows less than 150 ft³/s, and no violations are simulated for flows above 220 ft³/s.

Solar Insolation

The solar insolation rate, averaged over a time scale at least as long as that of a typical algal bloom (5–20 days), is an important predictor of the level of algal photosynthetic activity in the Tualatin River. Light conditions affect the level

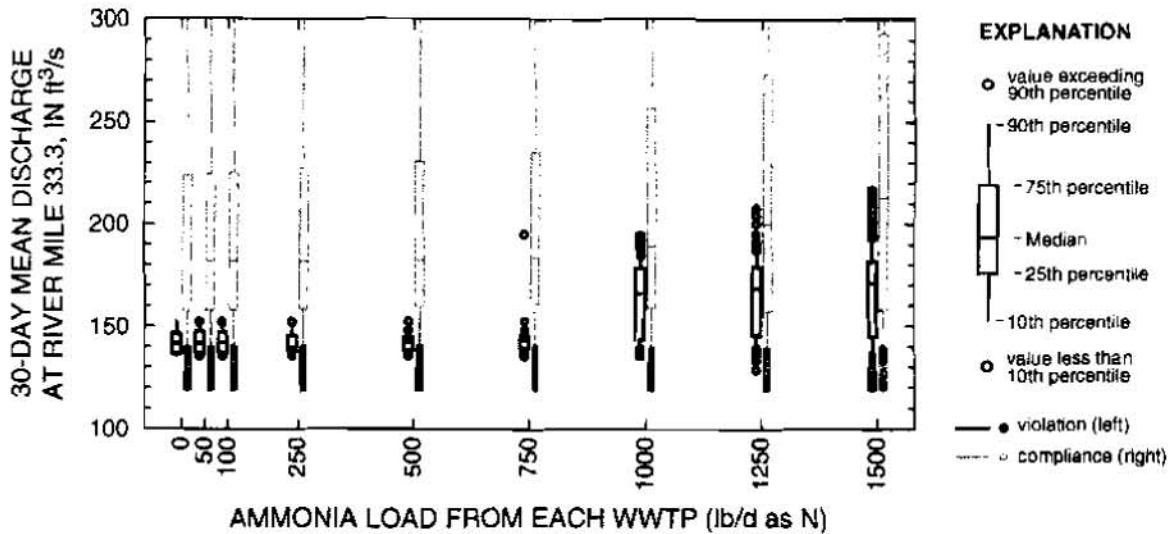


Figure 4. Box and whisker plot showing how compliance with or violation of the 30-day mean dissolved oxygen standard at river mile 16.2 varies as a function of both river discharge and the imposed WWTP ammonia load. (ft³/s, cubic feet per second; lb/d, pounds per day; WWTP, wastewater treatment plant)

of photosynthetic activity, and photosynthetic DO production is important in determining whether a given WWTP ammonia load will produce a DO violation within the reservoir reach of the Tualatin River. This dependence is illustrated in figure 5, in which the distribution of the 30-day mean solar insolation rate, measured at the Durham WWTP, is plotted against the imposed WWTP ammonia load for subsets of the modeled period that produced either compliance with or violation of the 30-day mean DO standard. The dependence is strong. Under low light conditions and high WWTP ammonia loads, DO violations are more likely; when light conditions are more favorable for algal growth, DO violations are less likely. For example, all violations for WWTP ammonia loads of 750 lb/d or less coincide with solar insolation less than 150 W/m² (watts per square meter), and no violations are simulated for solar insolation above 220 W/m².

The dependence of compliance with or violation of the DO standard on the solar insolation rate is stronger than that produced by river discharge and illustrates the importance of photosynthetic production in the DO budget of the Tualatin River during the summer low-flow period. All of the simulated DO violations for WWTP ammonia loads less than 500 lb/d occurred in October (table 1), for a combination of reasons. First, the seasonal variation in solar insola-

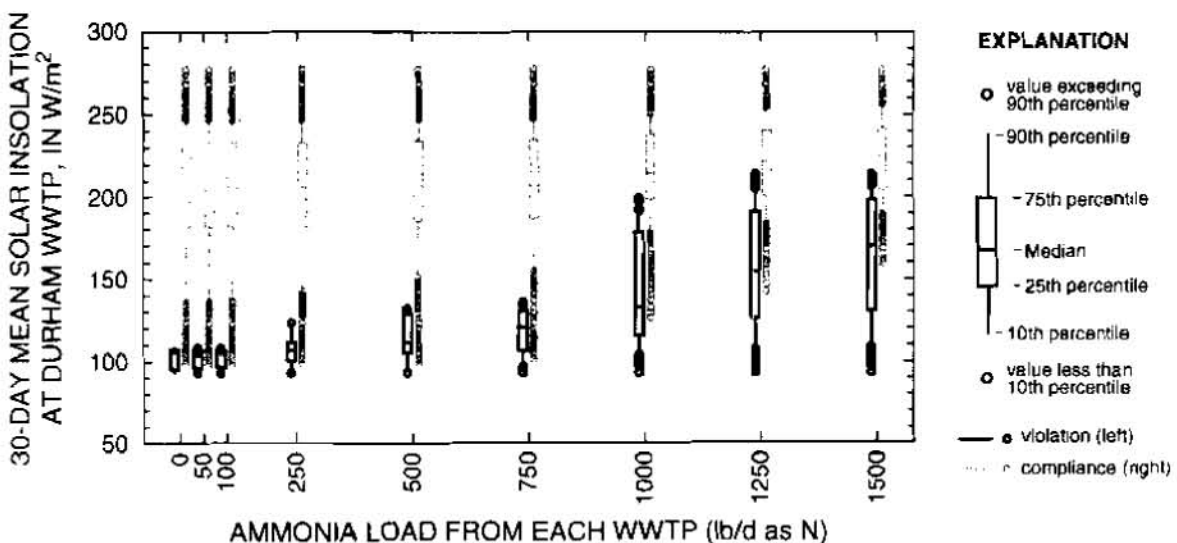


Figure 5. Box and whisker plot showing how compliance with or violation of the 30-day mean dissolved oxygen standard at river mile 16.2 varies as a function of both solar insolation and the imposed WWTP ammonia load. (W/m², watts per square meter; lb/d, pounds per day; WWTP, wastewater treatment plant)

tion, with shorter days and less intense light later in the summer, causes light conditions in October to be less favorable for algal growth and photosynthetic production. Second, the month of October is typically characterized by continuing low flow; sediment oxygen demand and carbonaceous biochemical oxygen demand continue to consume DO from the water traveling through the reservoir reach, depleting the DO to levels near the standard. The long travel time in the absence of significant photosynthetic production causes DO violations to be more likely in this period.

AMMONIA ASSIMILATIVE CAPACITY

Ammonia assimilative capacity is defined in this paper as the maximum load of ammonia that can be carried by a river without causing violations of a water-quality standard or criterion. For the Tualatin River, the relevant criterion is the State of Oregon minimum DO standard. Ammonia toxicity also may be a concern when large ammonia loads coincide with high pH and high water temperature. Under most conditions, however, prevention of DO violations also will prevent ammonia toxicity problems; therefore, the toxicity criterion is deemed secondary to the DO standard and is not addressed in this analysis.

The model results in table 1 and in figures 2–5 can be used to generate insight into the ammonia assimilative capacity of the Tualatin River. For example, table 1 shows, for the month of October in particular, that under certain conditions the Tualatin River has an ammonia assimilative capacity of zero; that is, it can carry no ammonia load from the WWTPs without decreasing a DO concentration that is already at or below the standard. Similarly, the model shows that under high-flow conditions (May and June, for example), the river can assimilate more than 1500 lb/d of ammonia from each WWTP without producing a DO violation. Indeed, the ammonia assimilative capacity may be as high as several thousand pounds per day under typical high-flow conditions. Furthermore, under low-flow and favorable light conditions in midsummer, photosynthetic production may exceed the nitrogenous oxygen demand produced by about 500 to 1500 lb/d of ammonia from each WWTP.

Under conditions where the ammonia assimilative capacity is zero, the Oregon Administrative Rules allow ODEQ, at its discretion, to allow the discharge of wasteloads that result in “no measurable reduction” of DO, where “no measurable reduction” is defined as approximately 0.2 mg/L (Oregon Department of Environmental Quality, 1997b). The 18 months of model output was analyzed to determine what level of WWTP ammonia load would result in a DO decrease of 0.2 mg/L under those conditions when the 30-day mean DO concentration was already at or below the standard in the absence of WWTP ammonia loads (fig. 6). Under these conditions, the effect of any additional ammonia load caused the greatest decrease in DO concentrations: when the 30-day mean DO concentration met or

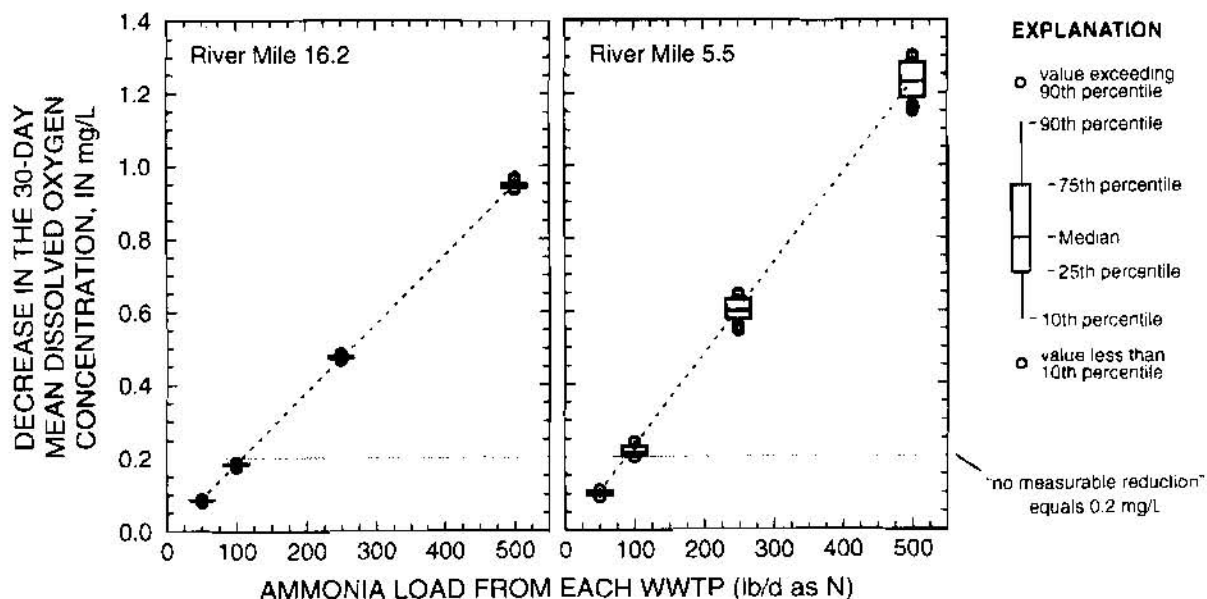


Figure 6. Box and whisker plots showing dissolved oxygen consumption due to ammonia nitrification as a function of the WWTP ammonia load. These plots include only conditions in the 18-month calibration period where the 30-day mean dissolved oxygen standard was violated in the absence of WWTP ammonia loads. (mg/L, milligrams per liter; lb/d, pounds per day; WWTP, wastewater treatment plant)

exceeded the standard, the same additional ammonia load caused less of a decrease in the DO concentration. Therefore, the data shown in figure 6 represent the most critical conditions for DO.

The dotted lines drawn through the medians of the distributions in figure 6 show that the predicted DO losses are linearly related to the imposed ammonia load. The slope of that line is slightly steeper for RM 5.5 than for RM 16.2 because RM 5.5 is downstream of both WWTPs, whereas RM 16.2 is downstream of only one WWTP (fig. 1). The slope of these lines depends mainly on river discharge and the instream nitrification rate, which is a function of water temperature. If the flow had been lower, the effect of instream ammonia nitrification would have been even greater and the slope of these lines would be steeper. Similarly, if the river flow could be augmented to maintain a higher minimum discharge, the slope of these lines would be more shallow. The results in figure 6 indicate that each WWTP could discharge about 100 lb/d of ammonia nitrogen under the most critical DO conditions and cause only a 0.2 mg/L decrease in the 30-day mean DO concentration. These results will aid in setting a new ammonia wasteload allocation for these two WWTPs under the revised ammonia TMDL.

These model results were used to generate a simple flow chart that illustrates the dependence of the Tualatin River's calculated ammonia assimilative capacity on measurable quantities such as river discharge (at a gage, RM 33.3) and solar insolation (fig. 7). The ammonia loads in the flow chart also depend on the instream nitrification rate, which is a

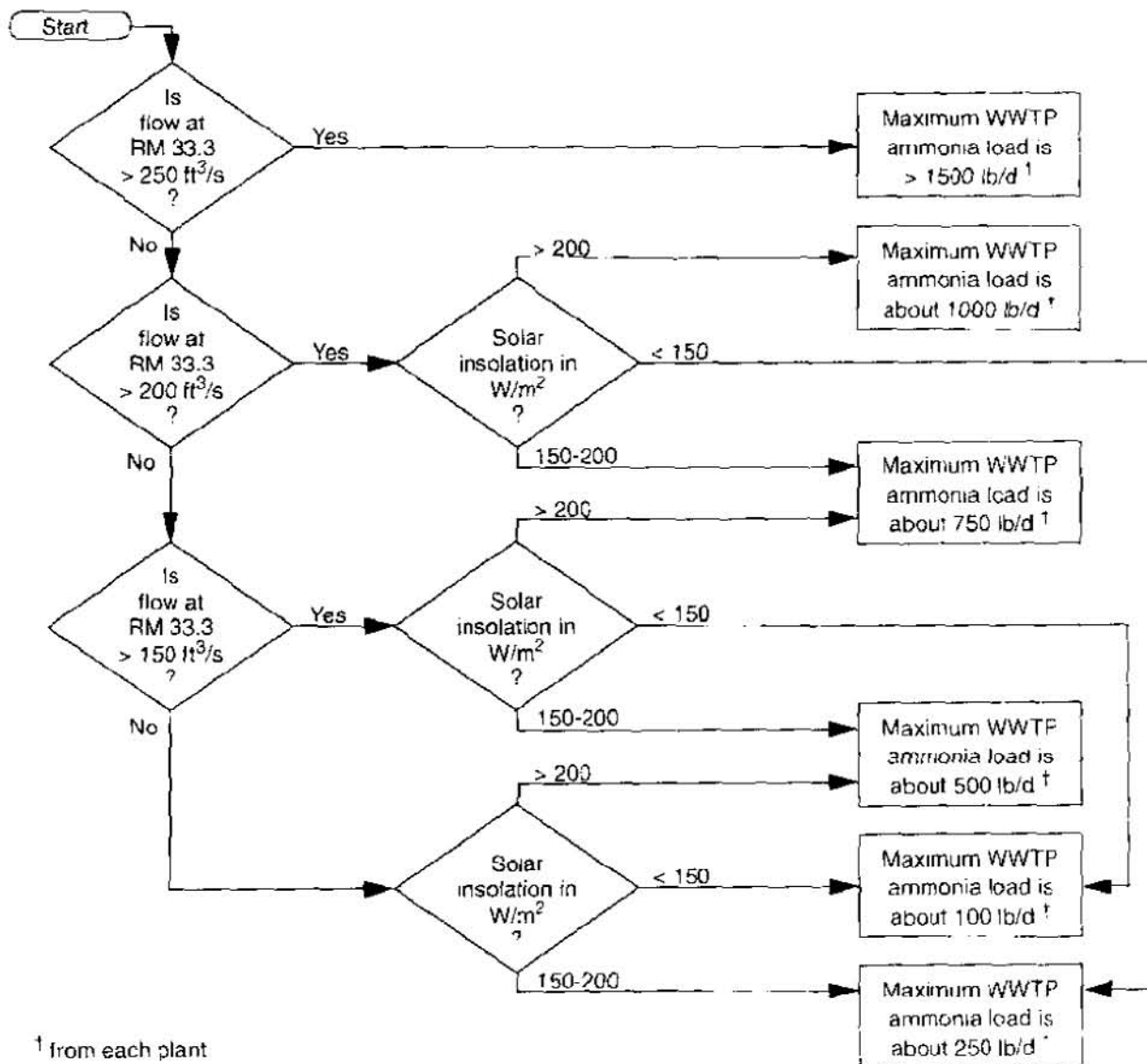


Figure 7. Flow chart illustrating the dependence of the ammonia assimilative capacity on flow and light conditions. (ft³/s, cubic feet per second; W/m², watts per square meter; WWTP, wastewater treatment plant)

function of water temperature, and on the averaging interval used for flow and solar insolation. The results in figure 7 are based on 30-day means of flow and solar insolation, as in figures 4 and 5.

Under the high-flow conditions encountered in May, the flow chart leads to an assimilative capacity greater than 1500 lb/d. In midsummer, when river discharge is typically between 150 and 200 ft³/s and the solar insolation rate is generally well above 150 W/m², several paths in the flow chart lead to assimilative capacities between 500 and 1000 lb/d of ammonia from each WWTP. In late summer, when river discharge typically is near 150 ft³/s and solar insolation is less than 150 W/m², the flow chart leads to an assimilative capacity of 100 lb/d, as calculated from figure 6.

SUMMARY

A two-dimensional, laterally averaged flow and water-quality model, CE-QUAL-W2, was used to simulate flow, water temperature, and water quality in the reservoir reach of the Tualatin River. The model was calibrated for an 18-month period encompassing the May 1 to October 31 periods of 1991, 1992, and 1993. Model calibration included flow, water temperature, and water-quality constituents such as ammonia, nitrate, DO, orthophosphate, phytoplankton, zooplankton, sediments, and dissolved and particulate organic matter. Once calibrated, the model was used to simulate the effects of various ammonia loads from two large WWTPs on DO concentrations in the lower reaches of the Tualatin River. These hypothetical ammonia loads were superimposed on the observed calibration conditions, therefore providing a realistic and wide range of hydrologic and meteorological conditions for testing. Simulations were run with constant ammonia loads between 0 and 1500 lb/d of ammonia nitrogen from each of the two plants; the total inorganic nitrogen loads (ammonia plus nitrate) from the WWTPs, however, were not modified from those used for the calibration in order to maintain the same overall nutrient load.

The results from these hypothetical scenarios were used to determine how the ammonia assimilative capacity of the Tualatin River depends on river discharge, water temperature, and solar insolation. That capacity was quantified on the basis of compliance with, or violation of, the State of Oregon minimum DO standard. Most of the simulated DO violations occurred when both river discharge and solar insolation were low. When light conditions are poor, photosynthetic production of DO is low and cannot offset the nitrogenous oxygen demand of a large load of ammonia. The long travel times through the reservoir reach during low-flow conditions allow much of that nitrogenous oxygen demand to be exerted before the ammonia exits that reach. Ammonia assimilative capacity was found to increase with increasing river discharge and solar insolation, and to decrease with increasing water temperature.

On the basis of a definition of "no measurable reduction" of dissolved oxygen (0.2 mg/l) for conditions when the DO standard was being violated in the absence of WWTP ammonia loads, the model results were used to calculate the maximum permissible ammonia load from each WWTP under the most sensitive conditions. That ammonia load, about 100 lb/d, is sensitive to the instream nitrification rate (which depends on water temperature) as well as the level of river discharge. Flow augmentation may be a useful tool to reduce the frequency of these violations and to increase the allowable WWTP ammonia loads under the most sensitive conditions.

The results of these model simulations provide insight into how the Tualatin River might be managed to reduce the number of future violations of the DO standard under various ammonia loading conditions. These results are being used by ODEQ to develop new wasteload allocations and a revised ammonia TMDL for the Tualatin River.

REFERENCES

- Cole, T.M., and Buchak, E.M., 1995, CE-QUAL-W2 — A two-dimensional, laterally averaged, hydrodynamic and water quality model, version 2.0; U.S. Army Corps of Engineers Instruction Report EL-95-1 [variously paged].
- Oregon Department of Environmental Quality, 1997a, Oregon Administrative Rules — Dissolved oxygen standard for the Tualatin River; Portland, Oregon, OAR 340-041-0445(2aE).
- Oregon Department of Environmental Quality, 1997b, Oregon Administrative Rules — Policies and guidelines generally applicable to all basins; Portland, Oregon, OAR 340-041-0026(3aCiii).

DEVELOPMENT AND APPLICATION OF A MUD TRANSPORT AND BED EVOLUTION MODEL FOR ESTUARY

By **Tran Thuc, Hydrologist, Institute of Meteorology and Hydrology, Hanoi, Vietnam**

INTRODUCTION

Coastal evolution is a ceaseless process therefore a dredging plan is necessary for the effective use of the available channel. The development of such type of plan demands a reasonably precise evaluation of the sediment movement in the area of interest. In the past hydraulic models have been used widely and quite successfully. With the advent and then rapid development in computer technology and efficient numerical techniques, mathematical modeling has emerged as an effective tool due to its economy in time and money along with a reasonable accuracy in determining even finer details of flow phenomenon.

A mathematical model was developed to compute sediment transport, siltation rate and bed evolution in the Chao Phraya Estuary, Thailand. The model was based on the solution of the three-dimensional diffusion-convection equation. Interaction of tidal current and wave action was taken into account. A two-dimensional depth-averaged hydrodynamic model was used to compute depth-averaged tidal currents and water levels. The shallow water wave model was used to compute the wave field. Measured data of water levels, tidal currents, sediment concentrations and siltation rates were used for model calibration. Very good agreement between the computed results and field data were obtained. The model was then applied to study the siltation rate in the designed navigation channel.

THEORETICAL CONSIDERATION

Hydrodynamic Model: Governing equations of the depth-averaged hydrodynamic model include the continuity equation and momentum equations in x- and y-directions as follows (Leendertse, 1967).

Continuity equation:

$$\frac{\partial \eta}{\partial t} + \frac{\partial hu}{\partial x} + \frac{\partial hv}{\partial y} = 0 \quad (1)$$

Momentum equation in x-direction:

$$\frac{\partial u}{\partial t} + u \frac{\partial u}{\partial x} + v \frac{\partial u}{\partial y} + g \frac{\partial \eta}{\partial x} + \frac{1}{\rho h} \tau_{bx} + \frac{1}{\rho h} \tau_{wx} - fv - \frac{1}{\rho h} \left[\frac{\partial}{\partial x} \left(h D_{xx} \frac{\partial u}{\partial x} \right) + \frac{\partial}{\partial y} \left(h D_{xy} \frac{\partial u}{\partial y} \right) \right] = 0 \quad (2)$$

Momentum equation in y-direction:

$$\frac{\partial v}{\partial t} + u \frac{\partial v}{\partial x} + v \frac{\partial v}{\partial y} + g \frac{\partial \eta}{\partial y} + \frac{1}{\rho h} \tau_{by} + \frac{1}{\rho h} \tau_{wy} + fu - \frac{1}{\rho h} \left[\frac{\partial}{\partial x} \left(h D_{xy} \frac{\partial v}{\partial x} \right) + \frac{\partial}{\partial y} \left(h D_{yy} \frac{\partial v}{\partial y} \right) \right] = 0 \quad (3)$$

where: u, v = depth-averaged velocities in x - and y -direction respectively, t = time, g = gravitational acceleration, η = water level, h = water depth, ρ = water density, f = Coriolis coefficient, τ_{bx}, τ_{by} = bottom shear stresses, τ_{wx}, τ_{wy} = surface shear stresses due to wind, D_{xx}, D_{yy}, D_{xy} = diffusion coefficients.

Bottom shear stresses are calculated based on Chezy equation as follows:

$$\tau_{bx} = \rho f_r u (u^2 + v^2)^{\frac{1}{2}}, \quad \tau_{by} = \rho f_r v (u^2 + v^2)^{\frac{1}{2}}, \quad f_r = \left(\frac{g}{C^2} \right) \quad (4)$$

A finite difference approximation is used to present the partial differential equations. The finite difference equations are expressed in an Alternating Direction Implicit (ADI) form with two successive time level operations being executed during each computing cycle. First stage: (i) implicit solution of $u^{n+1/2}$ and $h^{n+1/2}$ using the continuity and x -momentum equations, (ii) explicit solution of $v^{n+1/2}$ using the y -momentum equation, (iii) spatial smoothing of $u^{n+1/2}$ and $v^{n+1/2}$ using a velocity averaging scheme. Second stage: (i) implicit solution of v^{n+1} and h^{n+1} using continuity and y -momentum equations, (ii) explicit solution of u^{n+1} using x -momentum equation, (iii) spatial smoothing of u^{n+1} and v^{n+1} using a velocity averaging scheme.

Boundary conditions are specified as follows: Velocities perpendicular to solid boundaries are set to zero. At open boundaries either water levels or mean velocities are specified. For the initial conditions, water levels and velocities are prescribed at all grid points in the computation domain.

Wave Model: The RCPWAVE model developed by the Coastal Engineering Research Center (1986) is applied to compute the wave field in the study area. The model is based on the solution of the mild slope equation for combined refraction-diffraction as follows:

$$\frac{\partial}{\partial x} \left(c c_g \frac{\partial \phi}{\partial x} \right) + \frac{\partial}{\partial y} \left(c c_g \frac{\partial \phi}{\partial y} \right) + \sigma^2 \frac{c_g}{c} \phi = 0 \quad (5)$$

where: $c(x,y)$ = wave celerity, σ = angular wave frequency, c_g = group celerity, $\Phi(x,y)$ = complex velocity potential.

Sediment Transport Model:

1) Governing equation: The three-dimensional sediment transport model is based on the mass balance of material in suspension as follows:

$$\frac{\partial c}{\partial t} + \frac{\partial}{\partial x} (uc) + \frac{\partial}{\partial y} (vc) + \frac{\partial}{\partial z} [(w - w_s)c] - \frac{\partial}{\partial x} \left(D_x \frac{\partial c}{\partial x} \right) - \frac{\partial}{\partial y} \left(D_y \frac{\partial c}{\partial y} \right) - \frac{\partial}{\partial z} \left(D_z \frac{\partial c}{\partial z} \right) + \lambda c + S = 0 \quad (6)$$

where: c = sediment concentration, u, v, w = local velocities, D_x, D_y, D_z = diffusion coefficients in x -, y -, and z -direction respectively, w_s = settling velocity, λ = decay factor, S = source/sink term.

The three-dimensional sediment transport (Eq. 6) is integrated over each layer in the vertical, this yields the equation for multi-layer sediment transport model as follows:

$$\frac{\partial(h_k c_k)}{\partial t} + \frac{\partial}{\partial x}(h_k u_k c_k) + \frac{\partial}{\partial y}(h_k v_k c_k) + (w - w_s) [c_{k-1/2} - c_{k+1/2}] - \frac{\partial}{\partial x}(D_x h_k \frac{\partial c}{\partial x}) - \frac{\partial}{\partial y}(D_y h_k \frac{\partial c}{\partial y}) - \left[D_z \frac{\partial c}{\partial z} \Big|_{k-1/2} - D_z \frac{\partial c}{\partial z} \Big|_{k+1/2} \right] + \lambda c_k + S_k = 0 \quad (7)$$

where: k = layer index, c_k = layer-averaged sediment concentration, h_k = layer thickness, u_k, v_k, w_k = layer-averaged local flow velocities in x -, y -, z -direction respectively, S_k = source/sink term of layer k .

2) Local velocities: Local velocities $u(x,y,z), v(x,y,z)$ in the horizontal direction are described by logarithmic flow-velocity profiles as follows (Van Rijn, 1986):

$$u = \frac{U}{\left[\frac{z_0}{h} - 1 + \ln\left(\frac{h}{z_0}\right) \right]} \ln\left(\frac{z}{z_0}\right), \quad \text{and} \quad v = \frac{V}{\left[\frac{z_0}{h} - 1 + \ln\left(\frac{h}{z_0}\right) \right]} \ln\left(\frac{z}{z_0}\right) \quad (8)$$

where: z_0 = zero velocity level, U, V = depth-averaged velocity in x -, y -direction computed from the depth-averaged hydrodynamic model, h = water depth.

The local velocity in the vertical direction, $w(x,y,z)$, is computed from the equation of fluid mass balance as follows (Tsuruya et. al, 1990):

$$\frac{\partial h_k u_k}{\partial x} + \frac{\partial h_k v_k}{\partial y} + \frac{\partial h_k w_k}{\partial z} = 0, \quad \text{or:} \quad w_{k+1/2} = w_{k-1/2} + \frac{\partial h_k u_k}{\partial x} + \frac{\partial h_k v_k}{\partial y} \quad (9)$$

where: $w_{k+1/2}$ = vertical velocity at the interface of layer k and layer $k+1$.

3) Erosion: Bed materials are treated separately as sand and mud. The total rate of erosion of bed material, E , is the sum of erosion rate of sand, E_s (Van Rijn, 1986), and of mud, E_m (Partheniades, 1965).

$$E = P_s E_s + P_m E_m \quad (10)$$

$$E_s = - \left(D_z \frac{\partial c}{\partial z} \right)_{z=a} = w_s c_a = 0.015 w_s \frac{d_{50}}{a} \frac{T^{1.5}}{D_*^{0.3}}, \quad \text{and} \quad E_m = M \left(\frac{\tau_{cw}}{\tau_c} - 1 \right) \quad (11)$$

where: P_s, P_m = weight proportion of sand and mud respectively in bed material, τ_{cw} = effective bed shear stress by the combined action of wave and current, τ_c = critical shear stress for erosion of mud, M = coefficient, a = reference level above bed, c_a = bed boundary concentration of sand, T = bed shear stress parameter, D_z = vertical diffusion coefficient at reference level a , D_* = particle parameter.

4) Deposition: Deposition rate is estimated as the product of bed concentration and settling velocity of sediment particle. However, from the computation only the layer-averaged concentration is computed. The bed concentration is not available. An empirical relationship proposed by Sheng and Lick (1979) is used to estimate the bed concentration from the computed bed-layer concentration.

$$D = \beta w_s c_{Kmax} \quad (12)$$

where: c_{kmax} = layer-averaged concentration of the bed layer, β = correction factor

5) Diffusion coefficient: Diffusion coefficient in the vertical direction, D_z , includes current-related diffusion coefficient, $D_{z,c}$, and wave-related diffusion coefficient, $D_{z,w}$, (Van Rijn, 1986):

$$D_z = [D_{z,c}^2 + D_{z,w}^2]^{0.5} \quad (13)$$

Current-related diffusion coefficient:

$$\begin{aligned} D_{z,c} &= D_{z,c,max} = 0.25 \beta_1 \kappa u_{*c} h & \text{for } \frac{z}{h} \geq 0.5 \\ D_{z,c} &= D_{z,c,max} \frac{4}{h} z \left[1 - \frac{z}{h} \right] & \text{for } \frac{z}{h} < 0.5 \end{aligned} \quad (14)$$

where: $D_{z,c,max}$ = current-related diffusion coefficient in the upper half of the water depth, u_{*c} = current related bed shear velocity, β_1 = ratio of sediment and fluid mixing coefficient, κ = von Karman constant.

Wave-related diffusion coefficient:

$$\begin{aligned} D_{z,w} &= D_{z,w,bed} = 0.004 D_* \alpha_{br} \delta_s U_\delta & \text{for } z \leq \delta_s \\ D_{z,w} &= D_{z,w,max} = 0.035 \alpha_{br} h \frac{H_s}{T_s} & \text{for } z \geq 0.5h \\ D_{z,w} &= D_{z,w,bed} + \left(D_{z,w,max} - D_{z,w,bed} \right) \left[\frac{z - \delta_s}{0.5h - \delta_s} \right] & \text{for } \delta_s < z < 0.5h \end{aligned} \quad (15)$$

where: $D_{z,w,bed}$ = wave-related diffusion coefficient close to the bed, $D_{z,w,max}$ = wave-related diffusion coefficient in the upper half of the water depth, α_{br} = breaking coefficient, δ_s = thickness of near-bed mixing layer.

Horizontal diffusion coefficient, D_x and D_y , are assumed to follow the "four-third" law. For an open sea the equation is expressed as follows (Shuto, 1982):

$$D_x = 0.01L^{4/3} \quad (16)$$

where: L = mean size of the eddies participating in the diffusion process.

6) Settling velocity: Settling velocity is calculated separately for sand (Van Rijn, 1986) and for mud (Mehta and Dyer, 1986).

A finite difference approximation is used to present the partial differential equations. The ADI scheme is used with two successive time level operations during each computing cycle.

Initial concentrations are set to zero at all grid points in the computation domain. Boundary conditions are specified as follows: tidal currents and water levels are computed by using the hydrodynamic

model, waves are computed by using the wave model. At inflow boundaries the local equilibrium profiles are prescribed. At the outflow boundaries the normal derivatives of the concentrations are set to zero. Net vertical transport is considered to be zero at water surface.

Morphological Model: Bed level changes are computed basing on the sediment mass-balance equation. The equation is integrated over the water depth as follows (Van Rijn, 1986):

$$\frac{\partial z_b}{\partial t} + \frac{1}{(1-p)} \left[\frac{\partial}{\partial t} (h c_2) + \frac{\partial}{\partial x} (s_x) + \frac{\partial}{\partial y} (s_y) \right] = 0 \quad (17)$$

where: s_x = depth-integrated sediment transport in x-direction = $s_{sx} + s_{bx}$, s_{sx} = suspended sediment transport in x-direction, s_{bx} = bed load transport in x-direction, c_2 = depth-averaged concentration.

The continuity equation of sediment transport is solved by an explicit finite difference scheme. After each time increment the bed elevations are computed basing on the bed elevations of the previous time step and the sediment transport rates computed from the sediment transport model. The Modified Lax Scheme is applied as follows (De Vries, 1981).

$$\frac{\partial z_b}{\partial t} = \frac{z_{i,j}^{n+1} - \frac{\alpha_x}{4} (z_{i+1,j}^n + z_{i-1,j}^n) + \frac{\alpha_y}{4} (z_{i,j+1}^n + z_{i,j-1}^n) + \left(1 - \frac{\alpha_x}{2} - \frac{\alpha_y}{2}\right) z_{i,j}^n}{\Delta t_m} \quad (18)$$

where: Δt_m = time increment in morphological model, z_b = bed elevation, α_x, α_y = weighting factors.

Initial and boundary condition are specified as follows: At the river boundaries the bed elevations are considered unchanged. At the sea boundaries bed elevations are computed basing on the flow parameters and the explicit scheme. Initial bed elevations are specified basing on the measured data.

MODEL CALIBRATION

It is required that the grid system be fine enough in order to study detailed distribution of tidal current and sediment. However, due to the limitation of memory and speed of computer, very fine grid size cannot be applied for the whole Chao Phraya Estuary. The study area is then divided into several sub-areas in which grid systems of 5000 m x 5000 m, 500 m x 500 m, 250 m x 250 m and 50 m x 50 m are adopted. Computed results of the coarser grid are used as input data to the model of finer grid system.

Hydrodynamic Model: Measured data of water levels, tidal velocities and directions are used for the hydrodynamic model calibration. The computed results are found in very good agreement with the observed data both in water levels, velocity magnitudes as well as flow directions as shown in Fig. 1.

Sediment Transport Model: Field data of sediment concentration are used for the calibration of the sediment transport model. It is found that the computed results are in very good agreement with field data. Satellite images are also used to compared with the results of sediment concentration distribution in the study area.

Morphological Model: Annual siltation rates measured in the existing navigation channel (channel No.1) are used for morphological model calibration. Fig. 2 shows the comparison between the

computed results and the annual siltation rates measured in the existing navigation channel for the period of 1981-1985 and 1993. It is found that the model can give a very good prediction of annual siltation rate in the navigation channel.

A sample of sediment concentration distribution and flow field in the estuary are presented in Figs 3 and 4, respectively.

Through the computation it is found that the effect of wave action on the siltation process in the Chao Phraya Estuary is much stronger than that of tidal current. The main cause of siltation in the navigation channel is the sediment which has been deposited in the estuary in the past. Under the actions of wave and tidal current it becomes in suspension and deposits in the channel. River sediment does not seem to have strong influence on the siltation process in the navigation channel. This may be due to the fact that dams constructed in the upstream have stored most of sediment in river water and river water now contains less sediment than in the past.

APPLICATION

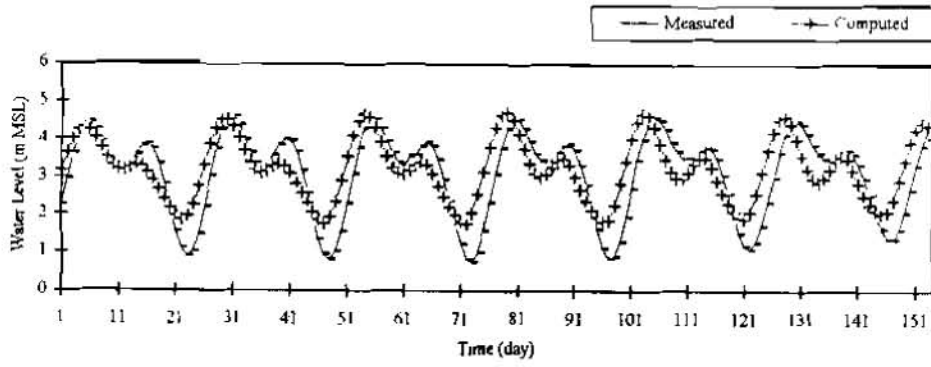
The model is applied to study the effect of the designed second navigation channel on tidal current and wave field in the estuary. It is found that with a small size, the effect of the channel is negligible.

The results show that when the second navigation comes into operation, a sediment amount of 1832,000 m³/yr has to be dredged annually in order to maintain water depth for navigation.

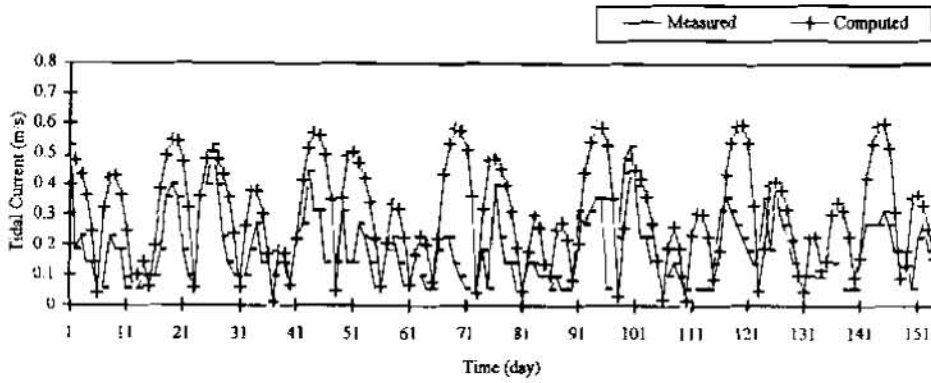
The model is also applied to estimate the spreading of the dredged spoil of the second channel. Recommendation on the location of the dumping place is then provided.

REFERENCES

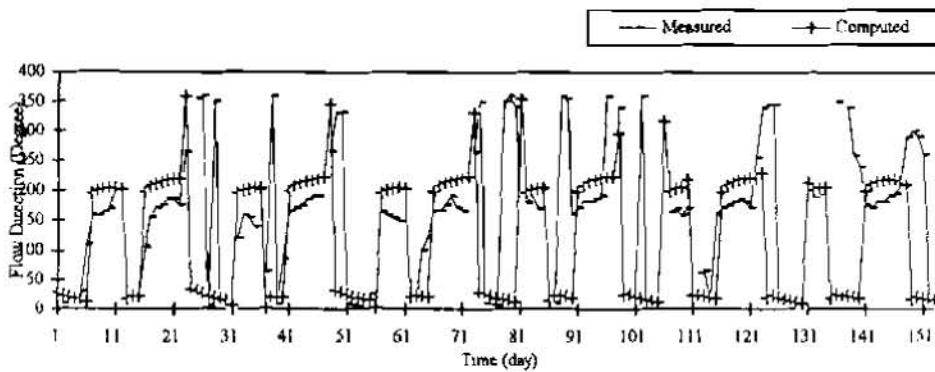
- Asian Institute of Technology, 1994, *Mathematical Model of Siltation in Second Navigation Channel of Bangkok Port*, Research Report, AIT, Bangkok, Thailand.
- De Vries, M., 1981, *Morphological Computation*, Lecture Notes fl0a Dept. of Civil Eng., Delft University of Technology, the Netherlands.
- Leendertse, J. J., 1967, *Aspects of a Computational Model for Long-Period Water-Wave Propagation*, Rand Corp. Mem., RM-5294-PR, Santa Monica, U.S.A.
- Partheniades, E., 1965, *Erosion and Deposition of Cohesive Solids*, Journal of Hydraulic Division, ASCE, Vol. 91, No.1, pp. 105-139.
- Sheng, Y. P., Lick, W., 1979, *The Transport and Resuspension of Sediments in a Shallow Lake*, J. Geophys. Res., Vol.84, pp. 1809-1826.
- Shuto, N., 1982, *Diffusion Process*, Lecture Note, Prepared for the Seminar on Tidal Hydraulics and Salinity Intrusion, Ho Chi Minh City, Vietnam.
- Tsuruya, H., Murakami, K., Irie, I., 1990, *Mathematical Modeling of Mud Transport in Ports with Multi-Layer Model - Application to Kumamoto Port*, Report of the Port and Harbor Research Institute, Vol. 29, No.1, Japan.
- Van Rijn, L. C., 1986, *Mathematical Modeling of Suspended Sediment in Non-uniform Flow*, Journal of Hydraulic Division, Vol.112, HY, pp. 433-455.



(a) Water Level



(b) Tidal Current



(c) Flow Direction

Fig. 1: Comparison between Computed and Measured Water Level, Tidal Current and Direction

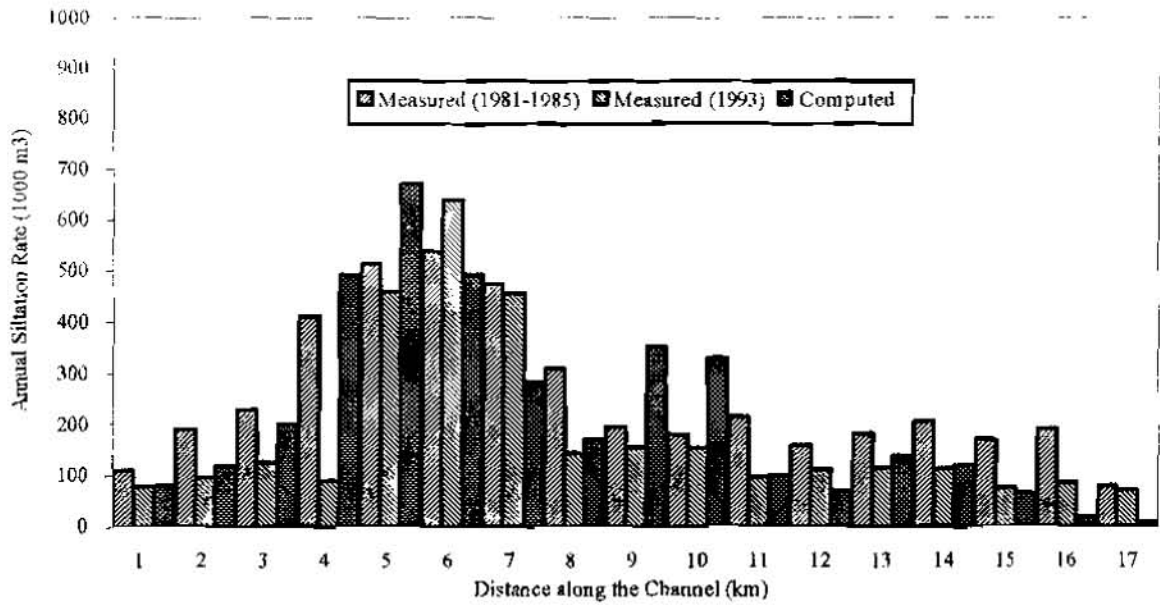


Fig. 2: Comparison of Computed and Measured Siltation Rates in the Navigation Channel

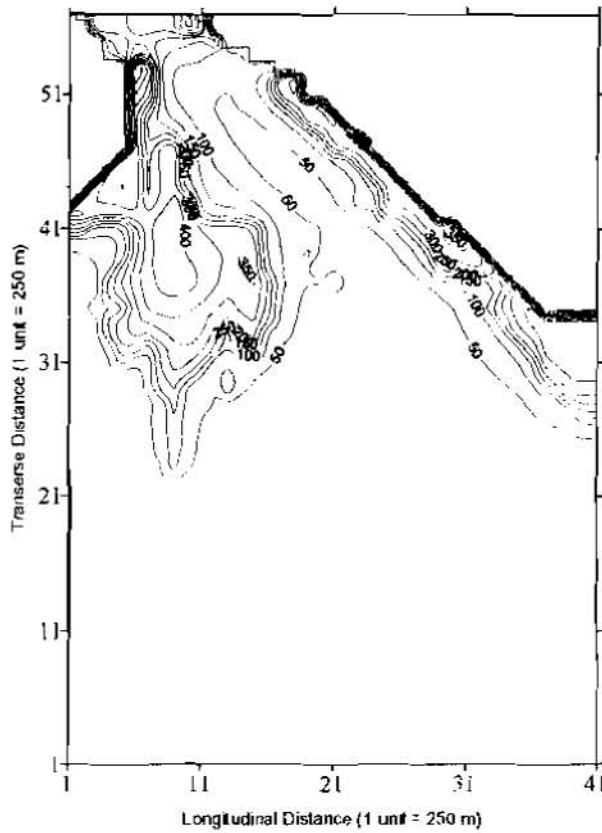


Fig. 3: Sediment Concentration Distribution

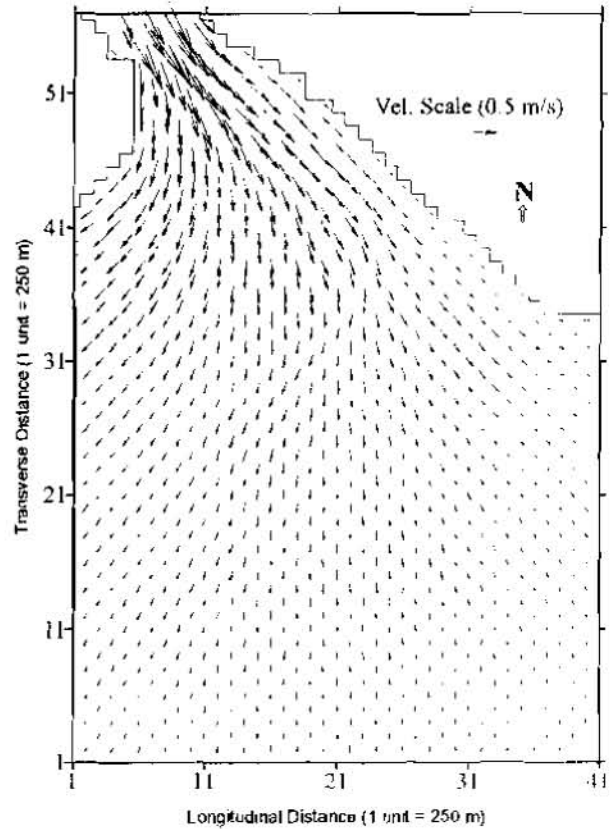


Fig. 4: Computed Tidal Current in the Gulf

USING CE-QUAL-W2 TO ASSESS THE EFFECT OF REDUCED PHOSPHORUS LOADS ON CHLOROPHYLL-a AND DISSOLVED OXYGEN IN THE TUALATIN RIVER, OREGON

Tamara Wood, Hydrologist, US Geological Survey, Portland, Oregon;
Stewart Rounds, Hydrologist, US Geological Survey, Portland, Oregon

INTRODUCTION

The Tualatin River drains a 712 square-mile basin on the west side of the Portland metropolitan area in northwestern Oregon. The basin supports a growing population of more than 320,000 people and a wide range of urban, agricultural, and forest-derived activities. The people who live in the Tualatin River Basin depend heavily on the Tualatin River for drinking water, irrigation water, recreation, and assimilation and transport of wastes. The economic prosperity currently enjoyed within the basin depends on the proper management of this surface water resource and the maintenance of its quality.

The streamflow of the Tualatin River reflects the seasonal rainfall, and the contribution of snowmelt is minimal. Most of the annual precipitation falls between November and June; seasonal streamflow is typically highest from December through April and lowest from July through October. The low-flow summer period is defined as May 1st through October 31st. Since January of 1975, Tualatin River streamflow has been augmented during this low-flow period with water releases from a man-made reservoir.

The reach of the river that is of primary concern meanders for approximately 30 miles over the floor of the basin, from river mile (RM) 38.4 to RM 3.4. This reach is characterized by a low slope (approximately 0.08 ft/mi) and backwater created by a low-head dam at RM 3.4. The river widens to 150 ft or more, exposing much of its surface to direct sunlight. In the summer, large populations of phytoplankton thrive in the warm, slow-moving water in which nutrients are usually abundant. The algal blooms and subsequent population crashes have historically contributed to violations of the State of Oregon minimum dissolved-oxygen standard (6.0 mg/L, pre-1996) and the maximum pH standard of 8.5. Several sites on the main stem also exceeded the 15 µg/L chlorophyll-a action level for nuisance phytoplankton growth.

In response to the Federal Clean Water Act (CWA) of 1972, the Oregon Department of Environmental Quality (ODEQ) in 1984 and 1986 listed the Tualatin River as a "water-quality limited" stream because of low dissolved-oxygen concentrations and nuisance levels of algae. One of the designated beneficial uses of the river, aesthetics, was listed as impaired by algal blooms. As required by the CWA, total maximum daily loads (TMDLs) were established for phosphorus and ammonia in order to limit algal blooms.

The establishment of TMDLs in the Tualatin River Basin prompted local and State agencies to be proactive in meeting their wasteload and load allocations. The urban area is served by four wastewater treatment plants (WWTPs), all of which are operated by the Unified Sewerage Agency of Washington County (USA). In 1990, the U.S. Geological Survey entered into a cooperative agreement with the USA to assess the water-quality conditions of the Tualatin River. One objective of that project was to construct and use a mechanistically based, process-oriented model of nutrients and dissolved oxygen for the main stem during the low-flow, high-temperature, summer period. The model was to be used as both a diagnostic tool to better understand nutrient and dissolved-oxygen dynamics, fate, and transport, and to assess the relative importance of various processes, and as a prognostic tool to evaluate the relative water-quality benefits of various management alternatives for the Tualatin River.

RESULTS OF MODEL CALIBRATION

A modified version of the U.S. Army Corps of Engineers model CE-QUAL-W2 was calibrated using data obtained during the May 1 to October 31 period of 1991, 1992, and 1993. These 3 years exhibited a wide range of hydrologic conditions, from very dry in 1992 to fairly wet in 1993. Because the water quality of the Tualatin River is closely coupled to its streamflow, the summers of 1991-1993 also exhibited a wide range of water-quality conditions, which allowed a robust model of the Tualatin River to be created when all three of the datasets were used for calibration. The calibration parameters represent the best fit of the model to a wide range of observed conditions.

Chlorophyll-a

The factors that control algal growth in the Tualatin River are well understood. When several days of bright sunlight are coupled with warm water, sufficiently-long travel times, and ample nutrients, an algal bloom occurs. The first step in model calibration, therefore, was to make sure that the model simulated both the streamflow and the water temperature in the river well in all 3 years (S. A. Rounds, U.S. Geological Survey, unpub. data, 1997). Once that was accomplished, the calibration of the algal growth in the river was accomplished by adjusting four rates—algal growth, algal respiration, algal excretion, and zooplankton grazing.

Rapid algal growth is typically observed as far upstream as a sampling site at RM 16.2. Blooms usually continue to expand, or may be eroded by zooplankton grazing, downstream to the dam at RM 3.4, but the results at RM 16.2 are representative and only those are presented in this paper. Simulated and observed concentrations of chlorophyll-a at RM 16.2 are shown in figure 1. The basic cycle in algal growth is captured by the model in all 3 years, even in 1992, which is characterized not so much by a succession of blooms as by an initial bloom followed by sustained, high concentrations of chlorophyll-a through the rest of the season. Model performance is degraded during time periods when zooplankton grazing is important (for example, during early August in 1991 and mid to late August in 1993).

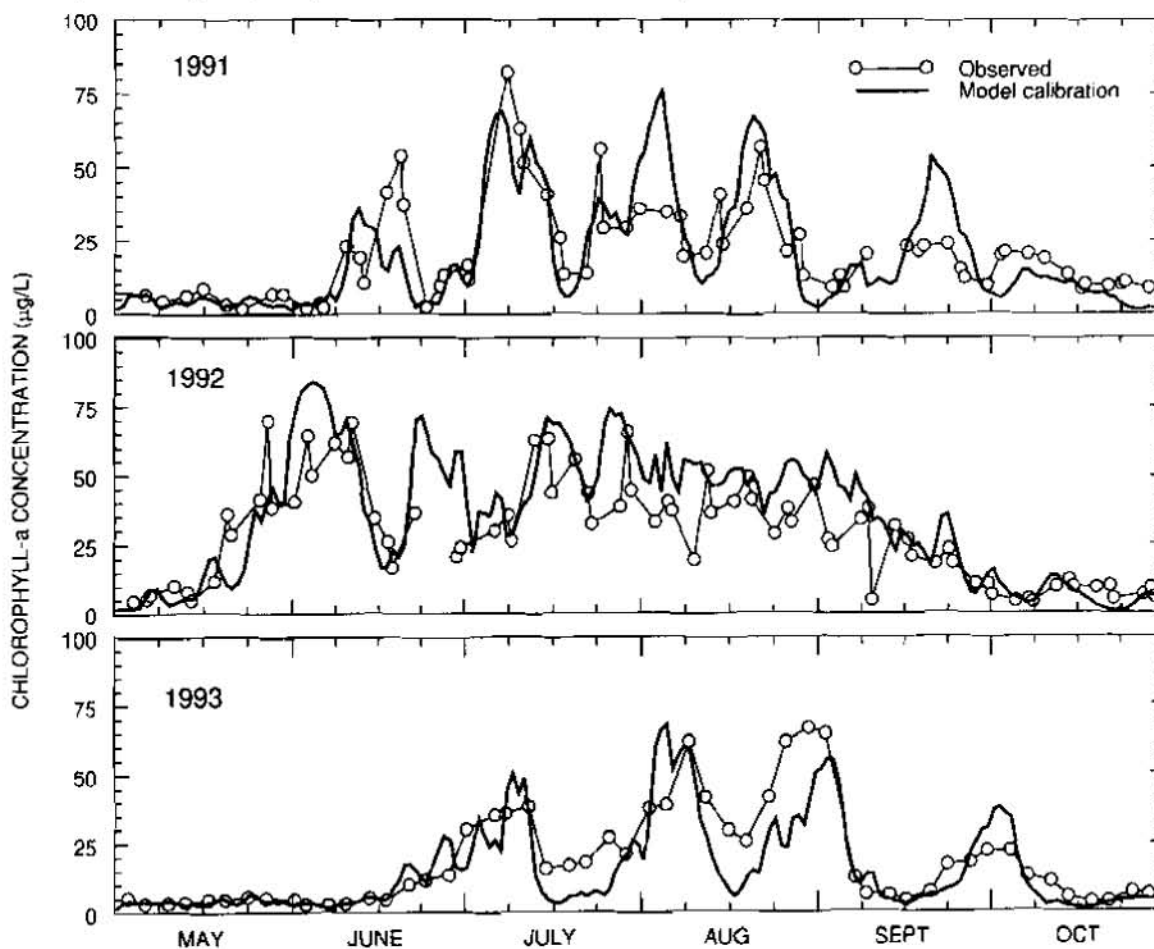


Figure 1. Measured and simulated chlorophyll-a concentration in the Tualatin River at RM 16.2.

Dissolved Oxygen

The largest oxygen demands in this system are: allochthonous carbonaceous biochemical oxygen demand (CBOD) entering at the upstream boundary and tributaries (including the WWTPs) in the form of detrital organic matter (OM); autochthonous CBOD produced within the model reach, primarily from the excretion of readily recycled organic material from viable cells; and sediment oxygen demand (SOD). Autochthonous

CBOD is significant only where algal growth occurs, but during algal blooms, this component of the CBOD dominates the other oxygen demands downstream of RM 16.2. Each type of demand dominates for short periods of time (days to weeks), but when demands are averaged from May to October, the largest oxygen demand comes from the SOD.

Sources of dissolved oxygen (DO) include reaeration, point and nonpoint sources of water containing DO, and photosynthesis. Reaeration is not a particularly important source (or sink) of DO in the Tualatin River, and is small compared to photosynthesis and inputs of oxygenated water. Inputs of oxygenated water can be important sources in some subreaches of the river, but only when those inputs are also important components of the water budget; for example, discharges from the WWTPs increase the DO concentration downstream of the plants at low-flow times of the year.

Downstream of RM 16.2, photosynthesis is by far the most important source of DO. Thriving algal cells under favorable light and nutrient conditions produce more DO through photosynthesis than they consume through the combined processes of respiration and the decay of excreted OM. Prolonged production of DO by photosynthesis has another consequence, however; when it abates, respiration and the bacterial decay of cells continue to consume oxygen. Thus, a period of overcast weather that precipitates a "crash" of a large algal population can also precipitate a drop in DO. Photosynthetic production and the consumption of oxygen by respiration and autochthonous CBOD make the algae of primary importance in determining the DO concentration, particularly on the daily and weekly time scales that are typical of the algal growth cycle. It is not surprising, therefore, that the bloom cycle seen in the observations of chlorophyll-a (figure 1) is also apparent in the observations of DO (figure 2). In general, where the model overestimates the chlorophyll-a at the peaks of blooms, it overestimates the DO as well. The converse is also true.

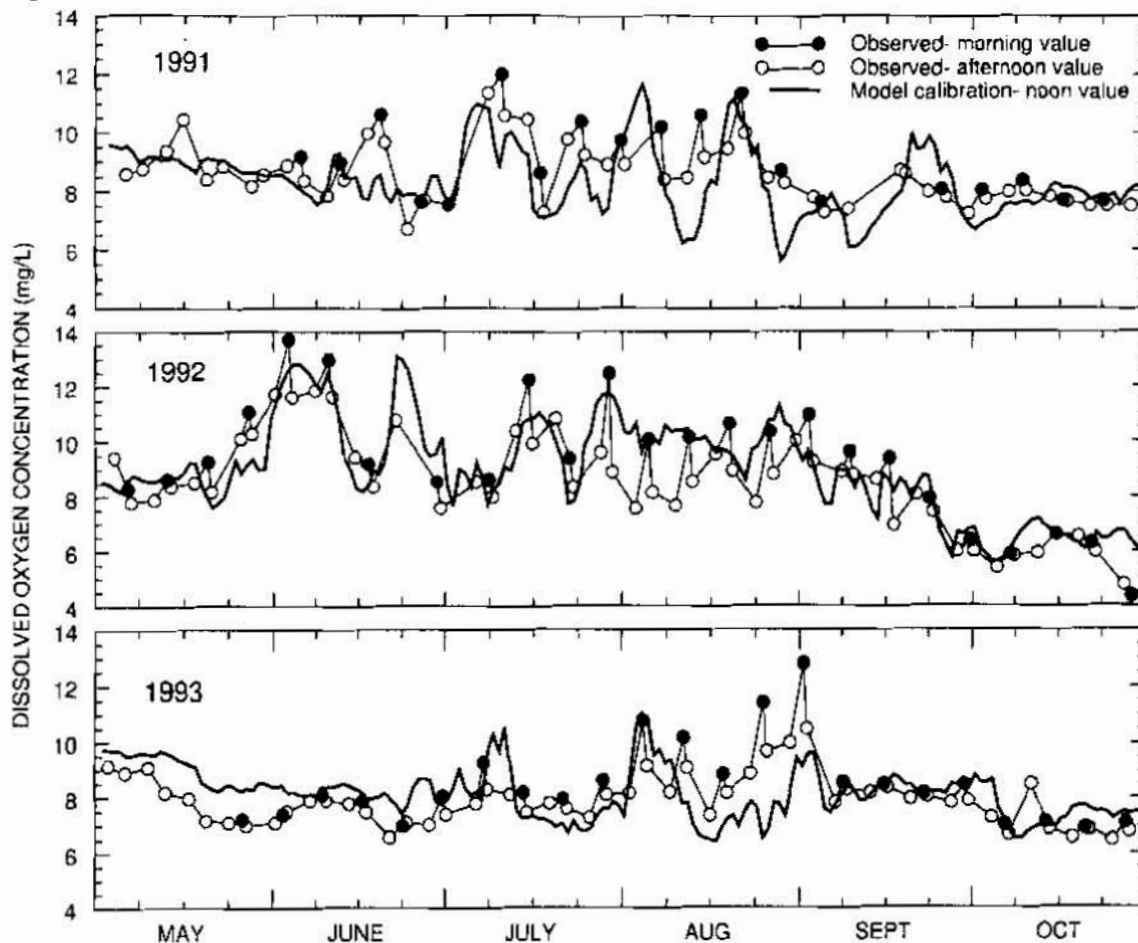


Figure 2. Measured and simulated DO concentration in the Tualatin River at RM 16.2.

It is important to distinguish between the daily to weekly effect of the algae on DO and their net *seasonal* effect. The algae clearly act to increase the DO concentration when they are growing and decrease it when they are in decline, but the magnitude of the increase or decrease is limited by residence time. The size of a bloom under continuously favorable light conditions is limited by the travel time through the reach between RM 16.2 and the low-head dam at RM 3.4, which usually does not exceed 9 days, even during low flows. Conversely, when light conditions become unfavorable for algal growth, the extent of oxygen depletion is also limited by travel time, because dead and respiring algal cells will eventually be advected out of the system. Dead algal cells that settle to the sediments continue to consume oxygen as they decay, but this does not significantly augment the high "background" SOD in the Tualatin River. The *duration* of a bloom, however, is not limited by travel time, but only by the duration of favorable light, temperature, and nutrient conditions. As a result, the effect of phytoplankton on the seasonal average of DO in the Tualatin River is largely a consequence of western Oregon's summer weather, which is characterized by favorable light conditions that often last for weeks at a time. The number of days that the algae are net producers of oxygen exceeds the number of days that they are net consumers; consequently the seasonally averaged concentration of DO downstream of RM 16.2 is increased over what it would be in the absence of primary production. A corollary is that if primary production were reduced, the SOD and allochthonous CBOD would remain largely unchanged over a single summer season, and the seasonally averaged concentration of DO downstream of RM 16.2 would likely decrease. It is important to remember this point when interpreting various management strategies for the river.

HYPOTHETICAL SCENARIOS

A primary goal of this application of CE-QUAL-W2 to the Tualatin River was to create a calibrated model that could be used to determine the probable efficacy of water-resources management decisions quickly and inexpensively by testing various hypothetical scenarios. The testing of hypothetical scenarios requires that the model be applied in a prognostic mode and, by definition, that it be applied under conditions to which it has not been explicitly calibrated. In order to ensure that the environmental conditions (including hydrology, meteorology, and water quality) of the hypothetical scenarios were small deviations from those under which the model was calibrated, and that the calibration parameters remain valid, the hypothetical scenarios were tested by using the same forcing functions and boundary data used in the calibration with the minor changes required for the scenario being tested. Each scenario was tested using all three (1991-1993) calibration seasons in order to simulate its effect for a wide range in hydrologic conditions. The strategy of testing the hypothetical scenarios by reusing the calibration datasets has the further advantage that the performance of the model has already been determined by a comparison with the observations. The accuracy of the hypothetical scenarios depends in large part on the accuracy of the calibration runs; for those time periods and river reaches that the calibration runs were more (or less) accurate, the hypothetical scenarios should also be more (or less) accurate.

Many of the hypothetical scenarios that have been tested with the model were designed to reduce the magnitude of algal blooms, either by reducing the length of time the algae are in the river (the travel time) or by making environmental conditions less favorable for growth. There are two reasons for the focus on reducing algal growth. The first is that the algae are a "nuisance" factor, and the second is the presumption that a reduction in algal growth will result in improved water quality, primarily as measured by DO and pH.

Four hypothetical scenarios that involve bringing the main stem and tributaries into compliance with the phosphorus TMDLs at the boundaries will be discussed, along with the changes in chlorophyll-a and DO concentration produced by each scenario. In order to quantitatively summarize each of the hypothetical simulations concisely, a table of the bimonthly means of four relevant concentrations resulting from each scenario was constructed (table 1). The 2-month periods are intended to roughly capture a seasonal pattern in the summer cycle. The first 2 months, May and June, are generally characterized by higher streamflow and smaller algal blooms than the July-August period, when low summer flows have been established, the weather is generally favorable for algal growth, and the size of algal blooms is the largest of the year. The September-October period is often an important period in terms of water quality because streamflow remains low through this period, but light conditions become less favorable for the algae. Very low oxygen concentrations (figure 2) are often observed during this period because low flows and high temperatures

result in continued strong oxygen demand from CBOD and SOD, but photosynthetic production of oxygen slows considerably. A very dry year presents an exception to this rough characterization of the bimonthly periods; in 1992, the May-June period behaves much like the July-August period because summer low flows were established earlier than normal. Bimonthly means for the model calibration run are also included in the table, and provide the base case against which the changes induced by the hypothetical scenarios are compared.

Tributary Phosphorus Reduction

In these scenarios, the total phosphorus entering the river at the upstream boundary and each tributary was reduced to the level of the regulated TMDL. The TMDL criteria are 0.07 mg/L total phosphorus for the three largest tributaries and 0.05 mg/L total phosphorus at the upstream boundary; the smaller tributaries do not have TMDLs, but were assigned concentrations of 0.07 mg/L for these scenarios. The reduction in total phosphorus was achieved in two ways. In the first case (scenario 1a), the phosphorus exceeding the TMDL was first removed from the detrital phosphorus compartment. If that compartment was depleted entirely, then the orthophosphate compartment was tapped for the remaining amount. This scenario amounts to a reduction primarily in allochthonous CBOD in order to achieve the phosphorus TMDL levels; a secondary decrease in orthophosphate occurs because less orthophosphate is released through CBOD decay. In the second case (scenario 1b), the process is reversed—the phosphorus is removed first from the orthophosphate compartment and then, if necessary, from the detrital phosphorus compartment. This scenario relies primarily on a reduction in orthophosphate and generally requires very little reduction in allochthonous CBOD to achieve TMDL levels at the boundaries. Both scenarios result in less orthophosphate in the water column, although scenario 1b reduces orthophosphate much more than does scenario 1a (rows 2 and 3 in table 1).

Although both scenarios reduce algal growth, preferentially removing orthophosphate (1b) to achieve TMDL levels reduces growth more than preferentially removing detrital phosphorus (1a) (compare row 12 with row 13 in table 1). Scenario 1a, however, results in a consistently higher bimonthly averaged DO concentration than scenario 1b, and for most of the 2-month time periods scenario 1a results in a higher bimonthly averaged DO concentration than the calibration run. In contrast, the bimonthly averaged DO concentrations from scenario 1b are almost always lower than in the calibration run because of reduced photosynthetic production (compare rows 16, 17, and 18 in table 1).

Tributary Phosphorus Reduction with Flow Augmentation

These scenarios combine scenarios 1a and 1b, in which phosphorus concentrations at the upstream boundary and in all tributaries were reduced to the TMDL criteria, with maintenance of a minimum streamflow of 150 ft³/s at the upstream boundary of the model grid (RM 38.4). In scenario 2a, phosphorus was preferentially removed from the detrital phosphorus compartment, as in 1a; in scenario 2b, phosphorus was preferentially removed from the orthophosphate compartment, as in 1b. The combination of phosphorus reduction at the boundaries and flow augmentation results in a greater reduction in algal growth than phosphorus reduction produces alone (compare rows 14 and 15 to rows 12 and 13 in table 1). Scenario 2a results in consistently higher chlorophyll-a (by 0.9 to 8.5 µg/L) and consistently higher DO (by 0.31 to 1.22 mg/L) than 2b.

Chlorophyll-a Reduction and Improvements in DO Concentration

Some important conclusions are illustrated by the comparison of two particular scenarios (1a and 2b) with the base case. Scenario 1a achieves the maximum *overall* increase in DO concentration, and 2b achieves the maximum *overall* decrease in chlorophyll-a. (These assessments were made by taking average values over the entire 6-month season and comparing with the average value for the calibration.) A plot of chlorophyll-a at RM 16.2 (figure 3) shows that the combination of flow augmentation with a significant reduction in orthophosphate (scenario 2b) can very effectively limit the size of algal blooms, often by as much as 50%. A comparison of figure 3 with figure 4 shows that the reduction in algal growth in scenario 2b manifests itself primarily as a much lower oxygen concentration during algal blooms. There is little evidence that this scenario results in increased DO concentration during algal crashes, probably because of their short duration

Table 1. Summary statistics for the phosphorus reduction scenarios.

[Bi-monthly mean concentrations for each constituent were derived from simulated, daily, 10-foot-average noon concentrations at RM 16.2. Concentrations given for the calibration simulation (c) are the model's best representation of observed conditions. The other runs superimpose combinations of phosphorus removal and flow augmentation on the calibrated conditions. In scenario 1a, total phosphorus concentrations were reduced to their target TMDL concentrations by removing detrital phosphorus first. In scenario 1b, the TMDL levels were achieved by removing orthophosphate first. The other two scenarios, 2a and 2b, removed phosphorus as in 1a and 1b while maintaining a minimum flow of 150 ft³/s at RM 38.4. Shaded cells highlight concentrations that would be in violation of a TMDL criteria, the DO standard, or the chlorophyll-a action level. M/J=May/June; J/A=July/August; S/O=September/October.]

Parameter	Scenario	1991			1992			1993			ROW
		M/J	J/A	S/O	M/J	J/A	S/O	M/J	J/A	S/O	
Ortho-phosphate (mg/L as P)	c	0.051	0.048	0.056	0.042	0.018	0.055	0.055	0.048	0.053	1
	1a	0.042	0.035	0.046	0.031	0.013	0.042	0.047	0.039	0.044	2
	1b	0.015	0.022	0.030	0.014	0.010	0.025	0.017	0.022	0.027	3
	2a	0.042	0.038	0.045	0.033	0.015	0.038	0.047	0.040	0.044	4
	2b	0.015	0.023	0.031	0.016	0.011	0.024	0.017	0.022	0.027	5
Total Phosphorus (mg/L as P)	c	0.115	0.110	0.098	0.100	0.076	0.104	0.113	0.102	0.100	6
	1a	0.055	0.063	0.063	0.057	0.051	0.061	0.060	0.066	0.064	7
	1b	0.056	0.065	0.064	0.059	0.055	0.063	0.060	0.067	0.065	8
	2a	0.055	0.063	0.063	0.058	0.053	0.060	0.060	0.065	0.063	9
	2b	0.056	0.065	0.063	0.059	0.056	0.061	0.060	0.067	0.064	10
Chlorophyll-a (µg/L)	c	8.4	36.7	13.9	35.5	50.4	18.3	6.7	25.9	12.9	11
	1a	8.1	33.4	13.6	31.2	43.6	16.4	6.6	24.5	12.5	12
	1b	5.3	22.7	10.1	24.6	33.4	12.1	5.7	17.0	9.2	13
	2a	8.2	28.4	10.2	27.5	40.0	11.5	6.6	21.4	8.2	14
	2b	5.3	20.1	8.4	23.2	31.5	9.1	5.7	15.0	6.9	15
Dissolved Oxygen (mg/L)	c	8.56	8.62	7.74	9.79	9.85	7.21	8.61	7.99	7.92	16
	1a	9.03	9.14	8.22	9.88	9.69	7.81	8.95	8.46	8.41	17
	1b	8.50	7.63	7.51	8.84	8.07	6.74	8.64	7.22	7.70	18
	2a	9.03	8.84	8.14	9.54	9.63	7.82	8.95	8.33	8.22	19
	2b	8.50	7.62	7.68	8.86	8.41	7.27	8.64	7.27	7.79	20

and because the background oxygen demands are so high that they dominate oxygen consumption even during algal crashes. The only time period when scenario 2b significantly increases DO concentration is October of 1992, when the flow augmentation decreases the time-of-travel enough that oxygen consumption by CBOD and SOD is reduced substantially. Therefore, the management strategy that most effectively reduces algal growth is not the same strategy that generates the greatest overall increase in DO concentration.

The phosphorus reduction scenario in which detrital phosphorus is removed preferentially (scenario 1a) is most effective at increasing DO because of the reduced concentration of allochthonous CBOD. This scenario also reduces orthophosphate somewhat because phosphorus release from the decomposition of detrital OM is reduced, but the ability of this scenario to limit algal growth is minimal, except at the peak of very large blooms. Algal growth is affected by this scenario somewhat more in 1992 because simulated phosphorus concentrations during the mid-summer months were already growth-limiting, so the effect of the small additional reduction in orthophosphate is enhanced. The effect of scenario 1a on DO is primarily a relatively constant positive offset (figure 4), especially during non-bloom periods, because of the reduction in the background oxygen demand from the decay of allochthonous CBOD.

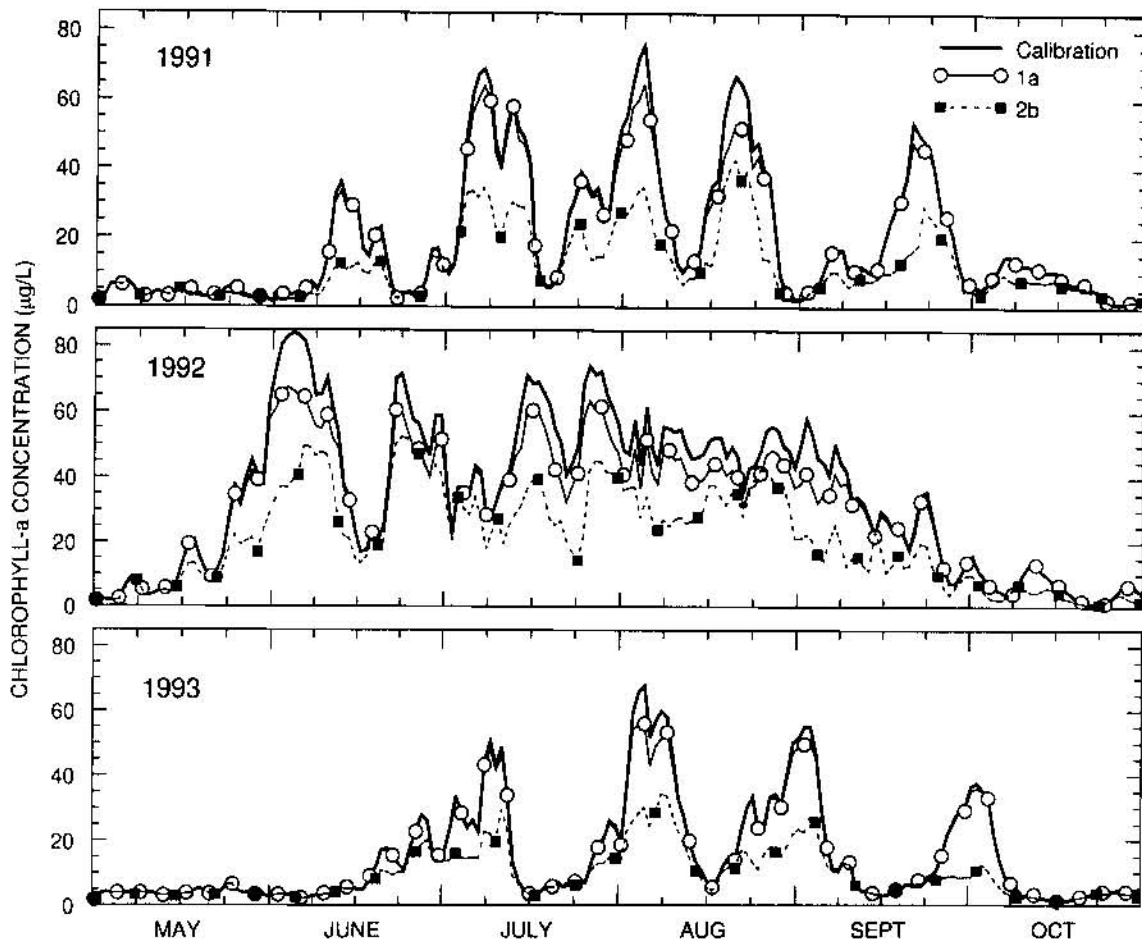


Figure 3. Calibrated chlorophyll-a at RM 16.2 compared with scenarios 1a and 2b.

The comparison of scenarios 1a and 2b demonstrates that the role of algae in determining the DO concentration is more often one of production than consumption; therefore, a reduction in algal growth more often reduces than increases DO concentrations. A reduction in the size of an algal bloom also will decrease the diel variations in DO and pH associated with that bloom that can cause stress to aquatic organisms. A reduced, but more stable, DO concentration during blooms may, therefore, be beneficial. The most effective way to increase DO concentrations during non-bloom periods, however, is to reduce the high background demand for oxygen.

SUMMARY

A modified version of the U.S. Army Corps of Engineers model CE-QUAL-W2 was used to simulate flow, temperature, and water quality in the Tualatin River, a low-gradient stream that meanders through a mixture of urban and rural landscapes on the west side of the Portland, Oregon, metropolitan area. Combined with warm temperatures and an ample nutrient supply, the travel time during the summer low-flow period is of sufficient duration to produce a thriving phytoplankton population that can cause large changes in the dissolved-oxygen (DO) concentration and the pH — large enough to violate Oregon State water-quality standards and degrade the designated beneficial uses. In 1988, the Oregon Department of Environmental Quality (ODEQ) established total maximum daily loads (TMDLs) for total phosphorus for the Tualatin River and its largest tributaries.

CE-QUAL-W2 was calibrated to the summer low-flow conditions observed from May through October of 1991, 1992, and 1993, and then used to evaluate the effects of various phosphorus loads and levels of flow augmentation on DO concentrations in the Tualatin River. These model simulations were run using the

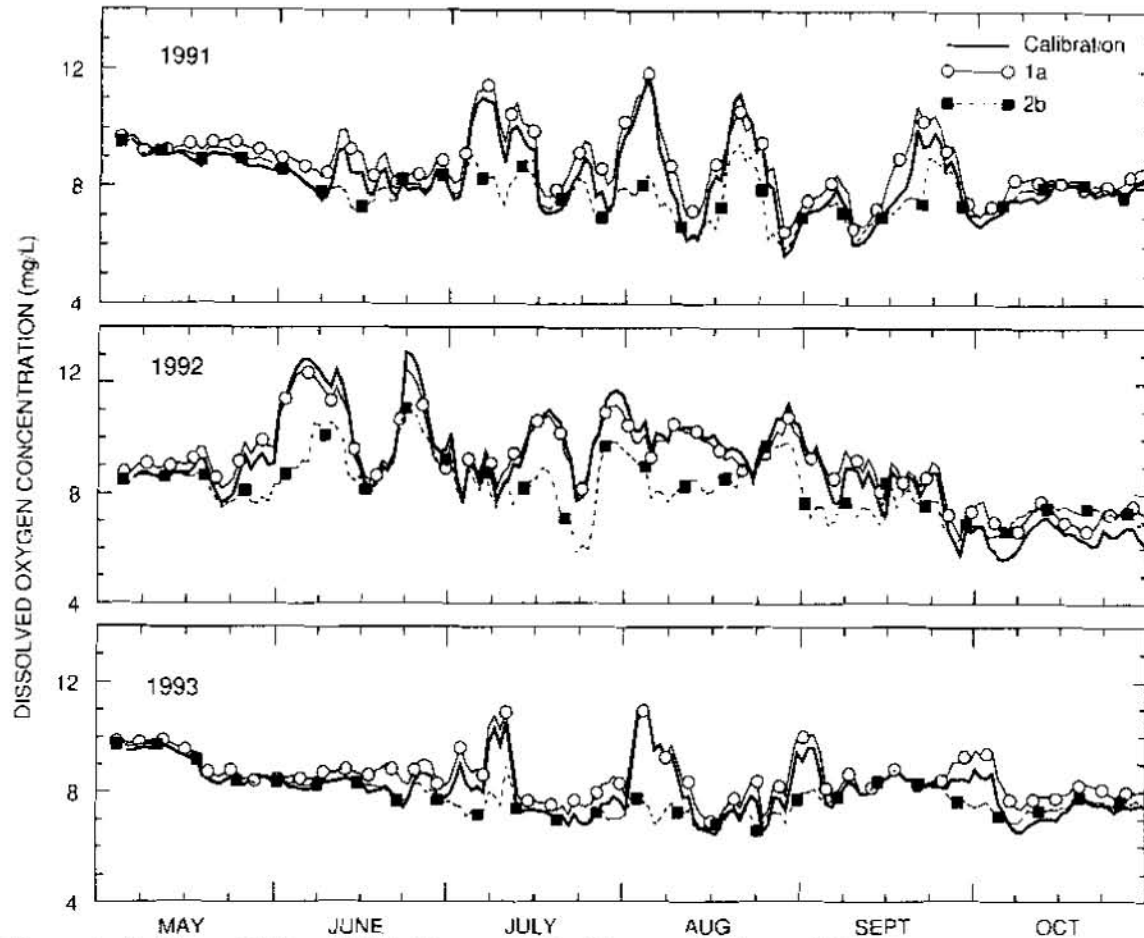


Figure 4. Calibrated DO at RM 16.2 compared with scenarios 1a and 2b.

same hydrologic and meteorological conditions under which the model was calibrated, thus providing a wide range of imposed conditions, from the very low-flow "drought" conditions of 1992 to the "wet" conditions of 1993. Several important results were obtained from these scenarios:

- ◇ For the period May through August, phosphorus-reduction scenarios showed some ability to limit algal growth during large blooms. When these scenarios failed to simultaneously reduce the background oxygen demands (carbonaceous biochemical oxygen demand [CBOD] and sediment oxygen demand), however, DO concentrations between algal blooms still decreased to near-problematic levels.
- ◇ Phosphorus reduction scenarios showed that if the total phosphorus TMDL was achieved in the tributaries and in the main stem at RM 38.4, the predicted effect on DO was unclear. If detrital phosphorus were removed preferentially, then DO conditions would improve, especially in October, because CBOD would be removed. If soluble orthophosphate were removed instead, then DO conditions actually would deteriorate due to reduced photosynthetic production of oxygen without a simultaneous loss of CBOD.
- ◇ During September and October, the most significant improvements in DO were obtained only through a large amount of flow augmentation, or through a lesser amount of flow augmentation combined with a reduction in the loads of CBOD from the boundaries.
- ◇ The model results indicate that the goals of limiting algal growth and reducing DO violations can be, at times, incompatible. (However, excursions to high pH values are also of concern, and reducing the number of pH violations is dependent on limiting algal growth.)

These results are being used by ODEQ to revise the total phosphorus TMDL for the Tualatin River.

AN ALTERNATIVE METHODOLOGY TO STUDY LOCAL SCOUR AT BRIDGE PIERS

Authors: Xibing Dou, Ph.D., Senior Research Engineer, GKY and Associates Inc., Springfield, Virginia; Yafei Jia, Ph.D., Research Assistant Professor, Center for Computational Hydroscience and Engineering, University of Mississippi, University, Mississippi; Sam S.Y. Wang, Ph.D., F. A. P. Barnard Distinguished Professor and Director, Center for Computational Hydroscience and Engineering, University of Mississippi, University, Mississippi; J. Sterling Jones, Research Hydraulic Engineer, Federal Highway Administration, McLean, Virginia

Abstract Local scour around bridge piers is caused by complex processes of interactions between three-dimensional turbulent flow and sediment. Downflow and vortices induced in front of a pier are the major contributors to local scour. Therefore, simulating secondary flow motions and using this information to predict sediment transport are critically important to numerical models that aim at simulating local scour. In order to capture the complex turbulent flow structures near piers, a stochastic turbulence closure-model is adopted in CCHE3D, a three-dimensional free-surface flow model. By using this model, anisotropic turbulence stresses, which are more realistic than the isotropic ones predicted by most existing eddy-viscosity models, are calculated. A sediment transport capacity formulation has been developed to estimate sediment transport rate for local scour. In this formulation, the dominant factors of local scour such as downflow, vortices, and turbulence induced or intensified by the piers are considered. Computational simulation of local scour around piers is conducted. The comparison of the simulation results and the experimental data have verified that both the turbulence model and the newly developed sediment transport formulation have enhanced the computational model's capability in simulating realistic local scour.

INTRODUCTION

Traditionally, local scour investigations have been conducted by physical modeling in the laboratory and field observations. These traditional methodologies have been costly, time-consuming, and subject to similitude or interpretation problems. Therefore, hydraulic researchers and engineers need a more effective alternative. With the dramatic advances of computer technology and numerical simulation methodology, simulating local scour processes by using numerical models has become a viable alternative. Local scour is a complex three-dimensional process with downflow and vortices induced in front of a pier as the major contributors. Simulating secondary flow motion to predict sediment transport are critically important to numerical models that aim at simulating local scour. However, from a comprehensive survey of previous studies of numerical simulation for local scour, it appears that the state of the art is far from adequate. Most of the numerical models used in simulating local scour are Eddy-Viscosity Models such as the Mixing-Length Models, the $k-\epsilon$ Models, etc. However, Eddy-Viscosity Models are based on the Boussinesq's hypothesis that implies the use of a scalar or isotropic eddy viscosity (Younis, 1991) and fail to simulate general three-dimensional flow in natural environments (Wilcox, 1993). In order to simulate secondary flow motion and, thereafter, local scour at bridge piers, a stochastic turbulence-

closure model, which predicts anisotropic turbulent stresses, has been incorporated into the three-dimensional flow model, CCHE3D, developed by the Center for Computational Hydroscience and Engineering (CCHE) at the University of Mississippi.

STOCHASTIC TURBULENCE-CLOSURE MODEL

Turbulence-Closure problems exist if Reynolds' statistical approach is used to describe turbulent flows. Because of the existence of unknown turbulent correlations, the system equations for turbulent flows do not form a closed set, therefore, turbulence-closure models are necessary. The turbulence-closure models which have been developed in the past can be broadly classified as Eddy-Viscosity Models and Reynolds-Stress Models in spite of various complexities among them.

Eddy-Viscosity Models are based on the Boussinesq's hypothesis:

$$\text{Turbulent stresses} = -\rho \overline{u'_i u'_j} = \rho \nu_t \left(\frac{\partial U_i}{\partial x_j} + \frac{\partial U_j}{\partial x_i} \right) \quad (1)$$

where u'_i and u'_j are the fluctuating velocity components; ρ is the density of water; ν_t is turbulent eddy viscosity, U_i and U_j are the time-averaged mean velocity components; x_i and x_j are the coordinates.

Boussinesq's hypothesis has some serious defects on its structure, which limit the range of the applicability of these models. For example, according to the definition of Boussinesq's hypothesis, eddy-viscosity ν_t is a positive coefficient between the turbulent stresses and the local rate of strain. A negative value of eddy viscosity would suggest that the shear stresses actually drive, rather than oppose, the fluid motion. Therefore, Boussinesq's hypothesis can not be applied to the flows in which the shear stress and velocity gradient have opposite signs; Boussinesq's hypothesis assumes that turbulent stresses are proportional to time-averaged velocity gradients and, thus, the turbulent stresses will be zero wherever the time-averaged velocity gradients are zero. This assumption does not agree with some laboratory experimental findings. For instance, the time-averaged velocity gradients are always zero at the center of a pipe. According to the hypothesis, the turbulent stresses have to be zero at this location. However, a lot of laboratory experiments have shown that the turbulent stresses at the center of the pipes are not zero. Besides, Boussinesq's hypothesis implies a scalar or isotropic eddy viscosity, but, there is ample experimental evidence, particularly from complex turbulent shear flows, to suggest the contrary (Hinze, 1975; Rodi, 1993). Wilcox (1993) summarized the flows Boussinesq's hypothesis fails to apply. He pointed out that Boussinesq's hypothesis can not be applied to three-dimensional flow and the flow in ducts with secondary motions.

A Stochastic Turbulence-Closure Model was proposed by Guoren Dou (hereafter referred to as G. Dou) in 1980. The turbulence fluctuating structures, the time-averaged flow structures and the drag coefficient for Newtonian and drag reduction flows in all states (laminar, transition, turbulent) and in all regimes (smooth, transition, rough) have been

studied through the model (also see G. Dou, 1987; 1996). In this model, the turbulent correlations, or the turbulent stresses, are calculated directly from the fluctuating velocities. The expression of fluctuating velocity was derived by G. Dou (1980) under the assumption that the change in an instantaneous velocity component at the center of an eddy is negligible within a certain distance. Taking the stochastic approach, G. Dou used the probability density function to calculate the statistical mean values and the correlation moments for the random variables and derived a general expression for the turbulent stresses:

$$\begin{aligned}
 -\overline{u_i' u_j'} = & -\left(\frac{1}{2} U^2 + 2M^2 L^2 \frac{\partial U_i}{\partial x_m} \frac{\partial U_j}{\partial x_l} \right) \delta_{ij} \\
 & + \frac{1}{2} \left[U^2 T - \frac{1}{2} M L^2 \left(\frac{\partial U_i}{\partial x_m} + \frac{\partial U_j}{\partial x_l} \right) \right] \left(\frac{\partial U_i}{\partial x_j} + \frac{\partial U_j}{\partial x_i} \right) \\
 & - \frac{1}{8} M^2 L^2 (3\delta_{lm} - 1) \left(\frac{\partial U_i}{\partial x_m} + \frac{\partial U_m}{\partial x_i} \right) \left(\frac{\partial U_j}{\partial x_l} + \frac{\partial U_l}{\partial x_j} \right)
 \end{aligned} \quad (2)$$

where U , L and T are the characteristic velocity, length and time; the subscripts m and l are the summation indices ($= 1, 2, 3$); δ_{ij} and δ_{lm} are the Kronecker deltas; M is a dimensionless parameter that represents viscous effects and can be expressed as:

$$M = \frac{z}{\alpha_0 \delta^*} \quad (3)$$

where z is the distance from solid wall; α_0 is a coefficient ($= 32.3$); δ^* is the thickness of viscous sub-layer ($= 11.6\nu / U_*$); ν is the kinematic viscosity of fluid; U_* is the bed-shear velocity.

The characteristic variables (U , L and T) for open-channel flow are determined by following equations (Dou, 1987):

$$U^2 = \alpha_1 \frac{z}{\delta^* + z} U_*^2 ; \quad M L = \alpha_2 \kappa z \sqrt{1 - \frac{z}{H}} ; \quad U^2 T = \alpha_3 \kappa U_* z \left(1 - \frac{z}{H} \right) \quad (4)$$

where κ is von Karman constant ($= 0.4$); H is the flow depth; α_1 , α_2 and α_3 are the coefficients which equal to 1.0, 0.39 and 1.96 respectively.

In 1997, Xibing Dou (hereafter referred as X. Dou) found that for three-dimensional flow simulation the coefficients, α_1 , α_2 and α_3 , in the above equation should be modified as:

$$\alpha_1 = 1 - e^{-\chi \left(\frac{B}{H} \right)^2} ; \quad \alpha_2 = 0.39 \left[1 - e^{-\chi \left(\frac{B}{H} \right)^2} \right] ; \quad \alpha_3 = 1.96 \left[1 - e^{-\chi \left(\frac{B}{H} \right)^2} \right] \quad (5)$$

where B is the minimum horizontal distance from any solid wall; χ is an adjustable parameter. It has been found that a stable three-dimensional flow field can be obtained if χ is taken as 0.01.

SEDIMENT TRANSPORT CAPACITY FOR LOCAL SCOUR

Sediment transport rate can be determined directly by establishing sediment transport functions. Yang (1996) discussed some of the commonly used transport functions. For example, based on power concept, G. Dou (1974) suggested that the rate of energy dissipation used by flowing water to keep sediment particles in suspension should be equal to that used by sediment particles in suspension, and proposed a formula for sediment transport capacity:

$$T_c = f_0 \frac{U_{av}^3}{gH\omega} \quad (6)$$

where T_c is sediment transport capacity; U_{av} is the depth-averaged velocity; g is the gravitational acceleration; ω is fall velocity; f_0 is a coefficient.

Similar to most of the sediment transport functions, G. Dou's sediment transport capacity formula was developed for the prediction of sediment transport rate for general scour. Because the mechanism of local scour is different from that of general scour, this formula can not be applied directly to local scour simulation. It must be modified by considering the factors that cause local scour (X. Dou, 1991). From the previous investigations of local scour, it has been found that the major factors are downflow, vortices, and turbulence induced by bridge piers. On the other hand, according to Yang (1973), the dominant factors governing the rate of sediment transport for general scour are velocity, depth, slope, resistance, shear stress, particle size, etc. Therefore, the general function of sediment transport capacity for both general scour and local scour is expressed as:

$$T_c = \psi(U_{av}, H, U_*, \omega, g, C, \gamma, \gamma_s, d_{50}, |W|, \Omega, b, i) \quad (7)$$

where C is Chezy's coefficient; γ_s and γ are the specific weights of sediment and water; d_{50} is median sediment particle size; $|W|$ is the magnitude of downflow; Ω is the strength of vortices; b is the width of pier; i is the turbulence intensity.

Applying non-dimensional variables and the superposition principle, the above function can be written as:

$$T_c = f_0 \sigma_0 + f_1 \sigma_1 + f_2 \sigma_2 + f_3 \sigma_3 \quad (8)$$

where $f_1, f_2,$ and f_3 are the coefficients; $\sigma_0, \sigma_1, \sigma_2,$ and σ_3 are the dimensionless parameters:

$$\sigma_0 = \frac{U_{av}^3}{gH\omega} \quad ; \quad \sigma_1 = \frac{|W| - |W|_{app}}{U_{av}} \quad ; \quad \sigma_2 = \frac{(\Omega - \Omega_{app})b}{U_*} \quad ; \quad \sigma_3 = \frac{i - i_{app}}{\omega} \quad (9)$$

where the subscript "app" indicates that the quantities are obtained from the approaching flow.

Assuming that the sediment transport capacity for general scour and the sediment transport

capacity for local scour are of the same order of magnitude and that their maximum values are equal, the general expression for sediment transport capacity is modified and rewritten as follows:

$$T_c = f_0 \sigma_0 + \left[\frac{(f_0 \sigma_0)_{\max}}{(\Sigma)_{\max}} \right] \Sigma \quad (10)$$

where Σ is the summation of the parameters, σ_1 , σ_2 , and σ_3 , normalized by their maximum values. The subscript "max" represents the maximum value in entire flow domain. Parameter Σ is expressed as follows:

$$\Sigma = \frac{F_1}{3} \left(\frac{\sigma_1}{\sigma_{1,\max}} \right) + \frac{F_2}{3} \left(\frac{\sigma_2}{\sigma_{2,\max}} \right) + \frac{F_3}{3} \left(\frac{\sigma_3}{\sigma_{3,\max}} \right) \quad (11)$$

$$F_1 + F_2 + F_3 \equiv 3$$

where F_1 , F_2 , and F_3 are proportion coefficients between 0 and 1.

It is noteworthy that the sediment transport capacity in equation (10) does not require calibration case by case.

NUMERICAL SIMULATION OF LOCAL SCOUR

Numerical simulations of local scour at cylindrical piers were conducted to compare with the physical experiments performed at the TFHRC Hydraulic Laboratory of FHWA and at the University of Alberta by Ahmed (1995). First, three-dimensional flow fields around cylindrical bridge piers were simulated by the model using the same boundary conditions used in the physical experiments. After the 3D flow field stabilized, the model simulated sediment transport in the channels and local scour around the piers in an uncoupled mode. The 3D flow field was adjusted after scour reached a preselected increment, then sediment transport computation resumed. The 3D flow field and sediment transport were alternately calculated until the scour hole reached equilibrium. Figure 1 shows the downflow and the horse-shoe vortex simulated by the model on the centerline of the channel. Figure 2 illustrates the shear stress ratio on the plane of symmetry prior to scouring around a pier. The model agrees well with laboratory measurements taken by Ahmed (1995). Figure 3 is a pictorial view of near-equilibrium scour hole that resulted from a 4603 minute simulation with the 3D model. Figure 4 illustrates the model capability for simulating local scour as a function of time. Again, the model agreed very well with several long duration experiments that were conducted in the Federal Highway Administration Hydraulic Laboratory and with the equilibrium condition that was documented by Ahmed (1995) under a carefully controlled laboratory experiment.

CONCLUSIONS

The implementation of the stochastic turbulence-closure model has enhanced the capability of the computational simulation model in prediction of anisotropic turbulence stresses. This

in turn predicts more realistic secondary motions induced by the presence of the structures or obstructions in the free surface flows. Due to the fact that traditional empirical functions predicting the sediment transport capacity were based on two-dimensional flow characteristics, they are not suitable for application to local scour studies. The modification of the sediment transport capacity function by considering the effects of downward velocity, vortices and turbulence intensity has greatly improved this function's applicability to the numerical simulation of local scour processes. Through the tests of numerical simulation of 3D flow field and local scour at piers, the model's potential in the application to local scour research has been demonstrated.

ACKNOWLEDGEMENTS

This work is a result of research sponsored by the USDA Agriculture Research Service under Specific Research Agreement No. 58-4431-9-075, the Federal Highway Administration through Dwight David Eisenhower Transportation Fellowship Program, and the University of Mississippi.

REFERENCES

- Ahmed, F., 1995, Flow and erosion around bridge piers, Ph.D. thesis, Department of Civil Engineering, University of Alberta.
- Dou, G., 1974, Similarity theory and its application to the design of total sediment transport model, Research Bulletin of Nanjing Hydraulic Research Institute, Nanjing, China.
- Dou, G., 1980, The stochastic theory and the general law of all flow regions for turbulent open channel flows, Proceeding of First International Symposium on River Sedimentation, Beijing.
- Dou, G., 1987, Mechanics of turbulent flows, High Education Publication, Vol. II, Beijing.
- Dou, G., 1996, Basic laws in mechanics of turbulent flows, China Ocean Engineering, Vol. 10, No. 1, pp 1-44.
- Dou, X., 1991, A numerical simulation of local scour process around rectangular piers, Master Thesis, University of Mississippi, Oxford.
- Dou, X., 1997, Numerical Simulation of Three-Dimensional Flow Field and Local Scour at Bridge Crossings, Ph.D. Dissertation, University of Mississippi.
- Hinze, J. O., 1975, Turbulence, McGraw Hill Book Company, New York.
- Rodi, W., 1993, Turbulence models and their application in hydraulics, Monograph, IAHR, Delft, The Netherlands.
- Wilcox, D. C., 1993, Turbulence Modeling for CFD, DCW Industries, Inc., La Canada, CA.
- Yang, C. T., 1973, Incipient Motion and Sediment Transport, Journal of Hydraulic Engineering, Vol. 99, No. HY10.
- Yang, C. T., 1996, Sediment Transport: Theory and Practice, The McGraw-Hill Companies, Inc.
- Younis, B. A., 1991, Applied turbulence modeling, Lecture Notes, University of Mississippi, Oxford, Mississippi.

NUMERICAL SIMULATION OF LOCAL SCOUR AROUND PIER
 Velocity vector on centerline prior to scour hole formation

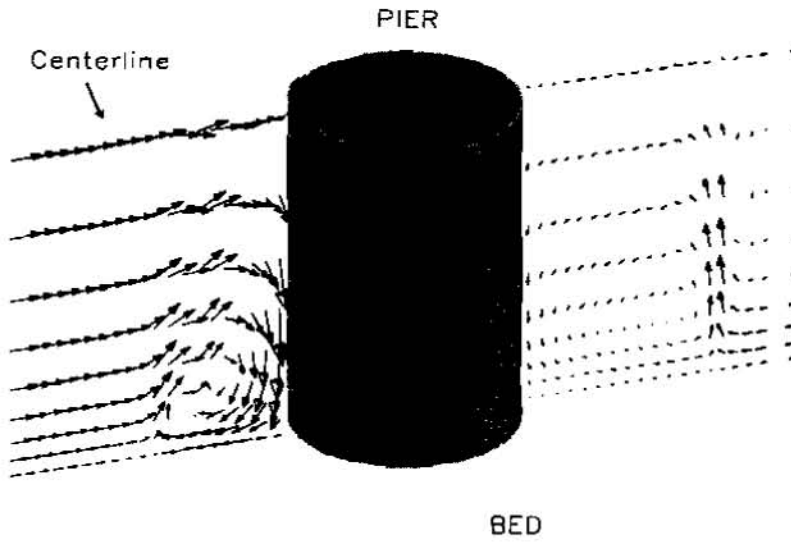


Figure 1. Downflow and horse-shoe vortex simulated in front of a pier

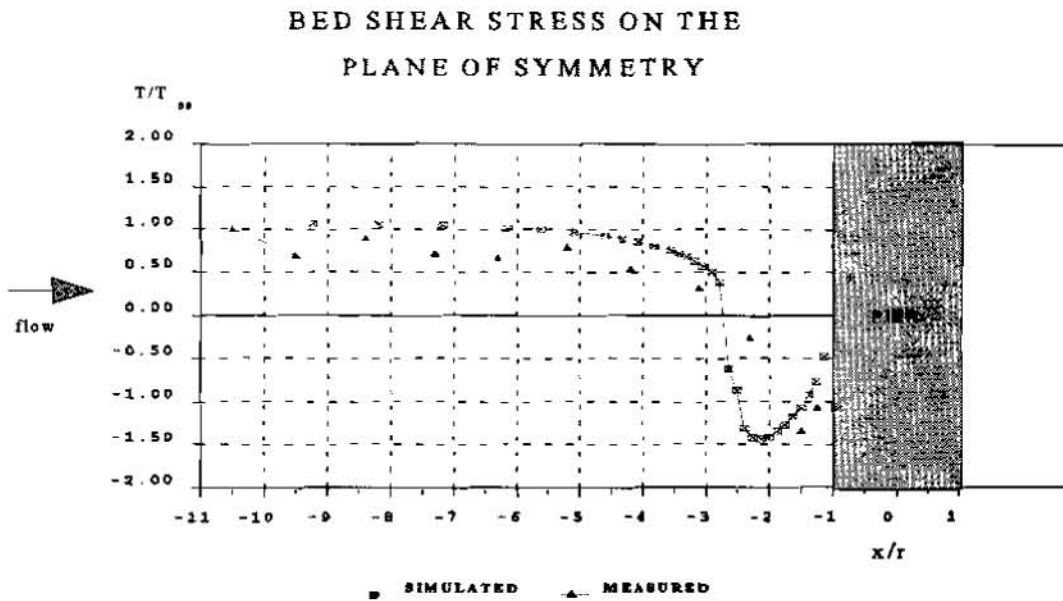


Figure 2. Comparison of shaer stress in front of a pier

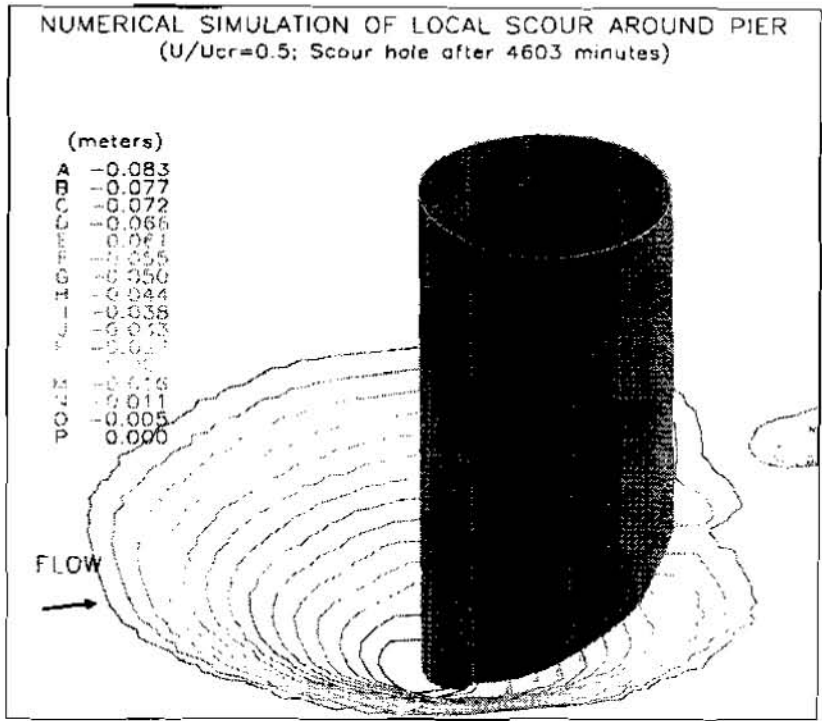


Figure 3. A near-equilibrium scour hole around a pier

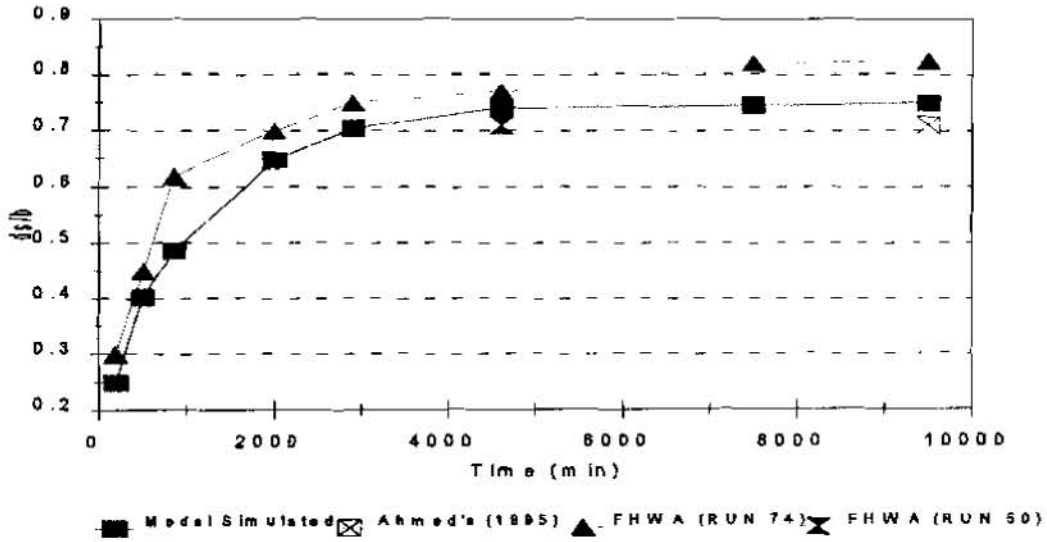


Figure 4. Comparison of scour depth vs time

**SEDIMENT TRANSPORT ANALYSIS OF THE ATHENS, OHIO LPP
AND A COMPARISON OF TWO
CORPS SEDIMENT TRANSPORT COMPUTER MODELS**

**Jon B. Fripp¹, Kenneth C. Halstead², Dr. Surya Bhamidipaty³
and Jerry W. Webb⁴**

Abstract Channel improvements are a common means of providing flood protection for many communities. Many older channel improvement projects consisted of enlarging the existing channel cross section in order to increase conveyance. While this technique proved to be effective in lowering flood depths, the associated reduction in channel velocities often cause these projects to be susceptible to sediment deposition. As a result, excessive maintenance dredging is then required to maintain the design conveyance. One such local flood protection project is located on the Hocking River in Athens, Ohio. Since this project was completed in 1971, approximately 95,000 yd³ of material has been removed from the channel at a cost in excess of \$325,000.

At the request of the Hocking Conservancy District, the local sponsor of the project, the Huntington District of the U.S. Army Corps of Engineers investigated potential alternatives to the continuation of the current dredging requirements. These alternatives included structural modifications to the channel that would either reduce sediment deposition, or localize it within easily maintainable areas. The Corps computer programs HEC-2 and HEC-6 were used to assess the sediment transport capability of the river with the various alternative scenarios that were studied.

Due to budgetary and scheduling constraints, many Corps studies do not have sufficient time or funding to conduct a fully involved and detailed sedimentation study. For these situations, the computer software package, SAM, was developed for use in the initial assessment of sedimentation trends. This paper will compare and contrast the results which can be obtained using SAM with those that were obtained using HEC-6. The lessons learned from this analysis of sediment transport along the Hocking River and the comparison of the results of the two methods could prove to be useful in future studies of this type, and in the design of channel improvements.

¹Hydraulic Engineer, Baltimore District, Corps of Engineers

²Hydraulic Engineer, Water Resources Engineering Branch, Corps of Engineers, 502 Eighth St, Huntington, WV 25701-2070

³Chief, Engineering Division, Walla Walla District, Corps of Engineers

⁴Supervisory Hydraulic Engineer, Water Resources Engineering Branch, Corps of Engineers, 502 Eighth St, Huntington, WV 25701-2070

INTRODUCTION

The Athens, Ohio Local Protection Project (LPP) consisted of straightening and increasing the width of the original channel. The channel improvement begins upstream of the town at the remains of White's Mill Dam and extends downstream for approximately five miles. The LPP widened the Hocking River channel to 215 feet, more than twice its original width, and shortened the stream by approximately 1400 feet through the Athens reach. A plan view of the original meanders through the town and the alignment of the improvements are shown on Figure 1.

As is common in many older channel improvement projects, this project provided an enlarged channel cross section in order to increase conveyance for flood damage reduction purposes. Since its completion in 1971, the project is estimated to have prevented over 78 million dollars in flood damages. As evidenced by the magnitude of prevented flood damages, this project design is effective in reducing flood water surface profiles. However, as a consequence, the dramatic change in the river's geometry has caused the project to be susceptible to sediment deposition. Significant maintenance dredging has been required to maintain the design conveyance. Since project completion, more than 95,000 yd³ of material has been removed from the channel at a cost in excess of \$325,000. Typical cross sections of the Hocking River for the original project design condition and for the 1992 study condition are shown on Figure 2.

Several futile attempts have been made by the Hocking Conservancy District (HCD) to maintain the original design channel template. However, much of the deposition reappears at the same locations throughout the length of the project as soon as the next year. In 1992, the HCD entered into an agreement with the Huntington District of the U.S. Army Corps of Engineers to cost share a study to determine whether there are any viable alternatives to the continuation of the current dredging requirements.

Subsequently, the Huntington District conducted a detailed study using the computer programs, HEC-2 and HEC-6, field reconnaissance, and engineering judgement to quantify the sediment transport characteristics of the river for current conditions and for the various alternatives that were considered. Since the current depositional pattern appears to be consistent, the study also investigated whether the Hocking River has reached a quasi stable condition, and whether significant flood events would flush the deposited sediment through the system.

Following completion of the detailed study, the computer software package, SAM, was made available for use by Corps Districts in the initial assessment of sedimentation trends. In an effort to test the applicability of the new software, the Huntington District applied input data and parameters of the Hocking River and compared the results to the detailed study. The remainder of this paper describes both studies and their respective results.

DETAILED SEDIMENTATION STUDY WITH HEC-6

Existing Conditions An HEC-2 model was developed for a 12.6 mile reach of the Hocking River at Athens, Ohio, using cross section data from a 1992 field survey. A second HEC-2 model was developed for the original design geometry of the project. Both models employ the same Manning's "n" values and rating curve at the downstream end for starting conditions. Therefore, the difference between the two reflects the effects of deposition in the project. By comparing of the results of the two models for three large flood events, the reduction in conveyance, due to sediment deposition, induces an increase in flood profiles from 0.5 to 1 foot.

While more than 95,000 yd³ of material has been removed from the channel since project construction, comparisons of design and current cross sections show that the original channel cross sectional shape has been reduced. To regain the original conveyance of the project, either dredging efforts must be increased, the sediment transport capacity of the channel must be increased, or the amount of sediment that enters the channel must be reduced.

Development of the HEC-6 Model The Corps computer program, HEC-6, was used to model the erosion and depositional trends in the project. This program simulates the sediment transport capacity of a river by mathematically modeling the interaction between sediment inflow and the hydraulic characteristics of the study reach. The required input into HEC-6 includes such site specific information as geometry, inflow hydrology, sediment inflow, and sediment transport capacity.

The geometry for the HEC-6 model was obtained from the first HEC-2 model. Sediment samples were taken from the bed of the study reach and used to develop the bed gradation of the model. Forty years of streamflow records were obtained from local USGS stream gages for the hydrologic input to the HEC-6 model. The Corps's Sediment Weighted Histogram Generator (SWHG) program was used to reduce the 365 mean daily records of each year into blocked histograms of thirty events per year. The sediment yield of the watershed is required as input into the HEC-6 model. Using historical records of sediment inflow as a guide, Toffaleti's (1948) computational technique was selected to characterize the total sediment load and the sediment distribution by size fraction for various discharges. Results of this technique were adjusted to reflect local conditions by using the regression relation between mean annual sediment discharge and mean annual water discharge, as published in the USGS report titled "Summary of Fluvial-Sediment Studies in Ohio, Through 1987".

Madden's (1985) modification of Laursen's (1958) relationship was selected for the sand transport equation in the HEC-6 model. Several other sediment transport methods available in HEC-6 were tested, but each produced thalweg elevations that became progressively unstable with time. In HEC-6, the basis for simulating vertical movement of the bed in response to scour or deposition is the Exner equation for continuity of material. It was

determined that five iterations of the Exner equation produced the most stable results. Long term depositional trends of the model compared favorably to historic dredging records.

The results of the HEC-6 computations are dependent on the data used to calibrate the model and the initial assumptions regarding the equations used to model the interaction of sediment with stream flow. Where possible, each step in the development of the HEC-6 model was compared with available information. When adequate data is not available, it is necessary to conduct a sensitivity analysis to assess the impacts of potential errors in the initial assumptions. This causes the development and calibration of an HEC-6 model to be very labor intensive and time consuming. Depending upon the skill of the modeler and the available information, the development of an HEC-6 model to this point may require up to three months. In many situations, not all of the information is readily available, thus the creation of the HEC-6 model can take even longer.

Alternatives An array of conditions and channel maintenance options were analyzed in the this study. These included: 1) allowing the current conditions to continue without maintenance, 2) a compound channel through the project with a dry floodway on the right bank, 3) channel improvements downstream of the project, 4) an upstream sediment trap, 5) use of flood walls and/or levees, 6) reconstructing White's Mill Dam, 7) reconstructing White's Mill Dam with an upstream sediment trap, and 8) reconstructing White's Mill Dam with channel improvements downstream of the project. The performance of each alternative was measured by pulsing the peak discharges of three floods, the May 1990 event, the design flood, and a 100-year flood, through the HEC-6 model at short time increments, both at the beginning and the end of the 40 years of record. This provides a "before" and "after" water surface profile. The effect that the alternative has upon the sedimentation in the project is reflected in the relative elevation difference between these water surface profiles. The results of the analyses of selected alternatives are summarized in the following paragraphs. Of these alternatives, only those that involve a sediment trap provide a cost effective and practical solution.

Current Conditions Allowing current conditions to continue without maintenance dredging was modeled by running the HEC-6 model through the 40 years of flow records. The model indicates that a steady state condition will not be achieved in this time frame and that deposition will continue in the project. The results indicate that the rising limb of the hydrograph would deposit more material in the project and that the peak discharge would not erode a significant amount of material.

Compound Channel with a Floodway The objective of a compound channel with a floodway was to create a self cleansing pilot channel to carry the normal river flow and a floodway to pass the flood flows. The pilot channel was designed using regime theory and approximating the original channel dimensions of the Hocking River through Athens. The pilot channel meander was configured to coincide with the current sand bar deposition pattern. The HEC-6 model indicated that deposition in the pilot channel would be significantly reduced.

However, the size of the floodway is limited by existing bridge openings and roads. As a result, the overall conveyance in the project would be reduced and the flood profiles would be increased.

Downstream Channel Improvement An HEC-2 analysis indicates that improving the channel downstream of the project would reduce flood profiles through the project reach. However, the HEC-6 analysis indicates that the sediment deposition problems would not improve. While the downstream channel improvement remains relatively clear and stable, material continues to deposit in the existing project. Eventually, without continued dredging, the benefits of the downstream channel improvement would begin to diminish.

Sediment Trap Alternatives that included an upstream sediment trap were the most successful with respect to providing long term reductions in water surface profiles, and in reducing much of the maintenance required in the project. The concept of a sediment trap, a dredged hole in the stream bed, provides a local sink for inflowing sediment so that deposition is confined to one area. This alternative confines the maintenance of the project to monitoring and periodically removing material from a single location rather than over the length of the project. The HEC-6 model indicates that the sediment trap reduces much of the sediment transport into the project and that flood water surface profiles would be reduced over time. A sediment trap of 600 feet in length and 300 feet in width would require the removal of 20,000 yd³ approximately six times over a 40 year period

ESTIMATION OF SEDIMENTATION USING SAM

The computer software package, SAM, can be used to calculate sediment-discharge rating curves for given hydraulic parameters. These sediment rating curves can be integrated with flow-duration data to calculate the average annual sediment yield for a reach of river. Sediment yield is often calculated as part of a sediment impact assessment.

A sediment impact assessment study uses a sediment budget analysis to assess the potential for degradation or aggradation of sediment. With this procedure, the estimated average annual sediment load entering the project area is compared to the average annual sediment load that the proposed project is capable of transporting. If there is more material entering the project than the project is capable of passing, the difference will most likely be deposited in the project. If the project can transport more material than is entering the area, then erosion can be anticipated. A sediment budget analysis using the Corps computer program SAM is significantly less time consuming than a full scale HEC-6 study. However, when used for a sediment budget analysis, SAM provides results that are more qualitative, rather than quantitative in nature. The capability of SAM to quantify erosion or deposition at specific locations is limited. Since the objective of the Athens, Ohio sedimentation study was to investigate several options to continued dredging, the sole use of a sediment budget analysis

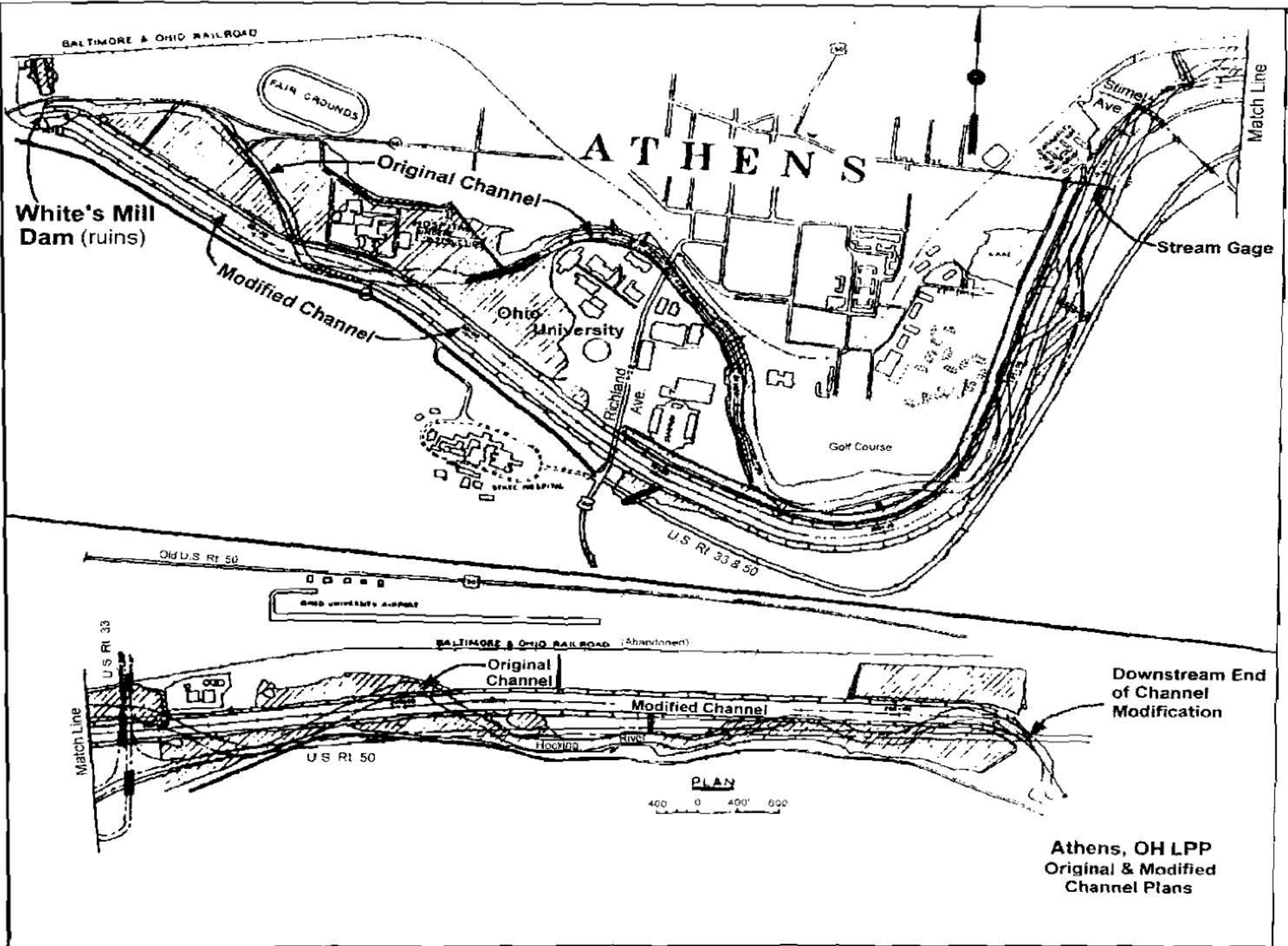
would not have been appropriate, even if the SAM package had been available.

To determine average annual sediment yield, it is necessary to calculate hydraulic characteristics of the stream for stream flows of specific exceedence intervals. These flows were obtained from the USGS water data report number OH-94-1 for 90%, 50%, and 10% exceedence. The required hydraulic properties are velocity, depth, stream width, and energy slope. These values were obtained from the HEC-2 model for the reach of the Hocking River upstream of the project and for the reach within the channel improvement project. For a SAM analysis, it is not necessary to conduct extensive sediment sampling as is required for an HEC-6 study. Only a bed gradation for the study reach is required. All of the input used in the SAM model are reach-characteristic values. They do not reflect the localized changes which are characteristic of the alternatives that were analyzed for the detailed HEC-6 study.

SAM contains a feature that provides guidance in the selection of sediment transport functions for the hydraulic parameters of the respective study reach. Both Yang's and Madden's modification of Laursen's equations were recommended by SAM to characterize the hydraulic parameters of the Hocking River in the project area. Since there is little evidence of armoring in the project reach, it was assumed that the entire sediment transport capacity is utilized. Both of these transport functions indicate that approximately 80% more material can be transported by the upstream reach of the Hocking River than can be transported through the project. This result agrees with the HEC-6 model insofar as indicating that the project reach will continue to experience significant sediment deposition. However, even if all of this excess material is assumed to deposit within the project, the SAM results slightly underestimate the deposition when compared to the dredging records and the results of the HEC-6 model. Nevertheless, as an order of magnitude approximation, SAM provides satisfactory results. The conclusion of the sediment budget analysis is that the current Athens, Ohio project is a depositional reach that will require significant dredging to maintain design conveyance. The most significant advantages that a SAM study has over HEC-6 study is cost and time. Depending upon the skill of the modeler and the available information, a sediment budget analysis could be completed in two to three weeks.

SUMMARY

The Corps sediment transport models, HEC-6 and SAM indicate that the Hocking River, through the Athens, Ohio local protection project, is a depositional reach and will continue to be so as long as current conditions persist. A sediment impact assessment using SAM can be used to arrive at this conclusion in a shorter amount of time and at a lower cost than an HEC-6 study. However, an HEC-6 study is necessary to quantify the deposition and to assess the relative merit of different options to continued dredging.



3-15

Figure 1

Athens, OH LPP - Cross Sections of 1992 Survey vs Original Design Template

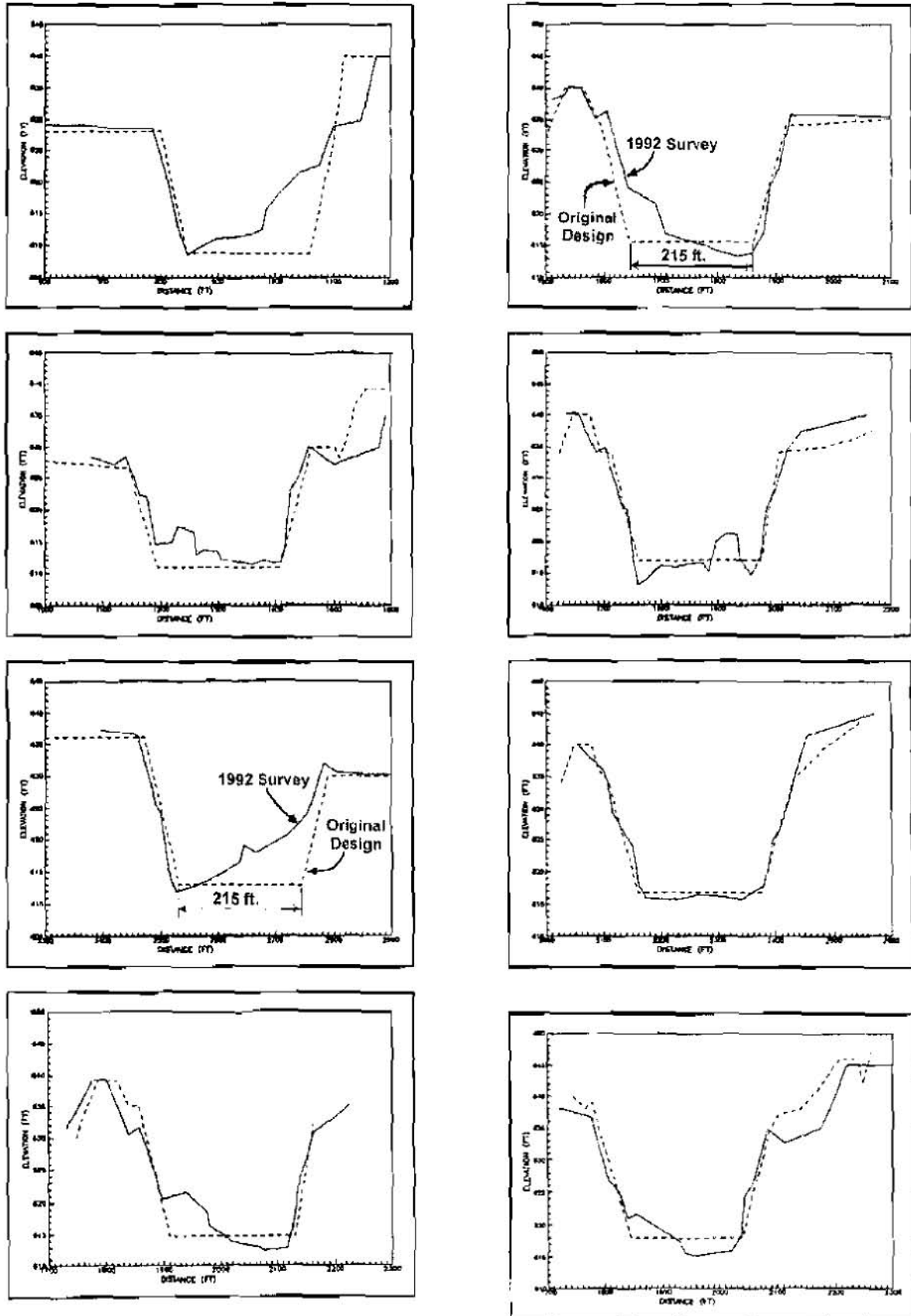


Figure 2

DESIGN OF CHANNEL RIPRAP USING OVERTOPPING FLOW METHODS

By: Terry L. Johnson, Senior Hydraulic Engineer, United States Nuclear Regulatory Commission, Washington DC; Steven R. Abt, Professor, Department of Civil Engineering, Colorado State University, Fort Collins, Colorado

Abstract: Using an empirically-based design method that was developed to determine riprap requirements for overtopping flow applications, a procedure has been developed for designing riprap for channels. To use this procedure, it is necessary to determine flow distributions through the channels and to apply these flow estimates to the overtopping flow method. Of particular importance is the application of the new procedure to channels with steep slopes. More common design methods, such as the Safety Factors Method, are sometimes more difficult to use and may overestimate riprap requirements for steep channels. The method is easily-applied and can be used to determine riprap requirements knowing only the discharge and slope of the channel.

INTRODUCTION

Design of riprap erosion protection for channels with hydraulically steep slopes can present a problem, because riprap sizes required for supercritical flows are generally very large. Further, because the depth of flow in steep channels is usually shallow (relative to the riprap size), many commonly-used design procedures, such as the Safety Factors Method (Richardson, et al. 1975), may have difficulty converging on an analytical solution. Difficulty in properly estimating Manning's 'n' values in turbulent flow regimes also leads to difficulty in estimating velocities that are used to size the riprap.

Recognition of basic difficulties in sizing riprap for overtopping flows at shallow depths led the staff of the Nuclear Regulatory Commission (NRC) to sponsor a series of near-prototype flume tests that were performed at Colorado State University (CSU). A testing program was performed over a period of several years to verify the adequacy of commonly-used methods for sizing riprap. One conclusion that was reached during these studies was that commonly-used methods may be overly conservative for embankments with slopes greater than a few percent (Abt, et al. 1987; Abt, et al. 1988).

DISCUSSION

The authors consider that one of the principal problems associated with riprap design on steep slopes is the use of Manning's 'n' values that may not be appropriate. Of necessity, designers must rely on estimates of 'n' values to determine parameters such as velocities, depths of flow, and shear stresses that become input parameters to other commonly-used design methods. Designers tend to rely on estimates of 'n' values that attempt to encompass various types of losses, including localized energy dissipation, expansion and contraction of flow, and normal friction losses. Very often, the assumed 'n' value is really an apparent 'n' value and its derivation has little or no basis, especially when the depths of flow are relatively small.

In an attempt to develop a design procedure with a limited number of variables, flume studies were performed at CSU. The tests were conducted on various slopes using riprap of various sizes. The outdoor flume facilities at CSU are very large and enable researchers to conduct studies under near-prototype conditions. The size of the flumes ensure that scale effects are insignificant and provide a great deal of confidence in the results of the testing. Because the flumes can effectively simulate overtopping and channel flows, the authors believe that extrapolation of the results can be performed with relative assurance of the validity of the analysis.

Using the results of these flume tests, a design method was developed for determining riprap requirements for rock-protected embankment slopes subjected to overtopping flows (Abt and Johnson, 1991). This method was based on a regression analysis of data developed in the flume tests. The equation used to determine the minimum average (D_{50}) riprap size required to prevent failure was provided as follows:

$$D_{50} = 5.23 S^{0.43} * q_f^{0.56}$$

where: q_f is the discharge at failure in cubic feet per second per foot of width (cfs/ft); S is the slope of the embankment (in feet/feet); and D_{50} is the minimum median stone size required to prevent failure (in inches).

This method also assumes that angular rock with a specific gravity of about 2.65 will be used. Other limiting assumptions related to porosity, angle of repose, and stability coefficients are discussed by Abt and Johnson (1991). In addition, procedures for increasing the rock size to prevent movement were also discussed. Abt and Johnson recommended that the failure discharge (q_f) be increased by a factor of 1.35 to prevent stone movement.

The design procedure previously derived is easily adapted to riprap design for trapezoidal channels. By assuming that the channel is merely an embankment subject to overtopping flows, the design procedure can be used to estimate riprap sizes for the channel. In channels where the width to depth ratio is large, flows along the side slope can be ignored, and the flow rate to be used is simply the design discharge divided by the channel bottom width. If normal depth occurs, the slope to be used in the design equation is the bottom slope of the channel. If normal depth does not occur, and the channel is subject to a downstream control, the slope to be used is the slope of the energy grade line (discharge is computed as before).

In cases where the channel width is small relative to the depth, the designer has the option to evaluate flows through various portions of the channel, including the center portion and along the side slopes. However, for ease of application, the authors recommend that the design discharge be computed similarly to the discharge if the channel were wide, although this will produce some additional conservatism.

For triangular channels, it is necessary to estimate the flows occurring in the center of the channel where the depth and discharge are greatest. At this point, it will be necessary to use Manning's 'n' value estimates to determine the amount of flow in a one-foot-wide strip in the deepest part of the channel.

For any trapezoidal channel, the riprap size will need to be increased for the side slopes. The side slope correction coefficient (K) is discussed in detail by the U. S. Army Corps of Engineers (USCOE, 1991), and the recommended relationship for the coefficient is a function of the side slope angle. For example, for a channel with side slopes of 1 Vertical (V) on 2 Horizontal (H), a side slope coefficient of about 0.88 is recommended. The calculated value of D_{50} should be divided by this coefficient to arrive at the proper rock size.

Thus, the equation to be used to design riprap for the channel side slopes is expressed as follows:

$$D_{50} = (5.23 * S^{0.43} * (q_f * 1.35)^{0.56})/K$$

where: D_{50} is the required median rock size (inches); S is the slope of the energy grade line (ft/ft); q_f is the discharge in the channel (cfs/ft); and K is the dimensionless side slope correction coefficient.

EXAMPLES OF PROCEDURE APPLICATION

To clarify the application of the design procedure discussed above, several design examples are presented. It is important to note that the examples are oversimplified, for the sake of clarity and ease of application. In reality, the authors expect that more complicated conditions will often exist in the field and that designers will be required to refine estimates of flows occurring in various parts of the channels. This is particularly true if the channels are irregularly shaped or have variable depth and roughness. Although not discussed in the examples, the authors expect that designers will elect to perform detailed computations of flow distributions in these channel segments.

Case I - Wide Trapezoidal Channel - Normal Depth

For a trapezoidal channel with side slopes of 1V on 2 H, a width of 100 feet, a discharge of 3000 cfs, and a slope of 0.03, the riprap requirements can be easily calculated. First, the failure discharge is estimated by dividing the flow by the bottom width of the channel. The design discharge is then increased by a factor of 1.35, to design for the prevention of stone movement. The resulting rock size is needed for the bottom of the channel. This size is then further increased by dividing the rock size by the side slope correction coefficient. The following example illustrates the method:

The design discharge (q) is the channel discharge (3000 cfs) divided by the width (100 feet) and multiplied by a factor of 1.35.

$$q = (3000/100) * 1.35 = 40.5 \text{ cfs/ft}$$

$$D_{50} = 5.23 * (0.03)^{0.43} * (40.5)^{0.56} = 9.2 \text{ inches} - \text{This size is required for the channel bottom}$$

For the side slopes of the channel,

$$D_{50} = 9.2/0.88 = 10.5 \text{ inches.}$$

Case II - Relatively Narrow Trapezoidal Channel - Normal Depth

For a trapezoidal channel with side slopes of 1V on 2H, a bottom width of 20 feet, a discharge of 2000 cfs, and a slope of 0.03, the minimum average riprap size is computed by ignoring the flows that occur along the channel side slopes:

For the channel bottom,

$$D_{50} = 5.23 * (0.03)^{0.43} * ((2000/20)*1.35)^{0.56} = 18.0 \text{ inches}$$

For the side slopes,

$$D_{50} = 18.0/0.88 = 20.5 \text{ inches.}$$

Case III - Trapezoidal Channel with Backwater Effects

In this example it is assumed that a channel with a bottom slope of 0.03 and side slopes of 1V on 2H is constricted at the downstream end, producing a backwater effect at the point where riprap is to be designed. The calculated slope of the energy grade line is used in lieu of the bottom slope in such cases. For a trapezoidal channel with a bottom width of 100 feet, a discharge of 5000 cfs, and a calculated energy grade line slope of 0.005, the riprap size is computed as follows:

For the channel bottom,

$$D_{50} = 5.23 * (0.005)^{0.43} * ((5000/100)*1.35)^{0.56} = 5.7 \text{ inches}$$

For the side slopes,

$$D_{50} = 5.7/0.88 = 6.5 \text{ inches}$$

SUMMARY AND CONCLUSIONS

Based on the results of near-prototype flume studies, a procedure has been developed for designing riprap for channels. The procedure eliminates the need for estimating Manning's 'n' values by requiring the designer to know only the slope and discharge of the channel. The method is restricted for applications using angular rock with a specific gravity of about 2.65.

The opinions expressed in this paper are the opinions of the authors and do not express the views of the Nuclear Regulatory Commission or Colorado State University.

REFERENCES

Abt, S. R., Khattak, M.S., Nelson, J.D., Ruff, J.F., Shaikh, A., Wittler, R.J., Lee, D.W., and Hinkle,

N.E., 1987, Development of Riprap Design Criteria by Riprap Testing in Flumes: Phase I. NUREG/CR-4651, U.S. Nuclear Regulatory Commission, Washington, DC.

Abt, S.R., Wittler, R.J., Ruff, J.F., LaGrone, D.L., Khattak, M.S., Nelson, J.D., Hinkle, N.E., and Lee, D.W., 1988, Development of Riprap Design Criteria by Riprap Testing in Flumes: Phase II. NUREG/CR-4651, U.S. Nuclear Regulatory Commission, Washington, DC.

Abt, S.R., and Johnson, T.L., 1991, Riprap Design for Overtopping Flows. Journal of Hydraulic Engineering, Vol. 117, No. 8.

Richardson, F.V., Simons, D.B., Karak, S., Mahmood, K., and Stevens, M.A., 1975. Highways in the River Environment-Hydraulics and Environmental Design Considerations. U.S. Department of Transportation, Washington, DC.

Stephenson, D., 1979, Rockfill in Hydraulic Engineering. Elsevier Scientific Publishing Co., New York, N.Y.

U.S. Army Corps of Engineers (USCOE), 1991, Hydraulic Design of Flood Control Channels. EM 1110-2-1601, July 1.

REDUCING LOCAL PIER SCOUR BY FLOW REDIRECTION

By J. R. Richardson and David M. Roberts, Department of Civil Engineering
University of Missouri, Kansas City, Missouri

Abstract: Laboratory investigations were conducted in a flume to investigate non-structural methods for reducing local pier scour. The results indicate that the normalized pier scour can be reduced by 10 to 30% by modifying piers with roughness elements that impede downward thrust of water in the vicinity of the pier face. Based on these results, it would be feasible to develop countermeasures that can be retrofitted to existing piers, which will measurably reduce local pier scour.

INTRODUCTION

Since the failures of Schoharie bridge in 1987 (killing ten people, NTSB, 1988); the Hatchie bridge in 1989, (killing eight people, NTSB, 1990); and the I-5 Bridge Failure (killing 8 people, Richardson, Jones, and Blodgett, 1997); the Federal Highway Administration launched an extensive effort to assess of the nation's bridges for scour. This effort calls for evaluating all bridges for scour, and either replacing or providing countermeasures to protect these bridges (FHWA 1988 & 1991).

According to the results of the National Bridge Inspection System (FHWA 1995), approximately 282,000, (61.1%) of the approximately 484,941 bridges nationwide over water have been analyzed for scour. Of the bridges receiving a complete analysis, approximately 9,846 (3.5% of the analyzed bridges) were found to be scour critical.

Currently, the only method to permanently protect scour critical piers is to found the pier deeper in the streambed by replacement of the pier or by underpinning. Although the best approach for long-term bridge protection, it is also the most costly. Given the number of bridges nationwide, this alternative will require significant expenditures. Alternatively, temporary countermeasures such as riprap can be employed to resist the erosive action of the fluid forces. However, it has been shown that riprap tends to be removed by the flowing water over time. Although riprap and channel bed protection is likely the least expensive to construct, the additional indirect costs of periodic inspection, monitoring and maintenance can be significant (Richardson and Davis, 1995).

It is clear that alternate strategies and countermeasures are needed. One potential methodology is to shape piers in a to inhibit the formation of adverse flow conditions at the streambed. For new bridges streamlining the piers is effective in reducing pier scour. For existing piers, streamlining is not usually an option. Alternatively, the vertical jet of water that initiates and maintains near-bed vortices can be impeded using horizontally aligned roughness elements. In order to determine the potential effectiveness of this type of countermeasure, a series of laboratory tests were performed in a flume at the University of Missouri from 1995 to 1997. A short summary of the findings this research is presented in this paper. Recommendations for continued study and ongoing development are also presented.

MECHANISIM OF LOCAL PIER SCOUR

Figure 1 illustrates the flow patterns, which form as a result of a pier obstructing the flow. As the pier blocks the horizontal flow, the horizontal velocity is converted to pressure head at the stagnation point immediately upstream of the pier face. This causes the water surface to rise at this location causing an adverse pressure gradient in the vertical direction. This pressure is released by the formation of a vertical jet of water with a vector pointed vertically downward parallel to the pier face. At the streambed, the vertical jet turns horizontally upstream, interferes with free stream flow, and is redirected downstream. The curvilinear path of the vertical jet forms a vortex (denoted the *horseshoe vortex*) near the bed, which is effective at eroding the bed and forming the cup-shaped erosion pattern indicative of local pier scour.

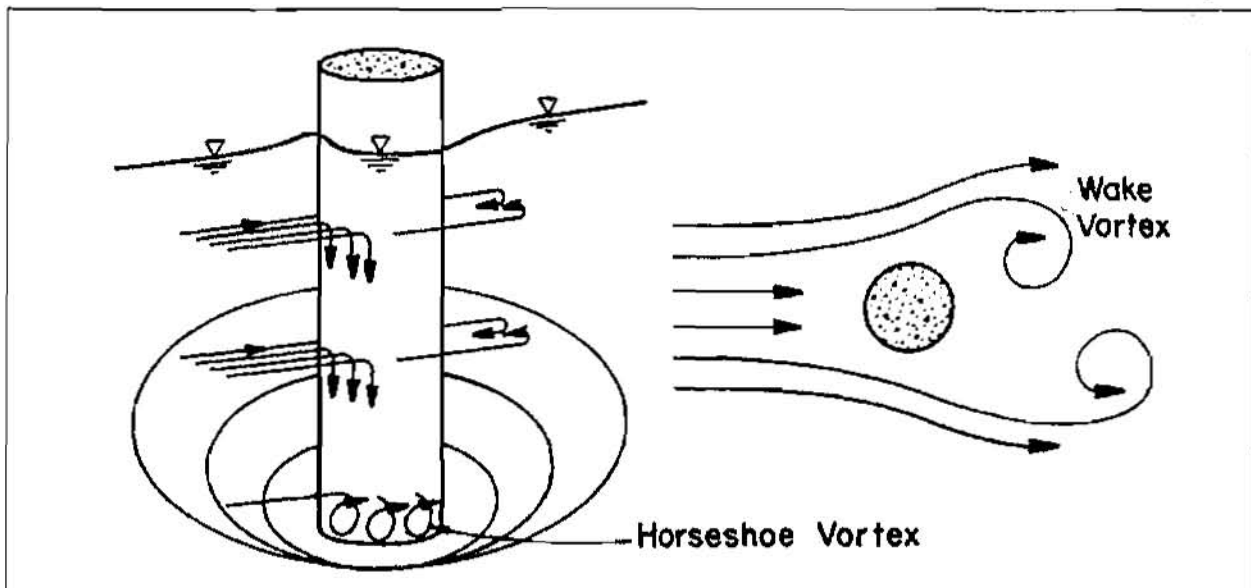


Figure 1 Pier Scour And Horseshoe Vortex, Richardson & Davis, 1995

The magnitude of local pier depends directly on the magnitude of the vertical jet of water caused by the obstruction. Therefore, hydraulic and pier geometry factors which tend to increase the magnitude of the vertical flow should be minimized. For example a sharp-nosed pier tends to split the flow, and has been shown to have approximately 10% less scour than a round or circular column, and approximately 20% less scour than a blunt faced pier.

The scour depth is also directly proportional to the flow velocity, pier width, and flow depth. In most cases it is not feasible to reduce flow velocity without enlarging the bridge opening. Likewise reducing the pier width is limited by the need to provide structural support of the bridge. Although the flow depth cannot be significantly reduced without increasing average flow velocity, the effective flow depth can be reduced by increasing the resistance to the vertical flow. This can be accomplished by installation of horizontal protrusions that allow horizontal flow to pass the pier relatively uninhibited, but resist vertical flow. This is the basis for the study reported in this paper.

LABORATORY SETUP

Equipment and Instrumentation: Testing was conducted in a 0.20-m wide by 3.0-m long by 0.28-m deep variable slope flume. The flume consists of a 1.82-m long rigid bed approach section; a 0.61-m long test section with a floor recessed 0.18-m (0.46-m deep); and a 0.61-m long downstream section. The test piers were mounted in the recessed test section and filled with

Kansas River Sand ($D_{50} \sim 0.5$ mm) to the elevation of the approach and downstream bed elevation. Kansas River sand was glued to the floor of the flume upstream and downstream of the test section to provide consistent boundary roughness for the entire channel length.

Two smooth Plexiglas circular model piers with diameters of 0.03175-m (1.25-inch) and 0.0254-m (1-inch) were used as a standard for comparison of the modified pier shapes. Respectively, these pier shapes were denoted *S* and *C*. All of the modified pier shapes were constructed from the 0.03175-m bar stock used for the *S*-shaped reference pier. Roughness elements were machined into the 0.03175-m stock to an inside diameter of 0.0254-m and resulted in roughness elements which protruded horizontally $L_p=0.0032$ -m from the pier. Respectively, the maximum and minimum diameter of the modified piers was equal to the diameters of the *S* and *C* reference piers.

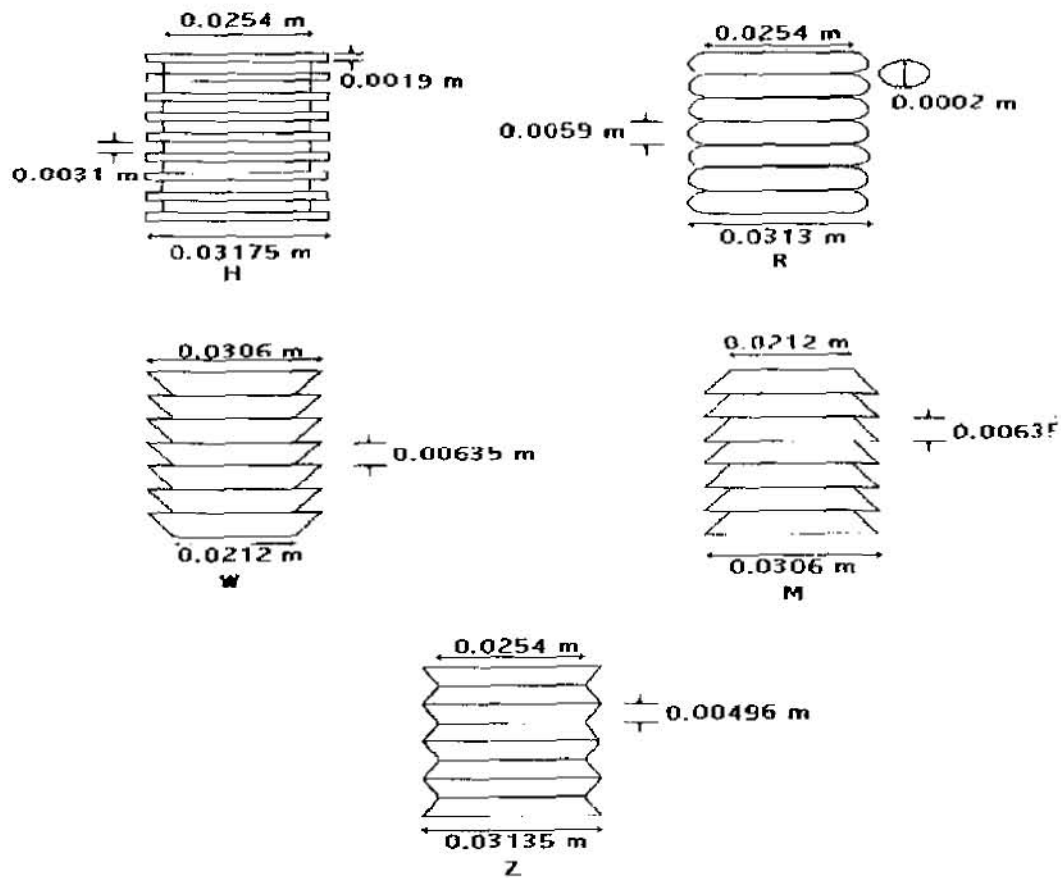


Figure 2. Series 1 Pier Shapes

The modified pier shapes were grouped into three different series based on the spacing of the roughness elements machined into the piers. For the first series, the spacing between roughness elements (defined as the vertical distance between pattern repeat (L_s)) ranged from 0.005-m to 0.00635-m. This produced a pier with horizontally aligned grooves with a ratio of L_s to protrusion length (L_p) of approximately 2.0. Initially, five modified pier shapes with $L_s/L_p \sim 2$ (Series 1) were tested. These shapes are denoted as: *R*, *H*, *Z*, *W*, and *M* shape (Figure 2). Based on the results of the series 1 testing, the *R*, *M* and *Z* shapes were eliminated. The remaining pier shapes (*H*,

and W) were tested with $L_r/L_p \sim 4.0$ and were denoted L , and N respectively (Figure 3). For the third series, the element spacing of the L pier was increased to $L_r/L_p \sim 8$ and denoted as K (Figure 3).

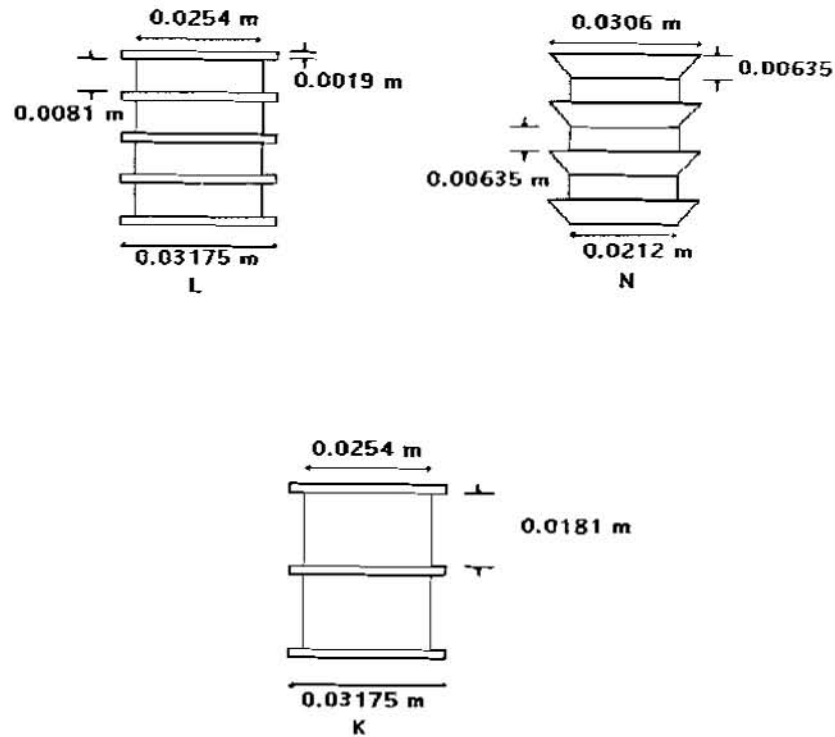


Figure 3 Series 2 and 3 Pier Shapes

TESTING PROTOCOL: Before each test the sand in the test section was mixed, pre-wetted, tamped and leveled. Extreme care was taken during start-up and shut down to insure that the scour hole which developed was the result of reported flow conditions and to insure that the scour hole was preserved for measurement and analysis. Start up procedures involved slowly filling the flume to a depth greater than the testing depth with the tail water gate closed. The discharge was then increased to the testing discharge as the tailwater was gradually opened. Test flow conditions were then established by adjustment of the tail water control to reduce the flow depth to the desired testing depth. Shut down was conducted in an opposite fashion and the flume was slowly drain prior to post-test measurement of the scour pattern.

A constant flow depth of 0.142-m was maintained for all tests. The approach Froud numbers ranged from approximately 0.175 to 0.25. All tests were conducted as clear-water tests to eliminate the variability in scour depth measurements associated with the movement of dunes and other bed forms.

Two long-term tests were performed using the 2.54-cm smooth pier and the Z pier to identify the time frame for the scour to fully develop. From these tests, it was found that the local scour reached a minimum of 93% of the maximum at testing durations of 75 minutes. In order to perform as many tests as possible the duration of each test was set to 75 minutes. It is acknowledged that the duration of each test was not sufficient to attain full equilibrium scour depths, however it was found that this duration was sufficient to achieve a scour hole, which was near equilibrium.

Discharges, flow depths and velocity measurements were periodically checked during each test. Average approach velocity was determined using continuity with the discharge determined from a precision venturi in the supply line of the flume. Additional point velocity measurements were made using a SonTek[®] acoustic Doppler velocity meter. Flow depth and scour depths were measured to the nearest 0.0005-m (0.5mm) using a point gage.

Periodic scour depth measurements were made on 10-minute intervals with the point gage during testing. Post test-measurements included re-measurement of the maximum scour depth, and preparing to-scale contour maps of the scour hole, and downstream deposition area. Each test was also photographed to further document the scour pattern.

RESULTS

General: To insure that during the course of testing that the bed material did not coarsen up due to winnowing of the bed material, periodic bed material samples were collected and analyzed for grain size. From this analysis, it was observed that there was no significant variation in the bed composition during the course of the testing.

Scour Results: The measured scour depths for each test was normalized by dividing the maximum measured scour depth (Y_s) by the minimum pier diameter (a). The minimum pier diameter was used to normalize the scour depth so that normalized scour depths plotting below the reference piers would indicate a reduction in scour depth relative to the 0.025-m reference pier. Figure 4 presents Y_s/a versus approach Froud number for the series 1 piers. Additionally, the pier scour depths for the two smooth reference piers (C and S) are also presented for comparison. The results indicate that the normalized scour for the reference piers plotted consistently with each other.

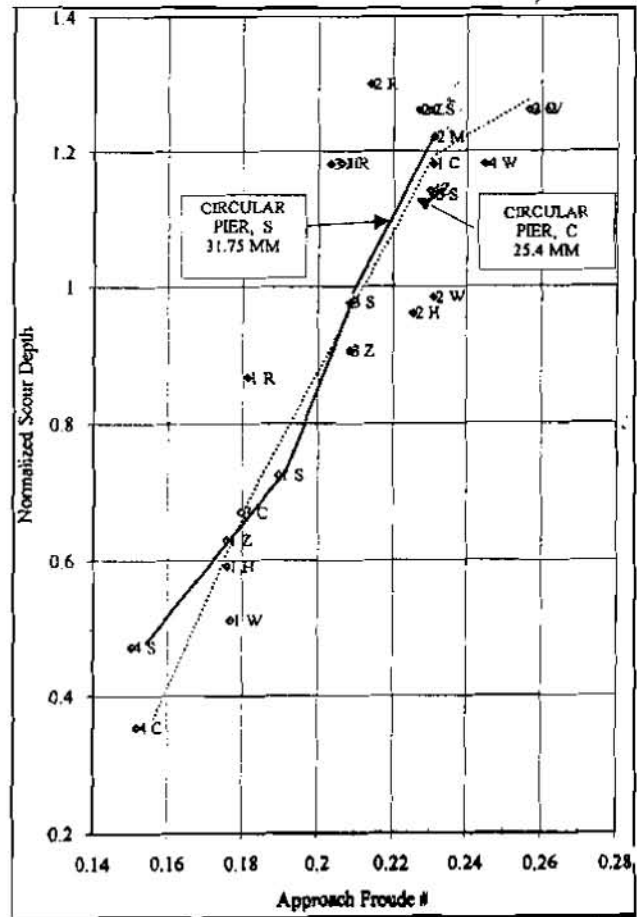


Figure 4. Y_s/a versus Froud
For Series 1 Pier Shapes

Of the shaped piers in series 1, the *R* pier indicated a tendency to increase scour depths at all Froud numbers. The normalized scour for the *M* shape was not significantly different than the smooth piers. The results of the *H*, *W* and *Z* patterns indicated that all of these patterns had an effect on reducing local pier scour with the *H* and *W* patterns displaying the greatest scour reduction. Considering these results, the shaping patterns that produced the most positive results were shapes in which the leading edge of the roughness element normal to the flow was sharp. This result was expected and indicated that sharp-edged protrusions were most effective at impeding the vertical flow.

The *R*, *M*, and *Z* piers were dropped from further consideration and additional tests of the *H* and *W* patterns were conducted. The spacing of the roughness elements of the *H* and *W* patterns were increased and re-tested. Spacing was increased by machining away alternate elements of the *H* pier and denoted as *L*. Similarly, the *W* pier was modified and denoted *N*. Figure 5 presents the results of testing for the series 2 piers of *L* and *N*. The results indicate that the *L* and *N* piers reduced the normalized scour depth by approximately 10% to 23% with a minimum reduction of approximately 10% for the *N* shape at a Froud number of approximately 0.26.

The normalized scour depth for the series 2 tests was less than for the same shapes tested in the series 1 tests indicating the importance of roughness element spacing. Additionally, increasing roughness element spacing resulted in more consistent scour reduction for the range of flows tested and than for the *H* and *W* piers. To further investigate the effect of pier shaping, alternate elements of the *L* pier were machined out to form the *K* pier (series 3). The results from testing the *H*, *K*, and *L* are plotted together for comparison (Figure 6). Increasing of the spacing from the *L* to the *K* pier resulted in increasing the reduction in normalized scour depth from approximately 20% to over 35% for Froud numbers ranging from 0.22 to 0.24. Outside this range, the scour reduction of the *K* pier was less than that of the *L* pier.

It should be noted that all of the documented reductions in local scour depth were referenced to the smaller diameter reference pier. This indicates that the reductions noted are actual reductions in scour depth and that the added diameter of the protrusions had no influence on increasing the scour depth. Consequently, the results indicate that it should be possible to fabricate and attach non-structural vertical flow inhibitors to existing bridge piers without increasing the effective width of the pier.

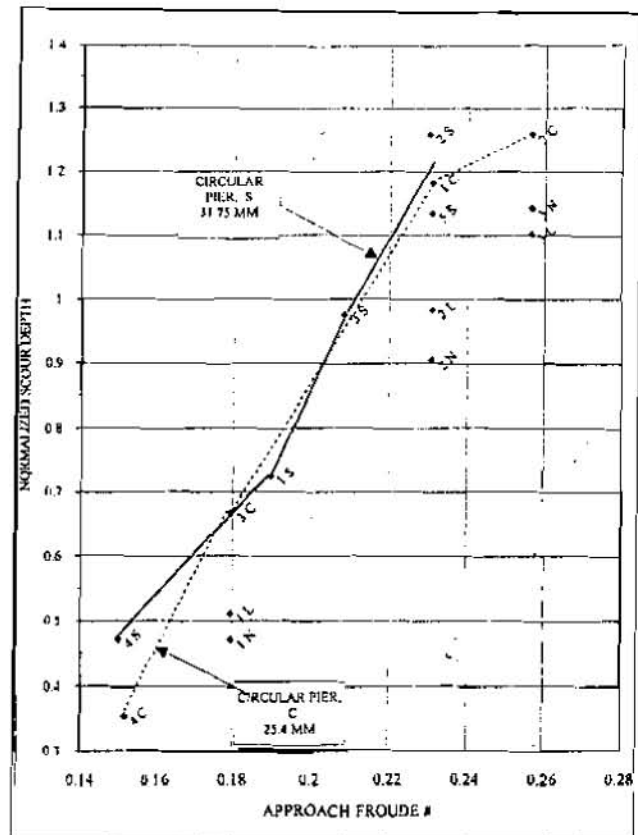


Figure 5. Y_s/a versus Froud For Series 2 Pier Shapes

Scour Hole Shape: Although the results are not presented in detail in this paper, the influence of pier shaping tended to reduce the extent of the scour hole. In the region downstream of the centerline of the pier most of the modified pier shapes resulted in increased deposition of sediments. For many of the tests, vertical erosion of the streambed was absent downstream of the pier centerline. This result bolsters the proposition that the roughness elements not only inhibited the vertical water jet at the face of the pier, but also tended to redirect the vertical flow downstream and reduced the magnitude of shedding wake vortices.

CONCLUSIONS

The results discussed above indicate that effective scour reduction can be achieved by inhibiting the vertical jet of water that sets up and maintains the horseshoe vortex. This resulted in a lessening of the maximum scour depth. The degree to which local scour can be reduced depends on the shape and spacing of the roughness element. Optimal shapes have abrupt edges that result in separation of the vertical jet of water and the formation of shedding vortices near the pier face. Spacing is also an important parameter in the design of this countermeasure. Based on this study, the optimal spacing is between $4 < L_s/L_p < 8$. Although not investigated, the distance that the roughness elements protrude from the pier should also strongly influence the magnitude of local pier scour reduction.

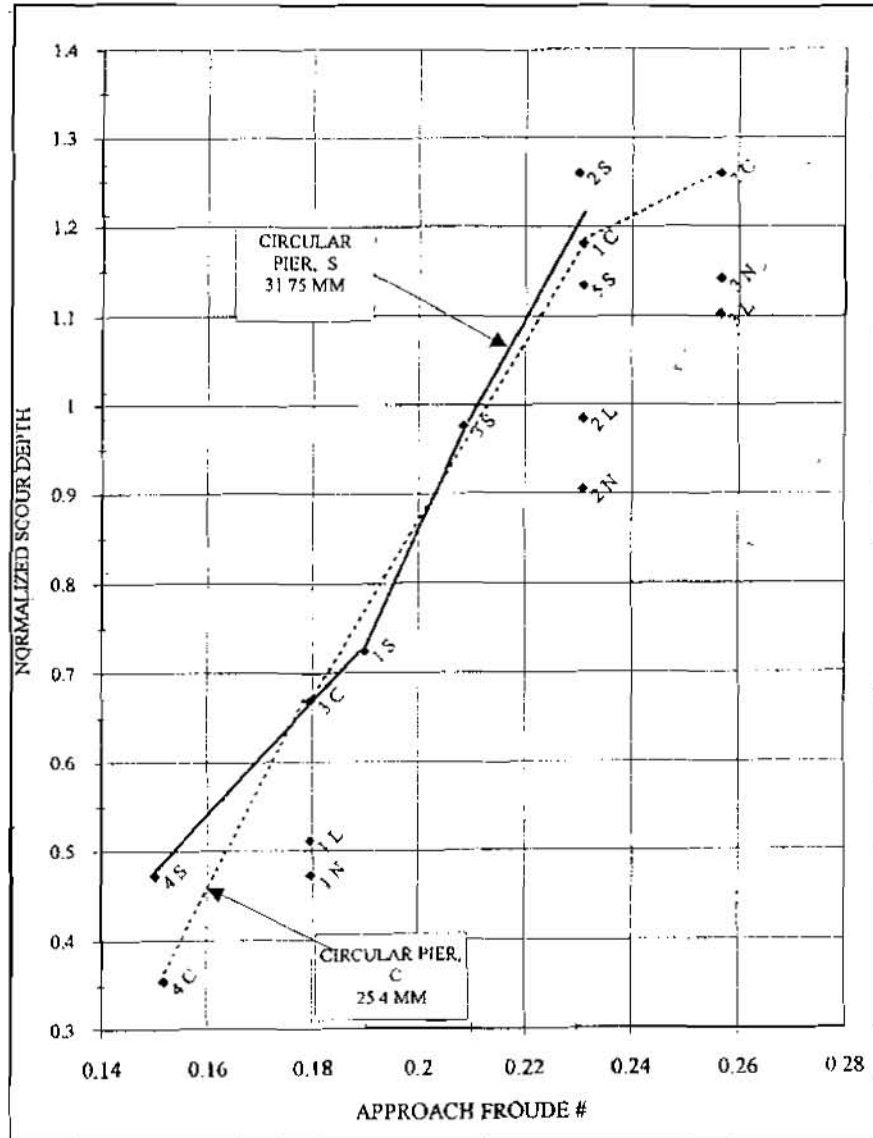


Figure 6 Y_s/a versus Froud For Series 3 Pier Shapes

The results of this preliminary study indicate that bridge piers can be modified by providing horizontal roughness elements to inhibit the vertical flow of water along the pier face. This investigation only provides proof of concept. Additional and more detailed research needs to be conducted before this countermeasure can be applied to an actual bridge. Further research needs

to be conducted at larger scale sizes, with a wider range in bed material conditions and for other pier geometry's.

Presently, there are few options and countermeasures that can be employed to protect the nation's existing bridge infrastructure from local pier scour. Existing options are either very costly (pier replacement/underpinning) or are limited in their reliability (riprap) and need constant monitoring. Further development of this countermeasure is recommended in order to develop and deploy it as an additional countermeasure technique for protecting the nation's bridges from the devastating and catastrophic effects of local pier scour.

Addition of pier retrofits to inhibit the vertical flow cannot eliminate local pier scour altogether. Furthermore this countermeasure cannot protect a bridge that has piers which the scour can severely undermine the pier. It is likely that a large percentage of the scour critical bridges nationwide are considered to be scour critical due to minimal geotechnical factors of safety. A reduction of 10 to 20% could be sufficient to upgrade these bridges in at minimal cost by using simple "strap-on" forms of this countermeasure. The resulting cost savings could be applied to targeting the most deficient and unsafe bridges in the nation.

Additional studies are ongoing. Currently the authors have completed laboratory testing at FHWA's Turner Fairbanks Hydraulics Laboratory to determine optimal L_s/L_p . Analysis and documentation of results are pending.

REFERENCES

- U. S. Department of Transportation, FHWA. Technical Advisory T5140.20, updated by Technical Advisory T5140.23, October 28, 1991. FHWA, Washington, D. C. 1988.
- NTSB. Collapse of the New York Thruway (I-90) Bridge over the Schoharie, Creek, Near Amsterdam, New York, April 5, 1987. NTSB/HAR-88/02, NTSB, Washington, D.C. 1988.
- NTSB. Collapse of the Northbound U. S. Rout 51 Bridge Spans over the Hatchie River near Covington, Tennessee April 1, 1989. NTSB/HAR-90/01, NTSB, Washington, D. C. 1990.
- Richardson, E. V. and Davis, S. R., Hydraulic Engineering Circular No. 18, Evaluating Scour at Bridges, Third Edition. FHWA-IP-90-017, FHWA, Washington, D.C. 1995.
- Richardson, E. V., Jones, J. S. and Blodgett, J. C. Findings of the I-5 Bridge Failure. ASCE Proceedings of the XXVII IAHR Congress. ASCE, Reston, VA. 1997.
- FHWA. Stream Stability and Scour at Highway Bridges, Instructors Guide. FHWA-HI-93-028, National Highway Institute, FHWA, Washington, D. C. 1995.

EROSION AND SEDIMENT TRANSPORT THROUGH RIPARIAN FOREST BUFFERS ^{1,2}

D.D. Bosch, Research Hydraulic Engineer, SEWRL, Tifton, GA ³; R.G. Williams, Agricultural Engineer, SEWRL; S. Inamdar, Agricultural Engineer, Biological and Agricultural Engineering Department, University of Georgia, Tifton, GA; J.M. Sheridan, Research Hydraulic Engineer, SEWRL; and R.R. Lowrance, Ecologist, SEWRL

Abstract: The Riparian Ecosystem Management Model (REMM) has been developed to examine effects of riparian buffer management on the flow of water and transport of sediment and agrichemicals through riparian systems. The model simulates physical, chemical, and biological processes in riparian areas. Computation of sediment movement begins at the field-riparian system boundary. Erosion via particle detachment and overland flow are calculated for three riparian zones using a modified USLE approach. Concentrated flow erosion, transport, and deposition are also simulated. Sediment moving with the concentrated flow can be deposited or transported out of the riparian area. The basis for this determination is the sediment transport equation, derived from the steady state continuity equation. The transport capacity is compared to the sediment available for transport and the difference is used to determine if channel deposition or erosion occurs. The effective transport capacity is computed using a modification of the Bagnold stream power equation. Verification and validation of the erosion and sediment transport components of REMM is nearing completion. Comparison of model output to observed data and other model predictions indicate the model is within acceptable ranges for most modeling efforts.

INTRODUCTION

Agricultural activities are a major source of non-point source water pollution in the United States. In conjunction with in-field conservation practices, the maintenance of riparian areas as buffer zones below agricultural fields can reduce sediment and agrichemical pollutants entering streams (Lowrance et al., 1983; Lowrance et al., 1984; Peterjohn and Correll, 1984). Although general guidelines are available on the management of stream-side areas (Welsch, 1991), information is lacking on how buffer zones should be designed to accommodate site-specific features. Options for managing riparian ecosystems may include decisions about application of fertilizers, upland loadings, widths of the buffers, composition of plant species, and timing and extent of grazing and harvesting.

¹ Contribution from the USDA-ARS, Southeast Watershed Research Laboratory, P.O. Box 946, Tifton, GA 31793, in cooperation with Univ. of Georgia Coastal Plain Exp. Stn.

² All programs and services of the USDA are offered on a nondiscriminatory basis without regard to race, color, national origin, religion, sex, age, marital status, or handicap.

³ USDA-ARS, Southeast Watershed Research Laboratory, PO Box 946, Tifton, GA 31793, phone: 912-386-3515, fax: 912-386-7294, email: dbosch@tifton.cpes.peachnet.edu.

The Riparian Ecosystem Management Model (REMM) has been developed to examine effects of riparian buffer management on the flow of water and transport of sediment and agrichemicals through riparian systems (Lowrance et al., 1998). REMM has four major components: hydrology, sediment, nutrients, and vegetative growth. This paper presents an overview of the erosion and sediment transport components of REMM and comparisons of model output to observed data. A complete description is provided in Altier et al., (in review).

METHODS

As with the overall model, the riparian system is divided into three zones for the erosion and transport calculations (fig. 1). REMM detaches and routes sediment eroded in the upland and riparian areas through the riparian system using established procedures. Sediment is delivered to the riparian area from the upland distributed into particle size fractions. These must be provided as model inputs. Sediment generated within the riparian area as sheet and channel erosion is estimated by the model considering each zone as a flow element.

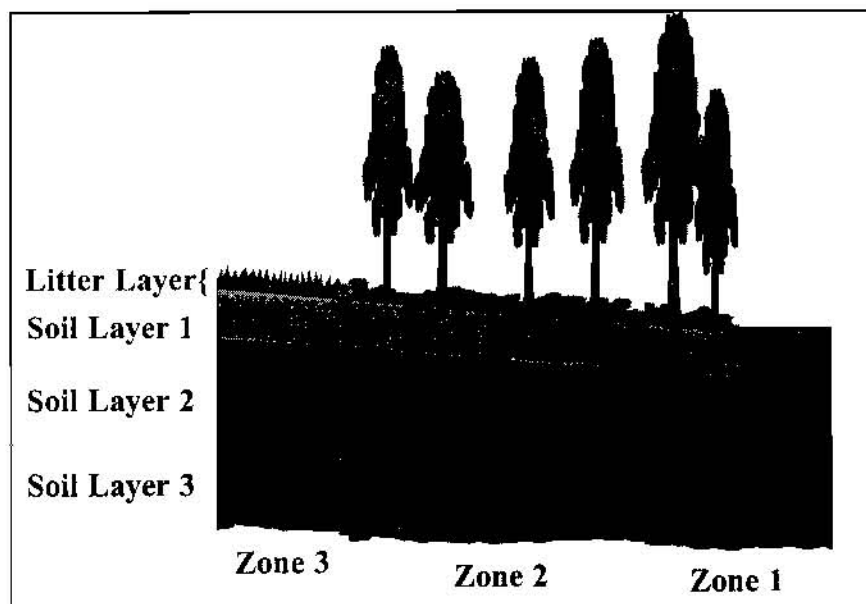


Figure 1. Schematic diagram of three-zone buffer system.

Computation of sediment movement begins at the field-riparian system boundary. Surface runoff from the field enters the riparian system as distributed flow, uniformly spread over zone 3 prior to computation of infiltration/runoff excess within the zone. Erosion via particle detachment and overland flow are calculated for each zone in the riparian system. Rill or channel and interrill areas are characterized for each zone (fig. 2). The fraction

of interrill eroded sediment which reaches the channel is determined by the interrill delivery factor (Foster, 1982), a function of interrill surface roughness.

Concentrated flow erosion, transport, and deposition are simulated for channels within each zone. This allows independent evaluation of the concentrated and overland flow components. Erosion and deposition are calculated separately for each of the three riparian zones. Flow is assumed to concentrate into a channel. The channel geometry can be used to more accurately represent flow conditions. A very wide channel can be used to approximate sheet flow. Sediment moving within the channel can be deposited or transported out of the riparian area. The transport capacity of the concentrated flow is calculated at the downslope end of the segment of each zone. The transport capacity is compared to the sediment available for transport and the difference is used to determine

if channel deposition or erosion occurs.

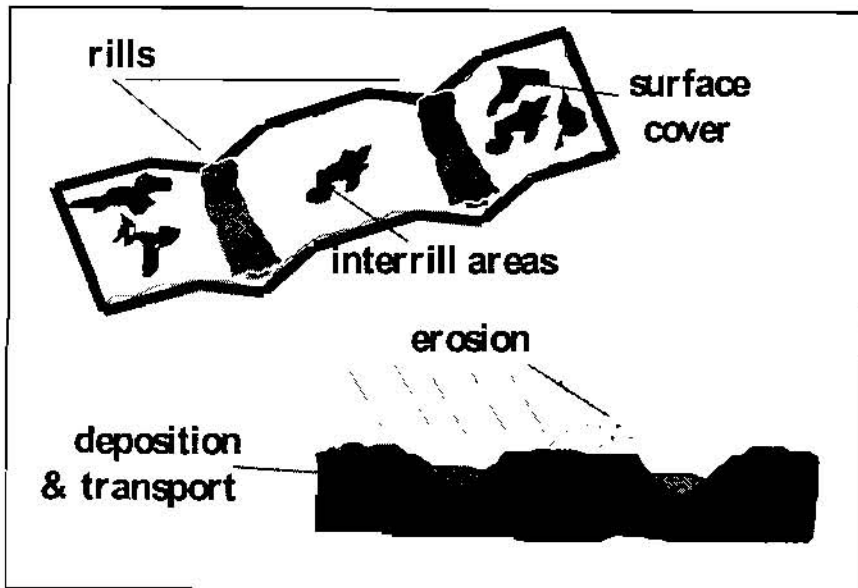


Figure 2. Characterization of erosion and sedimentation.

Overland Flow and Erosion: Lateral inflow of sediment within the respective zones, assumed to occur at all times during a storm, results from interrill erosion on overland flow areas or overland flow for channel areas. Daily sediment load into zone 3 from the field must be provided as user input, obtained through observations or modeling. Sediment is transported downstream by rill flow in the overland flow sequence, without deposition.

Characteristics of the A soil horizon are used to calculate the erosion within the riparian buffer for each storm event using a modified USLE approach (Wischmeier and Smith, 1978).

Sediment Routing and Channel Erosion: The potential sediment load and sediment transport capacity are used to determine whether erosion or deposition occurs in the channel. Potential sediment load is the lateral inflow load from rill areas plus that entering from upslope. If the potential load is less than the transport capacity channel erosion occurs until the transport capacity is satisfied or the limiting detachment rate is reached, whichever is less. The method used for sediment routing uses equations developed by Foster et al. (1981) and Lane (1982) and is applied in the AGNPS model (Young et al., 1989). The effective transport capacity is computed using a modification of the Bagnold stream power equation (Bagnold, 1966). A detailed presentation is made in Young et al. (1987).

Sediment Composition and Particle Size Relationships: A mixture of primary particles and aggregates make up eroded sediments. The volume of several chemicals transported with sediments are affected by particle size distribution. Due to the segregation that can occur in sediment transport, REMM routes sediment by particle classes to allow computation of soil-associated chemicals (Foster et al., 1985). The particle classes used are primary sand, silt, and clay and small and large aggregates.

Model Testing and Application:

The erosion and sediment transport algorithms used in REMM are from published sources in the literature (Wischmeier and Smith, 1978; Dissmeyer and Foster, 1984; Foster et al., 1981; Lane, 1982; Young et al., 1989). Comparison of the overland erosion and sediment transport components of REMM to predictions by the AGNPS model indicate good agreement between the two. The USLE

erosion approach has undergone extensive testing and has been found to yield acceptable long term results. While less testing has been conducted for forested conditions, good results have been observed for forested plots of various management conditions ranging in size from 0.09 to 1 ha (Dissmeyer and Foster, 1984). The sediment transport and deposition algorithms used in REMM have also been found to yield good results (Foster et al., 1981; Lane, 1982; Young et al., 1989).

The REMM erosion and sediment transport components were tested using a data set collected at a riparian site at the University of Georgia Gibbs farm near Tifton, Georgia (fig. 3). The soil in the riparian forest is an Alapaha loamy sand on a 2.5% slope. The adjacent 1.8 ha crop field is a loamy sand on a 1.5% slope. Corn was grown in the field in 1992, 1993, and 1994, millet and sorghum in 1995, and peanuts in 1996. Crops were grown using conventional agronomic production practices for the region, except in 1996. The peanuts were planted in small plots with bare alleyways.

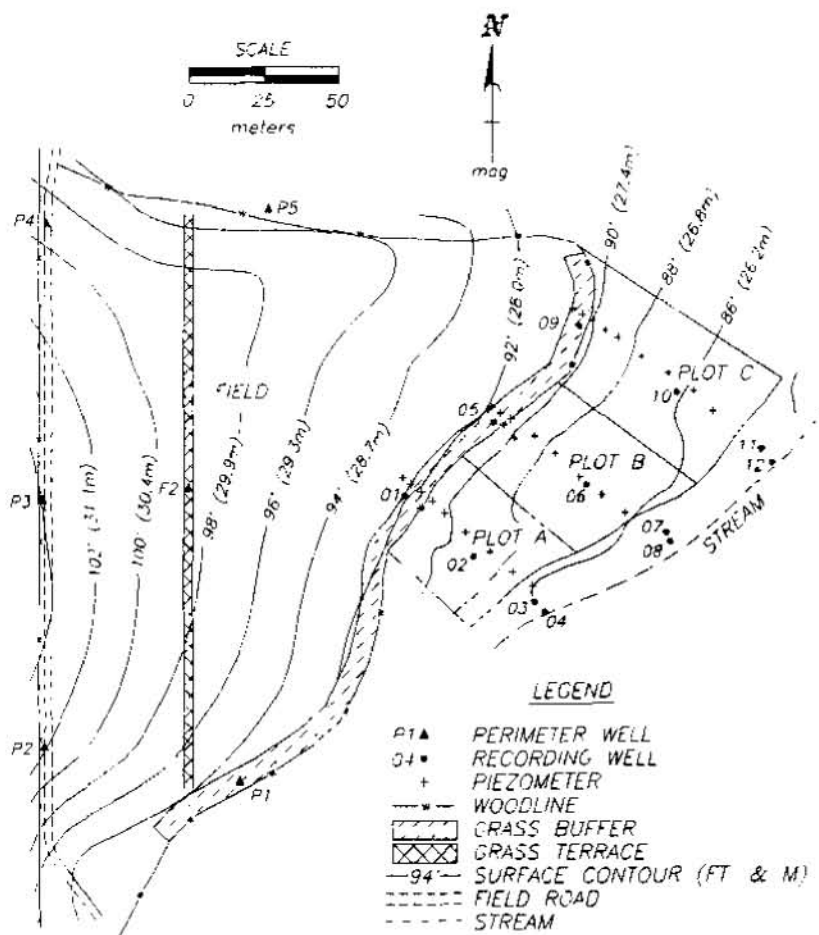


Figure 3. Location of the recording wells, middle transect of sample wells in riparian buffer, surface contours, and plot boundaries at the study site.

The area below the grass terrace in the field which contributes runoff to the riparian buffer is 0.9 ha in size. One third of this area, 0.3 ha, is assumed to contribute to each plot in the riparian buffer (fig. 3). The riparian buffer consists of a 8 m long grass filter in zone 3, a 50 m long managed pine

forest in zone 2, and a 10 m long hardwood forest in zone 1 (fig. 3). While three treatments were monitored at the site, only the mature forest treatment will be investigated here. The mature forest treatment, in plot A, was 40 m wide. A more complete overview of the site is presented in Lowrance et al. (1998).

Runoff and sediment transport data collected at the site were used for model testing. Data collected at the site from 1993 to 1996 were used for comparison to simulation results. Runoff collectors positioned at the edge of the field were used to collect the samples used for establishing the upland inputs for the riparian buffer simulations (Sheridan et al., 1998). Samples collected by runoff collectors positioned at the downslope edges of zones 3 and 2 were used to compare against model predictions. Samples were collected for each runoff producing event from 1993 to 1996.

Input data for the overland erosion component of the model was obtained from lookup tables in Wischmeier and Smith (1978) and Dissmeyer and Foster (1984). Rainfall intensity factors were calculated for each storm using relationships in Foster et al. (1980). A single channel was used to represent concentrated flow through the riparian buffer. Channel slopes were input as 2, 3.8, and 2.6% for zones 3, 2, and 1 respectively, with channel side slopes of 1%. The roughness coefficients for the channel reaches were input as 0.6, 0.5, and 0.4 for zones 3, 2, and 1 respectively. Interrill roughness was assumed to be 0.4, which corresponds to an interrill delivery factor of 94% for clay, 86% for silt, and 56% for sand particles.

RESULTS

The predicted mass of sediment delivered to the channel segment from interrill erosion for the four years of simulation was very low (table 1). Both the observed and simulated sediment yields for the Gibbs farm riparian buffer were also low (table 2). The accuracy of the runoff predictions varied from year to year and with position in the buffer. In general, simulated runoff exceeded observed runoff. A more detailed discussion on the runoff calculations is presented in Inamdar et al. (1998). Annual predicted sediment yields entering zone 2 were approximately double the observed values, while yields entering zone 1 were somewhat less than observed (table 2). The accuracy of the sediment predictions appears directly related to the accuracy of the runoff calculations (Inamdar et al., 1998).

Table 1. Observed annual precipitation and simulated interrill erosion totals in each of the zones.

Year	Precipitation (mm)	Zone 3 (kg)	Zone 2 (kg)	Zone 1 (kg)
1993	1002	0.2	1.6	0.6
1994	1488	0.7	3.3	1.5
1995	877	0.2	0.3	0.2
1996	1136	0.5	0.0	0.3

Sediment yields were calculated for each zone as a fraction of the mass entering the grass buffer (table 3). A sediment yield greater than 100% indicates more sediment leaving the zone than had entered from the field. This could be attributed to channel scouring or interrill erosion within the zone. For model simulations, approximately 70% of the sediment entering the grass buffer (zone 3) from the upland was predicted to be deposited there (table 3). This was slightly below the observed rate of 80 to 90% for most years. In 1993, the year in which a net of 0 deposition was observed in the grass buffer, more sediment left zone 2 than entered from the field. The total sediment load in 1993 was very low, 4.5 kg. Most of the yield leaving zone 2 was accounted for in a single storm on March 5. Deposition rates within zone 2 for both the observed and simulated values were approximately 95% for each year except 1993.

Table 2. Observed and simulated annual runoff and sediment totals at various positions in the riparian buffer.

year	Observed Data				Simulated Data		
	Runoff entering zone 3	Sediment entering zone 3	Sediment entering zone 2	Sediment entering zone 1	Sediment entering zone 2	Sediment entering zone 1	Sediment entering stream
	(mm)	----- (kg) -----			----- (kg) -----		
1993	22	4.5	4.6	4.9	1.3	0.9	1.2
1994	317	130.2	12.5	7.0	44.8	5.1	5.1
1995	109	42.6	7.4	1.5	14.6	2.1	2.0
1996	219	315.7	61.4	7.9	104.9	2.8	3.0

Table 3. Observed and simulated sediment yield rates at various positions in the riparian buffer as a percentage of sediment entering zone 3 from the field.

year	Observed Data		Simulated Data		
	Yield from zone 3	Yield from zone 2	Yield from zone 3	Yield from zone 2	Yield from zone 1
	----- (%) -----		----- (%) -----		
1993	102	109	28.9	20.0	26.7
1994	9.6	5.4	34.4	3.9	3.9
1995	17.4	3.5	34.3	4.9	4.7
1996	19.4	2.5	33.2	0.9	1.0

As with all sediment data from this site, the values are very low. Because of the design of the runoff collectors, the accuracy of the measurement decreases with decreasing sediment concentration. Arguably, the error in the observed data may mask any meaningful comparisons which could be made. Thus, it is difficult to compare event based data from this site. Additional model testing is being conducted on sites with higher sediment loads.

SUMMARY

REMM has been developed to examine the effects of riparian buffer management on the flow of water and the transport of sediment and agrichemicals through riparian systems. The model simulates physical, chemical, and biological processes in riparian areas. REMM is based on buffer system specifications recommended by the USDA Forest Service and the NRCS as a national standard (Welsch, 1991). It is intended for use by researchers as well as by planners as a decision tool to aid in the effective management of these areas.

Verification and validation of the erosion and sediment transport components of REMM is underway. Comparison of model output to observed data and other model predictions indicate the model is within acceptable ranges for most modeling efforts. Continued development and refinement of the model algorithms is currently underway.

REFERENCES

- Altier, L.S., R.R. Lowrance, R.G. Williams, S.P. Inamdar, D.D. Bosch, J.M. Sheridan, R.K. Hubbard, and D.L. Thomas. In Review. Riparian Ecosystem Management Model. USDA-ARS, Southeast Watershed Research Laboratory. USDA Conservation Research Report. U.S. Department of Agriculture, Agricultural Research Service.
- Bagnold, R.A. 1966. An approach to the sediment transport problem from general physics. Prof. Paper 422-J. U.S. Geol. Surv. Reston, VA.
- Dissmeyer, G. E., and G. R. Foster. 1984. A Guide for Predicting Sheet and Rill Erosion On Forest Land. USDA-Forest Service Technical Publication R8-TP 6.
- Foster, G.R. 1982. Modeling the erosion process. In Hydrologic Modeling of Small Watersheds. Eds. C.T. Haan, H.P. Johnson, and D.L. Brakensiek. ASAE Monograph 5. ASAE, St. Joseph, MI.
- Foster, G.R., R.A. Young, and W.H. Neibling. 1985. Sediment composition for nonpoint source pollution analysis. Trans. ASAE. 28(1):133-139, 146.
- Foster, G. R., L. J. Lane, J. D. Nowlin, J. M. Laflen, and R. A. Young. 1980. A Model to Estimate Sediment Yield from Field-sized Areas: Development of Model. In: Creams - A Field Scale Model For Chemicals, Runoff, and Erosion from Agricultural Management Systems. Vol I: Model Documentation. Conservation Research Report No. 26 USDA, Sci, and Educ. Admin. Chapter 3. pp. 36-64.
- Foster, G. R., L. J. Lane, J. D. Nowlin, J. M. Laflen, and R. A. Young. 1981. Estimating Erosion and Sediment Yield from Field-Sized Areas. Transactions of the ASAE 24:1253-1262.
- Inamdar, S., J. Sheridan, R.G. Williams, D.D. Bosch, and R. Lowrance. 1998. Hydrologic processes in riparian buffer zones. In Proceedings of the First Federal Interagency Hydrologic

- Modeling Conference. USDA, Las Vegas, Nevada. April 19-23, 1998.
- Lane, L.J. 1982. Development of a procedure to estimate runoff and sediment transport in ephemeral streams. In *Recent Developments in the Explanation and Prediction of Erosion and Sediment Yield*. Pub. No. 137. Int. Assoc. Hydro. Sci. Wallingford, Eng. pp. 275-282.
- Lowrance, R.R., L. Altier, R. Williams, S. Inamdar, D. Bosch, D. Thomas, and R. Hubbard. 1998. The riparian ecosystem management model (REMM): Simulator for ecological process in buffer systems. In *Proceedings of the First Federal Interagency Hydrologic Modeling Conference*. USDA, Las Vegas, Nevada. April 19-23, 1998.
- Lowrance, R.R., R.L. Todd, and L.E. Asmussen. 1983. Waterborne nutrient budgets for the riparian zone of an agricultural watershed. *Agric. Ecosys. Environ.* 10:371-384.
- Lowrance, R.R., R.L. Todd, J. Fail, Jr., O. Hendrickson, Jr., R. Leonard, and L. Asmussen. 1984. Riparian forests as nutrient filters in agricultural watersheds. *Bioscience*. 34:374-377.
- Peterjohn, W.T. and D.L. Correll. 1984. Nutrient dynamics in an agricultural watershed: Observations on the role of a riparian forest. *Ecology*. 65:1466-1475.
- Sheridan, J.M., R.R. Lowrance, and D.D. Bosch. 1998. Management effects on runoff and sediment transport in riparian forest buffers. *Trans. of the ASAE*. In review.
- Welsch, D.J. 1991. Riparian Forest Buffers. USDA-Forest Service Publication No. NA-PR-07-91. USDA-Forest Service, Radnor, PA. 20 pp.
- Wischmeier, W.H. and D.D. Smith. 1978. Predicting rainfall erosion losses - a guide to conservation planning. USDA, Agriculture Handbook No. 537.
- Young, R.A., C.A. Onstad, D.D. Bosch, and W.P. Anderson. 1989. AGNPS: A nonpoint-source pollution model for evaluating agricultural watersheds. *J. of Soil and Water Conservation*. 44:168-173.
- Young, R.A., C.A. Onstad, D.D. Bosch, and W.P. Anderson. 1987. AGNPS: Agricultural Non-Point-Source Pollution Model. A Watershed Analysis Tool. 1987. USDA, Cons. Res. Rept. 35. 80 p.

**Development of a Storm-Event based
Two-Dimensional Upland Erosion Model (CASC2D-SED)**

Billy E. Johnson¹, Pierre Y. Julien², and Chester C. Watson²

ABSTRACT

Modeling soil erosion is the process of mathematically describing soil particle detachment, transport, and deposition on land surfaces. In the United States, the prediction of upland erosion is commonly made by the USLE, developed by the USDA Agricultural Research Service in cooperation with the USDA Soil Conservation Service and certain other state experiment stations. The original USLE method is only able to compute annual soil loss due to sheet and rill erosion in tons per acre per year. The USLE has been the workhorse of the erosion prediction and conservation planning technology in the U.S. and even worldwide. Recent work has been done to improve the original USLE formula, namely the RUSLE and the MUSLE. However, from field tests, the use of these equations to predict sediment yield on an event or event-series basis, resulted in rather large errors from those measured in the field.

As a result of the limitations and errors involved in using the USLE equations, an increasing number of scientist and engineers are turning to distributed hydrologic models. Recent advances in hydrology, soil science, erosion mechanics, and computer technology have provided the technological basis for the development of physically-based erosion prediction technology. Work has been on-going at the Waterways Experiment Station with assistance from Colorado State University and the National Sediment Laboratory to develop a physically based single event upland erosion model and to verify the model on the watershed scale. The focus of this paper will be to describe the mechanics of the model and to present the model results.

INTRODUCTION

Every sediment particle that passes a given stream cross section must satisfy the following two conditions (Einstein, 1964): 1) It must have been eroded somewhere in the watershed above the cross section; 2) It must be transported by the flow from the place of erosion to the cross section.

The presence of sediment in streams and rivers has its origin in soil erosion. Erosion encompasses a series of complex and interrelated natural processes that have the effect of loosening and moving away soil and rock materials under the action of water, wind, and other geologic agents. In the long term, the effect of erosion is the denudation of the land surface, i.e., the removal of soil and rock particles from exposed surfaces, their transport to lower elevations, and eventual deposition. Sediment has a threefold effect on the environment : a) depleting the productive capacity of the land from which it is transported; b) impairing the quality of the water in which it is transported and the land on which it is deposited; and c) carrying chemical and biological pollutants.

That accelerated soil erosion is a serious global problem is widely recognized. What are difficult to assess reliably and precisely, however, are the dimensions (the extent, magnitude, and rate) of soil erosion and its economic and environmental consequences.

UPLAND EROSION

Langhaar (1967) defined dimensional analysis as a treatment of general forms of equations that describe natural phenomena. The application of dimensional analysis to any particular phenomena is based on the assumption that certain variables, which are named, are the independent variables of the problem, and that all variables, other than these and the dependent variables, are redundant or irrelevant.

¹Research Hydraulic Engineer, Waterways Experiment Station, 3909 Halls Ferry Rd., Vicksburg MS. 39180

²Professor, Department of Civil Engineering, Colorado State University, Fort Collins, CO. 80523

The purpose of dimensional analysis is to reduce information about a phenomena from a single premise, which is that the phenomena can be described by a dimensionally correct equation among certain variables. Sediment discharge by means of overland flow is a function of the hydraulic properties of flow, the physical properties of soil, and surface characteristics. Sediment transport as a result of erosion under simulated rainfall can be assumed to be related to a number of different variables. Elimination of some of the variables is possible since some are closely related to others, some are redundant, and some have relatively less effect than others on sediment discharge. Therefore, sediment transport is related to the following variables :

$$q_s = \phi(u, q_o, d, d_{50}, X, \nu, g, \rho, \rho_s, S_o, P) \quad (14)$$

where,

q_s = unit sediment discharge

u = longitudinal mean velocity

q_o = unit discharge

d = flow depth

d_{50} = grain size at which 50 percent of the particles are finer than the indicated size

X = longitudinal distance

ν = kinematic viscosity of water

g = gravity

ρ = mass density of water

ρ_s = mass density of solid particles

S_o = bed slope

P = porosity

In 1972 (Kilinc and Richardson) the mechanics of soil erosion from overland flow generated by simulated rainfall were studied experimentally and analytically. The experiments were conducted in a 4' deep, 5' wide, and 16' long flume at the Colorado State University Engineering Research Center. The results of this investigation resulted in the following sediment transport equation for sheet and rill erosion for bare sandy soil :

$$q_s = 25500q_o^{2.035} S_o^{1.664} \quad (15)$$

where q_s is in the units of (tons/m x s).

Considering various soil types, vegetation, cropping factors, and conservation practices yields the following equation (Julien, 1995a) :

$$q_s = 25500q_o^{2.035} S_o^{1.664} \frac{K}{0.15} CP \quad (16)$$

where K , C , and P are USLE coefficients.

The approach that is being used in this research is to use the modified Kilinc and Richardson equation to determine the sediment transport, transport the sediment from one overland grid cell to the next by three grain sizes (i.e., sand, silt, and clay), and then determine how much sediment stays in suspension and how much deposits on the receiving cell. In this scheme, the sediment transported out of a grid cell will first be assumed to come from sediment already in suspension, second from previously deposited sediment, and lastly from the soil surface (Figure 1).

Once the direction of flow (Figure 2) and the unit discharge have been computed, the upland erosion is broken down into three size fractions (sand, silt, and clay) and routed based upon how much sediment is in suspension, previous deposition, and how much sediment has been eroded from the soil surface (Figure 3). In order to determine how much sediment stays in suspension and how much is deposited on the receiving cell, the trap efficiency for each size fraction must be computed :

$$T_{E_i} = 1 - e^{-\frac{X\omega_i}{hv}} \quad (25)$$

where,

T_{ei} = trap efficiency for each size fraction

X = longitudinal length

ω_i = fall velocity for each size fraction

h = flow depth

V = flow velocity

The trap efficiency indicates how much sediment drops out for each size fraction, thus the remaining volume of sediment is assumed to stay in suspension.

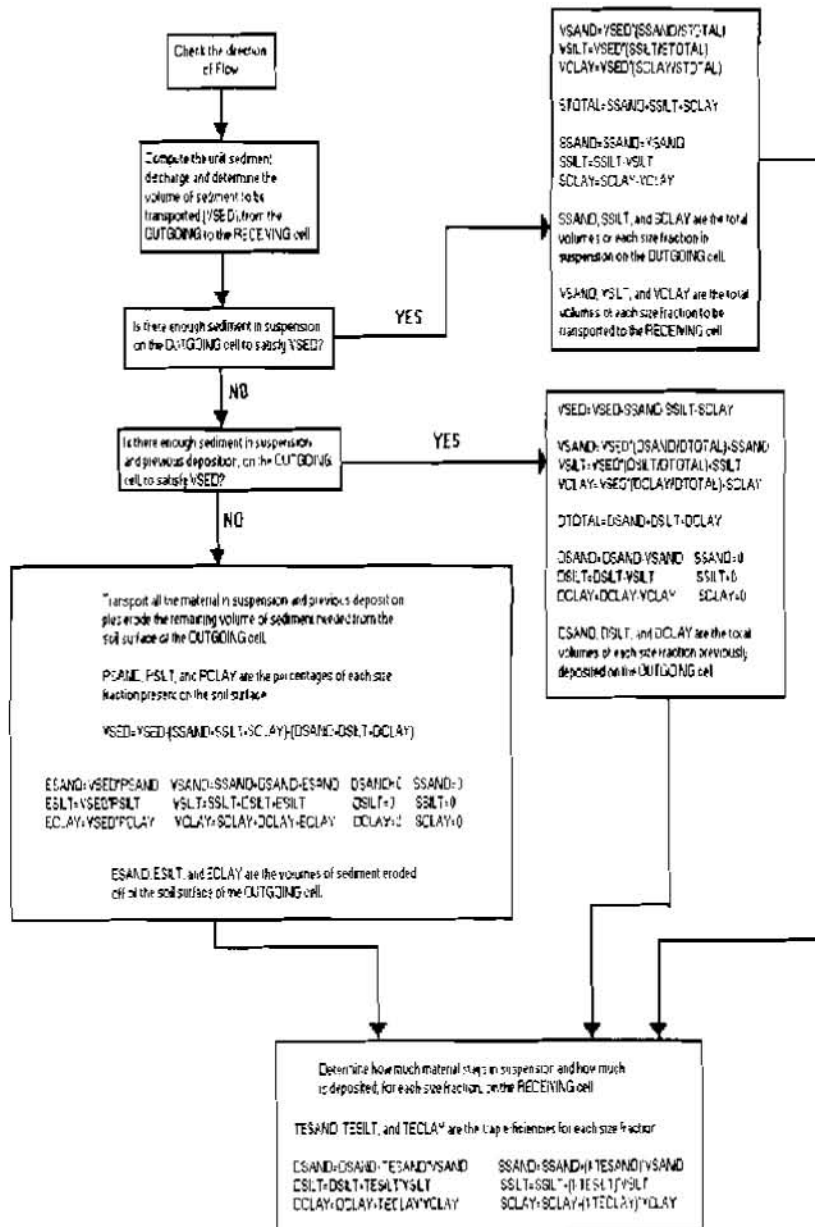


Figure 1 - Flow Chart for the Upland Erosion Scheme.

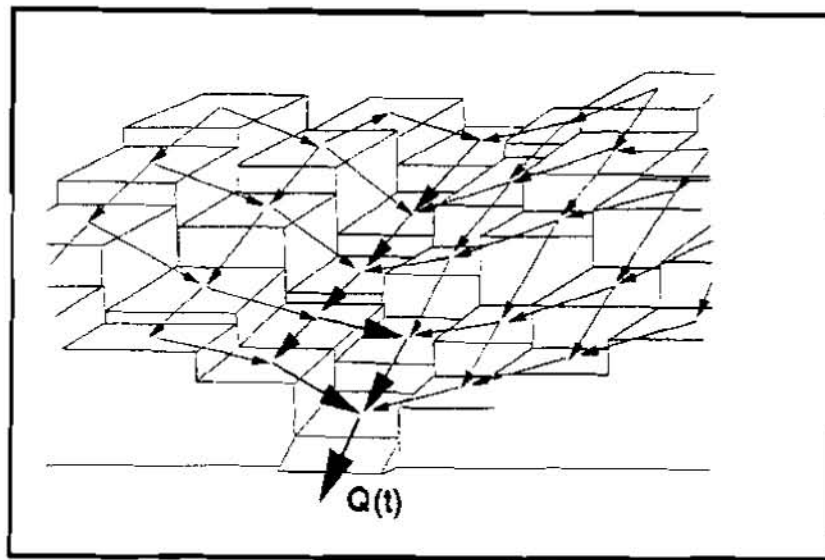


Figure 2 - Topographical Representation in Overland Flow Routing Scheme.

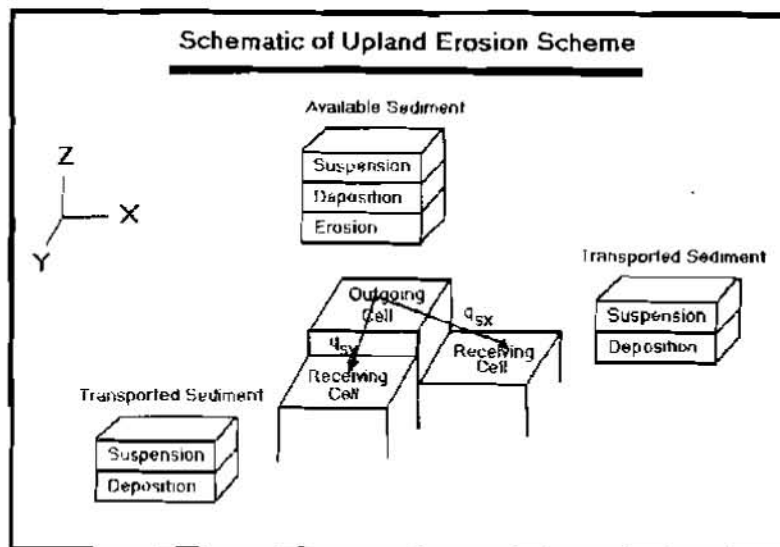


Figure 3 - Schematic of Upland Erosion Scheme

STUDY AREA

Goodwin Creek (Figure 4) is a tributary of Long Creek which flows into the Yocona River, one of the main rivers of the Yazoo River Basin. The Goodwin Creek watershed is located in North Mississippi, approximately 60 miles from Memphis, Tennessee and is extensively gaged by the Agricultural Research Service (ARS) as a research watershed in the areas of upland erosion, instream sediment transport, and watershed hydrology. The Vicksburg COE provided most of the construction funds when this watershed was originally established in 1977 (Blacknarr, 1995).

The Goodwin Creek watershed is divided into fourteen nested subcatchments with a flow measuring flume constructed at each of the drainage outlets. The drainage areas above these stream gaging sites

range from 0.63 to 8.26 square miles. Twenty-nine standard recording rain gages are uniformly located within and just outside the watershed.

Instrumentation at each gaging site includes an electronic data acquisition system which consists of a VHF-radio telemetry system with a microcomputer. This system collects, temporarily stores, and transmits the data at the predetermined intervals to a central computer at the National Sedimentation Laboratory (NSL).

The Climate of the watershed is humid, hot in the summer and mild in the winter. The average annual rainfall during 1982 to 1992 from all storms was 56.7 inches, and the mean annual runoff measured at the watershed outlet was 5.7 inches per year. Data from a standard climatological station near the center of the watershed is also transmitted through the telemetry system. This information complements climatological data available from the U.S. Weather station at Batesville, Mississippi. The

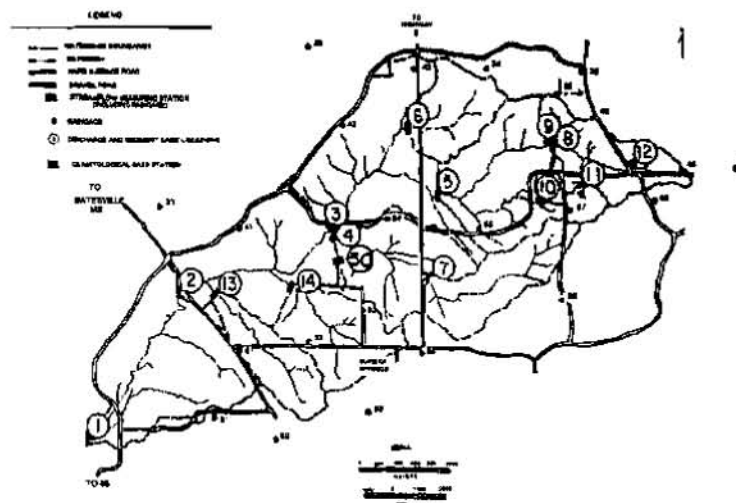


Figure 4 - Goodwin Creek Watershed

scope and quality of data being collected at the Goodwin Creek watershed has recently attracted the attention of scientists from NASA and NOAA working on large scale hydrometeorology.

The watershed flows approximately from northeast to southwest, it drains a total area of 8.26 square miles, with the outlet at latitude $89^{\circ}54'50''$ and longitude $34^{\circ}13'55''$. Terrain elevation ranges from 72 meters to 123 meters above mean sea level with an average channel slope of 0.004 in Goodwin Creek. Land use and management practices that influence the rate and amount of sediment delivered to streams from the uplands, range from timbered areas to row crops. The Goodwin Creek watershed is largely free of land management activities with 13 percent of it's area being under cultivation and the rest in idle pasture and forest land. Periodic acquisition of aerial photography and satellite data contribute to complete aerial coverage of land use and surface conditions. The predominant soil texture for Goodwin Creek watershed is silt loam with a small percent of sandy loam.

Measurements collected at each site and transmitted through the telemetry system includes water stage, accounting of automatically pumped sediment samples, air and water temperature, and precipitation. Manual sampling of total sediment loads is also carried out during storm events at stations 1 and 2 using bedload and depth-integrating suspended samplers. Surveys of channel geometry, bed material, bank geotechnical properties, and channel migration were conducted at periodic intervals to keep track of channel morphological change.

In evaluating the ability of CASC2D-SED to accurately simulate upland erosion on the watershed scale. Three storm events were used in the calibration and verification of the model, however only the results from the storm event occurring on October 17-18, 1981 will be presented.

Simulated streamflow hydrographs were compared to observed hydrographs at five locations on the main stem channel and one major tributary. Simulated sediment discharge hydrographs were compared to observed hydrographs at eleven locations along the main stem, tributaries, and upland areas. A total of seventeen rainfall gages were used to calculate overland flow runoff in the watershed.

The storm event of October 17, 1981 began at 9:19 pm and had a total rainfall duration of 3.5 hours with very little rainfall preceding this event. Total rainfall for this event varied from 2.55 to 3.11 inches with an average value of 2.85 inches. Total runoff varied from 0.87 inches at the upper streamflow gage to 0.64 inches at the downstream gaging location.

A comparison of the hydrograph plots and the hydrograph parameters (Table 1 to Table 3) show that CASC2D-SED had a varying degree of simulation success. CASC2D-SED was able to consistently simulate the overall shape and rate of rise. The time to peak was simulated within 3% at some places (gage 8 and gage 5), but was off by approximately 15% at gages 2 and 4. CASC2D-SED simulated the total volume of runoff low by approximately 20% across the watershed. The peak flows were within 1% to 8% throughout the watershed except at gage 3, which was off by 26%.

A comparison of the sediment discharge plots and the sediment yield parameters (Table 4 to Table 5) show that CASC2D-SED was able to predict upland erosion off of the Goodwin Creek Watershed within an acceptable range of -50% to 200% of the actual upland erosion. This range (-50% to 200%) is generally accepted by sedimentation engineers as being acceptable when comparing computed sediment yields versus actual sediment yields.

Table 1 - Goodwin Creek Watershed - Time to Peak (Minutes)

Gage I.D.	October 17-18 1981		
	Obs.	Comp.	Diff
1	266	254	12
2	239	223	16
3	207	213	6
4	195	181	14
5	191	188	3
8	181	179	2

Table 2 - Goodwin Creek Watershed - Total Runoff (Inches)

Gage I.D.	October 17-18 1981		
	Obs.	Comp.	% Diff
1	0.75	0.64	-14.7
2	0.71	0.70	-1.4
3	1.00	0.74	-26.0
4	0.77	0.66	-14.3
5	1.08	0.83	-23.1
8	1.08	0.87	-19.4

Table 3 - Goodwin Creek Watershed - Peak Flow (CFS)

Gage I.D.	October 17-18 1981		
	Obs.	Comp.	% Diff
1	1405.1	1385.3	-1.4
2	1286.5	1372.0	6.6
3	1050.6	820.1	-21.9
4	347.2	376.4	8.4
5	560.3	529.1	-5.6
8	260.2	248.7	-4.4

Table 4 - Goodwin Creek Watershed - Sediment Yield (Tons)

Gage I.D.	October 17-18 1981		
	Obs.	Comp.	C/O %
1	1394.4	420.6	30.2
2	1104.0	181.5	16.4
3	733.0	136.3	18.6
4	445.2	424.1	95.3
5	290.7	45.3	15.6
8	93.0	66.7	71.7
9	123.0	38.9	31.6
11	---	4.9	---
12	3.3	0.7	21.2
14	154.0	164.0	106.5

Table 5 - Goodwin Creek Watershed - Sediment Yield (Tons/Acre)

Gage I.D.	Drainage Area (Acres)	October 17-18 1981		
		Obs.	Comp.	C/O %
1	5286.4	0.26	0.08	30.2
2	4480.0	0.25	0.04	16.4
3	2176.0	0.34	0.06	18.6
4	889.6	0.50	0.48	95.3
5	1075.2	0.27	0.04	15.6
8	390.4	0.24	0.17	71.7
9	44.8	2.75	0.87	31.6
11	70.4	---	0.07	---
12	76.8	0.04	0.01	21.2
14	409.6	0.38	0.40	106.5

CONCLUSIONS

From the results of the three storm events discussed in this paper, CASC2D-SED was able to accurately simulate the rainfall-runoff processes on the watershed scale. The erosion and deposition patterns computed by the upland sediment scheme was accurate when compared to the field observations made on the Goodwin Creek Watershed. The upland erosion scheme implemented within CASC2D-SED computed sediment yield, in the upland areas, within a reasonable limit (-50% to 200%).

The linkage of CASC2D-SED with the GRASS GIS helped in the manipulation of input grids and the animation of output grids. These tools were essential in the verification of the upland erosion algorithm.

In the channel system, there are other components (i.e., gully erosion, bank failure, and bed erosion) that contribute to the total sediment yield. In order to compute total sediment yield, from the watershed, the estimation of sediment from these components will need to be implemented within CASC2D-SED.

This leads to the final conclusion, namely that CASC2D-SED was able to accurately estimate the sediment yield from the upland areas, however, if the goal is to compute total sediment yield from the overland and channel system, then the sediment contribution due to channel processes needs to be implemented and verified.

REFERENCES

- Beven, K. (1985). Distributed Models. Chapter 13 in Hydrologic Forecasting, Edited by M. G. Anderson and T. P. Burt. John Wiley & Sons, Chichester, UK.
- Blackmarr, W. A. (1995). Documentation of Hydrologic, Geomorphic, and Sediment Transport Measurements on the Goodwin Creek Experimental Watershed, North Mississippi, for the period 1982-1993 – Preliminary Release. National Sedimentation Laboratory - Research Report No. 3 - October 1995.
- Einstein, H. A. (1968). Deposition of Suspended Particles in a Gravel Bed. Journal of the Hydraulics Division, Proc. of the ASCE 94 (HY5) : 1197-1205.
- Foster, G. R. (1982). Chapter Eight of Hydrologic Modeling of Small Watersheds, Edited by C. T. Haan, H. P. Johnson, and D. L. Brakensiek. American Society of Agricultural Engineers. International Standard Book Number : 0-916150-44-5.
- Johnson, B. E. (1997). Development of a Storm-Event based Two-Dimensional Upland Erosion Model. PhD. Dissertation, Colorado State University.
- Julien, P. Y. (1995a). Erosion and Sedimentation. Press Syndicate of the University of Cambridge, New York, NY.
- Julien, P. Y. and Saghafian, Bahram, et al. (1995b). Raster-Based Hydrologic Modeling of Spatially-Variied Surface Runoff. Water Resources Bulletin, Vol. 31, No. 3, 523-536.
- Kilinc, M. and Richardson, E. V. (1973). Mechanics of Soil Erosion from Overland Flow Generated by Simulated Rainfall. Hydrology Papers No. 63, Colorado State University.
- Langhaar, E. M. (1967). Dimensional Analysis and Theory of Models. 8th Printing, John Wiley & Sons, Inc., New York, London, Sydney, 166.
- Philip, J. R. (1983). Infiltration in One, Two, and Three Dimensions. Proceedings of the National Conference on Advances in Infiltration. American Society of Agricultural Engineers. St. Joseph, MI., 1-13.
- Smith, R. E. (1976). Field Test of a Distributed Watershed Erosion/Sedimentation Model, Soil Erosion - Prediction and Control, Special Publication 21. Soil Conservation Society of America, Ankeny, IA., 201-209.

ANALYSIS OF THE TEMPORAL EVOLUTION OF THE SEDIMENT PRODUCTION OF THE PAMPULHA WATERSHED AND EVALUATION OF THE RESERVOIR SILTING

By Maria da Gloria Braz de Oliveira, Doctoral Student of Mining and Metallurgic Engineering at the Federal University of Minas Gerais and Professor at "Escola de Engenharia Kennedy" - Av. do Contorno 842 - Phone: (031) 238 1870 - Fax (031) 238 1001 - CEP 30 110 - 060 - Belo Horizonte - MG - Brazil

INTRODUCTION

The urbanization process brings about a great deal of human interference that causes various changes to the environment. Many of these interferences happen without any criteria. Erosion, for example, can bring about several serious environmental, economical and social problems if control measures are not considered.

In the Pampulha river basin located in Belo Horizonte, the third largest Brazilian city, the urbanization process is the main factor which influences the sediment production. Unplanned city growth, associated with the occurrence of major rainfalls, soil susceptibility to erosion processes, and the steep slopes, intensify the erosive processes as well as their consequences.

The temporal evolution of the sediment production is strictly linked to the urbanization process which is related to the process of urbanization and occupation patterns. These stages of evolution of the urbanization process, diversified along the urbanization process, are linked to various factors, such as soil susceptibility to erosion and steep slopes which allow for erosion source points. Associated with heavy rainfalls, those processes increase the production of sediments in the basin. (Oliveira, 1996).

The soil loss due to rainfall in the basin has been estimated by the Modified Soil Loss Equation (MUSLE), associating the sediment production with the evolution of urbanization in gradual scenarios of occupation.

Having the results of such studies in hand, it is possible to evaluate the sediment production in the basin under study and the silting of the reservoir from 1958 to 1994. The applicability of the model used has been considered adequate.

GENERAL ASPECTS OF THE STUDIED BASIN

The basin has an area of 97.6 km², 43 km² of which are in the district of Belo Horizonte and 54.6 km² are in the neighboring district of Contagem. It is drained by 40 water courses, that are distributed according to studies by Silva et al (1994), in eight sub-basins, as corresponding to the main tributaries to the basin: Água Suja, Baraúna, Paracatu, Tejuco, Mergulhão, Sarandi, Ressaca and Bom Jesus. The Sarandi and Bom Jesus sub-basins are in a later stage of urbanization, while the Ressaca sub-basin is practically fully urbanized with just a few industrial areas under development. These are the largest sub-basins in the Pampulha watershed.

The reservoir, bearing the same name as the basin's, was designed and built to store a volume of 18 million m³, as corresponding to a flooded area of 2.61 km² and a perimeter of 21 km.

The tropical climate of altitude presents a rainfall regime with an annual mean of 1500 mm. The rainy season occurs in the months of October through March, concentrating 90% of the annual total, and in December there is a monthly mean of 315 mm (Baptista et al, 1995).

According to studies by Silva et al (1994), the soil is a result of the excessive alteration and desiccation of the substrate of gneiss-granite composition, under the warm and humid tropical climate conditions, and it ranges from high to average erodibility patterns. As for the topography, it presents slopes with gradients of up to 40%.

URBANIZATION DEVELOPMENT

During the settlement period of the city of Belo Horizonte, the Pampulha area, as well as the surrounding areas of the Contagem district, consisted of zones of low demographic density and dominant rural activities. The construction of the Pampulha dam was carried out from 1936 to 1938, and following it the Leisure Complex of Pampulha was built in 1941. This resulted in the urban development of the area and several indiscriminate soil parcellings started to take place in its surroundings and neighbouring areas. However, urban occupation started in the 70's, even after some measures of soil use and urban occupation had been taken. It was in the 40's that there was considerable social and environmental impact. After the establishment of the industrial town of Cel. Juventino Dias, in Contagem, there was considerable social and environmental impact, since this area had got only rural characteristics.

At present, there are no empty areas in the portion of the river basin located in Belo Horizonte, as for soil parcelling or urbanization. The real estate business activity has already taken up the valleys and areas with steep slopes, taking off all the vegetation without any control. In Contagem, the dominant reminiscent areas have been inhabited in a disorderly fashion, and the matter concerning water pollution and sediment production was thoroughly disregarded (Oliveira, 1996). The predatory occupation has happened in both municipalities and it has raised serious consequences for the drainage network and the dam itself. After the dam was open to use, on January 31, 1958, the process of occupation of the upstream areas has been intensified, and so has the progressive process of environmental degradation of the water courses, whose main cause can be associated to the inflow of domestic and industrial sewerage, solid wastes and sediments carried along through the streams that make up the drainage network of the basin.

SILTING OF THE PAMPULHA RESERVOIR

The large sediment inflow happens mainly during the rainy seasons. The runoff from the rain water carries a significant amount of sediments, leading them into the drainage channels that will lead them into the pond, therefore causing its silting. Cross-sectional profiles carried out in 1958, 1984 and 1989 allowed Vignoli (1992) to perform studies on the evolution of the silting process and the reduction of the design life of the Pampulha reservoir. These are shown in Table 1. A 1994 cross-sectional profile indicates the volume of sediment stored in the reservoir is estimated as $8.1 \cdot 10^6 \text{ m}^3$.

Baptista et al (1995) pointed out that between 1979 and 1981, due to the urgency of adopting corrective measures in the short run, a sediment volume of about $1.2 \times 10^6 \text{ m}^3$ has been removed from the reservoir using drag-line equipment. In the subsequent period from 1989 to 1991, new dredgings were carried out, this time using hydraulic equipments; three million cubic meters have been removed. Disposal of the dredged material has been done in the reservoir area, forming islands, which if properly urbanized would allow for areas of community use.

Table 1 - Evolution of the Silting of Pampulha Reservoir

Year	1958	1984	1989
Total Area of the Water surface (km ²)	3.0	2.4	-
Volume (hm ³)	18.1	13.2	11.3
Silting (deposited volume- hm ³)	-	4.9	6.8
Solid Transport rate (10 ³ m ³ /year)	-	188.0	219.0
Number of years to silt 80 % of the volume	-	26.0	31.0
Unitary rate (m ³ /km ² x year)	-	1931.0	2247.0

EVALUATION OF THE SEDIMENT PRODUCTION PER EVENT IN THE PAMPULHA BASIN

The methodology adopted in the present evaluation of the sediment production per event in the Pampulha basin was based on the Modified Equation of Soil Loss below. The soil loss has been calculated for each sub-basin,

considering the extreme conditions of surface flow, in scenarios of urbanization evolution for the years of 1964, 1972, 1981, 1989 and 1994 (SILVA et al, 1996).

$$Y = R_w K LS C P \quad (1)$$

where:

Y = sediment production for an isolated event, in ton;
 R_w = flow factor;
 K = factor of soil erodibility, in $t h^{-1} MJ^{-1} mm^{-1}$;
 LS = conjugated factor of length and slope;
 C = factor of soil use;
 P = factor of preservation practices.

The R_w factor has been calculated by the following equation:

$$R_w = 89,6 (QS qp)^{0,36} \quad (2)$$

where:

QS = volume of surface flow in m^3 ;
 qp = peak flow in $m^3 s^{-1}$.

In order to estimate QS and qp , the urbanization process in the watershed has been mapped, as previously mentioned in this paper. The methodology used was the SCS triangular unit hydrograph, since it incorporates soil type and land use on the calculation of the maximum potential retention.

Due to the simplified idea of separating flow by the SCS model, the concentration of the rainy periods in a short period of time, as well as the impossibility to calibrate the parameter CN of this model from streamgauge data, the antecedent moisture condition III has been adopted (humid soil close to saturation), thus resulting in critical conditions of flow and consequently, a more unfavorable situation of sediments production in the basin under study. The CN'S have been estimated respecting the proposed scenarios and discretization of urbanization patterns. Having the CNIII values in hand, the average mean was used in order to find a common value, applicable to all the area of the sub-basin, presented in Table 2, along with the respective characteristics of each sub-basin.

For each year, it has been considered that at least a rainfall of 2 year-return period has occurred on each sub-basin. Generally, rainfall with intensity lower than 10 mm/h are not considered as erosive; in the Sarandi sub-basin, which is the largest one, the rainfall intensity of 2 year-return period has been estimated as 13 mm/h. On the top of that, rainfall of returns periods of 5, 10, 25, 50 and 100 years have been added according to the frequency of events.

Factor K evaluates the soil susceptibility to erosion, in function of the permeability and soil structure, % of organic matter and granulometry, and it has been calculated by the Wischmeier and Smith's equation (Paiva, 1995), as follows:

$$K = 2.1 M^{1,14} 10^{-4} (12 - ka) + 3.25 (kb - 2) + 2.5 (kc - 3) 0.001313 \quad (3)$$

where:

M = (% silt + % very thin sand) x (100 - % of clay);
 ka = % of organic matter;
 kb = relative coefficient of soil structure;
 kc = class of soil permeability.

A single value for K has been adopted for all sub-basins, since the present available data have come from the canal of the islands formed by the maintenance dragging of the reservoir which are 17% of clay, 50% of silt, 31% of thin sand and 2% of organic matter (Oliveira, 1996), resulting in parameter $ka = 2$. The soil was considered as a thin granular structure with moderate permeability, with values from $kb = 1$ to $kc = 3$, respectively (Paiva et al, 1995).

The land-use factor C was adopted according to the occupation patterns (Silva et al, 1996) and its weighted average mean has been used for each sub-basin, in each context of simulation. The corresponding factor to the conservation practices P was established according to the average slope of each sub-basin. The values of the factors C and P are based on studies of Lencastre and Franco (1984) and are shown in Table 3.

Table 2 - Characteristics and CNII of each Sub-basin

Data	Paracatu	Água Suja	Barauna	Bom Jesus	Sarandi	Ressaca	Tejuco	Mergulhão
A (km ²)	4.37	1.56	2.28	17.47	41.96	22.94	2.32	4.68
L (km)	3.25	1.19	2.87	8.74	16.76	9.58	1.59	4.02
H total (m)	85.80	18.00	85.80	126.00	204.00	157.20	52.00	168.00
H méd (m)	30.68	10.00	49.74	52.80	101.30	73.00	26.40	55.62
CN 1964	84.00	83.00	81.00	83.00	82.00	85.00	87.00	75.00
CN 1972	84.00	88.00	82.00	83.00	84.00	89.00	86.00	85.00
CN 1981	89.00	90.00	84.00	85.00	85.00	92.00	93.00	87.00
CN 1989	89.00	87.00	85.00	85.00	87.00	93.00	89.00	87.00
CN 1994	90.00	84.00	86.00	86.00	88.00	94.00	96.00	88.00

The value of the grouping factor and the length of the slope level (LS), was determined by the Williams and Berndt equation (Paiva, 1995), given by:

$$LS = \left(\frac{L}{22}\right)^m (0.065 + 0.0454 S + 0.0065 S^2) \quad (4)$$

where:

m = exponent, whose value varies according to S , adopting the value of 0.5, since $S \geq 4.5$ (Paiva et al, 1995)

S = % of slope;

L = length of the slope, in m, whose value was calculated as $\frac{1}{3}$ of the width of the equivalent rectangle of the basin, according to studies of Lencastre and Franco (1984) and Paiva et al (1995).

The values of sediment production per event, in tons, found for each sub-basins, are presented in Table 4. The evolution of the sediment production together with the growth of urbanization can be verified in Figure 1 and 2. These show present sediment production for an event with return period of 2 years for the two basins with the largest areas, one in the urbanization phase and the other practically fully urbanized, with some industrial areas.

Table 3 - Values of C and P for the Sub-basins

Sub-basin	P_{1964}	C_{1964}	P_{1972}	C_{1972}	P_{1981}	C_{1981}	P_{1989}	C_{1989}	P_{1994}	C_{1994}
Água Suja	0.50	0.56	0.50	0.42	0.50	0.37	0.50	0.06	0.50	0.19
Barauna	0.60	0.43	0.60	0.39	0.60	0.39	0.60	0.39	0.60	0.32
Bom Jesus	0.80	0.47	0.80	0.47	0.80	0.50	0.80	0.50	0.80	0.50
Mergulhão	0.60	0.43	0.60	0.43	0.60	0.34	0.60	0.34	0.60	0.34
Paracatu	0.60	0.40	0.60	0.68	0.60	0.35	0.60	0.45	0.60	0.17
Ressaca	0.80	0.62	0.80	0.59	0.80	0.59	0.80	0.39	0.80	0.35
Sarandi	0.80	0.47	0.80	0.53	0.80	0.43	0.80	0.48	0.80	0.48
Tejuco	0.50	0.86	0.50	0.62	0.50	0.18	0.50	0.14	0.50	0.09

Table 4 - Production of Sediments per Event in each Sub-basin of the Pampulha Watershed

Year, TR	Paracatu	Agua. Suja	Baraúna	Bom Jesus	Sarandi	Ressaca	Tejuco	Mergulhão
64, 2	6088	1374	2461	98176	199300	164212	6691	2937
72, 2	10349	1552	2434	98176	259718	207315	4451	7017
81, 2	7799	1598	2871	121065	226116	254179	2228	6468
89, 2	10028	205	3112	121065	289691	179628	1276	6468
94, 2	4077	508	2763	130109	309886	172275	1396	6970
64, 5	8077	1856	3377	130227	265167	214152	8703	4298
72, 5	13732	2000	3302	130227	339940	261926	5843	9225
81, 5	9913	2023	3822	157908	293579	313908	2751	8358
89, 5	12746	266	4105	157908	370374	220173	1630	8358
94, 5	5140	678	3614	168310	393249	209582	1680	8935
64, 10	9906	2302	4231	159540	325767	259550	10530	5616
72, 10	16840	2404	4110	159540	412977	310700	7111	11242
81, 10	11808	2404	4697	191284	354765	366607	3212	10065
89, 10	15182	322	5014	191284	442887	255804	1949	10065
94, 10	6087	836	4386	202800	467879	242241	1927	10697
64, 25	12816	3020	5615	206306	422284	331145	13402	7820
72, 25	21787	3039	5412	206306	528382	386436	9118	14435
81, 25	14760	2995	6093	244082	451027	447501	3921	12748
89, 25	18977	410	6454	244082	556086	310341	2445	12748
94, 25	7557	1088	5607	257091	583840	292082	2303	13458
64, 50	15444	3672	6884	248517	509617	395359	15977	9895
72, 50	26254	3604	6600	248517	632014	453359	10925	17317
81, 50	17373	3519	7357	291348	537167	518366	4541	15147
89, 50	22337	488	7755	291348	656695	357973	2887	15147
94, 50	8856	1317	6703	305546	686593	335479	2629	15915
64, 100	18497	4435	8374	297560	611157	469434	18948	12387
72, 100	31445	4254	7990	297560	751807	529735	13013	20647
81, 100	20362	4117	8823	345945	636402	598657	5244	17903
89, 100	26180	579	9259	345945	771970	411816	3392	17903
94, 100	10336	1583	7970	361327	804044	384450	2997	18734

ANALYSIS OF THE EVOLUTION OF THE SEDIMENT PRODUCTION AND THE SILTING OF THE RESERVOIR

In order to develop the calculations of the annual production of sediments of the sub-basins and, consequently, of the Pampulha watershed, it was necessary to gather data regarding the number of rain events which occurred in the region under study. Therefore, the series of rain gauge data have been abstracted for the period 1964 - 1994, for the Horto and the Gas Plant gauging stations, respectively. Data have been treated for each sub-basin and all events which happened in each sub-basin were specified for the different return periods. They were then quantified, and the total annual production of sediments for each sub-basin was calculated, by multiplying the number of recorded events by its respective production. The value of this sediment annual production of each sub-basin was estimated graphically.

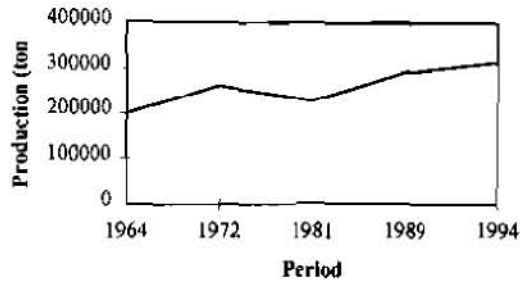


Figure 1 - Production of Sediments in the Sub-basin of the Sarandi Stream for Event 1, with TR = 2 years

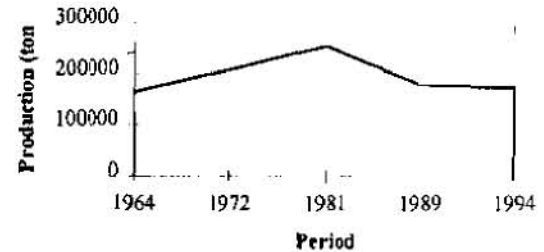


Figure 2 - Production of Sediments in the Sub-basin of the Ressaca Stream for Event 1, with TR = 2 years

The total annual production of sediments of the Pampulha watershed was calculated by adding the annual production of each sub-basin, allowing the plotting of Figure 3. Once this production has been estimated, and due to the lack of data to predict the propagation of these sediments along the water courses, the reduction factor Ef was used in order to obtain sediment inflow to the reservoir. According to Carvalho (1994), "... Ef represents a coefficient that transforms the total erosion of the basin in a portion that goes towards the outside." Therefore, knowing the values of the silting within the periods of 1957 - 1984 and 1984 - 1989, supplied by Vignoli (1992), the factor Ef was calibrated, within those periods, since it varies according to the changes which took place in the basin, due mainly to urbanization.

In the absence of data for the 1958-1963 period, the 2-year event for 1964 has been adopted (Oliveira, 1996). This can be justified since in 1957, the Pampulha leisure complex, the major focus of sediment production, had already been built. In order to calculate the total production of the sediments of the Pampulha Basin in the period of 1958 - 1984, the overall sum of the annual production in this period was conducted, resulting in a value of 14,340,000 m³. As the volume of silting was 4,900,000 m³, the value of Ef as being the ratio between the silting volume and the sediment production, can be estimated as $E_{f\ 57-84} = 0.342$. Similarly, the value of Ef for the years 1984 - 1989 was found to be $E_{f\ 84-89} = 0.470$, since the silting volume and the related production within such a period are 1,900,000 m³ and 4,040,000 m³, respectively.

Regarding the period 1990 - 1994 and in order to verify the validity of the MUSLE, the inflow of sediments was estimated, using the same value of $E_{f\ 84-89}$, reaching a value of 2,000,000 m³. Therefore, the value of inflow of sediments can be estimated in the period of 1957 - 1994 as 8,800,000 m³.

According to Champs (1991), the reservoir trap-efficiency was estimated as 94.8%. Supposing that a 100% trap-efficiency compensates for any dredging and sediment removal operations, the 5-year prediction of time variation of the reservoir silting has been performed by considering three scenarios from the year 1994. These correspond to minimum, average and maximum sediment inflows to the reservoir. According to these simulations, it is predicted that a complete silting of the reservoir will take place in the year 2012, for average conditions of sediment inflow.

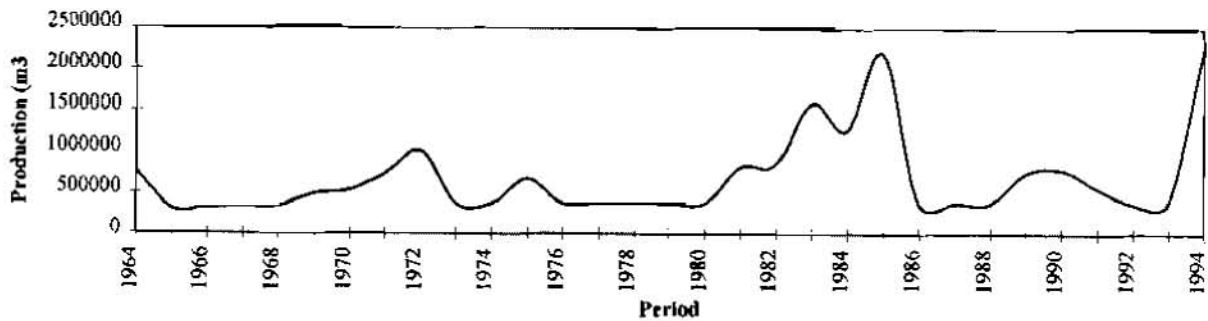


Figure 3 - Total Annual Production of Sediments in the Pampulha River Basin

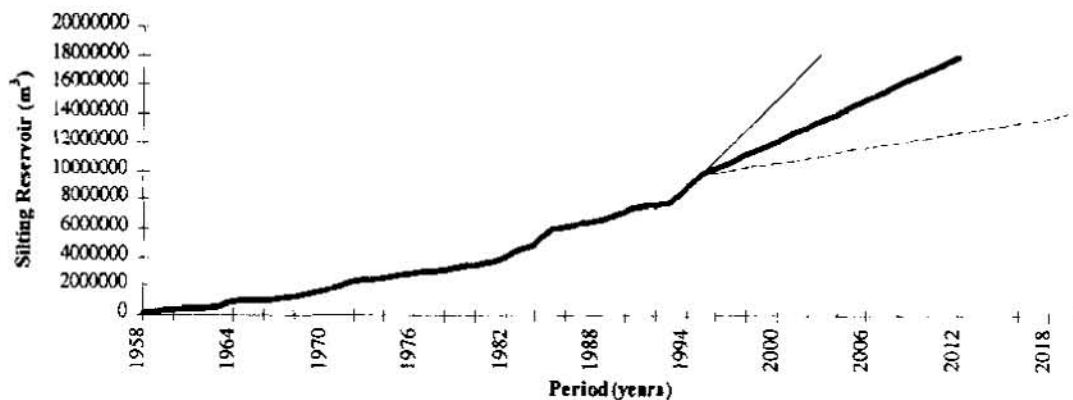


Figure 4 - Temporal Evolution of the Silting of the Pampulha Reservoir

CONCLUSIONS

This paper is the first consolidated study of the production of sediments in the Pampulha watershed and the volume of inflow into the reservoir. Only after a systematic hydro-sedimentometric monitoring of the tributaries of the reservoir under question, one will be able to estimate, with less uncertainty, the production of sediments and the silting volume. However, we can assure that the Modified Soil Loss Equation has fulfilled the expectations, considering that the volume obtained through this model has surpassed only by 10% the volume of the measured in 1994.

The Unity of the Pampulha Management Program - UGP, created by Belo Horizonte City Hall in 1995, has proposed the adoption of dredging operations for taking out the silting deposition from the pond with an estimate of 40,000 m³/month during 10 months. This figure was based on the study of Vignoli (1992), which represents an annual inflow of sediments around 380,000 m³/year. However, based on the results presented in this paper, the annual sediment inflow in the basin under study varies according to the intensity and frequency of rain events and also with the evolution of the urbanization process. It is not possible to adopt a volume of constant dredging from the reservoir, since it is known that there is always the uncertainty of large rainfall events.

It can also be stated that the increase of the sediment production is directly proportional to the evolution of urbanization, as depicted in Figure 1, mainly when it occurs in an indiscriminate and predatory way. Other physical

factors may influence the process, but the impact of the anthropic activities are presented as the major factor. It can be observed that as the urbanization process comes to a standstill, the production of sediments becomes stable as shown in Figure 2.

As adopting structural measures of silting control, when technically possible, carry partial and questionable efficiency, thus postponing the problem in time and space, besides bringing about environmental and financial losses to the community, it is obvious that non-structural measures are necessary to find a satisfactory solution for the problem. Therefore, the control actions in terms of erosion and silting of the reservoir should be linked to the characteristics of the sub-basins as for its preventive and corrective features, in spite of the difficulties to control the problems, considering the problems of erosion in the basin. (non-point sources).

As far as corrective measures are concerned, we recommend actions to recover the urban areas that have already been degraded by erosion, through remodeling the topography, whenever possible, through the construction of effective systems of stormwater drainage, together with the construction of the street network, conservation of the landscaped areas and last but not least, dredging out the silting from the drainage canals and reservoir.

REFERENCES

- Baptista, M.B., Pinheiro, M.C., Oliveira, M.G.B., Champs, R.B, 1995, Aspectos técnicos e econômicos do assoreamento de lagos urbanos -Análise do caso de Belo Horizonte. In: XI Simpósio Brasileiro de Recursos Hídricos e II Simpósio de Hidráulica dos Países de língua Oficial Portuguesa, , Recife/PE:ABRH.
- Carvalho, N.O, 1994, Hidrossedimentologia prática. 1 ed, Rio de Janeiro: CPRM.
- Champs, J.R.B., 1991, O problema de assoreamento da represa da Pampulha e as medidas adotadas para o seu controle, In: Encontro Nacional de Engenharia de Sedimentos, Ouro Preto, UFOP, ABRH.
- Lencastre, F.;Franco, F.M., 1984, Lições de hidrologia, Lisboa, Universidade de Nova Lisboa.
- Oliveira, M.G.B.,1996, Estudos dos processos erosivos e avaliação da produção de sedimentos na bacia hidrográfica da Pampulha - Dissertação de Mestrado, EEUFMG.
- Paiva,J.B.D., Paiva, E.M.C.D., Vilela, S.M., 1995, - Avaliação da descarga de sedimentos afluentes à captação da estação elevatória I do projeto de transposição das águas do rio São Francisco. In: Revista Brasileira de Engenharia, Cad. De Recursos Hídricos, vol.13, n.2.
- Vignoli, O.,1992, Investigações sedimentológicas na Pampulha - a evolução do assoreamento e seu controle. In: Seminário da bacia hidrográfica da Pampulha, Belo Horizonte, Anais...Belo Horizonte: SEGRAC.1992.
- Silva, A. B., Carvalho, E.T., Fantinel, L.M., Viana, C.S., Romano, A.W., 1994, Estudos técnicos para o levantamento dos focos de erosão e do risco geológico na bacia hidrográfica da Pampulha, Belo Horizonte, Relatório Técnico FUNDEP, IGC/UFMG.
- Silva, A. B., Carvalho, E.T., Fantinel, L.M., Viana, C.S., Romano, A.W., 1996. Estudos técnicos e assessoria nas áreas de geotecnia, hidrogeologia e geologia básica e outros projetos de intervenção urbanística, Rel. Téc. Final, PMBH, SMP, FUNDEP, IGC/UFMG.

PREDICTING SEDIMENT YIELD FROM ARID DRAINAGE AREAS

By

Timothy J. Randle, Hydraulic Engineer and Chih Ted Yang, Supervisory Hydraulic Engineer, U.S. Bureau of Reclamation, Sedimentation and River Hydraulics Group, Denver, Colorado

Abstract: The application of the unit stream power function for predicting the sediment yield from arid drainage areas is presented through a case study of three proposed reservoirs near Yuma, Arizona. The unit stream power function incorporates drainage area, length, slope, runoff, sediment particle size, and surface roughness characteristics. This function is thought to be an improvement over empirical formulas proposed for the southwestern United States.

INTRODUCTION

Sediment yields can be estimated from historical measurements of a stream's sediment load or from reservoir sedimentation surveys. In the absence of such measurements, sediment yields must be estimated from one or more predictive methods. The long-term prediction of sediment yields for arid drainage areas are often difficult because runoff and sediment load data are usually unavailable. Most empirical formulas are usually not applicable to arid drainage areas because they were developed for drainage areas with very different characteristics (i.e., rainfall, runoff, vegetation, etc.).

A physically-based procedure to predict sediment yields is presented based on a unit stream-power function that incorporates drainage area, length, slope, runoff, sediment particle size, and surface roughness characteristics. An example application of this procedure for three proposed reservoir sites along the All American Canal and Gila Gravity Main Canal near Yuma, Arizona is provided. The drainage areas of the proposed reservoirs are among the driest in the nation (Olmstead et al., 1973). Although rainfall runoff is infrequent in this arid region, the sediment yield during runoff can be significant due to the rainfall intensity and sparse vegetation.

PREDICTIONS OF SEDIMENT YIELD

The factors that determine sediment yield can be summarized as follows (Strand and Pemberton, 1982, and Yang, 1996):

- rainfall amount, intensity, and runoff;
- topography, soil type, and geologic formation;
- ground cover;
- land use;
- upland erosion rate, drainage network density, slope, shape, size, and alignment of channels;
- sediment characteristics, such as grain size and mineralogy; and
- channel hydraulic characteristics.

Unit Stream Power Equation for Sheet Erosion: The unit stream power theory stems from a general concept in physics that the rate of energy dissipation used in transporting materials should be related to the rate of material being transported (Yang, 1973 and 1996). The minimum rate of energy

dissipation theory states that when a dynamic system reaches its equilibrium condition, its rate of energy dissipation is at a minimum (Yang and Song, 1986 and Yang, 1996). The minimum value depends on the constraints applied to the system. The rate of energy dissipation per unit weight of water is

$$dY/dt = (dx/dt) (dY/dx) = VS = \text{unit stream power} \quad (1)$$

where Y is the potential energy per unit weight of water,
 t is time, and
 x is the reach length,
 dx/dt is equal to velocity (V), and
 dY/dx is equal to the energy slope (S).

For the equilibrium condition, the unit stream power (VS) will be at a minimum subject to the constraints of carrying a given amount of water and sediment. Sediment transport must be directly related to unit stream power (Yang, 1996).

The basic form of Yang's (1973) unit stream power equation for sediment transport is:

$$\text{Log } C = I + J \text{Log}(VS/\omega - V_{cr}S/\omega) \quad (2)$$

where C is the sediment concentration,
 I and J are dimensionless parameters reflecting flow and sediment characteristics and are determined from regression analysis of laboratory data,
 V is the flow velocity,
 S is the energy slope of the flow,
 ω is the sediment particle fall velocity, and
 V_{cr} is the critical velocity required for incipient motion.

Moore and Burch (1986) tested the application of equation (2) to sheet and rill erosion. They reported from experimental results that

$$I = 5.0105 \pm 0.0443 \quad (3)$$

and

$$J = 1.363 \pm 0.030 \quad (4)$$

Velocity was computed from Manning's equation because it is difficult to measure for sheet flow and they expressed unit stream power as

$$VS = (Q/B)^{0.4} S^{1.3} / n^{0.6} \quad (5)$$

where Q is the water discharge or runoff rate, in m^3/s ;
 B is the width of flow, in m ;
 S is the energy slope; and
 n is the Manning's roughness coefficient.

Moore and Burch (1986) also developed equations for rill flow. However, the average rill spacing must be specified. Only the equation for the simpler case of sheet flow was used in the case study because no site-specific data were available on rill spacing.

Yang's (1973) unit stream power equation was intended for open channel flow. The critical unit stream power required for incipient motion ($V_{cs}S$) may not be directly applicable to sheet and rill flow. For sheet and rill flows of very shallow depth, Moore and Burch found that the critical unit stream power required at incipient motion can be approximated by a constant (additional research is needed to determine if this constant can be universally applied):

$$V_{cs}S = 0.002 \text{ m/s} \quad (6)$$

Combining equations 4 through 8 yields:

$$\text{Log } C = 5.0105 + 1.363 \text{ Log } \left[\left\{ \frac{(Q/B)^{0.4} S^{1.3}}{n^{0.6}} - 0.002 \text{ m/s} \right\} / \omega \right] \quad (7)$$

Flood Hydrology Analysis: Application of the sheet erosion equation requires a prediction of the long-term hydrology for the drainage area. Flood hydrographs for various return periods were available for the case study. However, long-term sediment yield predictions must be based on all floods that are expected to occur over the period of study. The annual flood series accounts for only one flood per year, therefore, must be transformed into a partial duration series to account for all floods over the period of study.

The partial series is made up of all floods above some selected base value. The base value is chosen so that not more than a certain number of floods (N) are included for each year. The partial series can then indicate the probability of floods being equaled or exceeded N times per year (William Lane, Verbal communication, August 1996 and Linsley, et. al., 1975).

$$P_{\text{annual}} = 1/T_{\text{annual}} = 1 - (1 - P_{\text{partial}}/N)^N \quad (8)$$

where P_{annual} is the annual probability of floods being equaled or exceeded once per year,
 T_{annual} is the annual return period, in years, associated with the annual probability,
 P_{partial} is the probability of floods being equaled or exceeded N times per year, and
 N is the number of floods per year

Solving for P_{partial} , equation 10 can be expressed as

$$P_{\text{partial}} = 1/T_{\text{partial}} = N \left[1 - (1 - 1/T_{\text{annual}})^{1/N} \right] \quad (9)$$

where T_{partial} is the partial series return period, in years, associated with P_{partial}

CASE STUDY

The sedimentation volume of three proposed reservoirs near Yuma, Arizona was predicted for 100 years of future operations. The proposed reservoir sites are located beside the All American

Canal and Gila Gravity Main Canal. Both canals originate below Imperial Dam and flow along the edge of the foothills that border the flood plains of the Colorado and Gila Rivers (Bullard, 1994). These proposed reservoirs would be able to store available water for irrigation in the United States and to help provide required deliveries to Mexico. Available water would come from scheduled irrigation releases that are subsequently canceled due to rainfall over irrigated lands downstream and also from runoff into the Colorado River below Parker Dam.

The general drainage areas of the proposed reservoir sites are desert foothills with steep to very steep terrain (Bullard, 1994). Surface topography is composed of jagged rock, gravel, and sand. Little vegetation grows in these basins except for sparsely spaced desert brush and clumps of grass. Stream bottoms are steep and sandy. Bullard (1994) reported that the drainage areas appear to be capable of producing flash flood conditions and large sediment volumes in the event of intense rainfall. Drainage area characteristics for each of the proposed reservoir sites are summarized in table 1. The overall drainage areas of the two reservoirs along the All American Canal were each subdivided into three drainage areas and analyzed separately.

Table 1. Reservoir drainage area characteristics.

Proposed Reservoir	Drainage Area Name	Drainage Area (mi²)	Drainage Length (mi)	Average¹ Width (mi)	Drainage Slope (ft/mi)
All American Canal East	Unnamed Wash East	8.50	6.77	1.26	110.0
	Mission Wash	7.10	7.20	0.99	154.0
	Mission Wash East	2.20	1.50	1.47	317.0
All American Canal West	Picacho Wash	43.70	16.20	2.70	47.3
	Unnamed Wash	30.20	12.60	2.40	73.4
	Picacho Wash East	2.00	3.44	0.58	75.6
Gila Gravity Main Canal	Reservoir drainage area	10.10	4.31	2.34	119.0

These drainage areas are in a very warm desert climate where the frequency of rainfall events, that actually produce runoff, is expected to be one to two times per year (Earl Burnett, Verbal communication, August 1996).

Flood hydrographs with return periods of 100, 50, 25, 10, and 5 years were computed by Bullard (1994) for each drainage area. These hydrographs were determined from regional rainfall data because there were no site specific measurements. The flood hydrographs were computed using 5-minute time steps with the total durations ranging from 2.3 to 14 hours. Sediment concentrations were computed for each discharge using the unit stream power equation for sheet erosion (eq. 7).

¹The average drainage width was computed as the ratio of the drainage length to area.

The Manning's n roughness coefficient in equation 7 was assumed to be a constant of 0.030. The width (B) and slope (S) for each drainage area are listed in table 1. Sediment load was computed from each concentration and discharge value. Sediment loads was converted to volume assuming a bulk density of 70 lbs/ft³. Using this procedure, sediment volumes were accumulated for each flood hydrograph and for each drainage area.

The soils of the drainage areas are primarily sand and coarser (Bullard, 1994). The median sediment particle size was assumed to be within sand-size range but the size was not precisely known for any of the drainage areas (Earl Burnett, Verbal communication, August 1996). Therefore, sediment volumes were computed assuming a range of sand sizes (0.06 mm to 2.0 mm) .

Sediment concentrations (computed from eq. 7) were found to be sensitive to particle size. Example results for the All American Canal East Reservoir, Mission Wash drainage area are presented in table 2. The range of possible particle sizes was reduced by examination of the computed peak sediment concentrations. A maximum probable concentration of 300,000 ppm was assumed for the sand sizes of the study area. This is a reasonable limit based on other streams where long-term measurements exist. For example, the maximum mean daily concentration of record for the Rio Puerco near Bernardo, New Mexico (a major sediment producing tributary of the Rio Grande) is 230,000 ppm.

Table 2.—All American Canal East Reservoir, Mission Wash sediment yields.

Recurrence Interval (years)	Peak Discharge (ft ³ /s)	Sediment Volume (acre-feet) for Various Assumed Particles Sizes					
		0.06 mm	0.1 mm	0.2 mm	0.5 mm	1 mm	2 mm
100	3,409	430.64	130.58	28.99	6.04	2.36	1.18
50	2,510	259.94	78.82	17.50	3.65	1.42	0.71
25	1,768	145.68	44.17	9.81	2.04	0.80	0.40
10	1,005	56.85	17.24	3.83	0.80	0.31	0.16
5	579	22.50	6.82	1.51	0.32	0.12	0.06
100-year volume				255.74	53.32	20.81	10.35
Recurrence Interval (years)	Peak Discharge (ft ³ /s)	Peak Sediment Concentration (ppm)					
		0.06 mm	0.1 mm	0.2 mm	0.5 mm	1 mm	2 mm
100	3,409	2,350,000	713,000	158,000	33,000	12,900	6,420
50	2,510	1,960,000	595,000	132,000	27,500	10,800	5,360
25	1,768	1,590,000	482,000	107,000	22,300	8,720	4,340
10	1,005	1,130,000	341,000	75,800	15,800	6,170	3,080
5	579	795,000	241,000	53,500	11,200	4,360	2,170

Equation 9 was used to compute the partial duration series for a range of return periods assuming no more than two floods per year, for a total of 200 floods over a 100-year period (see table 3). The

largest flood considered was that associated with the 200-year return period because, of all the floods larger than the 100-year flood, half would be greater than the 200-year flood.

Table 3.—Transformation of annual flood series to a partial duration series assuming no more than two floods per year.

Annual Peak Flood Series				Partial Duration Series		
Flood Return Period (years)	Number of times exceeded in 100 years	Number of floods in 100 years	Flood Return Period (years)	Flood Return Period (years)	Number of Times Exceeded in 100 Years	Number of Floods in 100 Years
> 200.00	< 0.500				< 0.501	
100.00	1.000	1.000	200.00	199.505	1.003	1.003
90.00	1.111	0.111	95.00	94.749	1.114	0.112
80.00	1.250	0.139	85.00	84.749	1.254	0.140
70.00	1.429	0.179	75.00	74.749	1.434	0.180
60.00	1.667	0.238	65.00	64.749	1.674	0.240
50.00	2.000	0.333	55.00	54.749	2.010	0.336
40.00	2.500	0.500	45.00	44.749	2.516	0.506
30.00	3.333	0.833	35.00	34.748	3.362	0.846
25.00	4.000	0.667	27.50	27.248	4.041	0.679
20.00	5.000	1.000	22.50	22.247	5.064	1.023
15.00	6.667	1.667	17.50	17.246	6.782	1.718
10.00	10.000	3.333	12.50	12.245	10.263	3.482
7.00	14.286	4.286	8.50	8.242	14.836	4.573
5.00	20.000	5.714	6.00	5.738	21.115	6.279
4.00	25.000	5.000	4.50	4.234	26.795	5.680
2.00	50.000	25.000	3.00	2.720	58.579	31.784
1.50	66.667	16.667	1.75	1.445	84.530	25.951
1.30	76.923	10.256	1.40	1.073	103.923	19.393
1.10	90.909	13.986	1.20	0.839	139.698	35.775
1.00	100.000	9.091	1.05	0.608	200.000	60.302
Total		100.000		Total		200.000

The sediment volumes for the flood return periods listed in table 3 (5th column) were computed from regression equations (specific to each drainage area). The regression equations were determined from the logarithms of the sediment volumes (dependent variable) and the logarithms of the corresponding flood return periods (independent variable). The 100-year sediment volume was computed by accumulating the products of the sediment inflow volume, corresponding to a given range of floods, and the number of times floods in that range that are expected to occur during a 100-year period (see table 3, last column). Since the proposed reservoirs would normally be operated to completely contain runoff from local storms, they are expected to contain all of the sediment. Therefore, the trap efficiency for each reservoir was assumed to be 100 percent.

Results: Summary results for the three different reservoirs are presented in table 4. The finest sediment particle size (0.06 mm) was eliminated for all three drainage areas entering two of the reservoirs because the computed peak concentrations exceeded 300,000 ppm. Also, the 0.1 mm-

particle size was eliminated from two of the three drainage areas entering All American Canal East Reservoir and the 0.06 mm-particle size was eliminated from two of the three drainage areas entering All American Canal West Reservoir.

Table 4.—Summary results of 100-year sediment volumes by three methods.

Reservoir	100-Year Sediment Volume (acre-ft)					
	0.06 mm	0.1 mm	0.2 mm	0.5 mm	1 mm	2 mm
All American Canal East		1,000 ²	500	100	40	20
All American Canal West	1,000 ²	800	200	40	10	7
Gila Gravity Main Canal		500	100	20	8	4

Discussion: Results from the sheet erosion equation provided the lowest sediment yield estimates of other methods tried. The sheet erosion equation is potentially the most accurate method because it takes into account the important variables of drainage slope, width, roughness, and sediment particle fall velocity and the runoff velocity, duration, and frequency. The drainage slope (S), runoff velocity (V), and sediment particle fall velocity (ω) are represented as dimensionless unit stream power (VS/ω), which has been shown by Yang (1996) to be applicable to a wide range of conditions.

The sheet erosion equation is especially applicable to the drainage areas of the proposed reservoirs for the following reasons:

- the drainage surface is mostly composed of sand and particle cohesion can be ignored,
- there is little or no vegetation to resist erosion of sediment particles or complicate estimates of roughness,
- a reasonable estimate can be made for the total number of the runoff events over a 100-year period in this very arid climate, and
- a maximum probable limit on sediment concentration can be applied to reduce the range of sediment particle sizes.

The accuracy of the method could be improved if field measurements were available for runoff, the average sediment particle size distribution, and the surface area of the drainage that can be considered non-erodible (e.g., exposed bedrock).

²The sediment yield was computed assuming the next coarser sediment-particle size for two of the three drainage areas so that the computed peak concentrations would not exceed 300,000 ppm.

CONCLUSIONS

Application of the unit stream power equation for sheet erosion accounts for all of the important variables affecting sediment yields in arid drainage areas (i.e., drainage topography, runoff, sediment particle size, and surface roughness). For the case study, a reasonably accurate range of sediment yield predictions is provided by the sheet erosion equation. The method accounts for 200 floods, occurring over a 100-year period and a reasonable range of sediment particle sizes. The maximum 100-year sediment volumes could only be greater if peak sediment concentrations exceeded 300,000 ppm or if the runoff magnitudes or their frequencies are greater than expected.

REFERENCES

Bullard, K.L., August 1994. "Lower Colorado River Regulatory Storage Study, Probable Maximum Floods and Frequency Floods, All American Canal East Reservoir, All American Canal West Reservoir, Gila Gravity Main Canal Reservoir, Yuma Mesa Reservoir," Flood Hydrology Group, U.S. Bureau of Reclamation, Denver, CO.

Linsley, R.K. Jr., Kohler, M.A., and Paulhus, J.L.H., 1975. Hydrology for Engineers, McGraw-Hill Book Company, New York, pages 355-356.

Burnett, Earl, Verbal communication, August 1996. U.S. Bureau of Reclamation, Yuma, AZ.

Lane, William, Verbal communication, August 1996. U.S. Bureau of Reclamation, Denver, CO.

Moore, I.D. and Burch, J.G., 1986. "Sediment Transport Capacity of Sheet and Rill Flow: Application of Unit Stream Power Theory," *Water Resources Research* Vol. 22, No. 8.

Olmsted, F.H., Loeltz, O.J., and Irelan, Burdge, 1973. "Geohydrology of the Yuma Area, Arizona and California," *Water Resources of Lower Colorado River--Salton Sea Area*, Geological Survey Professional Paper 486-H, United States Government Printing Office, Washington D.C..

Strand, R.I., and Pemberton, E.L, October, 1982. "Reservoir Sedimentation, Technical Guideline for Bureau of Reclamation," Sedimentation and River Hydraulics Section, U.S. Bureau of Reclamation, Denver, CO.

Yang, C.T., 1971. "Potential Energy and Stream Morphology," *Water Resources Research*, vol. 7, no. 2, pp. 311-322.

Yang, C.T., 1973. "Incipient Motion and Sediment Transport," ASCE, *Journal of the Hydraulics Division*, Vol. 99, No. HY10.

Yang, C.T. and Song, C.C.S, 1986. "Theory of Minimum Energy and Energy Dissipation Rate," Chapter 11, *Encyclopedia of Fluid Mechanics*, Gulf Publishing, Co.

Yang, C.T., 1996. Sediment Transport Theory and Practice, McGraw-Hill.

RESEARCH ON ICE REGIME IN YELLOW RIVER

By Ke Sujuan, Engineer, Bureau of Hydrology, YRCC, Zhengzhou, China; Zhang Xuecheng, Engineer, Bureau of Hydrology, YRCC, Zhengzhou, China; Lu Guangqi, Senior Engineer, Bureau of Hydrology, YRCC, Zhengzhou, China

Abstract: Research on ice regime in Yellow River has been developed and considerable research positive results have been made since 50s. In this paper, the generalization and summation of ice regime research achievements was presented. It would be the basis for further research on ice regime in Yellow River.

Key Words: Ice regime, Ice Jams, Forecasting schemes and models, Yellow River

INTRODUCTION

Ice regime is a natural phenomena in rivers in the cold regions. As the biggest river in north China, ice regime in Yellow River is serious and disaster by ice jams or dams is often taken place because of the complicated river facies, the geographical position, high sediment concentration etc. Ice regime includes mainly ice slush run, freeze-up, ice jams, ice dams, broken-up. Among them, ice jams and ice dams are the major factors forming the disaster in ice slush run period. Research on the conditions, rules and mechanism creating ice regime would be useful for ice control and defending.

Research on ice regime in Yellow River was started in the middle period of 50s. Its main aim was to forecast ice slush run and freeze-up date. The broken-up date and the highest water stage of broken-up forecasting were added in 60s. The freeze-up period, the biggest discharge of broken-up and the tendency of freeze-up and broken-up forecasting had been added since 70s. At that time, the forecasting schemes were mainly through empirical correlation curves and formula. The forecasting statistic models based on the physical mechanism were established and the forecasting mathematical models being of close theoretical basis were developed in 90s.

Research on ice jams in Yellow River was started in 60s for observing and studying ice jams at Liujiaxia to Yabguoxia reach in the upper Yellow River. In 80s, research on ice in water was added, and a great development was obtained. But research on ice dams was still on the tentative stage up to now. It would develop the research level on ice dams to a new step if 97's National natural fund project "The formation mechanism, harm and defending measures of river ice and ocean ice" could be performed successfully.

In this paper, the generalization and summation of ice regime research achievements was presented. It would be the basis for further research on ice regime in Yellow River and be significance for decreasing ice disaster in Yellow River.

ICE REGIME FORECASTING SHEMES

Index method:

For the condition of ice slush run: Ice slush run would be started if one of the following three formulations was satisfied:

$$T_{a1} < -5^{\circ}\text{C} \quad \text{and} \quad T_{ap} \leq 0^{\circ}\text{C} \quad (1)$$

$$T_{ah} < 0^{\circ}\text{C} \quad \text{and} \quad T_{ap} \leq -5^{\circ}\text{C} \quad (2)$$

$$T_{ah} < 0^{\circ}\text{C} \quad \text{and} \quad T_{a1} \leq -10^{\circ}\text{C} \quad (3)$$

Where T_{a1} indicates daily minimum air temperature, T_{ap} indicates daily average air temperature, T_{ah} indicates daily maximum air temperature.

For the condition of freeze-up: If the following formulations could be satisfied the river would be froze-up:

$$C_i > 80\% \quad \text{and} \quad T_w = 0^{\circ}\text{C} \quad \text{and} \quad T_{ah} < 0^{\circ}\text{C} \quad \text{and} \quad T_{a1} < -10^{\circ}\text{C} \quad (4)$$

$$C_i > 80\% \quad \text{and} \quad T_{ah} < -5^{\circ}\text{C} \quad \text{and} \quad T_{a1} < -15^{\circ}\text{C} \quad (5)$$

Where C_i indicates ice slush run concentration, T_w indicates water temperature.

For Luokou to Lijin reach in the lower Yellow River, the conditions of freeze-up are as follows from analyzing the observed data:

- (1). Daily discharge at Lijin section is less than $350\text{m}^3/\text{s}$ and the average velocity less than 0.6m/s at the same day;
- (2). Daily average negative air temperature gets upon 6 days steadily;
- (3). The accumulated value of daily average negative air temperature gets upon 35°C ;
- (4). Daily average air temperature get less than -7°C and daily minimum air temperature gets less than -11°C at the same day or previous day.

Empirical correlation method: It includes mainly building correlation figures, correlation between the forecasting factors at upper section and the lower section, auto-correlation between the previous factors index and the forecasting factors etc. The forecasting factors include the date of ice slush run, ice slush run concentration, the date of freeze-up, the date of broken-up etc.

Practical ice regime forecasting schemes:

For forecasting the date of ice slush run: The thermal factors is mainly considered in forecasting the date of ice slush run. With the thermal factor action viewpoint, ice slush run would be started when water temperature gets or less than 0°C .

The heat flux of water body could be indicated as:

$$Q_T = Q \times T_w \quad (6)$$

Where Q_T indicate the heat influx of water body, Q indicates flow discharge and T_w indicates water temperature.

From equation (6), we know that the heat flux being direct proportion to water temperature. When air temperature becomes negative, great amount of heat of water body loss, so water temperature becomes higher, the heat flux becomes greater, then the date of ice slush run

becomes later. The qualified percent of the forecasting scheme is between 80 and 95%. But the intensity of temperature fall is not appeared in this method, it is inadequacy in this method.

For forecasting the date of freeze-up: The thermal factors and hydraulic factors are considered in this type of forecasting schemes. After ice slush run has started, when air temperature decreases continuously or keeps under 0°C , water body begins loss heat, the concentration of ice slush run becomes greater continuously, water flow begins to be obstructed and flow velocity decreases. When the concentration amount of ice slush run gets a limited value, flow velocity decreases to limited value and the negative air temperature gets a limited value, the freeze-up of river starts. Because of water temperature keeps near 0°C after the beginning of ice slush run, it could not reflect the thermal changes, so only air temperature could be used to represent the thermal factors, and water discharge is used to represent the hydraulic factors. These two factors are used to establish correlation curve to the date of freeze-up. The qualified percent of the forecasting scheme is between 78 and 91%.

For forecasting the date of broken-up: Here the thermal factors and hydraulic factors are mainly considered. The thermal factors include air temperature at previous period or accumulated air temperature, the hydraulic factors include the average flow discharge at the limited time interval before river broken-up, water storage and ice frozen depth. These factors are used to establish correlation curve to the date of broken-up. The qualified percent of the forecasting scheme is between 78% and 100%.

For forecasting the maximum water stage of broken-up: Here the hydraulic factors are mainly considered. Sometimes the thermal factors are also considered. The factors include water stage at previous period, air temperature, water storage, the date of freeze-up, ice frozen depth, broken-up regime etc. These factors are used to establish correlation curve to water stage of broken-up. The qualified percent of the forecasting scheme is between 76 and 94%.

For forecasting the maximum water discharge of broken-up: The hydraulic factors are the main factors affecting the maximum water discharge of broken-up. Here water stage at previous period, discharge and water storage are used to establish correlation curve to the maximum discharge of broken-up. The qualified percent is between 72 and 79%.

For forecasting the tendency of freeze-up and broken-up: Here only the lower Yellow River is considered. The forecasting scheme of the tendency of freeze-up and broken-up in the lower Yellow River is based on establishing inequalities curve and equation between the month average discharge at Luokou section and the month average air temperature at Beizhen section.

Ice regime forecasting statistic models: The thermal factors, hydraulic factors and topography of river channel are three main factors affecting ice regime. For the same reach, the thermal factors and hydraulic factors are the main factors. The thermal factors include solar radiation, the

heat exchange between gas and water, net radiation and evaporation condensation etc. Here the air temperature and water temperature represent the thermal factors, the discharge or velocity represents the hydraulic factors. It is to establish one dimensional or multivariate regression equation between these factors for forecasting ice regime.

For forecasting the date of ice slush run: Equations of forecasting the date of ice slush run on deferent reaches are deferent. The follows show that equations at Shizuishan, Zhaojunfen and Toudaoguai sections:

$$\text{Shizuishan section: } R_1=3.4537+1.2649x_1+2.26x_2 \quad (7)$$

Where R_1 indicates the date of ice slush run, x_1 indicates the date that water temperature equals to air temperature, x_2 indicates water temperature on the same day. The qualified percent is 85%, the average forecasting period is 15 days, the longest period is 30 days.

$$\text{Zhaojunfen section: } R_1=30.8957+0.2382x_1+2.1579x_2 - 1.4515x_3 \quad (8)$$

Where R_1 indicates the date of ice slush run, x_1 indicates the date of daily minimum air temperature becoming negative, x_2 indicates the minimum water temperature on the same day, x_3 indicates water temperature on the same day. The qualified percent is 95%, the average forecasting period is 15 days, the longest period is 22 days.

$$\text{Toudaoguai section: } R_1=31.0097+0.1796x_1+2.5819x_2 - 1.3538x_3 \quad (9)$$

Where R_1 indicates the date of ice slush run, x_1 indicates the date of daily minimum air temperature becoming negative, x_2 indicates the minimum water temperature on the same day, x_3 indicates water temperature on the same day. The qualified percent is 95%, the average forecasting period is 15 days, the longest period is above 20 days.

For forecasting the date of freeze-up: Equations of forecasting the date of ice slush run on deferent reaches are deferent. The follows show forecasting equations at Shizuishan, Zhaojunfen, Toudaoguai sections and for the lower Yellow River:

$$\text{Shizuishan section: } R_f=50.0809+0.6957x_1+1.9413x_2 \quad (10)$$

Where x_1 indicates the date that air temperature getting 0°C , x_2 indicates average water temperature on the same day. The qualified percent is 95%, the average forecasting period is 24 days, the longest period is above 30 days and the shortest period is 16 days.

$$\text{Zhaojunfen section: } R_f=-1.9292+0.6716x_1+47.035x_2 + 1.5203x_3 \quad (11)$$

Where x_1 indicates the date that air temperature becoming negative, x_2 indicates average flow velocity on the same day, x_3 indicates the minimum air temperature on the same day. The qualified percent is 95%, the average forecasting period is 19 days, the longest period is above 28 days and the shortest period is 6 days.

$$\text{Toudaoguai section: } R_f=7.7805+0.8913x_1 \quad (12)$$

Where x_1 indicates the forecasting date of freeze-up at Zhaojunfen section. The qualified percent is 90%, the average forecasting period is 22 days, the shortest period is 12 days.

For the lower Yellow River, the inequalities are showed in follows:

$$\begin{aligned} \text{December: } & \text{If } T_{B12} < 1 - \bar{Q}_{L12}/270 \quad \text{Then freeze-up} \quad \text{Else no freeze-up} \\ \text{January: } & \text{If } T_{B1} < 1 - \bar{Q}_{L1}/185 \quad \text{Then freeze-up} \quad \text{Else no freeze-up} \end{aligned}$$

Here, T_{B12} , T_{B1} indicate monthly average air temperature in December and January at Beizhen section respectively. \bar{Q}_{L12} , \bar{Q}_{L1} indicate monthly average discharge in December and January at Luokou section respectively.

There are many schemes for forecasting the date of freeze-up in lower Yellow River. For example,

follows show two schemes:

$$R_f = -3.4446 + 1.05115x_1 + 10.9498x_2 \quad (13)$$

Where x_1 indicates the date that daily average air temperature at Jinan section becoming negative steadily, x_2 indicates average flow velocity at Lijin section on the same day. The qualified percent is 84.4%, the average forecasting period is 6.2 days, the longest period is 14 days.

$$R_f = -1.0922 + 1.0513x_1 + 7.22198x_2 + 0.9297x_3 \quad (14)$$

Where x_1 indicates the date that daily average air temperature at Beizhen section becoming negative steadily, x_2 indicates average flow velocity at Lijin section on the same day, x_3 indicates the date difference between the dates that daily average air temperature at Jinan and Beizhen sections becoming negative steadily. The qualified percent is 84.4%, the average forecasting period is 12 days, the longest period is above one month.

For forecasting the date of broken-up: Equations of forecasting the date of broken-up on deferent reaches are deferent. For the upper Yellow River, the date is estimated from 1 March, for the lower Yellow River, the date is estimated from 1 January. The follows show forecasting equations at Shizuishan, Zhaojunfen, Toudaoguai sections and for the lower Yellow River:

$$\text{Shizuishan section: } R_k = 12.2725 + 43.5507x_1 - 0.027x_2 - 0.0675x_3 - 1.2296x_4 \quad (15)$$

Where R_k indicates the date of broken-up, x_1 indicates the maximum depth of ice cover, x_2 indicates the discharge at Lanzhou section in the last ten-days of February, x_3 indicates the accumulated value of the maximum positive air temperature from 1 January to 15 February, x_4 indicates the predicted value of air temperature in the first ten-days of March. The qualified percent is 95%, the average forecasting period is 16 days, the longest period is 23 days and the shortest period is 5 days.

$$\text{Zhaojunfen section: } R_k = 17.4708 + 17.7433x_1 - 0.9849x_2 \quad (16)$$

Where x_1 indicates the depth of ice cover before melting, x_2 indicates the maximum air temperature in the first ten-days of March. The qualified percent is 100%, the average forecasting period is 20 days, the longest period is 27 days and the shortest period is 11 days.

$$\text{Toudaoguai section: } R_k = 28.7527 + 0.2165x_1 - 0.2242x_2 \quad (17)$$

Where x_1 indicates the date that air temperature becoming positive, x_2 indicates the accumulated value of air temperature in 10 days after becoming positive. The qualified percent is 100%, the average forecasting period is 24 days, the longest period is 35 days and the shortest period is 14 days.

$$\text{For the lower Yellow River: } R_k = 2.8667 + 0.7793x_1 + 0.0295x_2 + 4.4949x_3 \quad (18)$$

Where x_1 indicates the date of daily average air temperature becoming positive, x_2 indicates frozen-up length, x_3 indicates the stage difference between frozen-up maximum stage and broken-up maximum stage at Lijin section. The qualified percent is 70%, the average forecasting

period is 17 days, the longest period is 40 days.

For the lower Yellow River, the inequalities are showed in follows:

Sunkou - Luokou reach:

$$\text{If } \sum_1^3 \bar{T}_{Ji} < 0.024 \sum_1^3 \bar{Q}_{Si} - 61 \text{ Then fighting broken-up Else verbal broken-up}$$

Luokou - Lijin reach:

$$\text{If } \sum_1^3 \bar{T}_{Ji} < 0.06 \sum_1^3 \bar{Q}_{Li} - 124 \text{ Then fighting broken-up Else verbal broken-up}$$

Where \bar{T}_{Ji} indicates the average air temperature at Jinan section, \bar{Q}_{Si} and \bar{Q}_{Li} indicate the discharges at Sunkou and Luokou sections respectively. The qualified percent is 80% to 90%.

Ice regime forecasting mathematical models: Ice regime forecasting mathematical models being of close theoretical basis were developed in 90s. At present, thermodynamics, dynamics theories and empirical methods are mainly applied in establishing mathematical models. Now the mathematical models have been established for the lower Yellow River and are being studied for the upper Yellow River.

For discharge routing: There are hydrological and hydraulic methods for discharge routing. In hydraulic method, one-dimensional equations for no steady flow, i.e. St. Venant equations are mainly applied for discharge routing with numerical solution. It could be solved by explicit and implicit methods.

In hydrological method, St. Venant equations are solved by simplifying as water balance equation and channel storage equation.

For forecasting the date of ice slush run: Generally, the date of water temperature getting 0°C point could be regarded as the date of ice slush run. So the key problem is to solve water temperature value. Here, one-dimensional convective-diffusion equation is applied:

$$\frac{\partial(\rho C_p A T_w)}{\partial t} + \frac{\partial(Q \rho C_p T_w)}{\partial x} = \frac{\partial(A E x C_p \partial T_w / \partial x)}{\partial x} + \Phi B \quad (19)$$

Where ρ indicates water density, C_p indicates water specific heat, T_w indicates water temperature, Ex indicates the coefficient of vertical diffusion. If vertical diffusion was neglected, the vertical distribution of water temperature could be written as:

$$\frac{\partial(\rho C_p A T_w)}{\partial t} + \frac{\partial(Q \rho C_p T_w)}{\partial x} = + \Phi B \quad (20)$$

By finite difference method, water temperature could be solved.

For forecasting the date of freeze-up: Here, ice slush run concentration, discharge and air temperature are mainly considered. Discharge can be solved by discharge routing method, air temperature can be solved by its forecasting method. Ice slush run concentration can be solved by applying one-dimensional convective-diffusion equation. Substituting $\rho_i L_i C_i$ for $\rho C_p T_w$ in equation (18), equation solving ice slush run concentration can be written as:

$$\frac{\partial(A \rho_i L_i C_i)}{\partial t} + \frac{\partial(Q \rho_i L_i C_i)}{\partial x} = \frac{\partial(A E x \rho_i L_i C_i / \partial x)}{\partial x} + B \Phi_T \quad (21)$$

Where ρ_i indicates ice density (917 kg/m³), L_i indicates potential heat flux shaping ice (80 cal/g), C_i indicates ice slush run concentration, Φ_T indicates heat exchange ratio per unit area. By applying finite difference method, ice slush run concentration can be obtained.

For the lower Yellow River, with analyzing observed data, the condition of freeze-up can be written as: $C_i T_a \geq \alpha Q$, where $\alpha = 0.008$, T_a indicates negative air temperature.

For ice cover thickness calculation: After shaping ice body, the growth of ice cover thickness mainly depend on the heat exchange between ice and gas. So the following equation can be applied in ice cover thickness calculation:

$$\begin{aligned} dh_i/dt &= \alpha \Phi_T / \rho_i L_i \\ \Phi_T &= K_{ia}(T_s - T_a) - K_{wi}(T_w - T_m) \end{aligned} \quad (22)$$

Where T_s indicates ice surface temperature, T_m indicates melt point temperature, K_{ia} indicates the coefficient of heat exchange between ice surface and gas, K_{wi} indicates the coefficient of heat exchange between ice surface and water body, h_i indicates ice cover thickness. T_s and T_m are both close to 0°C while calculating ice cover thickness.

For forecasting the condition of broken-up: When air temperature warms back to above 0°C, ice cover is melt continuously by heat, ice cover thickness becomes thinner, its intensity becomes weaker. The critical condition breaking ice cover can be indicated by the following inequality:

$$2(\tau_c h_i + \mu_1 f) + 2\mu_1 \sigma h_i < (\tau_i + \tau_g) B \quad (23)$$

where τ_c indicates the stress of river bank, h_i indicates ice cover thickness, f indicates the vertical stress of ice slush, μ_1 indicates the rubber coefficient of river bank, τ_i indicates the shear stress of bank to water body, τ_g indicates the gravity component of ice cover, B indicates ice cover width.

For practical application, because of limited condition, inequality (23) needs be simplified suitably, i.e., substituting ice cover thickness, discharge, positive air temperature for ice cover intensity, the stress acting on breaking ice cover, ice cover melt ratio respectively. The simplified inequality is written as: $Q_m \geq 10\alpha h_i^\gamma / (\sum T_{a+} + 1)$. Here Q_m indicates upstream inflow, h_i indicates ice cover thickness when air temperature becoming positive, $\sum T_{a+}$ indicates the accumulated value of air temperature after becoming positive, α indicates the coefficient of broken-up (4 for fighting broken-up and 22 for verbal broken-up), γ is a index (0.95 for the lower Yellow River).

Ice jams and dams research: Research on ice jams in Yellow River was started in the beginning of 60s when observing ice jams factors at Liujiaxia reach. Research on ice dams has not been developed yet, only some qualitative analysis was in progress. For example, for the lower Yellow River, the conditions shaping serious ice dams include: flow discharge on the date of freeze-up is less than 400m³/s, the maximum ice storage in ice covered reach is more than 500 million m³, the ratio of discharge at the date of freeze-up to the maximum discharge above the cross section shaping ice dams is less than 0.03 and ice thickness in freeze-up reach is more than 0.2m.

CONCLUSION

From above description, we can conclude the follows:

- (1). Research on ice regime in Yellow River has been developed and considerable research positive results have been made since 50s.
- (2). Ice damage in Yellow River is often taken place with complicated ice regime, few observed data and few ice regime mechanism mastered completely by us.
- (3) Research on ice jams and dams which often lead to ice damage are developed in primary level. They are the main objects in further study.

REFERENCES

- Bureau of Hydrology, YRCC, 1989, The Practical Hydrological Forecasting Schemes for Yellow River Basin.
- Bureau of Hydrology, YRCC, 1994, The Practical Ice Regime Forecasting Schemes for Yellow River Basin.

Authors:

Ke Sujuan, Bureau of Hydrology, YRCC

Address: East No. 12, Chengbei Road, Zhengzhou, 450004, China

Tel: +86+371-6304163

Zhang Xuecheng, Bureau of Hydrology, YRCC

Address: East No. 12, Chengbei Road, Zhengzhou, 450004, China

Tel: +86+0371-6304163

Fax: +86 -10-63202978

E-mail: Wangzhy@public3.bta.net.cn

Lu Guangqi, Bureau of Hydrology, YRCC

Address: East No. 12, Chengbei Road, Zhengzhou, 450004, China

Tel: +86+371-6303269

PRELIMINARY ANALYSIS OF THE INFLUENCE OF CLIMATE CHANGES IN CURRENT DECADE ON WATER AND SEDIMENT IN THE UPPER AND MIDDLE YELLOW RIVER

By Peng Meixiang, senior Engineer; Qiu Shuhui, assistant Engineer; Zhao Yingli, Engineer.
Hydrology Bureau of Yellow River Conservancy Commission, Zhengzhou, 450004

Abstract: Aimed at the abnormal phenomena of that there was the minimum average runoff of 50 years since the new China is established in the upper and middle Yellow River area from 1986 to 1995 and however the sediment into the yellow river was not decreased correspondingly, the climate background is analyzed and emphasized in the paper, and find that there were enormous changes in many climate factors, including precipitation, air temperature in the river basin, and relative to them, the subtropical high pressure in western Pacific, height field over the Tibet Plateau and India and Burma trough, typhoon activities, and so on. There had been long ENSO phenomenon and three times of ENSO events in the Pacific tropical region since 1990s, which are exceptional over a century. It is the abnormal of those factors that lead to the less runoff and much sediment in the upper and middle Yellow River.

INTRODUCTION

In recent years the on-coming flow to the Yellow River was reduced by a wide margin, additional due to great continuous water diversion, the phenomenon of flow cutoff often occurred in non-flood season. It is statisticed that annual average runoff was reduced by 35% than the annual mean, however the sediment into the Yellow River was not decreased correspondingly. Aimed at this phenomenon, this paper analyzed and emphasized the influence of climate background of climate changes on the sediment and flow in the upper and middle Yellow River beyond Sanmenxia area.

THE MAIN CHARACTERISTICS OF SEDIMENT AND FLOW VARIATION

It is analyzed that the annual average runoff in current 10 years of the upper and middle Yellow River has main characteristics as follows: (1) Lanzhou station in the upstream and Jinghe, Luohe and Weihe in the midstream possessed the minimum value since 1950s, as well as the runoff since 1990s was less to varying degrees than of the preceding 40 years. (2) The degrees of runoff decrease in all the year and flood season of Jinghe, Luohe and Weihe were similar, while the station of Lanzhou, flood season obviously exceeds the annual. If deduct the section of decrease in flood season, the general tendency of runoff of Lanzhou station in non-flood season is increasing also. It is indicated that the runoff decrease of the upstream is concentrated in flood season. (3) Although the runoff of the reach between Hekou tower and Longmen (following called for short Helong reach) in flood season or all the year was not as great as that of 1950s and 1960s. It also possessed increasing progressive tendency, especially obvious in flood season compared with 1980s.

Since 1980s, the sediment into Jinghe, Luohe and Weihe in flood season was more stable, although of the current 6 years (1990-1995) slightly increased compared with 1980s. However the sediment into Helong reach in flood season presents the same increasing tendency progressively as the runoff. In current 6 years it was increased by 1,300 million tons compared with 1980s. If we consider that water and soil conservation could reduce sand 300 million tons annually, the natural sediment into Helong reach in flood season during the current 6 years would be higher than the normals by 37 million tons or more.

ANALYSIS OF INFLUENCE OF CLIMATE CHANGES ON THE SEDIMENT AND FLOW

It is analyzed and indicated that the volume of water and sediment of the upper and middle Yellow River mainly depends on the precipitation and time distribution, while the conditions on the influence of the air temperature on the volume of sediment and flow is more complex. The tendency of regional climate changes in current years is analyzed preliminary as follows, of which the purpose is that provide a comprehensive climate background.

Influence of precipitation sudden change in the upstream on the runoff: Figure 1 presents a yearly developing curve of the precipitation (real line) and runoff (dotted line) in flood season of the area beyond Lanzhou station.

It is found that from Figure 1 the two curves show the identical varying tendency, which indicates that the volume of the runoff in flood season beyond Lanzhou area mainly depends on the precipitation in the valley; Round about 1986, both runoff and precipitation appeared a sudden change, i.e. turned the period between flood and low flow spell into the continuous period only of low flow. This kind of changes was the first time in recent 45 years. Since 1990s the runoff and precipitation are on the small side in the continuous 6 years, especially to the precipitation, the mean value of 6 years is less by 14% than normal years, which is very rare in history of the area beyond Lanzhou station with little variation.

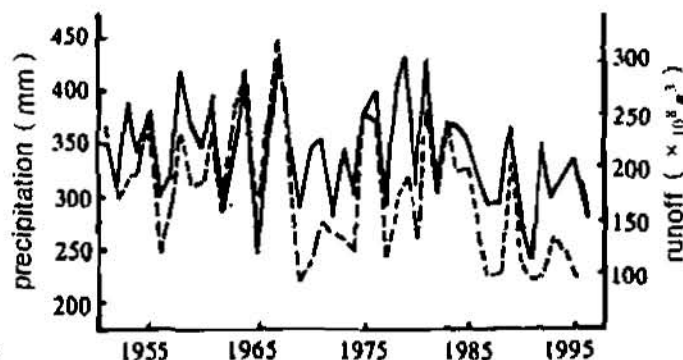


Figure 1. The developing curves of the precipitation(real line) and runoff(dotted line) in flood season beyond Lanzhou area.

The precipitation in 1991 (236mm) is the minimum since 1950s, while in 1990 (276mm) it took the third place from the end in history. Another obvious characteristics is drought and long duration and strong intensity. The runoff of the upstream in recent 10 years is rather low by 40% compared with normal years, due to the little persistence precipitation in the area beyond Lanzhou station.

Influence of the precipitation variation in the midstream on the sediment and flow: It is statisticed that the average precipitation in flood season in current 10 years of the midstream area beyond Sanmenxia station possessed the minimum value (335mm) since 1950s, which was lower than normals by 5%. However, the distribution of precipitation was very unevenly, more in North and less in South was main feature of it, the area with rather little precipitation was mainly concentrated in the flow-producing area of midstream---Jinghe, Luohe

and Weihe valley. Especially in the current 6 years the average precipitation in flood season is only 326mm, of which the minimum value (256mm) since 1950s appeared in 1991, the value of 1994 (271mm) which occupied the third place from the end in history was a little larger than of 1991 and 1972 (259mm). This is the main reason that the volume of stream flow in the middle Yellow River in current 10 years considerably decreased obviously.

The area with great precipitation mainly focused in Helong reach, especially in midsummer (from July to August) possessed the most obvious greater precipitation than normal years. The developing process between precipitation in midsummer and sediment in flood season (oblique line) of Helong reach is presented in Figure 2. It is quite obvious that this two curves assume synchronous changes but of their better relationship of correlation before 1974. The proportion coefficient between precipitation and sediment increased obviously after 1974.

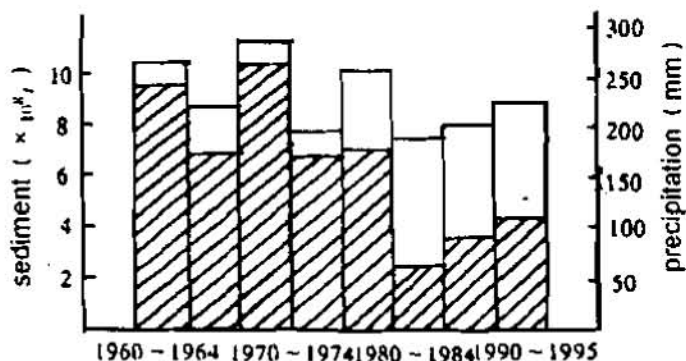


Figure 2. Developing chart of the precipitation in midsummer and sediment in flood season (oblique line) of Helong reach.

Table 1 lists out the average percents of precipitation per 10 days in midsummer of current 10 years of Helong reach. It is shown that from the figures and tables the precipitation in midsummer of Helong reach in 1986-1995 appeared the slowly increasing tendency, and assumed much more concentrated precipitation and increased intensity. For example, the precipitation during the first ten days of August in 1994 reached 102mm that was the highest record in history. While the rain in the first ten days of August in 1992 was 84mm which was only secondary to that of 1964 (94mm) and occupied the third place in history, the sediment corresponding to them.

Table 1. The statistical table on the anomaly percent of precipitation of ten days of Helong reach in current 10 years.

Years	J u l y (ten days)			A u g u s t		
	first	second	last	first	second	last
1986	-27	-81	-43	-46	-19	-66
1987	+3	-52	-98	-38	+3	+49
1988	+124	+84	-5	+81	+51	-46
1989	-70	+16	-14	-65	-8	-83
1990	+78	-61	+7	-89	-14	+9
1991	-70	-16	-21	-86	-70	-54
1992	-68	-32	+43	+127	+24	+60
1993	-27	+10	-19	+30	+27	-29
1994	+49	-45	-38	+176	-14	-26
1995	-92	+158	+7	+73	-43	+77
recent 6 years	-22	+3	-2	+38	-14	+6
annual mean	37	31	42	37	37	35

According to the average characteristic value of hard rain and gust in midsummer of each decade of Helong reach, it is found that the day-time and cover area of hard rain in current 10 years both increased obviously, especially in current 6 years, the rainy day-time reached 3.8 times averagely, which is equal with the late 1950s. The day-time of gust was not obviously increased but the intensity and cover area were shown the maximum value of the corresponding period in history, that indicates the times of gust in current 10 years was not as many as that of the preceding 30 years, but there was an outstanding characteristics---cover area was large. For the reasons above, the sediment into the channel of the upper and midstream increased obviously.

Relationship of air temperature variation and runoff: The decrease of runoff in the upper and middle Yellow River was affected by the changes of dry and thermal climate to a great extent. The precipitation and isothermal value in flood season of each decade beyond Sanmenxia area are presented in Table 2. It is found that the high temperature and great precipitation in 1950s and 1960s lead to the warm and wet as principal weather characteristics. Cold and dry was taken as main feature in 1970s and 1980s, i.e. the air temperature was low and precipitation was little. However, the tendency which air temperature gradually increased and precipitation gradually decreased in current ten years appeared acting out of character. The author considers that the climate in the upper and middle Yellow River area is developing toward the direction of warm and drought.

Table 2. The precipitation and sum of air temperature level in flood season of each decade in the area beyond Sanmenxia station.

Decade	Precipitation (mm)	Temperature level sum
50	315	122.3
60	319	135.6
70	311	140.9
80	307	140.9
annual mean	313	134.9
current 10 years	289	121.8
anomaly	-24	-11.1
current 6 years	285	120.7
anomaly	-28	-14.2

Notes: Temperature level is cited from the data of northwestern regions (6th station) statisticed by National Meteorology Service. 1st level is of megatherm, 5th level is of microtherm.

ANALYSIS OF CLIMATE BACKGROUND

From the analysis above, we know that in current 10 years the precipitation and runoff in flood season of the main flow-producing area of the upper and middle Yellow River, the regions beyond Lanzhou station and Jinghe, Luohe and Weihe valleys, both possessed the minimum value in the corresponding historical period. The main silt-producing area--Helong reach did not reduced on precipitation and sediment in flood season, on the contrary presenting an increasing tendency. This kind of abnormal phenomenon showed by precipitation and sediment is necessary to connect with the large scope of the climate background, the basic situation of the subtropical high

pressure in western Pacific, height field over the Tibet Plateau and India and Burma trough, typhoon and sea temperature field and so on are analyzed preliminary as follows.

Analysis of periodic climate of the subtropical high pressure: The changes of the location and intensity of the subtropical high pressure is an important factor that respect to the occurrence of the precipitation distribution in flood season and large scope of drought or excessive rain in China. The yearly change route of the location of ridge line of the subtropical high generally is that moving northward from winter to summer and withdraw southward from summer to winter, the latitudes in midsummer is highest. This kind of interannual changes sometimes appears abnormally that the northeastern location is not in midsummer but in July or September. That is to say, the interannual changes have two types (figure 3) : single-peak (type of I) and double-peak (type of II). But in general, the interannual changes of the ridge line

location of the subtropical high is taken the single-peak as principal ones, during recent 45 years there has 30 years being the type of single-peak which constituted 65%. In fact, the development of this two types has certain periodicity. Of current 45 years, the period of 1951-1979 took the single-peak as priority which constituted 76%. Correspondingly, the precipitation in flood season of the upper and middle Yellow River was on the great side and so did the sediment and flow correspondingly. For example, the nine of the sandy years which the sediment in flood season of Helong reach was in excess of 1,000 million tons meanly appeared in this period.

In 1980s the double-peak was changed as priority that constituted 70% during ten years, correspondingly the precipitation and the air temperature were

both on the low side, the sediment decreased obviously in flood season of the upper and middle Yellow River; Since 1990s the type of single-peak was resumed as main period, there had 5 years during the recent 6 years being the type of single-peak.

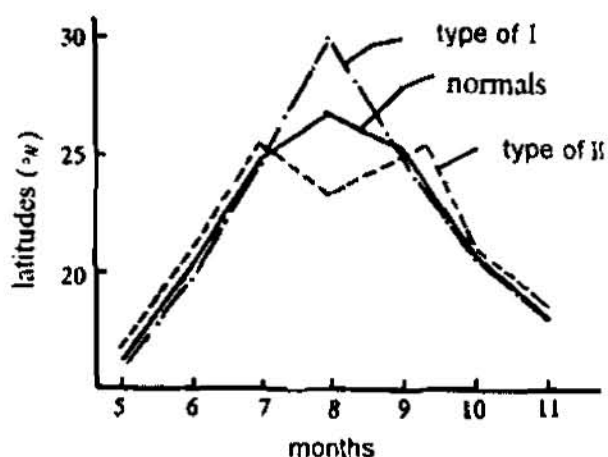


Figure 3. The two types of climate changes of the ridge line of subtropical high pressure.

In fact, the intensity and extent of westward extension of the subtropical high also occurred a sudden change in current 10 years. It is statisticed that the intensity and area of the subtropical high were both maximum since 1950s, there were persistence 3 years of 1993-1995 broke the historical record and in 1995 created the maximum value in history. In the meantime, the ridge point of the subtropical high stretched westward was also to the west abnormally. It reaches 7 of longitudes to the west in recent 6 years compared with normal years. The area beyond Lanzhou station and Jinghe, Luohe and Weihe valleys were almost controlled by the sphere of influence of the subtropical high, so the midsummer possessed dry and less rain as main characteristics. However the reach of Helong was right in the zone of northwestern front of the subtropical high, which characterized that much

precipitation and more process of hard rain and gust in midsummer. Naturally the sediment and flow also increased correspondingly.

Analysis of climate oscillation of the height field over the Tibet Plateau and Indian and Burma trough:

Figure 4 presents the yearly developing curve of geopotential height of the 500hPa Tibet Plateau (25-30°N, 80-100°E) and India and Burma trough (15-20°N, 80-100°E). We can clearly find from the figure that this two height fields have the oscillation period with around 40 years, which presents the better relationship of positive correlation with the runoff in flood season of the upper and middle Yellow River before 1981. For instance, the height field over Plateau was slightly high in 1950s and 1960s, the geopotential height field over India and Burma trough was normal and a little higher. Therefore much more flood occurred in the upper and middle stream, its correlation possibility reached 78%; In the end of 1960s this two height fields were changed rather low obviously, correspondingly the upper and middle Yellow River occurred much more low flow which possibility was 70%.

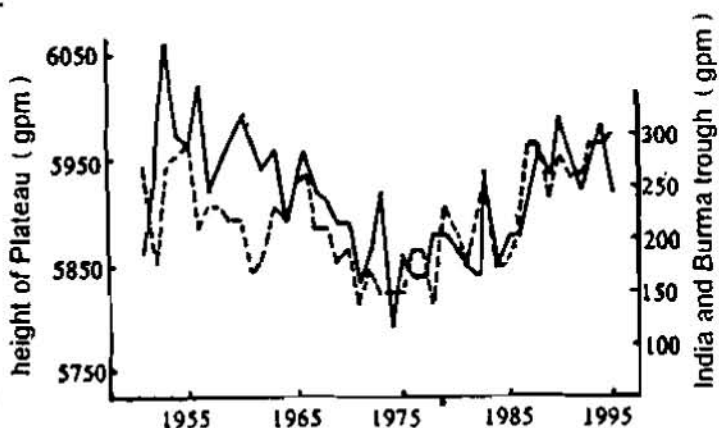


Figure 4. Yearly developing curves of geopotential height over Plateau(real line) and Indian and Burma trough in flood season.

Since 1987 this kind of relationship has been changed that the two height fields were both obvious higher than normal years, while the runoff of the upper and middle Yellow River was obvious less than normal years. It is analyzed and found that the sudden changes was also occurred in India and Burma trough in current 10 years, the height field was persistently high. There had 5 years (1987, 1988, 1993, 1994, 1995) during the ten years occupied the highest value in the corresponding period in history, of which the continuous 3 years of 1993-1995 broke the historical record. It is fully indicated that India and Burma trough was very weak unusually. The summer southern branch trough was not active corresponding to the southwestern monsoon (followed by numerous warm wet air flow) that influenced on the upper and middle Yellow River was obvious weaker than normal years. In addition, the height field over the Tibet Plateau was a little higher than normal years and small high pressures over the Plateau moved eastward and combined with the subtropical high, which impels the subtropical high to strengthen step by step the extension westward and arisen northward. As a result, it is necessary to lead to that the area beyond Lanzhou station and Jinghe, Luohe and Weihe valleys would be often controlled by the subtropical high pressure, the weather is more drought and less rain.

Analysis of the characteristics of typhoon activities: As well we know, typhoon that stretched northward to interland relates to the occurrence of considerable floods in history of the middle Yellow River. Therefore typhoon is an important climate factor which influences on the precipitation and silt production of the upper and middle Yellow River, especially to the midstream area. However, see from the landing location of typhoon in current 10 years, basically in the regions of Zhuangdong, Zhuangxi and Southern sea which landing location is to the south

for a little bit northern landing location in 1994. Moreover, there had no typhoon landing directly to north which influences the middle and lower Yellow River area.

Analysis of sudden changes in the sea temperature field: Professor Wang Shaowu of Beijing University points out in his paper "The simulation and forecasting research of ENSO" that in China the drought or excessive rain only of Hetao region in the Yellow River area was of consistent rate of 65%-70% with ENSO, drought occurred when ENSO appeared. The author also found in the past research that the better relationship lies in between ENSO and precipitation in flood season of the upper and middle Yellow River. Since 1980s, the obvious sudden change of climate appeared in the sea temperature field of the tropical Pacific, the interaction of atmosphere and sea leads to the rare abnormal phenomena since half or one century recently. Its main characteristics presents: (1) The events of ENSO since 1980s are of western types, i.e. the increase of the sea temperature firstly occurred in the middle equator and eastern Pacific, the center of warm water was spread to the offshore of western Peru from west to east which duration is 14.7 months; However most of the ENSO events in the preceding 30 years were of eastern types, which duration was only 12 months. (2) In the beginning of 1990s, the persistence long ENSO events occurred in the tropical Pacific, which the period of occurrence was shorten considerably and possessed the varying characteristics same as annual period. For example, from February of 1990 to 1995, the phenomena which the sea temperature of tropical Pacific was persistence higher appeared a long time of 5 years. The sea level pressure of the tropical southern Pacific continued the anomalous type of west high and east low, the index of southern oscillation experienced negative anomaly of 5 years. Likewise, there also had 5 years or more which the convection of the middle Pacific area was very active. This kind of anomalous conditions of the atmosphere and sea was not resumed all long although, it was continuously appeared three times of ENSO events in 1991/1992, 1993, 1994/1995, which this anomalous characteristics is very rare during centuries. (3) The sea temperature of the tropical Indian Ocean sustained the type of anomalous cold, compared with the cycle of ENSO occurred in the past, the sea temperature in the equatorial Indian Ocean presents the periodic variation with same phase as of the equatorial Pacific. However, since 1990s it appeared the periodic variation with inversion phase, i.e. when the sea temperature of the equatorial Pacific increased abnormally, the equatorial western Indian Ocean was anomalous cold.

REFERENCES

- Guishu Xiong , et al., 1988. Forecasting for Silt-reducing Action of Water Conservancy Project in the Upper and Middle Yellow River. *Journal of Yellow River* (1).
- Jijia Zhang. 1991. Development of research on a long-range weather forecast. Meteorological Publication of Beijing.

Peng Meixiang, Qiu Shuhui and Zhao Yingli
Address: No.12 East Chengbei Road, Zhengzhou 450004, China
Tel: 0371-6303281.
Fax: 0371-5958244.

ANALYSIS OF CHARACTERISTICS OF FLOW AND SEDIMENT IN THE YELLOW RIVER

By Qian Yunping, Engineer, Hydrology Bureau, YRCC, Zhengzhou, China; Dong Xuena, Engineer, Hydrology Bureau, YRCC, Zhengzhou, China; Lin Yinping, Engineer, Hydrology Bureau, YRCC, Zhengzhou, China

Abstract: The Yellow River is the second longest River in China. Its flow and sediment changes are becoming more complicated, more flexible due to human activities, changeable climate and geographical features. The flow and sediment characteristics may be roughly described as less water with more sediment; different sources of flow and sediment; unbalanced distribution of flow and sediment during the year and great annual fluctuation. Since the 1970s especially in the 1990s, some new variations and changes have been added to flow and sediment features of the Yellow River. Fast growing economic development, pressing situation of supply and demand of water resources, frequent cut-outs in the lower reaches, serious river course deposits and shrinking. All this, we will account for the new variations of flow and sediment of the Yellow River.

1 A General Survey of the Basin's natural Geography

The Yellow River originates from Yueguzhonglie Basin, which is 4500 m above the sea level and in the north of Bayankala Mountain. The River covers 9 provinces of Qinghai, Sicuan, Gansu, Ninxia, Inner Mongolia, Shanxi, Henan, Shandong etc. Its total Length is 5464 km with an area of 75200 km².

The Yellow River is divided into three reaches. The upper, middle and lower reaches. A). The upper reaches begin from the River's origin to Hekouzhen in Inner Mongolia. This river course is 3472 m long, with an area of 428000 km². The region from Lanzhou upward is high above the sea level, cold and wet. The major branches have Huangshui River and Tao River. Its annual rainfall is 500 to 700mm. The region between Lanzhou and Hekouzhen is arid and semi-arid. The annual rainfall is 200 to 300mm, but its vaporization is 1800 to 2000mm, with small inflow. This region owns advanced diversion works. It has the well-known Ningxia irrigation Zone and Inner Mongolia irrigation Zone. B). The middle reaches cover the area from Hekouzhen to Taohuayu in Henan province. The river course is 1206 km, with an area of 344000 km². Along the two banks of the River between Hekouzhen and Longmen, there are a lot of minor branches, flowing into the Yellow River in a shape of feather. The main branches are Hong River, Kuyie River, Wuding River and Yanshui River. The loess hills and gullies cover 70 percent area of this region. The loess layer is very thick, soft and spongy. The terrain condition is bad, with sparse regulation cover. In summer, it often storms with great intensity, but short duration, Water loss and soil erosion is very serious. Most of the region belongs to the area with much and coarse sediment. Most of the area is mountainous area, with an annual average rainfall of 456mm. There have few diversion works in the Yellow River. The area from Longmen to Sanmenxia is 191000 km², the River length is 244 km, with loess plateau terrace along the two banks. The major branches are Jing River, Luo River, Wei River and Fen River. Most of the area is loess plateau gullies, with the annual rainfall of 539

mm cover most areas. The region between Sanmenxia and Huayuankou is semi-wet, with a total area of 41600 km². The River course is 257 km. The major branches are Yiluo River and Qin River. The annual average rainfall is 649 mm, with frequent storms in flood season, which result in the most flood sources of the Yellow River. C). The Lower Reaches begin from Taohuayu downwards. The River course is 786 km. The region along the lower reaches is wet and semi-wet, with an annual average rainfall of 500 mm to 700 mm. The river course is well known "suspended river" with few inflows. The major branch is Dawen River. Since the 1950s, with the fast development of diversion works, the amount of drawing water from The Yellow River is growing very rapidly, in the 1990s, It has come to $110 \times 10^8 \text{ m}^3$.

2 Flow and sediment features of the Yellow River basin

2.1 Less water, More sediment

Most regions covered by the Yellow River Reaches are arid, semi-arid and poor in water resources. According to statistics of 1950 to 1995, the natural runoff at Huayuankou Station is $574 \times 10^8 \text{ m}^3$. The surveyed runoff of annual average is $425 \times 10^8 \text{ m}^3$. The total sediment discharge of Sanmenxia station, Heishiguan station and Wuzhi Station is 13.55×10^8 tons. The annual average sediment discharge and sediment concentration has made the highest record among all the rivers in China. In contrast to the Yangtze River, the Yellow River's water amount is only 1/17 of the Yangtze River's, but its sediment discharge is three times higher than that of the Yangtze River. It is quite evident that the Yellow River has more sediment, less water. In the 1990s, the Yellow River basin has suffered sustained drought periods. The surveyed runoff from 1990 to 1995 is only $287 \times 10^8 \text{ m}^3$, which is much lower than averaged data. Shortage of water resources is becoming more serious. Large quantity of sediment is transporting by insufficient water. This leads to serious sediment accumulation in the lower reaches and terrible shrinking of river course.

2.2. Different sources of flow and sediment

The Yellow River's flow distribution and sediment distribution are quite uneven and they have different origins. The region from Lanzhou upward occupies 29.6% of the total River's area. The annual average inflow is $336 \times 10^8 \text{ m}^3$, holding up 58.5% of the river's total inflow amount. The region has the main water resources of the Yellow River, but its sediment inflow is only 1.19×10^8 tons, taking up 7.2 percent of the River's to total sediment inflow. The area between Hekouzhen and Longmen holds up 14.8% of the total area of the River basin. Its inflow is $66 \times 10^8 \text{ m}^3$ occurring only 12% of the river's inflow, but its sediment amount has come to 8.88×10^8 tons, holding up 53.5% of the River's total sediment amount. The region offers the major sediment sources of the Yellow River. The region from Longmen to Sanmenxia holds up 17.9% of the River's total area. Its water amount and sediment amount is respectively $95.4 \times 10^8 \text{ m}^3$ and 5.24×10^8 tons, holding up respectively 16.9% and 31.6% of the River's total amount. The region is also a major sediment origin of the Yellow River. The district between Sanmenxia and

Huayuankou take up 5.5% of the River's total area. Its inflow is $59 \times 10^8 \text{ m}^3$, sediment inflow is quite small, only 0.4×10^8 tons. As flow and sediment have their own sources, plenty or low of water is inconsistent with much or less of sediment. Statistics shows there have four kinds of major compose (see table 1).

The Yellow River's flow and sediment have different sources. The River's origin and the lower reaches have ample water. This refers to the river reach from Lanzhou upwards and the area between Sanmenxia to Huayuankou. In the middle reaches,

Table 1 The Yellow River's runoff-sediment compose in typical years

Compose	contents	Typical years		
		1954	1958	1967
More water and more sediment	year Runoff (10^8 m^3)	571	644	699
	Sediment amount (10^8 t)	27	31.1	30
More water and less sediment	Year Runoff (10^8 m^3)	567	540	590
	Sediment amount (10^8 t)	13.3	9.86	7.01
Less water and more sediment	Year Runoff (10^8 m^3)	374	355	347
	Sediment amount (10^8 t)	22.3	15.4	24.7
Less water and less sediment	Year Runoff (10^8 m^3)	298	287	220
	Sediment amount (10^8 t)	5.33	6.18	2.88

there comes large quantity of mud and sand. This refers to area between Hekouzhen to Longmen area and Jing River, Luo River and Wei River reaches. So the sediment from the Yellow River's benches is experiencing a process of small quantity to large quantity and large quantity to small quantity. The river stretch from the River's origin to Lanzhou increases its annual average sediment amount gradually from 0.1 kg/m^3 to 3 kg/m^3 . The river reach from Lanzhou to Hekouzhen is from 3 kg/m^3 to 32 kg/m^3 . From Longmen to Sanmenxia the sediment amount at this river stretch is between 30 kg/m^3 to 35 kg/m^3 . At Huayuankou station, it diminishes to 29 kg/m^3 . At the river stretch from Huayuankou to Linjin station, due to serious sediment accumulation, sediment amount is brought down to 25 kg/m^3 .

3 Analysis of flow and sediment variations

3.1 Yearly changes of flow and sediment

Table 2 is a list which offers us average rainfall of the river stretch from HuaYuanKou upwards, runoff amount at HuaYuanKou Station and three stations' [SanMenXia station, HeiShiGuan station, WuZhi station] sediment discharge in different years.

Table 2 A List of the rainfall, runoff and sediment in different years

Item	1950~ 1959	1960~ 1969	1970~ 1979	1980~ 1989	1990~ 1995	1950~ 1995	Remarks
Rainfall (mm)	450	458	438	433	388	436	Rainfall and runoff are from the river stretch at Huayuankou station upwards. Sediment discharge is the total amount of three stations (Sanmenxia, Heishiguan, Wuzhi station)
Natural runoff (10^8 m^3)	575	646	542	591	474	574	
Surveyed runoff (10^8 m^3)	482	506	381	413	287	425	
Obstructed sand and Sediment discharge (10^8 t)	19.7	15.1	20.1	13.3	12.8*	16.6*	
Surveyed sediment discharge (10^8 t)	17.7	11.3	13.8	8.2	7.4*	12.3*	

In the light of above-mention information, we come to know that the rainfall is major supplementary water resource of runoff of the Yellow River. So natural runoff and rainfall share roughly the same changing pattern. However, the surveyed runoff is quite different. The highest runoff of the Yellow River basin appeared in the 1960s. The natural runoff at Lijin station came to $674.7 \times 10^8 \text{ m}^3$. It was $646.3 \times 10^8 \text{ m}^3$ at Huayuankou station. Most of water came from Lanzhou upwards. The natural runoff at Lanzhou station was $365 \times 10^8 \text{ m}^3$, holding up 57 percent of the inflow at Huayuankou station. The Yellow River enjoyed abundant water resources in the 1950s and 1980s. However, in the 1990s, water amount begins to shrink, and in recent years, the basin areas have suffered sustained years of drought. Between 1990 to 1995, The annual average runoff by practical survey at Huayuankou station is only $287.1 \times 10^8 \text{ m}^3$, $176.5 \times 10^8 \text{ m}^3$ at Lijin station, which a very big lower that average level. There exists a very big difference between the changing trend of natural runoff and the changing trend of surveyed runoff. And this changing deviation has a tendency to grow and increase since the 1970s. This is consistent with the fast-growing irrigation demand. The diverted water amount from the Yellow River is increased from $113 \times 10^8 \text{ m}^3$ of the 1950s to $300 \times 10^8 \text{ m}^3$ in the 1990s. So rapidly growing demand of diverted water for irrigation is the main reason resulting in the diminishing runoff by practical survey.

Yearly changes of sediment have much to do with runoff changing pattern. From the annual average sediment discharge of Sanmenxia, Heishiguan and WuZhi station in different period of time, we've got to know that the maximum of 17.7×10^8 tons in the 1950s, the minimum of 7.4×10^8 tons is in the 1990 to 1993 period. The surveyed annual average sediment discharge is 26% smaller than the annual average sediment discharge and obstructed sediment put to gather. Among all the things, 7% was risen in the 1950s. In sixties, it was reduced by 32%, in seventies the reduction is 17%; in eighties it came to 51%. In the early 1990s. it has brought down to 55%. The sediment storage in the 1950s increased from 1×10^8 tons 5×10^8 tons. So it is obvious that the surveyed diminishing sediment discharge has much to do with the increasing sediment storage. The sediment storage mainly refers to the diverted sediment for irrigations, water preservation projects and reservoirs' sediment storage.

3.2 Annual Distribution of flow and sediment

The Yellow River's runoff amount is mainly depending on precipitation, which is

concentrated in flood seasons [from July to October]. The annual average value holds up 60% of the whole year's runoff amount.

In fifties and sixties, the runoff amount from July to October occupied 60% of the annual total amount of the whole basin. In seventies and eighties, great changes took place. First, the percentage of July-Oct. runoff in the whole year is reduced. For instance, in the upper reaches, reduce to 53%. Meanwhile the monthly runoff in non-flood seasons was increasing. In the nineties, the percentage of runoff in the whole year in non-flood seasons continues to rise. The percentage of July-Oct runoff is making a sharp plunge. In the upper reaches, it is reduced from 53% to 39% in eighties. In the middle reaches. It is brought down to 43% from 58% in the 1980s. The lower reaches also see ten point percentage decrease.

There are two reasons accounting for the changes mentioned above. One is reservoirs' regulation. That means store water in flood seasons, discharge water in non-flood seasons. The other one is the yearly distribution change of the diverted water for irrigation in each river stretch. Reservoirs' storage regulations make great impact upon the annual distribution of runoff surveyed by the station on the trunk river. Before Liujiaxia Reservoir was built (before 1968). The July-Oct runoff at Lanzhou station held up 64.5% of the annual yield. When Liujiaxia reservoir began to store water in the 1968 to 1986 period, Lanzhou station's runoff from July to October occupied 52.4% of the yearly yield. After Longyangxia Reservoir was finished in 1986, from 1986 to 1995, the percentage of July-Oct. Runoff at Lanzhou station was brought down to 43% of the yearly crop. Since the establishment of the two reservoirs, the percentage of runoff in flood seasons has been cut down by 20 points percent.

The annual distribution of sediment is roughly the same as runoff's yearly distribution, which is concentrated in flood seasons. Sediment discharge in flood seasons is 80% of the annual to total amount, in the months which has the most large rainfall amount. The most large sediment discharge is in July and August. It is also the time when the Yellow River obtains its 40% rainfall of a whole year. Also in July and August, some trunk streams' sediment discharge hold up 50% of the annual yield, 70% at some trunk river' station; 80% to 90% at some trunk river' of loess plateau.

4 The affect on flow and sediment changes by human activities

4.1 Rapidly growing water demand of industries and agriculture is the main reason, which leads to the decreasing flow.

The provinces, regions and people living along the Yellow River valley mainly depend on the Yellow River's water resources for their economic development and daily life. With the fast-growing economic development, the irrigated area by drawing water from the Yellow River and the lower Yellow River is increased from 1.403 million hm^2 in the 1950s to 4.38 million hm^2 in the 1990s. In fifties, average water consumption for agriculture in the region from Huayuankou upwards is $103 \times 10^8 \text{ m}^3$, but in the 1990s, it has come to $185.3 \times 10^8 \text{ m}^3$, almost 80% increase. In the 1950s, average water

consumption for agriculture in the region from Huayuankou downwards is $19 \times 10^8 \text{ m}^3$, but in eighties and nineties it has reached $100 \times 10^8 \text{ m}^3$. Meanwhile, the lower Yellow River suffers frequent cut-outs. At present, the percentage of runoff utilization has come to 53%, which is much higher than that of other countries. But it is still insufficient to meet the needs of agricultural and industrial development in the lower Yellow River. This problem has been clearly reflected by frequent cutouts in the lower reaches.

4.2 Reservoirs' regulation function

Many water conservancy projects have been built on the Yellow River's trunk streams since the 1950s. For example, Longyangxia, Liujiaxia, Babanxia, Gingtongxia, Sanmenxia reservoirs. These projects and reservoirs have changed the yearly distribution of flow and sediment. This also makes the flow process more balanced and sediment more concentrated. Longyangxia, Liujiaxia and Sanmenxia reservoirs perform great regulation function upon the Yellow River's flow and sediment. Longyangxia and Liujiaxia reservoir control clear water resources. Sediment sources come mainly from the middle Yellow River. The inflow from the upper reaches can dilute sediment concentration. The two reservoirs store water in flood seasons, discharging water in non-flood seasons. This has changed the annual water distribution and made flowing process well distributed. The two reservoirs' storage in the upper reaches, to some extents, has increased the sediment concentration of the middle and lower reaches. The practice of "store clear water, discharge muddy water" by Sanmenxia Reservoir makes little impact upon the annual water regulation. Its main function is to regulate sediment. The sediment discharge in non-flood seasons is quite small, but in flood seasons, the discharge is bigger.

4.3 Affect on the reduction of flow and sediment by water and soil conservation

In the early seventies. In the middle of the Yellow River, people launched a drive to build traced fields, open up sand bank arid plots in order to preserve water and soil. In some other places, people started to populace the benefits off building dams by water force, opening up terraced fields by machines and afforest a wild stretch of land by plane seeding. This greatly improved water and soil preservation. The sediment-control dams built in this period had played an important part. The comprehensive regulation and management improved the ecological environment and the local people's living conditions. And they also performed the function upon reduction of water and sediment.

In the 1980s, in some sediment contributing areas, if storm intensity was not so strong, the annual reduction of water is $20 \times 10^8 \text{ m}^3$ to $30 \times 10^8 \text{ m}^3$, sediment reduction is 3×10^4 tons to 4×10^4 tons. By practical survey, the percentage of sediment reduction was about 40 percent to 50 percent on account of the comprehensive regulations we adopted. However, at present, the comprehensive measures and regulations we've adopted have really played key roles in preserving water and reducing sediment, but only on condition of mild storm intensity. But if the storm intensity becomes stronger, their functions will not be so evident. Even water calamity might take place. and this would increase the sediment amount of the Yellow Rive. So the Yellow River's sediment is far from being

reduced steadily and smoothly. We still have a long way to go.

Add it all up, Human activities have made great impact upon the flow and sediment variation of the Yellow River. The environment of the Yellow River Basin has been greatly changed. Human activities are interfering with the nature. The emerging new problems and variations that the Yellow River's flow and sediment are confronting are still expecting further study and investigation.

**Address: Hydrology Bureau, YRCC, No.12 Chengbei Road,
Zhengzhou, China**

Phone Number: 86-0371- 6304903

Postcard: 450004

Fax Number: 86-0371-6304903

E-mail: qyplyp@public.zz.ha.cn

INFLOW AND SEDIMENT YIELD OF THE YELLOW RIVER BASIN AND SEDIMENT REDUCTION THROUGH WATER CONSERVATION

By Xu Jianhua, Engineer, YRCC, Zhengzhou, China; Li Xuemei, Engineer, YRCC, Zhengzhou, China; Cui Qing, Engineer, YRCC, Zhengzhou, China; Zhangzheng, Engineer, YRCC, Zhengzhou, China; Liu Zhihong, Engineer, YRCC, Zhengzhou, China

Abstract: Flowing through the vast Loess Plateau, the Yellow River (Y.R.) is of concentrated sediment sources and with 74% of total sediment coming from an area of 100 thousand km² where soil and water conservation has been carried out in large scale to control soil and water loss. According to analysis, sediment to the Yellow River has been significantly reduced in current 20 years, and the annual sediment reduction by water conservation projects in the main sediment yield areas in the middle Yellow River is 370 to 490 million tons.

1 Properties of Sediment in the Yellow River Basin and Its Harmfulness in the Lower Reaches

The Yellow River flows through the Loess Plateau with area of 430,000 km² in the upper and middle reaches, and is famous in heavy sediment load of annual average sediment discharge of 1.6 billion tons for the Loess Plateau is of dry climate, frequent storms, sparse vegetation, dense gullies and poor erosion-resistant loess. The distribution of sediment yield is uneven in time and space. There are 74% of the sediment concentratedly yielded from the region of Hekouzhen to Longmen of around 100,000 km² area where the tributaries of the Yellow River very often happen hyperconcentrated flows with sediment content of 1,500 to 1,700 kg/m³, which bring about severe silt in Sanmenxia reservoir and lower reaches. The distribution of sediment to the Yellow River also is varied in time with 85% of yearly sediment yield in flood season. There is poor water resource in the Yellow River basin of annual total 58 billion m³ of water flow that is mainly from the region of upper Lanzhou where it is of less sediment, and there is only 60% in flood seasons. The status of heavy sediment load with less water resource, different sources of water and sediment, and serious imbalance of the percentages of water and sediment make the lower Yellow River channel heavily silted and became a famous "suspended river", which brings about difficulty to flood protection.

According to the properties of the water and sediment of the Yellow River, it is recognized in the paper that key for harnessing the Yellow River is sediment control, and the flood disaster can be fundamentally alleviated only if the management in severe soil and water loss areas are speeded up, the sediment into the Yellow River is decreased, and the probability of happening hyperconcentrated flows is reduced, the sediment content of the tributaries in the middle Yellow River is lowered, the sediment and water are adjusted in the lower reaches, and sediment transporting capacity is increased. In order to achieve the purposes, China central and local governments have invested a lot to developing soil and water conservation in large scale, and have made great improvement on the land surface conditions.

2 Achievements in Harnessing the Upper and Middle Yellow River and the Change of Water and Sediment

2.1 Soil and Water Conservation Achievements

There have been 7 hydraulic electricity stations in the stem of the Yellow River with total installed capacity of 3,310 thousand kw, 15 reservoirs of each with storage of over 100 million m³ in the stem and tributaries, 130 reservoirs of each with storage of 10 to 100 million m³, 819 reservoirs of each with storage of 1 to 10 million m³, the total reservoir storage is 52.3 billion m³ (Longyangxia and Sanmenxia reservoirs are not included), and the effective irrigated area in and out the river basin is 4.38 million hm² up to 1995. The acculated controlled areas have reached to 14.41 million hm², in which there are terraced land of 3.81 million hm², afforestation of 7.87 million hm², warping land of 0.38 million hm², and grassland of 2.34 million hm². The status of water and sediment in the Yellow River has been changed significantly because of development of water conservancy and hydraulic electricity and enlargement of controlled area of soil and water loss in the middle reaches.

2.2 Change of Runoff and Sediment Transport Records

Table 1 shows that the runoff records of stations in the middle Yellow River are changed greatly, i.e., the recorded runoff are 24.2 billion m³, 15.8 billion m³, 16.7 billion

Table 1. Statistics of annual runoff and sediment in the middle Yellow River

Item	River	Region	1950	1960	1970	1980	1990	1986	1950	1970	1950	
			to									
			1959	1969	1979	1989	1995	1995	1969	1995	1995	
Runoff ($\times 10^8$ m ³ /a)	Yellow River	Upper Hekouzhen	242.8	265.7	230.0	238.1	174.4	180.0	254.2	220.3	235.0	
		Hekouzhen	to	77.1	69.4	53.9	37.1	43.9	42.3	73.3	45.1	57.4
		Longmen										
		Upper Longmen	319.9	335.1	283.9	275.2	218.3	222.3	327.5	265.4	292.4	
	Weihe	Upper Huaxian	85.1	95.8	59.2	79.0	50.6	54.8	90.5	64.8	76.0	
	Fenhe	Upper Hejin	17.5	17.8	10.3	6.6	4.3	5.1	17.7	7.6	12.1	
	Beihuo	Upper Zhuangtuo	6.7	8.8	5.9	7.4	7.2	7.2	7.7	6.8	7.2	
	Yiluo	Upper Heishiguan	40.0	35.3	20.5	30.0	13.4	16.6	37.7	22.2	29.1	
	Qinhe	Upper Xiaodong	15.7	14.0	8.2	7.3	2.8	3.3	14.8	6.6	10.2	
	Yellow River	Middle reaches	242.1	241.1	158.0	167.4	122.2	129.3	241.7	153.1	192.0	
Sedime nt discharg e ($\times 10^8$ t/a)	Yellow River	Upper Hekouzhen	1.53	1.79	1.14	0.98	0.45	0.52	1.66	0.91	1.24	
		Hekouzhen	to	10.36	9.53	7.54	3.71	5.18	4.88	9.94	5.53	7.44
		Longmen										
		Upper Longmen	11.89	11.32	8.68	4.69	5.63	5.40	11.60	6.44	8.68	
	Weihe	Upper Hua-xian	4.29	4.36	3.84	2.76	2.95	2.79	4.32	3.22	3.70	
	Fenhe	Upper Hejin	0.70	0.34	0.19	0.05	0.02	0.02	0.52	0.10	0.29	
	Beiluohc	Upper Zhuangtuo	0.93	1.03	0.89	0.50	0.89	0.72	0.98	0.73	0.84	
	Yiluohe	Upper Heishiguan	0.36	0.18	0.07	0.09	0.005	0.02	0.27	0.06	0.15	
	Qinhe	Upper Xiaodong	0.13	0.07	0.04	0.03	0.003	0.01	0.10	0.03	0.06	
	Yellow River	Middle reaches	16.77	15.51	12.57	7.14	9.05	8.44	16.13	9.67	12.48	

m³, and 12.22 billion m³ respectively in 1950s to 1960s, 1970s, 1980s, and 1990 to 1995; and so be the sediment discharge, the recorded sediment discharges are 1.613 billion tons, 1.257 billion tons, 0.714 billion tons and 0.905 billion tons respectively in 1950s to 1960s, 1970s, 1980s, and 1990 to 1995. It can be seen from mentioned above that the inflow and sediment in the middle Yellow River has changed a lot.

3 Analysis of Factors Causing Water and Sediment Change in The Middle Yellow River

3.1 Climate

Soil erosion in the middle Yellow River is dominated by storm floods, therefore, climate factors, precipitation and rainfall intensity and their distribution in space and time, and their change are directly related to runoff and sediment yield. The annual average precipitation of statistics in the main sediment erosion area of from Hekouzhen to Longmen is 510 mm, 479 mm and 449 mm respectively in before 1969, 1970s and 1980s. The accumulations of daily rainfall over 10 mm are 360 mm, 326 mm and 317 mm respectively in 1950s to 1960s, 1970s and 1980s. All above demonstrate that there have been decrease in precipitation in current 20 years, which is advantageous to the natural runoff and sediment yield decrease and bringing the hydraulic and water and soil conservation projects into a full play in sediment deduction in the area. According to estimation, the runoff deduction from climate is 600 to 700 million m³ in 1970s and 1980s in the middle Yellow River that accounts for 11 to 13 percent of total runoff reduction, and sediment deduction is 120 to 240 million tons that is 20 to 40 percent of total sediment reduction, thus, runoff and sediment reduction are mainly caused by human activities.

3.2 Runoff and Sediment Reduction from Hydraulic and Water and Soil Conservation Projects

3.2.1 Fundamentals of Runoff and Sediment Reduction from Hydraulic and Water and Soil Conservation Projects

The hydraulic and water and soil conservation measures in the area are mainly terraced land, afforestation and grassland, warping land, reservoirs, irrigation, and so on. Terraced land is leveled land of severe soil and water loss to stress water infiltration, and there will be no runoff as well as no soil and water loss in normal rainfalls. However, the sediment reduction effect is less in large storms with some damages of terraced land.

Forest and grassland protect the under soil from splash erosion of raindrops and flow erosion from runoff through dead leaves and turf. Leaves of growing plants have also the effects of rainfall interception, and the roots can increase infiltration and decrease runoff. Experimental research of plots in Suide and Lishi show that the sediment reduction effect is evident and stable if there is 70% vegetation cover, but there will be less runoff reduction effect without vegetation covering the land surface all and without deep dead leaves.

Warping land is formed through silting the warping dams built in gullies for block sediment (such as check dams, warping dams and small reservoirs, and so on). Those gully erosion control projects are aimed at storage of water and sediment eroded from upper areas. The effects for block water and sediment will be ended as soon as the storage capacity is silted up, and after that, the only benefit come from the protection of collapse in the silt influence area. Reservoirs store sediment in dead storage or silt storage, the principle for sediment reduction is as same as warping land before silted up. Irrigation through drawing water from large rivers can more or less carry some sediment into the land, thus reduce water and sediment discharge in the rivers.

3.2.2 Evaluation of the Effect of Runoff and Sediment Reduction from Hydraulic and Water and Soil Conservation Projects

Calculation of runoff and sediment reduction from hydraulic and water and soil conservation projects is currently through two methods, hydrological method and water and soil conservation method. The water and soil conservation method is based on the principles of water and sediment reduction by each measures and calculated item by item. The hydrological method is based mainly on that the influence of human being on watersheds is reflected in the recorded processes of runoff and sediment. Runoff and sediment are characterized by rainfall and land surface conditions. The hydraulic and water and soil conservation projects can improve the land surface conditions but can not change the climate in the area, therefore, rainfall is considered without influence by water and soil conservation measures. On these basis, the basic point of hydrological method is to establish the mathematical model or expirical formula through the water and sediment records before artificial water and soil conservation, then the rainfall data after water and soil conservation measures carried out can be substituted in the above mentioned formula or model, and the comprehensive sediment reduction process can be obtained by comparison of the calculation with the corresponding records. Table 2 shows the calculated effects of water and sediment reduction through water and soil conservation measures by both hydrological and water and soil conservation methods.

The average runoff reduction in the middle Yellow River in 1970s to 1980s is around 4.8 billion m^3 , sediment reduction is 368 to 492 million tons. Based on hydrological method, the regions of runoff reductions percentages of the total in the same period are as following in proper order: the upper Xianyang region of Weihe river is 40.3%, Fenhe river is 30.9%, and the region from Hekouzhen to Longmen is 27.8%, in which the reductions of Weihe and Fenhe are mainly from water utilization in irrigation and relatively less from water and soil conservation projects; and the regions of sediment reduction percentages of the total are as following in proper order: the region from Hekouzhen to Longmen is 61.8%, the upper Xianyang region of Weihe river is 13.4%, Fenhe is 10.4%. The region from Hekouzhen to Longmen is the one of overloaded with coarse sediment in the Yellow River basin, so the maximum sediment reduction is of advantage to the river's silt reduction in the lower reaches. According to the calculation by some specialists, the silt in the lower Yellow River channel will be decreased 50 to 70 million tons with 20 to 30 million tons of coarse sediment of size equal to or larger than 0.05 mm if there is sediment reduction of 100 million tons in the region from Hekouzhen to Longmen, but the major project for sediment reduction in the region is warping dams

and reservoirs which is made up of 90% of the total. There are 6.9 billion m³ of storage for sediment silt in the region, in which 4.45 billion m, accounting for 64%, had been silted up till 1989. Thus, it is very difficult to deal with the unlimited sediment only on these limited storage.

Table 2 shows that there is relative less sediment and runoff reduction by climate factor in 1970s and 1980s which is only 13% in runoff reduction and 20% in sediment reduction, and the most is by human's activities but it will be hard to maintain effective relying on the existing dams and reservoirs. Therefore, it is necessary to increase investment, speed up further the management in the areas of serious water and soil erosion, and make the Yellow River to bring more benefit to mankind.

Table 2. Effects of water and sediment reduction through water and soil conservation measures in the middle Yellow River

Item	River	Region	Hydrological method			Water and soil conservation method			
			1970 to 1979	1980 to 1989	1990 to 1993	1970 to 1979	1980 to 1989	1970 to 1989	
	Y.R.	Hekouzhen Longmen	to 11.63	14.86	10.07	13.25	11.52	14.49	13.00
Runoff ($\times 10^8 m^3$)	Jinghe	Upper Qingyang	0.17	0.34		0.26	0.17	0.37	0.26
	Beiluohu	Upper Liujiahe	0.39	-0.01		0.20	0.39	0	0.20
	Weihe	Upper Xiayang	25.19	13.27		19.23	21.36	23.67	22.52
	Fenhe	Upper Hejin	13.60	15.90		14.75	13.77	12.20	12.99
		Total	50.98	44.36		47.67	47.21	50.73	48.96
	Y.R.	Hekouzhen Longmen	to 2.75	3.32	3.73	3.04	1.94	1.83	1.89
Sediment discharge ($\times 10^8 t$)	Jinghe	Upper Qingyang	0.36	0.35		0.35	0.36	0.35	0.35
	Beiluohu	Upper Liujiahe	0.45	0.28		0.36	0.45	0.28	0.36
	Weihe	Upper Xiayang	0.46	0.86		0.66	0.50	0.60	0.55
	Fenhe	Upper Hejin	0.61	0.42		0.51	0.58	0.48	0.53
		Total	4.63	5.23		4.92	3.83	3.54	3.68

Address: Hydrology Bureau, YRCC, No.12 Chengbei Road,
Zhengzhou, China

Phone Number: 86-0371- 6303422

Postcard: 450004

THE NECESSITY OF MODELLING NON-UNIFORM SEDIMENT IN AN 1-D MORPHOLOGICAL MODEL FOR A GRAVEL BED AND A SAND BED RIVER IN THE NETHERLANDS

By Don Duizendstra, Project Engineer Morphological Research, Ministry of transport, Public Works and Water Management , Institute for Inland Water Management and Waste Water Treatment, Arnhem, The Netherlands;

Cor Flokstra, Senior Project Engineer Mathematical Modelling, WL|DELFT HYDRAULICS, Delft, The Netherlands

Abstract:

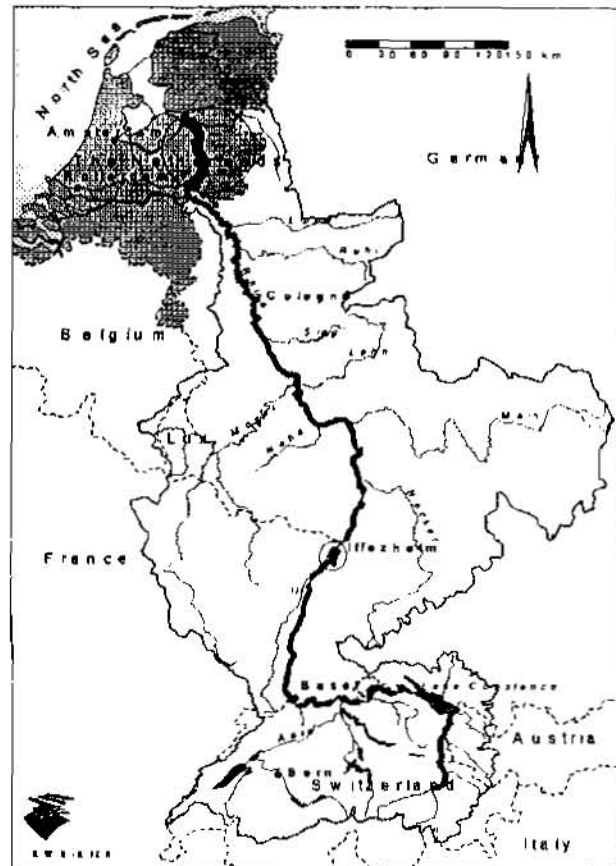
For a gravel bed river and a sand bed river with coarse and fine sediment with different geometric standard deviations morphological computations have been made with an uniform and a graded 1-dimensional numerical model. For the gravel bed river the river bed development is calculated for a period of 15 years with both models. The computations with the uniform model show severe erosion along the river reach, while the computed erosion with the graded model is less severe. Along the river reach the differences between the bed levels computed with both models vary between -0.2 and 3.0 metre. For the sand bed river these differences are much smaller and vary between -0.40 and 0.40 metre. The erosion and the sedimentation computed by the graded model show a more gentle behaviour with less extreme values. Further two series of computations are carried out for the gravel bed river with varying sediment mixtures. In the first series the sediment mixture is varied from very coarse gravel to very coarse sand and in the second series the geometric standard deviation of the sediment mixtures is varied between 1.0 and 2.73. The results of these computations show a large influence of the grain size and a small influence of the geometric standard variation on the bed levels computed by the uniform and the graded model.

INTRODUCTION

The complexity of computer models to simulate river morphology is still growing, accounting for more and more describing parameters and their interactions. The required computation time will increase, but also the data to be collected to run the model and the calibration time of the model. To reduce the required effort it has to be decided which effects can be neglected. The present paper concerns 1-D morphological modelling of rivers and the question when the effect of graded sediment on the bed level can be neglected. allowing the use of a model for uniform sediment. In a number of cases it is quit clear that a graded sediment model should be used, for example in case of dominant armouring and grain sorting or when erosion will expose bed layers of quite different composition. The present considerations are restricted to the less clear cases to choose the adequate model.

Computations have been carried out with both a model based on uniform sediment transport and a model based on graded sediment transport. The sediment has been specified by the mean diameter and the geometric standard deviation of the sediment mixture and different values of these parameters were used. The computations have been applied to the river IJssel, being a sand bed river, and to a reach of the river Rhine with a gravel bed. To illustrate the effect of changing the mean diameter and the geometric standard deviation of the sediment mixture a new model has been built. In this model the cross section is uniform

and the bed slope is constant. For each sediment mixture the changing bed slopes and Chézy values were computed.



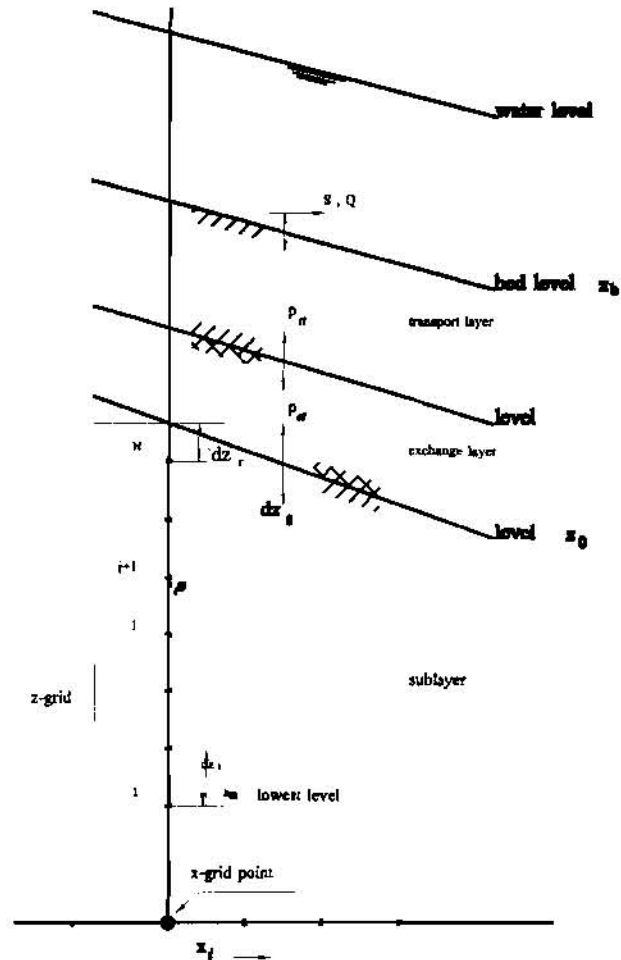
1-DIMENSIONAL MORPHOLOGICAL MODELLING

Since several decades a number of computer codes were developed at WL|DELFT HYDRAULICS to simulate 1-D modelling of the flow and morphology of a network of rivers and channels. At the same time Rijkswaterstaat/RIZA developed a code for 1-D flow modelling. Since one decade WL|DELFT HYDRAULICS and RIZA closely cooperate in generating the computer code SOBEK aimed to replace the models developed before.

The SOBEK modelling system simulates the morphology of network of rivers and channels for uniform sediment. The mathematical model is based on the St. Venant flow equations and a continuity equation for the bed level and sediment transport. A coupling between the bed and flow variation leads to a dynamical simulation of the river morphology. In SOBEK-uniform the sediment mixture of the bed can be described in the way required for the specific sediment transport relation. These parameters (characteristic grain sizes) may vary in space but will not be changed during the simulation as an effect of the model equations.

Since a few years WL|DELFT HYDRAULICS and RIZA have extended the SOBEK model to simulate the varying sediment composition of the bed. The used model corresponds to the model described by Ribberink, but has been extended with a bookkeeping system for the underlayer. The graded sediment will be split in a number of classes of strictly uniform sediment. For each class a separate mass balance is applied and the vertical mixing takes place within one or two active layers, called the transport and exchange layer. The vertical mixing within each layer is immediate and the layer thickness is fixed or related to the dune height. In SOBEK-graded the underlayer composition can vary both in horizontal and vertical direction, where the top side can be adapted by sedimentation or erosion and the applied bookkeeping system guarantees conservation of sediment. In the present computations the Meyer-Peter and Müller sediment transport relation has been used for the computations with SOBEK-uniform. In SOBEK-graded the sediment transport per fraction is calculated according to the same formula but the critical Shields parameter has

been corrected for the hiding and exposure effect, using the expression derived by Egiazaroff (1965) and improved by Ashida and Michiue (1972).

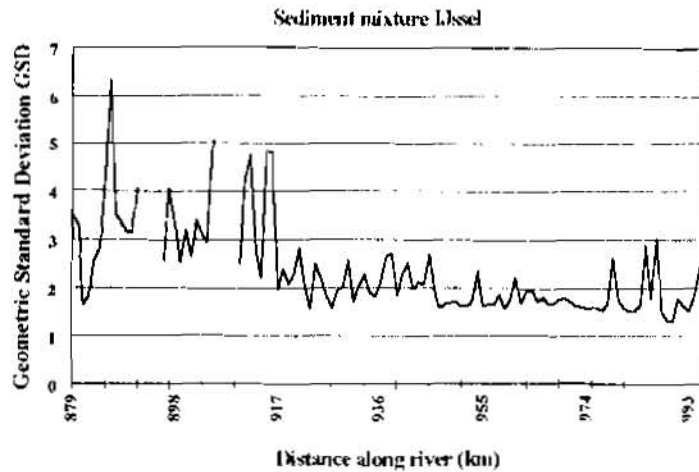


Definition sketch layer system

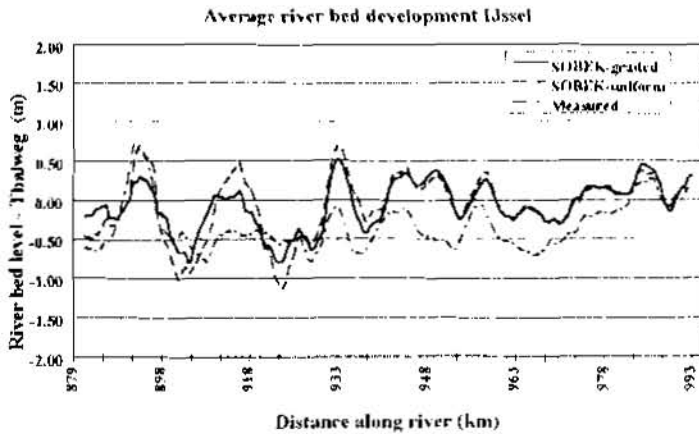
SAND BED RIVER

Description model area: The river IJssel in the Netherlands is a branch of the river Rhine running from the bifurcation at Westervoort to the IJssel lake. The length of the river till Kampen is 106.514 km. The width of the river varies between 60 metre at Westervoort to 178 metre at Kampen and the average slope is $0.8 \cdot 10^{-4}$. The discharge varies from 124 m^3/s to 1780 m^3/s with an average of 350 m^3/s . A number of lateral discharges are present, some dredging takes place and the upstream sediment supply is about 60.000 to 100.000 $m^3/year$. The grain size varies from about 7 mm upstream to 0.55 mm downstream and the geometrical standard deviation from 3.5 to 1.7 (excluding some peaks). This means that armouring layers can occur. The possible effects of these layers are supposed to be minor. The model schematization is known to be rough.

Computations: For the computations with the graded and the uniform model the models are only tuned on basis of the water flow. The model was primarily developed for flow simulation. The height of dikes and floodlands is not accurate in all cases. This means that the exchange flow between the floodlands and the main channel is not schematised accurately which has considerable effects on the morphological development. The morphological activities are restricted to the area within the summer dikes. The characteristic grain sizes used in the uniform model have been derived from the data used in the graded model, which were derived from field measurements. The computational grid comprises 428 grid points. In the computations the one-layer option was used with a constant composition of the underlayer and 8 sediment fractions were taken into account. The thickness of the transport layer was fixed and set to 0.015 metre. In both models the same overall tuning constant (0.5) was used for the computation of the sediment transport. The simulation time runs from January 1st 1971 to December 27th 1991. Upstream a time-series of discharges and bed levels were imposed and downstream a time-series of waterlevels.



Results: The differences between the measured and the computed bed levels are substantial but the differences between the results of the graded and the uniform model are modest. On the basis of these results no preference can be given to either a graded sediment or uniform sediment model for the IJssel. Apart from two unrealistic peaks at km 897 and km 910 the graded-sediment model seems to perform equally well or slightly better than the uniform model. In spite of the large differences in model concepts and computation time the effect of the gradation of the mixture on the bed level is small for the present case. The differences between both models can be further reduced by increasing the thickness of the transport layer. The river bed levels were computed after a simulation period of 20 years and averaged over 4 km.



GRAVEL BED RIVER

Description model area: The Rhine river downstream of the weir near Iffezheim in Germany has the typical characteristics of a gravel bed river with coarse sediment. The modelled river reach has a length of 12.3 kilometre, a width varying between 135 and 175 metre and an average slope of $5 \cdot 10^{-4}$ and starts 1 kilometre downstream of the weir Iffezheim. The model schematization is known to be rough.

By the weir the sediment transport is interrupted and huge erosion is expected. With success in Germany a sediment management program was developed and carried out by which the river was artificially supplied with sediment and by which the expected huge erosion downstream of the weir was reduced considerably. This well documented case was used for several computations with the 1-dimensional numerical morphological models SOBEK-graded and SOBEK-uniform. In these computations two situations are schematised, a situation in which

sediment was supplied and a situation in which no sediment was supplied. In this paper the computations in which no sediment was supplied will be described. The computed river bed development with the graded and the uniform model will be described and compared with each other.

Computations: For the computations with the graded and the uniform model the models are only tuned on basis of the water flow. An important goal of these computations is to get a picture of the differences between the results of the graded and the uniform model for a coarse sediment mixture. The computational grid comprises 17 grid points. An one-layer model was used for the computations with the graded model. At the upstream model boundary the sediment transport was set to zero and at the downstream boundary a Q-h (discharge-water level) relation was applied. The calibration constant in the sediment transport relation in both models was set to 1.0. The sediment mixture in the graded model is schematised with four classes and in the uniform model with the characteristic grain size diameters, D_m and D_{90} . The computations are carried out for a period of 15 years. For the first period of 5 years a flow curve was available. This flow curve is used 3 times.

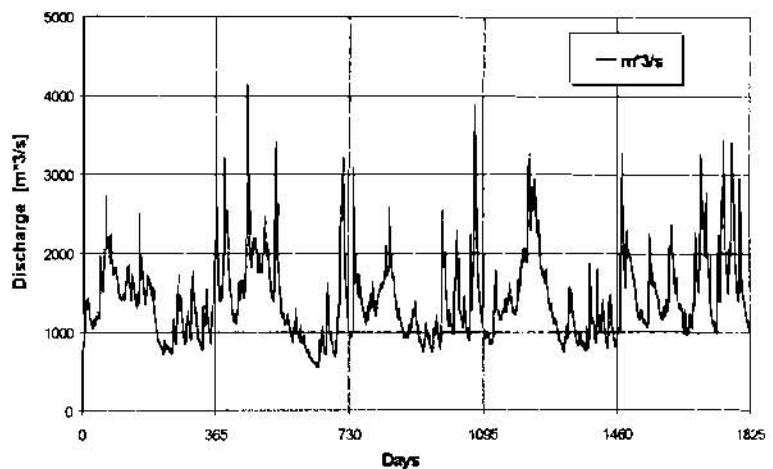
Schematization of sediment mixture by SOBEK-graded

Class of grain sizes metre	Percentage
0.002 - 0.006	13
0.006 - 0.016	21
0.016 - 0.035	42
0.035 - 0.048	24

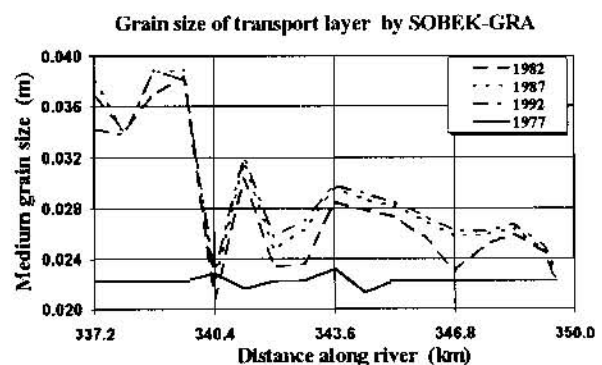
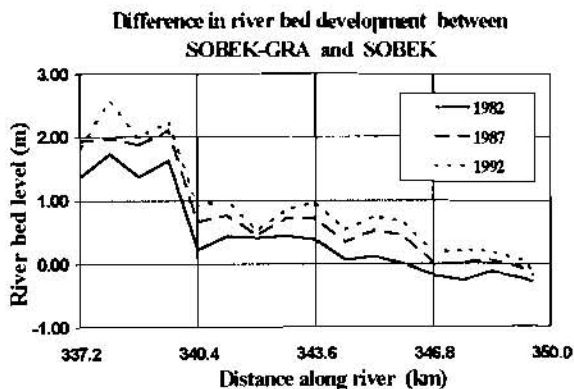
Schematization of sediment mixture by SOBEK-uniform

Characteristic grain sizes (metre)	
D_m	0.0235
D_{90}	0.0426

Course of discharge 1 March 1977 - 28 February 1982



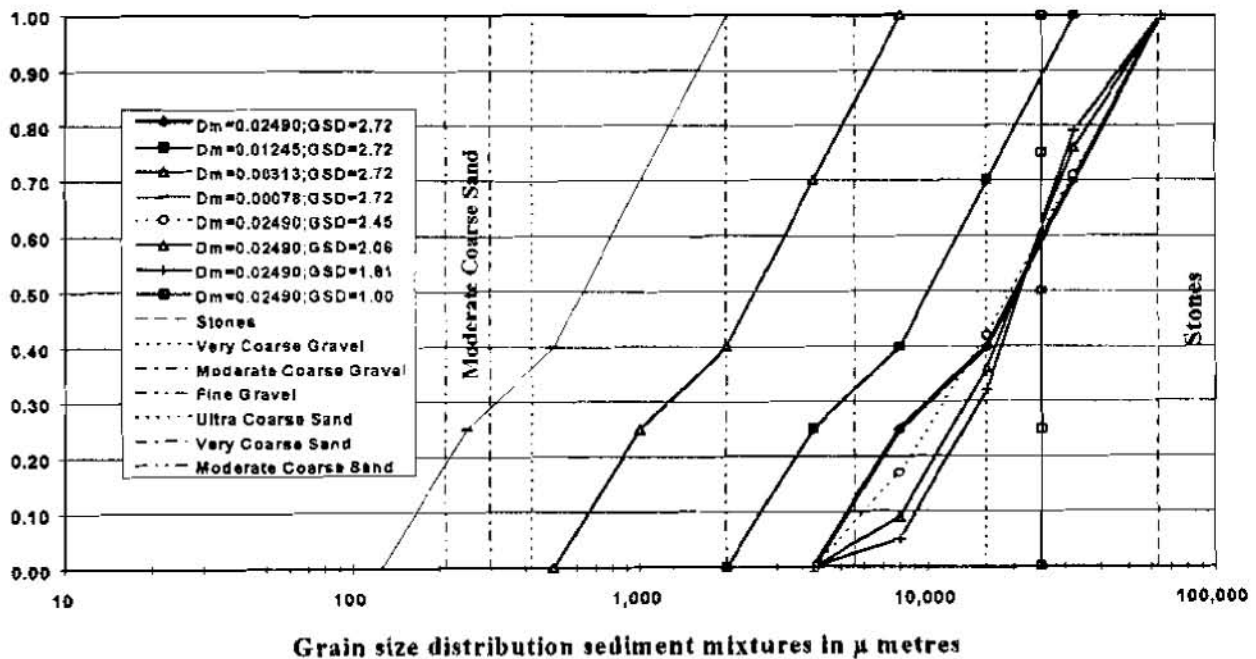
Results: The differences in the computed sediment transport and the corresponding erosion of the river bed by the graded and the uniform model are substantial. The computed sediment transport by the uniform model is 50% larger than the sediment transport computed by the graded model. After 15 years the erosion downstream of the weir is overrated by the uniform model with 2.5 metre and reduces in downstream direction. The reduced sediment transport and the corresponding erosion computed by SOBEK-graded are explained by the formation of armour layers. The computed composition of the transport layer after 15 years has coarsened and indicates that an armour layer is formed.



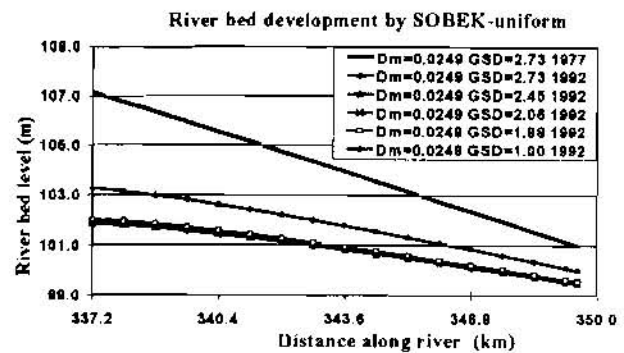
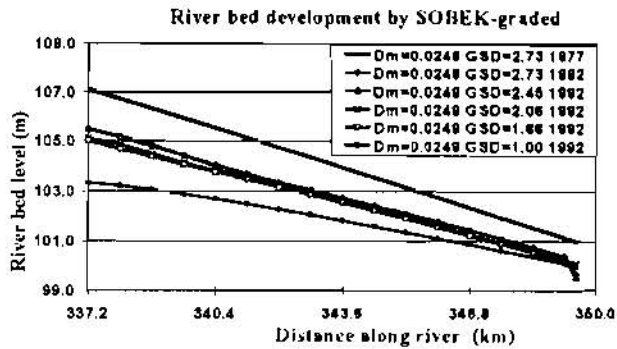
FROM A GRAVEL BED RIVER TO A SAND BED RIVER

Introduction: The differences in the computed bed levels by the graded and the uniform model after 15 years are quite large for a gravel bed river and are quite small for a sand bed river. An explanation for this different behaviour is found in the representation of the sediment mixtures in both models. The sediment mixtures are described by the grain sizes and the geometric standard deviation (GSD). To analyse the influence of the grain size and the GSD several computations were carried out in which the grain size and the GSD were changed.

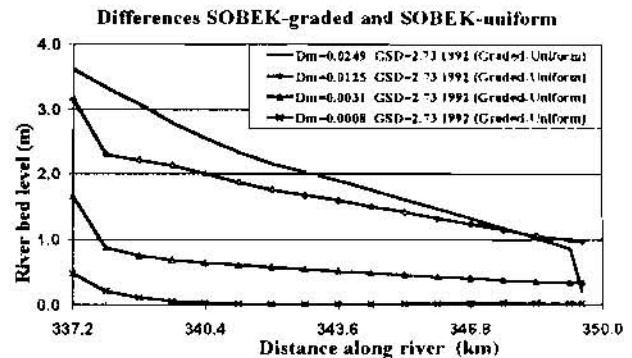
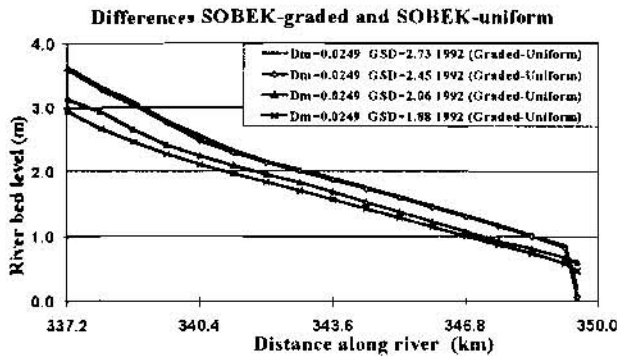
Computations: To analyse the influence of the grain size and the grain size distribution two series of computations were carried out with a simplified model based on the Iffezheim model, with a constant width (150 metre) and a constant slope. In the first series computations were carried out with four sediment mixtures with mean diameters varying from very coarse gravel (0.0249 metre) to very coarse sand (0.00078 metre) with a constant GSD (2.73). For the very coarse gravel mixture the initial bed slope is $5 \cdot 10^{-4}$ (Iffezheim case) and for the very coarse sand mixture the initial bed slope is $0.8 \cdot 10^{-4}$ (IJssel case). For the intermediate sediment mixtures the bed slopes are linear interpolated with respect to the mean grain size of the mixture. For each sediment mixture and corresponding bed slope, the corresponding Chézy values and water depths were computed as a function of the corresponding Shields value with the roughness predictor of Engelund and Hansen (1967). The Q-h relation (Iffezheim case) is adapted and the thickness of the transport layer is kept constant (0.06 metre). In the second series the GSD of the sediment mixture is changed from 2.73 till 1.00. A sediment mixture with a GSD value of 1.00 is an extremely uniform mixture, this mixture only consists of one grain size. In the computations with SOBEK-graded four classes of grain sizes were used while in the computations with SOBEK-uniform the corresponding characteristic grain sizes D_{90} and D_{10} are used.



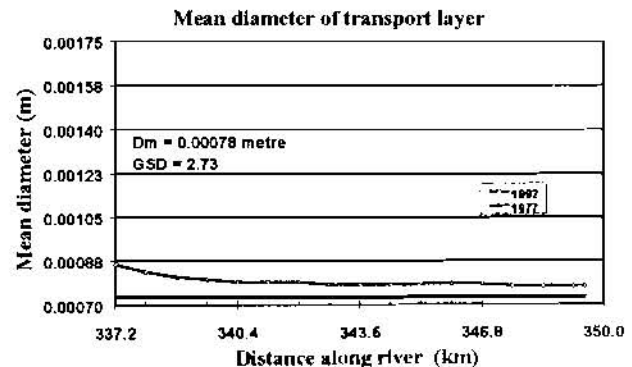
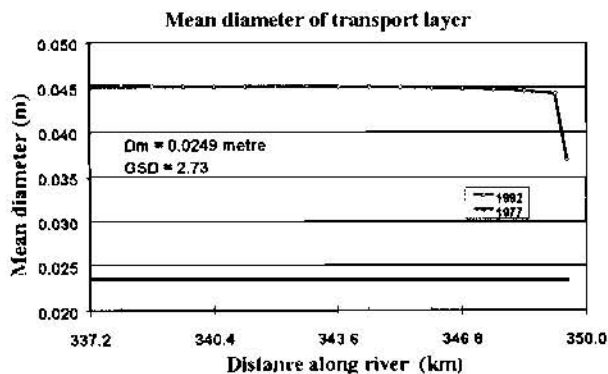
Results: With the graded and the uniform model computations were carried out for the gravel sediment mixture with a GSD varying from 2.73 till 1.00. The graded model shows less erosion (approximately 4 metre at the upstream model boundary) and shows differences for the varying GSD values and a large difference for the extreme uniform mixture with GSD=1.00. The uniform model shows minor differences for the varying GSD values but a large difference for the extreme uniform mixture with GSD=1.00. The bed levels computed by both models for the extreme uniform mixture are almost identical.



The differences in the computed bed levels are caused by the different representations of the composition of the sediment mixture. To illustrate the effects of the varying GSD values, the computed bed levels were reduced with the computed bed levels for the extreme uniform mixture (GSD=1.00). The differences between these adapted bed levels illustrate the differences between the graded and the uniform model. It is shown that for the gravel mixture there are some differences for varying GSD values. To illustrate the effects of varying mean grain sizes the computed bed levels for the four sediment mixtures were adapted in the same way. It is shown that the influence of the D_m is large. The differences between the computed bed levels by both models almost disappear completely for the fine mixture of very coarse sand.



There is a large difference between the results of the graded and the uniform model for the coarse mixture and a small difference for the fine sediment mixture. This has to be related to the reduction of the sediment transport by the formation of an armoured layer. To illustrate this effect the composition of the transport layer is computed for both mixtures after a period of fifteen years. For an easy comparison the initial and final mean grain sizes of both transport layers are drawn at comparable scales.



EVALUATION

The differences in the computations for the gravel bed and the sand bed river with the graded and the uniform model as shown in the figures are discussed step by step in this section.

- Sediment transport: In the transport relation of Meyer-Peter and Müller the sediment transport depends on the Shields value and the critical Shields value. The Shields value is adapted by the ripple factor $(C/C_{90})^{1.5}$ and in the case of the graded model the critical Shields value is adapted by the hiding and exposure correction after Egiazaroff, Ashida and Michiue. The computed sediment transport depends on the difference between the adapted Shields value and the adapted critical Shields value. The Shields values vary for the gravel bed river between 0.026 and 1.0 and for the sand bed river between 0.28 and 0.9. With a critical Shields value of 0.047, it is obvious that in the case of the gravel bed river during a substantial part of the computation time there will be no transport or just a little transport of the finer fractions of the sediment mixture. For the sand bed river at all times there will be transport of sediment and all fractions will be included.

- River bed development (gravel bed river): The river bed development by SOBEK-uniform shows little differences for a varying GSD between 2.73 and 1.88. These little differences are explained by the fact that in the uniform model the sediment transport only depends on the D_m and the D_{90} of the sediment mixture. The D_m is constant for the varying GSD values and the D_{90} values for these mixtures show only minor differences. For the extreme uniform mixture (GSD=1.00) the D_{90} value is reduced with a factor 2, resulting in a far less reduction of the ripple factor computed as $(C/C_{90})^{1.5}$ with $C_{90} = 18 \log(12 \cdot h / (3 \cdot D_{90}))$, leading to a reduction of the sediment transport, resulting in less erosion and a higher bed level. Also for these low Shields values the effect of the hiding and exposure correction is more substantial by which the transport of the larger grain sizes is stimulated with respect to the smaller grain sizes. The computed bed levels by SOBEK-graded show differences for all GSD variations and show also a greater variation for the extreme uniform mixture (GSD=1.00). The course of the bed level variation for the various GSD values is in one direction and is smooth. In the case of SOBEK-uniform this is not the case.

- Differences SOBEK-graded and SOBEK-uniform: The differences between the bed levels computed by SOBEK-graded and SOBEK-uniform for the very coarse gravel mixture vary from 3.0 to 3.6 metre at the upstream boundary and reduce in the downstream direction. Within the applied variation range of the GSD value (1.88-2.73), as is found in the IJssel river, the differences (0.0-0.6 metre) at the upstream boundary of the model are rather small. The differences for the intermediate GSD values fall within this range. For the varying mean grain sizes of the sediment mixture from 0.00078 till 0.0249 and a constant GSD (2.73) the differences between the computed bed levels are much larger. For the coarse gravel mixture at the upstream boundary these differences are approximately 3.6 metre. For the very coarse sand mixture these differences are only 0.5 metre. For the intermediate mean grain sizes (0.0125 and 0.0031 metre) the differences are approximately 3.1 and 1.7 metre.

- Composition of transport layer: For the very coarse gravel mixture over approximately the full length of the model the transport layer has coarsened with a factor 2. For the very coarse sand mixture the transport layer is coarsened only by a factor 1.1. The larger coarsening of the transport layer in the gravel bed is explained by the low range of Shields values. At low Shields values particularly the coarse fractions of the sediment mixture will not be transported and thus coarsen the remaining sediment mixture. The hiding and exposure correction adapts the critical Shields value for each fraction. For the fine fractions the critical Shields value will be raised and for the coarse fractions these value will be lowered thus stimulating the transport of the coarser fractions. It is obvious, that in the case of low ranges of Shields values, the effect of the hiding and exposure correction will be more effective, than in the case of high ranges of the Shields value. At very high Shields values the effect of the critical Shields value is minor and leads to equal mobility of all fractions.

CONCLUSIONS

These computations for the extreme boundary condition ($S=0$) show that the effect of an extreme variation in the GSD of the sediment mixture from 2.73 till 1.00 is less substantial than the effect of reduction of the D_m of the mixture. For the gravel bed river ($D_m=0.0249$ metre) large differences in the computed bed levels by the graded and the uniform model are shown. For the sand bed river ($D_m=0.00078$) the results of the graded and the uniform model are comparable and are not substantially influenced by variation of the GSD.

The differences between the results of the graded and the uniform model are explained by the ranges of the Shields values for both rivers. The Shields value in the gravel bed river varies between 0.026 and 1.0, for the sand bed river these values vary between 0.28 and 0.9. With a critical Shields value of 0.047 under which value no sediment transport will occur, it is obvious, that in the gravel bed river during a substantial part of the computation time there will be no transport or only transport of the finer fractions. These circumstances will lead to less erosion and to coarsening of the transport layer. For the sand bed river at all times there will be transport and all fractions will be included. This will lead to less reduction of the sediment transport and less erosion of the river bed and to a transport layer that is still coarsened but to a lesser extent.

These computations were only carried out for the extreme upstream boundary condition $S=0$. Downstream of weirs in rivers the on-going sediment transport will be partially or completely blocked. For this extreme situation the computations have shown the large influence of the mean grain size and the small influence of the GSD of the sediment mixture. Leading to the conclusion that in case of a coarse sediment mixture the application of a graded model is to be preferred above the application of an uniform model. It is clear that these computations have to be repeated for the more common and less extreme upstream boundary condition in which the bed level is maintained or varied as a function of time.

Obviously, the application of graded morphological models have many advantages. The transport process of the sediment is formulated in a more sophisticated way, the actual composition of the sediment mixtures is formulated in a more proper way and the relation between underlayer and transport layer is roughly prescribed. In the cases of dominant armouring and non-uniform vertical composition of the underlayer, only graded models can be applied.

REFERENCES

- Ashida, K., Michiue, M. (1972), Study on hydraulic resistance and bed load transport rate in alluvial streams, Transactions, Japan society of civil Engineers, 206, 59-69
- Duizendstra, H.D. and C. Flokstra (1997), Graded sediment in SOBEK, joint research RIZA and WL|DELFT HYDRAULICS, research report, working document 95.193X, research report Q2128
- Duizendstra, H.D. and K. Vermeer (1996), Graded sediment in SOBEK, joint research RIZA and WL|DELFT HYDRAULICS, Continued research 1995-1996, working document 95.162X, research report Q2128
- Duizendstra, H.D. and M. Laguzzi (1996), A modified numerical scheme implemented in SOBEK-GRA, joint research RIZA and WL|DELFT HYDRAULICS, research report, working document 95.192X, research report Q2128.10
- Duizendstra, H.D. and K. Vermeer (1995), Graded sediment in SOBEK, joint research RIZA and WL|DELFT HYDRAULICS, working document 95.078X, research report Q1841/Q1987
- Egiazaroff, I.V., 1965, Calculation of non-uniform sediment concentrations, J.Hydr.Division, Vol.91, No. 12
- Engelund, F. und Hansen, E. (1967), A monograph on sediment transport in alluvial streams, Teknisk Forlag, Copenhagen.
- Khin NiNi Thein (1989), One dimensional morphological modelling of graded sediments, WL|DELFT HYDRAULICS, Report Q697
- Laguzzi, M. (1994), Modelling of sediment mixtures, WL|DELFT HYDRAULICS, report Q1660
- Ribberink, J.S. (1987), Mathematical modelling of one-dimensional morphological changes in rivers with non-uniform sediment. Communications on Hydr. and Geotech. Engrg., No.87-2, Delft Univ. of Technol., ISSN 0169-6548
- H.D. Duizendstra, RIZA, P.O. Box 9072, 6800 ED Arnhem, The Netherlands, Phone +31263688559/911, Fax /678, E-mail d.duizendstra@riza.rws.minvenw.nl
- C. Flokstra, WL|DELFT HYDRAULICS, P.O. Box 177, 2600 MH Delft, Phone +31152858634/ 8585, Fax /8602, E-mail cor.flokstra@wldelft.nl

STABLE CHANNEL ANALYSIS OF THE RIO GRANDE IN THE UPPER REACHES OF ELEPHANT BUTTE RESERVOIR

By: Cassie C. Klumpp, Hydraulic Engineer, U.S. Bureau of Reclamation, Technical Service Center, Sedimentation and River Hydraulics Group, Denver, Colorado; Dr. Mohammed A. Samad, Hydraulic Engineer, U.S. Bureau of Reclamation, Technical Service Center, Sedimentation and River Hydraulics Group, Denver, Colorado

INTRODUCTION

The Middle Rio Grande flows through wide valleys of New Mexico carrying large quantities of sediment to Elephant Butte Reservoir (Figure 1). The river has been aggrading for the last 11,000 years. Although two large dams (Cochiti and Abiquiu Dams) limit sediment supply in the basin, tributaries such as the Rio Puerco and other smaller ephemeral washes deliver large quantities of sediment to the Rio Grande south of Albuquerque. Much of this sediment has been deposited in the upper reaches of Elephant Butte Reservoir. Coupled with a highly variable hydrologic cycle varying from long wet to long dry periods, sediment management in the delta of Elephant Butte Reservoir has proven to represent a difficult engineering task.

In the midst of a drought in the 1950's, a conveyance channel was constructed from San Acacia to Elephant Butte Reservoir to more efficiently transport water to the reservoir (Figure 2). Without the Low Flow Conveyance Channel, large quantities of water would have been lost due to seepage, evaporation and evapotranspiration as the river crossed the delta. The conveyance channel conserved between 50,000 and 60,000 ac-ft of water per year when the channel was in operation (1960-1980). The conveyance channel was designed to carry up to 2000 cfs. Diversions to the conveyance channel were discontinued in 1980 because of sediment accumulations. Since 1980, the conveyance channel functioned as a drain. A levee was built to contain the river channel, and separate it from the conveyance channel. However, since 1980 the river channel has aggraded more than 10 ft in some locations such that it is now at a much higher elevation than the conveyance channel.

The State of New Mexico had had to operate the conveyance channel to meet their water delivery under the Rio Grande Compact for many of the years between 1960 and 1980. Efficient delivery of water to Elephant Butte Reservoir is vital to the United States and Mexico.

Four basic design alternatives (river and conveyance channel) are under consideration to help meet New Mexico's water requirements in the future: two separate channels through the delta to the reservoir, a single channel through the delta, continuation of the current maintenance of the river using the conveyance channel as a drain, and discontinuance of all maintenance. A regime analysis was conducted for both a conveyance channel and river channel to gain insight into stable channel characteristics for future design alternatives.

Equilibrium slopes for different channel widths were determined for selected sediment transport relationships to see at what range of slopes the river or the conveyance channel could be operated. Equilibrium slope and width relationships of the conveyance channel also were analyzed with the dominant discharge and different sediment transport equations.

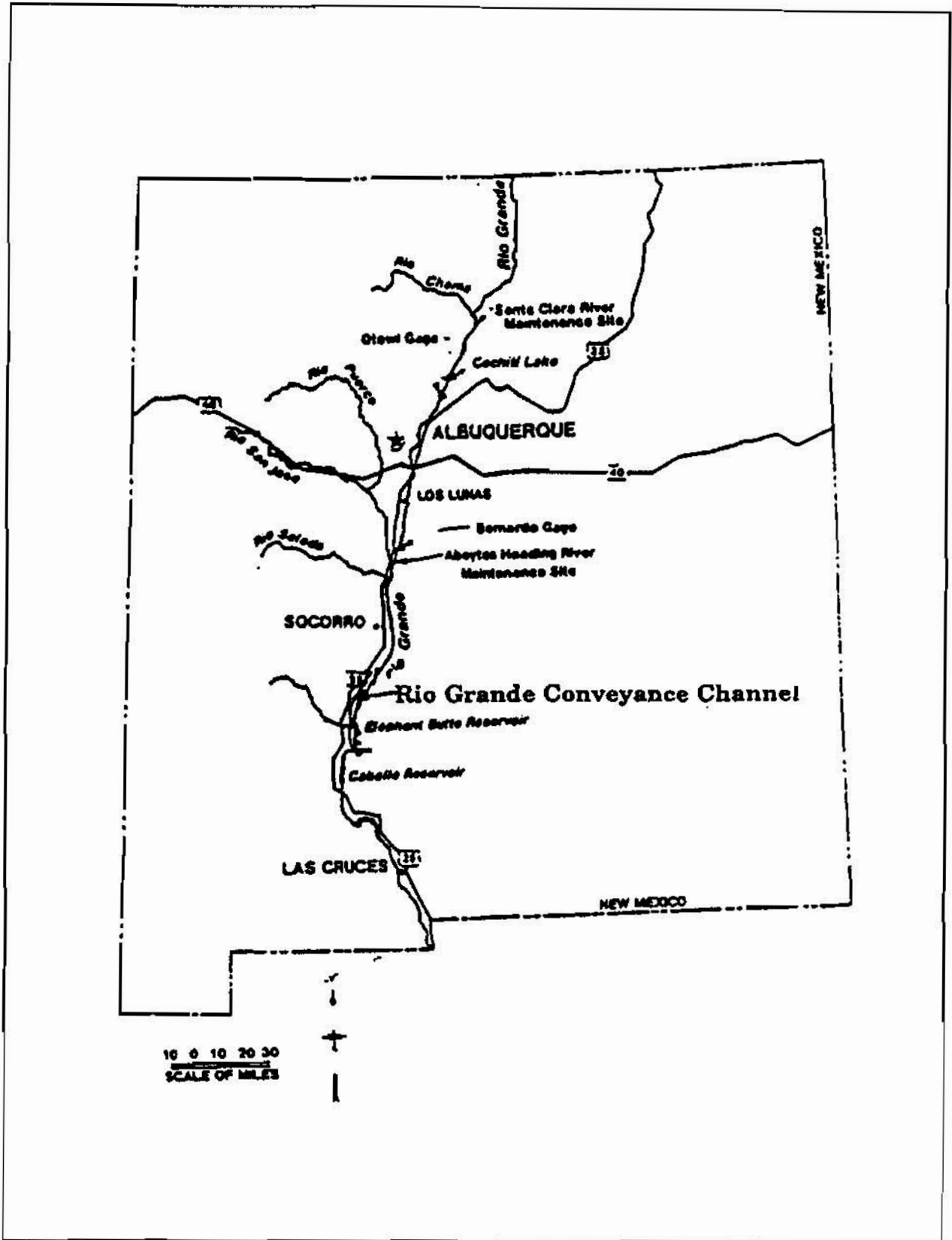


Figure 1 - Location map.

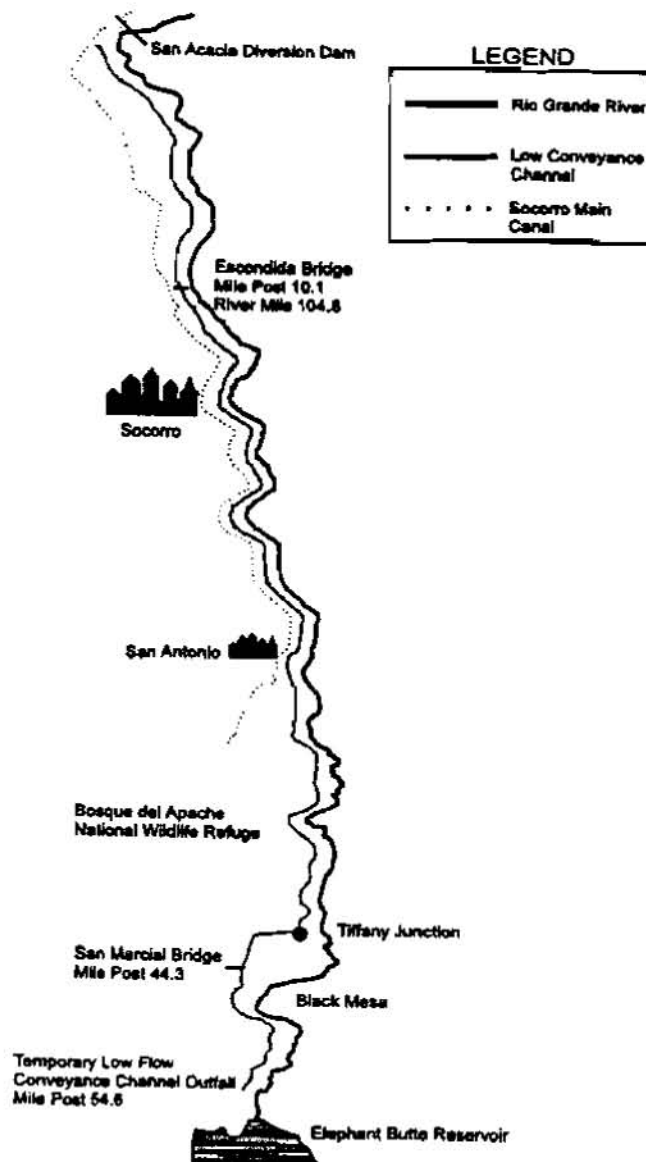


Figure 2-Configuration of the conveyance channel and Rio Grande near the headwaters of Elephant Butte Reservoir.

Regime theory has been utilized for more than 100 years for design of earth channels. During the early period, Kennedy, Lacey, Lindley, and Simons and Albertson focused on empirical canal design from the 1900's through the 1950's (Mahmood, 1971, Wargaladam, 1993). During the 1950's and the 1960's, a transitional period occurred because of the change from canal based regime analysis to a river regime analysis that was also more analytical than empirical in nature. This included equations developed by Chien, Chitale, Leopold and Maddock, Williams, and Klassen and Vermeer (Wargaladam, 1993).

From the 1960's to the 1980's, regime analysis focused on a combination of analytical and empirical approaches for river and canal regime analysis. Julien (1988) and Wargaladam (1993) developed four theoretical hydraulic equations for alluvial

channels based on discharge, sediment size, and a Shields parameter for sediment mobility. Julien used four basic equations to derive his relationships based upon continuity, flow resistance, longitudinal shear stress, and radial shear stress to account for natural channel bends. He combined the longitudinal and radial shear stress into one term which was expressed as a Shield's parameter for sediment mobility. When you solve Julien's equations iteratively relationships for depth, width, slope and velocity are obtained. When the slope is fixed, relationships can be derived for depth, width, slope and shear stress.

Equations by Kennedy, Lindley, and Lacey, were used to analyze a canal section similar to the original conveyance channel. Equations developed during the transitional period were also used to evaluate the conveyance channel including equations by Chien, Leopold and Maddock, Chitale, and Williams. Julien's theoretical equations were also used to evaluate a trapezoidal channel like the conveyance channel with a discharge of 1500 cfs, a particle size D_{50} of 0.2 mm, and a concentration of 1730 mg/L. Equations developed during the early period did not consider sediment particle size or concentration and were based on relationships between discharge and width, discharge and velocity, discharge and slope, discharge and depth or hydraulic radius. The results shown in Table 1 are highly variable, channel widths ranged from 37 to 100 ft and slopes from as steep as 0.001 to as flat as 0.00006.

Table 1.— Conveyance channel Regime Analysis for 1,500 cfs

Rio Grande conveyance channel					
Discharge (cfs)	D_{50} (mm)	Sed. conc. (mg/L)	Fall vel. (ft/s)	Kin. vis. (ft/s)	
1,500	0.20	1,730	0.075	0.000012	
Kennedy					
Depth (ft)	Hydraulic Radius (ft)	Perimeter (ft)	Width (ft)	Velocity (ft/s)	Slope
10.63	--	--	37.22	3.8	0.000146
Lindley regime equation for sand-silt channels					
6.64	--	--	80.29	2.8	0.000141
Lacey					
--	5.97	103.29	95.4	2.38	0.001001
Leopold and Maddock					
8.97	--	--	38.73	4.32	0.000961
Simons and Albertson					
--	6.17	109.93	109	2.21	6.55E-05
Chitale					
--	5.88	100.22	100	0.26	0.00015
Williams					
4.64	--	--	100.22	3.73	--

Table 2.—Rio Grande Channel Regime Analysis for a Discharge of 6,000 cfs

Rio Grande Channel					
Depth (ft)	Hydraulic Radius (ft)	Perimeter (ft)	Width (ft)	Velocity (ft/s)	Slope
Leopold and Maddock					
13.6	--	--	77.46	5.7	0.000257
Simons and Albertson					
--	10.17	223.56	--	2.64	4.1E-05
Williams					
6.21	--	--	240.01	4.79	--
Ackers					
--	--	--	--	--	0.000272
Klassen and Vermeer					
2.458431	--	--	803.18	6.99484	--

The river channel was also analyzed with applicable regime equations to determine a range of widths, velocities and slopes. Estimates for the channel forming flow for the river channel vary between 3000 and 9000 cfs. Since the construction of Cochiti Reservoir, the channel forming flow was estimated to be 6,000 cfs, along with a particle size D_{50} of 0.22 mm, and a sediment concentration of approximately 5000 mg/l. Again, results of the analysis shown in Table 2 are highly variable.

Table 3.—Julien's semitheoretical equations for the Rio Grande Conveyance channel

Q (cfs)	D50 (mm)	Slope	Depth (ft)	Width (ft)	Velocity (ft/s)
1,500	0.20	0.002 ¹	3.55	92.26	4.58
1,500	0.20	0.0019 ¹	3.61	93.73	4.44
1,500	0.20	0.0017 ¹	3.71	96.19	4.22
1,500	0.20	0.001 ¹	4.11	105.87	3.45
1,500	0.20	0.00093 ²	3.94	131.33	2.90
1,500	0.20	0.00084 ²	4.01	133.53	2.80
1,500	0.20	0.000704 ²	4.18	137.60	2.60
1,500	0.20	0.000512 ²	4.43	145.73	2.32

¹ slope is computed

² slope is fixed

**Table 4.—Julien's alternative semi-theoretical equations
for the Rio Grande Channel**

Q (cfs)	D ₅₀ (mm)	Slope	Depth (ft)	Width (ft)	Vel. (ft/s)
3,400	0.22	0.0005 ¹	6.13	205.51	2.70
6,000	0.22	0.0005 ¹	7.70	258.83	3.01
9,000	0.22	0.0005 ¹	9.05	305.51	3.25
3,400	0.22	0.00038 ²	6.81	178.97	2.79
6,000	0.22	0.00034 ²	8.76	230.68	2.97
9,000	0.22	0.00036 ²	10.21	269.13	3.28

¹ slope is fixed

² slope is computed

In the regime analysis, Julien's equations produced results that most closely matched observed conditions for both the conveyance channel and the river channel. These results are shown in Tables 3 and 4. The results for the conveyance channel, based on Julien's relationship, indicate a stable channel width of approximately 130 ft, with a velocity of 2.8 ft/s, a depth of 4 ft, and a slope of approximately 0.0008. The valley slope in the delta of Elephant Butte Reservoir is approximately 0.0005 which would require a channel on the order of 150 ft. with a depth of 4.5 ft and a velocity of 2.3 ft/s. The Middle Rio Grande conveyance channel is not in equilibrium. The heavy sediment loads contributed by the tributaries of the Rio Grande prevent equilibrium conditions. These results provide data for future channel designs, but artificial sediment removal and sediment exclusion will probably be necessary if the conveyance channel is going to operate for a 50-year design life.

As shown in Table 4, the results for the river channel based on Julien's regime equations indicate a river width of 300 ft, with a slope of 0.0005, and a velocity of 3 ft/s and a depth of approximately 7.7 ft. Actual river data in the vicinity of the delta for a discharge of 6,000 cfs indicate that widths vary from 200 to 800 ft, with velocities of 3 to 6 ft/s, and depths of 2 to 7 ft. If an artificial channel is designed through the delta, channel widths of approximately 300 ft. may provide a stable channel design for a shorter project life requiring sporadic sediment removal. The results of the regime analysis will be coupled with sediment transport modeling of the Rio Grande above Elephant Butte Reservoir for guiding channel designs. The regime approach developed by Julien provides an initial relationship of channel widths, depths and velocities for the given slope that can be used as a guide in the sediment transport modeling of different alternatives for a 50-year project design life.

SLOPE AND WIDTH RELATIONSHIPS BASED ON SEDIMENT TRANSPORT RELATIONSHIPS

The equilibrium slopes of the conveyance channel and the river channel were determined for selected sediment transport equations for comparison with the slopes and widths predicted by the regime equations. The equations selected were: Toffaleti, Laursen, and Yang. The slope was determined by fixing the width and Manning's n for the channel-forming discharge and varying the slope and depth until the sediment transport rate predicted by the equations matched the upstream supply. The parameters used in the analysis were: 1) a channel-forming discharge for the conveyance channel was 1,500 cfs and 6,000 cfs for the river channel, 2) a bed material size D₅₀ of 0.20 mm for the conveyance channel and 0.22 mm for the river channel, and 3) an upstream sediment supply for the conveyance channel of 7,000 tons/day and 84,000 tons/day for the river channel.

Results of the analysis for the conveyance channel and the river channel are summarized in Tables 5 and 6. The predicted slopes for the conveyance channel ranged between 0.0003 and 0.0008. The predicted slopes for the river channel ranged between 0.0012 and 0.0022.

**Table 5- Equilibrium Slope Relationships of the Conveyance Channel
for a Sediment Load of 7000 tons/day**

Width (ft)	Yang	Toffaletti	Laursen
30	0.00060	0.00030	0.00062
40	0.00062	0.00033	0.00063
50	0.00065	0.00036	0.00064
60	0.00068	0.00039	0.00066
100	0.00078	0.00053	0.00075

**Table 6- Equilibrium Slope Relationships of the river channel
for a sediment load of 84,000 tons/day**

Width (ft)	Yang	Toffaletti	Laursen
200	0.0014	0.0022	0.0013
300	0.0017	0.0012	0.0015
400	0.0018	0.0012	0.0016
500	0.0019	0.0013	0.0017

The predicted supply curves for each sediment transport equation were compared to the measured sand load calculated by the Modified Einstein equation. The Laursen and Yang equations followed the same trend as the supply curve but under-predicted the transport rates. The Toffaletti equation tended to greatly over-predict the sediment transport rates for the conveyance channel and slightly over-predict transport rates of the river channel. All of the results except for Toffaletti (conveyance channel) show that equilibrium slopes for the conveyance channel and the river channel for varying widths exceed the existing valley slope. These results show that for the existing sediment supply of the Rio Grande basin the river or conveyance channel slope would have to exceed the valley slope to transport the sediment supply.

CONCLUSIONS

1. The results of the evaluation of slopes predicted for sediment transport rates predicted by the sediment transport equations show that the equilibrium slope of the Middle Rio Grande exceeds the existing valley slope. The Laursen equation and Yang equation provide the best predictive results for modeling sediment transport.
2. The regime equations developed by Julien provide good data for development of a design for constructing one or two channel system through the delta. The Julien equations showed that for a two channel system like the one operated from 1960-1980, an optimal design for the conveyance channel may be approximately 150 ft wide with a depth of 4.5 ft and a velocity of 2 ft/s. The channel dimensions and velocities predicted by the Julien regime equations differ greatly from the present design of the conveyance channel. The existing conveyance channel has a bottom width varying from 20 to 40 ft, 2 to 1 side slopes, depths ranging from 5 to 8 ft, and velocities of 5 to 10 ft/s. Costs for construction of such a wide channel as predicted by Julien's regime equations may be too expensive.
3. The possibility of operation of a one channel system through the delta similar to the existing river channel may prove the most feasible. Although artificial removal of sediment will be necessary, operation of a one channel system is easier from an operation and maintenance standpoint. The stable channel dimensions shown from the Julien regime relationship for the river channel are similar to actual measured data in the Middle Rio Grande in the headwaters of Elephant Butte Reservoir.

REFERENCES

- Julien, Pierre, 1988, Downstream Hydraulic Geometry of Alluvial Channels, Engineering Research Center, Colorado State University, Fort Collins, Colorado.
- Lagasse, Peter, 1981, "Geomorphic Response of the Rio Grande to Dam Construction," New Mexico Geologic Society Special Pub. 10, pp. 27-41.
- Mahmood, K., 1971, "Regime Concept of Sediment-Transporting Canals and River., Chapter 30 in River Mechanics, edited by Shen.
- Wargaladam, Jayamurni, 1993, Hydraulic Geometry Equations of Alluvial Channels, Pd. D. Dissertation, Colorado State University, Fort Collins, Colorado.

MODELING OF LONG TERM CHANGES OF UNSTABLE STREAMS

By Eddy J. Langendoen, Research Assistant Professor, Center for Computational Hydroscience and Engineering, University of Mississippi, University, Mississippi; Ronald L. Bingner, Agricultural Engineer; Roger A. Kuhnle, Research Hydraulic Engineer, USDA-ARS National Sedimentation Laboratory, Oxford, Mississippi

Abstract: Computer models may assist engineers in planning grade control structures and erosion control practices to reduce sediment yield from unstable watersheds. Bed and bank materials from channels largely contribute to the sediment yield. The numerical channel evolution model BEAMS is capable of predicting the long-term runoff of graded sediment through channel networks. BEAMS computes channel bed scour and fill, lateral erosion at the bank toe, and width adjustment due to mass wasting. Application of BEAMS to Goodwin Creek in northern Mississippi from a companion study indicates that BEAMS accurately predicts sediment yield.

INTRODUCTION

The dynamics and rate of stream channel adjustment to changes in the supply of water, sediment, and size of sediment are difficult to establish. Channels are transformed from one quasi-equilibrium state to another. Instream erosion control structures are commonly used to stabilize the channels and reduce sediment yield during this period of instability. Such is the case in the Demonstration Erosion Control (DEC) watersheds in the Yazoo river basin, Mississippi. Erosion control structures have a long-term impact, but there are no methods to adequately measure this impact on channels. Monitoring programs may take decades to collect sufficient data to determine the effectiveness of the remedial structures. Alternatively, numerical model simulations may assist long term evaluations of the structures, and may aid in determining the dimensions and location of new erosion control structures.

This paper describes efforts to develop a channel evolution model that is capable of predicting the response of stream networks to instream grade control structures and changes in the supply of sediments from upland areas in selected watersheds in the Yazoo river basin. Incised channel networks are extremely dynamic and tend to evolve toward a new state of equilibrium. Schumm *et al.* (1984), Harvey and Watson (1986), and Simon (1989) integrated their observations and earlier descriptions of the temporal development of unstable, incised channel systems to generate similar conceptual models of incised channel evolution. The models suggest that channels initially respond to base level lowering by deepening as knick points or zones migrate upstream. After bank heights exceed a critical threshold, rapid widening ensues. A successful channel evolution model therefore needs to include these processes.

The sediment transport model BEAMS (Bed and bank Erosion Analysis Model for Streams) has been developed for use in long-term (> 10 years) simulations of channel bed and bank processes. Combined with the landscape analysis model TOPAZ (Garbrecht and Martz, 1995), watershed model SWAT (Arnold *et al.*, 1993), and channel flow routing model DWAVNET (Langendoen, 1996), BEAMS forms the FRAME (Fluvial Routing Analysis and Modeling Environment) software. This paper presents the basic premise of BEAMS and results of model validation by simulating the morphology of Goodwin Creek Watershed channel network.

MODEL DESCRIPTION

BEAMS estimates stream degradation, aggradation, and widening in response to natural and man-induced changes within an ungaged watershed, and due to continuous storm water runoff. BEAMS includes two major submodels:

1. Sediment transport model performing routing of graded sediment, computing bed scour and fill, and hydraulic sorting. The local bed elevation changes are determined from the sediment continuity equation:

$$(1 - \lambda) \frac{\partial A_b}{\partial t} + \frac{\partial Q_s}{\partial x} + \frac{\partial AC_s}{\partial t} = q_s, \quad (1)$$

where A_b is volume of material stored in the bed per unit length, Q_s is total volumetric sediment discharge, A is flow area, C_s is total volumetric sediment concentration, q_s is total volumetric lateral inflow rate of sediment, λ is porosity of bed material, t is time, and x is longitudinal distance. The total volumetric sediment transport

rate Q_s is computed by the sediment transport predictor SEDTRA (Garbrecht *et al.*, 1995). Equation (1) is solved for each of the nine size classes represented by SEDTRA.

2. Bank erosion and stability model accounting for bank toe erosion and width adjustment due to mass wasting. Basal erosion is computed by the method of Osman and Thorne (1988) for cohesive soils. Mass wasting is computed by performing a slope stability analysis for steep banks assuming planar failure planes.

Sediment Transport Model: Equation (1) is discretized as

$$(1-\lambda) \frac{1-\psi}{\Delta t} \Delta A_{b_j} + (1-\lambda) \frac{\psi}{\Delta t} \Delta A_{b_{j+1}} - \frac{\theta}{\Delta x} \Delta Q_s + \left(\frac{1}{U\Delta t} + \frac{\theta}{\Delta x} \right) \Delta Q_{s,j+1} + \frac{1}{\Delta x} (Q_{s,j+1}^n - Q_{s_j}^n) = (1-\theta) q_{s,j+1}^n + \theta q_{s,j+1}^{n+1} \quad (2)$$

Subscript j indicates distance, superscript n indicates time, ψ and θ are spatial and temporal weighting factors, Δt is time step, and Δx is reach length. The third term on the left-hand side of Equation (1) was rewritten as $AC_s = Q_s/U$ in which U is a characteristic flow velocity. The symbol Δ represents the increment of the respective dependent variable from time level n to time level $n+1$, for example $\Delta A_{b_j} = A_{b_j}^{n+1} - A_{b_j}^n$.

The mixing layer concept introduced by Hirano (1971) is used to model the response of channel beds to imposed changes in the supply of sediments. Material exchanges between the mixing layer and the substrate when the bed aggrades or degrades; the substrate being either a disturbed layer of previously deposited material or the undisturbed sediment. This is formulated as

$$\begin{aligned} \text{mixing layer : } \quad & \frac{\partial \beta_k A_m}{\partial t} = \beta_k^* \left(\frac{\partial A_m}{\partial t} - \frac{\partial A_b}{\partial t} \right) + \frac{\partial A_{b_k}}{\partial t} \\ \text{subsurface layer : } \quad & \frac{\partial \beta_k^s A_s}{\partial t} = -\beta_k^* \left(\frac{\partial A_m}{\partial t} - \frac{\partial A_b}{\partial t} \right) \end{aligned} \quad (3)$$

where β_k is the fractional content of grain-size class k in the mixing layer, A_m is the volume of material stored in the mixing layer per unit length, A_s is the volume of material stored in the disturbed layer per unit length, β_k^s is the fractional content of grain-size class k in the disturbed layer, and β_k^* is β_k in case of aggradation and β_k^s in case of degradation.

Bank Erosion and Stability Model: The channel width adjustment model accounts for the combined effects of lateral erosion and mass instability. It is based on a slightly modified approach of Osman and Thorne (1988) for cohesive soils. This approach determines a critical shear stress and initial rate of soil erosion. Once the shear stress exerted by the flow on the bank toe surpasses the critical shear stress, the lateral erosion distance can be computed. BEAMS transforms the lateral erosion distance because of restrictions on the geometrical representation of cross sections imposed by BEAMS, see Figure 1a. The eroded bank material is added to the lateral sediment discharge.

The mass stability of the bank is calculated using a static equilibrium analysis of slab-type failure. A factor of safety, $FS = \text{Resisting Force}/\text{Driving Force}$, is computed. It is assumed that the bank fails when $FS < 1$. Following mass failure, debris accumulates at the bank toe in a conceptual storage. The debris is removed by lateral erosion prior to further oversteepening or degradation generating further mass failures.

Cross Section: The channel cross section changes due to scouring or filling of the bed, lateral erosion at the toe of the bank, and mass wasting. Figures 1b and 1c show how the cross section is updated in the case when the channel is aggrading and degrading, respectively. To prevent bank material from entering the flow, bank angles are kept constant and new bed coordinates are computed from the calculated ΔA_b . If the channel is degrading then bed slope remains constant, whereas for aggrading channels the thalweg is filled first. The previous section discussed updating the cross section in case of lateral erosion at the bank toe. Figure 1a shows that in case of inclined beds, no bed material will enter the flow in case of lateral erosion. In case of bank failure, the new bank angle is that of the failure plane angle, and new coordinates at the top of the bank are computed.

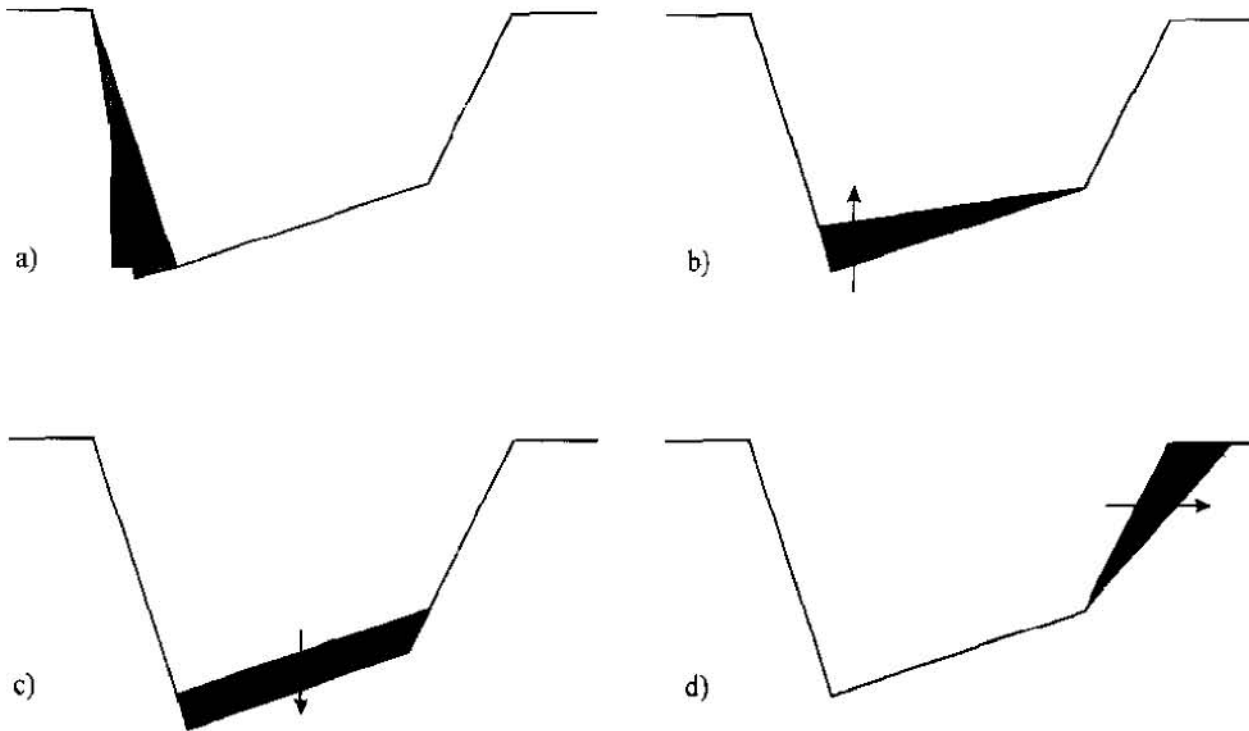


Figure 1 Sketch of cross section change due to (eroded material is shaded): a) lateral erosion at the toe of the bank, the originally eroded bank material has a dark shading, whereas the modified eroded bank material has a light shading; b) filling of bed; c) scouring of bed; and d) mass wasting.

Hydraulic Structure: Hydraulic structures affect the movement of sediment through the network. The upstream invert of structures is generally elevated above the channel bed. Structures may therefore obstruct the passage of sediment through or over them. BEAMS assumes that sediment transported in suspension will pass the structure, whereas the sediment transported as bed load will deposit upstream of the structure if the structure invert is above the bed. Because BEAMS employs total load formulations it uses the following criterion to determine whether a grain-size class is transported as suspended or bed load: if $u_* / \omega_k < 2$, where u_* is shear velocity and ω_k is particle fall velocity of size class k , the material of size class k belongs to the bed load, otherwise it is part of the suspended load.

Computational Sequence: BEAMS employs the following computational sequence:

- ↳ Loop over storm events.
 - ↳ Loop over time steps within a storm event.
 - ▶ Add sediment runoff from fields to q_s .
 - ▶ Compute volume of lateral erosion and add to q_s .
 - ▶ Compute sediment transport capacity Q_s .
 - ▶ Compute volume of sediment to scour from or deposit on the bed ΔA_b .
 - ▶ Determine bed material compositions β and β^s .
 - ▶ Update cross section.
 - ↳ End
 - ▶ Carry out slope stability analysis.
- ↳ End

MODEL APPLICATION

Goodwin Creek: The channel network of the 21.3 km² experimental watershed Goodwin Creek in northern Mississippi

was used to evaluate BEAMS (Figure 2). Fourteen hydraulic structures are present in the channel network: ten measuring flumes which act as grade control structures and four culverts. The computational mesh consists of 279 nodes; confluences and structures being represented by three nodes. Geometries of 86 cross sections are available from surveys conducted in 1977 by the Corps of Engineers. Bed slopes vary from 0.035 to 7.9 percent.

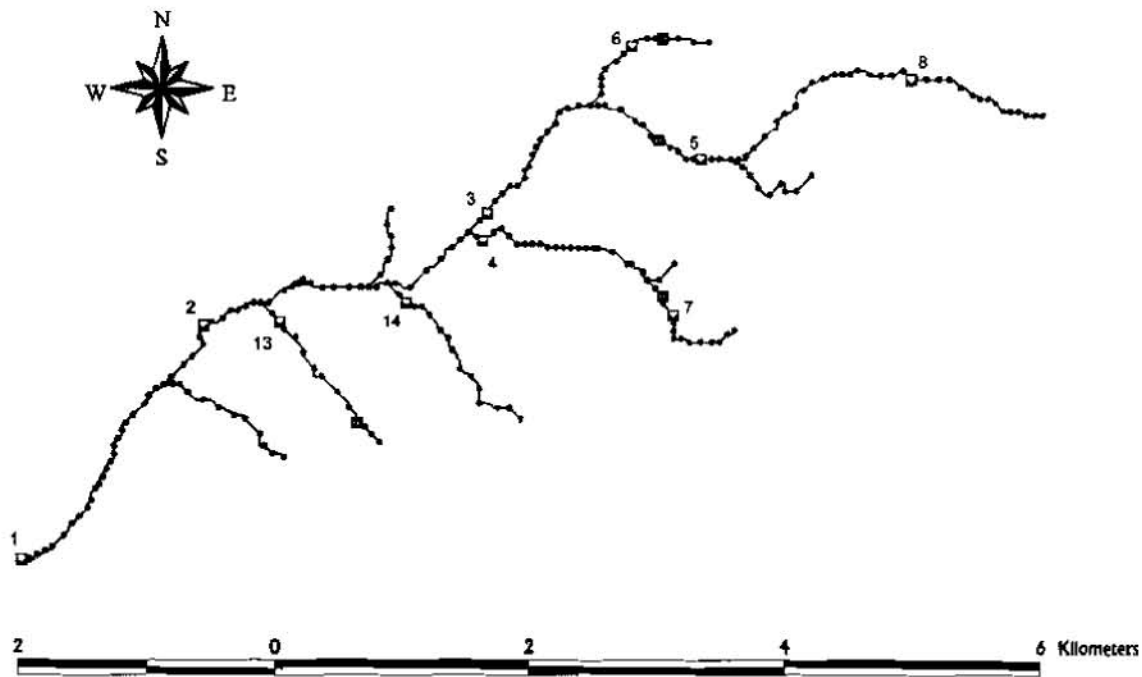


Figure 2 Channel network of Goodwin Creek Watershed, MS modeled by BEAMS. Culverts and measuring flumes are shown. The measuring flume numbers are shown next to the respective flumes.

Using data from the watershed model SWAT and the unsteady flow model DWAVNET, the evolution of the Goodwin Creek channel network was simulated from January 1, 1978 through December 31, 1995 using measured storm event rainfall. The simulation includes 1662 storm events. Storm events on Goodwin Creek during this period are defined as the continuous rainfall that occurs and separated from other rainfall by more than six hours. The average annual rainfall was 1460 mm, with the greatest amount of rainfall occurring during the spring months of the year. Most of the channels are ephemeral, with perennial flows occurring only in the lower reaches of the main channel.

Bed material composition for the channel network was not known at January 1, 1978. Therefore, data sampled in 1994 were used (Kuhnle, 1996). Median grain diameter of the bed material ranged from 0.5–7.4 mm over the watershed.

The bed material in the upper reaches of the watershed is predominantly composed of sand ($D_{50} = 0.5$ mm). In the central parts of the watershed, there are many sources of gravel and the size of the bed material coarsens. In the last three kilometers of the main channel, there are no major tributaries and the median size of the bed material decreases from 7 mm to 1 mm. Sources of sand and gravel to the channels originate from gullying in some of the upland parts of the watershed and bank erosion in the channels. Bank material properties comprised of friction angle, cohesion, dry bulk unit weight, and particle size distribution were obtained from studies by Little *et al.* (1982) and using Iowa Borehole Shear testing procedures (Lohnes and Handy, 1968) at selected sites within Goodwin Creek Watershed.

Results and Discussion: Figure 3 plots predicted profiles of the thalweg of the last three kilometers of Goodwin Creek between flumes 1 and 2. Figure 4 shows simulated changes in cross-sectional area along the same reach. Figures 5a through c show the evolutions of cross sections at 1945 m, 1285 m, and 435 m upstream of flume 1, respectively. The largest variations occur within the first eight years. After 1986 the channel appears to be in dynamic equilibrium. The general trend is: 1) enlarging channel downstream of flume 2; 2) channel fill approximately 1 km upstream of flume 1; and 3) enlarging channel upstream of flume 1.

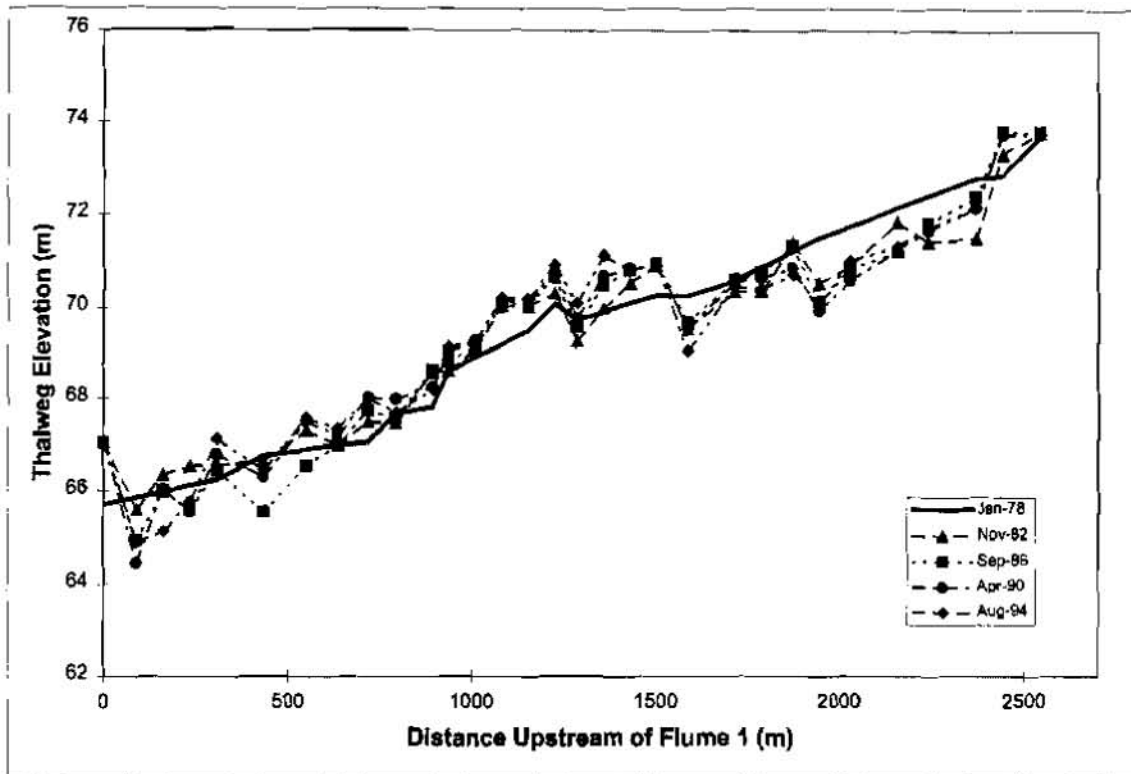


Figure 3 Evolution of thalweg profile along Goodwin Creek between flumes 1 and 2.

The loss of sediment is mainly caused by degradation. The cross sections do not show much lateral erosion. Some widening is observed at 1945 m upstream of flume 1 (Figure 5a), but is mainly caused by the extent of incision. The net loss (e.g., Figure 5b) or fill of sediment in a cross section is due to combined deposition and scouring of the bed. In general, degradation occurs when a flood wave is advancing, whereas aggradation occurs when a flood wave is subsiding.

Murphey and Grissinger (1985) observed the following channel responses to the installation of the measuring flumes in Goodwin Creek: 1) in general, reaches below flumes degraded; 2) those above flumes either aggraded or showed little response; 3) bendways eroded a great deal; but 4) straight reaches did not. The predicted cross-section changes reflect the above observations. Additionally, results obtained using BEAMS by Bingner *et al.* (1998) show the model accurately predicts total and fine sediment yield along with other channel evolution changes throughout Goodwin Creek.

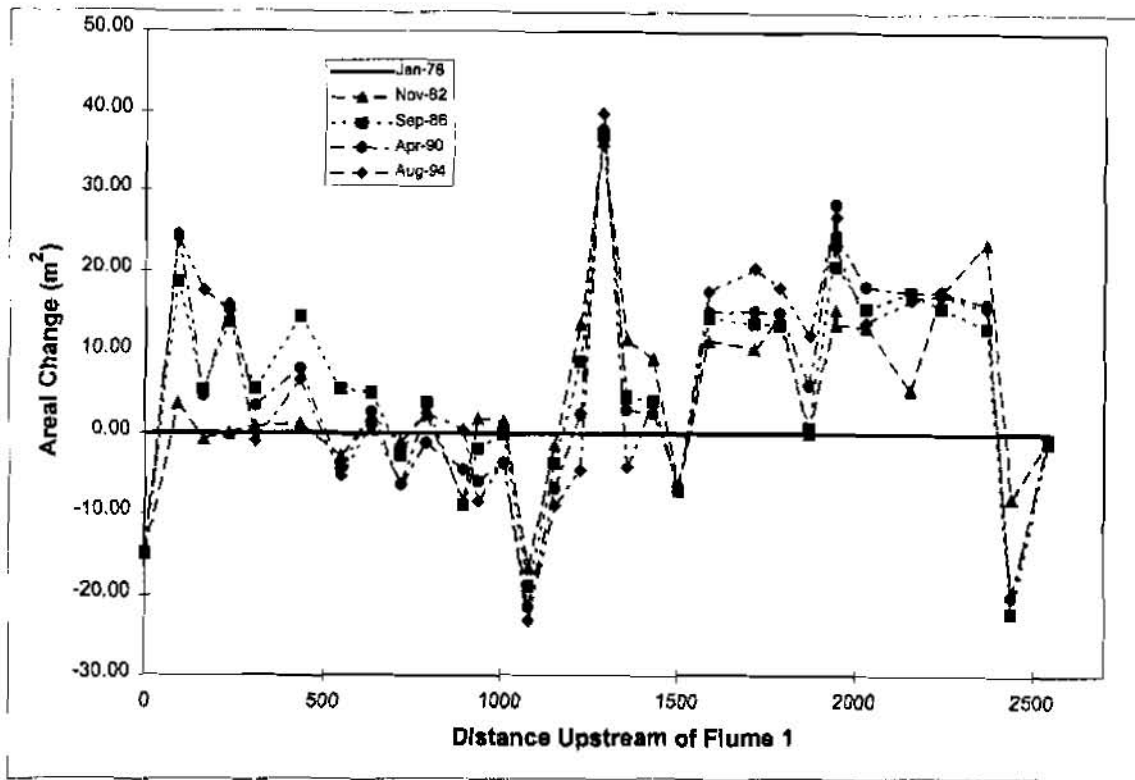


Figure 4 Changes in channel cross section area along Goodwin Creek between flumes 1 and 2.

CONCLUSIONS

The sediment transport model BEAMS is able to simulate evolution trends of channels affected by instream structures. Simplifying assumptions of equilibrium sediment transport, straight channels, lateral erosion being distributed over the entire flow depth, and planar bank failure, among others reduce the model complexity of the integrated processes. Because of large longitudinal variations in cross-sectional area, results show that narrow cross sections are susceptible to scour, whereas wide cross sections are susceptible to deposition of sediment. Further, migration of bendways can significantly contribute to the sediment yield of a watershed. Therefore, efforts are ongoing to implement a non-equilibrium sediment transport model to improve the transport of fines and sand, and to simulate planform changes.

ACKNOWLEDGMENTS

This work is a result of research sponsored by the USDA Agricultural Research Service under specific Cooperative Agreement No. 6408-13000-008-01S (monitored by the USDA-ARS National Sedimentation Laboratory) and the University of Mississippi. The work was carried out jointly by the Center for Computational Hydroscience and Engineering, The University of Mississippi and the USDA-ARS National Sedimentation Laboratory.

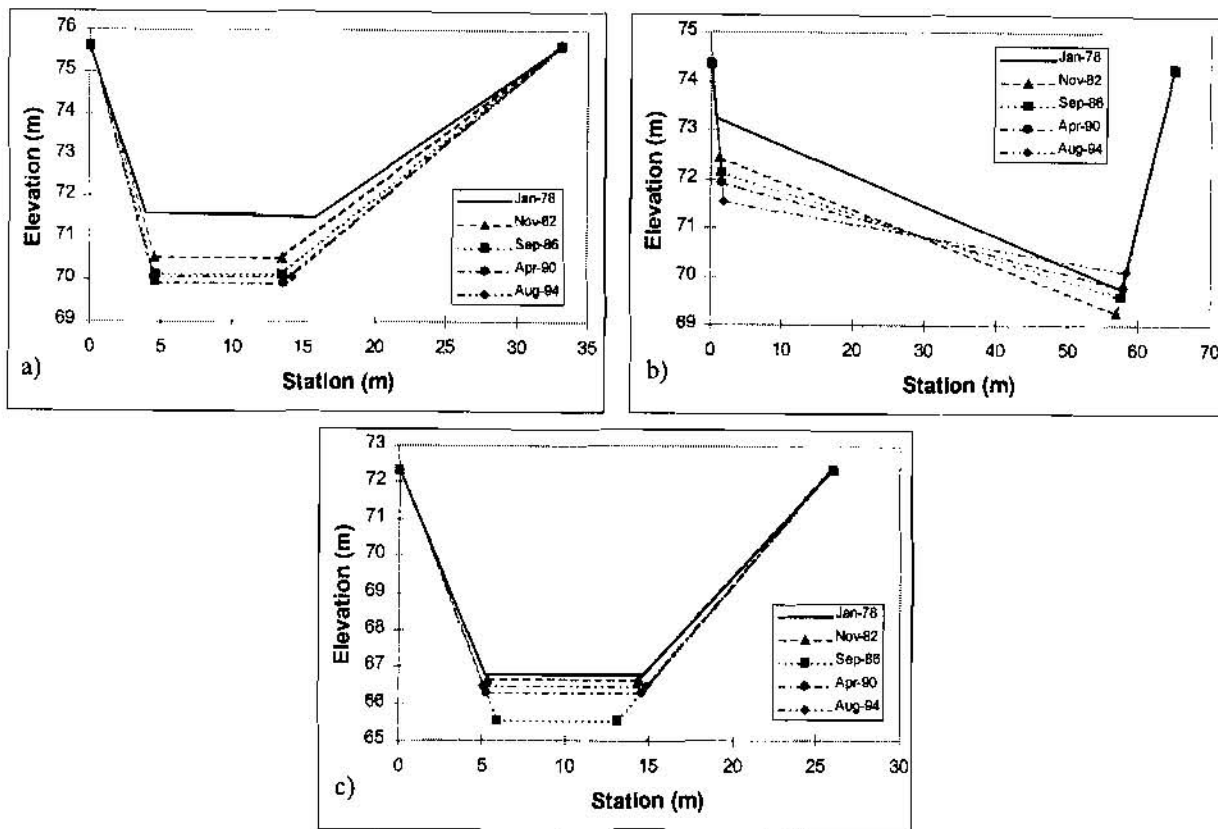


Figure 5 Evolution of channel cross sections: a) 1945 m, b) 1285 m, and c) 435 m upstream of flume 1.

REFERENCES

- Arnold, J. G., Allen, P. M., Bernhardt, G., 1993, A Comprehensive Surface-Groundwater Flow Model. *Journal of Hydrology* 142, 47-69.
- Bingner, R. L., Langendoen, E. J., Alonso, C. V., 1998, Development And Application Of A Watershed Evaluation Model Incorporating Incised Channel Processes. *Proceedings of the First Federal Interagency Hydrologic Modeling Conference, Las Vegas, NV.*
- Garbrecht, J., Kuhnle, R. A., Alonso, C. V., 1995, A Sediment Transport Formulation for Large Channel Networks. *Journal of Soil and Water Conservation* 50(5), 527-529.
- Garbrecht, J., Martz, L. W., 1995, An Automated Digital Landscape Analysis Tool for Topographic Evaluation, Drainage Identification, Watershed Segmentation and Subcatchment Parameterization. Report No. NAWQL 95-1, National Agricultural Water Quality Laboratory, USDA-ARS, Durant, Oklahoma.
- Harvey, M. D., Watson, C. C., 1986, Fluvial Processes and Morphological Thresholds in Incised Channel Restoration. *Water Resources Bulletin* 22, 359-368.
- Hirano, M., 1971, Riverbed Degradation with Armoring. *Proceedings Japanese Society of Civil Engineers* 195, 55-65.
- Kuhnle, R. A., 1996, Variations in Bed Material Size on Goodwin Creek. *Proceedings of the Sixth Federal Interagency Sedimentation Conference, Las Vegas, Nevada, II-68-II-74.*
- Langendoen, E. J., 1996, Discretization Diffusion Wave Model. Tech. Rep. No. CCHE-TR-96-1, Center for Computational Hydroscience and Engineering, The University of Mississippi, University, Mississippi.
- Little, W. C., Thorne, C. R., Murphey, J. B., 1982, Mass Bank Failure Analysis of Selected Yazoo Basin Streams. *Transactions of the ASAE* 25(5), 1321-1328.
- Lohnes, R. A., Handy, R. L., 1968, Slope Angles in Friable Loess. *Journal of Geology* 76, 247-258.
- Murphey, J. B., Grissinger, E. H., 1985, Channel Cross-Section Changes in Mississippi's Goodwin Creek. *Journal of Soil and Water Conservation* 40, 148-153.
- Osman, A. M., Thorne, C. R., 1988, Riverbank Stability Analysis. I: Theory. *Journal of Hydraulic Engineering* 114,

134-150.

Schumm, S. A., Harvey, M. D., Watson, C. C., 1984, *Incised Channels: Morphology, Dynamics, and Control*. Water Resources Publications, Littleton, Colorado.

Simon, A., 1989, The Discharge of Sediment in Channelized Alluvial Streams. *Water Resources Bulletin* 25, 1177-1188.

NUMERICAL SIMULATIONS OF SCOUR AND DEPOSITION IN A CHANNEL NETWORK

Authors : Hong-Yuan Lee, Commissioner, Water Resource Dept., Taiwan Provincial Government, Taichung, Taiwan, R.O.C. ; Hui-Ming Hsieh, Researcher, Disaster Prevention Research Center, National Cheng Kung Univ. Tainan, Taiwan, R.O.C. ; Sen-Yuan Lee, Graduate Student, Dept. of Civil Eng., National Taiwan Univ., Taipei, Taiwan, R.O.C. ; Jinn-Chuang Yang Prof., Dept. of Civil Eng., National Chiao Tung Univ., Hsinchu, Taiwan, R.O.C. ; Chih Ted Yang, Group Manager, Sedimentation and River Hydraulics, U.S. Bureau of Reclamation, Denver, CO 80225, U.S.A.

INTRODUCTION

A numerical model, which is capable of simulating scouring and deposition behaviors in a channel network, is developed in this study. The model adopts the stream tube concepts of GSTARS and USTARS, and hence is able to reflect the lateral variations of the channel cross section. It also treats suspended load and bed load separately and hence is able to simulate the deposition behaviors of the suspended sediment under a non-equilibrium process. The model solves the de Saint Venant equation, and thus can be applied in both steady and unsteady flow conditions. An internal boundary condition basing on the sediment transport capacity was proposed to distribute the incoming sediment load into the downstream links. The proposed measure is feasible based on cases study results. An assessment of this model's performance has been conducted through a comparison to an analytical solution. The application of this model to the Tanhsui river system in Taiwan and several hydraulic model studies also gave very convincing results.

THEORETICAL BASIS AND GOVERNING EQUATIONS

Stream tubes are imaginary tubes bounded by streamlines. Since the velocity vectors are tangential to the streamlines, no connective exchange occurs across streamlines. In this study, a one-dimensional hydrodynamic calculation is performed first to determine the hydraulic characteristics of the full channel cross-section, and then the channel is divided into a certain number of subsections or stream tubes within a section based on the principle of equal conveyance. The mobile-bed computation is then performed in each tube to calculate the channel bed evolutions, and hence it is able to reflect the lateral variations of channel cross-sections. The boundaries of the stream tubes are recomputed in every time step to reflect the uneven movement of the sediment particles in different tubes and lateral variations of the channel geometry.

Equations for Hydraulic Routing : The de Saint Venant equations are used in the unsteady flow computation. These include a continuity equation and a one-dimensional momentum equation.

$$\frac{\partial A}{\partial t} + \frac{\partial Q}{\partial x} = q \quad (1)$$

$$\frac{\partial Q}{\partial t} + \frac{\partial}{\partial x} \left(\beta \frac{Q^2}{A} \right) + gA \frac{\partial y}{\partial x} + gAS_f - \frac{Q}{A} q = 0 \quad (2)$$

where A = channel cross-sectional area; Q = flow discharge; t = time; x = coordinate in the flow direction; q = lateral inflow/outflow discharge per unit length; β = momentum correction coefficient; g = gravitational acceleration; y = water surface elevation; $S_f = Q|Q|/K^2$ = friction slope; $K = \frac{1}{n} AR^x$ = channel conveyance; n = roughness coefficient of Manning's formula and R = hydraulic radius.

Equations for Sediment Routing : The governing equations include a sediment continuity equation, a sediment concentration convection-diffusion equation and a bed load equation. The Rouse number $W/\kappa u_* = 5$, where W = fall velocity, κ = Karman's constant and u_* = shear velocity, is used to distinguish between bed load and suspended load. The sediment continuity equation is given as :

$$(1 - \beta) \frac{\partial A_{d,t}}{\partial t} + \frac{\partial}{\partial x} \sum_{k=1}^{N_{size}} q_k C_k + \frac{\partial Q_b}{\partial x} = 0 \quad (3)$$

where Q_b = bed load transport rate in the stream tube; q_k = flow discharge in the stream tube and C_k = depth-averaged concentration of the suspended sediment of size fraction k in the stream tube. The concentration C_k is calculated using the convection-diffusion equation shown as :

$$\frac{\partial (C_k A_i)}{\partial t} + \frac{\partial}{\partial x} (C_k q_i) = \frac{\partial}{\partial x} \left(A_i k_x \frac{\partial C_k}{\partial x} \right) + S_k + h k_z \frac{\partial C_k}{\partial z} \Big|_r^l \quad (4)$$

where k_x and k_z = longitudinal and transverse dispersion coefficients; A_i = area across the stream tube; h = flow depth; S_k = source term of the suspended sediment of size fraction k , and r and l = right and left boundaries of the stream tube. According to Van Rijn (1984) and Holly and Rahuel (1990), the source term S_k is the combination of deposition and resuspension, and can be expressed as :

$$S_k = S_{rk} + S_{dk} = a - b C_k \quad (5)$$

where S_{rk} and S_{dk} are the quantities of sediment resuspension and deposition, respectively. The bed load transport rate Q_b can be calculated using the following equation :

$$Q_b = \int_r^l q_b dB \quad (6)$$

where q_b = bed load discharge/unit width, which is calculated using Meyer-Peter and Muller formula.

Armoring Scheme : Most river beds consist of grains with a broad size fraction. Updating the bed composition at every time step is necessary and very crucial to a sediment routing model. Various techniques dealing with bed composition variation have been proposed. In this article, the model adopts the conventional sorting and armoring techniques which were proposed by Bennet and Nordin (1977). In that model the bed is divided into several layers, and bed deposition accounting is accomplished through the use of two or three armor layers depending on whether scouring or deposition occurs at the cross section during the time step.

COMPUTATIONAL PROCEDURES

The simulation processes consist of three parts in every time step, i.e., flow computations, stream tube computations, and sediment routing. Flow computation is performed first to provide the basis for determining tube boundaries. Then, sediment routing is performed for each stream tube to calculate the amount of channel bed variations. These procedures are described sequentially in the following sections.

Hydraulic Routing : Eqs.1 and 2 are transformed into difference equations using a Preissmann four points finite difference scheme. The difference equations are :

$$\frac{\phi}{\Delta t} (A_{i+1}^{n+1} - A_{i+1}^n) + \frac{(1-\phi)}{\Delta t} (A_i^{n+1} - A_i^n) + \frac{\theta}{\Delta x} (Q_{i+1}^{n+1} - Q_i^{n+1}) + \frac{(1-\theta)}{\Delta x} (Q_{i+1}^n - Q_i^n) - q_i = 0 \quad (7)$$

$$\begin{aligned} & \frac{\phi}{\Delta t} [Q_{i+1}^{n+1} - Q_{i+1}^n] + \frac{1-\phi}{\Delta t} [Q_i^{n+1} - Q_i^n] + 2 \left[\alpha \theta \left[(1-\phi) \frac{Q_i^{n+1}}{A_i^{n+1}} + \phi \frac{Q_{i+1}^{n+1}}{A_{i+1}^{n+1}} \right] + \alpha (1-\theta) \left[(1-\phi) \frac{Q_i^n}{A_i^n} + \phi \frac{Q_{i+1}^n}{A_{i+1}^n} \right] \right] \\ & \left[\frac{\theta}{\Delta x} [Q_{i+1}^{n+1} - Q_i^{n+1}] + \frac{1-\theta}{\Delta x} [Q_{i+1}^n - Q_i^n] - \alpha \left[\theta \left[(1-\phi) \frac{Q_i^{n+1}}{A_i^{n+1}} + \phi \frac{Q_{i+1}^{n+1}}{A_{i+1}^{n+1}} \right]^2 + (1-\theta) \left[(1-\phi) \frac{Q_i^n}{A_i^n} + \phi \frac{Q_{i+1}^n}{A_{i+1}^n} \right]^2 \right] \right] \\ & \left[\frac{\theta}{\Delta x} [A_{i+1}^{n+1} - A_i^{n+1}] + \frac{1-\theta}{\Delta x} [A_{i+1}^n - A_i^n] \right] + g \left[\theta \left[(1-\phi) A_i^{n+1} + \phi A_{i+1}^{n+1} \right] + (1-\theta) \left[(1-\phi) A_i^n + \phi A_{i+1}^n \right] \right] \\ & \left[\frac{\theta}{\Delta x} [y_{i+1}^{n+1} - y_i^{n+1}] + \frac{1-\theta}{\Delta x} [y_{i+1}^n - y_i^n] \right] + g \left[\theta \left[(1-\phi) A_i^{n+1} + \phi A_{i+1}^{n+1} \right] + (1-\theta) \left[(1-\phi) A_i^n + \phi A_{i+1}^n \right] \right] \\ & \left\{ \theta \left[\beta \frac{Q_i^{n+1} |Q_i^{n+1}|}{(K_i^{n+1})^3} + (1-\beta) \frac{Q_{i+1}^{n+1} |Q_{i+1}^{n+1}|}{(K_{i+1}^{n+1})^3} \right] \right\} + \left\{ (1-\theta) \left[\beta \frac{Q_i^n |Q_i^n|}{(K_i^n)^3} + (1-\beta) \frac{Q_{i+1}^n |Q_{i+1}^n|}{(K_{i+1}^n)^3} \right] \right\} \\ & - \left\{ \theta \left[(1-\phi) \frac{Q_i^{n+1}}{A_i^{n+1}} + \phi \frac{Q_{i+1}^{n+1}}{A_{i+1}^{n+1}} \right] + (1-\theta) \left[(1-\phi) \frac{Q_i^n}{A_i^n} + \phi \frac{Q_{i+1}^n}{A_{i+1}^n} \right] \right\} q_i = 0 \end{aligned} \quad (8)$$

where ϕ and θ are the weighting factors of space and time, respectively, and the subscripts i and $i+1$ represent the downstream and upstream ends of the simulated reach, respectively.

Stream Tube Computation : The algorithm for stream tube computation used for this model is same as that of the GSTARS model developed by Molinas and Yang (1986). Following the initial flow computations at each computational point, stream tube locations across the channel satisfying equal conveyance requirements can be determined. After the number and the location of stream tubes are known, the sediment routing procedure is carried out for each tube along the channel at each time step.

Sediment Routing : The difference equation for the sediment continuity equation, i.e., Eq.3, is shown as :

$$\Delta Z_i = \frac{-4\Delta t}{(1-p)(2P_i + P_{i+1} + P_{i-1})} \cdot \frac{\sum_{k=1}^{N_{st}} [qC_k]_{k,t} - \sum_{k=1}^{N_{st}} [qC_k]_{k,t-1} + Q_{b,k,t} - Q_{b,k,t-1} - q_{st,k,t}\Delta X_i}{(\Delta X_i - \Delta X_{i-1})/2} \quad (9)$$

where ΔZ_i = variation of the bed elevation for every size fraction and P_i = wetted parameter. The concentration C_i is obtained by solving the convection-diffusion equation, i.e., Eq.4. The split operator approach is used in solving this equation. The governing equation is separated into four portions, i.e., advection, longitudinal diffusion, transverse diffusion and reaction. They are solved subsequently in one time step. The C_i and CX_i values, where $CX_i = \partial C_i / \partial x$, obtained in the previous computation are served as the known values for the next computation. The computational techniques are described as the following : (To simplify the expression, C_i is replaced by C from here on.)

Advection-step : The advection portion of Eq.4 can be written as :

$$\frac{\partial C}{\partial t} + U \frac{\partial C}{\partial x} = 0 \quad (10)$$

where U = average velocity. Using the Holly-Preissmann two-point four-order scheme, the difference equation of Eq.10 can be obtained, when the Courant Number, $U\Delta t / \Delta x$ is less than 1 :

$$C_{i+1}^{n+1} = C_i^n = a_1 C_i^n + a_2 C_{i+1}^n + a_3 CX_i^n + a_4 CX_{i+1}^n \quad (11)$$

$$a_1 = r'^2(3 - 2r') ; a_2 = 1 - a_1 ; a_3 = r'^2(1 - r')\Delta x ; a_4 = -r'(1 - r')^2 \Delta x ; r' = \frac{U_i^n \Delta t}{\Delta x}$$

Differentiating Eq.10 with respect to x , the difference equation thus obtained is :

$$CX_{i+1}^{n+1} = CX_i^n \frac{1 - \frac{\Delta t}{2} \frac{\partial U}{\partial x} \Big|_{i,t'}}{1 + \frac{\Delta t}{2} \frac{\partial U}{\partial x} \Big|_{i+1,t^{n+1}}} \quad (12)$$

$$CX_i^n = b_1 C_i^n + b_2 C_{i+1}^n + b_3 CX_i^n + b_4 CX_{i+1}^n ; b_1 = \frac{6r'(r'-1)}{\Delta x} ; b_2 = -b_1 ; b_3 = r'(3r'-2) ; b_4 = (r'-1)(3r'-1)$$

When Courant Number is greater than 1, Eq.10 can be written in a different form :

$$C_{i+1}^{n+1} = C_i^n = A_1 C_i^n + A_2 C_{i+1}^{n+1} + A_3 CX_i^n + A_4 CX_{i+1}^{n+1} \quad (13)$$

$$A_1 = s'^2(3 - 2s') ; A_2 = 1 - A_1 ; A_3 = -U_i^n s'^2(1 - s')\Delta t ; A_4 = U_{i+1}^{n+1} s'(1 - s')^2 \Delta t ; s' = \frac{U_{i+1}^{n+1} - U_i^n}{\Delta t}$$

Differentiating Eq.14 with respect to t , and then transforming CT to CX , the difference equation becomes :

$$CX_{i+1}^{n+1} = CX_i^n \frac{U_i^n + \frac{s'\Delta t}{2} \frac{\partial U}{\partial t} \Big|_{i,t'}}{U_{i+1}^{n+1} - \frac{s'\Delta t}{2} \frac{\partial U}{\partial t} \Big|_{i+1,t^{n+1}}} \quad (14)$$

$$CX_i^n = B_1 C_i^n + B_2 C_{i+1}^{n+1} + B_3 CX_i^n + B_4 CX_{i+1}^{n+1}$$

$$B_1 = \frac{6s'(s'-1)}{\Delta t U_i^n} ; B_2 = -B_1 ; B_3 = \frac{U_i^n}{U_i^n} s'(3s'-2) ; B_4 = \frac{U_{i+1}^{n+1}}{U_i^n} (s'-1)(3s'-1)$$

Longitudinal diffusion step : The longitudinal diffusion portion of Eq.4 can be written as :

$$\frac{\partial C}{\partial t} - \frac{1}{A} \frac{\partial}{\partial x} \left(A k_x \frac{\partial C}{\partial x} \right) = 0 \quad (15)$$

Using the Tee Scheme finite difference method, Eq.15 can be discretized as :

$$C_i^{n+1} - C_i^n = f_1 [C_{i+1}^{n+1} - C_i^{n+1}] - f_2 [C_i^{n+1} - C_{i-1}^{n+1}] \quad (16)$$

$$f_1 = \frac{\Delta t}{\frac{1}{2}(x_{i+1} - x_{i-1})A_i} \frac{\left[\frac{1}{2}(A_i k_{x,i} + A_{i+1} k_{x,i+1}) \right]}{(x_{i+1} - x_i)} ; \quad f_2 = \frac{\Delta t}{\frac{1}{2}(x_{i+1} - x_{i-1})A_i} \frac{\left[\frac{1}{2}(A_i k_{x,i} + A_{i-1} k_{x,i-1}) \right]}{(x_i - x_{i-1})}$$

Differentiating Eq.15 with respect to x , and then using the Tee scheme, the difference equation becomes :

$$CX_i^{n+1} - CX_i^n = g_1 CX_{i+1}^{n+1} - (g_2 + g_3) CX_i^{n+1} + g_4 CX_{i-1}^{n+1} \quad (17)$$

$$g_1 = \frac{\Delta t}{\frac{1}{2}(A_{i+1} + A_i)} \frac{A_{i+1} k_{x,i+1}}{\frac{1}{2}(x_{i+1} - x_{i-1}) \cdot (x_{i+1} - x_i)} ; \quad g_2 = \frac{\Delta t}{\frac{1}{2}(A_{i+1} + A_i)} \frac{A_i k_{x,i}}{\frac{1}{2}(x_{i+1} - x_{i-1}) \cdot (x_{i+1} - x_i)} ;$$

$$g_3 = \frac{\Delta t}{\frac{1}{2}(A_{i-1} + A_i)} \frac{A_i k_{x,i}}{\frac{1}{2}(x_{i+1} - x_{i-1}) \cdot (x_i - x_{i-1})} ; \quad g_4 = \frac{\Delta t}{\frac{1}{2}(A_{i-1} + A_i)} \frac{A_{i-1} k_{x,i-1}}{\frac{1}{2}(x_{i+1} - x_{i-1}) \cdot (x_i - x_{i-1})}$$

The values of C and CX can be obtained by using Gaussian elimination method to solve the tri-diagonal matrix formed by Eqs.16 and 17.

Transverse-diffusion step : The transverse-diffusion portion of Eq.4 can be written as :

$$\frac{\partial C}{\partial t} = \frac{1}{A} \left(h k_z \frac{\partial C}{\partial z} \right) \quad (18)$$

Using the same method as shown for the longitudinal diffusion step, Eq.18 can be discretized as :

$$C_{i,j}^{n+1} - C_{i,j}^n = r_1 [C_{i,j+1}^{n+1} - C_{i,j}^{n+1}] - r_2 [C_{i,j}^{n+1} - C_{i,j-1}^{n+1}] \quad (19)$$

$$r_1 = \frac{\Delta t}{\frac{1}{2}(A_{i,j+1} - A_{i,j})} \frac{\left[\frac{1}{2}(h_{i,j} k_{z,i,j} + h_{i,j+1} k_{z,i,j+1}) \right]}{(z_{i,j+1} - z_{i,j})} ; \quad r_2 = \frac{\Delta t}{\frac{1}{2}(A_{i,j+1} - A_{i,j})} \frac{\left[\frac{1}{2}(h_{i,j} k_{z,i,j} + h_{i,j-1} k_{z,i,j-1}) \right]}{(z_{i,j} - z_{i,j-1})}$$

Differentiating Eq.18 with respect to x , and then using the Tee scheme, the difference equation is shown as :

$$-r_1 \cdot CX_{i,j+1}^{n+1} + (r_1 + r_2 + 1) CX_{i,j}^{n+1} - r_2 CX_{i,j-1}^{n+1} = CX_{i,j}^n + q_1 + q_2 \quad (20)$$

$$q_1 = -\frac{(A_{i+1,j} - A_{i,j})}{\Delta x} \cdot \frac{1}{A_{i,j}} \left[r_1 (C_{i,j+1}^{n+1} - C_{i,j}^{n+1}) - r_2 (C_{i,j}^{n+1} - C_{i,j-1}^{n+1}) \right] ;$$

$$q_2 = -\frac{h_{i+1,j} k_{z,i+1,j} - h_{i,j} k_{z,i,j}}{\Delta x} \cdot \frac{1}{(h_{i,j} k_{z,i,j})} \left[r_1 (C_{i,j+1}^{n+1} - C_{i,j}^{n+1}) - r_2 (C_{i,j}^{n+1} - C_{i,j-1}^{n+1}) \right]$$

The values of C and CX can be obtained by using Gaussian elimination method to solve the tri-diagonal matrix formed by Eqs.19 and 20.

Reaction step : The reaction portion of Eq.4 is shown as :

$$\frac{\partial C}{\partial t} = a_p - b_p C \quad (21)$$

where $a_p = a/A$ and $b_p = b/A$. There exists an analytical solution for Eq.21, and shown as :

$$C_i^{n+1} = \frac{a_p}{b_p} + \left(C_i^n - \frac{a_p}{b_p} \right) e^{-b_p \Delta t} \quad (22)$$

Differentiating Eq.21 with respect to x and the difference expression form for CX_i^{n+1} becomes :

$$CX_i^{n+1} = \frac{1}{(1 + b_p \Delta t)} \left[CX_i^n + \left(\frac{a_{p,i} - a_{p,i-1}}{\Delta x} \right) \Delta t - \left(\frac{b_{p,i} - b_{p,i-1}}{\Delta x} \cdot C_i^{n+1} \right) \Delta t \right] \quad (23)$$

NETWORK ALGORITHM AND BOUNDARY CONDITIONS

The definition sketch of the channel network is shown in Fig.1, where the computational point represents the

channel cross section, the reach is the path between two computational points, the node is the junction of the river tributaries and the link represents the flow path between two nodes. The network algorithms adopted in this model is similar to those of CHARIMA(Holly et al., 1990) with modification on sediment treatment and some numerical schemes. It consists of two portions, namely, hydraulic computation and sediment routing, are discussed separately as follows.

Hydraulic Routing : The flow discharge at the nodal point has to satisfy the continuity equation, i.e., the summation of the inflow and outflow discharges from all the tributaries at a nodal point must be zero, or there is no storage at the nodal point. The node continuity equation is :

$$Q_m^{n+1} + \sum_{j=1}^{L(m)} Q_{m,j}^{n+1} = 0, \quad m = 1, 2, \dots, M \quad (24)$$

where $L(m)$ = number of the links at node m , M = number of the nodes, j = identity of the links, Q_m^{n+1} = discharge at node m during time $n+1$ and $Q_{m,j}^{n+1}$ = discharge from link j . The network algorithm for the hydraulic routing used for this model is same as that of CHARIMA model developed by Holly et al. It comprises three phases for each iteration : namely, link forward sweep, node matrix loading and link backward sweep. For detail description of the solution algorithm, please refer to Holly et al.(1990).

Sediment Routing : Assuming the bed elevation at a nodal point is in an equilibrium condition, i.e., there is no scouring and sediment deposition at the nodal point and total sediment flux at the nodal point equals to zero. Assuming the incoming sediment is fully mixed at the nodal point and then is distributed, according to the sediment transport capacity, to the downstream links. Bed load and suspended load are calculated using different governing equations and hence are also treated separately at the nodal point. They are discussed as follows.

Bed Load Transport : Using the bed load equation to calculate the bed load transport capacity at the first section downstream of the nodal point and establish a rating curve describing the relationship between the flow discharge and the bed load sediment transport capacity, $Q_b = A_c Q^B$. Where Q_b = the bed load transport capacity, and A_c and B_c = constants to be calibrated. The outflowing bed load transport rate is distributed according to the bed load transport capacity obtained from the rating curve. The nodal bed load continuity equation and the corresponding distribution principle are listed as follows.

$$Q_{b,m}^{n+1} + \sum_{j=1}^{L_{in}(m)} Q_{b,m,j}^{n+1} = \sum_{j=1}^{L_{out}(m)} \frac{A_{c,j} Q_{out,j}^{B_c}}{\sum_{k=1}^{L_{out}(m)} (A_{c,k} Q_{out,k}^{B_c})} \left(Q_{b,m}^{n+1} + \sum_{j=1}^{L_{in}(m)} Q_{b,m,j}^{n+1} \right) \quad (25)$$

where, $L_{in}(m)$ = number of the links incoming toward the node m , $L_{out}(m)$ = number of the links leaving the node m and $Q_{out,k}$ = discharge leaving node m through link k .

Suspended Load Transport : The suspended load is calculated by solving sediment convection-diffusion equation using the split operator method. There are four portions, namely advection, longitudinal diffusion, transverse diffusion and reaction, involved in the split operator method and each portion had to be treated differently at the nodal point.

Advection : The sediment concentration C_k and corresponding concentration gradient are assumed to be fully mixed at the nodal point and then distributed according to the weight of the flow discharge. The equations are expressed as :

$$C_{k,out} = \frac{\sum C_{k,in} Q_{in}}{\sum Q_{out}} ; \quad C X_{k,out} = \frac{\sum C X_{k,in} Q_{in}}{\sum Q_{out}} \quad (26)$$

Longitudinal diffusion : Assuming net flux of the suspended sediment due to the longitudinal diffusion effect equals to zero at a nodal point. The relation is expressed as :

$$\sum k_x A_i C X_k = 0 \quad (27)$$

Transverse diffusion and reaction : Since the suspended sediment is assumed fully-mixed at the nodal point and hence transverse diffusion and reaction treatments are not needed at the nodal point.

The numerical scheme for suspended load computation has been assessed by comparing it with an analytical solution and a set of experimental data (Lee and Yu, 1991). It indicates that the algorithm performs well and the overall agreement is satisfactory. Please refer to Lee et al., (1997) for details of the assessments.

APPLICATION TO TANHSUI RIVER SYSTEM

The Tanhsui River system passes through Taipei area, and is one of the most important river in Taiwan. It consists of three branches, namely, Keelung River, Hsindan Creek and Tahan Creek, and one flood by pass channel, is a typical channel network. The location map is shown in Fig.2. The study network consists of 5 links, 6 nodes and 88 cross sections and is in the estuarine area. The schematic diagram is shown in Fig.3. There are five gage stations, namely, Hsiehchitou (link 1, Sec.3), Tachi bridge (link 2, Sec.20), Taipei bridge (link 3, Sec.13), Chongcheng bridge (link 4, Sec.10) and the entrance weir of the flood by pass channel (link 5, Sec.1), in the study area. These data, including water stages and channel bed variations, can be used to calibrate and verify the model. Field data from 1989, including geometric cross-sectional data and bed material data, are used as the initial condition. The test simulation was performed using data between 1989 to 1991. Data from 1989 to 1990 were used to calibrate the model and data from 1990 to 1991 were used for verification. Past experience and field observation indicate that there is insignificant sediment transport for flow discharge smaller than $100m^3/sec$. Therefore, only discharges greater than $100m^3/sec$ are selected as the input flow conditions. The upstream inflow suspended sediment concentrations versus the inflow water discharge rating curves obtained by the Taiwan Provincial Water Resources Department are used for the upstream boundary conditions. At the downstream boundary, which is located at Tudigonbi (link 1, Sec.1), the measured stage hydrographs are used as the down stream boundary conditions. The measured cross-sectional data in 1990 were used to compare with the simulation results as the basis for parameter examination. The stream tube number was set to be 5, a time interval of 1 hour was used in the simulation and the total simulation period is 1489 hours.

Parameter Examination : For the flow simulation, the energy loss coefficient is the key parameter for the model calibration. The measured water stage data from five different gage stations were used to calibrate the Manning's n value of the model. The agreements are very good. The diffusion coefficients in both longitudinal and lateral directions have to be examined for the simulation of suspended load transport. However, due to the lack of sufficient field data no calibration was made. The relations $k_r = 5.93u_*h$ and $k_s = 0.23u_*h$ suggested by Elder (1959) were used. Same relations were also adopted in the authors' previous study (Lee, et al., 1997). Agreements of the simulated bed elevation are satisfactory.

Verification : Using the parameters determined in the previous analysis, the model is applied to simulate the channel bed evolutions of Tanhsui River System from 1990 to 1991. The comparisons of the longitudinal bed profiles and cross-sectional bed profiles are shown in Figs.4 and 5 respectively. The overall accuracy is good. Five tubes were used in the simulations. The transverse variations of the bed profiles can be reflected by the stream tube concept and the accuracy is very satisfactory.

APPLICATION TO CHICHI HYDRAULIC MODEL STUDY

The Chichi common water intake project, which is currently under construction, is a water supply system in central Taiwan. One of the key facilities in this project is the sediment desilting basin. It consists of 12 subchannels and hence is able to flush sediment separately. Series of hydraulic models studies were conducted by Taiwan Provincial Water Resource Department to investigate the sediment flushing efficiency of this layout, and these studies provide a very good data set to verify NETSTARS. The layout of this sedimentation basin is shown in Fig.6. It consists of 14 links, 4 nodes and 199 cross sections. The particles used in the model studies ranges from 0.125 mm to 4.0 mm and the mean particle size is 1.0 mm. The distance between Sec.1 and Sec.4 is about 40 m and an adverse slope, with a slope of 1/50, is constructed to generate a uniform flow condition. The elevation varies from 0 to 2.5 m and then drops to -1.2 m. The design flow discharge was 44.5 cms and three different inflow concentrations, which equals 5000, 3000 and 1000 ppm, respectively, were tested in the experiments. The corresponding experimental duration equals to 10, 16 and 36 hours, respectively. The stream tube number is set to be 1 in every subchannel and Δt is set to be 10 min. in the simulation. The measured water

surface variations were used as the downstream boundary conditions. The simulated bed profile of sub-channel *F* for concentration equals 5000 ppm is shown in Figs.7. The agreement is acceptable.

CONCLUSIONS

A numerical model, which is capable of simulating scouring and deposition behaviors in a channel network under an unsteady flow condition, is developed in this study. This model integrates the stream tube concept with a state-of-the-art sediment routing algorithm which is capable of simulating suspended and bed loads separately. An internal boundary condition basing on the sediment transport capacity was proposed to distribute the incoming sediment load into the downstream links. The proposed measure is proved to be feasible. The model's performance and applicability have been demonstrated through an application to the Tanhsui River system and the hydraulic model study of the sediment desilting basin of the Chichi water supply project. Convincing results from the simulations are obtained.

REFERENCE

- Bennet, J.P. and Nordin, C.F., 1997, Simulation of Sediment Transport and Armoring., Hydrological Sciences Bulletin, XXII.
- Elder, J.W., 1959, The Dispersion of Marked Fluid in Turbulent Shear Flow., J. Fluid Mechanics 5, 544-560.
- Holly, F.M. and Preissmann, A., 1977, Accurate Calculation of Transport in Two Dimensions., Journal of Hydraulic Division, ASCE, Vol.103 (HY11), 1259-1277.
- Holly, F.M. and Rahuel, J.L., 1990, New Numerical / Physical Framework for Mobile-Bed Modeling, Part I., Journal of Hydraulic Research, Vol.28, NO.4.
- Holly, F.M., Yang, J.C., Schovarz, P., Scheefer J., Hsu, S.H. and Einhellig, R., 1990, CHARIMA Numerical Simulation of Unsteady Water and Sediment Movements in Multiply Connected Networks of Mobile-Bed Channels., IIHR Report No.0343, The University of Iowa, Iowa City, Iowa, U.S.A..
- Lee, H.Y., Hsieh, H.M., Yang, J.C. and Yang, C.T., 1997, Quasi-Two-Dimensional Simulation of Scour and Deposition in Alluvial Channels. Journal of Hydraulic Engineering, ASCE, Vol.123, No.7, 600-609.
- Meyer-Peter, E. and Muller, R., 1948, Formulas for Bedload Transport., IAHR, 2nd Meeting, Stockholm.
- Molinas, A.M. and Yang, C.T., 1986, Computer Program User's Manual for GSTARS., U.S. Department of Interior Bureau of Reclamation Engineering and Research Center, Denver, Colorado.
- Van Rijn, L.C., 1984, Sediment Transport, Part I: Bed Load Transport., Journal of Hydraulic Engineering, ASCE, Vol.110, No.10.
- Van Rijn, L.C., 1984, Sediment Transport, Part II: Suspended Load Transport., Journal of Hydraulic Engineering, ASCE, Vol.110, No.11, 1613-1641.

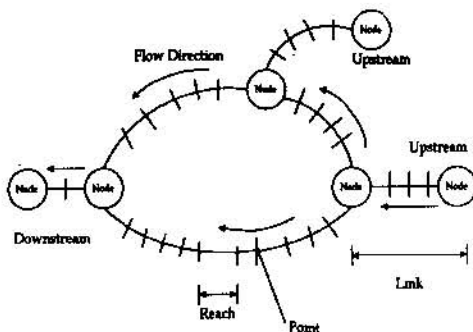


Fig.1 The definition sketch of the channel network

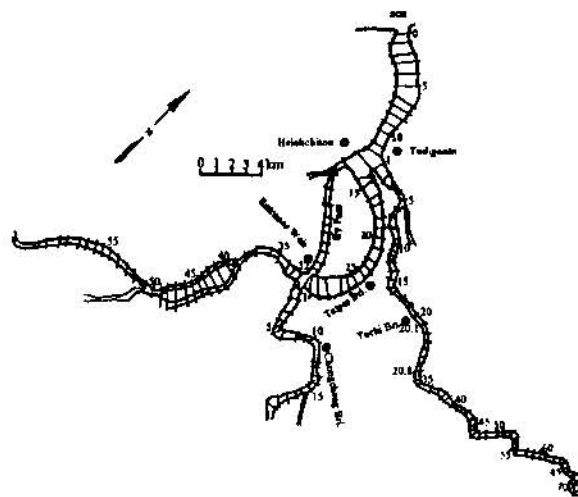


Fig.2 The location map of Tanhsui River

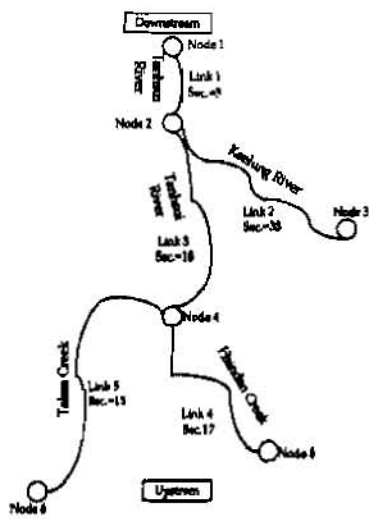


Fig3 The schematic diagram of Tanhsui River network

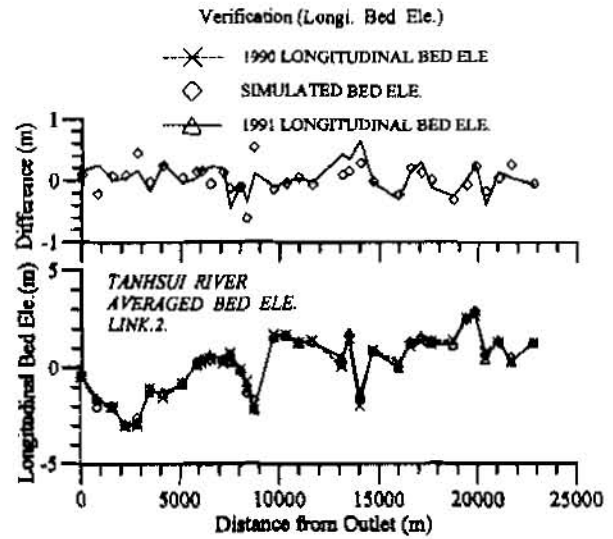


Fig.4 The simulated longitudinal bed elevation for link 2 (verification)

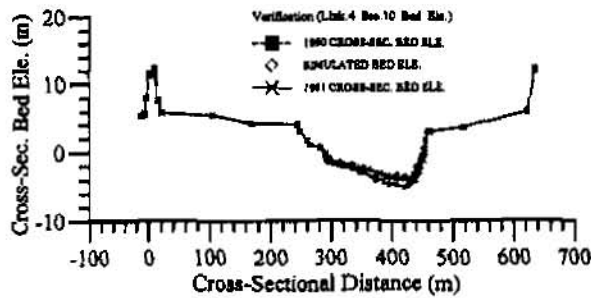


Fig.5 The simulated transverse bed profiles for link4, sec.10 (verification)

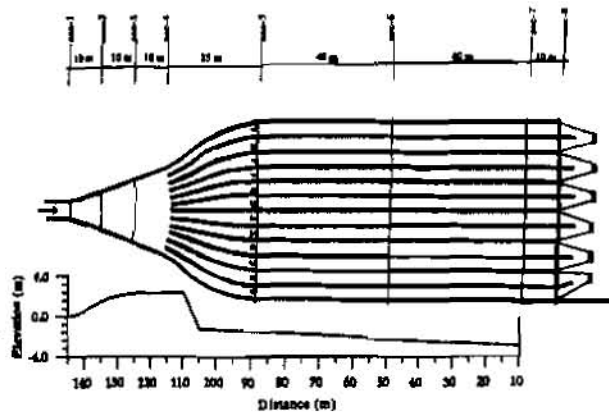


Fig.6 Layout of the sediment desilting basin of Chichi Water Supply Project.

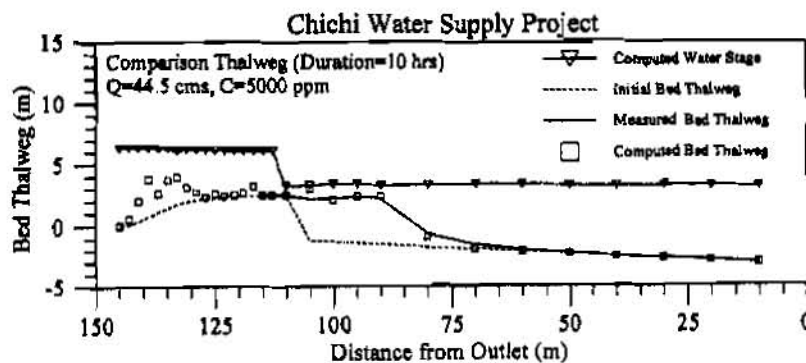


Fig.7 The simulated channel bed variations of subchannel F (C=5000 ppm)

Hildebrand Lock & Dam Sedimentation Problem and Solution

Walter Leput P.E., Chief, Hydraulics & Hydrology Section, U.S. Army Engineer District, Pittsburgh, PA

Howard Park P.E., Hydraulic Engineer, U.S. Army Waterways Experiment Station, Vicksburg, MS

Abstract: This paper presents a brief report outlining the results of an U. S. Army Waterways Experiment Station (WES) sediment study for the upper approach to Hildebrand Lock and Dam on the Monongahela River in West Virginia. Through the use of physical and numerical modeling, a durable and cost effective design was formulated to reduce costly maintenance dredging in this lock approach.

INTRODUCTION

The Hildebrand L/D is located on the left descending bank of the Monongahela River approximately 108 miles above Pittsburgh, PA. The project is just downstream of and on the inside of a bend in the river. The principal structures at the site include a 84' wide by 600' long lock, two weir sections and six 60' wide by 20' high gates (See Figure 1). The lock lift is 21'. Navigation depth for this river is 9'. Maximum navigation flow is 120,000 cfs. When the project was built in 1960, the lock was constructed land-ward of the left bank, widening the river by almost 50% in the upper approach. This project has experienced navigation delays and temporary shutdowns due to very fine sediment accumulations in the upper approach (See Figure 1). This area is on the inside of a bend and sheltered from normal velocity currents. The deposition was determined to be continual and not necessarily a function of high discharges. Because of the deposition in the approach, most tows stay to the center of the river and make very sharp turns into and out of the lock to avoid the sediment. Approximately two to three million dollars were spent every three years to remove this deposition and to assure the proper navigation depth.

The Waterways Experiment Station was contracted by the Pittsburgh District to model test and formulate a plan to keep sediment suspended past this upper lock approach. The adopted plan would also have to be compatible with navigation within this reach. After a cursory review of the problem and all existing pertinent data, WES concluded that the most feasible plan would include a submerged dike field in the upper approach. Because of the location downstream of a very sharp bend and the uniqueness of the depositing sediments, a physical model in conjunction with a numerical model was necessary to develop a plan that would eliminate or reduce sediment depositing in the approach.

PROTOTYPE FIELD DATA FOR MODELING

Modeling for this study required good prototype field data. Updated river soundings were added to existing mapping. Velocities were measured for a range of river discharges. Sediment samples were obtained by several methods in the upper reach. The sediment was found to be very fine material with a high percentage of organic matter. Navigation was documented by video for several months.

Based on the sediment analysis conducted at WES, the critical shear stress for deposition to be used in this study was 0.08 Pascals (n/m^2) and the critical shear stress for erosion used in this study was 0.50 Pascals (n/m^2). The average particle setting velocity was 0.00012 m/sec. WES concluded that the critical river velocity required to move or keep sediment moving past this approach was 1 fps. A flow of 10,000 cfs was determined to be the design discharge that could be utilized several times a year to flush sediment from the approach.

PHYSICAL MODELING

A fixed bed model was built to an undistorted linear scale of 1 (model) to 80 (prototype) at WES. The model reproduced the lock, dam and 1.7 miles of the river upstream of the project. This scale allowed for

accurate reproduction of water surface profiles, current magnitudes, cross-currents and eddies that would affect sediment deposition tendencies and navigation conditions.

The model was calibrated by verifying prototype water surface profiles and velocities for a range of discharges. The majority of the current magnitudes and directions were determined with cylindrical floats drafted to the depth of a loaded barge that were tracked with a computer program utilizing overhead video cameras. Miniature velocity meters were utilized to obtain all other velocity data. Surface current directions were observed in the model using confetti. A synthetic material scaled to the prototype was used as sediment to determine sediment deposition patterns. A remote controlled model towboat was used to determine the effects of currents on tows entering and leaving the upper lock approach

For base conditions a range of flows from 5,000 cfs to 120,000 cfs were tested and documented. At the upper end of the approach, the highest velocities were determined to be at the left bank and center of the channel then crossing over to the right bank. The model indicated very low velocities in the approach. See Figure 2 for base condition velocities for a flow of 10,000 cfs. The synthetic sediment indicated deposition patterns in the approach similar to the prototype. Besides sedimentation, no adverse navigation conditions were documented except for a slight out-draft at the entrance to the lock.

After several trial schemes, a dike plan was developed that increased the velocities along the lock approach reach. The plan consisted of three submerged dikes along the rightbank (See Figure 3). These dikes are submerged 12' below the normal pool. They are 10' wide at the top, have 1:1.5 side slopes and are 180 to 200' long. The approach area was assumed to be cleaned of sediment prior to construction of these dikes.

The model indicated that the dike plan significantly increase velocities along the left bank approach reach. Figure 3 shows the velocities for a flow of 10,000 cfs. The model suggested that the dikes would increase the approach velocities to the magnitude that would initiate movement and/or keep the sediment moving past the approach. Navigation tests indicated no adverse currents or eddies.

NUMERICAL MODELING

The 2-D numerical model study was conducted using TABS-2 modeling system. This system provides 2-D solutions to open-channel and sediment problems using finite element techniques. A 2-D depth-averaged hydrodynamic numerical model, RMA-2V, was used to generate the flow field. The flow field was then used with the sediment properties of the river as input to a 2-D sedimentation model, STUDDH. The other programs in the system perform digitizing, grid generation, data management, graphical display, output analysis and model interfacing tasks. The sediment model requires hydraulic parameters from RMA-2V, sediment characteristics, inflow concentrations and sediment diffusion coefficients. The sediment is treated as cohesive and deposition rates were calculated with the equations of Krone.

Finite element grids were developed to simulate the Monongahela River for a distance of 1.7 miles. The overall grid was modified only to accommodate submerged dike plans within the dike field. All other areas of the model grid were identical for all testing. Both grids consisted of 2832 elements and 8751 nodes.

The model testing included four steady state hydrodynamic boundary conditions (5,000 cfs - 50 days, 10,000 cfs - 30 days, 20,000 cfs - 10 days, and 40,000 cfs - 5 days). For each condition, a discharge was specified at the upstream boundary and water level at the downstream boundary. Within the study reach, Manning's n values ranged from 0.025 in the main river channel to 0.10 over the submerged dikes in the plan tests. Because of the limited prototype velocity data, the adjustment procedure was based on comparison to the physical model's water level and velocity distribution results for discharges of 5,000 cfs, 10,000 cfs, 20,000 cfs and 40,000 cfs. The primary adjustment parameters required by the hydrodynamic code as model input were Manning's n values and turbulent exchange coefficients. These parameters were adjusted within reasonable limits until the velocity distribution in the study reach agreed

with observations in the physical model for each discharge tested. Flow fields generated by the numerical model appeared reasonable.

The boundary information required for the sedimentation modeling study were suspended sediment concentrations at the upstream boundary and bed sediments within the model. Primary input parameters required were dispersion coefficients, critical shear stresses for deposition and erosion, critical concentrations and erosion rate constants. Suspended sediment concentrations used at the upstream boundary were generated from sediment rating information obtained by the Pittsburgh District. Sedimentation adjustment was restrained by the limited field data for verification. The only available field data consisted of the bed sediment samples in the deposition zone in the lock approach channel. The procedure in setting up the sediment code was based on the laboratory measurements of deposition and erosion shear stresses for the bed sediment samples collected on site. Once the observed sediment parameters were set in the model, the results appeared reasonable for the conditions tested.

The test procedure selected for the existing condition versus dike plan evaluation was to step through the sediment model using the four steady-state discharges sequentially. Each test started with 50 days of 5,000 cfs discharge, followed by 30 days of 10,000 cfs discharge, then 10 days of 20,000 cfs discharge, and then finally 5 days of 40,000 cfs discharge. During testing it was determined that the 20,000 and 40,000 cfs steps were unnecessary for plan evaluation, since these rare-event discharges were erosional in the approach channel rather than depositional and the fact that the approach channel was excavated in rock and non-erodible.

Existing-condition and Dike Plan bed-shear-stress patterns for the 10,000 cfs discharges are given in Figures 4 and 5. As demonstrated by these figures, the with plan condition results in significantly increased bed shear stresses over the existing condition in the vicinity of the lock approach.

Accumulated deposition in the vicinity of the lock approach after 50 days of 5,000 cfs discharge followed by 30 days of 10,000 cfs discharge demonstrated that the Dike Plan deposition in the vicinity of the lock approach is only a small fraction (about 20%) of that observed under the existing condition. Based on these numerical model results, it was concluded that the proposed dikes would be effective to significantly reduce deposition of fine material in the lock approach.

CONCLUSIONS

Through the combined use of physical and numerical modeling a cost effective sediment management plan was developed for the upper approach to Hildebrand L/D. The dike plan was constructed in 1996. Although the approach has not been dredged clean, prototype velocity measurements indicate that the dikes are altering the flow patterns as modeled. Recent approach bed soundings suggest that the sediment deposition has stabilized.

REFERENCES

Thomas, W.A., and McNary, W. H., Jr. (1985). "User's manual for the generalized computer program system: open-channel flow and sedimentation. TABS-2, main text and appendices A through O," Instruction Report HL-85-1, U.S. Army Engineer Waterways Experiment Station, Vicksburg, MS.

Park, Howard (1996). "Hildebrand Lock and Dam", Draft Technical Report, U.S. Army Engineer Waterways Experiment Station, Vicksburg, MS.

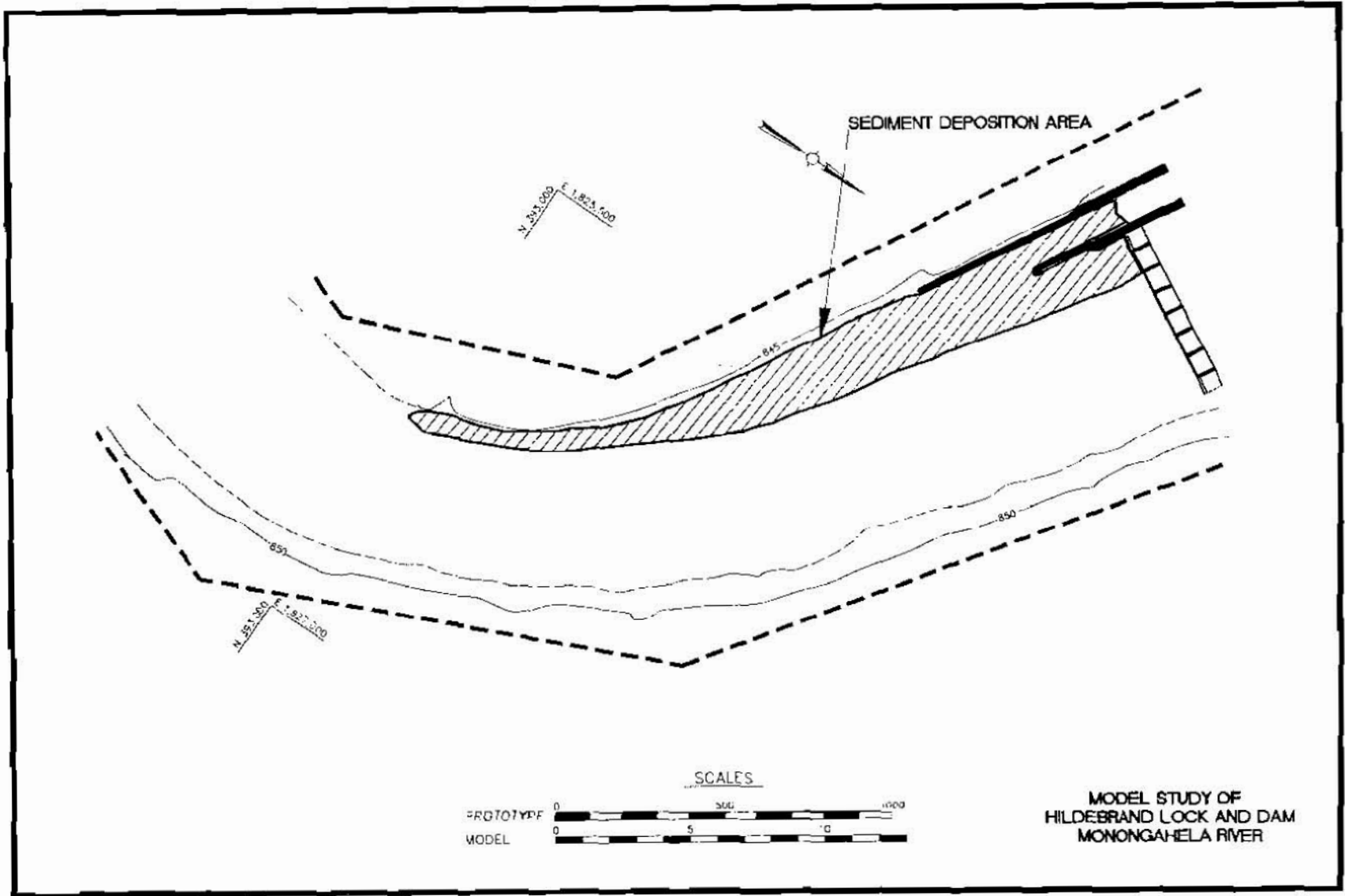
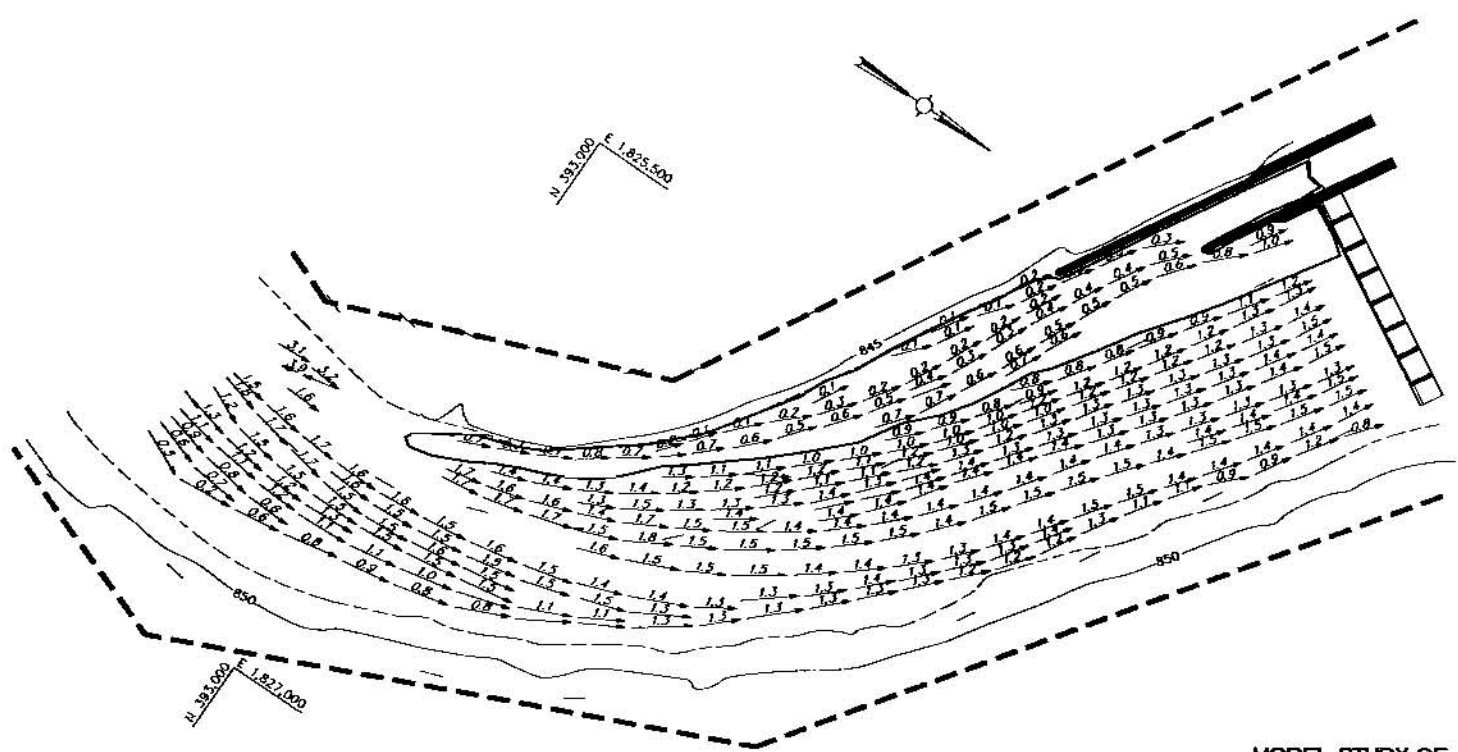


FIGURE 1

N. 593,000 E. 1,825,500



N. 593,000 E. 1,827,000

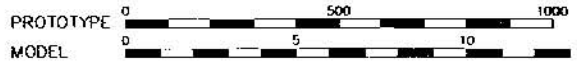


LEGEND

- 0.5 - VELOCITY IN FEET PER SECOND
- - - - VELOCITY LESS THAN 0.5 FEET PER SECOND

NOTE : VELOCITIES AND CURRENT DIRECTION OBTAINED WITH FLOAT SUBMERGED TO DRAFT OF LOADED BARGE (9.0 FT)
ALL CONTOURS AND ELEVATIONS ARE IN FEET REFERRED TO NGVD

SCALE(S)



**MODEL STUDY OF
HILDEBRAND LOCK AND DAM
MONONGAHELA RIVER**

**VELOCITIES AND
CURRENT DIRECTIONS**

BASE TEST

DISCHARGE: 10,000 CFS
UPPER POOL EL: 835.0 FT

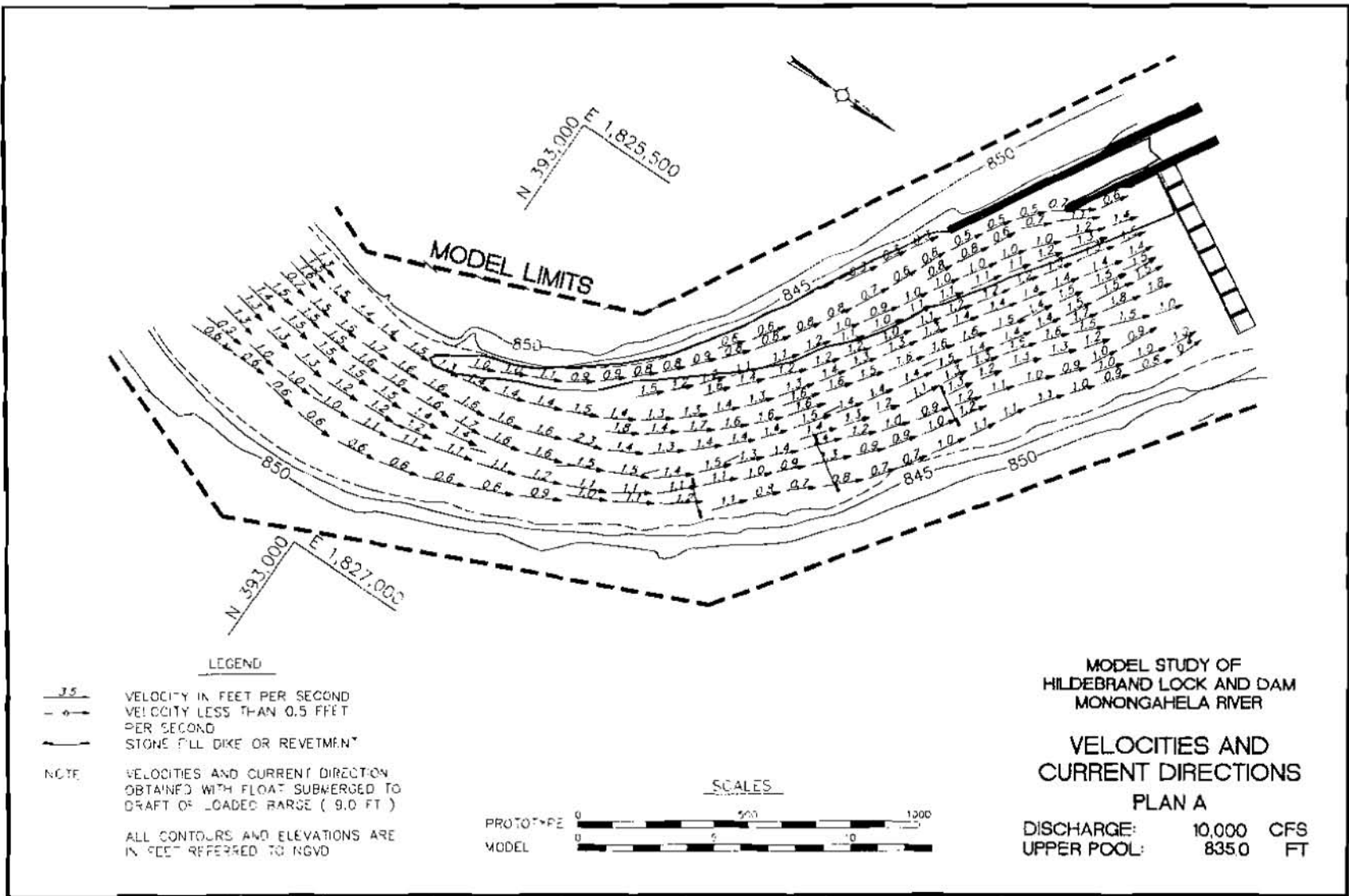
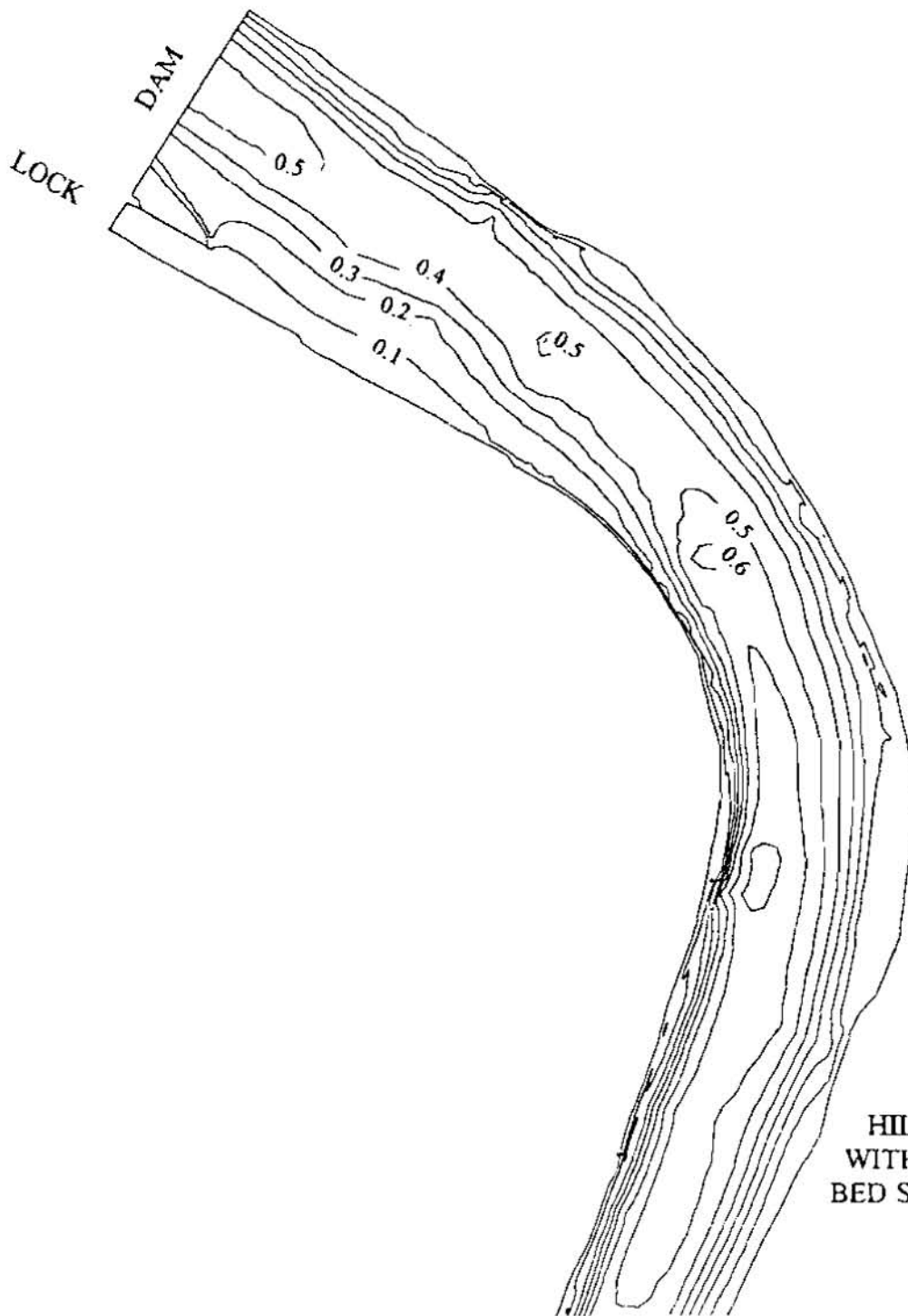
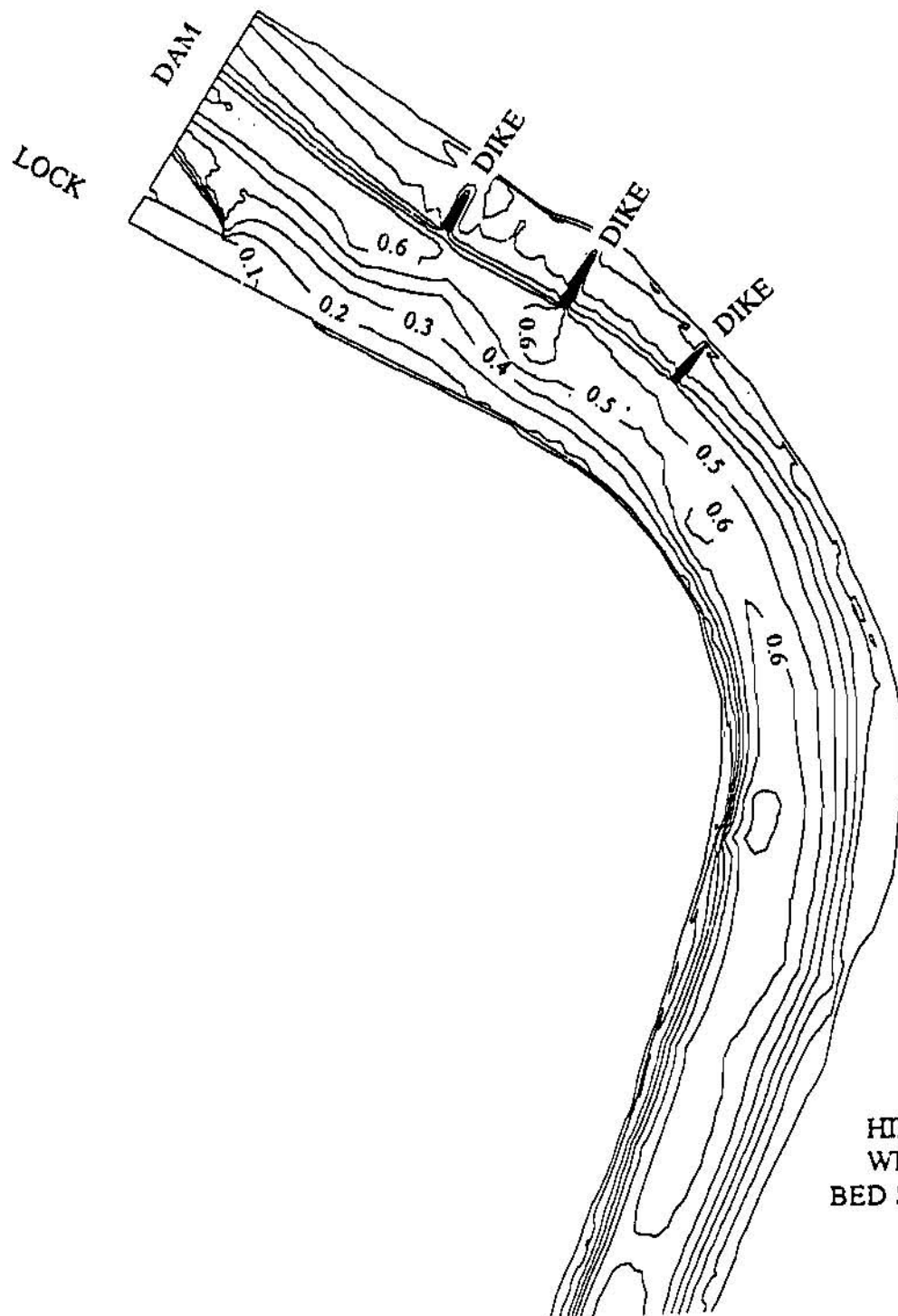


FIGURE 3



HILDEBRAND L/D
WITHOUT DIKE PLAN
BED SHEAR IN PASCALS

FIGURE 4



HILDEBRAND L/D
WITH DIKE PLAN
BED SHEAR IN PASCALS

FIGURE 5

GEOMORPHIC ANALYSIS OF THE RIO GRANDE SAN ACACIA TO THE NARROWS OF ELEPHANT BUTTE RESERVOIR

Paula W. Makar, Hydraulic Engineer, Bureau of Reclamation, Denver, CO; Robert I. Strand, Consultant, River Engineering and Sedimentation, Lakewood, CO; Drew C. Baird, Senior Hydraulic Engineer, Bureau of Reclamation, Albuquerque, NM

ABSTRACT

The study was undertaken to identify and quantify the historic geomorphic responses of the Rio Grande in the upper reaches of Elephant Butte Reservoir and the riverine reach extending to San Acacia, New Mexico. The river has responded to multiple natural and man induced changes in hydrology, channelization, vegetation management, impoundment, and sediment management. These parameters have been evaluated to determine their relative impact on the present day river system. The results of this study will be used in predicting the response of the river system to changes in the parameters and to plan water resource management activities in the Rio Grande Basin.

INTRODUCTION

The objective of this study was to identify and quantify the historic geomorphic responses of the Middle Rio Grande in the reach from San Acacia Diversion Dam to the Narrows of Elephant Butte Reservoir (see Figure 1). The Middle Rio Grande is defined as the reach from where the river exits White Canyon in northern New Mexico to Elephant

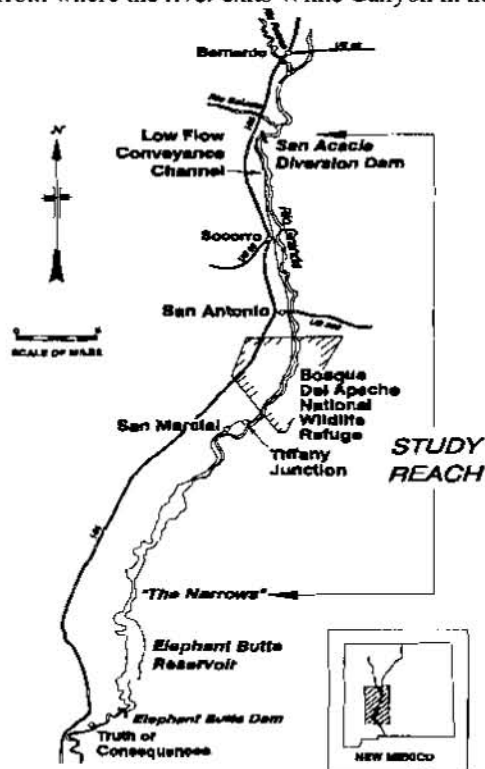


Figure 1. Location map

Butte Reservoir. This reach of river flows through a linked series of intermontane basins and canyons or "narrows" located on the Rio Grande Rift. The Rift is the primary source of historic tectonic and possible neotectonic activity in the area. To the west, the Colorado Plateau has been marked by volcanic activity with uplift and the surrounding highlands to the east have also been uplifted. The basins in-between have been downfaulted and then filled with alluvium as the Rift subsided. The Socorro basin, which runs from San Acacia to San Marcial, is about 38 miles long and 8 to 12 miles wide. It is bordered by mountains on the west and highlands on the east. The portion of the basin incised by river flow is 1 to 3 miles wide. Downstream of San Marcial the valley is much narrower, less than 3 miles wide. Here, the river has worked the entire valley floor between the mountains and mesas. The reach from

San Marcial to the Narrows of Elephant Butte is about 22 miles long (USBR, 1977). There are no major tributaries in the reach from San Acacia to the Narrows. The ephemeral nature of the upstream tributaries has strongly influenced the reach under study. Sediment loads from these tributaries are often in amounts larger than can be moved by normal river discharges and so delta deposits are created. Floods move these sediment obstructions into the Rio Grande and carry them until sediment transport capacity is diminished. So much sediment is moving through the system to the main stem that the bed is aggrading. Current average total load concentration in the Rio Grande is about 8,000 mg/l, down from past highs of 24,000 mg/l. The natural river bank levees rise with the bed and in some cases the river has become perched above the rest of the valley. Sand bars, built particularly on the falling stages of the hydrograph, can deflect flow against the banks. Channel aggradation combined with current directed toward the banks can cause the river to avulse and jump to a new course in the valley. The river migration has caused general aggradation across the valley. This aggradation has been continuing for over 10,000 years (Hawley, 1976) with periods of channel stability until the next avulsion. This long-term state of disequilibrium has made analysis of the Rio Grande problematic and predictions of the future very difficult.

RIVER AND CONVEYANCE CHANNEL OPERATION AND MAINTENANCE ACTIVITIES

The activities of man have had significant influence on the geomorphology of the study reach. Some of these actions have occurred within the study reach; others have taken place considerably upstream, but are no less significant in their impact on the river morphology. Water and sediment have been diverted from the river for hundreds of years both in Colorado and New Mexico. This irrigation development reached its peak in 1880. For the next 40 years the general trend in diversions was downward due to river instability, increased sedimentation and waterlogging of irrigated lands (USBR, 1947). These diversions not only reduced the natural water and sediment loads, but undoubtedly altered the relative proportions of each in the streamflow.

In 1915 a reservoir was formed by the closure of Elephant Butte Dam. With extended drought conditions by about 1951, there was no longer a defined channel through the delta of the reservoir. The delta area was covered with non-native tamarisk trees. Average annual water loss between the San Marcial gauge and the pool of Elephant Butte was about 140,000 ac-ft per year (USBR, 1953). In response to this severe water loss, the US Bureau of Reclamation constructed a channel from San Acacia through the delta downstream about 25 miles into the reservoir. The river was altered to be, in effect, a canal (Low Flow Conveyance Channel) and a flood overflow channel (Floodway). The Conveyance Channel was designed to carry all river flows up to 2,000 ft³/s with the remainder traversing the Floodway. This mode of operation was generally followed until 1979 when the reservoir rose significantly for the first time since the 1940s. The Floodway was confined to the eastern edge of the valley from San Acacia to the Narrows by the spoil levee created by excavating the Conveyance Channel. Continued aggradation and levee raising has resulted in a Floodway channel perched up to 10 feet or more higher than the rest of the valley for several miles upstream from the reservoir pool as shown in Figure 2.

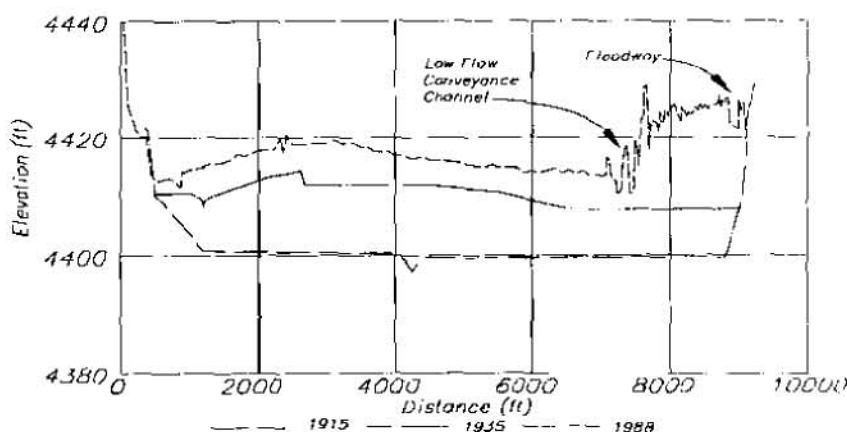


Figure 2. Historic Cross Sections - Reservoir Sedimentation Rangeline 12

During the period of channelization in the study reach, the Rio Grande was undergoing a stabilization program

upstream as well. The channel was confined to a managed width with the aid of steel (Kellner) jacks and the development of pilot channels. The area between the jack lines was kept clear of obstruction by vegetation management until recently. This stabilization program improves the efficiency of transporting water and sediment throughout the Middle Rio Grande reach of the river. Subsequent dams on the Jemez River, Galisteo Arroyo, and the Rio Grande mainstream (Cochiti) have further altered the sediment loads and river discharge patterns.

HISTORICAL OPERATION OF ELEPHANT BUTTE RESERVOIR

Elephant Butte Dam is part of the multipurpose Rio Grande Project that controls floods, generates power, and stores and delivers irrigation water. The reservoir filled once in 1942, again at the end of 1985, and remained full through 1988, and then filled again in 1992.

Figure 3 shows that the river bed elevation at San Marcial gauge had been rising continuously from 1895 to 1937. The water surface of 200 ft³/s is assumed to be similar to the average bed elevation. Between 1895 and 1915, the river bed rose about 4 feet. This clearly shows that the river bed above Elephant Butte Reservoir was rising steadily prior to the construction of the dam. The bed rose very slowly until the early 1920s. High flows occurred in the mid 1920s and the river bed elevation increased rapidly as the reservoir was filling. The bed continued to rise at a slower rate from the late 1920s until the mid 1930s. The trough in bed elevation on Figure 3 from 1937 to 1942 is largely attributed to the major flooding and avulsions in 1937 and 1941. The high water from snow melt and rain continued for months. After 1942, the bed rose at a very rapid rate until it reached the elevation that the trend line from 1928 to 1936 would have predicted and continued along that trend line until the late 1940s. The bed elevation was relatively stable until 1958 and then declined from 1958 to 1967 about 3 feet. This degradation at San Marcial gauge from 1958 to 1967 is ascribed to the reestablishment of the river channel through the delta of Elephant Butte Reservoir. The gauge elevation stayed about constant from 1967 to 1978. However, in 1979 the reservoir began to

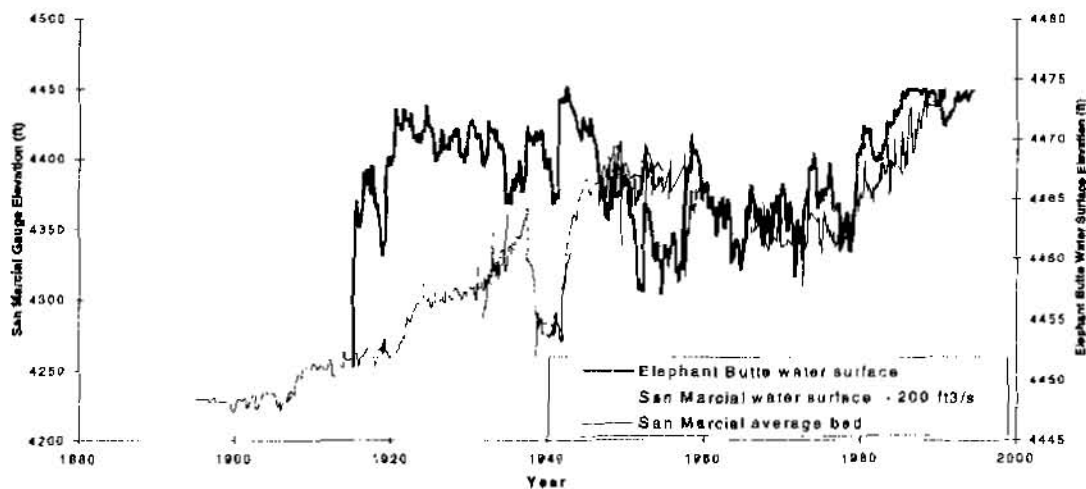


Figure 3. Comparison of San Marcial Gauge and Elephant Butte Water Surface Elevations

rise, filling in 1985, and remaining essentially full until 1989. During this period the river bed rose 10 ft. This can be largely attributed to the rise in water surface in the reservoir due to the abundant water supply. The river bed has risen about 24 ft over 94 years between 1895 and 1989, or a long term average of 0.23 ft/yr. Vanoni (1975) presents data which shows that in the period 1895-1954 the natural rate of aggradation not attributed to the Reservoir was 0.27 ft/yr or 15.9 ft. It was further determined that the rate attributed to the reservoir was only an additional 2.5 ft, for a total aggradation of 18.4 ft. In other words, over this period 86 percent of the aggradation is attributed to the natural aggradation rate and only 14 percent is attributed to the reservoir. Without the extensive Conveyance Channel and river channel construction and maintenance the river bed would likely have continued to aggrade at the natural rate of 0.27 ft/yr or at a reduced rate due to decreased sediment supply from the upstream channel.

EVALUATION OF MEASURED CHANGES OF AGGRADATION AND DEGRADATION

The distribution of deposited sediment is strongly dependent upon the operating reservoir surface elevation and to a lesser extent on particle size. Sediment deposition is heavily influenced by the channel construction and maintenance between San Marcial and the Narrows from 1951 to 1980. This channel resulted in degradation at the San Marcial gauge as noted earlier, and sediment in the main channel was remobilized and transported further into the reservoir during the low reservoir periods from the 1950's through the mid-1970's. In addition, the increased sediment transport by the Conveyance Channel decreased sediment deposition in the 22 miles of river from San Marcial to the Narrows, and thereby transferred sediment deposition downstream.

River Surveys: Numerous estimates of the possible amount of change have been made from various sedimentation surveys. Studies have been completed to determine the quantities of sediment accumulated in or removed from the Middle Rio Grande Valley over a period of 56 years (1936 - 1992). Figure 4 presents the aggradation from San Acacia to San Marcial over time. Two reaches are compared, upstream of the Bosque Del Apache National Wildlife Refuge (Refuge) and downstream including the Refuge. Significant differences in aggradation rates are evident over both time and space. The downstream reach shows much greater rates before 1962. A sharp decrease in the rate of deposition in the lower reach occurs after 1962 when Conveyance Channel construction was essentially complete. At that point the difference in rates of the upstream and downstream reaches becomes quite small. The total volume calculated for the years 1972 - 1992 was just over 11,000 AF. This compares to 16,000 AF calculated from the difference in total load transport at San Acacia and San Marcial for those years.

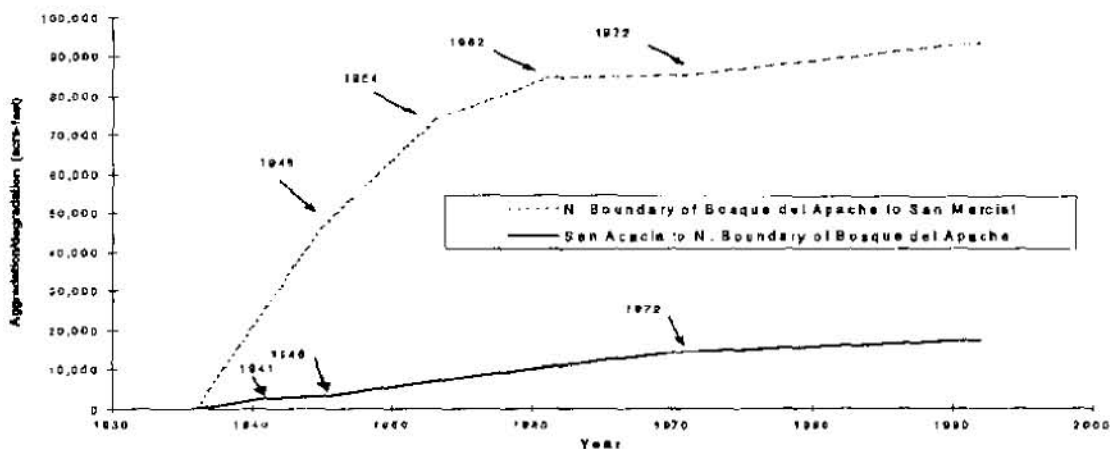


Figure 4. Cumulative Aggradation/Degradation by Reach

Reservoir surveys: The proposed reservoir pool was surveyed in 1907 and 1908, and silt survey lines established. In 1915 and 1916 additional lines were added in the San Marcial area referred to in the river surveys. Additional lines have been added over the years for a total of 92 lines. Surveys were carried out in 1920 and 1925, but apparently the results were not published. The SCS resurveyed the silt lines in 1935 and USBR published the results. Resurveys by USBR in 1949, 1957, 1969, 1980, and 1988 (USBR, 1988) have been published. Data for all silt lines are not available until 1980, but profiles and capacities are available for each year. The original storage capacity was 2,634,800 ac-ft. This has been reduced by sediment deposition to 2,065,010 ac-ft as of the 1988 reservoir resurvey. The original reservoir pool was 42 miles long. Sediment deposition in the upper reaches has reduced the reservoir pool length to about 32 miles.

WATER AND SEDIMENT BUDGET FOR THE STUDY REACH

At the present time, river discharge and suspended sediment loads are measured at two locations within the study reach, San Acacia and San Marcial. At each site, one gauging station measures discharge and suspended sediment in the Conveyance Channel and the other measures river or Floodway flows. The Conveyance Channel discharge records at both locations begin in 1958 and continue through the present, with some periods of unreported data. The

Floodway records begin in 1964 and are continuous to the present. As a single channel, San Acacia has data from 1936 to 1964 while at San Marcial the record runs from 1895 to 1964, with gaps in the very early data. The suspended sediment records are of significantly shorter period than the water discharge records. At San Acacia, the sediment record spans the period July 1946 to present (except for July 1956 through December 1958) and, at San Marcial, the record is from January 1925 to the present. These records have been compiled into tables and graphs representing the monthly, annual, and cumulative totals of streamflow and suspended sediment at both sites for the entire period of record (Strand, 1997).

Sediment Budget: The concurrent period of daily sediment records at San Acacia and San Marcial is from 1959 to the present. During this period several hundred special measurements were made which included sufficient hydraulic and sediment data required to compute total sediment loads with the Modified Einstein Procedure (USBR, 1955). From these computations a relationship was developed between measured suspended sediment and computed total sediment for the Conveyance Channel and Floodway at both sites. These relationships indicate that the unmeasured sediment load averages 30 - 35 percent of the measured suspended sediment load.

The transport of water and sediment in the Conveyance Channel has not always been continuous from San Acacia to San Marcial. For the period September 1974 to February 1975, the Conveyance Channel was breached at Tiffany Junction and water was diverted into the floodway upstream of the San Marcial gauge. This condition was made permanent in December 1975. In 1979 the levee at Tiffany Junction was overtopped and the Conveyance Channel filled with sediment. The Conveyance Channel was restored and put back into operation for the period November 1983 to February 1985. Since that time, no diversions have been made to the Conveyance Channel due to high reservoir levels. For all other periods since September 1974, the Conveyance Channel at San Marcial has acted as a drain and the discharge and sediment records at that station reflect drainage flows only. Figure 5 contains plots of the accumulated discharge and total sediment load at both gauging stations.

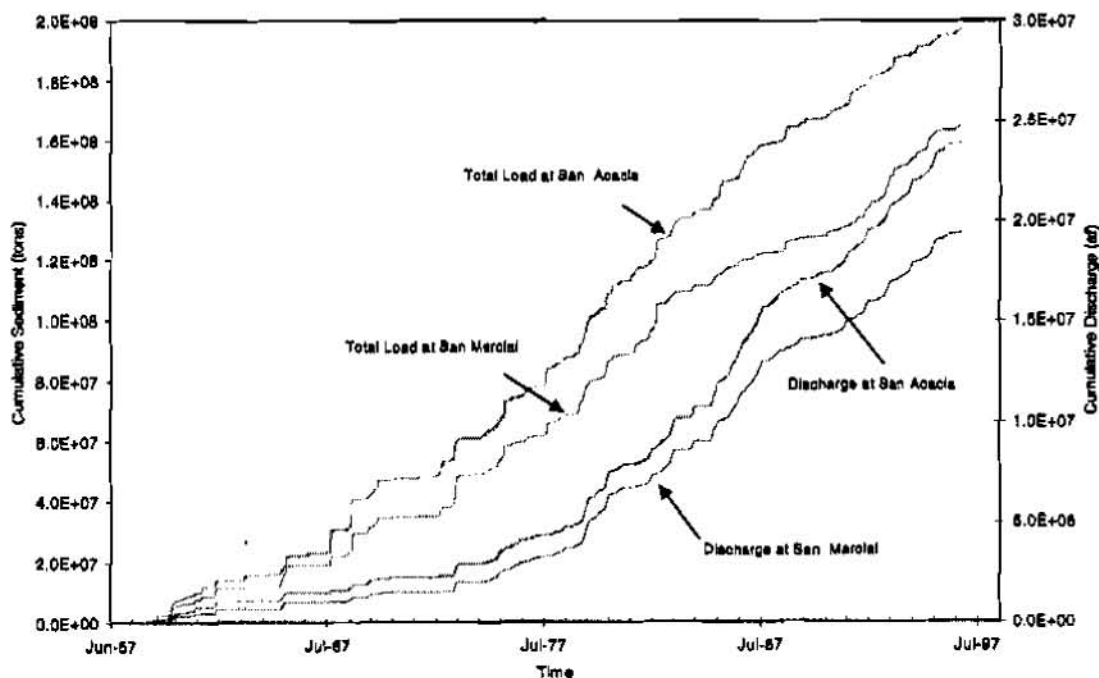


Figure 5. Total Load and Discharge Mass Curves

Figure 6 is a plot of the difference in total sediment load passing each gauging station 1959 to present, that is, San Acacia load minus San Marcial load. As would be expected, the load at San Marcial is generally less due to the ongoing aggradation in that portion of the study reach. Surprisingly, the 1991 to 1995 period shows a rapid reversal in that trend. This phenomenon is being investigated.

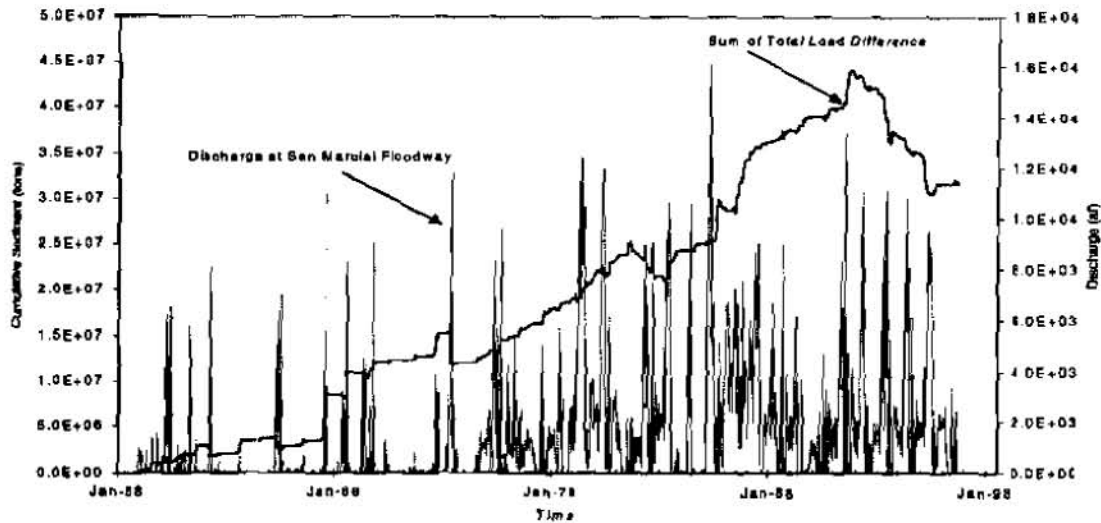


Figure 6. Comparison of Discharge and Difference in Total Load Transport

EVALUATION OF HISTORICAL AERIAL PHOTOGRAPHIC SETS AND SURVEY DATA

The recognition of serious sedimentation issues in the Middle Rio Grande Valley early on has led to a wealth of historic data. A plane table survey was conducted in 1914 in the reservoir pool and in 1918 for the reach from Cochiti Dam to San Marcial. Contour maps are available from these surveys, but maps for the reservoir reach are in microfiche only.

Aerial photos of the river were taken in 1935, 1949, 1962, 1972, 1985, and 1992. The purpose of the aerial survey in 1962 was to provide a record of Floodway and Conveyance Channel conditions at the end of construction and to establish a base for use in future evaluation of the channelization works. The later surveys provided the information to track changes over time. The accuracy varies from photomosaics in 1936, 1949 and 1962, to ratio-rectified photomosaic mapsheets in 1972, to orthophoto mapsheets in 1985 and 1992. Planform information has been digitized for each of the surveys. Specific features of interest to this study include the active river channel, recent change, vegetated islands, and the thalweg of the river. The active river channel is defined as the channel of the current river flow which is usually free of vegetation depending on the magnitude of the flows and recent change is where the current river flow is no longer clearing vegetation from the channel and vegetation is beginning to grow or the current channel flow has not yet cleared all vegetation from the channel.

The 1918 data were from topographic maps based on plane table surveys and the true active channel could not be positively determined. However, the river water surface and surrounding sand and vegetation areas were identified. It was assumed that the river plus the immediately adjacent sand was similar to the active river channel and so digitized. Figure 7 shows an example of the general narrowing of the active channel over the years. Figure 8 compares the average width with annual maximum mean daily flows. A definite correlation between channel width and discharge peaks is evident. A linear regression analysis of the average reach width to the average peak flows of the previous 5 years shows a strong relationship over the entire period of record. This emphasizes the degree to which annual peaks have influenced the river width.

CONCLUSION

The Middle Rio Grande has been undergoing a general aggradation trend for the last several thousand years. The aggradation combined with flooding causes the river to experience periodic avulsions and corresponding channel planform changes. The activities of man have had a mixed impact of exacerbating and reversing this long term trend

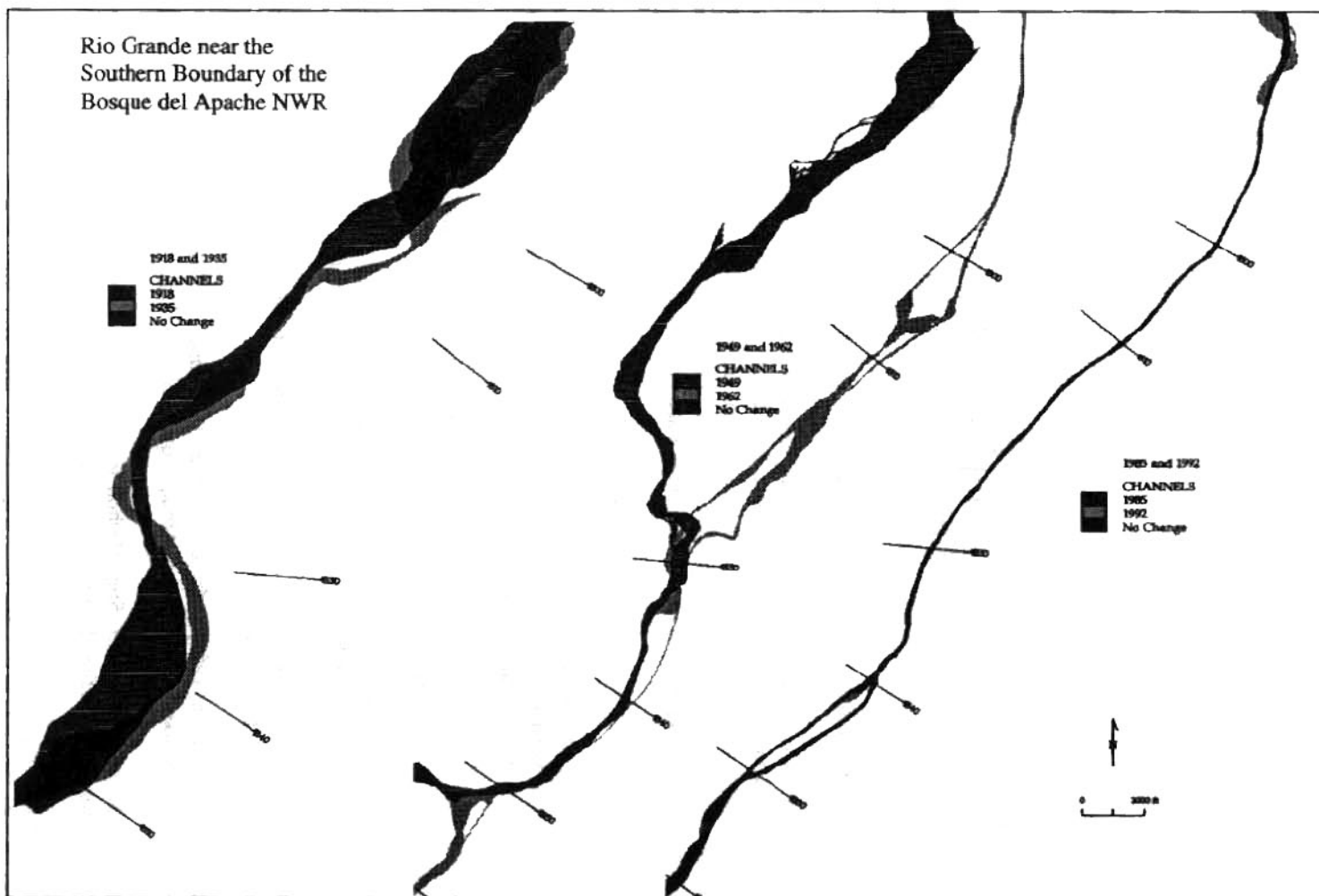


Figure 7. Planform comparison of active channel: 1918 to 1935, 1949 to 1962, and 1985 to 1992

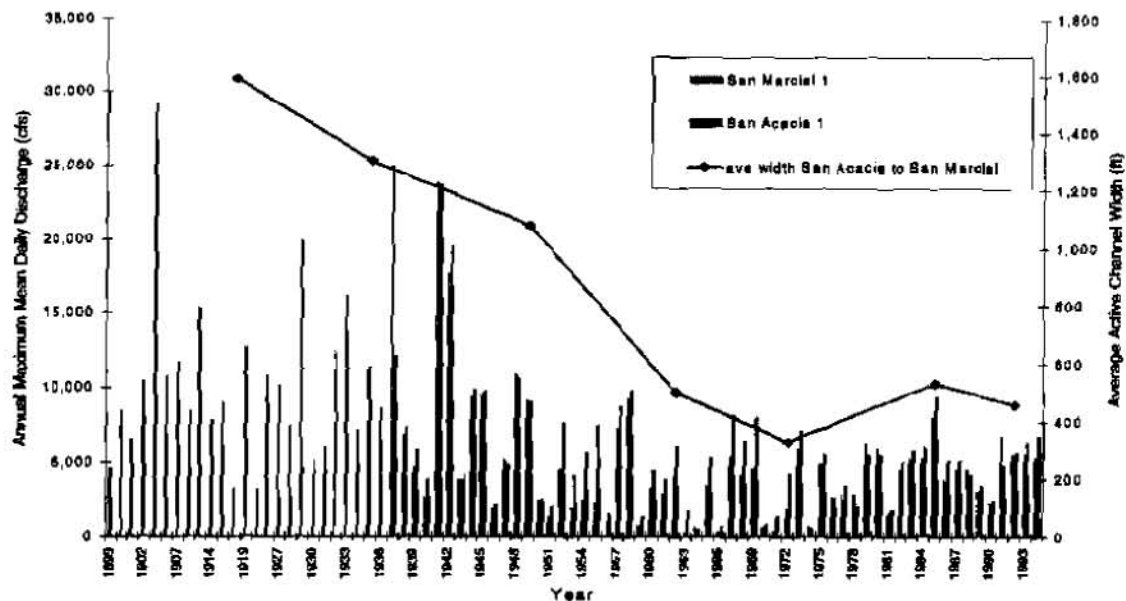


Figure 8. San Acacia and San Marcial Peak Discharges and Average Active Channel Width

in the shorter time periods. River migration upstream of the reservoir delta has decreased in recent times for four main reasons: 1) a decrease in flood peaks, 2) a decrease in sediment load, 3) man's activities to stabilize the channel, and 4) an infestation of tamarisk whose dense understory and root structures stabilized the banks. The studies described have quantified some of these impacts and will provide guidance for future river management activities to minimize impacts of aggradation and maximize the water conservation and habitat management goals.

REFERENCES

- Hawley, J.W., Bachman, G.O., Manley, K., 1976, "Quaternary Stratigraphy in the Basin and Range and Great Plains Provinces, New Mexico and Western Texas", in Mahaney, W.C. (ed) *Quaternary Stratigraphy of North America* Dowden, Hutchinson & Ross, Stroudsburg, Pennsylvania
- Orvis, C.J., 1989, *Elephant Butte Reservoir - 1988 Sedimentation Survey*. Sedimentation Section, United States Bureau of Reclamation, Denver, Colorado
- Strand, R.I., 1997, *Compilation of Historical Discharge & Suspended Sediment Data at the San Acacia & San Marcial Gauging Stations*, A report for the Bureau of Reclamation, Denver, Colorado
- United States Bureau of Reclamation, 1947, *Plan for Development, Middle Rio Grande Project, Rio Grande Basin, New Mexico. Region 5 Project Planning Report No. 5-15.1-2.*
- United States Bureau of Reclamation, 1953, *Definite Plan Report, Volume 1B, General Plan and Drainage, Middle Rio Grande Project, Rio Grande Basin, New Mexico. Albuquerque Projects Office, Albuquerque, New Mexico.*
- United States Bureau of Reclamation, 1955, *Step Method for Computing Total Sediment Load by the Modified Einstein Procedure*. Sedimentation Section, Engineering and Research Center, Denver, CO.
- United States Bureau of Reclamation, 1977, *Final Environmental Impact Statement, Operation and Maintenance Program for the Rio Grande - Velarde to Caballo Dam*. Albuquerque, NM. Vol. I.
- Vanoni, V.A. ed., 1975, *Sedimentation Engineering, Manuals and Reports on Engineering Practice No. 54*. American Society of Civil Engineers, New York, NY.

RIVER CHANNEL CHANGES DOWNSTREAM OF COCHITI DAM MIDDLE RIO GRANDE, NEW MEXICO

By Viola Sanchez, Civil Engineer, U.S. Bureau of Reclamation, Albuquerque, New Mexico

Abstract: The alluvial middle Rio Grande in New Mexico has changed significantly over the past 80 years. The ancestral middle Rio Grande was a relatively wide, aggrading channel with a shifting sand bed and shallow banks. The planform was braided, relatively straight, or slightly sinuous (Crawford et. al. 1993). Since at least 1918, the Middle Rio Grande has become narrower. This paper documents geomorphic channel changes since 1918 and attempts to determine what has caused the different changes. Cochiti Dam operations, channelization, and reductions in flood peaks from the watershed are investigated as reasons for channel changes, which are documented using historic hydrologic, cross sectional, bed material, GIS, and aerial photography data.

HYDROLOGIC HISTORY

It is estimated that the Middle Rio Grande Valley in New Mexico (Figure 1) has not been in a state of dynamic equilibrium for the last 11,000 to 22,000 years. The maximum degradation is believed to have occurred about 22,000 years ago, when the Rio Grande was about 60 - 130 ft below the current valley floor. Since then, the Rio Grande has been slowly aggrading because tributary inflows contribute more sediment than the river can remove (Crawford et. al. 1993). A consequence of the aggrading river is that levees had to be built to contain the river in its channel and prevent avulsions from forming in surrounding farmlands and inhabited areas. The levees exacerbated aggradation by confining sediment deposition to a smaller area. As the river continued aggrading, the levees had to be raised to maintain channel capacity. Table 1 lists the largest known flood events in the Middle Rio Grande Valley.

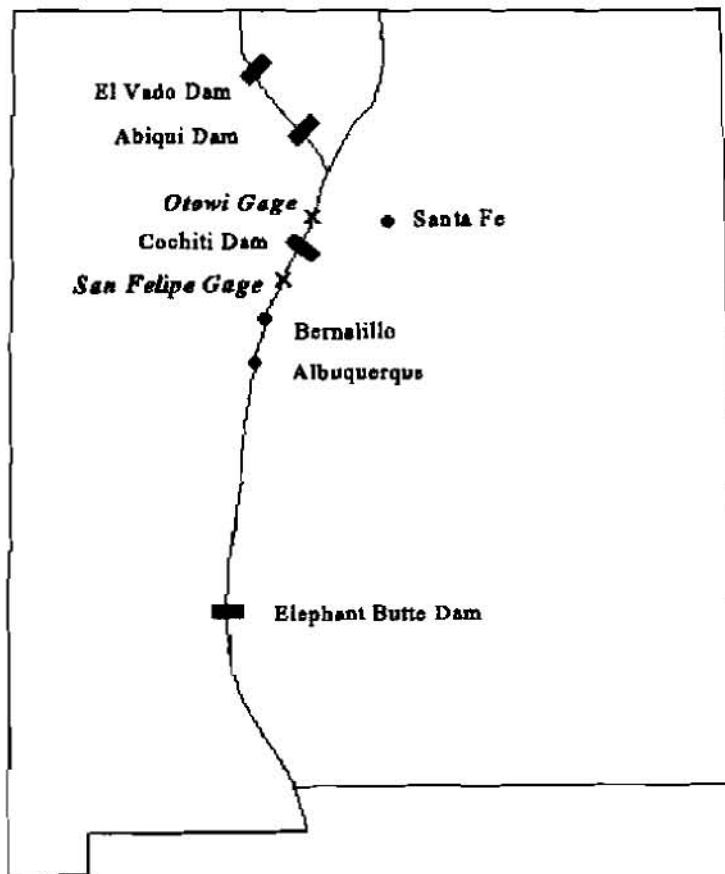


Figure 1. Location Map, Rio Grande and Rio Chama, New Mexico.

Table 1. Major Floods Through the Middle Rio Grande Valley.

Sources: Development Statement, p. II-1; House Document No. 243, p.33 ; USGS ADAPS Records.

Spring 1874, Albuquerque	120,000 cfs (MRGCD estimate)
	45,000 cfs (SCS estimate)
Spring 1884, Albuquerque	40,000 cfs
Spring 1920, Otowi	28,800 cfs
Spring 1941, Otowi	22,500 cfs
Spring 1941, Albuquerque	20,600 cfs

Photographs of the Flood of 1941 document the extensive changes created in both the floodway and surrounding riverside riparian forest (bosque). Figures 2 and 3 show the extensive sedimentation deposited as the flood wave receded. The channel shows widening at the expense of the surrounding bosque. During this and other similar flood events in the first part of this century, much of the bosque was destroyed. Often, salt flats were left in place of the willow and cottonwood bosque because of the subsequent high water table.

Completed in 1975, Cochiti Reservoir has significantly altered downstream river flows. Peak discharges have been reduced to the maximum that the river between Cochiti and Elephant Butte is capable of passing without harming riverside facilities and causing flooding. All flood control storage at Cochiti must be released downstream as soon as possible. During high inflow years, reservoir operations store inflows in excess of that which the river downstream can convey without damaging riverside facilities. Lower flows are then discharged for a longer duration. Figure 4 shows how outflows from Cochiti, as measured at the USGS San Felipe stream gage, have lower peaks and longer durations than inflows as measured at the USGS Otowi station. Flow peaks at San Felipe have been lowered considerably below the historical unregulated two year return period peak or channel-forming discharge of 11,166 cfs. Since flow regulation began at Abiquiu Dam on the Rio Chama in 1963, and Cochiti Dam on the Rio Grande in 1975, the regulated two-year return flow has decreased to 5,650 cfs, or about half of the unregulated peak flow (Bullard and Lane, 1993). Figure 5 shows the annual peak discharges between 1895-1996 at the Otowi gage, which correlates well with the San Felipe gage. Figure 5 shows 15 annual peak discharges greater than or equal to the channel forming discharge from 1895 to 1949. There are only two annual peak discharges greater than or equal to the channel forming discharge from 1950 to 1996.

By impounding sediments in the reservoir, it was hoped that the Rio Grande in the middle valley would degrade instead of aggrade. This would alleviate drainage problems by lowering the water table and lessen flood control problems because of increased channel capacity between the levees. Even before Cochiti Reservoir was built, the Bureau of Reclamation undertook channelization projects in the 1950's and 1960's to improve channel capacity, efficiency of water deliveries, and sediment transport capabilities. Figures 6 and 7 show how Kelner jacks and channelization were used to move the river away from an oxbow. An effort is underway among State and Federal Resource Management Agencies to quantify the effects of human activities on the environment. Of special interest are the impacts on endangered species (the silvery minnow and Southwestern willow flycatcher) and preservation of the bosque.

GEOMORPHOLOGY

The changing geomorphology of the Rio Grande below Cochiti Dam is evident from planform, sinuosity, and cross sectional data. Figure 8 shows the active channel planform of the Rio Grande just below Cochiti Dam in 1918, 1935/1936, 1984, and 1992. These planforms show a trend from a wider braided channel to a narrower single channel. The width of active channel for the river reach from Cochiti Dam to the New Mexico Highway 44 bridge in Bernalillo N.M. was obtained for the different years (Figure 9). Results show a consistent downward trend in active channel width between 1918 and 1992. Between 1918-1936 the river sinuosity was 1.10 and increased to 1.13 in 1949. Between 1949 and 1972 the sinuosity decreased to 1.07 due to the combined effects of channelization activities and the reduced peak flows from the watershed. Channelization activities occurred between 1953 and 1972. After 1972 the sinuosity has increased and the channel width has continued to decrease due to channel degradation and reduced sediment supply below Cochiti Dam. The river response in general coincides with the general geomorphic responses below major reservoirs as described by Schumm (1977). The increased sinuosity, channel migration, and channel incision is threatening to erode riverside levees in numerous areas. The levees protect riverside irrigation facilities, farmlands, and residential areas.

Figure 10 shows a typical cross section near Bernalillo in 1972 and 1995, showing channel degradation. The degradation extends downstream about 125 river miles. Thalweg degradation is highly variable and ranges from 1.8 ft. to 10.3 ft. with an average of 5.9 ft. between 1973 and 1995. In the first 22 miles downstream from Cochiti Dam, the bed material median size increased from an average of about 0.4 to about 3 mm between 1970-1980 (Lagasse, 1994). Additional bed material particle size data collected in this reach since 1980 shows that the median size is 20 mm or more in some areas.

CONCLUSION

The altered hydrograph and reduced sediment load below Cochiti Dam have caused some but not all of the geomorphic changes in the middle Rio Grande since 1972. The trend towards a narrower channel was present since at least 1918 and the narrowing rate has not accelerated since construction of Cochiti Dam. Although channelization of the Rio Grande has resulted in a narrower floodway, it has also allowed the bosque to flourish by stabilizing sediments long enough for vegetation to grow. While sinuosity has increased since 1972, it has still not reached the recorded peak in 1949. The historical channel forming discharge of 11,166 cfs has never been released from Cochiti Dam. However, this discharge has only been available twice during the 21 year period of reservoir operations, in 1985 (12,000 cfs at Otowi) and 1979 (11,500 cfs at Otowi). The lack of these larger peak flows since the late 1940's accounts for a portion of the channel narrowing that has occurred since 1942, in addition to the effects of channelization and construction of Cochiti Dam.

In summary, the flood history of the Middle Rio Grande has played a significant role in the development of geomorphic characteristics and surrounding habitat which are evident today. These changes are not solely due to human activities on the environment.

REFERENCES

Bullard, K.L., and Lane, W.L., (1993) "Middle Rio Grande Peak Flow Frequency Study," U.S. Department of the Interior, Bureau of Reclamation, Flood Hydrology Group, Denver Technical Center, Denver, CO.

Crawford, C.S. et. al. (1993) "Middle Rio Grande Ecosystem: Bosque Biological Management Plan." Biological Interagency Team, Albuquerque, New Mexico.

Development Statement, Middle Rio Grande Conservancy District, Albuquerque, NM, 1980 p. II-1

Lagasse, P.F. (1994) "Variable Response of the Rio Grande to Dam Construction," *The Variability of Large Alluvial Rivers*, ASCE Press, New York, New York.

Schumm, S. A., (1977), "The Fluvial System," John Wiley and Sons, New York, NY.

U. S. Congress. Rio Grande and Tributaries. New Mexico. House Document No. 243, 81st Congress, 1st Session. United States Government Printing Office, Washington: June 27, 1949.

U.S. Geological Survey ADAPS records.

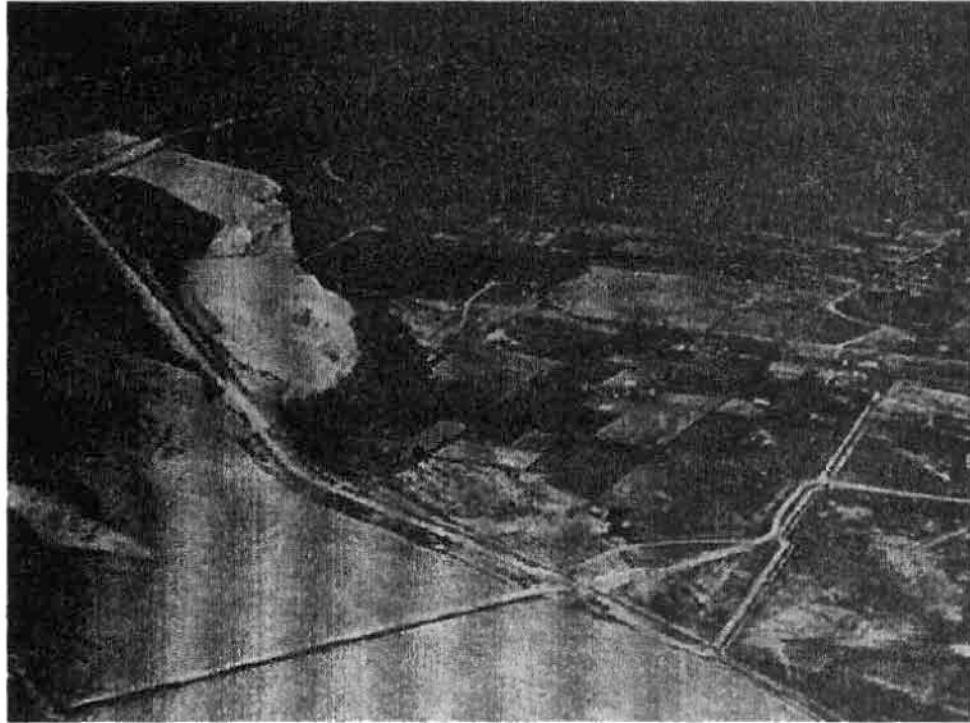


Figure 2. Channel avulsion, levee breaches, sedimentation, and bosque destruction resulting from the Flood of 1941.

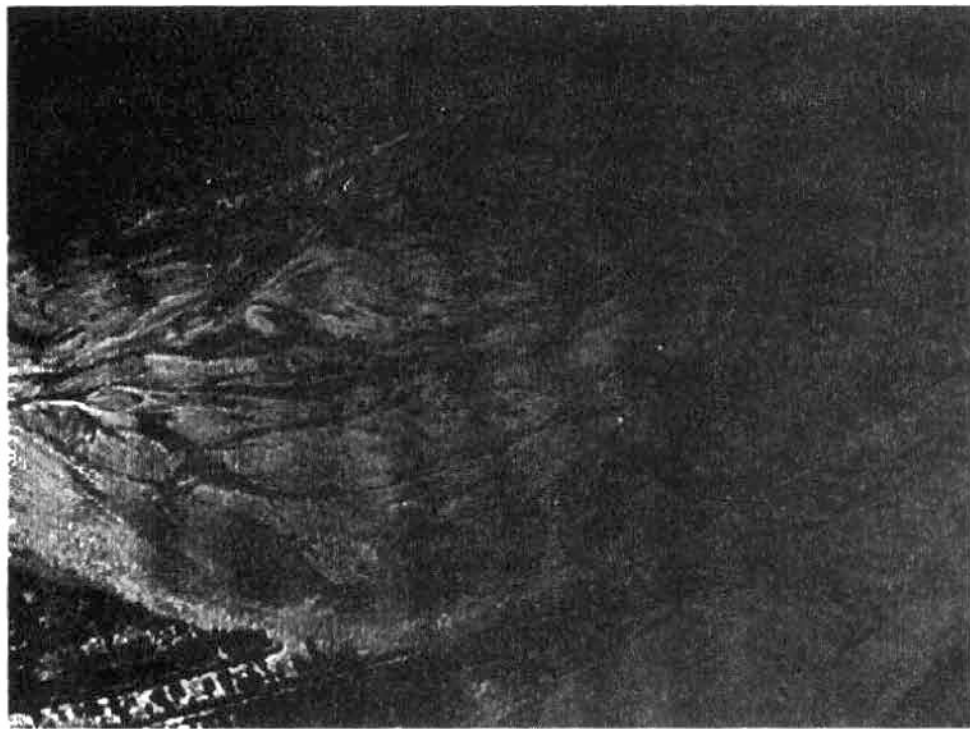


Figure 3. Channel widening, levee breach, sedimentation, and bosque destruction resulting from the Flood of 1941.

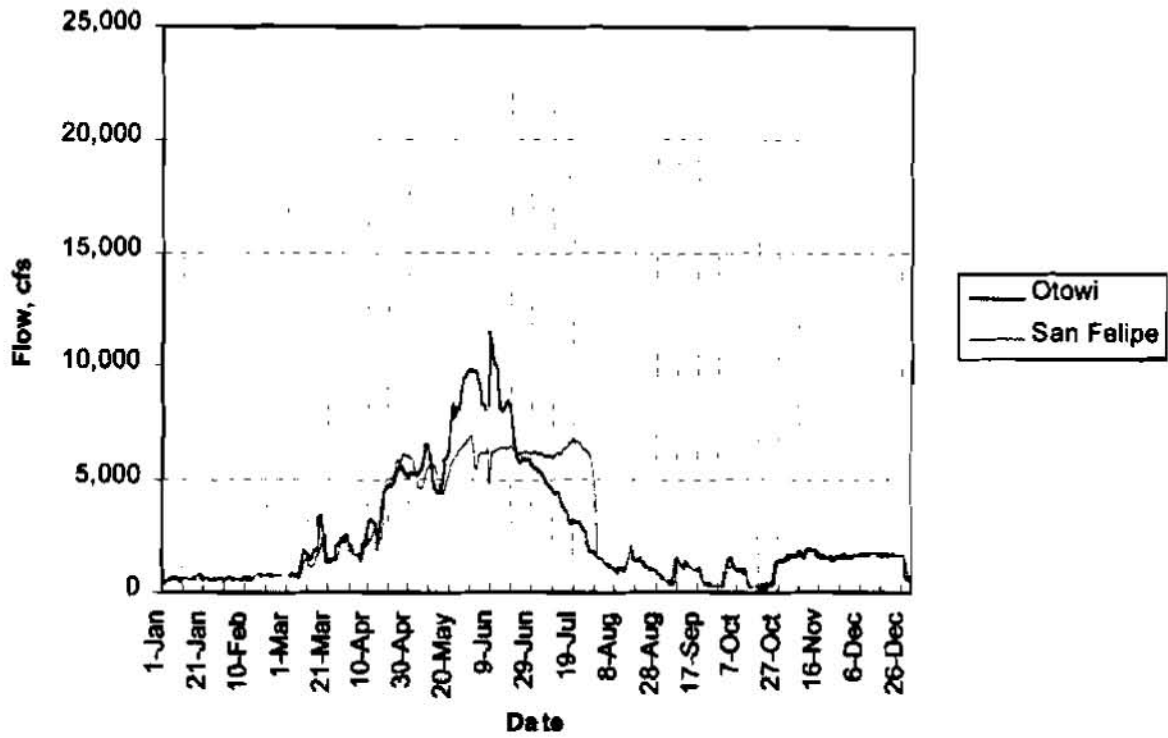


Figure 4. Cochiti Reservoir Inflow (Otowi) and Outflow (San Felipe) 1979 Hydrographs.

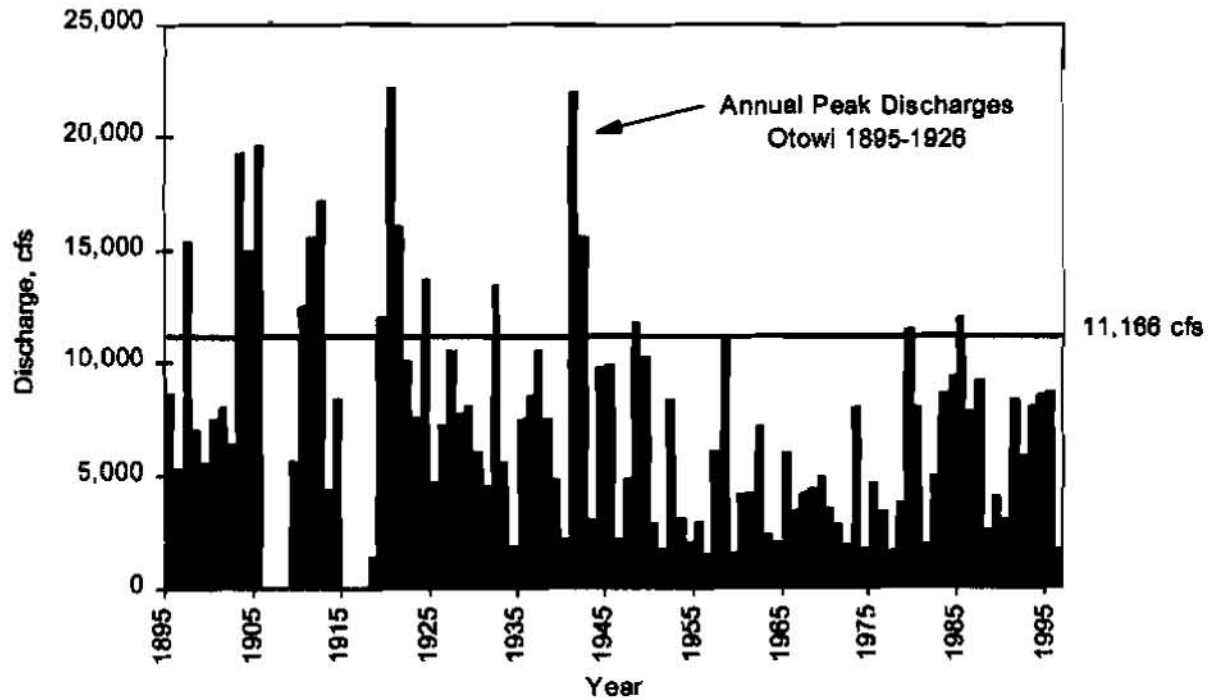


Figure 5. Historical Flow Peaks at Otowi with Channel-Forming Discharge of 11,166 cfs.



Figure 6. Oxbow near University of Albuquerque in the 1960's, showing meandering and bank erosion. Channelization to bypass oxbow is at left. Kelner jacks appear as faint lines parallel to the new channel and through the oxbow.

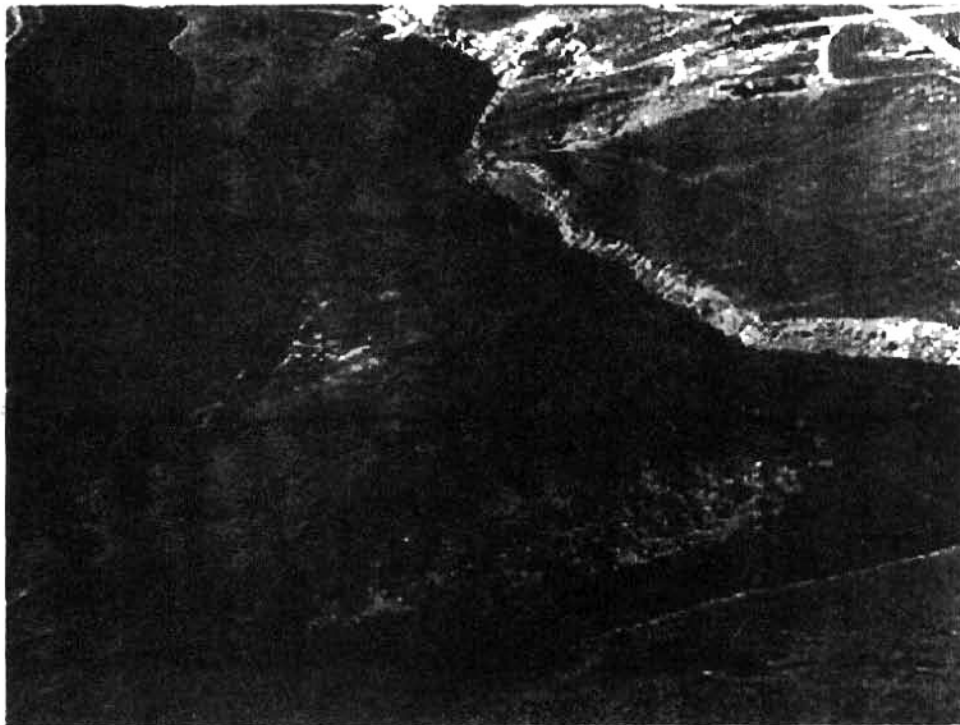


Figure 7. Oxbow near University of Albuquerque several years after channelization. Kelner jacks have succeeded in depositing sediments and vegetation is now flourishing. River is flowing in constructed channel.

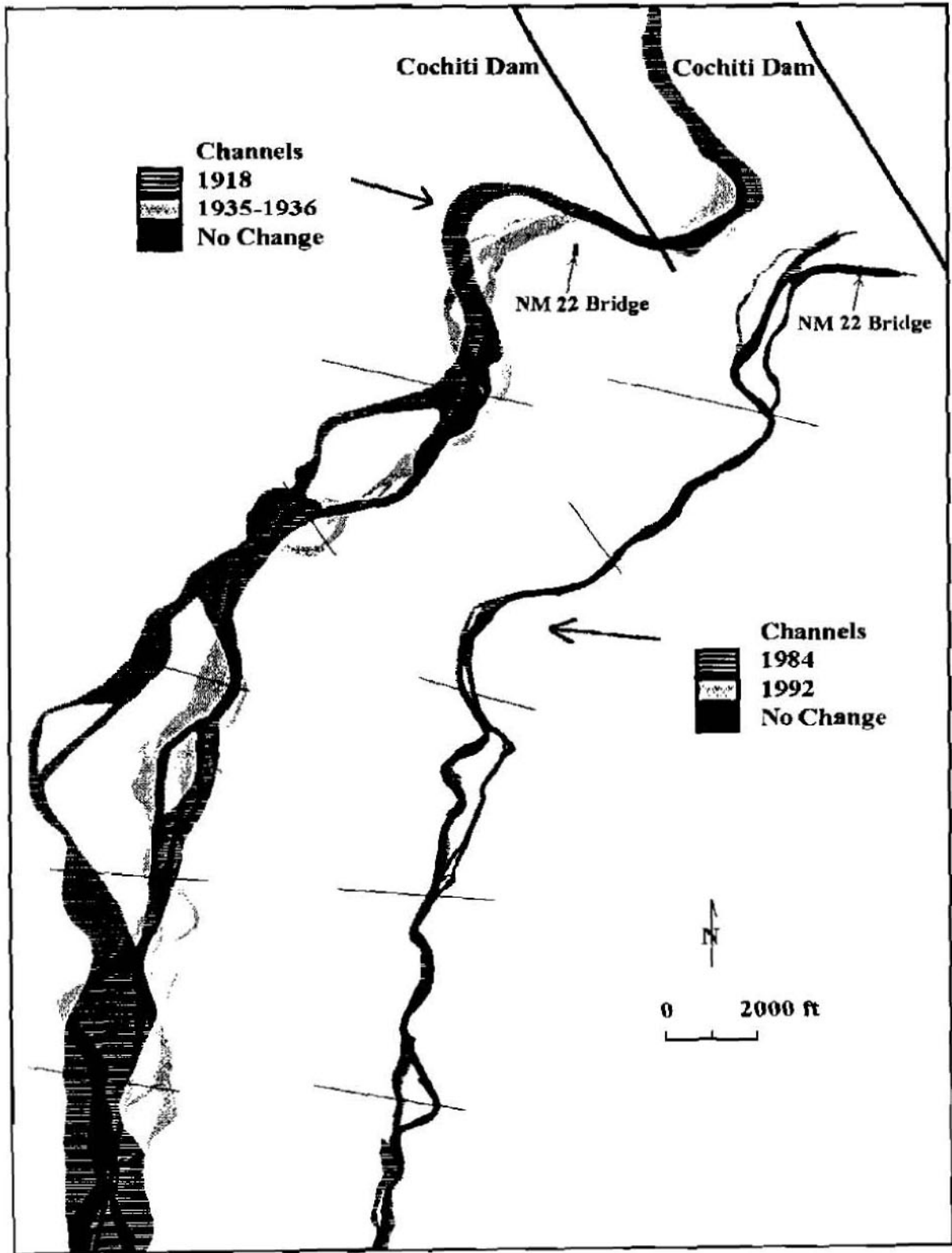


Figure 8. Rio Grande Planform Comparison below Cochiti Dam.

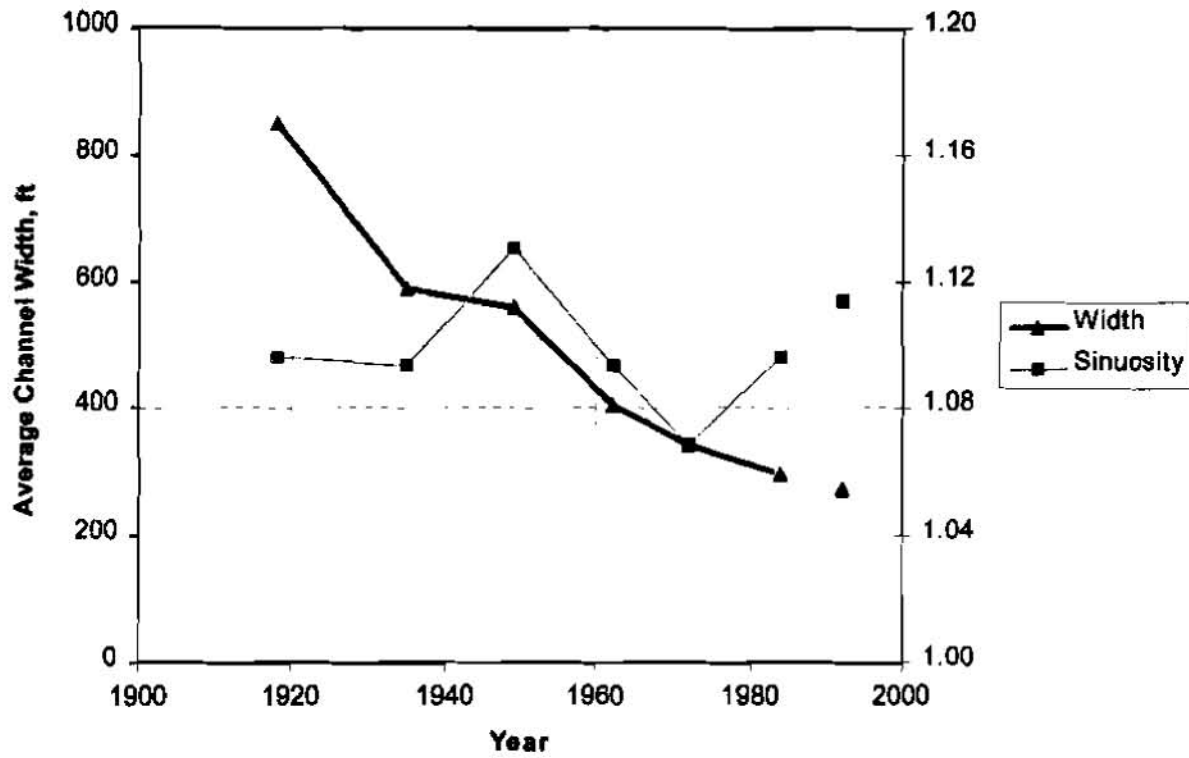


Figure 9. Rio Grande Active Channel Average Width and Sinuosity below Cochiti Reservoir.

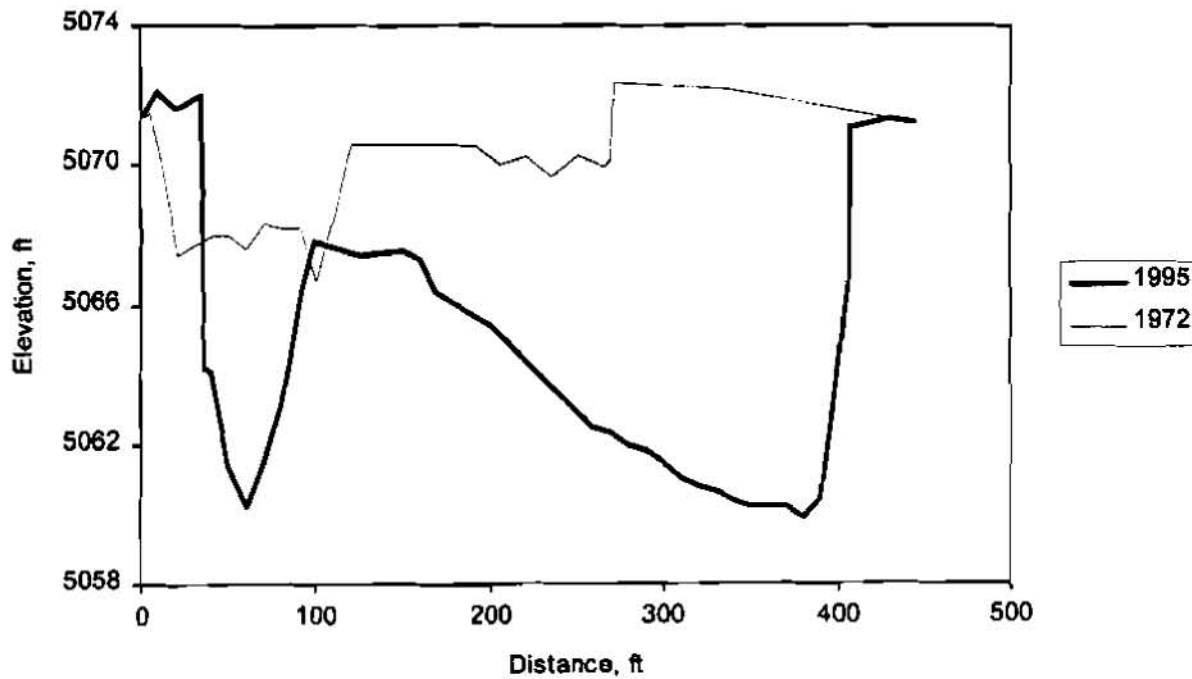


Figure 10. Typical Rio Grande Cross-Section near Bernalillo.

ALTERNATIVES ANALYSIS FOR REDUCTION OF MAINTENANCE DREDGING OF A TIDAL INLET

by

**Conor Shea, Senior Water Resources Engineer;
Michael Ports, Principal Water Resources Engineer; and
David Froehlich, Senior Water Resources Engineer;
Parsons Brinckerhoff, Inc., Baltimore, Maryland**

Abstract: Little Lagoon Pass is a tidal inlet located in Gulf Shores, Alabama. The Pass is the only permanent connection between Little Lagoon and the Gulf of Mexico. The Pass is subject to frequent infilling and blockage as sand is transported into the inlet by daily tidal cycles and occasional storm surges. When the inlet is blocked, water levels rise in the Lagoon causing flooding problem. Lagoon water quality may also be impaired due to loss of tidal flushing action. Dredging is required on a regular basis to maintain the Pass and is performed for extended periods about six time per year.

An investigation was conducted to examine the Pass and to examine the feasibility of alternatives to reduce the amount of required dredging. Three alternatives were developed and examined: The alternatives were evaluated through hydraulic and sediment transport modeling using the FHWA Finite Element Surface Water Modeling System - Flow in a Two Dimensional Horizontal Plane (FESWMS-2DH) computer model. Pass reconfiguration was selected as the preferred alternative based on a economic and feasibility analysis of the alternatives.

INTRODUCTION

Little Lagoon is a small tidal Lagoon located in Gulf Shores, Alabama. At the present time, the Lagoon possesses a single outlet to the Gulf of Mexico called Little Lagoon Pass (the Pass). The Pass is a 400 meter (1,300 feet) long, artificial channel that was constructed at the location of a intermittent channel in 1981. The Pass allows tidal flows to mix with the Lagoon and provides positive drainage for flood relief during major precipitation events. In addition, the Pass provides access for recreational and commercial fishing boats traveling between Little Lagoon and the Gulf of Mexico.

The Pass experiences chronic sand deposition, blocking flow from entering and leaving Little Lagoon. Closure of the Pass, either permanent or short term, is undesirable. The Pass must be kept open to maintain a positive drainage outlet and to provide flushing of Little Lagoon. There are concerns that the water quality of Little Lagoon may be severely impacted if the Pass becomes blocked because the shoreline of Little Lagoon is heavily developed with residential and vacation homes, some of which employ septic tanks for sewage treatment. If the daily tidal action that flushes the Lagoon were to be lost, it is possible that the effluent

from the septic tanks and organic loading from freshwater lakes would degrade the water quality of the Lagoon.

The State of Alabama Department of Transportation (ALDOT) is responsible for maintaining the Pass. Dredging must be started when sand deposition within the Pass results in the bed elevation at any point within the Pass to rise above a threshold elevation of -0.91m (-3.0 feet) NGVD. ALDOT must restore a cross section throughout the Pass to a depth of -1.52m (-5.0 feet) NGVD. Currently, ALDOT employs a floating dredging to clear the Pass. Sand from the dredging operations is deposited on the beach front down drift from the Pass. The volume of dredging is approximately 84,000 cubic meters per year (110,000 cubic yards per year). Total dredging costs to maintain the Pass are approximately \$22,000 per month or about \$3.08 per cubic meter (\$2.35 per cubic yard). Costs are high because a dredge must be maintained on station for immediate response at any time.

Parsons Brinckerhoff, Inc. was contracted by ALDOT to conduct a hydraulic analysis of the Pass and to examine alternate measures for maintaining the Pass (Parsons Brinckerhoff, Inc., 1997). The goal of the study was to identify a less expensive method of maintaining the Pass that did not result in reduction of flow through the Pass or result in undesirable sand deposition or beach erosion. Both structural and nonstructural measures were examined.

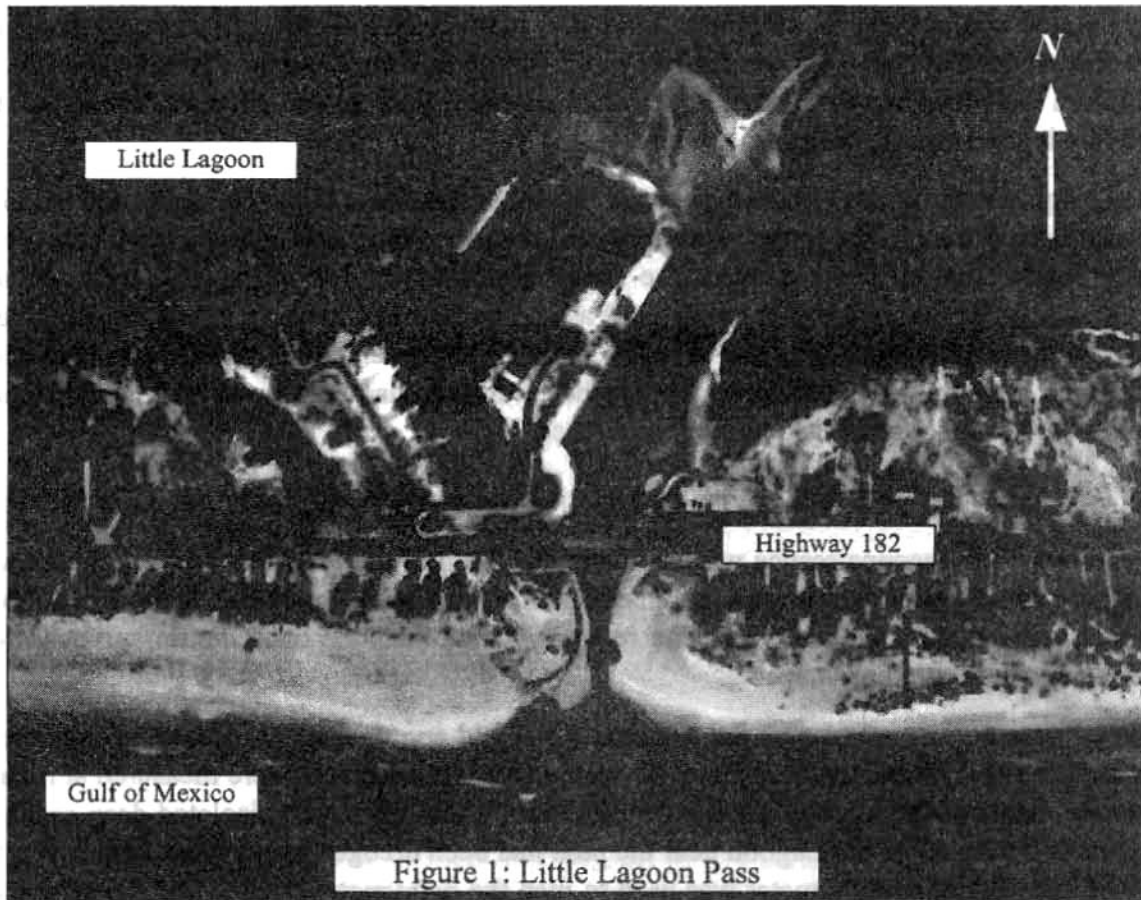
The study was conducted in four phases. Phase I consisted of field reconnaissance, bathymetric survey, and data collection. Phase II consisted of the development, calibration, and validation of a two-dimensional, dynamic hydraulic and sediment transport model of Little Lagoon. Phase III consisted of the formulation and simulation of three alternate solutions and baseline conditions. Phase IV consisted of an economic and feasibility analysis and comparison of the alternate solutions.

SITE DESCRIPTION

Little Lagoon: Little Lagoon is located in the extreme southern tip of Baldwin County, Alabama. The Lagoon is about 13 km (8 miles) in length and about 0.8 km (0.5 miles) in width. The Lagoon is shallow. Maximum depth is less than 4.2 m (14 feet) and most of the Lagoon has depths less than 2m (6 feet). The bottom profile running perpendicular to the Gulf of Mexico suggests that the Lagoon was originally part of the Gulf shoreline. A spit or bar was formed or deposited in front of the original shore and eventually formed the Lagoon.

The contributing drainage area into Little Lagoon is approximately 40 km² (15 square miles) Three freshwater lakes known as Little Lake, Middle Lake, and Lake Shelby are in the upper part of the drainage area, east of Gulf Shores. Drainage from the lakes into Little Lagoon is regulated by a recently installed weir. The weir has improved water quality in the Lagoon by trapping organic particulates within the freshwater lakes.

The Gulf Coast on the south side of the Lagoon is heavily developed. Development is most intense at the eastern end where the commercial area of the City of Gulf Shores is located. Multistory hotels, apartment buildings, and condominiums are common. Moving west along the Gulf Shore development becomes less dense. Development tapers into duplexes, vacation



cottages, and single family homes. The northern side of the Lagoon is developed in single family homes on large lots. The northern side is also heavily wooded. The extreme western end of the Lagoon is undeveloped. The City of Gulf Shores now requires all new development to connect to the City's sewage treatment system. Existing homes that are not connected to the system are required to connect into the system if septic systems fail.

Prior to construction of Little Lagoon Pass, there was not a permanent outlet channel from the Lagoon. Two ephemeral channels existed. One was located at the present location of the Pass. The other was located about 5 km (3 miles) further to the west. Anecdotal information suggests that usually only one channel would be open at a time. At times, the channels would be blocked by sand deposition in the channels completely closing the outlets from the Lagoon. Without an outlet, water levels in the Lagoon would rise until hydraulic forces were sufficient to reopen one of the channels. The Lagoon would drain and the cycle would be repeated.

Little Lagoon Pass: Little Lagoon Pass is located about a third of the way from the eastern end of the Lagoon. The Pass is oriented perpendicular to the Gulf Shore and curves as it enters Little Lagoon (Figure 1). The Pass is crossed by Alabama State Highway 182, a pedestrian walkway to the south of the highway bridge, and an elevated water line. The inlet varies in width from between 12 to 50 m (40 to 164 feet) and is about 0.4 km (1/4 mi.) long. The narrowest section of the inlet is at the Gulf entrance. Between the Gulf shoreline and the Highway 182 Bridge, both sides of the Pass are bounded by concrete seawalls. On the

Lagoon side of the Pass, an aluminum bulkhead seawall extends the full distance along the west side of the Pass between the Highway 182 Bridge and the Lagoon. On the east side, an aluminum bulkhead seawall extends a partial distance then stops. The remainder of the shoreline is sand transitioning into a marsh.

When originally built, the Pass had seawalls that extended about 60m (200 feet) into the Gulf beyond the shoreline. The jetties were removed to the existing shoreline in 1991 because of severe beach erosion to the west of the Pass. Removal of the jetties is thought to have increased the amount of sand entering the Pass. The beaches to the west of the Pass have recovered somewhat since the removal of the jetties. Improvement is attributed to placement of dredged sand from the Pass onto the beaches, but may also be a result of improved dune management practices such as plantings and fences.

SITE RECONNAISSANCE

An extensive site reconnaissance was conducted as the first phase of the study. The purpose of the site investigation was to gain an understanding of existing conditions in the Pass for use in modeling proposed alternatives. The reconnaissance included bathymetric surveys, flow monitoring, and sediment sampling.

Surveys were performed to map the Lagoon, Pass, and approaches. A recording fathometer was used to survey the Lagoon. A total of twenty five cross sections were measured at regular intervals. Most of the Lagoon is naturally shallow. There are several isolated deep sections. An area in the center of the Lagoon near the pass had been dredged to replenish beaches to the west of the Pass. The fathometer was used to map the bathymetry of the Gulf shore near the Pass. Cross sections were taken that extended 1 km (0.6 mile) into the Gulf from the shoreline. Extensive wading surveys were performed in and near the Pass. Surveys in the Pass are time sensitive. Sand transport rates are sufficiently high to cause the bed of the Pass to change on a daily basis. The general trend is towards deposition.

A sediment sampling program was conducted to help identify the sources and sinks of sand in transport through the Pass and the Lagoon. Samples showed an accumulation of organic materials in the samples taken from the east end of the Lagoon near the inflow from the Freshwater lakes. Moving towards the Pass, the sediment becomes cleaner and of more uniform characteristics. Sand size particles dominate. The grain size distribution measurements provide a strong indication that sand is transported from the Gulf into the Pass and Lagoon. The median grain size decreases moving into the Pass from the Gulf. The flood shoal is finer than Lagoon sediments. The ebb shoal has coarser sediment than adjacent Gulf samples. Flow over the ebb shoal is very shallow (less than 0.5m or 1.5 feet), resulting in stripping of fines from the surface sediment.

A set of manually read, tidal gages were established in the Pass, Lagoon, and at the Gulf Entrance. Simultaneous measurements were taken over a three week period to establish the change in water surface elevations across the Pass. Velocity and stage in the Pass were measured at four cross sections over the course of four tidal cycles. The tidal gage and velocity measurements also were used for calibration of the hydrodynamic model.

The tidal stage observations provide useful insights. On one occasion, the remnants of a hurricane caused sustained, heavy winds from the southwest for a three day period. During this time, the normally placid Gulf had heavy surf conditions. The normal tidal cycle was interrupted by the wind driven waves. There was no ebb flow through the Pass. Instead water levels in the Lagoon rose as the Lagoon was flooded by flow entering from the Gulf. The Gulf flows also brought in a large amount of sand that was deposited in the Pass.

The velocity measurements also pointed out an important characteristic of the Pass. The Pass is narrowest at the Gulf Entrance. Flow velocities are highest in this section. Approaching the Highway 182 Bridge, the Pass widens by a factor of three. Velocities drop in the expanded section. The Pass then travels beneath the Highway 182 Bridge which has four piers in the channel and the adjacent water pipeline which has four piers in the water. Flow velocities drop further due to pier resistance. As the Pass approaches the Lagoon, flow velocities drop again as the channel widens. The overall trend is for the competence of the Pass to transport sediment to undergo a steady decrease from the Gulf entrance to the Lagoon entrance.

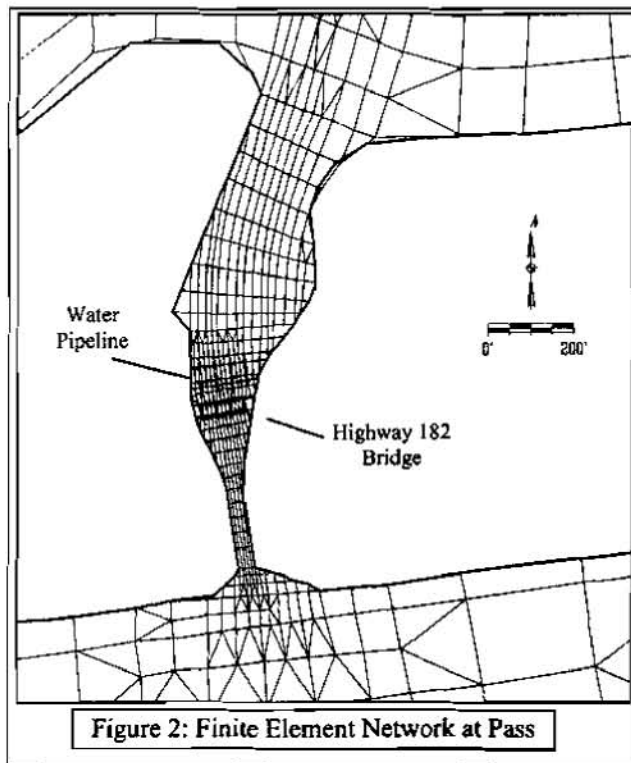
In addition to field observations, a review of dredging records was performed. As part of the maintenance program for the Pass, a bed elevation survey of the Pass is performed about once or twice a week. The survey consists of several point observations of bed elevation in the center of the channel at scattered locations throughout the Pass. Review of the records show some interesting patterns. Almost immediately after dredging is completed, the bed elevations begin to rise in the section of the Pass between the Highway 182 Bridge and the Lagoon. The bed elevations rise continuously in this section, but not at a consistent rate. Sudden increases occur which may be the result of strong winds from the southeast and southwest. As soon as one part of the Pass becomes filled in, the remainder of the Pass rapidly infills.

A general conclusion of the field investigations is that the Pass experienced infilling due to the expansion of the channel and head loss through the bridge crossings. Not all of the sand carried into the narrow deep channel at the Gulf entrance can be carried through the entire length of the Pass into the Lagoon resulting in deposition within the Pass.

HYDRODYNAMIC MODELING

A two-dimensional, dynamic hydraulic model of Little Lagoon was developed using the FHWA Finite Element Surface Water Modeling System - Flow in a Two Dimensional Horizontal Plane (FESWMS-2DH) computer model (Froehlich, 1996). FESWMS-2DH employs a finite element network to solve the momentum and energy equations and compute the direction and depth of flow at each node point in the finite element network. Dynamic conditions are simulated by the model so that the circulation through the Pass induced by tidal fluctuations may be modeled. The two dimensional model provides accurate resolution of the two dimensional flow field and is able to account for the complex bathymetry of the Lagoon.

A beta version of FESWMS-2DH Version 3.0 which incorporates sediment transport functions was employed for this study. The sediment transport functions model both



deposition and scour. The grain size distributions of the sediment in the study area has low variability, so armoring would not occur and an average grain size could be used in the model to represent the sediment.

The solution domain for the model included Little Lagoon, Little Lagoon Pass, and a portion of the Gulf of Mexico extending 1 km (0.6 mile) into the gulf and 1 km (0.6 mile) to either side of the Gulf entrance to the Pass. A portion of the finite element network for the area of the Pass is shown in Figure 2. Inflow from the freshwater lakes was assumed to be zero. It was assumed that the water in the Lagoon was saline. Modeling of fresh water/salt water mixing was not performed.

The hydrodynamic portion of the model was calibrated and validated using the field measured stages and flow velocities. Sufficient data was collected to allow for calibration of the hydraulic model over several tidal cycles. The model was run in a dynamic mode with a time step of 3 minutes. Boundary conditions for sediment transport and along shore currents were developed through use of Shore Protection Manual guidelines and methodologies (U.S. Army Corps of Engineers, 1977), and based on results from the field reconnaissance. The model was judged to provide an accurate simulation of existing conditions in the Pass.

DEVELOPMENT AND TESTING OF ALTERNATIVES

Development of Alternatives: In Phase III, conceptual alternatives for modifying the Pass were identified, developed, and tested. It was determined that the conceptual alternatives had to possess (or potentially possess) the following characteristics:

- (1) The flow through the Pass is sufficient to provide circulation to the Lagoon through the normal tidal cycle;
- (2) Longshore sand transport is not interrupted and no beachfront erosion occurs; and
- (3) The Pass is self-maintaining or able to be maintained with a limited amount of maintenance and dredging.

Three alternatives were identified:

- (1) Modification to existing dredging methods;
- (2) Installation of a groin system with sand bypassing; and

(3) Reconfiguration of the Pass to improve hydraulic efficiency.

The finite element network was modified to represent each of the alternatives. In addition, a Baseline model, representing conditions immediately after completion of current dredging procedures, also was generated. Each model was run through two tidal cycles. Analysis of the model results generated the following conclusions:

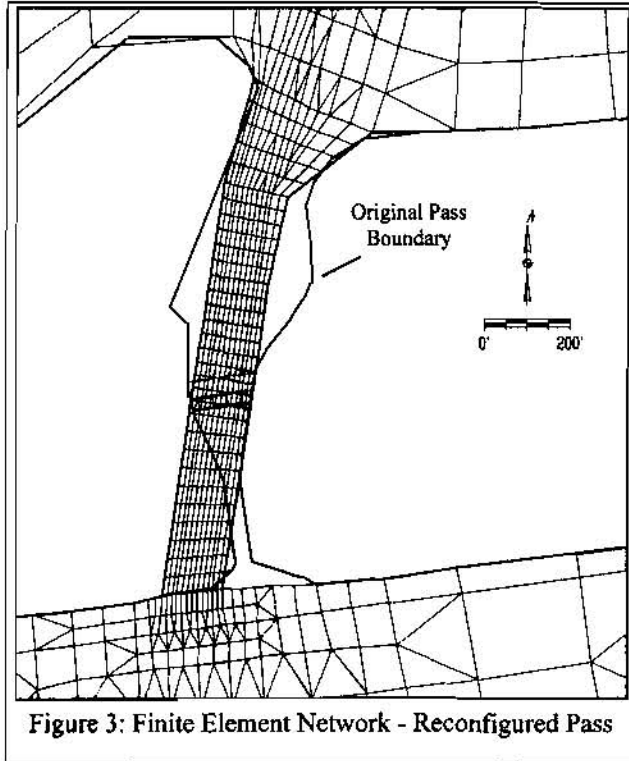


Figure 3: Finite Element Network - Reconfigured Pass

Revised Dredging Pattern: The revised dredging pattern deepened but did not widen the existing dredging cross section. Discharge through the inlet remained very close to the Baseline conditions, but flow velocities dropped dramatically. This result is somewhat intuitive because flow through the Pass is generated by the same water surface differential. It was concluded that deepening the cross section resulted in making the Pass a more efficient sediment trap.

Jetties with Sand Bypassing: The model simulated installation of the jetties, but did not incorporate the sand bypassing plant. Flow was not substantially altered. Sand inflow into the Pass was lowered due to lower velocities at the entrance to the jetties.

Pass Reconfiguration: The model simulated an angled inlet with no bends (Figure 3). The reconfigured Pass increased discharge on both flood and ebb tides. Most importantly, it resulted in a significant reduction in the amount of sand deposited in the Pass. Total sand discharge, measured as the difference between sand entering and exiting the Pass was increased greatly on both flood and ebb tides.

ECONOMIC AND FEASIBILITY ANALYSIS

An economic and feasibility analysis was conducted for each of the alternatives. The economic analysis was based on cost estimates for construction and annual maintenance costs. The Feasibility analysis considered the practicality of the alternative, local acceptance, and environmental impacts. The findings of the analysis were:

Revised Dredging Pattern: The revised dredging pattern could not be shown to effectively reduce maintenance costs. In addition, the dredging program at the Pass is closely monitored by local residents. Hence, any changes to existing procedures might draw objections. It was judged that a revised dredging pattern did not offer any significant advantages over existing procedures.

Jetties with Sand Bypassing: Sand bypassing was often touted as a fix. The feasibility analysis shows that it is not practical for three of reasons. First, the cost is very high in terms of initial investment and annual operation costs and bypassing may not completely eliminate the need for periodic dredging. Second, the Pass is a very popular tourist destination. Installation of sand bypassing plant may introduce a safety hazard to beach goers and create noise and sight impacts on an attractive beach. Third, sand transport rates at the Pass are highly variable. Major hurricanes and storm surges might deliver too much sand and cause the plant to fail, or otherwise damage the plant.

Pass Reconfiguration: Initial construction costs for reconfiguring the Pass are high, but reconfiguration could substantially reduce dredging costs. There may be local objections to any action at the Pass, but the reconfiguration appears to satisfy objectives of beach front properties and Lagoon concerns. Long term impacts of Pass reconfiguration are unknown. The reconfiguration greatly increases the potential sand transport rates through the Pass.

CONCLUSIONS

Review of the alternatives has led to the selection of Pass reconfiguration as the preferred alternative. Studies are now underway to optimize a reconfiguration design and examine long term impacts on the Lagoon, Pass, and beach front. Use of FESWMS-2DH to model the hydrodynamics and sediment transport proved to be an effective tool to examine the effects of alternative measures to improve the Pass.

REFERENCES

- Coastal Planning and Engineering, Inc., 1991, *An Evaluation of Possible Impacts that Shore Perpendicular Structures May Have Had at Little Lagoon Pass*, Prepared for the Alabama Department of Transportation by Coastal Planning and Engineering, Inc., Boca Raton, FL.
- Froehlich, D. C., 1996, *Finite Element Surface Water Modeling System: Two-dimensional Flow in a Horizontal Plane, Version 2 Draft User's Manual*, U.S. Federal Highway Administration, McLean, VA, 1996.
- Parsons Brinckerhoff, Inc., 1997, *Little Lagoon Pass Hydraulic Study and Feasibility Analysis*, Report prepared by Parsons Brinckerhoff, Inc., Baltimore, MD for the Alabama Department of Transportation.
- Richardson, T.W. 1991, "Sand Bypassing," Chapter 16 in *Handbook of Coastal and Ocean Engineering*, Volume 2, J.B. Herbich, editor, Gulf Publishing Company, Houston, Texas.
- U.S. Army Corps of Engineers, 1981, *Reconnaissance Report, Little Lagoon at Gulf Shores Alabama*, prepared by the Mobile District, Corps of Engineers, Mobile, AL, May, 1981.
- U.S. Army Corps of Engineers, 1977, *Shore Protection Manual*, U.S. Army Coastal Engineering Research Center, Washington, D. C.

INVESTIGATION OF PHYSICAL MECHANISMS UNDERLYING THE PREDICTABILITY OF DROUGHTS

T. T. Burke, Jr., Water Resources Engineer, Christopher B. Burke Engineering, Ltd., Rosemont, IL 60018; A. Ramachandra Rao, Professor, School of Civil Engineering, Purdue University, W. Lafayette, IN; and Khaled Hamed, Assistant Professor, Irrigation and Hydraulics Department, Faculty of Engineering, Cairo University, Giza, Egypt

Abstract: The regional predictability of Palmer's Drought Severity Index (PDSI) has been investigated by using spatial principal components of PDSI by Burke and Rao (1996). However, such an analysis does not provide any insight into the physical mechanisms underlying the predictability of the processes. The spatial structure of the patterns which can be predicted for the PDSI and precipitation variables are examined in this paper. An investigation of these patterns and the causal variable prior to the time at which the variable is predicted is useful. Usually, three or more patterns of the predicted variable are needed to make accurate predictions. Examining the patterns to gain insights into the physical mechanisms leading to the predictability of a process is neither easy nor usually possible. Consequently, a compact method of describing the connection between the process which is being predicted and the causal variable is needed. A method of compact representation of data, called "Principal Estimator Pattern", has been developed for this purpose by Davis (1977 and 1978). Davis' method is used in the present study to gain insight into the causal connections between precipitation and PDSI. The theory behind the method is described first. Data used and the results of the study are presented next. A set of conclusions are given in the end. The results of the study demonstrate the fact that principal estimator patterns can be successfully used to investigate the cause-effect relationships between spatio-temporal hydrologic variables. In particular, relationships between the present and past regional PDSI values and between regional precipitation and regional PDSI demonstrate the importance of both the persistence of droughts and of rainfall in predicting droughts.

INTRODUCTION

Both precipitation, which is the causal variable in this study, and droughts, which is the effect variable, vary both in space and time. Characterizing spatio-temporal variables, either to investigate their individual characteristics or their causal connections require special techniques. One such technique is based on principal estimator patterns. The technique of estimating principal estimator patterns was developed by Davis (1977 and 1978) to characterize oceanographic data, and is used in the present study.

The first objective of the present study is to investigate the spatio-temporal characteristics of droughts and precipitation by using principal estimator patterns. The second objective is to investigate the causal connections between precipitation and droughts by using the principal estimator patterns of the two processes. Monthly Palmer's Drought Severity Index (PDSI) and precipitation are used in the present study.

The method of computation of principal estimator patterns is discussed in the next section. The data used in the study and the results are given in the third section. A set of conclusions is given in the last section.

COMPUTATION OF PRINCIPAL ESTIMATOR PATTERNS

A time lag τ , at which the physical mechanisms of the processes are investigated, is selected first.

The time lag may be between the observations of the same process or between different processes. The principal estimator patterns are computed by using the spatial and temporal principal components. The spatial and temporal principal components of the data are computed by using methods discussed in Burke and Rao (1996). Let the principal spatial components of precipitation and PDSI data be denoted by $P_n(x)$ and $d_n(y)$ respectively. Similarly the principal temporal components of precipitation and PDSI data are denoted by $\pi_n(t)$ and $\theta_n(t+\tau)$. The precipitation and PDSI fields are approximated as in eqs. 1 and 2.

$$\tilde{P}_{x,t} = \sum_{n=1}^{M^*} \pi_n(t) P_n(x) \quad (1)$$

$$\tilde{d}_{x,t+\tau} = \sum_{n=1}^M \theta_n(t+\tau) d_n(y) \quad (2)$$

In equations 1 and 2 M and M^* are respectively the number of significant principal components used to model PDSI and precipitation data. The principal estimator patterns of precipitation data are computed by using principal amplitudes $h_m(t)$ and the associated spatial patterns $H_m(x)$ as given in eq. 3. The temporal components $\pi_n(t)$ and $h_m(t)$ are related as in eq. 4.

$$\tilde{P}_{x',t} = \sum_{m=1}^{M^*} h_m(t) H_m(x) \quad (3)$$

$$\pi_n(t) = \sum_{m=1}^{M^*} v_{nm} h_m(t) \quad (4)$$

Coefficients v_{nm} are computed by using eq. 5.

$$v_{nm} = \left[\pi_n^2(t) \right]^{1/2} \mu_{nm}, \quad n, m = 1, 2, \dots, M^* \quad (5)$$

The coefficients μ_{nm} in eq. 5 are computed by using eq. 6 with the constraints in eq. 7, where

$$\sum_{j=1}^{M^*} A_{nj} \mu_{jm} + \lambda_m \mu_{nm} = 0, \quad n, m = 1, 2, \dots, M^* \quad (6)$$

$$\sum_{i=1}^{M^*} \mu_{ni} \mu_{mi} = \sum_{i=1}^{M^*} \mu_{in} \mu_{im} = \delta_{nm} \quad (7)$$

δ_{nm} is the Kronecker delta. A_{nj} in eq. 6 are analogous to cross correlation coefficients between the temporal principal components $\theta_k(t)$ and $\pi_n(t)$ of PDSI and precipitation data. These are defined in eq. 8.

$$A_{nj} = \frac{\sum_{k=1}^M \left[\theta_k(t+\tau) \pi_n(t) \right] \left[\theta_k(t+\tau) \pi_j(t) \right] \left(\left[\pi_n^2(t) \right] \left[\pi_j^2(t) \right] \right)^{-1/2}}{\sum_{k=1}^M \left[\theta_k^2(t+\tau) \right]} \quad (8)$$

The expressions in square brackets indicate the mean over time. An example is given in eq. 9

$$\left[\Pi_m^2(t) \right] = \left(\sum_{t=1}^N \Pi_m^2(t) \right) / N \quad (9)$$

The $h_m(t)$ values in eq. 3 are estimated by using eq. 4 and $H_m(x)$ by eq. 10. $H_m(x)$ is the principal estimator pattern of the precipitation data.

$$H_m(x) = \sum_{n=1}^{M^*} v_{nm} P_n(x) \quad (10)$$

In order to compute the principal estimator pattern of the effect data PDSI, we first estimate $\bar{\alpha}_{nm}$ by using eq. 11.

$$\bar{\alpha}_{nm} = \sum_{k=1}^{M^*} \alpha_{nk} v_{km} \quad (11)$$

where

$$\alpha_{nm} = \frac{[\theta_n(t+\tau) \Pi_m(t)]}{[\Pi_m^2(t)]} \quad (12)$$

and v_{km} is defined in eq. 5. By using $\bar{\alpha}_{nm}$ and $d_n(y)$, $W_m(y)$ is estimated by eq. 13. $W_m(y)$ is the principal estimator pattern for PDSI. By using the known $W_m(y)$ and $\bar{d}_{x,t+\tau}$, the temporal components $w_m(t+\tau)$ are computed by using eq. 14.

$$W_m(x) = \sum_{n=1}^{M^*} \bar{\alpha}_{nm} d_n(x) \quad (13)$$

$$\bar{d}_{x,t+\tau} = \sum_{m=1}^{M^*} w_m(t+\tau) W_m(y) \quad (14)$$

Contour maps developed from the principal estimator patterns $H_m(x')$ and $W_m(x)$ are used to investigate their characteristics and causal connections. The principal estimator patterns may be computed by using both unrotated and rotated principal components. The rotation of principal components is discussed in Burke and Rao (1996).

DATA USED IN THE STUDY AND RESULTS

Monthly Palmer's Drought Severity Index and Precipitation Series were used in the study. The data were from the states of Illinois, Indiana, Ohio and surrounding areas. Data from January 1895 through December 1993 were analyzed. The locations of the forty nine stations from which the data were analyzed are shown in Fig. 1. The relationships between precipitation and PDSI and between lagged values of PDSI were investigated.

Relationships Between Precipitation and PDSI Case: The time lag τ value used in the study for predicting the present PDSI by using only the present monthly precipitation is 0. The reason for using only this τ value is that it is associated with the largest forecast skill (or accuracy) for the monthly time scale (Burke and Rao, 1996). In other words, the present monthly droughts can be most accurately forecast by using present monthly precipitation. Both unrotated and rotated data are analyzed.

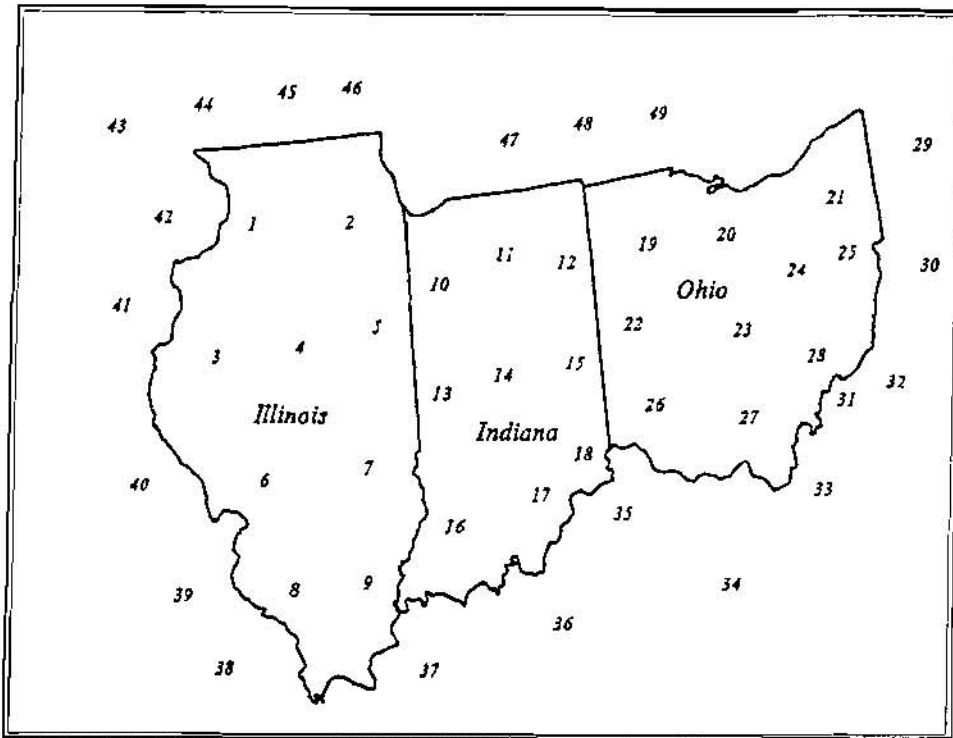


Figure 1. Locations of the forty-nine stations

The efficiency of the principal datum estimator is shown in Table 1 for the monthly precipitation-PDSI process. In Table 1, $S(\tau)$ is the forecast skill or accuracy. The largest forecast skill is 0.2132, which occurs at $\tau = 0$. $S_1(\tau)$ is the forecast skill of precipitation-PDSI case computed by using only the first datum amplitude $h_1(t)$. τ is the time lag between precipitation and PDSI process. r and r' are the correlation coefficients between the first principal amplitude $h_1(t)$ and the first principal estimated amplitude $W_1(t + \tau)$ and between $H_1(x)$ and $W_1(y)$, respectively.

From the results shown in Table 1, the skill, $S_1(\tau)$, obtained by using only the first principal datum amplitude $h_1(t)$ is 32% of the total attainable accuracy for the unrotated case and 27% for the rotated case. All four of the principal datum amplitudes carry nearly the same variance which is the reason the skills for each of these is low. Consequently, using only the first principal datum amplitude of precipitation to predict PDSI, nearly twice the magnitude of forecast skill is obtained, compared to using 4 or more precipitation PCs to predict PDSI in different time scales. The correlation, r , between the temporal components of the principal estimator patterns, $h_1(t)$ and $w_1(t)$ is practically the same for the unrotated and rotated cases. The correlation r' between $H_1(x)$ and $W_1(y)$ is very high. In other words, the spatial correlation between precipitation and PDSI processes is very high.

The first principal datum and estimated patterns, $H_1(x)$ and $W_1(y)$ respectively, of monthly precipitation-PDSI cases are shown in Figures 2 and 3. The precipitation-PDSI case with unrotated and Figure 3 for rotated data are shown in Figure 2. In these figures, the first principal datum pattern $H_1(x)$ of precipitation and the first principal estimated pattern of PDSI, $W_1(y)$ are plotted in solid and dashed lines respectively.

Table 1. Efficiency of the first principal datum estimator for precipitation-PDSI case

Case		τ	$S(\tau)$	$S_1(\tau)$	$\frac{S_1(\tau)}{S(\tau)}$	r	r'
Precip.- PDSI	Unrotated	0	0.2132	0.0541	0.3166	0.4771	0.9797
Precip.- PDSI	Rototated	0	0.2182	0.0461	0.2698	0.4760	0.9876

In Figure 2, the first principal datum (precipitation) pattern has a high value (0.4) at western Illinois and a decreasing trend toward the east. The first principal estimated PDSI pattern also has a high (0.2) in western Illinois and a decreasing trend to the east. The more accurately the contour lines match, the higher is the prediction level between the cause and effect variables. Consequently, it is possible to predict monthly PDSI by using only monthly precipitation.

However, since the values of the contour lines are different, the accuracy in predicting monthly PDSI by using only monthly precipitation is not high. These same features are shown in Figure 3 where the rotated data is used. There is not a significant difference between the unrotated and rotated results.

PDSI-PDSI Case: The efficiency of estimating PDSI using only PDSI data is illustrated in Table 2 for the monthly PDSI data. $S(\tau)$ is the forecast skill for the PDSI-PDSI case (Burke and Rao, 1996). For example, from Figure 4, the largest forecast skill is 0.8795, which occurs at $\tau = 1$. $S_1(\tau)$ is the forecast skill of PDSI-PDSI case by using only the first datum amplitude $h_1(t)$. The first principal datum amplitude explains 17 and 21 percent of the total skill $S(\tau)$ of PDSI-PDSI case for monthly unrotated and rotated data, respectively. The low ratio of $S_1(\tau) / S(\tau)$ is due to the fact that all the principal datum amplitudes are approximately the same and hence, explain nearly the same variance. The correlation coefficients between the first principal datum and estimated amplitudes, $h_1(t)$ and $W_1(t+\tau)$ respectively, are much higher than the precipitation-PDSI case.

The first principal datum and estimated patterns for predicting the present PDSI by using only the previous month's PDSI are plotted in Figures 4 and 5 for unrotated and rotated data respectively. As seen in Figure 4, the first principal datum and the estimated patterns are very similar. Both patterns have a high in southwestern Illinois and decrease to the northeast. As $H_1(x)$ and $W_1(y)$ values approach zero, the patterns are practically on top of each other. Figure 5 shows similar results for the rotated data, as the contour lines are very close. Both $H_1(x)$ and $W_1(y)$ patterns have high values in northwestern Illinois and lows in the far south (mostly below the region). The $H_1(x)$ and $W_1(y)$ values increase moving from central Indiana to central Ohio.

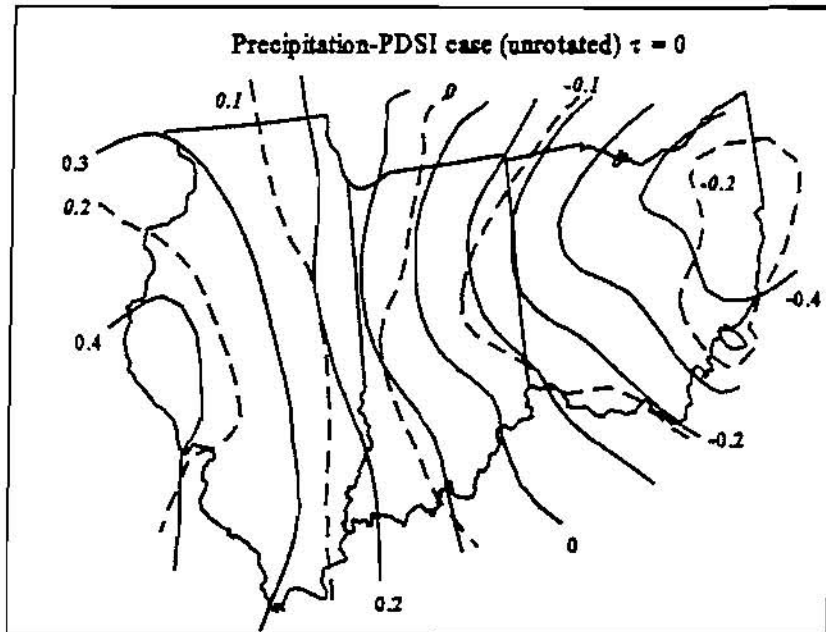


Figure 2. First principal datum of precipitation $H_1(x')$ (solid lines) and estimated $W_1(x)$ (dashed lines) patterns for predicting present monthly PDSI from present monthly precipitation using unrotated data.

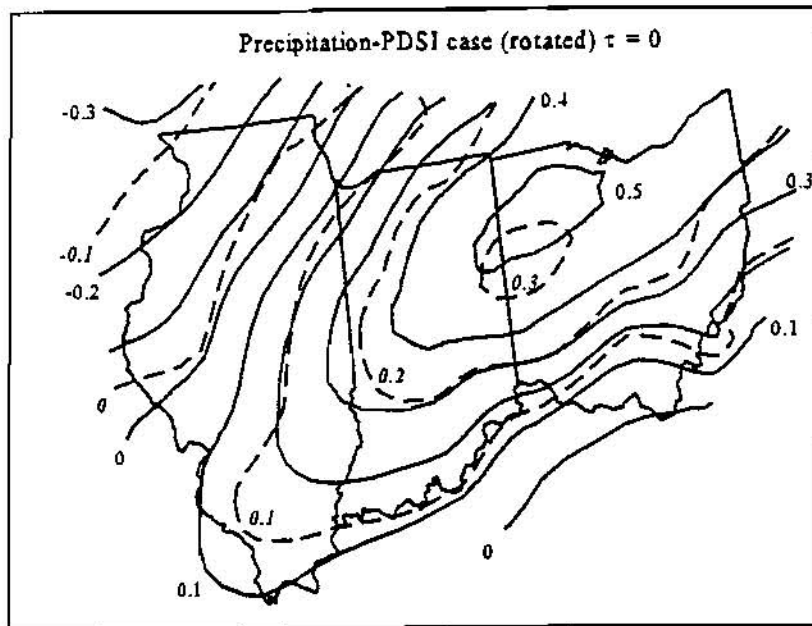


Figure 3. First principal datum of precipitation $H_1(x)$ (solid lines) and of PDSI estimated $W_1(y)$ (dashed lines) patterns for predicting present monthly PDSI from present monthly precipitation using rotated data.

Table 2. Efficiency of the first principal datum estimator for PDSI-PDSI case

Case		τ	$S(\tau)$	$S_1(\tau)$	$\frac{S_1(\tau)}{S(\tau)}$	r	r'
PDSI-PDSI	Unrotated	1	0.8795	0.1489	0.1693	0.9019	0.9999
PDSI-PDSI	Rotated	1	0.7940	0.1686	0.2122	0.9086	0.9997

The above results show that the previous months PDSI values can be used to get an accurate prediction of the present months PDSI. In other words, the PDSI values on the monthly scale have a lot of persistence.

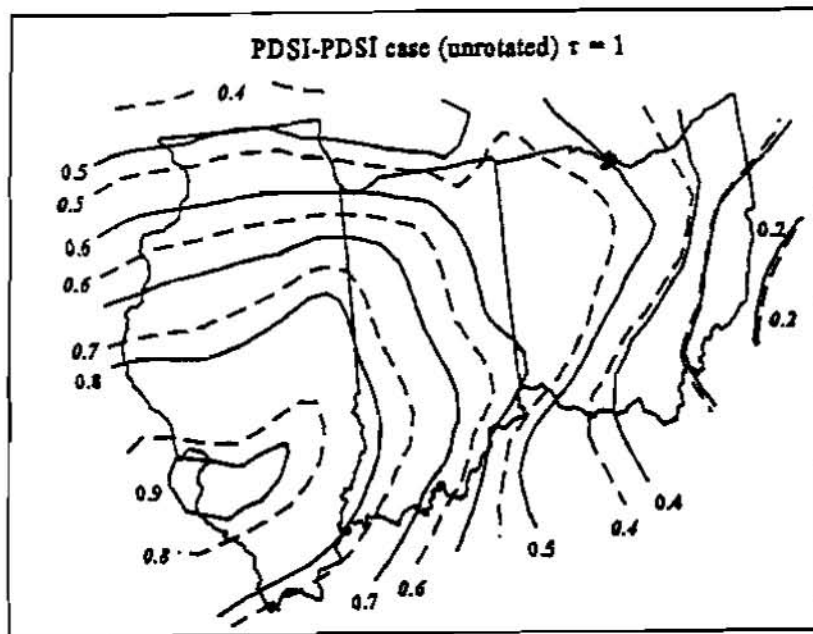


Figure 4. First principal estimator patterns of present PDSI $H_1(x)$ (solid lines) and of PDSI one month earlier $W_1(y)$ (dashed lines) for predicting present monthly PDSI from previous monthly PDSI using unrotated data.

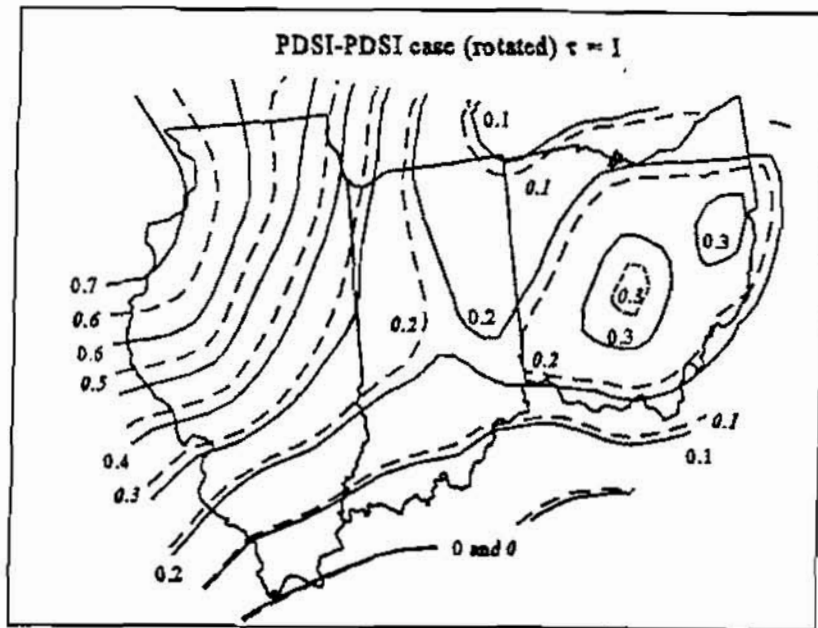


Figure 5. First principal estimator patterns of present PDSI $H_1(x)$ (solid lines) and of PDSI one month earlier $W_1(y)$ (dashed lines) for predicting present monthly PDSI from previous monthly PDSI using rotated data.

CONCLUSIONS

On the basis of results presented in this study we may conclude:

1. There is a very close causal relationship between regional droughts and precipitation.
2. There is practically no benefit in using rotated data, as the unrotated and rotated cases give results which are very close to each other.
3. In all the cases analyzed, the first principal datum estimator represented nearly the same portion of the variance as the remaining principal datum estimators.
4. The first principal datum estimator represents between 17% and 32% of the total forecast skill. Consequently, the first principal datum and estimated patterns, $H_1(x)$ and $W_1(y)$ respectively, represent the same relationships underlying the predictability of precipitation-PDSI or PDSI-PDSI cases, as the remaining principal datum and estimated patterns.

REFERENCES

1. T.T. Burke, Jr., and A.R. Rao, "Characterization and Predictability of Droughts in the Midwest", *Tech. Report CE-EHE-96-01*, School of Civil Engineering, Purdue University, W. Lafayette, IN 47907, pp. 208, 1996.
2. Davis, R.F., "Techniques for Statistical Analysis and Prediction of Geophysical Fluid System", *Geophysics, Astrophysics and Fluid Dynamics*, Vol. 8, pp. 245-277, 1977.
3. Davis, R.E., "Predictability of Sea Level Pressure Anomalies over the North Pacific Ocean", *Journal of Phys. Oceanography*, Vol. 8, pp. 233-246, 1978.

APPLICATIONS OF GIS FOR A DROUGHT STUDY

Tiao J. Chang, Professor

Civil Engineering Department, Ohio University, Athens, Ohio

Richard Germain, Former Graduate Student

Civil Engineering Department, Ohio University, Athens, Ohio

Timothy A. Bartrand, Graduate Student

Civil Engineering Department, Ohio University, Athens, Ohio

Abstract: Water allocation for the management of droughts is involved with many uncertain factors. One of the most uncertain elements is the amount of evaporation during time periods of drought for a large basin where there is still no reliable estimation. By applying the geographic information system, this study developed the procedure to form the image to express the unavailability of water during periods of drought for a selected drainage basin. Gaging stations of precipitation and streamflow in the studied basin were selected to spatially represent the area. Based on the method of truncation level, 70, 80, 90, and 95% truncated values of precipitation and streamflow were estimated at each gaging station. A 70% truncation level means that 70% of historic records at the corresponding gaging location were greater than the truncated value. The greater the truncation level, the lower the availability of precipitation or streamflow. Hence, these truncation levels were used to reflect the levels of drought severity. It is noted that precipitation was recorded by the depth of water and streamflow was expressed by the equivalent water depth. Since hydrologic records were taken at gaging locations, truncation levels of precipitation and streamflow were location-dependent variables. Assuming that these truncation levels at all gaging locations are regionalized variables, the kriging method was applied to estimate their regional distribution. The analysis of kriging, a spatial interpolation technique, was based on the minimum variance unbiased estimation. The kriging analysis of these truncation levels yielded vector values of precipitation or streamflow for a grid of points covering the studied drainage basin. These point values were converted into a grid of raster-based values and were expressed by a spatial image. The mathematical function of subtraction was used to subtract the streamflow image from the precipitation image for each level of drought severity. These were done on a cell-by-cell basis to create new attribute values for the new image to represent the unavailability of water at each corresponding level of drought severity.

INTRODUCTION

Estimation of water losses in a drainage basin can be valuable for reservoir sizing, calculation of irrigation demands, and flow modeling during periods of drought. However, water losses including evaporation and infiltration are complex phenomena depending on myriad conditions. Deterministic calculations for evaporation at a given location depend upon reliable measurements of temperature, wind speed, insolation, soil temperature and other data. Hatfield (1996) suggested that for conditions of deficient water supply, the Priestly-Taylor or Penman-Monteith models produce reasonable estimates of evapotranspiration, but are highly dependent upon model calibration. Other means for estimating evapotranspiration when data are unavailable include the Blaney-Criddle method and use of evapotranspiration rates for regions with similar climate and topography (Shih and Cheng, 1991).

As an alternative to deterministic approaches which depend on knowledge and measurement of many factors, this study proposes a means for deducing combined evapotranspiration and infiltration based on commonly measured data of precipitation and streamflow. The procedure was first used by Germain (1996). In the procedure, precipitation and streamflow data are regionalized throughout an entire basin by the kriging analysis, then a Geographic Information System (GIS) was used to manipulate the results and produced evaporation/infiltration images. To best model drought conditions, truncation levels were used for streamflow and precipitation. Values of truncation levels were estimated from a set of gaging stations in and around the basin of interest and the kriging analysis was introduced to form a regionalized coverage for the entire basin.

Studies using GIS to manipulate spatial variables of hydrologic components generally fall into the two categories, drainage analysis and groundwater modeling. Common applications of GIS on drainage analysis include urban storm sewerage management, mapping hydrologic variables of the region, calculating input parameters of existing models, and flood control for river basins (DeBarry and Carrington, 1990; Greene and Cruise, 1995; Leipnik et al., 1993; Lipschultz and Glaser, 1992; Smith and Vidmar, 1994; Bhaskar et al. 1992; Ross and Tara, 1993; Shea et al. 1993). For groundwater modeling, GIS was used to map groundwater elevations for wellhead protection and management

and to trace groundwater contamination for pollution control and for site remediation ((Baker et al. 1993; El-Kadi et al. 1994; Merchant, 1994).

GIS allows a spatial analysis and complex overlays of data concerning the location, topology and attributes of spatial objects. Two types of GIS, raster-based and vector-based, were developed for different applications. The raster system assigns values denoting an attribute to a grid of cells. This system simplifies mathematical functions but tends to memory intensive. The vector-based system defines the attributes with a series of points and lines. This leads to more accurate portrayals of the attributes and smaller files than the raster system. Unfortunately the vector-based system results in an image which is incompatible with many mathematical functions (Bonham-Carter 1994). Applications for both types of systems occur in the field of hydrology. Equivalent water depths as discussed in this study can be easily modeled using the raster-based approach while stream networks are vectors in nature.

METHODOLOGY

Streamflow and precipitation truncation levels are used to distinguish levels of drought severity. Values of truncation levels were determined by sorting the historic data in ascending order at each gaging station. A truncation level of T% is the value that corresponds to the i^{th} position of the sorted record with a length N, where i is expressed as

$$i = \frac{(100 - T)N}{100} \quad (1)$$

From this definition, it follows that at the T% truncation levels of streamflow or precipitation, T% of historic data exceed the truncation level. Thus, drought events of a given severity level occur when observed data are lower than the specified truncation level. Truncation levels of 70%, 80%, 90% and 95% were selected to demonstrate the proposed method for investigating water losses in periods of drought (Chang et al., 1995; Chang and Stenson, 1990). These streamflow truncation levels were expressed by equivalent water depths, which are assumed to be regionalized variables at centroids of their corresponding drainage basins.

By assuming that equivalent water depths of streamflow and precipitation at a given truncation level are regionalized variables, the kriging method was used to estimate their corresponding spatial distribution. The kriging method is based on the linear minimum variance unbiased estimation (Kitanidis, 1983; Delhomme, 1978). Given n measurements of a random variable, Z , at spatial locations, x_1, x_2, \dots, x_n , an estimator using a linear combination of n variables is formulated as:

$$Z_o^* = \sum_{i=1}^n \alpha_i Z(x_i), \quad (2)$$

where Z_o^* is an estimation of a true value Z_o and α_i is the weight of the observed value at location x_i . The goal is to find a set of weights which give the best estimation so that the estimation is unbiased with a minimum variance. The unbiased condition means that

$$E[Z_o^* - Z_o] = 0, \quad (3)$$

where E is the expectation operator. The minimum variance condition means that

$$E[(\sum_{i=1}^n \alpha_i Z(x_i) - Z_o)^2] = \text{minimum} \quad (4)$$

In order to satisfy the unbiased condition, coefficients $\alpha_1, \alpha_2, \dots, \alpha_n$, must be selected so that

$$\sum_{i=1}^n \alpha_i - 1 = 0 \quad (5)$$

Based on Eqn. 4, the estimation error, e , which is the difference between the estimated and true values, can be written as follows:

Therefore, the problem of kriging technique is reduced to minimizing Eqn. 4 subject to the constraint of Eqn. 5. Using

$$e = \sum_{i=1}^n \alpha_i Z(x_i) - Z_0 \quad (6)$$

the Lagrange multiplier, the necessary conditions for the minimization yields $n+1$ equations with as many unknowns:

$$\sum_{j=1}^n \alpha_j \tau(x_i - x_j) = \tau(x_i - x_0) + \mu, i=1,2,\dots,n, \quad (7)$$

$$\sum_{j=1}^n \alpha_j = 1, \quad (8)$$

where τ is the semi-variogram, which is the expectation of $(Z(x_i) - Z(x_j))^2$ and μ is a Lagrange multiplier. By solving these equations simultaneously, the optimum weights α_i can be obtained. The variance of this estimation is given by

$$\sigma^2 = - \sum_{i=1}^n \sum_{j=1}^n \alpha_i \alpha_j \tau(x_i - x_j) + 2 \sum_{i=1}^n \alpha_i \tau(x_i - x_0), \quad (9)$$

When x_0 coincides with a data location at x_i , the system solution yields $\alpha_i = 1$. This results in $Z_0 = Z(x_i)$ at location x_i and $\sigma^2 = 0$. Therefore, the kriging estimator is an exact interpolation at the observed point. If the semi-variogram cannot be estimated without bias due to nonstationarity, Delhomme (1978) provided an extended solution by using higher order differences to filter out the nonstationarity. Then, the solution to the problem can be obtained in a similar fashion.

The GeoEAS (Geostatistical Environmental Assessment) software (Erlunder and Sparks, 1991) was used to perform the kriging. For precipitation, inputs to the program included precipitation gage locations and precipitation depths corresponding to the 70%, 80%, 90%, and 95% truncation levels. For streamflow, inputs to GeoEAS were the equivalent water depth at the same truncation levels and the centroids for the drainage areas of each streamflow gage. Output from the analysis was files of vector-valued precipitation and streamflow on a regularly-spaced grid. Variogram models chosen for the kriging process were all cross-validated and normalized estimates at all gaging stations fell within a 95% confidence interval.

The point-valued values produced in kriging were converted to raster files and manipulated in a GIS to produce images showing evapotranspiration and infiltration. The ArcView GIS program (ESRI, 1996) was used to interpolate point values of precipitation and streamflow and produce raster images of those values. The raster images of streamflow equivalent water depth were subtracted from those of precipitation to produce images showing equivalent depth of evapotranspiration and infiltration at corresponding truncation levels. The evapotranspiration image was then divided by precipitation depth to yield images showing the percentage of water losses at a given drought severity level. These analyses were carried out using a grid cell size of roughly 450 m.

APPLICATION AND RESULTS

To illustrate the proposed GIS method, eighteen streamflow gaging stations and twenty-one precipitation gages are selected in the Scioto River basin, which is located in central Ohio and empties into the Ohio River as shown in Figure 1. The Scioto basin experienced significant drought in 1988, though typically rainfall is regular and water shortages are rare. The largest metropolitan area in the basin is the city of Columbus, Ohio, located roughly in the center of the basin. The Northern portion of the basin is generally flat and agricultural. The Southern portion of the basin is hillier than the North and includes regions of forest. Major tributaries to the Scioto River include the Olentangy River, Big Walnut creek, Big Darby creek, Deer creek, Paint creek and Salt creek. Several reservoirs are located in the basin, including the Alum creek and Delaware reservoirs in the Northern part of the basin and the Deer creek and Paint creek reservoirs in the Southern part of the basin.

Since the phenomenon of drought is of interest, streamflow and precipitation truncation levels of 70, 80, 90, and 95% were estimated based on Eqn. 1 to express levels of drought severity. The value of 70% truncation means that 70% of recorded flows or precipitations are greater than or equal to the level. In general, values of 70% truncation level or above are significantly lower than their corresponding mean values. To represent these truncated streamflows in a spatial format, equivalent water depths were estimated and assigned at their centroids of corresponding drainage basins. It can be expressed by

$$EWD = \frac{Q_g}{A_b} * 2.628 * 10^6, \quad (10)$$

where EWD stands for the equivalent water depth in millimeters, Q_g represents the truncation value at the gaging station in m^3/sec , and A_b is the drainage area of the gaging station in km^2 .

Next, EWD and precipitation records at varied gauges were assumed to be location-dependent. Hence, EWD and precipitation estimated at different truncation levels, i.e., 70, 80, 90, and 95%, were treated as regionalized variables and analyzed by the kriging method to obtain the spatial distribution at each truncation level. The results of the kriging analysis were vector-based, which were converted to a raster-based file, and expressed by a GIS image. Apply the mathematical function of image operation to substrate the image of EWD from that of precipitation to obtain the image of water losses at a given level of drought severity. Finally, the image of water losses was then divided by that of precipitation to yield the new image that express the percentage of water losses for the level of drought severity.

The example in Figures 2a and 2b show images of water losses at the 70% level of drought severity, respectively, in depth and percentage. Figure 2a shows that the dark-colored portions of the drainage basin, i.e. the South and Northeast of the basin, indicate higher levels of losses. A comparison made with an image of precipitation at the 70% truncation level showed that contours of losses closely match those of precipitation (Germain, 1996). In order to better identify the impact of water losses, they were expressed as a percentage of precipitation given in Figure 2b. In Figure 2b, the darker the shade, the greater the percentage of water losses. The fraction of water losses at the 70% truncation level ranges from a low of around 88% in the center of the basin to a high of around 94.5% in the Northwest corner of the basin. This trend is consistent with the low relief and intensive agriculture of the Northern portion of the basin. A portion of the Southern part of the basin also experiences great loss of available precipitation. This is likely related to higher temperatures in the Southern part of the basin compared with the North.

Figures 3a and 3b show water losses in depth and in percentage of the precipitation at the 80% level of drought severity. Water loss in depth are less in Figure 3a than in Figure 2a, mainly because the precipitation at the 80% level is less than at the 70% level. In addition, the region of highest losses shifts to the west of the basin at the 80% truncation level. A comparison of Figures 3b and 2b shows that the water losses in percentage increases as the drought severity increases. At the 80% truncation level, the highest water losses in percentage are again in the Northern portion of the basin. The range of water losses at the 80% level of drought severity is roughly 91 - 97%.

CONCLUSION

Despite the complicated physics involved in both evapotranspiration and infiltration, the proposed method in this study provides an alternative for estimating water losses during periods of drought. Furthermore, the use of equivalent water depths at varied truncation levels in the proposed method reflects the surface water availability of a basin. These equivalent water depths spatially represented at the centroids of their corresponding drainage areas enable the kriging analysis and the image expression of GIS. The results from this study also provide important information for regional water management in case of drought.

ACKNOWLEDGMENTS

This paper is based on the data obtained for the research supported by the U.S. Army Corps of Engineers, under agreement ED-W-8160-030, and is in part supported by Ohio University

REFERENCES

- Baker, C.P., Bradley, M.D., and Bobiak, S.M.K., 1993. "Wellhead Protection Area Delineation: Linking Flow Model with GIS," *Journal of Water Resources Planning and Management*, vol. 119, no. 2, pp. 275-287.
- Bhaskar, N.R., James, W.P., and Devulapalli, R., 1992. "Hydrologic Parameter Estimation Using Geographic Information Systems," *Journal of Water Resources Planning and Management*, vol. 118, pp. 492-511.
- Bonham-Carter, G.F., 1994. *GIS for Geoscientists: Modeling with GIS*, 1st Ed., Love Printing Service, Ltd., Ontario.
- Chang, T.J., Kleopa, X., and Teoh, C.B., 1995. "Use of Flood-Control Reservoir for Drought Management," *Journal of Irrigation and Drainage Engineering, ASCE*, Vol. 121, No.1, pp.34-42.
- Chang, T.J. and J.R. Stenson. 1990. "Is It Realistic to Define a 100-Year Drought for Water Management ?" *Water Resources Bulletin, AWRA*. Vol. 26, No. 5, pp. 823-829.
- DeBarry, P.A., and Carrington, J.T., 1990. "Computer Watersheds," *Civil Engineering*, vol. 60, pp. 67-70.
- Delhomme, J.P., 1978, "Kriging in the Hydrosociences," *Advances in Water Resources*, Vol. 1, no. 5, pp. 251-266
- El Kadi, A.I., Oloufa, A.A., Altahan, A.A., and Malik, H.U., 1994. "Use of a Geographic Information System in Site-Specific Groundwater Modeling," *Ground Water*, vol. 32, no. 4, pp. 617-625.
- Erlunder, E. And Sparks, A, 1991, "Geostatistical Environmental Assessment Software," USEPA document EPA 600/4-88/033, Office of Research and Development, U.S. Environmental Protection Agency, Las Vegas, NV
- ESRI, 1996. "ArcView Geographic Analysis System," Environmental Systems Research Institute, Redlands, Ca.
- Germain, R.J., 1996, "Drought Management Using a Geographical Information System," M.S. thesis, Ohio University, Department of Civil Engineering, Athens, Ohio
- Greene, R.G., and Cruise, J.F., 1995. "Urban Watershed Modeling Using a Geographic Information System," *Journal of Water Resources Planning and Management*, vol. 121, no. 4, pp. 318-325..
- Hatfield, G.L., and Allen, R.G., 1996, "Evapotranspiration Estimates Under Deficient Water Supplies," *J. of Irrigation and Drainage Engineering*, vol. 122, no. 5, Sept/Oct 1996, pp. 301-308
- Kitanidis, P.K., 1993. "Statistical Estimation of Polynomial Generalized Covariance Functions and Hydrologic Applications," *Water Resources Research*, vol. 19, no. 4, pp. 909-921.
- Leipnik, M.R., Kemp, K.K., and Loaiciga, H.A., 1993. "Implementation of GIS for Water Resources Planning and Management," *Journal of Water Resources Planning and Management*, vol. 119, no. 2, pp. 184-201
- Lipschultz, M.S., and Glaser, D.E., 1992. "Rainy Season Flooding Being Tracked by GIS," *Water Resources Engineering and Management*, vol. 139, pp. 22-25.
- Merchant, J.W., 1994. "GIS-Based Groundwater Pollution Hazard Assessment: A Critical Review of the DRASTIC Method," *Photogrammetric Engineering and Remote Sensing*, vol. 60, no. 9, pp. 1117-1127.
- Ross, M.A., and Tara, P.D., 1993. "Integrated Hydrologic Modeling with Geographic Information Systems," *Journal of Water Resources Planning and Management*, vol. 119, no. 2, pp. 129-140.
- Shea, C., Grayman, W., Darden, D., Males, R.M., and Sushinsky, P., 1993. "Integrated GIS and Hydrologic Modeling for Drainage Study," *J. of Water Resources Planning and Management*, vol. 119, no. 2, pp. 112-127.
- Shih, S.F., and Cheng, Kc. S., 1991. "Evapotranspiration Estimation for Data-Short Environment," *J. of Irrigation and Drainage Engineering*, vol. 117, no. 1, Jan/Feb 1991, pp. 107-122
- Smith, M.B., and Vidmar, A., 1994. "Data Set Derivation for GIS-Based Urban Hydrological Modeling," *Photogrammetric Engineering and Remote Sensing*, vol. 60, no. 1, pp. 67-76.

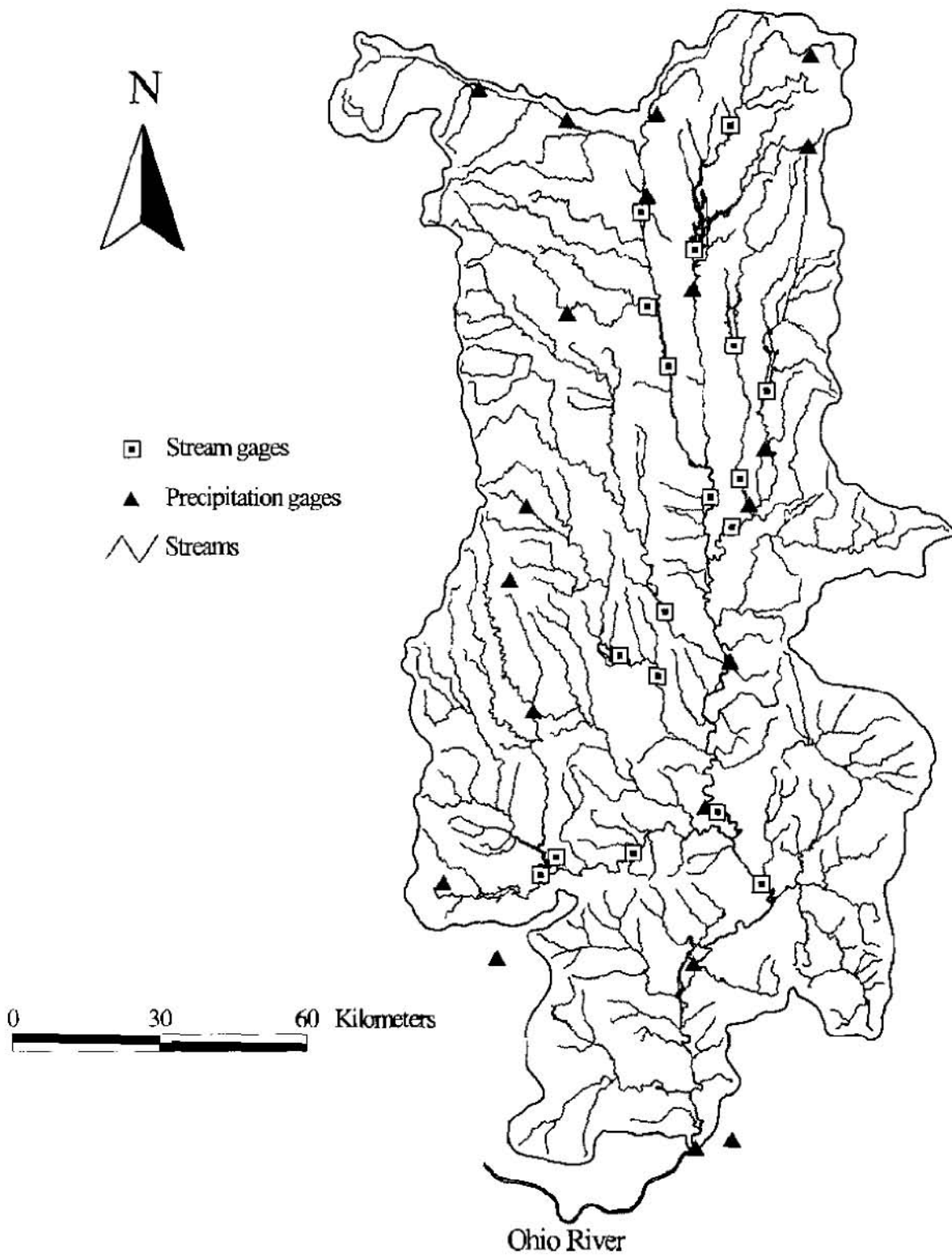
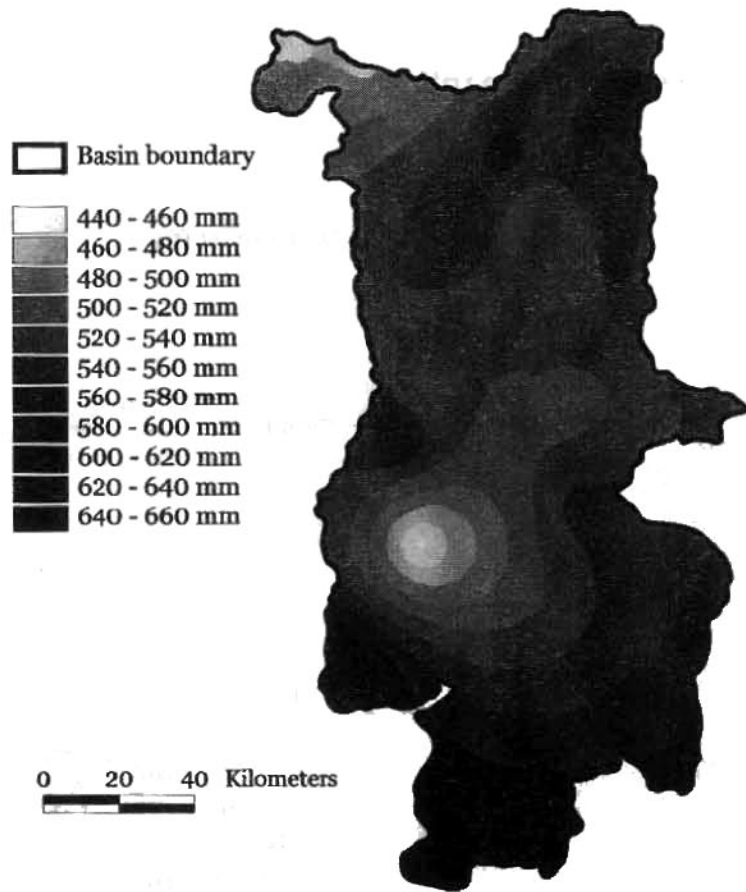
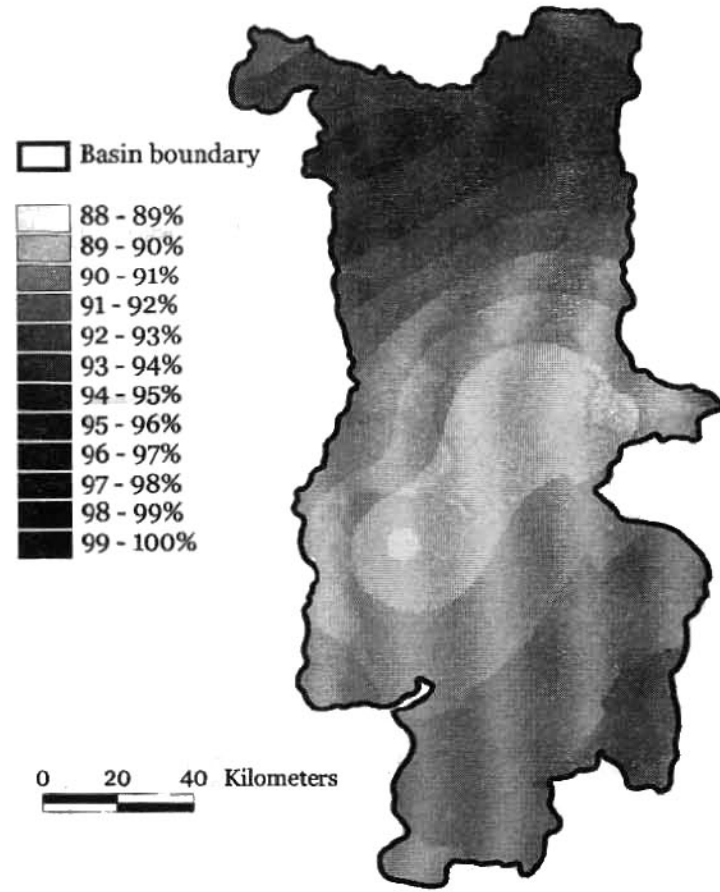


Figure 1: Scioto River Basin and Gaging Stations

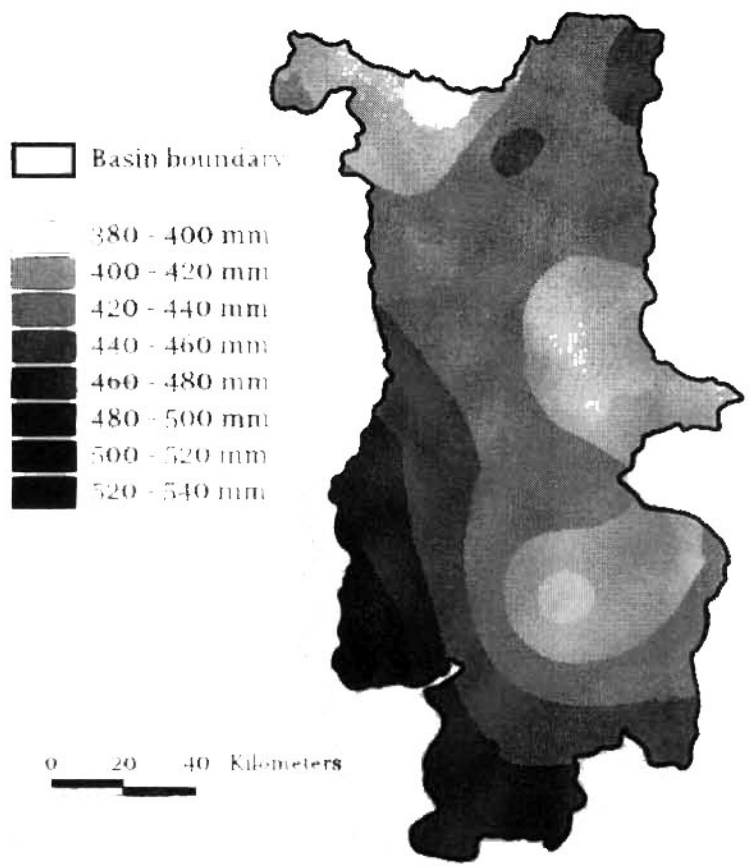


(a) Losses in mm/yr

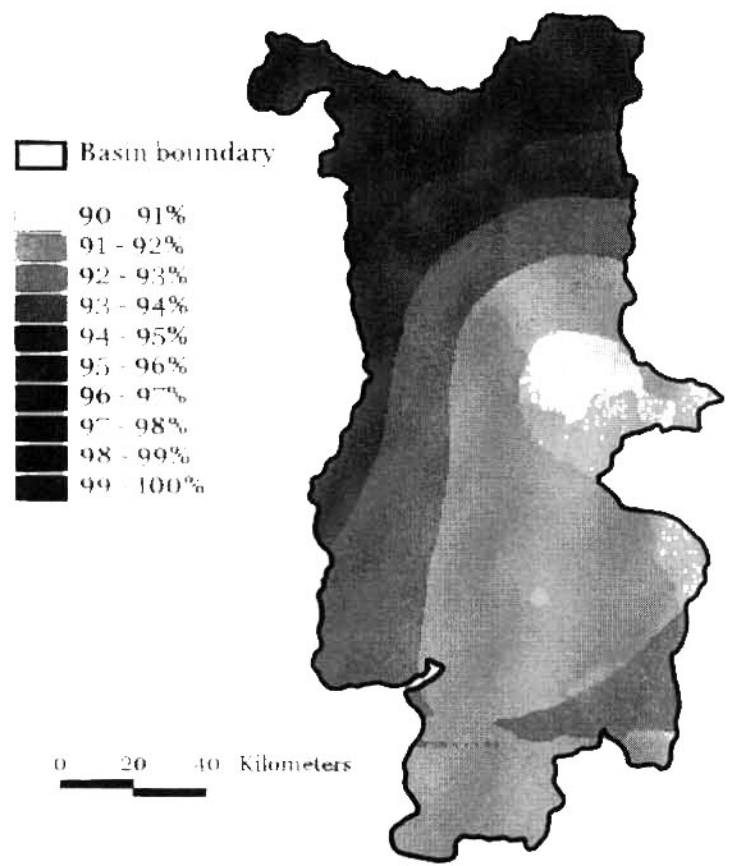


(b) Losses as percentage of precipitation

Figure 2: Losses at the 70% Truncation Level



(a) Losses in mm/yr



(b) Losses as percentage of precipitation

Figure 3: Losses at the 80% Truncation Level

APPLICATION OF SIMULATING METHOD ON THE REGIONAL DROUGHT ANALYSIS

By Gu Ying Senior Engineer, Liu Pei Engineer, Nanjing Institute of Hydrology & Water Resources, Ministry of Water Resources, 1 Xikang Road, Nanjing, China

Abstract: The modeling technique is applied in the water resources study widely, but this technique has not in common use in the agricultural drought study. In the paper, a simulating method is introduced on regional drought study. The results of study shown the drought modeling is a useful tool on the drought study in the area, and it is effective way for the drought real-time monitoring.

The drought simulating model was constructed, which based on the principle of water balance, it simulate the process of crop growth, calculate the variation of moisture, describe the water exchange in the atmosphere — crop — soil and groundwater, the drought modeling reflect the interaction in the factors affecting drought.

A study area was selected , the drought simulating in the area provide very useful information for drought study. Based on the information of agricultural drought characteristics which obtained from the drought modeling, we can find out the occurrence、development and mitigation process of drought, determinate the serious degree of drought and evaluate the possible loss of crop product according to the sensitive of crop to the water. In the paper author discuss the water shortage case during the crop growth in a serious drought year, analyzes the rule of regional drought, i.e. temporal and spatial distribution of agricultural drought on the study area .

SIMULATION MODEL OF AGRICULTURAL DROUGHT

Based on the water balance principle, simulation model use the mathematics method to calculate the soil moisture during the crop growth. Through the simulation of water exchange between the atmosphere-crop-soil, we can obtain many information about the water shortage of crop, according to these information and the crop sensitivity to water, analysis the water shortage effect to crop yield, assessment the serious degree of agricultural drought.

Agricultural drought simulation composed with two parts, one is drought characteristics simulation, another is crop yield decrease simulation.

Agricultural Drought Characteristics Simulation : The simulation of agricultural drought characteristics is the process of crop growth modeling, from which many information about drought obtained and found out the developing process of drought.

In the drought characteristic model, follow Water balance formula be used:

$$W_{t+1} = W_t + P_t + G_t - SD_t - F_t - R_t \quad (1)$$

Here W_i , W_{i+1} , the soil moisture at time i and $i+1$; P_i , the precipitation at time i ; G_i , the recharge of groundwater at time i ; F_i , the leakage of surface water at time i ; R_i , the surface runoff at time i ; SD_i , the water supply from soil at time i .

In the formula (1), precipitation and recharge of groundwater are main input items, the main output item is water supply from soil, and the soil moisture is regulation item. The happening of crop water shortage result from the water movement in the farm field unbalance.

The two layer and two stages mode have been used to construct the drought simulating model, which can simulate the process of water exchange between the atmosphere, soil and crop, describe the variation process of soil moisture. Fig.1 shows the structure of model.

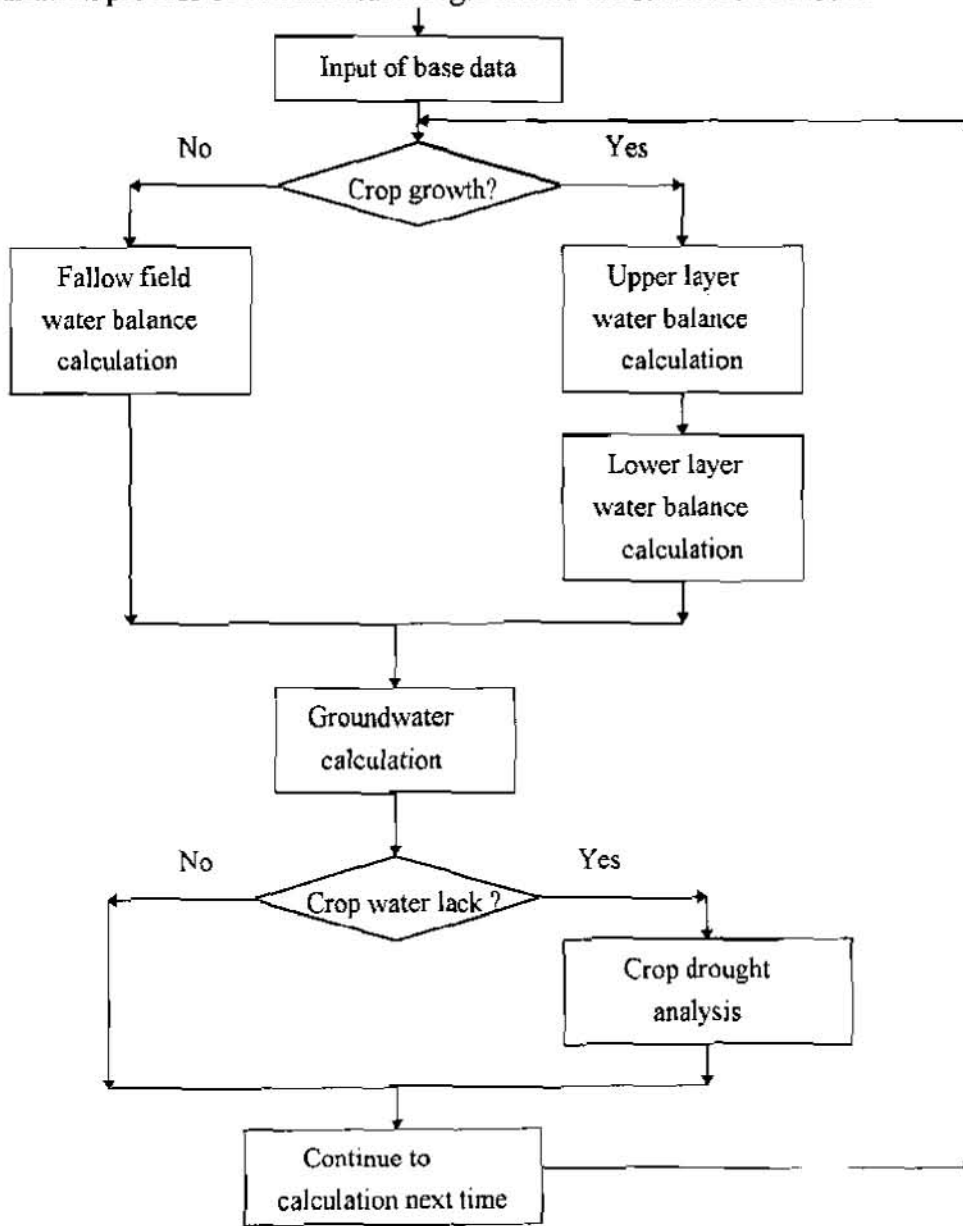


Fig 1 Sketch of Drought Simulation Model Structure

Two layer mode considerate the soil moisture exchange in vertical direction. In simulating calculation, the crop root layer has been divided into upper layer and lower layer. rainfall first recharge to the upper layer then lower layer, ground water receive the seepage from lower layer, and recharge to the soil as phreatic evaporation. Drought will occurrence if the crop cannot get enough water from soil

Two stages mode is a method of water supply from soil. In the modeling, taking the capillary capacity as the limit point, when soil moisture greater than capillary capacity, crop can absorb the water from soil freely, when soil moisture less than capillary capacity, means soil cannot supply enough water for crop demand, water shortage happening, if soil moisture reach wilting point, drought is coming.

By the agricultural drought characteristics simulation, we can realize the drought characteristics quantity, such as the time that drought start and end, water shortage volume in each crop growth stage, frequency of drought occurrence, variation of soil moisture and so on.

Crop Yield Decrease Simulation: In order to evaluation the degree of crop drought quantity, and water shortage effect to crop yield in different volume and time, the sensitive index method be applied to modeling the crop yield decrease, which based on the crop sensitivity for water and drought characteristics simulating results.

Crop hardness of drought has great difference for variety crop, and even for the same crop, the effect will also be not same since crop water shortage happened in different growth stage.

Follow formula used in the sensitive index method:

$$Y / Y_M = \prod_{i=1}^n (E_i / E_{Mi})^{\lambda_i} \quad (2)$$

Here Y, the crop yield under actuarial water supply condition (calculating), Y_M , the crop yield under sufficient water supply condition; n, the number of crop growth stages; E_i , the actuarial crop Evapotranspiration (calculating) i.e. the actual water supply from soil; E_M , the maximum crop Evapotranspiration; λ_i , the crop sensitivity index to water at crop growth stage i.

The magnitude of λ reflect the sensitivity of crop to water shortage. The value of λ is determined from the experiment. The decrease of crop yield is $(1 - Y / Y_M)$, according to the value of $(1 - Y / Y_M)$, drought degree of crop was divided into four class: extreme drought, severe drought, light drought, normal. The crop yield decrease modeling provide the reference for drought analysis and evaluation.

The simulating results shows the drought simulation model mentioned above is valid.

APPLICATION OF DROUGHT SIMULATION MODEL

In this study, drought simulation model be used to modeling the process of crop growth, in order to find out the occurrence, development and mitigation process of drought, and the regional

drought distribution in the time and space.

An Hui province in China was selected as study area. In the area, the annual precipitation is 800 ~ 1600 mm, and the precipitation are increased from north to south of Anhui. This area belong to three basin: Huaihe basin, Yangtz River basin and Xinan Jiang basin.

The input of simulation model were about 40 years precipitation and evaporation data, and taken the maize and wheat for study object, in order to discuss drought rule in the area. according to the feature of water resources and climate in this area, study area was divided into 14 subarea to calculate separately.

Analysis of Drought Regional Distribution : Many information were obtained from drought modeling, such as the frequency of agriculture drought during the past 40 years, annual water shortage ratio of crop, number of drought happened in each season, water lack quantity for each subarea and so on. Based on the puzzle principle, the multi-index comprehensive analysis method was applied to sum up all these information, we found out drought happened rule in the area, and its temporal and spatial variation (Fig 2).

Fig 2(a) shows, in the north of Anhui, drought happening was have high probability, second was in the region between Huaihe River and Yangtz River, in the Xin Anjiang basin drought happen chance was a few. Fig 2(b) shows drought happened in the season was of high frequency. In the north of study area was spring, in the region between Huaihe River and Yangtz River was summer, and there were no drought season obviously in the south of Yangtz River region.

The Simulation of Drought Developing in Dry Year : The drought model can modeling the whole crop water shortage process and the soil moisture variation process. These process reflect the drought occurrence, development and mitigation process, follow is example for drought process modeling.

The year 1966 was a severe dry year in Anhui province, drought severe region first was Huaihe basin, second was Yangtz River basin. in this year, drought happened mainly in the summer so for maize, water shortage was more severe than for wheat (maize growth from June to September, wheat growth from October to May), in view of whole study area, drought in Huaihe basin was more serious than other basin.

The whole drought process was describe by variation of soil moisture. Fig 3 shown the distribution of moisture ratio it was actual soil moisture to crop suitable soil moisture. It reflect the drought development is different duration.

Fig 3(a) shows the moisture ratio γ distribution at March 1 and March 11 in 1966, at beginning of March, there were ten subarea soil moisture ratio less than 1.0, it means drought already happen in these region, only four subarea's moisture great than 1.0, after ten days, soil moisture increase, due to rainfall, drought was relaxed. Fig 3(b) shows drought occurrence、development process during the June, we can knew drought developed from north to south, and drought become severe as the time coming, this figure let's found out the drought development process not only in time

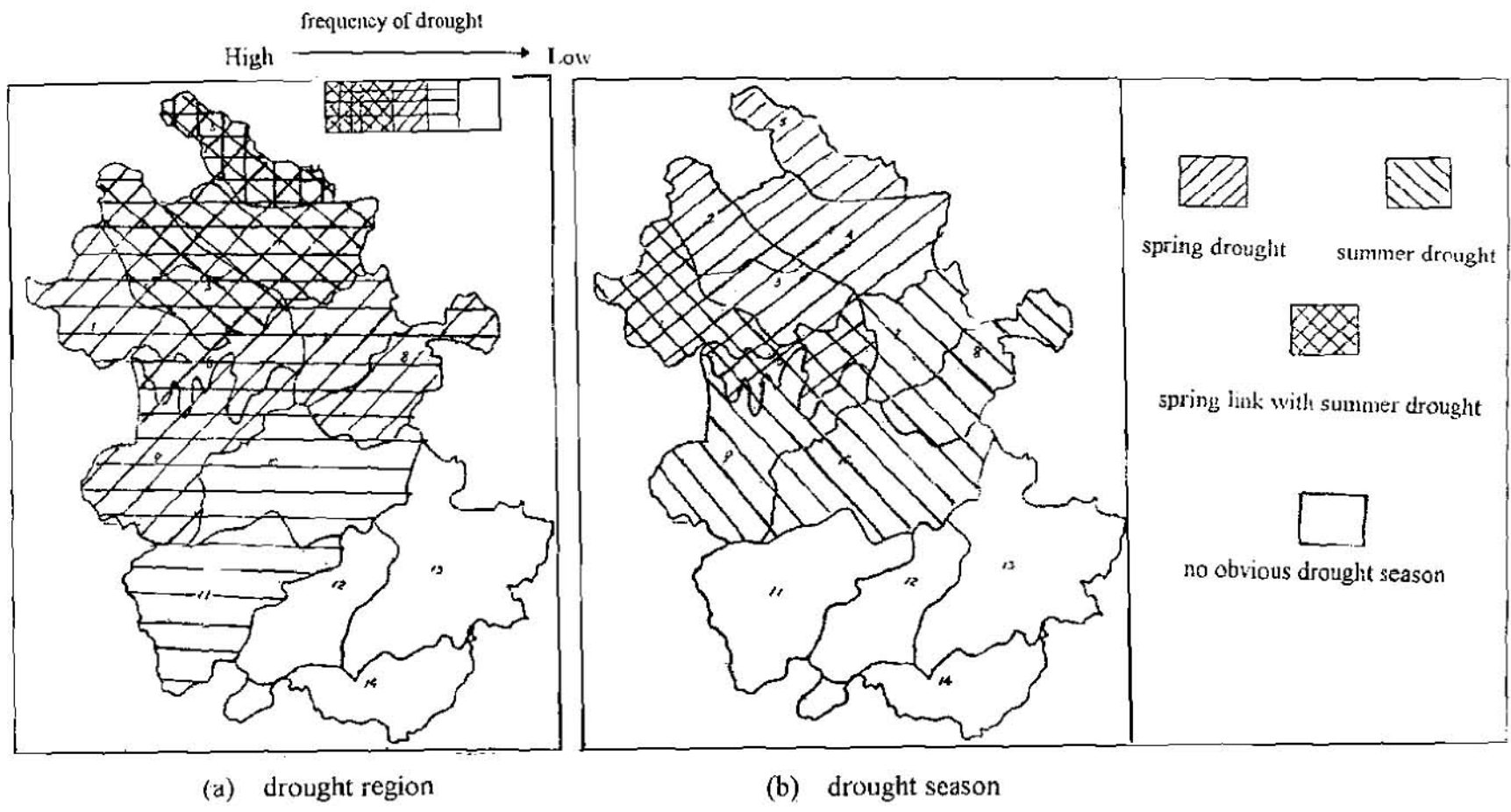
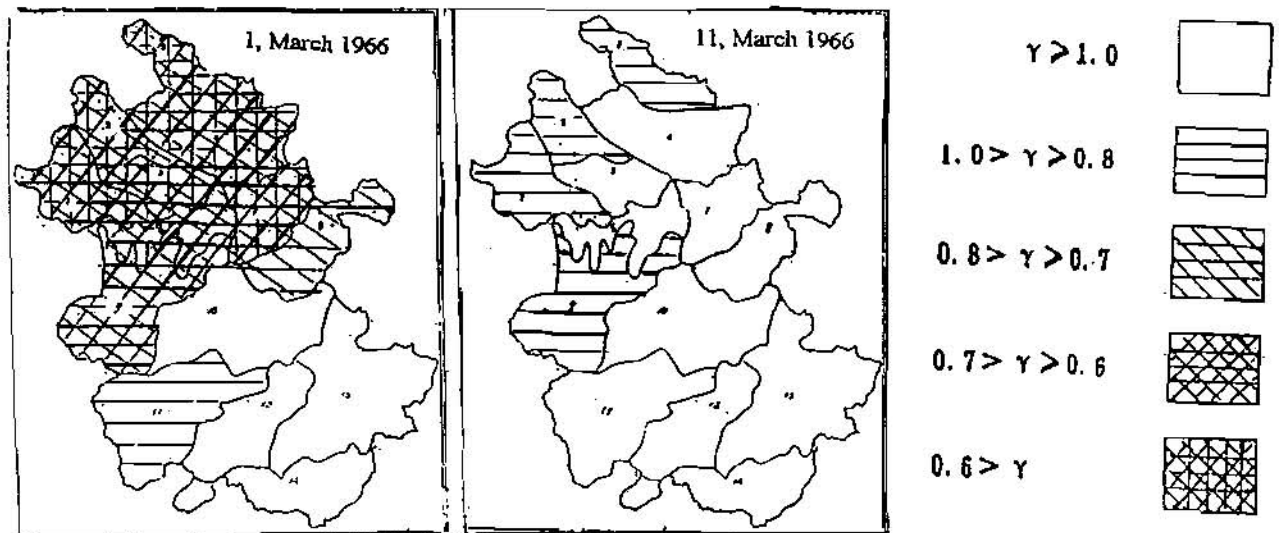
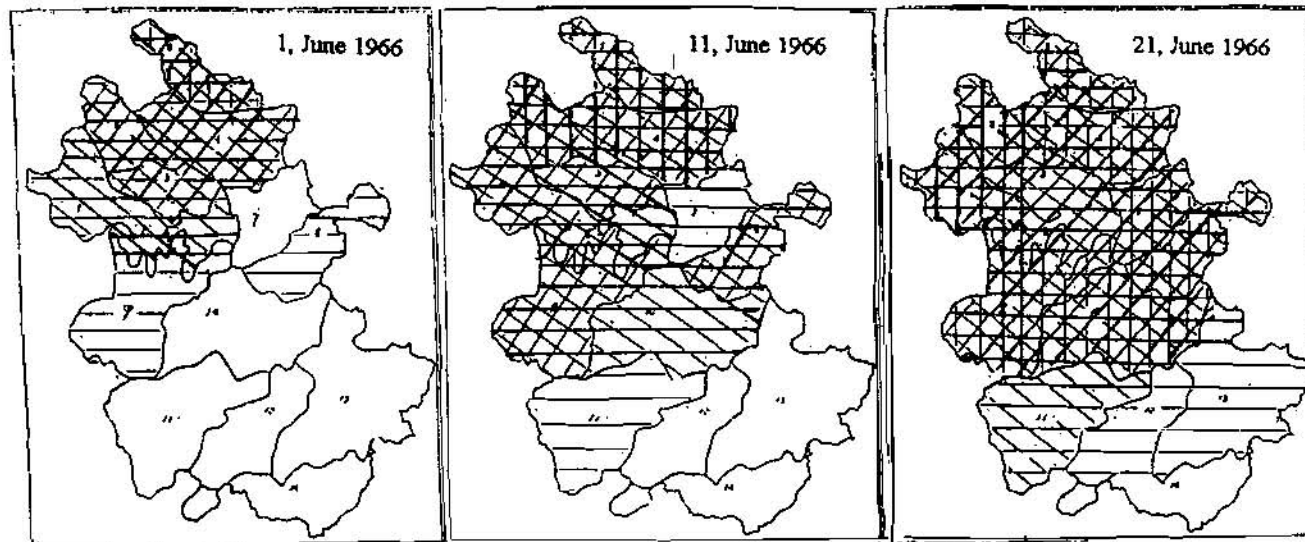


Fig 2 Distribution Map of Drought



(a) drought mitigation



(b) drought developing

Fig 3 γ Distribution Map

but also in space.

CONCLUSION

To sum above mention, the application of simulation technique provide a useful method for regional drought study. By drought simulation, we can study the regional layout of drought region and drought season , providing the background data for cope with agricultural drought, description the regional drought occurrence, development and mitigation process for special year, in order to understand the drought rule. Drought simulation open up possibility for agricultural monitoring. It is believed the technique of drought simulation will be applied for regional drought study widely.

REFERENCE

- Gu Ying, 1993. Study of agricultural drought simulation, Journal of Advances In Water Science China. 93(4): 253-258
Wang Xushen, 1990. Drought analysis of crop in North of China, Water Planning, 90(1): 22-30
Yu Shuangen, 1991. Discussion of crop water function, Water Resources Study 90(4): 25-30
Cheng Shouyu, 1992. Puzzle theory of hydrology and water resources system. Da Lian Publish House

Gu Ying , Mailing addresses: Nanjing Institute of Hydrology & Water Resources, 1 Xikang Road, Nanjing, China.

Tel: (025) - 3720331

Fax: (025) - 3737861

E - mail: nihwr@nj.col.co.cn

THE APPLICATION OF MEAN VALUE GENERATION FUNCTION MODEL IN REGIONAL DROUGHT RESEARCH

By Zhang Xuecheng, Engineer, Bureau of Hydrology, YRCC, Zhengzhou, China; Zhu Xiaoyuan, Senior Engineer, Department of Hydrology, MWR, Beijing, China

Abstract: Drought research is an important part of floods and droughts disaster countermeasure research. It is of very important meaning for predicting objectively future drought events and carrying out relative accurate decision that simulating historical drought events and their evolution regular in better approach. Based on one dimensional random process analysis pattern, a new concept meaning “mean value generation function” is introduced in this paper. According to mathematical derivation, the mean value generation function model is established too. The result of applying this model in regional drought research shows that mean value generation function model could simulate and predict drought events tendency in better approach.

Key Word: Mean value generation function, Orthogonal selection, Drought index simulation and prediction

INTRODUCTION

Disaster occurred by floods and droughts often cause considerable losses in social economics and human-being life. It is of very important meaning for carrying out relative accurate decision by the central and local governments that recognizing floods and droughts occurring regular in better approach. Traditional floods and droughts analysis approach often use statistic characteristic value tools. Up to now, there is no applicable mathematical model. Drought events may form random process with extending time. Based on mathematical analysis pattern, the mean value generation function model is established in this paper. This model is applied in regional drought research, that is, severe drought events occurred in Yulin and Guanzhong regions of Shanxi province. The results show that mean value generation function model could simulate and predict drought events evolution tendency in better approach.

THE DEFINITION OF MEAN VALUE GENERATION FUNCTION AND ITS MODEL ESTABLISHMENT PRINCIPLE

Assuming there is one dimensional random process, $x_{(t)} = \{x_1, x_2, \dots, x_n\}$, where t is the time. Its mean value can be computed by:

$$X = (1/n) \sum_{t=1}^n x_{(t)}$$

Where n indicates the sample volume. Defining mean value generation function as follows:

$$X_{K(i)} = \frac{1}{E} \sum_{j=0}^{E-1} x_{(i+jK)} \quad i=1,2,\dots,K \quad 1 \leq K \leq m \quad (1)$$

Where E indicates the maximum integer satisfying $E \leq [n/K]$, m indicates the maximum integer no exceeding $n/2$, that is, $m = [n/2]$. When n is the even number, $[n/2] = n/2$, when n is the odd number, $[n/2] = (n-1)/2$.

Let $K=1,2,\dots,m$, we can get $X_{1(i)}, X_{2(i)}, X_{3(i)}, \dots, X_{m(i)}$, where $X_{1(i)}$ is called the mean value of one-dimensional random process, $X_{2(i)}$ is called mean value generation function with 2 interval, reasoning out the rest by analogy. As one 'basis function', mean value generation function may be extended periodically. So we can obtain extended matrix F:

$$F = (f_{ij})_{n \times m} \quad (2)$$

$$f_{ij} = f_{K(i)} = X_{K(i)} \quad t=1,2,\dots,n$$

$$t = i[\text{mod}(L)]$$

where f_{ij} indicate matrix elements, the symbol mod indicates congruence.

Applying the mean value generation function, we can establish regression selection program step by step, orthogonal selection program, empirical orthogonal function selection program etc. The orthogonal selection program is chosen in this paper. It can eliminate interact between mean value generation function in accordance with Gram-Schmidt orthogonal operation(Fengying Wei and Hongxing Cao,1990). It is advantageous to collect conveniently dominant periods items existed in random process and to avoid increasing linear model computation amount with increasing mean value generation function numbers, particularly for multi-dimensional random processes.

MEAN VALUE GENERATION FUNCTION MODEL ESTABLISHMENT STEPS

Assuming there is one dimensional random process, i.e., $x_{(t)} = \{x_1, x_2, \dots, x_n\}$. Mean value generation function model establishment steps are as follows:

1. To standardize original random process, that is, it can be written as $x'_{(t)} = (x_{(t)} - X) / \sigma$, where X and σ indicate the mean value and the standard error.
2. To compute mean value generation function of $x'(t)$, that is, to compute f_i , $i=1,2,\dots,m$, then to construct periodic extended matrix F. Here, f_1 has been become zero.
3. Let f_2 be the first vector for Gram-Schmidt orthogonalization, We can obtain (m-1) orthogonal series in accordance with orthogonalizing f_3, f_4, \dots, f_m . Here, the m-1 series are denoted by f_2, f_3, \dots, f_m .
4. We can establish linear equation about $x'_{(t)}$ by taking f_2, f_3, \dots, f_m as the self-variables. It can be written as:

$$x^{\wedge}(t) = \sum_{i=2}^m \varphi_i f_{i(t)} + e_{(t)} \quad (3)$$

Where $e_{(t)}$ denotes pure random component. If using vector matrix symbol, it can be written as:

$$X = \begin{matrix} F & \phi \\ n \times 1 & n \times (m-1) & (m-1) \times 1 \end{matrix}$$

5. To solve least square estimator, that is, $\phi = (F^T F)^{-1} F^T X$. Because there are orthogonal relations between f_i and f_j , so the covariance matrix would be diagonal matrix and $f_{ii} = |f_i|^2$, its inverse matrix G would also be diagonal matrix. Here, $G = (F^T F)^{-1}$ and $g_{ii} = 1/f_{ii}$, where g_{ii} are the elements of the inverse matrix.

6. To select orthogonal functions. So the coefficients of the linear model can be expressed as:

$$\varphi_i = g_{ii} \sum_{t=1}^n f_{i(t)} x'(t) \quad i=2,3,\dots,m \quad (4)$$

Here, we use the absolute value magnitude of the coefficients to reflect the significance degree of mean value generation functions, arrange φ_i from small to big with its absolute value magnitude, so we can take f_i into equation (3) by selecting φ_i from big to small. Then the numbers of mean value generation function selected by equation (3) are determined by using double-scoring criterion (abbreviated by DSC), that is, both from quantity prediction scoring criterion and trend prediction scoring criterion. It differs from well known F-test, remainder error square accumulation criterion, prediction square accumulation criterion, AIC criterion and BIC criterion etc. This is a kind of transforming of the academic thought. Obviously, the excellent model may be chosen while DSC value becoming the minimum and N_k value becoming the maximum, where N_k denotes trend scoring value.

7. To determine prediction model. Assuming the number of selected mean value generation function is k , so the relationship between $x^{(t)}$ and $f_{i(t)}$ can be written as follows:

$$x^{(t)} = \varphi_0 + \sum_{i=1}^k \varphi_i f_{i(t)} \quad (5)$$

where φ_i indicates the i -th original coefficient, $x^{(t)}$ denotes the computed value of $x'(t)$. Trending mean value generation function for q steps, we can get:

$$x^{(n+q)} = \varphi_0 + \sum_{i=1}^k \varphi_i f_{i(n+q)} \quad (6)$$

That is, the prediction result for q steps can be determined by using equation (6).

THE APPLICATION OF MEAN VALUE GENERATION FUNCTION MODEL IN REGIONAL DROUGHT RESEARCH

The computation of drought index: Here two severe drought events occurred in Ynlin region and one severe drought event occurred in Guanzhong region of Shanxi province are chosen. Their duration are from 1965 to 1967, 1972 to 1974 and 1977 to 1979 respectively. The drought index computation method is developed by 'Flood and Drought' editorial room set up in the Bureau of Hydrology, Yellow River Water Conservancy Commission.

The formulation of the drought index is as follows:

Let $B_{(i,j)}$ denote drought index, the subscript i and j indicates year and month respectively. If $\theta_{(i,j)} < CD_{(j)}$, then

$$B_{(i,j)} = 6 \times [\theta_{(i,j)} - CD_{(j)}] / \theta_m \quad (7)$$

If the extreme drought events occur, then $\theta_{(i,j)} = 0$, so $B_{(i,j)} = -4$. Thus the follow inequality will be tenable for the general drought events:

$$-6 \times [CD_{(j)} / \theta_m] \leq B_{(i,j)} \leq 0 \quad (8)$$

Where $\theta_{(i,j)}$ denotes the soil average moisture capacity in humid soil zone, θ_m denotes field moisture capacity, $CD_{(j)}$ denotes crop water requirement. And

$$D_{(i)} = f[Z_{(i,T)}, T]$$

Where D denotes drought severity standard, $Z_{(i,T)}$ denotes drought index accumulated value, T denotes drought continuous duration. If T exceeds 50 ten-days but $Z_{(i,T)} \geq -20$, this kind events are belonged to normal events (i.e., $B > -0.5$); If $T > 50$ ten-days and $-60 \leq Z_{(i,T)} < -20$, this kind events are belonged to slight drought events (i.e., $-1.5 < B \leq -0.5$); If $T > 50$ ten-days and $-120 \leq Z_{(i,T)} < -60$, this kind events are belonged to severe drought events (i.e., $-2.5 < B \leq -1.5$); If $T > 50$ ten-days and $Z_{(i,T)} < -120$, this kind events are belonged to extreme drought events (i.e., $B < -2.5$).

So we can get three random processes by applying above described method, that is, the drought index series from 1965 to 1967 and from 1972 to 1974 in Yulin region, the drought index series from 1977 to 1979 in Guanzhong region. Their sample volume are all 36. These drought index values are regarded as practical values. For these three random processes, the mean value generation function models are established by using all the first 32 month drought index values. All the last 4 values are used to test prediction results calculated by equation (6).

The simulation and prediction of three droughts index series: Firstly, according to above description of mean value generation function model establishment steps, three drought index series are simulated respectively. Table 1 shows that the choice criterion of mean value generation function in three simulation model. For the drought index series from 1965 to 1967 in Yulin region, when the step gets 6, N_k value is from 19.5 up to 21.5 which being the maximum, DSC value is from 2.80 down to 2.57 which being the minimum, thus six mean value generation functions are chosen for taking part in the linear regression model. For the drought index series from 1972 to 1974 in Yulin region, when the step gets 10, N_k value is from 22.5 up to 23.0 which being the maximum, DSC value is from 2.28 down to 2.22 which being the minimum, thus ten mean value generation functions are chosen for taking part in the linear regression model. For the drought index series from 1977 to 1979 in Guanzhong region, when the step gets 7, N_k value is from 22.0 up to 22.5 which being the maximum, DSC value is from 2.87 down to 2.80 which being the minimum, thus seven mean value generation functions are chosen for taking part in the linear regression model.

The established linear regression equations are as follows:

For the drought series in Ynlin region from 1965 to 1967:

$$x^{(t)} = -0.0000027 + 1.1190f_{9(t)} + 1.2731f_{7(t)} + 1.3820f_{12(t)} - 2.0052f_{3(t)} - 0.3932f_{2(t)} + 1.0559f_{5(t)}$$

For the drought series in Ynlin region from 1972 to 1974:

$$\hat{x}^{(t)} = -0.0000013 + 1.4643f_{5(t)} + 0.8317f_{11(t)} + 1.0174f_{6(t)} - 0.3025f_{3(t)} + 0.9657f_{2(t)} + 0.0814f_{10(t)} \\ + 0.4761f_{4(t)} + 0.9644f_{16(t)} - 0.3336f_{8(t)} - 7.9437f_{15(t)}$$

For the drought series in Guanzhong region from 1977 to 1979:

$$\hat{x}^{(t)} = 0.00000026 - 0.1451f_{15(t)} + 0.3265f_{8(t)} + 0.5385f_{14(t)} + 0.8768f_{3(t)} + 0.7542f_{16(t)} + 0.1158f_{5(t)} \\ - 0.5308f_{2(t)}$$

The contrast results between simulated values and practical values of these three drought index series show that they being all very close except individual points. The evolution tendencies of the modeling curve and the practical curve for these three drought index series are almost complete consistent. The modeling average relative errors for three drought index series are 6.2%, 4.8% and 5.6% respectively. This shows that the application of mean value generation function model in region drought index series simulation being successful.

Table 1. The choice criterion of mean value generation function in three simulation models

STEPS	1	2	3	4	5	6	7	8	9	10	REMARKS
PERIODIC LENGTH	9	7	12	3	2	5	6	4	8	14	
DSC	2.83	2.90	2.77	2.76	2.80	2.57	2.72	2.67	2.66	2.67	Yulin
COEFFICIENT φ_i	23.71	19.48	18.34	17.82	17.24	15.59	14.04	13.83	13.51	12.08	1965
N_i	20.5	19.0	20.0	20.0	19.5	21.5	19.5	20.0	20.0	19.5	~1967
PERIODIC LENGTH	5	11	6	3	2	10	4	16	8	15	
DSC	3.18	3.02	2.81	2.83	2.83	2.58	2.44	2.34	2.28	2.22	Yulin
COEFFICIENT φ_i	30.16	24.66	22.06	20.11	20.11	16.93	13.29	11.22	10.17	9.41	1972
N_i	17.5	18.0	19.5	19.0	19.0	21.0	21.5	22.0	22.5	23.0	~1974
PERIODIC LENGTH	15	8	14	3	16	5	2	6	4	11	
DSC	3.60	3.14	3.09	3.02	2.98	2.87	2.80	2.94	2.83	3.06	Guanzhong
COEFFICIENT φ_i	28.96	28.14	25.60	25.53	22.08	21.37	20.07	17.46	16.92	15.28	1977
N_i	17.0	20.5	20.5	21.0	21.0	22.	22.5	20.5	19.5	19.0	~1979

Secondly, the prediction results of applying mean value generation function model in drought index series analysis are verified by contrasting practical drought index values. Here, for Yulin and Guanzhong regions, three practical drought index duration are all from September to December but in 1967, in 1974 and in 1979 respectively. From table 2, for these three drought index series, the average relative errors between predicted values and practical values are 5.6%, 4.5% and 8.7% respectively, that is, the prediction precision exceeds 90%. This shows that the application of mean value generation function model in region drought index series prediction being successful.

Table 2. The contrast between prediction results and practical values

month		9	10	11	12
Yulin region 1967.9.~12.	predicted value	-0.48	-0.26	-0.46	-0.36
	practical value	-0.5	-0.25	-0.47	-0.32
	relative error(%)	4.0	4.0	2.1	12.5
Yulin region 1974.9.~12.	predicted value	-0.58	-1.72	-1.66	-1.31
	practical value	-0.6	-1.8	-1.6	-1.4
	relative error (%)	3.3	4.4	3.7	6.4
Guanzhong region 1979.9.~12.	predicted value	-0.0089	-0.19	-0.71	-1.11
	practical value	-0.01	-0.2	-0.8	-1.2
	relative error (%)	11.0	5.0	11.2	7.5

CONCLUSION

We can obtain follow conclusions with above description:

1. Mean value generation function is based upon the mean values of the random process, it can conveniently increase or decrease the length of the random process for improving simulation and prediction results. For analyzing the random process, establishing mean value generation function model is one new approach.
2. Mean value generation function model can be applied in regional historical drought events simulation and prediction in better approach.

For further research, it would be interesting to improve model structure etc.

REFERENCE

Fengying Wei and Hongxing Cao, 1990, *The Mathematical Models For Long-Term Forecast And Their Applications*. Meteorology Publishing House, Beijing.

Authors:

Zhang Xuecheng, Bureau of Hydrology, YRCC
Address: East No.12, Chengbei Road, Zhengzhou, 450004, China
Tel: +86-371-6304163 Fax: +86-10-63202978
E-mail: Wangzhy@public3.bta.net.cn

Zhu Xiaoyuan, Department of Hydrology, MWR
Address: No.2, Lane 2, Baiguang Road, Beijing, 100053, China
Tel: +86-10-63202624 Fax: +86-10-63202978
E-mail: Wangzhy@public3.bta.net.cn

CHANGING HISTORY AT ST. LOUIS- ADJUSTING HISTORIC FLOWS FOR FREQUENCY ANALYSIS

By Ronald J. Dieckmann, Hydraulic Engineer, and Gary R. Dyhouse, Chief, Hydrologic Engineering Section, Corps of Engineers, St. Louis, MO

Abstract In 1997, the Corps of Engineers embarked on a major re-evaluation of flood discharge and stage frequencies along the Lower Missouri and Upper Mississippi Rivers. The first step in the overall study, to be completed in 2000, is to develop a preliminary set of peak discharge data that is relatively homogenous. This requires that the effects of known biases, like historic flood discharge over-estimates and reservoir effects, be removed. For this data set, flood peak discharges at St. Louis prior to 1931 were adjusted downward to reflect the over-estimates made throughout the period when floats were primarily used for velocity measurements. Flood peak discharges recorded after 1957 were adjusted upward to remove the partial control by flood reduction reservoirs which came on line throughout the period to the early 1980's. Preliminary evaluations were made of peak discharge frequency at St. Louis using Bulletin 17B techniques and compared to the current discharge-frequency estimate for a no reservoir condition. The results using the revised data show a varying impact, ranging from almost nothing at common frequencies to about a 10% reduction for rarer events.

INTRODUCTION

Stages have been measured continuously at St. Louis, Missouri since the Civil War. Discharge data are available through periodic measurements made during this period, but the published values are the result of a variety of measurement techniques. The Corps took most discharge measurements at St. Louis prior to 1931, after which the USGS fully took over this task. The methods that the Corps used to obtain velocity measurements varied significantly from 1861-1931. Surface floats, single and double floats, rod floats, and various meters were used. Meter measurements were taken from both floating plant, subject to water movement, and from bridges. Only after 1931, when the USGS took over discharge measurements at St. Louis bridge sites using the Price Current Meter, have homogenous and reasonable accurate flood discharge measurements been available. Published peak discharges prior to 1931 for flood events have been found to be significantly over-estimated by several past investigations..

Similarly, changes in the upstream watershed, especially the construction of dozens of flood reduction reservoirs, have also had impacts on discharges at St. Louis. The first major reservoir, Fort Peck in Montana, was completed just prior to World War II, but reservoirs did not significantly impact the record at St. Louis until the late 1950's. Reservoir construction continued until the early 1980's and the record at St. Louis during the past 40 years includes lower flood peak discharges than would have occurred prior to reservoir construction.

Impacts of the 1993 Flood The 1993 flood produced record flood levels throughout all or portions of the five Corps Districts that comprise the Upper Mississippi River and Lower Missouri River Basins. The Lower Missouri River extends from the most downstream main stem reservoir (Gavins

Point) to the mouth, while the Upper Mississippi River is the entire reach upstream from the mouth of the Ohio River. Some locations experienced flood levels exceeding the 0.2% chance stage (500-year average recurrence interval) flood. Many questions were raised as to the frequency of the 1993 event. In addition, inconsistencies were noted at some locations in comparing recent flood records over the last two decades to the calculated stages of hypothetical floods, like the 1% chance event (100-year average recurrence interval). For example, the estimated 1% chance flood at Hannibal, MO had been exceeded on three occasions from 1965-1993, a highly unlikely occurrence. The hypothetical profiles currently in force were developed generally in the 1960's and 70's based on data available at that time. With the passage of time, at least 20 years of additional data, including the 1993 flood, is now available to re-evaluate frequency profiles on both the Lower Missouri and Upper Mississippi Rivers. Congress directed the Corps to undertake this re-analysis in 1997. The initial work is aimed at developing preliminary estimates of peak discharges at all main stem gages to evaluate the appropriateness of the current Federal standard for frequency analysis: the log Pearson Type III distribution. This paper addresses the effort to determine preliminary peak discharges at St. Louis, removing the impacts of measurement errors and upstream reservoir effects.

ACCURACY OF HISTORIC DISCHARGES

Early Work As early as 1944, it was known that a significant difference in calculated discharge at St. Louis existed between measurements using floats and those using meters. Field tests and discharge comparisons were made in 1944 of the gaging techniques used by the U.S. Geological Survey and the Corps of Engineers at St. Louis. These joint tests were performed simultaneously between the USGS, using the Price Current Meter suspended from a bridge (still the current standard today), and the Corps, using double floats and old style meters suspended from floating plant. For the double floats, differences with USGS results ranged from about 10% at discharges of 400,000–500,000 cfs to over 15% at discharges of 700,000 cfs. Extrapolations to higher discharges found that differences would exceed 20% at flowrates greater than 850,000 cfs. In all cases, the double floats resulted in higher discharges. Although not tested, surface floats would likely exhibit even higher velocity measurements and discharges. A similar finding was made between velocity measurements using a USGS Price meter suspended from a bridge and those using Corps of Engineers old style meters suspended from floating plant. The Corps measurements were considerably higher than GS results, ranging from 4% higher at a discharge of 530,000 cfs to 15% higher at a discharge of 670,000 cfs. Extrapolations to higher flows again illustrated a continuation of this trend, with differences of 20% or more at discharges exceeding 900,000 cfs. However, the field tests made no recommendations concerning any adjustment of the historic record, which was largely the result of Corps measurements until 1931. As a reference, a flow of about 500,000 cfs is roughly the bankfull capacity, while a flow of 850,000 cfs represents about a 4% annual chance event and is about equal to the peak discharge experienced in April 1973. The stage of 1973 event represented the flood of record at St. Louis until the 1993 flood occurred.

UMR Work The subject of the accuracy of historic flow measurements was again addressed by the University of Missouri–Rolla (UMR) in the late 1970's as a research effort funded by the St. Louis District (1). Actual measurements were taken at the Chester, Illinois gage, located 70 miles downstream of St. Louis, with a variety of historic techniques and compared to standard USGS

measurements taken from the nearby long-record gage site. While no great differences were noted for low and moderate flows within banks, important differences were found for higher in-bank flows and for one moderate flood. Measurements of high in-bank and flood discharges found that 83% of these measurements with historic methods were more than 5% higher and that 42% of the historic technique measurements were more than 10% higher (2).

Models Finally, the physical model of the Mississippi Basin constructed by the Waterways Experiment Station, Vicksburg, MS was utilized in 1986-87 to evaluate the impact of levees and reservoirs on flooding at and downstream of St. Louis (3). Part of the testing attempted to approximate the discharge of each of the two largest historic floods at St. Louis (1844 and 1903). This would be accomplished by matching about one dozen known highwater marks from each event through the St. Louis reach for the channel and overbank conditions existing at those times. The results of the testing found that highwater marks from both floods were very well matched with flows that were 33% (1844) and 23% (1903) lower than the published historic discharge estimates for the two floods (4). Neither historic flood was measured at St. Louis and published records simply represent estimates made after the 1903 flood. These findings were also confirmed through later analytic {UNET, (5)} modeling of the Mississippi River following the 1993 flood.

ADJUSTMENT OF HISTORIC FLOOD DISCHARGES

Since the comparison of USGS and Corps techniques performed by UMR generally found minor differences in discharges less than channel capacity and a conservative approach to adjusting the discharges was desired, it was assumed that flows less than the current channel capacity (approximately 500,000 cfs) did not require any modification (decrease). This decision left about one-half of the historic peak discharges prior to 1931 (after which the USGS performed discharge estimates exclusively) unchanged. The greatest historic floods prior to 1931 were the events of 1903 and 1844, neither of which were measured at St. Louis. These events were modeled with both physical and analytical techniques. All models gave similar results---the published values were too high. The three models found that discharges of 870,000-1,000,000 cfs (depending on the model used) reconstituted 1844 flood highwater marks very well, while peak discharges ranging from 790,000-875,000 cfs hit highwater marks from the 1903 event. Consequently, an initial, linear relationship between published flood peaks and adjusted flood peaks was developed and all historic flood discharges from the start of record to 1931 evaluated. This initial relationship was further simplified by reducing recorded flood discharges between 500,000-700,000 by 5% and discharges between 701,000-1,000,000 cfs by 10%. The adjustments are intended to be a conservative modification of the historic data; i.e., the adjusted value is likely to be the upper limit of the possible range of the actual value. With these guides, adjustments were made to the peak discharge in 34 of the 72 years of record prior to 1931. Table 1 illustrates some typical changes to St. Louis flows.

RESERVOIR IMPACTS

Reservoir construction that resulted in significant impacts to flood discharges on the Mississippi River at St. Louis did not really begin until well after World War II. Five of the six major reservoirs in the Upper Missouri Basin came on line in the 1950's and flood reduction reservoirs on major tributaries of the Missouri, especially the Kansas River Basin, were built in the 1950's and '60's.

TABLE 1
Comparison of Selected Historic Flood Discharges

Year	Published Value (cfs)	Adjusted Value (cfs)
1844	1,300,000	1,000,000
1903	1,019,000	875,000
1892	926,500	833,900
1908	850,000	765,000
1884	543,600	516,400

However, these reservoirs are several hundred miles upstream from St. Louis and large uncontrolled watersheds enter the Missouri River downstream of the reservoirs. Estimates of reservoir impacts at St. Louis from these reservoirs were generally a foot or less for most floods prior to 1978. The structures having the most impact on flood levels at St. Louis are the Truman Dam (completed in 1978) on the Osage River in west central Missouri and the Cannon Dam (completed in 1984) on the Salt River in northeast Missouri. Cannon Dam is one of four significant flood reduction structures on tributaries of the Upper Mississippi River and these came on line during the period from the late 1950's to the early 1980's. Again, the other three reservoirs, in east central Iowa, have little impact on Mississippi flows at St. Louis compared to Cannon Dam. Due to reservoir construction at the time, any given flood discharge throughout the period from the mid-1950's through the mid 1980's can show varying impacts from upstream flood reduction reservoirs. Only since about 1984 have records reflected a relatively homogenous period of reservoir effects. Precise knowledge of reservoir impacts is further complicated by a lack of adequate hydrologic models to firmly establish exact effects of the reservoirs at downstream points. Reservoir effects can only be estimated based on the results of limited Missouri River modeling, limited modeling of tributary reservoirs of the Mississippi and Missouri, and a maximum of engineering judgement. Estimates of the reservoir effects at St. Louis have been made for every significant flood since 1973, but detailed modeling has not been performed for any flood except 1993. Detailed hydrologic and hydraulic modeling of a no reservoir scenario was featured as part of the Flood Plain Management Assessment Study (6) performed after the 1993 flood, and these results were used as a basis for estimating the impacts of other events between the mid-1950's and today. Again, no adjustments were made for peak discharges less than channel capacity at St. Louis (approximately 500,000 cfs), assuming that locally heavy rainfall downstream of existing reservoirs could cause flows of this magnitude. This resulted in upward adjustments to 19 events from 1958-96. A simple linear relationship between channel capacity and the 1993 flood peak discharge was developed for existing vs. no reservoir conditions. An initial estimate of reservoir impacts for each flood from 1958 through 1996 was obtained from this relationship and then further adjusted, based on the knowledge of which reservoirs were on line during that specific flood year. These adjustments resulted in a no reservoir flow that was typically 2-15% greater than actual, except for 1993 which reflected a 20% increase. As with the previous adjustments for gaging techniques, these adjustments are intended to be conservative. Selected recorded and adjusted flows at St. Louis are shown in TABLE II.

Variations of adjusted flow for some events differ from later floods having a similar discharge, due to the presence of certain reservoirs which were built after the earlier flood. The detailed hydrologic and hydraulic modeling effort scheduled for the 1998-2000 time frame will greatly improve the estimates of reservoir effects on peak discharges. The figures in Table II should be viewed as an initial estimate for the evaluation of selected frequency distributions.

TABLE II
Comparison of Selected Flood Discharges for Reservoir Impacts

Year	Recorded Discharge (cfs)	Adjusted Discharge (cfs)
1995	800,000	925,000
1993	1,070,000	1,285,000
1979	694,000	755,000
1973	852,000	875,000
1969	618,000	650,000

PRELIMINARY ANALYSIS OF ADJUSTED DISCHARGES

These adjusted peak annual discharges are part of a set of similar discharges from all long-record stations on both the Missouri and Upper Mississippi Rivers that will be statistically evaluated during 1998. About 25-30 stations will be analyzed using at least four different statistical distributions to determine if one is superior for the evaluation of large river systems (over 5000 square miles). A recommendation will not be forthcoming until late in 1998. However, a statistical analysis of the adjusted St. Louis discharge data was performed using Bulletin 17B procedures (7). The Log Pearson Type III distribution was applied to the 136 years of record, including the adjusted data at St. Louis, and compared to previous estimates of discharge-frequency under no reservoir conditions. The analysis showed little change at the common flood frequencies (50%, 20% chance), however, estimates of rare floods like the 1% chance were considerably lower (about 10%) than the earlier estimates. Although this evaluation is for a no reservoir condition, presumably a with reservoir condition might be expected to show a similar result. If so, discharge and stage for a given frequency at St. Louis may be reduced when the overall re-evaluation of the hydrology and hydraulics of the Mississippi-Missouri Rivers is completed late in the year 2000.

SUMMARY

This effort was intended to provide a preliminary set of adjusted discharges at St. Louis for use in statistical analysis, testing a variety of distributions. Final discharge estimates will be obtained through major, detailed hydrologic studies now underway. Annual peak discharges at St. Louis for floods were decreased prior to 1931 to reflect gaging over-estimates, while annual flood peak

discharges after 1957 were increased to remove reservoir impacts. Preliminary analysis suggests that current estimates of discharge for rarer floods may be conservative.

REFERENCES

- (1) Stevens, G.L., 1979, SLD Potamology Study (S-3), Institute of River Studies, University of Missouri-Rolla.
- (2) Dyhouse, Gary R., 1985, Comparing Flood Stage-Discharge Data--Be Careful!, Hydrology and Hydraulics in the Small Computer Age, Volume 1, pp73-78
- (3) Waterways Experiment Station, 1995, MBM Letter Report, River Responses to Geomorphic Changes in An Alluvial Valley
- (4) Dyhouse, Gary R., 1996, Effects of Federal Levees and Reservoirs on 1993 Flood Stages at St. Louis, Transportation Research Board, Record No. 14553, pp 11-17
- (5) HEC, 1995, UNET: One-Dimensional Unsteady Flow Through a Full Network of Open Channels, User's Manual, Version 3.0
- (6) Corps of Engineers, 1995, Floodplain Management Assessment of the Upper Mississippi and Lower Missouri Rivers and Tributaries
- (7) Hydrology Subcommittee, 1982, Guidelines for Determining Flood Flow Frequency.

Authors Contact Points:

Address:

Corps of Engineers, St. Louis District
CEMVS-ED-HE (Dieckmann or Dyhouse)
1222 Spruce Street
St. Louis, MO 63103-2833

Telephone:

R. Dieckmann (314)-331-8363
G. Dyhouse (314)-331-8362

Fax:

(314)-331-8346

Inet:

DIECKMAN@SMTP.MVS.USACE.ARMY.MIL
DYHOUSE@SMTP.MVS.USACE.ARMY.MIL

A COMPARISON OF MOMENTS-BASED ESTIMATORS FOR FLOOD FREQUENCY ANALYSIS THAT INCORPORATE HISTORICAL INFORMATION

By John F. England, Jr., Hydraulic Engineer, U.S. Bureau of Reclamation, Denver, Colorado; José D. Salas, Professor, Colorado State University, Ft. Collins, Colorado; and Robert D. Jarrett, Research Hydrologist, U.S. Geological Survey, Denver, Colorado

Abstract: The use of historical and/or paleohydrologic (pre-gaging station) data to extend an existing streamflow gaging record is now an important addition to traditional Flood Frequency Analysis (FFA) methods. A new moments-based approach was recently developed that exploits this type of pre-gaging information. The Expected Moments Algorithm (EMA) is a simple and efficient method for incorporating historical and paleoflood information (Cohn et. al, 1997). This paper is focused on the testing of EMA by comparison with the existing Bulletin 17B Historical (B17H) approach. Two data sets from the United States were utilized to illustrate and compare the two estimation approaches. Results from this preliminary study indicate that EMA appears to be a viable alternative to current procedures from an operational perspective; performance was comparable for the two data sets analyzed. The Bulletin 17B document could be revised to include an option for EMA as an alternate to the existing historical weighting approach; additional testing is warranted to confirm these results.

INTRODUCTION

Flooding is a natural phenomenon that has plagued society for generations. Regulatory agencies in the United States require the estimation of the 100- and 500-year floods to promote sound floodplain management and minimize the risk to the public. The problem that the hydrologist faces in estimating the probabilities of infrequent events is an insufficient amount of data. Approximately 20 to 50 years of discharge data is available at typical stream gage sites; many areas are lacking stream gage data. Thus, extrapolation of the available at-site data by a factor of 10 to 50 (or greater) to estimate a large return period is common, but is not substantiated with actual data. Risk-based approaches for spillway design are currently being developed, and are dependent on long data records and probabilistic models. Historical and paleoflood information can significantly extend the data base and provide confidence on estimates of extreme events.

A new moments-based approach was recently developed that exploits historical and/or paleohydrologic (pre-gaging station) information. The Expected Moments Algorithm (EMA) is a simple and efficient method for incorporating historical and paleoflood information (Cohn et. al, 1997). This paper is focused on a simple comparison of EMA with the existing Bulletin 17B Historical (B17H) approach (USWRC, 1982). The specific objectives of this paper are:

- (1) presentation of two sites consisting of peak discharges with historical and/or paleoflood information measured at (or near) the gaging stations and discussion of data characteristics;
- (2) briefly outline the theoretical differences between B17H and EMA parameter estimation procedures;
- (3) fit a LP-III frequency function to each data set (at-site frequency analysis), using each estimation procedure and compare results of fitting over the range of observed flood quantiles.

The Bulletin 17B Work Group listed some additional, needed studies (USWRC, 1982 p. 27-28) for future work: they included a recommendation that alternative procedures for treating historic data be developed. Thomas (1985) reiterated this need for further study of approaches that use historical information. This paper directly addresses the treatment of high outliers (historical information) in Bulletin 17B (USWRC, 1982) by comparing the existing approach with a proposed, alternate method (EMA). The EMA-B17H comparison is nearly identical to the original approach used for selecting the log-Pearson Type III (LP-III) distribution for Bulletin 13 (Benson, 1968).

CENSORED DATA EXAMPLES

The types of pre-gaging station data that may be incorporated into flood-frequency analysis can be broadly categorized into historical data (e.g. Thomson et. al, 1964) and paleoflood data (e.g. Jarrett, 1991). In the context of this paper, historical data is defined as events which were directly observed by humans, generally in a non-systematic manner by non-hydrologists. These events usually occurred and were described in some qualitative and/or quantitative fashion prior to the systematic record. In contrast, paleoflood hydrology is the study of past or ancient floods which occurred prior

to the time of human observation or direct measurement by modern hydrologic procedures (Baker, 1987). Thus, paleoflood data may be distinguished from both historical and systematic (conventional gaging station) flood data by lack of human observation, regardless of the time of occurrence.

The method to incorporate pre-gaging station data into flood-frequency analysis is to consider the data to be a censored sample. By censored data we shall mean that, in a potential sample of size n , a known number of observations is missing at either end or at both ends (David, 1981). Historical and paleoflood information is utilized with a systematic gage record in a censored data framework as shown by many researchers (Leese, 1973; Hosking and Wallis, 1986; Stedinger and Cohn, 1986; Salas, et al., 1994; Francis et. al, 1994; and others). The data are described in historical/paleohydrologic (N_h) and systematic gage (N_s) periods (Figure 1), where $N_h + N_s = N_{tot}$. The number of known flood discharges are related to a threshold (Q_0); the number of exceedances above the threshold for the historical (eprim) and gaging (e) period are estimated and summed (k).

An assumption is made about the type of censored flood sample (Type I or Type II) one has observed. The distinction between Type I and Type II censoring is that in the former case the number of exceedances (k) is a random variable, while in the latter case it is fixed in advanced (Kendall and Stuart, 1973; Cohen, 1991). Type I censoring occurs whenever data is censored above or below a known, fixed threshold (Q_0). For Type II censoring, the threshold is assumed to be the random variable with a fixed number (k) of data observed.

Previous investigators have made different assumptions about the type of censored data for simulation experiments. Stedinger and Cohn (1986) assumed Type I censoring and found historical information to be valuable in virtually all cases considered. Hosking and Wallis (1986) assumed Type II censored data and that only the largest flood was observed. Their conclusions were nearly opposite to Stedinger and Cohn for a regional distribution, but they acknowledge information could be useful when estimating three parameters of an at-site distribution. Hirsch and Stedinger (1987) demonstrated that N_h was the most important factor to estimate. Guo and Cunnane (1991) indicated Hosking and Wallis' results were due primarily to their Type II censoring assumption. Frances et. al (1994) showed that the value of historical and paleoflood data could be small or large depending on 3 factors: the relative lengths of N_h and N_s , the return period (T) of the quantile of interest, and the return period of the discharge threshold. We are currently investigating flood recording mechanisms to determine what type of censored data is recorded at a particular site. Preliminary screening of a 36 gaging station data set with historical and/or paleoflood information indicates either assumption (Type I or II) may apply. In addition, multiple censoring (more than one threshold) and binomial-censored data (threshold-exceedance discharge values unknown, a special case of interval censoring) (Stedinger and Cohn, 1986) may be observed. Methods are needed that incorporate these potential censored data types.

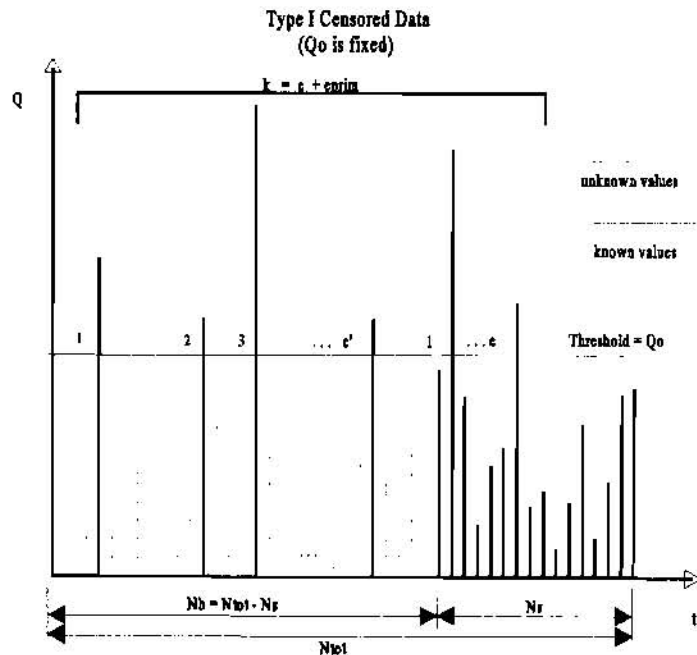


Figure 1 Data censoring framework.

Two sites were selected to illustrate and compare the EMA and B17H estimation procedures: Big Sandy River at Bruceton, Tennessee (USWRC, 1982) and Elkhead Creek near Elkhead, Colorado (Jarrett, in review). Three historical floods (eprim = 3) were observed prior to the establishment of a gaging station (USGS Gaging Station 03606500) on the Big Sandy River and were assumed to be the three largest floods in a 77-year period (USWRC, 1982 Appendix 6-1). If this information is correct, the sample is a Type II censored sample, as k is fixed. The threshold discharge (Q_0) was not specified in USWRC; a practical choice is equal to the smallest observed historic flood (18,500 cfs) if the sample is Type II. There is uncertainty in estimating N_h at this site; the historical period began at the first historic flood

occurrence. Hirsch and Stedinger (1987, p. 724) argue that this is a biased estimate and that N_h should be established on the quality of the historical information and not on the basis of the occurrence of the first extraordinary flood. In this paper, the data is analyzed assuming a Type II sample (k is fixed); no additional river stage information was available to determine if the floods were observed because they exceeded some fixed threshold (Type I). The threshold (Q_0) was set equal to 18,500 cfs, and is about 9 percent larger than the largest flood recorded in the gaging station record (17,000 cfs). The historical period, based on reconnaissance-level historical settlement information, was estimated to begin in 1860 (Figure 2); thus an additional 37 years of historical information was included.

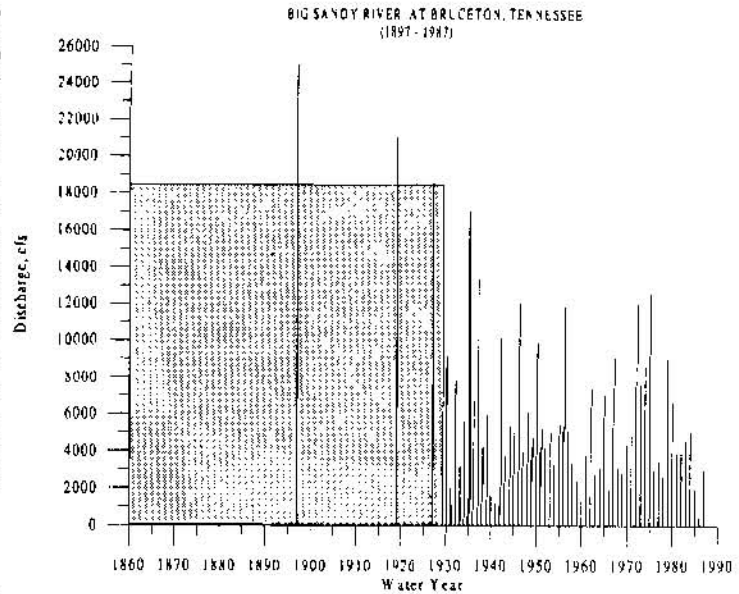


Figure 2 Big Sandy River peak discharge data. $N_s = 58$ years, $N_h = 70$, $N_{tot} = 128$ years, $Q_0 = 18,500$ cfs. The shaded area indicates censorship.

Large floods on Elkhead Creek near Elkhead, Colorado (USGS Gaging Station 09245000) arise from snowmelt runoff in the upper Colorado River Basin. One paleoflood ($e_{prim} = 1$) was estimated on Elkhead Creek at this location (Jarrett, in review), and represents the largest flood in approximately 1,000 to 10,000 years in the 64.2 mi² basin (Figure 3). The paleoflood (approximately 5,000 cfs) is 1.8 times the largest observed flood (2,850 cfs) in the 41-year gaging station record. Considerable uncertainty exists in the estimation of N_{tot} ; the largest flood may in fact be the largest in the Holocene period (10,000 years). For this paper, N_{tot} was assumed equal to 5,000 years. The paleoflood was assumed to be a Type II censored sample; with Q_0 equal to 5,000 cfs. No flood information was available below the threshold during N_h .

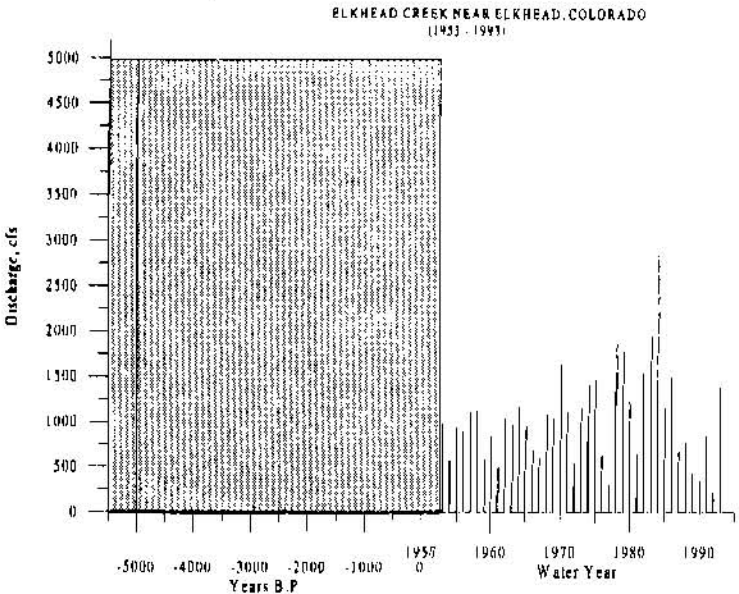


Figure 3 Elkhead Creek peak discharge data. $N_s = 41$ years, $N_h = 4959$, $N_{tot} = 5000$, $Q_0 = 5,000$ cfs. The shaded area indicates censorship.

Three important data assumptions were made as part of this study:

- (1) discharge estimates are explicitly known; no measurement errors or binomial-censored data are incorporated;
- (2) the historical period N_h is known perfectly, no errors in the paleoflood and/or historical record length exist;
- (3) a single threshold (Q_0) is known with accuracy and is appropriate to describe all exceedances.

While these three assumptions were made in this study for simplicity, they may be violated in practice. Refer to O'Connell et. al (1998, this volume) for a detailed discussion of a framework for incorporating data and model uncertainties.

The addition of historical and paleoflood data to frequency analysis is an essential element to obtaining realistic estimates of extreme flood quantiles (i.e., greater than a 50-year event), rather than relying exclusively on model extrapolations to rare probabilities. Continuing efforts in paleoflood data collection (e.g. Baker, 1987; Jarrett, 1990, 1991, in review;

Jarett and Costa, 1988; Enzel et. al, 1993; Ostenaar et. al, 1996, 1997) aid hydrologists and engineers to better understand the magnitude, occurrence, and distribution of extreme floods. A national paleohydrologic/flood data base is currently being developed (Hirschboeck and Baker, 1997); data will be archived at the National Geophysical Data Center's (NGDC) World Data Center A for Paleoclimatology.

FREQUENCY ANALYSIS METHODS

Two procedures that utilize historical information to estimate the parameters of a frequency distribution were compared: the historical adjustment presented in Bulletin 17B (B17H) (USWRC, 1982) and the Expected Moments Algorithm (EMA) (Cohn et. al, 1997). The log-Pearson Type III distribution was selected as the base flood frequency distribution to compare the two estimation procedures. Logarithms ($X_1, \dots, X_{N_{tot}}$) of the peak discharges ($Q_1, \dots, Q_{N_{tot}}$) were fit to a Pearson Type III (P-III) distribution, as recommended by the USWRC (USWRC, 1982). The P-III density function may be written as:

$$f(x; \alpha, \beta, \tau) = \frac{\left(\frac{x-\tau}{\beta}\right)^{(\alpha-1)} \exp\left(-\frac{x-\tau}{\beta}\right)}{\beta \Gamma(\alpha)} \quad (1)$$

where (α, β, τ) represent the shape, scale, and location parameters of the distribution. Properties and applications of the P-III distribution are presented elsewhere (Bobee, 1975; USWRC, 1982; Kite, 1988; Salas et. al, 1997).

The B17H historical weighting adjustment (USWRC, 1982) was designed to utilize pre-gaging information for two general cases (Cohn et. al, 1997): (1) a large flood occurring in a short systematic record and community knowledge that the flood was the largest in some longer time period; and (2) knowledge that one or more floods occurred prior to establishing a nearby gaging station. Three moments, mean (μ), standard deviation (σ), and coefficient of skew (γ) are estimated from the logarithms of the observed sample ($X_1, \dots, X_{N_{tot}}$) to estimate the parameters of the P-III distribution.

The first sample moment ($\hat{\mu}$), neglecting low outliers, is:

$$\hat{\mu} = \frac{W(\sum X_s - \sum X_e) + (\sum X_e + \sum X_{eprim})}{N_{tot}} \quad (2) \quad \text{with weighting factor} \quad W = \frac{N_{tot} - k}{N_s - e} \quad (3)$$

where X_s represent the logarithms of the systematic record peaks; X_e are the logarithms of the systematic peaks above the threshold, and X_{eprim} are the logarithms of the above-threshold historic/paleoflood peaks.

The B17H procedure is based on the concept of a threshold (Kirby, 1981), similar to a Type I censored data assumption, but the adjustment is not based on censored data theory. The key assumption is that the record is complete for all floods above Q_0 during the time period N_{tot} (Kirby, 1979 p. c-47). The weighting factor W is used to represent the unknown, below-threshold values and that they follow the same distribution as the below-threshold systematic observations (USWRC, 1982). The B17H adjustment, in effect, fills in the ungaged portion of the historic period with an appropriate number of replications of below-threshold (Q_0) portion of the systematic record (Kirby, 1981; Thomas, 1985). The technique is essentially the same as a fill-in method used by Benson (1950) for modifying a plotting position to account for historical information. Lane (1987) pointed out two shortcomings of this adjustment: (1) the assumption that the systematic record is representative of the entire historic period less the historic data; and (2) very little weight is given to the historic data. This second assumption is inappropriate for long historical/paleoflood periods in relation to the systematic record. For example, based on the Elkhead Creek data, $N_s = 41$, $N_h = 4,959$, $e = 0$ and $eprim = 1$: the systematic record is weighted 122 times ($W = 121.9$) to fill in the 4,958 unobserved (censored) observations.

In contrast, the EMA method was developed to utilize historical and paleoflood information in a censored data framework. This approach explicitly acknowledges the number of known and unknown values above and below a threshold. Three types of at-site flood information are used (Cohn et. al, 1997): systematic stream gage records; information about the magnitudes of historical floods; and knowledge of the number of years in the historical period when no large flood occurred. EMA moments are presented in (Cohn et. al, 1997); the first sample moment is:

$$\hat{\mu} = \frac{\sum X_s + \sum X_{eprim} + (N_h - eprim)E[X_h | (X_h < X_0)]}{N_{tot}} \quad (4)$$

where $E[X_h | (X_h < X_0)]$ is the expected value of a flood (X_h) given that it is below the threshold (X_0), and $X_0 = \log(Q_0)$. The term is then weighted by the number of

observations ($N_h - eprim$) below X_n . Cohn et. al (1997) present details of the EMA iterative solution algorithm, use of binomial and interval-censored data, and results from some limited Monte Carlo experiments.

The difference between B17H and EMA moment equations is the treatment of historical/paleoflood data. While B17H uses the systematic record to "fill in" the censored floods, EMA computes the expectation for data points below the threshold ($E[X_h|X_h < X_n]$) and weights this value by the number of censored (unknown) values ($N_h - eprim$). The assumption is made that the censored values arise from the same distribution as the uncensored values. EMA uses an iterative approach to estimate sample moments and distribution parameters. First, the sample moments are computed from X_s . Second, parameters are estimated from previously estimated sample moments. Third, new sample moments are estimated based on the current parameters to calculate $E[X_h|X_h < X_n]$. Steps 2 and 3 are iterated until the algorithm converges. Thus, the method specifically incorporates unknown, below-threshold (censored) historical values, which is fundamentally different from B17H.

METHODS FOR COMPARISON

Each estimation method was used to compute a flood discharge $\hat{Q}_i(T)$ for each observed flood (i), and each of the two flood series, where $T = (1/F(i))$. Comparisons were made between computed flood discharges $\hat{Q}_i(T)$ and data values $Q_i(T)$ for the L observed floods in each data set. This simple technique has frequently been used as a basis for comparing two estimation methods with empirical data sets (Benson, 1968; Bobee and Robitaille, 1977; Rao and Singh, 1987).

Two metrics were used to compute the relative goodness of fit between computed discharges $\hat{Q}_i(T)$ and data values $Q_i(T)$: a mean, absolute relative deviation ARD and a mean squared deviation MSD, where

$$ARD = \frac{1}{L} \sum |q_i(T)| \quad (5) \quad MSD = \frac{1}{L} \sum q_i^2(T) \quad (6) \quad \text{and} \quad q_i = \frac{\hat{Q}_i(T) - Q_i(T)}{Q_i(T)} \quad (7)$$

The statistics ARD and MSD are objective indexes of the goodness of fit of each method to sample data, throughout the recurrence intervals of interest for flood analysis (Bobee and Robitaille, 1977; Jain and Singh, 1987). Since one is interested in the performance of the estimation procedure to fit the extreme events on record as well, two additional comparisons were made: (1) q_i for the largest observed flood was used as a basis for comparison; and (2) ARD and MSD were estimated for the k largest floods. Probability of exceedance estimates $F(i)$ for the data values were computed via a Type I exceedance-based plotting position (Hirsch and Stedinger, 1987), with the distribution coefficient alpha (α) set equal to 0.4 as recommended by Cunnane (1978):

$$F(i) = \begin{cases} \frac{i - \alpha}{k + 1 - 2\alpha} (Pe) & i = 1, \dots, k \\ Pe + (1 - Pe) \frac{i - k - \alpha}{s - e + 1 - 2\alpha} & i = k + 1, \dots, g \end{cases} \quad Pe = \frac{k}{n} \quad (8)$$

DISCUSSION OF RESULTS

The results of the EMA-B17H average relative deviation (ARD) comparison for the two sites are presented in Table 1. The number of observed floods (L) and number of threshold exceedance floods (k) are listed for each location. The estimation method that corresponds to the lower value for ARD is considered best. Although not shown, similar results were obtained for the mean squared deviation (MSD) metric. Performance is nearly identical in terms of fitting observed floods on the Big Sandy River for both estimation methods. These results are illustrated in Figure 4, where the EMA and B17H frequency curves are indistinguishable. For Elkhead Creek, the estimation methods were nearly identical for the range of L observations. Frequency curves for Elkhead Creek are shown in Figure 5. The Weibull and Hazen plotting position parameter values ($\alpha = 0.0$ and 0.5 , respectively) were used to estimate different $F(i)$ values for each data set to determine the effects of a plotting position on the results. It was found that the choice of α had no effect on the results for the two data sets considered here. For ease of comparison and simplicity, regional coefficient of skew and

low outlier adjustments were not considered here.

Table 1 ARD comparison results

Data Set	No. observations (L)	Above threshold floods (k)	ARD (L observations)		ARD (Max observed)		ARD (Largest k)	
			EMA	B17H	EMA	B17H	EMA	B17H
Big Sandy River	60	3	0.036	0.037	0.084	0.096	0.044	0.052
Elkhead Creek	42	1	0.058	0.048	0.038	0.258	0.038	0.258

The descriptive ability of the method to match the extreme event of record and the above-threshold floods is of interest, in addition to matching the range of quantiles as discussed above. Benson (1968) suggested future work be conducted to handle 'outliers' or rare events. He cautioned (1968, p. 904) that "in any case, any major modifications ... would have to meet the test of conforming to the data satisfactorily". The relative deviations for the return period of the largest flood $q_i(N_{max})$ and for the k above-threshold floods for each data set are shown in Table 1. Here EMA performs nearly identically to B17H for the Big Sandy River, and better than B17H for Elkhead Creek; MSD results were similar. The results may be significant depending on the site, as B17H underestimated the maximum peak at Elkhead Creek by over 25 percent. While discharge measurement and dating errors were not considered in the estimation procedures, these results should still apply if the value is near the median estimate.

EMA performed equally as well or slight better overall than B17H for the two data sets and two metrics considered. Based on the data and comparison presented in this study, EMA performs comparably to the existing B17H approach for the range of quantiles considered, and may provide a better fit to the extreme events. The effects of the distribution (LP-III) assumption were not considered in this paper; based on Figures 4 and 5 the distribution appears adequate. Testing of the two methods to fit 34 additional data sets, in order to better confirm these results, is ongoing.

Thomas (1985) raised concerns about potential computational disadvantages with alternate approaches such as censoring theory, and that they must be weighed against any improvement in accuracy. The censored data EMA is an iterative

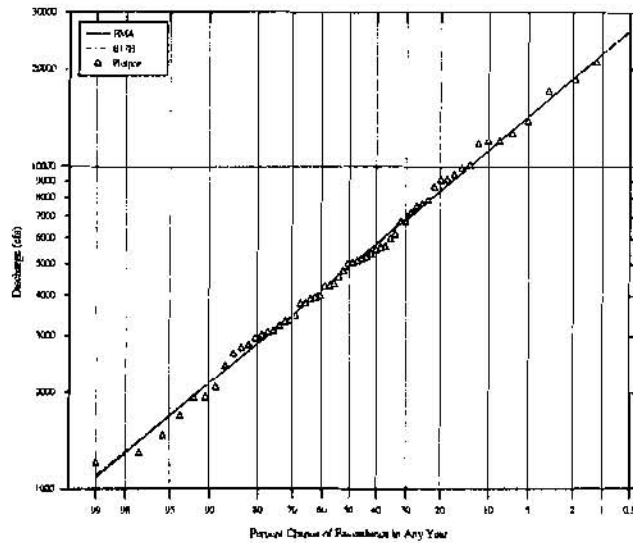


Figure 4 Flood frequency analysis probability plot for the Big Sandy River.

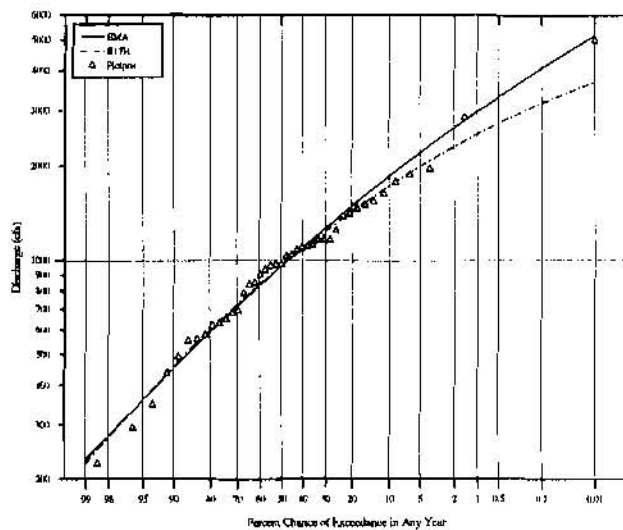


Figure 5 Flood frequency analysis probability plot for Elkhead Creek.

solution. For the two data sets analyzed as part of this paper, the number of iterations for solution convergence was 6 and 36 for the Big Sandy River and Elkhead Creek, respectively. On an Intel 486 PC processor and MS-DOS operating system, individual data set run times were 5 seconds on average. EMA computational disadvantages, as compared to B17H, are negligible for these data sets.

CONCLUSIONS

The following conclusions are made for this study:

Theoretical Differences: While both B17H and EMA are moments-based estimation procedures, historical and paleoflood information are used differently in each method. B17H was developed to address two specific community flood cases. It has two fundamental flaws: the "fill-in" method for censored data may be inappropriate for long records; and the method was not designed to incorporate the types of threshold-exceedance information now available such as interval censoring. EMA is more flexible than B17H as it was designed to incorporate the types of information currently being obtained. The EMA threshold-exceedance framework is an efficient way to utilize historical and paleoflood data.

Data Comparison: Two metrics of comparison (ARD and MSD) were used to demonstrate that EMA is an equal or better at-site estimator than B17H for the two data sets, quantile range and distribution considered in this study. EMA marginally outperformed B17H in estimating the maximum flood at each site.

Results from this study indicate that EMA appears to be a viable alternative to current B17H procedures from an operational perspective, and performed equally or better than the existing approach for the two data sets analyzed. We are encouraged by the results shown here. As EMA is moments-based, it is consistent with the Bulletin 17B guidelines. The Bulletin 17B document could be revised to include an option for EMA as an alternate to the existing historical weighting approach; additional testing is warranted to confirm these results. Further testing of these two methods by fitting to 34 additional data sets and monte carlo simulation is ongoing.

ACKNOWLEDGMENTS

The financial support of the United States Committee on Large Dams in the form of a graduate student scholarship for the first author is gratefully acknowledged. In addition, thanks are due to the NSF Grant CMS-9625685 on "Uncertainty and Risk Analysis Under Extreme Hydrologic Events" for their partial support of the second author. The advice and encouragement from Dr. William L. Lane (USBR, retired) and Dr. Timothy A. Cohn (USGS) in support of this work are much appreciated.

REFERENCES

- Baker, V.R. (1987) Paleoflood hydrology and extraordinary flood events. *J. Hydrology*, 96, pp. 79-99.
- Benson, M.A. (1950) Use of historical data in flood frequency analysis. *Transactions, American Geophysical Union*, 31(3), pp. 419-424.
- Bobee, B.B. (1975) The log Pearson Type III distribution and its application in hydrology. *Water Resour. Res.* 11(5), pp. 681-689.
- Bobee, B.B. and Robitaille, R. (1977) The use of the Pearson Type III and Log Pearson Type III distributions revisited. *Water Resour. Res.* 13(2), pp. 427-443.
- Cohen, A.C. (1991) *Truncated and censored samples*. Marcel-Dekker, NY, 312 pp.
- Cohn, T.A., Lane, W.L., and Baier, W.G. (1997) An algorithm for computing moments-based flood quantile estimates when historical information is available. *Water Resour. Res.* 33(9), pp. 2089-2096.
- Cunnane, C. (1978) Unbiased plotting positions - a review. *J. Hydrology*, 37, pp. 205-222.
- David, H.A. (1981) *Order Statistics*, 2nd ed., Wiley & Sons, New York, 360 pp.
- Enzel, Y., Ely, L.L., House, P.K., Baker, V.R., and Webb, R.H. (1993) Paleoflood Evidence for Natural Upper Bound to Flood Magnitudes in the Colorado River Basin. *Water Resour. Res.* 29(7), pp.2287-2297.
- Frances, F., Salas, J.D. and Boes, D.C. (1994) Flood frequency analysis with systematic and historical or paleoflood data based on the two-parameter general extreme value models. *Water Resour. Res.* 30(6), pp. 1653-1664.
- Guo, S.L. and Cunnane, C. (1991) Evaluation of the usefulness of historical and palaeological floods in quantile estimation. *J. Hydrology*, 129, pp. 245-262.

- Hirsch, R.M., and Stedinger, J.R. (1987) Plotting positions for historical floods and their precision. *Water Resour. Res.* 23(4), pp. 715-727.
- Hirschboek, K.K. and Baker, V.R. (1997) Global Paleoflood Database. Current research project, University of Arizona, Laboratory of Tree-Ring Research, sponsored by the National Oceanographic and Atmospheric Administration.
- Hosking, J.R.M., and Wallis, J.R.. (1986) Paleoflood hydrology and flood frequency analysis. *Water Resour. Res.* 22(4), pp. 543-550.
- Jain, D. and Singh, V.P.. (1987) Comparison of some flood frequency distributions using empirical data. In V.P. Singh (ed) *Hydrologic Frequency Modeling*, D. Reidel, pp. 467-485.
- Jarrett, R.D. (1990) Paleohydrologic techniques used to define the spatial occurrence of floods. *Geomorphology* (3), pp. 181-195.
- Jarrett, R.D. (1991) Paleohydrology and its value in analyzing floods and droughts. U.S. Geological Survey Water Supply Paper 2375, pp. 105-116.
- Jarrett, R.D. (in review) Regional interdisciplinary paleoflood approach to assess extreme flood potential, submitted to *Water Resour. Res.*, 37 pp.
- Jarrett, R.D. and Costa, J.E. (1988) Evaluation of the flood hydrology in the Colorado Front Range using precipitation, streamflow, and paleoflood data for the Big Thompson River Basin. U.S. Geological Survey Water Resource-Investigations Report 87-4117, 37 pp.
- Kendall, M.G. and Stuart, A. (1973) *The Advanced Theory of Statistics: volume 2, inference and relationship*. 3rd ed., Griffin, London, 723 pp.
- Kirby, W. (1981) Annual flood frequency analysis using U.S. Water Resources Council Guidelines (Program J407). Section C in Lepkin (and others), *WATSTORE User's Guide Vol. 4 Chap. 1* U.S. Geological Survey Open-File Report 79-1336-I, pp. C-1 to C-56.
- Kite, G.W. (1988) *Frequency and Risk Analysis in Hydrology*, Water Resources Publications, Littleton, Colorado, 257 pp.
- Lane, W.L. (1987) Paleohydrologic data and flood frequency estimation. In V.P. Singh (ed) *Regional Flood Frequency Analysis*, D. Reidel, pp. 287-298.
- Leese, M.N. (1973) Use of censored data in the estimation of gumbel distribution parameters for annual maximum flood series. *Water Resour. Res.* 9(6), pp. 1534-1542.
- O'Connell, D.R.H., Ostenaar, D.A., and Levish, D.R. (1998) Risk-based hydrology: bayesian flood-frequency analysis using paleoflood and data uncertainties. Proc. First Federal Interagency Hydrologic Modeling Conference, Las Vegas, Nevada, April 19-23, 1998 (this volume).
- Ostenaar, D.A., Levish, D., and O'Connell, D.R.H. (1996) Paleoflood Study for Bradbury Dam, Cachuma Project, California [unpubl]: U.S. Bureau of Reclamation Seismotectonics Report 96-3, Denver, CO, 86 pp., 1 folded plate, 4 appendices.
- Ostenaar, D.A., Levish, D., O'Connell, D.R.H., and Cohen, E. (1997) Paleoflood Study for Causey and Pineview Dams, Weber Basin and Ogden River Projects, Utah [unpubl]: U.S. Bureau of Reclamation Seismotectonics Report 96-6, Denver, CO, 69 pp., 3 appendices.
- Salas, J.D., Wohl, E.E., and Jarrett, R.D. (1994) Determination of flood characteristics using systematic, historical and paleoflood data; in: *Coping With Floods*, Rossi, G., Harmancioglu, N. and Yevjevich, V. eds.; Kluwer Academic Publishers, Netherlands, Ch.7, pp. 111-134.
- Salas, J.D., Smith, R.A., Tabios, G.Q., and Heo, J.H. (1997) *Statistical Computer Techniques in Water Resources and Environmental Engineering*, Chapters 1-14. Unpublished Manuscript of forthcoming book, Department of Civil Engineering, Colorado State Univ., Fort Collins, Colorado.
- Stedinger, J.R., and Cohn, T.A. (1986) Flood frequency analysis with historical and paleoflood information. *Water Resour. Res.* 22(5), pp. 785-793.
- Thomas, W.O. (1985) A uniform technique for flood frequency analysis. *J. Water Resour. Plann. Mgmt.*, ASCE, 111(3) pp. 321-337.
- Thomson, M.T., Gannon, W.B., Thomas, M.P., and Hayes, G.S. (1964) Historical floods in New England. U.S. Geological Survey Water Supply Paper 1779-M, 105 pp.
- U.S. Water Resources Council (USWRC) (1982) Guidelines for determining flood flow frequency. U.S. Interagency Advis. Comm. Water Data, Hydrol. Subcomm., Bull., 17-B (revised and corrected).

RISK IN MITIGATING HYDROLOGICAL DISASTERS

Dr. Shou-shan Fan
Adjunct Professor, University of Wisconsin, Milwaukee
Chair, ASCE Task Committee for Mitigating Hydrological Disasters
Reston, VA 20191-4400, USA

Abstract

Disasters caused by extreme hydrological events have been a major threat ever since the first human appeared on earth. Numerous human struggles against disasters have been documented in historical records since Biblical times. In today's highly developed society, the potential losses due to a major disaster are tremendous. As alternatives to counter such disasters increase, public tolerance for such disasters decrease. In this paper, based on the author's experience in working with the Federal Interagency Committee on Natural Disaster Reduction of the U.S. National Science and Technological Council and elsewhere, we address the following topics: (1) in-depth analysis of the problems and issues, (2) examination of the needs for modernizing existing mitigation measures, and (3) some cost-effective methods for conducting further studies.

This paper will underscore the fact that hydrological disaster reduction problems are interdisciplinary. Their ultimate solutions will require close cooperation of scientists, engineers, policy makers, and the public. We hope the conclusions of this paper will help reduce the uncertainty in estimating floods and provide the impetus for further research.

1. INTRODUCTION

Hydrological disasters, no matter how violent, need not cause major damage. Loss of lives can be prevented and economic impact minimized if a decision maker is provided with accurate prior information on major disaster characteristics, such as the magnitude and arrival time of the disaster and its potential damages. Therefore, prediction is very important to the success of disaster reduction.

At present, hydrological disaster reduction is not an exact science and it is still in a developmental stage. In spite of the many great achievements and advancements by scientists and engineers, disaster reduction remains highly subjective. It involves risks and uncertainty, and currently depends primarily on professional judgments.

Uncertainty and risk are closely related and are often used interchangeably. However, there are differences. For example, risk is predictable and uncertainty is not. Risk is the probability of an undesirable event. Uncertainty is the event to which risk cannot be predicted. Thus, when risk is zero, the event is certain and when risk is infinity, the event becomes totally uncertain.

There are several types of risk. They include socioeconomic, health related and technology induced risks. Due to page limitation, this paper is limited to the discussion of technology induced risk.

II. ANALYSIS OF TECHNOLOGY INDUCED RISK

We discuss below four aspects of technology induced risk: the complexity of disaster characteristics, complications created by human interventions, inadequacy of existing technologies and most importantly the lack of adequate data. For an easy demonstration, this paper has chosen the analysis of flood disaster reduction risk as an example to explain the complex problems and issues involved.

1. Complexity of Flood Characterization

The complexity of floods makes them very difficult to simulate and predict. They are complex because they are trinary and multidimensional:

- Floods are multidimensional because they are defined by either magnitude (discharge or stage), velocity, timing, duration, frequency, two-phase flow, degree of hazard, or a combination of these terms.
- Floods are trinary because they are products of three major factors, namely meteorologic, physiographic, and human intervention. These factors are closely interrelated.

The meteorological factors which influence flood flows in large rivers are the intensity, amount, and distribution of precipitation. The physiographic factors which influence floods can be divided into two major categories: basin characteristics and channel characteristics.

The basin characteristics are the size and slope of drainage area, permeability, land coverage and uses, and groundwater conditions that directly affect the flood run-off from the basin. The channel characteristics are the geometric and hydrodynamic properties of the channel that control the movement of flood waves.

2. Complications Due To Human Interventions

Flood characterization is further complicated by human interventions that may significantly modify the flood's complex nature previously discussed. Human interventions are of two major types:

a. Beneficial Actions - Flood Control and Mitigation

Generally, these measures are divided into two categories, engineering and administrative. The major engineering measures involve the construction of reservoirs to store floods, the building of levees to confine floods and to divert flows to minimize flooding, and the forecasting of floods to issue warnings. Administrative measures involve the zoning of floodplains and issuance of flood insurance.

b. Hazardous Intervention

Since 1936, the United States government has spent more than 13 billion dollars on flood control. Despite this vast governmental effort in flood control and floodplain management, the average annual flood loss in 1984 dollars, not counting death and suffering, has increased from less than 100,000 dollars at the beginning of the century to more than 3 billion dollars in 1984. The upward trend in flood losses is due not only to greater amount of floods but also to increased human encroachment onto the floodplains which are supposed to convey excess water during floods.

3. Inadequacies of Existing Technologies

a. A Review of Existing Flood Prediction Techniques

Presently, there are three frequently used inflow flood prediction techniques: probable maximum flood (PMF) approach, frequency analysis, and peak flood envelopment. All these techniques have been discussed elsewhere (Fan, 1990) and will not be developed further here.

The problems of flood prediction can be best illustrated by two case studies in the United States. One study is the probabilistic analysis of the annual peak floods of the Pecos River near Comstock, Texas, for the 53-year period from 1901 through 1954. In 1954, the Pecos River had a flood that was 8 to 9 times higher than any previously recorded.

The second study is the PMF derivation for the northeastern United States. The National Weather Service (NWS) in its 1956 Hydrometeorological Report (HMR) No.33, estimated the probable maximum precipitation (PMP) for a 24-hour duration, in a 200 square-mile basin of the Deerfield River to be 19.2 inches. Using the Corps of Engineers HEC-1 computer program, the PMF was estimated to be 248,700 cubic feet per second (cfs). In 1978, in its HMR-51, the NWS upgraded its previous PMP to 21.5 inches. As a result, the PMF was increased to 277,500 cfs.

b. Predicting Floods for Multiple Reservoir Systems

The estimation of design floods for each reservoir in a multiple reservoir system where the reservoirs are located in series, parallel, or both within the same basin should be performed systematically from the most upstream reservoir toward the downstream reservoirs. In a multiple reservoir system, the failure of a reservoir upstream by itself, may have very little impact immediately downstream. However, a breach flood may induce an unexpected sudden increase in flood flow and siltation to the next reservoir and this, in turn, may trigger a chain reaction of failure of one or more of the reservoirs downstream. Such an event would then have the potential to produce a much larger amount of damage.

c. Inundation Analysis

For water resources developments, the two phases of a reservoir failure inundation analysis involve the evaluation of breach parameters and determination of inundation boundaries by channel routing. This is accomplished by routing the floods from the reservoir through downstream channel to define the maximum water surface elevation on both sides of the channel on topographic maps. The end products will be utilized to determine the adequacy of floodwater disposal and to make a hazard evaluation.

d. Downstream Flood Hazard

Generally, downstream flood hazards can be estimated by either visual inspection or numerical modeling of a dam breaching flood. A dam breaching flood is determined primarily by the dam failure outflow hydrograph and characteristics of the channel downstream.

e. Upstream Hazards

Upstream from the dam, flood hazard may sometimes become dangerous when the fast-rising backwater inundates densely populated or extensively developed areas. Also, the delta formation caused by reservoir sedimentation may raise the nearby groundwater table during floods.

f. Sedimentation Hazards From Dam Breaching

When a dam fails suddenly, a high-speed flood wave moves the sediments accumulated in the reservoir into the flood plain downstream. The flood usually carries a large amount of collected sediment and debris as it sweeps the channel. Often, the swift current may wash away homes and destroy other properties. In rural areas, crops and livestock are frequently destroyed. Flooding may cause erosion in some areas and siltation in others.

g. Complications Arising From Special Nonpoint Interventions and Interaction with Natural Systems

- Global changes
- The effects of development of upper land on flood peaks
- The effects of land erosion on reservoir siltation (loss of storage)

h. Invalidation of Major Assumptions Embedded in Models

Human intervention and other factors previously discussed may at times invalidate key assumptions (linearization, data homogeneity and randomness, etc.) embedded in conventional disaster mitigation models and techniques.

In short, hydrological modeling techniques are still in a developing stage. They are not accurate and are at best approximations. For a complex hydrologic disaster reduction application, one has to make numerous simplifications and assumptions, such as linearity, homogeneity, randomness, etc.

4. Lack of Adequate Data

Data is an essential part of our life. For engineers, adequate hydrologic data are important for successful planning, designing, and operation of any water resources development. For modelers, data are critical in developing models. For model users, data are absolutely essential for calibration, verification, and the sound utilization of the models. Unfortunately, in the field of flood disaster reduction, the data we need are often nonexistent or not readily available. Therefore, we usually have to collect a great deal of field data.

In general, the inadequacy of data involves the lack of either or both quantity or quality of data. Data quantity and data quality problems are closely related and are usually treated together. The major categories of data problems are:

(1) monitoring; (2) sampling; (3) uncertainty and errors; (4) database management; (5) treatment, analysis, and interpretation; (6) processing, transmission, and dissemination; and (7) presentation. Each of these categories of data problems may involve one or more elements of uncertainties.

To illustrate the nature of the data problems, the issue of uncertainty in data monitoring is discussed below. In practice, since the data we need are often nonexistent or not readily available, we usually have to collect a great deal of field data ourselves. But data collection can be complex, expensive, and time consuming. Therefore, in resolving data problems, we often need to determine the worth of data by balancing the need, accuracy, and cost-benefit ratio of the plan. Sometimes, for a small project, it may not be economically justified.

a. In designing a data monitoring program, the following questions must be addressed:

- i) What parameters must be monitored?
- ii) What gages or instruments should be used?
- iii) Where should the gaging station be located and how many gages do we need at each station?
- iv) How many stations are needed, how should they be distributed, and how should they be operated?

The answers to these questions are not easy. They vary from problem to problem and are site-specific. In addition, the answers depend primarily on how well we understand the characteristics of the problems. Other critical factors involve the local environment, economics, and budgets.

b. Additionally, we often do not know exactly how to select the parameters that describe the phenomena or how to accurately measure the parameters once we select them. For example, channel roughness is one of the most important parameters in stream flow and sedimentation studies, but there is no accurate way to account for its true value.

c. For flows in a fixed-bed channel, channel geometry is a random variable in a spatial domain, independent of the flows. In an alluvial channel, however, the problems become much more complicated as channel geometry is random in both the spatial and the time domains and interacts continuously with random flows.

Therefore, the best we can do is to approximate a time and a spatial variable average through indirect means, using known values of channel geometry and flow characteristics.

III. CONCLUSIONS

We present the following conclusions in the hope that they may induce greater awareness of this subject and of the complications associated with these problems.

1. Hydrological disaster reduction is essential to the development and management of our nation's water resources. To reduce natural disasters, advanced knowledge of the characteristics of the disaster and the risk of their occurrences are essential.
2. Hydrological disaster is very hard to characterize because it is a product of many interrelated factors and can also be defined in many ways.
3. Predictions made using different analytical approaches, or even the same techniques applied by different persons, can yield significantly different results.
4. Disaster prediction research is a complex, dynamic, multidisciplinary, and multidimensional undertaking. It requires an understanding of the underlying physics and mathematics. Moreover it requires practical experience in many different disciplines, including meteorology, hydrology, hydraulics, environment, floodplain management (hazard evaluation, risk assessment), economics, and others.
5. Human intervention may at times invalidate key assumptions (linearization, data homogeneity and randomness, etc.) embedded in conventional disaster prediction techniques previously discussed.
6. Data accuracy and timely dissemination are keys to the success of disaster prediction. State-of-the-art technologies can improve data monitoring and more quickly disseminate information.
7. In data collection and modeling, we may never know the true values we are seeking, since we do not truly understand the natural phenomena. Under these circumstances, we should only expect to obtain approximate values.
8. A common national disaster data bases should be developed.
9. Disaster reduction remains highly subjective. It involves risks and uncertainty, and currently depends primarily on professional judgments.
10. Disaster reduction problems are interdisciplinary. Their ultimate solutions will require close cooperation of scientists, engineers, policy makers, and the public.

IV. REFERENCES

- Fan, Shou-shan; SCIENTIFIC EVALUATION OF PROBABLE MAXIMUM FLOOD RELATED STUDIES OF UPPER DEERFIELD RIVER, MASSACHUSETTS AND VERMONT; Staff Report, Federal Energy Regulatory Commission, Washington, D.C. 1984
- Fan, Shou-shan; RESERVOIR ENGINEERING, in "Civil Engineering Guidelines For Planning and Designing Hydroelectric Developments, American Society of Civil Engineers (5 vols.) , 1990
- Fan, Shou-shan; NATURAL DISASTER REDUCTION PLAN AT FERC; Paper presented at the International Water Power-91 Symposium, Denver, Colorado, 1991
- Fan, Shou-shan; NATURAL DISASTER AND ENVIRONMENTAL CONSIDERATION IN WATER RESOURCES PLANNING; Invited lectures, National Chiao-tung University, Taiwan, 1991
- Fan, Shou-shan; HYDRAULIC RISK OF FLOOD DISASTER REDUCTION OF DAMS; Proceedings, National Hydraulic conference, American Society of Civil Engineers, Baltimore, MD, 1992
- Fan, Shou-shan; A REVISIT TO DATA PROBLEMS AND DATABASES; Proceedings, 1993 International Water Power Conference, Nashville, Tennessee, August 10-13, 1993
- Fan, Shou-shan; PROBLEMS OF STREAM FLOOD SIMULATION AND PREDICTION; Proceedings, National Hydraulic Conference, American Society of Civil Engineers, Buffalo, NY, 1994
- Fan, Shou-shan and Nicholas C. Matalas; A LOOK AT TECHNOLOGICAL RISK AND UNCERTAINTY IN MITIGATION OF HYDROLOGICAL DISASTERS, Conference on Risk Assessment and Decision Making on Natural Hazards, National Science & Technological Council, White House Conference Center, Washington, DC; November 2-3, 1995

HYDROLOGIC MODELING OF TYGART LAKE FOR DAM SAFETY ASSURANCE EVALUATION REPORT

James A. Kosky, P.E., Hydraulic Engineer, U.S. Army Corps of Engineers, Pittsburgh District, Pittsburgh, Pennsylvania

Abstract: This paper discusses the hydrologic modeling effort of the Tygart River Lake for use in preparation of the Dam Safety Assurance Evaluation Report by the U.S. Army Corps of Engineers - Pittsburgh District. Extensive modeling was performed to analyze past flood events, including the Standard Project Flood (SPF), Threshold Flood (TF), Probable Maximum Flood (PMF) and various percentages of the PMF. The PMF was developed using current methods and compared to the original spillway design criteria. It was determined that the dam could not safely pass the PMF and some type of modification would be required.

INTRODUCTION

The Tygart Dam Project was authorized by the Rivers and Harbors Act of August 1935 as a navigation project and directed the Corps of Engineers to be responsible for the project. Tygart Lake is located in the northern part of West Virginia near the City of Grafton. The dam is a concrete gravity section type with a top length of 1,921 feet. The abutment section rises to a maximum height of 234 feet above stream bed. The outlet works consist of eight conduits controlled by two 5'-8" x 10' slide gates. The spillway has a crest length of 489 feet and is an uncontrolled concrete ogee type with a crest elevation of 1167 feet above National Geodetic Vertical Datum (NGVD).

The Tygart River originates in the mountainous region of northeastern West Virginia. It follows a long and sinuous course for approximately 113 miles and averages a slope of about 13 feet per mile. The tributaries are very steep and have average slopes greater than three times the main river channel. It joins the West Fork River to form the Monongahela River at Fairmont, West Virginia. The Tygart Dam is located approximately 23 miles upstream of the mouth of the Tygart River. The total drainage area upstream of the dam is 1,184 square miles. The Tygart dam basin is elliptical in shape with the north to south axis approximately 65 miles in length and the east to west about 25 miles wide.

The Tygart Dam is hydrologically and hydraulically deficient because it will not pass the Probable Maximum Flood without overtopping the dam. This discussion will summarize the methodology used in analyzing Tygart Dam for this hydrologic deficiency. Figure 1 shows the general location of Tygart Lake.

PAST FLOOD EVENTS

The November 1985 "Election Day" flood was the flood of record and provided the highest maximum elevation, runoff and pool storage recorded at Tygart Lake. The flood was caused by the remnants of Hurricane Juan which produced 6-7 inches of rainfall over three days in the

Tygart River basin. Tygart Dam used approximately 84% of its flood storage capacity and the lake level came within 9 feet of going over the spillway. This flood was estimated to be greater than the 200 year return frequency event.

The June 1972 flood resulted from Tropical Storm Agnes and was the second highest maximum pool consuming approximately 78% of the flood storage capacity. The November 1985 and June 1972 floods along with the floods of July 1958, March 1967 and a more recent flood of February 1994 were analyzed and used in calibrating the hydrologic model.

HYDROLOGIC MODELING

A hydrologic model was developed using the rainfall-runoff model, HEC-1, developed by the U.S. Army Corps of Engineers Hydrologic Engineering Center. A six hour unit hydrograph at the Tygart damsite was developed using past storms including the August 1945, November 1949 and October 1954 events. After the hydrologic model was calibrated, the floods were routed through Tygart Dam using the existing Reservoir Regulation Plan. Model results compared well to actual data.

The hydrologic model was then used to analyze the Standard Project Flood (SPF), Threshold Flood (TF) and the PMF. The SPF hydrograph was computed using the U.S. Army Corps of Engineers Engineering Manual (EM-1110-2-1411) -“Standard Project Flood Determinations”, March 1952. It was determined that the Tygart Dam could pass the SPF.

The Threshold Flood hydrograph was computed using the methods outlined in the U.S. Army Corps of Engineers, Institute of Water Resources “Guidelines for Evaluating Modifications of Existing Dams Related to Hydrologic Deficiencies.” The threshold flood is defined as ‘that flood that results in a peak reservoir water surface elevation equal to the dam crest less the appropriate freeboard.’ Therefore, this is the determination of the inflow event which exceeds the design criteria of the dam. The TF was computed as 77% of the PMF and a plot is shown in Figure 2.

The Probable Maximum Precipitation (PMP) was developed using the National Weather Service Hydrometeorological Reports (HMR) No. 51 and No 52. HMR No. 51 provides area-averaged Probable Maximum Precipitation (PMP) for the United States east of the 105th meridian. HMR No. 52 provides a procedure for distributing drainage area averaged PMP amounts from the storm areas using the PMP in HMR No. 51. The inflow hydrograph for the PMF was calculated using the HEC-1 model and distributing the PMP storm rainfall estimates over the Tygart Lake basin. The PMF inflow was computed to be approximately 398,000 cubic feet per second (cfs) and was routed through the reservoir outlets to establish a peak pool elevation of the PMF. Figure 3 is a plot of the PMF inflow hydrograph used in the analysis.

A sensitivity analysis was done to check the validity of the unit hydrograph developed by increasing it by 25% and 50% of the PMF and adjusting the volume to see the effects of the peak PMF elevation. The procedure is a check to see the stability of the unit hydrograph and showed an insignificant change in the PMF elevation when increased by these scenarios.

For the evaluation of the hydrologic deficiency at Tygart Lake, each flood condition was assumed to be composed of two flood events, an antecedent event and a main flood event. The initial water surface was determined by using a 30% of the main flood with a 3-day dry interval as the antecedent event as based on a NWS study of the Ohio River basin. The PMF was routed through the dam based on this antecedent event. The peak PMF elevation was computed at approximately 1198.0 feet above NGVD or about 4 feet above the top of the dam. As a result of this analysis, modification of the project is required to enable it to safely pass the PMF event in accordance with current hydrologic and hydraulic design criteria.

A NWS computer model, DAMBRK, an unsteady flow dam break model, was used in the hydrologic modeling to determine flood elevations at the downstream communities. The PMF and a hypothetical dam failure scenario was routed through the reservoir and inundation maps were developed illustrating the effects of with and without dam failure conditions at downstream points. This information was used to determine the potential loss of life and economic losses and to compute benefits provided by various modification alternatives investigated.

CONCLUSIONS

The PMF inflow hydrograph was used in analyzing various alternatives to enable the dam to safely pass the PMF. The six alternatives studied were the do nothing; use existing penstocks; construct auxiliary spillway; lower existing spillway; adding a pier and two rubber dams; overtopping; and raising the dam. The overtopping alternative was chosen after detailed analysis of all alternatives. The U.S. Army Corps of Engineers Waterways Experimental Station (WES) was contracted by the Pittsburgh District to build a prototype model and design the overtopping alternative. Results of the model have been completed and will be used in the final design. The extensive hydrologic modeling effort provided the information necessary to evaluate all of the alternatives and the basis for analyzing the safety of Tygart Dam.

REFERENCES

- Eugene Stakhiv, David Moser, Ph.D., 1986: "Guidelines for Evaluating Modifications of Existing Dams Related to Hydrologic Deficiencies", U.S. Army Corps of Engineers, Institute for Water Resources, Ft. Belvoir, VA under the Office of the Chief of Engineers, Washington, DC.
- E.A. Zurndorfer, F.K. Schwarz, E.M. Hansen, D.D. Fenn, and J.F. Miller, October 1986: Probable Maximum and TVA Precipitation Estimates With Areal Distribution for Tennessee River Drainages Less Than 3,000 Mi² in Area. "Hydrometeorological Report No. 56", National Weather Service, National Oceanic and Atmospheric Administration, U.S. Department of Commerce, for the Tennessee Valley Authority, Silver Spring, MD.
- Francis K. Schwarz, May 1973, Meteorological Criteria For Extreme Floods For Four Basins in the Tennessee and Cumberland River Watersheds. "Hydrometeorological Report No. 47", National Weather Service, National Oceanic and Atmospheric Administration, U.S. Department of Commerce, for the Tennessee Valley Authority, Silver Spring, MD.

Schreiner, L. C. and Riedel, J. T., 1978: Probable Maximum Precipitation Estimates, United States East of the 105th Meridian. "Hydrometeorological Report No. 51", National Weather Service, National Weather Service, National Oceanic and Atmospheric Administration, U.S. Department of Commerce, Washington, DC.

Hansen, E.M., Schreiner, L.C. and Miller, J.F., 1982: Application of Probable Maximum Precipitation Estimates - United States East of the 105th Meridian. "Hydrometeorological Report No. 52", National Weather Service, National Oceanic and Atmospheric Administration, U.S. Department of Commerce, Washington, DC.

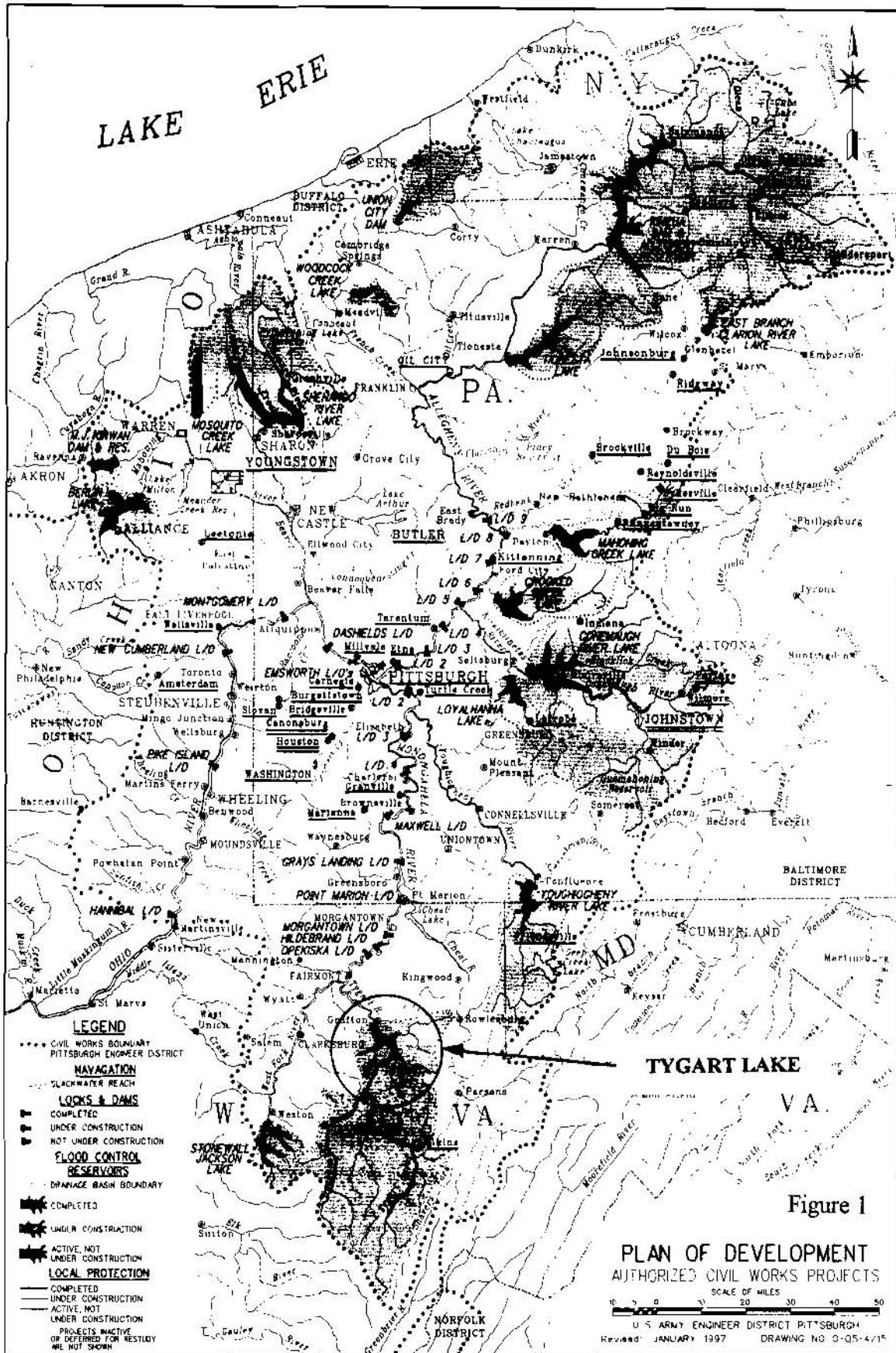
The Hydrologic Engineering Center, U.S. Army Corps of Engineers, "HMR52 Probable Maximum Storm (Eastern United States) Users Manual", March 1984.

The Hydrologic Engineering Center, U.S. Army Corps of Engineers, "HEC-1, Flood Hydrograph Package", Users Manual, September 1990.

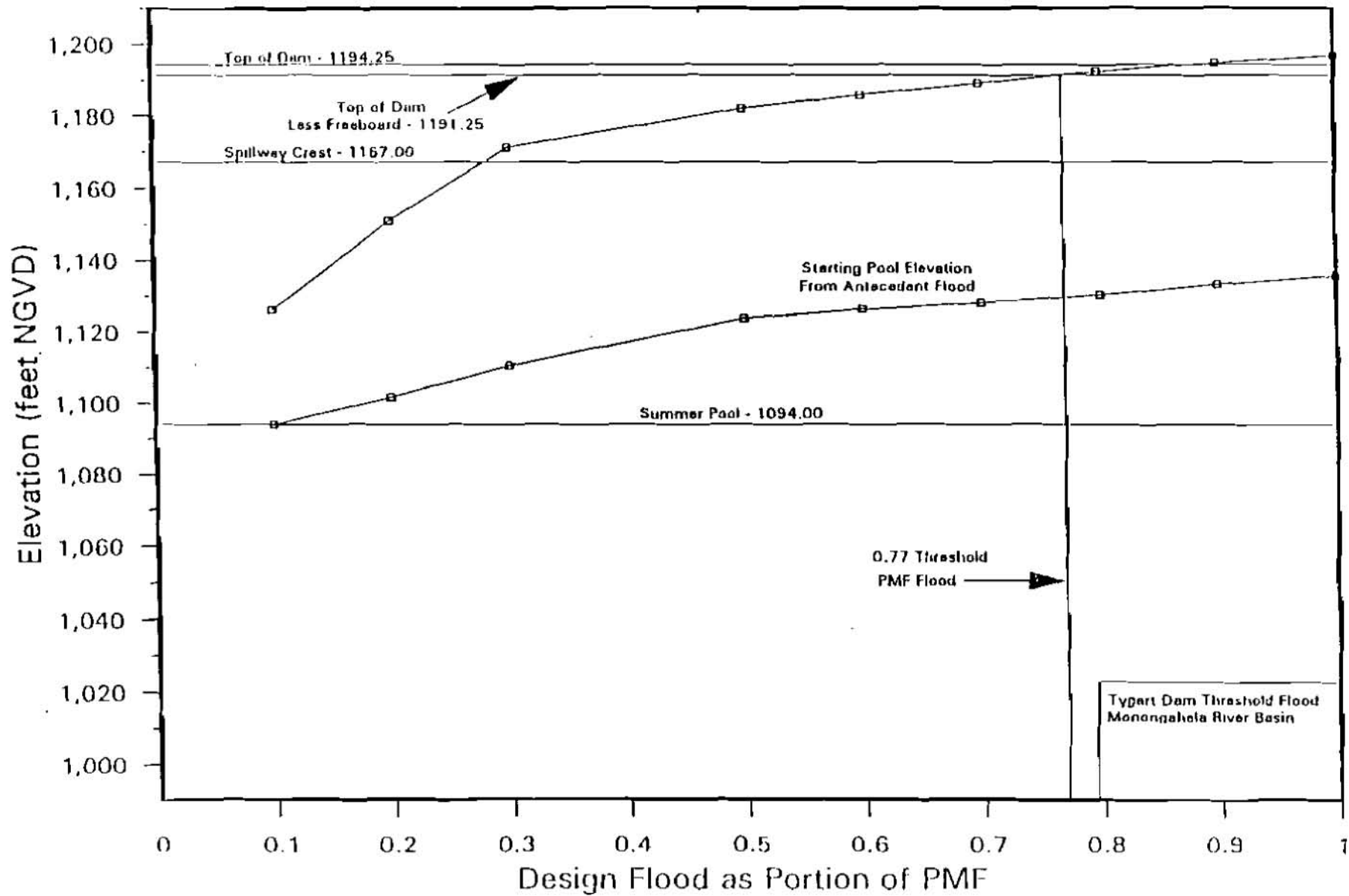
B.R. Bodine, M.T. Hebler, Waterways Experiment Station, U.S. Army Corps of Engineers, "H7780 - Wave Runup and Wind Setup - Computational Model", Program 723-F3-M007A, January 1986.

D.L. Fread, "The NWS DAMBRK MODEL: Theoretical Background/ User Documentation", August 1991 -Revised, The National Weather Service (NWS), NOAA, Silver Spring, MD.

Department of the Army, Office of the Chief of Engineers, Washington, DC, Civil Engineering Bulletin No. 52-8, EM 1110-2-1411, "Standard Project Flood Determinations", March 1952.



Determination of the Threshold Flood

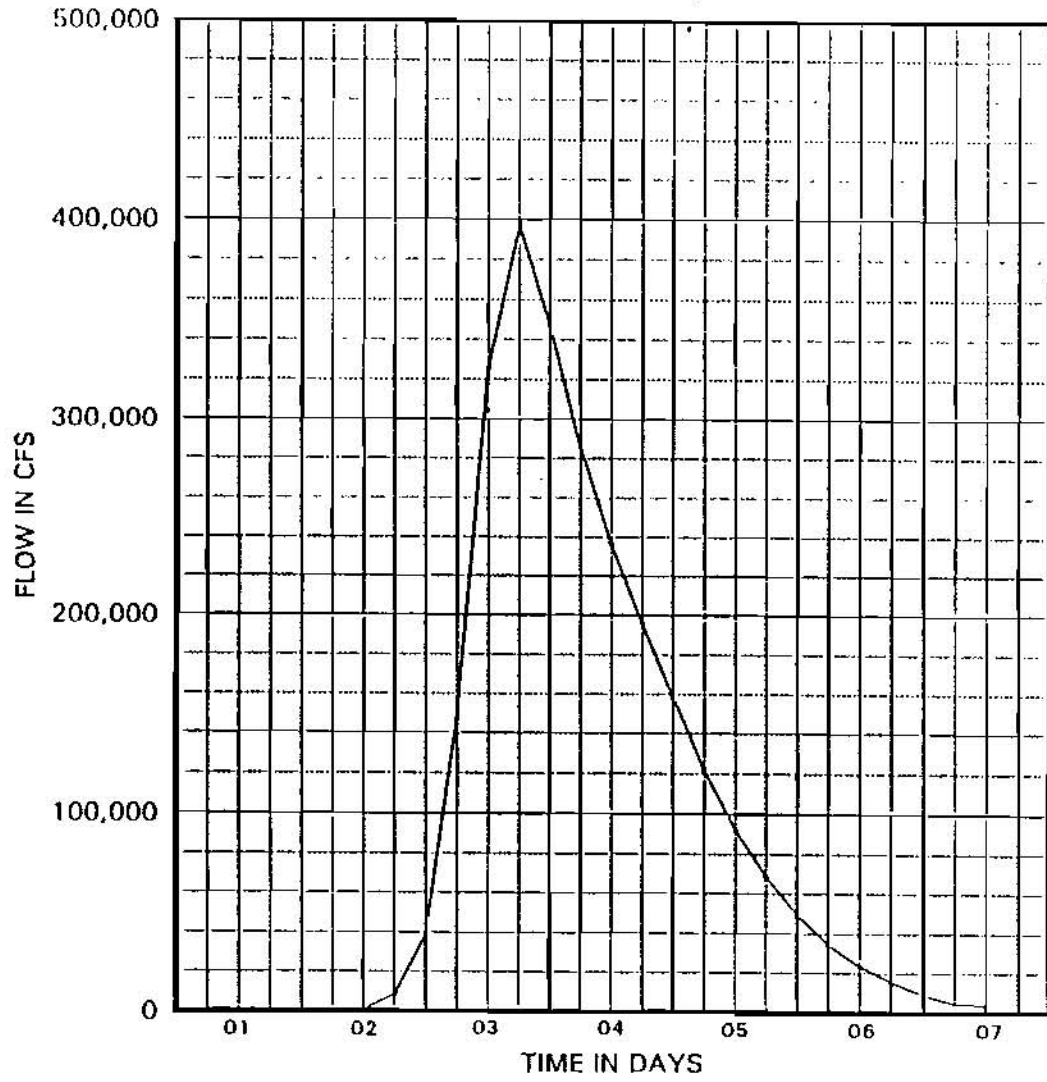


4-58

Figure 2

Tygart Dam Threshold Flood
Monongahela River Basin

Figure 3



Monongahela River Basin
TYGART DAM
PROBABLE MAXIMUM FLOOD
INFLOW HYDROGRAPH

THE RELATIONSHIP BETWEEN EXTREME RAINFALL DEPTHS AND FLOOD VOLUMES UNDER THE ASSUMPTION OF EXPONENTIALLY-TAILED PROBABILITY DISTRIBUTIONS

by Mauro Naghettini, Universidade Federal de Minas Gerais, Departamento de Engenharia Hidráulica e Recursos Hídricos, Avenida Contorno 842 - 8º andar, 30110-060 Belo Horizonte, MG, Brazil. Email : naghet@dedalus.lcc.ufmg.br.

INTRODUCTION

The fact that precipitation records are in many instances longer, more accurate, and more readily regionalized than flood discharge records has motivated the development of methodologies for incorporating the hydrometeorological information into flood frequency analysis. In particular, those described by *Guillot and Duband* (1967) and *Naghettini et al.* (1996) involve assumptions regarding the relationship between rainfall depths and flood volumes under extreme conditions, which are crucial for transferring the hydrometeorological information to flood frequency curves. These assumptions, common to both methodologies, are valid for rainfall probability distributions showing asymptotically exponential-like upper-tails and were introduced by *Guillot and Duband* (1967), as part of the so-called GRADEX method for flood frequency analysis.

The main objectives of this paper are : (a) to describe a mathematical model for the relationship between rainfall depths and flood volumes under the assumptions of GRADEX-based methodologies; (b) to fit it to extreme events in a given watershed, which have been obtained by using a calibrated hydrological model to simulate storms transposed to the area; and (c) to perform a sensitivity analysis on the parameters of the mathematical relationship between rainfall and flood volumes. The paper is organized as follows. A short description of the GRADEX method and the formulation of the mathematical relationship between rainfall and flood volumes are provided in the next two sections. Further, the model is applied to the Blue river basin, located in southeastern Oklahoma, followed by an analysis of the application results. Conclusions are given in the final section.

THE GRADEX METHOD

The GRADEX method - gradient of extreme values - was developed by the French electrical company "Electricité de France" and was first described by *Guillot and Duband* [1967]. The GRADEX method aims to extrapolate the flood volume frequency distribution using rainfall data and is based on simple physical and statistical assumptions. The first assumption refers to the relationship between rainfall and runoff volumes, as soil moisture storage in the watershed approaches saturation. It is assumed that at saturation conditions, any increase of rainfall volume tends to produce an equivalent increase of runoff volume. The second assumption refers to the upper tail of the rainfall volume distribution, which is assumed to be a simple decreasing exponential function of the form

$$1 - F(p) = \exp\left(-\frac{p - K}{a}\right) \quad (1)$$

where the positive constants K and a are the location and scale parameters, respectively. These are estimated by fitting a distribution that asymptotically exhibits an exponential upper tail (e. g. Gumbel, Gamma, or Log-Normal) to rainfall maxima. Combining these two assumptions causes the upper tail of the flood volume distribution to be exponential with the same scale parameter a (the GRADEX parameter) as the one estimated for the upper tail of the distribution of rainfall volumes.

Let P_i denote the maximum rainfall depth (for a specified duration d) over a watershed in a given month, season, or year. The duration d is usually specified as the average time-base of the watershed, estimated from observed flow hydrographs. Let X_i represent the flood volume (for the same duration d), associated with P_i , and let R_i be the "runoff deficit" defined by $R_i = P_i - X_i$. Figure 1 shows a schematic plot of X versus P . The points (P_i, X_i) are all below the line $X = P$, with the exception of a few relatively low values of X which have been affected by snowmelt. The values of R depend on many interdependent factors such as the antecedent soil moisture conditions, the groundwater storage, and the spatio-temporal distribution of rainfall over the basin. In the GRADEX method, R is treated as a random variable with distribution function, conditioned on P , characterized in Figure 1 by hypothetical quantile curves. The first assumption of the GRADEX method imposes these quantile curves tend asymptotically

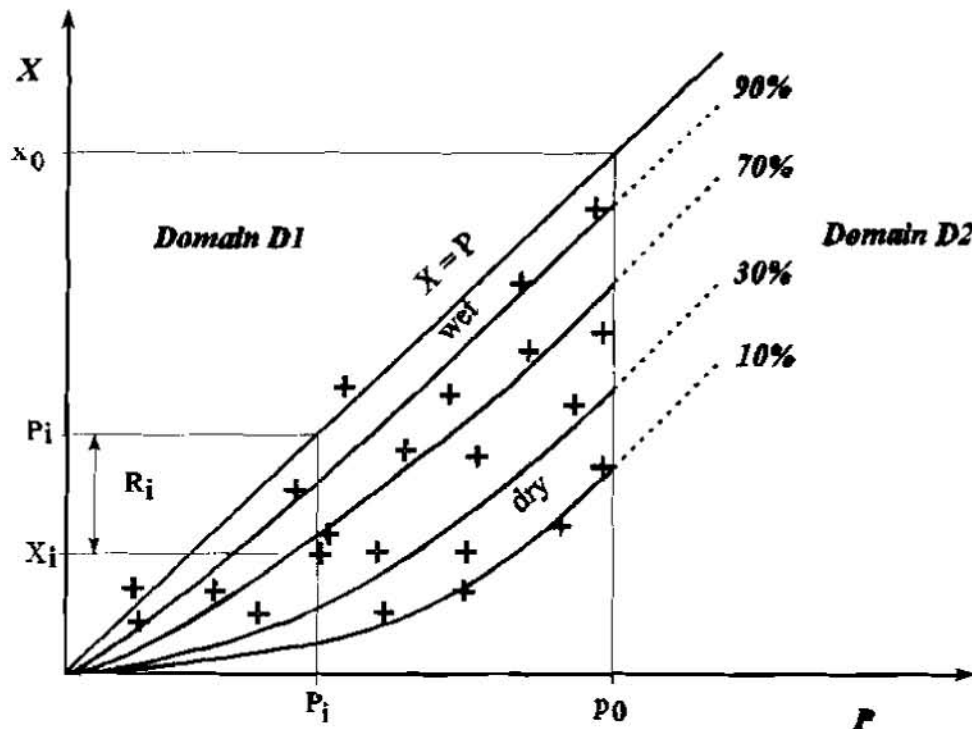


Figure 1 - Schematic Relationship Between Storm Rainfall (P) and Flood Volume (X).

to be parallel to the line $X=P$ as the watershed approaches saturation. The position of each asymptote depends on the basin initial conditions; for a given value of R , the quantile curves will become parallel to $X = P$ more rapidly in a wet terrain than in a dry terrain. In other words, the cumulative distribution function of R , conditioned on P , tends to have a stable shape and a constant variance for $P > p_0$.

The plane defined by the points (P_i, X_i) in Figure 1 may be divided in two domains :

- D1, defined by all points $P < p_0$ and $X < x_0$, where the probability distribution of R depends on P ; and
- D2, region where the quantile curves are parallel to the line $X=P$.

Let $f(p)$, $g(x)$, and $h(r)$ represent the probability density functions of P , X , and R respectively. The density function of X may be written as

$$g(x) = \int_0^{\infty} f(x+r) h_{X+R}(r) dr \quad (2)$$

where $h_{X+R}(r)$ is the conditional probability density function of R given $(X+R)$. In the domain D2 it is assumed that the distribution of R no longer depends on P , or in other terms, $h_{X+R}(r)$ becomes $h(r)$ and equation (2) may be rewritten as

$$g(x) = \int_0^{\infty} f(x+r) h(r) dr \quad (3)$$

The second assumption of the GRADEX method refers to the upper tail behavior of the cumulative distribution function $F(p)$, which is assumed to tend asymptotically to an exponential-like tail

$$1 - F(x+r) \approx \exp\left(-\frac{x+r-K}{a}\right) \quad (4)$$

where the location parameter K is a positive constant and the scale parameter a is referred to as the rainfall GRADEX parameter. In this case, the density $f(p)$ becomes

$$f(x+r) \approx \frac{1}{a} \exp\left(-\frac{x+r-K}{a}\right) = f(x) \exp\left(-\frac{r}{a}\right) \quad (5)$$

Substituting this expression in Equation (3) it follows that

$$g(x) \approx f(x) \int_0^{\infty} \exp\left(-\frac{r}{a}\right) h(r) dr \quad (6)$$

In this expression, the integral is definite and equal to a positive constant less than or equal to 1. Assuming this constant as being equal to $\exp(-r_0/a)$, it follows that for large x

$$g(x) = f(x+r_0) \quad (7)$$

Therefore, the probability density function $g(x)$ in domain D2 is deduced from $f(p)$ by a simple translation of the quantity r_0 on the variable axis, which is also valid for the cumulative distribution functions $G(x)$ and $F(p)$. The integral in equation (6) represents the expected value of $\exp(-R/a)$. As a result, the following equation may be written

$$r_0 = -a \ln \left\{ \mathbf{E} \left[\exp\left(-\frac{R}{a}\right) \right] \right\} \quad (8)$$

In traditional applications of the GRADEX method, *Guillot and Duband [1967]* recommend using the empirical distribution of the observed annual maximum flood volumes up to the 10 or 20-year flood in relatively impermeable watersheds and up to the 50-year flood in watersheds with high infiltration capacity. From that point on, the cumulative distribution functions of flood and rainfall volumes will be curves separated by the translation distance r_0 on the variable axis. Equivalently, in domain D2 the two distributions will plot on an exponential probability paper as straight lines, both with slope equal to the rainfall GRADEX parameter a .

The validity of equation (7) depends on the assumption that $F(p)$ is asymptotically an exponential function, and not only on the assumption that R and P are independent for $P > p_0$. In order to show it and following *CTGREF [1972]*, let us first equate expressions (3) and (7)

$$f(x+r_0) = \int_0^{\infty} f(x+r) h(r) dr \quad (9)$$

Denoting $(x+r_0)$ by τ , substituting it into equation (9), and rearranging it follows that

$$\int_0^{\infty} \frac{f(\tau+r-r_0)}{f(\tau)} h(r) dr = 1 \quad (10)$$

Differentiating with respect to τ

$$\int_0^{\infty} \frac{d}{d\tau} \left[\frac{f(\tau+r-r_0)}{f(\tau)} \right] h(r) dr = 0 \quad (11)$$

In order to equation (11) be satisfied, the ratio $f(\tau+r-r_0)/f(\tau)$ must be constant with respect to τ . The only functions which possess such a property are the functions of the form $A \exp(B\tau)$ where A and B are constants. As a result f and g must be exponential functions of this form. Among the probability distribution functions which exhibit an asymptotic exponential-like upper tail are the normal, the lognormal, the gamma, and the EV type I: the generalized Pareto distribution reduces to an exponential function when its shape parameter is equal to zero.

A MATHEMATICAL MODEL DESCRIBING THE RELATIONSHIP BETWEEN EXTREME RAINFALL DEPTHS AND FLOOD VOLUMES FOR EXPONENTIALLY-TAILED PROBABILITY DISTRIBUTIONS

The cumulative probability distribution of R , denoted by $H(r)$, is assumed to have the following form :

$$H(r) = \left(\frac{r}{D}\right)^E, \quad 0 \leq r \leq D \quad (12)$$

where parameter D is related to the maximum losses under extremely dry conditions and parameter E controls the shape of the curve. The density $h(r)$ is given by

$$h(r) = \frac{E}{D^E} r^{E-1}, \quad 0 \leq r \leq D \quad (13)$$

The relationship between rainfall and runoff volumes is modeled by the function proposed by *Guillot* [1993], which is given by

$$X = P - R \left[(1 - w) \tanh\left(\frac{P}{R}\right) + w \tanh\left(\frac{P}{D}\right) \right], \quad 0 \leq w \leq 0.4 \quad (14)$$

If $P(X, R)$ denotes the inverse of the function given by Equation 14, then the distribution function of flood volumes may be written as

$$G(x) = \int_{H=0}^{H=1} F[p(x, r)] dH \quad (15)$$

As previously shown, for large return periods $G(x)$ plots on an exponential probability paper as a parallel to $F(p)$. The parameter E of the distribution function $H(r)$ controls the relative positions of $G(x)$ and $F(p)$. On the other hand, the weighting parameter w controls the return period beyond which the flood-volume distribution becomes asymptotically parallel to the rainfall-volume distribution.

THE RAINFALL-FLOOD VOLUME RELATIONSHIP FOR THE BLUE RIVER BASIN

The Blue river basin near Blue (USGS gaging station 07332500) is an elongated basin of 476 square miles, located in southeastern Oklahoma. Streamflows are not influenced by significant diversions or reservoirs and have been continuously recorded since the 1937 water year. Hydrographs of the largest floods that have occurred in the Blue river basin show that the estimate of the average time-base is $d=5$ days. Rainfall data are available in 10 gaging stations in the nearby region with at least 80 years of record. *Naghattini et al.* (1996) used the data available at these stations to estimate the 5 day-rainfall GRADEX parameter over the watershed as $\hat{a} = 1.902$ inches, which is equivalent to 4869 cfsd.

In order to fit the model described by Equation 14, 36 storm rainfall events have been selected from the storm catalog compiled by the *U. S. Army Corps of Engineers* (1945) to be transposed to the Blue river basin. The main criterion for selecting those storms has been the location of their actual storm centers at some point inside a meteorologically homogeneous region as described by *Naghattini et al.* (1996). The HSP-F simulation model [*Johanson et al.*, 1984], calibrated over the 1980-1990 period, has been used to simulate the 36 transposed storms, each with 3 predefined schemes for temporal disaggregation. Five different scenarios for the initial conditions, ranging from extremely dry to saturated, have been imposed to the six HSP-F state variables. The resulting $5 \times 3 \times 36$ simulated 5-day flood volumes correspond to the additional flood events necessary to apply Equation 14 to the Blue river basin.

A first estimate of parameter D in Equation 13 has been obtained from a sample containing 138 pairs of observed rainfall and flood volumes, for 5-day duration, and 540 pairs of simulated flood volumes (from transposed storms) and associated 5-day rainfall volumes. Although simulated flood volumes do not constitute a random sample and cannot be used to estimate $H(r)$, they were employed only to have a first estimate of parameter D , which is a physically-based parameter. Observed five-day rainfall depths have been averaged to yield 138 rainfall volumes over the watershed, associated with the 138 largest 5-day flood volumes observed at the Blue streamgage. The pairs of simulated flood volumes correspond to 36 storms that have been transposed to the area. The observed and simulated values are shown in Figure 2.

The estimate of parameter D corresponds to the maximum difference between rainfall and flood volumes. The maximum difference among the observed and simulated values has been found to be 20773 cfsd. Since in Figure 2. the "runoff deficits" seem to increase with rainfall volumes, the final estimate of parameter D has been arbitrated as $\hat{D} = 30000$ cfsd. With this estimate of parameter D and with $\hat{a} = 4869$ cfsd, parameter E has been estimated such that the translation distance r_0 , calculated by substituting $h(r)$ in Equation 8, matches the distance (read on

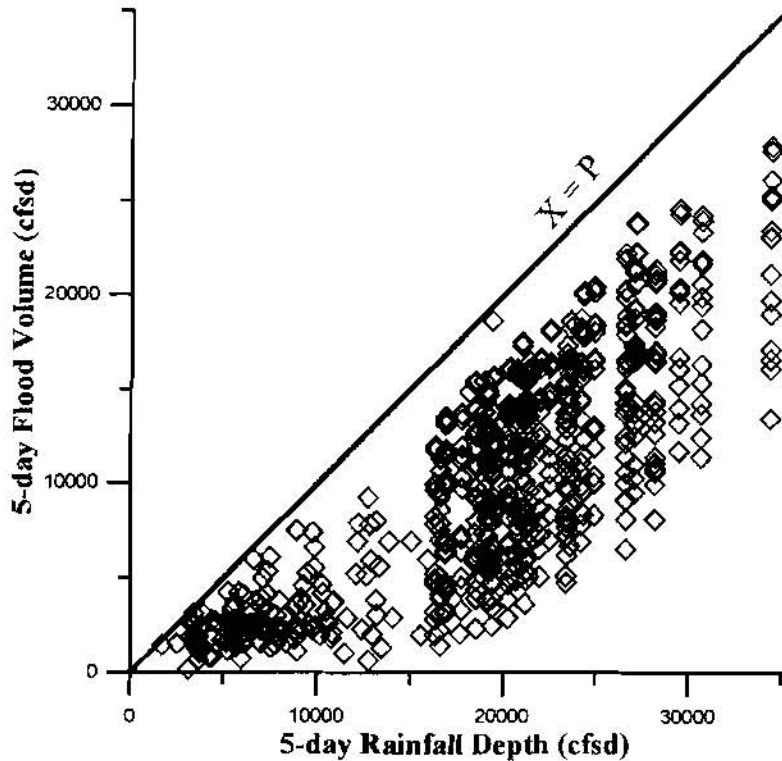


Figure 2 - Observed and Simulated 5-day Rainfall and Flood Volumes for the Blue River near Blue.

the variable axis) between the curves $F(p)$ and $G(x)$. This distance has been found to be 12804 cfds, which in equation 8 gives

$$-a \ln \left\{ \int_0^D \exp\left(-\frac{r}{a}\right) h(r) dr \right\} = -a \ln \left\{ \frac{E}{D^E} \int_0^D \exp\left(-\frac{r}{a}\right) r^{E-1} dr \right\} = 12804 \quad (16)$$

The solution to this equation yields $\hat{E} = 1674$. Hence, the estimate of the cumulative distribution function of the "runoff deficits" for the Blue river basin is given by

$$\hat{H}(r) = \left(\frac{r}{30000} \right)^{1674}, \quad 0 \leq r \leq 30000 \text{ cfds} \quad (17)$$

The weighting parameter w controls the point beyond which the asymptotic parallelism between $F(p)$ and $G(x)$ occurs. The Blue river basin has soils with low average permeability. As a result, $F(p)$ and $G(x)$ will become parallel on an exponential probability paper at a relatively low return period and parameter w has been estimated as $\hat{w} = 0.15$. Therefore, the estimated relationship between 5-day rainfall and flood volumes, valid for the Blue river near Blue, is given by

$$X = P - R \left[0.85 \tanh\left(\frac{P}{R}\right) + 0.15 \tanh\left(\frac{P}{30000}\right) \right] \quad (18)$$

where the "runoff deficit" R is specified according to its quantiles, calculated by the inverse of Equation 17. Figure 3 shows the estimated relationship between rainfall and flood volumes, with the observed and simulated events for the Blue river basin.

SENSITIVITY ANALYSIS OF E AND w ON THE RELATIONSHIP RAINFALL-FLOOD VOLUME

The model for the relationship between rainfall and flood volumes is very sensitive to changing values of parameter E . This parameter controls the distance the quantile curves have from the line $X=P$. On a probability plot of $F(p)$ and $G(x)$ versus p and x , this is equivalent to say that parameter E controls the distance that separates

the upper tails of the two distributions. The influence of parameter E on the rainfall-flood volume model, valid for the Blue river basin, is shown in Figures 4a, 4b, and 4c. For constant $\hat{D} = 30000$ cfsd, $\hat{a} = 4869$ cfsd, and $\hat{w} = 0.15$, parameter E has been specified as 1.0, 2.0, and 3.0. The distances that separate the quantile curves from the line $X=P$ change considerably with changing values of E , especially in the lower tail of $H(r)$.

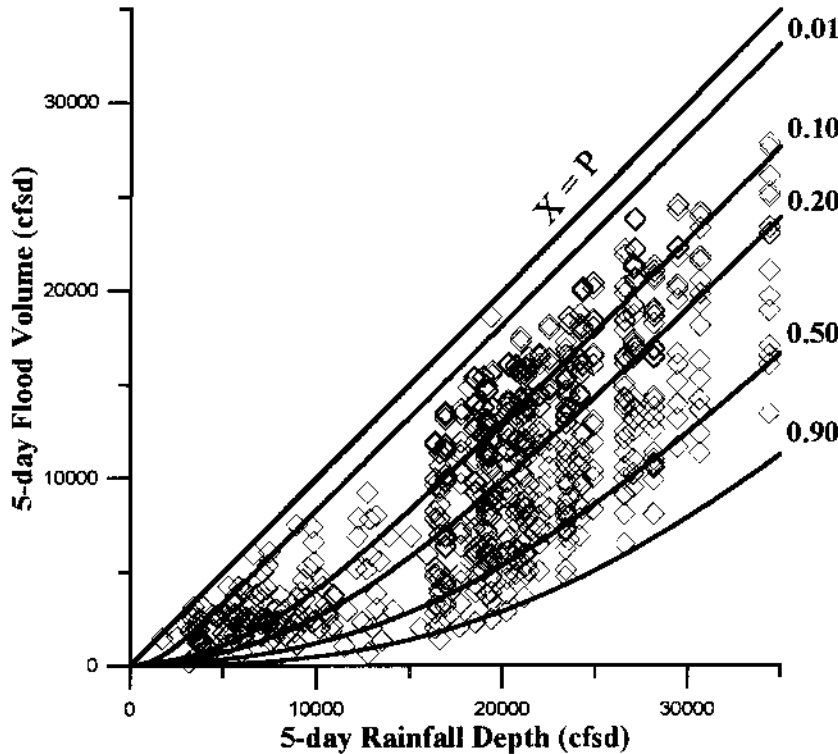


Figure 3 - Relationship between 5-day rainfall depth and 5-day flood volume for the Blue River near Blue. Final parameters are $w = 0.15$, $D = 30000$ cfsd, and $E = 1.674$.

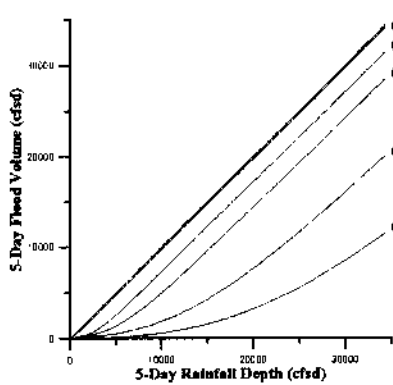


Figure 4a - $E=1.0$.

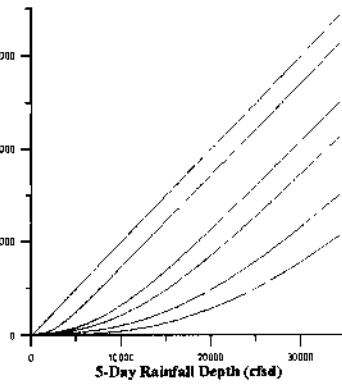


Figure 4b - $E=2.0$.

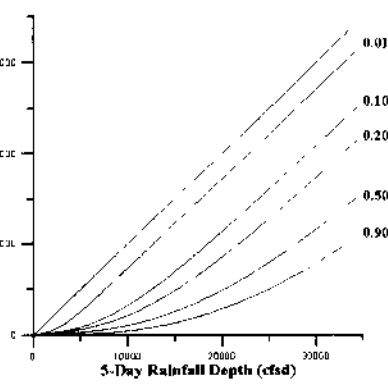


Figure 4c - $E=3.0$.

As opposed to parameter E , the model for the relationship rainfall-flood volume is not very sensitive to parameter w . This parameter controls the point beyond which the quantile curves tend to become parallel to the line $X=P$. The effect of changing values of w on the rainfall-flood volume relationship, estimated for the Blue river basin, is shown in Figures 5.a to 5.c. In these figures, parameter w has been specified as 0.10, 0.30, and 0.40, while the other parameters remained constant ($\hat{a} = 4869$ cfsd, $\hat{D} = 30000$ cfsd, and $\hat{E} = 1.674$).

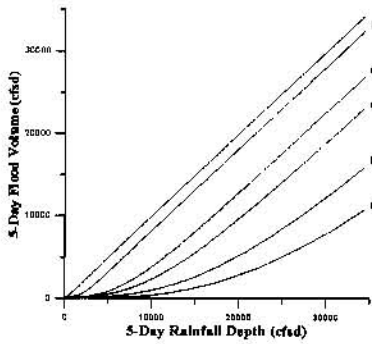


Figure 5a - $w=0.10$.

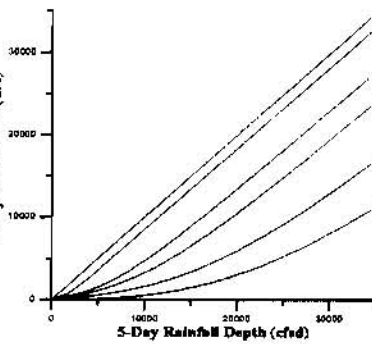


Figure 5b - $w=0.30$.

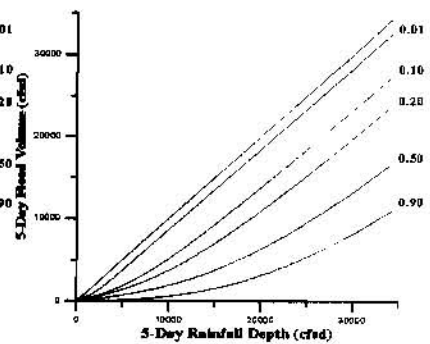


Figure 5c - $w=0.40$.

CONCLUSIONS

Equation 14 is formulated so that it becomes $X=P-R$ as P tends to infinity. Therefore, for large values of p , equation 15 becomes

$$G(x) = \int_{H=0}^{H-1} F(x+r) dH \quad (19)$$

Omitting K in Equation 1 and substituting it, along with Equation 12, into Equation 19, it follows that

$$1 - G(x) = \int_{r=0}^{r=D} \exp\left(-\frac{x+r}{a}\right) E \frac{r^{E-1}}{D^E} dr \quad (20)$$

By replacing E for $\Gamma(E+1) / \Gamma(E)$, Guillot [1993] showed that Equation 20 may be written as

$$1 - G(x) = \exp\left(-\frac{x}{a}\right) \left(\frac{a}{D}\right)^E \frac{\Gamma(E+1)}{\Gamma(E)} \int_{t=0}^{t=\frac{D}{a}} \exp(-t) t^{E-1} dt \quad (21)$$

where $t=r/a$. In this equation and for frequently used values of D , E , and a , the incomplete gamma integral is very close to 1. Hence,

$$G(x) = 1 - \exp\left(-\frac{x+r_0}{a}\right) = F(x+r_0) \quad (22)$$

where, r_0 - the translation distance- is given by

$$r_0 = a \ln \left[\frac{\left(\frac{D}{a}\right)^E}{\Gamma(E+1)} \right] \quad (23)$$

This is another way to demonstrate the basic principles of the GRADEX method. Table 1 displays the values of the translation distance r_0 , as calculated by Equation 23, along with the mean and median values of the "runoff deficits" r for the Blue river basin, with $\hat{a} = 4869$ cfsd, $\hat{D} = 30000$ cfsd, and \hat{E} ranging from 1.0 to 2.0.

Table 1 - Translation distance r_0 , mean and median values of r for the Blue river near Blue. Values in cfsd.

E	r_0 (cfsd)	r_{mean} (cfsd)	r_{median} (cfsd)
1	8853	15000	15000
1.2	10150	16364	16840
1.5	11890	18000	18900
1.674	12804	18781	19829
1.8	13420	19286	20410
2	14330	20000	21210

From Table 1, it is clear that the translation distance r_0 refers to a value which is much smaller than the mean or median value. In fact, because $X=P+(-R)$ and the upper tail of P is much heavier than the upper tail of $(-R)$, or in other words the lower tail of R , the sum of the two independent random variables for large return periods is then dominated by the upper tail of P . Hence, the translation distance r_0 and the position of $G(x)$ practically do not depend on the definition of the distribution function $H(r)$ for medium or upper values of R . Actually, they depend only on the low values of R , associated with large flood events that have occurred under wet or near-saturation antecedent conditions.

REFERENCES

- CTGREF, L'application de la méthode du GRADEX à l'estimation des crues de faible fréquence, Centre Technique du Génie Rural, des Eaux et des Forêts, Ministère de l'Agriculture, Paris, France, 1972.
- Guillot, P. and D. Duband, La méthode du GRADEX pour le calcul de la probabilité des crues à partir des pluies, in *Floods and their Computation - Proceedings of the Leningrad Symposium*, pp 560-569, IASH Publication no. 84, 1967.
- Guillot, P., The arguments of the GRADEX method : a logical support to assess extreme floods, in *Extreme Hydrological Events : Precipitation, Floods, and Droughts, Proceedings of Yokohama Symposium, I.A.S.H. Publication 213, 287-298, 1993.*
- Johanson, R. C., J. C. Imhoff, J. L. Kittle, Jr., and A. S. Donigian, Jr., Hydrological Simulation Program-Fortran (HSPF) : User's Manual for Release 8.0, U.S. Environmental Protection Agency, EPA-600/3-84-066, 1984.
- Naggettini, M., K. W. Potter, and T. Illangasekare, Estimating the upper-tail of flood-peak frequency distributions using hydrometeorological information, *Water Resources Research*, 32(6), p. 1729-1740, 1996.
- U. S. Army Corps of Engineers, Storm Rainfall in the United States, Office of the Chief of Engineers, Washington, D.C., 1945.

COWLITZ RIVER FLOOD HAZARD STUDY

By **Hilaire W. Peck, Hydraulic Engineer, Corps of Engineers, Portland, Oregon** and
Bruce J. Duffe, Hydraulic Engineer, Corps of Engineers, Portland, Oregon

Abstract: The eruption of Mount St. Helens, spring of 1980, resulted in deposition of vast quantities of sand-sized sediment which created a threat of flooding in Southwest Washington and navigation disruption on the lower Cowlitz and Columbia Rivers. Corps of Engineers levees on the Cowlitz River, a Sediment Retention Structure (SRS) on the North Fork Toutle River (a Cowlitz River tributary), and a dredging program were designed to reduce these threats.

In November 1995 and February 1996, large floods occurred on the Cowlitz River. There was considerable local concern that these events deposited sediment and decreased the flood protection afforded by the levees along the lower 17 miles of the Cowlitz River. The Federal Emergency Management Agency (FEMA) provided the Corps of Engineers, Portland District, funds to update the discharge-frequency curve, to determine risk of flooding, and to map flooded areas.

The frequency of events was estimated at a USGS gage at Cowlitz River at Castle Rock (RM 17.1). Since 1968, flows at this gage have been regulated by Mossyrock Dam at river mile 65.5. The previous frequency curve was developed using annual peak instantaneous flow data from 1928-1962. For this study, flow data provided by the USGS were used to estimate natural (unregulated) flood peaks at Castle Rock. A regulated discharge-frequency curve was revised from the updated natural discharge-frequency curve and a new natural versus regulated discharge relationship.

With the deposition of debris flow material during the eruption of Mount Saint Helens, the lower Cowlitz changed from a gravel bed to a sand bed stream. Following the closure of the SRS in 1987, the bed has gradually been returning to its pre-eruption gravel bed characteristics. For flood plain planning purposes, the *existing* risk of flooding (1997) reflecting existing channel bed characteristics and the *long-term (called "permanent" for this report)* risk of flooding reflecting the expected change of the stream bed back to primarily gravels are required.

The Corps of Engineers backwater application HEC-RAS (River Analysis System) was used to develop elevation-frequency data for existing and long-term conditions. The Corps HEC-FDA (Flood Damage Reduction Analysis) Monte Carlo simulation techniques were applied to the elevation- and regulated discharge-frequency curves. These computations resulted in the expected value of the events that would exceed the safe levee elevations accounting for the uncertainty in the derivation curves. The existing and long-term safe protection provided by the levees was estimated from these data.

INTRODUCTION

Authorization: This study was authorized by the Federal Emergency Management Agency (FEMA) following a request by the Cowlitz County Board of Commissioners. Authorization came through Mission Assignment No. COE-NPD-14 dated 17 May 1996.

Purpose and Scope: The purpose of this study was to provide new estimates of existing and permanent (long-term condition) safe protection afforded by the Kelso, Longview, Lexington, and Castle Rock

levees and to provide a new estimate of the median¹ 1.0 percent chance exceedance² flood plain. These new estimates were to make use of additional discharge data that have been recorded since the last discharge-frequency curve was developed (July 1982) and cross-section surveys on the Cowlitz River obtained in the summer of 1996.

DISCHARGE-FREQUENCY ANALYSES

The previous discharge-frequency curve was developed in July 1982 and used natural (without project) annual peak instantaneous flow data from water years³ (WY) 1928-1962. In this 35-year period, only two annual peak flows exceeded 80,000 cfs; 139,000 cfs in 1934 and 85,100 cfs in 1947. By contrast, in the 34 year period from WY 1963-1996, six annual peak flows exceeded 80,000 cfs and five of these were *after significant flow regulation* was in place through operation of Mossyrock Dam (i.e. WY's 1969 and beyond). It was important that the discharge-frequency be updated with these new data.

Natural Discharge-Frequency Curves: Short-interval data (1 hour or less) were needed to develop accurate estimates of the natural peak discharge from flow hydrographs during the period of significant regulation by Mossyrock Dam (WY 1969-1996). These short-interval data were provided by the USGS. Some of these data had been lost (WY's 1979-1987). Therefore, natural annual peak discharge was estimated for 19 of the 28 years during which Mossyrock Dam was in operation. A total of 60 years of systematic natural peak discharge data was available for the analyses (WY's 1928-1978 and 1988-1996). Historic information indicated that the natural peak discharge of the February 1996 flood was the largest at least since a large flood that occurred in November 1896. Thus, it is known that the February 1996 flood is the largest flood in 100 years (1897-1996).

A new estimate of the unregulated annual instantaneous peak discharge-frequency curve of the Cowlitz River at Castle Rock was developed based on Bulletin 17B [1] guidelines. The computer application HEC-FFA⁴ was used, incorporating the 59⁵ years of systematic natural peak discharge data and additional historic information.

Regulated Discharge-Frequency Curves: Eight significant natural/regulated data pairs were available from WY's 1969-1996. A natural versus regulated discharge relationship was developed from these data. This relationship and the median value natural discharge-frequency curve were used to develop the median and expected value regulated discharge-frequency curves. The median value regulated discharge-frequency curve was used to develop new flood profiles for the Federal Emergency Management Agency. The expected value regulated discharge-frequency curve was used to estimate existing and permanent safe protection afforded by the levees.

¹ Also referred to as the 'computed value'.

² In the remainder of this paper, '[x] percent chance exceedance flood' will be shortened to '[x] percent flood.' The [x] percent flood has one chance in [100/x] of being exceeded in any given year.

³ A "water year" runs from 1 October to 30 September. Thus, WY 1996 ran from 1 October 1995 to 30 September 1996.

⁴ The Corps of Engineers Hydrologic Engineering Center (HEC) Flood Frequency Analysis computer program (HEC-FFA), May 1992 was used in this study.

⁵ The February 1996 event is treated as an historic event in the analysis and is not, for analysis purposes, considered part of the systematic record.

HYDRAULIC ANALYSES

Flow profiles were estimated using backwater computations with the HEC-RAS⁶ model. The backwater model extended from RM 0 at the confluence with the Columbia River to RM 19.7 at the confluence with the Toutle River. Discharge at the upper end of the study reach was set equal to the discharge at the USGS gaging station at Castle Rock (Station Nr. 14243000). At three downstream locations, the flow was incrementally increased to account for tributary inflow. Tributary contribution was estimated as a drainage area ratio to the natural discharge at Castle Rock. The starting elevation was set equal to the Columbia River stage elevation at the confluence with the Cowlitz River. For hypothetical events, the starting water surface elevation was for the same frequency event on the Columbia River as the discharge at Castle Rock (e.g., a one percent chance stage on the Columbia River was used as the starting elevation for a one percent chance discharge at Castle Rock). This methodology maintained consistency with previous Corps analyses of the Cowlitz River.

Fifty-three cross-sections, surveyed in 1996, were used to define the channel geometry. In general, these cross-sections were about ½ mile apart. The left and right channel banks were set approximately where overbank vegetation greatly increased, using 1996 ortho-photographic contour maps as a guide. These bank stations were usually at the break in grade between the main channel and the overbank.

Five overbank areas that would become effective at carrying flow at some discharge equal to or less than the median 0.2 percent flood were identified. The length and topography of these overbank areas indicate that it would be likely that they would act differently hydraulically than the main channel. These overbank areas were treated as split flows. Due to modeling requirements, eight split flows were required in HEC-RAS to model these five overbank flow areas. Cross-sections for the split flows were obtained from 1996 ortho-photographic contour maps. A trial and error process was required to determine the amount of flow in the flow splits.

Six bridges were modeled. These were bridges at (1) RM 1, (2) RM 1.1, (3) RM 5 (Allen St. Bridge), (4) RM 5.01, (5) RM 6.7, and (6) 17.1 (Castle Rock Bridge). All flow profiles through the bridges were calculated with the energy method, except at Allen Street Bridge. For a discharge of about 145,000 cfs, as measured at Castle Rock, flow at the Allen Street Bridge reaches the bottom chord of the bridge and becomes pressurized. At the Allen Street Bridge pressure and weir flow were used to calculate the profile through the bridge at discharges greater than 145,000 cfs. Below 145,000 cfs, the energy method was used.

Model Roughness Factor Calibration: Eight high water marks between RM 6.3 and 19.7 were used to calibrate the backwater model to existing conditions. These high water marks were located immediately after the February 1996 flood.

High water marks on the lower 5 to 6 miles are too greatly influenced by backwater from the tidally affected Columbia River to be used in calibration of a steady flow backwater model. The high water marks at RM 6.3 and 7.2 were used to calibrate the roughness factor of the main channel from RM 0 to 6.7. This resulted in an *existing* conditions Manning's 'n' of 0.023. The high water mark at RM 7.2 and the other six upstream high water marks were used to calibrate the roughness factor of the main channel from RM 7.7 to 20.8. This resulted in a constant *existing* conditions 'n' value of 0.025 for this entire

⁶ The HEC River Analysis System computer program (HEC-RAS) has replaced HEC-2 for backwater computations. HEC-RAS Version 1.0. July 1995 was used in this study.

reach. Roughness factors of the split flows and overbank areas were set using the guide in the HEC-RAS documentation for Manning's 'n' values in flood plains. The ortho-photographs and experience from field visits to the study area were used to determine the type of vegetation in the split flows.

The peak discharge of the November 1995 flood (104,600 cfs) was used in the verification of *existing* condition model and compared to 14 high water marks obtained immediately after the peak of this flood.

Conclusions: The model calibrated very well to the February 1996 event. The model also reproduced the profile of the November 1995 flood. At locations unaffected or only marginally affected by Columbia River backwater, the model tended to slightly over-predict November 1995 measured high water marks. This *may* be because the channel bed was slightly less rough in November 1995 than in February 1996. This would result in a lower water surface than would have occurred had the bed been as rough as in February 1996. It could also be due to in-accuracy in high water mark measurements, model calibration, or both.

A detailed review of the data and methodologies (early 1980's study) that were used to arrive at the permanent conditions Manning's 'n' estimate of 0.027 was not performed for this study. However, it is unlikely that good high water marks or measured profiles were available at anywhere near as high a discharge as the February 1996 event. The roughness factors *may already* be at pre-eruption conditions and the existing condition values estimated in this study are simply better estimates of high discharge conditions. Further monitoring, sediment sampling, and analyses are planned to determine if the channel is in fact at permanent conditions. Until that time, the previously estimated Manning's 'n' of 0.027 will continued to be used for permanent conditions.

RISK AND UNCERTAINTY ANALYSES

Analyses Methodologies: The HEC-FDA⁷ program was used to perform the analyses. This program applies Monte Carlo simulation, a numerical-analysis procedure that computes expected value frequencies while explicitly accounting for the uncertainty in the basic value. Uncertainty was accounted for in the discharge-frequency curve, the natural versus regulated discharge transform relationship, and in the stage-discharge relationship.

Discharge-Frequency Uncertainty: With one exception, which is described in the remainder of this paragraph, the log Pearson Type III curve obtained for the natural frequency curve (see Section 2.1) was used for the risk and uncertainty analyses. As indicated in section 2.1, the natural discharge-frequency analysis considered a systematic record of 59 years and the February 1996 event as a historic discharge that was the largest in at least 100 years. The 5- and 95-percent confidence limits from the frequency analysis are based on the 59 years of systematic record length. The HEC-FDA program requires input of "equivalent record length." If historic information were not used in the frequency analysis, then the "equivalent record length" would be equal to the Bulletin 17B [1] systematic record length. Historic information, while not generally considered as good as systematic data by the Bulletin 17B [1] Interagency Advisory Committee on Water Data, does have intrinsic value. Thus, for the risk and uncertainty analyses, an "equivalent record length" of 80 years was chosen.

⁷ The HEC Flood Damage Reduction Analysis computer program (HEC-FDA), Provisional Version 1.0, December 1996, was used to perform all risk and uncertainty calculations.

Using an “equivalent record length” of 80 years and the remaining log Pearson Type III, statistics that were obtained for the natural discharge-frequency curve, discharge-frequency uncertainty was estimated as described in Bulletin 17B [1].

Natural versus Regulated Discharge Relationship Uncertainty: Upon the recommendation of the Hydrologic Engineering Center (HEC), a triangular error distribution about the natural versus regulated relationship was applied. The “maximum” limit of the regulated curve was graphically estimated from the data from which the curve was developed. The difference between the natural versus regulated curve and the “minimum” limit was taken as half the difference between the “maximum” limit and the natural versus regulated curve.

Stage-Discharge Uncertainty: A normal error distribution was assumed for the uncertainty about the stage-discharge relationship. The standard deviation of the error was estimated following EM 1110-2-1619 [2] guidelines. Uncertainty about the stage-discharge relationship includes (1) modeling uncertainty and (2) “natural” uncertainty.

The standard deviation of modeling uncertainty is defined in EM 1110-2-1619 based on Manning’s ‘n’ value reliability and the quality of the geometry data. Manning’s ‘n’ value reliability is thought to be good for existing conditions, which gave a standard deviation of 0.3 feet. The permanent conditions Manning’s ‘n’ value was previously estimated with pre-eruption data. Pre-eruption high water mark data were not available at discharges as great as the February 1996 event. Thus, for permanent conditions, the ‘n’ reliability was rated as between “good” and “fair” which gave a standard deviation of 0.5 feet.

Six discharge measurements that were above bankfull (70,000 cfs) and that were used to develop the existing USGS rating curve were available. The standard deviation of error of the “natural” uncertainty was obtained with these six discharge measurements using Equation (5-3) of EM 1110-2-1619. The total standard deviation was taken as the square root of the sum of the model standard deviation squared and the natural standard deviation squared (Equation (5-6) of EM 1110-2-1619). This gave a standard deviation of 0.63 feet for existing conditions and 0.74 feet for permanent conditions.

The one percent flood water surface profile was estimated with HEC-RAS using a Manning’s ‘n’ of 0.030 and compared to the permanent conditions results (‘n’ of 0.027). The ‘n’ of 0.030 produced a profile about one foot higher than the permanent conditions profile. Since it is believed to be very unlikely that the permanent conditions ‘n’ would get as high as 0.030, the standard deviation of 0.74 feet obtained for permanent conditions was considered reasonable.

Existing and Permanent Safe Protection: The ‘safe levee height’, which is defined as “the surface below which the levee will not fail [3],” remains the same as in 1992. This is because “... there has been no change in the physical attributes or condition of the levee features themselves [3].” The ‘critical point’ in the levee is the x,y,z coordinate of the levee where, as discharge is gradually increased, the water surface first reaches the ‘safe levee height.’ Backwater profiles were compared to the ‘safe levee height’ profile to obtain the critical point for each levee

As in previous Corps studies of the Cowlitz River, the *existing* safe protection is the expected-value frequency of the discharge (under regulated conditions) that just reaches the critical point given *existing* channel conditions. Permanent safe protection is obtained in a manner analogous to existing safe protection. The only difference is that expected permanent channel conditions (Manning’s ‘n’ of 0.027)

are used in the analysis rather than existing channel conditions. The HEC-FDA expected value frequency results were used to define existing and permanent safe protection.

Levee Certification: The water surface elevations at the critical points were noted for the median one percent chance flood profile (regulated conditions), both existing and permanent conditions. The permanent conditions results were provided to the Soils Engineering Section, Portland District to obtain their recommendation on certification.

Results:

Existing and Permanent Safe Protection: The authorized⁸ levels of protection and study results are shown in the following table.

Levee	Percent Chance Exceedance Flood		
	Authorized Safe Protection	Study Results, Existing Safe Protection	Study Results, Permanent Safe Protection
Kelso	0.70	0.51	0.75
Longview	0.60	0.75	1.36
Lexington	0.60	0.49	0.64
Castle Rock	0.85	0.70	0.95

Under existing conditions, only the Longview levee does not provide the authorized level of safe protection. It is estimated that, under existing conditions, the critical point of the Longview levee has one chance in 133 of being exceeded in any given. If the level of protection on the Longview levee was at authorized safe levels, then there would be one chance in 167 of the critical point being exceeded in any given year. None of the levees provide permanent safe protection that meets authorized safe levels. However, the permanent safe protection of all levees except the Longview levee are near the authorized safe levels. The discharge corresponding to the authorized permanent safe protection was obtained from the expected value regulated discharge-frequency curve. The backwater model was then operated for this discharge. The results showed that the water surface elevation at the Longview levee for a 0.60 percent chance flood is 0.9 feet higher than the critical point elevation.

Levee Certification: All levees (Longview, Kelso, Lexington, and Castle Rock) were certified under existing conditions for the administration of the National Flood Insurance Program.

Three levees (Kelso, Lexington, and Castle Rock) were certified under permanent conditions. The 0.60 percent chance flood in the permanent conditions backwater model produced a water surface elevation at the critical point of the Longview levee that was 0.3 feet higher than the safe levee height. The safe levee height is essentially a no risk elevation. An increase of the safe levee height by 0.3 feet may not significantly increase the risk. However, an evaluation of the safe levee height at this location would be required before the safe levee height could be raised. Such an evaluation is not within the scope of this study.

⁸ Authorized levels of safe protection are documented in DM No. 15, *Base - Plus Dredging.*" [4]

FLOODED AREA MAPPING

Methodology: Flooded areas were drawn on 1:200 scale ortho-photographic contour maps. In general, the median one percent chance flood profile, permanent conditions, is about one foot lower than the February 1996 flood profile and the median one percent chance flood profile, existing conditions, is about 2 foot lower than the February 1996 flood profile. Thus, relative to the accuracy of the ortho-photographic map contours (+/- 2 feet above RM 10.5 and +/- 1 foot below RM 10.5), the February 1996 flood profile is close to the median one percent chance flood profiles.

The spacing between contour intervals at a 1:200 scale did not allow significant differentiation between the median one percent chance flood profiles and the February 1996 flood profile. Thus, where photographic or first-hand information of the February 1996 flooded area was available, this information was given priority. Cowlitz County personnel, who took photographs of the flooded areas from the air shortly after the peak of the February 1996 event and the November 1995 event, assisted with this effort.

At most locations, the elevation of the median one percent chance flood and the elevation of the February 1996 flood obtained from the backwater profiles match the elevation of the flooded area boundary that one could obtain from the 1:200 foot ortho-photographic contour maps. That is, within the accuracy of what one could read off the contour maps. In all cases, flood elevations should be obtained from the profiles, not from flooded area maps. The flooded area maps are only intended to show the areal extent of flooding within mapping accuracy limits.

Results:

Median One-Percent Chance, Existing Conditions, and February 1996 Flooded Areas: At all locations except one, the February 1996 flooded area is identical to the median one percent chance flooded area, existing conditions.

At the left overbank at RM 15.1, the median one percent chance flooded area, existing conditions, is more extensive than the February 1996 flooded area. In February 1996, left overbank flow occurred just upstream of RM 15.1. However, sand bagging efforts limited the amount of flooding and the water elevation in this overbank area was less than on the Cowlitz River [personal Communication with Cowlitz County]. The portion of the left bank that was sand bagged in February 1996 is not a Corps certified levee and could not ordinarily be expected to withstand a flood of this elevation without more extensive failure. Thus, the left overbank area here was mapped to the same elevation as the Cowlitz River for the median one percent chance flood, existing conditions.

Median One-Percent Chance, Permanent Conditions, Flooded Areas: The flooded areas obtained for existing conditions (see previous paragraph) are also the median one percent chance, permanent conditions, flooded areas with one exception. Because the Longview levee is not certified for permanent conditions, additional flooded areas will need to be mapped behind the levee unless (1) further geotechnical analyses indicate the levee is certifiable, (2) further monitoring, study, or both indicates that the channel is already at permanent conditions, or (3) channel dredging or structural improvement of the levee improves conditions to the extent the levee is certifiable.

REFERENCES

1. Interagency Advisory Committee on Water Data, September 1981, Bulletin 17B, Guidelines for Determining Flood Flow Frequency.
2. U.S. Army Corps of Engineers, August 1996, Engineering Manual 1110-2-1619, Risk-Based Analysis for Flood Damage Reduction Studies.
3. U.S. Army Corps of Engineers, Portland District, Memorandum from Chief CENWP-PE-G to Chief CENWP-PE-H,
25 February 1997, Subject: Request for Safe Levee Height Information for Kelso, Longview, Lexington, and Castle Rock, Cowlitz County, Washington.
4. U.S. Army Corps of Engineers, Portland District, September 1987, Mount St. Helens, Washington Toutle, Cowlitz and Columbia Rivers, Design Memorandum No. 15, SRS Base - Plus Dredging.

REGIONAL FREQUENCY & EXTREME EVENT ANALYSIS, MUSKINGUM RIVER BASIN, OHIO

By Jerry W. Webb, Chief Water Resources Engineering Branch, U. S. Army Corps of Engineers, Huntington District, Huntington, West Virginia

Abstract: The Huntington District Corps of Engineers has responsibility for operating sixteen flood control reservoirs within the Muskingum River Basin. The Muskingum River Basin, situated in the east central part of Ohio, drains 8,051 square miles which equates to 20% of the land area of the state. More than half of the drainage basin is controlled by the existing system of reservoirs. The Corps of Engineers has placed significant emphasis on the evaluation of anticipated conditions for extreme storm events. Huntington District developed frequency of filling curves for the existing reservoirs in 1992, utilizing design storm concepts. Continued emphasis on evaluation of project performance for extreme storm events led to a recent study performed by Dr. David Goldman of the Hydrologic Engineering Center (HEC). The purpose of the investigation was to develop regionalized skew values for the Muskingum River Basin and regulated frequency curves for reservoir control points within the basin. His contributions and guidance in this study are truly appreciated. This paper presents a variety of approaches and guidance in the evaluation of extreme storm events.

INTRODUCTION

General Background: Three studies have been performed in this basin in an attempt to determine the frequency of protection offered by the existing reservoir system. The original analysis performed by Huntington District was driven by the significant level of interest expressed over encroachments that have occurred into the easements of reservoirs over time. Current policies have resulted in the removal of some dwellings, and additional dwellings will be removed unless constraints on pool usage can be developed to allow dwellings to remain in the flood control pool. Huntington District was tasked with performing a frequency of filling study for use in establishing an encroachment policy for all of the Muskingum River Basin reservoirs. The purpose of the subsequent study performed by HEC was to develop both regional skew values for peak-annual flow frequency analysis and regulated frequency curves for the basin. The analysis is complicated by the existing reservoirs which cause a significant portion of the historic record to be regulated. The limitations and lessons learned through a traditional approach and absence of reliability studies for the stochastic methods exemplify the challenge to today's hydrologic engineer in the assessment of regional frequency analysis. The methodology that was applied in this study was the subject of considerable discussion within the Corps' technical community. The initial proposal involved use of a stochastic rainfall approach of derived distributions. It was determined that the approach would be appealing from the research and development perspective, but it posed several technical obstacles and would exceed time and funding limitations:

Frequency of Filling Analysis: The study performed by Huntington District utilized a systematic design storm approach. This involved the generation of hypothetical rainfall events for each project in the Muskingum Basin and graphical extrapolation for extreme storm events from generally accepted antecedent precipitation conditions through a review of historical storm

infiltration rates for each project site. Maximum emphasis was placed on utilizing historic frequency data for developing the 5-year to 50-year component of the curves. All parameters used in the extrapolation of the curves were calibrated to the observed statistics associated with the historic operations. The study represents a systematic and consistent approach to the analysis of elevation frequency relationships.

Regional Skew Analysis: The analysis of regional skew performed by HEC focused on three techniques documented in “Guidelines for Determining Flood Flow Frequency, Bulletin 17B” including: 1) skew mapping; 2) regional regression and 3) development of regional means. The intention of the study was to select the regional skew estimates from the approach with the minimum mean square error. Application of the regression and mapping approaches proved to be unsuccessful. Given the failure of the regression and mapping application, regional skew was calculated from an area average.

Regulated Frequency Curve Development: The estimation of regulated flow values required estimates of volume-duration-frequency (VDF) curves and simulation of design hydrographs with a watershed model. The regulated frequency curves were computed by simulating the impact of study area reservoirs on design flows. Setting the initial reservoir water surface elevation and dam releases for the design storm inflows were critical aspects of performing simulations. The probable initial water surface elevations were inferred from a frequency analysis of the antecedent precipitation prior to major historical storms. The dam releases were determined from regulation policy provided by Huntington District.

FREQUENCY OF FILLING ANALYSIS

General Background Analysis: Regional frequency analysis of natural discharges and implementation of real-time flood forecasting capability were developed in the early to mid 1980's. The results of these studies were used in the initial phase of the frequency of filling study. The basic approach used in this study required that estimates for reservoir inflow volumes and their corresponding pool elevations be determined for a full range of frequency events. Reservoir inflow volume frequencies could be estimated using several techniques including: 1) graphical plotting position analysis of annual peak storage volumes, 2) annual frequency analysis of peak storage volumes using Bulletin 17B techniques, 3) frequency analysis of observed inflow gaging stations, and 4) use of an HEC-1 watershed model (Flood Hydrograph Package developed by HEC, Davis, CA) with hypothetical storms. All of these techniques only approximate inflow volumes associated with rare storm events and are only as good as the extrapolation techniques used.

Regional Natural Discharge Frequency Analysis: The original fourteen reservoirs were constructed in the 1930's. Therefore, a significant database of hydrologic data exists upon which several studies have been performed. A regional natural discharge frequency analysis for the entire basin was performed in 1982. A Log-Pearson type III distribution was fitted to the annual event series at 54 gaging stations with an average of approximately 40 years of record to derive generalized relationships. A map of the entire region was drawn to delineate isolines showing areas of equal skew. Peak discharges from this regional study were used in the frequency of filling study for initial calibration of runoff parameters associated with the design storms.

Real Time Flood Forecasting and Reservoir Control Analysis: A detailed study of the basin was performed in 1986 to establish real time forecast capability for water control purposes. The unit hydrographs and maximum routing times determined in that study were used as the basis for the adopted design storm hydrologic model.

Graphical and Bulletin 17B Annual Frequency Analysis: A graphical plotting position approach was employed to analyze the actual peak annual storage volumes at each project. The results of this procedure provided meaningful results up to the highest plotting position, which in this case utilizing the median plotting formula is equivalent to approximately a 75-year storm event. The upper end of the graphical plots were sensitive to potential high outliers and assignment of plotting positions to the largest five events in the historic record. This sensitivity produced inconsistencies in skewness associated with the graphical plot between the 10-year and 75-year event. A Bulletin 17B analysis of annual peaks was performed as a check against the graphical plotting position. Problems were experienced in the evaluation of high outliers and inconsistent shape of curves for rare storm events.

Hypothetical Design Storm Approach: The plan of study adopted a design storm approach to the subject analysis. It was assumed that this approach would provide the basis for determining the stage frequency relationships for all reservoirs within the system. Considerable effort was devoted to establishing a working hydrologic model that could be operated in a system mode to determine the response of the basin to the design storms. As the study progressed, additional techniques utilizing historic data were used to determine the sensitivity of the computed reservoir responses to the initial assumptions.

Rainfall Data, Distribution and Infiltration: National Weather Service (NWS) rainfall data provided historically related frequencies of depth-duration rainfall amounts for the Muskingum Basin. These rainfall amounts were used to generate hypothetical storm distributions. A sensitivity analysis of duration was performed resulting in the decision to utilize a 4-day storm to be used in this study. In order to establish initial assumptions for the hydrologic simulation of the design storm events, the peak discharges determined from the regional natural discharge frequency analysis were used to calibrate the rainfall losses associated with the 10-, 25-, 50-, 100-, 200-, and 500-year events. Loss rates were estimated for each frequency until the natural discharges were reproduced within reasonable error limits.

Antecedent Conditions: The design assumptions used in this study were established with reasonable engineering judgment and consistent policy. Due to lack of historic data for extreme events, a method consistent with the synthetic design storm approach was necessary. It was determined that an antecedent event proportional to the design storm would precede the main event. Starting pools and channel flows throughout the basin would be established, based on the response to the antecedent event, and then the design storm would follow. This concept acknowledges the potential for antecedent conditions to impact flood control pools prior to a major storm event. The similarity between these assumptions and the generally accepted, standard procedure for developing antecedent conditions for a PMP storm (30% with 3-day dry conditions or 39% with 5-days dry conditions) provides a consistent procedure that maintains a relationship with the frequency storm events. As previously discussed natural condition computer models were developed to calibrate the synthetic storms to the natural peak discharge condition. Infiltration rates for the entire storm were derived from

this process. Runoff for the antecedent condition utilized these infiltration rates on a 50% rainfall event over the basin prior to the actual synthetic storm event with a 2-day dry period between storm events. Most of the reservoirs were capable of passing flows associated with the antecedent storm event and return to normal pool prior to the main event for all but infrequent storm events.

Evaluation Procedures: The basin hydrology followed the design storm methodology used by Hydrologic Engineering Center (HEC) for determining regulated flow-frequency estimates. The initial phase of the study was based on calibrated natural condition rainfall based on 50 years of data. When these results were compared to the graphical historical frequency analysis and the Bulletin 17B analysis, it appeared that the calibrated losses for rare storm events were inconsistent with extrapolated values from the 50-year period of record graphical method. The resulting disparities indicated the need for a study of the historical duration of runoff volumes in the Muskingum Basin. HEC was tasked with performing a volume frequency analysis for various uncontrolled inflow gaging stations. The resulting volume frequency analysis indicated that there were inconsistencies in the skewness and extrapolation of the curves beyond the 50-year storm event. Since the basin can experience frozen, snow-covered conditions and since antecedent conditions can fluctuate dramatically, it was decided that more conservative loss rates should be used for extreme events. Utilizing some degree of engineering judgement, losses were estimated and applied to a basinwide hydrologic model. An initial loss rate of 1.25 inches was used for the 100-, 200-, and 500-year events with uniform loss rates of 0.05, 0.025, and 0.00 inches per hour, respectively. Review of the results of the rare storm simulation with the revised loss rates indicated that a combination of techniques / results would be the best approach to representing a complete pool elevation frequency relationship for each reservoir. The consistency of these relationships relative to the different reservoirs was maintained through development of a ranking factor and plotting procedure for combining the results from the different analyses.

Plotting Procedure: All analyses and curve plotting were performed on reservoir volumes and then the final curves were converted to elevation frequency. The graphical plotting position analysis of the historic annual peak storage volumes was used to define the lower portion of the curves. Results from this analysis were plotted and considered accurate up to approximately the 50-year frequency. The upper component of the curve was defined through a comparison / combination of an extrapolation of the graphical plotting position analysis and the hypothetical reservoir simulation results. A straight-line extrapolation of the curves was projected to the 100-year frequency. Reservoir operations for the 100-year event with 1.25-inch initial loss and 0.05 inch uniform loss were simulated. If the results of the reservoir simulation were lower than the straight-line extrapolation, the values from the reservoir simulation were ignored. If the simulation values were above the straight-line extrapolation, a curve fitting procedure was applied between the 50-year and 200-year events. The 200-year storm event with 1.25-inch initial loss and 0.025 inch uniform loss significantly impacted the final shape of the extrapolated curves.

Final Results and Conclusions: The final curves represent a consistent, defensible regional frequency analysis. The results from these procedures were plotted for each of the projects. In some cases, the shape of the stage volume relationship causes the elevation frequency curve to look significantly different from the volume frequency relationship. Another major factor is the computed plotting positions applied to the largest five storm events in the historic record.

Anomalies in the shape of the curves, which appear predominantly between the 10-year and 75-year event, are directly related to the plotting position formula. The upper portion of the curve is based on the largest five storm events. High outliers which could exceed a 75-year event or events of essentially equal magnitude introduce a strong influence on the skewness of the curve. The operational scenarios for storm events within this range may also influence the shape of the curve. The resulting curves indicate that the frequency of filling within the basin varies from a 180-year to a 550-year return period.

REGIONALIZED UNREGULATED FREQUENCY ANALYSIS

General Concept: Regional skew (often referred to as generalized skew) is weighted with at-site estimates of skew to obtain an adopted skew that results in improved estimates of flow-frequencies. The improvement is obtained because the regional skew is based on numerous stations which, presumably, increases the effective record length and decreases sampling error. Unfortunately, field conditions usually do not correspond to an ideal textbook example. Bulletin 17B provides very little guidance in the development of regional skew values. The guidelines suggest that at least 40 stations with at least 25 years of record within a 100 mile radius be used in the computation of regional skew. Regression, mapping, and regional mean approaches are recommended as methodologies for computing the regional skew values.

Regression Approach: In the regression approach, skew coefficient is related to various meteorologic and topographic variables. The standard error of the regression squared can be used as an estimate of the mean square error. The regional skew estimate is selected from the approach with the minimum mean square error. The regressions found that the correlation of skew with basin characteristics was insignificant. Most disappointing was the negative correlation between skew and stream slope which is contrary to results found from other regional studies.

Mapping Approach: The mapping approach involves plotting skew values on a map and isolines of skew are drawn. The difference between isoline and plotted values is used to compute mean square error. The distribution of skew coefficient values and isolines for the basin were estimated. The isolines estimates were rejected because mean square error could not be reasonably computed, given the lack of smooth regional variation. Actually, calculation of mean square error with these isolines would not be very different than calculating mean square error for an average skew value obtained for the entire basin.

Regional Mean Approach: In the regional mean approach, the regional skew value is the mean value of all the stations in the study region and the mean square error is computed as an average of the squared differences between the mean and station skew values. At-site estimates of Log-Pearson III statistics were obtained from both systematic and historic observations. The data used for computations of the at-site Log-Pearson III statistics were obtained from both the Water Control Section, Huntington District, and the USGS WATSTORE database. Huntington District provided unimpaired peak annual flows computed from regulated conditions based on a knowledge of operation characteristics of the reservoir systems. Annual peaks and random data from the continuous record were missing for the period from 1978 to 1986. Examination of the headwater gage data available from WATSTORE supports the conclusion that no major basin-

wide floods occurred during this period. Based on a review of all available records reasonable confidence can be placed in the completeness of the peak record during this period. Historic information was also provided for the 1913 flood event and the 1832 event with the 1913 being the largest event during this period.

Three different area averages shown in Table I were computed from the at-site statistics, and are compared to the value obtained from Bulletin 17B. As can be seen from this table, the estimate utilizing a historic period beginning in 1832 has the lowest mean square error. Consequently, the regional skew resulting from this data population should be selected based on guidance given the Bulletin 17B to utilize the estimate with the lowest mean square error. The extension of the historic period to 1832 was based on the observation that the 1913 event was the largest event of this period. The assumption was then made that this would be true at any other location where the 1913 event had been estimated as the maximum. This is a reasonable assumption, given the historically documented severity of the event in the western portion of the watershed.

**TABLE 1
REGIONAL SKEW VALUES**

SOURCE	REGIONAL SKEW	MEAN SQUARE ERROR
Records with 1913 Event	0.33	0.32
Records without 1913 Event	0.21	0.28
Records with 1913 Event beginning w/1832	0.26	0.24
Bulletin 17B	-0.2 - 0.0	0.31

VOLUME DURATION FREQUENCY ANALYSIS

Computation: The volume-duration-frequency curves were estimated by: 1) computing the Log-Pearson III statistics from the raw data; and 2) smoothing the computed standard deviation and skew values as a function of the mean flow for each duration. VDF curves computed from the flow data may intersect due to the sampling error in the statistics. Smoothing is performed to redistribute the sampling error between frequency curves and prevent the intersection of the curves. The estimation of the VDF frequency curves was a minor problem due to missing data in the systematic record and the availability of historic information. The computer program STATS developed by HEC was modified to smooth statistics by: 1) identifying dates of missing data; 2) including historic information in the computation of the frequency curves; and 3) adding an automatic smoothing algorithm for the sample standard deviation and skew values.

A regression routine was added to STATS to automatically smooth the relationship between the computed mean and standard deviation or skew for different durations.

Stream Flow Records: Daily stream flow records were computed at reservoir locations by the Huntington District and obtained from the USGS WATSTORE data base for headwater basins. The analysis of the computed daily values at reservoir locations was hampered by periods of missing data and shortness of the systematic record (1963-present). As in the case of the peak annual flow analysis, historic information for the 1913 and 1959 flood events was available in the

development of the VDF curves. The assumption was made that if the peaks associated with the estimated historic floods were the largest in the historic period then the flood volumes would be as well. Inclusion of the estimated historic events involves a tradeoff between the potential inaccuracy of the estimates and the knowledge that the recorded history of flood volumes does not include information on the most severe known flooding.

Adopted Frequency Curves: Generally speaking, the expectation is that skew should decrease as the duration increases, with the peak flow frequency curve having the largest skew value. Under this constraining requirement, the upper bound skew estimate is obtained by the peak flow analysis. This seems reasonable because the systematic record lengths for the historic peak flow analysis are much greater than for the VDF analysis. The frequency curves were computed for 1,3,5,7, and 10-day durations. The maximum duration of 10-days is the time base for design floods used in computing regulated frequency curves and was determined from the duration of consequential historic floods. The other durations were used to provide data for smoothing VDF curves, and to provide volumes of design hydrographs for the regulated frequency curve study. The VDF analysis resulted in regional skew values for the 1 and 3-day durations that were greater than the values obtained from the peak flow analysis which is not physically reasonable. Consequently, the 1 and 3-day duration skew values were set equal to the values obtained from the peak flow analysis. Table 2 provides the final results of the regional skew analysis for the different scenarios that were considered. The adopted skew values are a result of constraining the regional skew values obtained using the historic period beginning in 1832 by the regional skew values obtained from the peak flow analysis. Final regression curves based on the sample mean, a standard deviation smoothed via regression with the mean for each duration and the adopted skew from Table 2 were provided for each reservoir location.

**TABLE 2
REGIONAL SKEW FOR DIFFERENT RECORD LENGTHS & DURATIONS**

SCENARIO	G1 ¹	MSE ²	G3 ³	MSE	G7 ⁴	MSE	G10 ⁵	MSE
Systematic Record	0.38	0.54	0.28	0.52	0.11	0.52	0.03	0.53
Historic-1913	0.54	0.51	0.43	0.49	0.28	0.49	0.20	0.52
Historic-1832	0.42	0.46	0.28	0.42	0.08	0.36	-0.02	0.35
⁶ ADOPTED	0.26	0.24	0.26	0.24	0.11	0.40	-0.02	0.35

¹ Regional skew value for 1-day duration

² Mean square error of skew estimate

³ Regional skew value for 3-day duration

⁴ Regional skew value for 7-day duration

⁵ Regional skew value for 10-day duration

⁶ Adopted skew value results from constraining VDF estimates by peak flow skew

REGULATED FREQUENCY ANALYSIS

Development of Unimpaired Flows: Design hydrographs provide hypothetical flows for a particular exceedance frequency flood, and attempt to capture both the frequency characteristics

determined from a VDF analysis and the precipitation-runoff characteristics of the watershed. Design hydrographs were estimated by calibrating the HEC-1 basin model for natural conditions to the estimated VDF curves. Information provided by these sources was made compatible by considering depth-area adjustments of design storm precipitation and by using a regression between drainage area and mean flow to improve VDF estimates. This process promoted consistency between the HEC-1 model and frequency analysis predictions.

Development of Regulated Frequency Curves: HEC developed a methodology for estimating regulated peak-annual flow frequency curves by using a design storm approach. The computation of the regulated frequency curves involved both VDF analyses and watershed modeling. The strategy involved development of unimpaired flow design hydrographs that could be used in the watershed model to calculate regulated flow frequencies. The design hydrographs for any particular exceedance frequency was based on a calibration of the HEC-1 model to VDF curves for unimpaired basin conditions. The VDF curves were based on the same type of analysis used in developing the peak-flow frequency curves derived from the regional skew analysis. Final regulated peak-flow frequency results were determined by using the HEC-1 watershed model results that represent the operational characteristics of the flood control system.

U. S. Weather Bureau rainfall from TP-40 was used in conjunction with the HEC-1 basin model to develop design storm hydrographs. The basin model was calibrated by adjusting loss rates so that hypothetical rainfall would reproduce estimated flows for various frequencies and durations. The calibration strategy focused on approximating the flow-frequency estimates for the 1 and 3-day duration flows at reservoir locations and peak flow estimates at Zanesville, OH by adjusting model loss rates. The 1 and 3-day durations were chosen because these durations corresponded to significant flow periods in the major events of 1913 and 1959 and would have major impact on reservoir operations. Regulated peak-flow frequency curve estimates were determined in this manner for all at-site gage locations and reservoirs.

Results: The analysis of regulated flows demonstrated that most of the reservoirs could contain runoff volumes for the maximum event analyzed, the 0.1% chance event, without releasing flows greater than channel capacity. Preliminary results of regulated annual peak flow frequency curves at control points within the watershed were provided with an equivalent record length of 82 years. It should be noted that the NWS is currently updating the TP-40 rainfall for this area which could impact the results of this study.

CONCLUSIONS

There are obvious inconsistencies and conflicts of data associated with various approaches to evaluating frequency of extreme storm events in a regulated basin. At this time the more conservative traditional approach used in the frequency of filling analysis is considered appropriate for addressing the encroachment issue in the Muskingum basin. The study certainly points out the need for additional guidance in the resolution of questions concerning antecedent conditions and extreme rainfall volumes that may be anticipated..

PALEOFLOOD INVESTIGATIONS TO ASSESS EXTREME FLOODING FOR ELKHEAD RESERVOIR, NORTHWESTERN COLORADO

Robert D. Jarrett, Hydrologist, U.S. Geological Survey, Denver, CO 80225

Abstract: A regional paleoflood was conducted for Elkhead Reservoir in Elkhead Creek basin (531 km²) in northwestern Colorado to assist dam-safety officials assess the risk of large floods. Paleoflood data using bouldery flood sediments for 15 streams in the Elkhead Creek basin were used to document maximum flood discharges that have occurred during at least the past 10,000 years. No evidence of substantial out-of-bank flooding was found in Elkhead Creek basin. The maximum paleoflood of 135 m³/s for Elkhead Creek is about 13 percent of the probable maximum flood (PMF) of 1,020 m³/s. Flood-frequency relations, which incorporate paleoflood data, were developed to assess the risk of extreme floods. The 10,000-year flood is about 170 m³/s at Elkhead Reservoir. A regional paleoflood study approach, which can be used in other hydrometeorologic settings, provides information about maximum flooding in many thousands of years.

INTRODUCTION

Estimating the magnitude of extreme floods is difficult because of relatively short streamflow-gaging-station records. For many streams, gaged records do not contain large-magnitude, low frequency floods. Estimates of large floods are needed to provide accurate flood-frequency relations for the design of structures such as dams and highway infrastructure located in floodplains and for flood-plain management. For about 50 years, the design criteria for construction of high-hazard structures such as dams has included the probable maximum flood (PMF). The PMF is an estimate of the maximum flood potential for a given drainage basin and is derived from an analysis of the probable maximum precipitation (PMP) (Cudworth, 1989). The National Research Council (1994) and Hansen et al. (1988) recognized the shortcomings of estimating extreme rainfall in the mountainous areas such as in the Rocky Mountains.

Interdisciplinary flood research in Colorado (Jarrett, 1987, 1990; Jarrett and Costa, 1988; Henz, 1991; Pitlick, 1994; Waythomas and Jarrett, 1994; Grimm et al., 1995; Pruess, 1996; Tomlinson and Solak, 1997) and in the Rocky Mountains (Jarrett, 1993; Parrett and Holnbeck, 1994; Buckley, 1995; Eastwood, 1995; Jensen, 1995; Brien, 1996) provides new insight into the hydrometeorology of extreme flooding in the Rocky Mountains. One focus of the USGS interdisciplinary research project "Paleohydrology and Climate Change" is to develop cost-effective paleoflood techniques that can be used to estimate the magnitude and frequency of extreme floods in the Rocky Mountains. In an analysis of U.S. Geological Survey streamflow-gaging station data in the Rocky Mountain region, which included stations in New Mexico, Colorado, Wyoming, Idaho, and Montana, Jarrett (1990, 1993) compared maximum unit discharges (maximum peak flow divided by drainage area) to gage elevation. Based on these plots, enveloping curves were drawn that identified elevation limits of topographic controls for large unit discharges, which are caused by large, intense rainstorms. Above the limit, no large rain-caused floods have been documented. For example, above about 2,300 m in Colorado, maximum unit discharge is about 1 m³/s/km² for basins less than about 10 km²; as basin size increases, unit discharge decreases (Jarrett, 1990). These relatively small floods at higher elevations are caused primarily by snowmelt runoff or relatively small amounts of rainfall (as compared to lower-elevation rainfall amounts). Below about 2,300 m in eastern Colorado, unit discharges as large as 38 m³/s/km² have occurred. Jarrett (1990) also developed a relation between rainfall and elevation for Colorado from documented extreme rainstorms during about the last 100 years in Colorado. Above about 2,400 m in Colorado, maximum observed 24-hr

rainfall is about 100 mm; in eastern Colorado at lower elevations, maximum observed 24-hr rainfall is about 610 mm (Jarrett, 1990).

Because of these interdisciplinary research results, most state agencies in the Rocky Mountain region recently began hydrometeorologic and paleoflood studies to revise methodologies to estimate extreme precipitation and flooding for dam safety. The Bureau of Reclamation also recently began a program to use a risk-based assessment, which incorporates paleoflood investigations to provide estimates of the magnitude and frequency of extreme floods, to assist with dam safety decision making (Levish et al., 1994). Thus, it is important to develop methodologies that can be used by dam-safety officials to make decisions about the probabilities of extreme floods. A regional paleoflood study was conducted in northwestern Colorado to assess the flood hydrology for Elkhead Reservoir in Elkhead Creek basin near Craig. The objective of the paleoflood study was to estimate prior maximum flooding in the basin from evidence preserved in the floodplain to help dam-safety officials utilize study results in a risk-based assessment. A lack of flood evidence, particularly of extremely rare floods, in one basin such as Elkhead Creek basin could result from pure chance. Thus, it is essential to ascertain the flood history for other basins in the region by analyzing available flood and precipitation data and conducting paleoflood investigations for many streams within a hydroclimatic region. Regional analysis extends hydrologic records and provides a tool to estimate discharge at ungaged sites and decrease time-sampling errors at one site. Major drainages within the regional study area (10,900 km²) are the Yampa and White River basins. Results presented in this paper only are for 15 sites within the Elkhead Creek basin of the 86 paleoflood sites for streams in the regional study area of northwestern Colorado. The paleoflood study was conducted for the Colorado River Water Conservation District to complement a site-specific PMP/PMF study for Elkhead Reservoir by North American Weather Consultants in Salt Lake City, Utah, and Ayres Associates Inc. in Fort Collins, Colorado.

STUDY AREA

Elkhead Creek basin, which has a drainage area of 531 km² at Elkhead Reservoir, is located in northwestern Colorado. Hydroclimatic conditions are relatively homogeneous in northwestern Colorado (Kircher et al., 1985). Elkhead Creek has its headwaters in the Elkhead Mountains and flows southwesterly to Elkhead Creek's confluence with the Yampa River about 10 km east of Craig. Elevations in the basin range from about 3,307 m at the highest peak of the Elkhead Mountains to about 1,890 m at its confluence with the Yampa River. Distinct mountains and ridges define the boundaries of the basin. Most annual precipitation falls as snow in the winter months. Within the larger context of the regional study area, localized, convective rainstorms during summer months have produced localized flooding in small, steep basins at lower elevations in northwestern Colorado (Jarrett, 1987).

METHODOLOGY

Paleoflood hydrology is the study of past or ancient floods preserved in stream channels (Baker, 1987; Jarrett, 1990, 1991). Paleoflood data are particularly useful in providing probable upper limits of the largest floods that have occurred in a river basin (Jarrett, 1990). Floods leave distinctive deposits and landforms in and along stream channels, as well as botanic evidence (Baker, 1987; Jarrett, 1990, 1991). Slack-water deposits of sand-sized particles and bouldery flood-bar deposits most commonly are used to estimate past flood levels called paleostage indicators (PSIs). Paleoflood evidence is relatively easy to recognize and long lasting in the Colorado Rockies because of the quantity, morphology, and structure and size of sediments deposited by floods (McCain, et al., 1979; Jarrett, 1987; Jarrett and Costa, 1988; Waythomas and Jarrett, 1994). The slope-conveyance method (Barnes and Davidian, 1978) was used to estimate paleoflood discharge. Discharge is determined from estimates of flood width and depth

corresponding to the PSIs, channel slope, maximum-particle size of flood-deposited sediments located on the channel and floodplain obtained during onsite visits to streams. Flood depth is estimated by using the elevation of the top of flood-deposited sediments (or PSIs) in the channel or on the floodplain above the channel-bed elevation. Flow-resistance coefficients and velocity were estimated from analysis of data for mountain rivers (Jarrett, 1985).

Age estimates for paleoflood deposits are based on relative-age criteria (Waythomas and Jarrett, 1994). Relative-age techniques used for this study were degree of soil development, boulder weathering, and boulder burial. An important point for using relative-age dating techniques is to obtain ages using these different techniques and several samples within a reach of channel. The strategy of a paleoflood investigation is to visit the most likely places where evidence of out-of-bank flooding, if any, might be preserved. Where possible paleoflood estimates are obtained in bedrock controlled channels that minimize changes in channel geometry; there is little evidence that major changes in channel geometry have occurred in channels in this study. Onsite paleoflood data were collected for sites on Elkhead Creek and its tributaries.

To help facilitate risk assessments of rare floods, a flood-frequency relation was developed from an analysis of annual peak flows through 1996 for Elkhead Creek near Elkhead (09245000) using a Log-Pearson Type III (LPIII) frequency distribution (Interagency Advisory Committee on Water Data, 1981). The gage is located at an elevation of 2,086 m, has a drainage area of 166 km², and has 44 years of record. Paleoflood data (magnitude and ages) were incorporated into the flood-frequency analysis to extend the gaged record. Because the Elkhead gage is operated about 10 km upstream from the reservoir, regional flood-frequency relations for the northwest region of Colorado (Kircher et al., 1985) were used to estimate flood characteristics for Elkhead Creek at Elkhead Reservoir.

RESULTS

Paleoflood data were collected for 15 streams in Elkhead Creek basin. Few coarse-grained sediments have been mobilized and deposited as flood bars and slack-water deposits in streams in the study area (e.g., fig. 1). Where present, paleoflood deposits are either associated with the record snowmelt runoff in 1984, or the deposits are very old based on extensive pitting, grain relief, and extensive boulder burial (50 to 75%), and probably reflect glacial outwash. Thick, clay-rich, well-developed soils on flood-plain and hillslope surfaces and a lack of substantial flood-deposits (fig. 1) indicate that the age of maximum paleofloods is at least 500 years to about 10,000 years (since glaciation). No evidence of substantial out-of-bank flooding was found in any investigated stream in Elkhead Creek basin. The maximum paleoflood discharge in Elkhead Creek upstream from Elkhead Reservoir is 95 m³/s and downstream from Elkhead Reservoir is 135 m³/s. Maximum paleofloods provide physical evidence of an upper bound on maximum peak discharge for any combination of rainfall- or snowmelt-runoff in Elkhead Creek, in at least 10,000 years.

A flood-frequency relation for Elkhead Creek near Elkhead was developed using the recorded annual peak-flow data and paleoflood data (fig. 2). Flood-frequency analyses were done using the paleoflood discharge, which was varied by the estimated error of 25 percent to help define confidence limits. The historic-record length for the ages of paleofloods used in the analysis ranged from a maximum of 10,000 years to 100 years based on relative-age dating criteria (the latter age estimate reflects an extremely conservative or short-historic period). The flood-frequency relation for Elkhead Creek at Elkhead Reservoir (fig. 2) was estimated from the regional flood method developed by Kircher et al. (1985). The flood-frequency relation for the Elkhead Creek gage, which has about 30 percent of the drainage area at the reservoir, is similar to the regional relation likely because the majority of the basin between the gage and the reservoir contributes little runoff from snowmelt or rainfall. The 100-year flood estimate for Elkhead

Creek is $76 \text{ m}^3/\text{s}$ at the gage and is about $82 \text{ m}^3/\text{s}$ at Elkhead Reservoir.

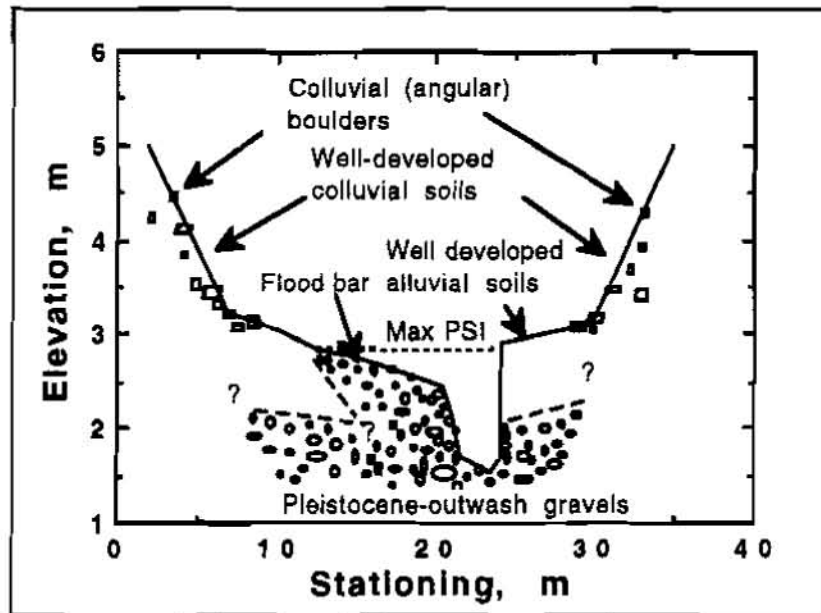


Figure 1. Graph of channel cross section for Elkhead Creek downstream from North Fork Elkhead Creek. Paleoflood discharge is $95 \text{ m}^3/\text{s}$.

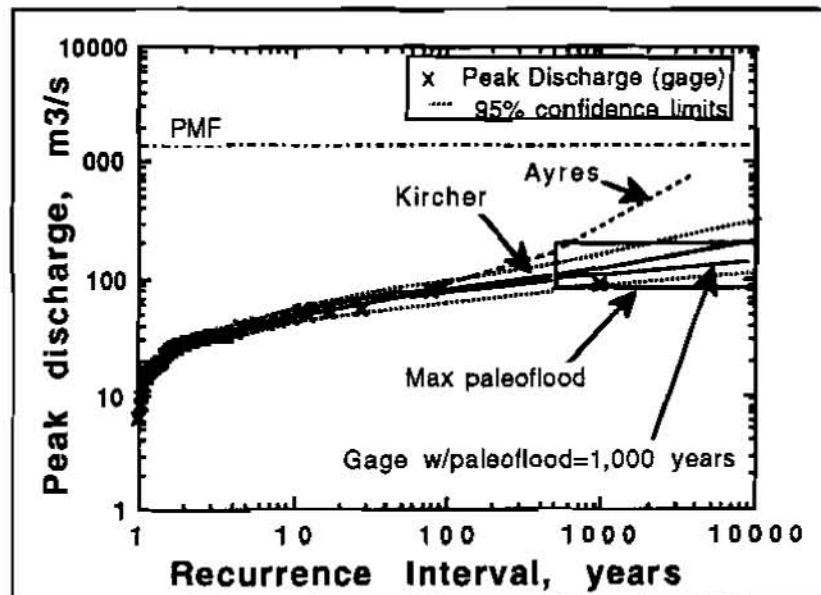


Figure 2. Flood-frequency relations for Elkhead Creek near Elkhead gage (092445500) with paleoflood data of $85 \text{ m}^3/\text{s} \pm 25\%$ with the age ranging from 500 to 10,000 years (shown as rectangle) with 95-percent confidence limits. Flood-frequency relations varied by less than 20 percent for the range of historic period length of 100 years and 10,000 years, probably because the maximum paleoflood is not much larger than the flood of record. The regional flood-frequency relation for Elkhead Creek at Elkhead Reservoir (Kircher et al., 1985) also is shown. The flood-frequency relation and probable maximum flood for Elkhead Reservoir (Ayres Associates, Inc., written commun., 1996) are shown for comparison.

The flood-frequency relation for Elkhead Creek at Elkhead Reservoir developed by Ayres Associates, Inc. (written commun., 1996) (fig. 2) essentially is the same as the flood-frequency relations from this study up to about the 100-year flood. The Ayres relation sharply increases above the 100-year flood and falls outside the confidence limits of the regional flood-frequency relations above the 200-year flood. The difference for larger recurrence intervals primarily results from transposition of rainstorms to Elkhead Creek basin and using rainfall-runoff modeling to estimate the upper end of flood-frequency relation.

Extensions of flood-frequency relations to rare floods (e.g., 10,000-yr recurrence interval) are tenuous for short-streamflow records, but are enhanced when paleoflood data are included in flood-frequency analysis (Kochel and Baker, 1982; Jarrett, 1987; Jarrett and Costa, 1988). The frequency curve for Elkhead Creek (fig. 2) was extended linearly and is constrained by the maximum paleoflood of 135 m³/s. The estimated recurrence interval for the maximum paleoflood near Elkhead Reservoir is about 2,500 years, and the 10,000-year flood is about 170 m³/s. For comparative purposes, the PMF estimate shown for Elkhead Creek at the dam (Ayres Associates Inc., written commun., 1996) is 1,020 m³/s and far exceeds a 10,000-year flood (fig. 2). Although such extrapolations of flood-frequency relations are imprecise, they demonstrate the probability of a flood similar to the magnitude of the PMF in Elkhead Creek basin is extremely small.

DISCUSSION

Bouldery flood deposits provide recognizable flood evidence preserved for many thousands of years had large floods occurred in streams in Elkhead Creek basin. In the type of paleoflood investigations conducted in the Rocky Mountains, lack of physical evidence of the occurrence of floods is as important as discovering tangible onsite evidence of such floods (Jarrett, 1987, 1990; Jarrett and Costa, 1988; Levish et al., 1994; Ostenaar and Levish, 1995). Although paleoflood estimates also involve uncertainties, the estimates are based on interpretations of physical data preserved in channels and on floodplains during at least the past 10,000 years in the Rocky Mountains. These uncertainties primarily are related to possible post-flood changes in channel geometry and flood heights interpreted from PSIs. One of the largest sources of uncertainty in paleoflood reconstructions is actual flood height inferred from PSIs. A comparison of the elevation of the top of flood-deposited sediment (PSIs) and high-water marks (HWMs) of recent large flooding in streams of the western United States was made (unpublished data). Analysis of the differences in PSIs and HWMs indicates that the elevation of the top of flood-deposited sediments (PSIs) generally are within +/-0.2 m of flood HWM elevations for extreme floods in a wide range of hydraulic and sedimentologic channels. Therefore, use of the top of flood-deposited sediments as PSIs for streams in this study provides a reliable estimate of the paleoflood depth that is used to reconstruct the discharge of paleofloods.

More quantification (e.g., using step-backwater analyses to calculate paleoflood discharges, using absolute-age dating of flood deposits, more robust flood-frequency parameter estimation procedures, etc.) would slightly improve the accuracy of individual paleoflood estimates and flood-frequency analysis. However, the interpretation that little out-of-bank flooding has occurred in many thousands of years in Elkhead Creek would not differ substantially. Maximum paleofloods provide physical evidence of an upper bound on maximum peak discharge for any combination of rainfall- or snowmelt-runoff in northwestern Colorado, since glaciation. The maximum paleoflood in at least the last 10,000 years for Elkhead Creek near Elkhead Reservoir is about 13 percent of the PMF estimate. Several recent paleoflood studies, primarily conducted by the U.S. Geological Survey and Bureau of Reclamation (Jarrett and Costa, 1988; Levish et al., 1994; Grimm et al., 1995; Ostenaar and Levish, 1995), also demonstrate large differences between maximum paleoflood estimates in the Rocky Mountain region and PMF estimates. Thus, given the large differences in maximum paleoflood and PMF values in the Rocky

Mountains, it seems prudent to conduct additional hydrometeorologic and paleoflood research to help reduce the uncertainty in estimates of maximum flood potential. A regional paleoflood study approach, which can be used in other hydrometeorologic settings, provides information for a risk-based approach for hydrologic aspects of dam safety.

REFERENCES

- Baker, V.R., 1987, Paleoflood hydrology and extraordinary flood events. *Journal of Hydrology*, v. 6, no. 1-4, p. 79-99.
- Barnes, H.H., Jr., and Davidian, Jacob, 1978, Indirect methods, in Hershey, R.W., ed., *Hydrometry--Principles and Practices*. New York, John Wiley, p. 189-190.
- Brien, D.L., 1996, Paleoflood and streamflow data to describe the spatial occurrence of rainfall and snowmelt floods in Wyoming. M.S. thesis, University of Wyoming, Laramie, 82 p.
- Buckley, J.L., 1995, Evaluation of design criteria for hazardous dams. MS thesis, University of Wyoming, Laramie, 93 p.
- Cudworth, A.G., Jr., 1989, Flood hydrology manual. U.S. Bureau of Reclamation, A Water Resources Technical Publication, 243 p.
- Eastwood, D., 1995, Statistical analysis of extreme precipitation in Wyoming. MS thesis, University of Wyoming, Laramie, 119 p.
- Grimm, M.M., Wohl, E.E., and Jarrett, R.D., 1995, Coarse-sediment distribution as evidence of an elevation limit for flash flooding, Bear Creek, Colorado. *Geomorphology*, v. 14, p. 199-210.
- Hansen, E.M., Fenn, D.D., Schreiner, L.C., Stodt, R.W., and Miller, J.F., 1988, Probable maximum precipitation estimates--United States between the Continental Divide and the 103rd meridian: Silver Springs, Maryland, National Oceanic Atmospheric Administration, Hydrometeorologic Report 55A, 242 p.
- Interagency Advisory Committee on Water Data, 1981, Guidelines for determining flood-flow frequency (2nd ed., revised 1982). Reston, Virginia, U.S. Geological Survey Office of Water Data Coordination.
- Jarrett, R.D., 1985, Determination of roughness coefficients for streams in Colorado. U.S. Geological Survey Water-Resources Investigations Report 85-4004, 54 p.
- Jarrett, R.D., 1987, Flood hydrology of foothill and mountain streams in Colorado. Ph.D. dissertation, Colorado State University, Fort Collins, 239 p.
- Jarrett, R.D., 1990, Paleohydrologic techniques used to define the spatial occurrence of floods. *Geomorphology*, v. 3, no. 2, p. 181-195.
- Jarrett, R.D., 1991, Paleohydrology and its value in analyzing floods and droughts--Floods and Droughts. *in* National Water Summary 1988-89, U.S. Geological Survey Water-Supply Paper 2375, p. 105-116.
- Jarrett, R.D., 1993, Flood elevation limits in the Rocky Mountains. *in* Kuo, C.Y., ed., *Engineering Hydrology--Proceedings of the symposium sponsored by the Hydraulics Division of the American Society of Civil Engineers*, San Francisco, California, July 25-30, 1993; New York, American Society of Civil Engineers, p. 180-185.
- Jarrett, R.D., and Costa, J.E., 1988, Evaluation of the flood hydrology in the Colorado Front Range using precipitation, streamflow, and paleoflood data. U.S. Geological Survey Water-Resources Investigations Report 87-4117, 37 p.
- Jensen, D.T., 1995, Probable maximum precipitation estimates for short-duration, small-area storms in Utah. Utah Climate Center, Utah State University, Logan, Final Report, 75 p.
- Kircher, J.E., Choquette, A.F., and Richter, B.D., 1985, Estimation of natural streamflow characteristics in western Colorado. U.S. Geological Survey Water-Resources Investigations Report 85-4086, 28 p.
- Levish, Daniel, Ostenaar, Daniel, and O'Connell, D.O., 1994, A non-inundation approach to paleoflood hydrology for the event-based assessment of extreme flood hazards, *in* Association of State Dam Safety Officials, 11th Annual Conference Proceedings, Lexington,

- Kentucky, Association of State Dam Safety Officials, p. 69-82.
- McCain, J.F., Hoxit, L.R., Chappell, C.F., and Caracena, F., 1979, Meteorology and hydrology in the Big Thompson River and Cache la Poudre River basins, Larimer and Welds Counties, Colorado, Part A of Storm and flood of July 31-August 1, 1976. U.S. Geological Survey Professional Paper 1115-A, p. 1-85.
- National Research Council, 1994, Estimating bounds on extreme precipitation events. National Academy Press, Washington, D.C., 25 p.
- Ostenaar, D.A., and Levish, D.R., 1995, The application of a non-inundation approach of paleoflood hydrology for the assessment of extreme flood hazards on the Ogden River, Utah. *in* Environmental and Engineering Geology of the Wasatch Front Region, Utah Geological Survey Publication 24, Lund, W.R., ed., p. 495-508.
- Parrett, Charles, Holnbeck, S.R., 1994, Relation between largest known flood discharge and elevation in Montana. *in* Cotroneo, G.V., and Rumer, R.R., eds., 1994, Hydraulic Engineering--Proceedings of the symposium sponsored by the American Society of Civil Engineers, Buffalo, New York, August 1-5, 1994: New York, American Society of Civil Engineers, p. 870-874.
- Pitlick, John, 1994, Relation between peak flows, precipitation, and physiography for five mountainous regions in the western United States. *Journal of Hydrology*, v. 158, p. 219-240.
- Pruess, J.W., 1996, Paleoflood reconstructions within the Animas River basin upstream from Durango, Colorado. MS thesis, Colorado State University, Fort Collins, 192 p.
- Tomlinson, E.M., and Solak, M.E., 1997, Site-specific probable maximum precipitation (PMP) study of Elkhead drainage basin. TRC North American Weather Consultants, Salt Lake City, Utah, NAWC Report WM 95-6.
- Waythomas, C.F., and Jarrett, R.D., 1994, Flood geomorphology of Arthurs Rock Gulch, Colorado, paleoflood history. *Geomorphology* 11, p. 15-40.

Additional Information: Robert D. Jarrett, U.S. Geological Survey, P.O. Box 25046, MS412, Denver, CO 80225; 303-236-6447; rjarrett@usgs.gov

PALEOHYDROLOGIC BOUNDS AND LOW PROBABILITY FLOODS

By Daniel R. Levish, Geologist; Dean A. Ostenaar, Geologist; and Daniel R.H. O'Connell, Geophysicist, U.S. Bureau of Reclamation, Geophysics, Paleohydrology, and Seismotectonics Group, Denver, Colorado

Abstract

An expeditious way to evaluate the magnitude of low probability floods is to identify and assign ages to geomorphic surfaces adjacent to a stream that serve as limits for the paleostage of large floods over thousands of years. These paleostage limits can then be input into a hydraulic model to calculate the maximum discharge that would not significantly inundate, and therefore significantly modify, a particular geomorphic surface. This maximum discharge, together with the age of the surface, forms a conservative limiting bound on flood discharge through time that is input for flood-frequency analysis. These paleohydrologic bounds are not actual floods, but instead they are limits on flood magnitude over a measured time interval. In this way, these bounds represent stages and discharges that have not been exceeded since the geomorphic surface stabilized.

Examples from paleoflood studies conducted for Causey Dam on the South Fork Ogden River, Utah, and Bradbury Dam on the Santa Ynez River, California, illustrate the utility of paleohydrologic bounds in flood frequency analysis. In both cases, flood frequency analysis based on the record of annual peak discharge estimates and extrapolation to the Probable Maximum Flood (PMF) leads to substantial overestimates of the frequency of large floods, and to the conclusion that dam overtopping may be likely. In fact, in both cases with the inclusion of paleohydrologic bounds in the flood frequency analysis, floods with a magnitude equivalent to spillway capacity are extremely low probability events.

For the past several decades the estimated Probable Maximum Precipitation (PMP) and the calculated Probable Maximum Flood (PMF) have been used as measures of hydrologic dam safety. However, both the PMP and PMF are hypothetical maximums and by definition have no associated probability. The absence of probability for the PMP and PMF limits the utility of these hypothetical indices for risk-based dam safety decisions. In the western U.S., short historical and gage records afford little support for the hypothetical PMF, and hydrologic indices based on the PMP are thwarted by the numerous complex and poorly understood assumptions required to turn rainfall into runoff. Paleohydrologic techniques are a means to directly assess the probability of extreme floods and test the validity of the PMF and PMP-based models. The results of paleoflood studies in California, Oregon, Utah, and Wyoming demonstrate that discharges with calculated annual probabilities of one in 10,000 are in the range of five to 25 percent of the hypothetical PMF.

Paleohydrologic Bounds

A paleohydrologic bound is a time interval during which a given discharge has not been exceeded. In stable reaches, stage can be converted to discharge through hydraulic modeling. Both properties of the paleohydrologic bound, time and discharge, are independently determined from objective criteria in the field. This approach is appropriate for hazard assessment because paleohydrologic bounds provide extremely valuable information for improving estimates of the frequency of large floods because the data are a direct description of the largest floods. It is not

necessary to develop evidence of specific paleofloods to define paleohydrologic bounds, although it can be convenient for illustration.

The objective of studies of flood risk based on paleohydrologic bounds is to identify and assign ages to geomorphic surfaces adjacent to a stream that serve as limits for the paleostage of large floods. These paleostage limits can then be input into a hydraulic model to calculate the maximum discharge that would not significantly inundate, and therefore significantly modify, a particular geomorphic surface. The depth of significant inundation is calibrated based on the properties of the particular reach and comparison with the geomorphic impact of extreme floods (e.g., Baker and Costa, 1987). This maximum discharge, together with the age of the surface, forms a conservative bound on peak discharge through time for use in flood-frequency analysis. These bounds are not actual floods, but instead they are limits on flood magnitude over a measured time interval. In this way, these bounds represent stages and discharges that have not been exceeded since the geomorphic surface stabilized.

Paleoflood hydrology includes the study of the geomorphic and stratigraphic record of past floods (e.g., Baker, 1989; Jarrett, 1991). This record is a direct, long-term measure of the ability of a stream to produce large floods and may often be at least 10 to 100 times longer than the conventional record of annual peak discharge estimates. Paleohydrologic techniques offer a way to lengthen a short-term data record and, therefore, to reduce the uncertainty in hydrologic analysis (Jarrett, 1991). Obviously, this allows for a higher degree of assurance for dam safety when making decisions regarding floods with long return periods. Paleoflood studies allow a long-term perspective that can put exceptional annual peak discharge estimates in context and assist in reconciliation of conflicting historical records.

Most conventional estimates of the frequency of large floods are based on extrapolation from short records of annual peak discharge estimates, sometimes with the addition of historic information. Most magnitude estimates for extreme floods are made by extrapolation of the statistical model selected for flood-frequency to a given return period or annual probability, or by hypothetically maximizing rainfall-runoff models. Frequency estimates for maximized rainfall-runoff models are either arbitrarily assigned or are based on extrapolating the flood-frequency curve to the calculated discharge. No matter how many of these short-term records are statistically combined, they can never accurately characterize the probability of very infrequent floods because statistical confidence is directly related to the length of record. Further, due to short record length, many statistical distributions may fit the data, but the extrapolation to low probability floods is highly dependent on the choice of the distribution. Because each basin is unique, regionalizing or substituting space for time to compensate for short record length cannot completely substitute for the accurate characterization of the properties of a specific site or region, and may result in unwarranted confidence. Additionally, if the record of annual peak discharge estimates contains an exceptionally large flood(s), this event(s) is usually assigned an unrealistically short return period, omitted from the frequency analysis, or "weighted" in some arbitrary fashion. Thus, any estimate of a flood with a recurrence greater than several hundred years that is based only on short-term record of annual peak discharge estimates or even long historic records of a few hundred years, will have a large inherent uncertainty. Paleoflood hydrology offers a means of verifying return periods that are many times longer than the length of the gage or historic records (Costa, 1978).

There is a long history of paleoflood hydrology, in a wide variety of settings throughout the world (e.g., Costa, 1986; Patton, 1987; Baker et al., 1988). One widely used technique, slackwater studies, uses fine-grained sediment that accumulates in backwater areas to construct a detailed history of past floods (e.g., Patton et al., 1979; Kochel and Baker, 1988). Early studies by Mansfield (1938) on the Ohio River and Jahns (1947) on the Connecticut River, demonstrate another approach. They recognized that historic floods had overtopped sites not previously inundated in thousands of years. Lacking evidence of recent inundation, the age of a geomorphic surface is an estimator of the minimum return period of a flood that could inundate that surface (Costa, 1978; O'Connell et al., 1997).

Incorporation of long-term paleohydrologic information in flood-frequency studies does not depend on being able to reconstruct the complete record of all past floods. Statistical techniques that can incorporate paleohydrologic bounds are a useful way to take advantage of paleohydrologic information (Stedinger and Cohn, 1986). In this way, it is not important if floods of a specified recurrence are not recorded or included in the frequency analysis. What is important is that limits on flood magnitudes over time intervals can be identified. Sensitivity analyses show that the addition of only one or two paleohydrologic bounds that span a range of hundreds to thousands of years have a significant impact on the shape of the flood-frequency curve (Ostenaa et al., 1996; O'Connell et al., 1997).

The field expression of paleohydrologic bounds, stable geomorphic surfaces, are flood plains that have been abandoned due to stream incision. Once abandoned, their surface characteristics change with time. Two of the most easily recognized changes involve the modification of surface morphology and the development of soil. Through time, slope processes and weathering mute the expression of surface irregularities related to fluvial erosion and deposition. Once a surface has stabilized, that is, it is no longer episodically overtopped, soils form in a predictable sequence (Birkeland, 1984).

Disruptions in soil profiles and geomorphic features, such as eroded channels, that result from significant inundation by large floods are generally easily recognized. This is why these former flood plain surfaces are reliable indicators of flood stage through time. The limits of the surface define a maximum channel width through which a maximum discharge can be modeled. The ages associated with the geomorphic surfaces that form bounds for flood magnitude are almost always minimum ages because of the problems related to dating the precise time when a particular surface was abandoned. The result is an estimate of the maximum discharge during the minimum time interval since stabilization. These estimates are made even more conservative because through time, channels may downcut and erode laterally, resulting in apparently larger cross-sections and discharges. Therefore, a study goal is to locate stable reaches with the minimum channel capacity adjacent to geomorphic surfaces that place limits on paleostage through the reach.

Paleohydrologic Bounds and Flood Frequency - Two Examples

Examples from paleoflood studies conducted for Causey Dam on the South Fork Ogden River, Weber County, Utah, (Ostenaa et al., 1997) and Bradbury Dam on the Santa Ynez River, Santa Barbara County, California, (Ostenaa et al., 1996) illustrate the utility of paleohydrologic bounds for estimating the frequency of extreme floods. In both cases, conventional flood-frequency analysis based only on the short record of annual peak discharge estimates with extrapolation to

the PMF leads to substantial overestimates of the frequency of large floods. With the inclusion of paleohydrologic bounds in the flood frequency analysis, floods with a magnitude equivalent to spillway capacity are extremely low probability events at both dams.

Causey Dam impounds water in the mountainous upper 210 km² of the South Fork Ogden River basin. The dam is a 258-m-long, 66-m-high earthfill embankment with an ungated spillway capacity of about 214 m³/s. The calculated thunderstorm PMF for Causey Dam has a peak discharge of more than 3000 m³/s, with the calculated threshold for dam overtopping of 677 m³/s. Based on standard engineering flood frequency analysis (e.g., NRC, 1985), a discharge equivalent to the estimated threshold overtopping discharge has a return period on the order of 2,000 to 30,000 years. Significant overtopping of Causey Dam could result in dam failure, and dam failure would result in substantial and unacceptable consequences downstream.

Downstream from Causey Dam the flood plain of the South Fork Ogden River is characterized by two groups of Holocene geomorphic surfaces that form paleohydrologic bounds. Ages for the bounds are based on the geomorphology and stratigraphy of these surfaces and 19 radiocarbon ages. The discharges associated with these bounds are calculated from hydraulic modeling in a stable reach 6 km downstream of the dam. The "Holocene 2" paleohydrologic bound is formed by a group of surfaces that have not been significantly overtopped in 2500 years. Based on hydraulic modeling a discharge of 115 m³/s would significantly modify this surface and therefore is the discharge value for the paleohydrologic bound. The "Holocene 1" paleohydrologic bound is formed by a group of surfaces that have not been significantly overtopped in the last 400 years. A discharge of 70 m³/s would modify these surfaces based on hydraulic modeling.

Bradbury Dam is a 1020-m-long, 85-m-high embankment that impounds water in the mountainous upper 670 km² of the Santa Ynez River basin. Bradbury Dam has a gated spillway with a capacity of 4533 m³/s. The calculated PMF for Bradbury Dam is 13,060 m³/s. Based on standard engineering flood-frequency techniques (e.g., NRC, 1985), the PMF has an extrapolated return period as frequent as less than 100 years. If the PMF were possible this flow would overtop the dam which could result in dam failure. Dam failure would result in substantial and unacceptable consequences downstream.

Between Bradbury Dam and the town of Lompoc 65 km downstream there are two Holocene surfaces that form useful paleohydrologic bounds. Ages for these bounds are based on the geomorphology and stratigraphy of these surfaces and 17 radiocarbon ages. The discharges associated with these bounds result from hydraulic modeling in two stable reaches, 2 km and 55 km, downstream of the dam. The "t1" paleohydrologic bound is formed by a group of surfaces that have not been significantly overtopped in 2900 years. Based on hydraulic modeling a discharge of 2550 m³/s would significantly modify this surface and therefore is the discharge value for the paleohydrologic bound. The "fp2" paleohydrologic bound is formed by a group of surfaces that have been significantly overtopped once in the last 700 years. A discharge of 1980 m³/s would modify these surfaces based on hydraulic modeling. Based on historical information a third bound can be constructed that spans from 1862 to 1907 at a discharge of 1275 m³/s.

For flood frequency calculations, the information from the paleohydrologic bounds is combined with the record of annual peak discharge estimates (O'Connell et al., 1997). The relative amounts of time spanned by the paleohydrologic bounds and the record of annual peak discharge estimates

for both the South Fork Ogden River and the Santa Ynez River is shown on Figure 1. To calculate flood-frequency statistics, the maximum likelihood (MLH) method of Stedinger and Cohn (1986) and Stedinger et al. (1988) is modified and incorporated into a Bayesian approach (Tarantola, 1987; O'Connell et al., 1997). For both the South Fork Ogden River and the Santa Ynez River the impact of the paleohydrologic bounds is dramatic. For the South Fork Ogden River the analysis indicates that a flow of spillway capacity has a probability of much less than one in 10,000, with an extrapolated probability less than one in 500,000. This indicates that overtopping of the dam is an extraordinarily unlikely event. For the Santa Ynez River the incremental advantage of adding more information can be demonstrated by calculating flood-frequency statistics from various data sets. The addition of paleohydrologic bounds has the greatest impact on the flood frequency calculations (Table 1). Table 1 illustrates the difference in the conclusion drawn from different sets of data. Once again, for the Santa Ynez River paleohydrologic information shows that a discharge equivalent to spillway capacity of Bradbury Dam is a very remote event with an extrapolated probability of less than one in 6,000,000.

Table 1: Mean Annual Probability and Return Period of Discharges Exceeding the Capacity of the Bradbury Dam Spillway (4533 m³/s)

Data Set	Mean Annual Probability	Return Period (years)
Gage	5.74×10^{-4}	1740
Historic + Gage	1.43×10^{-4}	7000
Paleoflood + Historic + Gage	1.57×10^{-7}	>6,000,000

Paleohydrologic bounds influence flood frequency calculations by extending the length of record. Inferences about low probability floods based only on short gage and historic records (less than 150 years in the western U.S.) depend on assumptions of the statistical distribution chosen to portray flood frequency (e.g., O'Connell et al., 1997). However, these short term records contain no information about the long term behavior of floods. In fact, many gage and historic records are hampered by trapping a low probability or long return period event in a short record. This adds significant bias to flood frequency estimates and in many instances in the western U.S. leads to an over estimate of flood magnitude for a particular probability or return period.

Paleohydrologic Bounds and the Calculated Probable Maximum Flood

The Probable Maximum Flood (PMF) has been used as a standard for hydrologic analyses in dam safety for several decades (NRC, 1985). As originally defined, the PMF has no return period. However, this definition is not practical for dam safety decisions based on risk. As a practical matter, the PMF has often been arbitrarily assigned a return period of 10,000 to 1,000,000 years at the upper and lower confidence limits for flood frequency analysis (e.g., NRC, 1985).

Paleoflood studies are a basis for testing whether the calculated PMF and the associated extrapolated return period are realistic. Because the fluvial geomorphology and stratigraphy of flood plains adjacent to streams are recorders of the most extreme floods, paleoflood records should contain extreme floods that are a large percentage of the PMF, if such floods are physically possible. The shorter the estimated return period assigned to the PMF, the more likely it becomes

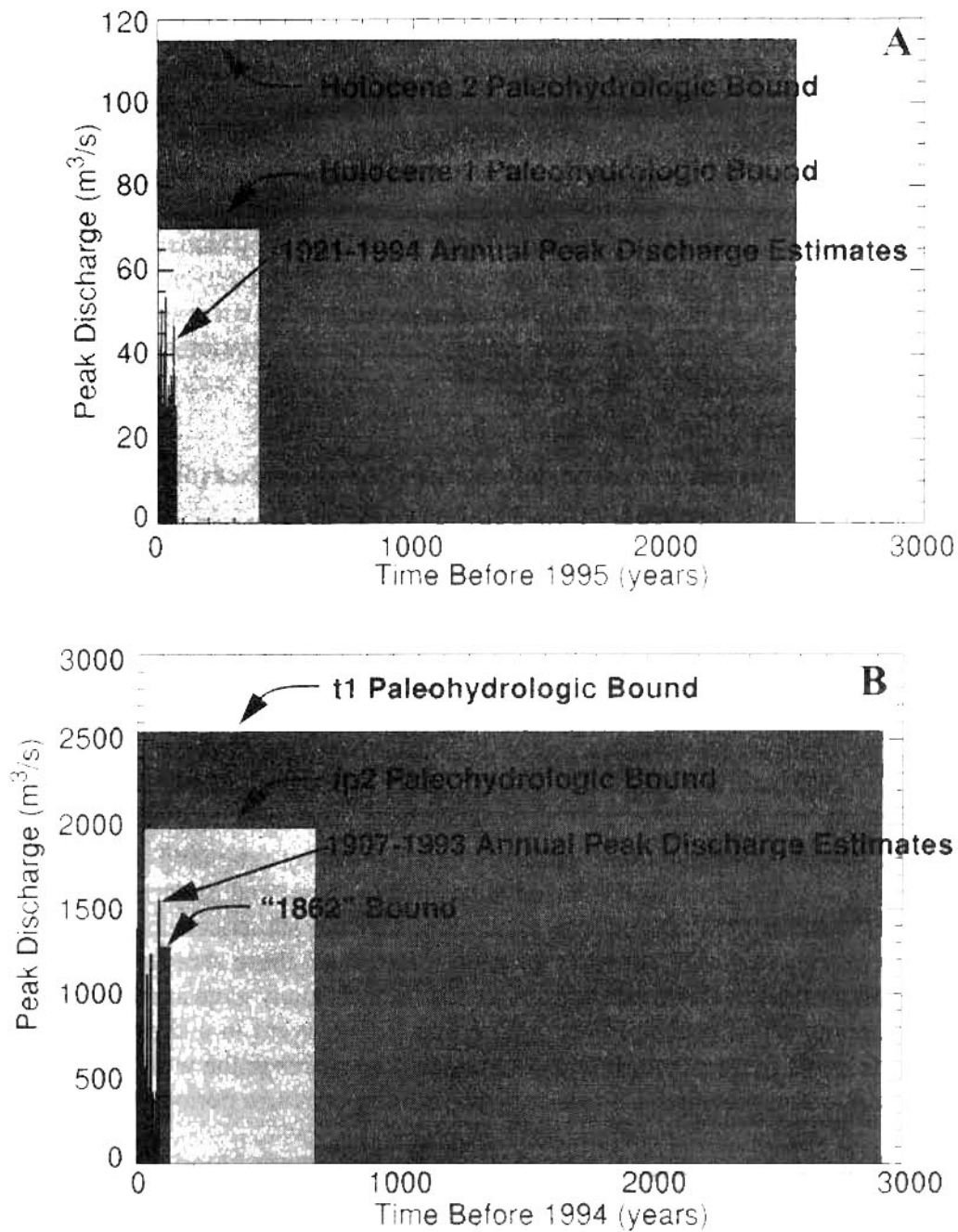


Figure 1 - Comparative time spanned by paleohydrologic bounds and the record of annual peak discharge estimates for A) South Fork Ogden River at Causey Dam and B) Santa Ynez River at Bradbury Dam. For the South Fork Ogden River there are no historic floods near the paleohydrologic bound. For the Santa Ynez River the 1969 flood exceeds the fp2 paleohydrologic bound. These plots illustrate that paleohydrologic bounds provide significantly more information about low probability floods than the record of annual peak discharge estimates.

that such large floods should be included in paleoflood records that are thousands of years in length. Considering the number of drainage basins present in an area the size of the western U.S., if there actually have been floods comparable to the hypothetical PMF, the numerous multi-thousand-year paleoflood records present along western streams are likely to record multiple PMF-scale floods.

The paleohydrologic bounds from the South Fork Ogden River and the Santa Ynez River are only a small percentage of the calculated PMF for Causey and Bradbury Dams. Data from other Reclamation paleoflood studies in the western U.S. shows a similar relationship to calculated PMF estimates (Table 2). It is clear that in a variety of hydrometeorological settings, the paleoflood record does not validate floods as extreme as the PMF nor does the paleoflood data validate estimates of PMF return period in the range of 10,000 to 1,000,000 years. Rather, the paleoflood data imply a potential upper limit for flood magnitude that is substantially smaller than implied by PMF calculations. The data in Table 2 indicate that in the western United States, peak discharges with an extrapolated return period of 10,000 years may be as little as five to 25 percent of the calculated PMF. These results have substantial impact when incorporated into dam safety decisions or criteria based on risk.

Table 2: Calculated Probable Maximum Flood Versus 10,000 Year Flood Estimated From Paleoflood Studies

Location	Drainage Basin Area (km ²)	Estimated 10,000 Year Paleoflood, 97.5 Percentile, Discharge (m ³ /s)	Probable Maximum Flood Peak Discharge (m ³ /s)	10,000 Year Paleoflood as Percentage of PMF
South Fork Ogden River, UT	210	150	3075	5
Santa Ynez River, CA	1080	2550	13,060	26
Ochoco Creek, OR	764	285	4785	6
Crooked River, OR	6825	1100	7225	15
North Platte River, WY	18,746	1275	10,600	12

Conclusion

The most reliable way to obtain probability estimates of extreme floods, floods with return periods of thousands of years, is to study the geomorphologic and stratigraphic record of extreme floods. Paleoflood hydrology is an event-based method for extending the length of the flood record in order to make realistic estimates of the probability of extreme floods. An expeditious way to gain paleoflood information is through the use of paleohydrologic bounds. For guiding hydrologic dam safety decisions, comparable levels of confidence cannot be obtained from analysis of short-term records of annual peak discharge estimates and historic information alone. Compared to conventional frequency analyses, incorporation of paleoflood data provides high assurance that the spillway capacity of Causey and Bradbury Dams will not be exceeded even at

long return periods. For many streams in the western U.S., paleoflood information does not validate PMF discharges derived from rainfall-runoff modeling, nor does it validate the range of PMF frequency commonly used in hydrologic risk decisions.

REFERENCES

- Baker, V.R., 1989, Magnitude and Frequency of Palaeofloods. In *Floods: Hydrological, Sedimentological, and Geomorphological Implications*, edited by K. Beven and P. Carling, New York: John Wiley and Sons, 171-183.
- Baker, V.R., and Costa, J.E., 1987, Flood Power. In *Catastrophic Flooding*, edited by L. Mayer and D. Nash, Boston: Allen and Unwin, 1-21.
- Baker, V.R., Kochel, R.C., and Patton, P.C., editors (1988). *Flood Geomorphology*. New York: John Wiley and Sons.
- Birkeland, P.W., 1984. *Soils and Geomorphology*. New York: Oxford University Press.
- Costa, J.E., 1978, Holocene Stratigraphy in Flood Frequency Analysis. *Water Resources Research* 14, 626-632.
- Costa, J.E., 1986. A History of Paleoflood Hydrology in the United States. *Eos (Transactions of the American Geophysical Union)* 67, (17), 425, 428-430.
- Jahns, R.E., 1947, Geologic Features of the Connecticut Valley, Massachusetts, as Related to Recent Floods. U.S. Geological Survey Water-Supply Paper 996.
- Jarrett, R.D., 1991, Paleohydrology and its Value in Analyzing Floods and Droughts. In U.S. Geological Survey Water-Supply Paper 2375, 105-116.
- Kochel, R.C., and Baker, V.R., 1988. Paleoflood Analysis Using Slackwater Deposits. In *Flood Geomorphology*, edited by V.R. Baker, R.C. Kochel, P.C. Patton, New York: John Wiley and Sons, 357-376.
- Mansfield, G.R., 1938. Flood Deposits of the Ohio River, January-February, 1937, a Study of Sedimentation. U.S. Geological Survey Water Supply Paper 838, 693-736.
- NRC (National Research Council), 1985. *Safety of Dams, Flood and Earthquake Criteria*. Washington, D.C.: National Academy Press.
- O'Connell, D.O., Levish, D., and Ostenaar, D., 1997, Bayesian Flood Frequency Analysis with Paleohydrologic Bounds for Late Holocene Paleofloods, Santa Ynez River, California. In *Twenty Years Later: What Have We Learned Since the Big Thompson Flood*, edited by E. Grunfest, Natural Hazards Research and Applications Information Center Special Publication, No. 33, University of Colorado, Boulder, Colorado, 183-196.
- Ostenaar, D.A., Levish, D.R., and O'Connell, D.R.H., 1996, Paleoflood Study for Bradbury Dam, Cachuma Project, California. Seismotectonic Report 96-3, Denver, CO: U.S. Bureau of Reclamation, Seismotectonic and Geophysics Group.
- Ostenaar, D.A., Levish, D.R., O'Connell, D.R.H., and Cohen, E.A., 1997, Paleoflood Study for Causey and Pineview Dams, Weber Basin and Ogden River Projects, Utah. Seismotectonic Report 96-6, Denver, CO: U.S. Bureau of Reclamation, Seismotectonic and Geophysics Group.
- Patton, P.C., 1987, Measuring Rivers of the Past: A History of Fluvial Paleohydrology. In *The History of Hydrology*, edited by E.R. Landa, E.R., and S. Ince, *History of Geophysics* 3, Washington, D.C.: American Geophysical Union, 55-67.
- Patton, P.C., Baker, V.R., and Kochel, R.C., 1979, Slack Water Deposits: A Geomorphic Technique for the Interpretation of Fluvial Paleohydrology. In *Adjustments of the Fluvial System*, edited by D.D. Rhodes, and G.P. Williams, Dubuque, Iowa: Kendall-Hunt, 225-253.
- Stedinger, J.R., and Cohn, T.A., 1986, Flood Frequency Analysis with Historical and Paleoflood Information. *Water Resources Research* 22, 785-793.
- Stedinger, J.R., Saurani, R., and Therival, R., 1988. *The MAX Users Guide*. Ithaca, New York: Department of Environmental Engineering, Cornell University.
- Tarantola, A., 1987, *Inverse Problems Theory: Methods for Data Fitting and Model Parameter Estimation*. New York: Elsevier.

Dan Levish, D-8330, Bureau of Reclamation, P.O. Box 25007, Denver, CO 80225 - E-mail - palcoflood@seismo.usbr.gov

RISK-BASED HYDROLOGY: BAYESIAN FLOOD-FREQUENCY ANALYSES USING PALEOFLOOD INFORMATION AND DATA UNCERTAINTIES

By D. R. H. O'Connell, Geophysicist, D. R. Levis, Geologist, D. A. Ostenaar, Geologist, U. S. Bureau of Reclamation, Denver, Colorado

Abstract: It is essential, and not particularly difficult, to rigorously incorporate observed data uncertainties in flood-frequency analyses. "Best fitting" (median, method of moments, maximum likelihood, etc.) flood-frequency distributions, particularly from analyses that do not explicitly include data uncertainties, have infinitesimal total probability and are irrelevant for risk-based hydrology. In contrast, a Bayesian approach incorporates data and parameter uncertainties. Peak discharge probability regions are calculated as a function of annual probability to quantify hydrologic hazards. Paleohydrologic bounds demonstrate that peak discharges of about 70,000 ft³/s and 90,000 ft³/s had not been exceeded on the Santa Ynez River in 700 years and 2900 years, respectively. These paleohydrologic bounds are combined with gage and historical data to estimate flood-frequency probabilities. If only gage and/or historical data are available, an inescapable conclusion is that a flow exceeding spillway capacity (160,000 ft³/s) is likely to occur in a 10,000 year period. Adding the paleohydrologic bounds to the Bayesian analysis shows that the probability of a flow exceeding spillway capacity in a 10,000 year period is less than 1 in 50,000 demonstrating the substantial statistical gain the paleohydrologic bounds provide. Paleohydrologic bounds reduce biases by putting large historic discharges in their proper long-term contexts and substantially reduce the range of possible discharges associated with long return periods. A Bayesian flood-frequency analysis for the Crooked River using paleohydrologic bounds shows that traditional flood-frequency analysis using systematic data substantially underestimates peak discharges with return periods longer than several hundred years. It is now painfully obvious that entirely too much effort has been expended over the years in pointless and nonproductive pursuits of flood-frequency fitting procedures instead of acquiring valuable new data and physical understanding. Bayesian flood-frequency analyses incorporating paleohydrologic information demonstrate that the most cost effective way to reduce flood-frequency uncertainties for rare events is to acquire paleohydrologic data. Bayesian flood-frequency analyses with paleohydrologic data spanning thousands of years provides a consistent basis for risk-based decision making. A program for Bayesian flood-frequency analysis, FLDFRQ3, is made freely available at <ftp://ftp.seismo.usbr.gov/pub/outgoing/geomagic/src/fldfreq3>.

INTRODUCTION

One use of flood-frequency analyses is to determine the annual risk (probability) of a peak discharge exceeding the operational capacity of critical structures. Traditional approaches (weighted-moments, L-moments, expected moments) cannot incorporate observational data uncertainties (Hosking and Wallis, 1997) and fail to provide sufficient information to quantify risk. A Bayesian methodology (Tarantola, 1987) and likelihood functions modified from Stedinger and Cohn (1986) are used to incorporate data and parameter uncertainties. Parameter and flood frequency likelihoods and probability intervals are calculated directly by numerical integration to provide flood-frequency probabilities suitable for risk assessment. Systematic parameter-space searches provide the most powerful method to determine flood frequency probabilities. This is feasible using a PC computer, a systematic search of a parameter space of four or less can be completed without resorting to Monte Carlo methods of statistical sampling and integration. A public domain flood-frequency program incorporating these concepts, FLDFRQ3, is freely available in source code and executable forms. Two data sets from the Santa Ynez River in southern California (Ostenaar et al., 1996) and the Crooked River in central Oregon (Levis and Ostenaar, 1996) are used to illustrate important aspects of Bayesian flood-frequency analysis.

Mathematistry Versus Information: Traditional flood-frequency approaches (weighted-moments, L-moments, expected moments) can not naturally incorporate paleohydrologic nonexceedence bound information. Instead of recognizing the failure of the mathematics to effectively use paleohydrologic data, the common spurious conclusion is that paleohydrologic information is not useful. For instance, Hosking and Wallis (1997) suggest that historic and paleohydrologic data may have little value in flood frequency analyses because of some unspecified aspect of associated data uncertainties. However, Stedinger and Cohn (1986) developed likelihood functions to fully exploit paleohydrologic information in a maximum likelihood (MLH) approach for flood frequency estimation. Their derivation is extended here to fully incorporate data uncertainties in a likelihood approach. The Bayesian approach

presented here using likelihoods, which Hosking and Wallis (1997) acknowledge is the appropriate approach to incorporate data uncertainties, shows that their conjecture is false: The most cost effective way to reduce flood-frequency uncertainties for rare events is to acquire paleohydrologic data. Bayesian flood-frequency analyses with paleohydrologic data spanning thousands of years provides direct flood-frequency information suitable for hazard assessments (Levish et al., 1997)

BAYESIAN FLOOD FREQUENCY

Life is So Uncertain: Incorporating Data Uncertainties in Bayesian Flood-Frequency Analysis: The Bayesian approach used here explicitly acknowledges that parameters and data are never perfectly known. Both parameter and data uncertainties are incorporated into probability interval estimates of flood frequency. This approach quantifies how well the data constrain model parameters. The Bayesian paradigm is a special case of the more general information theory of Shannon (1948), Tarantola and Valette (1982), and Tarantola (1987). These approaches quantitatively rank how well particular models fit data sets. The Bayesian approach uses a "global" parameter integration grid, as outlined below, in a systematic quantitative framework to identify what ranges of frequency functions are consistent with the data at various probabilities. By selecting broad probability intervals, conservative evaluations of flood risk are obtained.

Two types of data are used to estimate flood frequency: 1) estimated annual peak discharges from gaging records, and 2) paleohydrologic bounds from geologic data. Paleohydrologic nonexceedence bounds define time intervals when a stage, and therefore a corresponding discharge, was not exceeded sufficiently to modify a terrace or abandoned flood plain surface (e.g., Levish et al., 1997). Uncertainties in dating these surfaces with radiocarbon methods suggest these time intervals actually fall within a range of values (Talma and Vogel, 1993).

Discharge and dating information are separated according to uncertainty characteristics into two groups:

Group 1. Normal uncertainties: Annual peak discharge estimates whose magnitudes and uncertainties can be accurately estimated and characterized by a Gaussian frequency distribution. The assigned probabilities for the true discharges about the observed values are discretized over a 3σ range (Figure 1a).

Group 2. Value in a range with potentially variable likelihood within the range: Discharges for paleohydrologic bounds and time intervals of paleohydrologic bounds. Values are determined to be within a range described by an upper and lower bound, and optionally, a proportionally higher likelihood prescribed for a point within the interval. An example for a paleohydrologic bound is shown in Figure 1b and a paleohydrologic bound time interval example is shown in Figure 1c. The skew of the maximum likelihood position toward larger flows in Figure 1b reflects information available about the maximum stage, such as maximum elevation of water levels from the geologic record. The shape reflects some of the uncertainties of converting surveyed stream profiles into discharges for various stage elevations.

These data parameterizations provide the ability to use the best information available about the distribution of discharges and to use appropriate weightings of various data components in frequency distribution fitting procedures. Both parameter and data uncertainties are incorporated into probability interval estimates of flood frequency to provide realistic estimates of statistical confidence.

The Bayesian approach outlined in Tarantola (1987) is used here. Let \mathbf{d} represent data and \mathbf{m} represent model parameters. Let the data consist of two general types, peak discharge data (including bound information), x , and associated ages, t , $\mathbf{d}=[x,t]$, with properties as defined in previous section. Let $\Theta(\mathbf{d}|\mathbf{m})$ represent the conditional probability (likelihood function) describing the theoretical relationship between \mathbf{d} and \mathbf{m} . In flood-frequency analyses, $\Theta(\mathbf{d}|\mathbf{m})$ represents arbitrarily selected frequency distributions that often define a limiting extreme value. FLDFRQ3 provides seven frequency functions to choose from; Generalized Extreme Value (GEV), Generalized logistic, Generalized Normal, Generalized Pareto, Pearson Type III, and Loge and Log10 Pearson Type III. See Hosking (1996) and Hosking and Wallis (1997) for details concerning specific frequency functions.

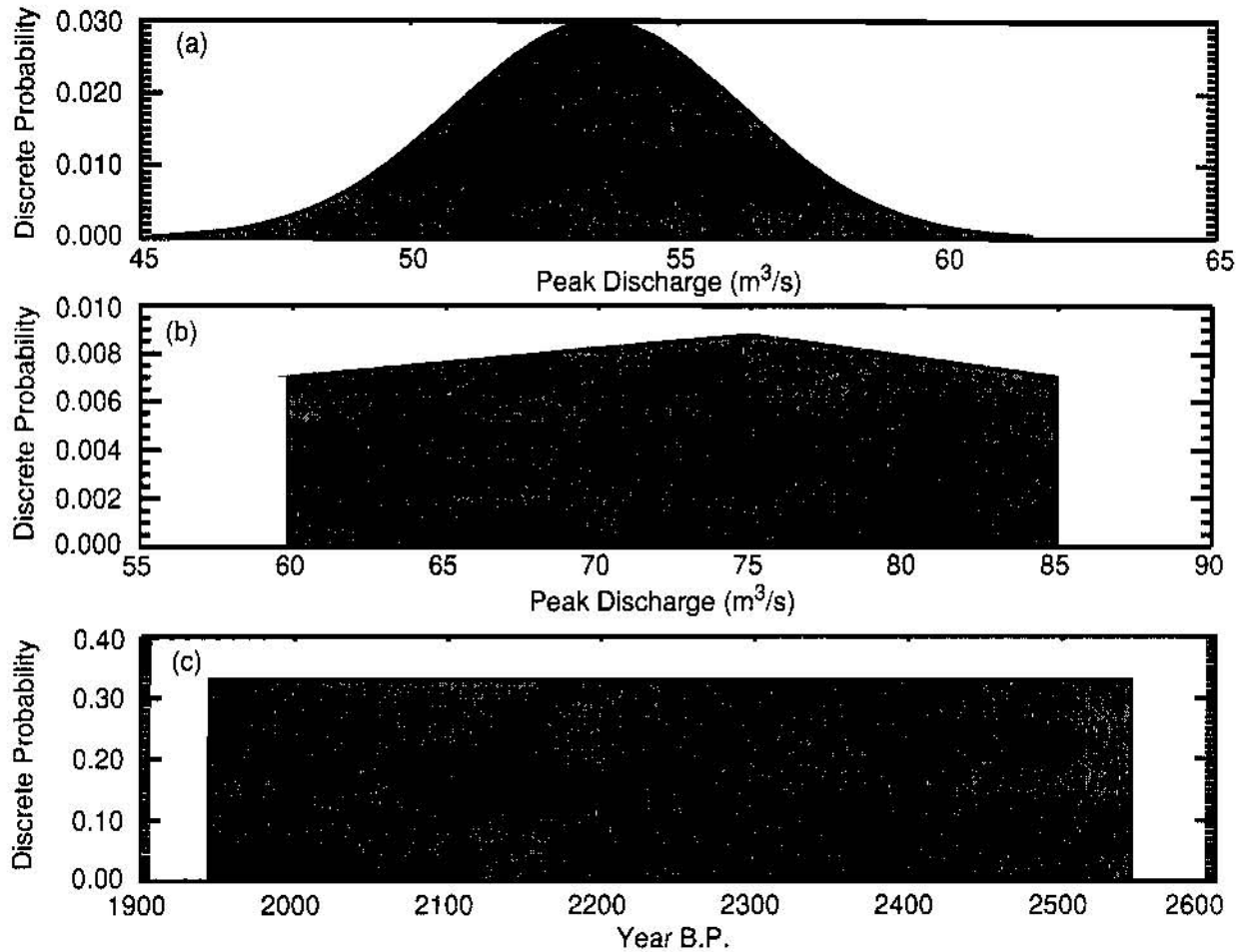


Figure 1. Examples of age and discharge uncertainty distributions. A group 1 annual peak discharge probability distribution is shown in (a) for a reported peak discharge of $53.5 \text{ m}^3/\text{s}$. A group 2 paleohydrologic peak discharge bound is shown in (b). A group 2 geologic age probability distribution is shown in (c).

Let $v(\mathbf{d}_{\text{obs}}|\mathbf{d})$ be the probability density for the output of a measuring system to be \mathbf{d}_{obs} when the input is \mathbf{d} . Then, the conditional probability density, $f_{D|M}(\mathbf{d}_{\text{obs}}|\mathbf{m})$, interpreted as the probability density for the observed data value to be \mathbf{d}_{obs} when the true model value is \mathbf{m} , is given by

$$f_{D|M}(\mathbf{d}_{\text{obs}}|\mathbf{m}) = \int_D d v(\mathbf{d}_{\text{obs}}|\mathbf{d}) \Theta(\mathbf{d}|\mathbf{m}) \quad (1)$$

The conditional *posterior* probability density for the model is (using EQ 1)

$$f_{M|D}(\mathbf{m}|\mathbf{d}_{\text{obs}}) = \frac{f_M(\mathbf{m})f_{D|M}(\mathbf{d}_{\text{obs}}|\mathbf{m})}{\int_M d\mathbf{m} f_M(\mathbf{m})f_{D|M}(\mathbf{d}_{\text{obs}}|\mathbf{m})} \quad (2)$$

where $f_M(\mathbf{m})$ are the prior probabilities for the model parameters. All statistical descriptions of the “solution” of the fitting function can be derived from (2), including MLH estimates, median, mean, and probability intervals. By optimizing parameter grid integration over the non-zero likelihood portion of the parameter model space using Nelder-Mead optimization, a “final”, numerically practical, $f_M(\mathbf{m})$ is defined to focus on nonzero likelihood regions of the model space.

What is of interest is the distribution function for a future observation x , $\hat{f}(x)$, given the *posterior* probability density for the model (2). Consider a quantity $y(\mathbf{m})$ which is a function of the model parameters \mathbf{m} , such as a peak discharge quantile X_T , or the probability that a peak discharge occurs that exceeds spillway capacity, $P_{>SW}$. To describe the uncertainty in such a quantity $y(\mathbf{m})$ due to uncertainty in the values of \mathbf{m} , one can compute (Stedinger, 1983):

$$P[y(\mathbf{m}) \leq y_0 | \mathbf{d}_{obs}] = \int_{\Omega} f_{M|D}(\mathbf{m} | \mathbf{d}_{obs}) d\mathbf{m} \quad (3)$$

where

$$\Omega = \{\mathbf{m} | y(\mathbf{m}) \leq y_0\} \quad (4)$$

Flood frequency statistics, such as annual probabilities for particular flows, are provided by (3 and 4).

Stedinger and Cohn (1986) and Stedinger et al. (1988) developed likelihood expressions for combining several data types which can be used to define $f_{D|M}(\mathbf{d}_{obs} | \mathbf{m})$. The likelihood and conditional probability expressions used here are similar, but are modified to incorporate the statistical data properties outlined above. For brevity, the log-likelihood (conditional probability) functions are discussed. Expressions for the corresponding likelihood functions can be obtained by applying the exponential function to these log-likelihood function expressions. For s systematic observations from group 1 data the log-likelihood function is:

$$\ln(f_{D|M}(\mathbf{d}_S | \mathbf{m})) = \sum_{i=1}^s \ln \left(\sum_j^S f_{ij}^S \Theta(x_{ij} | \mathbf{m}) \right) \quad (5)$$

where f_{ij}^S are discrete Gaussian probabilities for the annual peak discharge data. All j sums are over discrete data probabilities. For v observations of historic and/or paleoflood peak discharges the log-likelihood function is:

$$\ln(f_{D|M}(\mathbf{d}_R | \mathbf{m})) = \sum_{i=1}^v \ln \left(\sum_j^R f_{ij}^R \Theta(x_{ij} | \mathbf{m}) \right) \quad (6)$$

where f_{ij}^R are the discrete probabilities for group 2 historic and/or paleoflood peak discharges. For u time intervals of paleohydrologic bound observations, the log-likelihood function is:

$$\ln(f_{D|M}(\mathbf{d}_U | \mathbf{m})) = \sum_{i=1}^u \left(\sum_j^{Un} f_{ij}^{Un} n_{ij} \right) \ln \left[\sum_k^{Ud} f_{ik}^{Ud} \int_{x_{min}}^{U_{ik}} \Theta(x | \mathbf{m}) dx \right] \quad (7)$$

where f_{ik}^{Ud} are the discrete probabilities for group 2 paleohydrologic peak discharge bounds, U_{ik} are the ranges of upper x limits, n_{ij} are the ranges of time intervals, and f_{ik}^{Un} are the discrete probabilities for group 2 dating data. The log-likelihood function for v peak discharges with only a lower bound is:

$$\ln(f_{D|M}(\mathbf{d}_T | \mathbf{m})) = \sum_{i=1}^v n_i \ln \left[1 - \sum_k^{Td} f_{ik}^{Td} \int_{x_{min}}^{T_{ik}} \Theta(x | \mathbf{m}) dx \right] \quad (8)$$

where f_{ik}^{Td} are the discrete probabilities for group 2 paleohydrologic bounds, and T_{ik} are the ranges of maximum lower x limits for n_i events.

The log-likelihoods for the entire discharge record are the sum of each data type's log-likelihood function (from 6, 7, and 8)

$$\ln(f_{D|M}(d_{obs}|m)) = \ln(f_{D|M}(d_S|m)) + \ln(f_{D|M}(d_U|m)) + \ln(f_{D|M}(d_R|m)) + \ln(f_{D|M}(d_T|m)) \quad (9)$$

which is used in (1, 2, 3, and 4) to derive model parameter and flood frequency conditional probabilities.

DATA

Santa Ynez River: Bayesian frequency analyses are performed using three data sets (Ostenaar et al., 1996). The first data set, paleohydrologic, includes all annual peak discharge, historical, and paleohydrologic data representing about 2920 years of observation. The paleohydrologic data include two bounds, t1 and fp2, that provide discharge limits of 90,000 and 70,000 ft^3/s , that have not been exceeded in 2920 and 700 years, respectively (Figure 2). Historical data from the Lompoc area provide a limit on peak discharge since 1862 relative to the size of the large flood in 1907. The 57 year peak discharge record includes an exceptional flood in 1969 (peak of record). A second data set, historical, is derived by deleting the paleohydrologic data from the complete data set to provide 132 years of annual peak discharge and historical data. The third data set consists of the most recent 57 years of annual peak discharge estimates from the gage just downstream from the Bradbury Dam site (1935-1952), and the adjusted sum of the gages upstream of Lake Cachuma (1953-1993). Complete Bayesian frequency analyses are performed for each data set to evaluate the incremental value of acquiring historical and paleohydrologic data.

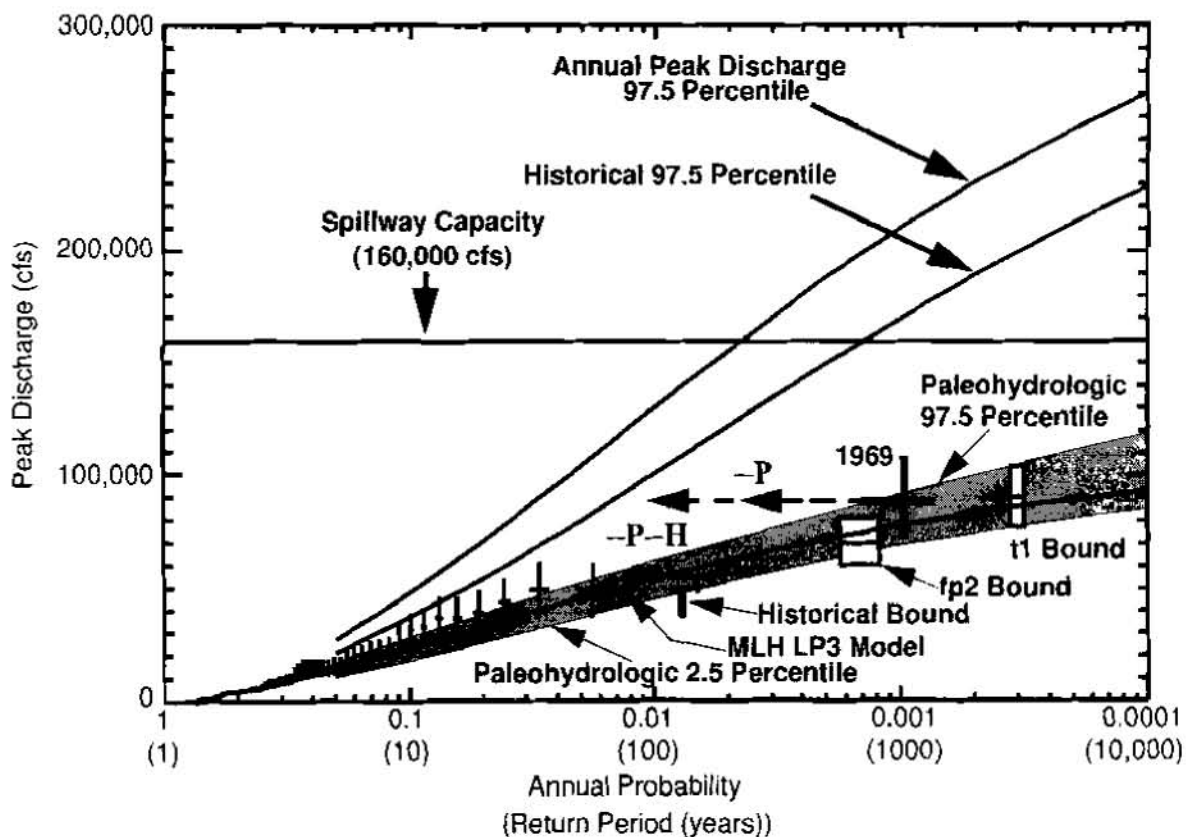


Figure 2. Flood frequency for the Santa Ynez River at Bradbury Dam. Annual peak discharges are shown with horizontal lines for plotting position ranges and vertical lines for 2σ measurement uncertainties. Paleohydrologic bounds are boxes denoting geologic age and discharge uncertainties. The 0.95 flood-frequency probability region using all data is shown in grey. The 1969 peak discharge is shown using thick lines and the dashed line arrows show the change in its plotting position when paleohydrologic (arrow with a $-P$ above it) and historical (arrow with a $-P-H$ below it) information are ignored.

Crooked River: Bayesian frequency analyses are performed using two data sets. Both data sets consist of the most recent 55 years of annual peak discharge estimates, an historical nonexceedence bound, and three paleohydrologic bounds shown on Figure 3 (Levish and Ostenaar, 1996). The four paleohydrologic bounds consist of a bound that has been exceeded numerous times, as indicated by field evidence, and three nonexceedence bounds (Figure 3.)

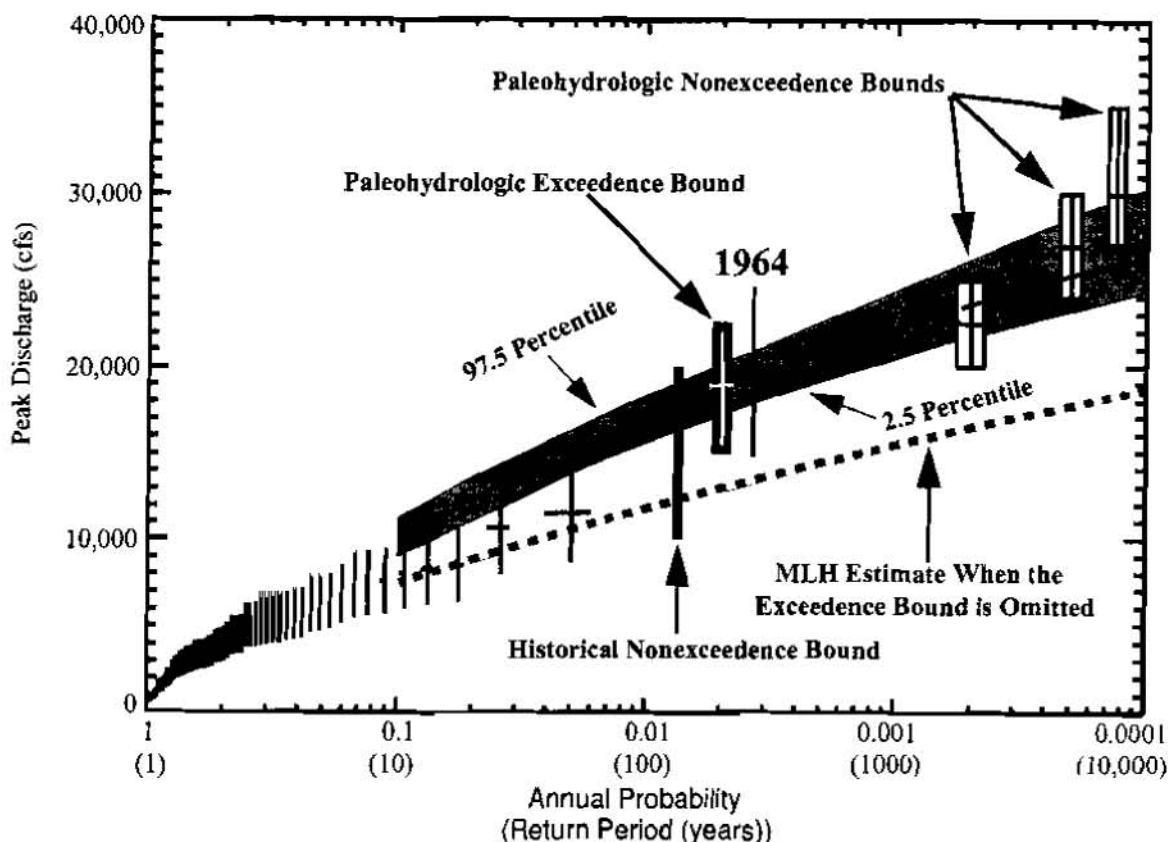


Figure 3. Flood frequency for the Crooked River at A. R. Bowman Dam. Annual peak discharges are shown with horizontal lines for plotting position ranges and vertical lines for 2σ measurement uncertainties. Paleohydrologic bounds are boxes denoting geologic age and discharge uncertainties. The 0.95 flood-frequency probability region using all data is shown in grey and this MLH estimate is shown as the long dashed line. The short dashed line shows the MLH estimate when the paleohydrologic exceedence bound is ignored.

RESULTS

Santa Ynez River: The paleohydrologic MLH flood frequency estimates and 0.95 probability region limits (lower 2.5 percentile to upper 97.5 percentile) are plotted in Figure 2 along with the upper 97.5 percentile limits from the historical and annual peak discharge data set calculations. The upper 97.5 percentile limits for the historic and annual peak discharge data demonstrate the weak constraints on long return period discharges afforded by such short time samples of peak discharge. In contrast, the paleohydrologic bounds constraints produce a much more contracted upper 97.5 percentile. Note, that neither the weighted-moment method of Bulletin 17B nor the MLH error estimation method of Stedinger et al.'s (1988) MAX program would provide these asymmetric (but more realistic) probability limits. These probability limits are more realistic because they incorporate the global information about the model's nonlinear probability distribution instead of local linearized estimates of model covariance at the MLH model position.

The substantial difference in the predictions of flood frequency by the three data sets can be understood in terms of each data set's plotting position for the peak discharge of record that occurred in 1969. With paleohydrologic data, the plotting position of the 1969 discharge is 1390 years (Figure 2); 191 years for the historical data, and 118 years for the

annual peak discharge data. Moving the plotting position of the 1969 discharge to the range of 100-200 years in Figure 2 explains the much wider upper probability limits of the annual peak discharge and historical data sets relative to the paleohydrologic data. A much steeper slope is required to fit the discharges if the 1969 discharge plotting position is less than 200 years. The difference between the paleohydrologic data predictions of flood frequency and the predictions of the historical and annual peak discharge data can be explained by the inability of annual peak discharge and historical data to place the largest 1969 discharge in its proper context (plotting position). The paleohydrologic bounds revealed that the 1969 flood was a rare event, larger than any flood in the past 700 years.

Crooked River: As shown in Figure 3, ignoring the paleohydrologic exceedence bound produces substantially lower MLH peak discharge estimates at long return periods. This illustrates a common pitfall of flood-frequency analysis (curve fitting). If too much irrelevant data are retained (small peak discharges), the three-parameter frequency function devotes too much importance to fitting irrelevant small peak discharges and almost completely ignores the most important data, the rare, but large peak discharges. The additional paleohydrologic information forces the frequency function to fit the rare, large flows more faithfully.

CONCLUSIONS

Something Versus Nothing: Stochastic Fabrication of Frequency: Stochastic hydrology was invented to “solve” a fundamental problem: how to plot something observed (actually inferred annual peak discharge from observed stage measurements) against something unknown (frequency). Traditional flood frequency analyses are basically obtuse (to transparent) attempts to provide fabricated frequencies (intrinsically unverifiable models) or plotting positions to be able to plot peak discharge versus frequency. Paleoflood hydrology provides both peak discharge (exceedence and nonexceedence bounds) and frequency (duration of nonexceedence) directly, eliminating the need to concoct frequencies with arbitrary and unverifiable models. Thus, the output of any flood-frequency analysis using paleohydrologic data (including Bayesian analyses) are inferior reproductions of the observed data because flood-frequency analyses were designed not so much to faithfully honor observed data, but to concoct missing information (frequency). At best, flood-frequency analysis with arbitrary frequency functions is just obtuse curve fitting; it can’t produce more information than is actually contained in the observed data. At worst, many times flood-frequency fitting procedures ignore important information because it doesn’t fit an arbitrary construction of mathematics or produces flood-frequency estimates from short duration systematic data with extreme (but unrecognized) biases.

The Bayesian flood-frequency analyses for the Santa Ynez and Crooked Rivers proves that paleohydrologic data provide the maximum statistical benefit for quantifying rare peak discharge probabilities. Paleohydrologic nonexceedence bounds provide direct flood-frequency information and reduce bias by placing rare observed systematic floods in their proper long-term frequency context. Hosking and Wallis’s (1997) conjecture that historical and/or paleoflood data do not provide significant flood-frequency information is false. It’s time to jettison the antiquated mathematics that is inconsistent with the data: The data are always right.

Stochastic hydrology is a mirage in a sterile desert of intellectual pursuits. The approach developed here is an evaporating watering hole, not an oasis. The path out of the desert is physical understanding of three-dimensional fluid flow being provided by Walters (this volume) and Denlinger et al. (this volume) coupled with frequency information (duration) provided by paleoflood hydrology. The Bayesian flood-frequency program, FLDFRQ3, is freely available from <ftp://ftp.seismo.usbr.gov/pub/outgoing/geomagic/src/fldfreq3>. However, plots of observed data including paleohydrologic nonexceedence bounds, such as shown in Figures 2 and 3 provide more meaningful information than any flood-frequency program, including FLDFRQ3, could ever provide about the statistics of rare floods.

Paleoflood hydrology provides information (frequencies of peak discharge nonexceedences) that is analogous to the output from a probabilistic seismic hazard analysis (PSHA) (frequencies of peak horizontal acceleration (PHA) nonexceedences). However, unlike PSHA analyses that require using several empirical functions to obtain PHA nonexceedence frequency estimates, paleoflood hydrology provides direct observational constraints on the frequencies of peak discharge nonexceedences for rare events. Thus, it is particularly ironic that paleohydrologic information has often been erroneously dismissed as irrelevant or unusable for quantifying the frequencies of rare, extreme floods. The Bayesian flood-frequency analyses incorporating paleohydrologic bound information

demonstrate that the most cost effective way to reduce flood-frequency uncertainties for rare events is to acquire paleohydrologic data. Bayesian flood-frequency analyses with paleohydrologic data spanning thousands of years provides a consistent basis for risk-based decision making.

REFERENCES

- Denlinger, R.P., Walters, R.A., Levish, D.R., and Ostenaar, D.A. (this volume), Robust methods for flood routing over highly irregular terrain.
- Hirsch, R.M., and Stedinger, J.R., 1987, Plotting positions for historical floods and their precision. *Water Resources Research*, 23, 715-727.
- Hosking, J.R.M., 1996, Fortran routines for use with the method of L-moments, Version 3, Research Report RC 20525 (90933), IBM Research Division, Yorktown Heights, New York, 157 p.
- Hosking, J.R.M., and Wallis, J.R., 1997, Regional frequency analysis: an approach based on L-moments. Cambridge, England: Cambridge University Press.
- Levish, D.R., and Ostenaar, D.A., 1996, Applied paleoflood hydrology in north-central Oregon. Guidebook for Field Trip 2, Geological Society of America Cordilleran Section, 92nd Annual Meeting, Portland Oregon, U. S. Bureau of Reclamation Seismotectonic Report 96-7, 182 p.
- Levish, D.R., Ostenaar, D.A., and O'Connell, D.R.H., 1997, Paleoflood hydrology and dam safety. WATERPOWER '97 Proceedings of the International Conference on Hydropower, August 5-8, 1997, D.J. Mahoney, ed., American Society of Civil Engineers, New York, 2205-2214.
- Ostenaar, D.A., Levish, D.R., and O'Connell, D.R.H., 1996, Paleoflood study for Bradbury Dam, Cachuma Project, California {unpub}. U.S. Bureau of Reclamation Seismotectonic Report 96-3, Denver, CO, 86 p., 1 folded plate, 4 appendices.
- Shannon, C.E., 1948, A mathematical theory of communication. *Bell System Tech. Journal*, 27, 379-423.
- Stedinger, J.R., 1983, Design events with a specified flood risk: *Water Resources Research*, 19, 511-522.
- Stedinger, J.R., and Cohn, T.A., 1986, Flood frequency analysis with historical and paleoflood information: *Water Resources Research*, 22, 785-793.
- Stedinger, J.R., Surani, R., and Therival, R., 1988, The MAX users guide {unpub}. Department of Environmental Engineering, Cornell University, Ithaca, New York, 51 p.
- Talma, A.S., and Vogel, J.C., 1993, A simplified approach to calibrating ^{14}C dates. *Radiocarbon*, 35, 317-322.
- Tarantola, A., 1987, Inverse problems theory: Methods for data fitting and model parameter estimation. Elsevier, New York, 613 p.
- Tarantola, A., and Valette, B., 1982, Inverse problems = quest for information. *Journal of Geophysical Research*, 50, 159-170.
- Walters, R.A., (this volume), A finite element model with moving boundaries: Application to floods and runoff.

D. R. H. O'Connell, D. R. Levish, and D. A. Ostenaar
U. S. Bureau of Reclamation
P.O Box 25007 D-8330
Denver, Colorado 80225-0007
geomagic@seisino.usbr.gov (DRHO)
dlevish@do.usbr.gov (DRL)
dostenaar@do.usbr.gov (DAO)

PALEOHYDROLOGY: LONG-TERM BOUNDS ON UNWARRANTED EXTRAPOLATION IN MODELING

By Dean A. Ostenaar and Daniel R. Levish

Geophysics, Paleohydrology, and Seismotectonics Group, U.S. Bureau of Reclamation

INTRODUCTION

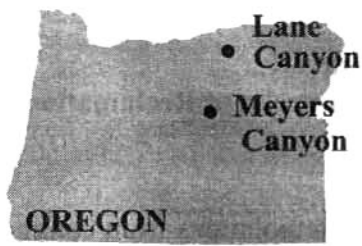
Perceptions of hydrologic risk are controlled by interpretations and extrapolations from common events to events well beyond the range of common experience. If measures of those common events are distorted or inaccurate, then so will be expectations of what constitutes a prudent level of conservatism. A common measure of hydrologic risk is peak discharge, a measure for which traditional estimates from early historic floods and floods in ungaged basins may be subject to considerable uncertainty. In many areas, the largest peak discharge estimates on record are from early historic floods or from indirect measurements of extreme floods in ungaged basins. Excessive conservatism in the characterization of these floods can lead to unwarranted perceptions of flood risk.

Paleohydrologic information can provide a long-term perspective on extreme events that is valuable to water resource modeling in two ways. First, in stable channel reaches, stage-discharge relationships for historic events and paleoflood events can be compared and evaluated. Discharge estimates for the historic events and paleoflood events can thus be directly compared to recent events that may be better constrained. Second, with paleohydrologic information extreme historic events can be placed in a long-term frequency context that cannot be developed from only the short period of historical observations. The paleohydrologic record is a direct indication of the magnitude and frequency of the most extreme floods over thousands of years.

Paleohydrologic studies can provide a compelling basis for reevaluation of published peak discharge estimates of extreme events. The previously reported discharge estimates for some of the most extreme floods in the western United States are substantial overestimates of the actual peak discharge for these floods. While these floods were significant, overstating the peak discharge from these events increased the perception of the flood risk in these regions. Paleohydrology provides a long term framework for assessing the frequency of the extreme events, regardless of the preferred value of peak discharge. Including paleohydrologic information in hydrologic risk assessments can change perceptions of the causative flood mechanism by demonstrating that long-term limits on peak discharge might exist. In other cases, including actual long term information on flood frequency and characteristics of extreme storms in that region may lead to a factual basis for developing operations and planning scenarios.

The impact of these data on perceptions of peak discharge issues are briefly illustrated below with results of paleohydrologic investigations at the sites of two extreme floods in eastern Oregon and from the Santa Ynez River in southern California. The Santa Ynez River data provide an illustration both of potential errors in peak discharge estimates of large floods, and the impact of paleohydrologic information on flood frequency estimates.

EXTREME FLOODS IN EASTERN OREGON



Eastern Oregon is the site of several significant convective storms that have produced large floods in small drainages. Particularly noteworthy are the Meyers Canyon flood of July 1956 and the Lane Canyon flood of July 1965. The discharge estimates for these floods are widely cited as amongst the largest flash flood peaks ever observed in the United States (e.g., Costa, 1987). As such, these floods are controlling data points for models of extreme events. On regional envelope curves of peak discharge (Hubbard and Harris, 1983), the estimates for these floods control the position of the curve, well above data from other floods. Likewise, the discharge estimates from these floods have been cited as evidence that floods nearly as large as the Probable Maximum Flood (PMF) have occurred historically (Bullard, 1986). The obvious significance of these discharge estimates in a regional context dictates that careful scrutiny be given to the accuracy of the original estimates (Levish and Ostenaar, 1996).

Revision of the peak discharge estimate values ascribed to the floods at Lane and Meyers Canyons does not change the fact that these floods were exceptional events. Geomorphic and stratigraphic evidence at both locations confirms that these floods were perhaps the largest in hundreds to thousands of years. The importance of the revised discharge estimates is in the use of the values for validating and calibrating models of extreme floods elsewhere.

Lane Canyon

On the afternoon of July 26, 1965, there was a dramatic geomorphic event in Lane Canyon. Some thirty years later, the geomorphic and stratigraphic record of this event is still quite clear. As originally interpreted by the U.S. Geological Survey the flood stands as one of the most spectacular ever reported. The discharge estimate of $810 \text{ m}^3/\text{s}$ ($28,500 \text{ ft}^3/\text{s}$) for a drainage basin of 13 km^2 (5 mi^2) leads to an incredible unit runoff of $62 \text{ m}^3/\text{s}/\text{km}^2$ ($5650 \text{ ft}^3/\text{s}/\text{mi}^2$). In any regional flood frequency analysis it is clear that Lane Canyon is a controlling flood. Our initial goals in revisiting Lane Canyon were twofold: first, to understand the possible return period of this event because of its regional importance; and second, to understand the potential uncertainty associated with this extraordinary discharge estimate.

After a brief reconnaissance and a review of the available information from the original USGS indirect estimate of peak discharge it appeared that $810 \text{ m}^3/\text{s}$ ($28,500 \text{ ft}^3/\text{s}$) must be a substantial overestimate of the actual peak discharge. The deposits in Lane Canyon clearly demonstrate that there were numerous debris flows coming down the canyon on the afternoon of the reported flood. It is also obvious that in spite of the fact that the high water marks were accurately surveyed near the mouth of Lane Canyon, there was no source for the flood. This strongly suggests that what was documented in the original two-section slope area estimate was a transient phenomenon such as channel blockage or aggradation due to debris flows rather than a true clear-water flood.

To provide a quantitative and definitive means to test this discharge estimate two study reaches were selected in Lane Canyon (Levish and Ostenaar, 1996). The first reach is near the mouth of the canyon and includes the site of the original indirect discharge estimate. The second reach is in the upper portion of basin and includes more than one-half the total basin area. In the upper reach

there is no obvious evidence of the stream being dominated by debris flows. High-water marks from the July 1965 flood can be estimated from geomorphic and stratigraphic evidence preserved in both reaches. These estimates can be confirmed in the lower reach with the aid of photographs taken by the USGS team that made the original indirect discharge estimate. New discharge estimates for each reach are obtained using a step-backwater model (HEC-2, Hydrologic Engineering Center, 1990) (Levish and Ostenaar, 1996). Additional hydraulic modeling, using methods described by Denlinger et al, (this volume); and Walters (this volume) are presently underway. The surveyed reach near the mouth of Lane Canyon is over 400 m (1310 ft) long and step-backwater modeling indicates 300 m³/s (11,000 ft³/s) as a maximum discharge assuming it was a clear water flood. Any consideration of the bulking effect of debris would reduce this estimate. The upper Lane Canyon reach is about 260 m (1850 ft) long. Step-backwater results from the upper reach in Lane Canyon show that 100 m³/s (3500 ft³/s) probably represents an upper limit peak discharge for clear water. This result appears consistent with the estimates from the lower canyon reach considering the difference in basin area.

It may never be possible to accurately estimate the peak discharge of the flood of 1965 because it is obvious from deposits in the channel that debris flows probably played an important role in controlling the water surface elevation near the mouth of the canyon. Without actual, direct observation of the flood it is not possible to absolutely determine what role the debris flows played in creating the high water marks at the site of the original indirect measurement.

Reexamination of the 1965 Lane Canyon flood indicates that the original indirect discharge estimate of 810 m³/s (28,500 ft³/s) is a substantial overestimate of the actual peak discharge, perhaps by more than 60%. At a site draining more than half the basin upstream of the location of the original indirect estimate there is no evidence of a peak discharge exceeding about 100 m³/s (3500 ft³/s) and there is no geomorphic evidence to suggest that the entire flood estimated at the original site could have originated from the remaining 5 km² (2 mi²) of basin area. At the site of the original indirect measurement, step-backwater modeling of a much longer reach does not support a peak discharge estimate greater than 300 m³/s (11,000 ft³/s). Downstream of the measurement site, post-flood photographs document deposition of a large volume of debris onto the Umatilla River floodplain at the mouth of the canyon. However, there is a general lack of evidence for continuation of a large flow downstream in the Umatilla River.

The 1965 flood in Lane Canyon clearly is an extraordinary geomorphic event, possibly as large as any event in Lane Canyon over the past several thousand years. The 1965 flood overtopped geomorphic surfaces underlain by deposits of Mazama Ash more than 7000 years old. Geomorphic and stratigraphic evidence in the canyon clearly show that other large debris flow events have occurred since that time, but also clearly indicate that none have been substantially larger. These relationships indicate that whatever discharge estimate used for the 1965 Lane Canyon flood, discharges only slightly larger have not occurred in more than 7000 years.

Meyers Canyon

Just as with Lane Canyon in 1965, the peak discharge estimate for the Meyers Canyon flood of 1956 is truly remarkable. The peak discharge estimate of 1550 m³/s (54,500 ft³/s) for a drainage basin of 33 km² (12.7 mi²) results in a very large unit discharge of 47 m³/s/km² (4290 ft³/s/mi²). This estimate was based on a three section slope area measurement. The significance of the flood was recognized at that time, and the original calculations were extensively reviewed and debated.

As a result there are numerous photographs of the area taken shortly after the flood to aid reconstruction of the flow. Our approach and goal in revisiting Meyers Canyon were similar to Lane Canyon; that is, because of the obvious regional significance of such a large flood it is important to understand the context of the flood, and the frequency with which similar floods might have occurred in the past to understand the possible return period of this event because of its regional importance (Levish and Ostenaar, 1996).

What is most striking upon visiting Meyers Canyon is small size of the channel immediately downstream of the indirect measurement site and of Bridge Creek at the confluence with Meyers Canyon. A brief site visit makes it clear that it is physically impossible for a peak discharge of $1550 \text{ m}^3/\text{s}$ ($54,500 \text{ ft}^3/\text{s}$) to have passed through Meyers Canyon and downstream to Bridge Creek. However, it is not immediately clear from review of the indirect computations and measurements what specifically led the estimate of peak discharge. After reviewing the U.S. Geological Survey indirect discharge estimate, field notes and photographs (USGS, 1956), and memorandum from Francis Hart of the U.S. Bureau of Reclamation (USBR, 1956), a picture started to emerge of a series of events that led to spurious high water marks in lower Meyers Canyon (Levish and Ostenaar, 1996). The high water marks are accurately recorded by the original survey, however, after visiting the site and reviewing the evidence, it seems clear that these high water marks are not directly associated with flow in the main channel of Meyers Canyon. It appears that the most likely explanation for emplacement of the high water marks in the area of the original slope area reach is channel blockage and breakout upstream of the measurement site coupled with tributary inflows on the left bank. Literal interpretation of the high water marks at the original measurement site leads to a completely anomalous estimate of peak discharge compared to any estimate that can be obtained immediately upstream or downstream. Thus, the original discharge estimate is of little meaning when used for regional comparisons.

In order to provide a quantitative and definitive basis for estimating a maximum discharge of the 1956 flood, two reaches in Meyers Canyon were surveyed for step-backwater modeling (Figure 1)(Levish and Ostenaar, 1996). In addition, a cross section in bedrock near the head of the arroyo in Meyers Canyon was measured, as well as cross sections on Bridge Creek upstream and downstream of its junction with Meyers Canyon.

Our strategy for understanding these outstanding peak discharge estimates was to determine the size of the flow upstream of the reach; how much water could be conveyed through the reach that contains the original indirect discharge estimate cross sections; and finally to assess the flow after it left the canyon. The upstream study reach step-backwater modeling indicates that about $200 \text{ m}^3/\text{s}$ ($7000 \text{ ft}^3/\text{s}$) would be about the maximum discharge possible, from approximately one-half the drainage area (Levish and Ostenaar, 1996). At the bedrock cross-section at the head of the arroyo, at a discharge estimated by the USGS indirect measurement ($1550 \text{ m}^3/\text{s}$) the water would be near the threshold for cavitation. The geomorphic characteristics of the channel document that this did not occur.

At the downstream end of lower Meyers Canyon, immediately downstream of the USGS indirect site, a peak discharge of $500 \text{ m}^3/\text{s}$ ($17,600 \text{ ft}^3/\text{s}$) appears to be a maximum value, based on a step-backwater model (Levish and Ostenaar, 1996). The fact that a peak discharge on the order of $1550 \text{ m}^3/\text{s}$ ($54,500 \text{ ft}^3/\text{s}$) never left Meyers Canyon is corroborated by cross sections of Bridge Creek above and below Meyers Canyon (Levish and Ostenaar, 1996). High water marks from the largest

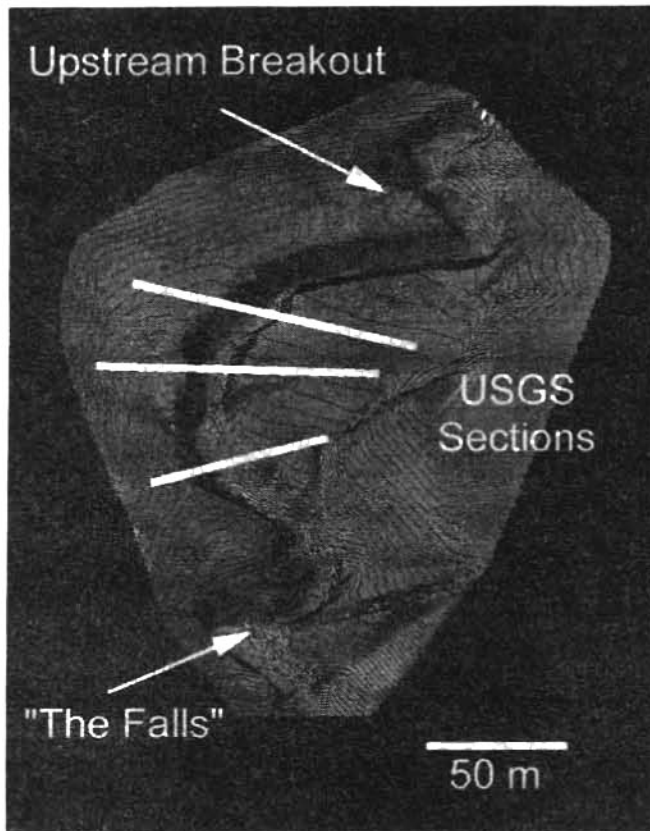


Figure 1 - Perspective view of the Meyers Canyon area. Contour interval is 1 m. The 1956 flood stayed within a similar-sized arroyo upstream of this reach, but broke out and flowed across the alluvial surface in the area of the USGS sections. All flow returned to the channel just downstream of the USGS sections. The entire flow was contained within the channel through the sharp bends in the area of "The Falls". The confluence of Meyers Canyon with Bridge Creek is about 200 m downstream.

floods on Bridge Creek upstream and downstream of Meyers Canyon indicate almost the same cross-sectional area. The fact that a flow on the order of $1550 \text{ m}^3/\text{s}$ ($54,500 \text{ ft}^3/\text{s}$) never exited Meyers Canyon is further supported by the morphology of Bridge Creek downstream of Meyers Canyon, where no evidence of such a large flood is present.

Just as with Lane Canyon, it may never be possible to accurately estimate a peak discharge for the flood of 1956 in Meyers Canyon. However, it is clear that a more realistic estimate of a maximum peak discharge is on the order of $500 \text{ m}^3/\text{s}$ ($17,600 \text{ ft}^3/\text{s}$) or roughly one third the original estimate. As with Lane Canyon, additional analysis with more robust hydraulic modeling methods is in progress.

PEAK DISCHARGE ESTIMATES FOR THE SANTA YNEZ RIVER, CALIFORNIA

As part of a paleohydrologic study of the Santa Ynez River for Bradbury Dam, the accuracy of several annual peak discharge estimates from the early part of the century at Lompoc became a significant issue (Ostenaa et al, 1996). Two of the three largest peaks of record for the Santa Ynez River at Lompoc are from 1907 and 1914. As originally reported, these peak discharge estimates are nearly as large or larger than the peak discharge reported for a large flood that occurred in 1969. The discharge estimate for the 1969 flood, $2270 \text{ m}^3/\text{s}$ ($80,000 \text{ ft}^3/\text{s}$), is based on the rating curve from the spillway at Bradbury Dam, upstream of Lompoc and the present-day gage at Lompoc. The older peak discharge estimates were called into question because there is a clear, ubiquitous geomorphic and stratigraphic record of the 1969 flood downstream of Bradbury Dam to Lompoc. The paleoflood record also documents the absence of similar-sized or larger floods for

at least 700 years prior to 1969. The magnitude of the resulting revisions to the previously reported peak discharge estimates illustrated in Table 1 is substantial. Ostenaa et al (1996) provide a detailed discussion of the data and basis for these revisions. The objective is to evaluate the impact these revisions on flood frequency estimates for the Santa Ynez River.

Table 1: Revised Peak Discharge Estimates for the Santa Ynez River at Lompoc

Date	Previously Reported Peak Discharge m ³ /s (ft ³ /s)	Depth of Flow m (ft)	Revised Peak Discharge m ³ /s (ft ³ /s)
January 9, 1907	3400 (120,000)	4.8 to 5.6 (16 to 18.5)	1560 (55,000)
February 7, 1909	646 (22,800)	3.2 (10.5)	637 (22,500)
January 25, 1914	2120 (75,000)	3.2 to 4.0 (10.6 to 13.3)	779 (27,500)
February 9, 1915	1176 (41,500)	1.5 to 1.8 (4.9 to 5.8)	425* (15,000*)
January 17, 1916	765 (27,000)	1.9 to 2.1 (6.4 to 7.0)	425* (15,000*)
February 20, 1918	445 (15,700)	2.0 to 2.5 (6.6 to 8.1)	425* (15,000*)
February 9, 1932	640 (22,600)	2.5 (8.2)	425* (15,000*)
March 3, 1938	1275 (45,000)	4.4 to 5.1 (14.4 to 16.8)	1275 (45,000)
January 25, 1969	2270 (80,000)	6.6 to 6.7 (21.8 to 22.2)	2270 (80,000)
*Maximum value from step-backwater modeling			

In the absence of the paleoflood information, flood frequency models for the Santa Ynez River and the surrounding region are required to account for the occurrence of three peak discharge values that exceed 2120 m³/s (75,000 ft³/s) in a record less than 90 years long. Regardless of the model, use of these data will lead to the conclusion that a 1/100 probability discharge might well exceed 2830 m³/s (100,000 ft³/s) (e.g., Pitlick, 1994). If these frequency models are used to extrapolate, the inevitable conclusion is that discharge values near the PMF are perhaps plausible within probabilities of 1/1000 to 1/10,000. Even if the early discharges are not used in the analysis or are revised, without paleoflood information the range of plausible discharge values for probabilities in the range of 1/1000 to 1/10,000 is not greatly diminished (Ostenaa et al, 1996). Only when the long period of record provided by the paleoflood data is included in the flood frequency models do estimates of peak discharge for probabilities of 1/1000 to 1/10,000 change substantially (O'Connell et al., 1997).

IMPLICATIONS OF REVISED PEAK DISCHARGE ESTIMATES AND PALEOFLOOD INFORMATION FOR MODELS OF EXTREME FLOODS

The validity of any model result depends on the quality and reliability of the data available to validate or confirm that result. As the National Research Council has previously noted, "*A modeling approach does not decrease the amount of data required; in fact it increases it. Modeling is not a replacement for observation*" (NRC, 1992, p. 14). Paleohydrologic data are of particular utility for testing models of extreme floods because the long geologic record provides an integrated sample of the many combinations of rare conditions necessary to produce extreme floods. As the examples from eastern Oregon illustrate, paleohydrologic methods provide a framework for evaluating the veracity of peak discharge estimates from extraordinary historic floods. These examples also illustrate the obvious point that data and models must fit the application for which they are intended. This point is well illustrated by the controversy regarding the extreme discharge estimates from Bronco Creek, AZ (e.g., House and Pearthree, 1995) and may be applicable to our assessments of the eastern Oregon floods as well. If the intended application of these extreme discharge values is for design of bridges or culverts, then an evaluation and modeling approach that reflects the maximum transient conditions at single unique sites that are significant to these applications is appropriate (Phillips and Hjalmarnson, 1996). On the other hand, where the application is directed towards the evaluation of regional flood size for use in developing inflow hydrographs for reservoirs, the evaluation and modeling approach must reflect an assessment of the flow through a river or channel system, independent of site-specific hydraulic anomalies. Likewise, if the application is to evaluate whether models of extreme floods such as the PMF are reasonable, the data used for such evaluations must reflect actual flow, not local transient conditions. For both of the latter applications, the revised estimates for eastern Oregon contained in this paper, and the estimates of House and Pearthree (1995) for Bronco Creek are most appropriate.

Similar conclusions follow for the use of peak discharge estimate in flood frequency calculations. Incorporation of paleohydrologic information in flood frequency calculations has significant impacts on the results (Stedinger and Cohn, 1986; O'Connell et al., 1997). The brief example from the Santa Ynez River illustrates the extent to which reliance on unquestioned data can lead flood frequency modeling astray. The context provided by paleohydrologic information is the only way to bring model results back into the proper focus.

REFERENCES

- Bullard, K.L., 1986, Comparison of Estimated Maximum Flood Peaks with Historic Floods: U.S. Bureau of Reclamation, Engineering and Research Center, Hydrology Branch, Denver, CO, 165 p.
- Costa, J.E., 1987, Hydraulics and Basin Morphometry of the Largest Flash Floods in the Conterminous United States: *Journal of Hydrology* 93, 313-338.
- Denlinger, R.P., R.A. Walters, D. Levish, and D. Ostenaar, this volume, Robust Methods for Flood Routing Over Highly Irregular Terrain.
- House, P.K., and P.A. Pearthree, 1995, A Geomorphologic and Hydrologic Evaluation of an Extraordinary Flood Discharge Estimate: Bronco Creek, Arizona: *Water Resources Research*, 31, 3059-3073.
- Harris, D.D., and L.E. Hubbard, 1983, Magnitude and Frequency of Floods in Eastern Oregon. U.S. Geological Survey Water Resources Investigations Report 82-4078.
- Hydrologic Engineering Center, 1990, HEC-2 Water Surface Profile User's Manual: Hydrologic Engineering Center (U.S. Army Corps of Engineers), Davis, CA.

- Levish, D.R., and Ostenaar, D.A., 1996, Applied Paleoflood Hydrology in North Central Oregon. Guidebook for Field Trip 2. Cordilleran Section, Geological Society of America 92nd Annual Meeting.
- O'Connell, D.O., Levish, D., and Ostenaar, D., 1997. Bayesian Flood Frequency Analysis with Paleohydrologic Bounds for Late Holocene Paleofloods, Santa Ynez River, California. In *Twenty Years Later: What Have We Learned Since the Big Thompson Flood*, edited by E. Grunfest. Natural Hazards Research and Applications Information Center Special Publication, No. 33, University of Colorado, Boulder, Colorado, 183-196.
- Ostenaar, D.A., Levish, D.R., and O'Connell, D.R.H., 1996, Paleoflood Study for Bradbury Dam, Cachuma Project, California. Seismotectonic Report 96-3, Denver, CO: U.S. Bureau of Reclamation, Seismotectonic and Geophysics Group.
- Phillips, J.V., and Hjalmarson, H.W., 1996. Implication of Translatory-Wave Phenomena for Engineering Design. River Tech 96 Conference Proceedings.
- Pitlick, J., 1994. Regional Flood-Frequency Analysis for the Santa Ynez River Basin and Adjacent Regions. Appendix A, In Ostenaar, D.A., Levish, D.R., and O'Connell, D.R.H., 1996, Paleoflood Study for Bradbury Dam, Cachuma Project, California. Seismotectonic Report 96-3. Denver, CO: U.S. Bureau of Reclamation, Seismotectonic and Geophysics Group.
- Stedinger, J.R., and T.A. Cohn, 1986, Flood Frequency Analysis with Historical and Paleoflood Information: Water Resources Research 22, 785-793.
- USBR (Bureau of Reclamation), 1956, Cloudburst Runoff in Mount Vernon and Mitchell, Oregon Areas {unpub.}: Memorandum from Head, Flood Studies Section to Chief, Hydrology Branch, November 23, 1956, Boise, ID, 8 p., 21 photographs.
- U.S. Geological Survey, 1956, Meyers Canyon near Mitchell, Oreg., flood of July 13, 1956, slope area determination, 252C {unpub.}: field notes, file documents, calculation sheets, and photographs in official file.
- Walters, R.A., this volume, A Finite Element Model with Moving Boundaries: Application to Floods and Runup.

Dean Ostenaar, D-8330, Bureau of Reclamation, P.O. Box 25007, Denver, CO 80225 - Email - paleoflood@seismo.usbr.gov

HEC-RAS (RIVER ANALYSIS SYSTEM)

Vernon Bonner, P.E.; Chief, Training Division
Gary Brunner, P.E.; Senior Hydraulic Engineer
Hydrologic Engineering Center, US Army Corps of Engineers
609 Second Street; Davis, CA 95616

INTRODUCTION

The *HEC-RAS River Analysis System* (HEC, 1997a,b,c) is a one-dimensional river modeling system designed for interactive use in a multi-tasking environment. Version 1, released in July 1995, provided steady-flow water surface profile calculations for a river network with sub-critical, supercritical, or mixed-flow regime on computers with MS Windows™ operating system. The program has been developed based on a single definition of the river geometric data for all modeling. River networks are defined by drawing, with a mouse, a schematic of the river reaches from upstream to downstream. As reaches are connected, junctions are automatically formed by the program. After the network is defined, reach and junction input data can be entered. The data editors are called by pressing the appropriate icons in the *Geometric Data Window*, or reach data can be imported from HEC-2 data sets (HEC, 1990).

Cross sections are located by river, reach, and river station. Pressing the cross-section icon provides the data entry editor. Data are defined by station-elevation coordinates, up to 500 coordinates are allowed. There is no maximum number of cross sections. The section data are stored in a downstream order based on their river-station number. Cross sections can be easily added or modified in any order. Cut, copy, and paste features are provided, along with separate expansion or contraction of the cross section's two over banks and channel. Cross-section interpolation can create additional computational sections based on a "string model" linearly linking adjoining sections. User-defined chords can be added to relate portions of each section to the next section.

HEC-RAS, Version 2, provides several added capabilities including the option to import and utilize three-dimensional (3D) river reach and cross-sectional data from a data exchange file. This paper highlights some major new features in Version 2 of the program.

HEC-RAS Version 2.0

Bridges. All bridges are modeled using the same physical definition of the bridge. The user can select one or several modeling methods to apply for low-flow and high-flow conditions. Low-flow methods included friction, momentum, and Yarnell methods. High-flow options included friction or pressure and weir equations. Pressure flow provides a gate equation for free-surface tailwater and pressure equation for fully submerged conditions. With support from the Federal Highway Administration, HEC has added WSPRO (FHWA, 1990) low-flow bridge hydraulics to HEC-RAS. The approach is a variation of the friction-based calculations. The HEC-RAS Hydraulics Reference (HEC, 1997c) provides a complete description of the methods used in this option.

Culverts. Two additional shapes have been added to the culvert options: Low Profile Arch and High Profile Arch. As shown in the Culvert Data Editor (figure 1), the program now supports eight culverts shapes. Also, the editor has been modified to provide all culvert data entries in a group.

Culvert hydraulics utilize the Federal Highway criteria for inlet control (FHWA, 1985) and compute total energy loss for outlet control. The computations have been expanded to handle several limitations that existed in Version 1. Culverts can now have adverse or steep slopes, with subcritical, supercritical or mixed-flow profiles computed inside the culvert.

Profile plots can display the water surface profile computed inside of the culvert.

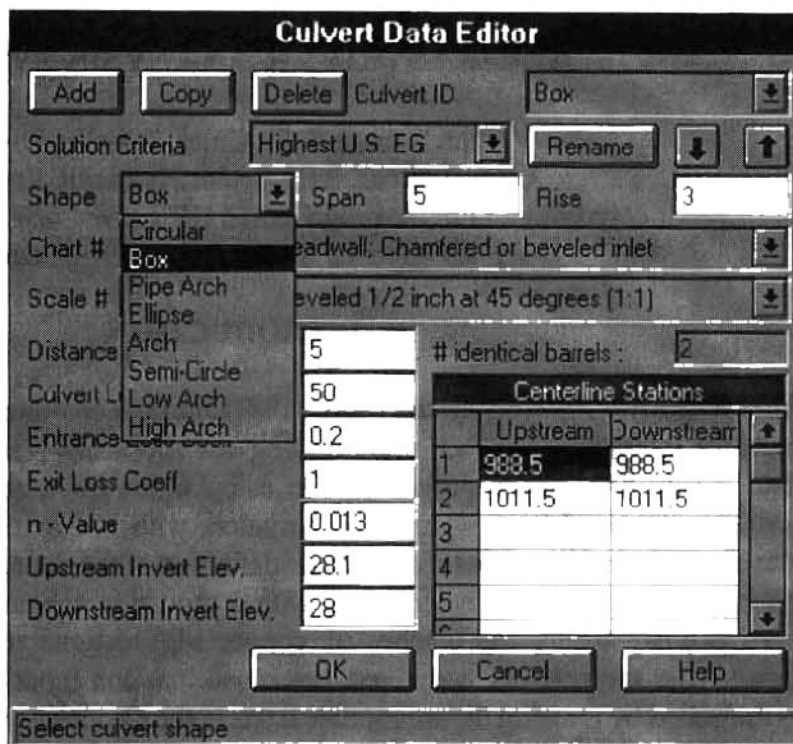


Figure 1. Culvert Data Editor

Gates and Weirs. The program can model inline gated spillways and overflow weirs. Gates can be radial (tainter gates) or vertical lift gates (sluice gates). The spillway crest of the gates can be either an ogee shape or a broad crested weir shape. In addition to the gate openings, the user can model a separate uncontrolled overflow weir. The weir (or dam) data are entered just like the roadway for a bridge or culvert, filling the cross section from the ground to top-of-weir. Gates are added with a Gate Editor, figure 2. The gates are placed into the section, by defining the dimensions, locations and coefficients. Like culverts, multiple identical gates can be defined by defining the number, the data for one, and the centerline location for each.

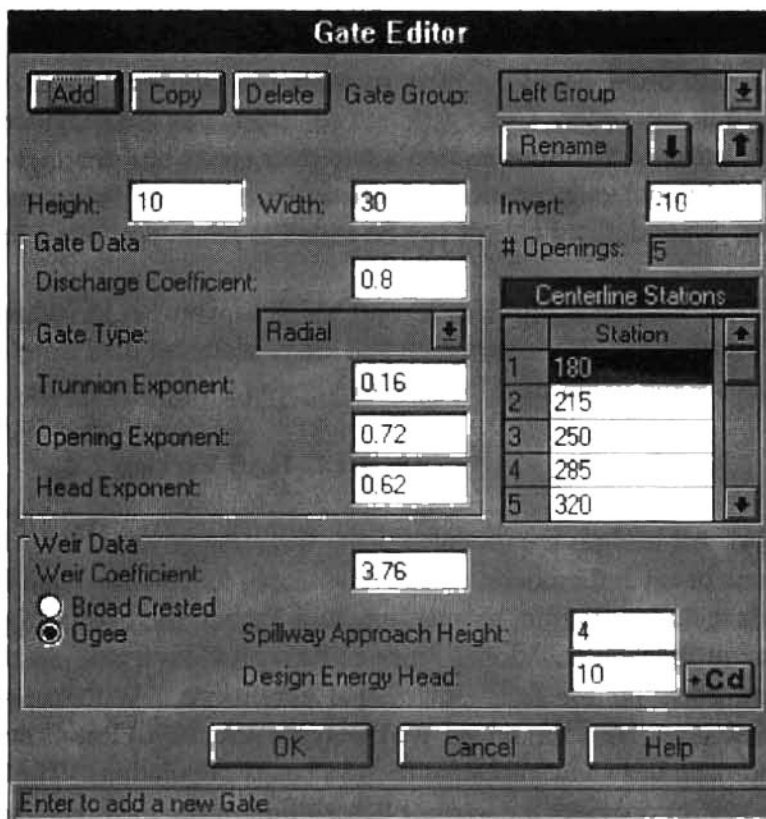


Figure 2. Gate Editor for Inline Gates and Weirs

Bridge Scour. Bridge scour is the first Hydraulic Design Option in HEC-RAS. The program feature was added with support from the Federal Highway Administration and it reflects the procedures presented in HEC 18, *Evaluating Scour at Bridges* (FHWA, 1995). After calibrating a model, water surface profiles are computed with the flow-distribution option. The results from this computation are the basis for the scour computation. The data entry screen provides tabs to input data for Contraction, Pier, and Abutment scour. As shown in figure 3, the computed scour is shown in the graphic. An output report can be generated, providing input summary and computed results.

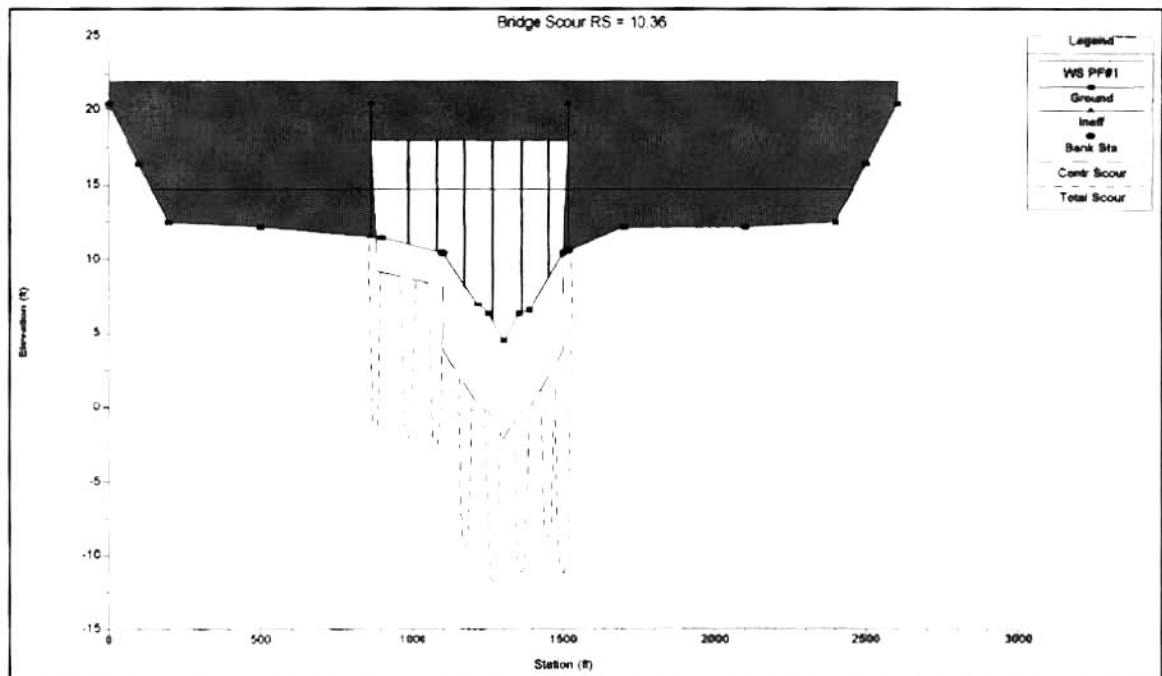


Figure 3. Bridge Cross Section with Computed Scour

Channel Modification. This option is the equivalent of the HEC-2 CHIMP routine. The modeler can evaluate the impact of channel modifications on the water surface profile by using the base geometry as one plan and the modified geometry as another. The data editor is accessed under **Options** in the **Geometric Data Editor**. Figure 4 is an example of the Channel Modification Editor.

A channel template is defined to apply to a selected range of cross-section data. Up to three trapezoidal channel templates can be defined by bottom width, invert elevation, side slopes, and location in the cross section. Channel 'n' values can be modified. **Center Cuts (y/n)** indicates whether the template will be centered between the section bank stations. If no, the station must be entered. The template can be extended on a constant slope down from the upstream section, or up from a downstream section.

Apply Cuts to Selected Range will define the channel modification data in the table at the bottom of the menu. Side slopes on the template are extended to the existing ground profile. Bank stations are redefined to match the template, when the section intercepts the ground outside of the existing bank station. The data for each section in the table can be modified. **Compute Cuts** applies the data

at the bottom of the table to the cross sections. As shown in figure 4, the sections and their cuts are displayed after the cut is applied. The modeler can interact with the channel modification until the desired results are achieved. The **Cut Fill Areas** produces a table of cut areas and volumes for the three cross-section elements, the total section, plus the total volumes for the reach.

The **Create Modified Geometry** computes a geometry file that can then be saved as a new geometry file. To compute profiles for the modified channel, a new plan is created with the new geometry and the flow data files. The results from profile computations can be compared in tables and graphics by selecting the existing and modified plan.

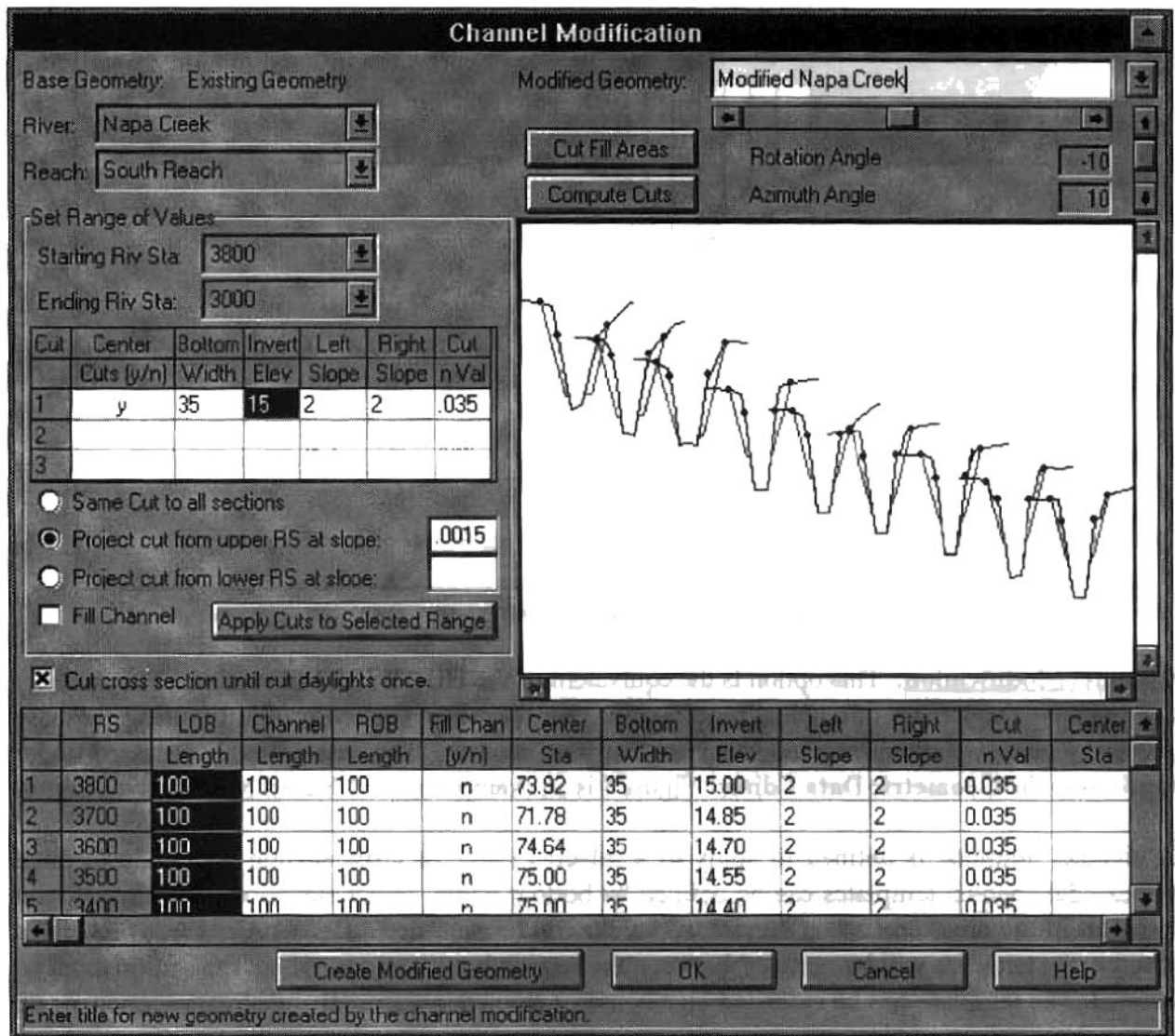


Figure 4. Channel Modification Menu with Computed Sections

Geometric Data Import. With a new data-exchange file format, the program can import and use 3D geometric data. Figure 5 shows the Geometric Data Editor with model data imported from a terrain model. The plan-form of the stream network and the cross-section locations and orientation

are preserved from the terrain data. The display is not distorted; therefore, cross-section widths and the distance between sections reflect the relative spacing of the physical data. Also, background maps can be added as a backdrop in the river-reach display and photographs can be linked with model cross-sections. Sections with photos attached display a marker that can be clicked on, with the cursor, to display the photograph. This option should be helpful for bridge and culvert modeling.

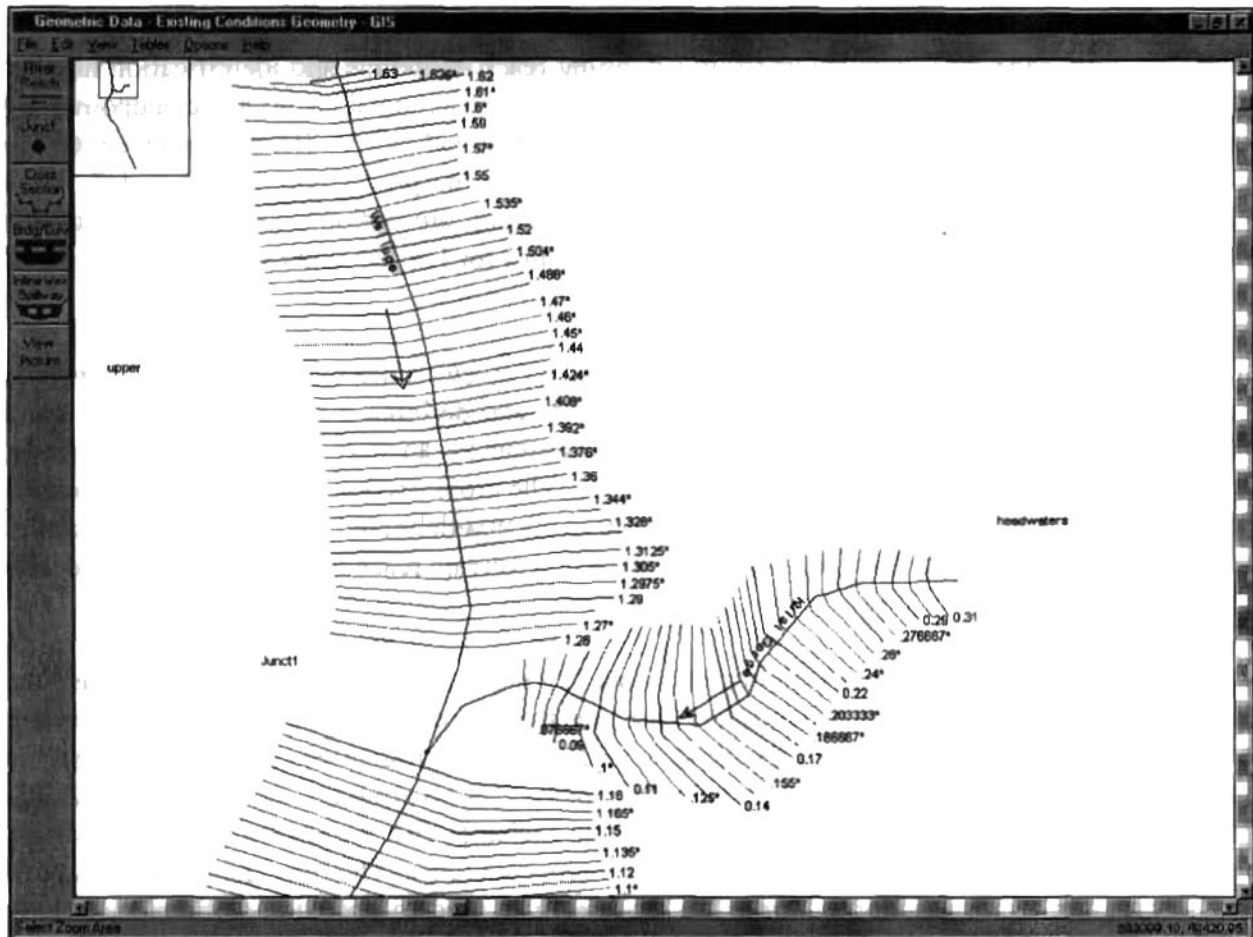


Figure 5. HEC-RAS Geometric Data Screen with Imported Terrain Data for Wailupe River, HI

Data Exchange File. HEC is developing a format standard for a general-purpose data exchange between CADD or GIS programs and its Next Generation computer programs (HEC, 1996). The goal is to facilitate data transfer between HEC models and the CADD and GIS software systems, without "adopting" any one system. Terrain data can include watershed boundaries, stream network definition, catchment area, river cross-sections, and similar model data. The initial focus has been to provide an interface with the *Hydrologic Modeling System*, HEC-HMS (HEC, 1995) and the *River Analysis System*, HEC-RAS. Data records have been defined to provide basic terrain data to these two program and new records will be added, as required.

The data exchange file is a formatted ASCII text file. Standard records in the file are composed of keywords and values. The use of keywords and a text-file format provides a self documenting file

which can be created or edited with a text editor, and is easily read and understood by reviewers. Records in the data file can be grouped into two types: file sections and objects. HEC-RAS can read geometric data from an exchange file composed of three file sections: (1) a header containing descriptions that apply to all data in the file, (2) the stream network containing reach locations and connectivity, and (3) model cross-sections containing their locations on the stream network and cross-section coordinates.

The stream network section contains records defining reach endpoints and identification number (ID), plus the reach data. At a minimum, the stream network must contain at least two endpoints and one reach. Each reach is defined by a multi-record object that includes: an ID, the stream centerline XYZ coordinates, and river stations. The XY values are the planar coordinates and Z is the elevation. In HEC-RAS, the elevation and river stationing are optional data in the centerline definition. River station values are assumed to be in miles for English units and kilometers for SI units.

The cross-section file section contains the cross-section objects. Each cross-section must include records identifying: the stream, reach and river station; and defining a 2D section cut line and a series of 3D locations on the cross-section. The cut-line object is an array of XY locations defining the cross section in plan view, as shown in figure 5. The cross-section object consists of a label "SURFACE LINE:" and the 3D coordinates, written as comma-delimited XYZ real-number triples. Also, the section's left and right bank stations and the downstream reach lengths can be defined with the cross sections.

Developing an HEC-RAS model with imported data first requires starting a new project. Then one would open the Geometric Data editor, select Files, and then select Import GIS Data. A file browser screen appears allowing you to select the data exchange file. The program reads the file and displays the river-reach graphic based on the imported data. The HEC-RAS program maintains the XYZ data for graphical displays and to provide output to the data exchange file. For hydraulic computations, the program translates the XYZ coordinates into 2D cross-sections. The translated data are shown in the program's cross-section editor. The modeler will need to provide additional data like: Manning's n , contraction and expansion coefficients, plus bank stations and reach lengths if they are not included in the exchange file. The modeler will also have to add data defining all hydraulic structures in the reach to complete the geometric data model. Flow data and boundary conditions are required for the flow-data file. Then, the model would be ready to compute profiles. The program operation and features are the same as they are for user input data, except for the XYZ graphic which displays the water surface in the 3D terrain model. Figure 6 is an XYZ display of the lower reach of the Wailupe River model, under flood-flow conditions.

HEC-RAS can write an output file in the data exchange file format. In the Main menu, under File, is an Export GIS Data option. Selecting this option allows you to write an exchange file with model results. In the file header section, the program writes the date and time for the output, the number of reaches, cross sections, and profiles. Version 2 allows the user to input a profile name, (e.g., 100-year) which is used as the profile identification label.

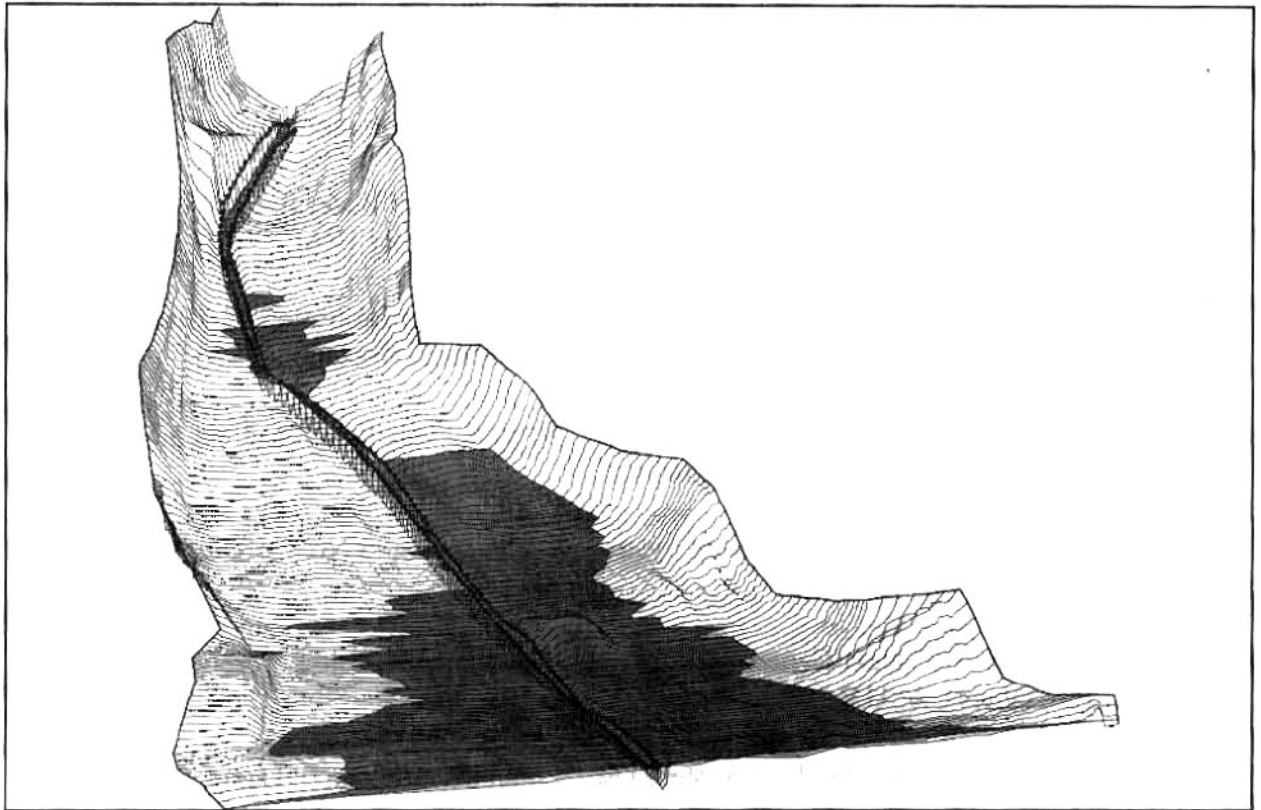


Figure 6. HEC-RAS XYZ Perspective Plot of Lower Wailupe River Reach, HI.

In the cross-section file section, the program writes the cross-section identification data and the 2D coordinate pairs for the section cut line. The computed water-surface elevation is written for each cross section. Following the cross-section data, the boundary polygons for each reach are provided by 2D coordinates. A reach's boundary polygon is composed of the most upstream cross section on the reach, the endpoints for each cross section in the reach and the most upstream cross-section of the downstream reach(es). If the cross-section geometry defines the limit of the water-surface inundation, no adjustments are made to the polygon boundary. The floodplain boundary will be determined in the terrain model by the intercept of the water-surface plane with the river-reach geometry. However, when the water surface is limited by levees, bridges and culverts, or floodways, the polygon is defined at the water's edge for those cross sections. Then when the polygon is used in the terrain model, the HEC-RAS knowledge of where the water is within each cross section is transferred to the CADD or GIS software. The adjusted polygon boundary will limit the floodplain definition to the polygon, rather than the water's intercept with the terrain data.

Version 2.1. An updated program was released in October 1997, providing error corrections to the Version 2.0 program and adding graphical editing of cross-section data. Also, options were added to model air entrainment effects on water surface elevation for high-velocity streams and to model floating debris accumulation on bridge piers. Both options are based on criteria used in the Corps' Los Angeles District and were added to develop a design model for the Santa Ana River.

REFERENCES

- Federal Highway Administration (FHWA) , 1985, Hydraulic Design of Highway Culverts, Hydraulic Design Series No. 5, U.S. Department of Transportation, September 1985.
- FHWA, 1990, User's Manual for WSPRO - A Computer Model for Water Surface Profile Computations, Publication no. FHWA-IP-89-027, September 1990.
- FHWA, 1995, Evaluating Scour at Bridges. Federal Highway Administration, Hydraulic Engineering Circular 18, FHWA # IP-90-017, 3rd Editions, November 1995.
- Hydrologic Engineering Center (HEC), 1990, HEC-2 Water Surface Profiles. User's Manual Davis CA: U.S. Army Corps of Engineers.
- HEC, 1995, The HEC Hydrologic Modeling System. Technical Paper No. 150, Davis CA: U.S. Army Corps of Engineers.
- HEC, 1996, Status of HEC Next Generation Software Development Project. Technical Paper No. 156, Davis CA: U.S. Army Corps of Engineers.
- HEC, 1997a, HEC-RAS River Analysis System User's Manual. Version 2, Davis, CA: U.S. Army Corps of Engineers.
- HEC, 1997b, HEC-RAS River Analysis System Hydraulic Reference Manual. Version 2, Davis, CA: U.S. Army Corps of Engineers.
- HEC, 1997c, HEC-RAS River Analysis System Application Guide. Version 2, Davis, CA: U.S. Army Corps of Engineers.

NEXT GENERATION FLOOD DAMAGE ANALYSIS PROGRAM

By Robert Carl, Hydraulic Engineer, U.S. Army Corps of Engineers Hydrologic Engineering Center, Davis, California; Michael Burnham, Chief, Planning Analysis Division, U.S. Army Corps of Engineers Hydrologic Engineering Center, Davis, California

Abstract: The Hydrologic Engineering Center (HEC) has developed a next generation Flood Damage Analysis computer program (HEC-FDA) for formulating and evaluating flood damage reduction plans. The program design is consistent with federal and Corps of Engineers policy and technical requirements. It includes risk-based analysis procedures. HEC-FDA calculates expected annual damage and equivalent annual damage using hydrologic, hydraulic, and economic data. It produces tabular and graphical output that can be used to evaluate the inundation reduction benefits of alternative plans and project performance. It uses Xbase formatted database files to store input data and output results which can be accessed by commercial programs. The graphical user interface (GUI) utilizes a cross-platform software library for easy porting to many platforms. The program operates on Microsoft Windows NT and Microsoft Windows 95 platforms.

INTRODUCTION

Background: One of the primary Civil Works Missions of the U.S. Army Corps of Engineers is to provide flood protection for communities in the United States. The Corps has reduced flood damage by implementing many structural and nonstructural measures. It has evaluated proposed alternative measures using a variety of tools ranging from hand calculations, mainframe batch computer programs, mainframe programs ported to personal computers, sophisticated Geographical Information Systems related programs, and now the new next generation HEC-FDA. Corps regulations dictate analysis procedures and reporting requirements. With time, these have changed to meet the changing needs of the country and to utilize new science and technology.

Requirements: The Corps recently enacted regulations requiring the use of risk-based analysis procedures for formulation and evaluating flood damage reduction measures (USACE, 1996b). Historically, without or existing conditions were evaluated using expected annual damage calculations which are computed by integrating a damage-frequency function. The damage-frequency function is derived from combining the discharge-frequency, stage-discharge, and stage-aggregated damage functions. Except for the discharge-frequency function, these functions all represented the best estimate — there was no attempt to quantify uncertainty in the functions other than to perform some sensitivity analyses. With the implementation of the risk-based regulations, all Corps studies must use the new procedures. The procedures require quantifying the uncertainty in the discharge-frequency, stage-discharge, stage-damage functions, and incorporating it into the economic and performance analyses of alternatives. HEC-FDA utilizes the Monte-Carlo numerical analysis procedure (Benjamin et al., 1970) to compute expected annual damage while explicitly accounting for the uncertainty in the basic functions.

RISK-BASED PROCEDURES

The damage-frequency function is derived from three basic functions: discharge-frequency, stage-discharge, and stage-damage. Alternatively, a stage-frequency function may be used in place of the discharge-frequency and stage-discharge functions. The uncertainty in the functions is quantified using a variety of parameters and techniques. For example, the uncertainty in the discharge-frequency functions is reflected in the equivalent length of record. If the function is computed using gaged data, the length of the gaging record is a good indication of the analyst's uncertainty in that function. At the other extreme, the stage-damage

functions are derived from Monte-Carlo simulations using uncertainties in several parameters including the first floor stage of structures, the estimated depreciated replacement value of the structure, etc. For every expected annual damage Monte-Carlo simulation, the three basic functions are sampled to derive the sampled damage-frequency function which is integrated to determine the expected annual damage. It may take several hundred thousand simulations before converging on the estimate of damage with an acceptable error.

PROGRAM STATUS

Provisional Version 1.0 of the HEC-FDA program was first released to only the U.S. Army Corps of Engineers in January 1997. Version 1.0 was released in January 1998 and is available to the public. During the last year, HEC (and their contractors) have made substantial changes to the database code, the GUI, and the calculation procedures. It has added new capabilities to analyze regulated frequency functions, interior-exterior stage functions, nonlinear geotechnical failure criteria, and levee wave overtopping.

SOFTWARE DESIGN

HEC-FDA is an object-oriented program written mostly in the C++ language. The software development was divided into four components which were written by different people including both HEC engineers and private contractors. There are four software components:

- (1) Databases - all interaction to the database is done through the database code.
- (2) Graphical User Interface (GUI) - all user input data are entered in the GUI screens.
- (3) Stage-Damage Monte-Carlo Simulations - all calculations for computing the stage-aggregated damage function with uncertainty is done in this component.
- (4) Expected Annual Damage Monte-Carlo Simulation - all the calculations to determine expected annual damage, equivalent annual damage and project performance is performed in this component.

The graphical user interface (GUI) software utilizes the Visix Corporation's "Galaxy" library (Visix Software Inc., 1994), and the database software utilizes the Sequiter Corporation's CodeBase library (Sequiter Software Inc., 1996). The stage-aggregated damage simulations are written in C++ using object-oriented design. The expected annual damage Monte-Carlo simulations are written in FORTRAN. The Galaxy library facilitates porting the GUI to multi-platforms including UNIX systems with minimal code changes. The CodeBase library enables storing the input and output data in standard Xbase formatted files which allow the user to edit the data using many commercial software programs (such as database or spreadsheet programs).

Before software coding began, HEC developed a requirements document. It provided a sound foundation upon which related design and development work could be built. In addition, a field group reviewed the design from a practitioner's standpoint. However, during software development, many substantial changes were made to all areas of the program design. The object-oriented design allowed concurrent modifications to all components of the program and facilitated the isolation of software bugs. Object-oriented development required new skills and new tools. Both have steep learning curves. To achieve project goals, HEC made a substantial investment in C++ training and the acquisition of software, particularly the Galaxy library. These were costly in time and staff resources. New code problems surfaced. For example, C++'s dynamic memory allocation and deallocation are powerful but difficult to program and the resulting software bugs have caused frequent execution failures in the early versions of the program.

STRUCTURE OF HEC-FDA ANALYSIS

Components and the GUI Structure: HEC-FDA is designed to be the primary tool for collecting, storing, and evaluating hydrologic, hydraulic, and economic input and output data for flood damage reduction studies. Specialists from different disciplines can use the program as a central collector of data and for turnkey analysis in these studies.

HEC-FDA is structured into several logical components which shadow the basic functions and provide structure to study management and access to evaluation results. These are the components:

- (1) File / Study management
- (2) Study Configuration
- (3) Hydrologic and Hydraulic Engineering
- (4) Economics
- (5) View
- (6) Evaluation
- (7) Results

Figure 1 displays the main HEC-FDA screen with an existing study open. The above components are shown as menu items with the exception of results which is located under the evaluation. The file / study management provides high level access to studies including creating new studies and opening existing studies. The study configuration provides the means to define the basic lists of

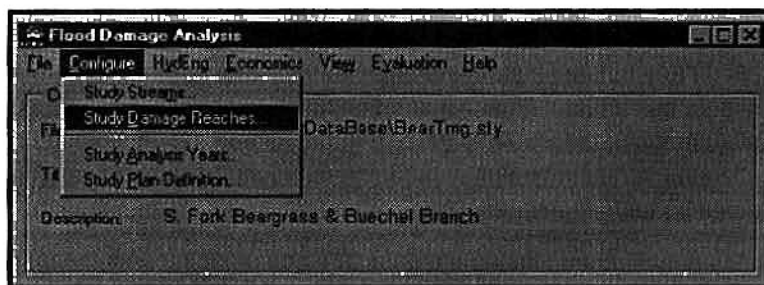


Figure 1: Study Configuration Screen

parameters such as streams, reaches, plans, and analysis years. The hydrologic and hydraulic engineering component accepts input data defining water surface profiles, frequency functions, stage-discharge rating functions, and geotechnical features such as levees. The economics component facilitates entry of structure attributes, damage potential functions, and calculation of stage-aggregated damage with uncertainty. The view component allows the analyst to view the basic lists (such as damage reaches) in modal windows. The evaluation component accesses data validation reporting and Monte-Carlo simulation for expected annual damage and equivalent annual damage. The results section displays expected annual damage and equivalent annual damage results in various formats as well as project performance information.

Overall Methodology: A flood damage reduction study requires the collection and analysis of hydrologic and economic data. The analyst creates a framework in which this data is categorized, stored, and manipulated. The framework of HEC-FDA requires the usual definitions for flood damage reduction studies such as alternative damage reduction plans, years of analysis, damage reaches, and damage categories. The three basic functions (discharge-frequency, stage-discharge, and stage-aggregated damage) are calculated from user input. The input and output (damage-frequency) functions are stored in the database from which plan formulation results are calculated and stored. They are stored by plan, year, stream-reach, and category if economics related. Detailed results are obtained by dividing the study area into reaches and an index location is established within that reach. The index location normally corresponds to a cross-section which is used for water surface profile calculations. The index location is established so that the three basic functions are developed for the same geographic location. Expected annual damage is calculated at the

damage reach level rather than for individual structures because Monte-Carlo simulation requires intense calculations requiring a significant amount of time.

The hydrologic and hydraulic input data is calculated outside of HEC-FDA but can be imported. The discharge-frequency functions may be computed using HEC-1 (USACE, 1987) or HEC-FFA (USACE, 1992). The stage-discharge functions are computed from water surface profiles which may be computed using HEC-2 (USACE, 1982) or HEC-RAS (USACE, 1997). Discharge-frequency and stage-discharge functions can be computed within HEC-FDA from the water surface profiles.

The economic stage-aggregated damage functions are computed within HEC-FDA. There is an additional framework for managing the input data for stage-damage calculations which includes damage categories, structure inventories, occupancy types, and structure modules. There is not a separate program for deriving the functions like there is for the hydrologic and hydraulic engineering functions.

STUDY CONFIGURATION

The study configuration includes the definition of study streams, damage reaches, analysis years, and alternative damage reduction plans. Figure 1 displays the configuration screen. Additional parameters should be considered as part of the configuration even though they are not attached to the "Configure" menu item. They include damage categories and structure modules. All configuration items should be defined early in the study. This allows two or more analysts to work on the study concurrently on different computers and then merge all data together into one database. Damage reaches are defined using stream stationing so that structures can be automatically assigned to reaches based on their geographic location with respect to water surface profiles.

HYDROLOGIC AND HYDRAULIC ENGINEERING

The hydrologic and hydraulic engineering component includes the entry of two basic functions: discharge-frequency and stage-discharge as well as water surface profiles, and levee criteria. Figure 2 demonstrates the functions which may be entered under "HydEng". Figure 3 depicts the screens for editing graphical frequency functions. The discharge-frequency, stage-discharge,

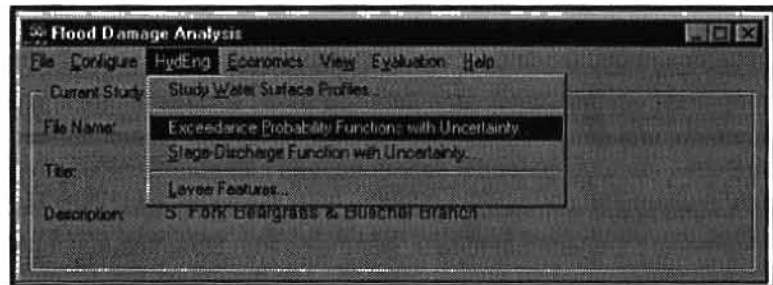


Figure 2: Hydrologic Engineering Components

and / or the stage-frequency functions can be computed from the water surface profiles. The analyst calculates eight water surface profiles which correspond to a wide range of exceedance frequencies - by default from 50% to 0.2% exceedance frequencies. HEC-FDA can then use the profiles to generate either a stage-frequency or discharge-frequency function. The computed stage-discharge function includes the invert stage at zero discharge. The analyst must then enter the uncertainty parameters for both functions.

ECONOMICS

The economics component includes data entry and calculation of stage-aggregated damage. The economics data entry consists of the configuration items of damage categories and structure modules as well as basic information such as occupancy types and structure inventories. Damage categories provide the framework for reporting damage by significant classes of damage such as single family residential, apartments, public

buildings, commercial structures, and industrial plants. For each of these categories, there are one or more global occupancy types and associated depth-damage functions. For example, the single family residential damage category may have the occupancy types of:

- (1) One story, no basement, wood frame, raised foundation
- (2) One story, no basement, masonry construction, slab floor
- (3) Two stories, with a basement, a wood frame, raised foundation
- (4) Etc.

For each of these occupancy types, there are separate depth-percent damage functions for the structure, contents, and "other". The depth-percent damage functions are global for every structure of that occupancy type and are entered as damage relative to the first floor stage as a function of the percent of value. For example, the structure depth-damage function may indicate that the damage at a depth of two feet above the first floor stage is 10 percent of the structure's value. The values of the structure (as well as contents and other) are entered with the individual inventoried structure. The occupancy type does include global parameters for the content and other values when they are expressed as a percent of the structure value. Also, the uncertainty parameters are

entered globally by occupancy type for the first floor stage, structure value, content value, and other value. Structure inventory allows the user to store either an exhaustive inventory of all structures in the study area or a sample. Current sampling techniques allow the user to enter data for one structure and indicate that it represents many identical structures. Structure inventory data includes the damage category, occupancy type, stream, structure identification, first floor stage, stream station, structure value, content value, and other value. If a unique depth-damage is required for a structure, then it may be entered with the structure inventory. Structure inventory data may be imported from other programs such as spreadsheets using tab-delimited text files. Structure modules may be used to alter structure characteristics (such as first floor stage) as a function of plan and year. This is especially helpful when levee alignments vary by plan and a structure may be protected only for some plans. Figure 4 depicts the entry of occupancy type information and Figure 5 depicts the entry of structure inventory data. When all economic data is complete, the stage-aggregated damage with uncertainty is computed for all damage reaches. During the early stages of a study, the stage-aggregated damage may be computed without using the risk-based analysis. This allows the user to debug the data faster and to get conventional results.

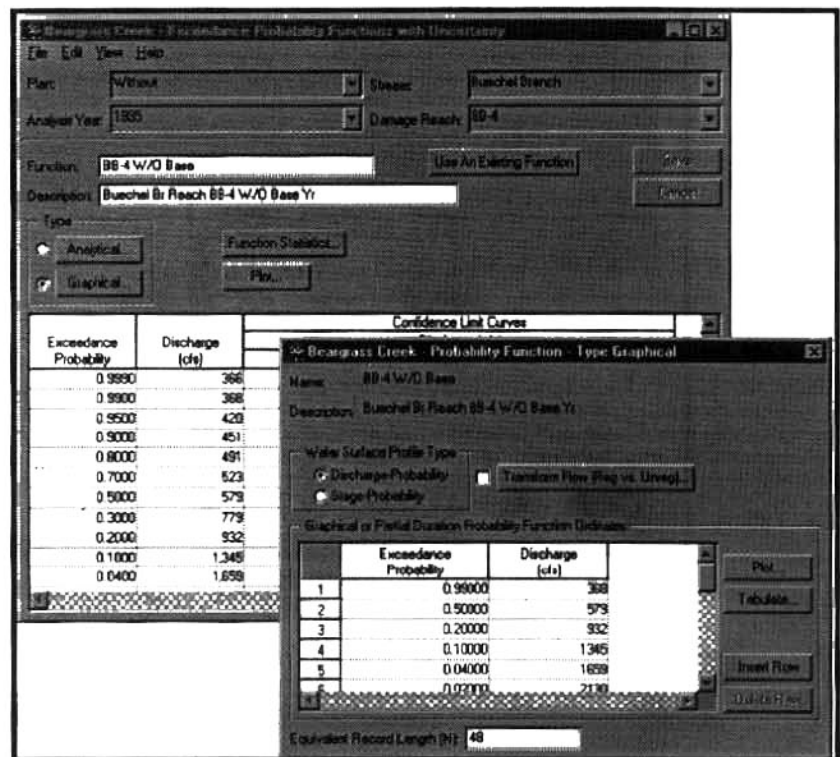


Figure 3: Editing Graphical Frequency Function

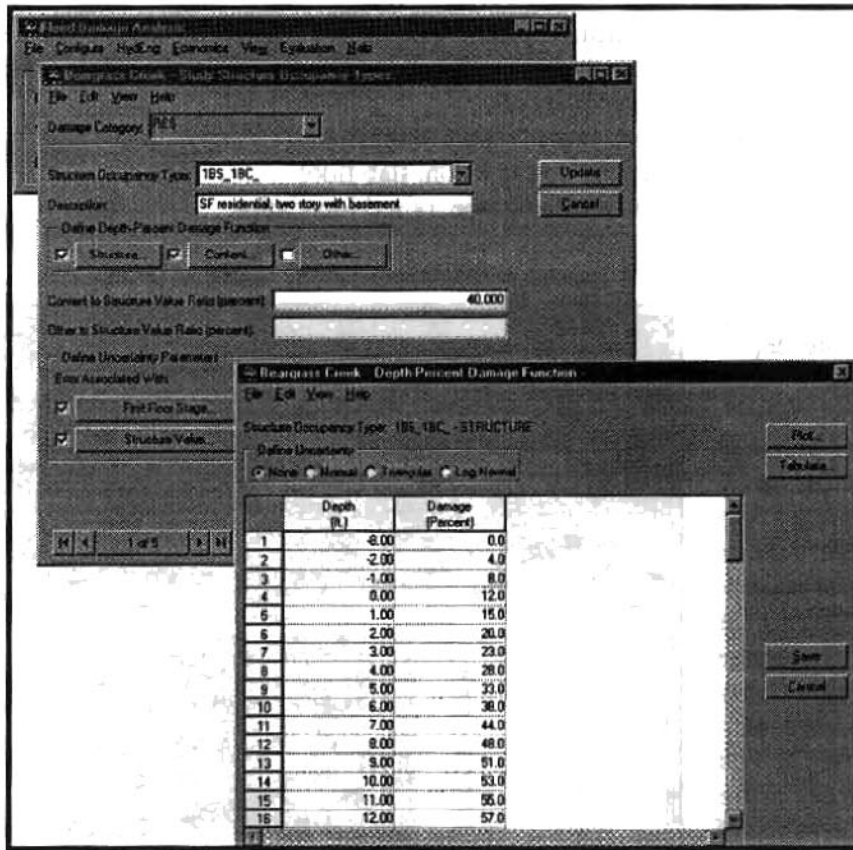


Figure 4: Occupancy Type Data Entry

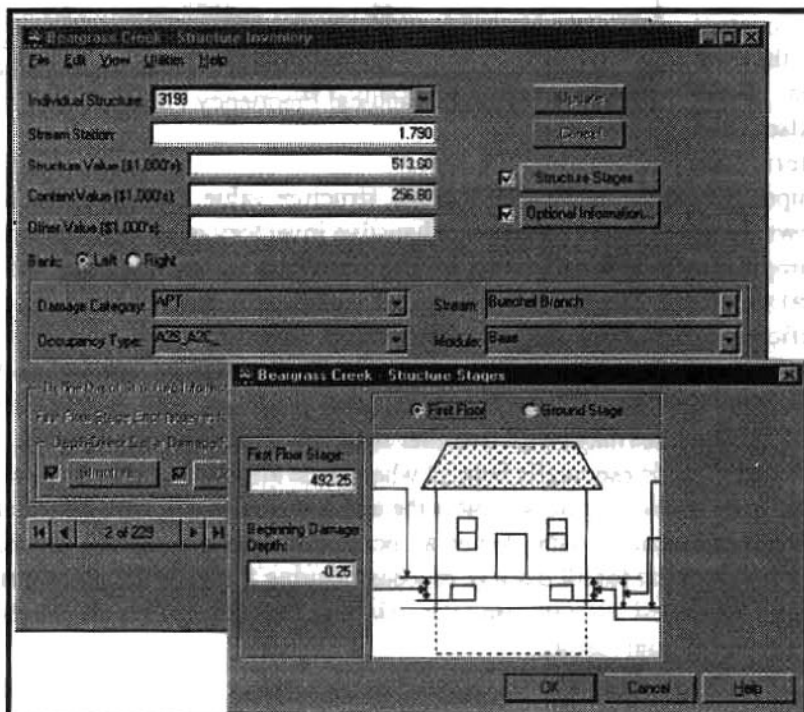


Figure 5: Structure Inventory In Form View

EVALUATION AND RESULTS

The evaluation component displays data validation information and facilitates the calculation of expected annual damage and equivalent annual damage. Before calculation, all supporting functions must be properly defined. HEC-FDA produces a table which indicates the plan / year combinations for which valid functions have been defined and which specific functions are not properly defined. It also tabulates the last computation date and time and indicates results that are out-of-date due to modification of supporting data such as discharge-frequency functions. The analyst can select those plan / year combinations for which calculations are performed.

The results component displays a wide variety of information including expected annual damage and equivalent annual damage by plan, year, reach, and category. The calculated functions such as damage-frequency can also be tabulated and plotted. The equivalent annual damage results are displayed including the discounted damage and amortization. Project performance tables display information that is used to measure the hydrologic efficiency of a flood damage reduction plan. Performance is measured in terms of the risk of flooding in any year, over a specified number of years, or if a specific hypothetical or historical event occurs. Plan performance uses the risk-based analysis of the hydrologic (not economic) functions.

CONCLUSIONS

The HEC-FDA program is a state-of-the-art computer program that provides a comprehensive analysis tool for formulating and evaluating flood damage reduction plans. It has a modern user interface and facilitates transfer of data between other commercial programs and databases. It includes a sophisticated risk-based analysis capability or it can be used for traditional calculations. The computational procedures and output reports are consistent with Federal and U.S. Army Corps of Engineers policy and technical regulations. "Version 1.0" was released in January 1998 and it includes a user's manual and test data.

REFERENCES

- Benjamin, J.R., and Cornell, A.C., 1970, *Probability, Statistics, and Decision for Civil Engineers*, McGraw-Hill Book Co., New York, N.Y.
- Sequiter Software Inc., 1996, *CodeBase Database Management for Programmers Version 6.2*, Sequiter Software Inc., Edmonton, Alberta, Canada.
- U.S. Army Corps of Engineers (USACE), 1982, "HEC-2: Water Surface Profiles, User's Manual".
- U.S. Army Corps of Engineers (USACE), 1987, "HEC-1: Flood Hydrograph Package, User's Manual".
- U.S. Army Corps of Engineers (USACE), 1990, "Guidance for Conducting Civil Works Planning Studies," Engineering Regulation (ER 1105-2-100).
- U.S. Army Corps of Engineers (USACE), 1992, "HEC-FFA: Flood Frequency Analysis, User's Manual," Engineering Regulation (EM 1110-2-1619).
- U.S. Army Corps of Engineers (USACE), 1996a, "Engineering and Design: Risk-Based Analysis for Flood Damage Reduction Studies," Engineering Manual (EM 1110-2-1619).
- U.S. Army Corps of Engineers (USACE), 1996b, "Risk-based Analysis for Evaluation of Hydrology/Hydraulics, Geotechnical Stability, and Economics in Flood Damage Reduction Studies," Engineering Regulation (ER 1105-2-101).
- U.S. Army Corps of Engineers (USACE), 1997, "HEC-RAS: River Analysis System".
- Visix Software Inc., *Galaxy Application Environment, Release 2*, 1994, Visix Software Inc., Reston, VA 22091.

THE HEC NEXGEN SOFTWARE DEVELOPMENT PROJECT

**Darryl W. Davis, Director, U.S. Army Corps of Engineers,
Hydrologic Engineering Center, 609 Second Street,
Davis CA 95616**

Abstract: The NexGen project is developing successor software packages to the existing family of HEC computer programs. Development is occurring via teams comprised of technical specialists, computer scientists, and consultants. Modern software engineering methods are being used and object-oriented program architecture is being employed. Begun in 1990, NexGen products are now emerging. Version 1.0 of the River Analysis System (HEC-RAS) was released in August 1995, and Version 2.0 in April 1997. Several Beta versions of the Hydrologic Modeling System (HEC-HMS) were released over the Spring, Summer, and Fall of 1997. The maiden Version 1.0 is expected by the end of 1997. A provisional version (internal to the Corps) of the Flood Damage Analysis package (HEC-FDA) was released in late 1996. The maiden Version 1.0 will be released in late 1997. This paper describes the evolution and status of the HEC family of programs, the objectives and management approach for NexGen, and findings and status of the project and products to date.

INTRODUCTION

The existing family of HEC programs is the result of 30 years of program development activities. The programs are operational in a batch mode on mainframe and minicomputers. For personal computers, major programs are assembled into packages comprised of one or more applications programs, supporting utilities, and a shell menu system for user interface. The programs include advanced computation and display capabilities. There are 91 programs in the existing family with 21 categorized as major software packages. The structure of the programs and their essential functioning remains batch. The programs are powerful, technical state-the-art software products. They will be supported for the near-term without further modifications.

The engineering applications computing environment is that of the desktop computer, both high-end personal computers and engineering workstations. The engineer-user expects software that is state-of-the-art in technical capability, highly interactive, supported by high quality graphics, and controlled via a graphical user interface. The historical HEC programs are not well structured for efficient adaptation to this new environment and the need to continually improve program capabilities dictates that computer code be easy to modify and maintain.

The NexGen project was formulated to respond to these needs; that is develop successor generation software to the present family of HEC programs. The project began in 1990 and the initial phase completed in 1995. The second phase is now underway.

NEXGEN PROJECT

Begun in October 1990, the NexGen project is now beginning the seventh year of work. The first year was devoted to forming project teams, investigating the array of software engineering issues, and documenting the technical requirements of the software packages. Technical teams developed preliminary requirements statements for the areas of hydrologic analysis, river analysis, reservoir analysis, and flood damage analysis. Software support teams developed preliminary concepts for the areas of software architecture and design, graphical user interface, data base support, graphics, and program development environment and standards.

The teams were each headed by a senior HEC engineer and comprised 3 to 5 technical staff. All 28 HEC technical staff served on at least one team. Staff participated in team activities on a part-time basis while continuing to perform their regular duties. The teams developed consensus on their respective assignments, developed plans for their accomplishment, and provided a study report of findings. The teams were encouraged to seek Center-wide participation through seminars and circulation of concept papers. Consultants from outside the Corps with specialized knowledge also participated. Management oversight is provided through a committee comprised of the team leaders and chaired by the Director. The oversight committee meets periodically to monitor progress, ensure coordination, and surface for resolution common issues that might impede progress. The project and associated management has been integrated with the Corps Water Control Data System (WCDS) (USACE, 1995) modernization project described by the author in another paper of these proceedings.

Team Findings: The technical teams confirmed the NexGen goal of developing a family of successor software packages to serve the U.S. Army Corps of Engineers into the next century. The packages would be designed for interactive use as single station programs or in multi-tasking, multi-user network environments. The river analysis, hydrologic modeling, and flood damage analysis software packages were designated for early development with development for reservoir systems delayed until later in the initial phase.

The Software Architecture and Design, User Interface, and Development Environment teams addressed the issues of computation environment, program architecture, coding language relationship to architecture, software engineering related to program design, and computer hardware and software industry standards. The teams concluded that development should target both RISC-chip based engineering workstations running Posix standard UNIX, and high-end Intel-chip based personal computers running in a Windows environment. Programs would employ a Graphical User Interface (GUI). In UNIX, the X Window standard using Motif for the GUI would be followed. In MS-DOS and successor systems, Microsoft Windows 3.1, Windows 95, and Windows NT would be the targets. Object-oriented programming using C++ and advanced features of Fortran 90 were recommended. Program architecture consistent with the above was formulated and recommended for testing. The program architecture includes deliberate separation of the GUI, graphics, compute engine, and data base. *Since the beginning of the project in 1990, new multi-platform GUI and graphics software development tools, Windows NT (Microsoft, 1994), and the Java (Arnold et al., 1996) programming language have emerged. It has proven to be a challenge to keep up with software industry changes - one has to be quick to field software before something associated therewith becomes obsolete!*

The Data Base Support team addressed the issue of providing for the data persistence necessary to support the GUI, graphics, and technical analysis envisioned for NexGen. The team concluded that the HEC-DSS system (USACE, 1995) best meets the time-series and paired-function data management needs. Model-parameter, and geometry data management needs were concluded to be relatively modest compared to the capabilities of commercial systems. Therefore, the need for a commercial data base management system was discounted. The team recommended continued monitoring of data management needs and emerging systems. Spatial and image data management support for NexGen is necessary with the emerging availability of NEXRAD (WSR-88D) spatial precipitation. HEC-DSS was targeted for extension to handle this data, and linkage to commercial GIS systems recommended for managing certain spatial-type data. HEC-DSS is undergoing modernization, with new GUI and display features being developed. Another paper in these proceedings describes HEC-DSS modernization.

The Graphics team addressed the issues of the nature and amount of data to display, types of displays, and approach to incorporate graphics into NexGen. The team concluded that graphics should follow published and de facto industry standards such as X Windows, and be targeted for common display and output devices. The team recommended use of high-level graphics packages rather than custom coding. The team recommended that a commercial package be tested for the UNIX environment and Visual Basic (Microsoft Inc., 1995) be tested for the Windows environment. Graphics is a particularly vexing problem when a commitment is made to platform portability, as in NexGen. More is said about this later.

NexGen Activities, Events, Time Line: Two development teams were formed in the second year to work on the hydrologic modeling and river analysis systems, the successors to HEC-1 and HEC-2 (USACE, 1995). Both teams focused on critical software development and technical decision items and development of early-stage working prototypes. Their initial efforts carried through the third year with functioning prototypes successfully developed. Although there has been some change in the composition of the teams, they continue to exist to the present.

The hydrologic modeling team took the lead in implementing object-oriented design and coding and worked in the UNIX operating system environment. UNIX and object-oriented development were both new areas for HEC and thus required substantial commitment change and learning. Until that time, HEC was a seasoned Fortran batch program developer. The river analysis modeling team focused on the DOS Microsoft Windows environment and Fortran 90.

At the end of the third year, we assessed: what we had learned; where we were; and identified critical technical and software development decision items. We learned 1) that developing GUI's and interactive graphics were hard and increased the development effort several fold, 2) that working in UNIX is particularly difficult, and 3) that undertaking object-oriented design and coding is not only difficult, but requires a change in approach to program design and coding. The change needed would amount to a software development cultural change for HEC. We concluded that we could make rapid progress toward a new river hydraulics package in the Microsoft Windows environment but the product would not be platform portable (e.g. would not run on UNIX workstations, etc.). It was also clear that object-oriented program development was desirable but would initially be slower, and staff skills would need to be enhanced. We also concluded that contrary to our earlier belief,

we should adopt a multi-platform development product for GUI development. The Galaxy development system (Visix, 1994) was selected. Had Java been in existence at the time of decision, we likely would have opted for it instead. Portability of interactive graphics continued to be a sticky issue that is settled for now with adoption of UNIRAS (Advanced Visual Systems, 1996).

A decision was made to move forward with the river hydraulics model (now named River Analysis System, HEC-RAS) to complete and field a Beta, then maiden version by the end of 1995. We needed a bonafide product from the NexGen effort to demonstrate good faith progress to Corps senior managers and other interested parties. To meet this target, HEC-RAS was to be fielded as a Microsoft Windows application. We decided to continue the HEC-HMS team as the lead in new software development concepts and operating system environments and thus targeted them to field the initial multi-platform product. This decision resulted in HEC-HMS development lagging HEC-RAS by more than a year. These decisions resulted in advancing HEC-RAS development to the Beta version by the end of the fourth year (over 200 testers world-wide participated) and fielding of Version 1.0 in the summer of 1995. Version 2.0, representing some major technical additions, was released in April 1997. HEC-HMS development continued on its pioneering path resulting in fielding an early multi-platform Beta version in the spring of 1997. Subsequent updated Beta versions were released through October 1997. The maiden Version 1.0 release is planned for late in 1997. In the mean time, we needed to accelerate development of the flood damage analysis software (HEC-FDA) because of a critical need to support the newly-adopted Corps policy of applying risk-based analysis in flood studies. The HEC-FDA team leveraged off work by the HEC-HMS and HEC-RAS teams to produce an early working version for Corps field offices.

RIVER ANALYSIS SYSTEM (HEC-RAS)

When completed, the HEC-RAS software package will include one-dimensional steady-flow, unsteady-flow, and sediment transport capabilities. It will thus be successor to HEC-2, HEC-6, and UNET (USACE, 1995). The program will use common geometry for all analyses, and hydraulic properties will be computed by the same routines. Version 1.0 implements the steady-flow model. Version 2.0 extended capabilities to include Federal Highway Administration methods for bridge flow and bridge scour, channel modification template, in-line weirs and gated structures, and GIS linkages for geometry data and inundation mapping. The next major emphasis is on unsteady flow analysis, to be followed by sediment transport analysis. HEC-RAS computes sub- and supercritical profiles, locating critical depth and hydraulic jumps as appropriate. The analysis for bridges has been improved and hydraulics of junctions added. The program is used through a GUI where data entry, editing, graphics, and computations are performed in an interactive environment. Because many thousands of HEC-2 format data sets exist, and large numbers of flood plains have been delineated with HEC-2, special care has been taken to permit importing existing data sets, and to reconcile HEC-RAS results with profiles computed with HEC-2. A large number of identical data sets have been run with HEC-2 and HEC-RAS to identify when different results might occur and to provide the basis for satisfactory reconciliation.

Technical computations routines are coded in Fortran 90 and the GUI is coded in Visual Basic. HEC-RAS is designed to run as a Windows 95 and Windows NT program thus taking advantage of features available in the Windows environment. Graphics are performed by calls to the Windows GDI (Microsoft Inc., 1995) so run-time licencing is not an issue. Version 2.0 is available for Intel-chip Personal Computers running Windows 3.1 or Windows 95 plus Intel-chip PC's and RISC-chip engineering workstations running the Windows NT operating system. At this time, we do not plan to port the complete HEC-RAS GUI and graphics for multi-platform applications - it is simply too costly to justify. Because the compute engine of HEC-RAS will be a component of the modernized Water Control Data System, a limited-scope GUI is being written in Java to accomplish the port to the Sun Solaris (UNIX) computer platform, a hardware component of WCDS. The Control and Visualization Interface of WCDS will handle tabular and graphic displays of HEC-RAS generated results, thus ported graphics are not an issue.

HYDROLOGIC MODELING SYSTEM (HEC-HMS)

The HEC-HMS program, when completed, will include single event and continuous record analysis capabilities. It will incorporate HEC-1, HEC-1C (continuous), elements of HEC-1F (forecasting), and several other limited scope programs. The several modes of analysis will use common time-series data and basin modeling routines. Version 1.0 will implement a basic continuous simulation capability along with existing single event model capabilities and will have spatial precipitation-runoff analysis capabilities. Subsequent releases will have additional capabilities.

Besides existing HEC-1 capabilities, notable technical additions will include accepting raster-spatial precipitation and associated runoff transform (such capability will be needed for analysis with NEXRAD radar output); soil moisture accounting for runoff estimation, and ready acceptance of GIS generated watershed boundaries, streams, and computation parameters. Significant innovations on the user side include interactive point and click, drag and drop model construction, interactive editing, results visualization and animation, and improved data management.

The model architecture is object-oriented and is coded in C++, technical routines are coded in C++ and Fortran 90, and the GUI is built using the Galaxy multi-platform system. Graphics for the Beta and maiden versions are developed via UNIRAS (Advanced Visual Systems, 1996) a proprietary multi-platform graphics development system.

The path to release of HEC-HMS has been an arduous if not an interesting and enlightening one. A prototype of a limited feature capability was built the first year to explore and test object-oriented concepts (here-to-fore HEC was a dyed-in-the-wool Fortran-based organization). After proof of concept, a functioning object-oriented prototype was built over the next two years. We learned enough by then to then re-code the prototype and commence Beta version construction - this over the next couple of years. Many issues of graphics, GUI, and other software issues were explored along the way. Unfortunately there were a number of false starts. In 1995, we began demonstrating the Beta version to limited audiences. To ensure that the first version would be a meaningful technical advance over HEC-1, we commenced research on spatial precipitation processing and associated runoff model architecture. These efforts culminated in the Beta version taught in an HEC course in the Summer of 1997. The class attendees and selected testers response was so

overwhelmingly positive, that we decided to make a release of that version as 1.0 before the year was out, even though other significant technical advances were being completed and coded. The last few months of 1997 were devoted to the industrial production part of new software - bullet proofing the code as much as possible, completing and publishing documents, preparing code and documents for electronic and hard copy dissemination, and preparing for the inevitable flood of inquiries, requests for support, and necessary training materials. Despite HEC being a small, engineering organization, we believe we have produced in HEC-HMS a current software industry technology state-of-the art product that will endure for many years to come. We'll have to wait and see if the effort ultimately pays off.

FLOOD DAMAGE ANALYSIS (HEC-FDA) SOFTWARE

The existing HEC-FDA package is recast in an object-oriented framework, linked to a generic data base file structure for inventory data, and enhanced to include capability for risk and uncertainty analysis in estimating expected annual damage and project performance. The risk-based analysis capabilities represent the result of several years of research into appropriate methods and algorithms for application of risk and uncertainty concepts in the Corps flood damage reduction project studies. Capability is included for inventory data storage and management (via an internal relational data base), uncertainty distribution development for flood plain structure inventory and flood elevation (rating) data, computation of expected annual damage via integration with Monte Carlo simulation, computation of conditional non-exceedance probabilities for flood protective works, and computation and display of uncertainty in project outputs. The program is an integrated piece of software rather than separate components that were previously executed separately. The HEC-FDA architecture is object-oriented and is coded in C++, technical routines are coded in C++ and Fortran 90, and the GUI is built using the Galaxy multi-platform system. CodeBase (Sequiter Software Inc., 1996) provides for internal data storage and management. Graphics for the Beta and maiden versions are being developed with a multi-platform graphics development system. An early version (referred to as Provisional Version 1.0) was released for Corps use in late 1996. The maiden Version 1.0 will be released in late 1997.

RESERVOIR SYSTEM SOFTWARE

Work is also underway on reservoir system software products of the NexGen project. The HEC-PRM prescriptive reservoir system analysis program (USACE, 1995) has been applied in several case-specific instances and continues to be tested for wider applications within the Corps. The program is a network-flow programming reservoir system optimization model with particular utility in study of reservoir system operation plans. A design and prototype development project is underway that is creating a GUI for both HEC-PRM and HEC-5. Both programs make use of similar physical system and operation specification data. Also, design and testing of an object-oriented reservoir simulation module with a focus on real time flood control operations has been initiated. This latter product will be a feature in the modernized WCDS, discussed in another paper.

CONCLUSIONS

The NexGen project is developing successor generation software packages for the U.S. Army Corps of Engineers. These packages are being made available as public domain software to the profession at large. Concepts of object-oriented software design and development offer significant potential benefit in NexGen software development and maintenance. Adherence to published hardware and software standards where available, and de facto standards otherwise, is critical to NexGen program platform portability. Developing prototype hydrologic and river analysis models proved to be essential to surfacing and resolving critical technical and software engineering issues. A structured management approach which employs investigative and development teams proved to be successful. The NexGen project is delivering the promised software products, serving the Corps and the larger water resources community into the next century.

REFERENCES

- Advanced Visual Systems, 1996. Toolmaster (UNIRAS) Release 6.5a. Advance Visual Systems Corporation.
- Arnold, Ken and Gosling, James, 1996, The Java Programming Language. Addison Wesley.
- Microsoft, 1995. Microsoft Visual Basic, Programmer's Guide, Version 4.0. Microsoft Corporation.
- Microsoft, 1994. Microsoft Windows NT, Version 2.4. Microsoft Corporation.
- Sequiter, 1996. CodeBase Version 6.2a. Sequiter Software Corporation.
- USACE, 1996. Annual Report. USACE Hydrologic Engineering Center.
- USACE, 1995. Water Control Data System (WCDS) Past, Present and Future, RD-39. USACE Hydrologic Engineering Center.
- Visix, 1994. Galaxy Application Environment. Visix Software Corporation.

HYDROLOGIC MODELING SYSTEM (HEC-HMS)

John C. Peters, Hydraulic Engineer and **Arlen D. Feldman**, Chief, Research Division,
Hydrologic Engineering Center, U.S. Army Corps of Engineers, 609 Second Street,
Davis, CA 95616

Abstract The Hydrologic Modeling System (HEC-HMS) is "new-generation" software for precipitation-runoff simulation that will supersede the Hydrologic Engineering Center's HEC-1 program. Technical capabilities and operational features of HEC-HMS are described, with emphasis on technical capabilities that differ from those in HEC-1. New features enable use of grid-based (e.g., radar) rainfall data and continuous simulation, and provide enhanced capabilities for parameter estimation.

INTRODUCTION

The Hydrologic Modeling System (HEC-HMS) is "new-generation" software for precipitation-runoff simulation that will supersede HEC-1. In addition to unit hydrograph and hydrologic routing options similar to those in HEC-1, the initial version of the program contains a quasi-distributed runoff transformation that can be applied with gridded (e.g., radar) rainfall data, and a simple "moisture depletion" option that can be used for continuous simulation. HEC-HMS is comprised of a graphical user interface, integrated hydrologic analysis components, data storage and management capabilities, and graphics and reporting facilities (Charley et al., 1995).

As presented by Charley et al., 1995, development of HEC-HMS took place utilizing a mixture of programming languages (C, C++, and Fortran). The software is built for multi-platform usage, primarily workstations and PC's. The computational "engine" and graphical user interface, GUI, are written in object-oriented C++. Hydrologic process algorithms (e.g., infiltration methods) are written in Fortran and have been incorporated into a library labeled *libHydro*. Although linked into a single executable, there are clear separations between the GUI, libraries, and databases and the main simulation engine. This design facilitates use of other components at later dates without having to revise the computational software.

All computations are performed in metric units. Input data may be English or metric and are automatically converted if necessary. The user selects either English or metric for the output results.

TECHNICAL CAPABILITIES

Hydrologic Elements Simulation with HEC-HMS is based on representing a watershed with *hydrologic elements*: subbasin, routing reach, junction, uncontrolled reservoir, diversion, source, and sink. The hydrologic and precipitation computation options are shown in Table 1.

Table 1. HEC-HMS Options

<u>Precipitation</u>	<u>Losses</u>	<u>Transform</u>
grid-based precipitation	initial/constant	ModClark
import hyetograph	deficit/constant	kinematic wave
specify gage weights	Green & Ampt	Clark unit graph
inverse-distance gage weighting	SCS Curve No.	Snyder unit graph
frequency-based design storm	gridded Curve No.	SCS Dimensionless unit graph
		user-specified unit graph
	<u>Routing</u>	<u>Baseflow</u>
	lag	exponential recession
	Muskingum	constant monthly
	Modified Puls	
	Muskingum Cunge	

A *subbasin* is conceptually an element that produces a discharge hydrograph at its outlet. Its properties include area and percent imperviousness. The discharge hydrograph is based on subtracting "losses" from input precipitation, transforming the resulting rainfall excess to direct runoff at the outlet, and adding baseflow. A *junction* is a location where two or more inflow hydrographs are combined to produce an outflow hydrograph.

A *river reach* is conceptually an element for which there is a "known" inflow hydrograph at its upstream end, and which produces an outflow hydrograph at its downstream end. A *reservoir* is similar to a river reach in that there is a "known" inflow hydrograph, and the reservoir element produces an outflow hydrograph. A *diversion* is an element for which a portion of the inflow to the element is diverted, and the remainder passes through. A *source* is an element with which a discharge hydrograph is imported into the basin network, e.g., an observed hydrograph or a hydrograph generated in a prior simulation. A *sink* is an element for which there is an inflow but no outflow.

Continuous Soil Moisture Accounting HEC-HMS includes the deficit/constant-loss method which permits simulation over extended time periods. It is similar to a method contained in the Interior Flood Hydrology Package (HEC, 1992). A moisture capacity for a subbasin must be filled for precipitation excess to occur. A moisture deficit is diminished by precipitation, and during precipitation-free periods is increased at a user-specified rate. Input requirements for the method include the moisture capacity (maximum moisture deficit), an initial moisture deficit, and recovery rates which can be specified with mean-monthly values.

Future versions of HEC-HMS will incorporate more comprehensive soil moisture accounting algorithms that account for evapotranspiration and enable simulation of subsurface contributions to total runoff using several soil moisture and groundwater storages.

Grid-based Modeling Option Traditional application of rainfall-runoff simulation has involved use of spatially-averaged (lumped) values of basin rainfall and infiltration (losses). This approach has been practically useful because rainfall data available from typically sparse gage networks are generally inadequate to justify more spatially-detailed simulation methods. The availability of grid-based (radar) rainfall enhances the attractiveness of modeling approaches that take into account spatial variations of runoff production. Also the availability of GIS for processing data associated with topography, soils, and land use greatly facilitates definition of spatially-variable watershed characteristics as depicted in Fig. 1.

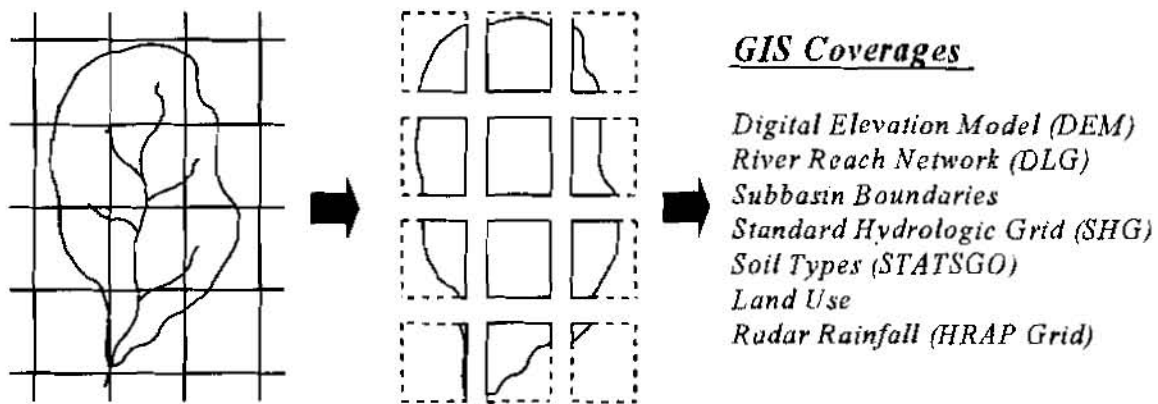


Figure 1. Grid-based Watershed with GIS Coverages

ModClark. The ModClark method (Peters and Easton, 1996; Kull and Feldman, 1998) is an option in HEC-HMS that enables grid-based runoff simulation. The method employs an adaptation of the Clark conceptual runoff model (Clark, 1943), by which direct runoff is represented very simply by two processes: translation and storage. Translation relates to the travel time for runoff contributions to reach the outlet, and storage relates to the attenuating effects of natural storage in the watershed. Two parameters of the method are T_c , time-of-concentration, and R , storage coefficient. T_c can be regarded as the time it takes for rainfall excess from the most remote location in the watershed to reach the outlet. R , a measure of the effects of natural storage, is the slope of the relation between storage and outflow for a linear reservoir. Like T_c , R has units of time.

With the ModClark method, the translation time to the outlet is unique for each grid cell and is based on the travel distance from the cell to the watershed outlet. Cell data needed are the area within the watershed of each cell, and the travel distance from the cell to the watershed outlet. Travel time for a cell is computed as a proportion of the basin travel time by multiplying by (cell distance to the watershed outlet divided by the distance from the most distant cell to the outlet). The lagged rainfall excess for each cell is then routed through a linear reservoir.

Gridded SCS Curve Numbers. With the ModClark method, losses (infiltration) are calculated individually for each grid cell, and are therefore dependent on the rainfall that is

associated with that cell. The potential for infiltration varies spatially in a watershed, and is a function of surface and subsurface characteristics. The Curve Number method of the Natural Resources Conservation Service (formerly Soil Conservation Service) relates losses to soil type and land use. Soils are categorized with relation to their infiltration potential, and land use reflects surface conditions such as forest, pasture, various types of urbanization, etc. Available data bases for soil and land use data can be accessed to provide data for analysis with GIS procedures to generate gridded values for Curve Numbers.

Grid-parameter File. Application of the ModClark method and gridded SCS Curve Numbers requires use of a grid-parameter file. The file associates grid cells with each subbasin, as depicted in Fig. 1, and for each grid cell, the following information is provided:

- cell x-coordinate (ID)
- cell y-coordinate (ID)
- travel distance to basin outlet, in *km*
- area of cell with basin boundaries, in *km²*
- SCS Curve No.

The file can be based on an HRAP grid (Reed and Maidment, 1994) or an SHG grid (Hydrologic Engineering Center, 1996a). The grid type used in specifying rainfall data must be the same as that used for application of the ModClark method. Generation of the grid cell file is achieved with automated procedures involving the use of ARC/INFO and associated macros. The procedures are labeled GridParm and SCSParm.

GridParm. GridParm consists of a sequence of Arc/Info macro language programs for generating cell areas and travel distances (HEC, 1996). The procedures require processing digital elevation model (DEM) data such as are available for the continental U.S. (via Internet) from the USGS EROS Data Center (USGS, 1990). An eight-direction "pour-point" algorithm defines the direction of flow from any grid cell to be in the direction of steepest descent from the cell to one of its eight neighbors. A flow path length (travel distance) is computed by summing the lengths of all segments along the path from the cell to the basin outlet. Area and travel distance are determined for DEM-based cells at a 100 meter resolution. The larger computational cells (e.g., a 2 km resolution for radar rainfall grids) are then superposed and their areas and travel distances are calculated by summing the areas and averaging the distances encompassed by the DEM cells.

SCSParm. SCSParm consists of a sequence of procedures to utilize soil and land use data to develop estimates for Curve Number for each grid cell. The soil data can be obtained from the State Soil Geographic (STATSGO) Data Base (SCS, 1993), which is accessible via Internet and also on a single CD-ROM disk for the continental U.S., Hawaii and Puerto Rico. Land Use and Land Cover (LULC) data can be downloaded over Internet from the U.S.G.S. EROS Data Center. Data from the two sources is intersected to develop areas with unique combinations of soil type and land use. A look-up table is accessed that relates the soil type/land use combinations to Curve Number. Finally, a grid overlay is used to associate a Curve Number with each grid cell.

HECPrePro. HECPrePro (HEC, 1996c) is a GIS preprocessor for developing basin model data for HEC-HMS. The preprocessor can be used to develop the following files for HEC-HMS as well as for general watershed information.

HEC-HMS basin file containing locational and connectivity information for hydrologic elements (as noted above for the grid-parameter file)

Text file listing attributes of hydrologic elements

Drawing Exchange File (DXF) of streams and subbasins that can be used as the basis for a background map in HEC-HMS

The preprocessor requires (as inputs) Arc/Info line coverages of subbasins and streams, and an Arc/Info elevation grid. The basin file generated by HECPrePro provides a schematic representation of a multi-subbasin watershed as illustrated in Fig. 2. The user of HEC-HMS must then provide the parameter data required for runoff simulation by each hydrologic element.

WATERSHED MODEL DEVELOPMENT

A graphical user interface (GUI) provides a means for constructing the watershed model and for specifying information to be retrieved or stored (e.g., importation of data from a previously developed HEC-1 input file), specification of application-specific information (data and execution instructions), and viewing of results. A significant component of the GUI is capability for schematic representation of a network of hydrologic elements (see Fig. 2). The schematic can be used in the initial configuration of a basin model by generating, dragging into place and connecting (graphically) icons that represent components of a basin network. Once a schematic is developed, pop-up menus can be invoked for input of data, to edit data, and to display simulation results.

The entering of data for a large number of hydrologic elements can be tedious if single-element editors are used. The GUI contains global editors for entering or reviewing data of a given type (e.g., values for Green & Ampt parameters) for all applicable elements. If the same data values are being displayed in more than one GUI screen, a change in one screen will automatically be reflected in the other(s).

APPLICATION

The execution of a simulation requires specification of three sets of data. The first, labeled *basin model*, contains parameter and connectivity data for hydrologic elements. The second set, labeled *precipitation model*, consists of meteorological data and information required to process it. The data may represent historical or hypothetical conditions. The third set, labeled *control specifications*, specifies a simulation time window and a fixed time interval for computations. A *project* can consist of a number data sets of each type. A *run* is configured with one of each type of data set.

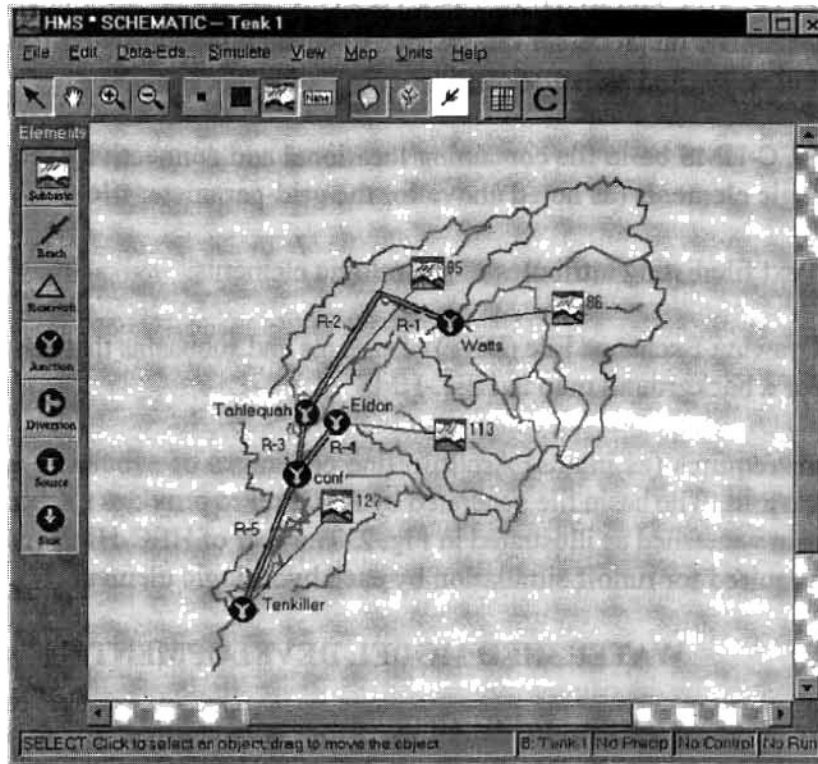


Figure 2. Basin Schematic

PARAMETER ESTIMATION

HEC-HMS provides capabilities for optimization (automated estimation) of the values for selected runoff parameters for situations where observed precipitation and discharge data are available. Parameter estimation is achieved by automated adjustment of the values for selected parameters to produce an *optimal fit* of a computed hydrograph to an observed hydrograph at a target location. The selected parameters may be associated with losses, runoff transformation, baseflow, or routing for any subbasins or reaches upstream from the target location.

The quantitative measure of optimal fit is the *objective function*, which is based on the degree of variation between the computed and observed hydrographs, and is equal to zero if the hydrographs match exactly. The key to automated parameter estimation is a *search procedure* for adjusting the selected parameters to produce an optimal fit; that is, to minimize the magnitude of the objective function. Constraints are imposed on parameter values to ensure that unreasonable values are not utilized.

Initial values for all parameters are required at the start of optimization. A hydrograph is computed at the target location (for which an observed hydrograph has been specified), and the value of the objective function is calculated. The search procedure adjusts values for the selected parameters (i.e., the parameters being optimized), and a new computed hydrograph and objective function are obtained. This cycle is repeated until the change in magnitude of the objective function is minimal, and the search is ended.

Objective Function An objective function is a quantitative measure of how well the computed hydrograph matches an observed hydrograph. The goal of optimization is to adjust parameter values so as to minimize the value of the objective function. Four objective functions are provided: 1) HEC-1 objective function (weighted squared differences between the observed and simulated discharges giving greater weight to differences associated with higher flows); 2) sum of squared residuals; 3) sum of absolute residuals; and 4) percent error in peak flow.

Search Methods You can choose between two methods for adjusting the selected parameters to obtain an optimal fit. The Univariate Gradient Method (HEC, 1982) varies the magnitude of one parameter at a time while holding the magnitude of the remaining selected parameters constant. The Nelder and Mead Method (Johnston and Pilgrim, 1976) changes the magnitude of all selected parameters each iteration. The search process takes longer than with the univariate gradient method, but may produce a more nearly optimal fit.

Initial Values and Constraints Initial values for parameters are required at the start of an optimization. The default initial values are those specified in the basin model. However, you can override any default initial value. *Hard constraints* limit the range of values that a parameter may have. Such constraints are used to keep the magnitude of a variable within physically reasonable limits, or to preclude values that cause instabilities or errors in computations. For example, negative loss rates are not allowed. When a search method attempts to use a value outside the range of hard constraints, the value is changed to the constraining value. You can specify *soft constraints* to keep parameter values to within tighter limits than those defined with the hard constraints. When a search procedure proposes a value outside of the soft constraints, the value is used, but the objective function is multiplied by a penalty factor.

Partial Derivatives Partial derivatives of the objective function are displayed as an aid for evaluating optimization results. A partial derivative is computed for a parameter by computing the objective functions at 0.995 and 1.005 times the optimal value of the parameter (with all other parameters held at their optimal values). The partial derivative is estimated as the difference between the values of the objective function divided by the difference between the parameter values. If a parameter value obtained by multiplying by 0.995 or 1.005 exceeds a hard constraint, the parameter value is set to the constraint, and the constrained value is used to calculate the partial derivative.

CONCLUDING REMARKS

A new generation of rainfall-runoff simulation models makes use of terrain-based data that cannot practically be developed by manual methods. GIS-based procedures enable efficient processing of such data to provide required parameters such as cell-based travel times and infiltration indices. Furthermore, GIS can be used to develop the configuration of multi-subbasin models as well as values for various watershed attributes. A simple continuous soil moisture accounting method is now available in HEC-HMS. Planned additions to HEC-HMS include: 1) comprehensive soil moisture accounting; 2) snow simulation; and 3) automated adjustment of discharge-frequency relationships to reflect land-use and project alternatives.

REFERENCES

- Charley, W., Pabst, A., and Peters, J., 1995, The Hydrologic Modeling System (HEC-HMS): Design and Development Issues. *Proc. Am. Soc. Civil Engrs. 2nd Congress on Computing in Civil Engineering*, Atlanta, Georgia.
- Clark, C.O., 1945, Storage and the Unit Hydrograph. *Trans. Am. Soc. Civil Engrs.*, 110:1419-1488.
- HEC, 1982, Hydrologic Analysis of Ungaged Watersheds Using HEC-1. Training Document No. 15, Hydrologic Engineering Center, US Army Corps of Engineers, Davis, CA.
- HEC, 1992, Interior Flood Hydrology Package, User's Manual. Hydrologic Engineering Center, US Army Corps of Engineers, Davis, CA.
- HEC, 1996a, HEC Proposes Standard Hydrologic Grid (SHG). *Advances in Hydrologic Engineering* (HEC March 1996 Newsletter), US Army Corps of Engineers, Davis, CA.
- HEC, 1996b, GridParm: Procedures for Deriving Grid Cell Parameters for the ModClark Rainfall-Runoff Method. User's Manual, US Army Corps of Engineers, Davis, CA.
- HEC, 1996c, HECPrePro - GIS Preprocessor for HMS. User's Guide and Reference Manual, prepared by Center for Research in Water Resources, University of Texas.
- Johnston, P.R. and Pilgrim, D.H., 1976, Parameter optimization for watershed models. *Water Resources Research*, 12(3), 477-486.
- Kull, D. W. and Feldman, A.D., 1998, Evolution of Clark's Unit Graph Method to Spatially Distributed Runoff. *Journal of Hydrologic Engineering*, Am. Soc. Civil Engrs., Vol. 3, No. 1, 9-19.
- Reed, Seann M. and Maidment, David R., 1994, Geographic Positioning of the HRAP Grid. Center for Research in Water Resources, University of Texas at Austin.
- Peters, J.C. and Easton, D.J., 1996, Runoff Simulation Using Radar Rainfall Data. *Water Resources Bulletin*, American Water Resources Association, Vol. 32, No. 4.
- Soil Conservation Service, 1993, State Soil Geographic Data Base (STATSGO) Data Users Guide. U.S. Department of Agriculture: Miscellaneous Publication Number 1492, Washington, D.C.
- USGS (US Geological Survey) 1990, Digital Elevation Models. USGS Data Users Guide 5, Reston, Virginia.

HYDROLOGIC ENGINEERING CENTER NEXGEN DATA STORAGE SYSTEM (HEC-DSS)

by

William J. Charley, Hydraulic Engineer, and
Arthur F. Pabst, Chief, Technical Assistance Division,
Hydrologic Engineering Center, U.S. Army Corps of Engineers, Davis, California;

Abstract: The Hydrologic Engineering Center's Data Storage System (HEC-DSS) enables the efficient storage and retrieval of time series and other data widely used in water resource studies. The HEC-DSS is used in many hydrologic and hydraulic computer programs, and is being incorporated into HEC's new NexGen suite of programs. There are currently approximately 15 utility and graphics programs available for both UNIX and PC operating systems. HEC is modernizing HEC-DSS with a Graphical User Interface (GUI), which will run on most of today's computer systems. The Java programming language was selected because of its multi-platform ability, quick development time, industry support, networking and GUI capabilities. The HEC-DSS GUI provides robust graphing and data manipulation capabilities. Data may be selected by means of tabular or map-based displays.

INTRODUCTION

Summary: The Hydrologic Engineering Center (HEC) developed the Data Storage System (HEC-DSS) to manage serial data for water resource engineering. The system enables fast and efficient storage and retrieval of time series and other data types for which storage in blocks of contiguous data is appropriate. The system consists of a set of computer library routines, which can readily be used with application programs, and a set of utility programs to manipulate, display, and maintain data stored in HEC-DSS database files. This database system is being used by programs being developed under the HEC NexGen program modernization project (HEC, 1995). A graphical user interface (GUI) program for HEC-DSS, which is near completion, uses the Java programming language to perform many of these utility functions.

History: The HEC-DSS (not to be confused with a Decision Support System) was the outgrowth of a need that emerged in the mid 1970's. At that time, most studies were performed in a step-wise fashion. Data was passed from one analysis program to another in a manual mode. While this was functional, it was not very effective. Programs that used the same type of data, or were sequentially related, did not use a common data format. Also, each program had its own set of graphics routines, or other such functions, to display results.

The Kissimmee River study, performed by HEC for the Jacksonville District of the Corps of Engineers beginning in 1978, required that an orderly approach be used to properly manage the data and results of analyses. The study involved the processing of a large number of alternative plans and conditions, and gave birth to the first version of HEC-DSS. The basic design provided for the storage of data in a standard form, independent of any particular program. The data was

provided to the programs when it was needed, and results were stored in the standard form for use by utilities and other application programs.

Current Applications: The current HEC-DSS version (version 6) includes a set of Java and C++ interface classes, as well as Fortran interface routines, for use by application programs. HEC-DSS has been installed on a variety of computers including PC's running Windows (95 and NT) and DOS, Apple Macintosh, UNIX workstations (Sun, Mips, Hewlett Packard, and Cray to name a few), and others. There are no licences or fees required for HEC-DSS or its utilities; the software is in the public domain.

The HEC-DSS is generally considered to be a "model-oriented" or a "working" database system. Currently HEC-DSS is used extensively in Corps offices for both project studies and real time water control and reservoir operations (HEC, 1993). In water control and reservoir operations, data (such as precipitation and stream flow data) are received from field data collections platforms via satellite and stored in a HEC-DSS database. When a modeling run is to be made, raw data is screened for missing and erroneous values. Validated precipitation data is processed to compute subbasin averages for a watershed. These are used by a rainfall-runoff model, along with validated observed flows and estimated future rainfall, to compute forecasted flows. The forecasted flows are retrieved by a reservoir operations model to compute the appropriate operations and modified flows. An economic benefits / flood impact model may then use these values to compute damages or project benefits. This procedure requires a number of exchanges of series data sets between the models. The HEC-DSS provides this capability, plus a set of utility programs to display, edit and maintain the database. Several Corps offices use a relational database, such as Oracle, in conjunction with the HEC-DSS, to store parameter data and other information that fits well into a relational construct.

HEC-DSS Characteristics: The HEC-DSS is designed specifically for data that occur as a series of numbers or text. Examples of data which are currently stored by HEC-DSS are time series (both regular interval and random reporting), curve coordinates (such as rating tables), radar images (such as NEXRAD radar data) (HEC, 1996), and text information (such as on-line documentation). HEC-DSS is not optimized for dealing with single data values, nor is it effective at conditional data searches common to relational database systems.

Internally, HEC-DSS provides efficient storage and retrieval of variable length data records based on unique user given record keys, called pathnames. A pathname consists of six parts that describe the data set, such as its watershed, location, parameter, beginning time and version. This convention makes the data set self-documenting. Time series data is stored in natural, manageable sized blocks. An example pathname for regular-interval flow data is:

`/SACRAMENTO RIVER/RED BLUFF/FLOW/01MAR1995/1HOUR/OBSERVED/`

The data for this pathname would consist of a month of hourly values, in this case 744 values. Although individual data sets are stored in time oriented blocks, user and application program interfaces and utility programs simply use a start and end date and time to identify a data sequence. Stored along with the data is other descriptive information, such as the units and type

(e.g., instantaneous or average), and an optional set of flags that describe each data value's quality or validation. Time series data can be stored in a compressed mode, with the compression and expansion accomplished internally by the software. Because HEC-DSS was initially designed to store data for long model simulation runs of hundreds of years, "year 2000" compliance is assured.

The pathname is the key to the data's location in the data base. A pathname is analyzed by the HEC-DSS to determine a "hash" index number. This index determines where the data set is stored within the database. The design ensures that very few disk accesses are made to retrieve or store data sets. One data set is not directly related to another, so there is no need to update other areas of the database when a new data set is stored.

Because of the self documenting nature of the pathname and the conventions adopted, there is no need for a data dictionary or data definition file as required with other database systems. In fact there is no database creation tasks or any database setup. By just providing a name to an application or utility program, a HEC-DSS database file will be generated and configured automatically. There is no pre-allocation of space; the software automatically expands the file size as needed.

An HEC-DSS database file has a user-specified conventional name, with an extension of ".dss". As many database files as desired may be generated and there are no size limitations, apart from available disk space. Corps offices have HEC-DSS files that range from a few data sets to many thousands. The HEC-DSS adjusts internal tables and hash algorithms to match the database size so that both small and very large databases are efficiently accessed.

Database Access: A principle feature of the HEC-DSS is that many users can read and write data to a single database at the same time. This multi-user access capability is implemented with system record locking and flushing functions. There is no daemon, or other background program, that manages accesses to a database. A database may exist on a Windows or Unix server machine, and can be accessed by users on PC's or other computers via NFS or the Microsoft network, as long as locking and flushing functions are implemented.

Unlike many commercial database systems, the HEC-DSS was designed to be easily added to a user's application program. In traditional "C" and Fortran programs, only two or three function calls are needed to access data. Those calls identify the database, the pathname, and a time window (if desired). Besides these languages, an extensive set of classes are available in both C++ and Java languages, the languages with which most new HEC "NexGen" programs are being developed. The NexGen programs make extensive use of HEC-DSS. However, these programs are designed so that users do not see the interaction with HEC-DSS; most of the time they will not know that it is being used.

Utility Programs: Currently there are several utility programs for HEC-DSS (HEC, 1995). These include a graphical display program, which provides report quality graphs of data; a mathematical manipulation program, which can perform a multitude of functions on data; a database utility program, which provides a mechanism to rename, edit, copy, import, export and

perform similar functions on data; a report generation program, which produces tables in a user specified format, and several data entry programs. These programs are relatively simple to use. For example, the graphical display program knows how to plot the data, and what the legends should contain, without additional information from the user. On the other hand, there are several commands that allow the user to customize a plot.

HEC-DSS GRAPHICAL USER INTERFACE

Overview: The current utility programs are windows based on Unix platforms, and “command prompt” based on computers running Microsoft Windows. Although none of the utilities are scheduled for retirement, a development project is nearing completion to produce a Java based graphical user interface to the HEC-DSS to provide user access to data and to perform common utility functions. This includes data display (both tabular and graphical), data entry and editing, mathematical manipulations, and database utility functions (such as deleting, copying, renaming, etc.). It has been designed to take into account “non-users”, inexperienced users and experienced users. It is intuitive to use, yet sufficiently robust to accommodate reasonable needs of most users. The Java programming language was selected because of its multi-platform ability, ease of use, industry support, networking and GUI capabilities (Cornell, 1997, and Flanagan, 1997). The interface is scheduled for release in 1998.

The HEC-DSS GUI has two primary interfaces for accessing data. The first is map-based, and the second is pathname list-based. The map-based interface, as depicted in Figure 1, is intended primarily for the display, tabulation (and editing) of data sets. Users identify data sets by selecting a location on a map displayed on the screen, and then choose the data parameter and version from selection boxes adjacent to the map. The HEC-DSS details (such as the pathname) are hidden from the user. In fact, the casual user may not even know that HEC-DSS is used as the database. The map interface requires a configuration file, which contains the map vectors (basin outline, river reaches, county boundaries, etc) in longitude/latitude or similar coordinates, whereas the list-based interface does not require a configuration file or setup. The map interface also has the potential to be used as a display interface for a user’s application program.

The list-based interface has two “views” of pathnames in the database. The first provides a list of sorted pathnames, while the second presents sorted pathnames separated into parts, as shown in Figure 2. A user may further refine the list by searching for a string in the pathnames, or by searching for a pathname part (for example, show all pathnames that contain “Flow” values for location “South Fork”). The list may be re-sorted by clicking on the pathname part title at the top of the list, in much the same way as Windows Explorer does for files.

Pathnames are selected and inserted into a sub-list similar to how files are selected in Windows Explorer. A pathname may be selected by double clicking the pathname, or by a single click then pressing the “Add” button. Multiple pathnames can be selected using the standard windows convention. Pathnames may be removed from the sub-list by selecting the pathname in the sub-list, then pressing the “Remove” button. Once the sub-list is complete, the user selects the operation to perform on pathnames in that list, such as graphing, tabulating, or other functions.



Figure 1. Preliminary Map-Based Interface

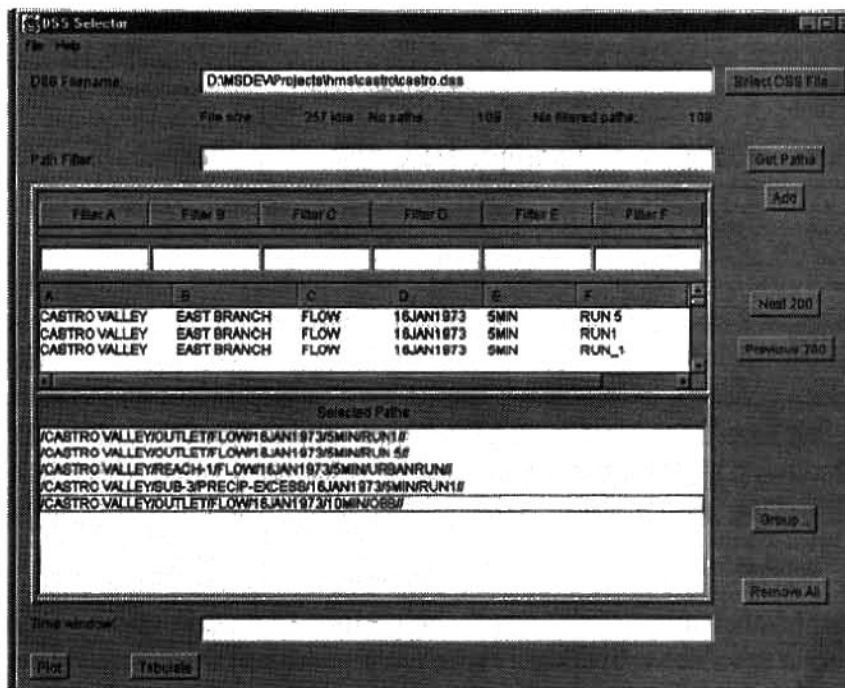


Figure 2. Preliminary Pathname Selector List

Data Display: The HEC-DSS GUI's graphing capability will generate a default plot of the data sets in the sub-list using pathname parts and the units from the header for labels. An example is shown in Figure 3. The user can customize the plot by selecting "graph options" from the menu. This brings up a window which allows the user to change curve and background colors; set the title, legend, font and a variety of other items. The customization settings can be saved in a "templates" file and can be applied to other data sets, if desired. The plot can be printed or saved as a postscript or "gif" file. Future versions of the GUI will allow data to be graphically edited using the mouse.

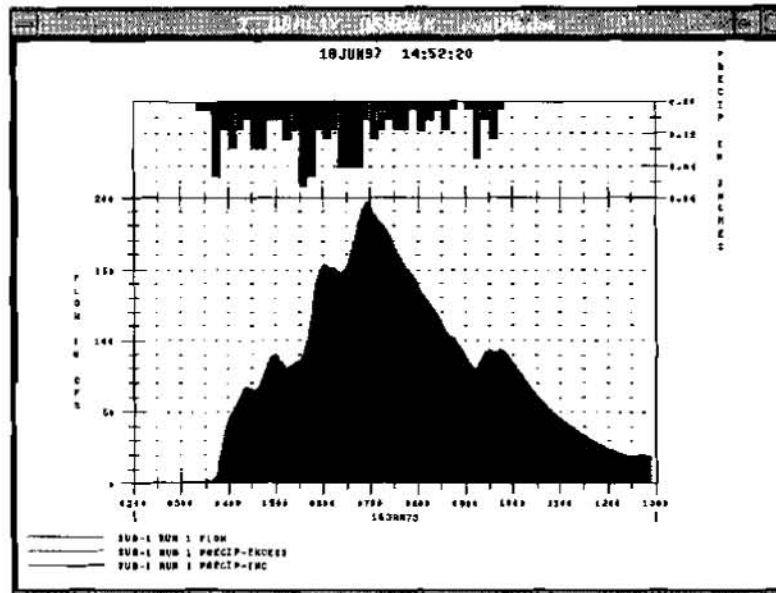


Figure 3. Example HEC-DSS Data Plot

Data sets are tabulated in a column-based approach, as depicted in Figure 4. For time series data, the date and time are in the left hand columns of each row, followed by values for each of the data sets in succeeding columns. A scroll bar can be used to scroll through the data. The tabulation window can be printed by selecting the "print" option from the menu. Data sets may be edited in this window, if the user has permission, by selecting a value with the mouse and changing the number. Data sets may also be edited through the main interface using a system editor.

Utility Operations: Mathematical functions can be performed on data sets by choosing the desired function from a drop down list box. There are several functions available: standard math functions, such as add, subtract, multiply and divide by a constant or another data set; unit conversion; record statistics (minimum, maximum, average); interpolation; smoothing; and others. Resulting data sets can be plotted or tabulated prior to saving.

Date	Time	Inflow (cfs)from Sub-1	Inflow (cfs)from Reach-1	Outflow (cfs)
16 Jan 73	0300	0.82	0.46	1.23
16 Jan 73	0305	0.82	0.46	1.28
16 Jan 73	0310	0.82	0.46	1.28
16 Jan 73	0315	0.82	0.46	1.28
16 Jan 73	0320	0.82	0.46	1.28
16 Jan 73	0325	1.15	0.46	1.61
16 Jan 73	0330	1.88	0.46	2.34
16 Jan 73	0335	2.66	0.46	3.12
16 Jan 73	0340	3.38	0.46	3.85
16 Jan 73	0345	16.03	0.47	16.50
16 Jan 73	0350	43.41	0.48	43.89
16 Jan 73	0355	62.82	0.54	63.36
16 Jan 73	0400	68.23	0.79	69.03

Figure 4. Example HEC-DSS Tabulation Window

The HEC-DSS GUI can perform several database utility operations. These include renaming, copying, deleting, and editing data sets; and import and export capability (e.g., from spreadsheet programs). The utility edit function will write several data sets to a text file, which the user may then edit with any text editor. This permits a global search and replace function and allows the user to be comfortable with their own editor.

Scripting: The scripting language NetRexx is built into the GUI, which provides a mechanism to automatically perform tasks and allows the program to be run in the background or on a timer schedule. In addition to the script, a command input window will be available for users who prefer to type in program commands rather than using the mouse to select operations. The script and command input are designed so that they will accept common commands and macros from the current suite of HEC-DSS utility programs.

Network Access: The HEC-DSS GUI is being developed to run as a standard stand-alone application or, optionally, as a client-server application using Java's Remote Method Invocation (RMI). The client-server implementation will permit users to view and modify data (if given permission) on their local computer from the database of a remote computer without relying on NFS or other disk sharing protocols. This, coupled with the map-based interface, provides a means for users to view data on a central computer or server without having to know about HEC-DSS. Under investigation is the possibility of offering this client-server capability in a browser environment such those provided by Netscape and Microsoft. The client portion of the program could either be downloaded as an applet or used by the browser as a "plug-in" program.

Conclusion: HEC-DSS provides an efficient database for storing and retrieving serial data for application and utility programs. Programs being developed under the HEC NexGen

modernization project use HEC-DSS for serial data storage. These programs, and portions of the HEC-DSS GUI where appropriate, will attempt to shelter details of the database from the user. The map-based interface will provide access to data for both novice and experienced users.

Development of the HEC-DSS GUI will continue. Plans for additional capability include the ability to generate spatial plots of data overlaid on the map screen. This includes color contours from discrete points (such as accumulated precipitation from gages) and gridded NEXRAD precipitation graphics.

REFERENCES

- Cornell, Gary, and Cay S. Horstmann, Core Java, Prentice Hall, Upper Saddle River, New Jersey, 1997.
- Flanagan, David, Java In A Nutshell, O'Reilly and Associates, Inc., Sebastopol, CA, 2nd Edition, 1997.
- HEC, "Application of Rainfall-Runoff Simulation for Flood Forecasting", TP-145, U. S. Army Corps of Engineers, Davis, CA, June, 1993.
- HEC, "HEC-DSS User's Guide and Utility Manuals, User's Manual", CPD-45, U. S. Army Corps of Engineers, Davis, CA, March 1995.
- HEC, "The HEC Hydrologic Modeling System", TP-150, U. S. Army Corps of Engineers, Davis, CA, November 1995.
- HEC, "Runoff Simulation Using Radar Rainfall Data", TP-155, U. S. Army Corps of Engineers, Davis, CA, August 1996.

OVERVIEW OF HYDRO-ENVIRONMENTAL MODELING AND SIMULATION SYSTEMS FOR THE U.S. DEPARTMENT OF DEFENSE

by J. P. Holland, PhD, PE
U.S. Army Engineer Waterways Experiment Station
Vicksburg, MS 39180-6199

Abstract: The U.S. Army is the lead within the U.S. Department of Defense (DoD) modeling and simulation (M&S) tool science and technology development in support of hydrodynamic, transport, and environmental quality (EQ). This research and development is led for the Army by the U.S. Army Engineer Waterways Experiment Station (WES). WES is an international leader in M&S for groundwater, estuaries, reservoirs, rivers, watersheds, and wetlands. Described below are a series of WES-developed M&S tools that directly support EQ. In addition, the technology and knowledge gaps that must be overcome in order to achieve the levels of EQ modeling technology required by DoD are overviewed.

INTRODUCTION

The U.S. Army Engineer Waterways Experiment Station develops a series of groundwater, surface water, and watershed modeling systems in support of military installation and Army civil works water resources project design, operation, and management. Applications of these systems are conducted by multiple organizations (e.g., U.S. Army Corps of Engineers field offices, U.S. Army, Navy, and Air Force installations, Department of Energy, Environmental Protection Agency (EPA), academia, etc.) and WES in support of environmental quality (EQ) and water resources management investigations. These investigations involve risk and tradeoff analyses for impact assessment, compliance and regulatory issues, risk reduction, and natural/cultural resource management. The tools overviewed below have all been developed through a partnership with other DoD and Federal agencies (particularly EPA, which often recommends and funds WES M&S tool development in the EQ area), and academia. Note that each of these tools is actually a computational system within itself, allowing access to multiple models, analysis tools, visualization, animation, parameterization, etc. Limited details for each of these systems is provided herein; more details are provided in Holland et al (1997) and Holland (1996).

GROUNDWATER MODELING SYSTEM - the GMS

The DoD GMS is among the state-of-the-art groundwater modeling systems in the subsurface modeling community. The GMS's ongoing development is under the auspices of the Groundwater Modeling Program. This program, led by WES for DoD, is a highly-integrated, partnered program with collaborators from five DOE laboratories, two EPA labs, and multiple DoD organizations. In addition, 20 academic institutions are partnering or have partnered in the effort. Version 2.0 of the GMS has been fielded and is in use by over 600 federal research groups within DOE, EPA, and DoD. The system provides access to five three-dimensional groundwater models presently; this number will increase to eight by mid-FY98, and to 12 by the end of FY98. As stated above, the system also has state-of-the-art visualization, conceptualization, and parameterization capabilities on-board. The GMS runs on UNIX workstations, personal

computers running Windows, and supercomputers. A key component of the system, the Map Module, increases the productivity of subsurface conceptualization, flow/transport modeling, and remedial design simulation by over a factor of 10. Ongoing research in the impacts of subsurface heterogeneity on subsurface flow/transport, development of remedial design/optimization modules for 15 cleanup technologies, and surface water / groundwater interaction M&S will continue through at least 2000. These GMS activities are discussed in more detail by Holland (1996). The desktop of the GMS, with a contaminant plume from Aberdeen Proving Grounds, MD visualized, is shown in Figure 1.

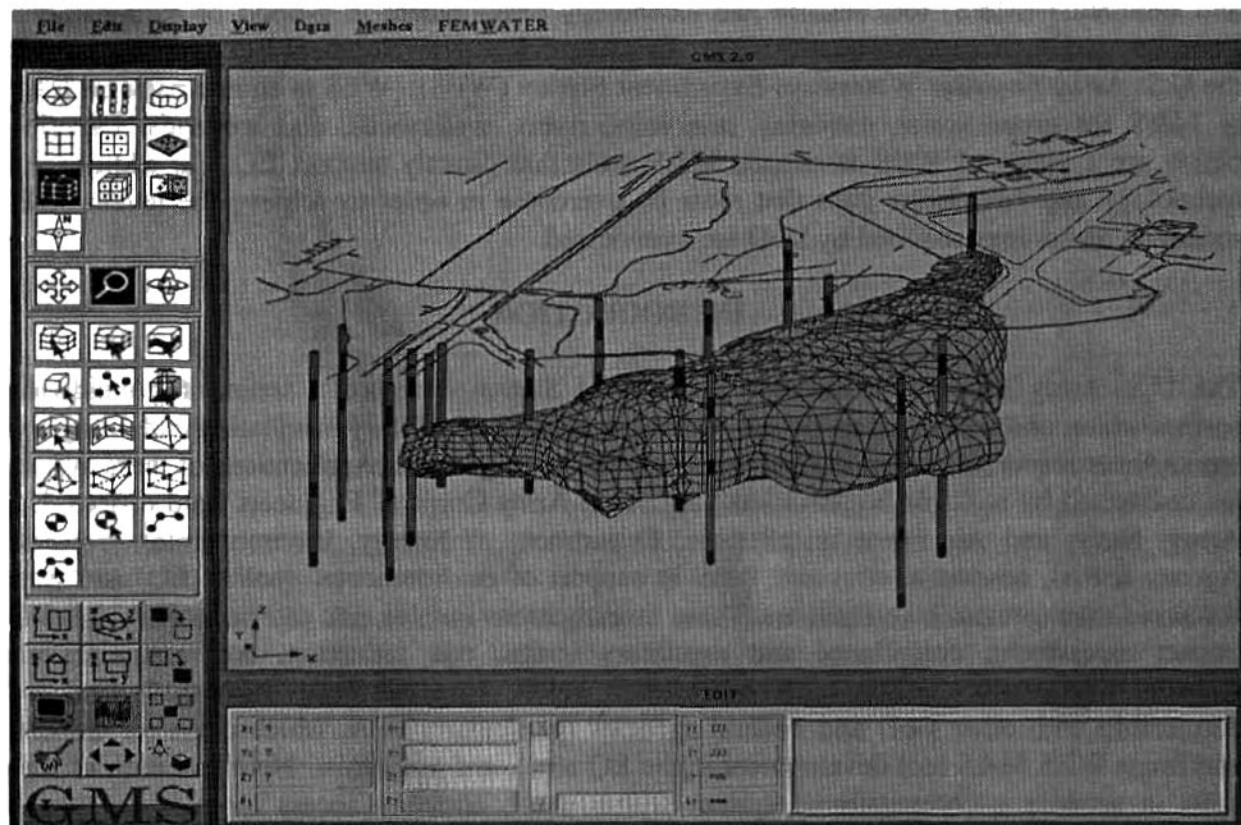


Figure 1. Desktop of the DoD GMS with Visualization of a Contaminant Plume

SURFACE WATER MODELING SYSTEM - the SMS

This surface water modeling system, developed primarily through Army Civil Works research and development, provides access to multiple incompressible Navier-Stokes (NS) solvers in both two and three spatial dimensions. The SMS has been developed for several multi-dimensional hydrodynamic and water quality models (including CH3D-WES, RMA10-WES, CEQUAL-ICM and the two-dimensional hydrodynamic/sediment transport system, TABS-MD) in concert with Brigham Young University (BYU, which provides analogous support to the GMS development) to address the need for efficient model setup, execution, and analysis. The system is mouse driven with pull-down menus and requires a minimum of manual data entry. The interface was designed to allow easy application of each of the models in the WES multi-dimensional

hydrodynamic modeling family. The interface provides access to several state-of-the-art visualization and animation capabilities. Several estuarine, riverine, and wetland sites have been modeled via SMS. SMS software runs on personal computers running Windows as well as multiple UNIX workstations. The system provides hydrodynamic, salinity, and sediment transport M&S capabilities in support of ecosystem management in estuaries, rivers, and wetlands. The graphical user environment for the SMS is directly analogous to its GMS counterpart. This M&S system has been used extensively in support of natural resources management strategy development for New York Harbor (Figure 2), Galveston, Chesapeake, and San Francisco Bays, the Mississippi River, South Florida Ecosystem Restoration, and numerous wetland environments. Details regarding the models within the SMS are given in Holland et al (1997), Johnson et al (1994), and Cerco and Cole (1995).

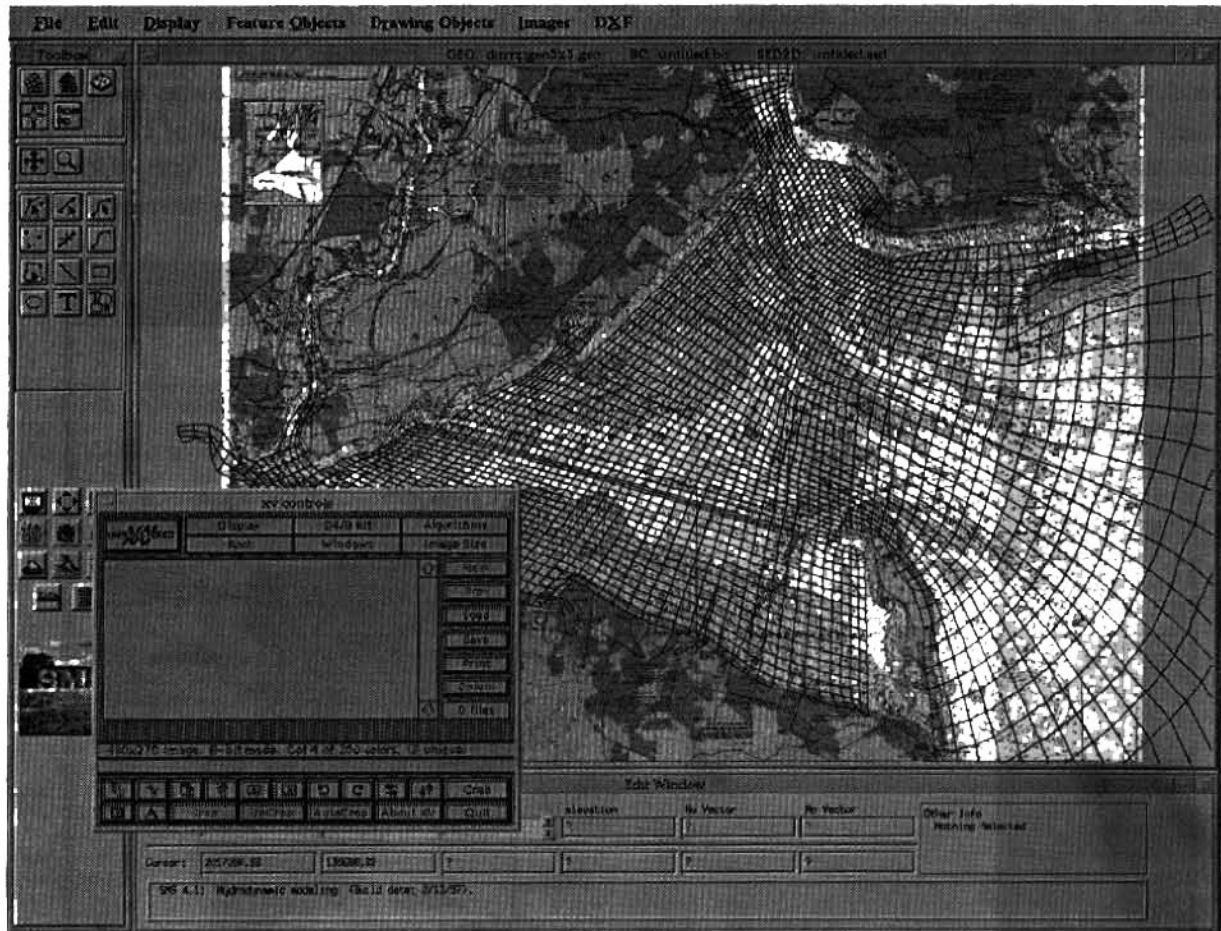


Figure 2. SMS Desktop with Numerical Grid Overlaying New York Harbor

WATERSHED MODELING SYSTEM - the WMS

The WMS provides DoD with the ability to productively conduct lumped-parameter and multi-dimensional watershed analyses in support of groundwater cleanup (infiltration boundary conditions) and resource management (e.g., computations of the impacts of runoff on erosional patterns, and corrections thereto, on DoD installations and Army civil works water resources

projects). Developed through leveraging military and Army Civil Works research, the WMS has been developed with the same look and feel as the SMS and GMS. Partnering with EPA has greatly extended the scope of this hydrologic modeling system.

Triangulated Irregular Networks (TINs) are employed within the WMS for defining the topography and calculating vital hydrologic statistics. TINs are created by inputting digitized data, either from digital topographical maps or from manually digitized data, and triangulating the points. Once the TIN is created, a continuous surface is modeled by interpolating between the corners of the triangles. After the surface is modeled, WMS automatically defines the stream network on the user's screen and calculates the contributing drainage area to each of the user-defined stream junctions. The WMS employs NEXRAD radar information in assessing precipitation intensities, durations, and distributions. The WMS then writes out the data into a form one of several watershed models (e.g., HEC-1, TR-20, or CASC2D) supported by the system accepts. The WMS is in use in support of Picatenny Arsenal, NJ, Ft. Hood, TX, Ft. Carson, CO, and Aberdeen Proving Grounds, MD. The system also continues to be used as the primary system for hydrologic predictions for the Sava River (Figure 3) in support of U.S. Forces in Bosnia. This latter study is being conducted in collaboration with the U.S. Army Corps of Engineers Cold Regions Research and Engineering Lab and the Topographic Engineering Center.

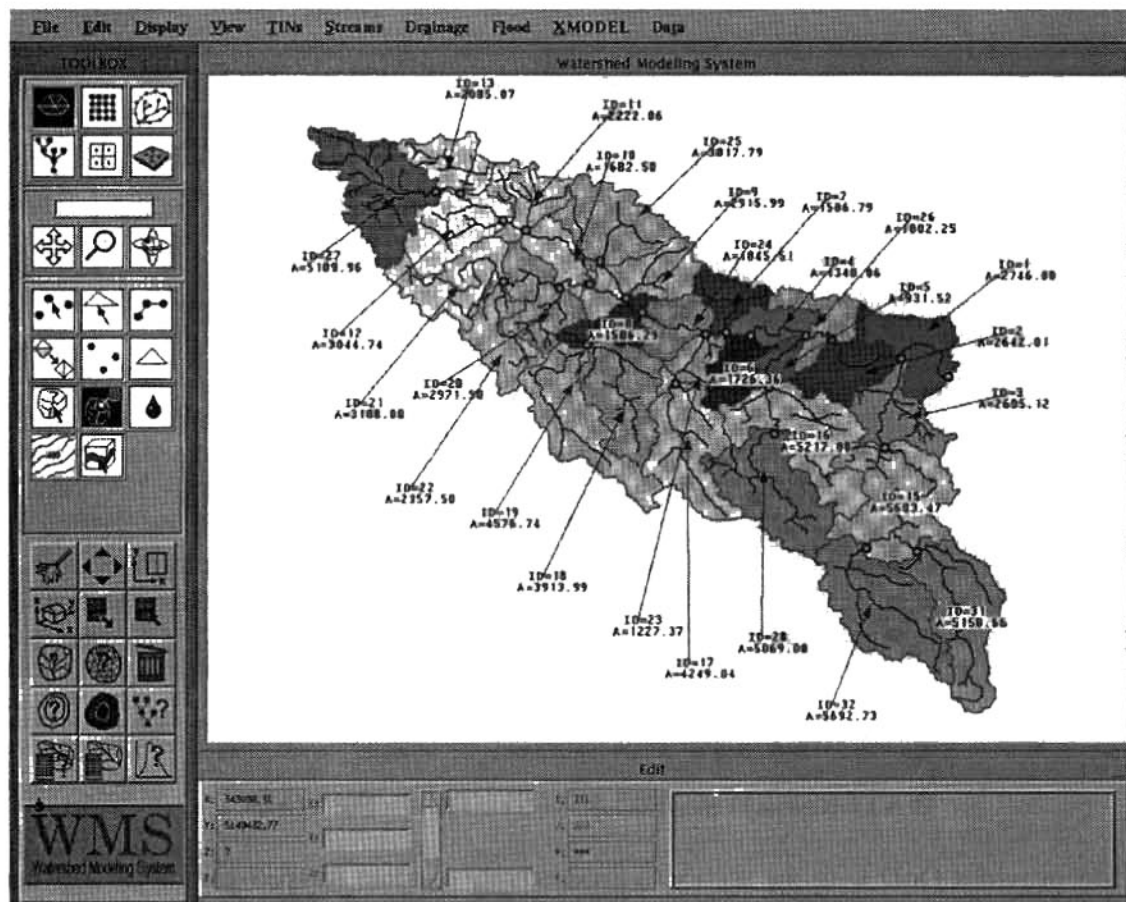


Figure 3. Sava River Attributes as Modeled within the WMS

M&S SYSTEM DEVELOPMENT PATH

Synopsized in the table below is the planned development path for the M&S systems presented above. This development path is specifically developed to produce coupled M&S systems in support of DoD EQ that provide an ever-increasing level of computational and scientific sophistication.

M&S System Capability	Deliverable Dates
Addition of optimal remedial design modules for fifteen technologies to the GMS.	FY96-00
Integration of watershed and groundwater modeling tools within the GMS and WMS.	FY96-98
Coupling of surface water and groundwater modeling tools for multi-scale phenomena. Integration of tools under a comprehensive modeling environment (CME).	FY98-99
Initial coupling of GMS and risk assessment for ecological impact.	FY98-99
Enhancement of SMS and WMS for full contaminants modeling and initial ecosystem response.	FY97-99
Incorporation of full decision support for risk reduction to both ecological endpoints and human receptors	FY98-01
Efficient M&S under CME for integrated surface water - groundwater - watershed investigations w/conceptual uncertainty and risk reduction.	FY99-01
Full ecosystem M&S under CME with risk and uncertainty for both human and ecological receptors.	FY00-02

TECHNICAL GAPS ASSOCIATED WITH M&S DEVELOPMENTS

The developments envisioned above will require, at a minimum, that the following technical gaps be overcome:

- Spatial heterogeneities are poorly handled in the current groundwater modeling formulations, thereby greatly reducing modeling confidence and risk reduction
- The uncertainties associated with physical site conceptualization and parameter estimation are poorly integrated in current modeling state of practice
- Limited information on a host of fundamental contaminant processes is

known, particularly for military-unique contaminants

- Similarly, limited quantification of ecological response to DoD practices in the environment has been investigated. In particular, linkage of hydrogeologic modeling with biological response and ecological modeling is needed to provide more complete feedback between water management decisions and environmental responses.
- Computationally-efficient linkages of surface water, groundwater, and watershed responses, each with vastly differing temporal scales, are required
- More rigorous testing of existing groundwater and watershed models is required
- New computational algorithms that take maximum advantage of scalable parallel computing architectures will be required to address high-resolution and integrated systems calculations
- Seamless linkage of remotely-sensed data, ground truth, and various forms of soft data with models is required to make most effective and efficient use of these technologies for decision making
- Improved interpretation of NEXRAD radar as a part of hydrologic simulation is needed

WES and its technical partners have embarked on a technical plan of attack which will greatly decrease these gaps over the next five years. It is equally clear that modeling technical support is needed. Water resources and installation managers have been reluctant to use advanced M&S tool developments. It is very possible that this reluctance is due to a lack of communication on the part of the research community concerning the worth of such tool development for resource conservation, compliance, and cleanup. As a means of increasing field awareness in groundwater modeling tool capabilities, the Army (through a partnership between the Army Environmental Center and the Corps of Engineers) has established a Groundwater Modeling Technical Support Program at WES. WES has found through years of hydro-environmental modeling that the modeling user community makes most effective use of such sophisticated modeling technology when properly supported by a trained and dedicated in-house technical staff.

SUMMARY

The Department of Defense, as a national leader in hydrodynamic and environmental quality modeling, has at its disposal an excellent cadre of M&S technology in support of hydro-environmental analysis and decision support. The effective use of this technology has been shown to result in significant cost savings, and results in more timely acceptance of DoD activities by regulatory agencies. The EQ modeling and simulation challenges of the future will require significant technical gaps to be overcome. These gaps can be overcome through the

conduct of focused research investigations planned and executed by the DoD services and its technical partners. Dedicated, in-house technical support for field use of M&S technologies as parts of their site-specific EQ activities is a key component in effective implementation of M&S technologies in the EQ area. Bringing these points to fruition will further stimulate DoD's leadership in hydro-environmental modeling well into the next century.

ACKNOWLEDGEMENT

This paper was prepared from research and development conducted by the U.S. Army Engineer Waterways Experiment Station, Vicksburg, MS. Permission was granted by the Chief of Engineers to publish this information.

REFERENCES

- Cerco, C. F., and Cole, T. M., 1995. "User's Guide to the CE-QUAL-ICM Three-Dimensional Eutrophication Model, Release Version 1.0," Technical Report EL-95-15, U.S. Army Engineer Waterways Experiment Station, Vicksburg, MS.
- Holland, J. P., 1996. "Department of Defense Groundwater Modeling Program: an Overview," Subsurface Fluid-Flow (Ground-Water and Vadose Zone) Modeling, ASTM STP 1288, J.D. Ritchey and J.O. Rumbaugh, Eds., American Society for Testing and Materials, Philadelphia, PA.
- Holland, J.P., Berger, R.C., and Schmidt, J.H., 1997. "Finite Element Analyses in Surface Water and Groundwater: an Overview of Investigations at the U.S. Army Engineer Waterways Experiment Station, " to be published in the Journal of Engineering Mechanics as a special publication for the Third U.S.-Japan Conference on Large Scale Computing and Finite Element Methods, Army High Performance Computing Research Center, Minneapolis, MN.
- Johnson, B.H., Kim, K.W., Heath, R.E., and Butler, H.L. 1994. "Development and Application of A Three-Dimensional Hydrodynamic Model," Chapter 9, Computer Modeling of Free-Surface and Pressurized Flows, Kluwer Academic Publishers, Boston, MA.

SURFACE WATER AND GROUNDWATER INTERACTION MODELING OF SOUTH FLORIDA

By H.C. Jerry Lin, Research Hydraulic Engineer, US Army Engineer Waterways Experiment Station, Vicksburg, Mississippi; D. R. Richards, Research Hydraulic Engineer, US Army Engineer Waterways Experiment Station, Vicksburg, Mississippi; M. Choate, Section Chief, US Army Engineer Jacksonville District, Jacksonville, Florida

Abstract: The rapid population growth and complex hydrologic conditions in South Florida has made the management of water resources much more complicated than a decade ago. A numerical model coupling 1-D canal flow, 2-D overland flow, and 3-D subsurface flow has been developed which will enable the Corps of Engineers to simulate the complex hydrologic system and determine the impacts of different water resources management plans in South Florida. This paper presents the results of the model application in South Florida.

INTRODUCTION

The US Army Corps of Engineers has been involved in water resources engineering in Central and South Florida for many years. Historically, the involvement has concerned the design and construction of drainage canals and other flood protection works. The rapid development of South Florida has made the use of surface and groundwater system much more complicated than the original designers of the flood protection works had planned. Many groups providing different plans for the use of limited water supplies include environmental naturalists that may want water resources systems restored to their original conditions, agricultural interests that may seek water to develop their businesses, and municipalists that have increasing populations that want a clean water supply, recreational facilities, and good flood protection at the same time.

It is not known to what degree these competing interests can be accommodated. It is known, however, that numerical models are essential in determining the impacts of various water resource management plans that are being considered. It is also known that the hydrology of Central and South Florida is exceedingly complicated with the water changing between overland flow to canal flow to groundwater flow with small changes in hydrologic conditions. Therefore, it is essential that numerical models must be able to model these complex conditions with some degree of accuracy.

The model under development for this purpose, under the sponsorship of the Jacksonville District of the Corps of Engineers and the South Florida Water Management District, will enable the modeler to simulate surface and subsurface interactions with a single modeling system. The codes employ finite element methods in coupling 1-D canal flow, 2-D overland flow, and 3-D subsurface flow. Simulations of 2-D overland flow are presented along with a development plan for future improvements.

MODEL DESCRIPTION

The model is designed to solve the following system of governing equations along with boundary conditions, which describe 3-D subsurface flow, 2-D overland flow, and 1-D canal flow. The model

has capabilities of simulating 2-D overland flow, coupling 2-D overland flow and 3-D subsurface flow, coupling 1-D canal flow and 3-D subsurface flow, and coupling 1-D canal, 2-D overland, and 3-D subsurface flow. The detailed descriptions of mathematical formulation and numerical formulation by the Galerkin finite element method of the model are given in Yeh *et al.* (1997).

3-D Subsurface Flow Module: The governing equation for 3-D subsurface flow is basically the Richard's equation.

$$F \frac{\partial h}{\partial t} = \nabla \cdot [\mathbf{K} \cdot (\nabla h + \nabla z)] + q; \quad F = \alpha' \frac{\theta}{n_e} + \beta' \theta + n_e \frac{dS}{dh} \quad (1)$$

where h is the pressure head; t is time; α' and β' are the modified compressibilities of the soil matrix and liquid fluid, respectively, n_e is the effective porosity, θ is the effective moisture content; S is the saturation; \mathbf{K} is the hydraulic conductivity tensor; z is the potential head, q is the source and/or sink.

Boundary Conditions: The boundary conditions for the flow equation are the Dirichlet conditions, Neumann conditions, Cauchy conditions, and variable conditions.

2-D Overland Flow Module: The 2-D overland flow module includes two systems: retention ponds and overland flow. The governing equation for retention pond is derived based on the concept of water budget, while the governing equation for overland flow is a spatial-temporal non-linear partial differential equation.

Governing Equation for Retention Ponds: The equation for retention ponds is described as

$$A(j) \frac{dH(j)}{dt} = QT(j) + QP(j) - QU(j) + QS(j) \quad j \in [1, N] \quad (2)$$

where $A(j)$ is the surface area of the j -th retention pond when the water surface elevation is $H(j)$; $H(j)$ is the water surface elevation of j -th retention pond; $QT(j)$ is the net volumetric flow rate through the water surface due to precipitation or evaporation to the j -th retention pond; $QP(j)$ is the net volumetric flow rate of pumping well to the j -th retention pond; $QU(j)$ is the net volumetric flow rate flowing out of the outlet of the j -th retention pond; $QS(j)$ is the net volumetric flow rate from the subsurface to dike or from the dike to subsurface of the j -th retention pond; and N is the number of retention pond in the region of interest.

The sources/sinks for each retention pond consist of (1) pumping from canal, (2) precipitation and evaporation, (3) seepage into/from surrounded dikes, (4) interaction with geologically-connected subsurface system, and (5) flow out of outlets of retention ponds.

Governing Equation for 2-D Overland flow: The continuity equation is represented as

$$\frac{\partial h}{\partial t} + \nabla \cdot (\mathbf{V}h) = r - i + q \quad (3)$$

where h is water depth; \mathbf{V} is a velocity vector; q is the flux rate from retention ponds, r is rainfall rate, and i is infiltration rate. The infiltration rate i is obtained by an iterative solution between 2-D overland flow and 3-D subsurface flow, as is the flux rate q between 2-D retention pond water budget and 3-D subsurface flow. Detail numerical implementation of this iterative procedure is

given in Yes *et al.* (1997). The velocity vector is calculated by the following equation.

$$\mathbf{V} = -\frac{a}{n} \left[\frac{h}{1 + (\nabla z_0)^2} \right]^{\frac{2}{3}} \frac{\nabla(h + z_0)}{\sqrt{|\nabla(h + z_0)|}} \quad (4)$$

where n is Manning's coefficient, a is a coefficient with the dimension $[L^{1/3}/T]$, and z_0 is ground-surface elevation.

Boundary Conditions for 2-D Overland Flow: The boundary conditions for the flow equation are the Dirichlet conditions (prescribed head), Cauchy conditions (prescribed flux rate), and radiation conditions (prescribed rating curve).

1-D Canal Flow Module: The governing equation for 1-D canal flow is derived based on the concept of water budget. A canal reach is defined as a canal section with two connectors at its two ends. A connector can be an upstream boundary gate, an interior gate, a downstream boundary gate, a weir, a dead end, or a structure-free joint.

Governing Equation for 1-D Canal Flow: The equation for 1-D canal flow is described as

$$B(j) \frac{dHRT(j)}{dt} = QT(j) + QP(j) + QUD(j) + QS(j) \quad j \in [1, \text{NORH}] \quad (5)$$

where $B(j)$ is the top surface area of the j -th canal reach; $HRT(j)$ is the water stage of the j -th canal reach; $QT(j)$ is the net volumetric flow rate into the j -th canal reach through the water surface due to precipitation and evaporation; $QP(j)$ is the net volumetric flow rate to the j -th canal reach through pumping; $QUD(j)$ is the net volumetric flow rate from the neighboring canal reaches through control structures to the j -th canal reach; $QS(j)$ is the net volumetric flow rate from the subsurface through the canal-subsurface interface to the j -th canal reaches; and NORH is the number of canal reaches discretized for simulation.

The sources/sinks for each canal reach include (1) pumping into/from other canal reaches or a specific location in the subsurface as well as pumping into a retention pond, (2) precipitation and evaporation, (3) discharge into/from neighboring canal reaches or through upstream/downstream boundaries, and (4) interaction with the geologically-connected subsurface system.

Boundary Conditions for 1-D Canal Flow: The boundary conditions for the flow equation are the upstream and downstream boundary conditions. The upstream boundary conditions are specified with a time-dependent flow rate profile. The downstream boundary conditions are specified with a time-dependent stage profile.

Interaction Between Subsurface Flow and Canal Flow System: The subsurface and canal interfaces can be conceptualized as lines and vertical planes describing the interface relative to the 3-D subsurface domain. To account for the interaction between the 3-D subsurface and 1-D canal flow system, the volumetric flow rates through each subsurface/canal interface segment are computed during each canal time step, and evenly distributed the fluxes to the nodes of the interface segment. These nodes will be served as point sources/sinks in computing subsurface flow.

Interaction Between Subsurface Flow and 2-D Flow System: The mechanism of linking the 2-D overland and 3-D subsurface flow system is basically assumed as a weak coupling (one time step lag between 2-D overland flow and 3-D subsurface flow).

MODEL APPLICATION

Site Description: The study area covers from south of Tamiami Trail to the boundary with Florida Bay and from west of C-111 canal system to the boundary with Gulf of Mexico (Figure 1). The area covers the entire Everglades National Park. The freshwater flows through the gates in the Tamiami Trail into Everglades National Park. Most of water flows through Shark River Slough into the Gulf of Mexico and small part of water flows through Taylor Slough into Florida Bay. The terrain elevation ranges from about 8 ft above mean sea level in the north and 0 ft at the boundary with the Florida Bay and Gulf of Mexico. The Everglades National Park is covered with dense vegetation. A report of evaluation of annual precipitation data showed that there are two distinctive wet (May-October) and dry (November-April) seasons in South Florida (Hayes and Radiola).

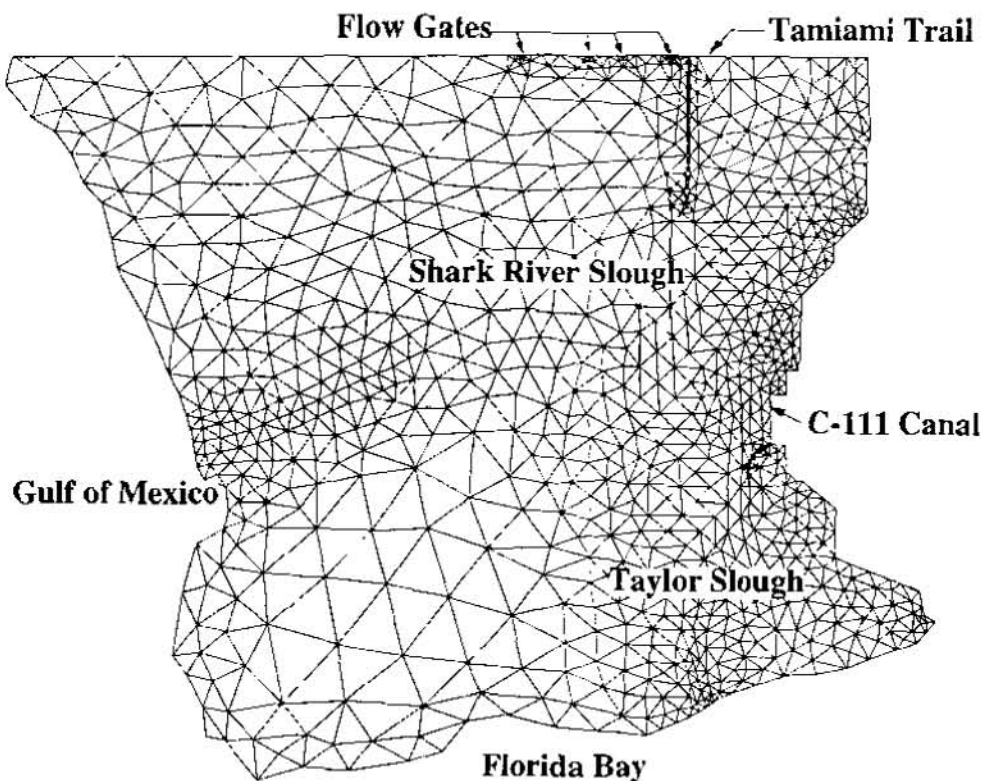


Figure 1. Location of Study Area

Comparison With Field Data: More than twenty gage stations (Figure 2) are located within the study area. These water level stations are maintained by the National Park Service (NPS), US Geologic Survey (USGS), US Army Corps of Engineers (COE), and South Florida Water Management District (SFWMD).

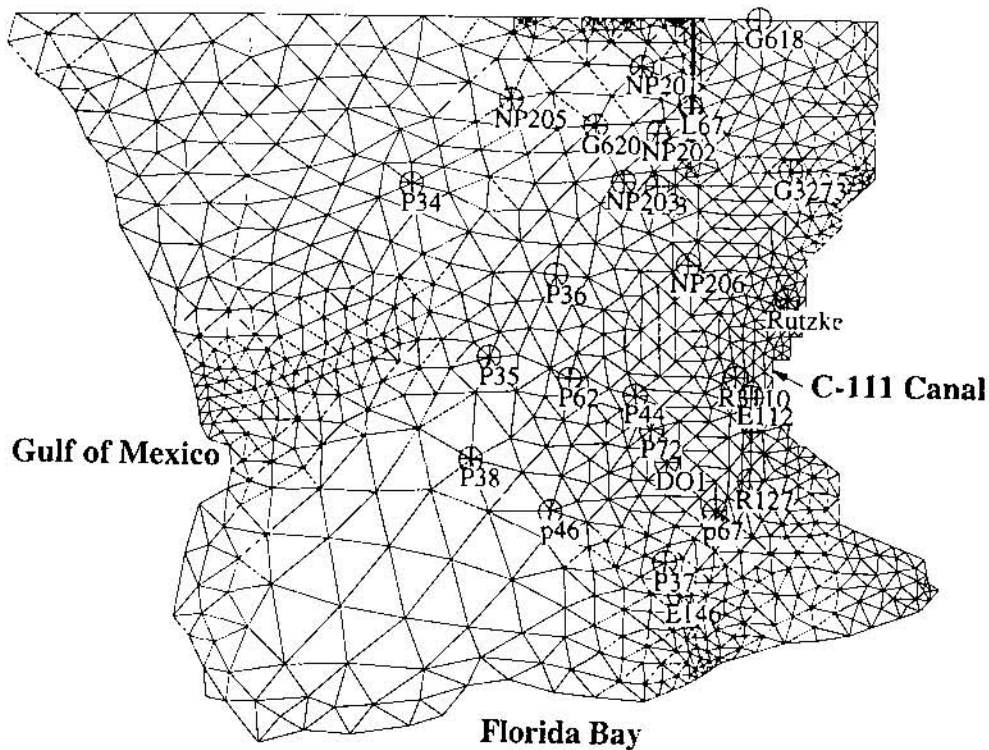


Figure 2. Location of Gage Stations

In evaluating the accuracy of the model simulating water surface elevation in the Everglades marsh, the model was run under 2-D overland flow mode. The model simulated water surface elevation for the period of one year. Simulated water surface elevations at the selected five gage stations (L67, P34, P36, P37, and P38) were compared to measured water levels (1994 field data). Plots of the simulated stages versus the observed data are shown in Figure 3 to Figure 7. A comparison of the simulated and observed water surface elevations indicated good agreement between model results and field measurement in wet season (time 3620 hr to 7300 hr). In dry season, the observed stages are below ground surface. The flow becomes subsurface flow. The model can not simulate subsurface flow when the codes are run under the 2-D overland flow-mode. In general, the model predicts with a reasonable accuracy of the water surface elevations in the Everglades National Park.

Summary and Future Development: The model was able to simulate water surface elevations with a reasonable degree of accuracy in the Everglades National Park. The water surface elevations during the dry season will be improved when the model runs under the 2-D overland and 3-D subsurface coupled-flow mode. The implementation of graphical users's interface for the model will enhance application of the model.

ACKNOWLEDGMENTS

The work reported herein was supported by the Civil Works Program of the U.S. Army Corps of Engineers. Permission was granted by the Chief of Engineers to publish the information.

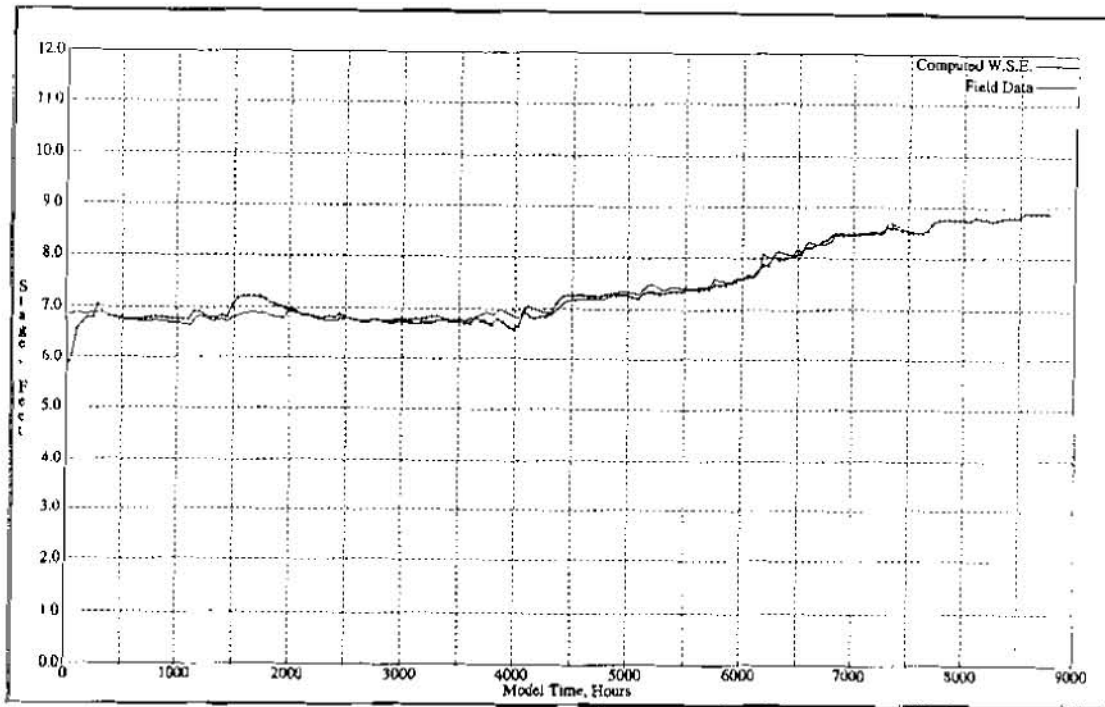


Figure 3. Computed versus Measured Water Surface Elevation at L67 Gage Station

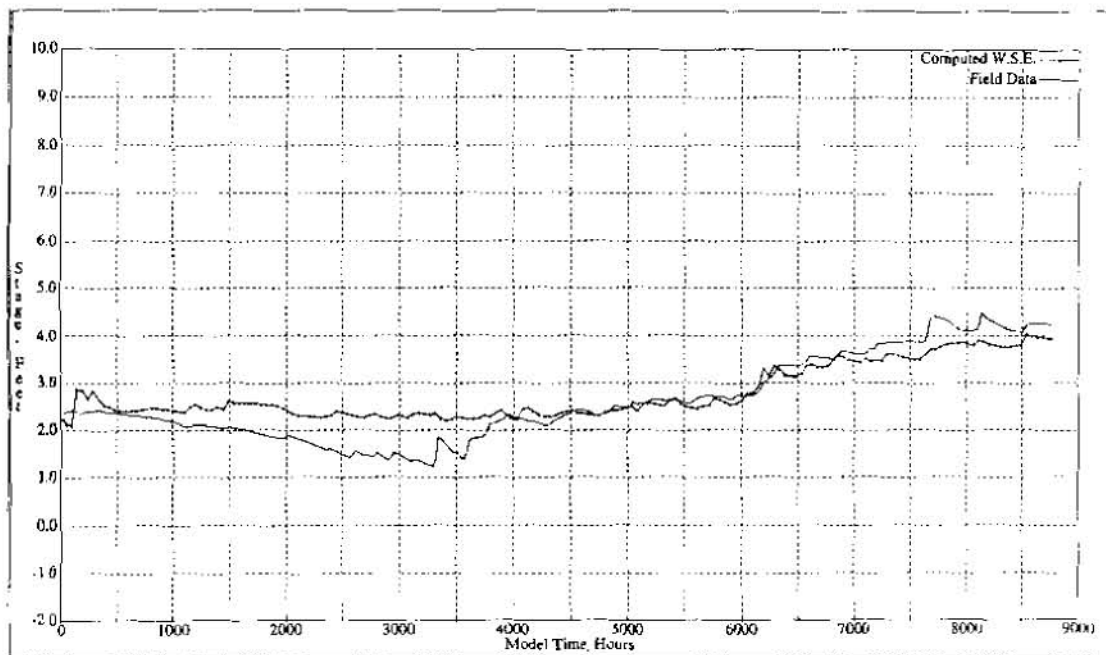


Figure 4. Computed versus Measured Water Surface Elevation at P34 Gage Station

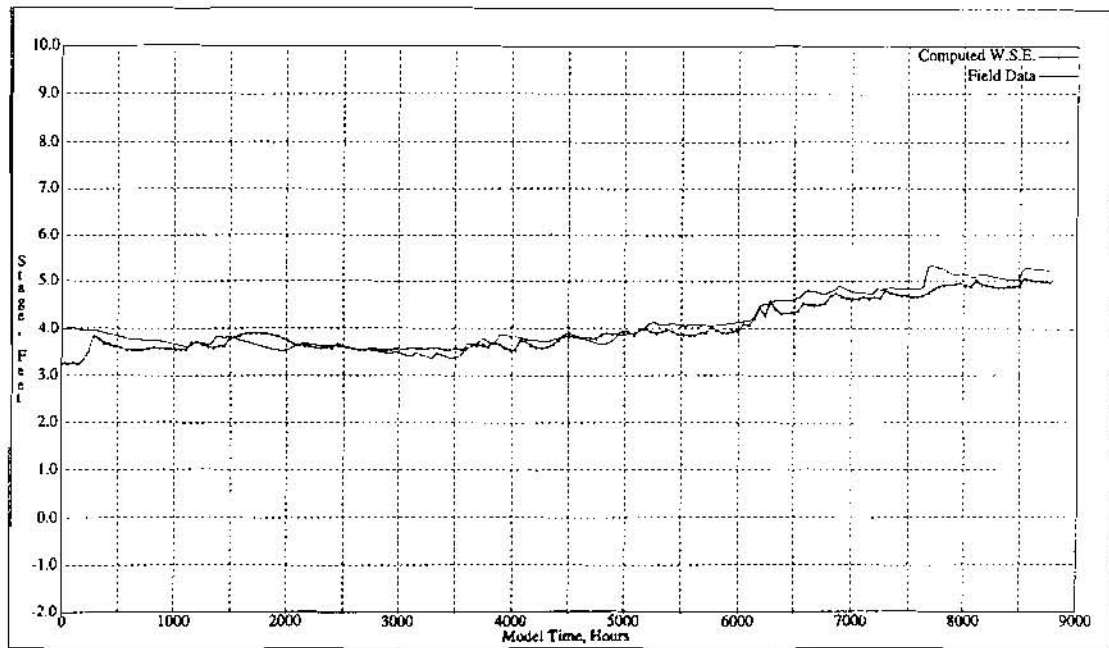


Figure 5. Computed versus Measured Water Surface Elevation at P36 Gage Station

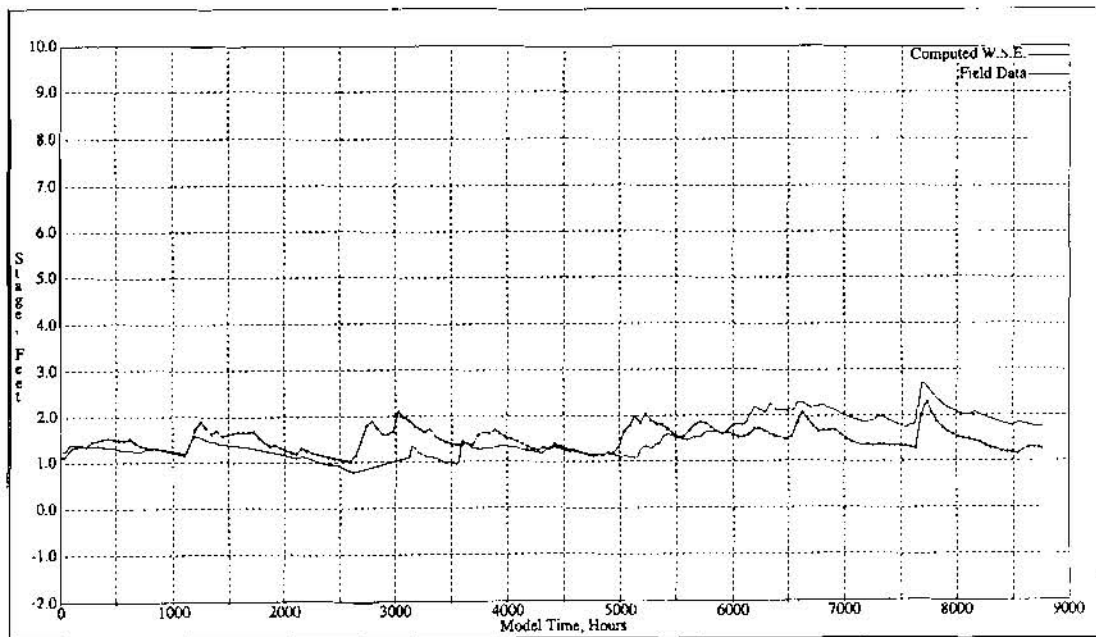


Figure 6. Computed versus Measured Water Surface Elevation at P37 Gage Station

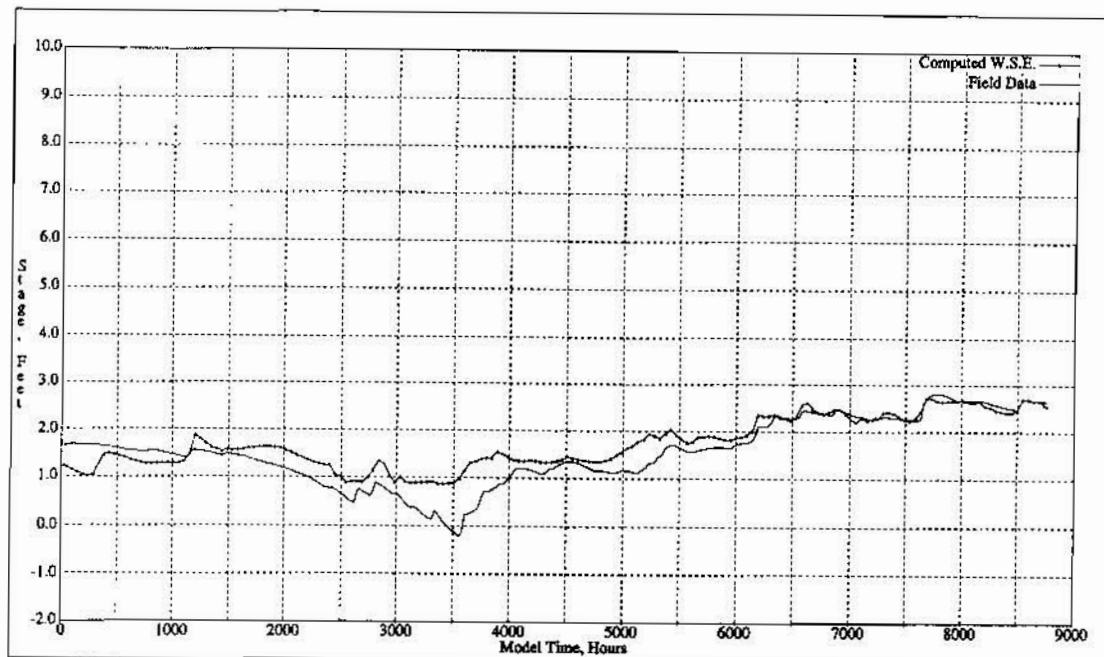


Figure 7. Computed versus Measured Water Surface Elevation at P38 Gage Station

REFERENCES

- Hayes, B.D., Radiola, M.M., 1997, South Florida Boundary Development. Progress Report, Rutgers, The State University of New Jersey.
- Yes, G.T., Cheng, J.R., Li, M.H., Cheng, H.P., Lin, H.C., 1997, COSFLOW: A Finite Element Model Coupling One-Dimensional Canal, Two-Dimensional Overland, and Three-Dimensional Subsurface Flow. Technical Report CHL-97-20, US Army Corps of Engineers Waterways Experiment Station.

INTEGRATION OF RIVERINE, ESTUARINE, AND COASTAL MODELS INTO THE SURFACE WATER MODELING SYSTEM

**By D. R. Richards, Research Hydraulic Engineer, U.S. Army Engineer
Waterways Experiment Station, Vicksburg, Mississippi**

INTRODUCTION

The US Army Corps of Engineers has developed numerous numerical models for the operation and design of Corps projects. Numerical hydrodynamic models were developed in the early seventies to address flood control and navigation problems in riverine and estuarine systems. Later, water quality simulation models that were coupled or uncoupled to hydrodynamic models were developed to address water quality issues at Corps projects. In recent years, when wetland remediation and creation became important, new simulation tools were developed to address these difficult to model systems. Unfortunately, each of the systems were developed for the prevailing computers, operating systems, and graphics tools of the day with little commonality between the systems. Recently, plans have been completed to integrate all of these tools into a single graphical user environment where water resource engineers and scientists can perform all of their analysis duties.

The tools that are being integrated include multi-dimensional models for hydrodynamic studies, coastal models for inlet analysis and wind wave simulation, water quality models, sedimentation models to minimize dredging costs, and wetland models for constructing and restoring wetlands. With one integrated surface water modeling system providing all of these capabilities, it will be easier to maintain useful software systems and well-trained personnel. Equivalent integration plans exist for groundwater and watershed systems as well. Therefore, it will soon be possible to have a trained workforce that can use a wide range of modeling systems that include watersheds, wetlands, groundwater, rivers, estuaries, and oceans.

The U.S. Army Engineer Waterways Experiment Station (WES) has been modeling rivers, estuaries, coastal seas, and wetlands for many years using a variety of numerical models. Prior to 1989, most of the models did not have modern graphical user interfaces (GUIs) that allowed user friendly operation of the models. In 1989, a graphical user interface called FastTABS was developed for the widely used TABS numerical modeling system. At that time, TABS was primarily a suite of two-dimensional, finite-element, numerical models used to model rivers, estuaries, and coastal seas. Since then, TABS has become a multi-dimensional suite of flow and transport models and renamed TABS-MD. Advancements in the TABS-MD models, as well as the inclusion of other surface water models, necessitated the development of the Surface Water Modeling System (SMS) from its predecessor the FastTABS system. Recently, plans for including coastal wave and water quality models have been formalized. The plan for their inclusion is the subject of this paper.

DESIGN PHILOSOPHY OF SMS

The Surface Water Modeling System (SMS) is a graphical user environment for performing model conceptualizations, mesh generation, statistical interpretation, and visual examination of surface water model simulation results. The software is written for personal computers using the Windows 95 and NT operating systems and for UNIX workstations. The input and output standards are published to allow the inclusion of new models into the system as they are developed. The intention is to provide a productive graphical user environment for new multi-dimensional models under development by the Corps of Engineers and its development partners.

MODELS CURRENTLY SUPPORTED BY SMS

The current capabilities of SMS include a suite of two-dimensional models for a variety of hydraulic applications. The applications vary from simulations of tidal circulation of coastal areas to rivers and wetlands to shock capturing simulations of high-velocity channels. A summary of the supported models and their capabilities follows.

RMA-2: RMA-2 is a two-dimensional, finite-element model, that simulates hydrodynamics of rivers, estuaries, coastal seas, and wetlands (Figure 1). It is particularly reliable and has been used on most of the larger rivers and estuaries in the United States. The code is quite robust in handling wetland wetting and drying problems (Figure 2).

RMA-4: RMA-4 is the conservative transport companion model for RMA-2. It too is a two-dimensional, finite-element code. First order decay functions can be assigned to source loadings to mimic natural transport processes. Several sources can be assigned at different points within the model domain.

SED2D: SED2D is a sediment transport companion model to RMA-2. Likewise, it is two-dimensional and finite-element based. It handles both cohesive and non-cohesive sediments in rivers and estuaries. It is derived from the STUDH sediment transport model.

FESWMS: FESWMS has similar capabilities to the RMA-2 model. It has a slightly different formulation but its most important difference is that it handles culverts and other forms of flows encountered at bridge crossings. It was designed for these problems by the Federal Highway Administration. It does not have sophisticated wetting and drying capability.

HIVEL2D: HIVEL2D is a free-surface, two-dimensional, finite-element code that is designed for flow fields that contain supercritical and subcritical regimes as well as transitions between the regimes. It has been used for spillway design and high velocity channel and bridge pier design that is common in the southwestern United States.

NEW MODELS TO BE SUPPORTED IN SMS

Development is under way to include a suite of coastal engineering codes that address short wave propagation, transformation and their interaction with beaches and coastal structures. Some of the codes to be included were previously supported in the Corps of Engineers Automated Coastal Engineering System (ACES). The ACES system contains a wide variety of coastal engineering tools both analytical and numerical not to mention connectivity to extensive coastal wave databases. ACES will continue to exist as a coastal engineering tool but some of its multidimensional models will now populate SMS. SMS will likely concentrate on multidimensional models as opposed to analytical methods and connection to databases as opposed to housing them. As in previous versions of SMS, connectivity to databases including GIS is considered important to enhance productivity.

Also to be included in new versions of the SMS are improvements to older codes and three-dimensional versions of two-dimensional codes. This includes the RMA-10 code which is essentially a three-dimensional version of RMA-2 with coupled hydrodynamics, salinity, and sediment. RMA-10 has already been used in many riverine and estuarine applications. Since much development is going into RMA-10 and it can be run in two-dimensional mode, it may at some point replace the RMA-2, RMA-4, and SED2D codes. This would only be done if the newer RMA-10 code contained all of the previous capabilities and there was a procedure to ensure some form of backward compatibility.

Coastal Models: The newly added coastal models will include the CGWAVE harbor oscillation model, the STWAVE spectral wave model, and the ADCIRC global circulation model. The implementation of these three models into SMS represents a suite of modeling tools that are important to coastal engineers and scientists. Additional models will be added as they are developed. They will certainly include more advanced wave current interaction models that are currently under development. A summary of the models to be included follows.

CGWAVE: CGWAVE is a two-dimensional, finite-element model that simulates the wave physics contained in the elliptic mild-slope wave equation, i.e. refraction, diffraction, and reflection (Panchang and Xu, 1995). These capabilities are important to the engineer especially if 100,000 node coastal problems can be solved on a personal computer. The implementation of CGWAVE will have this capability.

STWAVE: STWAVE is a steady-state, cartesian, finite-difference spectral wave model that solves the steady-state conservation of wave action equation (Smith, et al, in preparation). The model is typically used to quantify wave conditions at coastal inlets and is under development to allow wave current interaction with the ADCIRC long wave model also being included in the SMS.

ADCIRC: ADCIRC is a two-dimensional, finite-element, tidal circulation model that forms the basic circulation model under development in the Corps of Engineers Coastal Inlets Research

Program. It has been used along with STWAVE in wave-current interaction studies (Smith, et al, in preparation) and with a number of estuarine circulation studies using different tidal models because of its efficiency in generating offshore tidal boundary conditions on almost a global scale (Figure 3).

Water Quality Models: The new water quality models included are the CE-QUAL-ICM transport model and the CH3D-WES hydrodynamic model used frequently to provide hydrodynamics for CE-QUAL-ICM.

CE-QUAL-ICM: The CE-QUAL-ICM water quality model was originally developed as one component of a modeling package employed to study eutrophication processes in Chesapeake Bay and later generalized for wider applications. The following summarizes the model features (Cerco and Cole, 1995):

- one-, two-, and three-dimensional capabilities
- twenty-two state variables including physical properties; multiple forms of algae, carbon, nitrogen, phosphorus, and silica; and dissolved oxygen
- sediment-water oxygen and nutrient fluxes may be computed in a predictive submodel or specified based on observations
- state variables may be individually activated or deactivated
- computations may be restarted following interruption due to computer failure or similar circumstances
- internal averaging of model output over arbitrary intervals
- computation and reporting of concentrations, mass transport, kinetics transformations, and mass balances
- debugging aids include ability to activate or inactivate model features, diagnostic output, volumetric and mass balances

CH3D-WES: The CH3D-WES model is the numerical model used commonly to provide hydrodynamic input to the CE-QUAL-ICM model. CH3D-WES is a three-dimensional, boundary-fitted, finite-difference model (Johnson, et al, 1991). It can be used in either a z-plane version in which vertical cells are arranged in constant depth layers or a sigma-stretched version where a fixed number of vertical cells are stretched over the bathymetry. The z-plane version is most useful where there is significant salinity or temperature stratification in deepened channels next to shallow overbank areas. This allows the computation of vertical and lateral salinity gradients next to the deepened channels with a minimum of computational cells.

Chesapeake Bay is a notable example of a z-plane application (Johnson, et al, 1991). The sigma-stretched version is generally preferred provided that such salinity gradient difficulties are not observed. A good example of such a case is the New York Bight Study (Hall and Dortch, 1994). Versions of CH3D-WES are under development that have sophisticated sediment transport capabilities and they will be added to SMS as they become available (Figure 4).

SUMMARY

The Surface Water Modeling System (SMS) has now been in development in one form or another for almost ten years. In that time, the supported models have largely included two-dimensional, finite-element codes for riverine and estuarine flow and transport. Several new models are currently being implemented in SMS that will allow coastal engineers and water quality modelers more productive use their codes. The SMS has open input and output data standards that allow model developers to use the system with their codes if these standards are followed. The continued purpose of the SMS development is to provide a rich graphical user environment and sophisticated analysis tools that support the modeling activities of the Corps of Engineers and its development partners.

ACKNOWLEDGEMENTS

Support provided for the development of the SMS and the publishing of this paper were provided by several research programs of the Corps of Engineers and the support of several Corps of Engineers District offices through reimbursable studies. The Engineering Computer Graphics Laboratory at Brigham Young University were substantial research partners in the development of SMS. Permission to publish this paper was granted by the Office, Chief of Engineers, USACE.

REFERENCES

- Cerco, C. F. and T. Cole, 1995. Users Guide to the CE-QUAL-ICM Three-Dimensional Eutrophication Model, Release 1.0, Technical Report EL-95-15, U. S. Army Engineer Waterways Experiment Station, Vicksburg, Mississippi.
- Hall, R. W. and M. S. Dortch, 1994. New York Bight Study, Report 2, Development and Application of a Eutrophication/General Water Quality Model, U.S. Army Engineer Waterways Experiment Station, Vicksburg, Mississippi.
- Johnson, B. H., R. E. Heath, and B. B. Hsieh, 1991. Development and Verification of a Three-Dimensional Numerical Hydrodynamic, Salinity, and Temperature Model of Chesapeake Bay, Volume 1, Main Text and Appendix D, Technical Report HL-91-7, U.S. Army Engineer Waterways Experiment Station, Vicksburg, Mississippi, August, 1991.
- Panchang, V. G. and B. Xu, 1995. CGWAVE: A Coastal Wave Transformation Model for Arbitrary Domains, Technical Report, Department of Civil and Environmental Engineering, University of Maine, October, 1995.

Smith, J. M., A. Militello, and S. J. Smith, in preparation. Modeling Waves at Ponce De Leon Inlet, Florida. U. S. Army Engineer Waterways Experiment Station, Vicksburg, Mississippi.

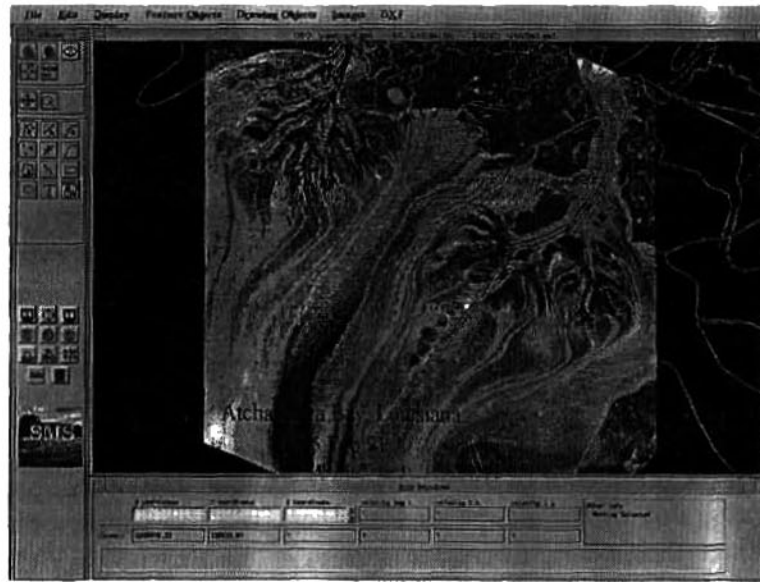


Figure 1. SMS desktop showing RMA-2 current velocities superimposed over a LANDSAT infrared image for the Atchafalaya Bay, Gulf of Mexico

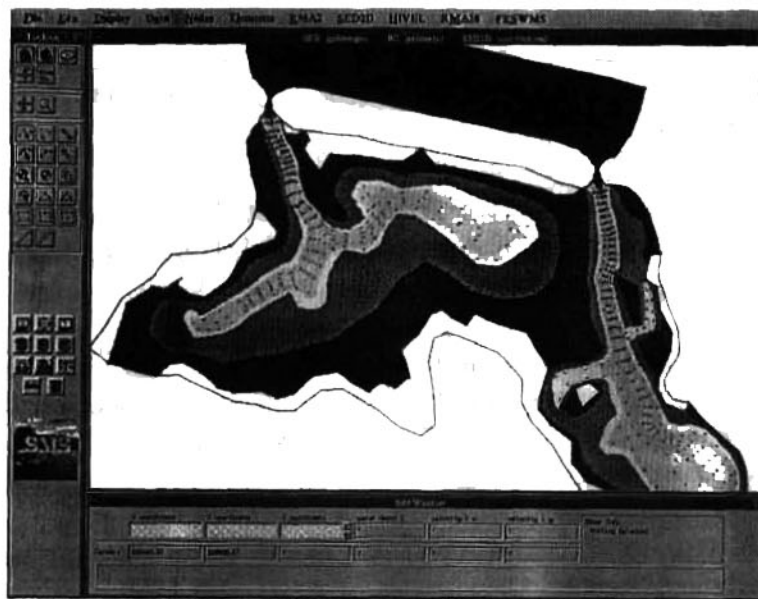


Figure 2. SMS desktop showing an RMA-2 estuarine wetland simulation displaying water depths, current velocities, and dry areas for Galilee Bird Sanctuary, Rhode Island

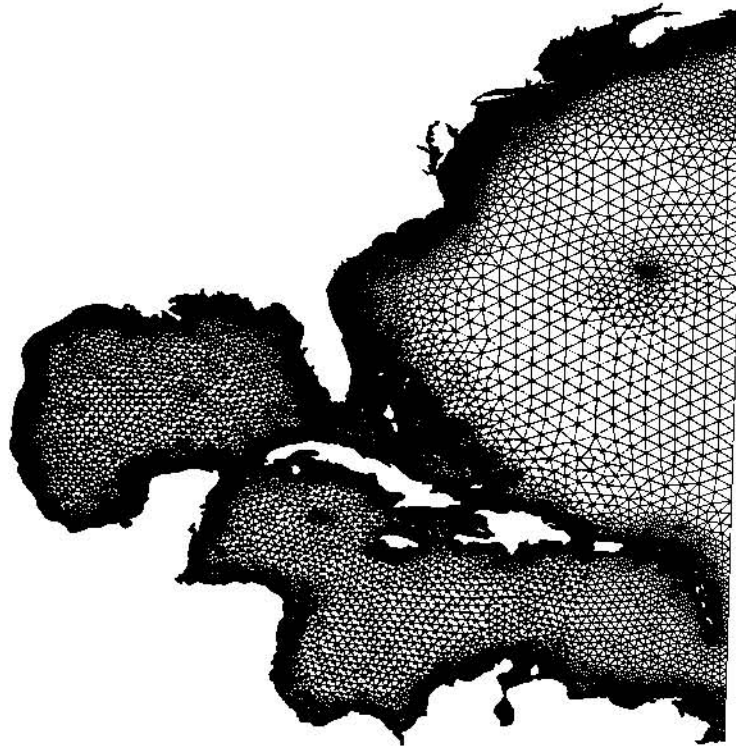


Figure 3. ADCIRC finite-element mesh of the Atlantic Ocean and Caribbean Sea

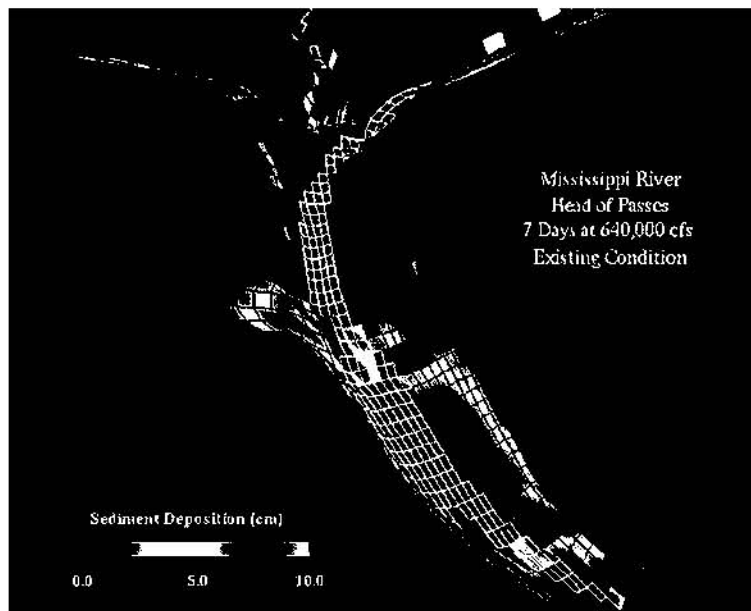


Figure 4. Sediment transport version of the CH3D-WES model showing sedimentation at the Mississippi River, Head of Passes, Louisiana

submitted by:

David R. Richards
US Army Engineer Waterways Experiment Station
Halls Ferry Road
Vicksburg, MS 39180
601-634-2126
richards@hl.wes.army.mil

WATERSHED AND RIVER SYSTEMS PLANNING MODEL IN THE SAN JUAN RIVER BASIN, COLORADO

**By P. Davidson, Hydraulic Engineer, Bureau of Reclamation, Salt Lake City, UT;
D. L. King, Hydraulic Engineer, Bureau of Reclamation, Denver, CO;
J. Ozga, Hydraulic Engineer, Bureau of Reclamation, Grand Junction, CO; and
J. Simons, Hydraulic Engineer, Bureau of Reclamation, Durango, CO.**

Abstract: A decision support system (DDS) was developed for use on the San Juan River basin near the four corners of Colorado, Utah, New Mexico, and Colorado to aid in long-term operation decisions in the watershed. The system includes a data base of hydrology and depletion data and a river and reservoir operating model developed by the Bureau of Reclamation (Reclamation). The river and reservoir system model was developed using RiverWare which was developed jointly by Reclamation and other agencies under contract to the Center For Environmental and Water Decision Support Systems (CADSWES) in Boulder, Colorado (Shane, et al, 1995). The system was used to examine various operating and hydrologic scenarios to study the effects on flows at selected locations in the watershed. The timing and shape of hydrographs was critical for fish spawning, habitat building and maintenance. The DDS enabled decision makers to efficiently examine the scenarios and select recommended operating criteria.

INTRODUCTION

The listing of two endangered species of fish, the humpback chub and the Colorado squawfish, have necessitated reexamination of river operations in the San Juan River Basin of Colorado, New Mexico, Arizona, and Utah. The Recovery Implementation Program (RIP) is in the seventh year of a seven year study to evaluate alternative operations of Navajo Reservoir in New Mexico to build and maintain fish habitat while allowing water development in the San Juan Basin. Elements of the study were development of natural flows, a baseline data set, and river system model that is being used to examine various operating, hydrologic, and depletion scenarios. This paper discusses development of the model and related data and use of same in the analysis.

BACKGROUND

A river and reservoir system model was being developed using RiverWare through an independent effort by Reclamation to demonstrate the feasibility of using a distributed rainfall model in conjunction with a relational database to support short-term operations and enhance fisheries (King, et al, 1998). It was intended that the prototype model use a daily time step. RiverWare is an object oriented river, diversion, and reservoir model building system that runs on a Unix work station. RiverWare currently has three operating modes which are the Simulation, Rule Based Simulation, and LP/Goal Programming controllers. A natural flow data set was developed for historic hydrology with which to validate and calibrate both modeling systems. The simulation controller was used to validate the RiverWare model, basically verifying that the physical configuration was correct and it served to catch spreadsheet errors. The Rule Based Simulator was used to implement operating decision criteria.

Prior to completion of this system, members of the development team were invited to participate on the Hydrology Team of the RIP. Other members of the hydrology team include Keller-Bliesner Engineering of Logan, Utah (consultant to US Bureau of Indian Affairs), United States Fish and Wildlife Service, Southwest Water Conservancy District, and Colorado and New Mexico. The purpose of the team is evaluate and recommend data inputs and model configuration. The model will be used to evaluate flow recommendations as alternative means of operating Navajo Reservoir to enhance the recovery of endangered species of fish.

In addition to the model and data set being built by Reclamation, the state of Colorado has developed a water rights model and data set for the San Juan basin. After considerable debate and evaluation, the hydrology team elected to use the RiverWare model because it could do a daily time step and because it was more dynamic in the ability to write operating policy rules.

DEVELOPMENT OF NATURAL FLOWS

Prior to selection of RiverWare by the hydrology team, natural flows were computed using standard Reclamation procedures. Natural flows on a grosser scale are calculated every five years for the entire Colorado River basin. The basic data used for these calculations was extended and revised to compute natural flows on the finer scale required for the fishery studies. This included updating of acres with 1993 Geographic Information System (GIS) coverage, additional demarcation of uses, and use of State of Colorado canal data available from Colorado River Decision Support System (CRDSS) website. The group responsible for calculation of natural flows elected to use spreadsheet computations because data for the five year computations existed in this form and RiverWare could not support the computations when the analysis was begun.

Subsequent to inclusion of the authors on the hydrology team, an attempt was made to reconcile differences between Colorado, New Mexico, and Reclamation regarding basic input data. Differences existed between irrigated acres (both GIS and annual), irrigation shortages, reservoir inventories, and other sources of depletions. Reclamation used spreadsheets to compute natural flows and only accounted for canal flows that involved imports, exports, or gages. Colorado used their model to compute natural flows. Because of the different approach to computation of natural flows, the team did not attempt to completely find closure on differences but to identify them, determine where the team could adjust the respective sides, and bring the computations to a reasonable proximity.

Another requirement of the team was that the data sets had to be extended back to 1929. 1928 was the year that the Colorado River Compact was signed and the period of 1929 through 1993 captures the drought periods of the 1930's and 1950's. The hydrologic data were extended by Keller-Bliesner using an algorithm developed by Dr. Upmanu Lall of Utah State University. Depletions were extended by running Blaney-Criddle with 1928-1993 climatological data. If climatological data were not available for a given period, similar data extension methods were used.

DEVELOPMENT OF MODEL AND OPERATING RULES

As previously noted, a RiverWare model of the San Juan Basin had been started prior to involvement with the hydrology team. The majority of this effort had been development of data handling

procedures. These included moving data from spreadsheets to text files for use on the work station, creation of a preprocessor to compute depletion volumes by RiverWare node, creation of files to map depletion and hydrology into RiverWare nodes, and creation of Data Management Interfaces (DMI's) to move data into and out of RiverWare. Prototype models of sub basins of the San Juan were developed to test these support procedures. Modeling consisted of three basic steps: configuration, validation, and calibration.

Configuration: Configuration consisted of mapping the natural flow and equivalent depletions into appropriate RiverWare objects and building the model in RiverWare. Reservoirs, river reaches, and confluences are straightforward. Depletions are modeled in RiverWare using Aggregate Diversion objects. Each aggregate diversion can have any number of "water users" whose water supply is affected by the behavior selected and linking of return flows. One method of providing water from one water user to the next is to automatically make unlinked return flows available to the subsequent water user. This method was used whenever possible to reduce modeling time and possible linking errors. Most "water users" also were aggregated through mapping and preprocessing. Again, this was done to reduce model complexity. However, it is possible to model every real water user in a watershed.

This application was the first to use the sequential linking structure type of aggregate diversion. The group found a few bugs in RiverWare that had to be corrected. In addition, the team decided that additional functionality was required. This included the addition of a new return flow method, the ability to separate return flow into a surface water and ground water component, and a creation of a primitive ground water object in which to store ground water. The variable efficiency method was created to better emulate the effect of water supply on an irrigation diversion's efficiency. It is assumed that an irrigation project increases in efficiency up to a maximum at which it is not possible to exceed. No reduction in depletions occur until maximum efficiency is reached.

Validation: Validation is the process of verifying that the configuration is correct. Natural flow, historic depletions and diversions, and historic reservoir releases are input, the model is run, and computed flows at natural flow nodes (which are river gages) is compared to gaged flows. This was not a trivial task because of the detail of modeling. Each sub basin of natural flow and depletion had to be mapped exactly from the natural flow and depletion data sets to achieve validation. This exercise also served the purpose of finding errors in the natural flow computations either due to spreadsheet equation errors or data errors.

Calibration: Calibration is the process of operating the river using rules. Natural flows and non shorted depletions are input but reservoir releases are established by operating rules. The initial objective of validation was to emulate historic operations to the extent possible. The three figures which we attempted to match were historic releases, historic storage, and historic depletions. We attempted to minimize differences from historic while respecting physical constraints. Once satisfactory progress was made on calibration, a parallel effort was begun to create a rule set for operating the river to enhance the endangered fisheries.

Creation of the rule sets and associated procedures was delayed by recomputations of the natural flow and other negotiated items such as what time step to use. The hydrology team elected to use a

monthly time step to be consistent with the natural flow data set. However, smaller time step data were needed for some of the fishery decisions. To support these requirements, a disaggregation algorithm was implemented in rules code using an algorithm developed by Dr. Upmanu Lall of Utah State University. RiverWare has the ability for every object and slot (data element of an object) to have it's own time step. We stored data to support disaggregation computations and rules in RiverWare data objects, objects whose sole purpose is to store data.

Initially, we used code from the Colorado River Simulation System (Frevert, et al, 1997) to prototype rules. We came to realize that the level of modeling in the San Juan Basin study required more detail. The team attempted to make these modifications so that eventually it could create a "generic" rule set, one that respected the basic operations of a reservoir including meeting downstream demands while obeying physical constraints and could be used with either a monthly or daily time step. In the process, we created a rule set which is robust and reasonably generic.

Our basic reservoir rule computes a target operation that respects downstream demands, flood control, target space, and filling criteria. This rule attempts to fill the reservoir during the runoff season and maintain a monthly target space the remainder of the year. A procedure was created that computes the minimum amount of water to release to meet demands which accounts for diversions that use return flow of upstream diversions, gains below a reservoir, imports, and exports.

In addition, a diversion rule was written to assign the water available to diversions based upon the supply. This rule has two major forks, depending upon the rule's dependency. The dependency of a rule determines when it is place on the queue for processing. The item upon which the rule is depended will be a RiverWare slot. For the diversion rule, we use an upstream dependency to tell the rule when the supply has changed and a downstream dependency to tell when the river below the diversions involved has changed.

If the supply has changed, the rule has sufficient knowledge to determine if a headgate shortage will occur. The rule sets the available water to aggregate diversions based upon the supply and adjustment algorithm. The current algorithm does the adjustment with a quasi water rights solution. If the downstream dependency placed the rule on agenda, the rule checks if a depletion shortage occurred. If so, the rule adjusts available water to diversions to respect water rights. If the location of shortages are unimportant, this rule does not need to used.

OPERATING RULES AND CRITERIA TO ENHANCE ENDANGERED FISHERIES

The final phase of the project was to establish operating criteria which would evaluate recommend flow that would enhance the fishery, implement these criteria as a rules set, and make model runs with extended hydrology and various operating scenarios. Operating criteria were based upon results of the first seven years of the overall study. Sedimentation, flow, habitat, fish counts, and other data were collected and analyzed during this period. These data were used to establish basic criteria for flow regimes that build or maintain fish habitat plus guidelines regarding the frequency that the respective hydrologies need to be achieved.

The RIP rules were not easy to implement. However, having the basic model and historic rules already implemented in RiverWare allowed the rules writers to focus on functionality and integrity of the implementation. RiverWare provides excellent diagnostics for rule debugging. Actual models could be used rather than using prototypes. The rules were implemented in a relatively short period of time and the team was able to make numerous scenario runs before the final operating recommendations were made. These recommendations are under review prior to June, 1998.

CONCLUSIONS AND RECOMMENDATIONS

RiverWare was an effective tool in implementing extremely complicated operating rules for the San Juan River basin. Furthermore, it provided efficient computation of various operating scenarios. RiverWare was excellent as a decision support tool in this study. Steps should be taken to use RiverWare to compute natural flows and as a tool in daily operations.

REFERENCES

- Frevert, D., Fulp T, Vickers, B., and King, D, 1997, "Development of a Data Centered Decision Support System for Multiple Purpose Water Resources Projects," Proceedings of the 24th Annual Water Resources Planning and Management Conference, American Society of Civil Engineers, Houston, TX.
- King, D.L., Parker, R., Kuhn, G, and Leavesley, G., 1998, "Watershed and River Systems Modeling in he San Juan River Basin, Colorado," First Fedearl Interagency Hydrologic Modeling Conference, Las Vegas, NV.
- Shane, R.M., Zagona, E.A, McIntosh, D. And Fulp, T.J., 1995, "Modeling Framework for Optimizing Basin Hydropower", Proceedings of WaterPower '95, American Society of Civil Engineers, NY.

WATERSHED AND RIVER SYSTEMS MANAGEMENT PROGRAM: CURRENT AND FUTURE APPLICATIONS IN THE BUREAU OF RECLAMATION

By Terrance J. Fulp, Operations Research Analyst, U.S. Bureau of Reclamation, Lower Colorado Region, Boulder, CO; and Don K. Frevert, Hydraulic Engineer, U.S. Bureau of Reclamation, Denver Technical Services Center, Denver, CO

Abstract: A data-centered decision support system (DSS) is being researched and developed that utilizes relational database and advanced modeling technologies to integrate water, power, and weather data, both historical and forecasted. The system facilitates the postulation, testing, and analysis of alternative operational and planning scenarios with respect to competing objectives and provides a practical tool to ensure the most efficient and responsible use of basin resources. The system is being developed using generic tools yet is easily customized to meet site-specific needs. Current applications include the Colorado, Yakima, and Rio Grande River basins, and it is anticipated that it will ultimately be applied to many other basins throughout the western United States.

INTRODUCTION

The demands placed on water resource systems have increased greatly over the past few decades. Meeting consumptive use demands, while still vitally important, is no longer the only objective to be considered in operational and planning decision making. Key issues in the management of Reclamation river basins include:

- flood control
- rainfall and snowmelt runoff forecasting
- increased consumptive use demands
- water quality (especially salinity)
- hydropower production
- recreational uses on reservoirs and rivers
- endangered species and other environmental concerns
- water rights (particularly for Native American Nations)

These issues are common Reclamation-wide. In order to address these and other issues, water managers need the ability to predict the outcomes of a wide range of water management actions under a wide range of hydrologic conditions. Necessary predictions range from long-term simulations of the operation of complete water resources systems under modified management strategies to short-term simulations involving forecasts of inflow and demand to predict the impacts of specific management actions. The entire hydrologic and water management processes must be represented by both models and data. System state variables to be examined include water quantity, water quality, and sediment transport and channel morphology. Furthermore, all of this information must be presented to the human decision maker in an intuitive format and in a timely manner.

Decision support systems (DSS) have been discussed in the literature since the early 1970's (Scott Morton, 1971), when it was recognized that "real world problems are often much more complex, much less structured, and require much more human input and judgment" than those contemplated by model developers (Loucks, 1995). Management of natural resources, particularly watersheds, falls into this category of problem. By the late 1980's, research in DSS applied to water management problems primarily focused on the use of artificial intelligence technology (Savic and Simonic, 1989), although many of these applications apparently did not prove to be successful in practice. Subsequent research focused on the development of "user-friendly" models (Fulp, et al, 1991).

It is our thesis that a decision support system is the best way to provide the tools to address these key issues. In particular, we have adopted the data-centered approach to decision support (Ryan and Sieh, 1993) which uses relational data base technology as the cornerstone for the decision making.

In this paper, we will briefly describe our research and development program, present an overview of the major components of the DSS, and describe how the system is being applied in the Colorado, Yakima, and Rio Grande River basins. We conclude with a discussion of some of the important issues that we have encountered for successful implementation of the system.

WATERSHED AND RIVER SYSTEMS MANAGEMENT PROGRAM (WARSMMP)

The goal of the Watershed and River Systems Management Program (WARSMMP) is the research, development, and implementation of a data-centered, decision support system for integrated watershed management. WARSMMP is a multi-year, cooperative effort between Reclamation and the U.S. Geological Survey (USGS) that was officially begun in Fiscal Year 1995. Current plans call for continued financial support through Fiscal Year 2000.

Our program strategy is governed by the premise that the water resources issues and our field offices' needs should dictate our research and development priorities. This interaction is depicted in Figure 1. This strategy calls for involvement of the potential users throughout all phases of the program (research, development, and implementation). Furthermore, following this strategy allows us to implement developed products and provide feedback to the development team in a timely manner. An important objective of the research program is the applicability of the developed products to basins other than those initially chosen for implementation. Clearly the products must be developed to have generic application, yet be able to be customized to meet site-specific objectives.

Throughout the duration of the program, partnering with other agencies has been and continues to be an important avenue to leverage limited funding. To this end, the Tennessee Valley Authority (TVA), the University of Colorado's Center for Advanced Decision Support for Water and Environmental Systems (CADSWES), the Electric Power Research Institute (EPRI), the National Oceanic and Atmospheric Administration (NOAA), and the Department of Agriculture have also participated in the development of certain aspects of the system.

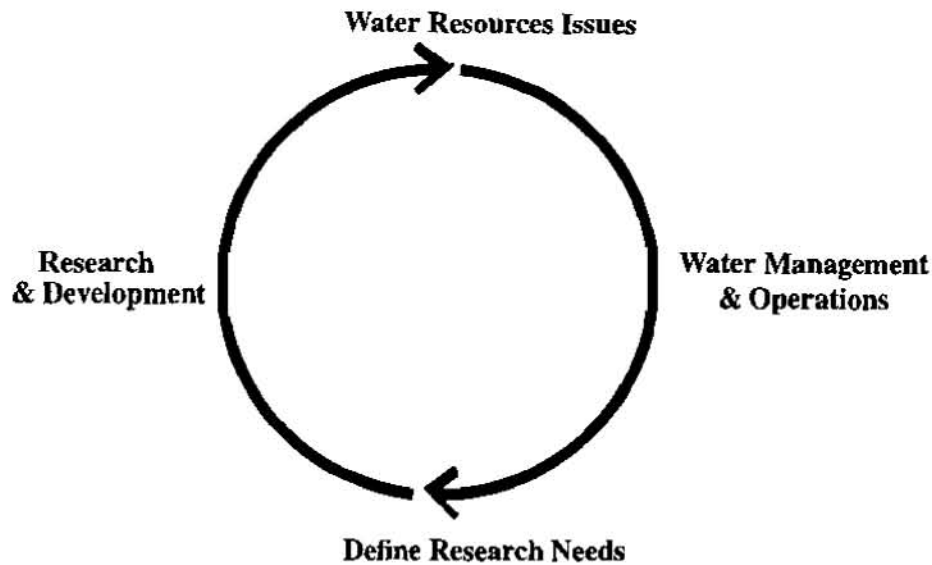


Figure 1. Interaction of research, development, and implementation phases in WARSMP.

MAJOR SYSTEM COMPONENTS

The major components of the system developed and implemented to date include the Hydrologic Data Base (HDB), the RiverWare reservoir and river system modeling environment, and the Modular Modeling System (MMS) environment. These components are shown in Figure 2. Companion papers in this conference cover each of these components in more detail, so only a brief overview is presented here.

The Hydrologic Data Base (HDB) has been designed for the storage of hydrologic time series data, attribute data, statistical information, and other types of data pertinent to water management activities. It was initially implemented using the Ingres Relational Database Management System (RDBMS), but has recently been ported to the Oracle RDBMS. The design includes a significant number of metadata tables for optimal storage and retrieval of data, and for the management of applications which use the data. The design also features a number of data integrity constraints to maintain data integrity. Currently, over 100 data types (i.e. average streamflow, power generation, maximum temperature, snow water equivalent, total dissolved solids, etc.) have been defined in HDB. Sites are categorized into object types (i.e. reservoir, powerplant, streamflow gage, etc.). HDB also allows the storage of modeled (forecasted) time series data. This data is stored in tables separate from the "real" data. Clearly, not all simulated data belongs in a database for long term storage; however, when significant forecasts of the state variables are obtained (such as an official operational forecast), these results are formalized by placing them in HDB for further reference. This ensures a consistent view of the projected state of the system throughout the organization.

The USGS Modular Modeling System (MMS) is an integrated modeling environment that can be used to simulate a variety of water, energy, and bio-geochemical processes (Leavesley, et al, 1996). To date, the primary use of MMS has been for the development and analysis of physical based,

precipitation-runoff models (PRMS) for the watersheds of interest. The PRMS component of MMS provides Geographic Information Systems (GIS) tools that can be used describe and analyze the spatial distribution of the hydrologic parameters needed for the runoff prediction. Various physical processes are available and users can even develop their own modules as needed.

RiverWare is a generic river basin modeling environment that can be used for both operations and planning. RiverWare provides point-and-click model building, user selection of engineering methodologies to customize the behavior of the modeling objects, and alternative solution algorithms to solve the resulting network (simulation, simulation with user-specified policies, and optimization/goal programming), all through a user-friendly interface. Timestep size ranges from hourly to yearly, with no limit on the time range of a model run (Zagona and Fulp, 1998).

By developing appropriate Data Management Interfaces (DMIs) to HDB, additional tools are being integrated into the DSS as needed. Many of these tools are “off-the-shelf” providing additional functionality with essentially no development cost. For example, a statistical package (S-Plus) has been integrated to facilitate the analysis of both historical and modeled data.

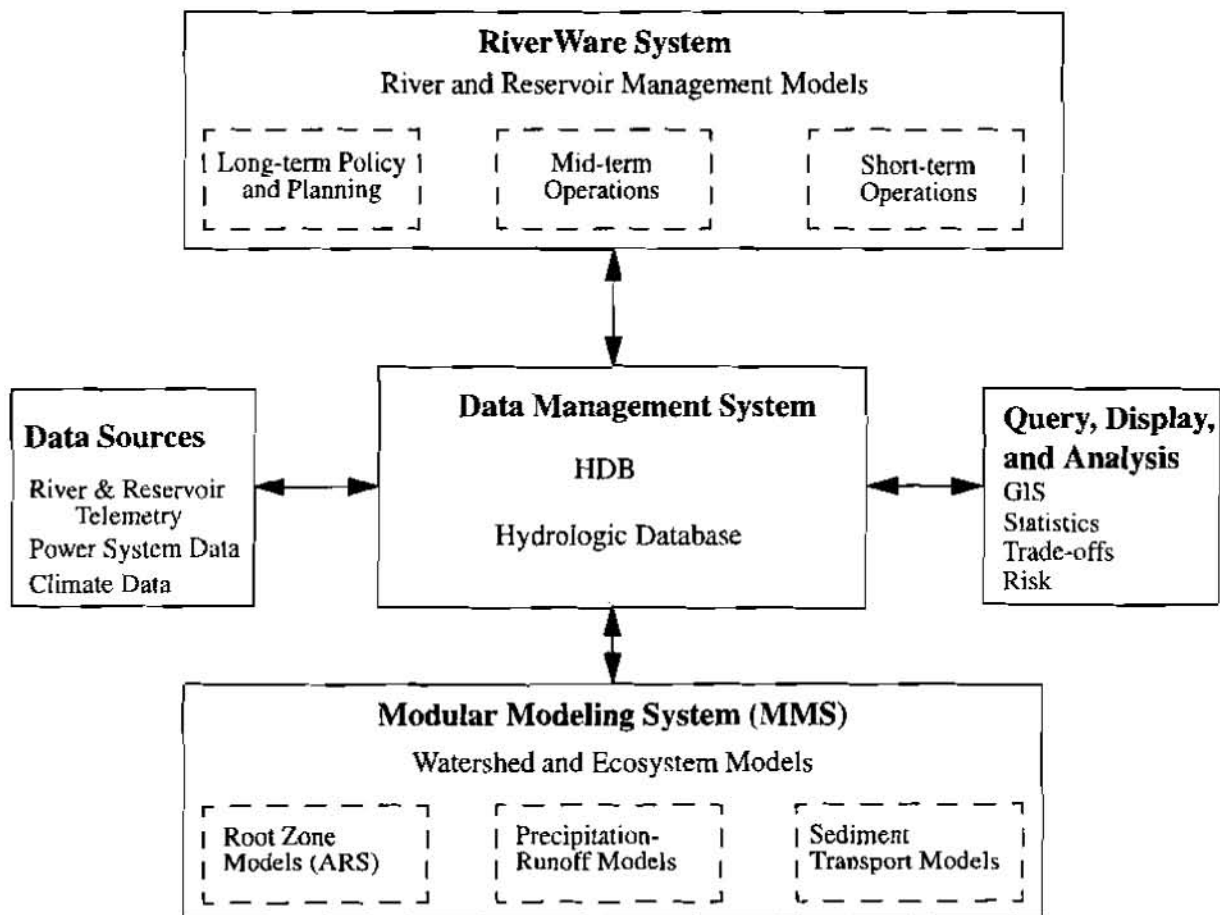


Figure 2. The data-centered decision support system.

CURRENT APPLICATIONS

To date, our main focus has been on the Colorado River. Starting in Fiscal Year 1997, we began implementation on the Yakima River basin in Washington and on the Rio Grande River basin in New Mexico. In this section we will briefly describe each of these applications.

Colorado River Basin: The Colorado River Basin is one of the most heavily legislated river basins in the U.S., covering seven states with a drainage area of some 245,000 square miles. Total storage in the basin (approximately 60 million acre-feet) is four times the average annual inflow. Operations and planning decision-making on the Colorado River is shared between the Upper and Lower Colorado Regions and their respective area and facilities offices. A hierarchical view of the decision making and some examples of models that were used to support these decisions is shown in Figure 3. The models included: a monthly time step policy and planning model of the entire basin used to assess the long-term effects of policy decisions with regard to water and energy supply, as well as salinity mitigation; a monthly time step operations model of the entire basin used to set the Annual Operating Plan and to adjust that plan throughout the year as hydrologic forecasts are updated; and a daily time step operations model for the Lower Basin which is used to set the daily releases to meet short-term water and energy demand, within the monthly targets. These models were used for a relatively long period of time (over two decades) and their results were trusted both within and outside our agency. However, they lacked the flexibility needed to model increasing demands and constraints on the system, as well as expanding operational objectives.

Through the WARSMIP program, we have successfully implemented HDB and RiverWare in both our Upper and Lower Colorado River regional offices for both operational and planning use. HDB is running as a "quasi-distributed" data base, in that both historical and forecasted data pertinent to each region is stored only in the HDB at that region and appropriate meta-data (such as site definitions) are automatically coordinated between the databases to ensure data sharing. RiverWare has been used to replace all three of the previously mentioned models, and in the case of the two operational models, is completely integrated with HDB. For example, each month the Upper Colorado Region receives the latest inflow forecasts from the National Weather Service Colorado River Forecasting Center (CRFC). These forecasts are automatically processed and entered into the database. RiverWare is then used by both regions to forecast the state of the system, given the updated forecasts, demands, and operational objectives. Upon agreement by each operations office, reports are generated automatically by extracting data from each database. MMS has been used successfully in a demonstration mode on the Gunnison Basin (Ryan, 1996) to generate alternative inflow forecasts throughout the runoff season. Further work is warranted to fully integrate these forecasts with the CRFC forecasts.

RiverWare has also been used to develop a model of the San Juan basin for use in consultations with other agencies regarding meeting endangered species habitat requirements. MMS has been used in that study to analyze the sediment transport requirements for building and maintaining appropriate habitat, as well as to generate inflow forecasts using the PRMS module. Based on the success of this planning application, implementation in an operational mode is anticipated.

Yakima River Basin: The Yakima River Basin in eastern Washington has a drainage of about 6100 square miles, with an average annual inflow of about 3.4 million acre-feet and about 1 million

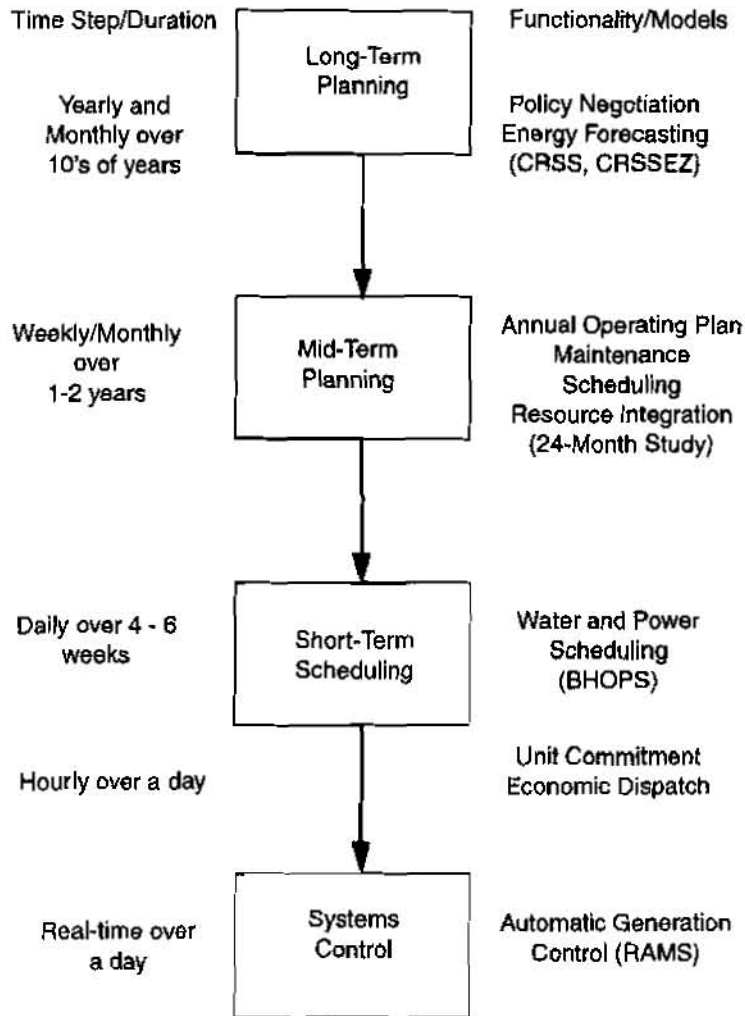


Figure 3. Hierarchical view of decision making on the Colorado River.

acre-feet of storage. It is a much smaller basin than the Colorado and presents a variety of new issues in terms of operational and planning strategies. For our program, it provides the opportunity to apply and extend the generic tools that have been developed to date, as well as to push the research and development with regard to new water management needs.

Our focus in the first year has been the implementation of HDB. In Fiscal Year 1997, our agency adopted the Oracle RDBMS as the agency-wide standard and we decided to port HDB to Oracle prior to installation at the Yakima Area Office. Although this caused some delays in our schedule, we were able to avoid a costly move to new hardware and software in the future. The HDB design has proven to be easily extended to incorporate new datatypes, such as fish monitoring data necessary for the anadromous fish, as well as new climatological data.

Application of the modeling components of the DSS also began in 1997. A PRMS model has been developed using MMS by USGS staff for use on the Yakima system and a basin planning model is under development using RiverWare. We anticipate development of an operational model in 1998.

Rio Grande River Basin: The Rio Grande River in New Mexico drains approximately 30,000 square miles and has an average annual inflow of about 660,000 acre-feet. The flow is augmented by a trans-basin diversion from the San Juan River of about 85,000 acre-feet annually. This diversion offers an opportunity to extend the DSS tools to incorporate the tracking of water ownership, as the diversion project "is operated to assure that there are no effects on the natural flow of the Rio Grande" (URGWOM, 1996). In 1997 our research focused on the extension of water ownership to RiverWare (Zagona and Fulp, 1998). This work will continue in 1998 and beyond, as well as the extension of HDB to store the state of each account over time.

SOME ISSUES FOR SUCCESSFUL IMPLEMENTATION

Movement to a computer-based, decision support system represents a major paradigm shift for our agency. We have encountered several major issues over the past three years, and although we cannot say that we have solved each and every one, we do feel that we have some experiences that may help others in similar pursuits.

A primary issue is whether an agency is really committed to making such a paradigm shift. Although having the commitment to an R&D budget is most important (and was a commitment that we had), we also realized that we needed to make available appropriate agency technical personnel if we were to succeed. Prior to entering into the program, several technical staff personnel formed a working group to discuss this and other issues and make a recommendation to management regarding the program. A key part of that recommendation was that management understand and make available the necessary staff time for technical program oversight. To date, we estimate that we have invested an average of 3.5 FTE (full-time equivalent) each year, primarily to define needs, review the proposed research, test the developed software, and transfer the technology.

Transfer of the technology is not guaranteed, however, even with up-front involvement of the target users. We have used a "side-by-side" approach to technology transfer where the Reclamation personnel involved directly in the program work with end users to solve real problems. Although this approach has proven successful, its drawback is that we cannot transfer the technology as rapidly as we would like. We are now moving to a more formal approach to technology transfer, including the development of formal training courses in use of the DSS.

Another critical issue is the long-term viability of the products that are being developed. This includes providing funding mechanisms for long-term maintenance and support. Our approach has been to provide mechanisms for some external funding (through the use of the products outside of our agency), as well as receiving a commitment from the operating groups involved to budget a share of the costs for the long term.

Finally, the real "proof of the pudding" will be if we become better water resource managers with use of the technology. Although we have received feedback indicating real improvement in our ability to reach new decisions in a timely manner, we are attempting to define metrics and collect the appropriate data so that we can more definitively answer this question in the future.

REFERENCES

- Fulp, T.J., Theobald, D.M., Williams, B., and Vickers, B., 1991, Decision Support for Colorado River Operations, Proceedings of the WaterPower '91 Conference, American Society of Civil Engineers
- Leavesley, G.H., Restrepo, P.J., Markstrom, S.L., Dixon, M., and Stannard, L.G., 1996, The Modular Modeling System (MMS) -- User's Manual, U.S. Geological Survey Open File Report 96-151
- Loucks, D.P., 1995, Developing and Implementing Decision Support Systems: A Critique and a Challenge, Water Resources Bulletin, Vol. 31, No. 4, American Water Resources Association
- Ryan, T.P., 1996, Development and Application of a Physically Based, Distributed Parameter, Rainfall Runoff Model in the Gunnison River Basin, Global Climate Change Response Program Report, U.S. Bureau of Reclamation, Denver, CO
- Ryan, T.P., and Sieh, D., 1993, Integrating Hydrologic Models, Geographic Information Systems, and Multiple Data Bases: A Data Centered Approach, Proceedings of the Federal Interagency Workshop of Hydrologic Modeling Demands for the 90's, U.S. Geological Survey Water Resources Investigations Report 93-4018, Denver, CO
- Savic, D.A., and Simonovic, S.P., 1989, A Pilot Intelligent Decision Support System for Reservoir Optimization, Proceedings of the 3rd Water Resources Operation Management Workshop: Decision Support Systems for Water Managers, American Society of Civil Engineers, NY
- Scott Morton, M.S., 1971, Management Support Systems, Computer-Based Support for Decision Making, Division of Research, Harvard University, Cambridge, MS
- URGWOM: Upper Rio Grande Water Operations Model Plan for Development, 1996, a joint report by the U.S. Army Corps of Engineers, U.S. Bureau of Indian Affairs, U.S. Bureau of Reclamation, U.S. Fish and Wildlife Service, U.S. Geological Survey, U.S. Section of the International Boundary and Water Commission
- Zagona, E., and Fulp, T., 1998, RiverWare: A General River and Reservoir Modeling Environment, to be published in the Proceedings of the First Federal Hydrologic Modeling Conference, Las Vegas, NV

RIVER OPERATIONS MODELING IN THE SAN JUAN RIVER BASIN

D. L. King, Hydraulic Engineer, Bureau of Reclamation, Denver, Colorado, R. S. Parker and Gerhard Kuhn, Hydrologists, U. S. Geological Survey, Denver, Colorado

Abstract: A decision support system (DSS) has been developed for use on the San Juan River Basin in Arizona, Colorado, New Mexico, and Utah through a collaborative effort by the Bureau of Reclamation and the U.S. Geological Survey. The DSS includes a watershed modeling framework, a river and reservoir-operations modeling framework, and a relational data base that links the two modeling frameworks. The Modular Modeling System (MMS), which is an interface to a variety of modules for simulating water, energy, chemical, and biological processes, data-analysis tools, and model-building tools, comprises the watershed modeling framework. The RiverWare Systems Model, which is a general purpose, interactive model-building tool that integrates multipurpose reservoir-operations, including flood control, navigation, recreation, water supply, water quality, and power economics, comprises the river and reservoir-operations modeling framework. The DSS developed for the San Juan River Basin provides water managers a useful tool to manage, utilize, and schedule delivery of water resources.

INTRODUCTION

The Bureau of Reclamation (Reclamation) and the U.S. Geological Survey (USGS) are collaborating on the Watershed and River System Management Program to couple a watershed modeling framework that simulates the physical hydrology of a river basin with a river and reservoir-operations modeling framework that simulates water use in a river basin. The Modular Modeling System (MMS) (Leavesley and others, 1996) is used for the watershed modeling framework, and the RiverWare Systems Model (RiverWare) (Fulp and others, 1995; Bureau of Reclamation, 1996) is used for the river and reservoir-operations modeling framework. These modeling frameworks are linked using a common data base [Hydrologic Data Base (HDB) (fig. 1)] that provides a comprehensive decision-support system (DSS) for use in the management of water resources. HDB also links ancillary tools needed by individual models, such as a geographical information system (GIS), statistical analysis, and data query and display capabilities (fig. 1).

This paper presents a brief description of the MMS and RiverWare models before presenting a more detailed description of the development, testing, and application of the DSS in the San Juan River Basin (fig. 2), which has an area of about 60,000 km². The San Juan River is a major tributary to the Colorado River and flows directly into Lake Powell, a Reclamation reservoir that regulates water between the seven states in the Colorado River Compact.

MODULAR MODELING SYSTEM

The MMS framework (Leavesley and others, 1996) is an integrated system of computer software for the development and application of models to simulate a variety of water, energy, chemical, and biological processes. MMS has three major components: pre-process, model, and post-process. The preprocess component provides tools to input, analyze, and prepare spatial and time-series

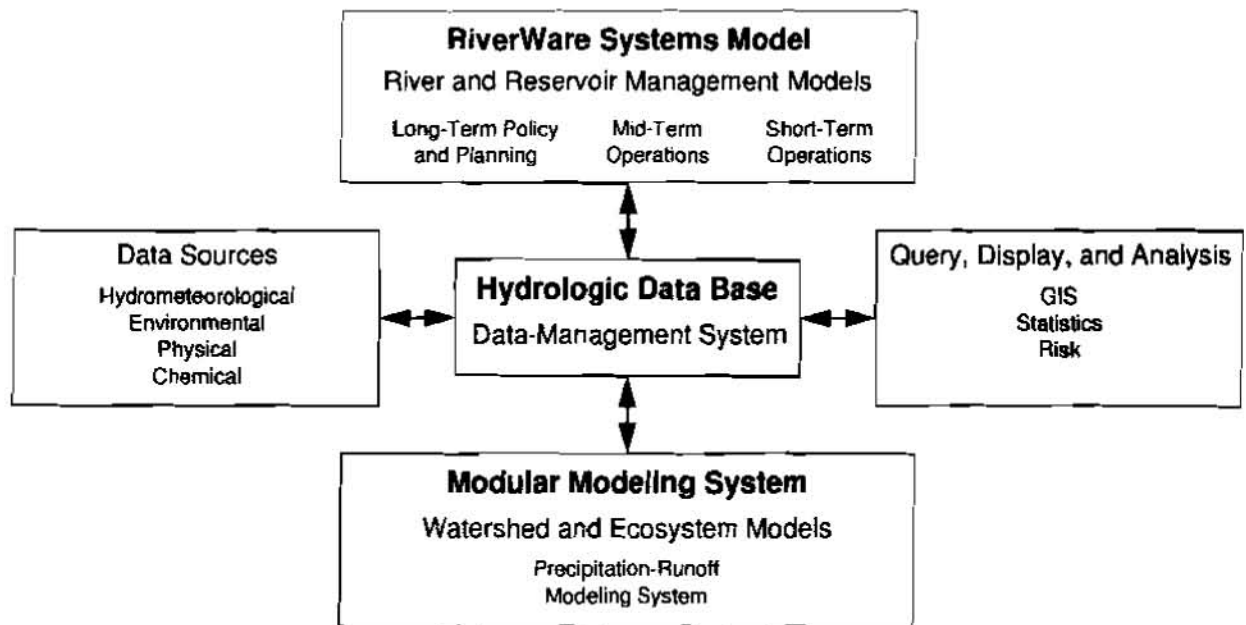


Figure 1. Data-base centered decision-support system.

data for use in model applications. The model component provides tools to develop and apply models. The post-process component provides tools to display and analyze model results and to transfer the results to other models or software. A major feature of the model component is the module library, which contains a variety of modules for simulating the various processes. For a given process, the library may contain several modules, each representing an alternative conceptualization or approach to simulating that process. Through an interactive model-builder interface, the user selects and links modules to create a specific model.

The model assembled within the MMS framework for application in the San Juan River Basin is the Precipitation-Runoff Modeling System (PRMS) (Leavesley and others, 1983). PRMS allows for spatial distribution of model parameters by partitioning the watershed into hydrologic response units (HRU's). Each HRU is assumed to have uniform physical and hydrologic characteristics; these characteristics, many of which can be related to the model parameters, are determined from information about climate, soils, topography, and vegetation. PRMS computes a daily water balance for each HRU by using daily inputs of air temperature, precipitation, and solar radiation. When appropriate, a snowpack is simulated for each HRU; the snowpack is modified twice a day on the basis of a calculated snowpack-energy budget.

RIVERWARE SYSTEMS MODEL

The RiverWare framework (Fulp and others, 1995; Bureau of Reclamation, 1996) is an object-oriented river, diversion, and reservoir operations model-building system developed jointly by Reclamation and other agencies under contract to the Center for Advanced Decision Support for Water and Environmental Systems (CADSWES) in Boulder, Colorado (Shane and others, 1995).

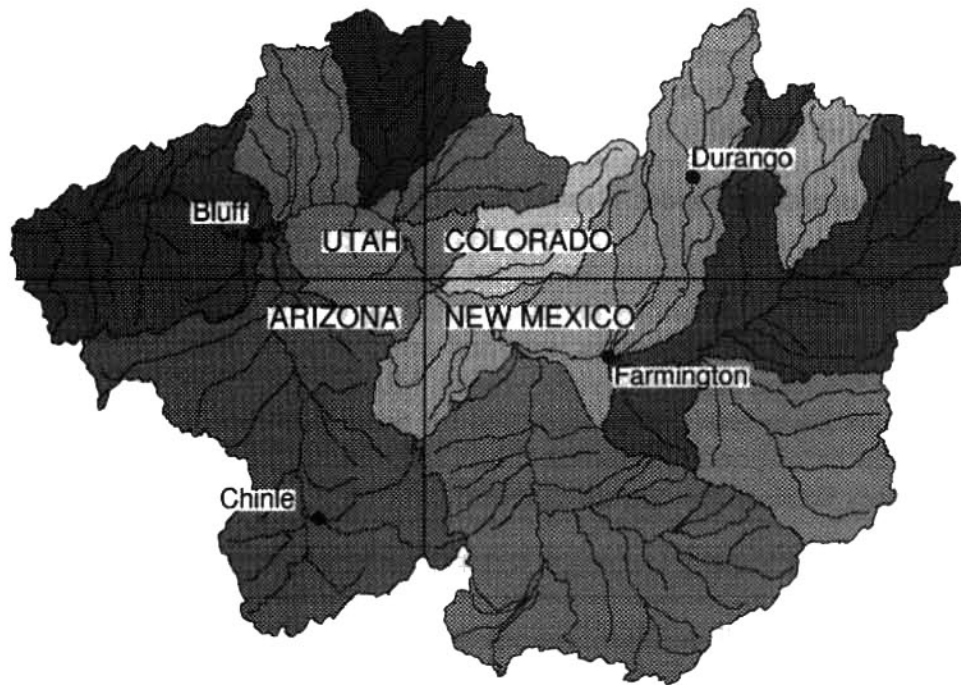


Figure 2. Location of San Juan River Basin.

RiverWare uses an object-oriented modeling and software approach that is data-centered; a specific river/reservoir system and its operating policies are defined by the data supplied to the model. This approach allows modification of a basin model to reflect new features or new operating policies and enables transportability to other river basins. The RiverWare software also provides extensibility, so that additional methods for computing new processes, additional objects for modeling new features, and additional controllers for providing new solution algorithms can be added easily to the software.

The user constructs a model by selecting reservoir, reach, confluence, and other “objects” from a palette; naming the objects; and linking them together to form the basin topology. Data associated with each object is typed in by the user or imported from files and engineering algorithms, such as power calculation, tailwater calculation, and river reach routing, are selected from a menu. Operating policy is added either through the constraint editor or the rulebase editor, depending on which controller the user wishes to use.

RiverWare currently has several modes of execution (controllers) that include simple simulation, rule-based simulation, linear goal-programming optimization, and multiple-run management controllers (Bureau of Reclamation, 1996). The simple solution controller was used to validate the RiverWare model for the San Juan River Basin, basically verifying that the physical configuration was correct and that the spreadsheet was error-free; the rule based simulation controller was used to implement operating-decision criteria.

HYDROLOGIC DATA BASE

The HDB software also was developed under contract to CADSWES. To a large extent, HDB is a repository of air temperature, precipitation, streamflow, and other time-series data (fig. 1) Near real-time data are populated from a hydrometeorological data-collection network that uses a combination of satellite and radio telemetry. To develop the DSS for the San Juan River Basin, a natural-streamflow data set was developed that could be used to calibrate the watershed model and to validate the river operations model. Natural streamflows are computed every 5 years on a large scale for the entire Colorado River Basin. The data and algorithms used for these computations were expanded and revised to compute the natural streamflows at the finer scale required for the San Juan River Basin. The revisions included updating of irrigated acreage with 1993 GIS coverage, demarcation of additional water uses, and use of detailed diversion data available from the Colorado River Decision Support System website. Monthly natural streamflow volumes for 28 sites in the San Juan River Basin were estimated for water years 1970-93 (King and others, in press). The 28 sites correspond to selected USGS streamflow-gaging stations in the basin and comprise the primary nodes in the operations model.

DEVELOPMENT OF SAN JUAN RIVER BASIN OPERATIONS MODEL

Development of the San Juan River Basin operations model primarily consisted of development of data-handling procedures. These procedures included moving data from spreadsheets to text files, creating a pre-processor to compute depletion volumes for each model node, creating files to map the depletions and other hydrologic characteristics to the nodes, and creating Data Management Interfaces to move data into and out of RiverWare. A prototype operations model for the Animas and Florida River subbasins also was developed to test these support procedures. Development of the San Juan River Basin operations model consisted of three basic steps: configuration, validation, and development of the operating rules.

Configuration: Configuration consisted of mapping the natural streamflows and equivalent depletions into appropriate RiverWare objects and building the operations model in RiverWare. Depletions were modeled by using aggregate diversion objects. Each aggregate diversion can have any number of water users, whose water supply is affected by the behavior selected and by the linking of return flows. Most water users were aggregated through mapping and preprocessing. Although it is possible to model every real water user in a watershed, aggregating greatly decreases model complexity and execution time.

Development of the operations model indicated that additional functionality was required in RiverWare. This included (1) adding a new return-flow method, (2) enabling separation of return flows into surface-water and ground-water components, and (3) creating a primitive ground-water object in which to store ground-water flow. A variable efficiency method also was created to better emulate the effect of water supply on the efficiency of an irrigation diversion. The method assumes that an irrigation diversion increases in efficiency up to a maximum; depletions are not reduced until the maximum efficiency is reached.

Validation: To validate the operations model, historical natural streamflow, depletions, diversions, and reservoir releases were input to the operations model; the model was run; and, the simulated

streamflows at the 28 model nodes were compared to the recorded streamflows at the gaging stations. The validation was a complex task because of the detail required for the modeling. The modeled depletions and streamflows for each subbasin had to correspond exactly to the depletions and natural streamflows in HDB to achieve validation. The validation also served the purpose of finding errors in the natural streamflow computations attributable to spreadsheet equation errors or data errors.

Development of Operating Rules: Initially, the river operating rules from the Colorado River Simulation System (CRSS) were used to derive prototype rules for the San Juan River Basin operations model (Frevort and others, 1997). Because the basin topology for the San Juan River Basin operations model was much more complex than the basin topology in CRSS, modeling the San Juan River Basin required some modifications of the CRSS operating rules. The creation of a “generic” rule set was attempted that could be used with a monthly or daily time step, and that could incorporate the basic operations of a reservoir, including the meeting of downstream demands, without modifying the physical constraints of the system.

To test the generic operating rules, the operations model was run by inputting the natural streamflows and non-shorted depletions in HDB and by using the operating rules being developed. The intent of the model simulations was to match historical releases, historical storage, and historical depletions by minimizing differences between the simulated and recorded values, without modifying the physical constraints previously defined.

The generic reservoir rule provides an operation that incorporates downstream demands, flood control, target storage quantities, and filling criteria. This rule attempts to fill a reservoir during the runoff season and maintain some target storage quantity for each month of the non-runoff season. A procedure also was developed which computes the minimum amount of water to release that will meet downstream demands and which accounts for gains downstream from a reservoir, exports, imports, and diversions that use the return flow from upstream diversions.

In addition, a generic diversion rule was written to assign the diversion quantity on the basis of the available water supply. This rule has two alternatives, depending upon the rule’s dependency. In the diversion rule, an upstream dependency is used to indicate when the supply has changed upstream from a diversion, and a downstream dependency is used to indicate when the supply has changed downstream from the diversion. If the supply has changed, the rule has sufficient data to determine if there will be a headgate shortage. The rule determines the amount of water available to aggregate diversions based upon the supply and adjustment algorithm. The current algorithm does the adjustment with a quasi water-rights solution. If the downstream dependency invokes the diversion rule, the rule checks for a depletion shortage. If there is a shortage, the rule adjusts the water delivered to the diversion.

OPERATING RULES TO IMPROVE ENDANGERED-FISH HABITAT

The final phase of the study was to establish revised operating rules that would improve the habitat for endangered fish, make model runs with the revised rules for various operating scenarios, and implement the revised rules. Two endangered species of fish, the humpback chub and the Colorado squawfish, have necessitated reexamination of operations in the San Juan River Basin. The

Recovery Improvement Program (RIP) is in the sixth year of a 7-year study to evaluate alternative operations of Navajo Reservoir in New Mexico that would build and maintain fish habitat while meeting downstream demands (King and others, in press). Sedimentation, discharge, habitat, fish counts, and other data were collected and analyzed as a part of the RIP study. The data for the first 6 years of the study were used to establish criteria for flow regimes that build or maintain fish habitat. Revised operating rules were developed on the basis of the flow-regime criteria.

The RIP criteria were not easy to implement in the operations model. However, having the basic model and historical rules already implemented in RiverWare allowed the rule revision to focus on the functionality and integrity of the implementation. Because RiverWare provides excellent diagnostics for rule debugging, actual models could be used rather than prototypes. The rules were incorporated into the operations model in a relatively short time, and numerous scenario runs were made develop the final revised operating procedures. These procedures are under review before implementation, which is intended for June 1998.

CONCLUSIONS

MMS, RiverWare, and HDB were effective tools in implementing extremely complicated operating rules for the San Juan River Basin. The San Juan River Basin operations model provides water managers a useful tool to manage, utilize, and schedule delivery of water resources. Furthermore, the operations model provides efficient computation of various operating scenarios. The combined system is a useful decision support system.

REFERENCES

- Bureau of Reclamation, 1996, PRYSM, Power and Reservoir System Model. Denver, Bureau of Reclamation Fact Sheet, 3 p.
- Frevert, D., Fulp, T. J., Vickers, W. B., and King, D. L., 1997, Development of a Data Centered Decision Support System for Multiple Purpose Water Resources Projects. Proceedings of the 24th Annual Water Resources Planning and Management Conference, American Society of Civil Engineers, Houston, 1 p.
- Fulp, T. J., Vickers, W. B., Williams, B., and King, D. L., 1995, Decision Support for Water Resources Management in the Colorado River Region: IN L. Ahuja, J. Leppert, K. Rojas, and E. Seely (eds.), Workshop on Computer Applications in Water Management. Colorado Water Resources Research Institute, Fort Collins, Colo., Information Series 79, p. 24-27.
- King, D. L., Davidson, P., Ozga, J., and Simons, J., [in press], Watershed and River Systems Planning Model in the San Juan River Basin, Colorado. Proceedings of First Federal Interagency Hydrologic Modeling Conference, Las Vegas, 7 p.
- Leavesley, G. H., Lichty, R. W., Troutman, B. M., and Saindon, L. G., 1983, Precipitation-Runoff Modeling System--Users Manual. U.S. Geological Survey Water-Resource Investigations Report 83-4238, 207 p.
- Leavesley, G. H., Restrepo, P. J., Markstrom, S. L., Dixon, M., Stannard, L. G., 1996, The Modular Modeling System (MMS)--User's Manual. U.S. Geological Survey Open-File Report 96-151, 142 p.
- Shane, R. M., Zagona, E. A., McIntosh, D., and Fulp, T. J., 1995, Modeling Framework for Optimizing Basin Hydropower. Proceedings of WaterPower 95, American Society of Civil Engineers, New York City, 1 vol.

PRECIPITATION DISTRIBUTION ALTERNATIVES IN APPLYING THE MODULAR MODELING SYSTEM IN THE SAN JUAN RIVER BASIN, COLORADO AND NEW MEXICO

**Gerhard Kuhn, R. S. Parker, L. E. Hay, and G. H. Leavesley
Hydrologists, U. S. Geological Survey, Denver, Colorado**

Abstract: The U.S. Geological Survey and the Bureau of Reclamation are collaborating to link a watershed modeling framework, the Modular Modeling System (MMS), with a routing and reservoir-management modeling framework, the RiverWare Systems Model, resulting in an integrated system of water-resource models and relational data bases that can be used in the management of water resources in the western United States. The joint effort is termed the Watershed and River System Management Program and the first study basin is the 18,750 square kilometer San Juan River basin in Colorado and New Mexico. Application of a watershed model to this large basin with extensive hydrologic and physiographic variability requires a realistic distribution of precipitation. An algorithm to distribute precipitation in the basin was developed that incorporated weather-type (WT) information and precipitation data from multiple National Weather Service precipitation stations in the basin. Distribution of precipitation estimated by using the WT algorithm was compared to the distribution estimated by using the algorithm provided within the MMS framework. Average error in simulated annual runoff for water years 1949-93, which was 16.5% when using precipitation distributed with the MMS algorithm, decreased to 11.4% when using precipitation distributed with the WT algorithm.

INTRODUCTION

In 1994, the U.S. Geological Survey and the Bureau of Reclamation began a collaborative program, termed the Watershed and River System Management Program. The purpose of the program is to develop, test, and implement an integrated system of water-resource models and relational data bases that can be used in the management of water resources in the western United States. The primary focus of the program is to link a watershed modeling framework that simulates the physical hydrology of a river basin with a routing and reservoir-management modeling framework that simulates water use in a river basin. The key to linking these models is a common data base that provides input to a decision-support system. The Modular Modeling System (MMS) (Leavesley and others, 1996) is used for the watershed modeling framework, and the RiverWare Systems Model (previously known as the Power and Reservoir Systems Model; Fulp and others, 1995; Bureau of Reclamation, 1996) is used for the routing and reservoir-management modeling framework. The first study basin for the program is the San Juan River basin in Colorado and New Mexico (fig. 1), and a second study basin has been established in the Yakima River basin in Washington.

The MMS framework (Leavesley and others, 1996) has three major components: pre-process, model, and post-process. The pre-process component provides tools to input, analyze, and prepare spatial and time-series data for use in model applications. The model component provides tools to develop and apply models. The post-process component provides tools to display and analyze model results and to transfer the results to other models or software. A major feature of the model component is the module library, which contains a variety

modules for simulating water, energy, chemical, and biological processes. For a given process, the library may contain several modules, each representing an alternative conceptualization or approach to simulating that process. Through an interactive model-builder interface, the user selects and links modules to create a specific model.

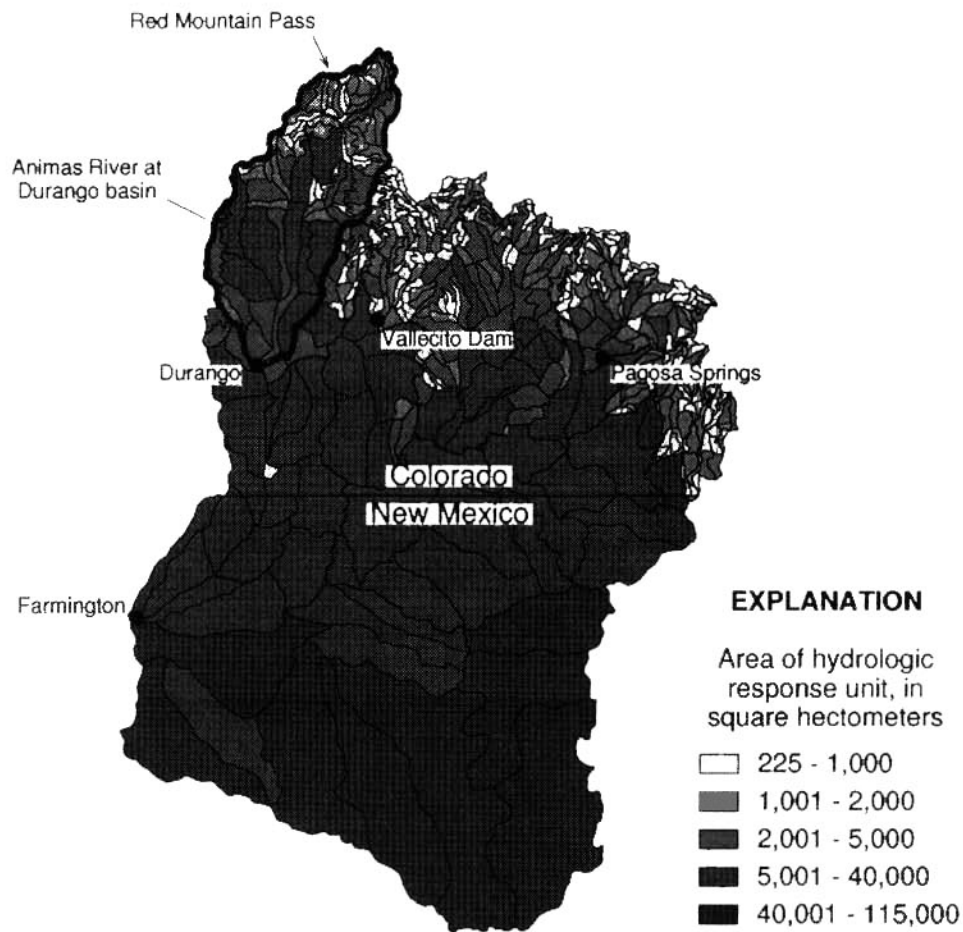


Figure 1. San Juan River basin upstream from Farmington, New Mexico, showing hydrologic response units.

The model assembled within the MMS framework for application in the San Juan River basin is the Precipitation-Runoff Modeling System (PRMS) (Leavesley and others, 1983); PRMS allows for spatial distribution of model parameters by partitioning the watershed into hydrologic response units (HRU's). Each HRU is assumed to have uniform physical and hydrologic characteristics; these characteristics, which are the model parameters, are determined from information about climate, soils, topography, and vegetation. PRMS computes a daily water balance for each HRU using daily inputs of air temperature, precipitation, and solar radiation. When appropriate, a snowpack is simulated for each HRU; the snowpack is modified two times a day on the basis of a calculated snowpack-energy budget.

In the San Juan River basin, PRMS was applied to the part of the basin upstream from Farmington, New Mexico (fig. 1), which has a drainage area of about 18,750 km². Most of the streamflow in this part of the basin is derived from snowmelt in the headwater drainages of the San Juan Mountains of Colorado, where elevation ranges from about 2,200 to 4,200 m. Precipitation, which is strongly affected by orography, has a large spatial variability, ranging from about 350 to 1,300 mm/yr. Applying PRMS to a large area with extensive hydrologic and physiographic variability creates a number of modeling problems related to scale. Some of the algorithms in PRMS are best used in small watersheds where parameters can be constrained in time or space. For large watersheds, hydrologic characteristics are highly variable, and some of the algorithms in PRMS are less functional. The purpose of this paper is to compare the linear precipitation-distribution algorithm within PRMS and the weather-type precipitation-distribution algorithm that was developed for applying PRMS to the San Juan River basin.

DISTRIBUTION OF PRECIPITATION

The hydrologic and physical characteristics of the San Juan River basin upstream from Farmington, New Mexico, vary substantially, requiring more than 400 HRU's (fig. 1) to represent the basin adequately. To simplify the analysis presented in this paper, application of PRMS to the Animas River at Durango, Colorado, a 1,790-km² tributary basin with 77 HRU's (fig. 1), was used to compare the precipitation-distribution algorithms.

Precipitation-Runoff Modeling System Algorithm: The precipitation-distribution algorithm provided in PRMS consists of two parameters used to estimate precipitation for each HRU. One parameter is used to adjust rain precipitation and one parameter is used to adjust snow precipitation; values for the two parameters can vary for each HRU and for each month of the year, but the parameter values remain constant for each year being simulated. Measured precipitation data at one or more sites in or adjacent to the basin (point data) are input to the model. Each HRU is specified to use the input data for a particular point-precipitation station, and the specified data are adjusted by the appropriate adjustment parameter, resulting in a varied distribution of precipitation on the HRU's (Leavesley and others, 1983, p. 13-14). Determining the appropriate values for the adjustment parameters becomes increasingly difficult with the use of multiple precipitation stations due to a general lack of high-elevation precipitation information; therefore, values for the adjustment parameters often are derived using a single precipitation station.

In the San Juan River basin, precipitation from October 1 through March 31 increases substantially with increasing elevation; therefore, the relation between winter precipitation and elevation was used to estimate values for the snow-adjustment parameters; all rain-adjustment parameters were assumed to be 1.0. A ratio of 1.83 was calculated between the long-term average snow-water equivalent (SWE) (653 mm) on April 1 at the Red Mountain Pass snowcourse (elevation 3,398 m) and the long-term average precipitation (356 mm) for October-March at the Vallecito Dam precipitation station (elevation 2,332 m). (Note: More years were used to calculate the long-term averages than those listed in table 1.) Based on the difference in elevation between the two sites, the change in the ratio per meter of elevation was calculated, and was used to estimate initial values for the HRU snow-adjustment parameter from the

difference in elevation between the HRU and the Vallecito Dam precipitation station. Because of data constraints and for simplicity, a single set of HRU snow-adjustment parameters was used for October-March. In calibrating the model for the Animas River basin, the snow-adjustment parameters were optimized, resulting in a ratio value of about 1.98 between the April 1 SWE at the Red Mountain Pass snowcourse and the October-March precipitation at the Vallecito Dam precipitation station.

October-March precipitation by HRU for two water years, estimated by using the PRMS algorithm and precipitation at the Vallecito Dam station, are shown in figure 2. The PRMS-distribution algorithm produced a linear distribution of precipitation that varied only on the basis of elevation; there is no spatial variability based on location of a HRU within the Animas River basin. Also, because the snow-adjustment parameter values are constant over time, the PRMS algorithm did not provide any temporal variability in precipitation beyond the temporal variability associated with precipitation at the Vallecito Dam station. The estimated precipitation for a particular HRU is adjusted by the same parameter value, resulting in an estimated precipitation for the HRU that is the same multiple of the input precipitation at Vallecito Dam. For example, estimated precipitation for an HRU at an elevation about equal to the elevation of Red Mountain Pass is computed to be about 2 times greater than the measured precipitation at Vallecito Dam (table 1); however, the ratio between measured precipitation at Red Mountain Pass and at Vallecito Dam had considerable annual variation (1.37 to 2.37 in table 1). Use of the same ratio each year resulted in estimated precipitation that, in some years, was substantially different from the trend of measured precipitation at snow-telemetry (SNOTEL) stations in and adjacent to the Animas River basin (water year 1993 in fig. 2).

Weather-Type Algorithm: To provide estimated precipitation distribution with greater spatial and temporal variability, a method with greater flexibility than the PRMS algorithm was needed. A method was developed that incorporated weather-type (WT) information and precipitation data from multiple National Weather Service precipitation stations (L.E. Hay, U.S. Geological Survey, written commun., 1997). The WT's were defined from daily sea-level pressure (SLP) data in a gridded (5x5-degree) format available from the National Center for Atmospheric Research. The SLP data from 16 points, covering an area from 30 to 45 degrees north latitude and from 100 to 115 degrees west longitude, were used in a map correlation procedure (Yarnal, 1984). A correlation coefficient that was significant at a 90-percent confidence level was used as the threshold for grouping the SLP data for water years 1949-93. This grouping resulted in six distinct WT's. Precipitation-elevation regression equations then were determined for the Animas River basin for each month and WT by using station elevation as the independent variable and monthly station precipitation as the dependent variable; the regressions were determined by using data for five precipitation stations that had continuous data for water years 1949-93. Mean station elevation and precipitation for each day were calculated using daily precipitation data. The mean station elevation and precipitation were used in the regression equations to distribute precipitation on a 5x5-km gridded surface based on the mean elevation of each grid cell. Lastly, a percent-area weighting scheme was used to interpolate the gridded precipitation to the HRU's.

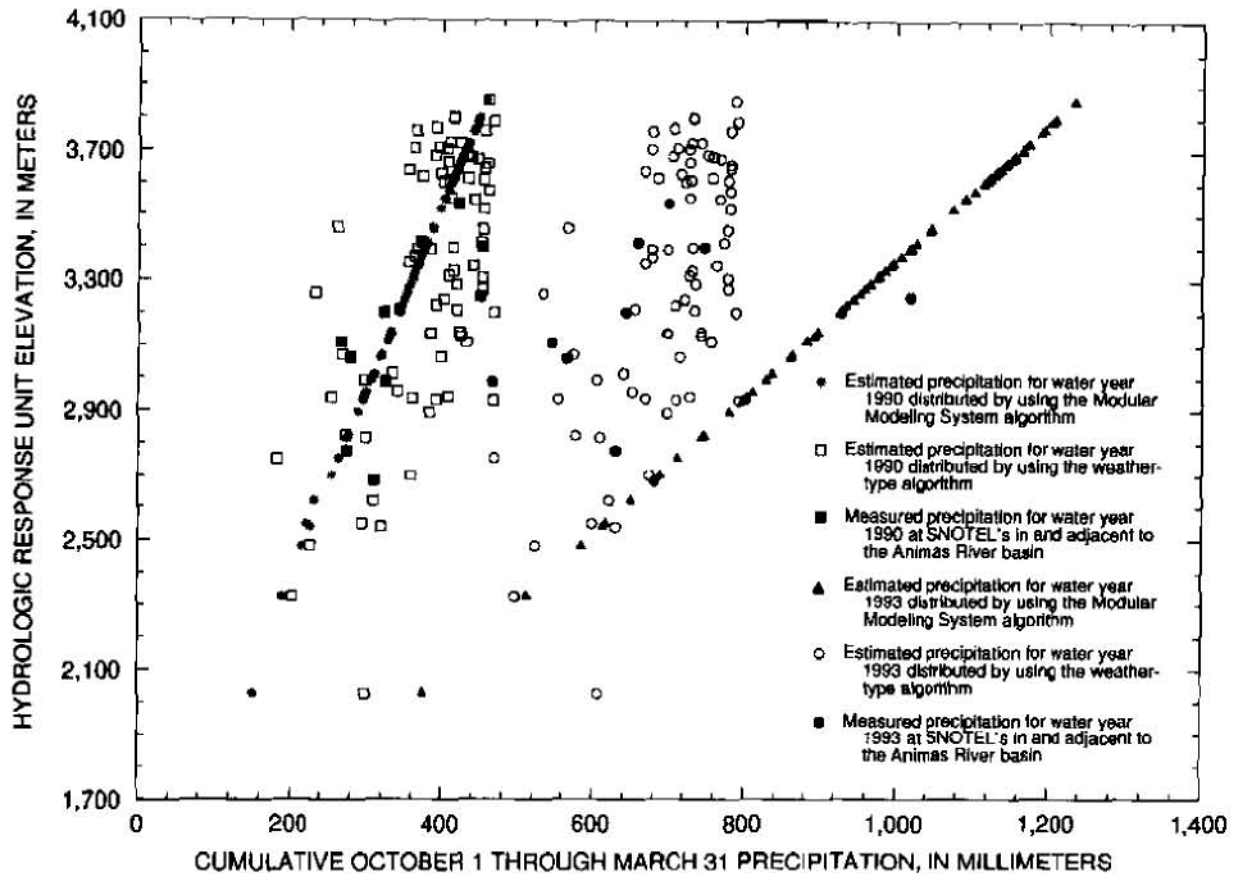


Figure 2. Distributions of precipitation for hydrologic response units in the Animas River basin.

October-March precipitation by HRU for two water years, estimated by using the WT algorithm, are shown in figure 2. The WT distribution algorithm produced a spatial distribution of precipitation that varied by elevation and by location (fig. 2). The variability by location results from use of the percent-area weighting scheme in which estimated precipitation on one or more of the 5x5-km grid cells is used to derive the estimated precipitation on the HRU. The spatial variability of precipitation distributed by using the WT algorithm generally is more similar to the spatial variability of measured precipitation at the SNOTEL stations in and adjacent to the Animas River basin than the distribution produced by using the PRMS algorithm (fig. 2). Precipitation estimated using the WT algorithm also had a temporal distribution that was different from year to year, and was closer to the trend of measured precipitation at the SNOTEL stations than the distribution produced using the PRMS algorithm (fig. 2). The differences between estimated October-March precipitation for an HRU adjacent to Red Mountain Pass (but with a mean elevation slightly higher than the pass) and measured October-March precipitation at Red Mountain Pass are substantially smaller for the WT algorithm than for the PRMS algorithm (table 1).

Table 1. Measured and estimated October 1 through March 31 precipitation at Red Mountain Pass
[Elevation of Red Mountain Pass = 3,398 meters; HRU = hydrologic response unit; PRMS = Modular Modeling System; WT = weather-type.]

Water year	Measured precipitation at Red Mountain Pass (millimeters)	Measured precipitation at Vallecito Dam (millimeters)	Ratio of Red Mountain Pass precipitation to Vallecito Dam precipitation ¹	Using PRMS algorithm		Using WT algorithm	
				Estimated precipitation for an HRU with an elevation of 3,413 meters (millimeters)	Percent difference ²	Estimated precipitation for an HRU with an elevation of 3,413 meters (millimeters)	Percent difference ²
1984	818	367	2.23	731	-10.6	636	-22.2
1985	770	521	1.48	1,038	34.8	765	-0.6
1986	630	382	1.65	762	21.0	653	3.7
1987	706	467	1.51	932	32.0	695	-1.6
1988	572	342	1.67	682	19.2	520	-9.1
1989	599	275	2.18	548	-8.5	574	-4.2
1990	452	191	2.37	380	-15.9	451	-0.2
1991	630	325	1.94	649	3.0	629	-0.2
1992	612	446	1.37	888	45.1	888	12.4
1993	747	515	1.45	1,026	37.3	772	3.3

$$^1\text{Ratio} = \frac{\text{measured precipitation at Red Mountain Pass}}{\text{measured precipitation at Vallecito Dam}}$$

$$^2\text{Percent difference} = \left(\frac{\text{estimated precipitation for the HRU} - \text{measured precipitation at Red Mountain Pass}}{\text{measured precipitation at Red Mountain Pass}} \right) \times 100$$

DISCUSSION

The estimated distributions of precipitation derived from the WT algorithm generally seem more realistic compared to the estimated distributions of precipitation derived from the PRMS algorithm because the WT algorithm resulted in a year-to-year distribution pattern similar to the year-to-year pattern of measured precipitation at SNOTEL stations. To evaluate the estimated precipitation distribution derived from the WT algorithm, the error in simulated runoff was used. The PRMS model was calibrated for the Animas River at Durango basin (fig. 1) by using the estimated distributions of precipitation derived from the PRMS algorithm, and by optimizing the snow-adjustment parameter values, as well as other model parameters. The resulting errors in annual simulated runoff for water years 1949-93 are shown in figure 3. The annual errors were less than 10% for 18 years and were more than 20% for 16 years (fig. 3); the mean of the absolute values of the annual errors was 16.5%.

Streamflow then was simulated by using the estimated distributions of precipitation derived from the WT algorithm and by using the same set of model parameters previously optimized, except that values for the snow-adjustment parameter were set to 1.0. The resulting errors in annual simulated runoff for water years 1949-93 are shown in figure 3. The annual errors were less than 10% for 26 years and were more than 20% for only 6 years (fig. 3); the mean of the absolute values of the annual errors decreased to 11.4%. Generally, the errors in annual simulated runoff were larger and more variable when the PRMS algorithm was used to distribute precipitation than when the WT algorithm was used to distribute precipitation.

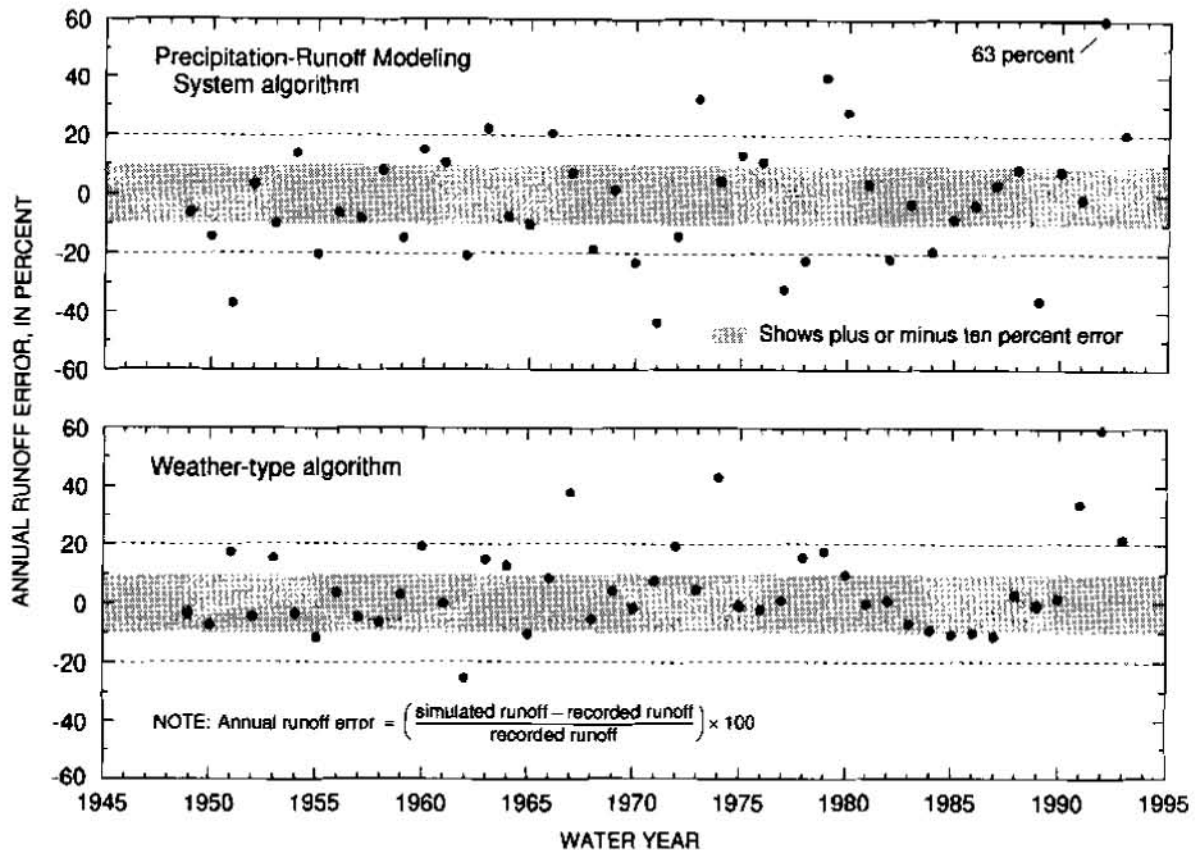


Figure 3. Annual runoff error for Animas River at Durango for two precipitation-distribution algorithms.

Use of estimated precipitation distributed by using the WT algorithm resulted in a substantially improved ability to simulate streamflow in the Animas River at Durango basin compared to use of estimated precipitation distributed by using from the PRMS algorithm. Application of the WT algorithm to other parts of the San Juan River basin needs to be done for a more complete evaluation of the method.

REFERENCES

- Bureau of Reclamation, 1996, PRYSM, Power and Reservoir System Model. Denver, Bureau of Reclamation Fact Sheet, 3 p.
- Fulp, T. J., Vickers, W. B., Williams, B., and King, D. L., 1995, Decision Support for Water Resources Management in the Colorado River Region: IN L. Abuja, J. Leppert, K. Rojas, and E. Seely (eds.), Workshop on Computer Applications in Water Management. Colorado Water Resources Research Institute, Fort Collins, Colo., Information Series 79, 24-27.
- Leavesley, G. H., Lichty, R. W., Troutman, B. M., and Saindon, L. G., 1983, Precipitation-Runoff Modeling System--Users Manual: U.S. Geological Survey Water-Resource Investigations Report 83-4238, 207 p.
- Leavesley, G. H., Restrepo, P. J., Markstrom, S. L., Dixon, M., Stannard, L. G., 1996, The Modular Modeling System (MMS)--User's Manual: U.S. Geological Survey Open-File Report 96-151, 142 p.
- Yarnal, B., 1984, A Procedure for the Classification of Synoptic Weather Maps from Gridded Atmospheric Pressure Surface Data. Computers and Geosciences 10(4), pp. 397-410.

THE MODULAR MODELING SYSTEM (MMS) – THE PHYSICAL PROCESS MODELING COMPONENT OF THE WATERSHED AND RIVER SYSTEM MANAGEMENT PROGRAM

G.H. Leavesley, S.L. Markstrom, M.S. Brewer, and R.J. Viger, Hydrologists, U.S. Geological Survey, Denver, Colorado

Abstract: The Modular Modeling System (MMS) is an integrated system of computer software that has been developed to provide the research and operational framework needed to support physical-process model development and application. MMS supports the development, testing, evaluation, and application of the wide range of modeling capabilities needed to address the issues associated with basin-scale water management. A geographic information system (GIS) interface, the GIS Weasel, has been integrated with MMS to support model development, application, and analysis. MMS has been coupled with RiverWare, an object-oriented reservoir and river-system modeling framework, using a shared relational database. The resulting database-centered, decision support system provides the tools needed for evaluating and applying optimal water-allocation and management strategies to complex, operational decisions on multipurpose reservoir systems and watersheds. The development and application of this decision support system are major objectives of a cooperative effort by the U.S. Geological Survey and the Bureau of Reclamation called the Watershed and River System Management Program.

INTRODUCTION

The interdisciplinary nature and increasing complexity of environmental and water-resource problems require the use of modeling approaches that can incorporate knowledge from a broad range of scientific disciplines. These modeling approaches must be flexible and able to address a wide range of study objectives, data constraints, and spatial and temporal scales of application. Models needed for river-basin management may include: (1) watershed models for simulating reservoir inflows and streamflow from unregulated basins; (2) one-dimensional and two-dimensional hydraulic models for application to selected river reaches where channel-flow characteristics may affect channel morphology or biological habitats; (3) sediment-transport and chemical-transport models to address a variety of water quality issues; (4) agricultural models to address land-management and irrigation practices and the fate and transport of nutrients and pesticides; and (5) biological and ecosystem models that address critical habitat issues.

The integration of this wide variety of modeling capabilities and their application to water-resources management is a major focus of the Watershed and River System Management Program (WARSMP). WARSMP is a cooperative effort between the U.S. Geological Survey (USGS) and Bureau of Reclamation (BOR) to develop an operational, database-centered, decision support system for application to complex, water-management

issues. The decision support system couples the U.S. Geological Survey's Modular Modeling System (MMS) (Leavesley et al., 1996a; Leavesley et al., 1996b) with the Bureau of Reclamation's RiverWare tools (Fulp et al., 1995) using a shared relational database. MMS facilitates the integration of a wide variety of models and their application to water- and ecosystem-resource management. RiverWare is an object-oriented reservoir and river-system modeling framework developed to provide tools for evaluating and applying optimal water-allocation and management strategies. The objectives of this paper are to provide an overview of the concepts and capabilities of MMS, the database-centered decisions support system, and their application to the WARSMP effort

MODULAR MODELING SYSTEM OVERVIEW

MMS is an integrated system of computer software that provides a common framework in which to focus multidisciplinary research and operational efforts to develop, evaluate, and apply a wide range of modeling capabilities across a broad range of spatial and temporal scales. MMS uses a master library that contains compatible modules for simulating a variety of water, energy, and biogeochemical processes. A model is created by selectively coupling the most appropriate process algorithms from the library to create an "optimal" model for the desired application. Where existing algorithms are not appropriate, new algorithms can be developed.

The conceptual framework for MMS has three major components: pre-process, model, and post-process (Fig. 1). All three components retrieve data from and store data in an underlying data storage scheme. The storage scheme may be composed of one or more data structures ranging from simple flat ASCII files to Structured Query Language (SQL) databases. Data management interfaces (DMIs) handle the transfer and reformatting of information among system components and the data structures. DMIs are essential to the interaction of the three components and are the only elements that are data-structure specific. Thus, changing data storage structures requires changing only the DMI.

The GIS Weasel supports MMS as a pre-processing component. However, it can also provide GIS post-processing capabilities for the visualization and analysis of spatial and temporal model output fields.

Graphical user interfaces (GUIs) provide access to all the features of MMS and the GIS Weasel. The present framework has been developed for UNIX-based workstations and uses X-windows and Motif for the GUIs. The GUIs provide an interactive environment for users to access model components, apply selected options, and graphically display simulation and analysis results. The current GUIs are being rewritten in the JAVA programming language to enable the application of MMS to a wider range of computer platforms.

Pre-process Component: The pre-process component includes all data preparation and analysis functions needed to meet the data and parameterization requirements of a user-selected model. A goal in development of the pre-process component is to take advantage

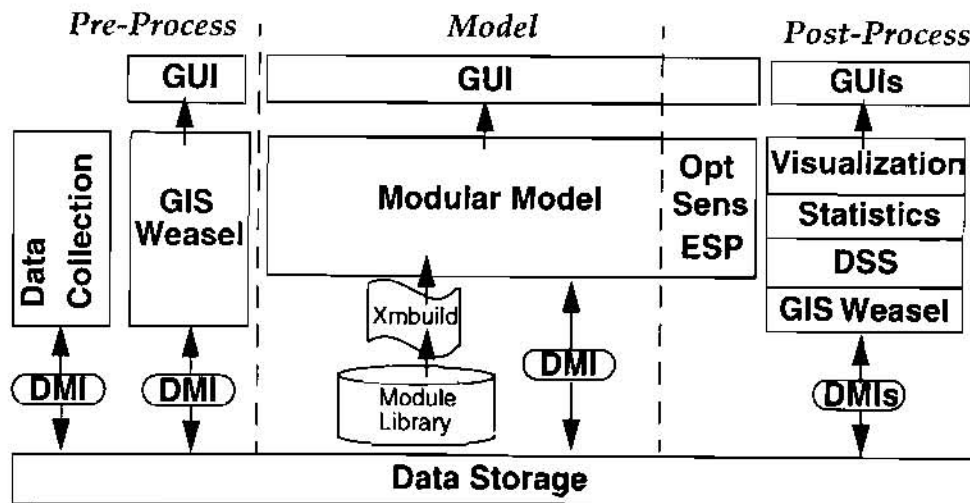


Figure 1. A schematic diagram showing the components of the Modular Modeling System (MMS).

of existing data-preparation and analysis tools and to provide the ability to add new tools as they become available. Spatial data analysis is accomplished using the GIS Weasel. Pre-processing functions provided by the GIS Weasel include the ability to (1) delineate and characterize watershed subbasin areas for distributed-parameter modeling applications, (2) estimate selected model parameters for these subbasin areas using digital elevation model (DEM) data and digital databases that include information on soils, vegetation, geology, and other pertinent physical features, and (3) generate an MMS input parameter file from these estimates.

Time-series data from existing databases and field instrumentation are organized and formatted for use in selected model applications. Additional tools are being developed to detect and replace erroneous or missing data values, aggregate data to longer time steps, disaggregate data to shorter time steps, and apply transform functions to produce a new time series. Methods to create simulated time series from model output or from the analysis and extrapolation of measured data to unmeasured points or gridded fields are also being developed.

Model Component: The model component is the core of the system and includes the tools to build a model by selectively linking process modules from the module library and to interact with this model to perform a variety of simulation and analysis tasks. The library can contain several modules for a given process, each representing an alternative conceptualization or approach to simulating that process. The user, through an interactive model builder interface (Xmbuild), selects and links modules to create a specific model. Once a model has been built, it may be saved for future use without repeating the Xmbuild step. This capability allows 'canned' versions of models to be provided to end users. User interactions with Xmbuild and the model are provided using a variety of X-window and graphical techniques.

An animation tool in the model component enables the visualization of the spatial and temporal variation of simulated state variables during a model run. Selected images from this animation for user-defined time periods can be stored and used in a post-modeling analysis to compare simulated and measured spatial and temporal variations in the selected state variable. Remotely sensed snow-covered area and soil moisture are examples of variables that can provide important additional independent measures of distributed-parameter model performance.

Post-process Component: The post-processing component contains the tools to analyze model results. These include a variety of statistical and graphical tools as well as the ability to interface with user-developed special purpose tools. Some tools are closely linked to the model component and are available as iterative procedures through the model component GUI. Optimization (Opt) and sensitivity (Sens) tools are provided to analyze model parameters and evaluate the extent to which uncertainty in model parameters affects uncertainty in simulation results. A modified version of the National Weather Service's Extended Streamflow Prediction Program (ESP) (Day, 1985) provides forecasting capabilities using historic or synthesized meteorological data. Other post-processing tools are stand-alone procedures. These include a variety of visualization and statistical tools, the GIS Weasel, and the ability to interface with resource management models and decision support systems (DSS).

GIS Weasel: The GIS Weasel has been designed to aid the preparation and analysis of spatial information for the estimation of parameters for lumped- and distributed-parameter models. It is composed of Arc/Info¹ (ESRI, 1992) GIS software, C language programs, and Unix shell scripts. All user interfaces are menu and map driven. The user is not required to have any knowledge of the command-line operating procedures of Arc/Info. However, the user should understand model assumptions regarding the treatment of spatial variations in watershed attributes.

The GIS Weasel provides tools to delineate, characterize, modify, and parameterize an area and its associated "model response units" (MRUs) using digital elevation model (DEM) and ancillary digital data. MRUs are areas delineated within a watershed, or region of interest, that reflect a model's treatment of spatially distributed attributes, such as slope, aspect, elevation, soils, and vegetation. An MRU may represent an area whose character or composition is assumed to be homogenous with respect to one or more attributes or it may be assumed to be heterogeneous with respect to all attributes. The GIS Weasel also delineates a drainage network and computes the connectivity of MRUs with this drainage network. The location of data-collection sites can also be overlaid with the MRU map to define associations between MRUs and the data sites.

¹ The use of trade, product, industry, or firm names is for descriptive purposes only and does not imply endorsement by the U.S. Government.

DATABASE-CENTERED DECISION SUPPORT SYSTEM

The physical process models in MMS are being linked with the reservoir and river management models of RiverWare via a common database, thus providing a database-centered decision support system (Fig. 2). A number of ancillary tools provide GIS, statistical analysis, and data query and display capabilities that are shared by MMS and RiverWare. In the current project, the database is termed the Hydrologic Data Base (HDB). Versions of HDB have been constructed using the commercial databases INGRES¹ (INGRES Corp., 1991) and ORACLE¹ (Oracle Corporation, 1987). However, this approach is not limited to INGRES and ORACLE, but can be used with any relational database system.

MMS and RiverWare access the database through user-written DMIs. Users can use a variety of standard DMIs, or write customized DMIs in any standard programming language that has database bindings, to access data from a variety of data repositories, including other relational databases. Changing the central database requires only that the DMIs be modified to support the selected database. No changes need to be made in MMS or RiverWare.

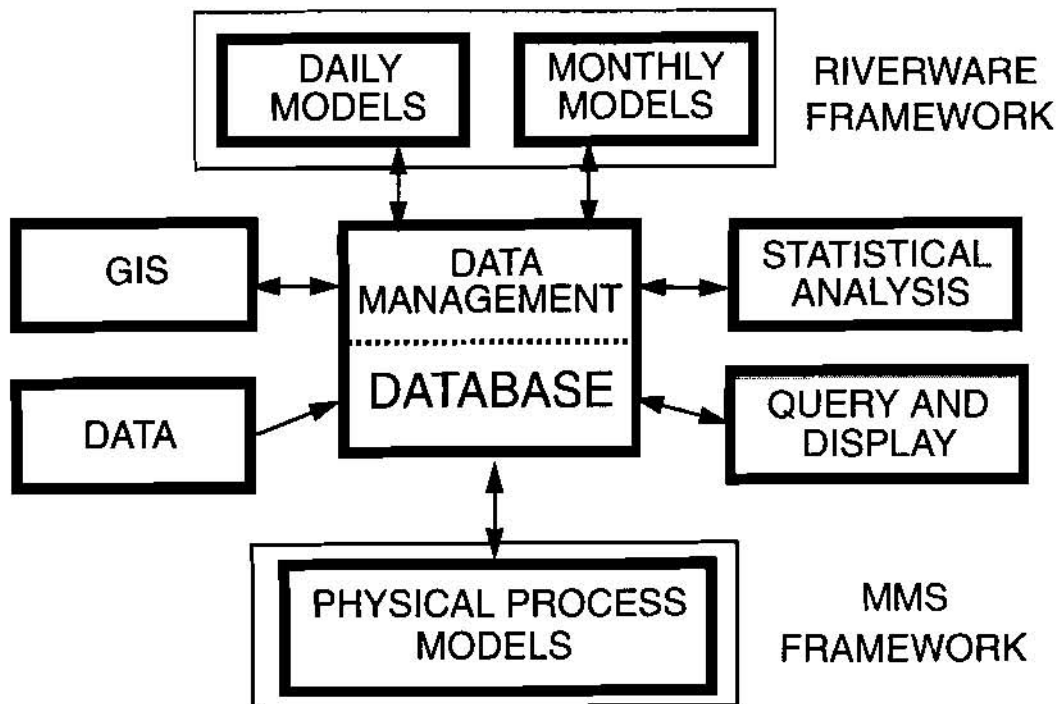


Figure 2. Schematic of the database-centered decision support system.

Communication between MMS and RiverWare is designed to use a scenario file in the database. A scenario is defined as a sequential list of modeling operations to be run using MMS and RiverWare. Different scenarios can be developed to address a range of resource-management decisions. The scenario file is accessed by both modeling systems and the specified models are executed in the order listed. A given resource-management decision may require the results of one or several models in both systems. Model results from MMS are written to the database for use as inputs to RiverWare and vice versa. This exchange of data and model results is an iterative procedure, the magnitude of which is dependent on the complexity of the decision process.

An example of such a procedure would be the management of a multi-reservoir river system within the constraints of competing water users and selected environmental constraints such as water-temperature limits or fisheries habitat needs. Here a scenario of MMS and RiverWare runs might begin with the execution of a watershed model in MMS to provide estimates of the daily time series of water inflows to all reservoirs in the system. Then RiverWare would be executed to use these inflows to develop a number of different management options and produce a time series of reservoir releases associated with each. These options might reflect different mixes of water use for power generation, agriculture, and municipal water supply.

Each release option has implications with regard to the environmental constraints on system operation and would need to be examined for those river reaches where these constraints apply. Thus, a one- or two-dimensional river hydraulic model would be run in MMS to assess the effects of the different reservoir-release options on the critical river reaches. Then RiverWare would be run again using the additional reach information to further refine the management options for these specific sets of conditions and constraints.

The generation of management options is not limited to RiverWare, but they can be developed within MMS as well. Using the ESP capability of MMS, alternative time series of water inflow to reservoirs can be developed, each with an associated estimate of a probability of occurrence. The manager could then select various levels of probability of occurrence to assess the effects of uncertainty on water management options. Alternatively, new time series of meteorological variables could be developed to reflect the potential effects of global climate change. These time series could be used as input to the watershed model to provide estimates of reservoir inflows for use in assessing the effects of climate change on basin management strategies.

The database-centered, decision-support system approach is being developed, tested, and implemented under WARSMP in the San Juan and Yakima River basins. The San Juan Basin has a drainage area slightly in excess of 23,000 mi² at Bluff, Utah, and is located in four-state area of Colorado, New Mexico, Arizona, and Utah. Water-management issues in the San Juan basin include efficiency of water-resources management, environmental concerns such as meeting flow needs for endangered species, and optimizing operations within the constraints of multiple objectives such as power generation, irrigation, and water conservation. The Yakima River basin has a drainage area of about 6,200 mi² at its point of discharge into the Columbia River and is located entirely in the state of Washington. The water-management issues in the

Yakima basin include the same issues as the San Juan basin, plus concerns regarding ground-water/surface-water interactions and water-quality issues related to irrigated agriculture.

SUMMARY

MMS is an integrated system of computer software that has been developed to provide the research and operational framework needed to support the development, testing, and evaluation of water, energy, and biogeochemical process algorithms and to facilitate the integration of user-selected sets of algorithms into operational models. MMS provides a common framework in which to develop and apply models that are designed for basin- and problem-specific needs. MMS is being coupled with the reservoir simulation and optimization software RiverWare using a common database interface to provide a database-centered decision support system for use in water-resources management. As the physical process modeling component of this decision support system, MMS provides a flexible framework in which to integrate these current activities and to easily incorporate any future advances in science and technology.

Given that different river basins may have different management objectives and operational constraints, the flexibility of MMS enables the development and application of those models determined to be most appropriate for a specific basin. Alternative modeling approaches can be evaluated to determine the optimal set of models for various management decisions. Coupled with RiverWare, the result is a very flexible set of water-resource management tools.

REFERENCES

- Day, G.N., 1985, Extended streamflow forecasting using NWSRFS. *Journal of Water Resources Planning and Management, American Society of Civil Engineers* 111, 157-170.
- Environmental Systems Research Institute, 1992, ARC/INFO 6.1 user's guide. Redlands, CA.
- Fulp, T. J., Vickers, W. B., Williams, B., and King, D. L, 1995, Decision support for water resources management in the Colorado River regions. *in* L. Ahuja, J. Leppert, K. Rojas, and E. Seely (eds.), *Workshop on computer applications in water management*. Colorado Water Resources Research Institute, Fort Collins, CO, Information Series No. 79, 24-27.
- INGRES Corporation, 1991, *INGRES/SQL Reference Guide for the UNIX and VMS Operating Systems*. Alameda, CA.
- Leavesley, G.H., Markstrom, S.L., Brewer, M.S., Viger, R.J., 1996a, The Modular Modeling System (MMS) -- The physical process modeling component of a database-centered decision support system for water and power management. *Water, Air, and Soil Pollution* 90, 303-311.
- Leavesley, G.H., Grant, G.E., Markstrom, S.L., Viger, R.J., Brewer, M.S., 1996b, A modular modeling approach to watershed analysis and ecosystem management, in *Proceedings of Watershed'96 A National Conference on Watershed Management*, U.S. Government Printing Office, 794-797.
- Oracle Corporation. 1987, *User documentation*. Belmont, CA.

THE WATERSHED AND RIVER SYSTEMS MANAGEMENT PROGRAM - AN OVERVIEW

**By Harry Lins, Hydrologist U.S. Geological Survey, Reston, Virginia, and
Donald Frevert, Hydraulic Engineer, U.S. Bureau of Reclamation, Lakewood, Colorado**

Abstract: Accurate and timely information is crucial to the planning, scheduling and operation of water and power resource systems. These data include the distribution of precipitation and inflow into the watershed, stream flows, reservoir levels and water and power demands.

A combined effort of the U.S. Bureau of Reclamation and the U.S. Geological Survey with support from other governmental, university and private entities is reviewed with emphasis on the modeling frameworks and data bases being developed and their areas of application throughout the western United States.

INTRODUCTION

The Watershed and River Systems Management Program, first conceived in 1992 is an interagency cooperative effort funded primarily by the U.S. Geological Survey and the U.S. Bureau of Reclamation. The overall objective of the program is improved water resources management in the United States. The program followed a successful cooperative modeling effort between the two agencies on the Gunnison River basin in 1989 and 1990.

The present effort combines the Modular Modeling System (MMS) developed by the U.S. Geological Survey with the RiverWare modeling framework developed by the U.S. Bureau of Reclamation (Reclamation), the Tennessee Valley Authority (TVA), the Center for Advanced Decision Support for Water and Environmental Systems (CADSWES) at the University of Colorado and the Electrical Power Research Institute (EPRI). The focal point of this combined effort is a data centered modeling approach using an Hydrologic Data Base (HDB) also developed by Reclamation with technical support from CADSWES.

Modeling capabilities include the combined use of these systems to simulate watershed runoff, reservoir inflow, the impacts of water resources management decisions on municipal, agricultural and industrial water users, environmental concerns, power users and recreational interests.

Initial development work occurred in the San Juan River basin of Colorado and New Mexico and basin wide modeling efforts are now being applied to management of the Colorado River system. New efforts are focusing on the Yakima River basin of Washington with future efforts planned for the Rio Grande basin of Colorado, New Mexico and Texas.

The remainder of this paper will provide a general description of the technology being developed and its application. Other papers in this and subsequent sessions will provide more detailed information about the technology and its implementation to deal with water resources management issues in the western United States.

MODULAR MODELING SYSTEM

The interdisciplinary nature and increasing complexity of environmental and water- resource problems require the use of modeling approaches that can incorporate knowledge from a broad range of scientific disciplines. Selection of a model to address these problems is difficult given the large number of available models and the potentially wide range of study objectives, data constraints, and spatial and temporal scales of application. Coupled with these problems are the problems of study area characterization and parameterization once the model is selected.

Guidelines for parameter estimation are normally few and the user commonly has to make decisions based on an incomplete understanding of the model developer's intent. To address the problems of model selection, application, and analysis, a set of modular modeling tools, termed the Modular Modeling System (MMS) has been developed by the U.S. Geological Survey.

The conceptual framework for MMS has three major components: pre-process, model, and post-process. A system supervisor, in the form of an X-window graphical user interface (GUI), provides user access to all the components and features of MMS. The present framework has been developed for UNIX-based workstations and uses X-windows and Motif for the GUI. The GUI provides an interactive environment for users to access model-component features, apply selected options, and graphically display simulation and analysis results. The current GUI is being expanded and enhanced into the full system supervisor, incorporating the linkages needed to access features in all the system components.

MMS began as a cooperative research effort between the USGS and the University of Colorado's Center for Advanced Decision Support for Water and Environmental Systems (CADSWES). As MMS took shape, interest in the MMS concepts was expressed by many national and international agencies and organizations. Agreements established with several of these groups have provided new ideas for system enhancement and the contribution of resources, in terms of money and/or people, to add these enhancements to the system. In addition, these groups continue to contribute their modeling expertise to the system by converting their models to MMS modules and by providing test sites for system evaluation and development. Reclamation has aided in the development of some of the GIS capabilities and the extended streamflow prediction tools.

MMS provides a common framework in which to focus multi disciplinary research and operational efforts. Continued advances in physical and biological sciences, GIS technology, computer technology, and data resources will expand the need for a dynamic set of tools to incorporate these advances in a wide range of interdisciplinary research and operational applications. MMS is being developed as a flexible framework in which to integrate these activities.

RIVERWARE MODELING FRAMEWORK

The RiverWare modeling framework has been developed over the past several years by technical experts at CADSWES with financial support from Reclamation, TVA and EPRI. RiverWare accesses information from the Hydrologic Data Base (HDB) and uses that information to perform general

simulation, rule based simulation and optimization analyses on simple and complex river systems using an object oriented modeling approach.

The RiverWare framework operates in a UNIX modeling environment on Sun-Sparc work stations. The object oriented approach allows managers and technical specialists the flexibility to deal with the rapidly changing operational constraints and hydrologic conditions being faced in the 1990s. These conditions were much more difficult to contend with using the older site specific main frame computer models - most of which had operational constraints hard wired into their FORTRAN code.

Technical capabilities of the RiverWare framework, including recent advances in the capability to do water accounting and ownership, uncertainty and risk analysis, multiple scenario management and recently implemented engineering capabilities such as sedimentation distribution and return flow simulation will be discussed in subsequent papers.

With these capabilities, RiverWare has fully replaced the old Colorado River Simulation System for use by Reclamation's water resource managers in the Colorado River basin. Colorado River basin applications include, among others, short term operational decisions at Hoover Dam and other facilities, intermediate length (24 month) basin wide operational studies and long range planning and policy analyses.

Future capabilities for RiverWare will be implemented on a need driven basis based on requirements in the new areas of emphasis - the Yakima River basin of Washington and the Rio Grande basin of Colorado, New Mexico and Texas.

COUPLING WATERSHED AND WATER MANAGEMENT MODELS

Many water management issues including fisheries and water fowl habitat, water quality concerns, and channel maintenance for river recreation, need reach-specific hydraulic and chemical information, conditioned on upstream stream flows. That is, the detailed hydrology of a given reach must include the constraints of the overall physical hydrology and water management within the basin. One way to include these constraints is to use reach-specific models within the modeling sequence. Several reach-specific models are included in MMS and can be linked with watershed model or RiverWare output.

For example, a one-dimensional hydraulic model using daily streamflow from RiverWare, along with detailed local topography and bed material information, can be used to predict a stage-discharge relation, reach-averaged vertical distributions of velocity, and stress at a cross-section. These relations provide the necessary hydraulic input to compute bed sediment discharge. Identifying sediment discharge and associated hydraulic conditions and predicting changes that occur with alterations in the hydrograph are critical to understanding channel and habitat maintenance.

SAN JUAN RIVER BASIN STUDY

During the original planning of the Watershed and River Systems Management Program in 1992, technical representatives of both USGS and Reclamation agreed that emerging issues on the San Juan

River basin would require the latest and best technology for solution. Accordingly, it was determined that the San Juan would be the focal point to improve capabilities of not only the MMS and RiverWare modeling systems and the HDB.

Capabilities of both modeling frameworks have been substantially improved on the San Juan basin. MMS capabilities have been refined both geographically and technically while capabilities of RiverWare to deal with ownership, diversions and return flow have resulted in better capabilities to deal with water rights issues raised by the states of Colorado and New Mexico. RiverWare has been recently applied by government and private sector technical specialists to fisheries and endangered species studies.

YAKIMA RIVER BASIN STUDY

Building on the experience gained in the San Juan basin, and recognizing that there were a number of water issues not considered in the San Juan study, USGS and Reclamation initiated a new investigation in the Yakima River basin of eastern Washington in 1997. Three issues in particular have major significance in the Yakima basin: recreational water use, junior versus senior water rights, and intrabasin topographic and climatic variability.

With more than 1 million recreational visits being made each year to the basin, recreation has become an important economic as well as water planning and management consideration. The effect of judicial law on water management in the Yakima basin is both complex and, at times, conflicting. In 1945 a Consent Decree established 'rules' for the operation of the Yakima Project by Reclamation, and for the allocation of water to junior or 'proratable' rights. Senior or 'non-proratable' rights are not reduced in years of water shortages unless the shortages are such that the senior rights cannot be met.

Recent actions by Congress have only increased the scope of judicial law's role. For example, the second phase of the Yakima River Basin Water Enhancement Project includes an analysis for determining biologically-based flows for anadromous salmon and steelhead fisheries, the latter being proposed for listing under the Endangered Species Act.

Finally, the high variability in topography and climate within the Yakima basin gives rise to broad spatial and temporal variations in the quantity and quality of streamflow. The humid, headwater parts of the basin produce the streamflow and the semi-arid to arid, lowland parts produce much of the water use. Thus, there are long distances between reservoirs and demands with travel times from reservoirs to lower-basin users and flow target points on the order of 12 to 48 hours.

The overall goal of the Yakima Basin study is to address these issues by improving: a) the management of water for the benefit of agricultural, recreational, wildlife, and water supply interests; b) flow for enhancing the quality of the resource; and c) the efficiency of the system-wide operations.

THE YAKIMA RIVER BASIN WATERSHED AND RIVER SYSTEM MANAGEMENT PROGRAM

**Authors: J.J. Vaccaro, Hydrologist, U.S. Geological Survey, Tacoma, Washington;
C.J. Lynch, Hydrologist, U.S. Bureau of Reclamation, Yakima, Washington;
K.M. Schurr, Hydrologist, U.S. Geological Survey, Tacoma, Washington;
W. Sharp, Hydrologist, U.S. Bureau of Reclamation, Yakima, Washington;
M.C. Mastin, Hydrologist, U.S. Geological Survey, Tacoma, Washington;
D. Schramm, U.S. Bureau of Reclamation, Yakima, Washington**

INTRODUCTION

The Watershed and River System Management Program (WARSMP) is a cooperative program between Department of the Interior agencies. The WARSMP is sponsored by the Water Resources Division of the U. S. Geological Survey (USGS) and the Science and Technology Research Program of the U.S. Bureau of Reclamation (USBR). The purpose of WARSMP is to develop, test, and implement a framework for the management of water resources in the Reclamation Act States (see Frevert and Lins, this volume). The framework is a fully-integrated data-centered decision-support system (DSS) of physical process models--Modular Modeling System (MMS; Leavesley and others, 1996), resource-management models--RiverWare (Fulp and others 1995), forecast models, data-management interfaces (DMIs) and graphical user interfaces (GUIs). The MMS and RiverWare are linked through a data management system--Hydrologic Database (HDB; Fulp and others, 1995, Leavesley and others, 1997), as are a point and click GIS tool-box (Leavesley and others, 1997), queries and displays, and real-time data and processing.

Beginning in fiscal year 1997, the collaborative work of the program focused on the Yakima River Basin. The Yakima River Basin is representative of water-use and water-resource management in the West, and management of its waters is one of the most difficult tasks the USBR undertakes in the western United States. Program elements are being accomplished jointly by the USGS and USBR.

STUDY AREA AND BACKGROUND

The Yakima River Basin is situated in eastern Washington (fig. 1), has a drainage area of about 6,200 square miles, and produces a mean annual regulated-runoff of 3,600 cubic feet per second. The basin's headwaters are on the east slope of the Cascade Range where annual precipitation is more than 90 inches, and the basin terminates where the river discharges to the Columbia River in the lower, arid part of the basin, which receives about 6 inches of precipitation annually. Most of the precipitation falls during the winter season as snow. The mean annual precipitation in the basin is about 27 inches (approximately 12,000 cubic feet per second) of which more than 80 percent falls in the upper part of the basin that encompasses about 3,660 square miles. Altitudes in the basin range from nearly 8,000 feet in the headwaters to about 400 feet near the mouth of the Yakima River. Although the highest altitudes in the basin are between 7,729 and 7,899 feet, most of the headwater regions lie between 4,000 and 6,000 feet. In the upper parts of the basin, the river has a medium to high slope as it passes through forested lands and deeply incised canyons. In the lower parts of the basin, the river follows a meandering course through hilly and flat agricultural lands to its mouth after traveling nearly 300 miles. Major tributaries to the Yakima River include the Cle Elum, Kachess, Teanaway, Bumping, American, Tieton, and Naches Rivers; there are also numerous small tributaries.

The average annual demand in the basin is about 2,500,000 acre-feet. This amounts to about 3,450 cubic feet per second or about 65 percent of the mean annual unregulated flow in the basin and nearly all of the mean annual regulated flow. Most of the demand is for irrigation of about 500,000 acres, mainly in low-lying semi-arid to arid parts of the basin. The demand is partly met by five major storage reservoirs in the headwaters that are capable of storing 1,065,400 acre-feet or about 28 percent of the mean annual natural flow of the river.

The basin has more than 80 canals, 5 diversion dams, 15 major return flows, and numerous smaller return flows. The major canals divert up to an annual rate of about 400 cubic feet per second, but the majority of the canals divert at an annual rate of 5 to 10 cubic feet per second. Nearly 45 percent of the water diverted for irrigation is eventually returned, at varying time-lags, as both surface and ground-water, to the river system. During the low-flow period, the return-flows account for about 70 to 80 percent of the water in the lower river stem.

WATER ISSUES

Water issues of many western basins are common to the Yakima River Basin. Included are Indian treaty rights, historical water rights, over-appropriation of water, reservoir and irrigation development, increasing population with a concomitant increasing municipal-industrial water use, increasing demand for wildlife and anadromous and resident fish, water quality of the surface and ground waters, and the interaction of ground water and surface water because all new demands are being met by ground-water. In addition, three other issues are of importance. First, with more than 1 million recreational trips per year to the basin, recreational use of water is becoming increasingly important, both with respect to basin-wide economics and competition for limited resources.

The second issue is how judicial law affects water management in the basin. For example, the 1945 Consent Decree established procedures or 'rules' for the operation of the Yakima Project by the USBR and for the allocation of water to junior or 'proratable' rights; senior or 'non-proratable' rights are not reduced in years of water shortages unless the shortages are such that the senior rights can not be met. Judicial law will continue to affect water management because of the current, basin-wide adjudication of water rights and the Congressionally mandated Yakima River Basin Water Enhancement Project (YRBWEP). Currently, the second phase of the YRBWEP includes an analysis for determining biologically-based flows for fisheries, mainly anadromous salmon and steelhead, the latter of which is proposed for listing under the Endangered Species Act.

The last issue is the intrabasin variability in topography and climate that results in spatial and temporal variations in the quantity and quality of streamflow. The humid, headwater parts of the basin produce the streamflow and the semi-arid to arid, lowland parts of the basin produce the need for much of the water use. Thus, there are long distances between reservoirs and demands with travel times from reservoirs to lower-basin demands and flow target points being on the order of 12 to 48 hours. This issue is further compounded by short-term variations in both inflows and demands.

Most of the above issues can be addressed by improving: a) the management of water for the beneficial use of the resource by agriculture, recreation, wildlife, and water supply; b) flows for enhancing the quality of the resource; and c) the efficiency of the system-wide operations. To provide a means for making these improvements is the essential part of this project. Long-term goals to address these means were identified during the planning stages of the project.

LONG-TERMS GOALS AND SCIENTIFIC ISSUES

The following long-terms goals of the project have been identified: 1) development of alternative runoff-volume forecasts; 2) development of runoff and streamflow forecasting for short-term operations and decision making; 3) enhancement of the operation simulation capability including long-term basin-wide planning models; 4) new capability to estimate quality parameters from operational actions--some quantity demands are affected by quality standards; 5) new capability to estimate water-budget components such as evapotranspiration to assist in irrigation management for quantity and quality for assessment of Total Maximum Daily Loads and Best Management Practices; 6) development of the system-wide relational HDB that is linked to MMS and RiverWare, contains historical and real-time data, GIS data layers, and operational rules, and is easily queried, updated, and linked to a graphical-statistical interfaces; and 7) overall improvement and development of analytical tools. By meeting some or all of these goals the 3 major improvements should be able to be accomplished.

There also are various scientific issues that need to be addressed. These issues include better methods for estimating forest-evapotranspiration, and snow accumulation and ablation. A pressing issue is the integration of ground-water and surface-water models within the decision support system because of the over-appropriation of water within the basin and the need for new supplies. Modeling physical processes in ungaged watersheds is important for providing

estimates of inflows to the river system; these inflows provide the initial water for irrigation during the reservoir refill season. Incorporation and analysis of habitat and biologically-based flow requirements is another scientific issue. The need to understand the affects of water-conservation measures on water quality and quantity in both space and time will be addressed by scaling up the results from the field-plot studies of best management practices to a basin-wide scale through the use of modeling. New methods for seasonal forecasting of runoff at different lead-times are also being explored.

TASKS, METHODS, AND PROGRESS

The following sections briefly describe the major tasks to be completed. The tasks fall into 5 general categories: 1) data and the HDB; 2) GIS and the GIS Weasel; 3) physical process modeling in the MMS; 4) river and reservoir management modeling in the RiverWare system; and 5) forecasting of streamflow. The tasks are described by identifying the goals, methods, and progress as of fiscal year 1997. Note that some of the planned work (goals) described may be limited by the overall scope of the program in the future.

Data and the HDB: The data being assembled fall into several categories: 1) daily streamflow, diversions, return flows, and reservoir stages, 2) climatological (daily precipitation, air-temperature, and snowpack, mean-monthly spatial distribution of precipitation, and snow-course data), 3) GIS layers, 4) real-time (HYDROMET, National Weather Service, NEXRAD, SNOTEL, and the agricultural community's AGRIMET), 5) daily and monthly estimates of unregulated streamflow at selected sites, 6) river channel characteristics, 7) historical water-quality, 8) historical fisheries (such as adult return counts for selected species), 9) habitat (such as benthic communities and woody debris), and 10) ground-water (shallow water-levels and pumpage). The first part of the project has focused on identifying, assembling, and assuring the quality (including potential error ranges) of some of these data.

A goal is to establish a consistent and long-term data-base to reside in the HDB, and be available for management of the system. Thus, not only will the complete historical data be assembled, but one consistent period of record, 1956-96, was identified for analysis and storage. For that period, most pertinent data series are being compiled with the missing values estimated and the records extended when necessary. For example, 37 weather sites have been identified and their records filled in for missing data and extended in time when needed. In addition, methods will be established to update the information in a timely manner. For example, the precipitation and air-temperature at National Weather Service (NWS) observer sites (part of the Hydroclimatology Network) will be updated regularly by an established method. Methods to both capture and update the USBR's HYRDOMET data in the HDB have already been developed as part of WARSMP.

The method planned for implementation of the HDB is two-fold. The complete HDB will reside in the USBR's Yakima Project Office, and a subset of the HDB will reside in the USGS's Washington office. The USGS HDB will be used to assure that MMS input and output is correctly being transferred to and from the HDB. In addition, parts of the HDB will be updated in the USGS office. These parts will mimic both the real-time capability of the HDB and the use of that data to drive the physical models in MMS. Thus, real-time linkages to HYDROMET, SNOTEL, NEXRAD, and other systems will not need to be implemented in the USGS office during this stage of the study, allowing for additional time to be focused on the scientific issues.

Last, as part of the data-assimilation stage, selected data were identified that needed to be collected. For example, one data item that is lacking is incoming solar radiation. This data item would provide valuable information for driving watershed and other physical-biological models. Thus, if new data collection is initiated, the data would be linked to the real-time network and to the HDB.

GIS and the GIS Weasel: The GIS and its associated data layers are an important component of the project, and allow for routine assessment of the landscape and water resources on a timely basis. The long-term goal is to provide a consistent GIS data-base of important spatial data for the Yakima River Basin for potential users. As part of the process, basin-wide data layers are continually being acquired and developed for the basin in a consistent manner. The tool being used to analyze much of the data is the GIS Weasel (Leavesley and others, 1997). The GIS Weasel is a point and click basin-analysis tool being developed by the USGS as part of the WARSMP project, and is an integral part of the data-centered approach.

Physical Process Modeling Using the MMS: This task includes several items. The first was to subdivide or delineate the Yakima River Basin into subbasins. Each of these subbasins generally represents a stream drainage or a part of a drainage. In turn, each subbasin then was characterized or further divided for application of a watershed model. This characterization and allied information will be incorporated in the MMS and within a watershed model. Last, the model will be constructed and used.

Subbasins: The subbasins that will be modeled using MMS or delineated and characterized for future work were defined using the GIS Weasel. Data layers used to delineate basins included gaging station locations, important river management locations, and landscape characteristics. The most important factor was that the subbasins correspond to the system-wide sites identified by the USBR for operational considerations and for use by RiverWare. A total of 59 subbasins were delineated (fig. 2), 4 of which represent the low-lying agricultural subbasins. The subbasins will be the basic modeling units for the study and for future operational use.

The delineation of the subbasins was completed at a scale compatible with the GIS data layers, data storage and handling ability, and preservation of the overall landscape characteristics of the basin. Delineations by the GIS Weasel were compared to several subbasins delineated by hand-drawn boundaries on different scale maps. The subbasins included a smaller, high-altitude basin that corresponds to a reservoir outflow point, and a larger basin with both high and low altitudes. Comparison of landscape characteristics, such as slope and location of stream networks was also done at several scales. Based on these comparisons, a 60 meter grid was selected to store and analyze the data layers in GIS, and to perform the subbasin delineation.

Modeling Response Units: Fifty-six of the subbasins (all the non-agricultural subbasins and the smallest agricultural subbasin) have been further divided (characterized) into modeling response units (MRUs) using the GIS Weasel. A MRU is considered to be a unit of landscape that has relatively consistent physical and climatological characteristics such that the hydrologic response to climate forcing is somewhat unique or homogenous. The initial MRU characterization is implicitly based on aspect because it was made by dividing a subbasin into 2-flow planes. That is, the GIS Weasel was used to define the flow planes (contributing areas) to the left and right banks of the stream network. These initial MRUs were then subdivided using altitude and mean annual precipitation. A final characterization was completed using soil characteristics. Land-cover and slope have generally been accounted for because of their strong relation to mean annual precipitation in most of the non-agricultural areas. All MRU delineation was done consistently so that MRUs in each subbasin could be interrelated. This is important for the physical modeling of ungaged watersheds so that model parameters can be transferred from calibrated models of gaged watersheds.

About 1,000 MRUs have been delineated for the 56 subbasins. However, watershed modeling does not lend itself to the 3 large low-lying agricultural subbasins, with minimal to no runoff. Thus, these major agricultural basins were only characterized by one MRU. In these areas the integration or linkage of ground-water, surface water, and land-surface-process models needs to be developed for addressing some of the major problems in the basin.

MMS Application and Module Selection: The initial physical modeling is focusing on part of upper Yakima River Basin (855 square miles) and most of the Naches River Basin (940 square miles). These 2 areas are above most diversions, account for about 90 percent of the runoff in the basin, and contain all of the reservoirs. They will be modeled with two separate models. The long-term goal is to extend the watershed models to all but the four low-lying agricultural subbasins.

The physical processes to be modeled are represented by modules in MMS. For this study, most of the modules are contained in the USGS Precipitation-Runoff Modeling System (PRMS; Leavesley and others, 1983). Additionally, several processes that are known to be important may need more appropriate algorithms. For example, two of the subbasins contain enough glacier area in the headwaters to affect summer streamflow, but MMS does not contain a module to account for glacier hydrology.

Model Construction and Use: Prior to parameter estimation, the periods of record for calibration and verification of the subbasin models will be selected from the 1956-96 period of record. Sensitivity of the model parameters will then be determined and analyzed for potential future work. The sensitivity of a particular parameter may indicate the need

for additional data-collection activities or module development in MMS. An error analysis will be completed in conjunction with the sensitivity analysis. The error analysis will focus on how errors propagate through the modeling system and how they may affect operational considerations using RiverWare.

The daily-model output will be linked to HDB for later input to RiverWare. The model output will be available at several levels. For daily operation, the model will calculate estimates of the next days' runoff for the major river-management points. These values will be input to RiverWare for helping to guide operations. Daily values of streamflow will also be calculated using 5-day forecasts of climate. These 5-day streamflow values should allow for improved operations on a weekly basis. Next, extended streamflow predictions will be made at selected times prior to and during the runoff season for input to RiverWare.

River and Reservoir Management Modeling Using the RiverWare System: RiverWare is currently being developed for simulation on a daily time-scale for both short-term and mid-term operations. The development is currently focusing on the same areas as the two watershed models, and will include similar river points, reservoir outflow locations, and ungaged watershed outflow locations. As part of relating between HDB and RiverWare, data management interfaces will be written into the system. Associated information for operational purposes in the RiverWare models includes such aspects as reservoir characteristics, diversions and associated return flow requirements, instream flows, flood rule-curves, stream routing, and basin water-rights information. This information will provide for improved daily short-term operations.

The need for mid-term operations will be met in several ways throughout each irrigation season. The extended and long-lead forecasts will be used by RiverWare to develop potential operational-strategies that will be available to USBR analysts for decision making. As a step in development of the long-term policy and planning model, a RiverWare model will be developed at a monthly time-step. The monthly model will complement the daily mid-term model. It is planned that the mid-term monthly model will use the same forecasts as the daily model but aggregated to monthly or weekly time-steps.

For long-term policy and planning, a monthly RiverWare model will use the historical data in HDB to calculate various scenarios. These will be readily available for decision making by analysts. The ability to have feedback between RiverWare and HDB should allow for a full range of long-term scenarios to be integrated into a planning process. Additionally, the need is recognized for a long-term planning model to have a resolution of a daily time-step, with reporting aggregated to weekly or monthly time-steps as is needed for mid-term operations. Daily estimated unregulated reservoir inflows and basin reach gains are currently being developed for this purpose.

The major new development in RiverWare to be completed under the aegis of the Yakima River Basin WARSMP is the writing of software code to account for prior appropriation doctrine. This development will not only allow for increased operational flexibility in the basin but also will enhance the transferability and usability of the RiverWare System to other basins throughout the United States.

Forecasting of Streamflow: There are four categories of forecasts that will be attempted during this study, these are 1) long-lead, 2) short-lead, 3) near real-time, and 4) extended forecasts. Long-lead forecasts are forecasts of monthly flows or seasonal (April-August) inflows made about 12 to 4 months prior to April 1. Two methods are being analyzed for long-lead forecasts. In the first, non-linear spline regressions are being developed by Lall (U. Lall, Utah State university, oral commun., 1997). This method uses both the historical monthly discharge time-series and atmospheric and sea-surface temperature data to forecast monthly time-series of streamflow. Initial results using this method are promising. In the second method, multiple-linear regression equations that use monthly climate-related indices to calculate the seasonal inflows are being developed by the USGS. It is planned to have both methods available to complement each other.

Short-lead forecasts are those for the seasonal inflows that are made March 1 and April 1 using April 1 snowpack, and antecedent weather and reservoir inflow information. The current short-lead forecast equation used by the USBR will be examined for possible improvement by including such factors as monthly climate-related indices. In addition, the

NWS April 1 forecast equation will also be examined. Together, the long- and short-lead forecasts should provide a reasonable analysis tool for system operations for the irrigation season, and they also will meet several of USBR's defined needs.

Near real-time forecasts use the real-time data that the USBR has linked to the HDB and that the USGS has used to construct the physical-hydrology models. These data are used to operate the models for short-term forecasts on a daily mode. These forecasts are linked to RiverWare through the HDB. This category of forecasts will also incorporate the NWS 5-day forecasts.

Last, the MMS has a modified version of the NWS's Extended Streamflow Prediction Program as a module. This module provides forecasting capabilities using historic or synthesized meteorological data. Thus, alternative time-series of inflows could be developed. These time series would have probabilities associated with them. In addition, based on the results of the long- and short-lead forecasts, the number of years of meteorological data used to drive the module will be constrained to be some subset of the historical record that has a higher probability of occurrence. That is, given both the forecasts and the climate-state during the winter, particular years of the historical record are more likely than other years to be representative of what will occur over the runoff season.

Additionally, under development is the use of NEXRAD information to make quantitative precipitation-forecasts and linkage of them to the HDB. When this technique is fully developed, these forecasts could be used to make improved short-term forecasts of inflows.

SUMMARY

The 6,200 square mile Yakima River Basin in eastern Washington is being studied under the collaborative work of WARSMP. Water-use and water-resource management in the Yakima River Basin is representative of that in the West. In keeping with WARSMP goals, the DSS is being applied to the basin and new tools are being developed to assess additional management and scientific issues. These issues include water rights-prior appropriation law, ground water and surface water interaction, and forecasting of streamflow.

Tools developed previously in WARSMP are being used regularly and have greatly expanded the ability to apply the DSS in a reasonable time-frame. These tools and new tools will be used in the remainder of the study to develop a comprehensive DSS that includes all of the major components: the MMS, HDB, and RiverWare. Increased efficiency in systems operations obtained from the DSS will be to the benefit of water use in the basin, and will allow for improved long-term resource planning.

REFERENCES

- Fulp, T.J., Vickers, W.B., Williams, B., and King, D.L., 1995, Decision support for water resources management in the Colorado River region: IN L.Ahuja, J. Leppert, K. Rojas, and E. Seely (eds.), Workshop on computer applications in water management, Colorado Water Resources Research Institute, Fort Collins, CO., Information series No. 79, pp. 24-27.
- Leavesley, G.H., Lichty, R.W., Troutman, B.M., and Saindon, L.G., 1983, Precipitation-runoff modeling system--Users manual: U.S. Geological Survey Water-Resources Investigations Report 83-4238, 207 p.
- Leavesley, G.H., Viger, R.J., Markstrom, S.L., and Brewer, M.S., 1997, A modular approach to integrating environmental modeling and GIS: IN Proceedings of 15th IMACS World Congress on Scientific Computation, Modeling, and Applied mathematics, Berlin, Germany.
- Leavesley, G.H., Restrepo, P.J., Markstrom, S.L., Dixon, M., and Stannard, L.G., 1996, The modular modeling system (MMS)--user's manual: U.S. Geological Survey Open-File Report 96-151, 142 p.



Figure 1. — Location of Study Area

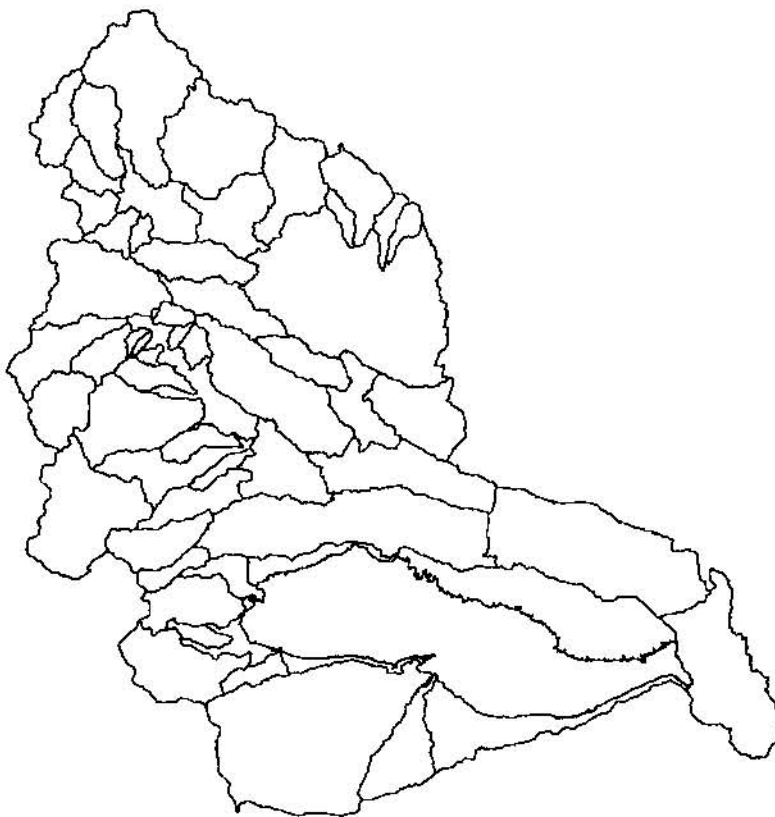


Figure 2. — Location of the 59 delineated subbasins

RIVERWARE: A GENERAL RIVER AND RESERVOIR MODELING ENVIRONMENT

By Edith A. Zagona, Research Associate, Center for Advanced Decision Support for Water and Environmental Systems, University of Colorado, Boulder, CO; Terrance J. Fulp, Operations Research Analyst, U.S. Bureau of Reclamation, Lower Colorado Region, Boulder, CO; H. Morgan Goranflo and Richard M. Shane, Technical Specialists, River System Operations, Tennessee Valley Authority, Knoxville, TN

Abstract: A general river basin modeling environment for operations and planning requires a high degree of software flexibility to allow users to model any river basin, manage data input and output efficiently enough for near real-time operations, and provide a selection of solution algorithms, all through a user-friendly interface. RiverWare is an extensible, maintainable software framework which provides a modeling environment to meet all the modeling needs of managers and operators of river and reservoir systems.

INTRODUCTION

Water management agencies and utilities face increasingly difficult challenges in managing water resources. Environmental considerations, increasing demands on dwindling water supplies, outspoken recreational interests, the specter of climate change, and the restructuring of the power utility industry all have converged at a time when federal resources for developing modeling tools are minimal. Planning and operational river basin models developed in the previous decades are often not adequate to represent the changing multiple objectives of the projects and cannot be updated without significant expense.

To meet this challenge, the U.S. Bureau of Reclamation (USBR) and the Tennessee Valley Authority (TVA) are investing in a project with the Center for Advanced Decision Support for Water and Environment Systems (CADSWES) at the University of Colorado (CU) in Boulder to develop a general river basin modeling tool which can be used for a wide range of applications. The tool, called RiverWare, has been developed and applied to several basins by the two sponsoring agencies, and continues to be enhanced and improved.

To meet the goal of providing a modeling tool that can be applied to any river basin for both operational and planning applications, the RiverWare software was designed to meet the following general requirements:

- Be flexible enough to use for a variety of applications including daily scheduling, operational forecasting and long-range planning. This requires a range of timestep sizes and appropriate physical process modeling variability to support this range.
- Support various modeling solution methodologies. An organization's decision as to which basic modeling approach to use, simulation or optimization, depends on the specific goals of the model as well as the traditional way of looking at their system. Offering a variety of approaches allows each organization to continue historical practices as well as explore new approaches.
- Allow tailoring of applications by providing many basin features and many alternative methods for modeling these features. Even more important than the range of available features and methods is the extensibility of the software to provide ease in adding new methods. It must be recognized that there will always be applications that require enhancing the software and that most

agencies have some computational methods to which they are wedded for institutional reasons.

- Represent policy as input data. Many older models are obsolete because the operating policies were hard-coded and mixed in with the physical process model where they cannot be easily changed, or in some cases, cannot even be understood. Easy policy evaluation and modification by the user must be seen as a basic requirement for all new modeling tools.
- Provide an easy-to-use interface. A water resources engineer should be able to build, run and analyze model results relatively quickly, easily and without excessive training requirements. An operations scheduler should be able to view selected data in a convenient format, make changes to the operation, rerun the model and analyze results quickly.
- Fit into existing data and model interfaces. Every water management organization has an existing framework of databases, real-time data, supporting models, reporting tools, etc. to which the model must be connected. A general modeling tool must be flexible enough to tailor the application to any existing or changing configuration.
- Be supported by an organization which provides continued maintenance, enhancements, user support and technology transfer.

In the remainder of this paper, we present several of the major features of the RiverWare modeling software.

MODEL CREATION

Objects and Slots: The basic building blocks of a RiverWare river basin model are *objects* which represent the features of the river basin. The objects are represented by icons on the workspace which can be opened to show the list of *slots*, which are the variables associated with the physical process model equations for that feature. For example, all reservoirs have slots, among others, called Inflow, Outflow, Storage and Pool Elevation.

The user constructs the model on the graphical workspace by selecting objects from a palette, dragging the objects with the mouse onto the workspace, naming the objects, and linking them together. Objects are linked together to form the topology of the river basin using the graphical link editor. Specifically, a slot on one object is linked to a slot on another object. During the simulation, the solution process involves propagation of the information among objects via the links. Currently, the RiverWare palette contains the following objects and the main water quantity physical processes which they model in a river basin:

- *Storage Reservoir* - mass balance, evaporation, bank storage, spill;
- *Level Power Reservoir*- Storage Reservoir plus hydropower, energy, tailwater, operating head;
- *Sloped Power Reservoir* - Level Power Reservoir plus wedge storage for very long reservoirs;
- *Pumped Storage Reservoir* - Level Power Reservoir plus pumped inflow from another reservoir;
- *Reach* - routing in a river reach, diversion and return flows;
- *Aggregate Reach* - many Reach objects aggregated to save space on the workspace;
- *Confluence*- brings together two Inflows to a single Outflow as in a river confluence;
- *Canal* - bidirectional flow in a canal between two reservoirs;
- *Diversion* - diversion structure with gravity or pumped diversion;
- *Water User* - depletion and return flow from a user of water;
- *Aggregate Water User*- multiple Water Users supplied by a diversion from a Reach or Reservoir;
- *Aggregate Delivery Canal* - generates demands and models supplies to off-line water users;

- *Groundwater Storage Object* - stores water from return flows;
- *River Gage* - specified flows imposed at a river node;
- *Thermal Object* - economics of thermal power system and value of hydropower;
- *Data Object* - user specified data: expression slots or data for policy statements.

Data required by the model is entered into the slots, of which there are three basic kinds. *Time Series Slots* contain data at specified times. The slot manages the time keeping and generates the time series for the data. The default time series inherits the start time, end time and timestep size from the Run Control dialog unless the user configures the time series differently on the slot. *Table Slots* contain functional relationship data such as area-elevation-volume tables, or simple parameter data required by the model equations. *Scalar slots* are single values. Data can be entered into slots manually by typing the number into the slot dialog, or by file import which can import an entire timeseries or table of values at once. Values can also be imported through the Data Management Interface (DMI) utility, which is described in a subsequent section.

Units: All internal representation of slot values and computations is done in the default SI units. However, the user may enter and display values in any selected unit of a similar type. For example, the internal RiverWare unit for all slots with unit type of FLOW is cubic meters per second (CMS). The user units are specified in the GUI and can be set to any other FLOW unit, e.g., cfs, acre-feet per day, etc.

Methods: Each object has a list of User-Selectable Method Categories. For each one, a method must be selected for the detailed modeling equations used in the physical process model. (Methods are described in detail in the Engineering Methods section below.)

Run Control: The intended model run is set up on the Run Control dialog. The start time and end time and the timestep size of the run are specified. Timestep size ranges from hourly to yearly. There is no limit on the range of the runs. RiverWare currently supports dates from 1800 to 2300 A.D. This time range could be extended easily without additional memory usage or performance deterioration. The user also selects the solution type or “Controller” on this dialog. The list of slots and User Methods which appear are dependent on the controller selection.

Saving Models: Models are saved as text files. All data including the objects and their names, their topologic arrangement on the workspace, all input data in the slots, user units, method selections, run control selections, and all GUI settings are saved in the model file. The results of a model run are saved optionally.

ENGINEERING METHODS

The objects on the workspace represent features of the river basin. Methods on each object contain the physical process model for the feature. The methods are flexible in handling a variety of input/output combinations of the basic data. In addition, the specific equations and physical representation of the processes are variable to accommodate a wide range of timestep sizes, data availability and resolution requirements, and modeling preferences.

To accomplish this flexibility, each object has two basic types of methods. *Dispatch Methods* map the input/output configuration specified by the user to the correct solution algorithm. *User Select-*

able Methods are alternative model representations which are selected by the user through the graphical user interface (GUI). For example, all reservoir objects have many dispatch methods for solving the mass balance equations. If Inflow and PoolElevation are known, the dispatch method for solving for Outflow and Storage is invoked. In addition, the user may select from a number of Evaporation methods, each of which calculates the evaporation loss in the reservoir as part of the mass balance calculation.

This object-oriented modeling approach mirrors the object-oriented software implementation and both benefit from this technology. From a software perspective, the benefit is extensibility: new methods can be added and integrated quickly and easily. From a modeling perspective, the benefit is the flexibility gained by selecting the physical process modeling methods individually on each object. Since the methods are easy to add, it is possible to have a large selection which includes some methods which may be quite particular to how one agency models one site, but necessary to that organization for institutional reasons. Table 1 contains a few examples of RiverWare's objects and User Methods.

Table 1: Selected User Methods in RiverWare

Object Type	User Method Category	User Methods	
Reservoirs	Evaporation & Precipitation	No Evaporation Pan and Ice Evaporation Daily Evaporation	Input Evaporation CRSS Evaporation
	Spill	Unregulated Spill Regulated Spill Unregulated Plus Regulated	Regulated Plus Bypass Unregulated Plus Regulated Plus Bypass
Power Reservoirs	Power	Plant Power Unit Generator Power	Peak Base Power LCR Power
	Tailwater	Tailwater Base Value Only Tailwater Base Value Plus Lookup Table	Tailwater Stage Flow Lookup Table Tailwater Compare Hoover Tailwater
Reaches	Routing	No Routing Time Lag Routing Variable Time Lag Routing SSARR	Muskingum Kinematic Wave Muskingum-Cunge MacCormack
Water User (on AggDiversion)	Return Flow	Fraction Return Flow Proportional Shortage	Variable Efficiency

In addition to water quantity modeling, RiverWare provides several options for water quality calculations. The user may select to model dissolved solids only, temperature only, or combinations of these and dissolved oxygen. If modeling total dissolved solids only, a simple, well-mixed model is available. Temperature and DO models use a 2-layer reservoir model and discretized reaches in which the water quality equations are coupled with hydraulic routing, either with or without dispersion.

A special object on the palette is the Thermal Object. This object evaluates of the avoided costs from replacement of thermal power by hydropower.

MULTIPLE SOLUTIONS AND CONTROLLERS

Alternative approaches to modeling multi-objective river basins have been developed, discussed and debated by water management agencies and academicians over the years. RiverWare endeavors to provide both prescriptive and descriptive techniques which are easy to formulate, analyze and apply to real planning and operations problems. Three fundamental solution methods are provided in RiverWare: simple simulation, rulebased simulation, and optimization. The first allows straight-forward scenario runs in which user-supplied inputs drive the solution. In the other two solution techniques, operational policies drive the solution. All operational policies are part of the input data set to permit easy modification and evaluation. In addition, the user may track water ownership by creating a network of water accounts in parallel with the river basin topology, and solve the accounting network independently of the simulation. The specific details of these solution methods have been designed and implemented to assure ease of use in solving a broad range of modeling application problems.

Simulation: Pure simulation solves a uniquely and completely specified problem. Each object must have enough information to invoke and solve a Dispatch Method, but may not have too much information. The solution is based on an object-oriented modeling paradigm: each object waits until it has enough information to solve, then it executes its Dispatch Method. The Dispatch Method solves for the unknown slots on the object, and information is propagated across links to other objects. Too much (conflicting) information results in an error state and termination of the run. Not enough information results in parts of the model left unsolved. In the cases where there are multiple links between objects, i.e., the boundary conditions are solved mutually by the two objects, the objects iterate until a solution meets the convergence criteria or the maximum iteration count is exceeded.

Although the simulation clock advances forward in time, the objects may solve for any timestep whenever they receive new information at that timestep. This allows some flexibility in specifying models where the solution is not propagating from upstream to downstream and forward in time. River reaches with time lags may solve for inflow given outflow, setting the inflow value at a previous timestep and propagating that value upstream. In addition, target operations on reservoirs may be specified, where a future target storage is met by adjusting the reservoir's outflow over a specified timeframe.

Rulebased Simulation: Whereas in pure simulation the model is exactly specified, in rulebased simulation there is not enough information on the objects to solve the system. The additional information is added by prioritized policy statements (rules) which are specified by the user, interpreted by the rule processor and which set slot values on the objects based on the state of the system. The rules themselves are basically if-then constructs which examine the state of system (functions of values of slots on the objects) in the antecedent (if) clause and then set slot values depending on that state. The rule set is global in that each rule has a unique priority even though it may pertain to only one or a few objects.

The rules are expressed through the graphical Structure Editor which helps the user formulate syntactically correct statements. The rule language permits the creation of functions which may perform complicated calculations to support the decisions made by the rules. The rule statements are parsed and interpreted, and the instructions are then executed by the Rule Processor.

The interaction between the simulation and the rules at each timestep is as follows. The model simulates until all objects have executed all the Dispatch Methods they can, given the user inputs. Then the Rule Processor fires the highest priority rule. The rule may fail if some of the slot values it needs are not yet set, or if it tries to overwrite values set by a higher priority rule. If the rule fails, the next highest priority rule is fired, and so on until a rule is successfully executed and new slot values are set on the model. After a rule fires, it is taken off the list of currently active rules until any of its dependencies (slots it accesses in the antecedent clause) change. After the rule fires, the simulation continues until it has solved everything it can, then the Rule Processor is invoked again. This continues until there are no more rules which can fire at that timestep, then the clock advances and the next timestep is executed. Just as in pure simulation, there is no guarantee of a solution. RiverWare provides diagnostic tools, however, to aid the analyst in understanding which rules successfully fired, as well as which objects dispatched which methods.

Optimization: RiverWare's optimization utilizes pre-emptive goal programming, using linear programming (LP) as an engine to optimize each of the prioritized goals input by the user. The optimal solution of a higher priority goal is not sacrificed in order to optimize a lower priority goal. The goals are input by the user through the graphical Constraint Editor tool. Each goal can be either a simple objective, or a set of constraints which is turned into an objective to minimize the deviations from the constraints. RiverWare accesses the CPLEX mathematical programming subroutine library for the solving engine.

One of the challenges of optimizing river basin operations using LP is representing the nonlinear processes. RiverWare provides automatic linearizing of nonlinear variables. The user may formulate goals or constraints on a wide range of model variables (slots). The underlying optimization software reformulates the objective as a linear expression in the basic decision variables. The nonlinear relationships are represented by table data entered by the user. The advanced user can select alternative linearization techniques and parameters which result in more accurate linearizations. RiverWare's optimization software also takes advantage of the basic model data available in the objects and links on the workspace to automatically generate the physical constraints of the system which reflect the mass balance, continuity and upper and lower bounds of the variables. These automatic features in RiverWare's optimization software allow the user to focus on expressing the policy in the goals, and make it possible for water resources engineers without an optimization background to generate and solve an appropriate goal programming formulation.

In addition to policies governing flows, elevations, spill and other variables in the physically-based model, power economic objectives may be brought into the analysis through methods developed on the Thermal Object. The user may specify an objective which involves maximizing the avoided thermal cost from hydropower generation. The economic value represents a trade-off of the value of immediate hydropower generation against future expected value of water in storage. The current value of hydropower is defined as the avoided costs of thermal power resulting from the addition of hydropower to the overall power mix. As the most expensive thermal units are replaced by hydropower, the marginal cost of power generation decreases.

When the optimization run is made, the physical constraints are generated and sent to the solver as the highest priority objective. Then each user-specified goal is interpreted, linearized, and solved. For each goal, the solutions of the higher priority objectives are maintained as constraints. The optimization solution, the values of the decision variables, are returned from CPLEX and entered

into the slots on the object. After an optimization run, the user can set up a post-optimization simulation run which automatically enters the optimal reservoir release schedule as inputs in the simulation and solves for storages, elevations, hydropower, etc. The simulation can be used to refine the optimization output.

Water Accounting: Water Accounts are created by the user on the objects. The sources of water to fill the accounts are supply links from other accounts and slots such as those which provide Hydrologic Inflow to the objects. Storage Accounts, Flow Accounts and Diversion Accounts all represent legal accounts in a water rights system. Pass-through accounts are created to keep track of the ownership of water in transit in the system.

In the initial prototype implementation of the water accounting system, the accounts calculate their balances as water is transferred from one account to another through the supply links. The account network solution behaves much like a spreadsheet in that it immediately updates the balances as data is entered. This allows for the accounting of water in an "after-the-fact" model. Future development will allow for prescriptive solutions of the network based on operations and water priorities.

Controllers: RiverWare's "controllers" are the software mechanisms for directing the model solution. The software architecture was designed to support any number of controllers. The controllers parallel the solution methods, but can also manage a combination of solutions. Currently the following controllers can be selected by the user on the graphical Run Control dialog where the user also specifies the begin and end dates of the run, and the timestep size.

- Simulation - can be run with or without Water Quality. Water Quality can be run in-line (at the end of each timestep) or post-process (at the end of the run).
- Rulebased Simulation - manages the interaction of the simulation with the Rule Processor. Water Quality can be coupled with rulebased simulation only in post processing mode.
- Optimization - pre-emptive linear goal programming solution; automatically sets up the post-optimization simulation if the controller is switched to "Simulation" after an optimization run.
- Accounting - executes accounting methods and solves accounts; currently this controller should be selected as a post-processor after a simulation run has been completed;
- Rulebased Simulation / Accounting InLine - solves each timestep for rulebased simulation then accounting, allowing the operational rules to access the previous timestep's accounting values.

DATA MANAGEMENT INTERFACE

The successful application of any model for operational scheduling requires the model's data to be updated quickly and easily to reflect current data such as real-time measurements, inflow forecasts, scheduled hydroplant operations, and special operations. For a general modeling tool, the data communications must be possible regardless of the specific database application or the sources of other data. Similarly, planning studies often require a large number of runs with varied data which may come from other sources such as historical databases. Automatic importing and exporting of data can be achieved through RiverWare's Data Management Interface utility.

The Data Management Interface (DMI) in RiverWare provides the means of using external programs to automatically load data into RiverWare. These routines are written by the user or the user's organization in any programming language and invoked through the RiverWare GUI.

Scenario-based DMI's execute a suite of individual routines to bring many data sources together into the model. The DMI can also be used to advance the run control start and end times.

MODEL ANALYSIS AND SCENARIO MANAGEMENT

The RiverWare modeling environment is designed to give the user the tools needed to build and run simulations to meet the needs of scheduling and planning activities. This is achieved through graphical user interface tools including the following:

- **Simulation Control Table:** a spreadsheet-like display of the data from a RiverWare model. The user constructs and configures an SCT, and can construct as many as needed to display various combinations of data. These can be iconified and brought up as different views on the model are needed. The SCT is interactive in that the user can specify inputs, run the simulation, and view the output from this interface.
- **Diagnostics:** information to assist the user in analyzing modeling problems during runs goes to an output dialog that saves the messages and offers searching and browsing features. The user may filter the information according to object, slot, time, etc. Warnings and errors are always displayed.
- **Dispatch Info Table:** a graphical tool showing what methods each object executed at each timestep and which slots were known and unknown. This is helpful to analyze over/under determination problems in simulation.
- **Expression Slots:** slots on the Data Object which hold user-defined expressions which are algebraic combinations of other slots, e.g., sum of all hydropower generation in the basin.
- **Plotting:** individual slots can be plotted quickly by selecting one button. Graphs with plot of many slots and/or many runs can be configured by the user. Plot set-ups can be saved.
- **Snapshot Manager:** the values of selected slots can be saved in this special data object for successive runs. If plotting the values, the new traces automatically are added to the plots. These data can also be accessed by the expression slots, the SCT and other output forms.
- **Multiple Run Management:** Many runs can be set up and executed in advance, automatically changing slot data or policies between runs. The runs can all have the same start/end times or be sequential. An Index Sequential setting on selected slots automatically permutes a series of historic data set as specified by the user (useful in using historic inflow data for planning studies).
- **Excel Writer:** a utility that takes outputs from RiverWare runs and creates an Excel input file for user-specific post-processing analysis.

TECHNOLOGY TRANSFER

RiverWare is under continued development at CADSWES, with new versions released several times a year. User support is provided to sponsors, and a web-based bug-tracking facility allows users to log problems directly. It is the intention of CADSWES and the sponsors to maintain the software in the future and provide enhancements as requested. In addition, formal training sessions are given at CADSWES. A three-day introductory training session is available, and new training courses for Rulebased Simulation and Optimization are anticipated.

RiverWare is a c++ application which runs on a Sun workstations under the solaris 2.3 (or greater) operating system.

GREAT LAKES ADVANCED HYDROLOGIC PREDICTION SYSTEM

Thomas E. Croley II, Research Hydrologist, Great Lakes Environmental Research Laboratory, Ann Arbor, Michigan

Abstract: The Great Lakes Environmental Research Laboratory's hydrology research over the past decade and a half addressed the Great Lakes community's forecasting needs and has culminated in a mature and tested Great Lakes *Advanced Hydrologic Prediction System*. Recently designed and tested technology properly incorporates multi-agency, multi-area, multi-period climate outlooks of meteorology probabilities into the package. This allows provision of 1- to 12-month (and longer) outlooks of probabilities for 25 hydrology variables over the entire Great Lakes basin, including simultaneous water levels on all lakes. It is important not to confuse probabilistic hydrology outlooks with currently available deterministic forecasts of lake levels, and to realize the much greater utility of the probabilistic hydrology outlooks. Probabilistic outlooks allow decision makers to incorporate some of the uncertainty inherent in forecasts, to properly consider the wide range of possibilities always present, and *to consider the risk associated with their decisions*, not possible with deterministic forecasts.

BACKGROUND

Extreme Great Lakes water levels cause extensive flooding, erosion, and damage to shorelines, shipping, and hydropower. Knowledge of even near-normal level expectations is important to riparians, recreational users, shipping, fishing, and many others. The International Joint Commission, at the request of the US and Canadian governments, recommended improving forecast methodologies, hydrological models, data collection, and communication of hydrological forecast information (IJC, 1993). While forecasts of meteorology, riverine flooding, and water level fluctuations are available for several hours to several days, the Great Lakes community requires water resource forecasts over large areas and time periods. Products must include nowcasts and 1-day to 3-month and future seasonal probabilistic outlooks of lake supplies, lake levels, and connecting channel flows. These require careful tracking of moisture storage variables and heat storage variables. The products must be relevant to users and delivered in a clear and understandable manner that aids in planning and decision making. They must make maximum use of all available information and be based on efficient and true hydrological process models.

Fortunately (for forecasters), the Great Lakes possess tremendous capacities for storage of mass and energy and respond slowly to changes in meteorology, making them amenable to hydrological forecasting. The dynamics of water supply components and basin and lake storages of water and heat must be understood before hydrological changes can be forecast. The Great Lakes Environmental Research Laboratory (GLERL) developed, calibrated, and verified conceptual model-based techniques for simulating hydrological processes in the Laurentian Great Lakes (including Georgian Bay and Lake St. Clair, both as separate entities). GLERL integrated the models into a system to estimate lake levels, whole-lake heat storage, and water and energy balances (Croley, 1990, 1993a,b; Croley and Hartmann, 1987, 1989; Croley and Lee, 1993; Hartmann, 1990). These include models for rainfall-runoff, evapotranspiration, and basin moisture storage [121 daily watershed models (Croley, 1982, 1983a,b; Croley and Hartmann, 1984)], overlake precipitation (a daily estimation model), one-dimensional (depth) lake thermodynamics [7 daily models for lake surface flux, thermal structure, evaporation, and heat storage (Croley, 1989a,b, 1992; Croley and Assel, 1994)], net lake supplies, channel routing [4 daily models for connecting channel flow and level, outlet works, and lake levels (Hartmann, 1987, 1988; Quinn, 1978)], lake regulation [a monthly plan balancing Lakes Superior, Michigan, and Huron and a quarter-monthly plan balancing Lake Ontario and the St. Lawrence Seaway (International St. Lawrence River Board of Control, 1963)], and diversions and consumption (International Great Lakes Diversions and Consumptive Uses Study Board, 1981). Details of these models are conveniently summarized by Croley et al. (1996). The modeling system is modularly-built, allowing model upgrades to be "dropped in" as developed and tested. It is coupled with near real-time data acquisition and reduction to enable representation of current system states. A new generation of interactively coupled models of the hydrosphere and atmosphere is forthcoming.

Forecasting efforts in the Great Lakes include the former US Lake Survey of the US Army Corps of Engineers, which began 6-month lake level forecasts in 1952. Since 1975, the Detroit District of the Corps has continued on a monthly basis. The Canadian Hydrographic Service (CHS) of the Department of Fisheries and Oceans began publishing monthly forecasts of levels in 1973. The Canadian forecasts are generated currently by the Great Lakes - St. Lawrence Regulation Office of Environment Canada and published by the CHS. See Table 1 for a chronology of recent Great Lakes forecasting developments. Both the US and Canadian monthly forecasts project water levels for each of the Great Lakes six months into the future. These forecasts are generated separately by each agency and then are coordinated to remove any differences. The Corps deterministic forecast is based upon extrapolations of recent

Table 1. Chronology of Recent Great Lakes Forecasting Developments.

Great Lakes Water Level Forecasting

1952:	US Lake Survey 6-month lake level forecasts
1964:	US Lake Survey develops "Trend Regression"
1973:	Canadian Hydrographic Service estimates levels from probabilistic supplies
1975:	US Army Corps estimates levels from supply statistics with Trend Regression
1977:	Environment Canada & Corps both publish combined levels forecasts
1996:	Bulletin distribution via the Internet
Now:	6,800 US & 2,600 Canadian bulletins coordinated by IJC

GLERL Advanced Hydrologic Prediction System (AHPS)

1982:	adapted runoff models to estimate supplies
1983:	Lake Superior installed for US Army Corps
1984:	Lake Champlain installed for NWS NERFC
1985:	identified weak evaporation estimates
1987:	all Great Lakes installed for 3 Corps offices
1988:	installed for New York Power Authority
1988:	delivered to Ontario Hydro
1990:	added improved 1-D evaporation models
1993:	altered deterministic outlooks, added an early form of probabilistic outlooks, re-evaluated & identified meteorology outlook as weakest part
1994:	installed for Midwest Climate Center
1995:	defined AHPS Product incorporated NOAA meteorology outlook probabilities built front-end AHPS Graphical User Interface (GUI) & public GUI built back-end AHPS GUI updated installation for Corps, NYPA, & MCC
1996:	expanded outlook products mixed agency outlook meteorology probabilities enhanced front-end AHPS GUI & public GUI assembled primitive back-end AHPS GUI demonstrated NRT AHPS at MCC on the WWW automated data downloading
1997:	AHPS outlooks produced at MCC & distributed via the Internet mixed multiple-area outlook meteorology probabilities developed method for lake-levels and connecting channel outlooks reinstalled for Ontario Hydro, NYPA, MCC, Corps demonstrated daily updates
Future:	development of improved AHPS distributed-parameter hydrology models incorporation of new & improved data streams expanded AHPS product dissemination revision & expansion of AHPS GUI & public GUI update Great Lakes AHPS lake regulation and channel routing routines

trends in water supplies for each of the lakes. Environment Canada's probabilistic forecast is computed from statistical analysis of historical water supplies. Neither the Corps nor Environment Canada use weather forecasts or antecedent hydrological conditions (current moisture and heat storages in the basins and lakes) in making their outlooks.

GLERL adapted runoff models to estimate supplies in 1982, installed their forecast package for the US Army Corps of Engineers on Lake Superior in 1983, for the NWS Northeast River Forecast Center on Lake Champlain in 1984, for 3 Corps offices on all Great Lakes in 1987, 1996, and 1997, for the New York Power Authority and Ontario Hydro in 1988, 1995, and 1997, and for the Midwest Climate Center in 1994, 1996, and 1997. GLERL identified weak

evaporation estimates in 1985, added improved one-dimensional evaporation models in 1990, altered deterministic outlooks, added probabilistic outlooks, and identified meteorology outlooks as the weakest component in 1993.

GREAT LAKES AHPS

Deterministic Hydrology Forecasts: GLERL developed the precursor to their present-day *Advanced Hydrologic Prediction System* (AHPS) as a semiautomatic software package to make deterministic forecasts of basin moisture storage, basin runoff, lake heat storage, surface water temperatures, lake surface evaporation, and lake water supplies (Croley, 1993b). These forecasts take advantage of the long-term memory of the Great Lakes system in the face of uncertain meteorology, and can be made for any number of months into the future. The package integrates modeling and near real-time data handling, is implemented in FORTRAN and PASCAL, and has been ported to several versions of MS-DOS, Windows, and UNIX. Inputs are daily meteorology (air temperature, dewpoint temperature, precipitation, wind speed, and cloud cover) for all available stations. Optional inputs are snow water equivalent, soil moisture, lake water temperature, and lake levels. Daily provisional point data are converted to areal averages for each watershed and lake surface by Thiessen weighting over digital maps of the areas (Croley and Hartmann, 1985). The areal averages are used by GLERL's runoff model (applied to all 121 Great Lakes watersheds) and their lake thermodynamics model (applied to each lake), to estimate basin moisture

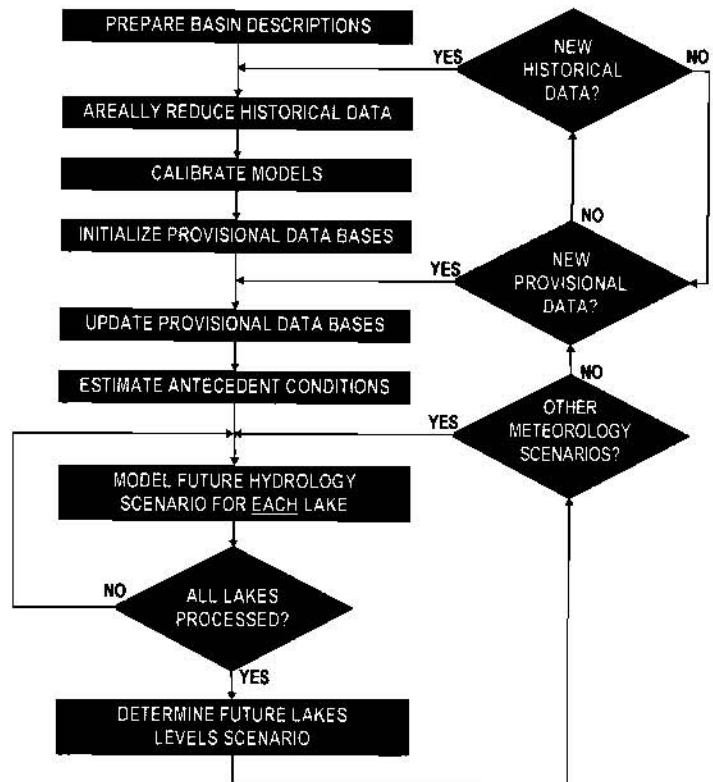


Figure 1. GLERL's Deterministic Hydrology Forecast.

and lake heat as antecedent (initial) conditions to a forecast. A deterministic "forecast" of all hydrology variables, including lake supply, may be made then by simulating the hydrology from the point of estimated initial conditions forward with a meteorology scenario (taken from the historical record, for example). The resulting lake supply scenarios, one for each lake, then are used with connecting-channel routing and lake regulation models to determine a lake levels scenario. This can be repeated for alternate meteorology scenarios. New provisional data are used as they become available; new historical data are also used as available to update models and databases. See Fig. 1.

Probabilistic Hydrology Forecasts: GLERL adapted this deterministic hydrology forecasting methodology to make probabilistic forecasts by considering historical meteorology as possibilities for the future. An *operational hydrology* approach [used also by the National Weather Service in their Extended Streamflow Prediction (ESP) forecasts] segments the historical record and uses each segment with models to simulate a possible "scenario" for the future. Sections of the historical meteorology record are input to hydrological, limnological, and other models, as in Fig. 1, as alternate meteorology scenarios, preserving observed spatial and temporal interrelationships. Corresponding hydrology variable scenarios are computed for the future, including lake supply scenarios. The resulting set of scenarios serves as a statistical sample for inferring probabilities and other parameters associated with both meteorology and hydrology; see Fig. 2. Probabilistic hydrology outlooks then are made from the sample for each variable of interest. Thus, the resulting probabilistic hydrology outlooks properly consider antecedent hydrological conditions, but they do not consider other-agency predictions of meteorology.

Probabilistic Meteorology Outlooks: Multiple long-lead probabilistic meteorology outlooks of improving skill (climate outlooks) are now available to the water resource engineer or hydrologist. They are defined over different time periods at different time lags; they forecast either event probabilities or most-probable events. The National Oceanic and Atmospheric Administration's Climate Prediction Center (CPC) recently (1 January 1995) changed from issuing a few relatively short-term outlooks of meteorology probabilities to a new multiple long-lead "climatic

outlook.” The outlook consists of a 1-month forecast for the next (full) month and thirteen 3-month forecasts, going into the future in overlapping fashion in 1-month steps. Each forecast predicts probabilities of average air temperature and total precipitation falling within selected intervals. Even more recently, the CPC began issuing an outlook of the most-probable intervals for 5-day air temperature and precipitation, set 5 days into the future (their 6-10 day outlooks). Likewise, the Atmospheric Environment Service’s Canadian Meteorological Center (CMC) of Environment Canada began issuing an outlook of the most probable interval for 30-day air temperature every half month (24 times per year). The CMC also issues outlooks four times per year of the most probable intervals for 90-day air temperature and precipitation. Although not operational yet, they are also issuing 3 experimental outlooks of the most probable intervals for 90-day air temperature and precipitation, going into the future in overlapping fashion in 3-month steps. More outlooks are coming on-line, including the NOAA National Center for Environmental Prediction’s ensemble forecasts.

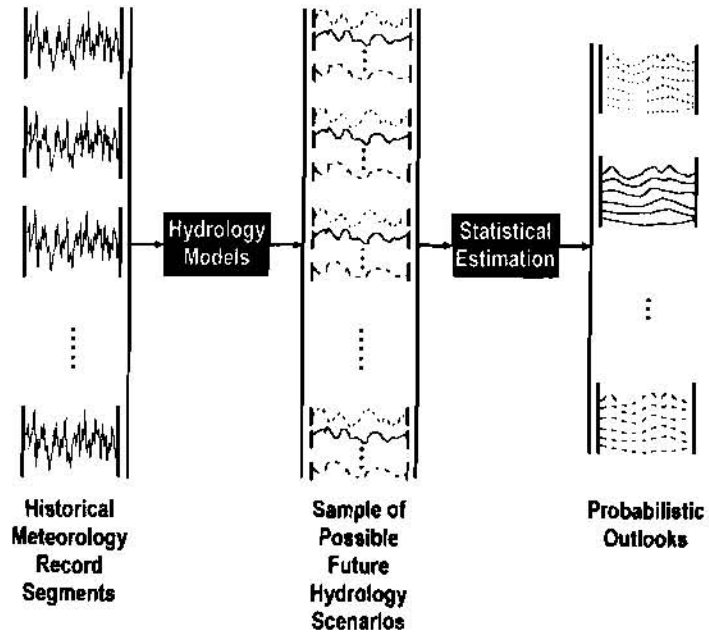


Figure 2. Operational Hydrology Approach.

Calculation of Weights: Users can interpret these probabilistic meteorology outlooks in improving their probabilistic hydrology outlooks. Recent work in the field used climatic indices from (other) long-range meteorology forecasts to estimate statistics subjectively (Smith et al., 1992) or coupled historical precipitation record segments with precipitation forecasts (Ingram et al., 1995). However, the relative frequencies of selected events (in the statistical sample of scenarios used in the operational hydrology approach) are fixed at historical values that are incompatible (generally) with those specified in the CPC’s or CMC’s probabilistic meteorology outlooks. Only by restructuring the set of scenarios can one obtain relative frequencies of selected events for a lake that match the CPC and CMC probabilistic meteorology outlooks over the lake. Recently, GLERL properly incorporated multi-agency, multi-period forecasts of meteorology probabilities by modifying their operational hydrology approach to generate probabilistic hydrology outlooks compatible with the meteorology outlooks. The hydrology variable scenarios, generated from corresponding segments of the historical meteorology record, are still used as a statistical sample for inferring probabilities, but the sample is first restructured. Croley (1996, 1997a,b) introduced a restructuring method that weights the scenarios and identifies boundary condition equations for the weights that correspond to probabilistic meteorology outlooks. The solution for the general case is shown to be an optimization problem. Now probabilistic hydrology outlooks consider both antecedent hydrological conditions and predictions of meteorology!

Simultaneous Spatial Outlooks: The probabilistic outlook of lake levels involves an additional complication. In a deterministic forecast, the forecast lake supply scenarios for each and all of the Great Lakes can be used as inputs to the connecting-channel routing and lake regulation models to determine the (simultaneous) lake level forecast scenarios on each lake. The connecting-channel routing and lake regulation models require water supplies on all lakes simultaneously to determine levels and outflows jointly on all lakes because all levels and outflows are interdependent. In a probabilistic outlook, the direct application of such a methodology might not be suitable for two reasons. 1) One cannot simply take the (say) 95th exceedance time series for water supplies as input to the connecting-channel routing and lake regulation models to determine the 95th exceedance time series for lake levels or outflows. There is not a simple one-to-one transform between quantiles of water supplies and lake levels. It is more appropriate to use the entire sample of water supply scenarios to create a sample of lake level scenarios from which to make probability outlooks. 2) However, since each lake (application area) involves a (generally) different set of probabilistic meteorology outlooks and set of weights, the water supply scenarios do not correspond to the same statistical sample from lake to lake. The use of all of the water supply scenarios for all of the Great Lakes, derived independently, as simultaneous inputs to the connecting-channel routing and lake regulation models then would not be representative of the same statistical sample when calculating lake level scenario forecasts.

As discussed earlier, the calculation of weights solves a set of equations representing multiple meteorology outlooks for a single lake to determine weights used in the solution for hydrology scenario probabilities. Because each lake's levels are not independent of the others, this method precludes the use of the independently derived weights in determining lake level probabilities. GLERL has been considering this issue for the past several years, and now have determined an appropriate method for determining joint lake level probabilities. The new extended methodology involves determining water supply (and other hydrology variable) scenarios on all lakes from the same historical record segments (as they existed on each of the lakes) and then solving all sets of equations (over all application areas) simultaneously to determine one set of weights that preserves all of the multiple meteorology outlooks over all of the Great Lakes. This of course requires that forecast parameters (such as start date and length of forecast) and historical meteorology record periods are the same over all application areas. The resulting weights can therefore be used directly in the solution for lake level probabilities, where the sample of lake level scenarios is derived from the appropriate simultaneous water supply scenarios on all the lakes; see Fig. 3. It is also useful to note here that, in Fig. 3, alternate meteorology outlooks (forecasts) may be considered without having to repeat provisional data updates, estimates of antecedent conditions, or any of the hydrology modeling required in sample building.

The methodology provides an objective and open-ended means of matching forecast meteorology probabilities in other forecasts besides the water resource forecasts considered here. This has opened the door on jointly considering additional multiple agency forecasts over multiple areas for multiple (different simultaneous) periods as they become available in the future.

Probabilistic Outlooks from Great Lakes AHPS: This physically-based approach for generating outlooks offers the ability, as compared to other statistically-based approaches, to incorporate improvements in the understanding of process dynamics as they occur in the future and to respond reasonably to conditions initial to a forecast (such as heat and moisture storages), not observed in the past. This allows GLERL to provide 1- to 12-month (and longer) outlooks of probabilities for 25 hydrology variables over the entire Great Lakes basin, including simultaneous lake levels on all Great Lakes, that consider meteorology outlooks. Probabilistic outlooks allow decision makers to *consider the risk associated with their decisions*, not possible with deterministic outlooks. Probabilistic outlooks for all variables, except for lake levels, currently are made with GLERL's technology on an operational basis by the Midwest Climate Center, available to the public via the Internet. Probabilistic outlooks for lake levels currently are made experimentally at GLERL, as part of their *Advanced Hydrologic Prediction System*. The methodology is also used operationally by the Midwest Climate Center, the New York Power Authority, and Ontario Hydro, and experimentally by the US Army Corps of Engineers in Buffalo and Detroit. A recent probabilistic lake level outlook is pro-

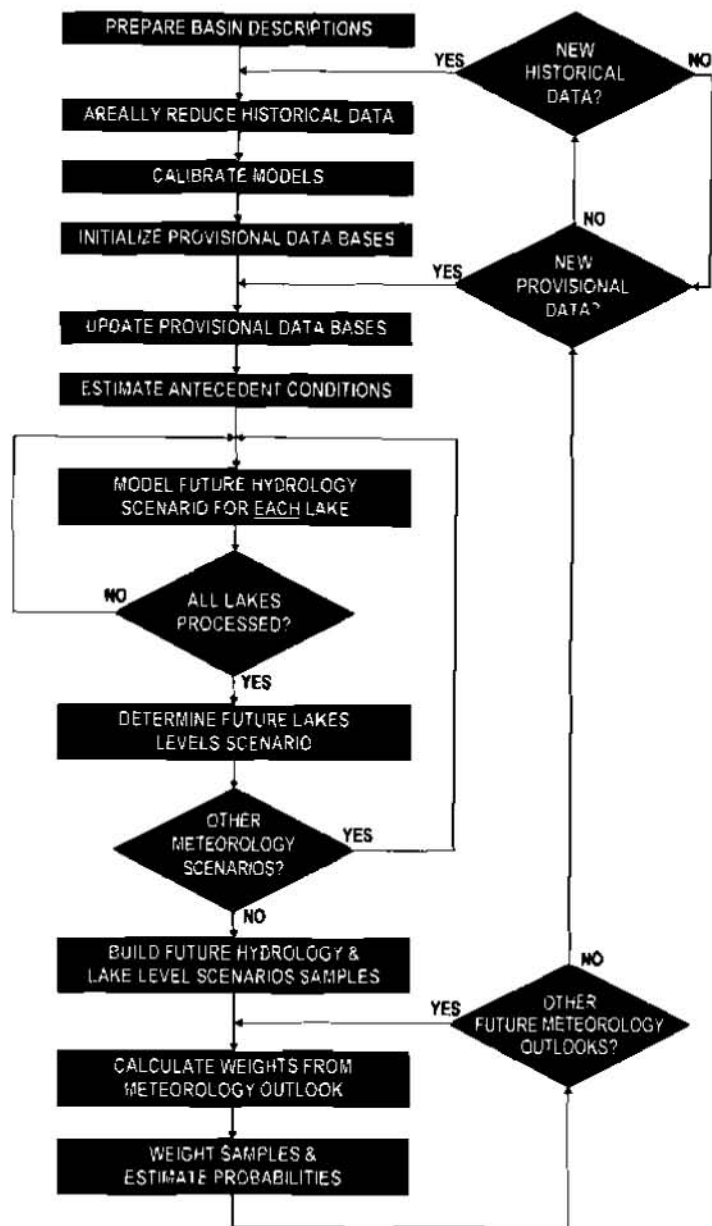


Figure 3. GLERL's Probabilistic Hydrology Forecast.

vided in Fig. 4. It is based on probabilistic meteorology outlooks from NOAA and Environment Canada. Both generally predicted near-normal September air temperature probabilities. NOAA forecast normal September precipitation probabilities and EC forecast above-normal September-October-November air temperature probabilities.

GREAT LAKES AHPS IMPACTS AND ASSESSMENT

Utility To Decision Makers: GLERL's probabilistic hydrology outlooks are state-of-the-art. They *a)* fully and correctly utilize the National Weather Service and Environment Canada probabilistic long range climate outlooks for multiple areas simultaneously, *b)* explicitly account for basin soil moisture and snow pack and lake heat storage and ice cover initial conditions, *c)* allow daily extended outlook generation, taking advantage of near-real-time data availability to offer continuously updated probabilistic outlooks, *d)* utilize hydrology models in a modularly-built package that allows upgrades to be "dropped in" as developed and tested, *e)* provide probabilistic outlooks for each lake and river watershed, capitalizing on improving weather prediction skill and hydrometeorology observations, *f)* offer the proper manner in which to consider the wide range of possibilities that always exist, *g)* incorporate some of the uncertainty inherent in forecast estimates, and *h)* allow consideration of risk by decision makers, as mentioned. Comparisons show that even deterministic outlooks from the GLERL forecast package (constructed by simply averaging probabilistic outlooks) have higher skill than the Corps and Environment Canada outlooks (Croley and Lee, 1993).

Multiple Great Lakes Outlooks: Would an additional forecast available to the public cause confusion, especially since the US Army Corps of Engineers and Environment Canada both concurrently publish "coordinated" deterministic forecasts? The desire to see simply what the future will be cannot be accommodated, particularly for extended forecast periods. Instead, we must educate the public on how to process a range of possibilities through expression as probabilistic outlooks. GLERL's probabilistic hydrology outlooks provide additional information to the public, not contained in either the coordinated or component forecasts. The probabilistic information can be used by the public to assess risk at several different levels from simple (similar to TV weather forecasts) to more sophisticated (similar to existing probabilistic meteorology outlooks). These risk assessments may be associated with decision making as shown in several Great Lakes case studies (Lee et al., 1997).

Lake Superior Average Lake Level (meters)

Forecast Start Date: September 2, 1997

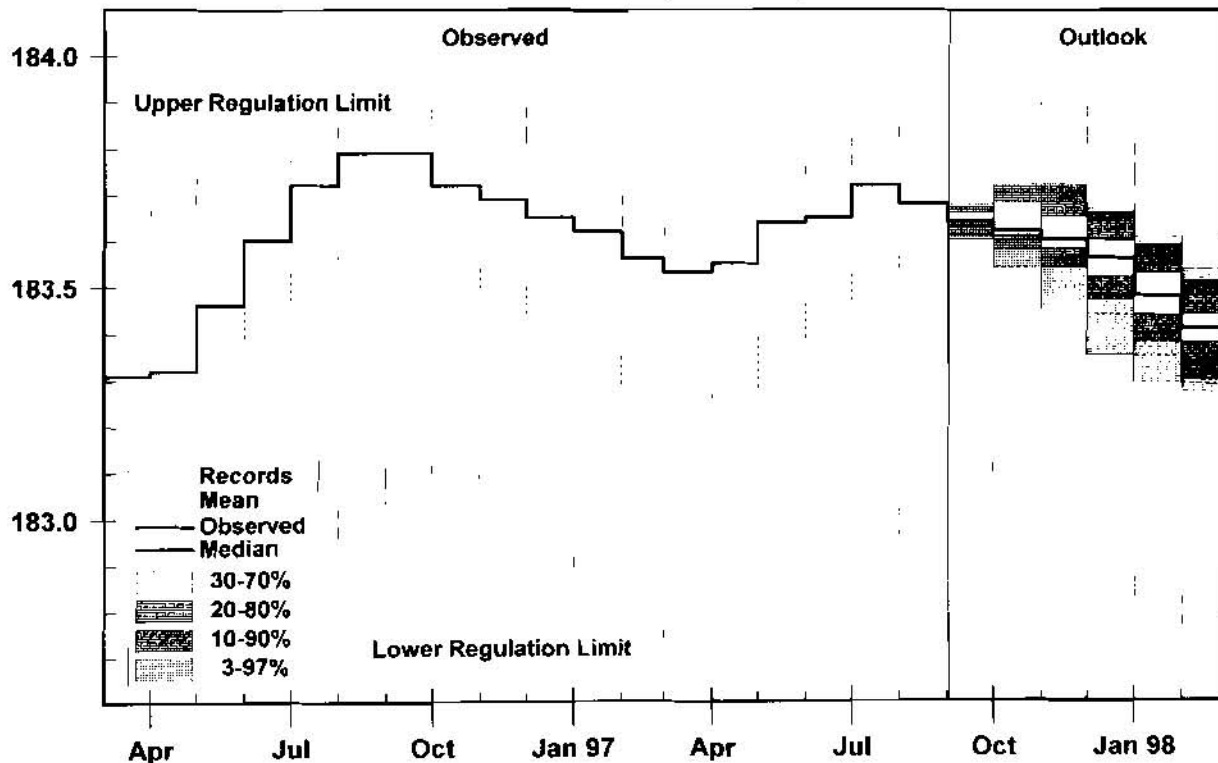


Figure 4. September 1997 Probabilistic Lake Superior Water Level Outlook.

It behooves all parties to ease possible confusion by introducing GLERL's probabilistic outlooks along side of the current deterministic ones, with appropriate explanation on the interpretation and use of outlook probabilities. This would help to educate decision makers on using outlook probabilities to assess risk in their decision making. This would also clarify the role of all of these outlooks in relation to one another. This is much preferable to forcing users to wonder if the different outlooks, that they discover independently available, are conflicting or are related to one another.

Responding To User Needs: Probabilistic hydrology outlooks address NOAA's 1995-2000 *Strategic Plan* component for the enhancement of environmental prediction. The plan calls for an integrated environmental observation, assessment, and forecast service that supports the Nation's economic and environmental agenda both by significantly improving short-term (immediate to 60 days) forecasts, and by implementing reliable seasonal to interannual (60 days-10 years) forecasts. GLERL has been providing that service on the Great Lakes, in terms of water quantity, through its AHPS program (see Table 1) for predicting Great Lakes hydrology variables, and through its Great Lakes Forecast System for predicting short-term wind-driven waves and setup on Lake Erie. Other NOAA offices (National Weather Service) have been providing both 1-2 day level outlooks (related to storm and wind setup) and 1 week level outlooks on all Great Lakes.

GLERL's probabilistic hydrology outlooks also address recommendation number 31 of the International Joint Commission to the US and Canada as a result of their Levels Reference Study (IJC, 1993). The 5-year study examined methods to alleviate problems associated with Great Lakes-St. Lawrence River Basin fluctuating water levels and outflows. They recommended development of improved lake operation and management tools. "[to] upgrade models used for simulation, forecasting and regulation in order to formulate a comprehensive water supply and routing model that includes the whole basin." In its report to the governments, the IJC supported the development of risk analysis techniques for application in management of water levels issues. The IJC recognized the usefulness of risk analysis techniques in its work under the Great Lakes Water Quality Agreement and supported their extension to lake level management.

REFERENCES

- Croley, T. E., II, 1982, Great Lakes basins runoff modeling. *NOAA Tech. Memo. ERL GLERL-39*, National Technical Information Service, Springfield.
- Croley, T. E., II, 1983a, Great Lakes basins (U.S.A.-Canada) runoff modeling. *J. Hydrol.*, **64**:135-158.
- Croley, T. E., II, 1983b, Lake Ontario basin (U.S.A.-Canada) runoff modeling. *J. Hydrol.*, **66**:101-121.
- Croley, T. E., II, 1989a, Verifiable evaporation modeling on the Laurentian Great Lakes. *Wat. Resour. Res.*, **25**(5):781-792.
- Croley, T. E., II, 1989b, Lumped modeling of Laurentian Great Lakes evaporation, heat storage, and energy fluxes for forecasting and simulation. *NOAA Tech. Memo. ERL GLERL-70*, Great Lakes Environmental Research Laboratory, Ann Arbor.
- Croley, T. E., II, 1990, Laurentian Great Lakes double-CO₂ climate change hydrological impacts. *Climatic Change*, **17**:27-47.
- Croley, T. E., II, 1992, Long-term heat storage in the Great Lakes. *Wat. Resour. Res.*, **28**(1):69-81.
- Croley, T. E., II, 1993a, CCC GCM 2xCO₂ hydrological impacts on the Great Lakes. In: *Climate. Climate Change, Water Level Forecasting and Frequency Analysis, Supporting Documents, Volume 1 - Water Supply Scenarios*, International Joint Commission, Washington, DC.
- Croley, T. E., II, 1993b, Probabilistic Great Lakes hydrology outlooks, *Wat. Resour. Bull.*, AWRA, **29**(5):741-753.
- Croley, T. E., II, 1996, Using NOAA's new climate outlooks in operational hydrology. *J. Hydrol. Eng.*, ASCE, **1**(3):93-102.
- Croley, T. E., II, 1997a, Water resource predictions from meteorological probability forecasts. *Proc. Sustainability of Water Resources Under Increasing Uncertainty*, IAHS Press, Institute of Hydrology, Wallingford, Oxfordshire, 301-309.
- Croley, T. E., II, 1997b, Mixing probabilistic meteorology outlooks in operational hydrology, *J. Hydrol. Eng.*, ASCE (in press, to appear Oct. '97).
- Croley, T. E., II, Assel, R. A., 1994, A one-dimensional ice thermodynamics model for the Laurentian Great Lakes. *Wat. Resour. Res.*, **30**(3):625-639.
- Croley, T. E., II, Hartmann, H. C., 1984, Lake Superior basin runoff modeling. *NOAA Tech. Memo. ERL GLERL-50*, National Technical Information Service, Springfield.

- Croley, T. E., II, Hartmann, H. C., 1985, Resolving Thiessen polygons. *J. Hydrol.*, **76**:363-379.
- Croley, T. E., II, Hartmann, H. C., 1987, Near-real-time forecasting of large lake supplies. *J. Wat. Resour. Plng. and Mgmt.*, **113**(6):810-823.
- Croley, T. E., II, Hartmann, H. C., 1989, Effects of climate changes on the Laurentian Great Lakes levels. In *The Potential Effects of Global Climate Change on the United States: Appendix A-Water Resources* J. B. Smith and D. A. Tirpak (Eds.), U.S. Environmental Protection Agency, Washington, D.C., pp 4-1 - 4-34.
- Croley, T.E., II, Lee, D. H., 1993, Evaluation of Great Lakes net basin supply forecasts. *Wat. Resour. Bull.*, **29**(2) 267-282
- Croley, T. E., II, Quinn, F. H., Kunkel, K. E., Changnon, S. A., 1996, Climate transposition effects on the Great Lakes hydrological cycle. *NOAA Tech. Memo. ERL GLERL-89*, Great Lakes Environmental Research Laboratory, Ann Arbor, 100 pp.
- Hartmann, H. C., 1987, An evaluation of Great Lakes hydraulic routing models. *NOAA Tech. Memo. ERL GLERL-66*, Great Lakes Environmental Research Laboratory, Ann Arbor, 9 pp.
- Hartmann, H. C., 1988, Historical basis for limit on Lake Superior water level regulations. *J. Great Lakes Res.*, **14**(3):316-324.
- Hartmann, H. C., 1990, Climate change impacts on Laurentian Great Lakes levels. *Climatic Change*, **17**:49-67.
- Ingram, J. J., Hudlow, M. D., Fread, D. L., 1995, Hydrometeorological coupling for extended streamflow predictions. *Proc. Conference on Hydro.; 75th Annu. Meeting of Am. Meteorological Soc.*, AMS, Boston, Massachusetts, 186-191.
- International Great Lakes Diversions and Consumptive Uses Study Board, 1981, *Great Lakes Diversions and Consumptive Uses*. International Joint Commission, Washington, D. C.
- International Joint Commission, 1993. *Methods of Alleviating the Adverse Consequences of Fluctuating Water Levels in the Great Lakes-St. Lawrence River Basin*. Report to the Governments of Canada and the United States. International Joint Commission, Washington, D.C. and Ottawa, Ontario, Canada.
- International St. Lawrence River Board of Control, 1963, *Regulation of Lake Ontario: Plan 1958-D.*, Washington, D. C.
- Lee, D. H., Clites, A. H., Keillor, J. P., 1997, Assessing risk in operational decisions using Great Lakes probabilistic water level forecasts. *Environ. Manag.*, **21**(1):43-58.
- Quinn, F. H., 1978, Hydrologic response model of the North American Great Lakes. *J. Hydrol.*, **37**:295-307.
- Smith, J. A., Day, G. N., Kane, M. D., 1992, Nonparametric framework for long-range streamflow forecasting. *J. Wat. Resour. Plng. and Mgmt.*, ASCE, **118**(1):82-92.

MODERNIZING THE U.S. ARMY CORPS OF ENGINEERS WATER CONTROL DATA SYSTEM

**Darryl W. Davis, Director, and Arthur F. Pabst, Chief, Technical Assistance Division,
U.S. Army Corps of Engineers, Hydrologic Engineering Center,
609 Second Street, Davis, CA 95616**

Abstract: The Water Control Data System (WCDS) is the data acquisition, management, modeling and decision support system that supports the Corps water control mission of regulating more than 500 dam and reservoir projects. The WCDS is a nationwide integrated system of hardware and software that allows user access to virtually any data and information in the system. The base system was operational in the 1988-1990 time frame. Advances in computer and related hardware and software provide the opportunity to upgrade WCDS and improve execution of the water control mission. The Corps is modernizing WCDS by replacing computer hardware, upgrading data acquisition hardware and software, creating a corporate water control database system, and upgrading and developing new modeling and decision support software. This paper describes the existing WCDS system, modernization activities, and current status.

INTRODUCTION

The WCDS is the automated information system (AIS) that supports the Corps of Engineers water control mission including the hardware, software, man-power and other resources required to acquire, develop, maintain, operate, and manage the system. The WCDS includes the collection, acquisition, retrieval, verification, storage, display, transmission, dissemination, interpretation and archival of data and information needed to carry out the water control mission of the Corps. Typically this data and information includes hydrologic, meteorologic, water quality, and project data and information. The system collects data on a near continuous basis from thousands of automated sensors throughout the nation. In addition, the system acquires spatial satellite and radar imagery, graphical products, text products, lab and field analyses of chemical, physical and biological samples. The system through its software incorporates this data and information into various user products and system outputs. The WCDS is a nationwide integrated system of hardware and software that allow user access to virtually any data and information in the system. A suite of software gives users the ability to display, manipulate, disseminate, interpret, and transmit this information throughout the Corps and to numerous other interested users.

The system supports the information needs for Corps water control decisions. There are hundreds of water control decisions made each day during normal hydrometeorological conditions. These include decisions of reservoir releases, power generation, navigation structure operation, facilities maintenance scheduling, special event operations - the list is quite long. The number and difficulty of these decisions, and consequently the information support needs, vastly increases during flood and other extreme events. Most day-to-day water control decisions are made at the staff level in district offices, with oversight and support at division level. In some situations, real-time decisions for main-stem projects that require a broad regional perspective are made at the division level.

Other Corps functions served by information from the WCDS include flood fight and emergency

management; environmental, land, and recreation system management; and the myriad of water-related interests of the Corps. Information is shared with other federal and local agencies to enable efficient, coordinated accomplishment of complementary activities. Local partners, users, and the general public are also consumers of the information provided by the WCDS.

EXISTING WCDS

The WCDS is an existing system, characterized as fully operational in the circa 1988-1990 time frame. The system evolved over the period 1975 to 1990. The system was then comprised of dedicated Harris mini-computers, data acquisition and communications hardware, and Corps-wide developed and fielded software, and locally developed software. Although guided by Corps-wide policy, the circa 1988-1990 WCDS was not a centrally planned and developed system except for the computer hardware. The Harris mini-computers, 24 total, were acquired via a centrally managed activity. A few offices used other computer equipment. The accumulated investment in the existing circa 1988-1990 system is estimated at \$80 million.

Software was developed to address various aspects of the basic WCDS functions. A portion of the software was developed for Corps-wide usage but substantial development took place in local district and division water control offices. The Corps-wide software was developed by the Corps Hydrologic Engineering Center (HEC) as reimbursable products for field offices. The software was subsequently generalized for Corps-wide application. A total of 54 HEC developed programs comprised of about 600,000 lines of code (mostly Fortran with some C) formed the Corps-wide WCDS software. Only a few Corps offices implemented the full suite of software but most offices make use of the HEC-DSS data storage system as the central data manager.

MODERNIZATION NEEDS AND OPPORTUNITIES

The circa 1988-1990 WCDS computer equipment was aged and data acquisition and processing requirements increased beyond capacity; operation and maintenance was costly; and staff requirements to continue useful service excessive. The water control decision process continues to increase in complexity and involve more interested parties. This in turn increases the need for improved responsiveness in information acquisition, processing, display, and communications/exchange. Recent extreme events, such as the Mississippi flood of 1993, taxed the limits of WCDS and exposed the need for improved capabilities. At the same time, substantial advances in network communications, computer and related hardware, and companion modern software, provide the opportunity to substantially improve execution of the water control mission. System modernization is planned to address both cost reduction and performance improvements.

Corps Corporate Perspective: Viewed from a corporate perspective, the existing WCDS was a patchwork of individual systems. The systems are largely locally maintained, managed and supported. Each system is a blend of user developed software, Corps developed and supported software, and commercial software. This independent development has produced great disparity in the level of performance and capability across the Corps. The existing systems can support needs given ample fiscal and manpower resources. However, many of the existing systems are inadequate to effectively move data and information through the Corps organization and to our customers. Data

acquisition, data management, communication, display, and report generation are generally cumbersome and labor intensive efforts. Modeling and forecasting are usually performed only on the most highly developed systems and even there these tools are often intermittently applied. The uniqueness of locally developed software to accomplish similar tasks at many districts frustrates effective technology transfer. Modernization is necessary to provide the tools needed in a reliable networked system of hardware and software that can be locally configured to meet the unique requirements of each user.

New Network and Workstation Technology: Workstations have processing capability orders of magnitude greater than the Harris mini-computers at a fraction of the cost. Likewise, communications and network hardware and software technologies have rapidly advanced. Network technology is common place within Corps offices and other cooperating federal and local government agencies. Integrated with appropriate software, network technology increases access to data sources, improves processing power for flow forecasting, impact analysis, and decision support modeling, and increases effectiveness in exchange of information.

New Data Sources: Important new data sources for input to real-time regulation decisions are now available. Geographic Information Systems (GIS) are commonly employed by the Corps and other state and local agencies to manage land-based information. Satellite imagery, and other spacecraft remote sensing data, are now routinely downloaded and displayed for scientific as well as general public information. Analysis methods to make use of such data continues to be developed in Federal government research laboratories, universities, and the private sector. Integrated with ground-based radar sensor data, in-situ measurements, and data handling and processing systems, these capabilities offer important advances in information support to the Corps real-time water control mission.

Improved Data Management Technology: Software for storing, retrieving, manipulating, and displaying a wide range of data has improved markedly over that of the last decade. The opportunity exists to develop a corporate Corps-wide water control data base system that would serve real-time as well as other water management information needs. Integration of data, models, and information management via the corporate data base would provide an order of magnitude improvement in overall data handling within the WCDS.

New Modeling, Forecasting, and Decision Support Tools: Advances in software that will take advantage of new and improved data sources and analytical analysis methods, implemented within state-of-the-art computer processing and network systems, would provide the critical element in improved information for water control decisions. Software to incorporate spatial precipitation data available from NEXRAD for forecasting, optimization algorithms for reservoir regulation, economic/flood damage impacts, and environmental effects are examples of advanced software tools that hold promise of significant contributions.

WCDS MODERNIZATION PROJECT

The WCDS modernization project includes replacement of pre-1990 computer and related hardware; upgrades to field instrumentation and communications equipment; and upgrading existing WCDS software including porting exiting products, modifying and upgrading existing products,

development of new software products, and acquisition and adaptation of Commercial Off-The-Shelf (COTS) software. Incorporated within the project are both centrally developed and maintained software and field developed software. Modernizing WCDS will standardize equipment, data handling, and software and thus ensure maintainability, upgradability, and usability. The project integrates activities among headquarters, field offices, and supporting offices.

The broad outlines of the modernized WCDS are documented in (USACE, 1995). On the hardware side, replacement of the Harris mini-computers began in the early 1990's and by 1996, all had been replaced by UNIX workstations. Technology insertion options in procurement contracts provide that as new workstations are acquired, state-of-the-art workstations are delivered. The Corps corporate communications system provides the basic network infrastructure that meets the modernized system connectivity requirements. The tasks requiring focused attention include software upgrades and additions, and hardware/software systems integration. The specific software requirements of the modernized system are documented in a series of 'Requirements Specifications' (USACE, 1997) that are guiding the system development. Figure 1 is a schematic for a prototype of the initial version of the modernized system. The prototype will be a limited capability but fully functional WCDS. The prototype diagram illustrates functional integration of the WCDS components. The meaning of abbreviations and acronyms in Figure 1 are defined in the sections that follow.

Data Acquisition: The data acquisition module will receive the suite of National Weather Service (NWS) products including text, graphics SHEF and digital products (including NEXRAD stage III data); GOES/DOMSAT text products, land-based radio, cooperating agency data, manual entry data, and direct (PUPIE) radar data. Processing capability will include decoding and transforming data received into usable forms and units via math functions; data verification; producing graphic products and reports; and delivering data acquisition products to the data base. Prototype data acquisition functions are depicted in the DA circle in Figure 1.

Data Base: The data base module will be comprised of an Oracle relational data base system and supporting temporary data cache and working files. Data to be stored includes: non-recurrent data such as documents, project data, imagery, text, notification lists, messages, WCDS component operational status, and gage status; recurrent data such as gage and radar products, NWS products and remote sensed data; and recurrent derived data such as model simulation results, transformed data, and software execution logs. Data objects for application usage include time series, spatial, hydraulics, documents, watershed, reservoir, GIS, economic impact, WWW interface, and gage accounting. Utility support includes a full suite of queries, import/export conversion and formats, and archiving. Data base management and performance tuning and data base security and access control will be provided. The data base function/module is depicted in Figure 1 by the DB circle.

Data Dissemination: Types of data to be disseminated include time series, paired, spatial, text, image, schematic, and multimedia. Delivery methods include World Wide Web technology (WWW), FTP, E-mail, fax, pager, and, recorded messages. Dissemination will occur locally within a Corps district office, among other district/division offices, Corps headquarters, cooperating agencies, and the general public. The data source will be the Oracle data base. Data recipients can retrieve and mathematically manipulate data, manipulate graphics, and generate tabular, graphic and text products. Specific report products will be developed for data acquisition and dissemination,

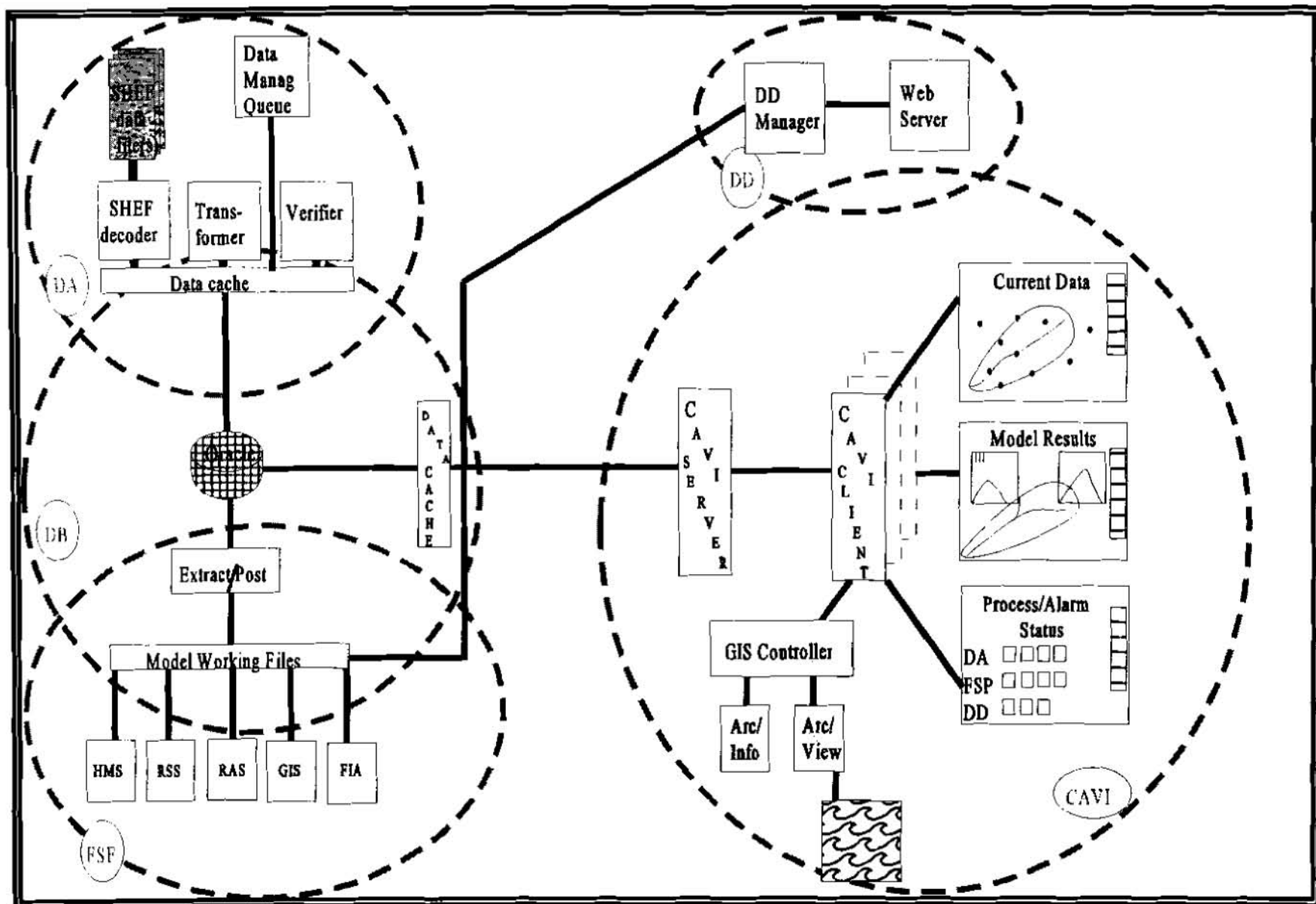


Figure 1 WCDS Version 1.0 Prototype Components

flood impact analysis, flow-stage forecasting, and reservoir simulation. Data dissemination is depicted in Figure 1 by the DD circle.

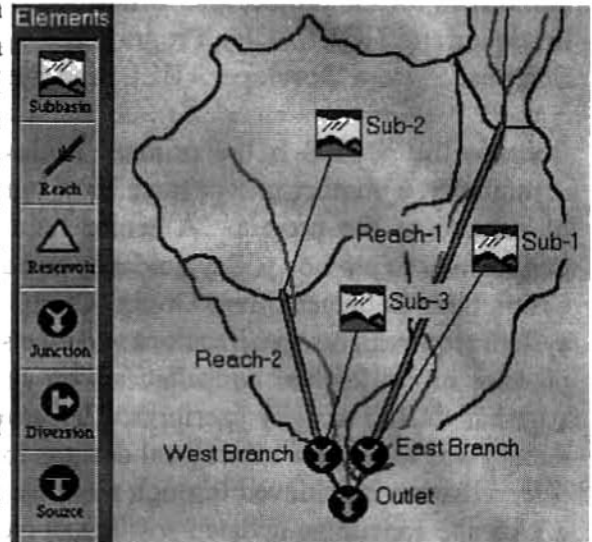
Flow-Stage Forecasting: Flow forecasting will be via grid-based precipitation/runoff continuous modeling for rainfall and snow melt using a suite of loss and runoff transform methods, supported by hydrologic and unsteady flow routing. Scenario evaluations to be supported include real-time gage and NEXRAD precipitation, QPF, and extended (long term) stream flow forecasts. Displays and reports may be locally generated and displayed and are also placed in the data base. Interactive user controlled forecasts and automated forecasts functioning in real time will be supported. Flow forecasting will employ the HEC-HMS (Hydrologic Modeling System) software package (USACE, 1996). Stage forecasting will be performed for steady and unsteady flow with flow data retrieved from the data base. Hydraulic structures accommodated include bridges, culverts, in-line weirs and gated spillways, lateral weirs, pump stations, levee overtopping and breaches including storage area connections, simple spillways, closed conduits, and navigation dams. Tabulations, reports, and charts are generated and may be displayed locally and also are placed in the data base. Stage forecasting will employ the HEC-RAS (River Analysis System) software package (USACE, 1996) and UNET (USACE, 1996). Later, HEC-RAS will have unsteady flow capability and will supplant early UNET applications, such as in the Mississippi Basin forecast model (USACE, 1997). Flow and stage forecasting are depicted in Figure 1 by the HMS and RAS boxes in the FSF circle.

Reservoir System Simulation: The reservoir simulation module will perform individual reservoir and reservoir system analysis for fixed/prescribed operation or rule-based operation at the option of the user. A major feature will be incorporation of a generalized rule editor capability to enable highly flexible (boolean-type) specification of operation rules. Typical reservoir physical features and operational characteristics will be accommodated to support flood, hydropower and other low-flow/conservation operations. Real-time/forecasted flow data will be retrieved from the data base and model working files, operations performed, and results (time series of reservoir storage, stage, releases, power generation, etc.) posted back to the data base. Reports may be generated locally and posted to the data base. A new object-based flood operation algorithm will be developed. Existing conservation/low-flow software packages are under consideration for integration into the WCDS.

Flood Impact Analysis: The flood impact module will estimate flood damage impacts from alternative forecast and operation scenarios, and post-flood event or flood season project accomplishment analysis. Flood stage and flooded area data will be retrieved from the data base and processed with flood plain information of infrastructure, damage potential, and population/occupancy to generate reports and displays by pre-defined polygon areas. These areas can be damage reaches, political jurisdictions, and habitat or other impact zones of interest. Urban, agricultural, and environmental loss/information functions form the basis for the analysis. The loss functions may be developed from structure/site specific inventories, or developed via GIS analysis. Report and graphics may be generated locally and are also posted to the data base. Flood impact and related analysis are depicted in Figure 1 as boxes labeled FIA and GIS within the FSF circle.

Control and Visualization Interface: This module performs the command functions. It provides the interface between the user and the various components and operations of WCDS to enable access, control, display, visualization, and management to be performed quickly and easily. The

CAVI will have two primary components: a visualization panel and a status/control panel. Secondary components include a menu bar, tool bar, and other windows. The CAVI has pages (visualization and status/control panels) for data acquisition, data visualization, model interface, CAVI administration, and CAVI configuration. Multiple instances of CAVI's will be operational within a Corps district/division office, for example for different watersheds and different technical users (model support staff). The primary user interface will be via a geographic representation of the water system displayed as a system schematic on a CAVI panel. The display might be augmented with map overlays as appropriate to the specific CAVI operation. The CAVI and decision support models will use a common schematic representation of the system to ensure seamless integration among WCDS component operations. Control will be exercised through appropriate panel and button activation, including model setup, sequencing, and execution. Visualization of status and results will be via a rich suite of tabulations, charts, plots, multi-dimensional displays, and graphic images. GIS will be enabled via the CAVI for such displays as flood inundation. WCDS module user access and security will be exercised through the CAVI.



Product Integration, Testing and Deployment: The modernized WCDS will be fielded as a distributed suite of hardware/software at Corps offices across the U.S., at as many as 44 sites, tied together by the Corps corporate communications network. The WCDS platform is the Sun Solaris system. The client-side platform is the Microsoft Windows NT system. The hardware and software configurations will be customized to each site but will include at least two Sun Sparcs and several Windows NT workstations and Windows 95 PCs. The components will initially be delivered as a Sun Solaris client-server system with the Sun as the server and CAVI client side delivered in both the Sun and Windows NT environments. Other WCDS components are being developed with possible/likely porting to Windows NT in the not-to-distant future. System development standards are documented in a software manual (file conventions, user selectable Metric/English units, universal time, development coding languages, and third party productivity software). Processing will be interactive, non-interactive, and script-driven. A messaging system will communicate status information and processing instructions among the CAVI and WCDS components. Alarm conditions are to be generated, monitored, and managed.

OVERSIGHT, MANAGEMENT, AND STATUS

The WCDS is an official U.S. Army Corps of Engineers Automated Information System (AIS) and as such, comes under Army policies of Life Cycle Management of Information Systems (LCMIS) (U.S. Army, 1989). LCMIS mandates certain formal management and oversight processes in which development is controlled by specific decision milestones. Documentation is required to support the management/decision process of the milestones. The milestone decisions (required before proceeding to the next phase) are at: initiation of development/modernization; planning/proof-of-

concept; development/testing; deployment; and operation and maintenance. Documentation required for milestone review and decisions includes: needs statement; economic analysis; management plan; system description; telecommunications/security plan; manpower/skills impact; testing/validation plan; and progress reporting metrics. The WCDS modernization project is in the proof-of-concept/development phase scheduled for a milestone decision early next year. This decision will validate concepts, approve full development, and authorize fielding of interim products. Responsible authorities for the project are: Milestone Decision Authority - Deputy Chief of Engineers, Corps headquarters (HQUSACE); Program Manager - Hydraulics and Hydrology Branch, HQUSACE; Software System Developer - HEC; and System Deployment/Support - HEC.

Because the WCDS is the primary decision support system of the Corps field water control community, a number of groups have been commissioned to ensure direct field input to and a degree of control of the project. A senior field advisory group drawn from division offices meets periodically to provide policy guidance and advise on critical corporate issues. Another group, the Corps User Representatives Group (CURG), drawn from district and division staff, prepared the system requirements specifications and meets periodically to update requirements, monitor progress, provide more detailed consultations on specific technical issues, and to later oversee testing. Another CURG activity (performed by groups formed into System Design and Testing - SDT - teams) was to prepare conceptual designs for the WCDS modules. Coordination and information dissemination is achieved through monthly nation-wide (call in) conference calls, maintenance of a Web site containing updated postings of meeting minutes, project documents, and draft/prototype products. An E-mail discussion group for the WCDS modernization project is also operational.

WCDS modernization is a decade-long project begun in 1991 and targeted for complete deployment in 2001. Hardware replacement began early and porting of existing WCDS software was completed shortly thereafter. Funding shortages hampered new software development until the project began in earnest in FY 1997. Development and deployment is now occurring on an incremental basis with a number of new products now being field tested. The WCDS modernization project will cost \$25 million with the software development component estimated to cost about \$5 million.

REFERENCES

- USACE, 1995. Water Control Data System (WCDS) Past, Present and Future, RD-39. USACE Hydrologic Engineering Center.
- USACE, 1995. Hydrologic Engineering Center 1995 Annual Report.
- USACE, 1997a. Water Control Data System Requirements Specifications. USACE Hydrologic Engineering Center.
- USACE, 1997b. Mississippi Basin Model System - Development and Application, Main Report. USACE, Washington, D.C. in press.
- U.S. Army, 1989. Army Life Cycle management of Information Systems.

PROBABILISTIC HYDROLOGIC FORECASTING METHODS AND TOOLS

D. J. Epstein, Water Resources Engineer, Riverside Technology, inc., Fort Collins, Colorado; E. Welles, Visiting Scientist, Hydrologic Research Lab, National Weather Service, Silver Spring, Maryland; G. N. Day, Director, Riverside Technology, inc., Fort Collins, Colorado

INTRODUCTION

The National Weather Service (NWS) has recently undertaken a demonstration project of the new Advanced Hydrologic Forecasting System (AHFS). The four objectives of this demonstration were to provide new probabilistic long-range forecast products, to integrate long-range meteorological climate forecasts into long-range hydrologic forecasts, to include short-term quantitative precipitation forecasts (QPFs) into the hydrologic forecasts, and to demonstrate a flood inundation mapping technology. This paper will address forecasting methods and tools that satisfy the first three objectives.

The NWS forecasting activities are supported by the National Weather Service River Forecast System (NWSRFS), a continuous forecasting system that provides real-time predictions of river flows and other variables used in producing river and flood forecasts. The system includes a Calibration System (CS), an Operational Forecast System (OFS), and an Extended Streamflow Prediction (ESP) component. ESP produces probabilistic forecasts of streamflow based on the assumption that historical meteorological data are representative of possible future conditions.

The Extended Streamflow Prediction Analysis and Display Program (ESPADP) was developed as part of AHFS to analyze ESP forecasts and to incorporate both short- and long-range climate prediction and QPF products into hydrologic forecasts. Products generated in ESPADP include time series realizations of future hydrologic conditions, also called traces, probability interval plots, expected value plots, and exceedance probability plots for selected variables over varying time intervals. Together, ESP and ESPADP provide tools for forecasters to generate, review, and produce probabilistic hydrologic forecasts which can incorporate climate forecast products.

NATIONAL WEATHER SERVICE RIVER FORECAST SYSTEM

Overview: The models and databases in NWSRFS comprise a continuous, conceptually-based, lumped parameter forecasting system. Forecasts can be produced on time steps ranging from 1 to 24 hours. The River Forecast System (RFS) databases manage four types of information: (1) observed data for all stations in the data network, plus some forecast and projected values; (2) parametric data for data preprocessing functions; (3) data in time series format as needed by the models; and (4) model parametric information, rating curves, and the state variables (carryover) needed to initiate computations.

The Calibration System: The calibration system is used to develop the model parameters that are used by the models in OFS. It also uses historical point precipitation and temperature data to produce historical time series of mean areal precipitation and temperature data which are used in ESP. The input data for the calibration system comes from historical records of meteorological data. When a watershed is calibrated, these historical data are used to make simulation runs at each forecast point for the historical record. By comparing these simulations to the flows that actually occurred, the user can manipulate the parameters of the various models in order to produce the parameter set which will most accurately reproduce the outflow from the basin. These parametric data are then stored and made available to the models in the operational forecast and ESP systems.

NWSRFS includes three programs that help support the calibration process: the Manual Calibration Program (MCP), the Automatic Parameter Optimization Program (OPT), and the Interactive Calibration Program (ICP). MCP is used during initial calibration and helps the user identify effects of parameter changes on the simulation. OPT contains automatic parameter estimation programs and is used to refine the best parameter set resulting from the MCP program. ICP provides a graphical user interface (GUI) based interactive tool for trial and error calibration.

The length of record to be used for model calibration depends on the location of the watershed. However, the record should be long enough to contain climatic and hydrologic variety (extremely dry to extremely wet conditions) and

recent enough to reflect current land use conditions. Experience with the model has shown that the most recent 20 years of record is a desirable calibration period for most watersheds; however, 10 years of data often will be sufficient. The preliminary steps in the calibration procedure consist of subdividing the basin and developing the mean areal estimates of temperature, precipitation, and evapotranspiration based on historical data sets.

Unit hydrograph models are then used to determine how the outlet hydrograph responds to a precipitation event within the basin. Initial unit hydrographs are developed for each sub-basin using historical data. During the calibration process, these initial estimates are refined during the trial and error adjustment process. The final step before calibration is a water balance analysis on each sub-area. The water balance analysis calculates and compares the precipitation, runoff, and evapotranspiration for each sub-area in order to provide a final validation of the data before calibration begins.

Experience with NWSRFS has shown that the best calibration strategy involves a combination of trial-and-error and automatic optimization procedures. The recommended procedure is a three-part calibration strategy designed to overcome the disadvantages associated with the manual and automatic methods. The three parts consist of an initial stage that includes initial parameter estimation and trial-and-error calibration, an intermediate stage employing automatic parameter optimization, and a final stage of manual and/or automatic parameter fine tuning.

Model simulation runs made with the initial parameter values typically reveal significant errors between observed and simulated streamflows. Manual calibration continues until consistent differences between the observed and simulated hydrographs have been removed. The initial stage of calibration should also provide parameter sensitivity information so that parameters having little effect on the model output will not be included in optimization.

In the final stage of calibration, the manual calibration program is run for the entire period of record. Simulated and observed streamflows are compared to determine if bias is present in any particular flow range. Occasionally, additional trial-and-error or automatic optimization model runs are performed. When no bias appears in the model results, the calibration is considered complete.

The Operational Forecast System: OFS is used to make real-time hydrologic forecasts for periods extending hours or days into the future. The system consists of a number of databases, programs, and utilities that store hydrometeorological observations, processed areal time series estimates of rain and temperature, network and model parameter information, and current model states. Preprocessor functions contain the software necessary to create the mean areal time series of precipitation, temperature, evapotranspiration, etc. The hydrologic, hydraulic, and utility software that produce the forecasts in NWSRFS are called operations. An operation can be a hydrologic or hydraulic model, a time series computation program, or a statistical computation or display tool.

Operations: The calibration, OFS, and ESP components all use an operations table concept for organizing the model computations. The operations table is a control structure that allows the hydrologic models to be executed in a sequence the user determines to be best for modeling a particular watershed. An operation can be any computational algorithm that produces or modifies a time series or displays results. Operations include the following:

1. Hydrologic or hydraulic models of processes, such as snow accumulation and ablation, soil moisture accounting, temporal distribution of runoff, channel routing, or river mechanics
2. Procedures for displaying model output or computing statistics involving model output or observations
3. Algorithms that perform basic computations with time series data, such as addition, subtraction, weighting data values, and changing time intervals

The operations table concept has other advantages for streamflow forecasting. The operations table allows new and existing models and procedures to be tested in parallel; results from the new technology can easily be compared to the old. Once a decision has been made to implement a new method over an entire basin, the process can occur in an incremental fashion. Different operations can be used in different parts of the watershed area, yet the user interface remains the same. Similarly, different operations can be used in different parts of a basin due to differences in hydrologic and climatic conditions. Example operations that may be included in modeling a basin are the NWS snow model, the Sacramento Soil Moisture Accounting model, and the NWS dynamic routing model.

Interactive Forecast Program: The Interactive Forecast Program (IFP) includes a GUI that lets the user make run-time adjustments, or MODS, to the system in order to fine tune the forecast based on the user's best judgment and knowledge of the watershed. This interface provides the user with information necessary to make decisions about the accuracy of the forecast and the capability to quickly and easily put those decisions into action.

The IFP displays include more than just a sub-basin hydrograph. A table of the plotted hydrograph values is provided, along with a map of the sub-basin boundaries and a schematic diagram showing the connectivity of the sub-basins. This schematic diagram shows the identifier of each sub-basin in a box. The color of the box represents the flow status of the main river in the sub-basin. When the forecasted stage or discharge in the river exceeds a predefined flood thresholds, the box changes color to immediately warn the user of the flow conditions. A similar situation can be enabled to warn of low flow occurrences.

The steps involved in preparing a forecast include:

- Storing real-time data on the appropriate databases
- Creating mean areal time series of precipitation and temperature
- Running the OFS programs to update current watershed states
- Running IFP to produce forecasts, display results, and make adjustments

Extended Streamflow Prediction: The ESP system uses the CS historical time series data and the OFS parameters and current conditions to produce long-range probabilistic hydrologic forecasts for user-specified periods. Implementation of ESP was a key element of the success of the AHPS demonstration project. ESP is linked to OFS and CS by databases and basin parameters. ESP uses the basin and network parameters and the current watershed states from OFS combined with the historical time series of precipitation, temperature, potential evapotranspiration, and river data from CS.

Simulations in ESP start with the current watershed states from OFS. The historical meteorological data time series are then applied to the basin, with each year of historical data producing a simulation trace. If, for example, 40 years of historical data are available, 40 individual traces would be generated, each trace conditioned on the current watershed states. These 40 traces can then be analyzed to produce probabilistic forecasts about watershed conditions ranging from 1 day to 1 year in the future based upon today's watershed states.

EXTENDED STREAMFLOW PREDICTION ANALYSIS AND DISPLAY PROGRAM

Objectives: ESPADP was designed and developed to provide a tool that would enhance the capability of NWS river forecast centers (RFCs) to produce accurate, extended water resources forecasts and increase user confidence in and understanding of probabilistic forecasting methods.

Overview: ESPADP is an analysis package designed to provide statistical and graphical analysis of time series data in general, and of ESP time series in particular. The package is intended to meet the needs of operational forecast hydrologists by providing meaningful data analysis and forecast products. ESPADP runs either through a GUI or in a command line batch mode. Both methods allow for interface with time-series data of a wide variety of type, duration, and time step. Temperature, precipitation, river stage, streamflow, and reservoir pool elevation are just a few of the data types that can be processed. Functionality within ESPADP allows for the development of custom analysis and for the inclusion of climatic forecast products within the hydrologic forecast. Users can compare model simulations (conditional simulations), calibration simulations (historical simulations) with observed data sets, and statistics over identical analysis and time intervals.

Analysis Tools: ESPADP provides a wide array of analysis capability. Data can be read in from ESP output or from ASCII file formats. Because of the probabilistic nature of ESP output, time series are broken up into sequences of realizations. ESP might be used to provide a forecast over 90 days using as many years of historical data as necessary. ESPADP processes each year of simulation as an independent trace. *Figure 1* presents the ESPADP analysis window with 43 years of traces originating from an ESP analysis. The traces, commonly referred to as a spaghetti plot, represent possible realizations of river stage at 14th Street in Des Moines, Iowa. The forecast period

covers December 9, 1996 to September 9, 1997. The analysis window can be shortened depending upon the forecaster's chosen products or analysis.

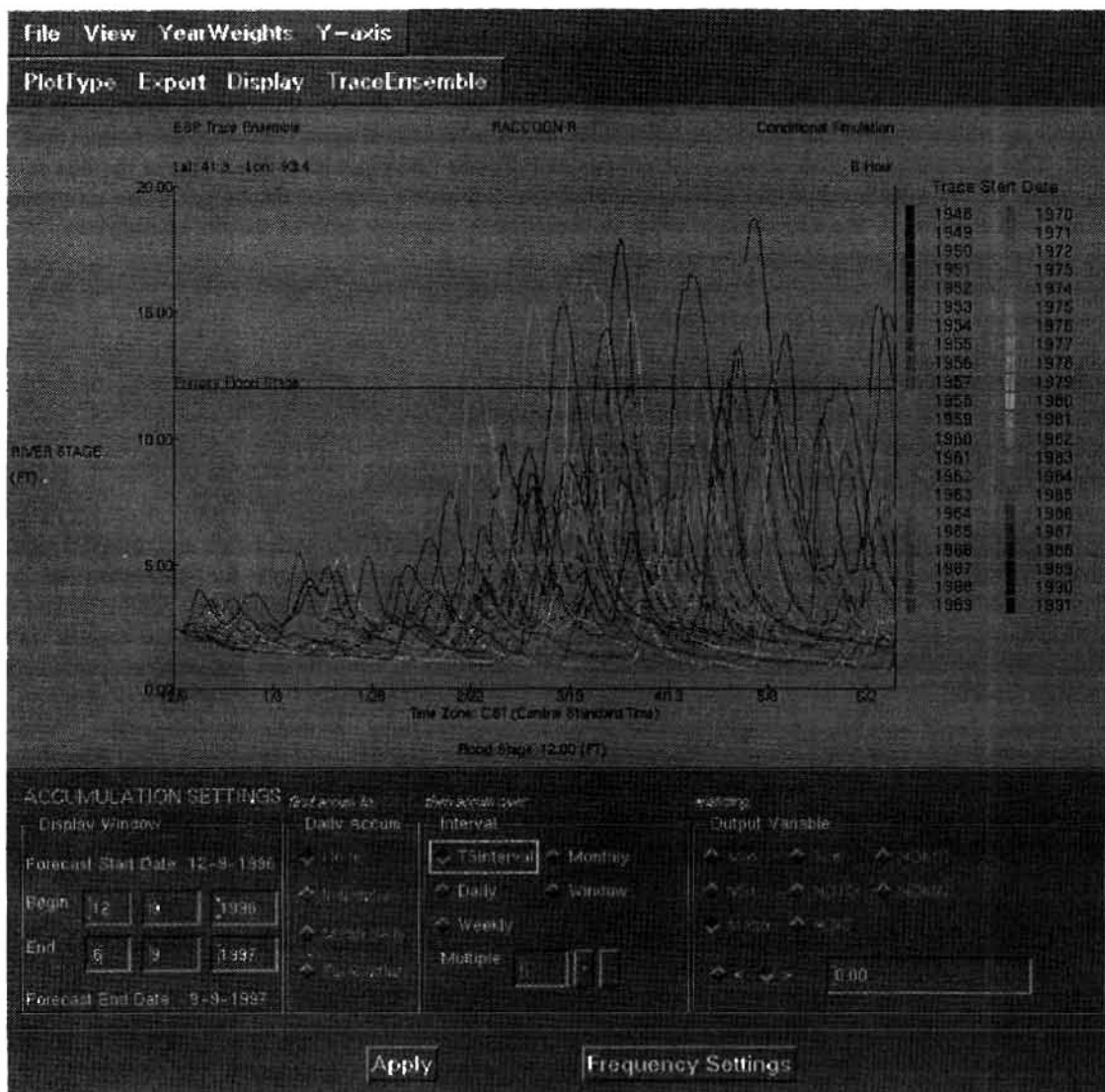
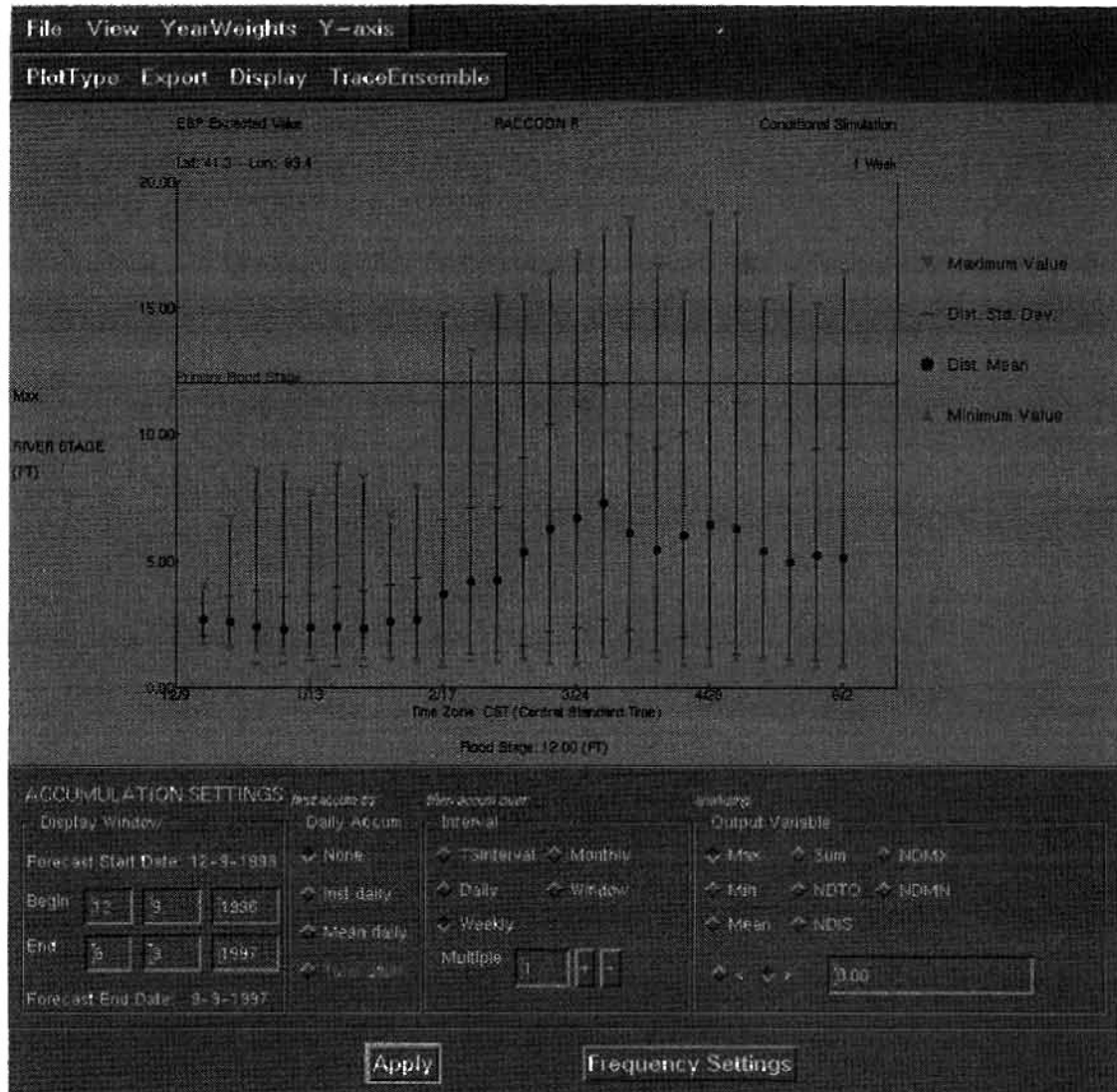


Figure 1. ESPADP Trace Display Shell - 14th Street Des Moines, IA
(Forecast period Dec. 9, 1996 to Sept. 9, 1997 using 43 years of historical data)

Data can be aggregated to larger time steps for analysis purposes. For example, hourly data can be processed to daily, weekly, or monthly time steps, some multiple of each, or it can span the entire forecast period. Analysis variables could include minimum values over some interval, maximum values, mean values, instantaneous values, accumulations (total values), the number of days to a maximum value, the number of days to a minimum value, the number of days to some threshold value, or the number of days below or above some threshold value.

Simple statistics over the ensemble of traces can be generated in an expected value plot (*Figure 2*). Minimum, maximum, mean, and standard deviation statistics are shown over the ensemble of years corresponding to each analysis variable over a specific interval. In *Figure 2*, the results were produced by first aggregating the data to weekly maximum stage values and then computing the statistics for each interval across the ensemble of traces.



**Figure 2. ESPADP Expected Value Plot - 14th Street, Des Moines, IA
(Statistics of weekly maximum river stage)**

Probability interval plots can be generated to capture some of the risk-based analysis required in probabilistic forecasting. The ensemble of traces over each analysis variable and user-specified interval can be converted into a distribution with exceedance probabilities displayed as a histogram. *Figure 3* shows the same 14th Street maximum stage variable broken out across 5 probability intervals. This example uses an empirical distribution for the analysis. Other distributions can be examined as well, including normal, lognormal, and wakeby distributions. From analysis such as this, information about risk of exceeding flood stage at a forecast point can be provided to decision makers.

Subsequent analysis allows the user to focus on a single analysis interval and examine, in detail, exceedance probability plots. These plots provide a picture of the risk over an interval across all exceedance probabilities within the current distribution. *Figure 4* details the exceedance probability plot at 14th Street examining maximum stage for an entire 60-day period. The relative shape of this curve details the relative risk of exceeding different river stages. Comparing historical calibration simulations with observed data provides measures of model bias. Bias can be adjusted in a regression-based, post-processing technique. The presence of consistent large bias in the results may be an indication that model recalibration is needed.

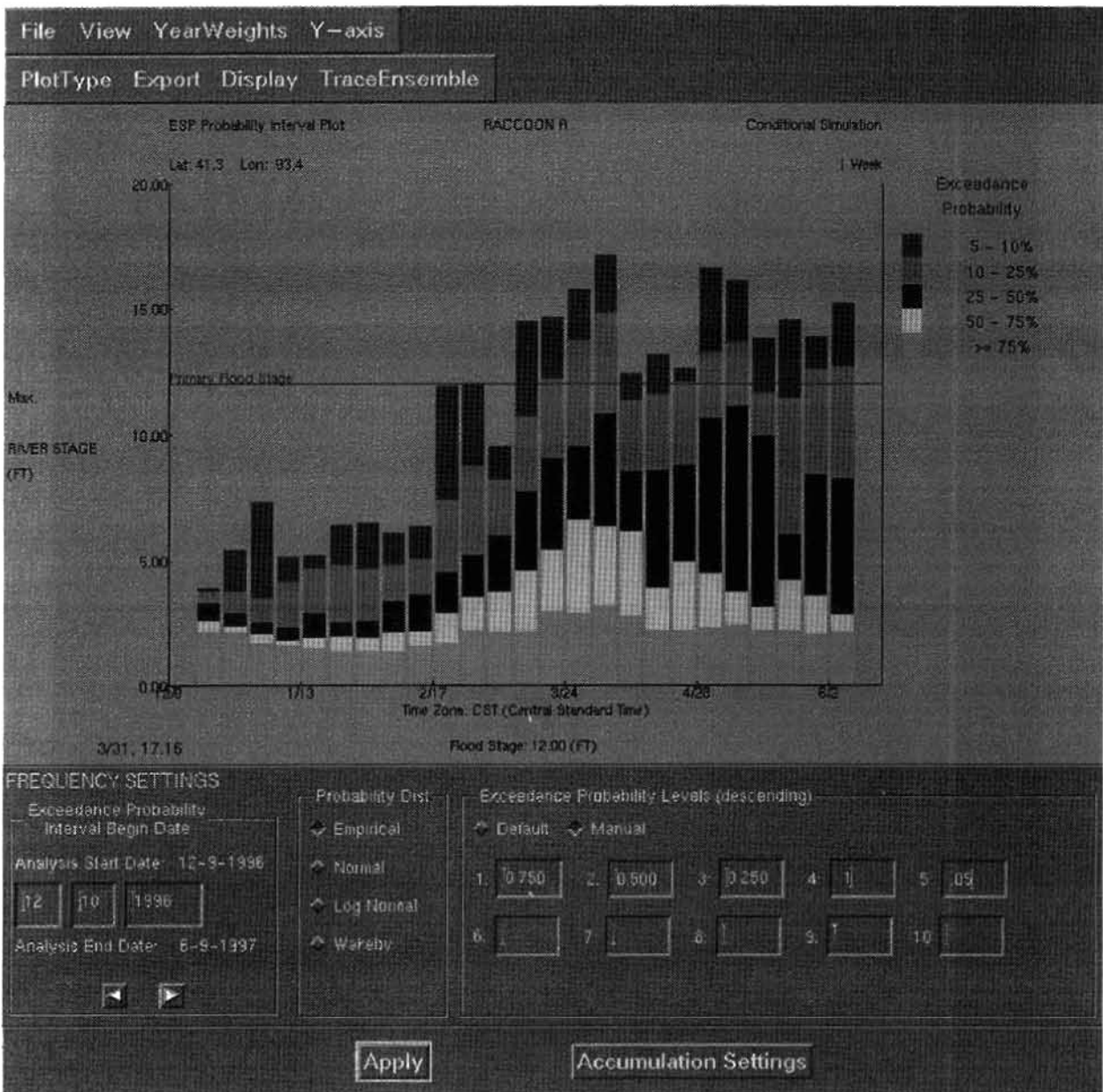


Figure 3. ESPADP Probability Interval Histogram - 14th Street, Des Moines, IA (Forecast of weekly maximum stage at 5 probability intervals)

Climatological Adjustments: Conditional simulations capture the climatology realizations based on initial model conditions at a given point in time. Through the ensemble of traces, the forecast represents what the hydrology might look like under each realization (or year) of historical climatology given current hydrologic conditions. It would be desirable to be able to condition the climatic input to the model based on a forecaster's assessment of future climate. If forecasters think that a subset of historical years might be more representative of future climate, they would like to be able to take advantage of that knowledge. ESP and ESPADP give the user several mechanisms to incorporate estimates of future climate into hydrologic forecasts.

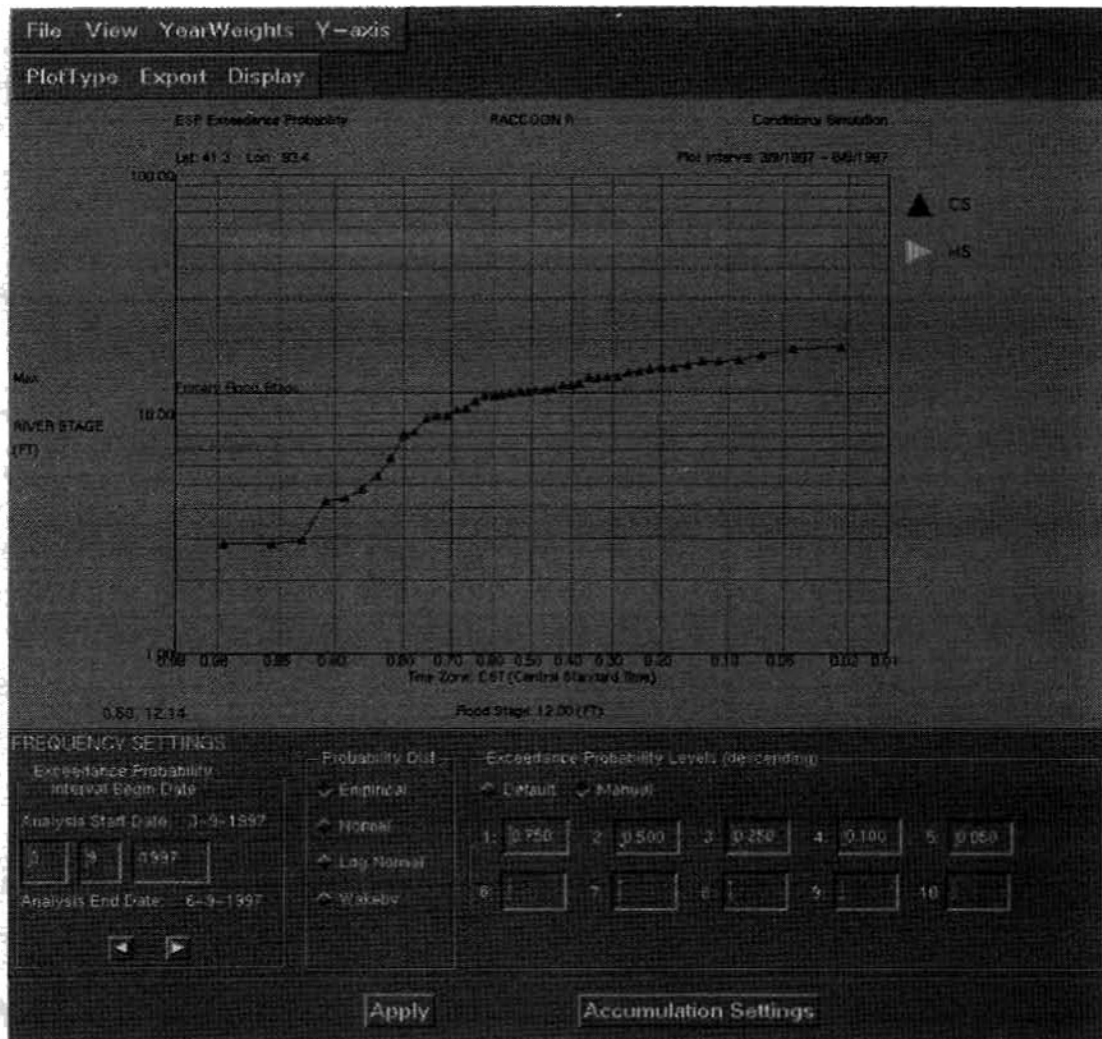


Figure 4. ESPADP Exceedance Probability Plot - 14th Street, Des Moines, IA (60-day forecast, March 9, 1997 to June 9, 1997, a maximum river stage exceedance probability)

First, ESPADP allows a QPF to be included directly into the conditional simulation. Within the simulation, the QPF is blended with historical precipitation for the short-duration precipitation forecast using adjustable blend parameters. The blending period provides a smooth transition between future values and the historical data. *Figure 5* shows the QPF blend parameters and how they are adjusted in ESPADP.

Next, ESPADP offers a mechanism to manually weight historical years. Using the entire historical period of interest, the user can define weights for each year depending upon an estimate of likelihood of occurrence. These weights are normalized, then incorporated into subsequent analysis of the ensemble of traces. Year weighting would help condition the hydrologic forecast to El Niño signatures by excluding or weighting historical years differently. Seasonal snowmelt forecasts can be shaped by forecaster knowledge of historical snowpacks, and temperature and precipitation patterns.

An additional year weighting technique, developed in the Alaska River Forecast Center, involves generating year weights based upon a monthly forecast from the Climate Prediction Center (CPC). Forecast shift anomalies are used to offset a distribution of the historical data. Conditional distributions for precipitation and temperature are used to compute year weights based on relative probabilities of occurrence in the current year.

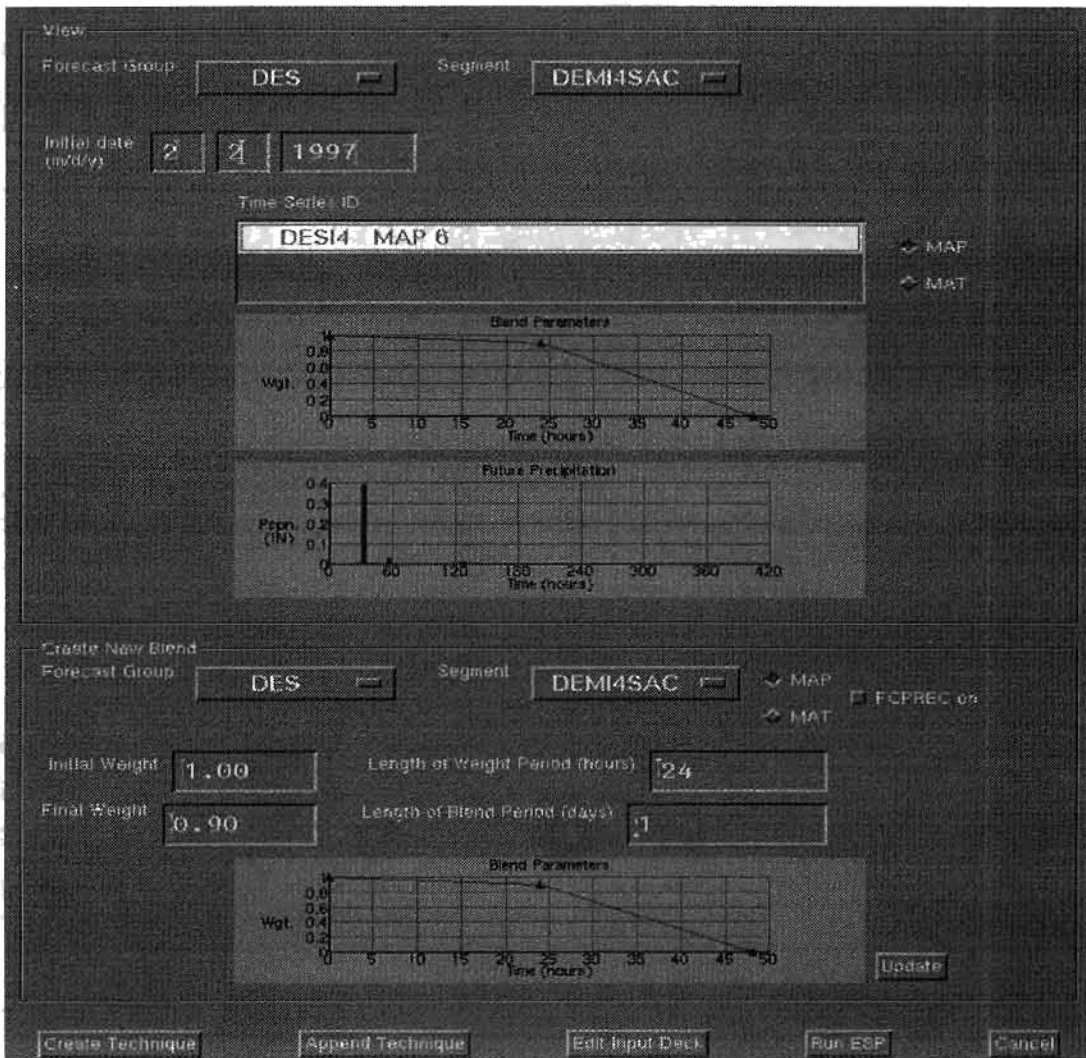


Figure 5. ESPADP QPF Interface To Adjust Weight And Blend Parameters For Future Precipitation

The year weighting techniques previously described are post-analysis techniques. ESP traces are generated and then conditioned upon knowledge of the future climate. An additional method was developed for incorporating CPC forecast information into ESP forecasts by modifying the input climate time series. In the pre-adjustment technique the historical precipitation and temperature data are adjusted based on the HPC 1- to 5-day forecast, the CPC 6- to 10-day forecast, and the CPC long-lead monthly and seasonal outlooks. This adjustment technique can be run to generate a new set of conditioned temperature and precipitation time series which are then used in ESP simulations.

CONCLUSIONS

As part of the AHPS demonstration project, the NWS has implemented tools and methods to help operational forecasters develop probabilistic hydrologic forecasts. Tools such as ESP and ESPADP allow the forecaster to include both short-term QPF and longer-term forecasts such as CPC 1-5, 6-10, monthly and seasonal forecasts into the hydrologic forecast. While hydrologic forecasting will never be an exact science, these tools and methods are helping forecasters provide more meaningful, probabilistic products that are appropriate for risk-based decision making. As longer-term climatic prediction techniques continue to improve, hydrologic forecasters will be able to better incorporate additional skill into the hydrologic forecasts.

APPLICATION OF A CONTINUOUS SIMULATION WATERSHED MODEL FOR NEAR REAL-TIME FLOW FORECASTING AND DAM OPERATION

By H. Vernon Knapp, Senior Hydrologist, State Water Survey, Illinois Department of Natural Resources,
Champaign, IL; William W. Rice, Engineering Studies Unit Manager,
Office of Water Resources, Illinois Department of Natural Resources, Springfield, IL

INTRODUCTION

The Fox Chain of Lakes and the Fox River, located 40 miles from Chicago in northeastern Illinois, have long been popular for boating, fishing, and other recreational activities. Over the years there has been considerable residential development along most of the flat shores of the lakes and river, thus floodwater levels have become an issue of great concern. During the warm season, high water levels also restrict recreational boating, which provides a valuable economic resource to the area. Stratton Dam, located on the Fox River seven miles downstream of the Chain of Lakes, partially controls the outflow of water from the lakes. The primary function of Stratton Dam has been to maintain the recreational pools in the lakes, but flood control management has become an increasingly important secondary function. Figure 1 shows the location of the dam, the Chain of Lakes, the watershed upstream of the lakes, and the hydrologic monitoring network.

The flow in the Fox River is sluggish, even during flood conditions. The average slope for most of the river's length is less than 0.5 feet per mile, and there is a considerable amount of off-channel storage of water. The time to peak following a uniform rainfall over the watershed is 3 to 4 days, but a substantial quantity of flow originating in the northern part of the watershed continues for an additional week. Most floods have composite hydrographs, combining successive rainfall/runoff events. Flood conditions are most common in early spring, and many of the largest flood events have occurred from a combination of rainfall and snow melt.

Previous analyses have indicated that the use of flow forecasting can have important benefits for reducing flood damages for the Chain of Lakes. Application of an unsteady flow routing model for the Chain of Lakes (Knapp and Ortel, 1991) has indicated that, with an advanced warning of an approaching flood, Stratton Dam could be operated to reduce lake levels by up to 0.5 foot prior to the arrival of most of the floodwaters. This would lead to a nearly equivalent reduction (0.4 foot) in the peak stage for major floods. This relatively small decrease in the peak stage produces a significant reduction in flood damages.

Most applications of flow forecasting systems make predictions of flow conditions for lead times of less than 24 hours, employing real-time data collection systems for measuring precipitation and streamflow, and preparing forecasts within minutes or hours after a rain event. Given the watershed characteristics and hydrodynamics of the Fox River, there is a greater need for longer flow forecasts, for as much as one week in advance. An existing continuous simulation watershed model of the Fox River basin (FRHM), developed at the Illinois State Water Survey (Knapp, et al., 1991), was modified for use in developing these forecasts. Parameter adjustment procedures were developed to more closely match model output with observed flows, thereby giving the model a near real-time forecast capability. The FRHM forecast is developed using the preexisting network of streamflow and precipitation gages. Two of the stream gages, at New Munster and Spring Grove, are located immediately upstream of the Chain of Lakes, and collectively measure flow from 80% of the watershed. Model calibration and parameter adjustment procedures focus on matching the observed flow at these two gages.

Given the hydrologic response of the watershed, it is possible to create forecasts the day following a precipitation event and still take advantage of most of the flood reduction capability provided by dam operation. By using precipitation data that has been measured within a 24-hour period, termed as *near real-time forecasting*, more common daily precipitation gages can be used to provide input into the model. These daily precipitation gages can provide a more complete coverage of total precipitation over the watershed with less need for installing a network of recording precipitation gages with telemetry.

This paper presents three aspects of the development and application of the model: 1) the parameter adjustment procedure used in forecasting, 2) use of available precipitation data for creating the flow forecast, and 3) the use of the forecasting results in the decision making process for operating the dam.

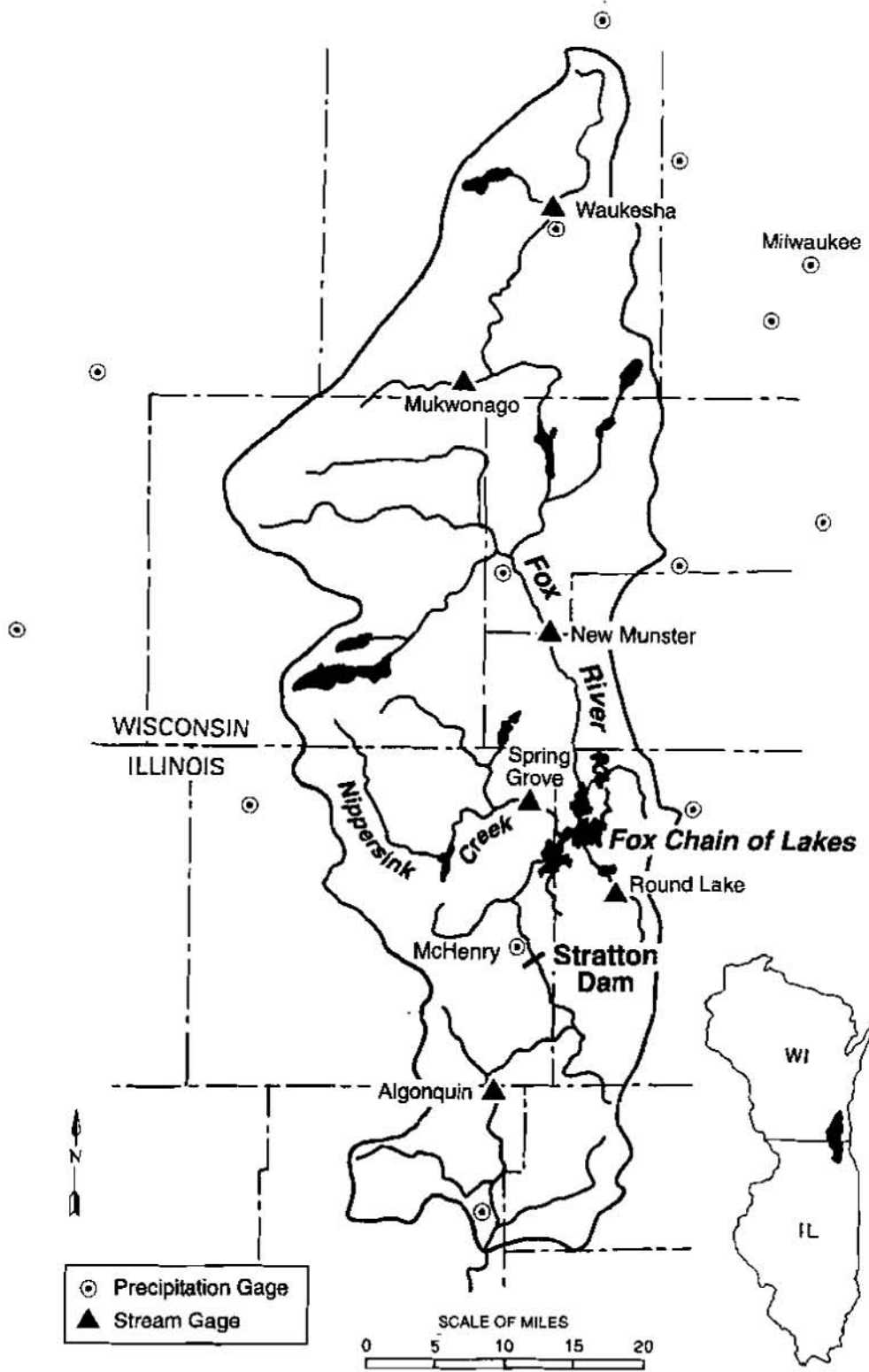


Figure 1. Location of the Fox Chain of Lakes and monitoring network

PARAMETER ADJUSTMENT PROCEDURE

Predicting the amount of streamflow associated with a given precipitation event (or set of events) is intrinsically an uncertain process. Even if accurate estimates of precipitation and other contributing climatic factors were available over the watershed, hydrologic prediction models would be unable to replicate all the complex responses that result in the generation of streamflow. Thus, the predicted streamflow amount will to some degree always differ from the coinciding observed flow in a stream.

Four basic errors can lead to an incorrect flow forecast: 1) inadequacy in the model's conceptual structure, 2) error or variation in the estimation of appropriate model parameters, 3) streamflow and precipitation measurement errors, and 4) error in estimating the average watershed precipitation, or other climatic variables, from point observations. The impact of any of these errors in the modeling process is persistent, such that an error that affects today's (or this hour's) streamflow prediction will also likely affect flow predictions for a limited amount of time into the future. The adaptive approach in modeling uses this persistence characteristic to improve the estimation of future flows. By adjusting the model parameters to more accurately portray the present flow conditions, it is expected that the same adjustment will reduce model error as applied to the short-term flow forecasts.

Emphasis was placed on identifying the type of hydrologic condition being simulated at any one time and the set of model parameters that can most effectively address the model error under this condition. This identification process was conducted using a manual process for adjusting parameters over portions of the historical flow record. The model operator was able to determine the parameters that would most efficiently produce the desired modifications and also make "hydrologic sense" given each set of circumstances. Also, by focusing on the most appropriate parameters for a given situation, the adaptive process required a relatively small number of iterations, with the potential for being more time-efficient for used in an operational framework.

Four parameters were identified as being most efficient in model adjustment over the range of all flow conditions: 1) BFADJ, which adjusts the baseflow release rate from the upper and lower subsurface storage, 2) SMXADJ, which adjusts the amount of infiltration and rainfall excess from a rain event, 3) SMULT, which adjusts the ratio that separates subsurface seepage going to interflow versus groundwater storage, and 4) TFADJ, which adjusts the average daily air temperature, which determines the separation of rainfall and snowfall during winter precipitation events, and influences the rate of snowmelt and ground thaw. Initially, there were no adjustments made that would alter the mass balance of water within the model, i.e. state variables such as soil moisture and groundwater storage were not adjusted. Thus, the integrity of the moisture accounting within the continuous simulation model could be maintained. This limitation was eventually considered too restrictive, and was relaxed to permit storage adjustments following extended periods of forecast overestimation or underestimation. Adjustments in precipitation amounts are also being considered in limited cases where parameter adjustment is ineffective.

For automated adjustment of parameters it is necessary to develop and use: (a) a mathematical routine to optimize the set of parameter values, (b) a set of rules to define which parameters to change and the magnitude of the modification, preferably in combination with, or (c) a combination thereof. The experiences in manual calibration suggested that use of optimization techniques alone would likely be inefficient and difficult to employ. An automated process was developed that uses a set of rules developed by the model operators to modify parameters. It is desirable that nonlinear optimization algorithms be added in the future, in combination with the existing set of rules, to reduce the number of iterations needed to arrive at an optimal set of parameters. As with most watershed model calibrations, there is generally no unique solution (or set of parameters) when adjusting parameters. The goal in parameter adjustment, therefore, is to come up with a credible set of parameters that cause the simulation error to be less than a set threshold value.

The magnitude of the reduction in the forecasting error associated with the manual and automated parameter adjustment processes has not been fully analyzed. However, several conclusions can be reached. First, the automated parameter adjustment process is not as reliable as manual adjustment for matching observed streamflows. Second, a model's operator should have routine experience its forecast applications and parameter adjustment procedures to most effectively use the model during flood events. Third, for best results the watershed upstream of the New Munster gage should not be adjusted in a lumped manner. Thus, the addition of one or two stream gages with telemetry upstream of New Munster would greatly improve the forecasting procedure, and may thereby reduce the dependence on manual adjustment.

EVALUATION OF PRECIPITATION DATA FOR USE IN FLOW FORECASTS

There are three basic categories of precipitation available for use in flow forecasting using the FRHM model: 1) that measured at precipitation gages located in and near the watershed; 2) precipitation estimated from radar data; and 3) quantitative forecasts of expected precipitation during the next 24- to 48-hours. The two basic concerns when analyzing the usefulness of precipitation data are the accuracy in both the precipitation data and the resulting streamflow forecast, and the lead time of the forecast. The precipitation gaging network provides accurate rainfall at the point of measurement, but only a few gages have telemetry and there may be a one-day delay before most other data is available. There is also the concern of whether this location-specific data provides the best spatial estimate of watershed precipitation. Radar-based data can provide a spatial estimate of the precipitation in a timely manner, but may lack the accuracy of gage measurements. The use of quantitative precipitation forecasts provide the greatest amount of lead time, but can introduce considerable uncertainty into the streamflow forecasting process.

Present Precipitation Gaging Network. Figure 1 presents the location of precipitation gages in and near the Fox River watershed that are active as of August 1997. Two additional gages, New Munster and Spring Grove, are located at USGS stream gages and provide real-time data during the warm season of the year. The Milwaukee and McHenry gages are recording gages which provide year-round, real-time data. The other gages shown in Figure 1 are measured daily.

For the eastern and southern portions of the Fox River watershed, the available gages provide precipitation data for roughly every 50 to 100 square miles, considered a good density of coverage for a watershed this size. In the northern and western portions of the watershed, in Wisconsin, the gage density is reduced to about 200 square miles per gage. Obtaining additional rainfall data from the central and western portions of the watershed should be a priority for developing accurate forecasts, as the estimation of watershed precipitation usually produces one of the largest errors in the flow forecasting process. It can also be expected that any errors in estimating the watershed precipitation will be magnified when calculating runoff. A doubling the number of gages in this region should reduce the error in the precipitation estimate by about 50%, as estimated by both Fontaine (1991) and Huff (1970).

Evaluation of Available Radar-based Precipitation Estimates. Radar-based precipitation (RP) estimates for the northeastern Illinois and southeastern Wisconsin area were obtained for the period August 1995 through May 1997. Twenty-four hour precipitation estimates were obtained to match the daily rainfall amounts available at most rain gages. RP estimates for over 50 precipitation events were gathered. Nineteen events, having either measured precipitation amounts or RP estimates in excess of 0.5 inches, were used in the following analysis.

The RP estimates and measured rainfall were compared for six gaging locations in or near the Chain of Lakes watershed. The average ratio between the RP estimate and the measured precipitation (defined as the radar/gage or R/G ratio) for the selected 19 events and 6 gaging locations was 1.78. The RP estimates overestimated the measured precipitation in 78 percent of the gage comparisons. Variations in the R/G ratio between gages do not appear to be related to distance from the radar or any other easily-identified geographic pattern. The tendency for the RP to overestimate precipitation was greatest during summer events (June through August), with an average R/G ratio of 2.14. The RP underestimated precipitation during the winter season (November through February), with a ratio of 0.88. This winter ratio matches closely with the findings of Fortune et al. (1995) for cool-season stratiform events in northeastern Illinois. R/G ratios for the spring and fall seasons were 1.53 and 1.94, respectively.

Table 1 compares the radar precipitation estimates with the observed precipitation for the six largest storms for which complete data were obtained. In most cases the RP estimates give a reasonable representation of geographic differences in the rainfall, even when the absolute magnitude of the RP estimates may be poor. The average R/G ratio for these six large events, 1.82, is not much different than the ratio for all storms.

Example of Error in the Flow Forecast using RP Estimates. The FRHM Model was used to produce flow forecasts for the May 10, 1996 event using: 1) RP estimates, 2) measured precipitation, and 3) the RP estimate adjusted using observed data from two real-time precipitation gages. In Figure 2, the flow forecasts using these two types of precipitation data is compared with the observed streamflow at the Fox River near New Munster. In general, the flow forecasts based on the measured rainfall compare favorably with the observed flows. The RP estimates are considerably higher than the measured precipitation. Thus, the flow forecasts using the RP estimates significantly overestimate the eventual observed flow.

Table 1. Comparison of Radar-Based Precipitation Estimates (RP) and Measured Precipitation (MP) for Six Major 24-Hour Events

Precipitation gage	August 29, 1995			May 10, 1996			July 18, 1996		
	RP (inches)	MP (inches)	R/G ratio	RP (inches)	MP (inches)	R/G ratio	RP (inches)	MP (inches)	R/G ratio
Mt. Mary College	1.5	1.85	0.81	2.2	0.86	2.56	2.5	0.48	5.21
Oconomowoc	2.2	0.71	3.10	2.0	0.93	2.15	2.0	0.66	3.03
Burlington	2.0	0.84	2.38	2.0	1.70	1.18	4.0	1.43	2.80
Harvard	1.0	0.19	5.26	2.5	1.44	1.74	3.0	1.89	1.59
Lake Villa	1.0	0.66	1.52	3.0	1.93	1.55	5.0	3.11	1.61
McHenry	0.6	0.22	2.73	2.5	1.66	1.51	3.0	2.20	1.36

Precipitation gage	October 17, 1996			February 21, 1997			May 1, 1997		
	RP (inches)	MP (inches)	R/G ratio	RP (inches)	MP (inches)	R/G ratio	RP (inches)	MP (inches)	R/G ratio
Mt. Mary College	0.8	0.51	1.57	1.0	1.02	0.98	0.9	0.94	0.96
Oconomowoc	2.0	1.13	1.77	1.3	1.41	0.92	1.0	1.20	0.83
Burlington	1.5	0.41	3.66	1.3	1.13	1.15	1.0	0.97	1.03
Harvard	1.5	0.91	1.65	1.3	1.43	0.91	1.0	0.87	1.15
Lake Villa	1.0	0.76	1.32	1.5	1.70	0.88	1.2	1.51	0.79
McHenry	1.0	0.51	1.96	1.5	2.06	0.73	1.0	0.96	1.04

Based on the present operation guidelines, the inflow forecast for the Chain of Lakes using the May 10 radar precipitation would be almost great enough to warrant the onset of flood operations at Stratton Dam. In other words, this would be close to creating a "false alarm," incorrectly estimating that flood conditions were impending. As shown in Figure 2, the accuracy of the flow forecast simulation using the RP estimates is much better when adjusted using additional "ground-truthing." In this example, the Milwaukee and McHenry precipitation gages were used to adjust the RP estimates. The use of only two gages to adjust the R/G ratios for the entire watershed was designed to most closely reproduce the present real-time forecasting capability of the watershed. As more measured

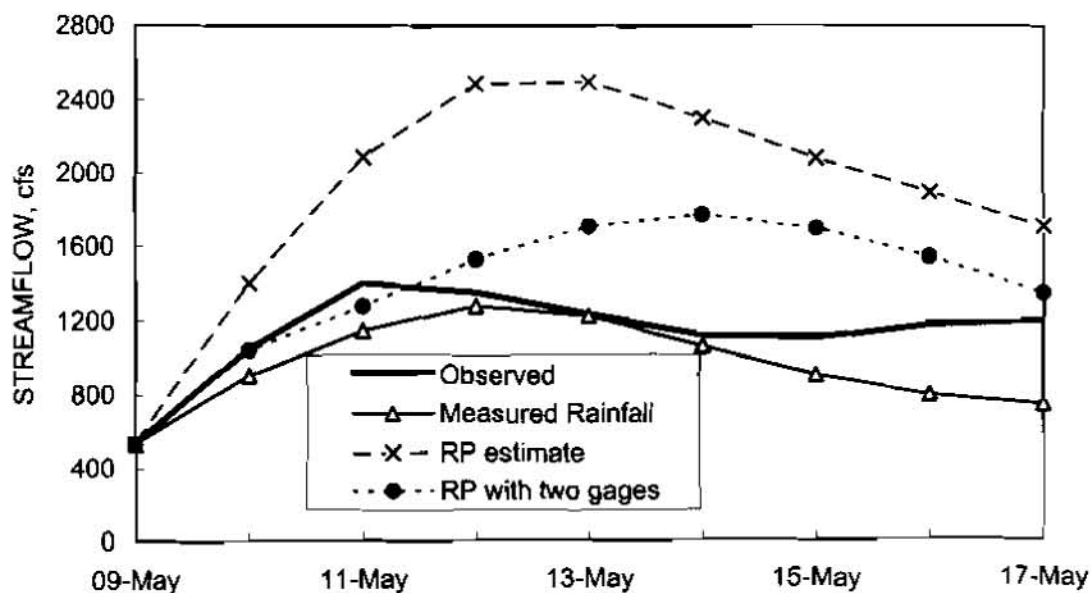


Figure 2. Forecasted and observed flows for the Fox River near New Munster; May 9-17, 1996.

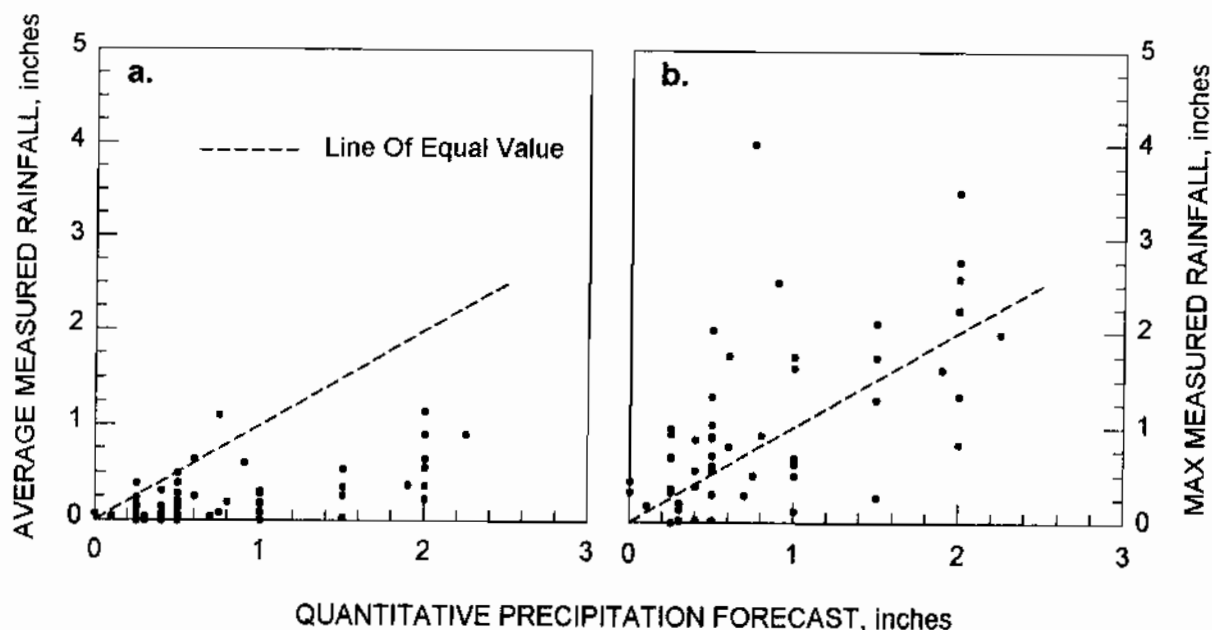


Figure 3. Comparison of QPF estimates with: a) Average, and b) Maximum Measured Point Rainfall.

precipitation data is used, the flow forecasts using the RP data more closely approach the observed flow values. However, the RP flow forecasts did not have similar accuracy to that produced using measured precipitation until five gages were used, providing a broad geographic coverage of the watershed. It is anticipated that future improvements in RP estimates may change this evaluation, and their utility in flow forecasting should be reexamined as these improvements occur.

Evaluation of the Quantitative Precipitation Forecasts. The 24-hour and 48-hour quantitative precipitation forecasts (QPFs), produced by the National Centers for Environmental Prediction (NCEP) of the National Weather Service, were obtained for selected precipitation events from the period April 1992 through May 1997. The QPF generally gives little spatial resolution across the Chain of Lakes watershed, therefore one value was always used as the average expected rainfall for the watershed. In general, measured daily precipitation is compared with the 24-hour QPF. In a few cases when precipitation occurred on consecutive days, the comparison was made between the two-day measured amounts and the 48-hour QPF. A total of 47 storms were evaluated, 25 of which were above 1 inch as either measured from any one rain gage data or as estimated from the QPF. The maximum QPF value in this sample was interpolated to be 2.25 inches. The maximum observed point rainfall in these storms was 4 inches, and the maximum average precipitation over the Fox River watershed for a single storm was 1.2 inches.

Figure 3 compares the QPF for these 47 storm events with the a) average measured watershed rainfall, and b) the maximum measured point rainfall. The average measured watershed precipitation was computed as the unweighted mean of all point rainfall estimates in and adjacent to the Fox River watershed. The values show that the QPF significantly overpredicts the watershed precipitation. For example, when the QPF is 2 inches, the average expected watershed precipitation is only 0.7 inches. The QPF underpredicts the watershed precipitation in only four cases, and in only one of these cases was the average measured watershed rainfall greater than 1 inch. The QPF corresponds much closer to the maximum point rainfall observed within the watershed, as shown in Figure 3b. Even then there is a considerable amount of scatter between the QPF and measured rainfall values, with an average difference of almost 60%.

The QPFs generally indicate the potential for heavy rainfall, and the possible maximum point rainfall to be expected from a storm, which can be useful for qualitative evaluations of flood potential. QPFs are most useful for forecasting situations which require short lead times. But at present, the QPFs do not provide sufficiently accurate estimates of the expected watershed precipitation to be used for major operation decisions at Stratton Dam, such as those that could cause downstream flood damages.

USE OF THE FLOW FORECASTS IN DAM OPERATION

The flow forecasts can be used for operation decisions in the two following manners. First, the flows can be used as input in an unsteady flow routing model (FEQ) that was developed for the Chain of Lakes, to predict the eventual stage of flooding and examine the impact of various operation policies. This use is highly dependent upon the parameter adjustment process, since flows predicted by the FRHM model must closely match observed conditions. The second use of the flow forecasts is as an indicator to predict the probability that flooding conditions will occur, thereby triggering a predetermined response for flood control operations. The second of these uses is discussed below. The estimation of flood probability currently uses the unadjusted flow forecasts, since the potential impact of parameter adjustment on this estimation has not yet been fully evaluated.

Schemes for dam operations are necessarily based on the probability of certain events occurring or not occurring, since none of the available information provides perfect foresight of future conditions. A primary goal in flood control operations at Stratton Dam is that the estimation errors do not cause flood damages above that which would occur without the use of the flow forecast. There is no vital need for the forecasting system to provide evacuation warnings, and the overall reduction of flood levels is the primary operation objective.

Flood forecasting terminology normally defines three categories of success or failure of the forecasting system: hits, misses, and false alarms. A "hit" is a flood that is properly forecasted as an oncoming flood event, a "miss" is a flood event that is not forecasted to reach flood levels, and a "false alarm" is an event that is forecasted to be a flood, but does not reach flood levels. For Stratton Dam operations, a false alarm is a potentially more harmful outcome than a miss. In the case of a false alarm, it is possible that the gates could be opened in advance of the expected flood waters, causing downstream flooding in situations where flooding would not have otherwise occurred. In the case of a miss, it is expected that the flood control operation at Stratton Dam will precede in essentially the same manner as it did without the use of the flow forecast system. Thus, while there is no advantage gained by such a forecast, there is no additional damage caused.

Relationship between the Flow Forecast Peak and Expected Flood Levels. Flows in the Fox River watershed were simulated for the 48 year period, 1948-1996, using the FRHM model. The unadjusted simulated flow values are used as surrogate values for the flow forecasts that would have been available in the days preceding flooding events. Over the 48-year period, there are 31 flooding events in which the peak stage in the Chain of Lakes exceeds the flood stage of 738.5 feet. In eighteen events, the peak stage exceeded 739.0 feet, and there are nine major flood events in which the level in the upper lakes equaled or exceeded 740.0. The duration of flooding has ranged from one day up to 39 days.

Table 2 shows the relationship between the peak discharge of the flow forecast and the maximum flood stage eventually observed in the Chain of Lakes. In all twelve historical cases when the forecast inflow peak exceeds 7000 cfs, the upper lakes exceed the flood stage of 738.5 feet, and in 10 of the 12 cases, the eventual flood stage exceeds 739.0 feet. As the magnitude of the inflow forecast decreases, the relative certainty of oncoming flood conditions also decreases. When the forecast peak is between 6000 and 7000 cfs, there is only a 70% chance that flood conditions will also arrive.

An examination of Table 2 indicates that in every case when the flow forecast exceeds 5000 cfs, the level in the upper lakes can be expected to exceed 738.0 feet. Based on historical operation practices, whenever the upper lakes reach an elevation of 738.0 feet, the outflow from Stratton Dam is increased to approximately 3000 cfs, which is the maximum outflow that will not cause downstream flood damage. Thus, it is recommended that the gate openings at the dam be increased to release 3000 cfs whenever the flow forecast exceeds 5000 cfs. Given this flow forecast there is a 70% probability that flood conditions will eventually develop, and by opening the gates early the lake storage can be reduced slightly, with the potential benefit of lessening or avoiding future flood damages.

Table 3 shows the relationship between the threshold value used to identify an oncoming flood event and the number of hits, misses, and false alarms created using that threshold value. Use of a higher threshold flow value (7000 cfs) for gate operations will provide for a conservative use of the flow forecast model but will assure that there are no false alarms. This conservative policy would still correctly anticipate of all major floods, even though fewer than half of all historical flood events would be forecasting "hits." Use of a more aggressive operation policy, using a lower threshold value, would increase the probability that gates were opened early for all flood events, but

Table 2. Probability of Flooding on the Chain of Lakes based on the Forecast's Peak Flow.

Flood stage in the Chain of Lakes is 738.5 feet

Peak discharge of forecast (cfs)	Maximum water level of flooding		
	>738.0	>738.5	>739.0
>7000	100%	100%	83%
6001-7000	100%	70%	50%
5001-6000	100%	69%	25%
4501-5000	67%	8%	0%
4001-4500	75%	12%	0%
3501-4000	68%	0%	0%
3001-3500	43%	0%	0%

Table 3. Flow Forecasting Success based on the Threshold Level used to Identify Flooding Conditions (when the water level in the Chain of Lakes exceeds 738.5 feet)

Threshold flow (cfs)	Hits	Misses	False Alarms
7000	12	19	0
6000	18	13	3
5000	29	2	6
4500	30	1	16
4000	31	0	31

would increase false alarms. It is recommended that the conservative forecast approach, using the 7000 cfs threshold value, be adopted until the potential flood damages of false alarms can be evaluated. Using this operation approach, all gates at the dam would be fully opened, allowing maximum outflow, whenever the forecast peak exceeds 700 cfs. Knapp and Ortel (1992) estimated that an advance warning of oncoming floods for the Chain of Lakes, forecasted within 24 hours following the observed precipitation, can lead to an average 0.4 foot reduction in peak levels in the Chain of Lakes for major flood events. As noted before, this stage reduction produces a significant decrease in flood damages. The average flood reduction potential for minor floods is approximately 0.2 foot.

Basic operation guidelines discussed herein include: 1) opening gates to the maximum setting when the forecast peak inflow exceeds 7000 cfs, 2) opening gates to produce the maximum outflow that will not cause downstream flood damages (3000 cfs), whenever the forecast peak inflow exceeds 5000 cfs, and 3) operating the dam following current procedures, based on observed inflows and lake stages, whenever a minor flood cannot be anticipated using the above condition. More complete dam operation guidelines using the flow forecast and existing hydrometeorological conditions in the watershed were developed and given in Knapp (1998).

REFERENCES

- Fontaine, T.A., 1991, Predicting Measurement Error of Areal Mean Precipitation During Extreme Events. *Water Resources Bulletin* 27(3), 509-519.
- Fortune, M.A., Labas, K., Westcott, N.E., 1995, Accuracy of Point Rainfall Estimates from an 88-D Radar in the Cool Season: The Illinois Experience. Preprints, 27th Conference on Radar Meteorology, American Meteorological Society, Vail, CO, October 9-13, 1995.
- Huff, F.A., 1970, Sampling Errors in Measurement of Mean Precipitation. *Jrnl. of Applied Meteorology* 9, 35-44.
- Knapp, H.V., 1998, Potential Influence of Streamflow Forecasts and Hydrometeorological Conditions on Stratton Dam Operations. Illinois State Water Survey Contract Report.
- Knapp, H.V., Ortel, T.W., 1992, Effect of Stratton Dam Operation on Flood Control Along the Fox River and Fox Chain of Lakes. Illinois State Water Survey Contract Report 533.
- Knapp, H.V., Ortel, T.W., Larson, R.S., 1991, Hydrologic Modeling of the Fox River Watershed. Illinois State Water Survey Contract Report 518.

A COMPREHENSIVE FLOW MODEL FOR FLOOD FORECAST/HINDCAST FOR TIDAL REACHES

CHINTU LAI Visiting Prof., Hydrotech Research Lab., National Taiwan Univ., Taipei, Taiwan
TSAN-WEN WANG Prof. and Assoc. Dean, Col. of Engrg., Nat'l Taiwan Univ., Taipei, Taiwan
NIEN-SHENG HSU Assoc. Prof., Dept. of Civil Engrg., National Taiwan Univ., Taipei, Taiwan
SHIANG-KUEEN HSU Director, Water Resour. Bureau, Minis. of Econo. Affa., Taipei, Taiwan

Abstract: Flow in tidal reaches is highly unsteady and the channel geometry is much complex. By describing its hydrodynamics with the St. Venant type equations, and its constituent and sediment concentrations with continuity equations, one can formulate a set of governing PDEs. Consideration of various constituent-distribution patterns gives different forms of continuity equation for constituent discharge, each reflecting different mixing patterns. These equations are subsequently transformed to a set of corresponding characteristic equations. Using the Multimode Method of Characteristics of the Second kind (MMOC-II), a comprehensive tidal flow model has been developed. The model performs its flow computation in two steps; computes the unknowns first at all junction and boundary points, and then at the interior grids reach by reach. Designed as a modular type, computational blocks for a certain numerical method can be replaced by those of other numerical methods. The model, intended for use in flood forecast and hindcast, should be built exact and precise, which is important in the real-time simulation. Because for an effective forecast the computation must start immediately with reliable initial conditions, must have sufficient computational resolution to determine accurate evacuation area and time, and so forth. The present comprehensive model can be applied to many other purposes than flood-flow simulation, and such model use is supposed to be more than just economical and efficient; for some applications it would mean performing better than a specialized model.

INTRODUCTION

Flows in estuaries and tidal reaches are exceedingly complex. As population density intensifies and industry, transportation, and other social activities congest in this area, the impact caused by natural hazards and the damage induced by human stresses multiplies. An efficient and reliable numerical model to simulate flows in tidal reaches is surely in great demand. The model must be sufficiently powerful to compute intricate estuarine flows, and also sufficiently comprehensive to simulate a variety of flows in a wide range of topographical conditions. The latter requirement is not merely for economy and flexibility, but a necessary condition for a truly workable, flood forecasting model, as may seem contrary to a common notion that a specialized program serves better for a specific task. The purposes of this study, therefore, are two fold: To develop a powerful numerical model by applying a newly derived numerical scheme; and to implement it as a comprehensive model that can serve continuously for long-term operations for varied flow regimes.

BASIC EQUATION SETS

A brief review of Lai and Wang (1995) states: If a third dependent variable, longitudinally varied fluid density, $\rho = \rho(x, t)$, is added to the original two dependent variables of the unsteady, fixed-bed, open-channel flow equations, e.g., flow depth, $h = h(x, t)$, and flow velocity, $u = u(x, t)$, a 3-unknown-3-equation system can be formulated for the movable-bed case. By further assuming different degrees of flow mixing or density stratification, can one derive four sets of unsteady open-channel flow equations for four different cases of longitudinally varied fluid density.

Flows of Well-Mixed Type: CASE I Constituents in the flow are assumed well mixed, varying only in the longitudinal direction. The three partial differential equations (PDE) are, respectively, the equation of continuity for constituent-laden flow, the equation of continuity for constituent discharge, and the equation of motion for constituent-laden flow,

$$h_t + uh_x + Hu_x + (H/\rho)\rho_t + (H/\rho)u\rho_x + (u/B)A_x^h - (\rho/\rho)(q/B) = 0 \quad (1)$$

$$h_t + uh_x + Hu_x + H/(\rho - \rho_w)\rho_t + H/(\rho - \rho_w)u\rho_x + (u/B)A_x^h - (c_i/c_c)(q/B) = 0 \quad (2)$$

$$gh_x + u_t + uu_x + (gh/\rho)\rho_x + (\rho/\rho)(qv/A) + g(S_f - S_b) = 0 \quad (3)$$

in which distance, x , and time, t , are the two independent variables, $A = A[h(x, t), x]$, is cross-sectional area, B , the channel top width, $H (= A/B)$, hydraulic depth of the cross section, $A_x^h \equiv (\partial A/\partial x)|_h$, the nonprismatic factor, q and ρ are the lateral inflow per unit length and its density, S_b and S_f are the bed slope and friction slope, respectively. The symbol ρ_w stands for density of clear water, c_c and c_i for constituent concentration in channel flow and in lateral inflow, respectively, g for the acceleration of gravity, \bar{h} for depth of the centroid of cross section, and $v = u - u'$, where u' is the x -component of lateral inflow.

Flows of Partially-Mixed Type - 1: CASE II In addition to advection of constituents, their dispersion effects are also assumed significant. The equation of continuity for constituent discharge in Case I, (2), is then replaced by:

$$\Delta\rho h_t + \hat{\Psi}_2 h_x + \Omega_2 H u_x + H\rho_t + \Phi_2 H\rho_x - q\Delta\rho/B + \Upsilon_2/BA_x^h = 0 \quad (4)$$

in which $\Delta\rho = \rho - \rho_w$, $\Delta\rho = \rho - \rho_w$, $\Upsilon_2 = \Delta\rho u - 2D_o\zeta$, $\hat{\Psi}_2 = \Upsilon_2 - D_o H\zeta_h$, $\Omega_2 = \Delta\rho - D_o\zeta_u$, $\Phi_2 = u - D_o\zeta_\rho$, $D_o =$ a longitudinal dispersion coefficient assumed as constant here, and $\zeta = \frac{\partial\rho}{\partial x}$ (applicable only to the dispersion term), $\zeta_u = \frac{\partial\zeta}{\partial u}$, ...

Flows of Partially-Mixed Type - 2: CASE III The third case is about the same as the second case except the longitudinal dispersion coefficient, $D_l = D_l(x, t)$, is assumed linearly dependent on the longitudinal constituent gradient, $\partial c_c/\partial x$. The equation of continuity for constituent discharge can be derived as:

$$\Delta\rho h_t + \hat{\Psi}_3 h_x + \Omega_3 H u_x + H\rho_t + \Phi_3 H\rho_x - q\Delta\rho/B + (\Upsilon_3/B)A_x^h = 0 \quad (5)$$

in which $\Upsilon_3 = \Delta\rho(u - K'\frac{\partial\theta}{\partial x}) - 2D_l\zeta$, $\hat{\Psi}_3 = \Upsilon_3 - D_l H\zeta_h - H K'\partial_h\zeta$, $\Omega_3 = \Delta\rho - D_l\zeta_u - K'\partial_u\zeta$, $\Phi_3 = u - D_l\zeta_\rho - K'\partial_\rho\zeta$, where K' is a parameter defined in Lai et al. (1995). This is again to replace (2) of Case I.

Flows with Constituent Deposit and Resuspension: CASE IV The fourth case allows the constituents/sediments to deposit or to be suspended depending on the degree of saturation. If $\zeta = \zeta(x, t)$ is the thickness of deposited constituent/sediment layer, the three basic PDEs will contain four unknowns, h, u, ρ , and ζ (Lai et al. 1995). Instead of seeking a fourth equation, the system is simplified to a case of 3-C, to match with the preceding three cases. Hence, $D\rho/Dt \approx 0$ is assumed in the equation of continuity for sediment-laden flow, and the effect of $gh\frac{1}{\rho}\frac{\partial\rho}{\partial x}$ is very small in the equation of motion. The resulting set is:

$$h_t + uh_x + Hu_x + (\rho_d/\rho)\zeta_t + (u/B)A_x^h - (\rho/\rho)(q/B) = 0 \quad (6)$$

$$\hat{\Psi}_4 h_t + \hat{\Psi}_4 u h_x + \hat{\rho}_u H u_t + \Omega_4 H u_x + \hat{p}'\zeta_t + \Delta\hat{\rho}(u/B)A_x^h - \Delta\rho(q/B) = 0 \quad (7)$$

$$gh_x + u_t + uu_x - (\rho_d/\rho)(u/H)\zeta_t + g\zeta_x + (\rho/\rho)(qv/A) + g(S_f - S_b) = 0 \quad (8)$$

in which ρ_d = density of deposited constituent layer, $\hat{\Psi}_4 = \Delta\rho + \rho_h H$, $\Omega_4 = \Delta\rho + \rho_u u$, and $\hat{p}' = (\rho_c - \rho_w)p'$, where p' = volume of sediment in unit volume of constituent/sediment layer.

CHARACTERISTIC EQUATION SETS

The four sets of governing PDEs are now transformed to the corresponding characteristic equation sets (Lai et al. 1995). These are the compatibility equations, J_j , $j = I, \dots, IV$, and the characteristic-direction equations, λ_i , $i = 1, 2, 3$.

CASE I: A linear combination of the three PDEs leads to

$$J_I = (\mu + 1)\frac{Dh}{Dt} + \nu\frac{Du}{Dt} + \left(\frac{\mu}{\rho} + \frac{1}{\Delta\rho}\right)H\frac{D\rho}{Dt} + F_1 = 0 \quad (9)$$

in which F_1 = aggregation of nonhomogeneous terms; μ, ν = combination factor; and

$$D/Dt = d/dt = \partial/(\partial t) + (dx/dt)\partial/\partial x = \partial/\partial t + (\lambda)\partial/\partial x \quad (10)$$

Because the fluid is incompressible and in this case nondiffusive, $D\rho/Dt = 0$, and (9) becomes decoupled two characteristic-equation systems:

$$L_{\pm} = \frac{Dh}{Dt} \pm \frac{c}{g}\frac{Du}{Dt} + F'_1 = 0 \quad \text{along } \lambda_{\pm} = \left(\frac{dx}{dt}\right)_{\pm} = u \pm c \quad (11)$$

$$\text{and} \quad D\rho/Dt = 0, \quad \text{along } \lambda_3 = u. \quad (12)$$

The latter system accounts for transport/advection of the constituents.

CASE II: A similar linear combination leads to the following compatibility equation,

$$J_{II} = (\mu + \Delta\rho)\frac{Dh}{Dt} + \nu\frac{Du}{Dt} + \left(\frac{\mu}{\rho} + 1\right)H\frac{D\rho}{Dt} + F_2 = 0 \quad (13)$$

where F_2 and D/Dt have the same meaning as in Case I.

CASE III: With exactly the same way as in Case II,

$$J_{III} = (\mu + \Delta\rho)\frac{Dh}{Dt} + \nu\frac{Du}{Dt} + \left(\frac{\mu}{\rho} + 1\right)H\frac{D\rho}{Dt} + F_3 = 0 \quad (14)$$

Case IV: For the fourth set of characteristic equations

$$J_{IV} = (\mu + \hat{\Psi}_4)\frac{Dh}{Dt} + (\hat{\rho}_u H + \nu)\frac{Du}{Dt} + \left(\mu\frac{\rho_d}{\rho} + \hat{p}' - \nu\frac{\rho_d}{\rho}\frac{u}{H}\right)\frac{D\zeta}{Dt} + F_4 = 0 \quad (15)$$

The last three characteristic systems are all coupled. After μ , ν , and the characteristic λ are determined for each case, the λ should yield three distinct real values, representing three distinct wave components. Generalizing, the last three compatibility equations

$$L_i = S_i\frac{Dh}{Dt} + T_i\frac{Du}{Dt} + P_i\frac{D\rho}{Dt} + F_i = 0, \quad i = 1, 2, 3 \quad (16)$$

where $L_i = J_{II}, J_{III}, J_{IV}$, can be defined along the three characteristics,

$$\left(\frac{D}{Dt}\right)_i \equiv \left(\frac{d}{dt}\right)_i = \frac{\partial}{\partial t} + \left(\frac{dx}{dt}\right)_i \frac{\partial}{\partial x} = \frac{\partial}{\partial t} + \lambda_i \frac{\partial}{\partial x}, \quad \text{along } C_i \quad i = 1, 2, 3 \quad (17)$$

NUMERICAL ALGORITHM FORMULATION

Applying the multimode method of characteristics (MMOC) (Lai, 1988a; 1994) to the characteristic equation sets displayed earlier, the corresponding four simulation models can be developed.

CASE I MODEL:—Advection-Dominated Flow Model: From (11) with appropriate boundary conditions, $h(x, t)$ and $u(x, t)$ can be found for any (x, t) point using the MMOC (Lai 1988a). Density particles, and thus concentrations, $c_c(x, t)$, can then be obtained from $D\rho/Dt = 0$. For the particle transport, either Eulerian or Lagrangian approach can be used.

CASE II MODEL:—Advection-Dispersion Model (1): (Constant Dispersion Coefficient) For a less well mixed flow the dispersion term is not negligible, and the three-equation set becomes a coupled system having three distinct wave components (Lai, 1994) – two hydrodynamic waves similar to the Case I model, and a third wave which is a modified flow velocity accounting for the nonhomogeneity of the fluid density. The three dependent variables are numerically integrated along the characteristics, $\lambda_1, \lambda_2, \lambda_3$ through use of (16).

CASE III MODEL:—Advection-Dispersion Model (2): (Variable Dispersion Coefficient) The third model can be treated in a similar manner as in the second model, but it is generally more strongly coupled, difficult to handle, and prone to numerical instability than the second.

CASE IV MODEL:—Movable-Bed Model: If $\rho \approx \rho_d \approx \varrho$ is assumed, this set becomes essentially the same as the governing equation set in Lai (1991) for unsteady movable-bed flow analysis, and the same modeling technique applies.

MODEL DEVELOPMENT FOR A COMPOUND-COMPLEX CHANNEL SYSTEM

Equations for Compound-Complex Channels: A main stream annexes a number of tributaries and branches upstream and divides into delta and braids or form islands or networks downstream. To adequately simulate unsteady flow in the whole riverine and estuarine system, a model capable of handling a compound-complex channel system must be developed. Basic equations for some junction problems are assembled herein.

Two-way Junction: The boundary conditions to be satisfied at the junction are,

$$u_1 A_1 = u_2 A_2 \quad (18)$$

$$Z_1 + \frac{u_1^2}{2g} = Z_2 + \frac{u_2^2}{2g} + h_f = Z_2 + (1 + \alpha) \frac{u_2^2}{2g} \quad (19)$$

in which subscript 1 or 2 indicates point before or after the junction, and α is the minor head-loss coefficient.

Multiway Junction: The boundary conditions to be satisfied at the junction are,

$$\sum_{i=1}^n u_i A_i = 0 \quad (20)$$

$$Z_1 + (1 + \alpha_1) \frac{u_1^2}{2g} = Z_2 + (1 + \alpha_2) \frac{u_2^2}{2g} = \dots = Z_n + (1 + \alpha_n) \frac{u_n^2}{2g} \quad (21)$$

A Comprehensive Model for Large-Scale Flood Flow Simulation: Based on the array of flow and transport equations displayed in the previous sections and subsections, a comprehensive coupled model can be assembled for large-scale floods, as well as other types of riverine and estuarine flow simulation. Individual routines and models, such as the four models discussed before, are first written, run, and tested; then they are assembled, each individual one as a building block, into

a comprehensive, large-scale model; which will eventually be consolidated to one coupled system for better approximation of the real world. More concrete procedures for model implementation are discussed below.

IMPLEMENTATION AND APPLICATION

Implementation of Four Individual Models: As has just been mentioned, for the first step toward a comprehensive model development, the four numerical models were each implemented separately. The first model essentially involves use of two separate ready models, — an unsteady open-channel flow model and a transport model — and hence, was first to be put to use. The fourth model, being closely similar to Lai's alluvial channel flow model (Lai, 1991), was implemented immediately following. The second and third models, both new and fraught with numerical difficulties, required some efforts to accomplish the development.

Applications: Because the model implementation time and stage, and the input and boundary data requirements all vary, a variety of application examples exist. Only a few examples are outlined.

Case I Model: — (a) Delaware River reach between Torresdale and Delair [DLW] (Reach length = 9.14 km; Aug. 15-16, 1962) was used for model testing. The simulation results of hydrodynamic part are similar to any previous runs (e.g., see Lai, 1988a). For the transport part, the Eulerian approach was applied.

(b) Threemile Slough near Rio Vista, CA [TMS] (Reach length = 5.19 km; July 15-16, 1959) For the transport part, a combined set of actual and hypothetical data were used, and the Lagrangian approach was applied for density-particle tracing.

(c) Tamsui River estuary between Kwantu Bridge and River Mouth, Taiwan. [TAM] (Reach length = 7.65 km; April 14, 1995) Sufficient data were gathered for a short period of hydrodynamic simulation. Hypothetical (or design) data were used for the transport simulation, by applying the Lagrangian approach. [See Wang, et al. (1997)]

Case IV Model: — (a) [DLW] Stage and discharge hydrographs, and a graph of time variation of bed-layer thickness were generated for a movable-bed open-channel conditions.

(b) Sacramento River, CA. [SCM] (Reach length = 34.3 km; Feb. 13 - March 20, 1980) Three kinds of hydrographs were generated: Time variation of depth; of flow velocity; and of sediment-layer thickness.

Case II Model: — (a) [DLW] Using the hydrodynamic data of the Delaware River reach and design data for the longitudinally varied density, a series of test runs were made. Physically reasonable results were obtained. Comparison of the third characteristic, λ_3 , of Case II Model, i.e., the speed of "density-wave" propagation, with the model-simulated flow velocity indicates that the density-wave is retarded/accelerated when the density gradient opposes/overlaps the pressure gradient (i.e., the ebb/flood flow).

Case III Model: — (a) [DLW] The simulation work with this model parallels that with Case II Model, except increased numerical instability was noticed.

Implementation of the Compound-Complex Channel Model: In general, the implementation begins with the schematization of the entire study area. A typical CCC model consists of a main stream, tributaries, reaches, and subreaches (or segments), that are systematically arranged in sequential, dendritic, or network forms. (e.g., see Figs. 1 & 2.) The unsteady flow simulations are to be carried out according to the computational algorithms described earlier. To this end, a set of channel geometry and property data, a set of initial-value data, and a time series of boundary-value data must be acquired, organized or reduced to the computer acceptable/compatible forms.

Applications: The application of CCC models can be proceeded in ascending stages, first by treating the system as of homogeneous-density flow with fixed-bed channels, then as of variable-density flow with fixed or movable-bed channels, but under decoupled modeling conditions, and thirdly, the same flow condition as the preceding case, but with the use of a coupled model. The first application case has been tried extensively on the Tamsui River estuarine system, that includes the severe flood flow caused by the 1996 Typhoon Herb. Copious computer outputs have been generated from this simulation. Figures 1 and 2 give a few examples of the simulation results.

Implementation of a Comprehensive Model: The four variable-density models can be placed loosely together for easy access and execution by the operator/computer. This is the comprehensive model of the first type, and does exist any time when the four models are ready. However, the four models can be closely tied together and put under the control of a well-designed supervisory program. Then the whole package works more like a single unit. This is the comprehensive model of the second type. A far better alternative is to replace the four working programs with a single 4-C (4 characteristics) program that handles 4 unknowns, h, u, ρ, ζ , or 4 components, simultaneously. This is the comprehensive model of the third type; the development of which is underway (also, see the preceding section on the CCC modeling).

EXAMINATION AND DISCUSSION

Two special features of the MMOC are its ability to accommodate a set of characteristics of great disparity (Lai, 1991; 1994), and its ability to properly adjust the modeling scale for optimum simulation (Lai, 1988b). However, these two features may show conflicting effects sometimes. In treating longitudinally-varied-density flow, separation of density-wave curve and velocity curve may be difficult (i.e., insufficient resolution). These are the things to heed when implementing a program for 4 unknowns, h, u, ρ, ζ .

A common notion for a comprehensive model is that it is efficient and economical when one has diverse problems to solve. However, a comprehensive model sometimes could function better than a specialized one even it is used for a single-purpose project. Suppose one has to compute and provide stream flow data for a tidal reach all the year round. A hydrodynamic/sediment-transport coupled model may not show the sediment effects in a short period of time, it could reveal considerable channel aggradation after six months or a year. If the model is to be used for flood forecast in addition to the routine operation, the model will be well equipped with ready initial values and boundary conditions when the flood arrives at any unspecified time. This is still true even the routine flow computation is not intended. Because when a typhoon hits, there is no time to prepare a decent set of initial values, nor time to design a set of hypothetical data to make an idle computer run for convergence.

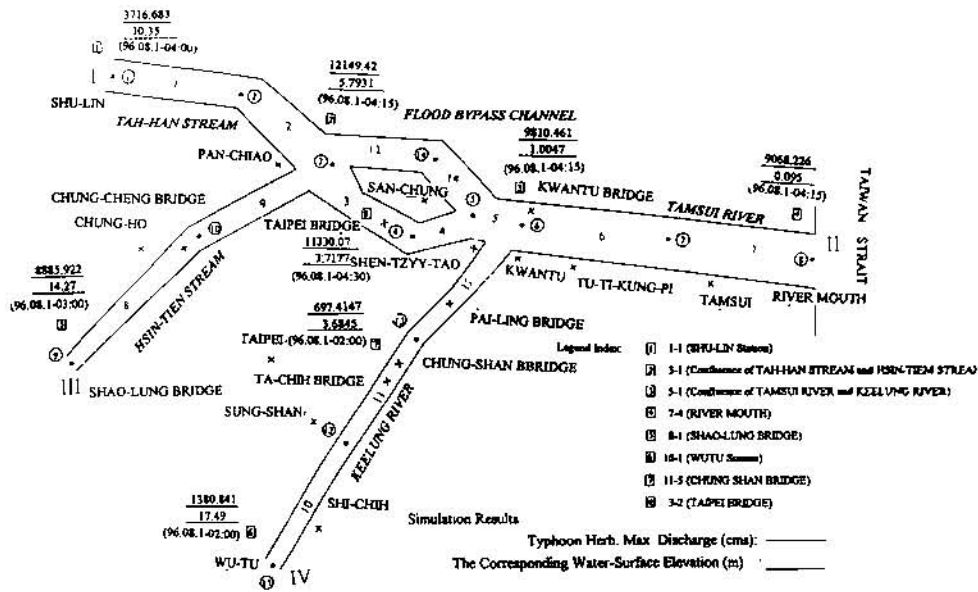
CONCLUDING REMARKS

Unsteady flow in tidal reaches can be described by the St. Venant type equations, for its hydrodynamics and by another form of continuity equation for its constituent concentration/movement. Four different sets of PDEs have been derived for varied constituent distribution patterns. These PDE sets are subsequently transformed to the corresponding characteristic equation systems, suitable for MMOC schematization, and finally, to the development of four tidal flow models. The first model consists of two decoupled subsystems, whereas the remaining three are all coupled; each yielding three characteristics, i.e., three model components. These models have been tested using various field data. Simultaneously, a large-scale tidal-hydraulics model to compute unsteady flow in

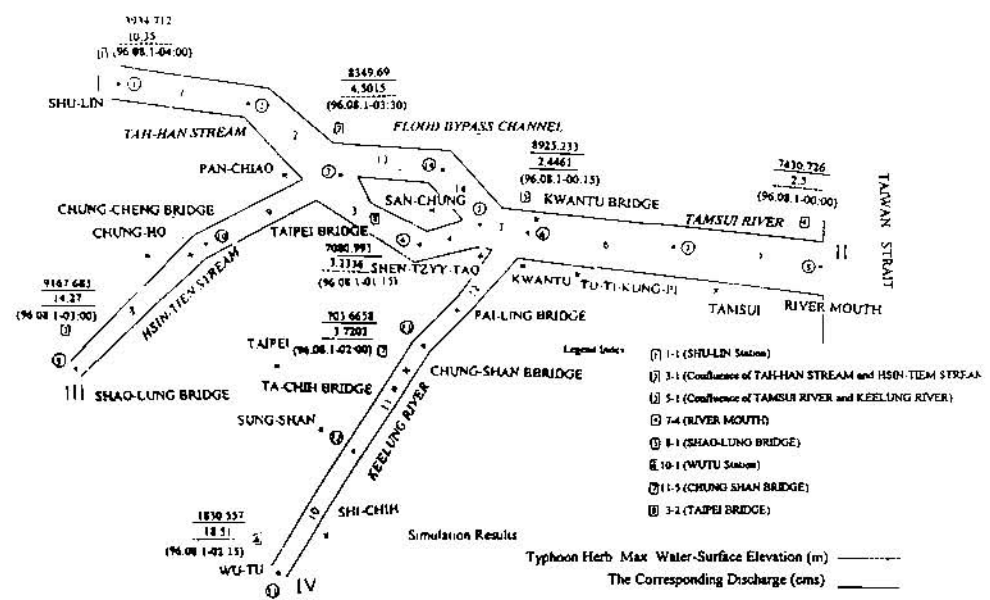
a compound-complex channel system has been developed. The model is highly powerful, and capable of treating severe storm floods such as one caused by the 1996 Typhoon Herb. A comprehensive CCC model that accommodates the four individual models functionally is under development. Such a model is expected to have advantages of more than just economical and efficient for application to diverse problems; but will function better, even used for a single purpose such as flood forecast, than a specialized model for some applications.

REFERENCES

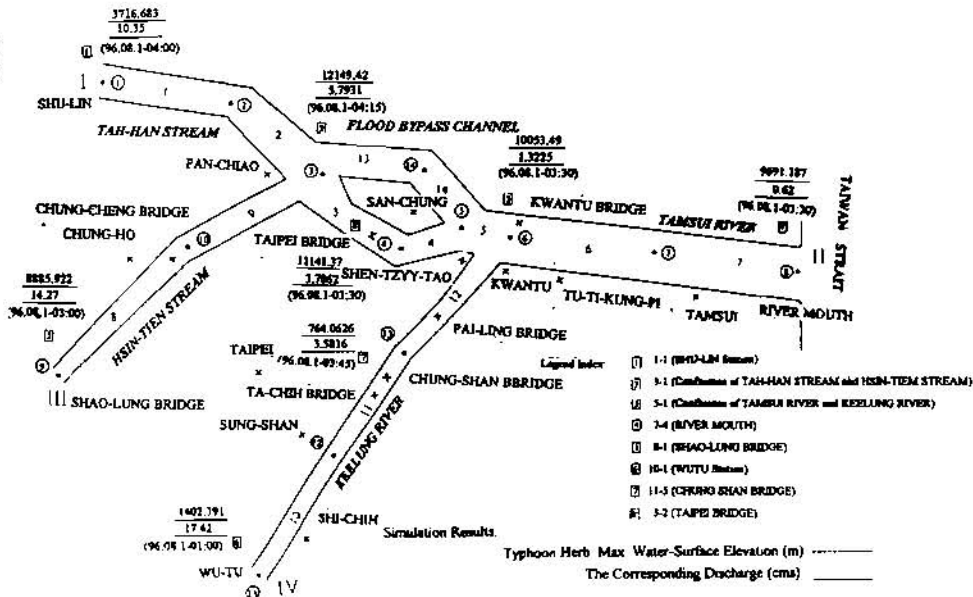
- Lai, C. (1988a). "Comprehensive method-of-characteristics models for flow simulation." *J. Hydr. Engrg.*, ASCE, 114(9), 1074-1097.
- Lai, C. (1988b). "A numerical scale model for simulating unsteady-alluvial channel flow." *Twelve selected computer stream sedimentation models developed in the United States*, S.S. Fan, ed., Federal Energy Regulation Commission, Washington, D.C. 179-260.
- Lai, C. (1991). "Modeling alluvial-channel flow by multimode characteristics method." *J. Engrg. Mech.*, ASCE, 117(1), 32-53.
- Lai, C. (1994). "Multicomponent-flow analyses by multimode method of characteristics." *J. Hydr. Engrg.*, ASCE, 120(3), 378-395.
- Lai, C., Wang, T. W., and Lai, K. Y. (1995). "Developing Multicomponent Riverine Flow Models Using the Multimode Method of Characteristics — Unsteady Flows with Longitudinally Varied Fluid Density." *Research Report No. NSC83-0410-E-002-038*, Dept. of Civil Engrg., National Taiwan Univ., Taipei, Taiwan.
- Wang, T.W., Hsu, N.S., Lai, C., Liu, M.S., and Lai, K.Y. (1996). "A study of flood control measures in tidal reaches (I)." *Research Report No.85EC2A043004*, Hydrotech Research Institute, National Taiwan Univ., Taipei, Taiwan.
- Wang, T.W., Hsu, N.S., Lai, C., and Lin, Y.H. (1997). "A study of flood control measures in tidal reaches (II)." *Research Report No.86EC2A040043*, Hydrotech Research Institute, National Taiwan Univ., Taipei, Taiwan.



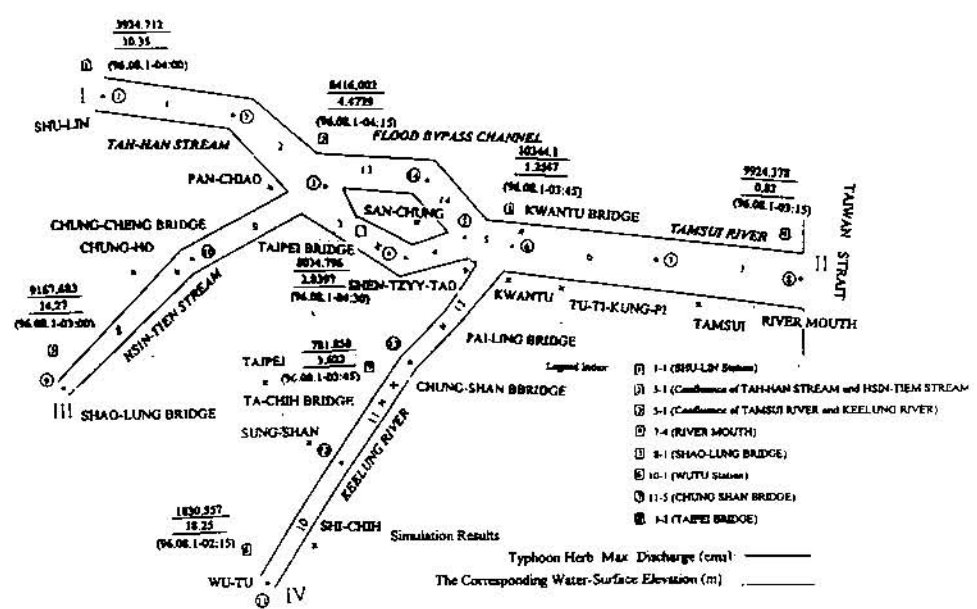
(a) Maximum Discharges



(a) Maximum Water-surface Elevations



(b) Maximum Water-surface Elevations



(b) Maximum Discharges

Figure 1 A List of Maximum Hydrologic Records During the 1996 Typhoon Herb, ---- Flood Bypass Channel Closed
(a) Maximum Discharges, (b) Maximum Water-surface Elevations

Figure 2 A List of Maximum Hydrologic Records During the 1996 Typhoon Herb, ---- Flood Bypass Channel Open
(a) Maximum Water-surface Elevations, (b) Maximum Discharges

A Summary of the National Weather Service Advanced Hydrologic Prediction System Demonstration in Des Moines, Iowa

Lee Larson, Chief, Hydrologic Research Lab, Office of Hydrology, National Weather Service, Silver Spring, MD. Edwin Welles, Visiting Scientist, Hydrologic Research Lab, Office of Hydrology, National Weather Service, Silver Spring, MD

INTRODUCTION

Floods are the leading weather related hazard. Our nation's most recent and prominent events, such as "The Great Flood of 1993" in the mid-west and subsequent flooding events in the western, eastern, and upper mid-western states, remind us that major floods will occur frequently and are devastating. Preparedness for these events can lead to saving billions of federal disaster relief dollars. Floods cause an average of nearly \$4 billion in damages annually, and over 75 percent of Presidential disaster declarations are in response to flooding events. It is, therefore, important to make the mitigation of this hazard a high-priority task.

Droughts, while generally not life-threatening in the United States, do have a serious impact on agriculture, ecosystems and water management, and the economy in general. With the Advanced Hydrologic Prediction System (AHPS) implemented nationwide, the National Weather Service (NWS) will have the tools to provide drought related hydrologic information to users. This improved capability builds on the traditional expertise and responsibility of the NWS flood forecasting program, and will provide the public with a full set of water resources information.

Recognizing this hydrologic forecasting requirement, the NWS has developed, implemented, and demonstrated AHPS for the Des Moines River basin in Iowa. This is the first phase towards the national implementation of AHPS. The Des Moines basin was chosen for this first phase because of the devastating impacts of the "Great Flood of 1993," which included severe flooding in the city of Des Moines, Iowa.

Our Nation's floods and droughts have forced the need for improved predictions to support flood/drought management and damage mitigation. It is imperative that AHPS products be provided to assist the mitigation of these hazards. Furthermore, the allocation of water among competing demands looms as a national problem requiring improved water quantity forecasts for sustainable development. By increasing lead times and the content of hydrologic forecasts, AHPS products will greatly improve the Nation's capability to take timely and effective actions that will significantly mitigate the impact of major floods and droughts. AHPS will also provide products to water resource managers for the optimal use of water and appropriate allocation for water supply, agriculture, navigation, hydropower, and ecosystems.

AHPS implementation began in 1995 through a significant commitment by personnel of the North Central River Forecast Center (NCRFC), Chanhassen, Minnesota; the Regional Hydrologist and other staff of the NWS Central Region Headquarters, Kansas City, Missouri; the Des Moines Weather Forecast Office (WFO), Johnston, Iowa; and the NWS Office of Hydrology, Silver Spring, Maryland. The March 1997 demonstration successfully met the implementation goals to demonstrate an operational long-term probabilistic forecast system. Furthermore, the demonstration revealed that AHPS is mature enough for implementation in other regions of the nation.

DEMONSTRATION DEVELOPMENT

In order to solicit input from the intended users of the new AHPS products, a meeting was held at the Weather Service Forecast Office (WSFO) Des Moines, October 2-3, 1996. Attendees at all or part of the 2-day meeting included NWS representatives from the Office of Hydrology, Hydrologic Research Laboratory; the National Operational Hydrologic Remote Sensing Center (NOHRSC); the North Central and Missouri Basin RFCs; WSFO Des Moines; and the Regional Hydrologist, Central Region. Other attendees represented the U.S. Geological

Survey, Rock Island Army Corps of Engineers (USACE), City of Des Moines, City of Des Moines Water Works, State of Iowa, and Iowa State Emergency Managers.

Through consultation with the users, it was decided that the following products would be issued once per week. It was also decided that these products would include the use of Quantitative Precipitation Forecasts and climate coupling. The selected products were:

- ESP probability Time Series (weekly) for flow, volume, and stage out to 60 days for 21 forecast locations in the Des Moines basin.
- 60-day Exceedance Probability Plot for flow and stage for all forecast locations.
- Flood inundation map showing 25, 50, and 75 percent probability of flooding at 60 days. Area covered by the map would be approximately downstream of Saylorville Dam to 14th Street in Des Moines, and up the Racoon River from the Des Moines River to the confluence of Walnut Creek.

In addition, it was decided that the Internet would be the primary system for issuing AHPS products to users. The WSFO Des Moines home page would provide access to the products. The NCRFC would also continue to produce all previous routine products during the AHPS demonstration. The AHPS products would be in addition to the usual hydrologic products prepared by NCRFC such as flash flood guidance, River Forecast, and Extended Streamflow Guidance products.

The specific goals of the demonstration were reiterated to be as follows:

- Use Quantitative Precipitation Forecasts (QPF) in the short-term forecasts.
- Use climate coupling and Ensemble Streamflow Prediction (ESP) techniques in long-range hydrologic products.
- Provide probability information in hydrologic products.
- Demonstrate a flood inundation mapping capability.

Lastly, the methods for evaluating the forecasts were determined. Verification of the AHPS demonstration would be based on a comparison of observed crests with Spring Flood Outlooks based on ESP procedures. Also included would be a summary of user evaluations as to the quality and usefulness of ESP-type products.

DEMONSTRATION DESCRIPTION

Computation of Forecasts

Forecasts distributed during the AHPS demonstration in Des Moines, Iowa, were computed using the ESP technique. To forecast with the ESP technique, an ensemble of possible streamflow hydrographs are calculated by initializing hydrologic models with the current states of the hydrologic system and then forcing those models with historical precipitation and temperature time series. A distribution is then fit to a sample taken from this ensemble of streamflow hydrographs. The fitted distribution describes the likelihood of an event occurring. It is from this fitted distribution that forecast products are derived. An empirical distribution was used as the underlying distribution for all the AHPS demonstration forecasts.

For the demonstration, a method was developed to integrate long-range meteorological forecasts into the streamflow forecasts. This method consists of shifting the historical precipitation and temperature time series by daily λ values prior to using them as input to the hydrologic models. The daily λ 's were calculated from the 2- to 6-

day Hydrometeorological Prediction Center precipitation and temperature forecasts, the 7- to 11-day Climate Prediction Center (CPC) precipitation and temperature forecasts, the 1-month climate outlook from CPC, and the seasonal climate outlooks from CPC. WSFO preceded the 24-hour QPFs that were also blended into the ESP forecasts.

Description of Forecast Products

The NCRFC provided AHPS forecast products for 20 locations during the demonstration and also the 5-day deterministic forecasts for all 20 locations. (See figure 1 for a map of the forecast point locations.) Examples of the 5 day forecast product is presented in figure 2, the Probability Interval plots with weekly intervals in figures 3-5, and Exceedance Probability plots for the 60-day forecast period in figures 6-7. The NOHRSC was responsible for providing the Inundation Map an example of which is presented in figure 8.

Probability Interval Plots for Maximum Flow, Maximum Stage, and Volume. These plots show the probability that the variable of interest at a point on a river will exceed a particular value in a 7-day period. The vertical axis shows flow measured in cubic feet per second and the horizontal axis shows time. Each vertical bar represents the probabilities for a 7-day period. The three probability levels are: greater than 75 percent, 75-50 percent, and 50-25 percent. The variable of interest can be either the Maximum Flow at a point, the Maximum Stage at a point, or the Volume passing a point. Examples of these products may be found in figures 3, 4, and 5.

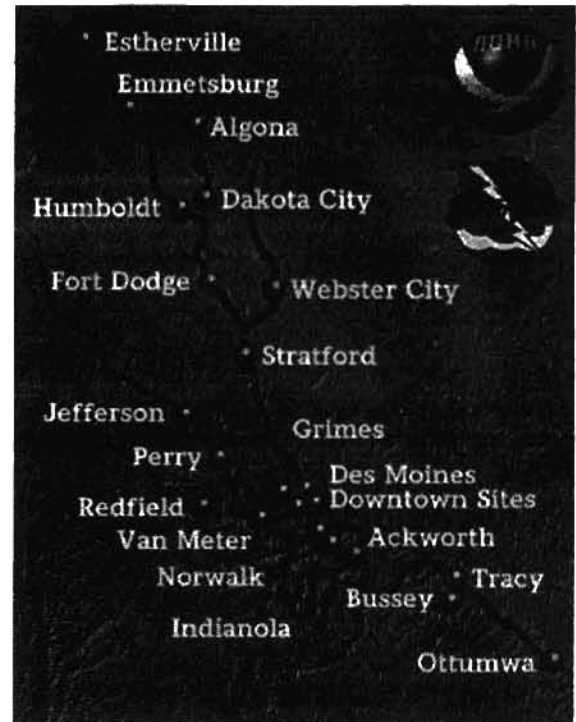


Figure 1

60-day Exceedance Plot for Maximum Flow and Maximum Stage. These plots show the probability distribution for the Maximum Flow or Maximum Stage over the identified 60-day period. The vertical axis shows the flow values measured in cubic feet per second, and the horizontal axis shows the probabilities. The triangles indicate sample points, and the line through the points represents the distribution that has been fit to those sample points. A point on the line indicates the probability that a specific flow will be exceeded some time during the identified 60-day period. Examples of these products may be found in figures 6 and 7.

Inundation Map for Maximum Stage. The AHPS Flood Inundation Map is intended only to demonstrate the capability of generating real-time inundation maps derived from NWS hydrologic forecasts. The inundation map depicts the probabilities that specific areas around Des Moines will be flooded during the identified 60-day period. Any given area is assigned one probability range for the specific 60-day period: a greater than 75 percent chance of flooding; a 50-75 percent chance of flooding; a 25-50 percent chance of flooding; or a less than 25 percent chance of flooding. The map does not give information about flood depth above the ground, river stage, or flood return interval and is not related to any hypothetical 25-, 50-, or 75-year return-interval flood. The inundation map is based on the best digital elevation model (DEM) data available. If a DEM of greater resolution and accuracy were available, it could be used with the demonstration software and procedures to produce a more accurate flood inundation map based on the NWS hydrologic forecasts. An example inundation map may be found in figure 8.

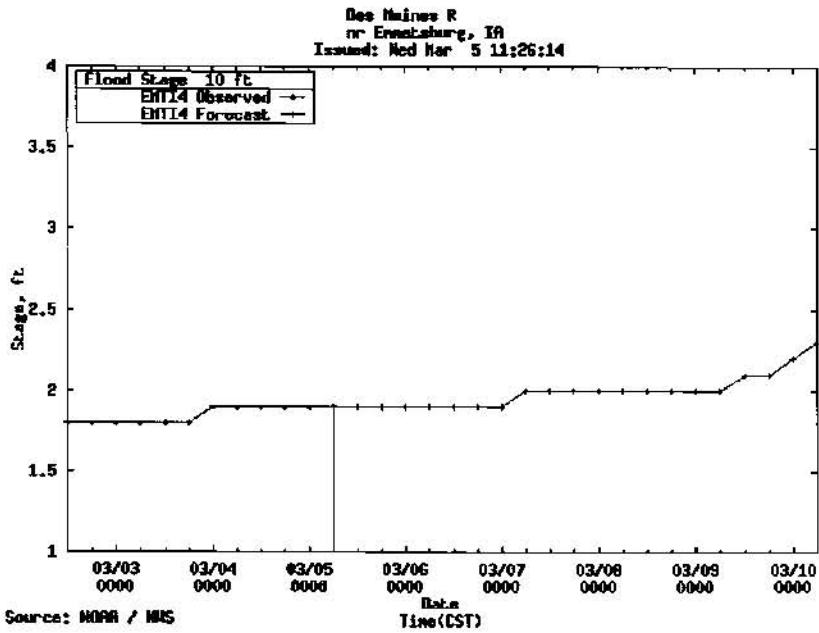


figure 2

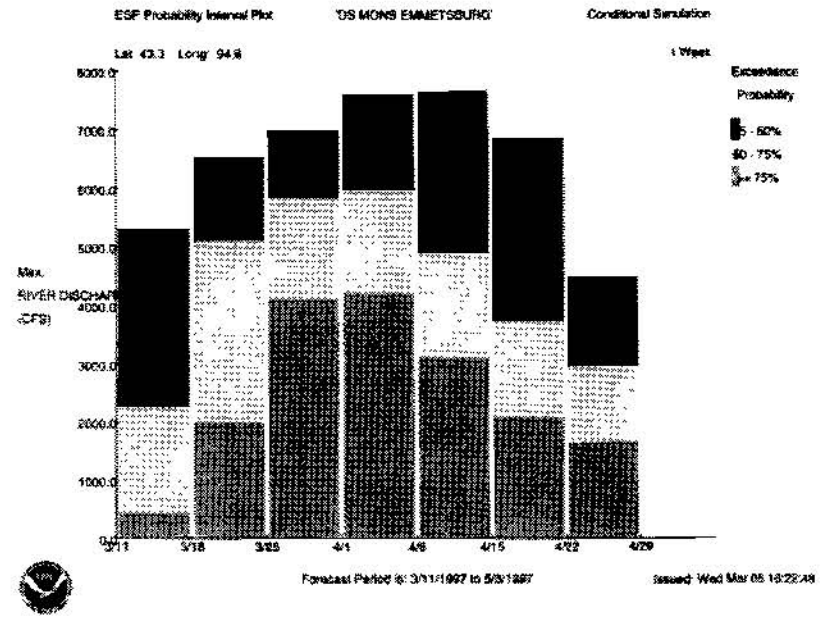


figure 3

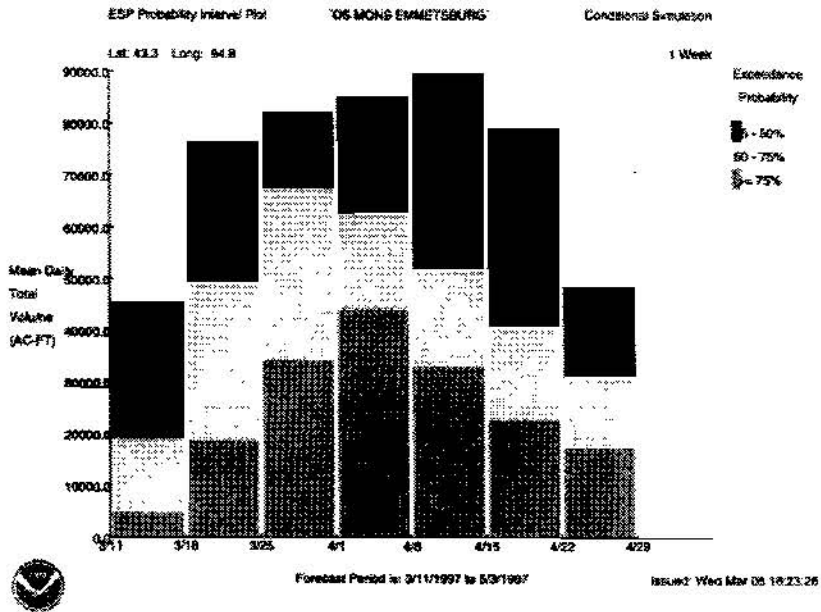


figure 4

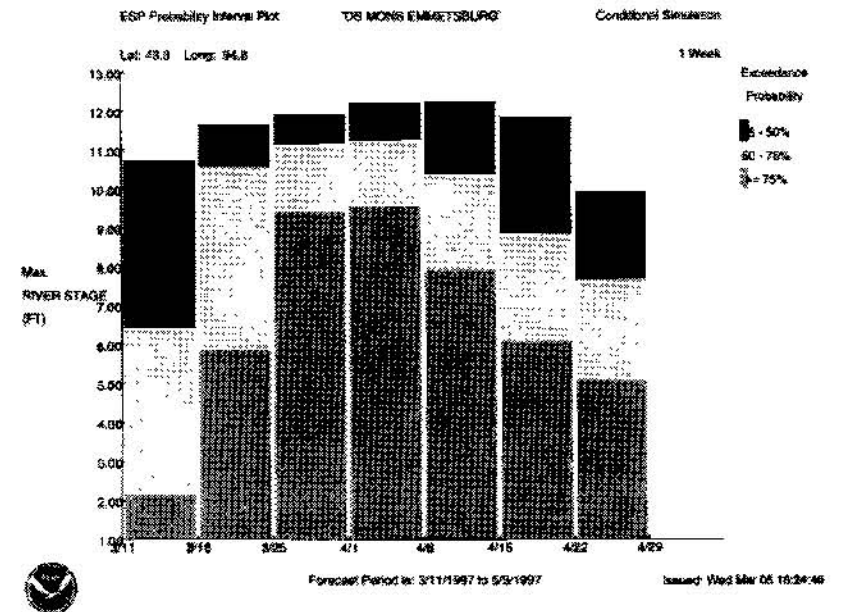


figure 5

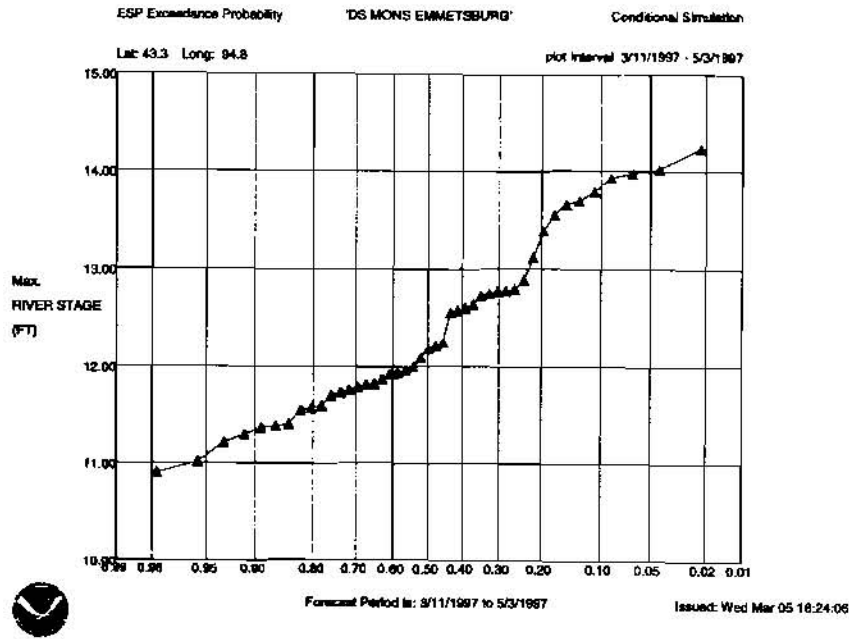


figure 6

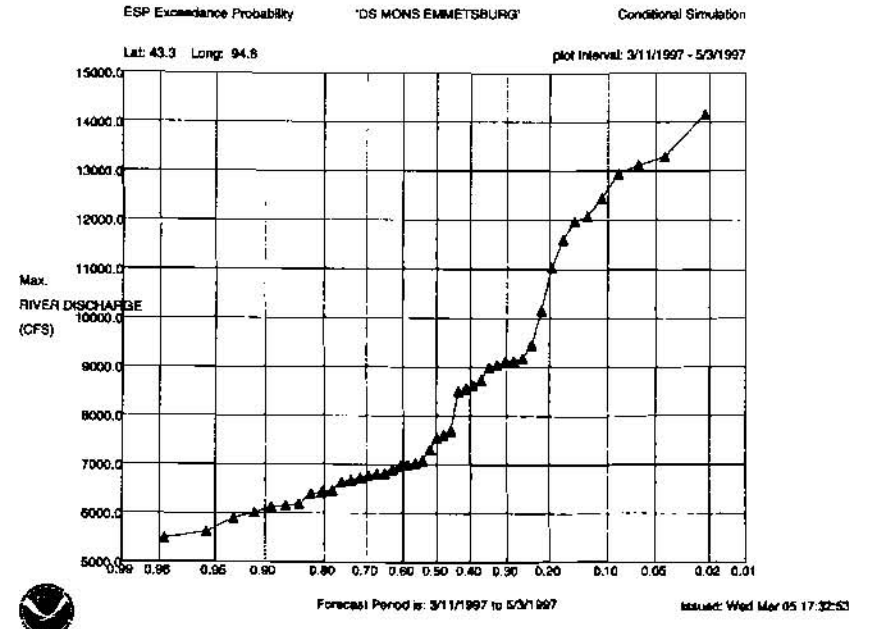


figure 7

6-45

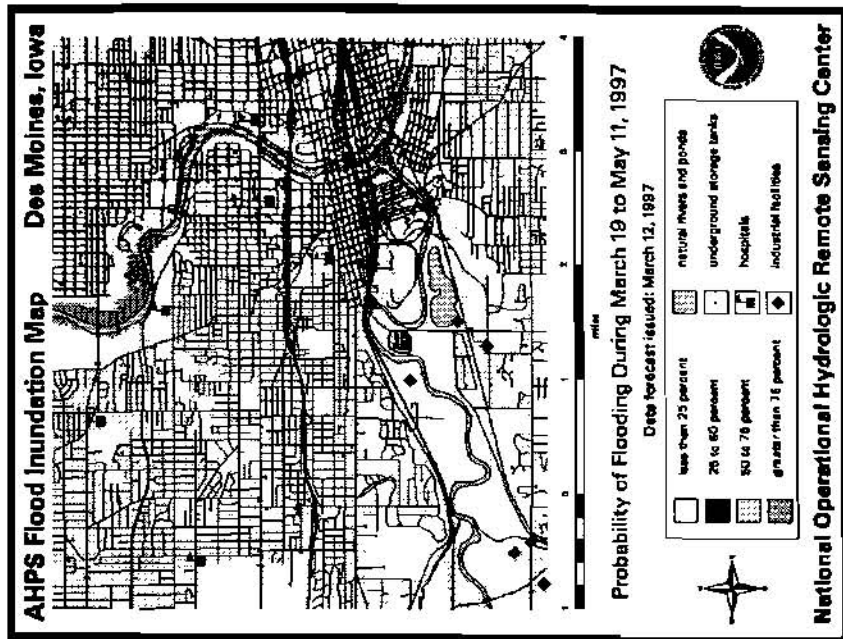


figure 8

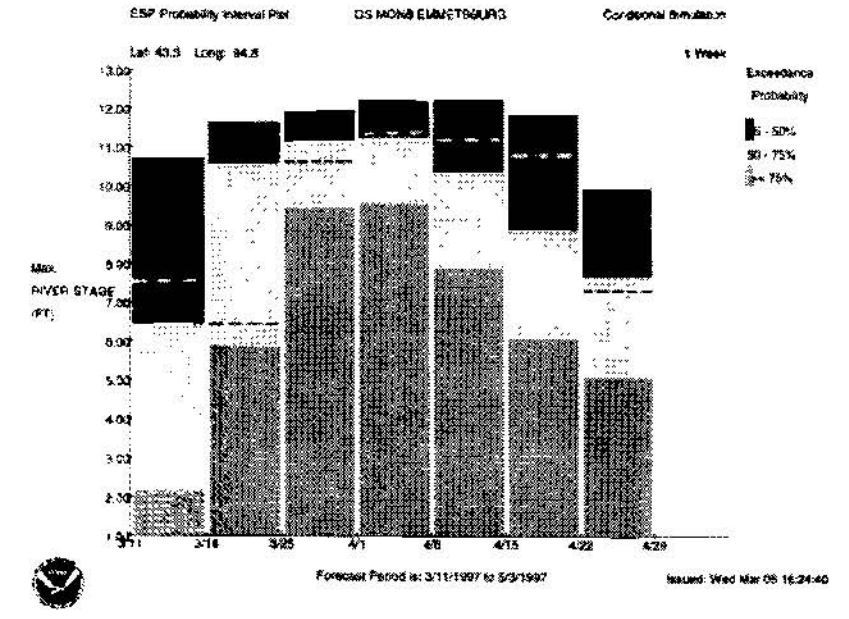


figure 9

AHPS PRODUCT EVALUATION

Hydrologic conditions during the demonstration

Snow conditions at the beginning of March were 8-13 inches of snow for the Upper Des Moines river basin, with unusually high water equivalents of 3- 6 inches; central and southeast Iowa had 2-4 inches of snow, with less than 2 inches of water equivalent. Average temperatures across the Des Moines river basin ranged from around 30 degrees in the northwestern sections in Minnesota to the lower 40s in southeastern Iowa. This was between 2-4 degrees below normal in the northwest to around 4 degrees above normal in the southeast. Precipitation amounts ranged from 0.5-1 inch in the Minnesota sections to 1-2 inches in Iowa. This was 50-75 percent of normal. Most of the precipitation fell the first week of March when Des Moines received almost an inch and a quarter of precipitation.

These conditions led to a few minor flood events within the Des Moines river basin during the month of March, with the majority of forecast points remaining below flood stage. Nine locations experienced minor above-flood stage conditions; however, at least three of these were largely due to ice affects (Algona, Jefferson, and Perry). It should be noted that an early melt occurred just prior to the beginning of the AHPS demonstration period. The benign hydrometeorologic conditions during the demonstration period, and the short period involved, minimized the amount of data analysis that was possible.

Evaluation

Analyzing the daily 5-day deterministic forecasts indicates diminishing skill after day 3 of the forecast period and significant variations in forecast values on days 4 and 5 of the forecast period. This can be primarily related to the fact that only 1 day of QPF was available.

To evaluate the Probability Interval plots, the observed data were overlaid on the plots for verification. The 60-day probability interval plots were examined by comparing observed hydrographs for the 60-day period to the interval plots issued on March 5. See figure 9 for an example. It was found that most of the observed maximum stages for each week were distributed almost equally in the 25-50 percent and 50-75 percent intervals; this is what would logically be expected. However, the number of observed stages in the greater than 75 percent interval was zero, while the number in the less than 25 percent interval was 11. This was probably a result of below-normal precipitation during the demonstration period. The observed stages for each interval for the 12 sites were as follows.

<u>Interval</u>	<u>No. of weekly maximum stages</u>
less than 25%	11
25%-50%	36
50%-75%	37
greater than 75%	0

The 60-day exceedance probabilities for a given observed data value were determined directly from the ESP output. Examining the 60-day products indicates that, in some cases, the observed data had exceedance probabilities in excess of 70 percent, with some observations having probabilities greater than 98 percent.

User Response

In order to evaluate the AHPS products from a user perspective, surveys were given to emergency management and other critical customer groups along the Des Moines basin. The following external customers returned an AHPS survey: West Des Moines Fire and Civil Preparedness; USACE; Des Moines Water Works; USACE, Rock Island; Emmet County EMD; Kossuth County EMD; Wright County EMD; Marion County EMD; Calhoun County EMD; Madison County EMD; Polk County EMD; Clarke County EMD; and an unknown.

Survey Results.

Question 1 - *How often did you access the AHPS products?*

multiple times per day	2
daily	0
every few days	2
weekly	0
less often than weekly	5 -- (due to lack of flood threat)
never	4 -- (due to lack of flood threat)

Question 2 - *For the following, please rate 1 to 10 with 1 being "unsatisfactory", 5 being "satisfactory" and 10 being "outstanding".*

	External Mean Responses
Ease of access to AHPS products	7
Understandability of AHPS products	7
Quality of AHPS products	7
Display of AHPS products	7
Timeliness of AHPS products	8
Usefulness of AHPS products	8

Question 3 - *Please rate the following WSFO Des Moines Home page products:*

	Not Useful	Useful	Essential
Current stages	0	1	7
5-day forecasts	0	2	6
Probability time series			
Stage	0	1	6
Flow	0	1	6
Volume	0	2	4
60-day Exceedance probabilities			
Stage	0	5	3
Flow	1	4	3
Site information	0	5	2
Site map	0	3	3
Gauge information	0	0	7
Inundation map	1	2	4
Help products	0	4	2

Question 4 - *What do you like best about AHPS?*

- The information was right before you and then you could plan your strategies.
- Rainfall potentials.
- Accuracy, timeliness, uncertainty, length of future forecast, ease of graphics.
- Timely information.

Question 5 - *What do you like least about AHPS?*

- No Internet access.
- Did not use since flooding was not a problem during the demonstration.
- Occasional trouble accessing.
- First time user - I found it confusing.
- Download slow.

- Timeliness of access.

These users rated AHPS products as 7 or 8 (on a scale of 1 to 10). They evaluated most AHPS products as "essential" to their operations. These users stated that what they especially liked about AHPS was "the information was right before you and then you could plan your strategies."

At a later time a more rigorous verification and comparison with other procedures could be made. However, even a cursory review of the types of products made available to the public, and an examination of Figures 2-8, shows the obvious advantages of AHPS because of the wealth of additional probabilistic information available through AHPS techniques. The user response before, during, and after the demonstration clearly showed the usefulness and applicability of ESP probability type hydrologic products.

SUMMARY

It should be remembered that the primary purpose of this demonstration was to show that all the necessary operations required for AHPS could be developed, implemented, and operated in an operational real-time environment. From that perspective, the AHPS demonstration was a total success.

The ESPADP software was developed and implemented at NCRFC. The Sacramento soil moisture accounting model had to be calibrated and running at NCRFC for the Des Moines basin. The capability to utilize QPF and climate information in long-range hydrologic forecasting was demonstrated. All of the necessary software and data necessary for inundation mapping had to be acquired by the NOHRSC and tailored for the Des Moines basin. Staff at WSFO Des Moines and NCRFC had to design a home page for disseminating the AHPS products, become familiar with the products, and work with the local users of the products. All of these many varied and critical requirements were accomplished on schedule.

All of the required AHPS products began flowing from NCRFC and NOHRSC to WSFO Des Moines and then to the public on schedule on March 5, 1997, and continued through March 26, as planned.

While the lack of significant flooding activity in the Des Moines basin during the demonstration was disappointing, it was not a problem for the overall project. In the early implementation stages of AHPS, the primary goals were to implement the AHPS at NCRFC, generate the forecast products as required, produce the inundation maps, and transfer all of this information to WSFO Des Moines. At WSFO Des Moines, the AHPS products were placed on the Internet home page, along with significant amounts of additional hydrologic information (E-19 information such as site history, location, maps, historical flood data, stage damage information, etc.) for access by outside users. All of this was accomplished and successfully demonstrated during this project.

This critical demonstration showed that all of the necessary pieces of AHPS are viable. The positive user response provides a critical impetus for the NWS to continue in its efforts to implement the AHPS across the nation.

COMPARING METHODS FOR FORECASTING TOTAL SUMMER FLOWS ON TRIBUTARIES OF THE COLORADO - BIG THOMPSON SYSTEM

by

M. MARKUS, Research Hydrologist, National Weather Service, Silver Spring, Maryland;
J. D. SALAS, Professor, Colorado State University, Fort Collins, Colorado

Abstract: The operation of the Colorado - Big Thompson (CBT) System in the Rocky Mountains of northern Colorado relies on the accuracy of predicting the future system inputs. One of the variables used by the CBT is total predicted summer streamflow on several headwater basins/tributaries of the system. Various linear regression models have been used in the past for streamflow prediction in the referred system.

The goal of the study was to determine if more complex methods, such as nonlinear neural networks and ARMAX models, could improve the forecasting performance of the existing linear regression models. It has been reported in literature that neural networks often provide better solutions when applied to complex and noisy systems. Besides neural networks, several ARMAX model were applied to the same forecasting problem, and the results of all the methods were compared.

The models were applied to predict the total summer flow at the Fraser River above the confluence, and the St. Vrain River above Lyons, based on the previous hydrologic conditions, snow, precipitation, and streamflow. In the case of the Fraser River, the linear regression produced as accurate forecasts as any other method; in the case of the St. Vrain River, the ARMAX(1,1,1) model produced more accurate forecasts than neural networks, which were, in turn, more accurate than the linear regression.

INTRODUCTION

Accurate predictions of the inflows to the CBT System in the Rocky Mountains of northern Colorado are critical for system planning and operation. The CBT operation models use the total predicted summer streamflow on several headwater basins/tributaries of the system. The inputs to the forecasting models are the current snowpack, cumulative precipitation, and the November flow of the previous year. The output is the total summer flow.

Artificial Neural Networks (ANNs) have been developed since the 1940s, but in recent decades, with current algorithms that overcome the limitations of early networks, they have raised a greater interest in practical applications. There is a wide variety of ANN algorithms; however, the main function of all ANN paradigms is to map a set of inputs to a set of outputs. An ANN is described as an information processing system composed of many nonlinear and densely interconnected processing elements or neurons. ANNs have been expected to provide better solutions when applied to: (1) complex systems that may be poorly described or understood; (2) problems that deal with noise or involve pattern recognition, diagnosis, abstraction, and generalization; and (3) situations where input

is incomplete or ambiguous by nature. It has been reported that ANNs have the ability to extract patterns in a phenomena and overcome difficulties due to the selection of a model form such as linear, power, or polynomial. ANN algorithms are capable of modeling the rainfall/snowmelt-runoff relationship, due to their ability to generalize patterns in noisy and ambiguous input data, and to synthesize a complex model without prior knowledge or probability distributions. The ANN models are calibrated using automatic calibration techniques. Thus, ANN models eliminate subjectivity and lengthy calibration cycles.

ANNs have also been applied to various engineering problems in recent years. In hydrology and water resources, ANNs have been applied frequently to forecasting and other problems.

Traditionally, for forecasting the total summer streamflow, various linear regression equations have been used. A goal of this research was to determine if a nonlinear, neural network model could improve the forecasting performance of the existing linear model.

In addition, several various ARMAX (autoregressive moving average with exogenous input) models were used for the same purpose.

The results of all the methods were compared in the following sections.

THE FORECASTING MODELS

Northern Colorado Water Conservancy District (NCWCD) in Loveland, Colorado, uses linear regression models to predict the total summer flow on tributaries of the CBT system. Forecasts are computed four times a year: February 1, March 1, April 1, and May 1. The total flow is defined as the sum of the monthly flow volumes for April, May, June and July. The inputs to the forecasting model are the current snowpack, cumulative precipitation between October 1 and the beginning of current month, and the November flow from the previous year. The output is the total flow between April 1 and July 31 (or May 1 and July 31 if the forecast is issued on May 1).

The models used in this study: multiple linear regression, ARMAX, and neural networks, are described in the following section.

The Multiple Linear Regression Model

The existing model is a multiple linear regression and has the following form (for April 1)

$$Q_{Apr-Jul} = a P_{Oct-Mar} + b Q_{Nov} + c S_{Apr-01} + d \quad (1)$$

where Q indicates flow, P stands for precipitation, S is snow water equivalent, and a, b, c, and d are the regression constants obtained based on the least square method.

Artificial Neural Networks (ANN)

ANN models were tested and compared with the multiple linear regression model given by Eq. (1). The ANN model had three inputs and one output, the same as the linear regression model. One hidden node was in a single hidden layer, reflecting a number of sigmoids superimposed, and in turn the complexity of the activation function.

The model equation is:

$$Q_{Apr-Jul}(i) = \frac{W2(1)}{1 + \exp(-(W1(1)P_{Oct-Mar}(i) + W1(2)Q_{Nov}(i-1) + W1(3)S_{Apr-01}(i) + B1))} + B2 \quad (2)$$

where index i denotes a particular year. The parameters of ANNs are $W1$, $W2$, $B1$, and $B2$. In this case, three inputs and one hidden node were used, so the parameter matrix $W1$ had size 3×1 . Other parameters were scalars (or matrices with dimensions 1×1) due to the presence of only one hidden node and one output. The model parameters were computed through minimization of the approximation error based on the back-propagation method (e.g. Hertz et al., 1991; or Muller and Reinhardt, 1990).

ARMAX Models

Another model type used in this study can be expressed by the following equation:

$$A(q)Q(t) = B(q)S(t-nk) + C(q)e(t) \quad (3)$$

where $Q(t)$ is the output time series predicted by the model, $S(t-nk)$ is the input time series shifted by nk , and $e(t)$ is noise. The numbers n_a , n_b , and n_c are orders of the shift operators $A(q)$, $B(q)$, and $C(q)$, respectively. Various values of the shift operators in Eq. (3) give different ARMAX models. For estimation of parameters in Eq. (3) see Ljung (1987).

Multiple linear regression, ANN, and ARMAX models were applied to the Fraser River above the confluence with the Colorado River, and the St. Vrain River above Lyons.

FORECASTING THE FRASER RIVER

The forecasting procedure was applied using data measured at the gaging station above the confluence of the Fraser River and the Colorado River. The Fraser River (Fig. 1) is a tributary of the Colorado River on the west slope of the Rocky Mountains in Colorado. The input time series contained 42 water years of data, over the period 1949-1993, with data for the years 1984-1986 missing. Precipitation data was obtained as an average from the Berthoud Pass and Granby gages. Flow data was measured at the station at the basin outlet, while snow data was an average of snow observations from six sites in the basin: Arrow, Berthoud Summit, Granby, Vasquez Creek, Lapland, and Ranch Creek.

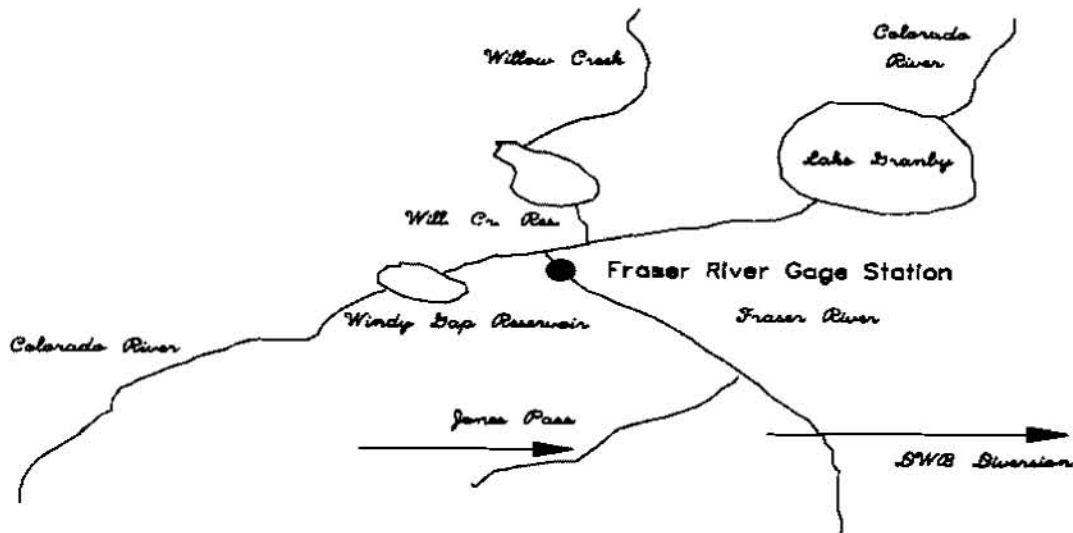


Figure 1 The schematic of the Fraser River

The multiple linear regression model for April 1 was given by:

$$Q_{Apr-Jul} = 2.072 P_{Oct-Mar} + 854.06 Q_{Nov} + 11796.35 S_{Apr-01} - 49284 \quad (4)$$

while the final model based on ANNs was:

$$Q_{Apr-Jul}(i) = \frac{0.73}{1 + \exp(- (0.41 P_{Oct-Mar}(i) + 0.58 Q_{Nov}(i-1) + 4.71 S_{Apr-01}(i) + 0.04))} - 0.24 \quad (5)$$

Other (ARMAX type) models are described in the following text. The meaning of $Q(t)$ is in this case total summer streamflow, $S(t)$ is snowpack on April 1, and $e(t)$ is a noise term in year t .

ARMA(1,1) Model. By assuming that there is no exogenous input in Eq. (3), that $n_a=1$, and that $n_c=1$, an ARMA(1,1) model was obtained. The model was not causal as the solutions were outside the unit circle.

ARMAX(1,0,1) Model. Assuming $n_a=1$, $n_b=1$, $n_k=0$, and $n_c=0$ in Eq. (3), an ARMAX(1,0,1) model was obtained. The final model has the following shape:

$$Q(t) = -0.025 Q(t-1) + 12582 S(t) + e(t) \quad (6)$$

ARMAX(0,0,1) Model. By setting $na=0$, $nb=1$, $nk=0$, and $nc=0$ in Eq. (3), an ARMAX(0,0,1) model was obtained. The model is:

$$Q(t) = 12473 S(t) + e(t) \quad (7)$$

ARMAX(1,1,1) Model. With $na=1$, $nb=1$, $nk=0$, and $nc=1$, the following ARMAX(1,1,1) model was obtained:

$$Q(t) = 0.042 Q(t-1) + 11936 S(t) + e(t) + 0.050 e(t-1) \quad (8)$$

Multivariate AR(1) Model. A bivariate AR(1) model given by Eq. (9) was assumed. The model parameters were estimated based on the Durbin-Levinson algorithm (Brockwell and Davis, 1990), and the final form was:

$$\begin{vmatrix} S(t+1) \\ Q(t) \end{vmatrix} = \begin{vmatrix} -0.155 & -0.93 \times 10^{-5} \\ 12320.0 & -0.0175 \end{vmatrix} \begin{vmatrix} S(t) \\ Q(t-1) \end{vmatrix} + \begin{vmatrix} e_1(t) \\ e_2(t) \end{vmatrix} \quad (9)$$

where $e_1(t)$ and $e_2(t)$ are independent normally distributed noise terms.

For each model, the root mean square error (RMSE) and squared correlation coefficient (R^2) were compared and shown in Table 1.

Table 1. Performance of various forecasting methods on the Fraser River summer forecast

Model/Criterion	MSE	R^2
ANNs	24441.0	0.666
Linear Regression	24502.7	0.661
ARMAX(1,0,1)	24488.0	0.662
ARMAX(0,0,1)	24502.7	0.661
ARMAX(1,1,1)	24587.0	0.660
Multivariate AR(1)	24485.8	0.662

All the models produced fairly similar results in terms of the RMSE and R^2 . ANNs were as good as linear regression and any ARMAX model. On the other hand, the linear regression was simpler and required less computational time. In addition, the chosen method based on neural networks had six parameters, while the linear regression had four parameters.

FORECASTING THE ST.VRAIN RIVER

Another watershed used to apply the forecasting procedures was the watershed of the St. Vrain River above Lyons in Colorado. The St. Vrain River (Fig. 2) is a tributary of the South Platte River, on the east slope of the Rocky Mountains in northern Colorado.

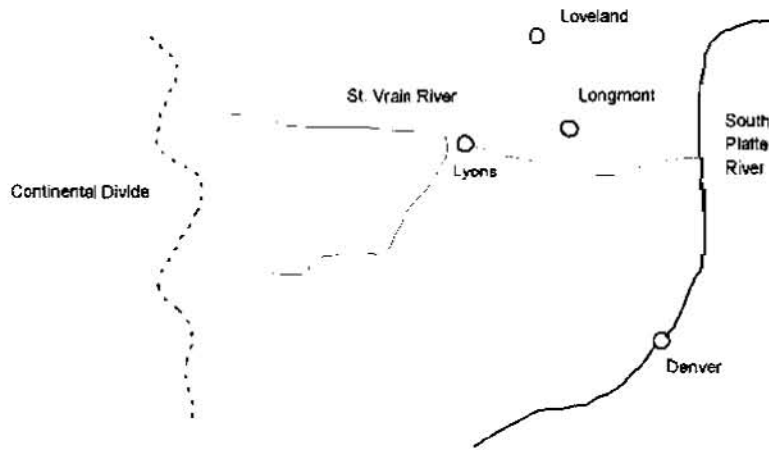


Figure 2 The St. Vrain River Basin Location

The input time series contained 42 water years of data, covering period 1951-1992. The precipitation data were obtained as the average from two observation sites: Estes Park and Allenspark Lodge. The flow data was measured at Lyons, Colorado, while snow data was the average of snow observations at five sites in the basin: Copeland Lake, University Camp, Wild Basin, Ward Basin, and Longs Peak in Colorado. Table 2 shows the performance of the forecasting models.

Table 2 Forecasting performances of various methods for forecast of the St. Vrain River summer flows

Model/Criterion	RMSE	R ²
ANNs	16550.9	0.6154
Linear Regression	16833.6	0.6022
ARMAX(1,0,1)	17051.4	0.5920
ARMAX(0,0,1)	16833.6	0.6022
ARMAX(1,1,1)	15773.0	0.6523
Multivariate AR(1)	17039.6	0.5924

In this case, ARMAX(1,1,1) was somewhat better based on RMSE and R^2 . Other models, including the linear regression and ANNs, were similar.

CONCLUSIONS

In the case of the Fraser River, the linear regression method produced as accurate forecasts as any other method. In this particular case, it is not very clear that using more complex models would significantly improve the forecast. However, in the case of the St. Vrain River, it appears that the ARMAX(1,1,1) model might be somewhat more accurate. The ARMAX(1,1,1) gave the smallest RMSE and the largest correlation coefficient between the observed and predicted streamflow.

ACKNOWLEDGEMENTS

Thanks are due to NSF Grant CMS-9625685 on "Uncertainty and Risk Analysis Under Extreme Hydrologic Events" for the partial support concerning this research.

Thanks are also due to Dennis Baker and Dr. John Scott from the Northern Colorado Water Conservancy District, Loveland, Colorado, for providing the financial support and a valuable advice and expertise.

REFERENCES

- Brockwell, P.J. and Davis, R.A., Time Series: Theory and Methods, Springer-Verlag, 1987.
- Haltiner, J.P. and Salas, J.D., Short-term Forecasting of Snowmelt Runoff using ARMAX Models, Water Resources Bulletin, Vol. 24, No. 5, 1988.
- Hertz, J., Krogh, A., and Palmer, R., Introduction to the Theory of Neural Computation, Addison-Wesley Publishing Company, 1991.
- Kohonen, T., An Introduction to Neural Computing, Neural Networks 1, 3-16, 1988.
- Lapedes, A. and Farber, R., Nonlinear Signal Processing Using Neural Networks: Prediction and System Modeling, Technical Report LA-UR-87-2662, Los Alamos National Laboratory, 1987.
- Liu, N., Baker, D., Scott, J., and Leaf, C., Streamflow Forecasting by Snowmelt-Runoff Models for the Fraser River Basin, Technical Report, Northern Colorado Water Conservancy District, Loveland, Colorado, 1991.
- Ljung, L., System Identification: Theory for the User, Englewood Cliffs, NJ : Prentice-Hall, 1987.
- Markus, M. and Baker, D., The Fraser River, Streamflow Forecasting and Simulation, Technical Report, Northern Colorado Water Conservancy District, Loveland, Colorado, 1994.
- Markus, M., Salas, J.D., and Shin, H., Predicting Streamflows Based on Neural Networks, Proceedings of the First International Conference on Water Resources Engineering, Water Resources Engineering Division of the American Society of Civil Engineers, San Antonio, Texas, 1995.

- Mood, A.M., Graybill, F.A., and Boes, D.C., Introduction to the Theory of Statistics, McGraw-Hill, New York, 1974.
- Muller, B. and Reinhardt, J., Neural Networks. an Introduction, Springer-Verlag, 1990.
- Raman, H. and Sunilkumar, N., Multivariate Modeling of Water Resources Time Series Using Artificial Neural Networks, Hydrological Sciences Journal, 40, 2, 1995.
- Salas, J.D., Delleur, J.W., Yevjevich, V., and Lane, W.L., Applied Modeling of Hydrologic Time Series, Water Resources Publications, 1980.
- Tokar, A.S. and Markus, M., Artificial Neural Networks and Conceptual Models in Water Management of Small Basins in the Central United States, FRIEND International Conference, Postojna, Slovenia, Europe, 1997.

INTEGRATION OF QUANTITATIVE PRECIPITATION FORECASTS WITH HYDROLOGIC MODELS AND RIVER BASIN DECISION SUPPORT SYSTEMS

By David Matthews,¹ Curtis Hartzell,² and Arlin Super,² River Systems and Meteorology Group, Bureau of Reclamation, Denver, Colorado

and

Tom Carroll³ and John Schaake,⁴ Office of Hydrology, National Weather Service, National Oceanic and Atmospheric Administration

Abstract: This paper describes plans for a system that will integrate key components of current research applications of quantitative precipitation forecasts, evapotranspiration analysis and forecasts, and NEXRAD precipitation algorithm research into the National Weather Service River Forecast System. The system will also provide operational forecasts to the Bureau of Reclamation's water managers' decision support systems. It is based on current decision support tools for water conservation, analysis of snow water equivalent and snow depth from the National Weather Service Snow Estimation and Updating System, and NEXRAD WSR-88D precipitation algorithms. It outlines other planned collaborative research with the National Operational Hydrologic Remote Sensing Center. Implications for the Advanced Hydrologic Prediction System and potential applications of emerging research tools from the Global Energy and Water Cycles Experiment—Continental-Scale International Project are discussed.

INTRODUCTION AND BACKGROUND

Accurate and timely hydrometeorological information is essential for reservoir and river basin management operations conducted at the Bureau of Reclamation's (Reclamation) facilities. Reclamation serves over 31 million Americans in 17 Western States and provides over 9.3 trillion gallons of water and 45 billion kilowatthours of electricity each year. River basin managers must have timely data from remote areas that are often inaccessible in winter, and the managers must have a means of quickly analyzing the impacts of precipitation and snowmelt on streamflow for routine river system management and emergency responses to extreme events. Consequently, Reclamation operates and maintains a variety of hydrometeorological observing systems and cooperates with other agencies in collecting additional data.

This paper presents an overview of: (1) current and planned applications of hydrometeorological data for water resources management within Reclamation and (2) collaborative partnerships planned with the National Weather Service (NWS) Office of Hydrology and the National Centers for Environmental Prediction. The overview includes brief descriptions of Reclamation's hydrometeorological and early warning observing systems, decision support tools, and interactions with other cooperating agencies. The cooperating agencies who collect, transmit, and analyze hydrometeorological information include the National Oceanic and Atmospheric Administration (NOAA), U.S. Geological Survey, U.S. Army Corps of Engineers, Natural Resources Conservation Service (NRCS), Agricultural Research Service, and National Aeronautics and Space Administration.

Other remotely sensed information from NOAA's National Operational Hydrologic Remote Sensing Center (NOHRSC), NWS NEXRAD, the NRCS SNOTEL, and the U.S. Geological Survey streamgauge observations will be discussed in the context of integrated application of these data to solving practical water resources management challenges.

¹ Manager, River Systems and Meteorology Group

² Research Meteorologist

³ Director, National Operational Hydrologic Remote Sensing Center

⁴ Chief Scientist, Office of Hydrology

The purpose of this paper is to show the types of integrated information systems Reclamation currently uses and establish a basis for further collaborative partnerships to apply information from other sources and emerging technologies to meet our water resources and related resources management responsibilities to the American public.

Reclamation's Responsibilities: Maintaining an equitable, balanced use of water among agricultural, industrial, recreational, and municipal water users, while maintaining the riparian habitat and conserving water, requires careful water resources management. Reclamation area offices and regional offices are responsible for the daily operation of reservoirs and the implementation of integrated resource management plans to equitably balance the distribution of water to users. At the same time, Reclamation must meet the legal constraints of the "Law of the Rivers" and provide for public safety during periods of extreme events such as floods and droughts.

Reclamation's water managers use a variety of tools to assist in developing long-range plans and annual operating plans and making monthly and daily operational decisions. Reclamation's Research and Technology Transfer Program addresses methods to apply emerging technologies to river system operations management tools. Our teams are developing an integrated observation and decision support systems to improve the efficient use of water from Federal reclamation projects for the general public. These programs include river basin management, irrigation district water conservation, flood early warning systems (EWS), and special NEXRAD algorithms. The following sections describe these efforts.

WATERSHED AND RIVER SYSTEM MANAGEMENT PROGRAM

The interagency Watershed and River System Management Program, sponsored by Reclamation's Science and Technology Program and the U.S. Geologic Survey's Water Resources Division, provides an excellent example that integrates hydrometeorological data with advanced technologies for decision support. The system uses a relational hydrologic data base that provides a central source of information that drives: (1) physically based process models, (2) river system simulation and optimization models, (3) planning and other special graphical analyses, and (4) and data tabulation displays.

Physical process models such as Leavesley's (1995) Modular Modeling System compute streamflow from precipitation over gridded hydrologic response units. Figure 1 shows a schematic of the program and how it integrates various sources of hydrometeorological information into a central relational Hydrologic Data Base (HDB) from which models access initial conditions, run simulations, and provide tabular and graphical analyses that river managers and planners may use to make decisions.

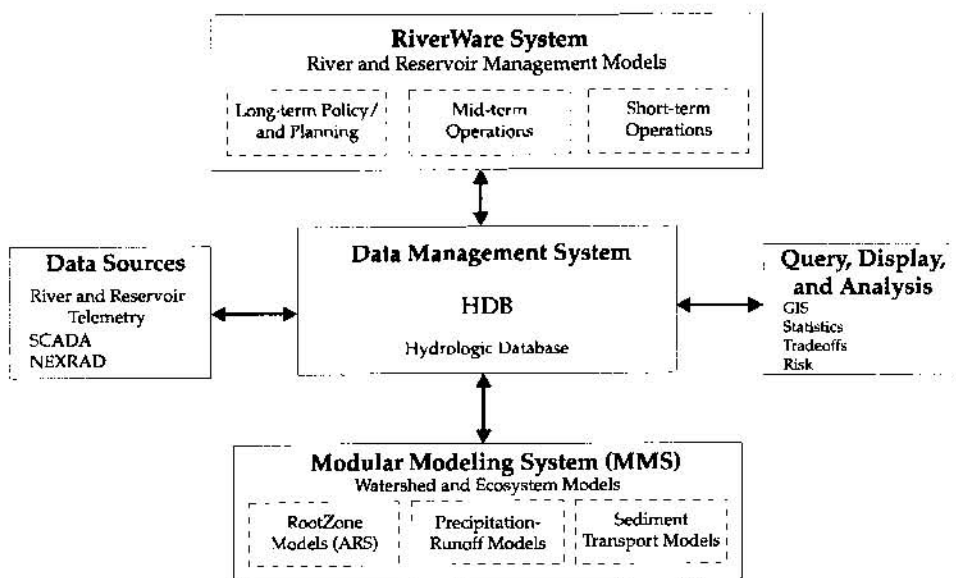


Figure 1.—Data Centered Decision Support System used in the Watershed and River System Management Program to assist water managers.

This HDB is linked to observing systems through data collection platforms that transmit to base stations and Geosynchronous Operational Environmental Satellites and radio relay links. Internet and other Reclamation communication networks bring data into the HDB from Reclamation and other agencies.

Models such as the Modular Modeling System (MMS), developed by Leavesley, simulate snowpack evolution, runoff, and resulting streamflow from the hydrometeorologic data. This streamflow data then drives the Power and Reservoir Systems Model (Zagona, Fulp, and Vickers, 1996) that is used by river operations managers to control irrigation deliveries and hydropower dispatches and maintain the equitable and sustainable use of vital water resources.

Efficient and effective management of river basin resources within the "Law of the River" requires careful and accurate decisions that balance limited water supplies with ever increasing demands for human and ecosystem water use. Ryan (1996) applied a similar modeling system to the Gunnison River Basin and showed that in 1994 more accurate conventional precipitation data produced better streamflow forecasts that resulted in additional power revenues of over \$100,000.

This user friendly MMS with graphical user interfaces, data management interfaces, and analytic tools is described in detail by Zagona et al. (1996).

AGRICULTURAL DECISION SUPPORT - THE AWARDS SYSTEM

Reclamation's initial work on making operational use of NEXRAD rainfall estimates was the development of an automated system to assist water users by providing easy access to rainfall and daily crop water use estimates. The result was the **Agricultural Water Resources Decision Support (AWARDS)** system.

The purpose of the AWARDS system is to improve the efficiency of water management and irrigation scheduling by providing guidance on when and where to deliver water and how much to apply.

The AWARDS system is based on modern remote sensing, communication, computer, and Internet technologies. The current AWARDS system works as summarized below.

- NEXRAD Doppler radar systems measure equivalent reflectivity factor (Z_e). The data are input to the Precipitation Processing System (PPS). The PPS produces the hourly Digital Precipitation Array for each radar system (Level II), Stage 1).
- Automated surface weather stations collect real-time data.
- Radar and surface weather data are transmitted and input to central computers for processing; the NWS River Forecast Centers produce NEXRAD Level III, Stage 2 and 3 products.
- The AWARDS system computer automatically collects digital format data files of Level III, Stage 3 radar rainfall estimates, weather station data, and NWS precipitation forecasts from the central computers.
- The AWARDS system computer prepares the rainfall image and chart products, making them available in near real time for Internet access.
- Reservoir operators, water managers, and on-farm water users access the AWARDS system products via the Internet.
- Reservoir operators, water district staff, and on-farm irrigators make operational decisions based on the information provided by the AWARDS system.

The AWARDS system works with 24-hour surface weather station data:

- Mean temperature
- Mean relative humidity
- Mean wind speed
- Point rainfall accumulation
- Total solar radiation

The AWARDS system uses the NEXRAD radar rainfall estimates and surface weather station data with:

- Crop evapotranspiration (ET) equations
- Local terrain and soil information
- Effective rainfall estimates
- Local daily maximum and minimum normals
- Quantitative precipitation forecasts
- Watershed/reservoir systems
- Irrigation water distribution systems

The AWARDS system provides the water managers and users with:

- NEXRAD rainfall and watershed rainfall water volume estimates
- Effective rainfall estimates
- ET estimates for determining crop water use

The above information is available from Reclamation's NEXRAD Web page: <http://www.usbr.gov/rsmg/nexrad>.

Figure 2 is an example of an interactive AWARDS system image for the Lugert-Altus Irrigation District, located in southwestern Oklahoma. The NEXRAD Hydrologic Rainfall Analysis Project (HRAP) (Greene and Hudlow, 1982) grid cells (about 4 by 4 kilometers) in figure 2 show the estimated 24-hour (midnight to midnight local time) average rainfall (inches) for each cell. Also shown (at + signs) are the locations of two Oklahoma Mesonet weather stations (Crawford et al., 1992). The irrigators can click a computer mouse on the HRAP grid cells within the dashed line boundary for popup estimated Crop Water Use (ET) charts and can click on the weather stations for popup daily weather charts.

EARLY WARNING SYSTEMS

Reclamation is designing EWS for Reclamation and Bureau of Indian Affairs (BIA) dams to provide enhanced public safety to populations at risk downstream from the dams. The EWS designs are comprised of the following components: (1) a method for **detecting** flash-flood events; (2) a **decisionmaking** process; (3) a means of **communicating** warnings between operating personnel and local public safety officials; and (4) a means for local public safety officials to effectively communicate the **warnings** to the public and carry out a successful **evacuation** of the threatened population (Fisher, 1993).

The ability to quickly respond to heavy rainfall and a potential flash-flood event depends upon adequately detecting the event and transmitting the data to the decisionmaker in near real time. There is a need to accurately estimate the rainfall water volume in the subbasins of the watershed above the dam. There is a further need for a reliable communications path for transmitting the data or an alert to the decisionmaker for the purposes of water management and issuing flash-flood warnings.

The goal behind this research is to develop a methodology, based on NEXRAD (WSR-88D) radar rainfall estimates, that provides reservoir and river system managers with high-resolution, mean rainfall accumulation and water volume estimates. This information can be automatically transmitted via a reliable satellite paging system to the decisionmaker. It is anticipated that, in the future, this methodology will be available to enhance EWS at many



Figure 2.—NEXRAD Level III Stage 3 rainfall accumulation estimates (4- by 4-kilometer grid) over the Lugert-Altus Irrigation District for the 24-hour period ending August 22, 1997, 12 UTC.

Reclamation and BIA dam-reservoir-watershed systems throughout the 17 Western States. However, such implementation of the NEXRAD-enhanced EWS will depend on the radar coverage over mountainous terrain and near real-time data availability. These estimates are provided hourly and for storm totals.

NEXRAD ALGORITHM APPLICATIONS

Reclamation has recently developed the means to use Level III reflectivities as input to a snow algorithm. Reclamation meteorologists and programmers began development of a Snow Accumulation Algorithm (SAA) for the NEXRAD Operational Support Facility in June 1995. The ongoing SAA development was described in detail by Super and Holroyd (1996, 1997a), and an overview was presented by Super and Holroyd (1997b).

The SAA was tested in real time during the 1996-97 winter at the Cleveland and Minneapolis National Weather Service Forecast Offices where Level II reflectivities were available as input. Reasonable results were obtained as discussed by Naistat et al. (1988) for the Minneapolis region. But Reclamation will not have Level II data available, so the SAA has been modified to use Level III reflectivities decoded from the 16 level graphical product. Further testing is needed, but initial SAA runs with both Level II and Level III data for Minnesota snowstorms indicate quite reasonable agreement. That is, degrading the Z_e measurements from 0.5 to 5.0 dBZ resolution does not appear

to result in serious degradation of snow water equivalent (SWE) estimation over several hours. Similar tests should be made with rain over shorter intervals to determine whether Level III reflectivity observations are adequate for use with EWS.

Because the NWS needs to merge or mosaic observations from adjoining radars across the entire nation, the single PPS precipitation algorithm is currently used by *all* radars for *all* seasons. This “lock-step” approach does not allow for the maximum use of *individual radar* observations over portions of the total area scanned by the radar; e.g., drainage basins. It is generally not possible, for example, to adjust the Ze-R relationship (where R=precipitation) to the optimum relation for specific regions, or to adjust for different rain types, such as thunderstorm and widespread stratiform rain.

Another example of PPS inflexibility is the inability to use the lowest practical radar beam elevation angle (beam tilt) for each ground location relative to the radar. The current scanning practice, designed for rain from high-based convective clouds, uses radar observations too high above the surface for accurate stratiform rain or snow estimation **except near the radar**. For such precipitation, it is best to scan as near the ground as possible, while not causing too much ground clutter contamination, because a vertical profile of Ze exists in such storm clouds with maximum values near the ground. Scanning too high in such layer clouds results in underestimation of surface rainfall **at mid to far ranges from the radar**. Consequently, Reclamation plans to convert its SAA into a rain algorithm which will allow more flexibility than the PPS when used with an *individual radar*.

USE OF NEXRAD WSR-88D RADAR ESTIMATION OF SNOW WATER EQUIVALENT TO IMPROVE OPERATIONAL WATER RESOURCES MANAGEMENT

Reclamation proposes to significantly improve estimation of SWE distributions and snow cover. Procedures will be developed in the upper Mississippi and upper Missouri River Basins, each an area of interest to the Global Energy and Water Cycles Experiment—Continental-Scale International Project. Improved estimation will be accomplished by incorporating NEXRAD *radar estimates of SWE and snow cover* into current NWS estimation methodology. NWS estimates are now based on integration of surface SWE measurements, airborne SWE sampling, and satellite snow cover mapping (but not radar). The SWE distribution and snow cover estimates are vital for initialization of various models used to predict *snowmelt and streamflow*. These predictions are of great importance to Reclamation's water management decisionmakers.

NEXRAD radar estimates will be produced by Reclamation's new SAA, being developed for the tri-agency NEXRAD Operational Support Facility. The SAA was successfully tested in real-time at Cleveland, Ohio, and Chanhassen, Minnesota, during the 1996-97 winter. Radar estimates of SWE and snow cover will be provided in the same gridded field format used by the NWS NOHRSC, tasked with making and disseminating national estimates of SWE and snow cover distributions. The NOHRSC will then integrate the radar fields into their Snow Estimation and Updating System (SEUS), which is used to initialize snow accumulation and ablation models. The latter provides streamflow predictions to Reclamation and other water management agencies.

Initial work will take place in the nonorographic regions of the Upper Midwest, where special surface SWE observations are available, allowing SAA "calibration" for that region. By the third year, emphasis will shift to mountains and plains of the Upper Missouri River Basin. Special surface observations in all studied areas will provide documentation of radar SWE accuracy and uncertainty, both needed to properly incorporate radar estimates into the SEUS. Methodology also will be developed to reduce known far-range underestimation by radar and to merge SWE and snow cover estimates from adjoining radars. This research will be coordinated with the NWS River Forecast System development team and with the Advanced Hydrologic Prediction System's implementation team.

SUMMARY AND CONCLUSIONS

Reclamation is partnering with other Federal, State and local agencies to integrate hydrometeorological information into data bases that can be used by operation managers of reservoirs and river systems and associated irrigation

district managers and emergency response teams to manage water and related resources more effectively. We look forward to continuing and improving our partnerships and enhancing our application of emerging technologies through these partnerships.

- Reclamation is designing EWS to provide enhanced public safety to populations downstream from dam structures who would be at risk during flash-flood events.
- The AWARDS system demonstrates a methodology that integrates NEXRAD Level III, Stage 3 rainfall estimates with modern computer, communication, and Internet technologies for improved water resources management.
- A NEXRAD-enhanced EWS is being planned for the Olympus Dam watershed near Estes Park, Colorado. This system will integrate the existing EWS stations with NEXRAD Level III, Stage 3 rainfall estimates and a reliable satellite paging system.
- Using NEXRAD Level III reflectivity data received from a NEXRAD Information Dissemination Service (NIDS) vendor and modifying the Reclamation-developed SAA for rain has the potential to improve both the spatial and temporal resolutions of the radar rainfall estimates. However, the accumulation resolution of estimated rainfall would be degraded.
- Various options for rain estimation are offered by NIDS products, the PPS algorithm, and Reclamation's more flexible algorithm. These options involve a number of tradeoffs between spatial, temporal, and accumulation resolutions of rainfall estimates. It is not yet apparent what the best approach will be for use with Reclamation's EWS.

The authors recommend that Reclamation's SAA be modified for rain and used with NIDS Level III reflectivities. Tests should be conducted to determine how well this approach estimates rainfall, as observed by reasonably dense gage networks. Comparisons between the same algorithm's runs with Level II and Level III Z_e observations for heavy rainstorms should reveal how much accuracy is lost by using the Level III "degraded" observations. Comparisons of PPS algorithm rain estimates, Reclamation algorithm estimates using Level III data and customization for a particular mountain watershed, both against rainfall measured from a reasonably dense gage network, would also be useful.

Comparisons with the NWS River Forecast System will be conducted to evaluate operational forecasts and the enhancements using SEUS with NEXRAD algorithm improvements and other products of cooperative research efforts.

REFERENCES

- Albers, S. C., McGinley, J. A., Birkenheuer, D. L., and Smart, J. R., 1996, The Local Analysis and Prediction System (LAPS): Analysis of Clouds, Precipitation and Temperature. *Wea. Forecasting* **11**, 3 pp. 273-287.
- Anthes, R. A., Hsie, E. Y., and Kuo, Y. H., 1987, Description of the Penn State/NCAR Mesoscale Model Version 4 (MM4). NCAR Tech. Note, NCAR/TN-282+STR, 66 pp.
- Fisher, D. B., 1993, Reclamation's design process of Early Warning Systems for dam safety. *Hydraulic Engineering '93*, Vol. 1, American Society of Civil Engineers, pp. 690-695.
- Bleck, R., and Benjamin, S. G., 1993, Regional weather prediction with a model combining terrain-following and isentropic coordinates. Part 1: Model description, *Mon. Wea. Rev.*, **121** pp. 1770-1785.
- Crawford, K. C., Brock, F., Elliot, R., Cuperus, G., Stadler, S., Johnson, H., and Doswell, C., III, 1992: The Oklahoma Mesonet: A 21st century project. Preprints, Eighth Int. Conf. On Interactive Information and Processing Systems for Meteorology, Oceanography, and Hydrology, Atlanta, Georgia. Amer. Meteor. Soc., pp. 27-33.
- Greene, D. R., and Hudlow, M. D., 1982, Hydrometeorologic Grid Mapping Procedures. Presented at the AWRA International Symposium on Hydrometeorology, Denver, Colorado.

- Hunter, S. M., 1996, WSR-88D Radar Rainfall Estimation: Capabilities, Limitations and Potential Improvements. National Weather Digest, **20**, June, pp. 26-38.
- Klazura, G. E., and Imy, D. A., 1993, A description of the initial set of analysis products available from the NEXRAD WSR-88D system. Bull. Amer. Meteor. Soc., **74**, pp. 1293-1311.
- Leavesley, G. A., Restrepo, P. J., Stannard, L. G., Frankoski, L. A., and Sautins, A. M., 1993, The Modular Modeling System - MMS. In proceedings of the Second International Conference/Workshop on Integrating Geographic Information Systems and Environmental Modeling, Breckenridge, Colorado, Sept. 26-30, 1993.
- Naistat, R. J., Super, A. B., and Effertz, D. W., 1998, Real-Time Testing of a Snow Algorithm in the Upper Midwest During the 1996-1997 Winter Season. Preprints, 16th Conference on Weather Analysis and Forecasting, Amer. Meteor. Soc., Phoenix, Arizona, January 11-16, 3 pp.
- Pereira A. J., Crawford, K. C., and Hartzell, C.L., 1996: Statistical objective analysis scheme for improving WSR-88D rainfall estimates. Bureau of Reclamation report R-96-08 (2 Vol.), Denver, Colorado.
- Pereira, A. J., Crawford, K. C., and Hartzell, C. L., 1996, How can we improve Stage 3 precipitation processing? Fifth National Heavy Precipitation Workshop. Department of Commerce/NOAA/NWS, p. 60.
- Ryan, T., 1996, Development and application of a physically based distributed parameter rainfall runoff model in the Gunnison River basin. Final Report, Global Climate Change Response Program, U.S. Bureau of Reclamation, Denver, Colorado, 64 pp.
- Super, A. B., and Holroyd, E. W., III, 1996, Snow accumulation algorithm for the WSR-88D radar, version I. Bureau of Reclamation Report R-96-04, Denver, Colorado, June, 133 pp.
- Super, A. B., and Holroyd, E. W., III, 1997a, Snow accumulation algorithm for the WSR-88D radar: Second Annual Report. Bureau of Reclamation Report R-97-05, Denver, Colorado, 79 pp.
- Super, A. B., and Holroyd, E. W., III, 1997b, Snow accumulation algorithm development for the WSR-88D radar.
-

Corresponding author address: David A. Matthews, D-8510, PO Box 25007, Technical Service Center, Bureau of Reclamation, Denver CO 80225-0007; email: dmatthews@do.usbr.gov

DEVELOPMENT OF AN UNSTEADY FLOW HYDRAULIC MODEL OF THE LOWER MISSOURI RIVER

**By Rebecca R. Allison, Hydraulic Engineer, U. S. Army Corps of Engineers
Kansas City District, Kansas City, Missouri**

INTRODUCTION

In the aftermath of the 1993 Flood, many questions were raised regarding the impact of environmental factors and structural systems on flood stages. In order to examine some of these questions, Congress authorized the Floodplain Management Assessment (FPMA) as a comprehensive study of the Missouri and Mississippi River Basins, and how they reacted to the conditions of the 1993 Flood. As part of this study, the Kansas City District of the U. S. Army Corps of Engineers developed an unsteady flow hydraulic model of the lower Missouri River and its tributaries using the mathematical computer model program UNET. This model extends from Rulo, Nebraska, at river mile 498, to the mouth of the Missouri River at its confluence with the Mississippi River. Following FPMA, development of the UNET model continued under the auspices of the Mississippi Basin Modeling System (MBMS). The UNET model of the lower Missouri River developed for the MBMS will be used by the U. S. Army Corps of Engineers Missouri River Region - Reservoir Control Center for reservoir operations.

UNET is a one-dimensional, unsteady flow program which simulates unsteady flow through a full network of open channels and reservoirs. New algorithms were developed for UNET to simulate hydraulic conditions and structures unique to the lower Missouri River. Algorithms were developed to simulate levee systems as storage areas or active flow areas, to simulate dike fields, and to account for ungaged inflow to the river system.

GEOGRAPHIC COVERAGE OF THE LOWER MISSOURI RIVER UNET MODEL

The Missouri River originates in the northern Rocky Mountains at Threeforks, Montana, and flows south and east for 2,315 miles to join the Mississippi River at a point approximately 15 miles above St. Louis, Missouri. The Missouri River Basin, which drains 74 percent of the upper Mississippi River Basin, is the largest of the United States' major water resource regions, embracing 513,000 square miles within the United States and 9,715 square miles in Canada. Hydrologically, the Missouri River Basin is divided into upper and lower portions with demarcation at Sioux City, Iowa. The lower Missouri River Basin contains 214,700 square miles.

The Missouri River Basin drainage area within the Kansas City District amounts to 110,445 square miles, which includes all of the lower basin drainage area from river mile 498.1 at Rulo, Nebraska, to the mouth near St. Louis. The Missouri River contributes 42 percent of the long-term average annual flow of the Mississippi River at St. Louis and is the major contributor of sediment in the upper Mississippi River Basin. Between Rulo, Nebraska, and the mouth at St. Louis, the Missouri River has a total fall of about 451 feet and the average slope varies from 0.8 to 1.0 foot per mile. The floodplains are comparatively wide and for the most part are under cultivation. The width of the floodplain varies from a maximum of approximately thirteen miles to a minimum of approximately

1.5 miles. The actual flow way decreases to less than 0.5 mile in reaches with urban levees at Kansas City and St. Charles.

Tributaries: Most of the major tributaries of the Missouri River are included as separate routing reaches in the UNET model. Inclusion depends on the existence of U. S. Geological Survey (USGS) gaging stations on the tributaries. Tributaries are modeled from the last downstream rated gage on the tributary to the confluence with the Missouri River, in order to reproduce the effects of backwater on the outflows. Major tributaries of the Missouri River which have the requisite gaging, and are therefore included in the Kansas City UNET model as routing reaches, are the Big Nemaha, Nodaway, Platte, Kansas, Big Blue, Little Blue, Grand, Chariton, Little Chariton, Blackwater/Lamine, Osage, and Gasconade Rivers.

Reservoirs: The Missouri River Basin contains numerous reservoirs and impoundments. All reservoirs within the Kansas City District are constructed on tributaries of the Missouri River. These include eighteen multiple-purpose lake projects constructed by the U. S. Army Corps of Engineers (Corps) and eleven lake projects constructed by the Bureau of Reclamation (Bureau). Seven Corps reservoirs are located in the Kansas River Basin, six are in the Osage River Basin, two are in the Little Blue River Basin, and there is one reservoir each in the Platte, Chariton, and Little Chariton river basins. The eleven Bureau lake projects are all on the Republican and Smoky Hill Rivers in the Kansas River Basin. The Bureau operates these lake projects primarily for the storage and distribution of water for irrigation, while the Corps is responsible for the flood control operation of the Bureau's lakes as part of the lower Missouri River flood control system.

Levees: The Kansas City District has constructed seventeen Federal levees along the Missouri River as part of the Missouri River Levee System (MRLS). All but four of the completed MRLS units are upstream of Kansas City. These units protect mostly agricultural lands plus some small towns. A combination of urban and agricultural land is protected in the St. Joseph, Missouri/Elwood, Kansas area by MRLS Levee Units R471-460 and L455. Flood protection in the Kansas City, Kansas/Missouri urban area is provided by seven Federal levee units constructed by the Kansas City District along the Missouri and Kansas Rivers. The units along the Missouri River are the Fairfax/Jersey Creek, Central Industrial District (CID), and East Bottoms Levee Units along the right bank, and the North Kansas City and Birmingham Levee Units along the left bank.

Within the Kansas City District, the Missouri River is almost totally leveed from the mouth to Rulo, Nebraska. Non-Federal (privately owned) levees protect the majority of the agricultural lands from the mouth to Kansas City. Three non-Federal levees protect urban areas on the lower end of the river. They are the Chesterfield-Monarch, Riverport, and Earth City Levee Districts. Upstream of Kansas City, non-Federal levees fill in where there are unprotected areas around the MRLS units. Non-Federal levees along the Missouri River were devastated by the 1993 Flood. Approximately 99 percent of all non-Federal levees were breached from Brownsville, Nebraska, to the mouth, which is a distance of 535 river miles. At the peak of the flood, all non-Federal levees in the lower reach of the river, with the exception of Riverport and Earth City Levees, were completely inundated and the floodplain functioned as if the levees did not exist.

UNET MODEL DEVELOPMENT

The Kansas City-Missouri River UNET model was developed by the Kansas City District to represent the unique character of the lower Missouri River. The UNET model of the lower Missouri River consists of a network of tributary and mainstem routing reaches. There are a total of twenty-five routing reaches in all – twelve tributary and thirteen mainstem routing reaches. Reach No. 1 begins at the USGS gage at Rulo, Nebraska, on the Missouri River and runs to the first routed tributary, the Big Nemaha River. Reach No. 25 begins at the last routed tributary, the Gasconade River, and ends at the gage at St. Charles, Missouri. The data necessary to develop the UNET model includes Missouri River and tributary geometry, observed discharge and stage data, levee data, and dike field data. The model has been calibrated to 1986, 1993, and 1994 water year flows.

River Geometry: The geometry of the river system is described by cross-sections that extend from bluff to bluff. The overbank geometry of the cross-sections is from two-foot contour maps which were developed by photogrammetry. These maps were compiled in the 1970's for the Missouri River Restudy which utilized the Kansas City Backwater Program. The cross-sections were translated from Kansas City Backwater format into HEC-2 format, and then into UNET format. Some of the cross-sections did not extend beyond the Federal levee systems. Overbank geometry for these cross-sections was augmented from USGS 7.5 minute series quadrangle maps. The channel sections were developed from the 1994 hydrographic survey of the Missouri River. A computer program was written to merge the channel sections with the overbank geometry. The distance between cross-sections averages from 0.5 mile to 1.0 mile. Cross-sections in urban reaches average 0.1 mile apart. Total number of cross-sections on the mainstem exceeds 800. All tributary cross-sections were developed from USGS 7.5 minute series quadrangle maps. The distance between cross-sections on tributaries varies from approximately 5.0 miles to 0.5 miles.

Boundary Conditions: The stage hydrograph from the Rulo, Nebraska, USGS gaging station on the Missouri River at river mile 498.1 is the upstream boundary condition hydrograph for the beginning reach of the Kansas City-Missouri River UNET model. Discharge data from USGS gaging stations are used as the upstream inflow hydrographs for all the tributaries modeled as routing reaches. The downstream boundary condition for the UNET model is the stage hydrograph from the St. Charles, Missouri, gaging station located approximately 28 miles above the confluence of the Missouri and Mississippi Rivers. All stage and flow data are one-hour observed data obtained from the Missouri River Reservoir Control Center's database. Ungaged inflow is accounted for by application of the Null Internal Boundary Condition option, as described later in this report.

Levees: For the UNET model, the Missouri River agricultural levees are modeled as systems. Where levee districts are contiguous, the levees are considered to be part of one levee system which encompasses one protected area. The minimum protected area of a levee system in the model is considered to be 100 acres. Levee districts are aggregated into systems such that the protected area per levee system is greater than 100 acres. Levee properties, such as top of levee elevation, surface area encompassed by the levee, and upstream and downstream river mile, were determined for each individual levee system. These properties were used to build the UNET levee parameter file, called the "include" file, which the program refers to during a UNET run.

Simulation of Levees: During large flood events on the Missouri River, agricultural levees are overtopped and there is significant overbank flow. The method of handling levees from earlier UNET versions simulates levee systems as storage cells defined by surface area and height of levee above the ground elevation. Levees are breached in the UNET model based upon a "time of failure" defined as the time for a breach to attain maximum enlargement, or based upon river stage versus top of levee elevation. (In the context of this report, "failure" of levees refers to any loss of normal levee function without consideration of the cause of the deficiency.) This earlier UNET methodology is inadequate for modeling multiple levee system failures along the Missouri River such as occurred in the 1993 Flood. To overcome this problem, a unique levee algorithm was developed and programmed for UNET. This new UNET levee algorithm simulates the unique behavior of the Missouri River levee systems that occurs during large flood events.

The behavior of levees along the Missouri River during the 1993 Flood was studied and used in developing the new levee algorithm. Missouri River levees were overtopped or breached early in the 1993 Flood event, and subsequently the protected areas behind the levees filled with water from the river. During the final crest, the levees degraded and the floodplain behind the levees actively conveyed flow. The Missouri River functioned under two geometric conditions: one in which levees constrained the flow to the channel, but provided storage behind the levees; and the second in which the levees no longer constrained the flow, and the overbank actively conveyed flow as if the levees did not exist.

With the new levee algorithm, levees are modeled in UNET in the following manner: When a levee overtops or breaches and the protected area subsequently fills, the flow through the breach in the levee depends on the elevation of the river and the elevation of the water in storage behind the levee. The water surface inside the levee interior is assumed to be horizontal. When the river discharge exceeds a specified flow, or when the river elevation exceeds a specified elevation, then the levee storage cross-sectional area and conveyance are added to the river cross-sections and the program routes flow through the channel and the entire width of the floodplain. When the flow falls below a specified discharge, or the river falls below a specified elevation, the levee storage cross-sectional area and conveyance are subtracted from the cross-sections and the river once again interacts with the levee interior through the breach.

The point at which the model changes from storage routing to floodplain routing is specified by flow. UNET uses elevation only if a flow is not specified. These flow values can be determined from rating curves observed at the gages. Plate 1 (located at the end of this report) is a rating curve at the Boonville gage. In this figure, the flow dramatically increases with stage beginning at approximately 300,000 cfs. This point, at which the slope of the graph changes dramatically, is the point where the floodplain actively begins to convey flow.

Dike Fields: The Missouri River Bank Stabilization and Navigation Project between Sioux City, Iowa, and the mouth, traverses the 498.1 river miles within the Kansas City District. This project entails the use of bank revetments and dikes to achieve a free-flowing navigation channel. A dike field is a system of rock embankments or timber structures that protrude from the bank. The dikes block the flow along the bank, concentrating the flow along the opposite bank, deepening the channel. The slack water areas behind the dikes eventually fill with sediment, burying the dike and forming a

narrower but deeper river channel. Dikes are generally located on the point bars on the inside of a river bend.

A cross-section with a typical dike on the left bank of the river is shown in Figure 1. The dike field creates a channel with a design width at a low flow profile which is called the construction reference plane (CRP) on the Missouri River. The target topwidth of the channel (TWCH) extends from the opposite bank to the end of the dike. The dike can have two steps - a lower step and an upper step. The lower step has a set width (TWSTEP) with a crest elevation (ZSTEP) defined by a distance below the CRP elevation (ZCRP). The width of the upper step is the remaining distance from the bank. The crest elevation of the upper step (ZDIKE) is an increment (DZSTEP) above the lower step.

Simulation of a Dike Field: A dike field is defined as a system of structures that contract the low flow cross-section to the design width of the channel. The model is one-dimensional; therefore, the effect of each individual dike cannot be simulated. Rather the cross-sections are contracted to simulate the contraction of the dike field. The area blocked by the dike field can be modeled as storage area or as a dead area which is deducted from the cross-section. The storage area simulates the condition where the area behind the dike has not as yet filled with sediment and the area stores water. When the water exceeds the top of the dike, the storage area is assumed to return to active flow area, since the submerged dike field has little impact on the conveyance of high flow. The added form roughness of the dike is part of the calibration of the model. The dead area simulates the condition when the area behind the dike has been filled with sediment and the area has been lost for all river stages.

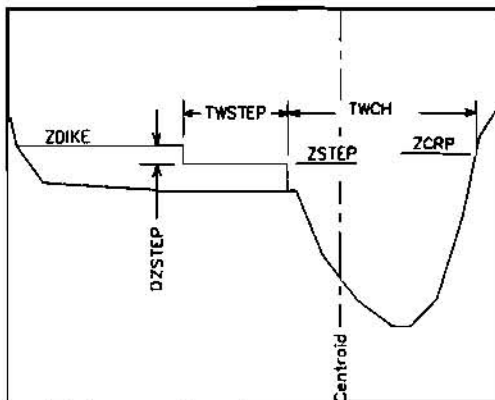


Figure 1. Dike on the left side of the channel. The dike is positioned on the left side of the channel because the centroid is within the right 40% of the channel.

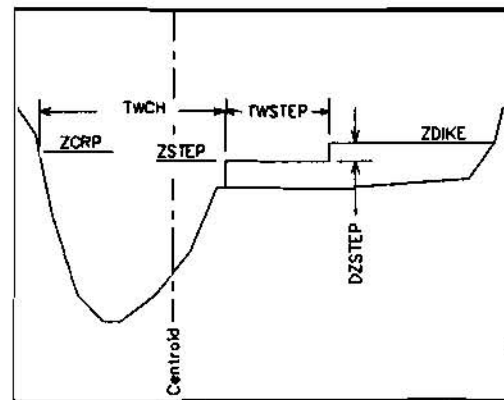


Figure 2. Dike on the right side of the channel. The dike is positioned on the right side because the centroid of the channel is within the left 40% of the channel.

The dike field may be positioned either on the left or the right bank. The modeler can specify the bank or the modeler can allow the program to choose the appropriate bank. The program always attempts to place the dike field on the point bar opposite the channel. The program uses the centroid of the area about the left bank station to locate the dike. When the centroid is located within the right or left 40% of the cross-section topwidth, the dike field is located on the opposite bank, which is

where a point bar is located for a pool cross-section. (See Figure 1 and 2.) For a crossing cross-section where the cross-sectional area is uniformly distributed, the centroid is located within the middle 20% of the topwidth and the dike field is located on the side opposite the channel invert or minimum elevation of the channel (ZMIN). (See Figure 3.)



Figure 3. At this crossing cross-section, the dike is located on the left side because the centroid is in the middle 20% of the topwidth and the minimum elevation is on the right side.

Calibration: The Kansas City-Missouri River UNET model has been calibrated to reproduce observed stages at river gages for the 1986, 1993, and 1994 water year flows. Currently, work is being done to calibrate the model for flow and stage data from water year 1990 up to the present. The primary factor for adjusting the model is Manning's n which is an estimate of the friction force of the boundaries on the flowing water. For large rivers, Manning's n varies with depth, because the relative size of the roughness elements, such as the dunes in the river bed, the height of vegetation, etc., declines with increasing depth. The object of the calibration process is to determine the variation of Manning's n with depth. The effect of the friction force from downstream is shown in the rating curve (stage versus flow) at a gaging station; hence, the variation of Manning's n with depth is represented in the relationship. The automatic calibration option of the UNET program adjusts conveyance at the cross-sections between gaging stations, such that the model reproduces the stages at the upstream rating curve under steady flow during the initial calculations of the program's execution. The Missouri River rating curves were developed at the principal gaging stations from observed stage data and computed flow data for the years 1986, 1993, and 1994. The model was calibrated to reproduce these rating curves.

Null Internal Boundary Condition: The final step in the calibration of the model is the application of the Null Internal Boundary Condition (NIBC). The NIBC is a tool for estimating ungaged lateral inflow into a major river system. For a reach of river of any length, the NIBC is inserted at the principal gage locations where the stage records are the most accurate. Generally, these locations are the USGS gaging stations. The NIBC is inserted at interior gage locations, creating the same number of NIBC independent routing reaches as interior gages. For the Missouri River between Rulo, Nebraska and St. Charles, Missouri, NIBC's are inserted at the USGS gages at St. Joseph, Kansas City, Waverly, Boonville, and Hermann. This breaks the model into five NIBC independent routing reaches.

The NIBC estimation procedure is an iterative process where the NIBC is applied in three steps. First, observed stage hydrographs are applied at all the NIBC and the upstream flow is routed to the NIBC. At the NIBC, the flow routed from upstream is missing the ungaged inflow. The flow hydrograph computed for the downstream reach at the NIBC from a stage boundary condition, does contain the ungaged inflow. The first estimate of the ungaged inflow hydrograph is the difference between the computed flow hydrograph downstream of the NIBC and the routed flow hydrograph upstream of the NIBC. To use the ungaged inflow, the flow is lagged backward in time (usually one day) and inserted in the model as a uniform lateral inflow. Next, UNET is executed with observed stage hydrographs applied at all the NIBC and ungaged inflow entered. This condition may be executed many times, with each iteration improving the estimate of the ungaged inflow. For the last step of the NIBC procedure, the ungaged inflow hydrographs are perceived to be correct and the stage hydrographs are removed. UNET is executed with ungaged inflow entered and no observed stage hydrographs applied at the NIBC.

CONCLUSION

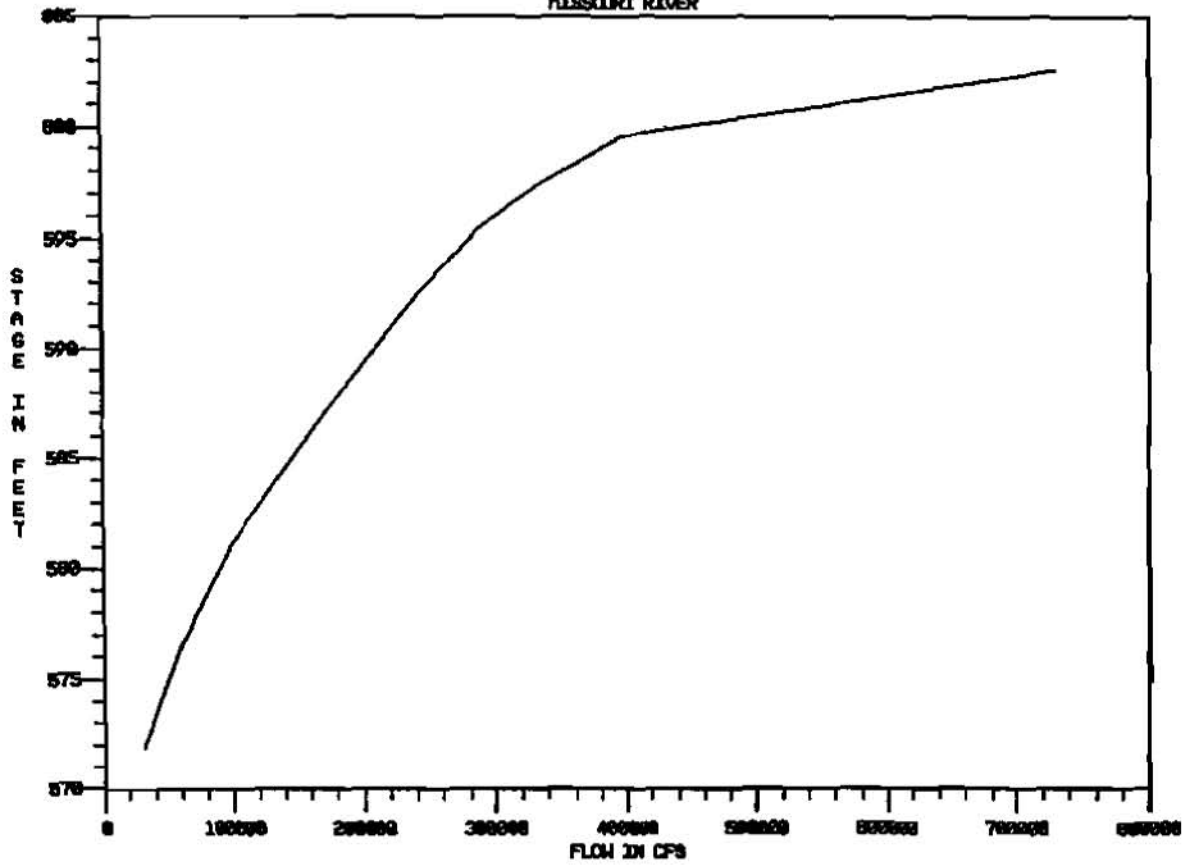
The Kansas City UNET model of the lower Missouri River produced for the MBMS is part of a forecast system developed primarily to improve and facilitate coordination among Corps water control activities. The Kansas City UNET model will be operated by the U. S. Army Corps of Engineers Missouri River Region - Reservoir Control Center (RCC) for reservoir operations and for real-time forecasting of the Missouri River. RCC will transfer flow and stage data computed by the model at Hermann, Missouri, to water control personnel at St. Louis District for use as a boundary condition in their UNET model. The Kansas City UNET model has also been used for a frequency study based on proportioned 1993 Flood flows. Future use of the model will incorporate the UNET sediment transport routine to predict bed material transport.

REFERENCES

- Barkau, R. L. Impact of Levees on the Middle Mississippi River: A report prepared for the Strategic Assessment and Strategy Team, July 15, 1994.
- Barkau, R. L. UNET: Unsteady Flow through a Full Network of Open Channels, February 24, 1992.
- Interagency Floodplain Management Review Committee. Sharing the Challenge: Floodplain Management into the 21st Century, June 1994.
- U. S. Army Corps of Engineers, Floodplain Management Assessment of the Upper Mississippi and Lower Missouri Rivers and Their Tributaries, Appendix A (Hydraulic Modeling), June 1995.
- U. S. Army Corps of Engineers, Kansas City District. The Great Flood of 1993 Post-Flood Report: Lower Missouri River Basin, Omaha District, Appendix E, September 1994.
- U. S. Army Corps of Engineers, Omaha District. The Great Flood of 1993 Post-Flood Report: Lower Missouri River Basin, Appendix D, September 1994.
- U. S. Army Engineer District, Kansas City, Corps of Engineers. Missouri River Basin, Kansas and Missouri: Design Memorandum No. 1A, Preliminary Master Plan, March 1964.
- U. S. Army Engineer District, Kansas City, Corps of Engineers. Missouri River Restudy. Missouri River Backwater Computations, 1977 through 1979.

27APR65 10:07:31

MISSOURI RIVER



BOONVILLE GAGE

Plate 1. Boonville Gage Rating Curve.

MODELING SUBSTANCE SPREADING ON 2D(IN PLANE) STEADY STREAM

By A. V. Babayan, Rostov State University, Rostov-on-Don, Russia;
K. A. Nadolin, Rostov State University, Rostov-on-Don, Russia

Abstract: A problem about spreading of admixture low concentrated in 2D steady stream of viscous fluid is considered, taking account of dissipation and diffusion processes. The area of stream is a channel given by its horizontal projection. The channel is assumed to be arbitray low-twisted and extended in one direction. i.e ratio of average width to its length may be considered as a small parameter. Proposed mathematical model of the process is derived by the small parameter method starting from 2D steady Navier-Stokes equations for incompressible fluid and unsteady diffusion equation in the moving medium. The main character feature of this model is considering of the wide-cross structure of the stream. The finite element method is used for numerical modeling.

INTRODUCTION

The description of the substance spreading is a main part of the water ecological systems modeling. Usually the problems of the water ecology are limited to considering of the passive admixture, when the change of substance concentration doesn't affect to the model hydrodynamical properties – fields of velocity and pressure. This simplified assumption is excused for the small admixture concentration or when the physical-mechanical substance properties are close to water properties. It conforms to many ecological problems. Now the 'having chamber' models are used widely. In this models the whole modeling area is divided to relatively homogeneous chambers. In bounds of each chambers the ecosystem descriptions are assumed constant and equal to average values. The interaction between neighboring chambers is described by the boundary balance conditions. However necessity of considering processes inside chambers often appears. In this case more detailed 'distribution models' are used.

One of such models, oriented to the river ecological system research, is considered in this paper. The proposed model is derived by the small parameter method starting from 2D steady Navier-Stokes equations for incompressible fluid and unsteady diffusion equation in the moving medium. This model represents the initial-boundary problem for the main term of decomposition of the unknown variables by the parameter, equal to the ratio of average width to its length. The main character feature of this model is considering of the wide-cross structure of the stream. It allows to research the particulars of the substance transferring in case of wind effect. This analysis is impossible for the distribution models, dealing with the integral or average characteristics of the flow (flow rate, average velocity etc.). On the strength of assumption for the admixture to be passive the field of velocity and pressure are derived from the independent subsystem, solved analytically. The equation for concentration is solved numerically.

PROBLEM DEFINITION

Let nonconservation admixture spread in 2D steady stream definite shape. The Descartes system of coordinates is accepted as shown at the Fig.1

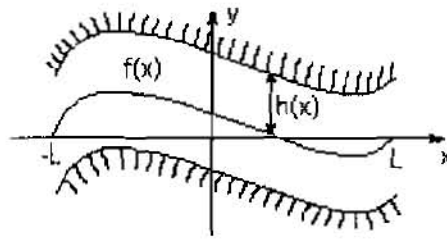


Fig.1

The channel is assumed arbitrary low twisted, so the coast line may be set as $f(x) \pm h(x)$. The function $f(x)$ defines the average line of the stream, and the function $h(x)$ - its halfwidth. The section of flow $(-L; L)$ is considered, and $f(-L) = f(L) = 0$ is caused by choice of the accepted system of coordinate (Fig.1).

The transport of admixture in the steady stream taking into account dissipation and diffusion processes may be written as [1]

$$(\mathbf{v}, \nabla_0) \mathbf{v} = -\frac{1}{\rho} \nabla_0 p + \nu \Delta_0 \mathbf{v} + \boldsymbol{\sigma}; \quad \operatorname{div}_0 \mathbf{v} = 0$$

$$\mathbf{v} \Big|_{y=f(x) \pm h(x)} = 0 \quad (1)$$

$$\int_{-h(x)}^{h(x)} \rho \mathbf{v}(-L, y) \mathbf{n} dy = Q$$

$$\frac{\partial c}{\partial t} + \mathbf{v} \nabla_0 c = D \Delta_0 c - \gamma c$$

$$\frac{\partial c}{\partial \mathbf{n}} \Big|_{y=f(x) \pm h(x)} = 0 \quad (2)$$

$$c(x, y, t) \Big|_{t=0} = c^0(x, y)$$

Unknown variables are: the vector of velocity $\mathbf{v}(x, y)$, the field of pressure $p(x, y)$ in the steady flow and the admixture concentration $c(x, y, t)$. The constant vector $\boldsymbol{\sigma} = (\sigma \cos \alpha, \sigma \sin \alpha)$ defines the external force (for instance, effect of wind), ρ and ν - the constant density and fluid viscosity respectively, Q - fixed stream of fluid at the entry of considered section, D and γ - coefficients of diffusion and admixture dissipation respectively. Function $c^0(x, y)$ defines the initial admixture distribution. The admixture is assumed to be inert, i.g. the density, viscosity and diffusion coefficient are not depended on substance concentration. The null index at the differential operators indicates the its 2D nature.

The purpose of further transformations of the task (1)-(2) is to obtain of the simplified equations, which allow implicit solution as it done in [2].

SWITCH TO DIMENSIONLESS VARIABLES

The field of velocity in equations (1) is accepted as $\mathbf{v} = \mathbf{V} + \delta\mathbf{v}$, where vector $\mathbf{V} = (U, W)$ and $\delta\mathbf{v} = (u, w)$. Hence

$$\begin{aligned} (\mathbf{V}, \nabla_0) \mathbf{V} &= -\frac{1}{\rho} \nabla_0 p + \nu \Delta_0 \mathbf{V} \\ (\delta\mathbf{v}, \nabla_0) \delta\mathbf{v} + (\mathbf{V}, \nabla_0) \delta\mathbf{v} + (\delta\mathbf{v}, \nabla_0) \mathbf{V} &= \nu \Delta_0 \delta\mathbf{v} + \sigma \\ \operatorname{div}_0(\mathbf{V} + \delta\mathbf{v}) &= 0 \\ \int_{h(-L)}^{h(-L)} \rho(U + u) dy &= Q \end{aligned} \quad (3)$$

The equations (2),(3) can be transformed into dimensionless equations, using characteristic channel length L as a linear scale in the x direction, and characteristic channel width H (for instance $H = h(-L)$) as a linear scale in the y direction. Value of the ratio $\varepsilon = H/L$ is small. Two velocity scales are used $U^* = Q(H\rho)^{-1}$ and $W^* = \varepsilon U^*$.

The scales of pressure and time are accepted as $P = \rho U^{*2} L H^{-1}$, $T = H(U^*)^{-1}$ respectively. As concentration unit of measurement $C = \max_{x,y} c^0(x,y)$ is used.

New dimensionless variables are introduced by formulae $x = L\tilde{x}$; $y = H\tilde{y}$; $t = T\tilde{t}$; $U = U^* \tilde{U}$; $W = W^* \tilde{W}$; $u = W^* \tilde{u}$; $w = W^* \tilde{w}$; $p = P\tilde{p}$; $c = C\tilde{c}$; $c^0 = C\tilde{c}^0$; $f = H\tilde{f}$; $h = H\tilde{h}$: The equations (2)(3) can be rewritten in the form (mark \sim is omitted):

$$\begin{aligned} \varepsilon U U_x + \varepsilon W U_y &= -p_x + \frac{\nu \varepsilon^2 U_{xx} + U_{yy}}{Re} \\ \varepsilon^3 U V_x + \varepsilon^3 W W_y &= -p_y + \varepsilon^2 \frac{\nu \varepsilon^2 W_{xx} + W_{yy}}{Re} \\ \varepsilon^2 u u_x + \varepsilon w u_y + \varepsilon U u_x + \varepsilon W u_y + \varepsilon u U_x + w U_y &= \frac{\nu \varepsilon^2 w_{xx} + w_{yy}}{Re} + \mu \cos \alpha \\ \varepsilon^2 u w_x + \varepsilon w w_y + \varepsilon U w_x + \varepsilon W w_y + \varepsilon^2 u W_x + \varepsilon w W_y &= \frac{\nu \varepsilon^2 w_{xx} - w_{yy}}{Re} + \mu \sin \alpha \\ U_x + W_y + \varepsilon u_x + w_y &= 0 \\ \int_{-1}^1 (U(-1, y) + u(-1, y)) dy &= 1 \\ c_x + (U(x, y) + \varepsilon u(x, y)) c_x + (W(x, y) + w(x, y)) c_y &= (D\varepsilon^2 c_{xx} + c_{yy}) / Pe - \lambda c \\ c_y + \varepsilon^2 (f'(x) \pm h'(x)) c_x \Big|_{y=f(x) \pm h(x)} &= 0; \end{aligned} \quad (4)$$

$$c(x, y, 0) = c^0(x, y)$$

Following dimensionless parameters are used here: $Re = HU/\nu$ – Reynolds number, $\lambda = \gamma T$ - admixture's decay parameter, $Pe = D/(W \cdot H)$ - Pekle's diffusion number.

EQUATIONS OF MAIN TERMS

The solution of the problem (4) is found as formal asymptotical sequences by the small parameter's ϵ powers. Equations for the main asymptotical terms are obtained substituting these sequences to (4) and grouping coefficients by the similar power. We have:

$$p_x = \frac{1}{Re} U_{yy} \quad (5)$$

$$p_y = 0 \quad (6)$$

$$u_{yy} = Re(wU_y - \mu \cos \alpha) \quad (7)$$

$$w_{yy} = \mu Re \cos \alpha \quad (8)$$

$$U_x + W_y + w_y = 0 \quad (9)$$

$$U|_{f(x) \pm h(x)} = u|_{f(x) \pm h(x)} = w|_{f(x) \pm h(x)} = 0 \quad (10)$$

$$\int_{-1}^1 (U(-1, y) + u(-1, y)) dy = 1 \quad (11)$$

$$c_t + U(x, y)c_x + (W(x, y) + w(x, y))c_y = \frac{1}{Pe} c_{yy} - \lambda c; \quad (12)$$

$$c|_{y=f(x) \pm h(x)} = 0$$

$$c(x, y, 0) = c^0(x, y)$$

The system (5)-(12) doesn't contain the second derivation W_{yy} , so the boundary conditions for this velocity component are replaced with integral:

$$\frac{1}{2h(x)} \int_{f-h}^{f+h} W(x, y) dy = 0 \quad (13)$$

Equation (5)-(12) are accepted as a simplified mathematic model of the explored process.

Main terms for velocity and pressure can be obtained by direct integration of the equations (5)-(9). Equations (5),(7) and (8) are integrated taking into account boundary conditions (10). We have:

$$U(x, y) = \frac{Re}{2} p'(x) [(y - f(x))^2 - h^2(x)] \quad (14)$$

$$u(x, y) = -\frac{Re}{2} \left\{ Re^2 p'(x) \mu \sin \alpha (y - f(x)) \left[\frac{(y - f(x))^4}{20} - \frac{h^2(x)(y - f(x))^2}{6} + \frac{7h^4(x)}{60} \right] + \mu \cos \alpha [(y - f(x))^2 - h^2(x)] \right\} \quad (15)$$

$$p'(x) = \mu \cos \alpha - \frac{3}{2 Re}; \quad w(x, y) = -\frac{1}{2} Re \mu \sin \alpha [(y - f(x))^2 - h^2(x)] \quad (16)$$

Following formula is obtained from relationship (9) and condition (13):

$$W(x, y) = -\frac{1}{2} Re \left\{ \left[(y - f(x))^2 + \frac{1}{3} h^2(x) \right] \left[f'(x) \left(\frac{3}{2} - \mu Re \cos \alpha \right) - \mu Re \cos \alpha \right] + 2 \left(\frac{3}{2} - \mu Re \cos \alpha \right) h(x) h'(x) (y - f(x)) \right\} \quad (17)$$

EQUATIONS FOR THE CONCENTRATION

Formulae (15)-(17) define main terms of the asymptotical form hydrodynamics characteristics of the flux, so the problem of finding admixture concentration can be considered as the following initial-boundary problem:

$$c_t + U(x, y)c_x + (W(x, y) + w(x, y))c_y = \frac{1}{Pe} c_{yy} - \lambda c; \quad (18)$$

$$c|_{y=f(x)+h(x)} = 0 \quad (19)$$

$$c(x, y, 0) = c^0(x, y) \quad (20)$$

$$U(x, y) = -\frac{1}{2} \left(\frac{3}{2} - \mu Re \cos \alpha \right) [(y - f(x))^2 - h^2(x)]; \quad (21)$$

$$W(x, y) + w(x, y) = -\frac{1}{2} \left[(y - f(x))^2 f'(x) \left(\frac{3}{2} - \mu Re \cos \alpha \right) + 2h(x)h'(x) \left(\frac{3}{2} - \mu Re \cos \alpha \right) (y - f(x)) - \frac{h^2(x)}{3} \left(f'(x) \left(\frac{3}{2} - \mu Re \cos \alpha \right) + 2\mu Re \sin \alpha \right) \right] \quad (22)$$

For numerical solution problem (18)-(22) area of the flow is turned to rectangle with substitution:

$$\tilde{x} = x; \quad \tilde{y} = \frac{f(x) - y}{h(x)};$$

Equations (18)-(22) can be rewritten in form (mark « » is omitted):

$$c_t + U(x, y)c_x + (W(x, y) + w(x, y))c_y = \frac{1}{Pe} c_{yy} - \lambda c$$

$$c_y|_{y=\pm 1} = 0; \quad c(x, y, 0) = c^0(x, y) \quad (23)$$

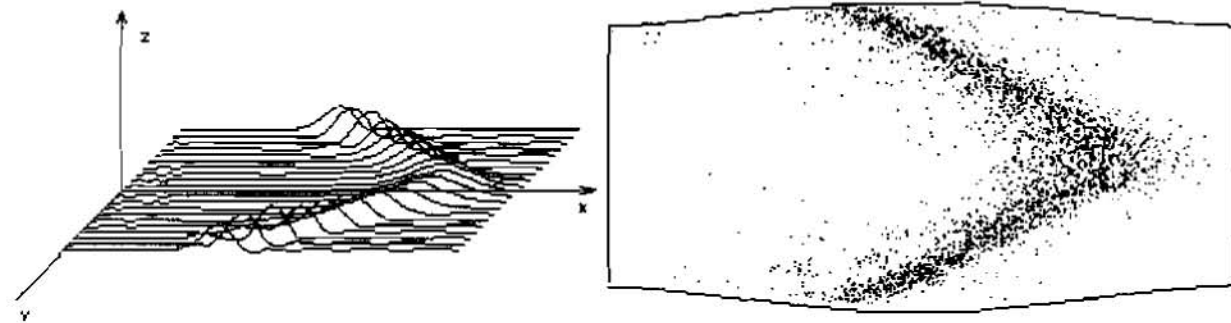
$$U(x, y) = -\frac{1}{2} \left(\frac{3}{2} - \mu Re \cos \alpha \right) h^2(x) (y^2 - 1)$$

$$W(x, y) + w(x, y) = -\frac{1}{2} h(x) \left[\left(1 - \frac{2}{3} \mu Re \cos \alpha \right) f'(x) + (-y^3 + 3y) h(x) - \frac{2}{3} \mu Re \sin \alpha \right]$$

Problem (23) was solved using finite element method with rectangular bilinear elements. The test problem about sewage discharge was considered. The discharge was modelled by the function:

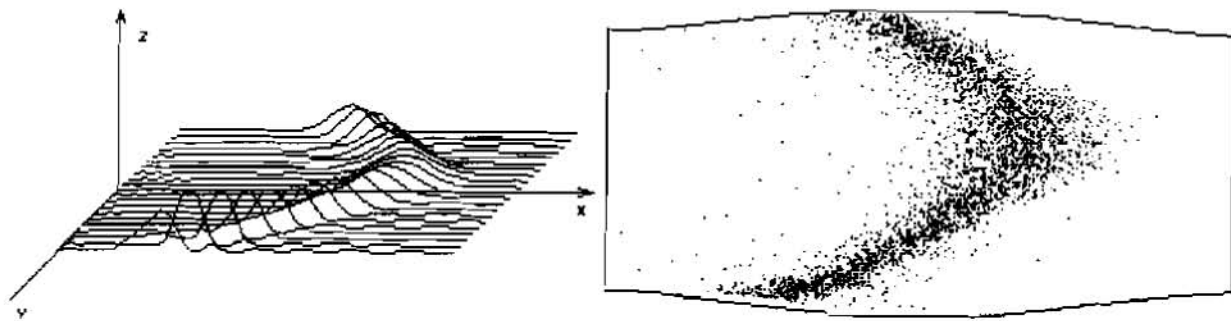
$$c^0(x, y) = \begin{cases} 1 - \frac{x}{l}, & 0 \leq x \leq l \\ 1 + \frac{x}{l}, & -l \leq x < 0 \\ 0, & |x| > l \end{cases}$$

Here l ($0 < l \ll 1$) defines admixture concentration in the wide-cross. Under $x = 0$ the concentration is maximum and equal to 1. The calculations were made for the channel shape as $y = \pm 0.2 \sin 2x$ and for following parameters: $Pe = 100$, $Re = 100$, $\lambda = 0.01$. At the figures (2)-(6) the graphics of the concentration and the charts of the admixture distribution along the channel are shown at the time $t = 1$. Parameters α and μ define the wind effect to the flow.



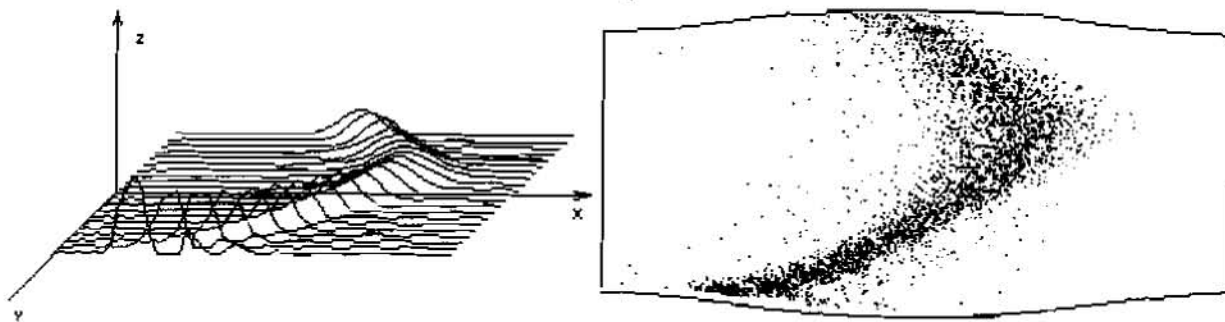
$\alpha = 0; \mu = 0;$

Fig. 2



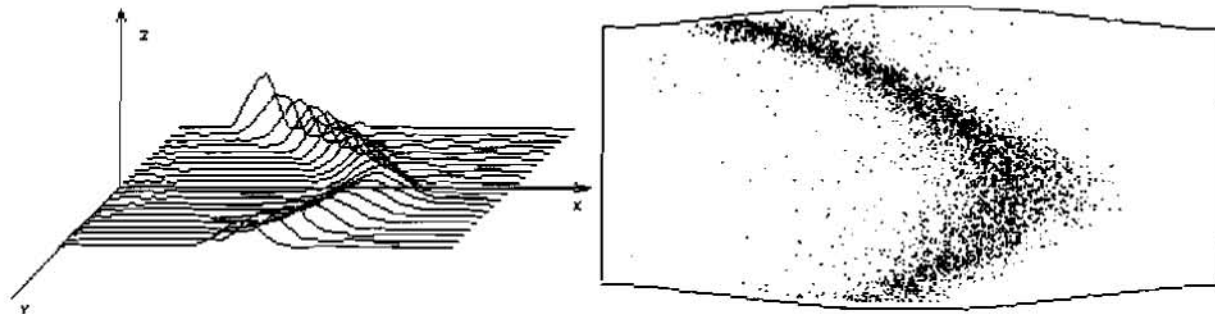
$$\alpha = \pi / 60; \quad \mu = 0.003$$

Fig. 3



$$\alpha = \pi / 40; \quad \mu = 0.003$$

Fig. 4



$$\alpha = -\pi / 40; \quad \mu = 0.003$$

Fig. 5

Here α is an angle of the wind effect and μ - its module.

CONCLUSIONS

The problem is representative for a large class of problems pertaining to situations where a leachate is going from the emitting source of finite length downward the river stream. Knowledge of where the compound can reach is paramount for water quality management. The model can be used to predict the horizontal transport and disposition of chemicals in rivers.

REFERENCES

1. Landau L.D., Lifshits E.M. Hydrodynamic. – M.: Nauka, 1986.
2. Bochev M.A., Nadolin K.A., Nikolaev I.A. Modelling of Substance Spreading in 2D Free-Surfaced Steady Stream. // Mathematical Modelling. 1996. V.8, N1. pp.11–24.

Contact points: A.V. Babayan Email: isaev@ns.unird.ac.ru

AN ANALYTICAL DIFFUSION MODEL AND ITS APPLICATION TO WATER LEVEL FORECAST

By Cheng Haiyun, Engineer, Changjiang Water Resources Commission, Wuhan, China;
Rui Xiaofang, Professor, Hohai University, Nanjing, China

Abstract: Based on the analytical solution of a linear diffusion wave equation in terms of water level, a flood routing model of channel is developed. This model has clear physical significance and takes into account all kinds of effects (backwater and lateral inflow) in the flood wave movement and it will find wide applications. It doesn't require detailed data of cross sections or river bed geometry. Good results are obtained when the model is applied to simulate flood flow conditions in 1981~1990 and verify in 1991~1993 in Jingjiang Reach of the Yangtze River of China.

INTRODUCTION

Flood routing of channel as a main content of hydrological study is to reveal the regularity of flood wave movement. The method of flood routing has been developed basically along two approaches, one way is based on the complete Saint-Venant equations for unsteady open channel flood, the other is based on water volume balance and storage equations such as Muskingum model. Normally it's difficult to forecast water level event for the hydrological method, but the applicability of hydrodynamics method is limited somehow due to the fact that this approach requires frequent cross-sectional and roughness information along the channel reach. Moreover, in most cases people are primarily concerned with water level just at a small number of sections rather than the discharges and levels at a large number of closely spaced intervals. There is considerable value in having an accurate lumped parameter flood routing model. In 1985, T. Tingsanchali put forward an analytical diffusion model for flood routing which could consider backwater effect and lateral flows. Following T. Tingsanchali, some further studies on this model have been carried out. Good results are obtained when applied to forecast water levels at Jinjiang Reach in middle and downstream Yangtze river of China.

DESCRIPTION OF THE ANALYTICAL DIFFUSION MODEL

The flood wave diffusion equation in terms of water level incorporating effects of channel irregularities and lateral flow can be expressed as⁽¹⁾:

$$\frac{\partial y}{\partial t} + w \frac{\partial y}{\partial x} = (DK + u') \frac{\partial^2 y}{\partial x^2} + Q_L(x, t) \quad (1)$$

in which, w = diffusion wave velocity; y = flow depth; DK = diffusivity due to channel irregularities; u' = diffusivity due to effects of hydrodynamics; $Q_L(x, t)$ = lateral discharge per unit width of the tributary and per unit width of the main channel; x = distance from upstream end; t = time.

The initial condition and boundary conditions are taken as;

$$y(x, 0) = H \quad (2)$$

$$y(0, t) = H + u(t) \quad (3)$$

$$y(l, t) = H + d(t) \quad (4)$$

where, H = uniform depth; $u(t)$ and $d(t)$ = water level variations above the initial depth H at the upstream and downstream ends; and l = the length of channel reach.

The tributaries and distributaries are treated as the sources and sinks distributed along the main channel. The contribution of lateral flows to momentum along the longitudinal direction of the channel have been neglected. The nonlinear diffusion equation is linearized to obtain an analytical solution by expressing the solution in the functional series⁽¹⁾.

$$y(x, t) = (H + h) \left(1 + \frac{\Phi_0}{(H + h)} + \frac{\Phi'_0}{(H + h)} + \dots \right) \quad (5)$$

in which h = the average height of the water level above H . Let $\Phi_0(x, t) = \Phi(x, t) + \Phi_3(x, t)$ and by substituting Eq. (5) into Eq. (1), and taking the first approximate solution, then

$$y(x, t) = H + h + \Phi(x, t) + \Phi_3(x, t) \quad (6)$$

in which $\Phi(x, t)$ is the solution of Eq. (7)~(10)

$$\frac{\partial \Phi}{\partial t} + \omega \frac{\partial \Phi}{\partial x} = u \frac{\partial^2 \Phi}{\partial x^2} \quad (7)$$

$$\Phi(0, t) = u(t) - h \quad (8)$$

$$\Phi(l, t) = d(t) - h \quad (9)$$

$$\Phi(x, 0) = -h \quad (10)$$

and $\Phi_3(x, t)$ is the solution of Eq. (11)~(14)

$$\frac{\partial \Phi_3}{\partial t} + \omega \frac{\partial \Phi_3}{\partial x} = \mu \frac{\partial^2 \Phi_3}{\partial x^2} + Q_L(x, t) \quad (11)$$

$$\Phi_3(0, t) = 0 \quad (12)$$

$$\Phi_3(l, t) = 0 \quad (13)$$

$$\Phi_3(x, 0) = 0 \quad (14)$$

in which $u = DK + u' = DK + (H + h)v_0/2s_0$ (15)

$$w = 3/2v_0 \quad (16)$$

$$v_0 = C[(H + h)s_0]^{1/2} \quad (17)$$

in which S_0 = bed slope; C = Chezy roughness coefficient.

Using a Laplace transformation technique, the solutions of Eq. (7) and (11) for the corresponding conditions are⁽²⁾:

$$\begin{aligned} \Phi(x, t) = & \frac{\exp\left[\frac{\omega x}{2\mu}\right]}{2\sqrt{\pi\mu}} \int_0^t \frac{u(t-\lambda)\exp\left[\frac{-\omega^2\lambda}{4\mu}\right]}{\lambda^{3/2}} \sum_{n=0}^{\infty} \left\{ (x + 2nl)\exp\left[\frac{-(x + 2nl)^2}{4\mu\lambda}\right] \right. \\ & \left. - [2(n+1)l - x]\exp\left[\frac{-[2(n+1)l - x]^2}{4\mu\lambda}\right] \right\} d\lambda + \frac{\exp\left[\frac{-\omega x'}{2\mu}\right]}{2\sqrt{\pi\mu}} \\ & \cdot \int_0^t \frac{d(t-\lambda)\exp\left[\frac{-\omega^2\lambda}{4\mu}\right]}{\lambda^{3/2}} \sum_{n=0}^{\infty} \left\{ (x' + 2nl)\exp\left[-\frac{(x' + 2nl)^2}{4\mu\lambda}\right] - [2(n+1)l - x'] \right. \\ & \left. \cdot \exp\left[\frac{-[2(n+1)l - x']^2}{4\mu\lambda}\right] \right\} d\lambda - h \quad (\text{in which } x' = l - x) \quad (18) \end{aligned}$$

and

$$\Phi_1(x, t) = \frac{1}{2\mu\sqrt{\pi}} \int_0^{\sqrt{u}} \exp\left[-\frac{\omega(x-\xi)^2}{2\mu}\right] \int_0^{2\sqrt{u}} Q_L[\xi, t - \frac{\rho^2}{4\mu}] \cdot \exp\left[-\frac{\omega^2\rho^2}{16\mu^2}\right] E(x, \xi, \rho) d\rho d\xi \quad (19)$$

in which

$$E(x, \xi, \rho) = \sum_{n=0}^{\infty} \left\{ \exp\left[-\frac{(2nl+x-\xi)^2}{\rho^2}\right] - \exp\left[-\frac{(2nl+x+\xi)^2}{\rho^2}\right] + \exp\left[-\frac{(2(n+1)l-x+\xi)^2}{\rho^2}\right] - \exp\left[-\frac{(2(n+1)l-x-\xi)^2}{\rho^2}\right] \right\} \quad (20)$$

If $u(t)$ and $d(t)$ are approximated by histograms

$$u(t) = u_j \text{ for } (j-1) < t \leq j, \quad j=1, 2, \dots, m_1;$$

$$d(t) = d_j \text{ for } (j-1) < t \leq j, \quad j=1, 2, \dots, m_2;$$

in which u_j and d_j are the changes in stepped water levels at the upstream and downstream ends, m_1 and m_2 are the corresponding flood durations, then Eq. (18) can be written as $\Phi(x, t) = \Phi_1(x, t) + \Phi_2(x, t) - h$, with

$$\Phi_1(x, t) = u_1 R_1(x, t) + \sum_{j=1}^{m_1-1} R_1(x, t-j)(u_{j+1} - u_j) \quad (21)$$

$$\Phi_2(x, t) = d_1 R_2(x, t) + \sum_{j=1}^{m_2-1} R_2(x, t-j)(d_{j+1} - d_j) \quad (22)$$

and Eq. (18) can be written as

$$\Phi_3(x, t) = q_{L1} R_3(x, t) + \sum_{j=1}^{m_3-1} R_3(x, t-j)(q_{L,j+1} - q_{L,j}) \quad (23)$$

in which q_{Lj} = stepped lateral discharge per unit width of the tributary and per unit width of the main channel, over its initial value, during the time period $(j-1) < t \leq j$. In Eqs (21), (22), and (23), $R_1(x, t)$, $R_2(x, t)$, $R_3(x, t)$ can be written as

$$R_1(x, t) = \exp\left(\frac{wx}{2u}\right) B(x, t) \quad (24)$$

$$R_2(x, t) = \exp\left(\frac{-wx'}{2u}\right) B(x', t) \quad (25)$$

$$R_3(x, t) = \frac{\exp\left(\frac{\omega x}{2\mu}\right)}{2\mu\sqrt{\pi}} \int_0^{2\sqrt{u}} \left[\exp\left(\frac{-\omega^2\rho^2}{16\mu^2}\right) \right]_0^{\rho} I(x, \xi, \rho) d\xi d\rho \quad (26)$$

in which $B(\rho, t) = \sum_{n=0}^{\infty} \left\{ S\left[\rho, \frac{2nl}{\rho} + 1, t\right] - S\left[\rho, \frac{2(n+1)l}{\rho} - 1, t\right] \right\} \quad (27)$

$$S(p, b, t) = \exp\left[-\frac{\omega\rho b}{2\mu}\right] - \frac{2b}{\sqrt{\pi}} \int_0^{\rho/2\sqrt{u}} \exp\left[-b^2\xi^2 - \frac{\omega^2\rho^2}{16\mu^2\xi^2}\right] d\xi \quad (28)$$

$$I(x, \xi, \rho) = \exp\left[-\frac{\omega\xi}{2\mu}\right] \sum_{n=0}^{\infty} \left\{ I'(2nl+x-\xi, \rho) - I'(2nl+x+\xi, \rho) + I'[2(n+1)l-x+\xi, \rho] - I'[2(n+1)l-x-\xi, \rho] \right\} \quad (29)$$

$$I'(b, \rho) = \exp(-b^2/\rho^2) \quad (30)$$

The dimensionless coefficient, $R_1(x, t)$, represents the upstream effect at a location, x , due to a unit rise in water level at the upstream end of a long channel in which no lateral flow exists, when the flow at the downstream end is uniform with the depth of H . The same description can be used for the dimensionless downstream effect, $R_2(x, t)$, for a unit rise at the downstream end when the upstream end is uniform with the depth of H . The coefficient $R_3(x, t)$ has a dimension of time and represents the effect of lateral flow at the location, x , due to a unit rise in the lateral discharge per unit width of the tributary and per unit width of the main channel, when the two ends of the channel are uniform according to the given initial condition.

CHARACTERISTIC OF MODEL RESPONSE

The Limit of Model Response; For Eq. (24) if $x = \text{constant}$ and $t \rightarrow \infty$, then

$$R_1(x, t) = \sum_{n=0}^{\infty} \exp\left(-\frac{nlw}{u}\right) \left\{1 - \exp\left[-\frac{w(x-l)}{u}\right]\right\} \quad (31)$$

For Eq. (31) when w, u, x, l are constant, $R_1(x, t) \xrightarrow{t \rightarrow \infty} \text{constant}$. Using a similar approach

$$R_2(x, t) = \left\{\exp\left[-\frac{wx}{u}\right] - \exp\left[-\frac{wl}{u}\right]\right\} \cdot \sum_{n=0}^{\infty} \exp\left[-\frac{nw}{u}\right] \quad (32)$$

For Eq. (32), When w, u, x, l are constant, $R_2(x, t) \xrightarrow{t \rightarrow \infty} \text{constant}$ and for Eq. (26) $\partial R_3(x, t) / \partial x \xrightarrow{t \rightarrow \infty} 0$, then $R_3(x, t) \rightarrow \text{constant}$.

This means that for any given values of w and u , $R_1(x, t)$, $R_2(x, t)$ and $R_3(x, t)$ at a location x approach constant values as t increases.

Determination of n in the Converging Series Terms in Eq. (31) and Eq. (32); From Eq. (31) and Eq. (32) it is found that the n in the converging series only depends on wl/u . In general, for Yangtze River when wl/u is within 4.0~5.0, n is 0~1. When wl/u is smaller, $n = 3 \sim 5$.

For $R_3(x, t)$ it's found that t is more important than n , in general, satisfied accuracy can be reached for Yangtze River just when $n = 3 \sim 5$.

The Numerical Analysis of Response Function; Let river reach length l be 317km, A, B, C are three stations. The distances of A, B, C from the upstream end are 60.9km, 155km. and 249.0km. A tributary D is assumed at 40.6km from the upstream end. Let $w = 1.85\text{m/s}$, $u = 5 \times 10^5 \text{m}^2/\text{s}$, the typical curves of $R_1(x, t)$, $R_2(x, t)$ and $R_3(x, t)$, at different stations, are shown in Fig. 1 and Fig. 2 for given w and u . In Fig. 1 $R_1(x, t)$ represents the downstream propagation of a flood wave caused by introducing a rectangular hydrograph of water surface of 1 m height above the initial depth at the upstream end (KM 0), and no lateral inflow is considered in this case. $R_2(x, t)$ represents the upstream propagation of a flood wave caused by introducing the same hydrograph at the downstream end (KM 317) of the channel. The curve of $R_3(x, t)$ represents the effect of lateral flow and means a rectangular hydrograph of lateral inflow is introduced at 40.6km, by taking the depths at the

upstream and downstream ends to equal the initial uniform depth, the propagation of water surface wave in the directions upstream and downstream of the lateral inflow location is shown in Fig. 2.

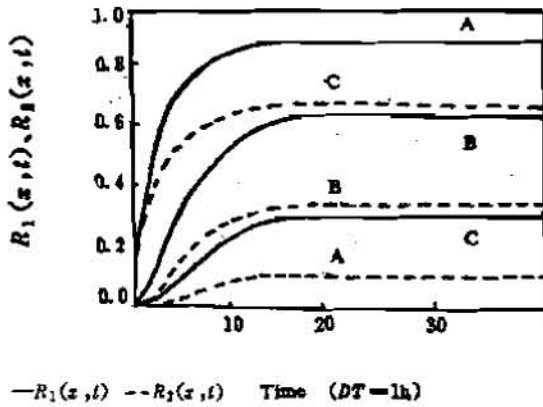


Fig. 1. Response curves of $R_1(x,t)$ and $R_2(x,t)$

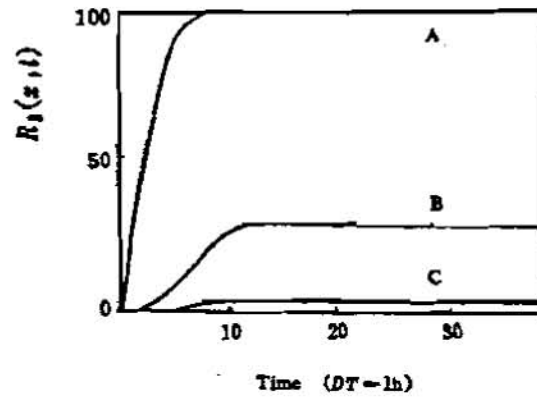


Fig. 2. Response curves of $R_3(x,t)$

APPLICATION TO THE JINGJIANG REACH OF THE YANGTZE RIVER

Reach Characteristics and Model Boundary: The Yangtze River is the longest river in China and one of the largest in the world. Located at the middle part of the Yangtze the Jingjiang Reach is a complex river network with many tributaries and distributaries as well as Dongting lake water system. On this reach flood disasters are frequent and severe. The flood threatened areas are economically important as they include some of the most developed industrial areas in China and are heavily populated.

Jingjiang Reach is about 340km long. The distance of model area is 317 km long from Yichang Station (km0) to Jianli station (km317) upstream the outlet point of the

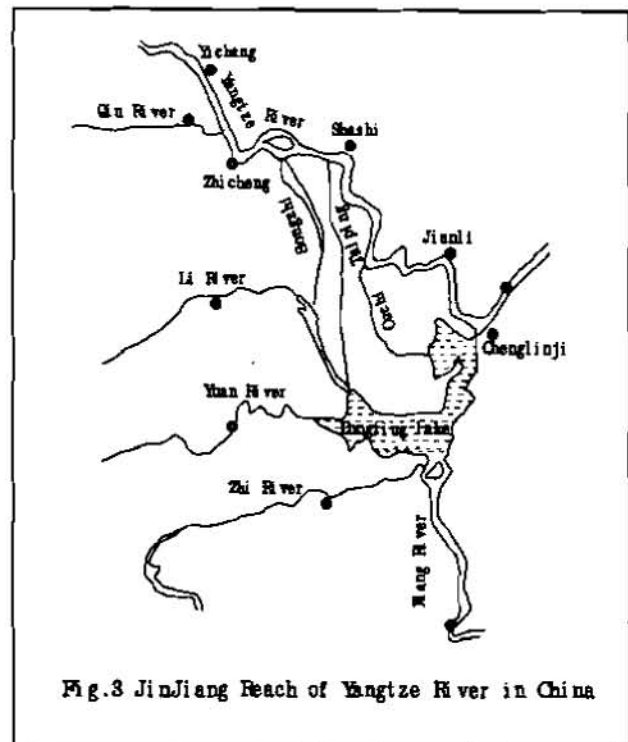


Fig. 3. Jingjiang Reach of Yangtze River in China

Dongting lake. Two tributaries Qin river and Zhu river discharge into the river at 40.6km, 147.6km. Three distributaries Songchi, Taiping, and Ouchi flow out the Yangtze river at 91.4km, 137.2km, and 238.7km, respectively, as shown in Fig. 3. Three gauging stations at Zhicheng (60.9km), Shashi (155km), and Shishou (248.9km) are considered for model calibration and verification. The average bed slope, S_0 , is about 0.61/10,000.

Collection and Processing of Data: During 1981~1990, 34 flood events have been collected, which represent all kinds of flood situations. In the light of the limitation of data collecting and transmitting in china, the time period of model calculation is considered as $\Delta t=6h$, therefor, the boundary discharges and water levels have been processed as $\Delta t=6h$.

Calibration and Verification of Model: For each flood case, parameters u' and w are computed according to Eqs. (15) and (16) in which H =the average initial depth along the river reach, and h =the average height of flood levels above the average initial depth, H , at the upstream and down stream ends of Jinjiang reach. For this model two parameters need to be calibrated, that is C , the chezy coefficient, and DK , diffusivity due to the channel irregularities. The calibration is based on physical analysis and combining trial-error-trial and optimization techniques, the parameters of model are shown in table 1, accuracy statistic of 34 flood cases are shown in table 2.

With the calibration parameters shown in table 1, the model is applied to test the flood events of 1991~1993. Here, 7 flood events have been verified, the results of model verification is also shown in table 2.

Table 1. Parameters of analytical diffusion model

Station Name	C	$DK (m^2/s)$
Zhicheng	40	1×10^7
Shanshi	45	0.6×10^7
Shishou	50	0.9×10^7

Table 2. Results of model calibration and verification

Station Name	Absolute error of peak water level (model calibration, in m)			Absolute error of peak water level (model verification, in m)		
	Max	Min	Average	Max	Min	Average
Zhicheng	0.34	0	0.11	0.30	0.05	0.12
Shashi	0.36	0	0.12	0.35	0.07	0.16
Shishou	0.32	0.01	0.13	0.28	0.02	0.11

Form table 2, we can find that the accuracy of water level computed for each station is high, the average errors of peak water level are about 0.15m. In our opinion, this results of model test is satisfaction for Mid-down Yangtze river flood control.

SUMMARY AND CONCLUSIONS

Proposed in the paper is an analytical diffusion model for flood routing with back water effects and lateral flows based on the linearization of the basic diffusion equation. The model applicability is tested by simulation in Jinjiang Reach in the Mid-down Yangtze River, and has a wide application. In addition, the model provides an excellent means to analyse individual or overall effects of the boundary conditions.

However, further refinement on linearization of the diffusion equation may be necessary when the model is applied to more nonlinear problem.

REFERENCES

- Hayami, s. , "On the Propagation of Flood waves. " Bulletin of Disaster prevention Research Institute, Vol. 1, No. 1, Dec. , 1951.
- Cheng Haiyun, "Study on the Method of Water Level Forecast to the Jinjing Reach in Yangtze River of China", thesis presented to Hohai University, Nanjing, China, in 1995, for the degree of Master of Engineering.
- Tingsanchali, T. , et. al. , Analytical Diffusion Model for Flood Routing. Journal of Hydraulic Engineering, 1985, 111(1):435~454.

ROBUST METHODS FOR FLOOD ROUTING OVER HIGHLY IRREGULAR TERRAIN

Roger P. Denlinger, Geophysicist, U.S. Geological Survey, Vancouver, Washington; Roy A. Walters, Oceanographer, U.S. Geological Survey, Denver, Colorado; Dan Levish, Geologist, U.S. Bureau of Reclamation, Denver, Colorado; Dean Ostenaar, Geologist, U.S. Bureau of Reclamation, Denver, Colorado.

Abstract

River flow and flooding over highly irregular terrain is usually dominated by fluid inertia, and this causes difficulties in solving for these flows. In this paper, we show that two dimensional models for flow provide accurate estimates of the inertial forces resisting flow as well as being robust enough for field scale problems. In addition, the flow may be routed over a digital model of the terrain without any arbitrary apriori choice of flow boundaries. We tested three two dimensional methods; a staggered finite difference method, and two finite element methods. The finite difference method and one finite element method were found to be unconditionally stable for inertially-dominated flows, and accurately modeled actual river flows in Oregon. The third method, though popular in modeling wave motion, was not well suited to inertially dominated flows, nor could it be modified to be usable.

INTRODUCTION

Floods are a serious environmental hazard, causing major losses of property and life each year. Current practice for flood hazard estimation uses one-dimensional models, hand picking the river gradients from topographic maps for input into each model. This practice is more art than science, and requires considerable experience to get reasonable results. The stage and discharge of the flow is commonly reset at each gauging station, in which case the model estimates the flow between gauging stations. Critical flow can be handled by existing one dimensional routines, but the transition to critical flow is assumed to be normal to the one-dimensional flow direction and the shock (or critical transition) must be stationary. These limitations are accepted because it is widely believed that the one-dimensional models are state-of-the-art in river hydraulics, belying the fact that robust, two dimensional models capable of solving shallow water flow have been reported in the literature since 1990.

In this paper we discuss comparisons between three tested methods of solving two dimensional shallow water flow, and indicate which of these methods are best for solving flood problems. In addition, all models use digital terrain data as input so that flow boundaries and stage are determined objectively by the terrain data and the discharge, and not subjectively. Comparisons between different methods of flow simulations with historical records of one flood in Oregon show that different methods produce the same results, and accurately capture the physics of flow behavior.

DESCRIPTION OF SHALLOW WATER FLOW

Shallow water flow is defined as flow in which the depth is much less than the characteristic length of the body of water, and in which the pressure is approximately hydrostatic.

With these assumptions, the flow equations are obtained by vertically integrating the Navier Stokes equations (Pinder and Gray, 1977) to obtain the following equations for continuity and momentum:

$$\frac{\partial U}{\partial t} + \nabla F = H \quad (1)$$

where

$$\begin{array}{cccc}
 h & uh & vh & 0 \\
 U = uh & F_x = u^2h + \frac{gh^2}{2} & F_y = uvh & H = -gh(Sf_x + So_x) \\
 vh & uvh & v^2h + \frac{gh^2}{2} & -gh(Sf_y + So_y)
 \end{array} \quad (2)$$

Here h is flow depth, u is horizontal velocity in the x direction, v is the horizontal velocity in the y direction, Sf is a friction term, So is bed slope, g is gravitational acceleration, and subscripts refer to the x and y components.

If velocities are defined with reference to a single point in space, the equation system is defined as Eulerian, and in this case the body forces acting on any fluid volume may be written

$$b = \rho g - \rho c \quad (3)$$

where b refers to body forces (i.e. forces per unit volume) and c is the total acceleration acting on a fluid volume, and is given by the total derivative in a fixed coordinate system, or

$$c = \frac{\partial \mathbf{u}}{\partial t} + (\nabla \cdot \mathbf{u} \tau) \mathbf{u} \quad (4)$$

This shows that even if the flow in question is steady (i.e. $\partial \mathbf{u} / \partial t = 0$), convective accelerations exist that oppose the forces due to gravity, increasing the resistance to flow. Herein lies the main difference with creeping flows, and the cause of the difficulties in obtaining solutions for river hydraulics as these convective terms usually dominate the flow (figure 1). One of the methods described below uses a moving coordinate system (or Lagrangian framework) for part of the solution, greatly simplifying the approximation of the inertial terms (the convective accelerations).

Equation (1) is just one form of these equations. There are many different forms for the shallow water equations depending upon the solution method used, and each form will have a different combination of the independent variables. For deviations from a slowly-varying lake level or sea level, it is convenient to split flow depth into a mean depth and additional surface elevation. For river hydraulics the form above in equation (1) is more convenient, particularly where flooding of dry areas may occur, since all variables gracefully go to zero as flow depth goes to zero.

METHODS OF SOLUTION

We will discuss three solution methods; a finite difference method, a semi-lagrangian finite element method, and a wave equation finite element method. The first method operates on structured (i.e. rectangular) grids, though an unstructured version is being developed by Vincenzo Casulli (Univ. of Trento, Italy) and Roy Walters (U.S. Geological Survey). The second and third methods, being finite element methods, operate on unstructured triangular grids that can follow the stream channel. The effectiveness of these methods depends upon what terms in the momentum equation dominate the problem under consideration. As we shall show, the first two methods are well suited to inertially dominated river hydraulics, where the convective accelerations fluctuate by many orders of magnitude within any given reach. In contrast, the wave equation method cannot be modified to handle inertially-dominated flows, and instead excels at modeling gravity waves due to the influence of tides, waves, and Coriolis forces in bays, estuaries, and along the continental shelf (Walters, 1995).

The wave equation form of the shallow water equations is obtained by differentiating the continuity equation with respect to time to form a wave equation, and then substituting in the momentum equation for the divergence term to separate the wave height from the velocities in the solution process (Lynch and Gray, 1978). This method has provided spectacular results in analyzing wave phenomena in harbors, estuaries, and around islands (Lynch, Werner, and Wolff, 1995; Walters, 1995). However the method results in convective acceleration terms both in the wave equation for height and in the momentum equation for velocity. For river hydraulics, these terms dominate, and we found that straightforward Galerkin weighting in the finite element formulation diverged unless the convective accelerations were less than 1% to 5% of the force balance. Part of this problem comes from the Galerkin weighting of the finite element procedure, as the central differences of this weighting method amplify disturbances in the solution by creating a "negative diffusion" (Hughes, Franca, and Mallet, 1986; Peraire, Zienkiewicz, and Morgan, 1986). This may be countered by a one sided weighting instead of Galerkin weighting in an attempt to create a "balancing diffusion" in an inertially dominated flow (Hughes, Franca, and Mallet, 1986; Lee, Peraire, and Zienkiewicz, 1987). However we found that this fix, though adequate for slow flows, would only allow us to obtain solutions where the convective accelerations were less than 5% to 6% of the force balance in the flow. When compared to other methods that allowed the convective accelerations to dominate (i.e. Shakib, Hughes, and Zdenek, 1991), this limitation proved to be completely inadequate for normal river flow.

In contrast to the difficulties with the wave equation, a semi-implicit finite difference method developed for estuaries (Casulli, 1990) was found to be unconditionally stable, and robust enough to handle the wide-ranging convective accelerations found in river flow. Briefly, it operates on a staggered, rectangular grid in which the velocities are defined on the sides of each rectangular cell and the depth is defined in the center. This staggered arrangement is the C-grid of computational fluid dynamics (Ferziger and Peric, 1996), and does not support spurious oscillations that may arise in the computation of the flow. A complete description is given for two-dimensional flows in Casulli (1990) and for three-dimensional flows in Casulli and Cheng (1992) and Casulli and Cattani (1994).

A third method, suggested by our failed attempts at upwinding the wave equation, was recently developed by Roy Walters and Vincenzo Casulli (1997). This method uses a discrete

form for the shallow water equations with a lagrange approximation for the convective accelerations. It requires elements devoid of spurious modes, and produces an accurate estimate of inertially dominated flow from element to element as shown by comparisons with analytical solutions. As it is a finite element method, it operates on unstructured grids and conserves mass between elements. This method also produces robust solutions to river flows, and compares well with the finite difference method of Casulli (1990) though the solution methods and form of the equations are entirely different.

RESULTS

All methods were tested using a quarter annulus wave tank problem (Lynch and Gray, 1978) and found to be free of spurious oscillations as well as to provide a close match to the analytical solution. The methods were then compared to each other on two field areas; one in Idaho and the other in Oregon.

For flows in the Big Lost river in Idaho, two significant results emerged from comparisons between the wave equation, the finite difference method, and the Lagrange-Galerkin method. The first result is that the convective accelerations, absent in the wave equation formulation, dominated the flow. The water surface elevation varied by more than 7 meters for the finite difference and lagrange methods, whereas the wave equation only produced 3 meters of head change over the same reach. Since all methods were constrained by the boundary conditions to produce the same discharge, the velocities obtained by the linear wave equation without advection were much higher, and unrealistically so. This reflects the absence of the braking action of the convective accelerations in the flow, and shows that with inertially-dominated flows the actual value of boundary friction (given by Manning's n or a Chezy coefficient) may be irrelevant. In addition, since the wave-equation model for flow was too shallow, significant areas of flooding were not modeled. The second result was that the finite difference method and the Lagrange-Galerkin method (Walters, this volume) produced identical results, despite the vastly different solution procedures.

On a simulation for the Crooked River in Oregon, the finite difference and Lagrange-Galerkin procedures again produced identical results. In this case we had actual flow data available (Levish and Ostenaar, 1996) for a flood with a discharge of 567 cubic meters per second (or 20,000 cubic feet per second). Both methods produced stages that matched stage observations for the flow for the measured discharge. In contrast, a one dimensional model (HEC-2) where boundary friction had been increased to obtain convergence produced a discharge of 30,000 cfs for the same stage at this location. Had this model been used to estimate a past flood discharge using field evidence such as terraces for a given flood stage, the estimated paleo-discharge would be 50% too high. In addition, such one dimensional models cannot account for flow in any direction except down the stream channel, and as a consequence misses a lot of resistance produced by flow in other directions (such as side channels and channels cutting across bars) that would otherwise provide a more accurate answer.

The contribution of the inertial forces to the total braking forces (inertia + friction) is plotted for the Crooked River in figure 1 for a steady flow of 567 cubic meters per second

(20,000 cubic feet per second). The steady flow insures that all forces are in balance, so that this figure shows both the variability and the dominate nature of the inertial terms in guiding the flow.

CONCLUSIONS

The physics of shallow water flow, combined with the bed slope and irregular geometry of river drainages, result in inertially-dominated (and often critical) flows. Of three methods tested to model these flows, only two were viable. The successful methods are a semi-implicit finite difference method operating on a staggered grid, and a Lagrange-Galerkin finite element method. The wave equation method that is so successful in modeling waves in harbors will not converge for an inertially-dominated flow, nor can it be made so with upwinding procedures.

The grossly inaccurate velocities obtained with the wave equation model in Idaho and the one dimensional model in Oregon are a direct result of ineffective treatment of convective accelerations in the flow. The wave equation is incapable of converging for an inertially-dominated flow. In the case of one-dimensional models, these cannot model convective accelerations that result from flow directions in any direction other than the chosen flow path down the stream channel.

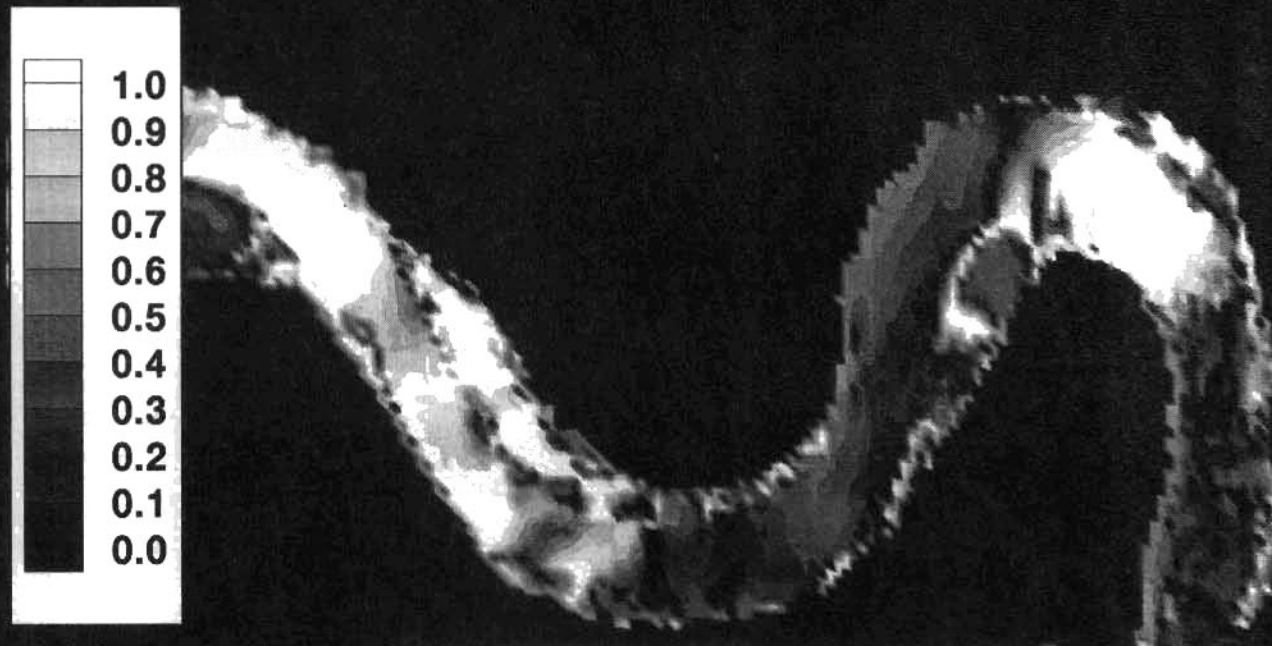
Paleo-flood studies are affected by inaccurate modeling procedures as well. Estimating discharge from stream terraces without effectively treating convective accelerations will lead to grossly overestimated velocities and discharges, and hence highly inaccurate estimates of the magnitude of past floods.

REFERENCES

- Casulli, V., 1990, Semi-implicit finite difference methods for the two-dimensional shallow water equations, *journal of computational physics*, 86, 56-74.
- Casulli, V. and Cattani, E., 1994, Stability, accuracy, and efficiency of a semi-implicit method for three dimensional shallow water flow, *Computers Math. Applic.*, 27, 99-112.
- Casulli, V. and Cheng, R., 1992, Semi-implicit finite difference methods for three dimensional shallow water flow, *Int. Journ. For Num. Meth. In Fluids*, 15, 629-648.
- Ferziger, J.H., Peric, M., 1996, *Computational methods for fluid dynamics*, Springer-Verlag, 356 p.
- Hughes, T.J.R., Franca, L.P., Mallet, M., 1986, A new finite element formulation for computational fluid dynamics: I. Symmetric forms of the compressible Euler and Navier-Stokes equations and the second law of thermodynamics, *Comput. Meth. Appl. Mech. Engrg.*, 54, 223-234.
- Lee, J.H.W., Peraire, J., Zienkiewicz, O.C., 1987, The characteristic galerkin method for advection dominated problems - an assessment, *Comput. Meth. Appl. Mech. Engrg.*, 61, 359-369.
- Levish, D.R., and Ostenaar, D.A., 1996, Applied paleoflood hydrology in North Central Oregon, *Guidebook for Field Trip 2, Cordilleran section*, 92nd Annual Meeting, Geol. Soc. America, Portland, Oregon, 182 pg.
- Lynch, D.R., Ip, J.T.C., Werner, F.E., Wolff, E.M., 1995, *Environmental Hydrodynamics: Comprehensive model for the Gulf of Maine*, in *Finite Element Modeling of Environmental Problems*, ed. Graham Carey, John Wiley and Sons, 17-33.

- Lynch, D.R., and Gray, W.G., 1978, Some analytical solutions to the linearized shallow water equations, *J. Hydraulics Div., ASCE*, 104(H 10).
- Lynch, D.R., and Gray, W.G., 1979, A wave equation model for finite element tidal computations, *Computers and Fluids*, 7, 207-228.
- Peraire, J., Zienkiewicz, O.C., Morgan, K., 1986, Shallow water problems: a general explicit formulation, *Int. Journ. For Num. Meth. In Engrg.*, 22, 547-574.
- Pinder, G.F., and Gray, W.G., 1977, *Finite elements in surface and subsurface hydrology*, Academic Press.
- Shakib, F., Hughes, T.J.R., and Zdenek, J., 1991, A new finite element formulation for computational fluid dynamics: X. The compressible Euler and Navier Stokes equations, *Comp. Meth. Appl. Mech. Engrg.*, 89, 141-219.
- Walters, R.A., 1995, Modeling surface water flow, in *Finite Element Modeling of Environmental Problems*, ed. Graham Carey, John Wiley and Sons, 1-13.
- Walters, R.A., and Casulli, V., 1997, A robust finite element model for hydrostatic surface water flows, submitted to *Comm. In Num. Meth. In Engrg.*

INERTIAL FORCES RESISTING STREAMFLOW CROOKED RIVER, OREGON



200 METERS

Figure 1. This plot shows the relative magnitude of convective accelerations (or inertial forces, as shown by equations 1, 3 and 4 in text) in the total force (inertia + friction) resisting streamflow, for a steady flow of 567 cubic meters per second (or 20,000 cubic feet per second).

UNSTEADY FLOW MODEL FOR FORECASTING MISSOURI AND MISSISSIPPI RIVERS

by

D. Michael Gee, Hydraulic Engineer, U.S. Army Corps of Engineers Hydrologic Engineering Center,
Davis, CA and

Ming T. Tseng, Chief Hydrologic Engineering Section, Headquarters, U.S. Army Corps of Engineers,
Washington, D.C.

Abstract: This paper describes the Mississippi Basin Modeling System (MBMS) and updates a previously published paper (Gee and Tseng, 1996). This system utilizes the UNET (HEC, 1997) unsteady flow model as a forecasting tool. Therefore, development of a graphical user interface (GUI) reflecting the unique needs of real-time forecasting and the consequent design of data protocols for storage, retrieval, presentation and transfer of forecast information from upstream to downstream offices were required. The data management system uses the Hydrologic Engineering Center's (HEC) Data Storage System (HEC, 1995). The modeling system was developed to encompass low flows and routine day-to-day forecasting needs (such as lock and dam operations), as well as the simulation and forecasting of flood events.

INTRODUCTION

The U.S. Army Corps of Engineers has built and operates a large number of reservoirs, levees, floodways and flow diversion structures in the Mississippi River Basin for flood control and navigation. These projects are operated and maintained by four Corps Divisions in a coordinated manner. Experiences during the Great Flood of 1993 concentrated the awareness of the need for a modeling system that could be used to improve operation of flood control projects during a storm system covering a geographic region as large as the upper Mississippi River basin (Interagency, 1994). Subsequent to the 1993 flood the Corps committed to the development of such a system to achieve the following objectives; 1) improve and facilitate communications between Corps offices, other agencies and Corps customers, 2) provide real-time discharge and stage data during flood events to support emergency management activities, 3) provide a means for assessment of impacts due to levee breaches, 4) provide displays of areal extent of flooding for various weather and levee breaching or overtopping scenarios, 5) identify navigation hazards, and 6) provide data for real-time damage assessment.

MISSISSIPPI BASIN MODELING SYSTEM

Geographic Coverage: The MBMS covers an extensive area. It extends from Anoka, MN to the Gulf of Mexico on the Mississippi River, from Gavins Point Dam to St. Louis (confluence with the Mississippi) on the Missouri River and from Lockport Lock & Dam to Grafton on the Illinois River. The model consists of a network of seven unsteady flow sub-models; four for the mainstem Mississippi River, two for the Missouri River and one for the Illinois River. Also included (although not simulated with UNET at this time) are the Ohio River and the Arkansas and White Rivers. It covers thousands of miles of river, including hundreds of inflow points and numerous gages. Portions of numerous smaller tributaries in the Basin are also modeled as unsteady flow routing reaches. A schematic representation of the system showing key locations is shown on Figure 1.

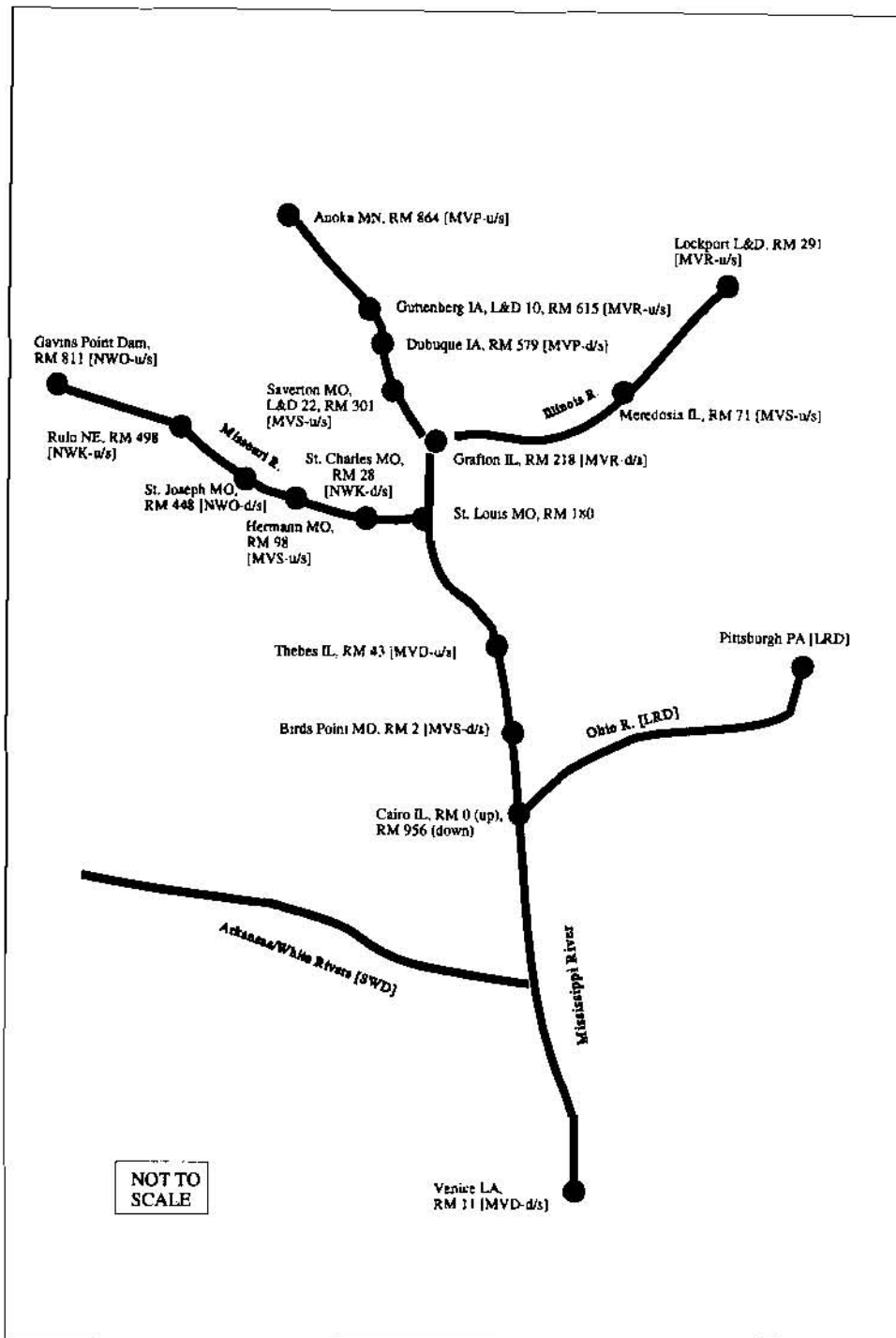


Figure 1. Schematic Diagram of MBMS Geographic Extent. (u/s = upstream location of UNET boundary condition, d/s = downstream location of UNET boundary condition.)

Components: The MBMS consists of many individual components that may be grouped into data bases and software modules. Among the data bases are: (1) Measured field data such as cross sections and hydrographs, (2) Predicted (forecasted) inflows to the system such as runoff generated by a rainfall event, (3) Project operation criteria such as navigation dam rule curves, (4) Calibration data such as observed stage and flow hydrographs, (5) Simulation parameters

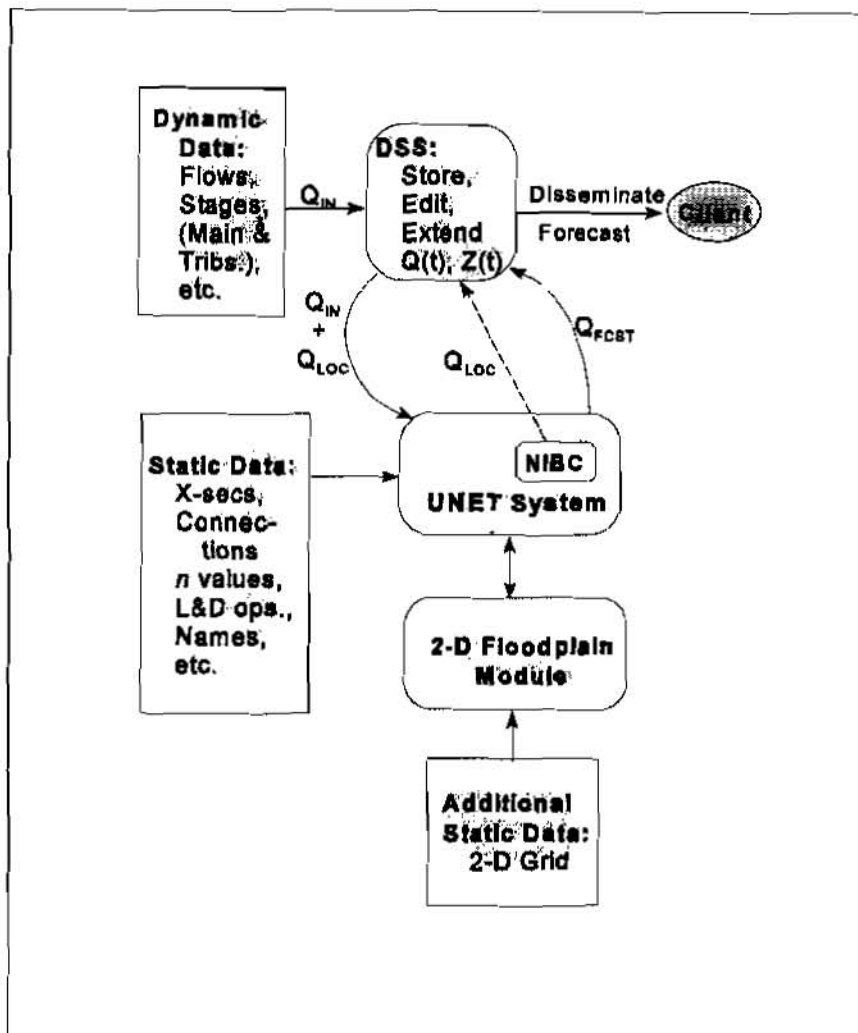


Figure 2. Components of the MBMS. NIBC = Null Internal Boundary Condition.

such as Manning's n values and discharge-conveyance relations, (6) Computed forecast flow and stage hydrographs, and (7) Geographic information system (GIS) data used for presentation of area maps, damage locations, gage locations, inundated areas, etc. The four primary software modules (each of which is composed of several sub-modules) comprising the MBMS are: (1) UNET, the one-dimensional unsteady flow hydrodynamic model, (2) A two-dimensional hydrodynamic model linked to UNET for overbank flow simulation, (3) HEC-DSS, the data management, manipulation and display module, and (4) the graphical user interface (GUI) that the forecaster uses to interact with the system. Also critical to successful operation of the MBMS are communication systems for the retrieval of real-time field data such as rainfall and gage readings, and the transmittal of forecasted information such as stage and flow hydrographs to other Districts and clients. The relationships among these components are depicted in Figure 2.

THE UNET MODELING SYSTEM

Description: UNET (HEC, 1997) is the primary hydraulic analysis tool used in the MBMS. It simulates one-dimensional unsteady flow through a network of open channels. One element of open channel flow in networks is the split of flow into two or more channels. For subcritical flow, that division of flow depends upon the capacities of the receiving channels. Those channel capacities are functions of downstream channel geometries and backwater effects. Another element of a flow network is the combination of flows, which constitutes a dendritic system. A dendritic situation is simpler than a flow split because flow from each tributary depends only on the stage in the receiving stream. An open channel flow network that includes single channels, dendritic systems, flow splits, and looped connections such as flow around islands, constitutes the most general case. UNET has the capability to simulate such a network. Another capability of UNET is the simulation of storage areas; e.g., lake-like regions that can either provide water to, or divert water from, a channel. In this situation the water surface elevation in the storage area will control the volume of water diverted. That volume, in turn, affects the shape and timing of downstream hydrographs. Storage areas can be the upstream or downstream boundaries of a river reach. In addition, a river can discharge laterally into storage areas over a gated spillway, weir, levee, through a culvert, or via a pumped diversion.

UNET Developments: Described below are several features that were added to UNET during development of the MBMS.

Levee Algorithms: Subsequent to the 1993 flood on the Missouri River, a new capability for simulating the effects of levee breaches was added to UNET. During 1993 virtually all of the agricultural levees along the Missouri were overtopped, resulting in significant overbank conveyance. This situation poses a peculiar modeling problem. For flows below a certain transition discharge, the levee interior acts as a storage cell which communicates with the river through a breach, or breaches, in the embankment. When flow exceeds the transition discharge the area behind the levee no longer acts as a storage cell but becomes part of the river, conveying flow. Therefore, there are two situations that must be modeled; a storage cell and a flowing river. An algorithm was developed that allows the overbank storage areas to change to conveyance areas (and back) based upon a triggering river flow or stage. Note, however, that this technique do not directly predict the location, size, or timing of a levee breach. Operationally, from forecasted stages, the forecaster may be able to hypothesize the locations and times of potential levee breaches and use the MBMS to rapidly evaluate impacts of various scenarios.

Dike Fields: A dike field is a system of structures that contracts the low-flow cross section to the design width of the navigation channel. Because UNET is a one-dimensional model the local effects of each individual dike cannot be simulated. Rather, the cross sections are numerically contracted to simulate the effects of the dike field. The area blocked by the dike field can be modeled as a storage area or as an area filled with sediment which is deducted from the cross-sectional area. Simulation of the added form roughness of the submerged dike field is done by the user as part of the model calibration.

Navigation Dam Algorithms: A major effort was undertaken to provide the ability to simulate lock and dam operations with the UNET system (Barkau, 1996). The capability to use operating rule curves at navigation dams as internal boundary conditions was developed and implemented for the MBMS project. Two types of navigation dam operation can be simulated; control point within the navigation pool (hinge-point operation) and control point at the dam. The hinge-point operation is defined by a set of functions which relate control point elevation to elevation at the dam for various discharges. Control at the dam relates target pool elevation to discharge and tailwater elevation. These functions may include seasonal effects (ice, wind, etc.) and other (environmental, legal, etc.) constraints. The concept is to provide the operator with the information needed to make decisions quickly and easily.

Null Internal Boundary Condition: The "null internal boundary condition" (NIBC) is a modification to the UNET system that is used to estimate residual (incremental) flows, which may be thought of as ungaged lateral inflows or outflows. This procedure uses two executions of UNET. The first execution assumes stage continuity at gages, with each gage location being an internal boundary condition. This execution produces computed flows both upstream and downstream of the gage, which will most likely differ. DSSMATH (an HEC-DSS utility) is then used to compute the residual flow (difference) for each reach between gages to achieve flow continuity at the gages. These residual flows are then distributed throughout the upstream reach (usually uniformly) and lagged in time as deemed appropriate. The second execution uses these flows as uniform lateral inflow hydrographs and removes the internal boundary conditions, resulting in an open river condition at the gages.

Graphical User Interface: The GUI developed for the MBMS was based on work done by the Corps' Cold Regions Research and Engineering Laboratory for the (then) Missouri River Division. That work involved management of releases from mainstem Missouri River dams to prevent damage to endangered species habitat. It was primarily a "simulation" application. That interface was expanded to meet the needs of forecasting applications. The enhancements to the interface included; consistent file management, implementation of a UNET hotstart capability, easy time window selection, and interaction with DSS-DSPY in a fashion consistent with and supporting water control needs. The GUI runs under UNIX. Figure 3 shows one of the initial screens. This screen provides the user with identification of the static data currently in use (e.g., River ID, CSect Template, and BC Template). The time period represents the entire simulation duration which includes a warm-up period prior to the time of forecast and the forecast interval. The warm-up period is used to blend in any changes to the system that may have occurred since the last forecast. An example would be updating the extrapolated local inflows to match the flows based on observed data from the last time of forecast to the present one. The execution of the UNET system is launched from this screen via the "Run UNET" button.

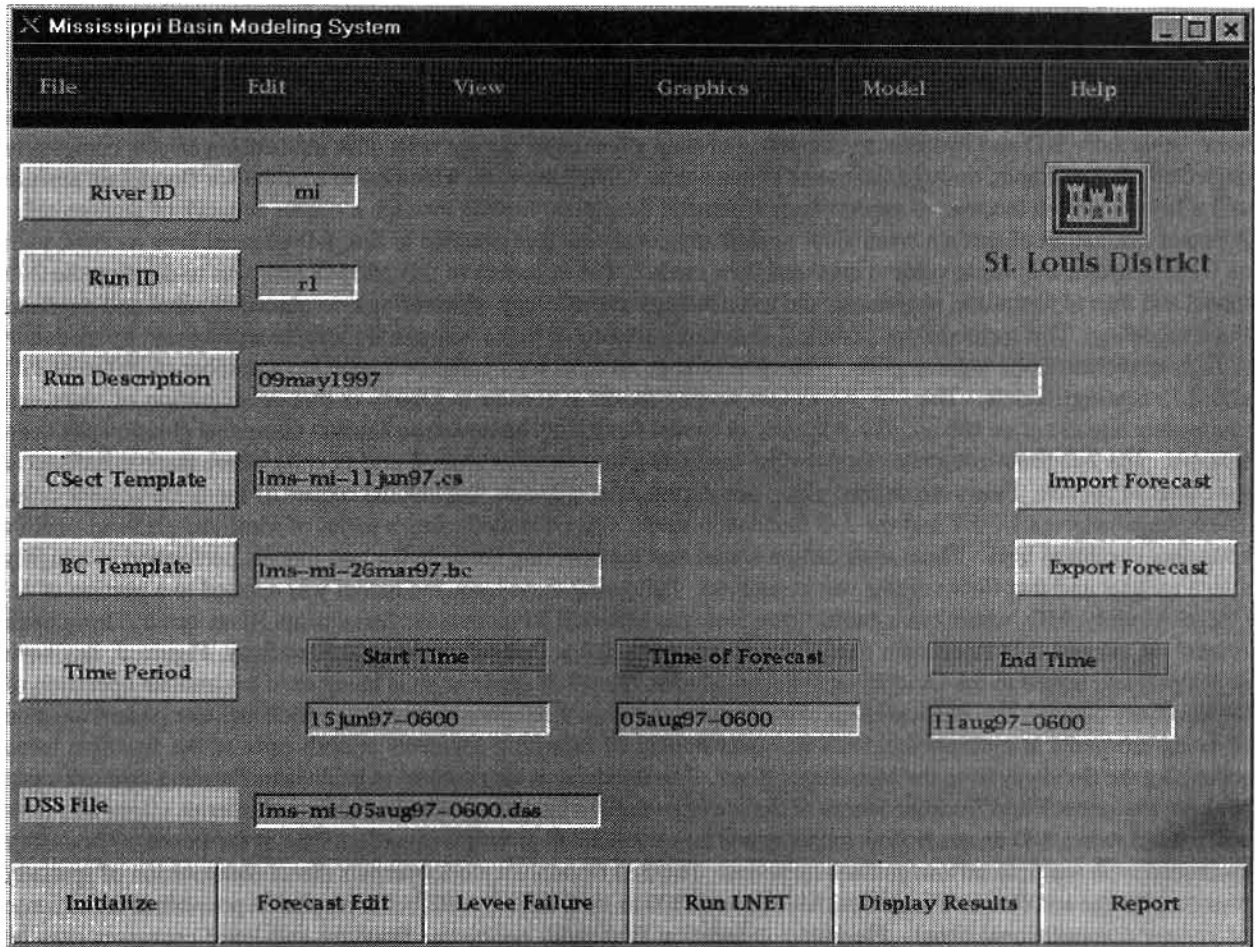


Figure 3. MBMS GUI Screen Obtained by Selecting the “Model” Button on the Entry Screen.

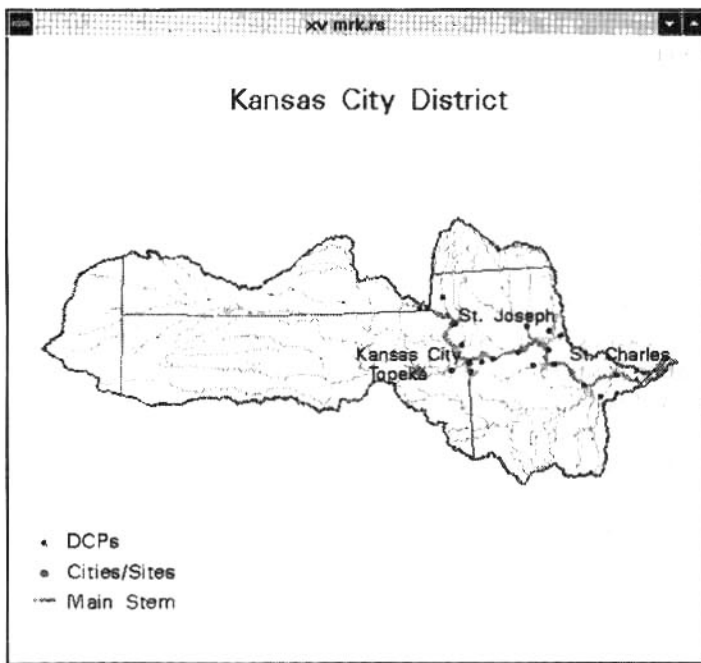


Figure 4. Example Display of a Drainage Basin from the GIS.

The “Forecast Edit” button allows the forecaster to edit the forecasted flows either graphically or by entering their new values. “Display Results” allows selection of a gage station, location, or profile for display of computed hydrographs or water surface profile elevations. The “Levee Failure” button generates a scrollable display of the levees defined as having potential for overtopping/breaching. The breach parameters, such as time of initiation, can be interactively changed from this screen.

The GUI also interfaces with a geographic information system (GIS) to provide map-based interaction with the data displays. Figure 4 shows an example of such a display. These displays are active in the sense that access to DSS data can be obtained by clicking on a location of interest.

TWO-DIMENSIONAL MODELING CAPABILITY FOR OVERBANK AREAS

An accurate description of combined channel and overland flood flow requires a blend of one- (1-D) and two-dimensional (2-D) surface water flow modeling concepts. Two-dimensional computations in a floodplain can range from being fully 2-D and dynamic to consisting of only a few large storage cells with momentum effects completely neglected. For example, through the use of storage cells, UNET provides a method to account for floodplain storage and allows a skilled modeler to approximate kinematic floodplain routing through a coarse network of storage cells. A recent evaluation of surface water flow models suggested that it is possible to link 1-D channel flow models, such as UNET, with a 2-D finite volume overland flow model. The objective of this MBMS task was to develop the 2-D model and then to formulate, implement, and test a linkage methodology which allows combined channel and overland flood modeling. This methodology permits 2-D dynamic routing of flows across a floodplain represented by moderate to high resolution finite volume grids. The same linkage methodology could be applied to a number of different 1-D and 2-D routing models. The 2-D floodplain routing model is similar to UNET in that conservation of mass and momentum equations are solved. For purposes of model flexibility, however, an explicit numerical solution has been selected. The 2-D finite-volume method divides the system into an unstructured grid of cells where stage is defined at the center of the cell. Flows are defined along one-dimensional channels that link the centers of the finite volume cells. The linkage between UNET and the 2-D floodplain model was evaluated using a series of idealized grid and interior boundary condition tests. These tests demonstrated that the coupling between the two models performed in a highly stable manner and that flow volume was conserved. Following these tests, the model was applied to a portion of St. Charles County, MO, where cross-basin flows from the Missouri River into the Mississippi River occur during large floods. A second 2-D floodplain model representing the Birds Point-New Madrid Floodway, Figure 5, has been developed and linked to the Ohio River Forecast Model. That 2-D application is being used to simulate operation of the floodway during a hypothetical flood. Floodway operation is a complex undertaking which includes phased creation of levee crevasses at multiple locations and overtopping of fuse-plug segments at both ends of the frontline levee separating the floodway from the Mississippi River. The floodway is also subject to backwater flooding through a gap between the setback and frontline levees at the lower end of the floodway. Determination of interior stages and flow distribution with a 1-D unsteady flow model would be very difficult given the irregular shape of the floodway boundary combined with multiple inflow/outflow locations. The 2-D floodplain model permits direct computation of spatially distributed stage and flow at a horizontal resolution of 300 to 1000 meters (with better resolution possible at the expense of greater computational time). Floodway inundation from both backwater flooding and levee crevasses may be visualized by creating animations directly from the stage computed by the 2-D model. This work was performed by the Corps' Waterways Experiment Station

DATA REQUIREMENTS

A continuing area of concern is the trade off between the cost of obtaining increased accuracy of topographic data and the accuracy of the results computed from those data. This has been studied and documented for the use of HEC-2, a steady flow model (HEC,1986). That study determined that the primary source of uncertainty in computed results was the estimation of energy loss coefficients, not topographic data accuracy using normal surveying standards at that time. Experience with one-dimensional unsteady flow models, such as UNET, has confirmed and expanded that conclusion. It is important, in the application of an unsteady flow model, that storage as well as conveyance be properly represented. This requires accurate definition of the conveyance and the flow-controlling elevations and locations (e.g., levees, weirs, etc.). Ground elevations in storage areas such as overbanks and leveed areas are not as critical if the volumetric capacity of those areas is correct. Information based on topographic maps with 1.5m (5 ft.) contours is usually adequate for overbank areas for systems with broad floodplains. When applying a two-dimensional flow model, however, the ground topography becomes more important, particularly in areas of little vertical relief. The MBMS team decided that 0.5m (2 ft.) vertical resolution was needed in the cross-over area between the Missouri and Mississippi Rivers for reliable two-dimensional modeling. This requirement depends on the relationship between water depth and the magnitude of changes in bed elevation. When applying any of these hydraulic modeling approaches, one must be aware that there is substantial uncertainty in past inflows to the system as well as the forecasted inflows, all of which will influence the accuracy of the computed results.

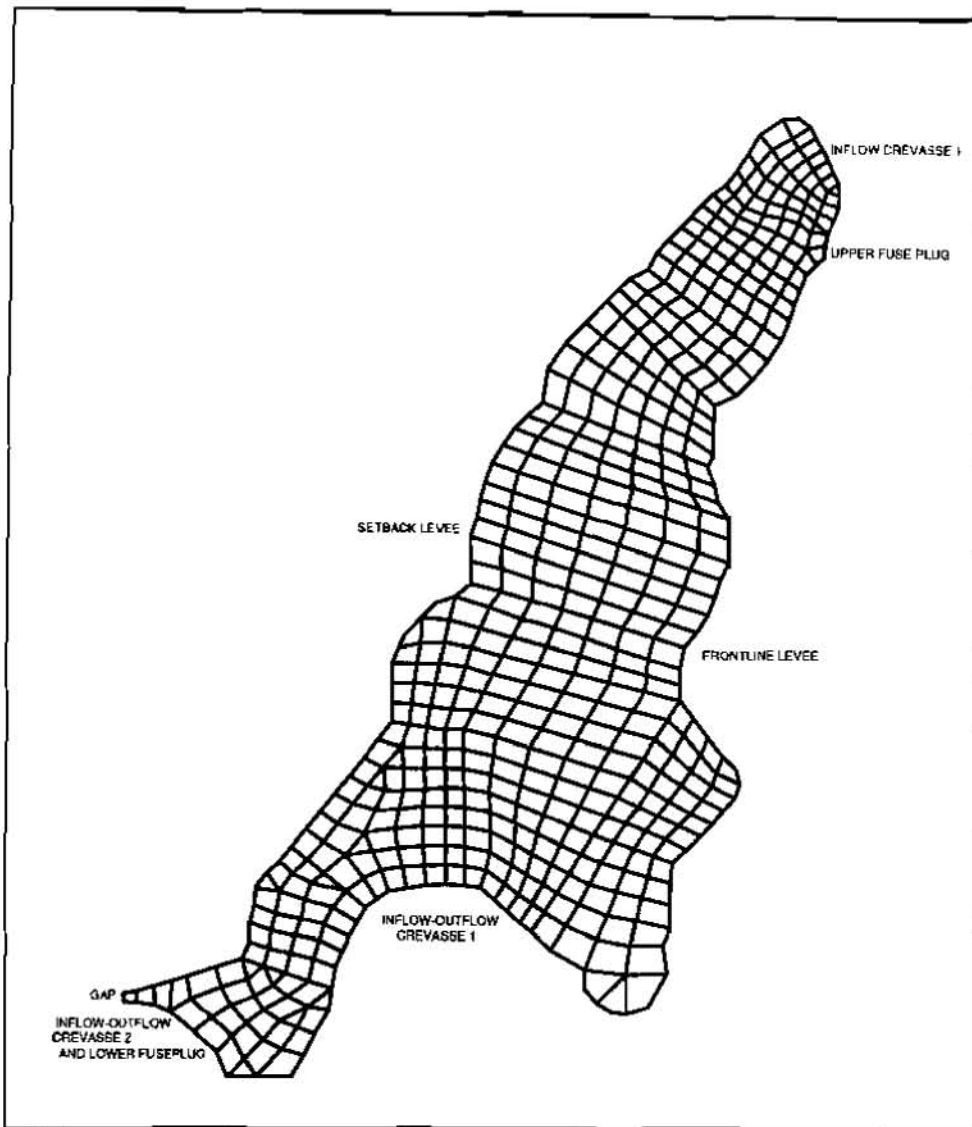


Figure 5. Two-Dimensional Grid Representing the Birds Point-New Madrid Floodway.

COORDINATION

The Mississippi Basin Modeling System development team consisted of representatives of the St. Paul, Rock Island, Omaha, Kansas City and St. Louis Districts; and the Mississippi Valley, Great Lakes and Ohio River, and Southwestern Divisions. Research and development were performed by the Waterways Experiment Station, Cold Regions Research and Engineering Laboratory and Hydrologic Engineering Center. Technical guidance and study coordination was provided by the Corps of Engineers Headquarters Hydraulics and Hydrology Branch. Dr. Robert Barkau served as a consultant to the team and individually to several of the offices involved. It is anticipated that future coordination will expand outside of the Corps to include the National Weather Service and, possibly, others. Coordination and data exchange were also accomplished with the Corps Floodplain Management Assessment (USACE, 1995) teams and the interagency Scientific Assessment and Strategy Team (Freeman and Frazier, 1997). These were two complementary efforts to study the impacts of levees on the Mississippi Basin system. The former used UNET to analyze the effects of an array of levee placement options on flood heights and the latter used an interdisciplinary approach to evaluate consequences of levee placement on wetlands, environmental quality, agricultural use, local economies, etc.

APPLICATIONS OF THE MODELING SYSTEM

The St. Paul District applied the MBMS during the 1997 flood to forecast water surface elevations on the Mississippi River within the District and to provide the (downstream) Rock Island District with predictions at Lock and Dam No. 10. The results of these forecasts were also used to coordinate emergency response activities. The results were posted on the District's water control home page. Preparation and dissemination of a UNET forecast, using the GUI, required about 20 minutes.

The Rock Island District also used the MBMS during the spring flood of 1997. The accuracy of St. Paul District's forecast at Lock and Dam 10 and careful base calibration of the MBMS were key factors in the production of accurate forecasts. The MBMS was run daily by Rock Island District's water control personnel from April 10 to May 7, 1997. This experience demonstrated both the accuracy and reliability of the MBMS in a real-time flood application.

The St. Louis District tested the MBMS in May 1996 during a flood. It was noted that stages at St. Louis were underpredicted by about 2 ft. Further investigation revealed that a shift in the rating curve had occurred. After the appropriate adjustment was made, the forecasted stages were within 1 ft. of observed. As this was a test application, no further refinements were made. After further calibration, GUI development and implementation of Lock & Dam algorithms, the MBMS was extensively used during the spring 1997 flood. Generally, the model results deviated from observations by less than 1 ft. A file transfer system was used to obtain forecasts from upstream on the Mississippi and Missouri Rivers. St. Louis' forecasts were then delivered to downstream Corps offices.

The Mississippi Valley Division tested the MBMS during the 1997 flood. The flow forecasts were deemed to be reasonable and, therefore, were used to estimate the duration of the Bonnet Carre Spillway operation.

ACKNOWLEDGMENTS

The Corps team assembled to execute this effort was composed of representatives of five Districts; St. Paul, Rock Island, St. Louis, Omaha and Kansas City. Also active in this study were the Mississippi Valley Division, Great Lakes and Ohio River Division and the Southwestern Division. Technical support was provided by the Waterways Experiment Station, Cold Regions Research and Engineering Laboratory and Hydrologic Engineering Center. Study management, guidance and coordination was provided by Corps of Engineers Headquarters Hydraulics and Hydrology Branch. The opinions expressed herein are those of the authors and not necessarily those of the U.S. Army Corps of Engineers.

REFERENCES

- Barkau, R.L., 1996, Navigation Dam Algorithm, a report submitted to the Hydrologic Engineering Center, December 1996.
- Freeman, G.E., and Frazier, A.G., 1997, Proceedings of the Scientific Assessment and Strategy Team Workshop on Hydrology, Ecology, and Hydraulics, v. 5 of Kelmelis, J.A., ed., Science for Floodplain Management into the 21st Century: Washington, D.C., U.S. Government Printing Office.
- Gee, D.M., and Tseng, M.T., 1996, Unsteady Flow Model for Forecasting Missouri and Mississippi Rivers. *Proceedings RIVERTECH '96 1st International Conference on New/Emerging Concepts for Rivers*, September 22-26 1996, Chicago, Illinois, pp. 869-876. International Water Resources Association, Urbana, IL, USA. (Also published as HEC Technical Paper No. 157, February 1997.)
- Hydrologic Engineering Center (HEC), 1986, Accuracy of Computed Water Surface Profiles, RD-26, U.S. Army Corps of Engineers, Davis, CA, December 1986.
- HEC, 1995, HEC-DSS User's Guide and Utility Manuals, User's Manual, CPD-45, U.S. Army Corps of Engineers, Davis, CA, March 1995.
- HEC, 1997, UNET One-Dimensional Unsteady Flow Through a Full Network of Open Channels, User's Manual, CPD-66, U.S. Army Corps of Engineers, Davis, CA, August 1997.
- Interagency Floodplain Management Review Committee, 1994, Sharing the Challenge: Floodplain Management into the 21st Century, Report to the Administration Floodplain Management Task Force, U.S. Government Printing Office, Superintendent of Documents, Washington, D.C., 189 pp., June 1994.
- USACE, 1995, Floodplain Management Assessment of the Upper Mississippi and Lower Missouri Rivers and Their Tributaries - Main Report, U.S. Army Corps of Engineers, Washington, DC, June 1995.

ESTIMATING ICE-AFFECTED STREAMFLOW BY EXTENDED KALMAN FILTERING

By D.J. Holtschlag, Hydrologist, U.S. Geological Survey, Lansing, Michigan; M.S. Grewal, Professor of Electrical Engineering, California State University, Fullerton, California

Abstract: An extended Kalman filter was developed to automate the real-time estimation of ice-affected streamflow on the basis of routine measurements of stream stage and air temperature and on the relation between stage and streamflow during open-water (ice-free) conditions. The filter accommodates three dynamic modes of ice effects: sudden formation/ablation, stable ice conditions, and eventual elimination. The utility of the filter was evaluated by applying it to historical data from two long-term streamflow-gaging stations, St. John River at Dickey, Maine and Platte River at North Bend, Nebr. Results indicate that the filter was stable and that parameters converged for both stations, producing streamflow estimates that are highly correlated with published values. For the Maine station, logarithms of estimated streamflows are within 8% of the logarithms of published values 87.2% of the time during periods of ice effects and within 15% 96.6% of the time. Similarly, for the Nebraska station, logarithms of estimated streamflows are within 8% of the logarithms of published values 90.7% of the time and within 15% 97.7% of the time. In addition, the correlation between temporal updates and published streamflows on days of direct measurements at the Maine station was 0.777 and 0.998 for ice-affected and open-water periods, respectively; for the Nebraska station, corresponding correlations were 0.864 and 0.997.

INTRODUCTION

U.S. Army Corps of Engineers (USACOE) is responsible for mitigating flood damages and for maintaining navigable conditions in streams by operation of dams throughout the United States. Decisions affecting the day-to-day operation of these dams are based on real-time streamflow data obtained by telemetry from streamflow-gaging stations typically operated by U.S. Geological Survey (USGS). Ice effects, associated with variable blockage of the channel by ice and increased flow resistance, reduce the accuracy of real-time streamflow data. To improve controllability of streamflow during ice-affected periods, Cold Regions Research and Engineering Laboratory of USACOE supported this study to improve real-time estimates of ice-affected streamflow.

USGS operates a network of about 7,000 continuous-record streamflow-gaging stations nationwide. Although stage (water-surface elevation of the stream) is continually recorded, direct measurements of streamflow and stage are obtained only at about 6-week intervals. The average (monotonically increasing) relation between stage and streamflow during open-water conditions (no ice cover) is referred to as the "stage-discharge rating." Streamflow indicated by the rating for a particular stage is referred to as the "apparent streamflow." Deviations in the average relation between stage and streamflow, which are interpreted from individual direct measurements of streamflow and stage, are described by shifts in the rating. Together with hourly or more frequent measurements of stage, the rating and shifts are used to compute streamflow records for annual publication, following a comprehensive analysis of streams in a network of gaging stations.

During open-water conditions, uncertainty associated with shifts in the rating are usually small with respect to the need for information affecting dam operations. Thus, real-time estimates of streamflow, traditionally determined directly from the rating and possibly the shift defined from the most recent direct measurement, provide sufficient accuracy. However, during ice-affected periods, the accuracy of real-time streamflow estimates are degraded by rapidly varying ice-backwater conditions and large time-varying shifts. In these conditions, the ratio of the true streamflow to the apparent streamflow, referred to as the "streamflow ratio," can vary from 1 during open-water conditions to a value near zero. These shifts create sufficient uncertainty in traditional real-time streamflow estimates that dam operations can be degraded.

FORMULATION OF THE PROBLEM

Based upon analysis of historical streamflow characterizations developed by traditional methods for estimating ice-affected streamflow, the dynamics of ice effects were classified into three modes. Mode 1 dynamics are associated with the sudden formation/ablation of ice effects as indicated by abrupt changes in apparent

streamflow. Mode 2 dynamics are associated with stable ice conditions and are approximated by a first-order difference equation relating the streamflow to air temperature. Finally, mode 3 dynamics are associated with the eventual elimination of ice effects at warm air temperatures. Each mode corresponds to a unique process (state) model.

The process model for mode 1 dynamics is an algebraic equation of the form

$$x_1(k) = \frac{h(k-1)}{h(k)} x_1(k-1), \quad (1)$$

where $x_1(k)$ (or $x_1(k-1)$) is the estimated ratio of the actual to apparent streamflow at time indexed by variable k (or $k-1$). The variable h corresponds to the apparent streamflow. Mode 1 dynamics were applied for either of two conditions: (1) if the one-day change in apparent streamflow increased by more than $q_dl\%$ and the average air temperature was less than t_lo , or (2) if the one-day change in apparent streamflow decreased by more than $q_dl\%$ when the streamflow ratio was less than 1. Because of the lack of derivative information in equation 1, parameters q_dl and t_lo were included among five threshold parameters estimated outside the extended Kalman filter.

The process model for mode 2 dynamics is a first-order difference equation driven by air temperature, u . The form of the process model for mode 2 dynamics is

$$x_1(k) = x_2(k-1) + x_3[x_1(k-1) - x_2(k-1)] + x_4(k-1)[\bar{u}(k-1) - x_5(k-1)], \quad (2)$$

which indicates that at times of ice effect and constant air temperature x_5 , the streamflow ratio (x_1) is in equilibrium about a nominal value x_2 . Changes from the equilibrium value are described by a difference equation that includes an autoregressive component with parameter x_3 and a forcing function term associated with daily air temperature. Air temperatures that vary from a nominal value of x_5 change the streamflow ratio from its nominal value of x_2 at a rate of x_4 . This form of a difference equation is nonlinear in parameters because rate parameters (x_3 and x_4) and offset parameters (x_2 and x_5) are estimated simultaneously. Prior information on the distribution of streamflow ratios during periods of ice effect was used in hope of facilitating the solution of this inherently difficult estimation problem. Air temperature, \bar{u} , indicates an exponentially weighted average of temperature from the three previous days. An exponential weighting factor, t_wt , used in computing \bar{u} , was included among threshold parameters because it did not occur explicitly in equation 2.

The process model for mode 3 dynamics is an equation of the form

$$x_1(k) = x_1(k-1) + \frac{\bar{u}(k-1) - t_hi}{t_ou - t_hi} [1 - x_1(k-1)]. \quad (3)$$

The mode 3 dynamic model is applied when the exponentially weighted air temperature value exceeds t_hi . Then, the streamflow ratio increases from its value at time $k-1$ to a value of one when the exponentially weighted air temperature equals t_ou . Because t_hi and t_ou occur explicitly in the process model, they could be included as parameters in the state vector. However, because of dangerous conditions for direct measurement of streamflow during mode 3 dynamics and correspondingly limited direct measurement data, t_hi and t_ou were included among threshold parameters estimated outside the filter. Estimates of streamflow ratio for all dynamic modes were constrained to an interval between a maximum of 1 and a minimum greater than zero. In this analysis, the minimum was the minimum ratio of published to apparent streamflow determined from historical record.

The process models for the three dynamic modes were developed so that the first (only) element in the state vector was the signal element (the estimated streamflow ratio). For this application, change in mode affected only the signal element. In contrast, the state parameter vector was treated as if mode 2 dynamics were always applied. Although this convention can create uncertainty in the state parameter vector, the uncertainty is minimized because updates affecting the parameter vector are computed only for days of direct streamflow measurement. Direct measurements are not generally possible during conditions of mode 1 or 3 dynamics because of unsafe measuring conditions associated with these ice conditions.

APPLICATION OF EXTENDED KALMAN FILTERING

Grewal and Andrews (1997), Bar-Shalom and Li (1993), and Brown and Hwang (1997) provide detailed information on the mathematical development and general application of Kalman filtering. A Kalman filter is an estimator of the state of a dynamic system given measurements that are related to the state. The extended form of the Kalman filter was selected because the state vector was formulated to include both a signal element (the streamflow ratio) and unknown parameters. In addition to the unknown parameters in the state vector, five threshold parameters are estimated externally to the extended Kalman filter.

A discrete-time extended Kalman filter was developed to account for effects of ice on streamflow. The filter consists of two models, a nonlinear process model and a linear measurement model. The general form of the nonlinear process model is

$$x(k) = f(x(k-1), k-1) + w(k-1), \quad (4)$$

where

$x(k)$ is the state vector. In this paper, the state vector is partitioned into two components. The first component is the streamflow ratio and is referred to as the "state signal element." The second component is referred to as the "state parameter vector." The total number of elements in the state vector is referred to as the "dimension of the state space."

$f(x(k-1), k-1)$ is a nonlinear function of the state at the previous time step plus other information on auxiliary variables available at time $k-1$.

$w(k-1)$ is a value from a random sequence representing process noise at time $k-1$. (In the analysis of dynamic systems, noise refers to random inputs that cannot be directly measured or controlled). The sequence w is assumed to be independent and normally distributed with a mean of zero and a covariance structure, $Q(k-1)$, commonly written $w \sim N(0, Q(k-1))$. In this application, only the variance of $x_1(k)$ was assumed to be nonzero; no process noise was associated with the state parameters.

The time-varying linear measurement model is of the form

$$z(k) = H(k)x(k) + v(k), \quad (5)$$

where

$z(k)$ is the streamflow at time k ,

$H(k)$ is the time-varying measurement sensitivity matrix that is represented by the vector

$[h(k) \ 0 \ 0]$, where $h(k)$ is the apparent streamflow, and

$v(k)$ is a value from a random sequence representing measurement noise at time k . The sequence v is assumed to be independent and normally distributed, with a mean of zero and variance $R(k)$. The subset of days indexed by k on which direct measurements of streamflow were obtained is denoted as k' . For the purpose of developing an estimate, the variance $R(k)$ was assumed to be proportional to the published streamflow on days of direct streamflow measurement. In open-water conditions, the standard error was assumed to be 2.5% of the published streamflow; during ice-affected conditions, the standard error was assumed to be 8.0% of the published streamflow. On days for which direct measurements were not made, published streamflow data were not used to update the estimate of the streamflow ratio.

IMPLEMENTATION

The extended Kalman filter was implemented by recursively computing daily updates to the state vector x and the state error covariance matrix P , given an initial estimate of the state vector x_0 and P_0 . The update is done in two steps: a temporal update and an observational update. The temporal update is computed at each time step; the observational update is computed only on days of direct streamflow measurement. The magnitude of P increases with temporal updates and decreases with observational updates. Bootstrap estimates of x_0 and P_0 were computed by iteratively replacing $x_0^{(j+1)}$ with $x_f^{(j)}$ until $x_f^{(j+1)} \equiv x_f^{(j)}$, where x_0 and x_f indicate the initial and final values for the state vector for the j or $j+1$ iteration of the extended Kalman filter, respectively.

Temporal Updates: The temporal update represents the best linear estimate of the state at time k on the basis of measurements of z available through $k-1$. The form of the general state equation is

$$x^{(-)}(k) = f(x^{(+)}(k-1), k-1). \quad (6)$$

In case of mode 1 dynamics, the signal element is computed as follows:

$$x^{(-)}_1(k) = \frac{h(k-1)}{h(k)} x^{(+)}_1(k-1). \quad (7)$$

For mode 2 dynamics, the temporal update of the state vector is computed as follows:

$$\begin{bmatrix} x^{(-)}_1(k) \\ x^{(-)}_2(k) \\ x^{(-)}_3(k) \\ x^{(-)}_4(k) \\ x^{(-)}_5(k) \end{bmatrix} = \begin{bmatrix} x^{(+)}_2(k-1) + x^{(+)}_3 [x^{(+)}_1(k-1) - x^{(+)}_2(k-1)] + x^{(+)}_4(k-1) [\tilde{u}(k-1) - x^{(+)}_5(k-1)] \\ x^{(+)}_2(k-1) \\ x^{(+)}_3(k-1) \\ x^{(+)}_4(k-1) \\ x^{(+)}_5(k-1) \end{bmatrix}. \quad (8)$$

Finally, in the case of mode 3 dynamics, the signal element is computed as

$$x^{(-)}_1(k) = x^{(+)}_1(k-1) + \frac{\tilde{u}(k-1) - t_{hi}}{t_{ou} - t_{hi}} [1 - x^{(+)}_1(k-1)] \quad (9)$$

for specified threshold parameters t_{hi} and t_{ou} .

A temporal update of streamflow is computed by multiplying the apparent streamflow by the estimated streamflow ratio; or, for consistency with the extended Kalman filter notation, by multiplying the time-varying measurement sensitivity matrix, $H(k)$, by the temporal update of the state vector as

$$\hat{z}^{(-)}(k) = H(k) x^{(-)}(k) = [h(k) \ 0 \ 0] x^{(-)}(k). \quad (10)$$

A temporal update of the error covariance matrix is computed as

$$P^{(-)}(k) = \Phi^{(1)}(k-1) P^{(+)}(k-1) \Phi^{(1)T}(k-1) + Q(k-1). \quad (11)$$

A first-order approximation of the state transition matrix is

$$\Phi^{(1)}(k-1) = \frac{\partial}{\partial x} f[x, k-1] \Big|_{x=x^{(+)}(k-1)}. \quad (12)$$

The estimate of the transition matrix used in this analysis is

$$\Phi^{(1)}(k-1) = \begin{bmatrix} x^{(+)}_3(k-1) & 1 - x^{(+)}_3(k-1) & x^{(+)}_1(k-1) - x^{(+)}_2(k-1) & \tilde{u}(k-1) - x^{(+)}_5(k-1) & x^{(+)}_4(k-1) \\ 0 & 1 & 0 & 0 & 0 \\ 0 & 0 & 1 & 0 & 0 \\ 0 & 0 & 0 & 1 & 0 \\ 0 & 0 & 0 & 0 & 1 \end{bmatrix}. \quad (13)$$

The value of Q was determined such that

$$\text{Prob}(\hat{z}^{(-)}(k) \pm Z_{\alpha=0.1} P^{(-)}_{1,1}(k) > z(k)) \sim 0.9, \quad (14)$$

where $Z_{\alpha=0.1}$ is the standardized normal deviate equal to 1.64.

Observational Updates: Observational updates were computed for days of direct streamflow measurement.

First, the Kalman gain matrix was computed as

$$\bar{K}(k) = P^{(-)}(k) H^T(k) [H(k) P^{(-)}(k) H^T(k) + R(k)]^{-1}. \quad (15)$$

Then, the covariance matrix was updated as

$$P^{(+)}(k) = [I - \bar{K}(k) H(k)] P^{(-)}(k). \quad (16)$$

The state vector update was computed as

$$\mathbf{x}^{(+)}(k) = \mathbf{x}^{(-)}(k) + \mathbf{K}(k) [z(k) - \hat{z}^{(-)}(k)]. \quad (17)$$

Finally, the observational update was computed as

$$\hat{z}^{(+)}(k) = H(k)\mathbf{x}^{(+)}(k) = [h(k) \ 0 \ 0]\mathbf{x}^{(+)}(k). \quad (18)$$

On days for which direct streamflow measurements were not made, observational updates were set equal to the temporal updates computed for that time step. Thus, estimated values computed by use of the extended Kalman filter were equal to the observational updates on days of direct streamflow measurement and were equal to the temporal updates otherwise. No adjustment was included for uncertainty in the apparent streamflow values.

AVAILABLE DATA

Sites in Maine and Nebraska were selected for application. The St. John River at Dickey site is in northern Maine, about 160 mi (miles) north of Bangor. Seventeen years of hydrologic data were obtained from USGS streamflow-gaging station 01010500. Drainage area at the gage is 2,680 mi² (square miles); average streamflow is 4,771 ft³/s (cubic feet per second). Climatic data were obtained from Fort Kent, Maine, which is about 25 mi east-northeast of the site. Within the selected periods, 37.1% of the daily values were ice affected. The Platte River at North Bend site is in east-central Nebraska, about 45 mi northwest of Omaha. Twenty-seven years of hydrologic data were obtained from USGS streamflow-gaging station 06796000. Drainage area at the gage is 70,400 mi²; average streamflow from 1949 through 1995 was 4,569 ft³/s. Climatic data for the site were obtained from Fremont, Nebr., which is about 15 mi east of the site. Within the period analyzed, 28.9% of daily streamflow values were affected by ice.

RESULTS

Filter estimates generally refer to estimates at time k based on measurements up to and including time k . In contrast, forecast estimates refer to estimates at time k based on data up to, but not including, time k . In this paper, extended Kalman filter estimates of streamflow are usually forecasts determined on the basis of the temporal updates. However, on days of direct measurement, more accurate filter estimates are computed by use of observational updates.

St. John River at Dickey, Maine: The extended Kalman filter was initialized to St. John River data by manually adjusting preliminary estimates of threshold parameter values to minimize the sum of squared errors in the extrapolated streamflow ratio, $x_1^{(+)}(k) - x_1(k)$, where k indicates days of direct streamflow measurements. Once satisfactory estimates of the threshold parameters were obtained, they were fixed and the filter was run repetitively using the state vector and error covariance matrix computed on the last iteration of the previous run to initialize the subsequent run. The filter was run repeatedly until elements in the state parameter vector were virtually constant. In this process, initial estimates for the state error covariance matrix converged.

Final estimates for the state parameters indicate that mode 2 dynamics are highly autoregressive, as indicated by the parameter $x_3=0.981$, about a streamflow ratio offset of $x_2=0.544$. Streamflow ratios increase at a rate $x_4=0.000855$ °C⁻¹ (degrees Celsius⁻¹) from the temperature offset $x_5=-3.19$ °C. (Note, for consistency with the natural correspondence between the freezing point of water and the zero of the Celsius scale, temperature values are referenced in the International System of Units rather than the English System of Units. To convert from Celsius to Fahrenheit, multiply the value reported in Celsius degrees by 9/5 and add 32.) Although the value for x_2 is higher than 0.15 (the mode of the distribution of empirical streamflow ratios) it is physically realizable. Similarly, x_5 is consistent with the distribution of air temperatures during periods of ice effects, which generally ranged from -20.5 to 2.5 °C. However, analysis of the state error covariance matrix indicates a large positive correlation (>0.99) between x_2 and x_5 and a large negative correlation (< -0.93) between x_3 and x_4 . Thus, although the form of the difference equation used to describe mode 2 dynamics resulted in parameters with physically realizable values, the large correlations indicate ambiguity concerning their true values. The high correlations in the state error covariance matrix indicate a potential

for reducing the dimension of the state parameter vector without loss of filter accuracy.

Sensitivities for threshold parameters were estimated as the change in the sum of squared errors in the streamflow ratio divided by the change in the corresponding parameter near the selected values. Results of simulations indicate that filter computations were most sensitive to changes in the q_dl parameter and least sensitive to the t_lo parameter. Formal optimization of the threshold parameters could lead to further improvement in filter performance.

One measure of the estimation accuracy of the filter is the relation between temporal updates of streamflow, $z^{(j)}(k)$, and published daily streamflow values, $z(k)$, where k indexes days of direct streamflow measurement. Although this value is modified by observational updates to more precisely estimate streamflow on days of direct measurement, $z^{(j)}(k)$ provides a conservative indication of the filter accuracy. The temporal update is considered a conservative indicator of accuracy because the variance of the estimation increases monotonically with time from the previous measurement and the length of the forecast lead is maximum just before the observational update. Results for St. John River indicate that the correlation between log-transformed values of $z^{(j)}(k)$ and $z(k)$ is 0.777 based on 40 days of ice-affected measurements and 0.998 based on 63 days of open-water measurements. Time between measurements at St. John River used in this analysis averaged 8.6 weeks.

Another measure of filter accuracy is the relation between published and estimated streamflows during periods of ice effects. The relation between published and estimated values is linear in the logarithm of transformed values. Uncertainty occurs in both the published and estimated values. Published streamflow values during periods of ice effects are typically rated "fair" or "poor" on a subjective basis. A rating of "fair" implies that about 95% of the daily values are within 15% of the true value; a "poor" rating indicates that daily streamflow values have less than "fair" accuracy (Novak 1985). Discrepancies between published and estimated values during periods of ice effects were computed as

$$e(k) = \frac{\log(z^{(j)}(k)) - \log(z(k))}{\log(z(k))} \quad (19)$$

Analysis of the distribution of discrepancies shows that 87.2% of the time, the absolute value of elements in the e sequence is less than 8%; 96.6% of the time, it is less than 15%.

Streamflow and climatic data for the St. John River at Dickey, Maine site from November 1986 through April 1987 are shown on Fig. 1. Upper and lower estimations were computed by adjusting the variance of Q to 0.0035 so that interval formed between the upper and lower estimations about the temporal updates at k contained the published values 90% of the time.

Platte River at North Bend, Nebraska: Following the protocol developed for St. John River, the extended Kalman filter was applied to Platte River data by manually adjusting preliminary estimates of threshold parameters to minimize the sum of squared errors in the temporal updates of the streamflow ratio for days of direct streamflow measurement. Again, once apparently satisfactory estimates of the threshold parameters were obtained, they were fixed and the filter was run until convergence was indicated. In this process, initial estimates of the state error covariance matrix converged.

Results for Platte River data also indicate that mode 2 dynamics are highly autoregressive, as indicated by the parameter $x_3=0.990$. Streamflow ratios increase at a rate $x_4=0.000939$ $^{\circ}\text{C}^{-1}$ about a temperature offset $x_5=-9.37$ $^{\circ}\text{C}$, a lower temperature than that estimated for St. John River in Maine. Unfortunately, the estimated streamflow ratio offset of $x_2=-0.068$ is not physically realizable. Analysis of the state error covariance matrix indicates a maximum positive correlation of 0.81 between x_3 and x_5 and a maximum negative correlation of -0.74 between x_3 and x_4 . The magnitudes of these correlations are not thought to be sufficient to cause significant degradation of parameter estimates. However, given the small magnitude of the estimated x_2 value, in future applications it may be possible to eliminate (set to zero) the streamflow ratio offset from the difference equation for mode 2 dynamics. Such an elimination would reduce the dimension of the state space, which would also likely reduce parameter ambiguity caused by high correlations in the state error

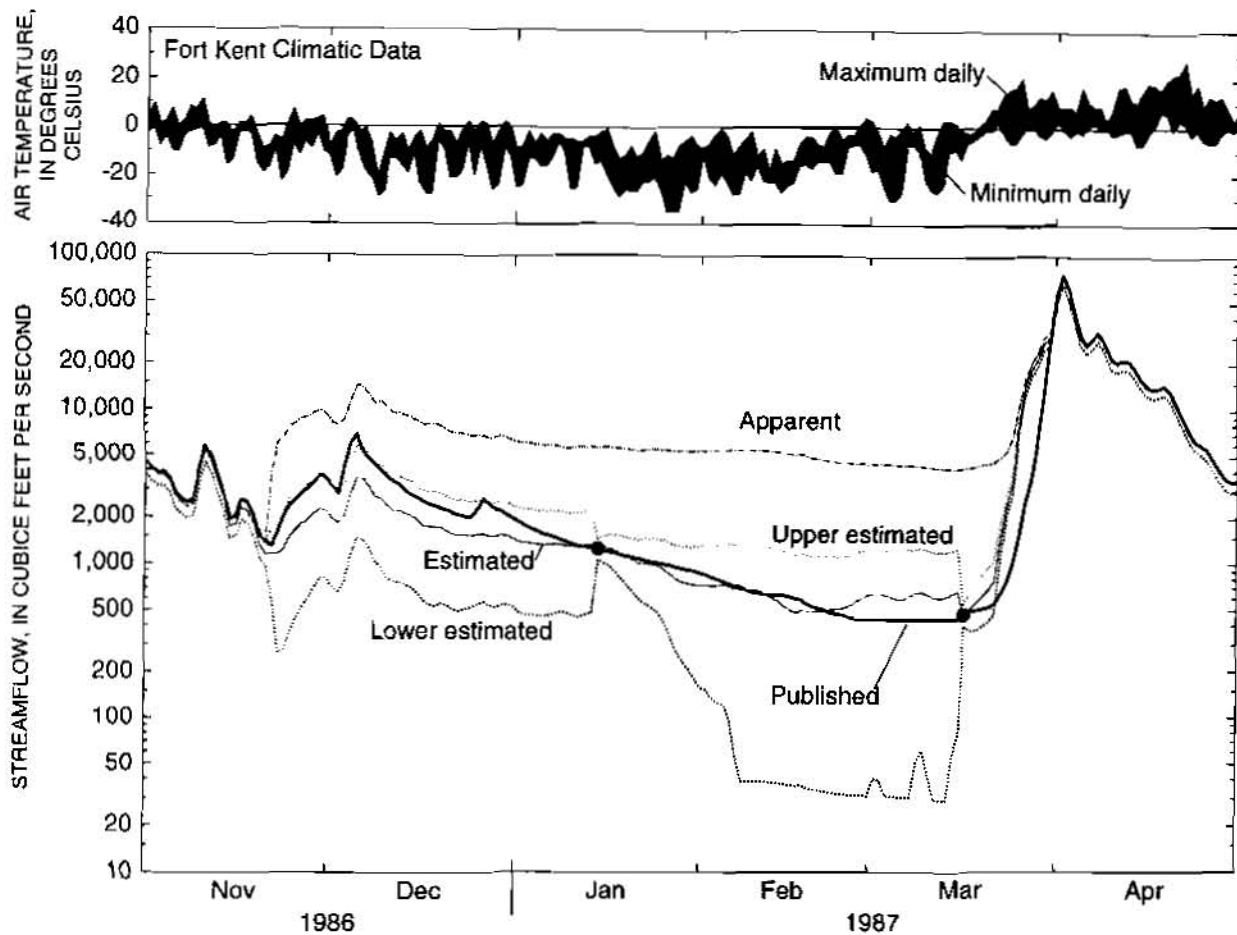


Figure 1. Streamflow and climatic data for the site near St. John River at Dickey, Maine

covariance matrix. Suboptimal values for the threshold parameters also present a possible explanation for the discrepancy between the estimated value of x_2 and the conceptualized value at the mode (0.30) of the empirical distribution of discharge ratios. Sensitivities for threshold parameters were estimated as the change in the sum of squared errors in the streamflow ratio estimate divided by the change in the corresponding parameter near the selected values. Results of simulations indicate that estimates are most sensitive to changes in the q_{dl} parameter and least sensitive to the t_{lo} parameter. Again, formal optimization of the threshold parameters could lead to further improvement in filter performance.

The temporal updates of streamflow on days of streamflow measurements compare closely with published daily mean streamflows. Results indicate that the correlation between log-transformed values of $z^{(j)}(k)$ and $z(k)$ is 0.864 based on 87 days of ice-affected measurements and 0.997 based on 345 days of open-water measurements. Time between measurements at Platte River used in this analysis averaged 3.2 weeks. The relation between published and estimated streamflows at Platte River during periods of ice effects is linear and unbiased in the logarithms of streamflow. Analysis of the distribution of discrepancies between published and estimated values during periods of ice effects by use of equation 19 indicates that 90.7% of the time, the absolute value of elements in the e sequence is less than 8%, and that 97.7% of the time, it is less than 15%.

Streamflow and climatic data for the Platte River at North Bend, Nebr. site from November 1977 through April 1978 are shown in Fig. 2. Upper and lower limits for estimates were computed by adjusting the variance of Q to 0.0039 so that the interval formed by the upper and lower estimate about the temporal update at k included the published values 90% of the time.

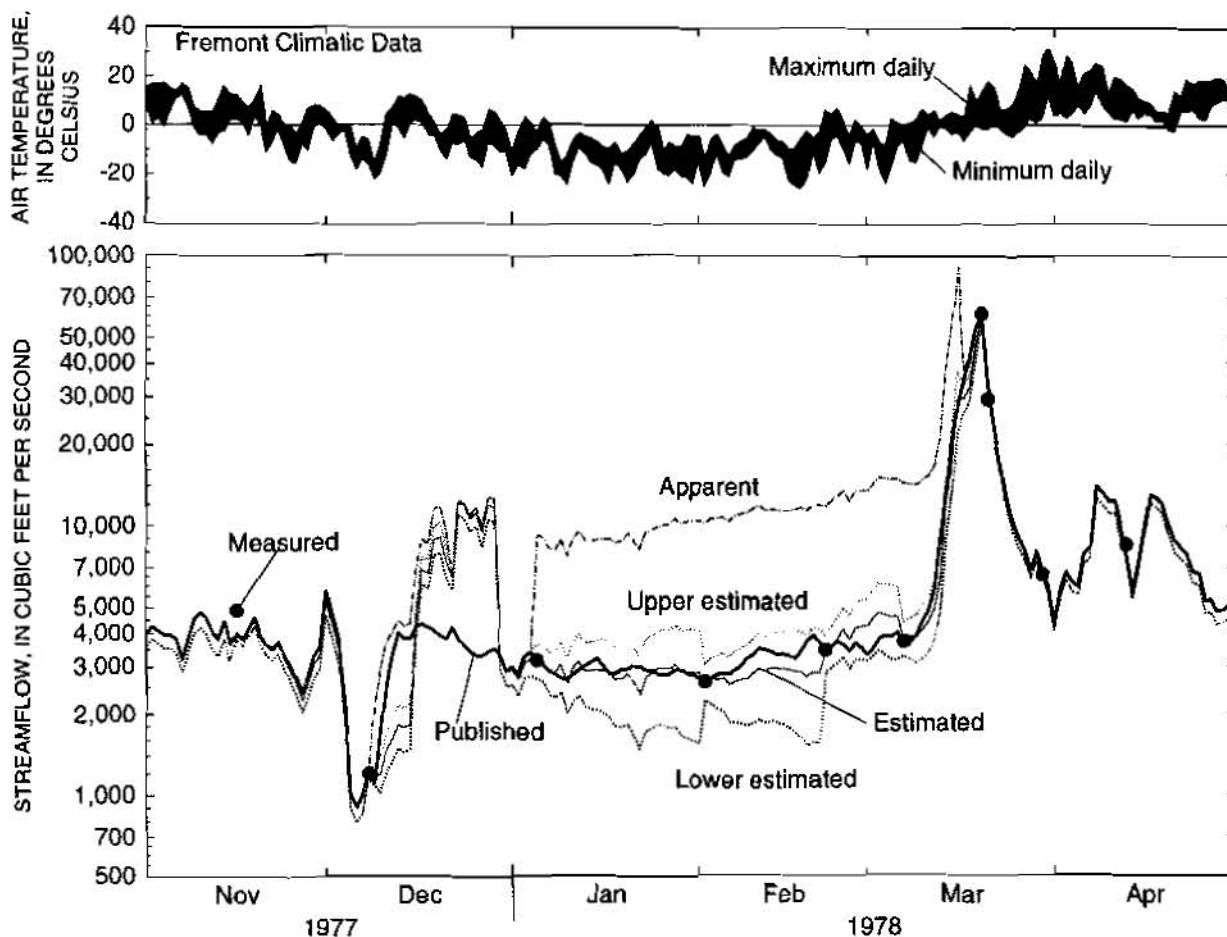


Figure 2. Streamflow and climatic data for the site near Platte River at North Bend, Nebraska

CONCLUSIONS

Three dynamic modes of ice effects were identified on the basis of historical interpretations of ice-affected streamflow records. The first mode is associated with rapid transitions in ice effects related to ice formation and ablation processes, as indicated by abrupt changes in apparent streamflow. The second mode is associated with gradual changes in ice effects with changes in air temperature. The third mode is associated with elimination of ice effects at warm air temperatures. Equations for these dynamic modes were developed within a discrete-time extended Kalman filter to estimate daily values and uncertainties of ice-affected streamflow. The utility of the filter was evaluated by application to historical data from two long-term streamflow-gaging stations. Results indicate that the filters were stable and that parameters converged for both stations. Estimates of ice-affected streamflow were highly correlated with published values. The extended Kalman filter developed in this paper provides a basis for estimating ice-affected streamflow at other gaging stations by adjusting filter parameters to site-specific conditions. The filter can be used to estimate daily mean streamflow during periods of ice effects by use of real-time climatic and hydrologic data.

REFERENCES

- Bar-Shalom, Y., and Li, X.-R., 1993, Estimation and tracking: principles, techniques, and software. Artech House, Boston, Mass.
- Brown, R. G., and Hwang, P.Y.C., 1997, Introduction to random signals and applied Kalman filtering, 3rd Ed. John Wiley, New York.
- Grewal, M. S., and Andrews, A.P., 1997, Kalman filtering theory and practice, 4th Ed. Prentice Hall Information and System Sciences Series, Englewood Cliffs, N.J.
- Novak, C.E., 1985, WRD data reports preparation guide. Open-File Rep. 85-480 U.S. Geological Survey.

MISSOURI RIVER FORECAST MODEL FROM GAVINS POINT DAM TO RULO, NEBRASKA

By Daniel Pridal, Hydraulic Engineer, U.S. Army Corps of Engineers, Omaha, Nebraska; Joel Knofczynski, Hydrologic Engineer, U.S. Army Corps of Engineers, Omaha, Nebraska

Abstract: This paper describes the process of developing a UNET unsteady flow model for use with forecasting flows and stages on the Missouri River within the Omaha District Corps of Engineers. The unsteady flow model is a portion of a larger Corps of Engineers effort to implement a comprehensive system wide forecasting tool of the Missouri River, Mississippi River, and significant tributaries. The Missouri River unsteady flow model study area extends from Gavins Point Dam at river mile 811.1 downstream to Rulo, NE, at river mile 498.0. The UNET unsteady flow model includes several tributaries as routing reaches, numerous lateral inflows, simulation of levee failure, and the inclusion of ungaged inflows. This paper describes the process of UNET model development, calibration, and verification using available geometry and observed flow and stage data. In addition, this paper describes the procedure and the data required to utilize the UNET model in a forecast mode for daily operation.

INTRODUCTION

The 1993 flood event resulted in catastrophic damages in large portions of the upper Mississippi River, lower Missouri River, and major tributaries. Although reservoirs were operated effectively during the flood, the Corps of Engineers did not have an integrated river model or procedure specifically designed and implemented for the Missouri River, Mississippi River and its tributaries to analyze and predict system wide impacts and various alternative actions during the flood. The objectives for development of a forecast model were established based on past flood experience and are listed in order of priority: a) improve and facilitate the coordination, communication, and sharing of data and forecasts among water control activities along the mainstem, b) assess impacts of levee breaching and floodway operations on local and downstream areas, c) support emergency management activities through timely prediction of stage and rate of rise, d) display areal extent of flooding potential for various predicted weather scenarios and levee failures, e) identify navigation hazards and, f) provide data for real-time flood damage assessment.

Following the 1993 flood event, the Corps of Engineers conducted a comprehensive system wide study to assess flood control and floodplain management practices known as the Floodplain Management Assessment Study (FPMA) (USACE, 1995). Corps District offices involved in the FPMA study along the Mississippi River include St. Paul, Rock Island, and St. Louis. Corps District offices along the Missouri River include Omaha and Kansas City. To achieve the FPMA study objectives, an unsteady flow model was constructed of the Mississippi, Missouri, and significant tributary rivers.

Following the FPMA study, the Corps initiated a study effort to translate the developed unsteady flow model into a forecasting tool. The UNET unsteady flow forecast model is known as the Mississippi Basin Modeling System (MBMS) (HEC, 1997). While coordinating with all involved Corps Districts, each unsteady flow model was developed independently. This report pertains to the hydrologic model development, calibration, and forecasting performed by the Omaha District. The forecast model is capable of being operated in at least two modes: 1) operational as a routine forecast model providing flows and stages and, 2) to evaluate the impacts of physical modifications to the system such as levee breaches or construction, channel changes, etc.

STUDY AREA

Basin Description: The Missouri River originates in the northern Rocky Mountains along the continental divide and flows south and east to join the Mississippi River near St. Louis, Missouri. The Omaha District encompasses approximately 414,900 square miles of the drainage basin upstream of Rulo, NE, to the river headwaters in the Rocky Mountains. The most significant flood control project constructed within the basin are the six main stem Missouri River Dams constructed by the Corps. The six dams, which were completed by 1964, provide flood protection by controlling runoff from the upper most 279,000 square miles of the drainage basin. The reservoir system has a total combined capacity in excess of 73 million acre-feet of which more than 16 million acre-feet is for flood control. Gavins Point

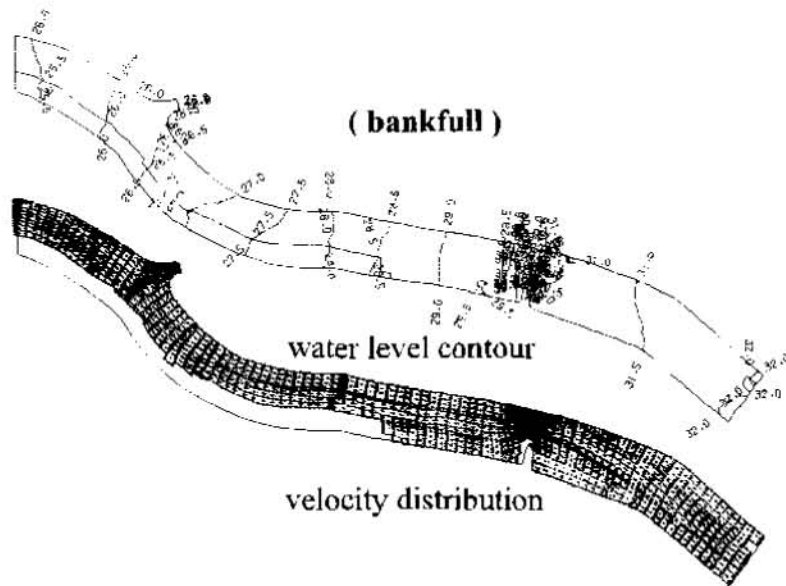


Fig. 7 The velocity distribution and water level contour

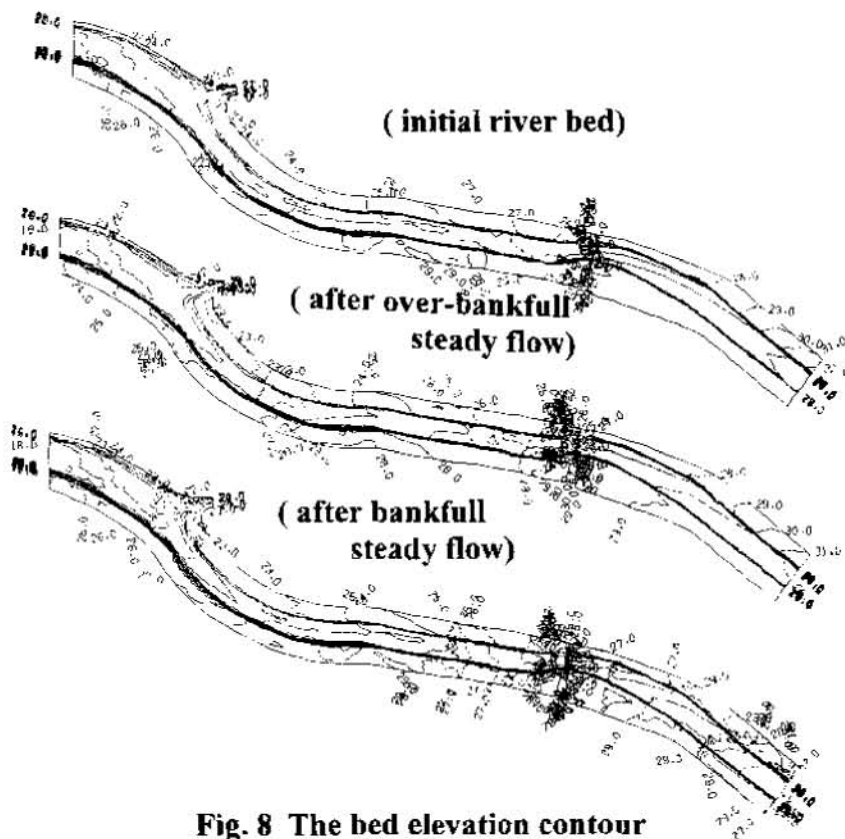


Fig. 8 The bed elevation contour

MO. The system of federal levees within the study area begins at Omaha, NE, and extends downstream. The majority of the area upstream of Omaha, NE, is protected by private or non-federal levees with varying degrees of protection. Downstream of Omaha, federal levee protection is not continuous and the level of protection varies. A notable area without any federal levees is the left bank in the Rulo area between river mile 515.2 and 482.2. All of the levee units on the Missouri River were designed to operate in conjunction with the six main stem dams to reduce flood damages as part of the Pick-Sloan plan. Federal levees were constructed in the 1950's and are usually set-back from the river bank a distance of 1000-5000 feet. Survey data for the federal levees consists of 35 to 45 year old profiles or as-builts. Total federal levee length is estimated as 250 miles in the reach from Omaha, NE, to St. Joseph, MO.

Following levee construction and chute closure, deposited sediment filled many areas riverward of the federal levees. Farming of these areas became extensive. To prevent crop damages caused by normal high flows on the Missouri River, farmers constructed secondary levees at or near the river bank. Many of the secondary private levees tie directly into the federal levees. Private levees have also been constructed along the river bank in areas where federal levees were not constructed. The left bank reach from river mile 515.5 to river mile 498.1 near Rulo, NE is protected solely by private levees. Survey data for the private levees is virtually non-existent. Private levee height appears to be near the same height as the federal levee. Total length of private levees along the Missouri River, interior levees, spoil banks, and tiebacks is unknown but is substantial.

Tributaries: Within the UNET model, major tributaries which enter within the study area are included as routing reaches from the tributary USGS gaging station location downstream to the confluence with the Missouri River. Separate tributary routing reaches and the river mile (RM) of the Missouri River confluence include the James River (RM 797.7), Vermillion River (RM 772.2), Big Sioux River (RM 734.2), Little Sioux River (RM 669.2), Soldier River (RM 664.0), Boyer River (RM 635.2), Platte River (RM 594.8), Weeping Water Creek (RM 568.6), Nishnabotna River (RM 542.0), Little Nemaha River (RM 527.8), Big Nemaha River (RM 494.8), and the Nodaway River (RM 463.0). With a drainage area of approximately 90,000 square miles, the Platte River is the largest of all tributaries. The Platte River is also a major contributor of sediment.

HYDRAULIC UNSTEADY FLOW MODEL UNET

UNET Model: A UNET unsteady flow model was constructed for use with the forecast model. UNET is a one-dimensional unsteady flow program (HEC, 1997) which includes the capability of simulating flow through a full network of open channels and storage areas. The dynamic wave routing method was used for this analysis because it has the ability to account for critical backwater effects in the routing and can directly simulate flows that spill over or breach a levee and pond behind the levee in predefined storage areas. River geometry is described for each cross section by station-elevation data using X1-GR cards similar to HEC-2 (HEC, 1990) format. All stage and flow hydrographs required by the UNET program are read from an HEC-DSS database file.

Model Extent: Model limits extend from downstream of Gavins Point Dam at river mile 811.05 to St Joseph, MO, at river mile 448.2. The UNET model contains approximately 1750 cross sections, 27 separate reaches, 12 tributary routing reaches, 24 storage areas, and over 50 connections between the Missouri River and the storage areas. Hydrologic data utilized by the model includes 14 upstream inflow hydrographs, 21 lateral inflow hydrographs, and 11 interior stage and discharge hydrograph locations on the mainstem.

Missouri River Geometry: Cross section data for the Missouri River was compiled from existing HEC-2 data developed in conjunction with a flood hazard study on the Missouri River (USACE, 1978). Cross section data for the flood hazard study were based on 4 foot contour interval surveys which were surveyed in 1974. Hydrographic surveys for the Missouri River that were completed in 1994 were integrated into the existing cross sections. These hydrographic surveys are only of the navigation channel and do not include the overbank area. Significant changes to the overbank area have occurred since the 1974 survey date. Check sections surveyed at three locations in 1994 illustrated a significant conveyance reduction within the overbank area. Cross section interval on the Missouri River is roughly 1000 feet. Within each cross section, bank stations were typically set at the top of natural bank or private levee adjacent to the river. X3 record stationing and elevations are required to reflect levee locations, effective flow areas modeled, and to correctly reflect the storage-conveyance relationship within each cross section.

Dam, located near Yankton, SD, at river mile 811.1, forms Lewis and Clark Lake and is the most downstream of the projects. An illustration of the study area is shown on figure 1.

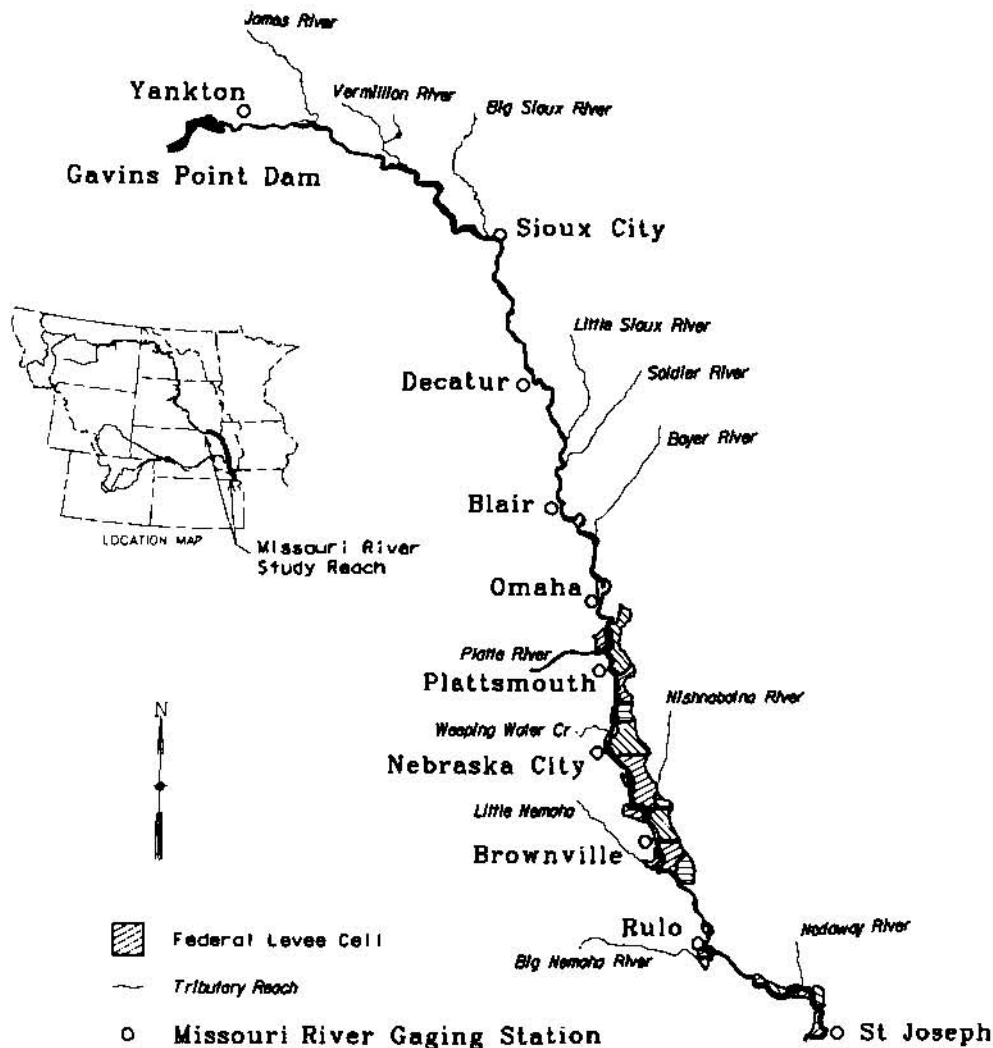


Figure 1

Missouri River: Between Gavins Point Dam and Rulo, NE, the Missouri River drainage area increases from 279,000 to 414,900 square miles. Average channel gradient within the reach varies from 0.8 to 1.2 feet/mile. Total valley width usually averages 5-10 miles between the bluffs. The Missouri River generally follows the right (west) bluff line.

Navigation Structures: Existing navigation structures within the Missouri River channel affect conveyance. There were seven acts of Congress which provided for the construction, operation and maintenance of a navigation channel and bank stabilization works on the Missouri River. The most recent was authorized in 1945 which provided for bank stabilization and a 9-foot deep and not less than 300 feet wide navigation channel for the Missouri River from its confluence with the Mississippi River at St. Louis, MO to Sioux City, IA for a total distance of 734.2 river miles. This was accomplished through revetment of banks, construction of permeable dikes, cutoff of oxbows, closing minor channels, removal of snags and dredging.

Levees: The Missouri River levee system was authorized by the Flood Control Acts of 1941 and 1944 to provide protection to agricultural lands and communities along the Missouri River from Sioux City, IA to the mouth at St. Louis,

Levee and Storage Area Data: Areas to the landward side of the federal levees were modeled as storage areas within UNET. Large overbank areas behind the federal levees will affect model timing and computed results if the storage cells have a significant amount of flow through them. Within the UNET model, levee storage areas are represented by a stage-volume relationship. All storage area data was derived from available USGS 7.5 minute quadrangle topographic maps. Features such as levees, roads and railroads were utilized to subdivide the storage cells. Interconnections between adjacent storage cells is based on elevation and assumed weir flow.

Levee Failure and Overtopping: The simulation of levee failures is performed utilizing the simple embankment failure record, (SF card) within the UNET model. Simulation of levee failure requires the collection of data for levee failure mechanisms, breach section geometry, areas inundated, and time to fill the inundated areas. Data from the 1993 event for L-550 indicated that the levee breach formed at a rate such that the interior storage area filled within 24 to 36 hours. While performing model calibration for the 1993 event, actual levee failure times and breach parameters were specified within the UNET model.

In the forecast model operation, levee failures within the model are determined to occur when top of levee elevations are exceeded. For each storage cell, an existing top of levee elevation and location is required to model each individual overflow/breach. In order to simulate potential levee failure within the forecast model, overtopping locations are provided at the upstream and downstream end of each levee cell. During forecast simulation, levee failure will automatically occur if computed stages exceed the specified levee top elevation. The distance between overflow locations varied from 5 to 10 river miles. If a breach occurs which is not predicated by model stage, the time of levee failure is included in the forecast to simulate flow into the storage area.

Rulo Overflow Reach: The Rulo overflow reach refers to the section of the Missouri River from river mile 482.8 to 515.5. Within this reach, the left bank is protected by a series of private levees. The level of protection from the private levees is estimated as 10 to 20 year. Floodplain width from the Missouri River to the bluff along the left bank varies from 3-9 miles. The floodplain contains the Squaw Creek National Wildlife Refuge and the Big Lake recreational area. A Missouri River USGS gaging station is installed on the U.S. Highway 159 bridge at Rulo, NE (RM 498.0). During the 1993 event, the private levees in the Rulo, NE, reach experienced considerable damage with numerous breaches. A significant amount of flow occurred in the overbank area. For the July, 1993, peak discharge measurement of approximately 300,000 cfs at Rulo, estimates are that approximately 30-40% of the flow bypassed the Rulo gaging station. In order to simulate the large amount of flow in the overbank, an additional conveyance reach was included in the UNET model for the left overbank. A series of artificial storage cells were constructed between the Missouri River channel reach and the Rulo overbank reach in order to simulate flow transfer from the mainstem Missouri River to the overbank. Numerous connections between the storage cells and adjacent reaches were established. Also, for reasons of model stability, the constructed Rulo overbank reach was a prismatic channel and did not resemble actual geometry.

UNET MODEL CALIBRATION

Calibration efforts employed discharge/conveyance relationships and an automated calibration feature found in UNET on a reach by reach basis. Model calibration centered on three flow events; high, normal navigation service, and low flows. The high flow period includes the flood event from June through August 1993. The calibration event for the navigation target level flows was September 1994 and the low flow calibration event was November 1989.

UNET Model Calibration: Calibration of the UNET model was an iterative process performed in several stages. Calibration efforts focused on reproducing observed stage hydrographs at gaging stations along the Missouri River and verifying with discharge measurements. Calibration efforts employed the NC record for channel and overbank roughness, the X3 record to set conveyance and storage within the cross section, and the conveyance change and discharge-conveyance relationships which may be applied for separate reaches within the model. Once the model is nearly calibrated, the UNET model automated calibration routine is performed. The calibration routine pairs observed stages at the stream gages on the Missouri River with routed flow and fits a fifth order polynomial to the paired data to create a rating curve and write it to DSS. Using a KR record in the UNET cross section data at each stream gage location, this relationship is then applied to the ordinates in the cross section tables. A total of 9 rating curves and

corresponding KR records were developed in the model calibration process. During forecast operation, the conveyance change and discharge conveyance relationship can be used in conjunction with the KR card rating curves to adjust model calibration as needed. An example of model calibration at the Nebraska City, NE, gaging station for the month of July 1993 is shown on figure 2.

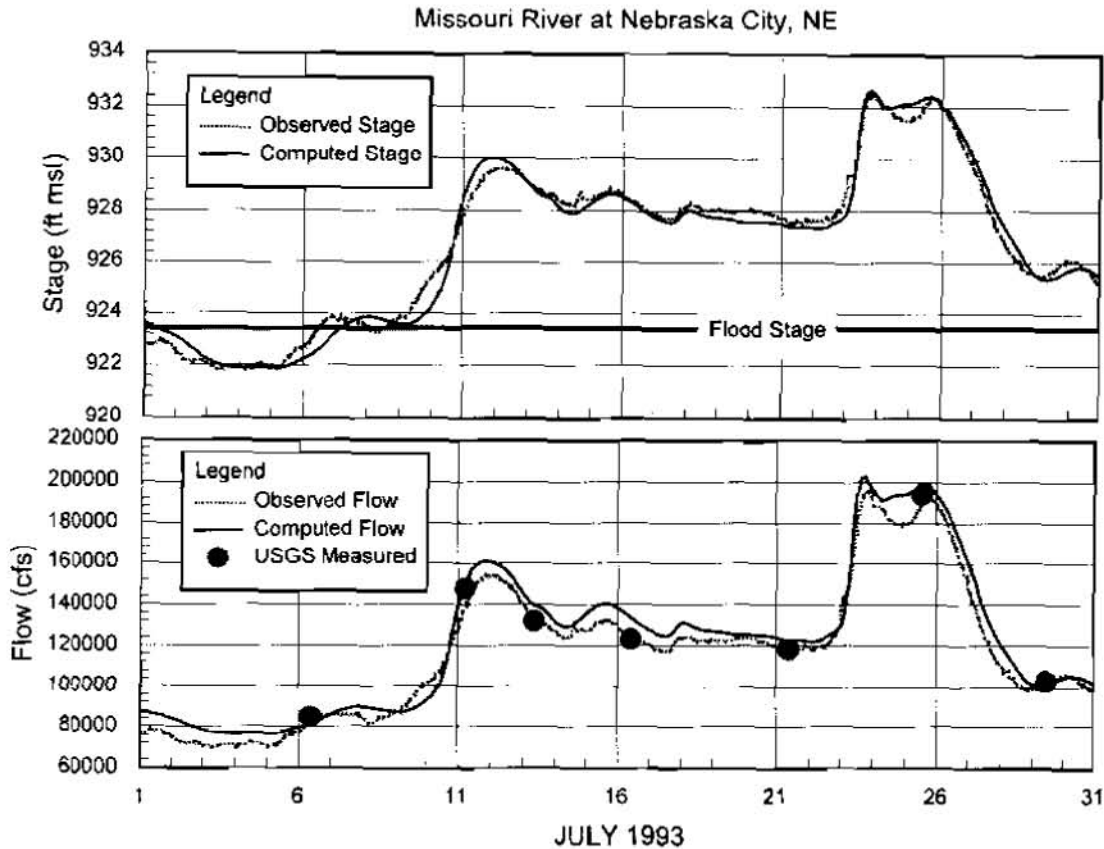


Figure 2

Model Stage Calibration: Calibration of computed model stages was performed employing stage hydrographs at Missouri River gaging stations located from Yankton, SD, downstream to St. Joseph, MO. Calibration was considered complete when computed model stages were within 0.5 feet of observed stages. Calibration of tributary routing reaches was not performed. Stage calibration was performed on a system wide basis for the entire hydrograph. Calibration of peak stages at the Rulo, NE, gage were particularly difficult for the 1993 event due to the large amount of flow within the overbank. Modeling methods at Rulo, NE, attempted to account for the complex flow phenomena which occurred with simplified techniques.

Model Flow Calibration: While the UNET model was calibrated to observed stage hydrographs, discharges still need to be verified to assure model accuracy. During an extreme flood such as 1993, problems were encountered using USGS discharge hydrographs that are based on a rating curve and shifts to the rating curve based on a single discharge measurement. Discharge measurements are taken at least once a week on the mainstem Missouri River. Generally, the calibrated model discharge is within 10% of the measured discharge data at the Missouri River gaging stations.

Calibration Accuracy: A final calibration of the UNET model for all three flow events was accomplished. However, several problems arose during calibration to all three flow events simultaneously. When calibrating to each event separately, a final calibration of less than 0.5 feet was possible. However, when the model was calibrated to one event and then another event was modeled with the same calibration factors, the model did not calibrate as well, being off as much as 1.0 foot for periods of the stage hydrograph. The discharge conveyance factors could then be changed to cause

a better calibration, but then the calibration accuracy of the initial event decreased. Therefore, the calibration factors were weighted to not give necessarily the best calibration for any one of the three events, but instead factors were chosen to allow for the most accurate simulation of all three events.

There are several factors which explains why all three events did not calibrate to the same discharge-conveyance factors. The November 1989 low flow event was before the flood of 1993 and the large flow event significantly altered section conveyance in the form of channel degradation and overbank deposition in many areas. Another factor is the time of season when the event occurred. The Missouri River undergoes seasonal changes which affects the water viscosity, bed forms, and a variation in vegetation affects roughness. Therefore, the conveyance factors that were used to calibrate flows during the summer may not work for flows during the spring or fall. The model was not configured to account for seasonal variations in conveyance. The variation in calibration parameters is critical for acceptable performance of the UNET model as a forecasting tool. Periodic updates of the model calibration parameters are required to insure model accuracy. The calibration performed to date illustrates that the model can be operated with a minimum accuracy of 0.5 foot at all locations if calibration parameters are updated as required.

FORECAST MODEL OPERATION

The calibrated UNET model is available for operation in the forecast mode. Operation of the forecast model is facilitated with the use of the MBMS graphical user interface (GUI). Forecast operation is performed with updated inflow data from the DCP gaging stations for the desired forecast period. For forecast operation, model inflow hydrographs must be extended for the forecast period. The transition of the UNET model to a forecast model for use with the GUI required no additional UNET model development. The GUI provides an interface which couples operation of the UNET model with forecasting inflow data and processing UNET model results. By using the GUI, the forecaster can efficiently develop stage and flow forecasts for the desired period. GUI operation does not require detailed UNET model knowledge. The GUI provides for consistent file management, UNET model simulation, easy selection of historical and forecast time window, model result review, and report generation.

Forecast Operation: The initial step in forecast operation is the extraction of data by the GUI. The forecaster updates the UNET model data base to the current time of forecast by extracting data from the real-time DCP database at all required gaging station locations. Ungaged inflows are simulated by executing the UNET model employing the null internal boundary condition. The forecaster may edit all inflow hydrographs for the forecast period as desired. Current forecast model operation does not include any hydrologic models to forecast inflow data. Inflow data may be forecasted by extending current values or estimating a change in inflow based on upstream data, weather forecasts, and other available information. Levee failure data may be edited to reflect current conditions. Once forecasted inflows are determined, the UNET model is executed for the forecast period.

Forecast Results: The GUI also contains routines for presentation of forecast model results. Computed hydrographs may be reviewed at all gaging station locations. Levee failure data is also available for review. By comparing to observed stage and measured discharge data, the forecaster may adjust model calibration parameters as required to reflect seasonal changes in river conveyance. A report generator is available to summarize UNET model results in the format desired.

SUMMARY

A UNET model was developed of the Missouri River from Gavins Point Dam to St. Joseph, MO. The UNET unsteady flow model includes several tributaries as routing reaches, numerous lateral inflows, simulation of levee failure, and the inclusion of ungaged inflows. The process of UNET model development, calibration, and verification using available geometry and observed flow and stage data was described. In addition, the procedure and the data required to utilize the UNET model in a forecast mode for daily operation is also presented. Forecast model operation utilizes the MBMS GUI and may be utilized to forecast flow and stage at required locations for the desired period. In addition, the forecast model may employed to assess the effects of levee failure and changes in channel conveyance during routine operation.

REFERENCES

- U.S. Army Corps of Engineers (USACE). 1995. Floodplain Management Assessment of the Upper Mississippi and Lower Missouri River and Their Tributaries, U.S. Army Corps of Engineers, Washington, DC.
- USACE, 1978-1979, Special Flood Hazard Information, Missouri River, Gavins Point Dam to Rulo, Nebraska, Volumes I and II, U.S. Army Corps of Engineers, Omaha District.
- Hydrologic Engineering Center (HEC), 1997, UNET, One-Dimensional Unsteady Flow Through a Full Network of Open Channels, U.S. Army Corps of Engineers, Davis, CA.
- HEC, 1997, Mississippi Basin Model System Development and Application, U.S. Army Corps of Engineers, Davis, CA.
- HEC, 1990, HEC-2 Water Surface Profiles, User's Manual, U.S. Army Corps of Engineers, Davis, CA.

A FINITE ELEMENT MODEL WITH MOVING BOUNDARIES: APPLICATION TO FLOODS AND RUNUP.

By Roy A. Walters, Oceanographer, U.S. Geological Survey, Denver, Colorado

Abstract A finite element model is developed for the 2-dimensional shallow water equations using semi-implicit methods in time. A semi-Lagrangian method is used to approximate the effects of advection. A wave equation is formed at the discrete level such that the equations decouple into an equation for surface elevation, and a momentum equation for the horizontal velocity. The stability and computational efficiency of this model are examined with a field scale test case that is characterized by highly irregular geometry.

INTRODUCTION

This paper contains the development of a robust and computationally efficient model that can simulate extreme hydraulic events that are accompanied by extensive flooding and drying. The goal is to be able to simulate large floods over floodplains with rather general topography. The wetted inundation area is then determined by the model solution.

The method adopted here is to use the primitive shallow water equations and form a wave equation at the discrete level. This procedure carries through the properties of the original discretized equations so that the use of elements without spurious computational modes is essential. Toward this end, low-order elements are used such that continuity is satisfied both globally and locally, and wetting and drying are greatly simplified.

In the next section, the model is developed using the discretized shallow water equations. Following this, a test case is presented that simulates a large flood on the Biglost River in southeastern Idaho.

MODEL DESCRIPTION

The basic equations are the 2-dimensional shallow water equations. Using both the hydrostatic assumption and the Boussinesq approximation, these equations are derived by a vertical integration of the Reynolds equations (Pinder and Gray, 1977). The continuity equation becomes

$$\frac{\partial \eta}{\partial t} + \nabla \cdot (H\mathbf{u}) = 0 \quad (1)$$

and the momentum equation becomes

$$\frac{d\mathbf{u}}{dt} - \frac{1}{H} \nabla \cdot (H A_h \nabla \mathbf{u}) + g \nabla \eta - \frac{\tau_s}{\rho H} + \frac{\tau_b}{\rho H} = 0 \quad (2)$$

where the coordinate directions (x,y,z) are aligned in the east, north, and up directions; $\mathbf{u}(x,y,t)$ is the depth-averaged horizontal velocity; $h(x,y)$ is the water depth measured

from a reference elevation; $\eta(x, y, t)$ is the distance from the reference elevation to the free surface; $H(x, y, t)$ is the total water depth, $H = \eta - h$; g is the gravitational acceleration; ρ is a reference density; ∇ is the horizontal gradient operator ($\partial/\partial x, \partial/\partial y$); and $A_h(x, y, t)$ is the coefficient for the horizontal component of viscous stresses. The surface and bottom boundary conditions are given by

$$\frac{\tau_s}{\rho} = \gamma_T H(\mathbf{u}_a - \mathbf{u}) \quad (z = \eta) \quad (3)$$

$$\frac{\tau_b}{\rho} = C_D |\mathbf{u}| \mathbf{u} = \gamma_B H \mathbf{u} \quad (z = h), \quad (4)$$

where the surface and bottom stress are denoted as τ_s and τ_b , respectively, \mathbf{u}_a is the wind velocity, and C_D is a bottom drag coefficient. Essential boundary conditions on η or volumetric flux are set at open boundaries, and $(\mathbf{u} \cdot \mathbf{n}) = 0$ (no normal flow) is set on land boundaries.

These equations are discretized in time using an implicit method such that the equations are evaluated in the time interval (t^{n+1}, t^n) where the superscript denotes the time level. The distance through the interval is given by the weight θ . This approach yields

$$\frac{\eta^{n+1} - \eta^n}{\Delta t} + \nabla \cdot [H^n (\theta \mathbf{u}^{n+1} + (1 - \theta) \mathbf{u}^n)] = 0 \quad (5)$$

$$\frac{\mathbf{u}^{n+1} - \mathbf{u}^*}{\Delta t} + \theta \mathbf{G}^{n+1} + (1 - \theta) \mathbf{G}^* = \mathbf{F}^* \quad (6)$$

where

$$\mathbf{G} = \gamma_B \mathbf{u} - \gamma_T (\mathbf{u}_a - \mathbf{u}) + g \nabla \eta$$

$$\mathbf{F}^* = \nabla \cdot (A_h \nabla \mathbf{u})^*$$

Semi-Lagrangian methods are used in order to take advantage of the simplicity of Eulerian methods and the enhanced stability and accuracy of Lagrangian methods (Casulli, 1990; Staniforth and Cotes, 1991). Here the superscripts n and $n + 1$ denote variables evaluated at the fixed nodes in the Eulerian grid at times t^n and t^{n+1} . The superscript $*$ denotes a variable evaluated at time t^n at the end of the Lagrangian trajectory from a computational node (See Figure 1). At each time step, the velocity is integrated backwards with respect to time to determine where a particle would be at time t^n in order to arrive at a grid node at time t^{n+1} (Staniforth and Cotes, 1991). Thus the material derivative, the first term in Equation 6, has a very simple form.

The governing equations are approximated in space using standard Galerkin finite element techniques (Becker, Carey, and Oden, 1981). The equations are discretized after defining a set of 2-dimensional triangular elements in the horizontal plane (Figure 1). Mixed methods are used such that the elements use a piecewise constant basis for η , and a constant normal

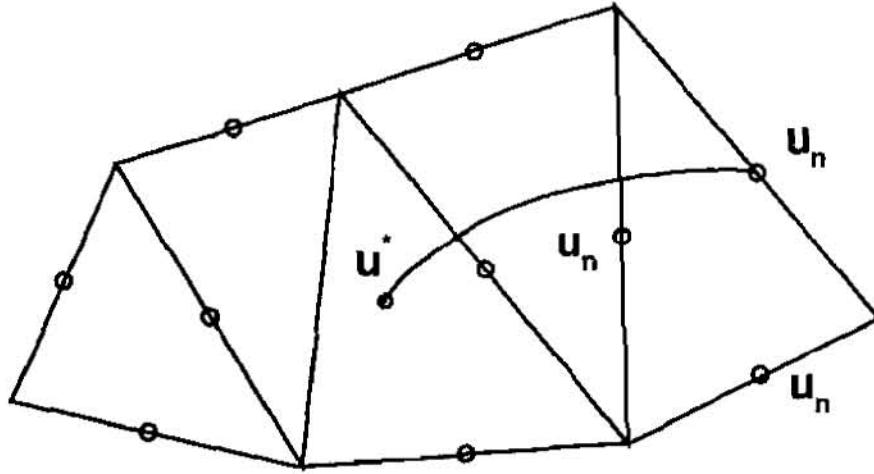


Figure 1: Definition of the elements and Lagrangian trajectories.

velocity along each edge with a linear variation in the element interior (Arbogast, 1995). For a piecewise constant interpolation for η , the finite element form of the continuity equation is

$$A_e \frac{\partial \eta_e}{\partial t} + \oint_{\Gamma_e} (H\mathbf{u}) \cdot \mathbf{n} d\Gamma = 0 \quad (7)$$

where A is the element area, Γ is the boundary of the flow domain Ω , and subscript e denotes the value for element e . Applying the discrete time operator in equation 5, the continuity equation can be written in terms of the normal component of velocity as

$$A_e \frac{\eta_e^{n+1} - \eta_e^n}{\Delta t} + \theta \oint_{\Gamma_e} H^n u_n^{n+1} d\Gamma = -(1 - \theta) \oint_{\Gamma_e} H^n u_n^n d\Gamma \quad (8)$$

where u_n is the normal component of velocity on the element side.

Next, the momentum equation is solved for u_n^{n+1} and this expression is used to eliminate u_n^{n+1} from equation 8. Integrating the finite element form of the momentum equation by using a 3 point quadrature at the midsides of the triangles, and using the discrete time operator given in equation 6

$$u_n^{n+1} = \frac{1}{C_1} [R_n - \theta N_n^{n+1}] \quad (9)$$

where

$$\begin{aligned}
R_n &= C_3 u_n^* + F_n^* + \gamma_T (\theta u_a^{n+1} + (1-\theta)u_a^*) - (1-\theta)N_n^* \\
C_1 &= \left[\frac{1}{\Delta t} + \theta(\gamma_B^{n+1} + \gamma_T^{n+1}) \right] \\
C_3 &= \left[\frac{1}{\Delta t} - (1-\theta)(\gamma_B^n + \gamma_T^n) \right] \\
N_n &= M^{-1} \left[\int_{\Omega} g \nabla \Phi \eta d\Omega - \oint_{\Gamma} g(\Phi \eta) d\Gamma \right]
\end{aligned} \tag{10}$$

where M is the mass matrix given by $M = \int_{\Omega} \Phi \Phi d\Omega$, and γ_B^{n+1} is extrapolated in time from the values at t^n . The continuity equation is put in the form of a wave equation at the discrete level by replacing u_n^{n+1} by the expression above.

$$\begin{aligned}
A_e \frac{\eta_e^{n+1}}{\Delta t} &- \frac{\theta^2}{C_1} \oint_{\Gamma_e} H^n N_n^{n+1} d\Gamma \\
&= A_e \frac{\eta_e^n}{\Delta t} - (1-\theta) \oint_{\Gamma_e} H^n u_n^n d\Gamma - \frac{\theta}{C_1} \oint_{\Gamma_e} H R_n d\Gamma
\end{aligned} \tag{11}$$

This equation contains only η at the $n+1$ time level. In practice, equation 11 is assembled and solved for η^{n+1} . Using these results, equation 9 is solved for u_n^{n+1} . The full velocity is recovered by calculating the velocity at the vertices of each triangle, then interpolating the tangential component of velocity at the midsides.

The stability analysis given by Casulli and Cattani (1994) is also applicable to this system of equations. Their results show that the linear system with constant coefficients is stable for $\frac{1}{2} \leq \theta \leq 1$ so long as a constraint on the viscous stress term is satisfied.

FIELD PROBLEM

This test case simulates transient flooding for a field-scale problem. The spatial domain is a segment of the Big Lost River in southeastern Idaho (Figure 2). The grid was created from digitized elevation data by C. Berenbrock (personal communication) using the grid generation methods of Henry and Walters (1993). The grid contains 12622 elements that have edges that vary in size from approximately 5 m in the river channel to 25 m at the edges of the floodplain.

Initially, the water was at rest with a surface elevation defined by the outflow surface elevation. The simulation was started by applying an input discharge of 210 m³/s at the inflow on the left boundary. A constant water level was specified at the outflow on the right boundary. In the simulations, a flood wave propagated through the river reach, progressively inundating areas adjacent to the river channel. The inundation area reached equilibrium in about 60 minutes of simulation time. The inundation area and surface elevation are shown in Figure 2. At this time there is flooding upstream of the first control point on the flow-

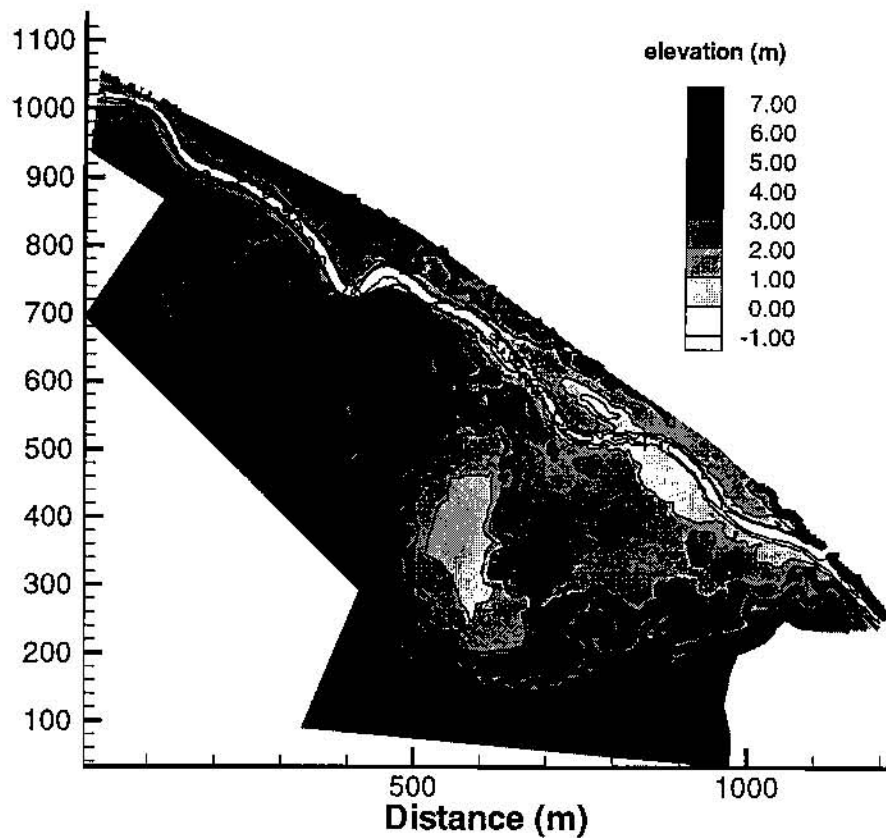


Figure 2: Topography for the Big Lost River simulation. The shaded contours are elevations in meters with respect to the water surface elevation at the outflow on the right. The heavy line indicates the edge of the inundated area after 30 minutes of simulation time.

a constriction. There is also flooding in the depression in the right-center of the domain caused by a constriction at the outflow. The advective terms cause a significant increase in water surface elevation at the control points because the flow must accelerate there.

A detail of the flow in the first sharp bend in the channel is shown in figure 3. A number of interesting flow features can be observed. A large eddy has formed on the inside of the bend where the flow passes over the shoulder of the channel. Another eddy occupies the inundated area on the left. A close examination of surface elevation indicates that there is a topographic low as the flow enters the bend, and there is a series of trailing waves farther downstream. These are hydraulic features that are expected with this complex topography. In general, these results indicate that the model is sufficiently robust to simulate highly transient flows with strong advective effects, and wetting and drying. Other tests have indicated that the model is accurate and converges at a rate $O(\Delta x)$, where Δx is an

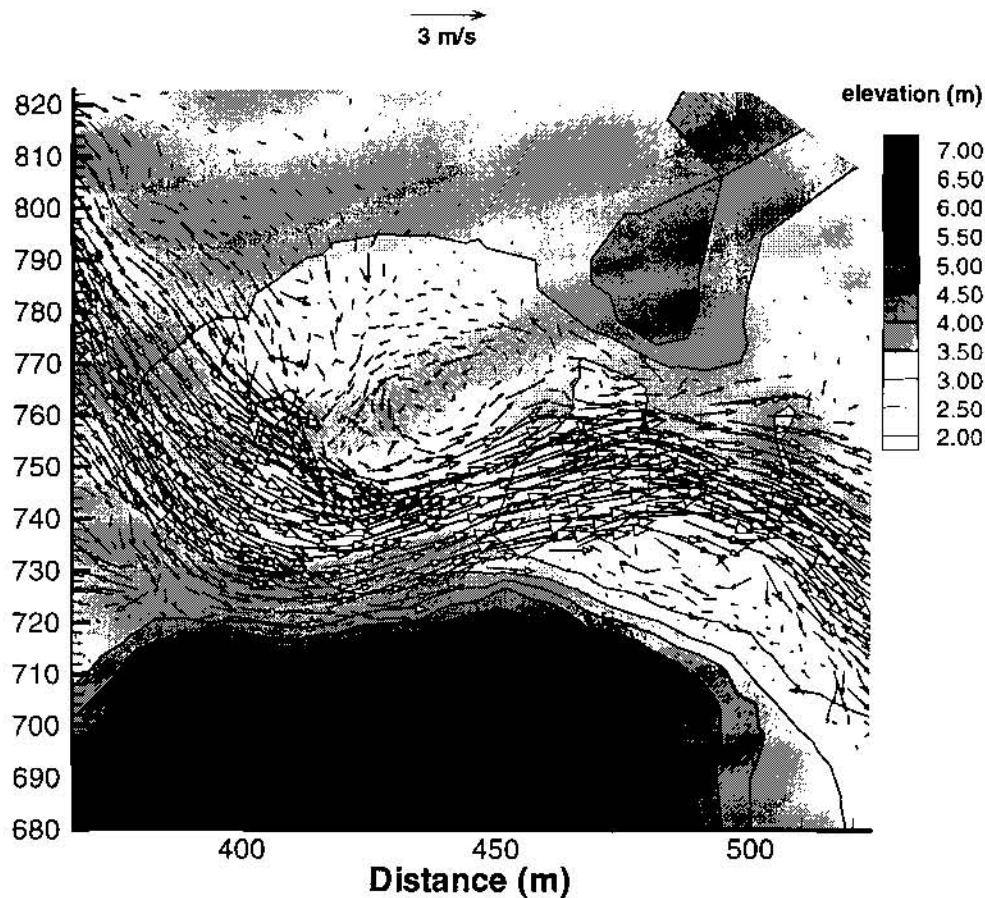


Figure 3: A flow detail in the sharp bend in the upper left part of the previous figure. The lines are elevation in meters with respect to the elevation at the outflow. Water surface elevation is shown in the inundated area that is recognized by the non-zero velocity vectors. Land elevation is shown in the dry areas.

element length scale (Walters and Casulli, 1997). This convergence rate is in agreement with theoretical predictions.

CONCLUSIONS

Using the shallow water equations, a discrete wave equation is formed from the discrete continuity and discrete momentum equations. With the mixed methods used here, there are no computational modes such as would occur with simple linear elements. An implicit time approximation coupled with a semi-Lagrangian calculation leads to a stable and robust model that treats both strong advection and moving boundaries. The method has $O(h)$ convergence rate. Results for a flood simulation highlight the efficiency and robust nature of the model.

REFERENCES

- Arbogast, T., 1995, Mixed Methods for Flow and Transport on General Geometry. In *Finite Element Modeling of Environmental Problems*, ed. G. F. Carey, Wiley, New York, 275-286.
- Becker, E., Carey, G. F., and Oden, J. T., 1981. *Finite Elements: An Introduction*, Prentice-Hall, Englewood Cliffs, New Jersey.
- Casulli, V., 1990, Semi-Implicit Finite Difference Methods for the Two-Dimensional Shallow Water Equations. *Journal of Computational Physics*, **86**, 56-74.
- Casulli, V. and Cattani, E., 1994. Stability, accuracy, and efficiency of a semi-implicit method for three-dimensional shallow water flow. *Computers Math. Applic.*, **27**, 99-112.
- Henry, R.F. and Walters, R. A., 1993. A geometrically-based, automatic generator for irregular triangular networks. *Communications in Numerical Methods in Engineering* **9**, 555-566.
- Pinder, G. F. and Gray, W. G., 1977. *Finite Elements in Surface and Subsurface Hydrology*, Academic Press.
- Staniforth, A., and Cote, J., 1991, Semi-Lagrangian integration schemes for atmospheric models-A review. *Monthly Weather Review* **119**, 2206-2223.
- Walters, R.A. and Casulli, V., 1997, A robust, finite element model for hydrostatic surface water flows. (Submitted to Comm. in Numerical Methods in Engineering).

UNET MODEL OF CONNECTED ESTUARIES IN COASTAL LOUISIANA

By Harley Winer, Hydraulic Engineer, US Army Corps of Engineers, New Orleans, Louisiana

Abstract: Prior to modern times, the lower Mississippi River regularly overflowed its banks nourishing the adjoining wetlands with sediment, nutrients and freshwater. Periodically the course of the river would change as channels became hydraulically inefficient. This process built all the land in the alluvial lower Mississippi River valley. Now, however, control structures and levees have been built to prevent the river from changing course and to prevent flooding. This has benefitted the region immensely in terms of flood protection, enhanced navigation and reliable freshwater supplies. However, this intervention has had the unintended consequence of cutting the supply of sediment, nutrients, and freshwater to the marshes of southern Louisiana.

The drastic reduction of freshwater flowing into the marshes, coupled with other activities such as canal construction, and subsidence, has resulted in significant salinity intrusion. To counter the devastating effects of salinity intrusion, freshwater diversions have been proposed and constructed as a means to maintain historical salinity gradients. On the west bank of the Mississippi River, these diversions range geographically from the Barataria Estuary to the Atchafalaya River. All of the west bank estuaries are connected by the Gulf Intercoastal Waterway (GIWW) which traverses the Gulf of Mexico coastal plain from Florida to Texas. This connectivity allows for flow into one estuary to be distributed into other estuaries.

To further our knowledge of where the water goes, a UNET model was constructed of the region. The UNET model is a solution of the unsteady flow equations with multiple linked channels. The capability of the model to handle time varying flow allows for the use of tidally driven boundary conditions as well as for time varying hydrographs due to storm runoff. There are two disadvantages to the choice of the UNET model. One is that overbank flow through the marshes can not adequately be modeled. UNET has the capability to model overbank flow but only in parallel to the main stream as in a flood plain situation but not as flow perpendicular to the channel which is a loss to the channel. The other disadvantage is that there is no constituent transport or salinity routine within the UNET package. These short-comings did not invalidate the choice of UNET. For many of the flow regimes of interest the flow is confined to within bank flow. In the extreme case where overbank flow is considered to be significant, compensations were made that enabled realistic answers to be obtained. Even though salinity modeling is not part of the UNET package, the UNET model was useful in obtaining hydrologic boundary conditions for salinity models of smaller areas.

A grid of 85 reaches was assembled linking all of the major channels between the Barataria Estuary in the east, the Atchafalaya River in the west, the GIWW to the north, and the Gulf of Mexico to the south. Numerous model runs were performed with variations in flows into the region. The same runs were also made with some proposed channel improvements. The model results established the distribution of flows into several receiving areas for various combinations of freshwater sources and flows.

INTRODUCTION

The coastal marshes between the Mississippi and Atchafalaya Rivers can be divided into several distinct areas. In the east between the Mississippi River and the Bayou Lafourche ridge is the Barataria Estuary with Barataria Bay at its seaward end (See Figure 1). West of the Bayou Lafourche ridge is the Grand Bayou marsh area, which is the marsh area between the GIWW and Terrebonne Bay in Figure 1. While east of the Atchafalaya River and west of the Houma Navigation Canal is the Terrebonne marsh area. Although these areas are all connected by the GIWW, such that one could get by boat from one area to another, they are separate distinct areas. Federal and state agencies have proposed several projects to benefit particular marsh areas within the region of interest. Because of the connection provided by the GIWW it is not clear how these proposed projects will influence other adjacent areas.

Two specific proposed projects were the impetus for construction of the UNET model of the region. One is a proposal to increase flow of Mississippi River water in Bayou Lafourche either through pumps or siphons or a combination of the two. The other is to enlarge Bayou l'Eau Bleu which is the connection between the GIWW and the Grand Bayou marsh area. The purpose of this enlargement is to increase the flow of freshwater into the Grand Bayou marsh area.

Bayou Lafourche was at one time the main channel of the Mississippi River, but it has filled in and at the turn of the century was but a small distributary that periodically shoaled at its mouth. Rather than repeatedly opening the connection between the River and Bayou, a decision was made to have the main line levee system completely close the connection. Because of water quality concerns, pumps with a total capacity of 340 cfs were installed in the 1950's to restore some river flow in the

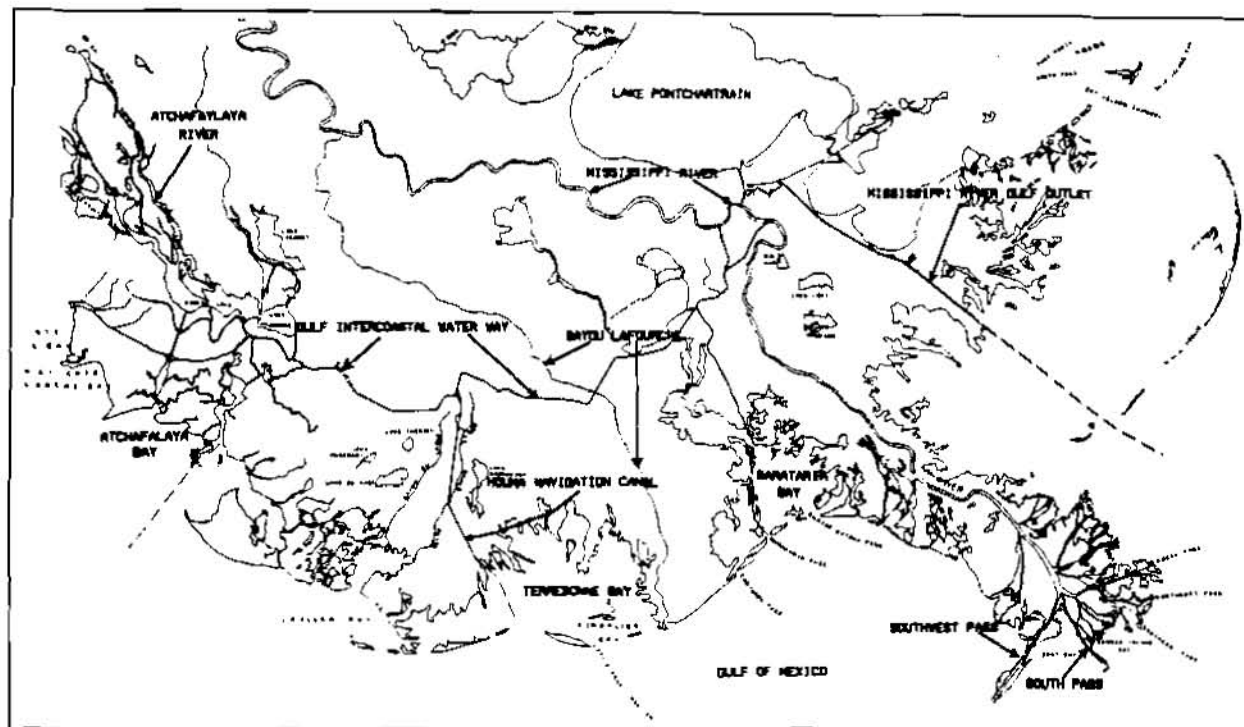


Figure 1: Major water bodies within the UNET study.

Bayou. There has been considerable development along the banks of the Bayou which precludes any large scale diversion of Mississippi River water. Consequently a modest diversion of one or two thousand cfs has been proposed along with channel improvements to prevent flooding.

Bayou l'Eau Bleu is a narrow waterway connecting the GIWW with the larger Cutoff Canal in the Grand bayou marsh area. The proposed project would increase the cross section of Bayou l'Eau Bleu by sixty percent. The project sponsor wanted to know whether the channel enlargement would be effective in increasing the flow of freshwater into the Grand bayou marsh area and whether the channel enlargement would promote salt water intrusion into the GIWW in periods of low freshwater inflow from Bayou Lafourche and the Atchafalaya River.

Freshwater inflow from the Atchafalaya River, of course, is seasonal; however in recent years a significant increase has been identified. This is due to two unrelated factors. First the Avoca Island Cutoff which freely connects the GIWW to the Atchafalaya River (the actual junction of the GIWW and Atchafalaya River has a navigation lock which prevents eastward flow) was recently enlarged to accommodate the manufacture of larger offshore oil rigs. This channel enlargement has allowed for greater eastward flows in the GIWW. The other factor is the growth of a delta at the mouth of the Atchafalaya which has raised the flow line along the river. The higher stages at the junction of the Atchafalaya River and the Avoca Island Cutoff pushes a greater flow eastward. This increased eastward flow in the GIWW can in high water season flow all the way to the Barataria Estuary.

A linear regression analysis of the annual means from a stage gage located at the junction of the Atchafalaya River and the Avoca Island Cutoff showed a .04 foot per year slope to the record. Other gages along the lower Atchafalaya River showed a similar slope. Linear regression analysis of records from stage gages in coastal Louisiana in marsh areas away from the influence of the growing Atchafalaya delta show a slope of .02 feet per year. This .02 feet per year is due to the influence of subsidance and relative sea level rise. The difference between this .02 feet per year and the .04 feet per year along the Atchafalaya is due to the growth of the delta extending the mouth of the river seaward and raising the flow line.

The issue then for the sponsors of the proposed projects is how increased Atchafalaya flows will interact with flows introduced by their project and by other projects. The other major factor is the Davis Pond Freshwater Diversion Structure which is currently in the initial stages of construction. This project, located at the head of the Barataria Estuary, is intended to control salinity gradients in the Barataria Estuary. The structure will have a design capacity slightly greater than 10000 cfs. This has the potential to induce freshwater flows via the GIWW to the areas west of the Barataria Estuary.

MODEL CONSTRUCTION AND VERIFICATION

The model was constructed and verified in three different sections. Since the primary purpose of the model was to address questions regarding a proposed diversion in Bayou Lafourche, greater detail was included in Bayou Lafourche and adjacent areas and less detail was provided in the areas more remote. The detail in the areas furthest from Bayou Lafourche was solely sufficient to provide proper influence in the Bayou Lafourche area. The three separate areas for initial grid construction were the Barataria estuary east of the Bayou Lafourche ridge, the Terrebonne marsh area west of the Houma

Navigation Canal, and Bayou Lafourche with the Grand Bayou marsh area to the west of Bayou Lafourche. These three separate sections will be referred to below as the eastern, western and central portions of the model. Grids for these three sections were constructed separately and then joined.

Sources of cross sectional information were limited for many of the reaches in the model. A few reaches (Barataria Waterway, Houma Navigation Canal, Avoca Island Cutoff) are maintained channels so recently dredged cross sections were available. Bayou Lafourche cross sections every 10,000 feet for the entire length of the channel exist thanks to a previous state survey. Precise reliable cross sectional data was available for but 16 reaches of the 85 total reaches or less than 20 percent of the entire grid. The GIWW which traverses the entire project area in 13 separate reaches is an authorized channel, however, there has been little or no maintenance dredging for decades. Detailed surveys are performed only when dredging is necessary, thus no cross sections were available for the GIWW. The only available information was the original dredge template, recent center line profiles, and aerial photographs. Since in some areas, there has been considerable bank erosion along the GIWW, a method of correlating the channel width obtained from aerial photos with the center line depth and original template was utilized to come up with an estimated cross section.

For the remaining reaches, synoptic cross sections were used wherever available. Field trip were taken to the Grand Bayou marsh area and the Terrebonne marsh area to obtain rough cross sectional data using a digital fathometer and a hip chain. Cross sections were also obtained from other agencies doing work in the area. The Soil Conservation Service (now Natural Resource Conservation Service) had commissioned twenty five cross sections within the Terrebonne marsh area. All of these were incorporated into the grid. USGS also provided cross sections for selected locations where they were doing discharge measurements. The results of these discharge measurements were also used in the verification of the model.

The western portion of the grid was verified using USGS synoptic discharge measurements. The USGS had conducted several synoptic discharge measurements along the GIWW to measure the eastward flow of Atchafalaya River waters along the GIWW distributary system. Since the most important factor as far as the area of interest adjacent to Bayou Lafourche was the flow in the GIWW east of the Houma Navigation Canal, the intent was to have the model match these flows. The USGS discharge measurements did not account for all of the flow measured at the head of the GIWW distributary system. This is because in high river flows large volumes of water are lost due to over bank flow over and through the low lying marshes and swamps in the Terrebonne marsh area. Because the UNET model does not account for over bank losses from a stream, flows in the western most distributaries were not matched to those reported by USGS. The UNET model tended to show greater flows in these distributary channels (such as Bayou Penchant and Bayou Copasaw) than the USGS measurements. By allowing for greater flow in these distributary channels to account for overland flow not included in the model, the net flow resulting at the eastern end of this section of the grid was matched to the USGS measurements. Problems are encountered with the use of the USGS synoptic discharge measurements. Each synoptic measurement is a snapshot in time of a tidally driven fluctuation in flow. Since there is little other information with which to correlate, it is impossible to know if the given measurement is a maximum, minimum or average condition. None-the-less, there is confidence in the model since there was general agreement with the model results and the eastern most discharge measurements.

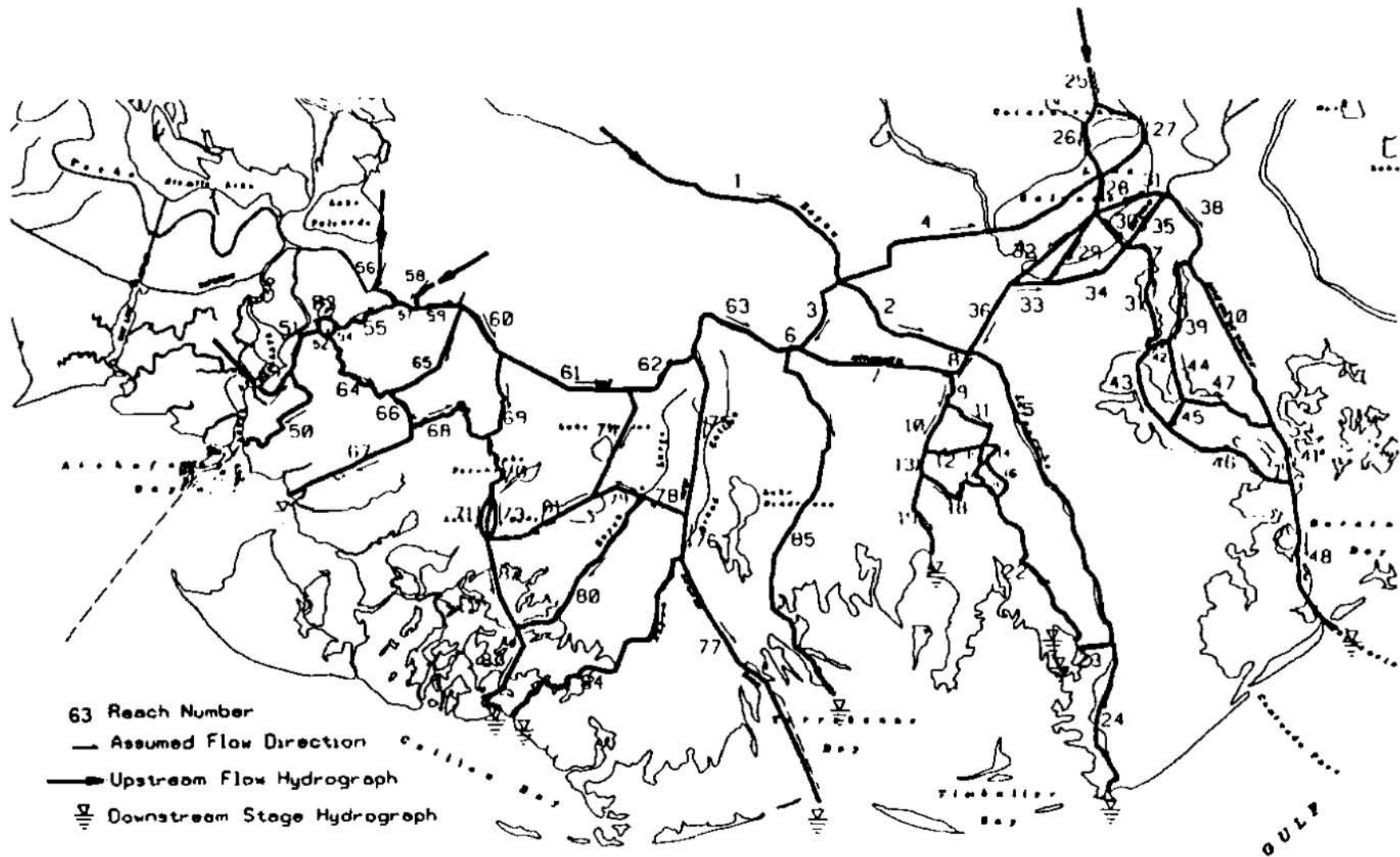


Figure 2: UNET model grid of Major Channels from the Atchafalaya River to the Barataria Estuary, from the GIWW to the Gulf of Mexico, superimposed on a regional map.

The central and eastern portions of the grid were verified using tide co-range and co-phase data that had been prepared by the National Ocean Service for a previous project. Since the UNET model solves shallow water or long wave equations, the assumption is that if the propagation of one long wave (the tide) is correctly modeled, the propagation of other long waves such as flood waves will also be correctly modeled. The UNET grid is shown in Figure 2 superimposed upon a map of the region.

RESULTS

Once the UNET grid was assembled and verified, the problem of data management needed to be addressed. Multiple runs were envisioned with numerous conditions of varying flows. The UNET model has the capability of outputting a time series of stage and flow for each and every position along each and every reach. A time series plot for a particular location is useful for visualizing a solution or for trouble shooting, but several thousand time series plots make for a very cumbersome report.

The solution to this dilemma was to make essentially steady state runs. UNET does not specifically have a steady state option, it is a program that solves time varying equations with time varying boundary conditions. The trick is to provide stage and flow hydrograph input conditions that are constant in time. Since the main interest was in the distribution of increased Bayou Lafourche flows, the output of the numerous runs was organized to show this distribution under the various combinations of input flows from Davis Pond and the Atchafalaya River. Small, medium and large discharges were selected for both the Barataria Estuary (Davis Pond) and the Atchafalaya River. Small medium and large for the Barataria Estuary were arbitrarily selected to be 500, 5000 and 10000 cfs; small medium and large for the eastward GIWW flow from the Atchafalaya River were arbitrarily selected to be 2000, 10000 and 20000 cfs. The increase of flow for the nine combinations of these flows are tabulated in Table 1 for the six reaches where introduced Bayou Lafourche flows could possibly go. These six reaches are Bayou l'Eau Bleu, the GIWW east of Bayou Lafourche, Bayou Lafourche south of the GIWW, Bayou Terrebonne, the GIWW west of Bayou Terrebonne, and Company Canal east of Bayou Lafourche. It should be noted that for the eastern and western reaches of the GIWW the increased flows reported in Table 1 may actually be decreases of reverse flow or rejected flow. It should also be noted that some of the combinations of flows may not actually occur. For example, it is highly improbable that Davis Pond structure will be operating at a high discharge at the same time that there are high discharges from the Atchafalaya River. This is because the Davis Pond structure is intended to maintain salinity gradients within the Barataria Estuary and would not be needed if there was a large influx of Atchafalaya River freshwater.

From Table 1 it is seen that between 5.5 to 10.3 percent of the increased Bayou Lafourche flow will go into Bayou l'Eau Bleu. The same combinations were run with the proposed enlargement of Bayou l'Eau Bleu. In these runs between 6.3 and 12.1 percent of the increased Bayou Lafourche flow went into Bayou l'Eau Bleu. The flows into the Grand Bayou marsh area through the improved Bayou l'Eau Bleu channel increased between 18% and 21% for all the various combinations of flows from the three major input (Bayou Lafourche, Atchafalaya, Davis Pond). The greatest increase occurred for the combination of high Barataria input and low Atchafalaya flow, whereas the least increase occurred with high Atchafalaya flow and low Barataria flow.

Table 1: Increased Flows Due to 2000 cfs Increase in Bayou Lafourche Flow

Increase in Flow in Bayou l'Eau Bleu For nominal 2000 cfs increase in Bayou Lafourche Flow			
	Barataria=500	Barataria=5000	Barataria=10000
Atchafalaya=2000	175	119	124
Atchafalaya=10000	193	169	110
Atchafalaya=20000	206	197	169

Increase in Eastward Flow in GIWW East of Bayou Lafourche For nominal 2000 cfs increase in Bayou Lafourche Flow			
	Barataria=500	Barataria=5000	Barataria=10000
Atchafalaya=2000	645	854	890
Atchafalaya=10000	686	764	980
Atchafalaya=20000	697	727	820

Increase in Flow in Bayou Lafourche South of GIWW For nominal 2000 cfs increase in Bayou Lafourche Flow			
	Barataria=500	Barataria=5000	Barataria=10000
Atchafalaya=2000	282	181	185
Atchafalaya=10000	301	252	155
Atchafalaya=20000	304	283	230

Increase in Westward Flow in GIWW West For nominal 2000 cfs increase in Bayou Lafourche Flow			
	Barataria=500	Barataria=5000	Barataria=10000
Atchafalaya=2000	776	726	669
Atchafalaya=10000	685	681	626
Atchafalaya=20000	640	641	628

Increase in Flow in Bayou Terrebonne For nominal 2000 cfs increase in Bayou Lafourche Flow			
	Barataria=500	Barataria=5000	Barataria=10000
Atchafalaya=2000	57	46	40
Atchafalaya=10000	71	67	52
Atchafalaya=20000	85	83	78

Increase in Flow in Company Canal East For nominal 2000 cfs increase in Bayou Lafourche Flow			
	Barataria=500	Barataria=5000	Barataria=10000
Atchafalaya=2000	63	74	91
Atchafalaya=10000	63	66	77
Atchafalaya=20000	67	69	74

Further analysis of the steady state results obtained from the UNET model showed that a significant portion of the increased westward flow in the GIWW west of the project area, ended up as increased flow down the Houma Navigation Canal. Since salinity intrusion along the Houma Navigation Canal continues to impact extensive areas of adjacent fresh water marsh, the increased freshwater flow in the HNC is an additional benefit for the proposed Bayou Lafourche Freshwater Diversion project.

The UNET model was also utilized to address the question of salinity intrusion north of the GIWW due to flow reversals in the proposed enlarged Bayou l'Eau Bleu channel during low water season. A salinity intrusion event in the first week of October 1996 was modeled using actual Gulf of Mexico and Atchafalaya River hourly stage records and measured Bayou Lafourche discharge as model input boundary conditions. The model was run for the period October 1 through October 15, 1996 with both the existing Bayou l'Eau Bleu channel and the proposed enlarged channel. The model was also run with the existing and proposed channels and various levels of introduced flow (as opposed to actual flow) in Bayou Lafourche. Analysis of the results of these simulations showed that the magnitude of flow reversals in Bayou l'Eau Bleu was considerable small compared to the Houma Navigation Canal. The magnitude of flow reversals in the channel north of the GIWW (the areas of particular interest as far as salinity intrusion) did not change with the enlarged Bayou l'Eau Bleu channel. The simulation also showed that with a Bayou Lafourche flow of 600 cfs there were no flow reversals in the channels north of the GIWW. The conclusion here is that a modest Bayou Lafourche diversion will prevent salinity intrusion north of the GIWW.

CONCLUSION

The UNET model of the major channels in the region from the Atchafalaya River to the Barataria Estuary was useful in addressing questions about flow distribution from a proposed freshwater diversion into Bayou Lafourche. It also answered questions about the efficiency of a proposed enlargement of the Bayou l'Eau Bleu channel connecting the GIWW and the Grand bayou marsh area.

In additional to the uses discussed above, flow output from the UNET model has been used as input in a habitat change model. The UNET model was also used to generate boundary conditions for a TABS salinity model of the Grand Bayou marsh area.

TWO-DIMENSIONAL FLOODPLAIN MODELING OF RIVERS IN TAIWAN

By Reuy-Bean Wu, Engineer, Planning Office, TPGWRD, Taichung, R.O.C.¹;

Yao-Tser Chang, Director, Planning Office, TPGWRD, Taichung, R.O.C.²;

Yih-Pin Cheng, Chief, Planning Office, TPGWRD, Taichung, R.O.C.³

Abstract

A two-dimensional horizontal finite numerical model (TABS2) was modified and applied to a 10 Km long channel-floodplain reach of Dah-Li Creek in Taiwan. Besides to proceed numerical model simulations but also to combine with the hydraulic model test and the long period measurements for verification and analysis, and to supply the reference and application for the latter design and planning of the low-water management. The results indicate the model may successfully estimate river stage and bed level in large-scale floodplain applications. Computed results compared well with observed data within expected ranges.

Review of the forerunner Applications

Two-dimensional flow models have been applied to certain classes of river channel problems. Applications have included detailed analyses of flow patterns near structures such as bridges (FHWA, 1989), dams (Gee & Wilcox), and floodplains (Samuels, 1985; Gee & Anderson, 1990), and many estuary studies which were of large scale such as McAnally et al. (1984), Gee et al. (1990). In addition, the two-dimensional sediment transport models also have been applied to the river studies such as Cache Creek (Deering, 1990). In Taiwan, those models were also applied to the simulations of the hydraulic characteristics and the bed aggregation-degradation on Keelung River (1993) and Dah-Li Creek (1994).

Model selection

The numerical model known as TABS2 including RMA-2 (King and Norton, 1978) and STUDH (Thomas and McAnally, 1985) was selected for use in this study. Hydrodynamic conditions were simulated and results determined with the aid of the two-dimensional finite element hydrodynamic model RMA-2, and sediment transport characteristics were modeled for selected cases using the sedimentation model. The depth-averaged two-dimensional flow model for river was according to the Galerkin finite element method. Meanwhile, the Newton-Raphson iterative method of simultaneous approximations is used to solve stages, velocities in river. This method can be used to consider the complicated boundaries, and the effects of the different constructions in river efficiently. In addition, this model adopted the marsh porosity method for some element in

the network is the intersection element that the portion was marsh and another portion was dry. The application described herein is the adequate proceeding of the marsh element formulation to a floodplain. Finally, the outcome hydraulic information was input to the movable bed model, and applied to predict bed elevations and sediment aggregation-degradation.

Study Reach

The study reach selected for the TABS2 application was that from Dah-Li Bridge (upstream) to Section No. 1 (estuary and merge into Woo River) of the Creek Dah-Li in Taiwan. Dah-Li Creek is a main river with about 13 Km long treated reach and 400.72 Km² basin area in the middle of Taiwan (Fig. 1). The research reach is about 10 Km long with a slope of 1/320. The improvement of this reach with a 320 m width was proceeded in the compound triangular profile with a 110-140 m wide meandering deep stream. The floodplain is about 100 m wide each side, has a slope of 1/50 orthogonal to the river, and is bounded by concrete bank. The floodplain use is prohibited for flood flow. Manning's *n* was estimated at 0.039~0.040 for the floodplain and the channel. Bed material *d_m* was sampled and estimated at 33~66 mm. Although the models allow detailed spatial variation of Manning's *n* and bed material parameters, this study used only two; one for the channel and one for the overbank. An observed event of approximately 2 years return period flood was used for test and verification. This flood rose from a base flow of 200 cms to a peak of 1,658 cms in 11 hrs at Shee-Nan Bridge. The discharge hydrograph at Shee-Nan Bridge and rating curve at Sec. No. 1 were obtained from TPGWRD, Taiwan.

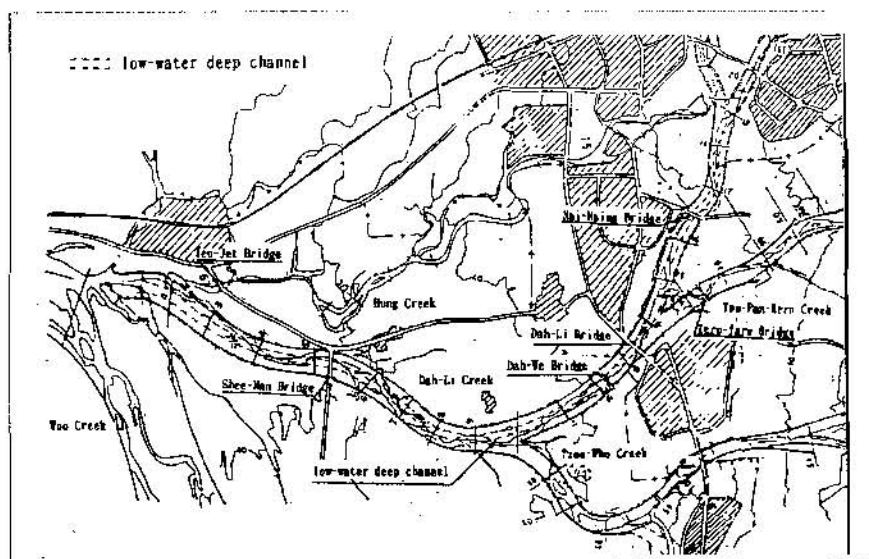


Fig. 1 Improved reach in Dah-Li Creek

System Schematization

TABS2 utilizes a finite element mesh composed of both triangular and quadrilateral elements. Ground elevations are defined at the corners of the elements and vary linearly between corner nodes. In this study, the channel was represented by a strip of six elements wide (Fig. 2) producing a triangular channel cross section. Overbank areas were represented by much larger elements. Ground elevations were determined from 0.5 m interval maps. The resulting finite element mesh was composed of 2,597 elements and 7,937 nodes (Fig. 3). The ratio of maximum to minimum areas was about 200 to 1. This variability in resolution demonstrates the flexibility of the finite element method for use in large-scale floodplain modeling. Turbulent exchange coefficients used varied with element size from 100 to 500 lb-sec/ft² (4,800 to 24,000 N-sec/m²) and effective diffusion coefficient used varied with element size from 500 to 2000 m²/sec.

The computations were performed with a 1 hr. time step. Three steady flow cases have been selected to compare with the series of physical model test besides the unsteady flow case was simulated. They were performed under the under-bankfull (2 years return period flood, the discharge of the main stream $Q_m = 1,470$ cms, the discharge of the branch stream $Q_b = 430$ cms), the bankfull (5 years return period flood with $Q_m = 2,350$ cms and $Q_b = 650$ cms) and the over-bankfull (100 years return period flood with $Q_m = 6,420$ cms and $Q_b = 2,020$ cms) flow. The computation between flow and sediment transport is uncoupled.

Results

The measured and computed water levels and velocity distributions of cross sections are shown in Fig. 4 and Fig. 5. In addition, the observed and computed bed elevation variation at Sec. No. 4 during the flood event is shown in Fig. 6. Note that, for water level and velocity distribution, both are approximately approach, but the lateral water surface slope (water level rising) of the computed is more explicit. The intentions of the bed elevation variation also are rather corresponding, only at the right floodplain locations, there are more difference between the computed and the observed (Fig. 6). It is possible that we suppose the floodplain bed material is same as the channel and with no protection so that we can probably predict the locations of bank protection and amend the layout.

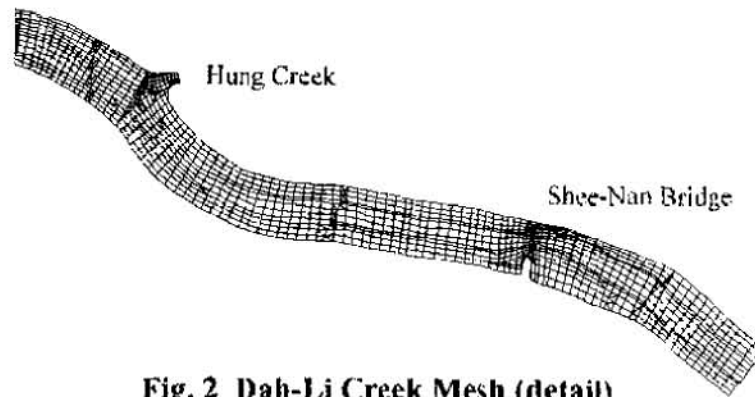


Fig. 2 Dah-Li Creek Mesh (detail)

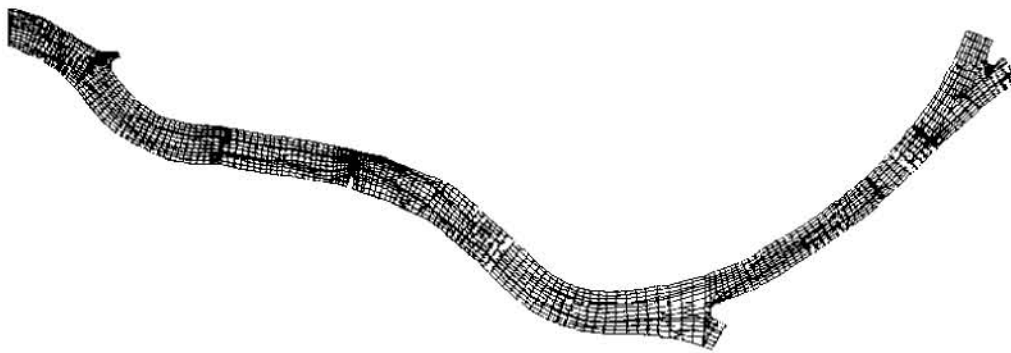


Fig. 3 Dah-Li Creek Mesh (flow is right to left)

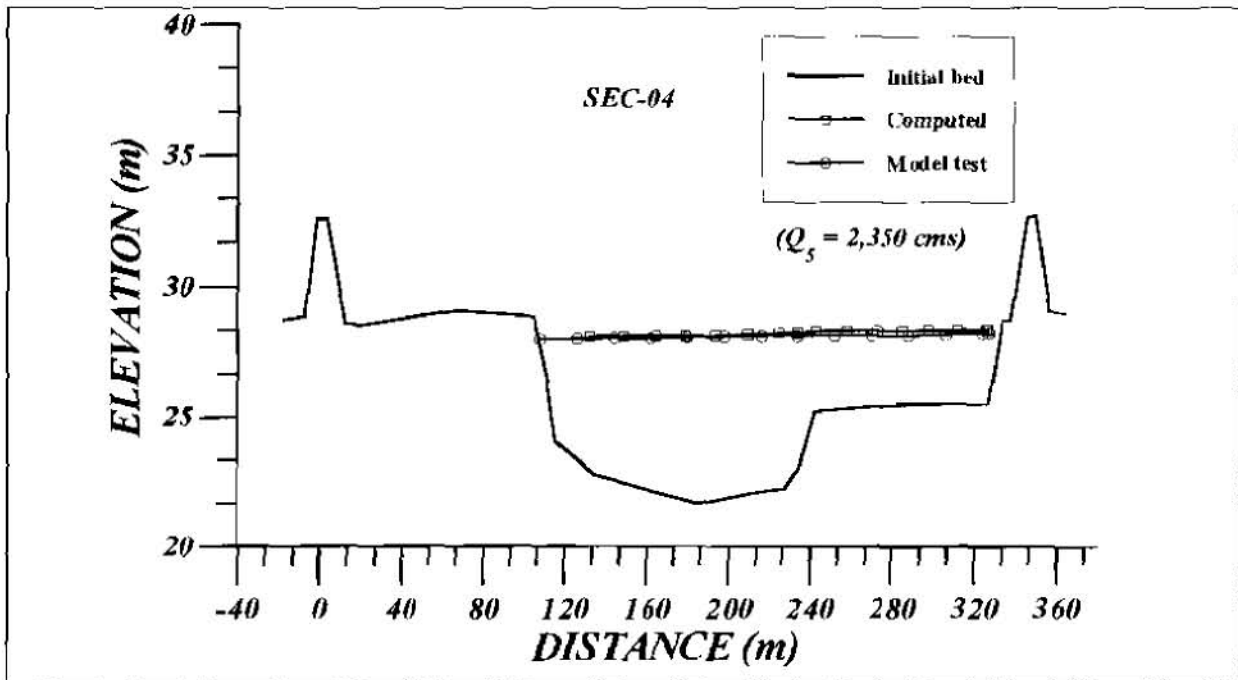


Fig. 4 The comparison of section water level

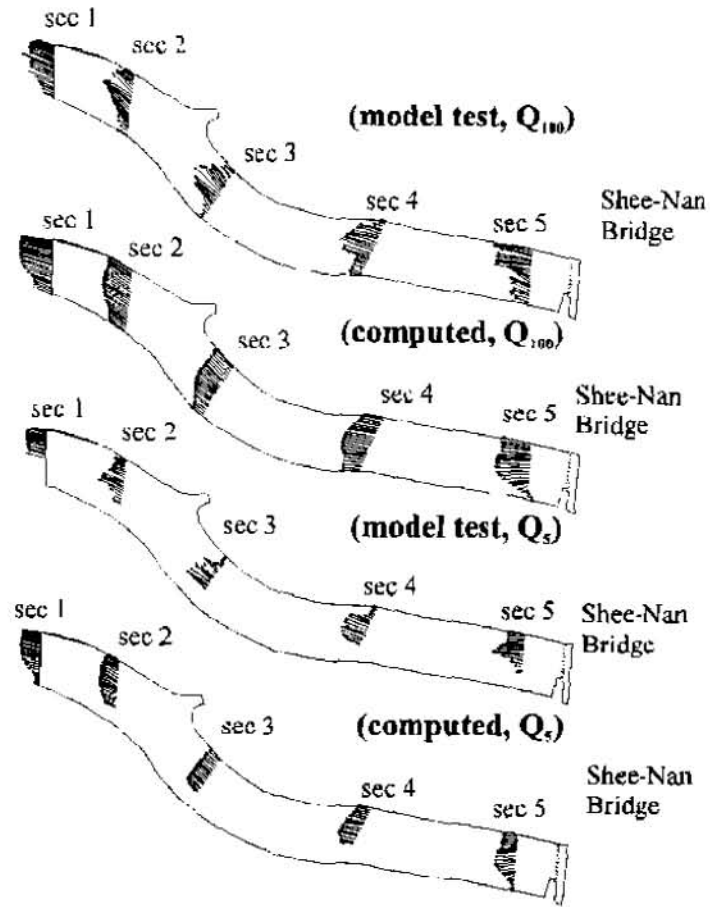


Fig. 5 The comparison of velocity distribution

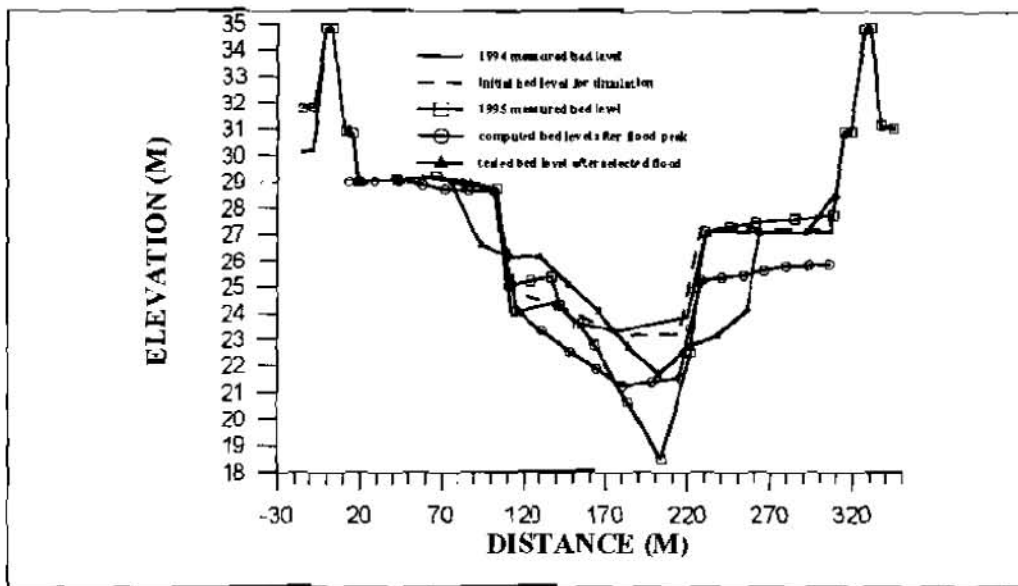


Fig. 6 The comparison of cross section bed level

Another results were shown in Fig. 7~8, which are the water level and the bed elevation contours and the velocity distribution of the flow field under two flow conditions. The velocity increased from 2.0 m/sec (under the under-bankfull flow) to 4.0 m/sec (under the over-bankfull flow). The maximum of the velocity took place at the location around bridge, which was up to over 7.38 m/sec. The two-dimensional solution obtained from RMA-2 yields velocity vectors in addition to stage at every computational node. Meanwhile, STUDH yields bed elevation variation and shear stress at every node. Examination of plotted velocity fields and bed elevation variation contours is useful for determining the layout of the deep channel of the improvement in river and the extent of inundation and velocity hazard areas within the floodplain at any particular time.

Computational Aspects

Previous applications of such models almost have been restricted to a river with milder slope than Taiwan. The results indicate that finite element schemes may successfully estimate the flow field and the bed elevation variation of river in the large-scale floodplain applications such as Taiwan. Due to the special bed contour with more difference between the computational nodes, it is need that the computational mesh was split by hand and AUTOCAD was used to digitize the grid. Although this is not a very computationally intensive problem for the simulation of steady flow conditions, the dynamics simulations performed (consisting of 98 time steps due to comparing with the model test) utilized significant computational resources. Fortunately, it is convenient that the simulations were performed on a personal computer at present. Each simulation took several hours of central processing time on computer. Relatively, due to the complicated bed contour that the coefficients should give more detailed during computing. The results and experience indicate that engineers contemplate two-dimensional floodplain modeling under these conditions and on this scale for dynamic flow events should carefully and properly plan their studies. The patience and practice for engineers is necessary.

Conclusions

Application of TABS2 to the Creek Dah-Li has demonstrated the applicability of finite element numerical models to the large-scale floodplain applications in Taiwan. The simulation results of this model were predicted reasonably well. Especially, it is very efficient in dealing with the complicated boundary flow field. It prevents that unsolvable problem of the computational node from occurring with water to the general numerical model. Hence, it is available for the hydraulic analysis and even the sediment transport simulation in natural rivers. The view of the relative accurate flow prediction, the high

compatibility, and the low computational costs these models seem suitable for the development of the morphological model in future.

Acknowledgements

Funding for this research came from Taiwan Provincial Government Water Resources Department (TPGWRD) through Planning Office awarded Hydraulics Laboratory. The direction and advice of Prof. Ming-His Hsu during the project of this study is appreciated. Permission to publish this paper was granted by the Chief of TPGWRD, Prof. Hong-Yuan Lee.

REFERENCE

- Ackers, P., and White, W. R., "Sediment Transport: New Approach and Analysis", Jour. of Hyd. Div., ASCE, No. HY11, 1973 (Nov).
- Graf, W. H., "Hydraulics of Sediment transport", McGraw Hill Book Co., New York, U.S.A., 1971.
- H. J. de Vriend, "Steady flow in Shallow Channel Bends", T. U., Delft, Netherlands, June, 1981.
- King, I. P. and Roig, L. C. (1988) "2-D Finite Element Models for Flood Plains and Tidal Flats," Proc. Int. Conf. on Computational Methods in Flow Analysis, Okayama, Japan.
- Thomas, A. R., and MacAnally, W. H., Jr., "User's Manual for The Generalized Computer Program System Open-Channel Flow And Sedimentation TABS-2", Hydraulics Laboratory, Waterways Experiment Station, Corps of Engineers, U.S. Army.

Office: 46 Pei-An RD. Chiu-Cheng, Wu-Feng, Taichung, Taiwan, R. O. C.

TEL : 886-4-3339256

FAX : 886-4-3393147

E-MAIL : rbwu@ms14.hinet.net

REMOTE SENSING OF DETRIMENTAL FLOW CONDITIONS AT LOCK AND DAM 24, UPPER MISSISSIPPI RIVER

By Robert D. Davinroy, Potamologist; David C. Gordon, Hydraulic Engineer; and David W. Kreighbaum, Senior Cartographer; US Army Corps of Engineers, St. Louis District, St. Louis, Missouri

Abstract: The use of modern day remote sensing software and standard image processing software to analyze aerial photography for surface flow pattern recognition on the Mississippi River was evaluated. This paper discusses the results of this analysis and summarizes future usage considerations for the engineer.

INTRODUCTION

Detrimental flow conditions at the downbound navigation approach to Lock 24 on the Upper Mississippi River have caused numerous accidents to barge tows. The flow conditions have been historically related to "outdraft", a term used to describe the effect of localized, diverted flow around the upstream pooled portion of a lock chamber. Between 1980 and 1991, records indicate that 36 accidents occurred as a result of outdraft conditions at Lock 24. Of these accidents, 23 involved damage to the lock or dam. The accident scenarios have usually involved either barges

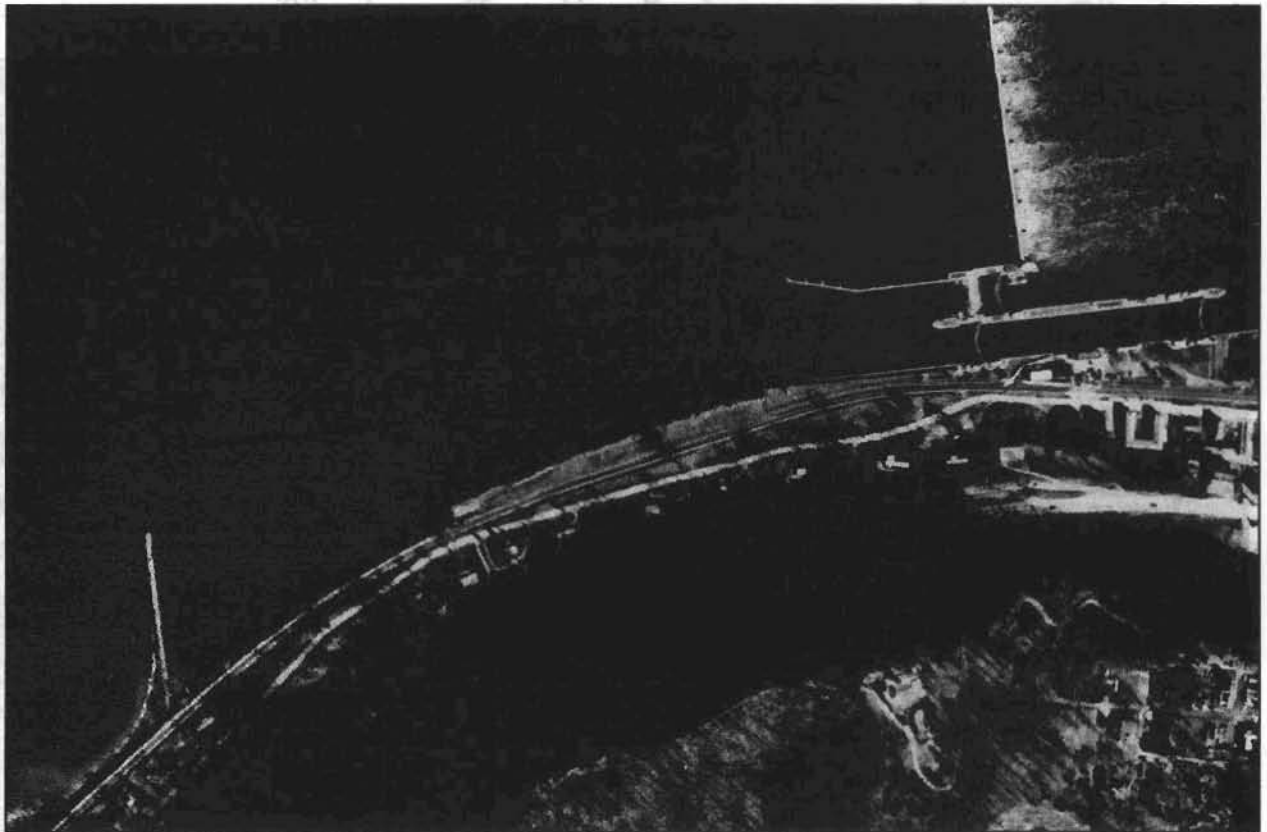


Figure 1: Color Aerial Photograph at Lock & Dam 24, Upper Mississippi River, Mile 273.5.

or towboats diverted toward the gates of the dam. Near loss of life and structural damage to the tainer gates have forced the St. Louis District Corps of Engineers to evaluate this problem and develop cost effective, river engineering design solutions.

The major obstacle that has faced river engineers at Lock 24 in the past has been the ability to discern the exact flow pattern in the river. Has there really been a major localized "outdraft" problem, or has some other factor been influencing flow effects? A somewhat modest amount of data has been collected near the lock and dam using traditional and modern velocity measuring systems to answer these questions. Unfortunately, the resolution of this data has limited the depiction or visualization of the detrimental flow conditions as they exist.

To rectify this problem, scanned color aerial photography taken in the study reach was used as an input to both a multispectral classification scheme and standard image processing software to investigate the possibility of remotely sensing currents. The effects of sediment load, surface roughness, and turbidity were expected to affect the spectral reflectance characteristics of the water, which could possibly lead to an analysis of currents on the river. Analysis of plan view current patterns of the Mississippi River using remote sensing techniques could become a valuable tool for pinpointing navigation problems and establishing base conditions for physical model studies.

A color aerial photo from December 1993 (Figure 1) was selected for this experiment because the color differences in the water were visually evident. These color differences occurred as a

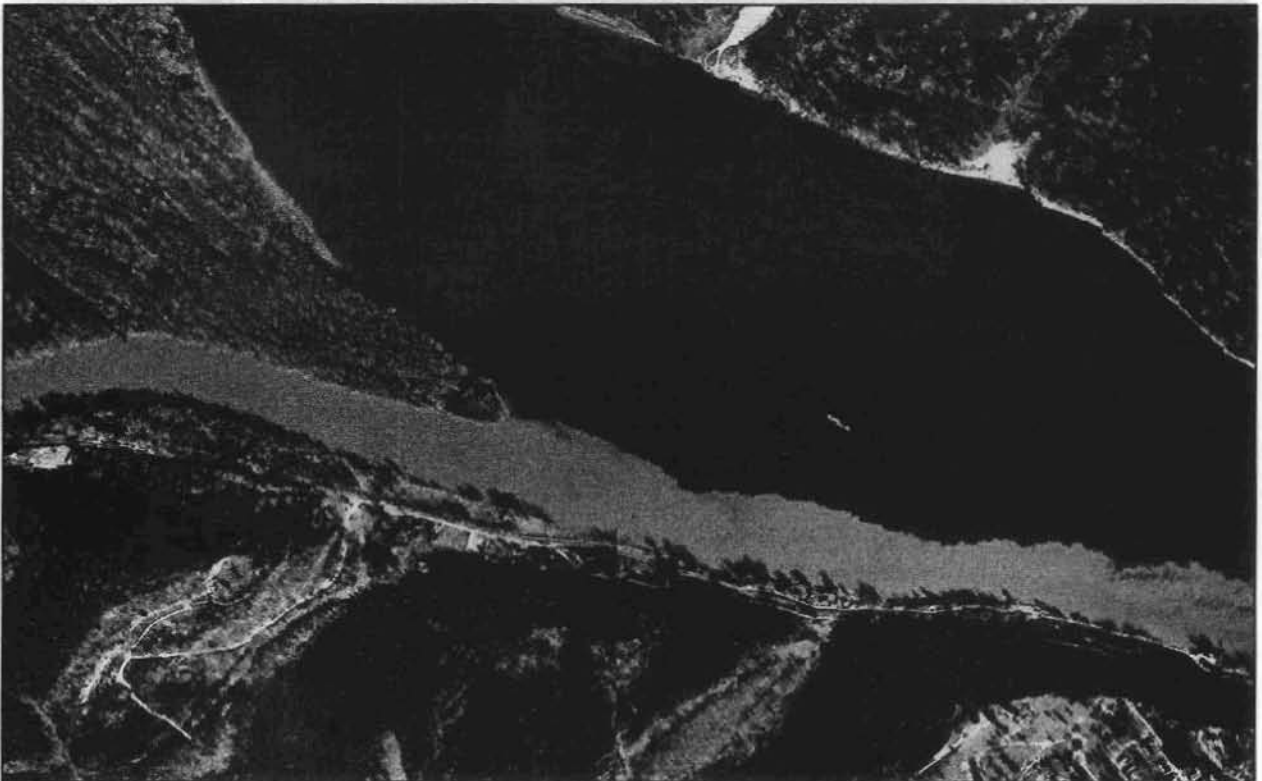


Figure 2: Tributary Supplied Seeding Source on the Mississippi River Upstream of LD 24.

result of a major influx of suspended sediment from a tributary 10 miles upstream of Lock and Dam 24. Figure 2 is an aerial photograph of the Salt River dumping into the Mississippi River with a large amount of light brown suspended sediment. The tributary supplied the study area with a seeding mechanism that allowed engineers to remotely sense flow patterns. The suspended sediment did not mix into the water column before reaching Lock 24. Therefore, the possibility existed for determining flow patterns because of the lack of homogenous suspended sediments in the study area.

The infrared aerial used for this study was taken in June of 1997 when the suspended sediment from the Salt River was not as prominent. A visual inspection of this aerial failed to show as much color variation as the color aerials from 1993.

TECHNIQUES

Remote Sensing Package Software: The original color and color infrared images were brought into two particular image processing software applications and post-processed for the possible extraction of meaningful information. The first application employed a full package remote sensing software scheme. The images were first scanned at 200 DPI and saved as TIFF format. The digital image files were then processed using Intergraph *Advanced Imager* software on a Pentium PC. Multispectral classification involved an unsupervised classification using ISODATA (Interactive Self-Organizing Data Analysis Techniques A) training. The training phase allows data to be clustered into like groups. Similar clusters are merged based on a specified number of iterations. The training data is used as the input to the classification scheme. Classification involves comparison of spectral reflectance for each pixel to statistical descriptions of each class in the selected training set. The classification algorithm decides which spectral class is closest to the pixel being analyzed, and assigns a value representing that class to the output image. Assignment of a color table to the output image from the classification allows interactive comparison with the original image. Classifications were run over two data sets covering the Lock and Dam 24 study reach, in visible and near-infrared wavelengths. The Minimum Distance classifier was chosen for its robustness, speed and simplicity. Other classifiers (Maximum Likelihood, Parallelepiped, and Para-MD) have been found in the past to yield similar results when using scanned aerial photography.

Standard Image Processing Software: A cheaper, more user-friendly methodology was attempted using *Corel Photopaint* on a Pentium PC. The color aerial photograph was scanned and converted to Bitmap format. Several different photo enhancement filters were used on the digital image to systematically determine which filter would best enhance the colors in the original photograph.

ANALYSIS

Remote Sensing Software Package: Comparison of classified imagery to the original color data sets was done visually, using hardcopy and softcopy data. Plots of classified data were compared with the original imagery. Individual areas were closely investigated on a pixel-to-pixel basis using *MGE Base Imager* image processing software.

Standard Image Processing Software: Comparison of the enhanced images were also compared visually with the original color data set and closely investigated on a pixel-to-pixel basis using *Corel Photopaint*.

RESULTS

Remote Sensing Package Software: Figure 3 displays the classification of the color aerial photograph. Some clarity of the image is lost due to the black and white format required by this paper, but the trends are still apparent. The black lines in all the classified images were added by the author to allow the reader to better interpret the trends. Using the remote sensing software, visual comparison showed distinct variance in the data sets using the classified color aerial. The effects of turbidity, surface roughness and suspended sediment are clearly evident on the classified data set. The minor differences in the classification (from the original color photos) were due mainly to the diverse lighting, which occurs on imagery containing water.

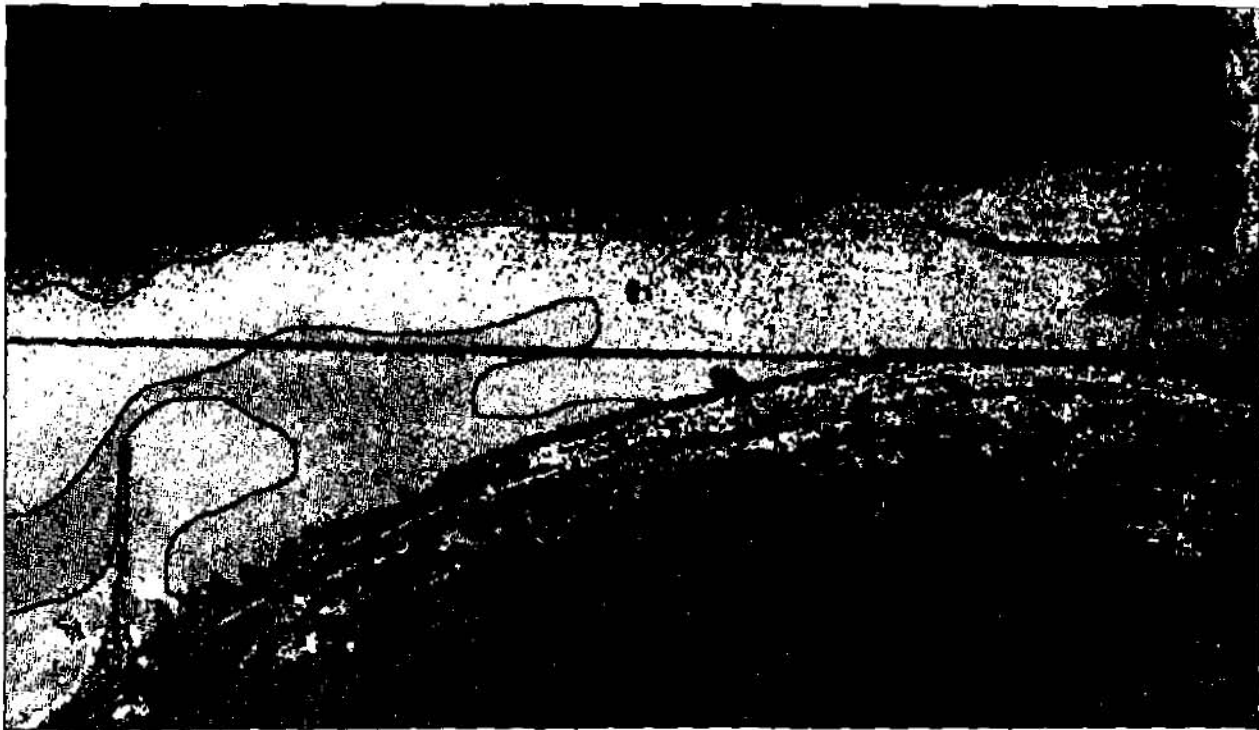


Figure 3: Aerial Color Classification Using Remote Sensing Scheme.

The addition of the near-infrared band to the classification did not make a difference, due to the fact that this band was represented by the red band in the classification. Scanned photography was digitally subdivided into red, green, and blue components. The difference in information between the infrared and visible band was not a factor in classification. Figure 4 shows the classification of the color infrared aerial. This classification was unable to enhance suspended sediments or flow patterns due the specular reflection of the photograph of the input photo. Specular reflection is a characteristic of water where light at similar incident angles is reflected in one direction, giving the surface a bright, overexposed look. Light entering a camera comes

through the lens at different angles, thus exposing the film at different levels. With surfaces such as water, these exposure differences can vary greatly. On river photography, similar areas of the river were visually different, based on the above-mentioned specular reflectance characteristics. The exposure differences led the classifier to believe that specular differences existed in areas where water characteristics were similar. Due to the specular reflectance of the photos, an aerial with the study area near the outer edges of the photo had to be used for this study. This scenario does not represent the ideal situation because of vignetting effects. Vignetting is a property of a lens where the edges of an exposed negative are softened due to the reduction of incident light coming through the outer edges of the lens. The light coming through the center of the lens is not affected as much as light coming through the edges of the lens. The circular pattern of color on this classified image represents this effect, therefore the desired results were not achieved.



Figure 4: Aerial Color Infrared Classification Using Remote Sensing Scheme.

Standard Image Processing Software: Image enhancements of the color aerial using *Corel Photopaint* did as good or better in splitting reflectance values into different classes. Figure 5 shows the enhanced output image from this scheme. The resultant image showed very distinct differences in color due to the suspended sediments tracing the flow patterns in the water column.



Figure 5: Aerial Color Enhanced Image Using Simplistic Filter (Corel Photopaint).

CONCLUSIONS

By using the classified and enhanced color aerial photography, engineers could, for the first time, visualize the detrimental flow patterns and cross currents that develop in the upstream-pooled area of the lock approach. The remote sensing methodology indicated that the navigation problem was mainly due to currents being subtly deflected off an existing rock bluff located on the right descending riverbank. The resulting cross current pattern has played havoc to downbound tows approaching the lock chamber. As pilots push through these cross currents, they run the risk being caught in these currents as they try to align their tow with the lock chamber. The danger continues as the tow enters the lock and the stern of the towboat is still vulnerable to the cross current pattern. The pilots must continually push their stern against these currents. There is absolutely no margin for error allowed during these critical periods. An additional push boat or helper boat is usually required for added safety. Failure to compensate for these currents during this scenario can cause the towboat to break away from the barges, endangering the lives of the crew and the structural integrity of the lock and dam.

The remote sensing data served as a critical reference for the development of a physical sediment modeling effort. Bathymetry and flow visualization collected from the model was compared to the remote sensing data during model calibration. Once base conditions were established in the model, engineers were then able to study a variety of design alternatives and arrive at the most

cost effective and efficient structural solution to the navigation problem. Figure 6 is a flow visualization photo of the model showing similar flow patterns during base test conditions. Notice the similar “shadow” of current immediately downstream of the dike as compared with the image enhanced photo. The flow visualization from the micro model, as well as field data, confirms the existence of the outflow problem as seen through remote sensing techniques.



Figure 6: Flow Visualization Showing Outdraft in the Lock & Dam 24 Micro Model.

FUTURE USAGE CONSIDERATIONS

The more simple approach using *Corel Photopaint* or other type standard image processing is a low cost option well worth the investment for the river engineer. The key in using any approach is to obtain high quality photography, which contains an upstream “flow seeding”, mechanism such as suspended sediment from a tributary, ice, drift, or turbulence. Without a seeding mechanism, the water column is homogenous throughout and the differences in color cannot be observed, therefore making the flow patterns unrecognizable.

The quality of aerial photography used as an input for a remote sensing scheme is critical. Information is lost between the surface of the earth and the camera, when exposing and printing the film, and during the conversion of the photographic hardcopy to digital imagery. Loss of information in the scanning process and differences in the incident angle of light entering the camera can greatly affect the ability to use both analysis schemes described in this paper. An all digital source, such as that flown using a multi-spectral scanner or thematic mapper could improve the aerial photographs collected for remote sensing. In this study, the classifier mainly assigned values based on red, green, and blue reflectance. A digital source would allow comparisons in more than three bands of the spectrum. Increased resolution at greater flying

height influences differences in exposure based on incident light angle. The ideal scene would contain no difference in specular reflectance of the water based on incident light angles, thus allowing suspended sediment, turbidity, and surface roughness effects on flow to be analyzed without interference. Hyperspectral digital scanner data (having hundreds of narrow spectral bands) could provide enough variance to enhance the classification.

REFERENCES

Colwell, Robert N., 1968, Remote Sensing of Natural Resources, Scientific American, January 1968, Vol. 218, No.1, PP.54-69.

US Army Corps of Engineers Interim Report, 1972, The Use of Remote Sensing to Obtain Data For Describing the Large River, Colorado State University Engineering Dept., CE Research # CER71-72MMS-32.

Collins, W.G., Nagarajan, R., and Marathe, G.T., 1993, Identification of Flood Prone Regions of Rapti River Using Temporal Remotely-Sensed Data, International Journal of Remote Sensing, Vol. 14, No. 7, 1297-1303.

Davinroy, Robert D., 1994, Potential For Remote Sensing of Rivers For Potamologic Applications, Project Report, Advanced Remote Sensing Course, University of Missouri-Rolla, Project Course Work.

Corel Photopaint, Version 5.0, 1995.

MGE Advanced Imager User's Guide, Intergraph Corporation, 1995.

Davinroy, Robert D., Gordon, David C., and Hetrick, Robert D., 1997, Navigation Study at the Approach to Lock and Dam 24, Upper Mississippi River, Hydraulic Micro Model Investigation, US Army Corps of Engineers Technical Report M2, St. Louis, Mo.

A DATA GATHERING TECHNIQUE FOR RIVER RESOURCE IDENTIFICATION

Dr. Marshall Flug, Water Resources Engineer
Biological Resources Division, US Geological Survey
4512 McMurry Avenue, Ft. Collins, CO 80525-3400

Heather L. H. Seitz, Research Assistant
Civil Engineering Department, Colorado State University
Ft. Collins, CO 80523-1372

Dr. John Scott, Research Associate
Civil Engineering Department, Colorado State University
Ft. Collins, CO 80523-1372

Abstract: Over the past twenty years, a variety of legislation has arisen which necessitates extensive data collection for many rivers, aquatic and riparian areas. A study conducted jointly by the United States Geological Survey (USGS)/Biological Resources Division (formerly the National Biological Service) and Colorado State University tested one method of taking measurements of a river system. Although this method is not new, published accounts of the procedure are not available. Recent interest in habitat, especially that of endangered species, has sparked a need to collect information about larger aquatic areas in an accurate, cost-effective and timely manner. Trials were run on two field trips to the Green River near Dinosaur National Monument (a tributary to the Colorado River in northeastern Utah), in June and August of 1995. Because the technique allowed river sections to be sampled faster and safer than with traditional survey techniques, many locations (transects) within a reach were evaluated. A large area of subsurface geometry and water depth was measured and recorded using a sonar scanner, an inexpensive and off-the-shelf piece of equipment. The paper will briefly describe the procedure followed during the field experiment; then the method of data retrieval and analysis will be reviewed, along with the results obtained; and lastly, a discussion on the use and applications of the sonar scanner for hydraulic and habitat studies.

Key Words: Sonar measurement, rivers, cross-sections, aquatic habitat, instream flow.

INTRODUCTION

The use of sonar to study underwater features is not a new practice (Smoot and Novak, 1969) although it has not yet become widely accepted. This experiment was performed to test the validity of the method for hydrologic and habitat measurements. A short explanation of the driving forces behind this and other studies will be followed by a summary of some traditional methods and other efforts with sonar equipment.

Why are so many rivers being studied so intensely anyway? Due to an increased awareness of anthropogenic impacts on the environment there has been a rise in the number of riparian and aquatic areas of concern to both environmental and government parties. Also, as a requirement of the Endangered Species Act, the factors which adversely impact a species and its habitat must be quantified. If a federally funded project will affect a habitat or species, then an Environmental Impact Statement must be completed, which requires extensive measurements. For most studies, the data to be collected consists of much more than just the water depths and temperatures. Many in the scientific community wish to know the substrate types and locations, water velocities, and

other features of the area such as shoreline vegetation.

In the past, several methods were used to collect data, with rods and sounding bombs being the most widely known. Sonar techniques which have been tried include combinations of strip charts and tag (or tie) lines (Rantz et. al., 1982). The Acoustic Doppler Current Profiler is an instrument which provides instantaneous discharge, depth, and velocities, continuously in a column of water from the surface to the bed. All of these systems have limitations, in terms of safety, cost, accuracy or the number of cross-sections which can be profiled in a reasonable amount of time. However, sonar sounders have been tested in a variety of applications, from checking for erosion around bridge piers (Landers et. al., 1993) to mapping of ocean floors (Limonov et. al., 1997) and are being recognized for their benefits.

SITE AND FIELD PROCEDURE

The site selected (Figure 1) was a stretch of the Green River in northeastern Utah near Dinosaur National Monument which was just over a mile in length. This reach has about four feet of depth, more than the required operational depth for the equipment during the planned study months; six transects that were previously surveyed by traditional methods and permanently marked with a bar and cap system; and was located just downstream of the USGS gage at Jensen, Utah, which is regularly surveyed in the summer months. Both of these prior surveys would be used to test the sonar for accuracy. Another major reason this particular site was chosen is its relevance as a habitat for the endangered Colorado Squawfish. Not only is it necessary to complete many cross-section profiles, but this must be done several times over the course of a spawning season in order to understand how the deposition and erosion of sediment affects the squawfish.

Procedure in the field evolved during several prior testing sessions, and indeed, even from the June trip to the August trip. The end result was a three person operation. Each crew member had a variety of responsibilities. Piloting the boat entailed the challenge of keeping a straight path across the river and, of course, ensuring a safe passage for all on board. For these river conditions a 16 foot flat-bottom boat with an outboard jet engine was used, which was capable of moving through both high currents and shallow waters. Near the front of the boat one person was responsible for the width measurements and communicating when preset width intervals were reached as the boat crossed the transect. These width measurements were generally identified with a hip chain at 5 meter (16.7 feet) intervals, except for the Jensen Gage transect which had the USGS overhead cable with marked widths at five foot (1.5 m) increments. The third person at the rear of the boat was responsible for the computer, checking that the file was receiving and recording output from the sonar sounder device, and also marking the widths on the sounder's monitor-keyboard, which are concurrently imprinted in the data file, as called out from the bow of the boat.

The connection between the sounder and the computer, an ordinary laptop, was made with a nine-pin cable wired to fit the connector included with the sounder. This wiring was the only adjustment made to any of the equipment, everything else was used straight out of the box. The transducer was mounted on the factory supplied bracket assembly which was then coupled to a metal rod, so that the depth of the transducer underwater could be controlled.

DATA RETRIEVAL AND ANALYSIS

Data from the sounder was received in a Terminal file in Windows, as ASCII text, with a single transect composing one file. These were easily imported into Quattro Pro where a Macro command was written to search out the lines containing depth, velocity, and temperature information, along with the coded markers. Once the data were pulled out of the files, charts could be created in which the depths and widths were linked via the markers.

Analysis of the data consisted of two parts, graphical and statistical. While specific results of these analyses will be discussed below, a few things should be mentioned about the analysis process. Most importantly is the fact that anyone with a spreadsheet program and a calculator should be able to perform a similar analysis on data from a sounder. There is no special equipment, program, or skill required other than a basic knowledge of graphing, command writing, and statistical equations. Analysis was performed on both sets of collected sonar data. Also comparisons between the sets, and testing of the relationship of the sonar data to previously collected traditional data surveys were evaluated. Lastly, graphs were made of points measured by the sonar sounder, with lines added to provide a continuous plot. The statistical analysis was accomplished using only measured data points, not from the graphic plots.

RESULTS

Both graphical and statistical analysis are presented in this section and are intended to show both the accuracy and the precision of this method. Figure 2 addresses the precision, or repeatability, in measuring with a sounder. Included are four traverses of Transect 1, performed on the same day, shown in feet of elevation. Each of these traverses included 21 measured transect points, with a sample variance for each traverse calculated by comparison to the average computed transect depth. The computed average of these four sample variances yields 0.24 ft (0.07 m) in an average water depth of 4.3 ft (1.3 m) or approximately 6% of the depth.

Accuracy is the distance from a "true" measurement, which in this case was presumed to be those measurements taken by the USGS. This is detailed for the Jensen Gage in Figure 3, a comparison of two Geological Survey measurements which bracket a set of three sonar measurements in both flow volume and time. The first USGS measurement on July 13, 1995 was at a flow of 14,400 cubic feet per second (432 cubic meters per second), the second was on August 29, 1995 at 1,740 cfs (52.2 cms), and the sonar data was collected on August 16 when the flow was 2,050 cfs (61.5 cms). Even with the differences in flow between the three dates, it is easy to see that the sonar average is very close to the Survey results for the middle 150 ft (45 m) of the transect. However, for a more quantitative analysis, it is best to throw out depths less than 2 ft (0.6 m) for all August measurements (due to equipment limitations), and then perform the statistical analysis. This corresponds to the widths from 70- 310 ft (21-93 m) and results in an average mean square deviation of 0.07 ft (0.021 m).

As with any study, these results are influenced greatly by the problems with the execution of the

method. The largest of these is that, by design, there is no tie line to keep the boat on a straight path. However, it would seem that near the shore, the captain would be able to keep the boat on the same line better due to lower velocities and better sight of the bar and cap marking the end-point, yet at the Jensen Gage transect, the opposite appears true. Two types of problems are related to the shoreline, the first is the coordination of the crew in pushing off, or coming to a stop, measuring widths and collecting data, each a task which requires concentration. Secondly is the limited accuracy of the sonar in shallow waters. Another opportunity for the introduction of errors at any point across the transect is related to the composition of bed material. Transect 1 has cobbles which, from traverse to traverse, can be measured either directly on top of or adjacent to the cobble. Likewise, an exact location in a transect may exhibit a different depth because the cobbles at that location have moved. For a sand bed channel, bedforms and moving sand contribute to variations among profiles which may measure changes in the depth by several inches.

APPLICATIONS

There are several applications for this technology in water resources. The first of these is for input into water resources models, in particular hydraulic routing models. A HEC-2 model was developed to assess the flow characteristics upon which to make recommendations on the operation of the major upstream Bureau of Reclamation reservoir in the Green River system, Flaming Gorge Reservoir. The standard HEC-2 model was revised to include sediment transport capabilities in addition to the hydraulic analysis. Within the reach of the Green River as it flows through the lower end of Dinosaur National Monument is a split-flow section as shown in Figure 1 and known to contain a gravel-bed area used by Colorado squawfish for spawning. It has been thought that this section, the right hand braid of the split-flow reach, experiences different hydraulic and sediment transport characteristics than the left hand and dominant braid of the channel. The timing of sediment deposition and transport is critical to the spawning of the squawfish and the continued population of the fish in the Green and Colorado River systems. The use of multiple transects at multiple times during the sediment deposition and scour periods as functions of the hydraulic conditions was necessary to calibrate the model and for use as a predictive tool for future reservoir operations. The use of the sonar device allowed for these multiple transects, efficiently and accurately. In addition, the output of the sonar device on the monitor indicated the nature of the bed composition, which was further checked by hand probes in the three to four feet deep channel. The sonar device and measurement technique provided for a non-intrusive approach to field data acquisition which left the gravel beds undisturbed and any deposited eggs intact.

A second application using this sonar technology is for habitat area quantification. Habitat studies routinely collect large amounts of depth, velocity, and temperature data for a river, often spending weeks in the field to do so. Width and depth measurements may be used to calculate the inundated area of a reach, commonly defined as the wetted bed surface area per 1,000 feet of river length. Using natural hydraulic or habitat features, the reach is divided up, with each length including a measured transect. Transect lengths are multiplied by the widths between marked points (i.e. every 5 m) to get the area of each point on the transect. The area above or below any depth is found by summing up the appropriate areas found in the previous step. Figure 4 shows a plot of the inundated area versus depth in the reach of river from Transect 1 to Transect 6, from data collected using the

sonar scanner in only a few hours. This could be used by biologists or others to determine the amount of suitable habitat for a species in a river reach, depending upon the species, its life stage and needs during each stage.

One final use of the data was to develop a three-dimensional figure of the habitat area from Transect 1 to Transect 6, Figure 5. It should be noted that each of these transects were measured multiple times on the same day, so those lines are averages. By referring back to Figure 1, a comparison in the amount of information gained by adding the depth measurements can be made. This information could include a variety of habitat and hydraulic features, such as the island in the middle of Transect 4, which traditional surveys might have difficulty with.

CONCLUSIONS

It is worthwhile noting that every method of measuring cross-sections has its faults. Some are less accurate, some less precise, others may be costly or take too long to be efficient. Using a sonar sounder to create a picture of the stream bed is faster than using a rod, safer than being tethered to an overhead line, and costs significantly less than the Acoustic Doppler Current Profiler. Perhaps the biggest advantage is not the cost or the speed, but the sheer amount of data which can be collected by a small group in as little as one day. More importantly, this data has been shown to be consistent, both from run to run on the same transect, as well as with surveys taken by alternate methods, by alternate groups. One suggestion for equipment modification to improve the collected data is the automatic recording of sonar echoes presently only displayed on the monitor, which identify the bed and substrate composition.

REFERENCES

Landers, M. N., Mueller, D. S., Trent, R. E., 1993, Instrumentation for Detailed Bridge-Scour Measurements. Proceedings of Hydraulic Engineering 1993, Specialty Conference of the American Society of Civil Engineers, San Francisco, CA.

Limonov, A. F., van Weering, T. C. E., Kenyon, N. H., Ivanov, M. K., Meisner, L. B., 1997, Seabed Morphology and Gas Venting in the Black Sea Mud Volcano Area: Observations with the MAK-1 Deep-Tow Sidescan Sonar and Bottom Profiler. *Marine Geology*, 137, 121-136.

Rantz, S. E., et. al., 1982, Measurement and Computation of Streamflow. USGS Water Supply Paper 2175, Chapter 5.

Smoot, G. F. and Novak, C. E., 1969, Measurement of Discharge by the Moving Boat Method. National Handbook of Recommended Methods for Water-Data Acquisition, Office of Water Data Coordination, USGS, Chapter 11.

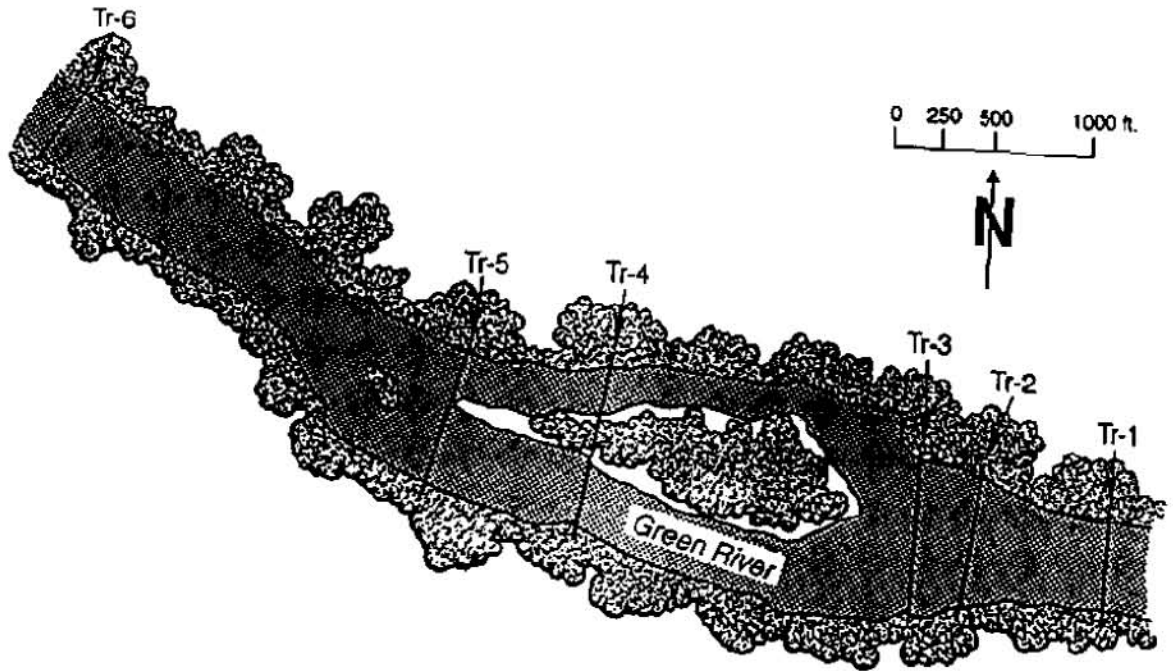


Figure 1. Green River near Dinosaur National Monument

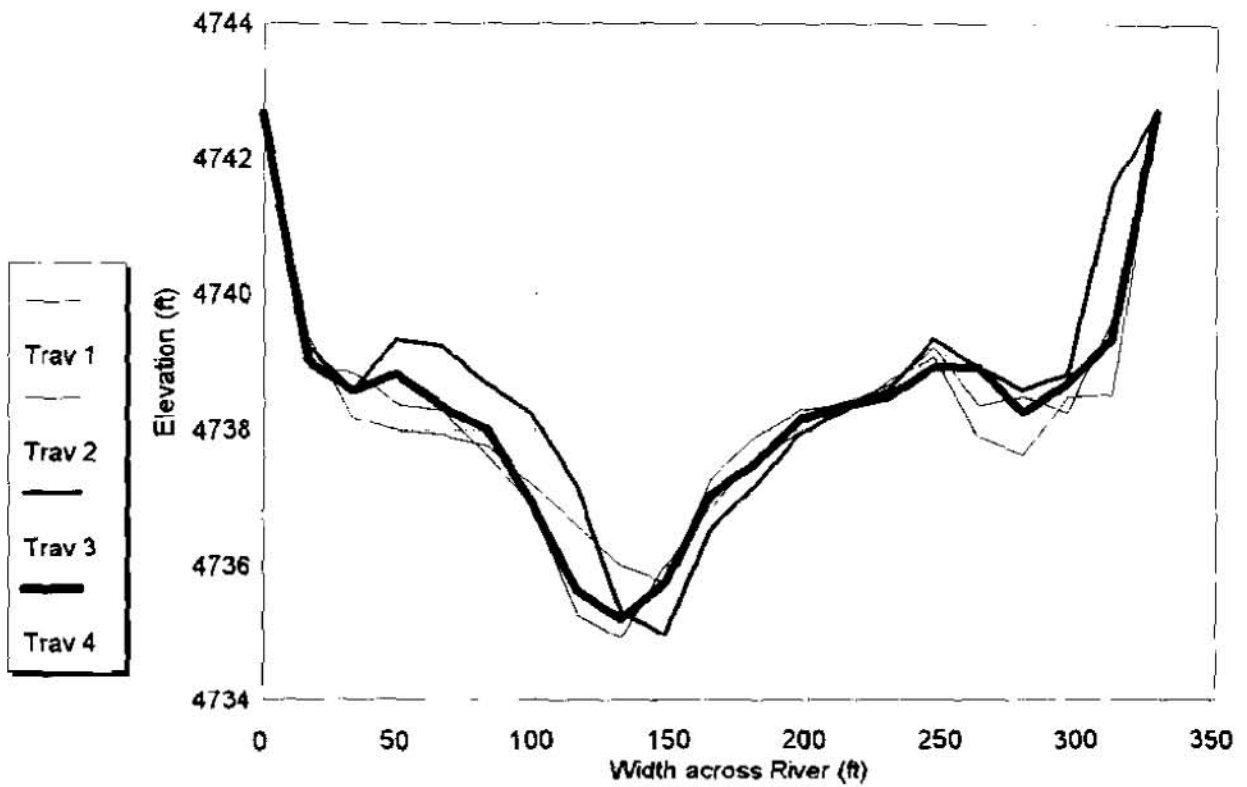
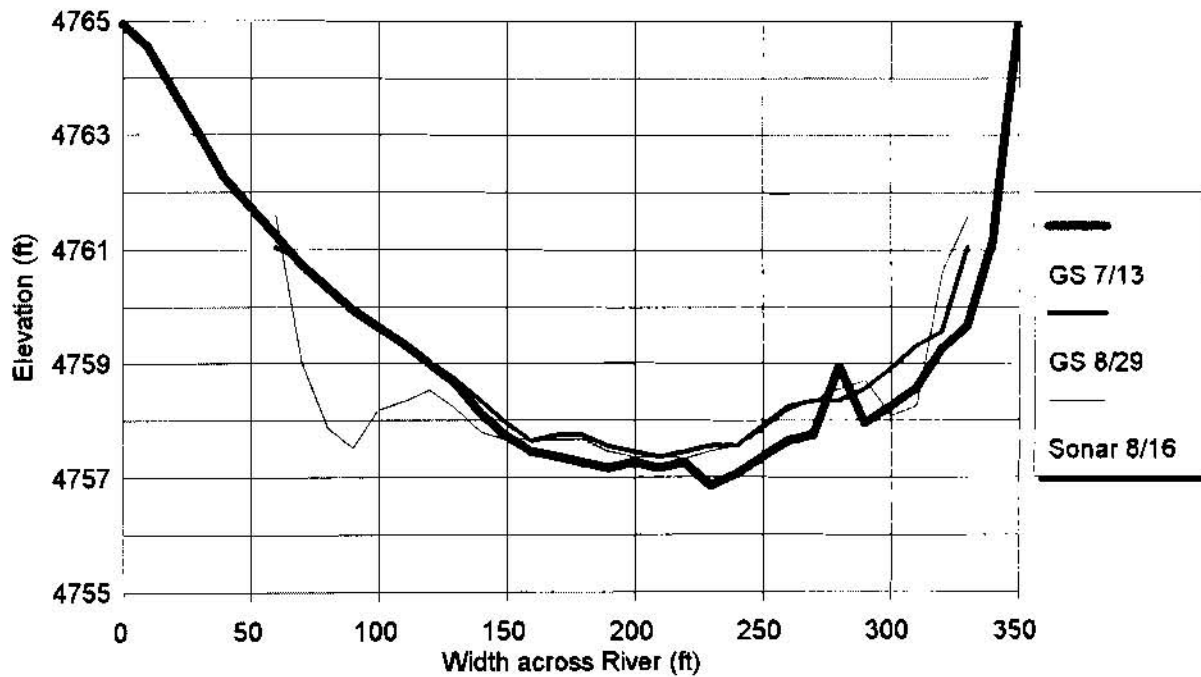


Figure 2. Elev. of Transect 1, 7/16/95



**Figure 3. Jensen Gage Transect:
USGS Data vs. Sonar Avg**

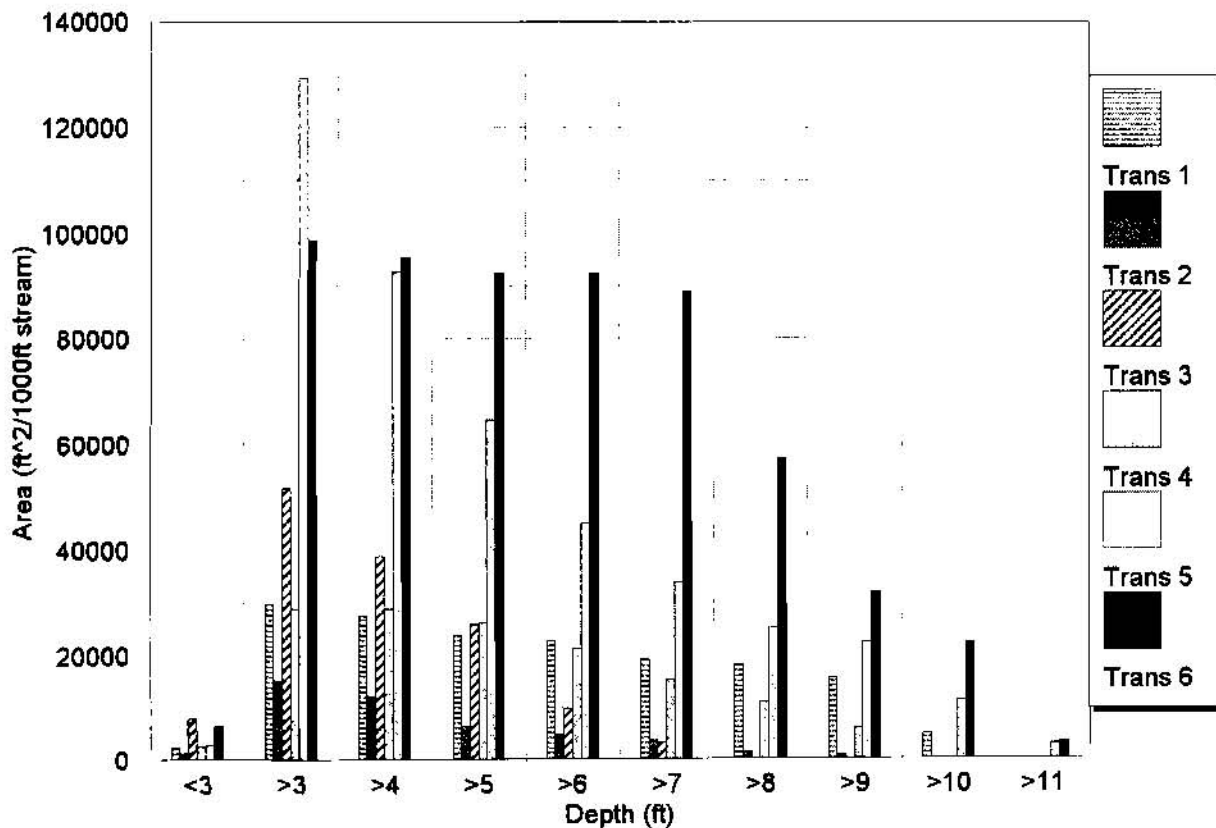


Figure 4. Inundated Area, Tr1-6, 6/29/95

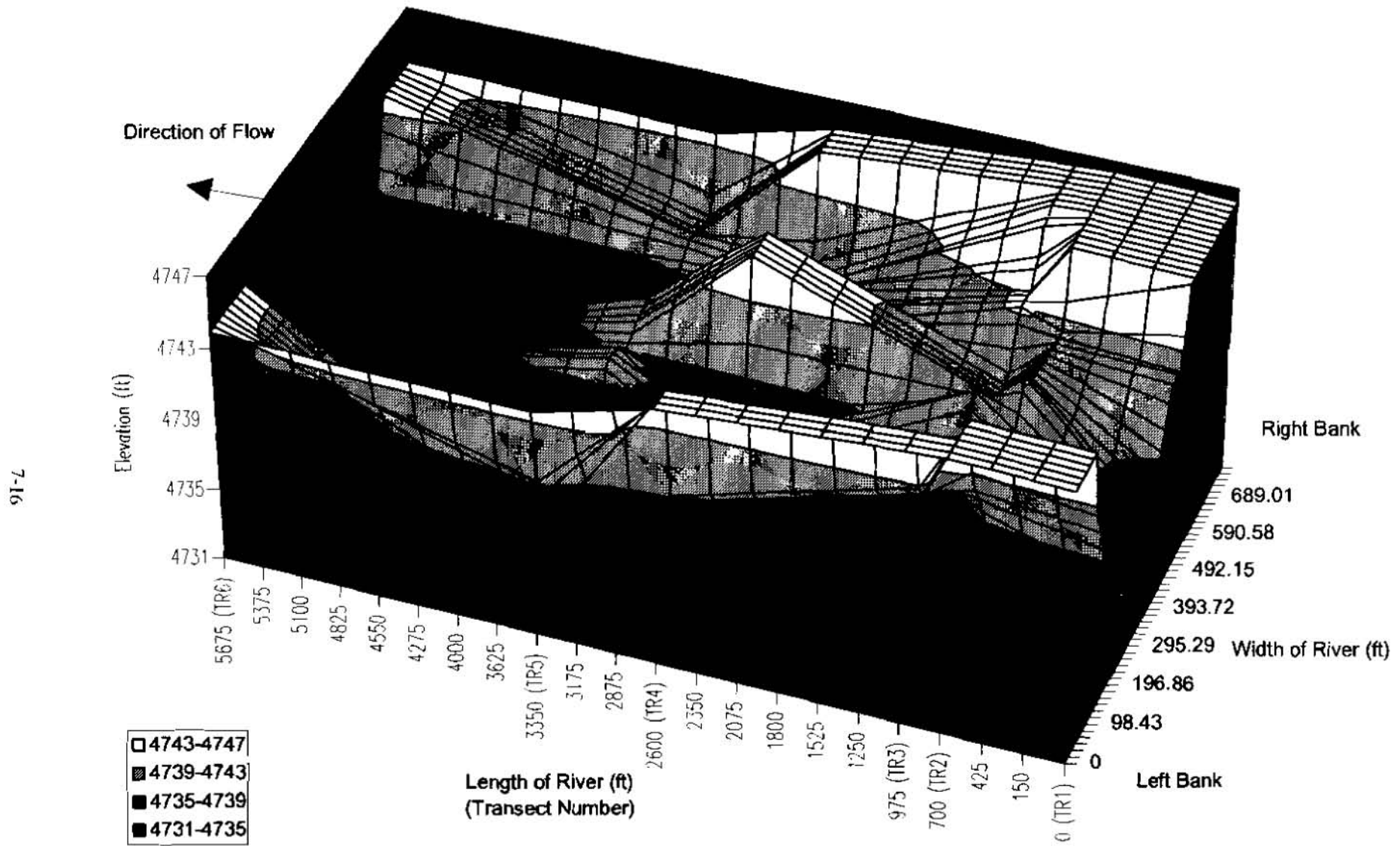


Figure 5. Three Dimensional Graph of Green River Stretch

THE RIPARIAN ECOSYSTEM MANAGEMENT MODEL (REMM): EVALUATION OF THE HYDROLOGY COMPONENT^{1,2}

**Shreeram Inamdar, PostDoctoral Associate ^{*,3}; Joseph Sheridan, Hydraulic Engineer ⁺;
Randy Williams, Agricultural Engineer ⁺; David Bosch, Hydraulic Engineer ⁺;
Richard Lowrance, Ecologist ⁺; L.S. Altier, Asst. Professor[@]; Dan Thomas, Associate Professor ^{*};
^{*} Biological and Agricultural Engineering, University of Georgia, Tifton, GA;
⁺ USDA-ARS, Southeast Watershed Research Laboratory, Tifton, GA;
[@] College of Agriculture, CSU, Chico, CA.**

INTRODUCTION

The Riparian Ecosystem Management Model (REMM) has been developed for natural resource agencies and researchers as a tool that can help quantify the water quality benefits of riparian buffers. REMM is based on buffer system specifications recommended by the U.S. Forest Service and the USDA-Natural Resources Conservation Service as a national standard (NRCS, 1995; Welsch, 1991). The riparian system is characterized in the model as consisting of three zones parallel to the stream and representing increasing levels of management away from the stream (see Figure 1 in Lowrance et al., 1998). These zones include a narrow, undisturbed forest area adjacent to the stream for protecting the stream bank and aquatic environment, an area with a managed woody vegetation for sequestering sediment and nutrients from upland runoff; and a grassed strip for dispersal of incoming upland surface runoff and sediment and nutrient deposition. The soil is characterized in three layers through which vertical and lateral movement of water and associated dissolved nutrients are simulated (Figure 1). The uppermost soil layer is covered by a litter layer which acts as a mixing layer and which interacts with surface runoff. A more detailed discussion of the model scope and structure is provided in the companion paper by Lowrance et al. (1998) and hence is not repeated here.

REMM simulates: (a) the movement of surface and subsurface water; (b) sediment transport and deposition; (c) transport, sequestration, and cycling of nutrients; and (d) vegetative growth. To simulate each of these processes REMM has four major modules: hydrology, sediment, nutrient, and vegetative growth. This paper is limited to the description and evaluation of the hydrology component.

MODEL DESCRIPTION

Water movement and storage is characterized by processes of interception, evapotranspiration, infiltration, vertical drainage, surface runoff, subsurface lateral flow, upward flux from the water table in response to evapotranspiration losses, and return flow. These processes are simulated for each of the three zones. The storage and movement of water between the zones is based on a combination of mass balance and rate controlled approaches. Each of these processes are simulated on a daily basis and are described briefly in the following paragraphs. For a complete description of the processes and the equations used, the reader is referred to Altier et al. (In press).

Interception losses occur in the vegetation canopy and litter layer. Canopy interception is an exponential function of the canopy storage capacity and the amount of daily rainfall and is simulated using a modified form of the Thomas and Beasley (1986) equation. Canopy storage capacity on any given day is a product of the leaf area index (LAI) on that day and a species-specific storage capacity per unit LAI. Precipitation falling through the canopy (throughfall) is subjected to litter interception. Similar to canopy interception, litter interception is determined by the depth of the litter at any given time and the litter storage capacity.

¹ Contribution from the USDA-ARS, Southeast Watershed Research Laboratory, P.O. Box 946, Tifton, GA 31793, in cooperation with University of Georgia Coastal Plain Experiment Station.

² All programs and services of the USDA are offered on a nondiscriminatory basis without regard to race, color, national origin, religion, sex, age, marital status, or handicap.

³ Biological and Agricultural Engineering, University of Georgia, P.O. Box 745, Tifton, GA 31793; phone: (912) 386 7210; fax: (912) 386 7294; Email: rivers@tifton.cpes.peachnet.edu.

While intercepted water is available on the vegetative canopy, evaporation of the intercepted water occurs. During this period all the radiant energy is used to evaporate the intercepted water. Transpiration proceeds after all moisture on the canopy has been evaporated. Potential rates of leaf evaporation and transpiration are both computed using a modified form of the Penman Monteith equation (Running and Coughlan, 1988), except that leaf evaporation is not constrained by stomatal resistance. Actual transpiration loss is limited by the availability of moisture in the soil and competition among the roots of the various plant types present. As the soil dries, water extraction depends on both the root distribution and the rate at which water can move to the roots. The maximum rate of water uptake from a layer is limited by its soil hydraulic conductivity. Unsaturated soil hydraulic conductivity is described by Campbell's (1974) equation. This allows any excess demand that is not realized by a layer to be transferred to the layer below. Litter evaporation is simulated using procedures similar to that used for evaporation of intercepted water on leaf surfaces. Radiation energy in excess of that consumed by litter evaporation is used to drive soil evaporation from the top mineral soil layer. Soil evaporation is computed in two stages (Gardner and Hillel, 1962).

The total depth of water available for infiltration at the soil surface within a zone is the sum of the throughfall depth and overland flow depth from the upslope zone or field. In most conditions the sum of incoming upland runoff and throughfall depth is less than the high infiltration capacity of the riparian soil. Under these conditions runoff will infiltrate at the rate of application. Only during high intensity storms does the runoff and throughfall rate exceed the infiltration rate. In such conditions, infiltration in the model is simulated using a modified form of the Green-Ampt equation (Stone et al., 1994). Water in excess of infiltration is assumed to be surface runoff. Surface runoff entering the riparian area is routed downslope using a simplified procedure based on the depth of runoff and flow velocity.

Vertical drainage from a soil layer occurs when soil moisture exceeds the field capacity. The amount drained also depends on the available storage capacity of the receiving layer. The rate of drainage is controlled by the lesser of the vertical hydraulic conductivities of the draining and receiving layer. Vertical unsaturated conductivity is simulated as a function of the soil moisture content using Campbell's equation (Campbell, 1974). In the presence of a shallow water table, overlying soil layers are maintained at a higher (less negative) matric potential and consequently higher soil moisture contents. Assuming that the soil layer is in equilibrium with the water table, the matric potential at the mid point of a soil layer can be determined by assuming that the pressure head at that point can be approximated by the height of the point above the water table. The moisture associated with this point can then be determined using the moisture retention curve relating matric potential to the soil moisture content and described by Campbell's equation.

In the absence of a shallow water table, evapotranspiration losses from a soil layer are limited by the soil moisture conditions within the soil layer (with wilting point moisture content being the lower limit). In the presence of a shallow water table though, a steady upward flux will occur from the water table to the soil layer to replenish ET losses from the layer. The rate of upward water movement is determined by the matric potential gradient, unsaturated hydraulic conductivity, and the depth of the water table below the soil layer. This evapotranspiration flux is determined using the Darcy Buckingham equation as described by Skaggs (1978).

Subsurface lateral movement is assumed to occur when a water table builds up over the restricting soil layer. The lateral movement of the water is simulated using Darcy's equation. In the model, saturated lateral soil conductivity is assumed the same as vertical saturated conductivity. Downslope subsurface flow between the component zones is driven by the gradient of the water table. The potential hydraulic gradient that determines the subsurface movement from zone 1 to the stream is assumed equal to the smaller of the surface slope of zone 1 and the gradient from the water table elevation from the mid point of zone 1 to the stream thalweg. Stream thalweg is a user defined input. Currently, the model does not simulate the influence of streamflow on the hydraulic gradient or the recharge of zone 1 from streamflow. Towards the downslope edge of the riparian slope subsurface moisture building up over the impeding soil horizon tends to reach the surface. In such conditions excess subsurface water is released to the surface as return flow or exfiltration. In addition, for a completely saturated soil profile any excess throughfall or upslope surface runoff contributions will not infiltrate but are considered as saturation excess overland flow.

MODEL EVALUATION

Parameterization

REMM hydrology component was evaluated using data collected at the riparian site at the University of Georgia Gibbs farm

near Tifton, Georgia. A detailed description of this site along with the type of data being collected and data collection facilities is provided in Lowrance et al. (1998), Sheridan et al. (1996; 1998), and Bosch et al. (1996). Essentially, this site has an upland contributing area and a three zone riparian buffer which are being monitored since 1992. The riparian buffer consists of a 8 m long grass filter in zone 3, a 50 m long managed pine forest in zone 2, and a 15 m long hardwood forest zone in zone 1 (Figure 1 in Lowrance et al., 1998). While the riparian buffer is being maintained under three different treatments, only data from the mature forest treatment are being used here for model evaluation (Figure 2 in Lowrance et al., 1998). Briefly, the data collected at this site included - [a] weather information such as solar radiation, air and soil temperatures, wind speed, and rainfall amounts and duration; [b] surface runoff at the field-grass zone interface, grass-pine forest interface, at mid point of the pine forest zone and at the conifer-deciduous forest interface (Sheridan et al 1998); and [c] water table elevations under the upland contributing field and each of the three component zones of the riparian buffer (Bosch et al., 1996).

To evaluate model performance, model predicted water table elevations and surface runoff were compared to those observed at the experimental site for years 93-96. Water table comparisons were made on a daily basis for recording wells 01, 02, and 03 located in zones 3, 2, and 1, respectively (Figure 2 in Lowrance et al., 1998). Surface runoff comparisons were made on an annual and monthly basis for positions 2 and 3 corresponding to surface runoff collectors at the grass-pine forest and pine-hardwood forest interfaces, respectively. A general evaluation of the model was also conducted by developing annual hydrology budgets for predicted results and comparing these budget values with available literature estimates. Results from each of these procedures are discussed in the following section.

Prior to evaluation runs, the model had to be initialized for: [a] daily weather information; [b] daily surface and subsurface runoff loading from the contributing field; and [c] parameter values representing the topographic, soil, and vegetative conditions with the riparian buffer. Daily weather data for the years 92-96 was provided as an input which includes: rainfall amount (mm), rainfall duration (hr), maximum air temperature (C), minimum temperature (C), solar radiation (langley's/day), wind speed (m/s), and dew point temperature (C).

Runoff collected by the surface runoff sampler at the field grass interface (position 1) was used to generate the daily surface runoff depth (mm per unit contributing area) to the model. Daily subsurface flow loading to the buffer (mm per unit contributing area) was computed using hydraulic gradient between upland wells P3 and P4 (Figure 2 in Lowrance et al., 1998) and recording well 01 (well in zone 3), water table thickness at well 01, and assuming a darcy flux rate of 48 mm/hr (Bosch et al., 1996). Values for parameters describing the buffer dimensions, soil, and vegetation characteristics were derived from currently measured data and previously published literature for the Gibbs farm site (Bosch et al., 1996; Perkins et al., 1986; Sheridan et al, 1996). A listing of the important selected parameters and the corresponding values used is provided in Table 1. For a listing of the parameters used to describe the grass/pine/hardwood vegetation the reader is referred to the companion paper by Altier et al. (1998). It is important to note that the values used to describe the topography, soil, and vegetation were best estimates based on measured data and were not adjusted or calibrated during evaluation runs.

Results and Discussion

Model predicted and observed daily water table elevations for wells 01 (zone3), 02 (zone 2), and 03 (zone 1) were compared for years 93-96. An annual average of the error between model predicted and observed elevations (Table 2) reveal that for the four years simulated, predicted water table elevations were closest to the observed during the drier years (95-96). During the wetter years (93-94) predicted water table elevations in zone 3 and zone 2 wells were much closer to the soil surface than those observed. A plot of the daily values for the year 96 reveals that observed water table elevations for zone 3 and zone 2 wells varied from 0 m from the surface during winter to a depth of 2 m or more during summer. This drop in water table is primarily attributed to high ET demands within these two zones (Bosch et al., 1996). In contrast, for zone 1 well this variation was limited to less than 0.9 m. Though model simulations were able to reasonably capture the drop of the water table during summer for zone 1 well, simulated water table depths for zone 3 and zone 2 wells were not as deep (below the surface) as those observed (Figure 1). This most possibly indicates that the model underestimated ET losses for zones 3 and 2. The largest fluctuations in the observed water tables for the three wells occurred during the summer months when the dry soil profile was subjected to high intensity convective storms. Model predicted water table elevations did not seem to reflect the flashy variations to the extent that were observed. Overall, the model predicted water table elevations are good considering that the soil parameters used in the model were based on best literature and measured estimates and were not calibrated.

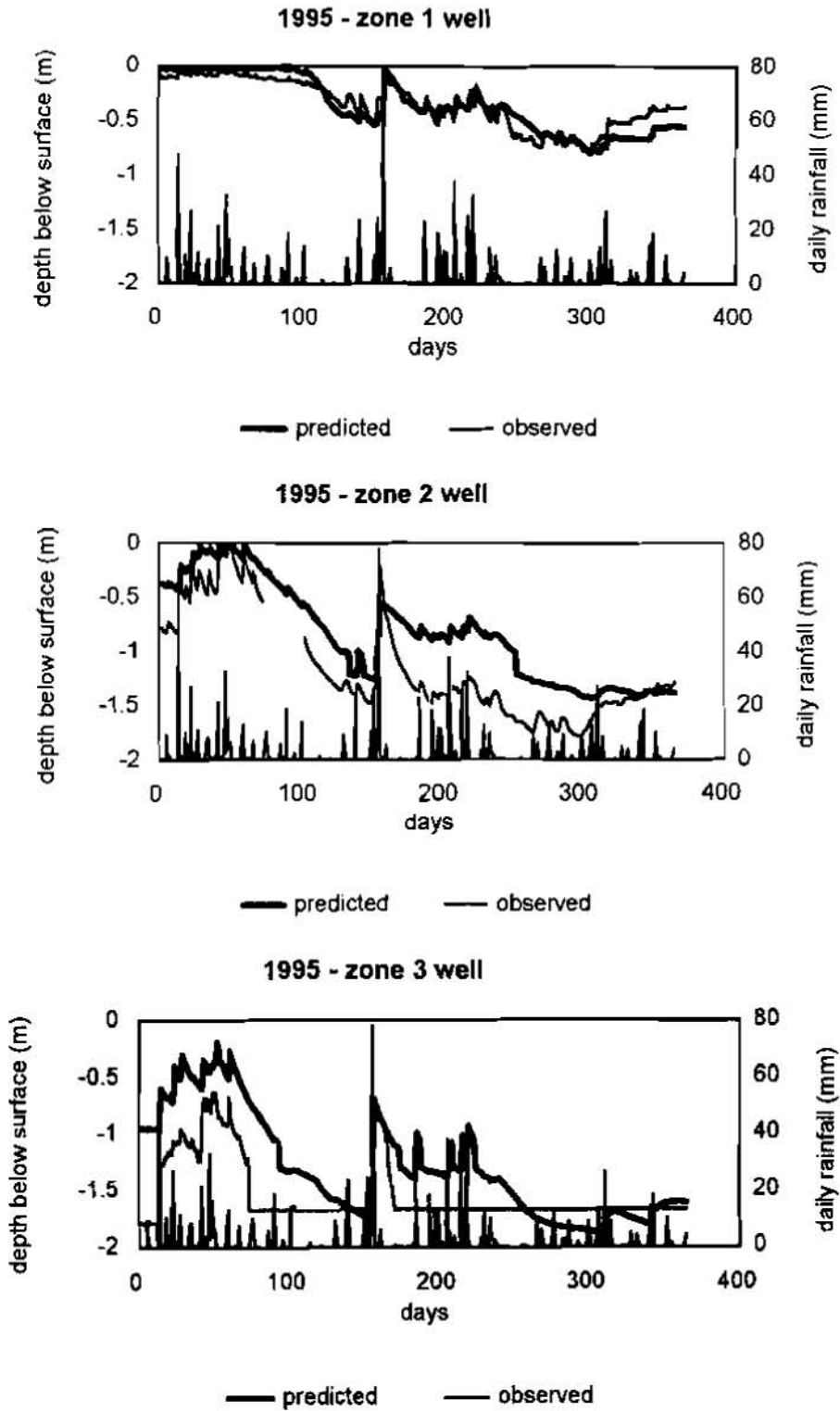


Figure 1: Model predicted and observed water tables for 1995 and zones 1, 2, and 3.

Table 1: Selected parameters and their values describing the three zone riparian buffer at Gibbs farm.

Parameter	units	zone 1 (hardwood forest)	zone 2 (pine forest)	zone 3 (grass filter)
length, width	m	15.24, 40.4	50.00, 40.4	7.60, 40.4
slope	%	2.0	3.8	2.62
manning's n		0.6	0.5	0.4
horizon thicknesses+	m	0.3, 0.7, 1.50	0.3, 0.90, 1.52	0.3, 1.00, 1.70
saturated conductivity	cm/hr	13, 11, 0.5	13, 11, 0.5	13, 11, 0.5
porosity	cm/cm	0.35, 0.38, 0.40	0.35, 0.38, 0.40	0.35, 0.38, 0.40
field capacity	cm/cm	0.15, 0.15, 0.15	0.15, 0.15, 0.15	0.15, 0.15, 0.15
wilting point	cm/cm	0.07, 0.07, 0.07	0.07, 0.07, 0.07	0.07, 0.07, 0.07
vegetation LAI*	m ² /m ²	0.0 - 4.0	3.5	0.0 - 2.5
Contributing field area	ha	0.3093		
seepage loss from aquiclude	mm/day	0.2		

+ each zone had three horizons, values are from the upper to the bottom horizon; & vegetation LAI are not predetermined but depend on simulated vegetative growth - values listed here are those that were observed during evaluation runs.

Model predicted annual surface runoff values exiting zones 3 (grass filter) and 2 (pine forest) were compared to that observed at runoff collectors at the grass-pine forest and pine-hardwood forest interface and are presented in Table 3. Prior to comparing the results it is important to point out that the surface runoff collectors are designed such that they are best suited for conditions where surface runoff primarily occurs as shallow sheet flow (Sheridan et al., 1996). Under conditions where flow is concentrated in channels, it is possible that observations made by these samplers may not be representative of the actual site conditions. At the Gibbs farm site, surface runoff typically occurs as a combination of concentrated flow and sheet flow.

Table 2: Annual average absolute error* in predicted and observed water tables (in meters)

recording well	93	94	95	96	4 yr Avg
annual rainfall (mm)	1100	1487	877	1119	1145
03 (zone 1 well)	0.131	0.070	0.080	0.116	0.101
02 (zone 2 well)	0.321	0.385	0.320	0.316	0.336
01 (zone 3 well)	0.377	0.666	0.300	0.374	0.431

* Annual average absolute error = $\sum_{nd} |W_p - W_o| / nd$ where W_p and W_o are predicted and observed values respectively, and nd is number of days in the year.

Observed values indicate that on an annual basis, except for year 93, surface runoff consistently decreased as it moved from the field to the pine-hardwood forest interface. For years 94-96 approximately 60% of the observed runoff entering zone 3 was lost to infiltration whereas for zone 2 this figure was approximately 44%. For year 93, there was a net gain of 42% and a loss of 58% of observed runoff for zone 3 and 2 respectively. Model predictions indicated similar trends for years 94-96, but underestimated the infiltration loss in zone 3 and overestimated the loss in zone 2 over the three year (94-96) period. Model predictions were best for year 95 when runoff values exiting both zones were reasonably close to those observed. The biggest difference between predicted and observed runoff values occurred for the year 93 and for runoff exiting zone

2. During this year most of the model simulated runoff from zone 2 was generated as saturation overland flow during late winter/early spring when the water table within zone 2 was at the surface and the buffer was subjected to large rainfall events. Overall, considering the annual variability in surface runoff totals, and accounting for the limitation of the runoff collectors (mentioned above) the model seems to provide good estimates.

When predicted runoff exiting each zone was plotted on a monthly basis (graphic not included here because of space limitation) the salient observations were - [a] surface runoff loading to the riparian buffer from field occurred either during wet winter condition or during high intensity storms during the summer; [b] during winter, a greater proportion of the field surface runoff loading was sustained as surface runoff along the length of the buffer and reached the pine-hardwood forest interface; [c] in contrast, most of the field surface runoff entering the buffer during summer was immediately lost to infiltration within the grass filter zone. These model predicted trends seem to follow those observed by the investigators at this site.

Table 3: Surface runoff comparisons (values in mm/year)

yrs	field ⁺ input	observed				predicted				% diff [@]	
		zone 3		zone 2		zone 3		zone 2		zone 3	zone 2
		runoff*	% inf ^{\$}	runoff	% inf	runoff	% inf	runoff	% inf		
93	21	30.7	-42	17.7	42	8.9	58	71.3	-697	70	-302
94	317	101.0	68	67.5	33	178.2	43	126.6	28	76	-87
95	108	20.7	64	55.9	46	38.6	48	20.0	64	44	-3
96	213	102.6	53	46.7	54	112.6	48	26.8	76	9	42

+ observed values -- used as input to the model; * runoff exiting zone (mm); \$ % infiltration of surface runoff = (inflow - outflow)*100/inflow; negative values indicate net gain of surface runoff within zone; @ % difference between observed and predicted surface runoff exiting zones = [(obs-pred)/obs]*100.

Beyond the water table elevations and surface runoff values there were no other specific data collected at Gibbs farm site which could be compared with model predictions. But annual estimates were available on parameters such as subsurface flow and surface runoff contribution to streamflow which could be used to compare model predictions to the Little River Watershed which contains the Gibbs Farm site. To allow for such a comparison the annual hydrologic budget of predicted values for the Gibbs farm site was developed and is presented in Table 4 and Figure 2. This budget also allows us to evaluate estimates for transpiration and interception for which annual estimates are more often available.

Over the four years of simulation the average annual surface runoff contribution to streamflow was 7% of the annual rainfall. This predicted value is slightly higher than 5% earlier reported by Sheridan et al. (1996) for the Gibbs farm site, but well within the range of 4-12% reported by Shirmohammadi et al. (1985) for Little River Watershed. Similarly, the subsurface flow contribution to streamflow predicted using the model was 7% of the annual rainfall. Again this value is higher than the value of 3% earlier estimated by Bosch et al. (1996) but less than the range of 14 to 22% reported by Shirmohammadi et al. (1984). The four year average also indicates that surface runoff decreases as a proportion of the rainfall from the field through the riparian buffer, whereas subsurface flow shows an increasing trend. This is expected since a large portion of the surface flow is lost to infiltration (and consequently added to subsurface flow) due the porous surface soil within the buffer.

The budget estimates presented in Table 4 also provide a salient result, that upland loadings to the buffer may not necessarily determine the magnitude of surface and subsurface runoff that is generated within the buffer and which is eventually lost to streamflow. This is obvious from budgets of years 93 and 96, where even though field loadings for 93 were much smaller than those of 96, streamflow contribution was higher in 93 compared to that of 96. A closer look at the budgets reveals that surface runoff contribution to streamflow during 93 was more than twice that of 96. A plot of the monthly rainfall, water

table, and surface runoff generated for zone 1 (graphic not included here due to space limitation) for years 93 and 96 reveals that for 93 most of the surface runoff which contributed to streamflow was generated during late winter/early spring. This was because there were a number of large rainfall events during late winter and early spring of 93 when the soil in zone 1 was already saturated and which resulted in saturation excess surface runoff. Compared to 93, 96 had a less rainfall during the early part of the year. This analysis indicates that, in addition to upland loadings, the amount of rainfall, its distribution during the year, and the soil moisture conditions in the alluvial zone (zone 1 in this case) are an important determinant of streamflow. In other words, the variable sources area mechanisms of runoff generation (especially within the alluvial zone) play a significant role in determining streamflow for this site. This result is consistent with conclusions of Shirmohammadi et al. (1986) who showed that generation of streamflow on Little River Watershed was largely controlled by the soil moisture conditions in the alluvial aquifer of the riparian zone.

Table 4: Model predicted annual hydrology budget (values in mm/year)

Variable		year 93	year 94	year 95	year 96	4 yr avg.
Rainfall (mm)		1100	1487	877	1119	1145
Field loadings* (mm)	surface runoff	21 (2)+	317 (21)	108 (12)	213 (19)	164 (14)
	subsurface flow	48 (4)	60 (4)	36 (4)	28 (2)	43 (4)
	total	69 (6)	377 (25)	144 (16)	241 (21)	207 (18)
Loss to stream* (mm)	surface flow	95 (9)	174 (12)	30 (3)	41 (4)	85 (7)
	subsurface	55 (5)	127 (8)	60 (7)	61 (5)	76 (7)
	seepage	40 (4)	41 (3)	23 (3)	13 (1)	20 (2)
	total	190 (18)	342 (23)	113 (13)	115 (10)	190 (16)
Transpiration (mm)^		676 (61)	823 (55)	709 (80)	734 (66)	735 (64)
Interception (mm)		166 (15)	182 (12)	180 (20)	172 (15)	175 (15)

* field loadings and loss to stream are based on the contributing area basis, field contributing area = 0.3093 ha; contributing area to stream = 0.6061 ha; + numbers inside bracket are % with respect to annual rainfall - rounded off to nearest whole numbers; ^ averaged across all three zones.

Annual transpiration loss of 751 mm/yr averaged over four years and the three vegetation types seems to be in the neighborhood of values reported in literature for similar site conditions (Riekerk, 1985; Ewel and Smith, 1992). The average annual interception loss of 15% predicted by the model is close to the value of 17% reported by Lowrance (1981) for riparian forests located on Coastal Plain watersheds.

REFERENCES

- Altier, L.S., Lowrance, R.R., Williams, R.G., Inamdar, S.P., Bosch, D.D., Sheridan, J.M., Hubbard, R.K., and Thomas, D.L. Riparian Ecosystem Management Model (REMM): Documentation. USDA Conservation Research Report, In Press.
- Altier, L.S., Lowrance, R.R., Williams, R.G., Inamdar, S.P. 1998. The Riparian Ecosystem Management Model (REMM): Plant growth component. In Proceedings of the First Federal Interagency Hydrologic Modeling Conference, Las Vegas, NV (this volume).
- Bosch, D.D., Sheridan, J.M., and Lowrance, R.R. 1996. Hydraulic gradients and flow rates of a shallow coastal plain aquifer in a forested riparian buffer. *Trans. of the ASAE*, Vol. 39(3):865-871.
- Campbell, G.S. 1974. A simple method for determining unsaturated conductivity from moisture retention data. *Soil Sci.* 117:311-314.
- Ewel, K.C., and Smith, J.E. 1992. Evapotranspiration from Florida Cypress swamps. *Water Res. Bull.* Vol. 28(2) 299-304.
- Gardner, W.R., and Hillel, D.I. 1962. The relation of external evaporative conditions to the drying of soils. *J. Geophys. Res.*

67:4319-4325.

- Lowrance, R.R., Altier, L.S., Williams, R.G., Inamdar, S.P., Bosch, D.D., Sheridan, J.M., and Thomas, D.L. 1998. The Riparian Ecosystem Management Model (REMM): Simulator for ecological processes in buffer systems. In Proceedings of the First Federal Interagency Hydrologic Modeling Conference, Las Vegas, NV (this volume).
- Lowrance, R.R. 1981. Nutrient cycling in an agricultural watershed: Waterborne nutrient input/output budgets for the riparian zone. Unpublished Ph.D. diss., Univ. of Georgia, Athens.
- NRCS. 1995. Riparian Forest Buffer, 392. NRCS Watershed Science Institute. Seattle, WA.
- Riekerk, H. 1985. Lysimetric measurement of pine evapotranspiration for water balances. In Advances in Evapotranspiration, 276-281. St. Joseph, MI, ASAE.
- Running, S.W., and Coughlan, J.C. 1988. A general model of forest ecosystem processes for regional applications I. Hydrologic balance, canopy gas exchange and primary production processes. *Ecol. Modelling* 42:125-154.
- Sheridan, J.M., Lowrance, R.R., and Bosch, D.D. 1998. Management effects on runoff and sediment transport in riparian forest buffers. Trans. Of the ASAE. In review.
- Sheridan, J.M., Lowrance, R.R., and Henry, H.H. 1996. Surface flow sampler for riparian studies. Applied Engineering in Agriculture, Vol. 12(2):183-188.
- Shirmohammadi, A.J., Sheridan, J.M., and Knisel, W.G. 1985. An approximate method for partitioning daily streamflow data. *J. Hydrol.* Vol. 74(3/4):335-354.
- Shirmohammadi, A.J., Sheridan, J.M., and Asmussen, L.E. 1986. Hydrology of alluvial stream channels in southern Coastal Plain watersheds. Trans. of the ASAE, Vol. 29(1):135-142.
- Skaggs, R.W. 1978. A water management model for shallow water table soils. WRR1, University of North Carolina Report no. 134., 178p.
- Stone, J. J., Hawkins, R.H., and Shirley, E.D. 1994. An approximate form of the Green Ampt infiltration equation. ASCE J. Irrigation and Drainage. Vol. 120(1):128-137.
- Thomas, D.L., and Beasley, D.B. 1986. A physically-based forest hydrology model I: Development and sensitivity of components. Trans. of the ASAE 29:962-972.
- Welsch, D.J. 1991. Riparian Forest Buffers. USDA-FS Publ. No. NA-PR-07-91. Radnor, PA.

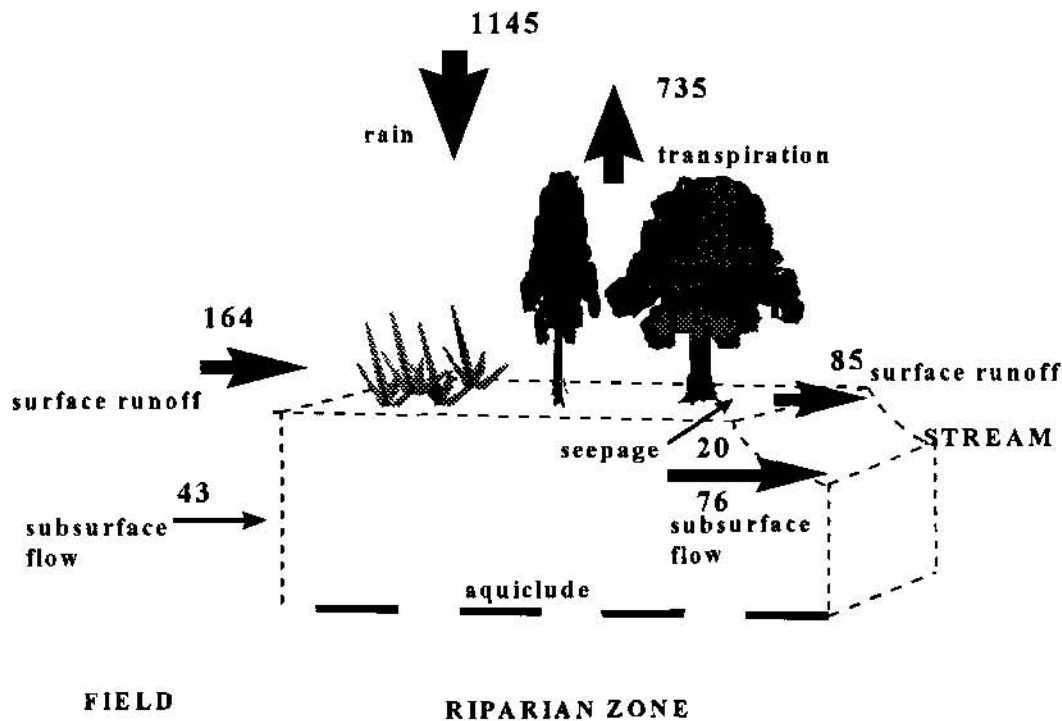


Figure 2: Model simulated annual hydrology values (mm/yr) averaged over the four year (93-96) simulation period.

COMPARISON OF RAINFALL RECORDS COLLECTED BY DIFFERENT RAIN-GAGE NETWORKS

Timothy D. Straub, Civil Engineer, U.S. Geological Survey, Urbana, Illinois;
Paminder S. Parmar, Student Trainee, U.S. Geological Survey, Urbana, Illinois

Abstract

The implementation of surface-water quantity and quality models is only as sound as the available data. In a study done by the U.S. Geological Survey (USGS), in cooperation with the Du Page County Department of Environmental Concerns, simulated runoff tended to be higher when monthly rainfall totals recorded by National Oceanic and Atmospheric Administration (NOAA) precipitation gages were used as compared to using monthly rainfall totals recorded by USGS rain gages. The purpose of this paper is to describe whether a significant difference was detected between rainfall recorded by the USGS rain-gage network and the NOAA precipitation-gage (a precipitation gage is designed to record snow and rainfall, whereas a rain gage only records rainfall) network located in and near Du Page County, Illinois. Rainfall data recorded from 1986 to 1995 at 10 USGS rain gages and 5 NOAA precipitation gages in and near Du Page County, Illinois, were analyzed. Further insight into the physical basis for possible differences is provided by a dual-gage (weighing- and tipping-bucket) setup installed at one site. Three statistical tests were completed to check the hypothesis of no difference in the rainfall data recordings: the Wilcoxon rank-sum test, the Kruskal-Wallis test, and the paired t-test. Results from the statistical tests indicated that significantly different rainfall amounts were recorded at USGS and NOAA gages. Fitting a straight, least squares trendline to the data comparing monthly records from each NOAA gage with monthly records from each USGS gage showed that on average, USGS gages were recording 86 percent of the total rainfall recorded at the NOAA gages. Similar results have been found in the dual-gage (weighing- and tipping-bucket) setup comparison of rainfall data.

INTRODUCTION

Three commonly applied techniques of recording rainfall include the universal-type weighing-bucket recording gage, tipping-bucket rain gage, and standard 8-in. nonrecording precipitation gage (National Weather Service, 1989, p. 8-17). The purpose of this paper is to describe the methods applied and results obtained in the determination of whether a significant difference is present between rainfall recorded by the USGS rain-gage network and the NOAA precipitation-gage network located in and near Du Page County, Illinois. Further insight into the physical basis for possible differences in recorded rainfall amounts is provided by a dual-gage (weighing- and tipping-bucket) setup.

DESCRIPTION OF STUDY AREA

The study area is 17 mi west of the city of Chicago. The study area includes all of Du Page County and portions of the surrounding counties (Fig. 1). Rapid urbanization has lead to appreciable changes in the hydrologic environment. Higher peak flows and increased flooding have resulted because of urbanization.

Climate

Northeastern Illinois has a temperate, humid, continental climate that is slightly modified by Lake Michigan. Long-term climate data in and near the study area were obtained from five NOAA precipitation gages (Fig. 1). The long-term average annual precipitation and long-term mean annual temperature for the study area is approximately 33 in. and 49°F, respectively (U.S. Department of Commerce, National Oceanic and Atmospheric Administration, 1990).

DATA COLLECTION AND SELECTION METHODS

National Oceanic and Atmospheric Administration Network

5 NOAA precipitation gages located in and near Du Page County, Illinois were used for the study (Fig. 1). 4 of these were 8-in. nonrecording gages. These consist of a large diameter outer can, a smaller diameter measuring tube inside the outer can, a funnel that connects the outer can and measuring tube, a measuring stick, and a support. The funnel directs precipitation into the measuring tube, which holds exactly 2 inches of rainfall (additional rainfall will flow into the overflow can) (National Weather Service 1989, p. 8). The other NOAA precipitation gage type is the universal weighing-bucket recording gage. Precipitation falls

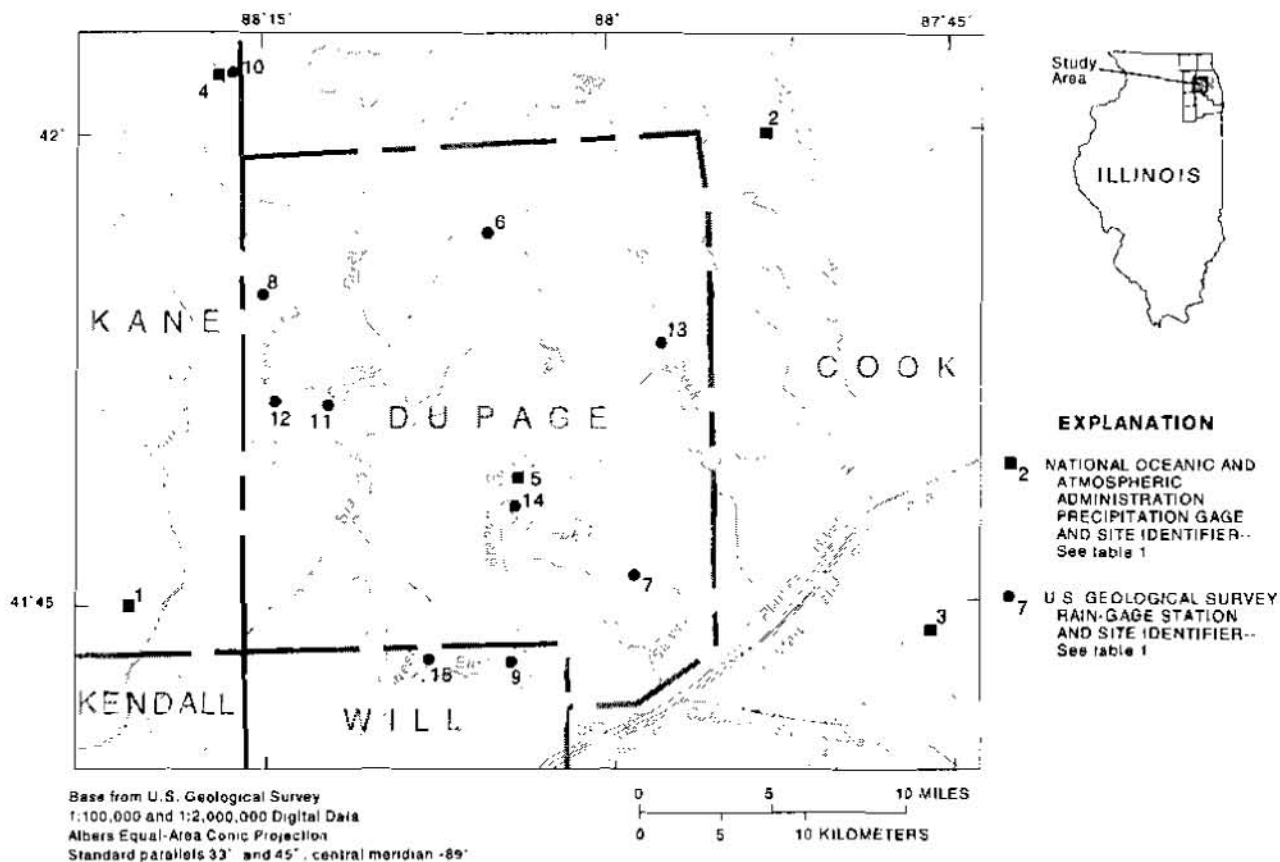


FIGURE 1: Locations of National Oceanic and Atmospheric Administration precipitation gauges and U.S. Geological Survey rain gauges in and near the study area.

TABLE 1: Precipitation Gages and Rain Gages Used in the Study

Site Identifier	Station Name and Abbreviation	Gage Type	Orifice Diameter, in inches	Accuracy, in inches	Months of Record Used
NOAA					
1	Aurora	Standard nonrecording	8	0.01	60
2	O'Hare	Universal weighing	8	.01	63
3	Midway	Standard nonrecording	8	.01	63
4	Elgin	Standard nonrecording	8	.01	60
5	Wheaton	Standard nonrecording	8	.01	63
USGS					
6	Bloomington Lift Station (BLOOM)	Tipping (Qualimetric) ¹	8	.01	28
7	Clarendon Hills Cemetery (CLARE)	Tipping (Qualimetric)	8	.01	51
8	Du Page County Airport (DPCA)	Tipping (Qualimetric)	12	.01	45
		Universal weighing with alter windshield	8	.01	11
9	East Branch Du Page River (EBDP)	Tipping (Qualimetric)	8	.01	45
10	Elgin Wastewater Treatment (ELGIN)	Tipping (Qualimetric)	8	.01	34
11	Kress Creek (KRESS)	Tipping (Qualimetric)	8	.01	57
12	National Accelerator Lab (NAL)	Tipping (Qualimetric)	8	.01	33
13	Salt Creek at Elmhurst (ELM)	Tipping (Climatronic)	8	.01	38
14	St. Joseph Creek at Hwy 34 (HWY34)	Tipping (Climatronic)	8	.01	33
15	West Branch Du Page River (WBDP)	Tipping (Qualimetric)	8	.01	35

¹ The use of brand names in this report is for identification purposes only and does not constitute endorsement by the U. S. Geological Survey, nor impute responsibility for any present or potential effects on the natural resources.

into the universal gage receiver, where it is funneled into a collector mounted on a weighing mechanism. The weight of the precipitation in the collector compresses a spring, which is connected to a pen (ink) arm. Ink from the pen leaves a trace on a paper chart, which is wrapped around a clock-driven cylinder. Ink tracings on the chart provide a "history of precipitation rates and amounts (National Weather Service 1989, p. 10). Gage information is listed in Table 1. Data used from the NOAA network were the monthly rain totals from March 1986 to September 1995 (U.S. Department of Commerce (1986-95)). Only the monthly totals for April through October were used for analysis so that snowfall-affected precipitation would not be a factor in the analysis.

U.S. Geological Survey Network

Between 1986 and 1990, the USGS installed a network of 14 tipping-bucket rain gages in and near Du Page County, Illinois. The 10 gages used in this study from this network are shown in Figure 1. Tipping-bucket rain gages work on the principle that rainfall collected by a funnel accumulates in a two-chambered bucket until the weight causes the bucket to tip on its pivot, dump the collected water, and move the other chamber under the funnel. The rain gages are connected to electronic data loggers that record the amount of rainfall in 0.01-in. increments at 5-minute intervals. Gage information for the 10 USGS gages used in the study is listed in Table 1. An insufficient amount of rainfall data for analysis were available at three gages and one gage did not operate properly. Monthly rainfall totals from the USGS network from March 1986 to September 1995 (Duncker and others 1993 and Straub and others 1997) were used in the study. Only the monthly totals for April through October were used for analysis so that snowfall-affected precipitation would not be a factor in the analysis.

U.S. Geological Survey Dual Gage Setup

Data have been collected by the USGS at Du Page County Airport, Illinois, where a tipping-bucket rain gage and a universal weighing-bucket recording gage have been installed within 5 ft of each other. Data used from this site were recorded from January 23, 1996, to December 11, 1997. Storms were selected for analysis when there were no equipment-related problems.

STATISTICAL TESTS

Statistical tests applied to the data were used to determine if there is a significant difference present between the amount of rainfall recorded for the same period of record between the USGS and NOAA gage networks. Three tests were selected to determine if the hypothesis of no difference in the measurements could be rejected. These were the Kruskal-Wallis test, the Wilcoxon rank-sum test, and the paired t-test. The Shapiro-Wilk test was randomly performed on the data to test for normality. A series of t-tests were performed and least squares trendlines were drawn for the dual-gage setup comparison in a manner similar to that used in the network comparison.

The Kruskal-Wallis test (Conover, 1980, p. 229-237) is a nonparametric test for comparing more than two groups of data. This test was used to determine if there were significant differences among rainfall amounts recorded at rain gages within the same group (differences within the NOAA and USGS networks). The Wilcoxon rank-sum test (Conover, 1980, p. 215-227) is a nonparametric test for comparing two independent groups of data. This test was used to determine whether one group of rain gages tended to record different rainfall amounts than another group of rain gages (differences between the NOAA and USGS networks). The two-sample t-test (Schlotzhauer and Littell, 1987, p. 191) is a parametric test to compare two independent groups of data. Unlike the nonparametric tests, the data are assumed to be normally distributed in a parametric test, with the variances assumed to be equal.

The hypothesis of all tests performed is that no difference is present between the amount each rain gage records (null hypothesis). The null hypothesis is tested by the calculation of a test statistic. The value of the test statistic is compared to reference values that would be expected if the null hypothesis were true. The result of this comparison is a probability level, or p-level, that tells you if the null hypothesis should be believed (Schlotzhauer, 1987, p. 126). The null hypothesis is either rejected or not rejected. The null hypothesis is never "accepted", it can only be "not rejected". In testing the given hypothesis, the maximum probability of rejecting the null hypothesis when it is correct is called the significance level (Spiegel, 1988, p. 207). For example, if it was determined that a difference was present between two rain gages at the 0.10

or 10 percent significance level, then there is a 10-percent chance that the conclusion of a statistical difference is incorrect.

For this study, 10-percent is considered moderately significant, whereas 1 percent is considered highly significant. The 10-percent level was used for tests among rain gages located at different sites. This results in less stringent criteria in rejecting the null hypothesis. This criteria was applied because the spatial variability related to rainfall distribution results in variations in rainfall totals between nearby rain gages even at the monthly time scale. The 1-percent level (0.01) was applied for the dual-gage setup. The rain gages in the setup were 5 ft apart. A lower significance level was chosen to make it more difficult to reject the null hypothesis (more difficult to conclude that there is a significant difference) as compared to the 10-percent level. This was applied because it was expected for storm totals to be nearly identical due to the proximity of the rain gages. At the 10-percent significance level, a p-level of greater than 0.10 results in failing to reject the null hypothesis, and a p-level of 0.10 or less results in rejecting the null hypothesis. The procedure of failing to reject or rejecting the null hypothesis is the same at the 1-percent significance level, except that a p-level of 0.01 is used in the analysis.

Results of Comparison Between the National Oceanic and Atmospheric Administration and U.S. Geological Survey Networks

First, the data were analyzed to determine if there were significant differences among rainfall amounts at the gages in each network. The Kruskal-Wallis test was performed on monthly rainfall totals for the entire NOAA precipitation-gage and USGS rain-gage networks (Table 2). In both tests, a p-level of greater than 0.10 was determined and the null hypothesis was not rejected. The next test was to combine both networks, with each rain gage considered separately (15 groups). Again the null hypothesis was not rejected. Next, NOAA gages were placed into one group and USGS gages were placed into another group for analysis with the Wilcoxon rank-sum test. From this analysis, the null hypothesis was rejected at the 10-percent significance level.

TABLE 2: Kruskal-Wallis and Wilcoxon Rank-Sum Test Results
Bold values indicate p-levels below the 10-percent significance level

Test	Comparison	P-Level
Kruskal Wallis	NOAA Network	0.810
	USGS Network	.979
	NOAA and USGS Network	.914
Wilcoxon Rank Sum	NOAA vs. USGS Network	.055

A series of t-tests were done to perform paired comparisons between the NOAA gages and the USGS gages for monthly rainfall totals. The p-levels of these tests are shown in Table 3. Data used in the t-tests were randomly checked for normality and it was concluded that the hypothesis of normality could not be rejected at the 5 percent significance level. In the first series of tests the 10 USGS rain gages were tested with the 5 NOAA rain gages for a total of 50 paired t-tests. At the 10-percent level, rejection of the null hypothesis resulted from 28 tests. For three USGS gages (BLOOM, CLARE, and DPCA), the null hypothesis was rejected in the comparison with all five NOAA gages; whereas for two USGS gages (ELGIN and WBDP), the null hypothesis was rejected in comparison with only one NOAA gage. An unevenness also resulted in the rejection of the null hypothesis in the NOAA gages. In tests involving the O'Hare, Midway, and Elgin, NOAA gages, the null hypothesis was rejected in comparison with only 3-4 USGS rain gages; whereas in tests involving the Aurora and Wheaton gages, the null hypothesis was rejected in comparison with 8-9 of the 10 USGS gages.

Paired t-tests were then performed within each network to determine if the rain gages in the same network were recording similar rainfall amounts. The results for the USGS network are shown in Table 4. The null hypothesis was rejected in 22 of 50 paired t-tests. The null hypothesis was rejected six times in comparisons with the rain gage at KRESS. Lastly, paired t-tests were performed among the NOAA gages. Out of the 10 possible tests, the null hypothesis was rejected in 3 tests, all involving Aurora gages (Table 5).

TABLE 3: P-Levels of Paired t-Tests Between National Oceanic and Atmospheric Administration and U.S. Geological Survey Rain-Gage Networks

Bold values indicate p-levels below the 10 percent significance level

Site	Aurora	O'Hare	Midway	Elgin	Wheaton
BLOOM	0.001	0.002	0.085	0.064	0.009
CLARE	.000	.096	.055	.031	.005
DPCA	.003	.032	.035	.041	.008
EBDP	.000	.304	.007	.180	.000
ELGIN	.165	.591	.315	.002	.290
KRESS	.045	.783	.644	.747	.074
NAL	.000	.504	.425	.227	.037
ELM	.008	.761	.228	.717	.031
HWY34	.016	.401	.217	.270	.021
WBDP	.034	.583	.296	.517	.144

TABLE 4: P-Levels of Paired t-Tests Between U.S. Geological Survey Rain Gages

Bold values indicate p-levels below the 10 percent significance level

Site	BLOOM	CLARE	DPCA	EBDP	ELGIN	KRESS	NAL	ELM	HWY34	WBDP
BLOOM		0.349	0.801	0.805	0.387	0.002	0.545	0.095	0.450	0.506
CLARE	0.349		.331	.072	.539	.317	.190	.023	.020	.038
DPCA	.801	.331		.459	.743	.080	.927	.503	.928	.276
EBDP	.805	.072	.459		.664	.005	.381	.714	.381	.206
ELGIN	.387	.539	.743	.664		.519	.929	.403	.818	.970
KRESS	.002	.317	.080	.005	.519		.000	.001	.002	.277
NAL	.545	.190	.927	.381	.929	.000		.305	.610	.386
ELM	.095	.023	.503	.714	.403	.001	.305		.860	.347
HWY34	.450	.020	.928	.381	.818	.002	.610	.860		.915
WBDP	.506	.038	.276	.206	.970	.277	.386	.347	.915	

TABLE 5: P-Levels of Paired t-Tests Between National Oceanic and Atmospheric Administration Precipitation Gages

Bold values indicate p-levels below the 10 percent significance level

Site	Aurora	O'Hare	Midway	Elgin	Wheaton
Aurora		0.076	0.040	0.096	0.405
O'Hare	0.076		.971	.845	.150
Midway	.040	.971		.813	.137
Elgin	.096	.845	.813		.288
Wheaton	.405	.150	.137	.288	

Investigation of the Difference in Recorded Rainfall Between Networks

The statistical test results indicated that some gages were recording different monthly totals than others. The magnitude of the difference was estimated by fitting a straight, least-squares, linear regression between monthly data from one gage to the monthly data of another gage. The relation between the USGS BLOOM gage and the NOAA O'Hare gage is shown in Figure 2. In this study, a trendline slope multiplied by 100 represents the percentage of rain that a USGS gage recorded as compared to a NOAA gage. A number of scattergraphs were plotted and analyzed. For each of these plots, a trendline was drawn. The mean trendline slope of the USGS rain gages averaged 0.86 relative to the five NOAA gages. The standard deviation was 0.05, with a coefficient of variation of 0.06 (Table 6). Slopes from 8 of the 10 USGS rain gages fall within one standard deviation of 0.86.

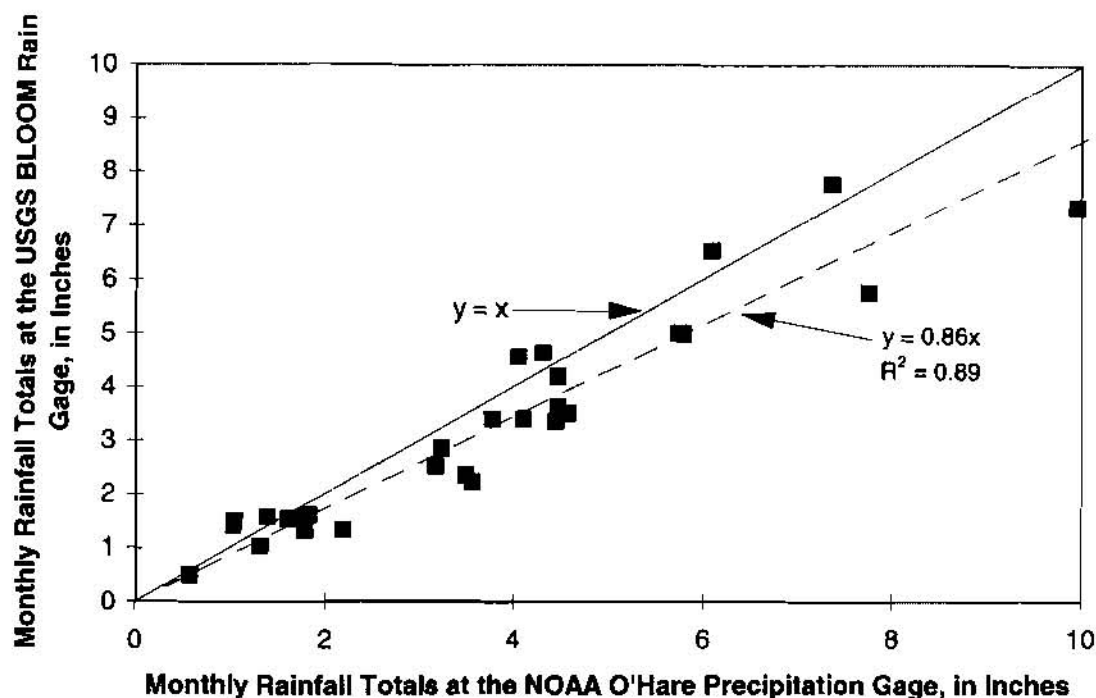


FIGURE 2. Comparison of monthly rainfall totals between the USGS BLOOM gage and the NOAA O'Hare gage.

TABLE 6: Trendline Slopes of U.S. Geological Survey versus National Oceanic and Atmospheric Administration Monthly Rainfall Totals

Site	Aurora	O'Hare	Midway	Elgin	Wheaton	Averages
BLOOM	0.792	0.858	0.782	0.807	0.802	0.808
CLARE	.811	.859	.828	.832	.836	.833
DPCA	.727	.687	.805	.804	.719	.748
EBDP	.848	.896	.882	.869	.875	.874
ELGIN	.823	.939	.807	.930	.874	.875
KRESS	.896	.916	.961	.964	.896	.927
NAL	.866	.892	.901	.868	.859	.877
ELM	.859	.948	.847	.917	.873	.889
HWY34	.878	.897	.867	.880	.897	.884
WBDP	.882	.904	.907	.898	.931	.904
Averages	.838	.880	.859	.877	.856	.862
Mean =	0.862					
St. Dev =	.052					
C. O. V. =	.060					

Dual-Gage Setup Comparison

A dual-gage setup comparison was performed between the USGS tipping- and weighing-bucket rain gages located at DPCA. The period for this comparison was from January to December 1996, this is a different time period than that used in the network analysis (April 1986-September 1995). In this study, it was discovered that there were scattered periods of time when the tipping bucket was not recording rainfall from storms or recording only during parts of a storm. For the dual-gage setup comparison, the data were analyzed for specific storms where the tipping-bucket rain gage was working properly. Storm totals were

analyzed in the dual-gage setup instead of monthly totals which were used in the network analysis. Rainfall data from 26 storms were used in the dual-gage setup analysis.

A series of t-tests were performed and least-squares trendlines were drawn for the dual-gage setup comparison in a manner similar to that used in the network comparison. A significance level of 0.01 was used in the dual-gage setup. The null hypothesis was rejected at the 1-percent significance level when all 26 storms were considered (Table 7). The fitted trendline for all storms was 0.91. It should be noted that the tipping-bucket rain gage at this location contains a 12-in. diameter cylinder instead of an 8-in. diameter cylinder used in all other USGS gages. Past research has shown that the 8-in. diameter rain gage averages 2.6 percent less rainfall than the 12-in. diameter rain gage (Jones, 1969).

A number of factors including temperature, wind speed, rainfall amount, and rainfall intensity for each storm was studied to examine why there was a difference in amount of rainfall recorded. No correlation was found between temperature or wind speed and the amount of rain recorded, but a relation was found between storm totals and the difference between amounts recorded at each gage. For storm totals with rainfall amounts greater than 1 in., the null hypothesis was not rejected. Upon further examination, it was determined that the storms producing greater than 1 in. of rain tended to have periods of more intense rain. Rainfall intensity was studied more closely. Four classes of rainfall intensity were considered: light, moderate, intense, and very intense. These were assigned based on the amount of rain recorded per 5-minutes. A criteria of greater than 0.27 in. per 5 minutes was selected for very intense rainfall. This was based on recommended corrections for tipping-bucket rain gages for periods when rainfall exceeded 0.27 in. per 5 minutes (Qualimetrics, Inc., 1986, p. 8). The criteria for other levels are listed in Table 7. Storms were classified according to the majority of the amount of rainfall. For example, a 2-hour storm with a total rainfall of 0.5 in. would be classified as intense if three 5-minute periods of intense rainfall resulted during the storm. The majority of the amount of rain in this storm would have been classified as intense, while only 15 minutes of the 2 total hours would have been an intense period of the storm. At the 1-percent significance level, light rain was the only category in which the null hypothesis could be rejected. Trendline slopes were established, and a relation was found between intensity and amount of rainfall difference among categories. Slopes of 0.88 and 0.97 were calculated for light rain and very intense rain, respectively. The 5-minute values for very intense rain were already corrected for the tipping-bucket rain gage as per manufacturer specifications, but the amount of the correction was small enough that these adjustments alone could not account for the result that an almost perfect trendline slope was determined for the very intense rainfall classification. Data from light storms are more sensitive to wetting losses (amount of rain required to moisten the funnel and inside surfaces). In the dual-gage setup, the tipping-bucket gage had a funnel, whereas no funnel was present for the weighing-bucket gage. It is estimated that 2-15 percent of each rain event measured at an initially dry gage is not recorded because of wetting losses in the summer (Sevruck, 1982). A shielded gage, such as the weighing-bucket in the dual-gage setup, records 3-5-percent greater amount of rain depending on the wind speed compared to unshielded gages, like the tipping bucket in the dual-gage setup (Linsley and others, 1975).

TABLE 7: Paired t-Tests Between Tipping- and Weighing-Bucket Gages at DPCA for Various Storm Classifications

Storm Classification	Trendline Slope	P-Level	Number of Storms
All Storms	0.91	0.002	26
Less Than 1 Inch Storm Total	.92	.005	21
Greater Than 1 Inch Storm Total	.91	.050	5
Light (0.01 - 0.04 inches per 5 minutes)	.88	.009	9
Moderate (0.05 - 0.09 inches per 5 minutes)	.92	.060	7
Intense (0.10 - 0.26 inches per 5 minutes)	.94	.200	4
Very Intense (Greater than 0.26 inches per 5 minutes)	.97	.400	5

CONCLUSIONS

Conclusions for the Network Comparison

From the results of the Wilcoxon rank-sum tests a statistically significant difference between monthly rainfall totals recorded by the two networks was determined, whereas there appeared to be no difference within a particular network, based on the results of the Kruskal-Wallis tests. Results from the paired t-tests indicated that within each network there were a few inconsistent rain gages, but for the most part, it can be concluded that some inherent difference in monthly rainfall amounts is present between the two networks and that the difference is not caused by variations within one particular network. Results of the least-squares regression showed that, on average, USGS rain gages recorded 86 percent of the total rainfall recorded at NOAA precipitation gages.

Conclusions for Dual-Gage Setup Comparison

The paired t-tests indicated that a statistically significant difference at the 1-percent significance level was present in the amount of rain recorded at the tipping-bucket gage as compared to the weighing-bucket gage when all storms were analyzed. On average, the tipping-bucket gage recorded 91-percent of that recorded by the weighing-bucket gage. The difference in the trendline slope (0.91) found in this analysis compared to the trendline slope found in the network comparison (0.86) can partly be explained in that only storms were selected when it was known that the tipping-bucket gage in the dual-gage setup was working under optimum conditions. In addition, the difference in the diameter of the rain gage at DPCA compared to other gages in the USGS network can result in a 2.6-percent increase for the rain recorded (Jones, 1969).

A difference was found between the two gages when different classifications of rainfall intensities were tested. As rainfall intensity increased, the difference in the amount of rainfall recorded between the tipping- and weighing-bucket gages decreased. These results should be considered with caution because only between four and nine storms were included for each rainfall classification. Two other factors in the setup of the gages can also affect the results when classifying by intensity. The weighing-bucket gage in the dual-gage setup did not contain a funnel which can decrease the losses due to wetting by 2-15 percent (Sevruk, 1982). Lastly, a shielded gage, such as the weighing bucket in the dual-gage setup, records 3-5-percent greater amount of rain depending on the wind speed compared to unshielded gages, like the tipping bucket in the dual-gage setup (Linsley and others, 1975).

REFERENCES

- Conover, W.J., 1980, Practical nonparametric statistics: New York, New York, John Wiley and Sons, Inc.
- Duncker, James J., Vail, Tracy J., and Earle, John D., 1993, Rainfall in and near Du Page County, Illinois, February 1986-September 1991: U.S. Geological Survey Open-File Report 92-485
- Jones, D.M.A., 1969, Effect of housing shape on the catch of recording gages: Urbana, IL, Monthly Weather Review, v. 97, no. 8, p. 604-606.
- Leighton, M.M., Ekblaw, G.E., and Horberg, Leland, 1948, Physiographic divisions of Illinois: Illinois State Geological Survey, Report of Investigations 129, 33p.
- Linsley, R.K. Jr., Kohler, M.A., Paulhus, J.L., 1975, Hydrology for engineers (2d ed.): New York, New York, McGraw-Hill, Inc., p. 69-70.
- National Weather Service, 1989, Cooperative station observations: Silver Spring, Maryland, National Weather Service Observing Handbook No. 2, Silver Spring, MD.
- Qualimetrics, Inc., 1986, Manual for precipitation gage calibrator model 60103: Sacramento, California, Manual No. 60103-001, October 1986, p. 8.
- Schlotzhauer, S.D., and Littell, R.C., 1987, SAS system for elementary statistical analysis: Cary, North Carolina, SAS Institute, Inc., 416 p.
- Sevruk, B, 1982, Methods of correction for systematic error in point precipitation measurement for operational use: Geneva, Switzerland, World Meteorological Organization, Operational Hydrology Report No. 21, WMO - No. 589, 91 p.
- Spiegel, M.R., 1988, Theory and Problems of Statistics (2d ed.): New York, NY, McGraw Hill Inc., 504 p.
- U.S. Department of Commerce, National Oceanic and Atmospheric Administration, 1986-95, Climatological data, Illinois: Asheville, N.C., Environmental Data and Information Service. (published monthly).

Boise Five Mile Drain - Future Flooding and Old Canal Crossings

**Kenneth L. Bullard, Hydraulic Engineer, U. S. Bureau of Reclamation,
Denver, Colorado**

ABSTRACT: Five Mile Drain is a 97-square-mile drainage basin located south and west of Boise, Idaho. Earlier in the century, several canals were constructed across the drainage basin to deliver water from Reclamation dams upstream to the primarily agricultural land south and west of Boise. In the 60 years since the original canal construction, much urbanization has occurred in the basin. The prospects for continued urbanization are great. This increased urbanization results in higher flood peaks and volumes. The original canal crossings constructed over Five Mile Drain are now hydraulically inadequate, and the canal banks act as unintentional flood detention dams. The problem will get much worse in the future. Private businesses and homes which were built safely out of the flood plain in the past are now subject to occasional flooding due to the increased volume of flood water and the now inadequate hydraulic structures used to pass the flood water under the canals.

This is a pilot study for Reclamation. Many other drainage basins in urbanizing areas of the western United States are crossed by canals built in support of Reclamation irrigation projects. Attempts to quantify the remaining flood problems resulting from urbanization upstream from Reclamation canals will be made and priorities set for future actions by Reclamation. Additional modeling and data needs are identified .

BASIN DESCRIPTION

The Five Mile Drain basin covers approximately 97 square miles of land to the south and west of the city of Boise, Idaho. This area includes the city of Meridian, and the rapidly urbanizing areas near the Boise International Airport, plus numerous areas of new housing developments and commercial lands. A field investigation of the site was made by the author of this report in October 1996.

In 1994, the land uses ranged from steep natural cover land south of Lucky Peak Reservoir and east of Interstate 84, to irrigated fields where sugar beets, corn, alfalfa, and other crops are grown in the relatively flat lands to the north and west of Meridian, Idaho. Much of the lower basin, west of the airport is crossed by numerous canals and drainage ditches. Many new housing developments ranging from town homes and apartments to small ranches of about 5 acres in size, are appearing in the flat areas of the basin, south and west of Interstate 84

The largest of the canals crossing the Five Mile Drain basin is the New York Canal, built by Reclamation, and currently maintained by a local agency. In this location many acres of flood ponding behind the canal bank can occur if the crossing of Five Mile Drain under the New York Canal is plugged.

Other locations of importance are at the Ridenbaugh Canal, crossing where the Five Mile Drain feeds directly into the Ridenbaugh Canal. A waste way for the canal exists at this point. Depending on what action is taken during potential flood events, some of the flood flows in Five Mile Drain may

enter the canal and be transported out of the basin, or the waste water from the canal may add to the flooding in downstream areas.

Near the downstream end of the study, the Phyllis Canal crosses Five Mile Drain. The canal bank is several feet above the natural and irrigated ground in this area. A large culvert structure under the canal exists at this point, but it may be insufficient to handle the large peak flows which may occur. Potential flooding of irrigated fields is likely for large floods behind the Phyllis Canal at this point. The study ends about 2 miles west of this point, where Five Mile Drain joins Ten Mile Drain. The combined flows enter the Boise River a short distance downstream from this confluence.

Some base flow appears to be in the drain below the Ridenbaugh Canal crossing at all times. This flow may come from sewage plant operations and from some irrigation return flow drains in the area. This base flow was measured and is included in the hydrologic model built to study this basin.

In numerous other locations, small culverts and pipes, ranging from 10 inches to 24 inches in diameter have their outfall in the Five Mile Drain channel. It is likely that each of these pipes drain some amount of developed area nearby, or they are the waste water outflow for some nearby industry or commercial site. It was not possible in this study to find the source of flow in each of these pipes. For this study, all potential flood flows resulting from heavy rainfall are considered to be overland and small channel flows until they reach the main channel of Five Mile Drain, or one of its main tributaries. It is not believed that any of the individual culverts or pipes would add very much to the Five Mile Drain flood flows for the return periods selected in this study. The effects of urbanization in each subbasin are taken into account in the whole subbasin, and include the effects of the many small culvert and pipe flows.

Numerous roads also cross this drain as it makes its passage across the southern and western city limits of Boise. Most of these road crossings are small CMP or concrete box type culverts. None of these road crossings has been individually considered in the development of the flood hydrographs in this study. The influence of each of these crossings will be best seen in the flood plain study which may follow from this study. It was not felt that any of these road crossings provided sufficient upstream ponding storage areas to influence the peak flows in any significant way and were thus eliminated from the flood hydrograph computations.

Nineteen subbasins were defined for this larger total basin. The subbasins were defined for each major tributary which could be defined on USGS (United States Geological Survey) topographic maps. The subbasins were further split to provide hydrograph information at each of the canal crossing points. Additional subbasins were defined for the upper basin where potential development in the steeper areas of the dry natural range land would appear to be limited.

PRECIPITATION

The HEC-1 model and the SCS TR55 method involve inputting a 24-hour series of incremental rainfall increments. The rainfall total for each desired return period for this study were obtained from the NOAA Atlas II for Idaho¹. This report provides basic rainfall data for various durations and provides procedures for reducing the rainfall for area size and for elevation. The Bureau of

Reclamation Flood Hydrology Group has produced a computer program titled PREFRE to produce data for numerous other durations and return periods using the NOAA ATLAS II data and procedures.

Rainfall incremental distribution was input at 15-minute increments based on the SCS procedures. The actual distribution is referred to as the SCS Type II rainfall distribution. This is the distribution preferred by the SCS in their flood hydrograph computation procedure. This distribution is recommended for all interior parts of the United States subject to thunderstorms.

LAG TIME COMPUTATIONS

The HEC-1 and SCS procedures for determining unit hydrographs require an estimate of the lag time for each subbasin. The SCS procedure involves estimating the longest travel time in each subbasin based on lengths of channel flow, shallow flooding, and overland flow in each subbasin. The total length of flow in each subbasin is for the longest water course. The upper 200 feet in each basin is considered to be overland flow. Flow velocity for this length of overland flow is determined from the estimated ground slope and from charts in the SCS TR55 Manual. The shallow flooding areas continue from the end of the overland flow length to the end of the main channel which appears on the USGS quadrangle maps. Flow velocity for this length of shallow flooding is determined from Mannings kinematic equation 3.3 in the SCS TR55 Manual. Estimates of Mannings n value, the shallow flooding reach slope, and the 2-year, 24-hour rainfall are needed for this equation. The remaining time to be added for flood hydrograph development in each subbasin is the travel time in the main channel as defined on the quadrangle maps. This time is estimated based on dividing the various main channel reach lengths by an estimated velocity. The sum of all of these estimated travel times is the subbasin time of concentration. In the HEC-1 procedure the SCS lag time is used. The SCS lag time is defined as 0.6 times the subbasin travel time. The SCS lag time is then used by the HEC-1 model to convert a dimensionless SCS unit hydrograph to unit hydrographs at the appropriate unit duration for each subbasin.

The flood hydrographs developed in each subbasin are combined or routed with the next downstream subbasins in order to determine the total flow at each point of interest at the bottom of each subbasin.

LOSS RATE AND CURVE NUMBER DETERMINATION

To estimate runoff from storm rainfall, the HEC-1 and SCS TR55 method uses the runoff curve number (CN) method². Determination of CN depends on the watershed's soil and cover conditions, which includes the hydrologic soil group, cover type, treatment, and hydrologic condition.

For this study the hydrologic soil groups in the Five Mile Drain basin were determined by using the SCS Soil Survey Series for Ada County, Idaho³. Copies of the map panels in the Ada County Soil Survey were taped together and the 19 subbasin boundaries for the Five Mile Drain basin were sketched on these maps. Each of the many soil types were identified by hydrologic group type in the SCS Ada County Soil Survey. On the copied map panels, each of the soil types were color coded based on the identified hydrologic soil group. Hundreds of individual soil groups were identified on the maps. By inspection of color coded map, it was determined that the majority of the soils in the

entire basin fell in hydrologic group C. Estimates of the other hydrologic group percentages in each subbasin were also made by inspection of the color coded maps. It was impractical to physically measure each of the hundreds of individual soil groupings. Small changes in the percent of coverage by any hydrologic group would have minimal effects on the computed curve numbers in any subbasin.

Urbanization changes a watershed's response to precipitation. The most common effects are reduced infiltration and decreased travel time, which significantly increase peak discharges and runoff. Runoff is determined primarily by the amount of precipitation and by the infiltration characteristics related to soil type, cover type, impervious surfaces, and surface retention. Other types of land use, such as irrigated crops and contoured farming, also tend to reduce surface runoff. The SCS TR55 method provides a means to estimate the CN for various land uses if the hydrologic soil group is known.

The main work involved in the selection of the curve number is determining the amount of land in each subbasin which is involved in each land use category. The Reclamation Snake River Project Office in Boise, Idaho, had good resources for the land use classification for this basin. This office provided land uses and the total acres in each use, broken into 12 categories, for each subbasin presented in this study. This land use classification was based on 1987 aerial photographs and adjusted by field inspections to 1994 land use conditions. With this information it was possible to determine the CN for each subbasin.

“ULTIMATE FUTURE CONDITION LAND USE”

“Ultimate future” development is defined, for this study, as the fully built, fully urbanized conditions, without specifying any date. To satisfy the needs of the scope of the study, some effort was needed to determine “ultimate future land use” and the increase in runoff likely to result from increased urbanization. Several sources of information were solicited: the local power company, the state highway department, and various county planning agencies. All of these sources had some projections for future population and needs of their agency in the area for future growth. The extent of the changes in land uses within the Five Mile Drainage Basin, based on these projections, were very difficult to ascertain.

The source of information which seemed to best suit the needs of this Five Mile Drain flood study was a 1993 provisional demography report for northern Ada County⁴. Several limitations on demography projections are listed in that report. With the limitations in mind, the report continues to break northern Ada County into several planning areas. This breakdown includes most of the Five Mile Drain basin area. In each planning area some population and employment projections for 5-year increments from 1990 to 2015 were made. For “ultimate future” build out conditions, it was decided that doubling the estimated rate of growth from 1990 to 2015, plus an additional 10 percent, and then multiplying this rate to the estimated population for the year 2015 would be appropriate. There is no scientific basis for this assumption and there is no future year associated with this estimate.

For use in this Five Mile Drain Study, the various subbasins defined for the HEC-1 flood model were assigned to the various planning areas in the Ada County demography report. The population estimates for the various districts were then applied to the subbasins. The ratio of the 1990 population to the estimated ultimate future population was calculated. The previously estimated

urbanized land area percentages were then multiplied by the ratio for the population increase. The increase in urbanized land area was calculated for each subbasin. The increase in the urbanized areas was then deducted from the non-urbanized land use categories in each subbasin. The urbanized areas were assumed to occur uniformly in each subbasin, taking up equal proportions of each non-urbanized category. In some cases the estimated increase in urbanized land uses added up to more than 100 percent of the total basin area using this technique. For those cases the resulting urbanized percentages were reduced such that the total subbasin area remained the same, but fully urbanized. The same procedure as was used with the 1994 land use analysis was used to convert the land uses to basin average curve numbers and impervious percentage for each HEC-1 subbasin.

As with all forecasts, the results are only approximate at best. They get worse as the amount of time increases between the date of the forecast and the forecasted date of some future event increases. The forecasts also get worse with smaller area size. The purpose of these forecast numbers is to give an indication of what the future may hold in terms of flooding along the entire Five Mile Drain. They are not intended to predict any specific future land use at any specific point in the basin. The results of the hydrologic modeling produced future condition 25-year hydrographs for each location that are approximately equal to the current condition 100-year hydrographs in peak and volume.

FLOOD STORAGE ROUTING CALCULATIONS

The flood plain portion of this study used discharges for the current (1994) conditions only and is considered **preliminary** in nature. There are three areas of possible large flood storage volume in the Five Mile Drain Basin. The largest potential flood storage site is at the New York Canal crossing, and the second largest is at the Interstate 84 crossing, and the third is the Pacific Railroad crossing near Meridian. In each case it was necessary to create information to perform storage routing in the HEC-1 model. In all cases the volume of storage was approximated using available USGS topographic maps. Contour lines behind the canals were measured and the surface areas and associated depths were converted to volumes in acre-feet. Additional ground survey information for the culverts and hydraulic structures was used for input the HEC-RAS model. This model then created the necessary rating curves for these structures, and these data were then input to HEC-1.

New York Canal Crossing of Five Mile Drain - The culvert providing cross drainage at this location is severely plugged. Only one of the original two barrels has any flow capability at all, and that opening has only about 1.5 feet of vertical open space which has not been silted in. Hydraulic computations performed with available survey data and the HEC-RAS model for this site indicate that only 154 ft³/s can be passed by this culvert prior to the west side canal bank being overtopped at elevation 2794 feet. Peak inflows for the current land use conditions at this point on Five Mile Drain are 1154 ft³/s and 641 ft³/s for the 100-year and 25-year flood events, respectively. In addition, significant flood volumes occur with both these events.

Interstate 80 near Eagle Road - The hydraulic structure available for passing potential Five Mile Drain flood flows under the main Interstate Highway at this point is limited to a single 6-foot diameter culvert, which is 520 feet in length, and has a relatively small head available on the upstream side. Hydraulic computations performed as part of this study show that this culvert is only capable of carrying about 320 ft³/s prior to the Interstate Highway being flooded at elevation 2644 feet. Peak

flood inflows calculated at this point are 2397 ft³/s and 1579 ft³/s for the 100-year and the 25-year floods, respectively. Eight Mile Drain, one of the major uncontrolled tributaries to Five Mile Drain provides a large portion of the peak flows just above Eagle Road near this point.

A major modeling complication for this crossing is that it does not show on the available USGS topographic maps. The interchange was sketched on the maps and approximate storage based on the contours upstream was calculated. Because of inconsistencies between the ground survey and the USGS topographic map, this storage computation is only approximate at best.

Pacific Railroad near Meridian - The railroad crossing at this location is the highest embankment in the area. This railroad crossing has two culverts, located about 220 feet apart, both with relatively small amounts of head available. In addition, the land just upstream to the south of this crossing is very flat. The calculated peak inflows at this site are 1753 ft³/s and 776 ft³/s, respectively, for the 100-year and the 25-year events. Hydraulic computations show that about 540 ft³/s can be passed by the existing culverts under the Pacific Railroad before overtopping the spur railroad to the west, at elevation 2614.3 feet. The potential exists at this point for flood flows to exit the Five Mile Drain floodplain and flow as shallow flooding to the west and into the populated areas of the City of Meridian. Insufficient mapping and survey cross section details exist at this time to completely analyze this problem. A spur railroad line serving the need of industries at this location provides some additional elevation to the west of the main crossing at this site. Additional mapping and survey data showing all the improvements in this area are needed to fully analyze this problem.

ADDITIONAL PROBLEMS WITH FLOODPLAIN ANALYSIS

For the most part, the hydraulic calculations appear to be good, but there are some anomalies which have not been resolved at the time of this report.

In many places the surveyed cross sections had to be extended, using available USGS topographic maps. In some areas, particularly in the lower portions of the study below Starr Highway and Phylliss Canal, the survey cross sections appeared to place the Five Mile Drain main channel 3 to 4 feet above the ground surface elevations determined on the USGS topographic maps. When the survey data were combined with extensions based on the maps, the apparent result was that the main channel banks were elevated above the surrounding ground, creating a levee effect. This creates some problems with the hydraulic computations. The apparent 100-year flood elevations are below the 25-year elevations in some places. This happens because the 25-year flood discharges can be contained in the main channel in most locations but the 100-year discharge cannot be contained in the apparent levee banks. Once the banks are overtopped the apparent 100-year flood elevation is lower than the 25-year flood elevation.

In other places the cross section extensions create very wide floodplain widths just above the elevation of the survey river banks. This also creates some anomalies in the relationship of the 100-year and 25-year floodplain widths. For purposes of plotting these preliminary floodplain limits, the data from the HEC-RAS output were used for all sections where it appeared reasonable. In those cross section locations where unreasonable results were computed, the floodplain limits were determined from the upstream and downstream sections. In all cases the limits of the floodplain

between cross sections are based on judgment and the realization that the survey cross section data may not match the topographic map.

Other problems with the USGS topographic maps used to plot the floodplain limits involve the age of these maps. Most of the USGS topographic maps were originally drawn in the 1950s with some revisions in the late 1970s. Much urbanization has taken place since these maps were last updated. In many places new roads and culvert crossings exist which are not shown on the maps. In particular the entire interchange of Interstate 80 with Eagle Road does not show on these maps. In some places the location of Five Mile Drain has changed by several hundred feet. These factors also make it difficult to consider these floodplain limits to be any thing but **preliminary** indications of where the actual floodplain should be drawn.

Other potential problems with drawing flood boundaries for Five Mile Drain involve the rapid pace of urbanization which is taking place at the time of the study. Many areas of this basin are under construction as this study is being undertaken. New housing developments, shopping malls, and industrial sites with road and channel improvements are constantly being created. These changes will affect both the discharges and the limits of the floodplain in most areas. Any floodplain limits which are delineated can be assumed to be accurate for only a limited amount of time.

MODELING NEEDS TO CONTINUE PROJECT IN THE NEXT CENTURY

In addition to the discharge and floodplain estimates for Five Mile Drain, this project produced the following data and modeling needs to improve the speed and accuracy of future estimates for similar projects in the future.

1. The use of digital elevation models to help improve the estimates of the basic hydrologic parameters for the flood hydrograph model, HEC-1 or a later version. It would be desirable to have such models be able to calculate reservoir storage behind urban type improvements such as railroad embankments, road crossings, canal crossings and small retention/detention basins in new subdivisions.
2. If available, the use of digital maps for computing composite curve numbers using SCS soil maps by overlaying the basin and subbasin boundary maps.
3. If available, use digital maps from county planning agencies to aid in the establishment of "ultimate future condition" land uses based on population projections. Most rural counties of this country do not have such information.
4. Possible inexpensive methods of improving digital floodplain mapping, especially in areas where recent development have altered the available USGS topographic map elevations and watercourse locations.
5. Improved and inexpensive methods of incorporating traditional survey data, regarding culverts and bridges, with digital or conventional USGS contour maps. Inconsistencies

between the two sets of data create major problems with hydraulic computations and floodplain mapping efforts.

6. Some computerized method of comparing future condition floodplain with existing conditions. Some method to develop and use stage-damage curves for the “ultimate future condition” is needed.

REFERENCES

- ¹ Miller, J. F., Frederick, R. H., and Tracey, R. J., NOAA ATLAS II - Precipitation-Frequency Atlas of the Western United States, Volume V - Idaho, United States Department of Commerce, National Oceanic and Atmospheric Administration, National Weather Service, Silver Spring Md, 1973.
- ² United States Department of Agriculture, Soil Conservation Service, National Engineering Handbook, Chapter 4- Hydrology, 1985.
- ³ United States Department of Agriculture, Soil Conservation Service, Soil Survey of Ada County, Idaho, 1980.
- ⁴ Ada County Planning Association, 1993 Provisional Demographic Report for Northern Ada County, Idaho, APA Report No. 16-93, August 1993.

EQUIVALENT RECTANGLE SIMPLIFICATION (ERS) METHOD AND ITS APPLICATION IN A DISTRIBUTED HYDROLOGIC MODEL

BY

Wilson Huaisheng Chen, Research Associate
Department of Environmental Science and Engineering
Oregon Graduate Institute, P.O.Box 91000, Portland, OR 97291-1000
Phone: (503) 690-1197, Email: wilson@ese.ogi.edu

AND

Robert. L. Beschta, Professor
Department of Forest Engineering
Oregon State University, Corvallis, OR 97331
Phone: (503) 737-4292, Email: beschtar@cmail.orst.edu

Abstract: In the field of distributed hydrologic models, the geometry of distributed grid cells represent a pre-defined condition and limitation associated with a particular model. Typically a square-cell geometry is adopted for distributed models since most terrain data is in a square-grid mesh. However, current methods for flow routing with a square-grid surface have limitations since such algorithms involve arbitrary flow directions (4 or 8 directions). There are continuing efforts to improve these problems. For example, TAPES-C model (Moore and Grayson, 1991) uses contour lines and flowpath lines as cell boundaries to form a flow net so that each cell has a naturally defined flow direction. However, hydrologic models developed based on TAPES-C can only be applied to a flow net type of cell format.

The Equivalent Rectangle Simplification (ERS) method is an effort to provide a general algorithm to handle slope flow routing for distributed hydrologic models without setting arbitrary flow directions or cell geometry requirement. For any polygon cell (triangle, rectangle, ...,etc.), the weight of each edge is defined as the proportion of drainage area that each edge has within the cell. The ERS calculates the weight for all the edges and generates a virtual rectangle called *Equivalent Rectangle* (ER) which has the same area, same slope angle, same aspect, same length, and same physical characteristics as the cell. An ER of a cell has only one edge (upper) receiving flow and one edge (lower) discharging flow. The hydrologic similarity between a cell and its ER is proven to have great approximation by pattern matching analysis and hydrograph comparison. Therefore, water balance and flow routing for the cell can be performed as an one-dimensional calculation whereby flow discharges through the edges of the cell are then distributed by their edge weights. Since one edge is shared by two cells, the discharging flow from one cell will become the receiving flow by the other cell. A forward routing scheme can then be applied over a distributed watershed from upper cells to lower cells.

The flexibility of the ERS methodology allows a variety of watershed cell distribution to be utilized for simulation purpose. As an example, the ERS is used in the Object Watershed Link Simulation (OWLS) model with application to the Bear Brook Watershed in Maine (BBWM). The watershed consists of both irregular triangular and irregular rectangle cells with different sizes. The simulation results are encouraging.

INTRODUCTION

Watershed hydrologic models are mathematical tools that can be used to simulate the water balance and transport processes within a basin. As the result of modern development in computer technologies, complicated and detailed simulations of a watershed become possible. There is a tendency in hydrologic model development to couple more and more physical rules and equations in the description of hydrologic processes. Since the variation of landscape characteristics within a basin are often large, the technique of subdividing a watershed into small, relative homogeneous land units (cells) become necessary. A model that employs physical rules for the description of hydrologic processes and sub-divides a watershed into many small cells is categorized as physically-based, distributed hydrologic model.

A cell is a small area in a watershed representing a relatively homogeneous characterization of geology, hydrology, soil, vegetation and topograph. Therefore, a natural cell may not have a regularly shaped boundary condition. Nevertheless, many hydrologic models require a certain pre-defined size and shape of cells, as well as their spatial orientations. For example, a square cell is one of the widely adopted shapes utilized by many distributed hydrologic models because of the format of terrain data (e.g. digital elevation model, or DEM data) and the convenience of making up the cell mesh. Inter-connections between cells and the distribution of flow to neighbor cells are accomplished through the hydrologic flow routing procedure. However, current methods for flow routing with a square cell surface may be inadequate since the algorithm involves arbitrary flow directions (4 or 8 directions). This arbitrary method may cause biased prediction of flow process in a basin. In an attempt to overcome this problem, the TAPES-C model (Moore and Grayson, 1991) uses contour lines and flowpath lines as cell boundaries to form a flow net so that each cell has naturally defined flow direction. However, hydrologic models based on this procedure are dependent on a flow-net cell format.

In this paper, we introduce a methodology called Equivalent Rectangle Simplification (ERS) to solve the arbitrary flow routing problems and to add flexibility to physically-based distributed hydrologic models.

THEORY

The ERS method is used to simplify the geometry of a cell, represented as a polygon with n edges and n nodes, into a rectangle which has the same soil and vegetation, same area, same slope, same center location, and same total length (or total width, or width-to-length ratio) as the original cell (Figure 1). Each edge of a cell has a weighting, which is determined by the relative area of a given cell providing water to that edge (Figure 2). This weighting was used to determine the amount of water that could cross a particular edge (zero when none, -9 identifies an upper edge that is receiving water from an upslope cell). By assuming that the physical performance of the cell can be approximated by that of its equivalent rectangle, hydrologic information can be calculated for the equivalent rectangle and then distributed to the edges of the cell by their relative weightings (e.g., discharge) or directly assigned to the edges (e.g., water depth).

The terminology *equivalent* means both cells have the same area, same slope, same soil and vegetation condition, same soil depth, same center location, same aspect and both are planar. They will also have same amount of precipitation inputs, solar radiation inputs, infiltration rate, surface water depth, soil moisture content, amount of flow generated from the surface, soil and macropore system. However, they can be different in shape and consequently the pattern of flow draining from each cell could be different. An equivalent rectangle for an irregular cell is constructed so that it satisfies these conditions. In order to implement a one-dimensional hydrologic calculation, the rectangle also needs to have two sides parallel to the aspect direction in addition to an upslope boundary and a downslope boundary.

There are an infinite number of rectangles that might satisfy the above requirements, however three types of rectangles are probably the most reasonable choices for an *equivalent rectangle* (Figure 1):

- A. A rectangle having the length equal to the projected length of the cell on the slope direction.
- B. A rectangle having the width equal to the projected width of the cell on the contour direction.
- C. A rectangle having the same length:width ratio to the projected length:width ratio of the cell.

Given these options, additional evaluations are needed before deciding which provides an appreciate hydrologic approximation of the original cell.

Figure 3 and 4 demonstrate an analysis of surface runoff routing for equivalent rectangles with type A (same length) and type B (same width) for several cell shapes (triangle and prism shapes were selected for ease of analysis). In both figures, an assumed rainfall event of 3 mm per time step with a duration of 3 time steps has been applied at time steps 2, 3, and 4. The cells of different shapes are assumed to be planar and no diffusion occurs during flow routing along the surface. For both figures, there are two groups of cells, one with shorter slope length and the other with longer slope length. In the group with shorter in slope length, the equivalent rectangular cell will take exactly one time step to route the generated flow out of the

cell. In the group with longer slope length, all cells requires more then one calculation time step to finish flow route. Each group has three types of cells with pyramid, triangle and prism shape respectively, representing the cells with wider downslope boundary, wider upslope boundary and wider center body. All the cells are assumed to be 10 cm^2 in area and are impermeable. Each cell will expect to generate 3 cm^3 of flow from each time step during the rainfall period. Taking into account the time consumed by flow routing; hydrographs were calculated using a spread-sheet.

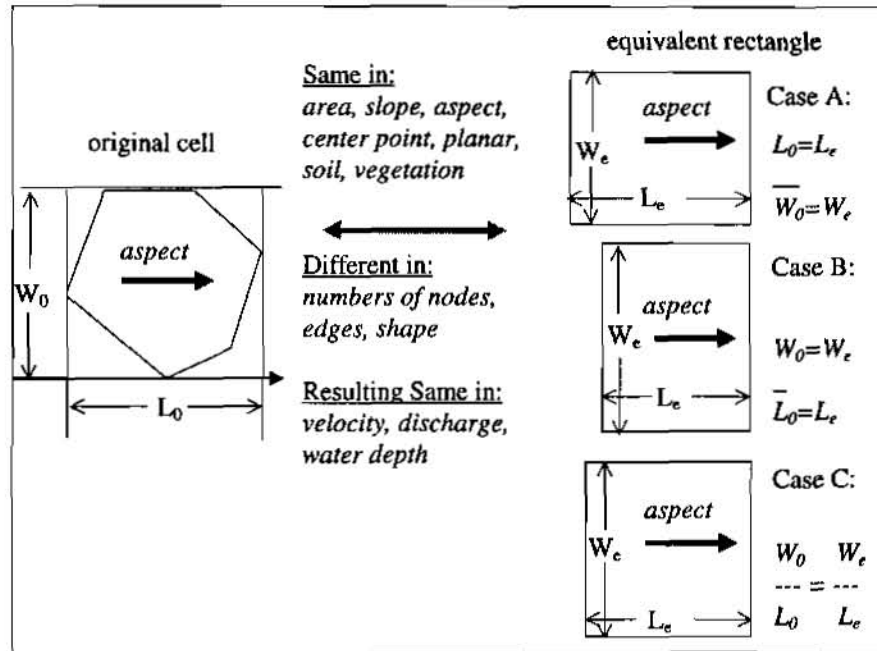


Figure 1. Equivalent rectangles.

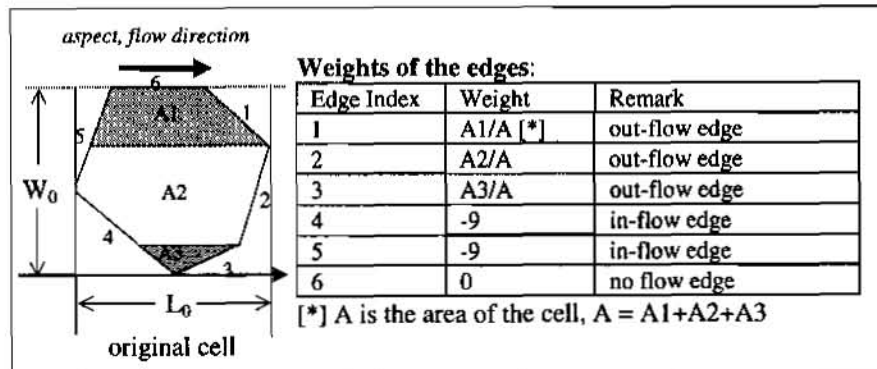


Figure 2. Edge weights of a cell.

In Figure 3, all cells within a given group have the same length even though shapes are varied. For the group of cells with a shorter slope length, runoff responses are instantaneous and all cells produce the same hydrograph. For the group of cells with relatively longer slopes, a pyramid-shaped cell tends to have a faster rising limb and slower falling limb. A triangle-shaped cell has a reversed runoff pattern and a prism-shaped cell tends to smooth the hydrograph peak. The duration of runoff for the different cell shapes are the same. The Equivalent Rectangle, however, produces flow in a linear manner and represents the average situation for the group of cells.

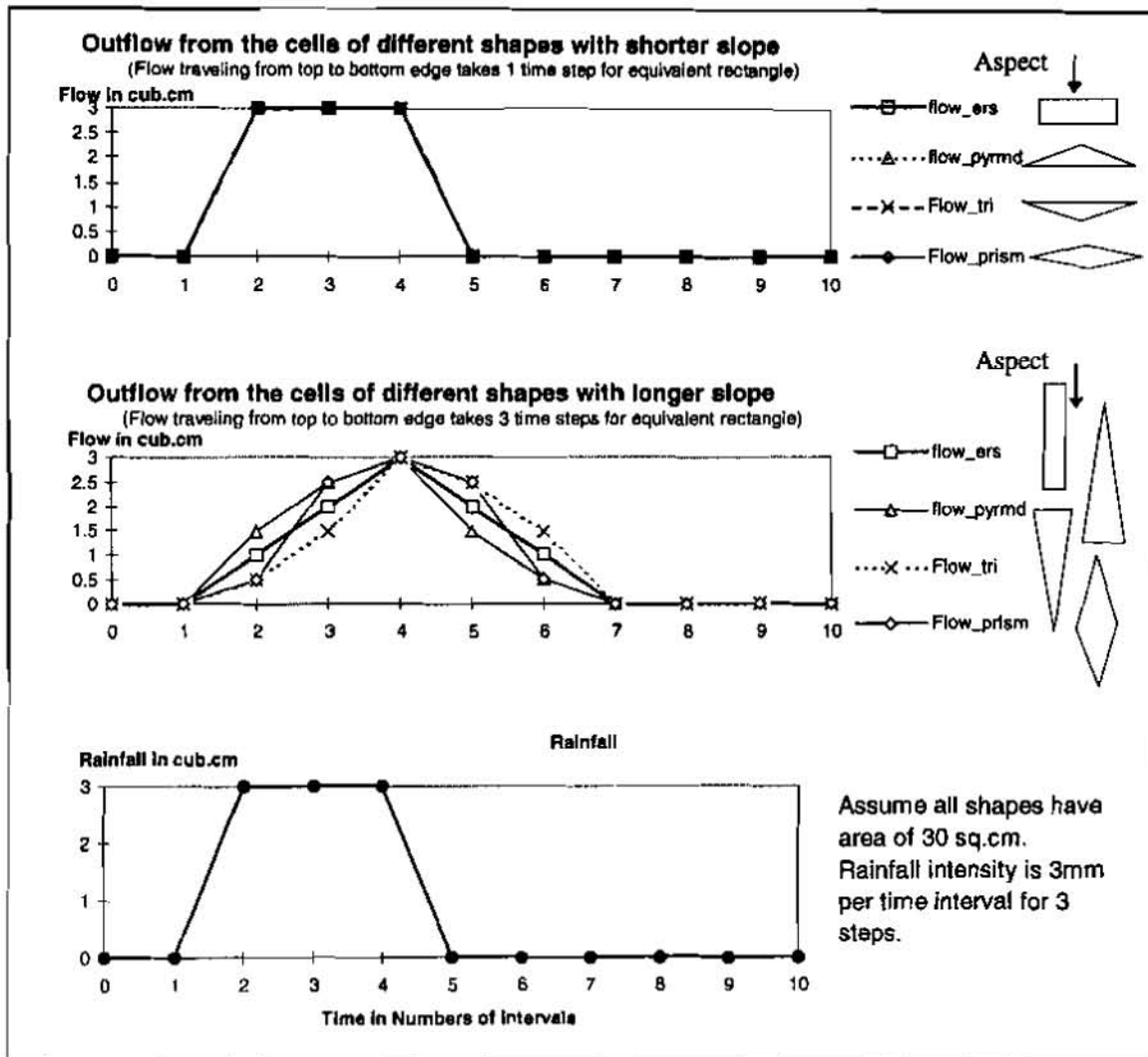


Figure 3. Equivalent Rectangle Simplification, Equal Length ERS.

In Figure 4, all cells with different shapes have been constructed to have the same width. For the group of cells with shorter slope length, runoff responses are quick but varied. Let us assume that the equivalent rectangle has a slope length such that one calculation time step is required to drain all its water, then all other cells will have longer length in order to have the same area. It will require more than one calculation time step to drain water from these cells. As shown in the Figure 4, the hydrograph of a pyramid-shaped cell can be reasonable equivalent by the rectangle, but hydrographs from triangle- and prism-shaped cells will be delayed about one time step in comparison to the equivalent rectangle. For the group of cells with relative longer slopes, this advanced outflow phenomenon of the equivalent rectangle becomes more obvious. In addition, flow from the equivalent rectangle tends to have a higher instantaneous peak than any other shapes.

For a type C rectangle, which has the same width-to-height ratio, we may expect outflow patterns to occur between those found for type A and B cells. Flow advancing and a higher peak of the equivalent rectangle may also be expected. Therefore, we can conclude that: an equivalent rectangle to a cell should have the same length as the slope length of that cell.

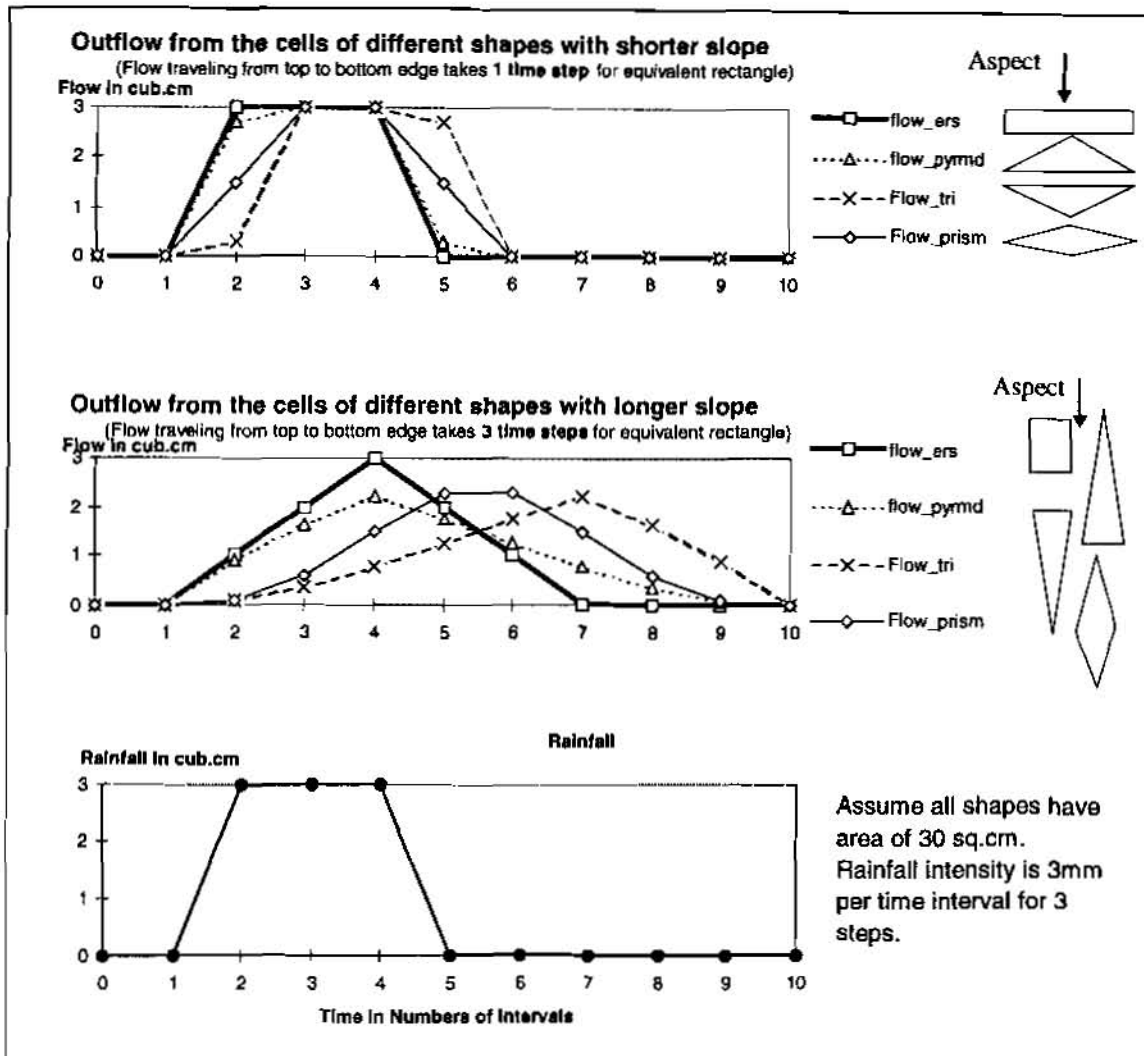


Figure 4. Equivalent Rectangle Simplification, Equal Width ERS.

APPLICATION

The ERS method has been used in the Object Watershed Link System (OWLS) model (Chen, 1996). The OWLS model is a physically-based, distributed, 3-D, vector-based watershed hydrologic model.

The Model Structure: The OWLS model is constructed using the concept of Object-Orientation methodology. A watershed is represented as a 3-D object, which consists of a group of linked 3-D cells (or basic land units), a 3-D boundary and a 3-D stream network. Each cell object consists of a group of linked 3-D edges and each edge is linked by two 3-D nodes. The hydrologic components are also expressed as linked objects. All objects in the OWLS model are distinct with their own characteristics. The structure of the OWLS model not only provides a higher computing efficiency, but also a greater flexibility and capability for watershed dynamic hydrologic simulation than traditional distributed hydrological models.

The Sub-Models: The OWLS model consists of four sub-models: (1) The Data Processing Model handles all data preparation for other sub-models. It converts data from raw ASCII format to the OWLS format, including DEM data conversion, precipitation distribution, air temperature interpolation, and air temperature extension; (2) The Geomorphological Model automatically delineates watershed boundaries, flow-paths, possible stream channels by a vector-based algorithm. It produces a vector-based database for watershed cells, boundaries and stream channels and provides a harmonious simulation base for the

hydrologic and visualization model; (3) The Hydrologic Model is represented by several layers in vertical dimension: the canopy layer, the surface layer, and the soil layer which also contains a macropore pipe component. The hydrologic model simulates processes that occur on a forested watershed, including rainfall, interception, solar radiation and associated evapotranspiration, snow accumulation and melting, infiltration, ex-filtration, macropore flow, surface overland flow, subsurface flow, and flow routing on hillslope and within channels. The ERS method is used in the hillslope flow routing, which includes flow routing for different types of horizontal flows (surface, subsurface and macropore flow). The horizontal 2-D flow routing problem is simplified into 1-D by the ERS method and routed by the non-linear kinematic wave finite differential calculations (Chow et al., 1988). The ERS technique dramatically reduces the complexity of the flow routing model and increases the flexibility and calculation speed of the model; (4) The Visualization Model is a significant component of the OWLS watershed model. It is specially designed for watershed hydrologic simulation and animation. The OWLS model also provides data outputs in text format for custom graphics.

The Watershed: The OWLS model has been applied to the Bear Brook Watershed in Maine (BBWM). The watershed is located in East Maine (44°52'15" Latitude, 68°06'25" Longitude), approximately 60 kilometers from the Atlantic coastline in the northeastern United States (Figure 5). The BBWM is a paired watershed study funded by the U.S.EPA since 1987 as part of the Watershed Manipulation Project (WMP) within the National Acid Precipitation Assessment Program (NAPAP). NAPAP was designed to assess the causes, effects, and strategies for controlling acidic precipitation.

The study site of the BBWM consists of two continuous first order streams: East Bear Brook (EBB) and West Bear Brook (WBB). On each stream, a catchment outlet was selected and gauged so that both streams have about the same catchment area (EBB=10.7 ha and WBB=10.2 ha). Both watersheds are topographically similar, and are thus ideal for a paired watershed study. Both watersheds have a maximum discharge of about 0.01 mm/ha/sec or 0.15 m³/s. Annual water yield relative to incoming precipitation for WBB ranges from 68 to 77% while EBB ranges from 62 to 68%. The soils in the two watersheds are thin spodosols developed from till (Erickson and Wigington, 1987). The bedrock consists predominantly of metamorphosed and deformed pelites, with minor calc-silicate gneiss, and dikes and sills of granite (Norton, et. al., 1992). Folists are common near and at the summit. Minor, poorly-drained soils are present in the upper part of EBB and a small area midway up the WBB. The depth of the watershed soils range from 0 to 5m, typically 1 to 2m. Vegetation of the BBWM is dominated by hardwoods including american beech, sugar maple, red maple, with minor amounts of yellow birch and white birch. Softwood, mixed, and hardwood stands cover approximately 25, 40, and 35% of the total watershed areas respectively. The climate at BBWM is cool and temperate, with a mild maritime influence. The mean annual temperature is about 4.9°C, with an observed range of +35°C to -30°C. Summer daily maximum temperatures commonly exceed 25°C and winter

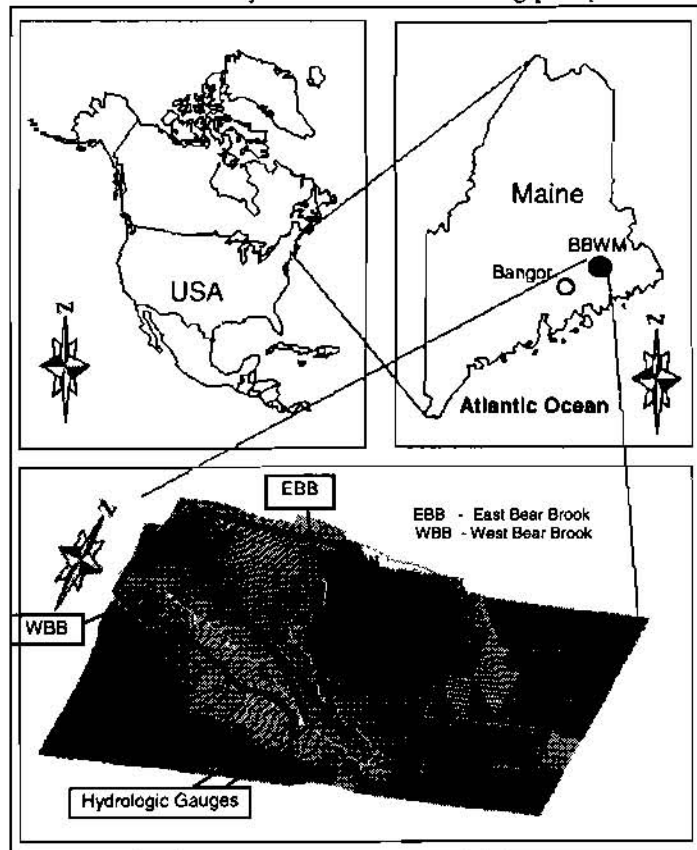


Figure 5. Bear Brook Watershed in Maine

minimum commonly reach -20°C. Precipitation for the period from 1987 to 1996 at the BBWM averaged about 1300 mm per year but locally has ranged from 700 to 1900 mm over the last 10 years. Typically about 20% to 25% of the precipitation is snow.

The Cells: In order to test the stability of the ERS method, we build two different kinds of cell networks for the BBWM watershed: (1) 50m-based triangular cells, which is developed from the 50m-based square cell network by linking two opposite corners to bisect the square (Figure 6); (2) irregular cells, which are constructed based on the points of a terrain land survey performed in the watershed. The range of distances between survey point is from 2 to 10m depending upon the complexity of the topograph (Figure 7).

The Simulation Results: The OWLS model was calibrated using the data from May 1989 at the EBB watershed using 50m-based triangular cells. The results of calibration are shown in Figure 8. The OWLS model has also been validated from different period and in the WBB watershed for additional details, see Chen (1996) or visit WEB site at hydromodel.com). The Same system parameters were also be used to test simulation results from the survey-based triangular cells. Results are presented in Figure 9 and indicate that the simulated hydrographs from different cell systems are basically equivalent. In the other words, the Equivalent Rectangle Simplification (ERS) method does produce stabilized simulation results for a physically-based distributed hydrologic model like OWLS.

CONCLUSION

The ERS method is a generalized approach for simulating flow routing associate with a variety of distributed cells. Simulation results from the OWLS model in the BBWM watershed indicate that this approach provides flexibility in watershed cell distribution and simplifies flow routing calculations.

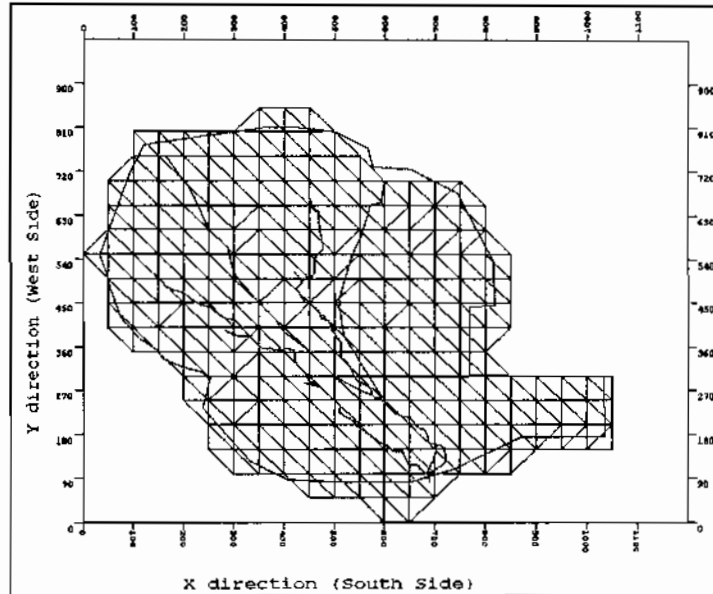


Figure 6. 50m-based Triangular Cells of BBWM

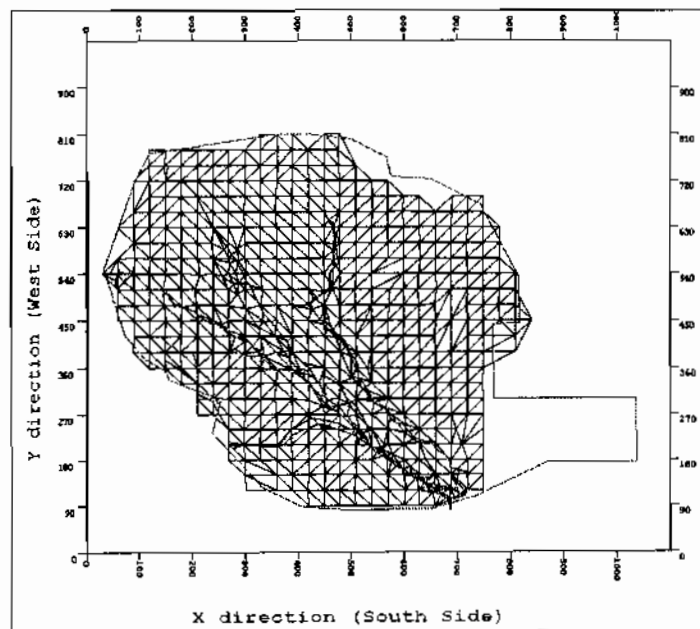


Figure 7. Survey-based Irregular Cells of BBWM

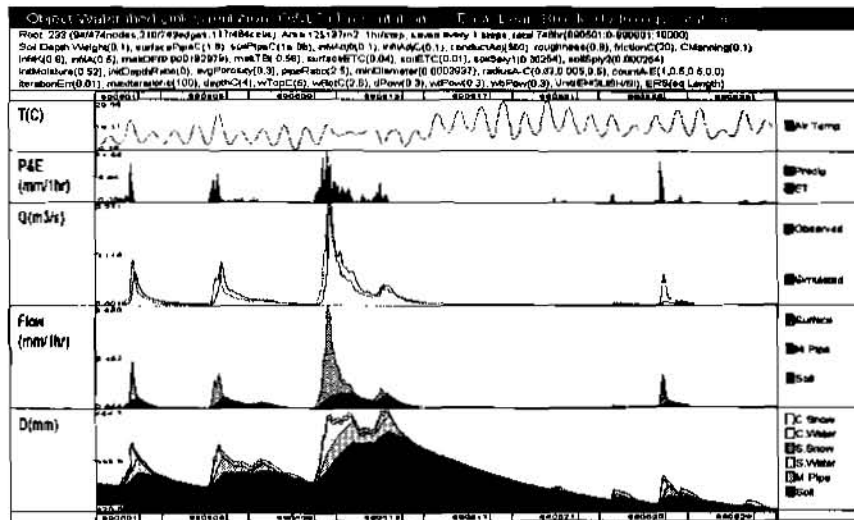


Figure 8. Calibration results from the OWLS model

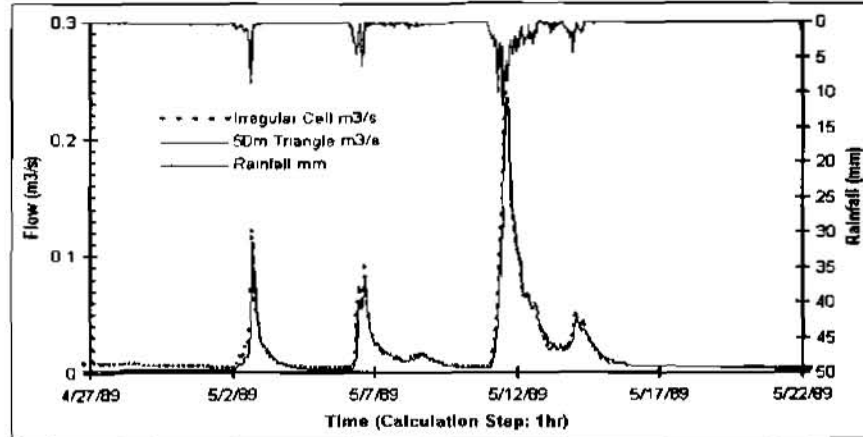


Figure 9. Comparison of Flow Simulation Results from Different Cell Patterns in the EBB.

REFERENCE

- Chen, Huaisheng, 1996, Object Watershed Link Simulation (OWLS), Ph.D. Dissertation, Oregon State University, Corvallis, Oregon, U.S.A. 174pp.
- Chow, V. T., D.R. Maidment, and L.W. Mays, 1988, Applied Hydrology, McGraw-Hill Book Company. 627pp.
- Erickson, H. and P.J.Wigington, 1987, The Bear Brook Watersheds: Site characterization and relation to DDRP watershed soils and NSWS Lakes in the Northeast, Unpublished manuscript.
- Moore, LD., and R.B.Grayson, 1991, Terrain-Based Catchment Partitioning and Runoff Prediction Using Vector Elevation Data. *Water Resources Research* 27(6):1177-1191.
- Norton, S.A.; R.F.Wright, J.S.Kahl, and J.P.Scofield, 1992, The Magic simulation of surface water acidification at, and first year results from, the Bear Brook Watershed Manipulation, Maine, USA. *Environmental Pollution* 77: 279-286.

STANDARD HYDROLOGIC GRID IN SPATIAL HYDROLOGIC MODELING

Authors: Tom Evans, Research Hydraulic Engineer, US Army Corps of Engineers, Davis, CA; Art Pabst, Chief of Technical Assistance Division, Hydrologic Engineering Center, US Army Corps of Engineers, Davis, CA

Abstract The US Army Corps of Engineers Hydrologic Engineering Center (HEC) is advocating the use of standard geographic grids for hydrologic analysis, and has defined a grid for this purpose in the conterminous United States. The proposed Standard Hydrologic Grid (SHG) has cells of equal area throughout its coverage, and is based on a coordinate system widely used for nationwide mapping of the US. These properties offer significant advantages for hydrologic analysis with distributed watershed models and data development with geographic information systems.

This paper presents the definition of the SHG and the rationale behind that definition.

INTRODUCTION

Developments in precipitation measurement and computer representation of the earth's surface make hydrologic modeling with distributed inputs and parameters--formerly the exclusive domain of researchers--viable for hydrologic practitioners. The National Weather Service's NEXRAD radar system provides spatially distributed precipitation data at most locations in the conterminous US. In addition, a growing number of public and private sources provide terrain, soil, land-use, and land-cover data that can be stored, retrieved, and analyzed in geographic information systems (GIS) to produce distributed parameters for hydrologic modeling.

Many distributed-input models simulate hydrologic processes on a grid, in effect breaking a watershed into a squares like a checkerboard and treating each square in that board as a separate and uniform (but not necessarily independent) region for hydrologic analysis. Since the squares in this checkerboard are much smaller than the watershed, this permits more detailed modeling of hydrologic processes than is possible with lumped parameter methods, like HEC-1, which treat the entire watershed as a uniform region. Each cell in the grid can have unique values for the parameters required by the model, and a unique value for precipitation depth at each time step as the model runs. Using this basic framework, a variety of models can be constructed employing different calculation methods and different assumptions--and requiring different parameters.

Using geographic grids introduces a new set of complications to hydrologic analysis. Where multiple grids are used in a model (e.g. a grid for precipitation depth, another grid for hydraulic conductivity of the soil) the grids must be aligned so that the cells in both grids refer to the properties of the same region of the earth's surface. Grids of different resolution (cell size) or based on different coordinate systems (map projections) can lead to misalignment of data and parameters and cause poor modeling results. Hydrologists using distributed models will be wise to learn some basic cartography.

Adopting a standard grid framework will enable hydrologists to exchange data and compare modeling results easily. Use of standardized grids will also allow hydrologic modelers who are not

well-versed in cartography to select data sets that are geographically compatible. For example, users of NEXRAD precipitation data do not need to know the definition of the HRAP grid to know that two data sets that cover the same range of HRAP cells cover the same region. By specifying a adhering to a set of standard data grids, hydrologists will save themselves a great deal of effort in data re-formatting and avoid degrading data through multiple coordinate system changes, which can distort data values much as many generations of photocopying reduce the quality of printed pages.

STANDARD HYDROLOGIC GRID OBJECTIVES

In developing a standard grid proposal, HEC set the following goals:

- The cells in the grid should be of equal area to avoid distortion of precipitation volumes.
- The underlying coordinate system should be one that is commonly used in US mapping.
- The underlying coordinate system should be continuous over the conterminous US, i.e. not divided into zones like the state plane or universal transverse Mercator (UTM) systems.
- The grid design should allow for a variety of cell sizes.

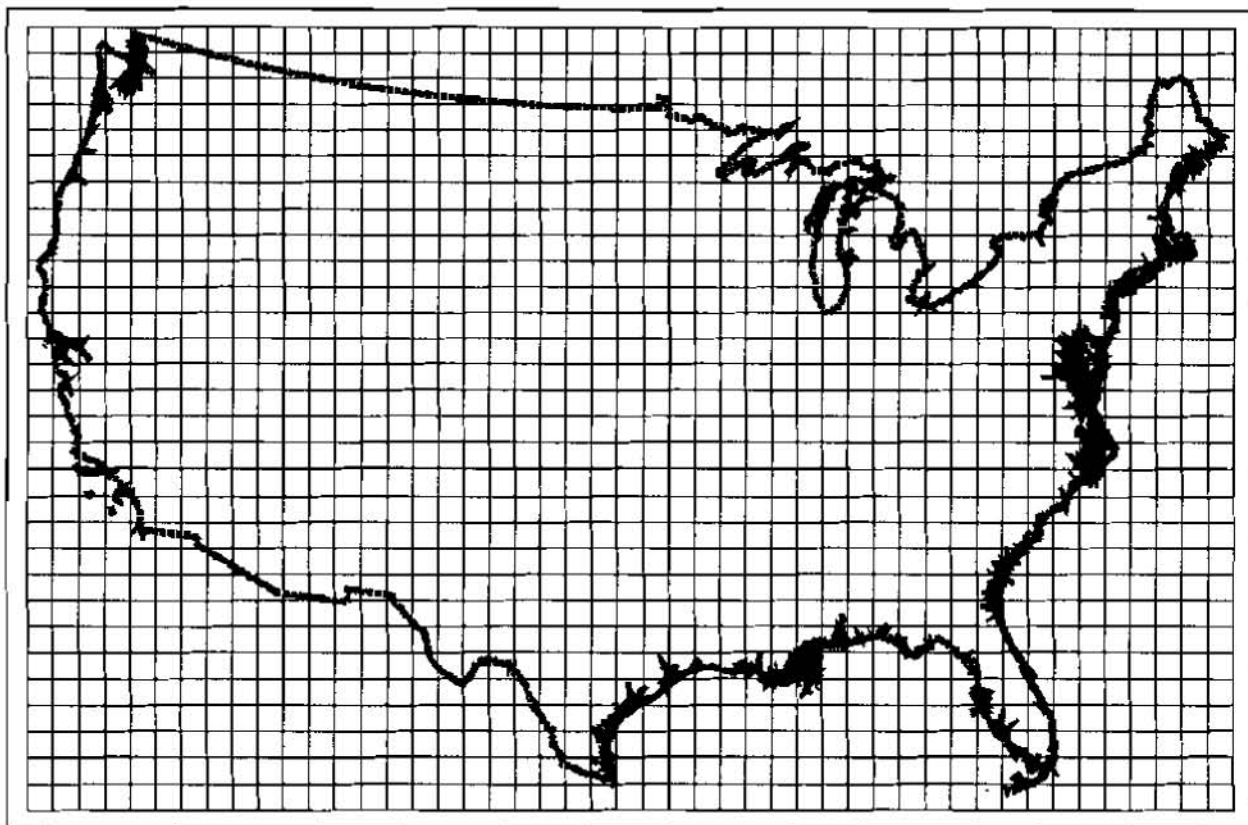
STANDARD HYDROLOGIC GRID DEFINITION

The proposed standard hydrologic grid (SHG) is a variable-resolution square-celled map grid defined for the conterminous United States. The coordinate system of the grid is based on the Albers equal-area map projection with the following parameters.

Units:	Meters
Datum:	North American Datum, 1983 (NAD83)
1st Standard Parallel:	29 degrees 30 minutes 0 seconds North
2nd Standard Parallel:	45 degrees 30 minutes 0 seconds North
Central Meridian:	96 degrees 0 minutes 0 seconds West
Latitude of Origin:	23 degrees 0 minutes 0 seconds North

No offsets, false northings, or false eastings are used. In this coordinate system, easting values range from approximately -2,360,000 m to 2,260,000 m, and northing values range from approximately 270,000 m to 3,175,000 m over the conterminous US.

Users of the grid can select a resolution suitable for the scale and scope of the study for which it is being used. For general-purpose hydrologic modeling with NexRad radar precipitation data, HEC recommends 2000 m cells, and HEC computer programs that use the SHG for calculation will select this cell size as a default. HEC will also support the following grid resolutions: 10,000 m, 5,000 m, 1,000 m, 500 m, 200 m, 100 m, 50 m, 20 m, 10 m. The grids resulting from the different resolutions will be referred to as SHG-2km, SHG-1km, SHG-500m and so on. The accompanying illustration shows cells in this map projection superimposed on the outline of the conterminous US (note that, for purposes of illustration, the cells are larger than the 10 km maximum SHG cell).



For identification, each cell in the grid has a pair of integer indices (i, j) indicating the position, by cell count, of its southwest (lower left, or minimum-x-minimum-y) corner, relative to the grid's origin at 96 W 23 N. For example the southwest corner of cell (121, 346) in the SHG-2km grid is located at an easting of 242000 m and a northing of 692000 m. To find the indices of the cell in which a point is located, find the point's easting and northing in the projected coordinate system defined above, and calculate the indices with the following formulas.

$$i = \text{floor}\left(\frac{\text{easting}}{\text{cellsize}}\right)$$

$$j = \text{floor}\left(\frac{\text{northing}}{\text{cellsize}}\right)$$

Where floor(x) is the largest integer less than or equal to x.

The equal-area property of the projection means that one inch of precipitation in any SHG-2km cell produces 82 acre-feet of water. The National Weather Service HRAP grid, in contrast, is based on a conformal map projection, and cells sizes range from 3.5 km to 4.5 km in the US (and the volume on one inch of precipitation varies from 252 to 417 acre-feet).

The Albers equal-area projection is probably the most common equal-area projection, and is supported by nearly all GIS packages. State Plane and UTM projections are more widespread, but

do not have the equal-area property, and cannot provide a uniform coordinate system over as large an area as the Albers.

The USGS and other federal agencies use the same Albers projection for a number of national mapping products including the national atlas, and the STATSGO soil database (produced by the Natural Resource Conservation Commission). Since the coordinates in these data sets can be converted directly to the Standard Hydrologic grid, data sampling for model parameter development is relatively simple.

Examples: As examples of cell identification in the SHG system, indices of cells containing points in the western US and the eastern US will be identified in the 1km, 2km, and 500 m SHG grids.

Western US: The location 121 degrees 45 minutes west, 38 degrees 35 minutes north (near Davis, California) projects to -2185019 m easting, 2063359 m northing, in the specified Albers projection. In the SHG-2km system the indices of the cell containing this point are

$$i = \text{floor}\left(-\frac{2185019}{2000}\right) = \text{floor}(-1092.5) = -1093$$

$$j = \text{floor}\left(\frac{2063359}{2000}\right) = \text{floor}(1031.7) = 1031$$

In the SHG-1km grid the indices are (-2186, 2063), and in SHG-500m they are (-4371, 4126)

Eastern US: The location 76 degrees 30 minutes west, 42 degrees 25 minutes north (near Ithaca, New York) projects to 1583506 m easting, 2320477 m northing, in the specified Albers projection. In the SHG-2km system the indices of the cell containing this point are

$$i = \text{floor}\left(\frac{1583509}{2000}\right) = \text{floor}(791.8) = 791$$

$$j = \text{floor}\left(\frac{2320477}{2000}\right) = \text{floor}(1160.2) = 1160$$

In the SHG-1km grid the indices are (1583, 2320), and in SHG-500m they are (3167, 4640).

GIS DATA EXCHANGE FOR HYDRAULIC AND HYDROLOGIC MODELS

Authors: Tom Evans, Research Hydraulic Engineer; John Peters, Senior Hydraulic Engineer; Gary Brunner, Senior Hydraulic Engineer, Hydrologic Engineering Center, US Army Corps of Engineers, Davis, CA;

Abstract The Hydrologic Engineering Center is developing the next generation of engineering software for hydraulic and hydrologic (H&H) studies in the Corps of Engineers. Two recent products are the *River Analysis System (HEC-RAS)*, a one-dimensional river modeling system, and the *Hydrologic Modeling System (HEC-HMS)*, a watershed rainfall-runoff model developed to replace the *Flood Hydrograph Package (HEC-1)*. Modeling with both programs begins with a definition of the physical system, which could be developed from a CADD or GIS program. HEC is developing a data-exchange format to provide a standard for transferring terrain data to their new H&H software packages. HEC-RAS, version 2.0, provides the ability to import and utilize XYZ cross-sectional data from terrain models to develop the geometric data. Upon completing the hydraulic calculations, the profile results can be written back to the terrain model. HEC-HMS can import the catchment boundaries and areas, river-reach definitions, and the connectivity of the basin from the data exchange file. This paper describes the file format and the associated terrain modeling routines developed to provide the connection between the H&H models and GIS/CADD software.

CADD AND GIS AT HEC

The Hydrologic Engineering Center (HEC) of the US Army Corps of Engineers is the creator of a number of widely used hydraulic and hydrologic computer models. The HEC-1 flood hydrograph model and the HEC-2 river hydraulics model are the best known and most widely used of these models. A number of companies, universities, and public institutions have attempted with varying degrees of success to link GIS programs with HEC-1 or HEC-2. Most of these efforts have taken the form of pre-processors that prepare input files for the models or post-processors that read and interpret their output files.

HEC is in the process of a major software modernization effort, called NexGen (HEC, 1993) directed at replacing batch-style programs like HEC-1 and HEC-2 with interactive programs. HEC-1 will be superseded by a new program called HEC-HMS (Hydrologic Modeling System), and HEC-2 will be superseded by HEC-RAS (River Analysis System). Although the old programs will be supported for the foreseeable future, there will be no new versions of HEC-1 or HEC-2, and improvements and new features will be added to the new programs, not to the old ones.

The NexGen programs make greater use of geographic information than the programs they are replacing. Although HEC-1 and HEC-2 used data that were derived from geographic sources (watershed areas, infiltration rates, stream cross-sections, etc.) the models themselves did not use or store any reference to location.

HEC's goals with respect to GIS are first that new programs, such as those developed in the NexGen project, should be able to take advantage of data provided by GIS but should not depend on a GIS for execution, and second that the NexGen models should be able to exchange data with any GIS

program. The second goal requires, among other things, that HEC models should not require that geographic data be available in any proprietary formats.

CURRENT EXAMPLES OF GEOGRAPHIC DATA USE IN HEC MODELS

HEC's present approach to data exchange between its models and CADD or GIS programs is to define simple file formats (so far they are all formatted ASCII text) that the models can read or write. These files contain geographic data and model parameters that can be derived from geospatial data, or model results that can be read into geographic data layers.

HEC's first use of GIS in conjunction with the NexGen models was the preparation of a parameter file for the modified Clark unit hydrograph rainfall-runoff transformation. This hydrograph method is designed to work with precipitation reported on a grid, like the National Weather Service's NEXRAD radar precipitation reports, and is part of HEC-HMS. The model requires a small number of parameters for each cell in the grid within the boundaries of the watershed where runoff is to be calculated. The parameters are read from a formatted ASCII file created by GIS programs. The number and type of parameters make it unlikely that these parameters could be calculated by hand, but they are fairly easy to generate with a GIS.

The best-documented example of HEC's approach to incorporating geospatial data in its models is the GIS import/export format devised for use with HEC-RAS, and implemented with version 2.0 of that model. HEC-RAS was already able to import HEC-2 input files, so preprocessors designed to work with HEC-2 could also be used with HEC-RAS. However, an expanded set of import and export functions now permit location data that was essentially thrown away in HEC-2—to be preserved in HEC-RAS.

The GIS import/export file for HEC-RAS is described in an appendix of the HEC-RAS user's manual (HEC, 1997). In summary, the files are formatted ASCII, constructed of keywords and values. The keywords identify the parameters being passed between the model and the GIS, essentially telling the model where to store the associated values. HEC-RAS can read the following information from the import file:

- Stream Network - Stream reaches, identified by stream and reach ID, with positions (in 3D coordinates) of reach centerlines and junctions
- Cross-sections - Locations of cross-sections (2D locations of cut lines, and 3D locations along the ground surface) with stream stationing and some hydraulic parameters

The 3D coordinates are used to plot the reach and cross-section positions in plan and perspective views. The 2D coordinates of the cross-section cut lines are stored in the model along with the station/elevation data common to both HEC-2 and HEC-RAS.

Once a model is run, results can be exported in a file very similar in format to the import file. The data exported from HEC-RAS are:

- Cross-sections - 2D cut lines with water surface elevations for one or several profiles

Water Surface Bounds - A set of polygons, one for each reach, limiting the extent of the water surface

The exported cross-section data can be read into a GIS layer and a water surface calculated between the cross-sections. Inundation areas can be mapped by comparing the interpolated water surface with the ground surface; the edge of the flooded area falls where the two elevations are equal. The bounding polygons are useful for locating the limits of inundated areas where the limits of the water surface are above the natural land surface as, for example, in laying out floodways.

FUTURE DIRECTIONS

The most probable course of the future of GIS activities at HEC a continuation and expansion of present efforts. HEC will focus on developing and improving hydrologic models, and will look for ways to incorporate geospatial data and methods, but will not tie its models to any particular GIS or CADD system. Near-term efforts will focus on designing a data exchange format for HEC-HMS and damage assessment models following the general form of that for HEC-RAS, and developing example methods in GIS programs to work with these models.

REFERENCES

- Hydrologic Engineering Center (HEC), 1996, The HEC NexGen Software Development Project (TP-138). Hydrologic Engineering Center, Davis, CA.
- Hydrologic Engineering Center (HEC), 1997, HEC-RAS River Analysis System User's Manual (CPD-68). Hydrologic Engineering Center, Davis, CA.

ESTIMATING WATER STORAGE POTENTIAL IN THE DEVILS LAKE WATERSHED USING HIGH-RESOLUTION, 7.5-MINUTE U.S. GEOLOGICAL SURVEY DIGITAL ELEVATION MODELS

Glenn G. Kelly, Cartographer, U.S. Geological Survey, Sioux Falls, South Dakota

Abstract

The Devils Lake Watershed is a 3,700-square-mile, closed drainage basin in northeastern North Dakota. Above average precipitation in the past several years has caused substantial flooding within the basin. Federal, State, and local entities have joined forces to coordinate flood control efforts and evaluate long-term options for the mitigation of future flooding.

One of the long-term flood control alternatives under consideration is the enhanced use of upper basin wetlands to intercept and store runoff. Most interested parties agree that the restoration and enhanced use of wetlands can and should be part of the long-term resolution of the Devils Lake water-balance problem; however, there is a lack of consensus as to the total volume of water that could be stored if all of the natural depressions in the Devils Lake Watershed were used to the fullest extent possible.

The U.S. Geological Survey (USGS) has suggested using high-resolution digital elevation models (DEM) derived from the existing 1:24,000-scale topographic maps as a cost-effective means of determining the potential storage capacity of wetlands within the Devils Lake Watershed. High-resolution DEM's differ from the standard 7.5-minute USGS DEM's in two ways: elevations are recorded at 10-meter, rather than 30-meter, horizontal intervals, and elevations are recorded in increments of one-tenth of a foot. In addition to determining basinwide storage capacity, these digital elevation data have the potential to help resolve many other local and basinwide hydrologic issues related to management of the Devils Lake Watershed.

To demonstrate the application of high-resolution DEM's to the study of the Devils Lake flooding issues, researchers selected a subbasin encompassing approximately 100 square miles as a representative test area. Ten high-resolution, 7.5-minute DEM's were produced to cover the subbasin. Using ARC/INFO to process the DEM's, researchers delineated the extent of the subbasin, computed the area of the subbasin, and determined the location, extent, and volume of each depression in the subbasin. Finally, the investigators calculated the average storage capacity per square mile and the total storage capacity for the subbasin.

Any use of trade, product, or firm names is for descriptive purposes only and does not imply endorsement by the U.S. Government.

INTRODUCTION

The Devils Lake Watershed is a 3,700-square-mile, closed drainage basin in northeastern North Dakota. The topography of the basin is gently undulating with numerous shallow depressions, wetlands, and lakes. Devils Lake is a large body of water lying at the low point in the watershed. Above average precipitation in the past several years has caused the lake to rise to record levels and has resulted in substantial flooding in the vicinity of Devils Lake, as well as in other areas of the basin.

The U.S. Army Corps of Engineers (COE), Bureau of Reclamation, Bureau of Indian Affairs, Federal Highway Administration, U.S. Fish and Wildlife Service, National Resource Conservation Service, Environmental Protection Agency, Federal Emergency Management Agency (FEMA), U.S. Geological Survey (USGS), North Dakota State Water Commission (NDSWC), and several county governments, municipalities, and local nongovernment organizations are cooperating in ongoing projects to contain the current flooding and to evaluate long-term options that will result in a more stable water balance and minimize future flooding within the basin.

Two possible long-term options have emerged for stabilizing the water balance in the Devils Lake Watershed. One option is to remove water from the Devils Lake Watershed by pumping water over the divide through an open channel into the Sheyenne River. The other option is to increase the water storage capacity of the watershed above Devils Lake by using the natural wetlands to a greater extent. The first option has been analyzed by the COE. The costs, results, and potential for success are relatively well known, but there are also several impediments to implementation of the project. Many downstream economic, environmental, and political issues are yet to be resolved. The issues related to the second option are even more complex and more difficult to quantify than are the issues involved in the first option. The COE and the NDSWC have investigated the second option, but there remains a lack of consensus as to the total volume of water that could be stored if the many hundreds of natural depressions in the Devils Lake Watershed were used to the extent possible.

To quantify this storage potential as well as address other issues relevant to the resolution of the Devils Lake flooding, the USGS proposed the use of high-resolution, 7.5-minute digital elevation models (DEM). To demonstrate the feasibility of the proposal, the USGS selected a representative subbasin within the Devils Lake Watershed and its Mid-Century Mapping Center produced 10 high-resolution DEM's covering the subbasin.

PURPOSE

Although the DEM's may have various applications, the purpose of this initial effort was to demonstrate and validate the use of high-resolution DEM's to determine the potential water storage capacity of the depressions and wetlands in the Devils Lake Watershed.

TEST BASIN

The subbasin chosen for the demonstration is known locally as St. Joe Coulee Basin (fig. 1). It covers an area of about 100 square miles, including parts of 10 different 7.5-minute quadrangles. St. Joe Coulee flows from north to south and empties into Chain Lake. The topography of the upper part of the basin is gently undulating with numerous small, shallow depressions and wetlands. The lower part of the basin has less local relief than the upper basin and fewer but larger depressions and wetlands, including some large, shallow bodies of water. The maximum elevation in the basin is 1,630 feet and the minimum elevation is 1,445 feet at the inlet to Chain Lake.

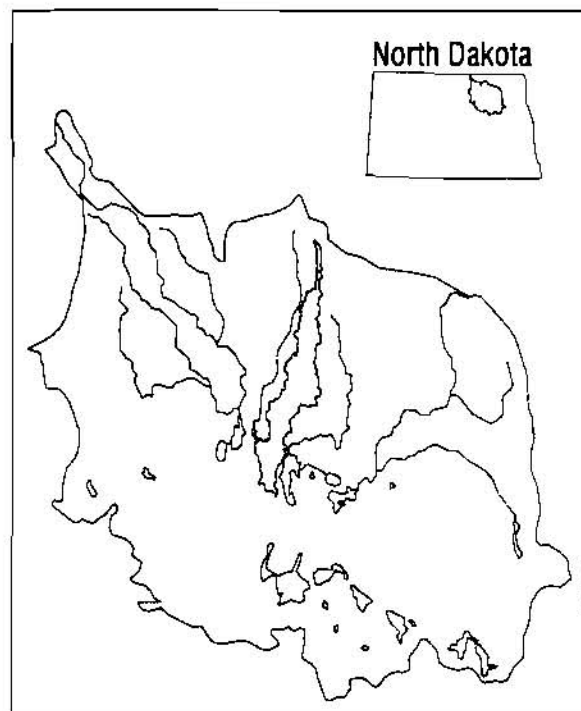


Figure 1.-- Devils Lake Basin. The shaded area is St. Joe Coulee Basin.

DATA

The existing 1:24,000-scale USGS topographic maps are the source of elevation information from which the high-resolution DEM's were derived. The maps were originally compiled between 1950 and 1971. The contours were compiled by both plane-table surveying and photogrammetric methods. The contour interval on all 10 quadrangles is 5 feet. Five of the quadrangles were revised in 1994. The revision did not apply to the hypsography except when it was necessary to alter contours in order to make them consistent with revisions in the hydrographic or planimetric features. The contours were modified to fit the shoreline of marshes, ponds, and lakes and the course of drainage ditches that had been added during the revision. The contours were also adjusted to fit the alignment of new roads. In addition to the topographic maps, a suite of USGS digital products is available for this site. A complete set of digital line graph (DLG) layers, a standard 7.5-minute DEM, and a set of four digital orthophoto quarter quadrangles are available for 6 of the 10 quadrangles covering St. Joe Coulee Basin. A digital raster graphic is available for each of the 10 quadrangles.

Six of the 10 high-resolution DEM's were generated from the DLG's. The remaining four DEM's were generated from tagged vector contour files that were created from the 7.5-minute quadrangles. The standard DEM production process, software, and editing tools were used to produce the DEM's. These high-resolution, 7.5-minute DEM's differ from standard USGS 7.5-minute DEM's in two ways: elevations are recorded in increments of 0.1 rather than 1.0 foot, and the elevations are placed at intervals of 10 meters rather than 30 meters.

PROCESSING

Given the necessary geographic information system (GIS) tools and a digital elevation data set, determining the volume of one or all of the depressions defined by the elevation data is a relatively simple procedure. Processing of the DEM's and subsequent derivative data and information was accomplished in ARC/INFO. The elevation data must be ingested into the GIS (demlattice),* individual elevation files must be merged into a single file (merge),* the value of each cell within each depression must be raised to a value equal to the elevation of the pourpoint of the depression (fill),* a difference data set must be created by subtracting the original elevation data from the newly created, filled elevation data, the extent of the study area must be defined (watershed),* and the volume of the difference data within the study area must be calculated (zonalsum).*

* ARC/INFO tools used in the processing

PRELIMINARY RESULTS

The area of the St. Joe Coulee Basin derived from the high-resolution DEM is 101 square miles. The area of the St. Joe Coulee Basin as interpreted by the North Dakota State Water Commission from USGS 1:24,000-scale topographic maps is 83 square miles. Nearly all of the spatial difference between the two basin delineations is the result of one area of difference at the southern end of the watershed (fig. 2). The correct delineation of the basin boundary through this area has not yet been determined. The total potential water storage capacity of the depressions in the St. Joe Coulee Basin computed from the DEM is 22,773 acre feet or 225.5 acre feet per square mile. This compares to a figure of 180 acre feet per square mile from the 1983 NDSWC study of the entire Devils Lake Basin. Two factors contributing to the difference are that the NDSWC study did not take into account the remaining storage potential associated with large water bodies, and the results from the high-resolution DEM include storage potential contributed by spurious depressions. Further analysis of the DEM and the topography of the area is necessary to identify and remove the spurious depressions associated with the surface generation process.

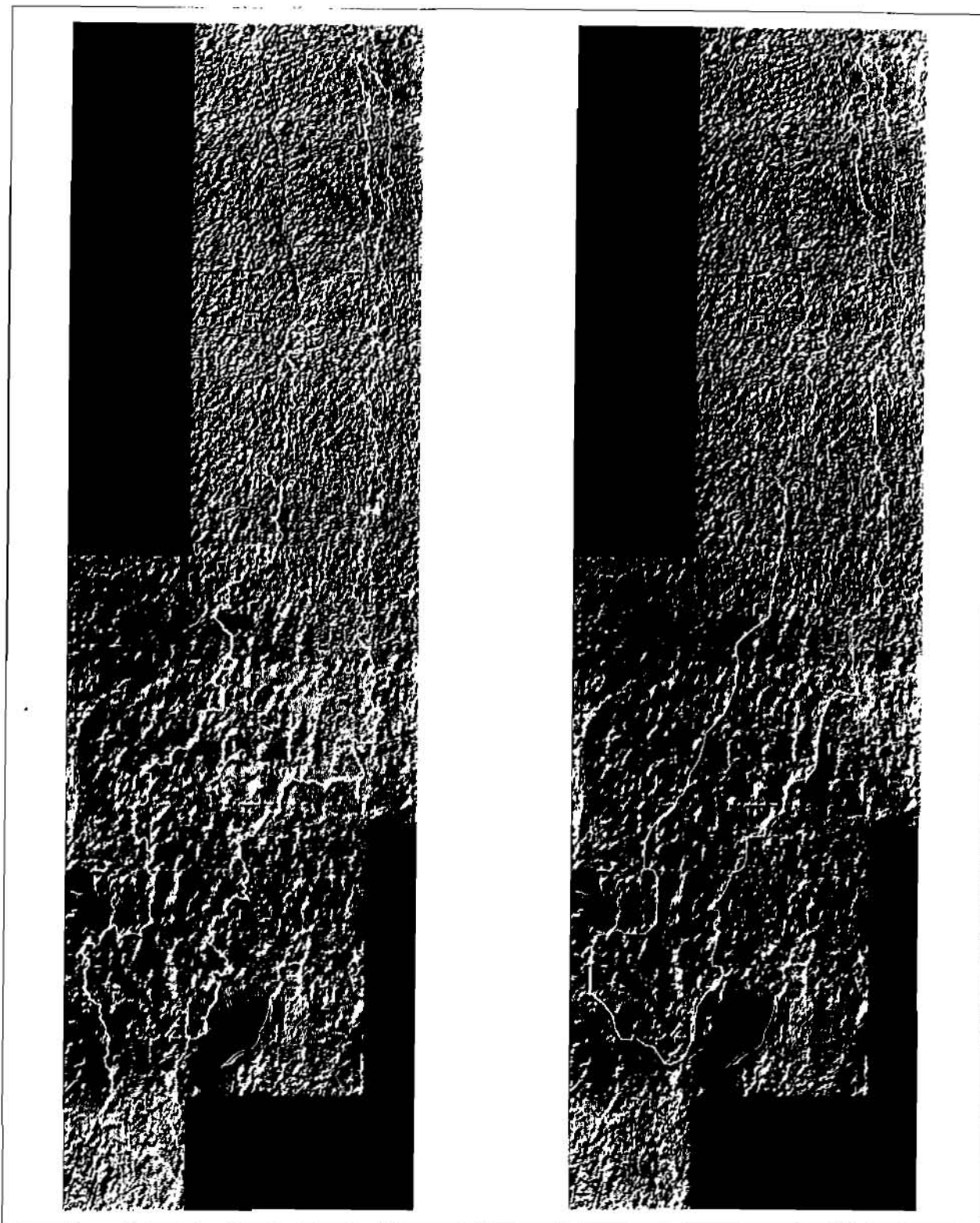


Figure 2. -- St. Joe Coulee Basin shown on a shaded relief image. The boundary on the left was generated from the high-resolution DEM. The boundary on the right was manually delineated by the NDSWC from 1:24,000-scale topographic maps.

VALIDATION

Although the results are not unreasonable, they do not correspond to the other information as well as it was hoped that they would. For this project, neither the time nor the resources were available to conduct a definitive analysis of the accuracy of the high-resolution DEM's, but an effort was made to demonstrate the quality and accuracy of the DEM's using existing products and information. In addition to the comparison of watershed boundaries noted in the Preliminary Results section, depression boundaries derived from the DEM were compared with wetland boundaries compiled in the National Wetlands Inventory, and they were compared with the depression boundaries compiled for several of the quarter-section test sites used in the 1983 NDSWC study. The depressions were also plotted on a digital orthophoto quadrangle to visualize correlation between the digital elevation data and the digital images (fig. 3).



Figure 3. -- The dark lines define the maximum extent of depressions derived from the high-resolution DEM. The depressions are superimposed on part of a digital orthophoto quadrangle.

More than 110 point elevations from a 1:24,000-scale map were compared with the corresponding points in the high-resolution DEM. The average difference was 0.6 feet and the root-mean-square-error (RMSE) was 1.5 feet. Elevations at four points established by a global positioning system survey were compared with the DEM. The maximum difference was 1.5 feet and the average difference was 1.0 foot. A small area (about 0.75 square miles) of the high-resolution DEM is coincident with a very accurate set of digital elevation data produced for FEMA and used for analysis of flooding in the community of Devils Lake. For the coincident area, a difference data set was created by subtracting the DEM from the FEMA data set. The resulting average difference between the FEMA data and the high-resolution DEM was 2.3 feet.

CONCLUSIONS

Although much work remains to be done to thoroughly understand the accuracy, applications, and limitations of the high-resolution DEM's, some conclusions can be drawn from the results. The most obvious advantage of the digital processing is the speed at which the data can be processed. Preprocessing of the DEM does require some one-time operator and computer time, but once the preprocessing is completed, delineation of any basin on a DEM of this size can be accomplished in only a few minutes on many personal computers or UNIX workstations. In contrast, it takes experienced technicians several hours to manually delineate a watershed like St. Joe Coulee Basin from 1:24,000-scale topographic maps. Also the results are repeatable, and as can be seen in the delineation of the St. Joe Coulee Basin, features are shown in greater detail than is usually shown when the basin delineation is manually interpreted from topographic maps. With a limited amount of intervention, the high-resolution DEM's can be used to delineate watersheds like the St. Joe Coulee Basin. The estimate for the total storage capacity of the depressions in the St. Joe Coulee Basin is probably as accurate as any of the other estimates, but the delineation of individual depressions and calculation of their potential storage capacity is not always reliable. The DEM's can be used to identify storage sites with potential for development, but more precise data are needed to accurately define the extent and volume of water storage that would result from a specific project.

The quality of the output is dependent on a large number of factors. Some of these factors can be adjusted to improve the results, but some cannot be changed. One problem that can be minimized with little effort is that of spurious depressions. The surface generation algorithm creates a number of depressions that are not real components of the landscape, and the DEM's contain many other depressions that are too small or too shallow to have been characterized by the original contour information. Intelligent selection of thresholds based on area, depth, or volume could be applied to remove these spurious depressions and improve the results. Two factors that cannot be changed are the date the contours were compiled and the contour interval. When the DEM's are compared with the digital orthophotos, it is apparent that some small, but relevant, depressions are not characterized in the DEM's. In most cases these features are positioned midway between contours, and even though the contour interval is only 5 feet, it is not adequate to portray these subtle features unless they are located near a contour.

An RMSE of 1.5 feet and an average difference of 2.3 feet or less between the high resolution DEM and the reference data sets are about what the investigators expected to achieve from source maps with a contour interval of 5 feet. The quality of the DEM's based on the visual comparisons is less

conclusive. There are some areas where the correlation is very good, and there are some examples of poorly correlated data. In cases of poor correlation, additional analysis is necessary to determine the cause of the poor results.

In areas like Devils Lake, the high-resolution DEM's are an adequate, efficient, and cost-effective means of estimating storage potential. The DEM's also have other applications related to surface hydrology and watershed management, but more investigation is needed to determine the specific applications for which these high-resolution digital elevation data are suitable.

REFERENCES

- Ludden, A.P., Frink, D.L., and Johnson, D.H., 1983, Water storage capacity of natural wetland depressions in the Devils Lake Basin of North Dakota: *Journal of Soil & Water Conservation*, v. 38, no. 1, p. 45-48.
- U.S. Geological Survey, 1993, Digital elevation models -- data users guide 5: Reston, Va, U.S. Geological Survey, 48 p.
- Wiche, G.J., 1986, Hydrologic and climatologic factors affecting water levels of Devils Lake, North Dakota: U.S. Geological Survey Water-Resources Investigations 86-4320, 62 p.
- Wiche, G.J., Jenson, S.K., Baglio, J.V., and Domingue, J.O., 1992, Application of digital elevation models to delineate drainage areas and compute hydrologic characteristics for sites in the James River Basin, North Dakota: U.S. Geological Survey Water-Supply Paper 2383, 23 p.

AUTOMATIC WATERSHED MODEL CALIBRATION WITH GEOGRAPHIC INFORMATION SYSTEMS

**By Rafael G. Quimpo, Professor; Jaber Al-Medeij, Graduate Student
Department of Civil and Environmental Engineering
University of Pittsburgh, Pittsburgh, PA 15261**

Abstract: The advent of high-speed microcomputers has abetted a quicker transfer of recent technology to hydrologic practice. In watershed modeling, extensive data bases have fostered the development of new software to exploit the speed and power of desktop computers in improving runoff prediction procedures.

This paper examines how current techniques for watershed analysis may be modified to take advantage of the availability of spatially distributed hydrologic data to drive and calibrate a watershed response function for a watershed. Starting from the Digital Elevation Model (DEM) for a drainage basin, the response function is developed using a modification of Clark's time-area distribution. The storage parameter is determined directly from an analysis of the flow paths as determined by the geomorphology of the basin. Watershed characteristics are extracted from data bases through the use of geographic information systems software. It is shown that using the method, one can quickly revise the watershed response function to incorporate changes in watershed characteristics due to urbanization.

INTRODUCTION

A major impact of geographic information systems on watershed hydrology is the accessibility and feasibility of rapidly processing of data on watershed characteristics. The high resolution capability of GIS data bases also permits the hydrologist to look into the feasibility of venturing into distributed systems modeling. Quimpo (1984) points out that the change from lumped hydrologic systems approach to distributed modeling may be examined as a matter of scale - of the detail that we examine the various processes in the hydrologic cycle. The choice of scale is constrained by the availability of data to validate a model formulation. Commensurability is another aspect which constrains this choice. One can have too much information in one aspect of the modeling exercise all to be obviated by the paucity of data on another aspect. Thus, while it is possible to consider hill-slope processes in developing the watershed response, since the available rainfall data do not have the resolution down to the hillslope level, this may suggest that one needs to exercise prudence in implementing elaborate theories of watershed behavior.

The response function approach would seem archaic in the light of our capability to handle distributed system formulations but data support systems for the latter just have not been developed to be practicable. For example, there is almost universal awareness of the shortcomings of using runoff curve numbers (U.S.S.C.S., 1972). Yet, they will be around for a long while because there is no better technology which is demonstrably better for a wide range of purposes.

Consider distributed watershed modeling. One can look into the details of the physical process which influence the hydrologic cycle as long as the necessary information needed to calibrate and verify a model formulations are available. With resolution currently dictated by the pixel size in GIS data bases, it follows that the level of sophistication in distributed modeling cannot go finer than the pixel size. This limitation is not overly restrictive. Compared to the availability of land use and soils data, topographic data as provided by current digital elevation models (DEM) provide more than sufficient information for all but the most theoretical treatment of watershed behavior.

All these arguments do not prevent us from attempting to improve our current technology. Research in the different aspects of the hydrologic cycle continues including refinements in the representation of spatial rainfall variability, detailed modeling of the abstraction processes including evapotranspiration and infiltration. It is therefore logical that similar work on the spatial representation of watershed characteristics is undertaken. Advances in rainfall estimation, database development and improved land use mapping all point to better data support systems that we can look forward to. Therefore, we must be prepared to make full use of them when they become available.

This paper focuses on the modeling of the response function of a watershed and examines some problems in relation to the availability of data and the attribution of physical significance to modeling the watershed response. The other motivation for us is to reduce the tedium and subjectivity in many of the tasks that currently confront the watershed modeler. The tools for doing these are now available and so we venture to develop the technique which exploits our computing capability and makes maximum use of current data resources. Another objective is to enable the rapid modification of the response function when watershed characteristics change due to development or urbanization. We also would like the hydrologist not to be too dependent on software expertise in order to use available technology. All too often we end up at the mercy of the software specialist.

Background: One of the major contributions in the evolution of watershed modeling was made by Clark (1945) when he introduced the concept of the time-area curve. The basic idea is that rainfall excess contributions generated from different parts of a watershed are transported to the outlet at different rates so that at any particular time after the inception of runoff, a certain fraction of the watershed contributes to the discharge. On the assumption that the rainfall excess continues, the areal contribution will increase until the whole watershed contributes to the basin outflow. If the rainfall excess is uniform in time, then the direct runoff reaches an equilibrium value at the time of concentration which is the time base of the time-area curve. The Rational Formula, as well as many other models of watershed behavior, makes this assumption. Dooge

(1959) articulated this in his classic paper on the theory of the unit hydrograph. The concept of the time-area plot has been institutionalized more or less in the HEC-1 Program of the Hydrologic Engineering Center. Its use is one of the options that is available to the hydrologist in the package. In the absence of other information which permits him to develop the basin response, HEC1 suggests that one may use the dimensionless equation:

$$AI = 1.414 T^{1.5} \quad 0 \leq T < 0.5$$

$$1 - AI = 1.414 (1 - T)^{1.5} \quad 0.5 \leq T \leq 1$$

where AI is the cumulative area as a fraction of the total subbasin area and T is the fraction of time of concentration. While this formula is useful, it is obvious that it does not consider the shape of the drainage basin nor the paths that rainfall excess increments take on their way to the outlet. This deficiency, hopefully, is somewhat mitigated by the routing of the time-area curve through a hypothetical reservoir to yield the instantaneous unit hydrograph. With the advent of DEMs, an alternative to this approach is now feasible. Algorithms are now available which can process DEMs to calculate the number of pixels that contribute to flow at any point in the drainage network. Thus, since the watershed outlet is the lowest point in the network this allows the automatic calculation of AI for T = 1 and hence, delineates the watershed.

Geographic Information Systems can improve on this procedure. They are able to display the drainage basin area as well as the drainage network as shown in Figure 1. But knowing the contributing area does not necessarily determine the time of concentration. Peculiarities of topography require that the time of travel from a contributing area to the outlet must be carefully estimated. The typical approach, if only surface runoff is considered, is to subdivide this travel time into overland and channelized components. Errors are introduced in modeling each of these two components and their travel times and hence the shape of the time-area curve is difficult to determine. However, even if the shape is difficult to derive, using DEMs to obtain an approximation would definitely be better than the use of Eq. 1. By using DEMs, at least some semblance of the basin shape is captured in the resulting time-area curve.

Everyone who has worked with Clark's method and unit hydrograph theory is aware of its limitations. The linear response approach is typically limited to small watersheds. There is no general agreement on the upper limit but hydrology textbooks suggest that unit hydrographs should be used for medium sized catchments of the order of perhaps 1000 km².

Case Study: In this study, we examined how we might adjust the basin response by subdividing the watershed into sub-watersheds and developing the time area curves for each sub-basin. Conceptually, there must exist an aggregation procedure such that the routed time area contributions from the sub-watersheds would result in a time-area curve for the basin which resembles the basin response. Without automatization however, determining the routing parameters to achieve this would be next to impossible. Because of GIS, this may now be attempted albeit without assurance of success.

To explore this procedure, a drainage basin in northwestern Pennsylvania was selected. Brush Creek drains a large portion of Cranberry Township which is a fast-growing community north of Pittsburgh. The digital elevation file for the Mars quadrangle was analyzed. Using routines developed by the Jenson(1991) and modified by Michelini (1994) and Bodnar, et al. (1996), the stream network for the whole quadrangle was first determined. This is shown in Figure 1. The Brush Creek watershed was next identified and its sub-watersheds were determined. In the program that was coded, this is simply done by specifying the coordinates of the outlet of the watershed or sub-watershed. The program automatically determines the contributing pixels and highlights the tributary area with a different color background as shown in Figure 2. The next step is to develop the time-area curve for the whole basin and for each of the subarea. Although this maybe done automatically, the time interval for plotting and calculating the time area contributions needs to be chosen judiciously. Too small increments of time result in too much information that obscures the shape of the curve. For example, a time interval of three minutes exhibited a time-area diagram which is so dispersed that no dominant mode can be identified. By successive trials, it was found that with a time interval of 30 minutes, one was able to develop reasonably shaped time area curves.

In calculating the travel times, a procedure must be developed to recognize that in the early stages, rainfall excess will be transported as overland flow whereas after it has accumulated to a certain amount flow maybe channelized. This distinction is important because it significantly affects the shape of the time area curve. For automatic processing, it was found that the most convenient method of estimating the time for overland flow is through the use of a threshold value for overland flow area. In calculating 'flow accumulations' most routines consider the flow direction in each pixel by examining the elevation of its boundaries or corners. These will determine the slope and hence the direction of flow. Following this approach, the travel path across each pixel is determined and hence the flow accumulations at each junction may be calculated. It is then assumed, and this may be subject to revision, that if the flow accumulation is less than the threshold number of pixels, overland flow occurs and above the threshold value, flow is channelized. The time of travel during overland flow is then calculated using an overland flow formula.

If flow is channelized, the time of travel is calculated by dividing the distance by an average velocity. Several velocity equations may be used. Note that the choice of method for calculating travel time is subjective and other investigators may use different approaches. The point is that an algorithm must be included to partition the distance traversed into overland and channel flow segments. These are subject to refinements that may be implemented by other investigators.

In our study, this is the technique used to obtain the time-area curve. In Clark's method, the time area curve is routed through a linear reservoir to simulate the storage effect. This results in the instantaneous unit hydrograph from which the finite duration unit hydrograph is determined. How well this simulation reflects reality depends on the choice of the storage factor. If data on the rainfall excess and corresponding direct runoff are available, this storage factor may be determined through a parameter estimation algorithm. However, without the requisite data one must rely on a trial and error method.

If the unit hydrograph for a watershed and those for each of the sub-basins which form it are available then the aggregation of the component hydrographs with routing would result in the unit hydrograph for the whole watershed. The routing constants which result in a reasonable match are the routing parameters that we seek.

Effect of Watershed Changes: The other idea which the study wanted to explore is that with GIS, it should be feasible to update the unit hydrograph automatically as new information on the watershed becomes available. Thus, if developments in the watershed cause the land use to change, these can easily be used to modify the watershed response function. In the watershed being considered, there have been a lot of changes due to urbanization. Urban development in the watershed, which is located in a suburb of Pittsburgh, has caused farms and rural land to be developed into residential and commercial areas. These changes can be captured through the revision of land use maps. These maps can be processed automatically to determine revised runoff characteristics. In this study, the net result of this urbanization was the reduction of the travel times of excess runoff from the developed areas to the watershed outlet. This can be implemented by using revised Runoff Curve Numbers, if the Soil Conservation Service Method is used, to characterize the affected areas. In this example, the effect of urbanization was determined to result in shorter travel times as a result of land cover modifications, paving and grading of the terrain to accommodate residential and commercial development. These were incorporated in developing the time-area curve and then used to develop the response function. To focus on this aspect, we examined the response function at the junction of subwatersheds 1 and 2 in Figure 2. Under unchanged conditions, the unit hydrograph calculated using Clark's method is shown in Figure 3. To demonstrate the effect of land use changes on the response function, the travel times for the pixels in Subarea 2 were recalculated to account for faster travel times because of development. These changes resulted in a revised time area curve and hence, a different watershed response function. The revised response function is shown in Figure 4. It is seen that indeed, one can incorporate land use changes very quickly to update the watershed response.

DISCUSSION AND CONCLUSION

The objective of this study was to demonstrate that combined with an acceptable model for watershed response, geographic information systems can be used to develop an automatic method for predicting runoff. The response model used is the unit hydrograph because it lends itself to a quick method of incorporating the effect of land use changes through Clark's time-area curve. We conclude that indeed using this simple linear model, we can reduce much of the drudgery in the calculations for runoff prediction by processing watershed data automatically through a watershed model. Furthermore, changes in watershed characteristics can easily be incorporated to enable the quick revision of the response function. Conceivably, the automatic procedure may also be developed using a distributed formulation. Our initial experience with it however is that the parameter estimation problem is much more complicated. Furthermore, currently available data make it difficult to implement the distributed approach. This does not mean however that others may not find it more challenging and hence preferable.

REFERENCES

- Bodnar, R., M. Michelini and R. G. Quimpo, 1996, Field Verification of Hydrographs Automatically Generated from DEM-Derived Watershed Response, Proceedings, North American Water and Environment Congress, '96, Anaheim, CA.
- Clark, C. O., 1945, Storage and the Unit Hydrograph, Transactions, American Society of Civil Engineers, 110, 1419-1446.
- Dooge, J. C. I., 1959, A General Theory of the Unit Hydrograph, Journal of Geophysical Research, 64, 241-256.
- Jenson, Susan, K., 1991, Application of Hydrologic Information Automatically Extracted from Digital Elevation Models, Hydrologic Processes, 5, 31-44
- Michelini, M., 1994. Automatic Generation of Unit Hydrographs Using a Digital Elevation Model, M. S. Thesis, University of Pittsburgh, Pittsburgh, PA.
- Quimpo, Rafael G., 1984, Spatial Heterogeneity and Models of Surface Runoff, Journal of Hydrology, 68, 19-28
- U.S. Soil Conservation Service, 1972, "Hydrology," National Engineering Handbook, Section 4, U. S. Government Printing Office, Washington, D.C.

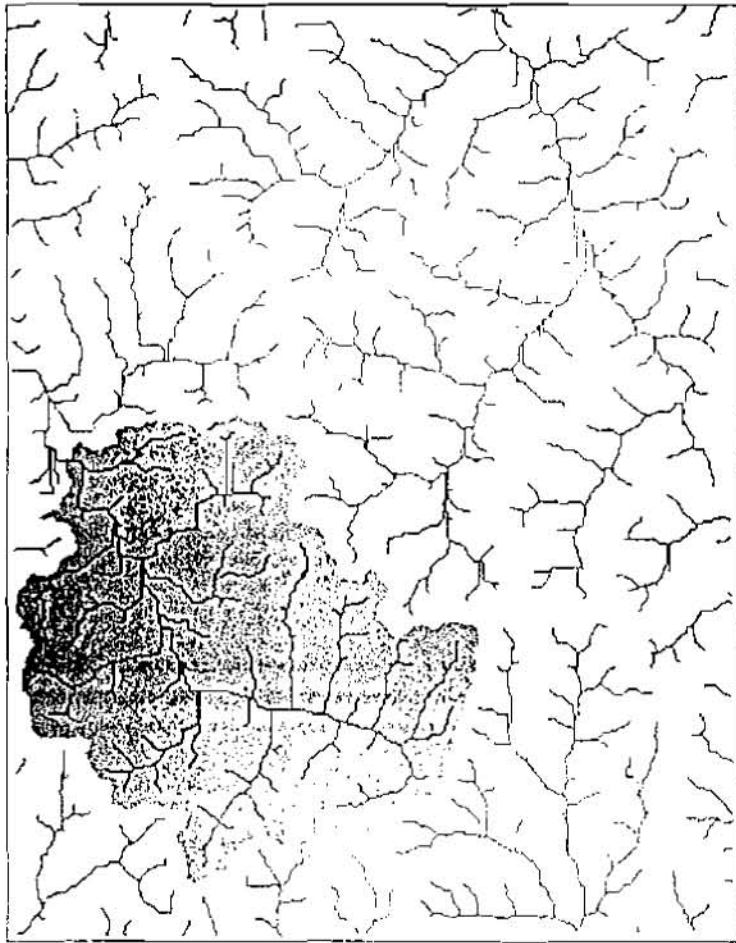


Figure 1. DEM with Brush Creek Watershed delineated

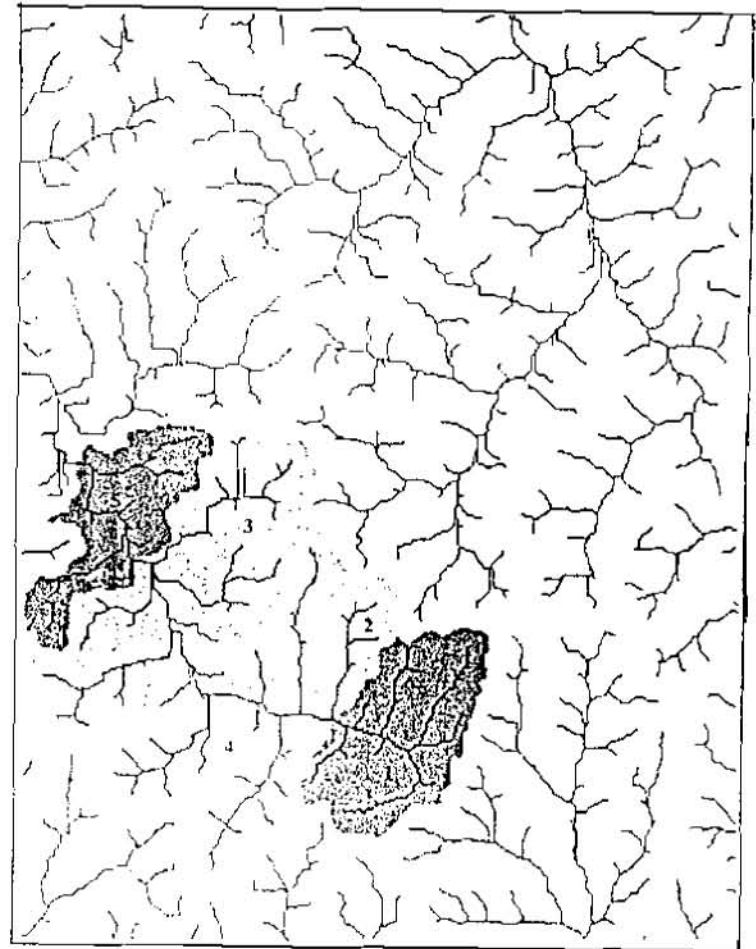


Figure 2. Subwatersheds of Brush Creek

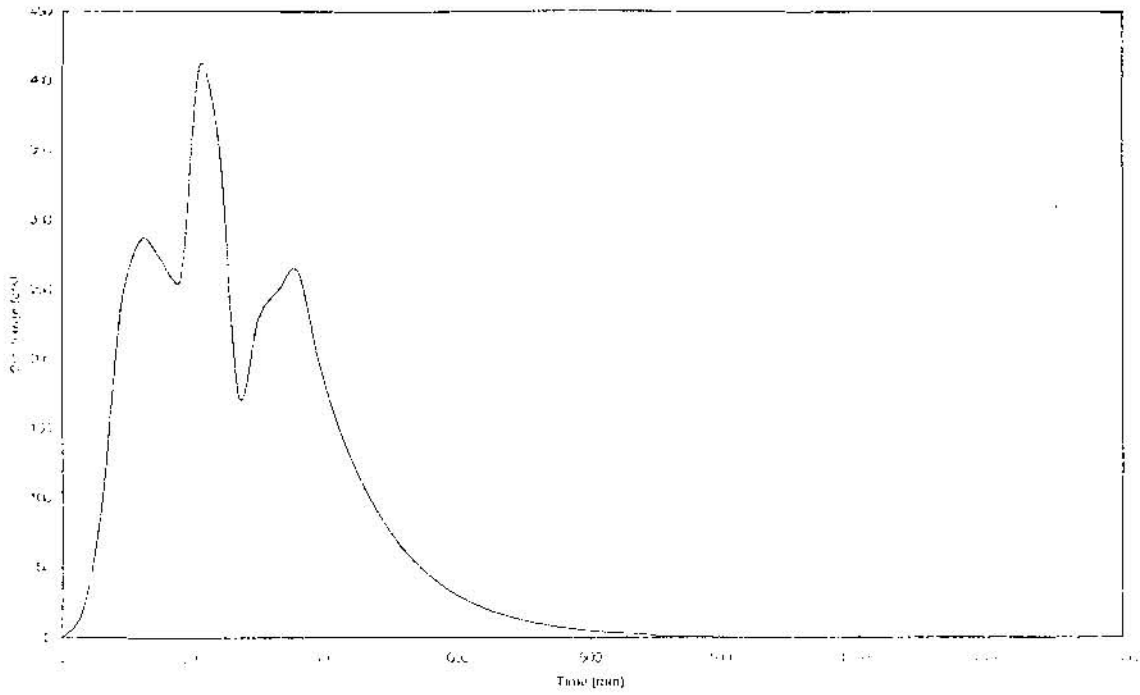


Figure 3. Clark Unit Hydrograph at Junction of Subwatershed 1 and 2

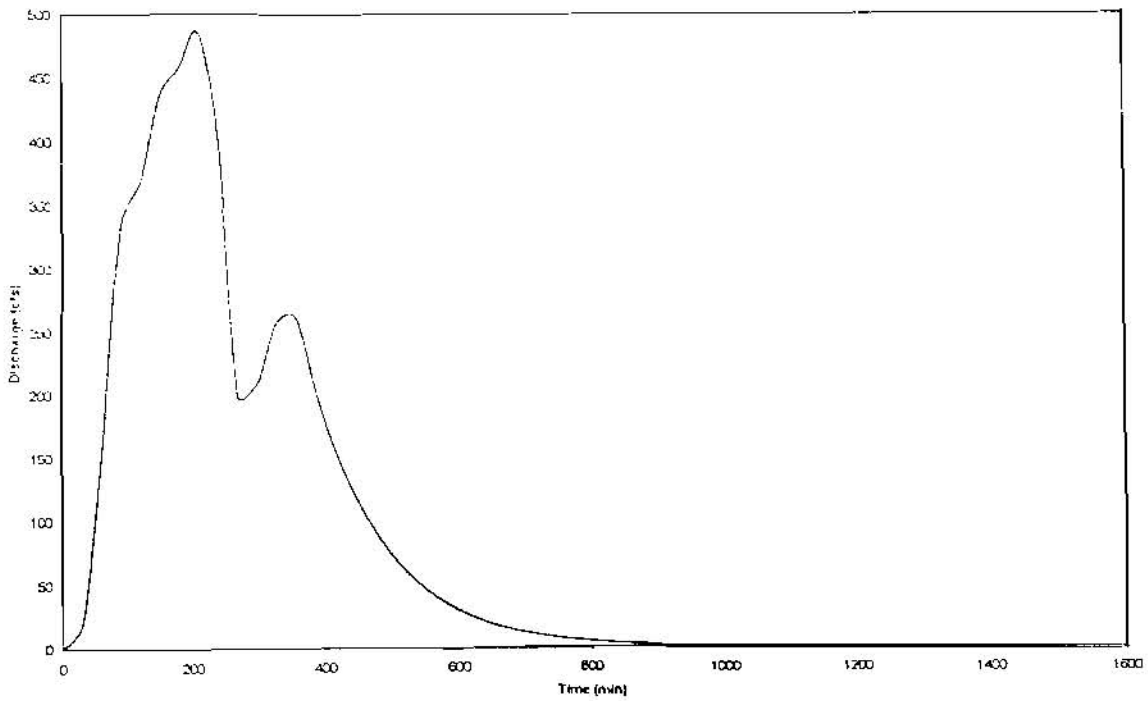


Figure 4. Unit Hydrograph with Land Use Changes in Subwatershed 2

The GIS Weasel - An Interface for the Treatment of Spatial Information Used in Watershed Modeling and Water Resource Management

R. J. Viger, S. L. Markstrom, and G.H. Leavesley

U.S. Geological Survey, Box 25046, MS 412, Denver Federal Center, Lakewood, CO 80225

ABSTRACT: The water resource modeling and management needs of the Watershed and River Systems Management Program require a variety of methods to account for spatial factors influencing water quality and quantity. Support of these needs is provided by the U.S. Geological Survey's GIS Weasel. The GIS Weasel is a graphical user interface (GUI) that is being developed to aid hydrologists and other physical process modelers in the delineation, characterization, and parameterization of an area of interest, drainage nets, and modeling response units (MRUs) for distributed and lumped parameter models. The GIS Weasel uses the Arc Macro Language, awk, C, and Unix shell scripts to provide an interface to the Arc/Info GIS software* for people with no GIS expertise. The GIS Weasel runs on all Unix platforms and the only data requirement is a digital elevation model describing the topography of the area of interest. The area of interest (AOI) to be modeled may be selected from an automatically generated set of watersheds, derived from a user-supplied pour-point (watershed outlet), or extracted from a pre-existing Arc/Info dataset. The drainage network is then derived based on a user-defined minimal sub-catchment area. Summary statistics and iterative trials allow the user to evaluate multiple areal thresholds before choosing a final value. Once the AOI and drainage network are established, MRUs can be delineated according to one of several different methodologies: 1) flow-planes associated with the drainage network; 2) elevation bands; 3) fixed-interval lattice of squares; 4) non-contiguous or "pixelated" zones (based on statistical similarities rather than spatial contiguity); 5) contributing areas associated with a coverage of points (e.g.: stream gages); 6) integrating pre-existing MRU maps. Tools for examining, modifying, and parameterizing the MRU map and its attributes are provided. Data derived from the original elevation grid (e.g. slope, aspect) or grids of other attribute data (e.g. vegetation, soils) can be examined on the basis of the AOI, MRUs, or grid cells using various queries and display tools. MRUs can be grouped, divided, created or eliminated. The GIS Weasel documents modifications of MRU delineations with metadata and the maintenance multiple MRU map versions. When a MRU map has been finalized, parameters can be generated using MRU attributes and their statistical measures.

*The use of trade, product, industry, or firm names is for descriptive purpose only and does not imply endorsement by the U.S. Government.

INTRODUCTION

The Watershed and River System Management Program (WARSMP) is jointly sponsored by the U.S. Geological Survey and the Bureau of Reclamation to develop a database-centered framework for water resources decision making. The Modular Modeling System (MMS) (Leavesley et al., 1996a) supports this program by providing a framework for building and applying interdisciplinary environmental and water resource physical-process models. The speed and accuracy of data preparation for use in an MMS modeling effort can be greatly improved by the use of geographic information systems (GIS), although the complexity of GIS technology can cause it to be infrequently used. The GIS Weasel provides an interface to Arc/Info that can be used to enhance applications of MMS and other WARSMP tools to any watershed or ecosystem by aiding the preparation and analysis of spatial information for model parameter estimation.

The GIS Weasel provides tools to delineate, characterize, modify, and parameterize a modeler's area of interest (AOI), usually a watershed and the area's constituent "model response units" (MRUs) using a digital elevation model (DEM) and ancillary digital data. MRUs are subdivisions of an AOI that reflect a model's treatment of spatially distributed attributes, such as slope, aspect, elevation, soils, and vegetation. An MRU may represent an area whose character or composition is assumed to be homogenous with respect to one or more attributes. The GIS Weasel also delineates a drainage network from the user-supplied elevation model and computes the connections between MRUs and the segments of the drainage network. A history of processing steps is recorded to enable the user to reenter the GIS Weasel's processing sequence at any previously completed point and proceed with an alternative computational procedure.

GIS WEASEL PROCESSING COMPONENTS

The GIS Weasel is composed of the Arc/Info geographic information system, C language programs, and Unix shell scripts. The software runs on all Unix platforms. An NT release of the GIS Weasel is planned for the spring of 1998. All user interfaces are menu and map driven. The user is not required to have any knowledge of Arc/Info commands. However, the user should understand model assumptions regarding spatial variations in parameters.

The GIS Weasel is roughly organized into halves: 1) the delineation component and 2) the characterization/modification/parameterization components (Fig. 1). The delineation component is an automated sequence of steps with limited user input. The characterization, modification, and parameterization components, however, are more interactive in nature and allow the user to explore the character of the modeling area. These three components are not a fixed sequence of processing steps, but rather an open editing session where a user can iteratively characterize, modify and parameterize the MRU map.

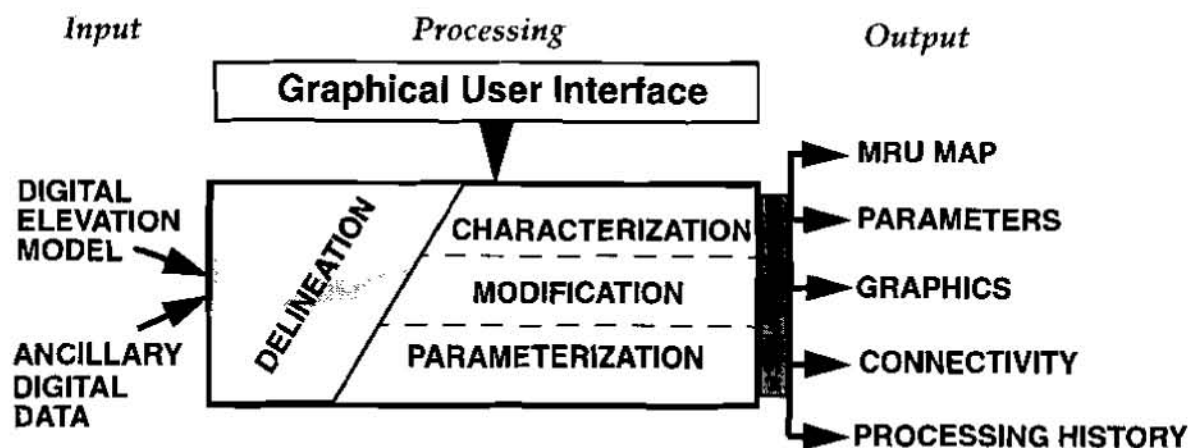


Figure 1. Schematic diagram showing the input, processing, and output components of the GIS Weasel.

DELINEATION COMPONENT: A DEM, in the Arc/Info GRID format, is used to define topographic surfaces, including the AOI and drainage network. The GIS Weasel first fills depressions in the DEM in order to insure that all paths of hydrologic flow will lead to the edge of the elevation model. Flow direction and accumulation surfaces are created using the filled DEM. The flow direction surface indicates the direction of steepest outflow for each cell. The flow accumulation surface uses the flow direction surface to compute the number of cells upslope from each cell.

The AOI is then delineated from a set of watersheds that are automatically extracted from the DEM, a user-specified watershed pour-point (watershed outlet), or a pre-existing Arc/Info coverage or GRID. The GIS Weasel has been developed with surface hydrology as the main emphasis, but by allowing the user to integrate a pre-existing Arc/Info geodataset (i.e. COVERAGE - vector, GRID - raster), a map of a groundwater or climate modeler's 'domain of interest' can be substituted for a 'watershed'. If the user wants to seed a watershed by specifying a pour-point from which to derive a watershed, point and vector COVERAGES can be superimposed on the DEM display for improved orientation. The user approves the delineated AOI to proceed. If a result is unsatisfactory, the user may redefine the area of interest.

A drainage network is extracted from the flow accumulation surface by selecting points on the surface that drain, according to the flow accumulation surface, an area equal to or greater than a user-specified threshold. The value of this threshold represents the minimum upslope area needed to initiate a first-order link in the drainage network (Jenson & Domingue, 1988). A link is defined as a segment of the drainage network that begins and ends with a node (nodes occur at the headwater point of first order links, at the confluence of two or more links, or at the pour-point for the AOI). As the threshold for the critical source is decreased, the number of source areas that will fit into a given watershed increases, as does the drainage network density. The drainage network density is directly related to the number of flow-plane type MRUs that will be found in an AOI (if the user were to choose one of these types of MRU delineation methodologies). The GUI allows

the user to experiment with different thresholds until an appropriate drainage network density, as defined by the user, is attained. The drainage network defined in the GIS Weasel may not need to be an exact representation of true stream morphology. The drainage net might only be needed for routing of hydrologic response through a watershed or as the basis for creating flow-plane MRUs. The interpretation of the Weasel-generated drainage network is left to the user.

The initial MRU map presented to the user upon completing the delineation component of the GIS Weasel will feature a single response unit, which is the AOI. Any subsequent subdivisions are optional.

CHARACTERIZATION COMPONENT: Exploration of the nature of the MRU map and any ancillary thematic information that may be associated with the AOI provides information from which decisions on MRU map modification and parameterization can be made. Data derived from the original elevation grid (e.g. slope, aspect) or other user-supplied grids (e.g. vegetation, soils) can be examined on the basis of individual grid cells, individual or groups of MRUs, or the entire AOI. User-created boolean logic can be used to query, display and evaluate various combinations of attribute constraints. Histograms of selected themes and plots of attribute occurrence by elevation (hypsothetic curves) can be created for selected MRUs. Attribute values at specific locations may be queried with a point-and-click tool.

MODIFICATION COMPONENT: A set of tools allowing the user to make revisions to the MRU map is available. These revisions may be based on information obtained from the characterization component or on the basis of potential changes in the characteristics of the AOI. For example, an MRU map reflecting current land cover conditions or management practices may be modified to reflect anticipated change. MRUs can be grouped, divided, created or eliminated. MRUs can be digitized on-screen, extracted by logical query, stream buffering or seeding new sub-watersheds. MRUs may be removed from the MRU map, effectively reducing the extent of the AOI. MRUs smaller than a user-specified area can be dissolved into the neighboring MRU sharing the most perimeter.

In addition to tools designed to make *specific* modifications of the MRU map, there are eight different methods currently available for the *automatic* subdivision of an AOI: three types of flow-plane MRUs; MRUs based on elevation bands; a fixed-interval lattice of square MRUs; non-contiguous or "pixelated" MRUs (highlighting statistical similarities rather than spatial contiguity); contributing areas upstream of pre-defined points (e.g.: stream gages); and use of a pre-existing Arc/Info COVERAGE or GRID of MRU boundaries.

The GIS Weasel provides version control and documentation to track modifications of MRU maps. Each version of the MRU map is named by the user. A sentence describing the derivation of each MRU map is automatically manufactured. This information is intended as a "memory refresher" for the user. Additional descriptors are automatically stored in ASCII files, which the user may edit directly. Although this descriptive information is not used by any of the GIS Weasel's automated routines, it can be

invaluable when the user returns to a study after an extended absence and needs to differentiate several MRU maps from each other.

PARAMETERIZATION COMPONENT: Parameters can be generated for all discrete spatial features associated with the AOI. Features include MRUs and the AOI itself (polygons), segments of the drainage network (lines), nodes in the drainage network, stream gages, meteorological stations and wells (points). In addition to creating parameters describing the spatial features independently, the establishment of relationships between different spatial features is needed to allow a physical-process model to simulate a whole system and its internal dynamics. Physical connections between these features can be calculated in some cases, and “coefficients of association” can be defined by the user in others. All of these data can be output to ASCII files for subsequent use in modeling software. Many users find it helpful to use the parameterization tools to generate files describing the MRUs prior to actually designating a “final” MRU map for use in modeling. These files can be used as a basis for further modification of the MRU map and then be discarded.

MRU attributes and statistical measures of these attributes are used to generate estimates of model parameters. Parameter estimates include, but are not limited to, frequency distributions and measures of central tendency. The GUI for parameter generation allows the user to specify the name of any GRID and one or more standard statistics which will be calculated for each response unit. All results are output to space-delimited ASCII files. This aspect of the parameter generation tool is intended to be generic. The same interface is used to parameterize the AOI.

Some MRU/AOI parameters related to geographic and topographic characteristics, such as area, elevation, and slope, are common among many models and can be easily derived from the filled DEM generated in the delineation component. In addition, there are specific routines for the Precipitation-Runoff Modeling System (PRMS), determination of the latitude and longitude for each MRU centroid, calculating the 10-85% slope (used in flood frequency regressions), calculating geomorphic routing coefficients for every point on the drainage network, generating soil parameters for TOPMODEL, and calculating the percent of an MRU's total area that intersects with zones of another GRID (useful for associating MRUs with climate model or NEXRAD data sets). The spatial parameter needs of the models that have been built in and are distributed with MMS, including PRMS and TOPMODEL, have been initial development targets. Refinement of these parameter generation routines and the development of routines for new parameters is driven by user demand and is intended to continue. Although some routines may not be necessary for a user's particular model, much of the parameter information generated can be useful for characterization. The GIS Weasel can generate, in addition to space-delimited ASCII parameter files, MMS formatted parameter files.

The GIS Weasel will define the arcs of the drainage network, including the direction “downstream” and up and downstream neighbors. The area weighted percentage of each MRU's total area that flows into a given segment of the drainage network also is calculated. This percentage serves as a “connector” between an MRU and a link in the

drainage network. The connection between MRUs and stream segments is needed for routing hydrologic or other responses through the AOI to the outlet, as well as calculating lag times in the arrival of the various MRU responses at the outlet of the AOI.

Currently under investigation is the use of parameters describing the locales surrounding meteorological stations as explanatory variables for the variation of time-series (point) data across a modeler's area of interest. These explanatory variables can be used to extrapolate observed values from the locations of the points to all cells within an AOI.

Specialized parameters, such as the rooting depth of vegetation in an MRU and the soil water-holding capacity, require the use of data layers in addition to the original DEM. Where possible, nationwide GRIDS of thematic information needed to support the derivation of these types of parameters have been collected by the GIS Weasel development team and are available on demand.

TIME-SERIES DATA

GIS coverages of points, representing any observed time-series data from precipitation at ground level to temperature at various altitudes to well measurements, can be associated with individual MRUs. While the measurements observed at the points will change with every time step of the model run, the associations between the MRUs and the points will be constant. Using the point coverage, the GIS Weasel can output a table that lists for each MRU the various points that apply to that MRU and a weighting factor between the point and the MRU. Two methods are currently available in the GIS Weasel to associate MRUs with points: 1) Thiessen polygons and 2) a simple point-and-click interface. The most current associations can be interactively edited by the user. Time-series data can also be distributed across an AOI according to a map of zones or polygons (e.g. a NEXRAD radar sweep). MRU-zone associations can be created using an automated overlay of the MRU map onto the time-series zone map, yielding area-weighted percentages.

INTEGRATED SYSTEMS APPLICATION

The integration of MMS and the GIS Weasel provides a flexible set of tools for application to a variety of environmental issues. One application of these two systems is the development of a water resources management decision support system that addresses a number of environmental concerns, including water quantity, water quality, endangered species, and the optimization of operational objectives such as power generation and irrigation within existing environmental constraints (Leavesley et. al., 1996b). The GIS Weasel provides the delineation, characterization, and parameterization tools for a number of models in MMS. These include watershed models that provide streamflow to water storage reservoirs, channel flow and sediment transport models for

routing water and sediment in selected channel reaches, and biological models that evaluate the effects of flow and sediment on stream biota.

A second application is the evaluation of the effects of alternative watershed and ecosystem management strategies (Leavesley et. al., 1996c). Landscape-generation models provide spatial representations of alternative land-use patterns associated with alternative forest-management scenarios. Management scenarios might range from maximum timber yield to maximum habitat protection. Scenario outputs from the landscape-generation models can be input to the GIS Weasel and used to characterize and parameterize each scenario for application with watershed and ecosystem-process models in MMS (Leavesley et. al., 1996d). The effects of these management strategies on issues such as streamflow, sediment, and selected chemical and biological processes can be evaluated by analyzing MMS model outputs for each scenario.

FUTURE DEVELOPMENT PLANS

While the GIS Weasel provides the mechanisms for delineating, characterizing, and estimating parameters for watersheds and MRUs, work remains to be done on the development, testing, and identification of the specific parameterization procedures that are most appropriate for each of the environmental processes that may be simulated using MMS.

Because many combinations of physical-process algorithms ("modules") are possible in MMS, many different models are possible. Each of these models have different parameter needs. It is the goal of the WARSMP development team that all spatial parameter needs of MMS modules are supported by the GIS Weasel.

As part of WARSMP's goal to integrate GIS and modeling, MMS has been modified to produce a list of parameter names when a model is built. Plans call for the GIS Weasel to be able to read this list of parameters and then automatically execute the appropriate parameter generation routines. This will further alleviate the expertise required on the part of the user.

The ability to recreate sets of spatial parameters for an AOI is crucial to isolating and comparing the physical response predictions of different models for the same AOI. The development of systematic methodologies for extracting spatial information would enable the comparison of physical responses of the different areas, and the extension of calibrated model parameters from areas with observed data to areas that lack observations.

Continued advances in physical and biological sciences, GIS technology, computer technology, and data resources will expand the need for a dynamic set of tools to apply these advances to a wide range of interdisciplinary research and operational environmental issues. MMS and the GIS Weasel provide a flexible framework for integrating and applying these tools.

REFERENCES

- Leavesley, G.H., Restrepo, P.J., Markstrom, S.L., Dixon, M., Stannard, L.G., 1996a, The Modular Modeling System (MMS): User's Manual, Open-File Report 96-151, U.S. Geological Survey.
- Jenson, S.K., Domingue, J.O. 1988, Extracting topographic structure from digital elevation data for geographic information system analysis, *Photogrammetric Eng. and Remote Sens.* 54, p. 1593.
- Leavesley, G.H., Markstrom, S.L., Brewer, M.S., Viger, R.J., 1996b, The Modular Modeling System (MMS) -- The physical process modeling component of a database-centered decision support system for water and power management, *Water, Air, and Soil Pollution* 90, p. 303.
- Leavesley, G.H., Grant, G.E., Markstrom, S.L., Viger, R.J., Brewer, M.S., 1996c, A modular modeling approach to watershed analysis and ecosystem management, in *Proceedings of Watershed '96 A National Conference on Watershed Management*, U.S. Government Printing Office, p. 794.
- Leavesley, G.H., Restrepo, P.J., Stannard, L.G., Frankowski, L.A., Sautins, A.M., 1996d, MMS: A modeling framework for multidisciplinary research and operational applications, in *GIS and Environmental Modeling: Progress and Research Issues*, GIS World Books, Fort Collins, CO, p. 155.

MODCLARK MODEL DEVELOPMENT, MUSKINGUM RIVER BASIN, OHIO

By Jerry W. Webb, Chief Water Resources Engineering Branch, U. S. Army Corps of Engineers,
Huntington District, Huntington, West Virginia

Abstract: The Huntington District Corps of Engineers has responsibility for operating sixteen flood control reservoirs within the Muskingum River Basin. The Muskingum River Basin, situated in the east central part of Ohio, occupies 8,051 square miles which equates to 20% of the land area of the state. More than half of the drainage basin is controlled by reservoirs. Currently daily operational forecasts for these reservoirs are generated using software developed by the Hydrologic Engineering Center (HEC) which uses point precipitation data and stage measurements transmitted by data collection platforms to the Water Control Data System in the Huntington District. A watershed model is used to develop runoff which is calibrated to basin response represented by actual stage data measured at gaging stations at the time of forecast. The ModClark computer program is a new tool developed by HEC that incorporates NEXRAD precipitation data into rainfall-runoff modeling. ModClark is relatively easy to implement since most of the tasks required for model development are similar in scope to those associated with the HEC-1, Flood Hydrograph Package. The most significant difference between the models is the requirement by ModClark to develop a digital elevation model (DEM) using a geographic information system (GIS). In hilly terrain, this task is readily performed through a series of user-friendly Arc/Info macros developed at HEC. For flat regions, as are considered in this study, some additional GIS manipulation is necessary. The final product is a series of input files that are used by ModClark to transform radar-measured precipitation into subbasin outflow. The comprehensive spatial coverage provided by NEXRAD weather-radar represents an improvement over the fields of point values associated with rain-gage networks. The enhanced representation of natural rainfall patterns into a rainfall-runoff model greatly improves real-time flood forecasting. This paper discusses development of a ModClark model by HEC staff and potential benefits and problems associated with application of this state-of-the-art forecasting technique in a complex multi-reservoir system.

INTRODUCTION

Acknowledgment. The Huntington District, Corps of Engineers, contracted with HEC to develop a ModClark model for the Muskingum River Basin. The study was performed by Daniel Kull with primary study guidance and management by Troy Nicolini. John Peters, David Goldman, and Arlen Feldman provided additional study guidance and management. Thomas Evans performed most of the Arc/Info GIS related tasks, while providing guidance for GIS tasks performed by others. Carl Franke retrieved and managed all NEXRAD radar data. Jerry Webb and James Schray of the Huntington District provided valuable assistance in supplying information and assembling data.

Model Development: The ModClark computer program is a new tool that incorporates NEXRAD precipitation data into rainfall-runoff modeling (USACE 1995b). ModClark is relatively easy to implement since most of the tasks required for model development are similar in scope to those associated with the HEC-1, Flood Hydrograph Package (USACE 1990). The program does require a high degree of technical effort when working with the digital elevation model (DEM) while using a geographic information system (GIS). The final product will eventually be used for real-time flood forecasting purposes in the Huntington District.

The methodology by which real-time forecasting models are developed consists of four basic steps; (1) calibration of parameters from historical events, (2) adoption of parameters, (3) verification of adopted parameters, and (4) parameter adjustment in operations forecast mode. The HEC-1F flood forecasting model of the Muskingum River Basin is well established and its parameters have been verified in an operational mode (USACE 1986;1989) over a long period of time. Two assumptions were made concerning unit hydrograph parameters in the original HEC-1F model; they are appropriate for the Muskingum subbasins and are adequate for the ModClark modeling effort.

Although Stage 3 (ground-truthed) NEXRAD radar data was unavailable at the time HEC developed the model for the Muskingum River Basin, Stage 1 NEXRAD data was available to initiate the model development. Based on experience gained from a previous study by HEC (USACE 1996), no attempt was made to adjust and calibrate unit

hydrograph parameters in the ModClark model based on Stage 1 radar-measured precipitation. Stage 3 data is now available and calibration will be performed by the District.

Unit Hydrograph Parameters: The HEC-1F model used by the Huntington District contained the Snyder unit hydrograph parameter for 40 of the 41 Muskingum subbasins. HEC-1 was used to transform the Snyder unit hydrograph parameters to equivalent Clark parameters. Subbasin areas and Clark parameters of time of concentration (T_c) and the storage attenuation coefficient $\text{\textcircled{R}}$ were extracted from the existing model for each subbasin.

Snyder's parameters were not available for the contributing area local to the outlet of the Muskingum River into the Ohio River at Marietta (LMT0H6). For this subbasin, equations developed as part of a separate regional regression analysis were used. These equations are:

$$T_c = 5.22 DA^{0.246} S^{-0.258} \quad \text{and} \quad T_c + R = 6.58 DA^{0.081} S^{-0.539}$$

where DA represents the drainage area in square miles and S is the slope in feet per mile. These equations were applied to LMT0H6 subbasin using $DA = 616 \text{mi}^2 (1595 \text{km}^2)$ and $S = 2 \text{ft/mi} (0.38 \text{m/km})$. The slope was measured between the upstream watershed boundary and outlet gage location.

Basin Characteristics File: The basin characteristics file is of the same format as the standard HEC-1 input file. Total subbasin area, Clark's unit hydrograph parameters, loss rate parameters, and base flow parameters for individual subbasins are included in the basin characteristics file. Parameters were kept the same as those used in the original HEC-1F model (with the Snyder's changed to Clark's). The basin characteristics file also specifies the pathnames for storage of generated flow hydrographs. For all ModClark output, the A, B, C, D, and E pathnames used in HEC-DSS (USACE 1994) are the same as those generated by HEC-1. The F part is set to "ModClark".

Grid-Cell Characteristics File: To develop the grid-cell characteristics file, the GridParm-DEM2HRAP (USACE 1995a) procedure was performed using the Arc/Info GIS system. This procedure evaluates runoff parameters for Hydrologic Rainfall Analysis Project (HRAP) cells from USGS digital elevation models. Seven USGS DEM quadrangles covered the Muskingum Basin: Canton-east, Canton-west, Clarkburg-west, Cleveland-west, Columbus-east, Marion-east, and Toledo-east. These quadrangles were downloaded from the USGS Earth Resources Observation Systems (EROS) Data Center through a file transfer protocol. When the subbasin and stream delineation generated from the DEM and the GridParm-DEM2HRAP procedure were compared to those supplied by the District, some major discrepancies were found. Most of the differences were in the north-west corner of the basin. Regions were modeled as draining into the wrong subbasins, and in some cases known Muskingum contributing areas flowed north into the Vermillion and Sandusky Rivers. Additionally, many of the delineated streams were not aligned with those in the U.S. Environmental Protection Agency Reach File #1 (RF1). The most noticeable errors were along the Lake, Black, and Clear Forks of the Mohican River flowing into Killbuck Creek instead of into the Mohawk Reservoir. These large delineation errors were due to the DEM representation of the extremely flat topography of north-central Ohio. In such flat terrain, even the slightest elevation error can change flow directions considerably.

A manual manipulation of the DEMs was used to overcome the stream and watershed delineation problems. To ensure proper stream locations, the RF1 streams were "burned" into the DEM through Arc/Info. Based on a suggestion by Dr. David Maidment of the University of Texas at Austin, a stream burn-in worked well when performed with the 1:100,000 digital line graph (DLG) stream network on a single subbasin. This resulted in satisfactory watershed delineation. The dense network represented by the DLGs forced errant contributing areas to flow in the proper direction. Figures 1 and 2 represent the final DEM with RF1 streams.

HEC concluded that efficient manipulation of DEMs could not yield satisfactory delineation for the flat area of the entire Muskingum River Basin. The DEMs were abandoned and a simpler approach to find the travel distances was used. The direct calculation of the distance from the grid-cells to their associated subbasin outlets was

obtained through Arc/Info. These cell-to-outlet distances were used to prorate the subbasin time of concentration, yielding a travel time for each grid-cell. The grid-cell characteristics file contains a list of the grid-cells with their x and y coordinates, area and average travel length to the subbasin outlet.

Verification: An HEC-1 model provided by the District was used for comparison with the ModClark model. Precipitation and flow data for 1995 and 1996 were sent to HEC. Point rainfall allowed basin-average precipitation to be calculated for input into the HEC-1 model. NEXRAD radar data provided the rainfall estimates for input into the ModClark model. NEXRAD data was needed from three sites: Pittsburgh, Cincinnati, and Cleveland. Each site has a sweep radius of approximately 230 km (143 mi).

Event Simulation: NEXRAD data availability forced simulation events to be constrained to the time period of October, 1995 to the present. Three events were available: April 22-28, April 29-May 7, and May 8-25, 1996 (Figures 5 and 6). These events were obviously not independent, but represented an opportunity to compare results of the ModClark model and the forecasts performed using established gage stations. During the ModClark and HEC-1 modeling runs, loss rate parameters were kept the same as those found in the HEC-1F model input files. Using the same loss rates for all subbasins and modeling runs allowed for easier comparisons between the ModClark, HEC-1, and observed hydrographs. In many cases, loss rate adjustments could have yielded more accurate model results. It was decided, however, that for the purposes of this study and considering the available data, using unadjusted global loss rates was preferred.

RESULTS AND CONCLUSIONS

General: The Muskingum Basin is the third basin to which the ModClark method has been applied. The first two were the Tenkiller (Peters and Easton 1996) and the Salt River (USACE 1996). Although this is a small number of applications, some commonalities have surfaced that are worth mentioning while describing observations unique to the Muskingum Basin. One conclusion evident from both the Salt River and Muskingum River is that Stage 1 radar rainfall is of limited value for flood forecasting. Runoff hydrographs generated using Stage 1 rainfall can be grossly in error compared to observed hydrographs, and even compared to hydrographs generated using gaged rainfall. In other cases, however, radar-rainfall generated hydrographs were significantly better than those generated using gaged rainfall. It appears that Stage 1 radar rainfall consistently produces inaccuracies in absolute magnitude (both over and under estimating). When storms are of a broader, more homogeneous nature, this inaccuracy can be amplified to produce discouraging results. When the storms are locally intense, two things differ. First, the actual Stage 1 inaccuracies - in the absolute sense - are in some cases smaller (this appears to be a characteristic of radar measurement), and second, any inaccuracies are somewhat masked by the superior spatial and temporal resolution compared to gaged rainfall. Because of this unpredictable performance of Stage 1 radar rainfall, it is recommended that forecasting for water control decisions should not be based solely on Stage 1 radar rainfall. Instead, superior radar rainfall products should be used, such as Stage 3 or equivalent commercial products, which includes ground truthing and other quality enhancements. Fortunately, as improved radar rainfall products become available, they can be used in the current ModClark model without modifications.

Another conclusion is that there are scenarios for which ModClark simulation of runoff using radar rainfall is superior to simulations based on gaged rainfall data. This was evident during verification modeling for the Muskingum with the Stage 1 data problems described above. The scenarios for which this was observed are characterized by locally intense rainfall occurring over portions of the watershed with few rain gages. The event occurring on May 17-18, 1996, was such an event (Figure 5 and 6). For these scenarios, the rain gages can misinterpret or completely miss the event. This is because locally intense storms produce rain cells that can travel between rain gage locations. Additionally, when subbasin-averaged precipitation is developed, localized rain-cells that track directly over a gage can result in the overestimation of basin-wide rainfall.

The above discussions lead naturally to the conclusion that the ModClark method has significant potential for improving forecast capability, when used with adequately accurate radar rainfall. A corollary to this is that at this point in the development of the ModClark procedure, it is important to separate evaluation of the method from that of the radar-rainfall product used.

Limitations: The application of ModClark to the Muskingum Basin revealed some limitation of various model components that did not surface during the first two applications to the Tenkiller and Salt Rivers. The GridParm-DEM2HRAP procedure, when performed as originally designed can yield erroneous results under certain conditions. In the case of the Muskingum Basin, these conditions appear to be restricted to the flat portions of the basin relative to the scale of the DEM. In other words, the magnitude of the errors in the DEM resulting from the scale of the DEM, was greater than the magnitude of the relief. The first two study basins were topographically "well defined" and the GridParm-DEM2HRAP procedure worked as designed. However, the flat portions of the Muskingum Basin necessitated the development of alternative approaches. These included alterations of the DEM using 1:500,000 and 1:100,000 scale river networks before application of GridParm-DEM2HRAP, and application of two simplified techniques for computing cell-to-outlet distances.

The findings from these activities were: 1) DEM alteration using the 1:500,000 River network produced poor results; 2) DEM alteration using the 1:100,000 river network produced good results but was time consuming; and 3) the more sophisticated of the two simplified cell-to-outlet techniques produced comparable results to those from using GridParm-DEM2HRAP on the DEM altered using the 1:100,000 scale river network. While the standard GridParm-DEM2HRAP procedure requires little Arc/Info experience, application of these alternative approaches requires a working knowledge of Arc/Info. As further experience warrants, these approaches may be incorporated into the GridParm-DEM2HRAP procedure.

FUTURE STUDIES

General Requirements: Although a major step towards the development of ModClark as a real-time flood forecasting tool has been completed for the Muskingum River Basin, there are still obstacles barring full implementation. At this point, only the actual rainfall-runoff model has been developed. The additional components and program enhancements that are needed for full forecasting realization all involve various software development issues.

The ModClark methodology is included in the NexGen HEC-HMS computer program for general use. This radar rainfall-runoff forecasting methodology was developed in conjunction with the Corps' Real Time Water Control (now the Water Control Data System) Research program. HEC-HMS, or a version thereof, will be further enhanced to include special features for real-time forecasting. It is envisioned that the basin model architecture of real-time forecasting with ModClark will be the same as the structure used in HEC-1F. The only difference will lie in the rainfall-runoff transformation. Rainfall data will be in a gridded format and be transformed to subbasin runoff through ModClark.

Stage 3 NEXRAD Data: The need for Stage 3 or equivalent NEXRAD data is evident in the testing and verification results of this report. The River Forecast Center (RFC) for the Muskingum Basin has now reached full NEXRAD development, Stage 3 data is now available for forecasting purposes.

Loss Rate Accounting: An obstacle that exists in using ModClark for forecasting revolves around loss rate accounting. When HEC-1F is used with basin-average precipitation, each subbasin's loss rate state is saved between model executions. This is not available for gridded precipitation and losses used by ModClark. Currently, ModClark requires all grid-cells within a subbasin to have the same loss-rates at the beginning of each simulation. ModClark tracks individual cell losses; grid-cell losses are unique because of the application of cell-specific radar rainfall data. During a forecasting run, these individual cell losses would need to be saved and used as initial state variables for the next forecast. The algorithms for this are currently under development.

Predicted Future Rainfall: The use of predicted future rainfall for forecasting is also an issue with ModClark. For full ModClark forecasting, predicted rainfall would need to be a grid-cell based data set. A question arises whether this level of detail for predicted rainfall is necessary or even realistic. One simple solution would be to use subbasin-averaged QPF (Quantitative Precipitation Forecast) of the National Weather Service values and distribute them evenly over the grid-cells within the subbasin.

REFERENCES

- Peters, J.C. , Easton, D.J., 1996, Runoff Simulation Using Radar Rainfall Data. *Journal of the American Water Resources Association (AWRA)*, 32(4), 753-760.
- U.S. Army Corps of Engineers, 1986, Real-Time Flood Forecasting and Reservoir Regulation for the Muskingum River Basin, Special Project Memo 86-1, Hydrologic Engineering Center (HEC), Davis, CA.
- U.S. Army Corps of Engineers, 1989, Water Control Software - Forecast and Operations, HEC, Davis, CA.
- U.S. Army Corps of Engineers, 1990, HEC-1 Flood Hydrograph Package, HEC, Davis, CA.
- U.S. Army Corps of Engineers, 1994, HEC-DSS User's Guide and Utility Manuals, HEC, Davis, CA.
- U.S. Army Corps of Engineers, 1995a, GridParm-DEM@HRAP: A Procedure for Evaluating Runoff Parameters for HRAP Cells from USGS Digital Elevation Models - Draft, HEC, Davis, CA.
- U.S. Army Corps of Engineers, 1995b, ModClark-Modified Clark Runoff Simulation Users Manual, HEC, Davis, CA.
- U.S. Army Corps of Engineers, 1996, A Pilot Application of Weather Radar-Based Runoff Forecasting, Salt River Basin, MO, PR-31, HEC, Davis, CA.

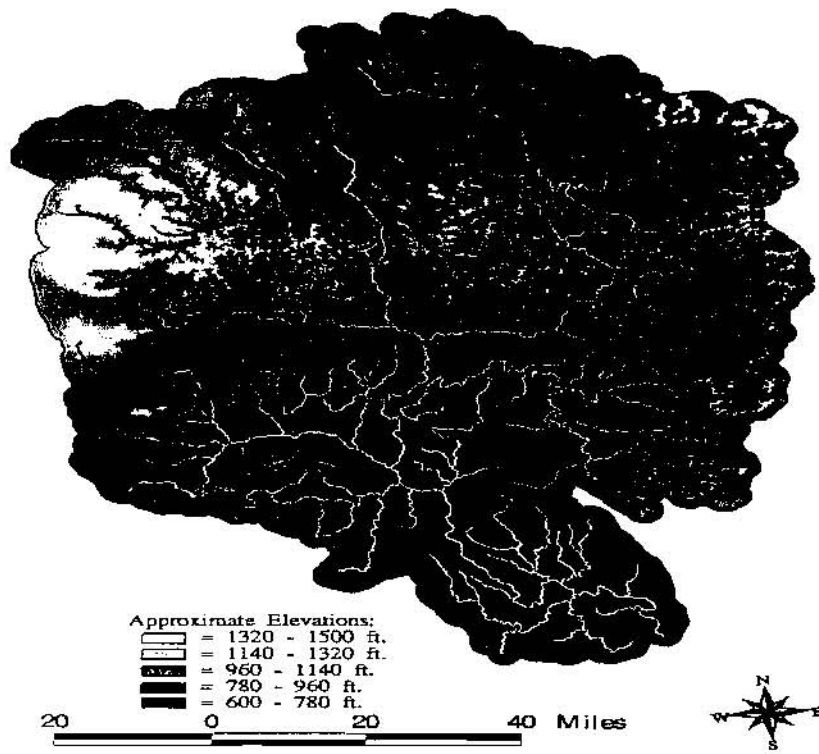


Figure 1
Muskingum River Basin DEM with RF1 Streams

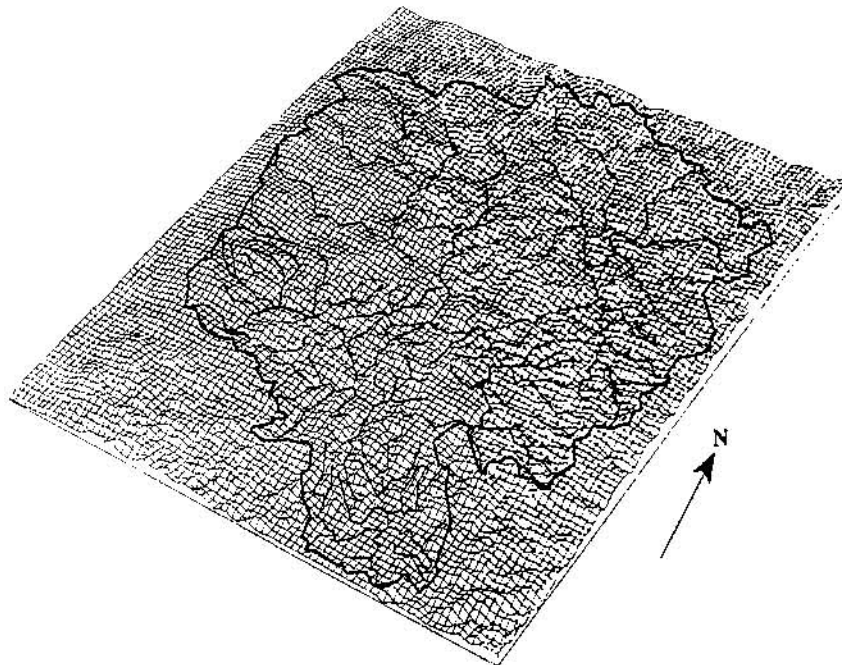


Figure 2
Perspective View of Muskingum River Basin DEM with RF1 Streams

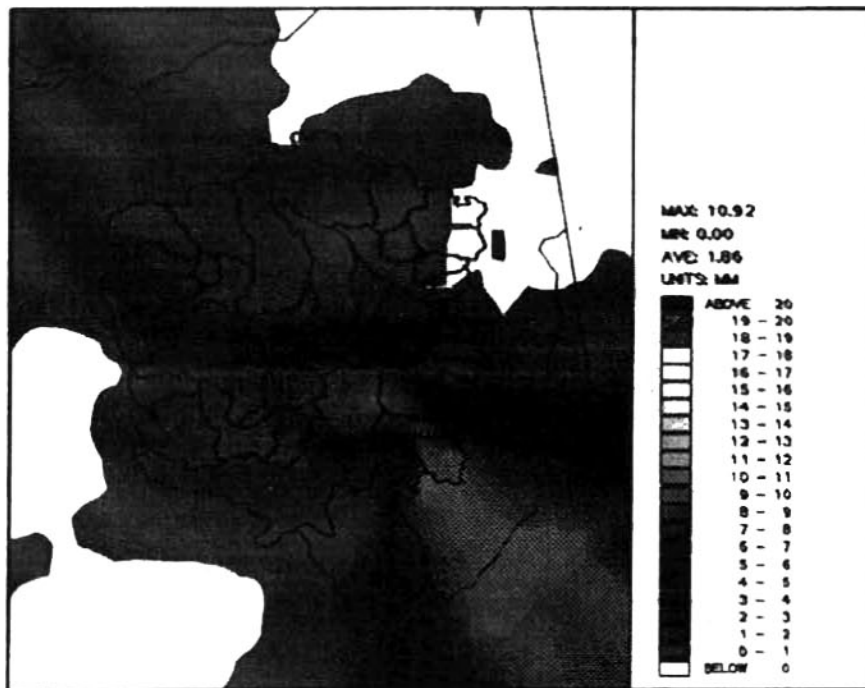


Figure 3
 Gage Measured Rainfall for 2100-2200 UTC, May 16, 1996

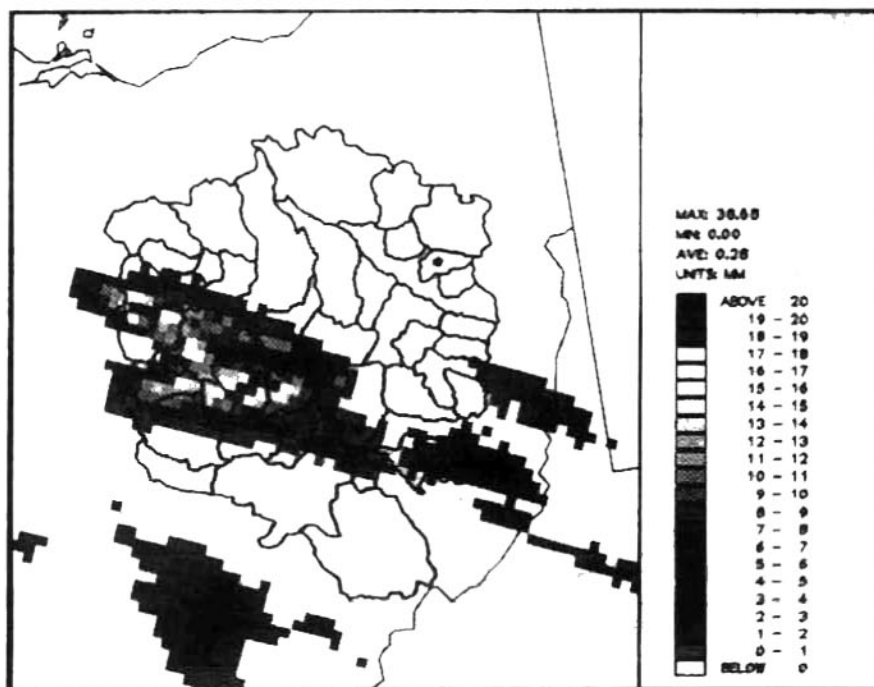


Figure 4
 Radar Measured Rainfall for 2100-2200 UTC, May 16, 1996

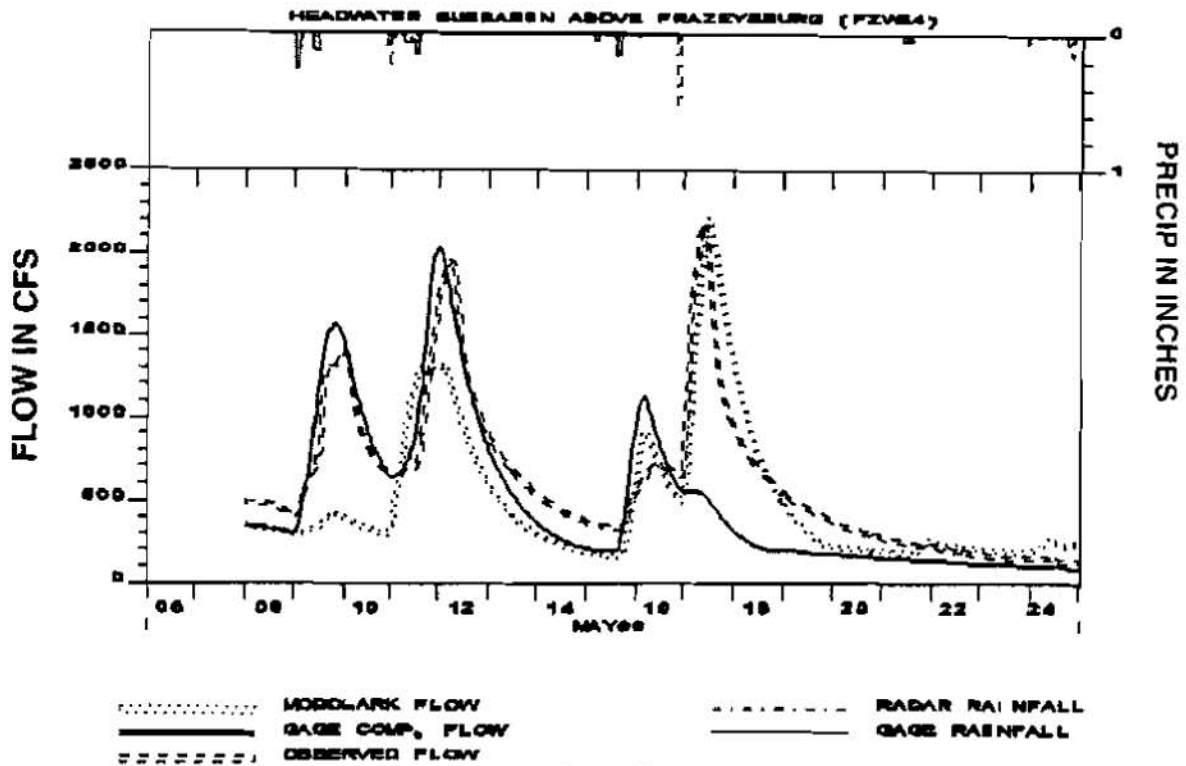


Figure 5
 Simulations for Frazeysburg Subbasin for May 8-25, 1996

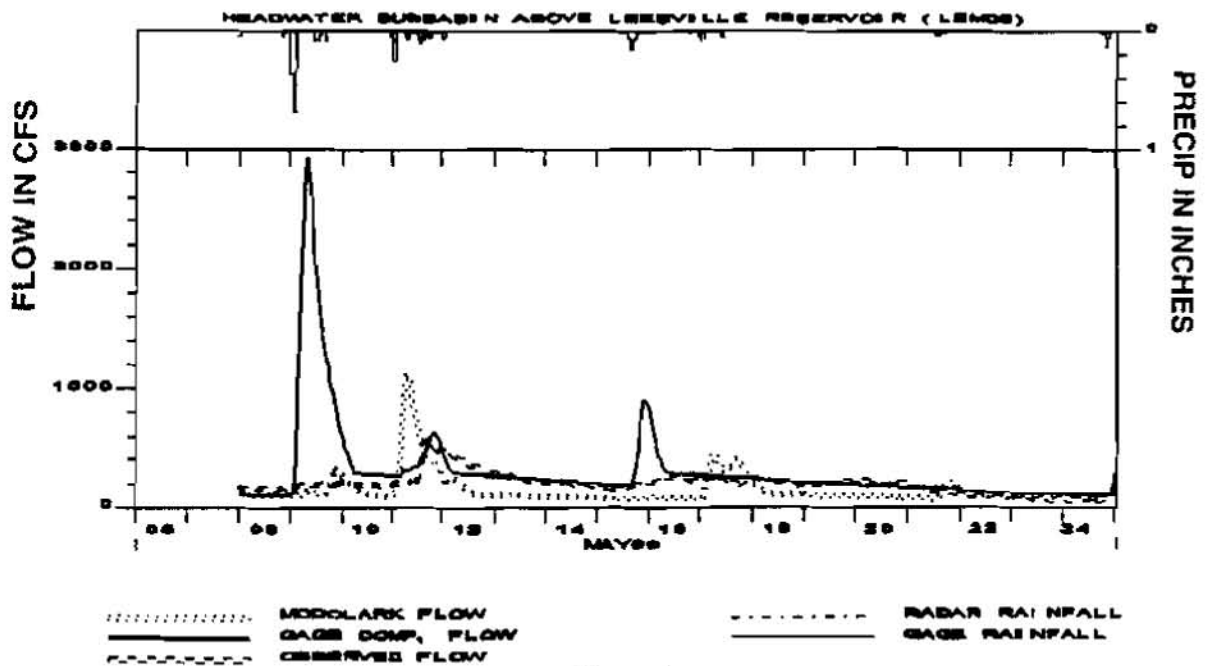


Figure 6
 Simulations for Leesville Reservoir Subbasin for May 8-25, 1996

A CONCEPTUAL MONTHLY RAINFALL RUNOFF MODEL

By Zhiming Chen*, Senior Engineer, Nanjing Institute of Hydrology & Water Resources,
Ministry of Water Resources, 1 Xikang Road, Nanjing, China

Abstract: A conceptual monthly rainfall runoff model with three free parameters is developed on the basis of the Xinanjiang model. The computed results show that in southern China and southern Belgium the model proposed in the paper with fewer parameters can reach as good results as the best of the other monthly models.

INTRODUCTION

Many rainfall runoff models strongly reflecting the physical process involved, can give very good results, but most of these require data on at least a daily basis. Less attention has been paid to monthly rainfall runoff models though these may be important and adequate in water resources assessment and planning, in decision making concerning the design and control of dams and other engineering works and in supplying information on availability of moisture for agricultural purpose. In this paper a conceptual monthly rainfall runoff model is suggested which is based on the Xinanjiang model (Zhao, 1980), the computation results are compared with those of other water balance models.

THE STRUCTURE OF THE MODEL

Brief description of the model: Many studies(Zhao et al.(1980,1992) and others) have found that in humid and semi-humid regions the concept of ' runoff formation on repletion' is workable. This means that runoff is assumed not to be produced until the soil moisture content of the aeration zone is restored to field capacity and, thereafter, the runoff equals the rainfall excess without further loss. Runoff so generated is subsequently separated into two components, surface runoff and groundwater runoff, each of which is routed to the outlet of the basin as through a linear reservoir. The flow chart of the model is shown in Fig.1.

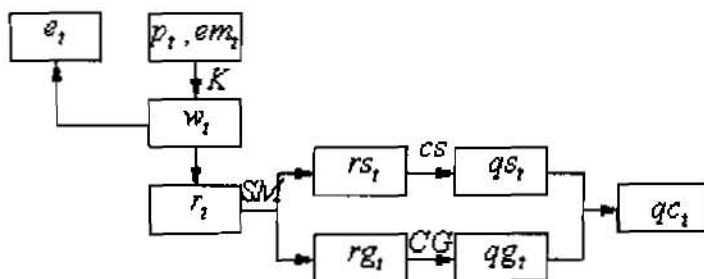


Fig.1 Flow chart for the monthly model

The inputs to the model are p_t , the measured areal mean precipitation and em_t , pan evaporation, or calculated evaporation at a free water surface on the basin (t is time in months). The symbols for outputs and state variables appear inside the blocks of Fig.1. Those for parameters are outside the blocks.

The meaning of these symbols in Fig.1 are as follows: e_t - the evapotranspiration in the month designated by t ; w_t - the tension water content at the end of the month designated by t ; r_t - the total amount of computed runoff in the month designated by t ; rs_t - the amount of computed surface runoff in the month designated by t ; rg_t - the amount of computed ground runoff in the month designated by t ; qs_t - the computed discharge of surface water in the month designated by t ; gg_t - the computed discharge of ground water in the month designated by t ; qc_t - the total computed discharge at the outlet of the basin in the month designated by t .

The parameters are: K - the ratio of areal potential evapotranspiration to pan evaporation or to calculated evaporation at a free water surface on a basin; SM - the areal mean free water storage capacity in a basin; CG - the recession coefficient for ground water; CS - the recession coefficient for surface water. It is taken as a constant

$CS = 0.3$. These two quantities, CG , CS are defined in the routing operation expressed through (14) and (15)

The computation of evapotranspiration: When rainfall exceeds $K \times em_t$, the evaporation is computed by

$$e_t = K \times em_t \quad (1)$$

When $K \times em_t$ is in excess of rainfall, the following equation is used to calculate the net evaporation rate:

$$e'_t = (K \times em_t - p_t) \times \frac{w_{t-1}}{wm} \quad (2)$$

where K is a parameter to be optimized. The effect of a change of wm on output can be offset by a corresponding change in K . For this reason, in optimization, for wm a constant value can be adopted.

Runoff production: In months, when rainfall exceeds evaporation, the excess is added to the tension water in the soil. When the soil moisture reaches the tension water capacity of the basin, runoff occurs. The formation of runoff is shown in Fig.2.

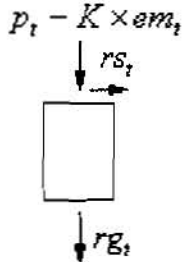


Fig.2 Formation of runoff

When $p_t - K \times em_t + w_{t-1} < wm$

$$w_t = w_{t-1} + p_t - K \times em_t \quad (3)$$

$$r_t = 0 \quad (4)$$

otherwise

$$w_t = wm \quad (5)$$

$$r_t = p_t - K \times em_t - (wm - w_{t-1}) \quad (6)$$

On the other hand, when computed evaporation is in excess of rainfall, no runoff occurs. The constant of tension water in the soil decreases:

$$w_t = w_{t-1} - e'_t \quad (7)$$

e'_t is net evaporation.

Runoff separation: The runoff r_t produced in accordance with eq.6 during months in which the rainfall exceeds evaporation is accumulated in storage and contributes to groundwater and surface runoff in a manner modeled by a tank with a free surface which can overflow to produce surface runoff and with an orifice in the bottom through which a contribution to groundwater flow is sustained. To consider an uneven distribution of free water capacity, a parabolic distribution is assumed

$$\frac{f}{F} = 1 - (1 - sm_t / smm)^{ex} \quad (8)$$

where f , the portion of basin area for which the free water capacity storage is less than or equal to sm_t , F , the basin area and ex , a coefficient, not a parameter and smm , the greatest free water capacity in the basin. It is

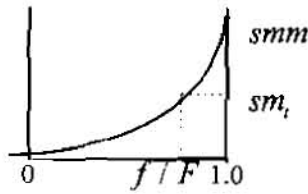


Fig.3 The distribution of free water capacity

assumed that the current state of free water storage in the basin can be represented by a point(ordinate sm_t on the parabola of Fig.3)implying that the part of the basin to the left of that point is at capacity storage and to the right the storage is constant below capacity level.

The area under the parabola is the areal mean of free water capacity SM , The following relationship can be obtained:

$$smm = SM \times (1 + ex) \quad (9)$$

The output of the model was found to be insensitive to the value of ex in the range of 0.5 to 2 and so was given a fixed value 1.5. From (8) and (9) sm_t can be expressed in terms of s , SM and smm

$$sm_t = smm \times \left(1 - \left(1 - \left(\frac{s_t}{SM}\right)^{\frac{1}{1+ex}}\right)\right) \quad (10)$$

The total runoff generated in accordance with equations (6) produced a contribution to surface water

When $r_t + s_{t-1} < SM$

$$rs_t = \int_{sm_{t-1}}^{sm_{t-1}+r_t} \frac{f}{F} ds_{t-1} = r_t - SM + s_{t-1} + SM \times \left(1 - \frac{(r_t + sm_{t-1})}{smm}\right)^{1+ex} \quad (11)$$

Otherwise

$$rs_t = r_t + s_{t-1} - SM \quad (12)$$

The remainder of r_t remain in the free water storage contributing to groundwater in succeeding months according to the equation

$$rg_t = s_{t-1} \times kg \quad (13)$$

The effect of a change of kg on calculated discharge can be offset by a corresponding changes in SM . This suggests dependence between these two parameters. When SM is chosen as parameter, then kg is decided by SM , and kg is not a parameter. The value of 0.07 is employed for kg .

Flow concentration: The routing of the surface water and groundwater to the outlet of a basin may be modeled by linear reservoirs, one for each component.

$$qs_t = qs_{t-1} \times CS + rs_t \times (1 - CS) \quad (14)$$

$$rg_t = qg_{t-1} \times CG + rg_t \times (1 - CG) \quad (15)$$

$$qc_t = qs_t + qg_t \quad (16)$$

where qs_t , qg_t , qc_t are computed surface water discharge, groundwater water discharge and total discharge at time t respectively. CS , CG are the recession coefficient of the linear reservoirs for surface water and ground water respectively.

It is found that monthly outputs are insensitive to the value of CS . The results with CS at 0.2 or 0.4 are nearly the same as those with CS at 0.3. This, perhaps, results from the times of flow concentration being very small, almost the same for all basins compared with the time step of one month. Henceforth CS is taken as a constant 0.3.

In application, the storage and state variables are taken at the end of the corresponding month. The physical units of all inputs, outputs and state variables are in mm. The values of wm , ex , kg , CS are fixed at 200, 1.5, 0.07, 0.3. Three parameters, K , SM , KG , remain to be optimized. Each has a clear physical meaning.

COMPUTATION RESULTS AND COMPARISON WITH OTHER MONTHLY MODEL

Data description: The basins under study in the paper are located in southern China (6 basins) and southern Belgium (6 basins). The climate of these two regions are quite different. In southern Belgium, precipitation (80 - 100 mm per month) do not show important seasonality. However potential evaporation is highly seasonal. In winter, potential evaporation is very low and in summer time it averages 100 mm per month. The six Chinese basins under study lie in the monsoon area, thus receiving plenty of rainfall, ranging from 1400 - 2000 mm per year. In the six months from April to September, about 80% of the total annual precipitation occurs. The basins studied in both regions have fairly good vegetation cover and basically lie in mountainous areas. In the 12 basins studied, there are no significant human activities which would interfere with hydrological activity. The main hydrological characteristics and data summary are given in Table 1. The table is taken from the paper by G.L.Vandewiele(1992).

Table 1 Data summary for the basins under study

Basin Code	Area (Km^2)	Data period (years)	runoff coefficient	Variation for runoff
Southern Belgium				
i8am	1044	16	52.0%	0.84
i8ho	68	8	58.6%	0.89
i8l2	1314	13	41.9%	0.85
i8ou	1597	12	45.2%	0.96
i8se	1235	16	53.1%	0.87
i8vi	554	16	44.4%	0.88
Southern China				
cej1	2000	16	55.3%	1.03
chl2	595	18	57.5%	0.99
cfh3	1556	17	76.1%	0.94
cxg4	1881	15	57.9%	0.90
cjz5	385	14	62.0%	0.96
cst6	1357	19	54.0%	0.95

Optimization and analysis of fit: It is assumed that: $\sqrt{qm_t} = \sqrt{qc_t} + u_t$, where qm_t , qc_t , u_t are the measured and computed runoff respectively at time t. u_t is normally distributed with zero expectation and constant variance.

The following objective function is used in optimization:

$$\min \sum (\sqrt{qc_t} - \sqrt{qm_t})^2 \quad (17)$$

For the elimination of the influence of assumed starting values, some length of take-off period is considered. It has been found that for this purpose 6 years is necessary though in most basins 3 or 3 y ears is sufficient.

The minimization was performed with the help of VA05A computer package(Hopper, 1978), and its efficiency was checked by plotting the sum of squares (16) versus each of the parameters. In that way it is possible to see whether a minimum was reached in the vicinity of given initial parameter values It is essential that the initial parameter values be chosen not far from the optimum values.

Minimization (17) with respect to parameter results in estimation of the parameter values. The model standard deviation is estimated by $\sigma = \sqrt{\frac{\text{minimum} \cdot \text{sum} \cdot \text{of} \cdot \text{squares}}{n-3}}$, where n is the number of terms in (17). The

half width of a 95% confidence interval for σ is approximately $HWCI = \frac{1.96\sigma}{\sqrt{2(n-3)}} = \frac{1.38\sigma}{\sqrt{n-3}}$. The

covariance matrix of the parameters is $\Delta = 2\sigma^2 H^{-1}$, where H is the Hessian of the sum of squares (17) at its minimum. From this covariance matrix the correlation matrix of parameter values can be computed. The correlation matrix of the optimized parameter values must be checked. A high correlation coefficient between the optimized values of two parameters suggests that a simpler model with less parameters might prove equally efficient, thus suggesting the necessity for a reexamination of the model structure.

The calibration period for all the basins studied is 10 years except for i8ho in southern Belgium, which has only 8 years of data, all of which is used in calibration. The rest of data for each basin except i8ho is test periods. The calculation results show that 10 years calibration period is necessary to reach good estimate of parameter values for same basin though 6-8 years calibration for most the basins studied is enough. The general behavior of residuals versus precipitation, evaporation and runoff have been checked for both calibration and test periods. The residuals do not show trends or heteroscedasticity. The correlation between the parameters are smaller than 0.9 in absolute value. The estimated mean runoff is nearly equal to the measured mean runoff for each basin. The residuals are satisfactory for all basins studied in the whole test period and in each of the four seasons (residuals in test period are non-significant). i8ho basin is an exception, having no test period.

Furthermore, some formal tests can be performed for the calibration and test periods to check the general agreement between calculated and measured discharge. It is to check whether

$$\frac{|\bar{u} \cdot \sqrt{n-k}|}{std.u} \leq 1.96 \quad (18)$$

where \bar{u} is the mean residual and $std.u$ is residual standard deviation. This test is at the 5% significant level. k is the number of parameters. This test can also be performed separately for all years to check whether the fitting is seasonally unsatisfactory. For example, to check the fitting between calculated and measured discharges in the spring season, the mean residuals and residuals standard deviation of discharges in all springs are obtained, and the test of (18) is performed. A year can be divided into four seasons: winter - January, February, March; spring - April, May, June; summer - July, August, September; autumn - October, November, December. Failure to pass the test of (18) means not-so-good agreement between calculated and measured discharges in the seasons tested. The test of (18) is performed for each of the four seasons separately in the calibration and test periods. There are 12 basins with four seasons each, so $12 \times 4 = 48$ test were performed, following the residuals analysis methodology described earlier. The significance level of all tests was taken at 5% level.

The efficiency of the model is measured by $Q = \frac{\text{measured} \cdot \text{cv} \cdot \text{of} \cdot \text{runoff}}{\text{estimated} \cdot \text{cv} \cdot \text{for} \cdot \text{mean} \cdot \text{runoff}} = \frac{ocv}{ecv}$,

where $ocv = \frac{\sqrt{\frac{1}{n} \sum (qm_i - \bar{qm}_i)^2}}{\bar{qm}_i}$, $ecv = \frac{2\sigma}{\sqrt{\bar{qm}_i}}$, \bar{qm}_i is the mean of measured discharges. σ is model

standard deviation and its computation is given in previous text. Model efficiency is a general expression of agreement between calculated and measured discharges for the whole calculated period. The greater the model efficiency, the better the general agreement. However, a high model efficiency do not always mean a good agreement between calculated and measured discharges for any shorter period such as season. Eq.18 however may be applied to the agreement or disagreement observed within any particular season.

Computation results and comparison with other monthly models: The ranges of the optimized parameter values

referring to different basins studied are quite different. The values of parameter SM for different basins in southern China and southern Belgium vary greatly from 4.5 to 135 mm. Prof. Zhao has pointed out that SM is not a physically realistic value in his research (zhao et al, 1988). Meanwhile, the ranges of values for parameter K or CG are 0.66 - 1.09 and 0.59 to 0.99 respectively. Parameters K , CG are dimensionless. Millimeter is the unit of parameter SM . The measurement is in months

Table 2 shows a comparison between the model proposed in the paper and some models from the literature. The results of the last five columns are taken from the paper by G.L.Vandewiele et al (1992). V-model means the model developed by G.L.Vandewiele et al (1992). T, Ta abcd, and P represents respectively T-model by Thornthwaite and Marthers (1955), Ta-model by Alley (1984), abcd-model by Thomas and P-model by Palmer(1965) and Alley (1984). P-model was first developed by Palmer(1965) and then modified by Alley (1984) in his comparative study of monthly water balance models. All of these four models are monthly models. The details of these models can be found in the paper by G.L.Vandewiele et al (1992). The two critical aspects of models: efficiency and number of seasons (out of four) with significant residuals are presented in Table 2.

Table 2 Model efficiency and number of seasons with significant residuals

Basin code	Model in the paper	V-model	T	Ta	abcd	P
Southern Belgium						
i8am	(2.88-0)	(3.02-0)	2.39-1	(2.84-0)	3.46-2	2.39-1
i8ho	2.16-0	2.37-0		2.28-0	(2.75-0)	
i8le	(2.85-0)	(2.39-0)	2.50-2	(2.71-0)	3.15-2	2.46-2
i8ou	(3.42-0)	(3.47-0)	2.58-1	2.86-2		2.51-2
i8se	(2.84-0)	(2.82-0)	2.59-2	2.71-2		2.54-2
i8vi	(2.78-0)	(3.10-0)	2.34-2	2.67-1	3.32-1	2.31-2
Southern China						
cej1	(4.35-0)	4.31-1	3.20-1	3.82-2	4.24-2	3.19-1
chl2	(4.54-0)	4.50-1			4.63-3	
cth3	3.87-1	(3.88-0)	3.02-2	3.13-2	(4.01-0)	3.02-2
cxg4	3.32-1	(3.57-0)		2.99-3	3.41-2	
cjz5	3.05-0	(3.40-0)	2.76-2	3.13-0	3.42-2	2.76-2
cst6	(4.25-0)	(4.27-0)	3.58-1	3.92-1	(4.34-0)	3.58-1

'good' fitting basins for each model are bracketed. The first figure in the group for each basin and each model refers to model efficiency, the second refers to numbers of seasons with significant residuals.

In model comparison, it should be noted that different model may have different numbers of parameters. The V-model and Ta have three parameters(for V-model, two other parameters implicitly), whereas models T and P have only two free parameters. The abcd model has four free parameters.

In Table 2, it can be seen that the model efficiency of abcd model is higher than that of other models. If considering only model efficiency, abcd model is the best. though in most cases the differences of model qualities between abcd model and other models also having high model quality are small. However, there are many seasons with significant residuals for abcd model. Significant seasonal residuals implies serious residuals seasonality. This in turn indicates not so good agreement between computed and measured discharges in one out of four seasons, perhaps caused by the model structure not adequately reflecting the hydrological process occurring in that season. If equal attentions are paid to seasonal fitting and general agreement, the following criteria may be used to define 'good' fitting: (1) the number of seasons with significant residuals is equal to the minimum number among six models and (2) the model efficiency belongs to the 95% confidence interval of the efficiency of the model with the highest model quality Q fulfilling the first condition.

By using these criteria, the number of 'good' fitting basins is 8 for the model proposed in Table 2. 9 for V-model, far more than other models, for example, 3 for abcd model. The proportion of seasons with significant residuals is 2 in 48 for the model proposed, the same percentage for V-model, much more for the other models listed in Table 2, for

example, 14 for abcd model. Thus it can be said that the proposed model and the V-model are the best, according to the proposed criteria. If the abcd model has four parameters and the V-model has five (two parameters implicitly) and the principle of parsimony are considered, the model proposed in the paper is superior in southern China and southern Belgium.

CONCLUSIONS

A conceptual monthly rainfall runoff model has been developed and computations have been made for humid region in southern China and southern Belgium. The model has fewer parameters (three) and yields results as good as the best of the other monthly water balance models tested.

ACKNOWLEDGMENT

This work was completed in Laboratory of Hydrology, Free University Brussels, Belgium. The author is indebted to Prof. G.L. Vandewiele, Laboratory of Hydrology, Free University Brussels, for his invaluable recommendations and guidance. Prof. A. Van der Beken, director of Laboratory of Hydrology, Free University Brussels is thanked for his support in the research. Special thanks is given to Prof. J.E. Nash for his many valuable suggestions and revisions of the paper. Without his kind assistance, the paper would not present this way.

REFERENCE

- Alley, W.M., 1984. On the treatment of evapotranspiration, soil moisture accounting and aquifer in monthly water models. *Water Resou. Research.* 80(8):1137-1149
- Hopper, M.J., 1978. Catalogue of subroutine. Harwell subroutine library. U.K. Atomic Energy Authority, Harwell, 69pp
- Palmer, W.C., 1965. Meteorological drought. Res. Pap., U.S. Weather Bur., 45-58
- Thomas, H.A., 1981. Improved methods for national assessment. Report, Contract WRJ 15249270, US Water Resources Council, Washington, S.C.
- Thornwaite, C.W. and Mather, J.R., 1955. The Water Balance. *Publ. Climatol. Lab. Climatol. Drexel Inst. Technol.*, 8(1):1-104
- Vandewiele, G.L., Xu, C-Y., and Ni-Lar-Win, 1992. Methodology and Comparative study of monthly water balance models in Belgium, China and Burma. *J. Hydrol.* 134:315-347
- Zhao, Renjun, Zhuang Yilin, Fang Lerun, Liu Xinren and Zhang Quangsheng, 1980. The Xinanjiang model. *International Association of Hydrological Science. Publ. NO. 129*, pp351-356
- Zhao, Renjun, Wang Pilan, 1988. Analysis on parameter values of the Xinanjiang model. *Journal of Hydrology*, N0. 6 (in Chinese)
- Zhao, Renjun, 1992. The Xinanjiang model applied in China. *J. Hydrol.* 135:371-383

** In January, 1998, the author will be in Iowa Institute of Hydraulic Research, University of Iowa, Iowa city, Iowa 52242-1585, U.S.A*

LANDSCAPE ASSESSMENT OF WETLAND FUNCTIONS (LAWF): A GEOGRAPHIC INFORMATION SYSTEM (GIS) MODEL FOR THE EVALUATION OF WETLAND FUNCTIONS

By M.S. Cheng, Ph.D., P.E, Section Head, Department of Environmental Resources Programs and Planning Division, Prince George's County, Maryland; N. Weinstein, R.L.A., AICP, Senior Environmental Engineer, Tetra Tech, Inc., Fairfax, Virginia; C. Victoria, Scientist, Tetra Tech, Inc., Laurel, Maryland.

Abstract: An innovative GIS wetland tool has been developed and to the watershed management program of Prince George's County, Maryland. The twofold purpose of this tool is to support the county's Nonpoint Source Pollutant Discharge Elimination System (NPDES) program and to help in the master planning and management of a Wetland Banking System (WBS) that is under development as a result of a Memorandum of Agreement (MOA) with the Baltimore District of the United States Army Corps of Engineers (USACE).

INTRODUCTION

Watershed Description: Prince George's County, Maryland, is a rapidly growing jurisdiction within the Washington, D.C., metropolitan area. The county has a population of approximately 750,000. Although there is a trend toward urbanization, with many housing, office, and industrial areas being developed, significant areas of agriculture and sand and gravel operations remain within the county. Located within the county are the Patuxent Wildlife Research Center and the Beltsville Agricultural Research Center, as well as several other major federal government facilities. The total area of the county is approximately 488 square miles, of which, or 31 square miles (6.3 percent) are wetlands and 12 square miles are open water. The three major drainage basins within the county are the Potomac, Anacostia, and Patuxent river basin. Each of these basins has significant natural, historic, and cultural resources.

Water Quality Programs: The county currently has an extremely effective NPDES program for water quality monitoring and an extensive GIS-based system for mapping and evaluating watershed hydrology and floodplain management. Significant water quality impacts are generated from a variety of sources including approximately 6,800 storm drain outfalls, as well as salt and sand applications to county roadways during the wintertime. Within the Anacostia River basin alone, the county has identified more than 100 sites for stormwater management water quality retrofits and wetland restoration. There are potentially hundreds of additional sites within the three major river basins that are candidates for retrofit and restoration.

Wetland Mitigation: In 1996 Prince George's County entered into an MOA with the USACE to establish a Wetland Banking System Master Plan. The Master Plan will identify sites within the three river basins and 11 subbasins that are to be used for potential mitigation bank sites. Final site selection and type and acreage of mitigation are determined by a Bank Oversight Team comprised of County and review agency officials. These sites are to be used to compensate for County Department of Public Works and Transportation and Maryland-National Capital Park and Planning projects.

Program Requirements: Because of the magnitude of information that needs to be processed and evaluated and the potential for numerous management scenarios a GIS-based data management and evaluation model is required. The GIS system will allow the county to quickly answer questions and develop management scenarios on both the subbasin and watershed levels. It can assist in the identification of wetlands at risk, mitigation issues, retrofit issues, identification of upland buffer areas, and identification of potential restoration sites.

LANDSCAPE ASSESSMENT OF WETLAND FUNCTIONS (LAWF) MODEL

Model Description: The LAWF model is an ARC/INFO based GIS system. Its main functions are to assist in the location and management of a WBS and to enhance the County's watershed management programs. The system is designed to evaluate wetland functions and values based on the existing GIS database and layer coverages. Wetland functions are the result of the combination of physical and chemical processes within the watershed. Values are the significance of each function to the overall processes within the ecosystem as well as the management goals and objectives. The user interface is designed to allow the user to define the management issues so that the system can define and organize the data for analysis. The functional assessment for each area in question is based on a ranking of criteria specific to the management issue or question. Each area, or watershed basin segment, is ranked according to the management question based on default or user-specified ranges of numbers.

Functional Assessment: The functional assessment for the model is based on modified criteria from the state of Maryland's Method for the Assessment of Wetland Function (Fugro East, 1995). The approach is predominately a desktop method that requires some field "truthing". The model is designed to evaluate the eight statutory functions listed in the State of Maryland Nontidal Wetlands Protection Act of 1989: (1) groundwater discharge, (2) flood flow attenuation, (3) sediment/toxic retention, (4) aquatic diversity/abundance, (5) production export; (6) sediment stabilization, (7) nutrient removal/transformation, and (8) wildlife diversity. The functional assessments are based on criteria and techniques from the Hydrogeomorphic Method (Brinson, 1993) and on the Wetlands Evaluation Technique (Adamus, et al., 1987).

To adapt the assessment methods for these functions into a GIS environment, the criteria and parameters to rate each function had to be reexamined and in some cases redefined so that they could be evaluated using the existing county GIS databases and coverages. The eight statutory functions were combined and redefined as follows:

- **Surface Water Processing:** Hydrologic and hydraulic processes within the wetlands, or potential wetlands site, and the contributing drainage area.
- **Water Quality Modification/Elemental Cycling:** Potential for water quality improvements through biological and chemical processes based on hydrologic and hydraulic parameters.
- **Groundwater Processing/Recharge:** Potential of the wetland, or mitigation/restoration site to act as a shallow aquifer recharge area.

- ***Groundwater Processing/Discharge:*** Potential of the existing wetland area to contribute to surface flow.
- ***Wildlife/Aquatic Diversity:*** Habitat potential of the area in question.

The user selects one or a combination of the above functions and then can examine an individual wetland polygon, user-defined assessment area, or subbasin. Each function comprises 5 to 15 variables. The scores from each variable are combined and weighted to arrive at an overall value for each function at the area in question. The results are then tallied and compiled in tabular format. In addition to the ranking of each area in question, the area and wetlands classification are listed. Potential threatened and endangered species locations, wetlands of special state concern, and historical or other cultural resources based on existing data layers are also identified. The end product allows the user to quickly assess the effectiveness of wetland functions in a watershed, to predict the effectiveness of potential restoration and mitigation projects, and to identify areas that will require additional fieldwork and studies.

REFERENCES

- Adamus, Paul R., Clairain, Ellis J., Smith, R. Daniel, and Young, Richard, 1987. Wetland Evaluation Technique (WET) Volume II: Methodology.
- Brinson, Mark M., 1993. A Hydrogeomorphic Classification for Wetlands. Wetlands Research Program Technical Report WRP-DE-4
- Fugro East, Inc., 1995. A Method for the Assessment of Wetland Function. Prepared for the Maryland Department of the Environment, Baltimore, Maryland

SPATIALLY DISTRIBUTED ENERGY BUDGET SNOWMELT MODELING IN MOUNTAINOUS REGIONS OF THE WESTERN UNITED STATES

By David C. Garen, Hydrologist, United States Department of Agriculture, Natural Resources Conservation Service, National Water and Climate Center, Portland, Oregon;
Danny Marks, Hydrologist, United States Geological Survey, Corvallis, Oregon

Abstract: A spatially distributed energy budget snow simulation model has been developed and applied to several areas in the western United States. This type of model takes advantage of the growing amount of GIS-based information on catchment characteristics and meteorological inputs. These modeling exercises have demonstrated the feasibility of detailed snow simulations in mountainous areas. The type of spatial information generated by such a model has significant potential in natural resource management. In addition, the snowmelt fields generated by the model can be used as input to a hydrologic model to simulate streamflow. It is envisioned that this model will become a practical tool for resource and water management.

INTRODUCTION

Where snow is an important part of the hydrologic water balance or where it plays a major role in resource management, it is valuable to have a modeling tool that can accurately simulate the dynamics of snow accumulation and melt, both temporally and spatially. Most models that are currently used for water management and other operational decision making are of the conceptual, spatially lumped type, originally developed two or three decades ago. With the data networks, computing facilities, and geographic information systems (GIS) available today, many new modeling possibilities are opening up. In this paper, we explore the applicability of a spatially distributed energy balance snow simulation model in mountainous areas that have, in varying degrees, important resource issues such as irrigation water supply, reservoir management, timber management, groundwater recharge, and recreation.

SNOWMELT MODEL

The model was originally developed and tested in the Sierra Nevada mountains of California (Marks, 1988; Marks and Dozier, 1992; Marks et al., 1992), but it has subsequently been used in the Wasatch mountains of Utah (Susong et al., 1996), the Cascade mountains of Oregon (Marks et al., 1997), and in the Boise River in Idaho (Garen and Marks, 1996). The model is thoroughly described in these previous papers, so only a brief description is presented here. The energy and water fluxes considered by the model are shown in Fig. 1.

The model is driven by inputs of net solar radiation, meteorological variables, and snowcover properties to compute the energy and mass balance of the snowcover at each grid cell in the area modeled. It predicts melt from two snowcover layers and runoff from the base of the snowcover, adjusting the snowcover mass, depth, and thermal properties at each time step. The surface layer is considered to be the active layer, with its thickness set to a constant value (0.25 m), representing the approximate depth of significant solar radiation penetration. All surface energy transfer occurs in this layer. The lower layer is simply the remainder of the snowcover below the surface layer. Both layers are assumed to be homogeneous and are characterized by their average temperature, density, and liquid water content.

The model assumes that energy is transferred between the surface layer and the lower layer and between the lower layer and the soil by conduction and diffusion. At each time step, the model computes the energy balance and the snow surface temperature and then adjusts the temperature and specific mass of each layer. If the computed energy balance is negative, the cold content, or the energy required to bring the temperature of the snowcover to 0°C, is increased, and the layer temperature decreases. If the energy balance is positive, the layer cold content is decreased until it is zero. Additional input of energy causes the model to predict melt. If melt occurs, it is assumed to displace air in the snowcover, causing densification and increasing the average liquid water content of both layers. Liquid water in excess of a specified threshold becomes predicted runoff. Though meltwater is usually generated in the

surface layer, mass lost to runoff is removed from the lower layer. The thickness of the surface layer remains constant until the lower layer is completely melted. At that time, the model treats the snowcover as a single layer.

The input data must be specified at a time resolution of 6 h or less, although better results are obtained with 3 h or less. The computational time step is normally 1 h, although under certain conditions, particularly when the snow layers become very thin, the model will use a smaller time step to ensure solution stability. The input data are interpolated internally to match the computational time step.

The model has a point version and a grid version. Both versions, along with many other physical modeling tools and image viewing and manipulation utilities, are implemented in a software package called Image Processing Workbench (IPW). This software is in the public domain and is fully documented (Marks and Domingo, 1997).

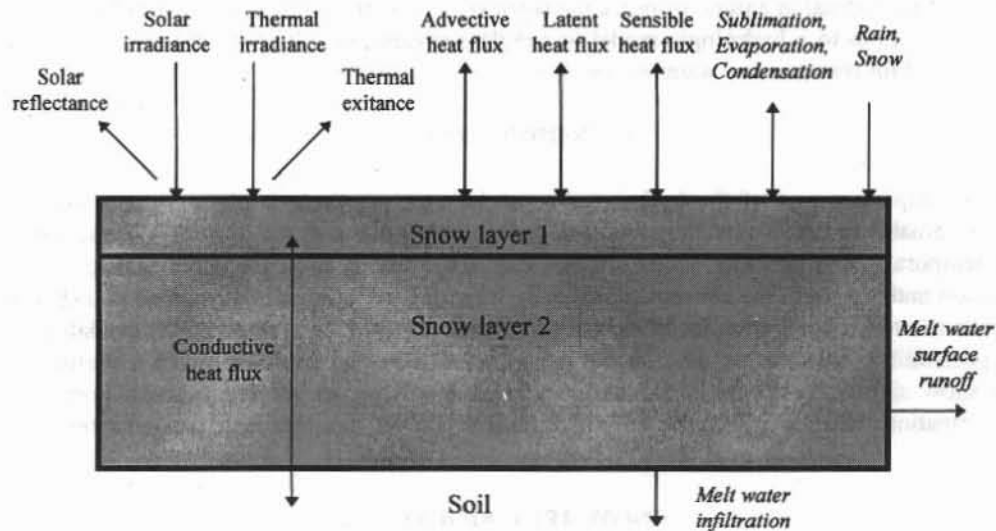


Fig. 1 Diagram of snow model components (energy fluxes in normal type, water fluxes in italics)

MODEL INPUT DATA

The static data required is a digital elevation model (DEM) for the area to be simulated. The resolution should be adequate to describe the important topographic features (elevation, slope, aspect) that would affect the energy budget of the snowpack, while at the same time having a manageable number of grid cells to keep the computations within reasonable time limits. Generally, the larger the area to be modeled, the larger the grid cell size. Examples of grid cell sizes are 75 m for the Wasatch mountain application and 250 m for the Boise River. This DEM is required for determining net radiation input to the snowpack, and it is used in the spatial interpolation of the meteorological input fields.

The meteorological data required include spatial fields of precipitation, air temperature, net solar radiation, incoming thermal (long-wave) radiation, vapor pressure, wind speed, and soil temperature for each time step in the period to be simulated. Some of these data are more readily available than others, so there is a varying degree of accuracy in the spatial fields of these variables, and some of them may have to be estimated. One of the main sources of these data is the Natural Resources Conservation Service (NRCS) SNOTEL network; other data sources include the National Weather Service (NWS) cooperative observer network, meteorological stations operated by the U. S. Bureau of Reclamation, and sites instrumented for research purposes, such as those in the Oregon Cascades installed by the U. S. Environmental Protection Agency.

Net radiation can be determined in different ways, depending on the data available. The starting point is to calculate fields of clear sky solar radiation using a model contained in IPW, with the DEM as input. If solar radiation

measurements are available, an adjustment factor based on the observed data can be applied to these fields. If no solar radiation measurements are available, adjustments can be made based on the difference between daily maximum and minimum temperatures, which is an index of cloud cover (Hungerford et al., 1989).

Vapor pressure can be derived from relative humidity and air temperature (there is a convenient IPW utility to do this). If no humidity data are available, one can often assume that the dew point is equal to the daily minimum temperature.

Precipitation and temperature fields can be interpolated from the station data using a procedure based on detrended kriging developed by Garen et al. (1994) and Garen (1995). If data are available at a time resolution greater than or equal to the data time step to be used in the model, these fields can be interpolated directly. Often, however, only daily data are available at many or all of the stations in the region. In this case, the daily fields can be calculated, then they must be disaggregated down to the required model time step. To do this, at least one representative station with the required time resolution must be available. For precipitation, one can disaggregate by applying a set of fractions to the daily total at each grid cell. The fractions represent the portion of the daily total occurring in each of the time steps within the day. A set of fractions for each day during the period to be modeled can be derived for each station with the higher time resolution data, then these can be averaged to arrive at a single set to apply over the whole region. For temperature, one can calculate values for each time step as a weighted sum of the maximum and minimum temperatures for the day. The weights can be derived to replicate a typical diurnal cycle for the location and time of year. These procedures were used by Garen and Marks (1996) and by Susong et al. (1996).

Depending on the amount of station data available for the other variables, the detrended kriging spatial interpolation procedure can be used, or, if there are insufficient stations, areal average values can be used to develop the necessary spatial fields of these elements.

MODEL OUTPUT

As output, the model produces two multi-band images, an energy and mass flux image (10-band) and an image of snow conditions (9-band). These can be output at any desired temporal frequency, generally less than the computational time step. The energy and mass flux image contains the following information (average or total refers to values since the previous output image):

- average net all-wave radiation (W/m^2)
- average sensible heat transfer (W/m^2)
- average latent heat exchange (W/m^2)
- average snow/soil heat exchange (W/m^2)
- average advected heat from precipitation (W/m^2)
- total evaporation (kg, or mm/m^2)
- total melt (kg, or mm/m^2)
- total predicted runoff (kg, or mm/m^2)
- snowcover cold content (J/m^2)

The snow conditions image contains:

- predicted depth of snowcover (m)
- predicted average snow density (kg/m^3)
- predicted specific mass of snowcover (kg/m^3)
- predicted liquid water in snowcover (kg/m^3)
- predicted temperature of surface layer ($^{\circ}\text{C}$)
- predicted temperature of lower layer ($^{\circ}\text{C}$)
- predicted average temperature of snowcover ($^{\circ}\text{C}$)
- predicted lower layer depth (m)
- predicted liquid water saturation (%)

Model output can be used in several ways. The images can simply be viewed to obtain a visual representation of the spatial distribution of the desired variable. They can also be made into a movie to provide an animated picture of

the snow accumulation and melt. The images can be analyzed to determine, for example, dates of maximum snow or melt out at selected locations in the region, or they can be used as input to a hydrologic model for simulating streamflow. Certainly there are other possibilities as well.

MODEL APPLICATIONS

Emerald Lake, California: This was the original test area for the model, located in Sequoia National Park in the southern Sierra Nevada mountains of California. It is a small (1.25 km²) alpine catchment, most of which is bare granitic rock, with elevations ranging between 2800 and 3416 m. This represented an intensive study, whose purpose was research, rather than an operational resource management application. The data monitoring and energy fluxes in this catchment are described in detail by Marks (1988), Marks and Dozier (1992), and Marks et al. (1992). The spatial version of the model was first applied to this basin in 1994. Two 10-day periods during the spring melt of 1986 were simulated. This simulation required 120 MB of input data, generated 200 MB of output, and took 9.5 h of computational time on a Sun Sparc-2 workstation.

Park City, Utah: This study was conducted to investigate groundwater recharge, most of which comes from snowmelt, in a 460 km² area near Park City, Utah, on the east side of the Wasatch Mountains (Susong et al., 1996). Elevations range between 2000 and 3100 m. Simulations were carried out for 1994 and 1995 using a data time step of 3 h and a grid cell size of 75 m (resulting in about 82000 grid cells). Meteorological input data came from six stations, four of which are NRCS SNOTEL sites, and two of which are NWS cooperative observer sites. The spatial fields were interpolated using the detrended kriging procedure mentioned previously. Each year of this simulation required about 1.5 GB of input data, generated 1 GB of output, and took about 12 h of computational time on a Sun Sparc Ultra-170E workstation.

Cascade Mountains, Oregon: The point version of the model was used to investigate the dynamics of rain-on-snow during a large flood event in the Willamette River basin in late January and early February 1996 (Marks et al., 1997). Data were taken from two of three ecological monitoring sites installed and operated by the U. S. Environmental Protection Agency, which form an elevational transect across the west slope of the Cascade Mountains, about 100 km east of Corvallis, Oregon. Three simulations were made, at open and forested locations at the high site (1142 m) and at an open location at the middle site (929 m). Data from six nearby NRCS SNOTEL sites were also used to help verify model results and check on their spatial representativeness. The various energy fluxes were analysed to obtain a thorough understanding of the processes that took place to create this flood and the contribution of snowmelt to it.

Boise River, Idaho: This was a modeling exercise to apply the model to a relatively large catchment that is an important source of irrigation water supply as well as having significant timber resources and recreational use. The idea was to begin working toward the use of the model operationally in the management of the extensive reservoir and water distribution system owned by the U. S. Bureau of Reclamation. The area modeled is the basin above the U. S. Geological Survey gaging station on the Boise River near Twin Springs, located about 45 km east of Boise, Idaho. The drainage area is 2150 km², with elevations ranging between 1000 and 3200 m. Garen and Marks (1996) carried out an initial application of the model, simulating a one month period (April 1990) using a data time step of 3 h and a grid cell size of 250 m (resulting in about 34400 grid cells). Meteorological data came from eight stations in and near the basin, five NRCS SNOTEL sites and three stations owned and operated by the U. S. Bureau of Reclamation. Again, the detrended kriging procedure of Garen et al. (1994) and Garen (1995) was used to prepare the spatial fields of precipitation and temperature. This one-month simulation required 500 MB of input data, generated 350 MB of output, and took 6.5 h of computational time on a Sun Sparc-10 workstation.

A second application to the Boise River is currently underway. Since the first model application, three of the SNOTEL sites in the basin have been enhanced with solar radiation, humidity, wind, and snow depth sensors to provide data that previously had to be estimated. This application covers the time period 1 October 1996 to 31 July 1997. Part of the goal of this work is to evaluate the worth of these additional sensors in improving the simulation of the snowpack. Longer-term, this model is being linked to a spatially distributed hydrologic model so that streamflow can be simulated (Schumann and Garen, 1998).

CONCLUSIONS

These applications have demonstrated that spatially distributed energy balance snow modeling is feasible and that, given good input data, the model can simulate the accumulation and melt of a snowpack quite accurately. It is essential, then, that reliable methods of spatial interpolation of meteorological inputs be used. The detrended kriging procedure used in two of these applications performed well, but there are some areas of refinement that could be pursued. As the preparation of the input data represents the major portion of the effort required to perform a snow simulation, any improvements in the accuracy of the input fields or in the convenience of preparing them is well worth it.

The spatial snow simulations required a significant amount of disk storage space and computational time. Constraints on these continue to diminish with the rapid advances in computer technology. Nevertheless, these requirements are somewhat demanding in an operational environment, and it may be possible to find ways to streamline the way the model processes data, at least to reduce the disk storage requirements. It is expected that computational times will fall steadily with the rapid leaps in computer processing speeds.

The future plans for the model include adding a forest canopy effects algorithm and linking the model to a spatially distributed hydrology model for simulating streamflow. It is envisioned that this model will become a practical tool useful for resource management decision making.

REFERENCES

- Garen, D. C., 1995, Estimation of Spatially Distributed Values of Daily Precipitation in Mountainous Areas. In: *Mountain Hydrology: Peaks and Valleys in Research and Applications* (proceedings of Canadian Water Resources Association conference, Vancouver, British Columbia), 237-242.
- Garen, D. C., Johnson, G. L., and Hanson, C. L., 1994, Mean Areal Precipitation for Daily Hydrologic Modeling in Mountainous Regions. *Water Resources Bulletin*, 30(3), 481-491.
- Garen, D. C., and Marks, D., 1996, Spatially Distributed Snow Modelling in Mountainous Regions: Boise River Application. In: *HydroGIS '96: Application of Geographic Information Systems in Hydrology and Water Resources Management* (proceedings of Vienna conference), IAHS Publication no. 235, 421-428.
- Hungerford, R. D., Nemani, R. R., Running, S. W., and Coughlan, J. C., 1989, MTCLIM: A Mountain Microclimate Simulation Model. Research Paper INT-414, U. S. Department of Agriculture, Forest Service, Intermountain Research Station, Ogden, Utah.
- Marks, D., 1988, Climate, Energy Exchange, and Snowmelt in Emerald Lake Watershed, Sierra Nevada. Ph.D. dissertation, Departments of Geography and Mechanical Engineering, University of California, Santa Barbara.
- Marks, D., and Domingo, J., 1997, Software Tools for Hydro-Climatic Modeling and Analysis -- Image Processing Workbench Version 2. U. S. Environmental Protection Agency, Corvallis, Oregon, World Wide Web page <http://ice.cor.epa.gov/~ipw/www/intro.html>.
- Marks, D., and Dozier, J., 1992, Climate and Energy Exchange at the Snow Surface in the Alpine Region of the Sierra Nevada: 2. Snow Cover Energy Balance. *Water Resources Research*, 28(11), 3043-3054.
- Marks, D., Dozier, J., and Davis, R. E., 1992, Climate and Energy Exchange at the Snow Surface in the Alpine Region of the Sierra Nevada: 1. Meteorological Measurements and Monitoring. *Water Resources Research*, 28(11), 3029-3042.
- Marks, D., Kimball, J., Tingey, D., and Link, T., 1997, The Sensitivity of Snowmelt Processes to Climate Conditions and Forest Cover During Rain-on-Snow: A Case Study of the 1996 Pacific Northwest Flood. *Hydrological Processes*, in press.

Schumann, A. H., and Garen, D. C., 1998, Spatially Distributed Hydrologic Modeling for Streamflow Simulation and Forecasting. Paper presented at First Federal Interagency Hydrologic Modeling Conference, Las Vegas, Nevada.

Susong, D. D., Marks, D., Garen, D., and Mason, J., 1996, Application of an Energy-Balance Snowmelt Model to Estimate Ground-Water Recharge in a Mountain Basin Under Varying Climate Conditions. Poster paper presented at American Geophysical Union fall meeting, San Francisco, California.

David C. Garen, United States Department of Agriculture, Natural Resources Conservation Service, National Water and Climate Center, 101 SW Main Street, Suite 1600, Portland, Oregon 97204-3224
Tel.: +1 503 414 3021 Fax: +1 503 414 3101 E-mail: dgaren@wcc.nrcs.usda.gov

Danny Marks, United States Geological Survey, 200 SW 35th Street, Corvallis, Oregon 97333
Tel.: +1 541 754 4484 Fax: +1 541 754 4799 E-mail: danny@heart.cor.epa.gov

SATELLITE BASED SOIL MOISTURE MEASUREMENT FOR HYDROLOGIC MODELING

**Thomas J. Jackson, Hydrologist, USDA ARS Hydrology Lab, 104 Bldg. 007 BARC-West,
Beltsville, MD 20705
(301) 504-8511, tjackson@hydrolab.arsusda.gov**

Abstract: The recognition of the role of soil moisture in hydrologic modeling has grown significantly in recent years, especially in linking hydrologic and atmospheric models. As a system state variable, soil moisture impacts evaporation and infiltration directly. It has been shown that microwave remote sensing can be used to measure soil moisture. The depth of the layer measured increases as the wavelength used increases. Current choices of satellite observing systems include single channel active microwave (radar) and multichannel passive microwave operating at short wavelengths. Radars generally offer high spatial resolution (~ 20 m) but the signal is difficult to interpret for soil moisture due to the equal or greater importance of other factors in determining the response. Passive microwave satellite systems have low resolution (~ 50 km) but are generally more adaptable to robust interpretation algorithms. None of the currently available satellite systems can be readily interpreted for soil moisture measurement, although under specific sets of conditions it is possible. The future promises improvements in both active and passive microwave sensing that will benefit soil moisture and hydrology. The next generation of passive microwave sensors, due for launch in 2 years, will offer a much longer wavelength than currently available. Other systems are being proposed that could provide both global and high resolution soil moisture measurements.

INTRODUCTION

The upper few centimeters of the soil are extremely important because they are the interface between soil science and land-atmosphere research and are also the region of the greatest amount of organic material and biological activity. Since spatially distributed and multitemporal observations of surface soil moisture are rare, the use of these data in hydrologic modeling has not been fully explored or developed. The ability to observe soil moisture frequently over large regions could significantly improve our ability to predict runoff and to partition incoming radiant energy into latent and sensible heat fluxes at a variety of scales up to those used in global circulation models. Temporal observation of surface soil moisture may also provide the information needed to determine key soil parameters such as saturated conductivity (Ahuja et al., 1993). These sensors provide a spatially integrated measurement which may aid in understanding the upscaling of essential soil parameters from point observations.

In this paper the basis of microwave remote sensing of soil moisture will be presented along with the advantages and disadvantages of different techniques. Currently available satellite sensor systems will be described. It should be noted that there are no satellite systems in operation that are truly capable of providing reliable soil moisture measurements.

MICROWAVE REMOTE SENSING

A general advantage of microwave sensors (as opposed to visible and infrared) is that observations can be made under conditions of cloud cover. In addition, these measurements are not dependent on solar illumination and can be made at any time of the day. Vegetation has an attenuating effect on microwave response functions which can often be removed. The sensor actually measures a shallow depth of the soil which is approximately 1/4 the wavelength (based on a range of wavelengths from 2 to 21 cm).

There are two basic approaches used in microwave remote sensing, passive and active. Passive methods measure the natural thermal emission of the land surface at microwave wavelengths using very sensitive detectors. Active methods or radars send and receive a microwave pulse. The power of the received pulse is compared to that of the pulse sent to obtain the backscattering coefficient. The backscattering coefficient is then related to the characteristics of the target. In the next section, common elements of the two approaches are presented followed by descriptions of the individual techniques.

The microwave region of the electromagnetic spectrum comprises the wavelengths between 1 and 100 cm. Within this region, there are various bands that are protected. These bands are often referred to by a lettering system. Some of the relevant bands that are used are: K (~0.8 cm), X (~3 cm), C (~5 cm), S (~10 cm), L (~20 cm), and P (~50 cm).

Fundamental Basis: Microwave sensors measure a variable that is ultimately related to an electrical property of the target called the dielectric constant. When the sensor is capable of seeing the soil, the dielectric constant is a composite of the values of its components: air, soil and water. Although the dielectric constant is a complex number, for most soil mixtures the imaginary part is small and can be ignored for computational purposes without introducing significant error. Values of the real part of the dielectric constant for air and soil particles are 1 and 5 respectively. Water has a value of about 80 at the longer wavelengths considered here (> 5 cm). The basic reason microwave remote sensing is capable of providing soil moisture information is this large dielectric difference between water and the other components. Since the dielectric constant is a volume property, the volumetric fraction of each component is involved. The computation of the mixture dielectric constant has been the subject of several studies and there are different theories as to the exact form of the mixing equation (Ulaby et al., 1986). A simple linear weighting function is typically used.

Passive Microwave Methods: Passive microwave remote sensing utilizes highly sensitive radiometers that measure the natural radio thermal emission at a particular wavelength. The measurement provided is the brightness temperature, T_B , that includes contributions from the atmosphere, reflected cosmic radiation, and the land surface. Atmospheric contributions are negligible at wavelengths > 5 cm (the microwave region of interest here). Cosmic radiation has known values and is easily incorporated into computations. Therefore, T_B is essentially dependent on the land surface condition.

The brightness temperature of an isothermal surface is equal to its emissivity multiplied by its physical temperature. If we independently estimate physical temperature, emissivity can be determined.

Microwave emissivity varies between 0.6 and 0.95 for most land surfaces. At these wavelengths the reflectivity is equal to 1 minus the emissivity. Emissivity is functionally related to the dielectric constant.

For natural conditions, varying degrees of vegetation will be encountered and this affects the microwave measurement. Vegetation attenuates the sensitivity of the interpretation algorithm to soil moisture changes and increases the possibility of significant error. The attenuation increases as wavelength decreases. This is an important reason for using longer wavelengths. At longer wavelengths it is possible to correct for vegetation using a vegetation water content related parameter. An algorithm for estimating surface soil moisture from T_B has been presented in Jackson (1993).

A problem with passive microwave methods is spatial resolution. For a given antenna size, the footprint size increases as wavelength and altitude increase. For realistic satellite designs at L band this might result in footprints as large as 100 km. Recent research has focused on the use of synthetic aperture thinned array radiometers which could decrease the footprint size from satellites down to 10 km.

Active Microwave Methods: A fixed position active microwave sensor that measures the sent and received power is called a scatterometer. These instruments measure the backscattering coefficient (σ^0). Through theory described in Ulaby et al. (1986), the backscattering coefficient can be related to the surface reflectivity. As described for the passive methods, these results can then be used to determine surface soil moisture. For active techniques, the step between the measurement of the backscattering coefficient and the surface reflectivity is a bit more involved. The geometric properties of the soil surface and any vegetation have a greater effect on these measurements and simple correction procedures are difficult to develop.

The signals sent and received by a radar are usually linearly polarized, either horizontal (H) or vertical (V). Combinations possible are HH, VV, HV and VH. More advanced multipolarization research systems can make all of these measurements simultaneously.

For bare soils, all models that relate the backscattering coefficient to soil moisture require at least two soil parameters, the dielectric constant and the surface height standard deviation (RMS). This means that in order to invert these models, the RMS must be determined accurately.

For a given sensor configuration (wavelength and viewing angle), different results are obtained at different polarizations but still depend on these same two variables. Current research approaches to determining soil moisture with active microwave methods utilize dual polarization measurements. With two independent measurements of two dependent variables, it is possible to solve for both the dielectric constant and the RMS. Algorithms incorporating this approach are presented in Oh et al. (1992), Shi et al. (1997) and Dubois et al. (1995). These do not work with vegetation nor can they be used with existing or near future satellites.

Active microwave sensors on aircraft and spacecraft typically employ synthetic aperture techniques radar (SAR) which utilize the motion of the platform to synthesize larger antennas. Exceptional

spatial resolutions with footprints on the order of 20 m can be achieved from satellite altitudes.

CURRENT AND NEAR FUTURE SENSOR SYSTEMS

To a large degree, research and applications utilizing microwave sensors are dependent on the instruments currently available. As the needs for soil moisture studies have developed, some new instruments have emerged to satisfy the need. However, soil moisture is a small voice in the crowd asking for new satellites. Therefore, for the most part we must take what we can get which is generally a nonoptimal system that limits the research and development that can be accomplished. Current and near future microwave sensors operating satellite platforms are described in the following sections.

Satellite based sensors offer the advantages of large area mapping and long term repetitive coverage. Revisit time can be a critical problem in studies involving rapidly changing conditions such as surface soil moisture. With very wide swaths it is possible to obtain twice a day coverage with a polar orbiting satellite. For most satellites, especially if viewing angle is important, the revisit time can be much longer. Optimizing the time and frequency of coverage is a critical problem for soil moisture studies.

Currently, all passive microwave sensors on satellite platforms operate at very short wavelengths (<1.5 cm). Of particular note is the SSM/I package on the Defense meteorological satellites (Hollinger et al., 1990). These satellites have been in operation continuously since 1987 and provide the following combinations of wavelength and polarizations: 0.3 cm H and V, 0.8 cm H and V, 1.3 cm V, and 1.5 cm H and V. The system was designed for estimating atmospheric parameters primarily over oceans and not land surface conditions. Therefore, interpreting the data to extract surface information will require accounting for atmospheric effects on the measurement. The atmospheric correction and the shallow contributing depth of soil for these short wavelengths make the data of limited value. Spatial resolution is 70 km at the longest wavelength and 15 km for the shortest.

The SSM/I utilizes conical scanning which provides measurements at the same viewing angle at all beam positions on a swath. This makes data interpretation more straightforward and simplifies image comparisons. These satellites have a polar orbit that provides two passes a day over most areas roughly 12 hours apart. Close to the poles there will be daily twice a day coverage. As latitude decreases, the coverage becomes intermittent. For instance, in the central U.S. there might be several days with twice a day coverage followed by a day or two of no data or a single pass. This potential gap in coverage is offset to a degree by the fact that there are currently four different satellites in operation with slightly different local coverage times. This also means that there could be coverage at up to eight times a day.

Although it is not designed for soil moisture studies, under limited conditions (basically no vegetation) the SSM/I satellite sensors can provide some very interesting information on soil hydrology. The results described by Heymsfield and Fulton (1992) and Teng et al. (1993) are good examples of qualitative analyses.

There has been only one quantitative evaluation of the SSM/I for measuring surface soil moisture (Jackson, 1997). In this study, data collected in two large scale experiments conducted over a mostly grassland watershed in Oklahoma were available for evaluating the capabilities of SSM/I data for soil moisture mapping. Physically based models were used to relate the satellite data to the ground observations. The results indicated that for this grass dominated subhumid area that a soil moisture-emissivity relationship with an error of estimate of 5.3% could be developed that incorporated the range of temperature and vegetation conditions encountered. Figure 1 summarizes the results using SSM/I as well as an aircraft sensor operating at a much longer (and better suited) wavelength. The key aspect of these results is that the range of response in T_B is quite limited under the low vegetation conditions of this particular study. This means that the algorithm is very sensitive to any uncertainties and/or errors in the various parameters and inputs required. Longer wavelengths provide more reliable and robust algorithms.

There is currently a passive microwave research sensor system on board the Russian MIR space station. This package called Priroda has only seen limited use due to the continuing problems with the platform. It does have a wide range of wavelengths including a C band (~5 cm) microwave radiometer. Some data has been collected over portions of the U.S., in particular Oklahoma.

Within two to three years two versions of a new passive microwave sensor system will be launched. This is the Advanced Microwave Scanning Radiometer (AMSR). The first scheduled for late 1999 will be on a Japanese satellite and the second will be on a NASA platform. This system will include many wavelengths including C band. There are plans by both Japan and NASA to produce soil moisture estimates as research level products for regions of low vegetation cover. AMSR will offer significant improvements beyond SSM/I, however, it is still not the optimal solution. An L band system is still a shortcoming of all the space programs.

At present there are three operational radar satellites. ERS-1 was launched by the European Space Agency in 1991 and provides C band VV synthetic aperture radar (SAR) data. Although numerous investigations have been conducted which attempt to utilize ERS-1 data, there have been few reported results in the area of soil moisture estimation. This is due to the limitations of using a single short wavelength and a single polarization SAR with an exact repeat cycle of 35 days. With this kind of temporal coverage, the data will be of little value in process studies. ERS-2 was launched in 1995 to provide continuing coverage and at the present time data may be obtained from both satellites. JERS-1 is operated by the Japanese and provides L band HH SAR data and also has a long repeat cycle. Some improvement may be provided by the Canadian RADARSAT sensor launched in 1995. This satellite has a C band HH SAR with a more frequent revisit interval.

As noted, the ERS-1 satellite has a C band VV SAR with a nominal incidence angle of 23° and has been in operation since 1991. It provides repeat coverage every 35 days. Based on the early work on soil moisture and σ^0 described in Ulaby et al. (1986), there is reason to believe that under the right conditions this satellite might be able to provide surface soil moisture. A number of investigators have evaluated this potential.

One rather extensive ERS-1 study was reported by Cognard et al. (1995). This investigation involved a total of 14 ERS-1 scenes collected over a two year period. The data were collected within the

context of a river basin study with 13 test sites. Based on field level analysis, the authors found that the σ° -soil moisture relationship was highly dependent on vegetation and associated tillage conditions. At this level, significant effort would be required to determine soil moisture. A significant improvement was made when the average σ° for the basin (12 km²) on each day was compared to the average soil moisture from the 13 sites. However, the sensitivity of σ° to soil moisture was very low, about 10% volumetric soil moisture for 1 dB σ° . Considering the absolute accuracy of the σ° values, this means that a considerable amount of uncertainty must be expected in the soil moisture estimates.

SUMMARY

Surface soil moisture can be measured using microwave sensors. The ability to monitor surface soil moisture over extended time periods and areas could provide valuable new information on soil parameters and processes related to hydrology. Depending on the platform and the sensor, the scale of application could range from a few meters to the globe.

There are limitations on microwave based soil moisture sensing. At the present time it is recognized that at some level of biomass the vegetation will mask the signal from the soil. The use of longer wavelengths can minimize this effect.

Passive and active microwave sensors each have advantages and disadvantages. The spatial resolution of passive instruments will limit the range of applications when used on a satellite. Sensitivity to other surface features could limit the usefulness of active systems. Selecting the best system will require tradeoffs and prioritizing applications. It may be that the optimal sensor system would include both an active and a passive instrument. This would allow a range of applications and the synergism of the two types of measurements to provide new information.

Wide scale research and application will continue to be severely hampered by the currently available and planned satellite instruments. All of these instruments have been designed for some other purpose. Although the optimal systems for soil moisture are known, the priority is not high within the current space agency programs. Discipline groups such as soil science and hydrology must be more aggressive with these agencies to make them recognize the need for appropriate long wavelength microwave sensors in space.

REFERENCES

- Ahuja, L. R., Wendroth, O., and Nielson, D. R., 1993, Relationship between the initial drainage of surface soil and average profile saturated hydraulic conductivity, *Soil Science Society of America Journal*, 5, 19-25.
- Cognard, A., Loumagne, C., Normand, M., Olivier, P., Ottele, C., Vidal-Madjar, D., Louahala, S., and Vidal, A., 1995, Evaluation of the ERS-1/synthetic aperture radar capacity to estimate surface soil moisture: two-year results over the Naizin watershed, *Water Resources Research*, 31, 975-982.

Dubois, P. C., van Zyl, J., and Engman, E. T., 1995, Measuring soil moisture with with imaging radars, *IEEE Trans. on Geoscience and Remote Sensing*, 33, 915-926.

Heymsfield, G. A. and Fulton, R., 1992, Modulation of SSM/I microwave soil radiances by rainfall, *Remote Sensing of Environment*, 29, 187-202.

Hollinger, J. P., Peirce, J. L., and Poe, G. A., 1990, SSM/I instrument evaluation, *IEEE Trans. on Geoscience and Remote Sensing*, 28, 781-790.

Jackson, T. J., 1993, Measuring surface soil moisture using passive microwave remote sensing, *Hydrological Processes*, 7, 139-152.

Jackson, T. J., 1997, Soil moisture estimation using SSM/I satellite data over a grassland region. *Water Resources Research*, 33, 1475-1484.

Oh, Y., Sarabandi, K., and Ulaby, F. T., 1992, An empirical model and an inversion technique for radar scattering from bare soil surfaces, *IEEE Trans. on Geoscience and Remote Sensing*, 30, 370-381.

Shi, J., Wang, J., Hsu, A., O'Neill, P. E., and Engman, E. T., 1997, Estimation of bare soil moisture and surface roughness parameter using L-band SAR image data, *IEEE Trans. on Geoscience and Remote Sensing*, 35, 1254-1266.

Teng, W. L., Wang, J. R., and Doraiswamy, P. C., 1993, Relationship between satellite microwave radiometric data, antecedent precipitation index, and regional soil moisture, *Int. J. of Remote Sensing*, 14, 2483-2500..

Ulaby, F. T., Moore, R. K., and Fung, A. K., 1986, *Microwave remote sensing: active and passive*, Vol. III, from theory to application, Artech House, Dedham, MA.

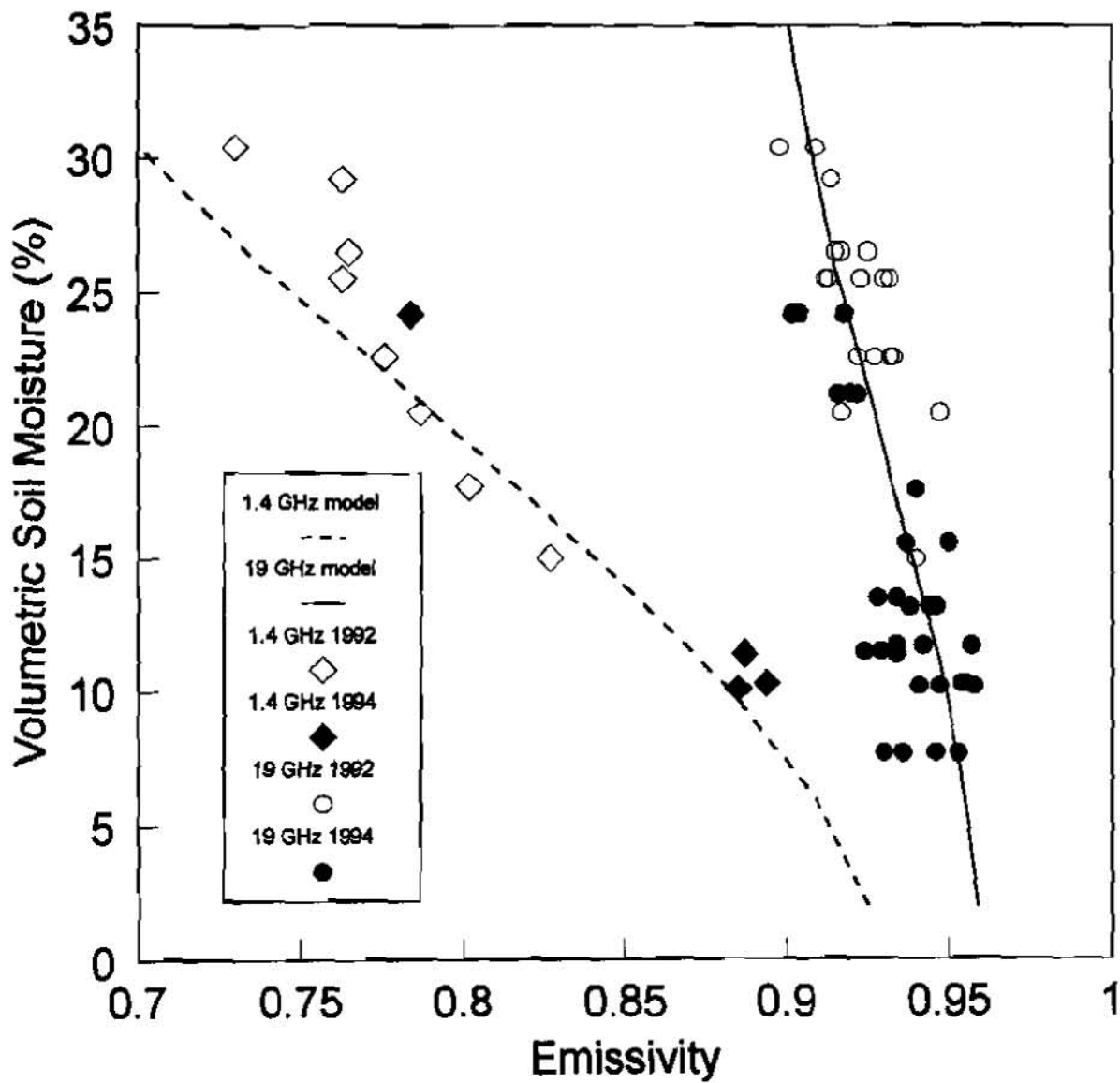


Figure 1. Relationships between passive microwave emissivity and volumetric soil moisture for SSM/I and L band.

A MODULAR APPROACH TO INTERACTIVE WATERSHED MODELING

By John L. Kittle, JLKittle Consulting, Decatur, Georgia; Paul R. Hummel, AQUA TERRA Consultants, Decatur, Georgia; Paul B. Duda, AQUA TERRA Consultants, Decatur, Georgia; Alan M. Lumb, U.S. Geological Survey, Reston, Virginia

Abstract: As the requirements for hydrologic modeling expand and change, the need for a flexible modeling system becomes essential. AQUA TERRA Consultants, in conjunction with the U.S. Geological Survey, is developing an interactive hydrologic modeling system known as GenScn (GENERation and analysis of model simulation SCeNarios). The system supports all aspects of modeling, from model setup and data management to model calibration to analysis of alternatives.

GenScn is intended for a wide range of hydrologic situations and locations. Thus, the ability to incorporate a suite of models within the system has been a continuing focus during development. Current technology allows existing model codes to be compiled into Dynamic Link Libraries (DLLs) which may then be accessed by the system. This allows model codes to be incorporated into the system as they are, without rewriting them in a different language.

In developing GenScn, care is being taken to develop reusable components to perform specific tasks such as mapping, plotting, and time-series data management. This results in clearly defined and easily tested module codes which may then be used within other modeling systems with minimal effort.

User interaction with GenScn is through a Graphical User Interface (GUI). Significant effort is being made to minimize a user's effort to perform tasks and to allow direct manipulation of the elements of the system. An on-line help system allows the user to access information about specific portions of the system's windows. A hypertext version of the model's user manual may also be accessed.

The system is being tested in several locations (Truckee-Carson River Basins, Guadalupe River Basin, DuPage County, IL) and can easily be adapted to other locations. Geographic Information System (GIS) data can be used in GenScn to generate maps and tables which aid in the analysis.

INTRODUCTION

Use of watershed models like the Hydrological Simulation Program-FORTRAN (HSPF) (Bicknell, 1997) traditionally involved using a text editor to build an input sequence to describe a watershed's physical and water management characteristics. For large, complex river basins, input sequences were often thousands of lines long when water quality was simulated in addition to the hydrology. The process of making changes was time consuming and complex. In addition, analyzing results from several model runs required manually and tediously keeping track of time-

series data sets from all scenarios at multiple locations for several constituents. The analyzer often had to reformat the results and use separate programs to analyze results and prepare the needed tables and graphs.

The development of GenScn came as a response to the need to make HSPF input sequences easier to build and HSPF output easier to analyze. The requirements for the software were refined based on experiences with ANNIE (Lumb, 1989 and Flynn, 1995) and the HSPF Expert System (Lumb, 1994). The scenario generator provides advanced interaction with the HSPF input sequence and integrated analysis capabilities. The program provides an interactive framework for analysis built around an established and adaptable watershed model. The results of different scenarios can be easily compared and analyzed because the model and analysis tools are linked in one package and use a common data base.

A scenario consists of an input sequence, its output reports, and associated time-series data. Each input sequence describes a scenario. Once the model is run for a particular scenario, output reports and time-series data specified in that scenario's input sequence are available for analysis. A new scenario is created by copying an existing input sequence, modifying this input sequence to describe the new scenario, and then running the model. Where specified by the input sequence, output files and time-series data are automatically generated when the new scenario is run for comparison with other scenarios.

When changes to the input are complete, the HSPF model can be executed. HSPF checks the validity of the input sequence. Changes that are incomplete or inconsistent are referred back to the user for further refinement.

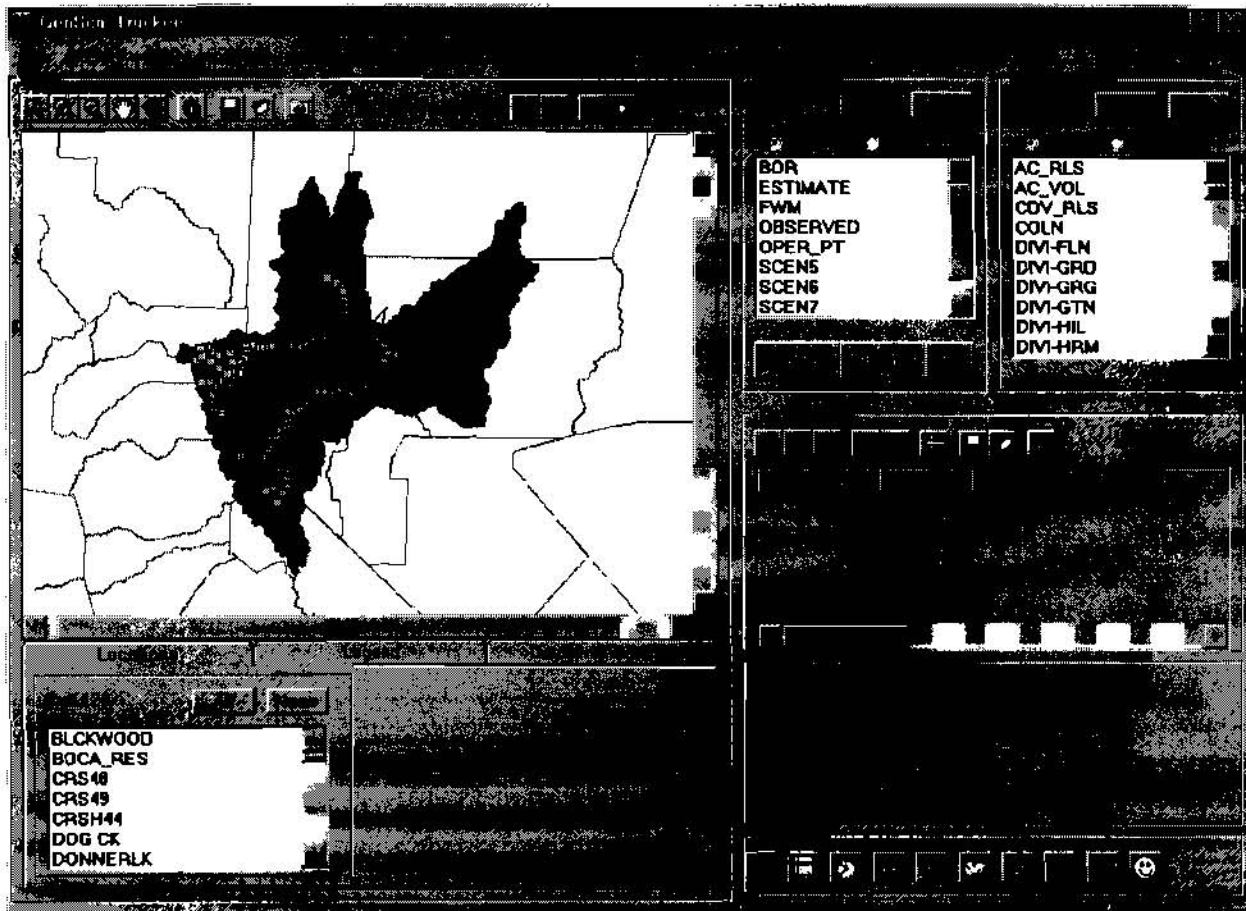
After execution is complete, the user may interactively specify results to be analyzed. Data to analyze may be specified by selecting scenario, location, and constituent names. Locations may also be specified graphically by clicking locations on a map. Results can be viewed either on the display screen or on printed output.

Results are available as tables and plots of the simulated data or results of statistical analyses of the data. A wide range of plots can be specified, including a standard time-series plot, a time-series plot of the difference between two time series, a bar chart, a flow-duration plot, a scatter plot of one time series versus the difference between two other time series, a scatter plot of two time series including an optional 45 degree line and regression line, and an event frequency plot. Statistical analyses include comparing two time series over a range of class intervals and constituent duration analysis. Included in the duration analysis is a lethality analysis methodology which links frequency data on instream contaminant levels to toxicity information resulting from both acute and chronic laboratory bioassays.

A METAPHOR FOR WATERSHED MODELING

A successful user interface for watershed modeling displays information to the watershed modeler in a manner consistent with the modeler's world view and needs. The goal of the

interface is to provide layers of information - a summary of information about the project in the main window along with a multitude of other windows which show additional information. This includes details about the watershed, model parameters and results along with complete documentation of the model's algorithms. The GenScn user interface has a main window which uses a map to show the watershed's spatial characteristics, text boxes which summarize locations where detailed information is available, scenarios which have been simulated (for model runs) or collected (for observed data), and constituents for which data is available. From the main window the user can activate a scenario, edit the description and parameters for the scenario, and run the model. The user may analyze results by selecting desired scenarios, locations and constituents and then selecting the time-series data available. A span of time and the analysis tool(s) are then selected to generate the desired tables, graphs, statistical summaries, or animations.



REUSABLE COMPONENTS

The design of reusable components has played a key role in the development of GenScn. The result of using these components includes (i) reusability within GenScn (references from different locations or with different parameter sets) (ii) reusability within other modeling systems, and (iii) more easily defined and tested modules.

A significant effort has been invested in developing a suite of modules for the graphical and tabular display of time-series data and other analysis results. The modules allow the programmer to set initial values for the parameters which define the plot or listing (e.g. data values, number of curves/columns, text labels). All plots and listings allow the end user to customize them to their liking using pull-down menus.

Initially GenScn used the Watershed Data Management (WDM) FORTRAN library of subroutines for time-series management. A set of subroutines were developed to interface between the Visual Basic GenScn code and the existing FORTRAN routines. This allowed the well-tested and well-documented WDM code to be preserved.

During development of GenScn, it was necessary to incorporate different types of time-series data (i.e. storage and model formats). To make GenScn work with these different data types in a consistent manner, a generic data structure was developed. Specific routines for each data type were written to fill the data structure. GenScn was then able to use this data structure in the same manner for all types of data.

Several other analysis tools were developed using existing FORTRAN codes which had already been tested and documented. The codes were compiled into DLLs and then called by GenScn using new code which interfaces to the DLLs. The duration and comparison analyses were both developed using this method. Another tool which allows the generation of new time series based on existing time series was also developed in this manner.

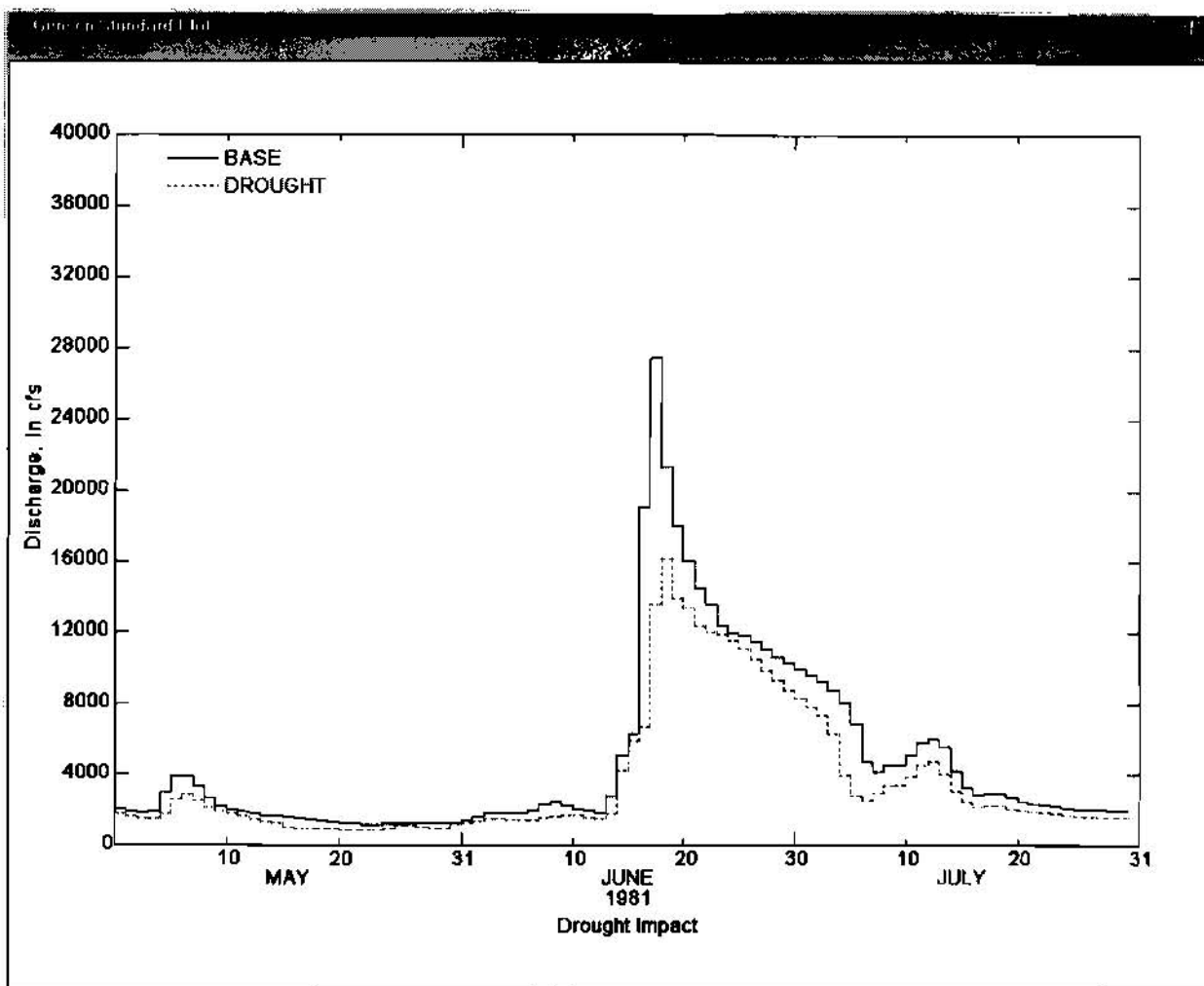
DEFINITION, SIMULATION AND ANALYSIS OF A SCENARIO

As an example of a possible scenario generator operation, assume we want to investigate the effect of severe drought. We might define this drought as a given period where precipitation is reset to three fourths of the normal amount. We will create a new scenario to simulate this drought period. We will perform this simulation using HSPF, and then we can analyze the results by comparing flows under normal conditions to flows under these drought conditions.

The steps to build the above scenario example are as follows. From the main scenario generator window, select the "BASE"(a calibration of the existing basin) scenario in the "Scenario" frame. Next, click the "Activate" button in the same frame. This brings up the GenScn Activate BASE window. Then click the "Save As" button to create a new scenario from this existing scenario. Call the new scenario "DROUGHT". Now we have a new scenario, but this scenario is identical to scenario "BASE" until we modify it. Select "EXT-SOURCES" in the "Block" frame. Change the multiplication factor for the precipitation source record to 0.75, representing three fourths of the normal precipitation. Click the "OK" button to save the revised ExtSources block. Next click the "Save" button to save this new drought scenario. Now we can click the "Simulate" button to run the HSPF model for this scenario. When the simulation is complete, return to the main window to begin the analysis of results.

The steps to view the results of the drought simulation (at one location) are as follows. In the "Locations" frame, select "GUADVICT". In the "Scenarios" frame, select "BASE" and "DROUGHT". In the "Constituents" frame, select "FLOW". Find time series which match

these criteria by clicking the "+" button in the "Timeseries" frame. Suppose we would like to see daily flows for the normal and drought conditions plotted together. Select the "Analysis:Graph" option from the menu bar or click the graph icon in the "Analysis" frame. Next, click the "Generate" button to produce the graph. The legend in the top left corner indicates which line is "BASE" and which is "DROUGHT". Compare the plots to see how much the flow is affected by these hypothetical drought conditions.



COMMUNICATION WITH OTHER SYSTEMS

GenSen is designed to work with data from other systems. Time-series input data can be used in GenSen in a variety of standard formats, including Relational Data Base (RDB - ASCII files of tab-delimited columns), WATSTORE (Hutchinson, 1977), and WDM. With these formats, data can be imported from various sources including the USGS NWIS database, commercially available data sets on CDs, the USGS World Wide Web site, and other sources used extensively within the USGS and EPA. The suite of tools produced through the USGS and EPA for the WDM system allow data in GenSen to be utilized by a wide range of other applications.

The data format used by the mapping capabilities of GenScn is the Environmental Systems Research Institute (ESRI) shape file. This format allows spatial data to be shared with GIS tools such as ArcView or ArcInfo.

GenScn is also designed to use GIS data as input for building the initial scenario. Data specifying characteristics of a watershed can be input interactively or through RDB formatted files. This characterizing data consists of basic watershed parameters such as stream segments, their connectivity, lengths, slopes, and contributing areas. The input formats for these data allow easy transfer from GIS to GenScn.

EXTENDING GENSCN TO NEW REGIONS

GenScn can be extended to new regions provided GIS coverages, time-series data, and characteristics of the stream network are available. The process of extending GenScn to a new region consists of building two files specifying the format and location of this data.

The first step toward setting up GenScn for a region is to create the new project file. This task is accomplished from within GenScn by selecting 'New Project' from the 'File' pull-down menu. The user will be prompted to specify the names of the WDM file, the HSPF message file, any RDB file of time-series data, and the map file. If the WDM file does not exist, GenScn will create it, and the user will have the opportunity to add observed data to this file as described below. The HSPF message file is provided with the GenScn software. The map file name should be specified, and if the file does not exist it may be created interactively. Once these file names are entered the user can click 'OK' and the project file will be created. Use 'Save Project' from the 'File' pull-down menu to save the project file.

The map file also can be created within GenScn. The map file contains information about the layers to be included on the map as well as other default map parameters. Layers to be displayed on the map must take the form of ESRI shape files. One of the map layers should be a shape file of gage locations.

Time-series data can be imported for use in GenScn by clicking on 'Observed' in the scenario list and then clicking 'Activate'. In the current release of GenScn the user will be presented with the option of entering observed data in RDB or WATSTORE daily values formats. Modules to import data from additional formats may be added at a clearly defined point in the GenScn code. After choosing one of these options the user proceeds to a window to enter information specifying the name of the file in which the data resides. Once specified the user may click on begin, and then for each data set in the file a set of parameters can be specified including the eight character scenario, constituent, and location attributes.

The GenScn 'New Scenario' feature converts a set of tabular input files which describe the characteristics of a watershed to a HSPF User Control Input (UCI) file. This feature is accessed by clicking on the 'New' button within the scenario frame in the main GenScn window. The user is prompted to specify the names of six input files, which are designed to be obtained from GIS coverages.

EXTENDING GENSCN TO OTHER MODELS

Although originally developed using the HSPF model, GenScn has been designed to be able to work with any surface water model which generates time-series results. GenScn does require each time series to be defined by a unique combination of scenario, location, and constituent. Several models have been incorporated into the GenScn system.

Results from the Full Equations (FEQ) routing model (Franz, 1996) were incorporated into GenScn by writing modules which read the time-series results from the FEQ output files and adapt them into the time-series data structure used by GenScn. This allows results from different FEQ scenarios to be compared. It also allows FEQ results to be compared with results from other models in GenScn. Future enhancements include building a DLL version of FEQ so that the model can be run from within GenScn.

Two additional examples of models which could be incorporated into GenScn are the Diffusion Analogy FLOW model (DAFLOW) (Jobson, 1989) and the Branched Lagrangian Transport Modeling system (BLTM) (Jobson, 1997). DLL versions of these models could be developed allowing them to be called from within GenScn. Their results could be adapted to the GenScn time-series data structure to allow GenScn's analysis tools to be used on them.

REFERENCES

- Bicknell, B.R., J.C. Imhoff, J.L. Kittle Jr., A.S. Donigan, Jr. and R.C. Johanson, 1997, Hydrological Simulation Program -- FORTRAN, User's Manual for Version 11, EPA/600/R-97/080, U.S. EPA, National Exposure Research Laboratory, Athens, GA.
- Flynn, K.M., P.R. Hummel, A.M. Lumb and J.L. Kittle, Jr., 1995, User's Manual for ANNIE, Version 2, a Computer Program for Interactive Hydrologic Data Management, Water-Resources Investigations Report 95-4085. U.S. Geological Survey, Reston, VA.
- Franz, D.D., C.S. Melching, 1997, Full Equations (FEQ) Model for the Solution of the Full, Dynamic Equations of Motion for One-Dimensional Unsteady Flow in Open Channels and through Control Structures, Water-Resources Investigations Report 96-4240, U.S Geological Survey, Urbana, IL.
- Hutchinson, N.E., Stuthmann, N.G., Merk, C.F., and Isherwood, W.L., Jr., 1977, WATSTORE User's Guide, Volume 5: U.S. Geological Survey Open-File Report 77-729-I, U.S. Geological Survey, Reston, VA.
- Jobson, H.E., 1989, Users Manual For an Open-Channel Streamflow Model Based on the Diffusion Analogy, Water-Resources Investigations Report 89-4133, U.S. Geological Survey, Reston, VA.

Jobson, H.E., 1997, Enhancements to the Branched Lagrangian Transport Modeling System, Water-Resources Investigations Report 97-4050, U.S. Geological Survey, Reston, VA.

Lumb, A.M., J.L. Kittle Jr. and K.M. Flynn, 1990, Users Manual for ANNIE, A Computer Program for Interactive Hydrologic Analyses and Data Management, Water-Resources Investigations Report 89-4080, U.S Geological Survey, Reston, VA.

Lumb, A.M., R.B. McCammon and J.L. Kittle Jr. 1994. Users Manual for an Expert System (HSPEXP) for Calibration of the Hydrological Simulation Program - Fortran. Water-Resources Investigations Report 94-4168. U.S. Geological Survey, Reston, VA.

RAIN INFILTRATION INTO CRACKING SOILS

S. N. PRASAD, PROFESSOR OF CIVIL ENGINEER, UNIVERSITY OF MISSISSIPPI, OXFORD, MS;
M. J. M. RÖMKENS, SOIL SCIENTIST, USDA-ARS, OXFORD, MISSISSIPPI; K. HELMING, SOIL
SCIENTIST, ZALF, MÜNCHENBERG, GERMANY

Abstract

Certain analytical solutions of rain infiltration into dry cracked soil are presented with particular emphasis on the calculations of ponding time. The morphology of cracks is identified by a rather simple geometric pattern whose scale, however, leads to a meaningful expression for ponding time. The analysis utilizes the wetting front solutions of horizontal diffusion governed by Richards' equation as developed by the present authors in a recent study. The soil matrix diffusion characteristics are represented by a set of two parameters given by Ahuja and Swartzendruber (1972). The ponding time estimates appear to agree well with the data currently being obtained at the National Sedimentation Laboratory for Mississippi Delta clay soils.

INTRODUCTION

Due to swelling and shrinking potentials, clay soils are highly dynamic in nature when subjected to varying hydrologic regimes. This leads to a hydrologic dependent morphology of field clay soils which generally consist of large aggregates (peds) which are separated from the adjoining peds by vertical cracks. The geometric patterns such as crack spacing, width and depth are strongly dependent on the historic events of wetting and drying as well as soil physico-chemical characteristics. Thus, the rain infiltration under these conditions consists of water movement both horizontally and vertically. When the vertical infiltration into the peds of the soil surface becomes smaller than the rainfall rate, runoff into the cracks take place which is absorbed by the soil matrix of the peds. The net result is an enhanced infiltration by cracking soil leading to much delay in overland flow generation, although the ponding on the ped surface may take place rather quickly.

Most of the hydrologic simulation models in existence assume that Darcy-type flow is applicable in which rain water is absorbed first by the surface layer, followed by downward movement dependent on soil physical (hydraulic) properties. The present study is intended to improve this assumption by considering rain infiltration which depends on the crack features of clay soils. The motivation for the model development is derived from an ongoing experimental research. Experiments are being conducted under laboratory conditions (Wells 1995) on shaly silty clay and other clay soils generally found in the Mississippi Delta. Existence of cracks produced major impact on the data for the ponding times and the cumulative infiltration values. It was found that when the surface is laden with deep cracks, the ponding time was escalated from the 5 to 20 minutes range to the hour range. This several fold increase in ponding time is the main focus of this paper. In as much as the crack morphology is quite complex, an attempt is made in the present model to reduce the infiltration dependence on a rather simple geometric parameter.

MODEL DEVELOPMENT

In dry clay soils whose surface consists of polygonal columns, rain infiltration primarily takes place through the cracks between the columns. As the surface water runs off along the crack walls, capillary action of the dry soil matrix in the polygonal columns absorbs this water and moves it horizontally. This is because the top surface of the columns under natural raindrop impact condition develops surface seal (crust) whose infiltration rate is significantly smaller than the hydraulic conductivity of the channels formed between the polygonal columns by the cracks. Thus, it is assumed that the top surface of the polygonal columns immediately attains saturation following the beginning of rainfall and runoff into the cracks takes place. Water entering the crack channels is imbibed into the column matrix by capillary and osmotic action forces at the crack-matrix interface and a process begins whose mathematical formulation and its solution is the main goal of this study.

In the past model development of the flow of fluid in fractured media has been in the area of porous rocks. Pruess and Tsang (1990) modeled steady flow in a variable fracture without a moisture exchange with the rock matrix. Kwicklis and Healy (1993) extended this steady flow model to a simple idealized discrete fracture network with impermeable

rock matrix. Other researchers modeled unsaturated flow by replacing the matrix fracture system with an equivalent porous medium (e.g. Wilson and Dudley 1987; Dykhuizen, 1987). Nintano and Buscheck (1991) modeled flow in a fracture idealized as two parallel plates with a coupling cross term accounting for the exchange of fluids between the fracture and the rock matrix. Gerke and van Genuchten (1993) modeled one-dimensional unsteady vertical flow in a two-porosity system with a coupling cross-flow moisture exchange term. In a related area of practical importance when surface connected macropores such as worm holes, root holes are present, preferred flow paths of water exist (Beven and German 1982). Various theoretical studies based on numerical solutions of the Richards' equation for unsaturated water movement coupled with certain model of flow in macropores have been carried out in the past. A Green-Ampt model of infiltration was suggested by Davidson (1984) into a soil containing regularly spaced water filled vertical cracks.

For the sake of simplicity here we assume that the soil surface consists of uniformly distributed cracks which result into columns of identical shapes in the form of solid cylinders whose lengths equal the depths of the cracks. We further simplify the geometry by assuming these polygonal columns to be squares in cross section of area ℓ^2 and height H . The infiltration process consists of receiving the rainfall of intensity i (cm/min) on the cross section of area ℓ^2 which provides runoff into the vertical sides of the column. The runoff is received by the vertical walls of the columns and develops into a saturated film of water on them, thereby giving rise to absorption by the soil matrix. Initial water content of the columns is assumed to be zero and from time $t = 0$ onward, it is assumed that the runoff from the column surface is constant and equals q_0 per unit length. From the continuity condition of the rainfall and runoff volume, q_0 may be given by

$$q_0 = \frac{i\ell}{4} \quad (1)$$

A sharp front, therefore, will develop which will separate the wetted from the unwetted region and will advance away from the top surface downward and away from the crack face horizontally. The shape of the front is primarily controlled by the conditions at the front but after the initial period the flow becomes essentially one-dimensional and takes place horizontally with a downward moving tip.

We consider the two-dimensional, unsaturated, crack matrix system with matrix block of half width $\ell/2$. Runoff water from the top surface enters into the crack opening region under a specific flux condition q_0 defined as the flux of water per unit distance along the crack edge. Lateral boundaries, $x = \ell/2$ at the midpoint of the matrix (column) are no-flow boundaries so that the system may be viewed as an infinite periodic system of cracks spaced ℓ apart. The effect of gravity on the flow in the matrix is assumed to be negligible compared to capillary and the analysis considers only half of the system by making use of the symmetry. The x -coordinate refers to the lateral distance (horizontal) from the crack face, and y coordinate is the vertical distance from the crack entrance (top surface).

As runoff into the cracks begins, the flow between the columns is in the form of vertical sheet flow whose front descends downward with a finite velocity. Let the front be located at $y = h(t)$; $x = 0$. Thus, the part of the crack surface, $0 \leq y \leq h$, boundary condition is given by $\theta = \theta_s$, where θ_s is the saturation water content (volumetric) of the soil matrix. Furthermore, matrix diffusion occurs along streamlines which are normal to the crack plane. The process of diffusion may be viewed to be taking place along one dimensional infinitely thin horizons perpendicular to the direction of sheet flow along the cracks. Each horizon is bounded on the end $x = 0$ by the crack face and, the other end is bounded by the wetting front $\delta(y,t)$. The diffusion process in this horizon is governed by Richards' equation of unsaturated flow with a concentration type boundary condition at $x = 0$. The entire infiltration cycle consists of various flow periods due to the existence of geometric constrains provided by changing boundary conditions. These periods are associated with the arrivals of the wetting front at $x = \ell/2$ and $y = H$. In the beginning, the flow along the crack is not much influenced by the diffusion into the soil matrix and is in the form of sheet flow driven by gravity at near zero matric potentials Ψ . In this period, a simple model of downward sheet flow may be assumed to be Poiseuille flow with a uniform thickness c . Applying the analysis of Bird et. al. (1960), the velocity profile results into a parabolic distribution whose average velocity, v , is given

$$v = \frac{\rho g c^2}{3\eta} \quad (2)$$

where g is the acceleration due to gravity, and ρ and η are the density and dynamic viscosity of water, respectively. The above result is rather simplistic, but considerably more complex surface velocity profiles result when specific geometry of fractured aggregate surfaces of soils as well as diffusion into the surface are considered.

Following the above mentioned initial period which we assume to be small, the water front travels downward but is retarded by the matrix diffusion. This period ends either when the front $\delta(0,t)$ of the horizon equals $l/2$ or when the downward travel depth $h = H$, whichever occurs first. The present analysis focuses on developing infiltration equation limited for the period, $0 \leq t \leq T$ where T is the penetration time to reach the crack depth $y = H$. It is, therefore, assumed that conditions are such that the time needed for $\delta(0,t) = l/2$ is larger than T . Certain simplistic infiltration equation may now be developed by considering mass integral balance equation of flow. Thus, we are concerned with finding the solution of flow of water downward and continuously diffusing into the column matrix when a constant runoff rate q_0 is introduced at the top, $y = x = 0$ at time $t = 0$. There is a sheet of water of constant thickness c adhered to the fractured surface where $\delta(y,t)$ is the position of the wetting front in the soil matrix. The mass balance equation, therefore, yields

$$q_0 t = \int_0^h (I+c) dh \quad (3)$$

where I is the cumulative water diffusion into the soil matrix at point $y = h$ at time t . It is obvious that I is primarily a function of the time water has been available for diffusion so that this time is the elapsed time since the arrival of the downward front. Thus, I is a function of $I(t - \tau)$ where τ is the value of t at which $y(t) = h$. Therefore,

$$\int_0^h I(t-\tau) dh = \int_0^t I(t-\tau) \frac{dh}{d\tau} d\tau \quad (4)$$

Equation (3) may now be written as an integral equation for the solution of h ,

$$q_0 t = ch + \int_0^t I(t-\tau) \frac{dh}{d\tau} d\tau \quad (5)$$

Equation (5) is similar to the Lewis-Milne equation which was developed for the infiltration advance in surface irrigation studies. Motivated by the success of the applications of Lewis-Milne solutions, we model the cumulative diffusion function I in such a way that the method of Laplace Transformation becomes a valid approach for the solution of the integral equation (5).

Analytical solutions of Richards' equation which are consistent with the objectives in developing infiltration equations for cracking soils, were developed by Römken and Prasad (1992). The spectral series solutions developed in this study utilizes soil water diffusivity function $D(\theta)$, of the type

$$D = \theta^n F(\theta) \quad (6)$$

where θ is the volumetric water content, $F(\theta)$ is a continuous function of θ and $F(0) \neq 0$, and n is a constant larger than unity. Diffusivity relationships which belong to these class of functions for certain loam and silty clay soils were investigated by Ahuja and Swartzendruber (1972). A particular relationship discussed there is given by

$$D(\theta) = \theta^n \frac{a}{(\theta_s - \theta)^{n/5}} \quad (7)$$

where θ_s is the saturated soil water content. Ahuja and Swartzendruber (1972) reported the values of a and n for fine silty clay in the range of 0.68 cm²/min to 1.4 cm²/min and 3.64 to 4.19, respectively. The saturated water content value for this soil was reported as $\theta_s = 0.5$. Römken and Prasad (1972) utilized the data given by these authors and found that the analytical solution for the water content profile compared quite favorably with the experimental data as well as other numerical solutions reported in the literature. In the following development of infiltration analysis of cracking soils, we adopt the three term solution given in Römken and Prasad (1992) for the case of horizontal flows into a single layer with saturation boundary conditions (IIIA).

The water content profile was given by

$$\theta(x,t) = \beta \left(1 - \frac{x}{\delta_1}\right)^\alpha + A_1 \left(1 - \frac{x}{\delta_1}\right)^{\alpha+1} + A_2 \left(1 - \frac{x}{\delta_1}\right)^{\alpha+2} \quad (8)$$

where

$$\alpha = \frac{1}{n} \quad (9)$$

$$\beta = \frac{1}{2}(\alpha+1)(\alpha+2)\theta_s \quad (10)$$

$$A_1 = -\alpha(\alpha+2)\theta_s \quad (11)$$

$$A_2 = \frac{1}{2}\alpha(\alpha+1)\theta_s \quad (12)$$

The wetting front penetration $\delta_1(t)$ is given by

$$\delta_1^2 = A^2 t \quad (13)$$

where

$$A^2 = \frac{2\alpha\alpha}{\theta_s^{n/s}} \left[\frac{1}{2}(\alpha+1)(\alpha+2)\theta_s \right]^n \quad (14)$$

The cumulative diffusion I may now be calculated from (8) as

$$I = \int_0^{\delta_1} \theta(x) dx \quad (15)$$

which leads to the following

$$I = \frac{3\theta_s}{3+\alpha} \delta_1 = \frac{3\theta_s A}{3+\alpha} \sqrt{t} = \lambda \sqrt{t} \quad (16)$$

where

$$\lambda = \frac{3\theta_s A}{3+\alpha} \quad (17)$$

In the above, (17), A is given by (14) so that λ reflects the soil matrix characteristics. From the data given by Ahuja and Swartzendruber (1972) for the case of fine silty clay an estimate of A is given by

$$A = 0.75 \text{ cm}/\sqrt{\text{min}} \quad (18)$$

so that the characteristic parameter is approximately equal to

$$\lambda = 0.35 \text{ cm}/\sqrt{\text{min}} \quad (19)$$

Thus, the cumulative diffusion function for fine silty clay yields

$$I = 0.35 \sqrt{t} \quad (20)$$

In (20) the time t is in minute. When (20) is utilized in (5) and Laplace Transformation is applied to (5), then after considerable simplifications, we have the following solution of the downward movement of the front h

$$\frac{h}{q_o} = \frac{4\sqrt{t}}{\Pi\lambda} + \frac{4c}{\Pi\lambda^2} \left[e^{-\left(\frac{\Pi\lambda^2 t}{4c^2}\right)} \operatorname{erfc} \left(\frac{\sqrt{\Pi\lambda\sqrt{c}}}{2c} \right) - 1 \right] \quad (21)$$

In the above erfc is the complimentary error function. For the purpose of an approximate estimate of the ponding time for cracking soils, we let $c = 0$ in (21) and substitute the values from (1) and (19) to obtain

$$\sqrt{t} = \frac{\pi \lambda h}{i e} = \frac{1 h}{i e} \quad (22)$$

where i is in cm/min. The experimental results reported in Wells (1995) were for the constant rainfall rate of 30 mm/hr = 1/20 cm/min. Thus, a comparison of the ponding times may be made based on

$$t = 400 \left(\frac{H}{\ell} \right)^2 \quad (23)$$

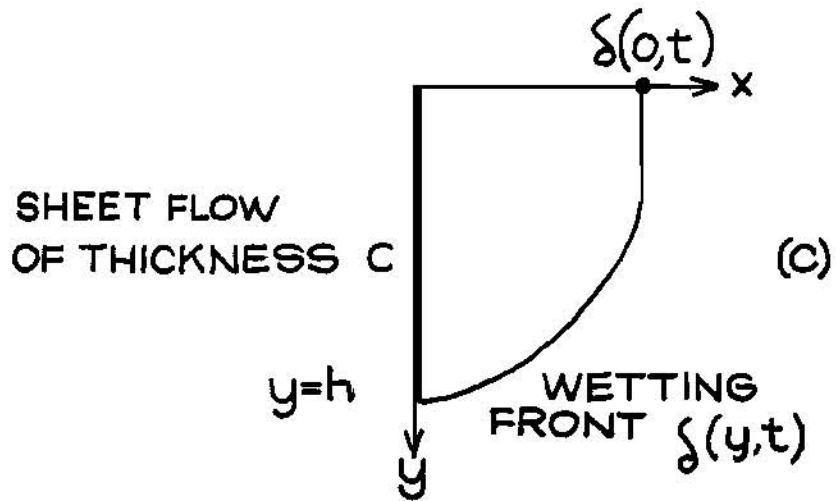
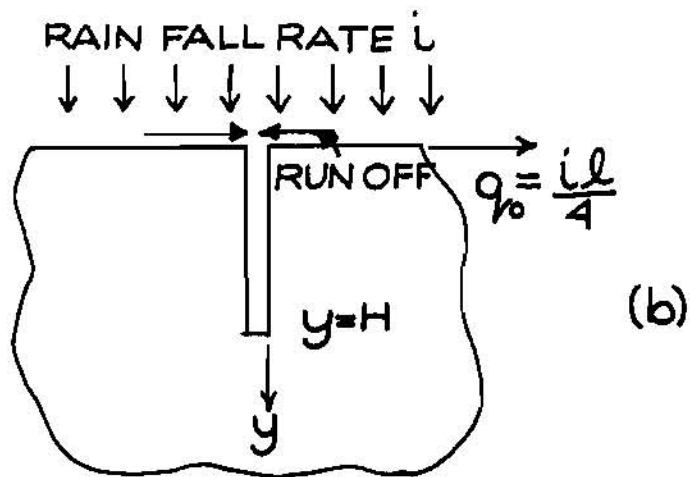
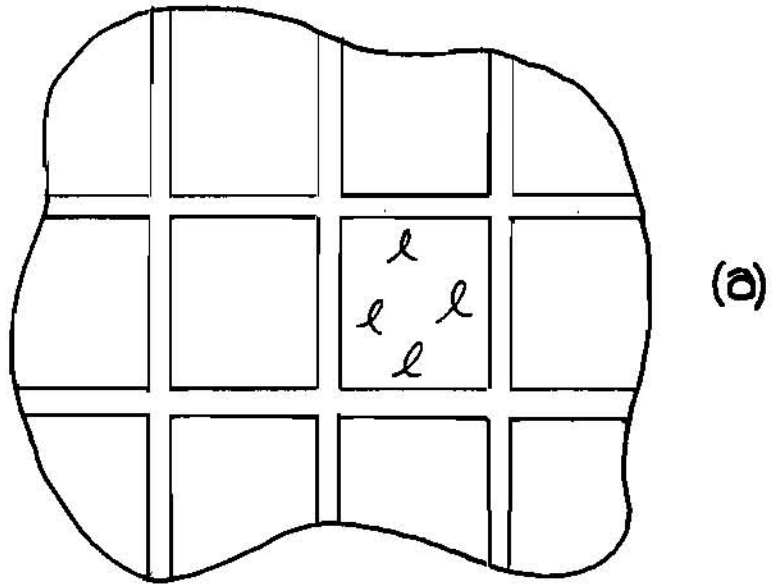
where H is an average depth of the crack and ℓ is an average length scale of the pedis. From the measurements on the size of the polygonal columns and an estimate of the crack depth the ratio ℓ/H is in the range of 2-4, whereas ponding times were in the range of 30-70 minutes. The comparison, therefore, appears feasible but a more accurate measurement of the crack geometry is essential for further improvement.

CONCLUSIONS

A rather simple model of infiltration process is proposed here from which ponding time calculations appear encouraging. In as much as the morphology of the surface of cracking soils is highly sensitive to hydrologic variations, it is desirable to develop infiltration equations which are based on geometric parameters reflecting certain average quantities. In this respect equation (23) may be viewed to be dependent on a parameter which is the ratio of two surface areas, namely the area of crack faces and the runoff contributing surface area. The development, however, is still in the elementary stage and needs further testing and improvements.

REFERENCES

- Ahuja, L. R. and Swartzendruber, D., 1972, An improved form of soil-water diffusivity function. *Soil Sci. Soc. Amer. Proc.*, Vol. 36, 9-14.
- Beven, K. and Germann, P., 1982, Macropores and water flow in soils. *Water Resource Res.* 18, 1311-1325.
- Bird, R. B., Stewart, W. E. and Lightfoot, E. N., 1960, *Transport phenomena*. pp. 37-41. John Wiley, N.Y.
- Davidson, M. R., 1984, A Green-Ampt model of infiltration in a cracked soil. *Water Resource Res.* 20(11) 1685-1690
- Dykhuizen, R. C., 1987, Transport of solutes through unsaturated fractured media. *Water Resource Res.* 21(12) 1531-1539.
- Gerke, H. H. and van Genuchten, M. T., 1993, A dual-porosity model for simulating the preferential movement of water and solutes in structured porous media. *Water Resource Res.* 29(2) 305-319.
- Kwicklis, E.D. and Healy, R. W., 1993, Numerical investigation of steady liquid water flow in a variably saturated fracture network. *Water Resource Res.*, 29(12) 4091-4102
- Nitano, J. J. and Buscheck, T. A., 1991, Infiltration of a liquid front in an unsaturated fractured porous medium. *Water Resource Res.* 27(8) 2099-2112.
- Pruess, K. and Tsang, Y. W., 1990, On two-phase relative permeability and capillary pressure of rough-walled rock fractures. *Water Resource Res.*, 26(9) 915-926.
- Römken, M. J. M. and Prasad, S. N., 1992, A spectral series approach to infiltration for crusted and non-crusted soils. *soil crusting: chemical and physical processes*. Edited by M. E. Sumner and B. A. Stewart, pp. 151-178. Lewis Publishers.
- Wells, R. R. 1995. Effect of cracks on rain infiltration in a Mississippi Delta clay soil, Master Thesis, University of Mississippi.
- Wilson, M. L. and Dudley, A. L., 1987, Radionuclide transport in an unsaturated fractured medium, in flow and transport through unsaturated fractured rock. *Geophys. Monogr. Ser. Vol. 42*, edited by D. D. Evans and T. J. Mickelson, pp. 23-29. AGU, Washington, D.C.



MODELING INFILTRATION AND STORM RUNOFF FROM SOILS WITH SHRINKAGE CRACKS

M. R. Savabi, Hydrologist, USDA-ARS, SEWRL, Tifton, GA, Stationed at USDA-ARS, Subtropical Horticultural Research Station, Mims, FL ; and C. W. Richardson, Agri. Engin., USDA-ARS, Grassland , Soil and Water Research Lab, Temple, TX.

Abstract: Soil surface crusting and shrinking cracks are common features of Vertisols. Although the Water Erosion Prediction Project (WEPP) infiltration component simulates the effects of surface crusting and macroporosity due to plant roots while adjusting the saturated hydraulic conductivity for soil surface conditions, the model does not simulate the effect of shrinkage cracks on infiltration. Therefore, the model was modified to simulate development of shrinkage cracks after a tillage practice and flow of water into the cracks. Hydrometeorological, soil, topography, and vegetation data from a pasture and a row-cropped watershed with highly shrinkage cracked Vertisols were used to test the WEPP hydrology component with and without a crack flow routine. The results indicate that the addition of a crack flow routine improved the ability of the model to predict storm runoff on watersheds with Vertisols, near Riesel, Texas.

INTRODUCTION

Accurate prediction of soil water intake and storm runoff is essential in any hydrologic modeling. Factors affecting infiltration rate such as soil surface crust, macropores, and vegetal cover need to be considered while modeling soil water intake and storm runoff. Although the effects of vegetal cover and soil surface crust on infiltration have been studied by several workers (Roth et al., 1988, Rawls et al., 1983) the effects of macroporosity and shrinkage cracks in particular on soil water intake have not been studied in depth. Beven and German (1982) reported that the theories of Darcian soil water flow that treats the soil as a homogeneous medium may not adequately describe infiltration and soil water redistribution in the presence of macropores such as shrinkage cracks. They grouped the macropores into four types: 1) pores formed by the soil fauna; 2) pores formed by plant roots; 3) cracks and fissures, and 4) natural soil pipes. Although all types of macropores may occur on different soil types to some extent, cracks and fissures due to shrinking and swelling of clay are common characteristics of Vertisols.

One of the major characteristics of Vertisols is their high coefficient of expansion, shrinking and swelling. Vertisols are known for their susceptibility to shrinking and swelling and extensive shrinkage cracks. The volume changes as much as 40% (based on oven-dry volume) by drying from field capacity to 15 atm. Godfery (1964) reported that fissures that exist in swelling clay soils may be the remnants of shrinkage cracks or slickenside boundaries. These natural fissures may have developed after long-term shrinking and swelling. Three shrinkage phases were reported by McGarry and Malafant (1987): 1) a structural phase at high water content, in which volume change is less than the volume of water removed, 2) the volume reduction is the same as the loss of water, and 3) at low gravimetric water content, volumetric reduction of the soil is smaller than the volume of water removed.

Shrinkage cracks have a significant effect on the soil water intake of Vertisols. Blake et al., (1973) studied the water recharge in soil with shrinkage cracks. They reported that water flow is likely to diverge sharply from "normal" when cracks extend to the soil surface. Kosmas et al., (1991) studied soil water distribution of swelling and shrinking soils under irrigation. They reported that a significant amount of irrigated water may move to lower layer soils without wetting the surface soil layers. Beven and German (1982) evaluated infiltration models which take into account the effect of macropores on infiltration simulations. They argued that none of the models are entirely satisfactory to simulate water flow into soil matrix and macropores. Furthermore, none of the models consider the spatial and temporal characteristics of the macropore system. This spatial and temporal variability of macropores is important, particularly in Vertisols where the shrinkage cracks may not be present all of the time due to swelling and/or tillage practices. Beven and German (1982) introduced a domain concept to model water movement in a combined macropore/matrix media. The water movement within the soil matrix is one domain and the water moving to macropores is the second domain.

The WEPP infiltration component (Savabi, et al., 1989) simulates the effects of surface crusting and macroporosity due to vegetation, while adjusting the saturated hydraulic conductivity for soil surface conditions. However, the model does not simulate the effect of shrinkage cracks on soil water intake and therefore, storm runoff infiltration. The objectives of this study were four fold: 1) to incorporate the simulation of developing shrinkage cracks after a tillage practice and/or complete swelling stage, 2) to simulate the temporal variability of the shrinkage crack area and depth as function of soil moisture fluctuation, 3) to simulate the flow of excess rainfall into the shrinkage cracks and its transmittion into lower soil layers, 4) to evaluate the model using hydrological data from a pasture and a crop watershed with Vertisols near Riesel, Texas.

MODEL DESCRIPTION

The WEPP hydrology model maintains a continuous daily hillslope water balance by linking infiltration, evapotranspiration, percolation, and subsurface drainage flow (Savabi et al., 1989). Excess rainfall is calculated as the difference between rainfall and infiltration. The infiltration equation used in the WEPP model is a solution of the single layer Green and Ampt equation (1911) for unsteady rainfall as presented by Chu (1978):

$$f_t = K_e \left(1 + \frac{N_s}{F} \right) \quad (1)$$

$$N_s = (\eta_e - \theta) \psi \quad (2)$$

where

f	=	infiltration rate, cm h ⁻¹
K _e	=	effective saturated hydraulic conductivity, cm h ⁻¹
t	=	time, h
N _s	=	effective matric potential, cm
F	=	cumulative infiltration depth, cm
η _e	=	effective porosity of 0-20 cm of soil, cm ³ cm ⁻³
θ	=	initial volumetric soil water content of 0-20 cm of soil, cm ³ cm ⁻³
ψ	=	the average wetting front capillary potential, cm

Rainfall excess is produced when the rainfall intensity exceeds the infiltration rate.

Effective saturated hydraulic conductivity (K_e) is an important parameter in determining storm excess rainfall and, therefore, runoff rate by the model. The effect of changes in vegetation cover and soil surface crusting on infiltration prediction is simulated by the WEPP hydrology model, using the partial area contribution method. The effective saturated hydraulic conductivity for the soil matrix may be provided by the user or estimated within the model using soil information provided by the user.

Simulation of Shrinkage Cracks Studies of the relationship between volume, occurrence of shrinkage cracks and soil properties are limited. In this study, we used the equations developed by Yassoglov et al., (1993) to predict fraction of area cracked and depth of shrinkage cracks. The cracked area at any given day after tillage is estimated by this equation:

$$CA = 2.04 * COLE e^{(C/\ln MC)} \quad (3)$$

where

CA	=	fraction of area cracked, m ² m ⁻²
COLE	=	coefficient of linear extensibility of top 350 mm of soil
C	=	clay content of top 350 mm of soil, percent
MC	=	volumetric moisture content of to 350 mm of soil, m m ⁻¹

The average crack width (CW in cm) was reported to be described by the following equation:

$$CW = CW_{max} * [1 - (MC/MCs)]^a \quad (4)$$

where

- CW_{max} = maximum average crack width, (assumed 0.75 cm, Yassoglov et al., 1993)
 MC_s = soil moisture at saturation, $m\ m^{-1}$
 a = constant, calculated for each soil (assumed 2.68 for Heiden soil)

Finally the average shrinkage crack depth (CD in cm) is related to the amount of clay, the field moisture content and the type of clay (Yassoglov et al., 1993):

$$CD = 93.4 * (COLE * C/MC)^{0.56} \quad (5)$$

Assuming that the shape of the shrinkage cracks resembles a cylinder, the equivalent depth of water which may remain in the cracks (cm) was calculated by this equation:

$$CS = CA * (CW/2)^2 * \pi * CD \quad (6)$$

The amount of excess rainfall leaving the hillslope, while cracks are filling, is determined by using the equation provided by Onstad (1984) for depression storage:

$$\begin{aligned}
 Q_i &= \frac{CS}{PR} * Er_i & FL < CS \\
 Q_i &= Er_i & FL \geq CS
 \end{aligned} \quad (7)$$

where

- Q = runoff rate leaving the profile, $cm\ h^{-1}$
 PR = rainfall excess required to fill all the cracks storage, cm
 Er = excess rainfall rate, $cm\ h^{-1}$
 i = interval of rainfall intensity distribution
 FL = $\sum Er_i - Q_i$, accumulated amount of excess rainfall filling the cracks, cm

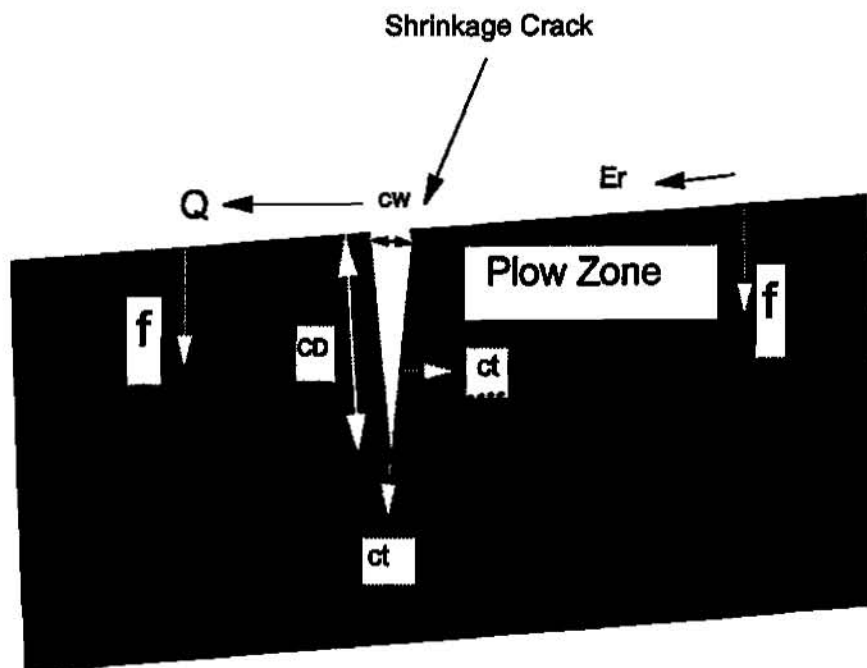


Figure 1 - Schematic representation of crack flow simulation. CW is crack width, CD is crack depth, CT is water penetrating into the crack walls, f is infiltration, Er is excess rainfall and, Q is excess rainfall after subtracting crack flow.

The depth of water filling the cracks for each rainfall event can be obtained by subtracting Q from Er. Equation 7 allows a portion of excess rainfall to pass between the cracks while the other portion will remain in the cracks. The excess rainfall flowing into the cracks is absorbed horizontally into the peds using a method developed by van der Ploeg and Benecke (1974). Calculated rainfall excess (Q) is then routed downslope to estimate the overland flow hydrograph using the kinematic wave method.

MODEL VALIDATION

Hydrometeorological records along with soil, vegetation, and topographic data from a pastured watershed (SW-12) and a row cropped watershed (W-12) located near Riesel, Texas, were used to evaluate the new crack routine. The model simulated storm runoff, with and without the crack flow routine was compared with measured storm runoff during 1987-1992.

Watershed Description The pasture watershed SW-12 is 2.97 acres in area with an average slope of 4 percent. The predominant herbaceous vegetation of the watershed are common broom weed (*Xanthocephalum dracunculoides*) and needlegrass (*Stipa ssp.*). Watershed W-12 is located near watershed SW-12 close to Riesel, Texas. The area of watershed (W-12) is 9.9 acres with an average slope of 1.5 percent. This watershed was planted with wheat, corn and sorghum during 1987, 1988, and 1989 respectively. The soils of the watersheds were developed from soft calcareous sediments which cover about 10 million ha in Texas. It is the most extensive swelling clay soil in the United States and it is closely related to the dark clay soils of the world (Godfery, 1964). The soil on the watersheds is classified as a Vertisol, Houston black clay series, recently named Heiden series. The soil is a fine montmorillonitic clay in the thermic family of Udic pellusterts (Richardson et al., 1979). This soil belongs to hydrologic soil group D. The shrinkage cracks are a common feature of this soil which are caused by alternative swelling and shrinking of the soil with changes in water content. A microloger weather station was used to monitor maximum, minimum, and average air temperature, total precipitation, storm duration and intensity. Storm runoff and sediment leaving each watershed were measured.

The WEPP input files were made based on field observations. Soil information provided by Elliot et al., (1989) for the top soil layer was used to make the soil data file (Table 1). The saturated hydraulic conductivity (Ks) of .47 cm/h was calculated from rainfall and runoff data reported by Elliot et al., (1989) for freshly tilled Heiden soil (Table 1).

Table 1, Soil data for Riesel watersheds, near Riesel Texas (after Elliot et al., 1989).

Depth cm	BD ^{1/} g/cm ³	Clay %	Sand %	Rock %	OM ^{2/} %	Ks ^{3/} cm/h	-33 kpa ^{4/} %	-1500 kpa ^{5/} %	COLE ^{6/}
23	1.33	53	10	0.0	2.0	.47	36	22	.101

1/ BD = soil bulk density, 2/OM= percent organic matter, 3/ Ks = saturated hydraulic conductivity, 4/ water retained at -33 kpa, 5/ water retained at -1500kpa, 6/ COLE = coefficient of linear extensibility

The management file and slope file were prepared for the cropped watershed and pastured watershed based on information provided by farm managers. Some of the climate information required by the model such as radiation, wind speed and direction, and dew point temperature was not available for the entire simulation period. Therefore, missing climate data was generated using the CLIGEN model (Nicks and Lane, 1989).

Although Equations 3-6 can be used to estimate the equivalent depth of shrinkage, the spatial variability of the shrinkage cracks and effect of farming practices on shrinkage cracks during the year were not studied by Yassoglov et al., (1993). For the cropped watershed, W-12, it was assumed that tillage practices such as Tandem disk or Moldboard plowing destroy any shrinkage cracks which may exist. However, on the pastured watershed, SW-12, shrinkage cracks were assumed not to be affected by any land practices. The development of shrinkage cracks after tillage on cropped watershed and for any given time for pastured watershed was assumed to be a function of soil water fluctuations, clay content and COLE.

RESULTS AND DISCUSSION

The WEPP hydrology model with and without a crack flow routine was tested on watersheds SW-12 and W-12. Only the measured storm runoff for the days with rainfall was selected for comparison with model simulated runoff. Regression analysis, Nash and Sutcliff coefficient (R), and standard error (Se) were used to compare the observed and model simulated storm runoff. Comparison of measured and WEPP predicted daily storm runoff, with and without a crack flow routine, from the watershed SW-12 between January 1987 to December 1989 is shown in Figure 2a and 2b. For watershed SW-12 the saturated hydraulic conductivity used by the WEPP model to predict infiltration was adjusted only for the effect of macropores due to roots, since bare area was reported negligible on this pasture watershed. The standard error of 11.3 mm and Nash and Sutcliff R of .48 indicates a fair agreement between WEPP-simulated and measured daily storm runoff (Fig. 2a). The Nash and Sutcliff coefficient of 0.58 vs. 0.48 and Se of 9.5 mm vs. 11.3 mm indicate that adding the shrinkage crack flow routine improved the ability of the WEPP model to predict storm runoff (Figs 2-a and 2-b).

For the W-12 watershed, the saturated hydraulic conductivity was adjusted for both crust effect and macroporosity due to roots. The Se and Nash and Sutcliff coefficient between the model predicted and the measured storm runoff are 8.2 mm and .33 respectively (Fig. 3a). For the case of the WEPP model with the crack flows routine, the Se and Nash and Sutcliff coefficient between the model simulated and the measured runoff were 6.6 mm and 0.57 respectively. The results indicate that adding a crack flow routine to WEPP hydrology reduced the discrepancy between model predicted and measured daily storm runoff (Figs 3a and 3b).

In general, the reason for the discrepancy between measured and WEPP simulated storm runoff on pasture and cropped watershed (Figs. 2 and 3) may be due to the Ks value for the Heiden soil matrix, adjustments of Ks for macroporosity, crusting effects, and/or crack flow simulations. The Ks of 4.7 mm/h was measured on freshly tilled plots (Elliot et al., 1989) and does not represent the Ks for the entire season on cropped watershed or for the pasture watershed. To improve the ability of the WEPP model to predict storm runoff with acceptable accuracy, work is underway to evaluate the Ks prediction and adjustments for various soil surface conditions. The information about the depth, volume, density and temporal and spatial variability of the shrinkage cracks was not available for the watersheds SW-12 and W-12 during 1987-1992. Therefore, the relationships developed by Yassoglov et al., (1993) were used in this study to predict crack storage on the watersheds. Information about the crack storage, as well as temporal and spatial variability of cracks is needed to improve estimation of storm runoff from watersheds with Vertisols.

CONCLUSIONS

Soil surface crusting and shrinking cracks are common features of Vertisols. Although the WEPP hydrology component simulates the effects of surface crusting and macroporosity due to plant roots while adjusting the saturated hydraulic conductivity for soil surface conditions, the model does not simulate the effect of shrinkage cracks on infiltration. Therefore, the model was modified to simulate development of shrinkage cracks after a tillage practice and flow of water into the cracks. The WEPP hydrology component with and without a crack flow routine was tested on watersheds with extensive shrinkage cracks near Riesel, Texas. The model simulated and the measured storm runoff was compared for the time period between 1987- 1992. The results indicate that the addition of a crack flow routine to the WEPP model improved the ability of the model to predict storm runoff on watersheds W-12 and SW-12 during 1987-1992.

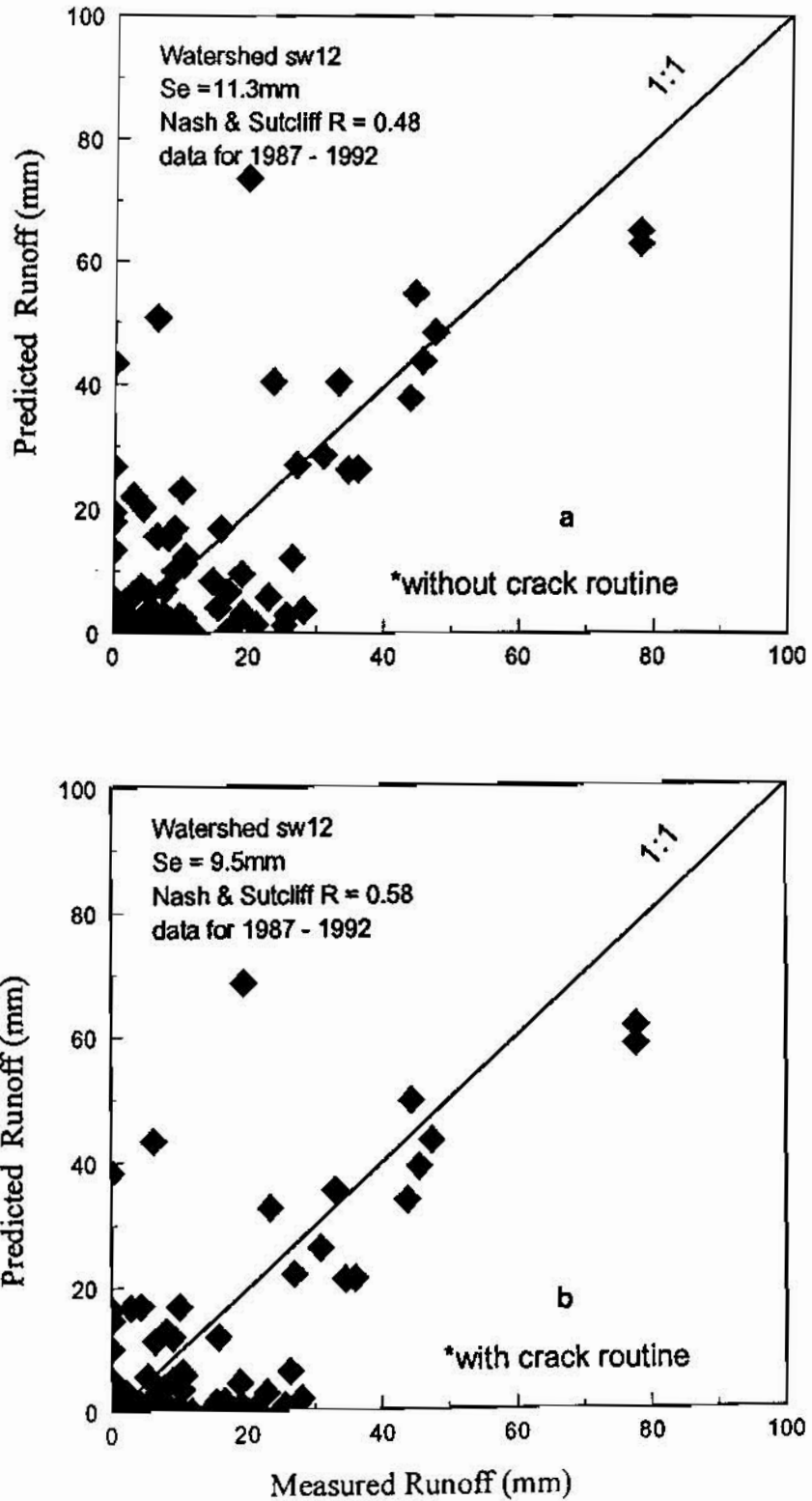


Figure 2 - Comparison of average measured and WEPP simulated storm runoff for pasture watershed (SW-12). Predicted storm runoff without crack flow simulation routine (a), and predicted storm runoff with crack flow simulations routine (b).

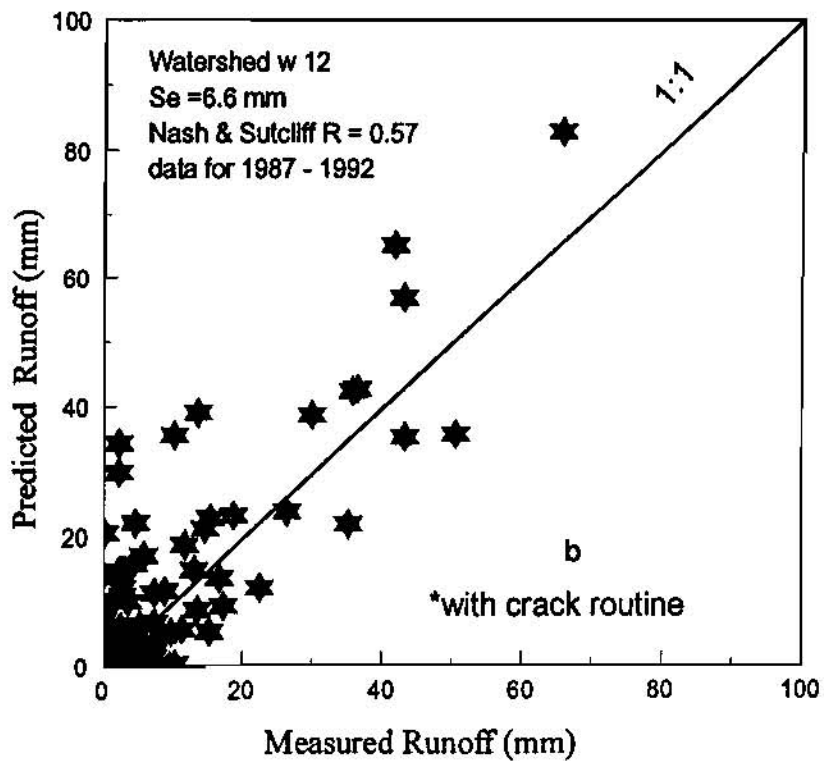
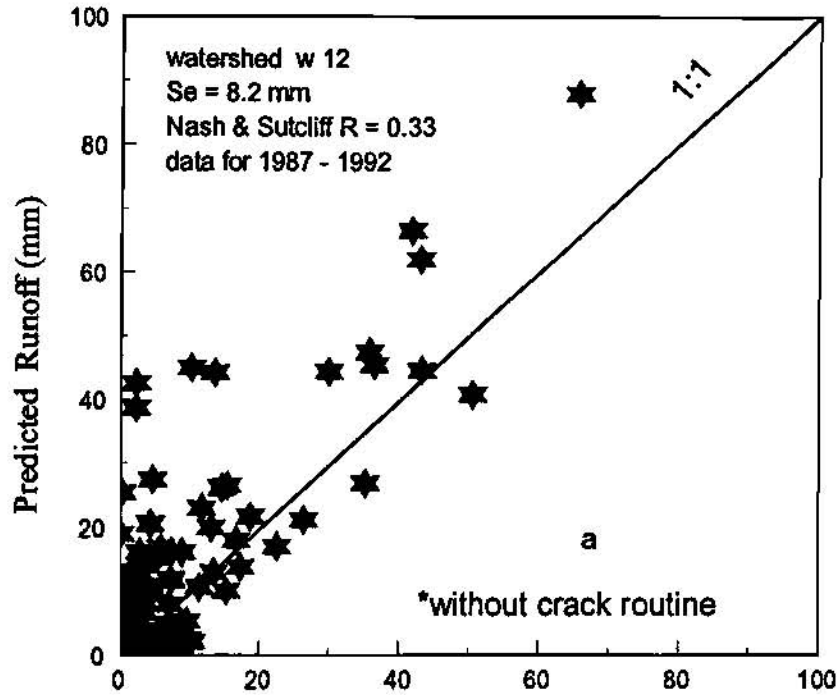


Figure 3 - Comparison of measured and WEPP simulated storm runoff for cropped watershed W-12. Predicted storm runoff without crack flow simulation routine (a) and, predicted storm runoff with crack flow simulations routine (b).

REFERENCES

- Beven, K., and German, P. 1982. Macropores and Water Flow in Soils. *Water Resour. Res.* 18:1311-1325.
- Blake, G., Schlichting, E. and Zimmermann, U. 1973. Water Recharge in a Soil with Shrinkage Cracks. *Soil Sci. Soc. Am. Proc.*, 37:669-672.
- Chu, S. T. 1978. Infiltration During Unsteady Rain. *Water Resour. Res.* 14(3): 461-466.
- Elliot, W. J., Liebenow, A. M., Lafen, J. M. and Kohl, K. D. 1989. A Compendium of Soil Erodibility Data from WEPP Cropland Soil Field Erodibility Experiments 1987 & 1988. USDA-ARS, National Soil Erosion Research Laboratory Report N0. 3.
- Godfery, C L. 1964. A Summary of the Soils of the Blackland Prairies of Texas. *Tex. Agr. Exp. Sta. Misc. Publ.* 698.
- Green, W. H. and Ampt, G. A. 1911. Studies in Soil Physics, I. The flow of Water Through Soils. *J. Agric. Science* 4:1-24.
- Kosmas, C., Kallianou, M. N. , and Yassoglou, N. 1991. Cracking Patterns, Bypass Flow and Nitrate Leaching in Greek Irrigated Soils. *Geoderma*, 49:139-152.
- McGarry, D. and Malafant, K. W. 1987. The Analysis of Volume Change in Unconfined Units of Soil. *Soil Sci. Soc. Am. J.* 51:290-297.
- Nicks, A. D and Lane, L. J. 1989. Weather generator . In: L. J. Lane and M. A. Nearing (Editor). USDA- Water Erosion Prediction Project: Profile Model Documentation. NSERL Report No. 2 USDA- ARS-National Soil Erosion Research Lab., W. Lafayette, IN. 49709. Chapter 2.
- Onstad, C.A. 1984. Depressional Storage on Tilled Soil Surfaces. *Transactions of the ASAE* 27(3):729-732.
- Rawls, W. J., Brakensiek, D. L., and B. Soni, B. 1983. Agricultural Management Effects of Soil Water Processes: Part I, Soil Water Retention and Green Ampt Infiltration Parameters. *Trans. ASAE* 26:1752-1763.
- Richardson, C. N., Burnett, E., and Bovey, R. W., 1979. Hydrologic Effects of Brush Control on Texas Rangelands. *Trans. of the ASAE* 22:315-319.
- Roth, C. H., Meyer, B., Frede, H. G., and Detsch, R. 1988. Effect of Mulch Rates and Tillage Systems on Infiltrability and Other Soil Properties of an Oxisol in Parana, Brazil. *Soil Tillage Res.* 11:81-91.
- Savabi, M. R., Engman, E.T. , Kustas, W. P. , Rawls, W. J., and Kanemasu, E.T. 1989. Evaluation of WEPP Water Balance Model for Watershed 1D in Konza Prairie, Kansas. In: *Proceedings of the 19th Conference, Agricultural and Forest Meteorology*, March 7-10, 1989, Charleston, SC, pp. 147-150.
- van der Ploeg, R. R., and P. Benecke. 1974. Unsteady, Unsaturated n-Dimensional Moisture Flow in Soil: A Computer Simulation Program. *Soil Sci. Soc. Am. Proc.* 38:881-885.
- Yassoglou, N., Kosmas, C. S., Moustakas, N., Tzianis, E., and Danalatos, N. G. 1993. Cracking in Recent Alluvial Soil as Related to Easily Determined Soil Properties. *Geoderma. An International Journal of Soil Science.* Pp 58-62.

SPATIALLY DISTRIBUTED HYDROLOGIC MODELING FOR STREAMFLOW SIMULATION AND FORECASTING

By **Andreas H. Schumann, Privatdozent, Lehrstuhl für Hydrologie, Wasserwirtschaft und Umwelttechnik, Ruhr-Universität Bochum, Germany;**

David C. Garen, Hydrologist, United States Department of Agriculture, Natural Resources Conservation Service, National Water and Climate Center, Portland, Oregon

Abstract: A GIS-based, spatially distributed soil moisture accounting and streamflow simulation model has been developed and applied to the Prüm catchment in western Germany and the Boise River in the U. S. state of Idaho. Parameter values for each grid cell are derived directly from a digital elevation model and GIS layers of soil type and land use / vegetation. Additionally, there are six calibration parameters controlling the surface runoff and the release of water from the soil moisture storages, which are determined by optimization. A spatial interpolation algorithm based on detrended kriging is applied to obtain gridded fields of meteorological input variables for each day in the simulation. Snowmelt is handled either by a degree-day approach, or the snowmelt output from a spatially distributed energy budget snow simulation model can be linked to the hydrologic model. This model has several advantages over traditional conceptual, spatially lumped models used for water management applications.

INTRODUCTION

The large amount of spatially detailed information derived from remote sensing, ground surveys, or interpolation of point measurements, and handled within a geographic information system (GIS), offers new opportunities for hydrologic modeling. An increasingly common approach is to use these data in distributed hydrologic models, where the catchment is divided into small, regularly or irregularly shaped, area elements based on catchment characteristics. The characteristics (e.g., land use, soil texture, topographic aspect, elevation) within the resulting elements are generally considered homogeneous. To describe hydrologic processes within each element, there exist physically-based models of micro- (or point-) scale processes, which were developed for well-defined physical conditions (e.g., infiltration in homogeneous soils with known hydraulic parameters), however, their use with spatial units of some hundred m² is not justified. The applicability of these models at the meso-scale is limited by unresolved problems of their parameterization (Grayson et al., 1993). As the needed model parameters (e.g., soil characteristics) cannot be measured for catchments on the order of hundreds of km² or larger, they must be derived using transfer functions and other assumptions from known catchment characteristics, e.g., from soil texture classes. This, however, increases the uncertainty of the parameter values considerably. Even if these parameters could be measured over large areas, it is questionable whether a single value (say, the mean) would adequately represent the behavior of the (relatively large) area elements. To overcome this problem, "representative" or "effective" values of parameters are commonly introduced to bridge the gap between a micro-scale model and its use at the meso-scale. The values of these "representative" or "effective" parameters depend strongly on the heterogeneity of the catchment and on the spatial scale. Since they usually have to be determined by calibration, the parameters lose their precise physical significance and may be of a magnitude quite different from measured values. Because of this, distributed hydrologic models are not truly physically-based but are a special category of conceptual models (Beven, 1989). (Actually, the concept of a truly physically-based model at the catchment scale is questionable [Grayson et al., 1992], but perhaps the physical basis of a model is really just a matter of degree.)

Considering these issues about physically-based models and parameter values, the question arises as to how GIS could be used to improve hydrologic models. Some options are:

- To use the GIS to improve the estimation of parameters in existing conceptual models, e.g., determining the composite runoff curve number for a drainage basin in the widely used SCS model (Maidment, 1993) from its land use data and digitized soil maps.
- To use a statistical distribution approach to consider the spatial heterogeneity of a catchment characteristic in the model parameterization. For example, the storage capacity of the upper, rooted soil zone could be described by an areal distribution function, which can be derived directly from an overlay of the vegetation and soil map within a GIS (Schumann, 1993).

- To subdivide the catchment into so-called "Hydrologic Response Units" (HRUs), which are similar with regard to selected characteristics and which are modeled separately, as in, e.g., the Precipitation-Runoff Modeling System (PRMS) of Leavesley et al. (1983).
- To subdivide the catchment into equally-spaced square grid elements and to represent the hydrologic processes in these units by a parameter set in which the physical characteristics of the units are considered. An example is the model for the Rhine, which is based on a subdivision of the river basin into 3 km-square grid elements (Kwadijk and Rotmans, 1995).

While the first option is certainly feasible and is a helpful improvement, it represents only a very limited use of the available information and the power of the GIS. There is no reason to limit ourselves to model parameterizations that were developed decades ago in an era without the information and computing facilities available today.

Subdividing a catchment into spatial units is very helpful in considering the areal distribution of meteorological inputs and the heterogeneity of catchment characteristics. We can divide the catchment into parts, each of which is similar in its physical characteristics (e.g., land use categories, soil texture classes, topography), however, the problem arises as to which characteristics should be considered as relevant to the hydrologic processes. If too many different characteristics are considered (e.g., all topographic characteristics relevant to hillslope processes), the partitioning will be very detailed. If we consider only some characteristics for this subdivision, we neglect the heterogeneity of the others. In addition, in a process-based subdivision of a catchment, the problem of heterogeneous distributions of meteorological variables (e.g., precipitation and temperature) remains.

This latter problem does not exist if we divide the catchment into grid-based units. For each grid cell the specific value of its precipitation or temperature can be estimated. The physical characteristics within each grid cell, however, may be heterogeneous. If we were to reduce the width of the grid cells, this heterogeneity would be reduced, but the disadvantages of a very detailed resolution are that the computational requirements are increased, and the model structure becomes more complex due to the need to describe more interactions among the small spatial units. The grid cell approach is very appealing, however, because it lends itself naturally to the GIS.

We believe that the grid cell approach is the most promising for the fullest and most convenient utilization of the GIS in hydrologic modeling. Below we present a model based on a coarse subdivision of a catchment into grid cells in which the heterogeneity of selected catchment characteristics within the grid cells is considered. Our goals in developing this model have been not only a good representation of the hydrologic processes, but also the direct utilization of spatially distributed catchment characteristics that are obtainable by the application of a GIS and the minimization of parameters requiring calibration. We envision this model being useful for streamflow forecasting and water management.

THE WATER BALANCE MODEL

General Structure: The model describes the spatially distributed water balance of a catchment on a daily time step. To parameterize the hydrologic process models, the following spatial catchment characteristics are considered:

- land use,
- soil texture classes,
- elevation and derived data (slope, aspect, topographic index, distances of flow paths).

These characteristics are stored within a GIS (ArcInfo) and are used in conjunction with other information to derive the model parameter values for each grid cell.

The spatial resolution of the model is based on a horizontal subdivision into regular grids of a width of one kilometer. This grid size was chosen based on the following considerations:

- each area element should be drained directly by a part of the river network to avoid the need to describe interactions among the grid cells,
- the computational requirements should be kept within reasonable limits so that the model is usable in practice,
- the spatial distribution of the meteorological variables within the catchment should be well represented.

Each 1 km² grid cell is characterized by:

- its location within the grid,
- a distribution function of the storage capacity of the upper, rooted soil zone, which can be derived from an overlay of land use and soil characteristics,
- average values of its elevation, slope, aspect, topographic index and distance to the catchment outlet.

For each grid cell the vertical water balance is computed by four interconnected submodels:

- an interception model,
- a soil storage model, which is the main steering component of the vertical and lateral water balance,
- an evapotranspiration model, which considers the available water and energy amounts to compute evaporation of intercepted precipitation and transpiration from the vegetation cover,
- a lumped model for the groundwater storage.

The model components are described below.

The Soil Moisture Storage Model: The main component of the water balance model is the upper soil storage, which represents the depth of water that is held in the root zone. To obtain the maximum capacity of this soil storage, the soil porosity is multiplied by the root depth for each grid cell. Porosity is determined from the soil texture class according to the values given by Rawls et al. (1983). The root depth depends on the type of vegetation and the seasonal development of the roots. Values of root depth by month of the year for the various land use classes were taken from different literature sources (e.g., from Disse, 1995).

Soil and land use GIS layers have a much finer spatial resolution than the 1 km² grid cell used for the hydrologic model. Within each 1 km² grid cell, therefore, we can determine that different types of soil and vegetation exist. We consider this heterogeneity by a distribution function. Similar to distribution functions in statistics, this function describes the fraction of each grid cell that is characterized by a storage capacity below a given value. We derive this function by overlaying the soil and the land use maps within the GIS. From this procedure, we derive a step function that mirrors the different types of vegetation and soil classes. This step function is approximated by a linear function to reduce computational requirements in the model. The approximated distribution function varies seasonally, due to the variation in the root depth. In Fig. 1, the estimation of this function is shown schematically.

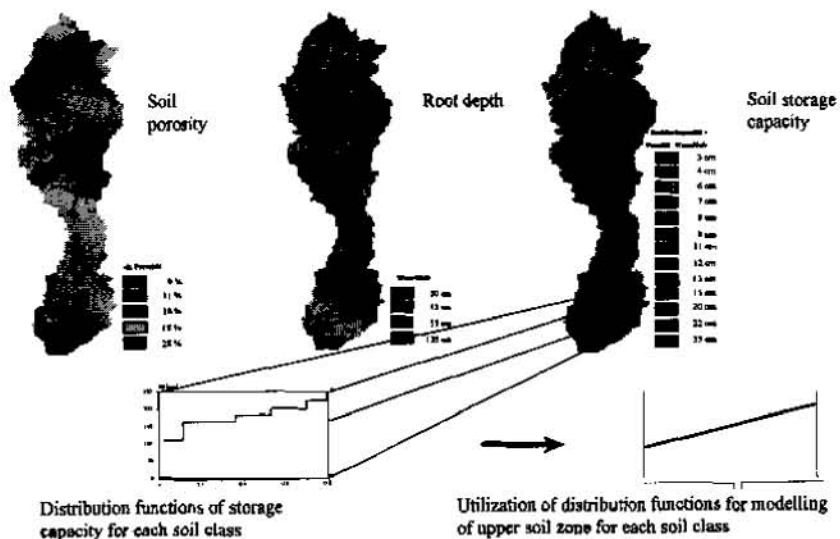


Fig. 1 Estimation of the distribution function of soil storage capacity

The approximated distribution function can be used in the same way as in the well-known Xinanjiang model (Ren-Jun, 1992) to describe the temporally changing portion of saturated area within each grid cell. The impacts of topography on the saturation of the upper soil zone should, however, also be considered. The $\ln(a/\tan\beta)$ topographic

index used in TOPMODEL, introduced by Beven and Kirkby (1979), is a widely-used characteristic to describe the relationship between the drainage area (a) and the slope ($\tan\beta$) at each point of a catchment. Under a given state of soil wetness within a catchment, the areas with a high value of the topographic index are more likely to be saturated than those with a lower value. In TOPMODEL, various simplifying assumptions are made to develop a quantitative relationship between the topographic index and saturated area. In our model, we prefer not to use this relationship, as we do not make the same assumptions used in TOPMODEL. Instead, we use the index in a different way, but still to consider the effect of topographic heterogeneity on saturation and runoff production.

If, after the addition of the effective precipitation (i.e., after subtraction of interception losses), the increase of the soil water content does not exceed the distributed soil storage capacity at any point of the grid cell, no saturated areas exist, and no surface runoff is produced (Fig. 2a). If the actual water content of the soil storage exceeds the storage capacity of a certain part of the grid cell, this part is saturated (Fig. 2b). To consider the influence of topography on the occurrence of saturated areas, the slope of the linear soil storage distribution function is adjusted. For each grid cell, the average of the topographic index $\ln(a/\tan\beta)$ is computed from the higher-resolution digital elevation data, and the mean value of the index for the catchment as a whole is also computed. We expect that the grid cells with a topographic index above (below) the catchment average will be saturated earlier (later) and to a greater (lesser) extent than those with a lower (higher) value. This is considered by an increase or decrease of the slope of the distribution function of soil storage capacity. The amount of this increase or decrease is a linear function of the difference between the grid cell topographic index and the catchment average index, and it is regulated by a calibration parameter. Fig. 2c shows the case where the saturated part of a grid cell is increased as the slope of its distribution function is increased. Increasing the slope therefore increases the dynamics of the soil water balance, as the amount of water that can be stored in the lower half of the range of soil storages is reduced, and the amount of direct runoff during rain periods is increased (Fig. 2d).

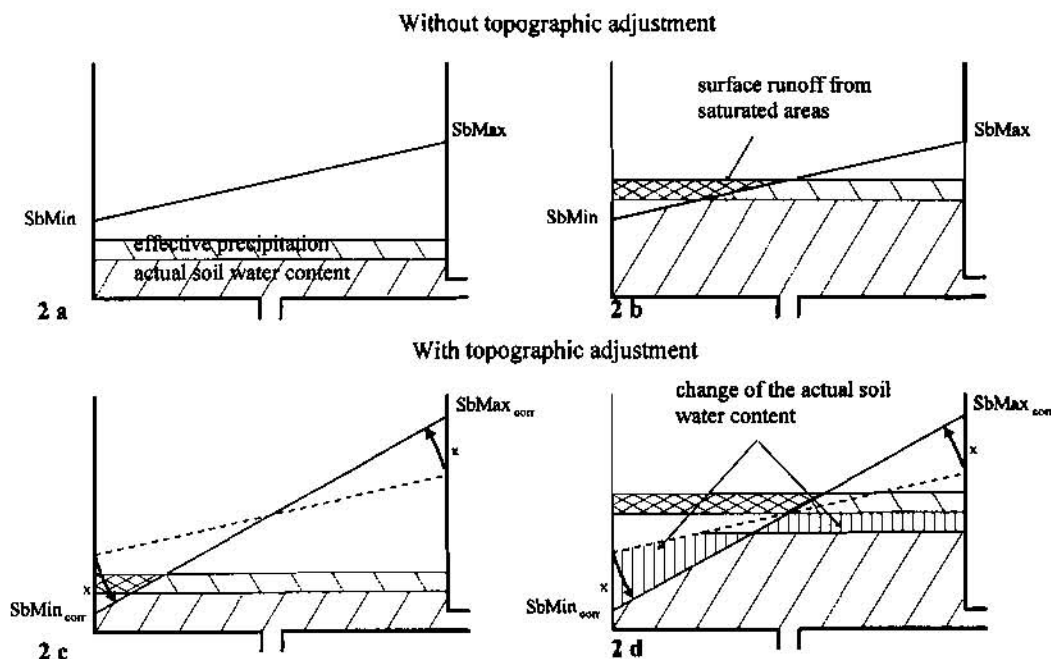


Fig. 2 Utilization of the distribution function of soil storage capacity

The soil storage controls not only the amount of surface runoff but also subsurface runoff (lateral flow) and the percolation into the deeper soil, which is not affected by transpiration. Lateral flow and percolation are governed by nonlinear equations of the form of Brooks and Corey (1964) but with (four) calibrated parameters. The storage of the percolated water and the base flow is described by a single linear storage for the catchment. As the area of each grid cell is small relative to the density of the natural drainage network and the daily computational time step, hillslope processes are neglected. Runoff is generated by each grid cell independently and is translated to the catchment outlet based on its flow path distance and an average channel flow velocity (which is a model parameter).

Other Model Components: The capacity of the interception storage is related to the Leaf Area Index (LAI) using an approach suggested by Hoyningen-Huene (1980). The LAI can be estimated from remote sensing data or can be related to the type of vegetation and its seasonal development. Evaporation of intercepted precipitation is considered to occur at the potential evaporation rate. For estimation of evapotranspiration from the soil storage, a reference evapotranspiration for grassland is computed according to a recommendation by Allen et al. (1994), based on the well-known Penman-Monteith formula. To consider different types of vegetation and the steering effect of soil moisture, crop factors are used, which were suggested for German climate conditions by Disse (1995). Snowmelt is handled either by a simple degree-day approach, or the results of a spatially distributed energy budget model (Marks and Dozier, 1992) can be read in.

Meteorological Input Data: Daily precipitation and temperature values are estimated for each grid cell from meteorological station data using a spatial interpolation procedure based on detrended kriging (Garen et al., 1994; Garen, 1995; Garen and Marks, 1996). This procedure accounts for both the effects of elevation and the horizontal spatial variability. Generally, only a limited number of meteorological stations with the other needed meteorological input variables (solar radiation or sunshine hours, humidity, wind) are available, so these are often represented by daily catchment average values, although they also can be represented by spatially distributed values if the station data are sufficient.

MODEL APPLICATION

The model is currently being tested on two catchments, one in Germany and one in the United States. A summary of these applications is given below.

Prüm catchment, Germany: The Prüm is in the western part of the central mountain region of Germany, with a drainage area of 577 km² at the gaging station at Prümzurley, and with elevations ranging from 170 to 700 m. The water balance can be characterized by an annual mean value of 894 mm of precipitation and 427 mm of runoff (period 1970 to 1987). Here, snow is a minor part of the overall water balance, but large flood flows can be generated by rain on snow. For this catchment, daily precipitation at 11 stations and runoff data at two gages were available. Other climate data (temperature, humidity, wind velocity, radiation) were available at three stations. The available period of observations was from October 1970 to September 1987.

In Fig. 3, the spatial variability of two catchment characteristics, the mean soil storage capacity and the mean topographic index, for the 1 km² grid cells of the subcatchment Echterhausen (drainage area 325 km²) are shown. An example of the computed spatial variability of the soil moisture is given in Fig. 4. It shows two different maps of the saturated portions of the grid cells on 1 January 1982. At the left side, the distribution of the soil storage capacity of each grid cell is computed considering the soil and vegetation characteristics only. On the right side, the same results after topographic adjustment of the soil storage distribution are shown. Obviously, considering the topography increases the spatial variability of the saturated areas considerably. Unfortunately, there exist no possibilities at present to evaluate this variability of the spatial patterns. The ability of our model to represent the water balance of the test catchment can, however, be validated by a comparison of the computed with the measured runoff. An example of this validation is given in Fig. 5. In general, the model represents the water balance of our test catchment well. The mean absolute errors during the simulated time period are 50.5 mm for yearly, 6.7 mm for monthly and 0.4 mm for daily values at the Prümzurley gage.

Boise River, Idaho, USA: The Boise River is in a mountainous region, with a drainage area of 2150 km² (at the Twin Springs gaging station, just above Arrowrock Reservoir), and with elevations ranging from 1000 to 3200 m. Most of the streamflow comes from spring and summer snowmelt. Digital elevation data were obtained from the U. S. Geological Survey at a cell size of 100 m, but this was smoothed and aggregated to 250 m because there were several digitizing artifacts in the data. Land use data were also obtained from the U. S. Geological Survey, and soil information was extracted from the STATSGO data base of the Natural Resources Conservation Service (NRCS, U. S. Department of Agriculture), both at a resolution of 100 m. Meteorological data were available for eight stations in and near the catchment.

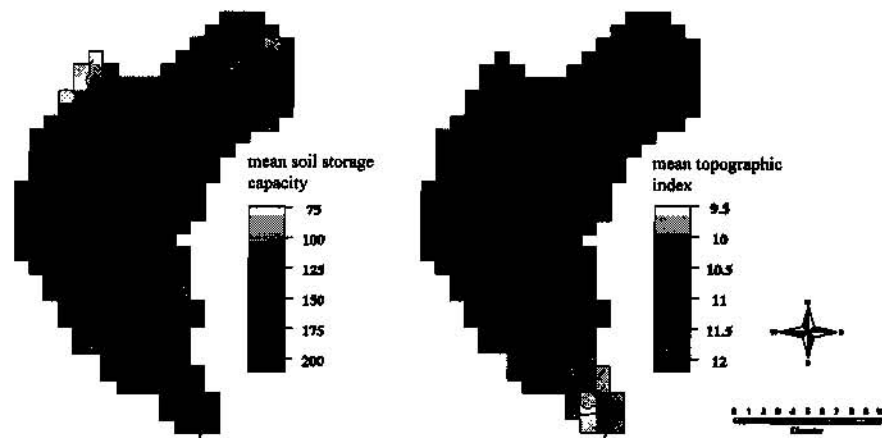


Fig. 3 Spatial heterogeneity of GIS-based estimated catchment characteristics for the catchment Echterhausen/Prüm

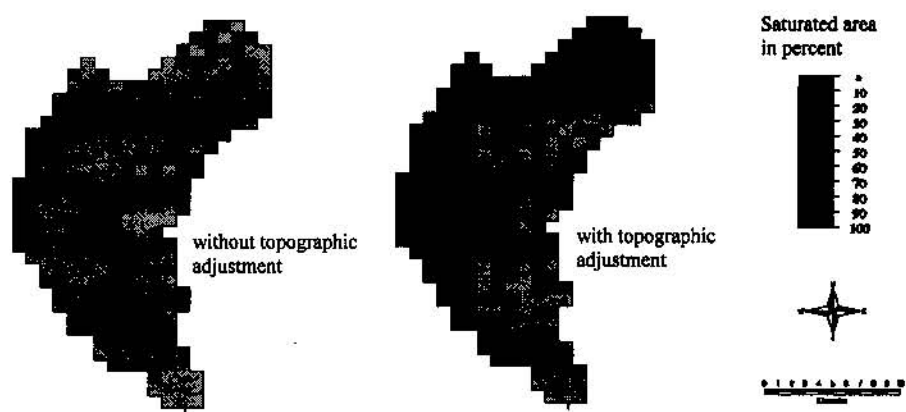


Fig. 4 Spatial variability of the computed soil moisture distribution for the catchment Echterhausen/Prüm, 1 Jan 1982

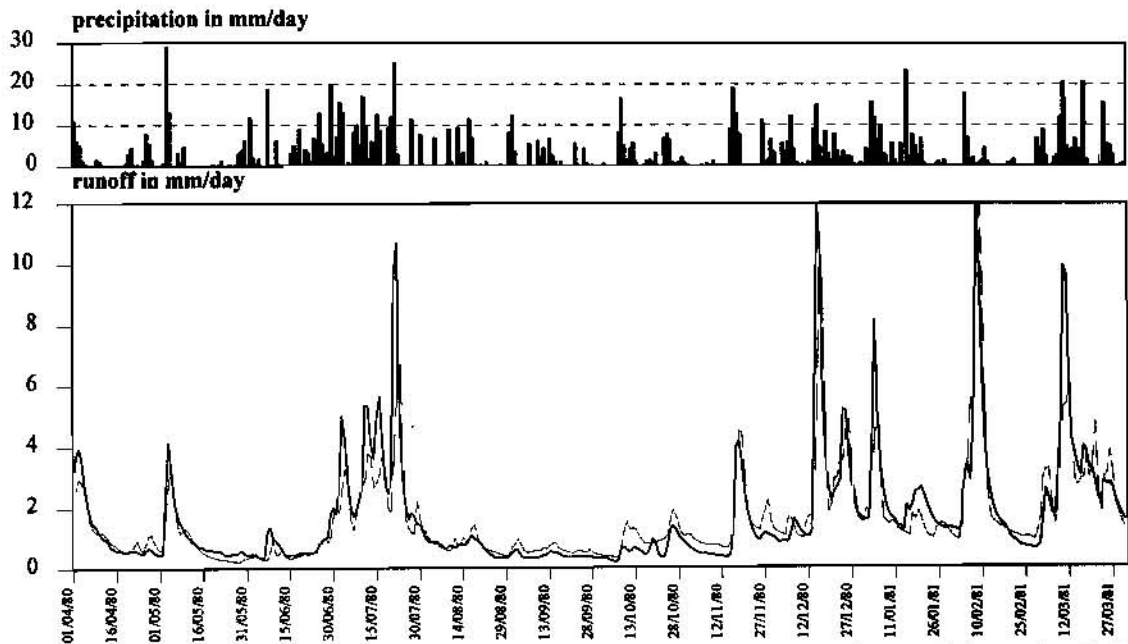


Fig. 5 Computed (dashed line) and measured (solid line) runoff for the catchment Prümzurley/Prüm, 1 Apr 1980 to 31 Mar 1981. (For improved visualization, peaks above 12 mm/day were truncated.)

This modeling is being conducted in conjunction with the application of a spatially distributed energy budget snow simulation model (Garen and Marks, 1998), which was previously applied to this catchment by Garen and Marks (1996). In the current application, the snow model is being used to simulate the development and melting of the snowpack during the period October 1996 - July 1997. The spatially distributed snow water equivalent and melt fields from this model will then be used as input to the water balance model, rather than using the degree-day method to handle snowmelt. As this snow modeling work is still ongoing, streamflow simulation results are not yet available. It is envisioned that the coupled models will also be tested on the 1997-1998 snow accumulation and melt season.

CONCLUSIONS

The water balance model described here represents a new type of hydrologic model for water management and streamflow prediction. By utilizing the abundant spatially distributed data now available, it has been possible to develop a model with several advantages over the previous generation of conceptual models used for these purposes. One of these advantages is that the spatial data provide much more information about catchment characteristics and meteorological inputs, which gives the model a greater physical basis and allows the number of calibration parameters to be reduced to a manageable level. A second advantage is that the model can potentially provide spatially distributed water budget information, such as runoff source areas, levels of soil moisture in different parts of the catchment, etc. More work needs to be done, however, to verify the spatially distributed output of the model. At present, we are only able to verify the streamflow computed by the model. We plan to continue refining the model and applying it to other time periods and catchments.

ACKNOWLEDGEMENTS

We would like to thank Joachim Geyer of the Ruhr-Universität Bochum for his substantial contributions to this work in the development and programming of the water balance model, carrying out the model runs for the Prüm catchment, and assisting in the application of the model to the Boise River. We would also like to acknowledge the funding assistance of the U. S. Department of Agriculture, Foreign Agricultural Service, who supported a two-week stay in Germany for D. Garen to help work on the model.

REFERENCES

- Allen, R. G., Smith, M., Perrier, A., Pereira, L. S., 1994, An Update for Definition of Reference Evapotranspiration. ICID (International Committee of Irrigation and Drainage) Bulletin 43, No. 2, 1-34.
- Beven, K., 1989, Changing Ideas in Hydrology -- the Case of Physically-Based Models. *Journal of Hydrology*, 105, 157-172.
- Beven, K. J., and Kirkby, M. J., 1979, A Physically Based, Variable Contributing Area Model of Basin Hydrology. *Hydrological Sciences Bulletin*, 24(1), 43-69.
- Brooks, R. H., and Corey, A. T., 1964, Hydraulic Properties of Porous Media. *Hydrology Papers*, No. 3, Colorado State University, Fort Collins, Colorado.
- Disse, M., 1995, Modellierung der Verdunstung und der Grundwasserneubildung in ebenen Einzugsgebieten. *Mitteilungen, Institut für Hydrologie Karlsruhe*, Heft 53.
- Garen, D. C., 1995, Estimation of Spatially Distributed Values of Daily Precipitation in Mountainous Areas. In: *Mountain Hydrology: Peaks and Valleys in Research and Applications* (proceedings of Canadian Water Resources Association conference, Vancouver, British Columbia), 237-242.
- Garen, D. C., Johnson, G. L., and Hanson, C. L., 1994, Mean Areal Precipitation for Daily Hydrologic Modeling in Mountainous Regions. *Water Resources Bulletin*, 30(3), 481-491.

- Garen, D. C., and Marks, D., 1996, Spatially Distributed Snow Modelling in Mountainous Regions: Boise River Application. In: HydroGIS '96: Application of Geographic Information Systems in Hydrology and Water Resources Management (proceedings of Vienna conference), IAHS Publication no. 235, 421-428.
- Garen, D. C., and Marks, D., 1998, Spatially Distributed Energy Budget Snowmelt Modeling in Mountainous Regions of the Western United States. Paper presented at First Federal Interagency Hydrologic Modeling Conference, Las Vegas, Nevada.
- Grayson, R. B., Blöschl, G., Barling, R. D., and Moore, I. D., 1993, Process, Scale and Constraints to Hydrological Modelling in GIS. In: HydroGIS '93: Application of Geographic Information Systems in Hydrology and Water Resources (proceedings of Vienna conference), IAHS Publication no. 211, 83-92.
- Grayson, R. B., Moore, I. D., and McMahon, T. A., 1992, Physically Based Hydrologic Modeling 2. Is the Concept Realistic? *Water Resources Research*, 26(10), 2659-2666.
- Hoyningen-Huene, J. v., 1993, Die Interzeption des Niederschlags in landwirtschaftlichen Pflanzenbeständen. In: Einfluß der Landnutzung auf den Gebietswasserhaushalt, Schriftenreihe des DVWK (Deutscher Verband für Wasserwirtschaft und Kulturbau), Heft 57, 1-53.
- Kwadijk, J., and Rotmans, J., 1995, The Impact of Climate Change on the River Rhine: A Scenario Study. *Climatic Change*, 30, 397-425.
- Leavesley, G. H., Lichty, R. W., Troutman, B. M., and Saindon, L. G., 1983, Precipitation-Runoff Modeling System -- User's Manual. U. S. Geological Survey, Water Resources Investigations Report 83-4238.
- Maidment, D. (ed.), 1993, Handbook of Hydrology. McGraw-Hill, 9.21-9.26.
- Marks, D., and Dozier, J., 1992, Climate and Energy Exchange at the Snow Surface in the Alpine Region of the Sierra Nevada 2. Snow Cover Energy Balance. *Water Resources Research*, 28(11), 3043-3054.
- Rawls, W. J., Brakensiek, D. L., and Miller, N., 1983, Green-Ampt Infiltration Parameters from Soils Data. *Journal of Hydraulic Engineering*, 109(1), 62-70.
- Ren-Jun, Z., 1992, The Xinanjiang Model Applied in China. *Journal of Hydrology*, 135, 371-381.
- Schumann, A. H., 1993, Development of Conceptual Semi-Distributed Hydrological Models and Estimation of Their Parameters With the Aid of GIS. *Hydrological Sciences Journal*, 38(6), 519-528.

Andreas H. Schumann, Lehrstuhl für Hydrologie, Wasserwirtschaft und Umwelttechnik, Ruhr-Universität Bochum, D-44780, Bochum, Germany
 Tel.: +49 234 7002688 Fax: +49 234 7094153 E-mail: Andreas.H.Schumann@rz.ruhr-uni-bochum.de

David C. Garen, United States Department of Agriculture, Natural Resources Conservation Service, National Water and Climate Center, 101 SW Main Street, Suite 1600, Portland, Oregon 97204-3224, USA
 Tel.: +1 503 414 3021 Fax: +1 503 414 3101 E-mail: dgaren@wcc.nrcs.usda.gov

Modeling the Hydrology of Wetland-Upland Systems on A Flat Terrain in Florida

By G. Sun, Forest Hydrologist, Southern Global Change Program, USDA Forest Service, North Carolina
H. Riekerk, N. B. Comerford, Associate Professor (retired) and Professor, University of Florida, Florida

INTRODUCTION

The southern United States has always been a center for soft wood timber production due to its ideal climatic and soil water conditions for tree growth (Sabine, 1994). More than 1 million acre of the land in the coastal area is classified as pine flatwoods (Cubbage and Flather, 1993). Important values of this ecosystem include timber production, wildlife habitat, and groundwater recharge (Brandt and Ewel, 1991). As human population and wood demands continue to increase in the South, forestry activities on pine flatwoods have become more and more intensified (Riekerk and Korhnak, 1984). Environmental concerns about forest management practices in the coastal areas include impact on water quality, hydrology (e.g., wetland hydroperiod) and resultant influences on wildlife habitat and long term cumulative impacts on soil productivity. Although the effects of forest management on upland watershed hydrology are well studied in the past century (Bosh and Hewlett, 1982; Swank and Crossley, 1988), little information is available for the low land and forested wetland landscape (Shepard et al., 1993).

Hydrologic computer simulation models are useful tools for scientists as well as land managers in decision making (Lovejoy et al., 1997). Although the procedures to construct hydrologic simulation models are the same including mathematical formulation, calibration, validation and testing, one model may be very different from another in its capability and applicability. For example, most of the available hydrologic models developed for hilly regions are not applicable for the Florida coastal conditions (Heatwole et al, 1987). Also, models developed for agricultural watershed conditions often need significant modification to apply for forests. Based on the agricultural drainage model DRAINMOD (Skaggs, 1978), a forest hydrology version, DRAINLOB was developed to model water management effects on the hydrology of loblolly pine flat in North Carolina (McCarthy, 1990). Heatwole et al (1987) modified the CREAMS model (Knisel, 1980) into CREAMS-WT to better represent the storage-based flatwoods hydrologic system of agricultural watersheds in South Florida. The DRAINMOD model was also modified to a new model, Field Hydrologic And Nutrient Transport Model (FHANTM), to simulate the hydrology and P movement on flatwoods fields (Campbell et al., 1995). Guo (1989) failed in directly applying a variable source area (VSA) based stormflow model, which was developed for upland hydrology, to a pine forest watershed. He suggested that the flat topography and large cypress wetland storage significantly reduced stormflow under most situations in the five runs. In existing forest ecological models for slash pine plantations, hydrologic cycles are included but water movement processes are not physically and explicitly modeled (Ewel and Gholz, 1991). In these kinds of lumped field scale models, runoff from a field was calculated as the precipitation excess, i.e. water will run off when the soil water storage is depleted. In recent years, there is a tendency to develop more physically based distributed models (Jensen and Mantoglou, 1992), which couple hydrologic processes with biological processes (Wigmosta et al., 1994). This development has been driven by the need for comprehensive large-scale (e.g., basin, globe) ecosystem studies, in which the hydrology is one of the most important components (Swank et al., 1994), and accelerated by the increase of computation power and advance of Geographic Information Systems (GIS) technology (Maidment, 1993).

The Florida flatwoods landscape includes a mosaic of cypress wetlands and forest uplands, so the hydrology of flatwoods is inherently complex. Slight spatial variations in topography cause significant changes in the water regime. The heterogeneous vegetation covers of wetlands and uplands and associated phenology may further complicate the interactions between surface water and groundwater. A new distributed flatwoods forest hydrologic model is needed to study the hydrologic processes of wetland/upland systems and provide a tool to evaluate the hydrologic impact of forest harvesting, specifically for this landscape.

Based on the COASTAL model (Sun, 1985), a FLATWOODS model was developed for pine flatwoods with the following specific objectives:

1. To predict spatial and temporal hydrologic effects (surficial groundwater table, runoff, soil water flux in the unsaturated zone, evapotranspiration) for forest management purposes.
2. To account for hydrologic heterogeneity and continuity of wetland/upland ecosystems and environmental

variables (e.g. precipitation);

3. To develop a tool for forest water management and hydrologic research using easily obtainable watershed and climatic information.

This paper describes model algorithms formulation, calibration, testing and are hypothetical simulation examples are given.

MODEL DEVELOPMENT

Structure Recognizing the heterogeneity, the model imposes a grid over the entire wetland-upland system to distribute the heterogeneous watershed into different, but homogeneous rectangular cells (Figure. 5.1). The physical properties of each cell are assumed to be uniform laterally for each soil layer, but non-uniform vertically in different soil layers. Each cell becomes a modeling unit that holds mathematical equations describing the physical properties. In practice, spatial data for forest lands are rarely available at high resolution with the exception of some readily available parameters such as surface elevation, vegetation and soil types (wetlands vs. uplands), etc.

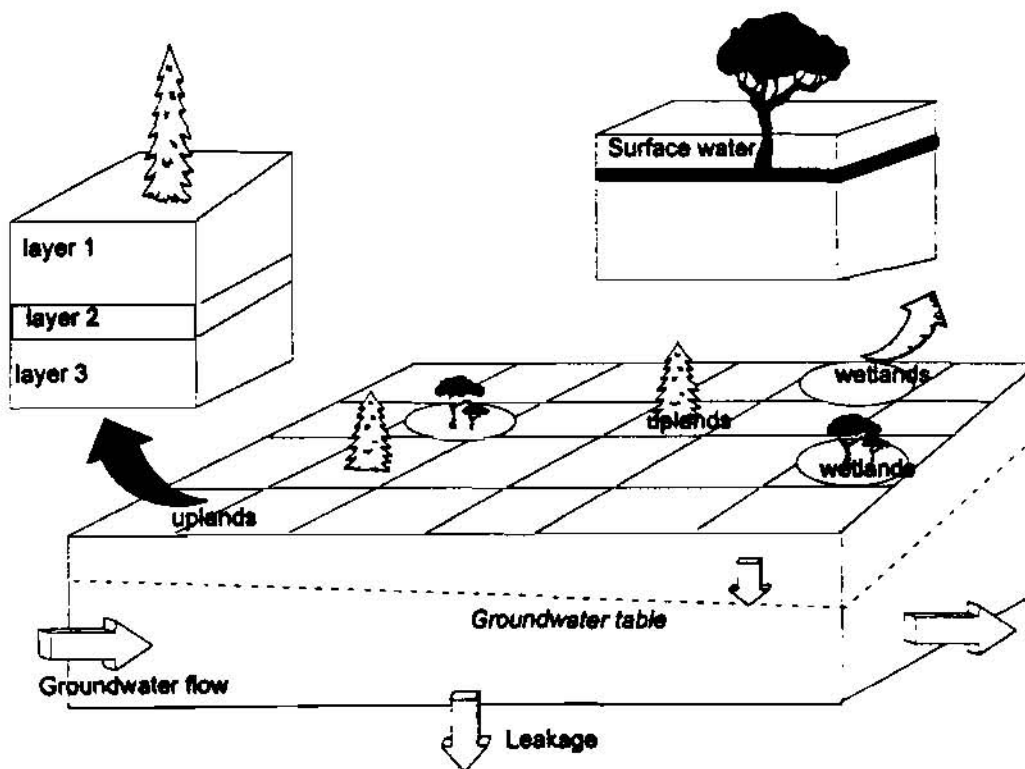


Figure 1. Structure of the FLATWOODS model showing the grid system and modeling units of pine uplands and cypress wetlands.

Hydrologic Components

Evapotranspiration Evapotranspiration is a highly significant part of the water balance of flatwoods. Driving forces for the hydrologic system are climatic variables including rainfall and air temperature (evapotranspiration). The daily rainfall and temperature data as model inputs are readily available from field recordings or a local weather station. Rainfall interception depends on daily rainfall, leaf area index (LAI) and available canopy interception storage or dryness of the forest canopy. The method by Hamon (1963) was adopted to estimate potential evapotranspiration (PET) with only daily temperature as a requirement. Evaporation of intercepted water on forest canopies has first demand on PET. Residual potential evapotranspiration (RET) is the difference between PET and evaporation from plant surfaces (intercepted rainfall on canopies). Actual evaporation (AE) from soil/water surfaces is dependent on atmospheric demand, soil water conditions and is affected by forest canopy shading. Actual transpiration (AT),

which involves physical and physiological processes, is the most difficult component to model. AT from each of the soil layer is a function of possible realized transpiration (PRT), soil water conditions, and root density. The concept of PRT is defined as the maximum transpiration that a crop can have for a certain atmospheric condition and LAI. PRT is a function of the residual potential evapotranspiration (RET), and stage of plant development indicated by LAI and root density.

Unsaturated Water Flow A maximum of three unsaturated soil layers have been used to simulate subsurface unsaturated water flow. The first layer (0-40 cm) represents the A horizon where most plant roots reside. The second layer (40-65 cm) represents the spodic horizon (B_h) where soil properties are distinct from the top layer. The third layer ranges from the 65-cm depth to the water table. The thickness in each layer varies throughout the simulation depending on water table depth. Drainage representing downward unsaturated water flow from an upper layer to a lower layer is estimated by Darcy's equation assuming a unit total potential gradient. Upward water flux represents water flow from a lower layer to an upper layer, driven by the water potential gradients induced by ET. This component is calculated in direct proportion to the ET flux in the layer. While evaporation from the soil surface takes place only from the first layer, plant roots extract water from all three unsaturated layers and the saturated zone. Soil moisture content is routed with the water balance in each layer. For some areas, such as wetlands, the soil profile may be fully saturated during part or all of the year. Percolation from the bottom of the third layer of the unsaturated zone becomes the input (source) to the underlying saturated subsystem.

Saturated Water Flow The base of the unsaturated zone becomes the upper boundary of the saturated zone. The bottom of the saturated zone has been set at the top of the clay layer about 2-3 m deep and which has a low conductivity < 10⁻³ m/day. Below this flow-restricting clay layer, which may be discontinuous in extent, often lies another intermediate aquifer composed of sands and sandy loams. Vertical flow (leakage) through the bottom of the saturated zone is estimated using an empirical function. Within the saturated zone, water moves horizontally from one cell to the surrounding four cells governed by a 2-D groundwater flow model with Dupuit assumptions (Bras, 1990). The two important parameters, specific yield and hydraulic conductivity in the groundwater flow equation, are not constant but vary depending on the position of the water table in the soil profile. The source term for the groundwater submodel is water percolation from the unsaturated zone. The sink of the groundwater flow model includes ET extracted from the aquifer, exfiltration (upward flux) from the saturated zone to the unsaturated zone, and/or surface flow from those cells if the water table is above a critical elevation.

Surface Water Flow Surface flow may occur from a grid cell under extreme wet conditions when the soil profile is saturated and the water table elevation is higher than the specified critical elevation. This situation happened in both wetlands and uplands at the study sites. Surface runoff leaving a flooded cell is modeled proportionally to the total saturated area of the entire watershed. The total daily runoff from the watershed was first simulated as a function of the average water table level, then equally distributed to each cell where overland flow occurred.

Governing Equations The core of the FLATWOODS model is the 2-D groundwater flow equation (Equation 1), which links the other two subsystems to describe the water flow in the vertical and lateral directions. In flatwoods uplands, surface flow rarely occurs unless the water table rises to the soil surface. Groundwater flow dominates the soil system during most of the time. In wetlands, however, surface water is periodically present and the overland flow may link otherwise isolated wetlands.

$$\frac{\partial(K_x \frac{\partial h}{\partial X})}{\partial X} + \frac{\partial(K_y \frac{\partial h}{\partial Y})}{\partial Y} - W = S_y \frac{\partial h}{\partial t} \quad (1)$$

where,

K_x, K_y = hydraulic conductivity along the horizontal X axis and Y axis (m/day);

h = hydraulic head (m);

W = water flux representing sources (e.g., drainage from unsaturated layers) and sinks (e.g., ET, surface runoff, leakage) (m³/day);

S_y = specific yield of the aquifer; it is not a constant, but varies with water table elevation;

Harvesting treatments were imposed from April 5 to May 31, 1994, followed by double bedding activities during the fall of 1994. The first block (16 ha) in the research area was designed as wetland + upland harvest and the second block (10 ha) as wetland harvest only. The third block (16 ha) was left untouched as a control. The harvested upland areas were planted with slash pine seedlings in January of 1995 and the cypress wetlands left for natural regeneration. Apparently, the most significant effect of the forest harvesting on model parameters was the reduction of the leaf area index. The leaf area index was assumed to be reduced to 0.5 for harvested wetlands and 0.1 for harvested uplands. Soil structure of the first layer also might have been altered due to compaction by the mechanical operations, but the change presumably was minor. Under these assumptions, the model was calibrated and validated with post-treatment data collected during June 1, 1994-May 31, 1995 (Figure 2b). The Pearson Correlation Coefficient was 0.88 and 0.82 for model calibration and verification periods, respectively.

Bradford Forest Watershed

The control watershed at the Bradford Forest in Bradford County, Florida has been monitored since 1978 (Riekerk, 1989). However, spatial water table data were limited for this study. In stead, runoff at the watershed outlet was used for model calibration and verification. The FLATWOODS model was calibrated with five years runoff data (1978-1982). The year of 1978 was a wet year (1453 mm rainfall) while the year of 1981 was a very dry year (916 mm rainfall). The model was verified with runoff data from 1983 to 1992 using the same parameters for the 5-year calibration (Figure 3). The model could not predict the extremely high flows very accurately causing underprediction of runoff in wet years (1983 and 1992). Two reasons have been hypothesized: (1) the boundary and outlet ditches in this artificially created watershed may generate higher peak flows during the wet seasons, especially in extreme years; and (2) the FLATWOODS model used a single runoff-water table level relationship independent of time to predict runoff, and no cell-by-cell surface flow routing procedures had been introduced. The assumption made in the runoff-groundwater table relationship seemed very effective since the model could also fit the low flow reasonably well during the two-year drought period of 1989 -1990.

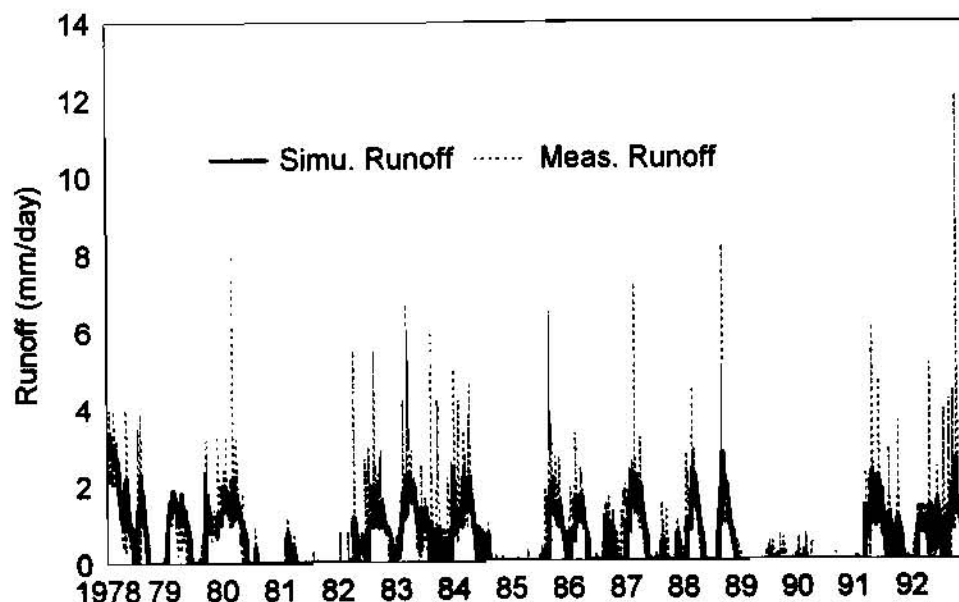


Figure 3. Flatwoods model calibration and validation using 15 years runoff data from the Bradford Forest site.

MODEL APPLICATION

Total thirteen scenarios were simulated to study the short-term (one year) and long-term (15 years) hydrologic effects of three forest management practices (wetland harvest only, upland harvest only, wetland + upland harvest) on a pine flatwoods landscape under three climatical conditions (dry, wet and normal).

Gator Nationals Forest - First Year Responses

In general, no significant difference ($\alpha = 0.001$) was found among the Control, Treatment 1 and Treatment 2 groups in affecting runoff and groundwater tables. However, wetland+ upland harvest method showed significant effects on the runoff and groundwater tables. Harvesting effects become more pronounced in a dry year than in a wet year (Figure 4). During a dry year, Treatment 1 and Treatment 2 apparently also caused significant hydrologic impacts, increasing runoff by 18-56% and the groundwater table level by about 60 cm.

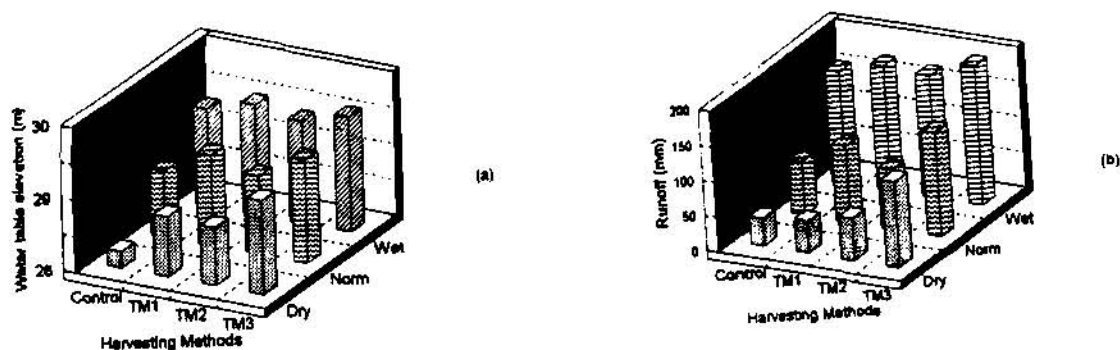


Figure 4 Simulated water table (a) and runoff (b) responses under three treatments and three climatic conditions.

Bradford Forest Watershed - Long Term Effects

The leaf area index (LAI), the only biomass accumulation indicator in the model, was assumed to reach 60% and 100% of the maximum for a mature stand at the age of five and fifteen years, respectively. Forest clear-cutting significantly raised groundwater table levels by 20-80 cm on an annual average (Figure 5). The most drastic increase occurred during dry years in 1981, 1984, 1989 and 1990 when the groundwater tables were down in the deepest soil layers, which had lower specific yield and porosity. Runoff substantially increased during the first six years 1978-1984 by an average of 200 mm after the treatment was imposed in 1978. The dry year of 1981 showed a maximum runoff increase of 12 folds during the 15-year simulation. Unlike the dry year of 1981, the two continuous dry years of 1989 and 1990 had no significant runoff increase due to the increased transpiration by recovered vegetation. The groundwater tables in 1989 and 1990 were elevated significantly but not high enough to cause the runoff to increase. The significant reduction of evapotranspiration loss of 100-300 mm after the forest removal apparently contributed to the runoff increase and the groundwater table elevation.

CONCLUSIONS

This case study suggested that pine flatwoods are storage-based hydrologic systems, where the groundwater table dictates the surface runoff and the groundwater level is controlled by both the precipitation input and the evapotranspiration output. Harvesting both wetlands and uplands showed the most significant effects on all runoff and water table compared to other treatments. Partial harvesting of wetlands or uplands also showed significant effects on the groundwater table depth, but mostly during dry seasons. Higher rainfall caused higher water table levels and runoff, but the harvesting effects decreased proportional to the increase of the rainfall amount. The 15-year long term simulation showed that runoff from the pine flatwoods had the highest increase during the first six years following treatments. The water regimes tended to recover to the norm by about the 10th year.

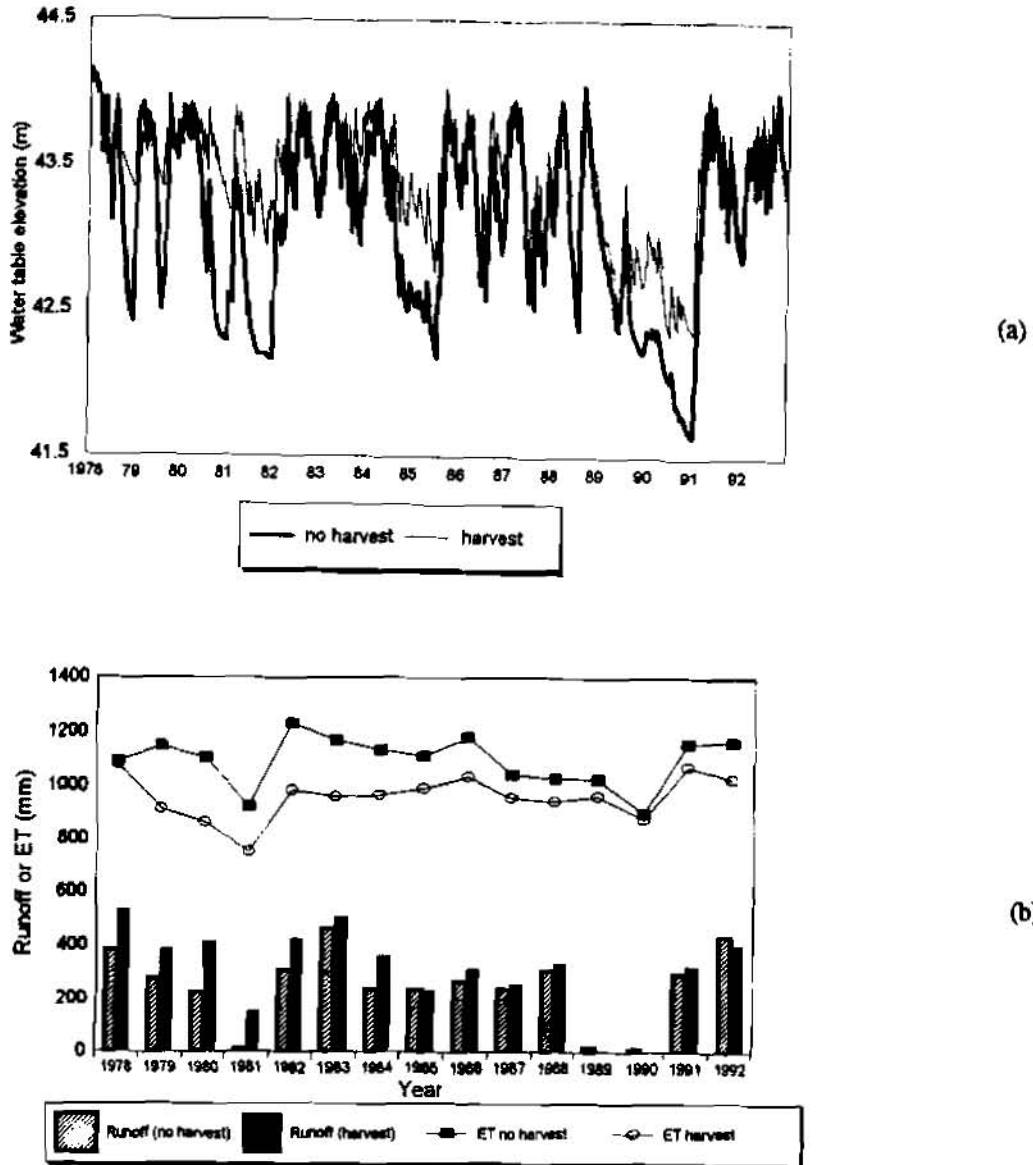


Figure 5 Longterm daily groundwater table (a) and annual runoff (b) responses at the Bradford Forest watershed.

References

- Bosch, J.M. and J.D. Hewlett. 1982. A review of catchment experiments to determine the effect of vegetation changes on water yield and evapotranspiration. *J. of Hydrology*. 55:3-23.
- Brandt, K. and K.C. Ewel. 1989. Ecology and management of cypress swamps: a review. Florida Cooperative Extension Service, IFAS, University of Florida, Gainesville.
- Bras, R.L. 1990. Hydrology - An Introduction to Hydrologic Science. Addison-Wesley Publishing Company. 633p
- Campbell, K.L., J.C. Capece, T.K. Tremwel. 1995. Surface/subsurface hydrology and phosphorus transport in the Kissimmee River Basin, Florida. *Ecological Engineering*. 5:301-330.
- Crownover, S.H., N.B. Comerford, and D.G. Neary. 1995. Water flow patterns in cypress/pine flatwoods landscapes. *Soil and Sci. Soc. Amer. J.* 59:1199-1206.
- Cubbage, F.W. and C.H. Flather. 1993. Forested wetland are and distribution: A detailed look at the South. *J. For.* 91:35-40.
- Ewel, K.C. and H.L. Gholz. 1991. A simulation model of the role of belowground dynamics in a Florida pine plantation. *Forest Science*. 37:397-438.
- Guo, W. 1989. Simulation of stormflow from a pine flatwoods watershed. M.S. Thesis, Univ. of Florida, 99p.
- Hamon, W.R. 1963. Computation of direct runoff amounts from storm rainfall. *Int. Assoc. Sci. Hydrol. Pub.* 63:52-62.
- Heatwole, C.D., K.L. Campbell and A.B. Bottcher. 1987. Modified CREAMS hydrology model for coastal plain flatwoods. *TRANSACTIONS of the ASAE* 30:1014-1022.
- Jensen, K.H., and A. Mantoglou. 1992. Future of distributed modelling. *Hydrological Processes*. 6:225-264.
- Knisel, W.G. 1980. CREAMS: A field-scale model for chemicals, runoff, and erosion from agricultural management systems. Conservation Research report No. 26. USDA, Washington, DC.
- Lovejoy, S.B., J.G. Lee, T.O. Randhir and B.A. Engel. 1997. Research needs for water quality management in the 21st century: A Spatial Decision Support System. *J. of Soil and Conservation*. 52(1):18-22.
- Maidment, D.R., 1993, GIS and hydrologic modeling. In *Environmental Modeling with GIS*. Goodchild, M.F., B.O. Parks and L.T. Steyaert, Eds, Oxford University Press, New York, 488 pp.
- McCarthy, E.J. 1992. Hydrologic model for drained forest watershed. *J. of Irrigation and Drainage Engineering*. 118:242-255.
- Riekerk, H. 1989. Influence of silvicultural practices on the hydrology of pine flatwoods in Florida. *Water Resour. Res.* 25:713-719.
- Riekerk, H. and L.V. Korhnak. 1984. Environmental effects of silviculture in pine flatwoods. In: Third Biennial Southern Silvicultural Research Conference, Ed. E. Shoulders, U.S. Forest Service, Gen. Tech. Report. SO-54:528-535.
- Sabine, J.B. 1994. Application of minor drainage on non-industrial private lands. In *Proceedings Water Management In Forested Wetlands*. USDA Forest Service, 158 p.
- Shepard, J.P., L.A. Lucier, and L.W. Haines. 1993. Industry and forest wetlands: Cooperative Research initiatives. *J. Forestry*. (91)5:29-33.
- Skaggs, R.W. 1984. DRAINMOD - a water management model for shallow water table soils. User's Guide. Univ. of North Carolina.
- Swank, W.T. and Crossley, D.A., Jr. 1988. Forest hydrology and ecology at Coweeta. *Ecological Studies*, Vol. 66., Springer-Verlag, New York, pp. 297-312.
- Swank, W.T., S.G. McNulty, and L.W. Swift. 1994. Opportunities in forest hydrology research from broad environmental perspectives. Ohta, T. (Ed.). In *Proceedings of the International Symposium on Forest Hydrology*. Tokyo, Japan, October. University of Tokyo, Tokyo. pp. 19-29.
- Wigmosta, M.S., L.W. Vail and D.P. Lettenmaier. 1994. A distributed hydrology-vegetation model for complex terrain. *Water Resour. Res.* 30:1665-1679.

Contact: gesun@unity.ncsu.edu; <http://sgcp.ncsu.edu/>

MODELING PRAIRIE SNOWMELT RUNOFF

Joseph A. Van Mullem, Hydraulic Engineer, Natural Resources Conservation Service, Bozeman, Montana

Abstract: Snow depth frequency and temperature-duration-probability (TDP) data were used with HEC1 to model snowmelt runoff on the prairies of eastern Montana. Snow water equivalent (SWE) was spatially distributed with pseudo elevation zones. A temporal distribution of temperatures was developed. The model was calibrated with volume-duration-probability data from snowmelt runoff. The effect of coincident frequencies of SWE and temperatures was determined.

INTRODUCTION

In the semi-arid northern Great Plains region of the US, snowmelt provides much of the annual water supply. Between 50 and 80 percent of the average annual runoff in eastern Montana occurs during February, March, and April primarily as a result of snowmelt (NRCS 1991). These snowmelt events are characterized as having longer duration and larger runoff volume than later spring and summer rainfall events. Because of this, they are more reliable for filling reservoirs and waterspreading systems. Snowmelt also provides most of the water for wetlands and contributes significantly to sheet, rill, and gully erosion.

This study adds to two previous studies which characterize snowmelt runoff in eastern Montana. One of these analyzed the frequency of snow depth (Van Mullem 1992), and the other described the runoff volumes from spring snowmelt (Van Mullem 1994). Snow depths ranged from six to 12 inches for the 50 percent chance and from 20 to 50 inches for the one percent chance. Most of the runoff events are less than seven days duration which corresponds to the time required to completely melt the snow. Most of the water infiltrates into the soil and the 25-year, 7-day runoff volume from a SWE which may exceed six inches, seldom exceeds one inch.

GOAL AND OBJECTIVES

The goal of this study was to improve our understanding of prairie snowmelt runoff. This information is to provide guidance in modeling techniques to the field engineers and hydrologists to develop snowmelt hydrographs. These can be used in design and analysis of hydraulic structures and land and water conservation measures in the area.

The objectives of this study were to:

1. Determine the temperature-duration-probability (TDP) characteristics in the eastern Montana prairie region.
2. Use this TDP data together with snow depth frequency data to produce runoff hydrographs with a model.
3. Calibrate the model output to fit watershed data obtained for the spring season by volume-duration-probability (VDP) analysis.

This will also provide a method for the field engineer to develop both the runoff volume and peak discharge frequency curves from the snow depth frequency curves. This has been a standard technique for many years with rainfall runoff, but has not normally been done with snowmelt probably because snow depth and temperature frequency data have not been readily available.

Temperature-Duration-Probability

The frequency analysis of maximum temperature for several duration's is termed Temperature-Duration-Probability analysis or TDP. TDP was done for nine stations in eastern Montana. The daily mean temperatures for the thirty year period 1961-1990 was obtained from the NRCS National Water and Climate Center. The maximum 1-, 3-, and 7-day values were found by month for February, March, and April by using a spreadsheet program. The month for the 3 or 7 day period was the month of the last day in the period (e.g., the period starting March 26 and ending April 1 was included in the April data). The Log Pearson III frequency distribution was used to determine the exceedance probability of the temperatures.

The variability of annual temperature maximum is not great. The coefficient of variation of the logarithms of the 7-day values averaged only 1.57. This means that the 50-year temperature is only 20% more than the 2-year temperature.

When degree-days at a particular frequency are plotted against days we get TDP curves as shown on Figure 1. Degree-days as used here is the sum of the temperatures for consecutive days in degrees above zero degrees F, and should not be confused with melting degree-days above 32 degrees F. The lines can be represented with a power function:

$$T_D = aD^b \quad (1)$$

where T_D is the accumulated degree-days for a duration of D days. It was found for the stations analyzed that the exponent b varied from 0.925 to 0.954 over all frequencies and all stations. That is, the lines are nearly parallel, as shown on Figure 1. The entire family of curves can be represented quite accurately with the exponent b of 0.935. The value of a in equation 1 is the 1-day maximum temperature.

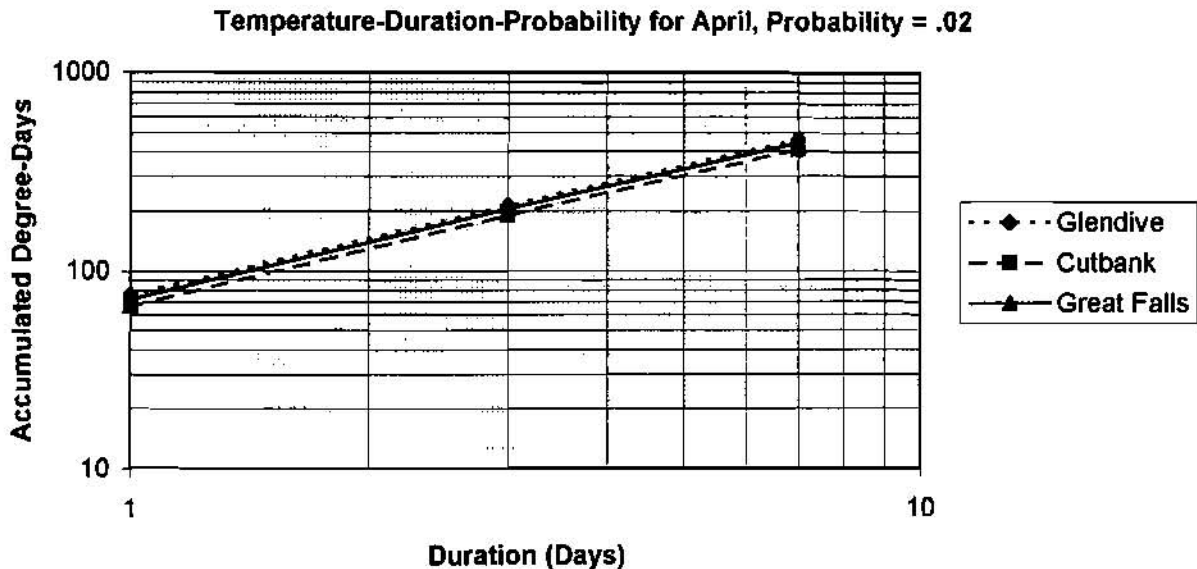


Figure 1. TDP curves for 50-year return period for April at three stations in eastern Montana.

The ratio of the 1-day to the 7-day can be found from equation 1, and results in the relationship:

$$T_1 = 0.162 T_7 \quad (2)$$

T_D for other duration's may be found in a similar manner from equation 1, and the temperature for the n^{th} day may be found by deducting the sum of the $n-1$ day. In this way a temperature is found for each day in the melt period from T_7 .

The 50-year, 7-day maximum degree-days for April is shown in Figure 2. The 7-day maximum degree-day temperature can also be estimated at a weather station with the equation:

$$T_{7.50} = 7.425 T_{\text{APRIL}} + 116.3 \quad (3)$$

where $T_{7.50}$ is the 50-year, 7-day maximum degree-days and T_{APRIL} is the mean April temperature at the station. The correlation coefficient, r , is 0.89, and the standard error of estimate is 6.8.

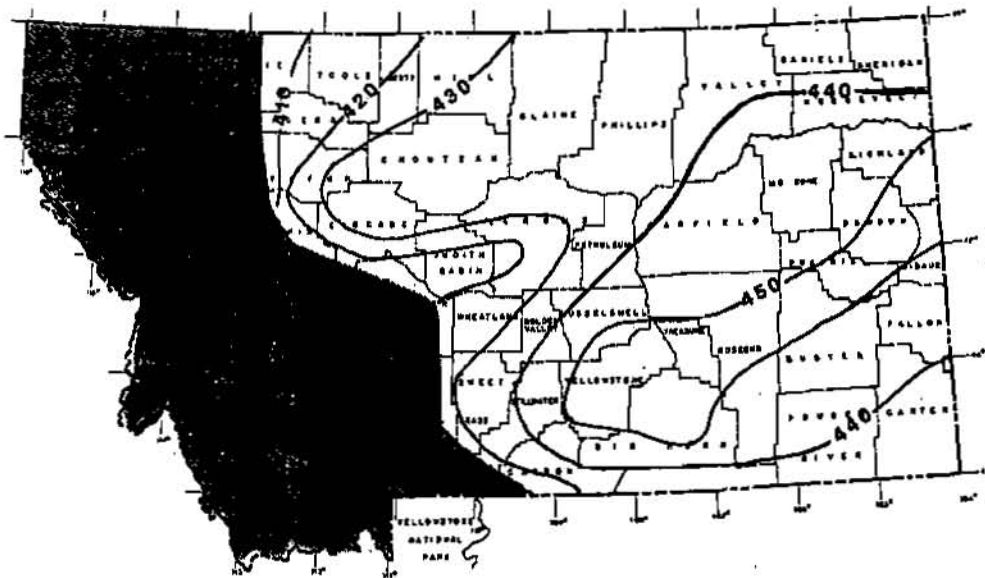


Figure 2. Maximum April 7-day temperature (degree-days), 50-year return period.

TEMPORAL DISTRIBUTION OF TEMPERATURE

Under actual conditions, it takes some time and heat to bring the snow to melting temperature, i.e., isothermal at 32 degrees F. The HEC1 model (Corps of Engineers 1990) does not consider this, nor does it allow the melt coefficient to be varied during the melt period. The snowpack is therefore considered to be isothermal at the start of the event. The most critical time for the temperature is the first or second day when all of the snow is available to melt.

It was observed that the maximum daily temperature does not normally occur on the first or second day of the melt period. An analysis of one station showed a wide variability with an average of six days of melting temperatures before the maximum day. For the modeling it was decided to have the maximum day occur on the fifth day. The second largest was placed sixth and the third largest fourth, etc., creating a temporal distribution with the highest values near the center.

The average diurnal variation for temperatures in April in the region is 30 degrees F. The HEC1 model distributes the daily temperature with a sine curve between the minimum and the maximum. This permits

the model to more accurately represent the diurnal variation of runoff and to more nearly predict the peak discharge.

Figure 3 shows the eight day temperature sequence that results from a 50-year, 7-day value of 450 degree-days. If a different 7-day value is needed, the values in figure 3 may be multiplied by the ratio of the desired 7-day value to 450.

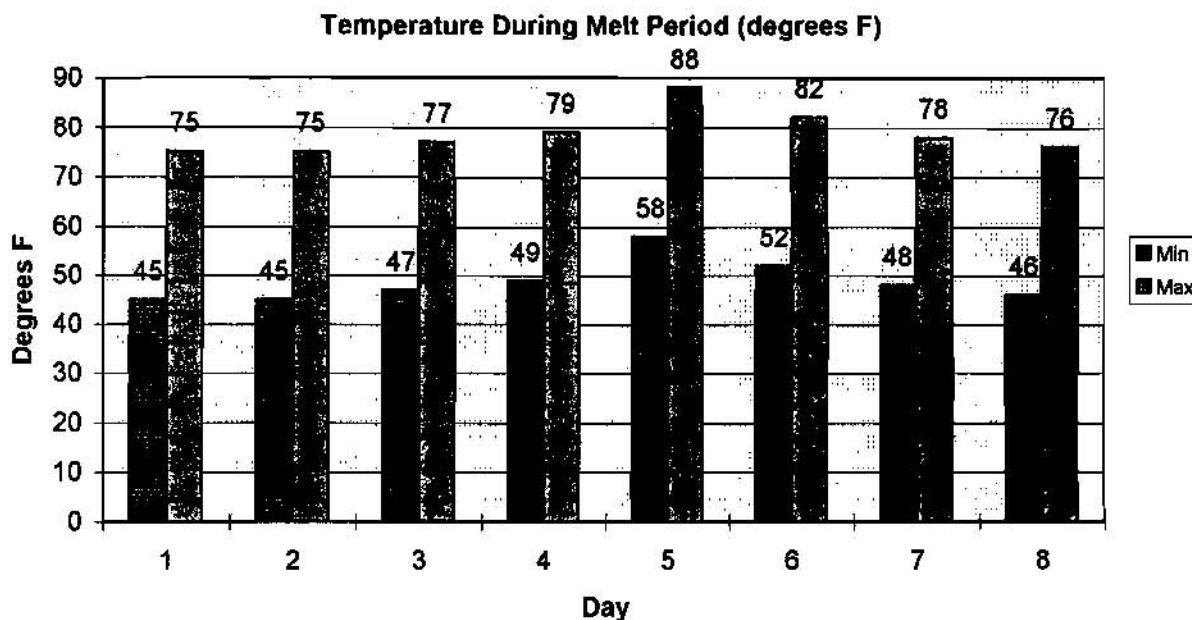


Figure 3. Temperatures during melt period for $T_7 = 450$.

Because of the uniformity found in temperature characteristics between stations, it is also possible to apply a ratio to the different return periods which may need to be analyzed. Table 1a lists these factors for common return periods. The temperature variation between months is also relatively uniform, and average values are shown in table 1b.

Table 1. Temperature factors for various return periods and months.

a. For return periods.		b. For months	
Return Period	Factor	Month	Factor
2-year	.832	February	.74
5-year	.900	March	.83
10-year	.930	April	1.00
25-year	.970		
50-year	1.00		
100-year	1.02		

For example, if the temperature distribution for a 25-year return period for March is needed for a location on figure 2 where the April 50-year, 7-day value is 430 degree-days, the following factor would be used:

$$430/450 \times .97 \times .83 = .77$$

Multiply 0.77 times each of the temperature in figure 3 to obtain the distribution.

SPATIAL VARIABILITY OF PRAIRIE SNOWPACK

The prairie snowpack is not uniform, but varies spatially over the watershed. Unlike mountain watersheds where snow depth is related to snowfall or elevation, prairie snow varies mostly because of aspect and wind. South facing slopes will have less and north facing slopes more snow, while windswept areas may be nearly bare and drifts in draws and coulees very deep. The spatial variability in wind blown areas has been related to vegetation type and height (Caprio et. al. 1986) (Donald et. al. 1995).

This spatial variability is important because it effects the contributing area during the melt period. The HEC1 model is set up with elevation zones and does not have a percent cover factor. Each sub-basin can have up to ten elevation zones, each with its own SWE at the start of the melt period. Although elevation differences in prairie watersheds may be only a few hundred feet, the elevation zones in the model permit us to vary the SWE in the watershed.

Pseudo elevation zones were used in the HEC1 model to represent the spatial variability of the SWE. Several distributions were tried to see which gave consistent and reasonable results. Specific field data was not available and only a general knowledge of the variability was used as a guide. If the snow is not distributed the model results show a discontinuity at lower SWE values. This results because the snow is gone all at once. When the snow lasts through the warmest day a high outflow results, but when it doesn't the outflow rapidly declines.

Figure 4 shows four distribution patterns tested with the model. The patterns shown in figure 4a and 4b fit the normal distribution while 4c is bimodal and 4d is uniform. Patterns with three and seven zones were also tested. No improvement was observed for using seven zones instead of five. The frequency of each SWE zone is equivalent to the fraction of the total area in that zone.

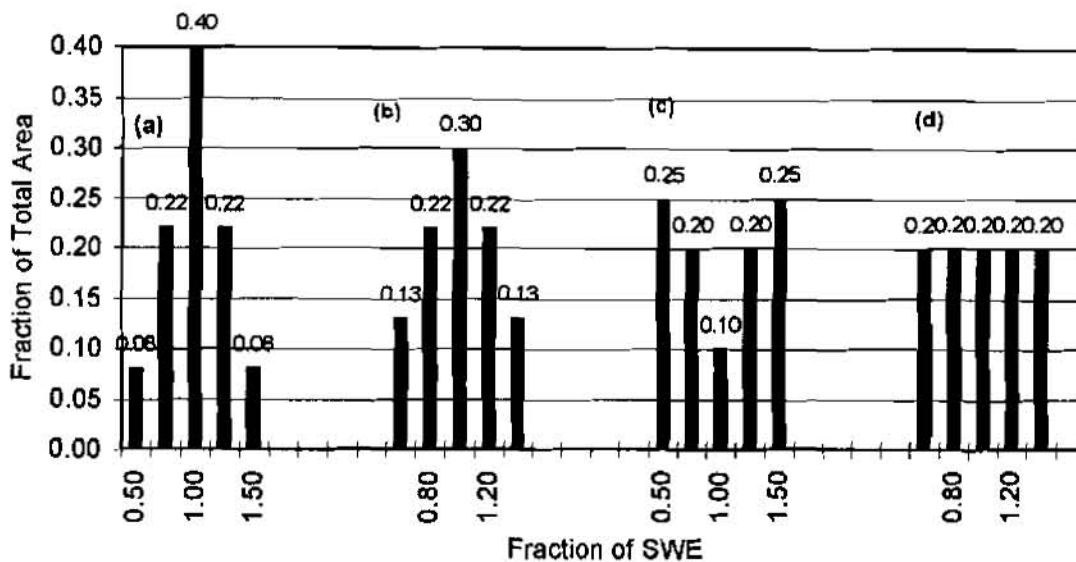


Figure 4. Snow distribution patterns.

In addition to the ratios of SWE to average SWE shown on the abscissa of figure 4, three other ratios sets were tested. These are shown in table 2. Each set of ratios is balanced so that the average SWE over the watershed is constant.

Table 3 shows the results of a series of runs with different snow distributions. All of the runs had an average SWE of 4.0 inches and used the same temperature distribution and other parameters. The 7-day runoff shown in the table does not vary much because all of the snow melted in all of the cases. The 1-day runoff shows some variation and the peak discharge shows more variation.

Table 2. Fraction of average SWE in each zone.

Zone	Factor (.5-1.5)	Factor (.6-1.4)	Factor (0-2.0)	Factor (uniform)
1	.5	.6	0.0	1
2	.8	.83	.6	1
3	1.0	1.0	1.0	1
4	1.2	1.17	1.4	1
5	1.5	1.4	2.0	1

Table 3. Effect of different spatial distributions of snow over a watershed on runoff

Distribution	SWE range	1-day (inches)	7-day (inches)	Peak Discharge (cfs)
Normal 1	.6-1.4	.402	.990	7026
Normal 1	.5-1.5	.392	1.005	6808
Normal 1	0.0-2.0	.338	1.080	5515
Normal 2	.6-1.4	.379	.999	6621
Normal 2	.5-1.5	.367	1.022	6404
Normal 2	0.0-2.0	.317	1.136	5090
Bimodal	.6-1.4	.327	1.019	5681
Bimodal	.5-1.5	.316	1.060	5468
Uniform	.6-1.4	.350	1.010	6084
Uniform	.5-1.5	.339	1.044	5871
Uniform	Uniform	.468	.960	7863

It is difficult to select one distribution over another since most of them can be calibrated to the desired results. However, the Normal 2 distribution with the SWE range of 0.5 to 1.5 times the average SWE was selected because it provided mid-range output over a range of snow depth frequencies. This distribution is similar to those described in southern Ontario (Donald et al 1995).

SNOW DENSITY

There was not enough data to do a frequency analysis on SWE so it was done on snow depth (Van Mullem 1992). It is therefore necessary to estimate snow density to convert these depths to SWE. The density of snow varies widely from about 0.1 to 0.5 in/in from the time it falls to the time it is melting. Because the maximum depth of the snow occurs just after a snowfall, it was assumed that most of the measured depth would be new snow. An average value of 0.15 in/in was used to convert snow depth frequency to SWE. The actual value is not as important as the assumption that the value is a constant over the range of snow depths used in the analysis. If the average value is in error that can be compensated for with calibration of the melt coefficient and the infiltration losses. If the density is not constant, the SWE frequency curve will have a different slope than the snow depth frequency curve.

MELT COEFFICIENT AND INFILTRATION LOSSES

The simple temperature melt model uses the equation:

$$M = C (T-32) \quad (4)$$

Where M is the daily snowmelt in inches of SWE, T is the temperature in degrees F., and C is the melt coefficient in inches/degree-day.

The melt coefficient for the study area was chosen so that 40 inches of snow at a density of 0.15 would completely melt in seven days with temperatures at the 10-percent probability level. This results in a factor of about 0.05 over most of the region.

The HEC1 model allows only two methods of computing infiltration loss from snowmelt. These are the initial loss-constant rate method, or the exponential loss rate method. The exponential rate method was selected because of its greater versatility. The values in the model were adjusted until the computed runoff volume matched the gauged data or map values developed in the previous study (Van Mullem 1994).

For the modeling of synthetic events it is intended to use the infiltration loss as the primary method of calibration from site to site. One of the difficulties of snowmelt modeling for the inexperienced user is in calibrating the model since almost any result can be obtained by varying the model parameters within their normal range. With the SWE distribution, temperatures, and melt coefficient fixed, it is only necessary to adjust the infiltration losses until the runoff volume is the desired amount.

The runoff is quite sensitive to the initial loss rate factor as shown for an example watershed in figure 5. The figure shows the typical range of variation for the 1-day and 7-day runoff values.

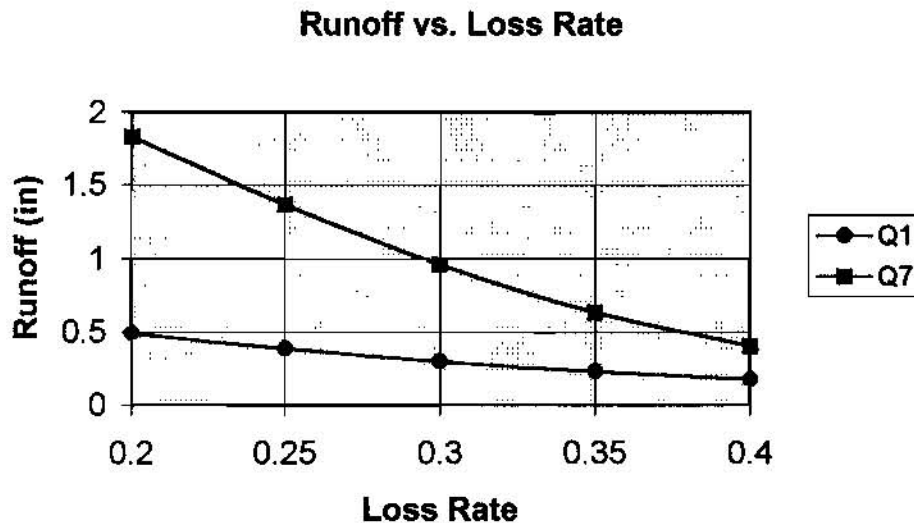


Figure 5. Example of typical runoff vs. initial loss rate.

COINCIDENT FREQUENCY

Snowmelt runoff is primarily the result of the interaction of two separate events: the amount of snow on the ground and the temperature during the melt period. Each of these conditions is independent of the other and each has its own magnitude-frequency relation. To determine the runoff for a specific probability it is necessary to analyze all probable combinations of SWE and temperatures. However, as with many other hydrologic events, it is not usually necessary to perform this much analysis, and some "average" condition is taken for one or more of the variables. To test the effect of coincident frequency on

snowmelt runoff in eastern Montana modeling was done over a wide range of temperature and SWE values.

The probability of two independent events occurring coincidentally is the product of the probability of each occurring (Johnson 1994). By using temperatures and SWE that varied from the two- to the 80-percent chance, a coincident frequency curve was developed for a watershed in the area. This was done by developing a coincident frequency table (Hansen 1988). Each modeled discharge represents a probability interval of both SWE and temperature. The probability of the event is the product of these two intervals. The probability of the discharge being greater than a certain value is the sum of all the entries that are greater than the value.

The coincident frequency curve for peak discharge was compared to frequency curves from a single temperature distribution applied to the range of SWE values. The 50-percent chance temperature resulted in a curve that fit the coincident curve very well between the 10- and 2-percent chance levels. However it resulted in much lower values at the 50-percent chance level. It is recommended to use the 20-percent chance temperature distribution to model snowmelt in eastern Montana. The resulting frequency curve has the same shape as the coincident curve and also more nearly matches the shape of the watershed gaged data.

SUMMARY

TDP data was developed for the eastern Montana prairie region. By using this data together with SWE probability data, snowmelt runoff modeling is much easier. Recommendations are made for the temporal distribution of temperature and the spatial distribution of SWE. When used in the HEC1 model, this information will enable the field engineer to develop realistic hydrographs for use in water resource design and evaluations.

REFERENCES

- Caprio, J. M., Grunwald, G. K., Snyder, R. D., and Cleary, E. C., 1986, Effect of Standing Small Grain Stubble on Snow Cover Characteristics. *Agronomy Journal* 78, 99-106.
- Corps of Engineers, 1990, HEC-1 Flood Hydrograph Package.
- Donald, J. R., Soulis, E. D., Kouwen, N., Pietroniro, A., 1995, A land cover-based snow cover representation for distributed hydrologic models. *Water Resources Research* 31, 995-1009.
- Hansen, W. W., 1988, Is normal high water really normal? *Floodplain Harmony, Proceedings of the 12th Annual Conference of the Association of State Floodplain Managers*, 315-320.
- Johnson, R. A., 1994, *Miller & Freund's Probability and Statistics for Engineers*, Prentice Hall, Englewood Cliffs, New Jersey.
- Natural Resources Conservation Service, 1991, *Water Yield for Beneficial Use, Montana Supplement 2, Engineering Field Manual Chapter 2*, Bozeman, Montana.
- Van Mullem, J. A., 1992, *Snow depth frequency in eastern Montana*, ASAE paper no. PNW 92104, Bozeman, Montana.
- Van Mullem, J. A., 1994, *Seasonal Runoff Volumes in Eastern Montana*, ASAE paper no. 942130, Kansas City, Missouri.

COMPARISON OF NINE UNCALIBRATED RUNOFF MODELS TO OBSERVED FLOWS IN TWO SMALL URBAN WATERSHEDS

By Phillip J. Zarriello, Hydrologist, U.S. Geological Survey, Ithaca, New York

Abstract: Nine uncalibrated runoff model results—CASC2D, CUHP, CUHP/SWMM, DR3M, HEC-1, HSPF, PSRM, SWMM, and TR20 were compared to observed flows in two small urban watersheds with distinctly different climatic and physiographic settings; a 3.10 mi² semiarid moderately-sloped watershed near Denver, CO, and a 0.14 mi² coastal watershed with steep slopes near Seattle, WA. All models were run by experienced modelers using identical data provided on selected basin characteristics and rainfall that are readily available to the engineering community. Observed streamflow was not provided, and thus the results are dependent on modelers' judgment and the ability to conceptually and quantitatively represent the hydrologic system. Data for six storms in each watershed (antecedent conditions, rainfall volume, intensity, and duration) were provided. Simulated peak flows differed from observed peak flows by as much as 260 percent and simulated storm volumes differed from observed storm volumes by as much as 240 percent. The average root mean square model error (RMS) was slightly larger for peak flows in the coastal watershed (68) than in the semi-arid watershed (55), whereas the RMS for storm volume was about the same in the two watersheds (54 and 56, respectively). In general, the models based on the SCS curve number had the poorest fit. Results indicate simulated flows from uncalibrated models have wide variability for both types of watersheds; this could result in over- or underdesign of stormwater-management structures.

INTRODUCTION

Planning and design of stormwater-drainage systems, culverts, detention basins, and other stormwater facilities requires information on storm peak flows and runoff volumes. Rainfall-runoff models, often utilized to estimate this information, vary in complexity, functionality, and applicability to a given region or storm type, but only through a process of calibration and verification can reliable results be acquired. Uncalibrated models are often used, however, because either the information needed for calibration and verification are unavailable, or the expense of these procedures can not be justified. Little information is available on the reliability and error associated with the use of an uncalibrated model.

To determine the variability of uncalibrated flow simulations across a range of model types, a simple comparison of nine selected, nonproprietary, runoff models were made for six storms in each of two small urban watersheds with distinctly different climatic and physiographic settings; Harvard Gulch, a semi-arid watershed near Denver, CO, and Surrey Downs, a coastal watershed in the Pacific Northwest near Seattle, WA. Each of the models were run by experienced modelers using only data provided on selected basin characteristics, antecedent storm conditions, and storm rainfall that are typically available to the engineering community. Observed streamflow were not provided and the models were run without being calibrated. Thus, model results are dependent on modelers' judgment and the ability to conceptually and quantitatively represent the hydrologic system. This paper describes the results of the uncalibrated models.

Acknowledgments: Numerous people provided their time and expertise to perform model simulations— Dr. Gret Aron, Penn State Univ. (PSRM); Darryl Davis, Arlen Feldman, Gary Brunner, Dr. David Goldman, and Stephen Breithaupt, U.S. Army Corps of Engineers (HEC-1); Richard Dinicola, U.S. Geological Survey (HSPF); Dr. Pierre Julien, Scott Hogan, Aaron Egbert, James White, and James Light, Colorado State Univ. (CASC2D); Tania McNutt, Colorado State Univ. (CUHP); Michael Schunidt, Camp, Dresser and McKee (SWMM). The ASCE Urban Water Resources Research Council, particularly Ben Urbonas, provided the initial idea and support for this study.

RAINFALL-RUNOFF MODEL CHARACTERISTICS

Runoff models differ mainly in the methods used to generate runoff and to route it through a basin; they also differ in the control options available, data handling, and user interface, but these differences generally have little or no effect on how the model computes runoff. The test models (summarized in table 1) calculate runoff (excess precipitation) by one of the following; (1) SCS curve number, (2) Horton's equation, or (3) continuous soil moisture accounting. The SCS curve number is the most widely used method because of its relative simplicity; it defines the watershed storage and is determined for a watershed or sub-watershed predominantly from the types of soils, vegetative cover, and land-use characteristics (Soil Conservation Service, 1986). Horton's equation assumes that the soil infiltration rate decreases exponentially as a function of time since the storm began. Some models account for soil-moisture stor-

age and infiltration using either the Green-Ampt or Phillips equation, or a variation thereof. The PSRM model uses the SCS curve number for determining soil infiltration, but uses soil moisture accounting to determine available storage. These models are either continuous or quasi-continuous (soil-moisture accounting is continuous, but routing is only performed only for a specified storm period), but continuous meteorologic data was not made available for this test, thus modelers were required to estimate initial starting conditions for each storm. Soil moisture accounting and infiltration procedures generally are more data-intensive than the SCS curve and Horton methods, and require a number of parameters corresponding to physical soil-water storage and infiltration characteristics.

Table 1. Characteristics of rainfall-runoff models [Some models have several options for runoff generation and flow routing, but only the option used for this study is identified].

Model	Simulation Type	Runoff Generation	Overland Flow	Channel Flow	Watershed Representation
CASC2D*	Event	Soil moisture accounting	Cascade	Diffusive wave	Distributed
CUHP†	Event	Horton	Unit hydrograph	Unit hydrograph	Lumped
CUHP/SWMM‡	Event	Horton	Unit hydrograph	Unit hydrograph	Distributed
DR3M**	Quasi-continuous	Soil moisture accounting	Kinematic wave	Kinematic wave	Distributed
HEC-1††	Event	SCS-curve no.	Unit hydrograph	Muskingum	Distributed
HSPF‡‡	Continuous	Soil moisture Accounting	Kinematic wave	Kinematic wave	Distributed
PSRM***	Quasi-continuous	SCS-curve no.& Soil moisture	Cascade	Kinematic wave	Distributed
SWMM†††	Event	Horton	Kinematic Wave	Kinematic Wave	Distributed
TR20‡‡‡	Event	SCS curve no.	SCS unit hydrograph	SCS unit hydrograph	Lumped

*. CASC2D - Cascade 2-Dimensional (Julian and Saghaian, 1991)

†. CUHP - Colorado Unit Hydrograph Procedure (Urban Drainage and Flood Control District, 1984)

‡. CUHP/SWMM - Subbasin application of CUHP linked together with SWMM

** DR3M - Distributed Rainfall Routing Runoff Model (Alley and Smith, 1982)

††. HEC-1 - Hydrologic Engineering Center (1990)

‡‡. HSPF - Hydrologic Simulation Program Fortran (Bicknell and others, 1993)

***. PSRM - Penn State Runoff Model (Aron and others, 1996)

†††. SWMM - Storm Water Management Model (Huber and Dickinson, 1988)

‡‡‡. TR20 - Technical Release No 20 (Soil Conservation Service, 1983)

Once excess precipitation is determined, surface runoff is calculated for overland flow and channel flow by one of the following methods: (1) unit hydrograph, (2) SCS triangular unit hydrograph, or (3) by solving equations for flow. The unit-hydrograph procedure derives a hydrograph by assuming a specific shape that represents land-use, soil, and geometry characteristics of the watershed, although techniques are available to derive the unit hydrograph from observed rainfall-runoff data, this data was not made available in this study. The SCS triangular unit hydrograph is an approximation of a nonlinear runoff distribution that is assumed to be constant in a unit hydrograph method. A number of methods exist for solving equations for flow. The Muskingum method is used for channel routing by determination of a wedge-shape channel storage in relation to inflow and outflow channel volume. Overland flow and channel routing is performed in some models by kinematic wave to solve the continuity equation for flow or by diffusive wave, which includes an additional pressure-differential term (Miller, 1984). The cascade method is a two-dimensional kinematic wave approximation for routing overland flow (Julien and others, (1995). Models that use the kinematic or diffusive wave routing differ by how overland flow and channel characteristics are specified.

MODEL DATA DESCRIPTION

Watershed Characteristics: Two small urban watersheds were selected for model simulations that differed in size, climate, and drainage characteristic. Information about the watershed that is typically readily available to the engineering community was provided to each modeler; this included a base map and tabular data on topography, buildings, roads, soils, and drainage characteristics.

Surrey Downs watershed (fig. 1A) is a 0.14 mi² area of mostly single-family residential land-use. The basin is about 2.5 times as long as wide and is drained entirely by a closed-pipe storm-sewer system. Base flow was given as 0.02 ft³/s. Most streets have curb and gutter that drain to the storm-sewer system. Relief is about 150 feet, with slopes upwards of 20 percent. Impervious area is about 30 percent of the watershed, with about 20 percent being effective impervious area. Modelers were provided with details on the types of impervious areas, but not by subbasin. Figure 1A does not show details of the storm-sewer system including pipe diameter, length, invert elevations, slope, material, and soil characteristics that were provided to the modelers. Soils are gravelly-sandy loam to fine-sandy loam. Additional details on the watershed are reported by Ebbert and others (1985).

Harvard Gulch watershed (fig. 1B) is a 3.10 mi² area of mixed urban land-use. The basin is about twice as long as wide and is drained by a combination of storm sewers and open channels. Base flow ranges from 2.1 and 5.6 ft³/s. Relief is about 150 feet with slopes generally ranging from about 2 to 0.5 percent. Impervious area covers about 38 percent of the watershed. Modelers were provided delineations, area, and percent impervious area for 33 subbasins, but were required to determine the effective impervious area where appropriate to the model. This task was made somewhat more difficult by a map of poor reproductive quality, a problem not uncommon in the real world. Soils are SCS Group B. (Ben Urbonas, Urban Drainage and Flood Control, Denver, C.O., written commun., 1990)

Storm Characteristics: Harvard Gulch and Surrey Downs watersheds are in distinctly different climatic regions. Harvard Gulch is in a semi-arid region with typically dry antecedent conditions and storms that are usually of short duration and high intensity. Surrey Downs is in the coastal Pacific Northwest, where antecedent conditions are typically wet and storms are usually of low intensity and long duration.

Table 2. Summary of storm characteristics used in runoff model test [All values are in inches].

Storm	Duration (hr:min)	Volume* (in)	Maximum Intensity (in) [†]			Antecedent Precipitation (in)			
			5 min	15 min	60 min	1 day	3 day	7 day	14 day
Harvard Gulch Watershed									
1981/5/8	00:50	1.04	0.63	0.99	1.56	-	-	-	-
1983/6/5	02:10	0.65	0.32	0.77	1.00	-	-	-	-
1985/5/17	01:05	0.39	0.26	0.32	0.62	-	-	-	-
1985/7/19	01:35	1.05	0.35	0.67	1.25	-	-	-	-
1987/6/9	01:00	0.27	0.11	0.24	0.40	-	-	-	-
1987/6/30	02:40	0.54	0.08	0.20	0.54	-	-	-	-
Surrey Downs Watershed									
1980/4/18	20:00	0.54	0.05	0.07	0.12	0.00	0.00	0.30	1.39
1980/8/17	08:00	0.58	0.08	0.18	0.34	0.03	0.03	0.03	0.03
1981/6/30	09:00	0.25	0.03	0.08	0.18	0.00	0.00	0.00	0.20
1981/9/20	09:00	0.12	0.03	0.06	0.09	0.04	0.48	0.48	0.40
1981/12/1	20:00	0.55	0.06	0.10	0.12	0.12	0.15	0.15	2.03
1981/1/15	24:00	0.97	0.02	0.04	0.14	0.00	0.05	0.36	0.36

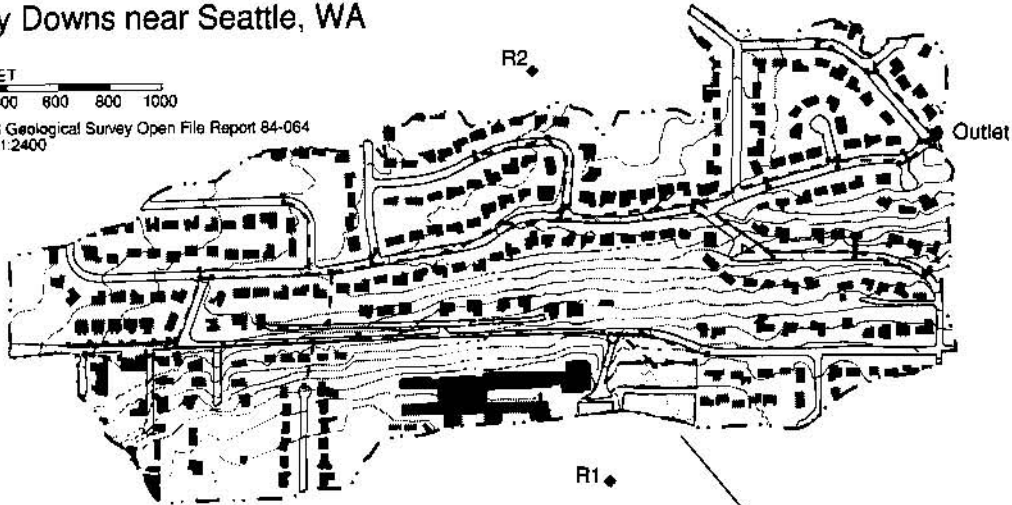
*. Volumes are the average for all rain gages.

†. Maximum intensity reported among all rain gages.

A. Surrey Downs near Seattle, WA

SCALE IN FEET
0 200 400 600 800 1000

Base from U.S Geological Survey Open File Report 84-064
Plate 1, Scale 1:2400

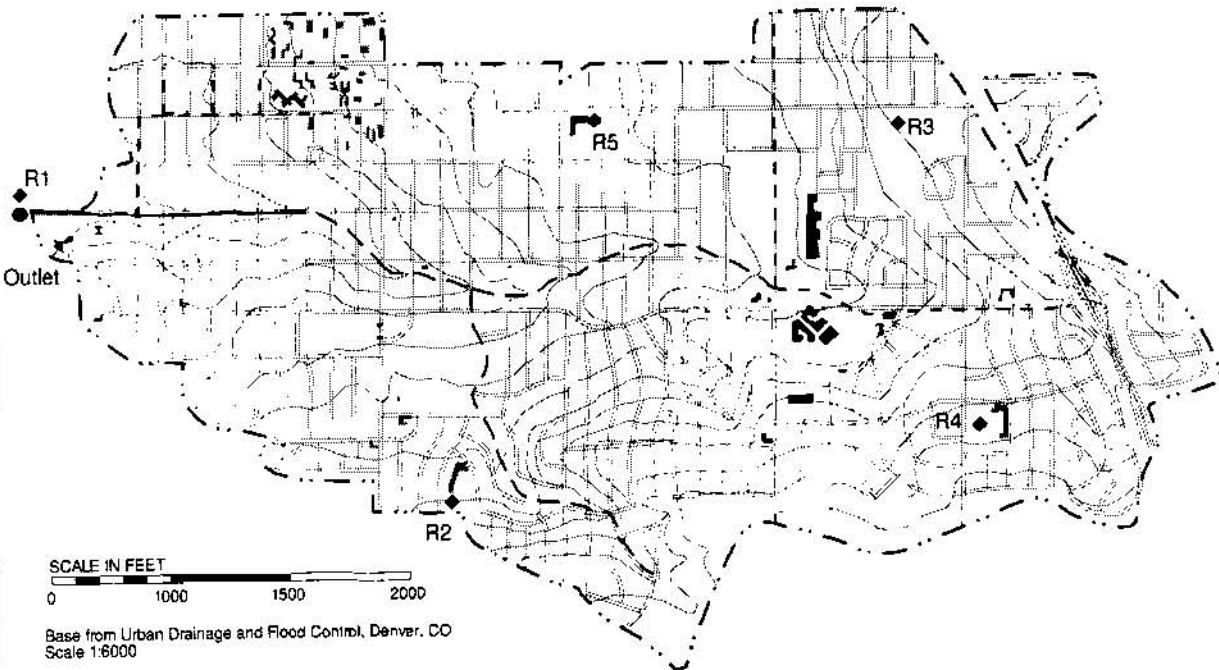


EXPLANATION

- | | |
|------------------------------|----------------------------|
| Concrete Lined Open Channels | Watershed Boundary |
| Grass Open Channels | Flow Gage |
| Storm Sewer | Rain Gage |
| Roads | 10 Foot Elevation Contours |
| | Buildings |



B. Harvard Gulch at Denver, CO



SCALE IN FEET
0 1000 1500 2000

Base from Urban Drainage and Flood Control, Denver, CO
Scale 1:6000

Figure 1.- Location and physical characteristics of (A) Surrey Downs and (B) Harvard Gulch watersheds.

Five-minute rainfall data for six storms for two gages at Surrey Downs (fig. 1A) and five gages at Harvard Gulch (fig. 1B) were provided. Information on antecedent conditions including the amount of precipitation in the past 1, 3, 7, and 14 days and the time since the last 0.0, 0.2, 0.5, and 1.0 in. of rain was provided for each storm at Surrey Downs. No antecedent conditions were reported for Harvard Gulch because of the semiarid climate, but it was reported that the area is routinely irrigated with 1.0 to 1.5 in/wk which is considered equal to the rate of evaporation. Daily evaporation at the Surrey Downs watershed ranged from about 0.30 inches in the summer to about 0.02 inches during the winter.

The rainfall and antecedent conditions for the storms simulated are summarized in table 2. Storms at the Harvard Gulch site averaged about 1.5 hours, and those at the Surrey Downs site averaged about 15 hours. Rainfall intensity in the Harvard Gulch watershed was generally 5 to 6 times greater on average than in the Surrey Downs watershed. Often, the 60-minute maximum intensity recorded in the Harvard Gulch watershed by a single raingage exceeded the average rainfall volume for all gages indicating a wide spatial variability. Rainfall in the Surrey Downs watershed was relatively uniform.

COMPARISON OF SIMULATED AND OBSERVED FLOWS

Results of the model-simulated flows and storm volumes (fig. 2 and 3) are summarized in terms of the percent error (departure from observed values) in table 3 (peak flows) and table 4 (storm volumes). The percent error is computed as:

$$r = \left(\frac{\text{Predicted} - \text{Observed}}{\text{Observed}} \right) \cdot 100 \quad (1)$$

where: predicted is the simulated value of flow or volume, and observed is the measured value of flow or volume

CASC2D results were obtained only for Harvard Gulch for the May 8, 1981 storm; the results are not included in the tables, but are shown in figure 2. Error for CASC2D simulations was -10 percent for peak flow and -39 percent for storm volume. Also, results of CHUP/SWMM, the distributed version of the CUHP model linked using SWMM, is only available for the Harvard Gulch watershed because no simulations were made of the Surrey Downs watershed.

Simulated peak flows differed from observed peak flows (table 3) by -100 to 260 percent at Harvard Gulch and by -100 to 200 percent at Surrey Downs. The RMS peak flow error ranged from 19 to 171 at Harvard Gulch and from 40 to 162 at Surrey Downs. The average RMS peak flow error for all models was 55 for Harvard Gulch and 49 for Surrey Downs. The standard deviation of the error in the predicted peak flow ranged from 17 to 92 at Harvard Gulch and from 20 to 85 at Surrey Downs. The average standard deviation in peak flow model error is about 40 percent greater at Surrey Downs (40) than at Harvard Gulch (31). In general, simulated peak flows at the Surrey Downs site tend to be overpredicted, whereas simulated peak flows for some models are overpredicted and some are underpredicted at Harvard Gulch.

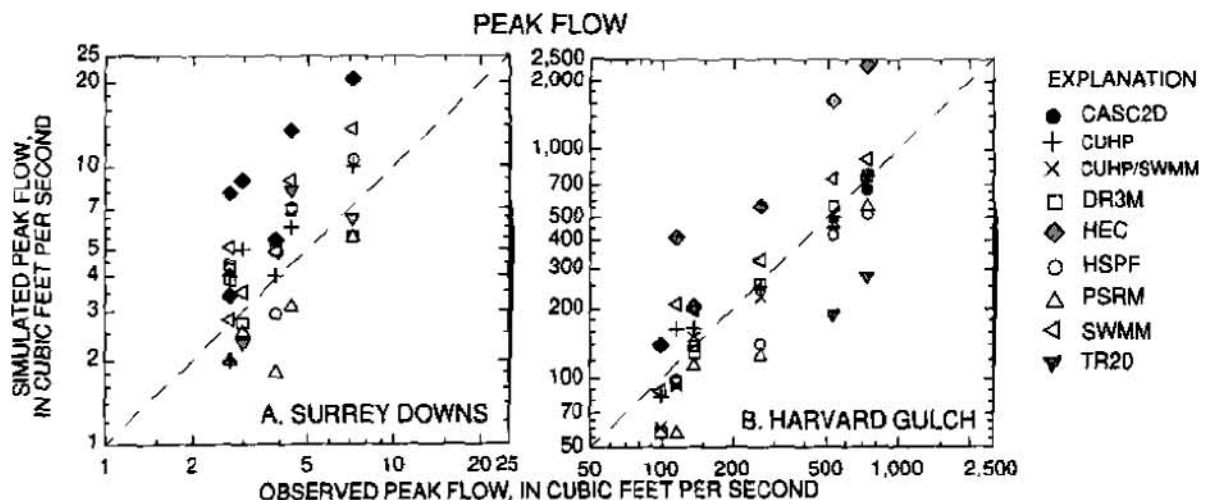


Figure 2.—Simulated versus observed peak flows at (A) Surrey Downs, WA and (B) Harvard Gulch, CO. for six storms [CASC2D results only available for one storm at Harvard Gulch, Locations shown in fig 1.]

Table 3. Error in simulated peak flow in relation to observed peak flow [All values in percent].

Storm	CUHP/ SWMM	CUHP	DR3M	HEC	HSPF	PSRM	SWMM	TR20
Harvard Gulch Watershed								
1981/5/8	2.8	3.8	3.7	220	-30	-24	22	-62
1983/6/5	-13	-5.0	-2.3	120	-46	-52	25	-98
1985/1/15	-18	43.	-16	260	-15	-50	83	-100
1985/7/19	-4.5	-6.0	6.0	210	-21	-12	40	-64
1987/6/9	-38	-15	-41	40	-52	-84	-10	-100
1987/6/30	11	22	-5.2	50	0.74	-17	46	-98
Mean	-10	7.0	-9.2	150	-27	-40	34	-87
RMS†	19	21	19	171	33	47	44	89
S.D.‡	17	22	18	92	20	27	31	18
Surrey Downs Watershed								
1980/4/18	-	48	62	200	-58	-26	89	-81
1980/8/17	-	39	-23	190	46	-24	89	-11
1981/6/30	-	2.6	27	38	-25	-54	26	-89
1981/9/20	-	-26.	44	26	-64	-67	3.7	-100
1981/12/1	-	3	57	200	60	-30	100	86
1981/1/15	-	68	-8.7	200	-	-16	17	-23
Mean	-	28	26	142	15	-36	54	-36
RMS	-	42	42	162	52	40	67	74
S.D.	-	34	35	85	56	20	43	70

*. Mean error

$$MEAN = \sum_{i=1}^n r_i$$

†. Root Mean Square error

$$RMS = \sqrt{\sum_{i=1}^n r_i^2 / n}$$

‡. Standard Deviation

where

$$r = \left(\frac{\text{Predicted} - \text{Observed}}{\text{Observed}} \right) \cdot 100$$

$n = \text{Number of Storms}$

Simulated storm volumes differed from observed storm volumes (table 4) by -100 to 190 percent at Harvard Gulch and by -100 to 240 percent at Surrey Downs. The RMS storm volume error ranged from 17 to 101 at Harvard Gulch and from 15 to 142 at Surrey Downs. The average RMS storm volume error is 56 at Harvard Gulch and 54 at Surrey Downs. The standard deviation of the error in the predicted storm volume ranged from 19 to 70 at Harvard Gulch and from 16 to 98 at Surrey Downs. The average standard deviation in storm volume error is also about 40 percent greater at Surrey Downs (62) than at Harvard Gulch (38). In general, simulated storm volumes tended to be overpredicted for larger storms and underpredicted for smaller storms at both sites, except for the largest storm at Surrey Downs which was underpredicted.

Models based on the SCS curve number (HEC-1 and TR20) for generating runoff generally had the poorest fit. HEC-1 simulations substantially overpredicted peak flows, and TR20 simulations substantially underpredicted peak flows; this may indicate the sensitivity of the simulations to user judgment of the SCS curve number. HEC-1 results presented represented simulations based on 6 subbasins; results also were provided for a simplified model that used only 3 subbasins. The simplified model produced slightly smaller peak flow error, but about the same runoff volume error. An additional HEC-1 analysis of the May 1981 storm at Harvard Gulch, performed by the CASC2D modelers, had only a -22 percent peak flow error which underscores the sensitivity of the model to the SCS curve number. A comparison of runoff simulation-techniques in west-central Florida indicated somewhat less, but comparable error, in simulated peak-flows and storm volumes for TR20 and HEC-1 simulations (Trommer and others, 1996). In that study, average uncalibrated-model peak-flow and storm-volume error averaged 45 and 43 percent, respectively, for TR20 simulations and 105 and 27 percent, respectively, for HEC-1 simulations.

The unit hydrograph method generally had about half error for simulations of the Harvard Gulch watershed than for simulations of the Surrey Downs watershed; this is attributed to its design for application in the Denver area. DR3M simulations of Harvard Gulch indicated an extended hydrograph recession compared to the observed recession; this resulted in relatively large storm-volume error for some simulations.

Table 4. Error in simulated storm volumes in relation to observed storm volume [All values in percent].

Storm	CUHP/ SWMM	CUHP	DR3M	HEC	HSPF	PSRM	SWMM	TR20
Harvard Gulch Watershed								
1981/5/8	30	29	98	39	-0.02	-6.3	15	-72
1983/6/5	25	9.7	100	61	1.3	-13	37	-96
1985/1/15	-12	50	15	190	11	-53	57	-100
1985/7/19	63	52	120	130	26	24	81	-57
1987/6/9	-18	-44	-13	3.5	-30	-81	-14	-100
1987/6/30	14	-14	35	43	-2.7	-37	16	-97
Mean	17	14	60	78	0.92	-28	32	-87
RMS	32	39	79	101	17	44	45	89
S.D.	30	38	55	70	19	37	34	18
Surrey Downs Watershed								
1980/4/18	-	-32	-5.2	-54	21	-31	-32	-82
1980/8/17	-	97	-9.4	150	28	-24	97	63
1981/6/30	-	61	20	70	-15	-36	61	-82
1981/9/20	-	-15	19	140	-63	-59	-15	-100
1981/12/1	-	39	-10	240	26	-27	39	69
1981/1/15	-	50	-20	110	1.0	58	50	-3.5
Mean	-	33	2.1	111	-0.14	-20	33	-23
RMS	-	55	15	142	35	42	16	73
S.D.	-	48	16	98	35	40	16	76

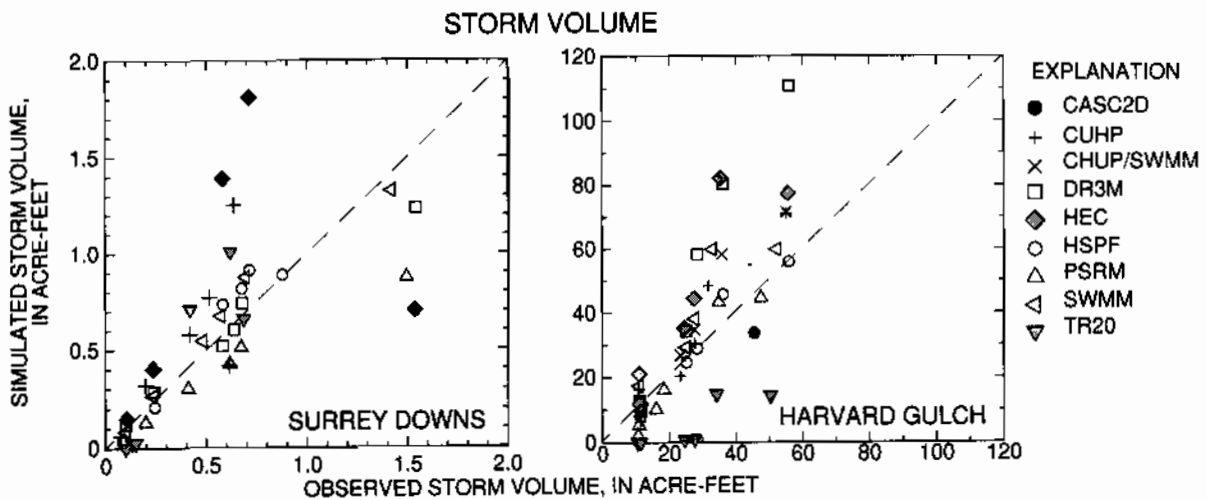


Figure 3.—Simulated versus observed storm volume at (A) Surrey Downs, WA and (B) Harvard Gulch, CO for six storms [CASC2D results only available for one storm at Harvard Gulch, Locations shown in fig 1.]

Model error was generally smaller for complex-distribution models DR3M, HSPF, PSRM and SWMM than for simple distribution-models CUHP, HEC-1 and TR20. The average peak-flow RMS error for the complex-distribution models was 36 at Harvard Gulch and 50 at Surrey Downs, in contrast the average RMS for the simple-distribution models was 75 and 92, respectively. The RMS storm-volume error for complex-distribution models averaged 46 at Harvard Gulch and 27 at Surrey Downs, in contrast to an average RMS for the simple-distribution models of 65 and 90, respectively. The error associated with the CUHP was generally similar to the error associated with the complex-distribution models, however. Michaud and Sorooshian (1994) also demonstrated that an uncalibrated complex-distribution model (KINEROS) was more accurate than a simple uncalibrated SCS-curve model.

The results of this test are not conclusive and do not indicate that one model performs better than another. The results merely show that the error associated with uncalibrated models can be substantial. The design of structures such as culverts, storm-sewers, detention basins, and other storm-water facilities based on uncalibrated model results could result in unnecessary costs when a model overpredicts peak flows and storm volumes, and perhaps result in even more severe consequences when these structures are underdesigned because the model underpredicts peak flows and storm volumes.

REFERENCES

- Alley, W.M. and Smith P.E., 1982, Distributed routing and rainfall-runoff model-- version II: U.S. Geological Survey Open-File Report 82-344, 201 p.
- Aron, Gret, Smith, T.A.3rd., Lakatos, D.F., 1996, Penn State Runoff Model, PSRM C96, User Manual: Environmental Resources Research Institute, Penn State, PA, Penn State Univ. 54 p.
- Bicknell, B.R., Imhoff, J.C., Kittle, J.L., Jr., Donigian, A.S., and Johanson, R.C., 1993, Hydrological Simulation Program--Fortran, Users Manual for Release 10: EPA-600/R-93/144, Environmental Research Laboratory, Athens, Ga., U.S. Environmental Protection Agency, Environmental Research Laboratory, 660 p.
- Ebbert, J.C. Poole, J.E., and Payne, K.L., 1985, Data collected by the U.S. Geological Survey during a study of urban runoff in Bellevue, Washington, 1979-82: U.S. Geological Survey Open-File Report 84-064, 256 p.
- Huber, W.C. and Dickinson, R.E. 1988, Storm water management model version 4, part A: Users manual: U.S. Environmental Protection Agency Report EPA/600/3-88/001a, 569 p.
- Hydrologic Engineering Center, 1990, HEC-1 Flood hydrograph package user's manual: U.S. Army Corps of Engineers, Davis CA, 410 p.
- Julian, P. Y. and Saghafian, Bahram, 1991, CASC2D: A two-dimensional watershed rainfall-runoff model, CASC2D user's manual: Report CER90-91PYJ-BS-12, Colorado State University, Fort Collins, CO, 66 p.
- Julian, P. Y. and Saghafian, Bahram, and Ogden, F.L., 1995, Raster-based hydrologic modeling of spatially-varied surface runoff: Water Resources Bulletin, Vol. 31, No. 3, p 523-536.
- Michaud, Jene and Sorooshian Soroosh, 1994, Comparison of simple versus complex distributed runoff models on a mid-sized semiarid watershed: Water Resources Research, Vol. 30, No 3, p. 593-606.
- Miller, J.E., 1984, Basic concepts of kinematic-wave models: U.S. Geological Survey Professional Paper 1302, 29 p.
- Soil Conservation Service, 1986, Urban hydrology for small watersheds: Technical Release No. 55, 210-VI-TR-55, 156 p.
- , 1983, TR-20 Project formulation-hydrology (1982 version), Technical Release No. 20, 296 p.
- Tommer, J.T., Loper, J.E., and Hammett, K.M., 1996, Evaluation and modification of five techniques for estimating stormwater runoff for watershed in West-Central Florida: U.S. Geological Survey Water-Resources Investigations Report 96-4158, 37 p.
- Urban Drainage and Flood Control District, 1984, Urban storm drainage criteria manual, Vol. 1 Chps. Rainfall and Runoff, 1984 revision, Denver, C.O., 120 p.

SIMULATING SEDIMENTATION IN SALMONID REDDS

By Carlos V. Alonso, Research Hydraulic Engineer, USDA-Agricultural Research Service, Oxford, MS; Fred D. Theurer, Agricultural Engineer, USDA-Natural Resources Conservation Service, Beltsville, MD; and Robert N. Havis, HAVIS Environmental Engineering, Fort Collins, CO

Abstract: Studies have shown that fine sediment intrusion can significantly impact the quality of spawning habitat. Fine sediment intrusion into streambed gravels can reduce permeability and intragravel water velocities, thereby restricting the supply of oxygenated water to developing salmonid embryos and the removal of their metabolic wastes. Excessive fine sediment deposition can effectively smother incubating eggs and entomb alevins and fry. This paper (1) presents a synopsis of models developed as management tools to evaluate the impact of stream sediment load on salmonid survival, and (2) discusses results obtained from field validation studies conducted in the Tucannon River in southeastern Washington and in the Salmon River in central Idaho.

INTRODUCTION

Commercial and sport benefits resulting from anadromous fisheries averaged \$434 million (US) annually in the Pacific Northwest in the 1970's. Because of reduced anadromous fish populations, this value represents less than half the potential (Theurer, 1985). Reduced spawning success because of watershed development is one of the major contributors to reduced populations of anadromous species. A large body of literature illustrates that fine sediment is detrimental to egg survival and developing embryos (Cooper, 1965; Chapman, 1988). Major reasons for increases in fine sediment loading to spawning areas are agricultural development (Theurer, 1985) and forest harvesting and associated road building (Platts and Megahan, 1975).

With increased land and hydropower development, Federal and State action agencies are concerned with the impacts of land management practices on instream sediment load and the effects on the spawning success of salmonid species. Field studies on sediment intrusion into spawning gravels are by nature site specific with limited geographic applicability. Because of the complexity and variability of environmental factors involved in salmonid survival, there is a need for a simulation tool applicable to widespread geographic locations capable of facilitating informed decisions on alternate land management practices upstream of salmonid spawning habitat.

The Sediment Intrusion and Dissolved Oxygen (**SIDO**) model developed by Alonso *et al* (1996) simulates the environmental variables controlling egg and fry survival in the redd habitat. Currently the chinook salmon and steelhead egg survival and fry emergence rates are simulated based on sediment particle size distribution, water temperature, and dissolved oxygen in the redd. This model was developed jointly by the USDA Agricultural Research Service and the Natural Resources Conservation Service (formerly known as the USDA Soil Conservation Service). A preliminary draft of the model documentation has been in circulation since 1988 and the final version was released in November of 1996. A complete set of documentation, Fortran 90 source code, and

associated executable software can be downloaded from the **SIDO** webb site www.sedlab.olemiss.edu/cwp_unit/Sido. The following introductory remarks present some background on the effects of fine sediment in salmonid spawning habitat, followed by a synopsis of the mathematical model, field applications, and comparison of results with field measurements.

SALMONID SPAWNING HABITAT

The incubation phase of many salmonid species coincides with periods of high flows carrying sediments that can penetrate in the gravel and affect intragravel flow. Conditions of spawning gravels prior to spawning and during the subsequent incubation period exhibit considerable time and space variability arising from climatic changes and the complexity of natural watersheds. To quantify this variability the chain of processes resulting in intragravel deposition and how their individual variabilities affect the substrate environment must be identified and translated into realistic, efficient algorithms.

The Redd Environment: Salmonid species spawn in the gravels of freshwater streams. The female deposits her eggs in the nest, or redd, which is a pocket of gravel from which the female has partially removed the sediment fines (Figure 1). Details of the redd construction process can be found elsewhere (Burner, 1951; Chapman, 1988). The newly hatched fry continue to live in the intragravel space until the egg-sac is absorbed. When they are ready to emerge from the gravel, they must struggle up through the gravel to the

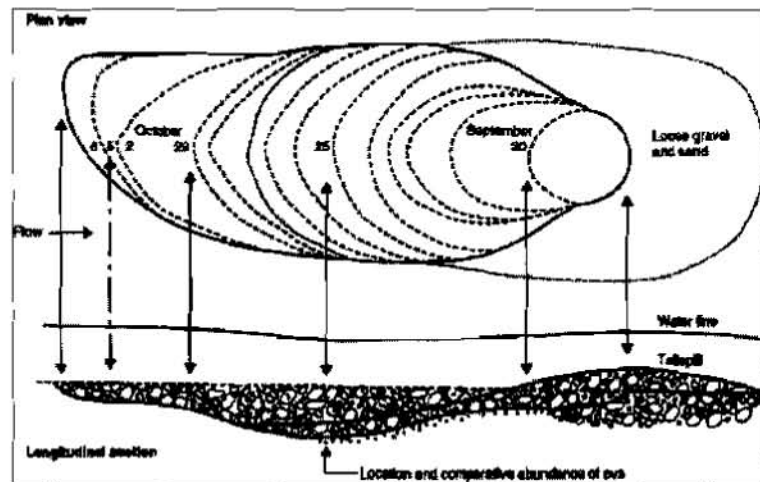


Figure 1. A fall chinook redd measured daily (Burner, 1951).

surface water. The intragravel growth stage represents a critical phase of their life cycle. During this period they are susceptible to damages from high levels of fine sediments. Incubating eggs and fry require appropriate levels of dissolved oxygen in the intragravel water for adequate survival and growth, and intragravel flows must be sufficient to remove the toxic metabolic wastes produced by the embryo. High levels of intruding fines reduce the permeability of the gravel substrate resulting in lower intragravel flows, as well as reduced interchange of water between the stream and the substrate. Intragravel water temperature must remain within a limited range to prevent further mortality. Finally, excessive amounts of fine sediments carrying organic matter exert a sediment oxygen demand that further reduces the available oxygen, and entrap the fry within the gravel as they try to emerge.

Sediment Intrusion Mechanisms: Large populations of spawners returning annually to a particular location serve to maintain a high quality spawning habitat. A large area of unconsolidated gravel, cleaner than the surrounding stream substrate, develops in these areas. However, fine material inevitably moves back into the redd environment after construction because the bed profile at a redd

site induces advective transfers in and out of the substrate. This intragravel circulation carries part of the fine sediments transported by the river into the gravel substrate, and the rate of intrusion depends on upstream sediment sources and precipitation or snow melt events. Fine sediments can infiltrate into clean gravel substrates in one of two ways. Finer grains settle down to the bottom of the substrate and fill the gravel pores from the bottom up (Einstein intrusion mode). Coarser grains are inhibited from infiltrating all the way to the bottom of the gravel bed. Instead they bridge the gravel framework voids creating a seal that traps further intruding fines at some distance between the gravel surface and the undisturbed underlying material (Beschta intrusion mode). Both modes of sediment intrusion have been encountered in the field as well as in the laboratory (Einstein, 1968; Beschta and Jackson, 1979; Carling, 1984; Diplas and Parker, 1985; Lisle, 1989). The specific impacts on the developing embryos and fry depend on particle size and composition. Clays and silts cause low intragravel hydraulic conductivity, and in excessive amounts they can entomb the eggs and fry in the gravel interstices. Larger intruding particles (0.85 mm to 9.50 mm) may create a seal or clogged layer within the gravel framework preventing fry from emerging into the stream.

SALMONID SPAWNING HABITAT MODELING

The **SIDO** model was designed to predict the daily movement of water, sediment, and dissolved oxygen within a salmonid redd when given the (a) stream discharge, (b) stream temperature, (c) sediment load rate and material composition, (d) local stream channel geometry, (e) initial composition of substrate material, and (f) salmonid species parameters. The model calculates the water surface profile over the redd, water and fine sediment intruding into the gravel substrate, and the daily sediment accumulation, water temperature, and dissolved oxygen status within the redd.

SIDO was developed to be used as part of a suite of modeling tools to analyze the relative effects of upstream management practices on salmonid spawning habitat. Hydrologic inputs to the model can be either from measured data or generated with daily models such as the ARS watershed model **AnnAGNPS** (Cronshey and Theurer, 1998) and the USF&W **Instream Water Temperature Model** (Theurer *et al*, 1984). The output from the **SIDO** model can be used with the fry emergence model presented by Miller *et al* (1998). This model incorporates procedures for determining pre-emergent fry survival rate as a continuous function of intragravel water temperature, dissolved oxygen concentration, and substrate particle size composition.

The spawning habitat is viewed in **SIDO** as a mixture of water and sediment moving through the habitat while interacting with each other and the habitat. Processes in the habitat are simulated in two distinct domains: a stream domain and a redd domain. Output from the stream simulation is passed on to the redd domain where the movement of water, dissolved oxygen (DO), and fine sediments through the gravel substrate is simulated. These two submodels exchange information on a daily time step, and are assumed uncoupled although, in practice, a certain amount of feedback always occurs, such as with processes involving bed scour and flushing of fines.

Streamflows are characterized by a one-dimensional representation, and inflows are treated as slowly varying and approximated as sequences of steady daily events. Scour and deposition of bed material are assumed not to alter the channel morphology to any significant degree during the intragravel growth stage. Backwater calculations yield the water surface profile for the channel reach and water depths over the redd. Sediment routing is restricted to determining the bedload and suspended

sediment transport rates in the neighborhood of the stream-redd interface. Modeling of transport processes in the redd is restricted to processes occurring on the plane of symmetry of the redd. This entails the assumption that the redd morphology remains, at all times, symmetric with respect to its longitudinal vertical section. A finite-difference grid overlaid on this section is used for the purpose of solving the water, sediment, and DO transport governing equations by means of finite difference schemes. The redd domain is divided into four compartments: the upstream pit zone left after the excavation, the disturbed zone which overlays the egg pocket, the egg pocket, and the undisturbed stream substrate beneath the redd. Differences in potentiometric head along the stream-redd interface drive the intragravel circulation which in turn carries fine sediments into the gravel bed. Sediment and dissolved oxygen are moved into the redd through advection and gravitational settling, neglecting the smaller dispersive transport mechanisms. As the infiltrating sediment settles in the interstices of the gravel framework, the pore space is gradually filled and the substrate permeability and intragravel flow are adjusted accordingly. The model computes the daily DO status as a function of the DO entering the redd with the intragravel flow and the DO consumption by eggs, fry, and organic carbon carried by the intruding sediment.

SIDO was developed to account only for the predominantly longitudinal geometric variability of short pool-riffle reaches, and sediment intrusion was modeled after conditions in the Tucannon River, southeastern Washington, where fines are able to settle unimpeded through the coarse gravel so that deposition occurs from the redd's bottom upwards. **SIDO** was subsequently extended in the **SSAM** model developed by Havis (1992) to accommodate the lateral streamflow variations and sediment intrusion of coarser particles resulting in seal formation encountered in the Salmon River, central Idaho. In the **SSAM** model the **HEC-6** river sedimentation model (HEC, 1977) was substituted for the original stream component in **SIDO**, and channel cross sections were divided into subsections where geometry and hydraulic variables are calculated in the vicinity of spawning locations of interest. To simulate the intrusion of larger sediment particles the Beschta intrusion mode was added. A seal is triggered in the gravel framework when the bedload material particle size statistics meet the Diplas-Parker criterium (Diplas and Parker, 1985) and the total bed load mass is sufficient to create a seal of finite volume.

SIDO and **SSAM** are deterministic models in which processes are linked by mathematical representations yielding uniquely defined cause-effect relations. Lisle and Lewis (1992) constructed a site-specific stochastic model in which the sediment infiltration rates are statistically dependent upon the variation of measured bedload transport. This study presents an interesting discussion of the relative uncertainty and variability of processes affecting gravel siltation.

FIELD EVALUATIONS

Tucannon River, Southeastern Washington: The **SIDO** model was applied to the Krouse Ranch site on the Tucannon River, southeastern Washington. The study reach is located about 1.7 km upstream of the Tucannon confluence with the Pataha Creek, and the area supports chinook and steelhead habitat. The reach is about 100 meters long, has an average bankfull width of about 18 meters, and a bankfull discharge of approximately 25 m³/s. The channel is fairly straight, with a bed profile incorporating a full pool, glide, and riffle sequence, and the average bed slope over several pool-riffle sequences is about 0.009. There was no appreciable vegetation on the channel banks,

with small trees and bushes growing on the overbank areas. The bed, banks, and transported sediment are all remarkably deficient in sand and fine gravel. During major storm events, suspended-sediment loads can be very high; generally, less than five percent of the total suspended sediment load is sand-sized material, and less than ten percent of the total sediment load is bed load. The model was calibrated using data collected at and near the study reach between 1979 and 1986 (Alonso *et al*, 1996). Streamflow data was used for the calibration of the one-dimensional stream submodel. Five surveyed channel cross sections were selected to characterize the geometry of the study reach. Water discharges and sediment loads for the period of September 1st, 1968, through March 30, 1969, were selected for this test because they cover the critical rearing period of Chinook salmon, and are representative of normal flow periods in the Tucannon River. Data from limited freeze-core sampling tests was used to calibrate the two-dimensional redd submodel. Freeze-core samples were extracted from artificial redds constructed in areas of the channel bed considered suited for spawning. Samples were extracted in the fall and again in the following spring.

Results from the streamflow calculations indicate that this part of the model reproduces quite well the hydraulics of the study reach for a typical range of upstream inflows. The concomitant evolution of critical substrate parameters was more difficult to test because of the limited scope of the available data. This part of the evaluation was largely confined to reproducing the main expected features of intragravel circulation and deposition patterns (Alonso *et al*, 1996). Some quantitative testing of gravel siltation was done by comparing the model response

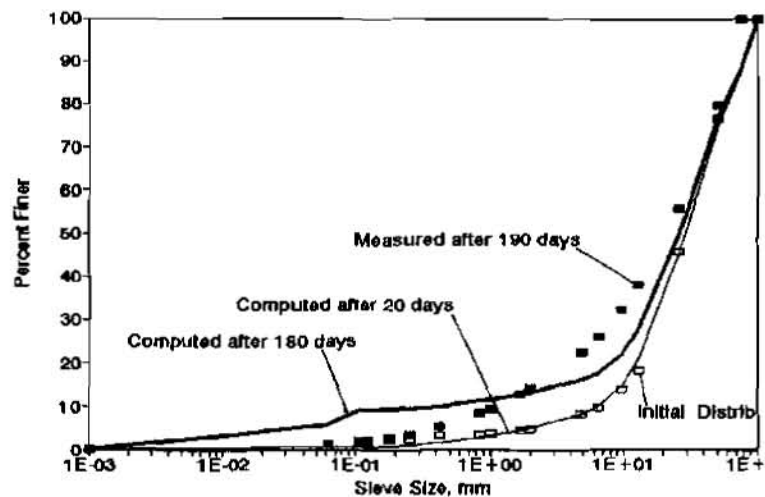


Figure 2. Changes in substrate composition with sediment intrusion, Tucannon River, Washington.

with the trends indicated by the freeze-core data. However limited, these tests lent credibility to the response exhibited by the intragravel calculations. The sequence of filling patterns indicates a definite correlation between the rate of deposition in the redd and the sediment loads imported by the streamflow. Redd filling is closely associated with the changes in the material composition of the gravel substrate. This effect is illustrated in Figure 2 which compares changes in particle-size distribution computed in a simulated redd with freeze-core data. Twenty days after construction very little fine sediment was observed in the redd. With time, clay, silt and fine sand accumulated in the voids and, gradually, the percentage of fines increases towards a maximum, reflected by the distribution attained by day 180 when the redd was totally filled with fines. Although the initial and final size distributions predicted by the model closely resemble the measured distributions, significant differences are evident between computed and observed populations. These differences are unavoidable given the level of uncertainty in the freeze-core data, and the expected variability between the actual and simulated redds.

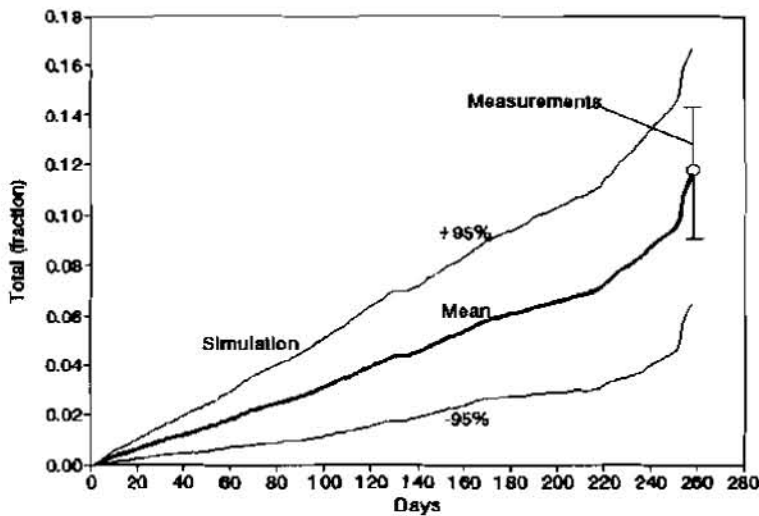


Figure 3. Computed and measured cumulative sediment intrusion, Salmon River, Idaho.

Salmon River, Central Idaho:

The Poverty Reach of the South Fork of the Salmon River in central Idaho was used to evaluate the SSAM model. The river bed is largely gravel and fluvial deposits which are rich in sands and gravels. The reach is about 1.5 km long and bank-to-bank distances average about 30 meters. The channel cross section geometry was measured at twenty three locations and a gaging station was installed and monitored at the reach outlet and at the confluence of a tributary. Sediment routing calculations employed these flow measurements as well as rating

curves developed from suspended and bed load monitoring at the reach and tributary inlets and measurements of the stream substrate particle size distribution. The period of study selected for analysis represents chinook salmon egg incubation from September 1990 to May 1991. This is a period of relatively low flow with a mean discharge of 3.17 m³/sec. A field monitoring program designed to evaluate sediment intrusion included freeze coring of artificial redds, and installation and monitoring of intrusion buckets.

HEC-6 calculations were evaluated by comparing simulated and measured water surface profiles, and bed loads and suspended loads collected at the reach outlet (Havis *et al*, 1996). The HEC-6 model tended to over-estimate sediment transport during low flows and to under estimate sediment load at higher flows. Silt transport simulations showed similar trends to sand transport. The calculated long-term flushing of sand-size particles from the bed substrate approximated quite well field measurements. The sediment intrusion and DO models were calibrated using data from 10 intrusion buckets and adjacent artificial redds with inserted pockets of chinook eggs (Havis *et al*, 1993). Under the relatively low flow regime of the study period, particle sizes in transport were too small to initiate sealing of the gravel interstices. Hence, the Einstein intrusion mode prevailed. Sediment intrusion simulations and field data are presented in terms of the fraction, by weight, of intruded material in a unit volume of substrate. This is the cumulative mass of sediment intruding the porous gravel framework divided

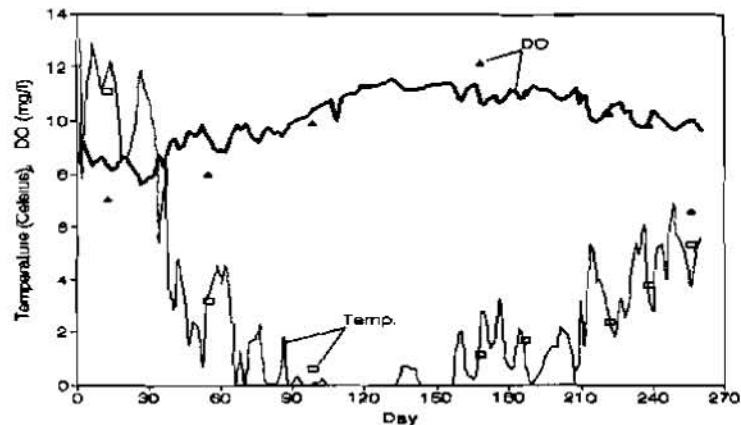


Figure 4. Simulated water temperature and DO concentration compared to measurements in the Salmon River, Idaho.

by the original gravel framework mass. The mean cumulative total sediment intrusion is displayed in Figure 3 along with the 95% confidence interval. The mean and standard deviations of the field measurements are given by the error bar. The increase in sediment intrusion rates during the last month of the study period is the result of increased bed load rates associated with the beginning of the Spring hydrograph. Model simulations of water temperature and DO concentrations are compared with field measurements in Figure 4. In the study area of relatively low organic loading to the aquatic environment, adequate oxygen was available to incubating eggs. DO concentrations appear to be mainly influenced by water temperature. Model predictions show general agreement with field measurements.

SUMMARY

Tools are available to evaluate the effects of upstream development, and increased sediment loads, on salmonid spawning habitat. Deterministic simulation models have general geographic applicability for evaluating the effects of fine sediment loads from agricultural areas and lands or the effects of coarse sediment loads from highland forested environments subject to logging and road building. The effects of hydrology, water temperature, and oxygen concentration are considered in predicting the success of salmonid egg incubation and emergence into the surface water environment. The models have been tested using field data and are available through the USDA, Agricultural Research Service.

REFERENCES

- Alonso, C.V., Theurer, F.D., and Zachmann, D.W., 1996, Sediment Intrusion and Dissolved-Oxygen Transport Model — SIDO, *Technical Report No. 5*, USDA-ARS National Sedimentation Laboratory, Oxford, Mississippi, 269 pp.
- Beschta, R.L., and Jackson, W.L., 1979, The Intrusion of Fine Sediments Into a Stable Gravel Bed, *Journal Fish. Res. Board Canada*, **36**: 204-210.
- Burner, C.J., 1951, Characteristics of Spawning Nests of Columbia River Salmon, *U.S. Fish & Wildlife Serv. Fish. Bull.*, **61**(52): 96-110.
- Carling, P.A., 1984, Deposition of Fine and Coarse Sand in an Open-Work Gravel Bed, *Can. J. Fish. Aquat. Sci.*, **41**: 263-270.
- Chapman, D.W., 1988, Critical Review of Variables Used to Define Effects of Fines in Redds of Large Salmonids, *Transactions*, American Fisheries Society, **117**:1-21.
- Cooper, A.C., 1965, The Effect of Transported Stream Sediments on Survival of Sockeye and Pink Salmon Eggs and Alevin, *Int. Pac. Salmon Fish. Comm., Bulletin No. 18*, 71 pp.
- Cronshey, R.G., and Theurer, F.D., 1998, AnnAGNPS—Non-point Pollutant Loading Model, *Proceedings*, First Federal Interagency Hydrologic Modeling Conference, Las Vegas, Nevada, April 19-23, 1998.

Diplas, P., and Parker, G., 1985, Pollution of Gravel Spawning Grounds due to Fine Sediment, *Project Report No. 240*, St. Anthony Falls Hydraulic Lab., University of Minnesota, 145 pp.

Einstein, H.A., 1968, Deposition of Suspended Particles in a Gravel Bed, *J. Hydraul. Div.*, ASCE, **94**(HY5): 1197-1205.

Havis, R.N., 1992, Salmonid Spawning Analysis Model (SSAM), *Project Completion Report and Model Documentation*, U.S. Forest Service, Boise, Idaho.

Havis, R.N., Alonso, C.V., King, J.G., and Russell, F.T., 1993, A Mathematical Model of Salmonid Spawning Habitat, *Water Resources Bull.*, **29**(3): 435-444.

Havis, R.N., Alonso, C.V., and King, J.G., 1996, Modeling Sediment in Gravel-Bedded Streams Using HEC-6, *J. of Hydraul. Eng.*, ASCE, **122**(10): 559-564.

Hydrologic Engineering Center, 1977, Scour and Deposition in Rivers and Reservoirs, *Computer Program HEC-6 Version 3.2*, U.S. Army Corps of Engineers, Davis, California.

Lisle, T.E., 1989, Sediment Transport and Resulting Deposition in Spawning Gravels, North Coastal California, *Water Resour. Res.*, **25**(6): 1303-1319.

Lisle, T.E., and Lewis, J., 1992, Effects of Sediment Transport on Survival of Salmonid Embryos in a Natural Stream: a Simulation Approach, *Can. J. Fish. Aquat. Sci.*, **49**: 2337-2344.

Miller, W.J., Theurer, F.D., and Alonso, C.V., 1998, A Computer Model to Predict Salmonid Fry Emergence, *Proceedings*, First Federal Interagency Hydrologic Modeling Conference, Las Vegas, Nevada, April 19-23, 1998.

Platts, W.S., and Megahan, W.F., 1975, Time Trends in Riverbed Sediment Composition in Salmon and Steelhead Spawning Areas: South Fork Salmon River, Idaho, *Transactions*, North American Wildlife and Natural Resources Conference, **40**:229-239.

Theurer, F.D., 1985, Evaluating the Impacts of Soil and Water Conservation Measures, Natural Resources Modeling Symposium, USDA Agricultural Research Service, *Public. ARS-30*, 1-6.

Theurer, F.D., Voos, K.A. and Miller, W.J., 1984. Instream Water Temperature Model, *Instream Flow Information Paper 16*, U.S. Fish and Wildlife Service, FWS/OBS-84/15.

INTERNET-BASED DECISION SUPPORT SYSTEMS OF HYDROLOGY TOOLS FOR WETLAND DETERMINATION.

**By R. L. Bingner, Agricultural Engineer, USDA-ARS, Oxford, Mississippi,
O. Butoi-Stanescu, Research Associate, University of Mississippi, Oxford, Mississippi,
P. B. Rodrigue, Wetland Hydrologist, USDA-NRCS, Oxford, Mississippi**

Abstract: Wetland hydrologic tools have been developed using scope and effect equations used by NRCS for application over the Internet to assist in the evaluation of drainage practices on wetland areas. The application of these tools over the Internet can provide users a common interface that is processed and maintained at a central location. The tools can be accessed with any computer operating system users may have available to them. This eliminates the need for users to update the program on their system as enhancements are added.

INTRODUCTION

Hydrologic and physical characteristics of a watershed are needed by USDA-NRCS to determine whether newly designed or existing drainage systems impact wetland hydrologic areas. Many tools have been developed by the USDA-NRCS to aid in the evaluation of the hydrology of potential wetlands. These tools are analytical techniques used to supplement the documentation of a wetland determination, often requiring access to extensive database information. The acquisition of this information can be difficult and tedious for even typical hydrologic applications, such as obtaining parameters needed from a climatic, soils, or landuse database. Computer-based technological tools have aided in the determination of potential wetland hydrologic characteristics.

Wetland hydrologic tools developed utilizing the Internet provides users of different computer operating systems a common interface. The tools and related information can be stored on a central computer, reducing user data storage and installation space requirements. This study presents the development of an internet-based decision support system (DSS) for use with hydrology tools applicable in evaluating a site for wetland hydrology. The appropriate tool must be selected to enable site conditions to be evaluated. These tools are derived from scope and effect equations used by USDA-NRCS and are developed from the Ellipse equation, (USDA, 1997), the Hooghoudt equation (Hooghoudt, 1937), the van Schilfgaarde equation (van Schilfgaarde, 1974), and Kirkham's equation (Kirkham, 1949). The use of these tools simplifies the procedures NRCS personnel use to calculate wetland hydrologic characteristics. Graphical results from the DSS can provide a quick presentation of wetland characteristics based on user-selected parameters.

DESCRIPTION OF EQUATIONS USED IN THE HYDROLOGIC TOOLS DSS

Ellipse Equation

The Ellipse equation may be used where wetland hydrology is the result of a high water table with a restrictive soil layer and the hydrology has been (or will be) altered with drains (surface or subsurface). If lowering of the water table for specified duration is all that is required to define wetland hydrology, then the ellipse equation is satisfactory to approximate this situation (a full description can be found in Chapter 19, EFH, "Hydrology Tools for Wetland Determination" (USDA, 1997)).

Application of Ellipse equation should be limited to the following conditions:

1. Where groundwater flow is known to be largely in a horizontal direction. Examples of this are stratified soils with relatively permeable layers acting as horizontal aquifers.
2. Where soil and subsoil materials are underlain by a barrier at relatively shallow depths which restricts vertical flow and forces the groundwater to flow horizontally toward the drain (the actual depth to the impermeable layer below the drain (a) is less than twice the drain depth (d), and is less than ten feet.)
3. Where open ditches are used, or where drains with sand and gravel filters or porous trench backfill materials are used (minimum restriction to and convergence of flow).

Hooghoudt Equation

The Hooghoudt equation is similar to the ellipse equation except that the depth to the impermeable layer from the free water surface in the drain (a), is replaced by an effective depth (de). This substitution makes the equation more accurate and widely applicable (greater range of a versus d). Also, the hydraulic conductivity is calculated separately for layers above and below the drainage feature. This equation is meant to be applied with no standing water above the tile line(s). Hooghoudt's equation (modified ellipse) should be used whenever the actual depth to the impermeable layer is greater than twice the drain depth ($a > 2d$) but where the calculated drain spacing (S) divided by the depth to the impermeable layer is greater than four ($S/a > 4$). If $S/a < 4$, the depth to the impermeable layer is considered infinite and other methods should be used (see Chapter 4, NEH 16, Drainage of Agricultural lands (USDA-NRCS, 1971)). In the Ellipse and Hooghoudt equations, drainage rate is the normal input, however for wetland determination purposes, the drainage rate is calculated from the drainable porosity, depth water table is lowered, and the time to lower the water table. The depth the water table is lowered and the time to lower the water table are established by the wetland hydrology criteria used.

van Schilfgaarde Equation

The van Schilfgaarde equation was developed for non-steady state conditions, as opposed to the ellipse equation (and Hooghoudt) which uses steady state assumptions. It includes a parameter for time (t) so that different lengths of time for the duration of saturation can be examined. A two-step iteration process is recommended to use the effective depth in place of actual depth, such as was described for the Hooghoudt equation. The van Schilfgaarde equation is meant to be applied with no standing water above the tile line(s) and where rainfall is sporadic (moist subhumid to arid climates) rather than constant (humid and superhumid climates).

Kirkham's Equation

The Kirkham's equation simulates the gradual lowering of the water ponded above a tile line or system. It is often combined with the Hooghoudt or van Schilfgaarde equation to describe the total removal of the water (ponded and water table). Kirkham's equation calculates the time to remove the ponded water, and the other drainage equation determines the time to remove the saturation to the specified depth. Kirkham's equation is meant to be applied where the tile line(s) lies directly under the wetland, but the site has no surface intake and water ponds.

Input Parameters

Hydraulic Conductivity (K, in/hr, all equations) is the saturated horizontal hydraulic conductivity. The horizontal K needs to be equal to or larger than the vertical K to apply the ellipse or Hooghoudt equations. For layered soils, a weighted value is used. Hydraulic conductivity should be obtained from field or laboratory methods, but can be approximated using the permeability information from a county soil survey, the National Soils database (www.statlab.iastate.edu/soils), or using MUUF data and computer program.

Drainable Porosity (f, dimensionless, van Schilfgaarde) is the volume of water that will be released per unit volume of soil by lowering the water table. Drainable porosity can be measured in the lab or can be calculated from the MUUF program. An adjusted drainable porosity (f') is used by NRCS to account for water trapped by surface roughness (s, inches), therefore $f' = f + s/(\text{depth of soil drained})$. The user may set $s=0$ if unsure of an appropriate surface storage value.

Drainage rate (q, in/hr, Ellipse, Hooghoudt) is the rate at which water must be removed to maintain the water table at the desired depth. In drainage design this value is normally precipitation and/or irrigation amounts. For wetland purposes it is used as the average rate at which the water table is lowered to a certain depth, over a certain time, with the removal of any infiltrated water over the drainage period, which is not the intended meaning of q in the equation. Therefore this value is often the combination of drainable porosity, depth water table is lowered, time to lower water table, and the amount of water from rainfall or irrigation that must be removed. Therefore q can be calculated by:

$$q = ((f' * (\text{depth water table lowered})) + \text{additional water}) / (\text{time to lower water table})$$

HYDROLOGY TOOLS INTERNET SITE

The Scope and Effect equations discussed above can be accessed over the Internet at the following site:

<http://www.sedlab.olemiss.edu/java/tools.html>

The site is interactive enabling input data to be entered directly on-screen with the results calculated on-screen without having to download the program.

Application Example

An example of the use of the ellipse equation will be used as shown in the "Hydrology Tools for Wetland Determination", Chapter 19, Engineering Field Handbook (1997).

For this example, the saturation will be removed in 14 days down to a depth of 12 inches. The drainable porosity of the soil is 0.05 ft/ft. The tile is installed at a depth of 7 feet with an impermeable layer located at 12 feet. The hydraulic conductivity is 1.14 inches per hour.

Step 1. Go to the Hydrology Tools Homepage:

<http://www.sedlab.olemiss.edu/java/tools.html>.

Step 2. Click on Ellipse (The image of the Ellipse screen is shown in Figure 1)

Step 3. Enter the values in the appropriate blocks:

$c=1$, $f=0.05$, $t=14$, $K=1.14$, $D=12$, $d=7$

Step 4. Click on compute after all values are entered

Note: you will be given a warning if a value is outside normal or suggested ranges. If you get a warning, click on OK to proceed with the calculation. Remember: garbage in, garbage out.

Step 5. The solutions for S and Le are displayed. (These values should be rounded to the nearest 5 feet to account for variability and precision of input values).

(S=495 ft, Le=247.5 ft)

Step 6. Individual input parameters can be changed, then click on compute to see the new results.

Step 7. Click on the Print command of your browser to obtain a copy of the solution screen(s) you want for documentation purposes.

Special Applications

In addition to being used to make wetland hydrology determinations, the scope and effect equations can also be used to evaluate other hydrology considerations related to wetlands. One of the most common situations involves evaluating if a new drainage system in the vicinity of a wetland will have any impact upon the hydrology of the wetland.

Impact of New Drainage System on an Adjacent Wetland

To use the scope and effect equations to evaluate the impact of a new drainage system on an existing wetland requires a new analysis of the input variables and what they represent.

In wetland determinations the critical period of concern was 14 days during the growing season for example (use the appropriate wetland hydrology criteria). However, in evaluating impacts, the goal is no impact at any time of the year. It is now necessary to establish the new criteria for the wetland of concern. A good starting point would be to determine the HGM (hydrogeomorphic) subclass of the wetland of concern. This will help establish the source of water and the critical period for the hydrology.

In a practical sense, "no impact" is probably unattainable. However, it is possible to look at negligible impacts, especially in comparison to other conditions in the watershed. Therefore, it has been suggested that the inputs should now represent the climatic conditions for the critical period of the wetland. For instance, the van Schilfgaarde equation could be applied with all inputs remaining the same except for time (t) which would now represent a time period of concern. This new "t" may be the average interval of time between rainfall events of 1" or more (time

between soil profile recharge). New "t" values could be based upon regional precipitation/evaporation records. Therefore for the same soils but different climates, the results would also be different, and yet results would be consistent across geo-political boundaries (county, state lines).

Evaluation of water table drawdown by Evapotranspiration

For some HGM subclasses of wetland, evapotranspiration may represent a significant driving force in the lowering of a water table near a wetland. The ET may in fact lower the water table to an extent that a drain installed in the soil profile may not have any impact on the adjacent wetland (Jacobsen and Skaggs, 1997).

Again, the inputs must be evaluated for what they now represent. For this situation, following the concepts presented by Jacobsen and Skaggs (1997), the new inputs for the Ellipse equation would be as follows. In the Ellipse equation, c would now equal the average ET rate (in/day) for the critical period evaluated. The time (t) would be 1, and the drainable porosity (f) would be 1. The value of d would now represent (see Jacobsen and Skaggs, 1997) the depth of the water table at which the upward flux can satisfy ET. This can be evaluated by the MUUF program. The equation is now solved for the lateral effect (L_e). This represents the distance from the wetland at which the water table is maintained at the depth d by the wetland. The water table will be lower further from the wetland because there is no replacement moisture to maintain the water table. Therefore in this situation, a drain placed at a depth less than or equal to d and at least L_e distance from the wetland will have no effect on the wetland. If a drain is placed deeper than d , additional analysis must be made.

Other Considerations

Often other changes in a watershed may completely overwhelm any changes in local drainage conditions. Changes in watershed landuse may increase (parking lots) or decrease (row crops to forest) runoff volumes and rates, thereby considerably changing the entire water balance of the wetland system.

It is important that the entire hydrology situation of the wetland be assessed to determine the relative impacts of various components of the water balance of the wetland and its watershed. Don't assume that a new drain is the only or most important hydrologic impact.

DISCUSSION

The Scope and Effect equations are not a miracle answer to wetland drainage questions that some people assume or others promote. Rather, the equations provide analysis to a set of parameters imposed. The user must verify that the equation(s) is applicable to the site and site conditions, that the underlying assumptions of the equation are met, that the source and degree of confidence in the input parameters are known, and that the results are applied in a practical manner knowing the physical system being studied. It is important to analyze the site to insure that drainage measures are the greatest impact on the wetland hydrology rather than natural (ET) or man-made (land use changes) impacts.

The use of the scope and effect equation with at least one other hydrology tool will strengthen the confidence in any evaluation made.

SUMMARY

Technology has been developed that integrates the simplicity of the Internet with scope and effect equations needed by NRCS for hydrologic evaluations of wetlands. Simple and easy to use graphical decision support systems enable users to apply parameters from any site requiring drainage evaluations. The development of Internet tools provides users with a common interface among many different operating systems.

The Internet tools described here provide one means that NRCS personnel can use for an effective evaluation of the hydrology from a site. Users unfamiliar with the scope and effect procedures can quickly learn and apply technology that is simply to utilize. As more tools and information is added to the Internet site users can simply revisit the Internet site without having to reinstall programs onto their computer.

Eventual implementation of this tool into NRCS field offices is one objective of a more comprehensive wetland modeling project supported by the USDA-NRCS Wetland Science Institute. This modeling effort involves development of wetland processes into the continuous version of AGNPS. Model evaluations of various management practices affecting wetlands can provide action agencies with additional information on which practice is more effective in improving water quality.

ACKNOWLEDGEMENTS

This bulletin was based upon the Hydrology Tools Coursebook (USDA, 1995) developed by Donald E. Woodward (ed.), National Hydrologist, Conservation Engineering Division, Washington, D.C., and the hydrology tools task group.

Included are the results of discussion of participants at the NRCS inter-region scope and effect meeting, November 18, 1997, Brookings, SD, on the use and applicability of the scope and effect equations to new drainage systems impacts on wetlands.

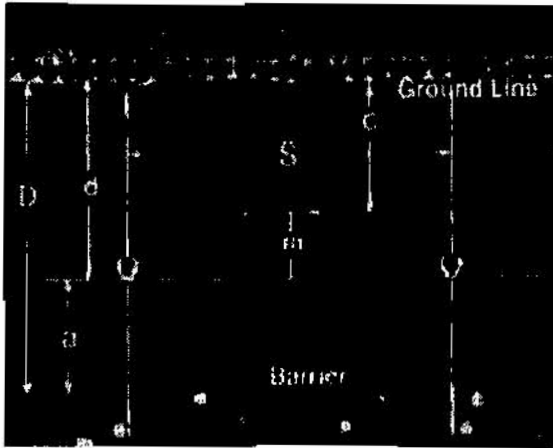
The Scope and Effect internet site was developed under a cooperative project agreement between the USDA, Agricultural Research Service, National Sedimentation Laboratory, and the NRCS Wetland Science Institute.

REFERENCES

- Hooghoudt, S. B., 1937, Bijdragen tot de kennis van eenige natuurkundige grootheden van den grond, 6. Versl. Landb. Ond. 43, 461-676.
- Jacobsen, S.M., and W.A Skaggs, 1997, Lateral Effect: What's Known and Unknown. Presented at the August 10-14, 1997, ASAE Annual International meeting, Minneapolis, MN. Paper No. 972034. ASAE, 2950 Niles Rd., St. Joseph, MI 49085-9659 USA.
- Kirkham, D., 1949, Flow of ponded water into drain tubes in soil overlying an impervious layer. Am. Geophys. Union, Trans. 30(3), 369-385.
- US Department of Agriculture, Natural Resources Conservation Service, 1997, Hydrology Tools for Wetland Determination, Chapter 19, Engineering Field Handbook. Donald E. Woodward (ed.). USDA, NRCS, Fort Worth, TX.
- US Department of Agriculture, Natural Resources Conservation Service, 1995, Hydrology Tools for Wetland Determination, Course Workbook, National Employee Development Center, USDA, NRCS, Fort Worth, TX.
- US Department of Agriculture, Natural Resources Conservation Service, 1971, Drainage of Agricultural Land, Section 16, National Engineering Handbook. USDA, NRCS, Washington, D.C.
- van Schilfgaarde, J., 1974. Nonsteady flow to drains. In: Drainage for Agriculture, Monograph 17, Am. Soc. Agronomy, J. van Schilfgaarde (ed.). Madison, Wisconsin. p. 245-270.
- The United States Department of Agriculture (USDA) prohibits discrimination in its programs on the basis of race, color, national origin, sex, religion, age, disability, political beliefs and marital or familial status. (Not all prohibited bases apply to all programs.) Persons with disabilities who require alternative means for communication of program information (Braille, large print, audiotape, etc.) should contact USDA's TARGET Center at 202-720-2600 (voice and TDD).

To file a complaint, write the Secretary of Agriculture, U.S. Department of Agriculture, Washington, D.C. 20250 or call 1-800-245-6340 (voice) or (202) 720-1127 (TDD). USDA is an equal employment opportunity employer.

Ellipse Equation



Example tile drainage system

Input Parameters

1	12
7	0.05
14	
1.14	<input type="checkbox"/> Calculate K
	N/A

Intermediary Results

5	6
0.0428 in/day	60000

Final Results

495	247.5
-----	-------

Figure 1. Ellipse equation as shown on the Hydrology Tools Internet site with example parameters.

AnnAGNPS INPUT PARAMETER EDITOR INTERFACE

**By R. L. Bingner, Agricultural Engineer, USDA-ARS, Oxford, Mississippi,
R. W. Darden, Supervisory Mathematician, USDA-ARS, Oxford, Mississippi,
F. D. Theurer, AnnAGNPS Project Manager, USDA-NRCS, Beltsville, Maryland,
C. V. Alonso, Supervisory Research Hydraulic Engineer, USDA-ARS, Oxford, MS
P. Smith, Hydrologic Unit Water Quality Project Manager, Ft. Collins, Colorado**

Abstract: AnnAGNPS has been developed cooperatively between USDA's ARS and NRCS as a replacement for AGNPS 5.0. Continuous watershed processes have been incorporated into AnnAGNPS, such as varying soil moisture, crop growth, climatic conditions, and operational management decisions. This requires many additional input parameters in order to utilize AnnAGNPS as a water quality management tool on large watersheds. A graphical user interface has been developed to aid users in the selection of appropriate input parameters describing watersheds and farming practices, and to run the simulation model. Automatic determination of many input parameters has also been incorporated into the interface. Enhancements to the USDA-NRCS HU/WQ model interface with AnnAGNPS will allow users a common interface for several watershed models.

INTRODUCTION

For large watersheds, the collection of necessary model input parameters can be tedious, time consuming, and error-prone. This study presents technology that combines geographical information systems (GIS) and AnnAGNPS model requirements to simplify and improve the accuracy needed in the development of a database for large ungaged watersheds for long-term evaluations of conservation management practices. An intuitive, PC-based, graphical user interface has been developed that leads users through the developmental steps needed to apply the water quality model, AnnAGNPS. This technology provides the user minimal involvement in the database management required to utilize AnnAGNPS. Compatibility with input parameter datasets developed for the single-event version, AGNPS 5.0, has been developed into the interface providing users the option of converting old input datasets into AnnAGNPS format. Additional parameter information can easily be added by the interface to provide a new AnnAGNPS input dataset.

By pinpointing major pollutant sources, AnnAGNPS helps planners focus their corrective actions at those source locations. Effective utilization of GIS and graphical user interface technology with water quality models can provide natural resource managers with simplified tools to evaluate best management practices within a watershed.

AnnAGNPS INPUT EDITOR INTERFACE DEVELOPMENT

Scientists at the U. S. Department of Agriculture (USDA), Agricultural Research Service (ARS) National Sedimentation Laboratory have developed a partnership with the USDA, Natural Resource Conservation Service (NRCS) to develop advanced technology needed to implement the AGNPS model and AnnAGNPS, the continuous version of AGNPS, in NRCS field offices and other locations. This cooperative effort is intended to produce a robust and accurate watershed parameter generator based on GIS that can also be added as an enhancement to the USDA-NRCS HU/WQ project.

The AnnAGNPS watershed input parameter editor is developed using standard ANSI FORTRAN 77 or higher and combined with MS Visual Basic. The current version is a stand-alone PC-based program requiring MS Windows 3.1 or later. The program also provides Windows-based GIS visualization of the watershed stream network and associated flow paths, along with other topographic features. The topographic dataset needed by AnnAGNPS to determine the flow directions for the water quality attributes and channel characteristics of each cell are automatically generated from a DEM. The interface then allows users to manually enter appropriate values for the rest of the input dataset parameters.

The interface is composed of a series of on-screen menus that guide the user through the process of entering the necessary watershed parameters. Titles to each series of screens are alphabetized into menus as shown in Figure 1. After a selection is made the appropriate screen is displayed. Input parameters can then be entered within each designated area. Each subwatershed area, which is designated as a cell, requires a significant level of inputs. For example, in the cell data screen shown in Figure 2, information on the soil, field, reach, and many of the topographic parameters are needed. As the user selects parameters that are within the range of values acceptable to the model, the background for that parameter space will turn blue. For parameters that are out of specified ranges or if no parameter is filled in that is required then the space turns red. The user has the option of accepting the values that are highlighted in red, but the interface at least informs the user of possible errors.

Additional cells can be created or modified while in each on-screen menu. If a certain set of parameters are duplicated among all of the cells then those parameters can easily be copied to other cells. Additional on-screen help is available as the user moves the cursor around the screen and over a parameter's input box. Suggested input ranges are also provided along with background information on the parameter of interest.

After the user has provided as much information to the input editor as needed to adequately describe the watershed, the interface will generate the input files needed to run the AnnAGNPS program. Modifications to input parameters can then be easily made from the interface for a series of evaluation runs.

FUTURE ENHANCEMENTS

For large watersheds with hundreds of subwatersheds, the current input interface can become cumbersome for the inputs that are not yet automatically generated. The HU/WQ project developed by USDA-NRCS provides a complete dataset required for the AGNPS 5.0 and SWRRB watershed models. Enhancements are planned to HU/WQ to incorporate AnnAGNPS as an option for input parameter development. Since HU/WQ currently only can be used on UNIX platforms, a PC-based version of HU/WQ is planned. This would provide an economical and efficient platform for watershed management planners to develop BMP's for large watersheds.

SUMMARY

A PC-based input parameter editor has been developed for use with the AnnAGNPS watershed model. The editor provides an intuitive Windows environment that allows entry or modification of input data parameters needed to describe the processes and management practices of a watershed. Future enhancements to the interface will involve incorporating AnnAGNPS to the HU/WQ interface currently used for AGNPS and SWRRB.

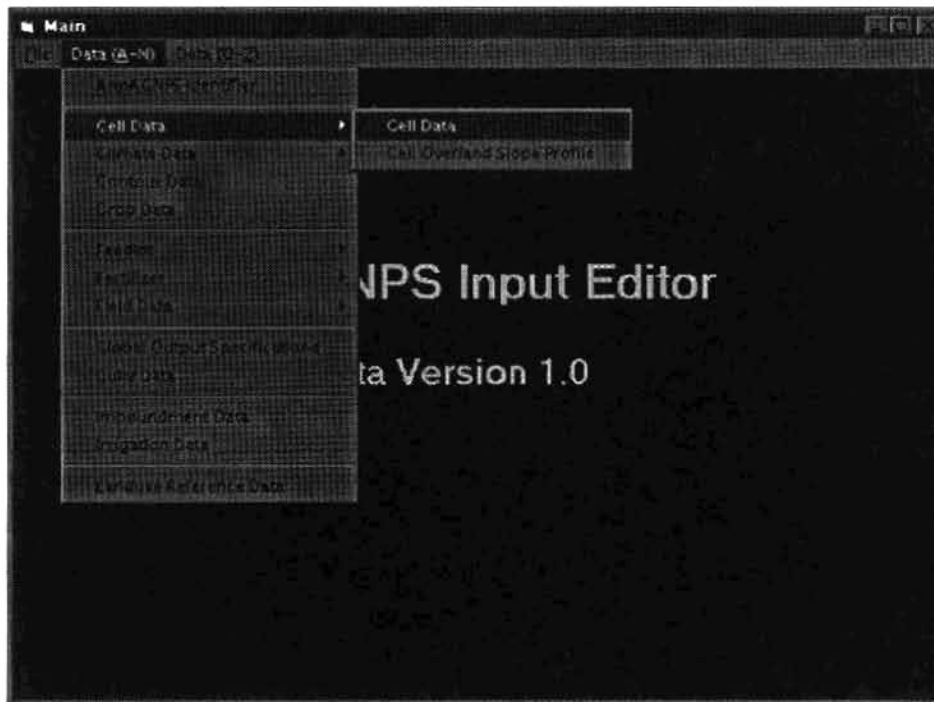


Figure 1. Example of the menu structure leading to the Cell Data form for the AnnAGNPS Input Editor.

Cell Data

Watershed No. Cells

Cell identifier	<input type="text"/>	BSFL flow L ² factor (rowing conditions)	<input type="text"/>
Cell Soil identifier	<input type="text"/>	Cell Slope identifier	<input type="text"/>
Cell Field identifier	<input type="text"/>	Overland flow Manning's "n"	<input type="text"/>
Cell Reach identifier	<input type="text"/>	Concentrated flow slope	<input type="text"/>
Reach Location code	<input type="text"/>	Concentrated flow length	<input type="text"/>
Cell Area	<input type="text"/>	Concentrated flow bottom width	<input type="text"/>
Cell time of conc.	<input type="text"/>	Concentrated flow side slope	<input type="text"/>
Cell average elevation	<input type="text"/>	Concentrated flow hydraulic depth	<input type="text"/>
		Concentrated flow Manning's "n"	<input type="text"/>

Current Cell

Cell average land slope	<input type="text"/>
Cell aspect	<input type="text"/>
BSFL L ² factor normal conditions	<input type="text"/>

Figure 2. The Cell Data form used by the AnnAGNPS Input Editor.

HEC-RAS (RIVER ANALYSIS SYSTEM)

Vernon Bonner, P.E.; Chief, Training Division
Gary Brunner, P.E.; Senior Hydraulic Engineer
Hydrologic Engineering Center, US Army Corps of Engineers
609 Second Street; Davis, CA 95616

INTRODUCTION

The *HEC-RAS River Analysis System* (HEC, 1997a,b,c) is a one-dimensional river modeling system designed for interactive use in a multi-tasking environment. Version 1, released in July 1995, provided steady-flow water surface profile calculations for a river network with sub-critical, supercritical, or mixed-flow regime on computers with MS Windows™ operating system. The program has been developed based on a single definition of the river geometric data for all modeling. River networks are defined by drawing, with a mouse, a schematic of the river reaches from upstream to downstream. As reaches are connected, junctions are automatically formed by the program. After the network is defined, reach and junction input data can be entered. The data editors are called by pressing the appropriate icons in the *Geometric Data Window*, or reach data can be imported from HEC-2 data sets (HEC, 1990).

Cross sections are located by river, reach, and river station. Pressing the cross-section icon provides the data entry editor. Data are defined by station-elevation coordinates, up to 500 coordinates are allowed. There is no maximum number of cross sections. The section data are stored in a downstream order based on their river-station number. Cross sections can be easily added or modified in any order. Cut, copy, and paste features are provided, along with separate expansion or contraction of the cross section's two over banks and channel. Cross-section interpolation can create additional computational sections based on a "string model" linearly linking adjoining sections. User-defined chords can be added to relate portions of each section to the next section.

HEC-RAS, Version 2, provides several added capabilities including the option to import and utilize three-dimensional (3D) river reach and cross-sectional data from a data exchange file. This paper highlights some major new features in Version 2 of the program.

HEC-RAS Version 2.0

Bridges. All bridges are modeled using the same physical definition of the bridge. The user can select one or several modeling methods to apply for low-flow and high-flow conditions. Low-flow methods included friction, momentum, and Yarnell methods. High-flow options included friction or pressure and weir equations. Pressure flow provides a gate equation for free-surface tailwater and pressure equation for fully submerged conditions. With support from the Federal Highway Administration, HEC has added WSPRO (FHWA, 1990) low-flow bridge hydraulics to HEC-RAS. The approach is a variation of the friction-based calculations. The HEC-RAS Hydraulics Reference (HEC, 1997c) provides a complete description of the methods used in this option.

Culverts. Two additional shapes have been added to the culvert options: Low Profile Arch and High Profile Arch. As shown in the Culvert Data Editor (figure 1), the program now supports eight culverts shapes. Also, the editor has been modified to provide all culvert data entries in a group.

Culvert hydraulics utilize the Federal Highway criteria for inlet control (FHWA, 1985) and compute total energy loss for outlet control. The computations have been expanded to handle several limitations that existed in Version 1. Culverts can now have adverse or steep slopes, with subcritical, supercritical or mixed-flow profiles computed inside the culvert.

Profile plots can display the water surface profile computed inside of the culvert.

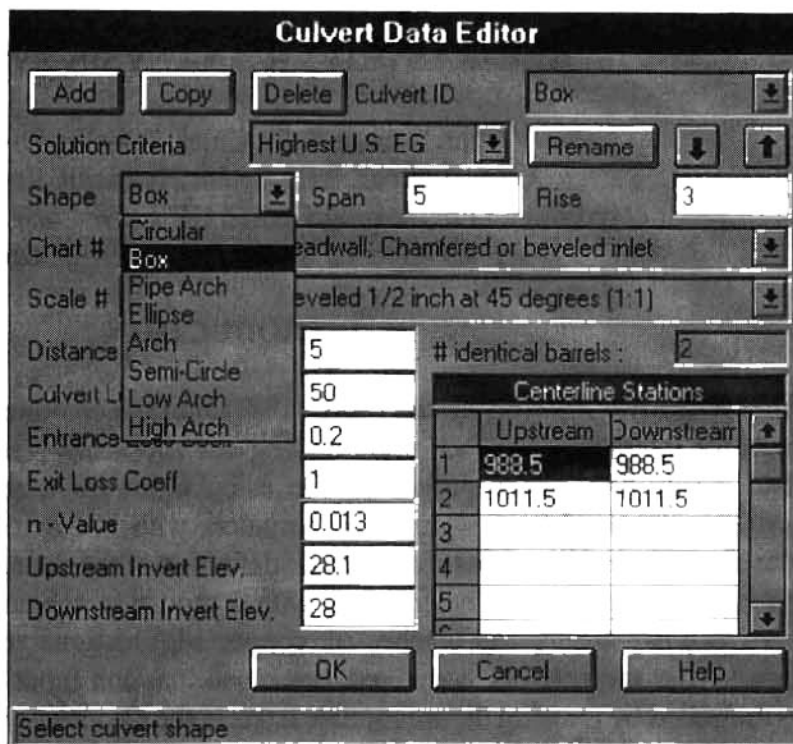


Figure 1. Culvert Data Editor

Gates and Weirs. The program can model inline gated spillways and overflow weirs. Gates can be radial (tainter gates) or vertical lift gates (sluice gates). The spillway crest of the gates can be either an ogee shape or a broad crested weir shape. In addition to the gate openings, the user can model a separate uncontrolled overflow weir. The weir (or dam) data are entered just like the roadway for a bridge or culvert, filling the cross section from the ground to top-of-weir. Gates are added with a Gate Editor, figure 2. The gates are placed into the section, by defining the dimensions, locations and coefficients. Like culverts, multiple identical gates can be defined by defining the number, the data for one, and the centerline location for each.

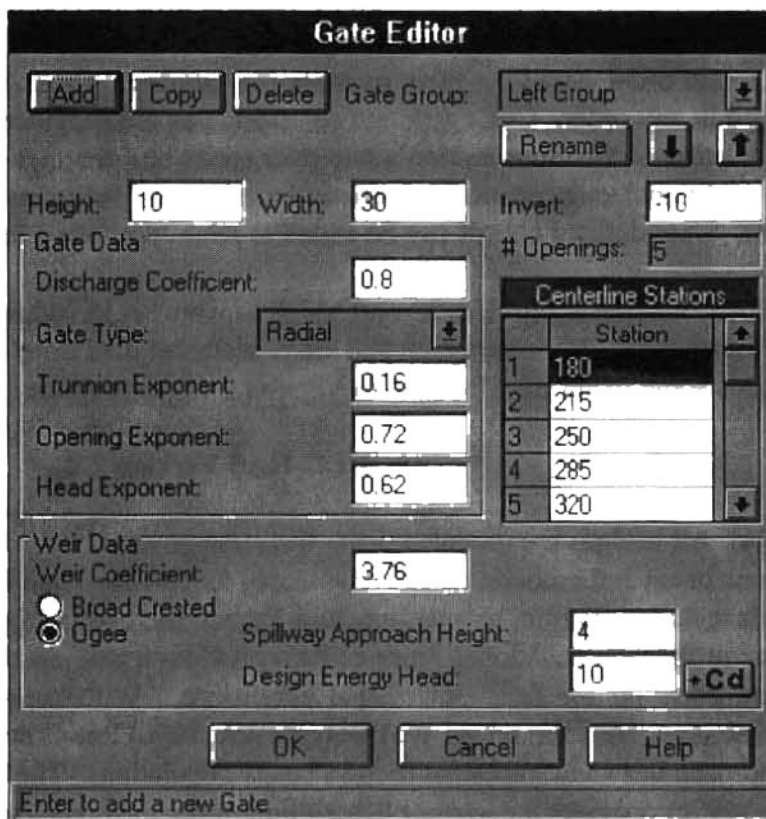


Figure 2. Gate Editor for Inline Gates and Weirs

Bridge Scour. Bridge scour is the first Hydraulic Design Option in HEC-RAS. The program feature was added with support from the Federal Highway Administration and it reflects the procedures presented in HEC 18, *Evaluating Scour at Bridges* (FHWA, 1995). After calibrating a model, water surface profiles are computed with the flow-distribution option. The results from this computation are the basis for the scour computation. The data entry screen provides tabs to input data for Contraction, Pier, and Abutment scour. As shown in figure 3, the computed scour is shown in the graphic. An output report can be generated, providing input summary and computed results.

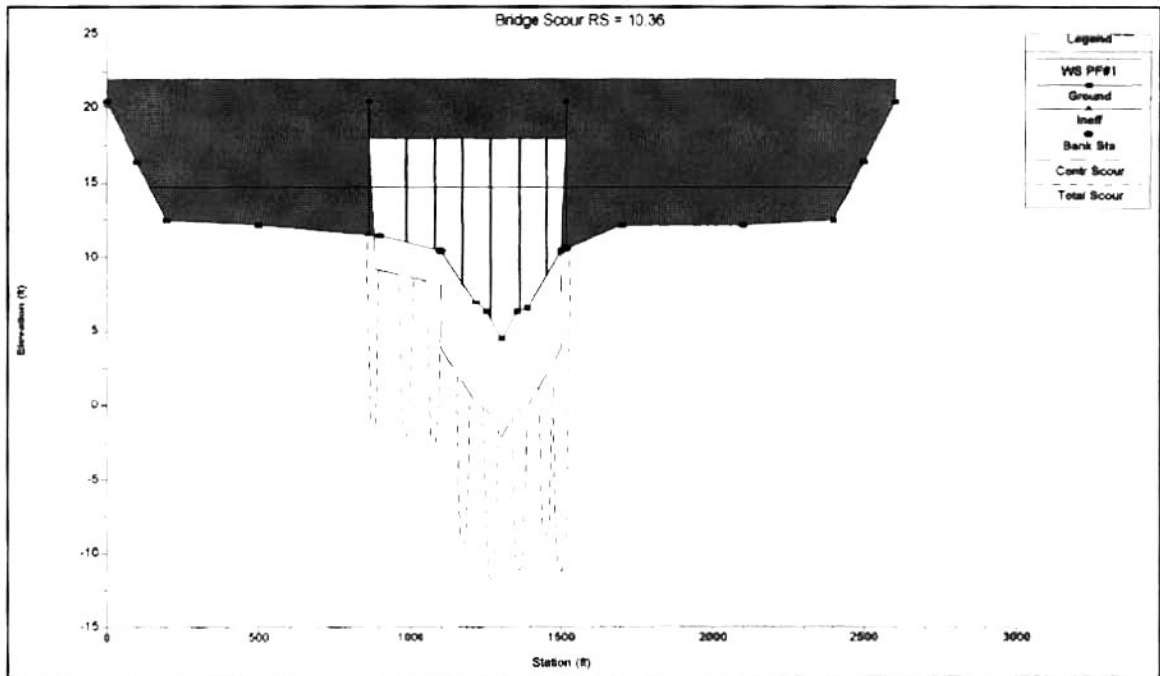


Figure 3. Bridge Cross Section with Computed Scour

Channel Modification. This option is the equivalent of the HEC-2 CHIMP routine. The modeler can evaluate the impact of channel modifications on the water surface profile by using the base geometry as one plan and the modified geometry as another. The data editor is accessed under **Options** in the **Geometric Data Editor**. Figure 4 is an example of the Channel Modification Editor.

A channel template is defined to apply to a selected range of cross-section data. Up to three trapezoidal channel templates can be defined by bottom width, invert elevation, side slopes, and location in the cross section. Channel 'n' values can be modified. **Center Cuts (y/n)** indicates whether the template will be centered between the section bank stations. If no, the station must be entered. The template can be extended on a constant slope down from the upstream section, or up from a downstream section.

Apply Cuts to Selected Range will define the channel modification data in the table at the bottom of the menu. Side slopes on the template are extended to the existing ground profile. Bank stations are redefined to match the template, when the section intercepts the ground outside of the existing bank station. The data for each section in the table can be modified. **Compute Cuts** applies the data

at the bottom of the table to the cross sections. As shown in figure 4, the sections and their cuts are displayed after the cut is applied. The modeler can interact with the channel modification until the desired results are achieved. The **Cut Fill Areas** produces a table of cut areas and volumes for the three cross-section elements, the total section, plus the total volumes for the reach.

The **Create Modified Geometry** computes a geometry file that can then be saved as a new geometry file. To compute profiles for the modified channel, a new plan is created with the new geometry and the flow data files. The results from profile computations can be compared in tables and graphics by selecting the existing and modified plan.

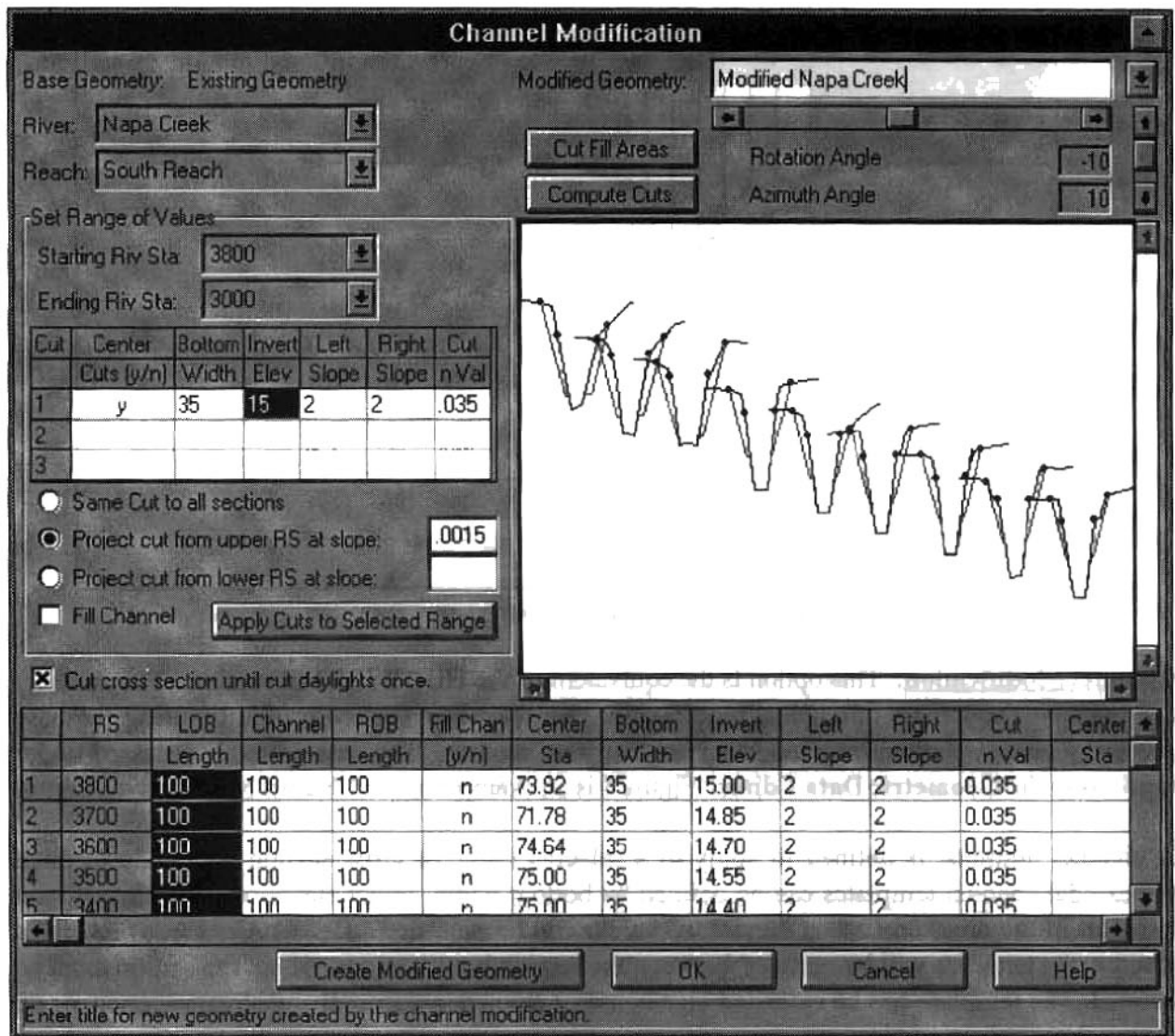


Figure 4. Channel Modification Menu with Computed Sections

Geometric Data Import. With a new data-exchange file format, the program can import and use 3D geometric data. Figure 5 shows the Geometric Data Editor with model data imported from a terrain model. The plan-form of the stream network and the cross-section locations and orientation

are preserved from the terrain data. The display is not distorted; therefore, cross-section widths and the distance between sections reflect the relative spacing of the physical data. Also, background maps can be added as a backdrop in the river-reach display and photographs can be linked with model cross-sections. Sections with photos attached display a marker that can be clicked on, with the cursor, to display the photograph. This option should be helpful for bridge and culvert modeling.

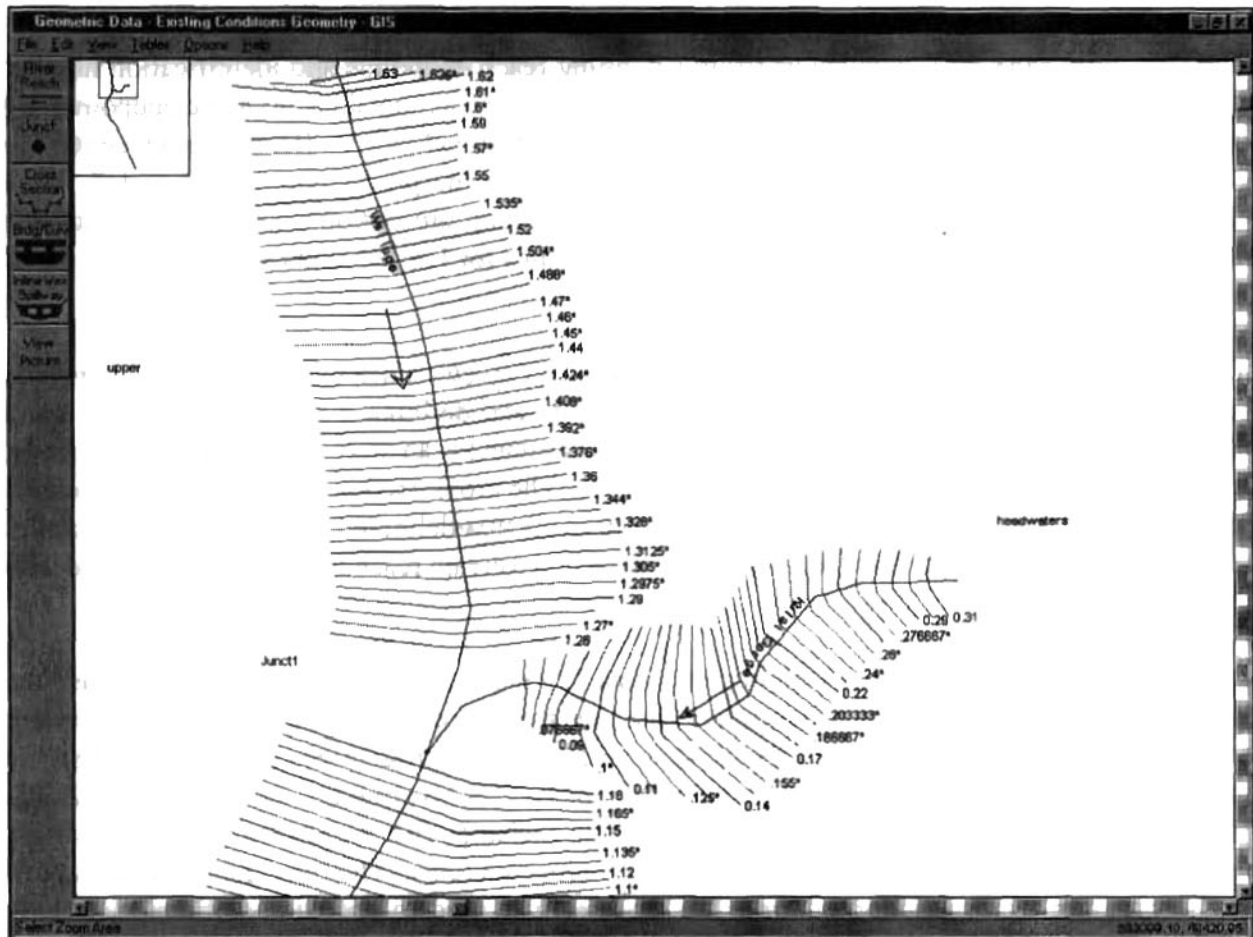


Figure 5. HEC-RAS Geometric Data Screen with Imported Terrain Data for Wailupe River, HI

Data Exchange File. HEC is developing a format standard for a general-purpose data exchange between CADD or GIS programs and its Next Generation computer programs (HEC, 1996). The goal is to facilitate data transfer between HEC models and the CADD and GIS software systems, without "adopting" any one system. Terrain data can include watershed boundaries, stream network definition, catchment area, river cross-sections, and similar model data. The initial focus has been to provide an interface with the *Hydrologic Modeling System*, HEC-HMS (HEC, 1995) and the *River Analysis System*, HEC-RAS. Data records have been defined to provide basic terrain data to these two program and new records will be added, as required.

The data exchange file is a formatted ASCII text file. Standard records in the file are composed of keywords and values. The use of keywords and a text-file format provides a self documenting file

which can be created or edited with a text editor, and is easily read and understood by reviewers. Records in the data file can be grouped into two types: file sections and objects. HEC-RAS can read geometric data from an exchange file composed of three file sections: (1) a header containing descriptions that apply to all data in the file, (2) the stream network containing reach locations and connectivity, and (3) model cross-sections containing their locations on the stream network and cross-section coordinates.

The stream network section contains records defining reach endpoints and identification number (ID), plus the reach data. At a minimum, the stream network must contain at least two endpoints and one reach. Each reach is defined by a multi-record object that includes: an ID, the stream centerline XYZ coordinates, and river stations. The XY values are the planar coordinates and Z is the elevation. In HEC-RAS, the elevation and river stationing are optional data in the centerline definition. River station values are assumed to be in miles for English units and kilometers for SI units.

The cross-section file section contains the cross-section objects. Each cross-section must include records identifying: the stream, reach and river station; and defining a 2D section cut line and a series of 3D locations on the cross-section. The cut-line object is an array of XY locations defining the cross section in plan view, as shown in figure 5. The cross-section object consists of a label "SURFACE LINE:" and the 3D coordinates, written as comma-delimited XYZ real-number triples. Also, the section's left and right bank stations and the downstream reach lengths can be defined with the cross sections.

Developing an HEC-RAS model with imported data first requires starting a new project. Then one would open the Geometric Data editor, select Files, and then select Import GIS Data. A file browser screen appears allowing you to select the data exchange file. The program reads the file and displays the river-reach graphic based on the imported data. The HEC-RAS program maintains the XYZ data for graphical displays and to provide output to the data exchange file. For hydraulic computations, the program translates the XYZ coordinates into 2D cross-sections. The translated data are shown in the program's cross-section editor. The modeler will need to provide additional data like: Manning's n , contraction and expansion coefficients, plus bank stations and reach lengths if they are not included in the exchange file. The modeler will also have to add data defining all hydraulic structures in the reach to complete the geometric data model. Flow data and boundary conditions are required for the flow-data file. Then, the model would be ready to compute profiles. The program operation and features are the same as they are for user input data, except for the XYZ graphic which displays the water surface in the 3D terrain model. Figure 6 is an XYZ display of the lower reach of the Wailupe River model, under flood-flow conditions.

HEC-RAS can write an output file in the data exchange file format. In the Main menu, under File, is an Export GIS Data option. Selecting this option allows you to write an exchange file with model results. In the file header section, the program writes the date and time for the output, the number of reaches, cross sections, and profiles. Version 2 allows the user to input a profile name, (e.g., 100-year) which is used as the profile identification label.

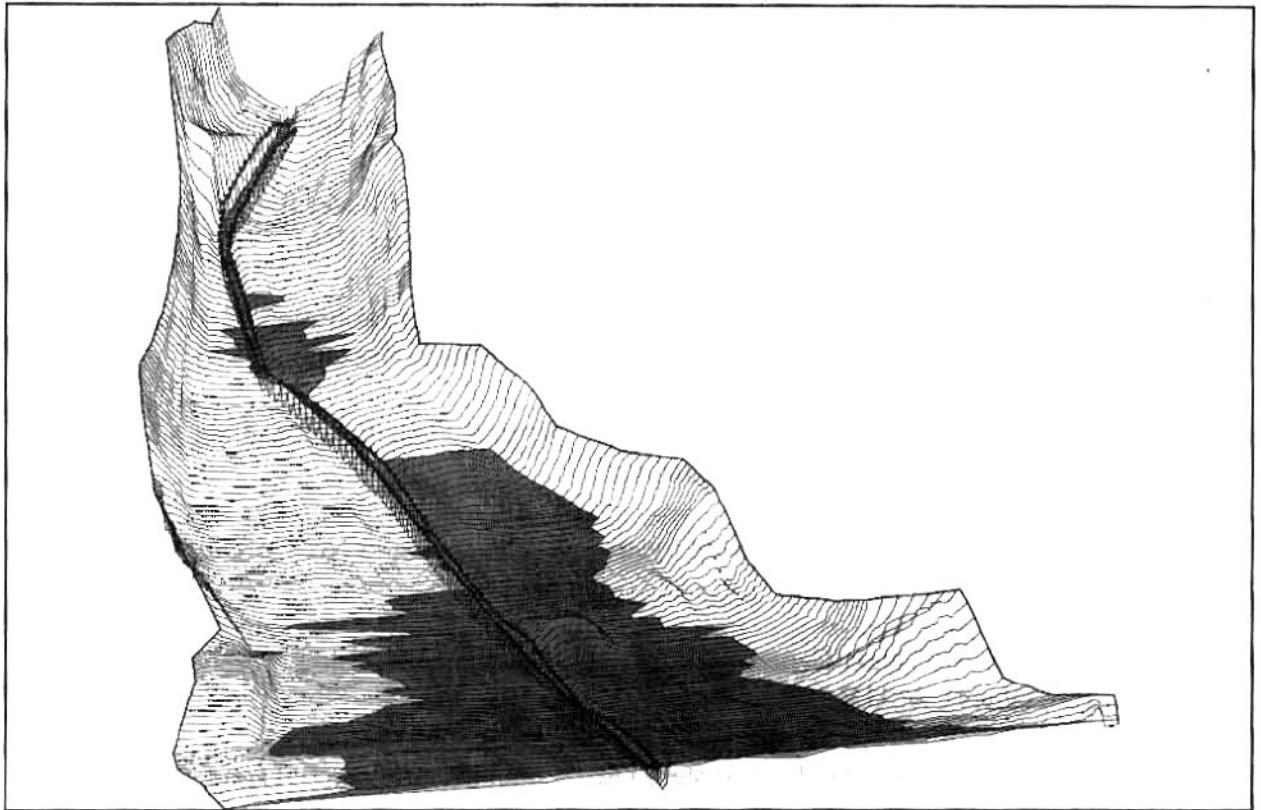


Figure 6. HEC-RAS XYZ Perspective Plot of Lower Wailupe River Reach, HI.

In the cross-section file section, the program writes the cross-section identification data and the 2D coordinate pairs for the section cut line. The computed water-surface elevation is written for each cross section. Following the cross-section data, the boundary polygons for each reach are provided by 2D coordinates. A reach's boundary polygon is composed of the most upstream cross section on the reach, the endpoints for each cross section in the reach and the most upstream cross-section of the downstream reach(es). If the cross-section geometry defines the limit of the water-surface inundation, no adjustments are made to the polygon boundary. The floodplain boundary will be determined in the terrain model by the intercept of the water-surface plane with the river-reach geometry. However, when the water surface is limited by levees, bridges and culverts, or floodways, the polygon is defined at the water's edge for those cross sections. Then when the polygon is used in the terrain model, the HEC-RAS knowledge of where the water is within each cross section is transferred to the CADD or GIS software. The adjusted polygon boundary will limit the floodplain definition to the polygon, rather than the water's intercept with the terrain data.

Version 2.1. An updated program was released in October 1997, providing error corrections to the Version 2.0 program and adding graphical editing of cross-section data. Also, options were added to model air entrainment effects on water surface elevation for high-velocity streams and to model floating debris accumulation on bridge piers. Both options are based on criteria used in the Corps' Los Angeles District and were added to develop a design model for the Santa Ana River.

REFERENCES

- Federal Highway Administration (FHWA) , 1985, Hydraulic Design of Highway Culverts, Hydraulic Design Series No. 5, U.S. Department of Transportation, September 1985.
- FHWA, 1990, User's Manual for WSPRO - A Computer Model for Water Surface Profile Computations, Publication no. FHWA-IP-89-027, September 1990.
- FHWA, 1995, Evaluating Scour at Bridges. Federal Highway Administration, Hydraulic Engineering Circular 18, FHWA # IP-90-017, 3rd Editions, November 1995.
- Hydrologic Engineering Center (HEC), 1990, HEC-2 Water Surface Profiles. User's Manual Davis CA: U.S. Army Corps of Engineers.
- HEC, 1995, The HEC Hydrologic Modeling System. Technical Paper No. 150, Davis CA: U.S. Army Corps of Engineers.
- HEC, 1996, Status of HEC Next Generation Software Development Project. Technical Paper No. 156, Davis CA: U.S. Army Corps of Engineers.
- HEC, 1997a, HEC-RAS River Analysis System User's Manual. Version 2, Davis, CA: U.S. Army Corps of Engineers.
- HEC, 1997b, HEC-RAS River Analysis System Hydraulic Reference Manual. Version 2, Davis, CA: U.S. Army Corps of Engineers.
- HEC, 1997c, HEC-RAS River Analysis System Application Guide. Version 2, Davis, CA: U.S. Army Corps of Engineers.

CCHE2D: A TWO-DIMENSIONAL FREE SURFACE FLOW AND SEDIMENT TRANSPORT MODEL FOR NATURAL RIVERS

By Randy Bowie, Coordinator of Computing Facility Operation, Center for Computational Hydroscience and Engineering, The University of Mississippi, University, MS 38677; Abdul Khan, Post-Doctoral Research Associate, same address; Yafel Jia, Research Assistant Professor, same address; and Sam Wang, F. A. P. Barnard Distinguished Professor, Director CCHE, same address.

Abstract: The CCHE2D is a computational software package, developed at the Center for Computational Hydroscience and Engineering (CCHE), University of Mississippi, for solving free surface, steady/unsteady, turbulent flows with sediment transport capability. CCHE2D is bundled with the graphical user environment known as HydroVision, also developed at the CCHE, which provides a graphical user interface (GUI) for grid generation, simulation control and scientific visualization.

The CCHE2D model along with the HydroVision GUI provide a robust software package for modeling practical river flow problems. The wetting and drying of the nodes during the simulation process allow for easy handling of submergence and exposition of the land during flood propagation with a specified discharge hydrograph at the upstream end. The model has been thoroughly tested by simulating both laboratory experiments and field situations and has been found to be both stable and accurate under a variety of conditions.

The model is targeted for use as a practical engineering tool for solving problems of natural rivers with or without hydraulic structures including bed aggradation or degradation, local scour, bank and bend migrations, etc. The model can also be used for assessing the impact of new or already present hydraulic structures, such as dike, bridge abutments and piers, grade control structures, etc., on the environment and ecology of a given river reach. In short the CCHE2D model along with HydroVision provides a robust, stable model for natural rivers with sediment transport. The model can be used both for determining the local flow and bed change details around the hydraulic structure and general flow and morphological conditions for a reasonably long river reach for steady or unsteady flow situations.

INTRODUCTION

The mathematical model is based on the depth-averaged Navier-Stokes equations for flow model and sediment continuity equation for bed and bank changes. The turbulent stresses are approximated with Boussinesq eddy viscosity concept. The turbulent eddy viscosity is approximated either by assuming parabolic distribution in vertical direction or by the mixing length hypothesis. The second approach is found to be more suitable for reverse flows, shear layers, and flow behind hydraulic structures. The sediment transport is modeled using van Rijn's bed load formula, however, the users can specify or input a different sediment transport formula valid for the case under investigation.

The above set of equations are solved using well documented efficient element method with explicit time stepping scheme. The spatial domain is discretized using structured grid with quadrilateral elements and quadratic interpolation functions.

Results are presented which demonstrate the application of the CCHE2D model and the HydroVision to a variety of situations. In particular the computed results of bed aggradation and degradation results are compared to experimental data. Simulations of Hotophia creek, a natural stream in north Mississippi, illustrate simulation of hydraulic structures and flood wave propagation.

The graphical user environment known as HydroVision provides a cross platform graphical user interface (GUI) for grid generation, simulation control and scientific visualization for the CCHE2D model. HydroVision's intuitive interface speeds the development of numerical simulations by providing automatic grid generation based either on cross section survey data or outer boundary geometry combined with a computer aided design interface for direct graphical editing of the efficient element grid; graphical input of initial conditions, such as bed roughness and initial surface elevation; graphical specification of boundary conditions; simulation control and simulation monitoring from the GUI; and scientific visualization and hard copy capabilities.

THE CCHE2D MODEL

Mathematical Model: The governing equations solved by the CCHE2D model are briefly explained here. For complete details the reader is directed to the CCHE technical report by Jia and Wang (1997a).

The momentum equations for depth-integrated two dimensional turbulent flows in a Cartesian coordinate system are:

$$\frac{\partial u}{\partial t} + u \frac{\partial u}{\partial x} + v \frac{\partial u}{\partial y} = -g \frac{\partial \eta}{\partial x} + \frac{1}{h} \frac{\partial \tau_{xx}}{\partial x} + \frac{1}{h} \frac{\partial \tau_{xy}}{\partial y} - \frac{\tau_{bx}}{\rho h} + f_{Cor} v \quad (1)$$

$$\frac{\partial v}{\partial t} + u \frac{\partial v}{\partial x} + v \frac{\partial v}{\partial y} = -g \frac{\partial \eta}{\partial y} + \frac{1}{h} \frac{\partial \tau_{xy}}{\partial x} + \frac{1}{h} \frac{\partial \tau_{yy}}{\partial y} - \frac{\tau_{by}}{\rho h} - f_{Cor} u \quad (2)$$

where u and v are depth-integrated velocity components in x and y directions, respectively, t is the time, g is the gravitational acceleration, h is the water surface elevation, ρ is the density of water, h is the local water depth, f_{Cor} is the Coriolis parameter, τ_{xx} , τ_{xy} , τ_{yx} , τ_{yy} are depth integrated Reynolds stresses and τ_{bx} , τ_{by} are shear stresses on the bed and flow interface.

Free surface elevation for the flow is calculated by the continuity equation:

$$\frac{\partial \eta}{\partial t} + \frac{1}{A} \int h s \bar{u} \cdot d\bar{n} = 0 \quad (3)$$

where h is the free surface elevation, A is the area of an element, s is the length of a line segment along a curved boundary of an element, h is the water depth at the segment and \bar{n} is the direction unit-vector of the segment pointing outwards.

The turbulence Reynolds stresses in the equations (1) and (2) are approximated according to the Bousinesq's assumption, as follows:

$$\tau_{xx} = 2\nu_t \frac{\partial u}{\partial x} \quad (4)$$

$$\tau_{xy} = \nu_t \left(\frac{\partial u}{\partial y} + \frac{\partial v}{\partial x} \right) \quad (5)$$

$$\tau_{yy} = 2\nu_t \frac{\partial v}{\partial y} \quad (6)$$

Two methods for calculating eddy viscosity are available in the current model. First, the eddy viscosity coefficient ν_t is calculated using the depth integrated parabolic eddy viscosity formula:

$$\nu_t = A_{xy} C_s \kappa u_* h \quad (7)$$

where

$$C_s = \int_0^1 \zeta(1-\zeta) d\zeta = \frac{1}{6} \quad (8)$$

and u_* is shear velocity, κ is the von Karman's constant (0.41) and V is the relative depth of the flow. A_{xy} is a coefficient to adjust the value of the eddy viscosity. Its default value is set to 1 and it can be adjusted by users from 1~10.

In addition to this approach, the depth integrated mixing length eddy viscosity model is also available:

$$v_t = \bar{l}^2 \sqrt{2\left(\frac{\partial u}{\partial x}\right)^2 + 2\left(\frac{\partial v}{\partial y}\right)^2 + \left(\frac{\partial u}{\partial y} + \frac{\partial v}{\partial x}\right)^2 + \left(\frac{\partial \bar{U}}{\partial z}\right)^2} \quad (9)$$

where

$$\bar{l} = \frac{1}{h} \int \kappa z \sqrt{\left(1 - \frac{z}{h}\right)} dz = \kappa h \int_0^1 \zeta \sqrt{(1 - \zeta)} d\zeta \approx 0.267 \kappa h \quad (10)$$

The depth integrated velocity gradient along vertical coordinate $\frac{\partial U}{\partial z}$ is introduced to account for the effect of turbulence generated from the bed surface. The eddy viscosity defined by (9) would be zero in the uniform flow condition without this term. It is determined in the way that eddy viscosity shall be the same as that of the uniform flow in absence of other terms. Assuming the flow is of logarithmic profile along the depth of the water, the vertical gradient should be

$$\frac{\partial U}{\partial z} = \frac{U_*}{\kappa z} \quad (11)$$

equation (11) is integrated vertically to obtain depth averaged vertical gradient, which is represented by

$$\frac{\partial \bar{U}}{\partial z} = \frac{1}{h} \int \frac{\partial U}{\partial z} dz = \frac{U_*}{h\kappa} \int_{z_0}^h \frac{1}{z} dz \approx C_m \frac{U_*}{h\kappa} \quad (12)$$

where U is total velocity, U_* is the total shear velocity and C_m is a coefficient. Instead of directly calculating C_m , this coefficient is assigned in such a way that equation (9) shall recover equation (7) in the absence of all the horizontal velocity gradients (uniform flow). Thus, the assigned value is 2.34375. Another important problem regarding both mixing length model and parabolic model is the wall effect. Very close to the wall, the distance to the wall should be used as the length scale instead of that to the bed. This is taken care of in the model.

Sediment transport modeling in the current version of the CCHE2D model is based on equilibrium bed load transport of uniform materials. The bed load transport formula developed by van Rijn (1993) is adopted,

$$q_b = 0.053 \left[\left(\frac{\rho_s}{\rho} - 1 \right) g \right]^{0.5} d_{50}^{1.5} D_*^{-0.3} T^{2.1} \quad (13)$$

where

$$D_* = d_{50} [(s-1)g/v^2]^{1/3} \quad (14)$$

$$T = (\tau - \tau_{cr}) \tau_{cr} \quad (15)$$

$$s = \rho_s / \rho \quad (16)$$

$$\tau_{cr} = (\rho_s - \rho) g d_{50} \theta_{cr} \quad (17)$$

and when D_* is the parameter, T is the bed shear stress parameter, s is the ratio of the density of the sediment to that of the water, and τ_{cr} is critical shear stress according to Shields .

Bed load q_b at solid walls and out let boundaries satisfies the condition

$$\frac{\partial q_b}{\partial n} = 0 \quad (18)$$

and at the inlet boundary, it is requires to prescribe $q_b = \text{constant}$.

Numerical Scheme: The aforementioned system of equations (1) and (2) are solved by using the Efficient Element

Method initiated by Wang and Hu (1992). A collocation approach is adopted in the finite element method to discretize the mathematical equations. In this version of the CCHE2D model, the mass conservation is expressed by the integral equation (3). Because the solution of the continuity equation is de-coupled from that of the momentum equations, it is very simple to solve equation (3) and update the water surface elevation.

All the unsteady governing equations are solved by the fourth order Runge-Kutta method. This explicit scheme makes it very simple to march in time. During the simulation, the time step Δt is adjusted automatically. The adjustment is controlled by the CFL number, which should always be less than one, and the error norm.

Verification and Applications: A few results are given to illustrate the model's capabilities, these results are taken from the CCHE technical report by Jia and Wang (1997b). Figures 1 and 2 show comparison of computed results obtained using CCHE2D with channel aggradation flume experiment data (Soni, 1981) and channel degradation experiment data (Newton, 1951) respectively. In both cases the trends of channel bed change agrees with those observed in physical experiments.

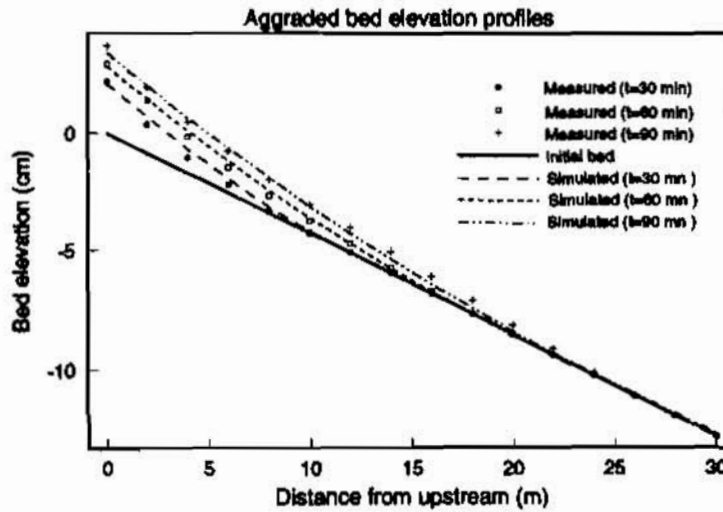


Figure 1 Verification of sediment transport model using aggradation experiments.

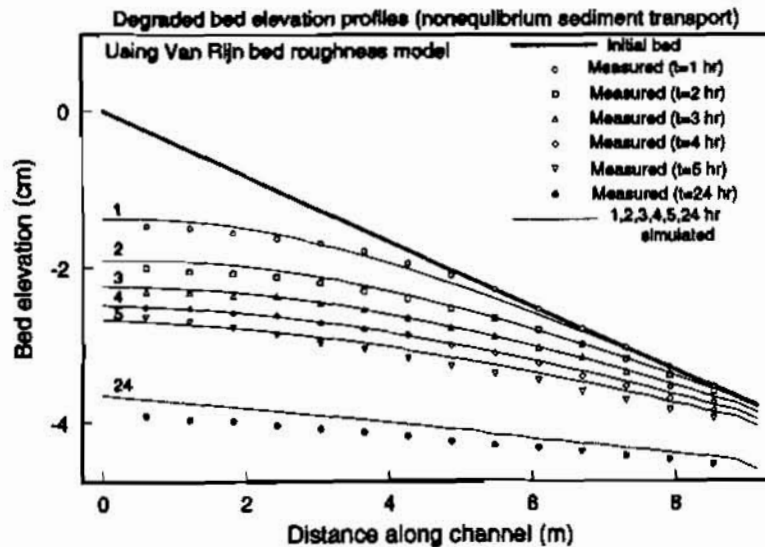


Figure 2 Verification of sediment transport model using degradation experiments.

The next two figures show application of the model to simulate flow in a natural channel. The vector plot in Figure 3 shows the flow patterns behind hypothetical spur dikes placed in a section of Hotophia creek. Figure 4 shows the

simulation of another section of the same creek with a flood wave passing through. Initially dry areas of the flood plains were submerged under the flooding and became dry again in the retreat period of the flood.

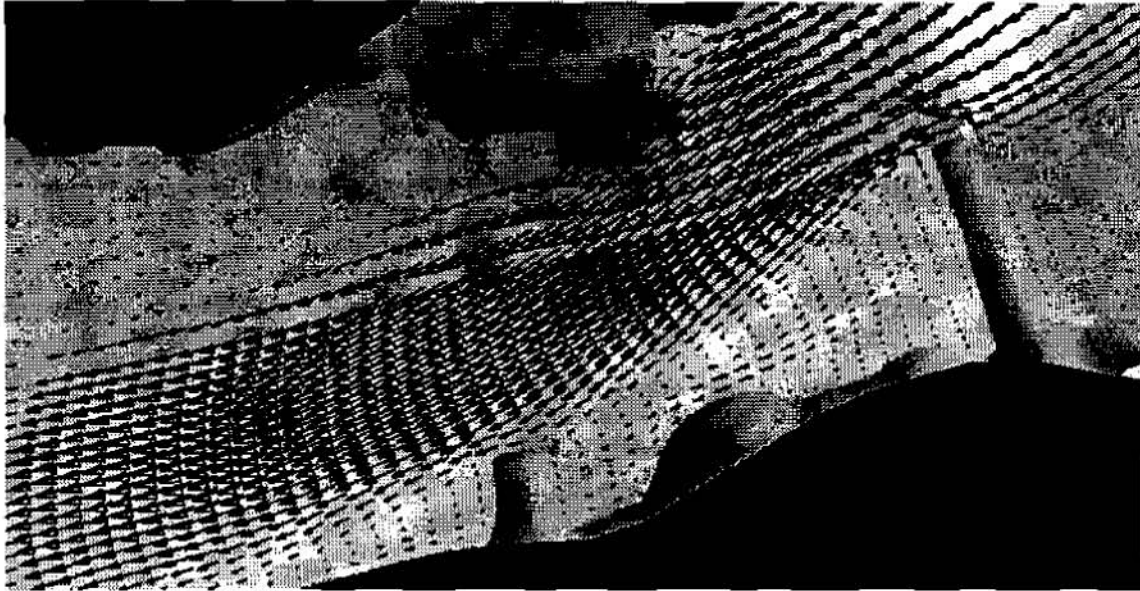


Figure 3 Simulated flow field around spur dikes in Hotophia Creek.

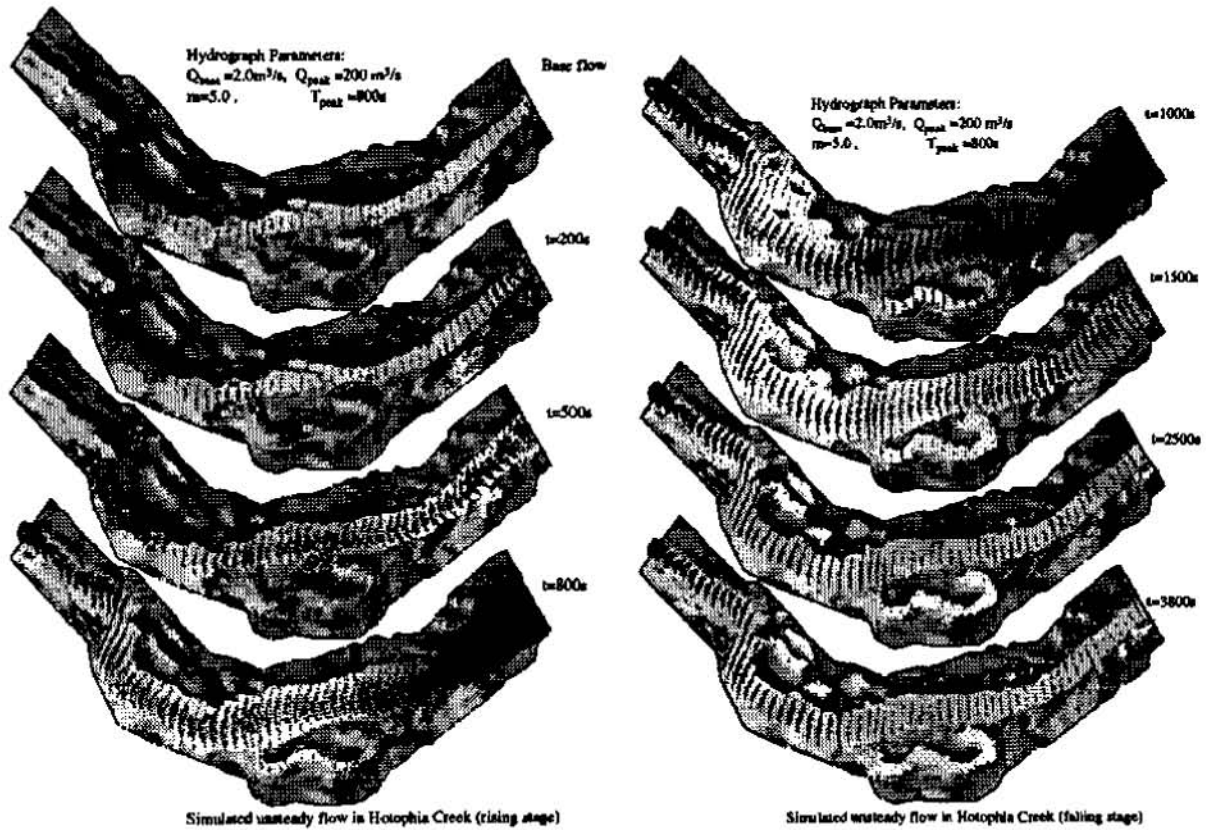


Figure 4 A Flood Wave Propagation

HYDROVISION

HydroVision is a highly interactive visual interface. It allows the user to generate a nonuniform structured mesh with quadrilateral elements, either via a computer aided design (CAD) interface, which allows for specification of elevations from a topographic map or automatically from cross-sectional data of natural rivers. The user can specify zones within the computational area having different roughness. A steady total discharge at the inlet section, specific discharge at boundary nodes or a discharge hydrograph at the inlet section, can be specified as inlet boundary conditions. Monitor stations can be specified in the computational domain and the time history plots of these points can be displayed while the simulation is underway. This feature helps in assessing the convergence of the model in case of steady flow simulation and yields useful information in the case of unsteady flow. At the same time a graphical display of the normalized maximum change of velocity and surface water elevation is provided to monitor the execution of the run. The final results of initial and final water surface elevation, velocity vectors and magnitude, bed shear stress etc., can be visualized and saved as a postscript file for printing and presentation.

The HydroVision interface with a generated grid is shown in Figure 5. In this case the grid was generated using cross section survey data. Figures 5, 6 and 7 show the setting of the boundary conditions, monitoring the error norms of an simulation in progress, and the visualization of a CCHE2D simulation. The entire interface is discussed in detail in CCHE technical report by Bowie and Khan (1997).

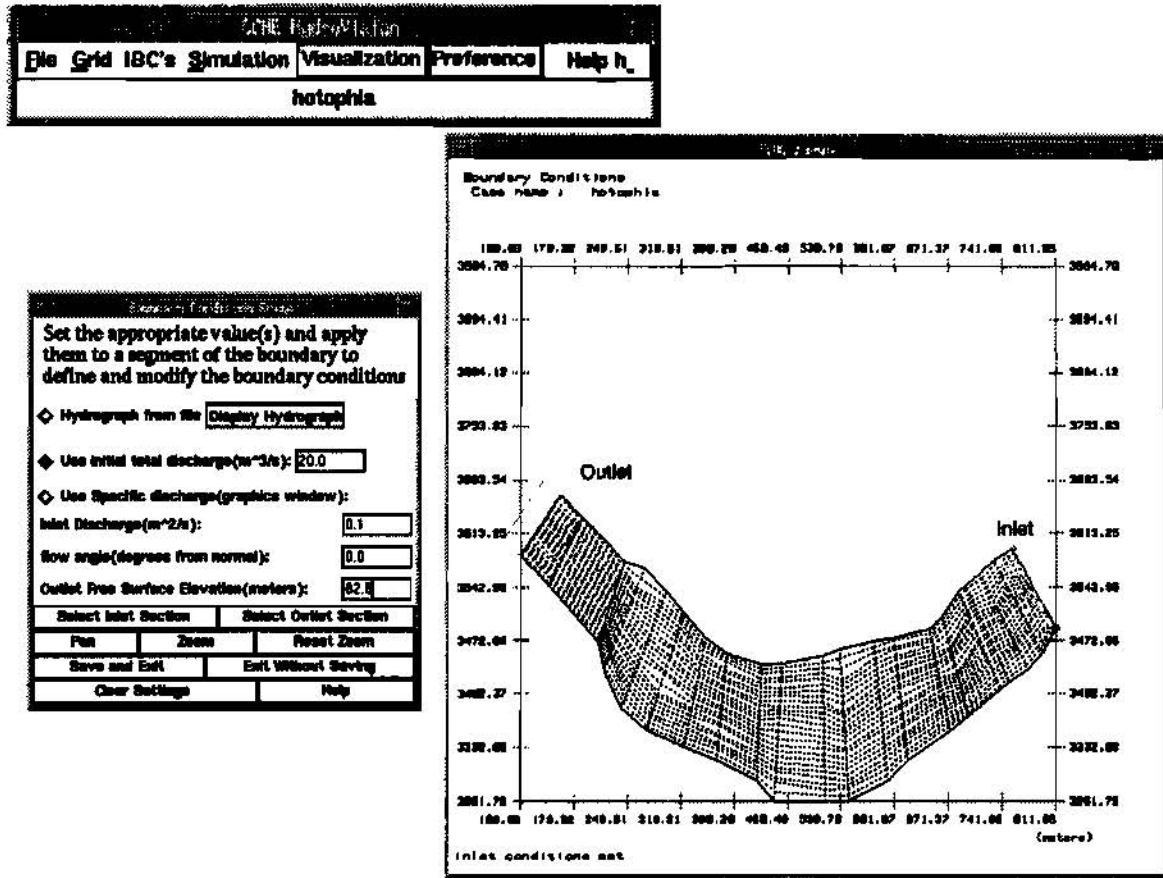


Figure 5 Setting Boundary Conditions in HydroVision

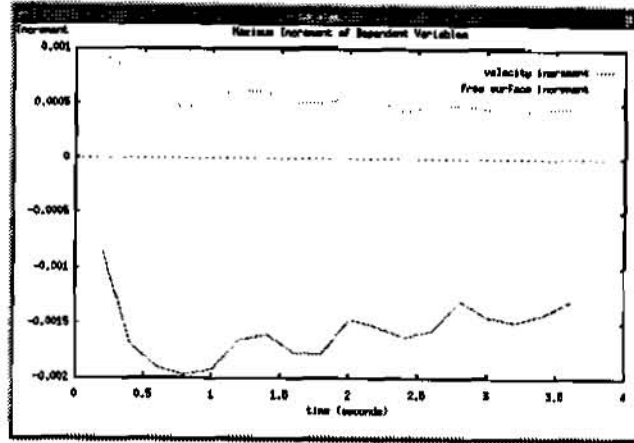
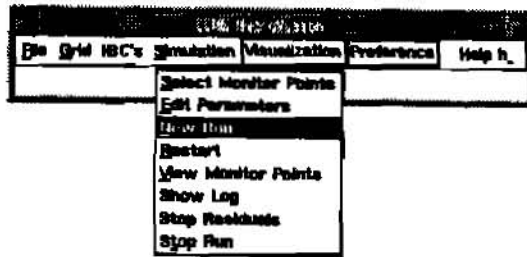


Figure 6 Monitoring the Error Norms of A Simulation

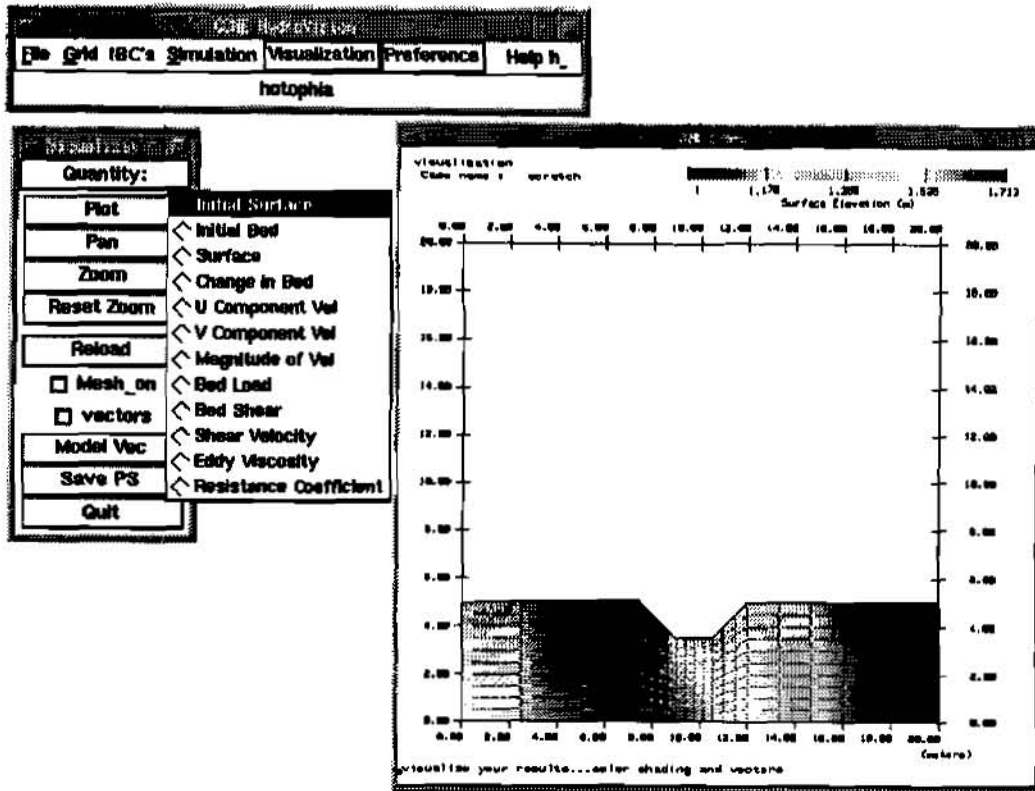


Figure 7 Visualization of CCHE2D Results Using HydroVision

SUMMARY

CCHE2D combined with the HydroVision GUI is an effective tool for studying natural channels. The model can be used to simulate the effectiveness of a hydraulic structure, the quality of fish habitat with a high degree of accuracy. The interface allows the user to make adjustments to the geometry or boundary conditions and perform new simulations very quickly.

BIBLIOGRAPHY

- Bowie R., and Khan A. A., 1997, "HydroVision: A Graphical User Environment Applied to the CCHE2D Model," CCHE-TR-97-5.
- Jia, Y., and Wang, S. S-Y., 1997, "CCHE2D: A Two Dimensional Hydrodynamic and Sediment Transport Model for Unsteady Open Channel Flows Over Loose Bed," CCHE-TR-97-2.
- Jia, Y., and Wang, S. S-Y., 1997, "CCHE2D Model Verification Tests Documentation," CCHE-TR-97-4.
- Newton, C.T., 1951, "An experimental investigation of bed degradation in an open channel", Trans. Boston Soc. Civ. Engrs., pp 28-60.
- Soni, J. 1981, "Laboratory study of aggradation in alluvial channels", J. Hydrol, 49, pp87-106.
- Van Rijn, L. C., 1993, Principles of Sediment Transport in Rivers Estuaries and Coastal Seas. Aqua Publications, The Netherlands.
- Wang Sam S.Y., and Hu, K.K., 1992 "Improved methodology for formulating finite-element hydrodynamic models", In T.J, Chung, (ed) Finite Element in Fluids, Volume 8, Hemisphere Publication Cooperation, pp 457-478.

NEXT GENERATION FLOOD DAMAGE ANALYSIS PROGRAM

By Robert Carl, Hydraulic Engineer, U.S. Army Corps of Engineers Hydrologic Engineering Center, Davis, California; Michael Burnham, Chief, Planning Analysis Division, U.S. Army Corps of Engineers Hydrologic Engineering Center, Davis, California

Abstract: The Hydrologic Engineering Center (HEC) has developed a next generation Flood Damage Analysis computer program (HEC-FDA) for formulating and evaluating flood damage reduction plans. The program design is consistent with federal and Corps of Engineers policy and technical requirements. It includes risk-based analysis procedures. HEC-FDA calculates expected annual damage and equivalent annual damage using hydrologic, hydraulic, and economic data. It produces tabular and graphical output that can be used to evaluate the inundation reduction benefits of alternative plans and project performance. It uses Xbase formatted database files to store input data and output results which can be accessed by commercial programs. The graphical user interface (GUI) utilizes a cross-platform software library for easy porting to many platforms. The program operates on Microsoft Windows NT and Microsoft Windows 95 platforms.

INTRODUCTION

Background: One of the primary Civil Works Missions of the U.S. Army Corps of Engineers is to provide flood protection for communities in the United States. The Corps has reduced flood damage by implementing many structural and nonstructural measures. It has evaluated proposed alternative measures using a variety of tools ranging from hand calculations, mainframe batch computer programs, mainframe programs ported to personal computers, sophisticated Geographical Information Systems related programs, and now the new next generation HEC-FDA. Corps regulations dictate analysis procedures and reporting requirements. With time, these have changed to meet the changing needs of the country and to utilize new science and technology.

Requirements: The Corps recently enacted regulations requiring the use of risk-based analysis procedures for formulation and evaluating flood damage reduction measures (USACE, 1996b). Historically, without or existing conditions were evaluated using expected annual damage calculations which are computed by integrating a damage-frequency function. The damage-frequency function is derived from combining the discharge-frequency, stage-discharge, and stage-aggregated damage functions. Except for the discharge-frequency function, these functions all represented the best estimate — there was no attempt to quantify uncertainty in the functions other than to perform some sensitivity analyses. With the implementation of the risk-based regulations, all Corps studies must use the new procedures. The procedures require quantifying the uncertainty in the discharge-frequency, stage-discharge, stage-damage functions, and incorporating it into the economic and performance analyses of alternatives. HEC-FDA utilizes the Monte-Carlo numerical analysis procedure (Benjamin et al., 1970) to compute expected annual damage while explicitly accounting for the uncertainty in the basic functions.

RISK-BASED PROCEDURES

The damage-frequency function is derived from three basic functions: discharge-frequency, stage-discharge, and stage-damage. Alternatively, a stage-frequency function may be used in place of the discharge-frequency and stage-discharge functions. The uncertainty in the functions is quantified using a variety of parameters and techniques. For example, the uncertainty in the discharge-frequency functions is reflected in the equivalent length of record. If the function is computed using gaged data, the length of the gaging record is a good indication of the analyst's uncertainty in that function. At the other extreme, the stage-damage

functions are derived from Monte-Carlo simulations using uncertainties in several parameters including the first floor stage of structures, the estimated depreciated replacement value of the structure, etc. For every expected annual damage Monte-Carlo simulation, the three basic functions are sampled to derive the sampled damage-frequency function which is integrated to determine the expected annual damage. It may take several hundred thousand simulations before converging on the estimate of damage with an acceptable error.

PROGRAM STATUS

Provisional Version 1.0 of the HEC-FDA program was first released to only the U.S. Army Corps of Engineers in January 1997. Version 1.0 was released in January 1998 and is available to the public. During the last year, HEC (and their contractors) have made substantial changes to the database code, the GUI, and the calculation procedures. It has added new capabilities to analyze regulated frequency functions, interior-exterior stage functions, nonlinear geotechnical failure criteria, and levee wave overtopping.

SOFTWARE DESIGN

HEC-FDA is an object-oriented program written mostly in the C++ language. The software development was divided into four components which were written by different people including both HEC engineers and private contractors. There are four software components:

- (1) Databases - all interaction to the database is done through the database code.
- (2) Graphical User Interface (GUI) - all user input data are entered in the GUI screens.
- (3) Stage-Damage Monte-Carlo Simulations - all calculations for computing the stage-aggregated damage function with uncertainty is done in this component.
- (4) Expected Annual Damage Monte-Carlo Simulation - all the calculations to determine expected annual damage, equivalent annual damage and project performance is performed in this component.

The graphical user interface (GUI) software utilizes the Visix Corporation's "Galaxy" library (Visix Software Inc., 1994), and the database software utilizes the Sequiter Corporation's CodeBase library (Sequiter Software Inc., 1996). The stage-aggregated damage simulations are written in C++ using object-oriented design. The expected annual damage Monte-Carlo simulations are written in FORTRAN. The Galaxy library facilitates porting the GUI to multi-platforms including UNIX systems with minimal code changes. The CodeBase library enables storing the input and output data in standard Xbase formatted files which allow the user to edit the data using many commercial software programs (such as database or spreadsheet programs).

Before software coding began, HEC developed a requirements document. It provided a sound foundation upon which related design and development work could be built. In addition, a field group reviewed the design from a practitioner's standpoint. However, during software development, many substantial changes were made to all areas of the program design. The object-oriented design allowed concurrent modifications to all components of the program and facilitated the isolation of software bugs. Object-oriented development required new skills and new tools. Both have steep learning curves. To achieve project goals, HEC made a substantial investment in C++ training and the acquisition of software, particularly the Galaxy library. These were costly in time and staff resources. New code problems surfaced. For example, C++'s dynamic memory allocation and deallocation are powerful but difficult to program and the resulting software bugs have caused frequent execution failures in the early versions of the program.

STRUCTURE OF HEC-FDA ANALYSIS

Components and the GUI Structure: HEC-FDA is designed to be the primary tool for collecting, storing, and evaluating hydrologic, hydraulic, and economic input and output data for flood damage reduction studies. Specialists from different disciplines can use the program as a central collector of data and for turnkey analysis in these studies.

HEC-FDA is structured into several logical components which shadow the basic functions and provide structure to study management and access to evaluation results. These are the components:

- (1) File / Study management
- (2) Study Configuration
- (3) Hydrologic and Hydraulic Engineering
- (4) Economics
- (5) View
- (6) Evaluation
- (7) Results

Figure 1 displays the main HEC-FDA screen with an existing study open. The above components are shown as menu items with the exception of results which is located under the evaluation. The file / study management provides high level access to studies including creating new studies and opening existing studies. The study configuration provides the means to define the basic lists of

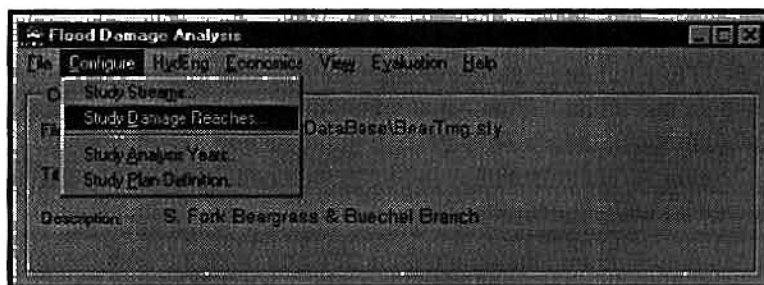


Figure 1: Study Configuration Screen

parameters such as streams, reaches, plans, and analysis years. The hydrologic and hydraulic engineering component accepts input data defining water surface profiles, frequency functions, stage-discharge rating functions, and geotechnical features such as levees. The economics component facilitates entry of structure attributes, damage potential functions, and calculation of stage-aggregated damage with uncertainty. The view component allows the analyst to view the basic lists (such as damage reaches) in modal windows. The evaluation component accesses data validation reporting and Monte-Carlo simulation for expected annual damage and equivalent annual damage. The results section displays expected annual damage and equivalent annual damage results in various formats as well as project performance information.

Overall Methodology: A flood damage reduction study requires the collection and analysis of hydrologic and economic data. The analyst creates a framework in which this data is categorized, stored, and manipulated. The framework of HEC-FDA requires the usual definitions for flood damage reduction studies such as alternative damage reduction plans, years of analysis, damage reaches, and damage categories. The three basic functions (discharge-frequency, stage-discharge, and stage-aggregated damage) are calculated from user input. The input and output (damage-frequency) functions are stored in the database from which plan formulation results are calculated and stored. They are stored by plan, year, stream-reach, and category if economics related. Detailed results are obtained by dividing the study area into reaches and an index location is established within that reach. The index location normally corresponds to a cross-section which is used for water surface profile calculations. The index location is established so that the three basic functions are developed for the same geographic location. Expected annual damage is calculated at the

damage reach level rather than for individual structures because Monte-Carlo simulation requires intense calculations requiring a significant amount of time.

The hydrologic and hydraulic input data is calculated outside of HEC-FDA but can be imported. The discharge-frequency functions may be computed using HEC-1 (USACE, 1987) or HEC-FFA (USACE, 1992). The stage-discharge functions are computed from water surface profiles which may be computed using HEC-2 (USACE, 1982) or HEC-RAS (USACE, 1997). Discharge-frequency and stage-discharge functions can be computed within HEC-FDA from the water surface profiles.

The economic stage-aggregated damage functions are computed within HEC-FDA. There is an additional framework for managing the input data for stage-damage calculations which includes damage categories, structure inventories, occupancy types, and structure modules. There is not a separate program for deriving the functions like there is for the hydrologic and hydraulic engineering functions.

STUDY CONFIGURATION

The study configuration includes the definition of study streams, damage reaches, analysis years, and alternative damage reduction plans. Figure 1 displays the configuration screen. Additional parameters should be considered as part of the configuration even though they are not attached to the "Configure" menu item. They include damage categories and structure modules. All configuration items should be defined early in the study. This allows two or more analysts to work on the study concurrently on different computers and then merge all data together into one database. Damage reaches are defined using stream stationing so that structures can be automatically assigned to reaches based on their geographic location with respect to water surface profiles.

HYDROLOGIC AND HYDRAULIC ENGINEERING

The hydrologic and hydraulic engineering component includes the entry of two basic functions: discharge-frequency and stage-discharge as well as water surface profiles, and levee criteria. Figure 2 demonstrates the functions which may be entered under "HydEng". Figure 3 depicts the screens for editing graphical frequency functions. The discharge-frequency, stage-discharge,

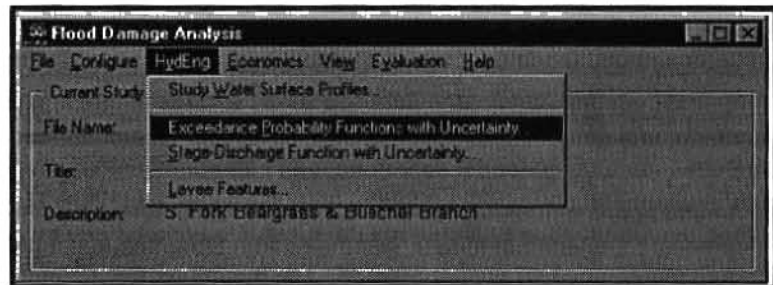


Figure 2: Hydrologic Engineering Components

and / or the stage-frequency functions can be computed from the water surface profiles. The analyst calculates eight water surface profiles which correspond to a wide range of exceedance frequencies - by default from 50% to 0.2% exceedance frequencies. HEC-FDA can then use the profiles to generate either a stage-frequency or discharge-frequency function. The computed stage-discharge function includes the invert stage at zero discharge. The analyst must then enter the uncertainty parameters for both functions.

ECONOMICS

The economics component includes data entry and calculation of stage-aggregated damage. The economics data entry consists of the configuration items of damage categories and structure modules as well as basic information such as occupancy types and structure inventories. Damage categories provide the framework for reporting damage by significant classes of damage such as single family residential, apartments, public

buildings, commercial structures, and industrial plants. For each of these categories, there are one or more global occupancy types and associated depth-damage functions. For example, the single family residential damage category may have the occupancy types of:

- (1) One story, no basement, wood frame, raised foundation
- (2) One story, no basement, masonry construction, slab floor
- (3) Two stories, with a basement, a wood frame, raised foundation
- (4) Etc.

For each of these occupancy types, there are separate depth-percent damage functions for the structure, contents, and "other". The depth-percent damage functions are global for every structure of that occupancy type and are entered as damage relative to the first floor stage as a function of the percent of value. For example, the structure depth-damage function may indicate that the damage at a depth of two feet above the first floor stage is 10 percent of the structure's value. The values of the structure (as well as contents and other) are entered with the individual inventoried structure. The occupancy type does include global parameters for the content and other values when they are expressed as a percent of the structure value. Also, the uncertainty parameters are

entered globally by occupancy type for the first floor stage, structure value, content value, and other value. Structure inventory allows the user to store either an exhaustive inventory of all structures in the study area or a sample. Current sampling techniques allow the user to enter data for one structure and indicate that it represents many identical structures. Structure inventory data includes the damage category, occupancy type, stream, structure identification, first floor stage, stream station, structure value, content value, and other value. If a unique depth-damage is required for a structure, then it may be entered with the structure inventory. Structure inventory data may be imported from other programs such as spreadsheets using tab-delimited text files. Structure modules may be used to alter structure characteristics (such as first floor stage) as a function of plan and year. This is especially helpful when levee alignments vary by plan and a structure may be protected only for some plans. Figure 4 depicts the entry of occupancy type information and Figure 5 depicts the entry of structure inventory data. When all economic data is complete, the stage-aggregated damage with uncertainty is computed for all damage reaches. During the early stages of a study, the stage-aggregated damage may be computed without using the risk-based analysis. This allows the user to debug the data faster and to get conventional results.

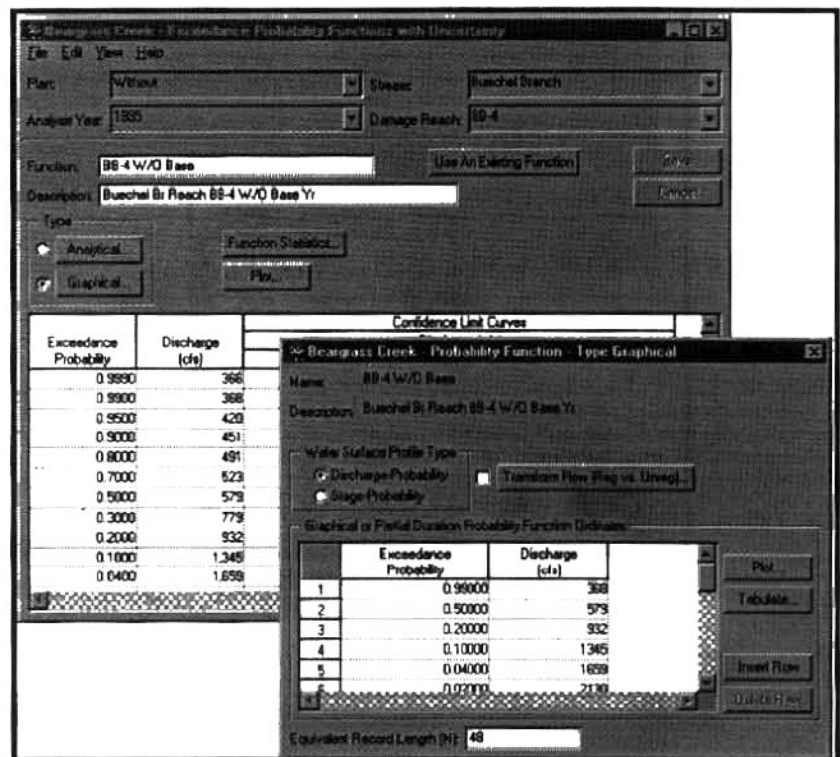


Figure 3: Editing Graphical Frequency Function

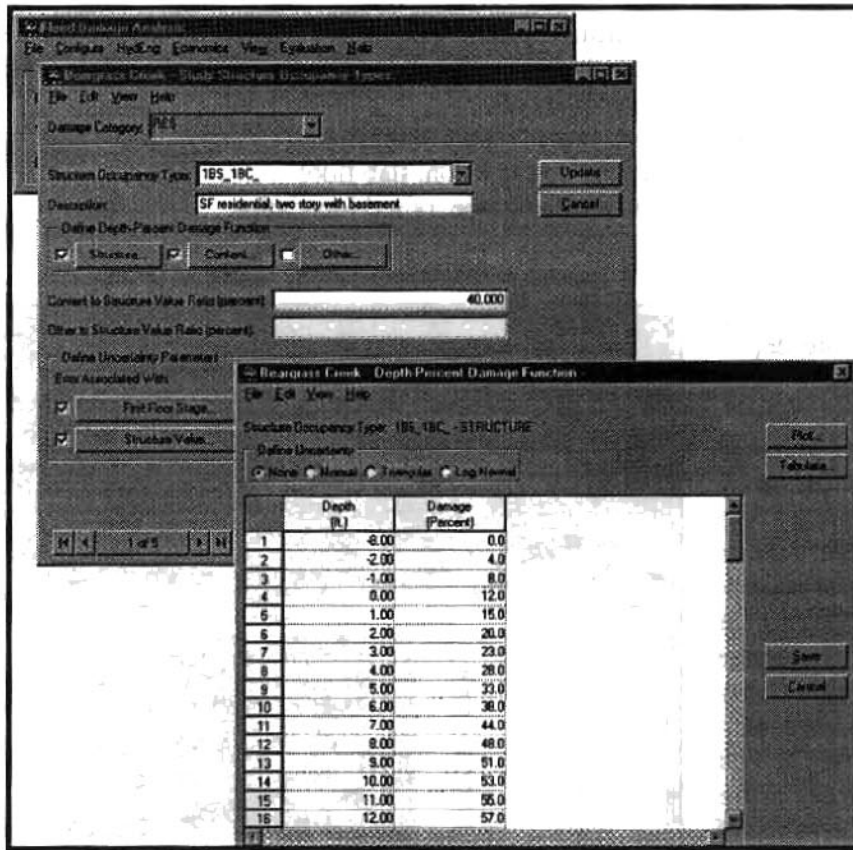


Figure 4: Occupancy Type Data Entry

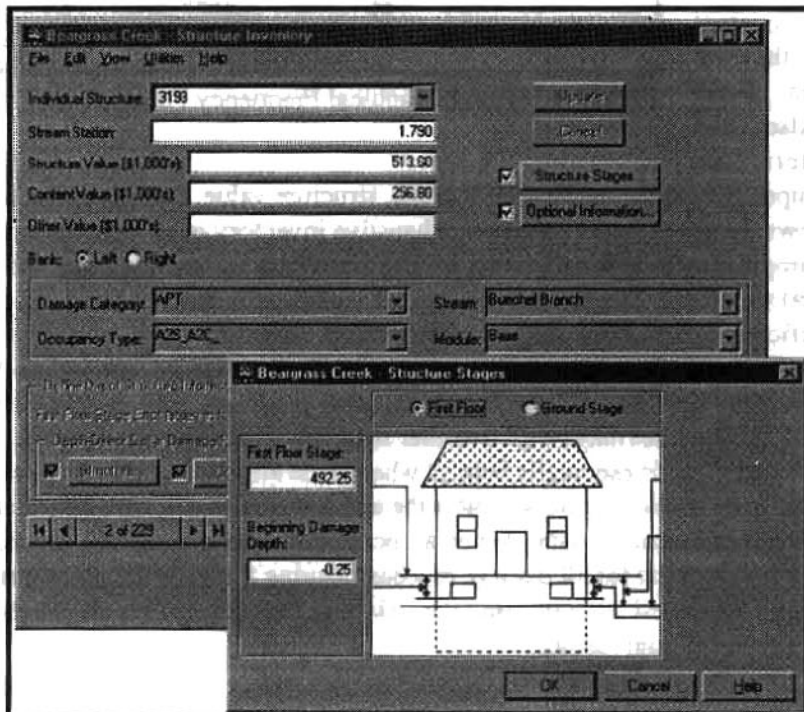


Figure 5: Structure Inventory In Form View

EVALUATION AND RESULTS

The evaluation component displays data validation information and facilitates the calculation of expected annual damage and equivalent annual damage. Before calculation, all supporting functions must be properly defined. HEC-FDA produces a table which indicates the plan / year combinations for which valid functions have been defined and which specific functions are not properly defined. It also tabulates the last computation date and time and indicates results that are out-of-date due to modification of supporting data such as discharge-frequency functions. The analyst can select those plan / year combinations for which calculations are performed.

The results component displays a wide variety of information including expected annual damage and equivalent annual damage by plan, year, reach, and category. The calculated functions such as damage-frequency can also be tabulated and plotted. The equivalent annual damage results are displayed including the discounted damage and amortization. Project performance tables display information that is used to measure the hydrologic efficiency of a flood damage reduction plan. Performance is measured in terms of the risk of flooding in any year, over a specified number of years, or if a specific hypothetical or historical event occurs. Plan performance uses the risk-based analysis of the hydrologic (not economic) functions.

CONCLUSIONS

The HEC-FDA program is a state-of-the-art computer program that provides a comprehensive analysis tool for formulating and evaluating flood damage reduction plans. It has a modern user interface and facilitates transfer of data between other commercial programs and databases. It includes a sophisticated risk-based analysis capability or it can be used for traditional calculations. The computational procedures and output reports are consistent with Federal and U.S. Army Corps of Engineers policy and technical regulations. "Version 1.0" was released in January 1998 and it includes a user's manual and test data.

REFERENCES

- Benjamin, J.R., and Cornell, A.C., 1970, *Probability, Statistics, and Decision for Civil Engineers*, McGraw-Hill Book Co., New York, N.Y.
- Sequiter Software Inc., 1996, *CodeBase Database Management for Programmers Version 6.2*, Sequiter Software Inc., Edmonton, Alberta, Canada.
- U.S. Army Corps of Engineers (USACE), 1982, "HEC-2: Water Surface Profiles, User's Manual".
- U.S. Army Corps of Engineers (USACE), 1987, "HEC-1: Flood Hydrograph Package, User's Manual".
- U.S. Army Corps of Engineers (USACE), 1990, "Guidance for Conducting Civil Works Planning Studies," Engineering Regulation (ER 1105-2-100).
- U.S. Army Corps of Engineers (USACE), 1992, "HEC-FFA: Flood Frequency Analysis, User's Manual," Engineering Regulation (EM 1110-2-1619).
- U.S. Army Corps of Engineers (USACE), 1996a, "Engineering and Design: Risk-Based Analysis for Flood Damage Reduction Studies," Engineering Manual (EM 1110-2-1619).
- U.S. Army Corps of Engineers (USACE), 1996b, "Risk-based Analysis for Evaluation of Hydrology/Hydraulics, Geotechnical Stability, and Economics in Flood Damage Reduction Studies," Engineering Regulation (ER 1105-2-101).
- U.S. Army Corps of Engineers (USACE), 1997, "HEC-RAS: River Analysis System".
- Visix Software Inc., *Galaxy Application Environment, Release 2*, 1994, Visix Software Inc., Reston, VA 22091.

EQUIVALENT RECTANGLE SIMPLIFICATION (ERS) METHOD AND ITS APPLICATION IN A DISTRIBUTED HYDROLOGIC MODEL

BY

Wilson Huaisheng Chen, Research Associate
Department of Environmental Science and Engineering
Oregon Graduate Institute, P.O.Box 91000, Portland, OR 97291-1000
Phone: (503) 690-1197, Email: wilson@ese.ogi.edu

AND

Robert. L. Beschta, Professor
Department of Forest Engineering
Oregon State University, Corvallis, OR 97331
Phone: (503) 737-4292, Email: beschtar@cmail.orst.edu

Abstract: In the field of distributed hydrologic models, the geometry of distributed grid cells represent a pre-defined condition and limitation associated with a particular model. Typically a square-cell geometry is adopted for distributed models since most terrain data is in a square-grid mesh. However, current methods for flow routing with a square-grid surface have limitations since such algorithms involve arbitrary flow directions (4 or 8 directions). There are continuing efforts to improve these problems. For example, TAPES-C model (Moore and Grayson, 1991) uses contour lines and flowpath lines as cell boundaries to form a flow net so that each cell has a naturally defined flow direction. However, hydrologic models developed based on TAPES-C can only be applied to a flow net type of cell format.

The Equivalent Rectangle Simplification (ERS) method is an effort to provide a general algorithm to handle slope flow routing for distributed hydrologic models without setting arbitrary flow directions or cell geometry requirement. For any polygon cell (triangle, rectangle, ...,etc.), the weight of each edge is defined as the proportion of drainage area that each edge has within the cell. The ERS calculates the weight for all the edges and generates a virtual rectangle called *Equivalent Rectangle* (ER) which has the same area, same slope angle, same aspect, same length, and same physical characteristics as the cell. An ER of a cell has only one edge (upper) receiving flow and one edge (lower) discharging flow. The hydrologic similarity between a cell and its ER is proven to have great approximation by pattern matching analysis and hydrograph comparison. Therefore, water balance and flow routing for the cell can be performed as an one-dimensional calculation whereby flow discharges through the edges of the cell are then distributed by their edge weights. Since one edge is shared by two cells, the discharging flow from one cell will become the receiving flow by the other cell. A forward routing scheme can then be applied over a distributed watershed from upper cells to lower cells.

The flexibility of the ERS methodology allows a variety of watershed cell distribution to be utilized for simulation purpose. As an example, the ERS is used in the Object Watershed Link Simulation (OWLS) model with application to the Bear Brook Watershed in Maine (BBWM). The watershed consists of both irregular triangular and irregular rectangle cells with different sizes. The simulation results are encouraging.

INTRODUCTION

Watershed hydrologic models are mathematical tools that can be used to simulate the water balance and transport processes within a basin. As the result of modern development in computer technologies, complicated and detailed simulations of a watershed become possible. There is a tendency in hydrologic model development to couple more and more physical rules and equations in the description of hydrologic processes. Since the variation of landscape characteristics within a basin are often large, the technique of subdividing a watershed into small, relative homogeneous land units (cells) become necessary. A model that employs physical rules for the description of hydrologic processes and sub-divides a watershed into many small cells is categorized as physically-based, distributed hydrologic model.

A cell is a small area in a watershed representing a relatively homogeneous characterization of geology, hydrology, soil, vegetation and topograph. Therefore, a natural cell may not have a regularly shaped boundary condition. Nevertheless, many hydrologic models require a certain pre-defined size and shape of cells, as well as their spatial orientations. For example, a square cell is one of the widely adopted shapes utilized by many distributed hydrologic models because of the format of terrain data (e.g. digital elevation model, or DEM data) and the convenience of making up the cell mesh. Inter-connections between cells and the distribution of flow to neighbor cells are accomplished through the hydrologic flow routing procedure. However, current methods for flow routing with a square cell surface may be inadequate since the algorithm involves arbitrary flow directions (4 or 8 directions). This arbitrary method may cause biased prediction of flow process in a basin. In an attempt to overcome this problem, the TAPES-C model (Moore and Grayson, 1991) uses contour lines and flowpath lines as cell boundaries to form a flow net so that each cell has naturally defined flow direction. However, hydrologic models based on this procedure are dependent on a flow-net cell format.

In this paper, we introduce a methodology called Equivalent Rectangle Simplification (ERS) to solve the arbitrary flow routing problems and to add flexibility to physically-based distributed hydrologic models.

THEORY

The ERS method is used to simplify the geometry of a cell, represented as a polygon with n edges and n nodes, into a rectangle which has the same soil and vegetation, same area, same slope, same center location, and same total length (or total width, or width-to-length ratio) as the original cell (Figure 1). Each edge of a cell has a weighting, which is determined by the relative area of a given cell providing water to that edge (Figure 2). This weighting was used to determine the amount of water that could cross a particular edge (zero when none, -9 identifies an upper edge that is receiving water from an upslope cell). By assuming that the physical performance of the cell can be approximated by that of its equivalent rectangle, hydrologic information can be calculated for the equivalent rectangle and then distributed to the edges of the cell by their relative weightings (e.g., discharge) or directly assigned to the edges (e.g., water depth).

The terminology *equivalent* means both cells have the same area, same slope, same soil and vegetation condition, same soil depth, same center location, same aspect and both are planar. They will also have same amount of precipitation inputs, solar radiation inputs, infiltration rate, surface water depth, soil moisture content, amount of flow generated from the surface, soil and macropore system. However, they can be different in shape and consequently the pattern of flow draining from each cell could be different. An equivalent rectangle for an irregular cell is constructed so that it satisfies these conditions. In order to implement a one-dimensional hydrologic calculation, the rectangle also needs to have two sides parallel to the aspect direction in addition to an upslope boundary and a downslope boundary.

There are an infinite number of rectangles that might satisfy the above requirements, however three types of rectangles are probably the most reasonable choices for an *equivalent rectangle* (Figure 1):

- A. A rectangle having the length equal to the projected length of the cell on the slope direction.
- B. A rectangle having the width equal to the projected width of the cell on the contour direction.
- C. A rectangle having the same length:width ratio to the projected length:width ratio of the cell.

Given these options, additional evaluations are needed before deciding which provides an appreciate hydrologic approximation of the original cell.

Figure 3 and 4 demonstrate an analysis of surface runoff routing for equivalent rectangles with type A (same length) and type B (same width) for several cell shapes (triangle and prism shapes were selected for ease of analysis). In both figures, an assumed rainfall event of 3 mm per time step with a duration of 3 time steps has been applied at time steps 2, 3, and 4. The cells of different shapes are assumed to be planar and no diffusion occurs during flow routing along the surface. For both figures, there are two groups of cells, one with shorter slope length and the other with longer slope length. In the group with shorter in slope length, the equivalent rectangular cell will take exactly one time step to route the generated flow out of the

cell. In the group with longer slope length, all cells requires more then one calculation time step to finish flow route. Each group has three types of cells with pyramid, triangle and prism shape respectively, representing the cells with wider downslope boundary, wider upslope boundary and wider center body. All the cells are assumed to be 10 cm^2 in area and are impermeable. Each cell will expect to generate 3 cm^3 of flow from each time step during the rainfall period. Taking into account the time consumed by flow routing; hydrographs were calculated using a spread-sheet.

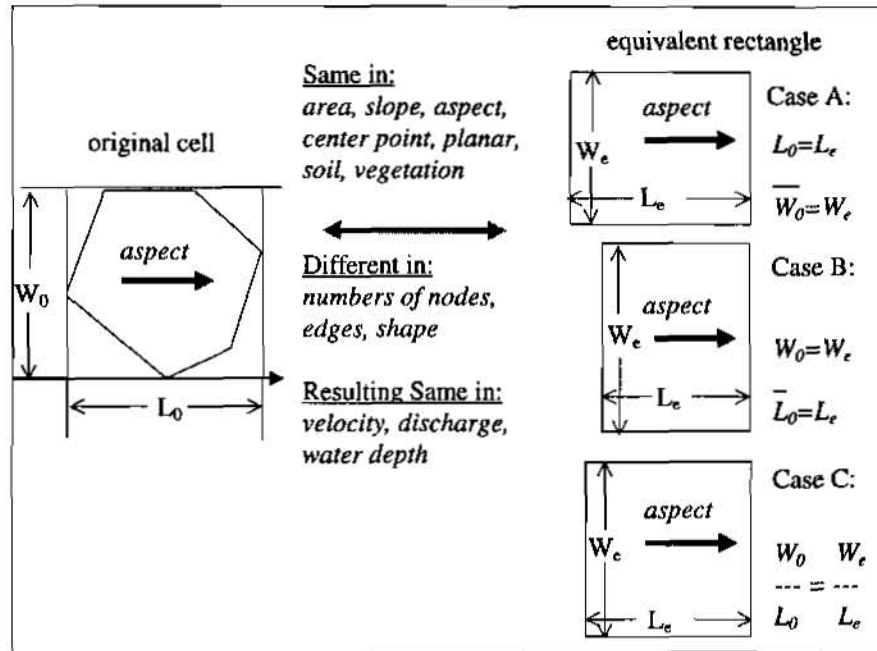


Figure 1. Equivalent rectangles.

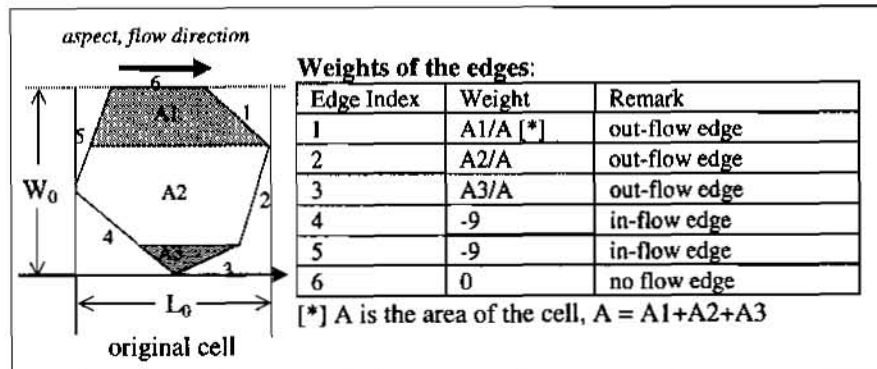


Figure 2. Edge weights of a cell.

In Figure 3, all cells within a given group have the same length even though shapes are varied. For the group of cells with a shorter slope length, runoff responses are instantaneous and all cells produce the same hydrograph. For the group of cells with relatively longer slopes, a pyramid-shaped cell tends to have a faster rising limb and slower falling limb. A triangle-shaped cell has a reversed runoff pattern and a prism-shaped cell tends to smooth the hydrograph peak. The duration of runoff for the different cell shapes are the same. The Equivalent Rectangle, however, produces flow in a linear manner and represents the average situation for the group of cells.

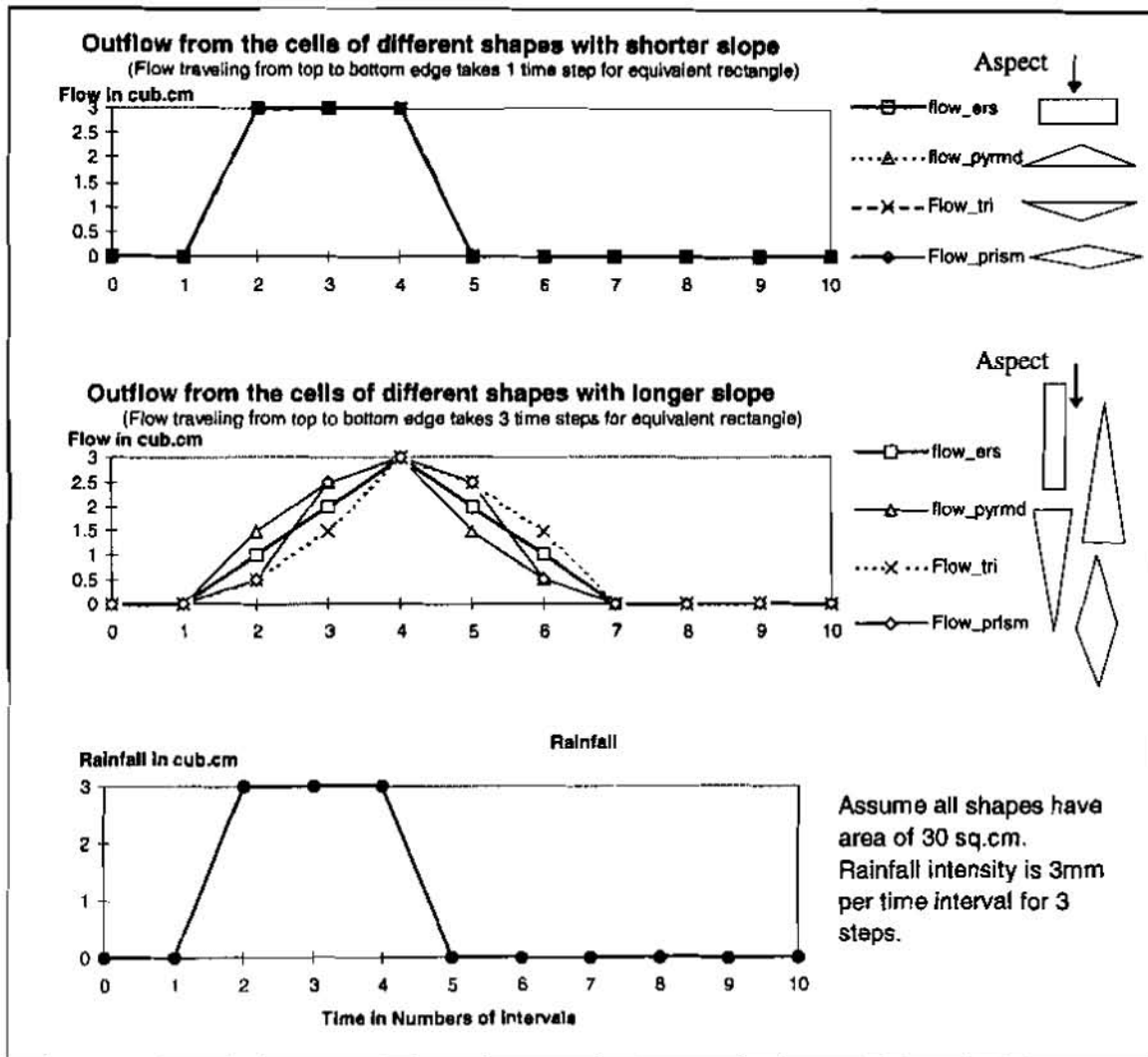


Figure 3. Equivalent Rectangle Simplification, Equal Length ERS.

In Figure 4, all cells with different shapes have been constructed to have the same width. For the group of cells with shorter slope length, runoff responses are quick but varied. Let us assume that the equivalent rectangle has a slope length such that one calculation time step is required to drain all its water, then all other cells will have longer length in order to have the same area. It will require more than one calculation time step to drain water from these cells. As shown in the Figure 4, the hydrograph of a pyramid-shaped cell can be reasonable equivalent by the rectangle, but hydrographs from triangle- and prism-shaped cells will be delayed about one time step in comparison to the equivalent rectangle. For the group of cells with relative longer slopes, this advanced outflow phenomenon of the equivalent rectangle becomes more obvious. In addition, flow from the equivalent rectangle tends to have a higher instantaneous peak than any other shapes.

For a type C rectangle, which has the same width-to-height ratio, we may expect outflow patterns to occur between those found for type A and B cells. Flow advancing and a higher peak of the equivalent rectangle may also be expected. Therefore, we can conclude that: an equivalent rectangle to a cell should have the same length as the slope length of that cell.

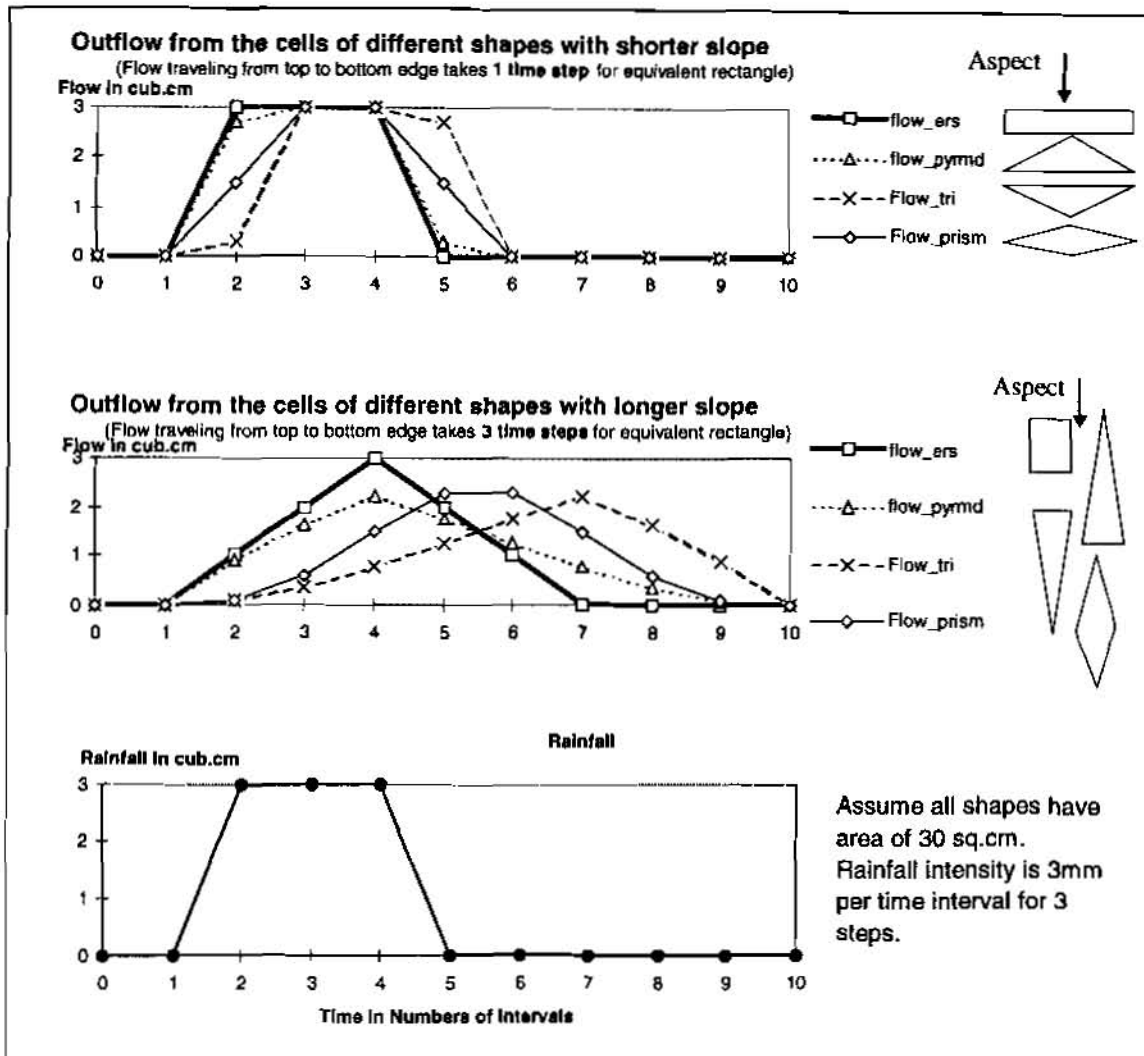


Figure 4. Equivalent Rectangle Simplification, Equal Width ERS.

APPLICATION

The ERS method has been used in the Object Watershed Link System (OWLS) model (Chen, 1996). The OWLS model is a physically-based, distributed, 3-D, vector-based watershed hydrologic model.

The Model Structure: The OWLS model is constructed using the concept of Object-Orientation methodology. A watershed is represented as a 3-D object, which consists of a group of linked 3-D cells (or basic land units), a 3-D boundary and a 3-D stream network. Each cell object consists of a group of linked 3-D edges and each edge is linked by two 3-D nodes. The hydrologic components are also expressed as linked objects. All objects in the OWLS model are distinct with their own characteristics. The structure of the OWLS model not only provides a higher computing efficiency, but also a greater flexibility and capability for watershed dynamic hydrologic simulation than traditional distributed hydrological models.

The Sub-Models: The OWLS model consists of four sub-models: (1) The Data Processing Model handles all data preparation for other sub-models. It converts data from raw ASCII format to the OWLS format, including DEM data conversion, precipitation distribution, air temperature interpolation, and air temperature extension; (2) The Geomorphological Model automatically delineates watershed boundaries, flow-paths, possible stream channels by a vector-based algorithm. It produces a vector-based database for watershed cells, boundaries and stream channels and provides a harmonious simulation base for the

hydrologic and visualization model; (3) The Hydrologic Model is represented by several layers in vertical dimension: the canopy layer, the surface layer, and the soil layer which also contains a macropore pipe component. The hydrologic model simulates processes that occur on a forested watershed, including rainfall, interception, solar radiation and associated evapotranspiration, snow accumulation and melting, infiltration, ex-filtration, macropore flow, surface overland flow, subsurface flow, and flow routing on hillslope and within channels. The ERS method is used in the hillslope flow routing, which includes flow routing for different types of horizontal flows (surface, subsurface and macropore flow). The horizontal 2-D flow routing problem is simplified into 1-D by the ERS method and routed by the non-linear kinematic wave finite differential calculations (Chow et al., 1988). The ERS technique dramatically reduces the complexity of the flow routing model and increases the flexibility and calculation speed of the model; (4) The Visualization Model is a significant component of the OWLS watershed model. It is specially designed for watershed hydrologic simulation and animation. The OWLS model also provides data outputs in text format for custom graphics.

The Watershed: The OWLS model has been applied to the Bear Brook Watershed in Maine (BBWM). The watershed is located in East Maine (44°52'15" Latitude, 68°06'25" Longitude), approximately 60 kilometers from the Atlantic coastline in the northeastern United States (Figure 5). The BBWM is a paired watershed study funded by the U.S.EPA since 1987 as part of the Watershed Manipulation Project (WMP) within the National Acid Precipitation Assessment Program (NAPAP). NAPAP was designed to assess the causes, effects, and strategies for controlling acidic precipitation.

The study site of the BBWM consists of two continuous first order streams: East Bear Brook (EBB) and West Bear Brook (WBB). On each stream, a catchment outlet was selected and gauged so that both streams have about the same catchment area (EBB=10.7 ha and WBB=10.2 ha). Both watersheds are topographically similar, and are thus ideal for a paired watershed study. Both watersheds have a maximum discharge of about 0.01 mm/ha/sec or 0.15 m³/s. Annual water yield relative to incoming precipitation for WBB ranges from 68 to 77% while EBB ranges from 62 to 68%. The soils in the two watersheds are thin spodosols developed from till (Erickson and Wigington, 1987). The bedrock consists predominantly of metamorphosed and deformed pelites, with minor calc-silicate gneiss, and dikes and sills of granite (Norton, et. al., 1992). Folists are common near and at the summit. Minor, poorly-drained soils are present in the upper part of EBB and a small area midway up the WBB. The depth of the watershed soils range from 0 to 5m, typically 1 to 2m. Vegetation of the BBWM is dominated by hardwoods including american beech, sugar maple, red maple, with minor amounts of yellow birch and white birch. Softwood, mixed, and hardwood stands cover approximately 25, 40, and 35% of the total watershed areas respectively. The climate at BBWM is cool and temperate, with a mild maritime influence. The mean annual temperature is about 4.9°C, with an observed range of +35°C to -30°C. Summer daily maximum temperatures commonly exceed 25°C and winter

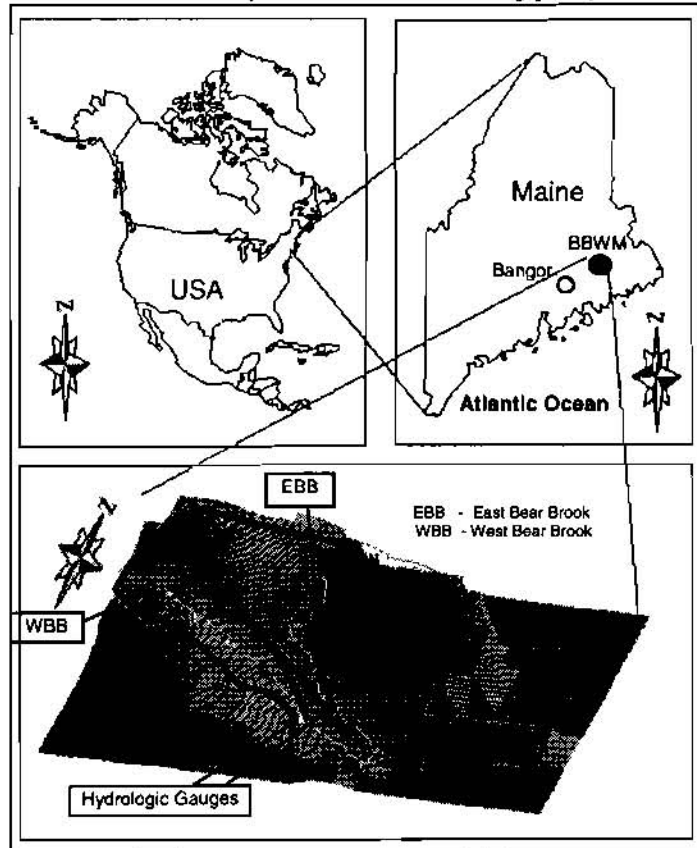


Figure 5. Bear Brook Watershed in Maine

minimum commonly reach -20°C. Precipitation for the period from 1987 to 1996 at the BBWM averaged about 1300 mm per year but locally has ranged from 700 to 1900 mm over the last 10 years. Typically about 20% to 25% of the precipitation is snow.

The Cells: In order to test the stability of the ERS method, we build two different kinds of cell networks for the BBWM watershed: (1) 50m-based triangular cells, which is developed from the 50m-based square cell network by linking two opposite corners to bisect the square (Figure 6); (2) irregular cells, which are constructed based on the points of a terrain land survey performed in the watershed. The range of distances between survey point is from 2 to 10m depending upon the complexity of the topograph (Figure 7).

The Simulation Results: The OWLS model was calibrated using the data from May 1989 at the EBB watershed using 50m-based triangular cells. The results of calibration are shown in Figure 8. The OWLS model has also been validated from different period and in the WBB watershed for additional details, see Chen (1996) or visit WEB site at hydromodel.com). The Same system parameters were also be used to test simulation results from the survey-based triangular cells. Results are presented in Figure 9 and indicate that the simulated hydrographs from different cell systems are basically equivalent. In the other words, the Equivalent Rectangle Simplification (ERS) method does produce stabilized simulation results for a physically-based distributed hydrologic model like OWLS.

CONCLUSION

The ERS method is a generalized approach for simulating flow routing associate with a variety of distributed cells. Simulation results from the OWLS model in the BBWM watershed indicate that this approach provides flexibility in watershed cell distribution and simplifies flow routing calculations.

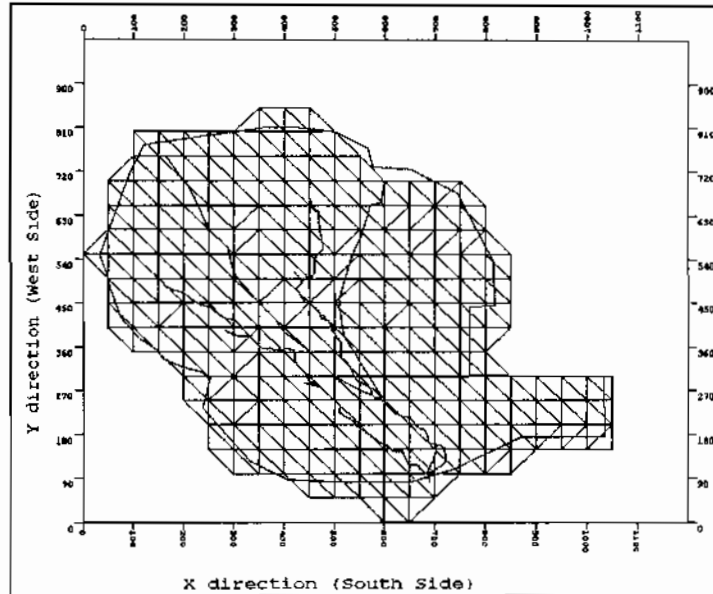


Figure 6. 50m-based Triangular Cells of BBWM

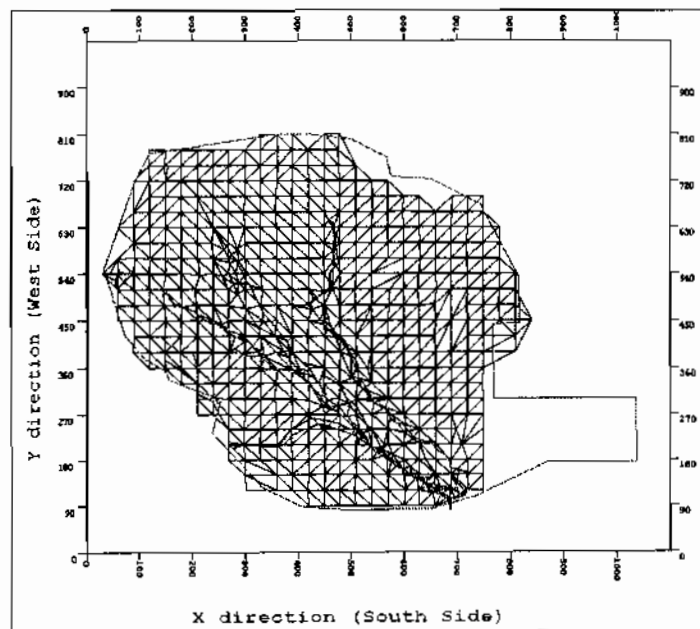


Figure 7. Survey-based Irregular Cells of BBWM

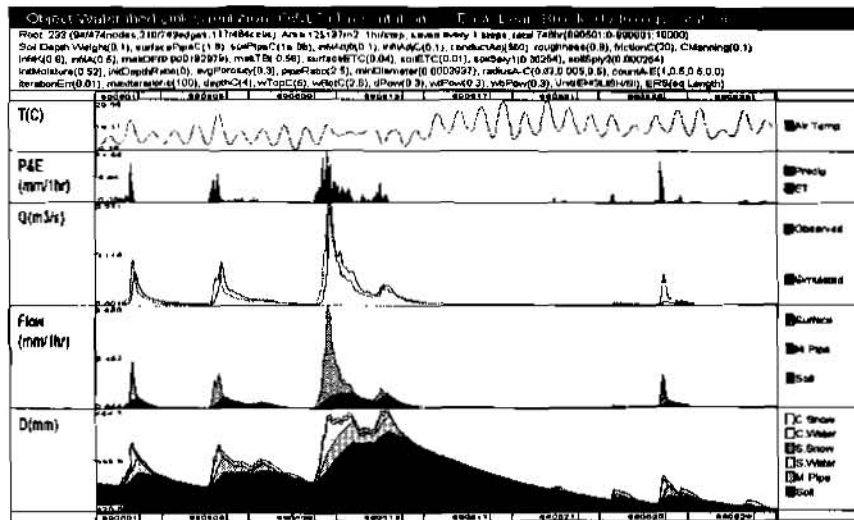


Figure 8. Calibration results from the OWLS model

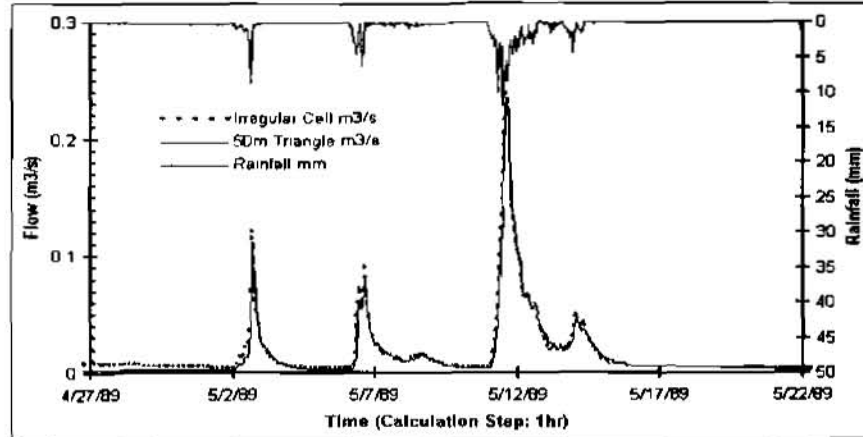


Figure 9. Comparison of Flow Simulation Results from Different Cell Patterns in the EBB.

REFERENCE

- Chen, Huaisheng, 1996, Object Watershed Link Simulation (OWLS), Ph.D. Dissertation, Oregon State University, Corvallis, Oregon, U.S.A. 174pp.
- Chow, V. T., D.R. Maidment, and L.W. Mays, 1988, Applied Hydrology, McGraw-Hill Book Company. 627pp.
- Erickson, H. and P.J.Wigington, 1987, The Bear Brook Watersheds: Site characterization and relation to DDRP watershed soils and NSWS Lakes in the Northeast, Unpublished manuscript.
- Moore, LD., and R.B.Grayson, 1991, Terrain-Based Catchment Partitioning and Runoff Prediction Using Vector Elevation Data. *Water Resources Research* 27(6):1177-1191.
- Norton, S.A.; R.F.Wright, J.S.Kahl, and J.P.Scofield, 1992, The Magic simulation of surface water acidification at, and first year results from, the Bear Brook Watershed Manipulation, Maine, USA. *Environmental Pollution* 77: 279-286.

SPATIALLY DISTRIBUTED MODELING OF THE HYDROLOGIC EFFECTS OF MECHANIZED MANEUVERS ON MILITARY TRAINING LANDS

William W. Doe III, Research Scientist, Center for Ecological Management of Military Lands,

Colorado State University, Fort Collins, CO; Pierre Y. Julien, Professor, Department of Civil Engineering, Colorado State University, Fort Collins, CO; Fred L. Ogden, Assistant Professor, Department of Civil and Environmental Engineering, University of Connecticut, Storrs, CT; Billy E. Johnson, Research Hydrologist, Hydraulics Laboratory, U.S. Army Waterways Experiment Station, Vicksburg, MS

Abstract: Advances in two-dimensional, raster-based hydrologic modeling, integrated with geographic information systems, offer military land managers a valuable decision-making tool to better understand and manage the impacts caused by intensive mechanized maneuver training on watersheds within military lands. CASC2D is a physically-based, distributed watershed model which has been integrated with GRASS, a geographic information system, to simulate the effects of multiple land use scenarios on large watersheds. The model can effectively simulate the effects of spatially varied rainfall events, surface and channel runoff and upland erosion/deposition. The CASC2D model has been applied to several watersheds on military lands to simulate the effects of multiple land use scenarios. The impacts caused by large-scale maneuver training, such as soil compaction and loss of vegetative cover, on hydrologic response can be spatially simulated in the model by adjusting critical parameter values based upon field measurements and tracked vehicle testing. This modeling approach was applied to a 50 square-mile watershed within the U.S. Army Pinon Canyon Maneuver Site in southeastern Colorado. The preliminary results suggest that the CASC2D model can provide land managers with visual and quantitative data on watershed processes that can assist them with mitigation approaches and best management practices to minimize erosion and water quality impacts of military training. The model's design also lends itself to a wide range of watershed modeling applications on federal lands.

INTRODUCTION

Military land managers must contend with the multiple environmental effects of large scale maneuver exercises on the landscape. Intensive training exercises involving hundreds of seventy-ton tracked vehicles and numerous off-road wheeled vehicles can cause severe disturbance to the soil surface and lead to degradation of vegetative cover, increased surface erosion, sediment production and deterioration of water quality in adjoining watercourses. Since land-based training exercises often impact thousands of acres of land it is difficult to account for the frequency and patterns of disturbance and to quantify their erosional effects. Nevertheless, land managers must comply with existing environmental statutes and be able to optimize land rehabilitation efforts to minimize future erosion problems.

Currently, the approaches to measuring and predicting soil erosion rely on the use of lumped-parameter, semi-empirical relationships such as the Revised Universal Soil Loss Equation (RUSLE). While such approaches provide an aggregate measure of sediment production at the watershed scale they do not account for internal watershed processes such as deposition on down-slope areas and sediment transport in stream channels. These latter processes can be significant in determining where to apply erosion control measures such as revegetation, sediment

control structures or bank stabilization.

The complex spatial and temporal distribution of military land disturbance, coupled with the spatial variability of rainfall-runoff processes in semi-arid regions where many maneuvers occur, dictate the need for more advanced hydrologic and erosion modeling capabilities that can better depict and predict the land use-watershed regime. The development of physically-based, distributed hydrologic/erosion models offer military land managers a valuable tool for simulating the complex relationships between military land use and watershed response. The compatibility of these two-dimensional models with raster (grid-cell) inputs, derived from geographic information systems, facilitates a more detailed understanding of the dynamic rainfall-runoff processes. This modeling approach was applied a 50 square-mile watershed within a military training area in southeastern Colorado where intensive maneuver activities occur. A two-dimensional, raster-based rainfall-runoff model, CASC2D, was integrated with a geographic information system, Geographic Resources Analysis Support System (GRASS), to demonstrate the potential for analyzing watershed responses under a variety of training impact scenarios (Doe, 1992).

DESCRIPTION OF WATERSHED

The Taylor Arroyo watershed encompasses a 50-square mile area of semi-arid grasslands and uplands in southeastern Colorado (Figure 1). It is located internal to one of several large training areas within the U.S. Army Pinon Canyon Maneuver Site (PCMS). The baseline hydrology of the watershed has been studied and documented by von Guerard et al. (1987,1993). Mean annual precipitation is 12 inches, distributed primarily as intense convective thunderstorms during the months of July-October and snowfall during the winter. The dominant hydrologic processes within the watershed are infiltration and channel flow. Infiltration is controlled primarily by the antecedent soil moisture conditions and the hydraulic properties of the surface layer. Subsurface flow from singular rainfall events is negligible. Runoff and sediment flow to the watershed outlet is controlled by a dense network of ephemeral channels. The 100-year peak discharge for the Taylor Arroyo has been estimated at 19,700 ft³/sec, with peak discharges of less than 1,000 ft³/sec typical for most Water Years. Annual suspended sediment loads have been computed between 400-4,000 tons/yr. A system of nine automated rain gauges and one stream gauge near the outlet is operated by the U.S. Geological Survey (USGS) (Figure 1a).

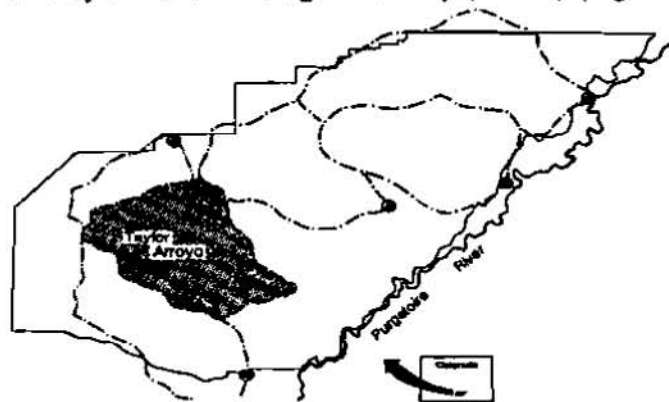


Figure 1. General location of the Taylor Arroyo watershed.

CHARACTERIZATION OF MANEUVER IMPACTS AND WATERSHEDS

Intensive land-use practices, such as tracked vehicle maneuvers, take place within military training areas with resulting impacts on the watershed regime. Typically, large maneuver tracts of land are subdivided into irregularly shaped areas, which are then allocated to and managed for training by military units based upon the scale of the exercise, diversity of terrain required and condition of the land. While the terrain may in some cases dictate the delineation of training area boundaries they are more likely determined by the alignment of major transportation roads, cultural features and live fire impact areas. Consequently, training area boundaries depict a land management unit that is inconsistent with analyzing hydrologic and erosional processes.

A watershed is a fundamental natural unit, the characteristics of which define the paths and rates of water and sediment movement across the landscape. Watershed boundaries are delimited by terrain form and can be easily derived from digital elevation model (DEM) data using GIS routines. In many cases, a natural watershed may cross several training area boundaries, or vice versa.

The notion of a "maneuvershed" can be used to conceptualize the hydrologic boundaries of a natural watershed within a military maneuver area (Doe, 1992). Since training frequency and distribution, hence disturbance, are characterized by training areas, the delineation and quantification of land use impacts within these boundaries can be superimposed upon the primary watershed boundaries. This approach was used to delineate the portions of the maneuversheds within the study which experience different intensities of land use impact. The spatial characterization of maneuver impacts is a critical consideration in managing the watersheds on military lands. This characterization can be effectively simulated in a spatially distributed model using a geographic information system. The changes in watershed response over time will be largely dictated by where and to what extent the watershed has been disturbed.

The characterization of maneuver impacts was accomplished by delineating a raster overlay of grid-cells where known or anticipated disturbance occurred. Field data collected from tracked vehicle impact studies within the watershed were then used to determine the intensity of disturbance, based upon the type, number and frequency of vehicle passes. The impact study data was combined with other data on soil texture and soil hydraulic characteristics to quantify the percent change in soil bulk density and porosity. This information was then used to quantify changes in critical soil hydraulic parameters for those grid cells in the model where disturbance occurred. The modified soils layer was then used as a data input to CASC2D, with the disturbed soil hydraulic conductivity values assigned. Using this approach a variety of land use scenarios were created and simulated using the CASC2D model.

The remaining data input layers, consisting of the watershed boundaries, soil texture, surface roughness and channel configuration, for each watershed were created in GRASS as described fully in Doe (1992); Doe, et al. (1996), Ogden (1992) and Saghafian (1992). The Watershed Modeling System (WMS) provides an efficient graphical user interface for running CASC2D (Nelson, 1996). WMS can be used both as a pre-processor to prepare grid-cell input files imported from GRASS and as a post-processor to display simulation results.

CASC2D RAINFALL-RUNOFF MODEL DESCRIPTION

CASC2D is a distributed, single-event, rainfall-runoff model. The model is fully documented in Julien and Saghafian (1991). CASC2D has been applied to several watersheds for hydrologic analysis. Saghafian (1992) calibrated and validated early versions of the model on a small, semi-arid watershed, the Mack's Creek in Idaho, to examine hydrologic response due to spatially-varied infiltration. Ogden and Julien (1993, 1994) used weather radar data with the model to test runoff sensitivity on both the Mack's Creek and Taylor Arroyo watersheds to temporally and spatially varied rainfall precipitation. Johnson et al. (1993) independently calibrated and tested CASC2D with observed data from five rainfall events on a small watershed in Mississippi.

The primary features of CASC2D include the Green and Ampt method for infiltration, a two-dimensional, explicit solution of the diffusive wave form of the de St.-Venant equations for overland flow, and a one-dimensional, explicit solution of the diffusive wave formulation for channel routing. Three hydraulic parameters (saturated hydraulic conductivity, capillary pressure head at the wetting front, and soil moisture deficit) are required to solve the Green and Ampt equation. The parameter values were determined from infiltrometer tests in the field, and compared with classifications of Rawls et al. (1983). The model also contains provisions to account for interception and detention storage, but these were not used in the simulations. To calculate surface runoff the model solves the two-dimensional equations of continuity and momentum which describe gradually-varied overland flow. Resistance to flow is described by Manning's equation. Finite-width channel flow routing is performed in a similar fashion but in only one direction along the channel path. The overland flow and channel flow are fully coupled to allow lateral inflows and outflows along the channel lengths.

The physical watershed domain in CASC2D is characterized by square (raster) grid cells. Raster data files for elevation, soil texture and surface roughness must be prepared. Although spatial variability is allowed from one grid cell to the next, each cell is represented as a homogeneous unit. The channel network is delineated in a file indicating the network connectivity and the physical characteristics of the various channel segments. The size of the surface feature files and channel network file is largely dictated by the user-selected grid cell resolution. For the simulations mentioned herein grid cell sizes of 300 meters were used initially due to computational power limitations. Advances in computing and user interfaces allow simulations to be easily performed at the 30-meter cell resolution.

Uniform or spatially-distributed rainfall data may be input to the model. For spatially-distributed rainfall data the inverse distance-squared algorithm is used to distribute the rainfall across the entire watershed. Simulations using both the distributed and uniform rainfall cases were performed. In the distributed rainfall case, data collected from nine rain gauges within the watershed for a 3-hour storm was input to the model.

Rainfall-runoff simulation is performed for each grid cell at a user specified time step. First, the existing surface depth, including the rainfall depth added during the time step, is reduced by the infiltration capacity of the grid cell's occupying soil, based upon the user specified Green and Ampt parameters. Then, the remaining surface depth, if any, is routed to adjacent cells according to the water surface slope. The overland flow is routed in two orthogonal directions within each grid cell. The model also enables simulation of run-on and subsequent re-infiltration, which occurs when surface runoff from upstream cells infiltrates into pervious downstream cells. Finally, the runoff from overland cells which reaches the channel cells is routed through the

channel network to the watershed outlet.

CASC2D provides the user with a number of simulation options to include a visual color display of both the static and dynamic characteristics of the watershed simulation. Spatial outputs from the model may be captured at grid-cell scale at any time during or at the conclusion of the simulation. These outputs include ponded depth of infiltration and depth of surface flow. The discharge over time at the watershed outlet can also be recorded to provide a cumulative measure of how the watershed response has changed for different land use scenarios.

EROSION AND SEDIMENT TRANSPORT ROUTINES

Modeling soil erosion is the process of mathematically describing soil particle detachment, transport and deposition on the land surface. Two important aspects of this modeling process are to determine the sediment sources from upland areas and the total sediment delivery to the watershed outlet. It is critical that land managers be able to determine those portions of the watershed which are most susceptible to the erosive forces of water so that appropriate intervention strategies can be undertaken.

Within CASC2D the mechanics of soil erosion from overland flow are calculated using a modified version of the Kilinc-Richardson equation. This equation was derived from flume experiments using simulated rainfall. The resulting equation was modified to consider various soil types, vegetation, cropping factors and conservation practices (Julien, 1995). The equation is calculated for each grid cell to determine the available sediment. The sediment transport and deposition is quantified by three grain sizes - sand, silt and clay. In the model's overland transport scheme a hierarchy for moving available sediment is applied. The priority for transport out of an individual grid cell is given to material already in suspension, followed by material previously deposited in the cell and finally, from the resident soil surface in the cell. The upland erosion routine is calculated for each grid cell towards the downstream outlet.

Johnson (1997) and Johnson, et al. (1997) applied the upland soil erosion scheme in CASC2D to both a small, 5-acre farm plot and to the 8.25 square-mile Goodwin Creek in Mississippi using actual storm event data with promising results. Proper calibration of the soil erosion scheme for Taylor Arroyo requires additional field measurements from known rainfall events. Sediment data from the Taylor Arroyo outlet gauge, monitored by the USGS, and from research data collected internally in the watershed provide an initial source of data for this purpose.

SIMULATION OUTPUTS AND ANALYSIS

Four different maneuver scenarios were developed and simulated for the Taylor Arroyo watershed. The scenarios were defined by the distribution and intensity of impacts within specified portions of the watershed. Although the scenarios do not represent any particular training event they are representative of the spatial extent and intensity of maneuver activities within the watershed. For purposes of quantifying the scenarios and changes in the values of critical soil hydraulic parameters in the model, three distributions of disturbance - 1) 24 percent, 2) 44 percent, and 3) 77 percent and three intensity levels of disturbance - 1) none, 2) medium, and 3) high, were defined (Doe, 1992). The disturbance for each scenario was spatially distributed to aggregate areas (grid-cells) within the watershed that have historically been damaged by maneuvers.

The three levels of disturbance were correlated to changes in porosity for different soil textures, based upon the methodology and Green-Ampt infiltration parameters defined in Rawls and Brakensiek (1983). The revised values for the Green-Ampt parameters were then assigned to those grid-cells in the model where the appropriate intensity level of maneuver disturbance occurred. It is important to note that other soil surface factors, such as surface roughness and depression storage, may be altered by intense land use activities. In the model simulations, these additional factors were not changed. However, if detailed field data were available, these parameters could be altered as well to account for disturbance effects.

Using combinations of the maneuver scenarios, as defined above, and selected rainfall scenarios, simulations in CASC2D were performed for the undisturbed and disturbed cases. The rainfall-runoff outputs from each simulation were then compared both graphically and spatially to determine the changes resulting from land use. The results are illustrated by the cumulative hydrographs (Figure 2).

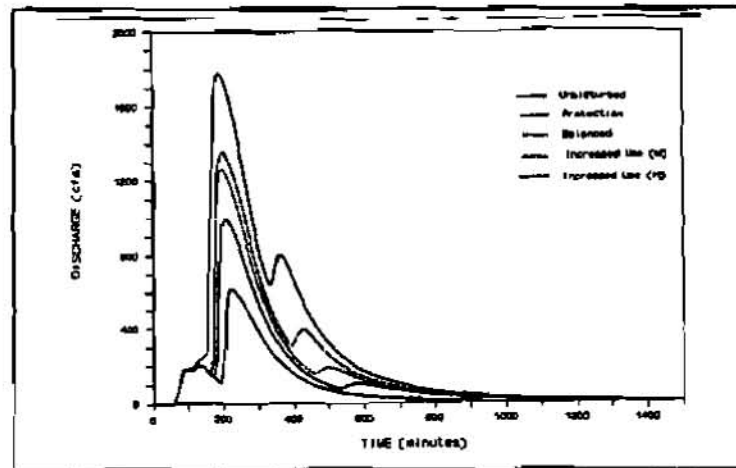


Figure 2. Hydrograph envelopes for maneuver disturbance scenarios on Taylor Arroyo watershed.

The results indicate that significant changes in watershed response occur under different impact scenarios. Similarly, the rainfall intensity, amount and distribution are also important controls on the watershed's behavior. The hydrograph envelopes portray the aggregated response of the watershed for particular maneuver events. As the level and intensity of maneuver impacts increase there is a corresponding increase in the peak discharge and output volume, and a decrease in the time to peak and infiltration volume. Another perspective on watershed response under different maneuver scenarios can be achieved by analyzing the spatial distributions of infiltration depth at grid-cell scale throughout the watershed. Using the inherent grid cell calculation capabilities of GRASS, the percent change in infiltration depth between the undisturbed case and maneuver was computed and spatially analyzed.

Another advantage of spatial modeling for land management is evident in performing data output analysis from the simulations. When the soil is compacted by maneuvers, the infiltration capacity is decreased. Intuitively, one would expect that in all of the disturbed areas (grid-cells) the resultant infiltration depth would therefore be less than in the undisturbed case. Likewise, for any given location internal to the watershed (e.g., a specified grid-cell), the resultant infiltration depth in that grid-cell would be the same for a given rainfall event, whether or not other portions of the watershed remain undisturbed or disturbed. However, the model results indicate that this does not hold true due to surface run-on from upstream portions (e.g., grid cells) of the

watershed. This so-called run-on effect is the result of differences in the infiltration properties of adjacent soils and their spatial position in the watershed. Up-slope soil areas (grid-cells) which have reduced infiltration properties, resulting from maneuver impact, will generate more overland flow than in their previously undisturbed state. As this additional overland flow is routed down-slope through the watershed it may encounter soil areas with higher infiltration capacities which can absorb the additional runoff and hence, exhibit an increase in infiltration depth. Such counterintuitive changes within the watershed would be impossible to detect in a one-dimensional, non-spatial model.

CONCLUSIONS

Spatial dynamic modeling of rainfall-runoff processes and erosion/deposition can provide military land managers with an increased understanding of the relationships between intensive land use, such as mechanized maneuvers, and their associated environmental impacts. The CASC2D model simulations on the Taylor Arroyo watershed illustrate the potential for analyzing the changes that occur in watershed response under a variety of land use scenarios. At the grid-cell scale, many of the watershed's internal processes, such as overland flow and sediment deposition, can be simulated and measured spatially as model outputs. Such information is very useful to identifying land management strategies that can mitigate the undesirable effects of land use.

ACKNOWLEDGMENTS

Preliminary development and research on CASC2D was conducted at the Army Center for Geosciences, Colorado State University, with funding support provided by the U.S. Army Research Office, Research Triangle Park, NC. The authors acknowledge the research efforts of Mr. Mark Jourdan, U.S. Army Waterways Experiment Station, Vicksburg, MS. The Watershed Modeling System (WMS) is a product of the Engineering Computer Graphics Laboratory, Brigham Young University, Provo, UT. Mr. Tom Warren, Directorate of Environmental Compliance and Management (DECAM), Fort Carson, Colorado and Mr. Doug Cain, Water Resources Division, U.S. Geological Survey, Pueblo, CO provided essential data for these efforts.

REFERENCES

- Doe, W. W., P. Y. Julien and F.L. Ogden, 1997. Maneuversheds and Watersheds: Modeling the Hydrologic Effects of Mechanized Training on Military Lands. Proceedings, American Water Resources Association/University Council on Water Resources Joint Symposium, June 29-July 3, 1997, Keystone, CO, pp. 767-776.
- Doe, W. W., B. Saghafian and P. Y. Julien, 1996. Land-Use Impact on Watershed Response: The Integration of Two-Dimensional Hydrologic Modeling and GIS, Hydrological Processes, Volume 10, November 1996, pp. 1503-1511.
- Doe, W. W., and B. Saghafian, 1992. Spatial and Temporal Effects of Army Maneuvers on Watershed Response: The Integration of GRASS and a Two-Dimensional Hydrologic Model, Geographic Information Systems: Proceedings of the Seventh Annual GRASS GIS Users Conference, National Park Service, Denver, Colorado, Technical Report NPS/NRGISD/NRTR- 93/13, pp. 91-105.

- Doe, W. W., 1992. Simulation of the Spatial and Temporal Effects of Army Maneuvers on Watershed Response, Ph.D. Dissertation, Department of Civil Engineering, Colorado State University, Summer 1992.
- Harrison, J.S., 1997. Erosion Modeling in Pinon Canyon Maneuver Site Using the Universal Soil Loss Equation and the GIS System-GRASS. Unpublished Master's Degree report, Department of Civil Engineering, Colorado State University, Fort Collins, CO, 56 pp.
- Johnson, B.E., 1997. Development of a Storm Event Based Two-Dimensional Upland Erosion Model, Ph.D. Dissertation, Department of Civil Engineering, Colorado State University, Spring 1997.
- Johnson, B.E., P.Y. Julien and D.K. Molnar, 1997. Advances in Soil Erosion Modeling on Goodwin Creek Watershed, Conference on Management of Landscapes Distributed by Channel Incision, May 20-22, 1997, Oxford, MS.
- Johnson, B.E., N.K. Raphael and J.C. Willis, 1991. Verification of Hydrologic Modeling Systems, Proc., Federal Water Agency Workshop on Hydrologic Modeling: Demands for the 90's, Fort Collins, CO, USGS Water Resources Investigations Report 93-4018, 9-20.
- Julien, P.Y., B. Saghafian, and F.L. Ogden, 1995. Raster-Based Hydrologic Modeling of Spatially-Variied Surface Runoff, Water Resources Bulletin, AWRA, Vol. 31, No. 3, pp. 523-536.
- Julien, P. Y. and B. Saghafian, 1991. A Two-Dimensional Watershed Rainfall-Runoff Model: CASC2D User's Manual, Colorado State University Report CER90-91PYJ-BS-12, March 1991, 66p.
- Ogden, F. L., B. Saghafian and W.F. Krajewski, 1994. GIS-Based Channel Extraction and Smoothing Algorithm for Distributed Hydrologic Modeling, Proceedings, ASCE Hydraulics Division Specialty Conference, Buffalo, NY, August 1994, pp. 237-241.
- Ogden, F. L. and P.Y. Julien, 1994. Runoff Model Sensitivity to Radar Rainfall Resolution, Journal of Hydrology, 158 (1994), pp. 1-18.
- Ogden, F. L., 1992. Two-Dimensional Runoff Modeling with Weather Radar Data, Ph.D. Dissertation, Colorado State University, Department of Civil Engineering, 1992.
- Rawls, W.J. and D.L. Brakensiek, 1983. A Procedure to Predict Green and Ampt Infiltration Parameters, Proceedings of the ASAE Conference on Advances in Infiltration, Chicago, IL, pp. 102-112.
- Saghafian, B., 1992. Hydrologic Analysis of Watershed Response to Spatially Varied Infiltration, Ph.D. Dissertation, Colorado State University, Department of Civil Engineering, 1992.
- von Guerard, P., P. Abbott and R. Nickless, 1987. Hydrology of the U.S. Army Pinon Canyon Maneuver Site, Las Animas County, CO, U.S. Geological Survey Water Resources Investigations Report 87-4227.
- von Guerard, P., R.S. Parker and R.G. Dash, 1993. Assessment of the Effects of Military Maneuvers on the Streamflow, Water Quality, and Sediment Yields at the U.S. Army Pinon Canyon Maneuver Site, Las Animas County, CO, U.S. Geological Survey Water Resources Investigations Report 91-4095.

THE SIMULTANEOUS HEAT AND WATER (SHAW) MODEL: A RESEARCH TOOL FOR MANAGEMENT DECISIONS

G.N. Flerchinger, Research Hydraulic Engineer, USDA Agricultural Research Service, Boise, Idaho; S.P. Hardegree, Plant Physiologist, USDA Agricultural Research Service, Boise, Idaho; and G.L. Johnson, Meteorologist, USDA Natural Resources Conservation Service, Portland, Oregon

INTRODUCTION

As computer simulation models become increasingly sophisticated, their ability to address complex problems is enhanced. Unfortunately, complex models are typically associated with complex input requirements and difficult interpretation of model results. Thus, as research models become more complex, the gap widens between models developed by researchers and models that a natural resource manager can use as a practical tool to make informed decisions. In many instances, however, the information gained and the benefit realized far outweigh the difficulty in applying a model. Additionally, input requirements can be simplified through development of a user-friendly interface to aid the user in applying the model.

The Simultaneous Heat and Water (SHAW) Model, originally developed to simulate soil freezing and thawing (Flerchinger and Saxton, 1989), simulates heat, water and solute transfer near the soil surface and has been used to predict climate and management effects on soil freezing, snowmelt, runoff, soil temperature, soil water, evaporation, and transpiration (Xu et al., 1991, Flerchinger et al., 1994, Hayhoe, 1994; Flerchinger et al. 1996a; Flerchinger et al. 1996b; Flerchinger and Pierson, 1997; Flerchinger and Seyfried, 1997). The detailed physics in the SHAW model coupled with its user-interface (ModShell for Model Shell) make it a useful tool to address many potential applications. The purpose of this paper is to demonstrate two applications where the SHAW model has been used as a decision aid for resource management. The first application used the SHAW model to simulate temperature and water conditions at the soil surface to assess the effects of climatic variability on establishment of native grass species after wildfire. In the second application, the model provided information to assess the potential risk posed by the migration of contaminants from an abandoned landfill site; the soil water balance, percolation to ground water, and contaminant transport were simulated at the site.

THE SHAW MODEL

The Simultaneous Heat and Water (SHAW) model simulates heat, water and solute transfer within a one-dimensional profile and includes the effects of plant cover, dead plant residue, and snow as illustrated in Figure 1. Unique features of the model include: simultaneous solution of heat, water and solute fluxes; detailed provisions for soil freezing and thawing; and simulation of transpiration and water vapor transfer through a multi-species plant canopy. Input to the model includes daily or hourly weather observations and parameters describing plant, snow, residue, soil and site characteristics. Daily or hourly predictions include evaporation, transpiration, percolation, surface energy fluxes, soil frost depth, snow depth, runoff and soil profiles of temperature, water, ice and solutes.

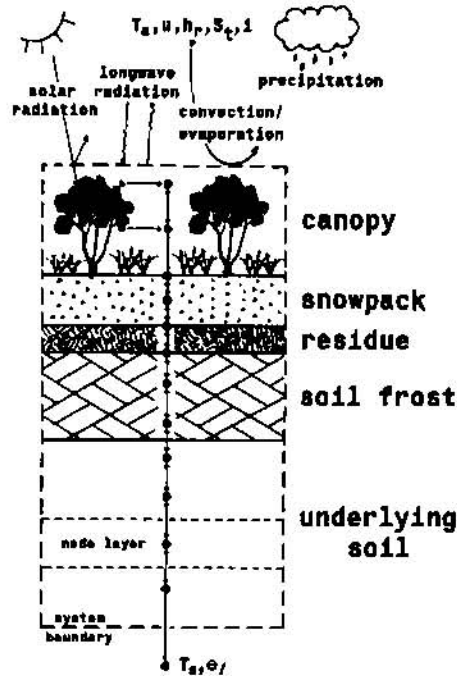


Figure 1. Physical system described by the SHAW model. (T_a is temperature, u is windspeed, h is relative humidity, S_s is solar radiation, i is precipitation, T_s is soil temperature, and θ_l is water content.)

APPLICATIONS FOR MANAGEMENT

Rangeland Revegetation: The Bureau of Land Management estimates that resource values are impaired or threatened on millions of acres of rangeland in the western United States. A major contributor to resource degradation on these lands is the spread of undesirable non-native annual weeds after wildfire. Current planning tools for rangeland restoration rely on gross approximations of species adaptation to mean annual precipitation and soil texture. Unfortunately, micro-climatic requirements for successful plant establishment are much more restrictive than those required for persistence of mature plants. This approach, which has had limited success, does not take into account seasonal and yearly variability in seedbed temperature and moisture, which are critical to germination and seedling establishment.

This application demonstrates the utility of the SHAW model to predict near-surface soil temperature and moisture conditions for assessment of native grass establishment after wildfire. Simulated soil temperature and moisture conditions were input into a seedling establishment model to assess probability of germination success for a spring planting scenario under historic weather conditions.

Model Validation: The site selected is near Orchard, Idaho located approximately 50 km southeast of Boise, Idaho where the USDA Agricultural Research Service maintains a microclimatic sensor network to provide input and validation data for the SHAW model. Three separate replications of soil temperature and water content profiles are collected for burned plots at each of three sites that vary in soil texture. Hourly observations of air temperature, wind speed, humidity, precipitation and solar radiation are also collected.

The SHAW model was parameterized with the aid of ModShell, which estimates soil hydraulic properties from soil texture. The model was initialized on November 1, 1994 using observed soil temperature and water content at the Orchard site. Figure 2 shows simulated and measured average daily soil temperature at a 2-cm depth for site 3, a silt loam soil, from November 1 through May of 1995. Model efficiency for this period at this site was 0.95; efficiencies for site 1 (a sandy loam) and site 2 (a loamy sand) were 0.85 and 0.91, respectively. Temperatures through the seedling germination period, which occurs in April and May, are most important. Simulated and measured hourly temperatures for the first half of May are plotted in Figure 3.

Model Application: Historic soil temperature and moisture information are not available for most wildland areas affected by fire. The SHAW model can be used to simulate post-fire soil temperature and moisture content using either observed or stochastically-generated weather time series from a nearby climate recording station. Recently, a methodology for spatially-interpolating the parameters of the GEM (Generation of weather Elements for Multiple applications) weather generator was developed and tested, enabling time series generation at any location, even where a representative climate station is not available (Johnson et al. 1997). For this example, a 30-year record of weather data from the Boise National Weather Service office, approximately 30 km from the Orchard site, was used for SHAW model input. The site was assumed to have burned in late summer, leaving a bare soil surface. The model was initialized using typical soil temperature and water content profiles in mid-August. A separate model run was then made for each year to simulate soil temperature and moisture for bare, post-burn conditions at the sandy loam site given an April 1st planting date the following spring.

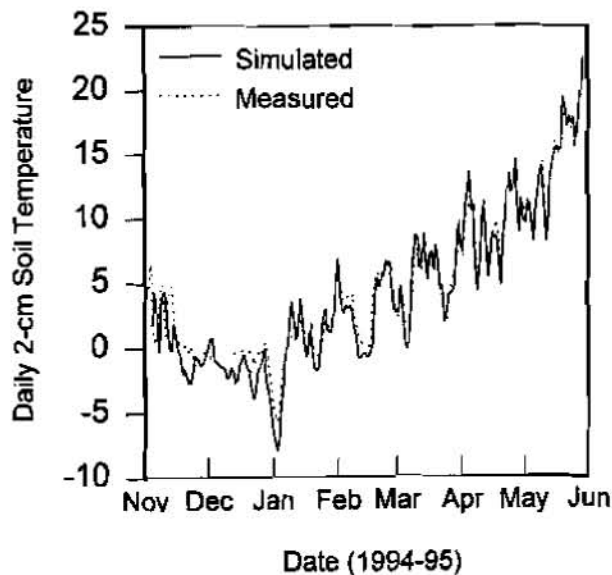


Figure 2. Simulated and measured average daily 2-cm soil temperature from November 1 through May for the silt loam soil at Orchard, Idaho.

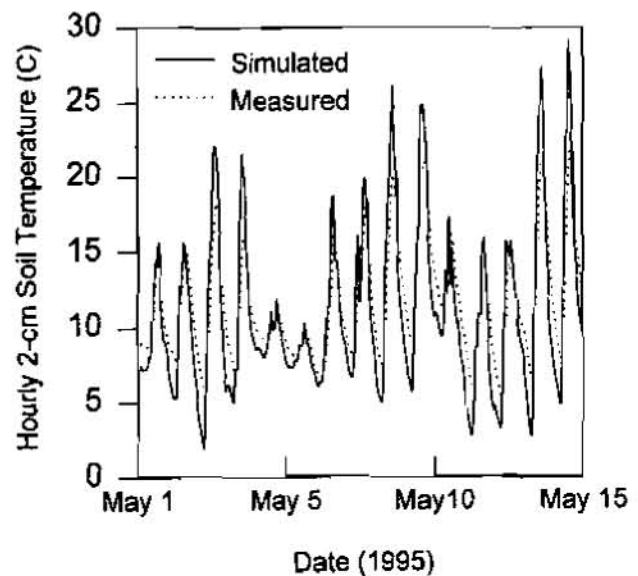


Figure 3. Simulated and measure hourly 2-cm soil temperature for early May for the silt loam soil at Orchard, Idaho.

Results from the Germination Model: Simulated soil temperature and moisture conditions for each of the 30 years were input to a hydrothermal germination response model to evaluate germination success for four native grass species: bottlebrush squirreltail, sandberg bluegrass, bluebunch wheatgrass, and thickspike wheatgrass. The germination model estimates germination rate as a function of seedbed microclimate for any temporally varying temperature regime between 0 and 35°C and water potential between 0 and 2.5 Mpa. Figure 4 shows the range of conditions over which these species are expected to germinate (Hardegee, 1996). Of the 30 years simulated, bottlebrush squirreltail was expected to successfully germinate only 17 % of the time. Probability of success for sandberg bluegrass was 7%, bluebunch wheatgrass was 33%, and thickspike wheatgrass was 17%. These results are consistent with the information contained in Figure 4, which shows that optimal germination conditions are narrowest for sandberg bluegrass (b).

Given the probability of germination success listed above, a land manager could make informed decisions about which grass species or mixture of species to seed. With additional information, such as soil moisture content prior to planting and long-term weather forecasts, seeding strategies could be tailored for the particular year to optimize probability of success.

Contaminant Transport Modeling: Small uncontrolled waste disposal sites are a known and perhaps significant source of ground-water pollution. Chemicals and waste products have historically been discarded at small landfill sites with little or no regulation. Many of these landfill sites have since been closed. One such site is the Murtaugh landfill located in southern Idaho. As with many abandoned landfill sites, the threat this site poses to water quality is uncertain.

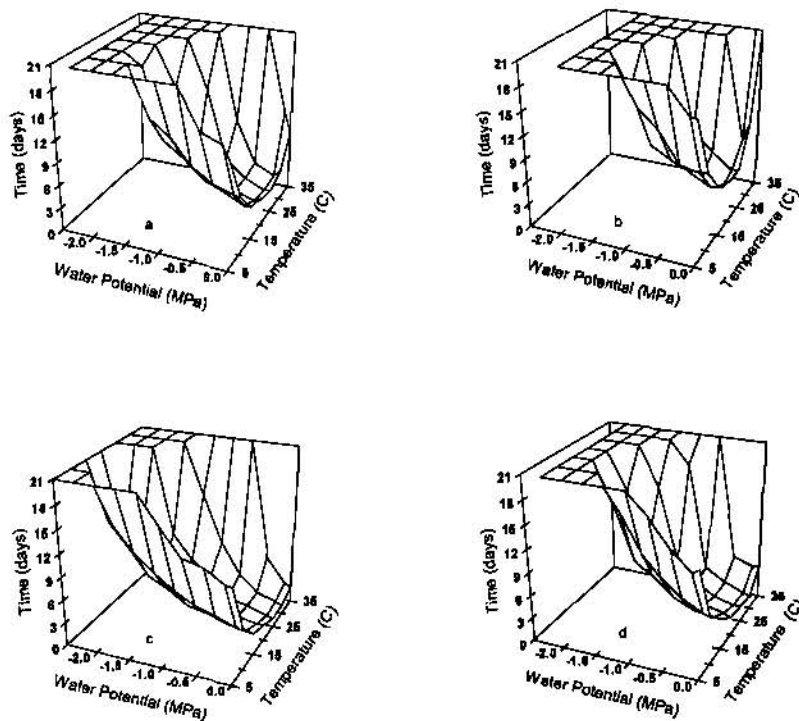


Figure 4. Days required to reach 3% total germination for (a) bottlebrush squirreltail, (b) sandberg bluegrass, (c) bluebunch wheatgrass, and (d) thickspike wheatgrass as a function of water potential and temperature.

Numerical models of contaminant fate and transport can be a cost-effective tool for assessing the potential hazards that a site may pose and for evaluating potential remediation measures, but seldom are models available which can simulate all aspects of contaminant fate and transport under complex site conditions. This application demonstrates the role that the SHAW model played in the site investigation and remediation of an abandoned landfill reported to contain unknown quantities of disulfoton, an acutely toxic pesticide. A detailed description of the contaminant transport modeling conducted at the site is given by Flerchinger et al. (1997).

Site Description: Murtaugh landfill is an approximately 2.4-ha (6-acre) tract of land owned by the U.S. Department of Interior Bureau of Land Management (USDI/BLM). The site was operated as an open landfill with little or no regulation from the 1920's until 1972. Large quantities of pesticides reportedly disposed in several trenches at the site prompted the BLM to initiate a site inspection (Weston, 1988). One drum sampled contained disulfoton, an acutely hazardous waste. Initial trench excavation estimated that somewhere between 10,000 to 27,500 containers were present in the trenches, each containing an estimated 5 to 10 L of contaminant. Area water wells were sampled with no detection of contamination.

Soil surveys indicated that the top soil at the site is about 0.3 m (1ft) thick (Wells, 1989). Below the top soil is a deep loess soil which rests upon the basalt formation and contains a relatively impermeable caliche layer, which is a hardened layer formed by the precipitation of calcium carbonate and other soil minerals. The caliche layer is between 4.6 to 6 m (15 to 20 ft) below the soil surface and varies from a 0.6-m (2 ft) thick hard layer to scattered broken pieces or absent. The basalt top follows the surface topography closely at 6 to 9 m (20 to 30 ft) deep.

Model Application: Because of the complexity of site conditions and contaminant properties, a combination of three models was applied to simulate the fate and transport of disulfoton and its metabolites at the Murtaugh landfill. Since a large percentage of the annual precipitation occurs in the winter months and frozen soil is commonly present during this period, the SHAW model was used to predict evapotranspiration, percolation and runoff at the site. The SHAW model was used to simulate a detailed water balance of the site along with aqueous-phase transport and degradation of disulfoton. Other models applied at the site included: a 3-dimensional aqueous-phase transport model applied to the depth of the ground water (approximately 160 m or 490 ft deep); and a 2-dimensional non-aqueous phase liquid (NAPL) transport model.

Trench excavation revealed that some buried containers had already corroded to rupture. Based on results from Walton et al. (1989) under similar climatic and soil conditions, it was conservatively assumed that the buried containers would fail over a 5-year period, during which all the chemicals currently present would leak out into the trenches. The maximum and minimum estimated volume of disulfoton was used to calculate a constant leaking rate spread uniformly over the 30 m x 100 m trench area as a steady-state influx boundary condition at a depth between 3.5 to 5.5 m. Deep percolation calculated by the SHAW model was used as input to the other models.

Weather conditions input to the model were supplied by the climate simulation model, CLIGEN (Nicks and Gander, 1994), which was used to generate daily weather data for the Burley, Idaho, located 30 km east of Murtaugh. A unit gradient boundary condition was set on the bottom of the

9-m (30-ft) simulated profile.

Model Results and Recommendations: The surface water balance simulated by SHAW indicated that the annual evapotranspiration averaged 262 mm from the Murtaugh landfill, which accounted for nearly all of the precipitation. Runoff averaged 11 mm annually and was most often associated with snowmelt and frozen soil. Percolation was zero most of the time, except for a few wet years which accumulated approximately 8 mm of percolation over 100 years, which was used as an upper boundary condition for the 3-dimensional aqueous phase and 2-dimensional non-aqueous phase transport models.

Figure 5 shows the concentration profiles from the SHAW simulation at end of the 5-year leaking period and after 10 years assuming the maximum estimated volume of contaminant. Much of the simulated transport occurred during the 5-year leaking. The maximum concentration was approximately 5,000 ppm, much higher than disulfoton water-solubility, indicating that soil water was insufficient to dissolve the leaking chemical and that a non-aqueous phase (NAPL) disulfoton would exist. When degradation of solutes was considered, disulfoton concentration drops to a very low level while its toxic metabolites remain at high concentration. Figure 6 shows the concentration profile of disulfoton and its toxic oxidative metabolite at the end of the 10-year simulation period based on the SHAW simulation. Simulations using the minimum estimated amount of contaminant showed very little migration.

Results of the contaminant fate and transport study are summarized as follows.

- (1) Only slight percolation was predicted at the Murtaugh site because of the low precipitation and relatively large potential evapotranspiration.
- (2) The low permeable caliche layer deters downward movement of dissolved chemicals. Without the caliche layer, however, contaminants can reach the fractured basalt very easily depending on the assumed volume of contaminants present.
- (3) When primary degradation is simulated, disulfoton disappears a few years after leaking. However, fate of toxic metabolites remains uncertain.

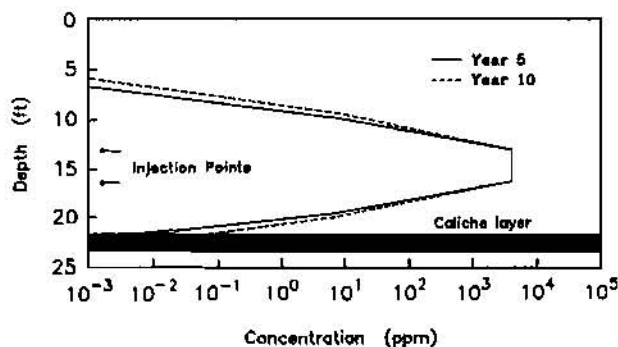


Figure 5. Concentration profile of disulfoton simulated by the SHAW model with maximum estimated amount of contaminant.

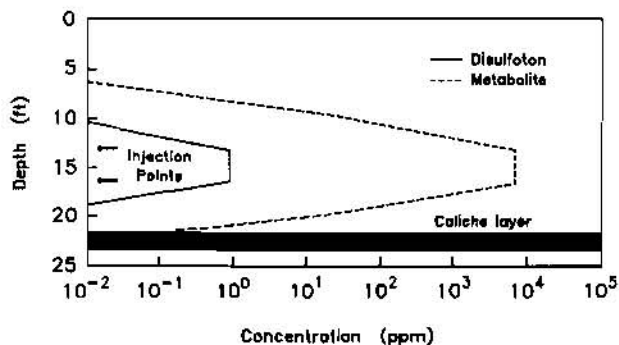


Figure 6. Concentration profile of disulfoton and its oxidative metabolite simulated by the SHAW model 10 yrs after the beginning of the 5-yr leaking period .

Site Remediation: Further site investigation revealed that the actual amount of contaminant present is close to the minimum estimates rather than the maximum. Based on the contaminant transport modeling, it was deemed that migration of contaminants to ground-water sources was not likely. Thus, costly removal of contaminants was not necessary. Closure of the site included access restriction and covering the site with 0.6 m (2 ft) of fill material to reduce the likelihood of surface contamination and subsurface exposure to rodents. Access wells were installed to sample contamination within the unsaturated zone beneath the trenches for monitoring of contaminant migration. Because this remedy results in hazardous substances remaining on-site above health-based levels, a review will be conducted by the BLM within five years after commencement of remedial action to ensure that the remediation continues to provide adequate protection for human and environmental health.

SUMMARY

The SHAW model simulates heat, water and solute transfer near the soil surface and within the soil profile. The flexibility and detailed physics incorporated into the SHAW model give it the ability to accurately simulate temperature, water and solute conditions for a myriad of applications including such complex problems as: runoff related to seasonally frozen soils; surface energy and water balance; percolation to ground water; evapotranspiration and plant water use by competing plants; and near-surface temperature and water conditions for such processes as seedling germination, plant establishment, and insect population dynamics. This ability enables natural resource managers to evaluate various management scenarios to make better-informed decisions which can lead to considerable cost savings. Two such applications of the SHAW model as a decision aid tool are presented in this paper.

MODEL AVAILABILITY

The SHAW model is freely available from the Northwest Watershed Research Center web site (<http://ars-boi.ars.pn.usbr.gov/index.html>) or by contacting the author (Gerald Flerchinger, 800 Park Blvd., Suite 105, Boise, ID, 83712; Phone: (208) 422-0716; Email: gflerchi@nwr.cars.pn.usbr.gov).

REFERENCES

- Flerchinger, G.N., Baker J.M., and Spaans, E.J.A., 1996a, A test of the radiative energy balance of the SHAW model for snowcover. *Hydrological Processes*, 10, 1359-1367.
- Flerchinger, G.N., Cooley, K.R., and Deng, Y., 1994, Impacts of spatially and temporally varying snowmelt on subsurface flow in a mountainous watershed: 1. Snowmelt simulation. *Hydrologic Science Journal*, 39, 507-520.
- Flerchinger, G.N., Hanson, C.L. and Wight, J.R., 1996b, Modeling evapotranspiration and surface energy budgets across a watershed. *Water Resources Research* 32, 2539-2548.
- Flerchinger, G.N. and Pierson, F.B., 1997, Modeling plant canopy effects on variability of soil temperature and water: Model calibration and validation. *Journal of Arid Environments* 35, 641-

- Flerchinger, G.N. and Saxton, K.E., 1989, Simultaneous heat and water model of a freezing snow-residue-soil system I. Theory and development. *Transactions of the American Society of Agricultural Engineers* 32, 565-571.
- Flerchinger, G.N. and Seyfried, M.S., 1997, Modeling Soil Freezing and Thawing and Frozen Soil Runoff with the SHAW Model. pp. 537-543 *In*: Iskandar, I.K., Wright, E.A., Radke, J.K., Sharratt, B.S., Groenevelt, P.H. and Hinzman, L.D. (eds.), *Proceedings of the International Symposium on Physics, Chemistry, and Ecology of Seasonally Frozen Soils*, Fairbanks, AK, June 10-12, 1997. CRREL Special Report 97-10. U.S. Army Cold Regions Research and Engineering Laboratory, Hanover, NH.
- Flerchinger, G.N., Deng, Y. and Gebhardt, K., 1997, Integrated modeling of disulfoton transport at an abandoned landfill site. *Applied Engineering in Agriculture* 13, 217-225.
- Hardegree, S.P., 1996, Optimization of seed priming treatments to increase low-temperature germination rate. *Journal of Range Management* 49, 87-92.
- Hayhoe, H.N. 1994. Field testing of simulated soil freezing and thawing by the SHAW model. *Canadian Journal of Agricultural Engineering*, 36, 279-285.
- Johnson, G.L., Daly, C.D., Taylor, G.H., Hanson, C.L., and Lu, Y.Y., 1997, GEM model temperature and precipitation variability, and distribution using PRISM. pp. 210-214 *In*: *Proceedings of the 10th Conference on Applied Climatology*. American Meteorological Society, Reno Nevada.
- Nicks, A.D. and Gander, G.A., 1994, CLIGEN: A weather generator for climate inputs to water resource and other models. pp. 903-909 *In*: *Proceedings of the Fifth International Conference on Computers in Agriculture*, Orlando, Florida. American Society of Agricultural Engineers, St. Joseph, Michigan.
- Walton, J.C., Rood, A.S., Baca, R.G., and Otis, M.D., 1989, Model for estimation of chlorinated solvent release from waster disposal sites. *Journal of Hazardous Material* 21, 15-34.
- Wells, R., 1989, Hydrogeology of the East Twin Falls County landfill, Draft Report, Prepared for the USDI-Bureau of Land Management, Burley, ID., Contract No. ID910-CT9-008, Geology and Geophysics Department, Boise State University, Boise, ID.
- Weston, Inc., 1988, Final Report: Twin Falls Landfill Site Inspection, Twin Falls County, Idaho. Prepared fro the USDI Bureau of Land Management, Burley, Idaho.
- Xu, X., Nieber, J.L., Baker, J.M., and Newcomb, D.E., 1991, Field testing of a model for water flow and heat transport in variably saturated, variably frozen soil. p 300-308 *In*: *Transportation Research Record No. 1307*, Transp. Res. Board, Nat. Res. Council, Washington D.C.

DEVELOPMENT OF WATER QUALITY MODELING FRAMEWORK

By: **Luis Garcia, David Patterson,**
Colorado State University, Integrated Decision Support Group, Fort Collins, Colorado,
Mertynn Bender,
U.S. Department of the Interior, Bureau of Reclamation,
Land Suitability and Water Quality Group, Denver, Colorado,
and Russell Kinerson,
U.S. Environmental Protection Agency, Office of Water, Washington, D.C.

Key Words: WASP, River, Water Quality, Model, Analysis Tools, Personal Computer, Metals

Abstract: Water Quality Analysis Simulation Program--5 (WASP5) is a computer program that provides a framework for modeling water quality. WASP5 can be used to evaluate intraphase or interphase exchange processes such as settling, suspension, adsorption, desorption, volatilization, or hydrolysis as well as contaminant transport. It can also simulate the partitioning of chemicals and metals in the air, water, or soil. However, assembling data for the WASP model is labor intensive. The time consuming data assembly process has created the need for a set of pre- and post-processors to integrate databases and simplify data manipulation.

Two modeling analysis tools have been developed as part of a system for use with WASP5. The Graphical Data Processor (GDP) was developed to process, aggregate, and evaluate the availability of large quantities of biological, ecological, and water quality data. WASP Builder was developed to graphically display the segment-node-linkages of a riverine environment. It also allows users to build and modify the data groups of the WASP5 input files in a Windows environment.

INTRODUCTION

Temperature, salinity, oxygen, and simple nutrient budgets can be modeled with existing water quality models. However, toxics change rapidly with time and distance, limiting the use of existing water quality models. The processes by which toxics react, transform, or are adsorbed onto suspended materials need to be incorporated into existing models. Water Quality Analysis Simulation Program--5 (WASP5) is a computer programming system for modeling toxics, nutrients, and metals. WASP5 can be used to evaluate which intraphase or interphase exchange processes can be used to simulate the partitioning of chemicals and metals in the air, water, and soil. These processes include settling, suspension, adsorption, desorption, volatilization, or hydrolysis.

Due to the complexity of these processes, correctly assembling data for WASP5 is difficult and time consuming. The first objective of this project was to develop data processing tools for assembling and processing riverine water quality, ecological, and biological modeling data sets. The second objective was to develop a user-friendly tool to assess toxic and metal transformation and transport in rivers. The Colorado State University Integrated Decision Support (IDS) Group with cofunding from the Bureau of Reclamation (Reclamation) Land Suitability and Water Quality Group and the U.S. Environmental Protection Agency (EPA) Office of Water is meeting these objectives by developing user-friendly analysis tools for EPA's WASP5 model. Two modeling

analysis tools, the Graphical Data Processor (GDP) and WASP Builder, have recently been developed for use in editing, aggregating, evaluating and displaying large amounts of water quality data for modeling projects. Both GDP and WASP Builder will be part of the WASP Analysis Tools (WASPAT) system. WASPAT contains additional tools for data pre- and post-processing.

GDP, a data pre-processor, allows users to identify time periods that have data suitable for a WASP5 analysis. The second tool, WASP Builder, allows the user to visualize the link-node layout of a riverine water quality model and edit the model input data sets in a Windows environment. Both tools allow users to more easily process data sets and apply them to the transport of toxics and heavy metals in a riverine environment. The current development efforts for WASPAT have focused on the toxic metals component (META) of WASP. The tools use an object-oriented Graphical User Interface (GUI) system developed with Microsoft Visual C++ on a MS-Windows-95 operating system. Graphics Server 4.50 supports the graphical displays in GDP.

This project focuses on application of the WASP5 model to a riverine environment. However, with slight modifications, these tools and GUI could be adapted for a variety of models, environments, and client needs. Future links to additional EPA models such as MINTEQ and BASINS (Better Assessment Science Integrating Point and Nonpoint Sources) are being investigated. Additional funding is sought to continue development, integrate existing water analysis tools into the framework, and expand the usefulness of the WASP model. For example, GDP currently processes data from EPA's STORET database, U.S. Geological Survey's WATSTORE database, and ASCII delimited files. This tool could be used "as is" or adapted to assemble and process a variety of data types for various models.

ANALYSIS TOOLS

Graphical Data Processor

GDP allows the user to determine the availability of STORET, WATSTORE, and ASCII delimited data for a WASP5 analysis. First, users select the data files that they want to analyze. This group of files is called a project. After selecting files for a project, a set of five windows appears in the main display window (Figure 1). The Project Files window displays the files associated (data files, parameter aggregation files, etc.) with the GDP project. The Units Conversion window allows users to convert data into comparable units of measure. The Data Aggregation window allows users to combine similar parameters from the same station or combine data for one parameter from different stations. The Notes window allows users to record notes or document their actions in the form of a text file. For example, the users could combine dissolved lead and total lead from one station into an aggregated parameter named "lead." The user could also combine total lead data from three different stations into an aggregated station named "Group 1." The Data Availability window allows users to create graphs that display time periods when data are available using daily or monthly time steps. It can also graph water quality data values in monthly time steps. The user can also determine periods of time where data are available for a given parameter from different stations or when a station has data regardless of parameter type.

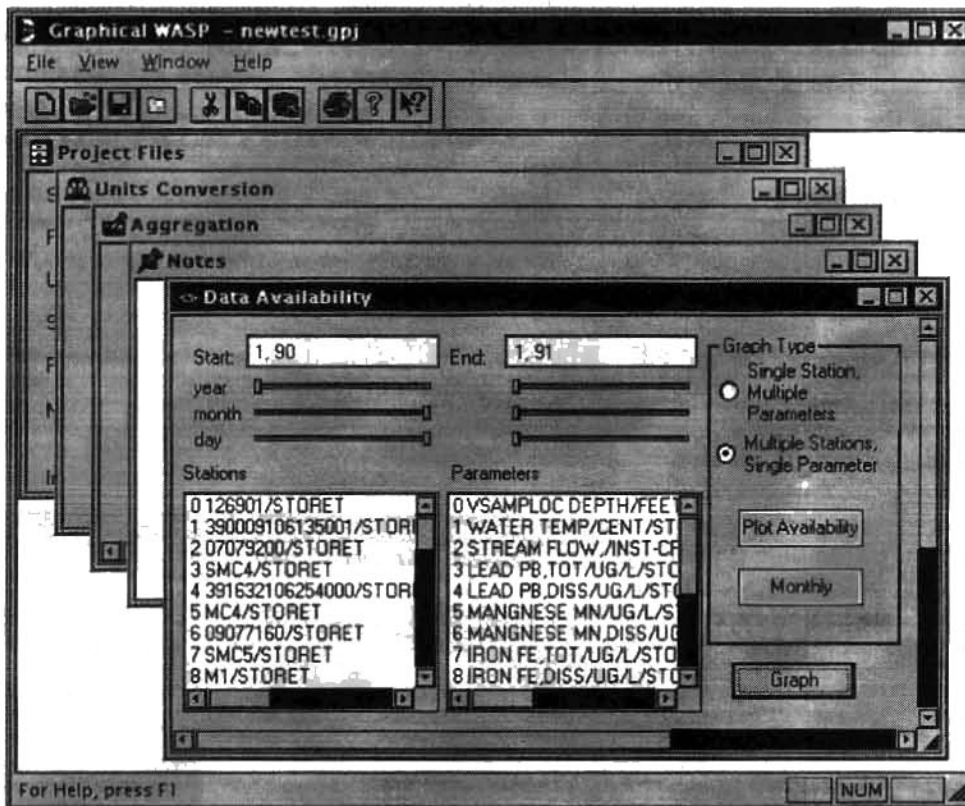


Figure 1. Cascade of five windows with the Data Availability window in the front.

After aggregating data and assessing its availability with GDP, the modeler can lay out the model segmentation and create the formatted input data sets using WASP Builder as an aid.

WASP Builder

WASP Builder allows the user to easily build and modify a link-node riverine model by modifying data groups. Figure 2 illustrates WASP Builder's representation of the air-water interface, the water-upper sediment interface, and the upper sediment-lower sediment interface. Each node on the screen describes a segment or a boundary between segments. Users can edit nodes individually, by selecting the node with the mouse, or globally, through the Edit Simulation Parameters function on the WASP Builder menu.

Depending on the WASP option users are running (EUTRO, TOXI, or META), the WASP data set is divided into different data groups. Currently, the WASP Builder supports files for WASP5 with the META4 option. To start a project, users open WASP input files created for the META option. Data groups A through J (Table 1) can be built and modified from the GUI (Figure 2). Since WASP Builder automatically formats data, it frees the user from the tedious task of building a formatted model input data set. Each data group can be separated into an individual file for temporary storage. These files can then be combined in different ways to create a single WASP input file. Descriptions of the data groups can be saved in each file.

In any project, the user can select different combinations of data groups and monitor how the changes affect model runs. For example, users could set up the network of segments and boundaries as a project. They could then create or import files with different flows (stored in Data Group C) without manipulating the other cards and compare outcomes. The system has been designed to insure that the selected cards are compatible. From the WASP Builder interface, a WASP5 input file can be generated from data groups.

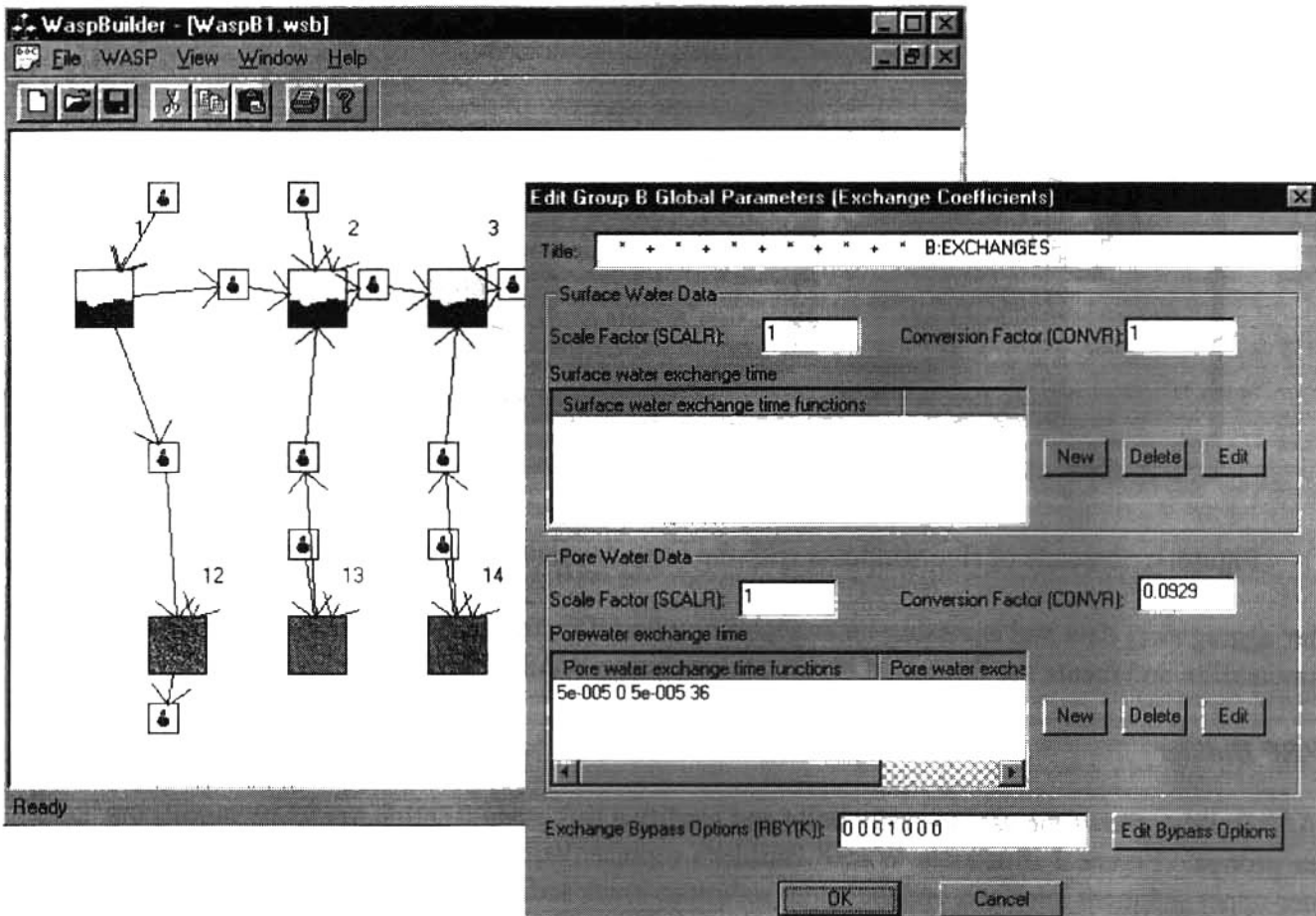


Figure 2. The WASP Builder representation of the link-nodes

Data Group	Data Group Function
Data Group A, Model Options	For model identification data and simulation control options.
Data Group B, Exchanges	Contains dispersive exchange information. Dispersion occurs between segments and along a characteristic length.
Data Group C, Volumes	Supplies initial segment volume information.
Data Group D, Flows	Supplies flow and sediment transport information between segments. Flows may be constant or variable.
Data Group E, Boundaries	Supplies concentrations for each system at the boundaries. All system concentrations must be supplied for each boundary.
Data Group F, Waste Loads	Defines the waste loads and segments that receive the waste loads for both point and diffuse sources.
Data Group G, Parameters	Contains appropriate environmental characteristics of the water body. Parameters are spatially variable.
Data Group H, Constants	Contains appropriate chemical characteristics or constants.
Data Group I, Time Functions	Contains appropriate environmental or kinetic time functions.
Data Group J, Initial Concentrations	Contains initial concentrations for each segment and each system.

Table 1. Descriptions of data groups (Ambrose et al. 1993).

FUTURE GOALS PENDING FINANCIAL SUPPORT

To date, efforts have concentrated on developing aids and graphical displays for input data. Some work is required to provide additional capabilities to the user for the input process. There is also a need to develop aids and graphical displays for model outputs, including sensitivity analysis and field verification. Given sufficient funding, potential areas of development could include:

- Linking to EPA's watershed management software, BASINS, to provide data input for the WASP model and provide BASINS users with modeling capabilities that the current steady-state toxics model, TOXIRoute does not have.
- Incorporating Geographic Information System (GIS) capabilities into WASPAT to allow users to visualize the linear representation (link-node) of the system and the location of sampling stations, streams and features such as cities, treatment plants, roads, etc.
- Allowing the user to run MINTEQA2 external from the WASPAT interface and exchanging files could help users determine the dominant chemical reactions and the data associated with them in the WASP METALS option. Presently, EPA's MINTEQA2 model is used to determine dominant chemical reactions and associated coefficients.
- Investigating expanding WASPAT to support the EUTRO and TOXI options. The present development focuses on the metals component of WASP. However, much of the data

required by META overlaps with the data required by EUTRO and TOXI. It is desirable to provide the capability of editing data sets for both EUTRO and TOXI using WASPAT.

- Developing the capability to fill in data using statistical approaches such as linear and non-linear interpolation, multivariate regression, and synthesis of data from surrounding stations could greatly enhance water quality models. Filling data gaps has been an important issue when working with existing data from STORET, WATSTORE, and project specific data.
- Allowing users to incorporate data from EPA's River Reach Files for Building Networks could improve modeling efficiency. EPA's River Reach Files include data for segment or reach numbers, sequence numbering, segment length, reach names, segment velocities at various flows, reach elevation differences, mean temperature, mean pH, roughness coefficient and other data that could be used to populate a WASP input file.
- Allowing the DYNHYD model to run interactively from the WASPAT interface to generate flows for a WASP run could prove beneficial. Tools developed for a WASP sensitivity analysis could also be used for DYNHYD to determine flow parameters.
- Developing screening tools. This includes developing linkages to remote sensing techniques such as AVIRIS and databases such as the USGS National Geochemical Data Base. Other screening tools could identify problem drainage areas by linking to the National Uranium Resource Evaluation (NURE) data for the Conterminous Western United States or compare indices, hazard protocols, baselines for metals, state and federal water quality standards, and detection limits.
- Developing a decision support system to integrate biological, recreational, economic, technical, legal, and political concerns could improve project planning.
- Developing error checks that detect improper input coefficients and input ranges would improve the confidence of modeling results. These value added features could be designed to detect the range of values physically possible for a parameter to have (screen for typos and bad data) and provide guidelines for values commonly used under different types of conditions.

Proposed Testing and Implementation

To demonstrate the usefulness of WASP, the system should be tested on a fast moving stream (high flow) dominated by colloidal loads of toxic metal compounds and a slow moving stream (low flow) dominated by dissolved species of toxic metals.

Proposed Graphical User Interface Window for Sensitivity Analysis

Developing an interface window that automatically generates a sequence of sensitivity runs to investigate major forcing functions and dominant coefficients would improve the understanding of the WASP model. This interface would provide the user with the ability to generate multiple input files for WASP runs and to analyze the differences in the output for user specified parameters. The user could select and graph the parameters and segments they wanted to track for a set of model runs generated with the sensitivity tool.

Proposed Documentation and Technology Transfer

As functions are added to GDP and WASP Builder hard copy and on-line documentation will be updated. In addition, documentation is needed for the most advanced research version of the WASP metals subprogram, META Version 2.0. A programmers reference has been generated to document the routines developed for the interface. Refereed journals and conferences will be used to transfer the technology to potential users in the public and private sectors. Technical appendices containing common combinations of chemical reactions in streams with toxic levels of metals could also be generated.

DEMONSTRATION

Interested parties are invited to request a demonstration version of the software.

Software Demonstration:

Dr. Luis Garcia
Colorado State University
Integrated Decision Support Group
601 South Howes Street, #410
Fort Collins, Colorado 80523 USA
E-mail: garcia@enr.colostate.edu
Telephone: (970) 491-5144
FAX: (970) 491-2293

Project Management:

Merlynn D. Bender
Bureau of Reclamation Technical Service Center
Land Suitability and Water Quality Group
Denver Federal Center, P.O. Box 25007 (D-8570)
Denver, Colorado 80225 USA
E-mail: mbender@do.usbr.gov
Telephone: (303) 236-8384 x 278
FAX: (303) 236-0199

SUMMARY

Simplifying the pre- and post-processing of WASP input data can save time and labor. Two data pre-processors, GDP and Wasp Builder have been developed. GDP allows the user to assess data availability for a modeling project. It also allows users to aggregate data from different stations and aggregate parameters. WASP Builder helps users visualize their model by displaying the node-link-segmentation. The Windows environment also simplifies data editing. Numerous ideas for simplifying WASP data processing remain.

REFERENCES

- Colorado State University Integrated Decision Support Group, 1997, "Graphical Data Processor User Manual Version 1.1", Fort Collins, Colorado.
- Colorado State University Integrated Decision Support Group, 1997, "WASP Builder User Manual Version 1.1, Fort Collins", Colorado.
- Colorado State University Integrated Decision Support Group, 1997, "Pre-Processor for WASP - Routine Descriptions", Fort Collins, Colorado.

Modeling System for Near Real-Time Flood Simulation for Salt Creek in Du Page County, Illinois

A.L. Ishii, Hydrologist, U.S. Geological Survey, Urbana, Ill.; T.J. Charlton, Principal Engineer, Du Page County Department of Environmental Concerns, Wheaton, Ill.; T.W. Ortel, Hydrologist, U.S. Geological Survey, Urbana, Ill.; C.C. Vonnahme, Senior Civil Engineer, Du Page County Department of Environmental Concerns, Wheaton, Ill.

Abstract

A near real-time flood-simulation system is being developed by the U.S. Geological Survey (USGS) in cooperation with Du Page County Department of Environmental Concerns for a 15-mile reach of Salt Creek in Du Page County, Ill. The Hydrologic Simulation Program-FORTRAN (HSPF) is being utilized to simulate rainfall-runoff for input to the Full EQuations (FEQ) model for dynamic-wave routing. The meteorological inputs for the rainfall-runoff simulation are obtained by Internet access and radio-telemetered precipitation gages. Boundary conditions for the dynamic-wave routing model are obtained from telemetered stream-elevation gages and rating curves. The interface for data-base management, developing and processing simulation files, and analysis of simulation results is the program GENeration and analysis of model simulation SCeNarios (GENSCN).

The flood-simulation system is being developed to estimate the downstream effects of diverting streamflow into or out of the Elmhurst Quarry Flood Control Facility, located about 10 miles from the downstream boundary, under various real-time or forecasted rainfall distribution scenarios. The flood-wave characteristics of the stream system are highly dependent upon the distribution of rainfall in time and space and, thus, the most effective management of diversions is dependent on the ability of facility managers to quickly simulate rainfall and snowmelt effects on the stream system.

The full benefit of understanding the complex model output from dynamic-wave routing can be realized only when the results can be quickly visualized and analyzed. Time series and model input files must be efficiently managed and the database made user friendly. Current operational procedures for the flood control facility are partly based upon operator intuition, which does not provide a systematic means to evaluate alternative operational schemes. The interfaced system makes it possible to test and compare various potential rainfall/diversion scenarios. This demonstration includes the GENSCN interface with operational HSPF and FEQ models for Salt Creek. The system includes clickable maps, animated water-surface profiles, and a variety of graphical and analytical tools for evaluating the output scenarios.

BACKGROUND

Du Page County is a rapidly urbanizing area about 17 miles west of the city of Chicago in Cook County, Illinois. Following heavy flooding in August 1987 that resulted in millions of dollars of damage in the metropolitan Chicago area, the State of Illinois gave the counties surrounding Cook County the responsibility to fund and implement storm-water management plans. Subsequent flooding has emphasized the value of both flood-mitigation facilities and data collection networks for planning and flood warning. Du Page County has designed and built one of the largest non-Federal off-line flood-control reservoirs in the Nation, the Elmhurst Quarry Flood Control Facility along Salt Creek (fig. 1). Storage provided in the quarry is about 8,300 acre-feet. The diversion works includes an 140-foot broad-crested fixed side weir, an 80-foot variable-elevation side weir, and a 7-foot by 7-foot sluice gate located at an elevation below the fixed weir. Water flows into a diversion conduit and then through two emergency shutoff gates to a vortex drop shaft. The shaft leads to a tunnel under a highway and into the quarry. After possibility of flooding has passed, the water stored in the quarry is pumped out through an aeration process and back into the creek.

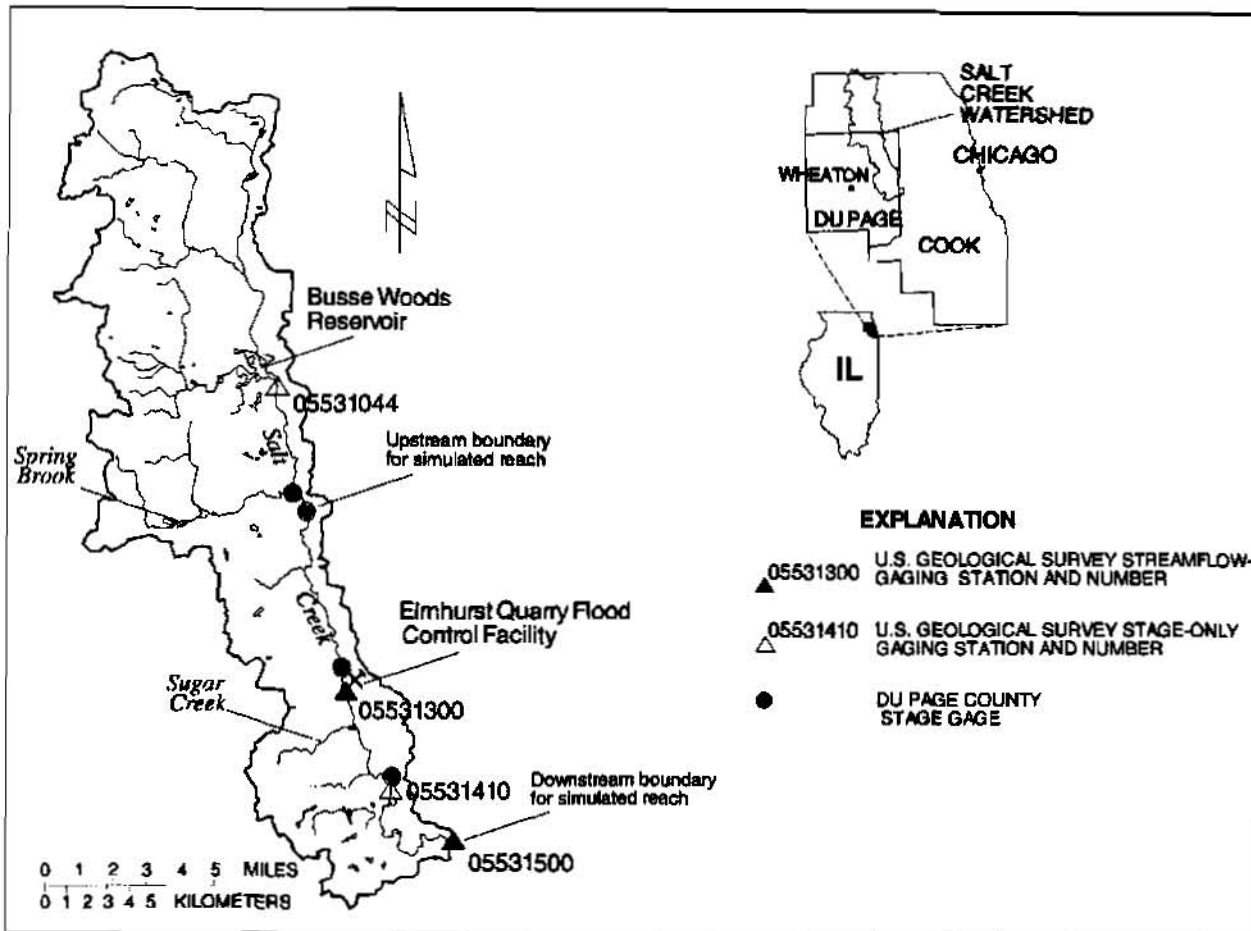


Figure 1. Salt Creek watershed and location of gaging stations on Salt Creek.

The Salt Creek watershed (fig. 1) area is 115 mi² to the U.S. Geological Survey streamflow-gaging station (05531500) located 8.8 miles upstream from the mouth. Based on the hydraulic characteristics of flooding, the watershed may be divided into three sections. The upper watershed (52 mi²) is the section upstream from Busse Woods reservoir. The middle section extends downstream to the junction of Sugar Creek and includes the narrow section from the junction of Spring Brook to the USGS streamflow-gaging station 05531300 (91 mi² area at the gage including the upper watershed). The Elmhurst Quarry Flood Control Facility is located in the narrow part of the middle section. The lower section may be considered to start at the junction of the Sugar Creek tributary with Salt Creek.

Continuous simulation rainfall-runoff simulation linked to dynamic-wave routing models were utilized to determine the flood-reduction potential of the Elmhurst Quarry project over its economic life span. Subsequent modeling has demonstrated that the unique hydraulic characteristics of the watershed require near real-time modeling to make effective decisions about planned diversions. The timing of the flood wave in the lower watershed is highly sensitive to the temporal and spatial distribution of rainfall; and consequently, the ability to generate scenarios in near real-time is needed. Hypothetical scenario generation based on predicted rainfall is valuable both to increase lead time in flood warnings and to allow for a safe return of flood waters to the creek. The purpose of this paper is to describe the application of the hydrologic, hydraulic, and scenario-generation programs to the near real-time flood-simulation system.

For intense, single storms of uniform rainfall, major flooding in the lower section of the watershed may be caused by local runoff from the downstream watershed tributaries, rather than by the flood wave traveling from upstream. For multiple or long-duration storms, the timing of the arrival of the flood wave from the upper watershed is also important because the effect of local inflows may be added to the flood wave arriving from upstream. The simulated

average travel time for the flood crest from the upstream boundary gage to the Quarry was about 11 hours for a uniform rainfall assumption for about 100 storms. The time-to-peak of the flood wave from the lower tributary areas to the mainstem was about 4-8 hours for selected events. Thus, the Elmhurst Quarry Flood Control Facility is of greatest benefit for the relatively rare multiple or long-duration rainfall event, which compounds the two flood waves. Snowmelt also has been a contributing factor to flooding in this area. Snowmelt routines are included in the continuous simulation rainfall-runoff model used, the Hydrologic Simulation Program—FORTRAN (HSPF) (Bicknell and others, 1997).

The ability to rapidly simulate flooding will improve the information base available for reservoir operation. Alternative strategies for operating the sluice gate on the flood control structure can be evaluated and compared prior to taking action. In order to achieve rapid hydrologic and hydraulic simulation, automated methods are needed for data retrieval, reformatting, error-checking and data estimation, and storage. Additionally, the links between the hydrologic and hydraulic models need to be streamlined, and graphical and other analyses of the modeled results must be available for quick review to aid in operational decision-making. These improvements form the basis of the flood-simulation system described in this paper.

HYDROLOGIC AND HYDRAULIC MODELS

Continuous rainfall-runoff simulation coupled with one-dimensional, unsteady-flow modeling has been mandated by Du Page County for flood-plain delineation and planning purposes. Design and operational planning have been accomplished using an approach based on the same hydrologic and hydraulic models that are used for flood-plain mapping. There are many advantages to this approach. Use of continuous simulation hydrologic models removes the need for estimating antecedent or initial moisture conditions because moisture balances are maintained continuously in the model for the extended period of the model run (usually many years). The development and use of a standard runoff time series incorporating the selected rainfall gage/land-use combinations and regionalized parameters throughout the county provides for consistency and reliability in projecting the effects of structures, diversions, and land-use changes on stream flows. The continuous runoff series can be coupled to a one-dimensional, unsteady-flow model that enables the simulation of backwater and flood-plain storage (Bradley and others, 1996). This is important where there are many control structures, and watersheds of low-gradient relief.

The continuous simulation rainfall-runoff model used in Du Page County, HSPF, is being modified by John Kittle, Jr., and others to meet the unique needs of the real-time flood-simulation mode (Alan Lumb, U.S. Geological Survey, written commun., 1996). A binary output file of unit runoff time series suitable for direct input as lateral inflows to the one-dimensional, unsteady-flow hydraulic model Full EQUations (FEQ) (Franz and Melching, 1997) has been added to HSPF version 12.0. HSPF is being modified to maintain the state variables in memory, so that the model can be stopped and updated without manually listing the starting state in the new simulation run.

The Full EQUations (FEQ) model, developed by Dr. Delbert Franz of Linsley, Kraeger Associates, Ltd., solves the full, dynamic equations of motion for one-dimensional, unsteady flow in open channels and through control structures. The FEQ model code and field test results have been documented by the USGS (Franz and Melching, 1997; Turner and others, 1996; Ishii and Turner, 1997). Equations for flow and elevation throughout the stream system resulting from the application of principles of conservation of mass and conservation of momentum are approximated by an implicit finite-difference approximation and solved in an iterative solution scheme that includes interpolation for function-table values at computational nodes. Thus, FEQ can output flow and water-surface elevation at any specified node in the modeled stream system. FEQ is uniquely adapted to model a wide variety of fixed and variable-geometry hydraulic controls including weirs, bridges, culverts, dams, and pumps using function tables computed with its companion program, Full Equation UTILities (FEQUTL) or other hydraulic models (Franz and Melching, in press). FEQ can be applied to simulate a wide variety of stream configurations including looped networks, lateral inflow, and wind-affected flow. FEQ has been utilized by the Illinois Department of Natural Resources Office of Water Resources for the operational management of an upstream reservoir on the Fox River in northeastern Illinois (William Rice, Illinois Department of Natural Resources Office of Water Resources, oral commun., 1996) and for planning and analysis purposes (Knapp and Ortel, 1992) in addition to the flood-plain mapping and project analysis work done in Du Page County (Lan and others, 1996).

In order to make the Salt Creek model operational for quick simulation for flood-warning purposes, several watershed tributary models that had been routed in detail for mapping and planning purposes required simplification. The effect of routing model detail reductions on the characteristics of the mainstem flood wave is under review, and continued testing is planned. A feature to provide hydrologic routing of watershed tributary flows has been implemented in FEQ, which may be used to improve the routing characteristics of the simplified tributary outflows (Delbert Franz, Linsley, Kraeger Assoc. Ltd., written commun., 1997).

NEAR REAL-TIME DATA ACQUISITION AND INPUT

The calibrated modules utilized in HSPF require precipitation, air temperature, dewpoint temperature, wind velocity, potential evapotranspiration, and solar radiation data to compute rainfall runoff and snowmelt. Precipitation is acquired from a precipitation network consisting of 26 gages installed throughout the county by the USGS. The network is operated in real time by spread-spectrum radio telemetry reporting to a base station located in the County offices in Wheaton. Stream elevation data at the four stage gages operated by the county on the mainstem of Salt Creek also are transmitted to the base station. The gages provide information on the flood-wave movement for warning and simulation. The status of pumps and reservoirs throughout the Salt Creek watershed is monitored by the supervisory control and data acquisition (SCADA) system. Next generation Doppler radar (NEXRAD) data provide storm tracking information for manual interpretation and warning.

Meteorologic data (air and dewpoint temperature, wind velocity, and solar radiation) are acquired from the Argonne National Laboratory Atmospheric Sciences World Wide Web page or from the emergency management office instruments at the County offices. The Meteorologic and hydrologic GENSCN Input Converter (MAGIC) program is used to convert the data as received to an HSPF format required for input to the Watershed Data Management (WDM) data base. Automated and manual methods for estimating missing or erroneous data are provided in the input interface. Potential evapotranspiration time series are computed by the methods utilized in calibrating the HSPF model for the county (Price, 1994). A sample window for the data input converter is shown in figure 2. Testing and implementation of the system are needed to verify the adequacy of the various data sources and estimation routines for short-term event simulations. The current plan is for the system to be operated with provisional data and to be updated as quality-assured data is received.

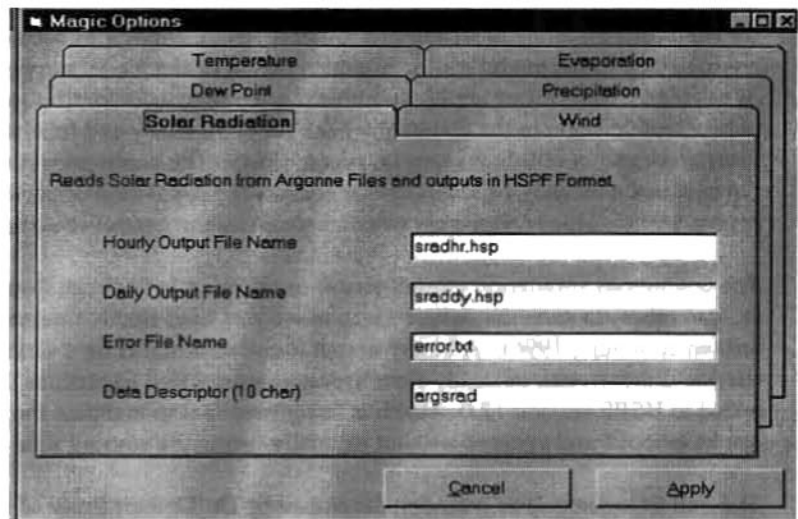


Figure 2. Meteorologic and hydrologic GENSCN Input Converter (MAGIC).

The upstream boundary condition for the FEQ model will be the stage hydrograph obtained from a stream-elevation gage operated by the county (fig. 1). These data are transmitted by radio telemetry. The location of the upstream boundary may be moved upstream in the future to increase the lead time for flood warning. Other data that can be obtained from the USGS real-time data page on the World Wide Web (WWW) includes the stream elevation at the three downstream streamflow-gaging stations along Salt Creek. Du Page County operates three additional stream-elevation gages with data transmitted by radio telemetry. These data are useful for determining the accuracy of the streamflow simulations. Discharge computed from a rating at the downstream boundary streamflow-gaging station (05531500) can be compared with the simulated discharge to determine overall accuracy of the simulation.

GENSCN GRAPHICAL USER INTERFACE

The application of hydraulic and hydrologic models to near real-time flood simulation requires an interface to streamline and unify pre- and post-processing of data input and output, linkage between the models, and analysis. The interactive computer program GENERation and analysis of model simulation SCeNarios (GENSCN) has been developed by John Kittle, Jr. and others (Alan Lumb, U.S. Geological Survey, written commun., 1996) in support of several USGS projects. A graphical user interface (GUI) currently is being developed for use on the personal computer platform. The GUI makes it possible to use the simulation and analysis features of GENSCN in a Microsoft Windows-based environment¹. GENSCN is being applied to the Truckee and Carson River Basins in Nevada and California to assess the effects of reservoir and diversion operations (Bohman and others, 1995), and to the Guadalupe River Basin in Texas as part of the National Water-Quality Assessment (NAWQA) program of the USGS (Marshall Jennings, U.S. Geological Survey, oral commun., 1997).

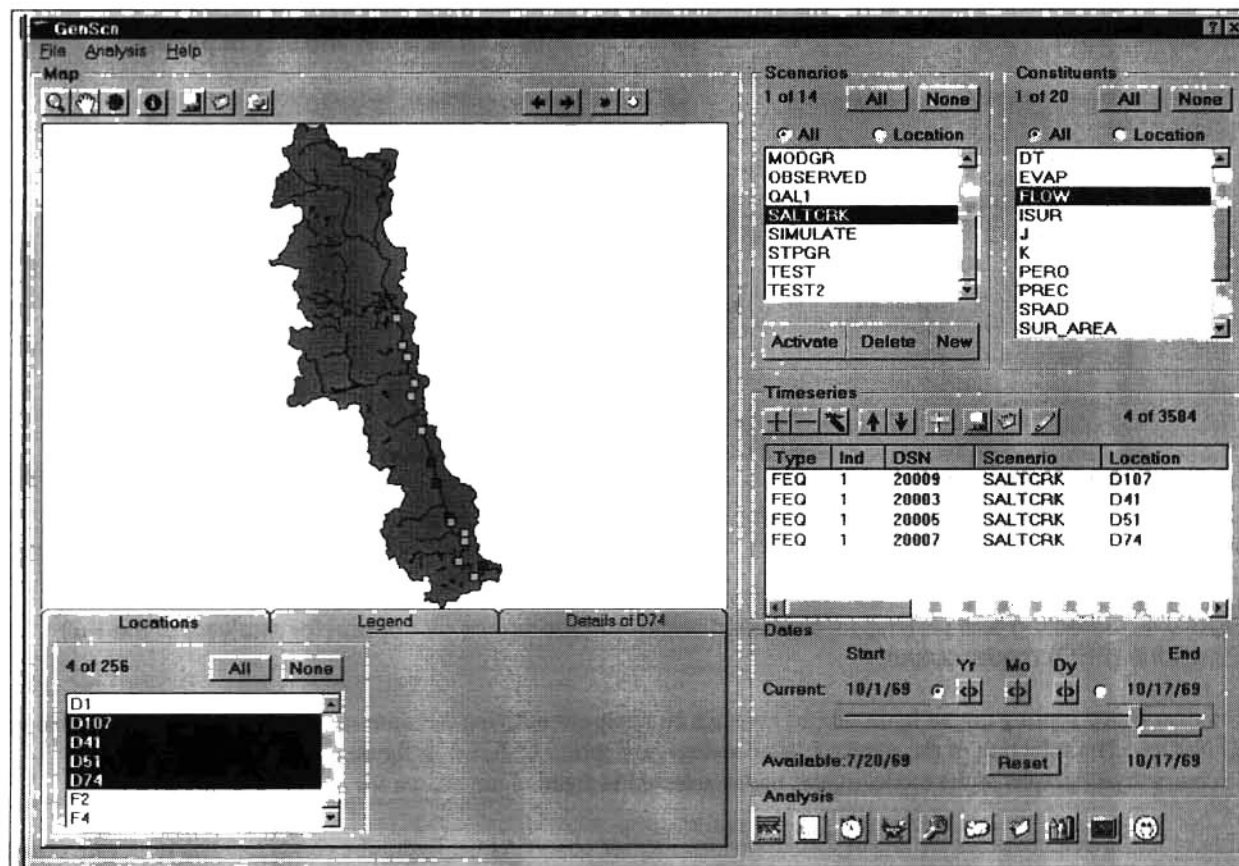


Figure 3. GENERation and analysis of model simulation SCeNarios (GENSCN) window showing selection of data set for processing and analytical option buttons (lower right).

The scenario generation and analysis options available in HSPF are fully implemented in GENSCN. The user can simulate previously developed scenarios, modify scenarios, or create new scenarios from within GENSCN. The HSPF program can be run from within the GENSCN interface. The analysis and plotting of output also is accomplished without exiting from the interface.

¹ The use of firm, trade, and brand names in this report is for identification purposes only and does not constitute endorsement by the U.S. Geological Survey.

Time series data sets, such as, flow, elevation, precipitation, storage, volume, and other data are referred to as constituents in the GENSCN interface. The user selects the scenarios (for example, simulated and observed data), the constituent (for example, flow or water-surface elevations), and the location for the desired data. The data sets, meeting all criteria are added to the buffer by choosing the add (+) button. The analytical options available for listing, plotting, comparing, and statistical analysis of the selected data are accessed through a drop-down menu or the button bar in the lower right panel (fig. 3). The GENSCN window displays shown in figures 3-5 are intended to illustrate features available in GENSCN and do not indicate citable or quantitative model results.

In order to analyze and display the results of unsteady-flow hydraulic modeling in GENSCN, an additional output format has been added to FEQ. The special FEQ output file, which includes water-surface elevation and discharge at each node specified in the FEQ input for each time step, is read in GENSCN. Additional values that can be plotted and listed with time include hydraulic channel and node properties such as cross sectional top width, area, conveyance, and volume available in level-pool reservoir nodes. GENSCN includes an animation option for viewing the time series at points along the river as an animated profile. The thalweg can be included and displayed. An example of the FEQ model output is shown as a profile plot in figure 4(b). The controls for running the animation are shown on the right in figure 4(a). The animation may be run forward and backward, or paused for a snapshot of the simulated profile at any time. The peak water-surface elevation at all locations also may be plotted.

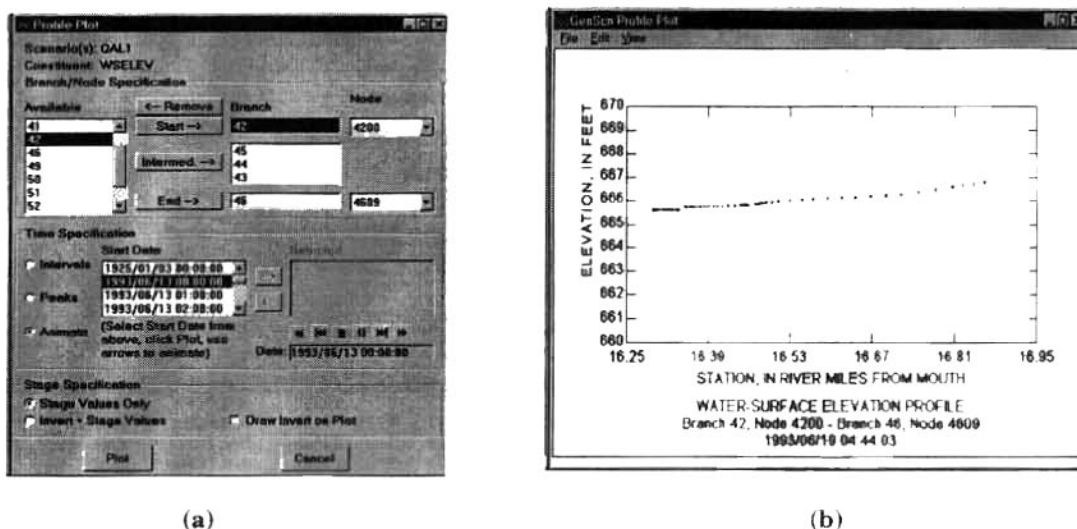


Figure 4. Selecting and plotting an animated water-surface profile plot option for analysis of the Full Equations (FEQ) model output.

The distributed routing output hydrographs also can be analyzed utilizing the time series output options available in GENSCN. The selection of the standard (time series) plot option is shown in figure 5. For this example, the discharge hydrographs at the model output nodes selected in figure 3 are shown for a particular simulation.

This example demonstrates the use of distributed routing for observing the hydraulic characteristics of the watershed. The most downstream hydrographs (at nodes D74 and D107) peak before the flood peak from upstream (D1 and D51) has arrived at the downstream locations. Local inflows from the subwatersheds in the lower watershed are the main source of inflow for the initial peak. This particular rainfall event was short and intense. Long duration or multiple storms result in local inflow peaks being added to the flood wave traveling from upstream, and, consequently, a larger downstream peak resulting later. This simulation is for the uniform rainfall case, and does not represent actual streamflow for the simulated period.

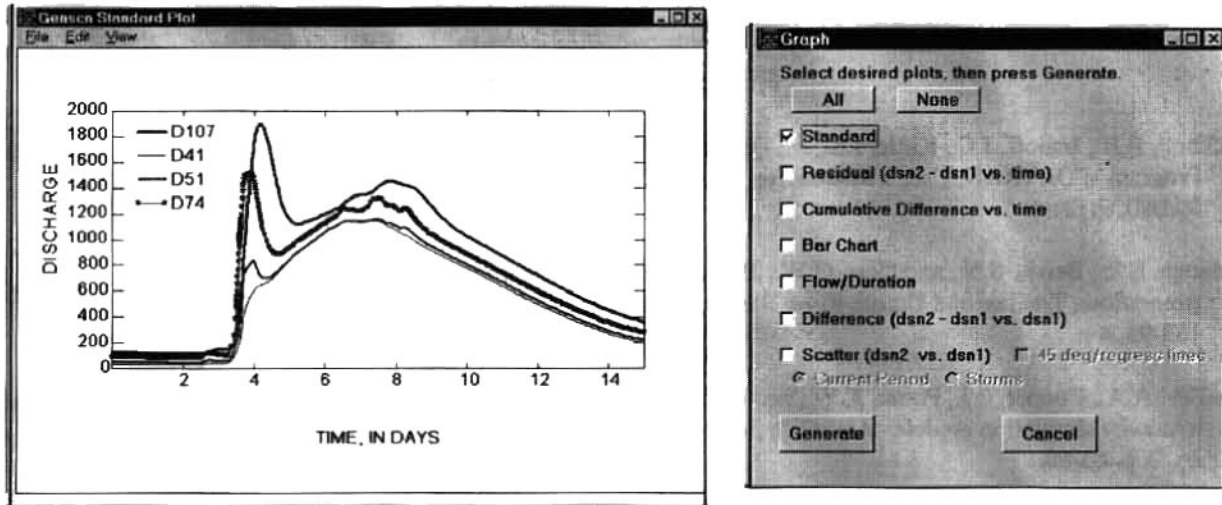


Figure 5. Standard plot option for analysis of time series data.

In addition to the time-series analysis options, GENSCN has the capability of displaying and animating spatial data through the map window. The selection of plotted nodes is illustrated in figure 3. Information regarding the constituents, scenarios, and time-series data available at the individual nodes may be selected. Additional geographic information system (GIS) coverages may be incorporated, and areas of interest may be enlarged through the zoom feature of the map window. The USGS Truckee-Carson program in Nevada and California utilizes animation to display time-series data on the map window. Different colors or line thickness are utilized to specify up to three different ranges of data on the river segments (Bohman and others, 1995). Future enhancements for the flood-warning system may include the ability to display and animate precipitation amounts throughout the County.

After the documentation and testing of the GENSCN system for near real-time flood warning are completed, the programs will be released and distributed for other applications to other watersheds. GENSCN is based on a modular design concept that allows for the efficient linking of other models and addition of new features and enhancements.

OPERATIONAL USE

The near real-time flood-simulation system for Salt Creek will be operated by the staff of Du Page County. Regular updates of the continuous simulation rainfall-runoff model will be needed in preparation for flood events. The fully routed results are not expected to be needed on a continuous basis but are to be implemented whenever elevations along Salt Creek are expected to approach flood stage. The major functions of the system are: (1) to simulate possible flood-stage creek elevations based on real-time or forecasted rainfall and snowmelt, (2) to simulate alternative operating strategies for the sluice gates at the Elmhurst Quarry and compare resulting creek elevations, (3) to simulate elevations in the creek resulting from pumped flows returned from the quarry with consideration of precipitation and other meteorologic conditions.

The system operator retrieves the hydrologic data from the WWW and the local base-station computer. The data input converter program is opened and the files are converted for input to the WDM data base. Errors and missing data reports are reviewed, automatic data revisions are either accepted or exchanged for data from other sources or estimates, and forecasted precipitation amounts may be entered. The GENSCN interface is used to write the data to the WDM; to run the hydrologic model, using updated initial conditions from the previous simulation; and to create the runoff files for hydraulic routing. The hydraulic model is run under one or more operational scenarios and the routed results are reviewed within the GENSCN interface for discharge, elevation, and storage at critical locations. Additional forecast precipitation scenarios then may be applied and the process repeated. Future enhancements to the system may include the display and animation of precipitation reported by the radio-telemetered precipitation network.

REFERENCES CITED

- Bicknell, B.R., Imhoff, J.C., Kittle, J.L., Jr., Donigan, A.S., Jr., and Johanson, R.C., 1997, Hydrological Simulation Program--FORTRAN, User's Manual for Version 11: U.S. Environmental Protection Agency EPA/600/R-97/080, in press.
- Bohman, L.R., Berris, S.N., and Hess, G.W., 1995, Interactive computer program to simulate and analyze streamflow, Truckee and Carson River Basins, Nevada and California: U.S. Geological Survey Fact Sheet FS-165-95, 4 p.
- Bradley, A.A., Cooper, P.J., Potter, K.W., and Price, T., 1996, Floodplain mapping using continuous hydrologic and hydraulic simulation models: American Society of Civil Engineers, Journal of Hydrologic Engineering, vol. 1, no. 2, p. 63-68.
- Franz, D.D., and Melching, C.S., 1997, Full equations (FEQ) model for the solution of the full, dynamic equations of motion for one-dimensional unsteady flow in open channels and through control structures: U.S. Geological Survey Water-Resources Investigations Report 96-4240, 258 p.
- Franz, D.D., and Melching, C.S., in press, Full equations utilities (FEQUTL) model for the approximation of hydraulic characteristics of open channels and control structures during unsteady flow: U.S. Geological Survey Water-Resources Investigations Report 97-4037.
- Ishii, A.L., and Turner, M.J., 1997, Verification of a one-dimensional, unsteady flow model for the Fox River in Illinois: U.S. Geological Survey Water-Supply Paper 2477, 65 p.
- Knapp, H.V., and Ortel, T.W., 1992, Effect of Stratton Dam operation on flood control along the Fox River and Fox Chain of Lakes: Illinois State Water Survey Contract Report 533, 79 p.
- Lan, Y., Rogers, S., Sikora, J., Cooper, P., and Klepp, C., 1996, Unsteady flow hydraulic modeling for flood plain mapping along the West Branch Du Page River, Du Page County, Illinois: International Water Resources Association Rivertech96 Proceedings of the 1st International Conference on New/Emerging Concepts for Rivers, Chicago, p. 204-211.
- Price, T.H., 1994, Hydrologic calibration of HSPF model for Du Page County—West Branch Du Page River at West Chicago, West Branch Du Page River at Warrenville, East Branch Du Page River at Maple Avenue, Salt Creek at Western Springs; including hydraulic evaluation—Salt Creek at Western Springs, Salt Creek at Rolling Meadows: Northeastern Illinois Planning Commission, 92 p.
- Turner, M.J., Pulokas, A.P., and Ishii, A.L., 1996, Implementation and verification of a one-dimensional, unsteady-flow model for Spring Brook near Warrenville, Illinois: U.S. Geological Survey Water-Supply Paper 2455, 35 p.

A MODULAR APPROACH TO INTERACTIVE WATERSHED MODELING

By John L. Kittle, JLKittle Consulting, Decatur, Georgia; Paul R. Hummel, AQUA TERRA Consultants, Decatur, Georgia; Paul B. Duda, AQUA TERRA Consultants, Decatur, Georgia; Alan M. Lumb, U.S. Geological Survey, Reston, Virginia

Abstract: As the requirements for hydrologic modeling expand and change, the need for a flexible modeling system becomes essential. AQUA TERRA Consultants, in conjunction with the U.S. Geological Survey, is developing an interactive hydrologic modeling system known as GenScn (GENERation and analysis of model simulation SCeNarios). The system supports all aspects of modeling, from model setup and data management to model calibration to analysis of alternatives.

GenScn is intended for a wide range of hydrologic situations and locations. Thus, the ability to incorporate a suite of models within the system has been a continuing focus during development. Current technology allows existing model codes to be compiled into Dynamic Link Libraries (DLLs) which may then be accessed by the system. This allows model codes to be incorporated into the system as they are, without rewriting them in a different language.

In developing GenScn, care is being taken to develop reusable components to perform specific tasks such as mapping, plotting, and time-series data management. This results in clearly defined and easily tested module codes which may then be used within other modeling systems with minimal effort.

User interaction with GenScn is through a Graphical User Interface (GUI). Significant effort is being made to minimize a user's effort to perform tasks and to allow direct manipulation of the elements of the system. An on-line help system allows the user to access information about specific portions of the system's windows. A hypertext version of the model's user manual may also be accessed.

The system is being tested in several locations (Truckee-Carson River Basins, Guadalupe River Basin, DuPage County, IL) and can easily be adapted to other locations. Geographic Information System (GIS) data can be used in GenScn to generate maps and tables which aid in the analysis.

INTRODUCTION

Use of watershed models like the Hydrological Simulation Program-FORTRAN (HSPF) (Bicknell, 1997) traditionally involved using a text editor to build an input sequence to describe a watershed's physical and water management characteristics. For large, complex river basins, input sequences were often thousands of lines long when water quality was simulated in addition to the hydrology. The process of making changes was time consuming and complex. In addition, analyzing results from several model runs required manually and tediously keeping track of time-

series data sets from all scenarios at multiple locations for several constituents. The analyzer often had to reformat the results and use separate programs to analyze results and prepare the needed tables and graphs.

The development of GenScn came as a response to the need to make HSPF input sequences easier to build and HSPF output easier to analyze. The requirements for the software were refined based on experiences with ANNIE (Lumb, 1989 and Flynn, 1995) and the HSPF Expert System (Lumb, 1994). The scenario generator provides advanced interaction with the HSPF input sequence and integrated analysis capabilities. The program provides an interactive framework for analysis built around an established and adaptable watershed model. The results of different scenarios can be easily compared and analyzed because the model and analysis tools are linked in one package and use a common data base.

A scenario consists of an input sequence, its output reports, and associated time-series data. Each input sequence describes a scenario. Once the model is run for a particular scenario, output reports and time-series data specified in that scenario's input sequence are available for analysis. A new scenario is created by copying an existing input sequence, modifying this input sequence to describe the new scenario, and then running the model. Where specified by the input sequence, output files and time-series data are automatically generated when the new scenario is run for comparison with other scenarios.

When changes to the input are complete, the HSPF model can be executed. HSPF checks the validity of the input sequence. Changes that are incomplete or inconsistent are referred back to the user for further refinement.

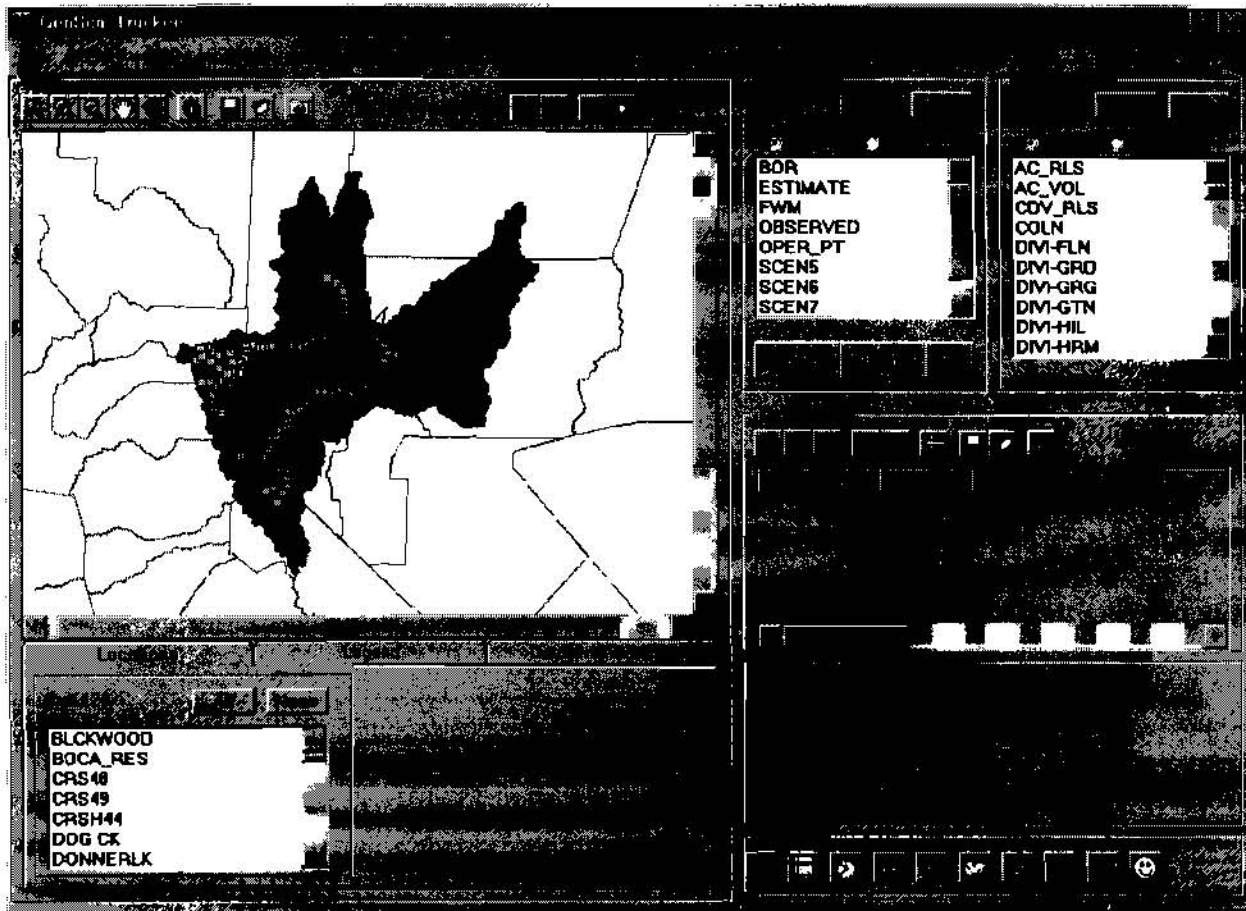
After execution is complete, the user may interactively specify results to be analyzed. Data to analyze may be specified by selecting scenario, location, and constituent names. Locations may also be specified graphically by clicking locations on a map. Results can be viewed either on the display screen or on printed output.

Results are available as tables and plots of the simulated data or results of statistical analyses of the data. A wide range of plots can be specified, including a standard time-series plot, a time-series plot of the difference between two time series, a bar chart, a flow-duration plot, a scatter plot of one time series versus the difference between two other time series, a scatter plot of two time series including an optional 45 degree line and regression line, and an event frequency plot. Statistical analyses include comparing two time series over a range of class intervals and constituent duration analysis. Included in the duration analysis is a lethality analysis methodology which links frequency data on instream contaminant levels to toxicity information resulting from both acute and chronic laboratory bioassays.

A METAPHOR FOR WATERSHED MODELING

A successful user interface for watershed modeling displays information to the watershed modeler in a manner consistent with the modeler's world view and needs. The goal of the

interface is to provide layers of information - a summary of information about the project in the main window along with a multitude of other windows which show additional information. This includes details about the watershed, model parameters and results along with complete documentation of the model's algorithms. The GenScn user interface has a main window which uses a map to show the watershed's spatial characteristics, text boxes which summarize locations where detailed information is available, scenarios which have been simulated (for model runs) or collected (for observed data), and constituents for which data is available. From the main window the user can activate a scenario, edit the description and parameters for the scenario, and run the model. The user may analyze results by selecting desired scenarios, locations and constituents and then selecting the time-series data available. A span of time and the analysis tool(s) are then selected to generate the desired tables, graphs, statistical summaries, or animations.



REUSABLE COMPONENTS

The design of reusable components has played a key role in the development of GenScn. The result of using these components includes (i) reusability within GenScn (references from different locations or with different parameter sets) (ii) reusability within other modeling systems, and (iii) more easily defined and tested modules.

A significant effort has been invested in developing a suite of modules for the graphical and tabular display of time-series data and other analysis results. The modules allow the programmer to set initial values for the parameters which define the plot or listing (e.g. data values, number of curves/columns, text labels). All plots and listings allow the end user to customize them to their liking using pull-down menus.

Initially GenScn used the Watershed Data Management (WDM) FORTRAN library of subroutines for time-series management. A set of subroutines were developed to interface between the Visual Basic GenScn code and the existing FORTRAN routines. This allowed the well-tested and well-documented WDM code to be preserved.

During development of GenScn, it was necessary to incorporate different types of time-series data (i.e. storage and model formats). To make GenScn work with these different data types in a consistent manner, a generic data structure was developed. Specific routines for each data type were written to fill the data structure. GenScn was then able to use this data structure in the same manner for all types of data.

Several other analysis tools were developed using existing FORTRAN codes which had already been tested and documented. The codes were compiled into DLLs and then called by GenScn using new code which interfaces to the DLLs. The duration and comparison analyses were both developed using this method. Another tool which allows the generation of new time series based on existing time series was also developed in this manner.

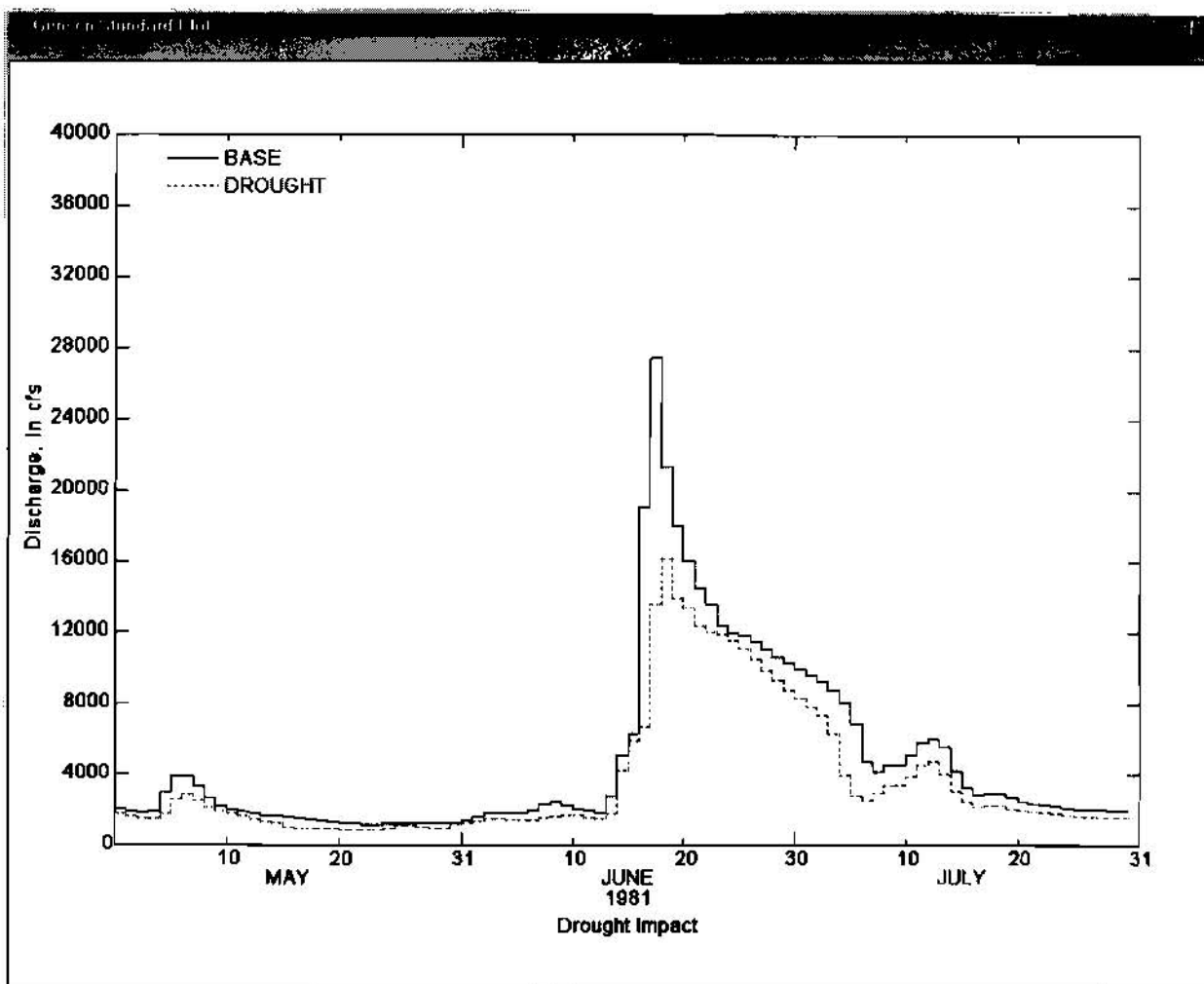
DEFINITION, SIMULATION AND ANALYSIS OF A SCENARIO

As an example of a possible scenario generator operation, assume we want to investigate the effect of severe drought. We might define this drought as a given period where precipitation is reset to three fourths of the normal amount. We will create a new scenario to simulate this drought period. We will perform this simulation using HSPF, and then we can analyze the results by comparing flows under normal conditions to flows under these drought conditions.

The steps to build the above scenario example are as follows. From the main scenario generator window, select the "BASE"(a calibration of the existing basin) scenario in the "Scenario" frame. Next, click the "Activate" button in the same frame. This brings up the GenScn Activate BASE window. Then click the "Save As" button to create a new scenario from this existing scenario. Call the new scenario "DROUGHT". Now we have a new scenario, but this scenario is identical to scenario "BASE" until we modify it. Select "EXT-SOURCES" in the "Block" frame. Change the multiplication factor for the precipitation source record to 0.75, representing three fourths of the normal precipitation. Click the "OK" button to save the revised ExtSources block. Next click the "Save" button to save this new drought scenario. Now we can click the "Simulate" button to run the HSPF model for this scenario. When the simulation is complete, return to the main window to begin the analysis of results.

The steps to view the results of the drought simulation (at one location) are as follows. In the "Locations" frame, select "GUADVICT". In the "Scenarios" frame, select "BASE" and "DROUGHT". In the "Constituents" frame, select "FLOW". Find time series which match

these criteria by clicking the "+" button in the "Timeseries" frame. Suppose we would like to see daily flows for the normal and drought conditions plotted together. Select the "Analysis:Graph" option from the menu bar or click the graph icon in the "Analysis" frame. Next, click the "Generate" button to produce the graph. The legend in the top left corner indicates which line is "BASE" and which is "DROUGHT". Compare the plots to see how much the flow is affected by these hypothetical drought conditions.



COMMUNICATION WITH OTHER SYSTEMS

GenSen is designed to work with data from other systems. Time-series input data can be used in GenSen in a variety of standard formats, including Relational Data Base (RDB - ASCII files of tab-delimited columns), WATSTORE (Hutchinson, 1977), and WDM. With these formats, data can be imported from various sources including the USGS NWIS database, commercially available data sets on CDs, the USGS World Wide Web site, and other sources used extensively within the USGS and EPA. The suite of tools produced through the USGS and EPA for the WDM system allow data in GenSen to be utilized by a wide range of other applications.

The data format used by the mapping capabilities of GenScn is the Environmental Systems Research Institute (ESRI) shape file. This format allows spatial data to be shared with GIS tools such as ArcView or ArcInfo.

GenScn is also designed to use GIS data as input for building the initial scenario. Data specifying characteristics of a watershed can be input interactively or through RDB formatted files. This characterizing data consists of basic watershed parameters such as stream segments, their connectivity, lengths, slopes, and contributing areas. The input formats for these data allow easy transfer from GIS to GenScn.

EXTENDING GENSCN TO NEW REGIONS

GenScn can be extended to new regions provided GIS coverages, time-series data, and characteristics of the stream network are available. The process of extending GenScn to a new region consists of building two files specifying the format and location of this data.

The first step toward setting up GenScn for a region is to create the new project file. This task is accomplished from within GenScn by selecting 'New Project' from the 'File' pull-down menu. The user will be prompted to specify the names of the WDM file, the HSPF message file, any RDB file of time-series data, and the map file. If the WDM file does not exist, GenScn will create it, and the user will have the opportunity to add observed data to this file as described below. The HSPF message file is provided with the GenScn software. The map file name should be specified, and if the file does not exist it may be created interactively. Once these file names are entered the user can click 'OK' and the project file will be created. Use 'Save Project' from the 'File' pull-down menu to save the project file.

The map file also can be created within GenScn. The map file contains information about the layers to be included on the map as well as other default map parameters. Layers to be displayed on the map must take the form of ESRI shape files. One of the map layers should be a shape file of gage locations.

Time-series data can be imported for use in GenScn by clicking on 'Observed' in the scenario list and then clicking 'Activate'. In the current release of GenScn the user will be presented with the option of entering observed data in RDB or WATSTORE daily values formats. Modules to import data from additional formats may be added at a clearly defined point in the GenScn code. After choosing one of these options the user proceeds to a window to enter information specifying the name of the file in which the data resides. Once specified the user may click on begin, and then for each data set in the file a set of parameters can be specified including the eight character scenario, constituent, and location attributes.

The GenScn 'New Scenario' feature converts a set of tabular input files which describe the characteristics of a watershed to a HSPF User Control Input (UCI) file. This feature is accessed by clicking on the 'New' button within the scenario frame in the main GenScn window. The user is prompted to specify the names of six input files, which are designed to be obtained from GIS coverages.

EXTENDING GENSCN TO OTHER MODELS

Although originally developed using the HSPF model, GenScn has been designed to be able to work with any surface water model which generates time-series results. GenScn does require each time series to be defined by a unique combination of scenario, location, and constituent. Several models have been incorporated into the GenScn system.

Results from the Full Equations (FEQ) routing model (Franz, 1996) were incorporated into GenScn by writing modules which read the time-series results from the FEQ output files and adapt them into the time-series data structure used by GenScn. This allows results from different FEQ scenarios to be compared. It also allows FEQ results to be compared with results from other models in GenScn. Future enhancements include building a DLL version of FEQ so that the model can be run from within GenScn.

Two additional examples of models which could be incorporated into GenScn are the Diffusion Analogy FLOW model (DAFLOW) (Jobson, 1989) and the Branched Lagrangian Transport Modeling system (BLTM) (Jobson, 1997). DLL versions of these models could be developed allowing them to be called from within GenScn. Their results could be adapted to the GenScn time-series data structure to allow GenScn's analysis tools to be used on them.

REFERENCES

- Bicknell, B.R., J.C. Imhoff, J.L. Kittle Jr., A.S. Donigan, Jr. and R.C. Johanson, 1997, Hydrological Simulation Program -- FORTRAN, User's Manual for Version 11, EPA/600/R-97/080, U.S. EPA, National Exposure Research Laboratory, Athens, GA.
- Flynn, K.M., P.R. Hummel, A.M. Lumb and J.L. Kittle, Jr., 1995, User's Manual for ANNIE, Version 2, a Computer Program for Interactive Hydrologic Data Management, Water-Resources Investigations Report 95-4085. U.S. Geological Survey, Reston, VA.
- Franz, D.D., C.S. Melching, 1997, Full Equations (FEQ) Model for the Solution of the Full, Dynamic Equations of Motion for One-Dimensional Unsteady Flow in Open Channels and through Control Structures, Water-Resources Investigations Report 96-4240, U.S Geological Survey, Urbana, IL.
- Hutchinson, N.E., Stuthmann, N.G., Merk, C.F., and Isherwood, W.L., Jr., 1977, WATSTORE User's Guide, Volume 5: U.S. Geological Survey Open-File Report 77-729-I, U.S. Geological Survey, Reston, VA.
- Jobson, H.E., 1989, Users Manual For an Open-Channel Streamflow Model Based on the Diffusion Analogy, Water-Resources Investigations Report 89-4133, U.S. Geological Survey, Reston, VA.

Jobson, H.E., 1997, Enhancements to the Branched Lagrangian Transport Modeling System, Water-Resources Investigations Report 97-4050, U.S. Geological Survey, Reston, VA.

Lumb, A.M., J.L. Kittle Jr. and K.M. Flynn, 1990, Users Manual for ANNIE, A Computer Program for Interactive Hydrologic Analyses and Data Management, Water-Resources Investigations Report 89-4080, U.S Geological Survey, Reston, VA.

Lumb, A.M., R.B. McCammon and J.L. Kittle Jr. 1994. Users Manual for an Expert System (HSPEXP) for Calibration of the Hydrological Simulation Program - Fortran. Water-Resources Investigations Report 94-4168. U.S. Geological Survey, Reston, VA.

FLOOD PLAIN MANAGEMENT, INTEGRATING NUMERICAL MODELS AND GIS

Author: Jesper T. Kjelds, General Manager, DHI Inc, Treveose, Pennsylvania

Abstract. A very important field in the regime of flood plain management is modeling of integrated catchment and flood plain hydrology and hydraulics. Numerical modeling tools applied for analysis of catchment and flood plain management is generally based on detailed spatial inputs. Integration of these modeling tools with Geographical Information Systems (GIS) greatly enhances the presentation and interpretation of the required input and produced outputs.

Application of the hydrological and hydraulic numerical modeling tool MIKE 11, developed by the Danish Hydraulic Institute (DHI), for flood plain management, analysis and flood forecasting can be seen as a strategic tool to support an integrated river basin management approach.

MIKE 11 is a professional engineering software package and uses an implicit numerical solution scheme for the simulation of flows, water quality, and sediment transport in rivers, channels, irrigation systems, and other water bodies. MIKE 11 is a dynamic, un-steady state, map-based Windows modeling tool for the detailed design, management, and operation of both simple and complex river and channel systems.

Merging the MIKE 11 river modeling system with GIS technology integrates an accurate and advanced mathematical modeling tool with a spatial analysis tool. The integrated system incorporates also advanced time series analysis tools and extreme value statistics, making it ideally suited as a core element in a “**Decision Support System (DSS)**” which can be efficiently applied for all aspects of Flood Plain and River Basin Management.

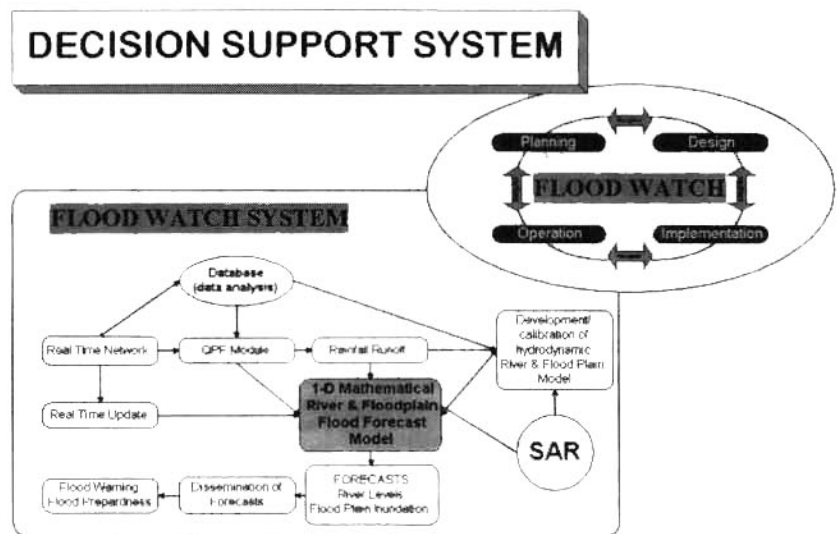
The real time Flood Forecasting module of MIKE 11 is an integral part of the new MIKE 11 Flood Watch system and interface developed within ArcView. Incorporating the system in an ArcView GIS environment provides a very powerful tool for real-time flood forecasting and flood warning applications.

INTRODUCTION

Combining advanced flood modeling with a GIS enables users and decision-makers at various levels to investigate and assess proposed flood mitigation options and preparing environmental impact assessments (Sørensen and Kjelds, 1996). The tasks encompassed in flood management (Syme and Paudyal, 1994) are not static but are usually of a very iterative nature. Related to present needs and future requirements the processes of flood management often develops following a cyclic pattern.

The integrated model approach is well suited for application at different stages of the frequently composite and complex tasks of flood management. MIKE 11 and MIKE 11 GIS finds its natural application at the planning, design, implementation and operation levels.

In the planning and design phase, the MIKE 11 system is a valuable tool for determining civil works design criteria, designing flood control and drainage structure operation rules, and providing inputs to flood preparedness programs.



At the implementation stage, MIKE 11 may be useful for a range of needs from scheduling flood prone construction works to a flood preparedness training aid.

The on-line monitoring and operation naturally succeeds the implementation application. Close supervision, control and the ability to initiate emergency relief requires that the developed MIKE 11 application be linked to a real-time reporting telemetry system. With the real-time linkage established, MIKE 11 can be applied on an operational basis for real-time flood forecasting, flood inundation mapping and eventually as an emergency response tool.

THE MIKE 11 MODELING SYSTEM

MIKE 11 (DHI-3, 1994) is a professional engineering software package for the simulation of flows, water quality and sediment transport in estuaries, rivers, irrigation systems, channels and other water bodies.

The applied implicit numerical methods yields unconditionally stable solutions and provide a complete and effective design environment for engineering, water resources, water quality management and planning applications. MIKE 11 is a windows (95 and NT) based fully dynamic, user-friendly, one-dimensional modeling tool for the detailed design, management and operation of both simple and complex river and channel systems. MIKE 11 includes basic modules for modeling and integrating rainfall runoff processes Advection-dispersion, cohesive/non-cohesive sediment transport and water quality with the advanced hydraulic kernel.

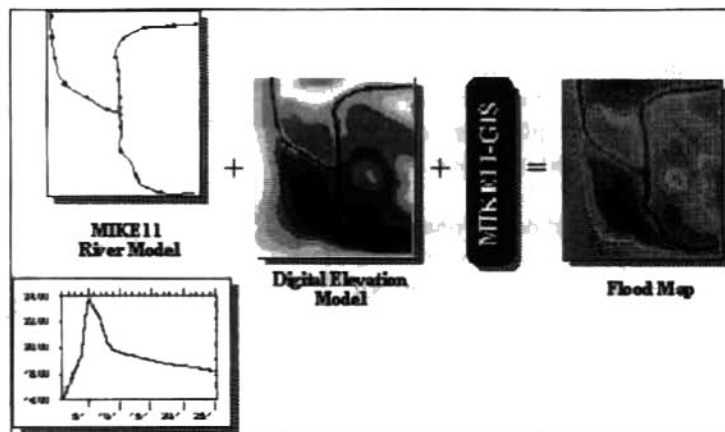
The suite of MIKE 11 water quality add-on modules is based on the Advection-dispersion model. The models simulate BOD-DO relations, chemical fate, eutrophication and temperature. The models allow their users to separate the impact of the various pollution loads and hence allow the identification of remedial measures, which meet pre-specified water quality standards at the lowest possible cost.

For modeling purposes which requires a detailed and distributed catchment description as well as an advanced river description the dynamic link between MIKE 11 and the MIKE SHE establishes an integrated hydrological modeling system. MIKE SHE (Refsgaard and Storm, 1995) is a deterministic, fully distributed, and physically based modeling system for describing the major flow processes of the entire land phase of the hydrological cycle. MIKE SHE solves the partial differential equations for the processes of interception; evapotranspiration and snow melt; overland and channel flow; unsaturated zone flow and saturated zone flow. The coupled approach allows for advanced modeling of a fully combined simulation of the water flow and solute transport and transformation processes in the entire land phase of the hydrological cycle.

The demand for means to control and predict floods has increased in many parts of the world in recent years, especially where major urban development has taken place in river flood plains. The MIKE 11 system includes also extensive functionality for real-time flood forecasting which recently has been integrated in an ArcView GIS environment. The MIKE 11 "Flood Watch" GIS interface has advanced data base functionality for storing, analyzing, retrieving, and applying information on real-time data in the study area.

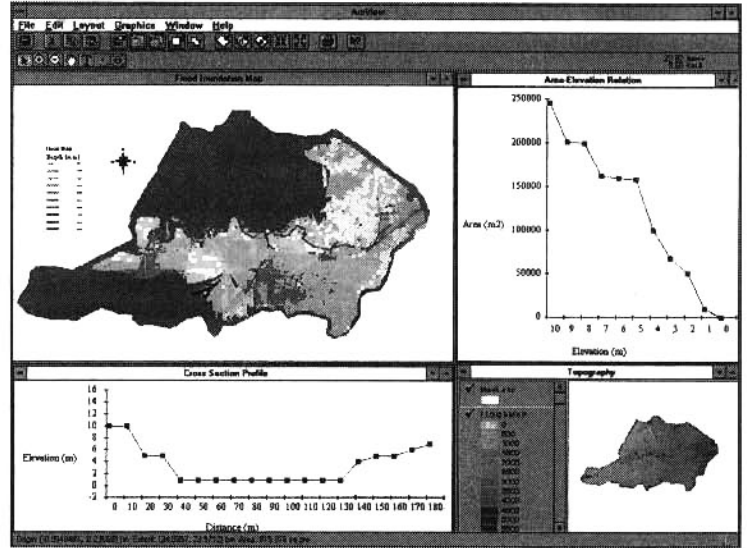
MIKE 11 GIS. (DHI-4, 1995) merges the technologies of numerical river modeling and Geographic Information Systems (GIS). It is developed as a fully integrated interface in ArcView GIS.

Development of a MIKE 11 GIS application requires information comprising a MIKE 11 river network, a MIKE 11 simulation and a Digital Elevation Model (DEM). For further analysis, information such as maps/themes of rivers, infrastructure, land use, satellite/radar images and other spatial data can be included.



The river network model is geo-referenced in MIKE 11 GIS through the Branch Route System (BRS). By linking a model simulation file to the BRS, MIKE 11 GIS produces three types of flood maps: depth/area inundation, duration and comparison/impact maps.

The flood maps are generated by applying an automatic and highly efficient interpolation routine. From a series of flood maps automatic routines allows for generation of highly visual video animation perfectly suited for presentation purposes. MIKE 11 GIS can also output water level hydrographs, terrain and water level profiles and flood zone statistics.



The topographical module facilitates accurate and automatic extraction of flood plain topography (flood plain cross-sections and area elevation relations) from the DEM. The extracted flood plain topography can readily be imported into a MIKE 11 cross section database.

MIKE 11 Flood Forecasting. The MIKE 11 FF system (DHI-2, 1994), is designed to perform the procedures required to simulate the future variation in discharge and water level in a river system as a result of catchment rainfall and inflow/outflow through boundaries in the river system. The MIKE 11 FF module includes the following components:

- Calculation of mean areal rainfall from point rainfall
- Calculation of discharge from water level data and rating curves or rating tables
- The NAM rainfall-runoff model, which calculates sub-catchment inflow to the river system
- The hydrodynamic module of MIKE 11 for routing the river flow and predicting water levels
- An automatic updating procedure which utilizes the measured and/or calculated discharge or water levels to minimize differences between observations and simulation at the time of forecast
- Specification of quantitative precipitation forecasts and predictions of boundary inflows
- The MIKE 11 GIS interface for mapping depth/area inundation.

The MIKE 11 FF module is dedicated to minimize the amount of information the operator is required to define in the daily forecast routine. The spatial inundation model allows for rapid and visual dissemination of flood warnings. Such a module is ideally suited for real-time applications, where reliability and fast performance are crucial. The MIKE 11 FF can be used in connection with either a manually based or a fully automatic data collection and processing system. All the model calculations required for issuing a forecast are done automatically by utilizing a number of individual modules. These are:

Mean area rainfall calculation. This module calculates the mean areal rainfall from point rainfall in a number of sub-catchments within the model area. The mean areal rainfall is used as input to the NAM module.

The rainfall-runoff module NAM. The NAM rainfall-runoff model (Nielsen and Hansen, 1973) is a deterministic, conceptual, lumped model representing the land phase of the hydrological cycle. It is based on both physical and semi-empirical formulations to describe the inter-relationship between surface storage intermediate storage and groundwater storage. Using the mean areal rainfall and evaporation as input the NAM model calculates sub-catchment inflow to the river system.

The automatic updating module. An important feature of the MIKE 11 FF is the automatic real-time updating procedure (Rungø, Refsgaard and Havnø, 1989). The updating routine applies an error prediction function to minimize the deviations between observed and simulated discharge/water levels at the time of forecast. The

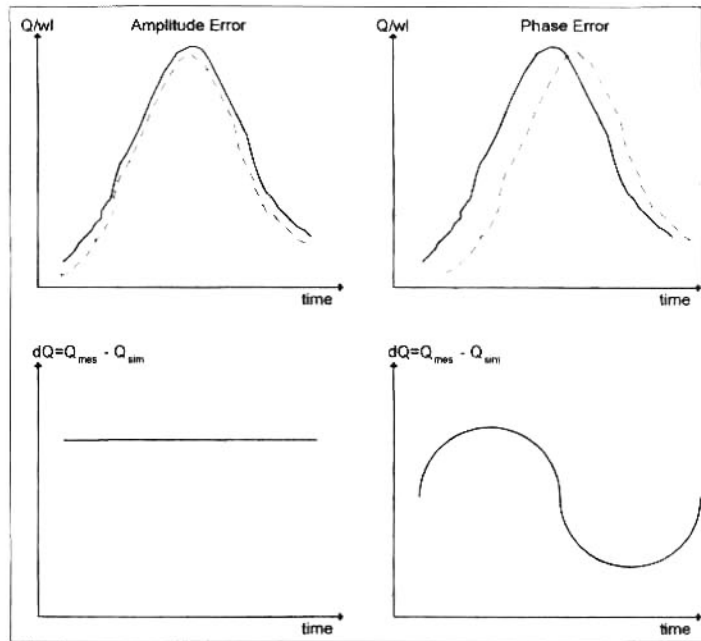
updating procedure in MIKE 11 FF identifies two different types of deviations or errors between measured and simulated data namely amplitude and phase error. Depending on the error types the function automatically make correction accordingly by minimizing the objective function given below:

$$\sum_{i=1}^n (F_i (M_i - (S_i + A_e - (S_i - S_{i+1}) / \Delta T * P_e)))^2$$

Where :

- A_e - amplitude error (m³/s)
- P_e - phase error (s)
- M - measured discharge (m³/s)
- S - simulated discharge (m³/s)
- F - weighting factor
- n - number of values included
- ΔT - timestep (s)

The minimum is found by differentiating the equation with respect to the amplitude error A_e and the phase error P_e and solving the equations subsequently. Based on phase errors and amplitude errors identified by the updating routine a series of correction discharges are calculated. The correction discharges are added as lateral inflow/outflow along the rivers at the updating points.



Updating can be specified on basis of discharge or water level measurements and can be carried out at any location in the river system where water level and/or discharge information is available in real-time.

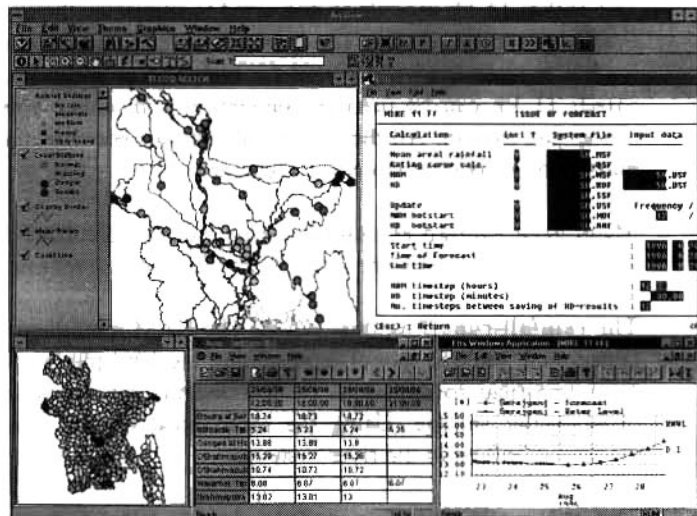
MIKE 11 FLOOD WATCH

Flood Watch is a framework for MIKE 11 Flood Forecast applications. The Flood Watch interface is an ArcView GIS application and serves as the central manager for acquisition of real time data, data pre – and post processing.

MIKE 11 Flood Watch consists of three main modules:

- The database management module,
- The data editing and presentation module
- The module for data preparation, numerical simulation and post-processing of results

The modeling module includes tools to setup and execution of hydrological and hydrodynamic model and to perform post-processing of the results. The setup tools provide facilities for fast data entry, receiving of telemetry data and options for data processing e.g. calculation of discharges from water levels and rating curves. Further the setup tools include pre-designed menus for specification of quantitative precipitation forecasts and prediction of boundary inflow in the forecast periods. The post-processing facilities allow the user to present results in tables, on graphs or on maps and interpolation of flood inundation maps.



Application of the integrated Flood Watch system enhances and facilitates data management and forecast routines. Integration of the MIKE 11 GIS interface enhances system capabilities for forecast of river levels and depth area inundation for selected areas, the system integrates seamless functionality for:

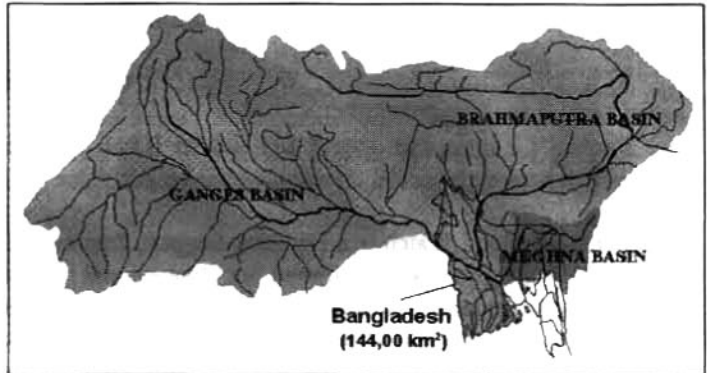
- real-time data base management including telemetric data collection
- real-time flood forecasting of water level and flood extent
- post-processing of results and formulation of flood warnings
- dissemination of flood warnings and flood information to end users incl. TV

The flexible and holistic approach encompassed in Flood Watch allows also for establishing a Flood Forecasting Warning and Response System for rapid and accurate dissemination that helps increase the level of awareness and preparedness.

APPLICATION OF THE INTEGRATED MIKE 11 FLOOD WATCH SYSTEM IN BANGLADESH

Bangladesh is located in the delta formed by three of the world's largest rivers, the Ganges, the Brahmaputra and the Meghna. Between them, they drain most of the eastern part of the Himalayas, a catchment of some 1.7 million square kilometers (Verwey, Havnø and Refsgaard, 1973).

The country's Flood Forecasting and Warning Centre (FF&WC) has since 1990 applied a mathematical river model to provide 24, 48 and 72 hours forecasts of changes in water levels in the major flood prone rivers at key locations throughout the country. The real-time information gathering network now consists of more than 60 stations from which continuous real-time measurements of rainfall and water levels are passed on to the FF&WC.

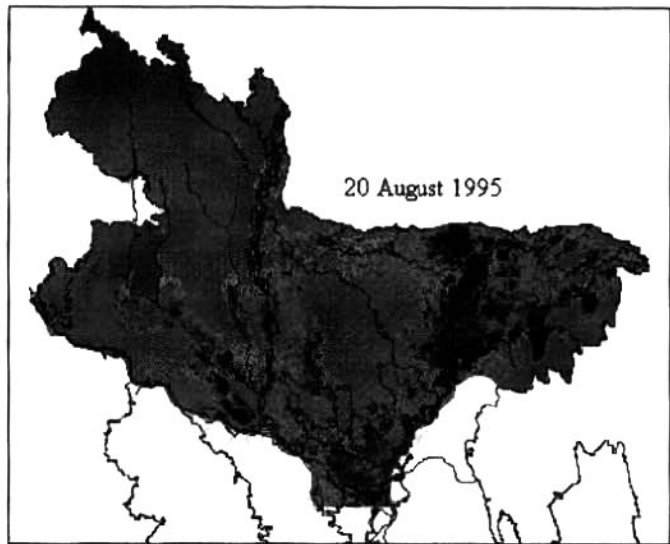


In 1995 DHI was contracted to provide "Expansion of the Flood Forecasting and Warning Services in Bangladesh" (DHI-1, 1995). It was immediately obvious that a complete GIS oriented system was required to handle the flood forecasting services. The new system, which became operational in the 1996 flood season, includes a hydrological and hydrodynamic MIKE 11 Flood Forecasting model covering in details the entire northern part of the country.

The model, one of the largest one-dimensional flood forecasting models presently in operation, comprises all major and secondary rivers in the northern part of Bangladesh, with a total catchment area on 82,000 km² delineated into more than 200 catchments. The schematized river system contains over 400 river branches and link channels with a total length of 7270 km. The hydraulic model describes a very complex river/flood plain flow pattern applying a Quasi 2-D schematization where flood plains are separated from the main river channels. The Quasi 2-D approach joins flood plains to the main rivers by a series of links. Flood plains which conveys flood water are modeled as flood plain branches while flood cells describes areas which also are subject to inundation, but in which water flow velocities are very small or zero. Flood plain branches and flood cells are also connected to each other using links. Based on the comprehensive model the flood forecasting system is used to predict river water levels and flood plain inundation depths and extents.

The flood forecast model is interfaced in the MIKE 11 Flood Watch system, this enables the local forecast officers to conduct all forecasting activities, ranging from telemetric data collection through to model simulations and production of flood maps from a single consistent user interface.

The model simulation results are analyzed in Flood Watch and used in MIKE 11 GIS for flood mapping. Flood inundation depths and extents for selected areas are produced as flood maps, which again are directly available in the Flood Watch system for further analysis and comparison with remote sensing data, such as satellite or SAR images. Comparison between simulated flood extents and flood extents delineated by satellite or SAR images is applied mainly to validate and to improve model calibration. Improved calibration of the complex flood plain model greatly improves the inundation model forecasts. Application of SAR images, which can penetrate could cover, permitting accurate data acquisition for calibration and validation seems very promising.



Initial trials of the new integrated MIKE 11 Flood Watch system indicate a high degree of acceptance by the users. Its use as a Decision Support tool is emphasized by the fact that the system is also installed in the Office of the Prime Minister of Bangladesh, from where rapid responses to adverse flooding conditions can be initiated.

CONCLUSION

The demand for means to control and predict floods has increased in many parts of the world in recent years, especially where major urban development has taken place in river flood plains.

The MIKE 11 Flood Watch is a Decision Support Framework for professionals involved in flood forecasting. The Flood Watch integrates an established one-dimensional hydrodynamic modeling system, MIKE 11. The MIKE 11 system includes extensive functionality for real-time flood forecasting integrated in an ArcView GIS environment composed as a single user-friendly interface. The system has been extensively tested in several case studies, including Bangladesh, one of the world's most complex hydraulic environments. The system has proven its capabilities in the fields of flood planning and structure design, as well as real time operation for flood forecasting. The user-friendly interface makes it an ideal Decision Support tool to decision-makers.

REFERENCES

- Danish Hydraulic Institute - 1, 1995, Expansion of Flood Forecasting and Warning Services, Inception and Project Report.
- Danish Hydraulic Institute - 2, 1994, MIKE 11 FF, Short Description.
- Danish Hydraulic Institute - 3, 1994, MIKE 11 User and Reference Manual.
- Danish Hydraulic Institute - 4, 1995, MIKE 11 GIS User Manual
- Nielsen, S.A. and Hansen, E., 1973, Numerical Simulation of the Rainfall-Runoff Process on a daily Basis. Nordic Hydrology, 4, pp 171-190.
- Refsgaard, J.C. and Storm, B., 1995, MIKE SHE. In: V.P. Singh (Ed): Computer Models of Watershed Hydrology, Water Resources Publications, pp 809-846.
- Rungø M., Refsgaard, J.C. and Havnø, K, 1989, Hydrocomp '89, Dubrovnik, Yougoslavia
- Syme, W.J., Paudyal, G.N., 1994, Flood Management Model, 2nd International Conference on River Flood Hydraulics York, UK.
- Sørensen H. R., Kjelds J.T., Deckers F., Waardenburg F., 1996, Application of GIS in hydrologic and hydraulic modelling. HYDRO GIS'96, 1996, Vienna, Austria.
- Verwey A., K. Havnoe, J. C. Refsgaard, 1988, Flood modeling in Bangladesh. International Seminar on Hydrology of Extremes, Floods and Low Flows

MODELING OF RIVER SYSTEMS USING THE SAMS PACKAGE

W. L. Lane,

Consultant, Golden, Colorado;

D. K. Frevert,

Hydraulic Engineer, U.S. Bureau of Reclamation Technical Service Center, Lakewood, Colorado;

J. D. Salas, and C. H. Chung,

*Professor and Graduate Student, respectively, Hydrology and Water Resources Program,
Department of Civil Engineering, Colorado State University, Fort Collins, Colorado*

Abstract The Stochastic Analysis, Modeling and Simulation (SAMS) Package is written in C and Fortran and runs under modern Windows Operating Systems such as Windows NT and Windows 95. Modeling capabilities in SAMS include single site and multisite systems such as univariate and multivariate Autoregressive Moving Average (ARMA), Periodic Autoregressive Moving Average (PARMA), and disaggregation approaches. An application to the Nile River basin in Africa is performed for demonstration in which a monthly multivariate model is first fitted to the historical streamflow sequences of three sites and a series of stochastic traces is then generated for each single site. In these synthetic series, the cross correlations between different sites as well as the autocorrelations of each site are preserved as desired.

INTRODUCTION

Stochastic modeling and simulation of hydrologic time series has been widely used in water resources system planning and management for various purposes including decision making and project assessment. Typical examples are determining the capacity of a reservoir, evaluating the reliability of a reservoir of a given capacity, and evaluating the performance of an irrigation system under uncertain irrigation water deliveries (Salas et al, 1980; Loucks et al, 1981).

Mathematical models are typically needed for stochastic simulation of hydrologic time series such as streamflow processes. For this purpose a number of stochastic models have been suggested in literature (Salas, 1993). Using one type of model or another for a particular case at hand depends on several factors such as, physical and statistical characteristics of the process under consideration, data availability, complexity of the system, and overall purpose of the simulation study. Given the historical record, the model should be able to reproduce the historical statistics. This is why a standard step in streamflow simulation studies is to determine the historical statistics. Once a model has been selected, the next step is to estimate the model parameters, then to test whether the model represents reasonably well the process under consideration. Thus, the needed simulation study can be performed based on the fitted model.

A variety of mathematical and statistical software have been developed since the advent of digital computers several decades ago for computations of varied degree of sophistication. For instance, IMSL, STATGRAPHICS, STATVIEW, ITSM, MINITAB, SAS/ETS, SPSS, and MATLAB, etc., are well known packages. These packages can be very useful for standard time series analysis of hydrologic processes. However, despite of the availability of such general purpose programs, specialized software for simulation of hydrologic time series such as streamflow have been attractive for several reasons. One is the particular nature of hydrologic processes in which periodic properties are important in the mean, variance, covariance, and skewness. Another one is that some hydrologic time series include complex characteristics such as long memory. Still another one is that many of the stochastic models useful in hydrology and water resources have been developed

specifically to fit the needs of water resources, for instance temporal and spatial disaggregation models. Examples of specifically oriented software for hydrologic time series simulation include HEC-4 (U.S Army Corps of Engineers, 1971), LAST (Lane and Frevert, 1990), and SPIGOT (Grygier and Stedinger, 1990).

The LAST package was developed in 1977 and 1978 by the Bureau of Reclamation for the purpose of modeling univariate and multivariate hydrologic time series. This package was originally designed to run on a mainframe computer, but later it was modified for use on personal computers. Even though various additions and modifications have been made to LAST over the past 20 years, the package has not kept pace with either advances in time series modeling or advances in computer technology. This is especially true of computer graphics.

Following is a description of the newly developed software package, SAMS, which is specially designed for the stochastic simulation of hydrologic time series such as monthly streamflows under modern personal computer operation system.

THE SAMS PACKAGE

SAMS, as expressed by its name, is a computer software package that deals with the Stochastic Analysis, Modeling, and Simulation of hydrologic time series. It is written in C and Fortran and runs under modern windows operating systems such as WINDOWS NT and WINDOWS 95. The package is designed in a interactive way that communicates with user through dialog windows and enables the user to choose different options that are currently available to carry out the task.

The main functions of SAMS can be classified into three categories: 1) statistical analysis of data, 2) stochastic model fitting including parameter estimation and testing, and, 3) synthetic data generation (see Fig.1). It has the capability of analyzing single site and multisite, annual and seasonal data and the results of the analysis can be presented in either graphical or tabular forms, or written to output files.

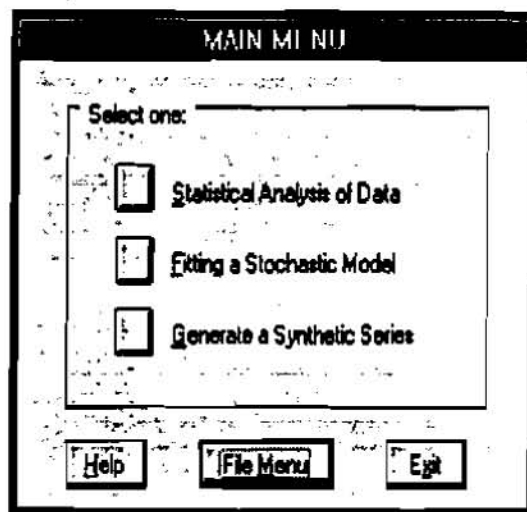


Fig. 1 SAMS main menu

The first major function (Data analysis) consists of plotting, normality checking, transformation, and statistical characteristics calculation. Plotting the data may help detect trends, shifts, outliers, or errors in the data. Probability plots are included for verifying the normality of the data. Data can be normalized by using different transformation techniques. Currently, logarithmic, power, and Box-Cox transformations are available. SAMS computes a number of statistical characteristics of the data including basic statistics such as mean, standard deviation, skewness, serial correlations (for annual data), season to season correlations (for seasonal data) and cross correlations (for multisite data). These statistics are important in investigating the stochastic characteristics of the data. Figure 2 displays the menu for showing the desired statistical characteristics of the data. Once an item is selected, SAMS will prompt the user to an output window that will present the results in tabular or graphical formats.

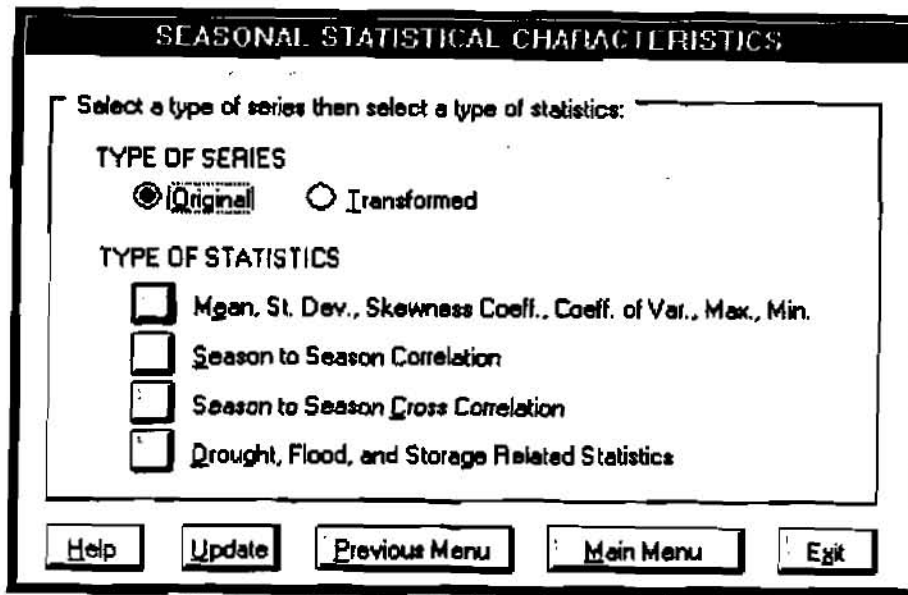


Fig. 2 Statistical analysis of seasonal data menu

The second main function of SAMS is model fitting. It includes parameter estimation and model testing for alternative univariate and multivariate stochastic models. The current version of SAMS includes the following models: 1) univariate ARMA(p,q) model, 2) univariate periodic PARMA(p,q) model, 3) multivariate autoregressive or MAR(p) model, 4) multivariate periodic autoregressive MPAR(p) model, 5) spatial disaggregation model, and 6) temporal disaggregation model. Two estimation methods are available, namely the method of moments (MOM) and the least squares method (LS). MOM is available for all the models while LS is available only for univariate ARMA(p,q) and PARMA(p,q) models. Figure 3 shows the menu for fitting an MPAR(p) model. Regarding annual disaggregation models, MOM is used for parameter estimation based on Valencia-Schaake or Mejia-Rousselle methods while for annual to monthly disaggregation Lane's condensed method can be used in addition to the above two.

For stochastic modeling and simulation at several sites in a stream network system based on disaggregation, two modeling-generation schemes are included which are based on defining a number of key stations, substations, and subsequent stations. Generally the key stations are the farthest downstream stations, substations are the next stations upstream, and subsequent stations are next further upstream stations. The first scheme fits a univariate ARMA(p,q) model to the sum of the annual data of all the key stations. Then, that sum is disaggregated into the key stations annual data. Then, such annual data at key stations are disaggregated into annual values at the substations which in turn are further disaggregated into annual data at the subsequent

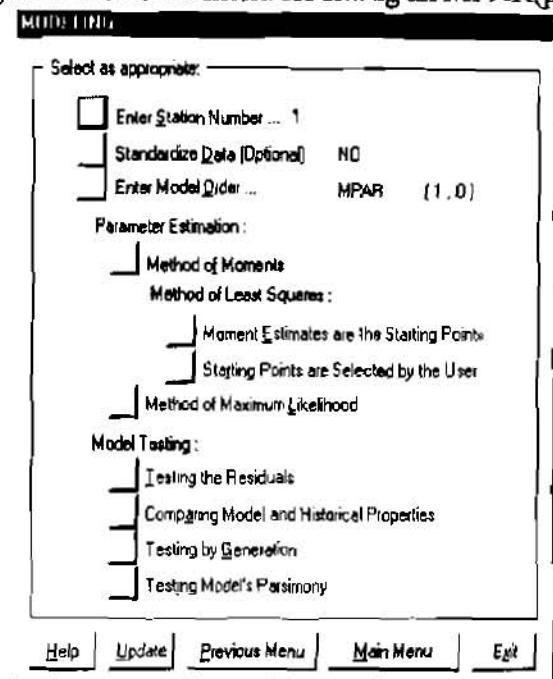


Fig. 3 Fitting a stochastic model menu

stations. The second scheme fits a multivariate MAR(p) model to the annual data for the key stations and the rest of the disaggregation into substations and subsequent stations is done in a similar manner as in the first scheme. In addition, if monthly data are desired, the annual values at all stations are further disaggregated based on temporal disaggregation approach.

The third main function of SAMS is data generation. Data generation is undertaken based on the models, approaches, and schemes as mentioned above. The model parameters for data generation can be those which are estimated by SAMS or they can be provided by the user. Figure 4 shows the menu for generating data from a seasonal multisite model. The statistical characteristics of the generated data are presented in graphical or tabular forms along with the historical statistics of the data. They can be printed and/or written on special output files.

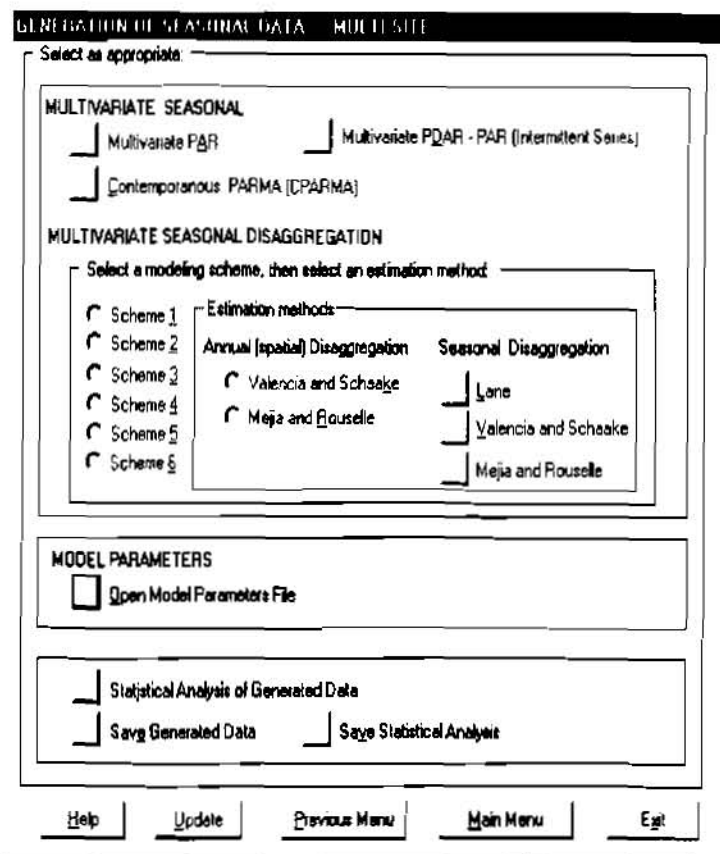


Fig. 4 Generation of multisite seasonal data menu

EXAMPLE

For demonstration's purpose, an analysis was conducted to the streamflows of the Nile River system. The monthly streamflow records of three sites for the period 1913-1989 were under modeling, of which Malakal is in the White Nile River basin, Khartoum is in the Blue Nile River basin, and Aswan is located in the downstream area of the Nile River basin. Since the White Nile River and the Blue Nile River are actually tributaries of the Nile River, these data are considered multivariate. Besides, the result of statistical analysis for the historical data show that the flow rates (with order of billions of m³/month) possess long memory. An MPAR(3) model was selected to fit the historical data in order to preserve their autocorrelations as well as the cross correlations between sites. Note that the data were transformed into normal domain by logarithmic transformation before being fitted by the model. The model parameters were estimated using method of moment (MOM) which were then used to generate synthetic series. One hundred samples of synthetic multivariate monthly flows each 77-years long were generated based on the fitted model. The average statistics computed from the generated samples can be compared to their historical counterparts by running the "Statistical Analysis of the Generated Data" function. As a result, it is shown that all the historical basic statistics including the monthly means, standard deviations, skewness coefficients, and coefficients of variance are well preserved in the synthetic series. Typically, the month-to-month correlations (as shown in Figures 5, 6, and 7) and month-to-month cross correlations (as shown in Figures 8, 9, and 10) are also well preserved in the synthetic

series. This indicates that the selected model is able to preserve both temporal and spatial dependencies of the multivariate data under study.

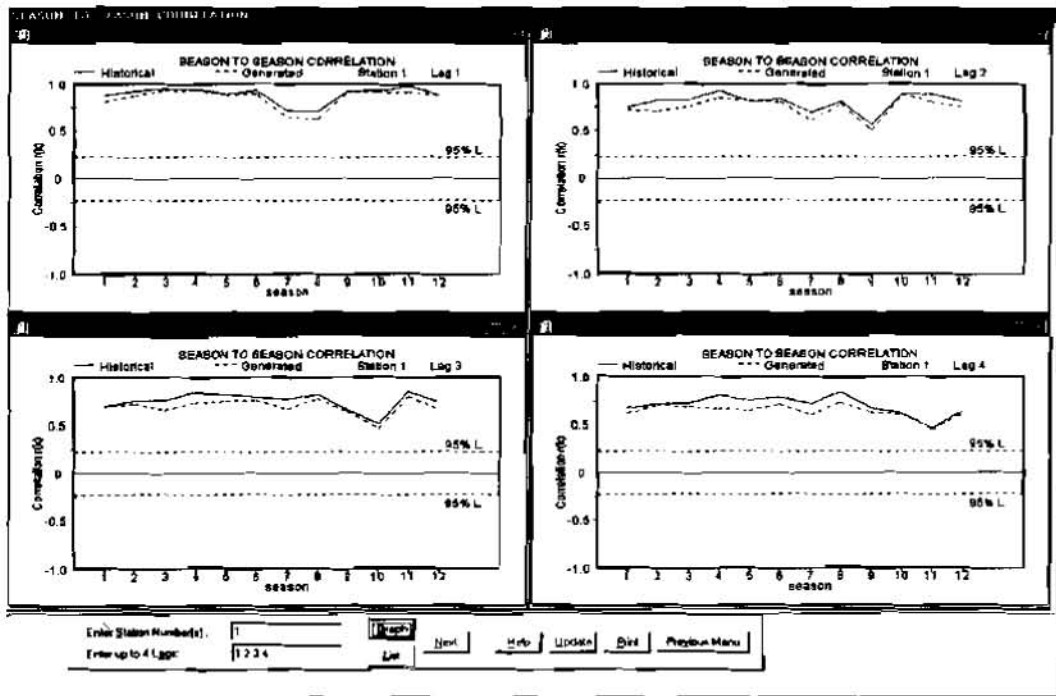


Fig. 5 Comparison of month-to-month correlations for Site 1 - Malakal

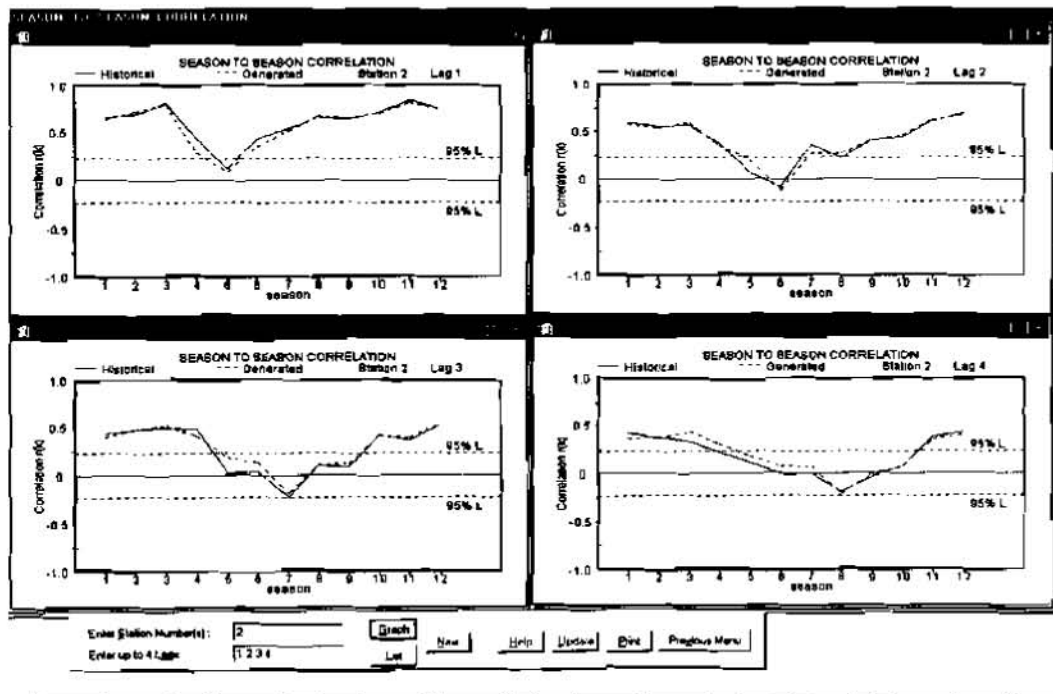


Fig. 6 Comparison of month-to-month correlations for Site 2 - Khartoum

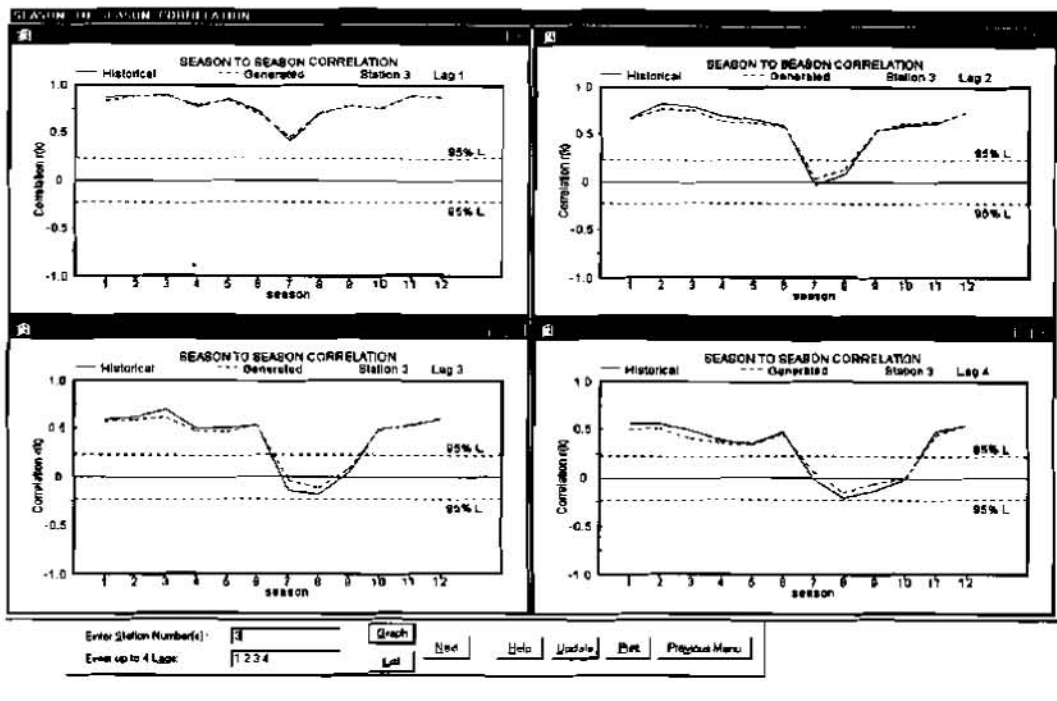


Fig. 7 Comparison of month-to-month correlations for Site 3 - Aswan

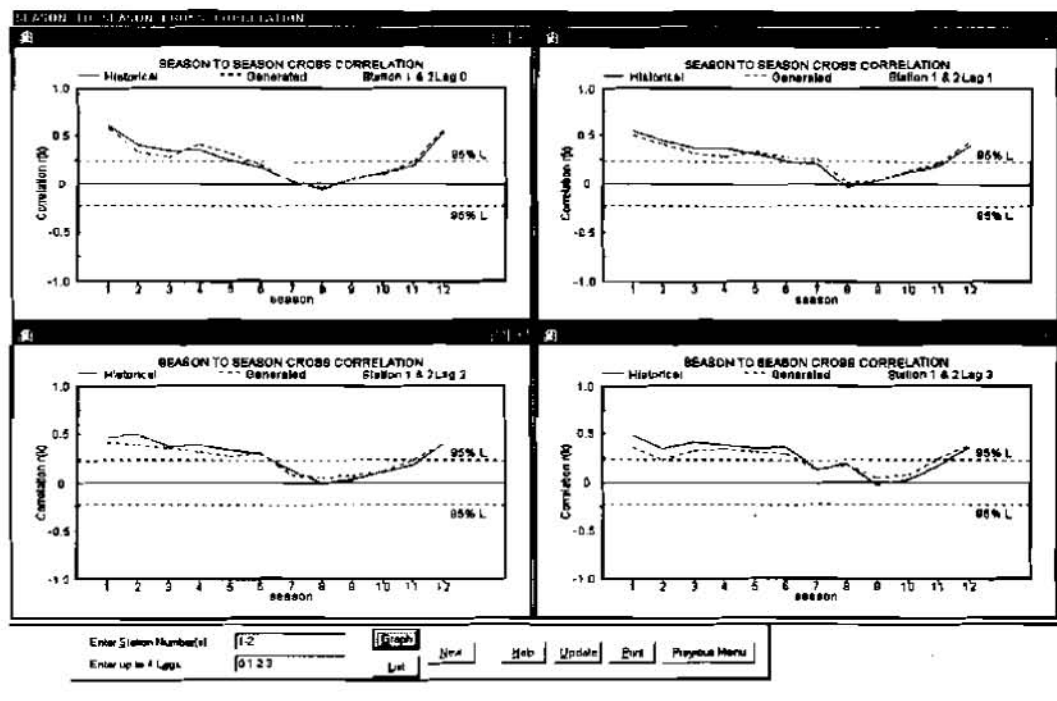


Fig. 8 Comparison of month-to-month cross correlations between Site 1 and Site 2

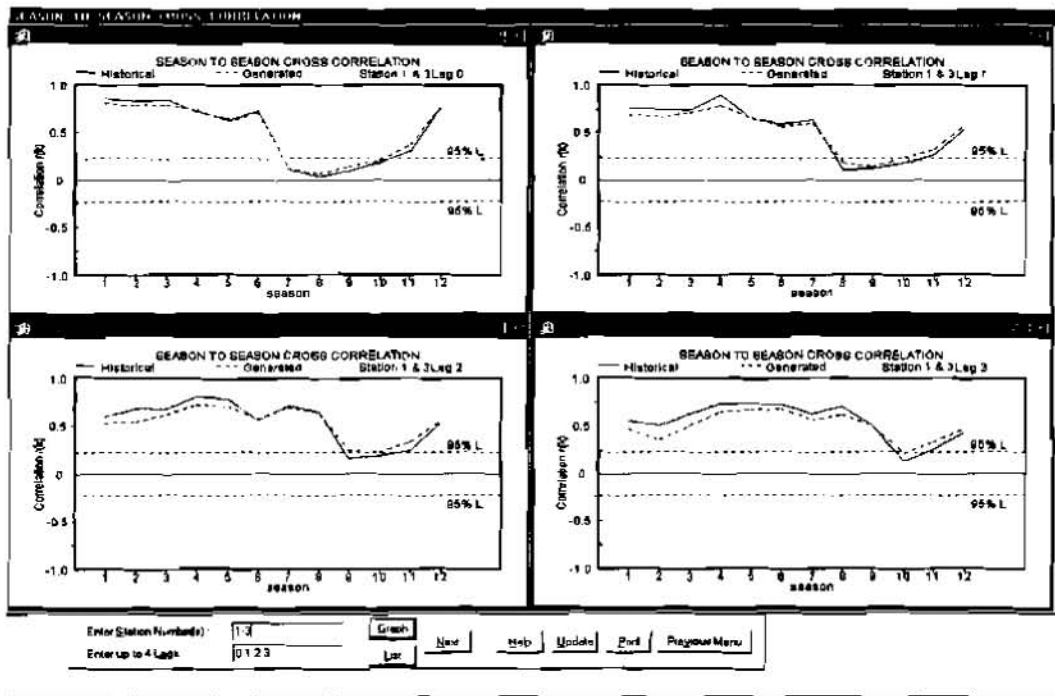


Fig. 9 Comparison of month-to-month cross correlations between Site 1 and Site 3

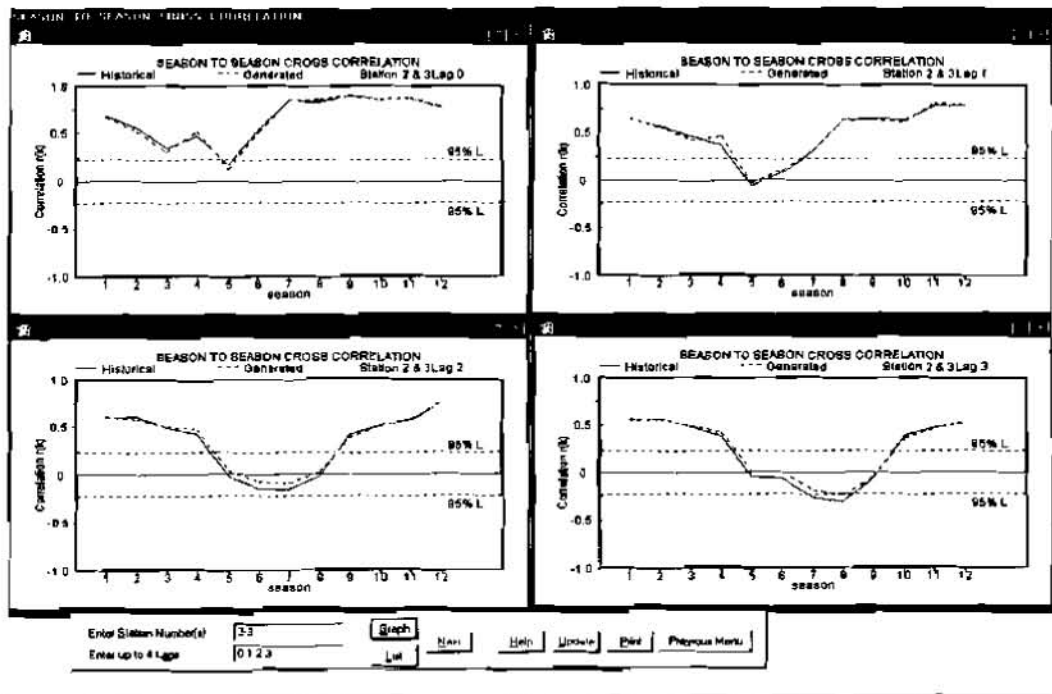


Fig. 10 Comparison of month-to-month cross correlations between Site 2 and Site 3

ACKNOWLEDGMENT

This paper was written with support of the U.S Bureau of Reclamation's research program under the advanced Hydrologic Techniques Project and computer support from the CCHE program of excellence in water resources of the Colorado State University Civil Engineering Department. Support from both these sources is greatly appreciated.

REFERENCES

- Grygier, J.C., and Stedinger, J.R., 1990., "SPIGOT, A Synthetic Streamflow Generation Software Package" , technical description, version 2.5, School of Civil and Environmental Engineering, Cornell University, Ithaca, N.Y.
- Lane W.L. and Frevert, D.K., 1990. Applied Stochastic Techniques, Personal Computer Version 5.2, User's Manual, Earth Sciences Division, U.S. Bureau of Reclamation, Denver, Colorado.
- Loucks, P., Stedinger, J.R. and Haith, D.A., 1981. Water Resources Systems Planning and Analysis, Prentice-Hall, Englewood Cliffs, NJ.
- Salas, J.D., Delleur, J., Yevjevich, V. and Lane, W., 1980. Applied Modeling of Hydrologic Time Series. Water Resources Publications, Littleton, Colorado.
- Salas, J.D., 1993. Analysis and Modeling of Hydrologic Time Series. In Handbook of Hydrology, D.R. Maidment Editor, McGraw Hill Inc., N. York.
- U.S Army Corps of Engineers, 1971. "HEC-4 Monthly Streamflow Simulation," Hydrologic Engineering Center, Davis, Calif.

MODSIM DECISION SUPPORT SYSTEM FOR RIVER BASIN WATER RIGHTS ADMINISTRATION

By Roger Larson, Hydraulic Engineer, U.S. Bureau of Reclamation, Boise, Idaho;
John Labadie, Professor, Dept. of Civil Engineering, Colorado State University, Ft. Collins, Colorado;
Marc Baldo, Research Associate, Dept. of Civil Engineering, Colorado State University,
Ft. Collins, Colorado

Abstract

The MODSIM general purpose decision support system is presented for integrating hydrological and institutional/administrative modeling capabilities in river basin management. MODSIM includes a powerful graphical user interface allowing interactive placement of river basin network objects on-screen in any configuration. Data import and editing is accomplished through familiar spreadsheet-style tools, with cross-platform implementation on Unix workstations and Windows-based PC's. MODSIM and the GUI development take advantage of C++ modularity and integration for future feature capability and maintenance. Capability is provided to distinguish between natural flow water rights and various storage contract arrangements for water entitlement accounting, exchanges, storage ownerships, water service contracts, and rent pool/water banking. MODSIM is also suitable for conjunctive use studies through an in-built stream-aquifer interaction model, or linkage with more realistic groundwater models such as MODFLOW through use of unit response functions. Spatially referenced graphical output of MODSIM results is provided, along with a scripting language for customized reporting. As a demonstration, MODSIM is applied to deriving relative yields from various proposed storage rental and reallocation scenarios in the Snake River Basin.

INTRODUCTION

Adjudication of natural flow rights, Native American water right claims, recovery efforts for recently identified endangered species, environmental quality, and changes in traditional water use and efficiencies are among some of the critical issues which may impact the future availability and distribution of water in many river basins of the Western U.S. Water resource investigators are challenged to provide detailed information to decision makers for predicting impacts on both physical river system features (i.e., river flows, reservoir contents, diversions, and hydropower generation) and entitlements (i.e., natural flow entitlements, storage accrual, and carryover storage). MODSIM is presented herein as general purpose decision support system for fully integrating the physical, hydrological, administrative, and legal aspects of these complex issues in river basin management.

MODSIM is applied to demonstrating the anticipated impacts of alternative water supply schemes, physical system features, flow and diversion entitlements, and water use scenarios in the Snake River basin as a case study. Accounting procedures are developed and incorporated into MODSIM which effectively simulate the administrative distribution procedures used by the Idaho Department of Water Resources and U.S. Bureau of Reclamation (USBR). The accounting procedures determine flow and diversion entitlements under appropriate doctrine natural flow rights and various reservoir storage contract rules, including storage ownership contracts, service contracts, and rent pool agreements.

Complex operational conditions that need to be addressed include maintaining target minimum streamflows at various points along the river system, adhering to reservoir rule curves, and satisfaction of Native American water right claims. River snails and chinook salmon are endangered species in the Snake River system for which recovery plans have introduced changes in reservoir and river operations. The USBR is actively seeking available water from willing sellers having storage ownership contracts and natural flow rights in excess of their needs. Available flow rights and reservoir space are targeted to help meet flow objectives and mitigation of endangered species recovery plans. In addition, irrigation practices in the Upper Snake River basin continue to improve in efficiency, resulting in reduced diversion demands and return flows, which in turn result in changes in reservoir release schedules. Urbanization in some areas of the basin have altered the use, demand and return flow timing patterns, as well as spatial distribution of groundwater storage in the system. Additional changes in ownership, use, and operation of the water resources of the Snake River are also being proposed. MODSIM provides a means of incorporating all these complex issues into an integrated decision making environment.

MODSIM DECISION SUPPORT SYSTEM

Decision support systems (DSS), as an appropriate methodology for water resource planning and management, have been described in Labadie, et al. (1989). The classic definition provided by Sprague and Carlson (1982) describes a DSS as "an interactive computer-based support system that helps decision makers utilize data and models to solve unstructured problems." The DSS includes: (i) model base management subsystem (MBMS); (ii) data base management subsystem (DBMS); and (iii) dialog generation and management subsystem (DGMS) for managing the interface between the user and the system.

A screen display of the graphical user interface for the MODSIM decision support system is shown in Fig 1. The MODSIM DSS operates under Microsoft Windows 95 and NT, although an X-Window version under UNIX is also available. The DSS is constructed around an open architecture permitting access to input and output data and allowing modification and verification at all levels of the modeling process. Where possible, the input and output data files for the various modules selected for use in the DSS are structured as ASCII data base text files. The graphical user interface for the DSS provides geo-referenced data base capabilities whereby the user can create and link river basin network objects on the screen, and then populate data for that object by simply using a mouse to activate the object and open a variety of data base windows. All data required for the DSS can be input in this manner, although lengthy sets of time series data for streamflows, demands, etc., can be input automatically via text files with the same name as the node.

The main menubar for the DSS is located at the top of the network editor window in the interface. The menus are used to load and save a MODSIM network, run the model, import and export data, select and display graphs; create, edit and generate tabular reports; access various utilities, and more. The interface contains tools (icons) for creating all nodes

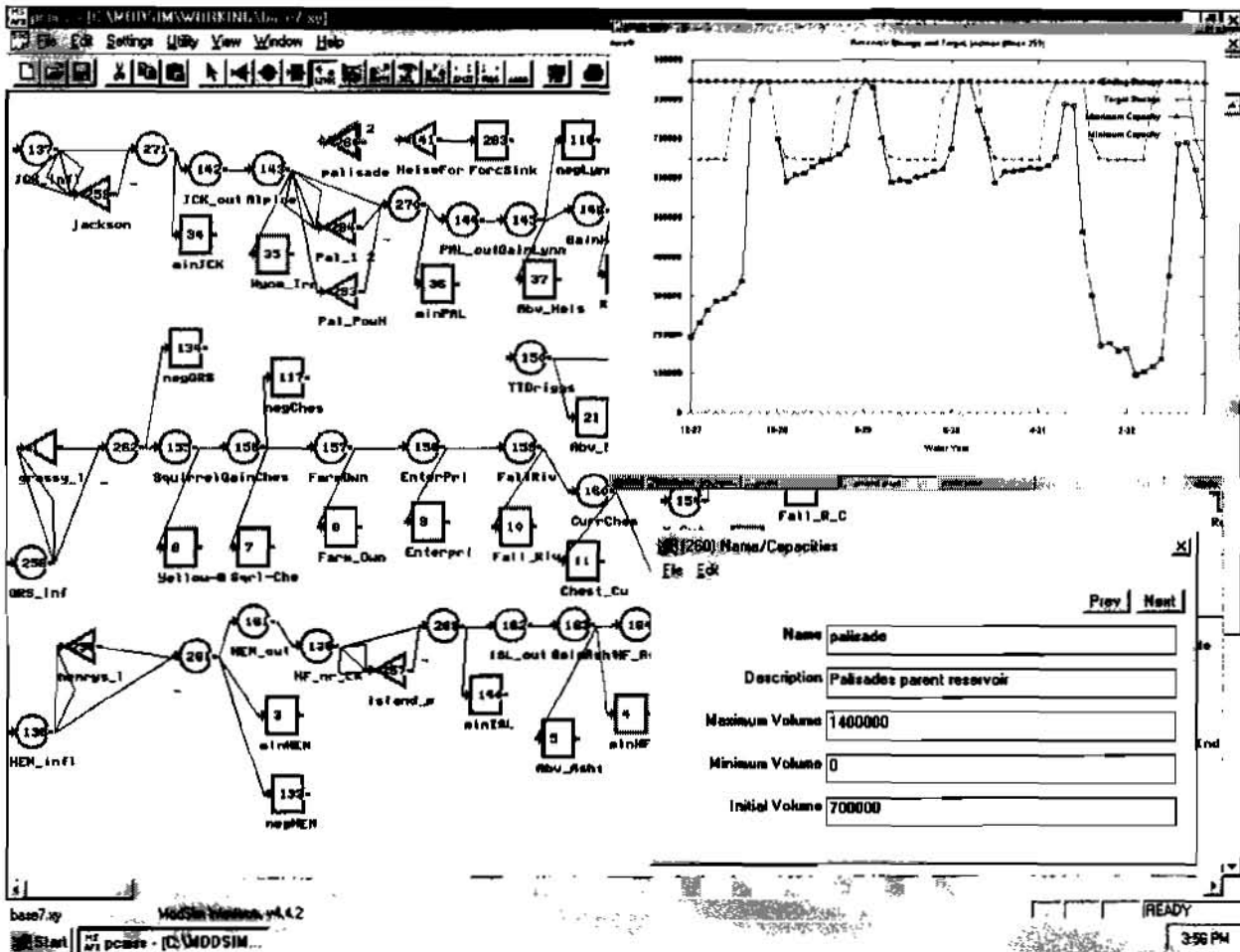


Figure 1. Graphical User Interface for MODSIM Displaying Upper Snake River Basin Network

and links in the network, as well as moving objects, deleting objects, providing annotation on the network for clarity, merging (and splitting) the display of multiple links between nodes for better graphical display, generating graphical plots of data associated with any object; and provides on-line MOSAIC help features documenting any aspect of the interface and model.

The drawing area displays the network which can be created and edited by the user. A zoom feature is provided allowing the user to resize the network to any desired factor for display clarity and convenience. Scroll bars are available on the edges of the drawing area that scroll the drawing area across the raster. Clicking with the left mouse button within the drawing area performs whatever task the current exclusive tool specifies. Clicking on an object in the drawing area with the right mouse button makes that object active, which is characterized by a change in color of the object. When the object is made active, an initial data base window associated with that object pops up. Next and Prev buttons in the the data base window can be activated to access all data base windows associated with that object (Fig. 1). The popup spreadsheets allow the user to edit data associated with the active object. Object types are nodes (both storage and nonstorage), links, and text annotations. Since nodes and links have many data values, several spreadsheet windows are available for each.

The Map Window allows display of physical representations of the geographic location of the network in either vector or raster formats. Each node in the network can be represented on the map with a user defined map symbol which can be selected among several different shapes and colors. Map Window Settings include: background color, symbol color, symbol size, and zoom factor. Map symbols can be used to locate nodes within the network editor window. Maps can be loaded into the map window using the File/Load map window menu item. A file requester appears, displaying any valid vector and raster files that can be loaded.

The Settings item in the Main Menu Bar displays numerous menu items, including Settings/Run Type [for management or calibration runs]; Settings/Time Scale [monthly, weekly or daily time increments; calender start date for run; total length of simulation run]; Settings/Conversions Table [units conversion options for input data files]; Settings/Groundwater Return [defining groundwater modeling parameters]; Settings/Hydrologic State [allowing users to edit the number of hydrologic states, the hydrologic state subsystems, and boundary values for targets]; Settings/Lag Factors [maximum number of lag factors in the stream-aquifer modeling; user generated or model generated lag factors]; Settings/Model Convergence [controls maximum number of iterations for convergence in groundwater calculations]; and Settings/Raster Dimensions [allowing editing of dimensions of the raster upon which the network is drawn].

Before attempting to access the on-line documentation or create a graph from the model output, certain preferences are set within the interface. These preferences can be edited using the File/Preference menu item. Once selected, this menu item displays a Preferences popup, which contains a standard menu bar, a text field box, a save button, and a list box containing settable preferences. One of the important preference items is External Utils. This preference is used to edit the list of external utilities that can be called from the interface. Selecting this preference displays the External Utilities Editor popup. This popup consists of a standard menu bar, a text field box, a list box containing the list of external utilities currently defined, an External Util Name text field, and a New button. The user can easily create a new External Utility, such as a utility for reformatting an output file or executing a spreadsheet software package. The DSS also includes a scripting language called SIMARGS allowing the user to develop customized output reports, graphical plots, and color-coded graphical displays.

MODSIM RIVER BASIN NETWORK FLOW MODEL

Network Flow Optimization Model: The simulation of large-scale, complex water resource systems requires efficient methodologies for analyzing system components in a fully integrated manner. The generalized river basin network model MODSIM employs a state-of-the-art network optimization algorithm for simultaneously assuring that water is allocated according to physical, hydrological, and institutional aspects of river basin management, including stream-aquifer interactions. Earlier versions of MODSIM have been successfully applied to a number of complex river basin systems, such as the Rio Grande River Basin (Graham, et al., 1986); the Poudre River Basin in Colorado (Labadie, et al., 1986); the Upper Colorado River Basin (Law and Brown, 1989); the Upper Snake River Basin (Frevert, et al., 1994), and South Platte River Basin (Fredericks and Labadie, 1995). In all of these cases, some form of priority-based water allocation dominates management of the system.

Although technically speaking, MODSIM is an optimization model, the attempt is to employ optimization methods as an efficient mechanism for performing simulation. The minimum cost network flow problem is solved via an efficient minimum cost network flow optimization algorithm over each successive time period in the simulation:

$$\text{minimize } \sum_{\ell \in A} c_{\ell} q_{\ell} \quad (1)$$

subject to:

$$\sum_{j \in O_i} q_j - \sum_{k \in I_i} q_k = 0; \text{ for all } i \in N \quad (2)$$

$$l_{\ell}(q) \leq q_{\ell} \leq u_{\ell}(q) \text{ for all } \ell \in A \quad (3)$$

where A is the set of all arcs or links in the network; N is the set of all nodes; O_i is the set of all links originating at node i (i.e., outflow links); I_i is the set of all links terminating at node i (i.e., inflow links); q_{ℓ} is the integer valued flow rate in link ℓ ; c_{ℓ} are the costs, weighting factors, or priorities per unit of flow rate in link ℓ ; l_{ℓ} is the lower bound on flow in link ℓ ; and u_{ℓ} is the upper bound on flow in link ℓ .

The link lower and upper bounds are depicted as themselves being functions of the arc flow in Eq. 3, which is necessary for inclusion of stream-aquifer interactions such as return flows during the current period. The solution procedure is to employ successive approximations, whereby a set of feasible flows is initialized, the bounds are set, and a new solution obtained which may differ from the initial solution. If so, the bounds are adjusted based on these new flows, and the procedure continues until convergence. All hydrologic information, both surface and subsurface, is represented in the network by appropriate specification of the arc bounds. Administrative and water right priorities are assigned by specification of the (negative) link costs in Eq. 1. The data base for the network optimization problem is completely defined by the link parameters for each link ℓ : $[l_{\ell}, u_{\ell}, c_{\ell}]$, as well as the sets O_i, I_i, N and A . The link parameters are automatically defined by MODSIM, based on hydrologic and administrative data provided by the user.

MODSIM employs an efficient dual coordinate ascent procedure based on Lagrangian relaxation, as developed by Bertsekas and Tseng (1994) for solving the network flow optimization problem. Comparative studies have shown Lagrangian relaxation to be far superior to the popular out-of-kilter (OKM) algorithm, as well as other primal-based network algorithms.

Reservoir Storage Targets and Priorities: The costs c_{iS} on the active storage links representing carryover storage in the network are computed as follows to reflect storage right priorities:

$$c_{iS} = - (50000 - 10 \cdot OPRP_i) \quad (4)$$

The user selects priority $OPRP_i$ as an integer ranking number between 0 and 5000. Notice that the computed cost c_{iS} is a negative number which, in a cost minimization objective, actually represents a benefit associated with carryover storage. This is not an actual economic benefit, but simply a mechanism for ranking water allocations according to decreed rights. An option available in MODSIM allows a water right decree date to be entered in place of the priority ranking $OPRP_i$, which is then automatically translated by MODSIM into the correct ranking order.

Evaporation loss is calculated in MODSIM as a function of average surface area in the reservoir over the current period, based on user input area-storage tables. Since average surface area in a reservoir is normally unknown until calculations are completed for the current period, an iterative process is usually required for accurate calculation of evaporation loss. However, this additional computational burden is avoided in MODSIM by a procedure whereby evaporation loss is included in the active storage links, and then subtracted from these values prior to providing initial storage levels for the next time period.

MODSIM provides numerous ways of specifying ideal target storage levels T_i and operating priorities $OPRP_i$. They may be directly input for each period, or conditioned on user-defined hydrologic states of the system. Multiple hydrologic states may be defined by the user, such as current storage levels in various selected reservoirs in the system. This allows consideration of a wide variety of reservoir operational strategies, including balancing storage between several reservoirs.

Consumptive Demands and Instream Flow Requirements: MODSIM automatically creates *demand links* which originate at each demand node and convey flows with demands assigned as upper bounds and lower bounds set at zero. This allows shortages to occur if water supply is limited and the demand is of junior priority. Demands may be defined as historical diversions, decreed water right amounts, predicted agricultural demands based on consumptive use calculations (performed outside the model), or projected municipal and industrial demands.

The link costs on the *demand links* are calculated using a formula similar to Eq. 4:

$$c_{iD} = - (50000 - 10 \cdot DEMR_i) \quad (5)$$

As with reservoir priorities $OPRR_i$, the user must select priorities $DEMR_i$ for demands between 0 and 5000. Again, if shortages must occur, then demands with lower priority (i.e., junior water rights) are denied flow first. For inefficient water application, MODSIM is capable of calculating return flows via groundwater or surface water, as described in more detail in Fredericks and Labadie (1995). Again, the option of entering a water right decree date may be used in place of directly entering the priority ranking $DEMR_i$. Multiple links may also be connected to a demand, representing several decreed water rights with different priorities. The maximum possible total delivery is dictated by the lower of the sum of the decreed water rights, the demand assigned to the node, and the capacity of the diversion structure or structures delivering the flow.

MODSIM also provides for demands for water which are not terminal; i.e., instream flow demands which *flow-through* the demand node and remain in the network for possible downstream diversion. In effect, this corresponds to demands with 100% return flow which is unlagged. This includes demands for instream flow uses for navigation, water pollution control, fish and wildlife maintenance and recreation which can be assigned water right decree priorities like any other demand. *Flow-through demands* are also useful for augmentation plans, exchanges between basin water users, and development of reservoir release operating rules. They have also been used for model calibration purposes, where a *flow-through demand* is assigned at a streamflow gaging station site, and the demands corresponding to actual measured flows are given the highest priority in the basin.

Water Exchanges and Credits: The ability of water users to formulate exchange agreements and plans for augmentation have become an important part of water administration in many over-appropriated river basins. For example, a water user may own storage rights in a reservoir from which it is physically impossible for the owner to directly receive releases. In this case, the owner may enter into an exchange agreement whereby direct river flow is diverted out of priority by the storage right owner, with an equal amount of flow released from the reservoir to satisfy senior water right holders that would be otherwise injured. MODSIM provides a variation on the flow-through demand allowing users to define *exchange demands* and *exchange links*.

An exchange demand is based on flow occurring in another link in the basin. The demand in this case is conditioned solely on the amount of flow in the link being *watched* by the demand. A credit demand is established based on flow in the watch link. Again, an *iterative structure* is required where, initially, the demand is set to zero. Upon solution of the network flow algorithm, the flow observed in the watch link is assigned as a demand at the exchange demand node, and the network solution is repeated. Since it is important that flow in the watch link agrees with the flow diverted to the demand, iterations proceed until the flows are equalized. An *exchange link* operates in much the same way as an *exchange demand*, except that the upper bound on the *exchange link* is based on the flow observed in the *watch link*.

Reservoir Storage Rights and Accounts: For reservoirs with storage right accounts, it is necessary to treat them as off-stream reservoirs, but in such a way as to be equivalent to an on-stream configuration. As shown in Fig. 2, the reservoir is represented as off-stream storage, with an accrual link and a release link returning to the river, as well as a bypass link representing flow passing directly through the reservoir. Each storage account in the reservoir is treated as a separate *child reservoir*. The *parent* reservoir is not directly connected to the network by the user, and is used only to maintain targets on total storage and total release, as well as account for total evaporation loss, total reservoir seepage, and hydropower production allocated to each *child* reservoir. In effect, nodes 2,3, and 4 all represent a single reservoir containing two storage accounts.

The accrual links can be assigned negative costs as related to a fill decree priority. They can also be specified as variable capacity links if there are time limitations on the fill period. Zero link capacities can be set for those periods

where the reservoir is not allowed to fill. In addition, accrual link can be assigned as seasonal capacity links, with the seasonal capacity corresponding to the amount of the fill decree. Refill priorities may also be assigned for any desired period.

Although accrual to the storage accounts via the accrual links in Fig. 2 are governed by the normal, priority based allocation process of MODSIM, once water is available in a storage account, it must be released to the owner as needed to meet demands. This implies a process which is *not* governed by a priority-based network flow allocation. The

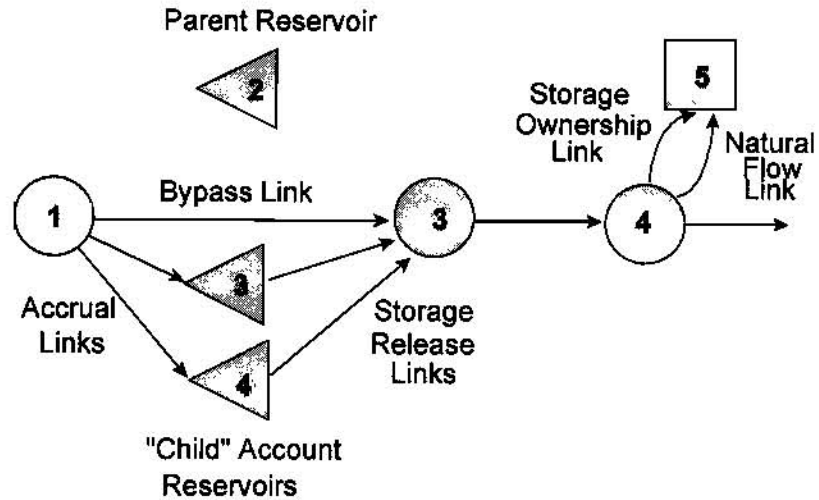


Figure 2. Storage Accounts and Storage Ownership

storage ownership link shown in Fig. 2 is related to one of the accrual links to the child account reservoirs. This guarantees that the owner of the storage right receives water from the correct account.

In order to allow for allocation of releases from storage accounts to the owners of those accounts, MODSIM includes an additional iterative step which is performed after allocation of all natural flows or direct diversions according to water right priority, including accruals to storage rights. The *storage allocation step* follows the *natural flow allocation step* in MODSIM. During the natural flow allocation step, releases are not allowed from the storage accounts, and diversions to the storage ownership links are also temporarily *turned off*. The storage allocation step is only performed in MODSIM if storage ownerships exist in the network. In those cases where owners of storage accounts are unable to physically receive reservoir releases from their accounts, MODSIM allows exchange mechanisms to take place whereby releases are made to downstream senior water right holders, and in return, the storage right owner is allowed to divert water out of priority.

IMPACTS FROM STORAGE ACQUISITION IN THE UPPER SNAKE BASIN

Management personnel at the USBR require information on relative yields and operational impacts from acquiring certain amounts of natural flow and storage contract water for proposed instream flow maintenance. Yield is dependent on the location of the water right or storage contract, the priority date, and the use of the water. Where and how the proposed water is to be used in the future will determine changes in river flows, reservoir contents, and impacts on other natural flow and storage water entitlements. MODSIM was applied to developing a network representation of the Snake River upstream of Brownlee Reservoir for these purposes.

A *base study* was completed as a basis for comparison which includes the existing physical features of the system, operational criteria, and water rights / storage contracts. Several studies were completed assuming different quantities and reservoir priority locations of storage water acquisition. Water is assumed to be purchased from various water users and used to meet an incremental instream flow objective at Milner Dam during August of each year. Storage water upstream of Milner Dam is currently regulated to satisfy demands upstream of this point in the river system. The nonexceedence curve shown in Figure 3 is an example of the results from one of these studies, showing how often and to what magnitude a 40,000 acre foot storage ownership in Ririe Reservoir could be made available at Milner as an incremental demand, assuming there no other deviations from the *base study* assumptions. Other information provided includes: changes in reservoir storage levels, streamflows at key locations, shortages, and storage accrual for other contracted space holders.

Table 1 is a summary of six scenarios where specified *blocks* of water have been reallocated to instream flow water requirements at Milner Dam. American Falls Reservoir provides the optimum yield characteristics in the system because of its location (and associated water supply) and its priority date relative to Palisades and Ririe Reservoirs, and has the most junior priority date of any reservoir in the basin. Column labels in Table 1 indicate the amount of storage space from the specified reservoir allocated to the instream flow function. For example, label *PAL100K* indicates that 100,000 acre-feet of Palisades Reservoir space is allocated to the Milner instream flow demand. Results show that, for the specified period of record, there is an 85% probability of yielding 36,000 acre-feet or more from allocating 40,000 acre-feet. For the same 85 percentile of years, a yield of the full 100,000 acre-feet is expected from an allocation of 100,000 acre-feet in American Falls. One could expect only 12,000 acre-feet (12% yield) from Palisades Reservoir allocation of 100,000 acre-feet in 5% of the years.

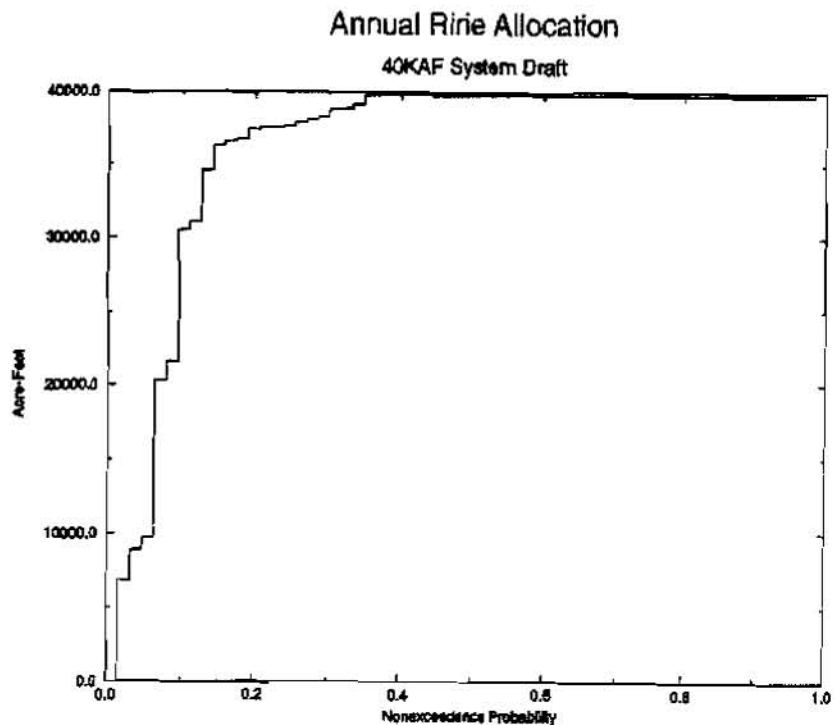


Figure 3. Nonexceedence Probability Distribution for Annual Ririe Allocation

CONCLUSIONS

The MODSIM river basin network model has been applied to integrating complex hydrological, operational, and institutional mechanisms in the Snake River basin. Information on relative yields and operational impacts from acquiring certain amounts of natural flow and storage contract water for proposed instream flow maintenance is obtained through application of MODSIM, which is able to fully incorporate the dependence of yield on the location of the water right or storage contract, the priority date, and the use of the water. These studies are crucial in determining where and how proposed available storage water is to be used in the future and its impact on river flows, reservoir contents, and impacts on other natural flow and storage water entitlements. MODSIM was applied to developing a network representation of the Snake River upstream of Brownlee Reservoir for these purposes. Since the Snake River system is operated in a manner in which many implicit exchanges take place in a given year, it is difficult to derive this kind of analysis information from historical data or other modeling tools that have been used in the past. The decision support structure of MODSIM allows these complex network structures to be easily constructed in a powerful graphical user environment. A variety of graphical plotting tools allows rapid assessment of the impacts of the various scenarios.

Table 1. Annual yield results for case study (acre-ft)

Annual Prob. (%)	PAL100K	PAL200K	AMF100K	AMF200K	RIR40K	RIR80K
100	100	200	100	200	40	80
40	100	200	100	200	40	80
35	100	200	100	200	40	77
30	100	200	100	200	39	75
25	100	200	100	200	38	75
20	100	198	100	200	37	73
15	97	180	100	190	36	72
10	96	175	100	185	31	64
5	95	165	98	180	20	28
2	12	30	93	175	7	0
0	12	30	93	175	0	0
Avg	96.4	190	99.5	197	37	73
Avg %	96.4	95.2	99.5	98.5	92.6	91.1

REFERENCES

- Bertsekas, D., Tseng, P., 1994, RELAX-IV: A Faster Version of the RELAX Code for Solving Minimum Cost Flow Problems. Dept. of Electrical Engineering and Computer Science, M.I.T., Cambridge, Mass.,
- Frevert, D., Labadie, J., Larson, R., Parker, N., 1994, Integration of Water Rights and Network Flow Modeling in the Upper Snake River Basin. Proceedings of the 21st Annual Conference, Water Resources Planning and Management Division, ASCE, Denver, Colorado.
- Fredericks, J., Labadie, J., 1995, Decision Support System for Conjunctive Stream-Aquifer Management. Completion Report for Grant No. 14-08-0001-G1551-04, Colorado Water Resources Research Institute, Colorado State University, Ft. Collins, Colo.
- Graham, L., Labadie, J., Hutchison, I., Ferguson, K., 1986, Allocation of Augmented Water Supply Under a Priority Water Rights System. Water Resources Research 22(7), 083-1094.
- Labadie, J., Bode, D., Pineda, A., 1986, Network Model for Decision-Support in Municipal Raw Water Supply. Water Resources Bulletin 22(6), 927-940.
- Labadie, J., Brazil, L., Corbu, I., Johnson, L. (eds.), 1989, Computerized Decision Support Systems for Water Managers. American Society of Civil Engineers, New York.
- Law, J., Brown, M., 1989, Development of a Large Network Model to Evaluate Yield of a Proposed Reservoir. Computerized Decision Support Systems for Water Managers, ASCE, New York, 621-631.
- Sprague, R., Carlson, E., 1982, Building Effective Decision Support Systems. Prentice Hall, Inc., Englewood Cliffs, New Jersey.

THE MODULAR MODELING SYSTEM (MMS) – THE PHYSICAL PROCESS MODELING COMPONENT OF THE WATERSHED AND RIVER SYSTEM MANAGEMENT PROGRAM

G.H. Leavesley, S.L. Markstrom, M.S. Brewer, and R.J. Viger, Hydrologists, U.S.
Geological Survey, Denver, Colorado

Abstract: The Modular Modeling System (MMS) is an integrated system of computer software that has been developed to provide the research and operational framework needed to support physical-process model development and application. MMS supports the development, testing, evaluation, and application of the wide range of modeling capabilities needed to address the issues associated with basin-scale water management. A geographic information system (GIS) interface, the GIS Weasel, has been integrated with MMS to support model development, application, and analysis. MMS has been coupled with RiverWare, an object-oriented reservoir and river-system modeling framework, using a shared relational database. The resulting database-centered, decision support system provides the tools needed for evaluating and applying optimal water-allocation and management strategies to complex, operational decisions on multipurpose reservoir systems and watersheds. The development and application of this decision support system are major objectives of a cooperative effort by the U.S. Geological Survey and the Bureau of Reclamation called the Watershed and River System Management Program.

INTRODUCTION

The interdisciplinary nature and increasing complexity of environmental and water-resource problems require the use of modeling approaches that can incorporate knowledge from a broad range of scientific disciplines. These modeling approaches must be flexible and able to address a wide range of study objectives, data constraints, and spatial and temporal scales of application. Models needed for river-basin management may include: (1) watershed models for simulating reservoir inflows and streamflow from unregulated basins; (2) one-dimensional and two-dimensional hydraulic models for application to selected river reaches where channel-flow characteristics may affect channel morphology or biological habitats; (3) sediment-transport and chemical-transport models to address a variety of water quality issues; (4) agricultural models to address land-management and irrigation practices and the fate and transport of nutrients and pesticides; and (5) biological and ecosystem models that address critical habitat issues.

The integration of this wide variety of modeling capabilities and their application to water-resources management is a major focus of the Watershed and River System Management Program (WARSMP). WARSMP is a cooperative effort between the U.S. Geological Survey (USGS) and Bureau of Reclamation (BOR) to develop an operational, database-centered, decision support system for application to complex, water-management

issues. The decision support system couples the U.S. Geological Survey's Modular Modeling System (MMS) (Leavesley et al., 1996a; Leavesley et al., 1996b) with the Bureau of Reclamation's RiverWare tools (Fulp et al., 1995) using a shared relational database. MMS facilitates the integration of a wide variety of models and their application to water- and ecosystem-resource management. RiverWare is an object-oriented reservoir and river-system modeling framework developed to provide tools for evaluating and applying optimal water-allocation and management strategies. The objectives of this paper are to provide an overview of the concepts and capabilities of MMS, the database-centered decisions support system, and their application to the WARSMP effort

MODULAR MODELING SYSTEM OVERVIEW

MMS is an integrated system of computer software that provides a common framework in which to focus multidisciplinary research and operational efforts to develop, evaluate, and apply a wide range of modeling capabilities across a broad range of spatial and temporal scales. MMS uses a master library that contains compatible modules for simulating a variety of water, energy, and biogeochemical processes. A model is created by selectively coupling the most appropriate process algorithms from the library to create an "optimal" model for the desired application. Where existing algorithms are not appropriate, new algorithms can be developed.

The conceptual framework for MMS has three major components: pre-process, model, and post-process (Fig. 1). All three components retrieve data from and store data in an underlying data storage scheme. The storage scheme may be composed of one or more data structures ranging from simple flat ASCII files to Structured Query Language (SQL) databases. Data management interfaces (DMIs) handle the transfer and reformatting of information among system components and the data structures. DMIs are essential to the interaction of the three components and are the only elements that are data-structure specific. Thus, changing data storage structures requires changing only the DMI.

The GIS Weasel supports MMS as a pre-processing component. However, it can also provide GIS post-processing capabilities for the visualization and analysis of spatial and temporal model output fields.

Graphical user interfaces (GUIs) provide access to all the features of MMS and the GIS Weasel. The present framework has been developed for UNIX-based workstations and uses X-windows and Motif for the GUIs. The GUIs provide an interactive environment for users to access model components, apply selected options, and graphically display simulation and analysis results. The current GUIs are being rewritten in the JAVA programming language to enable the application of MMS to a wider range of computer platforms.

Pre-process Component: The pre-process component includes all data preparation and analysis functions needed to meet the data and parameterization requirements of a user-selected model. A goal in development of the pre-process component is to take advantage

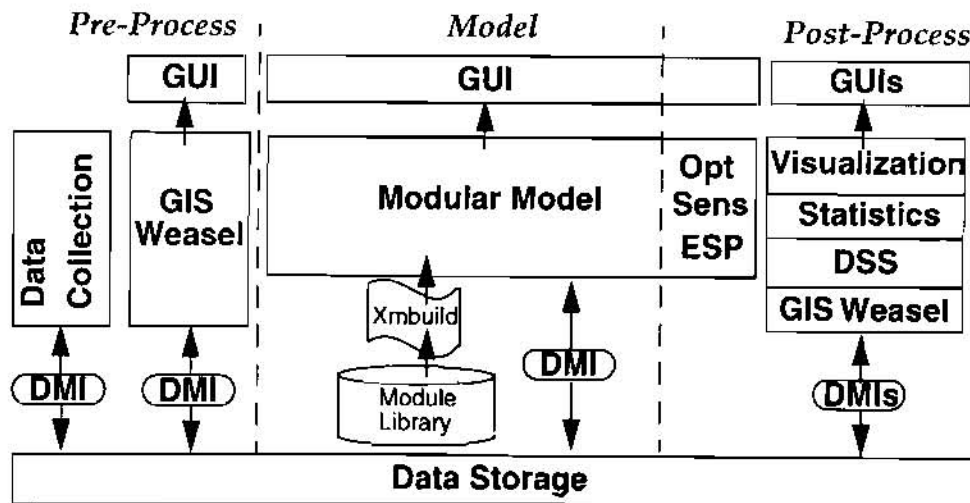


Figure 1. A schematic diagram showing the components of the Modular Modeling System (MMS).

of existing data-preparation and analysis tools and to provide the ability to add new tools as they become available. Spatial data analysis is accomplished using the GIS Weasel. Pre-processing functions provided by the GIS Weasel include the ability to (1) delineate and characterize watershed subbasin areas for distributed-parameter modeling applications, (2) estimate selected model parameters for these subbasin areas using digital elevation model (DEM) data and digital databases that include information on soils, vegetation, geology, and other pertinent physical features, and (3) generate an MMS input parameter file from these estimates.

Time-series data from existing databases and field instrumentation are organized and formatted for use in selected model applications. Additional tools are being developed to detect and replace erroneous or missing data values, aggregate data to longer time steps, disaggregate data to shorter time steps, and apply transform functions to produce a new time series. Methods to create simulated time series from model output or from the analysis and extrapolation of measured data to unmeasured points or gridded fields are also being developed.

Model Component: The model component is the core of the system and includes the tools to build a model by selectively linking process modules from the module library and to interact with this model to perform a variety of simulation and analysis tasks. The library can contain several modules for a given process, each representing an alternative conceptualization or approach to simulating that process. The user, through an interactive model builder interface (Xmbuild), selects and links modules to create a specific model. Once a model has been built, it may be saved for future use without repeating the Xmbuild step. This capability allows 'canned' versions of models to be provided to end users. User interactions with Xmbuild and the model are provided using a variety of X-window and graphical techniques.

An animation tool in the model component enables the visualization of the spatial and temporal variation of simulated state variables during a model run. Selected images from this animation for user-defined time periods can be stored and used in a post-modeling analysis to compare simulated and measured spatial and temporal variations in the selected state variable. Remotely sensed snow-covered area and soil moisture are examples of variables that can provide important additional independent measures of distributed-parameter model performance.

Post-process Component: The post-processing component contains the tools to analyze model results. These include a variety of statistical and graphical tools as well as the ability to interface with user-developed special purpose tools. Some tools are closely linked to the model component and are available as iterative procedures through the model component GUI. Optimization (Opt) and sensitivity (Sens) tools are provided to analyze model parameters and evaluate the extent to which uncertainty in model parameters affects uncertainty in simulation results. A modified version of the National Weather Service's Extended Streamflow Prediction Program (ESP) (Day, 1985) provides forecasting capabilities using historic or synthesized meteorological data. Other post-processing tools are stand-alone procedures. These include a variety of visualization and statistical tools, the GIS Weasel, and the ability to interface with resource management models and decision support systems (DSS).

GIS Weasel: The GIS Weasel has been designed to aid the preparation and analysis of spatial information for the estimation of parameters for lumped- and distributed-parameter models. It is composed of Arc/Info¹ (ESRI, 1992) GIS software, C language programs, and Unix shell scripts. All user interfaces are menu and map driven. The user is not required to have any knowledge of the command-line operating procedures of Arc/Info. However, the user should understand model assumptions regarding the treatment of spatial variations in watershed attributes.

The GIS Weasel provides tools to delineate, characterize, modify, and parameterize an area and its associated "model response units" (MRUs) using digital elevation model (DEM) and ancillary digital data. MRUs are areas delineated within a watershed, or region of interest, that reflect a model's treatment of spatially distributed attributes, such as slope, aspect, elevation, soils, and vegetation. An MRU may represent an area whose character or composition is assumed to be homogenous with respect to one or more attributes or it may be assumed to be heterogeneous with respect to all attributes. The GIS Weasel also delineates a drainage network and computes the connectivity of MRUs with this drainage network. The location of data-collection sites can also be overlaid with the MRU map to define associations between MRUs and the data sites.

¹ The use of trade, product, industry, or firm names is for descriptive purposes only and does not imply endorsement by the U.S. Government.

DATABASE-CENTERED DECISION SUPPORT SYSTEM

The physical process models in MMS are being linked with the reservoir and river management models of RiverWare via a common database, thus providing a database-centered decision support system (Fig. 2). A number of ancillary tools provide GIS, statistical analysis, and data query and display capabilities that are shared by MMS and RiverWare. In the current project, the database is termed the Hydrologic Data Base (HDB). Versions of HDB have been constructed using the commercial databases INGRES¹ (INGRES Corp., 1991) and ORACLE¹ (Oracle Corporation, 1987). However, this approach is not limited to INGRES and ORACLE, but can be used with any relational database system.

MMS and RiverWare access the database through user-written DMIs. Users can use a variety of standard DMIs, or write customized DMIs in any standard programming language that has database bindings, to access data from a variety of data repositories, including other relational databases. Changing the central database requires only that the DMIs be modified to support the selected database. No changes need to be made in MMS or RiverWare.

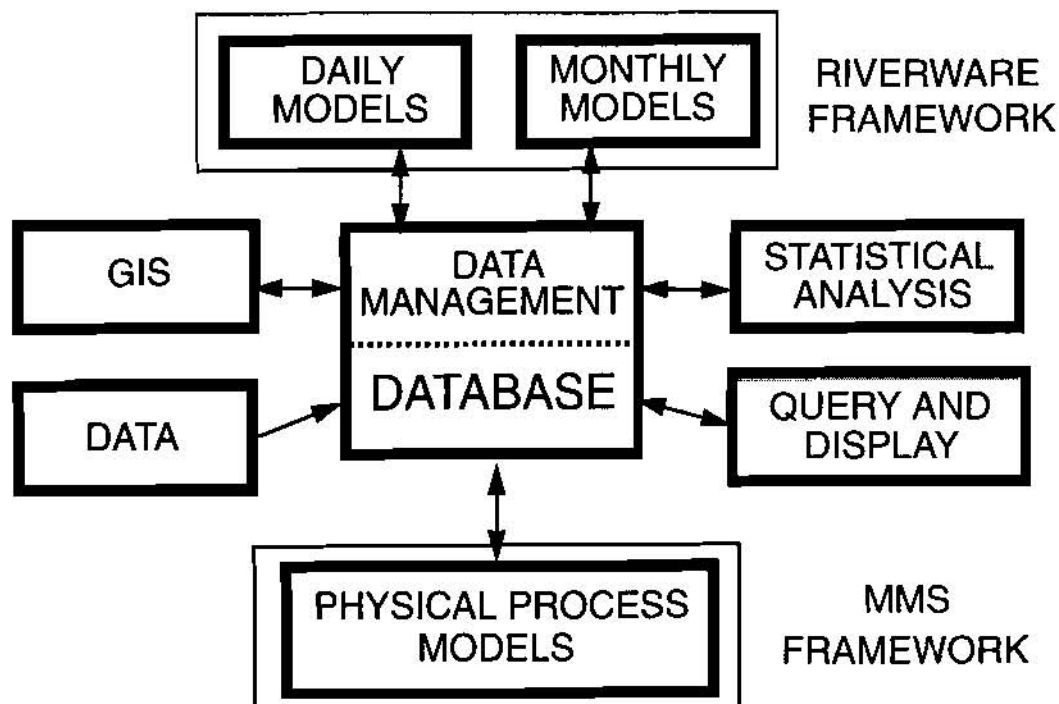


Figure 2. Schematic of the database-centered decision support system.

Communication between MMS and RiverWare is designed to use a scenario file in the database. A scenario is defined as a sequential list of modeling operations to be run using MMS and RiverWare. Different scenarios can be developed to address a range of resource-management decisions. The scenario file is accessed by both modeling systems and the specified models are executed in the order listed. A given resource-management decision may require the results of one or several models in both systems. Model results from MMS are written to the database for use as inputs to RiverWare and vice versa. This exchange of data and model results is an iterative procedure, the magnitude of which is dependent on the complexity of the decision process.

An example of such a procedure would be the management of a multi-reservoir river system within the constraints of competing water users and selected environmental constraints such as water-temperature limits or fisheries habitat needs. Here a scenario of MMS and RiverWare runs might begin with the execution of a watershed model in MMS to provide estimates of the daily time series of water inflows to all reservoirs in the system. Then RiverWare would be executed to use these inflows to develop a number of different management options and produce a time series of reservoir releases associated with each. These options might reflect different mixes of water use for power generation, agriculture, and municipal water supply.

Each release option has implications with regard to the environmental constraints on system operation and would need to be examined for those river reaches where these constraints apply. Thus, a one- or two-dimensional river hydraulic model would be run in MMS to assess the effects of the different reservoir-release options on the critical river reaches. Then RiverWare would be run again using the additional reach information to further refine the management options for these specific sets of conditions and constraints.

The generation of management options is not limited to RiverWare, but they can be developed within MMS as well. Using the ESP capability of MMS, alternative time series of water inflow to reservoirs can be developed, each with an associated estimate of a probability of occurrence. The manager could then select various levels of probability of occurrence to assess the effects of uncertainty on water management options. Alternatively, new time series of meteorological variables could be developed to reflect the potential effects of global climate change. These time series could be used as input to the watershed model to provide estimates of reservoir inflows for use in assessing the effects of climate change on basin management strategies.

The database-centered, decision-support system approach is being developed, tested, and implemented under WARSMP in the San Juan and Yakima River basins. The San Juan Basin has a drainage area slightly in excess of 23,000 mi² at Bluff, Utah, and is located in four-state area of Colorado, New Mexico, Arizona, and Utah. Water-management issues in the San Juan basin include efficiency of water-resources management, environmental concerns such as meeting flow needs for endangered species, and optimizing operations within the constraints of multiple objectives such as power generation, irrigation, and water conservation. The Yakima River basin has a drainage area of about 6,200 mi² at its point of discharge into the Columbia River and is located entirely in the state of Washington. The water-management issues in the

Yakima basin include the same issues as the San Juan basin, plus concerns regarding ground-water/surface-water interactions and water-quality issues related to irrigated agriculture.

SUMMARY

MMS is an integrated system of computer software that has been developed to provide the research and operational framework needed to support the development, testing, and evaluation of water, energy, and biogeochemical process algorithms and to facilitate the integration of user-selected sets of algorithms into operational models. MMS provides a common framework in which to develop and apply models that are designed for basin- and problem-specific needs. MMS is being coupled with the reservoir simulation and optimization software RiverWare using a common database interface to provide a database-centered decision support system for use in water-resources management. As the physical process modeling component of this decision support system, MMS provides a flexible framework in which to integrate these current activities and to easily incorporate any future advances in science and technology.

Given that different river basins may have different management objectives and operational constraints, the flexibility of MMS enables the development and application of those models determined to be most appropriate for a specific basin. Alternative modeling approaches can be evaluated to determine the optimal set of models for various management decisions. Coupled with RiverWare, the result is a very flexible set of water-resource management tools.

REFERENCES

- Day, G.N., 1985, Extended streamflow forecasting using NWSRFS. *Journal of Water Resources Planning and Management, American Society of Civil Engineers* 111, 157-170.
- Environmental Systems Research Institute, 1992, ARC/INFO 6.1 user's guide. Redlands, CA.
- Fulp, T. J., Vickers, W. B., Williams, B., and King, D. L, 1995, Decision support for water resources management in the Colorado River regions. *in* L. Ahuja, J. Leppert, K. Rojas, and E. Seely (eds.), *Workshop on computer applications in water management*. Colorado Water Resources Research Institute, Fort Collins, CO, Information Series No. 79, 24-27.
- INGRES Corporation, 1991, *INGRES/SQL Reference Guide for the UNIX and VMS Operating Systems*. Alameda, CA.
- Leavesley, G.H., Markstrom, S.L., Brewer, M.S., Viger, R.J., 1996a, The Modular Modeling System (MMS) -- The physical process modeling component of a database-centered decision support system for water and power management. *Water, Air, and Soil Pollution* 90, 303-311.
- Leavesley, G.H., Grant, G.E., Markstrom, S.L., Viger, R.J., Brewer, M.S., 1996b, A modular modeling approach to watershed analysis and ecosystem management, in *Proceedings of Watershed'96 A National Conference on Watershed Management*, U.S. Government Printing Office, 794-797.
- Oracle Corporation. 1987, *User documentation*. Belmont, CA.

THE RIPARIAN ECOSYSTEM MANAGEMENT MODEL: SIMULATOR FOR ECOLOGICAL PROCESSES IN RIPARIAN ZONES¹²

R. Lowrance, Ecologist, USDA-ARS, Tifton, GA³; L. S. Altier, Assistant Professor, California State Univ., Chico, CA; R. G. Williams, Agricultural Engineer, USDA-ARS, Tifton, GA; S. P. Inamdar, Post-Doctoral Associate, Univ. of Georgia, Tifton, GA; D. D. Bosch, Hydrologist, USDA-ARS, Tifton, GA; J. M. Sheridan, Hydraulic Engineer, USDA-ARS, Tifton, GA; D. L. Thomas, Associate Professor, Univ. of Georgia, Tifton, GA; R. K. Hubbard, Soil Scientist, USDA-ARS, Tifton, GA

Abstract: The Riparian Ecosystem Management Model (REMM) is a simulation model developed by USDA and university cooperators to provide comparisons among different field-scale buffer systems. The primary uses of REMM will be to simulate the water quality impacts of riparian and other edge of field buffer systems of different lengths, slopes, soils, and vegetation. Agencies such as USDA-NRCS and USDA-FS need this type model in order to provide specific guidance to landowners needing edge of field buffer systems. Although designed to simulate the specific type of multiple-zone buffer system recommended by USDA agencies, REMM is flexible enough to accommodate a wide range of buffer systems in a variety of land use settings. If hydrologic and pollutant loadings to the buffer system are available or can be estimated or modeled, REMM can be used to represent most edge of field buffers receiving diffuse inputs of water. This paper presents the general structure of REMM and information on the initial field testing site for the model. Operational aspects and details of model components and test simulations for REMM using field data from a riparian buffer system in the southeastern coastal plain are presented in five other papers in these proceedings,

INTRODUCTION

Agriculture continues to be a major contributor of nonpoint source pollution to the nation's waters and continues to limit the attainment of designated uses in many rural watersheds (USEPA, 1997). There is a growing realization that for agricultural watersheds to meet designated uses as defined under the Clean Water Act (CWA), there must be a combination of efforts to both control nonpoint source pollution and to restore aquatic ecosystems. Restoration and management of riparian ecosystems are essential to restoration of aquatic ecosystems and to attainment of water quality goals because of the multiple water quality functions performed by riparian ecosystems. Riparian forests are known to reduce delivery of nonpoint source pollutants to streams and lakes in many types of watersheds (Lowrance et al., 1997). In addition, riparian forests are known to be important in controlling the physical and chemical environment of streams and in providing detritus and woody debris for streams and near-shore areas of large water bodies.

The major United States Department of Agriculture efforts to restore riparian ecosystems are funded through the continuous sign-up of the Conservation Reserve Program (CRP) and the Conservation Reserve Enhancement Program/State Enhancement Program (CREP/SEP) authorized in the 1996

¹ Contribution from the USDA-ARS, Southeast Watershed Research Laboratory, P.O. Box 946, Tifton, GA, 31793, in cooperation with the University of Georgia and California State University.

² All programs and services of the USDA are offered on a nondiscriminatory basis without regard to race, color, national origin, religion, sex, age, marital status, or handicap.

³ USDA-ARS-SEWRL, P.O. Box 946, Tifton, GA 31793. Phone: 912-386-3894; fax: 912-386-7294; e-mail: lorenz@tifton.cpes.peachnet.edu.

Farm Bill. The continuous sign-up allows landowners to offer lands with high Environmental Benefits for the CRP at any time. Efforts spearheaded by Vice-President Gore to address the nation's lack of progress toward CWA goals have focussed on use of the CREP/SEP mechanism to address critical agricultural water quality problems (White House Memorandum, 10/18/97). The first project funded for CREP/SEP is an effort to have up to 100,000 acres of riparian land along Maryland's streams and rivers set aside and maintained to protect water quality (White House Press Release, 10/20/97). The Maryland CREP/SEP will spend about \$200 million over 15 years to restore riparian ecosystems. Clearly, USDA is planning to make large investments of funds in restoring streamside (riparian) ecosystems to control nonpoint source pollution, increase attainment of designated uses of streams, to provide wildlife habitat, and to restore aquatic ecosystems. An evaluation of whether goals are being met and an evaluation of alternative scenarios for achieving the environmental goals should accompany expenditure of public money to achieve environmental goals. Restoration and management of riparian ecosystems, while generally good for water quality, should be evaluated for their efficacy in controlling specific nonpoint source pollution problems. Although general guidelines are available from USDA action agencies on the management of riparian buffers (Welsch, 1991; NRCS, 1995), information is lacking on how buffer zones should be designed and managed to meet site-specific needs.

The Riparian Ecosystem Management Model (REMM) has been developed by USDA and university cooperators in order to provide a tool to assess the nonpoint source pollution control functions of riparian buffer systems. Unlike pollution control practices, which depend on engineering structures to control water or water-borne pollutants, riparian buffer systems are complex ecosystems. The control of nonpoint source pollution in riparian ecosystems depends on interactions among the hydrology, soils, vegetation, management, and climate of a specific riparian buffer system. Models which cannot account for effects of these factors on water and chemical transport in riparian systems will not be useful for comparisons of different scenarios of riparian buffer use to control nonpoint pollution. The series of papers presented at this symposium describe the functional elements of REMM and present validation results for the model. A demonstration will provide details on initializing and running the model. In this paper we provide an overview of the conceptual basis for REMM. In addition, we describe the general characteristics of an experimental riparian buffer system used for validation studies presented in the other papers.

GENERAL FUNCTIONS OF RIPARIAN BUFFER SYSTEMS

Riparian forests were the original streamside vegetation in most humid and sub-humid regions of the world, including the Eastern and Midwestern United States. Riparian forest is generally distinct from the surrounding landscape, even when the adjacent areas are in forest. In more arid areas, the riparian forest may be the only forest in a landscape, for example the gallery forests of the tall-grass prairie. In most cases, regardless of original or native vegetation, riparian ecosystems form an ecotone or edge between upland vegetation and land uses and aquatic ecosystems.

The general functions of riparian forest ecosystems have been reviewed and ranked for the Chesapeake Bay Watershed from most to least general based on the available scientific literature (Lowrance et al., 1997). These buffer system concepts are based on field observations, process studies, and experimental manipulations in a number of different riparian ecosystem studies. Because of the diverse nature of the Chesapeake Bay Watershed, the rankings probably apply to many humid regions in the U.S. The most general water quality function of riparian forests is to provide control of the stream environment. These functions include modifying stream temperature; controlling light quantity and quality; enhancing habitat diversity; modifying channel morphology; and enhancing food webs and species richness. All of these factors are important to the ecological health of a stream and are best provided by a riparian forest that approximates the original native

vegetation (Sweeney, 1992). These functions occur along smaller streams regardless of physiographic region. These functions are most important on smaller streams, although they are important for bank and near-shore habitat on larger streams and the shoreline of lakes and bays. Riparian forests contribute to bank stability and thus minimize sediment loading due to instream bank erosion. Depending on bank stability and soil conditions in the area immediately adjacent to the stream, management of adjacent areas for long-term rotations may be necessary for sustainability of stream environment functions. The next most general water quality function of riparian forests is control of sediment and sediment-borne pollutants carried in surface runoff. Properly managed riparian forests should provide a high level of control of sediment and sediment borne chemicals regardless of physiographic region. Natural riparian forest studies indicate that forests are particularly effective in filtering fine sediments and promoting co-deposition of sediment as water infiltrates. The slope of the riparian forest, the available water storage capacity, and the soil cover by litter are the main factors determining the effectiveness of sediment removal in mature riparian forests. In restored riparian forests, the degree to which enhanced infiltration typical of forest soils has been established might also determine effectiveness in controlling surface runoff pollutants. In all physiographic settings it is important to convert concentrated flow to sheet flow in order to optimize riparian forest function. Conversion to sheet flow and deposition of coarse sediment that could damage young vegetation can be enhanced by a vegetated filter strip upslope from the riparian forest.

The next most general water quality function of riparian forests is to control nitrate in shallow groundwater moving toward streams. When groundwater moves in short, shallow flow paths, such as in many Coastal Plain watersheds, 90% of the nitrate input may be removed. In contrast, nitrate removal may be minimal in areas where water moves to regional groundwater such as in Piedmont and Valley and Ridge areas. The degree to which nitrate (or other groundwater pollutants) will be removed in the riparian forest depends on the proportion of groundwater moving in or near the biologically active root zone and on the residence time of the groundwater in these biologically active areas. The presence of wetlands and the hydrologic connection between source areas and wetlands enhances the removal of nitrate via denitrification.

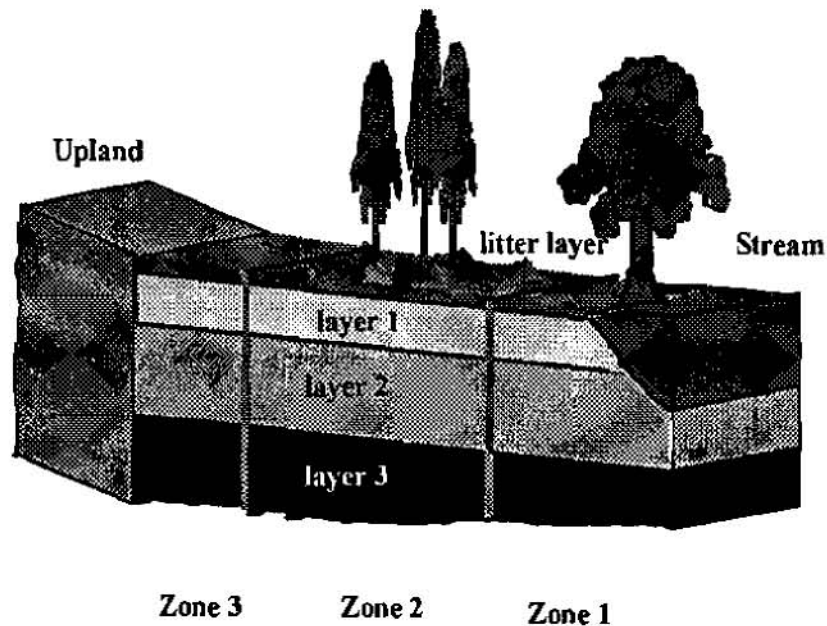
The least general function of riparian forests appears to be control of dissolved phosphorus in surface runoff or shallow groundwater. Control of sediment-borne P is generally effective. In certain situations, dissolved P can contribute a substantial amount of total P load. Most of the soluble P is bioavailable, so the potential impact of a unit of dissolved P on aquatic ecosystems is greater. It appears that natural riparian forests have very low net dissolved P retention. In managing for increased P retention, effective fine sediment control should be coupled with use of vegetation that can increase P uptake into plant tissue.

USDA's RIPARIAN FOREST BUFFER SPECIFICATION

Based on the general concepts described above, a riparian forest buffer system specification has been developed by USDA. (Welsch, 1991; Lowrance, 1992; NRCS, 1995) The riparian forest buffer specification is for a three zone riparian buffer system with each zone serving a particular major purpose and a number of secondary purposes (Figure 1). The buffer system consists of trees, shrubs, and herbaceous vegetation. The riparian forest buffer specification calls for a Zone 1 immediately adjacent to the stream which consists of permanent woody vegetation. In many cases, Zone 1 vegetation will be native hardwood species that occur on or near streambanks. The major purpose of Zone 1 is to provide shade and litter inputs for the aquatic ecosystem. The secondary function of Zone 2 is to retain nutrients. Zone 2 is on the upslope side of Zone 1. Zone 2 is an area of managed forest, which can be used for timber or biomass production by the landowner. The major function of Zone 2 is nutrient retention and infiltration of surface runoff. Secondary functions of

Zone 2 are to provide a buffer for Zone 1 vegetation and to retain sediment in surface runoff. Zone 3 is an herbaceous filter strip upslope from Zone 2. Zone 3 is similar to contour filter strips used as a field management practice. Management practices such as stiff grass buffers can also be incorporated in this zone. Zone 3 is generally immediately adjacent to the field or other pollutant source. The major functions of Zone 3 are sediment retention and conversion of channelized flow to sheet flow. Secondary functions of Zone 3 are infiltration of surface runoff and nutrient retention.

Figure 1: Cross section of riparian buffer system as simulated in REMM.



REMM was developed specifically to simulate hydrologic, chemical, physical, and biological processes in the type of riparian buffer system described above which has been adopted as a practice by USDA

agencies. REMM also provides flexibility to simulate functions of a wide variety of other field-edge and in-field buffer systems. Although the riparian forest buffer specification requires trees or shrubs in Zones 1 and 2, REMM can simulate up to twelve different vegetation types, and multiple vegetation types per zone. REMM can be used to simulate non-forest buffers and buffers in non-riparian positions, as long as the water, nutrient, and sediment inputs from the contributing area can be modeled or empirically determined.

GENERAL STRUCTURE AND FUNCTION OF REMM

REMM is designed to simulate daily processing of water, sediment, carbon, and nutrient inputs to a buffer system (Altier et al., In press). In general, inputs will be from agricultural lands, although inputs of water, sediment, and nutrients from other land uses could also be simulated. Water inputs are rainfall (or snowfall), surface runoff, subsurface flow (shallow groundwater), and seepage. Water outputs for each zone are calculated as subsurface flow, surface runoff, seepage, and evapotranspiration (ET). Nitrogen phosphorus, and carbon are input and output with each type of water input or output (except ET). Surface runoff carries sediment into and out of the zones. The output from Zone 1 is an estimate of the streamflow contribution of the entire contributing area, including the riparian buffer. In this sense, REMM is a watershed model when combined with modeled input from the upslope contributing area. REMM does not simulate the effects of channel expansion and overbank flooding during storm events. REMM assumes a lower confining layer for subsurface flow, although water can be allowed to move through the lower confining layer at a

constant rate. REMM does not allow simulation of groundwater flow paths that may make their way to stream discharge below the lower confining layer.

Much of the sediment transport module of REMM is based on AGNPS (Young et al, 1989). Sediment movement is simulated in rill and interrill erosion. Sediment is assumed to be composed of sand, large aggregate, small aggregate, silt, and clay. Sediment erosion, transport, deposition, and routing are done for each particle size class. Sediment deposition or transport is determined based on the transport capacity of the zone. Deposition or transport takes place through interaction with a litter layer, which is assumed to mix completely with surface runoff.

The dynamics of inorganic N and P in REMM are tied to estimates of either transformation rates or equilibrium concentrations for adsorbed ions. Nitrogen and phosphorus in initial soil organic matter (SOM) pools or N and P incorporated into plant biomass are cycled through SOM pools with different decomposition rates as done in the CENTURY model (Parton et al., 1987). N and P are mineralized as plant litter or SOM is re-synthesized into pools with a higher C/N or C/P ratio. N and P are immobilized from inorganic pools into either living plant biomass or SOM pools. As plant litter or soil organic matter are resynthesized into pools with higher C/N or C/P ratios, N and P are mineralized. Inorganic nutrients, whether from input sources or from mineralization of SOM, are available for plant uptake, microbial immobilization, water borne movement, or denitrification (N only). REMM does not simulate movement of pesticides, although it does simulate movement of dissolved and adsorbed carbon compounds that could be used as analogs of pesticides.

Vegetation growth is simulated on a stand basis. Vegetation in both an upper and lower canopy can be simulated for each zone and up to 12 different general vegetation types can be simulated. Plant growth is modeled based on estimates of the amount of gross photosynthesis and allocation of the photosynthate to growing plant parts and respiration depending on demand. If photosynthates are available, plant growth is limited by the availability of water and nutrients. Simulation of photosynthesis is based on the Forest-BGC model (Running and Coughlan, 1988).

TESTING AND VALIDATION OF REMM

Numerous research groups around the country where studies of riparian buffers in various settings have been conducted are currently testing REMM. Initial testing of REMM has been done by comparing simulated riparian buffers to data from actual riparian buffers studied by the Southeast Watershed Research Laboratory near Tifton, GA. This section of the paper describes the general characteristics of the field site used for validation of REMM. Subsequent papers in these proceedings will describe the specific results from the validation studies for hydrology, sediment transport, nutrient cycling, and plant growth.

Gibbs Farm Study Site: The study was done at a research farm (Gibbs Farm Site - GFS) which is part of the University of Georgia Coastal Plain Experiment Station near Tifton, GA. The site, referred to hereafter as the Gibbs Farm Site (GFS) is located in the Tifton-Vidalia Upland (TVU) portion of the Gulf-Atlantic Coastal Plain. The climate of the TVU is humid subtropical providing abundant rainfall and a long growing season. Because of both less permeable soil material at depth and the presence of a geologic formation (Hawthorn Formation) which limits deep recharge to the regional aquifer system, most of the excess precipitation in the TVU moves either laterally in shallow saturated flow or moves in surface runoff during storm events. The general hydrology of the region is reflected at the GFS and makes this region and the particular site ideal for the development of model testing data in a relatively simple hydrologic system.

The soil at the GFS riparian forest is an Alapaha loamy sand (fine-loamy, siliceous, acid, thermic Typic Fluvaquents). The soil of the adjacent upland area is a Tifton loamy sand (fine-loamy, siliceous, thermic, Plinthic Kandiudult). A three zone riparian buffer system as prescribed by the USDA-Forest Service specifications (Welsch, 1991) was established for this research project in 1992. Zone 3 is a herbaceous filter strip, Zone 2 is an area of managed forest where trees can be harvested, and Zone 1 is an area of permanent woody vegetation immediately adjacent to the stream channel. At the GFS (Figure 1), Zone 3 is an 8 m wide strip of common Bermudagrass (*Cynodon dactylon* L. Pers.) and Bahia grass (*Paspalum notatum* Flugge.). The grass strip was interplanted with perennial ryegrass (*Lolium perenne* L.) during its establishment. Zone 2 (before timber harvest) was a 40 to 55 m wide band of slash pine (*Pinus elliottii* Engelm.) and long leaf pine (*Pinus palustris* Mill.). Zone 1 is a 10-m wide band of trees with mostly hardwoods including yellow poplar (*Liriodendron tulipifera* L.) and swamp black gum (*Nyssa sylvatica* var *biflora* Marsh.). The entire buffer averages 55 m in width along an intermittent second-order stream channel. In early November 1992, one block of Zone 2 forest was clear-cut and one block was selectively cut. A third Zone 2 forest block was left as a reference area (Figure 2). The clear-cut Zone 2 blocks were replanted with improved slash pine in winter, 1993. No timber was harvested from Zone 1. The papers presented in this symposium will discuss model simulations and observations from the mature forest area only. The forest, with an average tree age of about 50 years, was considered to be in a steady state condition with very little net increase in biomass.

The field above the buffer system on the west side of the stream was in continuous corn (*Zea mays* L.) for the first three years of this study (1992-1994). In 1995, the field was planted in peanuts (*Arachis hypogea* L.). In 1996, the field was planted in millet (*Pennisetum glaucum* L.). All crops were grown using conventional tillage and conventional fertilizer and pesticide treatments. The exception is that the peanuts were grown in small test plots (4mx4m) which lead to high loadings of sediment in surface runoff.

Instrumentation and sample collection: Instrumentation at the experimental site was installed in late Fall, 1991 and Winter, 1992. Well sampling and surface runoff sampling began in January, 1992 and February, 1992, respectively. Recording well installations were completed in April, 1992. Samples were analyzed for sediment and N and P species using standard analytical techniques.

Surface runoff was collected using the dustpan shaped "Low-Impact Flow Event sampler (LIFE sampler, Sheridan et al, 1996). Two types of LIFE samplers are used to collect either 10% or 1% of the flow through a 30.48-cm wide dustpan. The 10% collection is made by splitting the flow into 10 pathways at the back of the collector and collecting flow from one pathway. The 1% sample is collected by connecting two 10% samples in series. The sample receptacle is large enough to contain runoff from approximately a 10-year return interval event in the 1% samplers. The receptacle is made from a 1m long piece of 10cm dia PVC pipe with capped openings at each end. PVC joints were welded using heated PVC to avoid possible interferences of solvents in PVC cement with the herbicide analysis. One of each type sampler is located at each zonal interface (six samplers per zonal interface). The samplers were positioned so as not to interfere with surface runoff collection at the next zonal interface (Figure 2). Six samplers are also in the middle of Zone 2. Having two types of samplers (10% and 1%) allows both large and small runoff events to be sampled and runoff volumes obtained. Surface runoff sample volumes were measured and subsamples collected for nutrient and sediment analysis on the work-day following each runoff event. Multiple events in a day were not collected separately. Samples were collected by pumping the receptacles with a peristaltic pump while agitating the sample by mixing with the inlet line of the pump.

Shallow groundwater movement of nutrients was determined using slotted monitor wells and a series of recording wells. A total of 115 slotted monitor wells were installed in the entire area (Figure 2) using Tri-loc slotted monitor pipe (Brainard-Kilman, Stone Mtn., GA). All PVC joints on monitor wells were welded using heated PVC. Paired wells were screened from 0-50 cm and 50-200 cm at

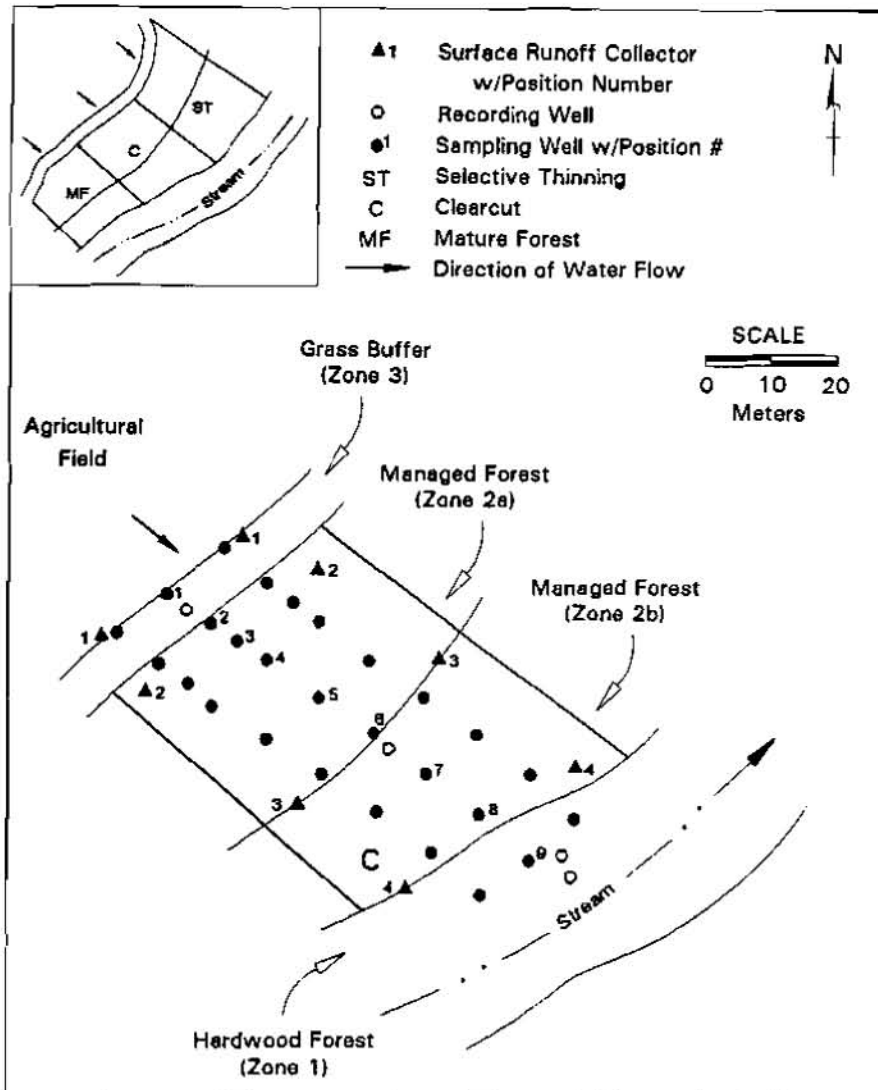


Figure 2. Layout of riparian forest plots in relation to upland field at the Gibbs Farm site.

the first four positions of each transect. The rest of the wells in each transect were screened from 0-200 cm depth. The first four positions are 5m apart and the rest of the well positions are 10m apart. Fully penetrating wells in the middle of each zone and the stream channel are instrumented with pressure transducers (Druck, Inc., New Fairfield, CT) connected to data loggers (Campbell Scientific, Logan, UT) so that water table levels can be monitored continuously. The soil water content and recording well data were used to calculate saturated thicknesses and ground water flux through the buffer system (Bosch et al., 1996). Wells were sampled bi-weekly. Before each well sampling, the depth of water below the ground surface was measured manually, and at least one well volume was removed and discarded.

Test Conditions and Reporting of Results: Four other papers presented as part of this symposium present simulation results for REMM with the model parameterized for the GFS. A final paper

discusses operational aspects of REMM. The test papers present results for hydrology, sediment transport, nutrient cycling, and plant growth for the mature riparian forest studied at the GFS. Where possible, key parameters from the GFS are compared to model simulation. For these tests of REMM, the GFS has been simulated as having a single vegetation type in each zone. Where possible, soil and water pools in REMM have been initialized with data from the GFS. When not possible, the pools were initialized from data collected at similar sites near the GFS or from literature values. Model simulations were done using weather data collected at the GFS and using estimates of upland inputs of water, sediment, and nutrients measured at the GFS. Very little calibration of REMM was necessary. Calibration of gross photosynthesis and soil organic matter turnover rates were done in order to stabilize the steady state or mature forest case. Other than that, the simulations presented in the companion papers are based on either field estimates of pools or rates or from literature values.

REFERENCES

- Altier, L.S., R. Lowrance, R.G. Williams, S. P. Inamdar, D.D. Bosch, J.M. Sheridan, R.K. Hubbard, and D.L. Thomas. Riparian Ecosystem Management Model (REMM): Documentation. USDA Conservation Research Report, In Press.
- Batten, H.L. 1980. Little River Research Watersheds. USDA Miscellaneous Publication, Southeast Watershed Research Lab, Tifton, GA. 17p.
- Bosch, D.D., J.M. Sheridan, and R. R. Lowrance. 1996. Hydraulic gradients and flow rates of a shallow coastal plain aquifer in a forested riparian buffer. Transactions of ASAE, 39, 865-871.
- Jacobs, T.C. and J.W. Gilliam. 1985. Riparian losses of nitrate from agricultural drainage waters. Journal of Environmental Quality 14, 472-478.
- Lowrance, R.R., R.L. Todd, J. Fail, Jr., O. Hendrickson, Jr., R. Leonard and L. Asmussen. 1984. Riparian forests as nutrient filters in agricultural watersheds. BioScience 34, 374-377.
- Lowrance, R., L.S. Altier, J.D. Newbold, R.R. Schnabel, P.M. Groffman, J.M. Denver, D.L. Correll, J.W. Gilliam, J. Robinson, R. Brinsfield, K. Staver, W. Lucas, and A. Todd. 1997. Water quality functions of riparian forest buffers in Chesapeake Bay watersheds Environmental Management 21, 687-712.
- NRCS. 1995. Riparian Forest Buffer, 392. United States Department of Agriculture/Natural Resources Conservation Service, Watershed Science Institute. Seattle, Washington.
- Parton, W.J., D.S. Schimel, C.V. Cole, and D.S. Ojima. 1987. Analysis of factors controlling soil organic matter levels in Great Plains grasslands. Soil Science Society of America Journal 51, 1173-1179.
- Peterjohn, W.T. and D.L. Correll. 1984. Nutrient dynamics in an agricultural watershed: Observation on the role of a riparian forest. Ecology 65, 1466-1475.
- Running, S.W. and J.C. Coughlan. 1988. A general model of forest ecosystem processes for regional applications I. Hydrologic balance, canopy gas exchange, and primary production processes. Ecological Modelling 42, 125-154.
- Sheridan, J.M., R.R. Lowrance, and H.H. Henry. Surface flow sampler for riparian studies. Applied Engineering in Agriculture 12, 183-188.
- Sweeney, B.W. 1992. Streamside forests and the physical, chemical, and trophic characteristics of Piedmont streams in eastern North America. Water Science & Technology 26, 2653-2673.
- USEPA. 1997. Clean Water Act Progress Report. United States Environmental Protection Agency, Office of Water. Washington, D.C.
- Welsch, D.W. 1991. Riparian Forest Buffers. USDA-Forest Service Publ. No. NA-PR-07-91.
- Young, R.A., C.A. Onstad, D.D. Bosch, and W.P. Anderson. 1989. AGNPS: A nonpoint-source model for evaluating agricultural watersheds. Journal of Soil and Water Conservation 44, 168-173.

IMPLEMENTING A WATER RESOURCE PLANNING MODEL WITHIN THE COLORADO RIVER DECISION SUPPORT SYSTEM

Steven Malers, Software Engineer, Riverside Technology, inc., Fort Collins, Colorado; Ray Bennett, CRDSS Project Manager, State of Colorado, Denver Colorado; Larry Brazil, President, Riverside Technology, inc., Fort Collins, Colorado

Abstract: The Colorado River Decision Support System (CRDSS) is a database and modeling system used by the State of Colorado to help water managers make informed decisions about Colorado water resources. Implementing the system has improved both the State's understanding of the data and its ability to analyze "what if" questions that are critical to water resources management in Colorado. The data-centered system allows different modeling and analysis tools to share the same data. This paper focuses on the implementation of the water resources planning component of the CRDSS.

INTRODUCTION

The CRDSS consists of databases and models that provide improved data and decision-making capability for the Colorado River and its tributaries within Colorado. It is being developed by the Colorado Water Conservation Board (CWCB) and the Division of Water Resources (DWR), under the overall guidance of the Department of Natural Resources. Initiated in 1993, the project is in the fifth and final year of development. The CRDSS Project Management Team consists of a contract project manager and senior staff of the CWCB and DWR. A Technical Advisory Committee of major Colorado River water users is helping guide the project. A consulting team headed by Riverside Technology, inc. (RTi) of Fort Collins was selected in January, 1994 to design and develop the CRDSS.

CRDSS was developed to allow Colorado to enter a new era of water management that emphasizes cooperation among state agencies, water providers, and water users. The CRDSS is a data-centered system that contains historic tabular data such as streamflow, climate and diversions; spatial data such as topography, hydrography, and irrigated acreage; and administrative data such as water rights and water management policies. Data are keyed to locations in the river basin using a geographic information system (GIS). This computer-based system allows decision makers to access water resource data, simulate potential decision and policies, and examine the consequences with regard to interstate compact policy, water resource planning, and water right administration.

This paper discusses one element of CRDSS: implementing a water resource planning (WRP) model using a data-centered approach. An extremely large scale application, CRDSS required the consistent development of five separate WRP model applications (White, Yampa, Colorado, Gunnison, and San Juan river basins) that, if desired, can be combined into one application that encompasses the entire western slope of the State of Colorado.

A DATA-CENTERED APPROACH

The CRDSS is a multi-year project requiring that various database and modeling components be developed and implemented over time. This required that the database design be scaleable and flexible enough to allow growth and enhancement. A model-generic approach was chosen, in which a core set of data are stored in a central database and are used by one or more applications. In this data-centered approach, the database becomes the repository for key data and consequently helps to maintain quality and consistency. **Figure 1** illustrates the CRDSS data-centered approach where various tools share common data.

In order to implement a data-centered system, there must be enough infrastructure in place to support and allow effective use of the system. The CRDSS database contains all of the key water resources data needed for planning and administrative purposes for the State of Colorado and allows for "one stop shopping" for Colorado water data users. Utilities have been written to format data files for models and provide effective data displays to users. Much of the data is available to Internet users via the CRDSS home page (see references). Utilities are available that allow users to quickly access and format data for use in other applications.

It is important to note that the implementation of a data-centered approach in the CRDSS has not precluded the use of modular tools. The WRP model and other tools can run stand-alone and are not tied directly to the database. This

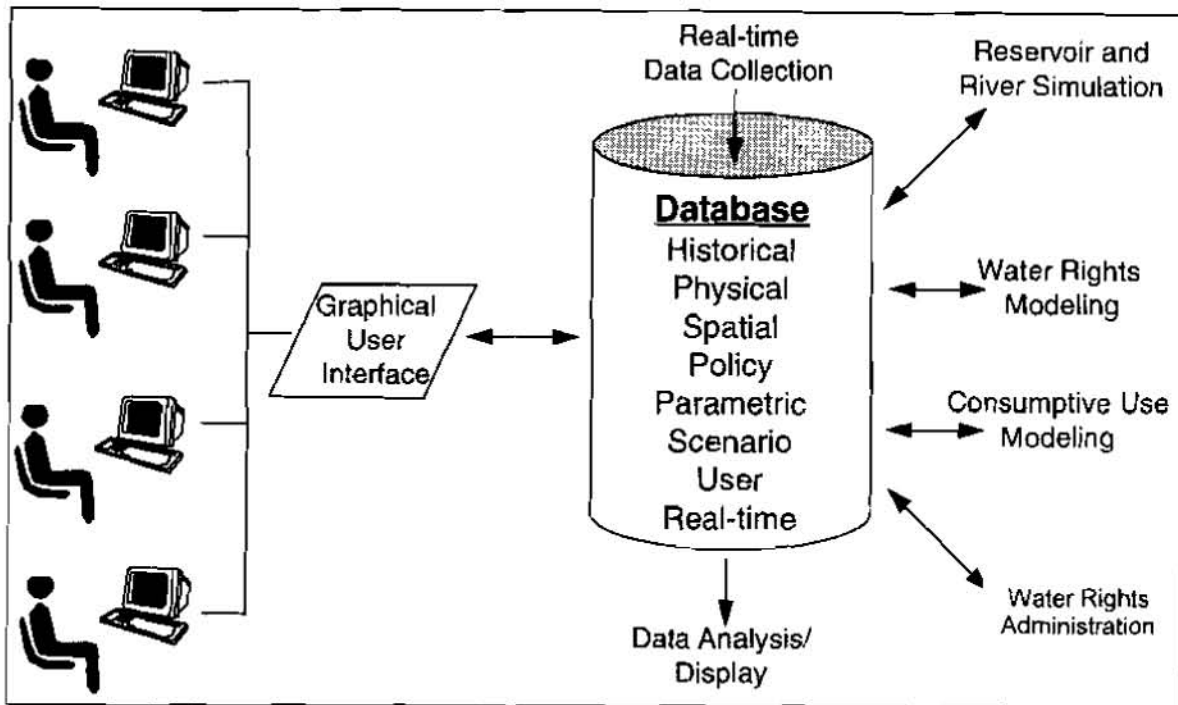


Figure 1. CRDSS Data-centered Approach

allows for distributed modeling efforts within the user community. In order to promote data sharing, standard data formats for time series and other data have been adopted. The data-centered approach, as adopted for the CRDSS, allows users to access data from a central location but perform analyses using accepted tools in a desktop environment. As a policy, model output is not currently stored in the database but is kept in the standard model output formats. This simplifies model use and database design and decreases the overall size of the database. Exchange of data between models occurs using standard data formats and file translation utilities, where necessary.

The main CRDSS database uses INFORMIX® on a server machine. Microsoft Access® versions of the database are being developed to further allow distribution and use of CRDSS data and tools for the PC environment. In this configuration, it is understood that the central database is the official repository of data for CRDSS that may only be changed by a database administrator.

Data Quality Issues: Despite the fact that State of Colorado staff had been maintaining a database of water rights and diversion data for many years, the CRDSS team quickly identified quality issues when data were loaded into the database and used for modeling. The new CRDSS database uses INFORMIX (which implements constraints and range checks), whereas the old database used a series of discrete files that often contained redundant data. The CRDSS team identified data coding problems such as miscoded structure types (a reservoir being called a diversion), use of the letter "O" instead of the number "0", and reservoir levels recorded as "full" or "half-full" instead of as a numeric value. Using a non-relational database resulted in a wide variety of data coding problems such as assigning the same structure different names ("XYZ DITCH" and "DITCH XYZ") and using different water coloring schemes (water coloring refers to the practice of identifying the different sources [river, storage, etc.] and uses [irrigation, power] of water). The CRDSS team detected some errors while populating the database, but often problems were detected only when the data was used for modeling. For example, if structure types were miscoded, then a request for all diversions might actually return a reservoir or instream flow. Some important (if simple) lessons were learned:

1. Ensure data quality, to the extent possible. For the State of Colorado, this meant using modern database tools to increase the scrutiny of data, as well as improving procedures to allow timely data corrections.

2. Enforce consistency and simplicity in data recording, to the extent possible. In a data-centered system, all data users and recorders should use standard practices so common tools can be used to share and use data, thus increasing efficiency.
3. Allow modeling tools to override official data, as needed. Because the modeling tools were meant to be generic, they could not effectively trap all data problems and implement fixes without becoming complicated and difficult to maintain. Therefore, utilities were implemented to allow the users to reset database values to correct problems. This overriding feature allows the State of Colorado to correct data problems in due time and lets modelers selectively edit data so that modeling can continue.
4. Understand the limitations of third-party data. The CRDSS database stores streamflow records from the U.S. Geological Survey (USGS), climate data from the National Oceanic and Atmospheric Administration (NOAA), and snow data from the Soil Conservation Service (SCS). In some cases, the CRDSS team found blatant errors in this data (for example, negative solar radiation, presumably from a badly calibrated gage). Rather than try to correct the data and compromise the tractability of the data, users of the system need to use good engineering judgment, as with any other engineering project.
5. Make the data available to as many people as possible. A common practice among the consulting community is to use USGS or other data and, if a problem is found (e.g., a water balance does not compute), make reasonable assumptions and continue with an analysis. There is seldom either time or budget to notify the data suppliers. However, for data that is controlled within the realm of the CRDSS (State of Colorado data), users (especially State of Colorado staff) who do find problems have a more direct channel of communication to allow data corrections. Additionally, CRDSS tools make it easier to detect data inconsistencies so that they can be corrected.

In summary, data quality problems were identified during both the database population and modeling activities. The quality problems have been prioritized, and the State of Colorado has invested resources to correct them. Techniques were developed to allow the modeling to proceed while data problems were corrected in a prioritized manner.

WATER RESOURCE PLANNING MODEL

The WRP model selected for use in CRDSS is called StateMod. This tool is a monthly water allocation and accounting model that had been developed for a series of projects by the State beginning in 1986. It is capable of making comparative analyses for the assessment of various historic and future water management policies in a river basin using the Prior Appropriation Doctrine (first in time, first in right). StateMod's operation is governed by hydrology, water rights, and operating rules. It recognizes four types of water rights: direct flow, instream flow, reservoir storage and operational. The direct flow, instream flow, and reservoir storage rights are self-explanatory. The operational rights are used to control complex, multi-structure activities associated with reservoir releases, exchanges, and carrier ditch systems. Key features of the model required to simulate the diverse operating conditions encountered on the western slope of Colorado include the following:

- Simulates tributaries and main stem river systems through the use of a tree-structured network
- Simulates direct flow, instream flow, storage and operation rights under the Prior Appropriation Doctrine as a function of water availability, priority, decreed amount, demand, structure capacity, and location
- Allows reservoirs to be operated with multiple accounts serving multiple users
- Allows instream flows to be operated as a point or river reach
- Simulates a wide variety of operating agreements and exchanges between several users or structures

- For a given structure, simulates one or more water rights, with one or more return flow patterns returning to one or more stream nodes
- Uses an efficient direct solution algorithm that recognizes the impact of a diversion's return flows during the current time step without having to iterate
- Estimates base or natural streamflows from gaged or estimated streamflow, diversion, and reservoir data

Baseflow Data: The generation of base or natural stream flows for a WRP application is necessary in order to analyze a "what if" scenario which includes a water right, structure, or operating strategy that might change in the future. Baseflow is a generic term defined herein to describe gaged stream flows that have been adjusted to remove a portion (0 to 100 percent) of human impact. If a user decides to remove all human activities (100 percent), then the baseflows generated are commonly called natural streamflow. If a user decides to remove only a portion of human impact, then the remaining impacts are "left in the gage."

Baseflows were created efficiently and consistently within CRDSS using the Baseflow module of StateMod. This module uses historic streamflow, diversion, and reservoir storage data to remove human impact for any number of structures that might be important for future development. Along with this historic data, the baseflow module uses the same water use parameters (efficiency, return flow timing, and return flow locations) that are used in the historic simulation. The key benefits resulting from the standard approach used to estimate baseflows within CRDSS include:

1. Parameter consistency: The same parameters used to estimate baseflows are used during the calibration to historic data.
2. Efficient baseflow generation: Baseflows can be quickly revised in response to calibration results or model refinements (e.g. include more historic structures).
3. Efficient calibration: Knowledge of historic data stored within the memory of the program provides an efficient mechanism to compare simulated to gaged stream flows, diversions and reservoir levels.

The Model Network: The model network describes the physical connectivity of the structures and gages being modeled. StateMod uses a network file that describes model nodes in an upstream to downstream fashion. **Figure 2** illustrates part of the network for the White River basin. This schematic representation of the network is useful for modeling and can be aligned to closely match the true orientation of the basin. Nodes are labeled with structure identifiers (State of Colorado identifiers or USGS stream gages). The figure illustrates the use of stream flow gages (e.g., 0903000), minimum streamflow reaches (e.g., upper terminus 432339 and lower terminus 432339_Dwn at top of figure), aggregate demands (e.g., node ADW_001 above the 09303000 gage), and the use of baseflow nodes, as discussed in the previous section.

The data used to plot the model network diagram shown in **Figure 2** is also used by utility programs to build most of the data files required by StateMod by querying the CRDSS database. The process begins with a single network file that describes the reaches and nodes in the model network. This file is processed to produce the network diagram, the StateMod-format network file, and several other files that contain structure and station information. These files are then processed by utility programs to create StateMod files containing data such as streamflow, diversion, demand, and water rights. During processing, command files can be used to override the database values, allowing the modeler to make adjustments for inaccurate or inappropriate data. The data flow sequence used to develop a StateMod network and supporting files has been fine-tuned to allow efficient modification and generation of data sets. Key benefits of this approach are the following:

1. Reproducibility: Model data sets can be reproduced quickly and accurately to react to new data, etc.
2. Documentation: Modeling assumptions are documented within the command files used to access the database.
3. Extensibility: Structures can be deleted or added and new data files build quickly and accurately.

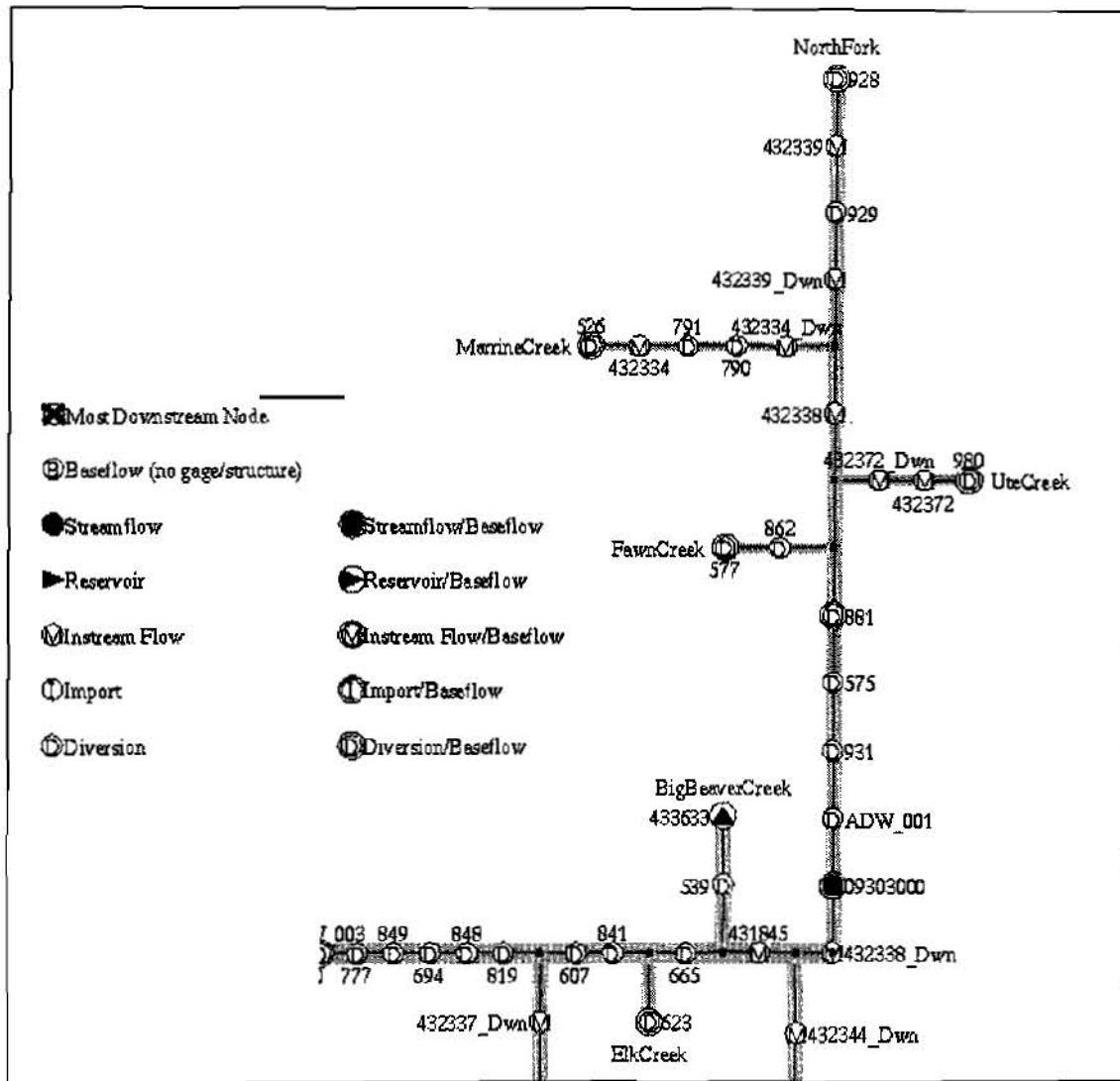


Figure 2. Example of Part of a StateMod Network Diagram - the North Fork of the White River

Model Size: To be cost-effective, meet deadlines, prove functionality, and meet the immediate needs of the State, the first phase of WRP development included only key structures. Key irrigation and municipal and industrial structures were selected for each river basin as follows:

1. A list of absolute decreed water rights for each structure was compiled and ranked.
2. The cumulative absolute decreed amount and percent of the basin total were determined.
3. Preliminary key structures were selected to represent 75 percent of the basin's cumulative absolute decreed amount.
4. Final key structures were determined after meeting with each basin's division and district engineers. These meetings resulted in the addition of new structures that were below the cut off but were considered important for administration. These meetings also resulted in the deletion of some structures that met the cutoff but which historically diverted significantly less than their decreed amount or they had been abandoned.

A similar approach was applied to reservoirs, instream flows, and stock ponds. The decision to explicitly model only key structures reduced the number of nodes included in each model from 80 to 90 percent, while simulating over 75

percent of each basin's water use. This version of modeling data used base flows that had been naturalized to 75 percent.

A second phase of WRP development, which is currently under development, is modeling the remaining water use in each basin by defining a number of spatially-located aggregated irrigation structures, reservoirs, stock ponds and municipal and industrial nodes. This version includes all instream flows that exist on the rivers and streams modeled. It includes aggregated irrigation structures, reservoirs, and stock ponds that were determined using GIS, based on their location relative to key streamflow gaging stations. It also includes aggregated municipal and industrial use that was determined to equal the difference between per capita water use estimates and explicitly modeled municipal and industrial structures. The enhancement from approximately 75 percent water use to 100 percent water use increased the number of modeled nodes by approximately 10 percent, still significantly less than explicitly modeling every structure. It was relatively easy to implement because of the data-centered approach discussed previously. Because this version of modeling data includes 100 percent of the basin water use, the base flows developed were natural flows.

Streamflow Data: Streamflow data is a key component to any WRP application. Unfortunately, it is typically available at a limited number of locations with a limited period of record. Therefore a mechanism is required to fill data gaps at gaged locations and distribute gaged data to ungaged portions of a watershed. To provide consistency and flexibility the following approach was used to develop streamflow data for the WRP within CRDSS:

1. Data filling parameters were developed. A control file containing data filling parameters was developed that allowed missing data at gaged locations to be filled on the fly when retrieving streamflow data from the centralized database. Key data filling parameters included the independent and dependent variables, regression type (linear or non-linear), and number of equations (annual - 1 equation versus monthly - 12 equations).
2. Proration factors were developed. For each gaged and ungaged location requiring streamflow data, the drainage area and average annual precipitation were developed using GIS. These proration factors thus provided a consistent, map-based approach to distribute gaged streamflow data to ungaged locations.

Diversion Data: Historic diversion data are used within the WRP model to estimate baseflows and to calibrate the model to historic observations. As discussed previously, one challenge was to develop a number of basin models in a cost-effective manner using data of varying quality. The diversion records available to CRDSS are of relatively high quality for large, key structures; small, less important structures typically have less frequent recordings. Similar to streamflow record filling, diversion records queried from the CRDSS database were filled on the fly using a control file provided by the user. Typical data filling approaches included the following:

1. If diversion records for a structure are not available at the beginning or end of the simulation period, fill with zeros.
2. If diversion records are unavailable during the study period, fill using the long-term historic average.
3. If neither of the simple data filling approaches just described are adequate, allow the user to provide a time series that overrides the information available in the database.

The last approach was used when the simpler data filling techniques were inadequate and when official database records were determined to be non-representative of current conditions. For example, the database records may indicate that a diversion was in place for 20 years with 3 years of missing record. Under the simple data filling approach, the missing years would be filled with the long-term average. However, if it is known that the diversion headgate was washed out during that period, a replacement time series having zeros during the 3 years could be specified.

Demand Data: Agricultural, municipal, and industrial demands are input to the StateMod model in order to divert and use water according to Prior Appropriation Doctrine. Demands are associated with diversions that are included in the network and may consist of explicitly modeled or aggregated structures. Municipal and industrial demands were estimated based on historic use. Irrigation demands were estimated from acreage, crop, and climate data.

Acreage data was developed in cooperation with the U.S. Bureau of Reclamation (USBR) by using aerial photography to construct GIS coverages of acreage for the entire western slope of Colorado for 1993. The State of Colorado then performed field surveys to verify the irrigated parcels, identify the crop grown, and tie each parcel of land to one or more headgates serving the land. The CRDSS team then assigned climate stations and weights to allow farm crop requirements to be estimated using the Blaney-Criddle approach. When combined with irrigation system efficiency estimates, river headgate demands were generated for each irrigation structure modeled.

System Efficiencies: One of the key pieces of data required by a WRP that is not generally gaged is the irrigation system efficiency (the ratio of water used to water diverted). For most WRP applications, irrigation system efficiencies are estimated based on agricultural practices, canal length, soil type, etc., but this approach requires significant knowledge of every diversion and can become highly subjective during the calibration process. As an alternative, the CRDSS team used consumptive use estimates in conjunction with historic diversion records to develop an average monthly efficiency for every irrigation structure modeled. For example, if a structure diverted 100 acre-feet of water in May, 1980, while the estimated demand is 30 acre-feet, then the system efficiency for that month is 30 percent (30/100). During a year, the annual efficiency might average 20 percent while monthly efficiencies might range from 10 to 40 percent. A similar range can be observed for one month from one year to the next. Therefore, these estimates could not be used without review because of data issues, irrigation practice variations, etc. However, once the data problems were resolved, the computed efficiencies seldom required adjustment during calibration.

One limitation of StateMod is that monthly efficiencies cannot currently be varied from one year to the next. Consequently, changing irrigation practices to reflect structural improvements or water management practices during water-short conditions cannot be fully reflected. A potential enhancement to StateMod might be to read in irrigation crop requirements and dynamically calculate monthly irrigation efficiencies.

SUMMARY

Previous sections illustrated some of the technical challenges that were addressed in implementing a WRP model into the CRDSS. Development efforts spent on constructing the centralized database and developing utility tools to access that data were only fully realized after applications to scenarios were implemented. For example, scenario data sets needed to be constructed to study different issues such as making a conditional water right absolute or inserting a new instream flow, diversion, or reservoir.

Figure 3 illustrates the Big Picture Plot feature of the StateMod graphical user interface (GUI). This graphic shows the difference in diversions between two scenarios, with upward bars indicating that the diversion received more water under the second scenario, and downward bars indicating a decrease. The size of the bar indicates the magnitude of the change. Consequently, WRP model users are able to see a basin's response to an input change. This type of display illustrates the power of the CRDSS and its potential for helping make decisions at different levels. The Big Picture Plot can be used by managers studying long-term average impacts, whereas hydrograph plots at a gage might be more useful to someone studying the time varying impact at a location on the river (such as an instream flow study). CRDSS offers display tools for various output levels to satisfy the needs of water managers.

REFERENCES

The CRDSS home page, <http://crdss.state.co.us>

Blaney(1952), Blaney, H.F., Rich, L. R., Criddle, W.D., et. al. (1952), "Consumptive use of water", Trans. ASCE, 117:948-967,

StateMod Users' Manual, on-line at <http://crdss.state.co.us/manuals/statemod/statemod.html>

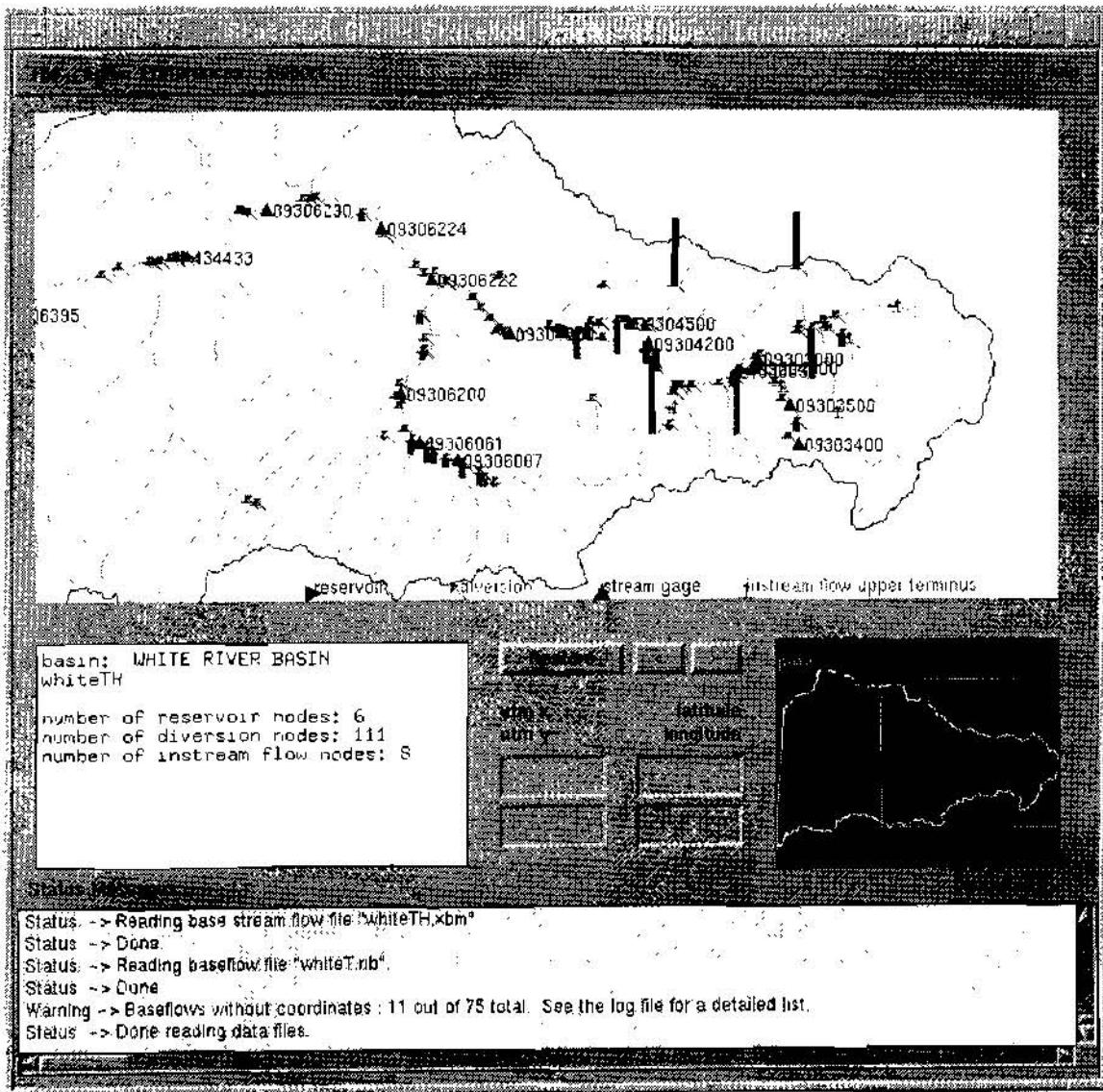


Figure 3. StateMod GUI Big Picture Plot

HYDROLOGIC FORECAST AND ANALYSIS MODELING (HFAM)

**Laura Mariño and Norman H. Crawford, Hydrocomp, Inc.,
3 Lagoon Drive, Suite 150, Redwood City, Ca 94065**

Abstract: Hydrologic modeling based on digital computers has been actively developed at research institutions for nearly forty years. Analog computer models for surface hydrology and groundwater systems were in use fifty years ago. Hydrologic models are "of an age" where their characteristic benefits and limitations might be well understood, yet hydrologic modeling still suffers from myths and misunderstanding. Some model users assume modeling results are reliable, irrespective of how the model was applied. Others distrust models and use "tried and true" formulas like $Q=CIA$, even though all hydrologic methods contain implicit modeling assumptions.

Hydrologic modeling has the obligation to calibrate and verify performance vs. field measurements, an obligation shared by all models of physical systems. In application a hydrologic model is a surrogate for watersheds and facilities. Failure to calibrate a model adequately makes all subsequent applications of the model suspect.

This paper outlines the scope and applications of continuous hydrologic simulation modeling for river basin planning and water resource facilities design and management. It defines the terms "conditional flood frequency" and "current value of release" explains their significance for flood control and reservoir management.

HYDROLOGIC MODELING

Hydrologic Processes

HFAM is a successor to Stanford Watershed Model series and Hydrocomp's HSP and HSPF models (Crawford and Linsley, 1966, Johanson et. al. 1980). Processes on the land surface; infiltration changes in soil moisture storage, actual evapo-transpiration, surface runoff, interflow and groundwater flow are simulated continuously. Streamflow is simulated by calculating continuous depth and velocity of flow in stream reaches using kinematic wave assumptions.

HFAM includes simulation of water resource facilities such as reservoirs and diversions and is developed to aid both facilities operation and design.

The data input requirements for modeling in Figure 1 are precipitation and potential evapo-transpiration. Precipitation data are from hourly and daily stations. Potential evapotranspiration is estimated from Class-A Pan records. Additional data are for topography, soils and vegetation in the watershed developed using GIS systems.

Snow accumulation and melt is modeled using 'theoretical melt' equations, where air-snowpack heat exchange due to convection, net solar radiation, long-wave radiation exchange, condensation and rain melt are included. Groundmelt is also included. In watersheds where snow is important

the additional data requirements are air temperature, wind movement and solar radiation (which may be calculated from cloud cover and clear sky radiation).

A flowchart for land surface/surficial processes in HFAM is shown in Figure 1.

Surficial Hydrologic Processes

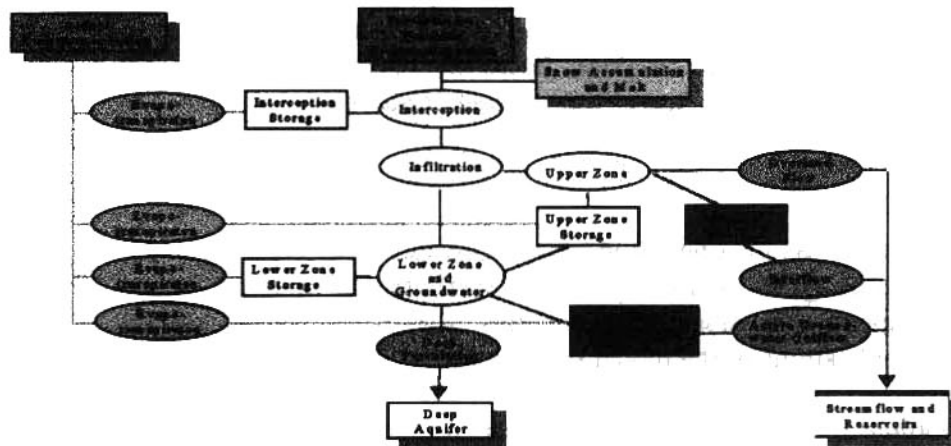


Figure 1

A flowchart for snow accumulation and melt processes is shown in Figure 2.

Snow Accumulation and Melt

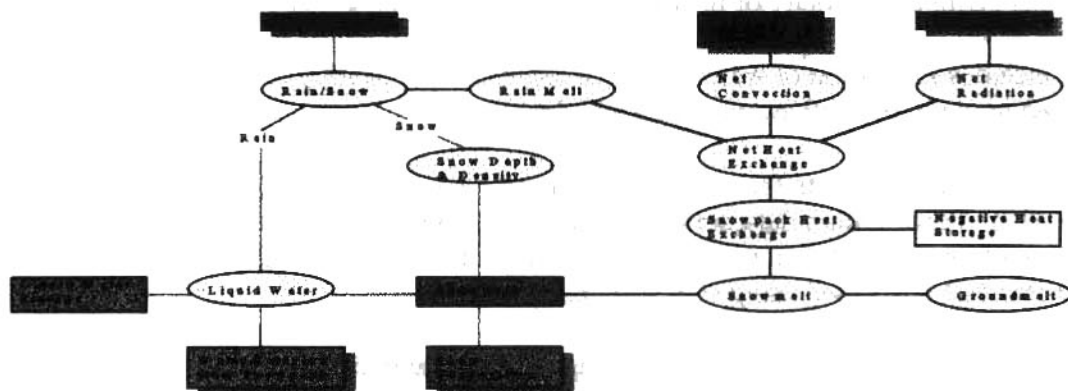


Figure 2

Management of Hydrometeorologic Data

Hydrometeorologic data is entered and is maintained in three HFAM databases, for *forecast*, *real-time* and *historic* data. Data storage is on daily and hourly intervals. Data input is from ASCII files, and commonly used data formats are supported. Data can be updated interactively, and can be inspected graphically. Data summaries of weekly, monthly, and annual time intervals are available.

Modeling results are available for the same time intervals as are model input data, and can be inspected graphically or printed in summary reports on weekly, monthly, and annual time intervals.

Modeling Water Resource Facilities

Water resource facilities are included in HFAM in by entering their characteristics on input screens. Types of facilities that are included are reservoirs, power plants, spillways, and diversions. Any number of facilities can be used.

HFAM does *Forecast*, *Probabilistic* and *Analysis* runs (Mariño, 1990). The results produced by each type of run are described in the following sections.

HFAM Forecast Runs

Forecasts for streamflow or inflow to reservoirs are typically made with a weather forecast, and are three to seven days in length. The current 'watershed state' or soil moisture, groundwater, and snowpack conditions are maintained by HFAM and are used as the forecast begins. During high flows or when major storms are expected, quantitative precipitation forecasts are used for model input. Since only one weather sequence is used for HFAM Forecast runs, the streamflow forecasts are single valued or deterministic.

Forecast runs require input of the 'watershed state', and meteorologic conditions for the period of the run, so they can be used to study extreme conditions. When HFAM is calibrated for a watershed, and when a historic watershed state that would cause maximum runoff is combined with probable maximum meteorologic conditions, a forecast run will create a probable maximum flood.

Forecast runs combining various historic watershed initial conditions with historic storms are a useful educational tool; e.g., "How large would the flood of 19xx have been if it occurred at a low watershed soil moisture initial condition?"

It is possible to augment meteorologic forecasts with historic meteorologic data to make longer forecast runs. For example, a user might assume that a historical very dry weather might be repeated and examine how reservoirs would behave over the next several months for this condition.

Forecast runs require only a few seconds to complete, and can easily be repeated for alternate weather forecasts. Figure 3 is a sample of HFAM Forecast run results.

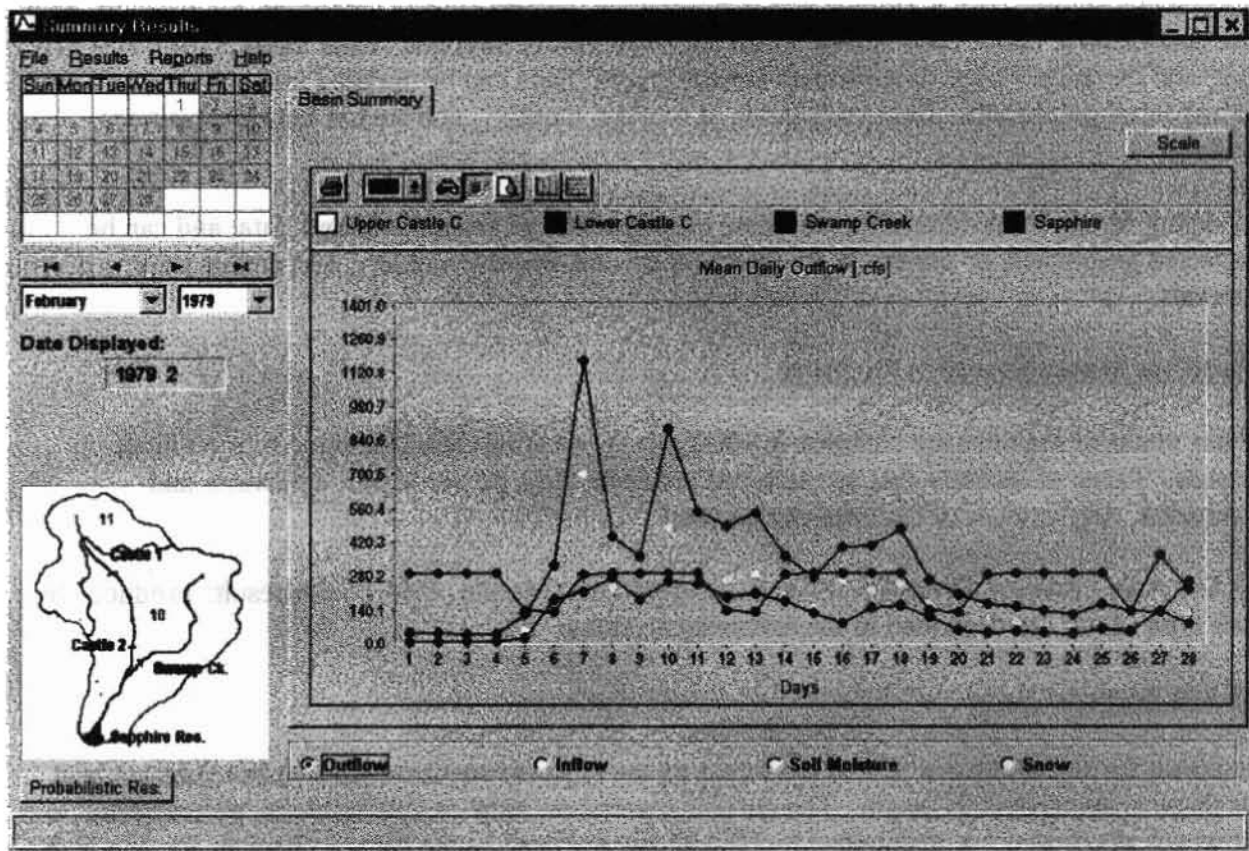


Figure 3

HFAM Probabilistic Runs

HFAM Probabilistic runs, like Forecast runs, use the initial or current 'Watershed State' of soil moisture, groundwater, and snowpack conditions that are maintained by HFAM. These runs are typically several weeks to one year in length. Since deterministic weather forecasts are not generally available for periods greater than one week, 'alternate future' weather sequences are used. Historic weather for the period of the probabilistic run is used. When a fifty to eighty year historic data base is compiled for a watershed, results from Probabilistic Runs show probability distributions for streamflows, reservoir levels, diversions, water deliveries for irrigation, hydroelectric generation, etc.

The initial watershed state is key to probabilistic runs. Streamflows with watershed initial conditions for June 1 1987, simulated with June to December weather from 1942 do not match streamflows measured in 1942. The mean and the variance of future simulated streamflows in a probabilistic run do not match the observed historic mean and variance, due to the unique watershed initial condition used in a probabilistic run. Historic observed streamflows have a range of watershed initial conditions on June 1st.

Figure 4 is a sample of HFAM Probabilistic Run results.

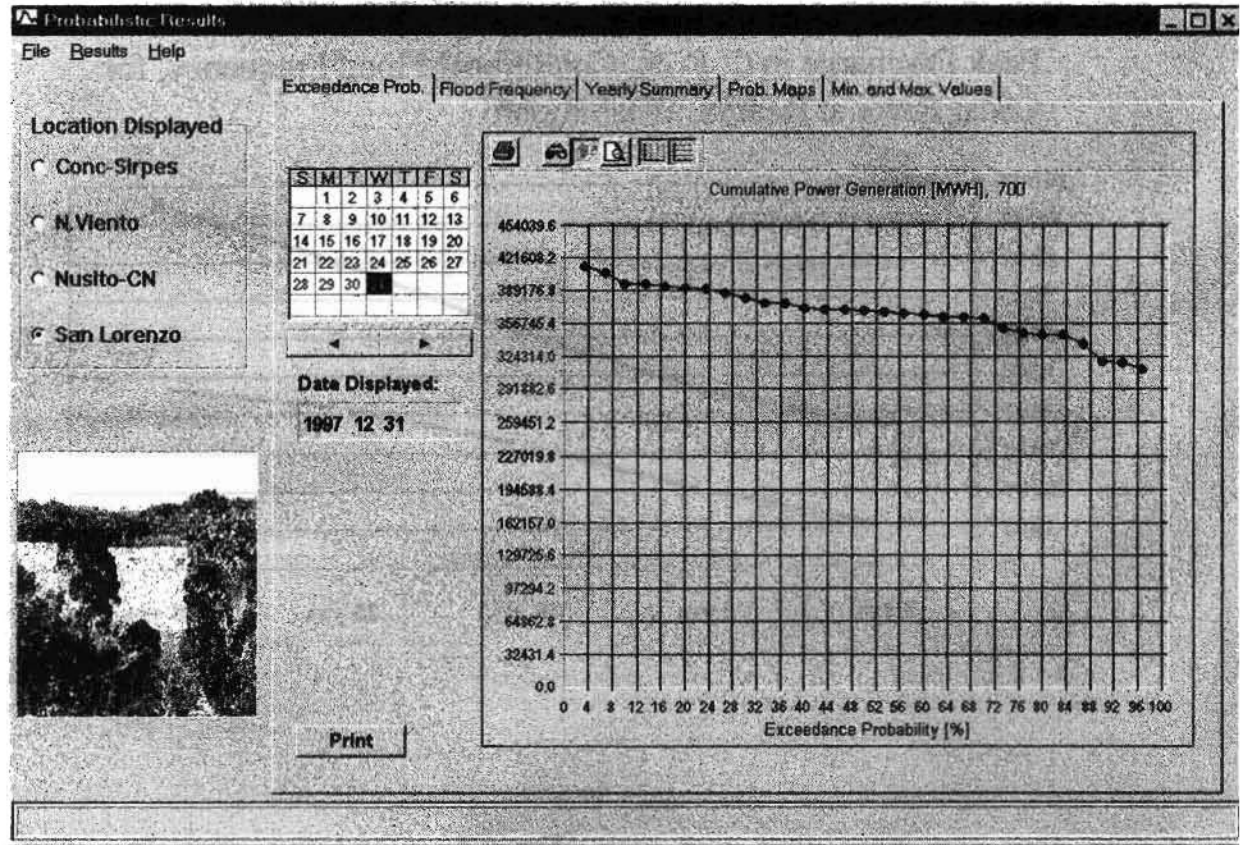


Figure 4

Conditional Flood Frequency:

HFAM Probabilistic Runs create "near-term" or "conditional" flood frequency. Conditional flood frequency depends on the watershed state as the model run begins - for example, the snowpack in a watershed may be at a historic maximum in late April. This watershed initial condition combined with 80 alternate historic weather sequences for May and June will show flood frequency for the current year. These conditional flood frequency results might be considerably larger than the long-term flood frequency found from stream gage records.

Figure 5 illustrates conditional flood frequency from HFAM Probabilistic runs for Cedar River at Renton, Washington (USGS 12119000). Conditional flood frequency for the period June 1st to September 30th is shown for June 1st initial conditions in 1975, a wet year, and in 1987, a dry year. It is logical to use conditional flood frequency for reservoir flood control operations and flood emergency planning. If current watershed initial conditions are such that the 1-% long-term peak

flow has a 5-% probability of occurring in the next six weeks, it is prudent to make use of this information.

Peak Discharge in C. F. S., Conditional Flood Frequency, for Cedar River at Renton, Washington

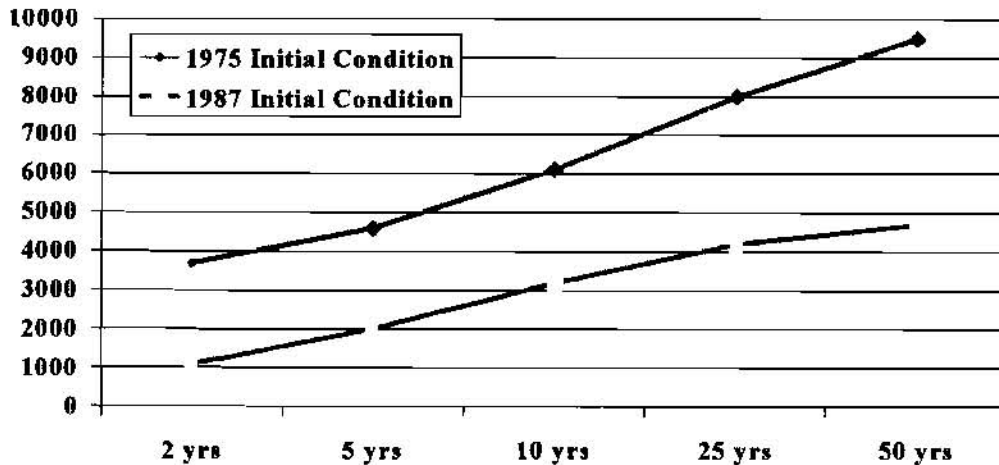


Figure 5

Current Value of Release at Reservoirs:

Probabilistic Run results are the basis for optimal analysis of reservoir operations. When future economic or environmental value of reservoir releases are defined, HFAM will show the 'current value of release', in \$/unit volume, and the current optimal release in cubic ft. per second or acre-feet per day. Releases greater or less than this optimal release will reduce future economic or environmental values below optimal levels.

HFAM Analysis Runs

HFAM Analysis Runs are used for two purposes, calibration of model parameters and long term continuous simulations of watershed and facilities.

Parameter Calibration:

Hydrologic models, like the meteorologic general circulation models (GCMs) and almost all models of physical systems, must be calibrated to verify their performance vs. field measurements.

This is a scientific obligation. It is not prudent to use a hydrologic model without analyzing its reliability for the problem at hand with through calibration. Calibration creates a model specific to a particular watershed. HFAM is calibrated for each application.

**Figura 4.4 Curvas de Duracion de Caudal Diario
Rio Concepcion - Los Sirpes,**

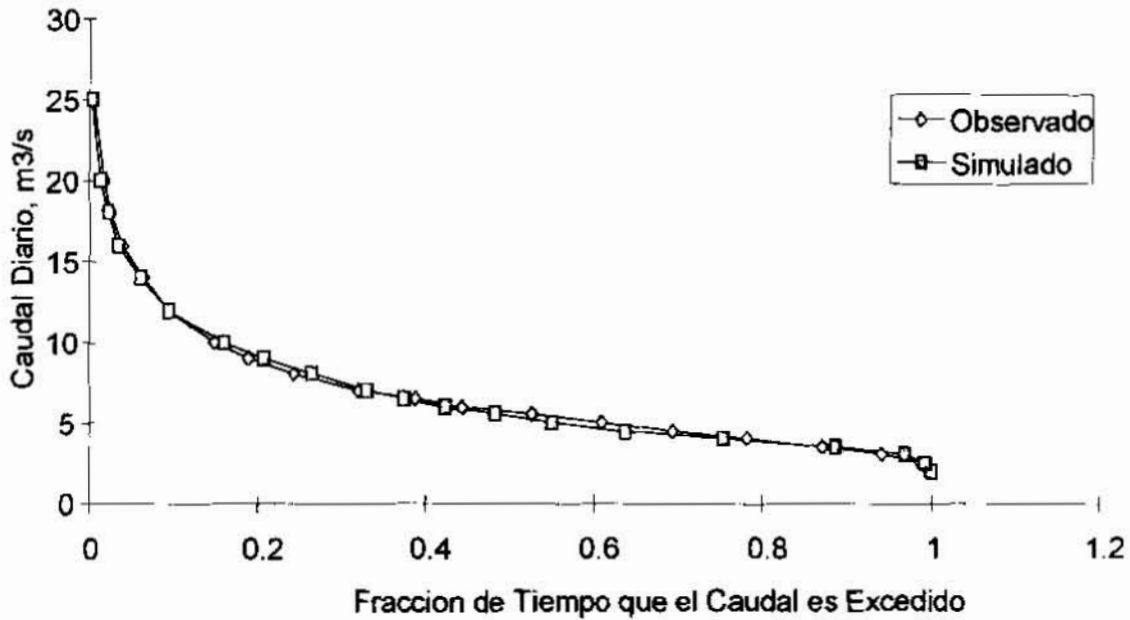


Figure 6

Peak Flow Frequency, Diamond River nr. Wentworth, N. H.

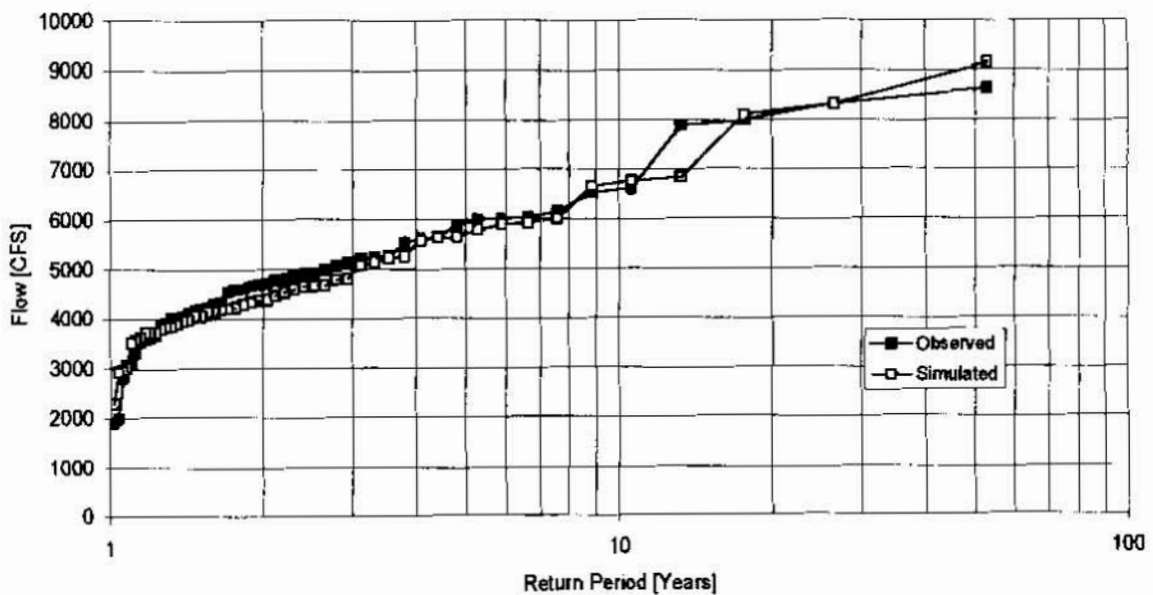


Figure 7

Continuous simulation models are calibrated with many years of hydrologic and meteorologic data. Typical 'simulated' and 'observed' results for daily flow duration are shown in Figures 6 for Rio Concepcion at Los Sirpes in Colombia. Figure 6 compares daily flow duration curves, simulated and observed for the period 1982 to 1996. Figure 7 compares simulated and observed flood frequency for Diamond River at Wentworth Location, N. H. for the period 1942 to 1993 (USGS 01052500).

Calibration methods for HFAM land and snowmelt parameters are outlined in the Hydrologic Journal on Hydrocomp's Web site, at <http://www.hydrocomp.com>.

Watershed and Facilities Simulation:

Long-term continuous simulations of watersheds and facilities over the historic hydrometeorologic data base that is available in a watershed, which in the United States is typically seventy to eighty years, are used for design studies. Water yield from reservoirs or diversions, drainage design, and flood frequency with and without detention basins are typical applications. Planning and environmental studies for effects of urban development, or the effects of agricultural or forestry operations in watersheds are done with HFAM Analysis runs. At water resource facilities, reservoir operating rules for power generation or environmental compliance can be studied.

Summary

Modeling hydrologic processes and the operation of water resource facilities is entering a new era. Powerful computer systems that were once expensive and limited to air-conditioned rooms are now widely distributed. We can now use computers to model physical processes in greater detail: Flood frequency is not a time-invariant watershed characteristic - its time dependency is due to season of the year and watershed state. Future streamflow probability *this year* is more relevant to environmental goals than long-term means. Operation of water resource facilities can be optimized continuously in time, and economic and environmental goals can both be enhanced when the dynamic nature of watersheds is taken into account.

REFERENCES

Crawford, Norman H. and Ray K. Linsley, Digital Simulation in Hydrology: Stanford Watershed Model IV, Technical Report No. 39, Department of Civil Engineering, Stanford University, July 1966

Johanson, Robert C. et al, Users Manual for Hydrological Simulation Program - Fortran (HSPF), EPA-600/9-80-015, Hydrocomp, Inc. April 1980

Mariño, Laura, Seattle Forecast Model (SEAFM), Users Manual, Hydrocomp, Inc. for the Seattle Water Department, 1990

Contact: **Laura Mariño, lmariño@stanford.edu**
Norman Crawford, norm@hydrocomp.com

PC HYDROSS Simulation System (PCHSS) A Graphical User Interface for the HYDROSS Model

By Nancy L. Parker, Bureau of Reclamation, Denver, Colorado, and
David A. Patterson, Computer Programming Contractor, Fort Collins, Colorado

Abstract: HYDROSS (Hydrologic River Operation Study System) is a surface water supply and hydrologic accounting model that has been used in the Upper Missouri/Great Plains Region of the Bureau of Reclamation for 20 years. Originally developed on a Cyber mainframe platform, it was ported in 1991 to run under DOS on a PC. In 1997, the Great Plains Region funded the development of a graphical user interface for HYDROSS. The intent of the GUI was to make HYDROSS easier to use by automating the preparation of highly formatted input files, to further automate the report process, and to facilitate the graphical display of output. An earlier attempt to develop a GUI for HYDROSS had succeeded in producing a good design concept, but the overhead of UNIX and Ingres database systems administration proved too cumbersome for most model users. This new effort changed little of the "look and feel", but took advantage of advancing PC technology to produce a product which can be used by anyone who can create an ascii text file and use common spreadsheet software. PCHSS was produced for minimal cost, it has proven to be a useful and therefore powerful tool for both experienced HYDROSS users and novice modelers, and it has also been a catalyst for the expansion of model capabilities.

INTRODUCTION

HYDROSS is a surface water supply model developed to assist in planning studies for evaluating existing and proposed demands on a river system. It is intended to operate over the period of record, simulating the effect of the existing and proposed features on the historical pristine flows and can be thought of as a hydrologic accounting model which allows the user the flexibility to conduct "what if" studies. The river system modeled is characterized by a flow network. The network includes nodes, called stations in HYDROSS, which represent reservoirs, demands, river confluences, and points of known flow. Links between nodes are symbolic of river reaches and canals. Basic input to the HYDROSS model consists of three data files; flow data, table data and network data. Conceptually, the Flow File contains the pristine monthly flow data at gaging stations in the system to be modeled. The Table File is a means for introducing operational parameters into the model. The Network File furnishes HYDROSS with a physical description of the study area: how the stations connect, physical facilities and supply requirement locations. HYDROSS operates on the data in a strict sequential order in time (results from one month depend on the system state at the end of the previous month), space, (results at one station depend on what is happening upstream and/or downstream), and priority (earlier water right dates are allowed water before later water right dates).

Water allocation in HYDROSS is structured so that flows are spatially and temporally allocated in accordance with *water right priorities*. Instream flows, reservoir power, storage demand, and diversions can be assigned a water right priority. An *instream demand* requires flow to be maintained in the river at a given station. A *power demand* is the flow required at a power plant associated with a reservoir. A *storage demand* is used to fill reservoirs. A *diversion demand* depletes water from the river and potentially denies water to other users with junior water rights. Diversions may occur

at any station, and there is no limit to the number of diversions per station. Up to 9,998 diversions can be assigned per river system. The user can assign efficiencies to both canals and diversion sites.

Reservoir operations in HYDROSS are controlled using five reservoir content levels. The *absolute maximum* and *absolute minimum* levels are based on the physical limitations of the dam and outlet works. The *maximum* and *minimum* levels are limits which can vary month to month and year to year. The *target* level is used to share water among several reservoirs at the end of each month via a pool maintenance routine which attempts to balance storage among a system of reservoirs. Power at a reservoir is computed using discharge, head, and efficiency data. Stored water can be called on to satisfy project demands and instream flow requirements. Reservoir seepage can be simulated as a function of elevation or capacity, or by using monthly values which can change year to year.

Return flows originate from diversions or reach losses and may return at any station within the river system. Return flows may be delayed up to 11 months. The user can assign efficiencies to return flows. The user can assign channel capacity at any station. HYDROSS will not willingly release stored water which exceeds channel capacity.

THE NEED FOR A GRAPHICAL USER INTERFACE

First developed nearly 20 years ago, HYDROSS was originally used in command line mode by preparing the input files and typing commands at an operating system prompt. A Graphical User Interface was first developed for HYDROSS in 1991-92, running on a UNIX workstation under XWindows, written in C and Motif, and using an Ingres database to store model data and manage scenarios. As PC-based software caught up to the graphical capabilities of the X environment and most HYDROSS users remained partial to the IBM-compatible PC, it became apparent that the overhead of the new GUI was prohibitive.

At the same time, HYDROSS was being used in an increasing number of modeling studies, and the old command line mode of operation was quickly becoming archaic due to the popularity of PC windowing environments. In 1997, a new effort was undertaken to produce a GUI which would satisfy the need to facilitate input preparation and the presentation of model output while not requiring the user to learn any cumbersome new software or procedures.

NETWORK BUILDER IMPROVEMENTS

The overall look and feel of the original interface had been well received and this was kept largely intact. All icon designs were retained and the basic functionality of the network builder remained the same - icons can be selected and placed on the screen and connected together to create the schematic diagram that represents the model. Some convenient enhancements were also added - some part of the initial new design and others at the suggestion of users who tested early versions. Icons can now be sized, links are color coded to distinguish station and demands, links anchoring labels and icons together and lines representing return flows can be toggled on and off to aid the system developer in keeping track of what has been done, and sections of the network can be "glued" together to make it easy to move icons around together. Popping up data editors, connections, disconnections, and

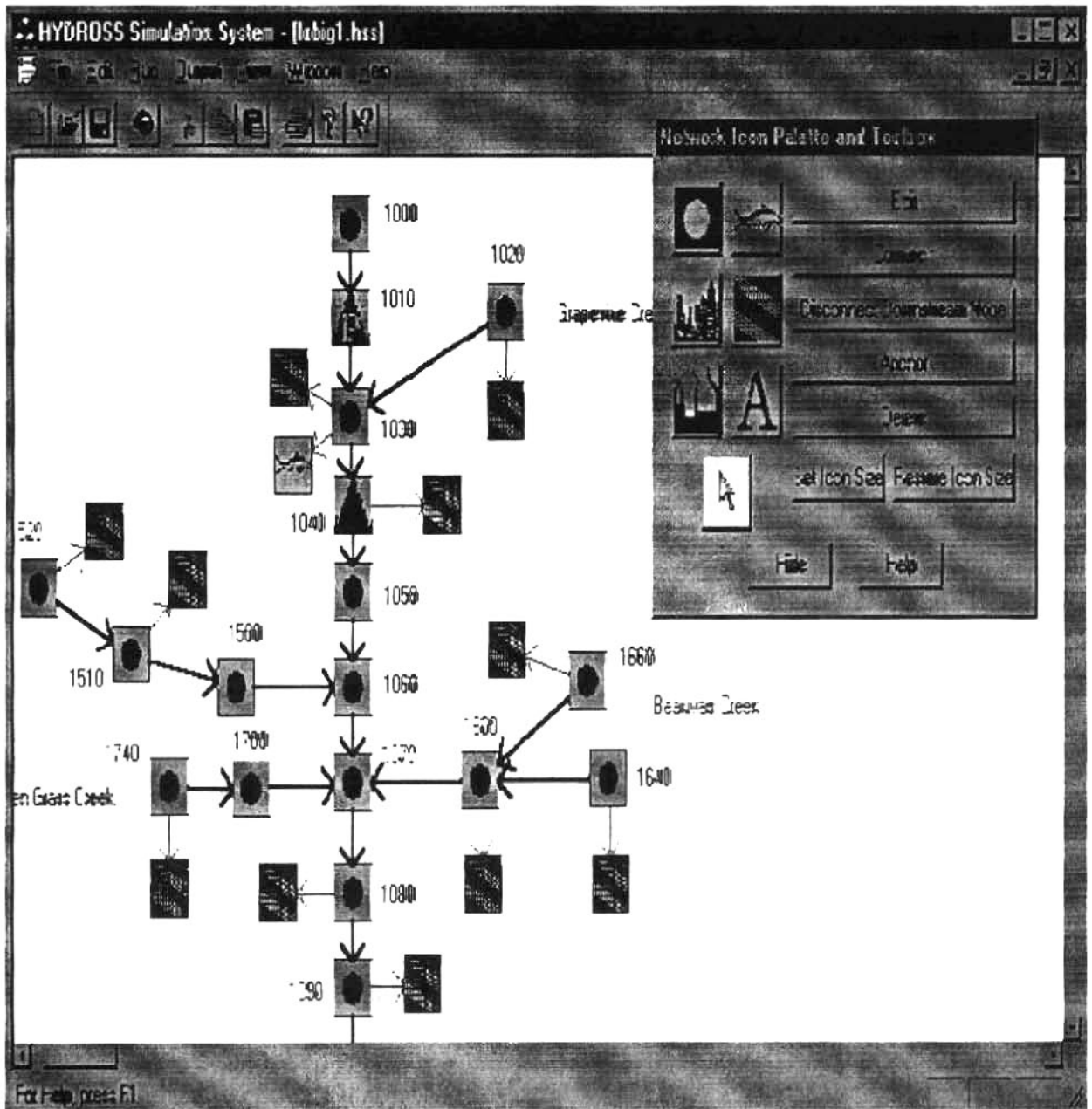


Figure 1 - A Network Schematic Diagram and the Network Builder Palette and Toolbox

anchoring can all be done in multiple ways (double clicking, left clicking, menus, buttons) to accommodate as many user habits as possible.

A NEW DATA STORAGE APPROACH

One of the intentions of the database design in the original GUI had been to conserve storage space. Given the proliferation of ever larger hard disk drives however, this objective had lost most of its importance. For the new system, it was decided that all data would be developed and stored in ascii

files that the users would maintain in whatever directory hierarchy suited their purposes. These files could be used by more than one scenario if appropriate, but separate copies could also be made for each scenario. It would be up to the user to be as conservative or excessive with his or her individual use of storage space as warranted by computer limitations.

HYDROSS requires data in three basic formats - time series data, table (parameter/function) data, and individual values. Two simple ascii formats were defined - one for time series input data and one for tables. For every data item that requires a time series or table, the user must prepare an ascii file and save it using a name they can associate with the data requirement. In the data entry screen, instead of importing or entering all of the data in some way, the whole path and name of the file is specified along with the units to be used for the file, as shown in Figure 2.

The interface data file which stores information about the connectivity etc... of the schematic network also stores all of the individual data values for the scenario and the paths and file names of the ascii files that have been specified for the various time series and table data items. This *.HSS file plus the set of ascii files that hold the time series and table data can be easily copied and transferred from one PC to another. Should a user want to use a different directory hierarchy to store the ascii files, there is a utility which strips the existing path strings from the *.HSS file and replaces them with new path strings. This allows users to maintain their individual preferences in storing data files as desired.

OUTPUT PROCESSING

The PlotFile utility enables the user to write selected output data items to a commas-and-quotes delimited file which can then be imported into any spreadsheet and graphed in the style desired. The design of the utility (Figure 3) allows output from two or more scenarios to be written to the same output file and then compared graphically. In this way, the automatic formatting of output data in a manner easily graphed goes significantly beyond the existing report options which only can extract data from the output of one scenario at a time.

HYDROSS has a good set of report options that extract requested data from the single output file and write it in a clearly labeled and easily readable format. Detailed reports are available for station activity, reservoir operations, diversion activity, station flows, shortages, limitation and constraints, and statistics. The original GUI automated the selection of these options, and displayed the written report on the computer screen. The option selection automation was kept largely intact in the new effort, although some archaic options were eliminated. The greatest change was that the new utility requires that the user enter the name of a text file to which the report will be written. The report can then be viewed with any text editor of the user's choice.

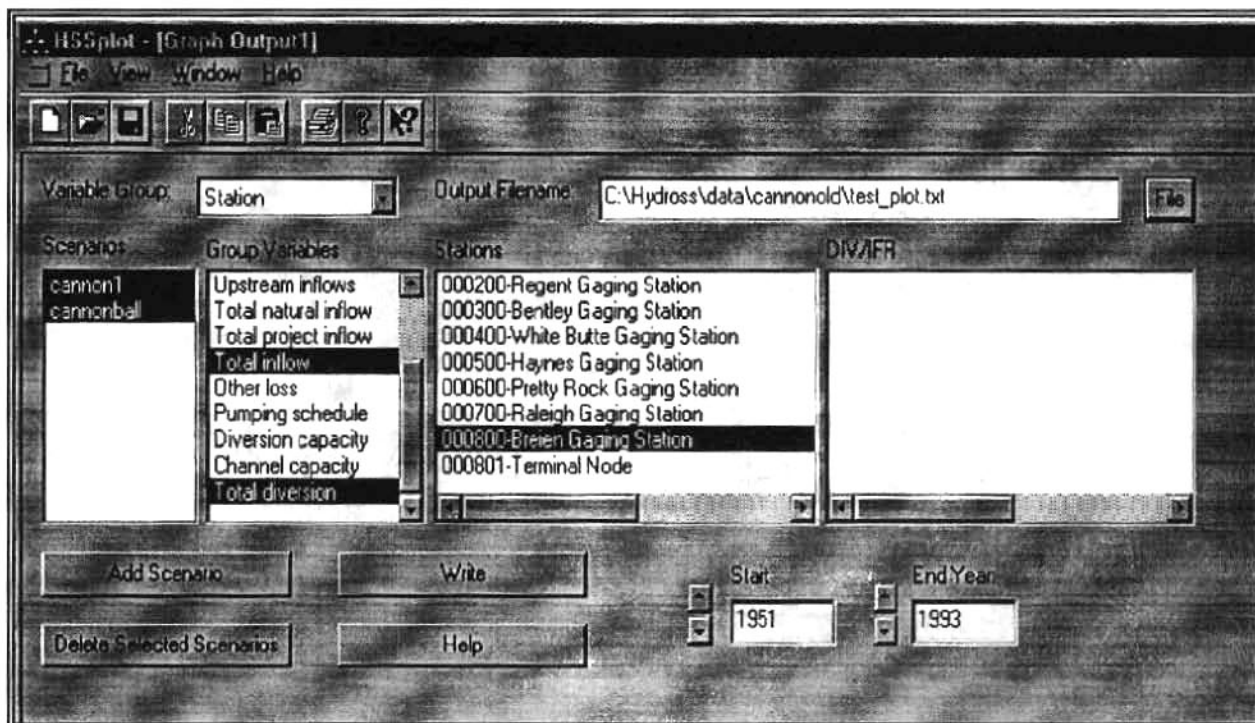


Figure 3 - PlotFile Utility Screen showing scenario/variable/station selection combinations.

SUMMARY

The PCHSS graphical user interface for HYDROSS remains completely separate from the HYDROSS model modules themselves. The GUI simplifies the preparation of input for the user by automatically generating the precisely formatted input files from space-delimited ascii files and individually entered values. Running the modules can then be done with the click of a button rather than issuing operating system commands with multiple arguments. These basic GUI elements open the model to many new users and facilitate the presentation of its output to the burgeoning number of water resources planners who rely on model study output to make decisions.

Reservoir Action Window

Station Name: Yellowtail Reservoir

Initial Content: 932 Units: kaf

Content At Spillway: 1070 Units: kaf

Share Flag

	Cont	Elev	Area	Disch Units
Content, etc:	lobig\yellowtail.txt File: kaf	ft	ac	CFS
Evaporation:	\lobig\y_evap.txt File: in			
Target Content:	lobig\y_target.txt File: kaf			
Min Content:	ta\lobig\y_min.txt File: kaf			
Max Content:	a\lobig\y_max.txt File: kaf			

Constant Seepage: Flow Units Type: Constant

Diversion Limits: Elev Units Flow Units

Buttons: OK, Cancel, Help

Note: An "Edit Power Data" button is visible to the right of the Target Content field.

Figure 2 - Reservoir Data Editor showing data file and individual value input.

HYDROLOGIC MODELING SYSTEM (HEC-HMS)

John C. Peters, Hydraulic Engineer and **Arlen D. Feldman**, Chief, Research Division,
Hydrologic Engineering Center, U.S. Army Corps of Engineers, 609 Second Street,
Davis, CA 95616

Abstract The Hydrologic Modeling System (HEC-HMS) is "new-generation" software for precipitation-runoff simulation that will supersede the Hydrologic Engineering Center's HEC-1 program. Technical capabilities and operational features of HEC-HMS are described, with emphasis on technical capabilities that differ from those in HEC-1. New features enable use of grid-based (e.g., radar) rainfall data and continuous simulation, and provide enhanced capabilities for parameter estimation.

INTRODUCTION

The Hydrologic Modeling System (HEC-HMS) is "new-generation" software for precipitation-runoff simulation that will supersede HEC-1. In addition to unit hydrograph and hydrologic routing options similar to those in HEC-1, the initial version of the program contains a quasi-distributed runoff transformation that can be applied with gridded (e.g., radar) rainfall data, and a simple "moisture depletion" option that can be used for continuous simulation. HEC-HMS is comprised of a graphical user interface, integrated hydrologic analysis components, data storage and management capabilities, and graphics and reporting facilities (Charley et al., 1995).

As presented by Charley et al., 1995, development of HEC-HMS took place utilizing a mixture of programming languages (C, C++, and Fortran). The software is built for multi-platform usage, primarily workstations and PC's. The computational "engine" and graphical user interface, GUI, are written in object-oriented C++. Hydrologic process algorithms (e.g., infiltration methods) are written in Fortran and have been incorporated into a library labeled *libHydro*. Although linked into a single executable, there are clear separations between the GUI, libraries, and databases and the main simulation engine. This design facilitates use of other components at later dates without having to revise the computational software.

All computations are performed in metric units. Input data may be English or metric and are automatically converted if necessary. The user selects either English or metric for the output results.

TECHNICAL CAPABILITIES

Hydrologic Elements Simulation with HEC-HMS is based on representing a watershed with *hydrologic elements*: subbasin, routing reach, junction, uncontrolled reservoir, diversion, source, and sink. The hydrologic and precipitation computation options are shown in Table 1.

Table 1. HEC-HMS Options

<u>Precipitation</u>	<u>Losses</u>	<u>Transform</u>
grid-based precipitation	initial/constant	ModClark
import hyetograph	deficit/constant	kinematic wave
specify gage weights	Green & Ampt	Clark unit graph
inverse-distance gage weighting	SCS Curve No.	Snyder unit graph
frequency-based design storm	gridded Curve No.	SCS Dimensionless unit graph
		user-specified unit graph
	<u>Routing</u>	<u>Baseflow</u>
	lag	exponential recession
	Muskingum	constant monthly
	Modified Puls	
	Muskingum Cunge	

A *subbasin* is conceptually an element that produces a discharge hydrograph at its outlet. Its properties include area and percent imperviousness. The discharge hydrograph is based on subtracting "losses" from input precipitation, transforming the resulting rainfall excess to direct runoff at the outlet, and adding baseflow. A *junction* is a location where two or more inflow hydrographs are combined to produce an outflow hydrograph.

A *river reach* is conceptually an element for which there is a "known" inflow hydrograph at its upstream end, and which produces an outflow hydrograph at its downstream end. A *reservoir* is similar to a river reach in that there is a "known" inflow hydrograph, and the reservoir element produces an outflow hydrograph. A *diversion* is an element for which a portion of the inflow to the element is diverted, and the remainder passes through. A *source* is an element with which a discharge hydrograph is imported into the basin network, e.g., an observed hydrograph or a hydrograph generated in a prior simulation. A *sink* is an element for which there is an inflow but no outflow.

Continuous Soil Moisture Accounting HEC-HMS includes the deficit/constant-loss method which permits simulation over extended time periods. It is similar to a method contained in the Interior Flood Hydrology Package (HEC, 1992). A moisture capacity for a subbasin must be filled for precipitation excess to occur. A moisture deficit is diminished by precipitation, and during precipitation-free periods is increased at a user-specified rate. Input requirements for the method include the moisture capacity (maximum moisture deficit), an initial moisture deficit, and recovery rates which can be specified with mean-monthly values.

Future versions of HEC-HMS will incorporate more comprehensive soil moisture accounting algorithms that account for evapotranspiration and enable simulation of subsurface contributions to total runoff using several soil moisture and groundwater storages.

Grid-based Modeling Option Traditional application of rainfall-runoff simulation has involved use of spatially-averaged (lumped) values of basin rainfall and infiltration (losses). This approach has been practically useful because rainfall data available from typically sparse gage networks are generally inadequate to justify more spatially-detailed simulation methods. The availability of grid-based (radar) rainfall enhances the attractiveness of modeling approaches that take into account spatial variations of runoff production. Also the availability of GIS for processing data associated with topography, soils, and land use greatly facilitates definition of spatially-variable watershed characteristics as depicted in Fig. 1.

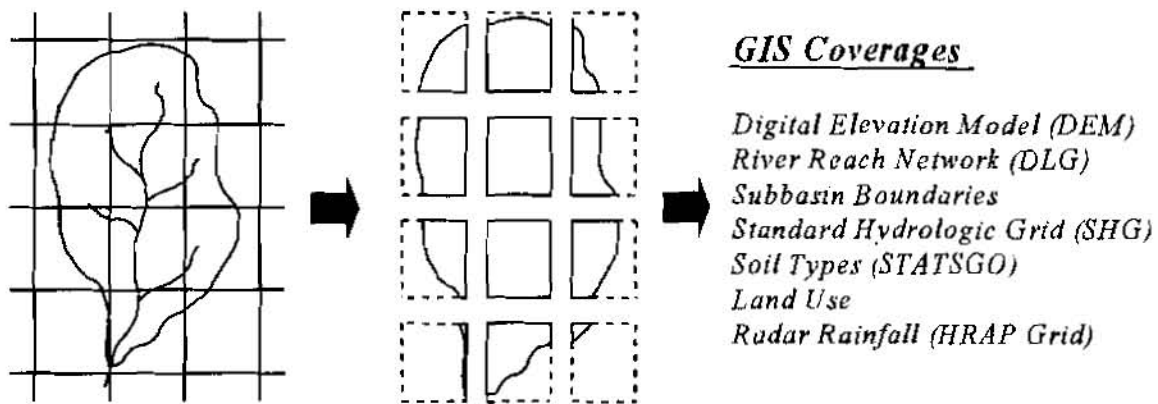


Figure 1. Grid-based Watershed with GIS Coverages

ModClark. The ModClark method (Peters and Easton, 1996; Kull and Feldman, 1998) is an option in HEC-HMS that enables grid-based runoff simulation. The method employs an adaptation of the Clark conceptual runoff model (Clark, 1943), by which direct runoff is represented very simply by two processes: translation and storage. Translation relates to the travel time for runoff contributions to reach the outlet, and storage relates to the attenuating effects of natural storage in the watershed. Two parameters of the method are T_c , time-of-concentration, and R , storage coefficient. T_c can be regarded as the time it takes for rainfall excess from the most remote location in the watershed to reach the outlet. R , a measure of the effects of natural storage, is the slope of the relation between storage and outflow for a linear reservoir. Like T_c , R has units of time.

With the ModClark method, the translation time to the outlet is unique for each grid cell and is based on the travel distance from the cell to the watershed outlet. Cell data needed are the area within the watershed of each cell, and the travel distance from the cell to the watershed outlet. Travel time for a cell is computed as a proportion of the basin travel time by multiplying by (cell distance to the watershed outlet divided by the distance from the most distant cell to the outlet). The lagged rainfall excess for each cell is then routed through a linear reservoir.

Gridded SCS Curve Numbers. With the ModClark method, losses (infiltration) are calculated individually for each grid cell, and are therefore dependent on the rainfall that is

associated with that cell. The potential for infiltration varies spatially in a watershed, and is a function of surface and subsurface characteristics. The Curve Number method of the Natural Resources Conservation Service (formerly Soil Conservation Service) relates losses to soil type and land use. Soils are categorized with relation to their infiltration potential, and land use reflects surface conditions such as forest, pasture, various types of urbanization, etc. Available data bases for soil and land use data can be accessed to provide data for analysis with GIS procedures to generate gridded values for Curve Numbers.

Grid-parameter File. Application of the ModClark method and gridded SCS Curve Numbers requires use of a grid-parameter file. The file associates grid cells with each subbasin, as depicted in Fig. 1, and for each grid cell, the following information is provided:

- cell x-coordinate (ID)
- cell y-coordinate (ID)
- travel distance to basin outlet, in *km*
- area of cell with basin boundaries, in *km²*
- SCS Curve No.

The file can be based on an HRAP grid (Reed and Maidment, 1994) or an SHG grid (Hydrologic Engineering Center, 1996a). The grid type used in specifying rainfall data must be the same as that used for application of the ModClark method. Generation of the grid cell file is achieved with automated procedures involving the use of ARC/INFO and associated macros. The procedures are labeled GridParm and SCSParm.

GridParm. GridParm consists of a sequence of Arc/Info macro language programs for generating cell areas and travel distances (HEC, 1996). The procedures require processing digital elevation model (DEM) data such as are available for the continental U.S. (via Internet) from the USGS EROS Data Center (USGS, 1990). An eight-direction "pour-point" algorithm defines the direction of flow from any grid cell to be in the direction of steepest descent from the cell to one of its eight neighbors. A flow path length (travel distance) is computed by summing the lengths of all segments along the path from the cell to the basin outlet. Area and travel distance are determined for DEM-based cells at a 100 meter resolution. The larger computational cells (e.g., a 2 km resolution for radar rainfall grids) are then superposed and their areas and travel distances are calculated by summing the areas and averaging the distances encompassed by the DEM cells.

SCSParm. SCSParm consists of a sequence of procedures to utilize soil and land use data to develop estimates for Curve Number for each grid cell. The soil data can be obtained from the State Soil Geographic (STATSGO) Data Base (SCS, 1993), which is accessible via Internet and also on a single CD-ROM disk for the continental U.S., Hawaii and Puerto Rico. Land Use and Land Cover (LULC) data can be downloaded over Internet from the U.S.G.S. EROS Data Center. Data from the two sources is intersected to develop areas with unique combinations of soil type and land use. A look-up table is accessed that relates the soil type/land use combinations to Curve Number. Finally, a grid overlay is used to associate a Curve Number with each grid cell.

HECPrePro. HECPrePro (HEC, 1996c) is a GIS preprocessor for developing basin model data for HEC-HMS. The preprocessor can be used to develop the following files for HEC-HMS as well as for general watershed information.

HEC-HMS basin file containing locational and connectivity information for hydrologic elements (as noted above for the grid-parameter file)

Text file listing attributes of hydrologic elements

Drawing Exchange File (DXF) of streams and subbasins that can be used as the basis for a background map in HEC-HMS

The preprocessor requires (as inputs) Arc/Info line coverages of subbasins and streams, and an Arc/Info elevation grid. The basin file generated by HECPrePro provides a schematic representation of a multi-subbasin watershed as illustrated in Fig. 2. The user of HEC-HMS must then provide the parameter data required for runoff simulation by each hydrologic element.

WATERSHED MODEL DEVELOPMENT

A graphical user interface (GUI) provides a means for constructing the watershed model and for specifying information to be retrieved or stored (e.g., importation of data from a previously developed HEC-1 input file), specification of application-specific information (data and execution instructions), and viewing of results. A significant component of the GUI is capability for schematic representation of a network of hydrologic elements (see Fig. 2). The schematic can be used in the initial configuration of a basin model by generating, dragging into place and connecting (graphically) icons that represent components of a basin network. Once a schematic is developed, pop-up menus can be invoked for input of data, to edit data, and to display simulation results.

The entering of data for a large number of hydrologic elements can be tedious if single-element editors are used. The GUI contains global editors for entering or reviewing data of a given type (e.g., values for Green & Ampt parameters) for all applicable elements. If the same data values are being displayed in more than one GUI screen, a change in one screen will automatically be reflected in the other(s).

APPLICATION

The execution of a simulation requires specification of three sets of data. The first, labeled *basin model*, contains parameter and connectivity data for hydrologic elements. The second set, labeled *precipitation model*, consists of meteorological data and information required to process it. The data may represent historical or hypothetical conditions. The third set, labeled *control specifications*, specifies a simulation time window and a fixed time interval for computations. A *project* can consist of a number data sets of each type. A *run* is configured with one of each type of data set.

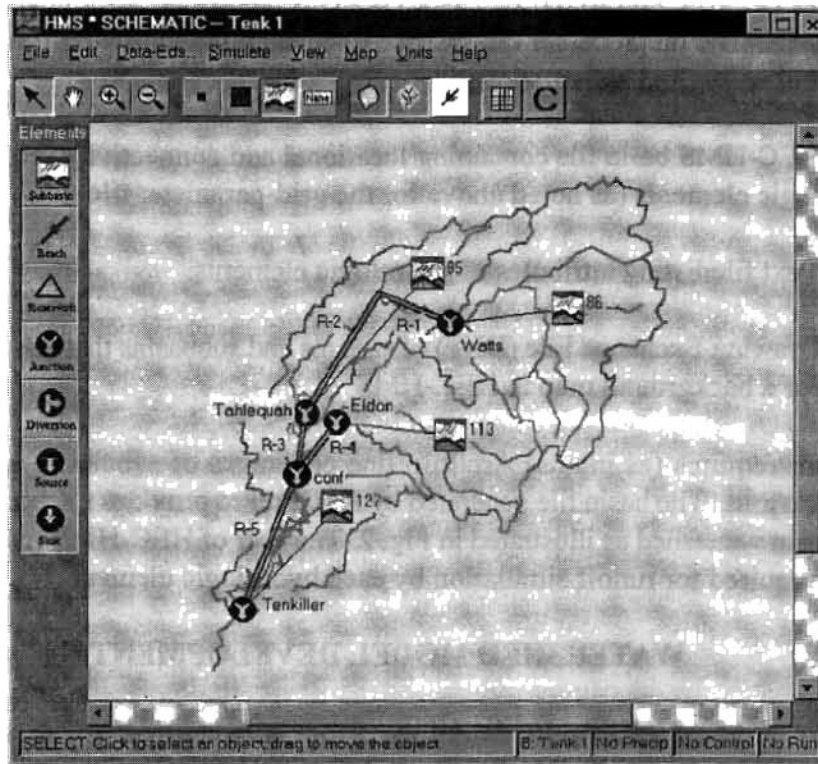


Figure 2. Basin Schematic

PARAMETER ESTIMATION

HEC-HMS provides capabilities for optimization (automated estimation) of the values for selected runoff parameters for situations where observed precipitation and discharge data are available. Parameter estimation is achieved by automated adjustment of the values for selected parameters to produce an *optimal fit* of a computed hydrograph to an observed hydrograph at a target location. The selected parameters may be associated with losses, runoff transformation, baseflow, or routing for any subbasins or reaches upstream from the target location.

The quantitative measure of optimal fit is the *objective function*, which is based on the degree of variation between the computed and observed hydrographs, and is equal to zero if the hydrographs match exactly. The key to automated parameter estimation is a *search procedure* for adjusting the selected parameters to produce an optimal fit; that is, to minimize the magnitude of the objective function. Constraints are imposed on parameter values to ensure that unreasonable values are not utilized.

Initial values for all parameters are required at the start of optimization. A hydrograph is computed at the target location (for which an observed hydrograph has been specified), and the value of the objective function is calculated. The search procedure adjusts values for the selected parameters (i.e., the parameters being optimized), and a new computed hydrograph and objective function are obtained. This cycle is repeated until the change in magnitude of the objective function is minimal, and the search is ended.

Objective Function An objective function is a quantitative measure of how well the computed hydrograph matches an observed hydrograph. The goal of optimization is to adjust parameter values so as to minimize the value of the objective function. Four objective functions are provided: 1) HEC-1 objective function (weighted squared differences between the observed and simulated discharges giving greater weight to differences associated with higher flows); 2) sum of squared residuals; 3) sum of absolute residuals; and 4) percent error in peak flow.

Search Methods You can choose between two methods for adjusting the selected parameters to obtain an optimal fit. The Univariate Gradient Method (HEC, 1982) varies the magnitude of one parameter at a time while holding the magnitude of the remaining selected parameters constant. The Nelder and Mead Method (Johnston and Pilgrim, 1976) changes the magnitude of all selected parameters each iteration. The search process takes longer than with the univariate gradient method, but may produce a more nearly optimal fit.

Initial Values and Constraints Initial values for parameters are required at the start of an optimization. The default initial values are those specified in the basin model. However, you can override any default initial value. *Hard constraints* limit the range of values that a parameter may have. Such constraints are used to keep the magnitude of a variable within physically reasonable limits, or to preclude values that cause instabilities or errors in computations. For example, negative loss rates are not allowed. When a search method attempts to use a value outside the range of hard constraints, the value is changed to the constraining value. You can specify *soft constraints* to keep parameter values to within tighter limits than those defined with the hard constraints. When a search procedure proposes a value outside of the soft constraints, the value is used, but the objective function is multiplied by a penalty factor.

Partial Derivatives Partial derivatives of the objective function are displayed as an aid for evaluating optimization results. A partial derivative is computed for a parameter by computing the objective functions at 0.995 and 1.005 times the optimal value of the parameter (with all other parameters held at their optimal values). The partial derivative is estimated as the difference between the values of the objective function divided by the difference between the parameter values. If a parameter value obtained by multiplying by 0.995 or 1.005 exceeds a hard constraint, the parameter value is set to the constraint, and the constrained value is used to calculate the partial derivative.

CONCLUDING REMARKS

A new generation of rainfall-runoff simulation models makes use of terrain-based data that cannot practically be developed by manual methods. GIS-based procedures enable efficient processing of such data to provide required parameters such as cell-based travel times and infiltration indices. Furthermore, GIS can be used to develop the configuration of multi-subbasin models as well as values for various watershed attributes. A simple continuous soil moisture accounting method is now available in HEC-HMS. Planned additions to HEC-HMS include: 1) comprehensive soil moisture accounting; 2) snow simulation; and 3) automated adjustment of discharge-frequency relationships to reflect land-use and project alternatives.

REFERENCES

- Charley, W., Pabst, A., and Peters, J., 1995, The Hydrologic Modeling System (HEC-HMS): Design and Development Issues. *Proc. Am. Soc. Civil Engrs. 2nd Congress on Computing in Civil Engineering*, Atlanta, Georgia.
- Clark, C.O., 1945, Storage and the Unit Hydrograph. *Trans. Am. Soc. Civil Engrs.*, 110:1419-1488.
- HEC, 1982, Hydrologic Analysis of Ungaged Watersheds Using HEC-1. Training Document No. 15, Hydrologic Engineering Center, US Army Corps of Engineers, Davis, CA.
- HEC, 1992, Interior Flood Hydrology Package, User's Manual. Hydrologic Engineering Center, US Army Corps of Engineers, Davis, CA.
- HEC, 1996a, HEC Proposes Standard Hydrologic Grid (SHG). *Advances in Hydrologic Engineering* (HEC March 1996 Newsletter), US Army Corps of Engineers, Davis, CA.
- HEC, 1996b, GridParm: Procedures for Deriving Grid Cell Parameters for the ModClark Rainfall-Runoff Method. User's Manual, US Army Corps of Engineers, Davis, CA.
- HEC, 1996c, HECPrePro - GIS Preprocessor for HMS. User's Guide and Reference Manual, prepared by Center for Research in Water Resources, University of Texas.
- Johnston, P.R. and Pilgrim, D.H., 1976, Parameter optimization for watershed models. *Water Resources Research*, 12(3), 477-486.
- Kull, D. W. and Feldman, A.D., 1998, Evolution of Clark's Unit Graph Method to Spatially Distributed Runoff. *Journal of Hydrologic Engineering*, Am. Soc. Civil Engrs., Vol. 3, No. 1, 9-19.
- Reed, Seann M. and Maidment, David R., 1994, Geographic Positioning of the HRAP Grid. Center for Research in Water Resources, University of Texas at Austin.
- Peters, J.C. and Easton, D.J., 1996, Runoff Simulation Using Radar Rainfall Data. *Water Resources Bulletin*, American Water Resources Association, Vol. 32, No. 4.
- Soil Conservation Service, 1993, State Soil Geographic Data Base (STATSGO) Data Users Guide. U.S. Department of Agriculture: Miscellaneous Publication Number 1492, Washington, D.C.
- USGS (US Geological Survey) 1990, Digital Elevation Models. USGS Data Users Guide 5, Reston, Virginia.

THE U.S. GEOLOGICAL SURVEY
HYDROLOGIC ANALYSIS SUPPORT SECTION
SOFTWARE SUPPORT SERVICES FOR
HYDROLOGIC MODELING AND DATA ANALYSIS

James Schornick, Hydrologist, Water Resources Division, U.S. Geological Survey,
Reston, Va.

Abstract. The U.S. Geological Survey (USGS) provides computer programs for surface-water, ground-water, and water-quality investigations. The programs include flow models, solute transport models, geochemical computation models, hydrologic computations, charting programs, data management, and utility programs. The purpose of this document is to provide instructions on how to obtain the software and documentation and to provide a brief description of the programs currently available.

INTRODUCTION

The USGS develops a variety of computer programs for the simulation and analysis of hydrologic processes. These programs include surface-water and ground-water flow models, solute transport models, geochemical computation models, hydrologic computations, water-quality and sediment computations, charting programs, data management, and utility programs. Information about USGS hydrologic software and documentation can be obtained from the following USGS Water Resources Applications Software home page:

<http://water.usgs.gov/software/>

The following listing provides brief descriptions of the software available.

SURFACE-WATER FLOW MODELS

- **BRANCH** - A weighted four-point, implicit, finite-difference model for the approximation of the unsteady-flow equations used to simulate steady or unsteady flow in a single open-channel or a dendritic branch network.
- **MODBRANCH** - A coupling of the MODFLW96 and BRANCH models to simulate leakage between surface-water and ground-water systems through a confining layer or riverbed.
- **DAFLOW** - A digital model for routing streamflow in upland channels or channel networks using the diffusion analogy form of the flow equations in conjunction with a Lagrangian solution scheme.
- **FESWMS-2DH** - A finite-element surface-water modeling system consisting of a

modular set of programs that simulate two-dimensional, depth-integrated, surface-water flows, including shallow rivers, flood plains, estuaries, and coastal seas.

- **FOURPT** - An unsteady one-dimensional, open-channel flow model that utilizes a four-point-implicit solution scheme. Simultaneous equations are solved by Gaussian elimination using an indexed, asymmetric, sparse-matrix solver useful for complex networks of interconnected channels.

SURFACE-WATER TRANSPORT MODELS

- **BLTM** - A Lagrangian solute transport model that is based on the one-dimensional convective-diffusion equation with reaction kinetics for up to 10 constituents.

WATERSHED MODELS

- **DR3M** - The Distributed Routing Rainfall-Runoff Model (Version II) is a watershed model for routing storm runoff through a branched system of pipes and (or) natural channels using rainfall as input.
- **PRMS** - The Precipitation-Runoff Modeling System is a modular, deterministic, distributed-parameter modeling system to evaluate the effects of various combinations of precipitation, climate, and land use on streamflow, sediment yields, and general basin hydrology.
- **HSPF** - The Hydrological Simulation Program uses continuous rainfall and other meteorologic records to compute streamflow hydrographs and pollutographs used to assess effects of land-use change, nonpoint source treatment alternatives, and flow diversions.
- **HSPEXP** - An expert system for calibration of the HSPF model, including 35 rules and 80 conditions for adjusting input parameters to improve calibration. Rules encompass four phases - annual volumes, low flows, storm flows, seasonal flows.

SURFACE-WATER HYDROLOGIC COMPUTATIONS

- **CAP** - The Culvert Analysis Program computes flows and stage-discharge relations for rectangular, circular, pipe arch, and other nonstandard shaped culverts.
- **FEQ** - The Full Equations Model simulates flow in a stream system

by solving the full, dynamic equations of motion for one-dimensional unsteady flow in open channels and through control structures.

- **GLSNET** - The Regional Hydrological Regression and Network Analysis Program uses generalized least squares and the analysis of residuals technique to estimate a regional regression equation to predict flow characteristics at ungaged sites.
- **MEASERR** - A program for determining the uncertainty and standard error for individual stream discharge measurements on the basis of a root-mean-square error analysis of the individual component errors.
- **NCALC** - A program for computing Manning's roughness coefficient from known discharge, water-surface profiles, and channel cross-sectional properties.
- **PEAKFO** - A program for flood-frequency analysis (based on Bulletin 17B) using method of moments to fit the Pearson Type III distribution to the logarithms of annual flood peaks.
- **SAC** - The Slope-Area Computation Program solves the one-dimensional steady-state energy and continuity equations for discharge by the slope-area method on the basis of given upstream and downstream water-surface elevations.
- **SWSTAT** - A program to compute surface-water statistics, including flow-duration tables and curves, annual n-day high/low flows, frequency analysis, and time series summary statistics, such as minimum, maximum, mean, standard deviation.
- **WSPRO** - A model for computing open-channel water-surface profiles for subcritical, critical, or supercritical flow assuming one-dimensional, gradually-varied steady flow.

SEDIMENT COMPUTATIONS

- **SEDSIZE** - A program to compute Inman, Trask, and Folk particle-size statistical parameters for fluvial sediments on the basis of phi values and percent finer values of selected sediment sizes. Also, computes percentages of gravel, sand, silt, clay, and the Meyer-Peter effective diameter.

GROUND-WATER FLOW MODELS

- **MODELW96** - A modular, three-dimensional, finite-difference ground-water flow model that simulates steady and unsteady flow in an

irregularly shaped flow system. Layers can be confined, unconfined, or a combination.

- **MODFLOW-GUI** - A pre- and post-processor graphical-user interface for preparing MODFLOW96 input data and viewing the model output. Designed for use within Argus Numerical Environments.
- **MODFLOWP** - The parameter estimation version of MODFLOW96 permits estimation of parameters by nonlinear regression, specifically, minimizing a weighted least-squares objective function by the modified Gauss-Newton method or by a conjugate-direction method.
- **MODPATH** - A particle tracking postprocessor for MODFLOW96 that uses a semi-analytical particle-tracking system to compute three-dimensional flow paths from the MODFLOW96 output.
- **CONTOUR** - A contouring program for uniform or variably spaced grids and that is designed for use with finite-difference models, such as MODFLOW96.
- **RADMOD** - A preprocessor to MODFLOW96 for a more precise computation of conductances and storage capacity related to cylindrical (axisymmetric) flow to wells.
- **ZONEBDGT** - A program for computing subregional water budgets using results from the MODFLOW96 model
- **MODEE** - A modular finite-element model that is based on the governing equations that describe two-dimensional and axisymmetric-radial flow in porous media.

GROUND-WATER SOLUTE TRANSPORT MODELS

- **ANALGWST** - A set of programs that calculate analytical solutions for one-, two-, or three-dimensional solute transport in ground-water systems with uniform flow.
- **HST3D** - A simulator for ground-water flow, heat, and solute transport in three-dimensional ground-water flow systems with variable density fluids.
- **HYDROTHERM** - A three-dimensional finite-difference model to simulate multiphase ground-water flow and heat transport in the temperature range of 0 to 1,200 Degrees Celsius
- **MOC** - A two-dimensional solute transport model that uses an iterative, alternating-direction implicit procedure to solve a

finite-difference approximation to the ground-water flow equation and the method-of-characteristics technique to solve the solute-transport equation.

- **MOC3D** - A three-dimensional single constituent transport model that is integrated with the MODFLOW96 model that uses the method-of-characteristics technique to solve the transport model.
- **MOC DENSE** - A two-dimensional, two-constituent solute transport model for ground-water that has variable density. An iterative, alternating-direction implicit procedure is used to solve a finite-difference approximation to the ground-water flow equation and the method-of-characteristics technique is used to solve the solute-transport equation.
- **MEI** - An interactive program for entering data into data files for use with the MODFLOW96, MODPATH, and MOC3D models.
- **SUTRA** - A hybrid, finite-element/integrated finite-difference model for the two-dimensional simulation of two principal processes - (1) saturated/unsaturated, constant or variable-density fluid flow, and (2) transport of thermal energy and single chemically reactive solute species.
- **YS2DT** - A two-dimensional, finite-difference model for simulating water flow and solute transport in variably saturated porous media.
- **AIRSLUG** - A program to generate type curves to interpret the recovery data from prematurely terminated, air-pressurized slug tests, which provide an efficient means of estimating the transmissivity and storativity of aquifers.

GEOCHEMICAL COMPUTATIONS

- **NETPATH** - An interactive program to calculate net geochemical mass-balance reactions and radiocarbon dating between water and minerals/gases along a hydrologic flow path.
- **PHREEQC** - A program that is designed to perform a wide variety of aqueous geochemical calculations, based on an ion-association model with capabilities for (1) speciation and saturation index- calculations; (2) reaction-path and advective-transport calculations, and (3) inverse modeling, which finds sets of mineral and gas-mole transfers that account for composition differences between waters of compositional uncertainties.
- **PHROPIZ** - A program to calculate geochemical reactions in brines and

other highly concentrated electrolyte solutions using the Pitzer virial-coefficient approach for activity-coefficient corrections.

WATER-QUALITY CALCULATIONS

- **SWPROD** - A program to calculate the daytime net productivity, night respiration, and total community metabolism from a diel series of dissolved oxygen, temperature, and salinity measurements.
- **BOD** - A program to compute nitrogenous and ultimate biological demand (BOD) and the rate constant, by using either linear or nonlinear fitting options.

CHARTING PROGRAMS (QWGRAF)

- **QWGRAF** - A collection of eight programs (see descriptions below) that share a common user-interface (HASS AIDE) and an underlying data management capability (see **DATMGR** description). The programs attempt to capture chart types or options within chart types that meet unique USGS needs that are not commonly found in third-party packages.
- **BOXPLT** - An interactive program to produce Box and Whisker plots. Options include hinge or quartile box boundaries, Tukey, Min/Max, or Percentile whiskers, and the ability to estimate percentile rankings from remarked data.
- **PRBPLT** - An interactive program to produce probability plots. Probability scales include plotting position (six models), quantile deviates, exceedance and nonexceedance cumulative probability percentiles, and recurrence interval.
- **EROPLT** - An interactive program to produce frequency distribution plots, including frequency, relative frequency, cumulative frequency, cumulative relative frequency, and the empirical distribution function.
- **LILIER** - An interactive program to produce a graphical test of the null hypothesis that a sample is normally distributed. The empirical distribution function of the standardized sample is compared to specified confidence-level bounds.
- **PIPER** - An interactive program to produce trilinear and quadlinear Piper (ternary) diagrams. Options for displaying samples include point symbols, partitioned point symbols (partitioning of samples within a diagram or between diagrams), sample density diagrams, and binary and ternary mixing diagrams.

- **DUROV** - An interactive program to produce Durov diagrams, which project the intersection points of two trilinear Piper diagrams as one of the two axes of an x/y coordinate plot. The other axis represents an additional user-defined variable.
- **STIEF** - An interactive program to produce Stief diagrams, which compare cation/anion pairs expressed in milliequivalents.
- **MAPPING** - An interactive program to produce maps of the USA, states, counties, hydrologic units, lat/long polygons with options for subarea overlays, extensive station labeling, and quantitative mapping of data to sites or areas.

DATA MANAGEMENT PROGRAMS

- **ANNIE** - An interactive program to store, retrieve, list, plot, check, and update spatial, parametric, and time-series data for hydrologic model and analysis. Uses binary, direct access Watershed Data Management (WDM) files.
- **IOWDM** - An interactive program to reformat various USGS file types for input to Watershed Data Management (WDM) files.
- **BSDMS** - An interactive program to store, retrieve, update, and display bridge scour and associated data.
- **DATMGR** - An interactive program to translate and modify rdb files, various USGS file types, and other ASCII-based flat files for input to QWGRAF programs or other applications that can accept these files types as input.

REFERENCES

- Alley, W.M., and Smith, P.E., 1982, Distributed routing rainfall-runoff model--version II: U.S. Geological Survey Open-File Report 82-344, 201 p.
- Bicknell, B.R., Imhoff, J.C., and Kittle, J.L., Jr., Donigan, A.S., Jr., and Johanson, R.C., 1997, Hydrologic Simulation Program--Fortran: User manual for version II: U.S. Environmental Protection Agency, National Exposure Research Laboratory, Athens, Ga., EPA/600/R-97/080, 755 p.
- Flynn, K.M., Hummel, P.R., Lumb, A.M., and Kittle, J.L., Jr., 1995, User's Manual for Annie, version 3, computer program for interactive hydrologic data management: U.S. Geological Survey Water-Resources Investigations Report 95-4085, 211 p.
- Harbaugh, A.W., and McDonald, M.G., 1996, User's documentation for MODFLOW-96, an update to the U.S. Geological Survey modular finite-difference ground-water flow model: U.S. Geological Survey Open-File Report 96-485, 56 p.
- Harbaugh, A.W., and McDonald, M.G., 1996, 1996, Programmer's documentation for

- MODFLOW-96, an update to the U.S. Geological Survey modular finite-difference ground-water flow model: U.S. Geological Survey Open-File Report 96-486, 220 p.
- Jobson, H.E., and Schoellhamer, D.H., 1987, User's manual for a Branched Lagrangian transport model: U.S. Geological Survey Water-Resources Investigations Report 87-4163, 73 p.
- Jobson, H.E., 1997, Enhancements to the Branched Lagrangian transport modeling system: U.S. Geological Survey Water-Resources Investigations Report 97-4050, 57 p.
- Kittle, J.L., Jr., Hummel, P.R., and Imhoff, J.C., 1989, ANNIE-AIDE, a system for developing interactive user interfaces for environmental models (programmers guide): U.S. Environmental Protection Agency, EPA/600/3-89/034, Environmental Research Laboratory, Athens, Ga., 166 p.
- Konikow, L.F., Granato, G.E., and Hornberger, G.Z., 1994, User's guide to revised method-of-characteristics solute transport model (MOC--Version 3.1): U.S. Geological Survey Water-Resources Investigations Report 94-4115,
- Lumb, A.M., Carsel, R.F., and Kittle, J.L., Jr., 1988, Data management for water-quality modeling development and use: Proceedings of the International Conference on Interactive Information and Processing systems for Meteorology, Oceanography and Hydrology.
- Parkhurst, D.L., 1995, User's guide to PHREEQC--a computer program for speciation, reaction path, advective-transport, and inverse geochemical calculation: U.S. Geological Survey Water-Resources Investigations Report 95-4227, 143 p.
- Plummer, L.N., Prestemon, E.C., and Parkhurst, D.L., 1994, An interactive code (NETPATH) for modeling NET geochemical reactions along a flow PATH--version 2.0: U.S. Geological Survey Water Resources Investigations Report 94-4169, 130 p.
- Plummer, L.N., and Parkhurst, D.L., Fleming, G.W., and Dunkel, S.A., 1988, A computer program incorporating Pitzers equations for calculation of geochemical reactions in brines: U.S. Geological Survey Water-Resources Investigations Report 83-4153, 108 p.
- Schaffranek, R.W., Baltzer, R.A., and Golddberg, D.E. 1981, a model for simulation of flow in singular and interconnected channels: U.S. Geological Survey Techniques of Water-Resources Investigations, book 7, chap. C3, 110 p.
- Schornick, J.C., and Place, M.C., 1997, User's manual for QWGRAF, computer programs for water-quality graphics: U.S. Geological Survey Water-Resources Investigations Report 97-4226,
- Voss, C.I., 1984, A finite-element simulation model for saturated-unsaturated, fluid-density-dependent ground-water flow with energy transport or chemically-reactive single-species solute transport: U.S. Geological Survey Water-Resources Investigations Report 84-4369, 409 p.
- Swain, E.D., and Wexler, E.J., 1993, A coupled surface-water and ground-water model for simulation of stream-aquifer interaction: U.S. Geological Survey Open-File Report 92-138, 162 p.

MODELING WITH MODSIM: KLAMATH RIVER WATER QUANTITY FOR PROTECTING FISH AND OTHER RESOURCE VALUES

Dr. John Scott, Research Associate
Civil Engineering Department, Colorado State University
Ft. Collins, CO 80523-1372

Dr. Marshall Flug, Water Resources Engineer
Biological Resources Division, US Geological Survey
4512 McMurry Avenue, Ft. Collins, CO 80525-3400

Abstract: A Water Quantity Model (WQM) was developed for the Klamath River Basin to assess water quantity related management alternatives in the recovery and maintenance of threatened and endangered fish species in the basin. The Biological Resources Division of the United States Geological Survey (USGS-BRD) contracted with the United States Fish and Wildlife Service, with additional support from PacifiCorp and the United States Bureau of Reclamation, to formulate this WQM primarily for the Technical Work Group of the Klamath River Basin Fisheries Task Force. The WQM is a monthly water simulation model of the operation of the Klamath River and reservoir system from Upper Klamath Lake to the mouth at the Pacific Ocean.

INTRODUCTION

The Klamath River Basin Fisheries Task Force (Task Force) represents Federal, state, and local county agency representatives, Native American Tribes, and anadromous fishery resource user groups in Oregon and California. The Task Force has been directed by Congress to work with the Secretary of the Interior to restore Klamath River Basin anadromous fisheries to optimum levels by 2006. Since 1994, the United States Geological Survey-Biological Resources Division (USGS-BRD, formerly the National Biological Service) has interacted with the Task Force, primarily through its Technical Work Group (TWG). In July 1995, the TWG identified a high priority need to support the development of a water quantity model for the Klamath River Basin, including the major tributaries (Shasta, Scott, Salmon, and Trinity Rivers).

The Bureau of Reclamation (BOR) is concurrently upgrading their KPOP (Klamath Project Operations Plan) model, which describes the features of a federal irrigation project and spatially simulates the river operation in the upper basin. This USGS-BRD project compliments that detailed effort, capitalizes on their data development, and coordinates the BOR project deliveries with a more in-depth study of the lower basin. Inputs to this WQM will utilize measured (i.e., historic records) or simulated flows for the upstream portion of the basin consistent with BOR operations. The range of annual net inflow conditions into Upper Klamath Lake (UKL) in acre-feet (AF) for the 1961-1992 period are:

	<u>Maximum (Year)</u>	<u>Minimum (Year)</u>	<u>Average (Yearly)</u>
Annual Inflow to UKL (AF)	2,119,000 (1965)	575,000 (1992)	1,350,000

The river points identified were the USGS gages shown in Figure 1, namely, the Link River at Klamath Falls; the Klamath River (KR) below Keno, OR; KR below John C. Boyle Power Plant, CA; KR below Iron Gate Dam, CA; KR near Seiad Valley, CA; KR at Orleans, CA; and the KR at Klamath, CA. The major tributaries (Shasta, Scott, Salmon, and Trinity Rivers) are not modeled

except as inflow points using USGS gage records at or near their confluence with the Klamath River. This configuration is expected to accommodate the needs of other water quality modeling studies and provide data for river reaches in support of fish habitat studies.

The simulation of the system shown in the flow network diagram provides several water management alternatives that can be investigated to change the flow patterns and volumes in the river. The total operational storage of the four PacifiCorp reservoirs originally proposed for inclusion in the model: Keno, J.C. Boyle, Copco and Iron Gate is only 13,555 acre-feet or about 1 percent of the average annual inflow to Upper Klamath Lake. By adding the active storage at Upper Klamath Lake, the available storage to manage river flow is increased to approximately 500,000 acre-feet or 37 percent of the inflows. Additionally, the only significant diversions from the system occur above Keno Dam in the BOR project area. The project annually diverts over 400,000 acre-feet in average annual diversions, while the annual returns or accretions to the system above Keno and below Upper Klamath Lake are about 235,000 acre-feet on average. The agricultural and wildlife refuge diversions account for an average net consumptive use of 165,000 acre-feet annually in the 1961-1992 time period. The inclusion of the upper basin is necessary to evaluate the system flexibility and to suggest and analyze potential management alternatives.

The modeling environment selected allows the system to be described and analyses performed through the use of data-sets. The model user can perform other model simulations of the Klamath River System for different sets of priorities, for different hydrologic sequences, and for adjustments to the data-set which alter other limitations on the flow network (e.g., increasing or decreasing turbine flows or by-pass flows).

WATER QUANTITY MODEL

The Water Quantity Model (WQM) for the Klamath River Basin is a computer software tool developed to simulate the hydrologic operation of the river and reservoir system on a monthly time step. MODSIM (Larson, 1997), the simulation model chosen, maintains mass balance at nodes for water flowing into and out of the system and account for the time step transition of storage in reservoirs, according to the system state equation,

$$S_{t+1} = S_t - O_t + I_t,$$

where, S is the storage in a reservoir node (for non-reservoir nodes, $S_{t+1}=S_t=0$); O is the total outflow from a reservoir or node; I is the total inflow to a reservoir or node; and t is the time period.

MODSIM is a general, multi-purpose, multi-reservoir simulation model, which will compute the amount of water at specified river points (nodes) and water flows through specific river reaches (links) of the Klamath River Basin for each defined time step. Operational features within the WQM can be defined by the user as varying in time, having seasonal or monthly values. Such Klamath River system operational features can include: reservoir storage volumes and controlled releases; physical limits on reservoir discharges (e.g., dependent upon outlet structures); limits on flows released to irrigation channels, diversion structures, or for delivery to consumptive use demands for agriculture, industrial, and municipal purposes; hydropower releases and power production levels; channel or river segment losses; legal apportionment of interstate allocations; and releases for instream purposes.

Water allocation based on water rights combined with measured, gaged, or synthetic river flows is the heart of MODSIM. MODSIM optimizes the water allocation process by meeting the user-

defined set of prioritized water demands in the Klamath River in each time step. This prioritizing allows the user to evaluate alternative water basin management strategies by comparing water deliveries and impacts to resources from different operating policies under several alternative flow scenarios (e.g., high flow years, low flow periods). The main output of the model, volumetric flows at various river locations, is needed to quantify impacts on fish habitats, water quality parameters, and other flow related resources important to restoration of anadromous fisheries in the Klamath River.

MODEL DEVELOPMENT PROCESSES

The process of model development includes the phases of verification, calibration, and validation. Additionally, the development of management alternatives is the final objective. An important aspect in performing a model study is to select a study period which reflects the conditions of the system being modeled and includes the range of hydrologic conditions experienced by the system and expected to occur in the future. The 1961 to 1992 period was selected to study the Klamath River Basin because it included the river flow conditions as a result of the construction and operation of the Klamath Project irrigation system and the hydroelectric operations of the PacifiCorp reservoirs. The time step used for this study is one month, which is appropriate for a model to analyze the decision making in planning for operations.

Verification is the first step in the model development process. The OTA report (1982) states that a model is "verified when it is determined that the designer's conception of the model is accurately embodied in the program written and run on the computer". MODSIM is a computer model written to simulate virtually any given river basin system with a properly defined data set. Therefore, for the Klamath River Basin, it is important to configure the physical system (links and nodes) correctly and then define the data. The configuration of the system network was coordinated with the TWG and various nodes along the river were included to meet study objectives. With the configuration defined properly the model was determined to be verified, but extensive work is required to gather the data and calibrate the model.

The major hydrologic inflow points in the system are flows into Upper Klamath Lake and tributary flows at the Shasta, Scott, Salmon, and Trinity Rivers. Accretions to the mainstem at ungaged points were calculated from the differences in known gage records proportionate to their corresponding tributary watershed area. Since MODSIM calculates evaporation losses as a function of reservoir surface area, this amount is added to all the net inflow and accretion values, where appropriate. Similarly, for accretions to reservoirs below Upper Klamath Lake where change in storage is known – for Copco and Iron Gate Reservoirs from 1967 to present– the gross accretions or inflows are calculated as the net sum of monthly change in storage, the evaporation losses as a function of end-of-month reservoir surface area, and the calculated differences between USGS gage flows at measured points in the Klamath Basin.

The input node, Large Springs, was included to reflect a known point source of inflows, the magnitude of which is estimated at 100 cubic feet per second (6,000 acre-feet per month). In several months, negative accretions or losses to the system occur as the difference between the gages, evaporation losses and/or change in storage at reservoirs, or due to the point inflow at the springs. Negative accretions are modeled as demands in the MODSIM model and are shown in Figure 1 as losses in the river reach.

The major reservoirs in the system are: Upper Klamath Lake, Copco Lake and Iron Gate Reservoir. The maximum and minimum levels for all the reservoirs have been set at their historical levels for the calibration and validation runs, although these levels are potential variables in the simulations of management alternatives. The major diversions from the basin are those for the Klamath Project in the upper basin at: A Canal, Lost River diversions and returns, North Canal, and ADY Canal. The input data for the Klamath Project operations have been coordinated with BOR and have been set at the historical levels for the calibration and validation runs.

The calibration process is the phase of model building where the outputs are compared to the historical operations of the river and reservoir system. The OTA report (1982) further defines this process as where the "model must be 'fitted' or 'fine-tuned' to the specific characteristics of the real-world system being studied. Each model contains a set of 'parameters,' i.e., values of coefficients, that establish the relationship between the model's predictions and the information supplied to the computer for analysis. A model is considered to be calibrated when model results match experimental observations taken from the particular system under investigation." There are very few parameters that must be estimated for this system during this process. The parameters may be more accurately characterized as additional data requirements that are time invariant for the system or for specific nodes in the system, i.e., reservoirs and demands. The parameters which are estimated for the Klamath Basin MODSIM model are: evaporation rates, reservoir area-capacity-elevation tables (to the extent these are not "known" quantities from BOR/PacifiCorp tables), power plant efficiency tables, and priorities on meeting demands and filling storage.

The principal method in performing the calibration process for water resources systems is to set two of the three sets of time series data in the system state equation at their historical values and then compare the third or remaining variable. For this reservoir system that means setting either the reservoir storage levels or the reservoir releases at historical levels, i.e., pre-determined targets with high priorities, in addition to knowing and using historical inflows. For the Klamath River Basin model, the storage targets were set at historical levels and the reservoir releases were calculated by the model. MODSIM will attempt to hit these storage targets before filling any other system demands. Additionally, the inflows at all other non-reservoir nodes and demands to the system, where they occur, are set at historical levels.

Since MODSIM calculates the reservoir releases and all other node outflows, the modeled Klamath River flow at these nodes is compared to the historical time series at USGS gage sites. Three river points were chosen for this comparison: first, the river point below Keno Dam where the USGS has maintained a gage continuously since October 1929; second, the USGS gage below Iron Gate Reservoir with a record of October 1960 to present; and third, the USGS gage at Seiad Valley with a continuous period of record from July 1951 to present. All three of these gages reflect the current development on the Klamath River.

The selected calibration period was 1970-1979, a period of low, average and high water years and for which excellent records on system hydrology were maintained. The differences in the modeled and gaged flows for the calibration period at the three river points are:

	<u>Ave Month (AF)</u>	<u>Ave Year (AF)</u>	<u>Max Month (AF)</u>
Keno USGS Gage	117	1404	1122
Iron Gate USGS Gage	125	1505	1159
Seiad Valley USGS Gage	158	1900	2719

The maximum monthly percent differences for these river points are less than 1 percent, whereas the average yearly percent differences are less than .1 percent. In addition to comparing flows at river points during the calibration process, the closeness with which MODSIM meets targets for reservoir storage and system demands must be checked to insure that flows are not met in deference to shorting these targets. In all cases the targets were met, for both storage and demands. The calibration is achieved based on these river flow point comparisons and because the storage and demand targets were met.

The validation process is the last step in model building. Its purpose is to develop general criteria and guidelines that the computer simulation model will use to produce acceptable operational results during the simulation of management alternatives. The OTA report (1982) defines validation as "the process of determining how accurately the model can predict real-world events under conditions *different* from those on which the model is developed and calibrated. To validate a model, a different set of field data is used as input to the model and the output is compared to actual observations of the new field conditions."

Whereas calibration uses the historical end-of-month storage values as targets at the reservoirs, during the validation process, rule curves are used to manage the reservoir storage. Storage rule curves are generally envelopes of storage levels that guide the reservoir operators in making release decisions based on the knowledge of present storage level and some expectation of future inflows. These rule curves are often developed and used by the reservoir managers and are specified as targets in simulation models; however, in this case they were not available. Therefore, to simplify the development process, rather than an envelope of curves for each reservoir, a general curve was developed for each of the major reservoirs for this study and effort was concentrated on analyzing the simulation results.

The time period from 1980-1989 was selected to test the model simulation during the validation process. This ten year period also has dry, wet and average hydrologic conditions. The specific points in the river basin chosen during the calibration process to compare the model results to historical time series data will also be used during this validation. The calibration parameters; i.e., evaporation rates; reservoir area-capacity-elevation tables, where needed; and power plant efficiency tables are maintained at the values determined during that model development process.

The differences in the modeled and gaged flows for the validation period at the three river points are:

	<u>Ave Month (AF)</u>	<u>Ave Year (AF)</u>	<u>Max Month (AF)</u>
Keno USGS Gage	125	1506	118,444
Iron Gate USGS Gage	112	1347	116,282
Seiad Valley USGS Gage	174	2092	116,277

The seasonal pattern of flow and the average flow conditions are modeled accurately, however, the differences in monthly flow vary greatly. The differences in modeled versus historical flow at river gages are mitigated as the volume of flow increases moving downstream and the affect of the reservoir system is diminished. The average monthly and yearly percent differences for these river points are less than 1 percent, however the maximum monthly percent differences are 84 percent at Seiad Valley and 132 percent at Keno. This large deviation from gage records is due to the change in rule curve operation from September 1986 to October 1986, which was going from a wet year to a dry year and the consequent attempt to reduce storage. All system demands, as

expected, are met in every year, but reservoir storage can deviate and does, especially in low water years when water is not available to meet all demands and reservoir storage targets.

Minimizing the differences between the model's outputs and the historical flows at the three river points was not as important to accepting the model validation as being able to explain the differences in river flow due to differences in reservoir storage as a result of rule curve operation. The validation is achieved based on these river flow point comparisons and the comparison of storage and demand targets. In all months water balance is maintained and the flow differences are explainable.

ANALYSIS OF MANAGEMENT ALTERNATIVES

The purpose for going through the model development processes is to have confidence in the model's simulation of different input conditions in the analysis of management alternatives. Possible management alternatives include analyzing the system with different Federal Energy Regulatory Commission (FERC) flow requirements below Iron Gate Reservoir or elsewhere in the system; investigating the effects of drought years; minimum or preferred flow alternatives for Tribal Trust species; and natural hydrograph patterned flows. The input time series or desired operational criteria selected for a management alternative may differ drastically from the historical operations and inputs used in the calibration and validation runs, but the MODSIM configuration is valid for these alternatives.

Minimum storage levels will be set at the physical minimums for Copco Lake and Iron Gate Reservoir for many of the runs and storage targets at the main reservoirs may be altered to effect various habitat objectives. The priorities for agricultural and refuge diversions will change relative to storage and in-stream demands depending on the management run.

Four management alternatives with two variations were identified and evaluated to date:

Alternative 1. October 1996 to September 1997 using current operations plan. Model used actual historical 1997 water year (WY) data.

Alternative 2. No diversions

Alt. 2A. Low water year (1992)

Alt. 2B. Average year

Alternative 3. Maximum diversions

Alt. 3A. Low water year (1992)

Alt. 3B. Average year

Alternative 4. Current operations-Average water year, but start out with Upper Klamath Lake at 4143 feet and decrease lake level one inch per month October 1-September 30 to lake level 4142 feet.

These management alternatives were simulated with MODSIM and the results (see completion report, Scott and Flug, 1997) are considered to be an accurate representation of the system's operation given the individual alternative's assumptions. Some configurations of hydrologic conditions, and in particular the effects of flow conditions on biological factors, may dictate that multiple year, either two or three consecutive years, should be analyzed. This is especially true for environmental criteria or limits that change depending on multi-year hydrologic conditions.

SUMMARY AND CONCLUSIONS

The network model developed will provide one integrated model of water flow for the Klamath River System and will allow individual users and interested parties to see the impact of a change in water use at one location upon other users elsewhere in the system. This link in hydrologic impacts should help sensitize cooperating parties to the importance of water flows on other vested interests. In the end, all parties should be in agreement on the technical analysis and quantification of water volumes and flows that move through the Klamath River System. The WQM has gone through the model development processes and several management alternatives have been analyzed.

The objective of developing this water quantity model was to assess recommended alternatives to the existing operation of the system to improve endangered species. The majority of alternatives will change one or more of the following time series quantities:

1. the historical water deliveries,
2. return flows from diversions,
3. tributary accretion flows,
4. reservoir physical characteristics, or
5. reservoir operational policies and resultant outputs.

The database developed for this project includes the historical data for all of the above time series or physical constants.

While the management alternatives were configured with existing data, future alternatives may require that additional analysis be performed to determine time series for the above quantities. If the historical deliveries to agricultural or refuge use are changed, then the return flows from these areas will need to be estimated by either statistical or physical modeling. Tributary accretion flows may need to be re-formulated for various management alternatives. These may be estimated from "typical" year flows or from statistical time series generation.

REFERENCES

Flug, Marshall and John F. Scott, November 1997. Completion Report for the Development of a Water Quantity Model, Klamath River Basin. United States Geological Survey-Biological Resources Division, Mid-continent Ecological Science Center, Fort Collins, CO.

Larson, Roger K., John L. Labadie, and Marc Baldo, April 1997. Decision Support System for River Basin Water Rights Administration. In: David H. Merritt, (Editor), Aesthetics in the Constructed Environment, Proceedings of the 24th ASCE WRPMD Specialty Conference, Houston, Texas.

Office of Technology Assessment, 1982. Use of Models for Water Resources Management, Planning, and Policy. U. S. Government Printing Office, Washington, D. C.

Figure 1. **SCHEMATIC FOR THE WQM**

- ← Inflow into Upper Klamath Lake
 - → A Canal Diversions
 - △ Upper Klamath Lake/Link River Dam
 - West and East Side Powerplants
 - Link River at Klamath Falls
 - △ Lake Ewauna
 - ← Lost River Diversion Channel: Diversions and Return Flows
 - → North Canal Diversions
 - ← Klamath Straits Drain
 - → ADY Canal Diversions
 - → Losses to Upper Basin
 - Klamath River Above Keno
 - △ Keno Lake and Dam
 - → Acc/Losses to Gage Reach
 - Klamath River below Keno
 - ← Trib Acc Keno to JC Boyle
 - → Losses to JC Boyle Reach
 - △ JC Boyle/Topsy Lake
 - ← Large Springs
 - JC Boyle Power Plant
 - Klamath River below JC Boyle Power Plant
 - ← Trib Acc JC Boyle to Copco
 - → Losses to Copco Reach
 - △ Copco Lake
 - Copco Power Plant 1
 - △ Copco 2 Forebay
 - Copco Power Plant 2
 - ← Trib Acc Copco to Iron Gate
 - → Losses to Iron Gate Reach
 - △ Iron Gate Reservoir
 - Iron Gate Power Plant
 - Klamath River Below Iron Gate
 - ← Bogus Creek Reach Acc
 - ← Willow Creek Reach Acc
 - ← Cottonwood Creek Reach Acc
 - → Losses to Shasta River reach
 - ← Shasta River near Yreka
 - ← Humbug Creek Reach Acc
 - ← Beaver Creek Reach Acc
 - ← Dona Creek Reach Acc
 - ← Horse Creek Reach Acc
 - → Losses to Scott River Reach
 - ← Scott River near Fort Jones and Acc to Confluence
 - → Losses to Seiad Valley Reach
 - ← Acc Scott River Reach to Seiad Gage
 - Klamath River near Seiad Valley
 - ← Salmon River at Somes Bar
 - ← Acc to Klamath River in Seiad to Orleans Reach (w/o Salmon)
 - Klamath River at Orleans
 - ← Trinity River at Hoopa
 - ← Acc to Klamath River in Orleans to Klamath Reach (w/o Trinity)
 - Klamath River near Klamath, CA
-
- Node Index**
- Gaged Flow
 - Input/Output Node
 - △ Reservoir
 - Power Plant

PREPARING THE ARS WATER DATABASE FOR THE TWENTY-FIRST CENTURY

By Jane L. Thurman, Computer Specialist, USDA-ARS Hydrology Laboratory, Beltsville, Maryland, and Ralph T. Roberts, Computer Specialist, USDA-ARS Hydrology Laboratory, Beltsville, Maryland

Abstract

The Water Data Center (WDC) is the group within the Hydrology Laboratory, Agricultural Research Service (ARS), U. S. Department of Agriculture, responsible for the storage, dissemination, and archival of water data collected by the agency. The ARS Water Database consists primarily of rainfall and runoff data from 333 experimental agricultural watersheds located in the United States. Data included in the base consist of variable time-series data from watersheds varying from .2 hectare (.5 acre) to over 1,200 square kilometers (463 square miles). Periods of record for some watershed stations extend to 50 years. Users of the database include hydrologists, modelers, engineers and students. As of October 1997 there were approximately 16,600 station years of rainfall and runoff available from the database. In an effort to make data readily available to the public in a timely and user-friendly environment, the WDC strives to develop state-of-the-art strategies to aid the end user in the retrieval of data from the ARS Water Database. This paper will present an overview of the World Wide Web pages developed for use on the Internet to help end users to select and to retrieve datasets useful to their research.

Key words: water data, hydrology, CD-ROM, Internet, information delivery system

INTRODUCTION

The U.S. Department of Agriculture, Agricultural Research Service (ARS) is one of the foremost sources of agricultural scientific expertise in the world. The agency provides innovative leadership for developing agricultural technology which can be used to address natural resource management and conservation questions. In support of these objectives, the ARS maintains a series of experimental watersheds, some of which have been monitored continuously for over 50 years. The resulting database of water-related information is useful for the development and validation of physically-based models for energy and water transfer in agricultural and rangeland systems, for studying the effects of various land management practices, for predicting the effects of future climate changes on agricultural and rangeland ecosystems, and for use in subgrid scale variability studies for global change models.

HISTORY OF THE ARS WATER DATABASE

The ARS has long understood the value of continuous monitoring to enhance our knowledge of the basic processes pertaining to water and land resources. Originally the ARS watershed research program was developed to explore the effects of alternative agricultural practices on the hydrology

of small watersheds. In support of this mission several research centers, representing contrasting land use areas, were established from the late 1920's through the mid 1960's. All the ARS experimental watersheds are heavily instrumented. Generally the watersheds consist of nested or paired study areas where alternative practices, land use, and climatic variability can be studied in a closely monitored environment. Many of the experimental basins include extensive rain gauge networks (Hershfield, 1971). Basic hydrologic parameters such as precipitation, streamflow, and temperature data are being collected continuously using various types of recording equipment. These data are recorded with variable time intervals sufficient to recreate storm hydrographs and rainfall hyetographs. ARS is currently collecting data at 140 distinct watersheds in 12 states. In addition to watersheds currently being monitored the WDC maintains data from about 200 watersheds where studies have been discontinued. Figure 1 indicates the study areas represented in the ARS Water Database.

The ARS Water Database consists primarily of precipitation and streamflow data. Readings included in the database consist of variable time-series data from watersheds varying from .2 hectare (.5 acre) to over 12,400 square kilometers (4,800 square miles). Periods of record for several watershed recording stations extend to 50 years. Rain gauge networks have from 1 to more than 200 recording stations per watershed. As of October 1997 there were approximately 16,600 station years of rainfall and runoff available from the database. In addition to the basic rainfall and runoff data, maximum-minimum daily air temperature data are generally available for each of the major study areas. Auxiliary data associated with the ARS Water Database include information about the watersheds such as latitude/longitude, area, and land use. Maps provide topographical information, location of significant physical features and the location of the rain gauges.

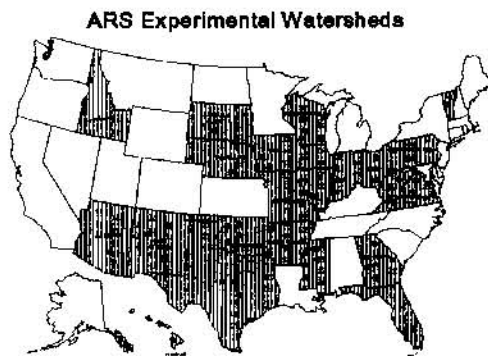


Figure 1: ARS Experimental Study Areas Represented in the ARS Water Database

DATABASE DISTRIBUTION

In the late 1950's ARS began to provide public access to its water data by publishing summaries of data collected by the watershed research centers. The WDC was established to compile, summarize and publish rainfall/runoff data. The result was a series of USDA Miscellaneous Publications numbering 22 volumes (Thurman and Roberts, 1989) and a database of rainfall/runoff data from the ARS experimental watersheds. Consequently the WDC became responsible for the storage, dissemination, and archival of water data collected by the agency. In an effort to make data readily available to the public in a timely and user-friendly environment, the WDC has developed various strategies depending upon the technological capabilities available at the time.

The distribution of information and data from the ARS Water Database have historically been dependent upon direct interaction with WDC staff. An USDA regional mainframe computer was first used to store and to process the database during the mid 1970's. In-house software was

developed to retrieve and transfer data to computer media which could be used by the researcher. Typical output media included magnetic tape, punch cards and printout.

During the early 1980's the WDC developed an on-line retrieval system called REPHLEX (Thurman et al., 1983) to enable users with access to the USDA mainframe computer to review and extract information from the database interactively. Later, as microcomputers became a viable alternative to the mainframe environment, the WDC developed and implemented a bulletin board system called REPHLEX II which used a microcomputer system with write-once, read-many optical disk storage.

The archival quality of the ARS Water Database led the WDC to develop a CD-ROM containing the base during the early 1990's. Generally, data are added to the database in minimum increments of a year. Typically, several years of data are added at various intervals for a specific location. The individual research facilities of ARS are responsible for quality control of the data collected at their location. Generally a 2-5 year lag time exists between data collection and inclusion in the ARS Water Database. During this interval the data are reviewed and corrected as necessary. Rarely are data modified after they arrive at the WDC. The CD-ROM is a user-friendly method of distribution because of the interactive software developed to interact with the database. This software has evolved to a Windows environment for maximum flexibility of features that include extraction, viewing, exporting and charting of data subsets.

In 1994 the WDC made the ARS Water Database available via anonymous file transfer protocol (ftp) on the Internet. A World Wide Web home page was generated for those with browsing software. A researcher using anonymous ftp to download portions of the ARS Water Database on the Internet may do so by connecting to the address: *hydrolab.arsusda.gov*. Internet browsing programs can reach a series of Web pages with the following command:

http://hydrolab.arsusda.gov/wdc/arswater.html

During the last two years the WDC has developed a comprehensive series of Web pages which facilitate the user's efforts to retrieve appropriate data subsets. Web pages showing the area, latitude-longitude, name, relevant rain gauges, and land use information for each watershed have been made available. Suggested single rain gauges are often listed for a watershed for those users who do not want or need to weight precipitation over the rain gauge network. Identifying rainfall, runoff, temperature, etc. by name rather than by the in-house coding structure makes it easier for a user to find the data that are needed and available. Maps of the watersheds have been made available with the data files on the Internet. These map files can be downloaded and printed to show features of the watershed such as topography and placement of recording stations.

PREPARING FOR THE NEW MILLENNIUM

Using the Internet the WDC has been able to centralize and summarize information that has generally been delivered through interaction with the users. As the year 2000 approaches the WDC will continue to make changes in our operations to best respond to our customer base and to the ARS.

Currently data files are organized by recording station and compressed to minimize download time for users using modems for their Internet access. With the development of tools to interact with databases the WDC will be able to develop interactive applications to extract and chart sub-portions

of the period of record for a recording station to web browsers. This development will give the Internet user the same capabilities now available to the CD-ROM users.

The Internet also supersedes the need to provide hardcopy publications. Reports, indices and summaries can be made available in html, ASCII text or as Adobe Acrobat Portable Document Format (PDF) format. Updated information can be made available in a timely manner. Reference materials and image data which provide visual illustration of the information can be made available. For example, the current WDC home page contains a mouse-sensitive map image to link the user to specific information and data files pertaining to a particular study area.

The WDC will also assertively use the ability to co-mingle information about the data from our centralized database with the distributed databases found at the individual watershed research centers of the ARS. While the ARS Water Database consists primarily of precipitation, streamflow and air temperature, there are often requests for other hydrologic and climatic parameters such as soil moisture, solar radiation, pan evaporation, groundwater levels and water quality parameters such as nutrient concentrations. These data may be available from the watershed research centers. By creating links in the WDC web pages, the distributed data become as easily accessible as the data from the centralized database.

CONCLUSION

The ARS maintains a series of experimental watersheds, some of which have been monitored continuously for over 50 years. The resulting database of water-related information is useful for the development and validation of physically-based models and for studying hydrologic processes on agricultural and rangeland ecosystems for time intervals of storm duration to 50 years. The ARS Water Database is an excellent source of information or data characterizing detailed hydrologic phenomena, long-term records, and intensive instrumentation. The WDC endeavors to make water data collected by ARS watershed research centers readily available to the research community in a timely and user-friendly environment. The thrust of these developments is currently concentrated on the Internet environment. Already the Internet has provided the capability to disseminate information electronically in lieu of that information historically provided through direct interaction with WDC staff. As web technology improves there exist varied opportunities to further improve the dialogue with users.

REFERENCES

- Hershfield, David M. (Editor), 1971. Agricultural Research Service precipitation facilities and related studies, U. S. Department of Agriculture, Agricultural Research Service, ARS 41-176, 117 pp., Washington, D.C.
- Thurman, Jane L., Roberts, R. T., and Burford, J. B., 1983. Retrieval procedures for hydrologic data from ARS experimental watersheds in the United States (REPHLEX). USDA, ARS, ARM-NE-9, 113 pp.

Thurman, Jane L., and Roberts, R. T., 1989. Hydrologic data for experimental agricultural watersheds in the United States, 1978-79. USDA Misc. Pub.. 1469, 613 pp.

Disclaimer

Trade names are used in this publication solely to provide information. Mention of a trade name does not constitute a guarantee or warranty of the product by the U. S. Department of Agriculture or an endorsement by the Department over other products not mentioned.

FRAME – AN INTEGRATED MODELING SYSTEM OF CHANNEL AND LANDSCAPE PROCESSES

By Dalmo A. Vieira, Research Associate; Eddy J. Langendoen, Research Assistant Professor, Center for Computational Hydroscience and Engineering, The University of Mississippi, University, MS; Ronald L. Bingner, Agricultural Engineer, USDA-ARS National Sedimentation Laboratory, Oxford, MS.

Abstract: FRAME (*Fluvial Routing Analysis and Modeling Environment*) is a software package to simulate watershed, channel flow and sediment transport processes. FRAME combines several component programs into a single package, creating an integrated modeling environment. FRAME manages all the computer programs of the watershed simulation, controlling their execution according to user input. FRAME facilitates the use of the modeling system by providing a context sensitive Graphical User Interface (GUI), and by performing automatic data format conversions and consistency checks. FRAME is a tool for personnel in federal action agencies, such as USDA-NRCS and USCOE, to perform long-term evaluations of runoff and erosion control management practices on ungaged watersheds. Effective planning can produce efficient designs to reduce project costs and total watershed sediment yield, thus improving water quality.

INTRODUCTION

FRAME is an integrated software package to simulate watershed, and channel flow and sediment routing processes. FRAME is composed of several modeling components, tied together by a control module that provides a Graphical User Interface (GUI) and manages all data sets and operations. FRAME uses the Geographic Information System ArcView[®] as the front-end interface (ESRI, 1996a, 1996b). FRAME is an extension to ArcView that provides the needed functionality. When the FRAME extension is active, sets of menu options are appended to the standard ArcView interface. These controls let the user perform all operations related to FRAME. Figure 1 shows FRAME's graphical user interface.

The core components of FRAME are the USDA-ARS models TOPAZ and SWAT, and the models DWAVNET and BEAMS developed cooperatively between CCHE and USDA-ARS. TOPAZ — TOPographic PArameteriZation — is an automated digital landscape analysis tool for identification of channels and subcatchments of drainage networks (Garbrecht and Martz, 1995). The computer model SWAT — Soil and Water Assessment Tool — simulates continuous watershed processes on a long-term basis with a minimum amount of input data requirements (Arnold et al., 1993). The flow routing model DWAVNET — Diffusion WAVE model for channel NETworks — simulates the long term, continuous runoff from storm events and may be applied to networks of channels with compound cross sections (Langendoen, 1996). Instream hydraulic and erosion control structures are integrated in the flow routing scheme. The sediment transport model BEAMS — Bed and bank Erosion Analysis Model for Streams — simulates the long term, dynamic response of streams to natural and man-induced changes in the watershed (Langendoen et al., 1998). BEAMS encompasses two major models. A sediment transport model performs routing of graded material and computes bed erosion and deposition and hydraulic sorting. A bank erosion and stability model accounts for bank toe erosion and width adjustment due to mass wasting.

FRAME has additional features that are not available in the original modeling software. These features include the generation of a computational mesh for the channel flow and sediment routing models, performed by a channel network analysis module (Vieira, 1997, Vieira et al, 1997).

FRAME distinguishes three steps in the simulation of watershed and flow routing problems. The *Landscape Analysis* phase deals with the automatic extraction of the channel network and the delineation of the watershed, and the definition of its subwatersheds. In the *Channel Network Analysis* part, FRAME manages the input of data for the channel flow and sediment transport models. FRAME is able to automatically create a computational mesh based on the extracted channel network. The third step is the *Channel Flow and Sediment Transport Analysis*. Using the data gathered during the first two steps, FRAME controls the flow and sediment transport models DWAVNET and BEAMS. FRAME manages the input data to these models, and provides a convenient GUI to help the user perform the channel flow simulations.

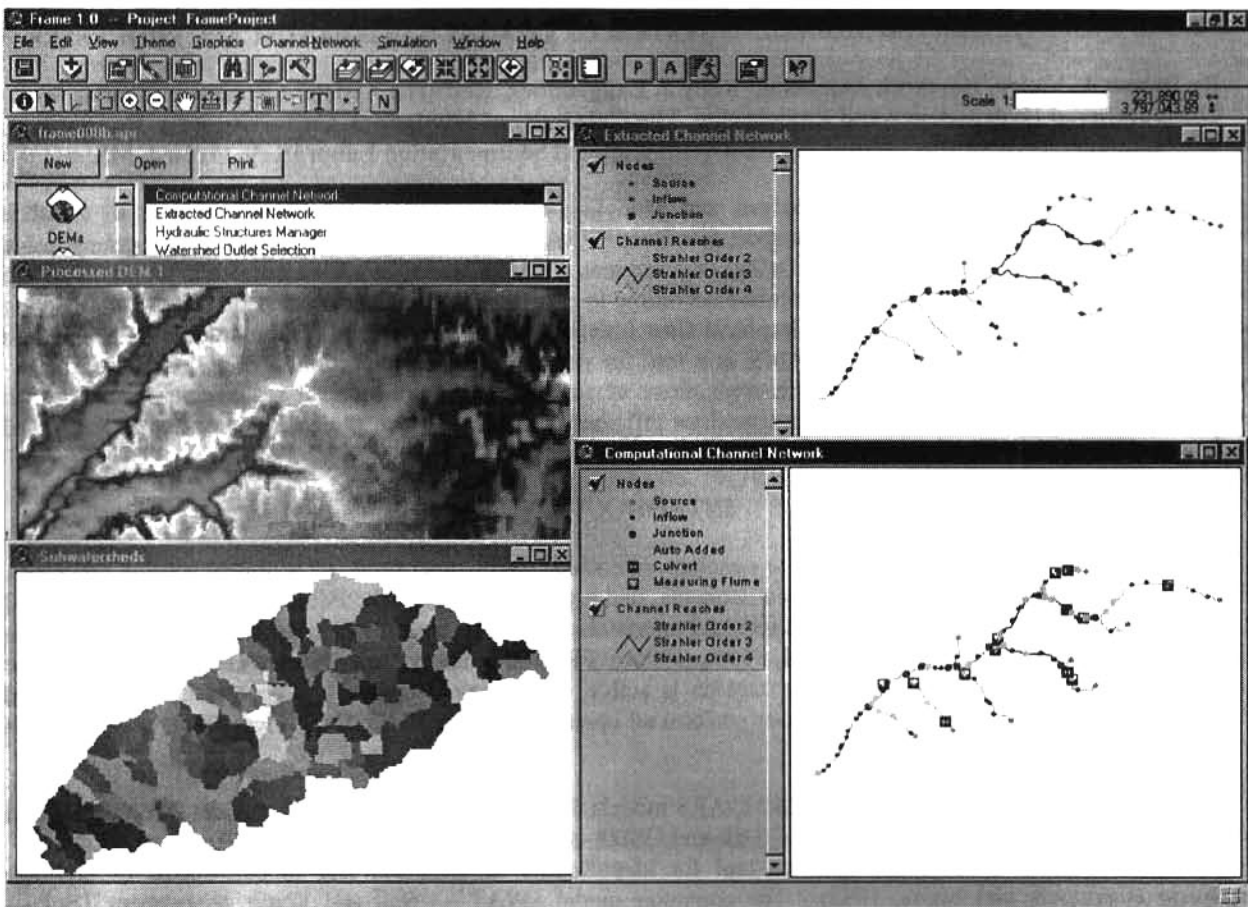


Figure 1. The FRAME Graphical User Interface

CHANNEL NETWORK EXTRACTION

FRAME provides the capability of extracting channel network and subwatershed information from a Digital Elevation Model (DEM). This capability is provided by the landscape analysis model. FRAME simplifies the preparation of input to TOPAZ by reducing the amount of information the user has to supply. The extraction of a channel network requires a sequence of preparation algorithms for the DEM. These algorithms ensure that the DEM is suitable for determining a convergent network of flow paths. The channel extraction algorithms require a DEM with clearly identifiable flow directions. Therefore, FRAME, through TOPAZ, ensures that depressions and flat areas are eliminated before the channel extraction process begins. Pits and depressions must be filled to the elevation of their local outlets. Flat areas are eliminated by imposing a relief that is based on the topography of the surrounding areas.

The user can control the appearance of the extracted channel network (channel density, minimum channel lengths, and subwatershed areas) through two calibration parameters. FRAME provides a convenient interface to guide the user in defining the parameters. FRAME also retrieves the necessary information about the DEM, reducing the amount of information the user has to input. Figure 2 shows an example of a channel network with first order cha

FRAME provides an additional option, which was not implemented in the TOPAZ module. The user can specify the minimum channel Strahler Order of channels to remain in the network. This option removes lower order channels after the channel network is extracted from the DEM. Lower-order channels are still considered when defining the subwatersheds. Since the flow in lower-order channels is often relatively small, its routing by the channel flow model can be regarded as unnecessary, and is carried out by the watershed model. The outflow of the subwatersheds corresponding to the removed channels is still considered as point inflow to the channel network.

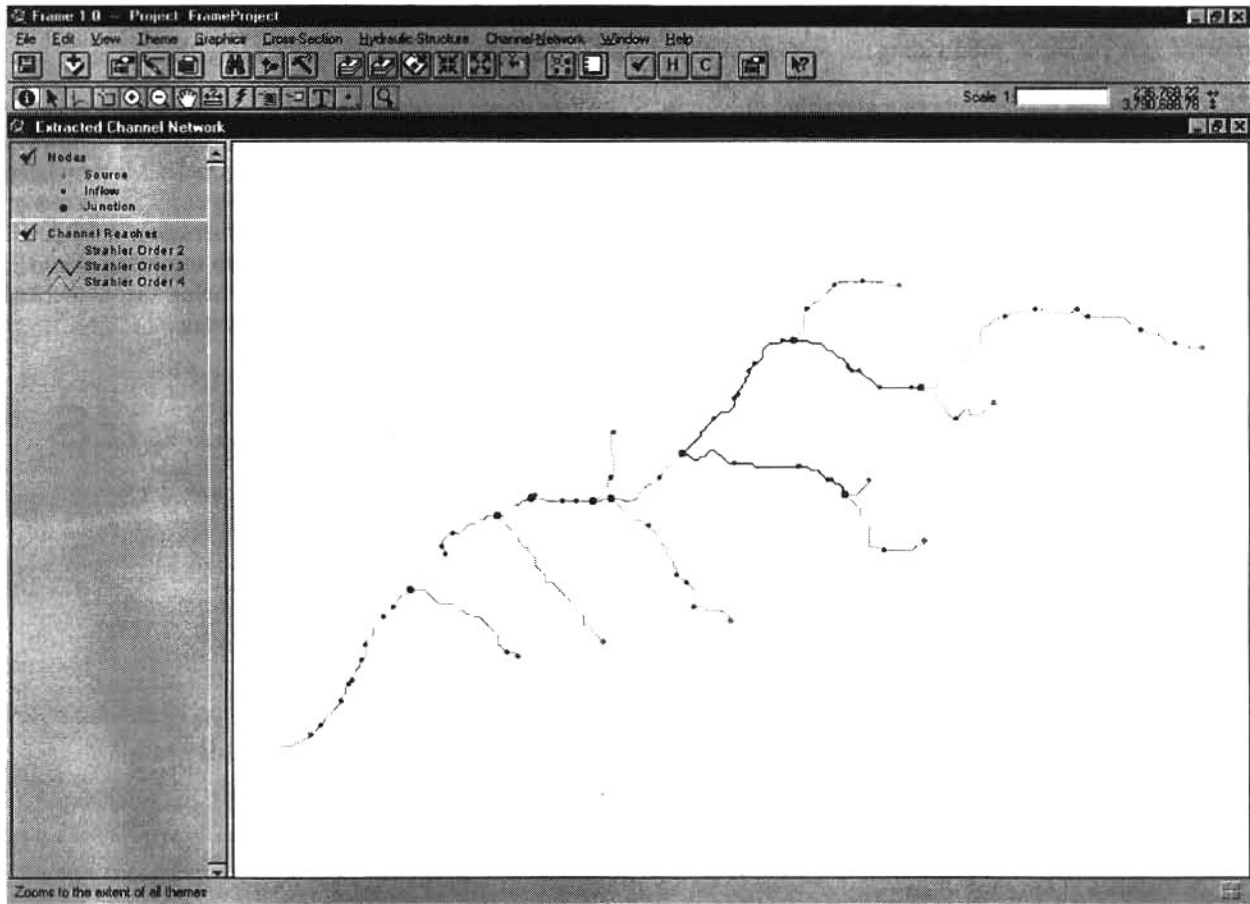


Figure 2 Channel network extracted from a Digital Elevation Model (DEM).

Frame Network Database: FRAME extends TOPAZ by creating a relational database to store the channel network and subwatershed data. This database eliminates the need of referencing to large, computer resource demanding, raster files. A series of tables are logically connected through indices, called IDs. FRAME manages the data relationships between these tables, updates their contents, and verifies their integrity.

The tables store data related to each of the following entities that compose the channel network: *Nodes*, *Reaches*, *Links*, *Channels*, *Subwatersheds*, and *Incremental Areas*. The FRAME database was designed so frequent operations, such as the addition of a node to the channel network, can be performed quickly, with a minimum of modifications to the tables. The database was designed to allow the addition of tables to describe future information. Figure 3 depicts the relationships among the database tables.

Channel Network Logical Description: A Node is a point in the network that represents a special feature. They mark the beginning and ending points of channel segments, location of channel junctions, point inflow, and hydraulic structures. They may also represent points in a computational mesh that represents the channel network, where flow and sediment transport variables will be computed.

The remaining entities represent channel segments. A Reach is a channel segment between two nodes. A Link is a logical entity, whose main purpose is to organize the numerical computation of flow in the network. A Link can assume two types: a container of Reaches or a single Hydraulic Structure. A Link is usually composed of several channel Reaches. A Channel represents the natural division of the network into streams.

The definition of subwatersheds is performed by TOPAZ, which identifies the drainage area for each stream in the network. *Subwatersheds* correspond to the segments called *Channel*, as defined above. FRAME divides the subwatersheds into portions called *Incremental Areas*. Incremental Areas are drainage areas that correspond to

channel segments between two nodes (Reaches). The purpose of incremental areas is primarily computational. They provide easy means of subdividing the outflow from a subwatershed among all nodes along its channel.

FRAME uses the node numbering algorithm present in TOPAZ to create its own numbering system, which is better suited to the flow and sediment transport simulations. A channel junction in the FRAME network is always composed of two incoming channels and one outgoing channel. Drainage networks extracted from DEMs may have more than two incoming channels, up to the theoretical maximum of seven. FRAME treats these cases as a series of consecutive channel junctions, each having two incoming and one outgoing channels. Furthermore, a FRAME junction is composed of three nodes, all at the exact same location: one node at the end of each incoming channel, and a node at the beginning of the outgoing channel. This approach of multiple nodes helps the numerical implementation of the discretization and solution methods of the flow and sediment transport models.

RELATIONAL DATABASE TABLES

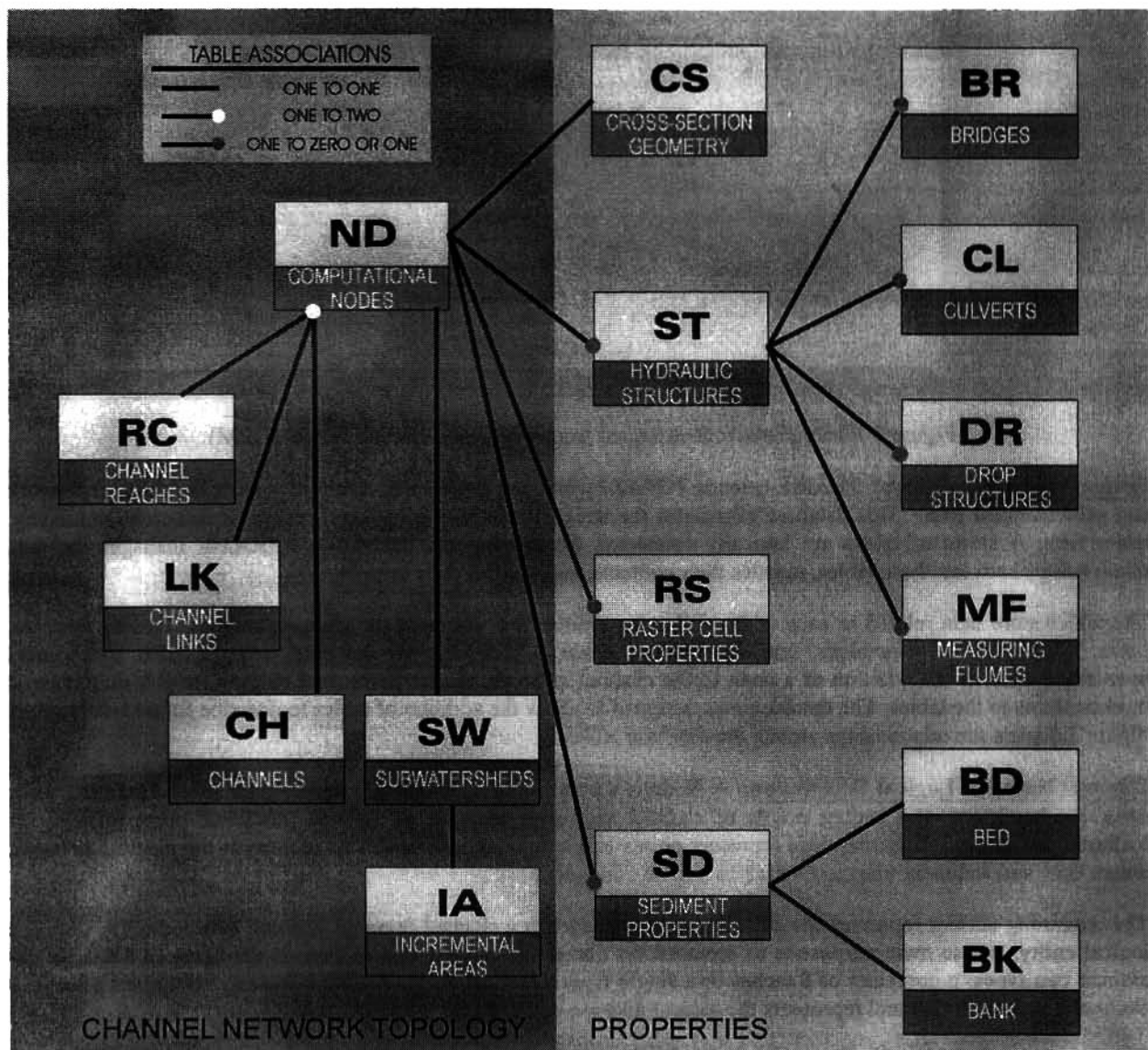


Figure 3. The FRAME Network Database.

CHANNEL NETWORK ANALYSIS

FRAME provides many features to help the user prepare the input data for the flow routing and sediment transport simulations. The input data for the simulation models can be classified into three categories:

- **Channel Network Definition** – Describes the channel network elements, such as channel segments, nodes, location of hydraulic structures, subwatersheds, etc.
- **Supplemental Data** – Includes all the data that is not a part of the channel network description, such as channel geometry data, hydraulic structure characteristics, bed and bank material description, etc.
- **Simulation Parameters** – Comprises user-defined options and parameters for the numerical simulations.

FRAME is able to automatically create the channel network and the corresponding subwatersheds. It also creates a logical description of all the network elements and their mutual relationships. The simulation models, however, usually require a more detailed topological schematization of the simulation domain. This spatial discretization depends on characteristics of the numerical analysis methods. For the flow simulation, the channel network is represented by one-dimensional channel segments and by nodal points. The simulation models impose certain conditions for the number, size, and distribution of these elements. FRAME is designed to automatically define a computational mesh that adequately describes the channel network, ensuring that the numerical simulation will meet the minimum requirements of accuracy and stability.

When a channel network is created, all channel segments and some nodal points are defined. The nodal points represent special features in the network, such as channel junctions, points of inflow, etc. For the numerical analysis, however, more nodal points are necessary to adequately describe the characteristics of the simulation domain. FRAME provides capabilities for the addition of nodal points to the channel network. FRAME performs an analysis of the network layout and selectively adds nodal points to improve the computational mesh characteristics. This analysis considers the length of channel segments, the positioning of hydraulic structures, and channel cross section properties. Therefore, to begin the channel network analysis, cross section and hydraulic structure data must be available.

FRAME provides a convenient interface for entering, editing, checking, and visualizing the input data. FRAME tries to minimize the input work by performing some tasks automatically.

Channel Cross Sections: The flow routing model requires that the channel cross section geometry be known for all computational nodes. FRAME relaxes this requirement by performing linear interpolation to supply the necessary information. The user is then required to supply cross section data only for the nodes at the beginning and ending of *Channels*, that is, for all Source Nodes and Channel Junctions.

In order to perform the numerical simulations in the channel network, all nodes should have cross section information available. Since a channel network usually has hundreds of nodes, the user rarely has information available for all the nodal points in the network. FRAME simplifies the input of data by using linear interpolation to supply the data for the nodes without information. FRAME uses the nearest upstream and downstream nodes with specified cross section for the interpolation. FRAME considers the subdivision into main channel, left and right floodplains when interpolating. During the search, FRAME does not navigate the network beyond channel junctions, since the cross section properties may vary significantly.

FRAME implements the cross section description format of the simulation models DWAVNET and BEAMS. Each cross section is represented by eight pairs of distance and elevation coordinates. The cross section is subdivided into three regions: main channel, left floodplain, and right floodplain. The floodplain regions are optional.

FRAME provides several ways to input cross sectional data. The user can select a node and then fill the appropriate fields with information when prompted by the program. Alternatively, the user may choose to create a separate data file containing the data for the required nodes. The data can be modified later using the various edit options. FRAME allows the selection of a particular node for editing or displays a spreadsheet-like table, where the user can see and edit cross section values for any node.

Hydraulic Structures: DWAVNET and BEAMS treat hydraulic structures in the channel network as a set of three nodes that occupy the same exact location. These nodes are used to implement the solution of the equations that describe the behavior of the hydraulic structure. The nodes represent the end of the channel reach upstream of the structure, the structure itself, and the beginning of the reach downstream of the structure.

Each hydraulic structure has its data stored in a database table. Since there are several types of structures, a different table is provided for each type. All tables are referenced in a master table called the *Structure Table*, which stores the location, type, and identification number of each structure. The connection to the rest of the database is made through this table.

FRAME provides a special window to guide the user in specifying the location and entering the characteristics of hydraulic structures. An interactive tool allows the user to click at the point where a hydraulic structure is to be inserted. FRAME will display an interface to select the type of structure and enter all the necessary data.

Computational Mesh Generation: The numerical flow routing in a channel network requires a well-defined set of computational nodes. A channel network, as extracted from a DEM, has very few nodes. The nodes only identify the beginning of channels and channel junctions. Furthermore, the spatial distribution of these features makes the resulting network inadequate for numerical computations. The flow model imposes restrictions on channel lengths and on the uniformity of their distribution in the network. The presence of junctions and hydraulic structures significantly affects the length of channel reaches. The channel network, as extracted from a DEM, shows great variations in reach lengths.

In order to have a channel network that is suitable for the numerical computations, many new nodes have to be defined. FRAME has a Channel Network Analysis module that inspects the channel network and determines improvements to create a computational network that is adequate to the flow routing model. This analysis module consists of a series of pre-defined rules, tuned to the simulation models of FRAME, which determine the number and location of new nodes to be added to the channel network.

The current version of FRAME has a set of three rules that analyze the channel network. They determine where extra nodes should be added in order to create a computational mesh that satisfies the accuracy and convergence requirements of the models DWAVNET and BEAMS.

The first rule to be applied is the verification of longitudinal variations in flow area. For locations where the flow area changes significantly, FRAME adds extra nodes so that the variation in area is reduced to acceptable values.

FRAME analyzes all channels to determine if the lengths of channel reaches are reasonably uniform. A large variation in the length of successive computational reaches can negatively affect the quality of the numerical simulations. FRAME adds nodes to the network to make the distribution of reach lengths more uniform.

Finally, FRAME inspects the neighborhood of channel junctions and hydraulic structures. Specialized algorithms compute the flow properties at these locations, and FRAME makes sure the computational network satisfies some special requirements.

FRAME provides a graphical interface to orient the user through this process. The interface consists of a new map window, where the user can create the Computational Channel Network. Besides the automatic, built-in rules procedure, the user can add or remove nodes interactively by clicking on the channel network map. Figure 4 shows the computational channel network window and its interface.

The interface for the Computational Channel Network window has a tool that allows the user to interactively add nodes to the computational network. When this tool is active, the user can just click at the point where a node is wanted. FRAME displays an interface where the user confirms the insertion of the node, and asks the user if there is cross section information to be input. The user can choose to input the data at the moment the node is added to the network, postpone the data entry, or let FRAME use its interpolation routines to supply the needed information.

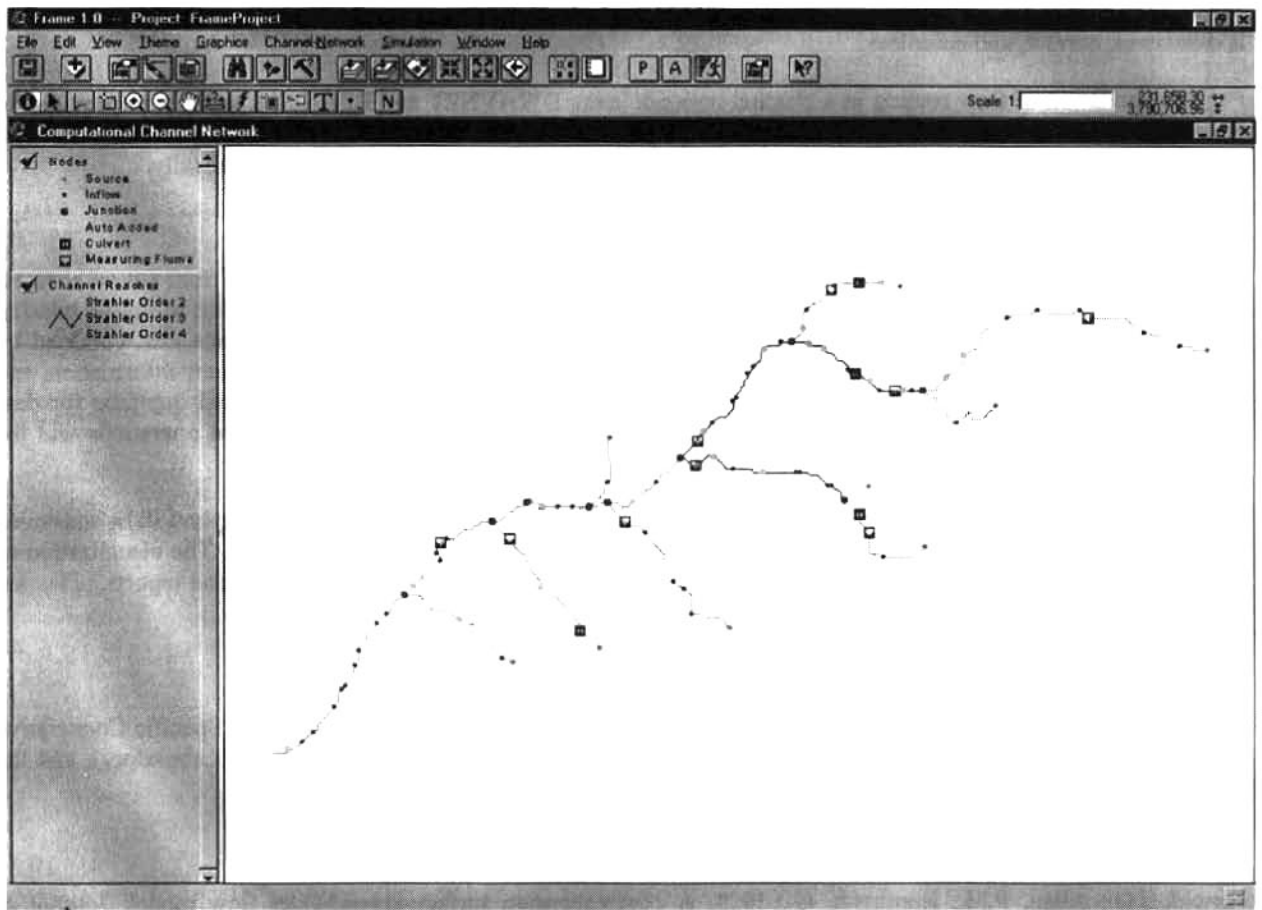


Figure 4. The Computational Channel Network.

When a new node is added, the database tables that describe the channel network are updated. The Node Table gets another record, and the node numbering is changed to account for the new node. The channel Reach containing the new node is split into two new reaches. The Link Table is modified only if the split Reach is the first or the last in the Link. The Subwatershed Table is modified to account for the addition of a new Incremental Area. The Incremental Area where the node was added is also split, a new record is added and the old Incremental Area has some properties altered. FRAME automatically inserts a record in the Cross Section Table to store data related to the newly added node. If the user has provided cross section data, FRAME stores the information in the table. Otherwise, the record is filled with the "No Data" value, and FRAME will later use the interpolation routines to complete the information.

FLOW SIMULATION

The simulation of flow and sediment transport in a network of channels requires the assembly of a large database. The database includes data from various sources, including the output of other modeling components, which is stored using different techniques, such as tables, raster images, and vector graphics. The exchange of information between modeling programs implies resource-consuming data format conversions. Another hurdle is the fact that the output of one modeling component does not usually provide all the input requirements of another. Extra effort must be spent in complementing the necessary information so that two or more programs can be used simultaneously or sequentially.

FRAME simplifies the modeling task since it controls the flow of information among the models, guiding the user through the process of data preparation and substantially reducing the amount of data handled by the user. FRAME organizes all data so that they are readily available for the simulation models. Data format conversions and

consistency checks are part of the process. The FRAME relational database is gradually built so that all information is consistent, correct, and complete.

For the simulation of flow routing in a channel network using DWAVNET and BEAMS, it suffices to provide the boundary conditions and a couple of parameters. FRAME provides the graphical user interface to guide the user through this process. FRAME controls the simulation models, performing all data input automatically.

SUMMARY

Modeling of a watershed system involves the tedious process of assembling a large database from varied sources. The collected data are rarely complete and ready for use by the simulation models, requiring effort to supply missing information and convert the data to formats suitable to the models. FRAME attempts to reduce this workload by integrating several data sets into a common database, analyzing the available data to produce new information, and by performing the necessary conversions. FRAME provides a convenient graphically oriented interface for data entry and checking. Furthermore, the interface guides the modeler, clarifying the sequence of operations and the available options.

The design of FRAME foresees the inclusion of other modeling components and tools. Data input will be improved by providing the user with digitizing capabilities and support for scanned and satellite images. The visualization of output data will be enhanced by the automatic production of maps, graphs, summary tables, and reports. Planned extensions to FRAME include water quality and groundwater simulation models.

ACKNOWLEDGMENTS

This work is a result of research sponsored by the USDA Agricultural Research Service under Specific Cooperative Agreement No. 6408-13000-008-01S (monitored by the USDA-ARS National Sedimentation Laboratory), and the University of Mississippi.

REFERENCES

- Arnold, J.G., Allen, P.M., Bernhardt, G., 1993, A comprehensive surface-groundwater flow model, *Journal of Hydrology*, 142, 47-69.
- Environmental Systems Research Institute, Inc., ESRI, 1996a, *Using ArcView GIS*, ESRI, Redlands, California.
- Environmental Systems Research Institute, Inc., ESRI, 1996b, *Avenue. Customization and Application Development for ArcView*, ESRI, Redlands, California.
- Garbrecht, J. and Martz, L.W., 1995, An automated digital landscape analysis tool for topographic evaluation, drainage identification, watershed segmentation and subcatchment parameterization, Report No. NAWQL 95-1, National Agricultural Water Quality Laboratory, USDA, Agricultural Research Service, Durant, Oklahoma.
- Langendoen, E.J., 1996, Discretization diffusion wave model, Tech. Rep. No. CCHE-TR-96-1, Center for Computational Hydroscience and Engineering, The University of Mississippi, University, Mississippi.
- Langendoen, E.J., Bingner, R.L., Kuhnle, R.A., 1998, Modeling of Long Term Changes of Unstable Streams, Proc. First Federal Interagency Hydrologic Modeling Conference, Las Vegas, NV.
- Vieira, D.A., 1997, FRAME - Control Module Technical Manual, Tech. Rep. No. CCHE-TR-97-7, Center for Computational Hydroscience and Engineering, The University of Mississippi, University, Mississippi.
- Vieira, D.A., Langendoen, E.J., Bingner, R.L., 1997, FRAME - A Modeling Environment for Watershed Processes. In Proc. Conference on Management of Landscapes Disturbed by Channel Incision, Oxford, MS, 709-715.

A FINITE ELEMENT MODEL WITH MOVING BOUNDARIES: APPLICATION TO FLOODS AND RUNUP.

By Roy A. Walters, Oceanographer, U.S. Geological Survey, Denver, Colorado

Abstract A finite element model is developed for the 2-dimensional shallow water equations using semi-implicit methods in time. A semi-Lagrangian method is used to approximate the effects of advection. A wave equation is formed at the discrete level such that the equations decouple into an equation for surface elevation, and a momentum equation for the horizontal velocity. The stability and computational efficiency of this model are examined with a field scale test case that is characterized by highly irregular geometry.

INTRODUCTION

This paper contains the development of a robust and computationally efficient model that can simulate extreme hydraulic events that are accompanied by extensive flooding and drying. The goal is to be able to simulate large floods over floodplains with rather general topography. The wetted inundation area is then determined by the model solution.

The method adopted here is to use the primitive shallow water equations and form a wave equation at the discrete level. This procedure carries through the properties of the original discretized equations so that the use of elements without spurious computational modes is essential. Toward this end, low-order elements are used such that continuity is satisfied both globally and locally, and wetting and drying are greatly simplified.

In the next section, the model is developed using the discretized shallow water equations. Following this, a test case is presented that simulates a large flood on the Biglost River in southeastern Idaho.

MODEL DESCRIPTION

The basic equations are the 2-dimensional shallow water equations. Using both the hydrostatic assumption and the Boussinesq approximation, these equations are derived by a vertical integration of the Reynolds equations (Pinder and Gray, 1977). The continuity equation becomes

$$\frac{\partial \eta}{\partial t} + \nabla \cdot (H\mathbf{u}) = 0 \quad (1)$$

and the momentum equation becomes

$$\frac{d\mathbf{u}}{dt} - \frac{1}{H} \nabla \cdot (H A_h \nabla \mathbf{u}) + g \nabla \eta - \frac{\tau_s}{\rho H} + \frac{\tau_b}{\rho H} = 0 \quad (2)$$

where the coordinate directions (x,y,z) are aligned in the east, north, and up directions; $\mathbf{u}(x,y,t)$ is the depth-averaged horizontal velocity; $h(x,y)$ is the water depth measured

from a reference elevation; $\eta(x, y, t)$ is the distance from the reference elevation to the free surface; $H(x, y, t)$ is the total water depth, $H = \eta - h$; g is the gravitational acceleration; ρ is a reference density; ∇ is the horizontal gradient operator ($\partial/\partial x, \partial/\partial y$); and $A_h(x, y, t)$ is the coefficient for the horizontal component of viscous stresses. The surface and bottom boundary conditions are given by

$$\frac{\tau_s}{\rho} = \gamma_T H(\mathbf{u}_a - \mathbf{u}) \quad (z = \eta) \quad (3)$$

$$\frac{\tau_b}{\rho} = C_D |\mathbf{u}| \mathbf{u} = \gamma_B H \mathbf{u} \quad (z = h), \quad (4)$$

where the surface and bottom stress are denoted as τ_s and τ_b , respectively, \mathbf{u}_a is the wind velocity, and C_D is a bottom drag coefficient. Essential boundary conditions on η or volumetric flux are set at open boundaries, and $(\mathbf{u} \cdot \mathbf{n}) = 0$ (no normal flow) is set on land boundaries.

These equations are discretized in time using an implicit method such that the equations are evaluated in the time interval (t^{n+1}, t^n) where the superscript denotes the time level. The distance through the interval is given by the weight θ . This approach yields

$$\frac{\eta^{n+1} - \eta^n}{\Delta t} + \nabla \cdot [H^n (\theta \mathbf{u}^{n+1} + (1 - \theta) \mathbf{u}^n)] = 0 \quad (5)$$

$$\frac{\mathbf{u}^{n+1} - \mathbf{u}^*}{\Delta t} + \theta \mathbf{G}^{n+1} + (1 - \theta) \mathbf{G}^* = \mathbf{F}^* \quad (6)$$

where

$$\mathbf{G} = \gamma_B \mathbf{u} - \gamma_T (\mathbf{u}_a - \mathbf{u}) + g \nabla \eta$$

$$\mathbf{F}^* = \nabla \cdot (A_h \nabla \mathbf{u})^*$$

Semi-Lagrangian methods are used in order to take advantage of the simplicity of Eulerian methods and the enhanced stability and accuracy of Lagrangian methods (Casulli, 1990; Staniforth and Cotes, 1991). Here the superscripts n and $n + 1$ denote variables evaluated at the fixed nodes in the Eulerian grid at times t^n and t^{n+1} . The superscript $*$ denotes a variable evaluated at time t^n at the end of the Lagrangian trajectory from a computational node (See Figure 1). At each time step, the velocity is integrated backwards with respect to time to determine where a particle would be at time t^n in order to arrive at a grid node at time t^{n+1} (Staniforth and Cotes, 1991). Thus the material derivative, the first term in Equation 6, has a very simple form.

The governing equations are approximated in space using standard Galerkin finite element techniques (Becker, Carey, and Oden, 1981). The equations are discretized after defining a set of 2-dimensional triangular elements in the horizontal plane (Figure 1). Mixed methods are used such that the elements use a piecewise constant basis for η , and a constant normal

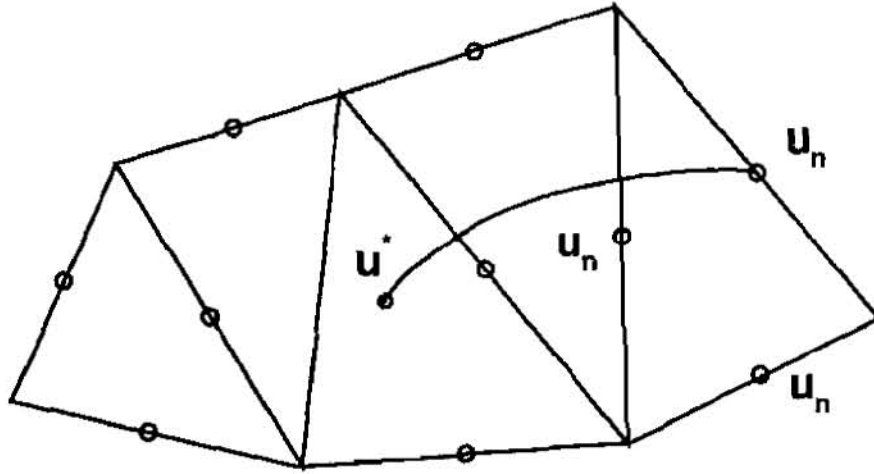


Figure 1: Definition of the elements and Lagrangian trajectories.

velocity along each edge with a linear variation in the element interior (Arbogast, 1995). For a piecewise constant interpolation for η , the finite element form of the continuity equation is

$$A_e \frac{\partial \eta_e}{\partial t} + \oint_{\Gamma_e} (H\mathbf{u}) \cdot \mathbf{n} d\Gamma = 0 \quad (7)$$

where A is the element area, Γ is the boundary of the flow domain Ω , and subscript e denotes the value for element e . Applying the discrete time operator in equation 5, the continuity equation can be written in terms of the normal component of velocity as

$$A_e \frac{\eta_e^{n+1} - \eta_e^n}{\Delta t} + \theta \oint_{\Gamma_e} H^n u_n^{n+1} d\Gamma = -(1 - \theta) \oint_{\Gamma_e} H^n u_n^n d\Gamma \quad (8)$$

where u_n is the normal component of velocity on the element side.

Next, the momentum equation is solved for u_n^{n+1} and this expression is used to eliminate u_n^{n+1} from equation 8. Integrating the finite element form of the momentum equation by using a 3 point quadrature at the midsides of the triangles, and using the discrete time operator given in equation 6

$$u_n^{n+1} = \frac{1}{C_1} [R_n - \theta N_n^{n+1}] \quad (9)$$

where

$$\begin{aligned}
R_n &= C_3 u_n^* + F_n^* + \gamma_T (\theta u_a^{n+1} + (1-\theta)u_a^*) - (1-\theta)N_n^* \\
C_1 &= \left[\frac{1}{\Delta t} + \theta(\gamma_B^{n+1} + \gamma_T^{n+1}) \right] \\
C_3 &= \left[\frac{1}{\Delta t} - (1-\theta)(\gamma_B^n + \gamma_T^n) \right] \\
N_n &= M^{-1} \left[\int_{\Omega} g \nabla \Phi \eta d\Omega - \oint_{\Gamma} g(\Phi \eta) d\Gamma \right]
\end{aligned} \tag{10}$$

where M is the mass matrix given by $M = \int_{\Omega} \Phi \Phi d\Omega$, and γ_B^{n+1} is extrapolated in time from the values at t^n . The continuity equation is put in the form of a wave equation at the discrete level by replacing u_n^{n+1} by the expression above.

$$\begin{aligned}
A_e \frac{\eta_e^{n+1}}{\Delta t} &- \frac{\theta^2}{C_1} \oint_{\Gamma_e} H^n N_n^{n+1} d\Gamma \\
&= A_e \frac{\eta_e^n}{\Delta t} - (1-\theta) \oint_{\Gamma_e} H^n u_n^n d\Gamma - \frac{\theta}{C_1} \oint_{\Gamma_e} H R_n d\Gamma
\end{aligned} \tag{11}$$

This equation contains only η at the $n+1$ time level. In practice, equation 11 is assembled and solved for η^{n+1} . Using these results, equation 9 is solved for u_n^{n+1} . The full velocity is recovered by calculating the velocity at the vertices of each triangle, then interpolating the tangential component of velocity at the midsides.

The stability analysis given by Casulli and Cattani (1994) is also applicable to this system of equations. Their results show that the linear system with constant coefficients is stable for $\frac{1}{2} \leq \theta \leq 1$ so long as a constraint on the viscous stress term is satisfied.

FIELD PROBLEM

This test case simulates transient flooding for a field-scale problem. The spatial domain is a segment of the Big Lost River in southeastern Idaho (Figure 2). The grid was created from digitized elevation data by C. Berenbrock (personal communication) using the grid generation methods of Henry and Walters (1993). The grid contains 12622 elements that have edges that vary in size from approximately 5 m in the river channel to 25 m at the edges of the floodplain.

Initially, the water was at rest with a surface elevation defined by the outflow surface elevation. The simulation was started by applying an input discharge of 210 m³/s at the inflow on the left boundary. A constant water level was specified at the outflow on the right boundary. In the simulations, a flood wave propagated through the river reach, progressively inundating areas adjacent to the river channel. The inundation area reached equilibrium in about 60 minutes of simulation time. The inundation area and surface elevation are shown in Figure 2. At this time there is flooding upstream of the first control point on the flow-

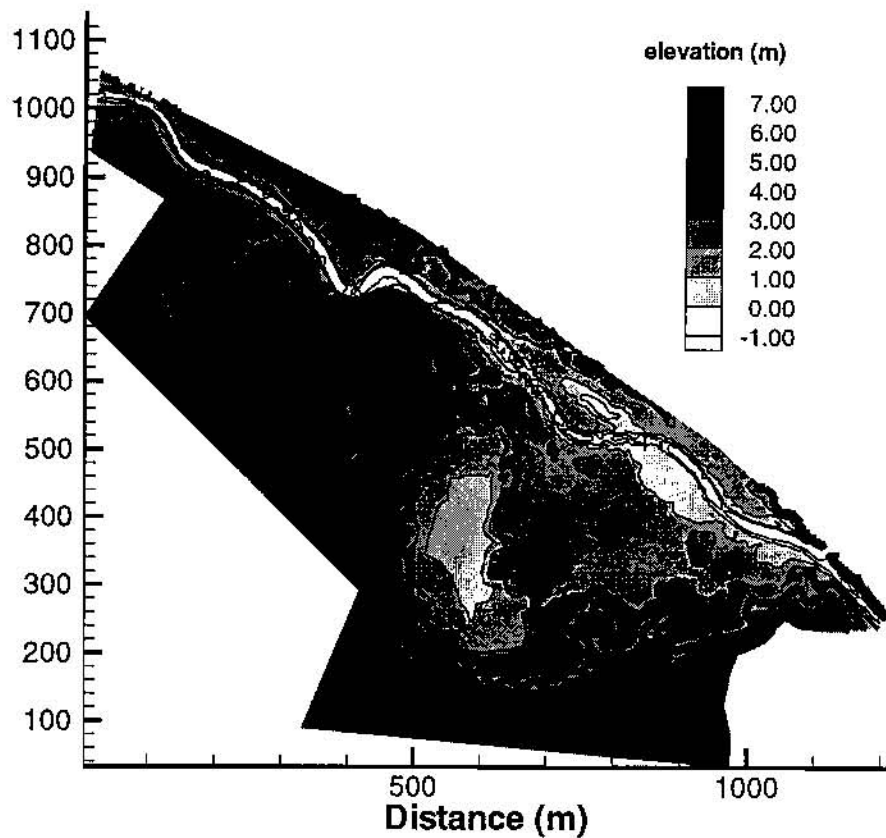


Figure 2: Topography for the Big Lost River simulation. The shaded contours are elevations in meters with respect to the water surface elevation at the outflow on the right. The heavy line indicates the edge of the inundated area after 30 minutes of simulation time.

a constriction. There is also flooding in the depression in the right-center of the domain caused by a constriction at the outflow. The advective terms cause a significant increase in water surface elevation at the control points because the flow must accelerate there.

A detail of the flow in the first sharp bend in the channel is shown in figure 3. A number of interesting flow features can be observed. A large eddy has formed on the inside of the bend where the flow passes over the shoulder of the channel. Another eddy occupies the inundated area on the left. A close examination of surface elevation indicates that there is a topographic low as the flow enters the bend, and there is a series of trailing waves farther downstream. These are hydraulic features that are expected with this complex topography. In general, these results indicate that the model is sufficiently robust to simulate highly transient flows with strong advective effects, and wetting and drying. Other tests have indicated that the model is accurate and converges at a rate $O(\Delta x)$, where Δx is an

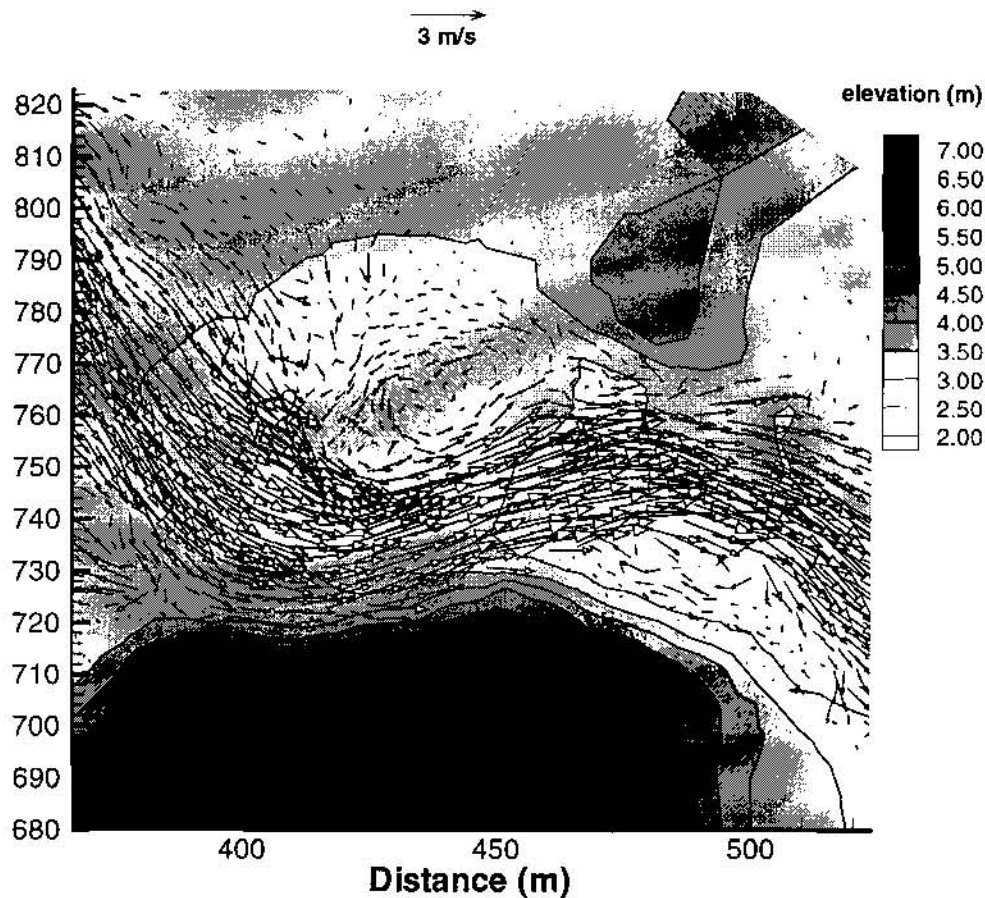


Figure 3: A flow detail in the sharp bend in the upper left part of the previous figure. The lines are elevation in meters with respect to the elevation at the outflow. Water surface elevation is shown in the inundated area that is recognized by the non-zero velocity vectors. Land elevation is shown in the dry areas.

element length scale (Walters and Casulli, 1997). This convergence rate is in agreement with theoretical predictions.

CONCLUSIONS

Using the shallow water equations, a discrete wave equation is formed from the discrete continuity and discrete momentum equations. With the mixed methods used here, there are no computational modes such as would occur with simple linear elements. An implicit time approximation coupled with a semi-Lagrangian calculation leads to a stable and robust model that treats both strong advection and moving boundaries. The method has $O(h)$ convergence rate. Results for a flood simulation highlight the efficiency and robust nature of the model.

REFERENCES

- Arbogast, T., 1995, Mixed Methods for Flow and Transport on General Geometry. In *Finite Element Modeling of Environmental Problems*, ed. G. F. Carey, Wiley, New York, 275-286.
- Becker, E., Carey, G. F., and Oden, J. T., 1981. *Finite Elements: An Introduction*, Prentice-Hall, Englewood Cliffs, New Jersey.
- Casulli, V., 1990, Semi-Implicit Finite Difference Methods for the Two-Dimensional Shallow Water Equations. *Journal of Computational Physics*, **86**, 56-74.
- Casulli, V. and Cattani, E., 1994. Stability, accuracy, and efficiency of a semi-implicit method for three-dimensional shallow water flow. *Computers Math. Applic.*, **27**, 99-112.
- Henry, R.F. and Walters, R. A., 1993. A geometrically-based, automatic generator for irregular triangular networks. *Communications in Numerical Methods in Engineering* **9**, 555-566.
- Pinder, G. F. and Gray, W. G., 1977. *Finite Elements in Surface and Subsurface Hydrology*, Academic Press.
- Staniforth, A., and Cote, J., 1991, Semi-Lagrangian integration schemes for atmospheric models-A review. *Monthly Weather Review* **119**, 2206-2223.
- Walters, R.A. and Casulli, V., 1997, A robust, finite element model for hydrostatic surface water flows. (Submitted to Comm. in Numerical Methods in Engineering).

USING ARC/INFO TO PROCESS AND ANALYZE RESERVOIR HYDROGRAPHIC SURVEY INFORMATION

By Paul Weghorst¹, Ron Ferrari², Sharon Nuanes³

Abstract: The Bureau of Reclamation, Technical Service Center's Water Resources Services Sedimentation and River Hydrologic Group, located in Denver Colorado, conducts reservoir sedimentation surveys. With recent advances in computer hardware and software, massive amounts of data can be collected and analyzed cost effectively, in timely fashion, with very accurate results. Final products are used to determine present reservoir capacity and long-term reservoir sedimentation rates.

The Sedimentation Group uses GPS (global positioning system) technology for its collection system and analyzes the collected data using ARC/INFO Triangular Irregular Network (TIN) software. ARC/INFO is a software package used in development and analysis of geographic information system (GIS) layers and the development of interactive GIS applications. GIS technology provides a means of organizing and interpreting large data sets. The hydrographic survey data collected during reservoir surveys are x,y,z coordinate data conforming to a recognized coordinate system such as UTM (Universal Transverse Mercator), Latitude/Longitude, State Plane, or other systems that represent the earth's 3-dimensional features on a flat surface. The data used to develop reservoir topography is usually from collected underwater and, or aerial data, but can come from digitized or scanned maps or photographs that cover the study area.

Contours for a reservoir area are computed from GPS compiled data using the TIN (triangular irregular network) surface modeling package within ARC/INFO. TIN is a set of adjacent, non-overlapping triangles computed from irregularly spaced points with x,y coordinates and z values. TIN was designed to deal with continuous data such as elevations. The TIN software uses a method where triangles are formed between all collected data points for interpolation purposes. Using options within ARC/INFO, a clip or polygon boundary of the study area is developed where no interpolation is allowed to occur outside the boundary. From the developed TIN a linear interpolation is used to develop contours along with computing the surface areas of the study area for specified elevations.

INTRODUCTION

Historically the Bureau of Reclamation (Reclamation) analyzed reservoir survey information using large main frame computers and complex programs resulting in expensive and time-consuming analysis. Advances in microcomputers and geographic information system software packages allow such analyses to be conducted much faster and more cost effectively. Reclamation developed an ARC/INFO based GIS application to assist in the analysis of survey data and subsequent generation of topographic contours of reservoirs. This paper presents an overview of the hydrographic survey process used by Reclamation and the methods used in the ARC/INFO based GIS analysis and mapping system.

HYDROGRAPHIC SURVEY EQUIPMENT AND METHOD

The hydrographic survey equipment used in the reservoir surveys is mounted in the cabin of a 24-foot tri-hull aluminum vessel equipped with twin in-board motors. The tri-hull boat is used for large reservoirs and small flat bottom boats or rafts are used for small reservoirs. The hydrographic system contained on the survey vessel consisted of a global positioning system (GPS) receiver with a built-in radio and an omni-directional antenna, a depth sounder, a helmsman display for navigation, a plotter, a computer, and hydrographic system software for collecting underwater data. Power to the equipment can be supplied by an on-board generator or two 12-volt batteries. The shore equipment includes a second GPS receiver with a built-in radio and an omnidirectional antenna. The GPS receiver and antenna are mounted on a survey tripod over a known datum point. The power for the shore unit is provided by a 12-volt battery.

1,2,3: Hydraulic Engineer, Bureau of Reclamation, Denver Technical Center, Water Resources Services, Mail Stops D-8520 and D-8540, PO Box 25007, Denver, CO 80225

GPS Technology and Equipment: The positioning system used is Navigation Satellite Timing and Ranging (NAVSTAR) GPS, an all-weather, radio-based, satellite navigation system that enables users to accurately determine a three-dimensional position. The NAVSTAR system's primary mission is to provide passive global positioning and navigation for land-, air-, and sea-based strategic and tactical forces and is operated and maintained by the Department of Defense (DOD). The GPS receiver measures the distances between the satellites and it self and determines the receiver's position from intersections of the multiple-range vectors. Distances are determined by accurately measuring the time a signal pulse takes to travel from the satellite to the receiver.

The NAVSTAR system consists of three segments:

- The space segment is a network of 24 satellites maintained in precise orbit about 10,900 nautical miles above the earth, each completing an orbit every 12 hours.
- The ground control segment tracks the satellites, determining their precise orbits. Periodically, the ground control segment transmits correction and other system data to all the satellites, and the data are then retransmitted to the user segment.
- The user segment includes the GPS receivers that measure the broadcasts from the satellites and calculate the position of the receivers.

The GPS receivers use the satellites as reference points for triangulating their position on earth. The position is calculated from distance measurements to the satellites that are determined by how long a radio signal takes to reach the receiver from the satellite. To calculate the receiver's position on earth, the satellite distance and the satellite's position in space are needed. The satellites transmit signals to the GPS receivers for distance measurements along with the data messages about their exact orbital location and operational status. The satellites transmit two "L" band frequencies (called L1 and L2) for the distance measurement signal. At least four satellite observations are required to mathematically solve for the four unknown receiver parameters (latitude, longitude, altitude, and time). The time unknown is caused by the clock error between the expensive satellite atomic clocks and the imperfect clocks in the GPS receivers. For hydrographic surveying the altitude and the reservoir's water surface elevation parameter are known, which realistically means only three satellite observations are needed to track the survey vessel; during the reservoir surveys, the best 6 available satellites are used for position calculations.

The GPS receiver's absolute position is not as accurate as it appears in theory because of the function of range measurement precision and the geometric position of the satellites. Precision is affected by several factors---time, because of the clock differences, and atmospheric delays caused by the effect on the radio signal of the ionosphere. Geometric dilution of precision (GDOP) describes the geometrical uncertainty and is a function of the relative geometry of the satellites and the user. Generally, the closer together in angle two satellites are from the receiver, the greater the GDOP. GDOP is broken into components: position dilution of precision (x,y,z) (PDOP) and horizontal dilution of precision (x,y) (HDOP). The components are based only on the geometry of the satellites. The PDOP and HDOP are monitored during the reservoir surveys, and for the majority of the time are less than 3, which is within the acceptable limits of horizontal accuracy for Class 1 and 2 level surveys (Corps of Engineers, 1991).

An additional and larger error source in GPS collection is caused by false signal projection called selective availability (S/A). The DOD implements S/A to discourage the use of the satellite system as a guidance tool by hostile forces. Positions determined by a single receiver when S/A is active can have errors of up to 100 meters. A method of collection to resolve or cancel the inherent errors of GPS (satellite position or S/A, clock differences, atmospheric delay, etc.) is called differential GPS (DGPS). DGPS is used during the reservoir surveys to determine positions of the moving survey vessel in real time. DGPS determines the position of one receiver in reference to another and is a method of increasing position accuracy by eliminating or minimizing the uncertainties. Differential positioning is not concerned with the absolute position of each unit but with the relative difference between the positions of two units, which are simultaneously observing the same satellites. The inherent errors are mostly canceled because the satellite transmission is essentially the same at both receivers.

At a known geographical benchmark, one GPS receiver is programmed with the known coordinates and stationed over the geographical benchmark. This receiver, known as the master or reference unit, remains over the known benchmark, monitors the movement of the satellites, and calculates its apparent geographical position by direct reception from the satellites. The inherent errors in the satellite position are determined relative to the master receiver's programmed

position, and the necessary corrections or differences are transmitted to the mobile GPS receiver on the survey vessel. For the reservoirs, position corrections are determined by the master receiver and transmitted via an ultra-high frequency (UHF) radio link every 3 seconds to the survey vessel mobile receiver. The survey vessel's GPS receiver used the corrections along with the satellite information it received to determine the vessel's differential location. Using DGPS resulted in positional accuracy of 1 to 2 meters for the moving vessel compared to positional accuracy of 100 meters with a single receiver.

The Technical Service Center (TSC) mobile and reference GPS units are identical in construction and consist of a 6-channel L1 coarse acquisition (C/A) code continuous parallel-tracking receiver, an internal modem, and a UHF radio transceiver. The differential corrections from the reference station to the mobile station are transmitted using the industry standard Radio Technical Commission for Maritime Services (RCTM) message protocol via the UHF radio link. The programming to the mobile or reference GPS unit is accomplished by entering necessary information via a notebook computer. The TSC's GPS system has the capability of establishing or confirming the land base control points by using notebook computers for logging data and post-processing software. The GPS collection system has the capability to collect the data in the surveyed area's coordinate system.

Survey Method and Equipment: The bathymetric survey was run using sonic depth recording equipment interfaced with a DGPS capable of determining sounding locations within the reservoir. The survey system software continuously records reservoir depths and horizontal coordinates as the survey boat moved across close-spaced grid lines covering the reservoir area. Data are also often collected along the shore as the boat traverses to the next transect and as it maneuvers in the open areas between the trees. Thick tree growth prevents the boat from reaching some areas of a reservoir, such as those near the shoreline or in shallow water areas in the main body of the reservoir. During each run, depth and position data are recorded on a notebook computer hard drive for subsequent processing by TSC personnel. The underwater data sets often average 50,000 points and have exceeded 150,000 points. The water surface elevation recorded during the time of collection is used to convert the sonic depth measurements to true lake bottom elevations.

For stationing the master GPS unit known benchmarks or datums are used. New benchmarks or datums are established where no benchmarks are available. The shore-based master GPS unit, which transmits the correction information to the mobile GPS unit on the survey vessel, is stationed at this site throughout a survey. During post-processing of the collected data points without differential correction are removed.

The underwater data is collected by a depth sounder that is calibrated by lowering a deflector plate below the boat by cables with known depths marked by beads. The depth sounder is calibrated by adjusting the speed of sound, which can vary with density, salinity, temperature, turbidity, and other conditions. The collected data are digitally transmitted to the computer collection system via a RS-232 port. The depth sounder also produces an analog hard copy chart of the measured depths. These graphed analog charts are printed for all survey lines as the data was collected and recorded by the computer. The charts were analyzed during post processing, and when the analog-charted depths indicate a difference from the recorded computer bottom depths, the computer data files were modified.

TOPOGRAPHY DEVELOPMENT USING ARC/INFO

The topography of reservoirs are developed from the collected underwater data and from the USGS quad maps. The upper contours of a reservoir are developed by digitizing contour lines from the USGS quad maps that cover the reservoir area. ARC/INFO V7.1.1 geographic information system software is used to digitize the USGS quad contours. A selected elevation contour that can be digitized from USGS quad maps or other maps is used to perform a clip of the triangular irregular network (TIN) such that contour interpolation is not allowed to occur outside the clipping contour. This clip is performed using the "hardclip" option of the ARC/INFO CREATETIN command. Using ARCEDIT, the underwater collected data and digitized contours are plotted to make sure that the clipping coverage includes the entire underwater data set. Using select and move commands within ARCEDIT, the vertices of the clipping coverage can be shifted to fit all the collected underwater data. A sample of underwater data and clipping coverage contours are presented on **figure 1**.

Contours for elevations below the clipping coverage are computed from collected underwater data using the TIN surface modeling package within ARC/INFO. TIN was designed to deal with continuous data such as elevations. The TIN software uses a method known as Delaunay's criteria for triangulation. Triangles are formed between all data points including all boundary points. This method preserves all collected survey points. The method requires that a circle

drawn through the three nodes of a triangle will contain no other point, meaning that sample points are connected to their nearest neighbors to form triangles using all collected data. Elevation contours are then interpolated along the triangle elements. The TIN method is discussed in great detail in the *ARC/INFO V7.1.1 Users Documentation*.

In creating a TIN, points that fall within a set distance of each other are weeded out to eliminate flat triangular elements (flat triangles occur where all three points making up a triangle have the same elevation). Elimination of redundant points helped to improve the performance of the contouring process and helped create more continuous contours in the lower elevations of the reservoir.

The linear interpolation option of the *ARC/INFO TINCONTOUR* command is used to interpolate contours from the reservoir TIN. In addition, the contours are generalized by weeding out vertices along the contours. This generalization process improves the looks of the resulting contours by removing very small variations in the contour lines. This generalization has little bearing on the computation of surface areas and volumes of a reservoir. Contours can be computed at a variable interval. A sample contour map is shown in **figure 2**. This map is a subset of a much larger map as shown in the upper right hand corner of **figure 2**.

Development of Contour Areas: Contour surface areas for a reservoir can be computed at any increment using the reservoir TIN discussed above. These calculations are performed using the *ARC/INFO VOLUME* command. This command computes areas at user-specified elevations directly from the TIN and takes into consideration all regions of equal elevation. Reclamation usually computes the surface areas at 1-foot increments but have on occasion computed the areas at 0.1-foot increments to help identify any data problems.

Storage Capacity: Storage-elevation relationships based on the computed surface areas are developed using the area-capacity computer program *ACAP85* (Bureau of Reclamation, 1985). Surface areas at determined contour intervals from a minimum reservoir elevation to a maximum elevation are used for computing reservoir capacity. The *ACAP85* program can compute area and capacity data at elevation increments of 0.01- to 1.0-foot by linear interpolation between the given contour surface areas. The program begins by testing the initial capacity equation over successive intervals to ensure that the equation fits within an allowable error limit. This capacity equation is then used over the full range of intervals fitting within this allowable error limit. For the first interval at which the initial allowable error limit is exceeded, a new capacity equation (integrated from basic area curve over that interval) tests the fit until it also exceeds the error limit. Thus, the capacity curve is defined by a series of curves, each fitting a certain region of data. Final area equations are derived by differentiating the capacity equations, which are of second order polynomial form:

$$y = a_1 + a_2x + a_3x^2$$

where:

y = capacity

x = elevation above a reference base

a₁ = intercept

a₂ and a₃ = coefficients

Sediment Analyses: Reclamation determines the total sediment volume by measuring the total change from the original reservoir volume at the time the dam closes to the new reservoir volume at the time of the new survey.

SUMMARY

Using *ARC/INFO* to process and analyze reservoir hydrographic survey information has stream lined the work process along with providing a more superior product over Reclamation's previous method. In the past Reclamation employed the use of large main frame computers and complex programs the resulted in expensive and time-consuming analysis of data. Such analyses still required hand drafting of final contour map products. *ARC/INFO* allows the use of much smaller computers and provides the utility to analyze large quantities of survey information quickly and more accurately. In addition to *ARC/INFO*'s contouring and volume analysis capabilities, the mapping capabilities of *ARC/INFO* allow the presentation of analysis results in final map form as a direct product of the analysis process. What used to take months to complete is now possible in a manner of days.

REFERENCES

Bureau of Reclamation, Surface Water Branch, 1985. *ACAP85 User's Manual*, Technical Service Center, Denver, Colorado.

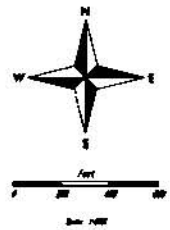
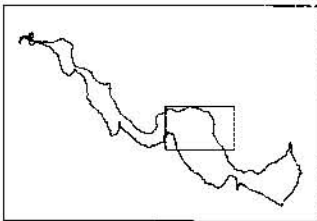
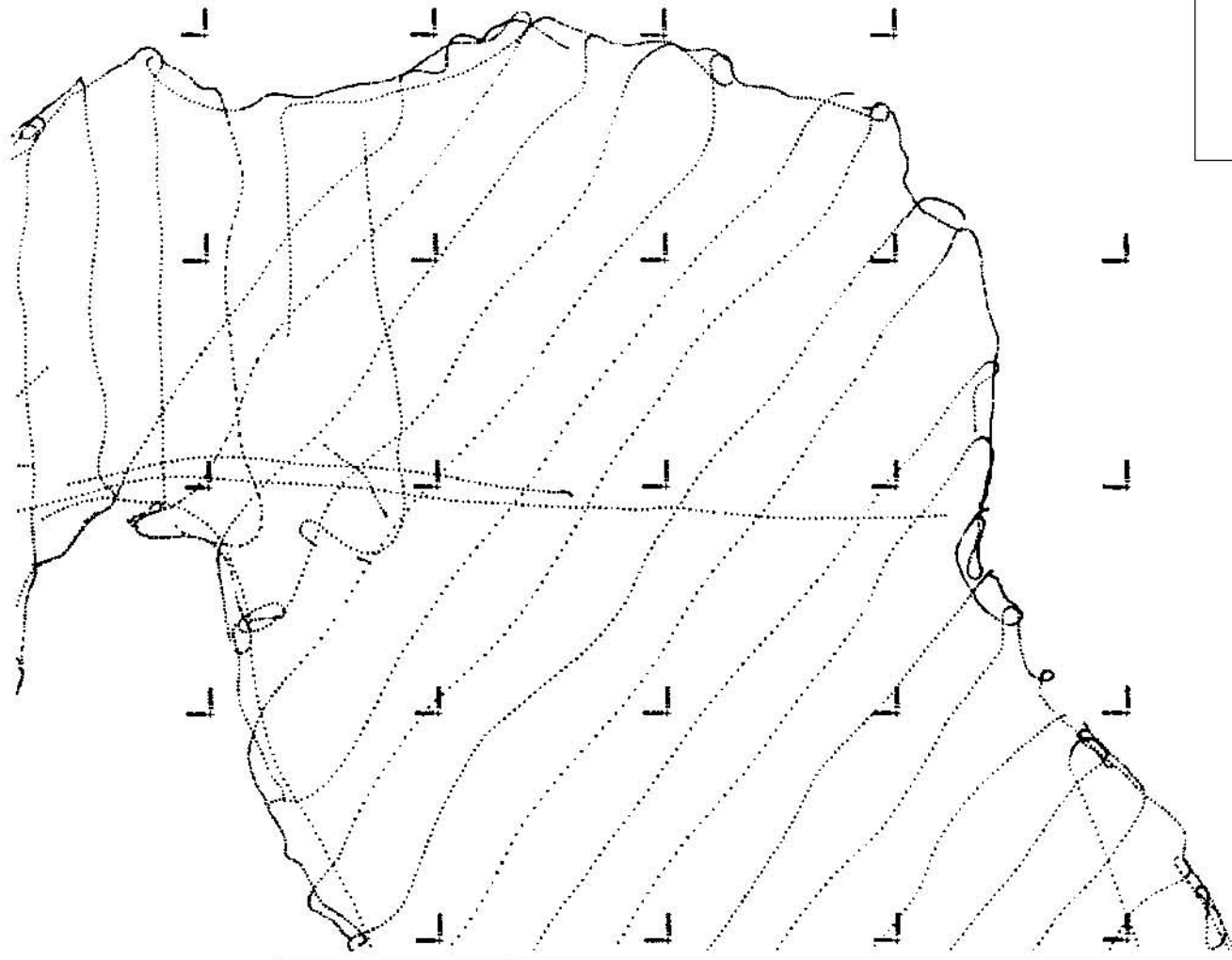
Bureau of Reclamation, 1987. *Design of Small Dams*, U.S. Government Printing Office, Denver, CO.

Bureau of Reclamation, 1987. *Guide for Preparation of Standing Operating Procedures for Bureau of Reclamation Dams and Reservoirs*, U.S. Government Printing Office, Denver, CO.

Corps of Engineers, March 1991. *Application of Differential Global Positioning System for Hydrographic Survey and Dredge Positioning*, ETL 1110-7-5 (FR), Department of the Army, Washington, DC.

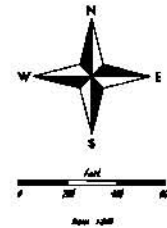
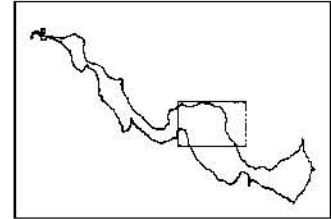
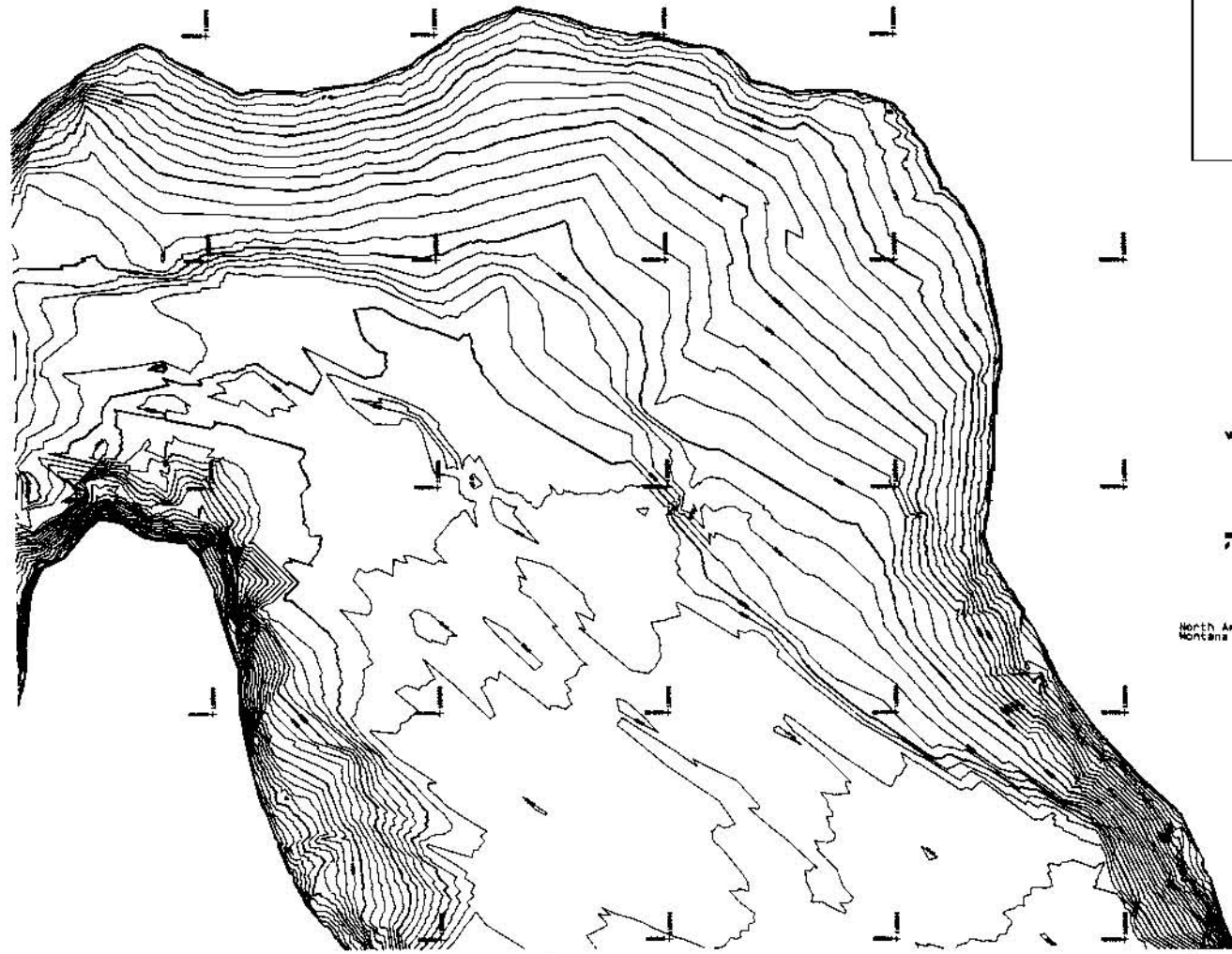
Environmental Systems Research Institute, Inc., 1992. *ARC Command References*.

Figure 1. - Sample Reservoir Survey Points and Clipping Coverage



STATE OF FLORIDA DEPARTMENT OF ENVIRONMENTAL PROTECTION WATER RESOURCES DIVISION	
DATE OF SURVEY: _____	CONTRACT NUMBER: _____
PROJECT: _____	SCALE: _____
DATE: _____	BY: _____

Figure 2. - Sample Reservoir Contours



North American Datum of 1927
Montana Coordinate System, Central

MONTANA DEPARTMENT OF TRANSPORTATION GARDEN RESERVOIR PROJECT	
DESIGNED BY _____	TECHNICAL APPROVAL _____
DRAWN BY _____	APPROVED _____
Bozeman, Montana 59717-0001	

RIPARIAN ECOSYSTEM MANAGEMENT MODEL (REMM): A DEMONSTRATION¹²

R. G. Williams³, Agricultural Engineer, USDA-ARS, Tifton, GA; R. R. Lowrance, Ecologist, USDA-ARS, Tifton, GA; L. S. Altier, Assistant Professor, California State University, Chico, CA; S. P. Inamdar, Post Doctoral Associate, University of Georgia, Tifton, GA

Abstract

The ability of riparian buffer systems to serve as filters to limit the quantities of eroded soil, organic materials, dissolved and adsorbed plant nutrients reaching the stream system has long been understood. What has not been understood, are the complex soil, water, and plant interactions that occur within the riparian system that controls the effectiveness of the filtering. The Riparian Ecosystem Management Model (REMM) has been developed to simulate these processes to gain an improved understanding of riparian systems and to give designers a tool to use to determine the characteristics of riparian buffers to meet water quality goals. REMM is a computer simulation model that operates under Windows 95. In REMM the riparian system is considered to be multiple zones between the field and the stream system. Each zone includes litter and three soil layers that terminate at the bottom of the plant root system and a plant community that can include six plant types in two canopy levels. Surface hydrology, erosion, vertical and horizontal subsurface flows, carbon and nutrient dynamics, and plant growth that occurs in these systems are modeled on a daily time step. This demonstration will be of REMM's operational characteristics. It will include data requirements, operation of the data input/output manipulation tools, model operation, and model output options.

INTRODUCTION

Managers, through system synthesis, use system operation predictions to develop optimized systems. Water resource managers use field or watershed system synthesis procedures to develop best management scenarios for evaluation of managed water resource systems or resource systems influenced by managed systems. System synthesis is usually accomplished through linking various mathematical models that define various components or sub-systems of the system. The mathematical model is a simple quantitative expression of the process being observed.

Overton and Meadows (1976) describe the modeling process as development of a concept then, through experimental, verification use observations to develop feedback to adjust the concept until the simulation objectives are fulfilled. Simulation objectives can be a simple process or a complex combination of processes. However, when complexity is added to the process or

¹ Contribution from the USDA-ARS, Southeast Watershed Research Laboratory, P.O. Box 946, Tifton, GA, in cooperation with the University of Georgia Coastal Plain Experiment Station.

² All programs and services of the USDA are offered on a nondiscriminatory basis without regard to race, color, national origin, religion, sex, age, marital status, or handicap.

³ USDA-ARS, Southeast Watershed Research Laboratory, P.O. Box 946, Tifton, GA; phone: (912) 386-3895; fax: (912) 386-7294; Email: randy@tifton.cpes.peachnet.edu

combination of processes, complexity is added to the computation and data requirements of the model. Computer simulation modeling is using computer computational and data management capabilities to simplify implementation of the combination process models.

Welsch (1991) indicates that riparian forests are complex ecosystems that can be depicted in three zones adjacent to stream systems consisting of undisturbed forest, managed forest, and runoff control. The Riparian Ecosystem Management Model (REMM) is a computer simulation model of riparian forest buffer systems. REMM uses field inputs from field data or outputs from field scale simulation models coupled with weather input from climate data or climate models to simulate hydrologic, carbon and nutrient cycling, and plant growth processes in riparian forest systems (Lowrance, et.al., 1998). The results of the simulations are the model output, which are the operational characteristics of riparian forest systems.

Since REMM is a complex model, from both a computation and data requirement standpoint, two principal methods to operate REMM are available for users. The first method includes a user interface to aid the user in development of input data sets and actual running of the model. The second method of using the model bypasses the user interface requiring the user to be more familiar with the input/output formats but giving the user increased flexibility in output. The first method is aimed at the general user who is interested in applying the model using either regionally developed data sets or local data. The second method of the model is intended for use by researchers who are interested in examining some of the internal dynamics of the various pools or individuals interested in linking REMM with other simulation models. The balance of this paper will be generally aimed at demonstrating the two methods, providing an overview REMM's process simulation, and the general structure of the REMM input/output file formats.

COMPUTATIONAL PROCESSES

Basic Overview

REMM is written in the C++ programming language and runs under the Microsoft Windows 95 operating system. REMM is designed to execute as a separate thread in a multi-tasking environment and is compiled as a Dynamic Link Library (DLL). A DLL is a runtime programming library (Swan, 1996). Previously it was indicated that there are two methods to operate REMM. This is not to imply that there are two versions of REMM but there are two controller programs for the REMM thread. Selection of the controller program depends on whether the user wants the controller program to assist in building or editing data sets or if the user prefers to use another editor.

Figure 1 shows the operational flow to execute a REMM simulation. The controller program starts a REMM execution and passes REMM the name of a file that contains a listing of the input/output file names that the simulation will be using. Input/output files will be described in the section on data files. This execution continues until complete or until the controller program signals to abort the simulation. At the end of the simulation the REMM thread stays active until the controller program requests that the thread be closed. The controller program monitors the simulation to determine simulation status. If an error has occurred the controller program

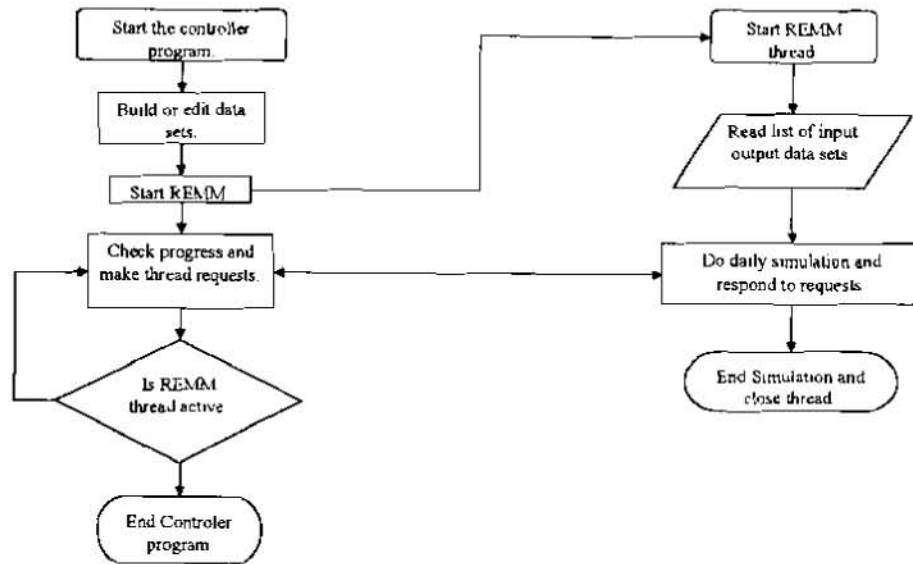


Figure 1. REMM controller process flow chart

notifies the user as to the type of error and terminates REMM's thread. If the simulation ends normally the controller program notifies the user and terminates the thread.

Computational flow

The computational flow of REMM is shown in Figure 2. A REMM simulation begins with reading a list of input/output file names. This list includes constants files, daily input files and daily, monthly, and yearly output files. The constants files are read prior to the beginning of the daily simulation loop. Inside the daily simulation loop the daily input files are read one line per day. The actual simulation processes are then performed and requests from the controller program are performed. Following the controller program requests, the output files are written.

DATA FILES

REMM uses data files for various data storage and manipulation functions. The three-letter file extension is used to designate the file type and the type can be classified as control, input or output. The functionality of these files is discussed below. These files are all in ASCII format and editable by any text editor. This provides the user with the capability to manipulate the files as needed or generate input files with another simulation program. Due to the limited space available here a detailed listing of the variables is not possible. A detailed list is available from the model developers.

Control

There is one main control file for REMM. This file has the extension .REM and is the first file read by REMM. The name of the .REM file is passed to the REMM thread when execution begins. In this file all the input and output file names are defined. Files are listed one per line

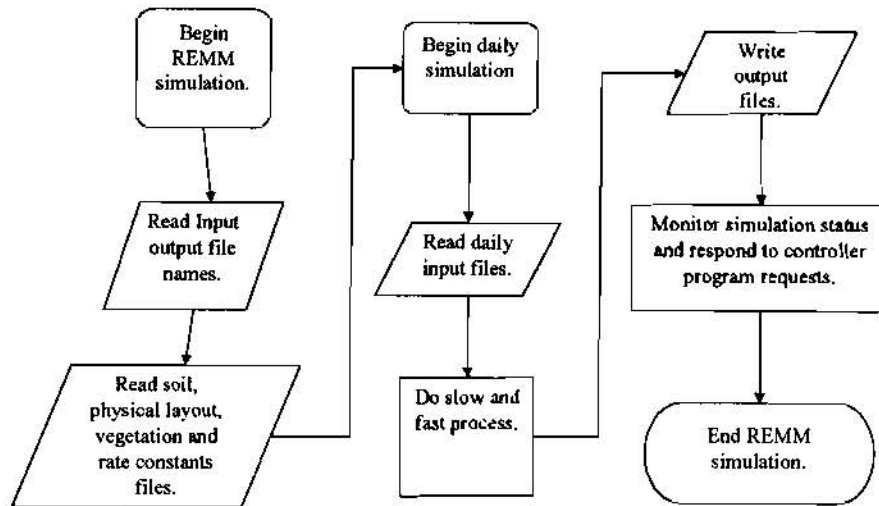


Figure 2. REMM process flow chart.

and the disk drive and full path must be included. A user can then save multiple files that contain the different riparian system configurations and run all simulations using one weather input data set or run one riparian system with various field input scenarios.

Input

There are two principal types of input files. There are the files that define the initial conditions, which are read at the beginning of the simulation and these that contain various daily inputs, which are read on a daily or as needed basis. The three initial condition files have the extensions .CN1, .CN2, and .CN3. There are three daily input files with the extensions .WEA, .FIN, and .CNG.

.CN1

The Constants 1 (.CN1) file is perhaps the main data file that the user will modify. This file has data arranged in blocks based on the functionality of the data. The initial block contains the basic data common to the riparian system. This block includes items such as the starting and ending dates, geographic information on the field above the riparian system and the stream outlet. The next three blocks of data are for zone specific information and starts with zone 1 (Lowrance, et. al., 1998). Clustered in these blocks is general, plant, litter and soil layer information. General information for each zone is length, width, and slope. The plant information is simply the fraction of the area covered by the plant. Litter data includes the basic erosion information, physical descriptors of the litter and initial carbon and nutrient levels. Following the litter data the initial conditions are set for the soil including physical descriptors, hydrologic properties, and initial carbon and nutrient levels.

.CN2

The Constants 2 (.CN2) data file contains plant specific information. This included basic physical information on the plant, factors related to photosynthesis, transpiration characteristics, nutrient content of plant part pools, and the initial size of the plant part pools. REMM allows up to six vegetation types in two canopy layers for each zone. The vegetation types include a herbaceous annual and perennial, five deciduous, and five conifers. Regional data sets are being developed that define plant characteristics typical to a region.

.CN3

The constants 3 (.CN3) file contains many of the rate coefficients used in the model. It is not anticipated that the general user would need to change any of these values. However, this file does provide the ability for refining rate coefficients without having to locate them in the computer code and then re-compiling the code.

.WEA

The weather (.WEA) input file contains the daily rainfall information. This includes rainfall, rainfall duration, maximum and minimum air temperatures, solar radiation, and wind velocity. This file can either be observed data or developed using a climate generator. The input format of the weather file is the same as that generated by CLIGEN for the WEPP model (Nicks et al., 1995).

.FIN

The field (.FIN) input file contains the daily outputs from the field draining into the riparian system. These data include surface runoff and associated eroded soil material, organic material, and plant nutrients. Also included are the daily subsurface drainage volumes and transported carbon and nutrients.

.CNG

The change (.CNG) file is designed to indicate when a major change has occurred in the riparian system. A tillage operation, timber harvest, or control burns are examples of major changes that can occur within the riparian system. Included in this data are the date of the change, type of change, and data that needed to be updated due to the change.

Output

REMM produces two principal types of output files. The first is a general report form and has the file name defined by the user in the REM file and the extension .OUT. This output is in the form of a report and contains initial conditions, monthly summaries, and annual summaries. The monthly and annual summaries include selected state variables including plant biomass, litter mass, soil nutrient level, and soil moisture levels. Also included in the summary information are fluxes of water, nutrient, and sediment through the system. The second type output is a tabular output with the file extension .TAB. The .TAB file contains either daily, monthly, or annual

outputs of user selected state variables and accumulated flux variables. This file is in a tabular format for import into the REMM user interface or whatever analyses program the user may prefer. This gives the user an easy way to capture model outputs in order to perform additional analysis on model outputs.

SUMMARY

Presented above are flow charts defining the REMM's basic operation. Also presented are descriptions of the input output files and the types of data they include. The purpose of this paper was to provide an overview of REMM's operation, data requirements and structure. Detailed listing of data in each file was not possible due to space limitations. Typically the user will not need the exact file structure of REMM and will use the user interface.

REFERENCES

- Lowrance, R. R., Altier, L.S., Williams R. G. , Inamdar S. P., Bosch, D. D., Sheridan, J. M., Thomas, D. L., and Hubbard, R. K., 1998, The riparian ecosystem management model: simulator for ecological processes in riparian zones. First Federal Interagency Hydrologic Modeling Conference, April 19-23, Las Vegas, NV, (in press)
- Overton, D. E., Meadows, M.E., 1976, Stormwater modeling. Academic Press, Inc., 111 Fifth Ave., New York, NY, 10003, 358 pp.
- Nicks, A. D., Lane, L. J. Gander, G.A., 1995. Chapter 2. Weather generator. In: USDA-Water Erosion Prediction Project (WEPP). NSERL Report No. 10. National Soil Erosion Research Laboratory, West Lafayette, IN, 47907.
- Swan, T., 1996. Mastering Borland C++ 5. Sams Publishing, 201 W. 103rd St., Indianapolis, IN 46290. 1058 pp.
- Welsch, D. J., 1991. Riparian forest buffers, function and design for protection and enhancement of water resources, USDA, Forest Service, Northeast area, Forest Resource Management, Radnor, PA, NA-PR-07-91.

OHIO RIVER DIVISION REAL-TIME MODELING/FORECASTING SYSTEM
Stanley M. Wisbith, P.E., Hydraulic Engineer and David P. Buelow, P.E., Chief, Reservoir
Control Center, Ohio River Regional Office, Great Lakes and Ohio River Division, U. S.
Army Corps of Engineers, Cincinnati, Ohio

INTRODUCTION

The Kentucky Lake-Barkley Lake (KY-BK) system is the single most important component of the flood protection system for the lower Mississippi River. The Ohio River Regional Office of the Corps of Engineers in Cincinnati, Ohio is responsible for regulation of the lakes during periods of flooding in the lower Ohio and Mississippi Rivers. Barkley is the first Corps' Nashville District lock and dam on the Cumberland River at mile 30.6. Regulation of Kentucky Lake, the first Tennessee Valley Authority project on the Tennessee River at mile 22.4, is addressed in Section 7 of the Flood Control Act of 1944. The projects are connected by an uncontrolled navigation canal and are regulated as a system at all times. The Cumberland River enters the Ohio River at mile 923 at Smithland, KY; the Tennessee enters 12 miles downstream at Paducah, KY. Priorities for flood control regulation are (1) safeguard the Mississippi River levee system; (2) reduce the frequency of use of the Birds Point-New Madrid floodway; and (3) reduce the frequency and magnitude of flooding of unprotected lands along the lower Ohio and Mississippi Rivers. Primary focal point is the stage at the mouth of the Ohio River at Cairo, IL at river mile 981.

Regulation of the KY-BK system for flood control requires near-real-time knowledge of the hydrologic status of the entire Ohio River Basin and the middle and upper Mississippi River Basins. A satellite-reporting network of stream and precipitation gages, direct access to NWS digital, graphical and text products, commercial weather radar, daily forecasts of tributary reservoir operations from Corps district offices and continuous coordination with NWS River Forecast Centers provides this intelligence. The modeling tool used is the unsteady flow model FLOWSED. Modeling is accomplished on Sun Ultra 1 workstations running under the Solaris operating system. A locally developed GUI provides full functionality for all aspects of the process from data compilation to presentation of results.

OHIO RIVER MODELING SYSTEM

The Ohio River Modeling System has a long history at the Cincinnati Reservoir Control Center. The current configuration based on data collection, distribution and main-stem Ohio River model was developed in 1983. At that time, the river model was added to the existing system to assist the operation and control of Barkley and Kentucky dams during flood operations on the lower Ohio and Mississippi rivers. The system has run reliably every working day since its inception. For the past 14 plus years, it has faithfully stood ready to be used for both everyday application and its primary purpose; regulation of the only two major projects capable of protecting the levee system on the lower Mississippi River. Although not infallible, the system has shown itself to be consistent, reliable and robust.

Since its initial deployment, the demand for the data produced by the Ohio River Modeling System has grown significantly. This increasing application has justified the continuing effort to develop and improve the modeling system, bringing it in line with developing technology. During its 14-year existence the model has been resident on four different platforms and has migrated from the Harris operating system to XENIX then to the UNIX operating system.

Control of the model is through a comprehensive software package. This package includes incoming and outgoing data streams, databases, database servers, hydrologic and hydraulic models, and visual display and editing capabilities. These items are interconnected by UNIX scripts and controlled by a flexible graphical user interface (GUI).

The Ohio River Modeling System is configured as a multi-layered package. Key components are a GUI program, HEC DISPLAY, HEC DSSUTL, an ungaged runoff model and the FLOWSED unsteady flow modeling module. In addition to these, there are several utility programs and scripts used to support and act as connections for the main programs. The scripting capability used for utilities and inter-process connection is the standard UNIX shell.

The FLOWSED module consists primarily of a time series database server and the actual unsteady flow model. The database server, called FLOWCON, is used to pass data between the unsteady flow model and the DSS databases. This program provides the input required by the model and stores the model output. FLOW22 is the unsteady flow model used to act as a river state transformation function. This function changes the river water surface elevations and flows with changing inflows and time.

FLOW22 generates a fully implicit solution to the one-dimensional St. Venant equations. This type of equation starts from an initial state then evolves through time with changing boundary conditions. No matter what starting state initially assumed, by using observed boundary conditions the model will eventually produce a realistic picture of the river, that is, assuming that the model has a long enough running duration. On the main-stem Ohio River this required duration is from two to three weeks.

It was decided during the initial development stage of the system to break the model run into two parts or phases. This was done to save computation time and to aid the distinction between real or observed boundary conditions and forecasted conditions.

The first phase of the process is the creation of the update or hot start data. This is a hindcast made using observed data up to the time of forecast. The model pre-loads all internal variables saved from the previous update run. Then, a run is made using observed boundary conditions from the time of the previous update until the time of forecast. The internal values are then saved to a database in order to provide starting conditions for both the forecasting phase and the next update phase. Update runs are made every working day, insuring that the model always reflects current river conditions.

The second phase of the process is the actual forecast run. Here the forecast boundary conditions are regularly used to produce a 5-day river forecast. This is the phase where the proposed Barkley and Kentucky operating schedules are refined.

Both phases of the model require three main types of input data. First are the headwater elevations and gate openings at all the mainstem navigation projects. This information is entered at each of the individual projects, passed through a navigation database and eventually resides in a DSS database. The second type is the flows at all gaged stream boundaries. This is provided to the regional office by the districts along the Ohio. This information will also eventually reside in a DSS database. The third type is the model inflow from the ungaged areas along the mainstem. This information is generated at the regional office and, as with the other two types of data, stored in a DSS database.

MODEL DEMONSTRATION

The Ohio River Regional Office model, in conjunction with the models run at the Corps' Pittsburgh, Huntington, Louisville and Nashville districts and the Tennessee Valley Authority, form a truly distributed modeling system. The demonstration will show this system in action during a flood event on the Ohio River. Data screening, update and forecast simulations, display of results, adjustment of reservoir discharges and briefing capabilities will be presented. The simplicity, flexibility and robustness of the model and its transportability to other river systems will become evident to the observer.

AN ENHANCED GENERALIZED STREAM TUBE MODEL FOR ALLUVIAL RIVER SIMULATION

By Chih Ted Yang, Mark A. Treviño, and Francisco J. M. Simões,
U.S. Bureau of Reclamation, Technical Service Center, Denver, Colorado

Abstract: Most of the sediment and water routing models were developed for solving one-dimensional alluvial river problems. Although two- and three-dimensional models exist for alluvial river simulation, they are too computational intensive and require extensive field data for engineering applications. The Generalized Stream Tube model for Alluvial River Simulation (GSTARS) was first developed by Molinas and Yang (1986) to simulate the flow conditions in a semi-two-dimensional manner and the change in channel geometry in a semi-three-dimensional manner. The original GSTARS was developed for Cyber mainframe computers. The revised and enhanced model, GSTARS version 2.0 (Yang, Treviño, and Simões, 1997) was developed for PC applications.

GSTARS version 2.0 (GSTARS 2.0) is applicable to subcritical, supercritical, and a combination of them regardless whether channel width is fixed or is a variable. Users can choose among eleven sediment transport functions with particle size ranging from clay to silt, sand, and gravel. This paper provides a general description of the concepts and approaches used in GSTARS 2.0 and examples are given to illustrate its engineering applications.

INTRODUCTION

Most of the sediment and water routing models, such as the HEC-6 (U.S. Army Corps of Engineers, 1977, 1993), were developed for solving one-dimensional alluvial river problems. Although truly two- and three-dimensional models exist for alluvial river simulation, they can be too computationally intensive for most engineering applications. The field data required for calibration and testing of these models may not be readily available. The Generalized Stream Tube model for Alluvial River Simulation (GSTARS) was first developed by Molinas and Yang (1986) to simulate the flow conditions in a semi-two-dimensional manner and the change of channel geometry in a semi-three-dimensional manner. The model was also used to simulate and predict river morphologic changes caused by manmade and natural events. As a result of these applications, GSTARS has been revised and enhanced. The original GSTARS was developed for a CYBER mainframe computer. The revised and enhanced model, GSTARS version 2.0 (GSTARS 2.0) (Yang, Treviño, and Simões, 1997), was developed for PC applications. This paper provides a general description of GSTARS 2.0. Examples of simulated and predicted results based on GSTARS 2.0 are given to illustrate model capabilities that can be useful in solving engineering problems and river morphology studies.

DIFFERENCES BETWEEN GSTARS AND GSTARS 2.0

The development of GSTARS 2.0 (Yang, Treviño, and Simões, 1997) is based on the original GSTARS (Molinas and Yang, 1986) and consists of four major parts. The first part is the development of a stream tube model or water and sediment routing with fixed width. Both energy and momentum equations are used in the GSTARS 2.0 model so the water surface profile computation can be carried out through combinations of subcritical and supercritical flows without

interruption. The second part is based on the stream tube concept. The stream tube concept is used for hydraulic computations in a semi-two-dimensional way. Once the hydraulic parameters in each stream tube are computed, the scour or deposition in each stream tube determined by sediment routing will give the variation of channel geometry in the vertical direction. The third part of development is based on the theory of a minimum energy dissipation rate (Yang and Song, 1986) or it's simplified version of minimum total stream power. This theory was used to incorporate the channel width as an unknown variable. The fourth part of development is to incorporate channel bank side stability criteria, based on an angle of repose and sediment continuity.

Improvements and revisions made in GSTARS 2.0 over GSTARS include but are not limited to:

1. Increase the number of user's selected sediment transport functions from 3 to 10,
2. Cohesive sediment transport capabilities,
3. Side stability subroutines based on an angle of repose,
4. Non-equilibrium sediment transport based on the decay function first published by Han (1980),
5. Transport function for sediment laden flows by Yang, Molinas, and Wu (1996),
6. Mass balance check and many debugging features,
7. Subroutines that add points to enable continued accurate modeling of cross-sections with an insufficient amount of measured points in any given stream tube,
8. Detailed users' guidelines,
9. Multiple examples based on publications available to the public, including Bureau of Reclamation's original GSTARS,
10. Increase in the number of cross-sections and cross-section points that can be input to describe the study reach,
11. The CYBER mainframe version of GSTARS was modified to operate on a PC using FORTRAN 77 and FORTRAN 90 syntax in GSTARS 2.0,
12. Error checking of an input data file,
13. Output plotting options, including graphic display capability for cross-sections and water surface profiles.

The following descriptions are based on GSTARS 2.0 only although GSTARS may also have some of the similar capabilities.

OVERVIEW OF GSTARS 2.0

GSTARS 2.0 consists of five main computation parts: (1) channel geometry, (2) hydraulics, (3) sediment routing and armoring, (4) channel width and depth adjustments, and (5) channel side stability.

1. Channel Geometry: GSTARS 2.0 can handle irregular channel cross-sections regardless of whether it is a single channel or it is separated by small islands and sand bars. A detailed description of channel geometry computation is given by Molinas and Yang (1985).
2. Hydraulics: Most water and sediment routing models are based on the energy equation using the standard step method. This method limits its applications to subcritical flows. If flow conditions

change from subcritical to supercritical, a critical depth is assumed. GSTARS 2.0 uses both the energy equation and the momentum equation. Consequently, it can handle both subcritical and supercritical flows, including hydraulic jumps (Molinas and Yang, 1985; Yang, Molinas, and Song, 1988).

3. **Sediment Routing and Armoring:** Once the hydraulic conditions are computed for each stream tube, the rate of sediment transport in each stream tube can be computed using the these methods:

- a. Meyer-Peter and Müller's 1948 formula
- b. Lauren's 1958 formula
- c. Toffaleti's 1969 method
- d. Engelund and Hansen's 1972 method
- e. Ackers and White's 1973 method
- f. Revised Ackers and White's 1990 method
- g. Yang's 1973 sand and 1984 gravel transport formulas
- h. Yang's 1979 sand and 1984 gravel transport formulas
- I. Parker's 1990 method
- j. Yang's 1996 modified formula for sediment laden flows
- k. Ariathurai and Krone's 1976 and Partheniades' 1965 methods for silt and clay transport

Yang (1996) made detailed descriptions and comparisons of sediment transport formulas and their limits of application. The armoring process computations are based on the method proposed by Bennett and Nordin (1977).

4. **Channel Width and Depth Adjustments:** These adjustments are based on the minimum energy dissipation rate theory (Yang and Song, 1986) or its simplified version of minimum total stream power. Whether a channel will adjust its channel width or depth at a given computation time step depends on which condition results in less total stream power (Yang, Molinas, and Song, 1988).

5. **Channel Side Stability:** Channel side stability depends on the bank materials and their angle of repose.

Detailed description of GSTARS 2.0 and examples of applications are given in the GSTARS 2.0 User's Manual (Yang, Treviño, and Simões, 1997).

POTENTIAL APPLICATIONS AND LIMITATIONS OF GSTARS 2.0

Potential applications of GSTARS 2.0 are:

1. The model can be used as a fixed-bed model to compute water surface profiles for subcritical, supercritical, and a combination of both flow conditions involving hydraulic jumps. These computations include but are not limited to:
 - a. Water surface profiles in manmade channels with no sediment.
 - b. Water surface profiles over spillways and wasteway.
 - c. Water surface profiles in rivers where bed elevation changes are negligible.

2. The model can be used as a movable-bed model to route water and sediment through alluvial channels.
3. The use of stream tubes allows the model to compute the variation of hydraulic conditions and sediment activities not only in the longitudinal but also in the lateral direction.
4. The model becomes one-dimensional with the selection of a single stream tube. Selection of multiple stream tubes allows more detailed simulation of changes in cross-section geometries in the lateral and vertical directions.
5. The armoring computations allow simulation of long-term riverbed changes.
6. The model can simulate channel widening and narrowing processes with the selection of the minimization procedure option.
7. The channel side stability option allows simulation of channel geometry change based on the angle of repose of bank materials.

GSTARS 2.0 is intended to be used as a general engineering tool for solving fluvial hydraulic problems. However, it does have the following limitations from a theoretical point of view:

1. GSTARS 2.0 is a quasi-steady flow model. Water discharge hydrographs are approximated by bursts of constant discharges. Consequently, GSTARS 2.0 should not be applied to rapid varied unsteady flow conditions.
2. GSTARS 2.0 is a semi-two-dimensional model for flow simulation and a semi-three-dimensional model for simulation of channel geometry change. It should not be applied to the situation where a truly two-dimensional or truly three-dimensional model is needed for detailed simulation of local conditions. However, GSTARS 2.0 should be adequate for solving most river engineering problems.
3. GSTARS 2.0 is based on the stream tube concept. The phenomena of secondary current, diffusion, and super elevation are ignored.

EXAMPLES OF APPLICATION

The Willow Creek Dam emergency spillway is an unlined spillway with a crest elevation at 4,144 ft. It discharges into a grass-lined channel with a length of approximately 2,900 ft before entering the Sun River Valley, Montana. The spillway consists of a 700-ft wide, 6-ft tall buried concrete cutoff wall that is protected by riprap on the sides and by 2 ft of rockfill at the crest.

Figure 1 shows the variation of longitudinal bed thalweg profile along the emergency spillway. This study reach consists of supercritical and subcritical reaches. Figure 2 shows the variation of channel width. Figure 3 shows the variation of channel cross-sectional shape changing from a fairly symmetrical to that typically found at a meandering bend.

The Lake Mesalero Dam and Dike were constructed in 1974 and are located at the confluence of Ciewegita and Carriage Creeks on the Mescalero Apache Indian Reservation about 2.5 miles southwest of Ruidoso, New Mexico. Reclamation conducted a detailed topographic survey along the unlined emergency spillway. Figure 4 shows a comparison between the predicted and the surveyed cross-sections after the December 1984 flood. Examples shown in this paper demonstrate some of the unique capabilities of GSTARS 2.0 for solving river engineering problems.

REFERENCES

- Ackers, P., and White, W.R., 1973, Sediment Transport: New Approach and Analysis, *Journal of the Hydraulics Division, American Society of Civil Engineers*, Vol. 99, No. HY11, 2041-2060.
- Ariathurai, R., and Krone, R.B., 1976, Finite Element Model for Cohesive Sediment Transport, *Journal of the Hydraulics Division, American Society of Civil Engineers*, Vol. 102, No. HY3, 323-338.
- Bennett, J.P., and Nordin, C.F., 1977, Simulation of Sediment Transport and Armoring, *Hydrological Sciences Bulletin*, XXII.
- Engelund, F., and Hansen, E., 1972, A Monograph on Sediment Transport in Alluvial Streams, Teknisk Forlag, Technical Press, Copenhagen, Denmark.
- Han, Q., 1980, A Study on the Nonequilibrium Transportation of Suspended Load, *Proceedings of the International Symposium on River Sedimentation, Beijing, China (in Chinese)*, D9-1-D9-8.
- Laursen, E. M., 1958, The Total Sediment Load of Streams, *Journal of the Hydraulics Division, American Society of Civil Engineers*, Vol. 84, No. 1, 1530-1-1530-36.
- Meyer-Peter, E., and Müller, R., 1948, Formula for Bed-Load Transport, *Proceedings of International Association for Hydraulic Research, 2nd Meeting, Stockholm*.
- Molinas, A., and Yang, C.T., 1985, Generalized Water Surface Profile Computations, *Journal of the Hydraulics Division, American Society of Civil Engineers*, Vol. 111, No. HY3, 381-397.
- Molinas, A., and Yang, C.T., 1986, Computer Program User's Manual for GSTARS (Generalized Stream Tube model for Alluvial River Simulation), U.S. Bureau of Reclamation, Denver, CO.
- Parker, G., 1990, Surface-Based Bedload Transport Relationship for Gravel Rivers, *Journal of the Hydraulics Research*, Vol. 28, No. 4, 417-436.
- Partheniades, E., 1965, Erosion and Deposition of Cohesive Soils, *Journal of the Hydraulics Division, American Society of Civil Engineers*, Vol. 91, No. HY1, 755-771.
- Toffaletti, F.B., 1969, Definitive Computations of Sand Discharge in Rivers, *Journal of the Hydraulics Division, American Society of Civil Engineers*, Vol. 95, No. HY1, 225-246.

- U.S. Army Corps of Engineers, The Hydraulic Engineering Center, 1977, HEC-6 Scour and Deposition in Rivers and Reservoirs, User's Manual, (revised 1993).
- Yang, C.T., 1973, Incipient Motion and Sediment Transport, Journal of the Hydraulics Division, American Society of Civil Engineers, Vol. 99, No. HY10, 1679-1704.
- Yang, C.T., 1979, Unit Stream Power Equations for Total Load, Journal of Hydrology, Vol. 40, 123-138.
- Yang, C.T., 1984, Unit Stream Power Equation for Gravel, Journal of the Hydraulic Engineering, American Society of Civil Engineers, Vol. 100, No. HY12, 1783-1797.
- Yang, C.T., and Song, C.C.S., 1986, Theory of Minimum Energy and Energy Dissipation Rate, Encyclopedia of Fluid Mechanics, Vol. 1, Chapter 11, Gulf Publishing Company, Edited by N.P. Chermisinoff, 353-399.
- Yang, C.T., Molinas, A., and Song, C.C.S., 1988, GSTARS - Generalized Stream Tube model for Alluvial River Simulation, Interagency Advisory Committee on Water Data, Subcommittee on Sedimentation, Twelve Selected Computer Stream Sedimentation Models Developed in the United States, Edited by S.S. Fan, U.S. Interagency Ad Hoc Sedimentation Work Group, Federal Energy Regulatory Commission, Washington, DC, 149-178.
- Yang, C.T., Molinas, A., and Wu, B., 1996, Sediment Transport in the Yellow River, Journal of Hydraulic Engineering, American Society of Civil Engineers, Vol. 122, No. 5, 237-244.
- Yang, C.T., Treviño, M.A. and Simões, F.J.M., 1997, Computer Program User's Manual for GSTARS 2.0 (Generalized Stream Tube model for Alluvial River Simulation Version 2.0), U.S. Bureau of Reclamation, Technical Service Center, Denver, Colorado.

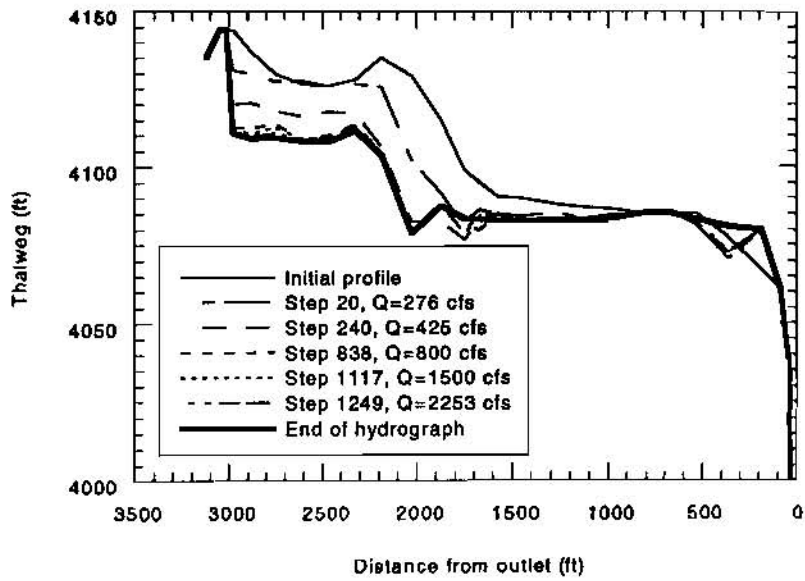


Figure 1. Evolution of thalweg profiles along the Willow Creek emergency spillway.

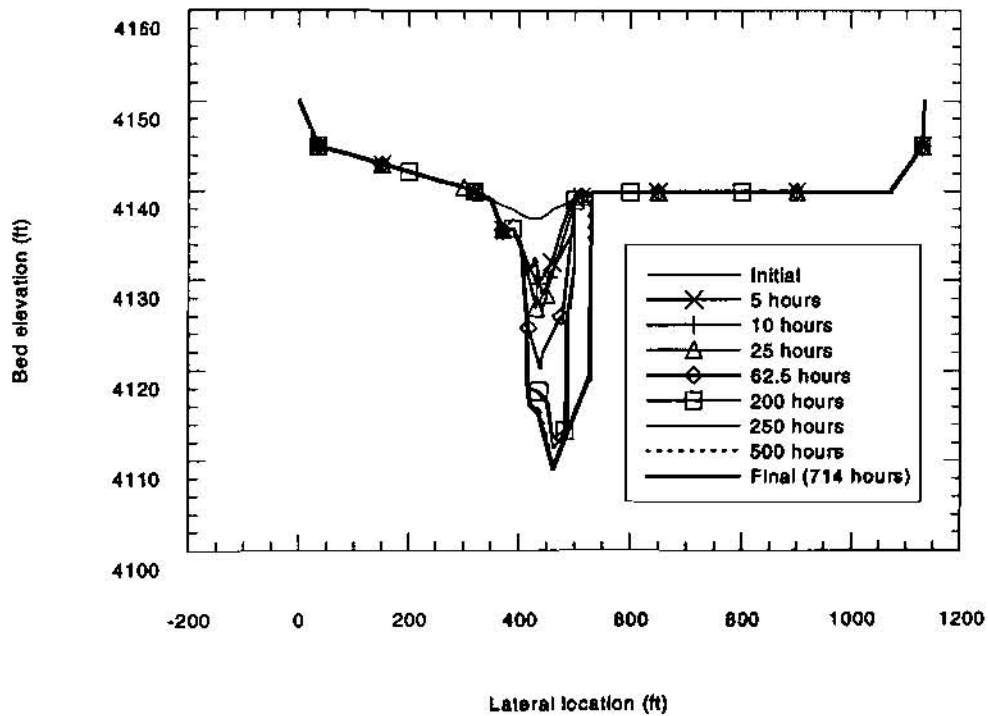


Figure 2. Evolution of cross-section at 2886 ft downstream of the Willow Creek Dam emergency spillway.

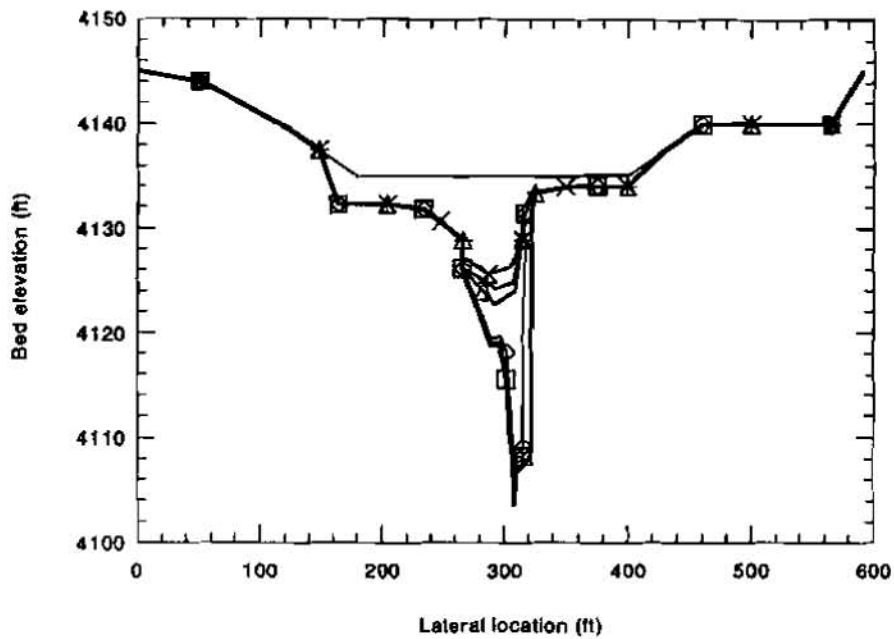


Figure 3. Evolution of cross-section at 2185 ft downstream of the Willow Creek emergency spillway.

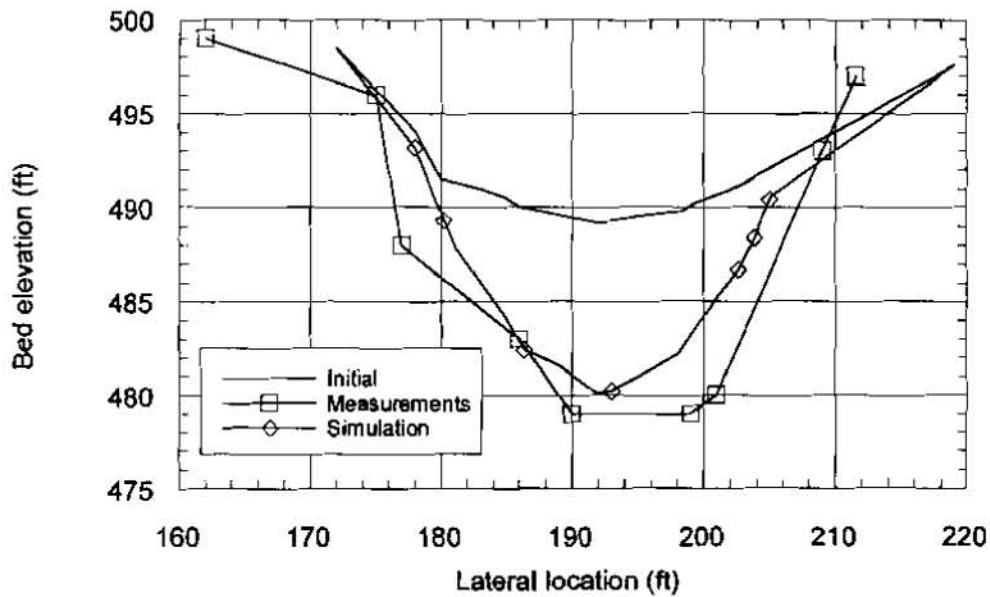


Figure 4. Comparison between predicted and surveyed cross-section at 60 ft downstream of the Lake Mescalero Dam emergency spillway.

RIVERWARE: A GENERAL RIVER AND RESERVOIR MODELING ENVIRONMENT

By Edith A. Zagona, Research Associate, Center for Advanced Decision Support for Water and Environmental Systems, University of Colorado, Boulder, CO; Terrance J. Fulp, Operations Research Analyst, U.S. Bureau of Reclamation, Lower Colorado Region, Boulder, CO; H. Morgan Goranflo and Richard M. Shane, Technical Specialists, River System Operations, Tennessee Valley Authority, Knoxville, TN

Abstract: A general river basin modeling environment for operations and planning requires a high degree of software flexibility to allow users to model any river basin, manage data input and output efficiently enough for near real-time operations, and provide a selection of solution algorithms, all through a user-friendly interface. RiverWare is an extensible, maintainable software framework which provides a modeling environment to meet all the modeling needs of managers and operators of river and reservoir systems.

INTRODUCTION

Water management agencies and utilities face increasingly difficult challenges in managing water resources. Environmental considerations, increasing demands on dwindling water supplies, outspoken recreational interests, the specter of climate change, and the restructuring of the power utility industry all have converged at a time when federal resources for developing modeling tools are minimal. Planning and operational river basin models developed in the previous decades are often not adequate to represent the changing multiple objectives of the projects and cannot be updated without significant expense.

To meet this challenge, the U.S. Bureau of Reclamation (USBR) and the Tennessee Valley Authority (TVA) are investing in a project with the Center for Advanced Decision Support for Water and Environment Systems (CADSWES) at the University of Colorado (CU) in Boulder to develop a general river basin modeling tool which can be used for a wide range of applications. The tool, called RiverWare, has been developed and applied to several basins by the two sponsoring agencies, and continues to be enhanced and improved.

To meet the goal of providing a modeling tool that can be applied to any river basin for both operational and planning applications, the RiverWare software was designed to meet the following general requirements:

- Be flexible enough to use for a variety of applications including daily scheduling, operational forecasting and long-range planning. This requires a range of timestep sizes and appropriate physical process modeling variability to support this range.
- Support various modeling solution methodologies. An organization's decision as to which basic modeling approach to use, simulation or optimization, depends on the specific goals of the model as well as the traditional way of looking at their system. Offering a variety of approaches allows each organization to continue historical practices as well as explore new approaches.
- Allow tailoring of applications by providing many basin features and many alternative methods for modeling these features. Even more important than the range of available features and methods is the extensibility of the software to provide ease in adding new methods. It must be recognized that there will always be applications that require enhancing the software and that most

agencies have some computational methods to which they are wedded for institutional reasons.

- Represent policy as input data. Many older models are obsolete because the operating policies were hard-coded and mixed in with the physical process model where they cannot be easily changed, or in some cases, cannot even be understood. Easy policy evaluation and modification by the user must be seen as a basic requirement for all new modeling tools.
- Provide an easy-to-use interface. A water resources engineer should be able to build, run and analyze model results relatively quickly, easily and without excessive training requirements. An operations scheduler should be able to view selected data in a convenient format, make changes to the operation, rerun the model and analyze results quickly.
- Fit into existing data and model interfaces. Every water management organization has an existing framework of databases, real-time data, supporting models, reporting tools, etc. to which the model must be connected. A general modeling tool must be flexible enough to tailor the application to any existing or changing configuration.
- Be supported by an organization which provides continued maintenance, enhancements, user support and technology transfer.

In the remainder of this paper, we present several of the major features of the RiverWare modeling software.

MODEL CREATION

Objects and Slots: The basic building blocks of a RiverWare river basin model are *objects* which represent the features of the river basin. The objects are represented by icons on the workspace which can be opened to show the list of *slots*, which are the variables associated with the physical process model equations for that feature. For example, all reservoirs have slots, among others, called Inflow, Outflow, Storage and Pool Elevation.

The user constructs the model on the graphical workspace by selecting objects from a palette, dragging the objects with the mouse onto the workspace, naming the objects, and linking them together. Objects are linked together to form the topology of the river basin using the graphical link editor. Specifically, a slot on one object is linked to a slot on another object. During the simulation, the solution process involves propagation of the information among objects via the links. Currently, the RiverWare palette contains the following objects and the main water quantity physical processes which they model in a river basin:

- *Storage Reservoir* - mass balance, evaporation, bank storage, spill;
- *Level Power Reservoir*- Storage Reservoir plus hydropower, energy, tailwater, operating head;
- *Sloped Power Reservoir* - Level Power Reservoir plus wedge storage for very long reservoirs;
- *Pumped Storage Reservoir* - Level Power Reservoir plus pumped inflow from another reservoir;
- *Reach* - routing in a river reach, diversion and return flows;
- *Aggregate Reach* - many Reach objects aggregated to save space on the workspace;
- *Confluence*- brings together two Inflows to a single Outflow as in a river confluence;
- *Canal* - bidirectional flow in a canal between two reservoirs;
- *Diversion* - diversion structure with gravity or pumped diversion;
- *Water User* - depletion and return flow from a user of water;
- *Aggregate Water User*- multiple Water Users supplied by a diversion from a Reach or Reservoir;
- *Aggregate Delivery Canal* - generates demands and models supplies to off-line water users;

- *Groundwater Storage Object* - stores water from return flows;
- *River Gage* - specified flows imposed at a river node;
- *Thermal Object* - economics of thermal power system and value of hydropower;
- *Data Object* - user specified data: expression slots or data for policy statements.

Data required by the model is entered into the slots, of which there are three basic kinds. *Time Series Slots* contain data at specified times. The slot manages the time keeping and generates the time series for the data. The default time series inherits the start time, end time and timestep size from the Run Control dialog unless the user configures the time series differently on the slot. *Table Slots* contain functional relationship data such as area-elevation-volume tables, or simple parameter data required by the model equations. *Scalar slots* are single values. Data can be entered into slots manually by typing the number into the slot dialog, or by file import which can import an entire timeseries or table of values at once. Values can also be imported through the Data Management Interface (DMI) utility, which is described in a subsequent section.

Units: All internal representation of slot values and computations is done in the default SI units. However, the user may enter and display values in any selected unit of a similar type. For example, the internal RiverWare unit for all slots with unit type of FLOW is cubic meters per second (CMS). The user units are specified in the GUI and can be set to any other FLOW unit, e.g., cfs, acre-feet per day, etc.

Methods: Each object has a list of User-Selectable Method Categories. For each one, a method must be selected for the detailed modeling equations used in the physical process model. (Methods are described in detail in the Engineering Methods section below.)

Run Control: The intended model run is set up on the Run Control dialog. The start time and end time and the timestep size of the run are specified. Timestep size ranges from hourly to yearly. There is no limit on the range of the runs. RiverWare currently supports dates from 1800 to 2300 A.D. This time range could be extended easily without additional memory usage or performance deterioration. The user also selects the solution type or “Controller” on this dialog. The list of slots and User Methods which appear are dependent on the controller selection.

Saving Models: Models are saved as text files. All data including the objects and their names, their topologic arrangement on the workspace, all input data in the slots, user units, method selections, run control selections, and all GUI settings are saved in the model file. The results of a model run are saved optionally.

ENGINEERING METHODS

The objects on the workspace represent features of the river basin. Methods on each object contain the physical process model for the feature. The methods are flexible in handling a variety of input/output combinations of the basic data. In addition, the specific equations and physical representation of the processes are variable to accommodate a wide range of timestep sizes, data availability and resolution requirements, and modeling preferences.

To accomplish this flexibility, each object has two basic types of methods. *Dispatch Methods* map the input/output configuration specified by the user to the correct solution algorithm. *User Select-*

able Methods are alternative model representations which are selected by the user through the graphical user interface (GUI). For example, all reservoir objects have many dispatch methods for solving the mass balance equations. If Inflow and PoolElevation are known, the dispatch method for solving for Outflow and Storage is invoked. In addition, the user may select from a number of Evaporation methods, each of which calculates the evaporation loss in the reservoir as part of the mass balance calculation.

This object-oriented modeling approach mirrors the object-oriented software implementation and both benefit from this technology. From a software perspective, the benefit is extensibility: new methods can be added and integrated quickly and easily. From a modeling perspective, the benefit is the flexibility gained by selecting the physical process modeling methods individually on each object. Since the methods are easy to add, it is possible to have a large selection which includes some methods which may be quite particular to how one agency models one site, but necessary to that organization for institutional reasons. Table 1 contains a few examples of RiverWare's objects and User Methods.

Table 1: Selected User Methods in RiverWare

Object Type	User Method Category	User Methods	
Reservoirs	Evaporation & Precipitation	No Evaporation Pan and Ice Evaporation Daily Evaporation	Input Evaporation CRSS Evaporation
	Spill	Unregulated Spill Regulated Spill Unregulated Plus Regulated	Regulated Plus Bypass Unregulated Plus Regulated Plus Bypass
Power Reservoirs	Power	Plant Power Unit Generator Power	Peak Base Power LCR Power
	Tailwater	Tailwater Base Value Only Tailwater Base Value Plus Lookup Table	Tailwater Stage Flow Lookup Table Tailwater Compare Hoover Tailwater
Reaches	Routing	No Routing Time Lag Routing Variable Time Lag Routing SSARR	Muskingum Kinematic Wave Muskingum-Cunge MacCormack
Water User (on AggDiversion)	Return Flow	Fraction Return Flow Proportional Shortage	Variable Efficiency

In addition to water quantity modeling, RiverWare provides several options for water quality calculations. The user may select to model dissolved solids only, temperature only, or combinations of these and dissolved oxygen. If modeling total dissolved solids only, a simple, well-mixed model is available. Temperature and DO models use a 2-layer reservoir model and discretized reaches in which the water quality equations are coupled with hydraulic routing, either with or without dispersion.

A special object on the palette is the Thermal Object. This object evaluates of the avoided costs from replacement of thermal power by hydropower.

MULTIPLE SOLUTIONS AND CONTROLLERS

Alternative approaches to modeling multi-objective river basins have been developed, discussed and debated by water management agencies and academicians over the years. RiverWare endeavors to provide both prescriptive and descriptive techniques which are easy to formulate, analyze and apply to real planning and operations problems. Three fundamental solution methods are provided in RiverWare: simple simulation, rulebased simulation, and optimization. The first allows straight-forward scenario runs in which user-supplied inputs drive the solution. In the other two solution techniques, operational policies drive the solution. All operational policies are part of the input data set to permit easy modification and evaluation. In addition, the user may track water ownership by creating a network of water accounts in parallel with the river basin topology, and solve the accounting network independently of the simulation. The specific details of these solution methods have been designed and implemented to assure ease of use in solving a broad range of modeling application problems.

Simulation: Pure simulation solves a uniquely and completely specified problem. Each object must have enough information to invoke and solve a Dispatch Method, but may not have too much information. The solution is based on an object-oriented modeling paradigm: each object waits until it has enough information to solve, then it executes its Dispatch Method. The Dispatch Method solves for the unknown slots on the object, and information is propagated across links to other objects. Too much (conflicting) information results in an error state and termination of the run. Not enough information results in parts of the model left unsolved. In the cases where there are multiple links between objects, i.e., the boundary conditions are solved mutually by the two objects, the objects iterate until a solution meets the convergence criteria or the maximum iteration count is exceeded.

Although the simulation clock advances forward in time, the objects may solve for any timestep whenever they receive new information at that timestep. This allows some flexibility in specifying models where the solution is not propagating from upstream to downstream and forward in time. River reaches with time lags may solve for inflow given outflow, setting the inflow value at a previous timestep and propagating that value upstream. In addition, target operations on reservoirs may be specified, where a future target storage is met by adjusting the reservoir's outflow over a specified timeframe.

Rulebased Simulation: Whereas in pure simulation the model is exactly specified, in rulebased simulation there is not enough information on the objects to solve the system. The additional information is added by prioritized policy statements (rules) which are specified by the user, interpreted by the rule processor and which set slot values on the objects based on the state of the system. The rules themselves are basically if-then constructs which examine the state of system (functions of values of slots on the objects) in the antecedent (if) clause and then set slot values depending on that state. The rule set is global in that each rule has a unique priority even though it may pertain to only one or a few objects.

The rules are expressed through the graphical Structure Editor which helps the user formulate syntactically correct statements. The rule language permits the creation of functions which may perform complicated calculations to support the decisions made by the rules. The rule statements are parsed and interpreted, and the instructions are then executed by the Rule Processor.

The interaction between the simulation and the rules at each timestep is as follows. The model simulates until all objects have executed all the Dispatch Methods they can, given the user inputs. Then the Rule Processor fires the highest priority rule. The rule may fail if some of the slot values it needs are not yet set, or if it tries to overwrite values set by a higher priority rule. If the rule fails, the next highest priority rule is fired, and so on until a rule is successfully executed and new slot values are set on the model. After a rule fires, it is taken off the list of currently active rules until any of its dependencies (slots it accesses in the antecedent clause) change. After the rule fires, the simulation continues until it has solved everything it can, then the Rule Processor is invoked again. This continues until there are no more rules which can fire at that timestep, then the clock advances and the next timestep is executed. Just as in pure simulation, there is no guarantee of a solution. RiverWare provides diagnostic tools, however, to aid the analyst in understanding which rules successfully fired, as well as which objects dispatched which methods.

Optimization: RiverWare's optimization utilizes pre-emptive goal programming, using linear programming (LP) as an engine to optimize each of the prioritized goals input by the user. The optimal solution of a higher priority goal is not sacrificed in order to optimize a lower priority goal. The goals are input by the user through the graphical Constraint Editor tool. Each goal can be either a simple objective, or a set of constraints which is turned into an objective to minimize the deviations from the constraints. RiverWare accesses the CPLEX mathematical programming subroutine library for the solving engine.

One of the challenges of optimizing river basin operations using LP is representing the nonlinear processes. RiverWare provides automatic linearizing of nonlinear variables. The user may formulate goals or constraints on a wide range of model variables (slots). The underlying optimization software reformulates the objective as a linear expression in the basic decision variables. The nonlinear relationships are represented by table data entered by the user. The advanced user can select alternative linearization techniques and parameters which result in more accurate linearizations. RiverWare's optimization software also takes advantage of the basic model data available in the objects and links on the workspace to automatically generate the physical constraints of the system which reflect the mass balance, continuity and upper and lower bounds of the variables. These automatic features in RiverWare's optimization software allow the user to focus on expressing the policy in the goals, and make it possible for water resources engineers without an optimization background to generate and solve an appropriate goal programming formulation.

In addition to policies governing flows, elevations, spill and other variables in the physically-based model, power economic objectives may be brought into the analysis through methods developed on the Thermal Object. The user may specify an objective which involves maximizing the avoided thermal cost from hydropower generation. The economic value represents a trade-off of the value of immediate hydropower generation against future expected value of water in storage. The current value of hydropower is defined as the avoided costs of thermal power resulting from the addition of hydropower to the overall power mix. As the most expensive thermal units are replaced by hydropower, the marginal cost of power generation decreases.

When the optimization run is made, the physical constraints are generated and sent to the solver as the highest priority objective. Then each user-specified goal is interpreted, linearized, and solved. For each goal, the solutions of the higher priority objectives are maintained as constraints. The optimization solution, the values of the decision variables, are returned from CPLEX and entered

into the slots on the object. After an optimization run, the user can set up a post-optimization simulation run which automatically enters the optimal reservoir release schedule as inputs in the simulation and solves for storages, elevations, hydropower, etc. The simulation can be used to refine the optimization output.

Water Accounting: Water Accounts are created by the user on the objects. The sources of water to fill the accounts are supply links from other accounts and slots such as those which provide Hydrologic Inflow to the objects. Storage Accounts, Flow Accounts and Diversion Accounts all represent legal accounts in a water rights system. Pass-through accounts are created to keep track of the ownership of water in transit in the system.

In the initial prototype implementation of the water accounting system, the accounts calculate their balances as water is transferred from one account to another through the supply links. The account network solution behaves much like a spreadsheet in that it immediately updates the balances as data is entered. This allows for the accounting of water in an "after-the-fact" model. Future development will allow for prescriptive solutions of the network based on operations and water priorities.

Controllers: RiverWare's "controllers" are the software mechanisms for directing the model solution. The software architecture was designed to support any number of controllers. The controllers parallel the solution methods, but can also manage a combination of solutions. Currently the following controllers can be selected by the user on the graphical Run Control dialog where the user also specifies the begin and end dates of the run, and the timestep size.

- Simulation - can be run with or without Water Quality. Water Quality can be run in-line (at the end of each timestep) or post-process (at the end of the run).
- Rulebased Simulation - manages the interaction of the simulation with the Rule Processor. Water Quality can be coupled with rulebased simulation only in post processing mode.
- Optimization - pre-emptive linear goal programming solution; automatically sets up the post-optimization simulation if the controller is switched to "Simulation" after an optimization run.
- Accounting - executes accounting methods and solves accounts; currently this controller should be selected as a post-processor after a simulation run has been completed;
- Rulebased Simulation / Accounting InLine - solves each timestep for rulebased simulation then accounting, allowing the operational rules to access the previous timestep's accounting values.

DATA MANAGEMENT INTERFACE

The successful application of any model for operational scheduling requires the model's data to be updated quickly and easily to reflect current data such as real-time measurements, inflow forecasts, scheduled hydroplant operations, and special operations. For a general modeling tool, the data communications must be possible regardless of the specific database application or the sources of other data. Similarly, planning studies often require a large number of runs with varied data which may come from other sources such as historical databases. Automatic importing and exporting of data can be achieved through RiverWare's Data Management Interface utility.

The Data Management Interface (DMI) in RiverWare provides the means of using external programs to automatically load data into RiverWare. These routines are written by the user or the user's organization in any programming language and invoked through the RiverWare GUI.

Scenario-based DMI's execute a suite of individual routines to bring many data sources together into the model. The DMI can also be used to advance the run control start and end times.

MODEL ANALYSIS AND SCENARIO MANAGEMENT

The RiverWare modeling environment is designed to give the user the tools needed to build and run simulations to meet the needs of scheduling and planning activities. This is achieved through graphical user interface tools including the following:

- **Simulation Control Table:** a spreadsheet-like display of the data from a RiverWare model. The user constructs and configures an SCT, and can construct as many as needed to display various combinations of data. These can be iconified and brought up as different views on the model are needed. The SCT is interactive in that the user can specify inputs, run the simulation, and view the output from this interface.
- **Diagnostics:** information to assist the user in analyzing modeling problems during runs goes to an output dialog that saves the messages and offers searching and browsing features. The user may filter the information according to object, slot, time, etc. Warnings and errors are always displayed.
- **Dispatch Info Table:** a graphical tool showing what methods each object executed at each timestep and which slots were known and unknown. This is helpful to analyze over/under determination problems in simulation.
- **Expression Slots:** slots on the Data Object which hold user-defined expressions which are algebraic combinations of other slots, e.g., sum of all hydropower generation in the basin.
- **Plotting:** individual slots can be plotted quickly by selecting one button. Graphs with plot of many slots and/or many runs can be configured by the user. Plot set-ups can be saved.
- **Snapshot Manager:** the values of selected slots can be saved in this special data object for successive runs. If plotting the values, the new traces automatically are added to the plots. These data can also be accessed by the expression slots, the SCT and other output forms.
- **Multiple Run Management:** Many runs can be set up and executed in advance, automatically changing slot data or policies between runs. The runs can all have the same start/end times or be sequential. An Index Sequential setting on selected slots automatically permutes a series of historic data set as specified by the user (useful in using historic inflow data for planning studies).
- **Excel Writer:** a utility that takes outputs from RiverWare runs and creates an Excel input file for user-specific post-processing analysis.

TECHNOLOGY TRANSFER

RiverWare is under continued development at CADSWES, with new versions released several times a year. User support is provided to sponsors, and a web-based bug-tracking facility allows users to log problems directly. It is the intention of CADSWES and the sponsors to maintain the software in the future and provide enhancements as requested. In addition, formal training sessions are given at CADSWES. A three-day introductory training session is available, and new training courses for Rulebased Simulation and Optimization are anticipated.

RiverWare is a c++ application which runs on a Sun workstations under the solaris 2.3 (or greater) operating system.

INDEX

<i>Allison, Rebecca R. – Development of an Unsteady Flow Hydraulic Model of the Lower Missouri River</i>	<i>6-65</i>
<i>Alonso, Carlos V. – Simulating Sedimentation in Salmonid Redds</i>	<i>8-1</i>
<i>Altier, L.S. – The Riparian Ecosystem Management Model (REMM): Plant Growth Component</i>	<i>1-33</i>
<i>Ascough, James C. II – Economic and Environmental Strategic Planning for the Whole Farm and Ranch: The GPFARM DSS</i>	<i>1-127</i>
<i>Babayan, A. V. – Modeling Substance Spreading in 2-D (in plane) Steady Stream</i>	<i>6-73</i>
<i>Bales, Jerad D. – Dynamic Modeling of Water-Supply Reservoir Physical and Chemical Processes</i>	<i>2-61</i>
<i>Binger, Ronald L. – AnnAGNPS Input Parameter Editor Interface</i>	<i>8-15</i>
<i>Bingner, Ronald L. – Internet-Based Decision Support Systems of Hydrology Tools for Wetland Determination</i>	<i>8-9</i>
<i>Bonner, Vernon – HEC-RAS (River Analysis System)</i>	<i>5-1</i>
<i>Bosch, D. D. – Erosion and Sediment Transport Through Riparian Forest Buffers</i>	<i>3-31</i>
<i>Bowie, Randy – CCHE2D: A Two-dimensional Free Surface Flow and Sediment Transport Model for Natural Rivers</i>	<i>8-19</i>
<i>Bullard, Kenneth L. – Boise Five Mile Drain - Future Flooding and Old Canal Crossings</i>	<i>7-33</i>
<i>Burke, T.T., Jr. – Investigation of Physical Mechanisms Underlying the Predictability of Droughts</i>	<i>4-1</i>
<i>Carl, Robert – Next Generation Flood Damage Analysis Program</i>	<i>5-9</i>
<i>Chang, Tiao J. – Applications of GIS for a Drought Study</i>	<i>4-9</i>
<i>Charley, William J. – Hydrologic Engineering Center NEXGEN Data Storage System (HEC-DSS)</i>	<i>5-33</i>
<i>Chen, C. C. – Using GIS and AgNPS Model to Study the Water Resources Conservation of Nan-Haw Reservoir Watershed in Taiwan</i>	<i>1-1</i>
<i>Chen, Songsheng – Modeling on Closure Discharge of the Main Stream of TGP</i>	<i>2-1</i>
<i>Chen, Wilson Huaisheng – Equivalent Rectangle Simplification (ERS) Method and Its Application in a Distributed Hydrologic Model</i>	<i>7-41</i>
<i>Chen, Zhiming – A Conceptual Monthly Rainfall Runoff Model</i>	<i>7-89</i>
<i>Cheng, Haiyun – An Analytical Diffusion Model and Its Application to Water Level Forecast</i>	<i>6-81</i>
<i>Cheng, M.S. – Landscape Assessment of Wetland Functions (LAWF): A GIS Model for the Evaluation of Wetland Functions</i>	<i>7-97</i>
<i>Conrads, Paul A. – Effects of Model Output Time-Averaging on the Determination of the Assimilative Capacity</i>	<i>2-93</i>
<i>Croley, Thomas E., II – Great Lakes Advanced Hydrologic Prediction System</i>	<i>6-1</i>
<i>Cronshey, Roger G. – AnnAGNPS -Non-Point Pollutant Loading Model</i>	<i>1-9</i>
<i>Davidson, P. – Watershed and River Systems Planning Model in the San Juan River Basin, Colorado</i>	<i>5-65</i>
<i>Davinroy, Robert D. – Remote Sensing of Detrimental Flow Conditions at Lock and Dam 24, Upper Mississippi River</i>	<i>7-1</i>
<i>Davis, Darryl W. – Modernizing the US Army Corps of Engineers Water Control Data System</i>	<i>6-9</i>
<i>Davis, Darryl W. – The HEC Nexgen Software Development Project</i>	<i>5-17</i>
<i>Denlinger, Roger P. – Robust Methods for Flood Routing Over Highly Irregular Terrain</i>	<i>6-89</i>
<i>Dieckmann, Ronald J. – Changing History at St. Louis – Adjusting Historic Flows for Frequency Analysis</i>	<i>4-31</i>
<i>DiLuzio, M. – The Combination of a Rainfall Event Model and a Continuous Simulation Model for a Better Assessment of NPS Pollution</i>	<i>1-135</i>
<i>Doe, William W. III – Spatially Distributed Modeling of the Hydrologic Effects of Mechanized Maneuvers on Military Training Lands</i>	<i>8-27</i>
<i>Dou, Xibing – An Alternative Methodology to Study Local Scour at Bridge Piers</i>	<i>3-1</i>
<i>Duizendstra, Don – The Necessity of Modeling Non-Uniform Sediment in an 1-D Morphological Model for a Gravel Bed and a Sand Bed River</i>	<i>3-63</i>
<i>Dziedzic, M. – Environmental Assessment of the Barigui River Watershed</i>	<i>2-101</i>
<i>England, John F. Jr. – A Comparison of Moments-Based Estimators for Flood Frequency Analysis That Incorporate Historical Information</i>	<i>4-37</i>
<i>Epstein, D. J. – Probabilistic Hydrologic Forecasting Methods and Tools</i>	<i>6-17</i>
<i>Evans, Tom – GIS Data Exchange for Hydraulic and Hydrologic Modeling</i>	<i>7-53</i>
<i>Evans, Tom – Standard Hydrologic Grid in Spatial Hydrologic Modeling</i>	<i>7-49</i>
<i>Fan, Shou-shan – Risk in Mitigating Hydrological Disasters</i>	<i>4-45</i>
<i>Feaster, Toby D. – Utilizing a Lagrangian-Eulerian Approach to Water-Quality Assessment of the Wateree River, South Carolina</i>	<i>1-41</i>

INDEX

<i>Feng, Xiangming – Effects of Hydraulic Projects in San-Hua Reach of the Yellow River to Floods and Runoff</i>	2-7
<i>Flerchinger, G. N. – The Simultaneous Heat and Water (SHAW) Model: A Research Tool for Management Decisions</i>	8-35
<i>Flug, Marshall – A Data Gathering Technique for River Resource Identification</i>	7-9
<i>Fripp, Jon B. – Sediment Transport Analysis of the Athens, Ohio, LPP and a Comparison of Two Corps Sediment Transport Computer Models</i>	3-9
<i>Fulp, Terrance J. – Watershed and River Systems Management Program: Current and Future Applications in the Bureau of Reclamation</i>	5-71
<i>Garbrecht, Jurgen – A GIS-Numerical Modeling Approach to Identify Regions with Suitable Water Resources for a Dual Crop Rotation</i>	1-49
<i>Garcia, Luis – Development of Water Quality Modeling Framework</i>	8-43
<i>Garen, David C. – Spatially Distributed Energy Budget Snowmelt Modeling in Mountainous Regions of the Western United States</i>	7-101
<i>Gee, D. Michael – Unsteady Flow Model for Forecasting Missouri and Mississippi Rivers</i>	6-97
<i>Geter, W. Frank – AnnAGNPS - RUSLE Sheet & Rill Erosion</i>	1-17
<i>Gu, Ying – Application of Simulating Method on the Regional Drought Analysis</i>	4-17
<i>Hayes, Richard J. – Large-Scale Reservoir System Modeling</i>	2-69
<i>Hess, Glen W. – Simulation of Selected Reservoir and River-Diversion Operations in the Truckee River and Carson River Basins, CA & NV</i>	2-29
<i>Holland, J. P. – Overview of Hydro-environmental Modeling and Simulation Systems for the U.S. Department of Defense</i>	5-41
<i>Holtschlag, D. J. – Estimating Ice-Affected Streamflow by Extended Kalman Filtering</i>	6-105
<i>Hsu, Shiang-Kueen – An Integrated Modeling for Water Resources Management Study in Taiwan</i>	1-57
<i>Huang, Wen-Cheng – Applicability of Decision Support System for Reservoir Operation in Taiwan</i>	2-37
<i>Hung, C. Y. – A Dynamic Model for Simulating the Long-Term Transport of Radionuclides from a Contaminated Land Surface to a Nearby Stream</i>	1-65
<i>Inamdar, Shreeram – The Riparian Ecosystem Management Model (REMM): Nutrient Dynamics</i>	1-73
<i>Inamdar, Shreeram – The Riparian Ecosystem Management Model (REMM): Evaluation of the Hydrology Component</i>	7-17
<i>Ishii, A. L. – Modeling System for Near Real-Time Flood Simulation for Salt Creek in Du Page County, IL</i>	8-51
<i>J. Izurieta D. – Water Quality Simulation in the Cazonas River, Mexico</i>	2-109
<i>Jackson, Thomas J. – Satellite Based Soil Moisture Measurement for Hydrologic Modeling</i>	7-107
<i>Jangaard, Loren – Additional Storage Study of Hanson Reservoir, Green River, WA</i>	2-77
<i>Jarrett, Robert D. – Paleoflood Investigations for Assessing Extreme Flooding for Elkhead Reservoir, Northwestern Colorado</i>	4-85
<i>Ji, Xuewu – Flood Disasters and the Three Gorges Projects on the Yangtze</i>	2-45
<i>Johnson, Billy E. – Development of a Storm-Event Based Two-Dimensional Upland Erosion Model (CASC2D-SED)</i>	3-39
<i>Johnson, Terry L. – Design of Channel Riprap Using Overtopping Flow Methods</i>	3-17
<i>Ke, Sujuan – Research on Ice Regime in Yellow River</i>	3-127
<i>Kelly, Glenn G. – Estimating Water Storage Potential in the Devils Lake Watershed Using High-Resolution, 7.5-min. USGS Digital Elevation Models</i>	7-57
<i>King, D. L. – River Operations Modeling in the San Juan River Basin</i>	5-79
<i>Kittle, John L. – A Modular Approach to interactive Watershed Modeling</i>	7-115
<i>Kjelds, Jesper T. – Flood Plain Management, Integrating Numerical Models and GIS</i>	8-59
<i>Klumpp, Cassie C. – Stable Channel Analysis of the Rio Grande in the Upper Reaches of Elephant Butte Reservoir</i>	3-71
<i>Knapp, H. Vernon – Application of a Continuous Simulation Watershed Model for Near Real-Time Flow Forecasting and Dam Operations</i>	6-25
<i>Kosky, James A. – Hydrologic Modeling of Tygart Lake for Dam Safety Assurance Evaluation Report</i>	4-53
<i>Kuhn, Gerhard – Precipitation Distribution Alternatives in Applying the Modular Modeling System in the San Juan River Basin, CO and NM</i>	5-85
<i>Lai, Chintu – A Comprehensive Flow Model for Flood Forecast/Hindcast for Tidal Reaches</i>	6-33

INDEX

<i>Lane, W. L. – Modeling of River Systems Using the SAMS Package</i>	8-65
<i>Langendoen, Eddy J. – Modeling of Long Term Changes of Unstable Streams</i>	3-79
<i>Larson, Lee – A Summary of the National Weather Service Advanced Hydrologic Prediction System Demonstration in Des Moines, IA</i>	6-41
<i>Larson, Roger – MODSIM Decision Support System for River Basin Water Rights Administration</i>	8-73
<i>Leavesley, G. H. – The Modular Modeling System (MMS) - The Physical Process Modeling Component of the WARSMF</i>	5-93
<i>Lee, Hong-Yuan – Numerical Simulations of Scour and Deposition in a Channel Network</i>	3-87
<i>Leput, Walter– Hildebrand Lock & Dam Sedimentation Problem and Solution</i>	3-95
<i>Levish, Daniel R. – Paleohydrologic Bounds and Low Probability Floods</i>	4-93
<i>Lin, H.C. Jerry – Surface Water and Groundwater Interaction Modeling of South Florida</i>	5-49
<i>Lins, Harry – The Watershed and River Systems Management Program - An Overview</i>	5-101
<i>Lowrance, R. – The Riparian Ecosystem Management Model: Simulator for Ecological Processes in Riparian Zones</i>	1-81
<i>Mach, Rodney – An Innovative Approach to Improving Water Quality Through Stormwater Management</i> ...	1-89
<i>Makar, Paula W. – Geomorphic Analysis of the Rio Grande San Acacia to the Narrows of Elephant Butte Reservoir</i>	3-103
<i>Malers, Steven – Implementing a Water Resource Planning Model Within The Colorado River DSS</i>	2-53
<i>Mao, Hongmei – Water Quality Modeling of Maopingxi Pollution Zone in Three Gorges Project Construction Zone</i>	2-117
<i>Marino, Laura – Hydrologic Forecast and Analysis Modeling (HFAM)</i>	8-81
<i>Markstrom, Eric J. – Probabilistic Forecasts in Multiobjective Analysis for Reservoir Operations</i>	2-85
<i>Markus, M. – Comparing Methods for Forecasting Total Summer Flows on Tributaries of the Colorado-Big Thompson System</i>	6-49
<i>Matthews, David – Integration of Quantitative Precipitation Forecasts with Hydrologic Models and River Basin DSS</i>	6-57
<i>Miller, William J. – A Computer Model to Predict Salmonid Fry Emergence</i>	2-125
<i>Naghetini, Mauro – The Relationship Between Extreme Rainfall Depths and Flood Volumes Under the Assumption of Exponentially-Tailed Probability Distributions</i>	4-61
<i>Nicholson, J. Patrick – Sustainable Soil, Water and Air Quality Mankind's Ultimate Challenge and Opportunity in the 21st Century</i>	1-95
<i>O'Connel, D.R.H. – Risk-Based Hydrology: Bayesian Flood-Frequency Analyses Using Paleoflood Information and Data Uncertainties</i>	4-101
<i>Oliveira, Maria da Gloria Braz de – Analysis of the Temporal Evolution of the Sediment Production of the Pampulha Watershed and Evaluation of the Reservoir Silting</i>	3-47
<i>Ostenaar, Dean A. – Paleohydrology: Long-Term Bounds on Unwarranted Extrapolation in Modeling</i>	4-109
<i>Parker, Nancy L. – PC HYDROSS Simulation System (PCHSS) A Graphical User Interface for the HYDROSS Model</i>	8-89
<i>Peck, Hilaire W. – Cowlitz River Flood Hazard Study</i>	4-69
<i>Peng, Meixiang – Preliminary Analysis of the Influence of Climate Changes in Current Decade on Water and Sediment in the Upper and Middle Yellow River</i>	3-135
<i>Peters, John C. – Hydrologic Modeling System (HEC-HMS)</i>	5-25
<i>Prasad, S. N. – Rain Infiltration into Cracking Soils</i>	7-123
<i>Preston, Stephen D. – Spatially Referenced Regression Modeling of Nutrient Loading in the Chesapeake Bay Watershed</i>	1-143
<i>Pridal, Daniel – Missouri River Forecast Model From Gavins Point Dam to Rulo, Nebraska</i>	6-113
<i>Qian, Yunping – Analysis of Characteristics of Flow and Sediment in the Yellow River</i>	3-143
<i>Quimpo, Rafael G. – Automatic Watershed Model Calibration with Geographic Information Systems</i>	7-65
<i>Randle, Timothy J. – Predicting Sediment Yield From Arid Drainage Areas</i>	3-55
<i>Richards, D.R. – Integration of Riverine, Estuarine, and Coastal Models into the Surface Water Modeling System</i>	5-57
<i>Richardson, J. R. – Reducing Local Pier Scour by Flow Redirection</i>	3-23

INDEX

<i>Rounds, Stewart – Using CE-QUAL-W2 to Assess the Ammonia Assimilative Capacity of the Tualatin River, Oregon</i>	2-133
<i>Sanchez, Viola – River Channel Changes Downstream of Cochiti Dam, Middle Rio Grande, New Mexico</i> ..	3-111
<i>Savabi, M. R. – Modeling Infiltration and Storm Runoff from Soils With Shrinkage Cracks</i>	7-131
<i>Schaffranek, Raymond W. – Simulation Model for Open-Channel Flow and Transport</i>	1-103
<i>Schornick, James – The U.S. Geological Survey Hydrologic Analysis Support Section Software Support Services for Hydrologic Modeling and Data Analysis</i>	8-95
<i>Schumann, Andreas H. – Spatially Distributed Hydrologic Modeling for Streamflow Simulation and Forecasting</i>	7-139
<i>Scott, John – Modeling with MODSIM: Klamath River Water Quantity for Protecting Fish and Other Resource Values</i>	8-103
<i>Shea, Conor – Alternatives Analysis for Reduction of Maintenance Dredging of a Tidal Inlet</i>	3-119
<i>Shenk, G. W. – The Chesapeake Bay Program Models</i>	1-111
<i>Slaughter, Charles W. – Hydrologic Modeling Approaches for Integrated Management of Stream Systems</i> ..	1-119
<i>Straub, Timothy D. – Comparison of Rainfall Records Collected by Different Rain-Gage Networks</i>	7-25
<i>Sun, G. – Modeling the Hydrology of Wetland-Upland Systems on a Flat Terrain in Florida</i>	7-147
<i>Theurer, Fred D. – AnnAGNPS - Reach Routing Processes</i>	1-25
<i>Thuc, Tran – Development and Application of a Mud Transport and Bed Evolution Model for Estuary</i>	2-141
<i>Thurman, Jane L. – Preparing the ARS Water Database for the Twenty-First Century</i>	8-111
<i>Truman, Clint – Influence of Rainfall Timing and Amount on Phosphorus Losses Associated with Runoff and Sediment - a GLEAMS Simulation</i>	1-151
<i>Vaccaro, J. J. – The Yakima River Basin Watershed and River System Management Program</i>	5-105
<i>Van Mullem, Joseph A. – Modeling Prairie Snowmelt Runoff</i>	7-155
<i>Vieira, Dalmo A. – FRAME - An Integrated Modeling System of Channel and Landscape Processes</i>	8-117
<i>Viger, R. J. – The GIS Weasel - An Interface for the Treatment of Spatial Information in Watershed Modeling and Water Resource Management</i>	7-73
<i>Walters, Roy A. – A Finite Element Model with Moving Boundaries: Application to Floods and Runup</i>	6-121
<i>Wang, Ling – Research on Flow Cut-outs in the Lower Yellow River</i>	2-13
<i>Webb, Jerry W. – ModClark Model Development, Muskingum River Basin, Ohio</i>	7-81
<i>Webb, Jerry W. – Regional Frequency & Extreme Event Analysis, Muskingum River Basin, Ohio</i>	4-77
<i>Weghorst, Paul – Using ARC/INFO to Process and Analyze Reservoir Hydrographic Survey Information</i> ..	8-125
<i>Williams, R. G. – Riparian Ecosystem Management Model (REMM): A Demonstration</i>	8-133
<i>Winer, Harley – UNET Model of Connected Estuaries in Coastal Louisiana</i>	6-129
<i>Wisbith, Stanley M. – Ohio River Division Real-Time Modeling/Forecasting System</i>	8-139
<i>Wood, Tamara – Using CE-QUAL-W2 to Assess the Effect of Reduced Phosphorus Loads on Chlorophyll-a and Dissolved Oxygen in the Tualatin River, OR</i>	2-149
<i>Wu, Reuy-Bean – Two-Dimensional Floodplain Modeling of Rivers in Taiwan</i>	6-137
<i>Xiong, Ming – A Comprehensive Summary on the Study of Flood Stochastic Simulation for Three Gorges Project</i>	2-21
<i>Xu, Jianhua – Inflow and Sediment Yield of the Yellow River Basin and Sediment Reduction through Water Conservation</i>	3-151
<i>Yang, Chih Ted – An Enhanced Generalized Stream Tube Model for Alluvial River Simulation</i>	8-143
<i>Zagona, Edith A. – RiverWare: A General River and Reservoir Modeling Environment</i>	5-113
<i>Zarriello, Phillip J. – Comparison of Nine Uncalibrated Runoff Models to Observed Flows in Two Small Urban Watersheds</i>	7-163
<i>Zhang, Xuecheng – The Application of Mean Value Generation Function Model in Regional Drought Research</i>	4-25